

**DISCLOSURE/CONFLICT OF INTEREST**

The ASBMR is committed to ensuring the balance, independence, objectivity and scientific rigor of all its individually sponsored or industry-supported educational activities. ASBMR receives its sponsorship of Continuing Medical Education through the Medical Education Collaborative (MEC). MEC is accredited by the Accreditation Council for Continuing Medical Education (ACCME) to sponsor continuing medical education for physicians. To ensure that this activity meets ACCME requirements, individuals who are in a position to control the content must disclose relationships with a commercial interest if the individual has the opportunity to affect CME content about the products or services of that commercial interest with which he/she has or has had a financial relationship within the past 12 months. Disclosure must be made by all planning committee members, speakers, authors, and others in a position to influence or control content. Failure to respond will make you ineligible to participate in the planning, development or delivery of content. This information will be disclosed to participants.

Disclosure should include any relationship that may bias one's presentation or which, if known, could give the perception of bias. These situations may include, but are not limited to:

**DISCLOSURE KEY**

- 1) Speaker's Bureau
- 2) Consulting Fees or other remuneration (payment)
- 3) Paid Research
- 4) Advisory Committee or other paid committee
- 5) Other

ABSTRACTS KEY	
1001-1300	Concurrent Oral Presentations
F#	Friday Plenary Poster Presentation
SA#	Saturday Poster Presentation
SU#	Sunday Poster Presentation
M#	Monday Poster Presentation
*(Asterisk)	Denotes Non-ASBMR Membership

## 1001

**Osteoblast-specific Deletion of *Lrp6* Reveals Distinct Roles for *Lrp5* and *Lrp6* in Bone Development.** C. R. Zylstra<sup>\*1</sup>, C. Wan<sup>\*2</sup>, K. K. VanKoeveering<sup>\*1</sup>, A. K. Sanders<sup>\*1</sup>, C. Lindvall<sup>\*1</sup>, T. L. Clemens<sup>2</sup>, B. O. Williams<sup>1</sup>. <sup>1</sup>Van Andel Research Institute, Grand Rapids, MI, USA, <sup>2</sup>University of Alabama Birmingham, Birmingham, AL, USA.

Mutations in the Wnt co-receptors *Lrp5* and *Lrp6* produce striking alterations in bone mass in both humans and mice, but precisely how these co-receptors mediate Wnt actions is unclear. Wnt ligands activate several signaling cascades, including the canonical pathway that inhibits APC-mediated degradation of Beta-catenin. Previously, we found that mice carrying conditional deletion of Beta-catenin in mature osteoblasts developed severe osteopenia accompanied by increased osteoclastogenesis. *Lrp5*-deficient mice have low bone mass, but are viable and fertile and do not exhibit alterations in osteoclast function. One potential explanation for these differences is that the highly related *Lrp6* might exert overlapping, or distinct, roles in bone development. Consistent with this, we previously found that mice carrying global mutations in both *Lrp5* and *Lrp6* display synergistic deficiencies in bone mass. However, the fact that these mutations were present in all cells of these mice did not allow us to unambiguously determine that these effects were due to altered regulation of osteoblasts. To gain insight into this question, we created mice carrying a conditional allele of *Lrp6* (*Lrp6*-flox). Offspring from matings of these mice with mice expressing Cre recombinase driven by the human osteocalcin promoter (OC-cre) have significantly lower bone mass demonstrating that *Lrp6* is required for the normal bone acquisition. When the OC-*Lrp6*-flox/flox mice are mated with mice globally deficient in *Lrp5*, the offspring develop severe osteopenia and essentially phenocopied mice lacking Beta-catenin in osteoblasts (OC-cre;Beta-catenin-flox/flox mice); mice die within four weeks of birth displaying severe osteopenia associated with reduced bone formation and increased bone resorption. These findings suggest that both *Lrp5* and *Lrp6* are required to fully activate beta-catenin in mature osteoblasts and provide the first direct genetic evidence for a role of *Lrp6* in osteoblast differentiation and/or function.

**Disclosures:** B.O. Williams, None.

## 1002

**G171V and A214V *Lrp5* Knock-in Mice Have Increased Bone Mass and Strength, and Can Help Precisely Define the In Vivo Functions of *Lrp5* During Bone Growth and Homeostasis.** Y. Cui<sup>\*1</sup>, P. J. Niziolek<sup>\*2</sup>, A. G. Robling<sup>2</sup>, M. L. Warman<sup>\*3</sup>. <sup>1</sup>Genetics, Case Western Reserve University, Cleveland, OH, USA, <sup>2</sup>Department of Biomedical Engineering, Purdue University, West Lafayette, IN, USA, <sup>3</sup>Departments of Orthopaedics and Genetics, Children's Hospital Boston and Harvard Medical School, Boston, MA, USA.

Low-density-lipoprotein receptor-related protein 5 (LRP5), a co-receptor in the Wnt signaling pathway, modulates bone mass. In humans, loss-of-function mutations in LRP5 reduce bone mass, while certain missense mutations increase it. In contrast to several strains of *Lrp5* knockout mice, only one mouse with a missense mutation causing increased bone mass has been published. In this mouse, the human LRP5 receptor (G171V) was over-expressed using a type I collagen promoter fragment. Consequently, this transgenic mouse may not accurately reflect the effect of an endogenous mutation. Therefore, we created two strains of mice with *Lrp5* knock-in mutations (G171V and A214V). In these knock-in mice the mutated *Lrp5* alleles are expressed at the same level as their wild-type counterparts. We compared 4-month-old male knock-in mice to their wild-type relatives. In mice with G171V or A214V mutations we observed significant increases in skull thickness (90-102%), L5 vertebral BV/TV (40-65%) and Tb.Th (35-51%), and decreases in L5 vertebral Tb. Sp (18-22%), with no change in Tb.N. We also found significantly increased bone strength as determined by three-point femur bending tests. Stiffness, ultimate force, and energy to failure were increased in the mutant mice by 50-100%. Similar patterns were observed in females and in 1 and 2-month-old animals. We next looked at younger animals to determine when these differences began to emerge. At 4-days-of-life we found no difference in the timing of secondary centers of ossification by alizarin red/alcian blue staining, but histomorphometric measurements revealed differences in trabecular bone volume. When creating these knock-in alleles, we noticed that the allele acted as a hypomorph when the floxed Neo selection cassette remained intact. Therefore, by removing the selection cassette using Cre recombinase that is expressed at different stages of osteoblast development, we can determine when expression of the mutant receptor is necessary or sufficient to cause the increased bone mass phenotype. In summary, we have created two strains of *Lrp5* missense mutant mice that model the human high bone mass phenotypes and can provide novel insights regarding the precise role(s) of *Lrp5* in the development and homeostasis of the skeleton. These mice can also be used to look at the non-skeletal consequences of *Lrp5* missense mutations that may enhance Wnt signaling.

**Disclosures:** Y. Cui, None.  
This study received funding from: NIH

## 1003

**Transgenic Over-Expression of the Wnt Antagonist Kremen-2 in Osteoblasts Leads to Severe Impairment of Bone Formation and Increased Bone Resorption.** J. Schulze<sup>\*</sup>, S. Seitz, M. Schneebauer<sup>\*</sup>, M. Amling, T. Schinke. Center for Biomechanics and Skeletal Biology, Department of Trauma, Hand, and Reconstructive Surgery, University Medical Center Hamburg-Eppendorf, Hamburg, Germany, Hamburg, Germany.

Since the identification of *LRP5* mutations in patients with either osteoporosis or osteosclerosis, the Wnt signaling pathway is considered to be of hallmark importance in the regulation of osteoblast differentiation and function. *Lrp5* encodes a co-receptor for ligands of the Wnt family, and its deletion in mice results in decreased bone formation. Interestingly however, mice with an osteoblast-specific inactivation of  $\beta$ -catenin, the major intracellular mediator of Wnt stimulation, display normal bone formation, but increased bone resorption, thereby demonstrating that the regulation of Wnt signaling in osteoblasts is more complex than previously anticipated. In this study we analyzed the role of Kremen-2 (*Krm2*), a transmembrane protein serving as a receptor for molecules of the Dkk family that antagonize Wnt signaling through binding to *Lrp5* or *Lrp6*. We first analyzed the expression pattern of *Krm2* in tissues and primary osteoblasts and observed predominant expression in bone and non-mineralized osteoblasts, but virtually no expression in mineralized cultures. Since the latter observation was exactly the opposite as observed for *Dkk1*, we asked the question, whether the transgenic over-expression of *Krm2* under the control of an osteoblast-specific *Colla1* promoter fragment would result in decreased bone formation, as it has been described for *Dkk1*-transgenic mice. The histologic analysis of the *Colla1-Krm2* mice revealed a striking reduction of bone mass compared to wildtype littermates (BV/TV:  $2.7 \pm 0.7$  vs.  $12.8 \pm 4.1$  % at 24 weeks of age), leading to reduced biomechanical stability. Dynamic histomorphometry revealed that bone formation was almost completely abolished in the transgenic mice at the age of 6 weeks and thereafter (BFR/BS:  $18 \pm 11$  vs.  $112 \pm 24 \mu\text{m}^3/\mu\text{m}^2/\text{y}$ ). In addition, we observed a three-fold elevation of osteoclast numbers, demonstrating that bone resorption is also affected in *Colla1-Krm2* mice. We next isolated primary osteoblasts and found lower levels of  $\beta$ -catenin in transgenic cultures, resulting in a decreased production of Opg. Moreover, we failed to detect Wnt3-dependent phosphorylation of *Lrp6* in transgenic cultures, thereby suggesting that the striking differences between *Colla1-Krm2* and *Lrp5*-deficient mice may be due to an additional inactivation of *Lrp6*-dependent signaling by *Krm2*. Taken together, our data demonstrate that *Krm2* is a potent inhibitor of bone formation and a potential target for osteoanabolic therapy.

**Disclosures:** J. Schulze, None.

## 1004

**Deletion of the Dkk1 Co-receptors Kremen 1 and Kremen 2 in Mice Leads to Increased Bone Formation and Bone Mass.** H. Saito<sup>\*1</sup>, K. Ellwanger<sup>\*2</sup>, P. Clément-Lacroix<sup>\*3</sup>, E. Hesse<sup>1</sup>, N. Maltry<sup>\*3</sup>, J. Niedermeyer<sup>\*2</sup>, R. W. Lee<sup>\*2</sup>, G. Rawadi<sup>\*3</sup>, H. Westphal<sup>\*4</sup>, C. Niehrs<sup>\*2</sup>, R. Baron<sup>1</sup>. <sup>1</sup>Oral Medicine Infection and Immunity, Harvard School of Dental Medicine, Boston, MA, USA, <sup>2</sup>DKFZ, Heidelberg, Germany, <sup>3</sup>Galapagos, Romainville, France, <sup>4</sup>National Institute of Child Health and Human Development, Bethesda, MD, USA.

Kremen1 and 2 (*Krm1*, -2) and LRP5/6 are transmembrane co-receptors for Dickkopf1 (*Dkk1*), an antagonist of Wnt/ $\beta$ -catenin signaling, a pathway that is essential for bone formation and bone homeostasis. We and others have previously shown that *Dkk1* haploinsufficiency leads to increased bone formation and bone mass whereas overexpression leads to osteopenia. However, the physiological relevance of Kremens in mammals as Wnt modulators is unresolved and their role in bone remodeling is unknown. We therefore generated and characterized *Krm* mutant mice and found that double mutants show enhanced Wnt signaling. To clarify the role of Kremens on osteoblast (OB) differentiation, mutant and wild-type mice calvarial OBs were cultured for 21 days and the expression of OB differentiation markers (*Runx2*, *Osx*, and *ALP*) was analyzed at day 0 and 3 by quantitative RT-PCR. OB differentiation markers were increased in mice lacking both *Krm1* and *Krm2* at both time-points in a gene dose-dependent manner. In vivo, single deletion of *Krm1* or *Krm2* was not sufficient to induce significant changes in bone volume (BV) or BFR but the double knockout mice showed a marked and significant increase in trabecular BV. A detailed histomorphometric analysis showed that trabecular BV/TV and trabecular number (Tb.N) were significantly increased and trabecular separation (Tb.sp) was significantly decreased in *Krm1*-/- *Krm2*-/- mice. Bone formation parameters (osteoblast surface: Ob.S/BS, number of osteoblast: N.Ob/BS, osteoid surface: OS/BS, bone formation rate: BFR/BV, BFR/BS, BFR/TV and mineral apposition rate: MAR) were significantly increased in *Krm1*-/- *Krm2*-/-. Bone resorption parameters (osteoclast surface: Oc.S/BS, number of osteoclast: N.Oc/BS and eroded surface: ES/BS) showed only a trend towards reduction, indicating that the high bone mass was primarily due to an increase in bone formation. Most importantly, triple knockouts in which *Dkk1* was haploinsufficient failed to show significant changes in BV/TV above and beyond the *Krm1*-2 double knockouts. Thus, our study provides the first genetic evidence for a functional interaction of Kremens with *Dkk1* as negative regulators of Wnt/ $\beta$ -catenin signaling and trabecular bone formation.

**Disclosures:** H. Saito, None.

## 1005

**Deletion of the Wnt Signaling Antagonist Secreted Frizzled Related Protein 4 (sFRP4) in Mice Induces Opposite Bone Formation Phenotypes in Trabecular and Cortical Bone.** H. Saito<sup>\*1</sup>, R. Hinkle<sup>\*2</sup>, D. Ebert<sup>\*2</sup>, C. Blanton<sup>\*2</sup>, N. Jaiswal<sup>\*2</sup>, L. Elenich<sup>\*2</sup>, D. Cody<sup>\*2</sup>, R. Baron<sup>1</sup>, G. Sabataskos<sup>2</sup>. <sup>1</sup>Oral Medicine Infection and Immunity, Harvard School of Dental Medicine, Boston, MA, USA, <sup>2</sup>Procter and Gamble Pharmaceuticals, Mason, OH, USA.

Both canonical and non-canonical Wnt signaling have been shown to increase bone formation rates (BFR) by increasing osteoblast (OB) proliferation, differentiation and activity. Consequently, components of the Wnt signaling pathway constitute potential drug target for osteo-anabolism. sFRP4 is a member of the sFRP family of Wnt inhibitors that functions as a Frizzled decoy receptor, antagonizing the activity of Wnt ligands and therefore, unlike Dkk1 and Sclerostin, suppressing both canonical and non-canonical pathway activation. To determine whether sFRP4 affected OB differentiation we transfected human Mesenchymal Stromal Cells (hMSC) with siRNA against sFRP4 *in vitro*. In the presence of BMP-2, down-regulation of sFRP4 mRNA expression in hMSCs resulted in a significant increase in alkaline phosphatase mRNA expression, suggesting that sFRP4 exerts a negative effect on OB differentiation. To further elucidate the role of sFRP4 *in vivo* we generated sFRP4 knock out mice. sFRP4 heterozygote (+/-) and homozygote (-/-) deficient mice are healthy, viable and develop normally. Femurs from male and female sFRP4 wild type, +/- or -/- mice were analyzed at 10, 22 and 44 weeks of age using uCT. A pronounced increase in trabecular bone (Tb) in sFRP4+/- and -/- mice was observed, with significant increases in bone volume (BV/TV) in the secondary spongiosa. Further investigation of the bone phenotype of the sFRP4 -/- revealed that the increase in Tb was associated with significant increases in Tb number and thickness and decreases in Tb separation. Static and dynamic histomorphometry further confirmed that this effect was due to increased OB differentiation and activity as demonstrated by significant increases in OB surface and number, mineralizing surface and mineral apposition rate (MAR). Consequently, at all ages and in both genders the BFR was increased over 250%. No changes were observed in bone resorption. Interestingly however, this marked increase in BFR and BV/TV in Tb was associated with a significant thinning of cortical bone in sFRP4+/- mice and an overall increase in the external diameter. The periosteal and the endosteal MAR were significantly reduced when in sFRP4+/- mice. Thus, deletion of sFRP4, which is expected to antagonize both canonical and non-canonical Wnt signaling, favors strongly BFR and BV/TV in Tb but may have opposite effects on cortical bone, at least in growing mice. This is in contrast with deletion of Dkk1 or Sclerostin which are expected to mostly activate canonical Wnt signaling.

**Disclosures:** H. Saito, Procter and Gamble Pharmaceuticals 3.

## 1006

**Mice Lacking the Wnt Receptor Frizzled-9 Display Osteopenia Caused by Decreased Bone Formation.** J. Albers<sup>1</sup>, M. Gebauer<sup>\*1</sup>, F. Friedrich<sup>\*1</sup>, J. Schulze<sup>\*1</sup>, M. Priemel<sup>1</sup>, U. Francke<sup>\*2</sup>, M. Amling<sup>1</sup>, T. Schinke<sup>1</sup>. <sup>1</sup>Center for Biomechanics and Skeletal Biology, Department of Trauma, Hand, and Reconstructive Surgery, University Medical Center Hamburg-Eppendorf, Hamburg, Germany, <sup>2</sup>Department of Genetics, Stanford University, Stanford, CA, USA.

The Wnt signalling pathway plays a key role in the regulation of bone formation, which is best underscored by the identification of mutations within the human *LRP5* gene causing either osteoporosis or osteosclerosis. *LRP5* encodes a co-receptor for ligands of the Wnt family, whose interaction with serpentine receptors of the Frizzled (Fzd) family is crucial for the initiation of intracellular signalling pathways. Thus, the identification of Wnt and Fzd family members specifically required for signalling in osteoblasts is one of the most important goals of current skeletal research. Using Affymetrix Gene Chip hybridization we observed that among the 10 known genes encoding Fzd receptors, only *Fzd9* is differentially regulated together with known osteoblast marker genes in primary mouse osteoblasts. To analyze, whether the expression of *Fzd9* in osteoblasts is required to regulate bone formation *in vivo*, we analyzed the skeletal phenotype of *Fzd9*-deficient mice. While we did not observe significant differences compared to wildtype littermates at the age of 6 weeks, our histomorphometric analysis at 24 and 72 weeks of age revealed a more than 40 % decrease of the trabecular bone volume in the *Fzd9*-deficient mice. Dynamic histomorphometry further revealed that this osteopenia is explained by a 50 % reduction of the bone formation rate, while bone resorption is unaffected. Likewise, *Fzd9*-deficient calvarial osteoblasts display a decreased rate of proliferation and a delayed matrix mineralization compared to wildtype cultures. Thus, to identify potential downstream targets of Wnt signalling in osteoblasts, we performed Affymetrix Gene Chip hybridization using wildtype and *Fzd9*-deficient cultures. In line with observations from *Lrp5*-deficient mice, we did not observe major changes in the expression of well-established osteoblast marker genes, such as *Runx2*, *Osteocalcin* or *Bone Sialoprotein*. We did however identify more than 200 genes, whose expression was reduced at least 2-fold in the absence of *Fzd9*, thereby suggesting that some of them may be relevant in the regulation of bone formation. Taken together, given the striking similarities between *Lrp5*- and *Fzd9*-deficient mice, our data suggest that *Fzd9* is one of the relevant Wnt receptors in osteoblasts, at least in mice. Since serpentine receptors are considered to be excellent drug targets, we believe that these data are also of immediate clinical relevance.

**Disclosures:** J. Albers, None.

## 1007

**Dlk1/FA1 Is a Novel Factor Enhancing Osteoclastogenesis and Inhibiting Bone Formation *in vitro* and *in vivo*.** B. M. Abdallah<sup>\*1</sup>, N. Ditzel<sup>\*1</sup>, G. A. Traustadottir<sup>\*1</sup>, A. F. Schilling<sup>\*2</sup>, M. Amling<sup>\*3</sup>, M. Kassem<sup>1</sup>. <sup>1</sup>Endocrine Research Laboratory (KMEB), Odense University Hospital, Odense, Denmark, <sup>2</sup>Center for Biomechanics, University Medical Center Hamburg, Hamburg, Germany, <sup>3</sup>Center for Biomechanics, University Medical Center Hamburg, Hamburg, Germany.

Dlk1/FA-1 (delta-like 1/fetal antigen-1) is a trans-membrane protein belonging to Notch family whose expression is known to modulate the differentiation signals of mesenchymal and hematopoietic stem cells in bone marrow. We have recently demonstrated an endocrine function of circulating soluble form of Dlk1 (named FA1) as an inhibitor of bone formation in adult mice. Here, we investigated the physiological role of gain and loss function of Dlk1/FA1 on skeletal remodeling using osteoblast-specific-Dlk1 over-expressing mice (Col1-Dlk1) and Dlk1-deficient mice. Interestingly, Col1-Dlk1 mice displayed growth retardation and significantly reduced total body weight and bone mineral density (BMD) by 30% and 23% respectively. The bone loss phenotype was due to the reduced trabecular bone volume fraction and the inhibitory effect of Dlk1/FA1 on bone formation rate. In contrast, Dlk1<sup>-/-</sup> mice displayed increased BMD and trabecular BV/TV fraction by 18% and 40% respectively. At cellular level, the total number of bone marrow (BM)-derived CFU-F as well as alkaline phosphatase positive (ALP+) CFU-F from Col1-Dlk1 mice were dramatically reduced compared to wild type mice (WT). In addition, FACS-sorted calvaria dlk1/FA1+ cells from Col1-Dlk1 mice displayed reduced *in vitro* osteoblast differentiation and impaired *in vivo* ectopic bone formation capacity. Histological analysis revealed increased bone resorption surfaces (stained positive for TRAP) in Col1-Dlk1 bones by 42% compared to WT. *In vitro*, higher osteoclast (OC) number and increased OC resorptive activity were observed in OC cultures derived from BM of Col1-Dlk1 compared to WT. Purified FA1 protein did not stimulate differentiation of BM cells into OC but osetoblastic-dlk1/FA1+ cells in co-culture system with BM cells, markedly increased the number of TRAP+ OC suggesting that dlk1/FA1 exerts its stimulatory effect on osteoclastogenesis via an osteoblast-mediated effects. In supporting to these data, our microarray analysis on osteoblastic dlk1/FA1+ cells vs WT control revealed marked stimulation of bone resorption-related inflammatory cytokines (approx. 33% of total up-regulated genes with >2 fold). In conclusion, our data demonstrate a novel role for Dlk1/FA1 in bone biology. Dlk1 exerts a dual role in bone remodeling: it inhibits bone formation and stimulates bone resorption and thus may function as resorption-formation "coupling factor".

**Disclosures:** B.M. Abdallah, None.

This study received funding from: Novo Nordisk

## 1008

**Twisted Gastrulation-Deficient Mice Exhibit Osteopenia through Enhanced Osteoclast Function.** J. Sotillo<sup>\*1</sup>, K. C. Mansky<sup>2</sup>, A. E. Carlson<sup>\*1</sup>, T. Schwarz<sup>\*2</sup>, B. MacKenzie<sup>\*3</sup>, E. Jensen<sup>\*1</sup>, A. Petryk<sup>\*4</sup>, R. Gopalakrishnan<sup>1</sup>. <sup>1</sup>Diagnostic and Biological Sciences, University of Minnesota, Minneapolis, MN, USA, <sup>2</sup>Developmental and Surgical Sciences, University of Minnesota, Minneapolis, MN, USA, <sup>3</sup>Pediatrics, University of Minnesota, Minneapolis, MN, USA, <sup>4</sup>Pediatrics and Genetics Cell Biology and Development, University of Minnesota, Minneapolis, MN, USA.

Bone morphogenetic proteins (BMPs), growth factors involved in skeletogenesis, are regulated by extracellular proteins like Twisted gastrulation (Twsg1). Using Twsg1-deficient (*Twsg1*<sup>-/-</sup>) mice, our goal was to assess the role of Twsg1 in postnatal bone homeostasis. Micro-CT analysis demonstrating the integrity of trabecular and cortical morphology showed severe reduction in bone of *Twsg1*<sup>-/-</sup> mice when compared to wild-type (WT) mice. Consistent with previous reports, *in vivo* and *in vitro* indices of osteoblast (OB) function, including mineral apposition rate and markers of OB differentiation (osteocalcin and alkaline phosphatase) assessed via qRT-PCR and ELISA were not significantly different between WT and *Twsg1*<sup>-/-</sup> mice. However, to our surprise, *Twsg1*<sup>-/-</sup> mice exhibit increased bone resorption compared to WT mice characterized by larger and increased number of osteoclasts (OCs), increased area of resorption pits and increased serum carboxy-terminal collagen crosslinks (CTX) and tartrate resistant acid phosphatase (TRACP 5b) levels. Furthermore, enhanced osteoclastogenesis *in vitro* was associated with upregulation of key genes involved in OC differentiation (nuclear factor of activated T-cells (NFATc1) and Cathepsin K) and enhanced precursor cell fusion as there was increased expression of dendritic cell-specific transmembrane protein (DC-STAMP), a molecule necessary for cell fusion, with concomitant increased nuclei number per multinucleated OCs. Interestingly, this phenotype is not due to altered ability of OBs to sustain osteoclastogenesis as both serum levels and gene expression of receptor activator for nuclear factor- $\kappa$ B ligand (RANKL) and osteoprotegerin were not different between genotypes. To see if the effects of Twsg1 deficiency could be reversed, *Twsg1*<sup>-/-</sup> OCs were treated with increasing concentrations of Noggin, a BMP antagonist. As expected, we observed dose-dependent attenuation of osteoclastogenesis, suggesting that (1) *Twsg1*<sup>-/-</sup> OCs exhibit enhanced BMP activity resulting in increased osteoclastogenesis and (2) during normal OC maturation, Twsg1 behaves as a critical BMP antagonist. Together, our results indicate that the osteopenia exhibited in Twsg1-deficiency is mediated through increased OC function and not through reduced OB activity. These novel findings suggest that by regulating BMP activity, Twsg1 is a key regulator of OC function.

**Disclosures:** R. Gopalakrishnan, None.

This study received funding from: NIH and University of Minnesota Academic Health Center.

## 1009

**In the Absence of NF- $\kappa$ B2, TNF Induces Osteoclast Formation *in vivo* Independent of RANKL/RANK and More Severe Arthritis in TNF-Tg Mice.** Z. Yao, L. Xing, B. F. Boyce. Pathology, University of Rochester, Rochester, NY, USA.

TNF plays a central role in bone loss following sex steroid deficiency and in rheumatoid arthritis. It induces osteoclast (Ocl) formation from Ocl precursors (OCPs) from RANKL $^{-/-}$  or RANK $^{-/-}$  mice *in vitro*, but not when it is administered to these mice *in vivo*; this discrepancy and why TNF induces fewer Ocls than RANKL *in vitro* remain unexplained, despite both of these cytokines activating NF- $\kappa$ B to induce Ocl formation. RANKL activates both the canonical and non-canonical NF- $\kappa$ B pathways, but TNF activates only the former. Activation of the latter pathway by RANKL leads to processing of the inhibitory NF- $\kappa$ B2 p100 protein to p52, which along with RelB goes to the nucleus to induce OCP differentiation. Here, we investigated the hypothesis that TNF induces NF- $\kappa$ B2 p100 expression to limit Ocl formation *in vitro* and *in vivo*. TNF induced strong p100 protein expression in RANK $^{-/-}$  or RANKL $^{-/-}$  OCPs *in vitro*, similar to wt cells, but RANKL did not. We generated RANK/nfkb2 or RANKL/nfkb2 double knockout (dKO) mice and found that TNF induced significantly more Ocls from their OCPs ( $436 \pm 17$  and  $442 \pm 23$ /well) *in vitro* than from wt cells ( $34 \pm 5$ /well), the maximal number reaching that of RANKL-treated wt cells ( $475 \pm 37$ ). TNF induced similar numbers of Ocls from TRAF6 $^{-/-}$  as from wt OCPs. We next injected TNF (0.5 $\mu$ g, twice daily for 5 d) over the calvaria of dKO and single RANK or RANKL KO mice. TNF induced only occasional Ocls in the RANK $^{-/-}$  and RANKL $^{-/-}$  mice, but importantly induced large numbers of actively resorbing ocls in the dKO mice. We generated TNF-transgenic (TNF-Tg)/nfkb2 $^{-/-}$  mice to determine the effect of absence of NF- $\kappa$ B2 on TNF-induced arthritis and osteoporosis. Arthritis occurred earlier and was more severe in the TNF-Tg/nfkb2 $^{-/-}$  than in TNF-Tg mice (inflammatory synovial tissue area  $0.28 \pm 0.09$  mm $^2$  vs.  $0.11 \pm 0.1$  mm $^2$ ; and Ocl number  $23.5 \pm 4.1$ /mm $^2$  vs.  $2.8 \pm 4.1$ /mm $^2$ ). TNF-Tg/nfkb2 $^{-/-}$  mice had significantly lower tibial cortical thickness ( $0.11 \pm 0.02$  mm vs.  $0.17 \pm 0.01$  mm) and trabecular bone volume ( $11.1 \pm 3.6$  % vs.  $15.8 \pm 3.8$  %) than TNF-Tg mice by  $\mu$ -CT analysis. Finally, TNF dose-dependently inhibited RANKL induced ocl formation from M-CSF-stimulated wt spleen and bone marrow cells ( $420 \pm 44$  vs.  $124 \pm 25$  and  $644 \pm 28$  vs.  $291 \pm 34$  per well). In summary, in the absence of NF- $\kappa$ B2, TNF induces ocl differentiation *in vivo* independent of RANKL-RANK-TRAF6 signaling and more severe arthritis and bone loss in TNF-Tg mice. We conclude that TNF-induced NF- $\kappa$ B2 p100 expression limits TNF and RANKL-mediated ocl differentiation and that p100 deficiency accelerates TNF-induced arthritis and bone loss. Thus, increasing NF- $\kappa$ B2 p100 levels in OCPs should limit bone loss in a variety of erosive bone diseases.

**Disclosures:** Z. Yao, None.

## 1010

**SLP-76 Couples Syk to the Osteoclast Cytoskeleton *in vitro* and *in vivo*.** J. Reeve<sup>1</sup>, W. Zou<sup>1</sup>, Y. Lu<sup>\*1</sup>, G. Koretzky<sup>\*2</sup>, F. P. Ross<sup>1</sup>, S. L. Teitelbaum<sup>1</sup>. <sup>1</sup>Pathology, Washington University in St. Louis, Saint Louis, MO, USA, <sup>2</sup>University of Pennsylvania, Philadelphia, PA, USA.

Optimal bone resorption requires organization of the osteoclast (OC) cytoskeleton into actin rings. These unique structures create a sealing zone between the cell surface and matrix, thereby isolating the resorptive microenvironment from the general extracellular space. Organization of the osteoclast cytoskeleton requires activation of the  $\alpha$ v $\beta$ 3 integrin, which in turn, forms a functional complex with a number of signaling molecules including the tyrosine kinase, Syk, and the guanine nucleotide exchange factor, Vav3. Both Syk and Vav3 are required for integrin-mediated OC spreading, actin ring formation and bone resorption. SLP-adaptor proteins (SLP-76 and BLNK) are Syk substrates in other hematopoietic cells and both contain Vav binding sites. We find that in OCs, integrin-engagement induces both SLP-76 and BLNK phosphorylation in a Syk-dependent manner, raising the possibility that SLP-76 or BLNK links Syk to Vav3 during integrin-mediated cytoskeletal reorganization. While BLNK $^{-/-}$  OCs are normal, SLP-76 $^{-/-}$  OCs exhibit retarded spreading and have decreased adhesion-induced Vav3 phosphorylation. Additionally, the ability of SLP-76 $^{-/-}$  OCs to resorb bone, *in vitro*, is reduced 2.3-fold, as measured by medium CTx. However, unlike Syk null OCs, those lacking SLP-76 retain some bone resorptive capacity *in vitro*, suggesting that another mediator, such as BLNK, also links Syk to the cytoskeleton. We confirmed such is the case by establishing that OCs lacking both BLNK and SLP-76 (DKO) have a substantially greater defect in spreading, actin ring formation and bone resorption than those deficient in only SLP-76. Furthermore, the defective DKO phenotype can be rescued by retroviral reconstitution with WT-SLP-76, but not SLP-76 in which three functional tyrosines are mutated to phenylalanine. Because absence of SLP-76 induces embryonic lethality we explored this issue *in vivo* by generating radiation chimera mice in which SLP-76 or SLP-76 and BLNK are absent in marrow cells. WT radiation chimeras served as control. Following marrow reconstitution, PTH(1-34) was injected to stimulate bone resorption. Confirming dysfunctional OCs, PTH-stimulated serum CTx in chimeric mice lacking only SLP-76, and those deficient in both SLP-76 and BLNK, was reduced 30% and 41%, respectively, relative to control. Collectively, both *in vivo* and *in vitro* studies demonstrate that SLP-76 plays an important role in OC function mainly through its role in cytoskeletal reorganization and is a potential anti-resorptive therapeutic target.

**Disclosures:** J. Reeve, None.

## 1011

**Cbl-PI3K Interaction Regulates Osteoclast Function, Differentiation and Survival.** N. Adapala\*, M. Barbe, M. Amin\*, F. Safadi, S. Popoff, A. Sanjay. Anatomy and Cell biology, Temple University, Philadelphia, PA, USA.

Cbl is an adaptor protein and an E3 ligase that plays both positive and negative roles in several signaling pathways that affect various cellular functions. Cbl has 22 tyrosines of which Y<sup>731</sup> is unique to Cbl (it is not present on Cbl-b, the other family member) and is phosphorylated by Syk and Src family kinases in response to growth factors, cytokines and integrin activation. Phosphorylated CblY<sup>731</sup> creates a binding site for the p85 regulatory subunit of phosphatidylinositol 3 kinase (PI3K) which also plays an important role in the regulation of actin cytoskeleton and bone resorption by osteoclasts. To further investigate the role of Cbl-PI3K interaction in bone homeostasis, we examined the knock-in mice (Cbl<sup>YF/YF</sup>) in which the PI3K binding site in Cbl is ablated due to the mutation in the regulatory tyrosine. Gross analyses revealed that the Cbl<sup>YF/YF</sup> mice are smaller in size than the wild type (WT) mice. The delayed growth was first apparent 3 days after birth; this trend continued for 2 weeks. The delay in growth occurred simultaneously with a lag in the growth of long bones. Histological analysis of the tibiae from 12 weeks old Cbl<sup>YF/YF</sup> mice showed that the amount of the cancellous bone was increased relative to the tibiae from the age matched WT mice. Histomorphometric analysis of the tibiae demonstrated an increase in the bone volume in the Cbl<sup>YF/YF</sup> mice as compared to the WT mice (WT,  $7.6 \pm 1.10$ ; Cbl<sup>YF/YF</sup>  $12.46 \pm 1.36$ ,  $p=0.001$  vs. WT). Interestingly, although the numbers of osteoclasts as compared to the WT mice were higher in Cbl<sup>YF/YF</sup> mice ( $WT\ 3.5/mm^2 \pm 0.7$ ; Cbl<sup>YF/YF</sup>  $7.5/mm^2 \pm 0.7$ ,  $p=0.029$  vs. WT), serum levels of C-terminal collagen telopeptide (CTX), a marker for osteoclast activity, were three fold less than in the WT mice ( $WT\ 1.8$  ng/ml  $\pm 0.5$ ; Cbl<sup>YF/YF</sup>  $0.66$  ng/ml  $\pm 0.12$ ;  $p=0.023$  vs. WT). This data suggest that Cbl<sup>YF/YF</sup> osteoclasts although more in numbers are inefficient in resorbing bone. Cbl and PI3K have been implicated in RANK-RANKL signaling, therefore to further investigate the role of Cbl-PI3K interaction, we examined *in vitro* osteoclast differentiation and survival in response to RANKL. Non-adherent bone marrow cells were cultured in the presence of 30ng/ml of M-CSF for two days and then with M-CSF and 50 ng/ml of RANKL. Two days after the addition of RANKL, 1.5-fold increase in multinucleated TRAP positive osteoclasts was seen in Cbl<sup>YF/YF</sup> cultures as compared to WT cultures in agreement with the *in vivo* data. Osteoclast survival in response to RANKL (50 ng/ml) was also enhanced 2.5-fold in the Cbl<sup>YF/YF</sup> osteoclasts as compared to WT osteoclasts. Cumulatively, these *in vivo* and *in vitro* results show that binding of Cbl to PI3K modulates osteoclast differentiation, survival and function.

**Disclosures:** A. Sanjay, None.

## 1012

**Wnt5a Regulates Osteoclast Differentiation in Physiological and Pathological Conditions.** K. Maeda<sup>\*1</sup>, Y. Kobayashi<sup>\*2</sup>, A. Ishihara<sup>\*2</sup>, N. Udagawa<sup>3</sup>, I. Takada<sup>\*4</sup>, S. Kato<sup>4</sup>, M. Nishita<sup>\*5</sup>, Y. Minami<sup>\*5</sup>, K. Marumo<sup>\*1</sup>, N. Takahashi<sup>2</sup>. <sup>1</sup>Department of Orthop. Surg., The Jikei Univ., Tokyo, Japan, <sup>2</sup>Institute for Oral Science, Matsumoto Dental Univ., Shiojiri, Japan, <sup>3</sup>Department of Biochemistry, Matsumoto Dental Univ., Shiojiri, Japan, <sup>4</sup>Laboratory of Nuclear Signaling, IMCB, Univ. of Tokyo, Tokyo, Japan, <sup>5</sup>Deptment of Physiology and Cell Biology, Kobe Univ., Kobe, Japan.

Wnts exert two types of signals,  $\beta$ -catenin ( $\beta$ -cat)-dependent (canonical) and  $\beta$ -cat-independent (non-canonical) pathways. The canonical pathway has been reported to suppress bone resorption due to up-regulation of OPG expression and suppression of RANKL expression in osteoblasts (OB). However, the roles of the non-canonical pathway in bone resorption are not elucidated. Here, we analyzed the effects of Wnt5a, a non-canonical Wnt ligand, on osteoclast (OC) formation *in vitro* and *in vivo*. (1) Wnt5a enhanced RANKL-induced OC formation from mouse bone marrow macrophages (BMM $\phi$ ). Wnt5a activated c-Jun N-terminal kinase and protein kinase C, but failed to increase the cytoplasmic accumulation of  $\beta$ -cat in BMM $\phi$ . (2) The role of Ror2, a co-receptor of Wnt5a, in OC formation was examined using short hairpin RNA interference. The knockdown of Ror2 abolished the stimulatory effect of Wnt5a on RANKL-induced OC formation in BMM $\phi$  cultures. (3) Semi-quantitative RT-PCR analysis revealed that the expression level of Wnt5a mRNA was much higher in OB than in BMM $\phi$ . (4) Addition of GST-soluble Ror2 (sRor2), a decoy receptor of Wnt5a, to BMM $\phi$  cultures also abolished the stimulatory effect of Wnt5a on RANKL-induced OC formation. sRor2 inhibited  $1\alpha,25$ -dihydroxyvitamin D $_3$  [ $1\alpha,25(OH)_2D_3$ ]-induced OC formation in co-cultures of OB and BMM $\phi$  in a dose-dependent manner. (5) The number of OC in the proximal portion of femora was significantly lower in Wnt5a $^{-/-}$  mice and Wnt5a $^{+/+}$  mice than in wild type (WT) mice at E18.5.  $1\alpha,25(OH)_2D_3$ -induced OC formation was significantly impaired in co-culture of WT-derived BMM $\phi$  and Wnt5a $^{-/-}$ -derived OB. The osteoclast formation was rescued when adding back Wnt5a to Wnt5a $^{-/-}$ -derived OB using a retrovirus expression system. These results suggest that Wnt5a secreted by OB promotes OC formation through Ror2. (6) Wnt5a has been shown to be expressed in rheumatoid arthritis (RA) synovium. We tested whether administration of sRor2 can prevent the bone loss associated with RA, using a type II collagen-induced RA model. Daily injection of sRor2 suppressed joint destruction and inhibited OC formation in the joint of RA mice. Taken together, our results suggest that Wnt5a is involved not only in physiological bone remodeling but also in pathological bone loss in RA.

**Disclosures:** K. Maeda, None.



## 1013

**$\beta$ -catenin Directly Binds to a Specific Intracellular Domain of PTH/PTHrP Receptor and Regulates the Signaling in Chondrocytes during Endochondral Ossification.** F. Yano<sup>1</sup>, U. Chung<sup>1</sup>, T. Ikeda<sup>1</sup>, Y. Kawasaki<sup>1</sup>, H. Kawaguchi<sup>1</sup>, H. A. W. Tawfeek<sup>2</sup>, M. J. Mahon<sup>2</sup>, G. V. Segre<sup>2</sup>, N. Ogata<sup>1</sup>.  
<sup>1</sup>Sensory & Motor System Medicine, Tissue Engineering, Univ. of Tokyo, Tokyo, Japan, <sup>2</sup>Endocrine Unit, MGH, Boston, MA, USA.

Although the PTH/PTHrP receptor (PTH1R) is known to be coupled to G $\alpha$ s and G $\alpha$ q pathways, involvement of other molecules that interact with the intracellular C-terminal domains in the signal transduction, cell surface localization, internalization, and recycling has been suggested. The present yeast two-hybrid assay to search for proteins that interact with the C-terminus has identified  $\beta$ -catenin, a critical regulator of cytoskeleton and canonical Wnt signaling. Further two-hybrid assays by deletion and mutagenesis in the C-terminus revealed that the region of amino acid sequence between L582 and W587 was essential for binding with  $\beta$ -catenin. Stably transfected GFP-labeled PTH1R in HEK293 cells was shown to be co-localized with endogenous  $\beta$ -catenin on the plasma membrane by immunocytochemistry. Immunoprecipitation / immunoblotting confirmed the physical association between PTH1R and  $\beta$ -catenin, which was decreased by PTH (1-34) treatment in the cells. The association was further shown to require binding of scaffolding peptides Axin and APC with the complex. The cAMP accumulation induced by PTH treatment was decreased by overexpression of constitutively-active  $\beta$ -catenin, whereas it was increased by knockdown of  $\beta$ -catenin by the siRNA. In addition, the cells overexpressing a PTH1R mutant with deletion of the  $\beta$ -catenin-binding region above enhanced the cAMP accumulation under the PTH stimulation. Finally, since PTH/PTHrP is known to be a crucial regulator of endochondral ossification by inhibiting hypertrophic differentiation of growth plate chondrocytes, we examined the involvement of the PTH1R /  $\beta$ -catenin signaling in chondrocyte differentiation. Immunohistochemical analyses of the mouse growth plate revealed that PTH1R and  $\beta$ -catenin, as well as Axin and APC, were co-localized mainly in the pre-hypertrophic chondrocytes. In cultured mouse chondrogenic ATDC5 cells transfected with luciferase-reporter gene construct containing the promoter of type X collagen (COL10), a representative marker of hypertrophic differentiation of chondrocyte, suppression of the COL10 transcriptional activity by PTH (1-34) treatment was abolished by the overexpression of constitutively active  $\beta$ -catenin. In addition, a decrease of endogenous COL10 mRNA level after the PTH treatment in ATDC5 cells was significantly restored by the constitutively active  $\beta$ -catenin overexpression. These lines of evidence provide a novel mechanism regulating the PTH/PTHrP signal through direct interaction of  $\beta$ -catenin with the C-terminus of the receptor in chondrocytes.

**Disclosures:** F. Yano, None.

## 1014

**PTH Signaling through LRP5/6 in Osteoblasts.** M. Wan<sup>1</sup>, C. Yang<sup>1</sup>, X. Wu<sup>1</sup>, J. Li<sup>1</sup>, H. Yuan<sup>1</sup>, X. He<sup>2</sup>, S. Nie<sup>1</sup>, C. Chang<sup>1</sup>, X. Cao<sup>1</sup>. <sup>1</sup>University of Alabama at Birmingham, Birmingham, AL, USA, <sup>2</sup>Harvard Medical School, Boston, MA, USA.

Recent studies demonstrated that PTH increased the expression level of  $\beta$ -catenin, a key component of the canonical Wnt pathway and a positive regulator of bone metabolism. Here we characterize a novel pathway through which PTH stabilizes  $\beta$ -catenin in osteoblasts. We found that PTH stimulated  $\beta$ -catenin-responsive luciferase reporter and enhanced the cytosolic abundance of  $\beta$ -catenin in UMR106 cells and mouse primary preosteoblasts. In both rat and mouse models, PTH single-dose treatment stimulated  $\beta$ -catenin expression within hours in most of the osteoblasts at trabecular bone. Importantly, treatment of preosteoblasts with conditioned medium containing Fz8CRD, a competitive inhibitor of Wnt, did not inhibit PTH-induced  $\beta$ -catenin stabilization. The results suggest the effect of PTH is not through sensitizing Wnt-stimulated signaling. To determine the mechanism underline this phenomenon, we found that PTH induced the formation of ternary complex of PTH ligand, PTH1R and LRP5/6 by immunoprecipitation assays, in vitro pull down assays and photo-bleaching based FRET approach. PTH-induced recruitment of LRP5/6 resulted in rapid phosphorylation LRP5/6, which is required for the subsequent binding of Axin to LRP5/6. In rats, PTH stimulated phosphorylation of LRP5/6 in osteoblasts at trabecular bone in 30 minutes and peaked at 8 hours after single-dose injection. We then examined the effect of sclerostin, an inhibitor of LRP5/6, on PTH-activated LRP5/6- $\beta$ -catenin signaling. Treatment of the cells with conditioned medium containing sclerostin dramatically inhibited PTH-induced LRP6/axin binding, indicating sclerostin is also an antagonist for PTH signaling. Interestingly, PTH, but not Wnt3a, single-dose treatment in mice suppressed the expression of sclerostin in osteocytes. The results implicate that PTH-suppressed sclerostin serves as a positive feed back for PTH-activated  $\beta$ -catenin signaling pathway. Mouse models of long term PTH administration were also analyzed. Levels of both  $\beta$ -catenin and phosphorylated LRP5/6 were significantly increased in the osteoblasts of trabecular bone sections when PTH was intermittently administered, but neither  $\beta$ -catenin nor phosphorylated LRP5/6 level was stimulated with continuous PTH treatment. These findings reveal a novel signaling pathway of PTH and also provide alternative interpretations of the effects of LRP5/6 and  $\beta$ -catenin on bone formation, which until now have been considered to affect the canonical Wnt signaling pathway exclusively.

**Disclosures:** M. Wan, None.

## 1015

**Parathyroid Hormone Stimulates Hematopoiesis and Increases Survival in Irradiated Mice.** Z. Zhang<sup>1</sup>, B. Li<sup>1</sup>, C. Fu<sup>1</sup>, X. Wang<sup>1</sup>, J. Tong<sup>1</sup>, D. Miao<sup>2</sup>, M. Qiu<sup>3</sup>. <sup>1</sup>Public Health School, Suzhou University, Suzhou, China, <sup>2</sup>Institute of Dental Research, Nanjing Medical University, Nanjing, China, <sup>3</sup>Department of Endocrine, General Hospital, Tianjing Medical University, Tianjing, China.

The mechanisms of bone and blood formation have traditionally been viewed as distinct, unrelated processes, but evidence suggests that they are interrelated. Based on observations that hematopoietic precursors reside close to endosteal surfaces, it was hypothesized that osteoblasts are a key component in the regulation of the hematopoietic stem cell (HSC) niche, and it has been shown that osteoblasts produce many factors essential for the survival, renewal, and maturation of hematopoietic stem cells (HSCs). It has been reported that hematopoiesis is severely altered in mice with an induced osteoblast deficiency. Parathyroid hormone (PTH) has been approved for the treatment of osteoporosis because it is highly effective stimulating bone formation and reducing fractures. In this study, we sought to determine whether PTH administration could enhance the hematopoietic recovery and survival of irradiated mice. C57Bl/6 male mice were exposed to sublethal and lethal doses of irradiation and human PTH (1-34) (80microgram/kg) was subsequently injected intraperitoneally once daily for four weeks in these mice. Whole blood was collected from the tails of mice on sequential days following irradiation and the blood cell numbers were determined by a hematocyte counter. Bone marrow progenitors were studied by determining colony forming units and hematopoietic stem cells were studied using the exogenous spleen colony assay. Histology and immunohistochemistry were also performed in tibia. PTH treatment facilitated the recovery of circulating white blood cell and platelet counts following radiation exposure. PTH-treated mice also demonstrated accelerated bone marrow cellular recovery, radioprotection of bone marrow progenitors and enhanced stem cell survival following irradiation compared with controls. In addition, increased staining of alkaline phosphatase, N-cadherin and osteopontin were found in sections of tibias from PTH treated mice and significantly increased mRNA expression of SDF-1 and VEGF in femurs. Remarkably, 60% of PTH-treated mice survived 1 month following 10Gy  $\gamma$ -ray exposure, which was 100% lethal in vehicle-treated mice. These data suggest that PTH, using a dosing schedule known to increase osteoblasts, can improve the hematopoietic recovery and survival of irradiated mice. PTH alteration of the bone marrow microenvironment might underly this effect.

**Disclosures:** Z. Zhang, None.

## 1016

**Knockout of the Parathyroid Hormone -Related Protein (PTHrP) Gene in Breast Cancer Cells Inhibits Tumor Progression and Metastatic spread in vivo: Modulation of Cell proliferation, Apoptosis and Angiogenesis Markers.** J. Li<sup>1</sup>, A. Karaplis<sup>2</sup>, P. M. Siegel<sup>3</sup>, W. J. Muller<sup>3</sup>, R. Kremer<sup>1</sup>. <sup>1</sup>Calcium Research Laboratory, McGill University, Montreal, QC, Canada, <sup>2</sup>Sir Mortimer B. Davis Jewish General Hospital, Montreal, QC, Canada, <sup>3</sup>Biochemistry, McGill University, Montreal, QC, Canada.

Previous studies suggest that PTHrP may promote growth and invasion of tumor cells. In this study, mice carrying a conditional PTHrP allele were crossed with the PyVMT transgenic mouse mammary tumor model and then with a separate transgenic strain expressing Cre in the mammary epithelium (MMTV-Cre). Homozygous (PyVMT-PTHrP<sup>fllox/lox</sup>-Cre<sup>+</sup>), heterozygous (PyVMT-PTHrP<sup>fllox/lox</sup>-Cre<sup>+</sup>) and control (PyVMT-PTHrP<sup>fllox/lox</sup>-Cre<sup>-</sup> and PyVMT-PTHrP<sup>fllox/lox</sup>-Cre<sup>+</sup>) animal models were generated. Tumors were harvested, minced trypsinized and 1X10<sup>6</sup> cells injected into mammary fat pads of syngeneic 5-week old FVB mice non-tumor bearing mice of the same strain. Tumor growth overtime of PyVMT-PTHrP<sup>fllox/lox</sup>-Cre<sup>+</sup> cells and of PyVMT-PTHrP<sup>fllox/lox</sup>-Cre<sup>+</sup> cells was reduced by 85% (P<0.01) and 45% (P<0.01) respectively as compared to tumor growth of control cells. Similar results were observed with cells isolated from PyVMT-PTHrP<sup>fllox/lox</sup>, PyVMT-PTHrP<sup>fllox/lox</sup> tumors, transfected with adeno-Cre GFP or adeno-GFP selected by flow cytometry and reimplanted into the mammary fat pad. Markers of tumor progression including Neu, cyclin D1 and Ki67 were reduced by over 80% and 40% respectively in animals transplanted with homozygous and heterozygous cells as compared to control cells. In addition, AKT signaling was markedly altered in both homozygous and heterozygous animals with a significant inhibition of AKT1 (30%) and stimulation AKT2 (50%). Finally, a strong inhibition of angiogenesis (over 50%) in adjacent blood vessels and a strong increase (3 fold) in apoptosis of tumor cells were observed in transplanted knockout tumors as compared to controls. We also compared metastatic spread to lungs independent of primary tumor growth by comparing animals with similar tumor size ( $\approx 2.3$  mm<sup>3</sup>) sacrificed at 7 weeks, 11 weeks and 13 weeks post-tumor implantation in animals transplanted with control PyVMT-PTHrP<sup>fllox/lox</sup>-Cre<sup>+</sup> and heterozygous PyVMT-PTHrP<sup>fllox/lox</sup>-Cre<sup>+</sup> and homozygous PyVMT-PTHrP<sup>fllox/lox</sup>-Cre<sup>+</sup> cells respectively. At sacrifice 100% control, 42% heterozygous and 14% homozygous animals had metastatic spread to lungs. Overall, our study demonstrates that PTHrP ablation strongly inhibits breast cancer progression through activation/inactivation of key signaling events of the cell machinery. These data suggest that PTHrP maybe a useful target to inhibit both breast tumor growth and its metastatic spread.

**Disclosures:** J. Li, None.

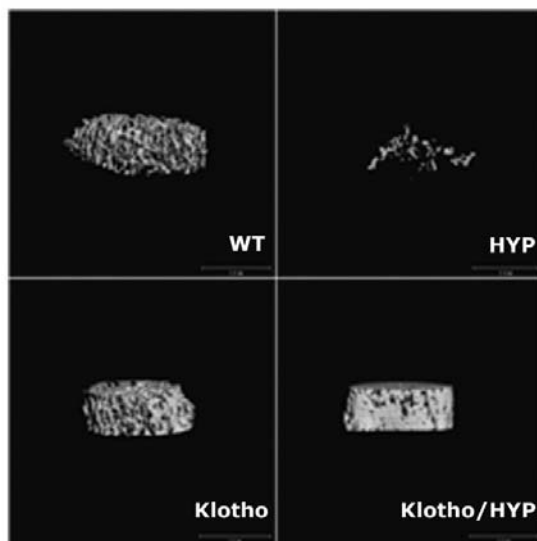
## 1017

**Increased Bone Volume and Correction Of HYP Mouse Hypophosphatemia in the Klotho/HYP Mouse.** C. Brownstein<sup>\*1</sup>, C. Gundberg<sup>\*2</sup>, R. Lifton<sup>\*1</sup>, T. Carpenter<sup>\*3</sup>. <sup>1</sup>Genetics, Yale University, New Haven, CT, USA, <sup>2</sup>Orthopaedics & Rehabilitation, Yale University, New Haven, CT, USA, <sup>3</sup>Pediatrics, Endocrinology, Yale University, New Haven, CT, USA.

Inactivating mutations of PHEX, the disease-causing gene in X-linked hypophosphatemia, result in increased circulating FGF23, a bone-derived phosphaturic factor. FGF23 is linked to Klotho, which converts FGFR1 into a specific receptor for FGF23. Knockout of Klotho (the Klotho mouse) results in a complex bone phenotype and hyperphosphatemia (Kuro-o, 1997), in distinct contrast to XLH.

We examined the effects of deleting both Klotho and PHEX by creating a double knockout (DKO) mouse line. Inactivating mutations in both Klotho and PHEX resulted in correction of low serum phosphate levels seen in PHEX null (HYP) mice, indicating that Klotho is epistatic to PHEX (Klotho  $12.5 \pm 1.9$  mg/dl, HYP  $3.9 \pm 1.3$  mg/dl, DKO  $11.6 \pm 2.2$  mg/dl). FGF23 levels remained elevated in all groups except wild-type (Klotho  $2688 \pm 102$  pg/ml, HYP  $1620 \pm 446$  pg/ml, DKO  $1533 \pm 35$  pg/ml), indicating that Klotho is necessary for FGF23 to have phosphaturic activity. 1,25 dihydroxyvitamin D (1,25D) levels in the DKO were indistinguishable from Klotho mice (Klotho  $173 \pm 21$  pg/ml, HYP  $27 \pm 19$  pg/ml, DKO  $195 \pm 81$  pg/ml), demonstrating that Klotho is a necessary mediator of FGF23's effect on lowering 1,25D. Moreover, the Klotho null phenotype and decreased lifespan persisted in DKO.

At age 6 weeks, PINP levels were dramatically reduced in DKO mice (Klotho,  $222 \pm 79$  ng/ml, HYP  $150 \pm 140$  ng/ml, wt  $432 \pm 217$  ng/ml, DKO  $22 \pm 12$  ng/ml;  $p = 0.013$ , wt vs. DKO). The addition of Klotho insufficiency resulted in correction of hypomineralization seen in HYP mice (trabecular apparent density: HYP  $63 \pm 88$  mg/ccm vs. DKO  $503 \pm 59$  mg/ccm, Klotho  $352 \pm 70$  mg/ccm, wt  $233 \pm 37$  mg/ccm,  $p < 0.015$  for all comparisons). Cortical porosity in DKO mice was improved in comparison to HYP (DKO  $2.6 \pm 1.7\%$ , HYP  $7.8 \pm 4.3\%$ ,  $p = 0.029$ ) and indistinguishable from Klotho (Klotho  $1.4 \pm 1.2\%$ , wt  $0.2 \pm 0.3\%$ ). Finally, DKO mice had greater trabecular bone volume (BV/TV) than all groups (DKO  $56.2 \pm 6.3\%$ , Klotho  $32.5 \pm 10.3\%$ , HYP  $8.6 \pm 7.7\%$ , wt  $21.4 \pm 3.4\%$ ;  $p < 0.004$ ); the overabundant unmineralized osteoid typical of HYP mouse appears to mineralize with the additional deletion of the Klotho gene, resulting in an extremely dense skeletal phenotype, moreso than in WT or even Klotho null mice. Paradoxically, by the time this phenotype is evident there is biochemical evidence of low bone formation.



**Disclosures:** C. Brownstein, None.

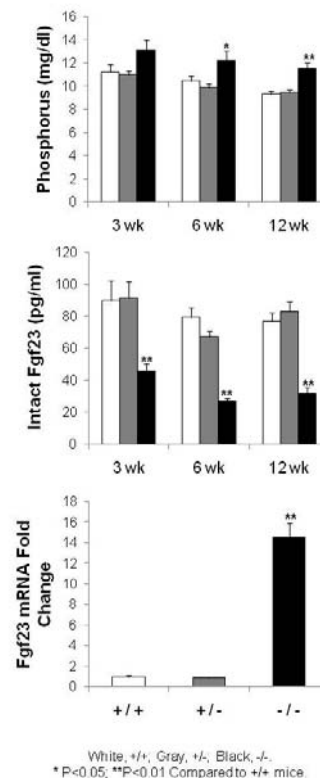
This study received funding from: Howard Hughes Medical Institute.

## 1018

**Ablation of the Galnt3 Gene in Mice Leads to Low Circulating Fgf23 Concentrations and Hyperphosphatemia Despite Increased Fgf23 Gene Expression.** S. Ichikawa<sup>\*1</sup>, A. H. Sorenson<sup>\*1</sup>, T. A. Fritz<sup>\*2</sup>, A. Moh<sup>\*3</sup>, D. S. Mackenzie<sup>\*1</sup>, S. L. Hui<sup>\*1</sup>, M. J. Econs<sup>\*4</sup>. <sup>1</sup>Medicine, Indiana University School of Medicine, Indianapolis, IN, USA, <sup>2</sup>Section on Biological Chemistry, NIDDK, National Institutes of Health, Bethesda, MD, USA, <sup>3</sup>Microbiology and Immunology, Indiana University School of Medicine, Indianapolis, IN, USA, <sup>4</sup>Medicine and Medical and Molecular Genetics, Indiana University School of Medicine, Indianapolis, IN, USA.

Familial tumoral calcinosis is characterized by ectopic calcifications and hyperphosphatemia. Three genes associated with this disease are fibroblast growth factor 23 (FGF23), Klotho (KL), and UDP-N-acetyl-alpha-D-galactosamine:polypeptide N-acetylgalactosaminyltransferase 3 (GALNT3). GALNT3 encodes an enzyme that O-glycosylates FGF23 in a furin-like convertase recognition sequence, thereby preventing proteolytic processing of FGF23 and allowing secretion of intact FGF23. Ablation of

Fgf23 and Kl in mice results in severe hyperphosphatemia as well as vascular and soft-tissue calcifications. In this study, we generated mice deficient in Galnt3. Mice with a homozygous deletion of Galnt3 were hyperphosphatemic as seen in patients with tumoral calcinosis. Galnt3-deficient mice also exhibited inappropriately normal 1,25-dihydroxyvitamin D [1,25(OH)<sub>2</sub>D] level and decreased alkaline phosphatase activity. In response to hyperphosphatemia, Galnt3-deficient mice had significantly increased Fgf23 expression in the bone, but decreased circulating intact Fgf23 levels, compared to wild-type and heterozygous mice. Renal expression of sodium-phosphate co-transporter IIa and Kl were also elevated in Galnt3-deficient mice. Histological and radiographic analyses of homozygous mice revealed no apparent calcifications or abnormalities in the tissues evaluated. Interestingly, Galnt3-deficient males, but not females, showed growth retardation, infertility, and significantly increased bone mineral density (BMD). In summary, ablation of Galnt3 enhanced expression of the Fgf23 gene, but impaired secretion of Fgf23, leading to decreased circulating Fgf23 and hyperphosphatemia. Our findings provide the evidence that Galnt3 plays an essential role in proper secretion of Fgf23 in mice.



**Disclosures:** S. Ichikawa, None.

## 1019

**Histomorphometric Changes by Teriparatide in Alendronate Pre-treated Women with Osteoporosis.** J. J. Stepan<sup>1</sup>, H. Dobnig<sup>2</sup>, D. B. Burr<sup>3</sup>, J. Li<sup>4</sup>, Y. L. Ma<sup>\*5</sup>, A. Sipos<sup>\*5</sup>, H. Petto<sup>\*5</sup>, I. Pavo<sup>5</sup>. <sup>1</sup>Institute of Rheumatology, Charles University Faculty of Medicine, Prague, Czech Republic, <sup>2</sup>Internal Medicine, Medical University, Graz, Austria, <sup>3</sup>Department of Anatomy and Cell Biology, Indiana University School of Medicine, Indianapolis, IN, USA, <sup>4</sup>Department of Biology, Indiana University-Purdue University, Indianapolis, IN, USA, <sup>5</sup>Lilly Research Laboratories, Indianapolis, IN, USA.

Teriparatide (TPTD) treatment increases trabecular bone volume similarly in postmenopausal women with osteoporosis irrespective of alendronate (ALN) pre-treatment or being treatment naïve (TN). Our aim was to investigate the effect of TPTD on osteoid matrix production and primary mineralization in patients after long-term ALN treatment. Sixty-six postmenopausal women with osteoporosis (mean age of 68.0 years, 62% with prevalent fractures) entered this prospective, non-randomized study and started with 20µg/day subcutaneous TPTD: thirty-eight stopped previous ALN treatment (mean duration of 63.6 months) while twenty-eight were previously TN. From 45 patients valid biopsies were available at baseline and after 24-month TPTD administration. At baseline, when compared with TN patients, the indices of matrix formation (osteoid perimeter) and primary mineralization (mineralizing surface) were significantly lower in the ALN group. After switching to TPTD, the indices of matrix formation and bone turnover increased and reached a similar level in both groups, resulting in a more marked percentage increase in the ALN group. Mineralizing surface also increased in both groups, however even a greater percentage increase in the ALN group could not fully compensate for the suppressed baseline. Consequently, after TPTD treatment, mineralizing surface was still significantly less in patients pre-treated with ALN (Table). Our results support the finding of a similar trabecular bone volumetric increase after 24 months by teriparatide irrespective of ALN pre-treatment driven by greater percentage changes of elevated bone formation activities.



	Baseline		After treatment with TPTD		Median of % Change from Baseline per Patients	
	Treatment naïve (n = 16)	Alendronate pre-treated (n = 29)	Treatment naïve (n = 16)	Alendronate pre-treated (n = 29)	Treatment naïve (n = 16)	Alendronate pre-treated (n = 29)
3D Bone volume/tissue volume (%)	18.1	18.6	20.3	20.5	17.8 <sup>b</sup>	28.4 <sup>b</sup>
Osteoid perimeter/trab.perim. (%)	6.24	3.96 <sup>a</sup>	11.29	9.82	67.5 <sup>b</sup>	230.9 <sup>b</sup>
Activation frequency (cycles/yr)	0.19	0.11	0.33	0.34	111.3 <sup>b</sup>	225.3 <sup>b</sup>
Mineralizing surface /bone surface (%)	4.97	2.13 <sup>a</sup>	8.19	3.81 <sup>a</sup>	25.8 <sup>b</sup>	119.1 <sup>b</sup>

Medians, <sup>a</sup> P<0.05 between groups (Mann-Whitney test), <sup>b</sup> P<0.05 from baseline (Wilcoxon signed rank test)

**Disclosures:** J.J. Stepan, None.

This study received funding from: Eli Lilly and Company.

## 1020

**Twelve Month Changes in Trabecular Microarchitecture Assessed by MicroMRI in Postmenopausal Women on Antiresorptive versus Anabolic Therapy.** S. L. Greenspan<sup>1</sup>, J. M. Wagner<sup>\*1</sup>, P. Greeley<sup>\*1</sup>, P. Seaman<sup>\*2</sup>, B. R. Gomberg<sup>2</sup>, M. Kleerekoper<sup>2</sup>, D. L. Medich<sup>\*1</sup>, K. T. Vujević<sup>\*1</sup>, S. Perera<sup>\*3</sup>.

<sup>1</sup>Department of Medicine, University of Pittsburgh, Pittsburgh, PA, USA,

<sup>2</sup>MicroMRI Inc., Philadelphia, PA, USA, <sup>3</sup>Department of Biostatistics, University of Pittsburgh, Pittsburgh, PA, USA.

Changes in bone mineral density (BMD) may only account for 30% of fracture risk reduction following therapy. Other factors including trabecular micro-architecture contribute to fracture risk. High resolution MRI (MicroMRI), examines trabecular microstructure and provides an index of the trabecular rods and plates. To examine trabecular changes in microarchitecture and conventional BMD (trabecular and cortical combined) in postmenopausal women with osteoporosis on antiresorptive versus anabolic therapy, we recruited 10 women on an antiresorptive bisphosphonate (risedronate, 35mg once weekly) and 10 women who just initiated anabolic treatment with teriparatide (20 mcg subcutaneous daily). The mean age was 70 years. Outcomes included BMD by DXA of the spine, total hip and right ultra distal radius (UD radius). MicroMRI was examined using a right bird cage wrist coil with a Sigma 1.5 Tesla MRI scanner and analyzed by MicroMRI Inc. (Philadelphia, PA). MicroMRI indices included: BV/TV (bone volume/total volume), Surf (topological surface density), Curv (topological curve density), Surf/Curv (surface to curve ratio, number of platelike to rodlike trabeculae, higher values indicate intact trabeculae); Erosion Index =(ratio of topological parameters that decrease with improvement).

Table: Percent Change Over 12 Months (Mean ± SEM)

Site	Risedronate (%)	Teriparatide (%)	Between Rx differences (p-value)
PA Spine BMD	0.6 ± 0.9	6.8 ± 1.8**	0.008
Total Hip BMD	-0.1 ± 0.6	3.3 ± 0.9 **	0.009
UD Radius BMD	0.9 ± 1.2	0.9 ± 1.0	0.968
BV/TV	7.3 ± 3.0*	1.4 ± 1.6	0.090
Surf	10.5 ± 4.0*	1.1 ± 3.1	0.078
Surf/Curv	14.8 ± 5.7*	5.3 ± 6.1	0.276
Erosion Index	-13.3 ± 3.2**	-2.4 ± 5.8	0.129

\*p < 0.05, \*\*p < 0.01 within group change

There were no significant differences in baseline BMD or microMRI indices between the 2 groups. After 12 months of therapy, indices of microMRI suggest improvement with an antiresorptive despite maintenance of conventional BMD. Anabolic therapy significantly improved hip and spine BMD without change in wrist BMD or microMRI trabecular indices. We conclude that measures of microMRI provide additional information about changes in structural integrity while on therapy that are not demonstrable with conventional BMD. New bone formation from teriparatide may require time to mineralize before structural changes are observed on microMRI. Further studies are needed to determine how these structural changes lead to fracture reduction.

**Disclosures:** M. Kleerekoper, MicroMRI Inc. 5.

This study received funding from: NIH/NCRR.

## 1021

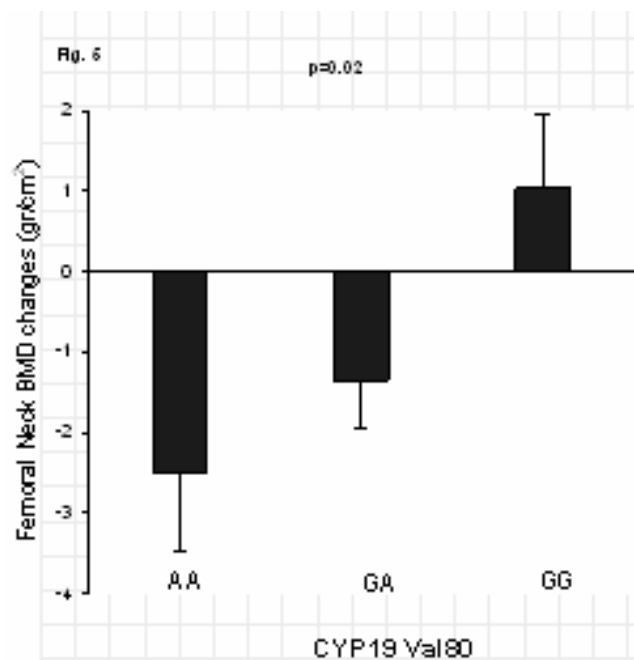
**The A Allele at Valine80 of the CYP19 Gene Is a Risk factor for Aromatase Inhibitors Associated Bone Loss.** N. Napoli, C. Ma\*, A. Rastelli\*, J. Yarramaneni\*, G. Moskowitz\*, M. Ellis\*, R. C. Villareal. Medicine, Washington University School of Medicine, St Louis, MO, USA.

Third generation aromatase inhibitors (AIs) have been reported to cause bone loss and increase the incidence of fractures. Genetic polymorphisms of the CYP19 gene are associated with differences in bone mineral density (BMD) and bone loss and even response to estrogen therapy. The objective of this study was to determine if polymorphisms of the CYP19 gene are also important determinants of bone loss in postmenopausal women taking AIs for breast cancer.

BMD was measured by dual energy x-ray absorptiometry, serum estradiol by radioimmunoassay, interleukin-6 (IL-6) and urinary N-telopeptide (NTx) by Elisa. DNA sequencing for 5 polymorphisms in the CYP19 gene were done by Pyrosequencing (Biotage AB, Uppsala, Sweden).

To date, 130 postmenopausal women with ER+ breast cancer (stage I-IIIa) participated in the study. In the 80 women who came for the 6-month follow-up, we found a significant reduction in estradiol (13.0±0.7 vs. 8.9±0.72 pg/ml, p<0.001) and a significant increase in IL-6 levels. A trend for an increase in urinary NTx (nmolBCE/mmolCre) in the 38 women with available urine samples (51.3±6.1 vs. 65.6±6.2, p=0.10) was also noted. Analysis of BMD (% change) at the 6-month follow-up showed minor bone loss in the lumbar spine, femoral neck and total hip (-1.02±0.4, -1.25±0.4, and 0.71±0.3, respectively). However, analysis according to the G/A base change at Valine80 showed significant bone loss in women carrying the A allele compared to those with the GG genotype in the femoral neck (AA=-2.75±0.9, AG=-1.37±0.6 and GG=0.66±0.8, p=0.02) and in the total hip (AA+AG=-1.1±0.4, GG=0.32±0.6, p<0.05). Moreover, IL-6 levels were significantly increased among the women carrying the AA genotype (AA= +528.2±132.8, AG=+90.9±76.7, and GG=+23.3±118.8, p=0.01). In the 45 women who returned for their one-year follow-up, a trend for greater bone loss in the femoral neck was once again observed (AA=-4.29±1.38, AG=-1.21±0.99, and GG=-0.12±1.37, p=0.08).

In conclusion our data suggest that patients with the AA genotype at Valine80 are at increased risk for AI-induced bone loss. This bone loss is perhaps mediated by the increase in proinflammatory cytokines resulting from profound estrogen deprivation. This subset of patients may represent as the best candidates for bone loss prevention at the initiation of AIs.



**Disclosures:** N. Napoli, None.

This study received funding from: NIH.

## 1022

**What Proportion of Older Women Would Receive Drug Treatment Under the New NOF Guidelines?** M. G. Donaldson<sup>1</sup>, P. M. Cawthon<sup>1</sup>, J. T. Schousboe<sup>2</sup>, K. E. Ensrud<sup>3</sup>, B. C. Taylor<sup>3</sup>, J. A. Cauley<sup>4</sup>, T. A. Hillier<sup>5</sup>, D. M. Black<sup>6</sup>, D. C. Bauer<sup>6</sup>, S. R. Cummings<sup>1</sup>. <sup>1</sup>San Francisco Coordinating Center, San Francisco, CA, USA, <sup>2</sup>Park Nicolette Health Services, Minneapolis, MN, USA, <sup>3</sup>Univ. of MN and CCDOR VA Medical Center, Minneapolis, MN, USA, <sup>4</sup>Univ of Pittsburgh, Pittsburgh, PA, USA, <sup>5</sup>Kaiser Permanente Center for Health Research, Portland, OR, USA, <sup>6</sup>Univ of California San Francisco, San Francisco, CA, USA.

The new National Osteoporosis Foundation (NOF) guidelines include drug treatment recommendations based on the WHO 10-year probabilities of hip and other osteoporotic fractures. The NOF recommends drug treatment for postmenopausal women aged 50 and older who have any of the criteria listed in the Table. It is not known what proportion of women aged 65 years and older would be recommended for drug treatment under those guidelines.

We used data from the Study of Osteoporotic Fractures (SOF) a prospective study of community-dwelling Caucasian women recruited from 4 US communities from population-based listings and mass mailings. The participants were recruited in 1986-7 before widespread publicity about osteoporosis and were not recruited on the basis of any risk factors for osteoporosis. Participants were  $\geq 65$  years (n=6025, mean age=71). Characteristics of the SOF participants are similar to those of white women  $\geq 65$  in the population-based NHANES III survey: for example, SOF participants had slightly higher FN BMD (0.65 vs 0.62 g/cm<sup>2</sup>) and similar history of fracture (17 vs 16%). We used baseline data to determine the proportion of women who would be recommended for drug treatment based on the NOF guidelines (except criterion A only history of hip fracture was included and E for which data were unavailable).

NOF guidelines would recommend 73% (n=4374) of women  $\geq 65$  years in SOF for drug treatment. Among those over 75 years, 94% would be recommended for treatment. Applying criterion B alone and D alone would recommend 43.6% and 57.1% of women respectively for drug treatment.

The NOF guidelines recommend drug treatment for about 73% of Caucasian women  $\geq 65$  years, and more than 90%  $\geq 75$  years. These results may underestimate the proportion of women recommended for drug treatment because history of clinical vertebral fracture and secondary causes of osteoporosis were not included. Before promoting widespread drug treatment of elderly women, it would be important to confirm the evidence and assumptions that underlie these recommendations.

NOF drug treatment criteria and proportion of women selected for treatment	
A: hip fracture	1.6 (99)
B: T-score $\leq -2.5$ at femoral neck, total hip or spine*	42.3 (2560)
Osteopenia (low bone mass)†: AND:	
C: other prior fractures	12.8 (769)
D: U.S. WHO 10-yr probability of:	
hip fracture $\geq 3\%$	9.6 (576)
any major osteoporosis-related fracture $\geq 20\%$	6.1 (370)
Total recommended for drug treatment	73% (4374)

\*after excluding secondary causes;

† -1.0  $\geq$  T-score  $> -2.5$  at the femoral neck, total hip, or spine

**Disclosures:** M.G. Donaldson, None.

This study received funding from: NIA.

## 1023

**Incorporating FRAX™ Algorithms in Models of Cost-effectiveness.** O. Ström<sup>\*1</sup>, F. Borgström<sup>\*1</sup>, E. McCloskey<sup>2</sup>, O. Anders<sup>\*2</sup>, H. Johansson<sup>\*2</sup>, J. A. Kanis<sup>2</sup>. <sup>1</sup>3/Innovus, Stockholm, Sweden, <sup>2</sup>WHO Collaborating Centre for Metabolic Bone Diseases, Sheffield, United Kingdom.

In modelling cost-effectiveness of osteoporosis treatments, fracture risk has generally been calculated with risk adjustments based on age, bone mineral density and previous fractures. The use of these components alone in case finding neglects other clinical risk factors (CRFs) which contribute to fracture risk and thus to cost-effectiveness. The aim of this study was to merge a previously published cost-effectiveness model (<http://www.iofbonehealth.org>) with a fracture risk algorithm (FRAX™) based on CRFs in individual patients.

The cost-effectiveness model based on Swedish data was merged with the FRAX™ fracture risk algorithm. The algorithm was used to calculate the individual risk contribution of the different CRFs, which were; prior fragility fracture, parental history of hip fracture, high alcohol consumption, rheumatoid arthritis, cigarette smoking and use of glucocorticoids. The algorithm produced relative risks for hip fractures and major non-hip fractures, which was used for vertebral, wrist and other fractures. Simulations comprised different combinations of CRFs, and a 5-year treatment costing 742 \$/year that reduced the risk of all fracture types by 35%. Residual linearly declining effect was assumed for 5 years.

The base-case scenario was a woman with T-score of -2.5 SD and no other CRFs. As seen in Table 1, the addition of any single CRF in 60, 70 and 80 year old women had a marked impact on the cost-effectiveness of treatment vs. no treatment.

The FRAX™ algorithm in combination with the cost-effectiveness model facilitates and improves estimation of the cost-effectiveness in patients with different combinations of clinical risk factors.

**Table 1. Cost/QALY gained in women with a T-score of -2.5 and different single CRFs**

Scenario	Cost/QALY (\$)		
	60 years	70 years	80 years
Base-case (T-score -2.5)	66,161	30,796	Cost-saving
Prior fracture	32,270	9,367	Cost-saving
Parental fracture history	40,880	354	Cost-saving
Current smoker	43,800	9,728	Cost-saving
Glucocorticoid use	32,388	3,850	Cost-saving
Secondary osteoporosis	45,693	14,390	Cost-saving
Alcohol (>3 units/day)	45,238	12,980	Cost-saving

**Disclosures:** O. Ström, None.

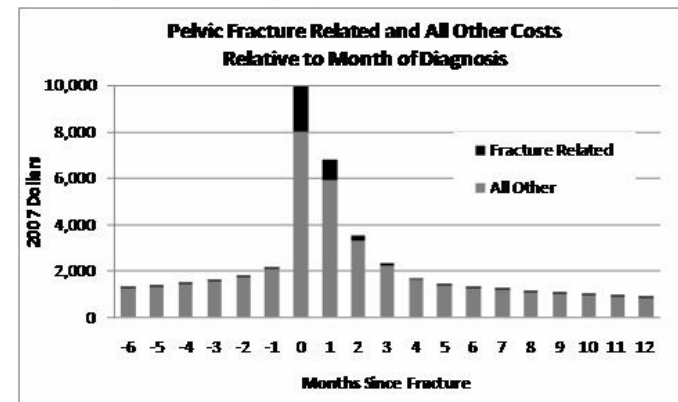
## 1024

**Incremental Costs Associated with Selected Skeletal Fractures.** M. L. Kilgore<sup>\*1</sup>, M. A. Morrissey<sup>\*1</sup>, D. Becker<sup>\*1</sup>, L. C. Gary<sup>\*1</sup>, H. Yun<sup>\*1</sup>, J. R. Curtis<sup>2</sup>, K. G. Saag<sup>2</sup>, R. Matthews<sup>\*3</sup>, W. Smith<sup>\*3</sup>, E. Delzell<sup>\*3</sup>. <sup>1</sup>Health Care Organization and Policy, UAB School of Public Health, Birmingham, AL, USA, <sup>2</sup>Medicine, UAB School of Medicine, Birmingham, AL, USA, <sup>3</sup>Epidemiology, UAB School of Public Health, Birmingham, AL, USA.

The purpose of this study is to estimate the costs of care for fractures that are or could be related to osteoporosis.

We used a national 5% sample of Medicare beneficiaries from 1999 to 2005. The data were structured longitudinally, with patient months as the units of observation. Time was indexed relative to incident hip, spine, forearm, leg, clavicle, pelvis, and humerus fractures identified using ICD-9 codes paired with physician service or inpatient claims. Costs were estimated using payments from all sources for Medicare covered services, expressed in 2007 dollars. Costs were characterized as directly related to fractures if the primary diagnosis code associated with the service was for the fracture. We examined patterns of costs over time relative to fractures and calculated associated incremental costs as the difference between payments for services subsequent to the fracture and average costs in the period preceding the fracture.

The pattern of costs relative to the month of a pelvic fracture diagnosis is similar to that for others and is presented as an example (figure).



Costs increased precipitously in the index month, then declined below baseline levels (reflecting zero costs for decedents).

The table shows average costs associated with fractures, incremental costs (change from baseline), and the direct fracture treatment costs (claims with a primary fracture diagnosis). Skeletal fractures were associated with substantial increases in costs for health services, most of which accrued in the first six months following the fracture.

	Number of Fracture Types and Associated Costs					Incremental Costs*	Direct Costs†
	Number	Baseline	6 Months	Year 1	Year 2		
Hip	90,039	7,823	36,180	41,275	8,188	28,357	14,045
Spine	69,867	7,643	19,542	25,000	9,246	11,899	2,913
Distal Forearm	37,998	4,955	12,903	17,008	7,905	7,948	1,601
Pelvis	27,661	8,750	26,873	32,284	8,755	18,123	3,229
Clavicle	8,125	7,556	18,007	24,043	8,627	10,451	1,073
Humerus	37,342	6,720	19,878	24,773	8,471	13,158	3,909
Forearm	47,833	5,087	13,340	17,537	8,009	8,253	1,823
Leg	43,475	7,897	30,192	35,282	8,599	22,295	4,002

\*Difference between first six months and baseline.

†Associated with a primary fracture diagnosis, first six months.

The higher proportion of costs were for health services not directly connected to fracture treatment; direct costs of care for a pelvis fracture, for example, accounted for only 17.8% of the incremental increase in average costs in the first six months following a fracture compared with baseline costs.

**Disclosures:** M.L. Kilgore, Amgen 3; Agency for Healthcare Research and Quality 3. This study received funding from: Amgen, Inc.

## 1025

**Bisphosphonates and Osteoporotic Fractures in Highly Compliant/Persistent Postmenopausal Women.** M. M. Wilkes<sup>\*1</sup>, N. J. Roberta<sup>\*1</sup>, W. W. Chan<sup>\*2</sup>, E. M. Lewiecki<sup>3</sup>. <sup>1</sup>Hygeia Associates, Grass Valley, CA, USA, <sup>2</sup>Novartis Pharmaceuticals Corporation, East Hanover, NJ, USA, <sup>3</sup>New Mexico Clinical Research & Osteoporosis Center, Albuquerque, NM, USA.

**Purpose:** Randomized clinical trials have demonstrated fracture risk reduction by bisphosphonate treatment in women with postmenopausal osteoporosis. The extent to which those results apply to routine clinical practice has remained uncertain. Recent observational studies have investigated fracture reduction by bisphosphonate using large clinical databases generated in the course of routine practice. These studies have created an opportunity to compare the magnitude of apparent treatment benefit in randomized trials with that in day-to-day clinical medicine. To capitalize on this opportunity, a cross-design synthesis has been conducted of placebo-controlled randomized trials and of observational studies assessing treatment effects in highly compliant/persistent patients.

**Methods:** Eligible studies of both types evaluated the effects of bisphosphonates on clinical fractures in women with postmenopausal osteoporosis. Standard meta-analytic methodology was applied. Twenty randomized trials with 44878 total patients and 7 observational studies with 107560 total patients were included in the meta-analysis.

**Results:** Data pertaining to all clinical fractures were available from 7 of the included randomized trials with 23769 total patients and 5 included observational studies with 68928 total patients. The pooled odds ratio (OR) for all clinical fractures in the randomized trials of 0.762 and 95% confidence interval (CI) of 0.680-0.855 indicated significant fracture reduction by bisphosphonate. The magnitude of the effect in the observational studies was closely similar (pooled OR, 0.776; CI, 0.721-0.835). The small difference in pooled OR between the two categories of studies was not statistically significant ( $p = 0.86$ ). The pooled OR for all 12 studies with data for all clinical fractures (0.763; CI, 0.715-0.815) indicated a significant 24% fracture reduction. The odds of nonvertebral, vertebral and hip fractures were also significantly lowered by bisphosphonate treatment both in randomized trials and observational studies.

**Conclusions:** Bisphosphonate treatment effects in randomized trials and observational studies coincided closely. These results suggest that the anti-fracture benefits of bisphosphonates among highly compliant/persistent patients in the "real world" are similar to those previously documented in randomized trials.

**Disclosures:** W.W. Chan, Employee of Novartis Pharmaceuticals Corporation 5. This study received funding from: Novartis Pharmaceuticals Corporation.

## 1026

**Subtrochanteric And Diaphyseal Femur Fractures in Patients Treated with Alendronate: A Register-Based National Cohort Study.** B. Abrahamsen<sup>1</sup>, P. Eiken<sup>\*2</sup>, R. Eastell<sup>3</sup>. <sup>1</sup>Department of Medicine F, Copenhagen University Hospital, Hellerup, Denmark, <sup>2</sup>Department of Cardiology and Endocrinology, Hillerød Hospital, Hillerød, Denmark, <sup>3</sup>Metabolic Bone Centre, Northern General Hospital, Sheffield, United Kingdom.

Recent reports (*NEJM* 2008;358:1303) have found alendronate(*aln*) use to be common in patients with subtrochanteric or proximal diaphyseal fracture of the femur, but it is unknown if these fractures are osteoporotic by nature or the result of excessive suppression of bone turnover.

We conducted a register-based cohort analysis in a tertiary prevention setting to test the hypothesis that the increase in the risk of these "atypical" femur fractures in patients treated with *aln* exceeded their increase in the risk of typical osteoporotic femur fractures.

All patients born 1945 or earlier who presented at Danish hospitals with fractures in the period 1996-2005 were identified. Fracture patients without baseline hip fracture were then entered into the tertiary prevention matched cohort analysis, where each patient who began *aln* and remained on treatment for at least 6 months ( $N=5187$ , mean exposure 2.5y) was assigned two untreated fracture controls ( $N=11160$ ). Matching was done by age, sex and location of index fracture.

	Subtrochanteric	Diaphyseal	Hip
Rate in alendronate treated vs untreated cohort (per 1000 person years)	1.9 vs 1.0	1.1 vs 0.6	17.0 vs 11.0
<i>Cox prop. hazards analysis:</i>			
OR, unadjusted	1.8 (1.0-3.1)	1.8 (0.9-3.7)	1.5 (1.3-1.8)
OR, adjusted for sex and age	1.8 (1.0-3.0)	1.8 (0.9-3.7)	1.5 (1.3-1.8)
OR, adjusted for sex, age, comedications and Charlson index	1.6 (0.9-2.8)	1.9 (0.9-4.0)	1.4 (1.2-1.7)

While *aln* use was associated with an increased risk of a new subtrochanteric fracture ( $p<0.05$ ), this was equally true for hip fracture ( $p<0.001$ ). The increased risk of diaphyseal fracture was not statistically significant ( $p=0.10$ ).

Our findings did not confirm the hypothesis that subtrochanteric or diaphyseal fractures with *aln* treatment occurred with a frequency over and above that expected for a typical osteoporotic fracture. These findings suggest that subtrochanteric fractures should be attributed to osteoporosis and not to *aln* treatment.

**Disclosures:** B. Abrahamsen, Nycomed 1, 4; Roche 1, 3; Servier 1; Novartis 2, 3. This study received funding from: Kaptajnlejnant Harald Jensen og Hustrus Fond.

## 1027

**Relationship of Bone Turnover Marker (PINP) and Changes in Femoral Neck Bone Mineral Density to Fracture Risk in Women with Postmenopausal Osteoporosis Treated with Once-Yearly Zoledronic Acid 5 mg (ZOL): The HORIZON-PFT Study.** P. D. Delmas<sup>1</sup>, F. Munoz<sup>\*1</sup>, F. Cosman<sup>2</sup>, S. Boonen<sup>3</sup>, D. Black<sup>4</sup>, N. B. Watts<sup>5</sup>, D. Kendler<sup>6</sup>, E. F. Eriksen<sup>\*7</sup>, P. Mesenbrink<sup>\*8</sup>, R. Eastell<sup>9</sup>. <sup>1</sup>INSERM Research Unit 831 and University of Lyon, Lyon, France, <sup>2</sup>Helen Hayes Hospital, West Haverstraw, NY, USA, <sup>3</sup>Katholieke Universiteit Leuven, Leuven, Belgium, <sup>4</sup>University of California, San Francisco, San Francisco, CA, USA, <sup>5</sup>University of Cincinnati Bone Health and Osteoporosis Center, Cincinnati, OH, USA, <sup>6</sup>Osteoporosis Research Centre, Vancouver, BC, Canada, <sup>7</sup>Novartis Pharma AG, Basel, Switzerland, <sup>8</sup>Novartis Pharmaceuticals Corp, East Hanover, NJ, USA, <sup>9</sup>University of Sheffield, Sheffield, United Kingdom.

Several studies have shown that reduction in bone turnover markers (BTMs) as a result of antiresorptive therapy, especially bisphosphonates, is associated with reduced risk of fracture. BTM change may be more predictive of fracture than bone mineral density (BMD) change. The associations between changes in BTM or BMD and fracture incidence were assessed in a subgroup of 1132 patients who had procollagen type 1 amino-terminal propeptide (PINP) levels measured at baseline and 1 year, from the randomized, double-blind, placebo-controlled HORIZON Pivotal Fracture Trial in which patients received three annual infusions of ZOL 5 mg. PINP (lower and upper quartile bounds) decreased from a median of 50 (33-67) at baseline to 18 (13-26) ng/ml at 1 year. The table shows the adjusted hazard ratio (HR)/odds ratio (OR) and 95% confidence interval (CI) associated with 1 standard deviation (SD) decrease in PINP level (1 SD of PINP is 27 ng/ml) at 1 year for risk of future fracture. Lower PINP levels were associated with a lower fracture risk after adjusting for baseline confounders. In contrast, femoral neck and total hip BMD increases (5.06 % at 3 years) were not consistently associated with fracture incidence. The HRs for the association between a 1% increase in BMD at 1 and 3 years and the incidence of all clinical fractures were 0.98 (0.94-1.01),  $P=0.19$  and 0.96 (0.92-0.99),  $P=0.03$ , respectively, and for nonvertebral fractures were 0.99 (0.95-1.01),  $P=0.62$  and 0.97 (0.93-1.01),  $P=0.09$ . In summary, PINP levels achieved after 1 year of therapy are significantly associated with the risk of vertebral and nonvertebral fracture, contrasting with the poor predictive value of BMD increase.

Table. Association between PINP level at 1 year and risk of future fracture.

Fracture category	Adjusted HR/OR <sup>2</sup> (95% CI)
Any clinical <sup>1</sup>	0.76 (0.59,0.96)*
Non-vertebral <sup>1</sup>	0.73 (0.56, 0.95)*
Hip	0.36 (0.20, 0.63)**
Morphometric vertebral <sup>2</sup>	0.60 (0.39, 0.99)*

<sup>1</sup> Cox model; <sup>2</sup> Logistic model

\* $P<0.05$ ; \*\* $P<0.01$

**Disclosures:** P.D. Delmas, Novartis Pharmaceuticals 1, 2; Amgen 1, 2, 3; Eli Lilly 1, 2, 3; Pfizer 1, 2.

This study received funding from: Novartis Pharma AG

## 1028

**Effect of Once-Yearly Zoledronic Acid 5 mg Infusion on Fracture Incidence in Postmenopausal Osteoporosis: Subgroup Analysis of the Horizon PFT Study.** R. Eastell<sup>1</sup>, D. M. Black<sup>2</sup>, S. Boonen<sup>3</sup>, S. R. Cummings<sup>2</sup>, P. D. Delmas<sup>4</sup>, L. Palermo<sup>\*2</sup>, P. Mesenbrink<sup>\*5</sup>, J. A. Cauley<sup>6</sup>. <sup>1</sup>University of Sheffield, Sheffield, United Kingdom, <sup>2</sup>University of California, San Francisco, San Francisco, CA, USA, <sup>3</sup>Katholieke Universiteit Leuven, Leuven, Belgium, <sup>4</sup>INSERM Research Unit 831 and University of Lyon, Lyon, France, <sup>5</sup>Novartis Pharmaceuticals Corporation, East Hanover, NJ, USA, <sup>6</sup>University of Pittsburgh, Pittsburgh, PA, USA.

In the 3-year, multicenter, double-blind, placebo-controlled HORIZON-PFT study, a once-yearly infusion of zoledronic acid (ZOL) 5 mg significantly reduced fracture risk in women with postmenopausal osteoporosis ( $n=3875$ ; mean age, 73 years). Patients were randomized to a single 15-minute infusion of ZOL or placebo at baseline, 12 and 24 months. Primary endpoint was incidence of new vertebral fractures and hip fractures at 3 years, with non-vertebral fractures as a secondary endpoint. In a subgroup analysis, fracture risk reduction and treatment-factor interaction were evaluated across 14 determinants of response. Preplanned subgroups (9 of 9) were age, bone mineral density (BMD) T-score and baseline vertebral fracture status, race, weight/body mass index, geographical region, prior bisphosphonate (BP) use, creatinine clearance, and baseline use of osteoporosis medications. *Post hoc* subgroups were hip BMD, smoking, height loss since age 25 years, fall in past 12 months, and daily activity. ZOL significantly reduced the risk of vertebral fractures in all subgroups of age, creatinine clearance and BMI (all  $P<0.0001$ ). Greater effects of ZOL on vertebral fracture risk were observed in younger women (adjusted odds ratio [OR], 0.18 [95% CI 0.10,0.31] in women  $<70$  years vs 0.37 [95% CI 0.27,0.52] in women  $\geq 75$  years), women with creatinine clearance  $\geq 60$  mL/min vs  $<60$  mL/min (OR, 0.21 [95% CI 0.14,0.29] vs 0.35 [95% CI 0.25,0.48]), and overweight or obese women (body mass index [BMI]  $\geq 25$  kg/m<sup>2</sup>; OR, 0.22 [95% CI 0.15,0.31] vs BMI 19-24.9 kg/m<sup>2</sup> (OR, 0.38 [95% CI 0.27,0.53])). Significant treatment-by-factor interactions ( $P<0.05$ ) were observed for ZOL with age, creatinine clearance and BMI. The most frequent treatment-related adverse events with ZOL were pyrexia (16.0%), myalgia (9.4%) and influenza-like illness (7.8%). In conclusion, once-yearly ZOL was effective in all subgroups analyzed for vertebral fractures, but was most effective at reducing risk of vertebral fracture in women younger than 70 years, with better renal function or with higher BMI.

**Disclosures:** R. Eastell, Novartis Pharmaceuticals 2, 3, 5.

This study received funding from: Novartis Pharma AG

## 1029

**Long-Term Treatment with Oral Bisphosphonates in Postmenopausal Women: Effects on the Degree of Mineralization and Microhardness of Bone.** G. Boivin, Y. Bala\*, R. D. Chapurlat, P. D. Delmas. INSERM Unité 831, University of Lyon, Lyon, France.

The degree of mineralization (DMB) is a major determinant of bone quality. In postmenopausal osteoporotic (PMOP) women treated with alendronate (ALN, 10 mg/day) for 2-3 yrs, DMB was significantly increased compared to placebo (PLA), accounting for the main part of the increase in bone density (1). Due to suggestions that long-term use of bisphosphonates (BPs) might be deleterious at the tissue level, we explored the DMB and microhardness in iliac bone biopsies obtained after long-term treatment with BPs in PMOP women from an outpatient clinic. Parameters of secondary mineralization were measured in bone samples from 45 PMOP women (age  $68 \pm 9$  yrs) after BPs therapy (32 on oral ALN only and 13 mainly on oral risendronate = RIS) for 3 to 12 yrs (mean  $6.5 \pm 2.0$  yrs). Results were compared with values from untreated control subjects (CTRL), from PMOP women treated with calcium and vitamin D (PLA) and PMOP patients treated for 3 yrs with ALN [3-ALN (1)]. Quantitative microradiography (2) of  $100 \pm 1 \mu\text{m}$ -thick sections allowed measurement of DMB ( $\text{g}/\text{cm}^3$ ) and Heterogeneity Index of the distribution of DMB (HI  $\text{g}/\text{cm}^3$ ), separately on cortical, cancellous and total bone (= cortical + cancellous). Vickers microhardness (Hv  $\text{kg}/\text{mm}^2$ ) was calculated in 18 3-ALN. DMB, HI and Hv of bone were similar in cortical and cancellous bone allowing results to be reported for total bone tissue. Among women treated long-term, DMB ( $1.13 \pm 0.07$  after ALN,  $1.10 \pm 0.07$  after RIS), but not HI ( $0.21 \pm 0.06$  after ALN,  $0.20 \pm 0.06$  after RIS), was significantly higher ( $p < 0.001$ ) than CTRL (DMB =  $1.09 \pm 0.08$ , HI =  $0.25 \pm 0.08$ ) and PLA (DMB =  $1.07 \pm 0.06$ , HI =  $0.28 \pm 0.12$ ), but DMB was significantly lower ( $p < 0.01$ ) than in 3-ALN (DMB =  $1.19 \pm 0.06$ , HI =  $0.23 \pm 0.07$ ). Hv in 3-ALN ( $42.77 \pm 1.82$ ) was similar to Hv from untreated osteoporotic patients ( $44.10 \pm 4.72$ ). There was no association between DMB, HI or Hv and the duration of BP-therapy and the parameters of bone remodeling (BFR, MS/BS, AcF). There was no difference between women treated with ALN or RIS. Although bone remodeling was markedly suppressed in these women treated long-term with BPs (3), no hypermineralization of bone tissue was found, and hardness was no different to controls. To conclude, after long-term treatment of PMOP women with oral BPs, DMB was preserved and there was no deleterious effect on bone microhardness. Our data show that mineralization increases during the first 3 yrs of BP therapy, then tends to decline to untreated values despite the persistence of low bone turnover.

1-Boivin et al. 2000, Bone 27:687; 2-Boivin & Meunier 2002, Calcif Tissue Int 70:503; 3-Chapurlat et al. 2007 J Bone Miner Res 22:1502

**Disclosures:** G. Boivin, None.

This study received funding from: INSERM.

## 1030

**Potential Mediators of the Reduction in Mortality with Zoledronic Acid after Hip Fracture.** C. Colón-Emeric<sup>1</sup>, P. Mesenbrink<sup>2</sup>, K. Lyles<sup>3</sup>, C. Pieper<sup>4</sup>, S. Boonen<sup>5</sup>, P. Delmas<sup>6</sup>, E. Eriksen<sup>7</sup>, J. Magaziner<sup>7</sup>. <sup>1</sup>Duke University Medical Center, Durham, NC, USA, <sup>2</sup>Novartis Pharmaceuticals Corporation, New Jersey, NJ, USA, <sup>3</sup>VA Medical Center, Durham, NC, USA, <sup>4</sup>Leuven University Center, Leuven, Belgium, <sup>5</sup>Hôpital Edouard Herriot, Lyon, France, <sup>6</sup>Novartis Pharma AG, Basel, Switzerland, <sup>7</sup>University of Maryland, Baltimore, MD, USA.

Zoledronic acid reduces the risk of death by 28% in patients with recent hip fracture, but the mediators of this effect are not completely known. We performed a retrospective analysis of the HORIZON-RFT clinical trial database using stepwise Cox-proportional Hazards modeling to characterize the causes of death, and explore potential mechanisms for the reduction in mortality. The analysis included 2111 patients with recent hip fracture randomized and treated with zoledronic acid or placebo infusion yearly. Causes of mortality were reported by the investigator and adjudicated by a blinded, central review committee. Models included baseline covariates associated with greater risk of death, and time-dependent covariates occurring during the study period including subsequent fracture, change in bone mineral density, infections, cardiac arrhythmias, and falls. In a model adjusted for baseline risk factors, zoledronic acid reduced the risk of death by 25% (95% CI 3-42%). Males experienced a greater mortality benefit (6.4% absolute risk reduction) than females (2.8%), with a particularly marked reduction in cardiac-related deaths (incidence 2.9% vs. 7.7%). Subjects living in a nursing facility at baseline, and subjects with greater levels of cognitive impairment did not experience a major reduction in deaths. Adding subsequent fractures to the model, we found that they were significantly associated with higher risk of death (HR 1.72, 95% CI 1.17-2.51), but explained only approximately 2% more of the zoledronic acid effect. Adjusting for other time-dependent risk factors decreased the death risk reduction by zoledronic acid; however, no treatment-by-factor interactions suggested treatment with zoledronic acid combined with the presence of any risk factors influenced the risk of death in any cohort. Compared to the placebo arm, there was a similar incidence of, but decreased death from pneumonia, neoplasms, and cardiovascular disease in subjects treated with zoledronic acid, suggesting that the drug may influence physiologic reserve. We conclude that zoledronic acid's death benefit is not fully mediated through a reduction in secondary fractures, but may also have an impact on physiologic reserve and ability to recover from acute illnesses.

**Disclosures:** C. Colón-Emeric, Novartis, Research Support from the Alliance for Better Bone Health 2, 3.

This study received funding from: Novartis Pharma AG, Basel, Switzerland.

## 1031

**New data on the impact of renal function on the relationship between 25-hydroxyvitaminD and Parathyroid Hormone.** B. Misra, D. J. McMahon, S. J. Silverberg, J. P. Bilezikian. College of Physicians and Surgeons, Columbia University, New York, NY, USA.

Although both low 25-hydroxyvitamin D [25(OH)D] levels and creatinine clearance <60 cc/min are causes of secondary hyperparathyroidism, little is known about how the relationship between 25(OH)D and PTH varies as a function of creatinine clearance (CrCl). The National Health and Nutrition Examination Survey (NHANES) in 2003-2004 measured parathyroid hormone (PTH), calcium, creatinine, and 25(OH)D in over 6000 individuals. We analyzed data from 2370 individuals  $\geq 45$  with corrected calcium concentration in the normal range (8.5-10.2mg/dL). We then determined mean PTH and % of subjects with elevated PTH ( $\geq 65\text{pg}/\text{mL}$ ) according to CrCl. In those with CrCl <60cc/min, mean PTH increases (even within the normal range) for each 5ng/mL decrease in 25(OH)D. In those with CrCl  $\geq 60\text{cc}/\text{min}$ , PTH levels do not begin to rise into the frankly abnormal range until 25(OH)D levels are markedly reduced. The % of subjects with elevated PTH increases as 25(OH)D falls regardless of renal function. Multiple regression models of PTH and 25(OH)D reveal significant linear, quadratic and cubic relationships for those with CrCl <60cc/min ( $R^2=0.1322$ ), while there is only a weak linear relationship in those with CrCl  $\geq 60\text{cc}/\text{min}$  ( $R^2=0.0891$ ). The stronger association between 25(OH)D and PTH when the CrCl is reduced could be a function of calcium intake, about which data are unavailable, or it may speak to the accumulation of PTH metabolites. The results of this study substantiate a complex relationship between 25(OH)D and PTH, suggesting that the association is stronger when renal function is impaired. The data demonstrate that PTH levels may rise within the normal range as 25(OH)D falls, and suggest an inflection point below which 25(OH)D insufficiency dramatically stimulates PTH levels in the CrCl <60cc/min group. Finally, in those with better renal function, PTH does not rise until vitamin D deficiency is marked. The data support the need for further investigation of the impact of renal function on the relationship between PTH and 25(OH)D.

25(OH)D (ng/mL)	CrCl $\geq 60\text{cc}/\text{min}$ Mean PTH (pg/mL)	CrCl $\geq 60\text{cc}/\text{min}$ %PTH $\geq 65$ (pg/mL)	CrCl <60cc/min Mean PTH (pg/mL)	CrCl <60cc/min %PTH $\geq 65$ (pg/mL)
0-4	106 $\pm$ 61	67	164 $\pm$ 98	100
5-9	57 $\pm$ 26	40	120 $\pm$ 91	72
10-14	56 $\pm$ 27	27	74 $\pm$ 40	48
15-19	48 $\pm$ 18	16	67 $\pm$ 40	36
20-24	45 $\pm$ 18	11	66 $\pm$ 35	43
25-29	44 $\pm$ 18	8	52 $\pm$ 26	20
$\geq 30$	38 $\pm$ 15	4	46 $\pm$ 22	12

**Disclosures:** B. Misra, None.

## 1032

**Pretransplant Parathyroid Function Predicts Laboratory and Bone Mineral Density Changes after Kidney and Kidney Pancreas Transplantation.** G. J. Elder<sup>1</sup>, R. Mainra<sup>2</sup>. <sup>1</sup>Centre for Transplant and Renal Research, Westmead Millennium Institute, Sydney, Australia, <sup>2</sup>Division of Nephrology, St. Paul's Hospital, Saskatoon, SK, Canada.

Patients with CKD stage 5 undergoing kidney (K) or kidney pancreas (KP) transplantation often have low calcitriol, suboptimal 25OHD and elevated iPTH levels. We investigated interactions of these hormones and biochemical responses over the 1<sup>st</sup> post-transplant year.

Of 346 patients undergoing transplantation (K: 234, KP: 112), 150 were followed for  $\geq 12$  months. Their median age was 42 years (range 18-68). Bloods were collected just before transplantation (baseline) and at 6, 12 and 52 weeks after transplantation for biochemistry, levels of 25OHD (adequacy  $\geq 60$  nmol/L), calcitriol (normal range 36-120 pmol/L) and iPTH (normal range 1-6.8 pmol/L). BMD by DXA was assessed at baseline and 12 months. Pre-transplant categories of iPTH <1, 1-3 and >3-times the upper normal range of the assay were used to evaluate influences of pre-existing parathyroid function on post-transplant laboratory data and BMD. Patients with 25OHD <60 nmol/L received cholecalciferol supplementation by 6 weeks. Values are shown as mean $\pm$ SD.

Baseline levels of 25OHD fell by 6 weeks (67 $\pm$ 33 nmol/L to 49 $\pm$ 23 nmol/L;  $p < 0.0001$ ) and were lower for KP recipients at these time points ( $p < 0.0001$  for each). Calcitriol levels rose from 36 $\pm$ 36 pmol/L (baseline) to 85 $\pm$ 56 pmol/L at 6 weeks and 111 $\pm$ 60 pmol/L at 12 weeks ( $p < 0.0001$  for each interval). The mean calcitriol level of 122 pmol/L at 52 weeks exceeded the assay upper range. Baseline iPTH was 45 $\pm$ 44 pmol/L. Pretransplant iPTH categories predicted post-transplant levels of iPTH and calcitriol ( $p < 0.0001$  and  $p = 0.028$  respectively; ANOVA repeat measures) and levels of phosphate (negative interaction;  $p = 0.04$ ). Pretransplant iPTH levels <1 and >3-times the assay upper normal range predicted 6 week levels of 25OHD (47 $\pm$ 23 vs. 59 $\pm$ 24 pmol/L;  $p = 0.0196$ ) and calcium (2.35 vs. 2.45 mmol/L;  $p = 0.002$ ). Higher pre-transplant iPTH levels predicted lower femoral neck BMD at baseline ( $p = 0.0028$ ) and 52 weeks ( $p = 0.0195$ ), but increased annual gain in BMD ( $p = 0.0003$ ), which remained significant after adjustment for transplant type and bisphosphonate use.

These data demonstrate that pre-transplant iPTH levels predict early post-transplant rises in calcitriol and changes in levels of iPTH, 25OHD, calcium and phosphate. The calcitriol response is inconsistent with a dominant early FGF-23 effect. Pretransplant parathyroid activity is an important influence on post-transplant laboratory indices and BMD.

**Disclosures:** R. Mainra, None.

## 1033

**Patients with Kidney Disease and Low 1/3 Radius and Femoral Neck BMD have Markedly Abnormal Cortical and Trabecular Microstructure by High-resolution Peripheral QCT.** T. L. Nickolas<sup>1</sup>, E. A. Stein<sup>1</sup>, V. Thomas<sup>\*1</sup>, H. F. Eisenberg<sup>\*1</sup>, D. J. McMahon<sup>1</sup>, M. B. Leonard<sup>2</sup>, E. Shane<sup>1</sup>. <sup>1</sup>Medicine, Columbia University, New York, NY, USA, <sup>2</sup>Pediatrics, Children's Hospital of Philadelphia, Philadelphia, PA, USA.

Fractures (FXs) are increased in end stage kidney disease (ESKD) and chronic kidney disease (CKD). In normal adults, areal BMD (BMD) of the spine and hip by DXA strongly predict FX. Associations between central DXA and FX in ESKD are weak, likely because concomitant hyperparathyroidism is associated with cortical (Ct) bone loss and preserved trabecular (Tb) bone. DXA does not distinguish Ct from Tb bone. BMD at the 1/3-radius (1/3R; 95% Ct bone) may be associated with FX in ESKD, but no data are available on relationships between 1/3R BMD and Ct and Tb microstructure in ESKD and CKD.

High resolution peripheral QCT (HRpQCT; XtremeCT, Scanco Medical AG; resolution 82 µm) distinguishes between Ct and Tb bone and quantifies Tb microstructure at the radius (RAD) and tibia (TIB). We performed RAD and TIB HRpQCT in 42 subjects with CKD (age 51-88, GFR 4-59 mL/min), hypothesizing those with low 1/3R BMD (T score ≤ -2.0) would have abnormal Ct and preserved Tb microstructure. We also assessed associations between HRpQCT and low BMD at the lumbar spine (LS), total hip (TH) and femoral neck (FN).

Low BMD was uncommon at the LS (10%) and TH (17%), while 45% had T-scores ≤ -2 at the 1/3R and/or FN. Subjects with low 1/3R or FN BMD were similar regarding GFR, race and gender (Table), but older than those with T<sub>z</sub> ≥ -1.9. Low 1/3R and FN BMD were associated with lower RAD Ct thickness (23% and 22%, respectively) and Tb density (30%; 21%), bone volume (29%; 21%) and number (15%; 10%), and higher Tb separation (TbSp) (40%; 27%) and standard deviation of TbSp (100%; 63%) reflecting inhomogeneity of the Tb network. Tb associations were weaker at the FN than 1/3R. Low LS and TH BMD were not associated with Ct or Tb structure. TIB HRpQCT relationships were similar to RAD at all BMD sites.

In summary, Ct and Tb microarchitecture at weight bearing and non-weight bearing sites are markedly abnormal in CKD patients with T scores ≤ -2.0 at the peripheral 1/3R and central FN. DXA of the 1/3R and FN may be more clinically relevant than LS and TH for identifying CKD patients with poor bone microstructure. Further studies are needed to elucidate relationships of these abnormalities to bone strength, and the ability of 1/3R and FN DXA, and HRpQCT Ct and Tb parameters at RAD and TIB to predict FX in CKD.

	T-Score 1/3 Radius < -2	T-Score 1/3 Radius > -2	p-value	T-Score Femoral Neck < -2	T-Score Femoral Neck > -2	p-value
N	19	23		19	23	
MDRD GFR (Median - Range)	13 (4 - 58)	23 (4 - 57)	NS	15 (4 - 50)	24 (4 - 59)	NS
Age (Median - Range)	75 (53-88)	70 (51-86)	NS	75 (56-85)	69 (51-88)	0.02
Gender (% Female)	45	23	NS	36	31	NS
Race (%)						
Non-Hispanic White	41	35		41	35	
African American	14	7	NS	9	11	NS
Hispanic	45	58		50	54	
<b>HR-pQCT Measurements Distal Radius (mean ± SD)</b>						
Cortical Density (mg HA/cm <sup>3</sup> )	755 ± 97	817 ± 80	0.02	744 ± 72	826 ± 91	0.002
Cortical Thickness (µm)	555 ± 212	716 ± 246	0.02	557 ± 191	714 ± 262	0.04
Trabecular Density (mg HA/cm <sup>3</sup> )	121 ± 35	172 ± 58	0.004	130 ± 48	165 ± 55	0.03
Trabecular Bone Volume (%)	10.1 ± 2.9	14.3 ± 4.8	0.004	10.8 ± 4.0	13.7 ± 4.6	0.03
Trabecular Number (n/mm)	1.7 ± 0.4	2.0 ± 0.3	0.008	1.8 ± 0.5	2.0 ± 0.3	0.1
Trabecular Thickness (µm)	60 ± 10	69 ± 20	0.1	60 ± 13	69 ± 18	0.07
Trabecular Separation (µm)	600 ± 276	429 ± 100	0.004	572 ± 286	452 ± 110	0.08
Trabecular Separation Standard Deviation (µm)	362 ± 362	180 ± 60	0.005	333 ± 366	204 ± 97	0.1

**Disclosures:** T.L. Nickolas, None.

## 1034

**Cardiovascular Manifestations of Mild Primary Hyperparathyroidism.** M. D. Walker<sup>1</sup>, J. Fleischer<sup>1</sup>, S. Homma<sup>\*1</sup>, T. Rundek<sup>\*2</sup>, D. J. McMahon<sup>1</sup>, A. Tineo<sup>\*1</sup>, J. Udesky<sup>\*1</sup>, R. Lui<sup>\*1</sup>, R. Sacco<sup>\*2</sup>, S. J. Silverberg<sup>1</sup>. <sup>1</sup>College of Physicians and Surgeons, Columbia University, New York, NY, USA, <sup>2</sup>University of Miami, Miami, FL, USA.

Severe primary hyperparathyroidism (PHPT) is associated with cardiovascular (CV) calcification and increased CV mortality. This prospective study of patients with PHPT seeks to determine whether the mild PHPT seen today still poses a risk to the CV system. Fifty patients (84% female; age ± SD 62 ± 8 yrs, range 48-75; serum calcium 10.5 ± 0.5 mg/dl; PTH 116 ± 50 pg/ml) have been enrolled. Blood pressure (BP) was 123 ± 17/ 75 ± 11 mm Hg. Lipids were mildly elevated: total cholesterol 210 ± 34, HDL 68 ± 17, LDL 123 ± 31, triglycerides 97 ± 56 mg/dl. Valvular calcifications, seen in classical PHPT, were uncommon (14%). Left ventricular (LV) mass was increased in 20 patients (40%), although only 8/20 had hypertension and none had diabetes. Systolic LV function and wall motion were normal. Carotid ultrasound showed plaque in 19 (38%), and increased carotid intima-medial thickness (IMT), a subclinical marker of atherosclerosis. On functional testing of the heart (diastolic function by mitral pulse wave velocity, deceleration time, isovolumic relaxation time, tissue doppler E velocity), peripheral vasculature (endothelial

function: brachial artery flow-mediated dilation, FMD) and carotid (distensibility), only carotid stiffness was abnormal.

CV Test	Mean ± SD	Normal Range	Abnormal
LV mass (g/m <sup>2</sup> )	99 ± 25	43-115	40%
IMT (mm)	0.96 ± 0.10 mm	0.7-0.9	66%
Mitral Pulse Wave E/A	1.1 ± .37	.75-1.5	33%
Deceleration Time (msec)	163 ± 30	>140	21%
Isovolumic relaxation time (msec) (IVRT)	83 ± 17	50-102	15%
Tissue Doppler E' Velocity (cm/sec)	11.4 ± 3	<15	15%
FMD (%)	4.8 ± 3.3	3-7%	32%
Carotid STRAIN (%)	10.2 ± 8.0	6-12%	6%
Carotid STIFFNESS	6.4 ± 3.0	< 6	44%

Higher PTH levels were associated with increased systolic (r = 0.4; p = 0.009) and diastolic (r = 0.3; p = 0.03) BP, and decreased vascular compliance (carotid stiffness: r = 0.4, p = .01; and strain r = -0.43, p = .005). Serum calcium levels correlated with IVRT (r = 0.36, p = 0.01) and strain (r = -0.29, p = 0.04). The relationships remained significant controlling for age and duration of PHPT. A regression model including calcium, PTH and their interaction explained 22.5% of the variation in IVRT and 17% of the variation in BP.

In summary, these patients had increased IMT and carotid stiffness which are risk factors for CV events. Increased LV mass, seen in severe PHPT, was also common. Some measures were associated with severity of PHPT: carotid compliance was lowest in those with highest PTH and calcium levels. In conclusion, patients with mild PHPT have structural and functional CV abnormalities consistent with increased vascular stiffness in the carotid vascular bed which may increase their CV risk.

**Disclosures:** M.D. Walker, None.

## 1035

**Abdominal Aortic Calcification (AAC) Detected on Lateral DXA Spine Images is Associated with Coronary Artery Disease.** J. T. Schousboe<sup>1</sup>, D. Clafin<sup>\*2</sup>, E. Barrett-Connor<sup>2</sup>. <sup>1</sup>Park Nicollet Clinic; Division of Health Policy & Management, Univ of Minn, Minneapolis, MN, USA, <sup>2</sup>Univ of Calif San Diego, San Diego, CA, USA.

**Background:** Abdominal aortic calcification (AAC) on lateral spine DXA images intended for vertebral fracture assessment (VFA) may be predictive of incident myocardial infarction or stroke. The association of AAC on VFA images with other subclinical measures of cardiovascular disease has not been reported.

**Methods:** 200 men and 223 women without prior history of clinical coronary disease had clinical cardiovascular disease risk factors assessed and coronary artery calcium (CAC) scored with electron beam computed tomography (EBCT) at the 8<sup>th</sup> study visit of the Rancho Bernardo long-term observational study of heart and other chronic diseases. Of these participants, 107 men and 116 women had VFA images done at the 9<sup>th</sup> study visit a mean 3.5 years later. 106 VFA's were fully evaluable for AAC using previously validated 24-point and 8-point semi-quantitative scores. The association between CAC quartile and AAC tertile was assessed by ordinal logistic regression models, adjusting for age, sex, blood pressure, total and HDL cholesterol, smoking status, presence of diabetes, and visceral to subcutaneous fat ratio. The sensitivity and specificity of AAC to detect those in the top quartile of CAC score was assessed with receiver operating curve (ROC) analyses.

**Results:** The multivariable-adjusted odds of CAC being one quartile higher with AAC scores in the top and middle tertiles, respectively compared to the bottom tertile of AAC are shown in the table

AAC Measure	AAC Tertile (Score)	Odds Ratio of Higher Quartile of CAC Associated with Elevated AAC (95% C.I.)
AAC-24	Bottom (0 or 1)	1.0 (Reference)
	Middle (2-4)	2.63 (0.85 - 7.91)
	Top (≥ 5)	7.36 (2.36 - 20.99)
AAC-8	Bottom (0 or 1)	1.0 (Reference)
	Middle (2)	1.97 (0.71 - 5.45)
	Top (≥ 3)	3.32 (1.17 - 9.40)

An AAC-24 score of ≥ 5 had sensitivity and specificity, respectively, of 65% and 70% to detect those in the highest quartile of CAC (score ≥ 400). AAC-8 score of ≥ 3 had sensitivity and specificity, respectively, of 45% and 78% to detect those in the top CAC quartile.

**Conclusions:** A high level of AAC detected on VFA images obtained with lateral DXA is strongly associated with coronary artery disease. Its presence should prompt re-assessment of the person's coronary risk disease profile and management of those risks that are modifiable.

**Disclosures:** J.T. Schousboe, Roche, Inc. 2.



## 1036

**PTH Reverses Abnormal Bone Remodeling and Structure in Hypoparathyroidism.** M. R. Rubin<sup>1</sup>, D. W. Dempster<sup>2</sup>, J. Sliney<sup>\*1</sup>, D. J. McMahon<sup>1</sup>, H. Zhou<sup>2</sup>, T. Nickolas<sup>\*1</sup>, E. M. Stein<sup>1</sup>, J. P. Bilezikian<sup>1</sup>. <sup>1</sup>Columbia University, New York, NY, USA, <sup>2</sup>Helen Hayes Hospital, New York, NY, USA.

Hypoparathyroidism (HypoPT) is characterized by atypical structural and dynamic properties of bone. We have reported that iliac crest bone biopsies show increased bone volume and suppressed bone turnover. We hypothesized that PTH treatment would restore these properties to normal. 16 HypoPT subjects (11 women; age 52 ± 12 yr) were treated with 100 µg of hPTH(1-84)[PTH] every other day for 2 yrs. Iliac crest bone biopsies were performed before (n=16) and after 1 (n=9) or 2 (n= 7) yrs of treatment. Bone remodeling variables were significantly increased at 1 yr, including osteoid thickness (2.2 ± 2 to 3.9 ± 2 lam #, p=0.02), mineralized perimeter (1.1 ± 5 to 7.9 ± 7%, p=0.001), mineral apposition rate (0.6 ± 0.3 to 0.9 ± 0.4 µm/d, p=0.01), bone formation rate (0.009 ± 0.1 to 0.08 ± 0.1 µm<sup>3</sup> / µm<sup>2</sup>/d, p=0.001), osteoid perimeter (2.5 ± 5 to 9.9 ± 7%, p= 0.002) and bone resorption rate (2.3 ± 19 to 24.2 ± 26 µm/d, p=0.004). At 2 yrs, some histomorphometric variables of bone remodeling remained significantly above baseline values including mineralized perimeter (1.1 ± 3 to 3.0 ± 4%, p= 0.001) and mineral apposition rate (0.6 ± 0.3 to 0.7 ± 0.4 µm/d, p= 0.03), although these were lower than the 1 yr values. Only osteoid perimeter continued to increase at 2 yrs (2.5 ± 9 to 13.9 ± 14%, p=0.006). After 2 yrs of treatment, structural parameters by histomorphometry revealed a decrease in cancellous bone volume (26.0 ± 6 to 21.7 ± 9%; p=0.04), an increase in trabecular separation (434.8 ± 8 to 499.1 ± 113 µm, p=0.01), and an increase in cortical porosity at both 1 (6.7 ± 4 to 10.2 ± 5%, p= 0.02) and 2 (6.6 ± 3 to 8.8 ± 4%, p= 0.03) yrs. Trabecular width, trabecular number and cortical width did not change. These data show that PTH treatment of HypoPT restores atypical structural and dynamic skeletal properties towards normal. The dynamic changes occur within the first year of therapy, with most markers of bone remodeling returning to baseline levels by 2 yrs. Further structural changes emerge after 2 yrs. Whether these changes have an impact on bone strength remains to be seen, but it would appear that PTH is a highly beneficial therapy in HypoPT.

**Disclosures:** M.R. Rubin, None.

## 1037

**Osteocyte-specific Ablation of Canonical Wnt Signaling Induces Severe Osteoporosis.** I. Kramer<sup>\*1</sup>, C. Halleux<sup>1</sup>, P. Brander Weber<sup>\*2</sup>, J. Q. Feng<sup>\*3</sup>, J. Boisclair<sup>\*2</sup>, H. Keller<sup>1</sup>, M. Kneissel<sup>1</sup>. <sup>1</sup>Musculoskeletal Disease Area, Novartis Institutes for BioMedical Research, Basel, Switzerland, <sup>2</sup>Pathology Laboratories, Novartis, Basel, Switzerland, <sup>3</sup>Biomedical Sciences, Baylor College of Dentistry, TX A&M Health Science Center, Dallas, TX, USA.

The potent osteocyte expressed bone formation inhibitor sclerostin encoded by the *Sost* gene appears to function as an inhibitor of canonical Wnt signaling by directly binding to Lrp5/6 Wnt co-receptors. Canonical Wnt signaling plays a crucial role in bone metabolism by controlling both osteoblast and osteoclast differentiation and activity. However, the role of canonical Wnt signaling in osteocytes remains to be elucidated. To investigate the *in vivo* function of the canonical Wnt signaling pathway in osteocytes we generated osteocyte-specific *beta-catenin* (*Ctnnb1*) deficient mice by crossing *Ctnnb1*<sup>loxP/loxP</sup> conditional mutant and *Dmp1-Cre* mice to obtain osteocyte-specific hetero- and homozygous (*Ctnnb1*<sup>loxP/loxP</sup>; *Dmp1-Cre*) *Ctnnb1* loss-of-function mice. We analyzed the bone phenotype in the appendicular and axial skeleton of male and female mice during growth at 6-12 weeks of age by *in vivo* and *ex vivo* peripheral quantitative and micro-computed tomography (pQCT and micro-CT) and DEXA. *Dmp1-Cre* induced *Ctnnb1* deficiency resulted in severe osteoporosis with a striking bone loss in the appendicular and axial skeleton, growth retardation and premature lethality by 2-3 month of age in both sexes. Total bone mass and density as measured by DEXA were strongly reduced by up to 60% in the tibia and femur and over 75% in lumbar vertebrae of osteocyte-targeted *Ctnnb1* mutant mice compared to control littermates. There was a progressive dramatic reduction in cancellous bone volume in both long bones with a strong decrease to complete loss of trabecular bone. Cortical bone thickness was reduced by about 50% with a concomitant outward drift and an increase in cross-sectional area in the metaphyseal region, while diaphyseal bone diameter was decreased. Histology revealed increased osteoclast activity. In contrast to homozygous *Ctnnb1* deletion *Dmp1-Cre* induced *Ctnnb1* heterozygosity caused only minor, mostly insignificant decreases in bone mass and density. Together, these results are reminiscent of the recently published bone phenotype of mice in which *beta-catenin* was deleted from the osteoblast stage onwards suggesting a previously underestimated role for canonical Wnt signaling in osteocytes in control of bone homeostasis that has not been addressed so far. In summary, we conclude that *Dmp1-Cre* induced loss of canonical Wnt signaling in osteocytes leads to severe bone loss and osteoporosis at young age.

**Disclosures:** I. Kramer, None.

## 1038

**PTH Receptor Signaling in Osteocytes Increases Bone Mass and the Rate of Bone Remodeling Through Wnt/LRP5-dependent and -independent Mechanisms, Respectively.** C. A. O'Brien<sup>1</sup>, C. Galli<sup>1</sup>, L. Plotkin<sup>1</sup>, K. Vyas<sup>\*1</sup>, P. Cazer<sup>\*1</sup>, J. J. Goellner<sup>1</sup>, S. Berryhill<sup>\*1</sup>, W. Webb<sup>\*1</sup>, A. Robling<sup>2</sup>, M. Bouxsein<sup>3</sup>, E. Schipani<sup>4</sup>, C. H. Turner<sup>5</sup>, R. S. Weinstein<sup>1</sup>, R. L. Jilka<sup>1</sup>, S. C. Manolagas<sup>1</sup>, T. M. Bellido<sup>1</sup>. <sup>1</sup>Department of Internal Medicine, University of Arkansas for Medical Sciences, Little Rock, AR, USA, <sup>2</sup>Anatomy and Cell Biology, Indiana University School of Medicine, Indianapolis, IN, USA, <sup>3</sup>Orthopedic Surgery, Beth Israel Deaconess Medical Center Harvard Medical School, Boston, MA, USA, <sup>4</sup>Endocrine Unit, Massachusetts General Hospital and Harvard Medical School, Boston, MA, USA, <sup>5</sup>Orthopedic Surgery, Indiana University School of Medicine, Indianapolis, IN, USA.

Chronic elevation of PTH increases bone remodeling and leads to either loss or gain of cancellous bone depending on the balance between resorption and formation. PTH also suppresses expression of the osteocyte-specific Wnt antagonist sclerostin, the product of the *Sost* gene. This evidence, together with the well-documented role of Wnt signaling on osteoblast production, survival, and function, suggests a mechanism by which PTH may increase osteoblast number and bone formation by acting on osteocytes. We addressed the functional consequences of PTH actions in osteocytes by generating transgenic mice expressing a constitutively active PTH receptor 1 exclusively in these cells using the osteocyte-specific dentin matrix protein-1 promoter (DMP1-caPTH1R1 mice). DMP1-caPTH1R1 mice exhibit a 2-fold increase in bone, detected at 3.5 weeks by histomorphometry and at 8 weeks by DEXA. Osteoblast number and trabecular width were elevated and osteoblast apoptosis was reduced in DMP1-caPTH1R1 mice. Surprisingly, osteoclast number was also increased. Transcripts for both osteoblast- and osteoclast-specific genes were elevated in bones from DMP1-caPTH1R1. Plasma levels of osteocalcin and CTX and urinary levels of DPD were increased, confirming that DMP1-caPTH1R1 mice exhibit high bone formation and resorption. *Sost* mRNA and sclerostin protein were strikingly decreased in the transgenic mice. Consistent with this, Wnt signaling was elevated, as demonstrated by increased expression of the Wnt/β catenin target genes Axin 2, SMAD6, BMP4, and naked, and by elevated β-galactosidase activity in bones from the Wnt reporter mice TCF-βgal crossed with DMP1-caPTH1R1 mice. Crossing DMP1-caPTH1R1 mice with mice lacking the Wnt co-receptor LRP5 attenuated the high bone mass phenotype but not the increase in bone remodeling. These findings demonstrate that PTH receptor signaling in osteocytes increases bone mass and the rate of bone remodeling through Wnt/LRP5-dependent and -independent mechanisms, respectively, revealing two previously unappreciated roles for osteocytes in the skeletal actions of PTH.

**Disclosures:** T.M. Bellido, Radius 5.

This study received funding from: NIH.

## 1039

**PTH-induced Bone Mass Gain Is Blunted But Not Abolished in *SOST* Overexpressing and Deficient Mice.** I. Kramer<sup>\*1</sup>, G. G. Loots<sup>\*2</sup>, H. Keller<sup>1</sup>, M. Kneissel<sup>1</sup>. <sup>1</sup>Musculoskeletal Disease Area, Novartis Institutes for BioMedical Research, Basel, Switzerland, <sup>2</sup>Biosciences and Biotechnology Division, Chemistry, Materials and Life Sciences Directorate, Lawrence Livermore National Laboratory, Livermore, CA, USA.

PTH signaling down-regulates expression of the bone formation inhibitor *SOST*. To test whether *SOST* suppression contributes to the bone anabolic action of intermittent PTH treatment, we subjected male BAC transgenic mice overexpressing human *SOST* and male mice lacking endogenous *SOST* (targeted knockout) to daily injections of 100 microg/kg hPTH(1-34) or vehicle for a two-month-period. Bone changes were monitored *in vivo* in the distal femur metaphysis and *ex vivo* in the entire femur by pQCT. Animals were sacrificed 4 hours after the final PTH application and RNA was extracted from long bone diaphyses for *SOST* expression analysis by real-time PCR. Consistent with its role as a bone formation inhibitor increased *SOST* gene dosage resulted in mild but significant osteopenia. Intermittent PTH treatment repressed endogenous mouse *SOST* by about 50%. Comparable suppression levels were observed for human *SOST* expressed from the BAC transgene under the control of its own proximal promoter and its downstream enhancer, resulting in a relative excess of *SOST* in PTH treated BAC transgenic mice. PTH treatment induced substantial increases in bone mineral content and density in wildtype mice due to cortical and cancellous bone gain. Both PTH-induced cortical and cancellous bone gain was significantly attenuated, but not abolished in *SOST* overexpressing mice. *SOST* deficient mice display a progressive distinct high bone mass phenotype. We hence initiated PTH treatment in these mice at 6 weeks of age to avoid a situation in which further intervention-induced bone gain might not have been achievable anymore. *SOST* was absent in knockout mice and was suppressed by about 50% in wildtype littermates following PTH application. PTH induced substantial increases in bone mass and density in the femur of growing wildtype mice. This was predominantly related to cortical thickening. *SOST* deficient mice showed small non-significant PTH-induced increases in bone mass and density and cortical thickening. In conclusion, our data support the hypothesis that bone mass gain induced by intermittent PTH treatment relies in part on *SOST* repression, since bone gain was attenuated in mice with higher *SOST* levels and in mice lacking *SOST*. Furthermore, the results from the BAC transgenic mouse model demonstrate that human *SOST* is regulated by intermittent PTH treatment in a similar manner as mouse *SOST*. The finding that PTH-induced bone gain is not completely abolished in *SOST* overexpressing or deficient mice is in line with the fact that PTH uses multiple pathways to promote bone formation.

**Disclosures:** I. Kramer, None.



## 1040

**Adenylyl Cyclase 6 Mediates Primary Cilia-Regulated Decreases in cAMP in Bone Cells Exposed to Dynamic Fluid Flow.** R. Y. Kwon<sup>\*1</sup>, S. Temiyasathit<sup>\*2</sup>, P. Tummala<sup>\*3</sup>, C. C. Quah<sup>\*3</sup>, C. R. Jacobs<sup>3</sup>. <sup>1</sup>Department of Mechanical Engineering, Stanford University, Stanford, CA, USA, <sup>2</sup>Department of Bioengineering, Stanford University, Stanford, CA, USA, <sup>3</sup>VA Medical Center, Palo Alto, CA, USA.

Primary cilia function as mechanosensory organelles in several tissue types. Recently, our lab showed that they mediate osteogenic and anti-resorptive responses in bone cells exposed to fluid flow. However, the second messenger system(s) involved has not been determined. In this study, our goals were to determine (1) whether exposing bone cells to dynamic flow alters intracellular levels of cyclic adenosine monophosphate (cAMP), a ubiquitous second messenger molecule, and (2) the role of primary cilia in mediating this process. To investigate this, we exposed MLO-Y4 osteocyte-like cells to oscillatory flow (1Hz, 1Pa) and quantified intracellular cAMP levels. We found that exposure to 2 minutes of flow induced a significant decrease in cAMP ( $0.62 \pm 0.07^{**}$ ;  $p < 0.001$ ;  $n = 17$ ). To assess the role of primary cilia in mediating this process, we treated the cells with siRNA targeted against polaris, a protein necessary for primary cilia formation. Treatment significantly lessened flow-induced decreases in cAMP (control siRNA:  $0.57 \pm 0.08$ , polaris siRNA:  $0.89 \pm 0.04$ ;  $p < 0.001$ ;  $n \geq 9$ ). To further investigate the relationship between primary cilia and cAMP, we immunostained the cells for all nine different membrane-bound isoforms of adenylyl cyclase (AC1-9), the enzyme that synthesizes cAMP. Interestingly, we found that one isoform, AC6, was highly localized to primary cilia, and treating the cells with siRNA targeted against AC6 significantly diminished flow-induced decreases in cAMP (control siRNA:  $0.57 \pm 0.08$ , AC6 siRNA:  $1.07 \pm 0.10$ ;  $p = 0.001$ ;  $n \geq 6$ ). Previous studies have shown that binding of  $Ca^{2+}$  to AC6 inhibits cAMP synthesis and that entry of  $Ca^{2+}$  through cilium-localized mechanosensitive ion channels is important for transduction of flow in renal epithelial cells and cholangiocytes. In our studies, blocking stretch-activated ion channels using gadolinium chloride eliminated flow-induced decreases in cAMP (no treatment:  $0.62 \pm 0.07$ , gadolinium chloride:  $1.02 \pm 0.08$ ;  $p = 0.001$ ;  $n \geq 9$ ). Taken together, our findings suggest that AC6 mediates primary cilia-regulated decreases in cAMP in bone cells exposed to short bouts of oscillatory flow, and that activation of mechanosensitive ion channels is necessary for this process. In addition, our findings are consistent with the hypothesis that flow-induced decreases in cAMP are due to inhibition of AC6 by  $Ca^{2+}$  entry through stretch-activated ion channels localized to primary cilia, although further investigation is necessary in this regard.

\*ST and RYK contributed equally to this work

\*\*all data expressed as mean  $\pm$  SEM of flow/no flow

**Disclosures:** R.Y. Kwon, None.

This study received funding from: National Institutes of Health Grant AR054156.

## 1041

**In Vivo Load Activated Propagation of  $\beta$ -catenin Signaling in Osteocytes through Coordinated Downregulation of Inhibitors of Lrp5.** N. A. Kim-Weroha<sup>\*1</sup>, A. Ferris<sup>\*1</sup>, B. Holladay<sup>\*1</sup>, S. P. Kotha<sup>2</sup>, M. A. Kamel<sup>1</sup>, M. L. Johnson<sup>1</sup>. <sup>1</sup>Oral Biology, UMKC School of Dentistry, Kansas City, MO, USA, <sup>2</sup>UConn School of Engineering, Storrs, CT, USA.

The Lrp5/Wnt/ $\beta$ -catenin signaling pathway is critical for bone formation in response to mechanical load. Osteocytes, thought to be the transducers of load, express two major inhibitors of Lrp5; Dkk1 and sclerostin. We have previously shown that the prostaglandin signaling pathway crosstalks with  $\beta$ -catenin signaling through Akt mediated inhibition of GSK-3 $\beta$  *in vitro*. Prostaglandin is essential for load induced bone formation and its release could enable osteocytes to respond rapidly to load, even in the presence of these Lrp5 inhibitors. To test this model *in vivo* we examined the timing of  $\beta$ -catenin signaling versus Dkk1 and sclerostin expression in bone subjected to loading (forearm compression, 100 cycles, 2 Hz, ~4000 $\mu$ E) in TOPGAL ( $\beta$ -catenin reporter) mice.  $\beta$ -catenin activity was monitored by  $\beta$ -gal staining and changes in Dkk1 and sclerostin were detected by immunostaining in the ulna midshaft region. The number of  $\beta$ -gal positive osteocytes in regions of maximal strain increased by 1.5, 1.8 and 2.6 fold, respectively, at 1, 4 and 24 hr post loading (N=4 per time) ( $p < .01$ ) to ~40% of the osteocytes (baseline ~15%), suggesting a rapid activation of  $\beta$ -catenin signaling in a subset of osteocytes and propagation to connecting osteocytes over time. Whereas osteocytes responded rapidly to loading,  $\beta$ -gal positive cells on the bone surface were not observed until 24 hr post loading suggesting slower propagation to the bone surface. At baseline, Dkk1/sclerostin were co-expressed in ~80% of the osteocytes in regions of maximal strain and >98% of the osteocytes in neutral strain regions. At 1 and 4 hours post loading, no statistically significant changes in the number of Dkk1 or sclerostin positive osteocytes were observed, but  $\beta$ -catenin signaling was observed in both Dkk1/sclerostin positive and negative osteocytes. However, by 24 hr post loading, the number of osteocytes positive for Dkk1/sclerostin was decreased by 50% ( $p < .01$ ) and most of the cells with activated  $\beta$ -catenin signaling expressed low or undetectable levels of these inhibitors, suggesting a reciprocal relationship between  $\beta$ -catenin activation and downregulation of the inhibitors in osteocytes over 24 hrs. The data support our model of a rapid activation of  $\beta$ -catenin signaling independent of Lrp5 thereby circumventing inhibition by Dkk1 and sclerostin, potentially through a PGE<sub>2</sub> crosstalk mechanism followed by a longer term Lrp5-dependent amplification of  $\beta$ -catenin signaling that requires the downregulation of Dkk1 and sclerostin. Such a model provides a molecular mechanism for the propagation of mechanical strain related responses.

**Disclosures:** N.A. Kim-Weroha, None.

This study received funding from: NIAMS RO1 AR053949-01.

## 1042

**Transcriptional Regulation of Connexin 43 by  $\beta$ -catenin, a Pathway Activated by PGE<sub>2</sub>-PI3K-GSK-3 Signaling in Mechanically Loaded Osteocytes.** X. Xia<sup>\*1</sup>, S. Harris<sup>2</sup>, L. F. Bonewald<sup>3</sup>, E. Sprague<sup>\*4</sup>, J. X. Jiang<sup>1</sup>. <sup>1</sup>Biochemistry, University of Texas Health Science Center, San Antonio, TX, USA, <sup>2</sup>Periodontics, University of Texas Health Science Center, San Antonio, TX, USA, <sup>3</sup>Oral Biology, University of Missouri, School of Dentistry, Kansas City, MO, USA, <sup>4</sup>Radiology, University of Texas Health Science Center, San Antonio, TX, USA.

Primary osteocytes and osteocyte-like MLO-Y4 cells express large amounts of connexin 43 (Cx43) which forms gap junctions and hemichannels. Osteocytes can only form gap junctions at the connecting tips of their dendritic processes leaving hemichannels along the extensive cell membrane surfaces of the dendrites and cell body. Fluid flow shear stress (FFSS) induces the opening of hemichannels in MLO-Y4 cells associated with the release of prostaglandin, an important bone modulator. The released prostaglandin E<sub>2</sub> (PGE<sub>2</sub>) binds to EP2/4 receptor activating the cAMP-PKA signaling pathway, which leads to an increase in the expression of Cx43 and consequently gap junction function. To identify the steps in this signaling cascade, we searched for potential crosstalk with the  $\beta$ -catenin pathway. Both FFSS and PGE<sub>2</sub> increased the phosphorylation levels of Akt suggesting that PI3 kinase (PI3K) signaling pathways are activated by FFSS through PGE<sub>2</sub> in MLO-Y4 osteocyte-like cells. PI3K specific inhibitor, LY294002, but not a MAPK inhibitor, PD98059 attenuated the stimulatory effect of PGE<sub>2</sub> on Cx43 expression. FFSS and PGE<sub>2</sub> stimulated the phosphorylation levels of glycogen synthase kinases 3 $\alpha$  and 3 $\beta$  (GSK-3 $\alpha/\beta$ ) and this increase was blocked by PI3K inhibitor, but not MAPK inhibitor suggesting that the inactivation of GSK-3 activity was also mediated by PI3K activation. Application of FFSS and PGE<sub>2</sub>, and subsequent PI3K activation led to the stabilization and nuclear translocation of  $\beta$ -catenin. Knockdown of  $\beta$ -catenin expression by siRNA resulted in a reduction in Cx43 protein expression. Furthermore, chromatin immunoprecipitation (ChIP) assay demonstrates the association of  $\beta$ -catenin with Cx43 DNA promoter, suggesting that  $\beta$ -catenin regulates Cx43 expression at the level of gene transcription. Together, these results suggest that FFSS through PGE<sub>2</sub> release activates PI3K-AKT signaling, which leads to GSK-3 inactivation and the activation of  $\beta$ -catenin pathway resulting in an increase in Cx43. Therefore, the PI3K-AKT/ $\beta$ -catenin signaling pathway plays an essential role in regulating gap junction and hemichannel function through transcriptional regulation of Cx43 expression in response to FFSS induced prostaglandin release.

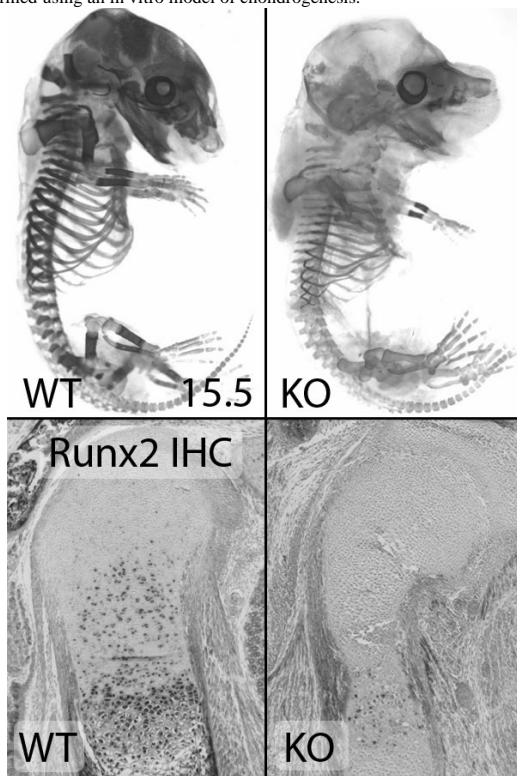
**Disclosures:** J.X. Jiang, None.

This study received funding from: National Institute of Health.

## 1043

**MIA3, a Novel Secreted Factor, Regulates Chondrogenic Differentiation in the Developing Mouse Embryo.** M. J. Solloway, D. Grant<sup>\*</sup>, K. Phamluong<sup>\*</sup>, A. Peterson<sup>\*</sup>. Molecular Biology, Genentech, Inc., South San Francisco, CA, USA.

MIA3 belongs to a family of four secreted proteins (MIA, MIA2, MIA3, OTOR) which are unique in that they contain an extracellular SH3 domain. These molecules have been implicated in regulating chondrogenesis via poorly characterized mechanisms: *Mia* is expressed exclusively in the developing skeleton, and treatment of differentiating mesenchymal stem cells with MIA protein stabilizes a chondrogenic phenotype while inhibiting osteogenic differentiation. However, null mice are viable and display subtle ultrastructural defects in collagen deposition. In order to further characterize the role(s) played by the MIA proteins in skeletogenesis, we generated an allele of MIA3 lacking the extracellular SH3 domain. Embryos lacking this ubiquitously expressed protein die near term and display a striking delay in the progression of chondrogenesis and mineralization as well as severe edema. This phenotype is overtly similar to that seen in embryos lacking the chondrocyte/osteoblast-specific transcription factor *Runx2*, and *Runx2* expression is strongly downregulated in the *Mia3* mutant bone anlagen. Several other markers of chondrogenic maturation are also severely misregulated in the mutant bone, including PTH/PTHrP receptor, *Ihh*, and Collagen type I. In support of this observation, treatment of differentiating ATDC5 teratocarcinoma cells with the purified MIA3 SH3 domain stimulates the early stages of chondrogenesis while delaying later chondrogenic maturation. In summary, our analysis of *Mia3* embryos uncovers a novel role for this gene in coordinating chondrocyte differentiation throughout the skeleton, and these observations are confirmed using an in vitro model of chondrogenesis.



**Disclosures:** M.J. Solloway, Genentech, Inc. 3.  
This study received funding from: Genentech, Inc.

## 1044

**PTHrP Prevents Chondrocyte Premature Hypertrophy by Inducing Cyclin D1-Dependent Runx2 and 3 Phosphorylation and Degradation.** R. Xie<sup>1</sup>, M. Zhang<sup>\*2</sup>, M. Zhu<sup>1</sup>, W. Hou<sup>\*1</sup>, R. Shen<sup>1</sup>, Q. Wang<sup>\*2</sup>, T. Zhu<sup>\*2</sup>, D. Chen<sup>1</sup>. <sup>1</sup>Orthopaedics, University of Rochester, Rochester, NY, USA, <sup>2</sup>Medical College of Nankai University, Tianjin, China.

PTHrP maintains chondrocytes in a proliferative state. In PTHrP KO mice, premature chondrocyte hypertrophy was observed. The mechanism by which PTHrP prevents chondrocytes from premature hypertrophy is not fully understood. *Runx2* and *3* are required for chondrocyte maturation. In *Runx2* and *3* double KO mice, chondrocyte hypertrophy was completely inhibited. We recently demonstrated that cell cycle protein cyclin D1 induces *Runx2* phosphorylation, ubiquitination and degradation. In the present studies, we tested the hypothesis that PTHrP regulates protein stability of *Runx2* and *3* through cyclin D1. We found that cyclin D1 induced *Runx3* degradation in a dose-dependent manner and *Runx3* directly interacts with CDK4. A conserved CDK recognition site, the SP motif, was identified in the C-terminal region of *Runx3* by sequence analysis (aa 356-359). Pulse-chase experiments showed that the mutation of *Runx3* at serine-356 to alanine (SA-*Runx3*) increased the half-life of *Runx3*. In contrast, a serine-356 to glutamic

acid mutation (SE-*Runx3*) accelerated *Runx3* degradation. In addition, SA-*Runx3* was resistant to cyclin D1-induced degradation. GST-*Runx3* was strongly phosphorylated by CDK4 in vitro. In contrast, CDK4 had no effect on the phosphorylation of SA-*Runx3*. While both WT and SE-mutant *Runx3* were ubiquitinated, the SA-mutant *Runx3* was not. The cyclin D1-induced *Runx3* degradation was completely blocked by the proteasome inhibitor PS1. SA-*Runx3* had a greater and SE-*Runx3* had a lesser induction of the 6xOSE2-Luc *Runx* reporter and ALP activity compared to WT *Runx3* in C3H10T1/2 cells. To investigate the role of cyclin D1 in chondrocyte proliferation and hypertrophy, we analyzed growth plate morphology and gene expression of cyclin D1 KO mice. The proliferating zone was significantly reduced and expression of chondrocyte differentiation marker genes and ALP activity were enhanced in postnatal cyclin D1 KO mice. PTHrP significantly suppressed protein levels of both *Runx2* and *3* in primary chondrocytes derived from WT mice. In contrast, the suppressive effect of PTHrP on *Runx2* and *3* protein levels was completely abolished in primary chondrocytes derived from cyclin D1 KO mice. Our findings demonstrate that the cell cycle proteins cyclin D1/CDK4 induce *Runx2* and *3* phosphorylation, ubiquitination, and proteasome degradation. PTHrP suppresses *Runx2* and *3* protein levels in chondrocytes through cyclin D1. These results suggest that PTHrP may prevent chondrocytes from premature hypertrophy by inducing degradation of *Runx2* and *3* in a cyclin D1-dependent manner.

**Disclosures:** R. Xie, None.

This study received funding from: NIH.

## 1045

**Transcription Factor Dmrt2 Controls Endochondral Ossification Through Regulating Type 10 Collagen (Col10a1) Gene Expression.** K. Ono<sup>\*1</sup>, K. Hata<sup>1</sup>, E. Nakamura<sup>\*2</sup>, A. Sugita<sup>\*1</sup>, K. Amano<sup>\*1</sup>, M. Nakanishi<sup>\*1</sup>, Y. Takigawa<sup>\*1</sup>, R. Nishimura<sup>1</sup>, S. Takenoshita<sup>\*3</sup>, T. Yoneda<sup>1</sup>. <sup>1</sup>Biochem, Osaka Univ Grad Sch Dent, Suita, Japan, <sup>2</sup>Biochem, Osaka Univ Sch Dent, Suita, Japan, <sup>3</sup>Surgery II, Fukushima Med Univ Grad Sch Med, Fukushima, Japan.

Dmrt (doublesex and mab-3-related transcription factor) genes encode a large family of transcription factors which play important roles in sex differentiation. Recent genetic studies have reported that loss of DMRT1/2 causes not only sex reversal but also growth retardation, scoliosis and malformation of fingers in human and that *Dmrt2*-deficient mice shows malformation of rib and sternum, suggesting that *Dmrt* genes are also involved in vertebrate skeletal development. In the present study, we investigated the role of *Dmrt2* in endochondral ossification that plays a central role in vertebral skeletal development. As a first approach to address this, we examined the expression of *Dmrt2* in chondrocytes. RT-PCR analysis revealed that *Dmrt2* was the only *Dmrt* family member strongly expressed in E11.5-E14.5 mouse hind limbs. Immunohistochemical analysis further demonstrated that *Dmrt2* was strongly expressed in pre-hypertrophic zone but weakly in proliferative and late-hypertrophic zone in E14.5 tibia. *Dmrt2* was also expressed in primary mouse chondrocytes in culture. The expression of *Dmrt2* was increased during chondrogenic differentiation in C3H10T1/2 cells treated with BMP2. We next investigated the effects of *Dmrt2* on chondrocyte differentiation. Overexpression of *Dmrt2* using adenovirus system reduced type 2 collagen (Col2a1) expression but increased Col10a1 expression in BMP2-treated C3H10T1/2 cells. *Dmrt2* also markedly increased Col10a1 expression in primary mouse chondrocytes in the presence of BMP2, whereas it decreased markers for early chondrocyte differentiation such as Col2a1, aggrecan and Col11a1. Moreover, knockdown of *Dmrt2* using siRNA suppressed Col10a1 expression. Finally, we studied the molecular basis of *Dmrt2* functions. *Dmrt2* reduced Sox9-induced Col2a1 expression. Reporter assay using Col2a1 promoter revealed that *Dmrt2* decreased Sox9 transcriptional activity. In contrast, *Dmrt2* directly transactivated Col10a1 gene promoter presumably through binding to the putative *Dmrt2* binding element in Col10a1 promoter. In conclusion, our results show that *Dmrt2* is expressed at high levels in pre-hypertrophic chondrocytes and inhibits Col2a1 expression and stimulates Col10a1 expression, suggesting that *Dmrt2* regulates cartilage differentiation through inhibiting early-stage and promoting late-stage chondrocyte differentiation. Further elucidation of *Dmrt2* function in chondrogenesis would contribute to better understanding of the mechanism underlying endochondral ossification.

**Disclosures:** K. Ono, None.

## 1046

**Conditional Deletion of Fibronectin Results in a Scoliosis-Like Phenotype.**Q. Chen<sup>1</sup>, H. Zhao<sup>\*1</sup>, J. Zhao<sup>\*1</sup>, D. M. Pacicca<sup>\*2</sup>, R. Fassler<sup>\*3</sup>, S. L. Dallas<sup>1</sup>.<sup>1</sup>Univ. of Missouri, Kansas City, Kansas City, MO, USA, <sup>2</sup>Children's Mercy Hospitals & Clinics, Kansas City, MO, USA, <sup>3</sup>Max Planck Institute of Biochemistry, Martinsried, Germany.

Congenital scoliosis is a condition of lateral curvature of the spine due to a developmental abnormality. Fibronectin (FN) is an extracellular matrix (ECM) glycoprotein that is expressed at sites of bone formation and is critical for osteoblast function. Although a role for FN in scoliosis has not been reported, we have generated transgenic mice in which FN is deleted in the osteoblast lineage. The mice exhibit a scoliosis-like phenotype, suggesting a potential role for FN in this disease. Mice with a floxed FN gene were crossed with mice expressing Cre recombinase driven by the 3.6kb Col1a1 promoter. Numbers of FNcKO mice were 60% less than expected, suggesting embryonic lethality. Surviving mice showed vertebral deformities resembling scoliosis. 100% of the FNcKO mice showed tail deformities (kinky tail), ranging from involvement of a single vertebra to all tail vertebrae. Deformities included fusions, hemivertebrae as well as block, asymmetric and abnormally segmented vertebrae. In a subgroup of mice with severe tail deformities, fusion of lumbar vertebrae, kyphosis and lateral spine curvatures were seen at birth and became more severe with age. FNcKO mice also showed significantly decreased bone mineral density and bone mineral content and a mild/moderate short stature. As FN controls assembly of several other ECM proteins, we next determined whether the phenotype of FNcKO mice was due to abnormal ECM assembly. Decreased FN in the skeleton was associated with decreased type I collagen and fibrillin-1, two ECM proteins implicated in scoliosis. FN deletion was also associated with reduced BMP signaling in osteoblasts, as shown by decreased phospho-Smad 1/5/8 staining. A key role for FN in assembly of bone ECM proteins was confirmed by infecting FN floxed osteoblasts with adenoviral Cre recombinase to delete FN in vitro. This resulted in a 90% reduction in FN, accompanied by impaired assembly of type I collagen, decorin, biglycan, LTBP1 and fibrillin-1, a known regulator of BMPs. Assembly of these matrix molecules was rescued by supplementation with FN. In the embryo, FN is localized at somite boundaries and disruption of FN in avian embryos inhibits somite formation. Conventional FN gene deletion is embryonic lethal at E8.5, with embryos failing to form somites. By examining FNcKO embryos, we found that the tail phenotype was apparent by E12.5, suggesting defective somitogenesis and/or resegmentation. These data suggest that misregulation of FN may play a role in scoliosis by regulating assembly of ECM proteins and/or altering ECM regulated growth factor pathways critical for axial skeleton patterning, bone growth and development.

**Disclosures:** Q. Chen, None.

This study received funding from: NIH (NIAMS) RO1 AR051517.

## 1047

**Activation of  $\beta$ -Catenin Signaling in Articular Chondrocytes Leads to Osteoarthritis-like Phenotype in Adult  $\beta$ -Catenin Conditional Activation Mice.**

D. Tang, M. Zhu, Q. Wu, M. Chen, C. Xie, R. N. Rosier, R. J. O'Keefe, M. Zuscik, D. Chen. Orthopaedics, University of Rochester, Rochester, NY, USA.

Osteoarthritis (OA) is a degenerative joint disease and the mechanism of its pathogenesis is poorly understood. Recent human genetic association studies demonstrate that mutations in the *Frzb* gene predispose patients to OA, suggesting that the Wnt/ $\beta$ -catenin signaling may play a key role in the development of OA. However, direct genetic evidence for  $\beta$ -catenin in this disease has not been reported. Since chondrocyte-specific activation of the  $\beta$ -catenin gene (targeted by *Col2a1-Cre*) is embryonic lethal, we have generated inducible  $\beta$ -catenin conditional activation (cAct) mice via breeding of  $\beta$ -catenin<sup>fl<sup>Ex3</sup>/fl<sup>Ex3</sup></sup> mice with *Col2a1-CreER<sup>T2</sup>* transgenic mice. Deletion of exon 3 of the  $\beta$ -catenin gene results in the production of a stabilized  $\beta$ -catenin protein which is resistant to phosphorylation by GSK-3 $\beta$ . In this study, tamoxifen was administered to the 3- and 6-month-old *Col2a1-CreER<sup>T2</sup>*;  $\beta$ -catenin<sup>fl<sup>Ex3</sup>/fl<sup>Ex3</sup></sup> mice and tissues were harvested for histologic analysis 2 months after tamoxifen induction. Over expression of  $\beta$ -catenin protein was detected by immunostaining in articular cartilage tissues of  $\beta$ -catenin cAct mice. In 5-month-old  $\beta$ -catenin cAct mice, reduction of Safranin O staining in articular cartilage tissue and reduced articular cartilage area were observed. In 8-month-old  $\beta$ -catenin cAct mice, cell cloning, surface fibrillation, vertical clefting and osteophyte formation were observed. Complete loss of articular cartilage layers and the formation of new woven bone in subchondral bone area were found in  $\beta$ -catenin cAct mice. Expression of chondrocyte marker genes, such as *aggrecan*, *Mmp-9*, *Mmp-13*, *Alp*, *Oc*, and *colX* was significantly increased (3 to 6-fold) in articular chondrocytes derived from  $\beta$ -catenin cAct mice. *Bmp2* but not *Bmp4* expression was also significantly up-regulated (6-fold increase) in these cells. In vitro studies further demonstrated that Wnt3a-induced expression of chondrocyte marker genes, such as *Alp*, *Oc* and *colX*, was completely inhibited by noggin in articular chondrocyte cell cultures, suggesting that Wnt3a regulates the expression of these chondrocyte marker genes in a *Bmp*-dependent mechanism. In addition, we also found that  $\beta$ -catenin protein is over expressed in knee joint samples from patients with OA. Our findings indicate that activation of  $\beta$ -catenin signaling in articular chondrocytes in adult mice leads to the premature chondrocyte differentiation and the development of an OA-like phenotype. This study provides direct and definitive evidence about the role of  $\beta$ -catenin in the development of OA.

**Disclosures:** D. Tang, None.

This study received funding from: National Institute of Health.

## 1048

**In vivo Knockdown of GEP, a Novel Growth Factor in Cartilage, Led to Defects in Cartilage and Osteoarthritis.**B. Jiang<sup>\*1</sup>, Y. Zhang<sup>\*2</sup>, Y. Xie<sup>\*1</sup>, L. Kong<sup>\*2</sup>, F. Guo<sup>\*2</sup>, Z. Cao<sup>\*1</sup>, J. Q. Feng<sup>1</sup>, C. Liu<sup>2</sup>. <sup>1</sup>Department of Biomedical Sciences, Baylor College of Dentistry, Texas A&M University System Health Science Center, Dallas, TX, USA, <sup>2</sup>Department of Orthopaedic Surgery, NYU Hospital for Joint Diseases, New York, NY, USA.

In searching for proteins critical for cartilage formation and function, we identified a previously unknown growth factor, granulin/epithelin precursor (GEP) in cartilage. In situ hybridization assays showed that GEP is highly expressed in growth plate and articular cartilage during both embryonic and postnatal development. Real time RT-PCR and Western blotting assays showed that GEP were upregulated by BMP2 during chondrogenesis. Additions of recombinant GEP into high-density human postnatal mesenchymal stem cell pellets, significantly increase expression levels of Sox9 (10-fold), Sox 5 and 6 (40-fold), Ihh (100-fold), and Runx2 (6-folds), Col II (30-fold), Aggrecan (50-fold), and Col X (120-fold), respectively. In contrast, GEP completely inhibits mRNA levels of PTHrP, and PTH receptor 1, two negative regulators of chondrogenesis. Furthermore, GEP is more potent than BMP2 in inducing chondrogenic markers such as Col X at an equivalent dosage level. We also created GEP knockdown mice where siGEP RNA is driven by the U6 promoter, a ubiquitous promoter that is disturbed by a loxP-flanked neomycin cassette (Note that the siGEP RNA expression will be activated only when crossed to Cre transgenic mice whose Cre removes the neomycin). Next, U6-ploxPneo-GEP transgenic mice were crossed to Sox2-Cre transgenic mice, where Cre enzyme is activated in early mesenchymal cells, for tissue-specific knockdown of GEP. GEP mRNA/protein levels in these mice were undetectable in cartilage, and these mice display a sharp reduction in skeletal length, bone volumes, and cortical bone thickness. The knockdown growth plate is only half size of that in WT, and shows a sharp reduction of Col II, alkaline phosphatase, and Col X. The 10-mo-old mice display an osteoarthritis phenotype in large and small joints such as joint space narrowing, reduction of articular chondrocytes in number, extracellular matrix and sclerotic subchondral bone formation, osteophytes, and subchondral sclerosis (increased bone density). Finally we showed that both mRNA and protein levels of GEP were upregulated in arthritis patients. Based on the above findings we conclude that GEP, a novel growth factor in cartilage, is critical for chondrogenesis; and that GEP null mice are a new arthritis model.

**Disclosures:** B. Jiang, None.

This study received funding from: NIH RO1 AR051587 (JQF) and RO3 AR052022 (CL).

## 1049

**Prolyl 3-Hydroxylase 1 and CRTAP are Mutually Stabilizing in the Endoplasmic Reticulum Collagen Prolyl 3-Hydroxylation Complex.**

W. Chang, A. M. Barnes\*, W. A. Cabral\*, J. C. Marini. Bone and Extracellular Matrix Branch, NICHD, NIH, Bethesda, MD, USA.

Osteogenesis Imperfecta is a heritable bone disease characterized by increased skeletal fragility and growth deficiency. Classical dominant OI is caused by mutations in the two genes encoding type I collagen. We recently identified null mutations in cartilage associated protein (CRTAP) and prolyl 3-hydroxylase 1 (P3H1/LEPRE1) as the cause of two novel recessive forms of OI, Types VII and VIII, respectively. CRTAP and P3H1, along with cyclophilin B, form a complex in the endoplasmic reticulum (ER) which modifies the  $\alpha 1$  chain of types I and II collagen by 3-hydroxylation of the Pro986 residue. The interactions of CRTAP and P3H1 in this complex are unknown. In this investigation, we used cultured dermal fibroblasts from type VII and VIII OI probands to demonstrate that CRTAP and P3H1 are mutually protective in the ER complex. P3H1 is absent on Western blots of CRTAP-null fibroblast lysates and, conversely, CRTAP is minimally detectable on Western blots of LEPRE1-null lysates. Real-time RT-PCR amplification yielded increased *LEPRE1* or *CRTAP* mRNA levels in cells which have null mutations and low levels of the other transcript. Therefore, absence of either CRTAP or P3H1 from cells with a null mutation in the other gene must be presumed to result from loss of normal mutual stabilization. In contrast, cyclophilin B, the third component of the complex, was equally abundant in control and both sets of mutant cell lines. Also, parental carriers of *CRTAP* or *LEPRE1* mutations have near-normal levels of the other protein. Stable transfection of a full-length *CRTAP* expression plasmid into *CRTAP* null fibroblasts restored both CRTAP and P3H1 protein levels. Stable transfection with a series of *CRTAP* deletion constructs demonstrated that deletions of portions of exon 1 or 4, which may be crucial for CRTAP folding or interactions with P3H1 in the complex, failed to restore P3H1 protein levels on Western blots. Expression of a construct with a deletion of the region encoding the only TPR-like motif in CRTAP results in partial restoration of P3H1 levels. We are also examining the trafficking of CRTAP in *LEPRE1*-null cells. Immunofluorescence microscopy demonstrated reduced levels of CRTAP in *LEPRE1*-null cells, while CRTAP localization in these cells is being determined. CRTAP is detectable in the conditioned media of control and *LEPRE1*-null fibroblasts. Since P3H1 has an ER retention signal, absence of the P3H1 may lead to increased CRTAP secretion. We are currently examining the levels of P3H1 secretion from *CRTAP*-null fibroblasts, as well as the proteosomal and non-proteosomal pathways of degradation that the null cells may be utilizing to handle the chronic ER stress from abnormally modified collagen.

**Disclosures:** W. Chang, None.

This study received funding from: NIH Intramural Research.

## 1050

**Defects in Mesenchymal Stem Cell Self-Renewal Lead to an Osteopenic Phenotype in *Bmi-1* Null Mice.** H. W. Zhang\*, J. Ding\*, J. L. Jin\*, D. S. Miao. The Research Center for Bone and Stem Cells, Nanjing Medical University, Nanjing, China.

Previous studies have demonstrated that the oncogene *Bmi-1* plays an important role in maintaining the self-renewal of neural and hematopoietic stem cells, but its role in maintaining the self-renewal of bone marrow mesenchymal stem cells (BM-MSCs) is currently unknown. In the present studies, we have analyzed the skeletal phenotype of *Bmi-1*<sup>-/-</sup> mice and determined the role of *Bmi-1* in BM-MSC function. Changes in cell proliferation and differentiation were examined in BM-MSCs isolated from 3-week-old *Bmi-1*<sup>-/-</sup> mice. *Bmi-1*<sup>-/-</sup> mice exhibited skeletal growth retardation associated with reduced chondrocyte proliferation and increased chondrocyte apoptosis, demonstrated by immunostaining for the proliferating cell nuclear antigen and by TUNEL staining, respectively. Histomorphometric analysis showed that bone mineral density, trabecular bone volume, osteoblast number, the alkaline phosphatase and type I collagen positive area of metaphyseal region and the mineral apposition rate were all significantly reduced in *Bmi-1*<sup>-/-</sup> mice. However, the number of adipocytes within bone marrow was increased in 2- and 4-week-old *Bmi-1*<sup>-/-</sup> mice. The reduced bone formation in *Bmi-1*<sup>-/-</sup> mice was associated with decreased gene expression of alkaline phosphatase, type I collagen and osteocalcin. The increased adipocyte formation was associated with increased expression of Ppar- $\gamma$  in bone tissue of *Bmi-1*<sup>-/-</sup> mice. In contrast, *Bmi-1* deficiency does not affect osteoclast formation. The numbers of TRAP-positive multi-nucleated osteoclasts and the ratio of RANKL and OPG gene expression were not altered in *Bmi-1*<sup>-/-</sup> mice. Bone marrow cell cultures showed that the efficiency of CFU-F formation was decreased. The percentage of alkaline phosphatase-positive CFU-F was significantly reduced accompanied by down-regulation of Runx2 protein expression. The efficiency of adipocyte formation was significantly increased associated with up-regulation of Ppar- $\gamma$  protein expression in BM-MSCs derived from *Bmi-1*<sup>-/-</sup> mice. Reduced proliferation and increased apoptosis of BM-MSCs were associated with up-regulation of the senescence-associated tumor suppressor genes including p16, p19 and p27 in *Bmi-1*<sup>-/-</sup> mice. Our results indicate that *Bmi-1* plays a critical role in maintaining the self-renewal of BM-MSCs by inhibiting the expression of tumor suppressor genes such as p16, p19 and p27. *Bmi-1* promotes Runx2 expression and BM-MSC differentiation into osteoblasts and down-regulates Ppar- $\gamma$  expression and inhibits their differentiation into adipocytes.

**Disclosures:** D.S. Miao, None.

## 1051

**Aberrant *Phex* Function in Osteocytes Has Limited Effects on Bone Mineralization in X-Linked Hypophosphatemia (XLH).** B. Yuan\*<sup>1</sup>, J. Q. Feng<sup>2</sup>, Y. Xing<sup>1</sup>, J. Meudt<sup>1</sup>, P. S. Rowe<sup>3</sup>, M. K. Drezner<sup>\*1</sup>. <sup>1</sup>University of Wisconsin, Madison, WI, USA, <sup>2</sup>Texas A&M Health Science Center, Dallas, TX, USA, <sup>3</sup>University of Kansas, Kansas City, KS, USA.

Patients with XLH and *hyp*-mice, with a deletion in the *Phex* gene, manifest hypophosphatemia, renal phosphate (Pi) wasting, and rickets/osteomalacia. Since targeted deletion of *Phex* in osteoblasts/osteocytes, using an *Osteocalcin* promoter Cre-loxP strategy, results in development of a classical *HYP* phenotype, osteoblast lineage cells alone are undoubtedly the physiologically relevant site for *Phex* mutations. Whether aberrant *Phex* function in both osteoblasts and osteocytes is necessary for the renal and bone phenotype in *hyp*-mice, however, remains unknown. Yet, novel therapeutic strategies for XLH are limited by such absent information. Thus, we generated mice with conditional DMP1-promoted *Phex* knockout, predominantly in osteocytes, (*DMP1-Phex*<sup>fllox/y</sup>) and compared their phenotype to that in normal and *hyp*-mice. Serum Pi in *DMP1-Phex*<sup>fllox/y</sup> (3.37 $\pm$ 0.27) and *hyp*-mice (3.32 $\pm$ 0.1) was significantly less ( $p < 0.001$ ) than in normals (6.16 $\pm$ 0.25). Moreover, the reduction in serum Pi in *DMP1-Phex*<sup>fllox/y</sup> mice was due to diminished renal Pi transport, associated with decreased renal Npt2 mRNA and protein levels, comparable to those in *hyp*-mice. Like *hyp*-mice, the *DMP1-Phex*<sup>fllox/y</sup> mice also exhibited increased bone FGF-23 production, evidenced by a 4.5 fold mRNA increase. With enhanced FGF-23 production, *DMP1-Phex*<sup>fllox/y</sup> mice had a significant increase in serum FGF-23 compared to normals (820 $\pm$ 58 vs 75.6 $\pm$ 5.7 pg/ml,  $p < 0.0001$ ) but, despite manifesting a substantial overlapping range of values with those in *hyp*-mice, had levels significantly less than in the mutants (1200 $\pm$ 61 pg/ml). Surprisingly, however, although femur radiographs documented *DMP1-Phex*<sup>fllox/y</sup> mice had a comparable rachitic phenotype to that in *hyp*-mice and an overlapping range of circulating FGF-23 prevailed, bone histomorphometrics revealed that targeted knockouts exhibited osteomalacia extraordinarily less severe than in the mutants with osteoid surface 3.5 fold less (8.7 $\pm$ 1.2% vs 30.0 $\pm$ 5.3%;  $p < 0.0001$ ). These data indicate that abnormal *Phex* function in osteocytes is sufficient to alone produce the renal XLH phenotype. However, the *Phex* mutation in osteocytes results in an extraordinarily mild osteomalacic mineralization disorder unlike that in *hyp*-mice or that reported in mice with *Phex* deletion in osteoblasts and osteocytes. Thus, together the data indicate that aberrant *Phex* function in the osteoblast exerts primary control over bone mineralization in XLH, most likely through downstream effects of *Phex* dysfunction, including release of local factors, such as ASARM peptides, potent mineralization inhibitors.

**Disclosures:** B. Yuan, None.

## 1052

**Deletion of the *GNAS* Antisense Transcript Results in Parent-Of-Origin Specific *GNAS* Imprinting Defects and Phenotypes Including PTH-Resistance.** S. Chillambhi<sup>\*1</sup>, S. Turan<sup>\*1</sup>, D. Hwang<sup>\*2</sup>, H. Chen<sup>\*2</sup>, H. Jüppner<sup>1</sup>, M. Bastepe<sup>1</sup>. <sup>1</sup>Endocrine Unit, Department of Medicine, Massachusetts General Hospital and Harvard Medical School, Boston, MA, USA, <sup>2</sup>Department of Nephrology, Kaohsiung Medical University, Kaohsiung, Taiwan.

Pseudohypoparathyroidism type-Ib (PHP-Ib) is characterized by renal resistance to parathyroid hormone (PTH) causing hypocalcemia, hyperphosphatemia, and increased PTH levels without Albright's Hereditary Osteodystrophy. Patients with PHP-Ib show imprinting defects of the *GNAS* locus, including either an isolated loss of A/B imprinting or broad epigenetic defects of the maternal allele. Deletions within the neighboring *STX16* locus have been identified in patients with isolated loss of A/B imprinting, whereas NESP55/*GNAS* antisense exon 3-4 deletions have been identified in familial cases with broad imprinting changes. We now identified a novel 5.1-kb deletion removing two exons of the antisense (AS) transcript in affected individuals and carriers of a not-yet-reported kindred with this disorder. The novel deletion overlaps with the previously identified NESP55/antisense exon 3-4 deletion by ~1.5 kb, but does not include NESP55. On maternal transmission the deletion leads to PHP-Ib and disrupts imprinting throughout the maternal *GNAS* allele, including partial gain of imprinting at NESP55 and complete loss of imprinting at the AS promoter, XL $\alpha$ s, and A/B. Unlike the previously described PHP-Ib deletions, the novel deletion also alters *GNAS* imprinting on paternal transmission, causing relaxation of imprinting at NESP55. Based on RT-PCR using total RNA from LCLs of one PHP-Ib patient and his mother, the mutant AS transcript is not expressed, consistent with the changes observed in NESP55 imprinting. In addition, individuals with paternal inheritance of the novel deletion exhibit a modest gain of A/B imprinting, which, based on data from previous mouse models, is predicted to de-repress paternal Gs $\alpha$  expression and, thereby, to increase its level in the proximal renal tubule. Accordingly, serum PTH was below the normal range in an individual who inherited the deletion paternally, suggesting increased PTH sensitivity. These findings redefine the boundaries of the *cis*-acting element that controls imprinting on the maternal *GNAS* allele and reveal a novel *cis*-acting mechanism underlying the tissue-specific silencing of paternal Gs $\alpha$  expression.

**Disclosures:** S. Chillambhi, None.

This study received funding from: National Institutes of Health.

## 1053

**7B2 Protein Mediated Inhibition of DMP1 Cleavage in Osteoblasts Enhances FGF-23 Production in *Hyp*-Mice.** B. Yuan<sup>1</sup>, J. Meudt<sup>\*1</sup>, J. Q. Feng<sup>\*2</sup>, M. K. Drezner<sup>1</sup>. <sup>1</sup>University of Wisconsin, Madison, WI, USA, <sup>2</sup>Texas A&M Health Science Center, Dallas, VT, USA.

Increased serum FGF-23 levels in *hyp*-mice, a murine homologue of X-linked hypophosphatemia (XLH), result from inhibition of FGF-23 degradation and enhanced production of FGF-23. We found previously that decreased *Phex*-dependent osteoblast production of 7B2, a helper protein for subtilisin-like proprotein convertase 2 (SPC2), decreases SPC2/7B2 proteolytic activity, causing elevated serum FGF-23 in *hyp*-mice. This elevation is due to diminished SPC2/7B2 proteolysis of FGF-23 and to downstream effects of SPC2/7B2, which increase FGF-23 mRNA. The mechanism by which decreased SPC2/7B2 activity exerts such effects on FGF-23 mRNA, however, remains unknown. Observations that DMP1 null mice have hypophosphatemic rickets with elevated FGF-23 mRNA and that DMP1 in osteoblasts/osteocytes is cleaved into N- and C-terminal fragments, which localize to the nucleus, suggest DMP1 cleavage may modulate FGF-23 gene expression. Therefore, we investigated if SPC2/7B2 proteolysis of DMP1 underlies increased FGF-23 production in *hyp*-mice. Transfection of full-length DMP1 into murine osteoblasts (TMOB) revealed FGF-23 mRNA was down regulated compared to that in controls (0.46 $\pm$ 0.1 vs 1.02 $\pm$ 0.1 fold;  $p < 0.001$ ). In contrast, transfection of DMP1 cDNA, mutated at the proteolytic cleavage site, caused no change in FGF-23 mRNA, indicating DMP1 cleavage is requisite for down-regulation of FGF-23 production. To determine if DMP1 cleavage is SPC2/7B2 dependent, we treated full-length DMP1 transfected TMOB cells with Dec, an SPC inhibitor. Such treatment dose dependently blocked DMP1 processing into N- and C-terminal fragments. In addition, cotransfection of TMOB cells with full-length DMP1, SPC2 and 7B2 constructs resulted in Western blot evidence of enhanced DMP1 cleavage into N- and C-terminal fragments (1.6 $\pm$ 0.2 vs 1.0 $\pm$ 0.2; 2.0 $\pm$ 0.1 vs 1.0 $\pm$ 0.1 fold;  $p < 0.01$ ). These data established that SPC2/7B2 cleavage of intact DMP1 may regulate FGF-23 mRNA. To assess if diminished DMP1 cleavage regulates FGF-23 production in *hyp*-mice with decreased SPC2/7B2 activity, we evaluated osseous production of DMP1 N- and C-terminal fragments. In *hyp*-mouse bone intact DMP1 is increased (2.8 $\pm$ 0.5 vs 1.0 $\pm$ 0.5 fold;  $p < 0.01$ ) while C- and N-terminal fragments are significantly reduced (1.6 $\pm$ 0.4 vs 3.7 $\pm$ 0.3; 1.8 $\pm$ 0.1 vs 2.8 $\pm$ 0.4 fold;  $p < 0.01$ ), consistent with decreased proteolysis of the intact protein. Thus, inactivating *Phex* mutations in XLH, and the resultant decreased osteoblast 7B2 concentration and diminished SPC2/7B2 activity, not only lessen FGF-23 degradation, but significantly limit DMP1 N- and C-terminal fragment production, decreasing the inhibitory effects of these fragments on FGF-23 mRNA and enhancing FGF-23 production.

**Disclosures:** B. Yuan, None.

## 1054

**Relative Efficacy of “Treating” versus “Preventing” Infantile Hypophosphatasia in Akp2<sup>-/-</sup> mice by Enzyme Replacement Therapy.** I. Lemire<sup>\*1</sup>, T. P. Loise<sup>\*1</sup>, P. Leonard<sup>\*1</sup>, G. Boileau<sup>\*2</sup>, H. Landy<sup>\*1</sup>, R. Hefi<sup>\*1</sup>, M. P. Whyte<sup>3</sup>, P. Crine<sup>1</sup>, J. L. Millan<sup>4</sup>. <sup>1</sup>Enobia Pharma, Inc., Montreal, QC, Canada, <sup>2</sup>University of Montreal, Montreal, QC, Canada, <sup>3</sup>Shriners Hospitals for Children and Washington University, St. Louis, MO, USA, <sup>4</sup>Sanford Children's Health Research Center, Burnham Institute for Medical Research, La Jolla, CA, USA.

Hypophosphatasia (HPP) is the inborn-error-of-metabolism that features rickets or osteomalacia due to loss-of-function mutation(s) within the gene that encodes the tissue-nonspecific isoenzyme of alkaline phosphatase (TNALP). TNALP null mice (Akp2<sup>-/-</sup>) phenocopy infantile HPP extremely well. We recently showed that enzyme replacement therapy (EzRT) using a bone-targeted recombinant form of human TNALP, i.e., sALP-FcD10, prevented the various manifestations of infantile HPP in this model. Now we have tested whether EzRT could rescue Akp2<sup>-/-</sup> mice with advanced disease. We evaluated a daily bolus s.c. injection of 8.2 mg/Kg sALP-FcD10 in Akp2<sup>-/-</sup> mice (n= 17) versus vehicle (n=16) starting at day 15 (at the 75th percentile of their life expectancy) and continued treatment until day 43-45 (“rescue” cohort). A “prevention” cohort of Akp2<sup>-/-</sup> mice (n=21) received the same bolus amount daily starting on day 1 while WT mice (n=30) without EzRT served as controls. None of the Akp2<sup>-/-</sup> mice receiving vehicle alone survived past day 24, while 9/17 of the mice in the rescue cohort survived to day 39, and 4/16 lived to day 43. In the prevention cohort, 20/21 mice survived to complete the study at day 44. The growth curve of the Akp2<sup>-/-</sup> mice on preventive treatment from day 1 was essentially identical to the growth curve of WT mice. For the rescue cohort, the growth rates were improved but the mice remained smaller than the controls. Radiographs of the feet at necropsy indicated that 2/16 (12.5%) of the Akp2<sup>-/-</sup> mice treated with vehicle and 7/17 (41.2%) of the Akp2<sup>-/-</sup> mice receiving sALP-FcD10 had normal x-rays, showing that EzRT brought a statistically significant improvement in bone mineralization. Next we evaluated different dosing intervals on the rescue of Akp2<sup>-/-</sup> mice. Mice were started on EzRT at day 12 and were injected s.c. with vehicle (RV), 8.2 mg/Kg daily to days 46/47 (RTx-1) or 8.2 mg/Kg daily for 7 days followed by 24.6 mg/Kg every 3 days (RTx-3) or followed by 57.4 mg/Kg every 7 days (RTx-7). The median survival was 19.5 days for RV, 21.0 days for RTx-7, 30.5 days for RTx-3, and 37.5 days for RTx-1. In all cases, survival was statistically increased when compared to the RV group. Thus, there is a clear benefit of bone-targeted EzRT in Akp2<sup>-/-</sup> mice with well-established HPP. Dosing less frequently than daily can also statistically improve their survival.

**Disclosures:** I. Lemire, Enobia Pharma, Inc. S.  
This study received funding from: NIH, Enobia.

## 1055

**World Health Organization (WHO) Absolute Fracture Models in Older Women: How Does Prediction Vary for Incident Hip and Non-spine Fractures Across T-Scores?** T. A. Hillier<sup>1</sup>, J. A. Cauley<sup>2</sup>, J. H. Rizzo<sup>\*1</sup>, K. L. Pedula<sup>\*1</sup>, K. K. Vesco<sup>\*1</sup>, B. C. Taylor<sup>\*3</sup>, D. C. Bauer<sup>4</sup>, K. E. Ensrud<sup>3</sup>, D. M. Black<sup>4</sup>, S. R. Cummings<sup>4</sup>. <sup>1</sup>Center for Health Research, Kaiser Permanente, Portland, OR, USA, <sup>2</sup>U Pittsburgh, Pittsburgh, PA, USA, <sup>3</sup>VAMC & U of MN, Minneapolis, MN, USA, <sup>4</sup>San Francisco Coordinating Center, CPMC Research Institute and UCSF, San Francisco, CA, USA.

Bone mineral density (BMD) is a strong predictor of fracture, yet most fractures occur in women with normal or low bone mass (LBM), not those with frank osteoporosis. Moreover, whether to treat the majority of women who have LBM is a clinical conundrum. The WHO Collaborative Metabolic Bone Disease group recently developed absolute probability of fracture models incorporating clinical risk factors with femoral neck (fn) BMD to enhance overall prediction of hip and other osteoporotic fractures, but it is unknown how the WHO model will predict fractures among women with LBM. To evaluate the overall sensitivity and specificity of the WHO 10-yr probabilities of hip and osteoporotic fracture models (U.S. Caucasian) to predict observed hip and non-traumatic non-spine fractures among women with normal or LBM, we stratified women age 65 and over in the Study of Osteoporotic Fractures (SOF) cohort based on initial DXA fnBMD: Normal (T-score [T]  $\geq -1.0$ ; n=1,154); LBM ( $-2.5 < T < -1.0$ ; n=3,791) and Osteoporotic ( $T \leq -2.5$ ; n=1,307). Receiver Operator Characteristics (ROC) curves assessed overall sensitivity and specificity to predict observed hip and other non-spine fractures with AreaUnder-the-Curve (AUC) using the 10 year probabilities of hip and other osteoporotic fractures, respectively, calculated by the WHO group which included clinical risk factors at baseline and fnBMD. Over a follow-up of 10.0 years, 368 women suffered an incident hip fracture and 1,734 women experienced at least one non-spine fracture. AUC for WHO 10 year probabilities for all women, stratified by initial fnBMD are in Table.

	Normal	Low Bone Mass	Osteoporotic	p-value
Hip Fracture				
Observed, n	14	176	178	
WHO AUC (95% CI)	0.79 (0.67, 0.90)	0.69 (0.65, 0.73)	0.59 (0.55, 0.64)	0.0003
Non-spine Fracture				
Observed, n	188	1034	512	
WHO AUC (95% CI)	0.59 (0.55, 0.64)	0.58 (0.56, 0.60)	0.63 (0.59, 0.66)	0.07

The WHO model predicted hip fractures better in women with normal and LBM than in those with osteoporosis. Prediction with the WHO model was similar across all BMD strata for non-spine fractures.

In summary, the WHO model predicted incident hip and other non-spine fractures even among women with normal and low bone mass. Although few women with normal bone mass suffered a hip fracture, the WHO model may offer particular utility to this group.

**Disclosures:** T. A. Hillier, None.

This study received funding from: The National Institute of Aging (NIA) and National Institute of Arthritis, Musculoskeletal, and Skin Diseases (NIAMS): 2 R01 AG027574-22A1, R01 AG005407, R01 AG027576-22, 2 R01 AG005394-22A1, AG05407, AG05394, AR35583, AR35582 and AR35584.

## 1056

**The Population Burden of First and Repeat Low-trauma Fractures: The Canadian Multicentre Osteoporosis Study.** S. A. Jamal<sup>1</sup>, L. Langsetmo<sup>2</sup>, R. G. Josse<sup>1</sup>, A. Papaioannou<sup>3</sup>, J. D. Adachi<sup>3</sup>, W. P. Olszynski<sup>4</sup>, D. A. Hanley<sup>5</sup>, C. S. Kovacs<sup>6</sup>, N. Kreiger<sup>7</sup>, D. Goltzman<sup>2</sup>. <sup>1</sup>Medicine, University of Toronto, Toronto, ON, Canada, <sup>2</sup>Medicine, McGill University, Montreal, QC, Canada, <sup>3</sup>Medicine, McMaster University, Hamilton, ON, Canada, <sup>4</sup>Medicine, University of Saskatchewan, Saskatchewan, MB, Canada, <sup>5</sup>Medicine, University of Calgary, Calgary, AB, Canada, <sup>6</sup>Medicine, Memorial University, St. Johns, NL, Canada, <sup>7</sup>University of Toronto, Toronto, ON, Canada.

Traditional T score risk categories fail to identify some men and women at high fracture risk, as the majority of fractures occur in men and women with T scores above -2.5. The objective of our study was to determine the contribution of first and repeat fractures, with and without consideration of T score risk categories, to the fracture burden among Canadian men and women.

We studied 2179 men and 5269 women, aged 50 to 90, participating in CaMos. We included all low trauma fractures that occurred over 7 years of follow up (incident fractures) and classified them as either first or repeat fractures. Analyses were stratified by sex, fracture status (first vs. repeat) and BMD categories based on T score ( $\geq -1$  normal;  $-1$  to  $-2.5$  osteopenic;  $\leq -2.5$  osteoporotic). All estimates were age-standardized using 2001 Canadian census data.

There were a total of 128 fractures in men and 577 fractures in women. The incidence of repeat fracture was at least double the incidence of first fracture within each 5-year age group, and each BMD category. An estimated 75% of all fractures in men were a first fracture and 25% were repeat fractures. Considering T score categories among men: 25% of all fractures occurred with normal BMD, 54% with osteopenic BMD, and 21% with osteoporotic BMD. An estimated 60% of all fractures in women were a first fracture and 40% were repeat fractures. Considering T score categories among women, 10% of fractures occurred with normal BMD, 51% with osteopenic BMD, and 39% with osteoporotic BMD. Only 13% of all fractures in men, and 19% of all fractures in women were a first fracture occurring with osteoporotic BMD.

Our findings demonstrate that repeat fracture is an important contribution to overall fracture burden, particularly among women. Indeed, the overall fracture burden of repeat fracture is similar to that of osteoporotic BMD in men and is greater than the contribution of osteoporotic BMD in women. Our results highlight the fact that while osteoporosis by BMD testing is a strong risk factor for fracture, additional factors, including prevalent fracture can strongly and independently contribute to fracture burden.

**Disclosures:** S. A. Jamal, None.

## 1057

**A Comparison of Prediction Models for Hip, Osteoporotic, and Any Clinical Fracture in Older Women: Is More Better?** K. E. Ensrud<sup>1</sup>, L. Lui<sup>2</sup>, B. Taylor<sup>\*1</sup>, J. Schousboe<sup>3</sup>, M. Donaldson<sup>2</sup>, H. Fink<sup>1</sup>, J. Cauley<sup>4</sup>, T. Hillier<sup>5</sup>, W. Browner<sup>\*2</sup>, D. Black<sup>\*6</sup>, S. Cummings<sup>2</sup>. <sup>1</sup>U of MN / VAMC, Mpls, MN, USA, <sup>2</sup>CPMCRI, SF, CA, USA, <sup>3</sup>U of MN, Mpls, MN, USA, <sup>4</sup>U Pitt, Pittsburgh, PA, USA, <sup>5</sup>Kaiser Permanente, Portland, OR, USA, <sup>6</sup>UCSF, SF, CA, USA.

While advanced age and low bone mineral density (BMD) are strongly associated with increased fracture (fx) risk, many other independent risk factors for fx have been identified. Thus, recent efforts by the WHO Metabolic Bone Disease Group have focused on developing a clinical risk factor index with and without femoral neck (fn) BMD to enhance fx prediction. However, it is uncertain whether prediction with models incorporating this index is superior to that based on a parsimonious model.

To compare the predictive validity of a simple model based on age and fnBMD alone (base model) with that of the more complex WHO models (10 year fx probabilities for hip and osteoporotic fx incorporating age plus WHO clinical risk factors, with and without fnBMD), we conducted a prospective cohort study in 6242 women aged ≥65 years enrolled in the Study of Osteoporotic Fractures. Fractures (including hip fx, osteoporotic [hip/clinical spine/wrist/humerus] fx, and any clinical fx) were ascertained during 10 years of follow-up. Area under the curve (AUC) statistics from receiver operating characteristic (ROC) curve analysis were compared for the base model vs. WHO models. The results were cross-validated using the 10-fold cross validation procedure.

AUC comparisons revealed no differences between the base model vs. the WHO model with fnBMD in discriminating hip, osteoporotic, or any clinical fx (table). However, the base model was superior to the WHO model without fnBMD in predicting these fx. For a given fx category, the proportion of fx events that occurred among women in the highest quartile of risk was similar across the 3 models. For example, the % of women experiencing a hip fx in the high risk quartile was 15.3 for the base model, 14.5 for the WHO model with fnBMD, and 14.1 for the WHO model without fnBMD.

In conclusion, a simple model based on age and fnBMD alone predicts 10-year risk of hip, osteoporotic, and any clinical fx in older women as well as more complex WHO models, suggesting that the addition of clinical risk factor information to age and fnBMD alone does not enhance prediction of these fx in older women.

AUC Statistic for Models Predicting 10 Yr Risk of Hip, Osteoporotic & Any Clinical Fracture

Model	Hip Fx*	Osteoporotic Fx†	Any Clinical Fx‡
Base model (age & fnBMD)	0.76	0.69	0.63
WHO model w/ fnBMD	0.75	0.69	0.64
WHO model w/o fnBMD	0.71‡	0.64‡	0.61‡

\*WHO models based on hip fx probability

†WHO models based on osteoporotic fx probability

‡p<0.05 compared to base model

**Disclosures:** K.E. Ensrud, None.

This study received funding from: NIH / NIA.

## 1058

**Differences in Fall Rates and Predictors of Falls by Sex?** R. L. Fullman<sup>1</sup>, P. M. Cawthon<sup>1</sup>, K. A. Faulkner<sup>2</sup>, K. L. Stone<sup>1</sup>, H. Fink<sup>3</sup>, E. Barrett-Connor<sup>4</sup>, K. Ensrud<sup>3</sup>, M. C. Nevitt<sup>\*5</sup>, E. Orwoll<sup>6</sup>, S. R. Cummings<sup>1</sup>. <sup>1</sup>CPMCRI, San Francisco, CA, USA, <sup>2</sup>University of Pittsburgh, Pittsburgh, PA, USA, <sup>3</sup>VAMC & University of Minnesota, Minneapolis, MN, USA, <sup>4</sup>UCSD, San Diego, CA, USA, <sup>5</sup>UCSF, San Francisco, CA, USA, <sup>6</sup>OHSU, Portland, OR, USA.

To examine differences in rates and predictors of falls by sex in older adults, we examined data from 9,289 Caucasian women from the Study of Osteoporotic Fractures (SOF) and 5,346 Caucasian men from the Osteoporotic Fractures in Men (MrOS) Study. Participants were aged ≥ 65, ambulatory and community living at enrollment. A number of predictors were assessed using similar protocols, including anthropometric and physical function measures, medical conditions and lifestyle factors, and were considered for inclusion in analyses. Incident falls during the first year of follow-up were ascertained on tri-annual questionnaires (response rate > 99%). Generalized Estimating Equations were used to calculate Risk Ratios (RR) and 95% Confidence Intervals (CI) for incident fall risk in each sex separately. Variables that were associated with fall risk in age adjusted models at the p<.05 level were included in multivariate (MV) models for each cohort.

The average age of women (73.8 years) and men (73.7 years) was similar (chi-square p value=0.07). During follow-up (average 0.99 years in both sexes), 25.7% of men and 26.3% of women reported a fall and 12.0% of men and 9.8% of women reported multiple falls. We identified several factors that were significantly related to fall risk or had similar RR estimates in men and women (Table). Walking for exercise was protective in men but associated with increased fall risk in women. Similarly, better physical performance, such as greater grip strength and faster walking speed, were associated with decreased fall risk in men, but were unassociated with fall risk in women. Factors not significant in either sex include: body mass index, height, self-reported health, visual acuity, using arms to stand, stroke, diabetes and current alcohol use.

In conclusion, fall rates in men and women are similar, but men report slightly more multiple falls. The predictors of falls in both sexes are generally similar with the history of falls being the strongest predictor in each cohort. However a few factors, such as walking for exercise, seem to differentially influence fall risk.

Predictor	Selected Predictors of Falls		p for interaction
	Men RR (95% CI)	Women RR (95% CI)	
Age (5 years)	1.03 (0.97, 1.09)	1.07 (1.01, 1.13)	0.52
Fall in the Past 12 months (yes)	2.80 (4.46, 3.18)	2.96 (2.68, 3.26)	0.63
Grip Strength (per SD, kg)	0.87 (0.81, 0.94)	0.96 (0.91, 1.02)	0.63
Walking Speed (per SD, m/s2)	0.90 (0.84, 0.98)	0.98 (0.92, 1.04)	<0.01
Trouble with Dizziness (yes)	1.27 (1.11, 1.45)	1.21 (1.07, 1.36)	0.01
Walking for Exercise (yes)	0.87 (0.77, 0.98)	1.16 (1.05, 1.28)	<0.01
> High School Education	1.14 (0.99, 1.33)	1.31 (1.18, 1.45)	<0.01

**Disclosures:** R.L. Fullman, None.

This study received funding from: NIA & NIAMS.

## 1059

**Substantial Adverse Outcomes Follow Non-Hip Non-Vertebral Fragility Fractures.** J. R. Center, D. Bliuc, T. V. Nguyen, J. A. Eisman. Bone and Mineral Research Program, Garvan Institute of Medical Research, Sydney, Australia.

Although osteoporosis and osteoporotic fractures are an important and growing public health problem, most of the attention and research has focussed on hip and vertebral fractures. The aim of this study was to examine the impact of non-hip, non-vertebral fractures.

All low trauma fractures occurring from April 1989 to May 2007 were recorded from 2245 women and 1760 men aged 60+ living in Dubbo, Australia and followed up for subsequent fracture and mortality.

There were 952 low-trauma fractures in women and 343 in men followed by 290 subsequent fractures in women and 74 in men with 461 deaths in women and 197 in men. Non-hip non-vertebral fractures accounted for almost 50% (n=659) of these initial fractures and preceded 54% (n=196) of subsequent fractures and 43% (n=200) of all deaths. Re-fracture rate following a non-hip non-vertebral fracture was increased 1.7-fold in women (95% CI 1.5-2.0) and a 2.3-fold in men (95% CI 1.6- 3.2). Similarly, standardised mortality ratios (SMR) were higher following non-hip non-vertebral fractures; SMR 1.50 (1.30-1.73) in women and 1.48 (1.18-1.85) in men. These were not as high as following hip or vertebral fracture [post hip and vertebral re-fracture rate increased 2.3-fold (1.9- 2.8) for women and 4.5-fold (3.2-6.3) for men and SMR 2.1 (1.8-2.4) for women and 2.6 (2.1-3.1) for men].

Non-hip non-vertebral fractures were particularly associated with increased mortality in those >70 years. In men, the associated mortality risk in those >70 was increased by 80% for the first 5 years post fracture [SMR 1.8 (1.2-2.7) for 70-79 year olds and SMR 1.9 (1.3-2.7) for 80+ year olds]. In women the SMR was 1.6 (1.2-2.2) for 70-79 year olds and 1.4 (1.1-1.8) for 80+ year olds. Of interest, rib fracture, which constituted a major grouping (31 in women and 31 in men), was associated with increased mortality risk that was significant in women, SMR 2.3 (1.6-3.2) and borderline in men SMR 1.4 (0.96-2.0).

Importantly the premature mortality following the non-hip non-vertebral fractures contributed to 28% of excess deaths in women and 31% of excess deaths in men and thus is clinically significant.

In summary this often ignored group of fractures not only constitutes half of all low trauma fractures but contributes significantly to the associated poor outcomes of re-fracture and premature mortality. Efforts to prevent non-hip non-vertebral fractures should be a priority and studies should include these fractures, as well as hip and vertebral fractures, as primary outcomes.

**Disclosures:** J.R. Center, None.

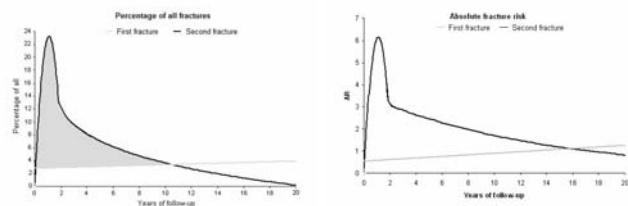
## 1060

**The Absolute Risk for Subsequent Fractures Fluctuates over Time.** T. van Geel<sup>\*1</sup>, P. Geusens<sup>2</sup>, K. Huntjens<sup>\*2</sup>, S. van Helden<sup>\*3</sup>. <sup>1</sup>Department of General Practice, Maastricht University, Maastricht, Netherlands, <sup>2</sup>Department of Rheumatology, Maastricht University Medical Centre, Maastricht, Netherlands, <sup>3</sup>Department of General Surgery and Trauma Surgery, Maastricht University Medical Centre, Maastricht, Netherlands.

The relative risk (RR) of subsequent fracture is double that of having a first fracture. Some studies indicate that this risk is even higher within short term after a first fracture. We analyzed the yearly absolute risk (AR) for a subsequent fracture, taking into account the time relation between menopause and first fracture and between first and subsequent fracture.

A population-based study in 4203 postmenopausal women aged between 50 and 90 years, who completed questionnaires about location and time of X-ray confirmed clinical fractures. The yearly AR and percentage (%) of all first and subsequent fractures were calculated over time using Cox regression, with a mean follow up of 40 years for a 1<sup>st</sup> fracture from menopause onwards and of 20 years for a subsequent fracture from the time of a first fracture onwards.

The mean 1-year AR of a first fracture was 1% and slightly increased over 40 years of follow up after menopause, resulting in 4% of all subsequent fractures occurring each year from menopause on. The 1-year AR of a subsequent fracture fluctuated over time and was 6% within 1 year after a first fracture, progressively decreasing to 2.5% during the 5<sup>th</sup> year and 1% during the 20<sup>th</sup> year. As a result, 23% of all subsequent fractures occurred within one year of a first fracture, and 50% within 5 years (Figure 1). The AR (1a) and % of all subsequent fractures (1b) of a 1<sup>st</sup> fracture (from onset of menopause) and a subsequent fracture (from the time of 1<sup>st</sup> fracture), indicating a window of opportunity to prevent subsequent fractures (grey area)



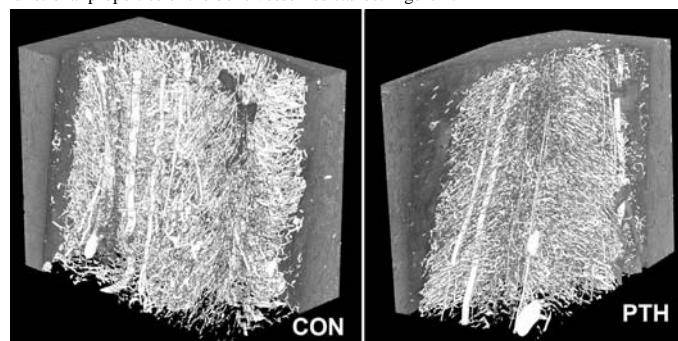
The yearly AR of a 1<sup>st</sup> fracture from menopause on slightly increases over time, but fluctuates over time for subsequent fracture after a first fracture. These results indicate a window of opportunity to prevent a subsequent fracture within short term after a first fracture.

**Disclosures:** P. Geusens, None.

## 1061

**Anabolic Daily Intermittent PTH 1-84 Reduces Bone Blood Vascular Bed and Induces Dramatic Changes in the Bone/Vessel Spatial Relationship.** R. Prisby<sup>1</sup>, Z. Peter<sup>2</sup>, A. Guignandon<sup>1</sup>, A. Vanden-Bossche<sup>1</sup>, L. Malaval<sup>1</sup>, L. Vico<sup>1</sup>, E. Peyrin<sup>2</sup>, M. Lafage-Proust<sup>1</sup>. <sup>1</sup>LBTO, INSERM 890, Saint-Etienne, France, <sup>2</sup>ESRF-Grenoble, INSERM- U630/CNRS/UMR- 5220, INSA, Lyon, France.

Intermittent parathyroid hormone (PTH) is a current treatment of osteoporosis. However, its mechanisms of action remain to be fully elucidated. PTH promotes osteoblastic expression of VEGF, an angiogenic factor. Bone vascularisation and osteogenesis are functionally coupled. Thus, we hypothesized that PTH might enhance bone mass via stimulation of bone angiogenesis. According to baseline tibial bone volume/tissue volume (BV/TV) assessed by  $\mu$ CT, 24 Wistar male rats (300g) were assigned to two groups: PTH and Control (CON) and were given either PTH 1-84 (100 $\mu$ g/kg/d) or 0.9% saline, respectively, 5 days/wk for 4 wks. After sacrifice, rats were perfused with a barium sulfate solution for opacification of bone vessels. Tibiae were processed for bone histomorphometry. Femora were collected for Synchrotron Radiation Computerized Tomography (SR- $\mu$ CT) imaging (voxel size: 2.8 $\mu$ m, energy: 25 keV). Expectedly, PTH treatment significantly increased tibial BV/TV (150%) in association with higher BFR (76%) and reduced (61%) osteoclast number compared to CON. Moreover, marrow adipocyte number was reduced 50% in the PTH group. The number of blood vessels in the II spongiosa was 46% lower in the PTH group. In contrast, the number of sinusoid bundles in the bone marrow was 33% higher than in CON. These results are illustrated in Figure 1: 3D image of bone marrow vascular bed in femur assessed by SR- $\mu$ CT. Blood vessel number negatively correlated ( $r^2 = -0.572$ ,  $p = 0.004$ ) with BV/TV. Histogram distribution of vessel distance from trabecular bone surfaces or osteoid seams was analyzed using ImageJ (NIH free software) on Goldner-stained sections ( $n=30$  fields/ group, X100). Overall, vessels from the CON group were closer to bone surfaces than those in the PTH group; however, vessels from the PTH group were closer to osteoid seams than in the CON group. Contrary to our hypothesis, these data demonstrate that while intermittent PTH 1-84 treatment enhanced osteogenesis, it did not induce bone angiogenesis. However, the spatial distribution of the vasculature within the IISF is markedly altered with PTH. Therefore the relation between the bone vasculature and osteogenesis may involve a modification of the functional properties of the bone vessel resistance. Figure 1:



**Disclosures:** R. Prisby, None.

This study received funding from: French National Research Agency.

## 1062

**Effects of Parathyroid Hormone on Fracture Repair in Glucocorticoid Treated Mice.** J. Li, A. R. Doyon<sup>\*</sup>, I. K. Ferries<sup>\*</sup>. Department of Biology, Indiana University-Purdue University Indianapolis, Indianapolis, IN, USA.

Long-term use of glucocorticoid (GC) reduces bone mass and strength which leads to a greater risk of fracture. GC treatment may also hinder fracture repair. In this study, we established a GC induced fracture nonunion animal model and investigated the effects of parathyroid hormone 1-34 (PTH) on fracture repair using this animal model. Four-month-old Swiss-Webster male mice were randomly divided into five groups. Three groups of GC treated mice were given with prednisolone that was slowly released from the

subcutaneously implanted pellets at the rate of 1.4 mg/kg/day. Placebo pellets were implanted into the animals in two placebo groups. Three weeks later, fracture surgery was carried out in all the animals. Osteotomy at midshaft femurs was performed under general anesthesia. Stainless steel pins were then inserted into the medullary cavity to stabilize the fracture site. Following fracture surgery, three GC groups were treated subcutaneously with vehicle, PTH at a low dose (40  $\mu$ g/kg/day) and a high dose (80  $\mu$ g/kg/day), respectively. Two Placebo groups were given vehicle and PTH at a dose of 40  $\mu$ g/kg/day, respectively. Radiographs, DXA, and mechanical testing (4-point bending) were used to evaluate the fracture repair at four weeks after fracture surgery. Compared to the placebo mice treated with vehicle, GC significantly reduced bone mineral density and bone mineral content of left intact femurs by 14% and 11% ( $p<0.05$ ) as well as decreased ultimate force by 22% ( $p<0.01$ ). Both low and high doses of PTH treatment prevented bone loss at the intact femurs in GC treated animals and preserved mechanical integrity, while PTH significantly enhanced bone mass of the intact femurs in placebo animals. Callus development at the fracture sites in GC animals treated with vehicle was significantly suppressed compared to that in placebo animals in term of callus area revealed by radiographs and callus mineral content (11%;  $p<0.05$ ) and density (14%;  $p<0.05$ ). In GC groups, PTH significantly increased callus mineral content compared with vehicle, despite the observation that callus under low dose PTH treatment was significantly less than that in placebo groups. Although PTH markedly improved ultimate force in placebo animals by 80% ( $p<0.001$ ), PTH did not increase ultimate bending forces in GC treated animals. These data indicate that PTH can restore GC induced bone loss and maintain mechanical properties of the intact bone. Normally PTH accelerates fracture repair. In GC treated mice, PTH increases callus formation but fails to improve mechanical properties compared to vehicle treatment, suggesting that the anabolic effect of PTH on fracture healing can be attenuated by GC administration in mice.

**Disclosures:** J. Li, None.

## 1063

**A Fusion Protein of Parathyroid Hormone (PTH) and a Collagen Binding Domain Shows Superior Efficacy and Longer Duration of Action Compared to PTH(1-34) as an Anabolic Bone Agent in Normal Female Mice.** T. Ponnappakkam<sup>1</sup>, R. Katikaneni<sup>1</sup>, A. Ponnappakkam<sup>1</sup>, E. Miller<sup>1</sup>, O. Matsushita<sup>2</sup>, J. Sakon<sup>3</sup>, R. C. Gensure<sup>1</sup>. <sup>1</sup>Pediatrics, Ochsner Clinic Foundation, New Orleans, LA, USA, <sup>2</sup>Microbiology, Kiseto University, Tokyo, Japan, <sup>3</sup>Chemistry, University of Arkansas, Fayetteville, AR, USA.

Osteoporosis affects nearly 10 million Americans. Despite application of current therapies, osteoporotic hip fractures result in costs of ~18 billion dollars per year. Anabolic agents such as parathyroid hormone show superior efficacy to antiresorptives (i.e. bisphosphonates), but have not been widely accepted in part because of inconvenient dosing (daily injection). We have developed a fusion protein of parathyroid hormone PTH(1-33) and a collagen binding domain (CBD) (PTH-CBD), designed to be retained in collagen-containing tissues and extend the duration of the anabolic bone effect. We compared the efficacy and duration of PTH-CBD to PTH(1-34) and vehicle control using a variety of dosing intervals in normal young female C57BL/6J mice (Jackson Laboratories). To determine the optimal dose of PTH-CBD, mice received a single subcutaneous injection of PTH-CBD at doses ranging from 0.05 mg/kg to 3 mg/kg, and BMD was measured each month. The optimal response (fastest time to reach peak BMD) was seen at 320 mcg/kg (molar equivalent to 80 mcg/kg of PTH(1-34)). Comparing the optimal PTH-CBD dose to that of PTH(1-34), monthly intraperitoneal dosing of PTH-CBD (320 mcg/kg) for 6 months achieved a higher peak BMD than did 2 weeks of daily administration of PTH(1-34) (80 mcg/kg) (PTH-CBD:  $81\pm3$ , PTH(1-34):  $75\pm3$ , vehicle:  $64\pm2$  mg/cm<sup>2</sup>,  $p<0.05$ ). These increases in BMD were sustained for an additional 6 months following the dosing interval (PTH-CBD:  $71\pm3$ , PTH(1-34):  $63\pm3$ , vehicle:  $54\pm2$  mg/cm<sup>2</sup>,  $p<0.05$ ). Serum alkaline phosphatase levels were elevated in the PTH-CBD group at the end of the study, indicating an anabolic mechanism of action (PTH-CBD:  $118\pm49$ , PTH(1-34):  $40\pm18$ , vehicle:  $32\pm8$  IU/L,  $p<0.05$ ). In a separate study, a single dose of PTH-CBD (320 mcg/kg) showed superior efficacy to 2 weeks of daily administration of PTH(1-34) (80 mcg/kg) (PTH-CBD:  $76\pm2$  vs. PTH(1-34):  $71\pm2$ , vehicle:  $67\pm1$  mg/cm<sup>2</sup>,  $p<0.05$ ). The gains in BMD were sustained for at least 5 months following the injection of PTH-CBD, while the BMD in the group which received PTH(1-34) returned to control levels (PTH-CBD:  $79\pm2$ , PTH:  $66\pm1$ , vehicle:  $63\pm1$  mg/cm<sup>2</sup>,  $p<0.05$ ). There was no additional benefit observed with administration of a second dose of PTH-CBD three months after the first one. The overall results suggest that a single dose of PTH-CBD provides superior efficacy and longer duration of action compared to daily PTH(1-34) in increasing BMD in normal female mice through an anabolic mechanism.

**Disclosures:** R.C. Gensure, None.

This study received funding from: Ochsner Clinic Foundation.



## 1064

**The Roles of Zoledronic Acid in Bone Healing and Osteoblast Functions.** J. Zhang\*, Q. Tu, J. Chen. General Dentistry, Tufts University School of Dental Medicine, Boston, MA, USA.

Recently the use of bisphosphonates has been linked to osteonecrosis of the jaw (ONJ). The mechanisms of how bisphosphonates possibly cause the development of ONJ remain to be determined.

To investigate the mechanisms of ONJ, 21 mice were divided into 3 groups which were injected with: zoledronic acid (250µg/kg), zoledronic acid (100µg/kg), and PBS, once a week for 4 weeks. One week after the last drug injection, the second and third right mandibular molars were extracted and bone defects were created in the diaphysis area of the right femurs using dental burs. One week after surgery, the bone tissues were isolated. H&E staining, TRAP staining, and ALP staining were performed. Moreover, MC3T3 cells were treated with zoledronic acid at different concentrations (0-5000ng/ml). Proliferation assay and real-time RT-PCR were performed. Mandibular bone healing was significantly retarded in 1 of the 7 mice (14.3%) injected with zoledronic acid (250µg/kg). There was no new bone formation and the bone defect was filled with inflammatory soft tissues. In PBS or zoledronic acid (100µg/kg) group, no wound healing delay was detected, which indicated that the dose of 250µg/kg is necessary to induce ONJ with an incidence similar to the reported clinical incidence (0.8% to 12%). There was no retardation in femoral bone healing process. TRAP staining showed that in the femurs from the zoledronic acid (250µg/kg and 100µg/kg) groups, Oc.N/BS was decreased by 32.27% and 8.93%, respectively, while in the mandibles, Oc.N/BS was decreased in zoledronic acid groups (250µg/kg and 100µg/kg) by 36.34% and 12.90%, respectively. ALP staining showed that in femoral growth plate area there was no significant difference in Ob. N/BS among the three groups. The proliferation rate of MC3T3 cells treated with zoledronic acid at lower concentrations (10ng/ml and 100ng/ml) was increased at earlier time points (24- and 48hrs) before being decreased by longer drug treatment (72hrs). The proliferation rate of MC3T3 treated with zoledronic acid at higher concentration (5000ng/ml) was decreased at all time points. Real-time RT-PCR demonstrated that MC3T3 cells treated with zoledronic acid at 10ng/ml showed an increase in the expression levels of BSP and EphB4, while cells treated with zoledronic acid at higher concentration (5000ng/ml) showed decreased levels of BSP and EphB4. In conclusion, zoledronic acid-induced osteoclast decrease in mandibles was more pronounced than that in long bones, suggesting a different response to zoledronic acid between these two distinct bone tissues. We speculate that a lower level of osteoblast proliferation and gene expressions in response to bisphosphonate therapy may delay the bone wound healing process in the mandible.

**Disclosures:** J. Zhang, None.

This study received funding from: NIH grants DE13745 and DE16710 to JC.

## 1065

**Studying Cellular Uptake and Distribution of Bisphosphonate *in vivo* Using Fluorescently-labelled Analogues of Risedronate.** A. J. Roelofs\*, E. P. Coxon\*, M. W. Lundy\*, F. H. Ebetino\*, J. F. Bala\*, B. A. Kashemirov\*, C. E. McKenna\*, M. J. Rogers\*. <sup>1</sup>Institute of Medical Sciences, University of Aberdeen, Aberdeen, United Kingdom, <sup>2</sup>Procter & Gamble Pharmaceuticals, Cincinnati, OH, USA, <sup>3</sup>Dept of Chemistry, University of Southern California, Los Angeles, CA, USA.

Bisphosphonates (BPs) are effective anti-resorptive agents due to their bone-targeting properties and efficient internalisation by bone-resorbing osteoclasts. However, it is still unclear exactly where BPs localise within the skeleton, and whether non-osteoclast cells are directly affected by these drugs *in vivo*. We have synthesised fluorescein-risedronate (FAM-RIS), Alexa Fluor 647-risedronate (AF647-RIS) and rhodamine-3-PEHPC (RHO-3-PEHPC) to help address these questions. Three-day old rabbits were subcutaneously injected with either 0.5 mg/kg FAM-RIS or 0.9 mg/kg AF647-RIS (both molar equivalent to ~0.2 mg/kg RIS) and sacrificed 24 hours later. Using confocal microscopy, FAM-RIS and AF647-RIS uptake could be detected in osteoclasts in histological sections or in osteoclasts that had been purified *ex vivo* using immunomagnetic beads. In addition, while uptake of FAM-RIS by bone marrow cells (BMCs) was hardly detectable by flow cytometry, preliminary experiments revealed uptake of AF647-RIS *in vivo* in a subpopulation of rabbit BMCs, a subset of which were CD14+. These findings confirm osteoclasts as the main cell type that internalises BPs *in vivo*, but suggest that bone marrow monocytes may also be directly affected by BPs.

Histological analysis of rabbit ulnae and vertebrae revealed strong labelling of FAM-RIS around vascular channels in cortical bone. Osteocytic lacunae in close proximity to these vascular channels also showed FAM-RIS binding. Moreover, FAM-RIS localized to the lacunae of newly embedded osteocytes. Similar results were obtained with adult mice. This supports the proposal that BPs may exert direct, extracellular effects on osteocytes *in vivo*, although our findings suggest that only a small subset of osteocytes may be exposed to BP. To investigate the effect of differences in bone affinity on skeletal distribution, rats were injected subcutaneously with a combination of FAM-RIS and RHO-3-PEHPC (an analogue of RIS with lower bone affinity), and sacrificed 1 or 7 days later. Some differences in localisation were observed after 1 day, but more strikingly, FAM-RIS, but not RHO-3-PEHPC, additionally labelled the surface of bone that had formed during the 7 days following injection. These observations illustrate the concept that BP can recycle to other bone surfaces *in vivo* and that this is dependent on relative bone affinity. These findings may help to explain differences in the duration of action of BPs with different bone affinities.

**Disclosures:** M.J. Rogers, Procter & Gamble 1, 2, 3; Novartis 3; Roche 3.

This study received funding from: Cancer Research UK; Alliance for Better Bone Health.

## 1066

**Risedronate Prevents Early Radiation-Induced Bone Loss at Multiple Skeletal Sites.** J. S. Willey<sup>1</sup>, E. W. Livingston\*, L. C. Bowman\*, M. E. Robbins\*, J. D. Bourland\*, T. A. Bateman<sup>1</sup>. <sup>1</sup>Bioengineering, Clemson University, Clemson, SC, USA, <sup>2</sup>Department of Radiation Oncology, Wake Forest University Baptist Medical Center, Winston-Salem, NC, USA.

Bone irradiation during cancer therapy can lead to atrophy and increased risk of fracture at several skeletal sites, particularly the hip. Late radiation-induced bone loss has been attributed to damaged osteoblasts and vascularity. In contrast, little attention has been given to increased osteoclast activity as a contributor to radiation-induced osteoporosis. Our aim was to identify if radiation increases osteoclast activity resulting in acute bone loss. Thirteen-week old C57BL/6 mice (n=6/group) received whole body radiation with 2 Gy X rays (140kVp). A 1 mm region of the proximal tibia distal to the growth plate was analyzed via microCT (µCT 80; Scanco). Relative to non-irradiated control, bone volume fraction (BV/TV; -42%), trabecular connectivity (ConnD; -82%) and number (Tb.N; -24%) were lower 2 weeks after exposure (P < 0.05). Circulating TRAP5b was significantly elevated on Days 1 (+50%) and 3 (+14%). TRAP-stained sections at Day 3 had increased osteoclast number (N.Oc/BS; +80%; P < 0.05) and osteoclast surface (Oc.S/BS; +210%; P < 0.001). Skeletally mature mice (twenty-week old; n=12/group) were then irradiated (2 Gy) with or without subcutaneous injections of risedronate (0.1 mg/kg/wk). MicroCT analysis was performed at 3 sites: Proximal tibia; distal femoral metaphysis extending 1 mm proximal to the growth plate; and a region of the body of the 5<sup>th</sup> lumbar vertebra (L5). Bones were collected 1, 2, and 3 weeks after irradiation. Body mass was not affected by treatments. From animals only receiving radiation, significantly lower BV/TV relative to control was observed at all three skeletal sites and at all three time points. ConnD was significantly lower after irradiation at all time points in the proximal tibia; at Weeks 2 and 3 in the distal femur; and at Week 3 in L5. Tb.N in the distal femur was significantly lower than control at all time points, and was lower in L5 at Week 2 and Week 3. Structure model index (SMI) values indicated more rod-like trabeculae after radiation in L5 at all time points, but starting at Week 2 at the distal femur. Evidence of bone loss or deterioration was entirely absent at all time points in animals receiving both radiation and risedronate. Overall, radiation + risedronate treatment resulted in more plate-like trabeculae in the femur and L5. This study demonstrated a rapid loss of trabecular bone after whole body radiation at several skeletal sites. Changes were preceded by an increase in osteoclast number. As risedronate prevented the atrophy, an increase in osteoclast activity likely contributed to the radiation-induced bone loss.

**Disclosures:** J.S. Willey, None.

This study received funding from: NSBRI/NASA; Procter and Gamble Pharmaceuticals; NIH

## 1067

**Finite Element Analysis Performed on Radius and Tibia HR-pQCT Images Provides New Insights for Fracture Status Assessment.** N. Vilayphiou\*, S. Boutroy\*, E. Sornay-Rendu\*, B. Van Rietbergen\*, F. Munoz\*, P. D. Delmas<sup>1</sup>. <sup>1</sup>INSERM Unit 831 and Université de Lyon, Lyon, France, <sup>2</sup>Department of Biomedical Engineering, Eindhoven University of Technology, Eindhoven, Netherlands.

The contribution to skeletal fragility assessment of cortical (Ct) and trabecular (Tb) bones properties, and of finite element analysis (FEA) derived mechanical properties have already been reported in patients with wrist fracture (fx) (Boutroy et al., JBMR 2008). We extended here the FEA to a larger population, including patients with vertebral and other peripheral fragility fx. This case-control study used both areal BMD measured by DXA, and FEA on *in vivo* HR-pQCT images of the distal radius and tibia (XtremeCT, Scanco Medical AG) in 101 women (74 ± 8 yrs) who previously sustained a fragility fx, and 101 age-matched controls, all from the OFELY cohort. The results were analysed by a principal component (PC) analysis (PCA) to test the contribution of FEA to fx status assessment.

We observed that areal and volumetric BMD, Ct thickness and Tb number, thickness, separation and distribution were significantly worse in cases than controls, with differences ranging from -6% to 37%. FEA-derived stiffness and failure load were 12% lower in cases than in controls (p<0.001). In both groups the load was mostly carried by the cortex, except at the very distal end of the tibia where the Tb bone carried more load. Tb bone carried 6 to 12% more load in controls than in cases at the distal radius (p<0.05), implying that the load distribution was more uniform in controls. Moreover many correlations were found between results of the radius and the tibia (|r|>0.6, p<0.01).

We conducted a PCA in the 202 women to reduce the number of variables. It resulted in defining 3 PCs, for which the odds ratio (OR) for fx occurrence were computed. One PC included stiffness, failure load, areal and volumetric BMDs and Ct thickness, explaining 52% of the variance at the radius and 48% at the tibia, with OR = 1.82 [1.33-2.49] and 1.87 [1.36-2.56] respectively. A second PC was made of Tb number and distribution, explaining 15% and 10% of the variance, with OR = 1.71 [1.28-2.29] and 1.87 [1.16-2.19]. A third PC explained respectively 10% and 20% of the variance, with OR = 1.61 [1.19-2.18] and 1.16 [0.88-1.54], and was composed by the distribution of load between Ct and Tb bone.

For this population including several kinds of fx, results at the radius confirm the previous study done only for wrist fx. Moreover and despite their limits, results obtained at the tibia are also associated with the fx status. In conclusion FEA applied on those two peripheral sites measured by HR-pQCT seems to provide useful information in addition to DXA and microarchitecture measurement for the assessment of fx risk.

**Disclosures:** N. Vilayphiou, None.

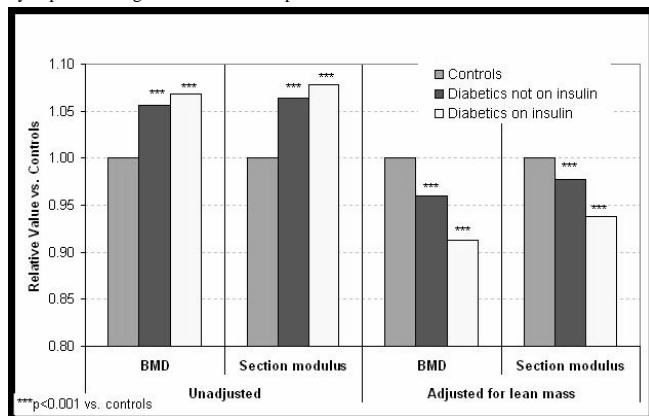


## 1068

**Geometric Evidence of a Modeling Defect in Type 2 Diabetic Women Enrolled in the Women's Health Initiative as a Potential Explanation for Increased Fracture Risk.** M. S. LeBoff<sup>1</sup>, R. Garg<sup>\*1</sup>, T. Beck<sup>\*2</sup>, J. Cauley<sup>3</sup>, G. Wu<sup>4</sup>, B. Lewis<sup>5</sup>, D. Nelson<sup>6</sup>, A. LaCroix<sup>7</sup>, Z. Chen<sup>4</sup>. <sup>1</sup>Endocrine, Diabetes, and Hypertension, Brigham and Women's Hospital, Boston, MA, USA, <sup>2</sup>Johns Hopkins University, Baltimore, MD, USA, <sup>3</sup>University of Pittsburgh, Pittsburgh, PA, USA, <sup>4</sup>University of Arizona, Tucson, AZ, USA, <sup>5</sup>University of Alabama, Birmingham, AL, USA, <sup>6</sup>Wayne State University, Detroit, MI, USA, <sup>7</sup>Fred Hutchinson Cancer Center, Seattle, WA, USA.

Diabetes increases the risk of fractures, yet bone mineral density (BMD) in patients with type 2 diabetes (T2DM) tends to be higher than in non-diabetic controls. We hypothesized that while BMD and the underlying geometry may be higher in an absolute sense, it is actually lower after accounting for the increased body weight in women with T2DM. Participants from the multi-ethnic, Women's Health Initiative Observational Study from the 3 BMD centers were included in this cross-sectional study. T2DM, defined by age at diagnosis > 20 years and no history of ketoacidosis, was self-reported. These analyses include 3 groups of women: 1) T2DM women on diet or oral hypoglycemic agents (n=299); 2) T2DM women on insulin therapy (with or without oral agents) (n=128); and 3) Non-diabetic controls (n=5520). Presence of undiagnosed diabetes in the control group cannot be ruled out. Hip structural analyses (HSA) in the femoral narrow neck (NN), intertrochanter, and shaft regions were done using the validated Beck's method on hip scans from dual energy x-ray absorptiometry (DXA). We compared HSA BMD and section modulus (SM) (bending strength) at the NN with and without correcting for total body DXA lean body mass as an index of hip muscle load. Women in all three groups were of similar ages (64.5, 64.3, 63.7 yrs, respectively) and heights, but those with T2DM were heavier, with greater lean body weight vs. controls (p<0.001). In both diabetic groups, absolute BMD and SM were higher vs. controls (Fig.). However, after adjusting for lean body weight, diabetic women had significantly lower BMD and SM. Among the diabetic women, women on insulin had the poorest bending strength.

Adjusted for lean body weight, the BMD and bending strength in the femoral neck are significantly lower in diabetic women vs. controls, with the poorest measures in those on insulin. This may be due to defective bone modeling adaptation in the diabetic women and may explain the higher fracture risk in patients with T2DM.



**Disclosures:** M.S. LeBoff, Eli Lilly 2; General Electric 5.  
This study received funding from: NIH.

## 1069

**Concentration of Insulin-Like Growth Factor (IGF-I) in Human Cortex Bone is Highly Correlated with Fracture Toughness of the Bone.** G. Sroga<sup>\*</sup>, D. Vashishth, Rensselaer Polytechnic Institute, Troy, NY, USA.

Insulin-like growth factor-I (IGF-I) is an abundant protein of bone matrix and is believed to play an important role during bone development and remodeling [1,2]. Any changes in IGF-I levels should therefore alter the amount as well as the quality of bone's extracellular matrix (ECM). Studies to date have only explored the relationships between IGF-I levels, bone mass and whole bone fracture properties and the effects of IGF-I on bone matrix quality remain unknown. In this study we report the age-related changes in bone matrix level IGF-I and its relationship to material level fracture properties indicative of bone's resistance to crack propagation.

Ten specimens of mechanically tested human cortical bone (posterior cortex) from male and female cadavers (age range 26 to 89 years) were used to isolate IGF-I (per g of dry weight bone) using methods published previously [1, 2]. Measurement of the concentration of IGF-I was conducted using an enzyme-linked immunosorbent assay (ELISA) (Oibt, GmbH, GE) according to the manufacturer's protocol. The normalized values of triplicate assays were then averaged and tested for correlation with fracture toughness of bone measured using crack propagation test [3].

The concentration of IGF-I in human tibial posterior cortex bone was inversely related to the age ( $R^2 = 0.69$ ;  $p < 0.05$ ). Concentrations of IGF-I in the eighth decade were on average about 2.4-fold lower than in the second decade of human subjects. IGF-I levels showed a positive and highly correlated non-linear relationship with fracture toughness of bone ( $r^2 = 0.83$ ;  $y = 0.85 + 0.004 \ln(x)/x^2$ ;  $y =$  fracture toughness,  $x =$  IGF-I bone matrix

concentration).

To our knowledge this is the first study on the relationship between bone matrix levels of IGF-I and material level measurement of bone quality. The results show a positive association between matrix level IGF-I and bone's resistance to propagation of fracture. As IGF-I level increase post-natally up to the juvenile phase and decrease thereafter well into the old age, these results suggest that IGF-I induced bone matrix changes may initially exert a protective influence on the skeleton and then become a source of weakness with aging. Further studies should be conducted to investigate the role of IGF-I on bone fracture.

## References

- [1]Seck T. et al. J. Clin. Endocrin. Metab. 83:2331, 1998.
- [2]Dong X. N. et al. Calcif. Tissue Int. 77:37, 2005
- [3]Vashishth and Wu. Trans. ORS. Vol. 29, 497, 2004

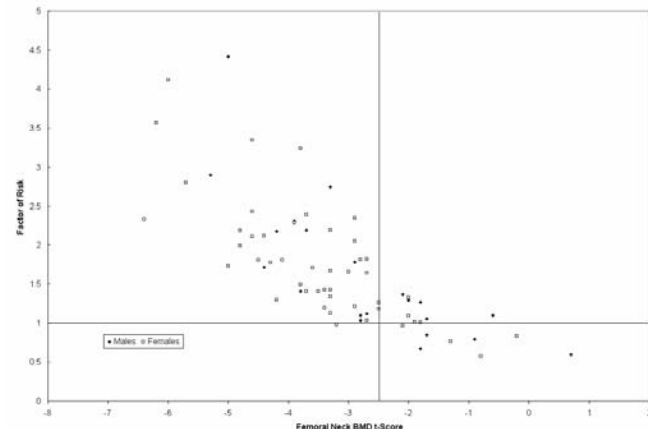
**Disclosures:** G. Sroga, None.

This study received funding from: NIH Grant AG20618.

## 1070

**Association Between Femoral Neck BMD and the Factor-of-Risk for Hip Fracture Derived from Direct Measurements of Strength In Human Cadaveric Femora.** B. J. Roberts<sup>\*</sup>, E. J. Thrall<sup>\*</sup>, M. L. Bouxsein, Orthopedic Surgery, Beth Israel Deaconess Medical Center / Harvard Medical School, Boston, MA, USA.

Areal BMD derived from DXA is currently the gold standard for diagnosis of osteoporosis; however, up to half of hip fractures occur in individuals who are not diagnosed as osteoporotic by DXA-based criteria. As fractures occur when the force applied to a bone exceeds its strength, a biomechanical approach to fracture risk assessment comparing the applied load-to-bone strength ratio, termed the factor of risk ( $\Phi$ ), may be useful. The aim of this study was to further explore this biomechanical approach by directly measuring femoral strength in elderly human cadaveric specimens and computing the factor of risk for hip fracture. We obtained 73 human cadaveric femurs (48 women and 25 men, aged  $74.2 \pm 8.7$ yr, range 55 to 98 yrs) with no evidence of prior fracture or metastatic lesions. We measured femoral neck (FN) aBMD by DXA, and then mechanically tested the femurs to failure at impact loading rates in a sideways fall configuration. The force applied to the hip during a sideways fall was computed from individual height and weight, after accounting for trochanteric soft tissue thickness which was estimated from body mass index using a previously published relationship (JBMR, 22:25-31, 2007). Women had lower FN aBMD ( $p=0.008$ ) and femoral failure load ( $4882 \pm 2209$  N vs  $2893 \pm 1099$  N,  $p < 0.001$ ), and higher  $\Phi$  (though not significantly) than men ( $\Phi = 1.76 \pm 0.74$  vs  $1.54 \pm 0.86$ ,  $p = 0.28$ ).  $\Phi$  was plotted against FN aBMD to determine the ability of a BMD-based diagnosis of osteoporosis to identify those specimens with a factor of risk greater than 1 (Figure). 53/ 54 (98%) specimens that had a FN aBMD t-score below -2.5 also had a  $\Phi > 1$ . However, 10/19 (53%) specimens with FN aBMD t-score above -2.5 had  $\Phi > 1$ . These data indicate that whereas a BMD-based diagnosis of osteoporosis is highly correlated with fracture risk, as assessed by the factor of risk, in our sample about 50% of individuals not designated as 'osteoporotic' would be at high risk for hip fracture should they experience a sideways fall. In sum, our findings strongly support the investigation of new methods of fracture risk prediction that consider the loads applied to the hip during a fall, and that incorporate other characteristics, such as bone geometry and/or microarchitecture, to improve estimates of bone strength.



**Disclosures:** M.L. Bouxsein, Merck & Co. 3.  
This study received funding from: Merck & Co.

## 1071

**Increased Non-enzymatic Glycation of Cancellous Bone due to Decrease in Remodeling During Alendronate Therapy of Osteoporotic Women.** D. Vashishth<sup>1</sup>, C. Bertholon<sup>\*2</sup>, E. Gineyts<sup>2</sup>, P. Chavassieux<sup>2</sup>, G. Boivin<sup>2</sup>, P. D. Delmas<sup>2</sup>. <sup>1</sup>INSERM Unit 831 University of Lyon & Rensselaer Polytechnic Institute, Troy, NY, USA, <sup>2</sup>INSERM Unit 831 University of Lyon, Lyon, France.

Treatment of osteoporotic postmenopausal women by alendronate (ALN) increases bone mineral density (BMD) by reducing turnover and increasing the mean degree of mineralization (DMB) [1,2]. Canine studies, however, suggest that reduction in turnover also has the potential to reduce the efficacy of ALN treatment by causing collagen crosslink formation through the process of non-enzymatic glycation (NEG) and increasing the propensity of bone to fracture [3,4].

Here we conducted analyses on human iliac crest biopsies, obtained from an ALN clinical trial [1], to determine collagen modifications and their relationships to bone quality and remodeling. We quantified enzymatic [pyridinoline (PYD) and deoxypyridinoline (DPD)] and non-enzymatic [pentosidine (PEN)] crosslinks in cancellous and cortical bone compartments of 100 µm-thick transiliac bone biopsy sections obtained from women at 2 years from the start of the treatment with ALN at dose of 10 mg/day (N=9) or placebo (PLB, N=15). Collagen crosslinks were compared between ALN and PLB groups and tested for correlation with measures of bone structure (BV/TV, Tb.Th, Tb. Sp, Tb.N), mineralization (DMB) and remodeling (MAR, MS/BS, BFR/BS, AcF, FP). Based on outlier analysis, data from 4 women (3 PLB and 1 ALN) were eliminated for non-parametric analyses.

Compared to PLB, ALN group showed significant (p=0.006) accumulation of PEN, in cancellous (ALN=17±3; PLB=8±3 nmol/mol of collagen) and not in cortical bone tissue. PYD and DPD were not different in cancellous or cortical bone tissues between ALN and PLB groups (p>0.05). Out of all measures of bone quality and remodeling, PEN correlated with BV/TV (r' = -0.52; p=0.01), DMB (r' = 0.57; p=0.008), BFR/BS (r' = -0.49; p=0.03), AcF (r' = -0.43; p=0.07) and MS/BS (r' = -0.54; p=0.01). PYD and DPD showed no correlation with any of the measured variables.

In conclusion, this study demonstrates that two years of ALN therapy of postmenopausal women results in post-translational modification of bone collagen through PEN. These effects are evident in cancellous and not in cortical bone and are localized in bone matrix with higher levels of DMB. Moreover, accumulation of PEN can be explained partially by remodeling suppression and low bone volume fraction. Further studies should be devoted to collagen changes induced by antiresorptive therapy and to their potential impact on antifracture efficacy.

**References:** [1] Chavassieux et al., JCI 1997 100: 1475-80. [2] Boivin et al. Bone 2000 5 : 687-94. [3] Allen et al. Ost. Int. 2008 19: 329-37. [4] Tang et al. 2007 Tans. ORS 32: 264.

**Disclosures:** D. Vashishth, Merck 4.

This study received funding from: NIAMS AR 49635 & INSERM France.

## 1072

**Transition From Alendronate to Denosumab in Ovariectomized Cynomolgus Monkeys Maintained or Improved Cortical and Trabecular Bone Mass, Without Altering the Linear Relationship Between Bone Mass and Bone Strength.** M. S. Ominsky<sup>1</sup>, S. Y. Smith<sup>2</sup>, F. Vlasseros<sup>\*2</sup>, R. Samadfam<sup>\*2</sup>, P. J. Kostenuik<sup>1</sup>. <sup>1</sup>Metabolic Disorders, Amgen Inc., Thousand Oaks, CA, USA, <sup>2</sup>Charles River Laboratories Preclinical Services Montreal, Inc., Montreal, QC, Canada.

The safety and efficacy of transitioning from a bisphosphonate to denosumab (DMAb, a fully human RANKL Ab) were examined in ovariectomized cynomolgus monkeys (cynos). Adult cynos (> 7 years old) were ovariectomized (OVX) and treated with vehicle (Veh, n=20), alendronate (ALN, n=21; 50 µg/kg IV biweekly), or denosumab (DMAb, n=11; 25 mg/kg SC monthly). After 6 months, animals from each of the Veh (n=10) and ALN (n=11) groups were switched from their previous treatment to denosumab (Veh-DMAb and ALN-DMAb), while the remaining animals continued treatment on Veh or ALN. The original DMAb group remained on DMAb for 12 months total. Serum calcium and BMD were monitored throughout the 12-month study. Strength testing was performed at the femur diaphysis, femur neck, and lumbar vertebrae.

Initiation of ALN or DMAb treatment resulted in transient decreases in serum calcium relative to vehicle controls. Pretreatment with ALN significantly reduced the denosumab-mediated calcium decrease compared to the Veh-DMAb group. One year of ALN or DMAb treatment resulted in significant increases from baseline in BMD at cancellous (lumbar spine DXA) and cortical (tibia diaphysis pQCT) sites. BMD continued to increase at both sites in the ALN-DMAb group after transition to denosumab. Transition from ALN to DMAb was also associated with significantly greater whole body BMD (vs. baseline), which was not observed with ALN alone.

Destructive compression testing of lumbar vertebral trabecular cores revealed significantly greater peak load and stiffness in DMAb and ALN-DMAb groups (p<0.05 vs. Veh), but not in the ALN alone group. No significant differences were found in extrinsic bone strength parameters at the femur neck and femur diaphysis, or in intrinsic strength parameters derived from the femur diaphysis for any group. Further evidence of normal material properties was demonstrated by strong and similar linear correlations within and across each group for load versus BMC at the femur diaphysis (overall r<sup>2</sup>=0.80), femur neck (r<sup>2</sup>=0.53), vertebral bodies (r<sup>2</sup>=0.69), and vertebral trabecular cores (r<sup>2</sup>=0.83).

In summary, transition from ALN to DMAb in adult OVX cynos resulted in maintenance or improvements in cortical and trabecular bone mass parameters, with no apparent safety concerns regarding serum calcium or bone strength. The linear relationship between bone mass and bone strength was preserved in all groups, suggesting that bone mass continued to predict bone strength independent of these treatment regimens.

**Disclosures:** M.S. Ominsky, Amgen 5.

This study received funding from: Amgen.

## 1073

**Ccrn4l, A Peripheral Clock Gene, Influences Stromal Cell Allocation, Bone Mass, and Marrow Adiposity in Mice and Humans.** M. Kawai<sup>1</sup>, C. Ackert-Bicknell<sup>2</sup>, B. A. Lecka-Czernik<sup>3</sup>, J. P. Rodriguez<sup>4</sup>, A. M. Pino<sup>\*4</sup>, S. Rios<sup>\*4</sup>, C. B. Green<sup>\*5</sup>, C. J. Rosen<sup>1</sup>. <sup>1</sup>Research Institute, Maine Medical Center, Scarborough, ME, USA, <sup>2</sup>The Jackson Laboratory, Bar Harbor, ME, USA, <sup>3</sup>University of Toledo, Toledo, OH, USA, <sup>4</sup>Universidad de Chile, Santiago, Chile, <sup>5</sup>University of Virginia, Charlottesville, VA, USA.

Rosiglitazone (ROZ) treatment of mesenchymal stromal cells (MSCs) causes suppression of osteoblast (OB) specific genes and increased adipocytic pathway genes. One such transcript is *Ccrn4l* (also called *nocturnin*) a gene originally cloned from *Xenopus* retinae. *Ccrn4l* is a peripheral clock gene that encodes a deadenylase expressed in bone, fat, liver and stem cells. Hepatic *Ccrn4l* mRNA exhibits a circadian rhythm, being highest at ZT 1200, lowest at 2400. Aging, high fat feeding and ROZ induce hepatic *Ccrn4l* mRNA but decrease hepatic *Igf1*mRNA. Thus, we hypothesized that *Ccrn4l* was a downstream mediator of *Pparg*, and a negative regulator of both IGF-1 and osteoblastogenesis. To test that hypothesis, we characterized the time course of *Ccrn4l* expression in adipocytes, as well as human and mouse MSCs, and phenotyped the skeleton of *Ccrn4l* -/- mice. We cultured primary calvarial OBs from 1 wk Swiss Webster females in 10% FCS x 7 days, followed by β-GP + ascorbic acid. At day 0 by RT-PCR, *Ccrn4l* transcripts were present, but during OB differentiation, *Ccrn4l* mRNA was suppressed. If calvarial OBs were cultured in adipogenic media (MDI: IBMX, insulin, dexamethasone, ROZ), *Ccrn4l* transcripts increased and were related to adipocyte number. In 3T3-L1 cells exposed to MDI+ROZ, *Ccrn4l* expression and protein levels were increased by 9hrs, and sustained, as was *Pparg* mRNA while *Igf1* transcripts declined after 12hrs and remained low until day 5. In human MSCs isolated from patients undergoing hip replacement, with osteoporosis (OP) or without (OA), *Ccrn4l* expression was present at baseline and higher in OP vs. OA patients (p<0.05), as was *Pparg* mRNA; *Ccrn4l* mRNA was maintained when cultured in MDI, but suppressed in osteoblastic media. Addition of 1,25 (OH)D<sub>2</sub> did not alter *Ccrn4l* expression in MSCs with either media. In vivo, *Ccrn4l* -/- mice had increased cortical vBMD and trabecular distal femoral BV/TV vs. B6 (p<0.03), due to greater trabecular thickness (p<0.003). Bone marrow adipocytes were reduced by 50% in *Ccrn4l* -/- vs. B6 (p<0.05). In sum, *Ccrn4l* expression is maintained in MSCs that undergo adipogenesis, while it is suppressed during OB differentiation. Global deletion of *Ccrn4l* results in high bone mass and a phenocopy of *Pparg* +/- mice. We postulate that *Ccrn4l* is a downstream mediator of *Pparg* activation, essential for circadian clock regulation in bone. One gene target for *Ccrn4l* may be *Igf1*, thus providing a critical link between the fate of MSCs as adipocytes and nutrient status.

**Disclosures:** C.J. Rosen, None.

This study received funding from: NIH AR54604.

## 1074

**Osterix Is Required for Skeletal Growth and Bone Homeostasis after Birth.** X. Zhou<sup>\*1</sup>, Z. Zhang<sup>\*1</sup>, J. Q. Feng<sup>2</sup>, B. G. Darnay<sup>3</sup>, J. Kim<sup>4</sup>, B. de Crombrughe<sup>5</sup>. <sup>1</sup>M.D. Anderson, Houston, TX, USA, <sup>2</sup>Biomedical Sciences, Baylor College of Dentistry, Dallas, TX, USA, <sup>3</sup>Experimental Therapeutics, M.D. Anderson, Houston, TX, USA, <sup>4</sup>Molecular Medicine, Cell and Matrix Research Institute, Daegu, Republic of Korea, <sup>5</sup>Molecular Genetics, M.D. Anderson, Houston, TX, USA.

Osterix (Osx) is a transcription factor required for osteoblast differentiation and bone formation during embryonic development. We hypothesize that Osx is also needed for bone formation and bone homeostasis postnatally. Osx is expressed specifically in all osteoblasts and osteocytes and at a lower level in hypertrophic chondrocytes postnatally. To circumvent the neo-natal lethality of Osx-null mice, we successfully deleted Osx after birth using CAG-CreER: a tamoxifen-inducible cre recombinase under the control of the CMV/βactin promoter. By QPCR, the expression level of Osx in the humerus of day 24 tamoxifen-treated CAG-CreER; Osx-/flox mouse was about 1% of the tamoxifen-treated wild type control. Postnatal Osx-null mutants displayed a novel skeletal phenotype. These mice were characterized by the disappearance of bone trabeculae, thin and porous cortical bones, and a massive accumulation of mineralized cartilage tissue. Both primary osteoblasts isolated from calvaria and bone marrow stromal cells of Osx mutants failed to form any mineralized nodules in vitro; calcein incorporation was almost completely absent in lumbar vertebrae and long bones of tamoxifen-treated CAG-CreER; Osx-/flox mice, indicating that Osx is required for bone formation postnatally. By In situ hybridization, the Col2a1 expression pattern in the mutant remained unchanged comparing to the wild type controls, eliminating the possibility of ectopic cartilage formation due to loss of Osx. Osteoclasts, although reduced in numbers, appear to function normally. We postulate that the removal of mineralized cartilage is a function that is dependent on the presence of Osx, but the exact mechanism of this function is still unclear. Inactivation of Osx also inhibited expression of osteocyte markers and severely affected the morphology of osteocytes and their dendritic extensions, suggesting that Osx also plays a key role in regulating and maintaining osteocyte functions.

Taken together, our data substantiate the hypothesis that Osx is needed for skeletal growth and homeostasis after birth, and identify Osx as the first transcription factor required for osteoblast differentiation and new bone formation, as well as osteocyte function postnatally. These results provide new insights into postnatal skeletal morphogenesis and remodeling, which in turn should facilitate the development of preventive and therapeutic procedures for common bone diseases including osteoporosis.

**Disclosures:** X. Zhou, None.

## 1075

**Mice Lacking the Novel Transmembrane Protein Osteopotential Develop Catastrophic Defects in Bone Modeling.** M. L. Sohaskey<sup>\*1</sup>, Y. Jiang<sup>2</sup>, J. Zhao<sup>\*2</sup>, A. Mohr<sup>\*3</sup>, F. Roemer<sup>\*3</sup>, R. M. Harland<sup>\*1</sup>. <sup>1</sup>Molecular and Cell Biology, University of California, Berkeley, CA, USA, <sup>2</sup>Osteoporosis and Arthritis Lab, Dept. of Radiology, University of Michigan Medical School, Ann Arbor, MI, USA, <sup>3</sup>Osteoporosis and Arthritis Research Group, University of California, San Francisco, CA, USA.

In vertebrates, bone modeling coordinated by bone-forming osteoblasts and bone-resorbing osteoclasts generates and ensures the integrity of the developing skeleton. Dysregulation of this process leads to pathophysiological changes and metabolic bone disease. In an insertional mutagenesis screen for essential regulators of mammalian development, we identified *Osteopotential* (*Opt*), a gene encoding a novel transmembrane protein widely expressed in the developing embryo. Mice homozygous for an insertional mutation in the *Opt* locus die predominantly at birth of undetermined causes. Mice surviving this perinatal crisis period develop striking skeletal abnormalities similar to those seen in humans and genetically engineered mouse models having severe forms of the brittle bone disease osteogenesis imperfecta (OI), in particular OI type V. Abnormalities include hemorrhaging around limbs, deformation of long bones, and aberrantly healed fractures evidenced by the formation of hyperplastic calluses on ribs and long bones. Surviving *Opt* homozygous mutants exhibit a marked decrease in the amount of trabecular and cortical bone relative to normal littermates. Consistent with the hypothesis that this low bone mass results from a primary defect in osteoblast differentiation, *ex vivo* studies using primary calvarial osteoblast cultures reveal a cell-autonomous impairment of differentiation in *Opt* mutant osteoprogenitors, despite a normal proliferative index. Moreover, differentiating calvarial osteoblast cultures from *Opt*-deficient mice synthesize markedly reduced levels of Type I collagen protein despite normal transcription of *Col1a2*. Surprisingly, osteoclast function also appears to be compromised in *Opt* mutant mice, implying a state of low bone turnover in which increased bone resorption does not contribute to the fragility of the *Opt* mutant skeleton. When overexpressed in cultured cell lines and primary osteoblasts, *Opt* co-localizes with the endoplasmic reticulum markers Calnexin and PDI. In addition, *Opt* efficiently translocates across ER-derived microsomal membranes *in vitro*, suggesting that *Opt* is an integral membrane protein of the endoplasmic reticulum. Collectively, these data are important in establishing how mutagenesis of *Opt* results in a dramatic failure of bone modeling in the mouse. Our findings may also provide valuable mechanistic insight into the etiology of recessive forms of OI demonstrating no genetic linkage to either Type I procollagen locus.

**Disclosures:** M.L. Sohaskey, None.

## 1076

**Ligand Activation of the Engineered G<sub>s</sub>-coupled Receptor Rs1 in Osteoblasts Promotes Trabecular Bone Formation.** E. Hsiao<sup>1</sup>, S. Millard<sup>2</sup>, A. Louie<sup>\*2</sup>, B. Boudignon<sup>\*</sup>, C. Manalac<sup>\*1</sup>, W. Lu<sup>\*2</sup>, B. Halloran<sup>2</sup>, B. Conklin<sup>\*1</sup>, R. Nissenson<sup>2</sup>. <sup>1</sup>GICD, J. David Gladstone Institutes, San Francisco, CA, USA, <sup>2</sup>Endocrine Unit, VA Medical Center, San Francisco, CA, USA.

Osteoblasts express a number of G-protein coupled receptors (GPCRs) that regulate intracellular cAMP levels through the G<sub>s</sub> and G<sub>i</sub> pathways. We previously described a mouse model that expresses an engineered G<sub>s</sub>-coupled receptor, Rs1, in maturing osteoblasts using the Collagen 1 alpha 2.3 kb promoter fragment (Coll(2.3)-tTA/TetO-Rs1 mice). In this model, dramatic trabecular bone formation was induced by basal Rs1 signaling activity from embryogenesis through adulthood, but the bone growth was significantly attenuated if Rs1 expression was delayed until after 4 wks of age. In this study, we sought to identify whether the phenotypic changes resulting from basal Rs1 activity could be induced by activating Rs1 with the synthetic agonist RS67333. Rs1 expression in Coll(2.3)-tTA/TetO-Rs1 mice was suppressed until 4 weeks of age by administration of doxycycline. After an additional 4-6 weeks off of doxycycline to allow Rs1 expression, mice were treated with either continuous RS67333 infusion by osmotic pump (3 mg/kg/day for 10 weeks) or with daily injections of RS67333 (3 mg/kg/day as a single daily dose for 4 weeks). Mutant mice treated with continuous RS67333 showed a significant increase in whole body DEXA bone mineral density as compared to agonist-treated wildtype littermates (0.108 +/- 0.020 vs. 0.054 +/- 0.002 g/cm<sup>2</sup>, p=0.004). Examination of the left femurs from individual animals showed wide variation in the degree of bone formation, as observed by microCT analysis of total femur bone volumes (105.8 +/- 95.0 vs. 20.9 +/- 0.4 mm<sup>3</sup>, p=0.26). The most severely affected femurs showed expansion of trabecular bone with loss of cortical bone and bone marrow space, resembling the changes induced by basal Rs1 signaling when Rs1 was expressed during embryogenesis and throughout postnatal life. In contrast, a 4 week course of intermittent, daily administration of RS67333 caused no detectable changes in cortical thickness or bone volume, although 5 of 8 animals showed an increase in trabecular bone within the secondary spongiosum. Our data indicate that continuous activation of Rs1 by a synthetic ligand in adult animals can reproduce the trabecular bony expansion seen with basal Rs1 activity from gestation. In addition, this study indicates that engineered receptors activated solely by synthetic ligands (RASSLs) such as Rs1 can be used to control and examine the temporal effects of G-protein signaling in osteoblasts.

**Disclosures:** E. Hsiao, None.

## 1077

**Expression of an Engineered G<sub>s</sub>-coupled Receptor, Rs1, in Mature Osteoblasts is Sufficient to Drive A Dramatic Anabolic Skeletal Response.** S. M. Millard<sup>1</sup>, B. Boudignon<sup>1</sup>, A. Louie<sup>\*1</sup>, W. Lu<sup>\*1</sup>, B. P. Halloran<sup>1</sup>, B. Conklin<sup>\*2</sup>, R. A. Nissenson<sup>1</sup>. <sup>1</sup>Endocrine Research Unit, VA Medical Center, San Francisco, CA, USA, <sup>2</sup>Gladstone Institutes, University of California, San Francisco, CA, USA.

To examine the role of G<sub>s</sub>-coupled signaling pathways in osteoblasts we used targeted expression of an engineered constitutively active G<sub>s</sub>-coupled receptor, Rs1. Previously it has been described that expressing Rs1 in maturing and mature osteoblasts *in vivo* using the Collagen 1 alpha 2.3 kb promoter induces a dramatic anabolic skeletal response, including a striking expansion of what appear to be early osteoblast lineage cells. Conceptually, these cells may be derived from either an expansion of Rs1 expressing cells, which fail to subsequently fully differentiate, or from an osteoblast progenitor population which can respond to paracrine signals generated by Rs1 expressing cells. To distinguish between these possibilities we have expressed Rs1 under control of the osteocalcin promoter, to restrict transgene expression to mature osteoblasts. MicroCT imaging of femurs from OC:Rs1 mice show a massive and generalized increase in mineralized bone by 9 weeks of age. The precise extent of the mineralized expansion varied greatly, both between animals, and between different bones of the same animal. Histomorphometry showed a marked increase in bone cellularity and osteoid with disorganized trabecular bone. Expression of Runx2 and alkaline phosphatase (abundantly present in early osteoblast lineage cells) was upregulated 5 fold and 6.5 fold, respectively, in RNA isolated from the tibiae of 9wk old OC:Rs1 animals as compared to littermate controls. Osteocalcin expression (restricted to mature osteoblasts) was modestly upregulated by only 2 fold. These data support the notion that the increased bone cellularity observed in the OC:Rs1 animals resulted from a preferential expansion of early osteoblast lineage cells. The findings suggest that G<sub>s</sub> coupled signaling in mature osteoblasts generates a paracrine signal which positively regulates cells earlier in the osteoblast lineage. The expression of RANKL, a known target of cAMP dependent G<sub>s</sub> signaling, was upregulated by 7 fold in RNA from the tibiae of 9 wk old OC:Rs1 mice and the RANKL:OPG ratio, an important determinant of osteoclastogenic activity, was increased by 2 fold at the RNA level. Furthermore, histomorphometric analysis revealed a striking increase in TRAP positive staining cells in OC:Rs1 mice. Thus, G<sub>s</sub> signaling in mature osteoblasts drives a large increase in bone formation and bone resorption. The former appears to result from paracrine control of the number of early osteoblasts whereas the latter likely arises from a G<sub>s</sub>-induced increase in the osteoclastogenic activity of mature osteoblasts.

**Disclosures:** S.M. Millard, None.

This study received funding from: NIH.

## 1078

**Jagged1 Stimulation by Parathyroid Hormone(1-34) (PTH) in Mature Osteoblasts Is not Required for Hematopoietic Stem Cell (HSC) Expansion.** J. Weber<sup>\*</sup>, B. Gigliotti<sup>\*</sup>, R. Porter<sup>\*</sup>, A. Olm-Shipman<sup>\*</sup>, B. Frisch<sup>\*</sup>, J. Smith<sup>\*</sup>, L. M. Calvi. Department of Medicine, University of Rochester School of Medicine, Rochester, NY, USA.

Osteoblasts regulate HSC in the bone marrow microenvironment. Osteoblastic-HSC interactions could be exploited to expand HSC, however the signals required are unknown. We have defined a murine model in which PTH expands HSC. Our data suggested that PTH may expand HSC by stimulating the ligand Jagged1 in osteoblasts, activating its Notch receptor(s) in HSC and increasing their self-renewal. Moreover, PTH increased Jagged1 only in a subset of osteoblasts *in vivo*. Based on these data, we hypothesized that PTH may specifically stimulate Jagged1 in mature osteoblasts, and that the PTH-dependent HSC increase may require osteoblastic Jagged1. To test whether PTH regulates Jagged1 depending on osteoblastic differentiation, unmineralized vs mineralizing MC3T3-E1 (MC3T3) cells were treated with a single dose of PTH and Jagged1 was quantified by real time RT-PCR. As we hypothesized, PTH increased Jagged1 only in mineralizing, osteocalcin (OC) positive MC3T3 cells. In contrast, in spite of expression of the PTH receptor, unmineralized MC3T3s did not upregulate Jagged1 after PTH. The Adenylate Cyclase (AC) stimulator Forskolin and PTH(1-31), which preferentially activates Protein Kinase A (PKA), also increased Jagged1 in mineralizing MC3T3 cells, suggesting that this effect is AC/PKA-dependent. In contrast, the Protein Kinase C stimulating Phorbol Ester and PTH(13-34) did not induce Jagged1. To test *in vivo* whether expression of Jagged1 in mature osteoblasts is required for the PTH-dependent HSC expansion, mice expressing the Cre recombinase (Cre) under the control of the human OC promoter were crossed with mice in which LoxP sites flank the first 2 coding exons of the Jagged1 gene. Cre targeting to osteoblasts and osteocytes was confirmed *in vivo* by the enhanced GFP reporter mouse strain Z/EG. Mice lacking osteoblastic Jagged1 were fertile and viable, and did not have any dramatic bone or hematopoietic phenotype. Adult male mice lacking osteoblastic Jagged1 and control littermates were treated with intermittent PTH or vehicle (n=5/group). HSC from the bone marrow, quantified by flow cytometric analysis as Lin-Sca-1-c-kit<sup>+</sup> (LSK) cells, were similar in all vehicle-treated mice. PTH treatment increased LSK equally in controls and in mice lacking osteoblastic Jagged1. In summary, while PTH stimulates Jagged1 specifically in mature osteoblasts, Jagged1 expression is not required *in vivo* for the PTH-dependent expansion of HSC. These data challenge whether Notch mediates the PTH-dependent HSC increase. Further studies are in progress to establish *in vivo* whether the Notch signaling pathway is required for osteoblastic-HSC interactions.

**Disclosures:** J. Weber, None.

This study received funding from: NIDDK/NIH and the Pew Foundation.

## 1079

**Critical Role of TGF- $\beta$  Signaling Pathways in Skeletal Development.** T. Matsunobu<sup>\*1</sup>, A. B. Kulkarni<sup>\*1</sup>, S. Karlsson<sup>\*2</sup>, Y. Yamada<sup>\*1</sup>. <sup>1</sup>Laboratory of Cell and Developmental Biology, National Institute of Dental and Craniofacial Research/NIH, Bethesda, MD, USA, <sup>2</sup>Molecular Medicine and Gene Therapy, Lund Strategic Center for Stem Cell Biology and Cell Therapy, Lund University, Lund, Sweden.

Transforming growth factor- $\beta$  (TGF- $\beta$ ) initiates its diverse cellular responses during development by forming a specific cell surface complex consisting of TGF- $\beta$  and TGF- $\beta$  type I (T $\beta$ R/Alk5) and type II receptors, which activates downstream signaling through Smad-dependent and/or -independent pathways such as MAPK pathways. The precise role in vivo has not been fully understood since gene targeting of TGF- $\beta$  signaling-related genes in mice has resulted in phenotypes varying from early embryonic lethality to normal at birth. In this study, we conditionally deleted ALK5 in the skeletal progenitors by Dermo1-Cre to determine the role of TGF- $\beta$  signaling in skeletogenesis. The conditional ALK5 knockout mice (ALK5CKO) were perinatal lethal, and skeletal preparation and histological examinations revealed that ALK5CKO had severe bone and perichondrium formation defects with less mineralization, partial joint fusion, and abnormal cartilaginous ectopic protrusions formed from the resting/proliferative zones. Immunohistochemical analysis showed that osteoblast proliferation activity and the expression of osteoblast differentiation markers were systemically decreased in ALK5CKO calvaria and limbs. To understand the mechanism of the bone formation defect in ALK5CKO, we further generated genetically modulated mice with ALK5<sup>flox/flox</sup>; ROSA26 to visualize Cre-mediated ALK5 inactivation by X-Gal staining, and we carried out metatarsal organ culture and primary neonatal calvarial cell culture. The proliferation of perichondrial cells in the metatarsal explants as well as the primary calvarial cells was reduced in part through the inhibition of JNK-MAPK and Smad pathways when ALK5 was inactivated. We also found that ALK5-deficient calvarial cells showed inhibition of MAPKs activity, and reduced osteogenic differentiation activity as evident by reduced alkaline phosphatase activity and mineralization. In contrast, adipocytogenesis was elicited even though the cells were cultured in osteogenic differentiation conditions in part through the inhibition of p38-MAPK and Smad pathways. These results suggest that TGF- $\beta$  signaling positively regulates the commitment of common osteoblast/adipocyte progenitors toward osteoblast lineage and osteoprogenitor proliferation and differentiation during skeletogenesis through Smad-dependent and -independent pathways. Our findings demonstrate an important in vivo function of TGF- $\beta$  signaling pathways in bone development by selecting different downstream pathways.

**Disclosures:** T. Matsunobu, None.

## 1080

**TGF $\beta$  Inhibits BMP Signaling and Osteogenesis Through the TGF $\beta$  and BMP R-Smad Direct Interaction.** O. Korchynski, P. ten Dijke\*. Molecular Cell Biology, Leiden University Medical Center, Leiden, Netherlands.

Bone morphogenetic proteins (BMP) and transforming growth factors  $\beta$  (TGF $\beta$ ) belong to the same TGF $\beta$  superfamily of cytokines. Interestingly, signalling pathways mediating BMP and TGF $\beta$  signals were found to counteract each other in the multiple physiological situations including bone destruction due to periprosthetic osteolysis and inhibition of TGF $\beta$ -promoted metastasis formation by BMPs. BMPs and TGF $\beta$ s transduce most of their signals through the intracellular Smad proteins. In the current study we describe a novel molecular mechanism underlying the negative crosstalk between the BMP and TGF $\beta$  pathways. Upon ligand stimulation endogenous BMP pathway-restricted (R-Smad) Smad1 and Smad5 form a transient complex with the endogenous activated TGF $\beta$ /Activin R-Smads, namely Smad2 and Smad3. This complex formation leads to the inhibition of BMP6 and BMP7-driven transcription and their direct target genes Id1, Smad6 and Smad7 mRNA expression as well as of Id1 and Msx2 and Msx1 promoters activation. As a result BMP6/7-induced both early and late osteoblast differentiation is strongly inhibited by TGF $\beta$ . Neither Smad1/5/8 phosphorylation nor their affinity to DNA binding is affected upon TGF $\beta$  treatment. Ectopic expression of Smad2 and Smad3 strongly exacerbates the inhibitory effect of TGF- $\beta$  on BMP response and subsequently osteogenesis. Smad1 or Smad5 overexpression or treatment with the specific TGF $\beta$ R-I/ALK5 kinase inhibitor SB431542 completely rescue BMP signaling from being inhibited by TGF $\beta$ . shRNA-mediated knockdown of Smad2 and Smad3 expression converts TGF $\beta$  from the inhibitor of BMP response into an activator of BMP signaling. Adenovirally delivered shRNA constructs that knockdown Smad2 and Smad3 expression or treatment with SB431542 inhibitor efficiently rescue BMP-induced osteoblast differentiation from the inhibition by TGF $\beta$ . Chromatin immunoprecipitation assay (ChIP) performed with an RNA Polymerase II-specific antibody revealed that BMP-induced transcription is indeed inhibited with a TGF $\beta$  treatment. Interestingly, co-ChIP assay reveals both BMP R-Smads (Smad1/5/8) and TGF $\beta$  R-Smad, Smad2 to be a part of common transcriptional complex bound to the BMP target genes promoters. Thus, simultaneous activation of both BMP and TGF $\beta$  pathways causes a formation of the complex between activated BMP R-Smads and activated TGF $\beta$ /Activin R-Smads leading to the inhibition of both BMP and TGF $\beta$ -driven transcription.

**Disclosures:** O. Korchynski, None.

## 1081

**A BMP-2-stimulated Signaling Niche in Osteoblasts Comprising of Smad and PI 3 Kinase/Akt Regulates NFATc1 Expression and Its Nuclear Translocation.** C. C. Mandal<sup>1</sup>, G. G. Choudhury<sup>\*2</sup>, S. Ganapathy<sup>\*1</sup>, S. E. Harris<sup>3</sup>, N. Ghosh-Choudhury<sup>1</sup>. <sup>1</sup>Pathology, University of Texas Health Science Center at San Antonio, San Antonio, TX, USA, <sup>2</sup>Medicine, University of Texas Health Science Center at San Antonio, San Antonio, TX, USA, <sup>3</sup>Periodontics, University of Texas Health Science Center at San Antonio, San Antonio, TX, USA.

The transcription factor NFATc1 acts as a master regulator of osteoclast differentiation under the control of osteoblast-derived protein factors. However, its function in osteoblasts (OB) is still evolving. To study osteoblastic NFATc1 regulation, we generated OB-specific BMP-2 knock out (BMP-2 cKO) mice by crossing homozygous BMP-2 floxed mice with 3.6kb collagen type I-Cre mice. These mice have reduced bone mass, radio-opacity and bone mineral density. Immunohistochemical staining of bone sections showed significant reduction in NFATc1 expression. Phosphorylation of Smad 1/5, the downstream transcription factors in BMP-2 signaling, was also significantly prevented in the BMP-2cKO mice. To examine the mechanism of NFATc1 expression, we used cultured OB. BMP-2 increased NFATc1 mRNA and protein expression within 4 hours, resulting in its translocation to the nucleus as determined by real time qRT-PCR-PCR, immunoblotting and immunofluorescence, respectively. Actinomycin-D completely inhibited BMP-2-stimulated NFATc1 protein expression, indicating the involvement of a delayed early transcriptional mechanism. Transient transfection assays using a NFATc1 promoter-driven luciferase reporter plasmid (NFAT-Luc) showed 5-fold increase in NFATc1 transcription by BMP-2. Adenoviral expression of inhibitory Smad 6 blocked BMP-2-induced NFATc1 protein expression and its nuclear translocation. Furthermore, expression of Smad 6 prevented BMP-stimulated NFATc1 transcription. Transfection of Smad 5 increased NFATc1 transcription in the absence of BMP-2, confirming the involvement of BMP-specific Smads in the expression of NFATc1 in OB. We have established a requirement of PI 3 kinase/Akt signaling in OB differentiation. Therefore, we tested the involvement of this lipid kinase cascade in NFATc1 expression. Expression of dominant negative PI 3 kinase or Akt significantly inhibited BMP-2-induced transcription of NFATc1 as judged by the transient reporter transfection assays. Also PTEN (a lipid phosphatase), which acts as an inhibitor of PI 3 kinase signaling, and dominant negative Akt significantly blocked BMP-2-induced nuclear translocation of NFATc1. Together these data for the first time show a role of NFATc1 downstream of BMP-2 in mouse bone development. Furthermore, our results provide novel evidence for the presence of a cross-talk between Smad and PI 3 kinase/Akt signaling for BMP-2-induced NFATc1 regulation.

**Disclosures:** C.C. Mandal, None.

This study received funding from: NIAMS RO1 and VA MERIT Review.

## 1082

**Point Mutation of Endofin at PP1c-Binding Domain Induces Angiogenesis and Bone Formation in Mice by Sensitizing BMP Signaling.** F. Zhang\*, W. Shi\*, T. Qiu, X. Wu, C. Wan, Y. Wang, T. Clemens, M. Wan, X. Cao. University of Alabama at Birmingham, Birmingham, AL, USA.

We have identified Endosome-associated FYVE-domain protein (endofin) as a Smad anchor for receptor activation in BMP signaling. Endofin binds Smad1 preferentially and enhances Smad1 phosphorylation and nuclear localization upon BMP stimulation. Endofin contains a protein-phosphatase-binding motif, which recruits protein phosphatase1 (PP1c) to negatively modulate BMP signals through receptor dephosphorylation of the BMP type I receptor. Point mutation of endofin at PP1c-binding domain (F872A) virtually abolished the interaction between PP1c and endofin. As a result, BMP signaling was sensitized and osteoblast differentiation was enhanced. To further determine whether this endofin mutant affects osteoblast activity and bone formation *in vivo*, transgenic mice were generated in which this mutant (F872A) was overexpressed in osteoblasts driven by a 2.3 kb Col I promoter. The expression of the mutant endofin (F872A) was detected in 4 different transgenic lines by Western blot. X-ray analysis revealed that bone density of the entire skeleton was elevated at 4 months of age in all 4 transgenic lines. Analysis of femur by  $\mu$ CT showed that trabecular volume was increased by 11% compared to wild type litter mates. Consistently, the trabecular bone thickness and number are also significantly increased, whereas the trabecular bone separation was decreased. Immunostaining of tibia sections demonstrated that the level of phosphorylated Smad1 was enhanced in osteoblasts from the transgenic mice. To directly assess the impact of the mutation on bone vasculature we performed contrast-enhanced  $\mu$ CT imaging.  $\mu$ CT imaging of vasculature in Microfil-perfused bones revealed a striking increase in the density of the vasculature, with progressively increased vessel numbers with age. Quantitative analysis showed that vessel surface and volume were both increased in mutant mice relative to controls. These observations suggest that enhanced BMP signaling with consequent upregulation of the production of angiogenic factors promotes formation of the bone vasculature. Consistent with this idea, the expression of *Vegf* was upregulated in trabecular bone of the mutant mice. Taken together, disruption of PP1c binding motif of endofin elevates the level of phosphorylated Smad1 and augments bone formation partially by stimulating angiogenesis.

**Disclosures:** F. Zhang, None.

This study received funding from: NIH.

## 1083

**NADPH Oxidase / Nox Signaling Stimulates Myofibroblast Mx2 Transcription Via Hydrogen Peroxide.** C. Lai\*, E. Huang\*, J. Shao, O. Sierra, R. Cohen\*, D. Towler. Internal Medicine, Washington University in St. Louis, St. Louis, MO, USA.

Aortofemoral calcification is prevalent in type II diabetes (T2DM), increasing risk for lower extremity amputation. LDLR<sup>-/-</sup> mice fed high fat diets develop T2DM, and accumulate aortic calcium, mediated via osteogenic mechanisms. The TNF- $\alpha$  dependent low-grade inflammation of T2DM activates pro-calcific aortic Mx2-Wnt signaling. Since TNF- $\alpha$  promotes oxidative stress via NADPH oxidase (Nox), we examined contributions of reactive oxygen species and Nox isoforms to Mx2 expression. Treatment of aortic adventitial myofibroblasts with TNF upregulated Mx2 expression within 2 hours, achieving 5- fold induction by 3 hours. While IL1- $\beta$  could also induce Mx2, IL-1 $\alpha$  and IL-6 could not. Pretreatment of cells with 10  $\mu$ M diphenyliodonium (DPI) - an inhibitor of all Nox enzymes -- inhibited Mx2 induction. The effects of DPI were phenocopied by treatment with resveratrol or ebelen, cell-permeant reactive oxygen scavengers that mimic the activity of peroxidases. Antisense oligonucleotides (ASOs) specific for Nox1 and Nox2 significantly impaired signaling, reducing TNF induction of Mx2 by 50%. By contrast, Nox3 ASO enhanced Mx2 induction, while Nox4 ASO was without effect. Administration of 20 ng/gm Nox1 ASO + 20 ng/gm Nox2 ASO intraperitoneally for 5 days reduced aortic expression of Mx2 in SM22-TNF $\alpha$  transgenic mice by 54% (p = 0.002) as compared to cohorts receiving 40 ng/gm control ASO. SIN-1, a superoxide precursor, had no effect on myofibroblast expression of Mx2. However, H202 dose-dependently upregulated Mx2, recapitulating the response to TNF. Two major regions of the Mx2 gene - the BMP2 and Wnt regulated enhancer (BMPRE) located between -4660 and -2874 relative to the transcription start site, and the YY1-regulated 0.4 kb proximal promoter region - were evaluated for H202 responsiveness. In transfected CH310T1/2 cells, 0.2 mM H202 stimulated (2.4 - fold, p < 0.001) the transcription driven by the Mx2 promoter fragment -498 to +26 cloned upstream of the luciferase reporter of pGL2. H202 stimulated transcription driven by the Mx2 BMPRE 4.8 - fold (p < 0.001) when placed upstream of the RSV minimal promoter of RSVLUC (also in pGL2). By contrast, H202 did not stimulate RSVLUC activity, or transcription driven by several other promoters. Sequential 5'- deletion of the proximal promoter element mapped H202 responses to nucleotides -69 to +26 within the Mx2 gene. Two MEF2-like cognates were identified that assembled specific protein complexes increased by H202 treatment. Thus, Nox1 and Nox2 contribute to TNF induction of Mx2 in vascular myofibroblasts. H202 generated by Nox activity upregulates Mx2 gene transcription in part via the Mx2 BMPRE and novel regulatory elements in the proximal promoter.

**Disclosures:** D. Towler, Wyeth 2; GlaxoSmithKline 2; Barnes-Jewish Foundation 3; Kirin 5.

This study received funding from: National Institutes of Health.

## 1084

**Targeted Overexpression of the Nuclear FGF2 isoforms in Osteoblasts induces Hypophosphatemia via Modulation of FGF23 and Klotho in Mice.** L. Xiao<sup>1</sup>, J. Coffin<sup>\*2</sup>, T. Carpenter<sup>3</sup>, M. Hurley<sup>1</sup>. <sup>1</sup>School of Medicine, University of Connecticut Health Center, Farmington, CT, USA, <sup>2</sup>Biomedical and Pharmaceutical Sciences, University of Montana, Missoula, MT, USA, <sup>3</sup>School of Medicine, Yale University, New Haven, CT, USA.

We previously examined mice in which a 3.6kb fragment of the type I collagen 5' regulatory region (Col3.6) drives expression of the nuclear (HMW) FGF2 isoforms in pre-osteoblasts and osteoblasts (HMWTg). Vector only transgenic mice (Col3.6-IRES-GFPsaph, VTg) were also developed. The bone phenotype of HMWTg mice included osteomalacia, decreased bone mineral density (BMD) and dwarfism compared to VTg, which was associated with hypophosphatemia. In the current study we examined whether decreased serum phosphate (pi) in HMWTg mice was due to renal wasting. Twenty-four h urine Pi was significantly increased in HMWTg compared with VTg mice (0.10 $\pm$ 0.02 vs. 0.04 $\pm$ 0.01 mgs/24h, p<0.05). To determine whether an increase in dietary Pi could rescue the bone phenotype, 21 days old male VTg mice and HMWTg mice were fed a normal diet (1% calcium, 0.67% phosphorous and 4.4 IU vitaminD/g) or a high Pi diet (1.1% calcium, 2% phosphorous and 2.2 IU/g vitamin D) for 4 weeks. BMD was (0.047 $\pm$ 0.001; 0.036 $\pm$ 0.004; 0.046 $\pm$ 0.001 g/cm<sup>2</sup>) in VTg-Normal diet, HMWTg-Normal diet and HMWTg-High Pi diet respectively. Reduced BMD in HMWTg was reversed by the high Pi diet but not by a normal diet (compared with VTg-Normal diet). In addition, the dwarfism in HMWTg was partially reversed in HMWTg with High Pi but not a normal Pi diet. Since the HMWTg bone phenotype was similar to FGF23 transgenic mice (Larsson et al., 2004), FGF23 was measured. Serum FGF23 was significantly increased in HMWFGFTg mice compared with VTg mice (282 $\pm$ 56 vs. 97 $\pm$ 7 pg/ml, p<0.05). To explore the mechanism(s) involved in renal Pi wasting, RNA was extracted from marrow stromal cells (MSCs) or kidneys and genes of interest were determined by Real-Time PCR. There were significant increases p<0.05 in FGF23 (1.95 $\pm$ 0.39 vs. 1.00 $\pm$ 0.00); and PHEX (4024 $\pm$ 1297 vs. 264 $\pm$ 21), in MSCs from HMWTg vs. VTg. In kidneys, there were significant increases p<0.05 in mRNA normalized to VTg for FGFR1C (1.28 $\pm$ 0.06 vs. 1.00 $\pm$ 0.00); FGFR3C (1.73 $\pm$ 0.26 vs. 1.00 $\pm$ 0.00); and Klotho (4.95 $\pm$ 1.35 vs. 1.00 $\pm$ 0.00) in HMWTg vs. VTg. In contrast, mRNA of the renal Na<sup>+</sup>/Pi co-transporter Npt2a was decreased (0.61 $\pm$ 0.14 vs. 1.00 $\pm$ 0.00, p<0.05) in HMWTg vs. VTg mice. We propose that overexpression of HMWFGF2 resulted in increased FGF23 in bone, which was released into the systemic circulation. FGF23 exerted its effect on the kidney by signaling via FGFRs and Klotho to down regulate Npt2a, which in turn caused kidney Pi wasting, osteomalacia and decreased BMD. This study suggests that a Pi regulating system may be evident in mice, which involves a cascade of signals involving multiple FGFs.

**Disclosures:** L. Xiao, None.

## 1085

**Inhibition of HIF1 $\alpha$  Alone or Combined with TGF $\beta$  Blockade Prevents Breast Cancer Bone Metastases.** L. A. Kingsley<sup>1</sup>, K. S. Mohammad<sup>1</sup>, M. Niewolna<sup>\*1</sup>, T. LaVallee<sup>\*2</sup>, J. M. Chirgwin<sup>1</sup>, T. A. Guise<sup>1</sup>. <sup>1</sup>Endocrinology, University of Virginia, Charlottesville, VA, USA, <sup>2</sup>EntreMed, Rockville, MD, USA.

Cancer cells frequently metastasize to bone, which is hypoxic and rich in growth factors. Previously we showed bone metastases are hypoxic, and 1% O<sub>2</sub> increased hypoxia-inducible factor (HIF)1 $\alpha$  in MDA-MB-231 breast cancer cells. Combined treatment with 1% O<sub>2</sub> and TGF $\beta$  additively increased mRNA expression of prometastatic factors VEGF and CXCR4, suggesting that HIF1 $\alpha$  promotes bone metastasis via crosstalk with TGF $\beta$ .

Stable MDA-MB-231 clones expressing shRNA against HIF1 $\alpha$  (shHIF1 $\alpha$ ) with a  $\geq$ 90% decrease in HIF1 $\alpha$  mRNA and protein expression were selected. Expression of HIF-target genes VEGF and CXCR4 was decreased compared to parental and non-target shRNA (shCtrl) cells. Two stable shHIF1 $\alpha$  clones were inoculated into the left cardiac ventricle of female nude mice (N=5-10/group). HIF1 $\alpha$  knockdown improved survival compared to mice that received parental or shCtrl cells (16 or 8d, P<0.05) and decreased osteolytic area on x-ray (P<0.001).

In the MDA-MB-231 bone metastases mouse model, we tested a drug with anti-HIF1 $\alpha$  activity, 2-methoxyestradiol (2ME2), in a bioavailable formulation. As a preventive therapy, 2ME2 (150mg/kg/d ip) decreased osteolytic area (P<0.005) and hindlimb tumor area by histomorphometry (P<0.05), while bone volume was increased (P $\leq$ 0.0001), compared to vehicle-treated mice. 2ME2 increased BMD, measured by DXA, at the femur (P<0.05) and tibia (P $\leq$ 0.0001). Development of established lesions was unaffected when treatment was initiated 14d after cell inoculation. Hypoxyprom-1 immunostaining for hypoxia was decreased in bone metastases from 2ME2-treated mice compared to controls. 2ME2 inhibited mammary fat pad tumor growth 27d post tumor inoculation (P $\leq$ 0.001) and decreased mRNA expression of HIF1 $\alpha$  and VEGF.

Combined blockade of TGF $\beta$  signaling and HIF1 $\alpha$  was tested by stably expressing shHIF1 $\alpha$  in MDA-MB-231 cells carrying a dominant-negative TGF $\beta$  type II receptor (T $\beta$ R2 $\Delta$ cyt). These cells cause fewer bone metastases and have decreased expression of the osteolytic factor PTHrP. Survival of mice receiving T $\beta$ R2 $\Delta$ cyt/shHIF1 $\alpha$  cells was extended by 7d compared to mice receiving cells with T $\beta$ R2 $\Delta$ cyt alone and >14d compared to mice receiving parental cells (P<0.0001). Osteolytic area was decreased in T $\beta$ R2 $\Delta$ cyt/shHIF1 $\alpha$  tumor bearing mice compared to T $\beta$ R2 $\Delta$ cyt/shCtrl (P<0.05) and parental (P<0.001).

Our results show that hypoxia/HIF1 $\alpha$  signaling promotes bone metastasis, which were inhibited by preventively targeting HIF1 $\alpha$  with 2ME2. Bone metastases were further inhibited by blocking both HIF1 $\alpha$  and TGF $\beta$  signaling. Combined targeting of HIF1 $\alpha$  and TGF $\beta$  could treat bone metastases more effectively than single-agent interventions.

**Disclosures:** L.A. Kingsley, None.

## 1086

**Important Contribution of the Immune System in Regulating the Tumor/Bone Vicious Cycle Independent from Osteoclasts.** K. Zhang\*, A. Hirbe\*, K. Weilbaecher, D. Novack, R. Faccio. Washington University, St. Louis, MO, USA.

While blockade of OC activity has been shown to be effective in decreasing tumor burden and associated bone erosion in animal models of bone metastasis, one third of patients diagnosed with breast cancer develop recurrent bone metastases even when treated with bisphosphonates, potent inhibitors of osteoclastic resorption, suggesting that additional factors beyond the OC are controlling tumor growth in bone. Here, we provide new data demonstrating that broadly immune deficient animals with an accompanying defect in OC development and function (PLC $\gamma$ 2<sup>-/-</sup> mice), are more susceptible to tumor growth in bone compared to wild-type immunocompetent mice. Intracardiac injection of luciferase-labeled B16 melanoma cells (B16-FL) into PLC $\gamma$ 2<sup>-/-</sup> mice yields a 2-fold increase in bone tumor burden compared to WT mice at day 8 and 10 as measured by bioluminescence imaging (p<0.001) and by histologic analysis (p=0.03). Despite the fact that cancer cells almost completely replaced the bone marrow, PLC $\gamma$ 2<sup>-/-</sup> mice still showed a 3-fold decrease in OC number compared to WT littermates (p=0.007) and protection from tumor-associated bone destruction. Thus, in this model system, OC deficiency was not sufficient to prevent tumor growth in bone.

We hypothesized that a lack of tumor surveillance, caused by poor immune cell function, caused enhanced tumor growth in bone. To show that cells of hematopoietic origin were responsible for increased bone metastasis, we injected B16-FL cells in lethally irradiated C57BL/6 mice transplanted with bone marrow from WT or PLC $\gamma$ 2<sup>-/-</sup> donors. Similarly to the null animals, tumor growth was increased in the bones of PLC $\gamma$ 2<sup>-/-</sup> transplant recipients (p=0.004 Day 8, p=0.01 Day 10). To further explore the possibility the immune cells contribute to regulation of bone metastasis, we turned to Lyn deficient mice, which have a hyperactive immune system and more responsive OCs, the opposite of PLC $\gamma$ 2<sup>-/-</sup> mice. Lyn<sup>-/-</sup> animals display significant inhibition of cancer cell growth in the bones following either intracardiac (p<0.01 Day 10) or intratibial injection (p<0.03 Day 10) of B16-FL cells. Again, despite an OC phenotype which should encourage tumor growth in bone, immune hyperactivity predominated and decreased bone metastasis. These two models, in which alterations in immune and OC activities are expected to have opposing effects on bone metastasis, both demonstrate a dominance of immunity over bone resorption. Thus, our data challenges the paradigm of the vicious cycle activation of osteoclastic bone resorption by tumor cells releases tumor growth factors from bone, suggesting that the immune system plays a role in regulating tumor growth in bone independent from osteoclasts.

**Disclosures:** K. Zhang, None.

This study received funding from: NIH RO1.

## 1087

**TGF- $\beta$  Signaling in Stromal Cells Facilitates Osteoblastic Lesions in Prostate Cancer.** X. Li<sup>\*1</sup>, J. A. Sterling<sup>2</sup>, S. A. Munoz<sup>\*2</sup>, G. R. Mundy<sup>2</sup>, N. A. Bhowmick<sup>\*1</sup>. <sup>1</sup>Department of Urologic Surgery, Vanderbilt Center for Bone Biology, Vanderbilt-Ingram Cancer Center, Vanderbilt University, Nashville, TN, USA, <sup>2</sup>Department of Medicine, Vanderbilt Center for Bone Biology, Vanderbilt-Ingram Cancer Center, Vanderbilt University, Nashville, TN, USA.

Advanced prostate cancer metastasizes to bone in approximately 90% of patients to form predominantly osteoblastic lesions, although the factors that mediate this process remain unclear. We reasoned that TGF- $\beta$  signaling in the host stromal cells of the bone microenvironment may be important, since (i) active TGF- $\beta$  is present there in relatively large amounts; (ii) TGF- $\beta$  signaling in stromal cells has been shown to enhance tumor initiation and progression in other situations (Science 2004, 303: 848). To test this, we compared the different stromal effect on LNCaP prostate cancer tumor growth between conditional knockout of the TGF- $\beta$  receptor type II in the stromal compartment (Tgfr2<sup>flloxEx2/loxEx2</sup>) and control (Tgfr2<sup>flloxEx2/loxEx2</sup>) mice. We found LNCaP tumor growth in tissue recombination xenograft models in the context of either the prostate stromal cells or the bone from Tgfr2<sup>flloxEx2</sup> mice to be significantly increased ( $n \geq 4$ ). No tumor grew when LNCaP cells were xenografted alone. This suggested an important role for TGF- $\beta$  signaling in stromal cell regulation of prostate cancer growth. When similar tissue recombinants of LNCaP-C4-2 with prostate stroma were inoculated via intra-tibial injections, we observed the progression of lytic, mixed, and finally osteoblastic lesions in the bone injected with LNCaP-C4-2 cells alone during a 13.5 week study. In addition, the osteoblastic lesions were smaller than those by LNCaP-C4-2 with either Tgfr2<sup>flloxEx2</sup> or Tgfr2<sup>flloxEx2/loxEx2</sup> prostate stroma recombinants. Interestingly, the bone with LNCaP-C4-2/Tgfr2<sup>flloxEx2</sup> prostate stroma injection developed directly to mixed and osteoblastic lesions within seven weeks without an obvious osteolytic phase. In vitro analyses of LNCaP-C4-2 cells indicated that conditioned media from Tgfr2<sup>flloxEx2/loxEx2</sup> and Tgfr2<sup>flloxEx2</sup> stromal cells decreased the expression of the osteolytic factor, PTHrP, by 2 and 20-fold respectively, when compared to LNCaP-C4-2 cells alone, suggesting that the absence of TGF- $\beta$  signaling in the stroma reduces the expression of osteolytic factors by the tumor cells. Taken together, these data indicate that TGF- $\beta$  signaling in the host stroma suppresses prostate cancer growth and the nature of the subsequent osteoblastic lesions. Specifically, TGF- $\beta$  responsiveness of the bone modulates the transition from primarily osteolytic to osteoblastic lesions.

Note: The first and second author contributes equally to this work.

**Disclosures:** X. Li, None.

This study received funding from: NIH and NCI: CA126505, CA108646.

## 1088

**Host Bone Marrow-Derived Stromal Cells Promote Myeloma Initiation and Development of Osteolysis.** J. A. Fowler, G. R. Mundy, S. T. Lwin\*, C. M. Edwards. Vanderbilt Center for Bone Biology, Vanderbilt University, Nashville, TN, USA.

In multiple myeloma (MM), the interaction between neoplastic plasma cells and the bone marrow (BM) microenvironment results in malignant proliferation of these cells, and a characteristic osteolytic bone disease. The 5T Radl murine model of MM is a spontaneous model occurring in aged C57BL/KaLwRij (KaLwRij) mice and propagated by inoculation of myeloma cells (either freshly isolated or the established 5TGM1 cell line) into mice of the same strain. Since myeloma grows in KaLwRij mice, but not in closely related C57BL6 mice, this suggests the KaLwRij BM creates a unique and permissive milieu for MM and that host cells from this microenvironment promote myelomagenesis. To test this, we utilized an established murine bone marrow stromal cell line (BMSCs) isolated from myeloma-bearing KaLwRij mice. These cells express vimentin and FSP-1, but not  $\alpha$ -SMA, consistent with a fibroblast phenotype. However, these cells did not demonstrate osteogenic or adipogenic differentiation potential characteristic of mesenchymal stem cells. Non-permissive C57BL6 or permissive KaLwRij mice were inoculated with 5TGM1-GFP MM cells  $\pm$  BMSCs. There was no difference in tumor burden in KaLwRij mice co-inoculated with 5TGM1 MM cells and BMSCs compared with 5TGM1 cells alone, suggesting that BMSCs do not directly increase MM growth. In striking contrast, 4 weeks following inoculation, C57BL6 mice inoculated with 5TGM1 or BMSCs alone did not develop MM but C57BL6 mice inoculated with 5TGM1 and BMSCs developed MM identical to that of the syngeneic KaLwRij mice. Tumor burden was demonstrated by an increase in serum paraprotein (134.65% increase compared with mice inoculated with 5TGM1 cells alone) and GFP-positive tumor cells in BM (55%) and spleen (7.22%). Osteolytic bone disease was confirmed by  $\mu$ CT analysis, with a significant increase in osteolytic lesions and decrease in bone volume. Histomorphometric analysis confirmed myeloma associated bone disease demonstrated by a 40% increase in osteoclast number and a 62% decrease in osteoblast number, compared with mice inoculated with 5TGM1 cells alone. Taken together, our results suggest that BMSCs derived from KaLwRij mice promote MM in mice in which MM otherwise does not develop. Thus, in myeloma, BMSCs promote initiation of the disease and subsequent osteolysis, demonstrating a critical role for host-derived BMSCs in the pathogenesis of MM.

**Disclosures:** J.A. Fowler, None.

## 1089

**Stat3 Induces Osteoblastic Bone Metastases Through Up-regulating the Expression of Shh and a Calcium Channel TRPM8 in the LNCaP Human Prostate Cancer Cells.** H. Kanzaki, H. Yono\*, P. Williams\*, A. Farias\*, T. Yoneda. Medicine, Endocrinology, UT Health Science Center San Antonio, San Antonio, TX, USA.

Prostate cancer preferentially metastasizes to bone and develops osteoblastic lesions with infrequent osteoclastic lesions through yet-unknown mechanisms. Signal transducers and activators of transcription 3 (Stat3), which is one of the oncogenic signaling molecules, is constitutively activated in human prostate cancer. Moreover, Stat3 is known to be involved in the promotion of osteoblast proliferation. These results collectively suggest Stat3 plays a role in the development of osteoblastic bone metastases in prostate cancer. To study this, we introduced a constitutive-active Stat3 cDNA into the LNCaP human prostate cancer cells (LNCaP/Stat3c cells). LNCaP/Stat3c cells showed increased proliferation and anchorage-independent growth compared with parental LNCaP cells. Histological examination revealed that left cardiac ventricle inoculation of these cells into male nu/nu mice developed predominantly osteolytic lesions with numerous TRAP-positive osteoclasts in the tibiae at 12 week. Of note, osteoblastic lesions began to emerge after 16 weeks and the majority of bone marrow cavity was replaced by osteoblastic lesions after 20 weeks. Parental LNCaP cells failed to develop bone metastases. We then studied the role of sonic hedgehog (Shh) in the osteoblastic bone metastases in this model. Shh is shown to be an autocrine factor up-regulated in aggressive prostate cancer and a stimulator of bone development. RT-PCR showed increased Shh mRNA expression and its downstream signaling molecules including PTCH1, Gli1 and Gli2 in LNCaP/Stat3c cells and western analysis displayed elevated Shh production. Cyclopamine (5mg/kg), an inhibitor of hedgehog pathway, significantly decreased LNCaP/Stat3c tumor growth, tumor-associated osteoblastic lesions and TRAP-positive osteoclast number. Finally, we examined the role of TRPM8, a Ca<sup>2+</sup>-permeable channel which was initially identified in human prostate cancer, reasoning that extracellular calcium is critical to the development of osteoblastic bone metastases in prostate cancer. TRPM8 mRNA expression was elevated in LNCaP/Stat3c cells compared with parental LNCaP cells. TRPM8 overexpression induced Shh expression, whereas TRPM8 knockdown reduced it. Increase in extracellular calcium up-regulated Shh expression. In conclusion, we established an animal model of osteoblastic bone metastases of human prostate cancer. Our results using this model suggest Ca<sup>2+</sup>/TRPM8/Shh axis plays an important role in the development of osteoblastic bone metastases of prostate cancer.

**Disclosures:** H. Kanzaki, None.

## 1090

**DKK1 Is Regulated by mRNA Stability and Epigenetic Mechanisms in Bone Metastasis.** K. L. Clines\*, J. M. Chirgwin, T. A. Guise, G. A. Clines. Medicine, University of Virginia, Charlottesville, VA, USA.

Osteoblastic bone metastasis is a complication of advanced prostate and breast cancer, resulting in pain and pathologic fracture. Tumor-produced endothelin-1 (ET-1) activates the osteoblast endothelin A receptor and increases pathologic new bone formation. Dickkopf homolog 1 (DKK1), a secreted negative regulator of canonical Wnt signaling, is a target of ET-1. ET-1 reduces Dkk1 mRNA and protein secretion in murine primary osteoblasts. Human cancer cells in bone secrete DKK1, whose concentrations are inversely related to osteoblast activity in bone metastasis. We hypothesize that osteoblastic bone metastases depend on decreased DKK1 secretion from two sources in the microenvironment: from osteoblasts and from tumor cells. ET-1 suppresses osteoblast DKK1 expression, while tumor expression of DKK1 is not well understood.

DKK1 down-regulation by ET-1 in the osteoblast was explored using *Dkk1*/luciferase reporter constructs. ET-1 did not change *Dkk1* promoter (1.7 kb) activity in murine primary osteoblasts. We then examined whether ET-1 decreases *Dkk1* mRNA stability via the 3'UTR, a 1.3 kb segment containing consensus binding elements for AUF1 and miRNAs. ET-1 significantly reduced (0.52 X,  $p=0.0005$ ) luciferase activity in a construct containing the *Dkk1* 3'UTR indicating that ET-1 regulates osteoblast *Dkk1* via message stability.

We next examined relative expression of *DKK1* and its CpG island methylation in prostate and breast cancer cell lines. Using real-time RT PCR, we found C4-2B, C4-2, LNCaP prostate and T47D breast lines had low *DKK1* expression while ZR-75.1, MCF-7, MDA-MB-231 breast and PC3 prostate lines had significant *DKK1* expression. *DKK1* contains a 5' 233 bp CpG island encompassing the transcriptional start site with 18 potential cytosine methylation sites. Changes in CpG methylation patterns are one mechanism responsible for gene misexpression during tumorigenesis. Methylation-specific sequencing of the *DKK1* CpG island was performed on the human cancer cells. Methylation was detected in the cancer cell lines with the lowest *DKK1* expression while the sequence was unmethylated in cells with the highest *DKK1* expression.

These observations are consistent with a model for osteoblastic bone metastases in which DKK1 production is decreased in both cancer cells and osteoblasts. The mechanisms involve both static epigenetic promoter silencing and dynamic control of *DKK1* mRNA stability via its 3'UTR. *DKK1* mRNA stability can be regulated by tumor-produced ET-1, while the factors that control its basal promoter activity via CpG island methylation are presently unknown. Understanding the regulation of *DKK1* gene expression in tumor and bone may lead to novel therapies for osteoblastic metastases.

**Disclosures:** G.A. Clines, None.

## 1091

**Large-scale Meta-analysis of Genome-wide Association (GWA) Scans for Osteoporosis Traits: the GEFOS Consortium.** F. Rivadeneira<sup>1</sup>, F. Kavvoura<sup>2</sup>, D. Karasik<sup>3</sup>, B. Richards<sup>4</sup>, B. Halldórsson<sup>5</sup>, Y. Hsu<sup>6</sup>, S. Demissie<sup>6</sup>, A. Cupples<sup>6</sup>, C. Zillikens<sup>1</sup>, C. van Duijn<sup>1</sup>, K. Estrada<sup>1</sup>, J. van Meurs<sup>1</sup>, H. Pols<sup>1</sup>, U. Thorsteinsdóttir<sup>5</sup>, M. Brown<sup>7</sup>, T. Spector<sup>4</sup>, S. Ralston<sup>8</sup>, D. Kiel<sup>3</sup>, J. Ioannidis<sup>2</sup>, U. Styrkarsdóttir<sup>5</sup>, A. Uitterlinden<sup>1</sup>. <sup>1</sup>Erasmus MC, Rotterdam, Netherlands, <sup>2</sup>Ioannina University, Ioannina, Greece, <sup>3</sup>HSL, Harvard University, Boston, MA, USA, <sup>4</sup>Kings College, London, United Kingdom, <sup>5</sup>deCODE Genetics, Reykjavík, Iceland, <sup>6</sup>Boston University, Boston, MA, USA, <sup>7</sup>University Queensland, Brisbane, Australia, <sup>8</sup>University Edinburgh, Edinburgh, United Kingdom.

GWA is a hypothesis-free search for genetic determinants which has been successful identifying variants associated with disease. **GEFOS** is a consortium of GWA studies on osteoporosis and fracture. In this first effort, we performed meta-analysis of 56785 SNPs present in all genotyping platforms used by 6 GWA studies, summing to 18304 Caucasian subjects in relation to femoral neck (FN) and lumbar spine (LS) bone mineral density (BMD). The consortium included **deCODE** (n~6700;IS; Illumina317), **Rotterdam** (n~4900;NL; Illumina550), **Framingham** (n~3600; US; Affymetrix500), **Twins UK** (n~2300 women;UK;Illumina317), **ERF** (n~700;NL; Illumina317); and **AOGC** (n~140;AU;Illumina317) studies. SNPs with  $MAF < 0.05$ ,  $p_{HWE} < 0.0001$  and marker call < 0.95 were excluded. BMD measured by DXA was analyzed within-populations as absolute differences in mean gender- and age-adjusted standardized values across genotypes. **METAL** was used for a first meta-analytical screen to select hits associated at  $p < 1 \times 10^{-4}$ , which were then meta-analysed using inverse-variance meta-analysis (**IVMA**) of group-level data with fixed and random effects models using **STATA**. Evidence of genome-wide significance (**GWS**) was set at  $p < 5 \times 10^{-8}$  and suggestive evidence (**sGWS**) at  $p < 1 \times 10^{-5}$ . No **GWS** hits were identified by any independent study. Meta-analyses from the 6 studies returned 46 SNPs associated with LS (35 SNPs) and FN BMD (21 SNPs) at  $p < 1 \times 10^{-4}$ . After **IVMA** in the combined-sex analyses four loci remained **GWS** at  $2.8 \times 10^{-11} < p < 2.9 \times 10^{-8}$  (LS 4 and FN 2) while 7 more were **sGWS** at  $1.0 \times 10^{-7} < p < 3.9 \times 10^{-6}$  (LS 6 and FN 2). Effect sizes for the **GWS** hits ranged between .06 and .09 SDs per allele copy. Two of the **sGWS** observed sex-specificity in males. None of the **GWS** or **sGWS** hits revealed significant heterogeneity ( $pQ < 0.10$  or  $I^2 > 50\%$ ). All loci annotate to novel loci with exception of the **LRP5 rs3736228**, which was **sGWS** and replicated earlier at **GWS** level in a large-scale consortium (**GENOMOS**). In conclusion, we have identified 13 loci associated with LS and FN BMD. These SNPs and several more await further replication in independent **GENOMOS** samples (n > 50,000). Meta-analysis with extended genome coverage in **GEFOS** is underway for BMD, fracture and other bone traits.

**Disclosures:** F. Rivadeneira, None.

## 1092

**Genome-Wide Association Study of BMD and Hip Geometry Indices. The Framingham Osteoporosis Study.** Y. H. Hsu<sup>1</sup>, S. Demissie<sup>2</sup>, K. Cho<sup>2</sup>, Y. Zhou<sup>2</sup>, E. Bianchi<sup>3</sup>, S. L. Ferrari<sup>3</sup>, L. A. Cupples<sup>2</sup>, D. Karasik<sup>1</sup>, D. P. Kiel<sup>1</sup>. <sup>1</sup>Hebrew SeniorLife and Harvard Med. Sch., Boston, MA, USA, <sup>2</sup>Biostat., BU, Sch Public Health, Boston, MA, USA, <sup>3</sup>Div. of Bone Dis., Geneva Univ. Hosp., Geneva, Switzerland.

Despite significant progress in understanding the genetic basis for osteoporosis, efforts to identify genes associated with BMD and bone geometry traits have been incomplete. With the completion of the HapMap project, GWA became a promising tool to dissect complex diseases. We have undertaken a GWA study using the Affymetrix 550K SNP chips to localize susceptibility genes for BMD at the lumbar spine and femoral neck and geometric indices of the hip (femoral neck-shaft angle, femoral neck length and narrow-neck width) in the Framingham Osteoporosis Study. 433,510 SNPs passed quality control criteria (call rate  $\geq 95\%$ , HWE  $p \geq 10^{-6}$  and  $MAF \geq 0.01$ ) in 2073 women and 1554 men (mean age 62.5 yrs) from 677 extended pedigrees. We conducted population- and family-based analyses, using sex-specific residual trait values adjusted for age, height, BMI, and estrogen/menopause (women). For population-based analyses, we used linear-mixed effects (LME) models that account for individual correlations within families. A principle component analysis (EIGENSTRAT) for all SNPs was performed to explicitly model differences of individuals' ancestral genetic background. The first 4 principle components (PCs) were significantly associated with bone traits; therefore, to minimize spurious associations from population substructure, we adjusted for PCs in LME models. After adjustment, the  $\lambda_{GC}$  were  $\leq 1.02$ . Family-based association test (FBAT) weighted by rank order of LME statistics was used to estimate the genome-wide significance. To test whether associated genes were expressed in bone, we measured mRNA of PTH-differentiated primary osteoblasts and further examined an embryonic mouse gene expression database for in situ localization in skeletal tissue. Several associations with bone traits achieved genome-wide significance level ( $p < 10^{-8}$ ), i.e. SNPs on **BMP10**, **PTPRD**, **MYC**, **SLC16A4**, **IL6** and **PRKG1** genes. All excepted for **BMP10** and **MYC** were expressed in osteoblasts. In addition, a gene-set enrichment analysis by Gene Ontology annotation for the genes selected from the most significant SNPs suggested significant clustering of genes involved in central nervous system (CNS) development. The 100 most significant SNPs from each trait are being further evaluated in > 2650 men and 5850 women from 2 independent studies (Rotterdam and the UK Twins Studies). In conclusion, our results reveal novel candidate genes and pathways to further elucidate the etiology of osteoporosis through the determination of BMD and bone geometry. Our findings further suggest an interaction between the CNS and skeleton.

**Disclosures:** Y.H. Hsu, None.

This study received funding from: NIAMS, NHLBI.

## 1093

**Genome-wide Association Study (GWAS) and Subsequent Replication Studies Identified ADAMTS18 and TGFBR3 as Novel Osteoporosis Risk Genes.** D. Xiong<sup>1</sup>, L. Zhao<sup>2</sup>, R. R. Recker<sup>2</sup>, J. M. Zmuda<sup>3</sup>, H. Deng<sup>1</sup>. <sup>1</sup>Departments of Orthopedic Surgery and Basic Medical Sciences, University of Missouri - Kansas City, Kansas City, MO, USA, <sup>2</sup>Osteoporosis Research Center, Creighton University, Omaha, NE, USA, <sup>3</sup>Department of Epidemiology, Department of Human Genetics, University of Pittsburgh, Pittsburgh, PA, USA.

Osteoporosis is a most common, highly heritable bone disease leading to fractures that severely impair the health and life quality of patients. We conducted a genomewide association study (GWAS) and several subsequent replication studies to identify alleles associated with BMD (bone mineral density) and risk of osteoporosis. We first used DNA microarray technology to examine ~500,000 SNP markers in 1000 unrelated homogeneous Caucasian subjects and tested them for association with BMD. For replication, we genotyped significant SNPs from GWAS in a) one sample of 593 unclear families having 1972 Caucasian subjects; b) one Chinese cohort composed of 350 hip fracture (HF) patients and 350 healthy controls; and c) one cohort from the Caribbean Island of Tobago composed of 908 men of West African ancestry. The original GWAS detected two novel BMD genes, namely ADAMTS18 (ADAM metalloproteinase with thrombospondin type 1 motif, 18;  $P = 4.17E-07$  and  $5.75E-07$  for allelic association with hip BMD at rs11864477 and rs16945612) and TGFBR3 (transforming growth factor, beta receptor III;  $P = 3.47E-08$  for haplotypic association with spine BMD at rs17131547). Replication studies showed that the same SNPs consistently associated with BMD variation in the independent sample of Caucasian nuclear families ( $P$  values = 0.0071 and 0.033 for allelic association with spine BMD and hip BMD at rs16945612; and  $P = 0.021$  for allelic association with spine BMD at rs17131547); as well as significantly associated with hip fracture (HF) in the Chinese sample ( $P = 0.019$  at rs16945612). The significance of TGFBR3 to BMD phenotypes were also successfully replicated at rs17131547 in the Tobago sample of West African ancestry ( $P$  values = 0.0067 and 0.031 for lumbar spine BMD and total body BMD;  $P$  values = 0.0011, 4.93E-04, 0.0054, 0.013, and 2.82E-04 for BMD measured at total hip, intertrochanter, femoral neck, trochanter and Ward's triangle, respectively). Bioinformatics analyses based on the identified significant SNPs and their highly correlated SNPs suggest several novel potentially significant functional mechanisms underlying bone metabolism and bone mass variation. Our data, for the first time, clearly demonstrated that ADAMTS18 and TGFBR3 are critical genetic factors determining human BMD variation and osteoporosis fracture risk.

**Disclosures:** D. Xiong, None.

## 1094

**Use of Genetic Markers in Prediction of Fractures.** V. Gudnason<sup>1</sup>, T. Aspelund<sup>1</sup>, A. V. Smith<sup>1</sup>, K. Siggeirsdóttir<sup>1</sup>, G. Eiriksdóttir<sup>1</sup>, B. Y. Jonsson<sup>2</sup>, T. F. Lang<sup>3</sup>, L. J. Launer<sup>4</sup>, T. B. Harris<sup>4</sup>. <sup>1</sup>Icelandic Heart Association, Kopavogur, Iceland, <sup>2</sup>University Hospital, Malmö, Sweden, <sup>3</sup>UCSF, San Francisco, CA, USA, <sup>4</sup>NIA, Bethesda, MD, USA.

Modeling risk for low trauma fractures has been incorporated into risk calculators, such as the one from WHO (www.shef.ac.uk/FRAX/). There is increasing interest to add genetic information to these conventional risk prediction models of fractures. We assess the use of genetic markers from three genes previously shown to have independent and interactive effects enhancing the risk of fractures at a population level (JBM:21:1443). We used data from the AGES-Reykjavik study, a population based study of 2300 men and women recruited between September 2002 and February 2004. Average age was 76 (SD=6) years, with a mean follow up of 4.6 years. Information on measurements for the fracture prediction model (age, sex, height, weight, BMD, previous fracture, family history of fracture, bone medication and smoking) was available for 879 men and 1133 women with 158 low trauma incident fractures of which 47 were hip fractures all verified from medical records and X-rays. Markers from three unlinked genes, Estrogen Receptor 1 (ESR1) haplotype derived from rs6557170 and rs985694, Estrogen Receptor 2 (ESR2) rs7159462 and Insulin Like Growth Factor 1 (IGF1) rs10860861, were used for genetic association analyses. For risk modeling the genotype information was added as an ordinal predictor with categories 1, 2 or 3 according to the number of fracture associated genotypes carried. Power analyses showed that the AGES-Reykjavik sample can identify Hazard Ratio (HR) of at least 1.4 for the given frequencies of the SNPs. The fracture associated allele frequencies were ESR1 haplotype 0.15, ESR2 0.10, IGF1 0.49. All were in HW equilibrium and were associated with incident fractures with HR of 1.5, ( $p = 0.01$ ), 1.4 ( $p = 0.05$ ) and 1.5 ( $p = 0.02$ ) respectively, after adjustment for age, sex, medication use and previous fracture. The area under the ROC curve (AUC) was 0.73 for the model predicting fractures using the clinical risk factors. When the haplotype and SNP information was added as a genotype score 1, 2 or 3 there was a stepwise increase in their HR and with information from all three genes the AUC went up to 0.75 ( $p < 0.05$  for difference). Using solely the genetic markers with age for prediction gave AUC 0.63. Using clinical measurements is a reasonable way for prediction of fractures. Using genetic information cannot replace the clinical measurements and adds only 2% to the AUC associated with the prediction model which is of limited clinical value. However the increase in HR observed with increased number of genetic markers carried may suggest that a model including more genes could become of clinical relevance.

**Disclosures:** V. Gudnason, None.

This study received funding from: NIH contract number N01-AG-1-2100), the Icelandic Heart Association, the Icelandic Parliament.



## 1095

**Simply Ask Them About Their Balance - Fracture Prediction in a Nationwide Cohort Study in Twins.** K. Michaëlsson<sup>1</sup>, H. Wagner<sup>\*1</sup>, H. Melhus<sup>2</sup>, R. Gedeberg<sup>\*3</sup>, N. L. Pedersen<sup>\*4</sup>. <sup>1</sup>Section of Orthopaedics, Department of Surgical Sciences, Uppsala, Sweden, <sup>2</sup>Section of Clinical Pharmacology, Department of Medical Sciences, Uppsala, Sweden, <sup>3</sup>Section of Anesthesiology and Intensive Care, Department of Surgical Sciences, Uppsala, Sweden, <sup>4</sup>Karolinska Institutet, Department of Medical Epidemiology and Biostatistics, Stockholm, Sweden.

The principal causal components of an osteoporotic fracture are a fall and weakened bone strength. While bone quality measures have been frequently studied, the ability of simple measures of impaired balance to predict fracture risk has received less attention.

Computer-assisted telephone interviews were conducted between 1998 and 2000 among 24,598 (84% of eligible) Swedish twins, 55 years of age and older. An impaired balance at the time of interview was reported by 2757 (12%) of the twins. Efforts were made to interview members of a pair within a month. An identical second interview performed among 105 twins two weeks after the first interview enabled reliability testing. The kappa statistics for the question regarding impaired balance was 0.81 (95% CI 0.60-1.00) indicating almost perfect agreement. Hip, any osteoporotic and any fracture identified by linkage to the National Hospital Discharge Register were used as outcomes. Fracture risk associated with impaired balance was analyzed in pairs of twins discordant for impaired balance. For these associations, we used conditional logistic regression to estimate odds ratios (ORs), and 95 percent (%) confidence intervals (CIs). We wanted each twin in the pair to have a similar time at risk. Since mortality risk was associated with impaired balance, we adjusted for the unequal lengths of the follow-up periods due to death. Thus, twin pairs where one twin died before end of follow-up (15%) were excluded from the analysis.

In a pair-wise conditional logistic regression analysis, the odds ratio (OR) of hip fracture was 3.13 (95% CI 1.62-6.05) for twins with an impaired balance compared to the co-twin with a normal balance. This estimate was not attenuated if we also considered previously recognized clinical risk factors for osteoporotic fractures in the model (HR 2.96; 95% CI 1.27-6.90). Approximately one third of all hip fractures were attributable to an impaired balance. The population attributable risk was 0.37 (95% CI 0.15-0.59). The OR of any fracture and any osteoporotic fracture for a twin with an impaired balance was 2.00 (1.29-3.11) and 2.39 (95% CI 1.49-3.82) compared to the co-twin with a normal balance. The adjusted ORs for these outcomes were 2.26 (95% CI 1.34-3.85) and 2.96 (95% CI 1.55-5.67), respectively. These results imply that a self-reported impaired balance is a novel and readily assessed risk factor for fractures in the elderly.

**Disclosures:** K. Michaëlsson, None.

This study received funding from: The Swedish Research Council and NIH.

## 1096

**Proximal Femoral Fragility and Age-Related White Matter Lesions by Brain MRI in Elderly Subjects: the Age Gene/Environment Susceptibility Study-Reykjavik.** T. F. Lang<sup>1</sup>, T. Hughes<sup>\*2</sup>, G. Sigurdsson<sup>\*3</sup>, G. Sigurdsson<sup>4</sup>, T. B. Harris<sup>\*2</sup>, K. Siggeirsdottir<sup>\*3</sup>, V. Gudnason<sup>\*3</sup>, L. Launer<sup>\*2</sup>. <sup>1</sup>Radiology, University of California, San Francisco, San Francisco, CA, USA, <sup>2</sup>Laboratory of Epidemiology and Biometry, National Institute on Aging, Bethesda, MD, USA, <sup>3</sup>Icelandic Heart Association, Kopavogur, Iceland, <sup>4</sup>Endocrinology, Landspítali, Reykjavik, Iceland.

**Purpose:** White matter lesions (WML) correspond to age-related microvascular changes in the white matter fiber tracts of the brain which are thought to disrupt neural networks responsible for lower extremity motor control. Previous studies have linked increased WML load with impaired gait, falls and hip fracture. Because bone remodeling is also under partial neural control, we hypothesized that WML's would also correlate to altered bone mineral density (BMD) and bone structure.

**Methods:** 4091 study participants (aged 66-99 years, 2338 women, 1753 men) had full brain MRI (1.5T system, including PD/T2 and FLAIR sequences) to detect WML. Subcortical (sWML) and periventricular (pWML) lesion loads were assessed semi-quantitatively from the MRI and related to femoral neck (FN) and total femur (TF) trabecular BMD (tBMD) and cortical tissue to total tissue volume ratios (c/t, a measure of cortical thickness) derived from hip QCT. The cohort was stratified into quartiles of sWML and pWML, and multiple regression (SASv9.2) was used to examine trends across quartiles and to compare tBMD and c/t in the highest quartile (HI) to the other three quartiles (REF). Least square means were computed for each quartile with adjustment for age, height, body mass index, diabetes, stroke history, smoking, hypertension, education and coronary arterial calcium. Analyses were carried out separately by gender.

**Results:** Only women showed statistically significant relationships between bone variables and WML's. In women, all bone measures tended to decline with increasing WML quartile, but the decrease was significant only for TF c/t (sWML: 2.2%, p=0.016; pWML 2.5%, p=0.008). As shown in the Table, the HI quartiles of sWML and pWML had significantly lower TF tBMD, TF c/t and FN c/t than the REF group.

**Conclusions:** These findings suggest that WML's may affect skeletal as well as neuromuscular risk factors for fracture, potentially through effects on muscles that may load bone or through effects on neural control of bone remodeling.

**Table:** \*, p<0.05 ; ^, p<0.01

	FN tBMD	FN c/t	TF tBMD	TF c/t
sWML REF	0.022	0.393	0.054	0.348
sWML HI	0.020	0.387*	0.051*	0.341^
pWML REF	0.023	0.392	0.054	0.348
pWML HI	0.018*	0.367*	0.051*	0.341^

**Disclosures:** T.F. Lang, None.

This study received funding from: National Institute on Aging.

## 1097

**ER $\alpha$  Deletion in Cells of the Monocyte/Macrophage Lineage Increases Osteoclastogenesis and Abrogates the Pro-apoptotic Effect of E<sub>2</sub> on Osteoclasts.** M. Martin-Millan, M. Almeida, E. Ambrogini, X. Qui\*, A. Warren\*, R. S. Shelton\*, R. S. Weinstein, R. L. Jilka, T. Bellido, C. A. O'Brien, S. C. Manolagas. Center for Osteoporosis and Metabolic Bone Diseases, University of Arkansas for Medical Sciences and Central Arkansas Veterans Healthcare System, Little Rock, AR, USA.

Estrogens attenuate osteoclastogenesis and stimulate osteoclast apoptosis. It remains unclear, however, whether these effects are cell autonomous and whether are mediated via *cis* or *trans* interactions of the estrogen receptor (ER $\alpha$  or  $\beta$ ) with DNA or kinase-mediated extranuclear actions of the ERs. To resolve these issues, we selectively deleted ER $\alpha$  in cells of the monocyte/macrophage lineage. Specifically, we generated mice in which exon 3 of the ER $\alpha$  was flanked by loxP sites (ER $\alpha^{fl/fl}$ ) and subsequently crossed with mice that express the Cre-recombinase enzyme under the control of the murine M Lysozyme (LysM-Cre) gene that is expressed in early precursors of the monocyte/macrophage lineage. The efficiency and specificity of the deletion was determined by measuring mRNA levels of ER $\alpha$  in macrophages (generated by culturing non-adherent bone marrow (BM) cells with 100 ng/ml M-CSF), osteoclasts (generated by culturing non-adherent BM cells with 30 ng/ml M-CSF and 30 ng/ml RANKL), and other non-bone tissues by real time PCR. Whereas ER $\alpha$  mRNA in macrophages and osteoclasts from the ER $\alpha^{fl/fl}$ ;LysM-Cre mice was significantly decreased as compared to the ER $\alpha^{fl/fl}$  controls, ER $\alpha$  expression was indistinguishable between the ER $\alpha^{fl/fl}$ ;LysM-Cre and the ER $\alpha^{fl/fl}$  in spleen and liver. To determine the effect of the deletion on osteoclastogenesis, triplicate BM cultures from each of 7 animals per genotype were established in the presence of RANKL and M-CSF. After 4 d TRAPase positive cells with 3 or more nuclei were enumerated. The number of osteoclasts in the cultures from the ER $\alpha^{fl/fl}$ ;LysM-Cre mice was 2-fold higher than those from ER $\alpha^{fl/fl}$  mice (723  $\pm$  SD 210 per well versus 347  $\pm$  82). Moreover, 17 $\beta$ -estradiol (E<sub>2</sub>) at 10<sup>-8</sup> M or 10<sup>-7</sup> M had no effect on osteoclast apoptosis in the cultures from the ER $\alpha^{fl/fl}$ ;LysM-Cre, as measured by *in situ* end-labeling, whereas it induced a 2.5-fold increase of osteoclast apoptosis in the ER $\alpha^{fl/fl}$ . E<sub>2</sub> also stimulated osteoclast apoptosis in cultures from knock-in mice in which classical ER $\alpha$  signaling through ERE sites has been selectively eliminated while preserving non-classical signaling (ER $\alpha^{NEK1/-}$ ). These results provide compelling evidence that the effect of estrogens on osteoclastogenesis and osteoclast apoptosis are cell autonomous and mediated via an extranuclear function of the ER $\alpha$ .

**Disclosures:** M. Martin-Millan, None.

## 1098

**The Longevity Gene SIRT-1 Independently Controls Both Osteoblast and Osteoclast Function.** J. R. Edwards<sup>1</sup>, K. Zainabadi<sup>\*2</sup>, S. T. Lwin<sup>\*1</sup>, F. Eleftheriou<sup>1</sup>, S. Munoz<sup>\*1</sup>, M. M. Moore<sup>\*1</sup>, L. Guarente<sup>\*2</sup>, G. R. Mundy<sup>1</sup>. <sup>1</sup>Center for Bone Biology, Vanderbilt University Medical Center, Nashville, TN, USA, <sup>2</sup>Dept of Biology, MIT, Cambridge, MA, USA.

The normal aging process is associated with osteoporotic bone loss, occurring through combined defects in both osteoblast and osteoclast regulation. Since there is a strong genetic component in age-related bone loss, we have examined the effects of longevity-associated genes on maintenance of bone mass in genetic mouse models. We have focused on the sirtuin gene family, which directly regulate lifespan in lower organisms and are strongly linked to cell replication, proliferation and survival. The prototype of this gene family in vertebrates is the well-conserved histone deacetylase Silent Information Regulator T-1 (SIRT-1). We have previously shown that pharmacological manipulation of SIRT-1 in osteoblastic cells can alter mineralization rates and osteogenic gene expression, and also influence osteoclast formation rates from precursor cells. To determine the *in vivo* role of SIRT-1 in skeletal development and bone remodeling, we have now generated and characterized osteoclast-, osteoblast-specific and double knockout murine models, using  $\mu$ CT and Piximus scanning, histomorphometric analysis of lumbar vertebrae and long bones, and primary bone cell cultures. Germline deletion of SIRT-1 results in a dramatic bone loss in male and female mice at 1, 4 and 11 mths of age. This is associated with a 27% increase in osteoclasts (p<0.05) and a 39% decrease in osteoblast numbers compared to WT animals (p<0.05). SIRT-1 KO in cells of the osteoblast lineage using the 2.3 Coll1 $\alpha$ 1 promoter generated a mouse model with 25% less BV/TV than floxed control animals (4mth, p<0.01). This was accompanied by a decrease in osteoblast number and activity, evidenced by decreased ObS/BS (22%) and bone formation rate (23%)(p<0.05). Deletion of SIRT-1 in osteoclast precursor cells, including monocytes and macrophages, using the lysozyme M promoter, also resulted in decreased BV/TV (31%, p<0.01), but unlike the above SIRT-1 Ob KO model, osteoclast numbers were increased compared to control mice (34%, p<0.05). The combined breeding of these models to generate an osteoblast/osteoclast-specific SIRT-1 KO resulted in up to 29% less BV/TV than control animals. These findings indicate that SIRT-1 controls bone mass by independently regulating both the osteoblast and osteoclast lineage. These findings identify a novel molecular link between aging, osteoclast and osteoblast function and bone loss.

**Disclosures:** J.R. Edwards, None.



## 1099

**Oxidative Stress Stimulates the Synthesis of PPAR $\gamma$ 2, and Ligand-Activated PPAR $\gamma$ 2 Sequesters  $\beta$ -catenin Leading to Suppression of TCF-mediated Transcription: an Explanation for the Age-related Decrease in Osteoblastogenesis and Increase in Adipogenesis.** M. Almeida, E. Ambrogini, L. Han, S. C. Manolagas, R. L. Jilka. Center for Osteoporosis and Metabolic Bone Diseases, Central Arkansas Veterans Healthcare System, University of Arkansas for Medical Sciences, Little Rock, AR, USA.

Age-related bone loss is associated with decreased production of osteoblasts and increased production of adipocytes, but the molecular mechanisms underlying this phenomenon have not been elucidated. In C57BL/6 mice, age-related bone loss is temporally associated with reduced osteogenic Wnt/ $\beta$ -catenin signaling and increased expression of PPAR $\gamma$ 2, which is required for adipogenesis. Old mice also exhibit increased levels of reactive oxygen species (ROS), oxidized lipid ligands of PPAR $\gamma$  like 9-HODE, as well as 4-hydroxynonenal (4-HNE), a metabolite of oxidized lipids that increases oxidative stress. Moreover, the age-related decrease in Wnt/ $\beta$ -catenin signaling is due to diversion of  $\beta$ -catenin from TCF- to FoxO-mediated transcription in response to increased oxidative stress. In view of evidence that Wnt/ $\beta$ -catenin signaling suppresses the synthesis of PPAR $\gamma$ 2, we hypothesized that the age-related increase in PPAR $\gamma$  is due to the ROS-induced diversion of  $\beta$ -catenin to FoxO. In support of this hypothesis, 100  $\mu$ M H<sub>2</sub>O<sub>2</sub> or 20  $\mu$ M 4-HNE increased the expression of PPAR $\gamma$ 2 in the uncommitted C2C12 mesenchymal cell line; and this effect was reversed by activation of  $\beta$ -catenin with lithium or Wnt3a. Interestingly, 9-HODE and rosiglitazone promoted the association of PPAR $\gamma$ 2 with  $\beta$ -catenin in C2C12 cell in co-immunoprecipitation experiments, suggesting a mechanism by which increased levels of PPAR $\gamma$  and its ligands could further reduce Wnt/ $\beta$ -catenin signaling. Consistent with this notion, Wnt3a-induced activation of TCF-mediated transcription was reduced by PPAR $\gamma$ 2 overexpression in C2C12 cells. And, 9-HODE and rosiglitazone inhibited Wnt/ $\beta$ -catenin-mediated transcription in a PPAR $\gamma$ 2-dependent fashion in osteoblastic OB-6 cells that conditionally express PPAR $\gamma$ 2. Furthermore, rosiglitazone increased PPAR $\gamma$ 2 expression. Collectively, these results indicate that the age-related increase in oxidative stress not only reduces Wnt/ $\beta$ -catenin signaling but also stimulates PPAR $\gamma$ 2 gene transcription. The increased levels of PPAR $\gamma$ 2 combined with an age-related increase in oxidized lipid ligands of this receptor results in sequestration of  $\beta$ -catenin, which further reduces Wnt/ $\beta$ -catenin signaling; and further stimulates PPAR $\gamma$ 2 synthesis. The consequence of this self-amplifying cascade is reduced production of osteoblasts coupled with increased production of adipocytes which are invariable features of old age in mice and humans.

**Disclosures:** M. Almeida, None.

## 1100

**Overexpression of Secreted Frizzled-Related Protein 1 Inhibits Bone Formation and Attenuates PTH Bone Anabolic Effects.** W. Yao, Z. Cheng, C. Busse\*, A. Pham\*, M. Shahnazari\*, N. Lane. Center for Healthy Aging, UC Davis Medical Center, Sacramento, CA, USA.

**Introduction.** Secreted Frizzled-related protein 1 (sFRP1) is a soluble antagonist of the Wnt signaling pathway and sFRP1 null mice have less age-related bone loss as compared to their wild-type (WT) mice. Since Wnt signaling is critical for osteoblast maturation, skeletal acquisition and maintenance, we hypothesized that over-expression of sFRP1 (sFRP1-Tg) would reduce osteoblast number and activity such that these animals would have an altered bone phenotype and bone acquisition with PTH treatment compared to wild-type mice. To test these hypotheses we evaluated the bone phenotype of sFRP1-Tg mice and their response to the anabolic agent, PTH, compared to the WT in both female and male mice.

**Methods.** Three-month-old WT or sFRP1-Tg male and female mice (n=7-12/group) were treated with PTH (1-34) (40  $\mu$ g/d, 5x/wk) or Vehicle for 2 weeks. Osteoblastic and osteoclast maturation and function were accessed by primary bone marrow stromal cell and osteoclast cultures. Bone mass and micro architecture from the distal femoral metaphysis was measured by microCT. Bone turnover was assessed with biochemical markers (osteocalcin, OPG, TRAP5b and CTX-I). Real-time PCR was performed from whole bone extracts and used to monitor the expression of several genes that regulate osteoblast maturation and function (Runx2; osterix, osteocalcin). Statistical analyses were performed using a two-way ANOVA with genotype (sFRP1-Tg) and treatment (PTH) being the factors.

**Results.** Male, but not the females have lower trabecular bone mass (-32%) at 3 months of age. Genes associated with osteoblast maturation (Runx2, osterix) and function (osteocalcin), serum osteocalcin, surface based bone formation [mineral apposition rate (MAR) and bone formation rate (BFR)], were significantly decreased in sFRP1-Tg mice in both genders compared to WT mice. Bone resorption, measured by serum CTX-1 and osteoclast surface were similar between sFRP1-Tg and WT mice *in vivo* but was higher in sFRP1-Tg mice *in vitro* (p < 0.05). Human PTH (1-34) treatment for 2 weeks increased trabecular volume (female, +156% and male +319%) in WT mice as compared to 84% in female or 103% in male sFRP1-Tg + PTH mice (p < 0.05 for PTH and genotype). The magnitude of the increase in surface based bone formation (MAR and BFR) was lower in sFRP1-Tg + PTH mice compared to the WT + PTH (p < 0.05).

**Conclusion.** Overexpression of sFRP1 inhibited osteoblast maturation and function, and attenuated PTH's anabolic action on bone. The gender differences in bone phenotype of this sFRP1-Tg animal and gender specific response to PTH is being further investigated.

**Disclosures:** W. Yao, None.

This study received funding from: 1K12HD05195801, R01 AR043052-07.

## 1101

**The Neglected Role of Intracortical Remodeling in Age-Related Bone Loss.**

R. Zebaze\*, A. Ghasem\*, A. Bohte\*, S. Iuliano-Burns\*, B. Kim\*, E. Mackie<sup>1</sup>, R. Price<sup>2</sup>, E. Seeman<sup>1</sup>. <sup>1</sup>Endocrinology, University of Melbourne, Melbourne, Australia, <sup>2</sup>University of Western Australia, Perth, Australia.

Vertebral fractures and trabecular bone loss are the flagships of osteoporosis. However 80% of fractures are non-vertebral, 86% occur after age 60 yrs and 80% of bone is cortical. These contradictions challenge prevailing notions of 'accelerated' trabecular loss and 'slower' age-related cortical bone loss. We quantified trabecular, intracortical and endocortical microarchitecture at the subtrochanteric region in post-mortem specimens from 12 women aged 29 to 87 using high resolution (HR)-CT (Viva-CT, 12  $\mu$ m resolution) and scanning electron microscopy (SEM) and measured cortical and trabecular bone diminution in 123 healthy women aged 20 to 91 years using HR-pQCT at the distal radius (Scanco).

Specimens from women <50 yrs had similar amounts of surface (perimeter available for remodeling) enveloping trabecular (0.6m) and cortical (0.5 m) bone but intracortical surface was 4 fold higher than trabecular surfaces in 60-70 yr olds (2 vs 0.46 m) and 6 fold higher in 70-80 yr olds (2.3 vs 0.38 m). 80+ yr olds had mostly intra-cortical surface. This shift of surface from trabecular to cortical bone alone accounted for the age-related diminution of bone mass *in vivo*. At peak there was 226.1g of distal radial bone mass, 17.1g was lost during the first 15yrs after menopause (50-65 yrs); similar amounts of cortical (7.9g) and trabecular (9.7g) bone were lost because similar amounts of surface (~0.5 m) enveloped these compartments. However, this constituted relatively more trabecular (22% or 9.7/43.6g) than cortical (4.3%, 7.9/182.5g) bone loss because similar surface enveloped less trabecular (43.6g) than cortical (182.5g) bone.

At 65 yrs there remained 174.3g cortical and 34.7g trabecular bone. Twice the amount of cortical (55.2g) than trabecular (22.9g) was lost during the next 15 yrs because cortical bone had 4 times more surface. After age 80, the diminution in bone mass (16.3g) was largely cortical (14.6g).

As shown using 3D mapping, most cortical bone loss occurs by increasing intracortical porosity which increased the surface available for remodeling from 0.5 to >2 meters after 65 yrs. Adjacent to the marrow, coalesce of pores contributed to cortical thinning by 'trabecularizing' the cortex. In old age a large proportion (~ 70% after age 80) of the 'trabeculae' in the marrow contained osteons reflecting their cortical origin.

Thus, across age most bone loss was cortical (72.2g, 68%) and of the 106.5g lost from 50 yr, 84% was lost after 65 yrs, mostly by accelerated intracortical resorption rather than endocortical or trabecular bone resorption. These findings challenge prevailing views and reconcile the epidemiology of fractures to its pathogenesis and structural basis.

**Disclosures:** R. Zebaze, None.

## 1102

**Toward a Physiologically-Based Definition of Hypogonadism in Men: Dose-Response Relationship Between Testosterone and Bone Resorption.** J. S. Finkelstein, S. M. Burnett-Bowie, A. F. Moore\*, B. F. Jones\*, L. F. Borges\*, J. M. Youngner\*, C. W. Hahn\*, C. V. Barry\*, B. Z. Leder. Department of Medicine, Endocrine Unit, Massachusetts General Hospital, Boston, MA, USA.

Bone resorption increases and bone mineral density (BMD) decreases when adult men become severely hypogonadal i.e. when serum testosterone (T) levels are in the castrate range. Because T levels decline with aging, the decrease in T may be responsible, at least in part, for changes in BMD as men age. The T level at which these changes begins is unknown, however. To address this question, we clamped the T level of normal men at levels ranging from prepubertal to high normal and assessed changes in bone resorption. 237 healthy men, age 20-50, were treated with goserelin acetate (Zoladex®, AstraZeneca LP, Wilmington DE, 3.6 mg sc q4 wk) to induce severe hypogonadism and randomized to receive 1 of 5 T gel doses (AndroGel®, Solvay Pharmaceuticals, Marietta, GA) or placebo daily for 16 weeks (Group 1: placebo gel, Group 2: 1.25g, Group 3: 2.5g, Group 4: 5g, Group 5: 10g). A sixth group received placebo goserelin acetate and placebo T gel. Study subjects and investigators were blinded to treatment assignment. Serum total T, bio-available T, estradiol (E), and N-telopeptide (NTX) levels were measured every 4 wks. Spine and hip BMD were measured by DXA and spine BMD by QCT at 0 and 16 wks. Mean baseline T levels ranged from 506 to 575 ng/dL. Mean (SE) serum total T levels from all visits after baseline are shown in the Figure. Mean baseline E levels ranged from 18.9 to 23.6 pg/mL. Mean serum E levels during treatment were  $10.9 \pm 0.6$ ,  $11.2 \pm 0.7$ ,  $13.5 \pm 0.6$ ,  $17.7 \pm 1.1$ , and  $23.1 \pm 1.5$  pg/mL in groups 1-5, respectively. There was a strong relationship between T dose and the percent change in NTX (Figure). NTX began to increase when the T dose fell from 2.5 to 1.25 g/day. As expected in this short-term study, BMD did not change. These results demonstrate that there is a strong dose-response relationship between T dose and NTX in men. Bone resorption begins to increase at a T dose that results in a mean serum T level between 187 and 332 ng/dL and a mean serum E level between 11.2 and 13.5 pg/mL. It is likely that a similar T level would result in bone loss if sustained. These data provide a physiological framework for defining hypogonadism in men with respect to skeletal homeostasis and help provide an objective basis for determining an intervention threshold to prevent hypogonadal bone loss in adult men.



**Disclosures:** J.S. Finkelstein, Solvay Pharmaceuticals 3, 5; AstraZeneca Pharmaceuticals LP 5.

This study received funding from: National Institutes of Health (NIA and NIDDK), Solvay Pharmaceuticals, AstraZeneca Pharmaceuticals LP.

## 1103

**Preterm Birth and Bone Mineral Density in Young Adulthood: The Helsinki Study of Very Low Birth Weight Adults.** P. Hovi\*, S. Andersson\*, A. Järvenpää\*, J. G. Eriksson\*, S. Strang-Karlsson\*, E. Kajantie\*, O. Mäkitie\*. <sup>1</sup>Department of Health Promotion and Chronic Disease Prevention, National Public Health Institute, Helsinki, Finland, <sup>2</sup>Hospital for Children and Adolescents, University of Helsinki, Helsinki, Finland.

Very-low-birth-weight (VLBW, <1500 g) infants have compromised bone mass accrual during childhood. Whether this results in subnormal peak bone mass and increased risk of osteoporosis in adulthood is unknown.

The Helsinki Study of VLBW Adults is a multidisciplinary cohort study representative of all VLBW births within the larger Helsinki area 1978 - 1985. This study evaluated skeletal health in 144 subjects with VLBW, born at a mean gestational age of 29.2 weeks, mean birth weight 1126 g, and birth weight z score of -1.2, compared with 139 born at term, matched for sex, age, and birth hospital. Data on perinatal and neonatal characteristics were collected from hospital records. Present calcium and vitamin D intake and physical activity were assessed with a questionnaire. Lumbar spine, femoral neck and whole body bone mass and bone mineral density (BMD) and body composition were measured by dual energy x-ray absorptiometry (Hologic Discovery A) at age 18.5 to 27.1 years (mean 22.6 years).

The VLBW subjects had, in comparison to subjects born at term, 2.4-fold odds (95% confidence interval [CI], 1.5 to 4.1) of having a lumbar spine BMD z score within the osteopenic or osteoporotic range. After adjusting for VLBW subjects' shorter height, the odds ratio was 1.8 (95% CI, 1.1 to 3.2). The VLBW adults had a 0.51 unit (95% CI, 0.28 to 0.75) lower lumbar spine and a 0.56 unit (95% CI, 0.34 to 0.78) lower femoral neck z score for BMD. These differences remained statistically significant after adjustment for the VLBW adults' shorter height and lower self-reported exercise intensity: 0.26 units (95% CI, 0.01 to 0.51) for the lumbar spine and 0.40 units (95% CI, 0.17 to 0.64) for the femoral neck. Adjustment for calcium or vitamin D intake had no impact on the differences. None of the BMD values were associated with weight z scores at birth or at 36 or at 40 weeks of postmenstrual age, or with duration of assisted ventilation or oxygen therapy.

Young adults with VLBW, studied close to the age of peak bone mass, have significantly lower BMD than do their peers born at term. This indicates that compromised childhood bone mass accrual in preterm children translates into increased risk for osteoporosis at adult age. Our findings suggest vigilance in osteoporosis prevention in the increasing proportion of the population with VLBW.

**Disclosures:** O. Mäkitie, None.

## 1104

**Background UVB Exposure in Pregnancy and Skeletal Development in Childhood.** A. Sayers\*, J. Tobias. Academic Rheumatology, University of Bristol, Bristol, United Kingdom.

In a previous small prospective study, maternal vitamin D levels were found to be associated with bone mineral content (BMC) of the child at age nine, suggesting a possible role of maternal vitamin D status in programming of skeletal development (Javaid et al, 2006, Lancet 367). We investigated whether an equivalent association exists in the larger Avon Longitudinal Study of Parents and Children (ALSPAC), using erythral UV (eUV) derived from meteorological monitoring data during the third trimester of pregnancy as a proxy measure of background UVB exposure, and hence a surrogate for maternal vitamin D status. This followed a preliminary study in 346 expectant mothers from ALSPAC, in which we confirmed a strong association between eUV and serum 25-hydroxy-vitaminD, both measured in the last trimester of pregnancy ( $p=0.0075 \times 10^{-27}$ ,  $r^2=0.3127$ ).

We investigated associations between birth length, birth weight and eUV. There was a strong positive association between eUV and crown heel length ( $p=0.000038$ ,  $N=10584$ ), such that those in the lowest 5% of UV exposure (low winter) were 0.28cm shorter than those with the highest 5% (high summer). In contrast, there was no association between eUV and birth weight. Subsequently, we examined the relationship between eUV and skeletal parameters measured at age 9.9 years using total body DXA scans. Erythral UV showed a strong association with height ( $p=0.017$ ,  $N=7444$ ) which resulted in 0.5 cm difference between high and low summer. In addition, positive associations were observed with total body less head (TBLH) bone mineral density (BMD) ( $p<0.00001$ ), BMC ( $p<0.00001$ ), and bone area (BA) ( $p<0.00002$ ) ( $N=7336$ ). BMD, BMC and BA were 0.008 g.cm<sup>-2</sup>, 27.1 g and 22.9cm<sup>2</sup> higher respectively, in mothers with eUV levels in the highest 5% (high summer) versus lowest 5% (low winter). These effects were attenuated to varying degrees after adjusting for height, following which differences between high and low summer for BMD, BMC and BA were 0.005 g.cm<sup>-2</sup>, 15.0 g, 6 cm<sup>2</sup> respectively,  $p<0.001$  for every effect.

We conclude that maternal vitamin D status, as reflected by eUV, exerts an important influence both on longitudinal bone growth in utero, and skeletal growth in subsequent childhood, as reflected by height and TBLH BA measurements at age 9.9. In addition, maternal eUV showed strong associations with TBLH BMC and BMD, which were only partially attenuated by adjusting for height, implying that as well as influencing skeletal growth in childhood, maternal vitamin D status exerts persisting effects on those metabolic processes which regulate 'volumetric' bone density.

**Disclosures:** A. Sayers, None.

## 1105

**A Clinical Tool for Adjusting BMD Z-Scores for Body Size in Growing Children?** B. Zemel<sup>1</sup>, H. Kalkwarf<sup>2</sup>, V. Gilsanz<sup>3</sup>, J. Lappe<sup>4</sup>, S. Oberfield<sup>5</sup>, J. Shepherd<sup>6</sup>, S. Mahboubi<sup>7</sup>, M. Frederick<sup>8</sup>, K. Winer<sup>9</sup>. <sup>1</sup>Pediatrics, University of Pennsylvania, Philadelphia, PA, USA, <sup>2</sup>Cincinnati Children's Medical Center, Cincinnati, OH, USA, <sup>3</sup>Radiology, Los Angeles Children's Hospital, Los Angeles, CA, USA, <sup>4</sup>Creighton University, Omaha, NE, USA, <sup>5</sup>Columbia University, New York, NY, USA, <sup>6</sup>University of California San Francisco, San Francisco, CA, USA, <sup>7</sup>Radiology, The Children's Hospital of Philadelphia, Philadelphia, PA, USA, <sup>8</sup>CTASC, Baltimore, MD, USA, <sup>9</sup>NICHHD, Bethesda, MD, USA.

Body size has a strong influence on bone outcomes in children, yet there is no consensus on how to consider these effects in clinical assessment. Children at-risk for poor bone accrual frequently have poor growth and delayed maturation. In the clinical setting, commonly used adjustment techniques consist of substituting "height age" (Ht-Age) or bone age for chronological age (ChronAge) in the calculation of BMD Z-scores (BMD-Z). However, these approaches have never been validated. The goal of this study was to assess these techniques and test alternatives that can be applied in the clinical setting to assess the impact of growth status on BMD-Z.

Data on 1554 healthy children from the NICHHD Bone Mineral Density in Childhood Study (BMDCS) were used. Subjects were evaluated annually on 4 occasions (5875 observations). Lumbar spine DXA scans were obtained on Hologic Delphi/Discovery bone densitometers following standard techniques. Bone age was assessed by a single radiologist. HtAge was determined as the age at which a child's height was equal to the median for the CDC height charts. Height Z-scores (HAZ) were calculated using the CDC growth charts, and BMD-Z were calculated based on the BMDCS.

An adjustment method was considered to be biased if the adjusted z-score had a mean that was significantly different from zero among children with rapid/slow growth or maturation. BMD-Z results for substituting HtAge for ChronAge were:  $0.6 \pm 1.2$  ( $p<0.0001$ ) if  $HAZ<-1$  and  $-0.5 \pm 1.0$  ( $p<0.0001$ ) if  $HAZ>1$ . Results for substituting bone age for ChronAge to calculate BMD-Z were:  $0.6 \pm 1.1$  ( $p<0.0001$ ) for bone age delay  $<-2$  yrs and  $-0.8 \pm 0.9$  ( $p<0.0001$ ) for bone age delay  $>2$ . An alternative approach utilized age and gender-specific simple regression models of HAZ on BMD-Z to calculate a predicted BMD-Z. HAZ adjusted BMD-Z was defined as observed minus predicted BMD-Z. HAZ Adjusted BMD-Z was  $0.1 \pm 0.9$  if  $HAZ<-1$  and  $0.0 \pm 1.0$  if  $HAZ>1$ .

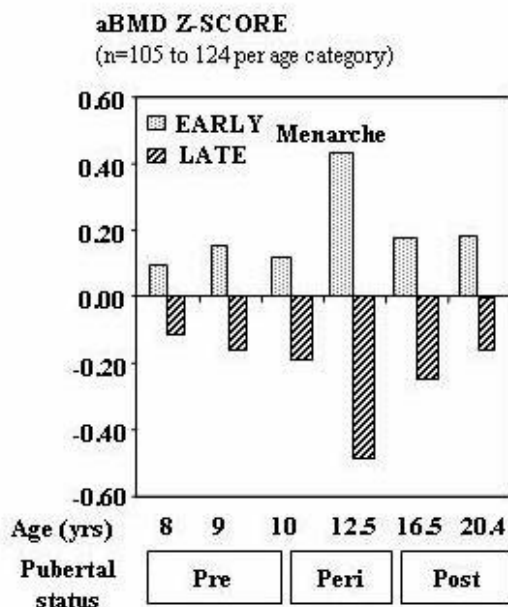
These findings discredit the substitution of bone age or Ht-Age for ChronAge to calculate an adjusted BMD-Z. Adjusting for HAZ gives an unbiased adjustment for the effects of growth on BMD-Z. This simple approach accounts for the age-specific relationship between height status and BMD, and avoids the comparison of children across different ages where stages of pubertal development may differ.

**Disclosures:** B. Zemel, None.

## 1106

**Influence of Pubertal Timing on Bone Trait Acquisition: Predetermined Trajectory Detectable Five Years Before Menarche.** T. Chevalley, J. P. Bonjour, S. Ferrari, R. Rizzoli. Service of Bone Diseases, Department of Rehabilitation and Geriatrics, University Hospitals of Geneva, Switzerland.

Late menarche is a risk factor for osteoporosis. It is associated with low peak bone mass (PBM) that may be due to reduced exposure time to estrogen. Nevertheless, menarcheal age (MENA) is under strong genetic influence, as shown by twin and familial studies. Therefore, it is possible that in addition to the mechanism of reduced estrogen exposure time from MENA to PBM time attainment, bone deficit may be present before any sign of pubertal maturation would become clinically patent. We tested this hypothesis in a cohort of healthy girls prospectively followed up from 8 to 20 yrs of age with intermediate bone assessment at 9.0, 10.0, 12.5 and 16.5 yrs. Mean MENA ( $\pm$ SD) was  $13.0 \pm 1.2$  yrs ( $n=124$ ). The cohort was segregated according to the median of MENA in EARLY ( $12.1 \pm 0.7$  yrs) and LATE ( $14.0 \pm 0.7$  yrs) subgroups. At  $20.4 \pm 0.6$  yrs, Z-scores of areal bone mineral density (aBMD) in EARLY and LATE were: Radial Metaphysis:  $+0.19$  vs.  $-0.17$ ,  $p=0.046$ ; Radial Diaphysis:  $+0.19$  vs.  $-0.18$ ,  $p=0.042$ ; Femoral Neck:  $+0.18$  vs.  $-0.18$ ,  $p=0.042$ ; Femoral Trochanter  $+0.10$  vs.  $-0.09$ ,  $p=0.282$ ; Femoral Diaphysis:  $+0.16$  vs.  $-0.15$ ,  $p=0.086$ ; Lumbar spine:  $+0.15$  vs.  $-0.14$ ,  $p=0.107$ . Differences in Z-score at 20.4 years of age between EARLY and LATE were observed not only at 16.5, 12.5 and 10 yrs, i.e. during pubertal maturation, but also before the onset of pubertal maturation. Indeed, between age 8 and 9 yrs two-way ANOVA indicated that the significant age-dependent bone growth ( $P=0.0001$ ) did not interact with the influence of future MENA ( $P=0.0042$ ). The figure illustrates the differences in mean Z-score of the 6 skeletal sites between EARLY and LATE MENA from prepuberty to PBM attainment at 20.4 yrs of age. In this group the reduced aBMD in LATE was associated with lower cortical volumetric bone density and thickness in both distal radius and tibia ( $P<0.05$ ) as measured by high resolution peripheral computerized tomography (HR-pQCT). In conclusion, in healthy female subjects, the negative influence of relatively later menarcheal age, 14.0 vs 12.1 yrs, on macro and microstructural bone traits observed at time of peak bone mass attainment, is associated with a predetermined deficit already observable a few years before the onset of pubertal maturation.



**Disclosures:** T. Chevalley, None.

## 1107

**A Three Year School-Curriculum-Based Exercise Program in Prepubertal Children Increases Bone Mineral Accrual and Bone Size but Do Not Influence Femoral Neck Structure.** B. Lofgren, G. Alwis\*, C. Lindén\*, H. G. Ahlberg, M. Dencker\*, P. Gardsell\*, M. K. Karlsson. Department of Clinical Science, Clinical and Molecular Osteoporosis Unit, Malmö, Sweden.

Most exercise intervention studies in children, evaluating the accrual of bone mineral content (BMC), include volunteers and specifically designed osteogenic exercise programs. No trial exceeds 24 months. The purpose of the this study was to evaluate if a population based 36 months moderate intense exercise program leads to skeletal benefits. 45 girls and 75 boys aged 7-9 years were included in a school-curriculum-based exercise intervention program of general physical activity for 40 minutes per school day. 42 matched girls and 54 boys assigned to the Swedish curriculum of 60 minutes training per week served as controls. BMC were estimated by dual X-ray absorptiometry of total body, lumbar spine, femoral neck and trochanter. Bone width was measured at third lumbar vertebra and femoral neck. Hip structural analyses (HSA) evaluated the structural properties of the femoral neck [cross-sectional area (CSA), section modulus (Z) and cross-sectional moment of inertia (CSMI)]. Height and weight were measured. Physical activity was estimated through questionnaires and by accelerometers. Children were followed annually for three years whereafter changes were calculated for each individual as the ratio of the slope fitted to all measurements. Group discrepancy was expressed in SD units (annual changes divided by SD for annual changes). No group differences were found at baseline in age, anthropometrics or bone parameters. Boys and girls in the intervention group had around double subjectively estimated weekly duration of physical activity (both  $p<0.001$ ) and by accelerometers measured most intense activities ( $>10000$  counts per minutes; both  $p<0.01$ ) than the controls. There were no group differences in accelerometer measured lower intensities. The BMC gain in the intervention girls was mean 0.8 SD higher in lumbar spine ( $p=0.003$ ), mean 0.5 SD higher in femoral neck ( $p=0.03$ ) and mean 1.1 SD higher in trochanter ( $p=0.0003$ ) and the gain in the third lumbar vertebra width mean 0.5 SD higher ( $p=0.05$ ) than in the control girls. The BMC gain in the intervention boys was mean 0.8 SD higher in lumbar spine ( $p=0.002$ ) and mean 0.7 SD higher in the trochanter ( $p=0.04$ ) while the gain in third lumbar vertebra width was mean 0.3 SD higher ( $p=0.04$ ) than in the control boys. No group differences were found in femoral neck structural changes. A school-based exercise program for three years in 7-9-year-old children is associated with a higher duration of total and intense physical activities, activities known as key features of osteogenic stimuli, and a higher accrual of BMC and bone width than in children at a lower level of exercise.

**Disclosures:** B. Lofgren, None.

## 1108

**Vitamin D Dose Response Study in Canadian Infants.** K. Trussler\*, C. Rodd<sup>1</sup>, S. Gallo\*, C. Vanstone\*, A. Khamessan\*, M. L'Abbe\*, H. Weiler<sup>1</sup>. <sup>1</sup>McGill University, Montreal, QC, Canada, <sup>2</sup>Europharm International Canada Inc, Montreal, QC, Canada, <sup>3</sup>Bureau of Nutritional Sciences, Health Canada, Ottawa, ON, Canada.

In 2004, Health Canada reaffirmed its policy recommendation that all breastfed infants receive a daily vitamin D<sub>3</sub> supplement of 400 IU/day in an effort to reduce vitamin D deficiency. However, clinicians continue to diagnose vitamin D deficiency in infants. It was hypothesized that this recommendation may be inadequate to achieve optimal vitamin D status for 97% of infants. Additionally, it has been proposed that 2000 IU/day may be beneficial for the prevention of chronic disease. Optimal status has not been defined for the infant population and value of 75 nmol/L was used based on adult literature. The primary objective of this study was to determine the serum concentrations (mean  $\pm$  SE) for 25(OH)D in each of the treatment doses (400 IU, 800 IU, 1200 IU, 1600 IU) in breastfed infants, 8 weeks after the start of supplementation. Breastfed infants ( $n=32$ ) were recruited from the greater Montréal area and were randomly assigned to one of four study groups (400, 800, 1200, or 1600 IU/d of vitamin D<sub>3</sub> provided in-kind from Europharm International Canada Inc). Supplementation began at 4 weeks of age and continued to 12 weeks of age. Blood samples obtained at baseline, 4 and 8 weeks thereafter were analyzed for total serum 25(OH)D (Osteia ELISA, Immunodiagnostic systems Ltd, UK). Repeated measures ANOVA accounted for the within-subject serial correlations and demonstrated that treatment ( $p<0.003$ ) and time ( $p<0.001$ ) were significant predictors of serum 25(OH)D levels. Mean values for each treatment-time are given in Table 1. While after 8 weeks of supplementation, the mean serum 25(OH)D concentration in the 400 IU/day group exceeded 75 nmol/L, 3 infants receiving 400 IU/day and 3 receiving 800 IU/day did not achieve this level. In contrast only 1 infant in the 1200 IU/day group and 0 infants in the 1600 IU/day group failed to meet the 75 nmol/L cutoff. This data represents pilot observations from the first dose response study using the Vitamin D<sub>3</sub> isoform. Continued evaluation to one year of age will establish optimal intakes in association with measures of bone health.

Table 1 Mean serum 25(OH)D (nmol/L) at baseline, 4 and 8 weeks of supplementation

	400 IU/day	800 IU/day	1200 IU/day	1600 IU/day
Baseline	82.9 $\pm$ 8.0	69.7 $\pm$ 14.6	53.7 $\pm$ 7.3	97.1 $\pm$ 10.9
4 weeks	100.5 $\pm$ 17.1	149.4 $\pm$ 8.2	133.4 $\pm$ 23.7	202.0 $\pm$ 31.3
8 weeks	76.7 $\pm$ 4.6	139.3 $\pm$ 37.5	202.6 $\pm$ 35.7	332.0 $\pm$ 71.3

**Disclosures:** K. Trussler, None.

This study received funding from: Canadian Institutes of Health Research, Nutricia Research Foundation.

## 1109

**Deletion of Zfp521, an Antagonist to Runx2 and Ebf1 Transcriptional Activity, Leads to Osteopenia and a Defect in Matrix Mineralization in Mice.** R. Kiviranta<sup>1</sup>, H. Saito<sup>\*1</sup>, D. Correa<sup>\*1</sup>, L. Neff<sup>\*1</sup>, G. C. Rowe<sup>\*1</sup>, E. Hesse<sup>1</sup>, S. Warming<sup>\*1</sup>, N. A. Jenkins<sup>\*2</sup>, W. C. Horne<sup>1</sup>, N. G. Copeland<sup>\*3</sup>, R. Baron<sup>1</sup>. <sup>1</sup>Harvard Schools of Medicine and Dental Medicine, Boston, MA, USA, <sup>2</sup>Cancer Genetics Laboratory, Institute of Molecular and Cell Biology, Singapore, Singapore, <sup>3</sup>Cancer Genetics Laboratory, Institute of Molecular and Cell Biology, Boston, Singapore.

We recently identified a novel zinc-finger protein 521 (Zfp521) that is expressed at high levels in prehypertrophic chondrocytes and in osteoblasts (Ob). Zfp521 interacts with Runx2 and early B-cell factors (Ebfs) and antagonizes their transcriptional activity. Surprisingly however, overexpression of Zfp521 in vivo lead to a dramatic increase in Ob numbers, bone formation rates and bone mass with no changes in bone resorption. To further elucidate the role of Zfp521 in Ob differentiation we used shRNA to knockdown Zfp521 expression in MC3T3-E1 cells and in primary osteoblasts. In MC3T3-E1 cells knockdown of Zfp521 resulted in increased Ob differentiation and depletion of Zfp521 in primary cells lead to increased bone nodule formation. As Zfp521 also regulates early B-cell factor (Ebf) activity during B-cell differentiation and Ebf1 and Ebf2 knockout mice have opposing bone phenotypes, we determined whether Ebf1 or Ebf2 were targets of Zfp521 in osteoblasts. Overexpression of Ebfs in MC3T3-E1 cells and in primary Obs enhanced, whereas overexpression of Zfp521 repressed, Ob differentiation. To better establish the physiological role of Zfp521 in bone we then analyzed Zfp521 knockout mice. At 3 weeks of age the trabecular bone volume and cortical thickness were markedly decreased in Zfp521<sup>-/-</sup> tibias despite increased expression levels of a highly homologous family member Zfp423, another inhibitor of Ebf transcriptional activity. Osteopenia was associated with an increase in N.Ob/BS and N.Oc/BS. There were also more Ob precursors in the bone marrow of Zfp521<sup>-/-</sup> mice, as tested in a colony forming unit assay. The osteoid surface was highly increased, and matrix mineralization appeared to be impaired despite normal serum calcium and phosphate. In culture Zfp521<sup>-/-</sup> calvarial Obs formed more mineralized bone nodules than controls, confirming an increase in Ob precursors. In the knockout cells the expression of Ebf2, a known regulator of OPG expression, and Ebf1 were decreased at day 7 of the cultures, possibly explaining the increased number of osteoclasts and the osteopenia. In conclusion, inactivation of Zfp521 leads to enhanced Ob differentiation possibly via increased transcriptional activity of Runx2 and Ebfs, and to increased osteoclast numbers leading to low bone mass. We conclude that Zfp521 is a novel regulator of bone homeostasis.

**Disclosures:** R. Kiviranta, None.

## 1110

**Altered Long Bone Structure in Recessive Null and Dominant Negative Connexin43 (Gjal) Mouse Mutants.** S. K. Grimston<sup>1</sup>, M. Watkins<sup>1</sup>, M. D. Brodt<sup>\*2</sup>, M. J. Silva<sup>2</sup>, R. Civitelli<sup>1</sup>. <sup>1</sup>Division of Bone and Mineral Diseases, Washington University in St. Louis, St. Louis, MO, USA, <sup>2</sup>Department of Orthopedic Surgery, Washington University in St. Louis, St. Louis, MO, USA.

Connexin43 (Cx43) is the major gap junction protein present in bone cells and it is involved in bone development and adult skeletal growth. We and others have observed large marrow area and thin cortices in the tibial diaphysis of *Gjal* deficient mice. To gain further insight on such structural abnormalities, we analyzed femora of 3 different *Gjal* mouse mutants; conditional knockout driven by either a 2.3kb fragment of the  $\alpha_1(I)$  collagen promoter (*ColCre;Gjal*<sup>-flox</sup>; or ColcKO, n=13), or the *Dermo1* promoter (*DM1Cre;Gjal*<sup>-flox</sup>; or DM1cKO, n=5), and conditional induction of an oculodentodigital dysplasia mutation, also driven by DM1 (*DM1Cre;Gjal*<sup>+G138R</sup>; or DM1cODDD, n=7). Relative to wild type (WT) littermates,  $\mu$ CT scans revealed a consistent pattern of significantly thinner cortices (87 $\pm$ 17%\*, 84 $\pm$ 7%\*, 91 $\pm$ 6%\* of WT) and larger marrow area (162 $\pm$ 41%\*, 169 $\pm$ 26%\*, 131 $\pm$ 37%\*) in ColcKO, DM1cKO and DM1cODDD, respectively. While there were no differences in cortical area among the 3 mutants, femoral total tissue area was larger (131 $\pm$ 23%\*, 139 $\pm$ 13%\*, 119 $\pm$ 18%\*) and second area moment of inertia was greater (175 $\pm$ 53%\*, 161 $\pm$ 36%\*, 129 $\pm$ 29%\*) in ColcKO, DM1cKO and DM1cODDD relative to their WT littermates, respectively. Although these findings are compatible with greater resistance to bending, 3-point bending test showed that ColcKO actually have a significantly decreased ultimate force relative to WT (78.2 $\pm$ 6.6%\*), implying that Cx43 deletion alters the material properties of long bones. Larger but thinner bones also suggest increased endocortical bone resorption with only partial compensatory increase in periosteal bone apposition. Consistent with this hypothesis, endocortical porosity, measured as a percent of total cortical area, was significantly higher in DM1cKO, relative to their WT littermates (13.8 $\pm$ 10.8%\* vs 2.9 $\pm$ 2.7%), however histological analyses showed no significant differences in osteoclast number. These common structural abnormalities of long bones observed in 3 different *Gjal* mutant models demonstrate that deficiency of, or interference with Cx43 alters bone architecture in a manner similar to what is observed in aging or disuse. The less severe phenotype of DM1cODDD mice is consistent with a dominant negative action of the Cx43 G138R mutant protein. Finally, the similar degree of structural changes in DM1cKO and ColcKO, relative to their respective WT littermates, suggests that Cx43 in osteoblasts and/or osteocytes is key for maintaining normal cortical bone structure and resistance to load.

\*p<0.05 vs. WT littermates.

**Disclosures:** S.K. Grimston, None.

This study received funding from: NIH grant AR041255.

## 1111

**Notch Inhibits Nuclear Factor of Activated T-Cells (NFAT) Transactivation in Osteoblast Cultures.** S. Zanotti, A. Smerdel-Ramoya, E. Canalis. Research, Saint Francis Hospital and Medical Center, Hartford, CT, USA.

Notch are transmembrane receptors that determine cell differentiation, and in bone, Notch inhibits osteoblastogenesis and osteoclastogenesis. In the Notch canonical pathway, interactions with Notch ligands result in the release of the intracellular domain of Notch (NICD), which translocates to the nucleus where it interacts with the CSL family of nuclear factors to activate the transcription of target genes, such as *hair enhancer of split 1 (hes1)*. Notch inhibits Wnt signaling and NICD interacts with Runx2; however, not all of the effects of Notch on osteoblastogenesis are explained by these interactions. NFATs are transcription factors that determine cell differentiation and function. Dephosphorylation of specific serines by calcineurin induces NFAT translocation to the nucleus and transactivation, whereas their phosphorylation induces NFAT nuclear export, inhibiting transactivation. NFATc1 and c2 regulate osteoblastogenesis and osteoclastogenesis. Consequently, we asked whether Notch inhibited these cellular events by regulating the activity of NFAT. In mesenchymal cells, Forkhead Box Protein O1 (FoxO1) forms a complex with NICD/CSL, and is required for the inhibitory effects of Notch on myotube differentiation. Since FoxO1 can inhibit NFAT signaling, we examined its role in Notch signaling and in the effects of Notch on NFAT activation. To study Notch/NFAT/FoxO1 interactions, ST-2 stromal cells were transfected with an NICD expression vector, and osteoblasts from *Rosa<sup>notch</sup>* mice, where NICD is induced following the deletion of a STOP cassette by CRE recombination, were used. The effects of NICD on NFAT transactivation and localization were examined. NICD inhibited the transactivation of a reporter construct containing nine copies of an NFAT binding motif, both in ST-2 cells and *Rosa<sup>notch</sup>* cells. In accordance with the inhibition of NFAT transactivation, NICD increased cytoplasmic and decreased nuclear levels of NFATc1. To determine whether FoxO1 participates in the inhibition of NFAT by Notch, the activity of Notch was tested in the context of FoxO1 downregulation by RNA interference. Notch induced the transactivation of CSL and the transcription of its target gene *hes1* in ST-2 cells and in *Rosa<sup>notch</sup>* osteoblasts. These effects were inhibited by FoxO1 downregulation, indicating that FoxO1 is necessary for the activation of the Notch canonical signaling pathway in osteoblasts. However, FoxO1 downregulation did not rescue the inhibitory effect of NICD on the transactivation of the NFAT reporter construct. In conclusion, Notch inhibits NFAT transactivation through a CSL and FoxO1 independent mechanism, and induces the nuclear export of NFATc1.

**Disclosures:** S. Zanotti, None.

This study received funding from: NIH Grant # DK45227.

## 1112

**FOXO1 Signaling in the Control of Bone Mass.** M. Rached<sup>\*1</sup>, M. Ogita<sup>\*1</sup>, R. A. DePinho<sup>\*2</sup>, J. P. Bilezikian<sup>1</sup>, S. Kousteni<sup>1</sup>. <sup>1</sup>Department of Medicine, Division of Endocrinology, College of Physicians & Surgeons, Columbia University, New York, NY, USA, <sup>2</sup>Dana-Farber Cancer Institute, Harvard Medical School, Boston, MA, USA.

Regulation of development, metabolic homeostasis and oxidative stress responses share many features. Several molecules that regulate responsiveness to oxidative stress are also utilized by signaling cascades that are associated with prolongation of lifespan. Molecules that well exemplify this point are a family of ubiquitous transcription factors known as FOXOs. FOXO1, one of three FOXO homologs, regulates cell proliferation, differentiation and survival in response to oxidative stress and increases lifespan in model biologic systems. We show that FOXOs, and in particular *Foxo1*, are expressed in osteoblastic cell lines, calvaria-derived osteoblastic cells and also in osteoblasts and osteocytes in the bone of young (10-day old) and adult (2 month-old) mice. Treatment of osteoblastic cell lines and calvaria-derived osteoblastic cells with the oxidative stress inducer H<sub>2</sub>O<sub>2</sub> had a dual effect on FOXO1 activity. Initially, it promoted *Foxo1*-mediated transcription as measured by the expression of endogenous *Foxo1* transcriptional targets Superoxide Dismutase 2 (*Sod2*), *Gadd45*, and a *Foxo1* reporter. At the same time, H<sub>2</sub>O<sub>2</sub> induced changes to inactivate FOXO1 (phosphorylation, cytoplasmic retention). Moreover, in this setting, FOXO1 maintained a balance between proliferation and survival of osteoblasts as measured by cell based assays and the expression or activity of cell-cycle (*cyclins D1* and *D2*, *p27kip1*), DNA damage (*Gadd45*) or anti-oxidant defense (*Sod2*) genes. FOXO1 also counteracted the adverse effects of H<sub>2</sub>O<sub>2</sub> on osteoblast survival. *In vivo*, *Foxo1* expression progressively decreased with age in C57Bl/6 mice. The decrease in *Foxo1* expression correlated with increased levels of Reactive Oxygen Species (ROS) in bone marrow cells derived from the aging animals. The expression and activity of *Sod2* were also reduced in femoral extracts with age. Moreover, *Foxo1* haploinsufficiency decreased bone mass and compromised bone microarchitecture in adult mice. Structural changes representing loss of trabecular connectivity and thus, reduced bone strength, concomitantly with increased bone diameter resemble the phenotype of aging bone. Deletion of *Foxo1* specifically from osteoblasts decreased *Sod2* activity in bone extracts, indicating attenuation of FOXO1 activity in bone. Further, it reduced osteoblast numbers, bone formation rate and bone volume without affecting the osteoclast numbers. These studies provide a link between pathways that regulate oxidative stress, longevity and skeletal homeostasis under the control of FOXO1 signaling. They also suggest that FOXO1 may prevent or delay skeletal aging.

**Disclosures:** S. Kousteni, None.

## 1113

**Age-related Bone Loss in Mice Associated with Ubiquitin Ligase Smurf1 Degradation of JunB Protein and Reduced Osteoblast Proliferation.** L. Zhao<sup>\*1</sup>, J. Huang<sup>\*2</sup>, R. Guo<sup>\*1</sup>, D. Chen<sup>2</sup>, Y. E. Zhang<sup>\*3</sup>, B. F. Boyce<sup>1</sup>, L. Xing<sup>1</sup>. <sup>1</sup>Department of Pathology and Lab. Medicine, University of Rochester Medical Center, Rochester, NY, USA, <sup>2</sup>Department of Orthopaedics, University of Rochester Medical Center, Rochester, NY, USA, <sup>3</sup>Laboratory of Cellular and Molecular Biology, Center for Cancer Research, National Cancer Institute, Bethesda, MD, USA.

Bone mass and bone formation rates are increased in Smad ubiquitin regulatory factor 1 (Smurf1) <sup>-/-</sup> mice (aged 4-8 months), suggesting that the ubiquitin ligase, Smurf1, negatively regulates bone volume with age. Smurf1 negatively regulates differentiated osteoblast functions by promoting ubiquitination and proteasomal degradation of bone morphogenetic protein (BMP) signaling molecules. However, it is not known if Smurf1 regulates the stability of other proteins in osteoblasts. We hypothesized that Smurf1 may target factors that regulate cell growth. Thus, we screened for a PY motif, the Smurf1 targeting sequence, in proteins known to control cell growth and found a PPXY sequence in JunB, suggesting that JunB may be a new target for Smurf1. Here, we used a combination of biochemical and genetic approaches to determine if Smurf1 affects JunB protein ubiquitination and degradation and has functional consequences in osteoblasts. We found that bone marrow cells from Smurf1<sup>-/-</sup> mice formed more (96 ± 1/dish vs. 52 ± 4, p<0.05) and more extensive (4943 ± 573 mm<sup>2</sup> vs 2053 ± 341, p<0.05) ALP<sup>+</sup> colonies than WT cells. JunB protein levels were increased (2.2-fold) in calvarial and bone marrow osteoblasts derived from Smurf1<sup>-/-</sup> mice compared to WT cells. Smurf1 over-expression decreased steady-state levels of JunB protein (21.6-fold), and this was attenuated by the proteasomal inhibitor, MG132. Over-expression of WT Smurf1, but not a catalytically inactive mutant Smurf1, increased the accumulation of ubiquitinated JunB protein. Immunoprecipitation experiments indicated that Smurf1 binds directly to JunB through its PY motif. Mutated JunB (PPVY to PPVF) abolished the interaction between Smurf1 and JunB as well as Smurf1-mediated JunB ubiquitination and degradation. JunB promotes cell growth in several cell types by regulating transcription of cyclins. We found that the expression level of cyclin D1 and the activity of a cyclin D1-luciferase reporter construct were significantly increased in Smurf1<sup>-/-</sup> osteoblasts compared to WT cells. Furthermore, knock-down of JunB with RNAi abolished the increase in cyclin D1 levels in Smurf1<sup>-/-</sup> cells. Thus, we have identified JunB as a new target of Smurf1 E3 ligase in osteoblasts and demonstrated that the regulation of JunB protein stability via proteasomal degradation affects osteoblast function. Inhibition of Smurf1 in osteoblasts could be a mechanism to limit age-related osteoporosis.

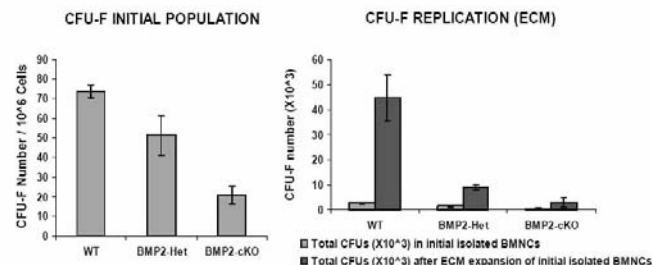
**Disclosures:** L. Zhao, None.

This study received funding from: National Institutes of Health.

## 1114

**Conditional Deletion of BMP2 Gene in Early Osteoblasts Leads to Reduction in the Total Bone Marrow (BM) Mesenchymal Stem Cells and Their Capacity to Form Osteoblast Precursors.** W. Yang<sup>1</sup>, M. A. Harris<sup>1</sup>, Y. Cui<sup>\*1</sup>, C. Skinner<sup>\*1</sup>, X. Chen<sup>1</sup>, Y. Lai<sup>\*1</sup>, A. Lichtler<sup>2</sup>, B. Kream<sup>\*2</sup>, Y. Mishina<sup>3</sup>, S. E. Harris<sup>1</sup>. <sup>1</sup>U Texas HSC San Antonio, San Antonio, TX, USA, <sup>2</sup>U Connecticut Medical CTR, Farmington, CT, USA, <sup>3</sup>NIEHS, Research Triangle Park, NC, USA.

BMP2 is thought to be essential for multipotential mesenchymal stem cells (MSCs) fate direction to osteogenic precursors. BMP2 has also been reported to mobilize osteogenic stem cells to the site of bone formation. However, the role and mechanism of endogenous BMP2 in MSCs fate and capacity is unrevealed. Using an early osteoblast selective BMP2 conditional knockout (BMP2-cKO) mouse model (3.6col1a1-cre), we have previously demonstrated that BMP2 is necessary for postnatal bone formation. Bone marrow from 3-month BMP2-cKO mice demonstrates reduction of both hematopoietic and stromal cells (BMSCs) components. We compared the BMSCs obtained from femurs and tibiae of BMP2-cKO mice to those from BMP2 heterozygous (BMP2-Het) and wild-type (WT) mice. The total BMSCs from the BM of BMP2-cKO mice is reduced 50%. Mesenchymal colony-forming unit (CFU) assays with BMSCs were then performed. CFU-F assays indicate there is a BMP2 gene dose-dependent reduction of MSCs population with 86% reduction for BMP2-cKO and 44% reduction for BMP2-Het compared to WT mice. CFU-OB assays demonstrate BMP2-cKO mice have a 90% reduction in osteogenic-potency compared to WT. The replication capacity of MSCs was examined by replating assays. MSCs were first expanded by plating on WT BM cell - derived extracellular matrix (ECM) that has the capacity to maintain MSC multipotential state. Equal numbers of expanded MSCs from BMP2-cKO, BMP2-Het and WT were then tested for CFU-F and CFU-OB. Replication capacity of MSCs with deletion of BMP2 is reduced 60% and differentiation capacity reduced 48%. Defects of MSCs capacity to form CFU-F in the absence of BMP2 could be caused by deficient BM microenvironment or intrinsic to the MSCs. Thus, we compared MSCs' self-renewal in ECM microenvironment to those on plastic. The results show that BMP2-cKO MSCs cannot be rescued by normal BM microenvironment. This suggests the defect in the MSCs of the BMP2-cKO animals is intrinsic to the MSCs population. One hypothesis is that BMP2 dependent gene expression in early osteoblasts is sending signals to the MSCs niche and population and affecting the stem cell quality and state of these multipotential precursors.



**Disclosures:** W. Yang, None.

This study received funding from: R01-AR054616, F32-DE018865

## 1115

**Class IA Phosphatidylinositol 3-kinases Are Indispensable for Osteoclast Function by Regulating Cytoskeletal Organization and Cell Death.** M. Nakamura<sup>1</sup>, M. Iwasawa<sup>1</sup>, Y. Nagase<sup>1</sup>, T. Nakamura<sup>2</sup>, S. Kato<sup>2</sup>, K. Ueki<sup>\*3</sup>, J. Luo<sup>\*4</sup>, L. C. Cantley<sup>\*4</sup>, K. Nakamura<sup>1</sup>, S. Tanaka<sup>1</sup>. <sup>1</sup>Department of Orthopaedic Surgery, Faculty of Medicine, The University of Tokyo, Tokyo, Japan, <sup>2</sup>Institute of Molecular and Cellular Biosciences, the University of Tokyo, Tokyo, Japan, <sup>3</sup>Department of Endocrinology, the University of Tokyo Faculty of Medicine, Tokyo, Japan, <sup>4</sup>Department of Systems Biology, Harvard Medical School, Boston, MA, USA.

Phosphatidylinositol 3-kinases (PI3Ks) are a family of enzymes that phosphorylate phosphatidylinositol lipids at the 3' position. They are divided into 3 classes based on their structures and substrates. Class IA PI3Ks regulate signaling pathways downstream of receptor-type and non receptor-type tyrosine kinases such as c-Fms and Src. They consist of an adaptor subunit p85 (α and β), and a catalytic subunit p110 (α, β, δ). Previous studies have reported that class IA PI3Ks play an important role in osteoclast activity by using specific inhibitors such as wortmannin although the exact role of the molecules in the skeletal tissue in vivo still remains unknown. To elucidate the role of class IA PI3Ks in osteoclasts, we generated osteoclast-specific p85α and β double knockout mice. Since conventional p85α knockout mice die within 3 weeks, we generated osteoclast-specific p85α knockout (p85α cKO) mice by crossing *pik3r1* (p85α, p55α, p50α) flox mice and cathepsin K-Cre knockin mice. In p85α cKO mice, p85α expression was specifically reduced in osteoclasts but not in osteoblasts or other tissues. They were then crossed with *pik3r2* (p85β) knockout mice to generate osteoclast-specific p85α&β double knockout (p85 dKO) mice. Akt activation in response to M-CSF stimulation was reduced in osteoclasts derived from p85α cKO mice, and almost completely abolished in p85 dKO osteoclasts. Radiological and histological analysis showed an increased bone mass in p85α cKO mice compared to control littermates with no statistical significance. While no abnormality was observed in the skeletal tissue of p85β KO mice, p85 dKO mice exhibited about 1.5 fold increase in bone mass compared to p85β KO littermates (p<0.05). Eroded surface was reduced by 50% while there was no significant difference in osteoclast number. Osteoclasts differentiated from p85α cKO and p85 dKO mice bone marrow cells (αKO OCs and dKO OCs) showed impaired spreading and actin ring formation, and their bone-resorbing activity was remarkably suppressed. dKO OCs exhibited an increased cell death after cytokine withdrawal, and the proapoptotic phenotype was completely restored by M-CSF treatment, which activated Erk but not Akt in the cells. From these observations, we conclude that class IA PI3Ks are indispensable for osteoclast function by regulating cytoskeletal organization and cell death.

**Disclosures:** M. Nakamura, None.

## 1116

**The Role of LIM kinase 1 in Osteoclast Cytoskeletal Remodeling and Bone Resorption.** T. Kawano\*, M. Zhu\*, K. Insogna. Department of Medicine, Yale University, New Haven, CT, USA.

LIM kinase 1 (LIMK1) is a serine/threonine kinase that phosphorylates and inactivates the actin-severing protein, cofilin. Depending on the cellular context, inactivation of LIMK1 has been reported to either increase or reduce cytoskeletal remodeling and cell motility. The role of LIMK1 in regulating the activity of osteoclasts has not been explored. We therefore examined the skeletal phenotype of 8-9 week-old LIMK1 k/o mice and found that total body and femur BMD were lower in the knock-out animals (428 vs. 447 10<sup>-4</sup> grms/cm<sup>2</sup> and 623 vs. 670 10<sup>-4</sup> grms/cm<sup>2</sup>; p<0.05 and p=0.06 respectively). Dynamic bone histomorphometry did not indicate changes in the rate of bone formation in the k/o animals, however serum levels of CTX tended to be higher (40±8 vs. 29±3 ng/ml) suggesting the possibility of higher rates of resorption. Consistent with this hypothesis, osteoclasts generated by co-culture from LIMK1 k/o mice resorbed significantly more bone in 48 hrs when plated on dentine slices than did osteoclasts from heterozygous animals as quantified by the concentration of CTX in the supernatant of these cultures (p=0.02). Since LIMK1 regulates actin remodeling, the cytoskeletal response to CSF1 was assessed in mature osteoclasts freshly isolated from LIMK1<sup>-/-</sup> and LIMK1<sup>+/-</sup> mice. LIMK1 k/o osteoclasts demonstrated a significantly greater increase in cell area in response to treatment with CSF1 for 15 min than the LIMK1<sup>+/-</sup> cells (62±10 vs. 29±4 %, p<0.001). In other cells, LIMK1 inactivates cofilin and we next sought to determine if the exaggerated cytoskeletal response to CSF1 observed in the LIMK1 k/o osteoclasts reflected increased amounts of unphosphorylated (i.e. activated cofilin) present in the cytosol of these cells. Western blot analysis demonstrated that, in untreated cells, there was 50% less phosphorylated cofilin present in the LIMK1<sup>-/-</sup> osteoclasts than in cells prepared from LIMK1<sup>+/-</sup> mice. In response to 15 min of treatment with CSF1, the amount of phosphorylated cofilin present increased in both groups of cells but the ratio of phosphorylated/dephosphorylated cofilin remained lower in the LIMK1<sup>-/-</sup> osteoclasts. Thus, after 15 minutes, there was 45% less phosphorylated cofilin present in the k/o cells. These data indicate that, in the genetic absence of LIMK1, osteoclasts resorb more bone and, as a likely consequence, bone mass is reduced in LIMK1 k/o mice. One reason for this cellular phenotype may be an increase in the amount of active cofilin in LIMK1<sup>-/-</sup> osteoclasts resulting in increased responsiveness to proresorptive cytokines such as CSF1 that are known to induce cytoskeletal remodeling and motility as a part of the resorptive process.

**Disclosures:** T. Kawano, None.

## 1117

**TSH Inhibits the Expression of High Mobility Group Box Protein (HMGB), a Regulator of TNF $\alpha$  Transcription, in Osteoclastogenesis.** R. Baliram\*, K. Yamoah\*, H. Amano\*, E. Abe\*. <sup>1</sup>Endocrinology, Mt. Sinai School of Medicine, New York, NY, USA, <sup>2</sup>Pharmacology, School of Dentistry, Showa University, Tokyo, Japan.

We have previously shown that enhanced osteoclast formation in TSHR (thyroid stimulating hormone receptor)-null mice is due to TNF $\alpha$  overexpression in osteoclast progenitors. The crucial role of TNF $\alpha$  is further evidenced by additional experiments indicating that cultures of bone marrow cells from TSHR<sup>-/-</sup>TNF $\alpha$ <sup>-/-</sup> mice exhibit normal osteoclast formation. Therefore, we sought to elucidate the molecular mechanism of TNF $\alpha$  expression in osteoclast progenitors by mapping a *cis* regulatory element in the mouse TNF $\alpha$  promoter (using 5' deletion analysis) and by analyzing protein binding to the mapped sequence by EMSA (electrophoretic mobility shift assay). Our results indicate that nucleotides -157 bp to -137 bp in the TNF $\alpha$  promoter are responsible for RANKL-induced transcriptional activity and that the binding of the nuclear factors to this sequence is enhanced by RANKL and IL-1/TNF $\alpha$  treatment. We called this sequence RSS, for RANKL-responsive sequence, and we purified the binding proteins by affinity column chromatography and identified them by mass spectrometry. The proteins were high mobility group box proteins (HMGBs: HMGB1 and HMGB2), which are responsible for transcription, replication, recombination and DNA repair. These proteins are secreted in pathological conditions such as inflammation and sepsis. Further experiments showed that (1) binding of HMGBs to the RSS occurs only in the presence of RANKL (ChIP, chromatin immunoprecipitation), (2) TSH inhibits HMGB1 and HMGB2 expression in osteoclast progenitors, (3) knocking down of the expression of either HMGB1 or HMGB2 with siRNAs results in a significant reduction in the expression of TNF $\alpha$  and TRAP (tartrate resistant acid phosphatase), and (4) treatment with recombinant HMGBs significantly enhances TNF $\alpha$ , IL-1 and IL-6 expression, as well as osteoclast formation, in RAW-C3 cells and bone marrow cell cultures. Moreover, we found a direct correlation between HMGBs and TNF $\alpha$  expression and osteoclast formation in TSHR-null mice and TNF $\alpha$ -null mice. These results indicate that TSH inhibits osteoclastogenesis in bone remodeling by altering the expression of HMGBs and TNF $\alpha$ .

**Disclosures:** E. Abe, None.

*This study received funding from: NIH.*

## 1118

**Three RANK Cytoplasmic Motifs, IVVY<sup>535-538</sup>, PVQEET<sup>559-564</sup> and PVQEQG<sup>604-609</sup>, play a Critical Role in TNF $\alpha$ /IL-1-mediated Osteoclastogenesis.** J. Jules, Z. Shi\*, X. Feng. Pathology, University of Alabama at Birmingham, Birmingham, AL, USA.

RANK contains 3 TRAF-binding motifs (T1: PFQEP<sup>369-373</sup>; T2: PVQEET<sup>559-564</sup> & T3: PVQEQG<sup>604-609</sup>) that regulate osteoclast biology. RANK also has a TRAF-independent motif (IVVY<sup>535-538</sup>) that commits bone marrow macrophages (BMMs) to the osteoclast lineage. Notably, TNF $\alpha$ /IL-1-induced osteoclastogenesis requires priming of BMMs by RANKL. Using chimeric receptors, we have shown that the IVVY motif primes BMMs in TNF $\alpha$ /IL-1-induced osteoclastogenesis (ASBMR 2007). Briefly, we developed 2 chimeras: WT & Mu. While WT comprises the human Fas external domain linked to the transmembrane & intracellular domains of normal RANK, Mu has inactivating mutations in the IVVY motif. The chimeras are activated by a human Fas activating antibody (Fas-AB), specific to human Fas, without affecting endogenous RANK or Fas. BMMs expressing WT or Mu were pre-treated with Fas-AB/M-CSF for 18h, followed with TNF $\alpha$  or IL-1 plus M-CSF for 96h. WT, but not Mu, promoted osteoclastogenesis, supporting a vital role for the IVVY motif in priming BMMs in TNF $\alpha$ /IL-1-mediated osteoclastogenesis. Here, we further addressed the issue by inserting the IVVY motif to TNFR1 to determine if the addition of this motif renders TNFR1 capable of mediating osteoclastogenesis. TNFR1 or TNFR1-I (bearing IVVY motif) was expressed in BMMs from TNFR1<sup>-/-</sup>R2<sup>-/-</sup> mice. While TNFR1 failed to form osteoclasts in response to TNF $\alpha$ , TNFR1-I could mediate osteoclastogenesis, confirming the role of the IVVY motif in priming BMMs. Also, we have recently found that the IVVY motif and TRAF-binding motifs in the RANK do not function independently, inferring a functional crosstalk between them. This suggests that TRAF-binding motifs may also regulate TNF $\alpha$ /IL-1-mediated osteoclastogenesis by crosstalk with the IVVY motif in the lineage commitment. To test this, we prepared a chimera mutant bearing inactivating mutations in all 3 TRAF motifs (M). BMMs expressing WT or M were treated with hFas-AB/M-CSF for 18h, followed with TNF $\alpha$  or IL-1 plus M-CSF for 96h. While WT formed osteoclasts, M failed to do so, indicating that one or more of TRAF motifs are implicated in TNF $\alpha$ /IL-1-mediated osteoclastogenesis. Then, we generated M1, M2 and M3 which contain mutations in T1, T2, & T3, respectively. The abilities of M2 and M3 but not M1 to form osteoclasts were impaired, indicating that T2 & T3 are functional. This was further supported by a study with a mutant chimera containing mutations in both T2 and T3, which failed completely to mediate TNF $\alpha$ /IL-1-induced osteoclastogenesis. Thus, we conclude that 3 RANK motifs (IVVY<sup>535-538</sup>, PVQEET<sup>559-564</sup> & PVQEQG<sup>604-609</sup>) play a vital role in TNF $\alpha$ /IL-1-mediated osteoclastogenesis.

**Disclosures:** J. Jules, None.

*This study received funding from: NIAMS.*

## 1119

**Lyn, Opposite to c-Src, Negatively Regulates Osteoclastogenesis *in vitro* and *in vivo* via Its Interaction with SHP-1 and Gab2.** H. Kim\*, F. Ross\*, S. Teitelbaum\*, R. Faccio\*. <sup>1</sup>Pathology, Washington University, St. Louis, MO, USA, <sup>2</sup>Orthopedics, Washington University, St. Louis, MO, USA.

The non-receptor tyrosine kinase, c-Src, is a rate-limiting activator of osteoclast function and Src kinase inhibitors are therefore candidate anti-osteoporosis drugs. While c-Src is central to osteoclast activity, but not differentiation, by affecting  $\alpha$ v $\beta$ 3 integrin and M-CSF dependent pathways, we find Lyn, another member of Src family kinases is, in contrast, a negative regulator of osteoclastic bone resorption. Absence of Lyn enhances RANKL-mediated differentiation of osteoclast precursors without affecting M-CSF-dependent proliferation and survival. In further contrast to c-Src, Lyn deficiency does not impact the activity of the mature resorptive cell, indicating that the two Src family kinases exert opposite functions in the osteoclast. More importantly our data indicate that mice lacking Lyn undergo accelerated osteoclastogenesis and bone loss *in vivo* in response to RANKL. Daily, supracalvarial RANKL injections for 6 days, double the percent osteoclast surface in the calvaria of mutant mice as compared to WT ( $P < 0.01$ ) and significantly increase serum TRACP5b and collagen type 1 fragments, markers of global bone resorption, respectively 3.7 and 2.5 fold ( $P < 0.01$  compared to WT). Mechanistically, Lyn forms an intraosteoclastic complex with receptor activator of NF- $\kappa$ B (RANK), the tyrosine phosphatase SHP1 and the adapter protein Gab2. Upon RANKL exposure, Gab2 is phosphorylated and leads to activation of AP1 and NF- $\kappa$ B pathways, thereby promoting osteoclast differentiation. In Lyn<sup>-/-</sup> cultures, we found enhanced and prolonged Gab2 phosphorylation, and sustained JNK and NF- $\kappa$ B signaling. The effect of Lyn deficiency on Gab2 activation was specific for RANKL since we did not detect any difference in WT and Lyn<sup>-/-</sup> cells stimulated with M-CSF. Finally and consistent with our findings in Lyn null cells, analysis of osteoclasts from *me<sup>o</sup>/me<sup>o</sup>* mice, which bear a natural inactivating SHP-1 mutation, revealed enhanced Gab2 phosphorylation and JNK and NF- $\kappa$ B activation in response to RANKL stimulation. Thus, by activating SHP-1, Lyn modulates RANKL-evoked Gab2 phosphorylation, a critical event in OC development. Here, for the first time we establish that Lyn also regulates the osteoclast and does it in a manner antithetical to that of c-Src. Therefore, the most pragmatic aspect of our findings is that successful therapeutic inhibition of c-Src, in the context of the osteoclast, will require its stringent targeting.

**Disclosures:** R. Faccio, None.

*This study received funding from: NIH and Arthritis Foundation.*

## 1120

**Syk Tyrosine 317 Negatively Regulates Osteoclast Function.** W. Zou, J. Reeve, F. P. Ross, S. L. Teitelbaum. Pathology, Washington University School of Medicine, St. Louis, MO, USA.

The  $\alpha v \beta 3$  integrin and c-Fms, the M-CSF receptor, stimulate the resorptive capacity of the differentiated osteoclast by organizing its cytoskeleton via the tyrosine kinase, Syk in a process requiring the kinase activity of c-Src. Thus, Syk-deficient osteoclasts fail to spread or form actin rings, in vitro and in vivo. These cytoskeletal defects of Syk<sup>-/-</sup> osteoclasts arrest their bone resorptive capacity resulting in enhanced skeletal mass. Syk activation is associated with prominent phosphorylation of tyrosine (Y) 317, residing in the protein's linker region. To determine if this phosphorylated Syk residue regulates osteoclast function, we retrovirally transduced Syk<sup>-/-</sup> macrophages with WT Syk or non-phosphorylatable SykY317F and differentiated them into osteoclasts. As expected, expression of WT Syk rescues the cytoskeletal abnormalities of Syk<sup>-/-</sup> osteoclasts. Furthermore, and in keeping with unaltered osteoclast number in Syk<sup>-/-</sup> mice, SykY317F does not affect osteoclastogenesis. Surprisingly, however, SykY317F not only rescues the cytoskeletal abnormalities of Syk<sup>-/-</sup> osteoclasts, but cells expressing the non-phosphorylatable mutant actually spread more effectively than WT. Additionally, SykY317F osteoclasts form larger actin rings and resorptive pits than WT and demonstrate a 3-fold enhancement of bone resorption, as measured by medium CTx. These results establish that SykY317F negatively regulates osteoclast function. The amino acid sequence surrounding SykY317 mirrors the motif recognized by the phosphotyrosine-binding domain of c-Cbl, which acts as an E3 ubiquitin ligase. While SykY317F does not affect M-CSF- and integrin-induced Syk kinase activity and Cbl phosphorylation, it disrupts Syk/Cbl association as determined by immunoblot. Furthermore, SykY317F abolishes M-CSF- and integrin-stimulated Syk ubiquitination and degradation thereby enhance activity of the downstream cytoskeleton-organizing molecules, SLP76, Plc $\gamma$ 2 and Vav3, to levels higher than those seen with WT Syk. Thus, SykY317 negatively regulates the tyrosine kinase's ability to organize the osteoclast cytoskeleton by accelerating proteasome-mediated Syk degradation. Butressing this posture, blocking Syk degradation by the proteasome inhibitor, MG132, increases integrin-induced SLP76 activation. In summary, our data suggests a model that SykY317 negatively regulates osteoclast function via regulating Syk degradation by associating with ubiquitin ligase c-Cbl and its downstream molecules activation.

**Disclosures:** W. Zou, None.

## 1121

**Crosstalk Between Androgen Receptor and Wnt Signaling Mediates Sexual Dimorphism During Bone Mass Accrual.** Y. Gabet<sup>\*1</sup>, T. Noh<sup>\*1</sup>, J. Cogan<sup>\*1</sup>, A. Tank<sup>\*1</sup>, T. Sasaki<sup>\*2</sup>, B. Criswell<sup>\*1</sup>, A. Dixon<sup>\*1</sup>, J. Tam<sup>\*3</sup>, T. Kohler<sup>\*4</sup>, E. Segev<sup>\*3</sup>, L. Kockeritz<sup>\*5</sup>, J. Woodgett<sup>\*5</sup>, R. Müller<sup>\*4</sup>, Y. Chai<sup>\*2</sup>, E. Smith<sup>\*1</sup>, I. Bab<sup>\*3</sup>, B. Frenkel<sup>1</sup>. <sup>1</sup>Biochemistry & Molecular Biology, Institute for Genetic Medicine, Keck School of Medicine, University of Southern California, Los Angeles, CA, USA, <sup>2</sup>Center for Craniofacial Molecular Biology, Keck School of Medicine, University of Southern California, Los Angeles, CA, USA, <sup>3</sup>Bone Laboratory, Institute for Dental Sciences, Faculty of Dental Medicine, The Hebrew University of Jerusalem, Jerusalem, Israel, <sup>4</sup>Institute for Biomechanics, ETH Zürich, Zürich, Switzerland, <sup>5</sup>Ontario Cancer Institute, Princess Margaret Hospital, Toronto, ON, Canada.

In humans and mice alike, bone remodeling is strongly dependent on the Wnt signaling pathway. Androgen receptor (AR) mediates the sexual dimorphism observed in many tissues and here we demonstrate a protective skeletal effect of AR by interacting with Wnt. We investigated the role of *Lef1*, one of the four transcription factors that transmit Wnt signaling to the genome, in bone mass accrual *in vivo*. Because *Lef1*<sup>-/-</sup> mice die perinatally, we assessed the bone phenotype of *Lef1*<sup>+/-</sup> males and females at 4, 13, 17 and 34 weeks of age by  $\mu$ CT. *Lef1*<sup>+/-</sup> female mice showed significantly reduced bone mass accrual in the distal femoral metaphyses and lumbar vertebral bodies. This was attributable to a decreased bone formation, assessed by vital calcein labeling. Remarkably, bone mass was not affected in *Lef1*<sup>+/-</sup> males. We also analyzed femora of mice haploinsufficient for *Gsk3 $\beta$* , a negative regulator of the Wnt pathway. Similarly, females were substantially more responsive than males to *Gsk3 $\beta$*  haploinsufficiency, displaying in this case a high bone mass phenotype. In osteoblast cultures, real-time PCR revealed a 2.5-fold increase in *Lef1* expression induced by AR activation, suggesting interaction between AR and Wnt. Thus, to test if changes in *Lef1* expression affect Wnt signaling in bone, we transiently expressed *Lef1* in *Lef1*<sup>-/-</sup> primary osteoblasts resulting in strong stimulation of the transfected super-TOPFLASH Wnt reporter. Therefore, we hypothesized that lack of AR signaling leads to suboptimal Wnt activity in females, hence the relative sensitivity of the female skeleton to changes in Wnt signaling. Indeed, similar to female *Lef1*<sup>+/-</sup>, male *Lef1*<sup>+/-</sup> mice lacking functional AR (*Lef1*<sup>+/-</sup>;AR<sup>flm</sup>) also displayed a low bone mass (LBM) phenotype compared to *Lef1*<sup>+/-</sup>;AR<sup>flm</sup>, demonstrating that AR signaling protects against *Lef1*<sup>+/-</sup>-related LBM. Together, the gender-preferential effects of both *Lef1* and *Gsk3 $\beta$*  haploinsufficiencies suggest that the skeleton is more responsive to variations in Wnt signaling in females compared to males, and that crosstalk between AR and Wnt mediates gender differences in bone mass accrual.

**Disclosures:** Y. Gabet, None.

## 1122

**Osteoblastic Androgen Receptor Regulates Cortical Bone Mineral Density.** Y. Imai<sup>1</sup>, T. Nakamura<sup>2</sup>, T. Matsumoto<sup>\*2</sup>, K. Inoue<sup>\*3</sup>, S. Kondoh<sup>\*3</sup>, T. Sato<sup>\*4</sup>, K. Takaoka<sup>1</sup>, S. Kato<sup>2</sup>. <sup>1</sup>Department of Orthopaedic Surgery, Osaka City University Graduate School of Medicine, Osaka, Japan, <sup>2</sup>Nuclear Signaling, IMCB, University of Tokyo, JST/ERATO, Tokyo, Japan, <sup>3</sup>Nuclear Signaling, IMCB, University of Tokyo, Tokyo, Japan, <sup>4</sup>Laboratory of Molecular Traffic, Department of Molecular and Cellular Biology, Institute for Molecular and Cellular Regulation, Gunma University, Gunma, Japan.

Androgen and estrogen sex steroid hormones regulate bone homeostasis through their specific nuclear receptors, Estrogen Receptors (ERs) and Androgen Receptors (ARs). We previously reported that osteoclastic ERs control osteoclast lifespan through Fas/Fas ligand signaling in trabecular bone<sup>1</sup>. Moreover, results of bone analysis in conventional AR knockout mice (ARKO) revealed bone loss in both trabecular and cortical bone with a high rate of turnover in bone metabolism<sup>2</sup>. However, the molecular mechanisms of bone mass control by AR remain unclear.

To clarify the functions of AR in both osteoclasts and osteoblasts, we generated both osteoclast- and osteoblast-specific conditional ARKO mice (OcARKO and ObARKO) using Cathepsin K-Cre mice, Col1a1(2.3kb)-Cre mice, and AR floxed mice. Bone phenotypes were examined by soft X-ray, bone mineral density (BMD) measurement, and bone histomorphometry.

There were no differences in body weight between control mice and OcARKO or ObARKO, regardless of gender. At 8 weeks of age, OcARKO exhibited osteopenia in trabecular bone such as distal femur and a high rate of turnover in bone metabolism, in which bone resorption was more rapid than in control mice. On the other hand, female ObARKO exhibited no differences in BMD of the long bones such as femur and tibia when compared to the control mice, though the results of DEXA suggested a tendency for cortical bone of male ObARKO mice to be less in volume than that in male control mice. Although it has been believed that androgens have osteoprotective effects, especially in males, whether the effects of androgens in bone tissue are direct or indirect has not been determined. Our studies revealed that osteoclastic ARs participate in regulating trabecular bone resorption, osteoblastic ARs maintain cortical bone formation, and ARs have direct effects in bone tissue.

1) Nakamura, T., Imai, Y., Matsumoto, T., Sato, S., Takeuchi, K., Igarashi, K., Harada, Y., Azuma, Y., Krust, A., Yamamoto, Y., et al. 2007. Estrogen prevents bone loss via estrogen receptor alpha and induction of Fas ligand in osteoclasts. *Cell* 130:811-823.

2) Kawano, H., Sato, T., Yamada, T., Matsumoto, T., Sekine, K., Watanabe, T., Nakamura, T., Fukuda, T., Yoshimura, K., Yoshizawa, T., et al. 2003. Suppressive function of androgen receptor in bone resorption. *Proc Natl Acad Sci U S A* 100:9416-9421.

**Disclosures:** Y. Imai, None.

This study received funding from: Japan Science and Technology Agency.



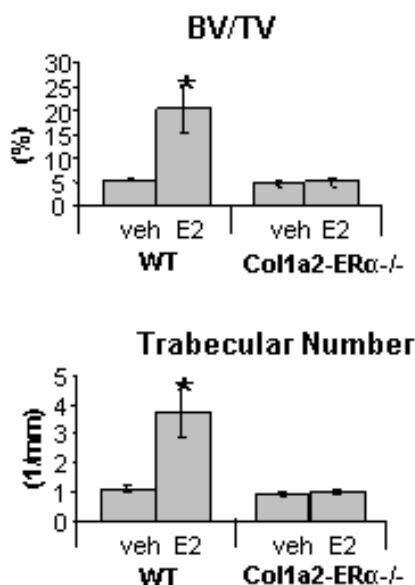
## 1123

**Estrogen Receptor- $\alpha$  Expression in Mesenchymal Cells Is Crucial for the Bone Protective Effects of Estrogen.** M. K. Lagerquist<sup>1</sup>, C. Håkansson<sup>\*1</sup>, S. H. Windahl<sup>1</sup>, A. E. Börjesson<sup>\*1</sup>, C. Jochems<sup>\*1</sup>, M. C. Antal<sup>\*2</sup>, A. Krust<sup>\*2</sup>, P. Chambon<sup>\*2</sup>, P. Angel<sup>\*3</sup>, H. Carlsten<sup>\*1</sup>, C. Ohlsson<sup>1</sup>. <sup>1</sup>Inst. of Medicine, Gothenburg, Sweden, <sup>2</sup>IGBMC, Illkirch, France, <sup>3</sup>DKFZ, Heidelberg, Germany.

Estrogen exerts bone protective effects by attenuating bone resorption in ovariectomized (ovx) mice. However, it is still debated whether osteoclasts, T-lymphocytes or cells of mesenchymal origin (e.g. osteoblasts and bone marrow stromal cells) are the primary target cells for this effect. The aim of this study was to *in vivo* investigate whether mesenchymal cells are involved in the bone protective effects of estrogen. For this purpose we used Col1 $\alpha$ 2-Cre mice in which expression of the Cre recombinase is driven by a P1-derived artificial chromosome that harbors the entire Col1 $\alpha$ 2 gene (Florin *et al*, Genesis, 2004). These mice were crossed with ER $\alpha$ -loxP mice to generate mice lacking ER $\alpha$  expression in osteoblasts, chondrocytes and fibroblasts but not in osteoclasts (Col1 $\alpha$ 2-ER $\alpha$ <sup>-/-</sup> mice). The Col1 $\alpha$ 2-ER $\alpha$ <sup>-/-</sup> mice and wild type mice were ovx at four months of age and treated with 17 $\beta$ -estradiol (E2) pellets (160 ng/mouse/day), or placebo for three weeks. Total body and spine bone mineral densities (BMD) were analyzed by dual-X ray absorptiometry. Trabecular BMD and cortical thickness were analyzed by peripheral quantitative computer tomography scans of femur while the trabecular bone structure (BV/TV, trabecular number and trabecular thickness) was analyzed by  $\mu$ CT.

In control mice, E2 increased total body BMD (+15%, p<0.01), spine BMD (+25%, p<0.01), trabecular BMD (+145%, p<0.05), cortical thickness (+16%, p<0.01), BV/TV (+267%, p<0.05), trabecular number (+233%, p<0.05) and trabecular thickness (+9%, p<0.01) compared to placebo treatment. Importantly, in the Col1 $\alpha$ 2-ER $\alpha$ <sup>-/-</sup> mice, E2 treatment did not have any effect on these bone parameters (Fig).

In conclusion, our results demonstrate that mesenchymal cells are important primary target cells for the effects of E2 on trabecular and cortical bone. These findings suggest that not only osteoclasts but also osteoblasts/bone marrow stromal cells are crucial primary target cells for the bone protective effect of estrogen.



**Disclosures:** M.K. Lagerquist, None.

## 1124

**A Novel Estrogen Receptor  $\alpha$  Variant Signals Rapidly from the Caveolae of Traditional ER $\alpha$ -negative Cells.** R. A. Chaudhri<sup>\*</sup>, R. Olivares-Navarrete<sup>\*</sup>, M. Liou<sup>\*</sup>, Z. Schwartz, B. D. Boyan. Biomedical Engineering, Georgia Institute of Technology, Atlanta, GA, USA.

Estrogen receptor alpha (ER $\alpha$ 66) regulates expression of many genes upon binding to its ligand 17 $\beta$ -estradiol (E2) in the cytosol. Recently, a novel variant of ER $\alpha$ , ER $\alpha$ 36, was identified, differing from ER $\alpha$ 66 by lacking both transcriptional activation domains but retaining the DNA-binding and ligand-binding domains as well as partial dimerization (Wang *et al.*, BBRC, 2005). We previously showed that rapid E2-dependent PKC activation in ER $\alpha$ -positive MCF7 cells, as well as in ER $\alpha$ -negative HCC38 cells, is membrane-mediated (Boyan *et al.*, Steroids, 2005). The membrane action of E2 is supported by studies using E2 conjugated to BSA (E2-BSA), which cannot cross the cell membrane, but elicits many similar effects as E2 such as PKC activation. E2 and E2-BSA rapidly increase PKC activity without new gene expression or protein synthesis and traditional ER $\alpha$  antibodies or ER antagonists do not block this effect (Boyan *et al.*, 2003). The goal of our study was to determine if ER $\alpha$ 36 is present in cell membranes and if it is responsible for E2-dependent PKC activation. We hypothesized that ER $\alpha$ 66-negative HCC38 cells carry ER $\alpha$ 36 and that it mediates the E2 membrane effect. ER $\alpha$  mRNA was

verified by RTPCR. Whole cell lysates and caveolae fractions from confluent cultures of MCF7 and HCC38 cells were examined by Western blot for the ER $\alpha$  variants. MCF7 and HCC38 cells were examined by immunocytochemistry for the localization of ERs. PKC activity was measured in confluent cultures treated with E2 for 9, 90 and 270 min. ER $\alpha$ 36 antibody was used to block the E2 effect. RTPCR showed both cell types express ER $\alpha$ . ER $\alpha$ 66 immunoblots showed that MCF7 cells have both ER $\alpha$  variants, but HCC38 cells do not contain ER $\alpha$ 66. Immunoblots also showed that ER $\alpha$ 36 exists in both cell types and is found in caveolae fractions of HCC38 cells. Immunocytochemistry showed ER $\alpha$ 36 throughout the cells, and peri-nuclear ER $\alpha$ 66 in MCF7 cells only. E2 caused a dose-dependent increase in PKC activity at 9 min in both cell types, which was inhibited when cells were treated with ER $\alpha$ 36 antibody. In contrast, ER $\alpha$ 66 antibody had no effect on PKC activity. Thus, HCC38 cells, traditionally negative for ER $\alpha$ , express ER $\alpha$  mRNA due to the shared sequence homology of the ER $\alpha$  variants. However, Western blot and immunocytochemistry show that ER $\alpha$ 66 exists only in MCF7 cells, while ER $\alpha$ 36 is present in both cell types, localized throughout the cell and exhibits colocalization to caveolin-1. This is consistent with previous literature showing that HCC38 cells are negative for ER $\alpha$  expression. PKC results demonstrate that E2-dependent PKC activity is present in HCC38 cells and is blocked by ER $\alpha$ 36 antibody, indicating that ER $\alpha$ 36 is responsible for the non-genomic, rapid effect of E2 on PKC activity.

**Disclosures:** R.A. Chaudhri, None.

This study received funding from: Children's Healthcare of Atlanta.

## 1125

**Estrogen Suppresses RANKL-induced Osteoclastic Differentiation of Human Monocytes Via an ER-alpha Associated Cytoplasmic Signaling Complex, but ER-alpha Is Downregulated During Osteoclastic Differentiation.** L. J. Robinson<sup>\*</sup>, B. B. Yaroslavskiy<sup>\*</sup>, R. D. Griswold<sup>\*</sup>, E. D. Zadorozny<sup>\*</sup>, H. C. Blair. Pathology and Cell Biology, University of Pittsburgh, Pittsburgh, PA, USA.

The effects of estrogen on bone cell survival and differentiation are controversial. Studies in mice have suggested that estrogen reduces bone resorption by inducing apoptosis of osteoclasts. Because there may be significant species differences, we studied this issue in human cells. Estrogen receptor expression was evaluated using quantitative real-time PCR. CD14-selected human monocytes lack estrogen receptor(ER)-beta; ER-alpha is expressed but levels decline markedly during osteoclastic differentiation, decreasing to essentially undetectable levels. Estrogen effects on non-transformed human monocytes were rapid and significant: inhibition of RANKL-induced osteoclastic differentiation occurred at 0.5 nM estradiol with 40-50% reduction in osteoclast numbers and activity at 10 nM estradiol. Apoptosis did not occur at significant frequency during human osteoclast differentiation *in vitro* with or without estrogen. Estrogen had acute effects on RANKL signal transduction in osteoclast precursors. Inhibition of NF-kB translocation was clearly seen within 30 minutes of RANKL stimulation. The estrogen effect was durable, with osteoclast differentiation suppressed 14 days after addition of RANKL when estradiol was withdrawn after 18 hours. An intermediate protein that binds ER-alpha in the presence of estrogen, BCAR1, was abundant in CD14 cells. Co-immune precipitation showed estrogen dependent formation of ER-alpha-BCAR1 complexes. Complex formation was enhanced by RANKL, and the RANK signaling protein Traf6 precipitated with the complex. Estradiol reduced RANKL stimulated phosphorylation of Ikb. This effect was abolished by knockdown of BCAR1, although osteoclast differentiation was also curtailed. Other studies suggested that deletion of ER-alpha under a cathepsin K promoter eliminate osteoclast apoptosis. At least in human osteoclasts, this approach would be problematical in that bone cells including mineralising osteoblasts produce cathepsin K (P<0.003) while unmodified osteoclasts bear little, if any, ER-a. We conclude that, in pure populations of human cells, estrogen reduces osteoclast formation, a cytoplasmic complex including ER-alpha and BCAR1 is a major mediator of this activity, and that BCAR1 is required for efficient osteoclast differentiation.

**Disclosures:** L.J. Robinson, None.

## 1126

**Biochemical Characterization of ERalpha Co-regulators in Multinucleated Mature Osteoclasts.** I. Takada<sup>\*</sup>, M. Youn<sup>\*</sup>, Y. Imai<sup>\*</sup>, S. Kato. Nuclear Signalling, Institute of Molecular and Cellular Bioscience, University of Tokyo, Tokyo, Japan.

Molecular basis of transcriptional regulation in osteoclasts at epigenetic levels is largely unknown, particularly no specific transcriptional co-regulators are characterized. Mature osteoclasts are multinuclear macrophage-like cells derived from the bone marrow hematopoietic stem cells. Recent studies show that several transcriptional factors regulate osteoclast differentiation. Selective ablation of ER $\alpha$  in mature osteoclasts in ER $\alpha$ <sup>Doc/Doc</sup> female mice resulted in trabecular bone loss caused by increased apoptosis due to upregulation of Fas ligand expression (Nakamura *et al.*, Cell 130:811-23, 2007). ER $\alpha$  is a member of nuclear hormone receptor superfamily and regulates the expression of target genes upon binding cognate ligands such as 17 $\beta$ -estradiol (E<sub>2</sub>) and SERMs (selective estrogen receptor modulators). Ligand-activated ER $\alpha$  binds to estrogen response elements and E<sub>2</sub>-bound ER $\alpha$  forms nuclear complexes with various co-activators including histone modifying enzymes (de-/acetyltransferases, methyltransferases, demethylases, Ub-ligases) and chromatin remodeling factors. In general, compositions of ER $\alpha$ -associated complex components and their expression levels are distinct among different tissues. However, transcriptional co-regulators of ER $\alpha$  in mature osteoclasts remain to be biochemically characterized.

To address this issue, we established a large scale osteoclast cell culture system to purify



ER $\alpha$ -associating proteins from multinucleated mature osteoclasts. First, we prepared nuclear extracts from osteoclasts and confirmed their purity by Western blotting using transcription factors as nucleus-specific markers. Then, we applied biochemical purification techniques by using a GST-fused ER $\alpha$  protein column or immobilized anti-ER $\alpha$  antibody column. Protein complexes eluted from these affinity columns were separated by SDS-PAGE and their components identified by MALDI-TOF/MS. Significantly, in addition to the known co-activators common for other ER $\alpha$  target cells, we have identified in these complexes new histone modifying enzymes and signaling factors. We showed that levels of these novel component-encoding mRNAs were induced in a RANKL-dependent manner during osteoclast differentiation. Finally, we tested modulation of the ER $\alpha$ -dependent transactivation by these novel components and identified several of them as transcriptional co-activators. Thus, in this study we demonstrated the existence of osteoclast-specific transcriptional co-regulators supporting ER $\alpha$  function.

**Disclosures:** I. Takada, None.

This study received funding from: ERATO.

## 1127

**The Predictive Validity of the WHO FRAX Model, Bone Mineral Density and Prevalent Vertebral Fracture for Incident Radiographic Vertebral Fractures.** M. G. Donaldson<sup>1</sup>, L. Palermo<sup>2</sup>, J. T. Schousboe<sup>3</sup>, K. E. Ensrud<sup>4</sup>, M. C. Hochberg<sup>5</sup>, S. R. Cummings<sup>1</sup>. <sup>1</sup>San Francisco Coordinating Center, San Francisco, CA, USA, <sup>2</sup>Univ California San Francisco, San Francisco, CA, USA, <sup>3</sup>Park Nicollet Health Services, Minneapolis, MN, USA, <sup>4</sup>Univ of MN and CCDOR VA Medical Center, Minneapolis, MN, USA, <sup>5</sup>Univ of Maryland, Baltimore, MD, USA.

The validity of the WHO 10-year probability of osteoporotic fracture model ('WHO FRAX model') for prediction of vertebral fracture has not been tested. We analyzed how well the WHO model for osteoporotic fractures (with and without femoral neck BMD (FN BMD)) predicted the risk of vertebral fracture. We also compared the predictive validity of the WHO FRAX model, femoral neck BMD, and prevalent vertebral fracture detected by radiographs at baseline alone or in combination.

We analyzed data from the placebo groups of FIT (3.8 yrs follow-up, n=3221) with odds ratios (OR) and areas under receiver operating characteristics (ROC) curves (AUC).

The WHO FRAX model, with and without FN BMD, predicted incident radiographic vertebral fracture (Table). The AUC was significantly greater for the WHO FRAX model with FN BMD (model C) than the WHO FRAX model alone (model B) (p=0.002). Prevalent vertebral fracture is significantly associated with incident vertebral fracture (model D) (RR 4.5). Prevalent vertebral fracture plus age and FN BMD (model F) predicted incident radiographic vertebral fracture as well as prevalent vertebral fracture combined with the WHO FRAX model with FN BMD (model G) (p= 0.76). However, baseline vertebral fracture status plus age and FN BMD (model F), predicted incident radiographic vertebral fracture a significantly better than the WHO FRAX model with FN BMD (model C) (p=0.0017), Table.

The WHO FRAX model (with and without FN BMD) predicts vertebral fracture. However, the WHO FRAX model alone does not significantly improve the prediction of vertebral fracture when FN BMD and age are known. A model including baseline radiographic vertebral fracture, FN BMD and age is the strongest predictor of future vertebral fracture. Given the strong association between prevalent vertebral fracture and incident vertebral fracture, it may be important to consider these in future revisions of the WHO FRAX model.

Predictors	OR*(95% CI)	AUC (95%CI)
A: FN BMD + Age	1.6 (1.7, 1.9)	0.71 (0.67, 0.74)
B: WHO 10-year risk of osteoporotic fracture <sup>†</sup>	1.8 (1.5, 2.0)	0.68 (0.65, 0.71)
C: WHO 10-year risk of osteoporotic fracture <sup>†</sup> + FN BMD	1.9 (1.7, 2.2)	0.71 (0.68, 0.74)
D: Baseline vertebral fracture	4.5 (3.4, 6.0)	0.68 (0.64, 0.71)
E: Baseline vertebral fracture + age	3.8 (2.8, 5.0)	0.73 (0.70, 0.76)
F: Baseline vertebral fracture + age + FN BMD	3.3 (2.5, 4.5)	0.76 (0.72, 0.79)
G: Baseline vertebral fracture + WHO 10-year risk osteoporotic fracture + FN BMD	3.3 (2.4, 4.4)	0.75 (0.72, 0.78)

\*OR: A (per 1SD decrease in FN BMD); B/C (per 1SD increase in WHO ); D/E/F/G (presence of baseline vertebral fracture)

<sup>†</sup>WHO models include age

AUC: Area Under the Curve

**Disclosures:** M.G. Donaldson, None.

This study received funding from: Merck.

## 1128

**Incident Vertebral Fracture is Predicted by Prevalent Vertebral Fracture as Identified by the Algorithm-Based Qualitative Method, but Not by Non-osteoporotic Short Vertebral Height. The Rancho-Bernardo Study.** G. Jiang<sup>\*1</sup>, E. Barrett-Connor<sup>2</sup>, D. L. Schneider<sup>\*2</sup>, R. Eastell<sup>1</sup>, L. Ferrar<sup>\*1</sup>. <sup>1</sup>Academic Unit of Bone Metabolism, NGH, University of Sheffield, Sheffield, United Kingdom, <sup>2</sup>Department of Family & Preventive Medicine, University of California San Diego, San Diego, CA, USA.

Osteoporotic vertebral fracture (OVF) is a strong predictor of incident fracture risk. The algorithm-based qualitative method (ABQ) identifies fewer prevalent vertebral fractures than other methods, because short height without depression at the central endplate is excluded as non-osteoporotic short vertebral height (SVH). The ABQ method has not been applied previously for the identification of incident OVF. The aims of this analysis were to 1) evaluate the identification of OVF by ABQ and 2) test the association between prevalent and incident OVF identified by ABQ.

An experienced radiologist applied the ABQ method to assess paired thoracic and lumbar spine radiographs (lateral projection) obtained over an average of 10 years follow-up in 255 men and 390 women (ages 49 to 88, mean 66 years, median 65 years) participating in the population-based Rancho Bernardo Study. For the identification of incident OVF, radiographs from both visits were assessed alongside each other. Participants were classified as follows: i) OVF, ii) SVH (no OVF) or iii) normal (no OVF, no SVH); participants with both OVF and SVH (in a different vertebra) were classified to the OVF group.

The prevalence of OVF was 10% (n = 62). There was a trend towards higher prevalence in men (12%) than in women (8%). The most common site of OVF was the thoraco-lumbar junction. The prevalence of SVH was 24% (n = 152) and was similar in men (27%) and in women (25%), with vertebral anterior height approximately 25% shorter than expected. These were mainly in the mid-thoracic region. The 10 year incidence of OVF was 5% (n = 35), tended to be lower in men (4%) than in women (7%). The incidence of OVF in those with prevalent OVF was much higher (18%) than in those with SVH (3%). The relative risk (logistic regression analysis) of incident OVF was 5.02 (95% CI: 2.33 to 10.8, P<0.01) and 0.74 (95% CI: 0.27 to 2.02, P=0.54) for participants with prevalent OVF and SVH respectively.

Conclusions: 1) OVF identified by ABQ had a trend towards higher incidence but lower prevalence in women than in men; 2) prevalent OVF by the ABQ method was a strong predictor of incident OVF; 3) SVH without evidence of OVF was more common than OVF but did not predict incident OVF.

**Disclosures:** G. Jiang, None.

This study received funding from: ARC, UK.

## 1129

**Spine Shape Predicts Vertebral Fractures in Postmenopausal Women.** M. Bruijine<sup>\*1</sup>, P. Pettersen<sup>\*2</sup>, A. Ghosh<sup>\*3</sup>, M. Sorensen<sup>3</sup>, M. Nielsen<sup>\*4</sup>. <sup>1</sup>Biomedical Imaging Group, Erasmus MC - University Medical Center Rotterdam, Rotterdam, Netherlands, <sup>2</sup>Center for Clinical and Basic Research, Ballerup, Denmark, <sup>3</sup>Nordic Bioscience, Herlev, Denmark, <sup>4</sup>Department of Computer Science, University of Copenhagen, Copenhagen, Denmark.

Early diagnosis and treatment of patients at high risk of developing fragility fractures is crucial in the management of osteoporosis. The purpose of this study was to investigate whether the shape of the spine as can be observed from lateral X-rays is indicative for the risk of future development of fragility fractures in the spine.

The study included 568 elderly women of whom 455 maintained skeletal integrity during the mean observation period of 4.8 years and 113 sustained at least one vertebral fracture in the same period. At baseline, none of the women had experienced a previous osteoporotic fracture, and the two groups were not significantly different in terms of age (66.2 ± 0.2 vs. 66.1 ± 0.4), spine BMD (0.77 ± 0.004 vs. 0.76 ± 0.008), body weight (64.7 ± 0.4 vs. 64.6 ± 0.8), height (160.6 ± 0.3 vs. 161 ± 0.5), and number of years since menopause. A radiologist annotated the corner points and mid points of the vertebral end plates of each vertebra from L5 to T4 on digitized lateral radiographs taken at the baseline visit. These points together describe a combination of factors characterizing the spinal shape, including the shape and the size of individual vertebral bodies and intervertebral disks, alignment of vertebrae, and spinal curvature. The positions of the points were subsequently used as the input features to train a pattern classification system to discriminate between spines of women maintaining skeletal health and spines sustaining a fracture in the near future (regularized linear discriminant analysis). Applied to an annotated X-ray image of an unfractured spine, this classification model then provides a measure of the probability that the spine will develop a fracture.

In a leave-one-out experiment, in which the classification models were constructed from a training set excluding any images of the patient under study, fracture probability measures were significantly different between the two groups at baseline (0.26 ± 0.02 vs. 0.18 ± 0.006, p < 10<sup>-6</sup>). Incident fractures could be predicted from the baseline image with 80% accuracy; the area under the ROC curve (AUC) was 0.65, and the odds ratio (OR) for fracture 5.2 [95% CI 2.3, 11.6]. Significant predictive value remained after adjustment for age and spine BMD (p < 10<sup>-6</sup>, AUC=0.66, OR=2.0 [1.0, 3.9]). Measures of spine shape can predict vertebral fractures in postmenopausal women, independent of age and spine BMD. The herein presented computer based diagnostic tool could be a useful supplement to existing approaches to fracture risk assessment.

**Disclosures:** A. Ghosh, None.

This study received funding from: Nordic Bioscience A/S.

## 1130

**Thoracic Kyphosis Index as a Risk Factor for Incident Vertebral Fractures and Alteration of Quality of Life in Postmenopausal Women with Osteoporosis.** C. Roux<sup>1</sup>, K. Briot<sup>1</sup>, S. Kolta<sup>1</sup>, R. Said-Nahal<sup>1</sup>, C. Benhamou<sup>2</sup>, J. Fechtenbaum<sup>1</sup>. <sup>1</sup>Rheumatology, Cochin Hospital, Paris, France, <sup>2</sup>Rheumatology, Orleans Hospital, Orleans, France.

Thoracic kyphosis, frequent in the elderly and in postmenopausal osteoporosis has been associated with impairment in global health, but limited prospective data exist. The objectives of this study were to assess quantitatively the thoracic kyphosis, the relationship between thoracic kyphosis and the risk of incident fractures, and the influence of thoracic kyphosis on quality of life in osteoporotic patients.

This study was performed on women with postmenopausal osteoporosis from the placebo groups of SOTI<sup>1</sup> and TROPOS<sup>2</sup> studies, aiming to demonstrate the efficacy of strontium ranelate against vertebral and non-vertebral fractures. Patients underwent lateral radiographs of the thoracic and lumbar spine at baseline and annually over 3 years (standardized procedures). Vertebral fractures were assessed (Genant score), and a kyphosis index at baseline (KI) was defined on lateral thoracic radiographs as the ratio BD/AC (AC= line from the anterior superior edge of T4 to the anterior inferior edge of T12; BD= perpendicular line from the furthest superior or inferior posterior point of T7, T8 or T9 vertebrae to AC line) expressed as a %. An assessment of quality of life was performed with the SF-36® generic questionnaire and the disease-specific QUALIOST® questionnaire.

The study was conducted in 2017 patients (mean age of 73.4±/6.1), with a mean lumbar spine T score of -3.06±/1.52; a mean hip T-score of -2.97±/0.66, and a mean KI of 25.41±/5.26. Patients in the highest KI tertile had significantly more new vertebral fractures (RR = 1.52 (95%CI 1.19; 1.96) p<0.001), over the study period (incidence 27.36%), compared to those in the medium tertile (incidence 19.07%) or in the lowest tertile (incidence 17.31%) (RR= 1.70 (95%CI 1.32; 2.21) p<0.001). The differences remained statistically significant after adjustment on the presence of prevalent fracture, confirming that the KI clearly participates in the risk for vertebral fractures. For both SF 36 and QUALIOST, changes in the physical score reflected significantly a better status for patients in the lowest tertile of KI as compared to patients in the highest tertile of KI.

These prospective results demonstrate that thoracic kyphosis is a risk factor for vertebral fractures over 3 years, and influences the quality of life in patients suffering osteoporosis. The thoracic kyphosis index is therefore a relevant tool for assessment of post menopausal women with osteoporosis.

References : <sup>1</sup> Meunier PJ et al. *N Engl J Med* 2004; <sup>2</sup> Reginster J.Y et al. *JCEM* 2005

**Disclosures:** C. Roux, None.

## 1131

**Three Methods of Lumbar Spine DXA Analysis as a Means to Predict Male Fracture.** K. E. Hansen<sup>1</sup>, L. Palermo<sup>2</sup>, A. N. Jones<sup>3</sup>, R. D. Blank<sup>1</sup>, H. A. Fink<sup>3</sup>, E. Orwall<sup>4</sup>. <sup>1</sup>U of WI School of Medicine & Public Health, Madison, WI, USA, <sup>2</sup>Epidemiology Department, UCSF, San Francisco, CA, USA, <sup>3</sup>VAMC, Minneapolis, MN, USA, <sup>4</sup>Oregon Health & Science University, Portland, OR, USA.

The DXA L1-L4 T-score (spine-T) is a weaker predictor of fracture (fx) in men than the femoral neck T-score (FN-T), likely from spurious elevation of bone mineral density (BMD) by spine osteoarthritis. We hypothesized that an osteoporosis diagnosis using the lowest vertebral body T-score (low-T) would predict fx better than spine-T, the International Society for Clinical Densitometry determined spine T-score (ISCD-T) or the L1-L4 T-score using female reference data (female-T).

We performed a case-control study within the Osteoporotic Fractures in Men (MROS) Study, a prospective cohort of men aged ≥65 years. Cases (n=484) were all men with incident clinical fracture by February 2007 and controls were randomly selected men without fx (n=1509). We determined four T-scores from each baseline BMD scan. An ISCD-T was possible for 1205 men. We determined sensitivity, specificity, positive and negative predictive value (PPV, NPV) and area under the curve (AUC) for each method of spine analysis. In logistic regression analysis, we controlled for other covariates that may influence fx risk, deriving odds ratios (OR) with 95% confidence intervals (CI) for fx based on an osteoporosis diagnosis by each analytic method.

Using a T-score threshold of -2.5 to diagnose osteoporosis, each analytic method demonstrated similar sensitivity, specificity, PPV and NPV. All four T-scores highly correlated (r=0.961 to 0.998). In 1993 men, the AUC for each method ranged from 0.529 to 0.558 (p=0.004, low-T vs. lumbar-T and p=0.003, low-T vs. female-T) with similar overlapping OR for fx (OR 1.99-2.68) in unadjusted analyses. In 1205 men for whom four T-scores were possible, the AUC ranged from 0.542 to 0.584 (p=0.002 for low-T vs. lumbar-T, p=0.01 for ISCD-T vs. low-T and p=0.002 for low-T vs. female-T) with similar OR for fx (OR 1.96-2.55) in unadjusted analyses. In analyses controlling for other covariates influencing fx risk including the FN-T, each method gave similar additional information on the OR for fx.

We conclude that lumbar spine T-scores provide additional information on fx risk in men beyond that provided by the FN-T. However, when using an arbitrary T-score threshold of -2.5 to diagnose spine osteoporosis, no lumbar spine analytic method is clearly superior to the others.

	Method	Sensitivity & Specificity	PPV & NPV	Adjusted OR (95% CI)
n=1993	Lumbar-T	14 & 93	38 & 77	1.56 (1.08, 2.27)
	Low-T	27 & 84	36 & 78	1.66 (1.26, 2.19)
	Female-T	10 & 96	45 & 77	2.10 (1.33, 3.32)
n=1205	Lumbar-T	22 & 88	38 & 76	1.47 (1.00, 2.17)
	ISCD-T	28 & 83	37 & 77	1.55 (1.09, 2.21)
	Low-T	41 & 76	37 & 79	1.81 (1.33, 2.47)
	Female-T	15 & 94	45 & 76	2.04 (1.28, 3.26)

**Disclosures:** K.E. Hansen, None.

This study received funding from: National Osteoporosis Foundation, NIH.

## 1132

**Cortical Porosity Is Increased in Male Osteoporosis with Vertebral Fracture.** A. Ostertag<sup>1</sup>, M. Cohen-Solal<sup>1</sup>, C. Marty<sup>1</sup>, D. Chappard<sup>2</sup>, M. C. de Vernejoul<sup>1</sup>. <sup>1</sup>606, INSERM and Paris 7 University, Paris, France, <sup>2</sup>922, INSERM and Angers University, Angers, France.

In men, vertebral fractures are poorly associated with bone density, and both cortical and trabecular micro-architectural changes could contribute to bone fragility. Bone histomorphometry makes it possible to investigate both the thickness and porosity of cortical bone, which has been reported to have a major impact on the biomechanical properties of bone. We therefore conducted a transversal study using iliac crest biopsies to investigate the trabecular and cortical bone structure in men with or without vertebral fractures. We selected 93 bone biopsies from male patients with idiopathic osteoporosis (defined as a T-score <-2.5), between 40 and 70 years of age. Patients were divided into two groups on the basis of the presence (n=46) or absence (n=47) of prevalent vertebral fracture (VFX). We measured micro-architectural indices in trabecular and cortical bone by histomorphometry at the iliac crest. Patients with VFX had lower trabecular bone volume (BV/TV: 12.4 ± 3.8 versus 14.7 ± 3.1 % (m ± SD)), p <0.01, higher trabecular separation (Tb.Sp: 871 ± 279 versus 719 ± 151 µm, p<0.01), and higher marrow star volume (V\*<sub>m.space</sub>: 16.17 ± 12.57 versus 9.45 ± 4.66 mm<sup>3</sup>, p<0.01). Cortical thickness was the same in patients with or without VFX, whereas cortical porosity (Ct.Po) was higher in patients with VFX (6.5 ± 2.6 versus 5.0 ± 2.0 %, p <0.01), because their Haversian canals had higher mean areas (8291 ± 4135 versus 5438 ± 2809 µm<sup>2</sup>, p<0.001). There was no correlation between any trabecular and cortical micro-architectural parameters. Using a logistic regression model, we evaluated the VFX as a function of the V\*<sub>m.space</sub> and Ct.Po, adjusted for age. The odds-ratio of having a VFX was 3.89 (95% CI 1.19-12.7, p=0.02) for the third tertile of V\*<sub>m.space</sub> (adjusted on age and Ct.Po), and 4.07 (95% CI 1.25-13.3, p=0.02) for the third tertile of Ct.Po (adjusted on age and V\*<sub>m.space</sub>).

Finally, we assessed the bone balance in the cortical bone. We observed that in patients with fractures, the osteon diameter was the same, but the Haversian canal diameter was non-significantly higher in patients with VFX. As a consequence, wall thickness was identical at the BMU level, and the balance was non-significantly lower in patients with fractures. In conclusion, our data show that both trabecular and cortical bone microarchitecture contribute independently to vertebral fractures in men with idiopathic osteoporosis. In contrast to data reported in women, in men it is cortical porosity, and not cortical width, that is associated with vertebral fractures. This suggests that the cortical deficit is different in men and in women with fragility fractures.

**Disclosures:** M.C. de Vernejoul, None.

## 1133

**Paget's Disease of Bone: A Histologic and Histomorphometric Analysis of Bone Biopsies from 754 Patients.** S. Seitz<sup>1</sup>, M. Priemel<sup>1</sup>, J. Zustin<sup>2</sup>, F. T. Beil<sup>1</sup>, T. Schinke<sup>1</sup>, K. Püschel<sup>3</sup>, J. Semmler<sup>4</sup>, H. Minne<sup>3</sup>, M. Amling<sup>1</sup>. <sup>1</sup>Center for Biomechanics, Experimental Trauma Surgery & Skeletal Biology, Department of Trauma, Hand, and Reconstructive Surgery, University Medical Center Hamburg-Eppendorf, Hamburg, Germany, <sup>2</sup>Department of Bone Pathology, University Medical Center Hamburg-Eppendorf, Hamburg, Germany, <sup>3</sup>Department of Forensic Medicine, University Medical Center Hamburg-Eppendorf, Hamburg, Germany, <sup>4</sup>Immanuel Hospital, Berlin, Germany, <sup>5</sup>Clinic Fürstenthof, Bad Pyrmont, Germany.

Paget's disease of bone (PDB) is the second most common metabolic bone disease. Although characteristic histological features of PDB are often described, quantitative analysis on the histological and especially on the histomorphometrical level is rare. Therefore, the aim of this study was to analyze, on the basis of the Hamburg Bone Register, PDB in terms of incidence, skeletal distribution, malignant transformation, as well as histological and histomorphometrical characteristics. Bone biopsies and patient files of 754 cases (330 women and 424 men) with histologically proven PDB were reviewed in a retrospective study. The peak incidence of PDB was between 70 and 80 years of age, and 72% of the patients with PDB were older than 60 years. The majority of monoostotic skeletal manifestation was localized at the pelvis, followed by the spine and the femur. Histological evaluation was performed on undecalcified sections of all cases. Quantitative static histomorphometry was performed on a representative subgroup of 247 biopsies derived from patients with manifestation of PDB at the iliac crest and compared to iliac crest bone biopsies of an age- and sex-matched control group from skeletal healthy patients using the Osteomeasure system according to ASBMR standards. Here we observed a more than 2-fold increase of bone volume in the biopsies derived from patients with PDB, accompanied by a 6-fold increase of osteoid volume, indicating a high turn over status or a defect of bone matrix mineralization. Cellular parameters demonstrated a more than 20-fold increase in osteoclast and osteoblast number. Paget sarcoma was diagnosed in 6 of 754

patients, suggesting a risk of malignant transformation in 0.8 % of the affected patients. Taken together, our study characterizes PDB in Germany on the basis of one of the largest cohorts of patients with histologically proven PDB. Moreover, for the first time a quantitative histomorphometric approach was taken for more than 200 cases, where we were able to demonstrate local high bone mass lesions as a result of an increase of both osteoclast and osteoblast indices.

**Disclosures:** S. Seitz, None.

## 1134

**Serum 25-OH-Vitamin D Measurement and Histomorphometric Analysis of Iliac Crest Biopsies from 1180 Patients Reveals a High Prevalence of Vitamin D Dependent Osteomalacia.** C. von Domarus<sup>\*1</sup>, M. Priemel<sup>1</sup>, S. Kessler<sup>\*1</sup>, T. O. Klatte<sup>\*1</sup>, S. Meier<sup>\*1</sup>, N. Proksch<sup>\*1</sup>, J. Schlie<sup>\*1</sup>, C. Netter<sup>\*1</sup>, F. Pastor<sup>\*1</sup>, T. Streichert<sup>\*2</sup>, K. Püschel<sup>\*3</sup>, M. Amling<sup>1</sup>. <sup>1</sup>Department of Trauma-, Hand- and Reconstructive Surgery, University Medical Center Hamburg-Eppendorf, Center of Biomechanics and Skeletal Biology, Hamburg, Germany, <sup>2</sup>Department of Clinical Chemistry, University Medical Center Hamburg-Eppendorf, Hamburg, Germany, <sup>3</sup>Department of Forensic Medicine, University Medical Center Hamburg-Eppendorf, Hamburg, Germany.

Although it is well established that bone mineral density decreases with age, a complete analysis of bone quality can only be achieved by a full histomorphometric evaluation of biopsies. This is especially important, since current techniques to quantify bone mineral density, such as DXA or qCT, cannot distinguish between low bone mass with normal matrix mineralization and osteomalacia. Thus, to evaluate bone status in Northern Germany, an area known for its high prevalence of vitamin D insufficiency, we examined 1180 iliac crest biopsies from male and female individuals aged between 20 to 99 years, excluding all patients who had signs of secondary osteopathies at autopsy. All biopsies were embedded undecalcified and processed histologically. Histomorphometric parameters, including bone volume, trabecular number, trabecular thickness, trabecular separation and osteoid volume, were quantified using the Osteomeasure system according to ASBMR standards. Statistical analysis was performed by student's t-test. Consistent with previously described studies involving less samples we found a significant reduction of the trabecular bone volume with age. This was mostly explained by a significant reduction of trabecular number, while trabecular thickness only changed moderately with age. Most importantly however, we observed that more than 25% of the individuals displayed a pathologic increase of non-mineralized bone matrix, i.e. an osteoid volume exceeding 2%. Interestingly, measuring the 25-OH-cholecalciferol levels in the serum of these individuals revealed that all of them had levels below 75nmol/l, while none of the patients above this threshold presented osteomalacia. Moreover, by combining the data of all individuals, we observed unexpected low serum levels of 25-OH-cholecalciferol (mean: 22.35 nmol/l SD:  $\pm 17.66$ ), which were even more reduced in individuals analyzed between October and March. Thus, since osteoid volume did not increase with age, it appears that the high prevalence of osteomalacia in Northern Germany is mostly caused by insufficient UV-light, as it has already been suggested in studies from countries with similar latitude relating vitamin D and PTH.

**Disclosures:** C. von Domarus, None.

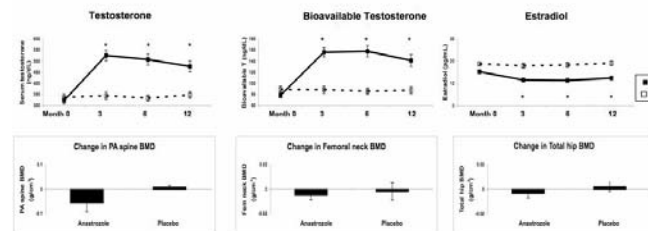
## 1135

**Effects of Aromatase Inhibitor Therapy on Bone Mineral Density in Hypogonadal Elderly Men.** B. Z. Leder, M. Dere\*, S. M. Burnett-Bowie. Endocrine Unit, Massachusetts General Hospital, Boston, MA, USA.

Androgens and estrogens independently regulate bone metabolism in men though the relative influence of each is unknown. Recently, aromatase inhibition (AI) has been proposed as a therapeutic intervention in older men with hypogonadism. Preliminary studies have demonstrated that aromatase inhibitors normalize serum androgens in hypogonadal men while lowering serum estrogens modestly. Whereas the combination of increasing serum androgens and decreasing estrogens may have advantages over standard testosterone (T) therapy in some organ systems (such as the prostate), the net effects on skeletal integrity are unknown.

To assess the effects of sustained AI on the skeleton in hypogonadal men age 60+, we randomized 69 men (mean age 66 $\pm$ 5) with T levels between 150-300 ng/dL on a single measure or between 300-350 ng/dL on two consecutive measures (mean 328 $\pm$ 92 ng/dL) to receive the aromatase inhibitor anastrozole (1 mg po QD) or matching placebo for 1 year. Gonadal steroids were measured at months 3, 6 and 12, while BMD of the spine, fem neck and total hip was measured at baseline and month 12 (DXA). Bone turnover markers are being analyzed and will be reported.

Subjects were well matched. The changes in hormone levels and BMD are plotted below. In the anastrozole group, mean T increased from 321 $\pm$ 94 ng/dL at baseline to 525 $\pm$ 139 ng/dL at wk 12 (p<0.0001 vs baseline and PBO). At wk 48, mean serum T remained significantly higher than baseline and PBO (476 $\pm$ 146 ng/dL) but lower than at wk 12 (p=0.03 wk 12 vs. wk 48). Changes in BioT (by direct measurement) revealed a similar pattern. As expected, anastrozole therapy modestly but significantly lowered estradiol levels; from 15 $\pm$ 4 pg/mL at baseline to 12 $\pm$ 4 pg/mL at month 3, remaining stable thereafter (p<0.001 vs baseline and PBO). BMD at all sites was unaffected by AI (P=NS compared to baseline and PBO)



In summary, anastrozole therapy significantly increased serum T and modestly lowered estradiol in men 60+ with symptomatic hypogonadism. Despite the decrease in estradiol, BMD at all sites remained stable. The lack of BMD changes suggests that AI therapy will not adversely affect skeletal integrity in older hypogonadal men. This lack of an effect may be due to the relatively small decrease in serum estradiol, the concomitant increase in T, or both. Assessment of bone turnover markers and geometry of DXA bone images may provide further insight into the effects of this intervention on the skeleton.

**Disclosures:** B.Z. Leder, Amgen 2; Novartis 1; AstraZeneca 5.

This study received funding from: National Institute of Health grants K23-RR-161310 (to BZL), R01-AG-025099-03 (to BZL), M01-RR-01066 (to the Mallinckrodt GCRC) and AstraZeneca Pharmaceuticals.

## 1136

**Mechanism of Action of the Anti-Aging Agent Resveratrol on bone.** M. Zhao<sup>1</sup>, S. Ko<sup>\*1</sup>, J. R. Edwards<sup>1</sup>, I. R. Garrett<sup>2</sup>, G. R. Mundy<sup>1</sup>. <sup>1</sup>Vanderbilt Center for Bone Biology, Medicine/Clinical Pharmacology, Vanderbilt University, Nashville, TN, USA, <sup>2</sup>Bone and Drug Device R&D, Orthobiologics Zimmer, Inc, Austin, TX, USA.

The anti-aging natural product resveratrol has been shown to increase bone mass in rats, but the mechanism of action is unknown. Recently, we have found that the longevity-associated gene SIRT-1, an NAD<sup>+</sup>-dependent histone deacetylase, is required for maintenance of normal bone mass, since mice null for SIRT-1 have decreased bone mass associated with decreased osteoblast differentiation and increased osteoclast activity. Independently, resveratrol has been shown to be an agonist of SIRT-1. Therefore, we determined if the mechanism of action of resveratrol on bone formation is mediated by agonist effects on SIRT-1 in osteoblasts. We examined the expression profile of the SIRT-1 gene in 2T3 osteoblastic cells, and found that SIRT-1 mRNA expression correlated with osteoblast differentiation. We then found that resveratrol treatment dose-dependently increased SIRT-1 mRNA expression in 2T3 osteoblasts and promoted osteoblast differentiation of these cells, as assessed by real time PCR and ALP activity. Next, we determined the relationship between SIRT-1, eNOS and resveratrol. Our reasons for doing this were several-fold. eNOS null mice have decreased bone mass (Armour et al, 2001), indicating that eNOS is required for normal postnatal bone formation, and the eNOS null mouse bone phenotype mimics that of the SIRT-1 bone phenotype. SIRT-1 has been shown to activate eNOS in other cell types, because of its deacetylase activity. Thus, we hypothesized that resveratrol, a SIRT-1 agonist, may sequentially increase both SIRT-1 and eNOS in osteoblasts. Therefore, we examined the effects of resveratrol on eNOS enzymatic activity and mRNA expression in osteoblasts. We found that resveratrol not only dose-dependently increased production of the eNOS product nitric oxide (NO), but also enhanced eNOS mRNA expression in osteoblasts. Next, we examined the effects of eNOS/NO on BMP-2 expression in osteoblasts. We found that incubation of 2T3 osteoblastic cells or calvarial bone organ culture with NO donors (SNP, NOC22) enhanced BMP-2 mRNA expression, osteoblast differentiation and bone formation. Using eNOS knockout mice, we found that eNOS deficiency in osteoblasts inhibited BMP-2 transcription and osteoblast differentiation. Importantly, we found that administration of resveratrol to eNOS null osteoblasts did not enhance BMP-2 gene expression and cell differentiation. Together, these data suggest that resveratrol increases SIRT-1 expression and activity, and in turn eNOS expression and activity, and by this mechanism, stimulates BMP-2 expression, osteoblast differentiation and bone formation.

**Disclosures:** M. Zhao, None.

## 1137

**Stimulation of Fracture Healing by Recombinant Human Platelet-Derived Growth Factor BB (rhPDGF-BB) Combined with  $\beta$ -Tricalcium Phosphate/Collagen Matrix in a Diabetic Rat Fracture Model.** L. Al-Zube<sup>1</sup>, E. A. Breitbart<sup>\*1</sup>, A. M. Simon<sup>\*1</sup>, J. P. O'Connor<sup>\*1</sup>, C. S. Young<sup>2</sup>, G. Bradica<sup>\*3</sup>, C. E. Hart<sup>\*2</sup>, D. S. Perrien<sup>2</sup>, S. Lin<sup>2</sup>. <sup>1</sup>NJMS-UMDNJ, Newark, NJ, USA, <sup>2</sup>BioMimetic Therapeutics, Inc., Franklin, TN, USA, <sup>3</sup>Kensey Nash Corporation, Exton, PA, USA.

Diabetes impairs fracture healing and has become a significant challenge in orthopedic surgery. rhPDGF-BB is a potent growth factor that is chemotactic and mitogenic to mature osteoblasts, osteoprogenitor cells and mesenchymal stem cells and synergizes with VEGF to enhance neovascularization. This study evaluated the use of rhPDGF-BB (PDGF), combined with an injectable  $\beta$ -TCP/collagen matrix formulation (GEM OS2), to enhance fracture healing in a diabetic rat. Male BB Wistar rats that spontaneously develop diabetes at ~85 days of age were used for the study. Upon diabetic conversion, blood glucose levels were maintained between 300 and 500 mg/dl representing poorly controlled Type 1 diabetes. 2 wk after conversion, rats were divided among 4 treatment groups: fracture alone (Untreated), fracture+buffer+ $\beta$ -TCP/collagen (Matrix), fracture+0.3 mg/ml PDGF+ $\beta$ -TCP/collagen (Low Dose), and fracture+1.0 mg/ml PDGF+ $\beta$ -TCP/collagen (High Dose). A closed mid-diaphyseal femoral fracture was created by blunt trauma and stabilized by an intramedullary Kirschner wire. After stabilization, the fracture was exposed, test compound implanted, and wound closed. BrdU staining at 4 d post-fracture revealed proliferation in the callus region was significantly higher for both PDGF groups compared to Untreated and Matrix groups ( $p < 0.05$ ). Torsion testing at 8 wk demonstrated a significant increase ( $p < 0.05$ ) in torque to failure as a percentage of the contralateral limb for the Low Dose group compared to Untreated and Buffer groups. Histological analysis at 12 wk showed a significant increase ( $p < 0.02$ ) in percent mineralized area in the calluses from the High Dose group compared to the other three groups. Diabetes impairs the fracture healing process beginning with a reduction in early cellular proliferation and ending with a decrease in biomechanical properties of the fracture callus. These data demonstrated that rhPDGF-BB can increase cellular proliferation in the early diabetic callus leading to improved mechanical properties and accelerated histological maturation at later time points. These results suggest a therapeutic potential for local rhPDGF-BB treatment in normalizing impaired fracture healing, specifically through stimulating cellular proliferation.

**Disclosures:** L. Al-Zube, BioMimetic Therapeutics, Inc. 3.  
This study received funding from: BioMimetic Therapeutics, Inc.

## 1138

**Anti-Sclerostin Antibody Increases Bone Mass by Stimulating Bone Formation and Inhibiting Bone Resorption in a Hindlimb-Immobilization Rat Model.** W. S. S. Jee<sup>1</sup>, X. Li<sup>2</sup>, X. Y. Tian<sup>\*1</sup>, C. Paszty<sup>2</sup>, H. Z. Ke<sup>2</sup>. <sup>1</sup>University of Utah, Salt Lake City, UT, USA, <sup>2</sup>Metabolic Disorders, Amgen Inc., Thousand Oaks, CA, USA.

Anti-sclerostin monoclonal antibody (Scl-Ab) has been shown to increase bone mass and bone strength by stimulating modeling-based bone formation in an ovariectomy-induced bone loss rat model. Experimental evidence has suggested that over-loading decreases sclerostin expression and under-loading/diuse increases sclerostin expression. The purpose of this study was to determine the effects of Scl-Ab in an immobilization/diuse-induced bone loss model in which there is both a decrease in bone formation and an increase in bone resorption in the immobilized limb. Ten-month-old male S-D rats were divided into normal weight-bearing (normal-loaded, NL) and right hindlimb immobilization (under-loaded, UL) groups. Both NL and UL animals were administered Scl-Ab at 5 or 25 mg/kg by s.c. injection, 2x/week for 4 weeks. Trabecular bone histomorphometric analyses were performed on proximal metaphysis of the immobilized right tibia. Compared with NL controls, short-term (4 weeks) UL in these adult male rats induced a significant increase in eroded surface (ErS/BS, +39%), an index of bone resorption, and a significant decrease in mineral apposition rate (MAR, -25%) and bone formation rate (BFR/BS, -30%), indices of bone formation. Treatment with Scl-Ab at 5 or 25 mg/kg in UL rats induced dose-dependent and significant increases in BV/TV by 45% and 59%, Tb.Th by 38% and 70%, mineralizing surface (MS/BS) by 73% and 121%, MAR by 53% and 76% and BFR/BS by 166% and 294%, and a dose-dependent and significant decrease in ErS/BS by 33% and 42%, respectively, compared with UL rats treated with vehicle. Bone mass and bone formation parameters of the immobilized hindlimb in UL rats treated with Scl-Ab at both doses were significantly higher than in NL rats treated with vehicle, indicating that Scl-Ab treatment not only prevents the UL-induced decrease in bone formation and increase in bone resorption, but also causes increases in bone formation and bone mass above and beyond what is found in the NL vehicle group. Interestingly, the impact of Scl-Ab on bone formation and bone resorption was less pronounced in the immobilized hindlimb of UL rats as compared to its effects on hindlimb of NL rats, suggesting a role for mechanical loading in the magnitude of the response to Scl-Ab treatment. Nonetheless, these data demonstrate that Scl-Ab treatment can significantly increase bone mass in unloaded bone and, additionally, that this is achieved by a simultaneous increase in bone formation and decrease in bone resorption.

**Disclosures:** X. Li, Amgen 5.  
This study received funding from: Amgen.

## 1139

**The Effects of Alendronate or Denosumab on Cortical and Trabecular Bone Mass, Bone Strength, and Bone Mass-Strength Relationships in Mice.** M. S. Ominsky<sup>1</sup>, X. Li<sup>1</sup>, H. Tan<sup>\*1</sup>, F. J. Asuncion<sup>1</sup>, M. Barrero<sup>1</sup>, X. Y. Tian<sup>\*2</sup>, K. S. Warmington<sup>\*1</sup>, D. Dwyer<sup>\*1</sup>, M. Grisanti<sup>1</sup>, M. Stolina<sup>1</sup>, W. S. Jee<sup>\*2</sup>, W. S. Simonet<sup>1</sup>, H. Z. Ke<sup>1</sup>, P. J. Kostenuik<sup>1</sup>. <sup>1</sup>Metabolic Disorders, Amgen Inc., Thousand Oaks, CA, USA, <sup>2</sup>University of Utah School of Medicine, Salt Lake City, UT, USA.

Denosumab (DMAb, a fully human anti-RANKL antibody) and alendronate (ALN, a bisphosphonate) have been shown to reduce bone turnover and to increase bone mass and bone strength in preclinical studies. The extent to which treatment-related increments in bone mass predict changes in bone strength with these two therapeutic classes has not been previously evaluated in the same study. DMAb does not recognize murine RANKL, so this study was performed with "huRANKL" knock-in mice that exclusively express a chimeric (human/murine) form of RANKL that is inhibited by denosumab. Female huRANKL mice (6-8-months-old,  $n = 9$ /group) were treated twice weekly with vehicle (Veh), DMAb (25 mg/kg IV), or alendronate (ALN, 100  $\mu$ g/kg SC) for 6 months. BMD was assessed by DXA, and lumbar vertebrae (LV), tibiae and femurs were collected for histomorphometry, micro-CT, and strength testing. DMAb and ALN each reduced trabecular and cortical bone turnover, as shown by significant reductions in mineralizing surface in LV-2 and at the endocortical surface of the tibia diaphysis. DMAb and ALN significantly increased DXA BMD of the leg and LV1-5, and both agents also increased cortical bone mass at the femur diaphysis and LV-5 by micro-CT. DMAb significantly increased trabecular bone volume and trabecular vBMD at the distal femur and LV-5 compared to Veh, while ALN did not. Three-point testing of femur diaphyses showed significant increases in peak load with DMAb and with ALN (+23 to +25%), whereas compression testing of LV-5 showed significantly greater peak load with DMAb (+53%) but not with ALN (+17% vs. Veh). Linear regression analyses of peak load versus vBMC at both sites revealed positive correlations for each treatment group, including Veh controls (combined  $R^2 = 0.56-0.66$ ). Peak load for each site also showed significant inverse correlations with bone turnover parameters such as serum TRACP-5b and mineralizing surface. These results suggest that bone strength in these mice was related to the degree of bone turnover suppression, with greater suppression predicting higher strength values. The linear relationship between bone mass and bone strength, which was evident in Veh controls, was not significantly altered by 6 months of DMAb or ALN, suggesting that material properties of trabecular and cortical bone were maintained. These data suggest that increments in bone mass with DMAb or ALN might be reasonable surrogates for improvements in bone strength under these conditions.

**Disclosures:** P. J. Kostenuik, Amgen Inc. 5.  
This study received funding from: Amgen Inc.

## 1140

**Androgen Receptor Disruption Increases the Osteogenic Response to Mechanical Loading in Male Mice.** F. Callewaert<sup>\*1</sup>, K. Venken<sup>\*1</sup>, A. Bakker<sup>\*2</sup>, J. Schrooten<sup>\*1</sup>, B. Van Meerbeek<sup>\*1</sup>, S. Boonen<sup>1</sup>, R. Bouillon<sup>1</sup>, G. Verhoeven<sup>\*1</sup>, D. Vanderschueren<sup>1</sup>. <sup>1</sup>Katholieke Universiteit Leuven, Leuven, Belgium, <sup>2</sup>Vrije Universiteit Amsterdam, Amsterdam, Netherlands.

Androgen receptor (AR) and estrogen receptor- $\alpha$  (ER $\alpha$ ) activation are both required to optimize bone mass in male mice. Bone tissue also responds to mechanical loading by increasing bone formation. ER $\alpha$  is involved in the adaptive response of bone to loading, albeit only shown in female mice. To what extent either AR or ER $\alpha$  or both affect the bone's osteogenic response to loading in male mice is not known. Therefore, the role of AR and/or ER $\alpha$  activation in the response to *in vivo* loading was investigated in male and female knockout (KO) mice. The left ulnae of 20-22 week-old male WT ( $n=9$ ), ARKO ( $n=7$ ), ER $\alpha$ KO ( $n=7$ ) and AR-ER $\alpha$  double KO (dKO,  $n=9$ ) mice, as well as the left ulnae of female WT ( $n=7$ ) and ER $\alpha$ KO ( $n=8$ ) mice were subjected to dynamic axial loading for 3 days a week during 2 weeks. Each loading session consisted of 40 cycles with a peak compressive load of 2.5 N. Following each load cycle, there was a rest period of 14.9 s. The right ulnae of these mice served as the nonloaded controls. Bone responses to loading were determined via dynamic histomorphometry, following calcein injections on day 3 and 12 of the loading period.

Compared with the nonloaded ulnae, mechanical loading significantly increased the periosteal bone formation rate (PsBFR) in male WT, ARKO, ER $\alpha$ KO and dKO mice ( $p < 0.05$ ). In female mice, a significant increase in PsBFR occurred only in WT ( $p < 0.01$ ), not in ER $\alpha$ KO mice ( $p = 0.21$ ). Bone formation on the endocortical surfaces of the ulnae was not significantly affected by mechanical loading. In male mice, the loading-induced increase in PsBFR was significantly higher in ARKO (+320%,  $p < 0.05$  vs. WT) and dKO mice (+256%,  $p < 0.05$  vs. WT) compared with WT mice (+114%). This resulted from a higher increase in the periosteal mineral apposition rate (PsMAR) in ARKO and dKO mice compared with WT mice, while the periosteal mineralizing perimeter (PsMinPm) increased to a similar extent in all male groups. ER $\alpha$  disruption did not affect the AR-related increase in PsBFR following loading in dKO mice. Inactivation of ER $\alpha$  in male mice had no apparent effect on the response to loading, since the PsMinPm, PsMAR and PsBFR increased to a similar extent in male ER $\alpha$ KO compared with WT mice. In contrast, ER $\alpha$  inactivation in female mice prevented the loading-induced increase of the PsBFR ( $p < 0.01$  vs. WT).

We conclude that ER $\alpha$  is required for the full osteogenic response to loading in female mice, while ER $\alpha$  disruption in male mice has no apparent effect. In contrast, AR inactivation increases the bone's response to loading in male mice, indicating that AR activation limits the response to loading.

**Disclosures:** F. Callewaert, None.

## 1141

**Low Bone Mass and Decreased Biomechanical Response in Beta 1 Adrenergic Receptor KO but not in Beta 2 Adrenergic Receptor KO Mice.** N. Bonnet, D. Pierroz, S. Ferrari. Geneva University Hospital and Faculty of Medicine, Division of Bone Diseases, Geneva, Switzerland.

Beta 2 adrenergic receptor-deficient mice (*Adrb2R* KO) have high bone mass consecutive to increased bone formation and decreased bone resorption, whereas mice deficient for both beta 1 and 2 adrenergic receptors (*Adrb1-2R* KO) have low bone mass. We raised the hypothesis that  $\beta 1$  and  $\beta 2$  adrenergic signaling may exert opposite effects on bone. To further investigate the role of *Adrb1R* and *Adrb2R* on bone, 3 month-old female *Adrb2R* KO, *Adrb1R* KO and their respective wild type (WT) littermates, as well as *Adrb1-2R* double KO mice were subjected to cyclic axial compression strain (40 cycles, peak 1500 microstrain) of the left tibia for 7 min, 3 days/week during 2 weeks (n=7 mice for each group). The non-loaded right tibia served as a paired control. Bone mass was analyzed by DXA and trabecular and cortical microarchitecture by ex-vivo microCT. Compared to WT littermates, *Adrb2R* KO had higher trabecular bone volume fraction (BV/TV) and thickness (Tb.Th) (+52% and +19% respectively,  $p<0.05$ ) but similar cortical bone volume (C.BV) at the non-loaded tibia, whereas *Adrb1R* KO had lower BV/TV, Tb. number (Tb.N) and C.BV (-45%, -14% and -12% respectively,  $p<0.05$  vs WT). Mechanical stimulation significantly increased BMD in WT littermates and *Adrb2R* KO mice, but not in *Adrb1R* KO nor *Adrb1-2R* KO mice (Table).

Group	Loaded-unloaded tibia BMD (mg/cm <sup>2</sup> )		Unloaded tibia BMD gain (%)		Loaded tibia BMD gain (%)	
	KO	WT	KO	WT	KO	WT
<i>Adrb2R</i>	6 ± 0.5 *	4 ± 0.5 *	0	+1.85	+8.1 *	+6.6 *
<i>Adrb1R</i>	0 ± 0.5 #	9 ± 0.5 *	-1.85	-1.72	+1.72 #	+7.4 *
<i>Adrb12R</i>	1 ± 1	NA	-1.75	NA	0	NA

\*  $p<0.05$  for compression effect; #  $p<0.05$  vs WT littermate. NA, not available.

Hence, the BMD response to compression was significantly greater in *Adrb2R* KO than *Adrb1R* KO and *Adrb1-2R* KO mice. Similarly, BV/TV and Tb.Th increased in loaded tibias of WT littermates and *Adrb2R* KO mice, but not in *Adrb1R* KO nor *Adrb1-2R* KO mice. Moreover, *Adrb2R* KO mice had a significant increase of C.BV at the tibial midshaft in response to mechanical stimulation (+11%,  $p<0.01$  by paired T-test), whereas other groups did not.

These results confirm that *Adrb2R* KO mice have high bone mass whereas *Adrb1R* KO mice have low bone mass. Furthermore, the response to mechanical loading was preserved and possibly increased in *Adrb2R* KO mice, consistent with  $\beta 2$ -adrenergic inhibitory effects on bone formation, whereas mechanical loading was not effective in absence of  $\beta 1$ -adrenergic signalling, consistent with *Adrb1* stimulatory effects on bone formation. The lack of mechanical response in *Adrb1-2R* KO mice further suggests that  $\beta 1$ -adrenergic effects on bone may predominate on  $\beta 2$ -adrenergic effects.

**Disclosures:** N. Bonnet, None.

## 1142

**Anabolic Response to Skeletal Loading in Mice with Targeted Disruption of Pleiotrophin Gene.** C. Kesavan, S. Mohan. Musculoskeletal Disease Center, Jerry L Pettis VA Medical Center, Loma Linda, CA, USA.

Bone formation induced by mechanical loading (ML) results from increased recruitment, proliferation and differentiation of osteoblast lineage cells. Pleiotrophin (PTN), an extracellular matrix associated protein, implicated in diverse functions, is also involved in recruitment of the osteoblasts to the site of bone formation. In a recently published study using whole genome microarray approach to identify the genes and the signal pathways responsible for ML-induced bone formation, we found that PTN expression was increased by 4-fold in response to ML in a good responder C57BL/6J (B6) mice. Furthermore, transgenic overexpression of PTN in mice resulted in increased bone formation. Therefore, we sought to determine whether the anabolic effects of ML on bone formation are mediated by PTN. We first evaluated time course effects of ML on expression levels of PTN gene using real time RT-PCR in 10 week old female B6 mice. A 9N load was applied using a four-point bending device at 2Hz frequency for 36 cycles, once per day for 2, 4 and 12 days on the right tibia and the left tibia was used as internal control. Four-point bending caused an acute increase in PTN expression (2-fold) within 2 days of loading and further increased (3 to 6 fold) with continued loading (4 to 12 days). The increase in PTN expression in response to ML was also seen in 16 and 36-week old mice. Based on these findings, we next used mice with targeted disruption of PTN gene to evaluate the cause and effect relationship between the change in PTN expression and ML induced changes in bone response. Since the mechanical strain produced by a given load depends largely on bone size, we measured periosteal circumference in the tibia of knockout (KO) and control mice and found no differences ( $4.55\pm 0.24$  vs  $4.69\pm 0.21$ ,  $p=0.50$ ). We, therefore, applied 9N load for both groups of mice (n=6-7). Quantitative analysis of ML-induced skeletal response measured by pQCT showed that two weeks of four point bending increased vBMD and bone size by 8% and 6% respectively in the PTN KO mice compared to the 11% and 8% increases seen in the littermate control mice. Although BMD and bone size response to ML were reduced by 23% ( $p=0.21$ ) and 18% ( $p=0.13$ ) respectively in PTN KO mice compared to control mice, these changes were not statistically significant. The issue of whether lack of significant difference in ML response between PTN KO and control mice is due to compensation by other members of PTN family is being pursued. In conclusion, our findings using PTN KO mice seem to suggest that PTN is not a key upstream mediator of the anabolic effects of ML on the skeleton.

**Disclosures:** C. Kesavan, None.

This study received funding from: U.S. Army.

## 1143

**Inhibition of Bone Biomechanical Response to Physical Activity and Loading in Mice Lacking Periostin.** N. Bonnet<sup>1</sup>, S. Conway<sup>\*2</sup>, S. Ferrari<sup>1</sup>. <sup>1</sup>Geneva University Hospital and Faculty of Medicine, Division of Bone Diseases, Geneva, Switzerland, <sup>2</sup>Indiana University School of Medicine, Wells Center for Pediatric Research, Indiana, IN, USA.

Periostin is an osteoblast-specific factor involved in cell recruitment and adhesion. We previously reported that periostin-deficient mice (POSTN <sup>-/-</sup>) mice have low bone mass and altered cancellous and cortical bone microarchitecture. Here we investigate the role of periostin on bone microstructure and strength in response to active and passive mechanical stimuli.

Three month-old female POSTN <sup>-/-</sup>, <sup>+/+</sup> and <sup>+/-</sup> mice were subjected to treadmill exercise (EXE) (45min/day, 5days/week) for 5 weeks or left untrained (UN). Another group of mice received direct mechanical stimulation by cyclic axial compression strain (40 cycles, peak 1500 microstrain), applied to the left tibia for 7 min, 3 days/week for a period of 2 weeks, while the right unloaded tibia served as paired control. Bone mass was analyzed by DXA, trabecular and cortical microarchitecture by ex-vivo microcomputed tomography, biomechanical properties by 3 point bending, and bone formation indices by histomorphometry of the tibia.

In <sup>+/+</sup> mice, EXE significantly increased BMD gain at the tibia compared to UN ( $+6.2\pm 3\text{mg/cm}^2$  vs  $+0.8\pm 2\text{mg/cm}^2$ ,  $p<0.05$ ), as well as trabecular bone volume fraction (Tb. BV/TV) and Tb. number (TbN) (+25% and +16%, respectively, in EXE vs UN,  $p<0.01$ ). Similar trends were observed on cortical bone volume (C.BV) and thickness (C.Th) at the tibial midshaft. Histomorphometric analysis indicated higher MAR, BFR and MP/BP at periosteum in EXE vs UN (+316%, +550% and +364%, respectively,  $p<0.01$ ). In contrast, exercise had no effect on BMD, BV/TV, TbN, C.Th, or bone formation indices in POSTN <sup>-/-</sup> nor <sup>+/-</sup> mice. As a consequence, the stiffness, elastic energy and the Young modulus were significantly higher in EXE vs UN among <sup>+/+</sup> mice (+36%, +25% and +30% respectively,  $p<0.05$ ), but not <sup>-/-</sup> nor <sup>+/-</sup> mice. Following axial compression, the loaded tibia had a significantly higher C.BV, C.Th, and periosteal MP/BP compared to the non-loaded tibia in both <sup>+/+</sup> and <sup>+/-</sup> mice, whereas <sup>-/-</sup> mice remained unaffected.

These results indicate that periostin plays an important role in the mechanotransduction of physical activity and loading stimuli. The cellular and molecular mechanisms by which periostin decreases the threshold for bone formation are currently under investigation.

**Disclosures:** N. Bonnet, None.

## 1144

**Regulation of Parameters of Bone Quality by MMP-2 and MMP-9.** J. S. Nyman<sup>1</sup>, S. Thiolloy<sup>\*2</sup>, C. C. Lynch<sup>\*1</sup>, C. A. Patil<sup>\*3</sup>, T. Yoshii<sup>\*1</sup>, E. O'Quinn<sup>\*1</sup>, A. Mahadevan-Jansen<sup>\*3</sup>, G. R. Mundy<sup>1</sup>. <sup>1</sup>Orthopaedics and Rehabilitation, Vanderbilt Center for Bone Biology, Nashville, TN, USA, <sup>2</sup>Cancer Biology, Vanderbilt University School of Medicine, Nashville, TN, USA, <sup>3</sup>Biomedical Engineering, Vanderbilt University, Nashville, TN, USA.

Bone quality is regulated independent of bone size, and one aspect of bone quality is type I collagen. Factors influencing collagen integrity have not been fully characterized. Gelatinases could be one such factor because they process denatured collagen and are expressed by bone cells. To test the hypothesis that gelatinases affect bone quality, we characterized the compositional, architectural, and biomechanical properties of bones in mice null for 2 gelatinases, MMP-2 and -9.

The left femur and left tibia of wild-type, MMP-2 or MMP-9 null mice (FVB background) were harvested at 16 weeks of age. Subsequently, we assessed 1) geometrical and structural properties of the diaphysis, trabecular bone architecture of the metaphysis and bone mineral density (BMD) by  $\mu$ CT; 2) compositional properties by Raman spectroscopy; and 3) biomechanical properties by three point bending. One-way ANOVA tested for statistically significant differences, followed by pair-wise comparisons when indicated. Femurs from MMP-2 null mice have reduced BMD and thinner cortices compared to wild-type controls. Raman spectroscopy further revealed that the tissue mineral of the null mice had poorer crystal structure (greater carbonate substitution) than that of controls. In addition, MMP-2 null femurs were 48% weaker and 32% less stiff than control femurs. When accounting for the structure of the diaphysis using the moment of inertia, the material yield strength and modulus was less in the MMP-2 null than in the control mice. In the tibia, MMP-2 deficiency caused a significant 30% decrease in bone volume fraction, and this loss was due to fewer numbers of trabeculae, not thinner trabeculae. Interestingly, MMP-9 deletion had a markedly different effect in that null femurs had a lower moment of inertia, greater BMD, thicker cortices, and higher modulus than the controls. MMP-9 did not have any effect on trabecular bone volume and architecture in the tibia. The present findings demonstrate that MMP-2 contributes to bone quality by influencing volumetric BMD, mineral lattice structure, and trabecular architecture independent of bone size. MMP-9 appears to influence bone structure and has modest effects on BMD and modulus of cortical bone. These differential roles for the gelatinases are surprising given the significant substrate overlap between the proteases. Our results have important implications in understanding how proteases contribute to bone quality and for the therapeutic development of protease inhibitors that could control specific aspects of bone quality.

**Disclosures:** J.S. Nyman, None.

## 1145

**NFATc1 Mediates HDAC-dependent Transcriptional Repression of Osteocalcin Expression During Osteoblast Differentiation.** M. K. Choo\*, H. Yeo\*, M. Zayzafoon. Department of Pathology, The University of Alabama at Birmingham, Birmingham, AL, USA.

Nuclear Factor of Activated T Cells (NFAT) is a transcription factor that plays a crucial role in the activation of T lymphocytes. We recently reported that the *in vivo* and *in vitro* pharmacologic or genetic suppression of NFAT signaling increases osteoblast differentiation and bone formation. To investigate the mechanism by which NFATc1 regulates osteoblast differentiation, we established an osteoblast cell line that overexpresses a constitutively active NFATc1 (ca-NFATc1). The activation of NFATc1 in ca-NFATc1 cells was demonstrated by the nuclear localization of NFATc1 protein using western blotting and immunofluorescence staining techniques and by an increase in NFAT transactivation (700 %) as compared to parent or GFP-transduced MC3T3-E1 osteoblasts. The activation of NFATc1 in osteoblasts dramatically inhibited osteoblast differentiation and function, demonstrated by inhibition of alkaline phosphatase activity and mineralization and by an 85% decrease in osteocalcin gene expression, a late marker of osteoblast differentiation. NFATc1-inhibition of osteocalcin gene expression was due to a 70% repression of the osteocalcin promoter activity and more specifically by an 80% decrease in TCF/LEF transactivation, which has previously been shown to be an important regulatory element of this promoter. This repression occurs through the action of histone deacetylase 3 (HDAC3). Here, we show the decrease in total HDAC activity during osteoblast differentiation that leads to hyperacetylation of histones H3 and H4 in MC3T3-E1 osteoblasts is completely blocked by the overexpression of NFATc1. Specifically, we demonstrate by immunoprecipitation assay that NFATc1 and HDAC3 can physically interact. Furthermore, we show by chromatin immunoprecipitation (ChIP) assay that the association of HDAC3 with NFATc1 at the TCF/LEF consensus sequence of the osteocalcin promoter is decreased in MC3T3-GFP cells during osteoblast differentiation. However, the overexpression of NFATc1 sustains the presence of HDAC3 at TCF/LEF sequence on the osteocalcin promoter resulting in hypoacetylation of histones H3 and H4, and ultimately causing a persistent inhibition of osteocalcin gene expression and osteoblast differentiation. These results indicate that NFATc1 acts as a transcriptional co-repressor of osteocalcin promoter in an HDAC3-dependent manner.

**Disclosures:** *M.K. Choo, None.*

*This study received funding from: NIH/NIAMS/ AR053898.*

## 1146

**Circulating Osteoblast Lineage Cells Increase with PTH Treatment of Hypoparathyroidism.** M. R. Rubin, D. Dempster, S. Cremers, H. Zhou, D. McMahon, J. Sliney\*, S. Kousteni, J. Shah\*, J. S. Manavalan\*. Columbia, New York, NY, USA.

It has been hypothesized that PTH increases bone formation by increasing the supply of osteoblast precursors. These cells can be detected in the peripheral blood (PB) by flow cytometry using antibodies specific for osteoblast-specific ligands, such as osteocalcin (OCN), CD34 (an early hematopoietic stem cell marker) and CD146 (an early mesenchymal stem cell marker). To evaluate the effects of PTH deficiency and replacement on these cells, we studied 9 hypoparathyroid (hypoPT) subjects (1 male; 4 postmenopausal; 53 ± 9 yrs) at baseline in comparison to 9 age-, sex- and menopause-matched controls (Ctls). HypoPT subjects were also studied after 1, 2, 3 and 6 months (mo) of PTH(1-84) treatment (100 µg qod). Changes in osteoblast precursors in HypoPT were correlated with changes in biochemical markers of bone formation at these intervals (n=9) and with dynamic histomorphometric variables of bone formation with quadruple-labeled iliac crest bone biopsies after 3 mo of PTH treatment (n=2).

At baseline, the percent of PB cells expressing OCN (%OCN+ cells) in HypoPT was significantly lower than in Ctls (1.1 ± 1 vs 2.3 ± 1%, p=0.004). With PTH treatment, % OCN+ cells increased from baseline (1.1 ± 1%), to 1 mo (2.5 ± 2%, p=0.009), peaked at 2 mo (4.5 ± 2%, p<0.0001), started to fall at 3 mo (2.9 ± 3%, p=0.002) and returned to baseline levels by 6 mo (0.9 ± 3%, p=NS). The proportion of OCN+ cells that did not express CD34 (OCN+/CD34-) rose with PTH treatment (baseline: 48 ± 17%; 1 mo: 68 ± 17%, p<0.0001; 2 mo: 76 ± 17%, p<0.0001; 3 mo: 78 ± 18%, p<0.0001; 6 mo: 73 ± 27%, p<0.0001). Within the OCN+/CD34- population, the proportion of cells that were CD146+ (OCN+/CD34-/CD146+) increased with PTH treatment from baseline to 6 mo (8.3 ± 14 to 19.2 ± 21%, p=0.02).

The increase in the %OCN+/CD34-/CD146+ cells with PTH treatment was associated with increases in biochemical markers of bone formation, including P1NP (slope 1.8 ± 0.8; p=0.04), BSAP (slope 0.45 ± 0.2; p=0.006) and osteocalcin (slope 0.30 ± 0.14; p=0.04). Increases in osteoblast precursors also predicted increases in histomorphometric variables of bone formation: as % total OCN+ cells increased, so did cancellous osteoblast perimeter (slope 0.75 ± 0.2; p=0.02), and as % OCN+/CD34- cells increased, so did intracortical mineralized perimeter (slope 0.20 ± 0.08; p=0.04).

HypoPT subjects have reduced osteoblast lineage cells compared to normals. With PTH treatment, they experience a clinically significant increase in the number of such cells, specifically those with a more mature (OCN+/CD34-) phenotype. Moreover, the close association with biochemical and histomorphometric indices suggests that these circulating cells with osteoblast characteristics might be representative of osteoblast activities in bone.

**Disclosures:** *M.R. Rubin, None.*

## 1147

**Telomerase Deficiency Leads to Decrease Bone Mass and Impaired Mesenchymal Stem Cells (MSC) Functions in Telomerase Deficient (TERC<sup>-/-</sup>) Mice.** H. Saeed\*, B. Abdallah, M. Kassem. KMEB lab, Department of Endocrinology, OUH, University of Southren Denmark, Odense, Denmark.

We have previously demonstrated that telomere shortening leads to *in vitro* replicative senescence of human mesenchymal stem cells (MSC) and telomerase over expression leads to telomere elongation, extended life span and enhanced bone formation (Simonsen et al (2002), Nature Biotechnology 20:592). In order to study the role of telomerase in MSC biology *in vivo*, we studied the phenotype of telomerase deficient mice caused by absence of telomerase RNA component (TERC<sup>-/-</sup>). TERC<sup>-/-</sup> displayed diminish bone mass already at 3 month of age and during 12 month follow up period (BMD (gm/cm<sup>3</sup>): TERC<sup>-/-</sup> 0.04173 vs. wild type (WT) 0.05941, p<0.0005). The decreased bone mass was associated with reduced total number of CFU-F and alkaline phosphatase positive (AP+) colonies compared to WT (P<0.005). Moreover, MSC revealed lower proliferation rate, accumulation of senescent cells, increased DNA damage (high levels of γH2AX staining) and decreased osteoblastic (OB) differentiation marker expression compared with WT. Similar impairment of *in vitro* OB differentiation of TERC<sup>-/-</sup> mouse embryonic fibroblast (MEF) was observed as well as decreased ectopic bone formation capacity when the cells implanted subcutaneously in immune deficient mice. Osteogenic super-array analysis of group of TERC<sup>-/-</sup> bone samples revealed decreased expression of several genes, like Tgfb1, Runx2, Tfp11, collagens, Igf1, Dmp1, Twist1, Phex, Tuf1 and more, known to be involved in osteoblast commitment, proliferation and maturation. Our data demonstrate that telomerase plays an important role in maintenance of stem cell functions and activation of telomerase in MSC can be a novel strategy for abolishing age-related bone loss.

**Disclosures:** *H. Saeed, None.*

*This study received funding from: Novo Nordisk Foundation.*

## 1148

**Targeted Disruption of PPARγ in Bone Marrow Stromal Cells Reveals Its Role in Aging-Induced Bone Loss.** G. Ou\*<sup>1</sup>, C. Isaacs<sup>2</sup>, M. Hamrick<sup>3</sup>, K. Ding<sup>1</sup>, S. Yang<sup>\*4</sup>, F. Gonzalez<sup>\*5</sup>, B. Kream<sup>6</sup>, X. Shi<sup>7</sup>. <sup>1</sup>Institute of Molecular Medicine and Genetics, Medical College of Georgia, Augusta, GA, USA, <sup>2</sup>Institute of Molecular Medicine & Genetics, and Department of Orthopaedics, Medical College of Georgia, Augusta, GA, USA, <sup>3</sup>Cell Biology, Medical College of Georgia, Augusta, GA, USA, <sup>4</sup>Department of Orthopaedic Surgery, Wayne State University, Detroit, MI, USA, <sup>5</sup>Laboratory of Molecular Carcinogenesis, National Cancer Institute, NIH, Bethesda, MD, USA, <sup>6</sup>Departments of Medicine and Genetics and Developmental Biology, University of Connecticut Health Center, Farmington, CT, USA, <sup>7</sup>Institute of Molecular Medicine & Genetics, and Department of Pathology, Medical College of Georgia, Augusta, GA, USA.

Peroxisome proliferator-activated receptor gamma-2 (PPARγ2), a key regulator of adipogenesis, has been implicated in osteoblast differentiation and bone formation. However, due to the embryonic lethality of global PPARγ gene knockout, the effect of tissue-specific PPARγ deficiency on bone development is unknown. Using a Cre/LoxP system we generated mice in which PPARγ gene is selectively ablated from the bone marrow stromal/progenitor cells (BMSCs), the precursors of the osteoblasts and the adipocytes, and examined the bone phenotype of these mice. We provide evidence to show that 1) the 3.6kb rat type I collagen promoter DNA fragment, which was previously thought to target preosteoblasts, is active and drives the expression of Cre recombinase robustly in BMSCs; 2) PPARγ null BMSCs attain significantly enhanced osteogenic differentiation capability in the expense of a complete loss of the ability for adipogenic differentiation; and 3) mice with BMSC-specific PPARγ gene knockout show increased bone mass preferentially at the spine of older mice, but not the younger ones, which is strikingly different from the PPARγ heterozygous mice as reported previously. Since bone remodeling is a key event maintaining the balance of bone metabolism throughout the life, these studies suggest that reducing the levels of PPARγ expression or inhibition of its activity would be promising strategies for reduction or prevention of bone loss induced by aging or medication such as anti-diabetic TZDs.

**Disclosures:** *X. Shi, None.*

*This study received funding from: Medical College of Georgia.*

## 1149

**Progressive Lipodystrophy in the Osteosclerotic Mice Over-expressing Fra1.** J. Luther<sup>\*1</sup>, M. Megges<sup>\*1</sup>, F. Driessler<sup>\*1</sup>, V. Mandic<sup>\*1</sup>, C. Zech<sup>\*1</sup>, G. Schett<sup>\*2</sup>, J. David<sup>\*2</sup>. <sup>1</sup>Bone Cell Differentiation, Deutsches Rheuma-Forschungszentrum, Berlin, Germany, <sup>2</sup>Department of Internal Medicine 3 and Institute for Clinical Immunology, University of Erlangen-Nuremberg, Erlangen, Germany.

A link between bone and fat mass has been established the last few years suggesting that common molecular mechanism are shared between osteoblast and adipocyte differentiation. We therefore analyzed the role the osteogenic transcription factor Fra1 in fat. *In vitro*, the adipogenic differentiation of primary osteoblast (POBs) isolated from the calvaria of pups over-expressing Fra1 (*fra1*-tg mice) was found to be drastically reduced when compared to wild type littermates. This effect was Fra1-dependent since constitutive or inducible over-expression of Fra1 in adipogenic cell line strongly inhibited adipocyte differentiation. It was not due to decreased cell growth. At the molecular level, the response to insulin as measured by ERK and AKT activation was unaffected. Although, the expression of key regulator of mesenchymal cell fate decision (i.e. *Runx2*, *Sox9* and *MyoD*) was unchanged; we found the adipogenic transcription factors *C/ebpβ* and *C/ebpα* to be down regulated in *fra1*-tg POBs and in adipogenic cell lines over-expressing Fra1. Consequently, *Pparγ* was also down-regulated in Fra1 over-expressing cells. The relevance of these observations was established by the finding that *fra1* transgenic (*fra1*-tg) mice that developed progressive osteosclerosis due to increased osteoblast differentiation are also developing a parallel drastic progressive lipodystrophy leading to total absence of fat tissue. The phenotype was found to be more pronounced in the females than in the males. Histologically, when present, the fat tissue appears to be immature and to be expressing high level of *Fra1* and lower level of the adipogenic marker *aP2* and *Glut4* as well as *C/ebpβ*.

Thus, our data suggest that Fra1 is promoting osteoblastogenesis and inhibiting adipogenesis this latter being caused by C/EBPβ and C/EBPα down-regulation. In addition, they demonstrate that increased bone mass can be observed in lean mice.

**Disclosures:** J. Luther, None.

This study received funding from: DFG-SFB760.

## 1150

**Abrogation of Cbl-PI3K Interaction in Mice Results in Increased Bone Volume and Osteoblast Proliferation.** T. A. Brennan<sup>1</sup>, N. Adapala<sup>\*1</sup>, Y. Yingling<sup>2</sup>, F. Safadi<sup>1</sup>, S. Popoff<sup>1</sup>, P. Marie<sup>\*3</sup>, M. Barbe<sup>1</sup>, A. Sanjay<sup>1</sup>. <sup>1</sup>Anatomy and Cell biology, Temple University, Philadelphia, PA, USA, <sup>2</sup>Kinesiology, Temple University, Philadelphia, PA, USA, <sup>3</sup>INSERM, Paris, France.

The mammalian members of Cbl family, Cbl and Cbl-b proteins function as E3 ubiquitin ligases and although both proteins are highly homologous in the tyrosine kinase binding and the RING finger domains, there are significant differences between the two proteins in the C-terminal half. One major difference is the presence of the regulatory tyrosine 731 in the C-terminal half of Cbl. When phosphorylated this tyrosine moiety binds to the p85 subunit of phosphatidylinositol 3 kinase (PI3K). PI3K is known to regulate osteoblast apoptosis and survival. We have shown that both the SH2 and the SH3 domains of p85 bind to Cbl. However, substitution of the tyrosine 731 to phenylalanine (Y731F) completely abolishes the binding between Cbl and PI3K indicating that the tyrosine 731 is the major PI3K binding site on Cbl. Recent report suggests that Cbl negatively regulates osteoblast differentiation modulating PI3K/AKT signaling. To investigate the impact of abrogation of Cbl-PI3K interaction on the mouse skeleton we examined the bone phenotype of the Cbl<sup>Y731F</sup> knock-in mice, in which the regulatory tyrosine is substituted to phenylalanine. In contrast to the adult Cbl<sup>-/-</sup> mice, which do not have any overt bone phenotype, micro CT analysis indicated that the bone volume in the Cbl<sup>Y731F</sup> was significantly increased as compared to the control mice (WT 7.45% ± 1.11; Cbl<sup>Y731F</sup> 12.17% ± 1.36; p=0.002 vs. WT). Similarly, trabecular thickness, separation, and numbers were also increased. In contrast to the Cbl<sup>-/-</sup> mice, in which the numbers of osteoblasts were similar to the control mice, there was a 2-fold increase in the numbers of osteoblasts in the age-matched Cbl<sup>Y731F</sup> mice (WT 53/mm<sup>2</sup> ± 2.8; Cbl<sup>-/-</sup> 57/mm<sup>2</sup> ± 0.7. p= n.s. vs. WT; Cbl<sup>Y731F</sup> 104/mm<sup>2</sup> ± 1.4; p=0.001 vs. WT). Increase in bone volume also affects the ability of bones to resist stress therefore we analyzed the mechanical strength of tibiae and femurs from the 12 week-old Cbl<sup>Y731F</sup> and WT mice. A three point bending strength test of whole bone comparing the WT and Cbl<sup>Y731F</sup> tibiae and femur suggested a trend towards increased stiffness (WT 1892 Nmm<sup>2</sup> ± 228; Cbl<sup>Y731F</sup> 2165 Nmm<sup>2</sup> ± 227) and peak moment (WT 29 Nmm ± 0.07; Cbl<sup>Y731F</sup> 28 Nmm ± 1.9) in the Cbl<sup>Y731F</sup> samples indicating increased strength of the adult Cbl<sup>Y731F</sup> bones. Ex vivo analysis of bone marrow-derived Cbl<sup>Y731F</sup> osteoblasts showed a 2-fold increase in proliferation as compared to the WT cells. Taken together, these results show that attenuation of Cbl-PI3K interaction results in increased bone volume and osteoblast proliferation.

**Disclosures:** A. Sanjay, None.

## 1151

**Akt Regulates Skeletal Development Through GSK3, mTOR, and FoxOs.** S. Rokutanda<sup>\*1</sup>, T. Fujita<sup>\*1</sup>, N. Kanatani<sup>\*1</sup>, C. A. Yoshida<sup>\*1</sup>, A. Mizuno<sup>\*2</sup>, T. Komori<sup>1</sup>. <sup>1</sup>Department of Cell Biology, Unit of Basic Medical Sciences, Nagasaki University, Nagasaki, Japan, <sup>2</sup>Department of Oral and Maxillofacial Surgery, Unit of Translational Medicine, Nagasaki University, Nagasaki, Japan.

Akt/protein kinase B is a serine/threonine protein kinase, that is stimulated by IGFs-IGF receptor signaling through PI3K. The lipid product of PI3K, PIP3, recruits PDK1 and Akt to the plasma membrane and Akt is subsequently phosphorylated by PDK1 and by mTORC2 leading to full activation.

The IGFs-IGF receptor-PI3K-Akt pathway plays key roles in skeletal growth and endochondral ossification. Mice deficient either in *Igf1*, *Igf1r* or *Akt1/Akt2* showed retardation of skeletal growth and endochondral ossification. However, the downstream signaling pathways through which Akt regulates those events remain to be clarified.

To shed light on these issues, we generated and analyzed chondrocyte-specific transgenic mice expressing constitutively active Akt (myristoylated Akt; myrAkt) or dominant negative (dn)-Akt under a *Col2a1* promoter. MyrAkt transgenic mice had thickened and shortened endochondral bones. Mineralization was reduced in the limbs but enhanced in the cranial base and vertebrae due to deceleration and acceleration of chondrocyte maturation respectively. Chondrocyte proliferation was stimulated by myrAkt in the resting layer of the limbs and in the vertebrae, but it was inhibited in the limb's proliferating layer. Akt also enhanced cartilage matrix production and cell growth in both limb and vertebral skeletons. On the contrary, dn-Akt transgenic mice had smaller skeletons than wild-type mice, and chondrocyte maturation, proliferation and cartilage matrix production were inhibited, indicating that Akt positively regulates chondrocyte maturation and proliferation, cartilage matrix production, and cell growth in skeletal development.

To understand how Akt regulates these cellular processes, we focused on major Akt downstream signaling molecules: GSK3, mTOR, and FoxOs. Using organ culture systems, we revealed that the Akt-mTOR pathway is responsible for positive regulation of all four cellular processes, that the Akt-FoxO pathway enhances chondrocyte proliferation but inhibits chondrocyte maturation and cartilage matrix production, and that the Akt-GSK3 pathway negatively regulates chondrocyte maturation, proliferation and matrix production in the limbs but not in vertebrae due to less GSK3 expression in the vertebrae.

These findings indicate that Akt positively regulates the cellular processes of skeletal growth and endochondral ossification, tuning the Akt-mTOR, Akt-FoxO, and Akt-GSK3 pathways accordingly to each skeletal element.

**Disclosures:** S. Rokutanda, None.

This study received funding from: The Japanese Ministry of Education, Culture, Sports, Science and Technology, the Uehara Memorial Foundation and the Japan Society for the Promotion of Science.

## 1152

**Dwarfism and Osteopenia in Mice with Inactivated Hypoxia-Response Element in the VEGF Gene Promoter.** C. Maes<sup>1</sup>, L. Coenegrachts<sup>\*1</sup>, I. Stockmans<sup>\*1</sup>, N. Smets<sup>\*1</sup>, P. Carmeliet<sup>\*2</sup>, R. Bouillon<sup>1</sup>, G. Carmeliet<sup>1</sup>.

<sup>1</sup>Laboratory of Experimental Medicine & Endocrinology, K.U.Leuven, Leuven, Belgium, <sup>2</sup>V.I.B. Vesalius Research Center, K.U.Leuven, Leuven, Belgium.

VEGF plays multiple crucial roles in cartilage and bone. One of the most potent inducers of VEGF expression is hypoxia, mediated largely through stabilization of the transcription factor hypoxia-inducible factor (HIF) that interacts with the hypoxia-responsive element (HRE) in the VEGF gene promoter. Previous studies provided evidence for important physiological functions for hypoxia and HIF in cartilage and bone. Here, we analyzed the contribution of HIF-mediated transcriptional regulation of VEGF, by investigating bone metabolism in mice lacking the HRE in the VEGF gene promoter (VEGF<sup>HRE</sup> mice).

VEGF<sup>HRE</sup> mice were born at ratios lower than the Mendelian expectation, but surviving mice (1/7) appeared healthy until past 6 months of age, when they started to develop neurodegenerative disease as reported. In newborn as well as 14-week-old mice, we documented 25-40% reduced VEGF protein levels in VEGF<sup>HRE</sup> bones compared with WT (P<0.001), without overt effects on the bone vascularization (histomorphometric analysis of PECAM-1 staining at 1 or 6 days after birth). Throughout life, VEGF<sup>HRE</sup> mice were smaller than their WT littermates. Body weights were reduced by 30% until postnatal day 6, but even by 60% at 4 weeks of age. VEGF<sup>HRE</sup> tibias were 20% shorter than those of 4-week-old WT littermates. The impaired postnatal growth was associated with significantly thinner growth plates displaying imbalanced differentiation, as evidenced by the reduced ratio of immature to mature chondrocyte zones. Strikingly, VEGF<sup>HRE</sup> mice displayed a severe deficit in mineralized bone mass at 4 weeks of age (bone volume/total volume (BV/TV) 3.89% versus 7.78% in WT; P<0.01) that drastically aggravated with age. By 14 weeks BV/TV was reduced to 20% (females) or 30% (males) of WT values, as measured by histomorphometry and micro-CT. This severe osteopenia in VEGF<sup>HRE</sup> mice was characterized by increased bone turnover. Parameters indicative of osteoclast formation (TRAP staining of bone sections, RANKL expression levels) or activity (urine DPD excretion) were significantly increased. Concomitantly, parameters denoting osteoblast differentiation or functioning were significantly higher as well (expression of Runx2 and osteocalcin, dynamic bone formation (MAR, BFR), relative osteoid surface). The underlying mechanism is our current focus of investigation.

In conclusion, the dwarfism and severe osteopenia of VEGF<sup>HRE</sup> mice underscore the importance of HIF-regulated VEGF expression in cartilage and bone metabolism and suggest a novel role for (mild changes in the levels of) VEGF in the development of age-related osteoporosis.

**Disclosures:** C. Maes, None.



## 1153

**Deletion of the Oxygen-sensor PHD2 in Chondrocytes Results in Increased Cartilage and Bone Mineralization.** K. Laperre<sup>\*1</sup>, P. Fraaij<sup>\*2</sup>, R. Van Looveren<sup>\*1</sup>, R. Bouillon<sup>1</sup>, P. Carmeliet<sup>\*2</sup>, G. Carmeliet<sup>1</sup>. <sup>1</sup>Laboratory of Experimental Medicine and Endocrinology, K.U.Leuven, Leuven, Belgium, <sup>2</sup>VIB Vesalius Research Center, K.U.Leuven, Leuven, Belgium.

During bone development, the avascular growth plate progressively enlarges resulting in a hypoxic centre. Consequently, hypoxia inducible factor (HIF $\alpha$ ) becomes stabilized which is crucial for chondrocyte survival and angiogenic invasion. When normoxia is restored, HIF $\alpha$  is targeted for proteasomal degradation after hydroxylation by prolyl-hydroxylase-domain containing proteins (PHD1, PHD2 and PHD3).

Here we analyzed the contribution of PHD2 in growth plate homeostasis. We therefore generated chondrocyte-specific PHD2 null mice by crossing PHD2<sup>fl/fl</sup> with collagen 2-cre mice (PHD2<sup>fl/Col2</sup><sup>Cre+</sup>) resulting in a selective and efficient deletion of PHD2. Accordingly, cultured PHD2 null chondrocytes displayed highly increased HIF1 $\alpha$  levels. PHD2<sup>fl/Col2</sup><sup>Cre+</sup> neonates were born at the expected Mendelian ratio and were morphologically indistinguishable from their littermates. However, they quickly became growth retarded and at the age of 14 weeks showed a significant decrease in body weight and femur length. Remarkably, this decreased bone length was associated with increased growth plate mineralization and enhanced trabecular bone volume. In vivo and in vitro analyses did not reveal major differences in osteoblast or osteoclast number or function. However, cartilage matrix was still abundantly present in trabecular bone suggesting impaired matrix remodeling. The chondrocyte phenotype was therefore further investigated.

The growth plates of PHD2<sup>fl/Col2</sup><sup>Cre+</sup> neonates were significantly shorter, due to a decreased length of the proliferating zone. The number and proliferation of chondrocytes was however not altered and no evidence was found for increased apoptosis. Gene expression of Ihh and PTHrP also did not differ between genotypes. On the other hand, the amount of matrix between chondrocytes was decreased in mutant neonates, and could explain the reduced length of this zone. The differentiation to hypertrophic chondrocytes seemed normal as the length of this zone and collagen 10 and MMP13 mRNA levels were similar in both genotypes. Yet, the cartilage matrix was more mineralized in mutant mice. This may be explained by the increase in metaphyseal vascularisation, likely resulting from enhanced VEGF gene expression in the growth plate. In addition, preliminary data suggest that chondrocyte aerobic metabolism is changed in PHD2<sup>fl/Col2</sup><sup>Cre+</sup> mice which may contribute to the altered matrix formation and mineralization.

Taken together, PHD2 expression in chondrocytes is important for normal matrix production and mineralization by regulating HIF-dependent angiogenic and metabolic pathways.

**Disclosures:** K. Laperre, None.

## 1154

**Chondrocyte-derived Ihh Is Required for Osteoblast Differentiation Despite Reconstitution of a Normal Growth Plate.** Y. Maeda<sup>\*1</sup>, E. Schipani<sup>\*2</sup>, B. Lanske<sup>1</sup>. <sup>1</sup>Developmental Biology, HSDM, Boston, MA, USA, <sup>2</sup>Endocrine Unit, MGH and HMS, Boston, MA, USA.

Indian hedgehog (*Ihh*) is essential for chondrocyte proliferation/differentiation and osteoblast differentiation during prenatal endochondral bone formation. We generated tamoxifen-inducible conditional *Ihh* knockout mice (*Col2a1-Cre ER*<sup>+</sup>; *Ihh*<sup>td/d</sup>), in which the *Ihh* gene was ablated from chondrocytes after birth. Our results demonstrated that *Ihh* expression in postnatal chondrocytes is essential for maintaining a growth plate, and for sustaining trabecular bone and eventual bone growth after birth. A decrease in expression of Wnt target genes suggested that *Ihh* activates osteoblast differentiation via the Wnt signaling pathway in postnatal life. However, loss of trabecular bone in the *Col2a1-Cre ER*<sup>+</sup>; *Ihh*<sup>td/d</sup> mutants could be secondary to their growth plate abnormalities. Therefore, to examine the direct role of *Ihh* on postnatal bone formation, maintenance of a growth plate in the mutants would be required. To rescue the growth plate of the *Col2a1-Cre ER*<sup>+</sup>; *Ihh*<sup>td/d</sup> mice we mated them to *col2a1*-constitutively active PTH/PTHrP receptor transgenic mice (Jansen, J). *Col2a1-Cre ER*<sup>+</sup>; *Ihh*<sup>td/d</sup>; J mice were born with the expected Mendelian ratio and subsequently injected with tamoxifen at P0 to produce *Col2a1-Cre ER*<sup>+</sup>; *Ihh*<sup>td/d</sup>; J mice. 7 days later, at P7, loss of *Ihh* and *patched* expression was confirmed. In contrast to the long bones of *Col2a1-Cre ER*<sup>+</sup>; *Ihh*<sup>td/d</sup> which exhibit a disorganized growth plate, the one of *Col2a1-Cre ER*<sup>+</sup>; *Ihh*<sup>td/d</sup>; J mice appeared to be relatively normal showing all layers of chondrocytes. Expression of coll X in the *Col2a1-Cre ER*<sup>+</sup>; *Ihh*<sup>td/d</sup>; J mice was found to be similar to control mice (*Ihh*<sup>fl/fl</sup>), whereas *Col2a1-Cre ER*<sup>+</sup>; *Ihh*<sup>td/d</sup> mice showed excessive coll X expression. Interestingly, expression of beta-catenin, a Wnt signaling target, was still decreased in the bone collar of *Col2a1-Cre ER*<sup>+</sup>; *Ihh*<sup>td/d</sup>; J mice when compared to normal mice, suggesting a direct role of chondrocyte-derived *Ihh* on osteoblast formation that was independent of loss of a growth plate. At P14, *Col2a1-Cre ER*<sup>+</sup>; *Ihh*<sup>td/d</sup>; J mice were smaller in size and displayed a disorganized growth plate with accelerated hypertrophic chondrocyte differentiation as demonstrated by increased collagen X expression, indicating an insufficient expression of the constitutively active *PTHrP* at this stage. In summary, we have demonstrated that a Jansen receptor expressed from chondrocytes can rescue the postnatal growth plate abnormalities in mice lacking *Ihh* expression in chondrocytes. Postnatal expression of *Ihh* in chondrocyte, however, is required for normal induction of Wnt signaling and, therefore, required for normal osteoblast differentiation.

**Disclosures:** Y. Maeda, None.

## 1155

**Regulation of Osteonectin/SPARC by microRNA-29.** K. Kapinas, C. B. Kessler<sup>\*</sup>, A. M. Delany. Center for Molecular Medicine, University of Connecticut Health Center, Farmington, CT, USA.

Matricellular proteins are fundamental regulators of bone remodeling, and the matricellular protein osteonectin (SPARC, BM-40) is the most abundant non-collagenous matrix protein in bone. Osteonectin is critical for the maintenance of bone mass. It promotes osteoblast differentiation and survival, and balances bone formation and resorption in response to PTH. However, the mechanisms regulating its expression remain poorly understood. We sought to characterize the post-transcriptional mechanisms regulating osteonectin in osteoblasts. Using luciferase-mouse osteonectin 3' untranslated region (UTR) reporter constructs, we found that the full length (1 Kb) 3' UTR repressed reporter gene expression by 80% in transiently transfected MC3T3-E1 osteoblasts. Deletion mutagenesis showed that this repression was mediated by the proximal 220 bases of the 3' UTR. The proximal 3' UTR contains a well-conserved motif with potential binding sites for microRNAs (miRs) -29a and -29c, and it repressed gene expression in MC3T3 cells by decreasing mRNA abundance and protein translation. qRT-PCR showed that miR-29a and -29c are expressed in osteoblasts. Transfection of miRNA inhibitors specific for miR-29a or -29c relieved repression mediated by the proximal 3' UTR, indicating that the miRNAs act on this region.

Since bioinformatics suggests that other genes important for osteoblast function may also be targets for miR-29, we determined whether miR-29a and -29c were regulated during osteoblastic differentiation in vitro. In MC3T3 cells, miR-29a, but not miR-29c, was increased 5 fold during osteoblastic differentiation. In parallel, osteonectin mRNA and protein levels were decreased. We previously showed that fibroblast growth factor-2 (FGF-2) decreased osteonectin mRNA stability in MC3T3 cells. Here, we found that FGF-2 increased the expression of miR-29a 3 fold, suggesting a means for controlling transcript stability.

Primary cultures of mouse calvarial osteoblasts were somewhat different from MC3T3 cells with respect to miRNA expression and osteonectin. Both miR-29a and -29c were increased 7 fold during osteoblastic differentiation. Osteonectin transcripts remained relatively unchanged during this time, whereas osteonectin protein levels were decreased. In these cultures, miR29 may repress osteonectin translation, in the absence of changes in transcript stability. Regulation of osteonectin, and likely other matrix components, by the miR-29 family may be critical for appropriate osteoblast differentiation and normal bone balance. Further, this important regulatory mechanism is probably active in other tissues where miR-29 and osteonectin are co-expressed, including adipose, brain, and eye.

**Disclosures:** K. Kapinas, None.

## 1156

**Conditional Knockout of the Ca<sup>2+</sup>-sensing Receptor in Osteoblasts Alters Regulators of Wnt Signaling, Delays Cell Differentiation, and Promotes Apoptosis in Bone.** W. Chang, C. Tu<sup>\*</sup>, T. Chen<sup>\*</sup>, D. Bikle, D. Shoback. Endocrine Unit, VA Medical Center, University of California San Francisco, San Francisco, CA, USA.

Extracellular Ca<sup>2+</sup>-sensing receptors (CaSRs) mediate cellular responses to changes in the extracellular Ca<sup>2+</sup> concentration ([Ca<sup>2+</sup>]<sub>e</sub>) in the parathyroid and kidney. High [Ca<sup>2+</sup>]<sub>e</sub> alter signal transduction, gene expression, and bone remodeling, and it is hypothesized that this occurs via CaSRs in osteoblasts (OBs) and other cells in the bone microenvironment. To test the role of CaSR in skeletal growth and development in vivo, we generated mice (<sup>OB</sup>CaSR<sup>Δflox/Δflox</sup>) with conditional knockout of the CaSR gene in OB lineage cells by breeding novel floxed-CaSR (CaSR<sup>lox/flox</sup>) mice with transgenic mice expressing Cre recombinase (Cre) under the control of 2.3 kb type 1 collagen promoter. <sup>OB</sup>CaSR<sup>Δflox/Δflox</sup> mice were growth-retarded and died within 3 weeks of birth. These mice showed severely undermineralized skeletons with excessive osteoid accumulation, as assessed by both micro-computed tomography and bone histology. Skeletal defects were evident at birth and persisted throughout life. Quantitative real-time PCR (qPCR) analyses demonstrated significant reductions in the expression of early and late markers of differentiation, type I collagen, alkaline phosphatase, dentin matrix protein-1, osteocalcin, and sclerostin by from 35 to 90% in bones from <sup>OB</sup>CaSR<sup>Δflox/Δflox</sup> vs control mice, confirming a delay in OB differentiation. The expression of transcription factors RUNX2 and Osterix was unchanged. Furthermore, CaSR knockout significantly suppressed expression of IGF1 and that of two survival genes -- BCL2 and BCL2-like 1 (BCL2L1) in bone. There was also increased expression of interleukin-10 (IL-10), an inducer of apoptosis. The changes in IGF1, BCL2, BCL2L1, and IL-10 expression are consistent with increased apoptosis, confirmed by enhanced TUNEL staining, in OBs and osteocytes in bone from <sup>OB</sup>CaSR<sup>Δflox/Δflox</sup> vs control mice. We next used a Wnt/β-catenin qPCR-based microarray to test whether changes in this pathway critical for OB survival and differentiation and bone formation were involved in the mediating phenotypic changes in bone from the CaSR knockout mice. There were statistically significant decreases in expression of critical effectors of the canonical Wnt pathway (LRP5, Lef, TCF, β-catenin) and increases in expression of pathway inhibitors (sFRP1 and 4). Several Wnts (10 of 17 assayed) were decreased including Wnts 1, 3a and 10, modulators of bone cell differentiation. Our data support the concept that CaSR signaling in OBs critically regulates survival, differentiation, and functions in bone by regulating a number of signaling pathways including IGF1 and Wnts.

**Disclosures:** W. Chang, None.

This study received funding from: NIH-NIA/NIAMS/NIDDK.

## 1157

**Post-mitotic Preosteoblasts Are the Targets of the Anabolic Actions of Intermittent PTH on Periosteal Bone.** R. L. Jilka<sup>1</sup>, C. A. O'Brien<sup>1</sup>, A. A. Ali<sup>1\*</sup>, P. Roberson<sup>1\*</sup>, A. DeLoose<sup>1\*</sup>, V. Dusevich<sup>2\*</sup>, L. Bonewald<sup>2</sup>, R. S. Weinstein<sup>1</sup>, S. C. Manolagas<sup>1</sup>. <sup>1</sup>Center for Osteoporosis and Metabolic Bone Diseases, Central Arkansas Veterans Healthcare System, University of Arkansas for Medical Sciences, Little Rock, AR, USA, <sup>2</sup>Dept. of Oral Biology, University of Missouri-Kansas City, Kansas City, MO, USA.

Intermittent administration of parathyroid hormone (PTH) stimulates bone formation on the surface of cancellous and periosteal bone by increasing the number of osteoblasts; and, at least in mice, the increase in cancellous osteoblasts is largely due to attenuation of their apoptosis. However, the mechanism responsible for the anabolic effect of PTH on periosteal bone is unknown. We report that daily injections of 100 ng/g of PTH(1-34) to 4-6 mo old mice increased the number of osteoblasts on the periosteum of lumbar vertebrae by 2-3 fold as early as after 2 days. However, the prevalence of apoptotic periosteal osteoblasts was only 0.2% in vehicle treated animals, which is ~20-fold lower than that of cancellous osteoblasts. Moreover, PTH did not have a discernable effect on periosteal osteoblast apoptosis. Osteoclasts were rarely seen on the surface of periosteal bone of either vehicle or PTH-treated mice, indicating that PTH anabolism at the periosteum is independent of osteoclasts. Administration of BrdU for 4 days failed to label periosteal osteoblasts under either basal conditions or following administration of PTH. Cancellous osteoblasts, on the other hand, were labeled under basal conditions, but PTH did not increase the percentage of BrdU-positive cells, arguing against a pro-proliferative effect of the hormone at either site. Consistent with the above, ganciclovir-induced ablation of replicating osteoblast progenitors in mice expressing thymidine kinase under the control of the rat 3.6kb Col1A1 promoter resulted in disappearance of osteoblasts from cancellous bone over a 7-14 day period, whereas periosteal osteoblasts were unaffected. However, 14 days of pre-treatment with ganciclovir prevented PTH anabolism on periosteal bone. Collectively, these results indicate that PTH increases periosteal osteoblast number by acting on post-mitotic progeny of replicating progenitors. We conclude that, in cancellous bone, attenuation of mature osteoblast apoptosis by PTH is responsible for increasing osteoblast number because their rate of apoptosis is high, making this effect of the hormone profound. However, in periosteal bone where the rate of osteoblast apoptosis is low, PTH must exert pro-differentiating and/or pro-survival effects on post-mitotic pre-osteoblasts. Targeting the latter cell is an effective mechanism for increasing osteoblast number in periosteal bone where the production of osteoblasts from replicating progenitors is slow.

**Disclosures:** R.L. Jilka, None.

## 1158

**Target Ablation of PTH/PTHrP Receptor (PPR) in Osteocytes Induces Hypocalcemia and Impairs Bone Structure.** P. P. Divieti<sup>1</sup>, W. F. Powell<sup>1\*</sup>, T. Kobayashi<sup>1</sup>, S. Harris<sup>2</sup>, F. Bringhurst<sup>1</sup>. <sup>1</sup>Endocrine Unit, Mass General Hospital, Harvard Medical School, Boston, MA, USA, <sup>2</sup>Department of Periodontic, University of Texas Health Center at San Antonio, San Antonio, TX, USA.

Osteocytes comprise over 90% of all bone cells, yet little is known of their function(s) or of the involvement of systemic hormones in regulating their activity. Parathyroid hormone (PTH), is a major physiologic regulator of calcium, phosphorus and skeletal homeostasis. Clinically, PTH is the only available anabolic agent to treat osteoporosis. Cells of the osteoblastic lineage are key targets of PTH action in bone, and recent evidence suggests that osteocytes might be important in the anabolic effects of PTH. To better understand the role of PTH signaling through PPRs in osteocytes and to determine the role(s) of these cells in mediating the effects of the hormone on bone we have generated mice in which PPR expression is specifically ablated in osteocytes. Transgenic mice in which the 10Kb-DMP1 promoter drives a tamoxifen-inducible Cre expression (10Kb-DMP1-Cre-ERT2) were mated with PPR(fl/fl) animals to create double heterozygotes, which then were mated with PPR(fl/fl) mice to generate DMP1-Cre/PPR(fl/fl) animals or osteocyte selective PPR-cKO mice, when given tamoxifen. PTH selectively inhibits sclerostin expression in osteocytes, and in the PPR-cKO mice, PTH no longer inhibits sclerostin. To further assess PTH signaling in osteocytes, we subjected 6 week old PPR-cKO and control mice to 2 weeks of low calcium diet (0.02% calcium) after a 1 week of pretreatment followed by continuous treatment with tamoxifen. Interestingly, PPR-cKO animals displayed a significantly lower ionized and total calcium levels compared to littermate controls. To further study the role of PPR in osteocytes in young animals we performed a series of experiments in which PPR-cKO and control littermates were injected with tamoxifen at day 3, 5 and 7 postnatally and then maintained on a weekly dose of tamoxifen for the length of the study. Mice were then either sacrificed at 21 days or subjected to a low calcium diet for 2 additional weeks. Blood was collected for calcium measurement and bones were fixed and processed for histological analysis. PPR-cKO mice were 18.5 % smaller than control littermates, as assessed by their body weights. Histological analysis revealed a reduction in trabecular bone and a delay in the secondary ossification center in PPR-cKO animals. Moreover, 5 weeks old PPR-cKO mice fed a low calcium diet had a plasma total calcium level that was significantly lower than in littermate controls, similar of what we previously reported for adult mice. This data further supports a key role of PTH signaling and PPR in osteocytes for proper bone modelling and remodelling, as well as a key role in calcium homeostasis.

**Disclosures:** P.P. Divieti, None.

## 1159

**The Impact of PTH on Cells of the Hematopoietic Lineage: *in vivo* and *in vitro* Studies.** F. Pirihi, A. Koh\*, J. Berry\*, P. Kamarajan\*, Y. Kapila\*, L. K. McCauley. Periodontics and Oral Medicine, University of Michigan School of Dentistry, Ann Arbor, MI, USA.

Parathyroid hormone (PTH) and parathyroid hormone-related protein function in diverse roles, from epithelial-mesenchymal interactions to skeletogenesis and carcinogenesis. PTH is currently under investigation for its potential as a therapeutic agent to stimulate hematopoiesis and bone marrow engraftment; however, the mechanisms for this action are unknown. IL-6 is upregulated by PTH and is also a major regulator of hematopoietic stem cells (HSCs); hence, it was hypothesized that IL-6 is important for the PTH-mediated hematopoietic cell expansion. *In vitro* and *in vivo* experiments were performed utilizing PTH and the tyrosine kinase receptor ligand FLT-3L, known to increase HSCs *in vivo*. Numbers of adherent and non-adherent hematopoietic cells increased after 8 days when whole bone marrow cultures were treated with a single application of FLT-3L. PTH alone did not alter cell numbers but acted synergistically with FLT-3L, further increasing adherent and non-adherent cell populations. In non-adherent cells, PTH combined with FLT-3L increased cyclinD1 mRNA levels while decreasing cell apoptosis as observed with FACS analysis by Annexin V and Propidium Iodide. To evaluate the PTH effect on hematopoietic cells *in vivo*, animals received daily injections of 50 µg/kg of PTH or vehicle for 3 weeks, bone marrow was isolated, and FACS analysis was performed. PTH increased the lin-sca1+ ckit+ population, reflecting increased HSCs. Subsequently, IL-6-deficient mice were utilized *ex vivo* to determine the IL-6 dependence for PTH-cell-expansion. In IL-6-deficient bone marrow cultures, adherent and non-adherent populations failed to amplify in the presence of FLT-3L and PTH. Using bone marrow derived from wild type mice, IL-6 synergized with FLT-3L to increase the non-adherent cell population, suggesting that IL-6 could mimic the PTH effect. In conclusion, PTH increases hematopoietic stem cells *in vivo*. PTH acts in conjunction with FLT-3L to increase hematopoietic and bone marrow stromal cells *ex vivo* through a decrease in apoptosis and an increase in proliferation. Moreover, IL-6 is a critical mediator of bone marrow cell expansion. These findings suggest that PTH mediates hematopoietic cell pool expansion through the upregulation of IL-6.

**Disclosures:** F. Pirihi, None.

*This study received funding from: NIH.*

## 1160

**Skeletal Dysmorphology of Mice Lacking the Mid-Region, Nuclear Localization Sequence and C-Terminus of Parathyroid Hormone-Related Protein.** R. E. Toribio<sup>1</sup>, H. A. Brown<sup>1\*</sup>, C. M. Novince<sup>2\*</sup>, L. M. Gooding<sup>1\*</sup>, S. T. Shu<sup>1\*</sup>, J. L. Werbeck<sup>1\*</sup>, L. K. McCauley<sup>2</sup>, J. Foley<sup>3\*</sup>, T. J. Rosol<sup>1</sup>. <sup>1</sup>College of Veterinary Medicine, The Ohio State University, Columbus, OH, USA, <sup>2</sup>School of Dentistry, University of Michigan, Ann Arbor, MI, USA, <sup>3</sup>School of Medicine, Indiana University, Bloomington, IN, USA.

Parathyroid hormone (PTH)-related protein (PTHrP) is a pleiotropic factor with multiple physiological functions, including regulation of morphogenesis, cell proliferation, differentiation, and apoptosis, and transplacental calcium transport. PTHrP exerts many of its skeletal actions by binding to the PTH-1 receptor (PTH1R) via its N-terminus. However, *in vitro* studies suggest that some of the effects of PTHrP on cell function may not be mediated by the N-terminus, but rather by the mid-region, a nuclear localization sequence (NLS), and the C-terminus.

The goal of this study was to determine if the mid-region, NLS, and C-terminus of PTHrP have *in vivo* functions on skeletal development. To address this question we engineered a knock-in mouse lacking PTHrP-(67-137) which encompasses these three domains (PTHrP<sup>Δ67-137</sup>). The presence of the mRNA and protein for PTHrP<sup>Δ67-137</sup> was demonstrated in fetal tissues.

PTHrP<sup>Δ67-137</sup> pups had an abnormal phenotype characterized by smaller weight at birth, a domed head, short snout, short limbs (chondrodysplasia), and a hunched back when compared to PTHrP<sup>Δ67-137/+</sup> and PTHrP<sup>+/+</sup>. Mutant pups failed to thrive and most of them died by day 5 (some lived up to 3 weeks). MicroCT and histomorphometry revealed decreased bone mass, trabecular thickness, trabecular number, and cortical bone thickness. PTHrP<sup>Δ67-137</sup> pups had craniofacial dysmorphology (spherical skull) with decreased calvarial bone density and thickness. Dental eruption was delayed (day 9 vs. day 7) and incisors were discolored and deformed. Long bones had shorter growth plates, decreased chondrocyte number, increased TUNEL labeling and TRAP+ cells, and decreased bone marrow cellularity. No *in vitro* differences in osteoblast or osteoclast proliferation were found. Bone and calvarial mRNA expression revealed overexpression of *Fgf1*, *Fgf3*, *tuftelin 1*, *IL-6*, *Itga3*, and *P63*, and underexpression of *Ambn*, *Mmp9*, *Bcl-2*, *Sost*, *Alp*, *Ocn*, *Phex*, and *Sox9*. Hematology and blood chemistry showed hypocalcemia, hypoglycemia, hypolipemia, hypoinsulinemia, and leukopenia. Serum osteocalcin was decreased in mutants, but no differences in serum PTH and TRAP 5b were found.

These findings support our hypothesis that the mid-region, NLS, and C-terminus of PTHrP have essential physiological functions in skeletal development and viability. It also suggests PTHrP plays a role in the interactions between hematopoietic precursors and skeletal development, and that PTHrP participates in the energy metabolism.

**Disclosures:** R.E. Toribio, None.

## 1161

**Cloning and Functional Analysis of Human Nurr1 (NR4A2) Promoter: Critical Role in the Regulation of CYP27B1 by Parathyroid Hormone and CREB Phosphorylation.** J. D. Sisler<sup>\*1</sup>, A. Maiti<sup>2</sup>, S. C. Ramage<sup>2</sup>, M. A. Forster<sup>\*3</sup>, M. J. Beckman<sup>\*1</sup>. <sup>1</sup>Biochemistry and Molecular Biology, Virginia Commonwealth University, Richmond, VA, USA, <sup>2</sup>Orthopedic Surgery, Virginia Commonwealth University, Richmond, VA, USA, <sup>3</sup>Physiology and Biophysics, Virginia Commonwealth University, Richmond, VA, USA.

Parathyroid hormone (PTH) is the central activator of renal proximal 1-alpha-hydroxylase (CYP27B1), the enzyme responsible for synthesis of 1,25-dihydroxyvitamin D<sub>3</sub> (1,25(OH)<sub>2</sub>D<sub>3</sub>). Involvement of the orphan nuclear receptor Nurr1 (NR4A2) was recently established in the PTH-mediated pathway of CYP27B1 activation. To determine the connection between NR4A2 and CYP27B1 in response to PTH, we created a murine proximal tubule epithelial cell model (MPCT), stably transfected with human PTHR1. In MPCT cells, transfected human CYP27B1 promoter activation, as well as endogenous mRNA and protein levels was optimally increased in response to 50nM of PTH at 12 hours. Transfection of MPCT cells with dominant negative constructs for CREB phosphorylation (CREB-133) and DNA-binding (K-CREB) abolished CYP27B1 promoter activity and blocked PTH-mediated increase in CYP27B1. Thus, regulation of CYP27B1 promoter was dependent on phospho-CREB activation. Next, a 1,938 bp segment of 5'-sequence upstream of the human NR4A2 start site was acquired by *in silico* screening from the Ensembl web interface, PCR cloned, sequence verified and subcloned into a pGL3-Luc reporter vector. A TF-Search analysis of transcription factor binding sites depicted a consensus CREB site at the promoter proximal end (-120 to +1 bp). Responsiveness of the full-length human NR4A2 promoter to PTH was maximal at 1 hour and diminished after 2 hours. The endogenous regulation of NR4A2 mRNA following PTH treatment correlated with the promoter activity and showed a maximal induction of 15-fold within the 2 hour period. Three distinct constructs were generated using site-directed mutagenesis of key bases within the putative CREB binding site of the human NR4A2 promoter and were used to establish the loss of PTH-mediated induction of NR4A2. In addition, knock-down of NR4A2 in MPCT cells by a specific siRNA obstructed the association between PTH-mediated early gene activation of NR4A2 at 1 hour and the increase of CYP27B1 at 12 hours. Taken together, these findings demonstrate that PTH control of immediate early induction of NR4A2 in renal proximal tubule epithelial cells is a critical step in the molecular mechanism to activate CYP27B1 gene expression, and provide new insights into the indirect link between phospho-CREB activation and stimulation of renal 1 $\alpha$ -hydroxylation by PTH.

**Disclosures:** M.J. Beckman, None.

This study received funding from: ARS USDA CRA 58-3625-6-103.

## 1162

**Mechanical Unloading Partially Rescues Hypophosphatemic Rickets in Dmp1-null Mice.** D. Ma<sup>\*1</sup>, S. Yu<sup>1</sup>, R. Zhang<sup>\*1</sup>, B. Yuan<sup>2</sup>, Y. Xie<sup>\*1</sup>, M. Drezner<sup>2</sup>, S. Dallas<sup>3</sup>, L. Bonewald<sup>3</sup>, J. Feng<sup>1</sup>. <sup>1</sup>Biomedical Sciences, Baylor College of Dentistry, TX A&MHSC, Dallas, TX, USA, <sup>2</sup>Medicine, School of Medicine, Univ. Wisconsin, Madison, WI, USA, <sup>3</sup>Oral Biology, School of Dentistry, UMKC, Kansas City, MO, USA.

Our recent studies suggest that the osteocyte is an endocrine cell that controls phosphate homeostasis through FGF23, as osteocytes in *Dmp1* null bone highly express FGF23, which is released into the circulation and causes severe hypophosphatemic rickets. To further validate these observations, neutralizing antibodies against FGF23 (kindly provided from Kirin, Japan) or PBS were injected into 6 day-old *Dmp1* null and control pups i.p. every other day starting at day 6. Mice were sacrificed at day 15. Serum phosphate (Pi) levels were significantly higher in the *Dmp1* null group injected with FGF23 antibody compared to the PBS injected group further supporting a physiological role of FGF23 in the control of Pi homeostasis. Not only did the Pi level return to normal (from 5.73 $\pm$ 0.47 mg% to 9.96  $\pm$ 0.3 mg%; age=15 day-old, N=5) but so did many of the bone defects. A significant improvement was seen in growth plate morphology, secondary ossification, long bone length, and bone mineralization. Histological analysis showed that defects in osteocyte maturation and morphology were greatly improved as reflected by alkaline phosphatase, E11, and FGF23 expression largely returning to normal. Osteocyte cell and lacunar morphology was also improved as determined by light and scanning electron microscopy.

Osteocytes are generally known and accepted to be the "professional" mechanosensory cells, sending signals of (re)modeling in response to loading. Therefore, we hypothesized that mechanical loading may regulate phosphate homeostasis through osteocytes. The tail suspension approach was used to determine if unloading of the hindlimbs of *Dmp1* nulls would improve or reverse the hypophosphatemic rickets. None of the unloaded tibias from the *Dmp1* null animals fractured (n=5) compared to 50% of the tibias from normal ambulatory *Dmp1* null animals (n=8). Therefore unloading ameliorates the tendency of tibias from the null animals to spontaneously fracture. Pi levels and the rickets phenotype were partially rescued from average 3.63 mg% (N=3, age=2-mo) to 4.98 mg% (N=2, age=2-mo) in the tail suspended null animals as was the morphology of the osteocyte lacuno-canalicular system as determined by resin-casted SEM images. These data support the concept that mechanical unloading and potentially loading may influence Pi homeostasis through osteocytes, and may have clinical implications for the treatment of children with hypophosphatemic rickets.

**Disclosures:** D. Ma, None.

This study received funding from: AR051587, AR046798.

## 1163

**Hip Fracture Patients at High Risk of Second Hip Fracture.** J. Ryg<sup>\*1</sup>, L. Rejnmark<sup>2</sup>, S. Overgaard<sup>\*3</sup>, K. Brixen<sup>1</sup>, P. Vestergaard<sup>2</sup>. <sup>1</sup>Dept of Endocrinology, Odense University Hospital, Odense, Denmark, <sup>2</sup>Dept of Endocrinology, Aarhus University Hospital, Aarhus, Denmark, <sup>3</sup>Dept of Orthopedic Surgery, Odense University Hospital, Odense, Denmark.

In hip fracture (Hfx) patients, little is known about time frame and risk factors of 2nd Hfx, as well as the ensuing mortality. The aim of study was to elucidate incidence of 2nd Hfx and subsequent mortality. A nationwide population-based cohort of all 169,145 patients with first Hfx in Denmark during 1977-2001 was followed for up to 25 years and compared with the background population. Data on fractures, vital status, and socio-demographic variables were retrieved from national registers and 2nd Hfx were validated against surgical procedures. Median [range] follow-up was 3.8 years [0-25 years] corresponding to 1,041,177 patient years. The majority of patients were women (72.4%) being older than males (78.6 $\pm$ 11.1 vs. 72.8 $\pm$ 16.3 years, p<0.05) (mean  $\pm$ SD). Any prior fracture was seen in 21.7% of women and 17.3% of men (p<0.05). A total of 27,834 patients (5,369 men; 22,465 women) suffered a 2nd Hfx during the study period. The cumulative incidence was 9% after 1 year and 20% after 5 years, being significantly higher than expected (2% and 12%, respectively, p<0.05). The RR of 2nd Hfx was increased by 11.8 (95% CI 11.2-12.5) 1 month after first Hfx, 2.2 (95% CI 2.0-2.5) at 1 year, and did not normalise until 15 years (RR 1.01, 95% CI 1.0-1.02). Adjusting for mortality revealed a significantly higher Hfx free 5-year survival in men and the youngest age-groups in both sexes (Table). Females (HR 1.36, 95% CI 1.32-1.40), age (HR 1.68, 95% CI 1.60-1.76 in patients above 85 years), alcoholism (HR 1.61, 95% CI 1.51-1.72), any prior fracture (HR 1.08, 95% CI 1.04-1.11), and living alone (HR 1.06, 95% CI 1.04-1.09) were significant risk factors for 2nd Hfx in a Cox' proportional hazard model. Both sexes had a higher mortality at 1 and 5 years following 2nd Hfx compared to the background population (men 1-year: 27% vs. 9%, p<0.05, 5-years 64% vs. 40%, p<0.05, women 1-year 21% vs. 10%, p<0.05, 5-years 58% vs. 41%, p<0.05).

Table: Hfx free 5-year survival (mean  $\pm$ SD) following first Hfx adjusted for mortality.

Age (years)	Men (%)	Women (%)	Total (%)	p (Men vs. Women)
<50	90.5 $\pm$ 0.5	84.1 $\pm$ 0.8	88.3 $\pm$ 0.4	<0.05
50-59	85.7 $\pm$ 0.7	80.6 $\pm$ 0.6	82.6 $\pm$ 0.5	<0.05
60-69	85.2 $\pm$ 0.5	80.6 $\pm$ 0.4	82.0 $\pm$ 0.3	<0.05
70-79	83.3 $\pm$ 0.4	78.8 $\pm$ 0.3	79.8 $\pm$ 0.2	<0.05
80-89	80.9 $\pm$ 0.6	76.7 $\pm$ 0.3	77.4 $\pm$ 0.2	<0.05
$\geq$ 90	79.6 $\pm$ 2.1	76.7 $\pm$ 0.8	77.2 $\pm$ 0.7	<0.05

In conclusion, patients with Hfx have a twofold risk of 2nd Hfx, the following mortality is significantly increased, and time span between fractures allow preventive measures in the majority of patients. We propose that programs for secondary prevention should be developed and tested.

**Disclosures:** J. Ryg, Eli Lilly, MSD, Nycomed, Roche, and Servier 5.

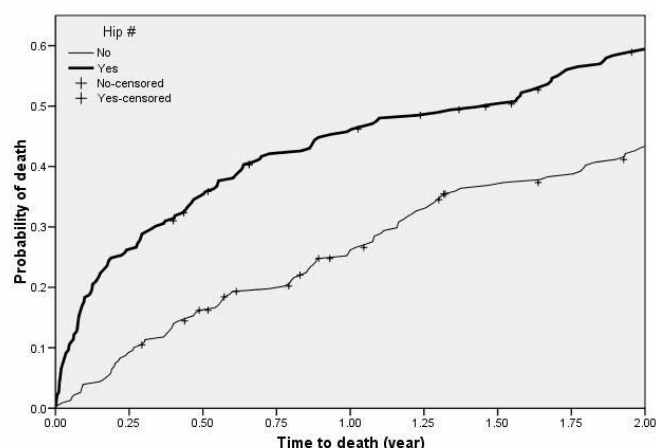
This study received funding from: University of Southern Denmark, Danish Centre for Evaluation and Health Technology Assessment, The family Christenson-Ceson's Family Foundation, and Helga and Peter Korning's Foundation.

## 1164

**Pattern of Death after Hip Fracture among Institutionalized Older People: 5 Year Followup.** P. N. Sambrook<sup>1</sup>, J. S. Chen<sup>\*1</sup>, L. M. March<sup>\*1</sup>, J. M. Simpson<sup>\*2</sup>, I. D. Cameron<sup>\*3</sup>, R. G. Cumming<sup>\*4</sup>, M. J. Seibel<sup>5</sup>. <sup>1</sup>University of Sydney, Institute of Bone & Joint Research, Sydney, Australia, <sup>2</sup>University of Sydney, School of Public Health, Sydney, Australia, <sup>3</sup>University of Sydney, Rehabilitation Studies Unit, Sydney, Australia, <sup>4</sup>University of Sydney, Centre for Education and Research on Ageing, Sydney, Australia, <sup>5</sup>University of Sydney, ANZAC Research Institute, Sydney, Australia.

An increasing risk of death post hip fracture has been well documented. However, the duration of the excess mortality remains unclear especially in very frail older people. In this study, we compared 229 hip fracture cases and 229 controls matched by age (within 5 years), gender, institution type and follow-up period from the FREE study cohort of 2005 institutionalized older people. The study sample consists of 90 males and 368 females with a mean age of 86 (range: 67-102) years followed for 5 years. Among the cases, death rates at 3, 6, 9 and 12 months were 26%, 35%, 42% and 45% respectively. The corresponding death rates for the controls were 9%, 16%, 20% and 27% respectively. The Kaplan-Meier survival curves for the cases and controls show that the greatest excess mortality occurred in the first three months after the hip fracture. This excess risk was reduced to zero at about 9 months after the fracture (see figure 1). The findings are supported by piecewise Cox regression analysis of the data. For example the hazard ratio of death for the cases compared to the controls was 3.25 (95% CI: 1.98-5.35; P<0.001) at 3 months, 1.93 (95% CI: 1.15-3.23; P=0.01) for the period of 3 - 9 months and 1.16 (95% CI: 0.87-1.55; P=0.32) for the period beyond 9 months following a fracture. Results remained unchanged after adjusting for age, gender, institution type, weight, cognitive function and number of medications. Conditional logistic regression analysis of the data gave similar results. In summary, among the frail elderly, mortality due to hip fracture is increased only for the first 9 months after the fracture. After that, death rates for those with and without hip fractures are similar for up to 5 years. Intensive medical attention should be given to frail older people to reduce mortality after a recent hip fracture.

Figure 1 Survival curves for cases and controls



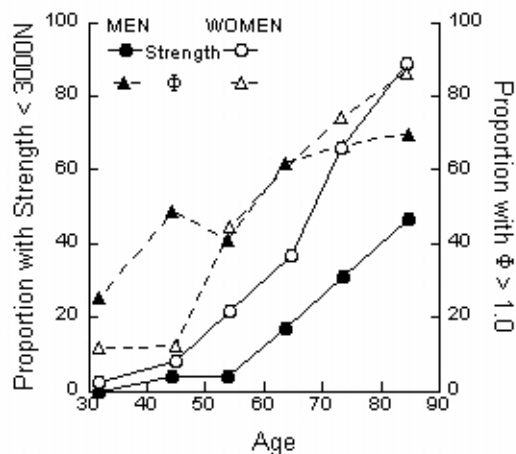
Disclosures: P.N. Sambrook, None.

## 1165

**Femoral Strength, Bone Density, and Aging in Women and Men.** T. M. Keaveny<sup>1</sup>, D. L. Kopperdahl<sup>1</sup>, P. F. Hoffmann<sup>1</sup>, S. Amin<sup>2</sup>, L. J. Melton<sup>2</sup>, S. Khosla<sup>2</sup>. <sup>1</sup>O. N. Diagnostics, Berkeley, CA, USA, <sup>2</sup>Mayo Clinic, Rochester, MN, USA.

Low bone mineral density (BMD) at the hip as measured by DXA is a well-established risk factor for hip fracture in both women and men but has only modest predictive sensitivity, and its relation to bone strength is not fully understood. Because femoral strength depends on volumetric BMD and 3D bone geometry, both of which differ by sex (Riggs, JBM 2004), the strength-BMD relation may depend on sex and the nature of the BMD measurement: areal BMD (in g/cm<sup>2</sup>), volumetric BMD (in g/cm<sup>3</sup>), or bone mineral content (BMC in g). Resolving these issues is critical to understanding the etiology of age-related hip fracture. Toward this end, we used finite element (FE) analysis of hip QCT scans to relate femoral strength, volumetric BMD (combined cortical and trabecular), areal BMD (femoral neck), and BMC (femoral neck) for an age-stratified (age 20-90 years) cohort of n=679 men and women, randomly sampled from the general population in Rochester MN. Strength was simulated for a sideways fall, and the load-to-strength ratio  $\Phi$  was also calculated using mass and height information and FE strength. Results (Figure) indicated that, by decade, the proportion of individuals having "low" bone strength (< 3000 N) was always greater for women; decreases in strength initiated during menopause for women and a decade later for men; and age-related strength loss was accentuated for women starting in the seventh decade. The proportion of those having high (worse) values of the load-to-strength ratio ( $\Phi > 1.0$ ) was greater in young men than in young women, was similar between the sexes in the fifth and sixth decades, and was higher in women starting in the seventh decade. For the same value of femoral strength, women had higher volumetric BMD and lower BMC than men (p<0.0001), but similar areal BMD. Taken together, these results provide new insight into the relation between femoral strength and clinical measures of bone density for men versus women, and suggest a structural mechanism based on integral bone strength for the known higher fracture incidence of women at advanced age.

### LOW BONE STRENGTH AND HIGH $\Phi$ VERSUS AGE AND SEX



Disclosures: T.M. Keaveny, O. N. Diagnostics 2.  
This study received funding from: NIH.

## 1166

**Secular Trends in Swedish Hip Fracture Incidence 1987-2002.** B. E. Rosengren<sup>1</sup>, H. G. Ahlberg<sup>1</sup>, M. K. Karlsson<sup>1</sup>, D. Mellström<sup>2</sup>. <sup>1</sup>Department of Clinical Sciences, Lund University and Department of Orthopaedics UMAS Malmö, Clinical and Molecular Osteoporosis Research Unit, Malmö, Sweden, <sup>2</sup>Departments of Internal Medicine and Geriatrics, The Sahlgrenska Academy at Göteborg University, Center for Bone Research at the Sahlgrenska Academy, Göteborg, Sweden.

The last fifty years, hip fracture incidence has been reported to increase in the western world. During the last decade, several studies have disputed this when reporting an unchanged or decreased hip fracture incidence. The aim of this study was to evaluate if a decline in hip fracture incidence was evident also in Sweden and how the growing population at risk influence the absolute number of hip fractures. The study evaluated the annual, gender specific, total number and age-adjusted incidence of hip fractures in all individuals aged 50 years or more in Sweden from 1987 to 2002 by use of central national data. Time-trend analysis was done by linear regression analysis. The annual number of hip fractures was unchanged over time in women with 10404 fractures year 1987 and 9866 year 2002 (-14.9 per year (95% CI=-41.4-11.6; p=0.25) but increased in men from 3699 year 1987 to 4190 year 2002 (39.1 per year (95% CI=21.6-56.7; p<0.001). The mean age when sustaining a hip fracture increased in women from 79.7 year 1987 to 81.7 year 2002 (0.13 per year (95% CI=0.12-0.14; p<0.001); and in men from 77.3 year 1987 to 79.1 year 2002 (0.11 per year (95% CI=0.10-0.13; p<0.001). Age-adjusted hip fracture incidence (per 10 000) declined over time in woman from 68.4 year 1987 to 51.9 year 2002 (-1.0 per year (95% CI=-1.1--0.89); p<0.001) and in men from 28.9 year 1987 to 26.0 year 2002 (-0.15 per year (95% CI=-0.27--0.04; p<0.05). This study infers that there has been a decreased age-adjusted hip fracture incidence in both women and men aged 50 years or older in Sweden between 1987 and 2002. Due to shifts within the populations at risk, the annual absolute number of hip fractures was unchanged in women but increased in men during the study period.

Disclosures: B.E. Rosengren, None.

## 1167

**Hip Strength Estimates by Finite Element Analysis and Fracture Prediction in Women and Men.** S. Amin<sup>1</sup>, D. Kopperdahl<sup>2</sup>, L. J. Melton<sup>1</sup>, E. Atkinson<sup>1</sup>, B. L. Riggs<sup>1</sup>, T. Keaveny<sup>3</sup>, S. Khosla<sup>1</sup>. <sup>1</sup>Mayo Clinic, Rochester, MN, USA, <sup>2</sup>O.N. Diagnostics, Berkeley, CA, USA, <sup>3</sup>University of California, Berkeley, CA, USA.

Hip bone density, a surrogate measure of bone strength at the hip, is an especially important predictor of fracture risk. Finite element [FE] analyses may provide better overall assessment of bone strength and, when combined with estimated bone loads from falls, offer improved site-specific fracture prediction. Whether FE estimates of fall load relative to bone strength at a specific site, such as the hip, will be equally useful predictors of overall or osteoporotic fracture risk is unclear. In an age-stratified, random sample of 580 community adults age  $\geq 35$  yrs, we measured femoral neck [FN] total volumetric BMD (vBMD, mg/cm<sup>3</sup>) using quantitative computed tomography, from which FE models were used to assess bone strength at the hip during a simulated sideways fall. The load to strength ratio for a fall (factor-of-risk [ $\Phi$ ]) was then estimated. We used age-adjusted logistic regression models to examine prediction of prevalent fractures, generally, and of osteoporotic fractures (fracture of the hip, vertebrae or distal forearm), specifically. Among 314 women (mean  $\pm$  SD) age: 61  $\pm$  15 yrs) and 266 men (62  $\pm$  16 yrs), 152 women and 131 men had a prevalent fracture after the age of 35 yrs. Two women and one man had a hip fracture. Estimates of FN vBMD, hip strength and  $\Phi$  were comparable predictors of both prevalent overall fracture and osteoporotic fracture (see Table). Odds ratios are presented per SD decrease in FN vBMD and hip strength, and per SD increase in  $\Phi$ . The c-statistic (the predictive probability of the model, and equivalent to the area under a ROC curve) from the different models were similar.

Women	Any Fracture		Osteoporotic Fracture	
	Odds Ratio (95% CI)	c-Statistic	Odds Ratio (95% CI)	c-Statistic
FN Total vBMD (mg/cm <sup>3</sup> )	1.5 (1.1, 2.1)	0.76	1.5 (1.0, 2.2)	0.81
Hip Strength (N)	1.3 (0.9, 1.8)	0.75	1.4 (0.9, 2.2)	0.80
$\Phi$	1.5 (1.1, 2.1)	0.76	1.5 (1.1, 2.1)	0.80
<b>Men</b>				
FN Total vBMD (mg/cm <sup>3</sup> )	1.6 (1.2, 2.2)	0.78	2.0 (1.3, 2.9)	0.71
Hip Strength (N)	1.3 (0.9, 1.8)	0.77	1.8 (1.2, 2.6)	0.70
$\Phi$	1.3 (0.9, 1.8)	0.77	1.9 (1.3, 2.6)	0.69

While FE model estimates of hip strength and  $\Phi$  are likely to provide better information than FN vBMD regarding hip fracture risk specifically, these estimates appear to be equally effective predictors of overall and osteoporotic fracture risk generally. Additional work on refining load estimation during falls may further improve fracture prediction.

Disclosures: S. Amin, None.  
This study received funding from: NIH.

## 1168

**Protective Effect of Total and Supplemental Vitamin C Intake on the Risk of Hip Fracture: A 17-Year Follow-Up from the Framingham Osteoporosis Study.** S. Sahni<sup>1</sup>, M. T. Hannan<sup>2</sup>, D. R. Gagnon<sup>\*3</sup>, J. Blumberg<sup>\*1</sup>, L. A. Cupples<sup>3</sup>, D. P. Kiel<sup>2</sup>, K. L. Tucker<sup>1</sup>. <sup>1</sup>JM USDA HNRCA, Tufts Univ., Boston, MA, USA, <sup>2</sup>Hebrew SeniorLife, Boston, MA, USA, <sup>3</sup>Boston Univ. SPH, Boston, MA, USA.

Vitamin C may influence bone health by reducing oxidative stress and subsequent bone resorption, and by playing a role in collagen formation. Therefore, we evaluated associations of vitamin C intake (total, dietary and supplemental) with incident hip fracture and non-vertebral osteoporotic fracture, over 15 to 17-y of follow-up in the Framingham Osteoporosis Study. 366 men and 592 women completed a food frequency questionnaire in 1988-89 and were followed for non-vertebral fracture until 2003 and hip fracture until 2005. Tertiles or categories of vitamin C intake (each for total, dietary and supplemental) were created, adjusting for total energy intake (residual method). Hazard ratios (HR) were estimated using Cox-proportional hazards regression adjusting for sex, age, BMI, height, smoking, physical activity index, total energy intake, alcohol intake, multivitamin use and current estrogen use (in women only). Supplemental and dietary vitamin C intakes were adjusted for each other. Final models were examined for attenuation by adding femoral bone mineral density (FN-BMD).

Mean age was 75 y  $\pm$  5.0. Over follow-up, 100 hip fractures and 180 non-vertebral fractures. Subjects in the highest tertile of total vitamin C intake had significantly fewer hip fractures or non-vertebral fractures compared to subjects in the lowest tertile (Table 1). Subjects in the highest category of supplemental vitamin C intake had significantly lower risk of hip and non-vertebral fracture compared to non-supplement users. Dietary vitamin C intake was not associated with risk of fracture (all  $P > 0.17$ ). The associations for hip fracture did not change after adjustment for baseline FN-BMD.

These results suggest that vitamin C may reduce the risk of fracture by 50% or more in elderly men and women, especially when vitamin C supplements are used. The observation that the risk for fracture may be independent of BMD suggests the possibility of effects on the bone matrix, muscle or other risk factors.

Table 1. Inverse association of carotenoid intake and the risk of hip fracture as well as non-vertebral osteoporotic fracture in the elderly men and women of the Framingham Osteoporosis Study.

Hip Fracture, HR (95%CI)	Tertile 1 (Lowest)	Tertile 2	Tertile 3 (Highest)	P-trend
Total vitamin C intake	Ref	0.73 (0.45-1.20)	0.56 (0.31-0.98)*	0.04
Supplemental vitamin C intake	Ref	0.50 (0.20-1.24)	0.31 (0.13-0.73)*	0.02
<b>Non-Vertebral Fracture, HR (95%CI)</b>				
Total vitamin C intake	Ref	0.98 (0.68-1.40)	0.64 (0.42-0.99)*	0.04
Supplemental vitamin C intake	Ref	0.81 (0.38-1.73)	0.58 (0.30-1.11) <sup>†</sup>	0.06

HR is significantly different from HR of tertile 1: \*  $P < 0.05$ , <sup>†</sup>  $P = 0.1$

**Disclosures:** S. Sahni, None.

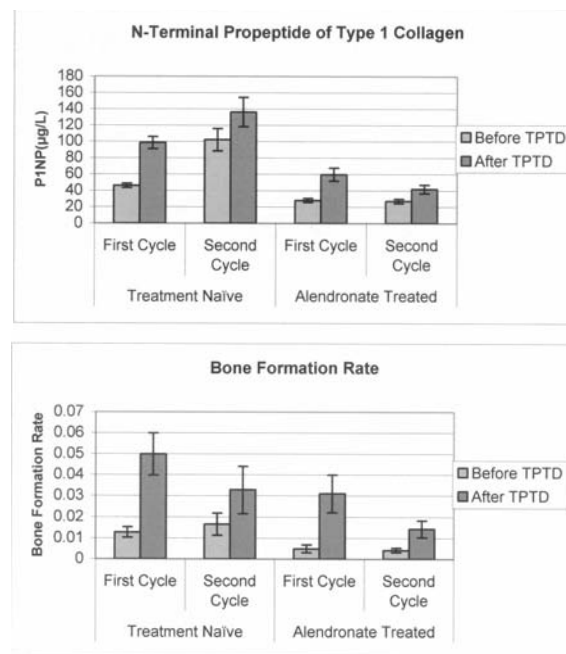
This study received funding from: NIH-NIAMS #AR/AG41398 and USDA-ARS Cooperative Agreement No. 58-1950-7-707.

## 1169

**Histomorphometric and Biochemical Bone Formation Responses to First and Second Cycles of Teriparatide Treatment.** R. Lindsay<sup>1</sup>, F. Cosman<sup>1</sup>, M. Boström<sup>2</sup>, H. Zhou<sup>1</sup>, J. Nieves<sup>1</sup>, D. W. Dempster<sup>1</sup>. <sup>1</sup>Helen Hayes Hospital, West Haverstraw, NY, USA, <sup>2</sup>Hospital for Special Surgery, New York, NY, USA.

We have shown that teriparatide (TPTD) given in 3 month (mos) cycles with 3 mos off intervals produces a similar BMD response after 15 mos compared to continuous treatment. Here, we performed iliac biopsies, using our quadruple labeling technique, during the first cycle of TPTD administration (7.5 weeks) and during the second cycle of TPTD administration (7.5 mos) in 37 women. Prior to TPTD administration, women were treatment naïve (n=18) or on prior and ongoing alendronate (n=19). In alendronate treated women, there was a greater relative increase in mineral apposition rate (MAR) during both the first (0.356  $\mu\text{m}/\text{d}$ ;  $p=0.002$ ) and second TPTD cycles (0.320  $\mu\text{m}/\text{d}$ ;  $p=0.001$ ) compared to the treatment naïve group (0.178  $\mu\text{m}/\text{d}$ , first cycle;  $p=0.001$  vs 0.114  $\mu\text{m}/\text{d}$ , second cycle;  $p=0.04$ ) but baseline MAR was lower in alendronate-treated than treatment-naïve women. Mineralized perimeter (Mdp) increased in both alendronate-treated (2.7%, first cycle and 0.93 %, second cycle; both  $p<0.01$ ) and treatment naïve women (3.87 %, first cycle;  $p=0.003$  and 1.59 %, second cycle;  $p=0.13$ ), but baseline Mdp was much lower on alendronate. Although bone formation rate (BFR= Mdp  $\times$  MAR) increased in both alendronate treated and treatment naïve women during both first and second cycles of TPTD treatment (Figure), it increased to a lesser degree in alendronate treated subjects than in naïve subjects during both TPTD cycles since this variable is heavily influenced by Mdp. The histomorphometric data are consistent with the biochemical changes in bone formation as assessed by P1NP (Figure).

These data indicate that TPTD can stimulate new bone formation during 2 discrete cycles of therapy in women who are both treatment-naïve and those on prior and ongoing alendronate therapy; however, in the presence of alendronate, the dramatic limitation of actively remodeling surface available for TPTD stimulation may provide a mechanism for the so-called blunting effect of alendronate on TPTD-induced BMD response.



**Disclosures:** R. Lindsay, Eli Lilly and Company 1.

This study received funding from: Eli Lilly and Company provided TPTD. NIH AR051454.

## 1170

**Treatment with Daily Subcutaneous Teriparatide (1-34) Compared with Daily Subcutaneous Parathyroid Hormone (1-84) in Women with Severe Postmenopausal Osteoporosis: A Randomized, Head-To-Head Study.** M. Bevilacqua<sup>\*1</sup>, L. J. Dominguez<sup>\*2</sup>, E. Chebat<sup>\*1</sup>, V. Righini<sup>\*1</sup>, M. Barrella<sup>\*1</sup>, M. Massarotti<sup>3</sup>, M. Barbagallo<sup>\*2</sup>. <sup>1</sup>Ospedale L. Sacco-Polo Universitario, Milan, Italy, <sup>2</sup>Geriatric Unit, University of Palermo, Palermo, Italy, <sup>3</sup>Humanitas, Milan, Italy.

**INTRODUCTION:** Teriparatide (TRP) and parathyroid hormone (PTH) are available for the treatment of severe osteoporosis. A 12-month, head-to-head study was performed to compare these two drugs in women with severe osteoporotic vertebral fractures. **SUBJECTS AND METHODS:** 70 patients from one single site were randomized to daily, self-administered, sc TRP (N=35, 20  $\mu\text{g}/\text{day}$ ) or PTH (N=35, 100  $\mu\text{g}/\text{day}$ ). Patients were admitted to the study after a comprehensive evaluation and eventual correction of vitamin D deficiency and secondary hyperparathyroidism. Endpoint was bone turnover markers change at 3, 6, and 12 months of treatment. Tolerability was evaluated by adverse experience (AE) reporting. **RESULTS:** After PTH treatment, there were significant increases at 6 and 12 months in N-Middle osteocalcin ( $\Delta\%$  +547% and +876%), P1NP (+270% and +493%) and N-telopeptide (+227% and +458%) ( $p<0.01$  for all vs. basal). The increases were greater than those observed with TRP (osteocalcin +260% and +550%; P1NP +277% and +457%; N-telopeptide +108% and +346%;  $p<0.01$  for all vs. PTH). Nevertheless, the increase in femoral BMD was similar for both treatments (PTH +3.8%, TRP +3.7%;  $p=NS$ ). The increase of osteocalcin was significantly correlated with  $i\text{Ca}^{++}$  increase ( $p<0.01$ ). Considering a cut-off point  $>1.3 \text{ mmol/L}$ , a similar number of patients in TRP- and PTH-treatment had a high ionized calcium (10 in TRP and 11 in PTH group). However, the mean concentration of ionized calcium was significantly higher at all three evaluations for PTH-treated group (TRP:  $1.18 \pm 0.02 \text{ mmol/L}$ ,  $1.32 \pm 0.08 \text{ mmol/L}$ ,  $1.32 \pm 0.05 \text{ mmol/L}$ ; PTH:  $1.21 \pm 0.02 \text{ mmol/L}$ ,  $1.35 \pm 0.1 \text{ mmol/L}$ ,  $1.41 \pm 0.1 \text{ mmol/L}$ ;  $\xi$  at 3, 6, and 12 months, respectively; \*means  $p<0.001$  vs. basal;  $\xi$  means  $p<0.01$  vs. TRP). Two patients withdrew from the treatment in the first month in each group because of vertigo with TRP, and because of nausea with PTH, and were replaced. No other significant differences were seen between treatment groups in the incidence of AE. **CONCLUSIONS:** TRP and PTH induced similar increases in femoral BMD after 12-month treatment, with significantly higher increases in ionized calcium with PTH. The implications and consequences of the significantly greater increase in bone turnover markers seen with PTH compared to TRP need to be further explored.

**Disclosures:** M. Bevilacqua, None.

## 1171

**Teriparatide versus Alendronate for Treatment of Glucocorticoid-Induced Osteoporosis: 36-month Results.** K. G. Saag<sup>1</sup>, J. R. Zanchetta<sup>2</sup>, J. P. Devogelaer<sup>3</sup>, R. A. Adler<sup>4</sup>, K. See<sup>5</sup>, G. P. Dalsky<sup>5</sup>, K. Krohn<sup>5</sup>, J. H. Krege<sup>5</sup>, M. R. Warner<sup>5</sup>. <sup>1</sup>University of Alabama at Birmingham, Birmingham, AL, USA, <sup>2</sup>Instituto de Investigaciones Metabólicas -IDIM, Buenos Aires, Argentina, <sup>3</sup>Université catholique de Louvain, Brussels, Belgium, <sup>4</sup>McGuire VAMC, Richmond, VA, USA, <sup>5</sup>Eli Lilly and Company, Indianapolis, IN, USA.

The purpose of this study was to compare the efficacy of teriparatide versus alendronate in patients with glucocorticoid-induced osteoporosis (GIOP). This was a multicenter, double-blind, 36-month clinical trial in patients who had taken glucocorticoids for  $\geq 3$  months (prednisone equivalent  $\geq 5$  mg/day). The 36-month results are reported here (18-month results reported by Saag et al. NEJM 2007). Patients were randomly assigned to teriparatide 20  $\mu$ g/day (n=214) or alendronate 10 mg/day (n=214). Bone mineral density (BMD) was measured by dual energy x-ray absorptiometry. A mixed model repeated measures analysis was used to analyze BMD at each timepoint and ANOVA was used to analyze endpoint BMD (last observation carried forward). At baseline, the median glucocorticoid dose was 7.5 mg/day in both groups, and the mean [ $\pm$ SE] lumbar spine BMD T-score was 2.4[0.1] and 2.5[0.1] in the teriparatide and alendronate groups, respectively. At the lumbar spine and femoral neck, BMD increased significantly more in the teriparatide compared with alendronate group (Table). Fewer patients had new radiographic vertebral fractures in the teriparatide (3/173, 1.7%) versus alendronate group (13/169, 7.7%) (p=0.007). The number of patients with new nonvertebral fractures was not significantly different between groups (teriparatide 16/214 [7.5%] versus alendronate 15/214 [7.0%]; p=0.843). There was no significant difference between groups in the number of patients with  $\geq 1$  adverse event (91% teriparatide versus 86% alendronate, p=0.116). Significantly more teriparatide patients reported nausea, dyspnea, insomnia, and viral infection; significantly more alendronate patients reported polyarthrititis, weight decreased, and hepatic enzyme increased. Hypercalcemia was reported as an adverse event in 1 patient in the teriparatide group and none in the alendronate group. In this 36-month trial of GIOP, patients treated with teriparatide had greater increases in BMD and fewer new vertebral fractures compared with patients treated with alendronate. Both treatments were generally well tolerated.

Mean % Change [ $\pm$ SE] from baseline in BMD (g/cm <sup>3</sup> )				
Time point (months)	n	Alendronate	n	Teriparatide
Lumbar Spine 18	148	3.8 $\pm$ 0.6*	156	8.0 $\pm$ 0.6*†
24	131	5.2 $\pm$ 0.7*	136	9.8 $\pm$ 0.7*†
36	112	5.3 $\pm$ 0.8*	123	11.0 $\pm$ 0.8*†
Endpoint	195	4.2 $\pm$ 0.9*	198	8.9 $\pm$ 1.0*†
Femoral Neck 18	145	2.8 $\pm$ 0.8*	156	4.4 $\pm$ 0.8*#
24	131	2.4 $\pm$ 0.8**	135	4.8 $\pm$ 0.8*‡
36	113	3.4 $\pm$ 0.9*	120	6.3 $\pm$ 0.9*†
Endpoint	177	2.6 $\pm$ 0.9**	185	5.1 $\pm$ 0.9*†

Within treatment: \*p<0.001, \*\*p<0.01; Between treatments: †p<0.001, ‡p<0.01, #p<0.05

**Disclosures:** K.G. Saag, Eli Lilly and Company 2, 3; Merck and Company 1, 2, 3; Novartis 1, 2, 3; Amgen 2, 3.  
This study received funding from: Eli Lilly and Company.

## 1172

**Teriparatide in Bisphosphonate-resistant Osteoporosis - Clinical and MicroCT Data. The "BBB-Study".** B. Mucche<sup>1</sup>, B. Jobke<sup>2</sup>, M. Hellmich<sup>1</sup>, J. Semler<sup>1</sup>. <sup>1</sup>Metabolic Diseases and Osteology, Immanuel-Krankenhaus, Berlin, Germany, <sup>2</sup>Dept. of Radiology - MQIR, UCSF, San Francisco, CA, USA.

There are cases of relevant progression of osteoporosis (OPO) despite of good compliance to at least 1 year of bisphosphonate treatment (BIS). Teriparatide (TPD) is an option, but used only in a minority with limited experience about the effects of previous treatments on lab, BMD and bone structure. Data of a 18months prospective study are presented. METHODS: 25 women (age 69 $\pm$ 9 ys) with progression of severe OPO during BIS (3.5 (1...7) ys; new fragility fractures = 14, BMD decline >3.5% = 11 pts, 12 ALN/13 RIS) were recruited for 18 months TPD treatment. All received 500 mg Ca & 400 IU D3. DEXA scans of lumbar spine and hip were performed every 6 months on a GE Lunar Prodigy, lab specimen (calcium, BAP and crosslaps) at months 0, 1, 3, 6, 12 & 18. Paired bone biopsies from the iliac crest by Yamshidi puncture were taken at M 0, 6 & 18. RESULTS: 20 pts finished the study. BMD T-scores M0/M6/M12/M18: LS -2.96/-2.56/-2.24/-2.10 (p<0.05, but NS between M12-M18), FN -2.21/-2.32/-2.29/-2.23 (NS), TH -2.23/-2.22/-2.19/-2.11 (NS). Lab M0/M1/M3/M6: calcium no clinically relevant change (p<0.001 only at M3 vs. M0; 4 pts with intermittend asymptomatic hypercalcaemia); BAP 14.4/20.5/20.3/28.4/24.7/21.1 (increase p<0.001 until M6 followed by a decrease; ULN=21.4 mg/l); crosslaps 239/350/553/850/594/469 mcg/l (increase p3.5ys delayed change of crosslaps slightly until M3. Neither use of ALN vs. RIS, nor fracture vs. BMD decline influenced the results. MicroCT(M0/M6/M18): BV/TV 6.31/8.24/8.16% (p<0.05 at M6, NS between M6/M18). Tissue density 1.074/1.065/1.024 (NS at M6, p<0.01 at M18). Connectivity density 2.09/3.12/4.75 (NS at M6, p<0.01 at M18). SMI 2.05/1.76/1.73 (p=0.05 at M6, NS at M18). TbN 1.09/1.24/1.15 (p<0.01 at M6 only). TbTh 0.121/0.129/0.118 (NS). TbSp 0.907/0.810/0.884 (NS). CONCLUSIONS: TPD proved to have positive anabolic effects on BIS resistant osteoporosis. Early (< M6), continuous increases of BAP and crosslaps were detected without correlation to duration or type of previous BIS. Afterwards bone turnover declined despite ongoing TPD. BMD at LS also increased already at M6. Bone structural

parameters (BV/TV, SMI, TbN) significantly improved early during treatment. Histological cellular turnover corresponded with lab turnover markers with increases in 75% (M6) followed by a decrease in 57% (M18). Bone structural parameters (BV/TV, SMI, TbN) significantly improved early during treatment followed by a marked increase in structural heterogeneity (SD TbSp) and intrabascular resorption in 84% at M18. Our data suggests further studies with remitting cycles of 6 months TPD followed by antiresorptive agents to optimize positive effects of teriparatide.

**Disclosures:** B. Mucche, Lilly GmbH, Germany - travel support 5.  
This study received funding from: Lilly Germany.

## 1173

**A Novel Calcium-sensing Receptor Antagonist Leads to Dose-Dependent Transient Release of Parathyroid Hormone after Oral Administration to Healthy Volunteers - an Initial Proof-of-Concept for a Potential New Class of Anabolic Osteoporosis Therapeutics.** L. Widler<sup>1</sup>, R. Gamse<sup>1</sup>, K. Seuwen<sup>1</sup>, T. Buhl<sup>1</sup>, R. Beerli<sup>1</sup>, W. Breitenstein<sup>1</sup>, S. Gyaw<sup>2</sup>, C. Reynolds<sup>3</sup>, G. Bruin<sup>3</sup>, R. Belleli<sup>3</sup>, L. Klickstein<sup>3</sup>, M. R. John<sup>3</sup>. <sup>1</sup>Novartis Institutes of Biomedical Research, Basel, Switzerland, <sup>2</sup>Parexel International, Baltimore, MD, USA, <sup>3</sup>Exploratory Development, Novartis Pharma AG, Basel, Switzerland.

Antagonism of the calcium-sensing receptor in parathyroid glands leads to parathyroid hormone (PTH) release via stimulation of an endogenous hormone-release mechanism. Calcilytics are a new class of molecules which aim to exploit this mechanism. In order to mimic the known bone-anabolic PK profile of s.c. administered PTH, a drug must release PTH transiently and robustly. In a dose-limited exploratory IND study, two compounds were tested for their ability to stimulate PTH-release. This report focuses on one compound, ATF936, a quinazolin-2-one derivative. ATF936 was administered orally to 12 healthy male volunteers in a randomized, within-subject dose-rising, double-blind, active comparator, placebo-controlled single dose study. Weekly dose-escalations occurred at 6, 20, 40, 70 and 140 mg. Blood samples for safety, PK, and pharmacodynamic analyses were obtained frequently over each 24-h post-dose period. Elevations in plasma intact and bioactive PTH closely followed the linear PK profiles of ATF936. The median time to maximum PTH concentration (Tmax) was 1 h and PTH concentrations decreased fairly rapidly after Tmax, reaching the placebo levels approx. 12 h post-dose. The maximum mean post-dose PTH concentration (Cmax) was increased 1.9 to 5.9-fold relative to the average individual baseline for doses between 40 and 140 mg. For the 140 mg dose, the geometric mean PTH Cmax was 18.6 pmol/L (CV 35.5%). 24-h post-dose PTH was within baseline levels. There were no significant effects on serum calcium. Only a small transient increase at 4 h post-dose was observed at 140 mg, similar to the effect of Forteo. ATF936 was well tolerated at all doses and no serious adverse events were reported. Adverse event frequency, safety laboratory values, vital signs or 12-lead ECG intervals did not suggest any compound-related adverse effects. In conclusion, the observed transient PTH-release after administration of a single dose of the oral calcilytic ATF936, which had a profile close to that observed with s.c. PTH, constitutes a proof-of-concept in man. Further development of this promising class of compounds might yield a novel pharmaceutical approach for oral bone anabolic osteoporosis therapy.

**Disclosures:** M.R. John, None.  
This study received funding from: Novartis.

## 1174

**Ronacaleret, a Novel Calcium-Sensing Receptor Antagonist, Demonstrates Potential as an Oral Bone-Forming Therapy in Healthy Postmenopausal Women.** L. A. Fitzpatrick<sup>1</sup>, E. Brennan<sup>\*2</sup>, S. Kumar<sup>1</sup>, C. Matheny<sup>\*1</sup>, B. Yi<sup>\*1</sup>, M. McLaughlin<sup>\*1</sup>, J. Phillips<sup>\*1</sup>, L. Skordos<sup>\*1</sup>, D. Ethgen<sup>1</sup>. <sup>1</sup>GlaxoSmithKline, Collegeville, PA, USA, <sup>2</sup>Previously with GlaxoSmithKline. Current address: IndiPharm LLC, Haverford, PA, USA.

Short-term antagonism of calcium-sensing receptors (CaR) on parathyroid cells results in the transient release of endogenous parathyroid hormone (PTH), which stimulates bone formation. The purpose of this study was to assess the safety, tolerability, pharmacokinetics (PK) and pharmacodynamics (PD) of ronacaleret, a CaR antagonist being investigated as an oral treatment for osteoporosis.

This 2-session, single-blind, placebo-controlled, randomized, parallel-group, dose-rising study was conducted in multiple US centers. Subjects were split into 3 cohorts plus placebo; each subject participated in a single-dose session and a 28-day repeat-dose session. Doses were 75 mg, 175 mg, or 475 mg. Bone biomarker measurements (osteocalcin [OC], type I procollagen [PINP], bone specific alkaline phosphatase [BSAP] and carboxy-terminal collagen crosslinks [CTX]) were performed prior to dosing and 24 h postdose for each session.

All subjects were postmenopausal women (mean age, 55 years). Bone biomarker analysis (n=65) indicated a net bone-formation effect with dose-dependent increases in the bone-formation markers OC, PINP and BSAP at day 28 (mean percent change from baseline of 63%, 79% and 35%, respectively, for 475 mg [ $p < 0.05$ ], relative to placebo) and no significant change in the bone resorption marker CTX.

Ronacaleret AUC and Cmax (n=53) increased with increasing dose, although slightly less than dose proportionally. Mean terminal half-life was 4 to 5 h, with negligible accumulation of ronacaleret with repeat dosing. Median Tmax ranged from 2 to 2.5 h following repeat dosing. There was a dose- and concentration-dependent increase in maximal postdose PTH concentration (adjusted mean change of PTH from baseline on day 28 of 287%, 551% and 885% for 75 mg, 175 mg and 475 mg ronacaleret, respectively; n=75) and total serum calcium.

In the safety population (n=81), all AEs were considered mild or moderate. Headache, constipation and diarrhea were more frequent in subjects who received ronacaleret than in those who received placebo; however, no obvious dose responses were observed and most subjects did not require treatment. No serious AEs or deaths were reported.

Single and repeat doses of ronacaleret were well tolerated. The dose-dependent increases in endogenous PTH, calcium and bone-formation markers support further investigation of ronacaleret as a novel oral bone-forming treatment for patients with osteoporosis.

**Disclosures:** L.A. Fitzpatrick, GlaxoSmithKline, Collegeville, PA, USA 5.

## 1175

**How Does Body Fat Influence Bone Health In Childhood? A Mendelian Randomisation Approach.** J. H. Tobias<sup>1</sup>, N. Timpson<sup>\*2</sup>, A. Sayers<sup>\*1</sup>, G. Davey-Smith<sup>\*2</sup>. <sup>1</sup>CSNB, University of Bristol, Bristol, United Kingdom, <sup>2</sup>Social Medicine, University of Bristol, Bristol, United Kingdom.

Fat mass may be a positive determinant of bone mass in children, but the evidence is conflicting, possibly reflecting the influence of confounding factors. The recent identification of common genetic variants related to obesity in children provides an opportunity to implement a Mendelian randomization study of obesity and bone outcomes in childhood, which is less subject to confounding and several biases than are conventional approaches. 7470 children from the Avon Longitudinal Study of Parents and Children (ALSPAC) who underwent total body DXA scans using a Lunar Prodigy at mean 9.9 years were matched to those who had been genotyped for the *MC4R* rs17782313 and *FTO* rs939609 markers of obesity previously identified from genome-wide association studies. The relationship between total body fat mass tertile as measured by DXA and total body, spinal upper and lower limb bone mineral content (BMC) was analysed by linear regression. Instrumental variable (IV) effects on BMC were derived from regressions in which *MC4R* and *FTO* markers were used in combination as markers of obesity; these estimate the causal effect of body fat on bone outcomes. 5192 and 2878 children were available for IV analyses involving total body and spinal BMC respectively. In linear regression analyses, total fat mass was strongly related to BMC of the total body (1.26, 1.25-1.27), spine (1.25, 1.23-1.26), upper limb (1.24, 1.23-1.25) and lower limb (1.30, 1.29-1.30) (effects shown as ratios of geometric means per fat mass tertile, with 95% CI). IV regressions revealed equivalent effects as follows: total body (1.22, 1.13-1.32), spine (1.25, 1.15-1.35), upper limb (1.23, 1.13-1.34) and lower limb (1.24, 1.15-1.34). Similar results were obtained after adjusting for height and puberty, when trunk fat mass was used in place of total fat, and when bone area was used instead of bone mass. However, in analyses where total body BMC adjusted for bone area was the outcome (reflecting volumetric bone density), linear regression with fat mass showed no association (0.999, 0.997-1.000), whereas IV regression revealed a weak positive effect (1.028, 1.005-1.051). In conclusion, when *MC4R* and *FTO* markers were used as IVs for fat mass, very similar associations with BMC were seen to those with fat mass as measured by DXA, confirming that fat mass is on the causal pathway for bone mass in children. In addition, whereas fat mass had little effect on volumetric density, IVs exerted a weak positive effect, implying that conventional estimates may under-estimate the true effect of body fatness or that both *MC4R* and *FTO* influence skeletal development via pathways that are independent of fat mass.

**Disclosures:** J.H. Tobias, None.

This study received funding from: Wellcome Trust.

## 1176

**Genetic Variation in *LRP5* Associates with Metabolic Characteristics in Healthy Prepubertal Children.** S. Lappalainen<sup>\*1</sup>, A. Saarinen<sup>\*2</sup>, P. Utriainen<sup>\*1</sup>, R. Voutilainen<sup>\*1</sup>, J. Jääskeläinen<sup>\*1</sup>, O. Mäkitie<sup>3</sup>. <sup>1</sup>Department of Pediatrics, Kuopio University and University Hospital, Kuopio, Finland, <sup>2</sup>Folkhälsan Institute of Genetics, Biomedicum Helsinki, and Department of Medical Genetics, University of Helsinki, Helsinki, Finland, <sup>3</sup>Hospital for Children and Adolescents, University of Helsinki, Helsinki, Finland.

Several studies have indicated that Wnt signaling plays a role in metabolism and in adrenocortical function. Polymorphisms in the low-density lipoprotein receptor-related protein 5 gene (*LRP5*) have been associated with obesity and hypercholesterolemia. Mice lacking *lrp5* have reduced glucose-induced insulin secretion and increased cholesterol levels. Both *LRP5* and *WNT4* are expressed in the human adrenal cortex, and *Wnt4* knockout mice show altered steroidogenesis. We hypothesized that genetic variation in *LRP5* associates with metabolic characteristics in children.

We performed a cross-sectional association study in 97 healthy prepubertal children. *LRP5* genotypes were determined by direct sequencing. Three single nucleotide polymorphisms (SNPs) in *LRP5* were selected for single marker analyses: c.1647C>T (p.F549F), c.3357A>G (p.V1119V) and c.3989C>T (p.A1330V). Single marker associations with clinical-metabolic characteristics, including adrenal function, glucose tolerance and lipid profile, were examined with age and gender as covariates.

Sixteen SNPs in *LRP5* were found in the 79 girls and 18 boys [age; mean (SD) 7.5 (0.9) yr]. SNP A1330V associated with higher dehydroepiandrosterone sulfate (DHEAS) levels [A/A, n = 87 vs. A/a, n = 9; mean (95 % confidence interval), 0.8 (0.7, 0.9) umol/L vs. 1.4 (0.8, 2.3),  $p = 0.01$ ]. It associated also with higher levels of total [4.2 (4.0, 4.3) mmol/L vs. 4.7 (4.1, 5.4),  $p = 0.02$ ] and low-density lipoprotein cholesterol [2.4 (2.3, 2.5) mmol/L vs. 2.9 (2.3, 3.6),  $p = 0.02$ ], as did SNP V1119V (n = 72 vs. n = 25;  $p = 0.04$  and  $p = 0.03$ , respectively). SNP F549F associated with higher systolic blood pressure [n = 91 vs. n = 6; 100 (98, 102) mmHg vs. 108 (95, 121),  $p = 0.04$ ]. There were no differences in the parameters of glucose metabolism, serum HDL or triglyceride levels between the genotype groups.

The observed differences in serum DHEAS levels between *LRP5* genotype groups suggest that altered Wnt signaling may modulate adrenal hormone profile during childhood. The significant associations between the *LRP5* genotypes and several metabolic characteristics provide further evidence for a significant role of the Wnt signaling pathway in regulation of multiple metabolic pathways. As novel pharmacotherapies targeting Wnt signaling are being developed for the treatment of osteoporosis it is important to recognize extra-skeletal implications of altered Wnt signaling.

**Disclosures:** O. Mäkitie, None.

## 1177

**Childhood Cortical Bone and Skeletal Age Show Bivariate Genetic Linkage to Chromosome 2p.** D. L. Duren<sup>1</sup>, J. Blangero<sup>\*2</sup>, R. J. Sherwood<sup>\*1</sup>, J. E. Curran<sup>\*2</sup>, T. Dyer<sup>\*2</sup>, S. A. Cole<sup>\*2</sup>, S. A. Czerwinski<sup>\*1</sup>, W. C. Chumlea<sup>\*1</sup>, M. Lee<sup>1</sup>, A. C. Choh<sup>\*1</sup>, E. W. Demerath<sup>\*3</sup>, R. M. Siervogel<sup>1</sup>, B. Towne<sup>\*1</sup>. <sup>1</sup>Community Health, Wright State University, Dayton, OH, USA, <sup>2</sup>Genetics, Southwest Foundation for Biomedical Research, San Antonio, TX, USA, <sup>3</sup>School of Public Health, University of Minnesota, Minneapolis, MN, USA.

The coordinated yet distinct processes of childhood skeletal growth, maturation, and mineralization are essential components of healthy children. The genetic regulation of each process appears to be distinct, but it is also likely that they have some shared genetic basis. We present an analysis of the genetic architecture of bone health in 10-year-old children, prior to the rapid changes in bone associated with puberty. We analyzed radiographic cortical thickness of the second metacarpal and skeletal maturation of the hand-wrist using the FELS method (Roche et al., 1988) in 600 children from the Fels Longitudinal Study examined at chronological age 10 years. These children are from 144 nuclear and extended families. An initial set of 440 of these individuals have been genotyped for ~ 400 autosomal markers spaced approximately every 10 cM. A variance components-based linkage analysis method (SOLAR; Almasy and Blangero, 1998) was used to obtain uni- and bi-variate multipoint LOD scores. Univariate linkage analysis of medial cortical bone revealed a suggestive LOD score (2.29) for linkage to markers on chromosome 2p. We followed this with a bivariate linkage analysis of medial cortical thickness and skeletal age, and found significant linkage (LOD = 3.07) to markers on chromosome 2p25 (between markers D2S319 and D2S2211), indicating an increased linkage signal over that of medial cortical thickness alone to the same chromosomal position. The location of this linkage is in close proximity to a region identified by independent studies of adult bone mass that have identified potential positional candidate genes. Given that results of the current study are based on bone mass and maturation in 10-year-old children, this replication of linkage to this region is both exciting and promising for future gene identification in this sample. Our future work will continue this research emphasizing the identification of specific genes or sets of genes that influence bone mass, strength, and maturation independently and jointly throughout childhood development.

**Disclosures:** D.L. Duren, None.

This study received funding from: NIH grants HD56247, HD36342, HD12252, and MH59490.



## 1178

**The Extracellular Matrix Protein Periostin Regulates Periosteal Apposition.** R. K. Fuchs<sup>1</sup>, M. Galley<sup>2\*</sup>, J. Doyle<sup>2\*</sup>, F. Klene<sup>1\*</sup>, S. J. Conway<sup>3\*</sup>, S. J. Warden<sup>1</sup>, D. B. Burr<sup>4</sup>. <sup>1</sup>Physical Therapy, Indiana University, Indianapolis, IN, USA, <sup>2</sup>Biomedical Engineering, Purdue University, Indianapolis, IN, USA, <sup>3</sup>Herman B. Wells Center for Pediatric Research, Indiana University, Indianapolis, IN, USA, <sup>4</sup>Anatomy and Cell Biology, Indiana University School of Medicine, Indianapolis, IN, USA.

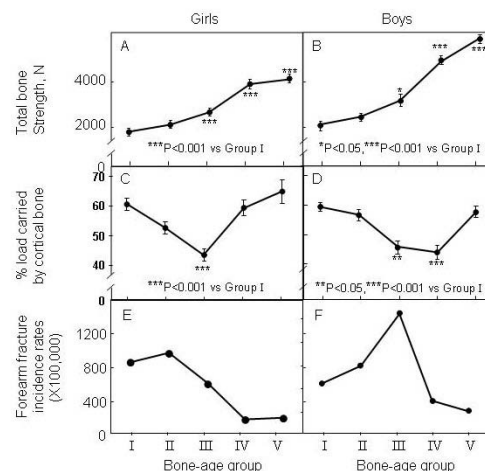
The identification of molecular pathways involved in regulating bone size is necessary to facilitate the development of novel therapies for preventing and treating osteoporosis. Periosteal expansion is well known to augment bone size during growth and aging, with resultant increases in bone strength; however, the genetic regulation of periosteal apposition remains unknown. The goal of this study was to examine the role of periostin (originally named osteoblast specific factor-2) in regulating cortical bone architecture and strength using a genetically-modified mouse model lacking a functional periostin gene. Periostin is an extracellular matrix protein preferentially expressed by immature osteoblasts located on periosteal bone surfaces. Based on the surface specificity of periostin we hypothesized that mice deficient in periostin (*peri*<sup>-/-</sup>) would have reduced bone size and strength when compared to wild-type controls (*peri*<sup>+/+</sup>). Ten mice per gender (male and female) and genotype (*peri*<sup>-/-</sup> and *peri*<sup>+/+</sup>) were evaluated. *In vivo* whole body bone mineral density (BMD; g/cm<sup>3</sup>) was assessed by dual energy x-ray absorptiometry (DXA) at 4-wk intervals from 4 to 16 wk. Upon euthanasia, the femur was excised and bone quantity of the total femur was assessed by DXA, geometry of the femoral mid-diaphysis was quantified by micro-CT, and biomechanical properties of the femoral diaphysis were evaluated by 3-point bending. *Peri*<sup>-/-</sup> mice had significantly reduced whole body BMD at 4, 8, 12, and 16 wk of age (all *p*<0.05). At 16 wk, femurs from *peri*<sup>-/-</sup> mice had significantly reduced BMD, cortical bone area, resistance to strain, and breaking strength when compared to *peri*<sup>+/+</sup> mice (all *p*<0.05). There were no significant genotype by gender interactions for any of the skeletal outcome measures (all *p*>0.05). Based on the surface-specificity of periostin, these data indicate that periostin may be involved in the regulation of bone size via periosteal apposition, and thus may be a novel target for the treatment of bone disease.

**Disclosures:** R.K. Fuchs, None.

## 1179

**Microfinite Element Modeling Reveals That Transient Deficits In Cortical Bone May Underlie The Adolescent Peak In Forearm Fractures.** S. Kirmani<sup>1</sup>, D. Christen<sup>2</sup>, G. H. van Lenthe<sup>2</sup>, P. R. Fischer<sup>1\*</sup>, M. L. Boussein<sup>3</sup>, B. L. Riggs<sup>1</sup>, L. J. Melton<sup>1</sup>, S. Amin<sup>1</sup>, J. Peterson<sup>1\*</sup>, L. McCready<sup>1\*</sup>, R. Müller<sup>1</sup>, S. Khosla<sup>1</sup>. <sup>1</sup>Mayo Clinic, Rochester, MN, USA, <sup>2</sup>ETH Zurich, Zurich, Switzerland, <sup>3</sup>Harvard Medical School, Boston, MA, USA.

The incidence of distal forearm fractures peaks during the adolescent growth spurt, but the biomechanical basis for this is unclear. Thus, we studied the distal radius of healthy 6-21 yr-old males (n = 61) and females (n = 66) using high-resolution pQCT (XtremeCT, Scanco, voxel size 82 microns). Subjects were classified into 5 groups by bone age (BA): Group I (pre-puberty, BA 6-8 yrs), Group II (early puberty, BA 9-11 yrs), Group III (mid-puberty, BA 12-14 yrs), Group IV (late puberty, BA 15-17 yrs) and Group V (post-puberty, BA 18-21 yrs). Compared to Group I, trabecular parameters (bone volume, density, trabecular number, and trabecular thickness) did not change in girls (*P* > 0.2), but increased in boys (*P* < 0.05) from late puberty onwards. Cortical thickness and volumetric BMD decreased from pre- to mid-puberty in girls (*P* < 0.01) but were unchanged in boys (*P* > 0.05) before rising to higher levels at the end of puberty (*P* < 0.001). Total bone strength, assessed using microfinite element (μFE) models, increased linearly across age groups in both sexes, with boys showing greater bone strength than girls after mid-puberty (*P* < 0.01) (Fig. A, B). Because the proportion of load borne by cortical vs. trabecular bone reflects, in part, the relative strengths of these compartments, we also evaluated how this changed during growth. As shown in Fig. C and D, the proportion of load borne by cortical bone (derived from the μFE models) decreased transiently during puberty in both sexes, mirroring the incidence of distal forearm fractures previously reported in this community (Fig. E, F). Since cadaveric studies (Osteoporosis Int 14:345, 2003) have demonstrated that cortical bone is a critical determinant of failure load at the wrist, the observed transient shift of load-bearing from cortical to trabecular bone in both sexes during puberty, and the concordance of this with the incidence of adolescent fractures, suggest that regional deficits in cortical bone may underlie the adolescent peak in forearm fractures. Further studies comparing adolescents with and without forearm fractures are needed to test whether children with fractures have greater deficits in cortical bone than children without fractures.



**Disclosures:** S. Kirmani, None.

This study received funding from: Thrasher Research Fund, NIH, Mayo Clinic Pediatric And Adolescent Medicine Research Committee.

## 1180

**Contribution of the Vertebral Posterior Elements in AP DXA Scans.** D. C. Lee, P. Campbell<sup>\*</sup>, V. Gilsanz, T. A. L. Wren. Childrens Hospital Los Angeles, University of Southern California, Los Angeles, CA, USA.

Because dual energy x-ray absorptiometry (DXA) is a two-dimensional projection technique, anterior-posterior (AP) measurements of the spine include the posterior elements as well as the vertebral body. This may be a disadvantage since the posterior elements likely contribute little to vertebral fracture resistance. This study used quantitative computed tomography (QCT) to quantify the impact of the posterior elements in DXA AP spine measures.

We examined 325 children (163 girls, 162 boys) age 6-21 yr, with both DXA and QCT. QCT data were acquired for a 10mm thick slice at the midportion of L3. QCT measures were calculated both including and excluding the posterior elements. DXA AP spine data were analyzed for the 10mm slice corresponding to the QCT scan region and for the entire L3 vertebra. Bone mineral content (BMC, g) and density (DXA aBMD, g/cm<sup>2</sup>; QCT vBMD, g/cm<sup>3</sup>) were determined and compared using Pearson's correlation. The posterior elements accounted for 51 ± 4% (range 39-65) of the total BMC. Nevertheless, the BMC measured by DXA and QCT correlated strongly for both the 10mm slice and the whole vertebra (*r* = .94). The relationships were weaker when excluding the posterior elements (*r* = .88). Weaker correlations were observed when comparing BMD measured by DXA and QCT (*r* = .73-.82). Our results indicate that even though the vertebral posterior elements account for half the BMC measured by DXA, the contribution of the posterior elements is relatively consistent. DXA therefore provides a reasonable measure of total BMC. However, DXA BMD values are less dependable, particularly as a measure of density of the vertebral body. We conclude that BMC is a more informative measure of bone in the lumbar spine of pediatric subjects than BMD and should therefore be the preferred measure.

	Correlation coefficients of DXA/QCT BMD/BMC measures.			
	DXA L3	DXA 10mm	QCT total	QCT vertebral body
DXA L3	1.00	.93 (BMC)	.94 (BMC)	.88 (BMC)
DXA 10mm	.91 (BMD)	1.00	.94 (BMC)	.88 (BMC)
QCT total	.79 (BMD)	.82 (BMD)	1.00	.95 (BMC)
QCT vertebral body	.73 (BMD)	.76 (BMD)	.90 (BMD)	1.00

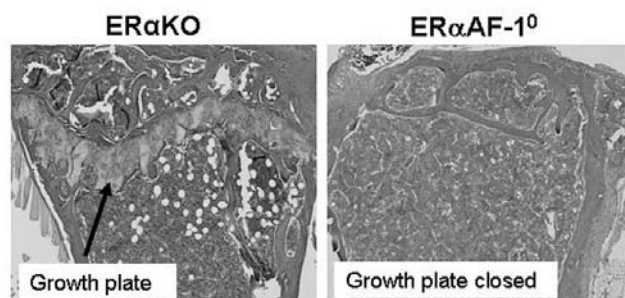
**Disclosures:** D.C. Lee, None.

This study received funding from: Dept of the Army.

## 1181

**Specific Inactivation of AF-1 in Estrogen Receptor- $\alpha$  (ER $\alpha$ ) Results in Growth Plate Closure while Total Inactivation of ER $\alpha$  Results in Increased Growth Plate Width in Elderly Female Mice.** A. E. Börjesson<sup>\*1</sup>, S. H. Windahl<sup>1</sup>, M. Antal<sup>\*2</sup>, A. Krust<sup>\*2</sup>, P. Chambon<sup>\*2</sup>, C. Ohlsson<sup>1</sup>. <sup>1</sup>Department of Medicine, Center for Bone Research, Sahlgrenska Academy, Göteborg University, Gothenburg, Sweden, <sup>2</sup>Institut de Génétique et de Biologie Moléculaire et Cellulaire, Illkirch, France.

Estrogen affects skeletal growth and promotes growth plate fusion in humans. In rodents, the growth plates do not fuse directly after sexual maturation, but prolonged treatment with high levels of estradiol has the capacity to fuse the growth plates. The DNA binding domain of estrogen receptor- $\alpha$  (ER $\alpha$ ) is surrounded by transcription activation function 1 (AF-1, N-terminal, ligand independent) and AF-2 (ligand dependent). AF-1 activity is promoter and cellular context dependent. The *in vivo* role of AF1 is unknown. The aim of the present study was to *in vivo* determine the role of AF-1 in the modulation of ER $\alpha$ -mediated effects in the growth plate. The skeletal growth and growth plate morphology of elderly (16-19 months of age) female mice with specific inactivation of AF-1 in ER $\alpha$  (ER $\alpha$ AF-1<sup>0</sup>) and mice with total inactivation of ER $\alpha$  (ER $\alpha$ KO) were compared with wild type mice. The lengths of both femur and tibia were increased in ER $\alpha$ <sup>-/-</sup> mice (Femur + 6.0%, Tibia +8.3%,  $p < 0.001$ ) but decreased in ER $\alpha$ AF-1<sup>0</sup> mice (Femur - 4.0%, Tibia -4.9%,  $p < 0.001$ ) compared with wild type mice. Importantly, the proximal tibial growth plate was closed in all ER $\alpha$ AF-1<sup>0</sup> mice, while it was open in all wild type mice (Fig). In contrast, ER $\alpha$ KO mice displayed increased growth plate width compared with wild type mice (ER $\alpha$ KO 111 $\pm$ 5  $\mu$ m, wild type 92 $\pm$ 4  $\mu$ m,  $p < 0.05$ , Fig). In conclusion, specific inactivation of AF-1 in ER $\alpha$  results in inhibited longitudinal bone growth due to growth plate closure while total inactivation of ER $\alpha$  results in enhanced bone growth in elderly female mice. Our data indicate that for the regulation of growth plate width/closure in elderly female mice, specific inactivation of AF-1 results in a hyperactive ER $\alpha$  AF2 transcription activation function, promoting growth plate closure.



**Disclosures:** A.E. Börjesson, None.

## 1182

**DNA Demethylation for Hormone-Induced Transcriptional Derepression.** M. Kim<sup>\*1</sup>, F. Ohtake<sup>\*1</sup>, I. Takada<sup>\*1</sup>, K. Takeyama<sup>\*1</sup>, H. Shibuya<sup>\*2</sup>, S. Kato<sup>1</sup>. <sup>1</sup>Institute of Molecular and Cellular Biosciences, University of Tokyo, Tokyo, Japan, <sup>2</sup>Department of Molecular Cell Biology, Mineral Research Institute and School of Biomedical Science, Tokyo Medical and Dental University, Tokyo, Japan.

Epigenetic modifications at the histone level affect gene regulation in response to extracellular signals. However, regulated epigenetic modifications at the DNA level, especially active DNA demethylation, in gene activation is not well understood. Here we report that DNA methylation/demethylation is hormonally switched to control transcription of the CYP27B1 gene. Reflecting the vitamin D (VD)-mediated transrepression of the CYP27B1 gene through the nVDRE, methylation of CpG sites (5mCpG) are induced by VD in this gene promoter. Conversely, treatment with PTH, a hormone known to activate the CYP27B1 gene, induces active demethylation of the 5mCpG sites in this promoter. Biochemical purification of a complex associated with the nVDRE-binding protein (VDIR) identified DNA methyl transferases, Dnmt1 and 3b for methylation of CpG sites, as well as a DNA glycosylase, MBD4. Phosphorylation of MBD4 by PTH-activated PKC potentiates its DNA glycosylase activity for 5mCpG. The association of DNA ligase I and polymerase  $\beta$  in the MBD4-bound promoter suggests a base excision repair process for DNA demethylation. Such PTH-induced DNA demethylation and subsequent transcriptional derepression are impaired in MBD4<sup>-/-</sup> mice. Thus, the present findings suggest that methylation switching at the DNA level contributes to, at least in part, the hormonal controls of transcription.

**Disclosures:** M. Kim, None.

This study received funding from: ERATO, Japan Science and Technology Agency.

## 1183

**Characterization of Interactions Between the Unliganded VDR and Effectors of the Canonical Wnt Signaling Pathway.** H. F. Luderer, M. B. Demay. Endocrine Unit, Massachusetts General Hospital and Harvard Medical School, Boston, MA, USA.

Ligand-independent functions of the Vitamin D Receptor (VDR) in keratinocyte stem cells are essential for normal hair follicle regeneration in mice. Previous studies demonstrated that the VDR is necessary for synergistic activation of Wnt reporter genes by LEF-1 and  $\beta$ -catenin in primary keratinocytes. Furthermore, when co-expressed in COS-7 cells, the VDR is present in a complex with  $\beta$ -catenin and LEF-1. While these data suggest that the VDR acts with  $\beta$ -catenin and LEF-1 to activate Wnt signaling in keratinocytes, the specific protein-protein interactions involved remain undefined. The purpose of this study was to identify and characterize the protein-protein interactions between the unliganded VDR and key effectors of the canonical Wnt signaling pathway. To determine if  $\beta$ -catenin and/or LEF-1 bind the VDR directly, a GST-fusion system was employed. An N-terminal GST-fusion of the wild type VDR was engineered in pGEX-5x-1 and expressed in bacteria. GST-VDR was bound to glutathione sepharose beads in the absence of ligand and then incubated with nuclear extracts isolated from COS-7 cells expressing endogenous  $\beta$ -catenin with or without LEF-1-HA. Proteins were eluted using reduced glutathione and subjected to Western analysis for detection of LEF-1-HA, endogenous  $\beta$ -catenin, and the VDR. While LEF-1 co-eluted with the GST-VDR,  $\beta$ -catenin did not. These data suggest that the unliganded VDR interacts with LEF-1 independently of  $\beta$ -catenin. To test whether the interaction between the VDR and LEF-1, was indeed ligand independent, similar experiments were performed using GST-L233SVDR, a VDR mutant unable to bind ligand. The L233SVDR mutant retained the ability to bind to LEF-1, demonstrating that ligand is not necessary for this interaction. This is in contrast with previous investigations demonstrating that liganded VDR interacts with  $\beta$ -catenin. Based on the observation that the effects of the VDR on the hair follicle are ligand-independent, it is likely that a VDR-LEF1 interaction plays a significant role in maintaining hair follicle homeostasis. Additional studies will be directed at determining which domains of the VDR are required and whether other effectors of canonical Wnt signaling also contribute to this interaction.

**Disclosures:** H.F. Luderer, None.

## 1184

**A Genetic Model to Study 1,25 dihydroxyvitamin D Action in Classical and Non-classical Target Tissues.** Y. Xue<sup>\*</sup>, J. Fleet. Dept. of Foods and Nutrition, Purdue University, West Lafayette, IN, USA.

1,25 dihydroxyvitamin D (VD) plays a vital role in maintaining calcium (Ca) and bone metabolism through vitamin D receptor (VDR) activation in the bone, kidney, and intestine. VD has been proposed to have effects in addition to the control of Ca metabolism but the function of VD in its non-classical target tissues is still unclear and the strong interdependency between VD action and Ca metabolism confounds studies in VDR knockout mice (KO) or vitamin D deficient mice. Previously, we recovered the disrupted Ca metabolism of VDR knockout mice by intestine-specific transgenic expression of human VDR (mVDR<sup>-/-</sup>, hVDR<sup>+/+</sup>; KO/TG). In this model, intestinal Ca absorption was recovered leading to normalized serum calcium, serum parathyroid hormone, and growth (bone length and body size) with improved femoral bone mass at 3 mo. To further study the role of VDR in its non-classical target tissues, we fed male mVDR<sup>+/+</sup> and KO/TG mice with AIN76A diet (0.5% Ca; 0.3% phosphorus (P)) and mVDR<sup>-/-</sup> with rescue diet (2% Ca, 1.2% P, 20% lactose (KO\_R)). At the 10 mo, serum calcium and PTH were recovered but urinary Ca was elevated (>8-fold) in both KO\_R and KO/TG (i.e. urinary Ca reabsorption requires VDR). Several parameters were normalized in KO/TG but not in KO\_R: duodenal calbindin D<sub>9k</sub> and TRPV6 mRNA (64% and 96% lower, respectively), body length (5% lower), femur length (8% lower), whole body bone mineral density (BMD) (22% lower), and heart size as % of body weight (BW) (30% higher). Thus, intestine-specific transgenic VDR recovery offers a benefit not met by the high Ca rescue diet. In contrast, body weight was reduced in KO\_R (34% lower) and partially recovered in KO/TG mice (20% lower). This was due to significant reductions in lean body mass (DEXA: KO\_R 19% lower; KO/TG 14% lower) as well as total body (DEXA), epididymal, and retroperitoneal fat mass (each 63% lower in KO\_R; 45% lower in KO/TG). This shows that has a VDR unique role in the control of fat and lean mass beyond that due to changes in Ca metabolism.

**Disclosures:** Y. Xue, None.

This study received funding from: NIH awards DK54111 and CA101113 to JCF.

## 1185

**Vitamin D Delays Breast Cancer Progression in the PyVMT Transgenic Mouse Model: Local Conversion of the Precursor 25(OH)<sub>2</sub>D<sub>3</sub> into 1,25(OH)<sub>2</sub>D<sub>3</sub> Is Safer and More Effective than Systemic Administration of 1,25(OH)<sub>2</sub>D<sub>3</sub>.** L. Rossdeutsch<sup>1</sup>, D. Haug<sup>1</sup>, J. Li<sup>1</sup>, T. Reinhardt<sup>2</sup>, W. Muller<sup>1</sup>, R. Kremer<sup>1</sup>. <sup>1</sup>Department of Medicine, McGill University Health Center, McGill University, Montreal, QC, Canada, <sup>2</sup>National Animal Disease Center United States Department of Agriculture Research, Ames, IA, USA.

Metabolic activation of 1,25(OH)<sub>2</sub>D<sub>3</sub> occurs at extra renal sites in several organs including breast. The purpose of this study was to determine if this local tumoral 25OHD<sub>3</sub>-1 $\alpha$ hydroxylase expression modulates any or all of the stages of breast tumor progression. For this purpose we used the PyVMT breast cancer mouse model in which the oncoprotein, polyomavirus middle T antigen (PyMT) is under the control of mouse mammary tumor virus LTR (MMTV LTR) and faithfully reproduces all stages of human breast cancer. Four week old females were treated prior to mammary intraepithelial neoplasia with either vehicle, 25OHD<sub>3</sub> (2000 pM/24h) or 1,25(OH)<sub>2</sub>D<sub>3</sub> (12pM/24h) for a total of 8 weeks. 1 $\alpha$ hydroxylase expression was measured and remained unchanged throughout the various stages of tumor progression. Kaplan Meier analysis indicated that mice treated with 25OHD<sub>3</sub> or 1,25(OH)<sub>2</sub>D<sub>3</sub> had a significant delay in tumor onset as compared to vehicle-treated animals (25OHD<sub>3</sub>=27days>1,25(OH)<sub>2</sub>D<sub>3</sub>=23days>Control =9days, P<.05). Furthermore, tumor growth overtime was significantly reduced in both 25OHD<sub>3</sub> and 1,25(OH)<sub>2</sub>D<sub>3</sub> treated groups in comparison to the placebo treated group (25OHD<sub>3</sub> 58.0  $\pm$  2.0 % (P<.002) >1,25(OH)<sub>2</sub>D<sub>3</sub> 45.1  $\pm$  2.2 % (P<.002)>Control). In addition, the expression of biomarkers and histological indices of tumor progression in 25OHD<sub>3</sub> and 1,25(OH)<sub>2</sub>D<sub>3</sub> treated animals were markedly delayed as compared to vehicle-treated animals. However, mean circulating 1,25(OH)<sub>2</sub>D<sub>3</sub> and calcium concentrations remained unchanged in 25OHD<sub>3</sub>-treated animals (2.39 $\pm$ .1mmol/L) but increased significantly in 1,25(OH)<sub>2</sub>D<sub>3</sub>-treated animals (3.19 $\pm$ .09 mmol/L P<.05) as compared to vehicle-treated (2.38 $\pm$ .02 mmol/L). Moreover, tumoral levels of 1,25(OH)<sub>2</sub>D<sub>3</sub> in mice treated with 25OHD<sub>3</sub> were significantly higher as compared to both 1,25(OH)<sub>2</sub>D<sub>3</sub> and vehicle-treated animals (25OHD<sub>3</sub>=390 $\pm$ 16.7pg/g>1,25(OH)<sub>2</sub>D<sub>3</sub>=326 $\pm$ .26.8pg/g>Control =182 $\pm$ .10.5pg/g, P<.05). Finally, 25OHD<sub>3</sub> and 1,25(OH)<sub>2</sub>D<sub>3</sub>-treated animals had a significant decrease in the mean number and surface area of lung metastases as compared to vehicle-treated animals (P<.05). Our data indicate that metabolic activation of 25OHD<sub>3</sub> in the mammary epithelium delays tumor progression and is more potent than systemic administration of 1,25(OH)<sub>2</sub>D<sub>3</sub> without inducing significant side effects. Our data suggest that strategies aimed at increasing local tissue concentrations of 1,25(OH)<sub>2</sub>D<sub>3</sub> may provide a novel and safe approach in the prevention of breast cancer.

**Disclosures:** L. Rossdeutsch, None.

This study received funding from: Candian Institue of Health Research, NSERC, Dairy Farmers of Canada.

## 1186

**The Rapid-Nontranscriptional Action of 1,25-(OH)<sub>2</sub>D<sub>3</sub> Induces IL-6 Production in Osteoclast Precursors Expressing Measles Virus Nucleocapsid Protein (MVNP).** Y. Hiruma<sup>1</sup>, S. Ishizuka<sup>2</sup>, G. D. Roodman<sup>3</sup>, N. Kurihara<sup>1</sup>. <sup>1</sup>Medicine/Hem-Onc, University of Pittsburgh, Pittsburgh, PA, USA, <sup>2</sup>Bone & Calcium Metab., Teijin Institute for Biomedical Research, Tokyo, Japan, <sup>3</sup>Medicine/Hem-Onc, University of Pittsburgh and VA Pittsburgh Healthcare System, Pittsburgh, PA, USA.

Osteoclasts (OCL) from patients with Paget's disease (PD) produce high levels of IL-6 and express MVNP. Targeting MVNP to the OCL lineage in transgenic mice results in formation of bone lesions and OCL characteristic of PD (PD-OCL). The capacity of MVNP to induce PD-OCL results in part from its capacity to induce both hyper-responsivity of OCL precursors to 1,25-(OH)<sub>2</sub>D<sub>3</sub> through increased expression of a VDR co-activator, TAF<sub>II</sub>-17, and high levels of IL-6 in the local bone microenvironment. However the molecular mechanisms responsible are still unclear. Since 1,25-(OH)<sub>2</sub>D<sub>3</sub> can induce both genomic and rapid-nontranscriptional actions of VDR, we determined the contribution of both activities of VDR to PD-OCL formation by human OCL precursors expressing MVNP. To determine the contribution of each pathway, we treated OCL precursors expressing MVNP or empty vector (EV) with either 1,24R-(OH)<sub>2</sub>-lumisterol<sub>3</sub> (1,24-Lu), which induces rapid-nontranscriptional actions of VDR, 1 $\beta$ ,25-(OH)<sub>2</sub>D<sub>3</sub> (1 $\beta$ ), a strong antagonist for the rapid-nontranscriptional effects of VDR, and (23S)-25-Dehydro-1 $\alpha$ -(OH)<sub>2</sub>-26,23-lactone (TEI-9647), a pure antagonist for the genomic actions of 1,25-(OH)<sub>2</sub>D<sub>3</sub>. 1,24-Lu increased OCL formation and bone resorption by MVNP transduced OCL precursors. However, in contrast to OCLs induced by 1,25-(OH)<sub>2</sub>D<sub>3</sub>, 1,24-Lu did not induce PD-OCL. Further, TEI-9647 inhibited the formation of PD-OCL (increased OCL number and nuclei per OCL) in OCL expressing MVNP. Thus, the genomic effects of VDR are required for development of PD-OCL. We confirmed that 1,24-Lu did not increase VDR mediated transcription in the presence of high levels of TAF<sub>II</sub>-17, using a modified mammalian two-hybrid assay. 1,25-(OH)<sub>2</sub>D<sub>3</sub> but not 1,24-Lu increased VDR mediated transcription in the presence of high levels of TAF<sub>II</sub>-17. We then examined which actions of VDR were responsible for the increased production of IL-6 by MVNP expressing OCL. 1,24-Lu induced IL-6 expression by OCL and this was blocked by either a p38MAPK inhibitor or by 1 $\beta$ . These results suggest that both the genomic and the rapid-nontranscriptional actions of VDR are required for MVNP to induce PD-OCL.

**Disclosures:** Y. Hiruma, None.

This study received funding from: NIH.

## 1187

**C/EBP $\beta$  / p57<sup>Kip2</sup> Signaling Maintains Transition from Proliferation to Hypertrophic Differentiation of Chondrocytes during Skeletal Growth.** M. Hirata, F. Kugimiya, S. Ohba, N. Kawamura, T. Ogasawara, Y. Kawasaki, T. Ikeda, K. Nakamura\*, U. Chung, H. Kawaguchi. Sensory & Motor System Medicine & Tissue Engineering, University of Tokyo, Tokyo, Japan.

This study investigated the role of CCAAT/enhancer-binding protein  $\beta$  (C/EBP $\beta$ ), a multi-functional transcription factor, in chondrocytes during skeletal growth. C/EBP $\beta$  was shown by immunohistochemistry to be localized mainly in late proliferative and pre-hypertrophic chondrocytes of the mouse growth plate. The homozygous deficient (C/EBP $\beta$ <sup>-/-</sup>) mice exhibited dwarfism from embryonic stages. The growth plate showed elongation of the proliferative zone and delay of the chondrocyte hypertrophy determined by BrdU uptake and type X collagen (COL10) immunostaining, respectively. In cultures of primary chondrocytes from C/EBP $\beta$ <sup>-/-</sup> ribs, cell proliferation determined by XTT assay was enhanced, while hypertrophic differentiation determined by COL10, MMP-13 and VEGF mRNA levels as well as ALP and Alizarin red stainings was suppressed. In contrast, retroviral overexpression of C/EBP $\beta$  in the wild-type chondrocytes suppressed the proliferation and enhanced the hypertrophic differentiation, suggesting the involvement of C/EBP $\beta$  in the transition from proliferation to hypertrophic differentiation of chondrocytes. A DNA cell cycle histogram in C3H10T1/2 cells revealed that the C/EBP $\beta$  overexpression caused accumulation of cells in the G0/G1 fraction. A microarray analysis identified several cell cycle factors as transcriptional targets of C/EBP $\beta$ , and among them p57<sup>Kip2</sup>, a cyclin-dependent kinase inhibitor, was shown by real-time RT-PCR to be most strongly up-regulated by the C/EBP $\beta$  overexpression and down-regulated by the C/EBP $\beta$  deficiency (C/EBP $\beta$ <sup>-/-</sup>) in chondrocytes. p57 was co-localized with C/EBP $\beta$  in the growth plate, which was dramatically decreased by the C/EBP $\beta$  deficiency. In HuH-7 cells transfected with a luciferase-reporter gene construct containing the p57 promoter region, the transcriptional activity was enhanced by C/EBP $\beta$  co-transfection. Deletion, mutagenesis, and tandem-repeat analyses of the luciferase assay identified the core responsive element to be between the -150 and -130 bp region containing a putative consensus site for C/EBP. The electrophoretic mobility shift assay revealed the binding of nuclear extracts of C/EBP $\beta$ -overexpressed COS7 cells with the oligonucleotide including this region, whose specificity was verified by the C/EBP $\beta$  antibody supershift. Finally, knockdown of p57 by siRNA inhibited the C/EBP $\beta$ -induced hypertrophic differentiation in cultured chondrocytes. We conclude that C/EBP $\beta$  directly transactivates p57 at a C/EBP element to maintain transition from proliferation to hypertrophic differentiation of chondrocytes during skeletal growth.

**Disclosures:** M. Hirata, None.

## 1188

**Dexamethasone Triggers Mitochondrial Apoptosis Through Bax in Proliferative Growth Plate Chondrocytes Causing Growth Retardation.** F. Zaman<sup>1</sup>, D. Chrystis<sup>\*1</sup>, K. Huntjens<sup>\*1</sup>, M. Takigawa<sup>\*2</sup>, B. Fadeel<sup>\*3</sup>, L. Savendahl<sup>\*1</sup>. <sup>1</sup>Woman and Child Health, Karolinska Institutet, Stockholm, Sweden, <sup>2</sup>Okayama University, Tokyo, Japan, <sup>3</sup>Institute of Environmental Medicine, Karolinska Institutet, Stockholm, Sweden.

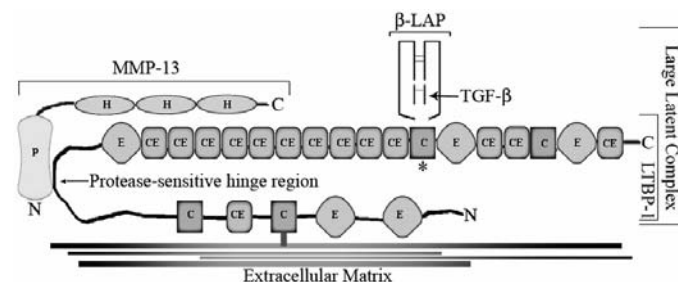
Dexamethasone (Dexa), a widely used glucocorticoid in children, causes severe growth retardation after long-term treatment. Investigating the deleterious effect of Dexa on growth, we have previously shown that Dexa induces apoptosis in proliferative chondrocytes. However, it is still unknown whether Dexa targets mitochondria by regulating the Bcl-2 family of proteins to induce apoptosis in proliferative chondrocytes. To address this, we have used an array of model system both in vitro (human HCS-2/8 proliferative chondrocytes, cultured fetal rat metatarsal bones) and in vivo (rat tibia growth plate). Fluorescent immunohistochemistry and Western immunoblot was performed to study the regulation of pro- and anti-apoptotic proteins. Apoptosis and cytochrome c release was quantified by ELISA. Gene silencing was performed with small interfering RNAs (siRNAs). When investigating mitochondrial-mediated apoptosis in HCS-2/8 proliferative chondrocytes, we found that Dexa (25 micromolar) induced conformational changes in Bax and increased its levels 3-fold (p<0.001 vs. control). We further verified Bax-conformational changes and its translocation into mitochondria in cultured fetal rat metatarsal bones and in the tibia growth plate of rats treated with Dexa. In addition, we observed greater mitochondrial depolarization (p<0.001 vs. control) and cytochrome c release (p<0.01 vs. control) in Dexa treated HCS chondrocytes. Interestingly, Dexa treatment in HCS cells not only altered the expression of Bcl-xS/L (p<0.01 vs. control) but also suppressed the levels of the inhibitor of apoptosis protein-2 by 25 % (p<0.01 vs. control). Suppression of the pro-apoptotic protein Bid with siRNA partially rescued chondrocytes from Dexa-induced apoptosis. Interestingly, Bax-suppression with siRNA completely rescued chondrocytes from apoptosis (p<0.01 vs. Dexa), suggesting Bax as a key regulator of apoptosis in these cells. In conclusion, we report for the first time that Dexa triggers apoptosis in chondrocytes by regulating the Bcl-2 family member of proteins. We found that the pro-apoptotic protein Bax acts as a key regulator of mitochondrial-mediated apoptosis. These results not only identify potential upstream and downstream therapeutic targets in Dexa-induced apoptosis but also indicate a significant role of the Bcl-2 family member of proteins. Based on these data, we speculate that glucocorticoid treatment in vitro and in vivo triggers mitochondrial mediated apoptosis in growth plate chondrocytes and thereby cause growth retardation.

**Disclosures:** F. Zaman, None.

## 1189

**Novel MMP13-derived Peptides Demonstrate Non-covalent Interaction of MMP13 with the TGF $\beta$  Large Latent Complex.** A. A. Selim<sup>\*1</sup>, S. M. Routson<sup>\*2</sup>, S. Lau<sup>\*2</sup>, M. D'Angelo<sup>2</sup>. <sup>1</sup>Biomedical Technology Research Group, KFUPM, Dhahran, Saudi Arabia, <sup>2</sup>Center for Chronic Disorders of Aging, Philadelphia College of Osteopathic Medicine, Philadelphia, PA, USA.

Dysregulated TGF $\beta$  activation has been indicated in the pathology of osteoarthritis. We have proposed a model of the mechanism of release of the TGF $\beta$  large latent complex by MMP13 that places the catalytic domain of MMP13 in alignment with the protease-sensitive hinge region of LTBP1, the site of release of this molecule from the extracellular matrix. Our bioinformatics-based model predicted that the hemopexin-like domains of MMP13 can non-covalently interact with the calcium-EGF-like domains of Latent TGF $\beta$  Binding Protein (LTBP1).



To test this proposed interaction, we designed three peptides from the hemopexin-like domain of MMP13 that are most likely to interact with LTBP1: MMP13-7, MMP13-10 and MMP13-19. We tested total binding of these fluorescence-labeled peptides with cartilage tissue extracts or LTBP1 immunoprecipitated proteins from cartilage tissue extracts. Specificity of binding was tested by displacement with 10-fold non-labeled peptide and controls included scrambled sequence of the same amino acid composition. Binding data demonstrated that MMP13-19 peptide had the most significant total binding and specific binding compared to the scrambled peptide. Hypertrophic cartilage extracts bound four times more MMP13-19 peptide than scrambled control and cartilage tissue extract immunoprecipitated with antibody to LTBP1 demonstrated three times more binding affinity for MMP13-19 peptide than the scrambled control. Specific binding was demonstrated by displacement of the MMP13-19 peptide binding in cartilage tissue extracts ( $p < 0.001$  compared to MMP13-19 fluorescent peptide binding). MMP13-7 had no significant total or specific binding and MMP13-10 had modest total and specific binding. These data suggest that the peptide sequence of the hemopexin-like domain, equivalent to MMP13-19, could competitively inhibit MMP13 non-covalent binding to LTBP1 in the TGF $\beta$  large latent complex resulting in decreased TGF $\beta$  activation. It is known that increased TGF $\beta$  activation plays an important role in osteoarthritis pathology. Therefore, these data indicate that the MMP13-19 peptide may have potential therapeutic applications for osteoarthritis.

**Disclosures:** M. D'Angelo, None.

This study received funding from: Center for Chronic Disorders of Aging and KFUPM.

## 1190

**Targeted Disruption of Nuclear Factor-E2 Related Factor-1 (Nrfl) in Osteoblasts Leads to Reduced Bone Size and Dramatic Alterations in Trabecular Bone Microstructure in Mice.** J. Kim<sup>\*1</sup>, W. Xing<sup>2</sup>, J. Chan<sup>\*3</sup>, S. Mohan<sup>4</sup>. <sup>1</sup>MDC, JLP VA Med Ctr, Loma Linda, CA, USA, <sup>2</sup>LLU, Loma Linda, CA, USA, <sup>3</sup>UC at Irvine, Irvine, CA, USA, <sup>4</sup>MDC, JLP VA Med Ctr, Loma Linda, CA, USA.

We recently showed that Nrfl is involved in mediating ascorbic acid (AA)-induced osterix expression and osteoblast (OB) differentiation via binding to antioxidant response element of mouse osterix promoter. Based on our *in vitro* data that Nrfl regulates genes critical for OB differentiation, we hypothesized that Nrfl expressed in OBs plays a key role in regulating bone formation (BF). To test this hypothesis, we used a Cre-loxP approach to disrupt Nrfl specifically in OB lineage cells. Transgenic mice expressing Cre recombinase under the control of the promoter/enhancer unit of Col1a2 gene were crossed with Nrfl loxP mice to generate Cre+ (Nrfl KO) and Cre- (WT) loxP homozygous mice. Disruption of Nrfl expression in OBs of KO mice was confirmed by real time PCR. Skeletal phenotypic measurements by PIXImus revealed 11% and 9% reduction ( $P < 0.01$ ,  $n = 9$ ) in total BMC and bone area in the KO mice at 8 weeks. Body weight or length was unaffected in the KO mice. pQCT analysis of femurs at 8 weeks revealed a 10% reduction in mid diaphysis cross sectional area in the KO mice.  $\mu$ CT analysis of the femur metaphysis revealed that trabecular bone volume/total volume and trabecular numbers were decreased by 65% and 53% respectively in the Nrfl conditional KO mice as compared with littermate controls ( $P < 0.01$ ). Trabecular separation was increased by 2.5-fold ( $P < 0.01$ ) in the KO mice. To determine if decreased peak bone mass in Nrfl deficient mice is caused by reduced BF, we performed *in vitro* nodule assay using primary cultures of bone marrow stromal cells derived from conditional KO and control mice. Alizarin red stained mineralized nodule area was reduced significantly in OBs derived from Nrfl KO mice compared to control mice ( $7 \pm 3\%$  versus  $22 \pm 5\%$ ,  $P < 0.05$ ). Because we previously found that suppression of Nrfl expression using siRNA blocked AA effects on osterix expression, we next determined if AA effect on osterix expression can be rescued by Nrfl overexpression in OBs derived from KO mice. Primary cultures of Nrfl deficient OBs

were infected with adenoviral (Ad) Nrfl or Ad-GFP prior to evaluation of AA effects on osterix expression. We found that Nrfl overexpression increased osterix expression by 4-fold compared to GFP overexpression ( $P < 0.01$ ) in AA dependent manner. In summary: 1) Targeted disruption of Nrfl in OBs results in decreased peak bone mass caused by reduced bone size and trabecular bone volume; 2) Lack of Nrfl influenced OB differentiation and osterix expression. In conclusion, our data provide the first *in vivo* experimental evidence that Nrfl produced by OBs is involved in regulating osterix expression, OB differentiation and BF.

**Disclosures:** J. Kim, None.

This study received funding from: Veterans Administration.

## 1191

**Mice Deficient in Bone Sialoprotein (BSP) Display Impaired Modeling and Remodeling and Respond to Ovariectomy but not to the Cortical Anabolic Effect of PTH.** N. Wade-Gueye<sup>\*1</sup>, M. Boudiffa<sup>\*1</sup>, N. Laroche<sup>\*1</sup>, A. Vandenbossche<sup>\*1</sup>, J. Aubin<sup>2</sup>, L. Vico<sup>1</sup>, M. Lafage-Proust<sup>1</sup>, L. Malaval<sup>1</sup>. <sup>1</sup>LBTO, INSERM 890, Saint-Etienne, France, <sup>2</sup>Dept. of Molecular Genetics, University of Toronto, Toronto, ON, Canada.

Bone sialoprotein (BSP) is a member of the Small Integrin-Binding Ligand N-Linked Glycoprotein (SIBLING) family, and highly expressed by bone cells. BSP interacts with both integrins and mineralized matrix, suggesting a role in osteogenesis and bone remodeling, but details remain unclear. We previously showed that adult BSP knockout (KO) mice exhibit a higher trabecular bone mass than wild type (WT), with lower bone formation and reduced osteoclast surfaces and numbers. To determine whether primary ossification is also affected by lack of BSP, we ablated femur bone marrow, an approach that induces intense medullar bone formation followed by resorption. Using longitudinal  $\mu$ CT, we found that 1 week after surgery, more primary bone was formed in the ablated marrow cavity of WT than KO mice (BV/TV:  $30.2 \pm 4.9\%$  vs  $13.8 \pm 3.8\%$ , mean  $\pm$  SEM,  $p < 0.05$ ,  $n = 10$ /group). In contrast, 2 weeks postsurgery, resorption of newly formed bone was more advanced in WT than in KO (BV/TV:  $-70\%$ , and KO:  $-17\%$ , wk1 vs wk2,  $p < 0.05$ ). We next asked whether the lower rate of bone turnover can be increased by catabolic (ovariectomy: OVX) or anabolic (intermittent PTH) hormonal challenges. Tibial trabecular bone volume was decreased 2 (WT:  $-40\%$ , KO:  $-28\%$ ,  $p < 0.05$ , vs baseline) and 4 weeks after OVX (WT:  $-46\%$ , KO:  $42\%$ ,  $p < 0.05$ , vs baseline). Bone formation rate (BFR) was transiently increased at 2 weeks only (WT:  $+49\%$ , KO:  $+52\%$ ,  $p < 0.01$  vs respective SHAM), while osteoclast numbers and surfaces were higher, 2 and 4 weeks after OVX in both genotypes. After one month of daily PTH 1-84 treatment, trabecular BV/TV was significantly decreased in WT ( $-30\%$ ,  $p < 0.05$ ,  $n = 8$ ) but not KO mice, while trabecular thickness increased ( $p < 0.05$ ) in tibia, femur and vertebra of both genotypes. In femur and vertebra, dynamic bone formation parameters (MAR, MS/BS and BFR/BS) and osteoclastic parameters were increased significantly by PTH in both genotypes. In contrast, femoral cortical bone area and thickness were significantly increased by PTH in WT ( $+10.7$  and  $13.2\%$ , respectively vs baseline,  $p < 0.05$ ) but not KO mice. In conclusion, BSP deficiency reduces both bone formation and resorption in both modeling and remodeling. However, the lower bone turnover can be stimulated by hormonal challenges. In particular, bone formation is increased, as shown transiently after OVX and in a more sustained way, although with site-specific differences, with PTH treatment. Our data suggest that the effects of BSP deficiency can be compensated, perhaps via overexpression of another SIBLING family member.

**Disclosures:** N. Wade-Gueye, None.

This study received funding from: Société Française de Rhumatologie.

## 1192

**In Vivo Downregulation of *Mustn1* mRNA Leads to Musculoskeletal Defects.** R. P. Gersch<sup>\*1</sup>, A. Kirmizitas<sup>\*2</sup>, G. Thomsen<sup>\*2</sup>, M. Hadjiargyrou<sup>1</sup>. <sup>1</sup>Biomedical Engineering, SUNY, Stony Brook, Stony Brook, NY, USA, <sup>2</sup>Biochemistry and Cell Biology, SUNY, Stony Brook, Stony Brook, NY, USA.

Previously, our lab reported on the isolation and characterization of the MusculoSkeletal Temporally Activated Novel Gene (*Mustang* or *Mustn1*), encoding for a 9.6 kDa nuclear protein that is involved in fracture repair. We further determined that *Mustn1* is necessary but not sufficient for pre-chondrocyte proliferation, differentiation, and matrix production *in vitro* via overexpression and RNA interference experiments. These data suggest that *Mustn1* may play a crucial role in the early stages of chondrogenesis, both during fracture repair as well as development. In the case of the latter, whole mount *in situ* analysis of *Mustn1* in wild type mice at stages 8.5-9.5dpc reveal expression in a broad range of tissues, such as the branchial arches, primitive heart, regions of the cranium, somites, and neural tube. During limb development 10.5-11.5dpc, *Mustn1* expression becomes restricted to areas promoting chondrogenesis, such as the craniofacial region, limb buds, and somites. At 12.5dpc *Mustn1* expression expands to include tissues undergoing endochondral and intramembranous ossification. These experiments were also repeated in *Xenopus laevis* and showed similar patterning of expression, with *Mustn1* localizing predominately to the craniofacial region as well as somites. This is not surprising considering *Mustn1*'s high protein homology (67%) between the two species. Further analysis of *Mustn1* temporal expression by RT-PCR revealed an increase during stages 14-19, corresponding to somite production and mesodermal development before reaching a plateau through stage 35. Lastly, morpholino oligonucleotides were designed against *Xenopus Mustn1* and injected into both blastomeres at the two-cell stage to ensure knockdown throughout the developing embryo. While control morpholino injected tadpoles were unaffected, gross morphological defects were observed in the craniofacial region of *Mustn1* morpholino treated specimens resulting in disruption of normal

craniofacial formation and an over production of tissue in the dorsal region of the head. In addition, tail and somite development were abnormal, with the presence of many "kinks" resulting in circular swimming by the tadpoles. Taken together, these experiments support the hypothesis that *Mustn1* expression is necessary for musculoskeletal development. Future work will focus on elucidating how *Mustn1* is involved in the regulation of chondrogenic genes and help to understand the process of cartilage and muscle formation both in *X. laevis* as well as mammals.

**Disclosures:** M. Hadjiargyrou, None.

## 1193

**Ablation of IGF-I Signaling in Osteoprogenitors Decreases Bone Formation and Blunts the Skeletal Response to PTH.** Y. Wang, R. K. Long\*, H. Z. Elalieh\*, D. D. Bikle. Endocrine Unit, University of California, San Francisco/ San Francisco VA Medical Center, San Francisco, CA, USA.

We and others have demonstrated that insulin-like growth factor-I (IGF-I) signaling regulates the functions of osteoblasts and osteoclasts, and mediates the anabolic actions of parathyroid hormone (PTH) on bone, although the cellular targets and mechanisms remain uncertain. To examine more specifically the cells involved, we generated mice with targeted knockout of IGF-I receptor (IGF-IR) gene in osteoprogenitors (OG) (<sup>OG</sup>IGF-IR<sup>-/-</sup>) by breeding loxP-flanked IGF-IR alleles in exon 3 (floxed-IGF-IR) mice with mice carrying the Cre recombinase transgene controlled by the osterix promoter (gift from Dr. Andrew McMahon). <sup>OG</sup>IGF-IR<sup>-/-</sup> mice grow normally with no difference in body weight at least through 7 weeks. A marked reduction of IGF-IR expression in osteoblasts was shown by immunohistochemistry in 2 day old <sup>OG</sup>IGF-IR<sup>-/-</sup> neonates. Compared with their wild-type (WT) littermates, osteoblast proliferation as assessed by the number of PCNA positive cells was reduced by 50%. At 3 weeks, histology revealed less trabecular bone (H&E staining) and mineralization (Von Kossa staining) in the <sup>OG</sup>IGF-IR<sup>-/-</sup> mice. Quantitative real-time PCR (Q-PCR) analysis demonstrated that the mRNA levels of alkaline phosphatase (ALP) decreased by 48% in the <sup>OG</sup>IGF-IR<sup>-/-</sup> mice compared with WT. At 7 weeks, micro-CT analysis showed significantly decreased trabecular bone volume (BV/TV), connectivity density, trabecular number and thickness (35%, 34%, 16% and 11%, respectively) and increased trabecular separation (23%) in the <sup>OG</sup>IGF-IR<sup>-/-</sup> mice compared to WT.

To evaluate the skeletal response to PTH, 3 week old <sup>OG</sup>IGF-IR<sup>-/-</sup> and WT mice were treated with vehicle or PTH (80 µg/kg bw) for 1 hr. As analyzed by Q-PCR, PTH significantly increased the mRNA levels of RANKL and ephrin 2 in the WT mice (13 fold and 3.7 fold, respectively), but these effects were blunted in the <sup>OG</sup>IGF-IR<sup>-/-</sup> mice. Our data indicate that the IGF-IR in osteoprogenitors is critical for osteoblast proliferation, differentiation and development/maintenance of normal trabecular bone volume and structure. The anabolic effects of PTH on bone require IGF-I signaling in the osteoprogenitors.

**Disclosures:** Y. Wang, None.

## 1194

**Ephrin B1 Reverse Signaling Regulates Bone Formation via Influencing Osteoblast Activity in Mice.** W. Xing, J. Kim\*, J. Wergedal, S. Mohan. Musculoskeletal Disease Center, Jerry L Pettis VA Medical Center, Loma Linda, CA, USA.

Interaction of ephrin B1 with its receptors via cell-cell contact leads to the activation of a bidirectional signal in which both the receptor-mediated forward signaling and the ephrin B1-mediated reverse signaling activate downstream signaling cascades. Because disruption of ephrin B1 gene in mice results in perinatal lethality and skull defects whereas double knockouts of ephrin B2 and B3 receptors, the key receptors for ephrin B1 ligand, fails to show overt bone phenotypes, we hypothesized that ephrin B1 might be a key member of ephrin family members in regulating bone formation. To study the function of ephrin B1 in bone, we recently generated osteoblast (OB) specific ephrin B1 conditional knockout (KO) and demonstrated that targeted disruption of ephrin B1 gene in OBs results in decreased bone size, BMD and trabecular bone volume. To identify the target cell types and cellular processes affected in the ephrin B1 conditional KO mice, we performed histomorphometric analyses at 4-weeks of age. Bone formation rate (BFR) decreased by 58% (P<0.05) at the endosteum of the femur midshaft in the KO mice. Because of reduced bone size in the KO mice, BFR was adjusted for bone surface (BS). BFR/BS was also decreased by 43% in the KO mice (P<0.05). To determine if the reduced BFR in ephrin B1 conditional KO mice is caused by impairment in the differentiated functions of OBs, we measured mineral apposition rate (MAR) in the KO and control littermates. MAR decreased by 43% (P<0.05) in the KO mice. Consistent with these data, measurement of BFR and MAR at another site of femur, third trochanter, revealed a 41% (P=0.01) and 29% (P=0.02) decrease in BFR/BS and MAR, respectively in the KO mice compared to gender-matched littermates. In order to determine if lack of OB produced ephrin B1 also influences osteoclasts, we measured bone resorption by evaluation of tartrate resistant acid phosphatase (TRAP) covered bone surface at the periosteum and endosteum of femur midshaft. The percentage of TRAP surface was not different in the KO mice compared to control mice neither at the periosteum (19.0 vs. 21.3, P=0.68) nor at the endosteum (11.9 vs. 12.9, p=0.78), thus suggesting bone resorption was not affected in the ephrin B1 OB-specific conditional KO mice. Based on our data, we conclude that ephrin B1 produced by OBs is an important regulator of OB activity, bone formation and peak bone mass.

**Disclosures:** S. Mohan, None.

This study received funding from: US Army.

## 1195

**Endorphins Regulate Bone Material Properties by Actions through Dynorphin.** P. A. Baldock<sup>1</sup>, I. Wong<sup>\*1</sup>, M. M. McDonald<sup>2</sup>, R. F. Enriquez<sup>\*1</sup>, C. Schwarzer<sup>\*3</sup>, D. G. Little<sup>2</sup>, A. Sainsbury<sup>\*4</sup>, H. Herzog<sup>\*4</sup>, J. A. Eisman<sup>1</sup>. <sup>1</sup>Bone and Mineral Program, Garvan Institute of Medical Research, Sydney, NSW, Australia, <sup>2</sup>Orthopaedic Research & Biotechnology, The Children's Hospital at Westmead, Sydney, NSW, Australia, <sup>3</sup>Pharmacology, Innsbruck Medical University, Innsbruck, Austria, <sup>4</sup>Neuroscience Program, Garvan Institute of Medical Research, Sydney, NSW, Australia.

Identification of sympathetic links from the hypothalamus to bone has increased our understanding of neural regulation of bone. Of these, leptin and neuropeptide Y remain major areas of interest. The dynorphins, a member of the endorphin family are known to regulate leptin and NPY. Dynorphins are predominantly expressed within the central nervous system, with actions via the kappa opioid receptor on pain, addiction and depression. Their peripheral expression appears limited to adrenal, testis and pancreas. In the hypothalamus, dynorphin is expressed in leptin-responsive neurons and pre-prodynorphin is co-expressed with neuropeptide Y.

To investigate its potential role in bone homeostasis, we examined the bone phenotype of Dynorphin knockout mice (Dyn<sup>-/-</sup>), which lack the pre-prodynorphin gene and thus all five dynorphin peptides.

Their body weight mice was not different to wild type despite a (17%) decrease in adipose mass. Dyn<sup>-/-</sup> mice showed reduced central NPY expression, a change shown previously to increase cortical bone mass and no changes in leptin, despite adiposity changes.

Cancellous bone volume was elevated in Dyn<sup>-/-</sup> mice compared to wild type (11.9% ±1 vs 8.8 ±0.6 p<0.02). Bone resorption was greater in Dyn<sup>-/-</sup> mice, as indicated by both osteoclast surface (11.9% ± 0.7 vs 7.9 ±0.7, p<0.01) and osteoclast number (4.4/mm ± 0.2 vs 3.3 ±0.3, p<0.05). However, these changes were overridden by an increased mineral apposition rate in Dyn<sup>-/-</sup> (2.4µm/d ±0.2 vs 1.6 ±0.1, p<0.02).

Cortical bone volume, in contrast, was reduced in Dyn<sup>-/-</sup> mice without change in bone length. Femoral BMD by DXA was reduced (60mg/cm<sup>2</sup> ±2 vs 72 ±4, p<0.05) as was BMC (23mg ±1 vs 30 ±2, p=0.05). A similar reduction in cortical BMD and BMC by pQCT across the femur was not accompanied by changes in bone dimensions or cortical thickness or area. These findings strongly indicate a change in bone material properties.

Importantly, Dyn<sup>-/-</sup> mice showed reduced central NPY expression, a change shown previously to increase cortical bone mass and no changes in leptin, despite adiposity changes. This study reveals for the first time a connection between the dynorphin system and bone. The loss of dynorphin signalling resulted in a change in bone material properties not explained by the NPY or leptin pathways. This study identifies a novel central mechanism for regulation of bone, with potential links to higher brain functions.

**Disclosures:** P.A. Baldock, None.

This study received funding from: NH&MRC

## 1196

**Wnt7a and Wnt7b Evoke Overlapping Yet Distinct Transcriptional Responses During the Osteogenic Programming of Mesenchymal Progenitors by Msx2.** S. Cheng, J. Shao, D. Towler. Internal Medicine, Washington University in St. Louis, St. Louis, MO, USA.

We previously demonstrated that paracrine Wnt/ beta-catenin signaling mediates the osteogenic activity of *Msx2* in vitro and in vivo. *Msx2* increases the expression of *Wnt7a* and *Wnt7b*, ligands for LRP5 and LRP6 that play crucial roles during skeletal development. In C3H10T1/2 cells, RNAi "knockdown" demonstrates that both *Wnt7a* and *Wnt7b* contribute to *Msx2* osteogenic actions via *LRP6*, quantifying alkaline phosphatase (ALP) as an osteoblast marker. Moreover, *Wnt7* co-localizes with *Msx2* in perivascular venues during the orthotopic and heterotopic mineralization induced by a *CMV-Msx2* transgene. Therefore, we examined the mechanisms whereby *Wnt7a* and *Wnt7b* control gene transcription in mesenchymal cells, using the C3H10T1/2 cell line as a model for study. Transient co-transfection of either *pcDNA3-Wnt7a* or *pcDNA-Wnt7b* upregulated activity of the TOPGLOW luciferase reporter, indicating that both ligands can activate canonical beta-catenin pathways in C3H10T1/2 cells. However, *Wnt7a* was consistently more effective than *Wnt7b* in upregulating either TOPGLOW or LEFLUC (5-fold vs. 2-fold; p < 0.05). By contrast, transcription driven by NFAT - a family of nuclear factors that dimerizes with osterix to enhance collagen synthesis and bone formation -- was induced only by *Wnt7b*, and not by *Wnt7a*. Western blot analysis and immunofluorescence confirmed that *Wnt7b* upregulated NFATc1 protein levels and NFATc1 nuclear accumulation. Both *Wnt7a* and *Wnt7b* inhibited *PPAR-gamma2* and *Osteopontin* promoter activities to similar extents. To better understand the impact of *Wnt7a* vs. *Wnt7b* signaling on osteoblast lineage allocation and differentiation, we generated *SFG-Wnt7a* and *SFG-Wnt7b* retroviral vectors, using transduced C3H10T1/2 cultured under osteogenic and adipogenic conditions. *SFG-Wnt7b* upregulated *Msx2* and *ALP*, suppressed adipogenic *PPAR-gamma* expression, and accelerated matrix mineralization and osteoblast maturation - including the induction of *Dkk2*. Moreover, *SFG-Wnt7b* profoundly suppressed the expression of *Dkk1* and *osteopontin* -- two negative regulators of osteoblast-mediated mineralized matrix formation. The suppression of *Dkk1* by *Wnt7b* is mediated via *Msx2*, since siRNA to *Msx2* substantially reversed inhibition. Detailed comparison with *SFG-Wnt7a* is ongoing. Thus, *Wnt7a* and *Wnt7b* exert overlapping yet distinct actions on osteoblast gene transcription. Given the differences of *Wnt7a* and *Wnt7b* on beta-catenin vs. NFAT transcription, these two Wnts provide distinct signals downstream of *Msx2* during osteogenesis. Along with NFAT and osterix, *Msx2* mediates aspects of *Wnt7b* actions, potentiating a "feed-forward" loop that accelerates mineralization and osteoblast differentiation.

**Disclosures:** S. Cheng, None.

This study received funding from: National Institutes of Health.

## 1197

**T Cells Amplify The Anabolic Action of PTH Through Wnt10b Signaling.** M. Terauchi<sup>1</sup>, M. S. Nanes<sup>1</sup>, M. Weitzmann<sup>\*1</sup>, M. Zayzafoon<sup>\*2</sup>, M. Weitzmann<sup>\*1</sup>, T. F. Lane<sup>\*3</sup>, R. Pacifici<sup>1</sup>. <sup>1</sup>Division of Endocrinology, Metabolism and Lipids, Emory University School of Medicine, Atlanta, GA, USA, <sup>2</sup>University of Alabama Birmingham, Birmingham, AL, USA, <sup>3</sup>University of California, Los Angeles, Los Angeles, CA, USA.

Intermittent PTH treatment promotes bone anabolism in part by activating Wnt signaling in osteoblasts (OBs). However, the nature and the source of the Wnt ligand involved are unknown. T cells express PTH receptors and produce Wnt10b, a Wnt ligand that stimulates osteoblastogenesis, suggesting the possibility that T cells may regulate the anabolic activity of iPTH by producing Wnt10b. To investigate this hypothesis 5 week-old TCR $\beta$  <sup>-/-</sup>, nude, RAG2 <sup>-/-</sup> and class I and II MHC <sup>-/-</sup> mice, strains which lack T cells, were treated for 4 weeks with iPTH via sq injection of human PTH 1-34, 80  $\mu$ g/kg/day (iPTH).  $\mu$ CT analysis of the femoral metaphysis showed that iPTH induced anabolism was blunted by 70-100 % in T cell deficient mice, as compared to WT controls. 4-point bending tests revealed that iPTH increased stiffness, failure load, and maximum load in WT mice but not in T cell deficient mice. Bone histomorphometry and serum osteocalcin (a marker of bone formation) and CTX (a marker of resorption), revealed that the lack of T cells blunts iPTH induced bone anabolism by blocking both formation and resorption. Mechanistic studies in TCR $\beta$  <sup>-/-</sup> mice revealed that in vivo iPTH treatment failed to stimulate CFU-ALP formation in bone marrow cultures, an index of the number of stromal cells with osteogenic potentials. iPTH increased proliferation, differentiation, life span, and Wnt-dependent gene expression in pre-OB derived from WT but not TCR $\beta$  <sup>-/-</sup> mice, suggesting that T cells regulate OBs at all levels of their life cycle. Moreover, iPTH increased Wnt10b production by CD8<sup>+</sup> T cells 3 fold and T cell produced Wnt10b activated Wnt dependent genes in OBs. Demonstrating that T cell produced Wnt10b plays a pivotal role, iPTH failed to promote bone anabolism in TCR $\beta$  <sup>-/-</sup> mice reconstituted with T cells from Wnt10b <sup>-/-</sup> mice, while it induced a full anabolic response in TCR $\beta$  <sup>-/-</sup> mice reconstituted with WT T cells. In summary, this study indicates that T cells represent a regulatory component of the BM microenvironment involved in the anabolic response to iPTH. Bone anabolism is induced by signaling in OBs, but T cells play a permissive role by producing Wnt10b in response to direct or indirect stimulation by PTH. Understanding the cross-talk between T cells and OBs may thus yield novel therapeutic strategies for potentiating bone anabolic agents.

**Disclosures:** R. Pacifici, Eli Lilly 1; P&G 1; Aventis 1; Novartis 1.  
This study received funding from: NIH.

## 1198

**High Bone Turnover in Mice Lacking the Growth Factor Midkine.** C. Neunaber, P. Catala-Lehnen, R. P. Marshall<sup>\*</sup>, T. Schinke, M. Amling. Center for Biomechanics and Skeletal Biology, Department of Trauma, Hand, and Reconstructive Surgery, University Medical Center Hamburg-Eppendorf, Hamburg, Germany.

Pleiotrophin (Ptn) and Midkine (Mdk) comprise a family of heparin-binding growth factors with similar activities on proliferation, survival and migration of various cell types. The physiologic function of both molecules is still not fully clarified, since mice lacking either *Ptn* or *Mdk* do not display major abnormalities, despite specific and rather mild behavioural defects. Interestingly, while the transgenic over-expression of *Ptn* in osteoblasts has been described to trigger increased bone formation, our own analysis of *Ptn*-deficient mice did not reveal any difference in terms of bone development or remodelling compared to wildtype littermates. Together with the results from an Affymetrix Gene Chip hybridization showing that *Mdk* expression increases with osteoblast differentiation, this observation prompted us to analyze the skeletal phenotype of *Mdk*-deficient mice at 6, 12 and 18 months of age. While the trabecular bone volume was not different from wildtype littermates in 6 months old mice, we observed a high bone mass phenotype in the *Mdk*-deficient mice starting at the age of 12 months (BV/TV: 24.1  $\pm$  4.8 % vs. 12.5  $\pm$  2.4 %). Dynamic histomorphometry further revealed that the bone formation rate was more than 2-fold increased compared to wildtype littermates (BFR/BS: 247  $\pm$  15  $\mu$ m<sup>3</sup>/ $\mu$ m<sup>2</sup>/y vs. 115  $\pm$  14  $\mu$ m<sup>3</sup>/ $\mu$ m<sup>2</sup>/y), indicating that Mdk is a negative regulator of osteoblast function *in vivo*. Surprisingly, the high bone mass phenotype of the *Mdk*-deficient mice was accompanied by an increase of bone resorption, as determined by measuring TRAP activities and collagen degradation products in the serum. Moreover, we observed increased cortical porosity and development of hyperostotic lesions in the *Mdk*-deficient mice, indicative of a high bone turnover phenotype. Interestingly, this phenotype developed with normal serum levels of Pth, Calcitonin, Rankl and Opg, thereby suggesting a direct effect of Mdk on bone cells. This is further supported by our previous observation that the gene *Piprz1*, encoding a tyrosine phosphatase whose action can be antagonized by Mdk binding, is strongly expressed in differentiated osteoblasts, and that *Piprz1*-deficient mice display an osteopenia at 12 months of age. Taken together, our results identify the growth factor midkine as an important regulator of both, bone formation and bone resorption, at least in mice. However, if such a function could also be demonstrated in human bone cells, Mdk would certainly be an attractive target for osteoanabolic therapy.

**Disclosures:** C. Neunaber, None.

## 1199

**PHEX Cleavage of SIBLING-ASARM Peptides as a Mechanism Underlying Osteomalacia in X-Linked Hypophosphatemia.** W. N. Addison<sup>\*1</sup>, Y. Nakano<sup>\*1</sup>, T. P. Loisel<sup>\*2</sup>, P. Crine<sup>2</sup>, M. D. McKee<sup>1</sup>. <sup>1</sup>Faculty of Dentistry, McGill University, Montreal, QC, Canada, <sup>2</sup>Enobia Pharma, Montreal, QC, Canada.

Mice with X-linked hypophosphatemic rickets (*Hyp*), caused by inactivating mutations of the *PheX* gene, have osteomalacic bones and a marked elevation of acidic, serine- and aspartate-rich motif (ASARM) peptides. ASARM peptides inhibit mineralization, and are derived from members of the SIBLING (small integrin-binding ligand N-linked glycoproteins) family of mineral-regulating proteins which include matrix extracellular phosphoglycoprotein (MEPE) and osteopontin (OPN). The mechanisms by which *PheX* inactivation leads to ASARM peptide accumulation, and inhibition of matrix mineralization, are still unknown. In the present study, we have examined the effects of PHEX interaction with OPN-derived ASARM (OpnASARM) and MEPE-derived ASARM (MepeASARM) peptides using an *in vitro* osteoblast culture model, mass spectrometry and mineral-binding assays. Treatment of MC3T3-E1 osteoblast cultures with phosphorylated OpnASARM peptides (with 5 phosphoserines [OpnAs5] or 3 phosphoserines [OpnAs3]) and a phosphorylated MepeASARM (with 3 phosphoserines [MepeAs3]) caused dose-dependent inhibition of mineralization. Binding of phosphorylated OpnASARM and MepeASARM to hydroxyapatite crystals was confirmed by a hydroxyapatite-peptide binding assay. Nonphosphorylated ASARM peptide showed little or no binding to hydroxyapatite and did not inhibit osteoblast culture mineralization, demonstrating the importance of ASARM phosphorylation in regulating mineralization. A recombinant, soluble secreted form of human PHEX enzyme rescued the inhibition of culture mineralization by OpnAs3 and MepeAs3 (but not by OpnAs5), and mass spectrometry of cleaved peptides obtained after incubations with PheX identified all forms of both OpnASARM and MepeASARM as substrates for PHEX. Enzymatic cleavage occurred at amide linkages between serine and glutamate, or between serine and aspartate. Cell proliferation (MTT assay) was normal after treatment with all peptides, and alkaline phosphatase activity and collagen deposition was unaffected by all peptides except OpnAs5 which slightly decreased collagen deposition. In conclusion, these data demonstrate for the first time that inhibition of mineralization by mineral-binding SIBLING ASARM peptides can be rescued by enzymatic degradation by PHEX, identifying a mechanism by which loss of PHEX activity can lead to extracellular matrix accumulation of ASARM resulting in the osteomalacia of XLH.

**Disclosures:** W.N. Addison, None.  
This study received funding from: Enobia Pharma.

## 1200

**Oxytocin Inhibits Bone Formation Through the Activation of the Sympathetic Tone: A New Candidate in the Central Regulation of Bone Formation.** C. Camerino. Dept. of Human Anatomy and Histology, University of Bari, Bari, Italy.

The neuropeptide Oxytocin (OT) is an hypothalamic hormone produced in the paraventricular (PVN) and supraoptic (SON) nuclei of the hypothalamus. It has been reported that oxytocin neurons in the PVN nucleus are a component of a leptin-sensitive signaling circuit between the hypothalamus and caudal brain stem. Indeed, hindbrain projection of OT neurons in the parvocellular paraventricular nucleus are hypothesized to transmit leptin signaling from the hypothalamus to the nucleus of the solitary tract. Knock out mice deficient in oxytocin (OTKO) display significantly increased body weight and 40% increase in fat pad weight compared to wild type (WT) littermates. This phenotype is evident at both 4 and 6 months of age. OTKO mice present also higher fasting glucose levels compared to WT. The results from Insulin Tolerance Test and Glucose Tolerance Test clearly show an insulin resistance state and lower ability to counteract the increase of glycaemia following a glucose bolus. Liver steatosis was also evident in the oldest animals thus confirming a diabetic status. Food intake did not show any significant difference between the OTKO and WT mice at both ages. Interestingly, OTKO mice displayed a 90% increase in plasma leptin concentration compared to the WT. Hyperleptinaemia is considered to reflect a state of leptin resistance that is accompanied by obesity, hypogonadism and paradoxically high bone mass. The paradox of leptin resistance has been the first evidence linking energy and skeletal homeostasis through the activation of the sympathetic nervous system. To investigate if hyperleptinaemia following OT deficiency had an impact on bone formation we measured the epinephrine levels and performed a  $\mu$ CT analysis of both vertebrae and long bones of OTKO mice. Interestingly, we found that in OTKO mice epinephrine levels were three times lower than in WT thus indicating a lower sympathetic tone. The results of  $\mu$ CT indicated that OTKO mice have a denser appendicular skeleton with increased mineralization of the lumbar vertebrae as well as of the femurs probably due to a *de novo* bone formation by osteoblast, which is a direct target of the sympathetic nervous system. The femurs of OTKO display a larger diameter of the medial diaphysis and a thicker skull. Based on these results we suggest that OT can be a new candidate in the central regulation of bone homeostasis and a mediator of the antiproliferative action of sympathetic tone on bone formation.

**Disclosures:** C. Camerino, None.

## 1201

**Rachitic Defects in *tcirg1*-Dependent Osteopetrosis Are Caused by Impaired Gastric Acidification.** T. Schinke<sup>1</sup>, A. F. Schilling<sup>1</sup>, A. Baranowsky<sup>\*1</sup>, A. Huebner<sup>\*1</sup>, A. Schulz<sup>\*2</sup>, J. Zustin<sup>\*3</sup>, M. Gebauer<sup>\*1</sup>, M. Priemel<sup>1</sup>, A. Villa<sup>4</sup>, A. Teti<sup>5</sup>, M. Amling<sup>1</sup>. <sup>1</sup>Center for Biomechanics, Experimental Trauma Surgery & Skeletal Biology, Department of Trauma, Hand, and Reconstructive Surgery, University Medical Center Hamburg-Eppendorf, Hamburg, Germany, <sup>2</sup>Department of Pediatrics, University Medical Center Ulm, Ulm, Germany, <sup>3</sup>Department of Bone Pathology, University Medical Center Hamburg-Eppendorf, Hamburg, Germany, <sup>4</sup>Human Genome Department, Istituto di Tecnologie Biomediche, CNR, Segrate, Milan, Italy, <sup>5</sup>Department of Experimental Medicine, University of L'Aquila, L'Aquila, Italy.

*TCIRG1* is the most commonly mutated gene in patients with autosomal recessive osteopetrosis (ARO). It encodes one subunit of the vacuolar proton pump, required for extracellular acidification by osteoclasts. Interestingly, while the initial characterization of *Tcirg1*-deficient *oc/oc* mice also revealed rachitic defects of the growth plates, a phenotype termed osteopetrorickets (OPR), the impact of *TCIRG1* on skeletal mineralization has been overlooked in ARO patients, since biopsies were only analyzed following decalcification. Thus, in order to estimate the prevalence of OPR, we performed histomorphometry on non-decalcified bone biopsies from ARO patients and observed an osteoid volume (OV/BV) above 5 % in half of the cases, which prompted us to elucidate the molecular basis of OPR using genetically modified mouse models. While we did not observe a pathologic enrichment of osteoid in osteopetrotic *Src*<sup>-/-</sup> mice, the OV/BV in *oc/oc* mice was above 20 %. The cause of this mineralization defect is a severe hypocalcemia, which is best underscored by the finding that the OV/BV was below 2 %, when serum calcium in the *oc/oc* mice was normalized by a high calcium diet. Since we did not observe increased renal calcium loss in the *oc/oc* mice, we next analyzed *Tcirg1* expression in the gastrointestinal tract. Here we found strong and specific expression in parietal cells of the stomach, which was confirmed by immunohistochemistry on human tissues. Moreover, we found that this expression is also of functional relevance, since the gastric pH was pathologically increased in *oc/oc* mice and in a patient with *TCIRG1*-dependent ARO. To demonstrate that this novel function of *Tcirg1* contributes to the OPR phenotype, we next analyzed achlorhydric *Cckbr*<sup>-/-</sup> mice, where we found no enrichment of osteoid, but a mild hypocalcemia accompanied by elevated PTH. In order to block PTH-induced bone resorption in these mice, we crossed them with *Src*<sup>-/-</sup> mice and observed that the combined deletion of *Cckbr* and *Src* led to OPR. Taken together, our data demonstrate a previously unknown function of *TCIRG1* in gastric acidification that contributes to the skeletal abnormalities caused by *TCIRG1* deficiency.

**Disclosures:** T. Schinke, None.

## 1202

**Impairment of Osteoblast lineage Differentiation leads to Increased Osteoclastogenesis in Osteogenesis Imperfecta Murine.** H. T. Li<sup>\*1</sup>, X. Jiang<sup>\*1</sup>, J. Delaney<sup>\*2</sup>, I. Bilic-Curcic<sup>\*2</sup>, D. W. Rowe<sup>1</sup>, I. Kalajzic<sup>1</sup>. <sup>1</sup>Dept. of Reconstructive Sciences, Uni. of Conn. Health Center, Farmington, CT, USA, <sup>2</sup>Dept. of Genetics and Dev. Biology, Uni. of Conn. Health Center, Farmington, CT, USA.

Osteogenesis imperfecta murine (OIM) is a mouse model that resembles severe type III human OI. Our study aims to address the prospective role of impairment of osteoblastic differentiation as a mechanism for this disease. Potentially, it is the combination of impaired osteogenic differentiation with increased bone resorption that leads to diminished bone mass. We have previously developed transgenic mice that express GFP at distinct stages of osteoblast differentiation; pOBCol3.6GFP (preosteoblast) and pOBCol2.3GFP (osteoblast/osteocytes). Using the crosses of these transgenic mice with the OIM model, we assessed osteoblast maturation and the mechanism of increased osteoclastogenesis. Cultures from the 2.3GFPoim/oim mice showed a marked reduction of cells expressing GFP relative to 2.3GFP<sup>+/+</sup> littermates. Similar number of 3.6GFP<sup>+</sup> cells between the <sup>+/+</sup> and oim/oim mice were observed. Conventional osteoblast differentiation markers as lower expression of AP, Col1a1, BSP, OC and mineralization in oim/oim mice confirmed the GFP data. Histological analysis of the 3.6GFPoim/oim mice showed an increased number of GFP positive cells lining the endocortical surface compared to 3.6GFP<sup>+/+</sup> mice. In contrast GFP expression was similar between 2.3GFPoim/oim and 2.3GFP<sup>+/+</sup> mice. These data indicate that the lineage is under continuous stimulation, while only a proportion of cells attain the mature osteoblast stage.

To assess the osteoclastogenic ability of cells at different stages during osteoblastogenesis, we co-cultured preosteoblasts (3.6GFP<sup>+</sup>) or mature osteoblasts (2.3GFP<sup>+</sup>) isolated by FACS with bone marrow derived osteoclast progenitors (BMMc). The immature osteoblasts exhibit a stronger potential to support osteoclast formation and differentiation, revealed by increased osteoclast number and activity. We confirmed the presence of a higher Rankl/Opg ratio in sorted immature osteoblasts. These results implied that the accumulated immature osteoblasts in oim/oim could be the driving force for augmented osteoclastogenesis. Indeed, increased osteoclast formation was observed when oim/oim derived osteoblasts were cocultured with osteoclast progenitors as compared with osteoblasts derived from <sup>+/+</sup> mice.

Our data indicates that the osteoblast lineage maturation is a critical aspect underlying the pathophysiology of the osteogenesis imperfecta.

**Disclosures:** H.T. Li, None.

This study received funding from: Children Brittle Bone Foundation and NIH AR053275.

## 1203

**ACVR1 Knock-In Mouse Model for Fibrodysplasia Ossificans Progressiva (FOP).** S. A. Chakkalakal<sup>\*1</sup>, D. Zhang<sup>\*1</sup>, T. Raabe<sup>\*2</sup>, J. Richa<sup>\*2</sup>, K. Hankenson<sup>3</sup>, F. S. Kaplan<sup>4</sup>, E. M. Shore<sup>5</sup>. <sup>1</sup>Department of Orthopaedic Surgery, University of Pennsylvania School of Medicine, Philadelphia, PA, USA, <sup>2</sup>Department of Genetics, University of Pennsylvania School of Medicine, Philadelphia, PA, USA, <sup>3</sup>Department of Animal Biology, University of Pennsylvania of Veterinary Medicine, Philadelphia, PA, USA, <sup>4</sup>Departments of Orthopaedic Surgery and Medicine, University of Pennsylvania School of Medicine, Philadelphia, PA, USA, <sup>5</sup>Departments of Orthopaedic Surgery and Genetics, University of Pennsylvania School of Medicine, Philadelphia, PA, USA.

Fibrodysplasia ossificans progressiva (FOP) is a rare genetic disorder of endochondral bone formation characterized by abnormalities of the developing embryonic skeleton, such as malformation of the great toes, and by progressive postnatal heterotopic ossification in soft connective tissues. All patients with these classic clinical features of FOP have the identical single nucleotide substitution (c.617G>A; R206H) in the gene encoding ACVR1/ALK2, a type I BMP receptor. The human and mouse ACVR1 genes are highly homologous and a mouse ACVR1 knock-in of the c.617G>A; R206H mutation would provide a much needed in vivo model for FOP. ACVR1 sequences from a C57BL/6 BAC library were inserted into the retrieval vector PL253 by a BAC recombineering strategy. Recombineering was also used to replace ACVR1 codon 206 (CGC>CAC) in murine exon 5, followed by addition of a neor marker gene flanked by FLP recombinase target sites. This targeting vector was electroporated into C57BL/6 ES cells that were then G418 (neor) selected. About 300 G418-positive colonies were isolated and grown, and homologous recombination was verified by Southern analysis in sixteen clones. Three positive ES cell clones were injected into blastocysts from Balb-c mice (white coat color) in order to detect genetically chimeric pups by chimeric black/white coat color. Twenty-seven chimeric pups were born, several with 70-90% black coat indicating a high proportion of cells with the mutant ACVR1 allele. Analysis of young chimeras through physical examination, histology, and X-ray/microCT analyses revealed phenotypes consistent with those of human FOP patients including malformed toes and post-natal heterotopic bone formation. These data provide the first direct in vivo evidence that the FOP c.617G>A; R206H ACVR1 mutation induces the characteristic clinical phenotype observed in FOP patients. Further development of this mouse model to obtain heterozygous germline transmission will generate a stable animal model to investigate the cellular and molecular mechanisms leading to the skeletal malformations and ectopic bone formation in FOP and provide a system for developing and testing treatments for FOP and other conditions of misregulated bone formation.

**Disclosures:** S.A. Chakkalakal, None.

## 1204

**Osteoblast and Osteoclast Involvement in the Pathogenesis of a Mouse Model for Craniometaphyseal Dysplasia (CMD).** I. Chen<sup>\*</sup>, J. Wang<sup>\*</sup>, B. Koczon-Jaremk<sup>\*</sup>, E. Reichenberger. Reconstructive Sciences, UCHC, Farmington, CT, USA.

Craniometaphyseal dysplasia (CMD) is a monogenic human disorder characterized by progressive thickening of craniofacial bones concurrent with widened and radiolucent metaphyses in long bones. Mutations for autosomal dominant CMD have been identified in the *ANK* gene (*ANKH*). A knock-in (KI) mouse model expressing the human *Ank* mutation (Phe377del) replicates many features of CMD. Here, we study the mutational effect on osteoblasts and osteoclasts in *Ank*<sup>KI/KI</sup> mice.

We performed skeletal analyses by biochemical markers and histomorphometry. We studied osteoblast defects using calvarial osteoblast and bone marrow stromal cell cultures by real time PCR, immunocytochemistry, alkaline phosphatase (ALP) and von Kossa/Alizarin red S staining. To study osteoclasts *in vitro*, we derived osteoclasts from mouse bone marrow macrophage precursors (BMMs) and human or mouse peripheral blood cultures. We determined osteoclast numbers and activity by TRAP staining and resorption assays.

*Ank*<sup>KI/KI</sup> mice have higher numbers of osteoblasts and osteoclasts, which, however, did not lead to increased bone formation or resorption. Serum ALP and TRAP5b were increased but levels of the N-terminal propeptide of type I procollagen (measure of bone formation) and the type I collagen cross-linked C-terminal telopeptide (marker of osteoclast activity) were normal. Histomorphometry showed increased osteoblast surface and osteoclast number in femoral and calvarial sections but mineral apposition and bone formation rates were comparable to *Ank*<sup>+/+</sup> mice. *Ank*<sup>KI/KI</sup> osteoblast cultures showed significantly reduced mineral nodules and expression of *Bglap*, *Phex* and *Mmp13* at the mineralization stage while ALP staining and other differentiation markers, such as *Col1*, *Bsp*, *Tnap* appeared comparable to *Ank*<sup>+/+</sup> cultures thus indicating defective osteoblast mineralization. *Ank*<sup>KI/KI</sup> BMM cultures formed significantly fewer TRAP<sup>+</sup> cells (nuclei ≥3) and showed decreased mineral resorption. Osteoclast-like cells of the same size generally carried significantly more nuclei in *Ank*<sup>KI/KI</sup> BMM cultures suggesting an enhanced fusion of precursors. However, *Ank*<sup>KI/KI</sup> multinucleated cells showed diminished actin ring formation and failed to enlarge in size. Results from peripheral blood cultures suggested that the degree of osteoclast formation depends on the available number of precursors in CMD patients and *Ank*<sup>KI/KI</sup> mice. Our study suggests that the CMD-like phenotype in mice and most likely CMD in humans is caused by a complex mechanism involving both, osteoblasts and osteoclasts. We believe that studies of this *Ank*<sup>KI/KI</sup> model could potentially lead to a novel therapeutic approach for CMD.

**Disclosures:** I. Chen, None.



## 1205

**Cardiovascular Diseases as Forecasters of Hip Fracture: A Nationwide Cohort Study in Twins.** K. Michaëlsson<sup>1</sup>, U. Sannerby<sup>\*1</sup>, H. Melhus<sup>2</sup>, R. Gedeberg<sup>\*3</sup>, L. Byberg<sup>\*1</sup>, N. L. Pedersen<sup>\*4</sup>. <sup>1</sup>Section of Orthopaedics, Department of Surgical Sciences, Uppsala, Sweden, <sup>2</sup>Section of Clinical Pharmacology, Department of Medical Sciences, Uppsala, Sweden, <sup>3</sup>Section of Anesthesiology and Intensive Care, Department of Surgical Sciences, Uppsala, Sweden, <sup>4</sup>Department of Medical Epidemiology and Biostatistics, Stockholm, Sweden.

Cardiovascular disease (CVD) and osteoporotic fractures are frequent health problems in the elderly. Recent studies indicate common etiologies for these diseases. However, the influence of different CVD diagnoses on fracture risk is uncertain. With a large twin analysis we can both examine the association between CVD, also in subcategories, and fracture risk, and evaluate the relative importance of genetics to lifestyle for this association.

We used a nation-wide cohort study, including all 33,432 Swedish twins born 1896-1944, and still alive in 1972. The Swedish Inpatient Registry identified twins with cardiovascular diseases and hip fracture. Cox's proportional hazards regression models were used with time-varying exposure of cardiovascular disease and covariate information including comorbidity to assess hazard ratios of hip fracture with 95% confidence intervals. Both twins in a pair were followed through an identical period of time, i.e. if one twin had a fracture or died, the co-twin was censored at the same date to avoid different follow-up time.

Of all women and men, 35% and 43%, respectively, had had a cardiovascular disease before censoring. A hip fracture was recorded for 1836 twins. CVD was associated with an increased future rate of hip fracture in both sexes. Any type of CVD, conferred a future adjusted HR of 1.71 (95% CI 1.51-1.92) for hip fracture, with similar estimates for women and men. The rate was three-fold higher within the first year after any CVD event. There was an especially increased risk of hip fracture after a diagnosis of heart failure (HR 2.86; 95% CI 2.31-3.53). This estimate was even higher within the first year after the diagnosis of heart failure (HR 14.52; 95% CI 10.35-20.37). We found a modest increased risk for hip fracture after a diagnosis of hypertension (HR 1.58; 95% CI 1.29-1.94) and ischemic heart disease (HR 1.36; 95% CI 1.15-1.62). Expectedly, there was an increased hip fracture risk after a history of stroke - HR 2.61 (95% CI 2.21-3.08). The increased risks were reduced by a within-pair comparison in monozygotic twins. This attenuation was especially marked for the diagnosis of heart failure but to a lesser degree for stroke.

Clinicians should have an increased awareness for the substantial increased risk of hip fracture after a recent diagnosis of CVD. Our generally attenuated estimates with the co-twin control analysis are an indication of shared genetic influences for CVD and osteoporotic fractures.

**Disclosures:** K. Michaëlsson, None.

This study received funding from: The Swedish Research Council and NIH.

## 1206

**Higher Bone Mineral Density is Associated with Increased Odds of Carotid Atherosclerosis in Postmenopausal Women Not Currently Using Estrogen Therapy.** G. A. Laughlin<sup>\*</sup>, E. Barrett-Connor. Family and Preventive Medicine, University of California San Diego, La Jolla, CA, USA.

Clinical and animal studies suggest that osteoporosis and atherosclerotic cardiovascular disease are biologically linked, perhaps through calcium-mediated processes or via reduced blood flow secondary to vascular disease. To test these hypotheses, we examined the association of bone mineral density (BMD) with a measure of overall atherosclerotic burden that is not directly calcium-dependent, intima media thickness (IMT) of the carotid arteries. Participants were 758 community-dwelling men and women, ages 55-97 (mean=75); 204 women were currently using estrogen therapy (ET), 245 were past or never users. IMT of the internal and the common carotid artery (ICA and CCA, respectively) was higher ( $p<.001$ ) in men (1.67 and 1.02 mm) than women (1.43 and 0.95 mm), but did not differ significantly by current ET. Carotid atherosclerosis was defined as IMT  $> 80^{\text{th}}$  sex-specific percentile for either the ICA or CCA, or stenosis  $\geq 25\%$ . In logistic regression analyses adjusting for factors common to osteoporosis and cardiovascular disease, higher BMD at the hip, femoral neck and lumbar spine was associated with significantly higher (not lower) odds of carotid atherosclerosis for women not using ET, but not for men or for women who were estrogen users (Table). In addition, the adjusted prevalence of osteoporosis (T-score  $\leq 2.0$ ) for women not using ET was significantly lower ( $p<.05$ ) at all three bone sites in those with carotid atherosclerosis versus those without. Osteoporosis prevalence did not differ by carotid atherosclerosis status for men or for women who were using ET. These results suggest that reduced blood flow secondary to atherosclerosis is not a biological basis for the widely reported association of osteoporosis and cardiovascular disease. The positive atherosclerosis-BMD association in women without ET was independent of factors common to bone and heart disease, and is unexplained.

**Table.** Odds Ratios for Carotid Atherosclerosis by 1 SD Increase in BMD

	Men (n=306)		Women on ET (n=204)		Women not on ET (n=245)	
	OR <sup>a</sup>	p-value	OR <sup>a</sup>	p-value	OR	p-value
<b>Total hip</b>						
Unadjusted	0.90	.36	0.94	.71	1.28	.09
Age-adjusted	0.97	.78	1.24	.21	1.59	.004
Multiply adjusted <sup>b</sup>	0.90	.49	0.99	.94	1.68	.009
<b>Femoral neck</b>						
Unadjusted	0.99	.92	0.97	.82	1.37	.047
Age-adjusted	1.04	.70	1.23	.22	1.76	.001
Multiply adjusted	1.03	.82	1.06	.76	1.82	.005
<b>Lumbar Spine</b>						
Unadjusted	1.11	.36	1.20	.24	1.52	.005
Age-adjusted	1.07	.58	1.23	.19	1.58	.004
Multiply adjusted	1.05	.72	1.08	.68	1.64	.008

<sup>a</sup> Odds ratios are for site- and sex-specific one standard deviation increase in BMD <sup>b</sup> Adjusted for age, weight, fasting insulin, triglycerides, osteoporosis medication use, smoking, physical activity

**Disclosures:** G.A. Laughlin, None.

## 1207

**Calcium Intake Is Not Associated with Increased Coronary Artery Calcification: The Framingham QCT Study.** E. J. Samelson<sup>1</sup>, J. M. Massaro<sup>\*2</sup>, C. S. Fox<sup>\*3</sup>, K. L. Tucker<sup>4</sup>, S. L. Booth<sup>\*4</sup>, T. J. Wang<sup>\*5</sup>, K. E. Broe<sup>1</sup>, S. D. Berry<sup>1</sup>, M. T. Hannan<sup>1</sup>, R. R. McLean<sup>1</sup>, L. A. Cupples<sup>\*2</sup>, C. J. O'Donnell<sup>\*3</sup>, D. P. Kiel<sup>\*1</sup>. <sup>1</sup>Inst for Aging Research, Hebrew SeniorLife, Harvard Med Sch, Boston, MA, USA, <sup>2</sup>Boston Univ School of Public Health, Boston, MA, USA, <sup>3</sup>NHLBI, Framingham, MA, USA, <sup>4</sup>Tufts Univ, Boston, MA, USA, <sup>5</sup>MA General Hosp, Harvard Med Sch, Boston, MA, USA.

Adequate calcium (Ca) intake is known to protect the skeleton. However, whether there is an increased risk of myocardial infarction (MI) among women taking Ca supplements compared to placebo is controversial. Even small, adverse effects of Ca intake on cardiovascular disease (CVD) could have major public health consequences since Ca supplements are widely used. We assessed the association between total Ca intake and coronary artery calcification (CAC), a direct measure of atherosclerosis that predicts risk of MI independent of other risk factors.

Participants included 690 women and 588 men in the Framingham Offspring Study (mean age 60 years, range 36-83 years) who attended clinic visits in 1998-2001 and completed food frequency questionnaires and CT examinations performed 4 years later in 2002-05. CAC was scored using the Agatston method. ANCOVA was used to calculate mean log-transformed CAC score across quartiles (1=low) of total Ca intake (from diet and supplements) adjusted for age, BMI, smoking, alcohol consumption, vitamin D supplement use, energy intake, and for women, menopause status and estrogen use.

Mean ( $\pm$ SD) total Ca intake was 1184 mg ( $\pm$ 565 mg) in women and 883 mg ( $\pm$ 456 mg) in men; 64% of women and 26% of men used Ca supplements. Mean CAC was 2.36 ( $\pm$ 2.44) in women and 4.32 ( $\pm$ 2.54) in men and ranged from 0 to 8.52.

While mean age-adjusted CAC score appeared to decrease with increasing total Ca intake, the trend was not significant after multivariable adjustment (Table). Results were similar for dietary Ca and Ca supplement use as well as for analyses that (1) additionally adjusted for diabetes, hypertension, CVD, total cholesterol, and aspirin use, (2) stratified by vitamin D intake from diet and/or supplements, and (3) excluded individuals with CVD.

While adequate Ca intake is important to bone health, effects on CVD risk are less clear. Our study does not support the hypothesis that high Ca intake increases coronary artery calcification, an important measure of atherosclerosis burden. Trials of Ca supplementation dosage used in clinical practice are warranted.

Mean Coronary Artery Calcification (CAC) Score by Quartile of Total Calcium (Ca) Intake				
Total Ca Intake Quartile	Women (N=690)		Men (N=588)	
	Age-Adjusted Mean CAC	Multivariable-Adjusted Mean CAC	Age-Adjusted Mean CAC	Multivariable-Adjusted Mean CAC
1 (low)	2.60	2.47	4.82	4.76
2	2.34	2.34	3.36	4.31
3	2.31	2.31	3.92	3.94
4 (high)	2.26	2.32	4.19	4.29
Linear Trend, p	0.12	0.58	<0.01	0.10

**Disclosures:** E.J. Samelson, None.

## 1208

**Subclinical Thyroid Disease Predicts Risk of Hip Fracture: The Cardiovascular Health Study.** J. S. Lee<sup>\*1</sup>, H. A. Fink<sup>\*2</sup>, J. A. Vu<sup>\*1</sup>, P. Buzkova<sup>\*3</sup>, L. D. Carbone<sup>4</sup>, Z. Chen<sup>\*5</sup>, A. R. Cappola<sup>6</sup>, J. Robbins<sup>1</sup>. <sup>1</sup>Internal Medicine, University of California Davis, Sacramento, CA, USA, <sup>2</sup>Internal Medicine, VA Medical Center, Minneapolis, MN, USA, <sup>3</sup>Biostatistics, University of Washington, Seattle, WA, USA, <sup>4</sup>Internal Medicine, University of Tennessee, Memphis, TN, USA, <sup>5</sup>Internal Medicine, University of Arizona, Tucson, AZ, USA, <sup>6</sup>Internal Medicine, University of Pennsylvania, Pittsburgh, PA, USA.

Thyroid hormone influences bone metabolism, but whether subclinical thyroid disease is related to risk of hip fracture is unclear. We evaluated whether biochemically-defined subclinical thyroid disease predicts the risk of incident hip fracture in older men and women. Participants were U.S. community-based men and women aged  $\geq 65$  years during 1989-90 in the prospective cohort Cardiovascular Health Study. Baseline serum thyroid-stimulating hormone (TSH) levels were measured in everyone, free thyroxine was measured if TSH was outside the reference 0.1-4.5 mU/L, and subjects were classified as subclinical hyperthyroidism, subclinical hypothyroidism, and euthyroid. 51 subjects with overt hyper/hypothyroidism were excluded from analyses due to small sample size. Incident hip fractures were validated by medical records (mean follow-up 12.5 y). Cox regression models were conducted to estimate hazard ratios for hip fracture by subclinical thyroid disease group. Risks of incident hip fracture were 2.07-fold higher in men with subclinical hypothyroidism and 3.31-fold higher in men with subclinical hyperthyroidism, while no associations were observed in women (Table). Additional adjustment for other risk factors of hip fracture and excluding those taking thyroid hormone or thyroid-altering medications did not materially alter the results. In conclusion, subclinical hypo- and hyperthyroidism are independent predictors for subsequent hip fracture in community dwelling older men.

**Hazard ratios (95% CI) for hip fracture**

Thyroid status	Number of Hip Fracture	Age-adjusted	MV-adjusted*
Men			
Euthyroid (n=1159)	58	1	1
Subclinical hypothyroid (n=184)	18	1.86 (1.09-3.15)	2.07 (1.16-3.67)
Subclinical hyperthyroid (n=29)	4	3.07 (1.11-8.48)	3.31 (1.01-10.85)
Women			
Euthyroid (n=1694)	198	1	1
Subclinical hypothyroid (n=359)	36	0.87 (0.61-1.24)	0.83 (0.57-1.21)
Subclinical hyperthyroid (n=142)	17	1.06 (0.65-1.74)	0.94 (0.54-1.63)

\*Adjusted for age, estrogen use, health status, frailty, smoking, alcohol.

**Disclosures:** J.S. Lee, None.

This study received funding from: NCRR Roadmap K12 and NHLBI.

## 1209

**Higher Bone Mineral Density Loss in Older Men with Diabetes: The Osteoporotic Fractures in Men Study.** E. S. Strotmeyer<sup>1</sup>, R. M. Boudreau<sup>\*1</sup>, L. M. Marshall<sup>2</sup>, A. V. Schwartz<sup>3</sup>, D. C. Bauer<sup>3</sup>, E. Barrett-Connor<sup>\*4</sup>, E. S. Orwoll<sup>2</sup>, J. A. Cauley<sup>1</sup>. <sup>1</sup>Epidemiology, University of Pittsburgh, Pittsburgh, PA, USA, <sup>2</sup>Oregon Health & Science University, Portland, OR, USA, <sup>3</sup>University of California, San Francisco, CA, USA, <sup>4</sup>University of California, San Diego, CA, USA.

Type 2 diabetes (DM) is associated with increased fracture risk despite generally higher bone mineral density (BMD) vs. non-diabetic adults. Older diabetic women have higher BMD loss (Schwartz et al 2005). We analyzed BMD change over 4.6 $\pm$ 0.4 years in 5,995 community dwelling men aged  $\geq 65$  years in the Osteoporotic Fractures in Men (MrOS) Study. DM was defined as self-report diagnosis, hypoglycemic medication use or fasting glucose (FG)  $\geq 126$  mg/dl. Impaired FG (IFG) was defined as FG  $\geq 100$  and  $<126$  mg/dl. Total hip and femoral neck BMD, total lean mass (LM) and fat mass (FM) were measured by DXA (QDR 4500W, Hologic Inc). Men missing BMD change or DM/IFG status were excluded. Of 4,094 men (age 72.8 $\pm$ 5.4 years; 91% white), 14% had DM and 37% had IFG. Adjusting for age, race, LM and FM, hip BMD was highest in DM and intermediately higher in IFG vs. normal FG at baseline (0.986 vs. 0.963 vs. 0.947 g/cm<sup>2</sup>; p<0.05) and follow-up (0.972 vs. 0.952 vs. 0.939 g/cm<sup>2</sup>; p<0.05). LM loss was highest in DM and intermediately higher in IFG vs. normal FG (-2.8 vs. -1.0 vs. 1.5 kg; p<0.05), with no FM change differences. Men with DM had significantly higher annualized % hip BMD loss vs. normal FG men after adjustment (Table). Higher hip BMD loss in DM occurred due to a concurrent higher BMC loss and lower area increase. Initial hip BMD did not attenuate results, suggesting that loss occurs regardless of initial BMD in DM. Adjusting for baseline fasting insulin level, smoking, drinking, physical activity, and medication use (corticosteroid, statin, thiazide, thyroid and osteoporosis medication) did not change associations. Thiazolidinedione (TZD) use in DM (N=48) was associated with 2x greater % BMD loss vs. DM not using TZDs (-1.028 vs. -0.496 %; p<0.05); however did not explain the higher BMD loss in DM vs. non-DM men. Results were similar for annualized % femoral neck BMD loss, though not significant for BMC or area. DM, but not IFG, was associated with 60% greater hip BMD loss, which was not explained by initial BMD, LM loss, or medication use. This BMD loss may have important implications for increased fracture risk in older diabetic adults.

Annualized % change	DM	IFG	Normal FG
Total hip BMD			
Unadjusted	-0.559 <sup>b</sup>	-0.331	-0.339
Adjusted*	-0.557 <sup>b</sup>	-0.313	-0.327
Adjusted* + initial BMD	-0.562 <sup>b</sup>	-0.313	-0.325
Total hip BMC			
Unadjusted	-0.458 <sup>b</sup>	-0.142	-0.154
Adjusted*	-0.456 <sup>b</sup>	-0.133	-0.134
Adjusted* + initial BMC	-0.451 <sup>b</sup>	-0.133	-0.136
Total hip area			
Unadjusted	0.147 <sup>b</sup>	0.236	0.227
Adjusted*	0.136 <sup>b</sup>	0.228	0.238
Adjusted* + initial area	0.123 <sup>b</sup>	0.228	0.242

\*adjusted for age, race, LM, FM, LM and FM changes <sup>b</sup>p<0.05 for DM vs. normal FG

**Disclosures:** E.S. Strotmeyer, None.

## 1210

**Predictors of Poor Outcomes Following Osteoporotic Fractures in Elderly Women and Men: An 18 Year Prospective Study.** D. Bliuc, N. D. Nguyen, T. V. Nguyen, J. A. Eisman, J. R. Center. Bone and Mineral Program, Garvan Institute of Medical Research, Sydney, Australia.

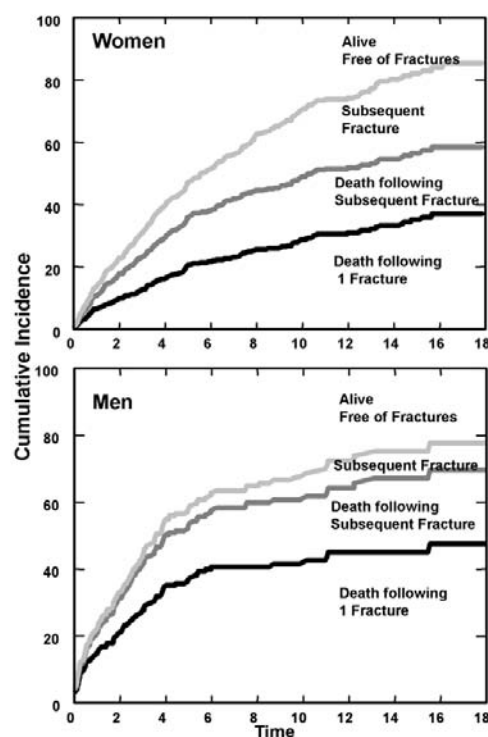
Osteoporotic fractures increase re-fracture and mortality risk. Although these severe outcomes are related, they are usually studied separately. The aims of this study were to examine the risk of either one or both of these outcomes following all osteoporotic fractures and to determine their predictors over 18-year in women and men aged 60+.

All subjects (n=1295) sustaining low trauma fractures from Dubbo Osteoporosis Epidemiology Study were followed (April 1989- May 2007). Bone mineral density, postural stability, quadriceps strength, physical activity, co-morbidities, calcium intake, smoking and anthropometric measurements were assessed 2-yearly in a subgroup (n=636) participating in the detailed study. Cumulative incidences of re-fracture and mortality were computed separately for women and men and the predictors for these outcomes were assessed by Cox Proportional Hazard Model for multiple events.

There were 952 fractures in women and 343 in men, followed by 290 subsequent fractures in women and 74 in men, and 461 deaths in women and 197 in men. The highest re-fracture and mortality risk was observed in the first 5-8 year period (Fig 1). By the end of 8 years 26 % women and 41% men had died and a further 37% women and 24 % men re-fractured. Approximately 50% of women and 75% of men with re-fracture died in the first 5 years post-fracture. Mortality risk was higher in men than women, but ongoing fracture continued to occur in those women who survived such that by the end of the study there were only 20% of subjects alive with no further fractures.

In the detailed study group, re-fracture independently increased mortality risk [HR: 4.32 (3.40- 5.49) and 2.32 (1.43- 3.48) for women and men, respectively]. Other independent predictors for mortality included older age, lower femoral neck BMD, physical inactivity and more falls in women and older age, low calcium intake, and quadriceps weakness in men.

This study has shown the cumulative risk of multiple adverse events following an initial fracture. Those who survive the initial fracture have increased re-fracture risk and further increase in mortality risk. These findings highlight the need for prevention of both initial and subsequent fractures.

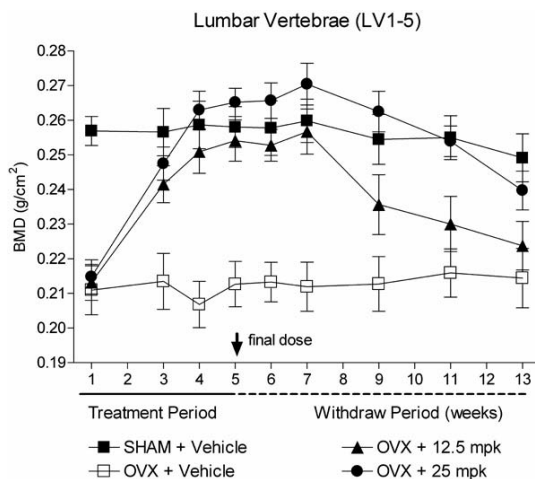


**Disclosures:** D. Bliuc, None.

## 1211

**Increases in BMD Observed with Anti-Sclerostin Antibody Treatment Are Reversible: A Longitudinal Ovariectomized Rat Study.** X. Li, K. Warmington\*, Q. T. Niu\*, M. Grisanti, H. Tan, D. Dwyer\*, M. Stolina, W. S. Simonet, P. J. Kostenuik, C. Paszty, H. Z. Ke. Amgen Inc., Thousand Oaks, CA, USA.

Anti-sclerostin monoclonal antibody (Scl-Ab) is a new anabolic agent that stimulates bone formation and increases bone mass and bone strength in animal models of osteoporosis. However, the effects of discontinuing treatment have not been studied in ovariectomized (OVX) rats. In this study, we examined the BMD response during treatment with Scl-Ab and after its discontinuation. Female SD rats at 5.5 months of age were sham-operated or OVX and left untreated for 7.5 months to allow for the development of osteopenia. OVX rats were then administered Scl-Ab at 12.5 or 25 mg/kg by weekly s.c. injection, for a period of 8 weeks (8-10/group). Thereafter, treatment was discontinued for another 16 weeks. BMD of lumbar vertebrae (LV-BMD) and of femur and tibia (FT-BMD) was determined before treatment, and at weeks 4, 6, 8, 10, 12, 16, 20 and 24 by DXA. OVX rats had significantly lower LV-BMD (-18%) and FT-BMD (-9%) than sham controls before the initiation of treatment. In OVX rats treated with either dose level of Scl-Ab, LV-BMD rapidly and significantly increased to the level of sham controls by the first 6 weeks of treatment (Figure). The LV-BMD was maintained at the increased level between the week 6 and week 12 time points. Thereafter, LV-BMD in the low dose group decreased by 8% at week 16, then by 10% and 13% at weeks 20 and 24, respectively, compared with the peak BMD at week 12. In the high dose group, LV-BMD decreased gradually by 3%, 6% and 11% at weeks 16, 20 and 24, respectively. Similarly FT-BMD rapidly and significantly increased, for both dose levels, to the level of sham controls by the first 6 weeks of treatment. In contrast to LV-BMD, FT-BMD was maintained at the increased level between the week 6 and week 20 time points. FT-BMD at week 24 was slightly decreased by 2.4% and 2.5% from those at week 20 in low and high dose groups, respectively. In summary, the increased BMD in lumbar spine and long bones, resulting from Scl-Ab treatment, was maintained for a period of time even after discontinuation of therapy. Thereafter, a decrease in BMD was observed. We conclude that increased bone mass induced by Scl-Ab treatment in OVX rats is reversible, with BMD decreasing over time upon discontinuation of treatment.



**Disclosures:** X. Li, Amgen 5.  
This study received funding from: Amgen.

## 1212

**A Short Treatment with an Antibody to Sclerostin Can Inhibit Bone Loss in an Ongoing Model of Colitis.** A. Eddleston\*, D. Marshall\*, A. Moore\*, P. Stephens\*, M. Muzylak\*, M. Marenzana\*, M. K. Robinson. Inflammation Biology, UCB-Celltech, Slough, United Kingdom.

Sclerostin is an osteocyte-produced protein which regulates the anabolic activity of osteoblasts. A neutralizing antibody to sclerostin has been reported to reverse ovariectomy-induced bone loss in a rats (Warmington et. al. 2005 J. Bone Miner Res 20 S22). The mouse CD4+CD45Rb<sup>high</sup> T cell transfer model of colitis is a chronic disease model in which animals develop inflammation-induced bone loss (Byrne et. al. 2005 Gut 54, 78-86). We have investigated the ability of a neutralizing antibody to sclerostin (Scl-ab) to inhibit bone loss in a modification of the model described by Byrne that features a more synchronous onset of colitis. CD4+CD45Rb<sup>high</sup> T cells isolated from Balb/c mice were cultured in vitro with IL-12 and anti-IL-4 to skew them towards a Th1 phenotype before transfer into SCID mice (5x10<sup>5</sup> cells per mouse). Scl-ab or an isotype-matched control antibody (Cntrl-ab) were dosed at 10mg/kg sc weekly starting at day 50 after cell transfer by which time colitis was apparent. At this point animals receiving T cells had significantly lower bone mass than a control group not receiving cells (day 50 femoral BMD in mice without cell transfer 80.8±1.5mg/cm<sup>2</sup> vs cell transfer group 73.2±2.6mg/cm<sup>2</sup> p<0.05). Antibody dosing continued until day 69 when the experiment was terminated. Dosing with Scl-ab had no effect on the severity of colitis (assessed by symptoms, weight loss and histology) however by the end of the experiment mice dosed with Scl-ab had significantly higher femoral and total BMD than mice dosed with Cntrl-ab (femoral BMD 73.4±3.4mg/cm<sup>2</sup> vs 64.5±2mg/cm<sup>2</sup> p<0.05, total

BMD 55.0±1.5mg/cm<sup>2</sup> vs 49.7±1.4mg/cm<sup>2</sup> p<0.01). Micro-CT at the distal femur in these animals showed that the Scl-ab treated animals had significantly more trabecular bone volume and increased trabecular thickness than Cntrl-ab treated animals (BV/TV+58% p<0.001, Tb.th +46% p<0.001). At the femoral mid-shaft cortical bone was significantly thicker (Cs.th +15% p<0.001) in Scl-ab treated animals. A four-point bending test showed that femurs from Scl-ab treated animals had significantly greater bone strength when compared with femurs from animals receiving Cntrl-ab (maximum load +67% p<0.01 and energy to failure +86% p<0.01). The Scl-ab treated animals also had significantly higher levels of circulating osteocalcin (p<0.01) but significantly lower levels of circulating TRAP5b (p<0.01) than those dosed with Cntrl-ab.

In conclusion a neutralizing antibody to sclerostin inhibits inflammation-induced bone loss in a chronic mouse model of colitis but does not reduce inflammation.

**Disclosures:** M.K. Robinson, UCB-Celltech 2.  
This study received funding from: UCB-Celltech.

## 1213

**Effects of Co-treatment with an Anti-Sclerostin Monoclonal Antibody and Alendronate in Ovariectomized Rats.** X. Li, K. Warmington\*, Q. T. Niu\*, E. Asuncion, M. Grisanti, D. Dwyer\*, H. Tan, W. S. Simonet, M. Ominsky, M. Stolina, P. J. Kostenuik, C. Paszty, H. Z. Ke. Amgen Inc., Thousand Oaks, CA, USA.

Anti-sclerostin monoclonal antibody (Scl-Ab) is a new anabolic agent which has been shown to increase bone formation, bone mass and bone strength in rodents and primates. More recently, in a placebo controlled Phase I trial in postmenopausal women, Scl-Ab was shown to increase serum markers of bone formation. For anabolic agents, there is general interest in determining whether or not anabolic activity is blunted by co-treatment with an anti-catabolic agent such as alendronate (ALN), which is known to inhibit bone resorption and preserve bone mass in animal models and in humans. In the current study, we examined whether co-treatment with ALN would result in a blunting of the anabolic effects of Scl-Ab in ovariectomized (OVX) rats. Female SD rats at 6.5 months of age were sham-operated or OVX and left untreated for 3.5 months, allowing for significant bone loss to occur. OVX rats were then treated for 6 weeks (10/group) with Scl-Ab (1x/week, s.c., 25 mg/kg), or ALN (2x/week, s.c., 0.028 mg/kg) alone or in combination. Micro-CT analysis of the 5<sup>th</sup> lumbar vertebrae revealed that, over the 6 week duration of the study, there was further trabecular bone loss in vehicle-treated OVX rats compared with pre-treatment OVX controls. As expected, ALN alone prevented this bone loss but did not restore bone mass in OVX rats. Scl-Ab alone not only prevented the further trabecular bone loss, but also restored trabecular vBMC, vBMD and trabecular bone volume, and improved trabecular architecture to levels of sham controls. In addition, Scl-Ab increased cortical area and cortical thickness of cortical shell to the levels higher than those of sham controls. Interestingly, trabecular bone mass and architecture, as well as cortical bone mass, did not differ significantly between the Scl-Ab alone and Scl-Ab plus ALN groups, indicating that ALN did not blunt the bone restorative effects of Scl-Ab in OVX rats. Consistent with this, histomorphometric analysis showed that Scl-Ab alone and Scl-Ab plus ALN were equally effective at increasing mineralizing surface, mineral apposition rate and bone formation rate, on both the periosteal and the endocortical surface of the tibial shaft. Furthermore, Scl-Ab alone and Scl-Ab plus ALN were equally effective at increasing serum osteocalcin, a bone formation marker. These results demonstrate that the anabolic responses to Scl-Ab treatment were not impaired by co-treatment with alendronate in OVX rats.

**Disclosures:** X. Li, Amgen 5.  
This study received funding from: Amgen.

## 1214

**Fully Human anti-DKK1 Antibodies Increase Bone Formation and Resolve Osteopenia in Mouse Models of Estrogen-Deficiency Induced Bone Loss.** H. Glantschnig\*, R. Hampton\*, N. Wei\*, K. Scott\*, P. Nantermet\*, J. Zhao\*, F. Chen\*, J. Fisher\*, Q. Su\*, B. Pennypacker\*, T. Cusick\*, P. Sandhu\*, A. Reszka\*, W. Strohl\*, O. Flores\*, F. Wang\*, D. Kimmel\*, Z. An\*. <sup>1</sup>Molecular Endocrinology, Merck Research Laboratories, West Point, PA, USA, <sup>2</sup>Biologics Research, Merck Research Laboratories, West Point, PA, USA.

Genetic studies have linked both osteoporotic and high bone mass (HBM) phenotypes to mutations within the LDL-receptor related protein 5 (LRP5). LRP5 and 6 are co-receptors for Wnt-ligands and bind inhibitory Dickkopf (DKK) proteins. Amino-acid substitutions leading to HBM-phenotypes desensitize LRP5 to the inhibitory function of DKK1. DKK1 is expressed in adult bone, and treatment modalities that diminish LRP/DKK1 binding may act as stimulators of bone mass accrual. Here we describe the development and the *in-vitro* and *in-vivo* characterization of functionally neutralizing anti-DKK1 monoclonal antibodies (mAbs).

Screening of CAT-libraries identified single-chain antibodies and full IgGs with high-affinity for *Rhesus macaque* and *Mouse sp.* DKK1, but not DKK2 and DKK4. Full IgGs were funneled through a series of functional *in-vitro* assays validating that selected antibodies block receptor-ligand interaction, neutralize DKK1-function in osteoblastic differentiation, and as expected, block DKK1 inhibition of Wnt-signaling. To evaluate pharmacologic efficacy *in-vivo*, selected anti-DKK1 mAbs were tested by sub-cutaneous injection in young and adult mice, and evaluated in a mouse model of estrogen-deficiency-induced osteopenia. Fully-human anti-DKK1 mAbs were found to have prolonged half-lives in mice (~17 days), dose-dependently reduced bioavailable DKK1 in serum and were tolerated well over treatment periods up to 8 weeks. mAbs (0.5 - 10 mpk/ 2x wk) elicited significant dose-dependent increases in BMD in young mice at the central and distal femur (4 wks).

Importantly, in osteopenic adult animals administration of DKK1-mAb (2 mpk/1-2x wk) resulted in significant stimulation of serum-PINP and new bone formation (2-fold) at endocortical surfaces and trabecular bone regions. This was paralleled by partial-to-complete resolution of osteopenia (BMD) in femur and lumbar-vertebral bones at 8 wks. Further, testing of antibodies in *Rhesus macaques* (10 mpk) resulted in a pharmacodynamic response (PINP), implicating that a bone-forming mechanism had been engaged.

In conclusion, we provide pharmacologic evidence for Wnt-pathway modulation by neutralizing DKK1-bioactivity resulting in resolution of osteopenia in animal models. Thus, fully-human anti-DKK1 mAbs exhibit the potential as bone-anabolic agents for the treatment of diseases characterized by low bone mass.

**Disclosures:** H. Glantschnig, None.

## 1215

**R-Spondin1 Reduces Bone Loss in Human TNF Transgenic and Ovariectomized Mice.** J. Zhao<sup>1</sup>, K. Kim<sup>\*1</sup>, M. Binnerts<sup>\*1</sup>, G. Kroenke<sup>\*2</sup>, J. Katzenbeisser<sup>\*2</sup>, A. Abo<sup>\*1</sup>, G. Schett<sup>\*2</sup>. <sup>1</sup>Research, Nuvelo, Inc., San Carlos, CA, USA, <sup>2</sup>Department of Internal Medicine 3 and Institute for Clinical Immunology, University of Erlangen-Nurnberg, Erlangen, Germany.

Wnt proteins are key mediators for bone formation and appear to protect the macro- and micro-architecture of periarticular bone during inflammation. Blocking of Wnts by natural antagonists, such as Dickkopf-1 (DKK1), results in enhanced breakdown of bone. To further explore the Wnt pathway during pathological bone remodeling, we investigated whether R-Spondin1 (RSp1), an inducer of the Wnt signaling pathway, reduces inflammatory bone resorption and postmenopausal bone loss in mouse models. RSp1 synergistically stimulated the activation of the Wnt pathway by Wnt3A by antagonizing DKK-1 using TCF reporter assay in osteoblastic C2C12 cells. RSp1 also amplified the Wnt-mediated osteogenic differentiation including alkaline phosphatase and osteoprotegerin in C2C12 cell line. Treatment with RSp1 achieved a significant protection of periarticular bone loss in arthritic human TNF transgenic (hTNFtg) mice. Bone erosions were smaller and osteoclast numbers were decreased upon RSp1 treatment in hTNFtg mice. RSp1 also protected cartilage loss and induced osteophyte formation although no effect on synovial inflammation was seen in hTNFtg mice. Likewise, RSp1 administration alleviated ovariectomy-induced bone loss in mice. We found that RSp1 substantially inhibited the suppressing effect of estrogen deficiency on femoral bone mineral density and content in mice. Moreover, RSp1 stimulated the new bone formation in trabecular bone in ovariectomized mice. In conclusion, RSp1 reduces bone loss during experimental arthritis and osteoporosis in mouse models by stimulating the bone anabolic pathway. Activation of Wnt signaling by RSp1 may thus be a potent strategy to protect the bone from pathological degradation. Currently, we are investigating the role of RSp1 in reducing ovariectomy-induced osteoporosis and collagen-induced arthritis in rat models.

**Disclosures:** J. Zhao, None.

## 1216

**Transition from Alendronate to Denosumab Resulted in Further Reductions in Local and Systemic Bone Turnover Parameters and Reduced Cortical Porosity in Ovariectomized Cynomolgus Monkeys.** M. S. Ominsky<sup>1</sup>, J. Jolette<sup>2</sup>, S. Y. Smith<sup>2</sup>, F. Vlasseros<sup>\*2</sup>, R. Samadpour<sup>\*2</sup>, P. J. Kostenuik<sup>1</sup>. <sup>1</sup>Metabolic Disorders, Amgen Inc., Thousand Oaks, CA, USA, <sup>2</sup>Charles River Laboratories Preclinical Services Montreal, Inc., Montreal, QC, Canada.

The effects of transition from the bisphosphonate alendronate (ALN) to the RANK ligand inhibitor denosumab (DMAb) on local and systemic bone turnover parameters were studied in adult ovariectomized (OVX) cynomolgus monkeys (cynos). OVX cynos (>7 years old) were treated with vehicle (Veh, n=20), ALN (n=21; 50 µg/kg IV 2/week), or DMAb (n=11; 25 mg/kg SC monthly). After 6 months, animals from each of the Veh (n=10) and ALN groups (n=11) were switched to DMAb for an additional 6 months (Veh-DMAb and ALN-DMAb), while the remaining 10 animals in these groups continued on Veh or ALN. The original DMAb group remained on DMAb for 12 months total. Serum biomarkers were monitored, and dynamic histomorphometry was performed at the rib, tibial diaphysis, proximal tibia, lumbar vertebra (L2), and ilium. Strength of L5-6 trabecular cores was tested by compression.

DMAb and ALN significantly reduced serum biomarkers of bone resorption (CTx) and formation (osteocalcin, OC) throughout the 12 month treatment period, with significantly greater reductions observed in the DMAb group. Upon transition from ALN to DMAb, serum CTx and OC levels were further reduced to the levels observed with DMAb alone. Dynamic histomorphometry of trabecular bone (iliac crest, L2 and proximal tibia) and of cortical bone (ribs, tibial diaphysis) showed significant reductions in bone turnover parameters after 12 months of DMAb or ALN. For most parameters at most skeletal sites, cortical and trabecular turnover suppression with DMAb and with ALN-DMAb was numerically or statistically greater than with ALN. Cortical porosity at the rib and tibial diaphysis was significantly lower with DMAb and with ALN-DMAb ( $p < 0.05$  vs Veh), but not with ALN alone.

Relationships between local bone turnover suppression and bone strength were studied by measuring peak load of L5-6 trabecular cores and by dynamic histomorphometry of trabecular bone from L2. Peak load of L5-6 trabecular cores was significantly greater in the DMAb and ALN-DMAb groups ( $p < 0.05$  vs. Veh), but not with continuous ALN. With all groups, L5-6 peak load was inversely correlated with L2 BFR ( $R = -0.53$ ) and osteoclast surface ( $R = -0.47$ ).

In summary, transition from ALN to DMAb resulted in further reductions in local and systemic bone turnover parameters compared to continuous ALN treatment in OVX cynos. Bone strength was maintained or improved by transition from ALN to DMAb, and bones

with the greatest strength values exhibited the lowest levels of bone turnover regardless of treatment.

**Disclosures:** M.S. Ominsky, Amgen 5.

This study received funding from: Amgen.

## 1217

**Loss of a Single Bim Allele Recovers the Defective Osteoclast Function in bcl-2-/- Mice but Does Not Restore the Anabolic Action of PTH.** Y. Nagase<sup>1</sup>, M. Iwasawa<sup>1</sup>, T. Akiyama<sup>1</sup>, Y. Kadono<sup>1</sup>, N. Ogata<sup>1</sup>, Y. Oshima<sup>1</sup>, M. Nakamura<sup>1</sup>, T. Yasui<sup>1</sup>, T. Miyamoto<sup>2</sup>, K. Nakamura<sup>1</sup>, S. Tanaka<sup>1</sup>. <sup>1</sup>The University of Tokyo, Tokyo, Japan, <sup>2</sup>Department of Orthopaedic Surgery, Cell Differentiation, Keio University School of Medicine, Tokyo, Japan.

Anti-apoptotic molecule Bcl-2 resides on the mitochondrial outer membrane, and inhibits apoptosis by suppressing cytochrome *c* release from mitochondria. We previously reported that Bcl-2 promoted the differentiation, activation and survival of both osteoblasts and osteoclasts by analyzing *bcl-2*<sup>-/-</sup> mice. However, *bcl-2*<sup>-/-</sup> mice die at about 2 weeks of age due to renal failure and immunodeficiency, and further analysis of the skeletal tissues of the mice is not possible. We found that loss of a single *bim* allele ameliorated the ill health and early death of *bcl-2*<sup>-/-</sup> mice. We therefore generated *bcl-2*<sup>-/-</sup>*bim*<sup>+/-</sup> mice by interbreeding with *bcl-2*<sup>+/-</sup> mice and *bcl-2*<sup>-/-</sup>*bim*<sup>-/-</sup> mice, and compared the skeletal tissue of *bcl-2*<sup>-/-</sup>*bim*<sup>+/-</sup> mice with that of *bcl-2*<sup>+/-</sup>*bim*<sup>+/-</sup> littermates (control) to analyze the role of Bcl-2 in the skeletal tissue. Although both mice grew normally into adults, *bcl-2*<sup>-/-</sup>*bim*<sup>+/-</sup> mice displayed an osteopenia compared to *bcl-2*<sup>+/-</sup>*bim*<sup>+/-</sup> mice. Bone histomorphometric analysis demonstrated that *bcl-2*<sup>-/-</sup>*bim*<sup>+/-</sup> mice reduced bone volume whereas they exhibited restoration of bone resorption which was impaired by *bcl-2* homozygous deficiency. Osteoclasts generated from *bcl-2*<sup>-/-</sup>*bim*<sup>+/-</sup> bone marrow cells displayed normal bone-resorbing activity, while the mineralization activity of osteoblasts generated from *bcl-2*<sup>-/-</sup>*bim*<sup>+/-</sup> calvarial cells was still impaired as well as *bcl-2* deficient osteoblasts. This indicates that inactivation of a single *bim* allele restores the defective function caused by *bcl-2* deficiency in osteoclasts, but is not enough to rescue the defective function in Bcl-2 deficient osteoblasts. We next examined the effect of intermittent PTH administration on bone mass in the mice. While intermittent PTH administration markedly increased the trabecular bone volume in *bcl-2*<sup>+/-</sup>*bim*<sup>+/-</sup> mice (control), it did not affect the bone volume of *bcl-2*<sup>-/-</sup>*bim*<sup>+/-</sup> mice. The osteoid surface was significantly increased in PTH administered *bcl-2*<sup>-/-</sup>*bim*<sup>+/-</sup> mice as compared to *bcl-2*<sup>+/-</sup>*bim*<sup>+/-</sup> mice, indicating that the mineralization of the mice is still attenuated. Collectively, these data indicate that loss of a single *bim* allele recovers the defective osteoclast function in *bcl-2*<sup>-/-</sup> mice but does not restore the anabolic action of PTH, and additionally Bcl-2 is indispensable for anabolic actions of PTH.

**Disclosures:** Y. Nagase, None.

## 1218

**R740S, a Dominant V-ATPase a3 Mutation, Causes Osteopetrosis in Mice.** N. Ochotny<sup>\*1</sup>, A. M. Fleniken<sup>\*2</sup>, C. Owen<sup>\*2</sup>, R. A. Zirngibl<sup>\*3</sup>, L. R. Osborne<sup>\*2</sup>, J. E. Henderson<sup>\*4</sup>, S. L. Adamson<sup>\*2</sup>, J. Rossant<sup>\*2</sup>, M. F. Manolson<sup>1</sup>, J. E. Aubin<sup>2</sup>. <sup>1</sup>Faculty of Dentistry, University of Toronto, Toronto, ON, Canada, <sup>2</sup>Centre for Modeling Human Disease, Samuel Lunenfeld Research Institute, Mt. Sinai Hospital, Toronto, ON, Canada, <sup>3</sup>Molecular Genetics, University of Toronto, Toronto, ON, Canada, <sup>4</sup>Bone Centre, McGill University, Montreal, QC, Canada.

Bone resorption involves osteoclast-mediated acidification via a vacuolar-type H<sup>+</sup>-ATPase (V-ATPase) localized to the ruffled border at the bone surface. V-ATPases are proton pumps composed of 13 subunits including the 'a' subunit. Of the 4 'a' isoforms in mammals a3 is enriched in osteoclasts where it is essential for bone resorption. Humans with homozygous a3 mutations are severely osteopetrotic and do not live past 6 years without treatment (bone marrow transplant), while their heterozygous parents have no detectable phenotype. Homozygous a3<sup>-/-</sup> mice have severe osteopetrosis and die by 6 weeks; a3<sup>+/-</sup> mice have no reported abnormalities. We identified an a3 missense mutation (R740S) during a mouse genome-wide ethylnitrosourea (ENU) mutagenesis screen for dominant point mutations affecting bone mineral density (BMD). The mouse a3 R740 residue is perfectly conserved in mammalian and yeast 'a' isoforms, and in yeast is essential for proton translocation. Our objective was to characterize the molecular and cellular mechanisms underlying osteopetrosis in Atp6i<sup>R740S/+</sup> mice. We employed DEXA, faxitron and micro-CT to quantify the BMD, visualize the skeleton and determine static histomorphometric parameters. Spleen cells were cultured with RANKL-MCSF and osteoclasts generated were replated onto dentine slices to quantify osteoclastogenesis and resorption respectively. Atp6i<sup>R740S/+</sup> intercrosses revealed that mice homozygous for the R740S mutation died at birth or soon after, in contrast to both a3<sup>-/-</sup> and a3<sup>+/-</sup> mice. Atp6i<sup>R740S/+</sup> mice have normal appearance, size and weight but exhibit higher BMD, greater trabecular bone mass and greater bone volume as percent of tissue volume compared with wildtype (WT) littermates, suggesting deficient bone resorption. Fewer and smaller (fewer nuclei/cell) osteoclasts formed in spleen cell cultures from Atp6i<sup>R740S/+</sup> versus WT mice and Atp6i<sup>R740S/+</sup> osteoclasts had decreased resorption activity on dentine slices. As heterozygote mice and humans with only one functional a3-encoding gene do not display any phenotype, the dominant R740S mutation is likely not related to haploinsufficiency of transcripts or translated protein. Also, there is only one copy of the a3 subunit per V-ATPase complex making it unlikely that mutant a3 interacts with and inactivates WT a3. R740S is the first dominant mutation of a3 that results in osteopetrosis.

**Disclosures:** N. Ochotny, None.

## 1219

**Mitogen-Activated Protein Kinase Phosphatase-1 Protects Bone Mass Via Negative Regulation of Osteoclast Differentiation and Activation.** J. Carlson<sup>\*1</sup>, F. Mercan<sup>\*2</sup>, Q. Zhang<sup>3</sup>, A. Bennett<sup>\*2</sup>, A. Vignery<sup>3</sup>. <sup>1</sup>Comparative Medicine, Yale School of Medicine, New Haven, CT, USA, <sup>2</sup>Pharmacology, Yale School of Medicine, New Haven, CT, USA, <sup>3</sup>Orthopaedics, Yale School of Medicine, New Haven, CT, USA.

Multinucleate osteoclasts (OC) are essential for bone development, homeostasis and repair and play a critical role in diseases such as osteoporosis and inflammatory arthritis. Mitogen-activated protein kinases (MAPK) transduce extracellular signals into cellular responses, which include gene expression, cell growth, differentiation, and apoptosis, and play a key role in OC formation and activation. While all MAPKs become activated during OCgenesis, p38 plays a central role in RANKL-induced OC differentiation and activation. MAPK phosphatases (MKP) are responsible for regulating MAPK signaling, yet their role in the differentiation of OC remains unknown. MKP-1 is an inducible nuclear MKP that inactivates all MAPKs, with a preference for p38 over JNK and ERK. We had discovered that MKP-1 transcripts are transiently induced at the onset of fusion in macrophages, and therefore asked whether MKP-1 regulates OC differentiation and/or activation. We first confirmed the induced expression of MKP-1 in spleen cell-derived mouse OC. We then found that in the absence of MKP-1, OC, as well as the actin ring they form to resorb bone, are smaller, yet resorb calcium-phosphate substrate more efficiently than wild-type OC. We then stimulated OC from MKP-1-null and wild-type mice with RANKL for increasing times, and subjected the cell lysates to western blot analysis. We found that absence of MKP-1 leads to potent hyper activation of p38, and to some extent ERK, which suggested that MKP-1 regulates MAPK signaling downstream of RANK in OC. To challenge OCgenesis *in vivo*, 2-month old MKP-1-deficient and wild-type mice were subjected to ovariectomy (OVX) or used as age-matched controls (n=8). We used soft X-ray, microCT, pQCT and dynamic histomorphometry to analyze distal femurs. MKP-1-null mice had a 19% lower trabecular density than wild types. While OVX decreased trabecular bone density in all mice, absence of MKP-1 led to 8% decrease in density and 12% decrease in thickness of cortical bone. Femurs from MKP-1-null mice had a lower number and a smaller surface area of trabeculae, and contained fewer OC that covered less bone surface than wild-types. These data strongly suggested that OC that lack MKP-1 become hyperactive in response to estrogen depletion. We conclude that MKP-1 regulates MAPK-dependent signaling and functions as a critical conduit for these kinases in the differentiation and activation of OC, with MKP-1 acting predominantly through p38 MAPK. MKP-1 might therefore offer a novel target to prevent bone loss in response to estrogen deficiency or inflammation.

**Disclosures:** A. Vignery, None.

## 1220

**Rac 1 and 2, in Combination, Mediate Osteoclast Function and Survival.** M. R. Croke<sup>1</sup>, H. Zhao<sup>1</sup>, D. A. Williams<sup>\*2</sup>, S. L. Teitelbaum<sup>1</sup>, F. P. Ross<sup>1</sup>. <sup>1</sup>Pathology and Immunology, Washington University, Saint Louis, MO, USA, <sup>2</sup>Hematology and Oncology, Children's Hospital Boston, Boston, MA, USA.

Osteoclastic bone resorption requires reorganization of the actin cytoskeleton, which, in other cells, is mediated by the Rho family of GTPases. One member of this family, namely Rac, is activated in osteoclasts by occupancy of surface receptors, including c-Fms and the  $\alpha\beta 3$  integrin, which polarize the osteoclast and promote formation of its unique cytoskeletal structure, the actin ring. However, whether Rac, itself, is required for osteoclast cytoskeletal organization and resorptive function is unknown. There are 3 known murine Rac GTPase isoforms, namely Rac1, 2 and 3. Because hematopoietic lineage cells, of which osteoclasts are derived, express only Rac 1 and 2, we utilized mice lacking these two isoforms in osteoclast precursors and/or the mature resorptive cell. Mice deficient in both isoforms (Rac dKO), in combination, develop severe osteopetrosis. Cells isolated from the marrow of Rac dKO mice differentiate into osteoclasts under the aegis of RANKL and M-CSF and their expression of the osteoclast differentiation markers, c-Src and cathepsin K is comparable to WT. On the other hand, Rac dKO osteoclasts fail to organize their cytoskeleton when generated on bone as manifest by a non-polarized phenotype, complete absence of actin rings and lack of ruffled membranes. The morphological abnormalities translate into dysfunctional resorption, exemplified by absence of pit formation on bone and diminished release of collagen degradation products into the medium. We also find that Rac dKO, osteoclast precursors, in the form of marrow macrophages, undergo accelerated apoptosis, as compared to WT, during initial exposure to RANKL, an event mediated by failure of the osteoclastogenic cytokine to activate Akt in the dual-deleted cells. Thus, Rac 1 and 2, in combination, not only are essential for organization of the osteoclast cytoskeleton, and hence the cells capacity to resorb bone, but also promote RANKL-mediated survival.

**Disclosures:** M.R. Croke, None.

## 1221

**The Cannabinoid Receptor GPR55 Affects Osteoclast Function *in vitro* and Bone Mass *in vivo***. L. Whyte<sup>\*1</sup>, E. Ryberg<sup>\*2</sup>, S. Ridge<sup>\*1</sup>, K. Mackie<sup>\*3</sup>, P. Greasley<sup>\*2</sup>, R. Ross<sup>\*1</sup>, M. J. Rogers<sup>1</sup>. <sup>1</sup>Institute of Medical Sciences, University of Aberdeen, Aberdeen, United Kingdom, <sup>2</sup>Dept of Lead Generation, AstraZeneca, MoeIndal, Sweden, <sup>3</sup>School of Medicine, University of Aberdeen, Aberdeen, United Kingdom.

Mice lacking either CB<sub>1</sub> or CB<sub>2</sub> cannabinoid receptors have been shown previously to have abnormal bone phenotypes, while synthetic and endogenous ligands for these receptors affect bone cell function *in vitro* and *in vivo*. GPR55 is structurally distinct from CB<sub>1</sub> and CB<sub>2</sub> but has recently been found to bind cannabinoids. The aim of this study was to investigate whether GPR55 plays a role in osteoclast function and bone physiology. Human osteoclasts were generated from peripheral blood monocytes of healthy donors. Using immunostaining and quantitative PCR we found that GPR55 is expressed in human osteoclasts and that GPR55 mRNA increases during differentiation. To study the functional role of GPR55, human osteoclasts were treated with O1602, a selective GPR55 ligand. In the presence of 1nM-1µM O1602 there was no effect on the formation of  $\alpha\beta 3$ -positive osteoclasts. However, when cells were cultured on dentine, O1602 increased the proportion of osteoclasts with F-actin rings (with 50nM, 236%±31 of control; p<0.01) and increased resorption area (217%±28 of control; p<0.01). Furthermore, the GPR55 antagonist cannabidiol (CBD, 1µM) significantly inhibited the increase in resorption and F-actin rings seen after treatment with 50nM O1602 alone (p<0.0001). Using a pulldown assay we also found that treatment of human osteoclasts with 1µM O1602 resulted in an increase in GTP-bound Rho. This is consistent with the proposed coupling of GPR55 to G $\alpha_{12/13}$  and with the stimulatory effects of O1602 on osteoclast polarisation. Consistent with the stimulatory effect of O1602 on osteoclasts *in vitro*, micro CT analysis of tibiae and femorae from male knockout and littermate control wildtype mice revealed that trabecular bone volume was significantly increased in GPR55<sup>-/-</sup> mice. In 12 wk old male mice, TBV was increased by 36% (p<0.01) in the tibia and by 71% (p<0.05) in the femur; in 8 month old male mice TBV increased by 33% (p<0.05) in the tibia and by 28% (p<0.05) in the femur. Consistent with this, bone surface increased by 46% (p<0.05) in the tibia and by 55% (p<0.05) in the femur of 8 month old male mice, while trabecular number also increased by 46% (p<0.05) in the tibia and by 55% (p<0.05) in the femur. This was not seen in female mice of the same age.

Taken together, these data demonstrate for the first time that, in addition to CB<sub>1</sub> and CB<sub>2</sub>, the cannabinoid receptor GPR55 plays a role in bone physiology. Further studies are now necessary to identify the endogenous ligands of GPR55 and its role in direct or indirect actions on osteoclasts or other bone cells *in vivo*.

**Disclosures:** M.J. Rogers, None.

This study received funding from: The Nuffield Foundation's Oliver Bird Rheumatism Programme.

## 1222

**PGC-1 $\beta$  and Iron Uptake in the Mitochondrial Activation of Osteoclasts.** K. Ishii<sup>\*1</sup>, K. Iwai<sup>\*2</sup>, S. Takeshita<sup>1</sup>, M. Ito<sup>3</sup>, N. Shimohata<sup>\*2</sup>, S. Taketani<sup>\*4</sup>, H. Aburatani<sup>\*5</sup>, C. J. Lelliott<sup>\*6</sup>, A. Vidal-Puig<sup>\*7</sup>, K. Ikeda<sup>1</sup>. <sup>1</sup>Dept of Bone and Joint Disease, National Center for Geriatrics and Gerontology, Obu, Japan, <sup>2</sup>Department of Molecular Cell Biology, Osaka City University, Osaka, Japan, <sup>3</sup>Department of Radiology, Nagasaki University Hospital, Nagasaki, Japan, <sup>4</sup>Department of Biotechnology, Kyoto Institute of Technology, Kyoto, Japan, <sup>5</sup>Genomescience Division, University of Tokyo, Tokyo, Japan, <sup>6</sup>R&D, AstraZeneca, Molndal, Sweden, <sup>7</sup>Department of Clinical Biochemistry, Cambridge University, Cambridge, United Kingdom.

Osteoclasts are acid-secreting polykaryons that are rich in mitochondria. The mechanism by which mitochondrial biogenesis is stimulated and how this is linked with the osteoclast differentiation program remain unknown. We found the transcription of PGC-1 $\beta$  (PPAR $\gamma$  coactivator) to be drastically induced during osteoclast differentiation by CREB in response to increased ROS, and that knockdown of PGC-1 $\beta$  inhibited the differentiation as well as mitochondrial gene expression in osteoclasts. PGC-1 $\beta$ -deficient mice exhibited impaired bone resorption with osteopetrosis-like histological features. In parallel, transferrin receptor (TfR) 1 mRNA, which was barely detectable in bone marrow macrophages (BMMs), was markedly induced along with osteoclast differentiation. Detailed biochemical analysis revealed that iron regulatory protein (IRP)2 senses a heightened iron demand in osteoclasts, and, by binding to the iron-responsive elements (IRE) of TfR1, leads to TfR1 upregulation through stabilization of its mRNA. By binding to the increased TfR1 on the cell surface, the addition of holo-Tf (i.e. preformed iron-Tf complex) as well as apo-Tf markedly and dose-dependently stimulated the formation of TRAP-positive osteoclasts from BMMs, along with an increased production of heme and iron-sulfur clusters in mitochondria. These effects were inhibited by iron chelation with desferrioxamine (DFO). The pit area resorbed by mature osteoclasts was also significantly increased by Tf and decreased by DFO, suggesting that iron uptake through TfR1 promotes osteoclast formation as well as the bone-resorbing function of mature osteoclasts. Treatment of female mice with DFO significantly inhibited bone resorption and bone loss following OVX, suggesting that iron is an important regulator of osteoclastic bone resorption *in vivo*. In conclusion, it is suggested that activation of CREB, a major osteoclastogenic signal downstream of RANK/ITAM, is deployed to induce the transcription of PGC-1 $\beta$ . PGC-1 $\beta$  drives mitochondrial gene expression, and, coupled with the increased iron uptake through the upregulated TfR1, plays an important role in bone resorption by coordinating the stimulation of mitochondrial biogenesis and respiration in osteoclasts.

**Disclosures:** K. Ishii, None.

## 1223

**Evidence for a Role of Prolactin in Calcium Homeostasis: Regulation of Intestinal TRPV6 and Intestinal Calcium Absorption by Prolactin.** D. V. Ajibade<sup>\*1</sup>, P. Dhawan<sup>1</sup>, B. S. Benn<sup>\*1</sup>, M. B. Meyer<sup>\*2</sup>, J. W. Pike<sup>2</sup>, S. S. Christakos<sup>1</sup>. <sup>1</sup>Biochemistry and Molecular Biology, UMDNJ, Newark, NJ, USA, <sup>2</sup>Biochemistry, University of Wisconsin, Madison, WI, USA.

Although 1,25(OH)<sub>2</sub>D<sub>3</sub> is an essential regulator of intestinal calcium (Ca<sup>2+</sup>) absorption, it has been suggested that prolactin (PRL) can also affect intestinal Ca<sup>2+</sup> transport. Increased Ca<sup>2+</sup> transport has been observed in vitamin D deficient pregnant and lactating rats, indicating that a factor besides 1,25(OH)<sub>2</sub>D<sub>3</sub> is involved in intestinal Ca<sup>2+</sup> transport. To investigate the possibility of PRL as a hormone involved in Ca<sup>2+</sup> homeostasis, vitamin D deficient male mice were injected with 1,25(OH)<sub>2</sub>D<sub>3</sub> (1ng/g bw), PRL (1ug/g bw), or PRL + 1,25(OH)<sub>2</sub>D<sub>3</sub> and changes in the expression of TRPV6, the apical Ca<sup>2+</sup> channel proposed to be a rate limiting step in the process of active intestinal calcium absorption, were examined. We found that PRL alone significantly induced duodenal TRPV6 mRNA levels 3 fold 4h after injection. Duodenal calbindin-D<sub>9k</sub> mRNA levels were unaltered by PRL. A single i.p. injection of 1,25(OH)<sub>2</sub>D<sub>3</sub> resulted in a 4-6 fold induction in both duodenal TRPV6 mRNA and calbindin-D<sub>9k</sub> mRNA 12h after injection. When a combination of 1,25(OH)<sub>2</sub>D<sub>3</sub> and PRL was given to vitamin D deficient male mice (12h and 4 h prior to termination respectively), a 2.5 and a 3-4 fold enhancement of the 1,25(OH)<sub>2</sub>D<sub>3</sub> induction of duodenal TRPV6 mRNA and calbindin-D<sub>9k</sub> mRNA levels respectively was observed (p<0.05 compared to 1,25(OH)<sub>2</sub>D<sub>3</sub> treatment alone). In addition, using the everted gut sac assay, combined treatment with PRL and 1,25(OH)<sub>2</sub>D<sub>3</sub> resulted in a significant enhancement in duodenal Ca<sup>2+</sup> transport compared to mice treated with 1,25(OH)<sub>2</sub>D<sub>3</sub> alone (1.5 fold enhancement; PRL +1,25(OH)<sub>2</sub>D<sub>3</sub>; p<0.05 compared to mice treated with 1,25(OH)<sub>2</sub>D<sub>3</sub> alone). Injection of PRL alone did not result in a significant induction in Ca<sup>2+</sup> transport. In order to further understand mechanisms that may be involved in the enhancement of TRPV6 expression by PRL, studies were done using the hTRPV6 promoter (-7000/+160). Using vitamin D receptor and PRL receptor transfected CV1 cells, 1,25(OH)<sub>2</sub>D<sub>3</sub> treatment (10<sup>-8</sup>M) alone or PRL treatment (1ug/ml) in the presence of STAT5 resulted in a 4-5 fold increase in TRPV6 transcription. A combination of PRL and 1,25(OH)<sub>2</sub>D<sub>3</sub> treatment in the presence of STAT5 resulted in a cooperative effect and a maximum induction of transcription of 20-25 fold. These findings indicate, for the first time, that PRL alone can regulate TRPV6 and that PRL has cooperative effects with 1,25(OH)<sub>2</sub>D<sub>3</sub> in regulating intestinal Ca<sup>2+</sup> transport proteins as well as intestinal Ca<sup>2+</sup> transport. These findings indicate that PRL is involved in Ca<sup>2+</sup> homeostasis and is an important modulator of the intestinal effect of 1,25(OH)<sub>2</sub>D<sub>3</sub>.

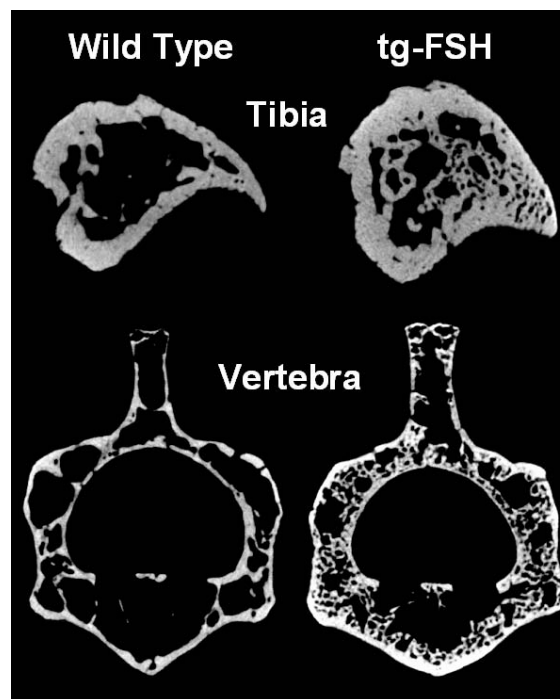
**Disclosures:** D.V. Ajibade, None.

## 1224

**Transgenic Expression of Human FSH in Female Mice Has an Anabolic Effect on Bone.** R. Kalak<sup>\*</sup>, C. M. Allan<sup>\*</sup>, K. J. McTavish<sup>\*</sup>, C. R. Dunstan, H. Zhou, M. J. Seibel, D. J. Handelsman<sup>\*</sup>. ANZAC Research Institute, The University of Sydney, Australia.

It was recently observed that female mice deficient in the FSH beta-subunit or receptor are protected from bone loss despite severe estrogen deficiency (1). The authors speculated that the postmenopausal elevation in FSH levels is responsible for the bone loss in women after the menopause. We previously developed a human FSH-expressing transgenic (tg-FSH) mouse model that features progressively increasing levels of circulating human FSH with increasing age (from 2.7 IU/L in 5 wk old mice to 6 IU/L in 6 month old mice) (2) independent of pituitary secretion, while serum estradiol levels remain normal. This model provides a unique opportunity to determine the in vivo effects of increased FSH activity on bone distinct from effects of estrogen deficiency.

We performed microcomputed tomography of the L3 vertebra and the tibia of 6-month-old female tg-FSH and wild-type (WT) mice (n= 10/ group). Trabecular bone was analysed for both vertebrae and tibiae. Cortical bone area and thickness were measured for tibiae. Vertebral trabecular bone volume (BV/TV) was increased by 50% (p=0.021) in tg-FSH as compared to WT mice due to increased trabecular number (TbN) (+42%, p=0.015) and reduced trabecular separation (TbSp) (-16%, p=0.004). Trabecular thickness (TbTh) was not significantly different between the two groups (Fig.1)



Tibial cortical bone area (+9%, p=0.024) and cortical thickness (+13%, p=0.034) were significantly increased in tg-FSH animals while tibial lengths were similar. In contrast, differences in tibial trabecular bone parameters were less pronounced: BV/TV (+88%, p=0.068), TbN (+76%, p=0.056), TbSp (-8%, p=0.364), TbTh (+3% and p=0.522) (Fig. 1). Changes in the different skeletal sites were correlated, consistent with a systemic effect. There was wider variation of vertebral and tibial BV/TV among tg-FSH compared with WT mice.

This study shows for the first time an anabolic effect of human FSH on mouse bone. While the mechanism of this effect remains uncertain, our data do not support the concept that FSH directly causes bone loss.

1. Sun L, et al. FSH directly regulates bone mass. *Cell* 2006; 125: 247-60.
2. McTavish KJ, et al. Rising follicle-stimulating hormone levels with age accelerate female reproductive failure. *Endocrinology* 2007; 148: 4432-9.

**Disclosures:** R. Kalak, None.

## 1225

**Local Osteocyte Defect in Dmp1 Null Mice Causes Overproduction of Fgf23.** S. Liu, J. Zhou<sup>\*</sup>, W. Tang<sup>\*</sup>, L. D. Quarles. The Kidney Institute, University of Kansas Medical Center, Kansas City, KS, USA.

Inactivating mutations of DMP1 leads to increased FGF23 expression in bone osteocytes and consequent FGF23-mediated renal phosphate wasting and impaired 1- $\alpha$  hydroxylase activity. The mechanism whereby inactivating DMP1-mutations stimulates FGF23 production by osteocytes is not clear. To determine if the increased FGF23 expression is due to an intrinsic abnormality of bone, we explanted long bones from 4.5 day-old wild-type (WT) and Dmp1-null/Fgf23 promoter-reporter mice (Dmp1<sup>-/-</sup>/Fgf23<sup>+/GFP</sup> and Dmp1<sup>-/-</sup>/Fgf23<sup>+/GFP</sup> respectively) into the back muscles of either WT or Dmp1-null recipients. By three weeks, the explanted bones had successfully engrafted and undergone linear growth in the recipients. GFP expression remained increased in osteocytes of Dmp1<sup>-/-</sup>/Fgf23<sup>+/GFP</sup> bone explanted into WT mice, whereas GFP expression remained low in Dmp1<sup>+/+</sup>/Fgf23<sup>+/GFP</sup> bone explanted into either Dmp1<sup>-/-</sup> or WT mice, consistent with an intrinsic abnormality leading to increased FGF23 expression. Paradoxically, GFP expression was suppressed when Dmp1<sup>-/-</sup>/Fgf23<sup>+/GFP</sup> bone was explanted into Dmp1<sup>-/-</sup> mice, suggesting an age-dependent suppression of Fgf23 by a systemic factor in adult Dmp1 null mice. To confirm the local abnormality of osteocyte function is responsible for increased Fgf23 expression in Dmp1 null mice, we cultured bone marrow stromal cells (BMSC) derived from Dmp1<sup>+/+</sup>/Fgf23<sup>+/GFP</sup> and Dmp1<sup>-/-</sup>/Fgf23<sup>+/GFP</sup> mice for 18 days under differentiating conditions. The Fgf23 promoter driven GFP expression was markedly increased in osteocyte-like cells embedded in mineralization nodules of Dmp1<sup>-/-</sup>/Fgf23<sup>+/GFP</sup> derived BMSC, but not in nodules generated by BMSC from Dmp1<sup>+/+</sup>/Fgf23<sup>+/GFP</sup> mice. To determine if Dmp1 directly regulates Fgf23 promoter activity, we cotransfected a full-length Dmp1 cDNA construct with an 8 kb Fgf23 promoter-luciferase reporter construct into Ros17/2.8 osteoblasts. We found that over-expression of Dmp1 had no significant effect on Fgf23 promoter activity *in vitro*, suggesting that the observed local effects of Dmp1 deficiency to increase Fgf23 gene expression *in vivo* and *ex vivo* may not involve direct Dmp1 transcriptional activity. Further studies are needed to determine whether the intrinsic increase in Fgf23 expression by osteocytes of Dmp1<sup>-/-</sup> mice represents Dmp1-dependent abnormalities in osteocyte development/function or alterations in extracellular matrix-derived autocrine/paracrine factors caused by Dmp1 deficiency.

**Disclosures:** S. Liu, None.

This study received funding from: NIH/NIAMS: RO1-AR45955.

## 1226

**The PTH 1 receptor (PTH1R) Stimulates Bone Formation Through a Distinct  $\beta$ -Arrestin Dependent Pathway Independent of G Protein Activation.** D. Gesty-Palmer, R. F. Spurney, P. J. Flannery\*, L. Yuan\*. Department of Medicine, Duke University Medical Center, Durham, NC, USA.

Intermittent administration of PTH (1-34) has anabolic effects on bone that have been conventionally attributed to classical G protein signaling mechanisms. Our recent studies have shown that PTH (1-34) stimulation of the PTH1R can activate two independent signaling mechanisms one G protein-dependent and the other  $\beta$ -arrestin-dependent (J Biol Chem 281:10856, 2006). Moreover, we have demonstrated that these two distinct signaling mechanisms (G protein *versus*  $\beta$ -arrestin) are pharmacologically separable through the use of biased ligands capable of preferentially activating one pathway or the other. To investigate  $\beta$ -arrestin dependent signaling in bone, we employed a " $\beta$ -arrestin biased ligand" (D-Trp<sup>12</sup>, Tyr<sup>34</sup>)-PTH(7-34), (PTH- $\beta$ arr), to determine whether G protein independent signals transmitted by  $\beta$ -arrestin contribute directly to the PTH1R stimulated anabolic response in bone. Our results show that PTH- $\beta$ arr induces bone formation in mice with an anabolic response similar to PTH(1-34), which activates both mechanisms. In  $\beta$ -arrestin 2 null mice, the increase in bone mass induced by PTH- $\beta$ arr is absent and the anabolic response to PTH(1-34) is attenuated by 50%. The  $\beta$ -arrestin dependent pathway enhances bone mineral density primarily by increasing trabecular bone mass with little effect on cortical bone. Additionally, while PTH- $\beta$ arr increases markers of bone formation such as serum osteocalcin, it does not appear to stimulate markers of bone resorption such as urine deoxypyridinoline (DPD). We conclude that G protein independent/ $\beta$ -arrestin dependent signaling contributes to a distinct anabolic component of PTH1R stimulated bone formation. Selective activation of this newly discovered mechanism may form the basis for a new class of pharmacologic agents which have valuable therapeutic properties for the treatment of metabolic bone diseases such as osteoporosis.

**Disclosures:** D. Gesty-Palmer, None.

This study received funding from: An Arthritis Foundation Investigator Award and by National Institutes of Health Grants HL16037, DK64353, AR46472 and HD43446.

## 1227

**Association between Cx43 and  $\beta$ -Arrestin is Required for cAMP-Dependent Osteoblast Survival Induced by PTH.** L. I. Plotkin, G. Frera\*, K. Vyas\*, S. C. Manolagas, T. Bellido. Endocrinology, Center for Osteoporosis and Metabolic Bone Diseases, Central Arkansas Veterans Healthcare System, Univ. Arkansas for Med. Sci., Little Rock, AR, USA.

Inhibition of osteoblast apoptosis via activating the cAMP/PKA pathway contributes, at least in part, to the increased bone mass induced by intermittent PTH administration to mice. This anabolic response is attenuated in mice with osteoblast-specific deletion of connexin (Cx) 43 or in heterozygous Cx43 null mice. Moreover, PTH-induced elevation of cAMP is blunted in osteosarcoma cells with reduced expression of Cx43. Based on these lines of evidence we aimed herein to determine whether Cx43 is required for prevention of osteoblast apoptosis by PTH. We report that PTH did not inhibit etoposide-induced apoptosis in osteoblastic Ob-6 cells expressing Cx45, which prevents Cx43 action, or Cx43 $\Delta$ 245 - a truncated Cx43 dominant negative (dn) mutant. Furthermore, PTH did not prevent apoptosis in Ob-6 cells in which Cx43 expression was silenced with a lentivirus containing a specific short-hairpin (sh) RNA (Cx43 $\Delta$  cells), whereas the hormone was effective in cells treated with scrambled shRNA (control) cells. Consistent with this, PTH increased the expression of the cAMP-responsive genes IL-6, RANKL, c-fos and Nur77 in control cells but not in Cx43 $\Delta$  cells. However, PTH receptor expression was not reduced in Cx43 $\Delta$  cells. Moreover, the stable cAMP analog dibutyryl cAMP (DBA) prevented apoptosis and increased the expression of cAMP target genes in both Cx43 $\Delta$  and control cells. Taken together, these results suggested that Cx43 levels modulate cAMP-mediated responses induced by PTH downstream of the PTH receptor. Cx43 interacts with  $\beta$ -arrestin and  $\beta$ -arrestin decreases PTH-induced cAMP responses in osteoblastic cells. This evidence raised the possibility that Cx43 plays a permissive role by sequestering  $\beta$ -arrestin, thereby allowing cAMP responses, including osteoblast survival, induced by PTH. Consistent with this hypothesis, we found that over-expression of  $\beta$ -arrestin blocked the anti-apoptotic effect of PTH, but not that of DBA, in control Cx43-expressing cells. Moreover, over-expression of Cx43 as well as a dn  $\beta$ -arrestin mutant rescued the anti-apoptotic effect of PTH in Cx43 $\Delta$  cells. We conclude that Cx43 is required for the anti-apoptotic effect of PTH on osteoblasts due to its interaction with  $\beta$ -arrestin and subsequent potentiation of PTH-induced cAMP responses. These findings provide a molecular explanation for the attenuated anabolic effect of intermittent PTH administration in Cx43 deficient mice.

**Disclosures:** L.I. Plotkin, None.

This study received funding from: NIH, NOF.

## 1228

**Inhibitory Role of G $\alpha$ q / PKC $\delta$  Signal in the Bone Anabolic Action of PTH.** N. Ogata<sup>1</sup>, F. Yano<sup>1</sup>, U. Chung<sup>1</sup>, N. Wettschureck<sup>\*2</sup>, S. Offerman<sup>\*2</sup>, G. V. Segre<sup>3</sup>, K. Nakamura<sup>\*1</sup>, H. Kawaguchi<sup>1</sup>. <sup>1</sup>Sensory & Motor System Medicine, Bone & Cartilage Regenerative Medicine, Univ. of Tokyo, Tokyo, Japan, <sup>2</sup>Pharmakologisches Institut, Univ. of Heidelberg, Heidelberg, Germany, <sup>3</sup>Endocrine Unit, MGH, Boston, MA, USA.

G $\alpha$ s-cAMP and G $\alpha$ q-PLC are the major signal pathways underlying G protein-coupled receptors. Contrary to the well-known bone anabolic action of the G $\alpha$ s signal in osteoblasts, we have reported that the G $\alpha$ q signal inhibits bone formation by analyses of transgenic mice with osteoblast-specific overexpression of a constitutively active G $\alpha$ q transgene (CA-G $\alpha$ q). The present study sought to examine the involvement of the G $\alpha$ q signal in the bone anabolic action of PTH whose receptor is known to be G protein-coupled. Although the subcutaneous injection of rhPTH (1-34) (0.08 mg/kg x 5 times X 4 weeks) caused about a 10% increase of bone volume in 8-week-old wild-type mice, this effect was not seen in the CA-G $\alpha$ q transgenic littermates. In the culture of osteoblastic MC3T3-E1 cells, stable overexpression of the CA-G $\alpha$ q inhibited their differentiation determined by ALP activity, which was abrogated by addition of GF109203X, an inhibitor of protein kinase C (PKC). Among the 13 PKC family members, PKC $\delta$  was shown to be most strongly induced by the CA-G $\alpha$ q overexpression by immunoblotting.

We further created double knockout (DKO) mice deficient in osteoblast-specific G $\alpha$ q and global G $\alpha$ 11, a G $\alpha$ q subfamily member that also activates PLC, by crossing COL1-Cre transgenic mice and mice with the G $\alpha$ q gene flanked by loxP / global ablation of G $\alpha$ 11 (G $\alpha$ q-*fl/fl*;G $\alpha$ 11<sup>-/-</sup>). Although histomorphometric analyses revealed that bone volume and turnover of the DKO mice were normal under physiological conditions, the bone anabolic effect of the rhPTH (1-34) injection shown above was significantly enhanced in the DKO mice as compared to that in the wild-type littermates, confirming inhibition of the PTH action by the endogenous G $\alpha$ q signaling as well. In the culture of primary mouse calvarial osteoblasts, intermittent treatment of rhPTH (10 nM) stimulated differentiation and matrix synthesis determined by ALP activity and mRNA levels of osteogenesis markers. These effects were markedly enhanced in the cells from the G $\alpha$ q/G $\alpha$ 11 DKO mice, which were restored by addition of PMA, an activator of PKC, to the levels of the wild-type osteoblasts. Protein level of PKC $\delta$  and its subcellular translocation to membrane enhanced by the rhPTH treatment in wild-type osteoblasts were suppressed in the DKO osteoblasts. Contrarily, cAMP accumulation in response to rhPTH was similar between cells of the two genotypes.

These lines of results demonstrate the inhibitory role of the G $\alpha$ q / PKC $\delta$  signal in the bone anabolic action of PTH, suggesting that suppression of the signal may lead to a novel treatment with PTH against osteoporosis.

**Disclosures:** N. Ogata, None.

## 1229

**Disruption of the Syndecan-1/Integrin Axis is a Novel Target for Myeloma Therapy.** Y. Yang<sup>1</sup>, J. P. Ritchie<sup>\*1</sup>, B. Ell<sup>\*2</sup>, A. C. Rapraeger<sup>\*2</sup>, R. D. Sanderson<sup>\*1</sup>. <sup>1</sup>Dept. of Pathology, Center for Metabolic Bone Disease, University of Alabama in Birmingham, Birmingham, AL, USA, <sup>2</sup>Pathology and Laboratory Medicine, University of Wisconsin-Madison, Madison, WI, USA.

In myeloma, malignant plasma cells invade and grow within the bone marrow microenvironment leading to osteolytic destruction of bone. Myeloma cell surfaces are enriched with the heparan sulfate proteoglycan syndecan-1 that via its extracellular core protein domain promotes activation of  $\alpha_v\beta_3$  and  $\alpha_v\beta_5$  integrins. The  $\alpha_v\beta_3$  integrin in particular drives myeloma progression by promoting tumor proliferation and angiogenesis and by regulating osteoclast differentiation and activation that leads to bone lysis. Synstatin is a peptide mimic of the syndecan-1 core protein that blocks the syndecan-1-mediated activation of  $\alpha_v\beta_3$  and  $\alpha_v\beta_5$  integrins. The purpose of this study was to assess the ability of synstatin to inhibit myeloma growth *in vivo*. Three mouse models of myeloma were utilized in this study --- a subcutaneous (s.c.) model in which human myeloma cells were injected s.c. into SCID mice (SCID-s.c.), a SCID-hu model, in which tumor cells were injected into fragments of human fetal bone implanted in SCID mice, and a syngenic model, in which murine myeloma cells are injected s.c. into Balb/c mice. Ten days after injection of tumor cells animals were treated with synstatin peptide for 4 weeks by constant delivery using Alzet osmotic pumps. Analysis of the levels of human immunoglobulin light chain in murine sera revealed that synstatin significantly ( $P < 0.002$ ) inhibited tumor growth 11-fold in the SCID-s.c. model and 3-fold in the SCID-hu model. In the syngenic model, tumor volumes revealed that synstatin reduced tumor growth by 17-fold ( $P < 0.002$ ). Immunohistochemistry performed on tumors from SCID-s.c. mice demonstrated that synstatin inhibits proliferation of cells within the tumor ( $1451 \pm 171/\text{mm}^2$  Ki-67 positive cells in treated vs.  $3111 \pm 148/\text{mm}^2$  positive cells in controls,  $P = 0.0001$ ). Synstatin also significantly inhibits angiogenesis, compared to controls (microvessel density of  $21 \pm 9/\text{mm}^2$  to  $39 \pm 10/\text{mm}^2$ , respectively;  $P = 0.01$ ) as assessed by CD34 staining of tumor tissue. We conclude that synstatin significantly inhibits myeloma tumor growth *in vivo* and thus may provide a novel therapeutic approach to this deadly cancer.

**Disclosures:** Y. Yang, None.

This study received funding from: NIH.



## 1230

**Prostaglandin E Receptor EP4 Antagonist Attenuates Growth and Metastases of Cancer.** M. Takita<sup>1</sup>, S. Yokoyama<sup>\*1</sup>, M. Inada<sup>1</sup>, T. Maruyama<sup>\*2</sup>, C. Miyaura<sup>1</sup>. <sup>1</sup>Department of Biotechnology and Life Science, Tokyo University of Agriculture and Technology, Tokyo, Japan, <sup>2</sup>Discovery Research Laboratory, Minase Research Institute, Ono Pharmaceutical, Co., Ltd., Osaka, Japan.

Bone metastasis of cancer is accompanied by severe bone destruction with increased bone resorption. We recently reported that prostaglandin E (PGE) produced by host cells play a key role in bone metastasis, and the PGE signal is mediated by EP4 receptor, a subtype of PGE receptors (EP1-EP4), expressed in host cells. EP4 antagonist suppressed osteolysis due to bone metastasis of mouse malignant melanoma B16 cells. In this study, we examined the role of host-derived PGE and EP4 receptor in tumor growth and visceral metastases in various tissues using B16 melanoma cells. When B16 cells were introduced to C57BL/6 mice by iv injection, metastases were detected as black spots in bone, lung, liver, and kidney on day 18 after injection. Bone mineral density (BMD) measured by DEXA showed significant decrease of BMD in femurs with B16 metastasis. When EP4 antagonist was orally administered to mice injected with B16 cells, metastases were markedly suppressed not only in bone, but also in lung, liver, and kidney. When B16 cells were implanted subcutaneously into C57BL/6 mice, B16 cells grew rapidly to form solid tumor with angiogenesis. Topical administration of EP4 antagonist markedly suppressed the growth of solid tumor on days 11-18 after sc implantation of B16 cells. Expression of cyclooxygenase-2 (COX-2), membrane-bound PGE synthase-1 (mPGES-1), EP4, and CD31 mRNAs was clearly detected in B16 tumor, but not in cultured B16 cells. Neither PGE2 nor EP4 antagonist affected the proliferation of B16 cells in vitro. In addition, cultured B16 cells did not produce PGE2 at all. When mPGES-1-null mice were used in this study, the growth of B16 solid tumor was limited compared with wild-type mice. Metastasis in various tissues also attenuated in mPGES-1-null mice lacking PGE synthesis. These results suggest that PGE2 produced by host cells binds to EP4 receptor expressed in host cells of various tissues, and enhances tumor growth and metastases of cancer in vivo. Here we show that EP4 antagonist is a possible candidate for the therapy of cancer with metastases.

**Disclosures:** M. Takita, None.

## 1231

**Activin A Mediates Multiple Myeloma (MM) Bone Disease which Is Reversed by RAP-011, a Soluble Activin Receptor.** S. Vallet<sup>\*1</sup>, S. Mukherjee<sup>\*2</sup>, N. Vaghela<sup>\*1</sup>, T. Hideshima<sup>\*3</sup>, S. Pozzi<sup>\*1</sup>, L. Santo<sup>\*3</sup>, D. Cirstea<sup>\*3</sup>, J. Seehra<sup>\*4</sup>, D. T. Scadden<sup>\*2</sup>, K. C. Anderson<sup>\*3</sup>, N. Raju<sup>1</sup>. <sup>1</sup>Massachusetts General Hospital, Dana Farber Cancer Institute, Boston, MA, USA, <sup>2</sup>Massachusetts General Hospital, Boston, MA, USA, <sup>3</sup>Dana Farber Cancer Institute, Boston, MA, USA, <sup>4</sup>Accelaron Pharma Inc, Cambridge, MA, USA.

MM is characterized by complex interactions between plasma cells and the bone microenvironment, resulting in imbalanced bone remodeling. This results in bone destruction which is a consequence of cytokine secretion inducing increased osteoclast (OC) function or decreased osteoblast (OB) formation. Activin, a member of the TNF- $\alpha$  superfamily, is a coupling factor in bone remodeling and our data suggest its potential role as a mediator of MM bone disease. We observed 4 fold increased activin A expression levels in bone marrow plasma of MM patients compared to normal controls (average  $103 \pm 132$  vs  $25 \pm 19.3$  pg/ml). Activin levels appeared to correlate with disease activity where more than 60% of MM patients at diagnosis had high activin levels, versus patients in remission who had levels comparable to normal controls. The main source of activin in MM were bone marrow stromal cells (BMSCs) and OCs (median levels in 72h culture supernatant are 2094 and 1396 pg/ml respectively), while OBs secreted low levels of activin (median:200 pg/ml). No activin was detected in MM cells. Interestingly, MM cells stimulated activin A secretion when cocultured with MM-derived BMSC (by  $109\% \pm 83$ ). This was associated with an increase in IL6 secretion by BMSCs resulting in MM cell growth. Moreover, activin A in combination with RANKL and M-CSF stimulated OC differentiation via induction of a three-fold increase in precursor cell proliferation. To test the role of targeting activin A with therapeutic intent, we used a chimeric antibody that binds activin via the extracellular domain of activin receptor IIA, RAP-011 (Accelaron Pharma Inc., Cambridge). In effect, RAP-011 inhibited MM cell growth induced by BMSCs with concomitant reduction in IL6 levels. RAP-011 impaired osteoclastogenesis by 40% ( $p < 0.05$ ) and almost completely abrogated OC function. Interestingly, RAP-011 enhanced OB activity (by 37.5%,  $p < 0.01$ ) of BMSCs differentiated in osteogenic media, assessed by mineral content at day 21. This was confirmed by quantitative-PCR analysis of osteocalcin and bone sialoprotein genes. These data therefore suggest that activin A is involved in development of MM bone disease and can be effectively targeted by a novel antibody. RAP-011 not only inhibits MM cell proliferation in the microenvironment, but has bone-anabolic effects via inhibition of OC formation and stimulation of OB differentiation. These effects of RAP-011 make it an attractive therapeutic tool to test in future clinical trials of MM.

**Disclosures:** S. Vallet, None.

## 1232

**Thrombospondin-1 and CD47 Regulate Osteoclastogenesis but have Distinct Effects on Bone Metastasis.** Ö. Uluçkan<sup>\*1</sup>, H. Deng<sup>\*1</sup>, J. L. Prior<sup>\*2</sup>, D. Piwnica-Worms<sup>\*2</sup>, W. A. Frazier<sup>\*3</sup>, K. N. Weilbaecher<sup>1</sup>. <sup>1</sup>Departments of Medicine and Cell Biology and Physiology, Division of Oncology, Washington University in St Louis, St Louis, MO, USA, <sup>2</sup>Molecular Imaging Center, Mallinckrodt Institute of Radiology, Washington University in St Louis, St Louis, MO, USA, <sup>3</sup>Department of Biochemistry and Molecular Biophysics, Washington University in St Louis, St Louis, MO, USA.

Thrombospondin-1 (TSP1) and its receptor CD47, a five-transmembrane protein of the Immunoglobulin superfamily, augment platelet aggregation by binding to  $\alpha$ IIb $\beta$ 3 integrin. We have previously shown that the  $\beta$ 3 integrins on platelets and osteoclasts (OC) play critical roles in bone metastasis. We thus hypothesized that TSP1 and CD47 will also augment  $\alpha$ v $\beta$ 3 function in OCs and thus affect bone metastasis. We observed that TSP1-/- mice have increased bone mineral density and decreased serum CTX levels compared to WT controls, consistent with an OC defect. OC defects are frequently associated with decreased tumor burden in bone. However, tumor burden in bone was unchanged in TSP1-/- mice after intra-cardiac delivery of luciferase labeled B16 osteolytic murine melanoma cells. Notably, loss of TSP1 is reported to enhance tumor angiogenesis through an interaction with CD36, not CD47, which could partially explain these unexpected results. Thus, we evaluated osteoclastogenesis and bone metastasis in CD47-/- mice. Compared to TSP1-/- mice, we observed a statistically significant but more modest increase in trabecular bone volume and decrease in CTX levels in CD47-/- mice. In vitro, the number of multinucleated TRAP-positive OCs formed by differentiating CD47-/- bone marrow macrophages was decreased. Tumor burden in bone after intra-cardiac and intra-tibial inoculation of tumor cells was decreased in CD47-/- mice, in contrast to TSP1-/- mice. We also observed a decrease in tumor-associated bone destruction in CD47-/- mice. Subcutaneous tumor growth was not different between WT and CD47-/- mice. Our results demonstrate that TSP1 and its receptor CD47 alter bone volume in mice but have distinct effects on bone metastasis. We postulate that the anti-angiogenic role of TSP1 could account for the difference in the tumor growth in bone between TSP1-/- and CD47-/- mice. Our results suggest that therapies aimed at inhibiting angiogenesis via TSP1 might have adverse effects on bone, whereas CD47 might be a safer target for the treatment of bone metastasis.

**Disclosures:** Ö. Uluçkan, None.

## 1233

**Fibroblast Growth Factor Receptor (FGFR) Signalling in the Pathogenesis of Osteosarcoma.** D. Weekes<sup>\*</sup>, T. Kashima, A. E. Grigoriadis. King's College London, London, United Kingdom.

Osteosarcoma (OS) is a highly malignant bone-forming tumour and is the most common primary malignancy of the skeleton, occurring primarily in children and adolescents, and also in the elderly as a secondary complication in Paget's Disease of Bone (PDB). There are no curative systemic therapies available for the treatment of OS, which currently relies heavily on surgical intervention and adjuvant chemotherapy, although many patients do not benefit from this treatment and develop recurrent or metastatic disease. The molecular mechanisms responsible for osteoblast transformation and tumour progression in both children as well as in PDB are not known, thus, identification of novel molecular therapeutic targets is of great importance.

Deregulated FGFR signalling has recently been implicated in the pathogenesis of breast and prostate cancer, however, whether it is also involved in skeletal malignancies has not been established. Our analysis of a transgenic mouse model of OS caused by overexpression of the c-Fos proto-oncogene demonstrated that induction of exogenous c-Fos expression in osteoblasts resulted in upregulation of FGFR1 RNA and protein expression, suggesting that FGFR1 is a novel c-Fos/AP-1 target gene. Further, immunohistochemistry studies showed high FGFR1 levels in tumours as well as at early sites of tumour formation, implicating deregulated FGFR1 signalling in tumour initiation. In murine osteoblasts, c-Fos and bFGF cooperated in stimulating anchorage-independent growth of non-transformed murine osteoblasts and c-Fos overexpression resulted in enhanced bFGF-dependent p38 and pERK MAPK signalling. Moreover, the FGFR signalling inhibitor, SU5402, as well as overexpression of dominant-negative FGFR1 constructs, inhibited anchorage-independent growth of c-Fos transgenic OS cells by over 50%.

These results in mice led us to investigate the role of FGF signalling in the pathogenesis of human OS. Treatment of U2OS human OS cells with bFGF stimulated colony growth in soft agar by 4-fold, and SU5402 completely abolished U2OS colony growth and inhibited MG63 cell colony growth by 75%, suggesting that FGF signalling is an important factor in the transformed state of human OS cells. To validate this notion, we performed Tissue Microarray analysis on primary human OS and demonstrated that over 60% of primary core biopsies expressed high levels of FGFR1, which increased to 85% for FGFR1 in matched biopsies taken after chemotherapy. These data implicate for the first time, signalling via FGFR1 as a possible mechanism of deregulated osteoblast growth during tumour initiation and for OS cell survival, and suggest that this pathway may represent a novel therapeutic target for OS treatment.

**Disclosures:** D. Weekes, None.

This study received funding from: Bone Cancer Research Trust.

## 1234

**Systemic Interleukin 8 Increases Bone Resorption *In Vivo*.** J. D. Dilley<sup>\*1</sup>, A. A. Carver<sup>\*1</sup>, J. M. Bracey<sup>\*2</sup>, N. S. Akel<sup>\*2</sup>, R. A. Skinner<sup>\*1</sup>, W. R. Hogue<sup>\*1</sup>, F. L. Swain<sup>\*2</sup>, P. Lahiji<sup>\*3</sup>, J. J. Maher<sup>\*3</sup>, M. S. Bendre<sup>\*4</sup>, D. Gaddy<sup>2</sup>, L. J. Suva<sup>2</sup>.  
<sup>1</sup>Orthopaedic Surgery, UAMS, Little Rock, AR, USA, <sup>2</sup>Orthopaedic Surgery & Physiology and Biophysics, UAMS, Little Rock, AR, USA, <sup>3</sup>Rice Liver Center Laboratory, UCSF, San Francisco, CA, USA, <sup>4</sup>Pathology, MD Anderson, Houston, TX, USA.

Skeletal metastases and the subsequent osteolysis connote a dramatic change in the prognosis for the cancer patient and significantly increase the morbidity associated with disease. Recently, we and others reported that breast and prostate cancer cells secrete the chemokine interleukin 8 (IL-8), and that IL-8 directly stimulates osteoclast formation *in vitro*, independent of any requirement for RANKL. IL-8 expression has also been negatively linked to the estrogen receptor (ER) status of cancer cell lines, implicating increased IL-8 expression in ER- breast cancer cells with the increased invasive potential of the tumor lines *in vivo*. In light of these studies, we examined IL-8 expression in primary human breast tumors in relation to ER status and determined the skeletal phenotype of male and female IL-8 transgenic (TG) mice. Tumor samples from 44 ER+ and 30 ER- invasive ductal breast carcinomas were immunostained for IL-8. All cases examined stained positive for IL-8 expression, with no significant differences observed in the intensity of IL-8 staining between ER+ and ER- samples, highlighting the important differences between primary tumors and tumor-derived cell lines. To investigate the osteoclastogenic activity of IL-8 *in vivo*, TG mice with a liver-specific transgene encoding human IL-8 were examined. Offspring were genotyped by quantitation of circulating human IL-8 levels in whole blood (84.5 ng/ml, versus 0.12 ng/ml in WT mice). IL-8 TG mice are profoundly osteopenic, with significantly increased bone resorption compared to WT mice, resulting in an inherently low bone volume, decreased trabecular number, increased trabecular spacing and significantly decreased cortical bone strength, related to the profound cortical thinning and increased endocortical resorption. Histological evaluation of the long bones demonstrated a dramatic increase in adipocyte numbers and apparent decreases in osteoblasts on the bone surface. These data demonstrate that IL-8 is expressed by primary breast tumors and suggest that tumor-derived IL-8 may play a role in tumor development and facilitate increases in bone resorption, leading to osteolytic bone lesions. In addition, IL-8 expression *in vivo* elicits profound increases in osteoclastogenesis and adipogenesis, suggesting a local role for IL-8 in the bone marrow microenvironment.

**Disclosures:** L.J. Suva, None.

This study received funding from: Carl L. Nelson Chair of Orthopaedic Surgery.

## 1235

**Osteoporosis Diagnosis and Incident Fracture as a Function of Prior Fractures Site in a Large Clinical Cohort.** W. D. Leslie<sup>1</sup>, J. F. Tsang<sup>\*2</sup>, L. M. Lix<sup>\*3</sup>.  
<sup>1</sup>Department of Medicine, University of Manitoba, Winnipeg, MB, Canada, <sup>2</sup>Department of Radiology, University of Manitoba, Winnipeg, MB, Canada, <sup>3</sup>Manitoba Centre for Health Policy, University of Manitoba, Winnipeg, MB, Canada.

Prior fractures are a known risk factor for future osteoporotic fractures. The objective of this study was to assess the importance of prior fracture site on the strength of this relationship.

We identified 21444 women age 45 y or older undergoing baseline hip assessment with DXA (1990-2002) from a population-based database which contains all clinical DXA test results for the Province of Manitoba, Canada. These were linked to longitudinal health service records for physician billings and hospitalizations to identify non-trauma ICD-9-CM fracture codes that preceded DXA (prevalent fractures from 1987 until testing date) or followed DXA (incident fractures from testing date until 2004). ICD-9-CM codes with fewer than 50 cases were excluded. Osteoporosis diagnosis (femoral neck [FN] NHANES-III T-score -2.5 or lower, N=6030 [28.1%]) and incident 'osteoporotic' fractures (hip, clinical spine, wrist, humerus during mean 4.2 y of follow up, N=1202 [5.6%]) were studied in age-adjusted multiple regression methods (logistic and Cox proportional hazards models) in relation to prior fracture site.

The number of prior fracture sites was correlated with lower FN T-score (p<0.0001) and higher risk for incident fractures (p<0.0001). The site most strongly associated with an osteoporotic FN T-score was ICD-820 Neck of femur (OR 1.76, 95% CI 1.53-2.02). In age-adjusted multivariate regression, only ICD-805 Vertebral (HR 2.65, 95% CI 2.12-3.30), ICD-812 Humerus (3.04, 95% CI 2.47-3.75), ICD-813 Radius/ulna (1.44, 95% CI 1.18-1.77), and ICD-820 Femur neck (1.51, 95% CI 1.07-2.12) were independently associated with incident osteoporotic fractures. Simultaneous adjustment for femoral neck BMD slightly only weakened these associations. Many common fracture sites did not contribute independent fracture risk information, including ICD-807 Ribs/sternum, ICD-814 Carpal bones, ICD-823 Tibia/fibula, ICD-824 Ankle, and ICD-825 Tarsal/metatarsal bones.

We conclude that site of prior fracture is an important consideration in identifying women at risk for osteoporosis and future osteoporotic fractures. Fracture risk assessment systems should emphasize the importance of prior fractures affecting the hip, spine, wrist, and humerus.

Prior Fracture Site (N)	Adjusted ORs (95%CI) for osteoporosis diagnosis and HRs (95%CI) for incident osteoporotic fracture		
	OR for T ≤ -2.5 (age-adj)	HR for incident fracture (age-adj)	HR for incident fracture (age+BMD-adj)
ICD-805 Vertebral (504)	<b>1.35 (1.22-1.49)</b>	<b>2.65 (2.13-3.30)</b>	<b>2.26 (1.82-2.82)</b>
ICD-807 Ribs, sternum (676)	<b>1.17 (1.07-1.27)</b>	1.08 (0.82-1.42)	0.96 (0.73-1.27)
ICD-808 Pelvis (135)	<b>1.46 (1.20-1.77)</b>	1.13 (0.69-1.87)	1.03 (0.63-1.68)
ICD-810 Clavicle (97)	<b>1.39 (1.11-1.74)</b>	1.03 (0.53-2.00)	0.93 (0.48-1.8)
ICD-812 Humerus (583)	<b>1.22 (1.11-1.34)</b>	<b>3.04 (2.47-3.75)</b>	<b>2.77 (2.25-3.41)</b>
ICD-813 Radius/ulna (1726)	<b>1.18 (1.11-1.26)</b>	<b>1.44 (1.18-1.77)</b>	<b>1.35 (1.1-1.65)</b>
ICD-814 Carpal (1071)	1.00 (0.93-1.09)	0.97 (0.75-1.26)	0.93 (0.71-1.2)
ICD-815 Metacarpal (259)	1.11 (0.96-1.29)	1.09 (0.68-1.76)	1.03 (0.64-1.65)
ICD-816 Phalanges hand (322)	0.94 (0.82-1.08)	1.06 (0.68-1.67)	1.19 (0.76-1.85)
ICD-818 Upper limb NOS (96)	1.09 (0.87-1.37)	0.69 (0.34-1.4)	0.68 (0.34-1.39)
ICD-820 Neck femur (399)	<b>1.76 (1.53-2.02)</b>	<b>1.51 (1.07-2.12)</b>	1.26 (0.91-1.77)
ICD-821 Femur NOS (173)	1.00 (0.82-1.24)	0.93 (0.56-1.54)	0.99 (0.60-1.62)
ICD-822 Patella (129)	1.14 (0.94-1.39)	1.43 (0.84-2.44)	1.57 (0.93-2.62)
ICD-823 Tibia/fibula (591)	1.04 (0.93-1.15)	0.81 (0.55-1.19)	0.73 (0.5-1.09)
ICD-824 Ankle (885)	0.89 (0.81-0.97)	1.01 (0.74-1.38)	1.11 (0.81-1.51)
ICD-825 Tarsal/metatarsal (901)	<b>1.09 (1.00-1.18)</b>	0.98 (0.73-1.31)	0.98 (0.73-1.3)
ICD-826 Phalanges foot (558)	1.01 (0.92-1.12)	1.17 (0.82-1.67)	1.17 (0.82-1.66)
ICD-827 Lower limb NOS (76)	1.05 (0.75-1.48)	0.87 (0.28-2.76)	0.93 (0.29-2.93)
ICD-829 Unspecified (121)	0.92 (0.92-0.92)	0.97 (0.53-1.77)	1.01 (0.55-1.85)

**Disclosures:** W.D. Leslie, None.

## 1236

**Fracture Risk and Incidence of Falls in Younger Postmenopausal Women (age 50-64 yrs): Rresults from National Osteoporosis Risk Assessment Survey (NORA).** E. Barrett-Connor<sup>1</sup>, S. G. Sajjan<sup>\*2</sup>, E. S. Siris<sup>3</sup>, T. Fan<sup>\*2</sup>, P. D. Miller<sup>\*4</sup>, S. S. Sen<sup>\*2</sup>.  
<sup>1</sup>University of California, San Diego, La Jolla, CA, USA, <sup>2</sup>Merck & Co., Inc, Whitehouse Station, NJ, USA, <sup>3</sup>Columbia University Medical Center, New York, NY, USA, <sup>4</sup>Colorado Center for Bone Research, Lakewood, CO, USA.

This study examined the association between the NORA-based tree algorithm for fracture risk (Chen et al., OI 2007) and self-reported future osteoporotic fractures and falls in postmenopausal women (PMW) between 50 and 64 years of age. Participants had no history of osteoporosis or bone-specific medication use at baseline, and completed year 1, year 2, and/or year 5 year follow-up surveys. Incident fracture rates (IFR) (see Table) were calculated dividing women with new fractures by person-years of follow-up. Relative risks (RR) for future fractures were calculated for women with the various combinations of risk factors for fracture using the Cox regression models. The tree algorithm for fracture risk included baseline personal history of fracture, a peripheral BMD T-score ≤ -1.1, and, self-reported fair/poor health status. A total of 3,192 women reported 3,451 future fractures. The prior history of fracture was the most important determinant of future fracture. The most important risk factors for falls were the prior history of fracture and fair/poor health status. Similar findings were observed for the algorithm without the BMD- T score. A simple 3 item tree-based algorithm identified relatively young PMW with a five fold increased risk of future osteoporotic fracture. Results were almost as good without a peripheral BMD measurement. Any PMW with a history of fracture and who reports fair or poor health should be evaluated for appropriate fracture prevention management.

Risk Factors	N	IFR (95% CI) Per 1,000 women-year follow-up	Relative risk of future fracture (95% CI)	% of Women reported a fall in the last 12-months at 1st follow-up survey
Prior history of fracture	5562	27.8 (25.6, 29.9)	4.9 (4.5, 5.5)	22.4
BMD-T score ≤ -1.1 with no fracture history	22710	12.6 (11.9, 13.3)	2.2 (2.0, 2.4)	16.6
Fair/Poor health with BMD-T score > -1.1 and no fracture history	8466	10.4 (9.3, 11.5)	1.8 (1.6, 2.1)	23.6
Excellent-Good health status with BMD-T score > -1.1 and no fracture history	54823	5.7 (5.4, 6.0)	Reference	16.2

**Disclosures:** E. Barrett-Connor, None.

## 1237

**Risk Factors for Subsequent Fractures within the Next Year in Patients Presenting with a Clinical Fracture.** P. Geusens<sup>1</sup>, G. Willems<sup>\*2</sup>, S. van Helden<sup>\*3</sup>.  
<sup>1</sup>Internal Medicine/Rheumatology, University Hospital, Maastricht, Netherlands, <sup>2</sup>University Hospital, Maastricht, Netherlands, <sup>3</sup>Surgery, University Hospital, Maastricht, Netherlands.

**Background:** Patients presenting with a clinical vertebral or non-vertebral fracture have a high risk of subsequent clinical fractures within one year.

**Objectives:** In a prospective study we investigated the association between baseline bone- and fall-related risk factors and the risk of subsequent clinical fractures within one year after a clinical fracture.

**Methods:** At baseline, clinical bone-related risks, bone mineral density (BMD, at the spine and hip) and fall risks were assessed, based on the Dutch guidelines of osteoporosis and fall prevention. Accordingly, the fracture nurse gave general instructions about life style and fall prevention. In addition, patients with osteoporosis were prescribed bisphosphonates, calcium and vitamin D. During follow-up fall and fracture incidence were recorded by telephone questionnaire.

**Results:** A total of 31 patients (3.6%) out of 866 consecutively evaluated patients had a subsequent fracture within 1 year (18 at the upper limb, 17 at the lower limb, 5 multiple simultaneous fractures and 1 other). An incident fall was reported by 185 (21.4%), 113

(13.0%) had one fall, 72 (8%) had two or more falls. Nearly all subsequent fractures (94%) resulted from a fall. In patients with an incident fall, fracture incidence was 15% in patients with osteoporosis, 18% in osteopenia and 8% when BMD was normal. In patients without an incident fall, the incidence was 0.6%, 0% and 1.2%, respectively. In a multivariate analysis including baseline age, sex, fall risks, BMD and incident falls, the only determinant of a subsequent fracture was an incident fall ( $p<0.001$ ). Incident falls were related to sex (relative risk (RR) of women versus men: 1.50, 95% confidence interval (CI): 1.08-2.08) and the presence of one or more fall risks at baseline (RR: 1.75, CI: 1.01-3.04).

**Conclusion:** We conclude that in patients presenting with a clinical fracture, fall risk evaluation contributes to the recognition of subjects who have an increased risk for a subsequent clinical fracture within one year.

**Disclosures:** P. Geusens, None.

## 1238

**Independent Contribution of Hip Geometry to Incident Fracture Prediction in a Large Clinical Cohort.** W. D. Leslie<sup>1</sup>, H. J. Prior<sup>2\*</sup>, P. Pahlavan<sup>3</sup>. <sup>1</sup>Department of Medicine, University of Manitoba, Winnipeg, MB, Canada, <sup>2</sup>Manitoba Centre for Health Policy, University of Manitoba, Winnipeg, MB, Canada, <sup>3</sup>St. Boniface General Hospital, Winnipeg, MB, Canada.

Although hip geometry is known to contribute to femur strength and fracture discrimination in cross-sectional studies, there are few data on prediction of incident fractures.

We assessed hip and non-hip osteoporotic fracture outcomes in 30,953 women aged 50 years or older (mean  $66\pm 10$ ) who underwent baseline hip DXA with a single scanner configuration (Prodigy, GE Lunar) through the Manitoba BMD Program. All hip scans were processed with a single version of analysis software (enCore v12) to generate multiple indices of hip geometry (hip axis length=HAL, cross sectional moment of inertia=CSMI, cross sectional area=CSA, strength index=SI) in addition to conventional BMD (total hip T-score=TH and femoral neck T-score=FN, NHANES III reference data). Population-based administration health data were linked to the scan results in order to determine fracture outcomes. During mean 3.7 years of follow up (range up to 9.6 years) we identified operated hip fractures (N=270) and non-hip osteoporotic fractures (clinical spine, wrist, humerus; N=1,269). Cox proportional hazards models constructed to assess the effect of hip geometry variables on fractures were sequentially adjusted for age, age+BMD, and age+BMD+weight+height.

Unadjusted mean values for HAL, CSMI, CSA, SI and TH were significantly different for hip fracture vs. non-fracture women (all  $P<0.0001$ ) and non-hip fracture vs. non-fracture women (all  $P<0.0001$ ). In age-adjusted models CSMI, CSA, SI and TH were significant predictors of hip and non-hip fractures; HAL was only significant for hip fractures. When fully adjusted (for age+BMD+weight+height), HAL (HR 1.22, 95% CI 1.06-1.40) and SI (HR 1.23, 95% CI 1.09-1.40) were still significant predictors of hip fractures but not of non-hip fractures. Similar results were seen when FN was substituted for TH in the fully adjusted model: HAL HR 1.32 (95% CI 1.17-1.50) and SI HR 1.16 (95% CI 1.03-1.30). Addition of HAL or SI to models that included BMD gave a significant improvement in hip fracture prediction (log-likelihood ratio test  $P<0.005$ ).

We conclude that some hip geometry parameters (HAL and SI) make a small but significant independent contribution to hip fracture prediction. Hip geometry does not affect non-hip fracture risk when adjusted for other factors.

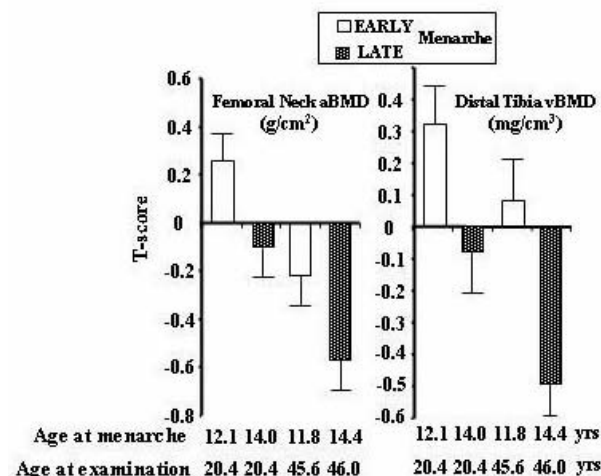
Hazard ratios for incident fracture per SD.		
	Hip fractures HR (95%CI)	Non-hip fractures HR (95%CI)
<b>Age-adjusted</b>		
Total Hip	2.46 (2.14-2.83)	1.60 (1.51-1.71)
HAL	1.33 (1.17-1.51)	1.05 (0.98-1.12)
CSMI	1.24 (1.09-1.41)	1.17 (1.10-1.24)
CSA	2.03 (1.74-2.36)	1.59 (1.47-1.71)
SI	1.31 (1.16-1.47)	1.14 (1.09-1.21)
<b>Age+BMD adjusted</b>		
HAL	1.29 (1.14-1.46)	1.04 (0.98-1.12)
CSMI	0.92 (0.81-1.05)	0.99 (0.93-1.05)
CSA	0.96 (0.77-1.19)	1.01 (0.91-1.11)
SI	1.19 (1.06-1.34)	1.09 (1.04-1.15)
<b>Age+BMD+height+weight adjusted</b>		
HAL	1.22 (1.06-1.40)	1.02 (0.95-1.10)
CSMI	0.96 (0.83-1.10)	1.04 (0.97-1.11)
CSA	1.04 (0.82-1.32)	1.07 (0.96-1.19)
SI	1.23 (1.09-1.40)	1.04 (0.99-1.11)

**Disclosures:** W.D. Leslie, None.

## 1239

**Deleterious Effect of Late Menarcheal Age on Bone Microstructure in Both Distal Radius and Tibia: No Interaction with Age Dependent Premenopausal Bone Loss in Weight-Bearing Skeletal Sites.** T. Chevalley, J. P. Bonjour, S. Ferrari, R. Rizzoli. Service of Bone Diseases, Department of Rehabilitation and Geriatrics, Geneva University Hospitals, Switzerland.

Late menarche is a risk factor for fragility fractures. We hypothesized that pubertal timing-dependent alterations in bone structural components would persist from peak bone mass (PBM) to menopause, independent of any premenopausal bone loss that can be observed in weight-bearing skeletal sites. The influence of menarcheal age (MENA) was examined in healthy young adult (YAD,  $20.4\pm 0.6$  ( $\pm$ SD) years,  $n=124$ ) and premenopausal middle-aged (PREMENO,  $45.8\pm 3.4$  yrs,  $n=120$ ) women. Areal bone mineral density (aBMD) was measured in both distal radius and femoral neck by DXA. Volumetric bone mineral density (vBMD) was measured by high resolution peripheral computerized tomography (HR-pQCT) in both distal radius and distal tibia. Median of MENA was  $13.0\pm 1.2$  and  $13.1\pm 1.7$  years in YAD and PREMENO, respectively. After segregation by the median of MENA in EARLY and LATE subgroups, the significant negative influence of LATE MENA was observed in both distal radius ( $P=0.039$ ) and femoral neck ( $P=0.004$ ) aBMD. Microstructure analysis indicated a marked deleterious effect of LATE MENA in vBMD of both distal radius ( $P=0.006$ ) and distal tibia ( $P=0.0005$ ). Cortical thickness was also reduced in LATE vs EARLY MENA in both distal radius ( $P=0.027$ ) and distal tibia ( $P=0.004$ ). As illustrated in the figure the negative effect of age between YAD and PREMENO was additive to LATE MENA in both femoral neck aBMD and distal tibia vBMD. In conclusion, in healthy women a 1.9-2.6 yrs later menarcheal age is negatively associated with areal and volumetric BMD as well as cortical thickness in both upper and lower limbs. This influence of pubertal timing is observed in early twenties and a few years prior to menopause. The negative influence of aging from early twenties to mid-forties on both aBMD and vBMD as assessed at weight-bearing skeletal sites does not attenuate the influence of MENA. Alterations in both bone mineral mass and microstructural components may explain the increased risk of fragility fractures associated with later menarcheal age.



**Disclosures:** T. Chevalley, None.

## 1240

**Performance of QUS In Comparison to DXA For Prediction Of Prospective Fractures Among Older Men and Women: The EPIC-Norfolk Study.** A. Moayyeri, S. Kaptoge, R. Luben\*, S. Bingham\*, N. J. Wareham\*, J. Reeve, K. T. Khaw\*. Public Health and Primary Care, The University of Cambridge, Cambridge, United Kingdom.

The role of quantitative ultrasound (QUS) in the management of osteoporosis is debated. Although QUS of the heel is known to be correlated with bone mineral density (BMD), the performance of QUS for prediction of fractures in comparison to dual-energy X-ray absorptiometry (DXA), the current reference standard for diagnosis of osteoporosis, is unclear. We examined this in a sample of men and women in the European Prospective Investigation into Cancer (EPIC)-Norfolk who had both heel QUS and hip DXA between 1995 and 1997 and were followed for incident fractures up to March 2007. From 1,454 participants (701 men) aged 65-76 years at baseline, 79 suffered a fracture over 15.567 person-years of follow-up (mean 10.3±1.4 years). In a sex-stratified multivariate Cox proportional-hazard model including age, height, weight, past history of fracture, smoking, alcohol intake and DXA total hip BMD, 1 SD decrease in BMD was associated with a hazard ratio for fracture of 2.28 (95% CI 1.75-2.98). In a multivariate model with heel broadband ultrasound attenuation (BUA) in place of BMD, hazard ratio for 1 SD decrease in BUA was 2.02 (95% CI 1.54-2.65). While the global measures of model fit (including Bayesian and Akaike's information criteria, LR chi-square, D-statistic, Nagelkerke's and Cox-Snell R-square) slightly favored the model with DXA measure, measures of discrimination (area under ROC curve 0.685 vs. 0.679) and calibration (Hosmer-Lemeshow statistic 0.82 vs. 0.45) showed relative superiority of the model with BUA. Using the alternate Cox models with DXA and BUA, we calculated exact 10-year absolute risk (probability) of fracture for all participants and categorized them in three groups of <5%, 5% to <15%, and ≥15%. Comparison of groupings based on DXA vs. BUA models showed a total reclassification of 24.9% of participants. The predicted risks for individual participants using BUA model were closer to the observed risks (especially among the 52.2% reclassified highest-risk group). This study shows that the power of QUS for prediction of prospective fractures and calculation of 10-year probability of fractures among the elderly is comparable to that of DXA. Given the ease and low cost of ultrasound, risk assessment tools (such as newly-developed FRAX tool) may include QUS measures in their algorithms to attain more accurate estimates of fracture risk. Further studies or meta-analyses are required to clarify whether QUS with clinical risk factors would be cost-effective for primary care case-finding when DXA is not available.

**Disclosures:** A. Moayyeri, None.

## 1241

**Strontium Ranelate Prevents the Progression of Thoracic Kyphosis in Postmenopausal Women with Osteoporosis.** C. Roux<sup>1</sup>, K. Briot<sup>1</sup>, S. Kolta<sup>1</sup>, R. Said-Nahal<sup>\*1</sup>, C. Benhamou<sup>2</sup>, J. Fechtenbaum<sup>1</sup>. <sup>1</sup>Rheumatology, Cochin Hospital, Paris, France, <sup>2</sup>Rheumatology, Orleans Hospital, Orleans, France.

Thoracic kyphosis, frequent in the elderly and in postmenopausal osteoporosis, has been associated with impairment in global health. It can be caused by vertebral fractures, and by degenerative spine changes (intervertebral disc space narrowing, deformities of the anterior part of the vertebrae and reduced spinal muscles strength). The objective of this study was to assess the effect on thoracic kyphosis progression over a 3-year treatment with strontium ranelate which reduces the risk of vertebral, non vertebral and hip fractures. This study was performed in women with postmenopausal osteoporosis from SOTI<sup>1</sup> and TROPOS<sup>2</sup> studies, aiming to demonstrate the efficacy of strontium ranelate against vertebral and non-vertebral fractures. Patients underwent lateral radiographs of the thoracic and lumbar spine at baseline and annually over 3 years (standardized procedures). The level of thoracic kyphosis was reflected by a kyphosis index, defined on lateral thoracic radiographs as the ratio BD/AC (AC= line from the anterior superior edge of T4 to the anterior inferior edge of T12; BD= perpendicular line from the furthest superior or inferior posterior point of T7, T8 or T9 vertebrae to AC line) expressed as a %.

The population consisted of 4055 women with postmenopausal osteoporosis (2038 in the strontium ranelate group and 2017 in the placebo group). Baseline characteristics were similar: mean age 73.5; mean lumbar spine T-score of -3.06; mean hip T-score of -2.97, and mean KI of 25.4. Over 3 years, there was a significant increase from baseline in kyphotic index for all patients. However, this increase was significantly lower (p=0.003) in patients treated with strontium ranelate: +3.71±7.69% than in the placebo group: +4.70±7.32%. After exclusion of patients having either prevalent or incident thoracic vertebral fractures, in a subset of 1193 patients (634 in the strontium ranelate group and 559 in the placebo group), the change in the strontium ranelate group was still lower (p<0.001) than in the placebo group (+ 2.72±7.17% versus 4.34±6.54%, respectively).

These prospective results demonstrate that thoracic kyphosis increases over time in postmenopausal women with osteoporosis. Strontium ranelate decreased the progression of this thoracic kyphosis over 3 years, regardless of the presence or not of vertebral fractures. This effect of strontium ranelate possibly reflects additional benefit on spinal components besides its efficacy in decreasing vertebral fractures.

References : <sup>1</sup> Meunier PJ et al. *N Engl J Med* 2004; <sup>2</sup> Reginster J.Y et al. *JCEM* 2005

**Disclosures:** C. Roux, None.

## 1242

**Prevention of Non-vertebral Fractures with Oral Vitamin D Is Dose Dependent: a Meta-analysis of RCTs.** H. A. Bischoff-Ferrari<sup>1</sup>, W. C. Willett<sup>\*2</sup>, J. B. Wong<sup>\*3</sup>, A. Stuck<sup>\*4</sup>, H. B. Staehelin<sup>\*5</sup>, J. E. Orav<sup>\*6</sup>, A. Thoma<sup>\*1</sup>, D. P. Kiel<sup>7</sup>, J. Henschkowski<sup>\*1</sup>. <sup>1</sup>Rheumatology and Institute of Physical Medicine, University of Zurich, Zurich, Switzerland, <sup>2</sup>Dept. of Nutrition, Harvard School of Public Health, Boston, MA, USA, <sup>3</sup>Division of Clinical Decision Making, New England Medical Center, Boston, MA, USA, <sup>4</sup>Geriatrics, University of Bern, Bern, Switzerland, <sup>5</sup>Geriatrics, University of Basel, Basel, Switzerland, <sup>6</sup>Biostatistics, Harvard School of Public Health, Boston, MA, USA, <sup>7</sup>Gerontology, Harvard Medical School, Boston, MA, USA.

**Background:** Anti-fracture efficacy with supplemental vitamin D (cholecalciferol = D3, ergocalciferol = D2) has been questioned by recent trials.

**Aim:** We performed a meta-analysis on the efficacy of supplemental vitamin D in preventing non-vertebral and hip fractures among older individuals (age 65+).

**Studies included:** We included double-blind randomized controlled trials (RCTs) of oral vitamin D with or without calcium supplementation compared with calcium or placebo. 12 RCTs (n=42,279) for non-vertebral fractures and 8 RCTs for hip fractures (n = 40,886) met our inclusion criteria.

**Results:** The pooled relative risk (RR) for prevention of non-vertebral fractures by vitamin D was 0.86 (95% CI, 0.77-0.96), and for hip fractures was 0.91 (95% CI, 0.78-1.05), but with significant heterogeneity for both endpoints. Including all trials, anti-fracture efficacy increased significantly with higher received dose (dose\*adherence) and higher achieved blood 25-hydroxyvitamin D levels (25(OH)D) for any non-vertebral fractures (dose\*adherence: p=0.003; 25(OH)D: p = 0.04) and for hip fractures (dose\*adherence: p=0.07; 25(OH)D: p = 0.009). Consistently, heterogeneity was resolved by pooling trials with a higher received dose of more than 400 IU/day separately. With the higher dose, the pooled RR for any non-vertebral fractures including 9 trial was 0.80 (95% CI, 0.72 -0.89; n = 33,265) and the pooled RR for hip fracture including 5 trials was 0.82 (95% CI, 0.69 - 0.97; n = 31,872). For the higher received dose, non-vertebral fracture reduction was significant among community-dwelling (-29%) and institutionalized older individuals (-15%), and was independent of additional calcium supplementation. **Conclusion:** Non-vertebral fracture prevention with vitamin D is dose-dependent, and a higher dose should reduce fractures by at least 20% for individuals over age 65 years.

**Disclosures:** H.A. Bischoff-Ferrari, None.

This study received funding from: Swiss National Foundations.

## 1243

**A Randomized Trial of Balloon Kyphoplasty and Nonsurgical Care for Acute Vertebral Fracture: Who Responds Best?** S. Cummings<sup>1</sup>, D. Wardlaw<sup>\*2</sup>, J. Van Meirhaeghe<sup>\*3</sup>, L. Bastian<sup>\*4</sup>, J. Tillman<sup>\*5</sup>, J. Ranstam<sup>\*6</sup>, R. Eastell<sup>7</sup>, P. Shabe<sup>\*8</sup>, K. Talmadge<sup>9</sup>, S. Boonen<sup>9</sup>. <sup>1</sup>University of California, San Francisco, CA, USA, <sup>2</sup>Woodend Hospital, Aberdeen, United Kingdom, <sup>3</sup>Algemeen Ziekenhuis St. Jan, Brugge, Belgium, <sup>4</sup>Klinikum Leverkusen, Leverkusen, Germany, <sup>5</sup>Medtronic Spine LLC, Sunnyvale, CA, USA, <sup>6</sup>Lund University Hospital, Lund, Sweden, <sup>7</sup>University of Sheffield, Sheffield, United Kingdom, <sup>8</sup>Advance Research Associates, Mountain View, CA, USA, <sup>9</sup>Katholieke Universiteit, Leuven, Belgium.

Balloon kyphoplasty aims to improve quality of life and reduce pain and disability by treating vertebral deformity and stabilizing the fracture with bone cement. We tested the efficacy of kyphoplasty versus nonsurgical care and analyzed 1 year outcomes to identify patients who may benefit most from the procedure.

Patients with 13 acute vertebral compression fractures were randomly assigned to kyphoplasty (N=149) or nonsurgical care (N=151). Overall, patients assigned to kyphoplasty had statistically significant improvements in quality of life; the SF-36 physical component summary (PCS) improved 3.4 (95% CI, 1.55.3) and Euroqol-5D (EQ-5D) improved 0.13 (95% CI, 0.050.22) points more than nonsurgical care. Kyphoplasty resulted in more pain relief (1.6 points; 95% CI 1.22.1), less Roland-Morris back disability (3.1 points; 95% CI, 1.94.3) and 2.4 (95% CI 1.13.7) fewer days of limited activity (within a two-week period). To identify patients who may benefit most from kyphoplasty, we analyzed the effect of kyphoplasty on outcomes in patients with higher (≥18 points) or lower (<18) baseline Roland-Morris disability scores (Table). We also tested the effects of kyphoplasty in patients above or below the median age of 74 years.

Each disability group had better improvement with kyphoplasty. A larger treatment effect of kyphoplasty was observed in those with greater disability; there was a significant treatment by subgroup interaction for Roland-Morris scores and disability days (p<0.05). The effects of kyphoplasty were similar for patients ≥74 years (range 74-95) and <74 years (range 44-73).

Compared to nonsurgical care, balloon kyphoplasty improved quality of life and reduced back pain and disability and did not increase the risk of vertebral fracture over 1 year. The effects may be somewhat greater in those with the highest Roland-Morris scores. The effects of kyphoplasty are similar for elderly and younger patients.

Outcome Measure (Range of the Scale)	12-Month Difference of Kyphoplasty Minus Control (Mean and 95% CI)	
	High Roland-Morris Disability (≥18 points at baseline)	Low Roland-Morris Disability (<18 points at baseline)
Roland-Morris (0-24 points)*	-4.6 (-6.2 to -3.0)	-1.5 (-3.3 to 0.2)
Roland-Morris (0-100 %)*	-23 (-33 to -13)	-13 (-23 to -2)
Back Pain (0-10 points)*	-1.8 (-2.4 to -1.2)	-1.4 (-2.1 to -0.8)
Disability Days (0-14 days)*	-3.6 (-5.4 to -2.1)	-1.0 (-2.9 to 0.9)
EQ-5D (0-1 point)	0.17 (0.05 to 0.29)	0.10 (-0.03 to 0.23)
SF-36 PCS (0-100 points)	4.4 (1.9 to 6.9)	2.4 (-0.5 to 5.2)

\*Demerit scales; lower scores are better

**Disclosures:** S. Cummings, Consultant to Medtronic Spine LLC 2.  
This study received funding from: Medtronic Spine LLC.

## 1244

**Effects of a Targeted Bone and Muscle Loading Program on QCT Bone Geometry and Strength, Muscle Size and Function in Older Men: An 18-month RCT.** S. Kukuljan<sup>\*1</sup>, C. Nowson<sup>\*1</sup>, S. Bass<sup>1</sup>, K. Sanders<sup>\*2</sup>, G. C. Nicholson<sup>2</sup>, R. M. Daly<sup>3</sup>. <sup>1</sup>School of Exercise and Nutrition Sciences, Deakin University, Melbourne, Australia, <sup>2</sup>Clinical and Biomedical Sciences, Barwon Health, The University of Melbourne, Geelong, Australia, <sup>3</sup>Department of Medicine, The University of Melbourne, Western Hospital, Melbourne, Australia.

We have previously shown that an 18 month community-based, multi-component exercise program, with or without additional calcium-vitamin D<sub>3</sub>, was effective for improving FN aBMD in older men. In this study we examine the effects of the exercise program on QCT measured bone geometry and strength, and muscle size and functional performance. Men (n=180) aged 61±7 years (±SD) were randomised to an exercise or non-exercise group with or without additional calcium-vitamin D<sub>3</sub> (fortified milk: 1000 mg/d calcium and 800 IU/d vitamin D<sub>3</sub>). The exercise consisted of high intensity (60-85% 1RM) resistance and power training (RT) and weight-bearing impact exercise (1.5-9.7 BW) performed 3 days/wk. QCT was used to assess mid-femur and mid-tibia total (TotAr), cortical (CortAr), medullary areas (MedAr), volumetric BMD (vBMD), polar moment of area (Ip), muscle cross-sectional area (CSA) and distal tibia trabecular vBMD. Gait (6-m walk), dynamic balance (step-test) and sway were also assessed. 172 men (95%) completed the study; exercise attendance averaged 63% and compliance with the fortified milk averaged 90%. Muscle CSA and gait speed improved in the exercise compared to non-exercise groups (1.0 vs -0.8%, p<0.01; -3.0 vs -1.1 seconds, p<0.05). ITT analyses revealed that there were no exercise-by-calcium-vitamin D<sub>3</sub> interactions, nor any main effects of exercise or calcium-vitamin D<sub>3</sub> on any QCT bone parameters. However, subgroup analyses of the exercise group revealed that the average number of jumps per session, but not the average RT load per session over the 18 month study, correlated with change in mid-femur CortAr (r=-0.32, p<0.001), MedAr (r=-0.30, p<0.01) and Ip (r=0.22, p=0.05). When expressed as tertiles, men who performed at least 65 jumps per session had a net 0.5 to 0.7% gain in mid-femur CortAr compared to those in the lowest two tertiles (≤35 or 36-64 jumps per session), independent of RT load, or the non-exercise group (all p<0.05). This can be attributed to reduced medullary expansion (net difference 0.5 to 1.2%) and not periosteal apposition. In conclusion, this study indicates that a multi-component resistance and weight-bearing exercise program can enhance muscle size and function in older men, and that bone geometry adapts to a given number of impact loads (≥65 jumps/session), and not the total resistance training load. In contrast, increased dietary calcium-vitamin D<sub>3</sub> had no effect on bone geometry or strength in this group of older well nourished men.

**Disclosures:** R.M. Daly, None.

## 1245

**Alendronate and Indapamid Alone or in Combination in the Management of Idiopathic Hypercalciuria Associated with Osteoporosis: a Randomized-Controlled Trial.** A. Giusti<sup>1</sup>, A. Barone<sup>\*1</sup>, G. Pioli<sup>2</sup>, G. Girasole<sup>3</sup>, V. Siccardi<sup>\*3</sup>, E. Palummeri<sup>1</sup>, G. Bianchi<sup>3</sup>. <sup>1</sup>Gerontology, Galliera Hospital, Genoa, Italy, <sup>2</sup>Gerontology, ASMN Hospital, Reggio Emilia, Italy, <sup>3</sup>Rheumatology, La Colletta, Genoa, Italy.

The role of bisphosphonates (BSF) in the treatment of patients with idiopathic hypercalciuria (IHC) associated with osteoporosis is still uncertain. To evaluate the effect of alendronate alone or in combination with indapamid on bone mineral density (BMD) and 24-hours calciuria (CaU), 67 post-menopausal women with IHC (CaU>4mg/kg/die) and low BMD [T-score<-2.0 at lumbar spine (LS), femoral neck (FN) or total hip (TH)] from two centres of Northern Italy, were randomised to receive: indapamid 2.5 mg daily alone (20 patients, IND group), alendronate 70 mg weekly alone (25 patients, ALN group) or the combination therapy (22 patients, ALIND group). Throughout the study, all subjects received daily calcium supplements, depending on their dietary intake, to maintain a daily input of 1,000 mg. Patients were instructed to increase water intake up to 2000 ml daily. The percentage change of BMD at LS, FN and TH, and the variation of 24-hours CaU from baseline at 1-year were the primary outcomes. Serum calcium, PTH and bone alkaline phosphatase were also measured. Patients in the 3 groups were similar with regard to baseline characteristics. After 1-year,

CaU values significantly decreased from baseline in all groups (IND, 239±78 vs. 364±44, p<.001) (ALN, 279±68 vs. 379±79, p<.001) (ALIND, 191±68 vs. 390±55, p<.001). The mean % decrease of CaU in ALIND group (-50%) was significantly greater compared to ALN (-24%, p<.001) and IND (-35% p=.012). BMD did not significantly changed from baseline after 1 year of treatment with indapamid (LS: +1±3.1%; FN: -0.3±3.5%; TH: -0.4±3.1%), while showed a significant increase from baseline in the other 2 groups (ALN; LS: +5.8±4.2%, p<.001; FN: +3.9±7.9%, p=.018; TH: +2±3.6%, p=.006) (ALIND; LS: +8.2±5.3%, p<.001; FN: +4.9±6.7%, p=.007; TH: +2.9±4.2%, p=.004). In addition, patients in the combination group (ALIND) showed a significantly higher increase of BMD at LS compared to ALN (p=.04).

These results show a benefit on BMD and CaU, of BSF<sup>†</sup> therapy in IHC associated with osteoporosis. The combination therapy demonstrated a reduction of CaU and an increase in LS BMD superior to that observed with alendronate alone. Our results support a new potential approach with BSF associated to thiazide diuretics in the management of post-menopausal women with IHC and associated bone loss.

**Disclosures:** A. Giusti, None.

## 1246

**Osteonecrosis of the Jaw: Zoledronic Acid 5 mg Experience in a Variety of Osteoporosis Indications.** J. Grbic<sup>1</sup>, D. Black<sup>2</sup>, K. Lyles<sup>3</sup>, D. Reid<sup>4</sup>, C. Bucci-Rechtweg<sup>\*5</sup>, P. Mesenbrink<sup>\*6</sup>, E. Orwoll<sup>7</sup>, E. Eriksen<sup>8</sup>. <sup>1</sup>Columbia University College of Dental Medicine, New York, NY, USA, <sup>2</sup>University of California, San Francisco, CA, USA, <sup>3</sup>VA Medical Center, Durham, NC, USA, <sup>4</sup>University of Aberdeen, Aberdeen, United Kingdom, <sup>5</sup>Novartis Pharmaceuticals Corporation, New Jersey, NJ, USA, <sup>6</sup>Novartis Pharmaceuticals Corporation, New Jersey, NJ, USA, <sup>7</sup>Portland VA Medical Center, Portland, OR, USA, <sup>8</sup>Novartis Pharma AG, Basel, Switzerland.

Currently bisphosphonates (BPs) constitute the primary therapeutic option for the treatment of osteoporosis, and the iv. BP zoledronic acid (ZOL), has demonstrated significant reduction of osteoporotic fractures at vertebral and non-vertebral sites. BPs have, however, been associated with Osteonecrosis of the Jaw (ONJ), characterized by exposed bone in the oral cavity. We have previously reported on the prospective assessment of ONJ incidence in the ZOL pivotal fracture trial (Study 2301) [J Am Dent Assoc. 2008 Jan;139(1):32-40]. In the current report, we analyzed the overall incidence of ONJ after completion of 3 additional studies ZOL studies, comprising a total of 11,000 patients. Moreover, we analyzed the distribution of the biomarker S-CTX, where levels below 0.1 ng/ml have been postulated as an indicator of increased ONJ risk [J Oral Maxillofac Surg. 2007 Dec;65(12):2397-410]. The studies included the uses of ZOL in the treatment of postmenopausal osteoporosis (N=7714), prevention of recurrent fracture after hip fracture (N=2111), treatment of glucocorticoid-induced osteoporosis (N=833), and male osteoporosis (N=302). The new studies included patients, thought to be at higher risk for the development of ONJ due to treatment with glucocorticoids and a high prevalence of diabetes. No spontaneous reports of ONJ were received for any of the additional studies. And after extensive review of all maxillofacial events with adjudication, the only two cases meeting the definition of ONJ remained the two cases previously described in patients with post-menopausal osteoporosis (one on placebo and one on ZOL). Among the 7714 patients enrolled in study 2301, the fraction of patients exhibiting S-CTX values < 0.1 ng/ml at months 6, 12, 24 and 36 were 60.8%, 30.9%, 20.4% and 16.1%, respectively. For the patient on placebo with adjudicated ONJ, S-CTX ranged between 0.26 and 0.37 ng/ml. S-CTX was not available for the patient on ZOL. In conclusion, in more than 11,000 patients, of which half were treated with zoledronic acid, no spontaneous reports of ONJ were received. Only 2 patients (1 on placebo, 1 on BP) met adjudication criteria for ONJ, thus no indication of increased risk of ONJ after treatment with ZOL. No association between low S-CTX and ONJ was established.

**Disclosures:** J. Grbic, Novartis, Research Support from the Alliance for Better Bone Health 2, 3.

This study received funding from: Novartis Pharma AG, Basel, Switzerland.

## 1247

**Loss or Gain of FoxO Function in Osteoclasts and Osteoblasts Alters the Rate of Apoptosis and BMD in Mice.** E. Ambrogini<sup>1</sup>, C. A. O'Brien<sup>1</sup>, M. Martin-Millan<sup>1</sup>, J. Paik<sup>\*2</sup>, R. A. DePinho<sup>\*2</sup>, L. Han<sup>1</sup>, A. Warren<sup>\*1</sup>, R. S. Shelton<sup>\*1</sup>, X. Qui<sup>\*1</sup>, J. Goellner<sup>1</sup>, R. L. Jilka<sup>1</sup>, M. Almeida<sup>1</sup>, S. C. Manolagas<sup>1</sup>. <sup>1</sup>Center for Osteoporosis and Metabolic Bone Diseases, University of Arkansas for Medical Sciences and Central Arkansas Veterans Healthcare System, Little Rock, AR, USA, <sup>2</sup>Center for Applied Cancer Science and Dept of Medical Oncology, Dana-Farber Cancer Institute, Depts of Medicine and Genetics, Harvard Medical School, Boston, MA, USA.

FoxO transcription factors influence cell proliferation, apoptosis, differentiation, metabolic responses, as well as resistance against oxidative stress (OS). Based on evidence that diversion of  $\beta$ -catenin from Wnt/TCF- to FoxO-mediated transcription by OS suppresses osteoblastogenesis, we investigated the role of FoxOs in bone metabolism *in vivo*, using mice in which we overexpressed FoxO3a in osteoblasts or mice with conditional deletion of FoxO1, 3a, and 4 (Mx-Cre<sup>+</sup>;FoxO1,3,4<sup>L/L</sup>). FoxO3a overexpression in osteoblasts was accomplished by creating a transgene with a transcriptional/translational stop cassette, flanked by loxP sites, inserted between the hybrid CMV-chicken  $\beta$ -actin promoter and a cDNA encoding an HA-tagged human FoxO3a. Mice carrying the transgene were then crossed with mice expressing the Cre recombinase under the control of the human osteocalcin promoter (OCN-Cre). Expression of the FoxO3a transgene was detected in calvaria and vertebrae but not liver or spleen, and resulted in increased expression of the FoxO-target genes Gadd45 and Bim. Importantly, these mice exhibited a significant increase in lumbar spine bone mineral density at 6 weeks. Deletion of FoxOs in Mx-Cre<sup>+</sup>;FoxO1,3,4<sup>L/L</sup> was achieved by induction of interferon using polyinosine-polycytidylic acid (pI-pC) injections. Four weeks later, mice were sacrificed and gene expression was determined. FoxO1, 3a, and 4 levels were decreased in liver (>98%), spleen (50-90%), as well as in calvaria and L4 (45-75%), as compared to Mx-Cre<sup>+</sup>;FoxO1,3,4<sup>L/L</sup> (control) mice. In addition, expression of the three FoxO isoforms was reduced (75-90%) in osteoblasts generated by culturing bone marrow derived stromal cells from Mx-Cre<sup>+</sup> mice for ten days in the presence of ascorbic acid, along with a decrease in the expression of the FoxO-target genes Gadd45 and p27<sup>Kip1</sup>. Finally, the expression of all three FoxOs was dramatically reduced (>99%) in mature osteoclasts from Mx-Cre<sup>+</sup>;FoxO1,3,4<sup>L/L</sup> mice obtained by culturing non adherent bone marrow cells in the presence of M-CSF and RANKL. FoxO deletion was associated with an increase in the basal rate of osteoclast apoptosis, as determined by caspase 3 activity. Collectively, these preliminary findings indicate that FoxOs play an important role in both osteoblasts and osteoclasts and influence bone mass.

**Disclosures:** E. Ambrogini, None.

## 1248

**Coactivator MBF1 Binds to JunD and Protects Its Transcriptional Activity Against Oxidative Stress to Prevent Age-Related Suppression of Osteoblast Differentiation.** S. Kido, R. Kuriwaka<sup>\*</sup>, T. Matsumoto. Department of Medicine and Bioregulatory Sciences, University of Tokushima Graduate School of Medical Sciences, Tokushima, Japan.

Oxidative stress reduces osteoblast number and suppresses bone formation, leading to the age-related loss of bone. We have demonstrated that anti-adipogenic cytokine, IL-11, was expressed in osteoblasts in an AP-1-dependent manner, and that DNA binding activity of JunD was reduced without change in its protein level in aged mice. Therefore, there is a possibility that reduced JunD activity may be caused by post-translational modification of JunD by an age-related increase in oxidative stress. MBF1, a transcriptional coactivator, directly binds to Fos and Jun to prevent oxidative damage and preserves their DNA binding activity. To determine potential roles of MBF1 in age-related reduction in bone formation, we first examined MBF1 expression in mice at different ages. In young mice, MBF1 protein was expressed in all tissues examined, whereas the amount of MBF1 decreased in many tissues including bone of aged mice. Cultured osteoblasts also expressed MBF1, and knockdown of MBF1 by siRNA in ST2 cells reduced the number of ALP<sup>+</sup> cells. In contrast, stable transfection of ST2 cells with MBF1 enhanced osteoblastogenesis and inhibited adipogenesis. When wild-type ST2 cells were treated with hydrogen peroxide, most cells died, whereas ST2 cells transfected with MBF1 survived even in the presence of hydrogen peroxide. DNA precipitation assay demonstrated that MBF1 forms complex with JunD on an AP-1 site of IL-11 promoter via binding to a basic region of JunD. MBF1 binding to JunD also enhanced AP-1-dependent IL-11 gene transcription even in the presence of hydrogen peroxide. These results demonstrate that MBF1 binds to a basic region of JunD and protects from oxidative damage to enhance transcriptional activation of IL-11 gene. It is suggested that reduced MBF1 protein expression in osteoblasts may play a role in age-related impairment of osteoblast differentiation by suppressing IL-11 transcription via a reduction in JunD activity, and that MBF1 can be a new target against age-related loss of bone.

**Disclosures:** S. Kido, None.

## 1249

**Changes in Marrow Cell Dynamics and Bone Geometry with Aging in Thrombospondin-2 Null Mice.** S. P. Terkhorh<sup>1</sup>, S. Tomassini<sup>\*2</sup>, C. Price<sup>\*1</sup>, R. A. Ruberte-Thiele<sup>\*1</sup>, J. A. Combs<sup>\*1</sup>, K. J. Jepsen<sup>\*2</sup>, K. D. Hankenson<sup>1</sup>. <sup>1</sup>Animal Biology, University of Pennsylvania, Philadelphia, PA, USA, <sup>2</sup>Leni & Peter W. May Department of Orthopaedics, Mount Sinai School of Medicine, New York, NY, USA.

Thrombospondin-2 is a 450 kDa trimeric matricellular protein that is highly expressed by mesenchymal lineage cells in bone, but not hematopoietic cells. Previous studies by our group have shown that thrombospondin 2 (TSP2) regulates marrow stromal cell (MSC) proliferation. When TSP2 is knocked out (TSP2-null) there is an increase in MSC number. Furthermore, TSP2-null mice examined at four months of age show increased endocortical bone formation and a reduction in marrow area. The purpose of this study was to assess the influence of TSP2 on the MSC pool and bone geometry in relationship to aging. Femurs and tibias were removed from wild type and TSP2-null mice, aged 14 and 20 months. Total bone marrow was extracted from one femur and tibia and plated for CFU-F assay. At 14 months there was a surprising reduction in the relative CFU-F number in the TSP2-null mice, but the TSP2-null mice show a 2-fold increase in total marrow cell number relative to wild type (WT). At 20 months of age the total marrow cell number in TSP2-null mice was actually less than the WT, but the relative CFU-F increased, suggesting that TSP2 regulates the MSC pool in an age-dependent manner. Next, microcomputerized tomography was used to assess bone geometry. In earlier experiments, we observed that bones of younger mice consistently show increased cortical thickness and reduced marrow area due to endocortical bone formation. In this study, at 14 months of age, the TSP2-null mice have an increased marrow area, because of endocortical expansion, as well as increased periosteal circumference when compared to WT mice. 20-month-old TSP2-null mice continued to demonstrate periosteal and endocortical expansion, but at this age, TSP2-null and TSP2 expressing mice exhibited similar geometric properties in bone. We conclude that TSP2 regulates the MSC pool in an age-dependent manner which corresponds to changes in bone geometry. TSP2-null mice have significant endocortical resorption, greater than WT mice, that occurs from 4 months to 14 months of age, with a concomitant decrease in CFU-F concentration. However, CFU-F concentration increases from the period of 14 to 20 months, and endocortical bone changes are equivalent during this period. Importantly, our results also show that TSP2 may influence hematopoietic cells in the marrow environment. There is two-fold increase in TSP2-null total marrow cells at 14 months relative to WT, but a reduction at 20 months. We propose that TSP2, produced by MSC in the marrow, could be an additional matricellular component of the HSC niche.

**Disclosures:** S.P. Terkhorh, None.

## 1250

**Endogenous Glucocorticoids Are Critical for the Development of Skeletal Fragility with Aging in Mice.** R. S. Weinstein, C. A. O'Brien, P. K. Roberson<sup>\*</sup>, S. C. Manolagas. Center for Osteoporosis and Metabolic Bone Diseases, University of Arkansas for Medical Sciences and Central Arkansas Veterans Healthcare System, Little Rock, AR, USA.

The adverse skeletal effects of hyperglucocorticoidism in humans and mice are well known, but far less is known of the contribution of glucocorticoids to the aging skeleton. Nonetheless, the decline in bone strength is disproportionately greater than the loss of bone mass with both glucocorticoid excess and aging. In addition, both conditions decrease bone vascularity and interstitial fluid volume. To establish whether endogenous glucocorticoids contribute to the development of skeletal fragility with aging, we searched for and found that aging increased serum corticosterone levels, adrenal weight and 11 $\beta$ -hydroxysteroid dehydrogenase type 1 expression (the enzyme that amplifies glucocorticoid activation) in murine bone and that dehydration compromised the resistance to deformation and energy required to break bones in young but not old mice. Next, we determined the impact of aging in transgenic mice overexpressing 11 $\beta$ -hydroxysteroid dehydrogenase type 2 (the enzyme that inactivates glucocorticoids) under the control of the osteocalcin promoter (OG2-11 $\beta$ -HSD2 mice), a model for deflecting glucocorticoid action from osteoblasts and osteocytes. At 21-months-of-age, vertebral and femoral strength were 18 to 19% greater in the OG2-11 $\beta$ -HSD2 mice when compared to the wild-type animals (WT) ( $p < 0.05$ ). In addition, the decrease in vertebral BMD observed between 16 and 21 months-of-age in the WT controls was less in the OG2-11 $\beta$ -HSD2 mice (-6.3% vs. -0.2%,  $p < 0.04$ ). Moreover, the OG2-11 $\beta$ -HSD2 mice had 9% more femoral BMD at 21-months-of-age than the WT animals. Bone volume and trabecular number in the vertebrae (as measured by  $\mu$ CT) were 10 to 16% greater and trabecular spacing was 13% lower in the OG2-11 $\beta$ -HSD2 mice than in the WT animals ( $p < 0.03$ ). The OG2-11 $\beta$ -HSD2 mice also demonstrated a 57 to 47% lower prevalence of osteoblast and osteocyte apoptosis when compared with WT animals ( $p < 0.02$ ). Furthermore, osteocyte-lacunar-canalicular fluid volume (as determined by quantitative epifluorescence of Procion Red injected into a tail vein) and vascular volume and surface area in the vertebrae and femora (as determined by  $\mu$ CT imaging of bones perfused with lead chromate) were 74 to 115% greater in the OG2-11 $\beta$ -HSD2 mice than in the WT animals ( $p < 0.02$ ). The attenuation of the adverse effects of age on bone strength, mass, cancellous architecture, osteoblast and osteocyte apoptosis, osteocyte-lacunar-canalicular fluid volume and vasculature in the 21-month-old OG2-11 $\beta$ -HSD2 mice strongly suggests that age-related hyperglucocorticoidism compromises bone strength, at least in part, through decreased bone fluid volume.

**Disclosures:** R.S. Weinstein, None.

## 1251

**Calorie Restriction Prevents Age-Related Trabecular Bone Loss via SIRT-1.** J. R. Edwards<sup>1</sup>, S. T. Lwin<sup>\*1</sup>, J. S. Nyman<sup>1</sup>, E. C. O'Quinn<sup>\*1</sup>, K. Zainabadi<sup>\*2</sup>, S. A. Munoz<sup>\*1</sup>, L. Guarente<sup>\*2</sup>, G. R. Mundy<sup>1</sup>. <sup>1</sup>Center for Bone Biology, Vanderbilt University Medical Center, Nashville, TN, USA, <sup>2</sup>Dept of Biology, MIT, Cambridge, MA, USA.

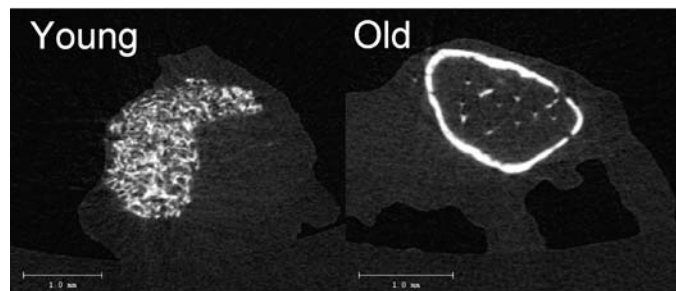
Calorie restriction (CR) increases lifespan in a variety of organisms including yeast, worms and flies. This effect is mediated by the longevity gene, Sir2. CR also prolongs lifespan in rodents and is associated with increased expression of the mammalian homologue of Sir2, SIRT-1. We have found that mice deficient in SIRT-1 have a low bone mass phenotype. Accordingly, we hypothesized that CR may enhance bone mass in mice via stimulatory effects on SIRT-1. To test this, we examined the effects of CR (~60% normal diet) under two circumstances, firstly in mice 16mths old after 4 mths CR, and secondly in mice 12 mths old after 8 mths CR (n=10). Cortical and trabecular bone mass was assessed by uCT scanning and histomorphometric analysis of undecalcified lumbar vertebrae and decalcified long bones. We found that aged mice subjected to CR were considerably leaner at  $23.4g \pm 1.1$  compared to AL-fed controls ( $31.9g \pm 1.5$ ,  $p < 0.001$ ). Consistent with the effects of CR to enhance SIRT-1 expression, CR-fed animals had a significantly higher total Bone Mineral Density (mg HA/ccm) at  $185.7 \pm 11.5$  compared to  $140.3 \pm 6.0$  in AL-fed controls ( $p < 0.01$ ). This corresponded with a significantly higher trabecular BV/TV in the CR mice ( $10.8\% \pm 0.4\%$  compared to  $6.7\% \pm 0.5\%$ ,  $p < 0.0001$ ), with no significant change in cortical bone. Next we determined whether these effects were dependent on SIRT-1. Mice lacking the SIRT-1 gene are significantly leaner than WT control animals ( $20.2g \pm 0.9$  compared to  $37.0g \pm 1.9$  respectively,  $p < 0.001$ ). In addition, SIRT-1 KO mice have a profound decrease in BMD (46%) and BV/TV (44%) compared to WT mice, along with a dramatic thinning of trabeculae ( $31.7\mu m \pm 1.5$  compared to  $63.2\mu m \pm 3.4$  respectively,  $p < 0.001$ ). However, SIRT-1 KO mice placed on a CR diet failed to demonstrate any retention of trabecular bone mass compared to AL-fed SIRT-1 KO animals. These studies describe the profound effects of a CR diet on bone mass, and indicate that part of this effect is dependent on the longevity-associated gene, SIRT-1.

**Disclosures:** J.R. Edwards, None.

## 1252

**Bone Marrow Stromal Cell Aging Directly Alters Bone Formation.** B. M. Boudignon, F. Lima<sup>\*</sup>, A. J. Gong<sup>\*</sup>, B. P. Halloran. Endocrine unit, Veteran Affairs Medical Center San Francisco, San Francisco, CA, USA.

Age-related or senile osteoporosis is characterized by a marked decrease in bone formation and disruption of the normal balance between bone formation and resorption. The changes in bone that occur with aging reflect autonomous changes in the BMSCs as well as changes in the systemic and marrow micro-environments which feedback to indirectly regulate BMSC activity. To begin to dissect out the autonomous and non-autonomous effects of aging on BMSC function, we implanted BMSC from animals of different ages into a common host. This normalized the systemic and marrow environments permitting us to focus on the effects of age on the ability of BMSC to form bone in vivo. BMSCs from young (6 weeks), adult (6 months) and old (22 months) C57Bl/6J mice were cultured for 10 days, harvested and implanted sub-cutaneously in collagen sponges (Gelfoam) in nude mice. After 2 months the sponges formed mineralized structures (ossicles). These were collected and examined using microCT analysis and histomorphometry. The morphology of the ossicles varied dramatically across age. Cells from young animals produced randomly distributed calcium deposits with little or no structure. Cells from old animals produced cortical bone-like shells surrounding a marrow cavity containing hematopoietic components and adipocytes. The cortical shell and marrow cavity were well vascularized and trabecular-like structures were found throughout the core. Active bone formation on trabeculae and on the inside (endocortical) surface of the shell was observed. Osteocytes were found throughout the cortical and trabecular bone. Cells from adult animals produced partial shell-like structures (old phenotype) along with regions of randomly distributed calcium deposits (young phenotype). Our data suggest that aging has a dramatic effect on the autonomous ability of BMSCs to form bone in vivo. This supports the idea that senescent changes in the mesenchymal stem cells contribute to the changes in bone associated with aging.



**Disclosures:** B.M. Boudignon, None.

## 1253

**Availability of Cytoplasmic  $\beta$ -Catenin Impacts Mechanical Signaling in Osteoblasts.** N. Case<sup>1</sup>, M. Ma<sup>\*1</sup>, B. Sen<sup>\*1</sup>, Z. Xie<sup>\*1</sup>, T. S. Gross<sup>2</sup>, J. Rubin<sup>1</sup>. <sup>1</sup>Medicine, UNC, Chapel Hill, NC, USA, <sup>2</sup>Orthopaedics, U. Washington, Seattle, WA, USA.

$\beta$ -catenin signaling is implicated in propagating the effects of mechanical loading on bone anabolism.  $\beta$ -catenin is found in membrane-bound and soluble cytoplasmic pools, suggesting compartmentalized roles. Tonic phosphorylation of  $\beta$ -catenin by GSK3 $\beta$  promotes degradation, decreasing cytoplasmic  $\beta$ -catenin under resting conditions. Here we compared the interrelated effects of GSK3 $\beta$  inactivation, membrane sequestration by caveolin-1 and mechanical strain on  $\beta$ -catenin signaling in CIMC-4 pre-osteoblast cells. LiCl treatment was first used to inactivate GSK3 $\beta$  causing cytoplasmic levels of active (dephospho) and total  $\beta$ -catenin to increase as expected. This was reflected by increased TopFlash  $\beta$ -catenin reporter activity ( $164 \pm 28\%$  of control) and upregulation of the  $\beta$ -catenin target gene WISP1 to  $183 \pm 13\%$ . We next established that alteration of caveolin-1, a membrane protein known to sequester  $\beta$ -catenin, affected  $\beta$ -catenin signaling. siRNA targeting caveolin-1 (siCav) increased cytoplasmic  $\beta$ -catenin levels, and Topflash activity was doubled in cells transfected with siCav compared to control siRNA transfected cells. Conversely, overexpression of caveolin-1 decreased  $\beta$ -catenin levels. Knockdown of caveolin-1 and LiCl had additive effects on  $\beta$ -catenin signaling: inhibition of GSK3 $\beta$  with LiCl increased TopFlash activity by ~3-fold in siCav transfected cells. Both of these independent regulators of  $\beta$ -catenin signaling further influenced mechanical control of  $\beta$ -catenin activation. Mechanical strain (2%, 0.17Hz) stimulated a rapid, transient  $\beta$ -catenin response. Active  $\beta$ -catenin translocated to the nucleus by 15 min, causing upregulation of WISP1 at 4 h ( $165 \pm 5\%$  of control). Total  $\beta$ -catenin protein was increased at 1 h and temporally followed a strain associated inactivation of GSK3 $\beta$ . Strain-induced  $\beta$ -catenin translocation was not sufficient to cause enhanced TopFlash activity but when LiCl was present, strain increased TopFlash activity ( $188 \pm 33\%$  of LiCl alone). Thus, a transient mechanical signal causing activation of  $\beta$ -catenin could be amplified by a state of decreased  $\beta$ -catenin turnover. Knockdown of caveolin-1 also enhanced the strain response: strain upregulation of WISP1 was absent in cultures treated with control siRNA, but strain-induced WISP1 was significantly increased in siCav treated cultures. In summary, alteration of  $\beta$ -catenin availability through decreased degradation or sequestration enhanced the ability of mechanical input to stimulate  $\beta$ -catenin signaling. These independent effects thus can combine to promote  $\beta$ -catenin action. This suggests that effects of exercise on the skeleton should be enhanced by strategies that increase the availability of cytoplasmic  $\beta$ -catenin.

**Disclosures:** N. Case, None.

This study received funding from: NIAMS NIH.

## 1254

**Deletion of the G Protein Subunit  $G\alpha$  in Early Osteoblasts Leads to Accelerated Osteoblast Maturation and Formation of Woven Bone with Abnormal Osteocytes, Resulting in Severe Osteoporosis.** J. Y. Wu<sup>1</sup>, C. Maes<sup>1</sup>, M. Chen<sup>\*2</sup>, L. S. Weinstein<sup>\*2</sup>, H. M. Kronenberg<sup>1</sup>. <sup>1</sup>Endocrine Unit, Massachusetts General Hospital, Boston, MA, USA, <sup>2</sup>Metabolic Diseases Branch, National Institute of Diabetes and Digestive and Kidney Diseases, Bethesda, MD, USA.

$G\alpha$  is a heterotrimeric G protein subunit which mediates cyclic-AMP-dependent signaling downstream of G protein-coupled receptors, including the parathyroid hormone (PTH)/PTH-related peptide (PTHrP) receptor (PPR). Deletion of  $G\alpha$  early in the osteoblast lineage in Osterix-Cre; $G\alpha$ (fl/fl) mice leads to severe osteoporosis with fractures at birth, the result of a low turnover state characterized by failure of bone formation and the abnormal persistence of woven bone. Markedly reduced expression of the terminally differentiated osteoblast marker osteocalcin suggested an impairment of osteoblastic maturation; however, primary calvarial osteoblasts isolated from mutant mice demonstrate accelerated mineralization when cultured under osteogenic conditions. Consistent with enhanced osteoblast maturation in vivo,  $G\alpha$  conditional knockout mice exhibit thicker cortical bone throughout late embryogenesis. Osteocytes, derived from mature osteoblasts embedded in mineralized matrix, are present at significantly increased density in mutant mice. However, the osteocytic canalicular network is disrupted in mutant mice, and transmission electron microscopy reveals abnormal morphology of mutant osteocytes. These findings confirm that mice lacking  $G\alpha$  in osteoblasts fail to produce lamellar bone. Furthermore, expression of characteristic osteocyte genes is disturbed in the mutant mice. Expression of E11, a protein normally localized to early osteocytes along the endosteal or periosteal surface, is found throughout the thickness of cortical bone. In addition, expression of Sost mRNA, a marker of late osteocytes that encodes the protein sclerostin and is suppressed by continuous PTH administration, is markedly increased in mutant mice. These results suggest that in the absence of  $G\alpha$ , osteoblast maturation may be pathologically accelerated, leading to the formation of exclusively woven bone with extreme fragility. Other consequences of the lack of  $G\alpha$  signaling, such as suppressed osteocalcin and enhanced Sost expression, may also contribute to abnormal bone structure and function.

**Disclosures:** J.Y. Wu, None.

This study received funding from: NIAMS.



## 1255

**Endogenous  $G_i$  Signaling in Osteoblasts Negatively Regulates Cortical Bone Formation.** S. M. Millard<sup>1</sup>, A. Louie<sup>\*1</sup>, C. Manalac<sup>\*2</sup>, W. Lu<sup>\*1</sup>, N. Cotte<sup>\*2</sup>, B. Boudignon<sup>1</sup>, B. P. Halloran<sup>1</sup>, B. Conklin<sup>\*2</sup>, R. A. Nissenson<sup>1</sup>.<sup>1</sup>Endocrine Research Unit, VA Medical Center, San Francisco, CA, USA,<sup>2</sup>Gladstone Institutes, University of California, San Francisco, CA, USA.

We have recently shown that expression of an engineered  $G_i$  coupled receptor under control of the Collagen I alpha 2.3 kb promoter results in severe trabecular osteopenia, yet little is known about the physiological role of endogenous  $G_i$  signaling in osteoblasts. In this study, we have investigated the skeletal effects of blocking  $G_i$  signaling in osteoblasts *in vivo*. This was accomplished by transgenic expression in osteoblasts of the catalytic subunit of pertussis toxin (PTX), which inhibits receptor-mediated activation of  $G_i$  signaling. Mice expressing PTX in osteoblasts under the control of the Collagen I alpha 2.3kb promoter were significantly smaller at weaning. These mice grew faster than their littermates immediately following weaning and maintained body weights at 85% of their littermate controls from 8wks of age (8wk males: 25.1±1.0 vs 29.0±0.2 gm, p<0.05; 8wk females: 21.1±0.4 vs 24.1±0.4 gm, p<0.001). MicroCT analysis of the femoral midshaft showed that despite their smaller stature the transgenic animals have an 8-12% increase in cortical bone volume (12wk males: 0.41±0.03 vs 0.36±0.01 mm<sup>3</sup>, p<0.05; 12wk females: 0.35±0.04 vs 0.32±0.01 mm<sup>3</sup>, p<0.05). The medullary volume was significantly reduced (by 22-28%), while total cortical volume at this site showed a non-significant trend to be reduced (by 6-10%). Col1(2.3):PTX transgenic mice displayed increased serum levels of osteocalcin, a marker of bone formation. Serum levels of pyridinolines, a marker of bone resorption, were unchanged. Furthermore, the expression ratio of RANKL:OPG, an important determinant of osteoclastogenesis, was found to be unchanged in RNA isolated from the tibiae of Col1(2.3):PTX mice. Together these data imply that increased cortical bone volume in the osteoblast-specific Col1(2.3):PTX transgenic mice results from increased cortical bone formation. Cancellous bone in the secondary spongiosa of the distal femur was also analyzed by microCT. Although data did not show any change in fractional bone volume (BV/TV) we found significant changes in structural indexes of the trabecular network. Mice expressing PTX in osteoblasts showed increased trabecular number and connectivity density associated with a reduced trabecular thickness. The present results indicate that signaling by endogenous  $G_i$ -coupled receptors in osteoblasts plays an important role in restraining endocortical bone formation and in modulating trabecular bone structure.

**Disclosures:** S.M. Millard, None.

This study received funding from: NIH.

## 1256

**Wnt/LRP5-Independent Inhibition of Osteoblastic Cell Differentiation by Sclerostin.** J. Caverzasio. Service of Bone Diseases, Dept of Rehabilitation and Geriatrics, University of Geneva, Geneva, Switzerland.

Bone diseases associated with mutations or deletions in the Sost gene indicate that sclerostin (SCT) is a major regulator of bone formation. SCT is a member of the DAN family of glycoproteins that shares the capacity to inhibit BMP activity but studies in osteoblasts indicated that SCT is not a classical BMP antagonist. Recent reports documented that SCT antagonizes canonical Wnt signaling by binding to the Wnt coreceptor low protein receptor-related protein 5 (LRP5). These studies have been performed in either *Xenopus* embryos or HEK293 cells transfected with plasmids encoding proteins of interest. So far, however, a direct antagonistic effect of SCT on activation of LRP5/6 by Wnts in osteoblastic cells has not been yet documented.

In the present study, we confirmed that SCT (2.5-10 µg/ml) inhibits alkaline phosphatase activity induced by either BMP-2 in MC3T3-E1 cells or by Wnt3a and BMP-2 in C3H10T1/2 cells (-40% to -60%). In C3H10T1/2 cells, SCT also decreased matrix mineralization induced by either BMP-2 (-60%) or Wnt3a (-50%). Surprisingly, however, a similar inhibitory effect of SCT (-80%) was also observed on matrix mineralization induced by the selective GSK3β inhibitor, SB216763, acting downstream of the Wnt/LRP5/6 receptor. In C3H10T1/2 cells, Wnt3a induced a time related increase in phosphoLRP5/6 (activated LRP5/6) that was maximal after 15 min and maintained for several hours. This effect preceded cytosolic accumulation of β-catenin at 6 h and 24 h measured by Western blot. Whereas DKK1 (2.5 µg/ml) completely blunted activation of LRP5/6, SCT had no effect on this response. In this analysis, we noted an early and transient activation of ERK1,2 by SCT. Therefore, we studied whether SCT can trigger activation of signaling molecules in MC3T3-E1 and C3H10T1/2 cells. Interestingly, in both cell lines, SCT rapidly and transiently (5'-60') activated Akt (4-5x), PKC (5-6x) and ERK1,2 (6-7x) suggesting activation of a receptor system. Studies are in progress to determine the receptor activated by SCT and its role in regulating osteoblastic cell differentiation.

In conclusion, this study failed to document an antagonistic effect of SCT on activation of LRP5/6 in response to Wnt3a in osteogenic cells. Moreover, inhibition of osteoblastic cell differentiation induced by SCT was observed in absence of activation of the Wnt/LRP5 receptor when β-catenin was activated by a selective GSK3β inhibitor. Finally, we found that SCT can activate receptor signaling pathways in osteoblastic and mesenchymal cells. These observations strongly suggest that in osteoblastic cells, SCT may activate a receptor system that negatively regulates osteoblastic cell differentiation induced by BMPs and Wnts.

**Disclosures:** J. Caverzasio, None.

## 1257

**Critical Role of Connexin43 (Cx43) in Postnatal Skeletal Growth and Bone Mass Acquisition.** M. P. Watkins<sup>1</sup>, S. Grimston<sup>1</sup>, D. Ornitz<sup>\*2</sup>, R. Civitelli<sup>1</sup>.<sup>1</sup>Bone and Mineral Diseases, Washington University in St Louis, St Louis, MO, USA, <sup>2</sup>Molecular Biology and Pharmacology, Washington University in St Louis, St Louis, MO, USA.

Cx43 is the major gap junction protein expressed in osteoblasts and osteocytes. Mice with conditional ablation of the Cx43 gene (*Gjal*) in mature osteoblasts and osteocytes - obtained using Cre driven by the 2.3kb fragment of the  $\alpha_1(I)$  collagen promoter (*ColCre;Gjal<sup>-/-</sup>*; *ColcKO*) - develop a lower than normal peak bone mass, but have no major skeletal malformations. However, craniofacial abnormalities are present in *Gjal* null mice and in oculodentodigital dysplasia, caused by loss of function *Gjal* mutations. To gain further insights on the cellular defects brought about by *Gjal* deficiency, we have used the *Dermol* promoter, which is active during embryogenesis, to ablate *Gjal* in osteochondroprogenitor cells (*DM1-Cre;Gjal<sup>-/-</sup>*; *DM1cKO*). We have previously reported that *DM1cKO* mice are more severely osteopenic than are *ColcKO*, but they also exhibit stunted postnatal growth, with >10% shorter long bones relative to wild type (WT) littermates. Consistent with decreased BMD we observed a 57±12% decrease in trabecular bone and a 62±11% decrease in cortical thickness by histomorphometry. Growth plate width was also significantly decreased in *DM1cKO* mice (34±10% of WT), with an apparent decrease in proliferating and hypertrophic chondrocytes, consistent with the short *DM1cKO* limb bones. Further  $\mu$ CT analysis confirmed decreased cortical thickness (84±7%) as well as a significantly larger marrow area (169±26%) in the *DM1cKO* compared to wildtype (WT) litter mates. However, no differences were observed in either static (osteoblast and osteoclast number per bone surface) or dynamic bone formation indices (mineral apposition or bone formation rate) in *DM1cKO* relative to WT litter mates. *In vitro* analysis of bone marrow progenitor cells using colony forming unit (CFU) assays revealed an unexpected 57±11% increase in CFU-fibroblast in *DM1cKO* compared to WT, and a similar increase in CFU-osteoblast (57±17% of WT). *Gjal* ablation in *DM1cKO* CFUs was confirmed by β-galactosidase staining. This increase in uncommitted and osteogenic bone marrow precursors may represent a compensatory mechanism that partially offsets an osteoblast differentiation defect consistently reported in *Gjal* deficiency. Our results also suggest that Cx43 is involved in both longitudinal bone growth, through an effect on growth plate chondrocytes, and in postnatal acquisition of normal bone mass and microarchitecture, via modulation of osteoblast differentiation.

**Disclosures:** M.P. Watkins, None.

This study received funding from: NIH AR041255.

## 1258

**Overexpression of Lef1ΔN Increases Bone Mass in Mice.** F. Secreto\*, L. H. Hoepfner\*, B. Stensgard\*, G. Evans\*, T. E. Hefferan, M. J. Yaszemski, J. J. Westendorf. Department of Orthopedic Surgery, Mayo Clinic, Rochester, MN, USA.

Activation of the canonical Wnt/beta-catenin pathway facilitates osteoblast specification from mesenchymal progenitors and enhances bone mass and strength. One unanswered question is how does canonical Wnt signaling promote proliferation of immature osteoblasts, but not expansion of mature osteoblasts and osteocytes, while at the same time promoting survival of these mature and terminally differentiated cells. Our preliminary data suggest that these stage-specific responses could in part be mediated by different isoforms of lymphoid enhancer binding factor-1 (Lef-1). Lef1 is a member of the T-cell factor family of transcription factors responsible for regulating Wnt-dependent gene expression. We previously reported that Lef1 protein levels decline with osteoblast maturation. We recently discovered that a naturally occurring N-terminal truncated isoform of Lef-1, called Lef1ΔN, increases significantly in MC3T3 cells and primary calvarial osteoblasts (COB) prior to osteocalcin gene expression. Because the expression profile of Lef1ΔN suggested that this transcription factor might contribute to terminal osteoblast differentiation, we developed transgenic mice expressing Lef1ΔN in a tissue-specific manner under the control of the (2.3)Col1a1 promoter. The FLAG-tagged Lef1ΔN was only detected in RNA isolated from calvaria and brain, with calvarial expression being 10-fold higher than in the brain. Primary COB cultures derived from neonatal mice carrying the Lef1ΔN transgene had increased expression of collagen 1α1 and bone sialoprotein RNAs as compared to cultures derived from wild-type mice. Additionally, the number of alizarin-positive nodules present in Lef1ΔN transgene-positive COB cultures was greater than in wild-type COB cultures. Micro-CT analyses of trabecular bone revealed that Lef1ΔN transgenic mice (as compared to wild-type controls) have increased bone volume density (Tibia: +9.44%, Femur: +7.92%), increased trabecular number (Tibia: +7.64%, Femur: +5.77%), and decreased trabecular separation (Tibia: -8.18%, Femur: -6.81%). No sex-linked differences were observed; however, the Lef1ΔN-dependent increases in bone parameters were lost in all mice following sexual maturation. Lef1ΔN retains a low-affinity beta-catenin binding domain and activates Lef1 responsive promoters *in vitro*, but at a 10-fold lower rate than full-length Lef1. In contrast to full-length Lef1, Lef1ΔN does not block Runx2-dependent activation of the osteocalcin promoter. Together these data suggest that Lef1ΔN promotes bone mass accrual and that the isoform switch from Lef1 to Lef1ΔN is crucial for proper osteoblast differentiation.

**Disclosures:** J.J. Westendorf, None.

This study received funding from: NIAMS AR50074.

## 1259

**TRIP-1 is eIF3i: A Key Regulator of Osteoblast Activity.** D. M. Metz-Estrella\*, T. Sheu\*, J. Puzas. Orthopaedics, University of Rochester, Rochester, NY, USA.

The overall control of bone formation by osteoblasts requires regulation of both gene expression for the control of cell number and protein synthesis for the control of cell activity. Numerous bone-related diseases such as osteomalacia, rickets, calcium deficiency, etc are characterized by increased numbers of osteoblasts yet the rate of new bone formation is very slow due to the inactivity of the cells themselves. Thus, control over the translation of structural and regulatory proteins in osteoblasts must play an important role. In this regard, translation initiation factors would be a central point of focus for regulating bone formation. eIF3 is a translation initiation factor complex of 750 kDa. The "i" subunit of eIF3 (i.e. eIF3i) shares identity with TRIP-1 (TGFbeta-Receptor-Interacting-Protein-1), a protein discovered to interact with tartrate resistant acid phosphatase (TRAP). The TRIP-1/TRAP interaction regulates the activity of osteoblasts within the resorption lacunae. Our hypothesis is that up-regulation of TRIP-1 will increase the overall synthetic pathways of osteoblasts and increase bone formation.

In order to explore this hypothesis, we performed in vitro protein:protein interaction experiments and cell culture assays to evaluate bone formation markers in osteoblasts. We have also created a doxycycline-inducible tissue-specific transgenic mouse that over expresses TRIP-1 in osteoblasts. These animals were analyzed with micro CT methodology.

Our results indicate that TRIP-1 is phosphorylation target of the TGFbeta receptor and that it has strong binding affinity for the MH1 domain of Smad3. Together, this complex can translocate into the nucleus. Perhaps more importantly, TRIP-1 can also be phosphorylated by mTOR, a central kinase in the regulation of energy utilization and protein translation. TRIP-1-transfected osteoblasts show little change in proliferation, however, mice treated with doxycycline to induce TRIP-1 show an increase in skeletal parameters. That is, preliminary experiments demonstrate that mice, when treated with doxycycline for three weeks, show a 48% increase in total bone volume; a 45% increase in bone volume/total volume; a 10-15% increase in trabecular number and trabecular thickness and a 60% increase in connectivity.

Our data support the hypothesis that the TGFbeta pathway, and perhaps other Smad-dependent pathways, can regulate post-transcriptional activity of osteoblasts. The molecular intermediate we have examined, i.e. TRIP-1, is perfectly positioned to participate in both transcriptional and translation regulation of osteoblast activity. Studying these processes as separate, yet coordinated, regulators of bone formation may provide a molecular explanation for the tissue-level changes seen in some bone diseases.

**Disclosures:** J. Puzas, Novartis 1; Lilly 1; Merck 1.

## 1260

**An Evaluation of Circulating Osteoprogenitor Cells During Fracture Healing Using Parabiotic Mice.** T. Barisic-Dujmovic\*, D. J. Adams\*, L. Wang\*, S. H. Clark\*. <sup>1</sup>Genetics and Developmental Biology, University of Connecticut, Farmington, CT, USA, <sup>2</sup>Department of Orthopaedic Surgery New England Musculoskeletal Institute, University of Connecticut, Farmington, CT, USA, <sup>3</sup>Department of Reconstructive Sciences, University of Connecticut, Farmington, CT, USA.

Osteoprogenitors are mesenchymal cells localized in the bone. Recent studies have suggested the existence of osteoblastic precursor cells in the circulation, but the origin of these cells in vivo is not clear. Parabiotic pairs of pOBcol2.3GFPcyan (a marker of mature osteoblasts and osteocytes) and pOBcol3.6GFPtopaz (expressed in preosteoblasts and osteoblasts) transgenic mice were created to determine if osteoblastic cells originating from one parabiont can home to a bone fracture site created in the other parabiont. Utilizing two different GFP isoforms (topaz and cyan) permits microscopic visualization of both transgene reporters within the same animal using fluorescence-specific filters.

Parabiotic pairs of mice were created by surgically joining two transgenic mice; one mouse carried the pOBcol2.3GFPcyan transgene while its partner carried the pOBcol3.6GFPtopaz transgene. Four weeks after parabiosis surgery a transverse fracture of the tibia was created in one parabiont with a blunt guillotine after an intramedullary pin had been placed in the bone. Two different sets of experiments were conducted. In the first set, the tibial fracture was created in the pOBcol3.6GFPtopaz parabiont. Samples from the fractured bone, as well as from the contra lateral bone, were examined for pOBcol2.3GFP transgene expression at time points ranging from day 14 to day 50 post-fracture. Microscopic analyses have shown no evidence of pOBcol2.3GFP transgene expression in the fracture callus or other long bones isolated from the pOBcol3.6GFPtopaz parabiont. In the second set of experiments, the tibial fracture was created in the pOBcol2.3GFPcyan parabiont. Bone samples from the fractured tibia were examined for pOBcol3.6GFPtopaz transgene expression. A weak GFP signal indicating the presence of cells bearing the pOBcol3.6GFPtopaz transgene was detected on the trabecular surfaces of the fracture callus isolated from the pOBcol2.3GFPcyan parabiont. These GFP positive cells were also present in the other long bones of the pOBcol2.3cyan parabiont. However, these pOBcol3.6GFPtopaz positive cells were not osteoblasts, as they did not deposit bone matrix and were positive for TRAP expression based on a fluorescence-based ELF97 TRAP staining assay. This cellular phenotype of the GFP+ engrafted cells is consistent with a myeloid lineage, specifically osteoclasts. This study demonstrated that circulating osteoprogenitor cells do not home physiologically to the fractured bone.

**Disclosures:** T. Barisic-Dujmovic, None.

## 1261

**Tissue-specific Knockout (KO) of the Ca<sup>2+</sup>-sensing Receptor (CaSR) in Chondrocytes Inhibits IGF1 Signaling and Delays Differentiation in the Growth Plate.** C. Tu\*, H. Elalich\*, T. Chen\*, D. Shoback, D. Bikle, W. Chang. Endocrine Unit, VA Medical Center, University of California San Francisco, San Francisco, CA, USA.

Raising the extracellular [Ca<sup>2+</sup>] ([Ca<sup>2+</sup>]<sub>e</sub>) promotes the terminal differentiation of cultured growth plate chondrocytes (GPCs) potentially by activating the CaSR. To examine the role of the CaSR in growth plate development in vivo, we generated cartilage-specific CaSR KO (CaSR<sup>lox/lox</sup>) mice using Cre/lox recombination by breeding floxed-CaSR (CaSR<sup>lox/lox</sup>) mice with transgenic (Tg) mice expressing Cre driven by a Col(II) promoter [JBM 22 (Suppl 1): S50, 2007]. The homozygous KO is embryonic lethal. Because of the death of CaSR<sup>lox/lox</sup> embryos in utero before embryonic stages E12-13, we generated a tamoxifen (Tam)-inducible KO model to study the role of CaSRs in late embryonic and postnatal development. CaSR<sup>lox/lox</sup> mice were bred with Tg <sup>Cre-ER</sup><sup>Tam</sup> mice which express cDNA encoding a fusion protein (Cre-ER<sup>Tam</sup>) containing Cre and a mutated ligand-binding domain of the estrogen receptor conferring Tam sensitivity. The Cre-ER<sup>Tam</sup> is controlled by a mouse Col(II) promoter for cartilage-specific expression. Homozygous <sup>Cre-ER</sup><sup>Tam</sup>/CaSR<sup>lox/lox</sup> mice are viable and fertile. A single maternal injections of 4OH-Tam 2-3 days before birth induced excision of CaSR gene in <sup>Cre-ER</sup><sup>Tam</sup>/CaSR<sup>lox/lox</sup> neonates. Immunohistochemistry and quantitative (q) PCR confirmed a marked reduction in CaSR protein and RNA expression, respectively, in growth plates from <sup>Cre-ER</sup><sup>Tam</sup>/CaSR<sup>lox/lox</sup> mice vs controls not injected with Tam or not containing Cre. Histology of cartilage sections from <sup>Cre-ER</sup><sup>Tam</sup>/CaSR<sup>lox/lox</sup> growth plates revealed 20% expansion of the hypertrophic zone and decreased mineralization in that zone. qPCR analyses of RNAs from the epiphyseal growth plates of the KO mice demonstrated decreased expression of type X collagen, RUNX2, and osteopontin -- markers of mature and terminally differentiated GPCs -- compared to controls. Expression of early differentiation markers -- aggrecan and type II collagen -- was unchanged, supporting a selective impact on chondrocyte maturation and terminal differentiation in the KO mice. There were also significant decreases in both RNA and protein levels for the IGF1 and IGF1 receptor (R) in growth plates from KO mice by qPCR and immunohistochemistry, respectively, suggesting that local IGF1/IGF1R signaling in GPCs might be reduced. This is supported by the observation that high [Ca<sup>2+</sup>]<sub>e</sub>-induced differentiation was significantly reduced in GPCs with IGF1Rs knocked-out in culture. This work demonstrates a critical role for CaSRs in growth plate development in vivo and an interaction between CaSR and IGF1/IGF1R signaling during GPC differentiation.

**Disclosures:** W. Chang, None.

This study received funding from: NIH-NIA/NIAMS/NIDDK.

## 1262

**ADAMTS-7, A Direct Targeting Molecule of PTHrP, Is a Novel Potent Mediator of Chondrogenesis.** X. Bai\*, D. Wang\*, Y. Luan\*, T. Kobayashi\*, H. M. Kronenberg\*, C. Liu\*. <sup>1</sup>New York University, New York, NY, USA, <sup>2</sup>Massachusetts General Hospital, Boston, MA, USA, <sup>3</sup>Massachusetts General Hospital, Boston, MA, USA.

We previously reported that ADAMTS-7, a metalloproteinase that belongs to ADAMTS family, was important for the degradation of cartilage oligomeric matrix protein (COMP) and its level was significantly elevated in arthritis (Liu, et al, *FASEB J.* 2006; 20(7):988). ADAMTS-7 contains a zinc catalytic domain followed by non-catalytic ancillary domains, including a disintegrin domain, a thrombospondin domain, a cysteine-rich domain, a spacer-1 domain, three thrombospondin motifs, a spacer-2 domain, and a C-terminal four thrombospondin motifs. Here we report the effects of these domains of ADAMTS-7 on the extracellular matrix interaction and proteolytic activities. The cysteine-rich domain was essential for ADAMTS-7 to interact with extracellular matrix. The weaker proteolytic activity was detected with the ADAMTS-7 catalytic domain alone and the sequential inclusion of each carboxyl-terminal domain influenced its activity against COMP. Our studies also suggest a critical role of ADAMTS-7 in chondrogenesis. Using RT-PCR and Western blotting assays, we showed that both mRNA and protein levels of ADAMTS-7 were upregulated during differentiation of chondrocytes. ADAMTS-7 significantly inhibited chondrogenesis, as revealed by mRNA levels of both early and later genes critical for chondrogenesis such as Sox9 (75% reduction), collagen type II (72% reduction), and collagen X (90% reduction) and Alcian blue staining. In addition, its inhibitory activity strictly depends on its enzymatic activity, since its point mutant lacking enzymatic activity failed to do so. To determine the potential mechanisms by which ADAMTS-7 negatively regulates chondrogenesis, we studied the effects of ADAMTS-7 on PTHrP/IHH signaling. ADAMTS-7 induced PTHrP 6- to 10-fold at all time points tested (day 3, 5, 7, 10) and inhibited IHH (45% reduction at day 7) during chondrogenesis. We further showed that PTHrP strongly induced mRNA and protein levels of ADAMTS-7 in chondrocytes. Importantly, knocking down ADAMTS-7 via the siRNA silencing or blocking ADAMTS-7 protein activity via anti-ADAMTS-7 antibodies almost abolished the effects of PTHrP on chondrogenesis in vitro. Using an immunohistochemistry assay, we showed that ADAMTS-7 was highly expressed in the proliferating and prehypertrophic chondrocytes of growth plates and that ADAMTS-7 was hardly detectable in PTHrP null growth plates at day E18.5 in vivo. Our findings demonstrate for the first time that ADAMTS-7, a downstream molecule of PTHrP in cartilage, is a novel negative regulator of chondrocyte differentiation.

**Disclosures:** C. Liu, None.

This study received funding from: NIH.

## 1263

**Expansion of Mesenchymal Progenitors in an *in vivo* Model of Constitutive Activation of the PTH/PTHrP Receptor.** M. Ohishi, L. E. Purton\*, E. Schipani. Massachusetts General Hospital, Boston, MA, USA.

Transgenic mice expressing constitutively active PTH/PTHrP receptors in osteoblasts (PPR\*Tg) show a considerable expansion of a stromal cell population in trabecular bone areas. A similar histological finding has also been described in hyperparathyroidism and in fibrous dysplasia in humans. In situ hybridization demonstrated that, differently from mature osteoblasts, PPR\*Tg stromal cells produce only modest amount of type I collagen mRNA, whereas osteocalcin mRNA is undetectable in these cells. In order to further characterize this population, PPR\*Tg mice were bred with transgenic mice that express green fluorescent protein (GFP) in mature osteoblasts but not in more immature cells (2.3kb Col1 GFP, kindly donated by Dr. Rowe UConn). Histological analysis of adult tibias isolated from PPR\*Tg/2.3kb Col1 GFP double mutant mice showed GFP accumulation in osteoblasts, but not in stromal cells. Collectively, these data indicate that PPR\*Tg stroma is enriched in immature cells at early stage of osteogenic differentiation. We thus investigated whether the stromal expansion observed in PPR\*Tg mice is associated to an increase in mesenchymal stem cells (MSCs)/progenitors. The number of CFU-Fs was significantly higher in the bone marrow (BM) isolated from 6-8 week old PPR\*Tg mice in comparison to controls, suggesting an expansion of the MSC/progenitor pool in mutants. Because CFU-Fs may include a heterogeneous population of cells, we explored the use of flow cytometry to identify MSCs/progenitors. The percentage of the BM Sca1+CD45-CD31- population, which has been reported to be enriched in MSCs/progenitors, showed no difference between control and PPR\*Tg. Since the specificity of CD45 as a marker of hematopoietic cells has been recently challenged, we then pursued a genetic approach, rather than the CD45/CD31 negative selection, to define BM mesenchymal cells by flow cytometry. Reporter mice expressing GFP upon excision of a stop cassette by Cre recombinase whose transcription was driven by the Prx1 mesenchymal enhancer (Prx1Cre/ZEG), were crossed with PPR\*Tg mice to generate PPR\*Tg/Prx1Cre/ZEG mice. Flow cytometry of BM cells isolated from PPR\*Tg/Prx1Cre/ZEG mice showed a dramatic increase in GFP-expressing cells when compared to controls (0.322±0.12% vs 0.0136±0.014%, p<0.01). Most of these GFP positive cells were also CD45 positive. More importantly, a subset of them expressed Sca1 and was significantly expanded in mutants. In summary, we have identified in the mouse BM a population that is likely of mesenchymal origin, expresses Sca1 and is expanded in PPR\*Tg. It will now be important to study whether this population differentiates *in vitro* into the various mesenchymal lineages.

**Disclosures:** M. Ohishi, None.  
This study received funding from: NIH.

## 1264

**Parathyroid Hormone Related Protein (PTHrP) Nuclear Localization Sequence and C-terminus Regulate Craniofacial Development.** C. M. Novince<sup>1</sup>, A. J. Koh\*<sup>1</sup>, H. A. Brown\*<sup>2</sup>, J. C. Hu\*<sup>1</sup>, T. J. Rosol<sup>2</sup>, L. K. McCauley<sup>1</sup>, R. E. Toribio\*<sup>2</sup>. <sup>1</sup>School of Dentistry, University of Michigan, Ann Arbor, MI, USA, <sup>2</sup>College of Veterinary Medicine, The Ohio State University, Columbus, OH, USA.

Parathyroid hormone related protein (PTHrP) plays an integral role in skeletal development, especially endochondral bone growth and tooth eruption, via intracrine, autocrine, and paracrine means. The PTHrP intracrine anti-apoptotic activity is mediated by a nuclear localization sequence (NLS) in the mid-region of the molecule. The purpose of this study was to determine the role of the PTHrP NLS and C-terminus in craniofacial development. Homologous recombination was used to knock-in (KI) full length PTHrP absent the coding region for amino acids 67-137 in mice. PTHrP KI mice and littermates were sacrificed at 2 days of age for tissue harvest. Skulls were imaged via micro-CT, and mandibles and vertebrae processed for histomorphometric analysis. Calvariae were digested and osteoblasts isolated for proliferation, and mineralization in culture. Spleens were dissociated and mononuclear cells analyzed for osteoclastogenesis. Femurs and tibiae were analyzed for gene expression via real time PCR, and cell populations via flow cytometry. The skulls of KI mice demonstrated doming of the cranium, and foreshortening and narrowing of the maxilla. Histologically, large islands of red blood cells were found in the bone marrow of KI mice. KI mandibles had reduced total bone area, reduced percent bone area, and fewer and more flattened trabeculae than wildtype (WT). KI mice had more TRAP+ osteoclastic cells per bone perimeter. Incisors of KI mice did not extend as far posteriorly in the body of the mandible, and KI molars had a haphazard cellular organization, decreased matrix accumulation, and abnormal cuspal formation. *In vitro*, PTHrP KI and WT calvarial osteoblasts were similar with respect to morphology, proliferation, and mineralization. KI and heterozygous (HET) spleen derived TRAP+ osteoclasts did not differ with respect to morphology or numbers. Interestingly, the bone marrow of KI mice had higher interleukin-6 expression versus WT, whereas PTH/PTHrP receptor expression was similar in WT and KI mice. The frequency of hematopoietic stem cells (Lin-Sca-1+c-Kit+ cells) showed a trend toward an increase in KI versus HET bone marrow. In summary, lack of the PTHrP NLS and C-terminus resulted in a severe skeletal phenotype characterized by reduced bone area, defective tooth development and altered hematopoietic marrow composition. The PTHrP 67-137 region appears to be a critical regulator of physiologic bone and tooth development. Additional cellular and molecular studies will further elucidate the roles and mechanisms of the PTHrP NLS and C-terminus in skeletal development.

**Disclosures:** C.M. Novince, None.

## 1265

**A Transcription Factor Znf219 Regulates Chondrocyte Differentiation Through Forming Transcription Factory Complex with Sox9.** Y. Takigawa<sup>\*1</sup>, K. Hata<sup>\*1</sup>, S. Muramatsu<sup>\*2</sup>, K. Amano<sup>\*1</sup>, K. Takada<sup>\*3</sup>, A. Matsuda<sup>\*2</sup>, R. Nishimura<sup>1</sup>, T. Yoneda<sup>1</sup>. <sup>1</sup>Biochem, Osaka Univ Grad Sch Dent, Osaka, Japan, <sup>2</sup>Asahi Kasei Pharma, Shizuoka, Japan, <sup>3</sup>Orthod, Osaka Univ Grad Sch Dent, Osaka, Japan.

Gene targeting approaches demonstrated that Sox9, an HMG-containing transcription factor, is necessary for chondrogenesis. Mutations of SOX9 gene in human result in Campomelic dysplasia characterized by severe chondrodysplasia. Sox9 regulates chondrogenic genes including type II (COL2a1) and XI collagen (COL11a2), and aggrecan by forming a molecular complex, namely transcription factory, with Sox5 and Sox6. Although these studies clearly indicate an essential role of Sox9 for chondrogenesis, molecular mechanism by which Sox9 regulates chondrogenesis is not fully understood. Especially, identification of the components of the Sox9 transcription factory has not been accomplished yet. As an approach to address this, we attempted to identify transcriptional partners of Sox9 and examine their functional roles in chondrocyte differentiation. We generated a full-length cDNA library from a chondrogenic cell line, ATDC5, and screened the cDNA library using the COL2a1 luciferase reporter construct. We isolated the Znf219 gene, which contains nine zinc finger domains. RT-PCR showed Znf219 mRNA expression in primary chondrocytes. Whole mount *in situ* hybridization using E11.5 mouse embryos demonstrated that Znf219 expression was specifically observed in the developing limb buds where COL2a1 and Sox9 were strongly expressed. Moreover, Znf219 markedly up-regulated the transcriptional activity of Sox9 for the COL2a1 gene promoter. Co-immunoprecipitation experiments showed that Znf219 physically associated with Sox9. In addition, DsRed-tagged Znf219 was well co-localized with Venus-tagged Sox9 in the nuclei. These results suggest that Znf219 forms transcription factory with Sox9 during chondrocyte differentiation. To examine the functional role of Znf219 in chondrocyte differentiation, we overexpressed Znf219 in the C3H10T1/2 mesenchymal cells using the adenovirus gene delivery system. Znf219 overexpression dramatically enhanced Sox9-induced mRNA expression of COL2a1, aggrecan and COL11a2 mRNA. Consistent with this, knockdown of Znf219 using micro RNA system inhibited Sox9-induced COL2a1, aggrecan and COL11a2 expression. Furthermore, overexpression of a dominant-negative Znf219 mutant inhibited BMP2-induced chondrocyte differentiation of C3H10T1/2 cells and mouse embryo limb bud cells. In conclusion, our results suggest that Znf219 functions as a molecular component of the transcription factory formed by Sox9 and plays an important role in early-stage of chondrocyte differentiation.

**Disclosures:** Y. Takigawa, None.

## 1266

**The Wnt Target Gene Twist1 Inhibits Sox9, the Master Regulator of Chondrogenesis.** S. Gu<sup>\*</sup>, M. Reinhold<sup>\*2</sup>, M. Naski<sup>3</sup>. <sup>1</sup>Biochemistry, University of Texas Health Science Center at San Antonio, San Antonio, TX, USA, <sup>2</sup>Pathology, University of Texas Health Science Center at San Antonio, San Antonio, TX, USA, <sup>3</sup>Pathology & Biochemistry, University of Texas Health Science Center at San Antonio, San Antonio, TX, USA.

Canonical Wnt signaling strongly inhibits chondrogenesis. Data show that lack of canonical Wnt signaling during early bone formation leads to expansion of chondrocytes, whereas augmented Wnt signaling represses chondrocyte differentiation. We hypothesized that Wnt-signaling strongly inhibits chondrogenesis through Wnt-dependent gene expression. In previous work we showed that Wnt signaling induces Twist1 and that Twist1 inhibits chondrogenesis. Here we provide evidence that Twist1 inactivates cartilage development by directly inhibiting the expression and activity of the master regulator of chondrogenesis, Sox9. We demonstrate a reciprocal relationship of Twist1 and Sox9 expression in chondrocytic cells and significantly, knockdown of Twist1 expression leads to increased Sox9 expression. In addition to regulating Sox9 expression, Twist1 inhibits the transcriptional activity of Sox9. Transcription assays show that Twist1 inhibits Sox9 activity and that the C-terminus of Twist1 is required for the inhibition. *In-vitro* binding experiments show that Sox9 and Twist1 form a stable complex. Complex assembly requires the C-terminus of Twist1 but not the C-terminal transactivation domain of Sox9. Dimerization of Twist1 with other basic-helix-loop-helix transcription factors is not required for the binding to or the inhibition of Sox9. The lack of a requirement for dimerization suggested that Twist1 may recruit a co-repressor and thereby represses Sox9. We find that Twist1 binds avidly to histone deacetylases, but this interaction does not appear to be required for the inhibition of Sox9 by Twist1. We hypothesize that Twist1 inhibits Sox9 through steps that alter DNA binding or the recruitment of co-activators. These data indicate that Sox9 expression and activity are tightly regulated by Twist1. This suggests that the earliest steps of chondrogenesis are decided by the balance of Twist1 and Sox9.

**Disclosures:** S. Gu, None.

## 1267

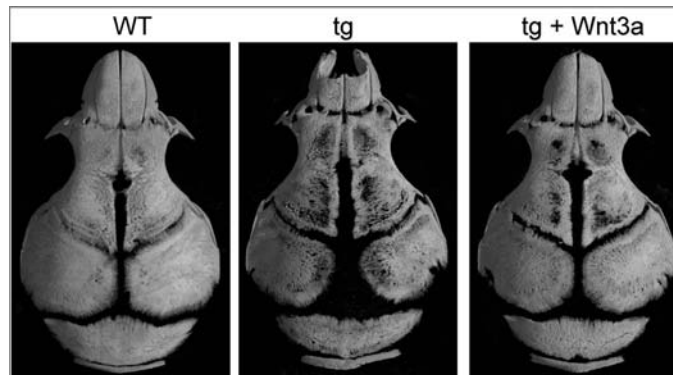
**Glucocorticoid Signalling Through Osteoblasts Is Essential for Cranial Skeletal Development.** H. Zhou, W. Mak\*, R. Kalak\*, J. Street\*, C. Fong-Yee\*, Y. Zheng\*, C. R. Dunstan, M. J. Seibel. Bone Research Program, ANZAC Research Institute, The University of Sydney, Sydney, Australia.

Glucocorticoids (GC) play an important role in bone cell differentiation and mesenchymal lineage commitment (1). Using Col2.3-HSD2 transgenic (tg) mice in which GC signaling is abrogated in mature osteoblasts, we investigated the role of endogenous GC signalling in early skeletal development.

Neonatal tg mice develop a distinct cranial phenotype characterised by bone hypoplasia and osteopenia, disorganised and poorly mineralised frontal, parietal and interparietal bones and increased suture patency. These changes were apparent as early as E15.5. In addition, ectopic differentiation of cartilage in the sagittal suture and a postnatal defect in parietal cartilage removal were observed in tg mice, resulting in ectopic cartilage below the sutures and abundant remnant cartilage underneath the parietal and inter-parietal bones. When compared to wild type (WT) mice, the cranial cartilage in neonatal tg animals demonstrated reduced cartilage removal and chondrocyte apoptosis. mRNA and protein expression of MMP14, an enzyme essential for calvarial cartilage removal, were also profoundly reduced in parietal bone and cartilage. Concurrently, the accumulation of  $\beta$ -catenin protein, an upstream regulator of MMP14 expression, was reduced in tg cranial chondrocytes and osteoprogenitor cells in suture areas; probably due to a lack of Wnt signaling from neighbouring osteoblasts. mRNA expression for Wnt9a and Wnt10b was reduced 40% and 50% respectively in osteoblasts of tg parietal bone compared to WT littermates. Also, Wnt9a was undetectable by in situ hybridisation in tg calvarial osteoblasts but was strongly expressed in the WT. Exogenous Wnt3a protein, delivered by supracalvarial injection, rescued the phenotype confirming Wnt signalling as a key mediator in this process (Fig. 1).

We conclude that endogenous glucocorticoids stimulate the expression and secretion of Wnt proteins in mature osteoblasts, in keeping with our previous results (1). Wnt signalling induces a) parietal cartilage chondrocytes to initiate MMP14-mediated cartilage degradation; and b) mesenchymal progenitor cells to differentiate towards the osteoblast lineage. Thus glucocorticoids and osteoblasts play an essential role in the intricate development of intramembranous bone.

1. J. Biol. Chem. 283:1936, 2008



**Disclosures:** H. Zhou, None.

This study received funding from: NHMRC Project Grant #402462.

## 1268

**Notch Signaling Inhibits Chondrogenesis and Subsequently Promotes Chondrocyte Maturation.** Y. Dong<sup>1</sup>, A. Jesse<sup>\*1</sup>, R. Kopan<sup>\*2</sup>, T. Gridley<sup>\*3</sup>, T. Honjo<sup>\*4</sup>, R. J. O'Keefe<sup>1</sup>, M. J. Hilton<sup>1</sup>. <sup>1</sup>Department of Orthopaedics and Rehabilitation, University of Rochester, Rochester, NY, USA, <sup>2</sup>Department of Developmental Biology, Washington University School of Medicine, St. Louis, MO, USA, <sup>3</sup>The Jackson Laboratory, Bar Harbor, ME, USA, <sup>4</sup>Department of Immunology and Genomic Medicine, Kyoto University Graduate School of Medicine, Kyoto, Japan.

The Notch signaling pathway governs differentiation and cell fate determination in many organ systems during development. Until recently the role of Notch signaling in the skeletal system has largely gone unexplored. While prior work has implicated Notch signaling, primarily via Notch 1 and 2 receptors, in regulating chondrocyte maturation and bone marrow mesenchymal progenitor cell differentiation, the molecular details remain unclear. Our current studies define the mechanisms by which Notch regulates chondrogenesis and chondrocyte maturation both *in vitro* and *in vivo*. We first characterized expression of all Notch pathway components during limb-bud cell micromass differentiation. *Notch1* and *Hes1*, a classical Notch target gene, were prominently expressed during the earliest stages of chondrogenesis. In contrast, *Notch2* and the molecular targets *Hey1* and *HeyL* were induced later during chondrocyte maturation. These data suggest potential early and late functions of Notch signaling during cartilage development that may be coordinated by separate Notch signaling mechanisms. Supporting this notion, micromass cultures treated with DAPT, a Notch signaling inhibitor, enhanced chondrogenesis and subsequently delayed chondrocyte terminal maturation. Furthermore, we analyzed the *in vivo* effect of Notch gain and loss-of-function specifically in the limb mesenchyme. Skeletal staining, histology, and molecular analyses of *Prx1Cre*;

*Rosa-NICD<sup>+/+</sup>* embryos, which sustain Notch signaling in the limb mesenchyme, show a significant inhibition of chondrogenesis as predicted by our *in vitro* data. To further assess whether Notch regulates various aspects of cartilage development via canonical signaling mechanisms, we removed the canonical Notch transcriptional effector, RBPJk, using the same *Prx1Cre* transgene. Analyses of *Prx1Cre*; *RBPJk<sup>+/+</sup>* embryos revealed an enhancement in chondrogenesis followed by a robust delay in the progression of chondrocyte maturation. Together these results demonstrate that RBPJk-dependent Notch signaling inhibits chondrogenesis and subsequently promotes chondrocyte maturation, likely via differential regulation of *Hes/Hey* target genes during cartilage development.

**Disclosures:** Y. Dong, None.

## 1269

**A Mouse with a Ser1386Pro Mutation in the C-propeptide Domain of *col2a1* Provides a Model for Spondyloepiphyseal Dysplasia Congenita.** C. T. Esapa<sup>1</sup>, T. Hough<sup>\*2</sup>, S. Testori<sup>\*1</sup>, R. Head<sup>\*1</sup>, E. Crane<sup>\*1</sup>, C. Chan<sup>\*1</sup>, M. Brown<sup>3</sup>, S. Brown<sup>\*2</sup>, P. Croucher<sup>4</sup>, R. Cox<sup>\*2</sup>, M. Cheeseman<sup>\*2</sup>, R. V. Thakker<sup>1</sup>. <sup>1</sup>University of Oxford, Oxford, United Kingdom, <sup>2</sup>MRC Harwell, Mammalian Genetics Unit and Mary Lyon Centre, Harwell, United Kingdom, <sup>3</sup>University of Queensland, Queensland, Australia, <sup>4</sup>University of Sheffield, Sheffield, United Kingdom.

Investigations of skeletal dysplasias which are often inherited have yielded important insights in the molecular mechanisms of bone development, osteoporosis and osteoarthritis. However, these studies have been hampered by the lack of available patients and affected families. To overcome this limitation, we have investigated mice treated with the chemical mutagen N-ethyl-N-nitrosourea (ENU) for hereditary bone disorders and established a mouse model designated, *Longpockets*. Mice were kept in accordance with national welfare guidelines and project license restrictions. Mice heterozygous<sup>+/+</sup> for the *Longpockets* mutation were found to have severely disproportionately short humeri that lead to shortened forelimbs. In addition, *Longpockets<sup>+/+</sup>* mice had moderately shortened hindlimbs and flattened vertebrae. Histology revealed gross disorganization and early closure of the humeral growth plate with flattened epiphyses, consistent with the features of spondyloepiphyseal dysplasia congenita (sedc). Micro-computed tomography scanning of *Longpockets<sup>+/+</sup>* mice revealed the development by 8 weeks of age, of knee erosions, consistent with arthritis. *Longpockets<sup>+/+</sup>* mice were found to die perinatally. Positional cloning studies mapped *Longpockets* to a 5Mb region on chromosome 15 which contains the cartilage-expressed genes *col2a1*, *wnt1* and *wnt10b*. We hypothesized that *Longpockets* may be due to a *col2a1* mutation. DNA sequence analysis identified a T to C transition at nucleotide 4156. This altered a highly conserved serine residue at position 1386 to a proline residue. Western blot analysis using a *col2a1* antibody and lysates from mouse embryonic fibroblasts (MEFS) of wild type<sup>+/+</sup> and *Longpockets<sup>+/+</sup>* embryos revealed an absence of the mature 100 kDa type II collagen protein in the MEFS<sup>+/+</sup>, which instead had lower molecular weight breakdown products. Transient transfection of wild type *col2a1* and Ser1386Pro mutant c-myc constructs in COS-7 cells and confocal microscopy revealed perinuclear aggregation and retention of the mutant protein in the endoplasmic reticulum. Thus, our studies have established a novel mouse model for a dominantly inherited form of sedc that is due to a missense mutation in the C-propeptide domain of *col2a1* and that is likely associated with arthritis of the knee. These results will help to elucidate further the *in vivo* role of the *col2a1* C-propeptide domain in the assembly and trafficking of type II collagen.

**Disclosures:** C.T. Esapa, None.

This study received funding from: Medical Research Council, UK.

## 1270

**The -301T/C of Sclerostin(SOST) Modulates Bone Mineral Density by Wnt and Estrogen Signaling Pathways.** Q. Y. Huang, G. H. Y. Li\*, A. W. C. Kung. The University of Hong Kong, Hong Kong, China.

Osteoporosis is a complex disease influenced by both genetic and environmental factors. Accumulating evidence shows that genes which cause monogenic diseases also contribute to similar complex disease in the general population. We sought to determine whether the allelic variation in seven monogenic bone disease genes (*CLCN7*, *TCIRG1*, *SOST*, *CA2*, *CSTK*, *TGFB1* and *SLC26A2*) contributes to osteoporosis / bone mineral density (BMD) variation in the normal Chinese population. We conducted a gene-wide and tag SNP-based association study in 1,243 case-control Chinese subjects. The cases were subjects with low BMD (Z-scores  $\leq -1.28$ , equivalent to the lowest 10 percent of the population) at either the L1-4 lumbar spine or femoral neck. Control subjects had high BMD (Z-score  $\geq +1.0$ ) at the corresponding sites. Twenty-two tag SNPs (tSNPs) from seven monogenic bone disease genes were selected based on the CHB panel of the Phase II HapMap Project ( $r^2 > 0.8$  and minor allele frequency  $> 0.2$ ), and were genotyped using the high-throughput sequenom platform. Allelic and haplotype association analyses were conducted by Haploview and binary logistic regression analyses. Gene-gene interactions were investigated using multifactor dimensionality reduction method. AlIBaba 2.1 was applied to predict the putative transcription factor binding sites at the promoter polymorphism. The promoter SNP rs1230399 (-301T/C) of *SOST* showed significant genotypic and allelic associations with BMD at all skeletal sites measured ( $P = 0.04$ - $0.001$ ), including the lumbar spine, femoral neck, trochanter and total hip. The haplotype CC consisting of rs1230399 and rs865429 showed consistent associations with high BMD at femoral neck and spine ( $P = 0.005$ ,  $0.002$ , respectively). Importantly, this association has been replicated in the Caucasian population. Functional analysis showed that the rs1230399 was located at the core consensus recognition site of two important transcription factors C/EBP $\alpha$  and FOXA1 which were involved in the Wnt and estrogen signaling pathway. T $\rightarrow$ C mutation abolishes the binding of both C/EBP $\alpha$  and FOXA1 to *SOST*. In addition, significant gene-gene interactions were identified for *SOST*/*CLCN7* and *TGFB1*. In conclusion, the C-allele of -301T>C variant of *SOST* was associated with high BMD. The variant may mediate BMD by Wnt and estrogen signaling pathways.

**Disclosures:** Q.Y. Huang, None.

This study received funding from: Hong Kong Research Grant Council (HKU7514/06M) and CRCG Grant, The University of Hong Kong.

## 1271

**Role of *Ostm1* in Bone, Hematopoiesis and Neuronal Development.** A. Griffiths\*, C. Héraud\*, M. Pata\*, B. Maranda\*, J. Yacher<sup>1</sup>. <sup>1</sup>Institut de recherches cliniques de Montréal (IRCM), Montreal, QC, Canada, <sup>2</sup>CHUL-CHUQ, Laval, QC, Canada.

Autosomal recessive malignant osteopetrosis is a rare disorder due to a failure of the hematopoietic lineage derived osteoclast. These active osteoclasts have the unique property to resorb bone matrix and a lack of bone resorption leads to an abnormal increase in bone mass characteristic of osteopetrosis. Our laboratory characterized the *grey-lethal* gene (*Ostm1*) from the spontaneous osteopetrotic *gl* mutant, and isolated the human *OSTM1* homologue and the first *OSTM1* mutation. This mouse mutant displayed a total absence of *Ostm1* transcript whereas it is normally detected at high levels in hematopoietic tissues and in the brain. In an attempt to correct the *gl* osteoclast phenotype we targeted *Ostm1* expression to committed osteoclasts with a TRAP-*Ostm1* transgene. However, this osteoclast expression was inefficient to correct *gl*/*gl* defects, suggesting that *Ostm1* is required in other or additional cell types. Functional rescue was then undertaken by directing *Ostm1* expression in all myeloid lineages including osteoclasts with a PU1-*Ostm1*-BAC transgene. All *gl*/*gl*-PU1-*Ostm1* BAC transgenic mice expressed *Ostm1* in hematopoietic cells and displayed full rescue of osteopetrosis and thrive normally at three weeks. However by 5 weeks of age these *gl*/*gl* transgenic mice became overtly ill and died prematurely with a lifespan of approximately 6-7 weeks compared to three weeks for *gl*/*gl* mice. Analysis of *gl*/*gl* PU1-*Ostm1*-BAC transgenic mice showed neurological anomalies with a significant neurodegeneration in brain cortex, hippocampus and cerebellum. Precisely, these *gl*/*gl*-PU1-*Ostm1* BAC transgenic mice accumulated with age neuronal cytoplasmic inclusions associated with cell loss. Our simultaneous characterization of a patient with an additional *OSTM1* mutation associated with neurodegeneration further supported a key role of *OSTM1* in the CNS. Taken together, our results demonstrated that the *Ostm1* gene plays a major functional role in neuronal development independently of the hematopoietic and osteoclast lineage.

**Disclosures:** A. Griffiths, None.

## 1272

**Molecular Consequences of a Mutant *Dlx3* Affecting Bone Homeostasis in Tricho-Dento-Osseous Syndrome.** O. Duverger\*, D. Lee\*, M. Q. Hassan\*, S. X. Chen\*, F. Jaisser\*, J. B. Lian\*, M. I. Morasso\*. <sup>1</sup>NIAMS/NIH, Bethesda, MD, USA, <sup>2</sup>UMass Medical School, Worcester, MA, USA, <sup>3</sup>College de France, Paris, France.

The homeodomain protein *Dlx3* plays a crucial role during embryonic development. *Dlx3* was shown to be expressed in diverse secretory cells of mineralized tissues: in craniofacial bone and tooth (intramembranous ossification) as well as in the appendicular skeleton (endochondral ossification). Functional studies have further demonstrated that *Dlx3* is a key regulator of bone differentiation. In humans, a frameshift mutation in the

coding sequence of the *DLX3* gene results in an ectodermal dysplasia called Tricho-Dento- Osseous syndrome (TDO). The main features of this autosomal dominant disorder are defects in hair, teeth and bone (increased density of both craniofacial and appendicular bone). In order to investigate the functional alterations caused by the mutated *Dlx3*<sup>TDO</sup> isoform *ex vivo*, we used a tetracycline-inducible osteoblastic cell line and calvarial-derived osteoblasts in which the expression of *Dlx3*<sup>WT</sup> and/or *Dlx3*<sup>TDO</sup> could be regulated and monitored. Immunocytochemical analysis revealed that both *Dlx3*<sup>WT</sup> and *Dlx3*<sup>TDO</sup> recombinant proteins are targeted to the nucleus. However, as demonstrated by Electrophoresis Mobility Shift Assay (EMSA), *Dlx3*<sup>TDO</sup> is not able to bind to the canonical *Dlx3* binding site. Furthermore, we demonstrate that the frameshifted C-terminal domain in *Dlx3*<sup>TDO</sup> is accountable for the loss of DNA binding activity since the C-terminal domain in *Dlx3*<sup>WT</sup> is not required for DNA binding activity. Although *Dlx3*<sup>TDO</sup> alone cannot bind to a *Dlx3* responsive element, when *Dlx3*<sup>WT</sup> and *Dlx3*<sup>TDO</sup> are co-expressed they form a complex that can bind DNA. Concomitant with the inability to bind DNA, *Dlx3*<sup>TDO</sup> has a defective transcriptional activity. Moreover, the transcriptional activity of *Dlx3*<sup>WT</sup> is significantly reduced in the presence of the mutated isoform, indicating that *Dlx3*<sup>TDO</sup> has a dominant negative effect on *Dlx3*<sup>WT</sup> transcriptional activity. The use of mouse models of the TDO syndrome will be an invaluable tool to understand how these functional effects of the mutation translate into the hair, teeth and bone phenotype in TDO syndrome.

**Disclosures:** O. Duverger, None.

This study received funding from: Intramural Research Program of the National Institute of Arthritis and Musculoskeletal and Skin Diseases.

## 1273

**T $\beta$ RI Inhibitor Rescues Uncoupled Bone Remodeling in Two Different Animal Disease Models.** X. Wu<sup>1</sup>, W. Lei\*, Y. Tang<sup>1</sup>, T. R. Nagy\*, W. Van Hul<sup>3</sup>, M. Wan<sup>1</sup>, X. Cao<sup>1</sup>. <sup>1</sup>Department of Pathology, University of Alabama at Birmingham, Birmingham, AL, USA, <sup>2</sup>Department of Nutrition Sciences, University of Alabama at Birmingham, Birmingham, AL, USA, <sup>3</sup>Department of Medical Genetics, University of Antwerp, Antwerp, Belgium.

Bone remodeling is a dynamic process beginning with resorption of a volume of bone by osteoclasts and replaced with new bone formation by osteoblasts throughout life. Bone resorption and formation in each remodeling cycle are precisely coupled to sustain bone mass and architecture. Disruption in coupling is often associated with bone diseases. The uncoupling mechanisms underlying these bone diseases have not been elucidated. TGF $\beta$ 1 is one of the most abundant cytokines deposited in the bone matrix. The active TGF $\beta$ 1 is released during bone resorption, and recruits osteoprogenitors during bone remodeling. Here we generated two different mouse models with uncoupled bone phenomenon and demonstrated that high levels of active TGF $\beta$ 1 in the bone marrow that cause the uncoupled bone remodeling. Camurati-Engelmann Disease (CED) is an inherited bon hyperparathyroidism mouse model e disease associated with amino acid substitutions in the latency-associated peptide (LAP), but not in the mature TGF $\beta$ 1 peptide. In examining cellular function of six different CED-derived TGF $\beta$ 1, we found that mutations in LAP cause premature release of mature TGF $\beta$ 1 upon secretion and TGF $\beta$ 1 mutants are hyperactive to induce phosphorylation of Smad2 and luciferase transcription activity. First we have established a mouse model, in which a CED-derived TGF $\beta$ 1 mutant was transgenic. High levels of active TGF $\beta$ 1 were detected only in bone marrow and matrix of the TGF $\beta$ 1 mutant mice. A typical progressive diaphyseal dysplasia in CED patients was observed in the long bones of CED mice with about 50% tibia fractures. CED-derived mutation-caused release of active TGF $\beta$ 1 in the bone marrow uncoupled bone resorption and formation. Most importantly, treatment of TGF $\beta$ 1 mutant mice with the TGF $\beta$  type I receptor (T $\beta$ RI) inhibitor for 6 weeks rescued the uncoupled bone resorption and bone formation and completely prevented tibial fractures in TGF $\beta$ 1 mutant mice. Furthermore, we examined hyperparathyroidism mouse model by continuous infusion of PTH(1-34). The mice had high bone turnover phenotype with uncoupled bone resorption and formation. Similar to CED mice, a high level of activated TGF $\beta$ 1 in the bone marrow of the mice was observed. Again injection of T $\beta$ RI inhibitor rescued the bone phenotype of hyperparathyroidism mice. Thus, abnormal activated TGF $\beta$ 1-induced uncoupled bone remodeling implicates a general pathological mechanism for bone coupling disorders. T $\beta$ RI inhibitor is implicated as a potential agent for the treatment of CED and hyperparathyroidism patients.

**Disclosures:** X. Wu, None.

This study received funding from: NIH.

## 1274

**CFTR Regulates Osteoblast Bone Formation Independent of Chloride Conductance.** L. A. Kingsley<sup>1</sup>, C. R. McKibbin\*, K. L. Clines\*, S. E. Gabriel\*, P. A. Friedman<sup>3</sup>, G. A. Clines<sup>1</sup>. <sup>1</sup>Medicine, University of Virginia, Charlottesville, VA, USA, <sup>2</sup>Pediatrics, University of North Carolina, Chapel Hill, NC, USA, <sup>3</sup>Pharmacology, University of Pittsburgh, Pittsburgh, PA, USA.

Low BMD and increased risk of fracture are associated with cystic fibrosis (CF), a recessive human genetic disease caused by mutations of the cystic fibrosis transmembrane regulator (CFTR). CF bone disease is an emerging complication of CF patients who are now living longer due to advances in lung disease management. Chronic illness, malnutrition, vitamin D deficiency, glucocorticoids and hypogonadism have all been proposed to be responsible for CF bone disease. However, recent epidemiological investigations and knockout animal models suggest a direct link between CFTR inactivation in bone and low BMD.

We investigated the biology of CFTR in bone. First, we assessed CFTR expression in bone and found by real-time RT PCR that it was expressed in the osteoblast but not the

osteoclast. Murine calvarial organ cultures from CFTR KO mice had reduced bone formation compared to calvariae from WT littermates ( $6430 \mu\text{m}^2$  vs.  $16440 \mu\text{m}^2$ ,  $p=0.0023$ ). Altered chloride ( $\text{Cl}^-$ ) conductance and secretory function are responsible for most CF-related diseases. However, the CFTR-specific  $\text{Cl}^-$  channel inhibitor CFTR<sub>inh</sub>-172 had no effect on bone formation in calvarial organ cultures. These results suggest that CFTR has effects in bone independent of  $\text{Cl}^-$  conductance. We then examined whether CFTR inactivation alters the expression of osteoblast differentiation markers. No significant differences in Runx2, osterix, collagen I and osteocalcin mRNA concentrations were observed between osteoblasts derived from CFTR KO and WT mice. These results suggest that the pool of KO and WT cultured osteoblasts were at a similar stage of differentiation.

We then tested direct effects of CFTR in the osteoblast. CFTR associates in a membrane macromolecular complex with NHERF-1 and NHERF-2 (PDZ adaptor protein  $\text{Na}^+/\text{H}^+$  exchanger regulatory factors). Another macromolecular complex between NHERF and the parathyroid hormone receptor (PTH1R) retards PTH1R endocytosis and recycling. We hypothesize the existence of a novel PTH1R-NHERF-CFTR macromolecular complex. Preliminary data show that CFTR inactivation decreases uptake of labeled PTH by osteoblasts compared to WT cells, suggesting that CFTR mutations may impair normal bone remodeling by dysregulating osteoblast PTH signaling. The direct actions of CFTR in bone are largely an unexplored area of CF research. Defining the mechanisms of bone loss and determining optimal treatments are critical because CF patients are now living longer and the incidence of fractures is expected to increase.

**Disclosures:** GA. Clines, None.

## 1275

**Alendronate Transiently Impairs Removal of Alveolar Bone and Healing of the Root Socket After Tooth Extraction in Rats.** J. I. Aguirre, M. K. Altman\*, S. E. Franz\*, A. C. F. Bassit\*, T. J. Wronski. Physiological Sciences, University of Florida, Gainesville, FL, USA.

Osteonecrosis of the jaw (ONJ) has been identified as a potential complication of bisphosphonate (BP) treatment. Although ONJ occurs most frequently in cancer patients treated IV with nitrogen-containing BPs, it has also been reported to occur, although with a much lower incidence, in postmenopausal women treated with alendronate (ALN). Since tooth extraction is one of the most important risk factors for ONJ, we performed this dental procedure in ALN-treated rats to evaluate its potential as a novel animal model for ONJ. For this purpose, 2 month-old rats were injected SC twice weekly with vehicle or a dose of ALN comparable to that used to treat postmenopausal osteoporosis ( $15 \mu\text{g/kg}$  bw). Treatments were administered for 4 weeks before the first mandibular molar was extracted, and continued during the post-extraction (PE) period until rats were sacrificed at 10, 21, 35, and 70 days PE. The left mandibles were collected to assess the effects of ALN on alveolar bone in the interdental area between the first and second molars, and on bone healing within the distal root socket by determining osteo- and angiogenesis using histomorphometry. We found that ALN-treated rats had increased alveolar bone volume and height at 10 days PE. The interdental alveolar bone appeared to protrude into the oral cavity in 30% of the ALN-treated animals. However, these parameters progressively decreased in ALN-treated rats to the level of vehicle-treated rats by 35 and 70 days PE. In addition, a 2.5-fold increase in the percentage of empty osteocytic lacunae was found in alveolar bone of ALN-treated rats at 10 days PE. ALN also induced decreases in osteoblast, mineralizing, and eroded surfaces in the alveolar bone at 10, but not at 21 days PE. Within the root socket, woven bone volume decreased by approximately 70% in ALN-treated rats only at 10 days PE. Decreases in osteoblast and eroded surfaces, but not in osteoclast surface and number, were also observed in ALN-treated rats only at 10 days PE. Remarkably, ALN-treated rats exhibited decreased blood vessel area, perimeter, and number within the root socket by 35-40% at 10 days PE, but not at later times. These findings indicate that ALN transiently impairs angiogenesis and bone formation during the early stages of bone healing after tooth extraction in rats. These data also indicate that ALN delays the removal of interdental alveolar bone after tooth extraction. Although ONJ was not detected in ALN-treated rats, it is possible that treatment with higher oncology doses of a more potent BP would result in the observed transient effects becoming more persistent and ultimately developing into an ONJ-like lesion.

**Disclosures:** J.I. Aguirre, None.

This study received funding from: Merck & Co.

## 1276

**The Recalculation of Genome Scans on a Common Genetic Map Enhances Our Ability to Identify Common Bone Density QTL in New and Historical Data.** C. L. Ackert-Bicknell<sup>1</sup>, S. Tsaih<sup>\*1</sup>, M. Marion<sup>\*1</sup>, Z. Lu<sup>\*1</sup>, A. Cox<sup>\*1</sup>, R. Smith<sup>\*1</sup>, R. Korstanje<sup>\*1</sup>, W. G. Beamer<sup>1</sup>, J. Wergedal<sup>2</sup>, G. A. Churchill<sup>\*1</sup>, B. J. Paigen<sup>\*1</sup>. <sup>1</sup>The Jackson Laboratory, Bar Harbor, ME, USA, <sup>2</sup>J.L. Pettis Memorial VA Medical Center, Loma Linda, CA, USA.

Many quantitative trait loci (QTL) for bone mineral density (BMD) have been reported in the mouse, covering nearly every chromosome. The genetic maps used in these studies have evolved over 85 years from assemblies of unrelated data sets. As a result, there are many inconsistencies with regards to marker order and relative positions. A new genetic map has been created based on 15,000 polymorphic markers genotyped 2293 mice from 80 separate pedigrees of a heterogeneous stock of outbred mice. In this new map, the order of and distance between markers have been corrected and this new genetic map shows high correlation with the physical map of the mouse genome. All published bone trait QTLs were mapped using the old genetic map, suggesting that the locations of the QTL peaks

may be mis-mapped: negatively impacting candidate gene identification and cross-species homology studies. We have recalculated the peak position and confidence intervals (CIs) for BMD QTLs using raw data from five of the original mapping crosses (B6x129, B6xC3H, B6xC3H, NZBxSM and NZBxRF). Across the genome, we found that 60% of the QTL peaks were shifted by more than 4 cM when recomputed on the new genetic map; 28.3% of the QTL peaks were off by more than 10 cM; and 3% of the peaks were off by 20 cM or more. We found one peak on Chr 11 that shifted by 49.5 cM and one peak on Chr 10 that shifted 60.3 cM, as compared to the peak location reported in the literature. This shift of QTL peaks was not uniform across all chromosomes as some original maps for individual chromosomes proved more accurate. We observed that for some chromosomes, such as Chr 1, little movement was observed for QTL peaks (average shift =  $2.37 \pm 0.44$  cM), whereas for other chromosomes, such as Chr 4, all QTLs were significantly shifted (average shift =  $16.81 \pm 1.6$  cM). Due the availability of the C57BL/6J reference sequence, we are now able to provide precise physical locations of the QTL peaks and CIs. In this study we have shown that computation of QTL locations from raw data using the updated genetic map can substantially improve the quality and consistency of historical QTL reports. As the identification of candidate genes relies on accurately projecting the genetic map onto the physical map, our results may partially explain the paucity of identified genes known to underlie these bone QTLs. The shifts observed in this study have encouraged us to expanded our analysis to include all available data sets used for the identification of BMD and bone strength QTLs. Our results from this QTL recalculation project will be deposited in a publicly accessible QTL database.

**Disclosures:** C.L. Ackert-Bicknell, None.

## 1277

**Serum 25 Hydroxyvitamin D (25(OH)D) and the Risk of Hip and Non-spine Fractures in Older Men.** J. A. Cauley<sup>1</sup>, N. Parimi<sup>\*2</sup>, K. Ensrud<sup>3</sup>, D. Bauer<sup>4</sup>, S. Cummings<sup>4</sup>, A. Hoffman<sup>\*5</sup>, J. Shikany<sup>\*6</sup>, E. Barrett-Connor<sup>7</sup>, E. Orwoll<sup>8</sup>. <sup>1</sup>Univ of Pittsburgh, Pittsburgh, PA, USA, <sup>2</sup>California Pacific Med Ctr Research Institute, San Francisco, CA, USA, <sup>3</sup>Univ of Minnesota, Minneapolis, MN, USA, <sup>4</sup>Univ of California at San Francisco, San Francisco, CA, USA, <sup>5</sup>Stanford Univ, Stanford, CA, USA, <sup>6</sup>Univ of Alabama at Birmingham, Birmingham, AL, USA, <sup>7</sup>Univ of California at San Diego, San Diego, CA, USA, <sup>8</sup>Oregon Health & Science Univ, Portland, OR, USA.

Vitamin D deficiency is common in older adults, including cases of acute hip fracture (fx). However, few prospective studies have tested the hypothesis that serum measures of total 25(OH)D predict fractures. We performed a case cohort study of 436 men with incident non-spine fx, 81 men with incident hip fx identified over an average of 5.3 years and a random sample of 1608 men. All subjects were enrolled in the Osteoporotic Fractures in Older Men Study (MrOS). 25(OH)D was measured in fasting baseline serum using LC-MS; interassay CV%, 4.4%. Modified Cox proportional hazards models were used to calculate the relative hazard (RH) (95% confidence intervals) of fx by one standard deviation (SD) increase in vitamin D and across quartiles of vitamin D. Nonparametric smoothing techniques (spline analyses) were used to evaluate the linearity of the models. Base models adjusted for age, season, clinic, race, height and weight. Subsequent models added in adjustments for neuromuscular function, total hip BMD or history of falls. The mean 25(OH)D was 24.6ng/ml in non-spine fx; 21.2ng/ml in hip fx and 25.2ng/ml in controls (non-spine fx vs controls,  $p=0.14$ ; hip fx vs controls,  $p<0.0001$ ). A one SD increase in 25(OH)D was associated with a 39% lower risk of hip fx (Relative Hazard (RH)=0.61; 95% confidence interval (CI), 0.46-0.83). Adjustment for neuromuscular function and falls had little effect. Men with the lowest 25(OH)D (Quartile 1) had greater than a two fold increased risk of hip fracture, Table. Further adjustment for BMD attenuated this association. However, spline analysis showed no significant threshold of 25(OH)D where fx risk was increased; risk of hip fx decreased with increasing 25(OH)D. Circulating 25(OH)D levels were unrelated to non-spine fractures. In conclusion, men with lower 25(OH)D have an increased risk of hip fx. The stronger association with hip fx may reflect a link between Vitamin D deficiency and frailty.

Table: RH(95%CI) of hip fracture across quartile of 25(OH)D

Quartile 25(OH)D ng/ml	Model 1 <sup>a</sup> RH (95% CI)	Model 2 <sup>b</sup> RH (95% CI)
1 (3.31 - <19.9)	2.49 (1.16, 5.36)	1.69 (0.76, 3.77)
2 (19.9 - <25.1)	1.49 (0.69, 3.26)	0.97 (0.43, 2.22)
3 (25.1 - <29.9)	1.01 (0.43, 2.34)	0.70 (0.28, 1.73)
4 ( $\geq 29.9$ )	referent	referent
p trend	0.006	0.058

<sup>a</sup>adjusted for age, clinic, season, race, height, weight

<sup>b</sup>Model 1 plus hip BMD

**Disclosures:** J.A. Cauley, Merck & Co, Inc, Eli Lilly & Co, Pfizer, Novartis 2, 3.

This study received funding from: The National Institute of Arthritis and Musculoskeletal and Skin Diseases (NIAMS), the National Institute on Aging (NIA), the National Center for Research Resources (NCRR), and NIH Roadmap for Medical Research.

## 1278

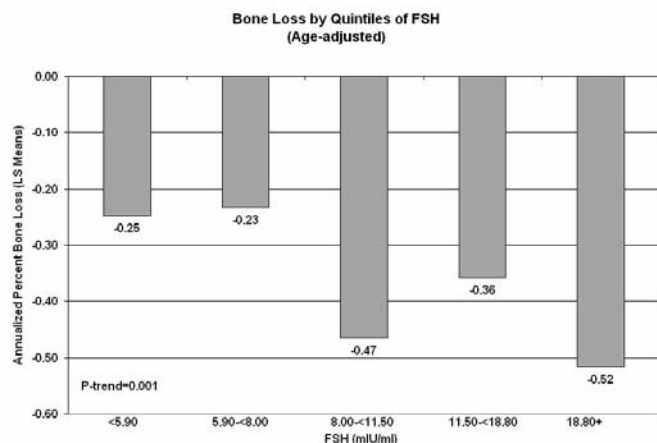
**Gonadotropins, Bone Loss and Fracture in Men: the MrOS Study.** D. C. Bauer<sup>1</sup>, S. L. Harrison<sup>2</sup>, J. A. Cauley<sup>3</sup>, S. R. Cummings<sup>2</sup>, H. A. Fink<sup>4</sup>, A. Hoffman<sup>5</sup>, E. Orwoll<sup>6</sup>. <sup>1</sup>UCSF, San Francisco, CA, USA, <sup>2</sup>California Pacific Medical Center, San Francisco, CA, USA, <sup>3</sup>University of Pittsburgh, Pittsburgh, PA, USA, <sup>4</sup>VA Medical Center, Minneapolis, MN, USA, <sup>5</sup>Stanford, Palo Alto, CA, USA, <sup>6</sup>OHSU, Portland, OR, USA.

Sex hormone deficiency is associated with bone loss and fracture in older men and women, but the independent effects of gonadotropin levels are unknown. Recent rodent studies suggest FSH may regulate bone mass via a direct effect on osteoclasts.

We performed a prospective case-cohort analysis in the Osteoporosis in Men (MrOS) study to determine if FSH or LH levels were associated with bone loss or non-spine fracture risk. At the baseline visit hip DXA (Hologic QDR4500) was measured and fasting serum was archived at -190C in 5995 men over 65. Incident non-spine fractures were confirmed centrally and repeat hip DXA was obtained after a mean follow-up of 4.6 yr. After excluding 73 men using hormonal or other bone-active therapy, we used baseline serum to measure FSH and LH (Beckman Coulter) in 320 men with non-spine fracture (including 62 hip fractures) and 1193 randomly selected men. Baseline sex hormone levels (free estradiol and free testosterone by mass spectrometry) were also available. Bone loss was examined using age-adjusted linear regression models in 872 men from the randomly selected cohort who returned for follow-up BMD, and fractures were examined using age-adjusted Cox models that account for the case-cohort sampling.

Both FSH and LH levels increased with age ( $r=0.26-0.27$ ,  $p<0.001$ ). Higher FSH levels were associated with greater hip bone loss (Figure); results were similar for LH and after adjustment for sex hormone levels. Compared to men without non-spine fracture, those with fracture were significantly older (74.9 yr. vs. 73.7), had lower leg strength (194.2 watts vs. 208.9) and had lower total hip BMD (0.90 gm/cm<sup>2</sup> vs. 0.96), but mean FSH ( $\pm$ SD) and LH were similar among men with and without fracture (FSH: 15.2 $\pm$ 16.6 mIU/ml vs. 14.2 $\pm$ 14.0,  $p=0.81$ ; LH: 7.0 $\pm$ 6.7 mIU/ml vs. 6.6 $\pm$ 5.3,  $p=0.73$ ). Neither FSH nor LH were associated with non-spine or hip fracture risk. For example, after adjustment for age the RH for non-spine fracture per SD increase in FSH was 1.01 (CI: 0.88, 1.17).

We conclude that in older men higher levels of FSH and LH are associated with greater hip bone loss, independent of sex hormone levels, but gonadotropin levels are unrelated to fracture risk in this population.



**Disclosures:** D.C. Bauer, Merck 4; Amgen 3; Novartis 3; P and G 3.  
This study received funding from: NIAMS and NIA.

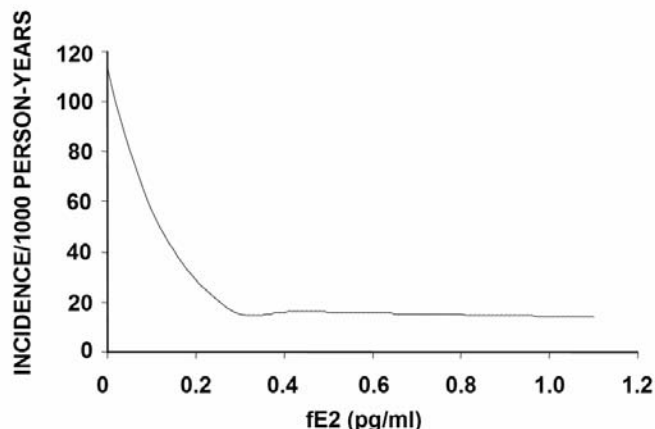
## 1279

**Older Men with Low Serum Estradiol and High Serum SHBG Have an Increased Risk of Fractures.** L. Vandenput<sup>1</sup>, D. Mellström<sup>1</sup>, H. Mallmin<sup>2</sup>, A. H. Holmberg<sup>3</sup>, M. Lorentzon<sup>1</sup>, A. Odén<sup>4</sup>, H. Johansson<sup>1</sup>, E. S. Orwoll<sup>5</sup>, F. Labrie<sup>6</sup>, M. K. Karlsson<sup>3</sup>, Ö. Ljunggren<sup>2</sup>, C. Ohlsson<sup>1</sup>. <sup>1</sup>Center for Bone Research at the Sahlgrenska Academy, Departments of Internal Medicine and Geriatrics, University of Gothenburg, Gothenburg, Sweden, <sup>2</sup>Department of Medical Sciences, University of Uppsala, Uppsala, Sweden, <sup>3</sup>Clinical and Molecular Osteoporosis Research Unit, Lund University and Department of Orthopaedics, Malmö University Hospital, Malmö, Sweden, <sup>4</sup>Consulting Statistician, Gothenburg, Sweden, <sup>5</sup>Bone and Mineral Unit, Department of Medicine, Oregon Health and Science University, Portland, OR, USA, <sup>6</sup>Laboratory of Molecular Endocrinology and Oncology, Laval University Hospital Research Center and Laval University, Québec, QC, Canada.

Osteoporosis-related fractures constitute a major health concern not only in women but also in men. To investigate the predictive role of serum sex steroids for fracture risk in men, serum sex steroids were analyzed by the specific gas chromatography-mass spectrometry technique at baseline in older men (n=2639, mean 75 years of age) of the prospective population-based MrOS Sweden cohort. Fractures occurring after baseline were validated (average follow-up of 3.3 years).

The incidence for having at least one validated fracture after baseline was 20.9/1000 person-years. Estradiol (E2; hazard ratio (HR) per SD decrease 1.34, 95% confidence interval 1.22-1.49), free estradiol (fE2; HR per SD decrease 1.41, 1.28-1.55), testosterone (T; HR per SD decrease 1.27, 1.16-1.39) and free testosterone (fT; HR per SD decrease 1.32, 1.21-1.44) were all inversely while sex hormone-binding globulin (SHBG; HR per SD increase 1.41, 1.22-1.63) was directly related to fracture risk. Multivariable proportional hazards regression models, adjusted for age, suggested that fE2 and SHBG ( $p<0.001$ ), but not fT, were independently associated with fracture risk. Further sub-analyses of fracture type demonstrated that fE2 was inversely associated with clinical vertebral fractures (HR per SD decrease 1.57, 1.36-1.80), non-vertebral osteoporosis fractures (HR per SD decrease 1.42, 1.23-1.65) and hip fractures (HR per SD decrease 1.44, 1.18-1.76). The inverse relation between serum E2 and fracture risk was non-linear with a strong relation below 16 pg/ml for E2 and 0.3 pg/ml for fE2.

In conclusion, older Swedish men with low serum E2 levels and high SHBG levels have an increased risk of fractures.



**Disclosures:** L. Vandenput, None.

## 1280

**Post-Fracture Mortality in Men: Contributions of Sex Hormones and Bone Mineral Density as Risk Factors.** T. V. Nguyen<sup>1</sup>, N. D. Nguyen<sup>1</sup>, C. Meier<sup>2</sup>, J. A. Eisman<sup>1</sup>, M. J. Seibel<sup>3</sup>. <sup>1</sup>Bone and Mineral Research Program, Garvan Institute of Medical Research, Sydney, Australia, <sup>2</sup>Division of Endocrinology, Diabetes and Clinical Nutrition, University Hospital Basel, Basel, Switzerland, <sup>3</sup>Bone Research Program, ANZAC Research Institute, the University of Sydney, Sydney, Australia.

Although mortality risk is increased among men with fracture, it is not clear what factors contribute to the risk. Moreover, the relationship between sex hormones and mortality in men is controversial, with some but not all studies suggesting that low levels of testosterone were associated with increased mortality risk. We examined the effect of sex hormones on the risk of post-fracture mortality.

Total testosterone and sex hormone-binding globulin (SHBG) were measured by tandem mass spectrometry in 609 men whose aged was at least 60 years (as of 1989) and whose health status had been monitored for 18 years with biannual clinic visits. During the follow-up period, fractures and mortality were ascertained. In addition to basic clinical and anthropometric variables, baseline bone mineral density (BMD, GE-Lunar Prodigy) was also measured in all men. The association between baseline testosterone and fracture or mortality was analyzed by the Cox's proportional hazards model with adjustment for covariates.

During the follow-up period, 113 sustained a fracture and 275 men died; among whom 69 died following a fracture. Fracture was associated with a 50% increase in the risk of mortality (RR 1.5, 95% CI: 1.4 - 1.6). Lower levels of testosterone were associated with an increased risk of mortality (RR 1.7, 95% CI: 1.2 - 2.6) and of fracture (1.5; 95% CI: 1.2 - 1.8) after adjusting for SHBG. More importantly, the risk of mortality after a fracture was significantly increased in those with lower total testosterone levels (RR 3.1, 95% CI: 1.4 - 7.0) after adjusting for SHBG, body weight and age. In multivariate analysis, lower total testosterone, lower BMD (or weight), lower SHBG and advancing age were independent risk factors of post-fracture mortality. These factors collectively accounted for ~60% of total mortality risk.

These results indicate that sex hormones were independent predictors of post-fracture mortality in elderly men, and that mortality should be considered as an important component of osteoporosis outcomes. These data also suggest that it is possible to identify men at high risk of post-fracture mortality.

**Disclosures:** T.V. Nguyen, None.

This study received funding from: National Health and Medical Research Council, Australia.



## 1281

**Cortical Cross Sectional Area in Young Adult Men Is Inversely Related to Risk of Hip Fracture in Their Older Relatives - The GOOD Study.** M. Lorentzon, R. Rudäng\*, D. Mellström, C. Ohlsson. Internal Medicine, Center for Bone Research at the Sahlgrenska Academy (CBS), Göteborg, Sweden.

Peak bone mass is to a large extent genetically determined and believed to be a predictor of future risk of osteoporosis. It is still unclear whether it is the volumetric bone mineral density (vBMD) or bone size at the age of peak bone mass that confers the risk of future osteoporotic fracture. The aim of the present study was to investigate which of these bone parameters in young men (age 18.9±0.6 years, n=1066) included in the Gothenburg Osteoporosis and Obesity Determinants (GOOD) study, that were associated with X-ray verified hip fractures in their parents and grand parents. Using the Swedish multi-generation register, 5901 relatives of the young men in the GOOD-study were identified. The Swedish in-patient care register was used to search for hip fracture data on these relatives. In total, 366 relatives had sustained a hip fracture. Bone parameters were measured in the GOOD-study subjects using both DXA and pQCT. The 320 GOOD-study subjects with a relative with at least one hip fracture had lower areal BMD (aBMD) of the lumbar spine (1.22±0.15 vs. 1.25±0.15 g/cm<sup>2</sup>; p<0.01), radius (0.57±0.06 vs. 0.58±0.06; p=0.04), and total body (1.24±0.10 vs. 1.25±0.10; p=0.04), than the 746 GOOD-study subjects without a relative with a hip fracture. The reduced aBMD at the radius, in the subjects with a relative with at least one hip fracture, was due to a smaller cortical cross sectional area (CSA; 94.8±12 vs. 96.7±12 mm<sup>2</sup>; p=0.02) and lower trabecular volumetric BMD (215±41 vs. 221±41 mg/cm<sup>3</sup>; p=0.02). Using a binary logistic regression (with age of relatives (age deceased or current age), GOOD-study subject age, height, weight, physical activity, calcium intake, and smoking as covariates) we found that lumbar spine aBMD (p<0.01) and cortical CSA (p<0.01) were inversely and independently related to risk of hip fracture in the relatives.

Every SD decrease in the radius cortical CSA, of the GOOD-study subjects, was associated with 1.25 (95% CI: 1.06-1.49) times increased risk of hip fracture in their relatives. Our results suggest that aBMD and especially cortical CSA at the age of peak bone mass are important determinants in predicting osteoporotic fractures in the elderly.

**Disclosures:** M. Lorentzon, None.

*This study received funding from: The Swedish Research Council.*

## 1282

**Distribution and Rate of Clinical Fractures in Older Men Without Osteoporosis: the Osteoporotic Fractures in Men (MrOS) Study.** H. A. Fink<sup>1</sup>, T. L. Blackwell<sup>\*2</sup>, B. C. Taylor<sup>\*1</sup>, K. E. Ensrud<sup>1</sup>, J. A. Cauley<sup>3</sup>, L. Marshall<sup>\*4</sup>, E. S. Orwoll<sup>4</sup>. <sup>1</sup>VA Medical Center, Minneapolis, MN, USA, <sup>2</sup>California Pacific Medical Center, San Francisco, CA, USA, <sup>3</sup>University of Pittsburgh, Pittsburgh, PA, USA, <sup>4</sup>Oregon Health Science University, Portland, OR, USA.

Low BMD strongly predicts future fractures (fx) in populations, but not all patients with fx have low BMD. We examined the proportion of older men with incident fx across BMD categories and, within each BMD category, the distribution of fx types.

We used data from MrOS, a prospective cohort study in men aged ≥65 yrs. From total hip, femoral neck and lumbar spine BMD measured by DXA, men were categorized as osteoporotic (T-score ≤-2.5 any site), normal (T-score ≥-1 all sites), or low bone mass. Self-reported incident fx collected every 4 months were centrally confirmed by radiology reports.

Of 5985 men with BMD measured at all sites, 36% had normal BMD, 54% low bone mass, and 10% osteoporosis. Rate of any clinical fx was lowest in men with normal BMD (9.4 per 1000 person-yr) and greatest in men with osteoporosis (38.3 per 1000 person-yr). However, among men with clinical fx (n=608), 78% were not osteoporotic at any site (21% normal BMD, 57% low bone mass). Analogously, among men with hip fx (n=104), 63% were not osteoporotic at any site (6% normal BMD, 57% low bone mass). Distribution of fx type differed as a function of BMD category. In fx cases with normal BMD (n=128), the most frequent fx types were rib/chest/sternum (23%), ankle/foot/toe (20%), spine (11%), and hand/finger (10%), with fewer men having wrist (6%) or hip (5%) fx. By contrast, in fx cases with osteoporosis (n=134), the most frequent fx types were hip (29%), spine (22%), rib/chest/sternum (19%), and wrist (13%), with fewer men experiencing fx of ankle/foot/toe (8%) or hand/finger (4%). These patterns were similar among men with traumatic fx (n=92), in that 85% were not osteoporotic at any site, and that of traumatic fracture cases with normal BMD, only 5.3% had fx at hip, spine or wrist, and of traumatic fx cases with osteoporosis, 29% had fx at hip, spine or wrist.

In this older male cohort, while incident fx rates were approximately 4-fold higher in men with osteoporosis than in those with normal BMD, nearly 80% of men with any fx and over 60% of men with hip fx were not osteoporotic at either hip or spine. Of men with incident fx, those with normal BMD infrequently had fx at hip, spine or wrist, a pattern appearing more pronounced for men with traumatic fx. In contrast, most incident fx in men with osteoporosis occurred at these "traditional" osteoporosis sites. Future studies should examine risk factors for fx, including for specific fx types, in men without osteoporosis.

**Disclosures:** H.A. Fink, None.

## 1283

**Elevated Production of Interleukin 1β (IL-1β) and Tumor Necrosis Factor α (TNF-α) by Peripheral Blood Mononuclear Cells (PBMC) is Associated with Increased Hip Fracture Risk in Elders: The Framingham Osteoporosis Study.** R. R. McLean<sup>1</sup>, R. Roubenoff<sup>\*2</sup>, M. T. Hannan<sup>1</sup>, L. A. Cupples<sup>\*3</sup>, D. P. Kiel<sup>1</sup>. <sup>1</sup>Hebrew SeniorLife & Harv Med Sch, Boston, MA, USA, <sup>2</sup>Friedman Sch of Nutr Sci & Policy, Tufts Univ, Boston, MA, USA, <sup>3</sup>BU Sch of Public Health, Boston, MA, USA.

Age-related bone loss may be partly mediated by the local skeletal effects of inflammatory cytokines, and previous studies suggest that elevated serum concentrations of inflammatory markers are associated with greater risk of osteoporotic fracture. Spontaneous cytokine production by PBMC, however, may provide a better indication of an individual's *in vivo* inflammatory activity than serum concentrations. We prospectively examined the associations of spontaneous PBMC production of the inflammatory markers IL-1β, interleukin 1 receptor antagonist (IL-1ra), TNF-α, and interleukin 6 (IL-6) with the risk of hip fracture among elderly participants in the population-based Framingham Study Original Cohort. Non-fasting blood samples were drawn from 274 men and 428 women (mean age 78 years, range 72-94) in 1992-94 (baseline) and total PBMC production (ng/mL) of IL-1β, IL-1ra, TNF-α and IL-6 were measured in unstimulated cells using radioimmunoassays. Quartiles of markers were created (Q1=low). Incident hip fractures were ascertained from baseline through December 2005. Sex- and age-adjusted hip fracture incidence rates (IR, per 1000 person-yrs) and 95% confidence intervals (CI) were calculated for quartiles of each marker. Hip fracture hazard ratios (HR) and 95% CIs were calculated across quartiles (Q1 referent) using Cox proportional hazards regression, adjusting for sex and baseline covariates: age (yrs), weight (lbs), height (in), alcohol consumption (oz/wk), current smoking (y/n) and daily use of aspirin or NSAIDs (y/n). Median follow-up time was 9.5 years (range 0.01-14.4) and 69 incident hip fractures occurred. Due to a consistent threshold effect after Q1, the upper three quartiles were combined (Q2-4).

Inflammatory marker ranges, sex- and age-adjusted hip fracture incidence rates (95% CI), and multivariable-adjusted\* hip fracture hazard ratios (95% CI) per marker quartiles.

Marker	Quartile	Range (ng/mL)	IR (per 1000 p-y)	HR
IL-1β	Q1	0.04, 1.84	7.4 (2.7, 12.0)	1.00
	Q2-4	1.88, 42.0	13.0 (9.6, 16.4)	1.98 (1.03, 3.81)
IL-1ra	Q1	0.11, 6.60	7.9 (2.9, 12.9)	1.00
	Q2-4	6.80, 72.0	12.8 (9.3, 16.4)	1.79 (0.95, 3.39)
TNF-α	Q1	0.04, 2.16	7.6 (3.1, 12.2)	1.00
	Q2-4	2.20, 40.0	13.0 (9.5, 16.4)	1.94 (1.01, 3.72)
IL-6	Q1	0.04, 1.96	11.1 (5.4, 16.7)	1.00
	Q2-4	2.00, 20.0	11.9 (8.6, 15.2)	1.15 (0.65, 2.03)

\*Adjusted for sex, age, weight, height, alcohol, smoking, and aspirin/NSAID use

Participants in Q2-4 of IL-1β and TNF-α had a two-fold increased hip fracture risk, while those with elevated IL-1ra tended to have 79% higher risk. IL-6 was not associated with hip fracture. Our results suggest that elevated PBMC production of IL-1β and TNF-α may be risk factors for hip fracture in older men and women, providing further evidence that inflammation may be an important mediator of osteoporotic fracture risk among community-dwelling elders.

**Disclosures:** R.R. McLean, None.

## 1284

**IGFBP-2 and Bone Loss in Aging Women and Men.** S. Amin, L. J. Melton, E. Atkinson\*, S. Achenbach\*, R. Robb\*, J. Camp\*, B. L. Riggs, S. Khosla. Mayo Clinic, Rochester, MN, USA.

Low estradiol does not fully explain age-related bone loss, and we have shown that high IGF binding protein-2 [IGFBP-2] predicts low bone density and high bone turnover, cross-sectionally, in aging men and women. We therefore examined the role of high IGFBP-2 on longitudinal bone loss assessed using QCT. In an age-stratified, random sample of community adults, we measured serum IGFBP-2 at baseline. At baseline and 3 yr follow-up, we measured trabecular volumetric bone mineral density [vBMD] (g/cm<sup>3</sup>) at the lumbar spine [LS] and femoral neck [FN], and cortical vBMD and thickness (mm) at the FN. Using peripheral QCT (Densiscan, Scanco), we assessed radius and tibia trabecular and cortical vBMD annually over the 3 yrs. We used unadjusted and age-adjusted Spearman correlations to describe the relation between IGFBP-2 and annualized rates of bone loss [% loss/yr], stratified by menopausal status in women, and age (< vs. ≥50 years) in men. We then adjusted for bioavailable estradiol [bio E<sub>2</sub>] (pg/ml), measured using mass spectroscopy. We studied 223 women (79 premenopausal, age range and mean IGFBP-2: 21-55 yrs, 545 ng/ml; 144 postmenopausal, 42-97 yrs, 593 ng/ml), and 303 men (119 men, 22-49 yrs, 302 ng/ml; 184 men, 50-91 yrs, 520 ng/ml), not on hormones or bisphosphonates, who had baseline and follow-up scans for at least one site. Adjusting for age, we found no association between IGFBP-2 and bone loss in premenopausal women or men <50 yrs. In postmenopausal women, high IGFBP-2 was associated with bone loss at all sites except the LS, whereas in men ≥ 50 yrs, it was associated with trabecular bone loss at the tibia and LS only. Following additional adjustment for bio E<sub>2</sub>, findings were unchanged in premenopausal women and men; however in postmenopausal women, high IGFBP-2 was then only associated with cortical bone loss at the tibia and FN (see Table).

	Postmenopausal Women		Men ≥ 50 years	
	Mean %Loss/Yr	Un-/Age-/Age+Bio E <sub>2</sub> - %Loss/Yr	Mean %Loss/Yr	Un-/Age-/Age+Bio E <sub>2</sub> - Adjusted Correlations
LS Trabecular vBMD	-1.6	0.02/-0.03/0.03	-1.3	-0.33*/-0.22*/-0.21*
FN Trabecular vBMD	-1.9	-0.30*/-0.28*/-0.16	-1.0	-0.24*/-0.08/-0.09
FN Cortical vBMD	-0.8	-0.26*/-0.31*/-0.24*	-0.04	-0.15/-0.06/-0.08
FN Cortical Thickness	-0.6	-0.30*/-0.19*/-0.14	-0.9	-0.23*/-0.06/-0.01
Radius Trabecular vBMD	-0.8	-0.07/-0.19*/-0.05	-0.5	-0.08/-0.14/-0.13
Radius Cortical vBMD	-0.5	-0.17*/-0.19*/-0.08	-0.4	-0.23*/-0.07/-0.08
Tibia Trabecular vBMD	-0.8	-0.35*/-0.25*/-0.11	-0.2	-0.12/-0.19*/-0.18*
Tibia Cortical vBMD	-0.6	-0.32*/-0.30*/-0.21*	-0.2	-0.10/-0.05/-0.03

\* p<0.05

In older women, cortical bone loss at weight-bearing sites is influenced by high IGFBP-2. In older men, who have greater cortical apposition with aging than women, IGFBP-2 did not influence cortical bone loss. In older women, low estradiol is likely dominant for trabecular bone loss, while in older men, who have higher estradiol than older women, high IGFBP-2 contributes to trabecular loss at the LS and tibia. These results provide further insights on likely differences in hormonal regulation of bone loss, not only by age and gender, but by bone compartment, and suggest a role of the IGF system in age-related bone loss.

**Disclosures:** S. Amin, None.  
This study received funding from: NIH.

## 1285

**Effect of Denosumab vs Alendronate on Bone Turnover Markers and Bone Mineral Density Changes at 12 Months Based on Baseline Bone Turnover Level.** J. P. Brown<sup>1</sup>, C. Deal<sup>2</sup>, L. H. de Gregorio<sup>3</sup>, L. C. Hofbauer<sup>4</sup>, H. Wang<sup>5</sup>, M. Austin<sup>5</sup>, R. B. Wagman<sup>6</sup>, R. Newmark<sup>5</sup>, C. Libanati<sup>5</sup>, J. San Martin<sup>5</sup>. <sup>1</sup>CHUQ Laval University, Quebec City, QC, Canada, <sup>2</sup>Cleveland Clinic, Cleveland, OH, USA, <sup>3</sup>SYNARC/CCBR, Rio de Janeiro, Brazil, <sup>4</sup>Technical University Medical Center, Dresden, Germany, <sup>5</sup>Amgen Inc., Thousand Oaks, CA, USA, <sup>6</sup>Amgen Inc. and Stanford University School of Medicine, San Francisco and Stanford, CA, USA.

Denosumab, an investigational RANKL inhibitor, suppresses osteoclast-mediated bone resorption by a different mechanism than bisphosphonates. We directly compared the effect of denosumab vs brand alendronate (ALN) on bone turnover marker (BTM) changes, and BMD changes based on the baseline levels of serum C-telopeptide (sCTX) and procollagen type 1 N-propeptide (PINP) in a phase 3 study of postmenopausal women with low BMD.

Postmenopausal women (lumbar spine or total hip T-score ≤ -2.0) were randomized 1:1 to receive subcutaneous (SC) denosumab injection (60 mg, every 6 months [Q6M]) + oral placebo weekly or oral ALN (70 mg) weekly + SC placebo injection Q6M. All received calcium and vitamin D. BTM changes from baseline were assessed over 12 months. BMD

gains at the total hip, lumbar spine, femoral neck, and radius at month 12 were compared across quartiles of baseline sCTX.

Subjects (N = 1189; 594 denosumab; 595 ALN; mean age 64 yrs) had a mean lumbar spine T-score of -2.6. With denosumab sCTX decreased by a median of 89%, 77%, and 74% vs 61%, 73%, and 76% with ALN at month 1, 6, and 12, respectively ( $P \leq 0.0001$  month 1 and 6;  $P = 0.5$  month 12). Median PINP decreases at these times were: 26%, 72%, and 72% for denosumab vs 11%, 62%, and 65% for ALN ( $P < 0.0001$  all times). As reported earlier, denosumab resulted in significantly greater gains in BMD vs ALN ( $P \leq 0.0003$  all sites). BMD increases at the total hip were greater for subjects in both groups with higher baseline bone turnover; BMD gains were significantly greater for denosumab vs ALN regardless of baseline bone turnover (table - sCTX; PINP not shown). Results were similar for BMD gains at the lumbar spine, femoral neck, and radius. Adverse events were similar for each group.

Denosumab suppressed bone remodeling and increased BMD at all measured sites more than ALN. BMD gains were consistent across different levels of baseline bone turnover. The differences in results between these drugs may be due to their different mechanism of inhibiting bone turnover.

	Table. Baseline sCTX by Quartile and Percent Change in Total Hip BMD at Month 12			
	sCTX < 0.447 ng/mL	sCTX 0.477 to < 0.631 ng/mL	sCTX 0.631 to < 0.836 ng/mL	sCTX ≥ 0.836 ng/mL
Denosumab				
N	136	135	145	159
Mean % BMD change at 12 months (95% CI)	2.7 (2.3 - 3.1)	3.2 (2.8 - 3.6)	3.6 (3.2 - 3.9)	4.3 (3.9 - 4.7)
Alendronate				
N	148	149	139	125
Mean % BMD change at 12 months (95% CI)	1.9 (1.5 - 2.3)	2.5 (2.1 - 2.9)	2.6 (2.2 - 2.9)	3.1 (2.7 - 3.5)
P-value	0.0089	0.0193	0.0002	<0.0001

**Disclosures:** J.P. Brown, Amgen 3, 4; Procter & Gamble and Sanofi-Aventis 1, 2, 3, 4; Novartis 1, 2, 3, 4; Merck 1, 3.

This study received funding from: Amgen Inc

## 1286

**A Phase III Study of the Effects of Denosumab on Vertebral, Nonvertebral, and Hip Fracture in Women with Osteoporosis: Results from the FREEDOM Trial.** S. R. Cummings<sup>1</sup>, M. R. McClung<sup>2</sup>, C. Christiansen<sup>3</sup>, E. Siris<sup>4</sup>, S. Adami<sup>5</sup>, S. Kutilek<sup>6</sup>, I. R. Reid<sup>7</sup>, J. R. Zanchetta<sup>8</sup>, J. San Martin<sup>9</sup>, C. Libanati<sup>9</sup>, S. Siddhanti<sup>9</sup>, A. Wang<sup>9</sup>, P. D. Delmas<sup>10</sup>. <sup>1</sup>San Francisco Coordinating Center, CPMC Research Institute & UCSF, San Francisco, CA, USA, <sup>2</sup>Oregon Osteoporosis Center, Portland, OR, USA, <sup>3</sup>Center for Clinical and Basic Research, Ballerup, Denmark, <sup>4</sup>Columbia University Medical Center, New York, NY, USA, <sup>5</sup>University of Verona, Verona, Italy, <sup>6</sup>Center for Clinical and Basic Research, Pardubice, Czech Republic, <sup>7</sup>University of Auckland, Auckland, New Zealand, <sup>8</sup>University of Salvador, Buenos Aires, Argentina, <sup>9</sup>Amgen Inc., Thousand Oaks, CA, USA, <sup>10</sup>Universite of Lyon 1 and INSERM Research Unit 831, Lyon, France.

Background: Denosumab, an investigational fully human monoclonal antibody to RANKL, is an inhibitor of osteoclast differentiation, proliferation, and function that is currently being investigated as a treatment for osteoporosis. Clinical trials completed to date have shown that denosumab rapidly decreased bone resorption and increased hip, spine, distal radius, and total body bone mineral density.

Methods: FREEDOM (Fracture REduction Evaluation of Denosumab in Osteoporosis every 6 Months) is a phase III trial for which the primary outcome is the effect of denosumab on risk of new vertebral fracture. Secondary outcomes include denosumab's effect on risk of nonvertebral fracture and hip fracture. A total of 7,868 women were recruited from 214 clinical centers in 32 countries. Subjects were between ages 60 and 90 years (mean age=72.3 years) and had osteoporosis (lumbar spine or total hip T-score <-2.5 and ≥-4.0). The mean lumbar spine T-score was -2.8, and 23% of subjects had prevalent vertebral fractures at baseline.

Participants were randomly assigned to receive denosumab 60 mg every 6 months by subcutaneous injection or matching placebo for 3 years. All participants received elemental calcium 1000 mg/d and vitamin D 400-800 IU/d.

The study remained blinded at the time this abstract was written. As of March 2008, 84% of participants either completed or are ongoing. The last patient visit will be completed in May 2008.

Results: The complete 3-year results, including the effect of denosumab on new vertebral, nonvertebral, and hip fractures, along with safety data, will be available for presentation at the time of the ASBMR meeting.

**Disclosures:** S.R. Cummings, Amgen, Pfizer, Novartis, Zelos 3; Eli Lilly, Procter & Gamble, Zelos, Amgen, Organon, Pfizer 2.  
This study received funding from: Amgen Inc.

## 1287

**The Effects of Lasofoxifene on Bone Turnover Markers: the PEARL Trial.**

**R. Eastell<sup>1</sup>, D. M. Reid<sup>2</sup>, S. Vukicevic<sup>\*3</sup>, J. Thompson<sup>\*4</sup>, D. Thompson<sup>4</sup>, S. R. Cummings<sup>5</sup>, P. D. Delmas<sup>6</sup>.** <sup>1</sup>Metabolic Bone Centre, Northern General Hospital and the University of Sheffield, Sheffield, South Yorkshire, United Kingdom, <sup>2</sup>Applied Medicine, University of Aberdeen Medical School, Foresterhill, Aberdeen, United Kingdom, <sup>3</sup>Department of Anatomy, Zagreb Medical School, Zagreb, Croatia, <sup>4</sup>Pfizer Inc, New London, CT, USA, <sup>5</sup>San Francisco Coordinating Center, CPMC Research Institute and University of California, San Francisco, CA, USA, <sup>6</sup>INSERM Research Unit, University of Lyon, Lyon, France.

Lasofloxifene (LASO) is a potent new selective estrogen receptor modulator that decreases bone turnover, improves bone density and reduces LDL-cholesterol levels. Phase II trials suggested that these effects may be stronger than observed with raloxifene. We tested the effects of LASO on bone turnover markers in the phase III Postmenopausal Evaluation And Risk-reduction with Lasofloxifene (PEARL) trial to examine the magnitude of response and the proportion of women returned to the lower half of the reference interval for young women (a putative goal of therapy). PEARL enrolled 8,556 women aged 59 to 80 years who had osteoporosis defined as a lumbar spine (LS) or femoral neck (FN) T-score < -2.5, and excluded women with a T-score < -4.5 at either site, > 3 radiographic vertebral fractures (VFX), or a VFX within the previous year. Participants received calcium (1,000 mg/d) and vitamin D (400-800 IU/d) and were randomly assigned to 0.25 mg/d, 0.5 mg/d of LASO or placebo. We measured serum bone alkaline phosphatase (b ALP) (Quidel), PINP, osteocalcin (OC), and CTX (Roche Elecsys) in 1104 women aged 59 to 80 (mean, 68 years) at baseline, 1, 3, 6, 12, 24 and 36 months. We found the nadir in bone turnover markers at 12 months and so we report these results in the table that shows the median % change and the median level on treatment (and 95% confidence intervals) and the reference interval in healthy young women (\*Glover et al, Bone 2008).

	LASO 0.25, % change	LASO 0.5, % change	Placebo, % change	LASO 0.25, Median	LASO 0.5, Median	Placebo, Median	Ref Interval*
b ALP, IU/L	-29 (-31, -26)	-27 (-29, -26)	-4 (-6, -1)	17 (16, 17)	16 (16, 17)	22 (21, 22)	9 to 29
PINP, ng/mL	-46 (-48, -44)	-46 (-50, -43)	-4 (-8, -1)	27 (26, 29)	25 (24, 27)	45 (42, 49)	16 to 69
OC, ng/mL	-45 (-47, -44)	-46 (-50, -43)	-6 (-8, -2)	11 (11, 12)	10 (10, 11)	18 (17, 19)	7 to 28
CTX, ng/mL	-48 (-51, -45)	-53 (-55, -48)	-1 (-5, 2)	0.23 (0.21, 0.25)	0.20 (0.18, 0.22)	0.40 (0.37, 0.42)	0.11 to 0.69

Thus, both doses of LASO induced significant reductions in bone turnover markers as compared to placebo. The median marker level on treatment was in the lower half of the reference interval for healthy young women, a level associated with low risk of fracture.

**Disclosures:** R. Eastell, PAREXEL 5; Procter & Gamble Pharmaceuticals 5; Organon Laboratories 5; Novartis 5.

This study received funding from: Pfizer, Inc

## 1288

**The Effects of Lasofoxifene on Fractures and Breast Cancer: 3-Year Results From the PEARL Trial.**

**S. R. Cummings<sup>1</sup>, R. Eastell<sup>2</sup>, K. Ensrud<sup>3</sup>, D. M. Reid<sup>4</sup>, S. Vukicevic<sup>5</sup>, A. LaCroix<sup>6</sup>, U. Sriram<sup>7</sup>, D. Thompson<sup>8</sup>, J. R. Thompson<sup>9</sup>, P. D. Delmas<sup>10</sup>.** <sup>1</sup>CPMC Res. Inst., San Francisco, CA, USA, <sup>2</sup>Northern General Hospital, Sheffield, United Kingdom, <sup>3</sup>U. of Minnesota, Minneapolis, MN, USA, <sup>4</sup>U. of Aberdeen Medical School, Aberdeen, United Kingdom, <sup>5</sup>Zagreb Medical School, Zagreb, Croatia, <sup>6</sup>U. of Washington, Seattle, WA, USA, <sup>7</sup>Saint Joseph Hospital, Chicago, IL, USA, <sup>8</sup>Pfizer Inc, New London, CT, USA, <sup>9</sup>Pfizer Inc., New London, CT, USA, <sup>10</sup>INSERM, U. of Lyon, Lyon, France.

Lasofloxifene (LASO) is a new potent SERM that decreases bone turnover and improves BMD. We tested the effects of LASO on clinical outcomes in the Postmenopausal Evaluation And Risk-reduction with LASO (PEARL) Trial. PEARL enrolled 8,556 women age 59 - 80 years with a lumbar spine (LS) or femoral neck (FN) T-score ≤ -2.5, and excluded women with a T-score < -4.5 at either site, >3 radiographic vertebral fractures (VFX), or a VFX in the previous year. Participants received calcium (1,000 mg) and vitamin D (400-800 IU) and were randomly assigned to LASO 0.25 mg/d, 0.5 mg/d or placebo (PBO). The primary outcome, time to new or worsening VFX, was assessed by ≥1 category change in semiquantitative (SQ) grade confirmed by ≥20% and ≥4 mm decrease in vertebral height or 'binary' SQ rating. Non-vertebral fractures (NonVFX), ER+ breast cancer (BrCa), venous thromboembolic events (VTE), stroke, and CHD were adjudicated by panels of external experts. Compared with PBO, 3 years of LASO improved BMD at the spine (3.3% for both doses, P < 0.001) and FN (2.7% for 0.25 mg and 3.3% for 0.5 mg/d, P < 0.001). LASO 0.25 mg and 0.5 mg reduced VFX by 31 and 42% (P<0.002; table). The 0.5 mg dose decreased the risk of NonVFX by 22% (P=0.02); a 14% decrease with 0.25 mg was not statistically significant (P=0.13). LASO 0.25 mg and 0.5 mg/d reduced the risk of ER+ BrCa by 84% and 67%, respectively. LASO treatment increased the risk of VTE, but not stroke or CHD. Two cases of endometrial cancer occurred in the PBO group, 2 in the 0.25 mg, and 1 in the 0.5 mg LASO groups. Hot flushes, muscle spasm, vaginal discharge, candidiasis, uterine polyps and prolapse occurred more often; back pain, arthralgia, insomnia, hyperlipidemia, hypertension, and gastritis occurred less often with LASO.

At 3 years LASO showed no increased risk of CHD or endometrial cancer and an increased risk of VTE. The benefits at 3 years demonstrated a decreased risk of VFX and ER+ breast cancer, and with the 0.5 mg/d dose, a significantly decreased risk of NonVFX.

Cumulative Outcomes of 3 years treatment with lasofloxifene versus placebo (Rate per 1,000 subjects over 3 years)

Outcome	PBO	LASO 0.25 mg	HR (95% CI)	P-value	LASO 0.5 mg	HR (95% CI)	P-value	LASO pooled	HR (95% CI)	P-value
VFX	64.2	47.2	0.69 (0.55,0.87)	<0.01	38.2	0.58 (0.45, 0.73)	<0.01			
NonVFX	73.3	63.5	0.86 (0.70, 1.05)	0.13	58.6	0.78 (0.64, 0.96)	0.02			
ER+ BrCa	4.4	0.7	0.16 (0.04, 0.73)	0.01	1.5	0.33 (0.11, 1.02)	0.04	1.1	0.24 (0.09, 0.65)	<0.01
VTE	3.5	9.1	2.60 (1.26, 5.40)	0.01	7.7	2.20 (1.04, 4.64)	0.03	8.4	2.40 (1.21, 4.74)	0.01
Stroke	7.0	4.9	0.70 (0.35, 1.38)	0.30	6.0	0.85 (0.44, 1.62)	0.62	5.4	0.77 (0.44, 1.36)	0.37
CHD	19.3	16.1	0.83 (0.56, 1.23)	0.36	15.1	0.78 (0.52, 1.16)	0.21	15.6	0.81 (0.58, 1.13)	0.21

LASO = lasofloxifene; PBO = placebo; HR = hazards ratio; CI = confidence interval.

**Disclosures:** S.R. Cummings, Amgen 2, 3; Novartis 2, 3; Lilly 2, 3; Pfizer 2, 3. This study received funding from: Pfizer, Inc.

## 1289

**Ergocalciferol Is Not Bioequivalent to Cholecalciferol In Vitamin D Insufficient Hip Fracture Cases.**

**P. Glendenning<sup>1</sup>, H. Seymour<sup>\*2</sup>, M. J. Gillett<sup>\*1</sup>, G. T. Chew<sup>\*2</sup>, P. Goldswain<sup>\*2</sup>, C. Inderjeeth<sup>\*3</sup>, S. Vasikaran<sup>\*1</sup>, M. Taranto<sup>\*1</sup>, A. Musk<sup>\*1</sup>, W. D. Fraser<sup>4</sup>.** <sup>1</sup>Biochemistry, Royal Perth Hospital, Perth, Australia, <sup>2</sup>Geriatric Medicine, Royal Perth Hospital, Perth, Australia, <sup>3</sup>Aged Care, Sir Charles Gairdner Hospital, Perth, Australia, <sup>4</sup>Clinical Biochemistry, University of Liverpool, Liverpool, United Kingdom.

Vitamin D insufficiency is commonly associated with hip fracture. In this patient group, the equipotency of ergocalciferol and cholecalciferol has not been studied in a randomised, double-blind, placebo controlled trial or with measurement of 25OHD by high performance liquid chromatography (HPLC) as the primary outcome variable.

Our study compared the effects of cholecalciferol and ergocalciferol supplementation on circulating 25-hydroxyvitamin D (25OHD) and parathyroid hormone (PTH) levels in vitamin D insufficient hip fracture patients. 95 hip fracture patients with vitamin D insufficiency (25OHD < 50 nmol/L) were randomised to treatment with either ergocalciferol 1000 IU daily plus matching placebo (n=48) or cholecalciferol 1000 IU daily plus matching placebo (n=47) for 3 months. The primary outcome variable was total 25OHD concentration measured by HPLC; secondary endpoints were total 25OHD measured by radioimmunoassay (RIA), intact PTH (iPTH) and bioactive (1-84) PTH (wPTH).

70 patients (73.7%) completed the study with paired samples for analysis. Cholecalciferol supplementation resulted in a greater increase in HPLC measured total 25OHD than supplementation with an equivalent dose of ergocalciferol (P = 0.010). Results were similar for total 25OHD measured by DiaSorin RIA (P < 0.001). Changes in iPTH and wPTH were not significantly different between treatments.

In vitamin D insufficient hip fracture patients, supplementation with cholecalciferol 1000 IU daily for 3 months was more effective in increasing circulating total 25 OHD than an equivalent dose of ergocalciferol.

**Disclosures:** P. Glendenning, Partial funding obtained from Boots healthcare who provided ergocalciferol tablets and placebo tablets for free. 3.

## 1290

**Case Finding for the Management of Osteoporosis with FRAX - Assessment and Intervention Thresholds for the UK.** J. E. Compston<sup>1</sup>, E. McCloskey<sup>\*2</sup>, H. Johansson<sup>\*3</sup>, O. Strom<sup>\*3</sup>, F. Borgstrom<sup>\*3</sup>, A. Oden<sup>\*3</sup>, J. Kanis & the National Osteoporosis Guideline Group<sup>\*3</sup>. <sup>1</sup>Department of Medicine, University of Cambridge, Cambridge, United Kingdom, <sup>2</sup>Northern General Hospital, Osteoporosis Centre, Sheffield, United Kingdom, <sup>3</sup>University of Sheffield, WHO Collaborating Centre for Metabolic Bone Diseases, Sheffield, United Kingdom.

The FRAX tool has recently become available to compute the 10-year probability of fractures in men and women from clinical risk factors (CRFs) with or without the measurement of femoral neck bone mineral density (BMD). The aim of this study was to develop a case-finding strategy for men and women from the UK at high risk of osteoporotic fracture by delineating the fracture probabilities at which BMD testing or intervention should be recommended. Fracture probabilities were computed using the FRAX tool calibrated to the epidemiology of fracture and death in the UK. Intervention thresholds, underpinned by cost-effectiveness analysis, were set by age, based on the fracture probability at which intervention became cost-effective in women with a history of a prior osteoporosis related fracture. Assessment thresholds for the measurement of BMD followed current practice guidelines in the UK where individuals are considered to be eligible for assessment in the presence of one or more CRF. An upper assessment threshold (i.e. a fracture probability above which patients could be treated without recourse to BMD) was based on optimisation of the positive predictive value of the assessment tool. The consequences of assessment and intervention thresholds on the requirement for BMD tests and interventions were assessed using the distribution of clinical risk factors and femoral neck BMD for women in the source cohorts used for the development of the FRAX. The intervention threshold at the age of 50 years corresponded to a ten-year probability of a major osteoporotic fracture of 7.5%. This rose progressively with age to 30% at the age of 80 years. Assessment thresholds (6-9% at the age of 50 years) also rose with age (18-36% at the age of 80 years). The use of these thresholds in a case-finding strategy would identify 6-20 % of women as eligible for BMD testing and 23-46% as eligible for treatment, depending on age. This study provides a method of developing management algorithms for osteoporosis from the estimation of fracture probabilities, rather than those based on BMD alone or BMD with single or multiple CRFs.

**Disclosures:** J.E. Compston, Servier 1, 3, 4; Procter and Gamble / Nycomed / Roche 1, 4; Novartis / Amgen / Wyeth / Eli Lilly 1, 4; Merck Sharpe & Dohme 1, 4.

## 1291

**A Randomized, Double-Blind, Placebo-Controlled Study of Odanacatib (MK-822) in the Treatment of Postmenopausal Women with Low Bone Mineral Density: 24-Month Results.** M. McClung<sup>\*1</sup>, H. Bone<sup>\*2</sup>, F. Cosman<sup>\*3</sup>, C. Roux<sup>\*4</sup>, N. Verbruggen<sup>\*5</sup>, C. Hustad<sup>6</sup>, C. DaSilva<sup>\*6</sup>, A. Santora<sup>\*6</sup>, A. Ince<sup>\*6</sup>. <sup>1</sup>Oregon Osteoporosis Center, Portland, OR, USA, <sup>2</sup>Michigan Bone and Mineral Center, Detroit, MI, USA, <sup>3</sup>Helen Hayes Hospital, West Haverstraw, NY, USA, <sup>4</sup>Cochin Hospital, University of Paris, Paris, France, <sup>5</sup>Merck Research Laboratories, Brussels, Belgium, <sup>6</sup>Merck Research Laboratories, Rahway, NJ, USA.

Odanacatib, a selective inhibitor of cathepsin K, has been shown to rapidly and reversibly decrease bone resorption in both preclinical and Phase I clinical studies. A randomized, double-blind, 1-year dose-ranging trial with a 1-year extension was performed in postmenopausal women with low bone mineral density (BMD) to evaluate the safety and efficacy of weekly doses of placebo, 3, 10, 25 or 50 mg of odanacatib on BMD and biochemical indices of bone turnover.

Postmenopausal women (N=399, mean age: 64.2 ± 7.8 years) with BMD T-scores ≤ -2.0 at the lumbar spine, femoral neck, trochanter, or total hip and ≥ -3.5 at all sites were randomized to receive placebo or 1 of 4 doses of odanacatib. All participants also received weekly 5600 IU vitamin D3 supplements and daily 500-mg calcium supplements if normal consumption was <1000 mg calcium/day. 320 women from the 12-month base study continued into the 1-year extension, and 280 women completed 2 years of treatment. Participants and investigators remained blinded to treatment allocation during the extension period. The primary endpoint was the percent change vs. baseline in lumbar spine BMD. Other endpoints included the percent change vs. baseline in BMD measurements at the proximal femur, total body, and distal forearm, as well as in biochemical markers of bone resorption and bone formation.

Twenty-four months of treatment produced progressive dose-related increases in BMD vs. baseline. With the 50-mg dose of odanacatib, lumbar spine and total hip BMD increased 5.5% and 3.2%, respectively, whereas BMD at these sites was essentially unchanged with placebo (-0.2% and -0.9%). Urinary N-telopeptide (NTx/Cr) and bone-specific alkaline phosphatase (BSAP) decreased 52% and 13%, respectively, with the 50-mg dose, whereas uNTx/Cr decreased 5% and BSAP increased 3% with placebo. The safety profile of odanacatib was generally favorable, with no dose-related trends in any adverse experiences. Rash was reported in 4.8% of those in the 50-mg group and in 7.9% of those in the placebo group.

These results show that 2 years of odanacatib treatment was generally well-tolerated and increased lumbar spine and total hip BMD in postmenopausal women with low BMD.

**Disclosures:** C. Hustad, Employee of Merck & Co., Inc., the sponsor of the study. 5. This study received funding from: Merck & Co., Inc.

## 1292

**C-telopeptide and Bone Alkaline Phosphatase Predict Morphometric Vertebral Fracture Risk in a Pivotal Phase III Trial of Toremifene in Men on ADT.** M. R. Smith<sup>\*1</sup>, R. A. Morton<sup>\*2</sup>, M. L. Hancock<sup>\*2</sup>, G. Barnette<sup>\*2</sup>, D. Rodriguez<sup>\*2</sup>, K. A. Veverka<sup>2</sup>, M. Steiner<sup>\*2</sup>. <sup>1</sup>Massachusetts General Hospital, Boston, MA, USA, <sup>2</sup>GTx, Inc., Memphis, TN, USA.

Hypogonadism is a primary risk factor for male osteoporosis. Castrate levels of testosterone and estrogen are rapidly achieved and sustained in men undergoing androgen deprivation therapy (ADT) for prostate cancer. We conducted a prospective trial to determine whether or not toremifene, a SERM, prevents fractures in men on ADT. A total of 1389 men with prostate cancer were randomly assigned to receive 80 mg toremifene or placebo once daily for 24 months. All subjects were on ADT for ≥6 months, had a serum PSA ≤4 ng/mL, were ≥70 years of age or were at or below WHO thresholds for spine or hip bone mineral density at baseline. The primary endpoint was met with a 54% reduction in new onset morphometric vertebral fractures (MVF; p=0.032) in the intent-to-treat population. An analysis of serum markers of bone turnover revealed a marked suppression of bone specific alkaline phosphatase (bALP), osteocalcin (OC), and C-telopeptides (CTX) in subjects taking toremifene relative to placebo and baseline values. The most common adverse events were joint pain, dizziness, back pain, and extremity pain. In addition, we evaluated whether the serum markers of bone turnover could predict fracture risk. bALP exhibited significantly greater increases from baseline to months 12 and 24 (0.04±1.64, p=0.05 and 4.33±3.06, p=0.01, respectively) among those subjects with a MVF compared to subjects with no MVF. Subjects not experiencing a MVF showed a decrease in mean bALP from baseline to both 12 and 24 months (-1.91±0.42 and -3.73±0.35, respectively). Absolute changes in CTx from baseline to both 12 and 24 months differed significantly (p=0.04 and p=0.02, respectively) between subjects who incurred a MVF and those who did not. CTx increased nearly 14% from baseline to 24 months (p=0.02) in patients who incurred MVF. The prognostic significance of the absolute and percent change from baseline of the three bone turnover markers on the development of a MVF were evaluated in a Cox regression model as time dependent covariates. Increases in CTx were associated with a significantly (p<0.01) greater hazard for the development of a MVF. Percent increases in bALP, though not absolute change, were significantly associated with increased hazard for developing a MVF (p<0.01). Changes in OC were similar to those observed for other bone markers though results did not reach statistical significance. In conclusion, these data indicate that the serum bone turnover markers CTx and bALP predict fracture risk in men on ADT.

**Disclosures:** M.R. Smith, Amgen 2; Novartis 2; GTx, Inc. 2; Merck 2.

## 1293

**Trabecular Risk of Fracture, Caused by Disuse, is Strongly Influenced by Baseline Morphology.** E. Ozcivici, S. Judex. Biomedical Engineering, SUNY Stony Brook, Stony Brook, NY, USA.

Genetic variations affect the magnitude of disuse induced bone loss. Here, a genetically heterogeneous mouse population was subjected to mechanical unloading to determine if specific aspects of the trabecular structure can predict changes in its mechanical properties when exposed to a strong catabolic stimulus (disuse). F2 female progeny of BALB (high mechanosensitivity) and C3H (low mechanosensitivity) inbred mouse strains (n=359) were hindlimb unloaded for 3 weeks. At baseline (16wk) and endpoint (19wk), the distal femoral metaphysis was scanned by in vivo microCT and converted into finite element models to simulate a uniaxial compression test. Disuse induced longitudinal changes in peak Von-Mises (VM) stresses were calculated for each mouse and stratified by their respective percentiles (Low Responders, LR: -10-14% change, n=54; Intermediate Responders, IR: 24-29% change, n=54; High Responders, HR: 42-92% change, n=54). F2 mice that were subjected to 3wk of hindlimb unloading lost 43% of their trabecular BV/TV, accompanied by losses in Conn.D, Tb.N, Tb.Th that amounted to 38%, 17%, and 18%, respectively (p<0.05). As a consequence of this deterioration, both peak stress levels and skewness of the stress distributions (an indicator of trabecular load bearing efficiency) increased by 27% and 104%, respectively (p<0.05). Disuse induced changes in peak stresses were normally distributed (R2>0.95). At baseline, no significant differences in trabecular structure were observed between the low (LR) and intermediate (IR) response groups. In contrast, those mice that experienced the greatest changes in VM stresses (HR) had significantly smaller BV/TV (-22%), Tb.N (-10%), and Tb.Th (-8%) than the IR group. Despite these differences in morphology, bone mechanical properties were similar between the three groups at baseline. Consistent with the changes in VM stresses, loss of BV/TV was much greater in HR mice (-58%) than in IR (-44%), or LR mice (-23%). Linear multiple regressions showed strong correlations between baseline Tb.Th and Conn.D and peak stresses altered by disuse (R2=0.70, 0.77 and 0.65 for HR, IR and LR respectively). This data indicate that peak stresses in healthy trabecular bone do not necessarily reflect the differences in its quantity and structure (i.e., connectedness, thickness and number). The results also demonstrate that a poor trabecular structure predisposes an individual to great tissue losses and a large increase in peak stresses upon the loss of weightbearing. Therefore, treatment of individuals with poor trabecular bone structures may also be protective against severe tissue losses caused by conditions like bedrest or space flight.

**Disclosures:** E. Ozcivici, None.

This study received funding from: NASA.

## 1294

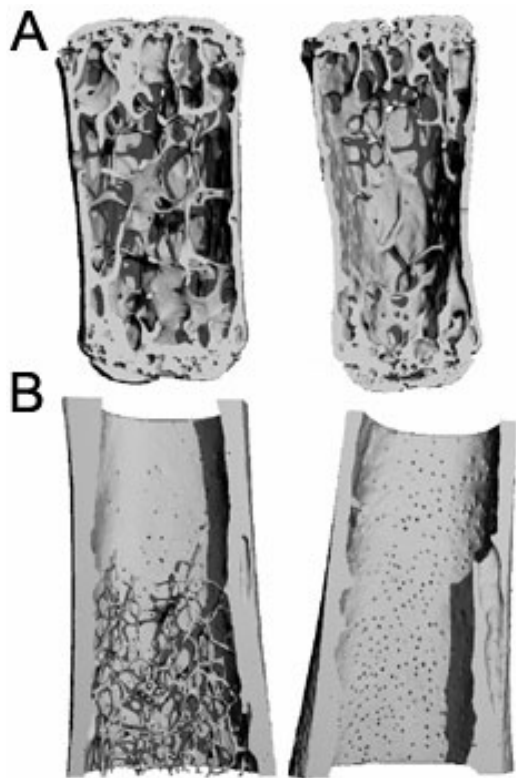
**Excessive Erythropoiesis Affects Bone Architecture.** G. Kuhn<sup>\*1</sup>, P. Schneider<sup>\*1</sup>, B. Schuler<sup>\*2</sup>, M. Meier<sup>\*1</sup>, J. Vogel<sup>\*2</sup>, R. Müller<sup>1</sup>. <sup>1</sup>Institute for Biomechanics, ETH Zurich, Zurich, Switzerland, <sup>2</sup>Institute for Veterinary Physiology, Vetsuisse-Faculty, University of Zurich, Zurich, Switzerland.

Excessive stimulation of hematopoiesis as found e.g. in polycythemia vera or erythropoietin (epo) treatment will cause an increase in space requirements and metabolic demands of red bone marrow. Expansion of hematopoietic tissue is limited by the surrounding bone. We investigated whether bone can adapt to increased marrow volume by increasing marrow spaces and to metabolic demands by allowing more vessels to penetrate the cortex.

Femur and sternum were obtained from male 12-13 week old transgenic mice (tg) that show an oxygen-independent constitutive over-expression of human epo cDNA, wild-type (B6) controls, and wild-type animals treated with the epo-analogue novel erythropoiesis stimulating protein (NESP) for 4 weeks. Hematocrit of the tg mice was 80% compared to 45% in controls and 69% in the NESP group. Synchrotron micro-computed tomography images were taken at the proximal femur, the femoral mid-diaphysis (42% femoral length) and the 3rd segment of the sternum and quantitatively analysed.

In both bones of tg animals we found either a high number of canals penetrating the cortex, or canals with very large diameters. Less and smaller canals were found in the controls. Preliminary quantitative analysis of the sternum showed a decrease in trabecular bone volume density by 40% and an increase in trabecular spacing by 50% in tg mice (Fig. 1a) compared to their wild-type control. Trabecular thickness was similar in both groups. Cortical thickness was significantly reduced in the femur shaft of tg animals. Areas of the femur shaft that were filled with trabecular bone in controls were devoid of trabeculae in tg mice (Fig. 1b). Values of the NESP-treated group were between controls and tg animals.

Our results show that chronic excessive erythropoiesis leads to an increase in marrow cavity volume with a concomitant reduction of cortical and trabecular bone as well as an increase in cortical porosity. One reason for inferior bone properties in tg animals might be increased intramedullary pressure due to the expansion of the red bone marrow. Angiogenesis might be stimulated to enable increased trafficking of erythrocytes and reticulocytes from bone marrow to peripheral circulation as well as by a high demand of protein, leading eventually to a higher vascularization of the cortex.



**Disclosures:** G. Kuhn, None.

## 1295

**Combined Effects of Irradiation and Unloading on Murine Bone.** E. R. Bandstra<sup>1</sup>, S. E. Riffle<sup>\*1</sup>, S. A. J. Lloyd<sup>\*1</sup>, J. S. Willey<sup>1</sup>, G. A. Nelson<sup>\*2</sup>, M. J. Pecaut<sup>\*2</sup>, T. A. Bateman<sup>1</sup>. <sup>1</sup>Bioengineering, Clemson University, Clemson, SC, USA, <sup>2</sup>Radiation Medicine, Loma Linda University, Loma Linda, CA, USA.

Radiation may have deleterious effects on the trabecular bone of astronauts in the spaceflight environment. Solar particle events have the ability to deliver 1 Gy of proton radiation. On long-duration missions, astronauts will be exposed to both radiation and microgravity, which is already a well-documented cause of bone atrophy. This study investigated the effects of whole body irradiation combined with skeletal unloading. Sixteen-week-old female C57BL/6 mice (n=15/group; 4 groups) were exposed to either 1 Gy of 250 MeV protons (IRR) or served as non-irradiated controls (NR). One day after exposure, half the irradiated mice and half the control mice were hindlimb suspended (HLS), with the remainder serving as normally loaded controls (LC). Mice were killed after 4 weeks of unloading. MicroCT analysis was performed on trabecular bone in the proximal tibia. Radiation treatment alone resulted in a significant loss of bone and deterioration of trabecular microarchitecture at 4 weeks (i.e., loss of vBMD). Similarly, HLS alone induced substantial deterioration of bone. HLS alone also resulted in increased circulating levels of TRAP5b at sacrifice. While IRR alone did not exhibit elevated TRAP5b at 4 weeks, HLS + IRR did result in an increase in TRAP5b relative to both non-irradiated control (P<0.01) and HLS alone (P=0.05). HLS + IRR resulted in generally lower values for BV/TV, Conn.D, vBMD, Tb.Sp, Tb.N, and SMI than both HLS and IRR independently. Overall, the combination of IRR + HLS resulted in greater bone loss and deterioration of trabecular microarchitecture than the two challenges separately. Although both skeletal challenges induced atrophy, bone loss due to HLS alone was substantially greater than IRR alone (i.e., a 90% lower vBMD relative to control for HLS vs. 16% lower vBMD for IRR). During spaceflight missions, astronauts typically lose on the order of 2.5% of trabecular bone per month. B6 are a low bone density mouse model, and thus small amounts of atrophy can be large percent bone loss. Future models of HLS + IRR would benefit from using animals with greater baseline amounts of trabecular bone. This would more appropriately model the skeletal challenges of combined microgravity and radiation experienced by astronauts in the spaceflight environment.

**Disclosures:** E.R. Bandstra, None.

This study received funding from: NSBRI/NASA.

## 1296

**NanoCT Can be Used to Assess Mechanically Related Modelling and Remodelling in the Mouse Fibula.** L. Saxon<sup>1</sup>, P. L. Salmon<sup>2</sup>, A. Sasov<sup>\*2</sup>, L. Lanyon<sup>1</sup>. <sup>1</sup>Royal Veterinary College, London, United Kingdom, <sup>2</sup>SkyScan, Kontich, Belgium.

**Introduction:** Nondestructive imaging of bone structure at the material level including imaging of osteocyte lacunae requires submicron resolution. NanoCT is a high resolution CT imaging technique that images voxel dimensions down to less than 150 nanometers. Using this method we set out to determine whether it can detect changes in osteocyte number, the contours of bone formation/resorption surfaces, and cortical bone geometry in the externally loaded mouse fibula.

**Methods:** Female C57BL/6 mice (n=5) at 17 weeks of age underwent two weeks of mechanical loading using a non-invasive tibia/fibula loading model that has been reported previously. The right fibula was exposed daily to 10 minutes of dynamic axial loads and the left fibula served as an internal non-loaded control. At the end of the two weeks of loading, the mice were killed and the fibulae were extracted and stored in 70% alcohol. High-resolution nano-CT was used to scan a region 2-3mm distal from the tibia-fibula junction (SkyScan 2011; SkyScan, Kontich, Belgium) at 0.400 nm voxel size (emission spot size 300 nm).

**Results:** Two weeks of mechanical loading to the right fibula resulted in significant side-to-side differences in cortical bone geometry, bone remodelling and osteocyte lacunar morphometry. There was a substantial increase in fibular volume and outward expansion of the fibular periosteum. There was also a sizeable increase in medullary volume indicating endocortical resorption; the net result on cortical thickness was no change. Elevated fractal dimension (0-40 um range) in the right fibulas signified increased surface irregularity due to surface remodelling, and a sharp drop in TB.Pf to negative values indicated extensive concave surfaces associated with resorption. Extensive low-density formation sites were also visible on the surfaces of the loaded right, but not the left, fibulas. There was a doubling of the percent volume occupied by osteocyte lacunae. Osteocyte diameter increased while separation decreased. The number density of osteocyte lacunae per fibular volume increased as did the volume of individual lacunae, in the loaded compared to non loaded fibulas.

**Conclusion:** NanoCT appears to be an effective tool for quantifying osteogenic changes in response to a mechanical loading in the mouse fibula; these changes involve outward cortical expansion and an increase in osteocyte lacunar number density and size.

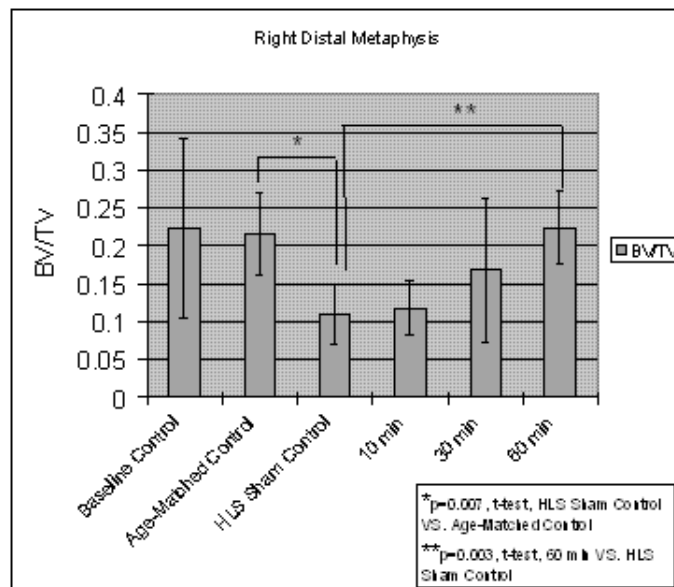
**Disclosures:** L. Saxon, None.

This study received funding from: SkyScan.

## 1297

**Loading Duration Influences the Degree of Inhibition of Bone Loss using Dynamic Muscle Stimulation in a Disuse Rat Model.** Y. Qin<sup>1</sup>, M. Malbani<sup>\*1</sup>, M. Shih<sup>2</sup>, W. Carroll<sup>\*2</sup>. <sup>1</sup>Biomedical Engineering, SUNY Stony Brook, Stony Brook, NY, USA, <sup>2</sup>RS Medical, Inc., Vancouver, WA, USA.

Musculoskeletal adaptations to aging and disuse environment have significant physiological effects on skeletal health, i.e., osteopenia and bone loss. Muscle stimulation (MS) via contractions has been shown to promote blood flow to bone, possibly by creating a pressure gradient within the microvasculature. The overall hypothesis for this study is that dynamic MS can enhance anabolic activity in bone, and inhibit bone loss in a functional disuse condition. Using a hindlimb suspension (HLS) rat model, electro-induced dynamic MS was applied as replacement of the normal weight-bearing activity of the hindlimb with two skin patch electrodes at the right quadriceps muscles for total of 30 animals. The stimulus was applied at 115 mA, 71 Hz, 0.2 ms pulse with 3s on and 8s rest. The animals were divided into six groups (5 per group), including 1) baseline control, 2) age-matched control, 3) hindlimb suspended (HLS) sham control, 4) HLS+10 min MS, 5) HLS+30 min MS, 6) HLS+60 min MS, 5days per week, for a total of 4weeks. Left and right femurs were harvested for micro-computed tomography analysis. Distal metaphyseal regions and one epiphyseal region of the femurs (0.75mm per region) were scanned at 15µm resolution and evaluated to obtain bone volume fraction (BV/TV), connectivity (Conn.D), and trabecular number (Tb.N). Disuse alone generated significant bone loss (-49.03% BV/TV, p=0.007, -58.55% Conn.D, -23.74% Tb.N, comparing to the age-match control). Dynamic muscle contraction at 30 min demonstrated anabolic effects at the metaphyseal regions (52.72% BV/TV, p=0.24, 76.38% Conn.D, 11.97% Tb.N, when comparing to the average HLS sham control). MS at 10 min showed a lesser response (7.31% BV/TV, 23.89% Conn.D, 3.17% Tb.N). The most significant response occurred at 60 min MS loading [103.43% BV/TV (p=0.003, Fig. 1), 164.65% Conn.D, 22.35% Tb.N]. These results demonstrated that dynamic electro-induced muscle contraction can indeed initiate adaptive response to inhibit bone loss under functional disuse environment with a dose dependent pattern, in which 60 min low-energy contraction is able to recover 100% of bone loss induced by disuse. These preliminary data suggest that low-level bone strain and/or increased fluid pressure induced by MS may be crucial factors in musculoskeletal tissue remodeling.



**Disclosures:** Y. Qin, None.

This study received funding from: NIH (AR052379) and RS Medical.

## 1298

**Dependence of Endosseous Implant Anchorage on Mechanostructural Determinants of Peri-implant Bone Trabeculae.** Y. Gabet<sup>\*1</sup>, R. Voide<sup>\*2</sup>, T. L. Mueller<sup>\*2</sup>, D. Kohavi<sup>\*3</sup>, R. Müller<sup>2</sup>, I. Bab<sup>1</sup>. <sup>1</sup>Bone Laboratory, Institute for Dental Sciences, Faculty of Dental Medicine, The Hebrew University of Jerusalem, Jerusalem, Israel, <sup>2</sup>Institute for Biomechanics, ETH Zürich, Zürich, Switzerland, <sup>3</sup>Oral Implant Center, Hebrew University-Hadassah School of Dental Medicine, Jerusalem, Israel.

Low bone mass is highly prevalent among patients receiving endosseous implants. In turn, the implantation prognosis in low density skeletal sites is poor. However, little is known about the mechanostructural determinants of the implant anchorage. Using metabolic manipulations that lead to low bone density and to its rescue, we show here critical anchorage dependence on the peri-implant bone (PIB). Titanium implants were inserted horizontally into the proximal tibial metaphysis of adult rats, 6 weeks postorchietomy (ORX) or sham-ORX. Systemic intermittent administration of parathyroid hormone iaPTH(1-34) or vehicle commenced immediately thereafter for 6 weeks. Implant anchorage was analyzed using micro-image guided failure assessment

(µIGFA) in pullout, which allows concomitant high resolution analysis of failure initiation and progression combining 3D µCT imaging and biomechanical testing. Reactive forces in the cortex were negligible. Failure of implant anchorage occurred mainly at the thinnest segment of individual trabeculae, 0.5-1.0 mm away from the implant. ORX-induced low density trabecular bone showed the poorest biomechanical properties, due mainly to decreased trabecular number. It presented the highest intratrabecular and lowest osseointegration (OI, bone-implant bonding) failure rates. Treatment with iaPTH(1-34) induced supranormal increases in bone density and biomechanical parameters. The increases in trabecular thickness (Tb.Th) and OI in these animals were of a similar magnitude and were associated with a remarkable shifting of failure to the OI. A particularly tight correlation was found between the Tb.Th and all the biomechanical parameters ( $r^2 = 0.862$ ,  $r^2 = 0.823$ ,  $r^2 = 0.737$  for ultimate force, stiffness and toughness, respectively). iaPTH(1-34) did not affect the trabecular number. These results provide a direct link between bone quality and its importance in determining implant mechanics, thus supporting a model wherein the anchorage failure involves buckling of the weakest trabeculae followed by a "domino reaction" leading to PIB collapse. iaPTH(1-34) minimizes this reaction thus portraying Tb.Th as a target for enhancing implant anchorage.

**Disclosures:** Y. Gabet, None.

## 1299

**Microdamage Repair and Remodeling Requires Mechanical Loading.** E. I. Waldorff<sup>\*1</sup>, K. B. Christenson<sup>\*1</sup>, L. A. Tesmer<sup>\*2</sup>, S. A. Goldstein<sup>1</sup>. <sup>1</sup>Orthopaedic Surgery, University of Michigan, Ann Arbor, MI, USA, <sup>2</sup>Rheumatology, University of Michigan, Ann Arbor, MI, USA.

Prior work demonstrates that bone remodeling in response to fatigue microdamage is altered with age, which may increase fracture risk. Furthermore, bone loss associated with aging may result from disuse due to reductions in physical activity or infirmity. The purpose of this study was to examine the effects of disuse on bone remodeling in response to microdamage, potentially providing clinically important insight into the relationship between microdamage accumulation and increased fracture risk in the elderly.

At day 0, 120 male 6-month old Sprague Dawley rats were assigned to 1 of 2 groups: weight-bearing (WB) or hindlimb suspension (HS). Within each group, the rats were further divided into 3 subgroups (n=20), corresponding to 3 sacrificial times (day 14, 18 or 35). At day 14, animals were anesthetized and their left tibia underwent cyclic 4-point bending in order to produce fatigue-induced microdamage (7200 cycles at 2 Hz, -7000 microstrain max. at the lateral mid-diaphysis for both WB and HS). At sacrifice, right/left pairs of tibiae were assigned to 1 of 3 treatments within each subgroup: flow cytometry for HSC and monocyte markers (n=6), basic fuchsin staining for microdamage assessment (n=7), or ELF97 (TRAP) fluorescent staining (n=7). Prior to staining, morphologic analysis was conducted on the last two groups using 3D microCT.

Morphologic examinations revealed that the damage induced a stress fracture response, which at day 35 resulted in a sig. increase in woven bone apposition for both WB and HS, with the WB group being sig. greater than the HS group. At day 35, the WB group had a sig. decrease in microdamage, while the HS group showed no change in damage remaining from day 14. Flow cytometry indicated that a shift in the osteoclast lineage had occurred due to an increase of HSCs, and a decrease of monocytes in the damaged leg for WB compared to HS at day 35. HS showed no difference between contralateral tibiae for both flow cytometry markers at any time points, indicating that the histological evidence of "no damage removal" at day 35 for HS was due to a lack of osteoclast activation, and not a change in the targeting mechanisms of remodeling.

This study demonstrated that disuse alters the microdamage response through a reduction in woven bone production and the lack of resorption of microdamage. The data suggests that elderly individuals with severe activity reductions may further accumulate microdamage. Most importantly, while a variety of studies have proposed that the repair of microdamage is triggered by cell apoptosis, these results suggest this mechanism may be insufficient without the stimulus associated with mechanical usage.

**Disclosures:** E.I. Waldorff, None.

## 1300

**Lovastatin Best Enhances Fracture Repair When Administered One Week Post-Fracture.** G. E. Gutierrez<sup>1</sup>, J. S. Nyman<sup>2</sup>, S. A. Munoz<sup>\*1</sup>, S. B. Jadhav<sup>\*1</sup>, G. R. Mundy<sup>1</sup>. <sup>1</sup>Center for Bone Biology, Vanderbilt University and Medical Center, Nashville, TN, USA, <sup>2</sup>Orthopaedics, Vanderbilt University and Medical Center, Nashville, TN, USA.

Statins stimulate osteoblast differentiation by their effects on BMP2 gene transcription. Retrospective clinical studies and animal models have suggested that statins may increase bone mineral density and reduce the risk of osteoporosis and fractures (Bauer DC, 1999).

The purpose of this study was to determine whether lovastatin (LV), when administered locally and/or systemically at the time of fracture or one week later, could positively affect bone healing using a closed femoral fracture model in rats.

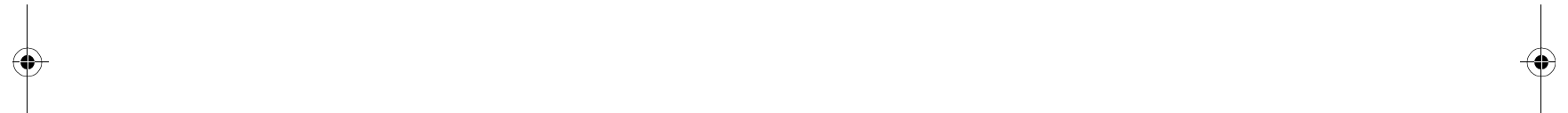
Methods: Femoral fractures were created, following intramedullary pinning in rats. Groups (n=12) included vehicle-treated (veh), and LV IM (1.5-1500 µg) administered once within 2 hours of fracture in a) close proximity to the fracture site (ipsilateral), b) in the contralateral limb, and c) ipsilateral one week after fracture (delayed). Radiographs were taken at day 0, 14 and 28 days after procedure. Animals were euthanized at day 28 and femora harvested for biomechanical testing and µCT.

Results: Compared to veh, radiographs showed increased bridging at the cortices with LV treatment at 2 and 4 weeks even when LV was administered in the contralateral side. By biomechanical testing, there was a dose-response increase in maximal force and stiffness (up 41% and 46% respectively when compared to veh) in bones treated with LV, and this increase was enhanced when administered one week after fracture (16% vs. 42% with 150

ug LV). There was also a positive effect when LV was injected in the contralateral side.  $\mu$ CT images showed a decrease in gaps within the bridging cortices of the callus when treated with LV (up to 26.4% improvement) and with delayed treatment (46.9% improvement) which correlated with the increases in biomechanical strength ( $r=0.56$ ). These results demonstrate that a single sustained-release injection of LV accelerates femoral fracture repair locally and systemically in rats, and that this effect is enhanced when LV is administered one week after fracture. It has been previously shown that fracture induces endogenous expression of BMP2 with maximal peak at one week. The delayed effect reported here may be due to LV inducing higher levels of BMP2 expression beyond one week with the consequent acceleration of fracture healing.

A pharmaceutical agent capable of accelerating fracture healing in patients, improve their outcome and quality of life, even when administered systemically, will be an important advance in orthopaedics and may be beneficial for other applications where BMP2 has been shown to be efficacious.

**Disclosures:** *GE. Gutierrez, OsteoGenix 2, 5.*





## F002

### BMP-2 Stimulates a Feedback Activation loop for Expression of NFATc1 in Osteoblasts. C. C. Mandal<sup>1</sup>, G. G. Choudhury<sup>\*2</sup>, N. Ghosh-Choudhury<sup>3</sup>.

<sup>1</sup>Pathology, University of Texas Health Science Center at San Antonio, San Antonio, TX, USA, <sup>2</sup>Medicine, Nephrology, University of Texas Health Science Center at San Antonio and South Texas Veterans Health Care System, San Antonio, TX, USA, <sup>3</sup>Pathology, University of Texas Health Science Center at San Antonio and South Texas Veterans Health Care System, San Antonio, TX, USA.

Bone remodeling is controlled by dual actions of osteoclasts and osteoblasts (OB). The calcium sensitive NFATc1 transcription factor, as an osteoclast signature gene, regulates its differentiation downstream of BMP-2-stimulated osteoblast-coded protein factors. Whether NFATc1 has any role in osteoblasts is yet to be confirmed. We showed that BMP-2, via receptor-specific Smad pathway, regulates delayed early expression of NFATc1 in osteoblasts. Under basal condition, NFATc1 is phosphorylated. Activation of NFAT requires dephosphorylation by calcium-dependent serine threonine phosphatase, calcineurin. We examined the role of calcium in BMP-2-stimulated regulation of NFATc1 in osteoblasts. BMP-2 induced calcium release from intracellular stores, as measured by Fura-2 fluorescence. BMP-2-stimulated intracellular calcium increased calcineurin phosphatase activity, which dephosphorylated NFATc1, resulting in its nuclear translocation. Since NFATc1 is expressed as a delayed early gene product in response to BMP-2, we tested the hypothesis whether a feedback loop regulates its expression. Immunosuppressant cyclosporine A (CSA), which inhibits calcineurin upstream of NFAT, blocked BMP-2-induced NFATc1 mRNA and protein expression, as determined by real time qRT-PCR and immunoblotting. Also, VIVIT peptide, an inhibitor of NFATc1, suppressed BMP-2-stimulated NFATc1 mRNA and protein expression. To directly investigate the involvement of NFATc1 in its expression, we used the NFATc1 promoter-driven luciferase reporter construct. BAPTA-AM, an inhibitor of calcium abundance blocked BMP-2-induced transcription of NFATc1. Expression of NFATc1 increased NFATc1 transcription. CSA as well as expression of VIVIT peptide inhibited transcription of NFATc1 in response to BMP-2, indicating the action of a feedback activation loop in expression of this transcription factor. Genomatix search of the 5' flanking sequence of NFATc1 revealed the presence of an NFAT binding site in its promoter. To test the function of this NFAT element, we performed electrophoretic mobility shift assay using nuclear extracts from BMP-2-treated OB in the presence of this DNA sequence. BMP-2 increased protein-DNA complex formation, which was inhibited by excess cold element, indicating specificity. Together these data for the first time demonstrate the presence of an NFATc1 autoregulatory loop in BMP-2-stimulated osteoblasts.

**Disclosures:** C. C. Mandal, None.

This study received funding from: NIAMS RO1 and VA MERIT Review.

## F004

### GPRC6A Null Mice Exhibit Osteopenia and Feminization. M. Pi<sup>1</sup>, L. Chen<sup>\*1</sup>, M. Huang<sup>\*1</sup>, W. Zhu<sup>\*1</sup>, B. Ringhofer<sup>\*1</sup>, J. Luo<sup>\*1</sup>, L. Christenson<sup>\*1</sup>, B. Li<sup>\*1</sup>, H. Zhang<sup>2</sup>, P. D. Jackson<sup>\*3</sup>, P. Faber<sup>\*3</sup>, K. R. Brunden<sup>\*3</sup>, J. J. Harrington<sup>\*3</sup>, L. D. Quarles<sup>1</sup>.

<sup>1</sup>Kidney Institute, Department of Medicine, KUMC, Kansas City, KS, USA, <sup>2</sup>Clinical Pharmacology, Vanderbilt University, Center for Bone Biology, Nashville, TN, USA, <sup>3</sup>Athersys, Inc, Cleveland, OH, USA.

GPRC6A is a widely expressed orphan G-protein coupled receptor that senses extracellular amino acids, osteocalcin and divalent cations *in vitro*. To determine the function of this receptor *in vivo*, we characterized the phenotype of GPRC6A null (GPRC6A<sup>-/-</sup>) mice. We observed a complex phenotype in GPRC6A<sup>-/-</sup> mice involving multiple organ systems. In this regard, we observed a decrease in bone mineral density (BMD) due to decreased mineralization of extracellular matrix, decreased lean body mass. In addition, we observed feminization of male GPRC6A<sup>-/-</sup> mice in association with increased circulating levels of estradiol, and reduced levels of testosterone. The bone phenotype appears to be due, at least in part, to a primary effect of GPRC6A on osteoblasts, since bone marrow stromal cell cultures and primary osteoblasts derived from GPRC6A<sup>-/-</sup> mice displayed a marked attenuation of extracellular calcium-stimulated ERK activation, diminished alkaline phosphatase expression and impaired mineralization *ex vivo*. The absence of GPRC6A was not associated with changes in serum TRAP, FGF23, PTH, calcium, 1,25(OH)<sub>2</sub>D levels or urine Dpd/Cr ratio. These data indicate that GPRC6A participates in the regulation of osteoblast-mediated bone mineralization and steroid biosynthesis, as well as other tissue-specific functions. The overall function of this receptor may be to mediate the anabolic effects of extracellular amino acids, osteocalcin and divalent cations in multiple tissues.

**Disclosures:** M. Pi, None.

This study received funding from: This work was supported by NIH R01-AR37308 (L. D. Q.) and COBRE grant P20 RR017686 (M. P.).

## F006

### The Adipocyte-secreted Protein URB Is a Potent Stimulator of Bone Formation. F. Tremblay<sup>\*1</sup>, S. Fukayama<sup>2</sup>, C. Huard<sup>\*3</sup>, R. X. Martinez<sup>\*3</sup>, R. Gimeno<sup>\*1</sup>. <sup>1</sup>Cardiovascular and Metabolic Diseases, Wyeth Research, Cambridge, MA, USA, <sup>2</sup>Women's Health and Musculoskeletal Biology, Wyeth Research, Cambridge, MA, USA, <sup>3</sup>Biological Technologies, Wyeth Research, Cambridge, MA, USA.

Osteoblasts (OBs) and bone marrow adipocytes share common progenitor cells. Increasing evidence suggests that these cells reciprocally regulate their functions via actions of secreted factors. Adipose tissue secretes a variety of factors, collectively named "adipokines" including leptin, adiponectin, PAI-1 or TNF- $\alpha$ . For example, it has been shown that leptin plays a pivotal role in bone metabolism. Conversely, it has recently been proposed that osteocalcin, a major OB-specific secreted protein, may have regulatory roles in energy metabolism. Together, it is an area of intense investigation to identify new adipokines and to characterize their functional roles in different target tissues. Using a combination of transcriptional profiling and bioinformatic analysis, we have identified expression of Urb as a ~150 kDa secreted protein in both human and mouse adipose tissues. Temporal analysis of Urb expression in mouse-adipose-like cell line, 3T3-L1, revealed a biphasic pattern with high mRNA levels in fully differentiated adipocytes. Expression of Urb in white adipose tissue was significantly decreased upon fasting and also was decreased in ob/ob mice. Treatment of ob/ob mice with insulin sensitizing agent rosiglitazone reversed the down-regulation of Urb. Using *ex vivo* neonatal calvaria organ culture, we next examined possible functional roles for Urb in bone formation/resorption. Incubation with 1% or 5% Urb conditioned medium (CM) for 7 days resulted in significant increase in total bone area (TBA) by 50-80%. Although the number of OBs was not altered, OBs became cuboidal in shape, suggesting that they were activated. Similar osteogenic actions/activities were observed when calvaria were incubated with FLAG-purified Urb protein. Histologically, enhanced bone resorption also was evident. Adenovirus-mediated gene transfer of Urb also induced similar calvarial responses. To investigate in more detail the mechanism(s) by which Urb protein stimulates bone formation, we next performed expression profiling studies using RNA samples prepared from calvaria after incubation with Urb protein for 4 days. Over 1,700 transcripts were modulated ( $P \leq 0.01$ ). Among all, we are currently evaluating functional significance of 38 genes in the osteogenic actions/activities of Urb.

We conclude Urb protein enhances bone remodeling (both bone formation and bone resorption) in favor of bone formation. Urb protein *per se* and/or modulation of its signaling pathways should enable us design treatments for bone disorders where bone formation lags behind bone resorption such as osteoporosis.

**Disclosures:** F. Tremblay, None.

## F008

### Osterix, a Positive Regulator in Adult Bone Formation. W. Baek<sup>\*1</sup>, M. Lee<sup>\*1</sup>, J. Oh<sup>\*1</sup>, S. Kim<sup>2</sup>, H. Akiyama<sup>\*3</sup>, B. de Crombrughe<sup>4</sup>, J. Kim<sup>1</sup>.

<sup>1</sup>Department of Molecular Medicine, CMRI, Kyungpook National University School of Medicine, Daegu, Republic of Korea, <sup>2</sup>Skeletal Diseases Genome Research Center Kyungpook National University Hospital, Daegu, Republic of Korea, <sup>3</sup>Department of Orthopaedics, Kyoto University, Kyoto, Japan, <sup>4</sup>Department of Molecular Genetics, University of Texas M. D. Anderson Cancer Center, Houston, TX, USA.

The transcription factor Osterix (Osx) is essential for osteoblast differentiation and bone formation, as mice lacking Osx die within an hour of birth with a complete absence of intramembranous and endochondral bone formation. Perinatal lethality by Osx gene disruption prevents the study for the role of Osx in bones that are growing or already formed. Here, the function of Osx was examined in developing bones at adults after bone collar formation using the time-specific and site-specific Cre/loxP system. Osx was inactivated in all osteoblasts by Col1a1-Cre with the activity of Cre recombinase under the control of 2.3-kb collagen promoter. Even though no bone defects were shown in newborn, Osx inactivation exhibited dramatically reduced bone phenotypes in growing mice. Bone mineral density and bone forming rate were decreased in vertebra lumbar of Osx-inactivated mice with Col1a1-Cre (Osx<sup>lox/+</sup>;Col1a1-Cre). Moreover, the thinner and more porous cortical bone of the diaphysis region of long bones was observed with the reduction of bone length. The increased trabecular bones were investigated but they were immature or premature. However, no functional defects were found in osteoclasts. The expression of early marker genes for osteoblast differentiation such as Runx2, osteopontin, and alkaline phosphatase (ALP) was markedly increased in Osx<sup>lox/+</sup>;Col1a1-Cre mice. On the other hand, late marker gene, osteocalcin was decreased. We propose that Osx inactivation in growing bones delayed osteoblast maturation, accumulated immature osteoblasts, and finally, reduced osteoblast function for bone formation, without apparent defects in bone resorption. Thus, these findings suggest that Osx plays a significant role in positively regulating osteoblast differentiation and bone formation in adult bone.

\*First two authors equally contributed to this work.

**Disclosures:** J. Kim, None.

This study received funding from: Korea Research Foundation Grant funded by the Korean Government (MOEHRD, Basic Research Promotion Fund) (KRF-2007-313-E00314) and also supported by the Brain Korea 21 Project in 2008.

## F010

**Inactivation of Dlx5 Gene Results in Altered Osteoblast-osteoclast Coupling Inducing Increased Bone Resorption and Reduced Cortical Thickness in Male Mice.** N. M. Samee<sup>\*1</sup>, V. Geoffroy<sup>1</sup>, C. Marty<sup>\*1</sup>, C. Schiltz<sup>\*1</sup>, M. Vieux-Rochas<sup>\*2</sup>, G. Levi<sup>\*2</sup>, M. C. de Vernejoul<sup>1</sup>. <sup>1</sup>INSERM U606, Paris, France, <sup>2</sup>CNRS UMR5166, Paris, France.

Dlx5 is an homeodomain transcriptional factor expressed in osteoblasts. Dlx5 inactivation in mice induces perinatal lethality. We investigated its function in late osteogenesis and bone remodelling in Dlx5-null mice at the end of gestation and in Dlx5 heterozygous adult mice using *in vivo* and *in vitro* approaches. Femurs of 18.5 dpc Dlx5-null mice exhibited a reduction of the total (Total BV/TV -21.4% ;  $P < 0.05$  ,  $n = 5$ ) and trabecular bone volume associated with increased trabecular separation and reduced trabecular number. Calvaria-derived Dlx5-/- osteoblasts displayed a reduced proliferation rate, a delayed differentiation state and a severe reduction of Runx2, Osterix, Osteocalcin and Bone Sialoprotein expression. In addition to the impaired osteoblast function that was demonstrated *in vitro*, we observed that Dlx5-/- femora exhibited an increase in osteoclasts number *in vivo*. As Dlx5 is not expressed by osteoclasts, we hypothesized that its expression in osteoblast could be involved in the control of osteoblast/osteoclast coupling. Cultured Dlx5-/- osteoblasts displayed a higher RANKL/OPG mRNA ratio and co-cultured Dlx5-/- osteoblasts with normal spleen cells induced a higher number of TRAP-positive multinucleated cells with an increased resorption pits area (Dlx5-/- :  $1534 \pm 119 \mu m^2$  versus Dlx5+/+ :  $680 \pm 32 \mu m^2$ ;  $n = 4$  wells). In 10- and 20-week-old adult mice, Dlx5 was still expressed at high levels in long bones. Bone mineral density (BMD) measured at the femurs of 10-week-old mice was lower in male Dlx5+/+ mice (-7.8%;  $P < 0.05$ ;  $n = 14$ ) but not in Dlx5+/- females compared to wild-type mice.  $\mu$ CT and histomorphometry analyses showed that the cortical thickness at the midshafts of Dlx5+/- male femurs was significantly lower (-14%;  $P < 0.01$ ,  $n = 13$ ) while no modifications of the micro-architecture were observed in trabecular bone. Unexpectedly, the cortical decrease was the result of an increased marrow diameter with a significantly higher number of endosteal osteoclasts per bone surface. Furthermore, the urinary level of deoxypyridinoline confirmed an increased bone resorption in Dlx5+/- male compared to WT male ( $29.7 \pm 3.12$  nmol /v/s  $22.1 \pm 1.46$  nmol;  $P < 0.05$ ). In conclusion, we show that the total or partial inactivation of Dlx5 triggered a bone phenotype resulting from an altered osteoblast/osteoclast coupling inducing an increased resorption activity. Moreover, Dlx5 significantly interferes with long bones remodelling mainly affecting the cortical thickness in adult male mice.

**Disclosures:** N.M. Samee, None.

## F012

**Mice Lacking NMDA Receptor Expression in Osteoblasts Have Pronounced Vertebral Bone Abnormalities.** S. Martinez-Bautista<sup>\*</sup>, N. Wang<sup>\*</sup>, G. Richards<sup>\*</sup>, T. M. Skerry<sup>\*</sup>. Clinical Sciences (South), School of Medicine and Biomedical Sciences, University of Sheffield, Sheffield, United Kingdom.

Cell-cell communication underlies the way in which populations of different cells interact in bone to regulate skeletal architecture and mass. For some years glutamate has been proposed as a signalling molecule in the skeleton because of demonstrations of expression of numerous components of glutamatergic synapses by bone cells, and effects of chemical antagonists on osteoblast and osteoclast function *in vitro*. However, the physiological role of glutamate has been hard to establish because full knockout animals have lethal phenotypes due to marked anomalies in brain function while most chemical antagonists administered *in vivo* have significant side effects because of their actions on the brain.

We obtained mice expressing the Cre recombinase under the control of the osteocalcin promoter, and others in which the obligatory NMDA type glutamate receptor subunit Grin1 had been flanked by lox-p sites. These mice were crossed to generate double heterozygotes, and then intercrossed to produce offspring with Cre<sup>+</sup>Grin1<sup>lox/lox</sup> genotypes, in which NMDA receptor expression in osteoblasts was effectively abrogated. Analysis has been performed by staining pups at term and by microCT measurements of pups and young adult skeletons ( $n = 4$  at different ages up to 4 months). Osteoblast specific deletion of a functional NMDA receptor results in mice with normal viability and size. While their long bones have slightly reduced trabecular bone mass and thickness, the most profound effects is that their lumbar vertebrae have dramatic reductions in bone volume of over 50%. Preliminary data suggests that the compressive strength of the vertebrae in mice lacking NMDA receptor expression is reduced dramatically. We interpret our current data to show that glutamate plays a significant role in vertebral bone formation in young mice. The effect of the deletion on bone at greater ages and on bone's response to challenge is yet to be determined, but this existing insight into a site specific difference between vertebral and long bone properties could be of considerable importance clinically.

**Disclosures:** S. Martinez-Bautista, None.

## F014

**CNBP Conditional Knockout Mice Show Severe Osteoporosis-like Phenotype.** S. Yang<sup>1</sup>, W. Chen<sup>\*1</sup>, L. Chen<sup>\*2</sup>, N. Li<sup>\*2</sup>, Y. Li<sup>1</sup>. <sup>1</sup>The Forsyth Institute-Harvard School of Dental Medicine, Boston, MA, USA, <sup>2</sup>The Forsyth Institute, Boston, MA, USA.

At any particular age and phase of life, genetic factors explain about 70% of the variance in bone phenotype after adjustment for major medical and disease factors. However, the genes underlying the genetic syndromes of osteoporosis remain largely unidentified. In order to identify genes that are important for bone formation and may be related to the genetic syndromes of osteoporosis, we have cloned a number of transcription factors that are predominately expressed in osteoblasts using Rat osteoblast cDNA differential screening. One of these transcription factors is a zinc-finger protein, cellular nucleic acid binding protein (CNBP). We found that CNBP is first expressed in early osteoprogenitor cells. Subsequently, CNBP is expressed throughout the osteoblast lineage, including osteocytes. We have generated CNBP null mutant mice. However, homozygous mutants die around E10.5 with forebrain truncation, which precludes the study of CNBP function in bone formation. To study CNBP function in bone development, we have generated conditional CNBP knockout mice (CNBP<sup>CNBP/Coll 1-Cre</sup>) by using bone tissue-specific targeted disruption of the CNBP gene using Cre/loxP technology. Bone tissue-specific targeted disruption of the CNBP gene was attained using the  $\alpha 1(I)$  collagen promoter to drive Cre expression, which allows us to examine the role of CNBP in osteoblast differentiation after birth *in vivo*. CNBP<sup>CNBP/Coll 1-Cre</sup> mice are viable, but are smaller in size with severely bended vertebral bone. Histological analysis and morphological analysis of the CNBP<sup>CNBP/Coll 1-Cre</sup> mice indicate that the mutant mice have severe skeletal defects both in newborn and adult mice. X-Ray examination and Micro-CT determination show that the mutant mice have lower bone density when compared to wild-type mice, suggesting an osteoporosis-like phenotype. Our results demonstrate that CNBP is essential to bone formation and mutation or change in expression level of CNBP may contribute the genetic syndromes of osteoporosis. This knowledge may be applied towards the development of new diagnostic and therapeutic alternatives for human osteoporosis.

**Disclosures:** S. Yang, None.

## F017

**Regulation of the Osteoblast-Specific Transcription Factor Osterix by NO66, a Jumonji Family Histone Demethylase.** K. M. Sinha<sup>\*1</sup>, H. Yasuda<sup>\*1</sup>, M. M. Coombes<sup>\*2</sup>, S. Y. R. Dent<sup>\*2</sup>, B. de Crombrughe<sup>1</sup>. <sup>1</sup>Molecular Genetics, M.D. Anderson Cancer Center, Houston, TX, USA, <sup>2</sup>Biochemistry and Molecular Biology, M.D. Anderson Cancer Center, Houston, TX, USA.

Osterix (Osx) is an osteoblast-specific transcription factor required for osteoblast differentiation and bone formation. Osx null mice have a normal cartilage skeleton but fail to form bone or to express osteoblast-specific marker genes. To better understand the control of transcriptional activation by Osx, we identified Osx-interacting proteins using affinity purification techniques. Here we report that a Jumonji C (JmjC)-domain containing protein, NO66, interacts with Osx in osteoblast cells. NO66 is expressed in all developing bones. Interactions between NO66 and Osx inhibit gene activation by Osx. Knockdown of NO66 in osteoblast cells triggers accelerated osteoblast differentiation and mineralization as well as a marked stimulation in expression of Osx target genes including *Coll1a1*, *Osteocalcin* and *Bone sialoprotein* (*Bsp*). NO66 exhibits a JmjC-dependent histone demethylase activity that affects both H3K4me and H3K36me *in vivo* and this activity is required for inhibition of transcriptional activation by Osx. Osx and NO66 colocalize at the *Bsp* promoter in undifferentiated preosteoblasts. BMP-2-induced differentiation of these cells causes a marked decrease in NO66 occupancy and an increase in trimethylation of H3K4 and H3K36 in the *Bsp* gene. Our results provide the first evidence that NO66 serves as a negative regulator of Osx target genes in osteoblasts by modulating histone methylation states.

**Disclosures:** K.M. Sinha, None.

## F020

**BMP2 Induces Osterix Expression through Up-regulation of Dlx5 and Its Phosphorylation by p38 MAPK.** M. J. Ortuño<sup>\*1</sup>, A. Ulsamer<sup>\*1</sup>, S. Ruiz<sup>\*1</sup>, A. R. G. Susperregui<sup>1</sup>, N. Osses<sup>\*2</sup>, J. L. Rosa<sup>\*1</sup>, F. Ventura<sup>\*1</sup>. <sup>1</sup>Barcelona University, Barcelona, Spain, <sup>2</sup>Pontificia Universidad Católica Valparaíso, Valparaíso, Chile.

Osterix (Ox) and Dlx5 are two of the osteoblast master transcription factors induced by bone morphogenetic protein-2 (BMP2) during osteoblast differentiation. Ox is a zinc-finger transcription factor specifically expressed in osteoblast and osteocytes of developing bones. Because no bone formation occurs in Ox-null mice, Ox is thought to be an essential regulator of osteoblast differentiation. Dlx5 is a homeobox-containing transcription factor expressed in developing skeletal elements. Dlx5-null mice have a delayed cranial ossification and abnormal osteogenesis, suggesting it also plays an important role in osteoblast differentiation. We report that BMP2 induces transcriptional activation of Ox through a homeobox sequence located in the proximal promoter region. Our results demonstrate that in response to BMP2, Dlx5 expression precedes Ox expression. In addition, Dlx5 binds to BMP2-responsive homeobox sequence both *in vitro* and *in vivo*. Finally, Dlx5 overexpression assays show its role in BMP2-dependent Ox expression. These data strongly suggest that Dlx5 is essential to mediate Ox expression by BMP2. Furthermore, we demonstrate that Dlx5 is a novel target of p38 MAPK, which has been shown to be relevant for osteogenic effects of BMP2. Our results show that Dlx5 is substrate for p38 both *in vitro* and *in vivo* and that Ser34 and Ser217 are the sites phosphorylated. The phosphorylation by p38 at Ser34/217 enhances Dlx5 transcriptional activity increasing Ox expression. Thus, we propose a novel activation mechanism of Dlx5 by BMP2 through p38-induced Dlx5 phosphorylation and its further transcriptional activity inducing Ox expression.

**Disclosures:** *M.J. Ortuño, None.*

## F024

**Overexpression of Glutathione Reductase in Osteoblasts Decreases Bone Formation and Partially Prevents Ovariectomy-induced Bone Loss.** M. Almeida, E. Ambrogini, M. Martin-Milla, L. Han, A. Warren<sup>\*</sup>, R. S. Shelton<sup>\*</sup>, J. Goellner, R. S. Weinstein, R. L. Jilka, C. A. O'Brien, S. C. Manolagas. Center for Osteoporosis and Metabolic Bone Diseases, University of Arkansas for Medical Sciences and Central Arkansas Veterans Healthcare System, Little Rock, AR, USA.

Loss of bone mass in mice either with advancing age or following gonadectomy is associated with increased oxidative stress, as well as increased osteoblast and osteocyte apoptosis; and administration of the antioxidant N-acetyl-cysteine (NAC) prevents all these changes in gonadectomized animals. Moreover, H<sub>2</sub>O<sub>2</sub> stimulates osteoblastic cell apoptosis *in vitro*, suggesting a direct effect of oxidative stress in these cells. To establish that oxidative stress influences the biology of osteoblasts in a cell autonomous manner *in vivo*, we have generated mice overexpressing the human form of the peroxide scavenging enzyme glutathione reductase (GSR) gene selectively in osteoblastic cells, using the 3.6 kb sequence of the rat collagen type 1A1 promoter (3.6Col1A1). Bone specific expression of the transgene was confirmed by RT-PCR in vertebrae and femurs, as well as in osteoblasts derived by culturing bone marrow cells in the presence of ascorbic acid. In addition, GSR activity was increased in both calvaria and bone marrow derived osteoblasts from transgenic animals. Moreover, Col-GSR female mice exhibited a decrease of BMD in the spine and femur at 2, 3, 4, 5, and 6 months of age, raising the possibility that lowering ROS with the transgene attenuated osteoblastogenesis. In support of this contention, administration of NAC for 28 d to 5 month-old C57BL/6 mice decreased osteoblastogenesis, as measured by the number of colony forming units-osteoblasts in *ex vivo* bone marrow cultures. Moreover, cell proliferation of three different osteoblastic cell models (OB-6, 2T3, and MC3T3) was attenuated after 3 d of culture in the presence of 1 nM NAC as determined by BrdU incorporation. Lastly, the loss of bone following 6 wk of OVX of 6 month-old mice was partially prevented in Col-GSR mice, as compared to the wt controls, perhaps reflecting attenuation of OVX-induced osteoblast apoptosis by the transgene. In agreement with this mechanistic scenario, bone marrow stromal cells from Col-GSR mice, cultured for 15 d in the presence of ascorbic acid, where protected against H<sub>2</sub>O<sub>2</sub>-induced apoptosis, as determined by caspase 3 activity. Collectively, these findings support our working hypothesis that at low levels intracellular H<sub>2</sub>O<sub>2</sub> is an important signal for the replication of osteoblast precursors while at high levels it promotes osteoblast apoptosis, as is the case in most other cell types including stem cells (Nature Reviews, 8:722, 2007).

**Disclosures:** *M. Almeida, None.*

## F026

**Fibroblast Growth Factor 2 Signaling in Osteoblasts: Connexin43 is a Docking Platform for Protein Kinase C delta.** C. Nigier, F. Lima, J. P. Stains. Orthopaedics, University of Maryland, Baltimore, MD, USA.

Gap junctional intercellular communication (GJIC) permits the direct transfer of small molecules between adjacent cells. We have previously shown that the gap junction protein, connexin43 (Cx43), plays a role in regulating signaling and transcriptional responses in osteoblasts. Recently, we have reported that increasing GJIC through Cx43 overexpression enhances the transcription response of the osteocalcin promoter to fibroblast growth factor 2 (FGF2) treatment. Conversely, an attenuation of the transcriptional response to FGF2 is observed when endogenous Cx43 is knocked down using siRNAs. A role for Cx43 as a docking platform for signal transduction machinery has begun to emerge in many cell types. In this study, we hypothesize that Cx43 influences the FGF2 responsiveness of cells by recruiting the signaling machinery to the gap junction plaque, where it acts to amplify signals initiated in one cell into adjacent, gap junctionally coupled cells. Accordingly, we have examined the protein-protein interactions that occur between Cx43 and downstream signal transducers of the FGF response in MC3T3 cells. We reveal that the effects of Cx43 on FGF2 signaling in osteoblasts are mediated by protein kinase C delta (PKCδ), as we can abrogate the synergistic effects of FGF2 and Cx43 using the inhibitor, rottlerin, or siRNAs against PKCδ. By immunoprecipitation, we are able to pull down PKCδ with antibodies directed against Cx43. In addition, anti-PKCδ antibodies are able to specifically pull down the phosphorylated form of Cx43, which is predominantly associated with Cx43 present at the plasma membrane. Using immunoprecipitations, we show that in the basal state PKCδ associates with Cx43. However, upon FGF2 treatment, the association of Cx43 and PKCδ diminishes rapidly (~15 minutes). By immunofluorescence, we demonstrate that upon FGF2 treatment, PKCδ translocates to the nuclei. Indeed, using chromatin immunoprecipitations, western blotting and luciferase reporter assays, we have shown that PKCδ phosphorylates Runx2 and impacts its recruitment and transcriptional activity on the osteocalcin proximal promoter. We propose that upon transduction of an FGF2 induced second messenger via GJIC, PKCδ becomes activated and is mobilized from the gap junction to the nucleus where it affects gene transcription. In total, our data show that Cx43 assembles the signaling machinery required for the propagation of signals generated by the FGF2/FGF receptor complex to adjacent cells in order to coordinate and amplify the cellular response. Understanding the association and regulation of these complexes will permit us to identify the second messengers that are transmitted by gap junctions.

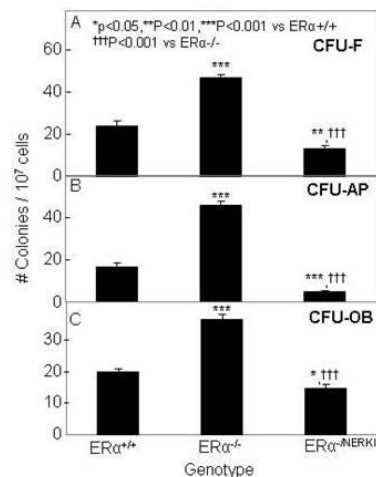
**Disclosures:** *J.P. Stains, None.*

*This study received funding from: NIAMS AR052719.*

## F029

**Loss of Classical ERE Signaling Results in Suppression of Early Commitment of Bone Marrow Stromal Cells to Osteoblasts.** F. A. Syed, D. G. Fraser<sup>\*</sup>, M. J. Oursler, S. Khosla. Endocrinology, Mayo Clinic College of Medicine, Rochester, MN, USA.

Estrogen signals either through the "classical" ERE pathway or the "non-classical", non-ERE pathway. We have previously shown that mice with a deleted ERE allele and a knock-in of a mutant ERα that cannot bind EREs on the other allele (ERα<sup>NERKI</sup>) have cortical osteopenia and decreased bone formation rates (JBMR 20:1992, 2005). We also established that these mice display a decrease in marrow fat content *in vivo*, which was in contrast to mice lacking complete ERα signaling (ERα<sup>-/-</sup>), which displayed an increase in adipocyte volume compared to their respective ERα<sup>+/-</sup> controls (JBMR 22:S109, 2006). In the present study, we have generated ERα<sup>+/-</sup>, ERα<sup>-/-</sup> and ERα<sup>NERKI</sup> mice on a C57/BL6 background and have compared the inherent potential of marrow-derived stromal cells (MSCs) obtained from three month old female mice to form early bi-potential osteoblastic/adipocytic (methylene blue positive) fibroblastic colonies (CFU-F), early committed pre-osteoblastic (alkaline phosphatase positive) colonies (CFU-AP), and fully differentiated (von kossa positive) mineralized nodule forming osteoblastic colonies (CFU-OB). MSCs derived from ERα<sup>NERKI</sup> mice exhibited a 45% reduction in CFU-F colonies and a 72% reduction in CFU-AP colonies (P<0.001) compared to ERα<sup>+/-</sup> mice. By contrast, MSCs derived from ERα<sup>-/-</sup> mice exhibited a 95% increase in CFU-F and a 173% increase in CFU-AP colonies (P<0.001) compared to ERα<sup>+/-</sup> MSCs. Interestingly, the ERα<sup>NERKI</sup> MSCs displayed a 72% and 90% reduction in their potential for CFU-F and CFU-AP colony formation, respectively, compared to ERα<sup>-/-</sup> MSCs (P<0.001). An essentially similar pattern of differentiation to mature mineralizing osteoblasts was observed in stromal cultures derived from these mice. While ERα<sup>NERKI</sup> cultures displayed a 26% reduction in total CFU-OB colonies compared to wild types, ERα<sup>-/-</sup> cultures displayed an 84% increase. When ERα<sup>NERKI</sup> and ERα<sup>-/-</sup> CFU-OBs were compared, a 60% reduction was observed in ERα<sup>NERKI</sup> cultures. These results suggest that loss of classical ER signaling has suppressive effects on commitment of early osteoblastic and adipocytic progenitors in the bone marrow stromal compartment, which results in suppression of later mineralized nodule formation *in vitro*. These results also explain our earlier observation of reduced marrow adipocyte parameters *in vivo* in ERα<sup>NERKI</sup> mice.



**Disclosures:** F.A. Syed, None.

This study received funding from: NIH RO1 AG-28936.

## F032

**hPTHrP 1-36 Stimulates PKA-Dependent Phosphorylation and Nuclear Translocation of  $\beta$ -Catenin In Neonatal Mouse Calvarial Bone Cells.** A. Bryan\*, D. Cullen, J. A. Yee. Biomedical Sciences, Creighton University, Omaha, NE, USA.

Treatment of humans or rodents with amino terminal PTH or PTHrP stimulates either bone resorption or bone formation depending on the whether administration of the peptide is continuous or intermittent. While the anabolic effect of intermittent treatment has been related to a decrease in osteoblast apoptosis and an increase in the size of the osteoblast population, the signaling pathway that mediates these changes is not well characterized. The binding of PTH or PTHrP to their receptor activates two intracellular signaling pathways, cyclic AMP/PKA and DAG/PKC. Recently, the canonical Wnt signaling pathway mediated by  $\beta$ -catenin has been associated with the elevated BMD that occurs as a consequence of the G171V mutation in the Wnt co-receptor Lrp5. As a result, it has been proposed that the canonical Wnt signaling pathway may contribute to the action of other bone anabolic factors. The purpose of this work was to test the hypothesis that PTHrP stimulation of the cyclic AMP/PKA pathway increases canonical Wnt signaling in mouse osteoblast-like cells *in vitro*. Calvarial bone cells were isolated from neonatal mice by digestion in collagenase and grown in DMEM plus 10% FBS. The effect of recombinant hWnt3a (5 ng/ml), synthetic hPTHrP 1-36 (200 ng/ml), 10 mM LiCl<sub>2</sub>, 1 mM dBcAMP, or 10  $\mu$ M forskolin (Fsk) on the cellular and nuclear levels of  $\beta$ -catenin and on PKA-dependent phosphorylation of  $\beta$ -catenin was determined by immunoblotting. Translocation of  $\beta$ -catenin to the nucleus in response to treatment was also examined by immunohistochemistry. The effect of hPTHrP 1-36 and hWnt3a on osteoblast differentiation was assessed by measuring alkaline phosphatase (AP) activity. The level of cellular and nuclear  $\beta$ -catenin was increased at 0.5, 1, and 6 hrs after exposure to hWnt 3a, LiCl<sub>2</sub>, hPTHrP 1-36, dBcAMP, and Fsk. Pre-treatment with the PKA inhibitor H89 prevented the increase in  $\beta$ -catenin observed in cells treated with hPTHrP 1-36. Immunohistochemical staining confirmed that treatment with hWnt3a, LiCl<sub>2</sub>, hPTHrP 1-36, and Fsk increased nuclear  $\beta$ -catenin. Treatment with hPTHrP 1-36 and Fsk, but not hWnt3a or LiCl<sub>2</sub>, stimulated PKA-dependent phosphorylation of  $\beta$ -catenin. Continuous exposure to hPTHrP 1-36 or Fsk for 5 days increased AP activity by 2-3 fold; however, neither hWnt3a or LiCl<sub>2</sub> affected AP activity. These results demonstrate that hPTHrP 1-36 stimulates PKA-dependent phosphorylation of  $\beta$ -catenin in calvarial bone cells. Moreover, PKA-dependent phosphorylation of  $\beta$ -catenin may be associated with its translocation into the nucleus of PTHrP target cells. We conclude that crosstalk between the cyclic AMP/PKA and canonical Wnt signaling pathways may contribute to the anabolic action of PTHrP in bone.

**Disclosures:** A. Bryan, None.

This study received funding from: NIH AR-051365.

## F034

**The Sympathetic Tone Mediates Leptin's Inhibition of Insulin Secretion by Modulating Osteocalcin Bioactivity.** E. Hinoi<sup>1</sup>\*, N. Gao<sup>2</sup>\*, T. Yoshizawa<sup>1</sup>\*, D. Jung<sup>3</sup>\*, J. K. Kim<sup>3</sup>\*, K. H. Kaestner<sup>2</sup>\*, G. Karsenty<sup>1</sup>. <sup>1</sup>Department of Genetics and Development, Columbia University, New York, NY, USA, <sup>2</sup>Department of Genetics, University of Pennsylvania, Philadelphia, PA, USA, <sup>3</sup>Department of Cellular and Molecular Physiology, Penn State Medical Center, Hershey, PA, USA.

The emerging relationship between bone and energy metabolisms that has been demonstrated over the last few years raised the prospect that leptin and osteocalcin may cooperate in regulating some aspects of glucose metabolism. To address this question we studied young *ob/ob* mice that are neither obese nor diabetic. These young *ob/ob* mice display a hyperinsulinemia that appears perinatally and is also present in lipodystrophic mice that have no adipocytes. Hyperinsulinemia is caused, in both mouse models, by an increase in beta-cell proliferation, insulin expression and secretion. Remarkably, sympathetic stimulation reduces hyperinsulinemia by 50% in both mutant mice demonstrating that the low sympathetic tone caused by leptin deficiency contributes significantly to its development but treatment of isolated islets with a sympathomimetic does not affect insulin gene expression or beta-cell proliferation. In contrast, ablating sympathetic signaling in osteoblasts only results in leptin-dependent hyperinsulinemia. In osteoblasts, sympathetic activity stimulates expression of *Esp*, a gene inhibiting the activity of osteocalcin, a powerful insulin secretagogue. Accordingly, *Osteocalcin* deletion halves hyperinsulinemia in *ob/ob* mice while *Esp* inactivation doubles it and also delays the onset of glucose intolerance in adult *ob/ob* mice. That leptin's ability to regulate insulin secretion depends largely on the level of osteocalcin bioactivity underscores the role of skeleton in glucose homeostasis.

**Disclosures:** E. Hinoi, None.

## F038

**Induction of Embryonic Stem Cell-Related Pluripotency Genes in Post Natal Stem Cells During Fracture Healing.** M. V. Bais\*, J. McLean\*, P. Sabastiani\*, M. Young\*, N. Wigner\*, T. Smith\*, D. N. Kotton\*, T. A. Einhorn, L. C. Gerstenfeld. Orthopaedic Research Laboratory, Boston University School of Medicine, Boston, MA, USA.

Fracture healing is defined by one round of endochondral bone formation followed by a period of coupled bone remodeling, and is generally considered to recapitulate the processes of embryological bone formation. Using Bayesian clustering of the temporal gene expression across fracture healing identified unique temporal relationships between Notch, TGF- $\beta$  and Wnt signaling pathways that could be selectively related to gene ontologies associated with skeletogenesis, vasculogenesis, neurogenesis and gametogenesis. A comparison of the ~12,000 genes showing greater than a three fold change in the fracture callus tissues from unfractured bone identified ~300 out of ~1000 expressed genes, that have been shown to be preferentially expressed in embryonic stem cells (ESC). Multiple regulators of pluripotency, self renewal, and epigenetic chromatin remodeling observed in ESCs, showed unregulated expression during fracture healing. One of the central epigenetic regulators associated with ESC self renewal that was observed during fracture healing was the homeotic gene *Nanog*. RT-PCR showed that *Nanog* was temporally induced ~30 fold between days three and five post fracture while in induced skeletal formation after surgical marrow ablation, a ~7 fold increase in *Nanog* expression was seen in the same post injury period. Marrow stromal cells (MSC) grown *ex vivo* showed that *Nanog* had a ~45 fold induction in expression relative to murine embryonic fibroblasts (MEF) at 6 days after being placed in culture. A comparison of the maximal levels of *Nanog* expression within the MSCs to those seen in induced pluripotent stem cells (IPS) showed that MSCs expressed 30 fold less *Nanog* than the IPS cells. Once the MSCs were placed in media that promoted osteogenesis, *Nanog*'s expression fell to those observed in freshly isolated marrow aspirates. Transfection of a lentiviral shRNA to *Nanog* into undifferentiated W20 murine marrow stromal cell line that has been previously used to test BMP2 induced osteogenic differentiation lead to a seven fold induction of osteocalcin expression in the absence of BMP treatment. In summary, approximately a third of the known genes that are upregulated in ESCs relative to differentiated lineages are upregulated in the stem cell populations that are recruited during fracture healing. These data for the first time suggest that one of the known epigenetic transcriptional regulators that impart stem cell maintenance of ESC, also may play a role in regulating and maintaining post-natal stem cells such as MSCs.

**Disclosures:** L.C. Gerstenfeld, None.

This study received funding from: PO1-AR049920.

**F041**

**Effect of Osteoblast Depletion on Hematopoietic Niches in the Bone Marrow.** K. Lamothe<sup>\*1</sup>, D. Rowe<sup>2</sup>, H. L. Aguila<sup>1</sup>. <sup>1</sup>Department of Immunology, University of Connecticut Health Center, Farmington, CT, USA, <sup>2</sup>Center for Regenerative Medicine and Skeletal Development, University of Connecticut Health Center, Farmington, CT, USA.

Cells of the osteoblastic lineage participate actively on defining hematopoiesis in the bone marrow. We have developed a transgenic mouse model (Col2.3ΔTK) in which osteoblasts can be selectively ablated after treatment with the drug gancyclovir (Gcv). This ablation affects hematopoiesis with a rapid loss of cells whose primary development depend on the bone marrow microenvironment. These include B cell progenitors, NK cells, myeloid progenitors and ultimately early progenitors including hematopoietic stem cells. We postulate that osteoblast depletion or alterations in bone remodeling homeostasis could be used as a way to modify hematopoietic niches.

To test this hypothesis we ablated osteoblasts in transgenic mice in the C57BL/6 (B6) background by treating them with Gcv for 10 days followed by injection of a limited number of hematopoietic stem cells from B6 transgenic mice bearing a GFP transgene driven by the H-2Kb MHC Class I promoter. These transplanted mice developed hematopoietic chimerism, scored by hematopoietic cells expressing GFP, to degrees equivalent to the observed in lethally irradiated control recipient mice. The chimerism is multilineage, including donor cells of myeloid and lymphoid origin. Moreover, sequential transplants of bone marrow from these primary chimeras to lethally irradiated recipients, congenic for the CD45.1 molecule, indicates that the initial transplant engrafted long-term hematopoietic stem cells. This was scored by the presence of GFP CD45.2 positive multilineage hematopoietic cells in the host animals.

In another set of experiments we prevented osteoblastogenesis in utero, through the injection of Gcv in pregnant wild type females mated with transgenic males. After injection of Gcv at the onset of osteoblast development (10-15 days of embryonic life) a fraction of the progeny was born with a non developed cartilaginous skeleton, that progressively generate bona fide bone after birth upon release of the Gcv pressure. These mice present drastic anomalies in the dose of hematopoietic progenitors in the bone marrow, with active hematopoiesis in periphery. Interestingly, as osteoblastogenesis initiate, hematopoiesis in the bone marrow began to establish. These results emphasize the fundamental role of osteoblastogenesis on defining hematopoietic development. They clearly show that controlled alterations in bone remodeling could be used as a regime to facilitate hematopoietic engraftment after bone marrow transplantation and provide a model to study the initiation of hematopoietic niches in the bone marrow post migration of progenitors from extramedullary sites.

**Disclosures:** H.L. Aguila, None.

**F044**

**Connective Tissue Progenitor Cell Contribution to Ectopic Skeletogenesis.** V. Y. Lounev<sup>\*1</sup>, E. M. Shore<sup>2</sup>, D. L. Glaser<sup>\*1</sup>, F. S. Kaplan<sup>3</sup>. <sup>1</sup>Department of Orthopaedic Surgery, Center for Research in FOP & Related Disorders, University of Pennsylvania School of Medicine, Philadelphia, PA, USA, <sup>2</sup>Departments of Orthopaedic Surgery and Genetics, Center for Research in FOP & Related Disorders, University of Pennsylvania School of Medicine, Philadelphia, PA, USA, <sup>3</sup>Departments of Orthopaedic Surgery and Medicine, Center for Research in FOP & Related Disorders, University of Pennsylvania School of Medicine, Philadelphia, PA, USA.

At least two populations of progenitor cells, one of hematopoietic origin, and one of connective tissue origin are necessary to form heterotopic bone. While cells of hematopoietic origin are critical for inducing heterotopic ossification (HO), the identity of the responding connective tissue progenitor cells is unknown. We have previously shown that cells of myogenic lineage (myoD-Cre) contribute minimally to the early fibroproliferative stages of heterotopic ossification, but not to the chondrogenic or osteogenic stages, while cells of vascular smooth muscle lineage (smMHC-Cre) do not contribute at all. In order to evaluate contributions of the vascular lineage expressing the early endothelial marker Tek/Tie2 to the various stages of BMP-induced HO, we crossed floxed lacZ reporter mice to a transgenic line that over-expresses BMP4 at neuromuscular junctions (under Nse promoter), then crossed these double transgenic mice with Tek/Tie2-Cre. In response to injury, this mouse model induced heterotopic ossification with an inflammatory muscle reaction that was physiologically similar to the inductive events experienced by patients who have fibrodysplasia ossificans progressiva (FOP), the most catastrophic form of heterotopic ossification in humans. We found that cells expressing Tek/Tie2 contributed to the fibroproliferative, chondrogenic, and osteogenic stages of the evolving endochondral anlagen. Connective tissue progenitor cells of the Tek/Tie2 vascular lineage are thus sufficient to respond to injury-induced triggers and to differentiate through an endochondral pathway to form heterotopic bone. Insight into the cellular pathophysiology of HO has important implications for the development of cell-targeted therapies for FOP and other conditions of dysregulated BMP-induced heterotopic ossification.

**Disclosures:** V.Y. Lounev, None.

**F047**

**Diet Induced Obesity Compromises the Osteogenic Potential of the Bone Marrow.** Y. K. Luu<sup>1</sup>, J. E. Pessin<sup>\*2</sup>, S. Judex<sup>1</sup>, C. T. Rubin<sup>1</sup>. <sup>1</sup>Biomedical Engineering, Stony Brook University, Stony Brook, NY, USA, <sup>2</sup>Medicine and Molecular Pharmacology, Albert Einstein College of Medicine, Bronx, NY, USA.

It is often presumed that the load bearing challenges inherent to obesity will have a beneficial impact on the skeleton. There is increasing evidence, however, that overweight individuals do not realize a proportionally greater bone mass, and thus are at a greater relative risk of fracture when falling. We hypothesized that the failure of the skeleton to keep pace of increased adiposity was not necessarily a failure of the extant bone cell population and bone remodeling, but that diet induced obesity actually hampered differentiation of osteoprogenitors, by diet-related reduction of the mesenchymal stem cell (MSC) pool available to build up the skeleton.

Starting at 7w of age, male C57BL/6J mice were maintained on either a regular chow diet (RD) or a 45 kcal% high fat diet (HFD). Following six weeks, animals were euthanized and bone marrow harvested from femurs and tibias. Relative to RD (n=8), flow cytometric analyses of the total marrow indicated that the number of stem cells present in HFD (n=8) animals was markedly suppressed, with the overall stem cell population - including both hematopoietic and MSCs - decreased by -54.8% (p<0.001), and the undifferentiated MSC population in the HFD down by -59.6% (p<0.001).

The phenotypic impact of this diminished progenitor pool was evident at 12w. While the adipose burden in HFD (n=10) was 52.8% greater than RD (n=15; p<0.001), bone volume fraction in the proximal tibia of HFD animals only increased 16.8% (p=0.03) relative to RD, and with body mass as a covariate, this increase in bone volume fraction was insignificant (p=0.51). Cortical bone volume in the mid-diaphysis was unaffected by the HFD (4.0%, p=0.11). However, the quality of the bone structure was significantly compromised in HFD animals, with a -40.0% (p<0.001) reduction in trabecular number, and -24.5% (p<0.001) decrease in trabecular thickness relative to RD. Overall, the data indicate that a high fat diet greatly disrupts the overall stem cell population, both in terms of number and differentiation patterns, providing additional insight into the interaction of adipogenesis and osteoblastogenesis, and the role that diet ultimately may have beyond "simply" caloric intake and increased adiposity. Indeed, the suppressed population of multipotent stem cells in the bone marrow of obese mice may reflect the origins of medical complications that parallel obesity, and complicate bone's responsiveness in the overweight population.

**Disclosures:** Y.K. Luu, None.

This study received funding from: NIH.

**F050**

**WNT-4 Acts Through the Non-Canonical Pathways to Stimulate Osteoblast and Bone Marrow Stromal Stem Cell Differentiation.** M. K. Bergenstock<sup>\*</sup>, J. Tamasi<sup>\*</sup>, N. C. Partridge. Physiology and Biophysics, UMDNJ-RWJMS, Piscataway, NJ, USA.

Parathyroid hormone (PTH) increases bone formation by directing changes in osteoblast function and is currently the only clinically available anabolic agent for treating osteoporosis. We discovered that non-canonical *Wnt-4* is PTH-regulated and expressed by bone lining cells, osteocytes, and hypertrophic chondrocytes after PTH stimulation. Wnt proteins are essential in development and are necessary for the acquisition of high bone mass. Wnts are divided into Wnt-1 and Wnt-5a signaling classes, which activate canonical (Wnt/β-catenin) and non-canonical intracellular pathways (Wnt/Ca<sup>2+</sup> and Wnt/Planar Cell Polarity, PCP), respectively. Primary osteoblastic cells treated with WNT-4 did not increase pre-osteoblastic proliferation when compared with controls but showed greater alkaline phosphatase activity and early stimulation of osteoblast marker genes (*runx2*, *alkaline phosphatase*, *osteocalcin*, *MMP-13*, *osterix*) as well as genes of the canonical pathway (*lef-1*, *tcf-1*, *β-catenin*, *groucho*, *wif-1*, *sfrp-4*) when compared with controls. Differentiating primary osteoblastic cells had significantly greater Von Kossa staining and a 2.5 fold increase in *osteocalcin* gene expression in WNT-4 treated cells compared with controls. In a non-osteogenic environment, we also found that WNT-4 significantly increased bone marker mRNA expression. WNT-4 only minimally activated the canonical pathway. In contrast, continuous WNT-4 treatment of mineralized rat primary cells resulted in a 12-fold increase in CamkII phosphorylation (Wnt/Ca<sup>2+</sup> pathway) and a 2-fold increase in JNK phosphorylation (Wnt/PCP pathway). Differentiating rat primary cells acutely treated with WNT-4 showed a significant 5-fold increase in CamkII phosphorylation 2 and 4 h after stimulation. Acutely stimulated MC3T-E1 cells showed significant phosphorylation of JNKs 1 h after WNT-4 stimulation in all three phases of osteoblastic development. Using specific inhibitors to CamkII and JNKs we found that WNT-4 stimulates bone marker gene expression through non-canonical means. WNT-4 treatment of bone marrow stromal stem cells showed induction of osteoblastic markers and inhibition of adipocytic markers, as well as increased colony forming units and mineralized nodules. Our data support a role for non-canonical Wnts and imply that the canonical pathway is not exclusively important in bone. We hypothesize that WNT-4 acts on immature osteoblasts to accelerate their differentiation, as well as on immature stromal stem cells in the bone marrow to stimulate osteoblastogenesis, thereby preventing differentiation to adipocytes.

**Disclosures:** M.K. Bergenstock, None.

This study received funding from: American Association of University Women (AAUW).

**F054****Deletion of *Mef2c* in Osteocytes Decreases *Sost* Expression and Increases Bone Mass.** I. Kramer<sup>\*1</sup>, O. Leupin<sup>1</sup>, S. Mundlos<sup>\*2</sup>, H. Keller<sup>1</sup>, M. Kneissel<sup>1</sup>.

<sup>1</sup>Musculoskeletal Disease Area, Novartis Institutes for BioMedical Research, Basel, Switzerland, <sup>2</sup>Max Planck Institut für Molekulare Genetik, Berlin, Germany.

Expression of the osteocyte-derived bone formation inhibitor *Sost* in adult bone requires a distant enhancer. We have recently shown that myocyte enhancer 2 (*Mef2*) transcription factors are present in osteocytes and control this enhancer and thus *Sost* expression indicating a putative role for *Mef2s* in the regulation of bone mass. To test this hypothesis we deleted *Mef2c*, one of three *Mef2s* demonstrated to activate *Sost* expression, from osteocytes by crossing *Mef2c<sup>loxP/loxP</sup>* conditional knockout mice with *Dmp1-Cre* mice to generate *Mef2c<sup>loxP/loxP</sup>; Dmp1-Cre* mice. We monitored the long bone phenotype of male and female *Mef2c<sup>loxP/loxP</sup>; Dmp1-Cre* and control littermate mice during growth and ageing (1-6 months) using peripheral and micro-computed tomography (pQCT, microCT). RNA was extracted from femoral cortical bone at necropsy for *Sost* expression analysis by real-time PCR. Animals grew to skeletal maturity with normal body weight and bone length. We found that deletion of *Mef2c* in osteocytes resulted in a reduction of *Sost* expression by about 60% in both sexes. pQCT measurements demonstrated that bone mass, cortical thickness and cancellous bone mineral density were significantly increased in the distal femur metaphysis of male mice during growth and ageing compared to controls. A similar but less pronounced phenotype reaching only borderline significance was observed in the proximal tibia metaphysis. Bone diameter was significantly increased in either long bone. MicroCT measurements revealed that cancellous bone volume and trabecular thickness were increased in the tibia metaphysis. *Ex vivo* measurements in the distal femur metaphysis and lumbar vertebra L3 demonstrated robust increases in cancellous bone volume due to trabecular thickening. Interestingly, female mice displayed a similar but distinctly more moderate cortical and cancellous bone phenotype in the femur metaphysis. Consistent with this finding increases in vertebral cancellous bone volume were also smaller. No appreciable cortical or cancellous bone gain was detectable in the tibia. In summary, osteocyte specific deletion of *Mef2c* leads to increased bone mass in male mice, while its impact on female mice is more modest. The observed *Sost* down-regulation in osteocyte specific *Mef2c* deficient mice is in line with our previous *in vitro* findings. Interestingly, while *Sost* repression occurs in both sexes to a similar extent, the bone phenotype is more distinct in male mice suggesting that *Mef2c* exerts its action on bone mass in part also via regulation of other genes. In conclusion, our data indicate a novel role for *Mef2c* in adult bone homeostasis.

**Disclosures:** I. Kramer, None.

**F058****Evidence that Differentiated Bone Cells Display an Autophagic Response Regulated by HIF-1 $\alpha$ .** A. M. Zahm<sup>\*</sup>, V. Srinivas<sup>\*</sup>, C. S. Adams<sup>\*</sup>, I. M. Shapiro. Orthopaedic Surgery, Thomas Jefferson University, Philadelphia, PA, USA.

It is now recognized that many cells can survive stressful conditions through the induction of autophagy, a process in which cellular components are re-utilized for maintenance of metabolic activity. We have previously shown that in the hypoxic environment of the growth plate, chondrocytes undergo autophagy prior to activation of apoptosis. The objective of the investigation was to determine if bone cells undergo autophagy, and whether the autophagic response is dependent on expression of HIF-1 $\alpha$ . Rat long bones were sectioned and stained for LC3, a microtubule-associated protein that localizes to autophagosomes. While few osteoblasts were positive for LC3, punctate LC3 staining was observed in many osteocytes, indicative of autophagic activity. To further investigate the mechanism regulating bone cell autophagy, MLO-A5 cells were maintained in culture and autophagy was evaluated by immunofluorescence and Western blot analysis. We found that LC3 II was expressed and LC3 protein was localized to discrete, punctate subcellular locations. These results and ongoing electron microscopic studies indicate that there is a baseline level of autophagy in the bone cells. To study the mechanism of autophagy, the MLO cells were treated with thapsigargin and the expression of LC3 was evaluated. As expected, this agent enhanced LC3 II expression and condensation. In addition, thapsigargin stabilized HIF-1 $\alpha$  even under normoxic conditions. To ascertain if HIF-1 was required for bone cell autophagy, we silenced this transcription factor and measured LC3 levels following thapsigargin treatment. We found that thapsigargin-induced autophagy was inhibited in the silenced MLO cells, suggesting that HIF-1 is required for induction of the autophagic state. Interestingly, treatment of the cells with 3-methyladenine, a potent inhibitor of autophagy, exerted a profound effect on the bone cells. Following treatment with this agent, there was a dramatic reduction in thapsigargin-induced HIF-1 stabilization. Together, these results suggest a complex interaction between HIF-1 and the autophagic response. A similar study was performed using MLO-Y4 preosteocytes. In contrast to the less differentiated MLO-A5 cells, these cells did not evidence stimulation of the autophagic response following thapsigargin treatment, despite exhibiting high baseline LC3 II protein levels. The results of the investigation indicate that *in vivo*, bone cells express an autophagic phenotype that is responsive to HIF-1 $\alpha$ . Based on these findings, we conclude that the autophagic response enables bone cells to differentiate and survive in a hypoxic environment.

**Disclosures:** A.M. Zahm, None.

**F062****Imaging of Mineralization Kinetics Suggests that the Transition from Osteoblast to Osteocyte Initiates Prior to Mineral Deposition.** S. L. Dallas<sup>1</sup>, Y. Lu<sup>\*1</sup>, J. L. Rosser<sup>\*1</sup>, D. W. Rowe<sup>2</sup>, I. Kalajzic<sup>2</sup>, L. F. Bonewald<sup>1</sup>, P. A. Veno<sup>\*1</sup>. <sup>1</sup>Univ. of Missouri Kansas City, Kansas City, MO, USA, <sup>2</sup>Univ. of Connecticut Health Ctr, Farmington, CT, USA.

Mineralization of osteoid matrix and differentiation of the osteoblast into an osteocyte are two processes that occur simultaneously during bone formation and are interrelated spatially and temporally. We have previously shown by live cell imaging with fluorescent lineage markers that the transition of an osteoblast towards an osteocyte begins just prior to mineralization. We have also identified a motile cell type on the bone surface that expresses *Dmp1*-GFP and *E11/gp38*, two osteocyte markers, and may represent a committed osteocyte precursor.

To further understand the dynamic process of osteoblast to osteocyte transition and its integration with mineralization, time lapse live cell imaging was performed in mineralizing primary osteoblasts and the late osteoblast/early osteocyte cell line, MLO-A5. Primary cells were isolated from mice expressing a *Dmp1*-GFP transgene as an osteocyte marker and/or a 3.6kb *Col1a1*-DsRed transgene as an osteoblast marker. Embryonic mouse calvaria were used for *in vivo* validation of *in vitro* observations. In primary osteoblasts, areas of mineral deposition, imaged vitally using alizarin red, were defined by clusters of highly motile cells switching on *Dmp1*-GFP expression, accompanied by membrane ruffling and shedding of vesicle-like structures. These cells also expressed the early osteocyte marker, *E11/gp38*. Quantitation of mineralization kinetics showed a wave of GFP induction preceding a rapid (10-14h) mineralization phase. Dual mapping of the motion trajectories and morphology of GFP+ve cells showed correlation of mineralization with transition from a motile polygonal cell to a stationary dendritic osteocyte-like morphology. Similar to the primary cells, mineralization in E15.5 mouse calvaria was exclusively associated with interconnected tracts of cells expressing *Dmp1*-GFP that preceded and patterned mineral deposition in a honeycomb-like trabecular structure. In MLO-A5, a clonal cell line representing the transitioning late osteoblast/osteocyte, mineral was deposited throughout the culture in a honeycomb-like pattern with mineralization kinetics similar to primary cells. Transfection with a *col1a2*-GFP fusion protein as a vital probe for collagen assembly, confirmed mineral deposition on collagen bundles, arranged in honeycomb structures analogous to the mineralization pattern in E15.5 calvaria. These data provide further *in vitro* and *in vivo* evidence that the transition towards an osteocyte is initiated prior to mineralization and that this transitioning cell type is responsible for triggering mineral propagation along a prepared, primed matrix.

**Disclosures:** S.L. Dallas, None.

This study received funding from: NIH (NIAMS)R21 AR054449.

**F066****Phex binds to SNARE-Associated Protein Snapin and Co-Localizes in Vesicle-Enriched, Extracellular Matrix Micro-Environment Mediating Mineral Crystal Nucleation.** J. P. Gorski<sup>1</sup>, N. T. Huffman<sup>\*1</sup>, Z. Xiao<sup>\*2</sup>, S. Liu<sup>\*2</sup>, D. Studer<sup>\*3</sup>, P. S. N. Rowe<sup>2</sup>, L. D. Quarles<sup>2</sup>. <sup>1</sup>Univ. of Missouri-Kansas City, Kansas City, MO, USA, <sup>2</sup>Univ. of Kansas Med. Ctr., Kansas City, KS, USA, <sup>3</sup>Univ. of Bern, Bern, Switzerland.

Mutations of *PHEX* are associated with abnormalities of mineralization as well as increased expression of phosphaturic factor FGF23. However, the mechanism of hypophosphatemia-independent impairment of extracellular matrix mineralization is unknown. The purpose of these studies was to determine if a functional Phex physically localizes to initial sites of mineralization in UMR 106-01 osteoblastic cultures, termed biomineralization foci (BMF). Phex proteolytic activity was found to be 2-3 fold higher in mineralized cultures versus non-mineralized controls or cultures treated with serine protease inhibitor AEBSEF. When mineralized BMFs were isolated by laser capture microscopy and subjected to western blotting, a 60 kDa fragment of Phex was specifically enriched within these complexes, co-localizing with biomarkers BAG-75 and bone sialoprotein, but not MEPE. Interestingly, high pressure freezing electron microscopy revealed that extracellular BMF complexes contain many vesicles which appear to undergo fusion prior to mineralization. Furthermore, proteomic peptide mapping studies on isolated BMF identified a 58 kDa gel band as synaptotagmin-7, a Ca<sup>2+</sup> binding vesicular membrane protein associated with SNARE complexes. Independently, we used the PGBKT7-Phex (E581V) bait construct containing residues 46-749 of the extracellular domain of mouse Phex containing an inactivating mutation to screen a pre-transformed mouse 17-day embryo Matchmaker cDNA library. We obtained three C-terminal clones of snapin that interacted with the Phex construct. Also, we found that snapin was expressed in osteoblastic cell lines by RT-PCR and that a FLAG-tagged full-length Phex was able to co-immunoprecipitate a V5-tagged full-length snapin in co-transfection experiments. Snapin, like synaptotagmin-7, is associated with neural SNARE complexes where they control intracellular docking/fusion of transport vesicles at the plasma membrane. These results indicate that formation and mineralization within the bone extracellular microenvironment involves multi-vesicular exocytosis and fusion. Identification of two SNARE-associated proteins at sites of mineral nucleation suggests such complexes may play a new role in extracellular vesicle fusion events in bone. This potentiality is strengthened since Phex was shown to interact directly with snapin. Whether the formation of 60 kDa Phex at sites of mineral nucleation promotes subsequent growth and propagation of the mineral phase or is a mechanism to limit the function of Phex remains to be determined.

**Disclosures:** J.P. Gorski, Founder, BoneMetrics LLC 5.

This study received funding from: NIH AR052775 (JPG).

## F069

**Deletion of CYP27B1 Reverts the Premature Aging Phenotype of the Klotho-null Mice.** X. Bai<sup>1</sup>, D. Qiu<sup>\*1</sup>, D. Panda<sup>\*1</sup>, D. Goltzman<sup>2</sup>, A. C. Karaplis<sup>1</sup>. <sup>1</sup>Department of Medicine, Lady Davis Institute, Montreal, QC, Canada, <sup>2</sup>Department of Medicine, Royal Victoria Hospital, Montreal, QC, Canada.

Mice homozygous for the null Klotho allele have a short lifespan and show biochemical and morphological features consistent with premature aging-like phenotype. In this study, we have used a mouse genetic approach to investigate *in vivo* the role of Cyp27b1 in the metabolic and skeletal derangements arising in the absence of Klotho. To this end, we crossed mice heterozygous for the hypomorphic Klotho allele (Kl<sup>+/-</sup>) to mice heterozygous for the null Cyp27b1 allele and obtained mice homozygous for both the Kl-hypomorphic and the Cyp27b1-null allele (Cyp27b1<sup>-/-</sup>/Kl<sup>-/-</sup>). Mice were sacrificed and serum and tissues were procured for analysis and comparison to WT, Cyp27b1<sup>-/-</sup> and Kl<sup>-/-</sup> controls.

From 4 weeks onward, Cyp27b1<sup>-/-</sup>/Kl<sup>-/-</sup> mice were clearly distinguishable from Klotho-null mice and exhibited a striking phenotypic resemblance to the Cyp27b1<sup>-/-</sup> controls. The life span of the double mutants increased from 10 weeks to 17 weeks as did their body weight, in parallel to the Cyp27b1<sup>-/-</sup> mice. Serum analysis for calcium, phosphorus, PTH, ALP activity, and creatinine confirmed the biochemical similarity between the Cyp27b1<sup>-/-</sup>/Kl<sup>-/-</sup> and Cyp27b1<sup>-/-</sup> mice and their distinctness from the Kl<sup>-/-</sup> controls. Interestingly, the extremely high serum FGF23 levels observed in the Klotho-null mice were almost completely suppressed in the double knock-out mice, similar to the serum levels in the Cyp27b1<sup>-/-</sup> mice. The characteristic skeletal changes associated with the absence of Klotho were also dramatically converted by the concurrent deletion of Cyp27b1. Hence, wide, unmineralized growth plates and osteomalacic abnormalities were apparent in trabecular and cortical bones of the Cyp27b1<sup>-/-</sup>/Kl<sup>-/-</sup> mice as in the Cyp27b1<sup>-/-</sup> controls. Moreover, widespread soft tissue calcification characteristic of the Kl<sup>-/-</sup> mice was absent in the double mutants.

In summary, our findings substantiate *in vivo* the essential role of Cyp27b1 in the Klotho-null phenotype as its ablation fully reverts the complete spectrum of biochemical and skeletal alterations arising from lack of Klotho. In addition, the results add *in vivo* credence to the proposed role of 1,25(OH)2D as a pivotal regulator of FGF23 expression.

**Disclosures:** X. Bai, None.

## F074

**Osteoclast-Independent Function of Cathepsin K: Regulation of Toll-like Receptor 9 Signaling in Autoimmunity.** K. Okamoto<sup>\*1</sup>, M. Asagiri<sup>\*1</sup>, T. Hirai<sup>\*2</sup>, T. Kunigami<sup>\*2</sup>, H. J. Gober<sup>\*1</sup>, K. Nishikawa<sup>\*1</sup>, K. Aoki<sup>\*3</sup>, K. Ohya<sup>\*3</sup>, S. Kato<sup>\*4</sup>, P. Saftig<sup>\*5</sup>, H. Takayanagi<sup>1</sup>. <sup>1</sup>Department of Cell Signaling, Tokyo Medical and Dental University, Tokyo, Japan, <sup>2</sup>Nippon Chemiphar Co., Ltd., Saitama, Japan, <sup>3</sup>Department of Hard Tissue Engineering, Tokyo Medical and Dental University, Tokyo, Japan, <sup>4</sup>Institute of Molecular and Cellular Biosciences, University of Tokyo, Tokyo, Japan, <sup>5</sup>Biochemical Institute, Christian-Albrechts-University Kiel, Kiel, Germany.

Cathepsin K is a lysosomal cysteine protease that plays a pivotal role in osteoclast-mediated degradation of the bone matrices. Thus, cathepsin K has been considered as a potential therapeutic target for the treatment of bone diseases such as osteoporosis and autoimmune arthritis. Because epoxysuccinic acid derivatives such as E-64 are known to inhibit a wide range of cysteine proteases, we examined a number of newly synthesized analogous compounds in rats treated with low calcium diet to obtain an orally bioavailable bone resorption inhibitor. Through this screening, we obtained a potent cathepsin K inhibitor named NC-2300, which suppresses osteoclastic bone resorption both *in vivo* and *in vitro*. To test the effects of the inhibitor on disease model, we treated adjuvant-induced arthritis in rats with oral administration of NC-2300 and compared the results with the effects of alendronate. NC-2300, but not alendronate, markedly suppressed bone erosion at the inflamed joints, whereas both compounds had a comparable inhibitory effect on periarticular osteoporosis. Surprisingly, NC-2300 also inhibited autoimmune inflammation even when administered after the onset of disease. Furthermore, cathepsin K-deficient mice were found to be resistant to experimental autoimmune encephalomyelitis, suggesting a more general function of cathepsin K in the immune systems. We found that pharmacological inhibition or targeted disruption of cathepsin K impaired Toll-like receptor (TLR) 9 signaling in dendritic cells in response to unmethylated CpG DNA, which in turn led to incomplete induction of the inflammatory T helper 17 cell polarization. While the antigen-presenting ability in dendritic cells was unaffected by cathepsin K inhibition, TLR9-induced secretion of pro-inflammatory cytokines, IL-6, IL-12 and IL-23 was attenuated by cathepsin K inactivation. On the other hand, neither TLR2 nor TLR4 signaling depends on cathepsin K. Therefore, our study indicates that cathepsin K, which was thought to be an osteoclast-specific enzyme, also functions as a dendritic cell-specific regulator of TLR9 signaling. Cathepsin K may serve as a potential target of therapeutic intervention to control autoimmune diseases, but immunological side effects should be carefully evaluated in inhibition of this enzyme in osteoporosis.

**Disclosures:** K. Okamoto, None.

## F079

**PIAS3 Negatively Regulated RANKL-mediated Osteoclastogenesis Directly in Osteoclast Precursors and Indirectly via Osteoblasts.** T. Hikata<sup>1</sup>, H. Takaishi<sup>1</sup>, A. Hakozaiki<sup>1</sup>, M. Furukawa<sup>1</sup>, S. Uchikawa<sup>1</sup>, J. Takito<sup>1</sup>, T. Kimura<sup>\*2</sup>, Y. Okada<sup>\*2</sup>, R. Nishimura<sup>3</sup>, S. V. Reddy<sup>4</sup>, M. Matsumoto<sup>\*5</sup>, Y. Toyama<sup>\*1</sup>. <sup>1</sup>Department of Orthopaedic Surgery, Keio University, Tokyo, Japan, <sup>2</sup>Department of Pathology, Keio University, Tokyo, Japan, <sup>3</sup>Department of Molecular and Cellular Biochemistry, Osaka University, Osaka, Japan, <sup>4</sup>Children's Research Institute, Medical University of South Carolina, Tokyo, SC, USA, <sup>5</sup>Department of Spine and Spinal Cord Disease, Keio University, Tokyo, Japan.

Protein inhibitor of activated STAT3 (PIAS3) not only inhibits the DNA binding activity of STAT3 in the JAK/STAT signaling pathway, but also interacts with MITF that is an important transcription factor for the osteoclast differentiation. Last year, we reported that PIAS3 negatively regulated RANKL-mediated osteoclastogenesis *in vitro* using gain of function and loss of function methods. Here we generated PIAS3 transgenic mice (Tg) using the tartrate-resistant acid phosphatase (TRAP) gene promoter. Two lines selected from 27 founders gave similar results. X-ray and microcomputed tomography analysis revealed an osteopetrotic bone phenotype in the 8-week-old PIAS3 Tg. Histological analysis showed that the osteoclast number was significantly reduced in the epiphyseal region and that the bone marrow was abnormally filled with trabecular bone in PIAS3 Tg. Bone histomorphometric analysis indicated an increase in bone volume associated with a reduced osteoclast number, a decrease in the indicators of osteoclastic bone resorption, and a normal level of bone formation in PIAS3 Tg. Consistently, bone marrow macrophages (BMMs) from PIAS3 Tg showed decreased *in vitro* RANKL-mediated osteoclastogenesis. Real-time RT-PCR revealed that c-Fos, NFATc1, cathepsin K, and TRAP gene expression were markedly attenuated in BMMs from PIAS3-Tg. Taken together, PIAS3 Tg mice showed an osteopetrotic phenotype due to an impairment of osteoclast differentiation. In primary osteoblasts isolated from mouse calvaria, PIAS3 overexpression downregulated the RANKL expression through inhibition of STAT3 DNA binding activity. In co-cultures with primary osteoblasts and BMMs in the presence of Oncostatin M, PIAS3-transduced osteoblasts supported less osteoclast formation than mock-transduced osteoblasts. These results suggested that PIAS3 negatively regulated RANKL-mediated osteoclastogenesis directly in osteoclast precursors and indirectly via osteoblasts.

**Disclosures:** T. Hikata, None.

## F081

**High Dose of RANKL Rescues Integrin  $\alpha_9$ - Osteoclast Phenotype.** G. Lu<sup>1</sup>, Y. Hiram<sup>1</sup>, F. Cackowski<sup>\*1</sup>, C. Boykin<sup>\*2</sup>, K. Patrene<sup>\*1</sup>, J. L. Anderson<sup>\*1</sup>, D. Del Prete<sup>\*1</sup>, J. J. Windle<sup>2</sup>, G. D. Roodman<sup>3</sup>. <sup>1</sup>Medicine/Hem-Onc, University of Pittsburgh, Pittsburgh, PA, USA, <sup>2</sup>Human Genetics, Virginia Commonwealth University, Richmond, VA, USA, <sup>3</sup>Medicine/Hem-Onc, University of Pittsburgh and VA Pittsburgh Healthcare System, Pittsburgh, PA, USA.

We have previously demonstrated that integrin  $\alpha_9$  plays a critical role in osteoclast (OCL) differentiation and function. Compared to wild type mice,  $\alpha_9$ <sup>-/-</sup> bone marrow cultures formed significantly less OCLs that are smaller in size and have a markedly reduced bone resorption capacity. Further, introduction of a full length  $\alpha_9$  cDNA into  $\alpha_9$ <sup>-/-</sup> cells rescued the OCL phenotype. Since  $\alpha_9$ <sup>-/-</sup> mice survive less than 2 weeks post-partum, the role of  $\alpha_9$  in adult bone is unknown. Therefore, we generated  $\alpha_9$ <sup>-/-</sup> chimeric mice by transplanting  $\alpha_9$ <sup>-/-</sup> bone marrow cells or WT cells into lethally irradiated mice. Genotyping confirmed that  $\alpha_9$ <sup>-/-</sup> transplanted mice were chimeric, with only their hemopoietic cells lacking  $\alpha_9$ <sup>-/-</sup>. Two months post stem cell transplantation, bone marrow cultures from the  $\alpha_9$ <sup>-/-</sup> chimeric mice showed similar phenotypes as those seen in the cultures from  $\alpha_9$ <sup>-/-</sup> mice. In addition, micro-QCT scanning of the proximal tibiae of chimeric mice, showed significantly increased trabecular bone volume/total tissue volume (BV/TV), trabecular numbers (Tb.N), trabecular thickness (Tb.Th), and decreased trabecular separation (Tb.Sp) compared to WT transplanted mice (WTT). However, these changes in micro-QCT parameters began to diminish with time and were not significant after 3 to 4 months post transplantation. In addition, bone marrow cultures from older chimeric mice formed increased numbers of normal sized OCLs. RANKL treated bone marrow cultures from chimeric mice 3-4 months post-transplant showed dramatically elevated phosphorylation of p38 and p44/42 compared to WT transplants, but had similar levels of integrins  $\alpha_9$  and  $\beta_3$  mRNA. We then tested if increased RANKL levels were present in the sera of chimeric mice 3-4 months post-transplant and found that RANKL levels were progressively increased compared to WTT. Further, treatment of  $\alpha_9$ <sup>-/-</sup> marrow cultures with the high concentrations of RANKL reversed the phenotypic abnormalities in OCL formed in  $\alpha_9$ <sup>-/-</sup> marrow cultures. These results suggest that increased RANKL signaling can reverse the abnormal OCL activity in  $\alpha_9$ <sup>-/-</sup> mice.

**Disclosures:** G. Lu, None.

This study received funding from: NIH.



## F083

**Tec Kinases, Therapeutic Targets for Bone Destructive Diseases.** M. Shinohara\*, T. Koga\*, K. Okamoto\*, K. Arai\*, H. Takayanagi. Cell Signaling, Tokyo Medical and Dental University, Tokyo, Japan.

Bone homeostasis depends on balanced action of bone-resorbing osteoclasts and bone-forming osteoblasts. Tipping the balance in favor of osteoclasts leads to diseases with a low bone mass such as osteoporosis as well as rheumatoid arthritis and periodontitis. Now, it is well documented that enhanced bone destruction by osteoclasts is observed in these diseases. Therefore, it is important to understand the mechanism of osteoclast differentiation. Osteoclasts are multinucleated cells that originate from bone marrow-derived monocyte/macrophage precursor cells (BMMs). The differentiation of BMMs to osteoclasts is mainly regulated by three signaling pathways activated by RANKL, M-CSF and immunoreceptor tyrosine-based activation motif (ITAM). We reported that Tec tyrosine kinases, Btk and Tec, regulate ITAM pathway in response to RANKL stimulation through PLC $\gamma$  activation in the last year's meeting. However, it remains unclear how Tec kinases link RANKL and ITAM signaling during osteoclastogenesis. To address this issue, we performed a system biology analysis and found that SLP adaptors interact with both Tec kinases and PLC $\gamma$  in an ITAM-dependent manner. *In vitro* osteoclast differentiation was severely abrogated in BMMs from mice deficient in SLP adaptors, suggesting that the crucial role of the RANKL-stimulated formation of the osteoclastogenic complex including Tec kinases, SLP adaptor proteins and PLC $\gamma$ . Furthermore, in the last year we also reported that Tec-/-Btk-/- mice are resistant to ovariectomy-induced bone loss, suggesting that Tec kinases are good therapeutic targets for bone diseases. Thus we analyzed therapeutic efficacy of Tec kinase inhibitor in bone disease models and found that Tec kinase inhibition reduced osteoclastic bone resorption in models of osteoporosis and inflammation-induced bone destruction. This study identifies the importance of osteoclastogenic complex and provides a molecular basis for a novel therapeutic strategy for bone diseases.

**Disclosures:** M. Shinohara, None.

## F085

**The Cholesterol Sensing Receptors, Liver X Receptor  $\alpha$  and  $\beta$ , Have Novel and Distinct Roles in Osteoclast Differentiation and Activation in Bone.** K. Robertson\*<sup>1</sup>, M. Norgård\*<sup>2</sup>, S. Windahl\*<sup>3</sup>, K. Hultenby\*<sup>2</sup>, C. Ohlsson\*<sup>3</sup>, J. Gustafsson\*<sup>1</sup>, G. Andersson\*<sup>2</sup>. <sup>1</sup>Karolinska Institute, Stockholm, Sweden, <sup>2</sup>Karolinska University Hospital, Stockholm, Sweden, <sup>3</sup>Sahlgrenska University Hospital, Gothenburg, Sweden.

The Liver X Receptor ( $\alpha$ , $\beta$ ) is primarily responsible for regulating cholesterol homeostasis within cells and the whole body. However, as recent studies show that the role for this receptor is expanding we investigated whether the LXRs could be implicated in bone homeostasis and development. pQCT was performed on both males and female LXR $\alpha$ -/-, LXR $\beta$ -/-, LXR $\alpha$ -/ $\beta$ -/- and WT mice at 4 months and 1 year of age. Then 4 month female mice were additionally analyzed using qPCR, immunohistochemistry, histomorphometry, transmission electron microscopy and also serum bone turnover markers were measured. At the mRNA level, LXR $\beta$  was more highly expressed than LXR $\alpha$  in whole femur. pQCT determined adult female LXR $\alpha$ -/- mice had a significant increase in BMD due to an increase in all cortical parameters. No difference was seen on trabecular BMD. Quantitative histomorphometry showed these mice had significantly more endosteal osteoclasts in the cortical bone; however, although SEM showed no difference in the size of the OC, their ruffled border or clear zone, they appeared to be less active than normal as suggested by a significant reduction in serum levels of CTX. Conversely, the female LXR $\beta$ -/- mice exhibited no change in BMD, presumably because a significant decline in the volume of the trabecular osteoclasts was compensated by an increase in the expression of the osteoclast markers Cathepsin K and TRAP and a larger ruffled border. These mice also had an increased expression of osteoblast associated genes and an increase in serum ALP and OC, suggesting increased bone turnover. Our study shows that both LXRs have distinct roles in cellular function within the bone; LXR $\alpha$  has an impact on osteoclast activity primarily in cortical bone whereas LXR $\beta$  modulates osteoclast differentiation and bone turnover in trabecular bone. These novel findings expand the role for the LXRs away from cholesterol metabolism.

**Disclosures:** K. Robertson, None.

This study received funding from: Swedish Research Council, the Swedish Cancer Fund, KaroBio AB, the Swedish Children's Cancer Fund, the Loo and Hans Ostermans Stiftelse.

## F087

**DC-STAMP Regulates Bone Metabolism Through Cell-cell Fusion of Osteoclasts.** R. Iwasaki\*<sup>1</sup>, T. Miyamoto\*<sup>2</sup>, H. Kawana\*<sup>3</sup>, T. Nakagawa\*<sup>3</sup>, T. Suda\*<sup>4</sup>. <sup>1</sup>Department of Cell Differentiation, Dentistry and Oral Surgery, Keio University School of Medicine, Tokyo, Japan, <sup>2</sup>Department of Orthopedic Surgery, Musculoskeletal Reconstruction and Regeneration Surgery, Keio University School of Medicine, Tokyo, Japan, <sup>3</sup>Department of Dentistry and Oral Surgery, Keio University School of Medicine, Tokyo, Japan, <sup>4</sup>Department of Cell Differentiation, Keio University School of Medicine, Tokyo, Japan.

Multinucleation by cell-cell fusion is a characteristic of osteoclasts. Recently, we have isolated DC-STAMP (Dendritic Cell Specific Transmembrane Protein), a seven transmembrane protein, as an essential molecule for osteoclast cell-cell fusion, and that osteoclasts in DC-STAMP deficient mice show complete lack of cell-cell fusion (J. Exp. Med. 2005). However, it is not yet characterized the role of osteoclast cell-cell fusion via DC-STAMP in bone homeostasis. Here we generated DC-STAMP transgenic mice (Tg) under the control of an actin(CAG) promoter to express DC-STAMP ubiquitously *in vivo*. The defects of osteoclast cell-cell fusion in DC-STAMP deficient mice was rescued by crossing with DC-STAMP Tg mice *in vivo* and *in vitro*, and DC-STAMP expression in the cells derived from DC-STAMP Tg mice was significantly upregulated compared to that from wild-type mice. *In vitro* osteoclast formation assay, the number of multinuclear cells as well as the number of nuclei in each multinuclear cell were significantly upregulated in osteoclasts of Tg mice compared with that of wild-type littermates. DC-STAMP expression was detected in various tissues of DC-STAMP Tg mice such as liver, muscle and brain, all of which do not express DC-STAMP physiologically. Interestingly, ectopic cell-cell fusion was not observed in liver and muscle, and the multinucleation of myotube was not stimulated by the forced expression of DC-STAMP in Tg mice. Thus, our results suggest that DC-STAMP promotes cell-cell fusion in a tissue specific manner under a stimulation of RANKL. The cell-cell fusion was not induced even in the cells derived from Tg bone marrow in the presence of M-CSF alone, while the addition of RANKL in turn induced hyper-multinucleation of osteoclasts. Interestingly, bone parameters such as bone volume per tissue volume and trabecular number were significantly downregulated in DC-STAMP Tg mice, whereas these parameters were significantly upregulated in DC-STAMP knockout mice, suggesting that cell-cell fusion of osteoclast via DC-STAMP plays a critical role in regulating bone metabolism.

**Disclosures:** R. Iwasaki, None.

## F089

**Inpp4b as a Regulator of Bone Mass.** M. Rashed\*, M. Arsenault\*, M. Ferron\*, M. Pata\*, J. Vacher. IRCM, Montreal, QC, Canada.

Osteoclasts are unique hematopoietic cells that derive from the monocyte lineage and are responsible for bone resorption. Loss of osteoclast activity leads to malignant osteopetrosis, a genetic disease characterized by increased bone mass and severe reduction in bone marrow compartment. In mouse and human, the grey-lethal (*gl*) gene is responsible for the most severe form of recessive osteopetrosis. We have identified a novel *gl* osteopetrosis-associated gene, the Inositol polyphosphate 4-phosphatase type II (Inpp4b) that is markedly repressed in *gl/gl* osteoclasts. The mouse Inpp4b cDNA encodes a 105kDa protein including a C2 domain and a consensus C(X)<sub>2</sub>R catalytic site. The Inpp4b phosphatase was shown to hydrolyse *in vitro* the second messenger PtdIns(3,4)P<sub>2</sub> to PtdIns(3)P which have been implicated as regulators of intracellular signaling in bone cells. Normally, Inpp4b is expressed throughout the osteoclast lineage and in osteoclast maturation/activation. To study the role of Inpp4b, we used the cell-based monocytic model RAW 264.7 that can be induced to differentiate upon RANKL stimulation into the osteoclast lineage. Enhanced *ex vivo* expression of native Inpp4b in these cells caused a significant decrease in differentiation into osteoclast-like cells. In contrast, overexpression of a phosphatase inactive Inpp4b mutant promoted differentiation. Moreover, we showed that differentiation was mainly regulated by NFATc1 activation, nuclear translocation and transcription of osteoclast-specific target genes. These results indicated that Inpp4b is a negative regulator of osteoclast differentiation and is dependent on its activity. We then investigated the role of Inpp4b *in vivo* and produced TRAP-Inpp4b transgenic mice that exhibited no obvious phenotype. By contrast, TRAP-Inpp4b-*gl/gl* transgenic mice displayed an increase in bone density with reduced osteoclast population, leading to a more severe osteopetrotic phenotype than *gl/gl* mice. Based on these results, analysis of the role of Inpp4b in bone mass regulation was undertaken independently of *gl* by production of a null allele. Together our results demonstrated that the Inpp4b phosphatase, potentially through the NFATc1 pathway, is a major regulator of the osteoclast lineage.

**Disclosures:** M. Rashed, None.

## F091

**Regulation of Bone Mass and Osteoclastogenesis by the Carcino-Embryonic Antigen Related Cell Adhesion Molecule 1 (CEACAM1).** S. Huang\*, M. Harris\*, M. Kaw\*, M. McInerney\*, N. Ebraheim\*, S. Najjar\*, B. Lecka-Czernik. Department of Orthopaedic Surgery, Center for Diabetes and Endocrine Research, University of Toledo Medical Center, Toledo, OH, USA.

The Carcino-Embryonic Antigen Related Cell Adhesion Molecule 1 (CEACAM1) represents a transmembrane glycoprotein belonging to a subgroup of the immunoglobulin superfamily. Among other functions, CEACAM1 promotes insulin clearance in liver and decreases inflammatory responses. Upon its phosphorylation by the insulin receptor tyrosine kinase, CEACAM1 takes part of the insulin-receptor endocytosis complex to increase the rate of receptor-mediated insulin endocytosis and degradation, which constitute the basic mechanism of insulin clearance in liver. Transgenic liver-specific overexpression of the phosphorylation-defective S503A *Ceacam1* mutant under the control of the ApoA1 promoter exerts a dominant-negative effect on CEACAM1 function in L-SACCI mice. The mice develop impairment of insulin clearance and hyperinsulinemia, which results in insulin resistance and increased hepatic triglyceride synthesis and secretion. L-SACCI animals have increased fat mass, with higher number of macrophages infiltrating fat tissue. Here, we demonstrate that the bone of 5 month-old L-SACCI male mice is larger and has more mass as compared to the bone of wild type (WT) animals. Trabecular bone of the L-SACCI tibia has increased volume (54%;  $p=0.037$ ), connectivity density (76%;  $p=0.008$ ) and trabeculae number (24%;  $p=0.048$ ). In addition, total area and cortical area in midshaft tibia are increased by 20% ( $p=0.003$ ) and 10% ( $p=0.04$ ), respectively. Although larger and thicker, L-SACCI bone is not osteopetrotic and has enlarged medullary area (42%,  $p=0.002$ ). In addition, the length of L-SACCI bone is not different from that of WT. This indicates that CEACAM1 regulates bone remodeling, rather than developmental bone growth. To determine the cellular basis for the altered bone phenotype, we have compared number of osteoclast progenitors in the bone marrow of L-SACCI and WT animals. Osteoclast progenitor number and their ability to form multinucleated TRAP+ cells were assessed in co-culture of non-adherent bone marrow cells with osteoclast-supporting mesenchymal U-33/γ2 cells. We found that adult L-SACCI animals possess 20-fold lower number of osteoclast progenitors than WT. This suggests that CEACAM1 plays an important role in osteoclast differentiation. Investigations are underway to determine whether alteration in the bone phenotype of L-SACCI mice results from systemic insulin resistance and lipid abnormalities or from impaired monocyte differentiation into osteoclasts.

**Disclosures:** B. Lecka-Czernik, None.

## F093

**CD47 (IAP) Is an Important Modulator of Osteoclast and Osteoblast Differentiation *in vitro* and *in vivo*.** V. E. DeMambro<sup>1</sup>, L. A. Maile<sup>2</sup>, E. T. Everett<sup>1</sup>, D. R. Clemmons<sup>1</sup>, W. G. Beamer<sup>1</sup>, C. J. Rosen<sup>1</sup>. <sup>1</sup>The Jackson Laboratory, Bar Harbor, ME, USA, <sup>2</sup>University of North Carolina, Chapel Hill, NC, USA.

CD47 (Integrin Associated Protein; IAP) and SHPS-1 are critical signaling molecules for IGF-1 activation of smooth muscle. The extracellular domains of IAP and SHPS-1 bind and this association is required for SHPS-1 phosphorylation. Also the presence of an intact IAP extracellular domain is important for macrophage differentiation. Since multiple cell types express IAP, and osteoclast-osteoblast (OC-OB) interactions are necessary for skeletal remodeling, we hypothesized that the absence of IAP would affect both OC and OB function, resulting in impaired peak bone acquisition. We raised *IAP*<sup>-/-</sup> mice on a C57BL/6J (B6) background and performed skeletal phenotyping at 16 wks. We also extracted bone marrow stromal cells (BMSCs) and evaluated their *in vitro* capacity to differentiate. *In vivo*, *IAP*<sup>-/-</sup> females were lighter, had less % fat than B6 (WT), had reduced total whole body aBMD (DXA), total femoral vBMD (pQCT) and cortical thickness (all  $p<0.01$  vs WT). MicroCT of the distal femur revealed that *IAP*<sup>-/-</sup> mice had reduced BV/TV ( $p=0.007$  vs WT) due to reduced trabecular thickness ( $p=0.02$  vs WT) but not number. *In vitro*, non-adherent BMSCs from *IAP*<sup>-/-</sup> mice were grown in 2.5% FCS with RANKL (30ng/ml); cells were counted by TRAP staining and # of nuclei per cell was assessed. Although total TRAP+ cell #'s were similar by genotype, the # of cells with >3 nuclei was reduced (WT:  $300 \pm 40$  vs *IAP*<sup>-/-</sup>:  $48 \pm 9$ ,  $p<0.01$ ). In WT cells, addition of anti-IAP antibody that disrupts IAP/SHPS-1 association reduced the # of multinucleated cells from  $402 \pm 65$  to  $137 \pm 25$ ,  $p<0.05$ . In WT cells without RANKL, IAP was completely cleaved, but this was prevented by addition of RANKL. Further, a MMP-2 inhibitor prevented IAP cleavage in WT cells, resulting in enhanced SHPS-1 phosphorylation, whereas *IAP*<sup>-/-</sup> cells showed no SHPS-1 phosphorylation. We also cultured adherent BMSCs from *IAP*<sup>-/-</sup> and WT mice in 10% FCS; at d7 *IAP*<sup>-/-</sup> BMSCs showed a significant reduction in ALP+ colonies vs WT. By d18 von Kossa staining revealed that the *IAP*<sup>-/-</sup> cultures did differentiate and mineralize though to a lesser extent than WT controls. We conclude intact IAP is required for SHPS-1 association and phosphorylation and that both events are necessary for complete osteoclastogenesis and OB recruitment. Global deletion of IAP caused impaired cortical and trabecular bone acquisition in both genders. In sum, we believe IAP may be critical for OC fusion. One mechanism whereby RANKL promotes osteoclastogenesis may be inhibition of IAP cleavage. Further studies are needed to delineate whether changes in osteoclastogenesis or OB recruitment in the *IAP*<sup>-/-</sup> mouse are the primary mechanisms for impaired peak bone acquisition.

**Disclosures:** V.E. DeMambro, None.

This study received funding from: NIAMS 45433.

## F098

**Mice Deficient in Pyk-2 Have Impaired Ovariectomy-Induced Bone Resorption.** E. Smith<sup>1</sup>, D. T. Crawford<sup>1</sup>, N. A. Hanson<sup>1</sup>, E. Purev<sup>2</sup>, R. Baron<sup>2</sup>, T. A. Brown<sup>1</sup>, L. Buckbinder<sup>1</sup>. <sup>1</sup>Pfizer Global R&D, Groton, CT, USA, <sup>2</sup>Harvard School of Dental Medicine, Boston, MA, USA.

Mice deficient in proline-rich tyrosine kinase 2 (Pyk2) on a C57BL/6 background have a high bone mass phenotype at 18 weeks of age characterized by increased bone formation and increased osteogenesis of marrow-derived stromal cells (Buckbinder L, et al. PNAS 104: 10619-10624, 2007). Recent evidence has also suggested that osteoclasts from 6-8 week old *Pyk2*<sup>-/-</sup> mice on a 129 background show diminished resorptive capacity due to impaired podosome formation (Gil-Henn H, et al. JCB 178: 1053-1064, 2007). Based on this, the objective of this study was to evaluate the ability of *Pyk2*<sup>-/-</sup> mice to undergo osteoclastic bone resorption stimulated by ovariectomy. Bone marrow macrophages from *Pyk2*<sup>-/-</sup> mice on a C57BL/6 background were differentiated into osteoclasts by co-culture with primary mouse calvarial osteoblasts. Consistent with cells from *Pyk2*<sup>-/-</sup> mice on a 129 background, these cells demonstrated a decrease in % area resorbed when plated on dentin slices as well as impaired podosome formation compared to cells from WT mice. Female *Pyk2*<sup>-/-</sup> and wild-type (WT) mice received ovariectomy (OVX) or sham surgery at 10 weeks of age and were euthanized after 8 weeks of bone loss. Trabecular BV/TV of lumbar vertebrae in *Pyk2*<sup>-/-</sup> mice was not significantly reduced in OVX vs. sham mice by μCT, while BV/TV in WT mice was reduced 29.6% ( $p=0.04$ ). Despite this, 2-way ANOVA did not detect a statistically significant interaction between genotype and OVX vs. sham surgery. Trabecular BV/TV in the distal femoral metaphysis was reduced by 59% in *Pyk2*<sup>-/-</sup> mice ( $p<0.0001$ ) and 74% in WT mice ( $p=0.04$ ) after ovariectomy as measured by μCT. In this case, the interaction between genotype and surgery was significant by 2-way ANOVA ( $p=0.008$ ). Serum CTx (RatLAPS, Nordic Biosciences Diagnostics) was increased 33% after OVX compared to Sham in WT mice ( $p=0.097$ ), which represented a 43% increase compared to 10 week old WT mice ( $p=0.012$ ). In contrast, serum CTx was not significantly increased after ovariectomy compared to either Sham or 10 week old animals in *Pyk2*<sup>-/-</sup> mice. Taken together, these data suggest that *Pyk2*<sup>-/-</sup> mice demonstrate reduced resorption responses when stimulated by estrogen deficiency. These data provide *in vivo* evidence that Pyk2 is involved in osteoclastic bone resorption in addition to osteoblastic bone formation and is therefore an attractive therapeutic target for osteoporosis.

**Disclosures:** E. Smith, None.

## F103

**Non-enzymatic Glycation Increases Bone Fragility Through Altered Microdamage Formation & Propagation.** S. Tang<sup>1</sup>, D. Vashishth<sup>2</sup>. <sup>1</sup>Orthopedic Surgery, University of California, San Francisco, San Francisco, CA, USA, <sup>2</sup>Biomedical Engineering, Rensselaer Polytechnic Institute, Troy, NY, USA.

The fracture resistance of bone in part depends on its ability to optimize the formation of microdamage such as microcracks and diffuse damage. Nonenzymatic glycation (NEG) occurs w/ aging and diabetes, and adversely affects bone matrix quality and bone's fracture resistance. We hypothesized that (1) NEG-mediated stiffening of the organic matrix of cancellous bone may alter the magnitude of microdamage production during pre-yield and post-yield loading; and (2) the differences may be the result of altered microdamage morphologies. Novel methods to segment and quantify microdamage are introduced. Bone cores from the tibial plateaus of a 64yo human donor were scanned by microCT, incubated in either a NEG or a control solution, subjected to unconfined compression to either 0.6% or 1.1% apparent strains, and stained for microdamage in a lead-uranyl acetate solution. Stained samples were rescanned by microCT to determine the magnitude of load induced microdamage. The ratios of damaged volume to bone volume (DVBV), a measure of microdamage quantity, and damaged surface to damaged volume (DSDV), an indicator of microdamage morphology, were used to characterize microdamage. During pre-yield loading, the NEG group incurred a 53% increase in total damage(DVBV) than the controls ( $p<0.05$ ) but was more crack-like as indicated by the higher DSDV ( $p<0.05$ ). Post-yield loading resulted in the controls incurring 18.6% higher DVBV but was morphologically more diffuse-like than the NEG group ( $p<0.001$ ). In summary, the new microCT based technique successfully allowed to measure and segment microdamage. Consistent w/ fracture mechanisms in brittle materials, NEG reduced microdamage formation in the post-yield region and altered microdamage morphology to more crack like than diffuse damage. These results have important implications for diabetes and antiresorptive bone therapies that cause accumulation of AGEs in bone.



**Disclosures:** S. Tang, None.

This study received funding from: NIH AG20618.

## F107

**Enzyme Replacement Therapy Prevents Dental Defects in the *Akp2*<sup>-/-</sup> Mouse Model of Infantile Hypophosphatasia.** M. D. McKee<sup>1</sup>, I. Lemire<sup>2</sup>, R. Heft<sup>3</sup>, P. Crine<sup>3</sup>, J. Millan<sup>4</sup>. <sup>1</sup>Faculty of Dentistry, McGill University, Montreal, QC, Canada, <sup>2</sup>Enobia Pharma, Montreal, QC, Canada, <sup>3</sup>Enobia Pharma, Montreal, QC, Canada, <sup>4</sup>Sanford Children's Research Center, Burnham Institute for Medical Research, San Diego, CA, USA.

Osteomalacia in hypophosphatasia (HPP) is attributable to loss-of-function mutations in the tissue-nonspecific alkaline phosphatase (TNALP) gene. In the absence of functional TNALP, one of its natural substrates - pyrophosphate (PPi) - accumulates extracellularly and inhibits skeletal and dental mineralization. HPP is classified according to age at diagnosis, and varies remarkably in severity, spanning (from most severe to mildest) perinatal, infantile, childhood, adult and odontohypophosphatasia forms. TNALP-null mice (*Akp2*<sup>-/-</sup>) phenocopy human infantile HPP remarkably well, as the mice are born with a normally mineralized skeleton, but develop rickets at about 1 wk of age, and die at about 2 wks of age having severe skeletal and dental hypomineralization and episodes of apnea and epileptic seizures. In the dentition of these mice, a delay in dentin mineralization and incisor eruption, and a deficiency in the amount of acellular cementum, have been documented. Following our previous work on the skeleton, here we report on the complete prevention of tooth mineralization and acellular cementogenesis abnormalities following treatment of *Akp2*<sup>-/-</sup> mice with daily subcutaneous injections of a mineral-targeting form of recombinant, secreted human TNALP (sALP-FcD10) given at a dose of 8.2 mg/kg for 15 days. Mandibles from wild type, sALP-FcD10-injected (treated) and vehicle-injected (untreated) mice were examined by radiography, micro-computed tomography, histology (including von Kossa staining for mineral) and transmission electron microscopy (TEM; including immunogold labeling for osteopontin). In addition to preventing osteomalacia in the *Akp2*<sup>-/-</sup> mice, daily sALP-FcD10 injections prevented the hypomineralization of dentin and cementum that occurs in the untreated *Akp2*<sup>-/-</sup> mice. Hypomineralized *Akp2*<sup>-/-</sup> molar root dentin and incisor root analogue dentin, which are particularly sensitive to the lack of TNALP, showed well-developed dentin and cementum structure and complete mineralization after the sALP-FcD10 injections. Ultrastructural analysis by TEM of the tooth root surfaces confirmed that the acellular cementum typically missing or reduced in *Akp2*<sup>-/-</sup> mice was restored by the sALP-FcD10 injections, and characteristic intense immunogold labeling for osteopontin was observed over the restored acellular cementum. In conclusion, a mineral-targeting, recombinant form of TNALP prevents dental hypomineralization, and restores acellular cementum, in TNALP-null mice.

**Disclosures:** M.D. McKee, Enobia Pharma 2, 3; Targanta Therapeutics 2, 3. This study received funding from: Enobia Pharma.

## F109

**Osteopontin Deficiency Reduces Aortic Calcification and Oxidative Stress in Diabetic LDLR<sup>-/-</sup> Mice.** J. Shao, C. Lai\*, R. Cohen\*, J. Cai\*, D. Towler. Internal Medicine, Washington University in St. Louis, St. Louis, MO, USA.

Osteopontin (OPN) is a matrix cytokine that binds calcium phosphate, inhibits epitaxial mineralization, and enhances calcium egress from pre-existing calcium deposits. When cleaved by proteases, a cryptic C-terminal peptide (SVVYGLR in humans, SLAYGLR in mice) is revealed that binds alpha-4 integrins. Previously, we showed that OPN, via this peptide, stimulates vascular Nox2 expression, increases oxidative stress, and upregulates arterial MMP9. Furthermore, we showed that OPN deficiency reduces aortic MMP9 activity and oxidative stress in male LDLR<sup>-/-</sup> mice fed high fat diets (HFD) - a model of type II diabetes and aortic calcification. Since MMP9 degrades arterial elastin -- necessary for medial artery calcium deposition in vivo -- we assessed the impact of osteopontin deficiency on diabetic vascular calcification. Two month old OPN<sup>+/+</sup>;LDLR<sup>-/-</sup> and OPN<sup>-/-</sup>;LDLR<sup>-/-</sup> mice were HFD (42% of calories from fat) for 3 months, then analyzed for (a) aortic valve and medial calcium staining using an Alizarin red histochemical score; and (b) aortic tissue calcium load, using formic acid calcium solubilization and measurement with an ion-selective electrode. Diabetes and dyslipidemia were equivalent in both genotypes. However, as compared to OPN-replete cohorts, OPN-deficient mice exhibited a 50% reduction in aortic histological calcification scores (OPN<sup>+/+</sup>;LDLR<sup>-/-</sup> = 7.9 +/- 0.9 vs. OPN<sup>-/-</sup>;LDLR<sup>-/-</sup> = 3.9 +/- 0.4, p < 0.05, two-tailed Mann-Whitney U-test). Aortic calcium tissue load was decreased by 30% (OPN-replete = 0.71 +/- 0.09 ug calcium/mg of dry aorta vs. OPN-null = 0.51 +/- 0.07 ug calcium / mg of dry aorta; p = 0.065). Reductions in aortic calcification with OPN deficiency were accompanied by reductions in aortic Nox2 and CD68+ macrophage accumulation (p < 0.05). Since pulsatile teriparatide administration down-regulates aortic OPN and calcium accrual, we examined whether teriparatide impacts vascular inflammation and oxidative stress. Two-month old OPN<sup>+/+</sup>;LDLR<sup>-/-</sup> mice were fed HFD for 1 month, treated with either vehicle or teriparatide (0.4 mpk/day s.c.). Teriparatide dosing reduced aortic OPN, Nox2, and CD68+ macrophage accumulation by 60% (all p < 0.05). This was accompanied by a 25% reduction in the serum oxidative stress marker, 8-F-isoprostane (75.4 +/- 7.5 pg/ml vs. 56.6 +/- 7.3 pg/ml, p < 0.05). Thus, aortic OPN participates in the inflammatory signals and matrix remodeling events that initiate vascular calcification. Teriparatide-induced down-regulation of aortic OPN mimics key vasculotropic features of OPN deficiency. Suppression of aortic OPN gene expression by pulsatile teriparatide may mediate the beneficial effects of teriparatide on vascular inflammation and oxidative stress in diabetic LDLR<sup>-/-</sup> mice.

**Disclosures:** D. Towler, Wyeth 2; GlaxoSmithKline 2; Barnes-Jewish Foundation 3; Kirin 5. This study received funding from: National Institutes of Health.

## F112

**Nkx3.2 Is an Important Mediator of Hypoxia-induced Chondrocytic Differentiation.** Y. Kawato\*, M. Hirao<sup>1</sup>, J. Hashimoto<sup>1</sup>, N. Tamai\*, N. Yamasaki\*, A. Nampei<sup>1</sup>, A. Myoui<sup>2</sup>, H. Yoshikawa<sup>1</sup>. <sup>1</sup>Orthopaedics, Osaka University Graduate School of Medicine, Suita, Japan, <sup>2</sup>Medical Center for Translational Research, Osaka University Hospital, Suita, Japan.

Recently, we reported that hypoxia promotes chondrocytic differentiation in mesenchymal lineage independently of Sox9 (J Biol. Chem. 281(41), 2006). Other papers also described that there is Sox9- independent pathway in hypoxia-induced chondrocytic differentiation (J Cell Biol. 177(3), 2007) (J Biol. Chem. 283(8), 2007). It is known that Nkx3.2, a novel chondrogenic transcription factor induced by Shh, suppresses Runx2 in mesenchymal lineage. Then, we hypothesized that hypoxia induces Nkx3.2 activation followed by Runx2 suppression, leading to promotion of chondrocytic differentiation, while osteoblastic differentiation is inhibited. C3H10T1/2 was cultured under normoxia (20% O<sub>2</sub>) and hypoxia (5% O<sub>2</sub>) with rh-BMP2 (300ng/ml). At first, we performed immunocytochemistry for Nkx3.2 protein using micromass culture samples. Nkx3.2 was expressed at the site of cell condensation and the number of nucleus with positive staining was increased by hypoxia. Real time RT-PCR revealed that Nkx3.2 gene expression was promoted by hypoxia from day1 to 10. On the other hand, Runx2 expression was suppressed from day3 to 7. Shh gene expression was up-regulated from 6hrs to 24hrs after hypoxic stimulation. Sox9 gene expression showed no difference between normoxia and hypoxia. Furthermore, because it is known that PTH-rP also positively regulates Nkx3.2 during endochondral ossification, we checked the gene expression of PTH-rP and found that it was promoted by hypoxia, while Ihh, a prehypertrophic chondrocyte marker, was down-regulated. From these observations, it is suggested that hypoxia up-regulates Shh and Nkx3.2 and induces subsequent Runx2 down-regulation, which in turn promotes chondrocytic commitment and inhibits chondrocyte hypertrophy during endochondral ossification. Next, we checked the specificity of Nkx3.2 in hypoxia using RNAi. Alcian blue staining showed that siRNA for Nkx3.2 abolished hypoxia-induced glycosaminoglycan (GAG) production of 10T1/2. We also confirmed that augmentation with wild-type Runx2 (WT-Runx2) completely restored suppressed alkaline phosphatase (ALP) activity by hypoxia. These results suggest that Nkx3.2 is a dominant regulator of chondrocytic differentiation induced by hypoxia, and that Runx2 down-regulation is the primary mechanism of suppression of osteoblastic differentiation. Although further confirmation on the relationship between Nkx3.2 and Runx2 in hypoxia is necessary, Nkx3.2 seems to play important roles in hypoxia-induced Runx2 down-regulation, inhibition of osteoblastic commitment and promotion of chondrocytic differentiation.

**Disclosures:** M. Hirao, None.

## F114

**Postnatal Deletion of PTH/PTHrP Receptor in Growth Plate Chondrocytes Leads to Growth Plate Fusion.** T. Hirai, A. S. Chagin, T. Kobayashi, S. Mackem, H. M. Kronenberg. Massachusetts General Hospital and Harvard Medical School, Boston, MA, USA.

PTH/PTHrP receptor (PPR) signaling regulates development during endochondral bone formation in fetal life. The PPR, however, is also expressed in the postnatal growth plate and its role there is unknown. PPR null mice have abnormal bones, but the physiological role of PPR signaling in postnatal chondrocytes can not be determined in PTH/PTHrP receptor null mice because of the embryonic lethality. We, therefore, generated a new mouse model in which deletion of the PPR gene in chondrocytes can be induced in a temporal- and tissue- specific manner. To selectively ablate the PPR gene in chondrocytes of the postnatal skeleton, floxed PPR mice were mated with mice in which a collagen type 2 (*Col2*) promoter drove a transgene coding for a fusion protein of Cre recombinase and an estrogen receptor ligand-binding domain with a point mutation (*ER<sup>T</sup>*). This point mutation in the fusion protein (*CreER<sup>T</sup>*) allows induction of Cre recombinase by tamoxifen. Therefore, injection of tamoxifen can be used to induce ablation of the PPR gene conditionally at any time point. We generated *Col2-CreER<sup>T</sup>;floxed PPR* (*PPR<sup>fl/fl</sup>*) mice. Mice were treated with 0.5 mg tamoxifen/body at postnatal day (P)3, and the effect on bone development was analyzed at P6, P10 and 4 weeks of age. We observed a decrease in growth of long bones in post-natal deletion of PPR (*Col2-CreER<sup>T</sup>; PPR<sup>fl/fl</sup>*) mice. Histological analysis of long bones of 4-week-old mice revealed abnormalities of the skeleton in *Col2-CreER<sup>T</sup>; PPR<sup>fl/fl</sup>*. Postnatal deletion of PPR in chondrocytes resulted in premature fusion of the growth plates and permanent deformity of bone epiphyses. To determine the mechanism of disappearance of the growth plate chondrocytes, we looked at early times after tamoxifen administration. Three days after treatment of tamoxifen, the columns of chondrocytes in the growth plate were disrupted, and ectopic hypertrophic chondrocytes expressing collagen X were found in the middle of the growth plate. The domain of expression of Indian hedgehog was also enlarged. The expansion of the hypertrophic zone was accompanied by a dramatic decrease in the number of proliferating chondrocytes in the columnar zone, as determined by BrdU labeling. Moreover, histological examination at P10 showed that the premature fusion of the growth plate in *Col2-CreER<sup>T</sup>; PPR<sup>fl/fl</sup>* mice had already occurred. Thus, PPR signaling is required postnatally for maintenance of the growth plate. We speculate that these findings may explain the premature closure of growth plates seen in human Albright hereditary osteodystrophy.

**Disclosures:** T. Hirai, None.

## F116

**Identification of a Transcription Factor p63 for Transactivation of Wnt9a and Gdf5 Causing Joint Cartilage Formation.** A. Kan, T. Ikeda, T. Saito, K. Nakamura, U. Chung, H. Kawaguchi. Sensory & Motor System Medicine, Tissue Engineering, University of Tokyo, Tokyo, Japan.

Joint cartilage formation is an essential step to realize a regenerative medicine against degenerative skeletal disorders like osteoarthritis. Wnt9a and Gdf5 are known to be representative crucial molecules for joint formation from mouse genetics findings. Using comparative mapping between human and mouse Wnt9a promoters within about 3 kb upstream of the transcriptional initiation site, we initially detected a highly conserved region between -158 bp and -117 bp, called Joint-Specific Enhancer (JSE). Screening from a phage display library of human tracheal cartilage by biopanning with tandem copies of the JSE construct identified a p53 family gene p63 as the most probable transcriptional factor for this region. In fact, the JSE contained a p53 family-binding motif. In both chondrogenic ATDC5 cells and non-chondrogenic HuH-7 cells transfected with luciferase-reporter gene constructs containing tandem-repeat of the JSE, the p63 overexpression stimulated the transcriptional activity depending on its repeat number, which was abrogated by site-directed mutagenesis in the binding motif above. Electrophoretic mobility shift assay (EMSA) showed binding of nuclear extracts from p63-overexpressed HuH-7 cells with the wild-type JSE oligonucleotide probe, but not with the mutated probe. The complex disappeared with an excess of unlabelled wild-type probe and underwent supershift by the p63 antibody, indicating a specific binding between JSE and p63. Overexpression of p63 was confirmed to increase the endogenous Wnt9a expression in ATDC5 and HuH-7 cells by real-time RT-PCR. Similarly, deletion, mutagenesis, and tandem-repeat analyses of the luciferase assay within the 3 kb Gdf5 promoter identified the core responsive element to p63 between the -1 bp to +63 bp region containing the binding motif. EMSA also showed the specific binding between this region and p63. Furthermore, the p63 overexpression in non-chondrogenic HeLa cells and de-differentiated mouse costal cells caused chondrogenic differentiation with induction of type II collagen (COL2) expression. In vivo expression of p63 was detected in all cartilaginous tissues of developmental limbs of mouse embryos by immunohistochemistry. When we further investigated the skeletons of p63-deficient (p63<sup>-/-</sup>) mouse embryos, they exhibited severe short limb deformities with suppressed COL2 and SOX9 expressions. Taken together, the present analyses of Wnt9a and Gdf5 promoters identified p63 as a crucial transcription factor for joint cartilage formation. Further understanding of the molecular network related to p63 and Wnt9a/Gdf5 will herald a new era of cartilage regenerative medicine.

**Disclosures:** A. Kan, None.

## F118

**Brachy-syndactyly Caused by Loss of *Sfrp2* Function.** R. Morello<sup>1</sup>, T. K. Bertin<sup>\*1</sup>, S. Schlaubitz<sup>\*1</sup>, C. A. Shaw<sup>\*1</sup>, S. Kakuru<sup>\*1</sup>, E. Munivez<sup>\*1</sup>, P. Hermanns<sup>\*2</sup>, Y. Chen<sup>\*1</sup>, B. Zabel<sup>\*2</sup>, B. Lee<sup>1</sup>. <sup>1</sup>Molecular and Human Genetics, Baylor College of Medicine, Houston, TX, USA, <sup>2</sup>Pediatric Genetics Section, Freiburg University Hospital, Freiburg, Germany.

*Sfrp2* belongs to the secreted frizzled related family of proteins that share a cysteine-rich domain (CRD) with the Wnt family of receptors, called frizzled. Since Wnt molecules bind the CRD domain of the frizzled receptors, the Sfrps proteins can function as soluble receptors for Wnt thereby modulating its downstream signaling. *Sfrp2* is highly expressed during mouse embryonic development of the eye, brain, neural tube, craniofacial mesenchyme, kidney, joints, testis, pancreas and sub-epithelial structures. We found that during mouse limb bud development, *Sfrp2* is expressed in perichondrium of the digits at E13.5, in all limb joints and mesenchymal tissue surrounding them at E15.5 and then in mesenchyme lining ossified diaphyses of autopod elements. We generated *Sfrp2* knock-out mice via homologous recombination. Although *Sfrp2*<sup>-/-</sup> pups are grossly indistinguishable from their WT counterparts and thrive into adulthood they show subtle limb defects with mesomelic shortening and consistent shortening of all autopodal elements that is clinically manifested as brachydactyly. Moreover, a selective hind-limb syndactyly, involving the 3rd and 4th digit, was also observed and showed variable penetrance depending on the mouse genetic background. The brachydactyly is caused by decreased chondrocyte proliferation and delayed differentiation in distal limb chondrogenic elements. These data suggest that *Sfrp2* can regulate both chondrogenesis and regression of interdigital mesenchyme in distal limb. *Sfrp2* can also repress canonical Wnt signaling by *Wnt1*, *Wnt9a*, and *Wnt4* in vitro. *Sfrp2*<sup>-/-</sup> and TOPGAL/*Sfrp2*<sup>-/-</sup> mice have a mild increase in beta-catenin and beta-galactosidase staining, respectively, in some phalangeal elements. This however does not exclude a potential concurrent effect on non-canonical Wnt signaling in the growth plate. In combination with what is known about BMP and Wnt signaling in human brachydactyly, our data establish an important role for *Sfrp2* in proper distal limb formation and suggest *SFRP2* could be a novel candidate gene for human brachy-syndactyly defects.

**Disclosures:** R. Morello, None.  
This study received funding from: NIH.

## F122

**Determinants of Humeral Bone Volume in Males: A Genome-wide Analysis.** L. L. Tosi<sup>1</sup>, F. Suer<sup>\*2</sup>, B. Harmon<sup>\*2</sup>, C. Brandoli<sup>1</sup>, H. Gordish-Dressman<sup>\*2</sup>, E. Hoffman<sup>\*2</sup>, J. Devaney<sup>\*2</sup>. <sup>1</sup>Bone Health Program, Children's National Medical Center, Washington, DC, USA, <sup>2</sup>Research Center for Genetic Medicine, Children's National Medical Center, Washington, DC, USA.

**Objective:** We sought to identify genetic markers for bone volume, a polygenic trait with critical implications for bone strength and quality, in men. Previous studies have suggested that genes for bone structure may be sex-specific, thus we began by focusing on a single sex. We chose to study the humerus because we believe that it may be a particularly sensitive bone for detecting genetic predispositions in bone health for two reasons: (1) it is a single bone and thus not subject to load sharing; and (2) it is not weight-bearing and thus less affected by confounding factors such as fluctuations in weight or activity. **Methods:** We calculated total bone volume in the distal 9.6 cm of the humeral diaphysis of the non-dominant arm from magnetic resonance images (MRI) using semi-automated software from Rapidia. Subjects were 303 young adult Caucasian males (23.68 ± 5.47 years) participating in the Functional Polymorphisms Associated with Muscle Size and Strength (FMS) study, a multi-center program designed to study the influence of genetic polymorphisms on bone geometry, fat volume, and skeletal muscle size and strength. We performed genome-wide screening for the 60 subjects with the highest and lowest bone volumes in the cohort, using the Affymetrix® Genome-Wide SNP Array 6.0. Results were analyzed using the bioinformatics software package Partek GS. **Results:** We identified 138 SNPs associated with bone volume in the study cohort. Among the most significant SNPs, 121 of 138 were in five linkage disequilibrium blocks and 129 fell on the X chromosome. In all, we identified eight regions of interest, with four SNPs falling in the UTR regions of genes, and one SNP falling in the coding region of a gene. The genes KCND1, DMD, TMEM 164, CHDR1, KAL 1, GEMIN8, RPGR, and DGKK contained the most statistically significant SNPs. **Discussion:** Many whole genome scans that have attempted to study bone density (a combination of bone size and mineral properties) have shown inconsistent results. By focusing on bone volume, we believe that we may be able to identify genetic markers that are consistent across multiple populations. As next steps, we plan to (1) validate the results of the whole-genome analysis by genotyping the most statistically significant SNPs in the entire FMS population, (2) fine-map and deep sequence the identified regions, and (3) develop hypotheses as to how these genes influence bone quality.

**Disclosures:** L.L. Tosi, Merck 4.  
This study received funding from: Merck.

## F127

**Expression of an Engineered G<sub>s</sub>-coupled Receptor in Osteoblasts Affects Intramembranous and Endochondral Bone Formation During Bone Repair.** E. Hsiao<sup>1</sup>, S. Lieu<sup>\*2</sup>, Y. Yu<sup>\*2</sup>, C. Manalac<sup>\*1</sup>, B. Conklin<sup>\*1</sup>, R. Nissenson<sup>3</sup>, C. Colnot<sup>2</sup>. <sup>1</sup>GICD, J. David Gladstone Institutes, San Francisco, CA, USA, <sup>2</sup>Dept. of Orthopedics, Univ. of California, San Francisco, CA, USA, <sup>3</sup>Endocrine Unit, VA Medical Center, San Francisco, CA, USA.

Activation of G-protein coupled receptors (GPCRs) in bone, such as the parathyroid hormone receptor (PTHr1) by recombinant PTH(1-34), has been associated with improved fracture healing; however, how GPCR signals regulate fracture healing is not well understood. We previously described mice expressing an engineered G<sub>s</sub>-coupled GPCR, Rs1, in maturing osteoblasts using the Collagen 1 alpha 2.3 kb promoter fragment (Coll(2.3)-tTA/TetO-Rs1 mice). Mutant mice showed dramatic skeletal expansion in both intramembranous and endochondral bones that was suppressed when Rs1 expression was delayed until after 4 wks of age. Since bone repair can recapitulate embryologic bone development, we hypothesized that Rs1 signaling in osteoblasts would accelerate and/or augment healing after bone injury. In this study, we used 14-16 wk old male Coll(2.3)-tTA/TetO-Rs1 mice where Rs1 expression was induced at 4 wks of age. A 1-mm tibia cortical defect model and a non-stabilized 3-point bending tibia fracture model were used to assess repair via intramembranous or endochondral ossification, respectively. Three mice per time point were analyzed at 7, 14, and 21 days after surgery and compared to littermate WT controls. In the cortical defect group, histomorphometry on the mutant mice showed significant increases in the total callous and trabecular bone volumes at 21 days (0.606 ± 0.159 vs. 0.262 ± 0.069 mm<sup>3</sup>, p=0.01 and 0.217 ± 0.026 vs. 0.130 ± 0.030 mm<sup>3</sup>, p=0.009) but not at 7 or 14 days after injury. These increases in trabecular bone were confirmed by microCT. In the non-stabilized fracture group, mutant mice showed a significant increase in callus volume at day 7 (41.383 ± 3.827 vs. 29.308 ± 1.963 mm<sup>3</sup>, p=0.004) but equal callous volumes at days 14 and 21 by histomorphometry. The proportion of cartilage within the callus was decreased at days 7 (0.044 ± 0.038 vs. 0.094 ± 0.025, p=0.07) and 14 (0.037 ± 0.010 vs. 0.091 ± 0.014, p=0.003) and was correlated with increased bone content within the callus at day 14 (0.499 ± 0.066 vs. 0.383 ± 0.022, p=0.02). These results show that constitutive Rs1 expression in adult osteoblasts stimulates callous and bone formation during healing of cortical defects and non-stabilized fractures, correlating with our prior results that Rs1 is anabolic in both intramembranous and endochondral ossification. Our findings also suggest that G<sub>s</sub> signals in osteoblasts may negatively regulate chondrogenesis during bone repair.

**Disclosures:** E. Hsiao, None.

## F131

**Impaired Bone Formation in Mice Lacking Lamin A/C Activation Leads to Severe Osteopenia.** D. Rivas<sup>1</sup>, W. Lee<sup>\*2</sup>, R. Akter<sup>1</sup>, J. E. Henderson<sup>2</sup>, G. Duque<sup>3</sup>. <sup>1</sup>Lady Davis Institute-McGill University, Montreal, QC, Canada, <sup>2</sup>JTN Wong Laboratories-McGill University, Montreal, QC, Canada, <sup>3</sup>Nepean Clinical School-University of Sydney, Penrith, Australia.

Nuclear lamina alterations occur in premature aging syndromes that include severe osteoporosis. The role of proteins of the nuclear lamina in bone remains to be elucidated. Our previous study demonstrated that knockdown of lamin A/C, a protein of the nuclear lamina, inhibits osteoblastogenesis and promotes adipocyte differentiation of mesenchymal stem cells (MSC) *in vitro*. In this study we used the Zmpste24-null progeroid mice, which exhibit nuclear lamina defects and lack active lamin A/C, to identify the role of lamin A/C in MSC differentiation *in vivo*. At four months of age, histological and micro computed tomography measurements of femurs in Zmpste24-null mice revealed a significant decrease in bone volume (BV/TV), trabecular number (Tb.N) and both cortical and trabecular thickness in Zmpste24-null mice compared with their wild type littermates ( $p < 0.001$ ). Osteoblasts surface and numbers are dramatically diminished by 75% in the Zmpste24-null mice. This phenotype occurred in the absence of alterations in osteoclast numbers or eroded surfaces. In contrast the number of marrow adipocytes and the amount of fat volume was significantly higher in Zmpste24-null mice compared to controls ( $p < 0.01$ ). The expression of osteoblast markers (alkaline phosphatase, osteocalcin) was found to be significantly down regulated in Zmpste24-null mice 60-70 % compared to WT littermates, and serum levels of parathyroid hormone, vitamin D and osteoclast markers remained unchanged. The differences were significantly higher in male than female Zmpste24-null mice ( $p < 0.01$ ). We also examined bone marrow stromal cells isolated from Zmpste24-null and WT mice and tested their ability to differentiate into osteoblasts. Colony forming unit-osteoblasts were significantly reduced in Zmpste24-null mice compared to WT mice. These data indicate that the presence of lamin A/C is necessary for normal osteoblast differentiation *in vivo*, possibly by preventing the differentiation of MSC into the adipocyte lineage.

**Disclosures:** G. Duque, None.

This study received funding from: University of Sydney Medical Foundation and Canadian Institutes for Health Research.

## F135

**Bone Microarchitecture Is Dependent Upon Collagen  $\alpha 1(XI)$  Expression During Development.** N. J. Hoskins\*, A. Pedracini\*, L. M. Mercer\*, J. T. Oxford. Biology, Boise State University, Boise, ID, USA.

Collagen type XI is an essential component of the collagen fibrils within the developing skeleton. It is a quantitatively minor member of the fibrillar collagens that plays a regulatory role in the assembly of embryonic collagen fibrils as the diameter of collagen fibrils is dependent on the presence of Collagen  $\alpha 1(XI)$ . However, very little is known about the role of collagen type XI in bone microarchitecture formation.

In this study, skeletal mineralization was evaluated in the absence and presence of Collagen  $\alpha 1(XI)$  comparing the chondrodysplasia (*cho*) mouse embryo to wildtype. The data presented support a role for collagen type  $\alpha 1(XI)$  in skeletal development that is distinct from its function in nucleating the formation and limiting the diameter of cartilage type II collagen fibrils.

Established characteristics of the *cho* mouse were apparent in the mouse included in this study, including a shortened snout, and short, wide long-bones with flared metaphyses. The *cho* mouse humerus was 55% the length of the wildtype humerus and approximately 35% wider at the diaphysis and metaphyses.

Quantification of the differences in the humerus, vertebral column, and ribcage of the *cho* and wildtype mice was carried out using high-resolution three-dimensional models that were created from x-ray microcomputed tomography images.

Analysis revealed differences in bone density, size and microarchitecture. The differences in skeletal properties between these mice were analyzed by determining bone mineral density (BMD) calculations and three-dimensional measures of microarchitecture (BV/TV, Tb.Th, Tb.N, Tb.Sp). Results indicated that bone mineral density was increased in the absence of collagen  $\alpha 1(XI)$  in humerus, vertebrae, and the anterior rib samples of the *cho* mouse. The increase in bone density correlated with an observed increase in trabecular number, trabecular thickness, and percent bone volume, as well as a decrease in trabecular separation in the humerus, ribs, and vertebrae. In contrast, cortical bone mineral density was similar in wildtype and *cho* mice.

A function for Collagen  $\alpha 1(XI)$  in the establishment of bone microarchitecture during embryonic development is supported by this data. Future studies will focus on Collagen  $\alpha 1(XI)$  in bone formation and mineralization by osteoblasts, and new functions for Collagen  $\alpha 1(XI)$  in non-cartilaginous tissues of the skeleton.

**Disclosures:** N.J. Hoskins, None.

This study received funding from: NIH RR016454.

## F141

**Nephroblastoma Overexpressed (Nov) Induces Gremlin Expression by Post Transcriptional Mechanisms.** A. Smerdel-Ramoya<sup>1</sup>, S. Zanotti<sup>1</sup>, A. N. Economides<sup>\*2</sup>, E. Canalis<sup>\*1</sup>. <sup>1</sup>Research, Saint Francis Hospital and Medical Center, Hartford, CT, USA, <sup>2</sup>Senior Director, Regeneron Pharmaceuticals, Inc., Tarrytown, NY, USA.

Nov, a member of the CCN family of proteins, inhibits osteoblastogenesis and causes osteopenia *in vivo*. Although Nov binds bone morphogenetic protein (BMP)-2/4 and decreases BMP signaling and activity, interactions of Nov with other extracellular proteins are possibly responsible for selected effects of Nov in bone. We postulated that Nov could induce the synthesis of BMP antagonists, and examined for their expression *in vitro* and *in vivo*. ST-2 stromal cells transduced with retroviral vectors to overexpress Nov under the control of the cytomegalovirus promoter (pLPCX-Nov) were compared to vector transduced cells. Gremlin mRNA levels increased in Nov overexpressing cells from *gremlin/gapdh* copy number of  $10 \pm 2$  in control to  $377 \pm 58$  in pLPCX-Nov cells. Conversely, down regulation of Nov in ST-2 cells by RNA interference (RNAi) reduced gremlin mRNA levels from  $3.4 \pm 0.6$  in control to  $1.2 \pm 0.2$  *gremlin/gapdh* copy number in Nov down regulated cells. To explore mechanisms of gremlin induction by Nov, a 2.1 kilobase fragment of the gremlin promoter was cloned and transfected into ST-2 cells overexpressing Nov (pLPCX-Nov), co-transfected with Nov expression vectors (pcDNA-Nov) or transfected into wild type ST-2 cells and treated with Nov protein. Gremlin promoter activity was not altered by Nov under any of these conditions. Furthermore, gremlin promoter activity was not changed in Nov down regulated cells. The results indicate lack of transcriptional control. To determine whether post transcriptional mechanisms were operational, ST-2 cells were transcriptionally arrested, using 5,6-dichlorobenzimidazole riboside (DRB), and the decay of gremlin transcripts determined. Gremlin mRNA half life was prolonged from ~12 h in control cultures to >48 h in pLPCX-Nov cells. Conversely, down regulation of Nov destabilized gremlin transcripts shortening the half life of gremlin mRNA from 11 h in control to 2.7 h in Nov down regulated ST-2 cells. Moreover, the half life of gremlin mRNA was shortened to ~25% in stromal cells from *nov* null mice when compared to wild type cells. The regulation of gremlin by Nov was confirmed *in vivo*, and gremlin mRNA levels in calvariae from Nov transgenic mice were 10 times higher than in wild type controls, whereas gremlin mRNA levels were reduced to 50% in *nov* null calvariae. The effect of Nov seemed to be selective to gremlin, and expression of noggin, another BMP antagonist was not modified. In conclusion, Nov induces gremlin expression in cells of the osteoblastic lineage by post-transcriptional mechanisms. This effect explains in part the inhibitory actions of Nov on osteoblastogenesis and bone formation.

**Disclosures:** A. Smerdel-Ramoya, None.

This study received funding from: NIH Grant # AR21707.

## F145

**Specific Forms of DMP1 Support Attachment and Haptotactic Migration via  $\alpha V\beta 3$  but not  $\alpha V\beta 5$  Integrin.** Z. von Marschall\*, L. W. Fisher. CSDB, NIH, Bethesda, MD, USA.

Mutations in dentin matrix protein-1 (DMP1) result in human skeletal disease. While the precise function(s) of DMP1 in mineralizing and metabolically active ductal epithelial tissues remains essentially unknown, the presence of a highly conserved integrin-binding RGD motif suggests that interaction with integrins is critical. Using a panel of relevant human cell types [primary dental pulp stem cells (DPSC), a salivary intercalated duct cell-line (HSG), and osteosarcoma cells (MG63)], we compared both integrin-specific attachment and haptotactic migration on various forms of DMP1 as well as two other SIBLINGs, bone sialoprotein (BSP) and osteopontin (OPN). DPSC and MG63 cells attached and migrated onto DMP1 using  $\alpha V\beta 3$ , while cells lacking this integrin (HSG) failed to do so. Contrary to reports using other cells, the  $\alpha V\beta 5$  integrin on HSG cells also failed to support attachment to OPN. As expected, HSG did attach to the much more integrin-promiscuous BSP. *De novo* expression of  $\alpha V\beta 3$  by adenoviral gene transduction induced HSG cells to attach to as well as migrate onto both DMP1 and OPN. Using a variety of DMP1 constructs, we found that neither 1) substituting the BSP-derived conserved amino acid residues flanking the RGD in DMP1, nor 2) replacing the first four coding exons of BSP for same in DMP1, nor 3) the lack of post-translational modifications changed integrin-binding specificity of DMP1 for  $\alpha V\beta 3$  integrin. In contrast to previous studies suggesting that the proteolytic processing of DMP1 is required to generate a functional C-terminal fragment, we did not observe significant differences in cell attachment or migration between the full-length and BMP-1-processed (57 kDa) form. However, the proteoglycan form of the full-length DMP1 exhibited a dramatically lower ability to support cell attachment and those that did attach failed to spread effectively. The migration onto DMP1 was also severely inhibited by the presence of the glycosaminoglycan (GAG) chain. Both attachment and spreading were rescued after the GAG chain was eliminated by an *in situ* treatment with chondroitinase ABC. In conclusion, attachment and migration on DMP1 and OPN are mediated by  $\alpha V\beta 3$  and not  $\alpha V\beta 5$  integrins. BSP can use either receptor but substituting the BSP RGD domain or the first four coding BSP exons into DMP1 did not engender BSP-like properties. Intact, BMP-1-processed, and nonpost-translationally modified forms of DMP1 were equally efficient at these processes, but the greatly diminished activity of the proteoglycan form suggests that the GAG chain may be critical for differential functions of DMP1.

**Disclosures:** Z. von Marschall, None.

## F149

**Changes in Bone Matrix Material Properties Due to Osteopontin Deficiency.** P. J. Thurner<sup>1</sup>, C. Chen<sup>\*2</sup>, S. Ionova<sup>\*3</sup>, J. W. Ager<sup>\*3</sup>, R. O. Ritchie<sup>\*3</sup>, T. Alliston<sup>2</sup>. <sup>1</sup>School of Engineering Sciences, University of Southampton, Southampton, United Kingdom, <sup>2</sup>Orthopaedic Surgery, University of California San Francisco, San Francisco, CA, USA, <sup>3</sup>Lawrence Berkeley National Laboratories, Berkeley, CA, USA.

Bone matrix material properties reflect the ability of bone matrix to resist deformation and fracture. Using advanced mechanical testing techniques we previously identified TGF $\beta$  as one of the first known regulators of the material properties of bone matrix, through mechanisms that remain unknown. TGF $\beta$  regulates the expression of several bone matrix proteins including osteopontin (OPN). Previous work by our group and others suggests that OPN contributes to the material quality of bone matrix by direct mechanical contributions and by regulation of mineralization. Therefore, we hypothesized that OPN is required for the regulation of bone matrix material properties by TGF $\beta$ . In the present study, we aim to determine if and how OPN participates in the specification of bone matrix material properties by TGF $\beta$ .

If OPN is downstream of TGF $\beta$  in the regulation of bone matrix material properties, then OPN expression should be disrupted in transgenic mice with altered TGF $\beta$  signaling that exhibit defective bone matrix material properties and bone from OPN deficient mice (OPN<sup>-/-</sup>) should resemble bone from DNT $\beta$ R11 mice which express a dominant negative TGF $\beta$  type II receptor in osteoblasts. Although TGF $\beta$  induces OPN expression in vitro, preliminary data reveal no TGF $\beta$ -dependent differences in OPN mRNA expression in 10-day old mouse calvarial bone. To evaluate the material properties of OPN<sup>-/-</sup> bone matrix, bones were harvested from 2-month old male mice (WT and OPN<sup>-/-</sup>) on a C57/bl6 background according to approved protocols. Notched three-point bending tests of femora showed a reduced fracture toughness ( $p \leq 0.03$ ,  $N=9/9$ ) in OPN<sup>-/-</sup> mice ( $3.87 \pm 0.79$  MPa m<sup>1/2</sup>, compared to WT mice ( $5.55 \pm 1.78$ ) MPa m<sup>1/2</sup>). Small angle X-ray scattering revealed a significantly smaller mean crystal thickness ( $p \leq 0.02$ ,  $N=9/7$ ) in OPN-KO mice ( $1.93 \pm 0.7$ ) nm compared to WT mice ( $2.02 \pm 0.07$ ) nm. Consistent with previous reports, the altered material properties of OPN<sup>-/-</sup> bone result in part from altered mineral organization. To examine the possible direct mechanical role of OPN, de-mineralized femora were evaluated by tensile testing. These tests show a possible decrease in ultimate tensile strength in OPN-KO mice compared to WT mice. Nanoindentation studies are currently underway. Although preliminary data do not reveal consistent similarities between DNT $\beta$ R11 and OPN<sup>-/-</sup> bone, we find so far that OPN deficiency results in lower fracture toughness and decreased mineral crystal thickness.

**Disclosures:** P.J. Thurner, None.

## F153

**Loss of MMP-9 Results in Improved Healing, and Remodeling of Adhesions in A Murine Model of Flexor Tendon Repair.** A. E. Loisel<sup>\*</sup>, M. J. Wolenski<sup>\*</sup>, J. A. Jacobson<sup>\*</sup>, D. J. Mitten<sup>\*</sup>, E. M. Schwarz<sup>\*</sup>, H. A. Awad<sup>\*</sup>, R. J. O'Keefe. Center for Musculoskeletal Research, University of Rochester, Rochester, NY, USA.

In a murine model of flexor tendon healing, we have previously demonstrated that MMP-9 expression is significantly increased at seven days post repair, returning to basal levels after this time. Biomechanically, flexion of the metatarsophalangeal (MTP) joint range of motion (ROM) was limited due to fibrous adhesion formation between 14 and 21 days post-repair. To gain a better understanding of the effects of MMP-9 and collagen catabolism during flexor tendon healing, we examined tendon healing in MMP-9<sup>-/-</sup> (KO) mice. Healing was evaluated based on biomechanical properties, histological evaluation and gene expression patterns using real-time RT-PCR up to 28 days post-repair.

MMP-9<sup>-/-</sup> mice had delayed synthesis of both reparative collagen 3, and mature collagen 1. Wild type (WT) mice had peak Col3 expression at day 10, while peak expression of Col3 was delayed until day 21 in KO mice. Interestingly, histology indicated that KO mice displayed an organized arrangement of collagen fibers earlier than WT mice (day 21, compared to day 28 wild type), suggesting an earlier transition from scar tissue to mature tendon tissue. Consistent with an earlier return to normal tendon architecture, expression of GDF-5 and Smad8 was observed earlier in KO mice. Expression of these two genes that have each been shown to induce neotendon formation was elevated beginning at day 7 post-repair in KO mice, with peak GDF-5 expression occurring at day 14 and the highest Smad8 expression on day 28. In WT mice there was no significant induction of GDF-5 or Smad8 until day 28 post-repair. Biomechanically, WT and KO mice both displayed a steady increase in maximum load at failure of the repair, but loss of MMP-9 resulted in significant increases in the maximum load at failure compared to WT at all time points post repair (44% of control for KO and 27% of control for WT at day 28). To quantify adhesion formation, MTP joint ROM was measured at incrementally applied loads, and the adhesion coefficient ( $[\alpha]$ , a measure of resistance to gliding) was calculated. MMP-9<sup>-/-</sup> mice exhibited earlier and more robust adhesion formation, with the greatest resistance to MTP joint ROM occurring at 14 days post-repair. ( $[\alpha]$  KO = 139,  $[\alpha]$  WT = 57) Notably, remodeling of adhesions occurred earlier and to a greater degree in MMP-9<sup>-/-</sup> mice. By day 21, adhesions in the KO tendons were completely remodeled and no significant loss in functional ability was present.

This data suggests that despite an early lag in healing, and more robust adhesion formation, loss of MMP-9 is beneficial in the later stages of healing, resulting in the presence of adhesions for a shorter period of time, as well as increase in the overall rate of healing.

**Disclosures:** A.E. Loisel, None.

## F158

**TGF $\beta$ - and BMP-Signaling Pathways Have Antagonistic Effects During Chondrogenesis.** B. Keller<sup>\*1</sup>, Y. Chen<sup>\*1</sup>, E. Munivez<sup>\*1</sup>, T. Bertin<sup>\*1</sup>, B. Zabel<sup>\*2</sup>, B. Lee<sup>3</sup>. <sup>1</sup>Molecular and Human Genetics, Baylor College of Medicine, Houston, TX, USA, <sup>2</sup>Centre for Pediatrics and Adolescent Medicine, University Hospital of Freiburg, Germany, <sup>3</sup>Molecular and Human Genetics, Baylor College of Medicine, Howard Hughes Medical Institute, Houston, TX, USA.

TGF- $\beta$ /BMP signaling is essential for normal development of almost all embryonic and extraembryonic tissues. Ligands of these pathways are involved in the development of cartilage and bone at multiple stages. BMPs are important during early condensation of the cartilaginous anlagen, proliferation and hypertrophy of chondrocytes. *Smad1* and *Smad5* are two mediators of the BMP signals and they are both expressed in the growth plate. Similarly, TGF $\beta$  signaling has been shown to exhibit diverse effects both *in vitro* and *in vivo*. To compare the role of these signaling pathways in the growth plate, we generated mouse models of loss of function of BMP vs. TGF $\beta$  signaling. To down regulate BMP signaling *in vivo*, we generated chondrocyte-specific deletions of *Smad1* on either a wild type or *Smad5* heterozygous background.

Mice deficient in *Smad1* in proliferating chondrocytes show only a slight shortening of the growth plate, while mice with an additional *Smad5* heterozygous background show a more severe phenotype with shorter prehypertrophic and hypertrophic zones and a diminished proliferation rate. *Ihh* expression in these mice is down-regulated. Morphologically, the conditional *Smad1* deletion with and without *Smad5* heterozygous background mice showed craniofacial alternations characterized by agenesis of the nasal septum. Interestingly, mineralization and extracellular matrix production were not affected.

To down-regulate TGF $\beta$  signaling, we generated transgenic mice over-expressing a dominant negative form of the TGF $\beta$  receptor I ( $\Delta$ T $\beta$ RI) in proliferating chondrocytes. The transgenic mice are smaller but show histologically an elongated growth plate with enhanced *Ihh* expression and an increased proliferation rate. The production of the extracellular matrix is disturbed. Morphologically,  $\Delta$ T $\beta$ RI transgenic mice also exhibited a craniofacial phenotype; the skull is smaller with a prominent mandible. Hence, during endochondral ossification, BMP and TGF $\beta$  signaling have antagonistic effects on cell proliferation and differentiation. While disruption of BMP signaling leads to a shortening of the growth plate with fewer proliferating cells, impairment of TGF $\beta$  signaling results in an increase in the proliferation rate and thus a longer prehypertrophic and hypertrophic zone.

**Disclosures:** B. Keller, None.

## F163

**Evaluation of Clinical Utility of Venous Sampling for FGF23 in Identifying and Confirming Responsible Tumors for Tumor-Induced Osteomalacia (TIO): Analysis of 15 Patients.** N. Ito, H. Suzuki<sup>\*</sup>, Y. Shimizu<sup>\*</sup>, T. Saito<sup>\*</sup>, S. Fukumoto, T. Fujita<sup>\*</sup>. Division of Nephrology & Endocrinology, Department of Medicine, University of Tokyo Hospital, Tokyo, Japan.

TIO is a paraneoplastic syndrome caused by overproduction of FGF23 by responsible tumors. This disease is completely cured by resection of responsible tumors. Therefore, the detection of responsible tumors for TIO is clinically very important. Several methods including MRI skeletal survey and Octreotide scintigraphy have been advocated for the detection of responsible tumors for TIO. However, the sensitivity of these methods is not 100%. Furthermore, even when tumors were found by these methods, none of these techniques can confirm that the detected tumors are responsible for TIO. On the other hand, venous sampling for FGF23 was reported to be useful for the detection and confirmation of responsible tumors in a few patients with TIO. Therefore, we further analyzed the clinical utility of venous sampling for FGF23 in consecutive 15 patients with typical features of TIO. Blood samples were collected either by using catheters inserted from femoral vein (average 15.5 samples/patient) or by venipuncture from the body surface (average 5.4 samples/patient), and FGF23 levels in these samples were measured by ELISA for intact FGF23 (Kainos, Japan). In 6 patients, previous imaging studies by CT or MRI had revealed suspicious tumors for TIO. In these patients, venous sampling (4 patients with catheters and 2 patients from the body surface) revealed the increase of FGF23 in the proximal regions of tumors and confirmed that the tumors are responsible for TIO in 5 patients. Resection of tumors resulted in the cure of TIO in these 5 patients. In contrast, the increase of FGF23 was not detected around the tumor in one patient and the resection of that tumor did not improve the clinical features in this patient. On the other hand, suspicious tumors had not been identified by previous studies in 9 patients. Venous sampling (4 patients with catheters and 5 patients from the body surface) indicated the increase of FGF23 in 6 of these patients and subsequent detailed imaging studies detected responsible tumors for TIO in all 6 patients. Collectively, sampling using catheters and from the body surface identified the responsible tumors in 6 out of 8 patients and 5 out of 7 patients, respectively. These results indicate that venous sampling for FGF23 is clinically useful for identifying and confirming responsible tumors for TIO.

**Disclosures:** N. Ito, None.

## F168

**Intermittent Injection of Recombinant Osteocalcin Improves Glucose Tolerance and Insulin Sensitivity.** M. Ferron<sup>\*1</sup>, G. Karsenty<sup>1</sup>, P. Ducy<sup>\*2</sup>.<sup>1</sup>Genetic and development, Columbia University, New York, NY, USA, <sup>2</sup>Pathology, Columbia University, New York, NY, USA.

We recently showed that the uncarboxylated form of the osteoblast-specific secreted molecule osteocalcin functions as a hormone favoring glucose handling and increasing energy expenditure. We also demonstrated that continuous subcutaneous infusion of recombinant uncarboxylated osteocalcin can increase insulin secretion,  $\beta$ -cell proliferation and energy expenditure in wild-type (WT) mice. As a result, it could prevent the development of obesity and type 2 diabetes in hyperphagic mice or mice fed a high fat diet. In a new set of studies, we tested the effect of recombinant osteocalcin administered intermittently once a day on energy metabolism. Daily injections of osteocalcin in WT mice at both 3 and 30 ng/g/day significantly improved glucose tolerance, as assessed by glucose tolerance tests (GTT). At 30 ng/g/day this effect was already significant after 3 weeks, peaked at 6 weeks and was no longer detectable after 12 weeks of treatment. In contrast, injection of osteocalcin at 3 ng/g/day induced a significant effect on GTT only after 6 weeks but this effect kept improving overtime. Insulin sensitivity, as assayed by insulin tolerance tests (ITT), was improved after 3 weeks at both concentrations. This effect was still detectable after 12 weeks of treatment in mice injected with 3 ng/g/day. Blood glucose after feeding was significantly reduced following 5 to 10 weeks of osteocalcin injections at 30 ng/g/day. Importantly, daily injections of osteocalcin had no effect on body weight, food intake or body temperature. Experiments are in progress to determine if intermittent injection of osteocalcin can improve insulin sensitivity in a diet-induced mouse model of type 2 diabetes.

**Disclosures:** M. Ferron, None.*This study received funding from: NIH, FRSQ.*

## F171

**Prostaglandin E2 as a Potential Mediator of Parathyroid Hormone (PTH)-dependent Regulation of Hematopoietic Stem Cells (HSC).** R. Porter<sup>\*</sup>, B. Frisch<sup>\*</sup>, J. Weber<sup>\*</sup>, A. Olm-Shpan<sup>\*</sup>, L. M. Calvi. Department of Medicine, University of Rochester School of Medicine, Rochester, NY, USA.

HSC are pluripotent cells responsible for the establishment and renewal of the entire hematopoietic system. We and others have established that osteoblastic cells in the bone marrow microenvironment regulate HSC cell fate decisions. Specifically, PTH expands HSC by activating osteoblasts in the HSC niche. However, the molecular mechanisms for this increase are unknown. PTH increases local production of prostaglandin E2 (PGE2) in osteoblasts by stimulating cyclooxygenase 2. We also recently found that treatment of MC3T3 cells with PTH ( $10^{-7}$  M) rapidly induces PGE2 Synthase expression, suggesting that PGE2 may be a mediator of the PTH effect on HSC. In fact, we have shown that *in vivo* PGE2 treatment increases lineage<sup>+</sup> Sca-1<sup>+</sup> c-kit<sup>+</sup> (LSK) cells within the bone marrow 2.75-fold compared with vehicle treated mice ( $p=0.0061$ ,  $n=8$ /group). This increase was specific to HSC as there was no effect on CFU-C or peripheral blood Hct, Plt or WBC counts. Bone marrow mononuclear cells (BMMC) from mice treated with PGE2 also had superior lymphomyeloid reconstitution in competitive repopulation analyses. However, this effect was specific to the short-term HSC responsible for repopulation 6-8 weeks after transplantation. To investigate the mechanism of PGE2 mediated expansion of short-term HSC, we analyzed the expression of the four PGE2 receptors, EP1-EP4, by quantitative RT-PCR. Reciprocal differential expression was found, with EP2 and EP4 transcript levels very low in long-term HSC and high in short-term HSC, and EP1 and EP3 showing the opposite pattern. These data suggest that PGE2 may act through EP2 and/or EP4 to cause expansion and increased repopulating ability of short-term HSC. It is known that HSC that reside in G<sub>0</sub> of the cell cycle have increased ability to reconstitute myeloablated recipient mice. Since PGE2 treatment resulted in superior reconstitution, we hypothesized that PGE2 may increase the percentage of HSC residing in G<sub>0</sub>. To test this hypothesis, we treated BMMC from wild type or EP2<sup>-/-</sup> mice with  $10^{-6}$  M PGE2 or vehicle for 90 minutes. The percentage of cells in G<sub>0</sub> vs. G<sub>1</sub> was determined by flow-cytometric analysis using the RNA and DNA dyes, Pyronin-Y and Hoechst 33342 respectively. PGE2 treatment increased the percentage of wild-type LSK cells in G<sub>0</sub> compared to vehicle-treated LSK cells (62% vs. 53.1%). However, this effect was not observed in the EP2<sup>-/-</sup> mice (67.2% vs. 58.1%). Taken together, these findings suggest that one mechanism of the PGE2-dependent regulation of short-term HSC activity may involve increasing the percentage of HSC that reside in G<sub>0</sub> by activation of EP2, thereby augmenting their ability to reconstitute the hematopoietic system of a myeloablated recipient.

**Disclosures:** R. Porter, None.*This study received funding from: NIH and the Pew Foundation.*

## F174

**Craniofacial Bone Defect in Nell-1 Mutant Mice Associated with Disregulated Runx2 and Osx Expression.** X. Zhang<sup>1</sup>, T. Ko<sup>\*1</sup>, D. Pathmanathan<sup>\*1</sup>, H. Lee<sup>\*1</sup>, F. Chen<sup>\*1</sup>, C. Soo<sup>\*2</sup>, C. T. Culiat<sup>\*3</sup>, K. Ting<sup>1</sup>.<sup>1</sup>Dental and Craniofacial Research Institute, University of California, Los Angeles, Los Angeles, CA, USA, <sup>2</sup>Plastic and Reconstructive Surgery, University of Southern California, Los Angeles, CA, USA, <sup>3</sup>Life Sciences Division, Oak Ridge National Laboratory, Oak Ridge, TN, USA.

Nell-1 has been verified as a factor capable of promoting osteochondrogenic differentiation *in vitro* and *in vivo* consistently. ENU-induced *Nell-1* nonsense mutant mice died immediately post-birth and exhibited major defects in skeletal system. Current study has focused on the contributions of Runx2 and Osx to the craniofacial defects in mice with *Nell-1* deficiency since both molecules were crucial in osteochondrogenesis and linked to *Nell-1*'s function in previous studies. To further clarify the craniofacial feature of the *Nell-1* mutant mice, the quantitative Micro CT and cephalometric analyses were applied on newborn mice. To verify the defects of craniofacial bone development in *Nell-1* mutant mice, *in situ* activities of Alp and TRAP as well as protein expression of the marker genes *Opn*, *Ocn*, *Bsp*, *Col X* and *Sox9* were evaluated by histochemistry or immunohistochemistry. To address the possible mechanisms of craniofacial bone defects associated with *Nell-1* deficiency, the expression level and tissue distribution of Runx2 and Osx were investigated in context with cell proliferation and differentiation status in craniofacial tissues of mouse embryos at multiple stages in addition to newborns by real time PCR, Western Blot and immunohistochemistry. The result showed significantly increased calvarial suture width, decreased calvarial bone mineralization, decreased mandibular bone density and altered mandible angle morphology in mutant over wild type mice. Mutants also exhibited markedly reduced Alp activity in bone forming regions, while TRAP activity remained unchanged. All osteoblastic marker proteins were consistently downregulated to various degrees in the calvarial bones and craniofacial cartilages in newborn mutants. In particular, altered Runx2 and Osx expression in mesenchymal condensation, the osteogenic fronts of cranial suture, bones and cartilages in mutant over wild type mice at different developing stages suggest *Nell-1* is important for normal Runx2 and Osx expression. In conclusion, *Nell-1* deficiency induces delay and malformation of craniofacial bone and cartilage, possibly through dysregulating Runx2 and Osx expression and/or protein functionality. Combined with previous findings, we conclude that *Nell-1* plays a significant role in modifying craniofacial membranous and endochondral skeletal growth and development.

**Disclosures:** X. Zhang, Bone Biologics, Inc 5.*This study received funding from: NIH DE016107-01, March of Dimes Birth Defect Foundation 6-FY02-163, Thomas R. Bales Endowed Chair.*

## F176

**Phospholipase C $\gamma$ 2 as a Promising Therapeutic Target in Rheumatoid Arthritis.** V. Cremasco<sup>\*</sup>, E. Benasciutti<sup>\*</sup>, D. B. Graham<sup>\*</sup>, M. Cella<sup>\*</sup>, R. Faccio. Washington University, St Louis, MO, USA.

Rheumatoid arthritis is a debilitating chronic autoimmune disease characterized by synovial inflammation of peripheral joints and progressive destruction of bone and cartilage. Thus, identifying common signaling molecules affecting the osteo-immune system is likely to lay the groundwork for future therapies.

We have shown that phospholipase C gamma 2 (PLC $\gamma$ 2) is required for osteoclast (OC) differentiation and function. To analyze the role of PLC $\gamma$ 2 in inflammatory mediated bone loss, we used an established model of LPS induced bone erosion, in which injection of LPS directly into the knee joint enhances OC formation by inducing production of proinflammatory cytokines. While WT mice exhibited profound OC activation and bone erosion, PLC $\gamma$ 2<sup>-/-</sup> mice were protected from LPS induced focal osteolysis.

These findings together with the previously reported role of PLC $\gamma$ 2 in B cells, suggested that PLC $\gamma$ 2 could be central to both the inflammatory and the osteolytic response during arthritis. We used an antigen induced arthritis model wherein WT or PLC $\gamma$ 2<sup>-/-</sup> mice were immunized with methylated bovine serum albumin (mBSA), and then challenged 21 days later by intra-knee injection with mBSA. We found that PLC $\gamma$ 2<sup>-/-</sup> mice were protected from bone loss and inflammation compared to WT mice. Despite the capacity of PLC $\gamma$ 2<sup>-/-</sup> T cells to be activated *in vitro* by PMA and ionomycin, *ex-vivo* activation of T cells, as assessed by production of TH1-TH2 cytokines, was impaired in KO animals.

To determine whether the defective B cell development may contribute to the protection from mBSA-induced arthritis, we adoptively transferred WT CD45.1 congenic B cells into PLC $\gamma$ 2<sup>-/-</sup> mice. Strikingly, despite the presence of functional B cells, PLC $\gamma$ 2<sup>-/-</sup> mice remained protected from arthritis and unable to activate T cells. Consistent with this finding, we observed that B cell deficient mice developed arthritis at similar rates as WT mice, suggesting that the diminished response observed in PLC $\gamma$ 2<sup>-/-</sup> is independent of B cells.

In the multifactorial pathogenesis of arthritis, dendritic cells (DC) play a crucial role in initiating T cell response as they are armed antigen presenting cells. To test whether PLC $\gamma$ 2<sup>-/-</sup> mice might have defective DC function, we employed a DC transfer model of arthritis, where WT mice were immunized with mBSA pulsed WT or PLC $\gamma$ 2<sup>-/-</sup> DC and then challenged by intra-knee injection with mBSA. We found that mice injected with PLC $\gamma$ 2<sup>-/-</sup> DC did not develop any signs of arthritis, while WT DCs potentially induced inflammation, bone erosion, and T cell activation.

In conclusion, our study indicates a novel role for PLC $\gamma$ 2 in inflammatory bone loss and DC induced T cell activation suggesting PLC $\gamma$ 2 as a promising target for the treatment of both inflammation and bone erosion during the arthritic disease.

**Disclosures:** V. Cremasco, None.*This study received funding from: Arthritis Foundation, NIH.*



## F181

**Mice Lacking the Growth Hormone Receptor (GHR) in Liver Have Normal Skeletal Growth and Bone Volume Despite Virtual Absence of Circulating IGF-1.** D. J. DiGirolamo<sup>1</sup>, M. Mavalli<sup>1\*</sup>, C. Wan<sup>1</sup>, Y. Fan<sup>2\*</sup>, M. A. Sperling<sup>3\*</sup>, T. L. Clemens<sup>1</sup>. <sup>1</sup>Pathology, University of Alabama at Birmingham, Birmingham, AL, USA, <sup>2</sup>Immunology, University of Pittsburgh, Pittsburgh, PA, USA, <sup>3</sup>Children's Hospital of Pittsburgh, Pittsburgh, PA, USA.

Growth hormone (GH) is thought to exert its effects on skeletal growth and mass through production of insulin-like growth factor-1 (IGF-1) from both liver and peripheral tissues. It is currently accepted that circulating IGF-1 produced in the liver, and peripheral IGF-1 produced in bone in response to GH, both play an important role in dictating linear growth and bone mass. However, limitations of previous models confound interpretation of the contribution of circulating versus peripheral IGF-1. To further explore the specific contribution of liver-derived and peripheral IGF-1 in mediating linear skeletal growth, we developed a model of tissue-specific GH receptor (GHR) deletion using the Cre-LoxP system. Liver-specific deletion of GHR (GHR<sup>LD</sup>) via albumin-driven Cre, resulted in >90% deletion of GHR as determined by quantitative RT-PCR and immunohistochemical analyses. Compared to controls, circulating IGF-1 was suppressed by 94% ( $23.9 \pm 4.2$  ng/ml;  $n = 13$  vs  $400 \pm 33.1$  ng/ml;  $n = 15$ ); IGFBP3 was suppressed by 80% ( $220.8 \pm 23.5$  ng/ml vs  $1083.2 \pm 125.1$  ng/ml); and acid labile subunit was suppressed by 84% ( $330.2 \pm 41.8$  ng/ml vs  $1992.6 \pm 163.9$  ng/ml;  $p < 0.001$  for each). Growth hormone was elevated ~4 fold in GHR<sup>LD</sup> mice ( $33 \pm 6.3$  ng/ml vs  $9.9 \pm 0.7$  ng/ml in controls;  $p < 0.001$ ) likely due to the absence of negative feedback by IGF-1. Despite virtual absence of circulating IGF-1, total body weight ( $23.45 \pm 0.67$  gm vs  $25 \pm 0.86$  gm), total length ( $8.88 \pm 0.11$  cm vs  $9.07 \pm 0.07$  cm) and tibial length ( $1.82 \pm 0.03$  vs  $1.8 \pm 0.02$  cm) were not different in GHR<sup>LD</sup> versus controls. Additionally, preliminary uCT studies showed no difference in bone volume between control and GHR<sup>LD</sup> mice at 16 weeks. To determine if normal linear growth resulted from a compensatory increase in IGF-1 from the growth plate, real-time PCR for IGF-1 was performed on RNA extracted from the growth plates of these mice. No difference in IGF-1 expression was seen between GHR<sup>LD</sup> and control mice. In summary, linear growth and bone volume are unchanged by >90% suppression of circulating IGF-1. These results challenge the prevailing view that circulating IGF-1 is required for normal bone growth and mass.

**Disclosures:** D.J. DiGirolamo, None.

## F186

**BMP2 Inactivates TAK1-ATF2 Signaling Pathway in Chondrocytes.** L. Gao<sup>\*</sup>, T. Li, Y. Zhang, T. Sheu<sup>\*</sup>, M. J. Zuscik, D. Chen, E. M. Schwarz, R. J. O'Keefe. Orthopaedics, University of Rochester, Rochester, NY, USA.

A concomitant increase in BMP and decrease in TGF $\beta$  signaling occurs in Smad3<sup>-/-</sup> chondrocytes and contributes to the pathogenesis of osteoarthritis in these mice. Since both TGF $\beta$  and BMP regulate the p38 MAP kinase pathway, the manner in which BMP2 modulates this pathway was investigated.

## Table of Contents

Primary sternal chondrocytes from Smad3<sup>-/-</sup>, ALK2<sup>fllox/fllox</sup>, ALK3<sup>fllox/fllox</sup> and Smad1<sup>fllox/fllox</sup> mice and C5.18 cells, C9 cells, and primary articular porcine chondrocytes were used. Transfection and luciferase reporter assays, Western blots and immunoprecipitation were performed. p38 kinase and ATF2 binding assays were performed.

TGF $\beta$  or constitutively active (ca) ALK5 enhanced while BMP2 and ca-ALK3/6 decreased ATF2 reporter activity. TGF $\beta$  and anisomycin stimulated p38 phosphorylation, an effect suppressed by BMP2. BMP2 also suppressed p38 kinase activity. Similar inhibition was also observed in porcine chondrocytes and in C9 cells that overexpress BMP2. Western blots showed that BMP2 prevented activation of TAK1, MKK3/6, p38 and ATF2, indicating inhibition of the MAPK pathway in chondrocytes at an upstream signaling event. To determine possible involvement of Smad1 and BMP type I receptors, phosphorylation of p38 was examined in Smad1, ALK2 or ALK3 deficient chondrocytes. Cre-mediated deletion of Smad1 and ALK3 completely abolished BMP2 mediated inhibition of the p38, including the ability of anisomycin and TGF $\beta$  to induce ATF2 binding to its response element. In contrast, deleting ALK2 had a minor role in the inhibitory effect of BMP2 on p38. Immunoprecipitation assays were done to determine where BMP2 inhibits the TAK1-ATF2 pathway. TAB1 formed a complex with TAK1 in anisomycin or TGF $\beta$  treated cells. BMP2 prevented formation of this complex. In the presence of BMP2, TAB1 instead formed a complex with phospho-Smad1. Subsequent experiments showed that the Smad1 linker region is responsible for interaction with TAB1. Ad-TAB1 greatly reduced, while Ad-Smad1 increased *colX* expression in mouse chondrocytes.

The findings demonstrate that BMP2 inhibits activation of TAK1-ATF2 signaling by anisomycin and TGF $\beta$ . The mechanism involves the classic ALK3-Smad1 pathway and targets the upstream signaling molecule, TAB1. In response to BMP2, phospho-Smad1 forms a complex with TAB1, and prevents interaction between TAB1 and TAK1. The findings provide novel insights regarding integration of TGF $\beta$ /BMP2 signaling and define the TAK1-ATF2 as a potential therapeutic target to modulate chondrocyte maturation in diseases such as osteoarthritis.

**Disclosures:** L. Gao, None.

## F188

**TGF $\beta$ 1 Induces Migration of Sca-1 and CD29-Positive Mesenchymal Stem Cells in Coupling Bone Resorption and Formation.** Y. Tang, X. Wu<sup>\*</sup>, W. Lei<sup>\*</sup>, L. Zhao<sup>\*</sup>, W. Chao<sup>\*</sup>, Z. Shi<sup>\*</sup>, X. Feng<sup>\*</sup>, X. Peng<sup>\*</sup>, M. Wan<sup>\*</sup>, X. Cao<sup>\*</sup>. Pathology, University of Alabama at Birmingham, Vestavia Hills, AL, USA.

The recruitment of osteoprogenitors to the bone resorptive sites is the initial event for coupling of bone resorption and formation. We demonstrate that TGF $\beta$ 1 released from bone matrix during osteoclastic bone resorption induces migration of stro-1 positive primary human bone marrow mesenchymal cells (MSC). Migration of MSCs was examined in coupling with *in vitro* osteoclastic bone resorption. Osteoclastic bone resorption-conditioned medium (CM) stimulates migration of MSCs, whereas CM from monocytes/macrophage or osteoclasts without bone slices had no effect. Importantly, addition of an antibody against TGF $\beta$ 1 inhibited the migration, CM prepared from bone slices of TGF $\beta$ 1<sup>-/-</sup> mice did not induce migration of MSCs with no detectable active TGF $\beta$ 1. The results indicate that TGF $\beta$ 1 released and activated during osteoclastic bone resorption.

Bone resorption was stimulated or inhibited in mice by injection with PTH (1-34) or OPG. Immunostaining of consecutive tibia sections with antibodies against CD29 and Sca-1, the markers for MSCs with osteogenic potential, revealed that PTH treatment resulted in a significant increase in the numbers of MSCs at the bone surface, and the numbers of the Sca-1<sup>+</sup> and CD29<sup>+</sup> MSCs at the remodeling surfaces were significantly reduced in the trabecular bone of OPG injected mice. Injection of the T $\beta$ R1 inhibitor in the rat tibia reduced bone formation dose-dependently as demonstrated by X-ray,  $\mu$ CT and histomorphometry, and the numbers of the Sca-1<sup>+</sup> and CD29<sup>+</sup> MSCs at the remodeling surfaces were significantly reduced. The TGF $\beta$ 1<sup>-/-</sup> mice was crossed with immunodeficient Rag2<sup>-/-</sup> mice to prevent the early death of the TGF $\beta$ 1<sup>-/-</sup> mice due to organ failure with inflammatory disease. Immunostaining showed lack of the Sca-1<sup>+</sup> and CD29<sup>+</sup> MSCs at the remodeling surfaces. Tracking of BrdU-labeled MSCs that were injected into the femur cavities of TGF $\beta$ 1<sup>-/-</sup>Rag2<sup>-/-</sup> and TGF $\beta$ 1<sup>-/-</sup>Rag2<sup>-/-</sup> mice demonstrates that TGF $\beta$ 1 induces migration of labeled STRO-1<sup>+</sup> MSCs to the bone remodeling sites *in vivo*. Therefore, active TGF $\beta$ 1 functions as a primary factor for recruitment of MSCs to the bone remodeling surface in the coupling process.

**Disclosures:** Y. Tang, None.

This study received funding from: NIH.

## F190

**Halofuginone Inhibits Melanoma Bone Metastases and TGF-beta Signaling.** P. Juárez<sup>1</sup>, J. Chirgwin<sup>1</sup>, K. Mohammad<sup>1</sup>, R. McKenna<sup>1\*</sup>, H. Walton<sup>1\*</sup>, M. Niewolna<sup>1\*</sup>, D. Javelaud<sup>2\*</sup>, F. Luciani<sup>3\*</sup>, V. Delmas<sup>3\*</sup>, L. Larue<sup>3\*</sup>, A. Mauviel<sup>2\*</sup>, T. Guise<sup>1</sup>. <sup>1</sup>University of Virginia, Charlottesville, VA, USA, <sup>2</sup>INSERM, Paris, France, <sup>3</sup>Institut Curie, Orsay, France.

TGF-beta derived from bone fuels a vicious cycle of osteolytic metastases by inducing tumor expression of prometastatic genes, whose products act on bone cells to enrich the skeletal microenvironment. The vicious cycle can be blocked with inhibitors of the TGF-beta pathway. Halofuginone (Hfg), is a plant alkaloid derivative that is orally active, extensively used in animals, and has entered Phase II clinical trials in cancer patients. It increases expression of inhibitory Smad7, decreases phosphorylation of Smads 2 and 3 and blocks TGF-beta-induced type I collagen synthesis. We tested Hfg against osteolytic bone metastases caused by melanoma and then showed that TGF-beta induction of prometastatic target genes was inhibited by Hfg in breast, prostate and melanoma cell lines.

Nude mice inoculated in the left cardiac ventricle with 1205Lu human melanoma cells developed osteolytic bone metastases in 5 weeks. Mice treated daily i.p. with 5 $\mu$ g of Hfg had significantly less osteolysis on radiographs compared with mice injected with PBS ( $0.08 \pm 0.03$  vs  $0.42 \pm 0.09$ ,  $p < 0.01$ ; lesion area (mm<sup>2</sup>) of fore- and hind-limbs;  $n = 12$ /group). In contrast, Hfg had no effect on the growth of subcutaneous 1205Lu tumors or on the capacity to invade Matrigel<sup>TM</sup> *in vitro*, suggesting that the effect of Hfg is specific to block tumor growth in the bone microenvironment.

Human 1205Lu melanoma, MDA-MB-231 breast and PC-3 prostate cancer cells (all of which cause osteolytic metastases) were treated with 5ng/ml TGF-beta1 for 24hrs +/- 4hr pretreatment with 200nM Hfg. All three cell lines showed similar responses. Hfg blocked TGF-beta activation of: a) the synthetic Smad-signaling reporter pGL3-(CAGA)<sub>3</sub> by dual luciferase assay (decreased 70-80%,  $p < 0.05$ ); b) phosphorylation of Smads 2 and 3, as measured by Western blotting (decreased 60-70%); c) transcription of Smad7 (by PCR +/- actinomycin D). It reduced mRNAs for TGF-beta1 and alpha1-collagen I 80-90% and significantly (all  $p < 0.05$ ) decreased TGF-beta induction of mRNAs encoding CXCR4, PTHrP and CTGF in MDA-MB-231 cells (5.25, 2.5, 11-fold), in PC-3 cells (5, 10, 15-fold) and in 1205Lu (3.5, 4, 15-fold) respectively. Finally, Hfg reduced TGF-beta receptor II expression, but not that of receptor I in all 3 cell lines.

Our results suggest that halofuginone may be particularly effective for treatment of TGF-beta-responsive bone metastases due to melanoma, breast and prostate cancer.

**Disclosures:** P. Juárez, None.

## F195

**Calcitonin Attenuates the Anabolic Effect of PTH *in vivo* and Rapidly Upregulates Sclerostin Expression.** J. H. Gooi\*, S. Pompolo\*, N. E. McGregor\*, E. Walker\*, M. T. Gillespie, J. M. W. Quinn, T. J. Martin, N. A. Sims. St. Vincent's Institute, Fitzroy, Australia.

There is increasing evidence for a role of osteoclasts in the anabolic action of PTH. To determine whether osteoclast activity contributes to PTH anabolic action, 3-week-old rats were treated with daily subcutaneous hPTH(1-34) (30ug/kg) and co-treated with 0.5ug/kg salmon calcitonin (sCT). The dose of sCT was identified by bioassay as the lowest dose required to lower serum calcium transiently ( $P < 0.01$ ), in order to inhibit osteoclast activation acutely without a prolonged effect on resorption. The anabolic effect of PTH, detected by pQCT and histomorphometry, was significantly impaired in rats co-treated with sCT ( $p < 0.05$  for both). Daily sCT alone had no effect on trabecular bone mineral density (Tb.BMD) or trabecular bone volume (BV/TV).

To identify inhibitors or stimulators of bone formation modified by sCT co-administration with PTH we examined gene expression in metaphyseal bone of 3 week old female rats treated with vehicle, 0.5ug/kg sCT, 30ug/kg hPTH(1-34) or co-administered sCT and hPTH(1-34). Bones were collected at 1.5, 4 and 6 hours after treatment and femoral metaphyseal mRNA analysed by quantitative real time PCR (qRT-PCR) and tibial sections prepared for immunohistochemistry. Several genes whose expression was affected by PTH were not modified by simultaneous sCT treatment, including RANKL, OPG, IL-6, c-fos and ephrinB2. In contrast, the reduction of mRNA for the osteocyte-derived bone formation inhibitor, sclerostin caused by PTH administration, was significantly diminished by sCT co-administration at all time points. Furthermore, sCT alone increased sclerostin mRNA at least 2.5-fold at 1.5, 4 and 6 hrs ( $p < 0.001$ ). This increase was confirmed by immunohistochemistry in samples from the same experiment: in the tibia, the number of sclerostin positive osteocytes in cortical bone was significantly increased at 4 hrs following sCT administration (vehicle:  $26\% \pm 4\%$ ; sCT:  $43\% \pm 3\%$ ,  $p < 0.01$ ). Also at 4 hrs, qRT-PCR analysis revealed that sCT reduced mRNA for other osteocytic gene products including MEPE ( $-1.4 \pm 0.06$  fold,  $p < 0.01$ ) and DMP-1 ( $-1.9 \pm 0.06$  fold,  $p < 0.001$ ).

These data indicate that calcitonin can promote sclerostin production, as well as influence production of other genes characteristic of the osteocyte, and suggest this is a pathway by which calcitonin might modify the anabolic effect of PTH. Since the only known target of CT in bone is the osteoclast, it seems likely that this effect of calcitonin on sclerostin production by osteocytes is the result of an indirect action, either through the osteoclast or through some non-skeletal site of calcitonin action, which could include the brain.

**Disclosures:** J.H. Gooi, None.

## F202

**Deprivation of Vitamin A Results in a Partial Rescue of the Mineralization Defects in Phex-Deficient Hyp Mice.** S. Seitz\*, F. Barvencik\*, M. Amling, T. Schinke. Center for Biomechanics, Experimental Trauma Surgery & Skeletal Biology, Hamburg, Germany.

Inactivation of the *Phex* gene causes severe defects of bone matrix mineralization and phosphate homeostasis in mice and humans. Although *Phex* encodes a transmembrane protein with significant homologies to endopeptidases, a physiologic substrate has not yet been identified. Moreover, *Fgf23*, the major gene regulating phosphate homeostasis downstream of *Phex*, is mostly affected at the transcriptional level, since its expression is increased in osteoblasts from *Phex*-deficient *Hyp* mice. Therefore, to analyze the possibility that changes in gene expression may be involved in the skeletal abnormalities caused by *Phex* deficiency, we compared primary osteoblasts from wildtype and *Hyp* mice using Affymetrix Gene Chip hybridization. Here we observed that the expression of about 200 genes, including *Fgf23*, *Mepe* and *Dmp1*, was more than two-fold increased in cultures from *Hyp* mice. Since several known target genes of retinoic acid signaling, but also genes involved in the uptake and intracellular processing of retinol, were also expressed at higher levels in osteoblasts from *Hyp* mice, we next asked the question, whether vitamin A-deprivation would influence their phenotype. Surprisingly, feeding a vitamin A-deficient diet until the age of 6 weeks led to an overall increased size of the *Hyp* mice, and their growth plate thickness was significantly reduced compared to *Hyp* mice on a normal diet ( $0.26 \pm 0.02$  mm vs.  $0.43 \pm 0.08$  mm) with a near absence of rachitic features. Moreover, osteoid volume and surface were significantly decreased in *Hyp* mice receiving the Vitamin A-deficient diet (OV/BV:  $20.4 \pm 5.9\%$  vs.  $42.2 \pm 8.9\%$ ), suggesting that increased retinoic acid signalling in osteoblasts contributes to the defects of bone matrix mineralization caused by *Phex*-deficiency. Interestingly, the improvement of the *Hyp* phenotype by deprivation of vitamin A occurred without normalization of phosphate homeostasis, since serum *Fgf23* and phosphate levels were not changed compared to *Hyp* mice receiving the control diet. Taken together, these data reveal a novel aspect in the pathogenesis of X-linked hypophosphatemic rickets and could help identify further molecules involved in the regulation of bone matrix mineralization.

**Disclosures:** S. Seitz, None.

## F205

**MEPE Regulates Bone Remodelling Independent of Serum Phosphate and Alters Renal Vascularisation.** V. David, A. Martin, A. M. Hedge\*, P. S. N. Rowe. Medicine, The University of Kansas Medical Center, Kansas, KS, USA.

Matrix extracellular phosphoglycoprotein (MEPE) like dentin matrix protein 1 (DMP1) is a SIBLING-protein involved in bone and phosphate mineral metabolism. In *HYP*, increased proteolysis of MEPE and DMP1 generates small protease-resistant ASARM-peptides that inhibit mineralization. Bolus or short-term infusion of MEPE and ASARM-peptides in normal mice inhibit intestinal and renal phosphate uptake. Remarkably, despite a major age-dependent low bone mass phenotype, transgenic mice over expressing MEPE (MEPE-tgn) are hyperphosphatemic with increased serum  $1,25(\text{OH})_2\text{D}_3$ . Unlike *HYP* mice, MEPE-tgn mice respond to constitutively increased levels of MEPE by markedly over expressing PHEX ( $3x$   $p < 0.01$ ) and this may contribute to the hyperphosphatemia. To clarify MEPEs role we fed MEPE-tgn mice (4 months) with a normal and low phosphate/ $1,25(\text{OH})_2\text{D}_3$  diet. The diets consisted of 1% phosphorus (1% PO4) and 2.4 IU/g  $1,25(\text{OH})_2\text{D}_3$  or 0.1% of phosphorus (0.1% PO4) and 1 IU/g  $1,25(\text{OH})_2\text{D}_3$ . As previously shown, MEPE-tgn mice were hyperphosphatemic on the 1%PO4 diet (WT:  $8.1\text{mg/dL}$  vs. MEPE-tgn:  $11.4\text{mg/dL}$ ,  $p < 0.01$ ) whereas the 0.1%PO4 diet induced a hypophosphatemia in both WT and MEPE-tgn animals (WT:  $7.3\text{mg/dL}$  vs. MEPE-tgn:  $7.4\text{mg/dL}$ ). Barium sulphate perfusion and  $\mu\text{CT}$  imaging revealed a marked increase in renal vascular number ( $+200\%$   $p < 0.03$ ) and decreased vascular diameter ( $-15\%$ ;  $p < 0.03$ ) in the MEPE-tgn mice (1%PO4 diet). This was accompanied by a 3 fold increase in bone-renal VEGF ( $p < 0.05$ ). Interestingly, by further reducing bone turnover in both WT and MEPE-tgn mice, the low 0.1% PO4 diet partially corrected the MEPE-tgn BMD defect (figure 1) and compensated for the growth delay and shorter bones. In contrast, MEPE-tgn mice still retained the cortical and trabecular bone thinning defect ( $-5\%$  Ct.Th. and  $-10\%$  Tb.Th.,  $p < 0.05$ ) and also the reduced bone remodelling (both diets). Consistent with this, serum measurements of osteocalcin ( $-40\%$  versus WT,  $p < 0.05$ ), and CTX (1% PO4:  $-40\%$ ; 0.1% PO4:  $-5\%$ , NS) were reduced. To conclude, MEPE dynamically modulates an age-dependent inverse relationship between BMD and serum phosphate. In contrast, MEPE lowers bone remodeling in a phosphate independent manner and significantly alters renal vascularisation. The altered vascularisation may contribute to the impaired renal-phosphate handling.

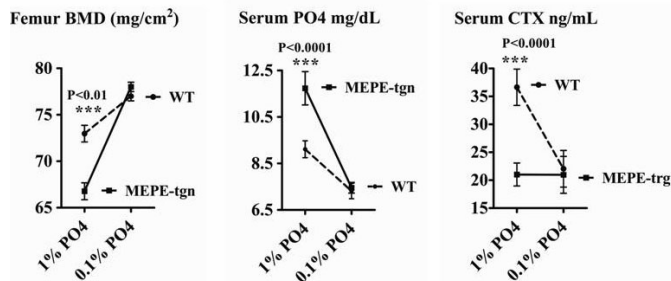


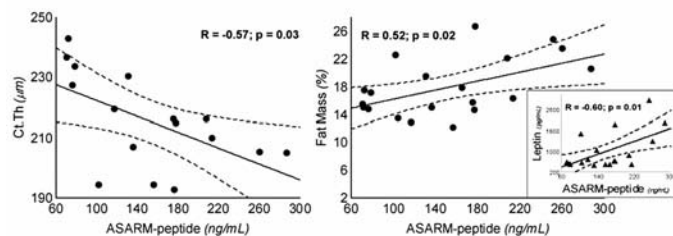
Figure 1 Transgenic and wild type bone-mineral and serum chemistry.

**Disclosures:** V. David, None.

## F207

**MEPE C-terminal ASARM-peptide, Promotes Hypophosphatemia, Bone Defects and Increases Adiposity.** A. Martin, V. David, A. M. Hedge\*, P. S. N. Rowe. Medicine, The University of Kansas Medical Center, Kansas, KS, USA.

ASARM is a protease resistant peptide belonging to several SIBLING proteins and was first described as a C terminal MEPE fragment. Proteolytic degradation of MEPE releases protease resistant ASARM peptide into the circulation. In hypophosphatemic rickets mice (HYP), increased protease activity and MEPE expression results in increased serum ASARM levels. We tested the hypothesis *in vivo* that circulating ASARM peptides were responsible for, at least in part, the hypophosphatemia and bone disorders noted in HYP. Male mice (8 weeks, C57/Bl6, n=5) were fed *ad libitum* for 2 months either with a 1% phosphorus /2.4 IUg<sup>-1</sup> 1.25(OH)<sub>2</sub>D<sub>3</sub> diet (1% PO<sub>4</sub>) or a 0.1% of phosphorus/1 IUg<sup>-1</sup> 1.25(OH)<sub>2</sub>D<sub>3</sub> diet (0.1% PO<sub>4</sub>). During the last month, animals were also infused either with ASARM peptide (5mg/d/Kg) or vehicle (V) using Alzet osmotic pumps. ASARM treatment induced a hypophosphatemia (-20% vs. V; p=0.03) and an increased fractional excretion of phosphate (FEP) on the 1% PO<sub>4</sub> diet (+50% vs. V p=0.004). Serum PO<sub>4</sub> was decreased with both V and ASARM treated groups on the 0.1%PO<sub>4</sub> diet. The hypophosphatemia and two-fold increase in serum ASARM (p=0.002) and 1,25(OH)<sub>2</sub>D<sub>3</sub> levels (V=48 pg/mL vs. ASARM=98 pg/mL; p<0.02) occurred without significant changes in serum FGF23 or PTH (1%PO<sub>4</sub> diet). ASARM-peptide treated mice also displayed a reduced cortical thickness (-30 %, p<0.01) and bone volume (-20%, p<0.01). Accordingly, ASARM treatment significantly reduced serum osteocalcin (-30%, p<0.01), osteopontin (-25%, p<0.01) and RANKL/OPG (-30%, p<0.01). On the 0.1%PO<sub>4</sub> diet, ASARM-treated mice did not show any significant changes in bone parameters, while 1.25(OH)<sub>2</sub>D<sub>3</sub> levels were decreased. Interestingly, on this diet, ASARM-treated animals presented with a higher body weight (+10% vs. V, p<0.05) related to an increase in fat mass (+40% vs. V, p<0.05). As a consequence, serum leptin levels were increased significantly in these mice (+72%; p=0.04) and correlated significantly with ASARM serum levels (Figure 1). To conclude, ASARM peptide induces hypophosphatemia and decreases bone turnover independent of serum FGF23 levels. Thus, in HYP, increased ASARM-peptides likely play a component role in the hypophosphatemia. The peptide also induces an increase in adiposity in a phosphate dependent manner that is regulated negatively by 1.25(OH)<sub>2</sub>D<sub>3</sub>.

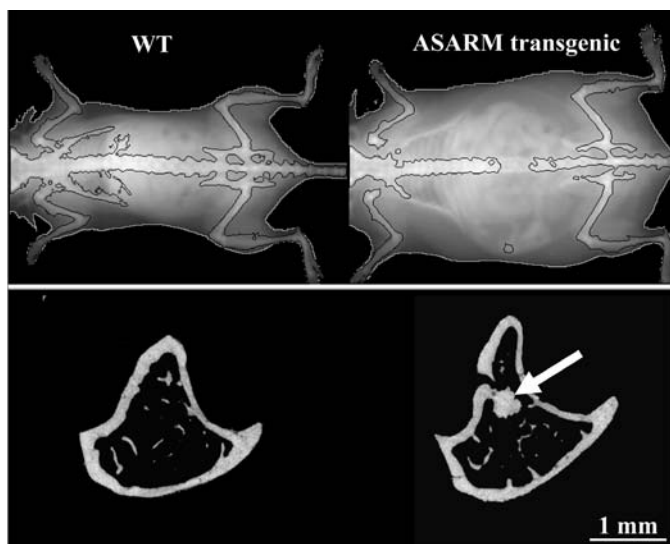


Disclosures: A. Martin, None.

## F210

**Transgenic ASARM-peptide Overexpression with Reduced Serum Phosphate and 1.25(OH)<sub>2</sub>D<sub>3</sub> Leads to Decreased Bone Mineral Density and Obesity.** A. Martin, V. David, A. M. Hedge\*, P. S. N. Rowe. Medicine, The University of Kansas Medical Center, Kansas, KS, USA.

ASARM is a protease resistant peptide belonging to several SIBLING proteins and first described as a C-terminal MEPE motif. Studies *in vitro* show both MEPE and ASARM peptide inhibit mineralization. In familial hypophosphatemic rickets (HYP, ARHR) or tumor-induced osteomalacia (TIO) MEPE expression is increased. We therefore used ASARM peptide over expressing transgenic mice (2.3 kb col1a1 promoter) to investigate the role of ASARM-peptides *in vivo*. Wild type (WT) and transgenic (Ap-tgn) mice (C57/Bl6 males, 4 and 8 months) were fed *ad libitum* with a 1% phosphorus/ 2.4 IUg<sup>-1</sup> 1.25(OH)<sub>2</sub>D<sub>3</sub> diet (1%PO<sub>4</sub>), or a 0.1% phosphorus/1 IUg<sup>-1</sup> 1.25(OH)<sub>2</sub>D<sub>3</sub> (0.1%PO<sub>4</sub>) diet. Ap-tgn mice on the 1%PO<sub>4</sub> diet, were hypophosphatemic (-14% vs. WT, p<0.05) and displayed a decreased cortical thickness (-5% vs. WT, p<0.05). An increased BMD also occurred in the older Ap-tgn animals (+10% vs. WT, p<0.05) with intra meta- and diaphyseal calcifications, reduced bone resorption (-50% sCTX vs. WT, p<0.005) and a marked increase in abdominal fat mass (+25% vs. WT, p<0.05). The increased fat mass was associated with increased leptin levels (+257% vs. WT, p<0.05) and unchanged body weight. When fed lower levels of phosphorus and 1.25(OH)<sub>2</sub>D<sub>3</sub>, ASARM peptide over expression induced a significant BMD decrease in 4 month-old mice (-10% vs. WT, femur and vertebrae BMD, p<0.05). Older, 0.1%PO<sub>4</sub> Ap-tgn mice displayed a higher body weight (WT: 31.4±2.9g vs. Ap-tgn: 36.3±3.0g, p<0.05), a striking increased fat mass (+70% vs. WT, p<0.05) and dramatically elevated serum leptin levels (+750% vs. WT, p<0.02). These older mice still had a very low global BMD (-10% compared to WT, p<0.05), but long bone defects were less pronounced compared to the younger Ap-tg mice (-5% vs. WT, NS). Notably, the 0.1%PO<sub>4</sub> diet Ap-tg mice sustained a major increase in leptin with a 2 fold increase apparent as early as 4 months. To conclude, ASARM peptide alters bone turnover and induces obesity when associated with low phosphate and 1.25(OH)<sub>2</sub>D<sub>3</sub>. The increased disordered body-weight/fat mass mirrors an age dependent evolution towards obesity status and central leptin resistance. This suggests non-collagenous matrix proteins actively regulate metabolism with bone functioning dynamically as an endocrine organ.



Disclosures: A. Martin, None.

## F213

**Parathyroid Hormone-related Peptide (PTHrP) Blockade Inhibits Tumor Progression in a Model of Human Breast Cancer.** D. C. Huang, X. F. Yang, R. Kremer. Department of Medicine, Center for Bone and Periodontal Research, McGill University, Montreal, QC, Canada.

Elevated production of parathyroid hormone-related peptide (PTHrP), the major mediator of malignancy-associated hypercalcemia, is usually associated with advanced metastatic breast cancer. It has been suggested that PTHrP plays a role in tumor invasion and metastasis independent of its role on tumor osteolysis. Here we analyzed the effect of PTHrP inhibition *in vitro* and *in vivo* on growth, invasion and metastasis. First, we used transient transfection of siRNA against human PTHrP designed against the N-terminal region of hPTHrP 1-7 and cloned into the pENTR<sup>TM</sup>/H1/TO vector. An 80% inhibition of PTHrP transcription and production was observed at 24 h and sustained up to 72 h in the MDA-MB 435 human breast cancer cell line. A 36% (p<0.01) inhibition of invasion through the matrigel coated filters in siRNA-treated cancer cells was observed compared with control cells. Next, we examined these effects using a monoclonal antibody (mAb) against human PTHrP. These mAbs were produced after immunization of BALB/c mice with synthetic human PTHrP (1-33). The mAb was then purified from the myeloma line FO fusion clone using protein G Sepharose columns. Specificity of the mAb was confirmed by ELISA using different fragment peptides. Addition of mAb to the cell cultures showed a significant inhibition of invasion as compared to cells treated with control mouse IgG. Next we analyzed breast tumor growth and metastasis in BALB/c nu/nu mice following injection of MDA-MB-435 cells into the mammary fat pad. Six weeks following tumor implantation and treatment with mAb (200 ug subcutaneously, every 2 days), a 60% inhibition (p<0.01) in tumor growth was observed as compared to animals injected with control IgG. Lung metastasis was also inhibited with only 33% of mAb-treated animals to 100% of control IgG-treated animals showing metastatic spread. Overall our data demonstrate that PTHrP blockade inhibits invasion *in vitro* and tumor growth and metastasis *in vitro* and *in vivo* in a model of human breast cancer. These data suggest that therapeutic strategies aimed at blocking PTHrP may be useful in the treatment of breast cancer growth and extra-skeletal metastasis.

Disclosures: D.C. Huang, None.

## F215

**Suppression of Canonical wnt Signaling by Dkk1 Attenuates PTH-mediated Peritrabecular Stromal Cell Response and New Bone Formation in a Model of Secondary Hyperparathyroidism.** J. Guo, M. Liu\*, D. Yang, C. C. Thomas\*, E. Schipani, F. R. Bringhurst, H. M. Kronenberg. Endocrine Unit, Massachusetts General Hospital and Harvard Medical School, Boston, MA, USA.

We have previously shown that PTH suppresses Dkk1 expression and activates canonical wnt signaling in bone. Transgenic mice that overexpress Dkk1 under the control of the 2.3 Kb collagen  $\alpha 1(I)$  promoter exhibit attenuated canonical wnt signaling and low bone mass. Either continuous infusion of PTH or feeding mice a low calcium diet that induces secondary hyperparathyroidism causes extensive peritrabecular stromal cell responses and new bone formation. To determine whether the suppression of Dkk1 is required for the peritrabecular stromal cell responses to PTH, Dkk1 transgenic mice at weaning were fed a low calcium diet for three weeks, and bone was examined by histology with H&E, von Kossa and Masson-Goldner Trichrome stains, and by *in situ* hybridization analysis. As expected, wild type mice fed a low calcium diet displayed large amounts of disorganized bone and extensive peritrabecular stromal cell responses. Such stromal cells strongly express mRNAs encoding  $\alpha 1(I)$  collagen and osteopontin, and to a lesser extent osteocalcin, indicating that they are preosteoblasts. Masson-Goldner Trichrome stain

demonstrated that the disorganized bone contained a high density of osteocytes and irregularly deposited mineral, suggesting that such disorganized bone is very similar to woven bone and presumably represents poorly organized, newly formed bone. Dkk1-overexpressing mice, when fed the low calcium diet, exhibited elevated serum PTH and a rachitic expansion of hypertrophic chondrocytes like those found in the wild type mice, but also uniquely exhibited tibial fractures and failed to develop a peritrabecular stromal cell and woven bone response seen in the wild type mice. Our findings indicate that activation of canonical wnt signaling at least in part by suppression of Dkk1 is essential for PTH-mediated peritrabecular stromal cell responses and new bone formation.

**Disclosures:** J. Guo, None.

*This study received funding from: NIDDK and NHLBI.*

## F217

### Safety and Efficacy of Long-Term Parathyroid Hormone Replacement in a Pediatric Patient with Inherited Hypoparathyroidism: Skeletal and Renal Outcomes.

T. A. Theman<sup>\*1</sup>, M. T. Collins<sup>1</sup>, D. W. Dempster<sup>2</sup>, H. Zhou<sup>2</sup>, J. C. Reynolds<sup>3</sup>, J. S. Brahimi<sup>\*4</sup>, P. Roschger<sup>5</sup>, K. Klaushofer<sup>5</sup>, K. K. Winer<sup>\*6</sup>.

<sup>1</sup>Skeletal Clinical Studies Unit, Craniofacial and Skeletal Diseases Branch, NIDCR, NIH, Bethesda, MD, USA, <sup>2</sup>Regional Bone Center, Helen Hayes Hospital, West Haverstraw, NY, USA, <sup>3</sup>Nuclear Medicine, CC, NIH, Bethesda, MD, USA, <sup>4</sup>CC, NIH, Bethesda, MD, USA, <sup>5</sup>Ludwig Boltzmann Institute of Osteology, Hanusch Hospital, Vienna, Austria, <sup>6</sup>ENGB, NICHD, NIH, Bethesda, MD, USA.

Autosomal dominant hypocalcemia (ADH) is an inherited form of hypoparathyroidism caused by activating mutations in the calcium-sensing receptor (CaR). Features include hypocalcemia, hyperphosphatemia and hypercalciuria, which can lead to nephrocalcinosis and renal insufficiency. Treatment with PTH(1-34) may be superior to conventional therapy but is contraindicated in children, and long-term effects on the skeleton are unknown.

The patient is a 20-year-old female with ADH treated with PTH continuously since age 6/12. Serum and urine mineral levels and were measured regularly. A bone biopsy was obtained at age 19 for histomorphometry and quantitative backscattered electron imaging (qBEI). Her data were compared to one age, sex, and length of hypoparathyroidism-matched control not on PTH, and two sex-matched ADH controls before and after one year of PTH.

The patient's growth was normal. Despite normal or below normal serum calcium and magnesium levels on PTH, persistent hypercalciuria and hypermagnesuria were observed. Nephrocalcinosis, without evidence of impaired renal function, developed by age 19. Cancellous bone volume was dramatically elevated in the patient as well as both ADH controls after one year of PTH. Bone mineral density distribution (BMDD) by qBEI of the patient and ADH controls was strikingly shifted towards lower mineralization compared to the non-ADH control. Moreover, the ADH controls exhibited a further reduction in mineralization after one year of PTH. These findings imply a role for CaR in bone matrix mineralization. Notably, there were no fractures or osteosarcoma.

Long-term PTH replacement in a child with ADH was safe, increased bone mass without negatively impacting mineralization, and improved serum and renal mineral control but did not prevent nephrocalcinosis. Additionally, this is the first direct evidence of a role for CaR in human bone.

**Disclosures:** T.A. Theman, None.

*This study received funding from: The Intramural Research Program of the NIH, NIDCR, and NICHD, the NIH/Pfizer Clinical Research Training Program (TAT), and the AUYA, WGKK, and FWF project P19009-N20 (PR, KK).*

## F219

### Pthrp-Induced Wnt Signaling Specifies the Mammary Mesenchyme.

M. Hiremath<sup>\*</sup>, J. J. Wysolmerski. Internal Medicine, Yale University School of Medicine, New Haven, CT, USA.

PTHrP regulates mammary morphogenesis by specifying mesenchymal cell fate during embryonic development. Disruption of the PTHrP or PTHrP genes results in a lack of mammary-specific mesenchyme and a failure of the mammary buds to give rise to the mammary ducts, while overexpression of PTHrP in the epidermis (K14-PTHrP mice) induces ectopic mammary mesenchyme under the ventral skin and causes inappropriate differentiation of the ventral epidermis into nipple skin. Previous studies demonstrated that PTHrP secreted by the mammary epithelial cells induced the expression of  $\beta$ -catenin and Lef1 in the mammary mesenchyme, suggesting that PTHrP signaling might modulate Wnt signaling in these cells. To test this hypothesis, we bred a Wnt reporter transgene, TOPGAL-C, onto the PTHrP-null and K14-PTHrP overexpressing backgrounds. As reported previously, canonical Wnt signaling was active in the mammary mesenchyme of WT mice between embryonic day 12 and 18. Overexpression of PTHrP led to the induction of ectopic Wnt signaling in the ventral mesenchyme underlying the nipple-like epidermis of K14-PTHrP mice. Interestingly, both mesenchymal and epithelial TOPGAL-C expression was abolished in PTHrP-null mammary buds. In order to determine if Wnt signaling contributed to the ability of PTHrP to specify mammary mesenchyme fate, we crossed the K14-PTHrP transgene onto a Lef1-null background. Loss of Lef1 partially reversed the nipple-like differentiation of the ventral skin usually associated with overexpression of PTHrP, suggesting that TCF/ $\beta$ -catenin signaling acts downstream of PTHrP in these cells. Taken together, our studies suggest that PTHrP regulates mammary bud development by inducing mesenchymal Wnt signaling.

**Disclosures:** M. Hiremath, None.

## F221

### A Long-Acting PTH Ligand that Binds to a Distinct PTH Receptor Conformation (R<sup>0</sup>) Can Stimulate Increases in Markers of Both Bone Resorption and Bone Formation in Mice. M. Okazaki<sup>\*</sup>, J. T. Potts, T. J. Gardella. Endocrine Unit, Massachusetts General Hospital, Boston, MA, USA.

The mechanisms that govern the balance between the bone-anabolic and bone-catabolic effects of PTH are not fully understood, but it is clear that the timing (periodicity /duration) of ligand exposure is a critical parameter. Thus, the paradigm, that once-daily (intermittent) PTH stimulates a net increase in bone, while continuous infusion stimulates a net bone loss. We reported last year that the modified PTH ligand, M-PTH(1-28) (M = Ala1,Aib3,Gln10,Har11,Ala12,Trp14,Arg19), binds with high affinity to a PTHR conformation, R<sup>0</sup>, which, by mechanisms still under study, results in prolonged signaling due to continued receptor occupancy. We showed that the R<sup>0</sup> analogs induce prolonged hypercalcemic and hypophosphatemic effects in mice. Such long-acting ligands might be predicted to have enhanced effects on bone resorption, relative to bone formation, even when administered intermittently. We therefore examined the effects of a long-acting PTH ligand on markers of bone metabolism in mice. We injected (i.v.) into wild-type C57/BL6 mice (age 3 months), the R<sup>0</sup>-selective ligand, M-PTH(1-34), rat PTH(1-34), or vehicle control, once daily, for 14 days, and measured parameters of bone formation and resorption. Peptides were injected at a concentration of 5 nanomole per kg body weight, which produced equivalent rises in plasma cAMP for the two peptides. Serum markers of bone formation (PINP and osteocalcin) and resorption (CTX) were measured by EIA at days 7 and 14, and areal bone mineral density at the isolated femur was measured by PIXIMUS at day 14. Maximum effects on CTX occurred at day 14: relative to vehicle, rPTH(1-34) increased CTX 1.3-fold ( $P = 0.001$ ), and M-PTH(1-34) increased CTX 2.3-fold ( $P = 0.0002$ ). The effect of M-PTH(1-34) on CTX was greater than that of PTH(1-34) ( $P = 0.001$ ). PTH(1-34) tended to increase PINP at day 7 (~1.3 fold,  $P = 0.09$ ) but not at day 14, and did not significantly change osteocalcin. In contrast, M-PTH(1-34) significantly ( $P \leq 0.0004$ ) increased PINP at day 7 (1.6-fold) and day 14 (2.6-fold), and increased osteocalcin by 2-fold at day 14 ( $P = 0.048$ ). PTH(1-34) increased total femur BMD by 3 % ( $P = 0.003$ ), while M-PTH(1-34) increased femur BMD by 11% ( $P < 0.0001$ ). These data show that a long-acting PTH analog, when administered in a once-daily regimen, can stimulate a net increase in bone mineral density in mice. The analog, as expected, strongly increases markers of bone resorption, but also increases markers of bone formation, and thus increases BMD as well as the rate of bone turn-over to greater extents than does an equal dose of PTH(1-34), at least in this mouse strain.

**Disclosures:** M. Okazaki, Chugai Pharmaceutical Co. Japan 5.

## F224

### Identification and Optimization of Residues in PTH and PTHrP that Determine Altered Modes of Binding to the PTH/PTHrP Receptor. M. Okazaki<sup>\*</sup>, J. T. Potts, T. J. Gardella. Endocrine Unit, Massachusetts General Hospital, Boston, MA, USA.

PTH and PTHrP use the same G protein-coupled receptor, the PTHR, to mediate their distinct biological actions. Recent data, for example, from competition binding and FRET analyses, suggest that PTH and PTHrP bind to the PTHR via different mechanisms that involve altered selectivities for distinct PTHR conformations. Thus, PTH(1-34) has a greater capacity to bind to the G protein-uncoupled conformation (R<sup>0</sup>), than does PTHrP(1-36), whereas PTHrP(1-36) favors the G protein-coupled conformation (RG). To explore the molecular basis for this apparent differential binding and conformational selectivity, we compared the effects of substitutions in the N-terminal and C-terminal regions of PTH and PTHrP peptides on the interaction of the ligands with the PTHR. Unlike in PTH(1-14) where Ala substitutions at positions 1, 3, 10,11,12 and 14 increased cAMP activity, each Ala substitution in PTHrP(1-14) abolished activity in cells expressing PTHR. Thus, the (1-14) regions of PTH and PTHrP interact with the juxtamembrane (J) region of the PTHR differently. Both PTHrP(1-14) and PTHrP(1-36) were much less potent for cAMP activity in cells expressing a PTHR lacking the extracellular N-terminal (N) domain (delNT), as compared to their respective PTH(1-14) and PTH(1-34), counterparts. PTHrP(1-36) activity therefore depends more heavily on interactions between the C-terminal ligand region and the PTHR N domain than does PTH(1-34) activity. Ala -scan analysis of the C-terminal regions of PTH(1-28) and PTHrP(1-28) revealed for each peptide strong reductions in activity at positions Arg20, Trp/Phe23 Leu24 and Leu/Ile28, known in PTH to form the core N domain-binding motif. Enhancements in activity were found at several, but different positions in each scaffold: Leu18, Phe22, and His26 in PTHrP(1-28) and Asn16, Glu19 and Ala22 in PTH(1-28). The Ala substitutions at positions 16, 19, and 22 in PTH increased binding to delNT, whereas those at positions 18, 22, 26 in PTHrP decreased binding to delNT. The enhancing effects of the Ala substitutions at positions 16, 19, and 22 of PTH are thus mediated via the PTHR J domain, whereas, those at positions 18, 22, 26 of PTHrP require the PTHR N domain. Further type substitution analysis of positions 16, 19, 22, as well as 25 (neutral to Ala substitution) in PTHrP(1-28) resulted in the analog [Ala18,22,Leu25,Lys26]-PTHrP(1-28), which exhibits a cAMP potency and RG binding affinity that is greater than that of PTH(1-34) and among the highest of any PTH or PTHrP peptide studied so far. These data support the hypothesis that PTH and PTHrP interact with the PTHR via different mechanisms, and suggest new tactics for developing potent PTH and PTHrP ligands.

**Disclosures:** M. Okazaki, Chugai Pharmaceutical Co. Japan 5.

## F226

**The N-Terminally Extended XL $\alpha$ s (XXL $\alpha$ s) Acts as a Novel Heterotrimeric G Protein Subunit with an Ability to Transduce Receptor Activation into Intracellular Signaling.** C. Aydin\*, M. J. Mahon\*, M. Bastepe. Endocrine Unit, Department of Medicine, Massachusetts General Hospital and Harvard Medical School, Boston, MA, USA.

*GNAS* encodes both the  $\alpha$ -subunit of the stimulatory G protein (G $\alpha$ ) and its extra-large variant XL $\alpha$ s. Disruption of XL $\alpha$ s in mice results in poor adaptation to feeding and impairs the glucose and energy metabolism. Also disrupted in the XL $\alpha$ s knockout mice is an N-terminally extended XL $\alpha$ s variant, termed XXL $\alpha$ s, which results from 5' extension of the open reading frame. Furthermore, XXL $\alpha$ s is also predicted to be disrupted by most *GNAS* mutations associated with human disease, such as progressive osseous heteroplasia, Albright's osteodystrophy, and fibrous dysplasia of bone. Thus, impaired XXL $\alpha$ s activity may contribute, at least partly, to the phenotype of XL $\alpha$ s knockout mice and the pathogenesis of diseases caused by *GNAS* mutations. Nonetheless, the cellular role of this highly conserved XL $\alpha$ s variant remains unknown. Here we engineered cDNA encoding the full-length human XXL $\alpha$ s and investigated its functional properties in cultured HEK293 cells and *Gnas*<sup>E2-/-</sup> cells, i.e. MEFs that lack endogenous XXL $\alpha$ s, XL $\alpha$ s, and G $\alpha$  due to homozygous disruption of *Gnas* exon 2. By confocal indirect immunofluorescence microscopy, native XXL $\alpha$ s, an N-terminally FLAG-tagged XXL $\alpha$ s, and an XXL $\alpha$ s mutant in which the methionine corresponding to the initiator of XL $\alpha$ s is changed to a valine (XXL $\alpha$ s-M302V) were localized to the plasma membrane of transfected HEK293 cells. Basal cAMP accumulation was markedly elevated in *Gnas*<sup>E2-/-</sup> cells transiently expressing an XXL $\alpha$ s mutant carrying an arginine-to-histidine change in its GTPase core domain (XXL $\alpha$ s-R844H). Isoproterenol (10<sup>-5</sup> M) stimulation of *Gnas*<sup>E2-/-</sup> cells transiently expressing either XXL $\alpha$ s or XXL $\alpha$ s-M302V resulted in an approximately 10-fold increase in cAMP accumulation. Sequence analysis of an Est clone derived from E18.5 whole mouse embryo showed that XXL $\alpha$ s mRNA comprises the entire open reading frame. However, 5'-RACE using total RNA from newborn mouse heart and rat INS-1 cells determined that XXL $\alpha$ s mRNA starts either 307 bp or 297 bp downstream from the first ATG of the longest open reading frame, predicting an N-terminal truncation of 48 or 101 amino acids, respectively. Our findings indicate that XXL $\alpha$ s is a plasma membrane protein with an ability to signal as a G $\alpha$ - and XL $\alpha$ s-like protein and that the N-terminus of XXL $\alpha$ s varies in a tissue-specific manner. It will be necessary to determine whether the size of the N-terminal domain affects XXL $\alpha$ s activity and whether deficiency or overactivity of this protein due to paternally inherited *GNAS* mutations is involved in disease pathogenesis.

**Disclosures:** C. Aydin, None.

This study received funding from: NIH/NIDDK.

## F228

**PTHrP Regulates Mammary Gland Ductal Elongation During Puberty.** K. Boras-Granic\*, J. J. Wysolmerski<sup>1</sup>, M. Dunbar<sup>\*2</sup>. <sup>1</sup>Endocrinology, Yale University, New Haven, CT, USA, <sup>2</sup>Biology, Penn State Berks-Lehigh Valley College, Reading, PA, USA.

Pubertal development of the mammary gland is mediated by bulbous structures known as terminal end buds (TEBs) that develop at the tips of the growing ducts. Estrogen is necessary for the formation and maintenance of TEBs and acts to cause ductal growth, in part, by upregulating amphiregulin expression and shedding by epithelial cells and causing subsequent epidermal growth factor receptor activation in stromal cells. We have previously shown that transgenic overexpression of PTHrP inhibits the effects of estrogen on ductal extension. In this study we asked if endogenous PTHrP acted to modulate ductal growth during puberty. We first examined the normal pattern of PTHrP expression in the mammary gland using a PTHrP-lacZ knockin mouse. During puberty, the PTHrP gene was expressed within cap cells of the terminal end buds (TEBs) and in myoepithelial cells of the ducts. These cell-types are located adjacent to stromal cells bearing PTH/PTHrP receptors and are the same cell-types in which PTHrP was previously overexpressed using the human keratin 14 promoter. We next used the Cre-loxP recombination system to disrupt PTHrP gene expression in the mammary gland at the onset of puberty. MMTV-Cre (line D) mice direct recombination in both luminal and myoepithelial/cap cells beginning at day 21. At 5 weeks of age, we found that PTHrP expression was reduced by 50% in MMTV-Cre/PTHrPlox/lox mice and that elongation of the ductal tree was accelerated by 20-30% in these mice as compared to littermate controls. Thus, PTHrP serves as an endogenous inhibitor of mammary ductal extension during puberty. Finally, given the importance of EGFR signaling during ductal extension, we investigated the effects of PTHrP on this signaling system. Estrogen could not stimulate proliferation or phosphorylation of the EGFR in primary cultures of either mammary epithelial cells (MECs) or stromal cells alone. However, estrogen readily induced both proliferation and EGFR phosphorylation in co-cultures of MECs and stromal cells. Co-cultures of MECs and mammary stromal cells from K14-PTHrP mice were resistant to both proliferation and EGFR activation when treated with estrogen, as were co-cultures of WT cells treated with exogenous estrogen plus PTHrP. In summary, our data suggest that endogenous PTHrP, secreted by cap and/or myoepithelial cells, acts on surrounding stromal cells to inhibit EGFR signaling, thus modulating mammary ductal growth during puberty.

**Disclosures:** K. Boras-Granic, None.

## F233

**Glucocorticoid Signaling in Osteoblasts Maintains Normal Bone Structure in Mice.** R. Kalak\*, J. Street\*, R. E. Day\*, J. R. K. Modzelewski\*, P. Y. Liu\*, G. Li\*, C. R. Dunstan<sup>1</sup>, H. Zhou<sup>1</sup>, M. J. Seibel<sup>1</sup>. <sup>1</sup>Bone Research Program, ANZAC Research Institute, The University of Sydney, Australia, <sup>2</sup>Medical Engineering & Physics, Royal Perth Hospital, Australia, <sup>3</sup>Musculoskeletal Research Unit, Queen's University Belfast, United Kingdom.

The role of endogenous glucocorticosteroids (GC) in bone development is still ill-defined. Using a transgenic (tg) mouse model of osteoblast-targeted disruption of intracellular GC signaling, we examined the role of endogenous GC in bone growth and development and its dependence on age, gender and skeletal site. Tibiae and L3 vertebrae of 3 and 7-week-old, male and female wild type (WT) mice and their tg, age and sex matched littermates (n= 10/ group; 80 in total) were analysed by micro-CT and mechanical testing. Data were analysed separately for 3 and 7-wk-old mice by 2-way ANOVA using genotype (WT or tg), gender and their interactions as factors. No interaction between genotype and gender was found for any of the analysed parameters; therefore, we only present data which was statistically pooled across gender. Tibial trabecular bone volume (BV/TV) and trabecular number (TbN) were significantly reduced by 24% and 20%, resp., and trabecular separation (TbSp) was significantly increased by 23% in 7-wk-old tg mice when compared to their WT littermates. Analogous changes were observed in the tibiae of 3-wk-old-mice and in the vertebrae of 7-wk-old mice but not in the vertebrae of 3-wk-old mice, where trabecular bone structure did not differ between tg and WT animals. Tibial length and cortical bone area were significantly decreased by 3% and 14% in 7-wk-old tg vs. WT mice and similar changes were seen in 3-wk-old mice. When compared to WT animals, tibial strength of 7-wk-old tg mice was significantly reduced with a decrease in both maximum load (-27%) and stiffness (-32%). In contrast, differences in tibial strength of 3-wk-old tg and WT mice were not statistically significant. The lack of interaction between genotype and gender indicated that the effect of disrupted GC signaling on bone structure in both sexually immature and mature mice was independent of gender. However, the effect of genotype was modulated by age for vertebral BV/TV, TbN and TbSp (p< 0.02). Correction for body weight did not affect the difference between WT and tg animals in 7-week-old mice, but in 3-wk-old mice it removed the observed effects in tibial bone parameters. We conclude that GC signaling in osteoblasts is important in maintaining normal bone volume and strength, however its effects are likely to be modulated by other factors such as age and skeletal site but not gender.

**Disclosures:** R. Kalak, None.

This study received funding from: NHMRC #402462.

## F238

**Intestinal-Specific Vitamin D Receptor Null Mice Maintain Normal Calcemia but Display Severe Bone Loss.** L. Lieben\*, R. Masuyama, K. Moermans\*, R. Bouillon, G. Carmeliet. Experimental Medicine, KULeuven, Leuven, Belgium.

The signaling of 1,25(OH)<sub>2</sub>vitaminD<sub>3</sub> [1,25(OH)<sub>2</sub>D<sub>3</sub>] via the vitamin D receptor (VDR) is required for normal mineral and skeletal homeostasis, and its effect on intestinal calcium absorption is considered to be essential. To verify this hypothesis, intestinal-specific VDR null mice were generated by crossing VDR floxed (VDR<sup>fl</sup>) mice with mice expressing Cre recombinase driven by the Villin promoter. The VDR<sup>fl</sup>/Villin-Cre<sup>+</sup> mice (VDR<sup>int-/-</sup>) showed specific and efficient VDR inactivation in the intestine. VDR<sup>int-/-</sup> mice were born at the expected Mendelian frequency and developed normally until weaning, where after their weight gain gradually declined compared to VDR<sup>fl</sup>/Villin-Cre<sup>+</sup> mice. As expected, intestinal calcium absorption was decreased in 8-wk-old mutant mice evidenced by reduced accumulation of <sup>45</sup>Ca in serum after oral gavage (-60%) and decreased TRPV6 and calbindin-D<sub>9k</sub> mRNA expression. Surprisingly, serum calcium levels were normal suggesting compensatory mechanisms. Indeed, serum PTH and 1,25(OH)<sub>2</sub>D<sub>3</sub> levels were increased 1.8 and 6.5 fold in mutant mice. Accordingly, renal calcium reabsorption was enhanced as evidenced by decreased urinary calcium/creatinine levels (-50%) and increased TRPV5 (x1.6) and calbindin-D<sub>9k</sub> (x3.5) mRNA levels. In addition, both trabecular and cortical bone mass was manifestly reduced in mutant mice (-50%), often resulting in spontaneous bone fractures. This bone loss was associated with increased bone resorption as serum CTX levels (x3) were elevated. In particular, the number of TRAP<sup>+</sup> cells in the cortex of mutant mice was increased resulting in decreased cortical thickness and increased porosity. Moreover, serum levels and femoral mRNA expression of osteocalcin was significantly increased. Also, osteoid surface was tripled in VDR<sup>int-/-</sup> mice, indicative of enhanced bone formation and/or decreased mineralization, thereby contributing to lower mineralized bone mass. Unlike systemic VDR null mice, growth plate morphology was not altered in VDR<sup>int-/-</sup> mice. Despite high 1,25(OH)<sub>2</sub>D<sub>3</sub> levels, FGF23 serum levels were decreased in mutant mice (-40%). Treating cultured stromal cells with increasing PTH doses inhibited the 1,25(OH)<sub>2</sub>D<sub>3</sub>-induced FGF23 expression. This mechanism may have contributed to the normal renal NPT2a protein and serum phosphate levels in VDR<sup>int-/-</sup> mice. In conclusion, loss of the VDR in the intestine decreases intestinal calcium absorption even during normal calcium intake, resulting in compensatory mechanisms mediated by increased PTH, 1,25(OH)<sub>2</sub>D<sub>3</sub> and decreased FGF23 levels to maintain normal serum calcium and phosphate levels and normal growth plate structure, at the expense of severe bone loss.

**Disclosures:** L. Lieben, None.

## F240

**Evidence of a Role for the Human Vitamin D Response Element Binding Protein, Heterogeneous Nuclear Ribonucleoprotein (hnRNP) C1/C2 in Chromatin Remodeling and Transcript Splicing.** H. Chen<sup>1</sup>, M. Hewison<sup>2</sup>, M. Nanes<sup>1</sup>, J. S. Adams<sup>2</sup>. <sup>1</sup>Division of Endocrinology, Emory University School of Medicine, Atlanta, GA, USA, <sup>2</sup>Department of Orthopaedic Surgery, UCLA/Orthopaedic Hospital, Los Angeles, CA, USA.

Heterogeneous nuclear ribonucleoproteins (hnRNPs) are among the most plentiful proteins in the eukaryotic cell nucleus. Constitutive overexpression of hnRNP C1/C2 in humans results in clinical resistance to the active vitamin D metabolite, 1,25-dihydroxyvitamin D (1,25D). Resistance is legislated in part by the ability of C1/C2 to compete with the vitamin D receptor (VDR)-retinoid x receptor for occupancy of double-strand (ds), *cis*-acting, vitamin D response elements (VDREs) involved in 1,25D-directed transcriptional regulation. Because of the ability of C1/C2 to specifically interact with single-strand (ss) as well as ds nucleic acid with an AGGTCA-like motif, we theorize that C1/C2 is instrumental in marking the exposed, exterior surface of ds DNA as it wraps around the nucleosome, readying that stretch of ds DNA and its underlying histone for chromatin remodeling and transcription. In chromatin immunoprecipitation (ChIP) analysis of 1,25D-responsive cells the functional VDRE in the CYP24 proximal promoter was occupied by C1/C2 in the absence of added 1,25D. Re-ChIP assays demonstrated that: 1) chromatin assembly factor 1 (CAF1); a chaperone for histones H3/H4; 2) acetylated H4 itself; 3) the gene-silencing proteins, heterochromatin protein 1 (hp-1) and histone deacetylase (HDAC), were also associated with the C1/C2-bound VDRE. Following addition of 1,25D, C1/C2 and associated proteins were competitively displaced from the VDRE by VDR, and the RNA polymerase II (pol II) recruited. By contrast, in 1,25D-resistant cells the over-abundant C1/C2 was less readily displaced from the VDRE with concomitant dysregulation of associated proteins and pol II recruitment. These data suggest that C1/C2 tethers both chromatin assembly/remodeling and transcriptional proteins to specific *cis* elements in the CYP24 gene promoter. Furthermore, because C1/C2 also binds to an AGGUCA element in ss mRNA, we also assessed the ability of C1/C2 to affect splicing of a VDRE-driven growth hormone minigene reporter construct. 1,25D-directed minigene splicing was disrupted in a time-dependent fashion in 1,25D-resistant cells, suggesting that displacement of C1/C2 from the VDRE is also essential for subsequent processing of RNA transcripts. Collectively, these data demonstrate that C1/C2, by virtue of its ability to bind both ss and ds nucleic acid, can direct 1,25D-VDR-VDRE-directed gene expression at the level of chromatin remodeling, transcription and splicing.

**Disclosures:** M. Hewison, None.

This study received funding from: NIH grant AR037399-20 to JSA.

## F242

**Snail Downregulates VDR Expression by Recruiting Sin3A, HDAC1 and HDAC2 to Multiple Regions of VDR Promoter and Deacetylating Histone H3/H4.** H. Wang\*, J. Shen\*, S. Park\*, A. T. M. Adesanya\*, Y. Li, S. Refetoff\*, R. E. Weiss\*, M. J. Favus. Medicine, University of Chicago, Chicago, IL, USA.

Snail is a key transcription repressor that plays important roles in epithelial to mesenchymal transitions (EMTs) during embryonic development and tumor invasion. Snail also downregulates VDR expression in human colon cancer and cell lines to block the anti-tumor action of 1,25(OH)<sub>2</sub>D<sub>3</sub> analogs. We have found elevated VDR and suppressed Snail in intestine and kidney of genetic hypercalciuric stone-forming (GHS) rats and speculate on the potential mechanisms whereby Snail downregulates VDR gene expression. In this study, we tested the hypothesis that Snail repression of VDR is the result of Snail binding to novel sites in the VDR promoter. Using cell lines that differ in their level of VDR expression, we found that higher VDR expression was associated lower Snail expression at both the mRNA and protein levels. The electrophoretic mobility shift assay (EMSA) demonstrated that Snail binds to several VDR promoter sequences containing E-box (CACCTG or CAGGTG) *in vitro*. Moreover, the chromatin immunoprecipitation (ChIP) assay demonstrated that endogenous Snail, Sin3A, HDAC1 and HDAC2 bind to multiple VDR promoter regions containing the E-box sequence. Additionally, overexpression of Snail in HEK293 (kidney) and SW480 (intestine) cells resulted in greater deacetylation of histones H3 and H4 at the VDR promoter regions. As a result, VDR gene expression was down-regulated. Immuno-staining shows that Snail, Sin3A, HDAC1 and HDAC2 co-localize with VDR in the nuclei of both HEK293 and SW480 cells. In conclusion, we demonstrated that Snail binds to novel multiple E-boxes within the VDR promoter and recruits the co-repressor Sin3A, histone deacetylase HDAC1 and HDAC2 to suppress VDR expression in kidney and colon cancer cell lines.

**Disclosures:** H. Wang, None.

## F244

**Double Deletion of  $\alpha$ 2a- and  $\alpha$ 2c-adrenergic Receptors Results in a Phenotype of High Bone Mass and in Resistance to the Thyrotoxicosis-induced Osteopenia.** T. L. Fonseca\*, C. C. Costa\*, A. C. B. Moulattai\*, F. R. S. Freitas\*, P. C. Brum\*, C. H. A. Gouveia\*. <sup>1</sup>Department of Anatomy, Institute of Biomedical Sciences, University of Sao Paulo, Sao Paulo, Brazil, <sup>2</sup>Physical Education and Sports School, University of Sao Paulo, Sao Paulo, Brazil.

It is well known that thyrotoxicosis induces bone loss. Recent studies demonstrated that the activation of the sympathetic nervous system (SNS) also reduces bone mass, via  $\beta$ 2 adrenergic receptors (AR). To investigate if thyroid hormone interacts with the SNS to regulate bone mass, we studied the effect of triiodothyronine (T3) on bone of mice with disruption of both  $\alpha$ 2a-AR and  $\alpha$ 2c-AR ( $\alpha$ 2a/ $\alpha$ 2c-AR<sup>-/-</sup>), which present chronically elevated sympathetic tone, with high levels of plasma noradrenaline. Forty-day-old female wild type C57BL/6J mice (WT) and  $\alpha$ 2a/ $\alpha$ 2c-AR<sup>-/-</sup> mice (KO) were treated with a supraphysiological dose of triiodothyronine (T3; 3.5 $\mu$ g/100g/BW/day) for 80 days or left untreated. Surprisingly, we found that KO mice present 15-24% ( $p < 0.01$ ) higher bone mineral density (BMD) than WT mice in all skeletal regions analyzed [tibia, femur, vertebra and hind body (lumbar spine+pelvis+hind limbs)]. As expected, T3 treatment significantly decreased BMD (11-14%,  $p < 0.01$ ) in all skeleton sites, but did not induce osteopenia in KO mice. The Three-Point Bending Test showed that the maximum load was 8% and 17% increased in the femur and tibia, respectively, of KO versus WT mice. Bone histomorphometry analysis showed that trabecular volume, thickness and number were also increased in KO versus WT mice (92, 47 and 29%, respectively;  $p < 0.01$ ). By real-time PCR analysis, we found that  $\alpha$ 2a-AR and  $\alpha$ 2c-AR mRNAs are expressed and that  $\alpha$ 2c-AR mRNA was downregulated by T3 (33%,  $p < 0.05$ ) in the tibia of WT mice. Tibial  $\beta$ 2-AR mRNA expression did not vary between mice lineages (WT vs. KO) or by T3 treatment. The mRNA of tartrate-resistant acid phosphatase and receptor activator of nuclear factor kappa B (factors positively related to osteoclastic activity) presented a 2-fold lower expression in KO versus WT mice ( $p < 0.05$ ), which suggests that bone resorption is reduced in KO mice. Finally, we found that T3 downregulates (3-fold,  $p < 0.001$ ) the mRNA of osteoprotegerin, a protein that limits osteoclastic activity, in WT but not in KO mice. In conclusion, the phenotype of high bone mass presented by  $\alpha$ 2a/ $\alpha$ 2c-AR<sup>-/-</sup> mice suggests that  $\alpha$ 2a-AR and/or  $\alpha$ 2c-AR are important to mediate the osteopenic effects of the SNS. The resistance of KO mice to the T3-induced osteopenia suggests a T3-SNS interaction, which probably depends on  $\alpha$ 2a-AR and/or  $\alpha$ 2c-AR, to regulate bone mass.

**Disclosures:** T.L. Fonseca, None.

This study received funding from: FAPESP.

## F246

**A Key Mechanism Underlying the Immunosuppressive Effects of Vitamin D: 1,25dihydroxyvitamin D<sub>3</sub> Is a Transcriptional Modulator of IL-17.** S. Joshi\*, S. Youssef\*, S. Gaffen\*, L. Steinman\*, S. Christakos\*. <sup>1</sup>Biochemistry, UMDNJ-NJMS, Newark, NJ, USA, <sup>2</sup>Neurology, Stanford University, Stanford, CA, USA, <sup>3</sup>SUNY Buffalo School of Dental Medicine, Buffalo, NY, USA.

A new class of helper T cells producing IL-17 has recently been identified as a distinct inflammatory CD4+ helper T cell lineage (TH17). IL-17 has been reported to play a critical role in numerous inflammatory conditions and autoimmune diseases, including inflammation induced bone loss and multiple sclerosis. We report here for the first time that the active form of vitamin D, 1,25(OH)<sub>2</sub>D<sub>3</sub>, has a direct repressive effect on the expression of IL-17. 1,25(OH)<sub>2</sub>D<sub>3</sub> treatment (10<sup>-9</sup>-10<sup>-7</sup> M) for 24 - 96 h of activated mouse CD4+ T cells resulted in a dose dependent inhibition of IL-17 (maximum decrease, 66%). The murine model of multiple sclerosis, EAE, was used to test whether 1,25(OH)<sub>2</sub>D<sub>3</sub> inhibits IL-17 production *in vivo*. Treatment with 1,25(OH)<sub>2</sub>D<sub>3</sub> (50 ng/day/3 days) of mice with existing EAE (clinical score, 3.5) reversed paralysis, prevented the progression of the disease and resulted in a 50-60% decrease in the percentage of infiltrating IL-17 producing CD4+ T cells to the CNS. Correlated to the findings in mice, treatment of activated human CD4+ T cells with 1,25(OH)<sub>2</sub>D<sub>3</sub> also inhibited the production of IL-17. The mechanism of 1,25(OH)<sub>2</sub>D<sub>3</sub> mediated repression was found to be transcriptional repression mediated by VDR/RXR. When the human T cell line Jurkat was transfected with the human IL-17 promoter (-1,125/+5) and VDR and treated with PMA (10<sup>-7</sup> M) and ionomycin (200 ng/ml), there was a dose dependent inhibition of the transcriptional activation of IL-17 in the presence of 1,25(OH)<sub>2</sub>D<sub>3</sub> (activation levels were maximally reduced 70%). Deletion mutant analysis indicated that the region between -232 and -159 was required for the activation of the IL-17 promoter and for inhibition by 1,25(OH)<sub>2</sub>D<sub>3</sub>. Two NFAT sites are located within this region. Activation and inhibition by 1,25(OH)<sub>2</sub>D<sub>3</sub> were not observed using the -232/+5 construct with both NFAT sites mutated. Overexpression of NFAT was able to relieve the 1,25(OH)<sub>2</sub>D<sub>3</sub> dependent repression. EMSA showed that VDR/RXR binds to the NFAT sites and displaces NFAT from its site. ChIP analysis using the Hut 102 T cell line showed that activation by PMA/ionomycin can enhance recruitment of NFAT to the -232/-159 region of the IL-17 promoter. In the presence of 1,25(OH)<sub>2</sub>D<sub>3</sub> and VDR, recruitment of NFAT is inhibited and recruitment of VDR to this site is observed. These findings indicate that VDR mediates the suppression of IL-17 by blocking NFAT from binding to its sites on the IL-17 promoter and by associating with the NFAT element. The inhibition of IL-17 transcription by 1,25(OH)<sub>2</sub>D<sub>3</sub> may provide a key mechanistic explanation for the potent immunosuppressive action of 1,25(OH)<sub>2</sub>D<sub>3</sub>.

**Disclosures:** S. Joshi, None.



## F249

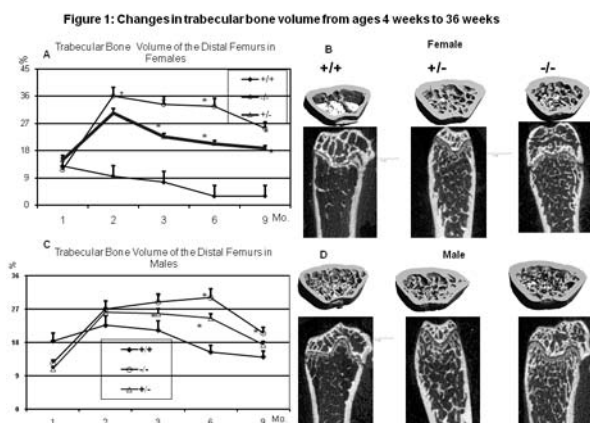
**Augmentation of Peak Bone Mass Occurs in Female and Male Mice without Progesterone Nuclear Receptors.** W. Yao, Z. Cheng, A. Pham\*, C. Busse\*, N. E. Lane. Center for Healthy Aging, UC Davis Medical Center, Sacramento, CA, USA.

Peak bone mass (PBM) is a strong determinant of incident osteoporotic fracture risk. We characterized skeletal acquisition and bone metabolism at the age of rapid skeletal acquisition in mice with the two nuclear progesterone receptors (PRA and PRB) rendered nonfunctional (PRKO).

**Methods.** We measured bone mass acquisition by repeated in vivo microCT scans of the distal femurs (DF) and mid-femurs in both female and male mice from all the genotypes (n=5-8/genotype: WT, PRKO +/-, PRKO -/-) from 1-9 months of age. At 2 months of age, when the rapid skeletal acquisition occurred, we characterized bone metabolism by measurement of biochemical markers of bone turnover (PINP, DPD/Cr), reproductive hormones/growth factors (FSH, Inhibin A, testosterone (T), progesterone (P), IGF1, TGFβ1), bone cell activities (primary osteoblast cultures for ALP and mineralization nodule formation; osteoclast maturation and activity by TRAP staining and dentin resorption).

**Results.** No differences were found between PRKO +/-, -/- and WT mice in body weight or femur length in both genders. PRKO -/- and +/- mice had an accelerated gain in BV/TV of the DF (between the ages of 1-3 months), greater PBM at age 3 months in both the female (+400%) and male (+95%; p < 0.05) PRKO mice compared to WT litter-mates. Mid-femur cortical thickness was greater in the PRKO -/- and +/- mice than the WT in both the males and females aged 6-9 months. At 2 months of age, FSH levels were higher in WT > PRKO +/- > -/- in both genders (p<0.05), while inhibin A levels were PRKO -/- > +/- > WT mice (p<0.05). P, T and IGF1 levels were similar among the genotypes. In the female mice, osteoblast maturation and activity (TGFβ1, PINP, in vitro ALP level and mineralization nodules) were PRKO -/- > +/- > WT mice (p<0.05); while the osteoclast maturation and activity (DPD/Cr, TRAP+ staining and dentin resorption) were similar among the genotypes. In male mice, osteoblast maturation (ALP, nodule formation) was higher in PRKO -/- > +/- = WT (p < 0.05); while osteoclast maturation and activity (DPD/Cr, TRAP+ staining, and dentin) were lower in PRKO -/- and +/- mice (p<0.05).

**Conclusions.** PRKO mice achieved a higher PBM than WT mice with females more affected than males. Elucidation of how progesterone mediates bone cell functions through its receptors may provide a novel pathway to augment PBM and reduce the burden of osteoporosis.



**Disclosures:** W. Yao, None.

This study received funding from: 1K12HD05195801, R01 AR043052-07.

## F253

**Lrp6 Loss of Function Impacts Bone Homeostasis and Responds to Folate Supplementation.** B. Slowinska\*, J. Monaghan\*, M. C. H. van der Meulen<sup>2</sup>, D. Chen\*, L. Lukashova\*, M. E. Ross\*. <sup>1</sup>Laboratory of Neurogenetics and Development, Weill Medical College of Cornell University, New York, NY, USA, <sup>2</sup>Mechanical and Aerospace Engineering, Cornell University, Ithaca, NY, USA, <sup>3</sup>Musculoskeletal Repair and Regeneration Core Center, Hospital for Special Surgery, New York, NY, USA.

Human mutations in the low-density lipoprotein receptor-related protein 5 (LRP5) gene are associated with clinical disorders of high bone mass (HBM, gain of function alleles) or low bone mass (osteoporosis-pseudoglioma, OPPG, loss of function alleles). LRP5 and LRP6 both function as co-receptors with Frizzled to transduce Wnt signals in the canonical pathway. Since Lrp6 is expressed in cells important for bone formation and remodeling, we examined its role in bone homeostasis. In addition, our previous studies of an Lrp6 mutant allele revealed that this gene can contribute to neural tube birth defects that can be prevented by dietary supplementation with the vitamin, folic acid (FA). We therefore sought to determine the effect of the Lrp6 null allele with or without FA supplementation on bone morphology of the femur, measured by microcomputed tomography (micro-CT), and on whole bone strength, measured by three-point bending assays. Mice from the

Lrp6<sup>+/+</sup> line were maintained on defined diets containing either 2 ppm (mg/kg) FA or 10 ppm FA. Subjects were F2-generation or beyond, male offspring of Lrp6<sup>+/+</sup> x Lrp6<sup>+/+</sup> parents maintained on one of the two diets. In age matched adults (50 wk) fed 2 ppm FA, micro-CT revealed significant differences in several parameters in femurs including trabecular number and spacing (Tb. N., 1.16±0.5 vs 2.34±1.4 p<0.015; Tb. Sp. 1.2±0.65 vs 0.45±0.03 p<0.01) comparing heterozygous Lrp6<sup>+/+</sup> with <sup>+/+</sup> siblings, respectively. Interestingly, no statistical differences existed between genotypes maintained on the high (10 ppm) FA diet. No significant differences in these parameters were found in Lrp6<sup>+/+</sup> mice on the 2 ppm vs 10 ppm diet, while Lrp6<sup>+/+</sup> mice fed the 10 ppm diet had Tb.N. and Tb.Sp. values indistinguishable from <sup>+/+</sup> on either diet. Whole bone strength and stiffness in bending were not significantly different between genotypes or diets. We conclude that Lrp6 haploinsufficiency alters bone homeostasis in trabecular bone but does not alter cortical bone mechanics. Dietary supplementation with FA can ameliorate the effects of genotype on trabecular bone.

**Disclosures:** M.E. Ross, None.

This study received funding from: NIH/NIAMS Core Center Grant AR046121.

## F256

**Camurati-Engelmann Disease (Progressive Diaphyseal Dysplasia): A Unique Variant Featuring a Novel, Heterozygous, Leucine Repeat Mutation in TGFβ1 Together with a Novel, Homozygous, Missense Change in TNFSF11 Encoding RANKL.** M. P. Whyte<sup>1</sup>, W. Totty<sup>2</sup>, D. Novack<sup>2</sup>, D. Wenkert<sup>1</sup>, X. Zhang\*, S. Mumm<sup>1</sup>. <sup>1</sup>Shriners Hosp for Children, St. Louis, MO, USA, <sup>2</sup>Washington Univ Schl Med, St. Louis, MO, USA.

We report what seems to be a unique disorder of skeletal homeostasis affecting a mother and son. Our molecular studies indicate that the condition derives from disturbances and dosage effects in two key genes that regulate bone turnover.

A 32-year-old man was self-referred for an undiagnosed disorder causing lower limb pain beginning in childhood. As a teenager, "osteopathia striata" was diagnosed, and he grew to 6' 10" by his late 20's. He had disproportionately long lower limbs, pseudoclubbing, deafness, torus palatinus, and hypomasculinization. Karyotype was normal. Skeletal survey revealed generalized osteosclerosis, widened bones, and cortical and trabecular bone thickening most closely resembling Camurati-Engelmann disease (CED). However, the changes extended to the ends of the long bones unlike CED (Fig). BMD z-scores were +7.7 and +4.4 in spine and hip, respectively. Markers of bone turnover were elevated. Calcium homeostasis seemed normal, except for marked hypocalciuria. Non-decalcified iliac crest revealed significant osteomalacia (Fig). His asymptomatic mother was 5' 9," and had similar, but distinctly more mild, clinical, radiological, and biochemical changes.

We amplified by PCR and sequenced exon 1 of *TNFRSF11A* (RANK) as well as all coding exons and adjacent mRNA splice junctions of *TNFRSF11B* (OPG), *TNFSF11* (RANKL), *SQSTM1* (sequestosome 1), and *TGFβ1* [transforming growth factor β1].

No mutations were detected for RANK, OPG, or sequestosome 1. However, in *TGFβ1*, we found a novel 12 bp duplication in exon 1 that would insert 4 Leu residues, reminiscent of a report (Nat Genet 26:273, 2000) of a 9 bp insertion at the same site adding 3 Leu residues in a patient with CED. Additionally, in our proband we identified in *TNFSF11* a homozygous, single-base change resulting in a non-conservative amino acid change (c.107C>G, p.Pro36Arg) in RANKL that was heterozygous in his mother. This *TNFSF11* change is not found in dbSNP (SNP Database), nor reported in several association studies of RANKL polymorphisms, but was detected in 1/22 alleles tested randomly from other patients. Hence, this change may reflect the impact of a gene dosage effect of RANKL that contributes to the novel skeletal phenotype in this family.



**Disclosures:** M.P. Whyte, None.

## F260

**Geometric Property QTLs in HcB/8 x HcB/23 F2 cross.** N. Saless<sup>1</sup>, S. Litscher\*, M. J. Houlihan\*, T. K. O'Neil\*, R. S. Kattappuram\*, S. Sudhakaran\*, K. G. Abdul Raheem\*, S. Olson\*, G. Lopez Franco\*, P. Demant\*, R. D. Blank\*. <sup>1</sup>Cellular and Molecular Biology, University of Wisconsin, Madison, WI, USA, <sup>2</sup>University of Wisconsin, Madison, WI, USA, <sup>3</sup>University of Minnesota, Minneapolis, MN, USA, <sup>4</sup>Roswell Park Cancer Institute, Buffalo, NY, USA, <sup>5</sup>Endocrinology, University of Wisconsin and Madison VAMC, Madison, WI, USA.

Fractures are an important health problem with a significant genetic component. We performed a reciprocal F2 intercross of the recombinant congenic mouse strains HcB/8 and HcB/23 including 603 animals, reporting whole bone biomechanical performance-related quantitative trait loci (QTLs). To elucidate the mechanisms leading to biomechanical performance in our animals, we now report femoral geometry QTLs in the same cross. Animals were maintained to 17 weeks under standard husbandry conditions. Following



sacrifice, we subjected femora to quasi-static 3-point bend testing to failure. We acquired cross-sectional digital images of the fracture surfaces and extracted of major and minor inner and outer axes, perimeter, cortical cross-sectional area, and cross-sectional moment of inertia. Linkage analyses were performed with QTL Cartographer and R-QTL. Experiment-wide 5% and 1% significance levels for linkage were established by permutation testing.

The main results are summarized in the table. On chromosome 4 in particular, a QTL for femoral size appears to underlie the previously identified QTL for yield load, maximum load, stiffness, and BMD. It is worth noting that our chromosome 4 QTL overlaps that identified by Beamer and colleagues for bone mineral density. Subsequent work by Robling and colleagues showed that the chromosome 4 locus contributes to differences in responsiveness to mechanical loading in vivo. Our experiment allows localization of the QTL to a short chromosomal segment centered at 67 cM.

Bone geometry is a major determinant of biomechanical performance, accounting for approximately 50% of whole bone strength in multiple regression analyses performed by multiple investigative teams. In addition to its importance in fracture susceptibility, geometric phenotypes are highly reproducible, making them ideal for linkage studies. More importantly, the relationship between long bone geometry and modeling during growth makes these phenotypes amenable to investigation of the cellular-level mechanisms by which biomechanical performance is established.

Geometric Property QTLs		
Location (Chromosome, cM)	Traits	Max LOD Score
1, 52-67	Outer Minor Axis, Shape Factor	3.7, 3.1
2, 27-31	Outer Major Axis, Perimeter, Cross-Sectional Area, Shape Factor	6.5, 5.8, 3.5, 6.5
3, variable	Outer Major Axis, Cross-Sectional Area, Moment of Inertia	3.7, 3.0, 3.22
4, 67	Outer Major Axis, Perimeter, Cross-Sectional Area, Moment of Inertia	12.2, 7.8, 12.9, 3.8, 17.7
6, variable	Outer Major Axis, Perimeter, Cross-Sectional Area, Moment of Inertia, Shape Factor	5.1, 3.5, 3.9, 3.3, 3.6
10, 29 & 44	Outer Minor Axis, Outer Major Axis, Cross-Sectional Area, Moment of Inertia, Shape Factor	3.4, 7.6, 3.4, 7.5, 4.2, 3.8

**Disclosures:** N. Saless, None.

## F265

**A Recombinant Congenic Strain (B.H-6) Establishes that Trabecular Bone Mass and Bone Marrow Adiposity Are Distinct and Heritable Phenotypes.** C. Ackert-Bicknell<sup>1</sup>, G. A. Churchill<sup>1\*</sup>, K. R. Shockley<sup>2\*</sup>, M. Horowitz<sup>3</sup>, E. Canalis<sup>4</sup>, C. J. Rosen<sup>5</sup>. <sup>1</sup>The Jackson Laboratory, Bar Harbor, ME, USA, <sup>2</sup>The Jackson Laboratory, B, ME, USA, <sup>3</sup>Yale University, New Haven, CT, USA, <sup>4</sup>St Francis Hospital and Medical Center, Hartford, CT, USA, <sup>5</sup>Research Institute, Maine Medical Center, Scarborough, ME, USA.

We previously reported a Quantitative Trait Locus (QTL) for serum IGF-I and vBMD on mouse Chr 6. This QTL was named *Igf1s1*. The B6.C3H-6T (6T) congenic mouse was generated such that C3H/HeJ (C3H) alleles for this QTL were moved onto a C57BL/6J (B6) background. The C3H-like region of the 6T congenic extended from 48.6 to 121 Mb (NCBI Bld 36). We also generated a second congenic strain for the *Igf1s1* QTL, i.e. B.H-6. The B.H-6 congenic strain is C3H-like for the region from 89.0 Mb to 125 Mb on Chr 6 and therefore is only C3H-like for the distal two-thirds region on Chr 6 that the 6T congenic is C3H. Female B.H-6 mice had more body fat than 6T ( $p<0.05$ ), but not different from B6 mice. B.H-6 mice had significantly greater trabecular BV/TV by  $\mu$ CT, whereas femoral vBMD by pQCT did not differ from B6; in contrast, 6T mice had low vBMD and reduced trabecular BV/TV vs. B6. Both strains exhibited a marked increase in marrow adiposity. We hypothesized there was a common genetic mechanism regulating marrow adiposity in the 6T and B.H-6 strains, but that a separate genetic pathway was involved in bone acquisition. To test this hypothesis we examined gene expression in the femur of the B.H-6 and the 6T mice by Illumina microarray. A total of 41 genes were found to have significantly different expression between the 2 strains. None were located within the B.H-6 congenic region suggesting that genes found within the 6T region, but not the B.H-6 locus were responsible for differences in BV/TV between 2 strains. Osteocalcin, also known as *Gpmb*, is located at 48.9 Mb on mouse Chr 6; this gene regulates both osteoblasts and osteoclasts. The 6T strain is C3H-like for this gene whereas B.H-6 is not, and *Gpmb* had 3.3 fold lower expression in the femur of 6T vs. B.H-6 ( $q<0.00001$ ). Previously, we showed that 6T lost bone but did not increase marrow fat on a high fat diet (HFD), while B6 did not lose bone but showed increased marrow adiposity on a HFD. We then compared gene expression from femorae of 6T and B6 mice on a HFD, by Illumina micro-array, and found *Gpmb* to be significantly suppressed in 6T vs. B6 (-1.5 fold;  $p<0.04$ ). Importantly, *Gpmb* has a non-synonymous SNP in the 2<sup>nd</sup> Exon of C3H, resulting in an asparagine to aspartic acid substitution in 6T. In conclusion, we showed differential genetic regulation of marrow fat and bone mass. This would imply that marrow adiposity is a distinct and heritable phenotype, independent of BV/TV. Polymorphic differences in *Gpmb* likely contribute to the low bone mass phenotype of the 6T congenic.

**Disclosures:** C.J. Rosen, None.

This study received funding from: NIH AR45433, and 54604.

## F270

**Drugs which Inhibit Osteoclast Function Suppress Tumor Growth and Alter Hematopoietic Cell Populations in Bone.** X. Li<sup>1</sup>, J. Liao<sup>1\*</sup>, A. Koh<sup>1\*</sup>, K. J. Pienta<sup>2\*</sup>, L. K. McCauley<sup>1</sup>. <sup>1</sup>Periodontics and Oral Medicine, University of Michigan, Ann Arbor, MI, USA, <sup>2</sup>Medicine, University of Michigan, Ann Arbor, MI, USA.

Inhibition of bone resorption is effective in reducing tumor burden in murine models and human prostate cancer patients. However, whether drugs which inhibit osteoclast function restrict tumor growth independent of inhibition of bone resorption is unclear. It was recently reported that increased osteoclast activity resulted in mobilization of hematopoietic stem cells (HSCs). The purpose of this investigation was to determine whether drugs which inhibit osteoclast function alter tumor growth directly or indirectly, and how they impact HSCs in the marrow.

Zoledronic acid (ZA), a bisphosphonate, and recombinant OPG-Fc, a RANKL inhibitor, (provided by Amgen), were administered to mice bearing vertebral implants (vossicles) containing Ace-1 osteoblastic prostate cancer cells. Vertebrae from 11d mice or gelfoam sponges were seeded with  $5 \times 10^5$  luciferase tagged prostate carcinoma (Ace-1<sup>luc</sup>) cells subcutaneously in athymic mice (2 vossicles, 2 gelfoam implants/mouse). Mice received ZA (5 $\mu$ g/mouse, twice/week), (OPG-Fc at 10mg/kg, 3 times/week) or vehicle, and luciferase activity measured weekly. At sacrifice, bone marrow cells were harvested and HSCs evaluated by flow cytometry. Histologic analysis of the tumors, vossicles and endogenous bones and serum biochemistry were performed.

Results showed: 1) There was a significant increase in tumor luciferase activity in vossicles versus gelfoam implants. The tumor size was also significantly larger in vossicles than in gelfoam. 2) ZA (versus vehicle) significantly inhibited tumor growth in bone but not in gelfoam implants, decreased serum TRAP5b and osteoclast numbers, increased tibia and vossicle bone areas, and increased the percent of HSCs (lin<sup>-</sup>, c-kit<sup>+</sup>, sca-1<sup>+</sup> cells) in the marrow. 3) OPG-Fc (versus vehicle) significantly inhibited tumor growth in bone but not in gelfoam implants, decreased serum TRAP5b and osteoclast numbers, increased tibia and vossicle bone areas, and increased the percent of HSCs in the marrow. The ZA studies were repeated in non-tumor bearing C57B6 mice and similar significant elevations in HSCs in the bone marrow were found.

These data suggest that tumors prefer to grow in bony sites and that the effect of drugs which inhibit osteoclast function on prostate carcinoma growth and osteoblastic lesions requires the bone microenvironment. Furthermore, these data resulted in the novel findings of an association of inhibition of bone resorption with elevated marrow HSCs. These studies begin to clarify the mode of action of drugs which inhibit osteoclast function in treating skeletal metastasis and shed light on the interactions of bone resorption, tumor growth and HSCs.

**Disclosures:** X. Li, None.

This study received funding from: NIH.

## F272

**2-Methoxyestradiol Blocks Prostate Cancer Bone Metastases.** K. S. Mohammad<sup>1</sup>, L. Kingsley<sup>1</sup>, T. La Vallee<sup>2\*</sup>, T. A. Guise<sup>1</sup>, J. M. Chirgwin<sup>1</sup>. <sup>1</sup>University of Virginia, Charlottesville, VA, USA, <sup>2</sup>EntreMed Inc., Rockville, MD, USA.

The majority of patients with hormone-refractory advanced prostate cancer develop bone metastases, where disorganized new bone formation results from paracrine stimulation of osteoblasts by tumor cells. Many secreted proteins that activate osteoblasts are regulated by the hypoxic response pathway. We hypothesized that anti-hypoxic therapy should be effective against bone metastases and tested this with 2-methoxyestradiol (2ME2), an inhibitor of microtubule polymerization and the Hif-1 pathway that is in clinical trials in cancer patients. 2ME2 was tested alone and in comparison and combination with two established treatments for bone metastases: zoledronic acid (ZA), and the endothelin A receptor antagonist, atrasentan.

Nude mice (n=15/group) received human prostate cells by intratibial injection. The LuCaP23.1 xenograft is androgen-dependent, secretes prostate specific antigen (PSA), and causes florid osteoblastic bone responses. Effects of treatments on bone and tumor burden were assessed in vehicle, 3 single-treatment groups, 3 double-treatment groups and one triple-treatment group. Atrasentan was given at 20mg/kg/d in drinking water. 2ME2 (EntreMed, Inc) was given at 150mg/kg/day by ip injection (of soluble bioactive dispersion formulation). ZA was given at 5ug/kg/3x per wk by sc injection. Mice were treated for 26 wks, while followed by X-ray, ELISA for serum PSA. No group that received 2ME2 alone or in combination showed bone lesions on X-ray, although direct effects on bone of the drugs can obscure the X-ray appearance of small tumor responses. More significantly, only one mouse out of the 60 receiving 2ME2 had detectable PSA, a surrogate marker of tumor burden secreted by prostate cancers and not present in mice. While all the mice in the other treatment groups showed a significant increase in PSA level starting at 8 weeks post-tumor inoculation.

Preliminary data suggest that 2ME2, while lacking substantial estrogenic activity, may be a moderately effective anti-androgen, consistent with loss of muscle mass seen in the 2ME2-treated mice. LuCaP23.1 xenografts are androgen-dependent; so the efficacy of 2ME2 against this tumor in bone may represent a combined anti-androgen and anti-hypoxic effect. Separating these two mechanisms, both of which would be beneficial in the clinic, requires testing 2ME2 in an androgen-independent model of prostate cancer bone metastases.

**Disclosures:** K.S. Mohammad, None.

## F275

**Combined Transforming Growth Factor  $\beta$  Receptor I Kinase Inhibitor and Bisphosphonates Are Additive to Reduce Breast Cancer Bone Metastases.** K. S. Mohammad<sup>1</sup>, E. Stebbins<sup>\*2</sup>, L. Kingsley<sup>1</sup>, P. G. J. Fournier<sup>1</sup>, M. Niewolna<sup>\*1</sup>, C. R. McKenna<sup>\*1</sup>, X. Peng<sup>\*1</sup>, L. Higgins<sup>\*2</sup>, D. Wong<sup>\*2</sup>, T. A. Guise<sup>1</sup>. <sup>1</sup>University of Virginia, Charlottesville, VA, USA, <sup>2</sup>Scios Inc., Fremont, CA, USA.

Breast cancer commonly metastasizes to and destroys bone to cause pain and fracture. Substantial data support central roles for bone-derived TGF- $\beta$  and tumor-derived osteolytic factors such as PTHrP in a vicious cycle of bone destruction. A small molecule inhibitor of TGF- $\beta$  receptor I kinase (TGF- $\beta$ RI), SD-208, inhibits signaling downstream of the TGF- $\beta$  receptor, reduced osteolytic lesion area and prolonged survival in mice. Bisphosphonates reduce skeletal morbidity in patients with bone metastases. Thus, we hypothesized that combined treatment of SD-208 and zoledronic acid (ZA) would be more effective for osteolytic bone metastases than either treatment alone.

Mice were inoculated with MDA-MB-231 breast cancer and randomized to receive the following treatments when osteolytic lesions were detected on radiographs: 1) SD-208 (60mg/kg/day); 2) ZA (5ug/kg/1/wk); 3) ZA (5ug/kg 3/wk); 4) SD-208+ZA; 5) SD-208+ZA or 6) vehicle. Osteolytic lesion area was reduced in mice treated with SD-208, ZA 1/wk ( $p<0.001$ ), ZA 3/wk ( $p<0.05$ ) vs. vehicle. Mice treated with combinations had significantly less osteolysis than vehicle or single treatment: SD-208+ZA 1/wk ( $3.11 \pm 0.091 \text{ mm}^2$ ) ( $p<0.001$ ) and SD-208+ZA 3/wk ( $2.19 \pm 0.47 \text{ mm}^2$ ) vs. vehicle ( $p<0.001$ ); Single treatment, SD-208 vs. SD-208+ZA 1/wk ( $p<0.001$ ), SD-208 vs. SD-208+ZA 3/wk ( $p<0.001$ ); ZA 1/wk vs. SD-208+ZA 1/wk ( $p<0.001$ ), ZA 3/wk vs. SD-208+ZA 3/wk ( $p<0.001$ ). Histomorphometric analysis showed a significant reduction in tumor burden and increase in total bone area with all single and combined treatment. Combined treatment with SD-208 + ZA 3/wk increased total bone area than SD-208 alone ( $p<0.01$ ) or ZA 1/wk alone ( $p<0.05$ ). This was accompanied by a reduction in osteoclast # by all single treatments. Combined treatment with SD-208 + ZA 1x/wk decreased OCL # than SD-208 alone ( $p<0.05$ ). SD-208 alone ( $p<0.01$ ) or in combination with ZA (ZA 1/wk  $p<0.05$ , ZA 3/wk  $p<0.05$ ) and not ZA alone increased osteoblast #.

To determine if the reduced osteolysis observed in mice treated with combined SD-208 and ZA was due to reduced expression of TGF- $\beta$  target genes. Quantitative RT-PCR analysis indicated that PTHrP, IL-1 and PMPA mRNA steady-state levels were decreased in response to combined SD-208+ZA more than either treatment alone. These data indicate that combination therapy with TGF- $\beta$  receptor I kinase inhibition and bisphosphonates reduce the progression of established osteolytic metastases more effectively than either therapy alone. This effect may be due to reduction in tumor factors which promote osteolysis.

**Disclosures:** K.S. Mohammad, None.

## F277

**Bortezomib, a Proteasome Inhibitor, Prevents Metastatic Breast Cancer Osteolysis and Reduces Mammary Fat Pad Tumor Growth in Mice.** M. D. Jones<sup>\*1</sup>, J. C. Liu<sup>\*2</sup>, J. Schoonmaker<sup>\*3</sup>, T. K. Barthel<sup>2</sup>, S. Mulay<sup>\*3</sup>, M. L. Bouxsein<sup>\*3</sup>, G. S. Stein<sup>1</sup>, S. Mukherjee<sup>\*2</sup>, J. B. Lian<sup>1</sup>. <sup>1</sup>Department of Orthopedics and Physical Rehabilitation, University of Massachusetts Medical School, Worcester, MA, USA, <sup>2</sup>Department of Cell Biology and Cancer Center, University of Massachusetts Medical School, Worcester, MA, USA, <sup>3</sup>Center for Regenerative Medicine, Massachusetts General Hospital and Harvard Medical School, Boston, MA, USA.

The selective proteasome inhibitor bortezomib (Bzb) inhibits the proliferation of several solid tumors and can increase osteoblasts in the bone marrow. Our goal was to test the efficacy of Bzb in preventing breast cancer metastasis to bone by directly inhibiting tumor cell growth and protecting the bone from osteolysis using experimental approaches in mice appropriate for translational studies. MDA-MB-231 metastatic breast cancer cells were injected into the mammary fat pad (MFP) or the right tibia of female NCr/SCID mice that received intraperitoneal injections of Bzb 3x/week at a dose of 0.3mg/kg or PBS injections (controls) following IUCAC approved procedures. Experimental groups were: 1) Bzb treatment initiated 24 hours following MDA-MB-231 cell inoculation; 2) Bzb treatment initiated 3 weeks prior to MDA-MB-231 cell inoculation, followed by withdrawal upon MDA-MB-231 cell inoculation, to assess protective effective on the skeleton; and 3) Bzb treatment initiated upon radiographic evidence of osteolytic disease as monitored by weekly radiography. At 6 or 8 weeks, tibias with tumors were examined by histology and  $\mu$ CT (Scanco, Inc) to quantify bone parameters. Tumors developed in the MFP were significantly reduced in volume in Bzb treated mice. Intratibial tumor growth progressed and osteolysis continued until the cortical bone was lost in the control mice. In contrast, osteolysis in Bzb treated mice progressed more slowly (group 1). Bzb pretreatment (group 2) resulted in significantly less bone loss compared to controls. Tumor size and osteolytic disease were reduced in the Bzb group treated after osteolytic disease was detected (group 3) compared to controls. The  $\mu$ CT images and calcein labeled bone indicated a replacement of lost bone occurred in Bzb treated mice. Additionally, examination of the contralateral tibias showed Bzb increased skeletal bone mass in mice of each treatment group. Our studies show that in the mouse, Bzb inhibits tumor growth and osteolysis and appears to regenerate lost bone. In patients with breast cancer, Bzb has the potential to increase bone renewal following tumor irradiation and can reduce osteolytic bone disease by inducing new bone formation through recruitment of progenitor cells into the osteoblast lineage as indicated by in vitro studies.

**Disclosures:** M.D. Jones, None.

## F279

**Ectopic Runx2 Expression Disrupts Normal Acini Structure in Mammary Epithelial Cells.** J. Pratap, K. Imbalzano<sup>\*</sup>, J. Underwood<sup>\*</sup>, N. Cohet<sup>\*</sup>, K. D. Veeraraj<sup>\*</sup>, A. J. van Wijnen, A. N. Imbalzano<sup>\*</sup>, J. L. Stein<sup>\*</sup>, J. B. Lian, J. Nickerson<sup>\*</sup>, G. S. Stein. Department of Cell Biology and Cancer Center, University of Massachusetts Medical School, Worcester, MA, USA.

The Runx2 transcription factor, essential for skeletal development, regulates mammary gland specific genes. Recent evidence shows that Runx2 is ectopically expressed in metastatic breast cancer cells and contributes to tumorigenic properties by increasing expression of VEGF and MMPs. To understand the role of Runx2 during early events of mammary gland formation, disruption of which results in a cancer cell phenotype, we utilized the three-dimensional culture system (20 days) of human MCF10-A normal mammary epithelial cells. These cells cultured on basement membrane (Matrigel) form polarized, growth-arrested acini-like spheroids that recapitulate in vitro several aspects of in vivo glandular architecture. We find low levels of Runx2 in nuclear extracts of MCF10A cells by EMSA and by in situ immunofluorescence. Here we show that ectopic expression of Runx2 by adenovirus in MCF10-A cells causes disruption of normal acini formation compared to controls. Ultrastructural analysis using electron microscopy revealed disorganized acini with absence of a lumen in the Runx2 overexpressed cells. We find that the disrupted structure is due to altered cell proliferation detected by increased Ki-67 staining and increased expression of cdc6, a cell proliferation marker and the anti-apoptotic marker Bcl-2. Interestingly, these disorganized structures do not show  $\beta$ 4-integrin staining indicating the loss of basement membrane. In complementary experiments, we depleted Runx2 in bone metastatic MDA-MB-231 breast cancer cells by lentiviral stable expression of shRNA-Runx2 and achieved more than 80% knockdown of endogenous Runx2. The parental MDA-MB-231 cells do not form organized acini when cultured in reconstituted basement membrane. Upon culture of MDA-MB-231-shRNA-Runx2 cells, we find a partial reversion to acini structures compared to the controls by 10 days of differentiation. In summary, our studies show that overexpression of Runx2 causes increased cell proliferation and decreased apoptosis of mammary epithelial cells in vitro and that depletion of Runx2 in cancer cells results in acquisition of the normal architecture of mammary glands. These novel findings provide direct evidence of the biological activity of Runx2 in early aspects of breast cancer progression, in addition to the Runx2 induction of metastatic genes in primary tumors. Together these findings suggest Runx2 as a potential therapeutic molecular target in breast cancer.

**Disclosures:** J. Pratap, None.

## F281

**Application of Preventive Measures Minimizes the Occurrence of Osteonecrosis of the Jaw in Patients with Bone Loss Treated with Bisphosphonates: A Single-Institution Series.** C. Ripamonti<sup>\*</sup>, M. Maniczo<sup>\*</sup>, E. Cislighi<sup>\*</sup>, T. Campa<sup>\*</sup>, E. Fagnoni<sup>\*</sup>, G. Salbene<sup>\*</sup>, C. Bareggi<sup>\*</sup>, L. Ascani<sup>\*</sup>, A. Pigni<sup>\*</sup>, C. Brunelli<sup>\*</sup>. IRCCS Foundation, National Cancer Institute of Milan, Milan, Italy.

Osteonecrosis of the jaw (ONJ) is an uncommon adverse event that has been reported in patients receiving complex cancer treatment regimens including bisphosphonates (BPs). Risk factors such as periodontal disease and dental trauma place patients at increased risk of ONJ; therefore, proactive monitoring of the oral cavity is recommended (Ruggiero et al. J Oral Maxillofac Surg. 2004;62:527-534). The occurrence rates of ONJ before and after the implementation of dental preventive measures were investigated in this study. Patients with bone loss treated with BPs and who did not receive preventive dental care ( $n = 812$ ; referred from January 1999 to February 2007; PRE group) were retrospectively compared with patients who received regular dental examinations every 6 months ( $n = 154$ ; POST group). POST-group patients received regular dental maintenance and care (dental visit  $\pm$  panoramic jaw radiograph) to assess potential dental pathologies throughout BP treatment. ONJ incidences are presented as raw percentages ([ONJ cases,  $n$ ]/[total patients,  $n$ ]  $\times$  100) and incidence rate (IR) ([ONJ cases,  $n$ ]/[monitoring time of all patients]). Differences between the PRE and POST groups were analyzed through 1-tailed Fisher's exact test and presented as IR difference (IRD) with 95% confidence interval (CI). Among 966 BP-treated patients assessed (male/female = 255/711), 73% had bone metastases from breast cancer. Patients received zoledronic acid (ZOL;  $n = 244$ ), pamidronate (PAM;  $n = 600$ ), PAM followed by ZOL ( $n = 79$ ), or clodronate (alone or with PAM;  $n = 43$ ). BPs were administered per institutional guidelines; ZOL was used per label. Overall, the observed ONJ incidence was 2.9% (ZOL/PAM + ZOL,  $n = 19$ ; PAM,  $n = 9$ ). ONJ incidence was significantly lower in the POST group ( $n = 1$ ; 0.6%) vs the PRE group ( $n = 27$ ; 3.3%) ( $P = .048$ ). Among both ZOL- and PAM + ZOL-treated patients, the incidence was significantly lower in the POST group (0.9%) vs the PRE group (8.7%) ( $P = .002$ ). For all BP-treated patients, IR of ONJ was 0.007/patient-yr for the POST group and 0.03/patient-yr for the PRE group, resulting in an IRD of 0.24 (95% CI = 0.006, 1.45). In conclusion, implementation of routine preventive measures before and during BP treatment reduced the frequency of ONJ by 76% relative to that of patients who did not receive preventive dental care. These data support the importance of preventive dental care in all patients undergoing BP treatment to maintain bone health.

**Disclosures:** C. Ripamonti, None.

## F283

**Inhibition of BMP Pathway and Osteoclast Activity in Osteoblastic Prostate Cancer Lesion in Bone.** M. S. Virk<sup>\*1</sup>, F. A. Petrigliano<sup>\*2</sup>, N. Q. Liu<sup>\*2</sup>, D. Stout<sup>\*3</sup>, A. F. Chatzioannou<sup>\*3</sup>, W. C. Dougall<sup>\*4</sup>, J. R. Lieberman<sup>1</sup>. <sup>1</sup>Orthopaedic Surgery, UCHC, Farmington, CT, USA, <sup>2</sup>Orthopaedic Surgery, UCLA, Los Angeles, CA, USA, <sup>3</sup>Pharmacology, UCLA, Los Angeles, CA, USA, <sup>4</sup>Amgen Inc., Seattle, WA, USA.

The purpose of this study was to investigate the influence of inhibition of BMP activity and osteoclast activity on the development and progression of an osteoblastic prostate cancer lesion in a murine model of bone metastasis. A total of 45 male SCID mice tibias were implanted with 200,000 human prostate cancer cells (LAPC-9) and divided into five groups. Osteoclast activity was inhibited with recombinant RANKL antagonist (RANK: Fc) and BMP inhibition was achieved by ex-vivo transduction of LAPC-9 cells with retrovirus expressing a BMP antagonist, noggin (RN). Group I: RANK: Fc treatment; Group II: Retronoggin treatment; Group III: combined treatment; Group IV: cells alone (control); Group V: empty vector control. Radiographs, hind limb measurements, micro PET-CT (<sup>18</sup>F- fluorodeoxyglucose [FDG] and <sup>18</sup>F-fluoride), and histology were performed at 2, 4 and 5 weeks. Osteoblastic lesions were present on radiographs in control groups (IV and V) & Group I tibias at 4 wks. However, blastic lesions were first detected in Group II & III tibias at 5 wks and these lesions were limited to the proximal tibia. The blastic lesions were quantified on microCT, which demonstrated a lower (p<0.001) percentage increase in bone volume in Group II & III but not in Group I tibias (p>0.05) at 4 & 5 wks compared to the controls. Micro PET with FDG, which correlates with glucose metabolism demonstrated significantly smaller signal volumes (p<0.001) in Group II & III tibias at 4 and 5 wks compared to the control animals. Hind limb measurements were smaller (p<0.001) in Group II & III tibias but not in Group I tibias (p>0.05) compared to the control group tibias at 2 and 4 wks. Serial micro PET scans with <sup>18</sup>F-fluoride tracer demonstrated a lower percentage difference in maximum fluoride signal intensity (p<0.05) in Group II & III tibias but not in Group I tibias (p>0.05) compared to the control group tibias at 2 and 4 wks. Histomorphometric analysis demonstrated a lower (p<0.001) bone area/tissue area in Group II & III tibias but not in Group I tibias (p>0.05) when compared to the control tibias. The number of osteoclasts/mm were significantly lower (p<0.001) in Group I & III tibias compared to the control group tibias. BMP inhibition by noggin delayed the development and progression of osteoblastic lesions. However, inhibiting osteoclast activity did not have a significant effect on the development or progression of osteoblastic lesion. Combined inhibition of BMPs and osteoclast activity was not superior to inhibition of BMPs alone in delaying the progression of osteoblastic prostate cancer lesions in this model.

**Disclosures:** M.S. Virk, None.

This study received funding from: NIH.

## F286

**Novel Splicing Variants of ADAM8 Stimulate Tumor-Induced Bone Metastasis by Increasing Invasion and Osteoclastogenesis.** I. Hernández<sup>\*1</sup>, J. L. Moreno<sup>2</sup>, C. Zandueti<sup>\*1</sup>, L. Montuenga<sup>\*1</sup>, F. Lecanda<sup>1</sup>. <sup>1</sup>Division of Oncology, Center for Applied Medical Research, Pamplona, Spain, <sup>2</sup>Orthopaedics, University of Maryland School of Medicine, Baltimore, MD, USA.

ADAMs (a disintegrin and metalloprotease) are type I transmembrane proteins involved in morphogenesis, cell proliferation, differentiation, migration, adhesion, fusion, and tumorigenesis. They form a large family of cell-surface proteins, characterized by containing a disintegrin domain displaying adhesive properties and a metalloproteinase domain with proteolytic activity. ADAM8 is highly expressed in osteoclast precursors and induces leukocyte adhesion and migration. Recently it has been associated with poor prognosis of lung cancer. To gain insight in the function of ADAM8 in the context bone metastasis, we screened a panel of lung cancer cell lines by RT-PCR. ADAM8 was downregulated in lung cancer cell lines as compared to normal epithelium cells (NHBE). However, several splicing isoforms were differentially upregulated in tumor cells vs NHBE. These data were confirmed by western blot analysis in cell lysates. We cloned and sequenced several new splicing isoforms. Two of them, Δ18a and Δ14', both lacking their transmembrane and cytoplasmic domains, were present in several tumor cell lines but they were expressed at low levels in normal NHBE. Only retroviral overexpression of Δ18a in two lung cancer cell lines showed enhanced invasive activity as compared to mock cells (p<0.001). Interestingly, ADAM8-shRNA markedly decrease invasive activity as compared to mock cells (p<0.05). In conditions that mimic the bone-marrow microenvironment by coculture of lung cancer cells with ST-2 stromal cell line, expression levels of ADAM8 and Δ14' isoform were markedly increased. Moreover, addition to osteoclast cultures of cell free supernatants from Δ14' overexpressing cells only, and not Δ18a or wild type, resulted in a significant increase in the area of TRAP+ cells in vitro (p<0.01). Furthermore, in a murine model of bone metastasis, intracardiac inoculation lung cells overexpressing Δ14' induced an increase in prometastatic activity with high tumor burden as assessed by X-Ray image analysis (p<0.05) and μCT scans. These data indicate that the expression of different truncated forms of ADAM8 by lung cancer cells may result in the specific up-regulation of their invasive and osteoclastogenic activity in the bone microenvironment. These findings suggest a novel mechanism of tumor-induced osteolysis in bone metastatic colonization.

**Disclosures:** I. Hernández, None.

## F288

**Role of Fibroblast Activation Protein (FAP) and Dipeptidyl Peptidase (DPP4) in Myeloma Bone Disease and Tumor Growth.** A. Pennisi<sup>\*1</sup>, X. Li<sup>\*1</sup>, D. Gaddy<sup>2</sup>, N. Akel<sup>\*2</sup>, N. Aziz<sup>\*3</sup>, S. Yaccoby<sup>1</sup>. <sup>1</sup>MIRT, UAMS, Little Rock, AR, USA, <sup>2</sup>Department of Physiology and Biophysics, UAMS, Little Rock, AR, USA, <sup>3</sup>Point Therapeutics, Wellesley Hills, MA, USA.

Fibroblast activation protein (FAP) and dipeptidyl peptidase 4 (DPP4) are related serine proteases which have been implicated as tumor microenvironmental factors. We found that these proteases were not expressed by myeloma (MM) cells, however, while DPP4 was highly expressed by osteoclasts, FAP was one of few genes consistently upregulated in osteoclasts after co-culture with MM cells. Inhibition of FAP in MM-osteoclast co-cultures using siRNA attenuated osteoclast-induced MM cell survival (*Ge et al., BJH 2006*). The aim of the study was to investigate the effect of two FAP/DPP4 inhibitors, PT-100 and PT-630, on MM cell growth and osteoclastogenesis in. Ex vivo MM cells from 6 patients were co-cultured with osteoclasts and treated with PT-100 or PT-630 (0.1-100 μM) for 7 days. Whereas PT-100 inhibited MM cell growth in all tested doses by 43%-72% (p<0.002 vs. 100 μM), PT-630 inhibited MM cell growth in a dose dependent manner reaching 49% growth inhibition with 100 μM (p<0.02). These compounds had no direct effect on MM cell growth, suggesting that FAP-induced MM cell survival depends on close contact between MM cells and osteoclasts. MMP-2 and MMP-9 have been associated with tumor metastasis and FAP activity. MMP-2 but not MMP-9 was reduced in co-culture conditioned media by 44±7% (p<0.04) following treatment with PT-100 while PT-630 had no significant effect. PT-100 and PT-630 inhibited formation of multinucleated osteoclasts by 70±4% (p<0.001) and 56±6% (p<0.003) respectively, through a mechanism involving reduced p38 MAPK activity. These compounds also reduced resorption pit area by osteoclasts on dentine slices by 92% (p<0.01) and 69% (p<0.04) respectively, indicating that reduced osteoclast differentiation by these compounds was accompanied by reduced resorption activity. In vivo, SCID-hu mice engrafted with MM cells from 5 patients were treated with PT-100 and PT-630. Overall, PT-100 and PT-630 reduced MM growth by 51% (p<0.05) and 66% (p<0.05) respectively. Bone mineral density (BMD) measurements of the myelomatous bone revealed prevention of bone loss by PT-100 or PT-630 (p<0.05). These agents markedly reduced number of multinucleated osteoclasts (p<0.02) but had no effect on number of osteoblasts in myelomatous bones. We conclude that FAP/DPP4 are involved in MM osteolysis and tumor growth and thus approaches to inhibit activity of these serine proteases in myelomatous bone may help control MM and its associated bone disease.

**Disclosures:** A. Pennisi, None.

This study received funding from: NCI, Point Therapeutics.

## F291

**Identification of RhoB as a Key Target Involved in Cell Motility and Bone Metastasis.** D. Luis-Ravelo<sup>\*</sup>, I. Antón<sup>\*</sup>, S. Vicent<sup>\*</sup>, I. Hernández<sup>\*</sup>, C. Zandueti<sup>\*</sup>, J. Agorreta<sup>\*</sup>, M. J. Pajares<sup>\*</sup>, L. Montuenga<sup>\*</sup>, F. Lecanda. Division of Oncology, University of Navarra, Pamplona, Spain.

Lung cancer disseminates to a variety of organs including the skeleton. This process is associated with significant morbidity and dismal prognosis. The aim of this study was to identify and functionally characterize key target genes involved in the deleterious process of bone metastasis. Using an in vivo model of bone metastasis after intracardiac inoculation (i.c.) of a lung cancer cell line, we isolated highly metastatic subpopulations (HMS) derived from parental cells. Transcriptomic profiling and robust bioinformatics analysis identified RhoB as a significant overexpressed gene in HMS. Rho B is a membrane associated GTPase involved in cell transformation, survival, stress fiber formation and angiogenesis. RhoB was validated by real-time RT-PCR and Westernblot analysis in HMS. To delineate its functional role in bone metastasis, we lentivirally transduced lung cells with several shRNA against RhoB (shRhoB). Westernblot analysis showed abrogation of RhoB levels as compared to scramble control cells. Cell proliferation in vitro was unaffected in shRhoB and scramble transduced cells. Interestingly, chemotactic assay in Boyden chamber showed a dramatic decrease in motility of shRhoB cells as compared to control cells (p<0.001), whereas RhoB overexpressing cells showed increased motility, consistent with its role in cytoskeletal remodelling. Conditioned media of shRhoB or RhoB overexpressing cells did not show any difference in their proosteoclastogenic or metalloproteolytic activities in vitro. Interestingly, i.c. inoculation of shRhoB cells in nude mice induced a dramatic decrease in their prometastatic activity, including a severe reduction of osteolytic lesions and tumor burden (p<0.01), assessed by X-ray image analysis, bioluminescence imaging, and μCT scans, as compared to control cells. Finally, to assess the relevance of these findings, immunohistochemical analysis of RhoB in a panel of human lung tumor samples revealed significant decrease in survival by Kaplan Meier curves in patient lung cancer biopsies with high RhoB as compared to low RhoB staining (log Rank test p<0.01). Taking together these data indicate that RhoB plays a critical role in bone metastasis, by increasing motility and promoting bone colonization. These data suggest that Rho B may represent a good prognosis marker in lung cancer and a potential therapeutic target in bone metastasis progression.

**Disclosures:** D. Luis-Ravelo, None.

This study received funding from: FIS & RTICC.

## F293

**Blocking TGF $\beta$  Signaling Reduces Gammopathy and Improves Bone Volume and Strength In Vivo.** A. J. Hart\*, J. A. Fowler, S. T. Lwin\*, S. A. Munoz\*, E. C. O'Quinn\*, J. S. Nyman, C. M. Edwards, G. R. Mundy. Vanderbilt Center for Bone Biology, Vanderbilt University, Nashville, TN, USA.

Bone disease caused by multiple myeloma (MM) results not only from increased osteoclast-mediated bone resorption, but also a marked impairment of bone formation by osteoblasts. Since TGF $\beta$  suppresses osteoblast differentiation in vitro, and blocking TGF $\beta$  signaling with a receptor kinase inhibitor antagonizes the inhibitory action of MM-cell conditioned media on osteoblasts, we hypothesized that inhibition of TGF $\beta$  would have beneficial effects on MM progression in vivo. To study this, we chose the 5T Radl murine model of myeloma, and the 1D11 monoclonal antibody (Genzyme) that has been shown to effectively block all three TGF $\beta$  ligands. We show that blocking TGF $\beta$  in vivo reduces MM serum paraprotein levels and significantly improves bone volume and strength. Fourteen Rag2<sup>-/-</sup> mice were injected with 1x10<sup>6</sup> 5TGM1 myeloma cells and monitored for the development of gammopathy. Starting on the day of MM cell injection, mice were injected IP every three days with 10mg/kg 1D11, or a control antibody, 13C4. At 22 days following tumor cell inoculation, there was a significant decrease in IgG2b levels in mice treated with 1D11 compared to 13C4, indicating a protective effect of anti-TGF $\beta$  treatment against MM progression. Examination of the bones by  $\mu$ CT after sacrifice showed a significant improvement in BV/TV, trabecular number, and cortical bone thickness in mice treated with 1D11 compared to 13C4. There was also a significant improvement in biomechanical parameters including stiffness, bending strength, and maximum force needed to fracture the bone when tested using three point bending. Thus, we have shown that anti-TGF $\beta$  therapy reduces paraprotein levels and improves bone volume and strength. We propose, based on these preclinical data, that anti-TGF $\beta$  therapy is worthy of evaluation in a prospective clinical trial in patients with MM.

**Disclosures:** A.J. Hart, None.

## F297

**Effects of Odanacatib on Bone Biomarkers in Ovariectomized Non-Human Primates.** G. A. Wesolowski, M. Pickarski, L. T. Duong. Molecular Endocrinology, Merck & Co., Inc, West Point, PA, USA.

Odanacatib (ODN) is a selective and reversible inhibitor of cathepsin K (Cat K) currently being developed for the treatment of osteoporosis. Other evidence on efficacy of ODN for the prevention of bone loss in the ovariectomized (OVX) rhesus monkey study has been reported [1, 2]. Female rhesus monkeys (12-19 yr-old) were ovariectomized or left intact, and assigned into four groups: Intact, OVX, OVX+6 and 30 mg/kg ODN. ODN was dosed, orally daily, in prevention mode. At 21 months, OVX-induced loss in bone mineral density at the spine and hip were shown to be fully protective by both doses. This study monitors the changes in bone turnover markers for the duration of treatment. Serum or urine collected at baseline, 6, 15, 27, 40, 48, 59, 72 and 91 weeks are analyzed for resorption markers, C-telopeptide of Coll (sCTX), N-telopeptide (uNTX) and total deoxypyridinoline (uDPD); and formation markers N-propeptide of Coll (sP1NP) and bone specific alkaline phosphatase (sBSAP). Two exploratory markers were assayed, tartrate resistant acid phosphatase (TRAP5b) as a marker for osteoclast number, and C-terminal peptide of Coll (ICTP), a marker generated by metalloproteinases and degraded by Cat K. CTX, NTX and DPD were increased 60, 100 and 80% above baseline respectively by week 6 in OVX, and gradually returned to baseline by week 72. All resorption markers were dose dependently restored to or below sham levels by ODN. TRAP5b was increased in OVX to 220% above baseline and remained elevated throughout the study. Unlike current antiresorptive therapies, ODN did not suppress TRAP5b, similar to what was observed in Cat K knock-out mice, suggesting pharmacological inhibition of Cat K had no effect on osteoclast formation or survival. Bone formation markers responded to OVX more slowly than resorption markers, reaching significance by 15 weeks post-OVX compared to sham. P1NP and BSAP peaked by 267% and 75% respectively, above baseline; and ODN treatment restored these markers to levels consistent with sham. ICTP is normally undetectable in post-menopausal women and not responsive to bisphosphonates. In monkeys, this marker also did not respond to OVX; however, as a direct substrate of Cat K, ICTP was dose dependently increased 50 and 100% by 6 and 30 mg/kg ODN respectively versus baseline, providing evidence of ODN engagement of Cat K. Together with the reported efficacy of ODN in prevention of BMD loss in the same study [2], here we show that ODN restored markers of bone resorption and formation to normal sham levels, further demonstrating ODN is a novel antiresorptive in blocking estrogen deficiency induced bone loss with no apparent effect on osteoclast number. [1] Masarachia et al, ASBMR, 2007, S126; [2] Cusick et al ASBMR, 2008 (submitted)

**Disclosures:** G.A. Wesolowski, Merck & Co., Inc 3.

## F301

**The Relationship of Urinary Excretion of C-Telopeptides to Growth in Children.** F. Gossiel<sup>\*1</sup>, R. A. Hannon<sup>1</sup>, N. J. Bishop<sup>2</sup>, P. Dimitri<sup>\*2</sup>, R. Eastell<sup>1</sup>. <sup>1</sup>Academic Unit of Bone Metabolism, University of Sheffield, Sheffield, United Kingdom. <sup>2</sup>Academic Unit of Child Health, University of Sheffield, Sheffield, United Kingdom.

The DG motif of the CTX epitope <sup>1207</sup>EKAHGDDR<sup>1214</sup> exists in the  $\alpha$  form in newly synthesised collagen. It undergoes non-enzymatic  $\beta$  isomerisation as collagen ages. Measurement of  $\alpha$ CTX and  $\beta$ CTX may allow us to distinguish between bone turnover in newly synthesised and mature bone.

The aims were a) to investigate the relationship between the ratio of  $\alpha$ - and  $\beta$  CTX fragments to age, and height velocity in children, b) to compare this to the ratio found in premenopausal women.

48 healthy boys and girls (mean age 10.5 years; range 4.3 to 16.6 years) were recruited. Height was measured at baseline and again 1 year later in a subset of 25 children and height velocity was calculated. 75 healthy premenopausal women (mean age 38 years; range 30 to 45 years) were also recruited. Second morning void urine samples were collected from all subjects at baseline.

$\alpha$  and  $\beta$  CTX were measured in urine (Alpha and Beta Crosslaps ELISA (Nordic Biosciences Diagnostics a/s, Copenhagen, Denmark)).

$\alpha$  and  $\beta$  CTX and  $\alpha/\beta$  CTX ratio decreased with age in children ( $\alpha$ CTX  $r = -0.46$ ,  $P < 0.001$ , 95% CI -0.66 to -0.21,  $\beta$ CTX  $r = -0.46$ ,  $P < 0.001$ , 95% CI -0.66 to -0.20;  $\alpha$ CTX /  $\beta$ CTX ratio  $r = -0.36$ ,  $P < 0.05$ , 95% CI -0.58 to -0.01).

In the subset of children  $\alpha$  and  $\beta$  CTX and  $\alpha/\beta$  CTX ratio significantly predicted height velocity, ( $\alpha$ CTX  $r = 0.68$ ,  $P < 0.001$ , 95% CI 0.36 to 0.85;  $\beta$ CTX  $r = 0.50$ ,  $P < 0.05$ , 95% CI 0.10 to 0.76;  $\alpha/\beta$  CTX ratio  $r = 0.72$ ,  $P < 0.0001$ , 95% CI 0.46 to 0.87).

	Children	Adults
$\alpha$ CTX ng/ml, median (CI)	11.5 (9.1-12.3)	0.29 (0.25-0.34)
$\beta$ CTX ng/ml median (CI)	12.2 (9.7-14.3)	1.47 (1.31-1.84)
$\alpha/\beta$ CTX ratio median (CI)	0.89 (0.80-0.96)	0.20 (0.19-0.21)

The median and 95% confidence interval (CI) of the urinary CTX measurements

We conclude  $\alpha$  and  $\beta$  CTX and the  $\alpha/\beta$  CTX ratio in the children are related to growth.  $\alpha$ CTX and the  $\alpha/\beta$  CTX ratio are more strongly associated and are better predictors of height velocity than  $\beta$ CTX, a marker of the degradation of mature collagen. The alpha/beta ratio was 4 times higher in children compared to adults, as this reflect the high level of degradation of immature collagen during growth.

**Disclosures:** F. Gossiel, None.

## F306

**Age Is the Key to Assessing Fracture Risk: FRAX.** C. Greenbaum\*, M. Greenwald. Desert Medical Advances, Palm Desert, CA, USA.

The World Health Organization (WHO) has developed FRAX, a computer model to estimate the risk of fracture using the density measurement and 10 clinical risk factors. Ideally the radiologic technician would enter this information into the computer program and relate the risk of fracture to the patient. In practice, the radiologic tech may not have medical history, other than age and sex. In a community osteoporosis program, we evaluated consecutively 97 men and 200 women naïve to prior osteoporosis treatment, and compared the results in two formats, using BMD and age, versus FRAX with all 10 clinical risk factors.

The average age of the women was 67 (range 55-96) and the average age of the men was 73 (range 55-96) and all were Caucasian. The bone density measurement evaluated was the femoral neck and the clinical risk factors were collected by questionnaire. Diagnostic threshold and intervention threshold was based on a 4% ten year risk of hip fracture. Using this cutoff, the diagnostic agreement was very high between the two formats. In women, the concordance between the two formats was 97.5% and in men the concordance between the two formats was 92%.

	Osteoporosis Treatment Indicated		
	FRAX (BMD+age)	FRAX (BMD+10 risks)	Agreement
Women (n=200)	59	64	97.5%
Men (n=97)	23	32	92%

Of interest, using bone density alone and no risk factors (assuming a threshold of -2.5 T score for the bone density) only 31 women were identified for treatment and only 11 men. The practical conclusion to this community screening program is that bone density measurement and age will approximate the FRAX diagnosis with all 10 risk factors and that a significant percentage will be more correctly assessed at risk and identified for treatment. This finding concurs with the finding that the current standard basing treatment decisions on bone mineral density alone has proven to be specific but not sensitive for the identification of patients at high risk of fracture. In NORA, nearly 50% of postmenopausal women in the community over the age of 50 years who developed a hip fracture were not identified by the BMD test (J Bone Miner Res 2004 Aug;19(8):1215-20).

**Disclosures:** M. Greenwald, None.

## F308

**Treatment Threshold in Men on Androgen Deprivation Therapy: T-score vs. FRAX.** R. A. Adler. Endocrinology, McGuire Veterans Affairs Medical Center, Richmond, VA, USA.

Men treated with androgen deprivation (ADT) for prostate cancer are at risk for osteoporosis and fracture. Which men should be treated with bisphosphonates? The new FRAX calculator uses secondary osteoporosis as a risk factor only if femoral neck bone density (BMD) is not available. We compared FRAX with and without femoral neck BMD in 115 consecutive men screened because of ADT (46 Caucasian, 67 African-American, 2 other). We used default settings on a Hologic Discovery densitometer (ethnicity-adjusted male database) to measure spine, hip, and forearm BMD. Using spine, total hip, and femoral neck only, 18 men had osteoporosis and 67 had osteopenia or low bone mass. Adding total forearm increased the number with osteoporosis to 39. Calculating FRAX using weight and height and checking off "secondary osteoporosis," 57 men met criteria for bisphosphonate treatment (at least 3% hip fracture or 20% osteoporotic fracture risk within 10 years). Of the 57, osteoporosis was found in 12 (spine and hip) or 29 (spine, hip,

or forearm). 8 men meeting FRAX criteria had normal BMD at all sites. We attempted to calculate FRAX with the femoral neck T-score, but FRAX uses a female normative database. Thus, to use the male database T-score, we adjusted it by 0.3 for Caucasian and 0.5 for African-American men. Calculating FRAX with the femoral neck BMD, only 12 men were recommended for treatment. Of these, only 5 had osteoporosis; the rest had osteopenia. Seven men with osteoporosis (spine and hip) and 4 men with osteoporosis (spine, hip, forearm) did not meet criteria for treatment with either FRAX calculation. Because we used an ethnicity-adjusted normative database for the T-scores, we analyzed only the white men and found similar results.

We conclude that while FRAX may turn out to be very useful for men in general, the specific group of men treated with ADT may need to be judged on clinical grounds and BMD for treatment decisions. Similar to previously reported results, adding forearm bone density increases the detection of osteoporosis in ADT patients. FRAX based on weight, height, and secondary osteoporosis may identify additional men who are at risk for fracture, despite normal BMD. Recalculating FRAX using a female database T-score (rather than the arbitrary adjustment to the male T-score we used) may improve the fracture risk prediction. Without fracture outcome studies in ADT patients, clinicians will need to use BMD, fall risk assessment, and possibly FRAX to identify those men who will likely benefit from bisphosphonate therapy.

**Disclosures:** R.A. Adler, None.

## F310

**Bone Mineral Density Shows no Peak from Birth to Youth as Measured by Quantitative Computed Tomography.** E. M. Hauge<sup>1</sup>, J. S. Thomsen<sup>2</sup>, A. Brüel<sup>2</sup>, K. Brixen<sup>3</sup>, A. Vesterby<sup>4</sup>, F. Melsen<sup>1\*</sup>. <sup>1</sup>Department of Rheumatology, Aarhus University Hospital, Aarhus C, Denmark, <sup>2</sup>Institute of Anatomy, Aarhus University, Aarhus C, Denmark, <sup>3</sup>Department of Endocrinology, Odense University Hospital, Odense, Denmark, <sup>4</sup>Institute of Forensic Medicine, Aarhus University, Aarhus C, Denmark.

Peak bone mass is a major determinant of fracture risk in senescence. Most of the growth-related increase in bone mineral density (BMD) as assessed by dual-energy X-ray absorptiometry (DXA) is due to an increase in bone size. In contrast to the area-dependent DXA-BMD, quantitative computed tomography (QCT) supplies a volumetric measurement of BMD, which is not influenced by bone size. Although DXA-BMD and QCT-BMD are correlated, data suggests that changes in QCT-BMD during growth differ from the increases seen in DXA-BMD.

We investigated the age-related changes in BMD measured in vitro by DXA and QCT using second lumbar vertebral bodies obtained during routine autopsy procedures, as approved by the regional ethical committee. The study comprised 126 individuals (53 women and 73 men) with an age range of 0.2-95 years and a median age of 60.5 years. The studied individuals had died suddenly from accidents or acute diseases. Individuals with known malignant, renal, or metabolic bone diseases were excluded as were vertebral bodies with fractures. The vertebral bodies were scanned with a Hologic Discovery A DXA-scanner and a Stratix XCT 960A pQCT scanner at a voxel size of 0.689x0.689x1 mm. Data were analyzed by linear regression, and reported as the squared Pearson correlation coefficient ( $r^2$ ) and the slope of the regression line (B) with its statistical significance (p).

Peak bone mass was reached at the age of approximately 25 years. During bone growth (0-25 years) DXA-BMD increased in both females ( $r^2$ : B, p) (0.99; 63 g/cm<sup>2</sup>/year, p<0.001) and males (0.61; 45 g/cm<sup>2</sup>/year, p<0.001). In contrast, QCT-BMD remained constant during the period from birth to peak bone mass, and was therefore not correlated with age neither in females (0.12; 0.10 mg/cm<sup>3</sup>/year, p=0.50) nor in males (0.08; -0.10 mg/cm<sup>3</sup>/year, p=0.31). After peak bone mass was reached, DXA-BMD decreased significantly with age for women (0.57; -142 g/cm<sup>2</sup>/year, p<0.001) and men (0.18; -106 g/cm<sup>2</sup>/year, p<0.01). This senescent decrease in DXA-BMD was paralleled by decreases in QCT-BMD for both women (0.63; -0.32 mg/cm<sup>3</sup>/year, p<0.001) and men (0.43; -0.38 mg/cm<sup>3</sup>/year, p<0.001). The discrepancy between BMD assessed by DXA and QCT confirms the confounding of bone geometry in DXA-scans. QCT may better reflect the mineral density of architecturally intact bone without being influenced by bone size. This is of particular importance when studying mineral density during bone growth, where the skeletal geometry changes substantially.

**Disclosures:** E.M. Hauge, None.

## F312

**Assessment of Absolute Fracture Risk and Osteoporosis in Chinese: Is There Any Difference Between the Application of Chinese Normative Database and NHANES III Caucasian Database?** E. Y. W. Chu\*, S. W. Y. Tsang\*, A. W. C. Kung. Medicine, The University of Hong Kong, Hong Kong, China.

WHO and ISCD recommend the use of a uniform Caucasian (non-race adjusted) female normative database for women of all ethnic groups as reference for BMD T-scores determination and fracture risk assessment. The objectives of the study were (1) to compare the Southern Chinese and NHANES III normative database in identifying subjects with osteoporosis and fractures in postmenopausal Southern Chinese women in Hong Kong; and (2) to examine the relation of BMD thresholds and clinical risk factors (CRF) evaluation and incident osteoporosis fracture rate and hip fracture rate. 2226 postmenopausal Hong Kong Southern Chinese women aged 45 and above were prospectively followed for incident low trauma fracture. Bone mineral density (BMD) was determined at the hip and spine by dual-energy X-ray absorptiometry (DXA). New fractures were recorded and verified by either retrieval of x-ray report or from the

computerised patient record system of the Hospital Authority of the Hong Kong Government.

The mean age at baseline was 62.1 ± 9.3 yr. After 4.3 ± 2.2 yr (range 3-12 yr) of follow-up, 137 new osteoporotic fractures were reported. Compared to Southern Chinese database, NHANES III Caucasian female database at the femoral neck overestimated the percentage of women with osteoporosis (18.2% vs 28.8%). However, the overall osteoporotic fracture rate and hip fracture rate were similar between the two reference databases. Although fracture rates were highest in women with femoral neck BMD T-score ≤ -2.5 SD, these women only experienced 56% of the osteoporotic fractures and 61% of the hip fractures. Addition of one or more CRF (>65 yr of age, BMI <19, previous fracture, 1 or more falls in the past 12 months, exercise <30min/day) improved the detection rate of osteoporotic fractures to 80% and hip fractures to 88%. Lowering the BMD T score threshold to -2.0 together with CRF further increased the detection rates to 86% and 91% respectively. The NHANES III Caucasian database can be applied to Southern Chinese for absolute fracture risk assessment. BMD T-score threshold at -2.0 together with CRF assessment could identify the majority of women at high risk of osteoporotic fracture.

**Disclosures:** S.W.Y. Tsang, None.

## F315

**Evaluating Bone Microstructure at the Distal Tibia in Children: An X-treme CT Study.** M. Burrows<sup>1</sup>, D. Liu<sup>\*1</sup>, Y. Ahamed<sup>\*1</sup>, S. Braid<sup>1</sup>, H. A. McKay<sup>2</sup>. <sup>1</sup>Dept of Orthopaedics, University of British Columbia, Vancouver, BC, Canada, <sup>2</sup>Dept. of Orthopaedics and Family Practice, University of British Columbia, Vancouver, BC, Canada.

A high resolution pQCT system permitting in vivo assessment of bone architecture has been developed (X-tremeCT, Scanco). X-tremeCT reference data is available for adults but not for children. Our aim was to develop reference data for X-tremeCT in children. We assessed the distal tibia with the X-treme CT at the 8% site in a cross-section of 77 girls and 94 boys (14-18 years). We provide data for cortical bone density (D.Cort, mg/cm<sup>3</sup>), trabecular bone density (D.Trab, mg/cm<sup>3</sup>), cortical thickness (Cort.Th, mm), total bone volume (BV/TV, 1), trabecular number (Tb.N, 1/mm), trabecular thickness (Tb.Th, mm), trabecular separation (Tb.Sp, mm) and inhomogeneity of the network (Tb.Sp SD, mm). Means and standard deviations are provided for sex and age (Tables 1 and 2). We used two-way ANOVA to test for main effects by age group and age-by-sex interactions (p<0.05). Within sexes, D.Cort was significantly greater for girls and boys across age (p<0.01). D.Trab increased significantly for girls and boys between 14 and 17-18 yrs (p<0.01). Cort.Th did not increase significantly in girls, but was increased significantly in boys across age (p<0.01). BV/TV increased significantly for girls from age 14 to 15-16 years (p<0.05) but was stable in boys. Tb.N, Tb.Th, Tb.Sp and Tb.Sp SD did not change significantly across age in boys or girls (p>0.05). Between the sexes, D.Cort was significantly greater for girls (p<0.01) compared with boys at all ages. Cort.Th was greater for girls at ages 14 and 15-16 years, after which boy's Cort.Th was significantly greater (p<0.01). We provide novel bone microstructure data for boys and girls using X-treme CT.

**Table 1.** Cortical, trabecular bone density and cortical thickness at the distal tibia (Mean(SD))

Group	n	Age (yr)	Height (cm)	Weight (kg)	D.Cort (mg/cm <sup>3</sup> )	D.Trab (mg/cm <sup>3</sup> )	Cort.Th (mm)
<b>Girls</b>							
14	13	14.2 (.1)	158.2(7.0)	46.6(8.1)	770.6(35.6)	172.4(25.7)	.8(.1)
15-16	41	15.3 (.5)	161.1(7.3)	54.7(8.3)	844.4(41.1)	189.8(26.0)	1.1(.2)
17-18	23	17.9 (.4)	162.0(5.1)	56.7(9.2)	882.1(24.7)	194.6(34.5)	1.2(.2)
Total	77						
<b>Boys</b>							
14	23	14.2(0)	166.2(1.0)	56.8(13.4)	707.9(75.8)	171.3(5.5)	.7(.3)
15-16	41	15.1 (.5)	170.4(7.2)	62.2(13.6)	771.1(51.6)	198.2(27.0)	.9(.2)
17-18	30	17.8(.5)	174.9(6.4)	71.4(10.7)	859.4(26.6)	206.3(29.4)	1.4(.2)
Total	94						

**Table 2.** BV/TV ratio, trabecular number (Tr.N, mm), thickness (Tb.Th, mm), separation (Tb.Sp, mm) and spatial density (Tb.Sp.SD) at the distal tibia (Mean(SD))

Group	n	Age (yr)	BV/TV (1)	Tb.N (mm)	Tb.Th (mm)	Tb.Sp (mm)	Tb.Sp SD (mm)
<b>Girls</b>							
14	13	14.2 (.1)	.09(.02)	1.37(.25)	.06(.01)	.66(.08)	.33(.04)
15-16	41	15.3 (.5)	.15(.02)	1.66(.23)	.09(.01)	.51(.08)	.23(.05)
17-18	23	17.9 (.4)	.16(.02)	1.72(.25)	.09(.01)	.49(.09)	.22(.04)
Total	77						
<b>Boys</b>							
14	23	14.2(0)	.14(.01)	1.66(.14)	.08(.01)	.51(.04)	.23(.02)
15-16	41	15.1 (.5)	.16(.02)	1.82(.29)	.09(.01)	.47(.08)	.21(.04)
17-18	30	17.8(.5)	.17(.02)	1.91(.28)	.09(.01)	.45(.09)	.21(.07)
Total	94						

**Disclosures:** M. Burrows, None.

## F317

**Measurement of T2\* Relaxation Time of the Trabecular Bone Network at 7T and 3T Compared to Topological and Structural Measurements from HR-pQCT.** R. Krug\*, A. J. Burghardt, A. S. Issever\*, M. Kentenich\*, G. Diederichs\*, T. M. Link, S. Majumdar. Radiology, UCSF, San Francisco, CA, USA.

In recent years, magnetic resonance imaging (MRI) has become increasingly the method of choice to assess bone architecture in vivo non-invasively and without ionizing radiation. In addition to resolve the trabecular microarchitecture directly by using high-resolution MRI, indirect methods like T2\* measurements can also be used. This method takes advantage of induced magnetism between the more diamagnetic bone and the bone marrow interface leading to signal cancellations. Thus, T2\* is expected to be very closely related to topological and structural bone properties. Previously, T2\* measurements were conducted at 1.5T of human vertebral bone specimens in vitro revealing a strong positive association between 1/T2\* and bone mineral density (BMD) measured by QCT. However, there is strong evidence that trabecular bone strength is a function of the bone's architectural make-up, rather than merely BMD. The relationship between T2\* measurements of trabecular bone and structural as well as topological parameters obtained from very high-resolution images has not yet been investigated.

In this work, we hypothesized that T2\* is more strongly related to topological and structural parameters than BMD and that new clinical ultra-high field MRI at 7T might have some advantages over lower field strength regarding T2\* measurements. To this end, we measured the T2\* relaxation time of trabecular bone at the wrist from five intact human cadaver hand specimens at both 7T and 3T MRI and compared the obtained results with structural and topological measurements using a new in vivo 3D high-resolution peripheral quantitative micro-CT (HR-pQCT) modality (isotropic voxel size of 41µm).

Highest correlations (R>0.7) were found for trabecular spacing and for the structure model index (SMI) which is a metric for topological classification. Correlations for BMD were significantly lower and very low for trabecular thickness. All correlations were significantly higher for 7T than for 3T. The correlation of T2\* between both field strengths was very high (R=0.98) and the absolute T2\* values were significantly lower at 7T. Our results indicated that T2\* measurement of bone density are well suited at ultra high field strength and correlate highly with topological and structural parameters as measured from HR-pQCT at high, isotropic resolution. The high correlations reflect the closer relationship of T2\* to bone structure than to BMD. Thus, T2\* has the ability to provide additional topological and structural information as compared to only BMD measurements.

**Disclosures:** R. Krug, None.

## F319

**Osteoporosis Risk Assessment: A Composite Index Combining Clinical Risk Factors and Biophysical Parameters.** M. Rachidi\*<sup>1</sup>, F. Richard\*<sup>2</sup>, H. Bierme\*<sup>2</sup>, C. Roux\*<sup>3</sup>, P. Fardellone\*<sup>4</sup>, E. Lespessailles<sup>5</sup>, C. Chappard<sup>1</sup>, C. Benhamou<sup>1</sup>. <sup>1</sup>CHR Orleans - IPROS, INSERM Unit 658, Orleans, France, <sup>2</sup>University Paris Descartes, MAP5, CNRS UMR 8145, Paris, France, <sup>3</sup>Rheumatology Service, Cochin Hospital, Paris, France, <sup>4</sup>INSERM Unit ERI 12, Amiens, France, <sup>5</sup>Rheumatology Service, IPROS, Orleans Hospital, Orleans, France.

The objective of this work was to develop a composite index including clinical risk factors, bone mineral density (BMD) and bone micro-architecture analysis to evaluate osteoporosis fracture risk in post-menopausal women. The protocol was a multi-center cross sectional case-control study of 169 healthy postmenopausal women without fracture and 122 age-matched women with osteoporotic fractures (20 hip, 41 vertebrae, 32 wrist and 29 other fractures). BMD was measured at the lumbar spine (LS) and the total hip (TH) by DXA. Radiographs of the calcaneus were obtained with a new X-ray high-resolution digital device (BMA, D3A, France). Several mathematical estimators [1] were used to extract trabecular bone texture properties. The method is based on the analysis of directional regularity of the image line by line, and on the field projections using anisotropic fractional Brownian fields. The results showed that combining different and complementary information related to several risk factors led to an improvement of the OR of osteoporotic fractures. For hip plus vertebral fractures a higher OR was obtained when the textural parameters were added to TH-BMD T-score  $\leq -2.5$  SD than with each parameter separately. The OR was 4.7 [95% CI, 2.5-8.9] with TH-BMD, 5.5 [95% CI, 2.9-10.4] using textural parameters and 13.9 [95% CI, 7.7-25.3] with both combined. When we added the age and body mass index to BMD and micro-architecture analysis the OR increased slightly to 15.9 [95% CI, 8.7-29.4]. When including other clinical factors (family history of fracture, tobacco and chair test) the OR shifted to 23.6 [95% CI, 12.4-44.8]. For all fractures globally, the improvement is lower. The OR was 2.4 [95% CI, 1.5-3.9] when TH-BMD values were combined to texture parameters and was 2.9 [95% CI, 1.8-4.8] when the clinical factors were added. These data reflect the multifactorial nature of osteoporosis and suggest that a composite index combining BMD, bone texture analysis and clinical risk factors may constitute a relevant tool in the field of osteoporosis.

[1] H. Bierme and F. Richard, Estimation of anisotropic Gaussian fields through Radon transform, ESAIM: Probability and Statistics, 12(1): 30-50, 2008.

**Disclosures:** M. Rachidi, None.

## F321

**Finite Element Analysis of Proximal Femur QCT Scans for the Assessment of Hip Fracture Risk in Older Men.** T. M. Keaveny<sup>1</sup>, L. M. Marshall<sup>2</sup>, C. M. Nielson<sup>2</sup>, S. R. Cummings<sup>3</sup>, P. F. Hoffmann\*<sup>1</sup>, D. L. Kopperdahl<sup>1</sup>, E. S. Orwoll<sup>2</sup>. <sup>1</sup>O. N. Diagnostics, Berkeley, CA, USA, <sup>2</sup>Oregon Health & Science University, Portland, OR, USA, <sup>3</sup>California Pacific Medical Center, San Francisco, CA, USA.

Finite element (FE) analysis of quantitative CT (QCT) scans provides an integrative measure of strength for the proximal femur and can be combined with estimates of the *in vivo* loads acting at the hip during a fall to calculate a load-to-strength ratio. We studied the relation of such biomechanical measures to the risk of incident hip fracture in men, alone and in combination with other fracture risk factors. A case-cohort design was used to identify a randomly selected subcohort of 225 men and 45 incident hip fracture cases from among 3549 community dwelling men (age  $\geq 65$ ) followed on average for 5.5 years after a baseline hip QCT scan. FE analyses of the QCT scans were performed (n=250 total, 40 with fractures), blinded to fracture status, to simulate a sideways fall and in vivo loads were estimated from mass and height data. Cox proportional hazards regression models were used to compute the hazard ratio (HR) per standard deviation (SD) change in FE outcome after controlling for age, study site, body mass index (BMI), and areal BMD (by DXA). The HR per SD change in FE-strength, load-to-strength ratio, and BMD were highly significant before and after adjusting for age (Table). When additionally adjusted for BMD (and study site and BMI, which had little effect), the HR for the load-to-strength ratio remained statistically significant. These results provide unique insight into hip fracture etiology and demonstrate the clinical potential of such a biomechanical approach to the assessment of hip fracture risk.

**Table:** Hazard ratio (HR) per standard deviation (SD) change\*.

VARIABLES	MODELS		
	Unadjusted	Age-adjusted	Age, BMI, Site, BMD-adjusted
FE-Strength (N)	13.1 (3.9-43.5)	8.0 (2.6-24.3)	2.7 (0.5-14.6)
Load-to-Strength Ratio	4.0 (2.7-6.0)	3.5 (2.4-5.2)	3.1 (1.6-6.1)
Total hip BMD (g/cm <sup>2</sup> )	5.1 (2.8-9.2)	4.6 (2.6-8.3)	

95% confidence interval shown in parentheses. Site - study site. \*Risk increased per SD decrease in FE-Strength and BMD, and per SD increase in Load-to-Strength Ratio.

**Disclosures:** T.M. Keaveny, O. N. Diagnostics 2.

This study received funding from: Amgen, Eli Lilly, and Merck.

## F323

**Towards an Understanding of The Mechanism of Femur Strength Improvement by Alendronate In Postmenopausal Women.** T. J. Beck\*<sup>1</sup>, J. Cauley\*<sup>2</sup>, H. Wang\*<sup>3</sup>, J. West<sup>3</sup>, A. DePapp\*<sup>3</sup>, K. Ensrud\*<sup>4</sup>. <sup>1</sup>Johns Hopkins Univ., Baltimore, MD, USA, <sup>2</sup>Univ. of Pittsburgh School of Public Health, Pittsburgh, PA, USA, <sup>3</sup>Merck Research Laboratories, Rahway, NJ, USA, <sup>4</sup>Minneapolis VA Medical Center, Minneapolis, MN, USA.

Alendronate (ALN) treatment reduces hip fracture rates compared to placebo among osteoporotic women, but appears unlikely to affect fall risk suggesting that ALN improves femur strength.

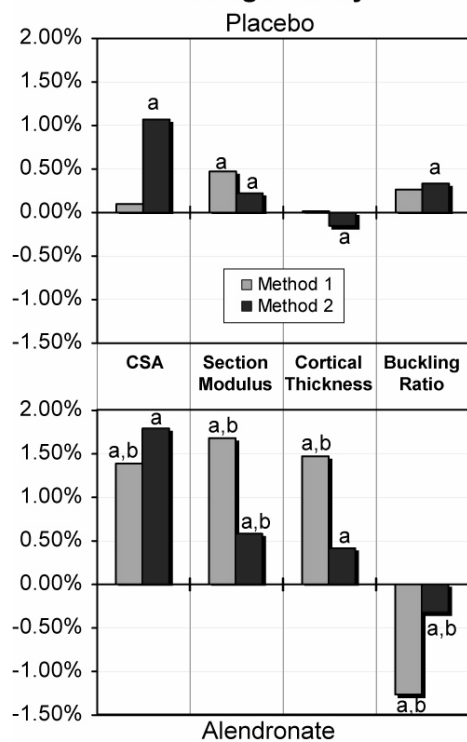
However, the mechanism underlying this association is uncertain. Potentially ALN may alter geometry to diminish load stresses and/or may improve tissue stress resistance. Some effect on the latter is evident from biopsy studies showing increased mean tissue mineralization in subjects treated with ALN. To examine the effect of ALN on bone geometry parameters separate from its mineralization effects, we compared differences in changes in geometric parameters with ALN treatment as defined by 2 different methods in 803 post-menopausal women with low bone mass (400 on placebo [PBO] and 403 treated with ALN 5-10 mg/d) enrolled in the FIT trial at Minneapolis and Pittsburgh sites. Method 1 derived from Hip Structure Analysis (HSA) assumed a fixed mineralization and Method 2 utilized cortical margin dimensions reliable in only thick cortex regions, but did not require a mineralization assumption.

Annual rates of change after 36 months of treatment in bone cross section analysis (CSA), section modulus, mean cortical thickness and buckling ratio for the two treatment groups by both methods are shown in the Figure. Among women taking PBO, mean rates of change in section modulus, cortical thickness and buckling ratio as defined by both methods were similar, although the increase in CSA was greater using Method 2.

Among women assigned to ALN, average rates of change in CSA were similar using both methods, but rates of change in section modulus, cortical thickness, and buckling ratio were smaller in magnitude using Method 2. Except for Method 2 CSA, differences in rates of change in parameters between ALN and PBO groups reached significance, irrespective of method (p<0.05).

Our findings suggest that ALN treatment improves femur shaft geometry independent of tissue mineralization effects, but geometric improvement is overestimated by 50-75% if mineralization effects are not taken into account. Bone strength improvement by ALN appears to combine geometric changes with greater tissue stress resistance.

### Annual rates of change in femur shaft geometry



<sup>a</sup>p<0.05 vs baseline, <sup>b</sup>p<0.05 vs placebo

**Disclosures:** J. West, Merck Research Laboratories 5.  
This study received funding from: Merck & Co., Inc.

### F327

**Frequent Apheresis for Platelet and Plasma Donations Constitutes an Independent Risk Factor for Decreased Bone Mineral Density.** K. Amrein<sup>1</sup>, C. Katschnig<sup>1</sup>, G. Lanzer<sup>1</sup>, H. Dobnig<sup>2</sup>. <sup>1</sup>Dept. of Blood Group Serology, Medical University Graz, Graz, Austria, <sup>2</sup>Div. of Endocrinology, Medical University Graz, Graz, Austria.

**BACKGROUND:** Modern medicine requires supply with single donor platelets and plasma products. Apheresis is the procedure of choice to obtain selective blood components, and citrate is used routinely for anticoagulation. In Austria, plasma and thrombocyte donations may be performed up to 50 and 26 times per year. The aim of the present study was to investigate whether frequent apheresis donations and thus substantial intermittent changes in acid-base homeostasis can be considered a safe long-term procedure for maintenance of skeletal health.

**METHODS:** We enrolled plasma and thrombocyte donors (>15 donations in the last six years) in an open, observational, single-center, cross sectional study. 70.3% of study subjects donated platelets only ("P"), 29.7 % donated both plasma and platelets ("PP"). 101 donors were included in the study group (76% m/24% f) and compared to 75 age, sex and BMI matched controls from similar socioeconomic status (74% m/26% f). The median number of donations was 51 for the entire group [(range 16 to 633), 46 for "P" and 105 for the "PP" group]. We performed bone densitometry by DEXA and measured lumbar spine and hip bone mineral density (BMD). A case report form including evaluation of calcium intake and physical activity was completed for every participant.

**RESULTS:** Statistical analysis adjusted for BMI, physical activity and daily calcium intake revealed a significantly lower BMI at the lumbar spine and femoral neck in the order of 4% at both measurement sites for the donor group (see table). Analysis of biochemical parameters relating to bone and mineral metabolism is in progress.

**CONCLUSIONS:** Regular blood donations by apheresis seem to constitute an independent risk factor for lower BMD at the lumbar spine and hip. Studies to further characterize bone turnover and calcium metabolism during and following the apheresis procedure are in progress. If results of our study can be confirmed in a prospective study design, effective strategies for prevention of detrimental long-term effects on bone mass must be formulated and/or the number of donations limited.

	Control Group	Donor Group	P-Value
L1-L4 g/cm <sup>2</sup>	1.251	1.190	<0.01
L1-L4 Z Score	0.183	-0.294	<0.01
L1-L4 T Score	0.215	-0.290	<0.01
Femoral neck g/cm <sup>2</sup>	1.025	0.984	<0.05
Femoral neck Z Score	0.145	-0.113	0.065
Femoral Neck T Score	-0.172	-0.440	0.059

**Disclosures:** H. Dobnig, None.

### F333

**Inflammatory Markers and the Risk of Hip Fracture: The Women's Health Initiative (WHI).** J. A. Cauley<sup>1</sup>, R. Boudreau<sup>1</sup>, K. Barbour<sup>1</sup>, D. C. Bauer<sup>2</sup>, J. S. Lee<sup>3</sup>, R. Jackson<sup>4</sup>, J. A. Robbins<sup>2</sup>, M. A. Allison<sup>5</sup>, N. Greep<sup>6</sup>, R. B. Wallace<sup>7</sup>, S. R. Cummings<sup>8</sup>, A. Z. LaCroix<sup>9</sup>. <sup>1</sup>University of Pittsburgh, Pittsburgh, PA, USA, <sup>2</sup>University of California, San Francisco, San Francisco, CA, USA, <sup>3</sup>University of California, Davis, Davis, CA, USA, <sup>4</sup>The Ohio State University, Columbus, OH, USA, <sup>5</sup>University of California, San Diego, San Diego, CA, USA, <sup>6</sup>University of California at Irvine, Orange, CA, USA, <sup>7</sup>University of Iowa, Iowa City, IA, USA, <sup>8</sup>University of California San Francisco, San Francisco, CA, USA, <sup>9</sup>Fred Hutchinson Cancer Research Center, Seattle, WA, USA.

To test the hypothesis that inflammatory burden confers a higher risk of subsequent hip fractures (fx), we conducted a nested case control study among 400 cases of incident hip fx and 400 controls matched on age, race and date of blood draw. Hip fxs were identified over an average follow-up time of 7.1 yrs. Subjects were selected from 38,795 women enrolled in the WHI Observational Study who had no prior hip fx and were not using estrogens or other bone active agents. Baseline soluble receptors of interleukin 6 (IL6sR) and tumor necrosis factor (TNFsR1 and TNFsR2) were measured with ELISA (CV%<16%). Conditional logistic regression was used to estimate the odds ratio (OR) and 95% CI. Multivariable models (MV) included age, BMI, fx history (hx), family hx of hip fx, diabetes, smoking, alcohol, calcium intake, NSAIDS use and corticosteroid use. Inflammatory markers were higher in cases versus controls, (IL6, p=0.08; TNFsR1, p=0.018; TNFsR2, p=0.006). Women with the highest cytokines (Quartile 4) had a 47-61% higher risk of hip fx compared to Quartile 1-3, Table. Because high levels of ≥2 inflammatory markers maybe more indicative of inflammatory burden, we compared women with 0 or 1 (referent), 2, or 3 markers in the highest quartile. 13% of cases compared to 6% of controls had all 3 cytokines in the highest quartile, p=0.001. Compared to women with 0 or 1 "high" cytokine, the OR (95%CI) of hip fx in women with 2 "high" cytokines was 1.47(0.95, 2.77); and for 3 "high", 2.66(1.48, 4.78) p trend <0.001. Adjustment for frailty score, falls, or bone turnover markers had little effect. Adjustment for bioavailable estradiol tended to strengthen the association: OR=3.06(1.66, 5.64). Both estradiol and inflammatory markers were independently related to hip fx. We conclude that elevated inflammatory markers are prognostic for hip fx.

MV odds ratio (95%CI) of hip fracture by inflammatory markers: Quartile 4 vs Quartile 1, 2 and 3 combined (referent)

	OR	(95%CI)
IL6sR	1.49	(1.05, 2.13)
TNFsR1	1.47	(1.04, 2.08)
TNFsR2	1.61	1.15, 2.27)

**Disclosures:** J.A. Cauley, None.

This study received funding from: The WHI program is funded by the National Heart, Lung and Blood Institute, National Institutes of Health, U.S. Department of Health and Human Services.



## F335

**Low Vitamin D Levels and Risk of Death in Older Men: A Prospective Study.** S. R. Cummings<sup>1</sup>, P. M. Cawthon<sup>1</sup>, N. Parimi<sup>1</sup>, E. Barrett-Connor<sup>2</sup>, K. E. Ensrud<sup>3</sup>, A. R. Hoffman<sup>4</sup>, J. Shikany<sup>5</sup>, E. S. Orwoll<sup>6</sup>. <sup>1</sup>Research Institute, California Pacific Medical Center, San Francisco, CA, USA, <sup>2</sup>UCSD, San Diego, CA, USA, <sup>3</sup>University of Minnesota, Minneapolis, MN, USA, <sup>4</sup>Stanford University, Palo Alto, CA, USA, <sup>5</sup>University of Alabama, Birmingham, Birmingham, AL, USA, <sup>6</sup>Oregon Health and Sciences University, Portland, OR, USA.

A low level of 25(OH)D (vitamin D) have been associated with an increased risk of fracture, falls, function and some diseases, including some types of cancer, but it is not known whether vitamin D deficiency increases mortality. We tested the hypothesis that low levels of 25(OH)D are associated with increased cause-specific mortality. We measured 25(OH)D levels with LC-MS in serum archived from 1608 men randomly sampled from the Osteoporotic Fractures in Men study (MrOS), a community-based cohort of men age 65 or older recruited from 6 U.S. cities. Follow-up for vital status was 97.7% during an mean of 6.1 years. Causes of death were adjudicated from medical records and death certificates. We used proportional hazards models to test the associations between 25(OH)D levels and overall mortality (N=258), non-cancer mortality (N=169) and cancer mortality (N=89). We also specifically analyzed cardiovascular (CV) death (N=91). Results were adjusted for age, BMI, season of blood draw, clinical center and education level and race.

Compared with 25(OH)D levels >30 ng/mL, men with vitamin D deficiency (≤15ng/mL) had a 2.2-fold increased risk of death due to causes besides cancer with no significant increased mortality for those with levels of 15 ng/mL -30 ng/mL (Table). The p-value for linear trend was 0.008. This increased risk with deficiency was due to both an increased risk of CV death, (RH=2.0: 0.9-4.2) and non-CV non cancer death (RH=2.3; 1.1-5.2). There was no significant association between 25(OH)D deficiency and death due to all types of cancer combined (RH=0.6; 0.2-1.4). Results for vitamin D deficiency were similar for to results men in the lowest quartile 25 (OH)D levels (≤ 20 ng/mL) compared to men in the highest quartile.

In conclusion, vitamin D deficiency is associated with an increased risk of death besides death due to cancer. In older men, vitamin D supplementation might decrease mortality from causes besides cancer.

Table. Relative Hazard (RH, 95% CI) of death by category of Vitamin D status

Mortality	Vitamin D status			p for trend
	Deficiency (≤15 ng/mL)	Insufficiency (>15 ng/mL to <30 ng/mL)	Sufficient (≥30 ng/mL)	
Overall	1.4 (0.9, 2.2)	0.9 (0.7, 1.3)	1.0 (ref)	0.246
Non-cancer	2.2 (1.3, 3.7)	1.2 (0.8, 1.8)	1.0 (ref)	0.008
CV	2.0 (0.9, 4.2)	1.1 (0.6, 2.1)	1.0 (ref)	0.098
Non-CV, non-cancer	2.3 (1.1, 5.2)	1.2 (0.6, 2.2)	1.0 (ref)	0.046
Cancer	0.6 (0.2, 1.4)	0.7 (0.4, 1.1)	1.0 (ref)	0.12

**Disclosures:** S.R. Cummings, None.

This study received funding from: NIH grants: U01AR45580, U01 AR45614, U01 AR45632, U01 AR45647, U01 AR45654, U01AR45583, U01 AG18197, U01-AG027810, and U11 RR024140.

## F337

**Lack of Seasonal Variation of Bone Resorption in Elderly Women in Relation to Periodicity of Sunlight Exposure at a Northerly Latitude (57° N).** A. Mavroei<sup>1</sup>, F. O' Neill<sup>2</sup>, A. J. Black<sup>3</sup>, W. D. Fraser<sup>4</sup>, B. L. Diffey<sup>5</sup>, D. M. Reid<sup>3</sup>, H. M. Macdonald<sup>3</sup>. <sup>1</sup>School of Medical Sciences, University of Aberdeen, Aberdeen, United Kingdom, <sup>2</sup>St Thomas Hospital, Twin Research & Genetic Epidemiology Unit, London, United Kingdom, <sup>3</sup>School of Medicine, University of Aberdeen, Aberdeen, United Kingdom, <sup>4</sup>Unit of Clinical Chemistry, Liverpool University, Liverpool, United Kingdom, <sup>5</sup>Institute of Cellular Medicine, Newcastle University, Newcastle, United Kingdom.

Although evidence is accumulating that vitamin D may influence many health outcomes there is still uncertainty regarding its role on bone health. It is assumed that healthy adults in the UK obtain most of their vitamin D by exposure of skin to sunlight with seasonality, latitude and lifestyle playing an important role. The aim of this study was to assess the contribution of sunlight exposure to bone resorption changes over a 15 month period.

365 Caucasian Scottish women (mean age 61.4 y ± 1.5 (SD)), participated in a 15-month longitudinal study examining the role of diet and sunlight on vitamin D status at a northern latitude of 57°. They were > 5 years postmenopausal and were not suffering from any disease or taking any medication that would affect their bone metabolism. Data were collected at 3 month intervals. The main outcome measures presented here were seasonal periodicities of ultraviolet radiation (using personal polysulphone film badges worn by the volunteers for one week every season as an objective method of measuring UV exposure), fasting serum parathyroid hormone (PTH) and fasting serum beta C-telopeptide (CTX). All data were log-transformed before General Linear Model repeated measures analysis.

	CTX (µg/L)	PTH (pmol/L)	Sunlight exposure (SED/wk)
Spring 2006 (Mar-May)	0.385 (± 0.167)	5.04 (±1.59)	4.4 (±5.0)
Summer 2006 (June-Aug)	0.382 (±0.163)	4.92 (±1.67)	7.6 (±6.2)
Fall 2006 (Sep-Nov)	0.379 (±0.161)	5.00 (±1.84)	1.3 (±2.2)
Winter 2006/07 (Dec-Feb)	0.379 (±0.162)	5.10 (±1.68)	0.4 (±0.5)
Spring 2007 (Mar-May)	0.376 (±0.155)	5.14 (±1.93)	4.1 (±4.3)

There was no significant seasonal variation in serum CTX, while periodicity in serum PTH peaked in the spring 2007 (p = 0.003). As expected, sunlight exposure was highest in the summer (p <0.001) followed by the two spring readings. When considering each season separately, sunlight exposure was a significant predictor of CTX explaining 2% of the variation during the summer period only (Beta = +0.063 P = 0.016).

These longitudinal data suggest that bone resorption is unaffected by season in postmenopausal women living in the North of the UK in spite of reduced quality of sunlight in the winter months.

**Disclosures:** A. Mavroei, None.

This study received funding from: Food Standards Agency.

## F339

**Bone Mass Recovers in Young Women with Anorexia Nervosa Who Are Both Weight and Menstrual Recovered.** E. J. Waugh<sup>1</sup>, B. Woodside<sup>2</sup>, D. E. Beaton<sup>3</sup>, P. Cote<sup>4</sup>, G. A. Hawker<sup>1</sup>. <sup>1</sup>Osteoporosis, Women's College Hospital, Toronto, ON, Canada, <sup>2</sup>Psychiatry, University Health Network, Toronto, ON, Canada, <sup>3</sup>Mobility Program, St. Michael's Hospital, Toronto, ON, Canada, <sup>4</sup>Rehabilitation Solutions, University Health Network, Toronto, ON, Canada.

We evaluated the effect of recovery from anorexia nervosa (AN) on BMD in a cohort of patients aged 17-40 yrs who had received inpatient treatment for AN over a 12-yr time period. A detailed illness history and key covariates were obtained by a Life History Calendar semi-structured interview. BMD at the lumbar spine L1-L4 (LSP), femoral neck (FN) and total body (TB) was measured by DXA. Low BMD was defined as a Z-score value ≤ -1.5 at one or more sites. Participants were considered recovered if they both achieved a BMI ≥ 18.5 kg/m<sup>2</sup> and resumed regular menstruation, for ≥ 1 year. Ill vs. recovered groups were compared by t-test or chi square; logistic regression was used to determine the odds of having low BMD adjusted for current weight, and duration and severity (lowest lifetime BMD) of illness.

We recruited 190 participants from two treatment centers: 77 were recovered, 113 were ill (91 never recovered; 22 relapsed). At interview, mean age of the participants was 27.2 ± 5.6 yrs and mean BMI was 19.4 ± 3.4 (11.1 - 35.5) kg/m<sup>2</sup>. Age at AN onset was 18.2 ± 4.2 (10-32) yrs, duration of illness was 5.9 ± 4.6 (1 - 25) yrs and lowest lifetime BMI was 13.9 ± 2.3 (7.2 - 18.0) kg/m<sup>2</sup>. Compared to ill participants, those recovered had shorter duration of illness (3.8 ± 2.7 vs 7.3 ± 5.1 yrs, p < 0.0001); only n=14 (18.9%) of those ill > 5 years were recovered. Among those recovered, mean duration of recovery was 5.1 ± 3.8 (1 - 26) yrs. Mean Z-scores were significantly higher in recovered vs ill patients at each skeletal site: LSP (0.07 ± 1.1 vs. -1.03 ± 1.2, p<0.0001), FN (0.17 ± 1.2 vs. -0.40 ± 1.2, p=0.008), TB (0.38 ± 1.0 vs. -0.13 ± 1.1, p=0.004). The prevalence of low BMD was 47.3% in ill patients who had never recovered, 27.3% in patients currently relapsed and 11.7% in recovered patients (p<0.0001, ill vs recovered). The adjusted odds of having low BMD in recovered vs ill patients was 0.22 (95% CI 0.09-0.53). Duration and severity of illness had minimal effect on the odds ratio (OR) associated with recovery status (weight only adjusted OR = 0.19). Participants who were only weight recovered (n=18) or only menstrual recovered (n=11) had similar odds of having low BMD compared to ill participants (p=0.62, p=0.58, respectively). Results indicate that significant recovery of BMD occurs in women with AN who achieve both weight and menstrual recovery. Neither duration or severity of illness appear to have a major influence on recovery of BMD; however those ill > 5 years are less likely to experience recovery from AN.

**Disclosures:** E.J. Waugh, None.

## F341

**Essential Fatty Acid and Fish Intake Is Associated with Higher BMD in Elderly Women and Men: The Framingham Study.** E. Farina<sup>1</sup>, D. P. Kiel<sup>2</sup>, R. Roubenoff<sup>3</sup>, E. J. Schaefer<sup>1</sup>, L. A. Cupples<sup>4</sup>, K. L. Tucker<sup>1</sup>. <sup>1</sup>Jean Mayer USDA Human Nutrition Research Center on Aging at Tufts University, Boston, MA, USA, <sup>2</sup>Institute for Aging Research, Hebrew SeniorLife, Harvard Medical School, Boston, MA, USA, <sup>3</sup>Schools of Nutrition and of Medicine, Tufts University, Boston, MA, USA, <sup>4</sup>Boston University School of Public Health, Boston, MA, USA.

Few studies have examined the relationship between essential fatty acid (EFA) intake and bone. Thus, we examined associations between both cross-sectional and longitudinal changes in hip BMD and EFA intake in the original cohort of the community-based Framingham Study. BMD was measured at the femoral neck (FN) and trochanter (TROCH) in 521 women (age 75.4 ± 4.8 y) and 334 men (age 75.3 ± 5.0 y) at baseline (exam 20) using dual-photon absorptiometry, and in 388 women and 235 men at 4-y follow-up (exam 22) using dual-energy x-ray absorptiometry (with adjustment for difference in scanners). Dietary intake was assessed by the previously-validated Willett food frequency questionnaire. EFA exposure variables consisted of α-linolenic acid (ALA,



18:3 n-3), docosahexaenoic acid (DHA, 22:6 n-3), eicosapentaenoic acid (EPA, 20:5 n-3), total n-3 fatty acids (sum of ALA + DHA + EPA + docosapentaenoic acid (22:5 n-3)), total n-6 fatty acids (sum of  $\alpha$ -linoleic acid (18:2 n-6) + arachidonic acid (20:4 n-6)), and n6:n3 ratio. BMD measures were regressed on energy adjusted quartile of EFA intake, with adjustment for age, BMI, height, dietary and supplemental intakes of calcium and vitamin D, physical activity, smoking, alcohol use, and estrogen use for women. In women, significant positive linear trends were observed with baseline BMD for total n-3 fatty acids (FN & TROCH) and total n-6 fatty acids (FN). Women with greater intakes of total n-6 fatty acids lost less BMD over 4-y (FN, P for trend=0.058) than those with lesser intakes. Women with fish intakes  $\geq$  the median (1.47 servings/week) lost less BMD over 4-y (-0.022 g/cm<sup>2</sup> vs -0.034 g/cm<sup>2</sup>) at the FN than those with lower fish intakes (P=0.024). In men, those with greater intakes of DHA as well as those with a lower n6:n3 ratio lost less BMD over 4-y than those with lesser DHA intakes and a higher n6:n3 ratio. Men with fish intakes  $\geq$  the median (1.47 servings/week) had higher mean baseline BMD (0.815 g/cm<sup>2</sup> vs 0.772 g/cm<sup>2</sup>) at the TROCH than those with lower fish intakes (P=0.005). These findings suggest a beneficial role for EFAs on skeletal health in the elderly.

	Q1	Q2	Q3	Q4
<b>Baseline BMD (g/cm<sup>2</sup>) by quartile of EFA intake in women</b>				
Tot n-3 FAs - FN, TROCH	0.720, 0.631	0.730, 0.652	0.728, 0.652	0.748 <sup>†</sup> , 0.663 <sup>†</sup>
Tot n-6 FAs - FN	0.713	0.728	0.741 <sup>†</sup>	0.744 <sup>†</sup>
<b>4-y change in BMD (g/cm<sup>2</sup>) by quartile of EFA intake in men</b>				
DHA - FN	-0.045	-0.032	-0.021 <sup>†</sup>	-0.015 <sup>†</sup>
N6:n3 Ratio - FN	-0.016	-0.013	-0.041 <sup>†</sup>	-0.034 <sup>†</sup>

<sup>†</sup> P < 0.05 relative to Q1. <sup>†</sup> P for trend < 0.05.

**Disclosures:** E. Farina, None.

## F345

**Women Who Fractured Their Hips Experience Greater Loss of Geometric Strength in the Contralateral Hip During the Year Following Fracture Compared to Age-Matched Controls.** L. Reider<sup>\*1</sup>, T. Beck<sup>1</sup>, M. Hochberg<sup>2</sup>, W. Hawkes<sup>\*2</sup>, D. Orwig<sup>\*2</sup>, J. YuYahiro<sup>\*2</sup>, R. Hebel<sup>\*2</sup>, J. Magaziner<sup>2</sup>. <sup>1</sup>Johns Hopkins University, Baltimore, MD, USA, <sup>2</sup>University of Maryland, Baltimore, MD, USA.

The majority of hip fracture research has focused on predicting fractures, interventions that reduce incidence, and the consequences on survival and quality of life. Limited attention has been given to changes in bone after a hip fracture, despite the propensity these patients have to fracture their contralateral hip. An understanding of changes in the contralateral hip after an index hip fracture is relevant to design of interventions to optimize recovery and to minimize the risk of additional fractures. This study compared femur geometry and its change over 12 months in women following hip fracture compared to women who had not sustained a hip fracture. Geometry of the contralateral hip was derived from DXA scan images obtained at baseline and 2, 6, and 12 months after fracture in 131 women 65 years and older participating in the Baltimore Hip Studies using the Hip Structural Analysis (HSA) program and compared with those from an age-matched group of 263 women enrolled in the Study of Osteoporotic Fracture (SOF) who had not suffered a hip fracture obtained a mean of 42 months apart. Multi-level mixed models were used to compare BMD, section modulus (Z), cross sectional area (CSA), outer diameter, and buckling ratio at baseline and over 12 months at the narrow neck, intertrochanteric, and shaft regions of the hip adjusted for age, height, weight, baseline value and HRT use. At baseline, wider bones and smaller CSA underlie the significantly lower BMD observed in women who fractured their hip resulting in more fragile bones expressed by a lower bone bending strength (Z) and higher buckling ratio. Relative to baseline, these women experienced a significantly greater net loss in CSA, Z and BMD and a greater increase in buckling ratio at all three regions over 12 months compared to women without a hip fracture. Not surprisingly women who have fractured a hip show much weaker geometry in the unfractured femur than in women without hip fractures but rates of further decline are considerably faster over 12 months following fracture compared to age matched controls. Results suggest little progression to an unfractured level and even greater susceptibility to a second hip fracture.

**Baseline means (SE) and annual net change in femur geometry in 131 women with hip fracture and in 263 age-matched controls**

	Baseline Mean		% Change/year	
	Cases	Controls	Cases	Controls
<b>Narrow Neck</b>				
Z (cm <sup>3</sup> )	0.88 (0.02)*	0.95 (0.01)	-1.5%	-0.3%
BMD (g/cm <sup>2</sup> )	0.59 (0.01)*	0.68 (0.01)	-2.5%*	-1.0%
CSA (cm <sup>2</sup> )	1.83 (0.03)*	1.96 (0.02)	-1.7%*	-0.2%
Outer diam. (cm)	3.24 (0.02)*	3.06 (0.02)	0.8%	0.8%
Buckling Ratio	16.2 (0.25)*	12.4 (0.18)	3.9%*	2.3%
<b>Intertrochanteric</b>				
Z (cm <sup>3</sup> )	2.71 (0.07)*	3.23 (0.05)	-4.1%*	-0.9%
BMD (g/cm <sup>2</sup> )	0.56 (0.01)*	0.68 (0.01)	-3.4%*	-1.00%
CSA (cm <sup>2</sup> )	2.92 (0.06)*	3.48 (0.04)	-3.3%*	-0.78%
Outer diam.(cm)	5.46 (0.03)*	5.43 (0.02)	0.1%	0.2%
Buckling Ratio	14.9 (0.52)*	11.4 (0.18)	5.7%*	1.8%
<b>Shaft</b>				
Z (cm <sup>3</sup> )	1.26 (0.03)*	1.83 (0.02)	-1.7%*	-0.1%
BMD (g/cm <sup>2</sup> )	0.94 (0.02)*	1.07 (0.01)	-2.8%*	-0.6%
CSA (cm <sup>2</sup> )	2.71 (0.05)*	3.06 (0.03)	-1.9%*	-0.4%
Outer diam. (cm)	3.05 (0.02)	3.02 (0.01)	0.8%*	0.1%
Buckling Ratio	5.2 (0.20)*	4.4 (0.09)	4.4%*	1.5%

\*p<0.05 vs. controls

**Disclosures:** L. Reider, None.

## F347

**Timing of Repeated Bone Mineral Density Measurements: Development of an Absolute Risk-based Prognostic Model.** S. A. Frost<sup>\*</sup>, N. D. Nguyen, J. R. Center, J. A. Eisman, T. V. Nguyen. Bone and Mineral Research Group, Garvan Institute of Medical Research, Sydney, Australia.

Osteoporosis is operationally defined in terms of bone mineral density (BMD), which is known to decline with advancing age. The present study attempted to address the following question: for an individual who is at present non-osteoporotic, given their current age and BMD level, when is the ideal time to repeat the BMD measurement?

To address the above question, data from the Dubbo Osteoporosis Epidemiological Study (DOES) were used. Non-osteoporotic women (n = 1008) and men (n = 750) over the age of 60 in 1989 were followed-up with bi-annually measurements of BMD until one of the following outcomes occurred: (1) osteoporosis at the femoral neck (T-score  $\leq$  -2.5), or (2) an incident low-trauma fracture. A modified Cox's proportional hazards model that accounted for a competing risk of death was used to estimate the probability of an outcome within 5-year and 10-year period.

At baseline (1989) there were 1008 women and 750 men whose femoral neck BMD T-scores were greater than -2.5 (non-osteoporosis). During the follow-up period (median 7.1 years), 346 women (34%) and 160 men (21%) developed osteoporosis or sustained a low-trauma fracture. As expected, the risk of either osteoporosis or fracture increased with advancing age (RR 1.3; 95%CI: 1.1 - 1.6 for women and 2.3; 95% CI: 1.7 - 2.9 for men) and lower BMD levels (RR 3.2; 95% CI 2.6 - 4.1 for women, and 2.6; 95% CI 2.0 - 3.3 for men). Using the predicted risk [of osteoporosis or fracture] of 10% as a cut-off level for repeating BMD measurement, the estimated time to reach the cut-off level varied from 1.5 years (for an 80-year old woman with a T-score of -2.2) to 10.6 years (for a 60-year old man with a T-score of 0). A nomogram was developed to facilitate the estimation of time for repeating BMD measurements.

Based on an individual's current age and BMD T-score, it is possible to estimate the average time to repeat BMD testing for the individual. The prognostic model and approach presented in this study may help improve the individualization and management of osteoporosis.

**Disclosures:** S.A. Frost, None.

## F349

**Development a Nomogram for Individualizing the Absolute Risk and Time to Recurrent Fracture.** N. D. Nguyen, S. A. Frost, J. R. Center, J. A. Eisman, T. V. Nguyen. Bone and Mineral Research Program, Garvan Institute of Medical Research, Sydney, Australia.

Some, but not all, individuals with a pre-existing fracture are at increased risk of subsequent fractures. However, the identification of those high-risk individuals (of re-fracture) is a challenge. This study sought to develop a prognostic model for individualizing the risk of and time to subsequent fracture.

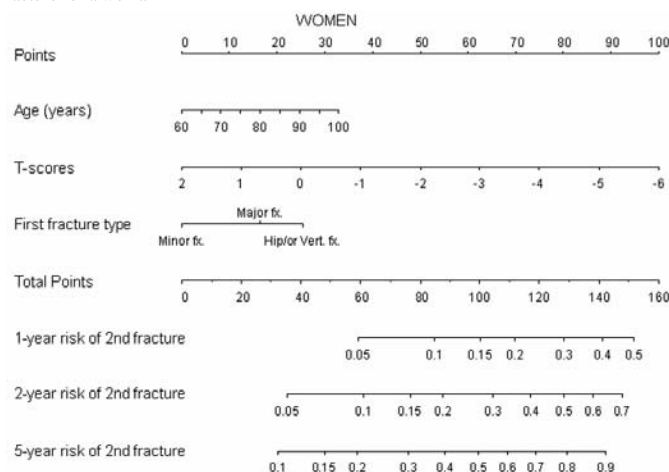
The model was developed from 2234 participants (1377 women) aged 60+ years as of 1989 in the Dubbo Osteoporosis Epidemiology Study, whose fracture incidence was ascertained between 1989 and 2007. Apart from anthropometric and demographic variables, femoral neck bone mineral density (BMD) was measured by DXA. A "counting process" model within the framework of the Cox's model was utilized to account for multiple fractures within an individual.

Between 1989-2007, 539 women (W) and 195 men (M) had sustained an incident fracture; among whom 193 W and 40 M sustained a recurrent fracture, 81 W and 11 M sustained 2 or more recurrent fractures. In women, advancing age (HR per SD: 1.1, 95% CI: 1.0-1.2) and low baseline BMD (1.4, 1.2-1.7) were consistently associated with an increased risk of recurrent fracture. Moreover, women with a pre-existing major clinical fracture (e.g. hip, vertebral, Colles' fracture) had a greater risk of subsequent fractures (2.0; 1.2-3.4). In men, advancing age (1.3; 1.2-1.5) and low BMD (1.5; 1.4-1.7) were independent risk factors for recurrent fractures.

For any given age and BMD, the time to reach an absolute risk of subsequent fracture was shorter than the time from fracture-free to a first fracture. For example, a 60-year old woman with BMD T-score = -2.5 was estimated to have a 17% 5-year risk of an initial fracture, but once fracture has occurred, the 5-year risk of subsequent fracture was increased to 26%. Based on age, BMD and types of fracture in women, a multivariable nomogram was developed for individualizing the absolute risk of subsequent fracture for any individual. Such a nomogram for women is illustrated in the figure below.

These results suggest that it is possible to identify men and women who are at high risk of subsequent fracture by considering their age, femoral neck BMD and fracture type in a prognostic model. The model can aid clinical decision making by estimating short-term and long-term absolute risks of re-fractures.

Figure: Nomogram for prediction of subsequent fracture risk given any first incident fracture for a woman



**Disclosures:** *N.D. Nguyen, None.*

*This study received funding from: National Health and Medical Research Council, Australia.*

## F351

**SSRI Use and Risk of Fracture in Older Women.** S. Diem<sup>1</sup>, T. Blackwell<sup>2</sup>, K. Stone<sup>2</sup>, J. Cauley<sup>3</sup>, T. Hillier<sup>4</sup>, E. Haney<sup>5</sup>, K. Ensrud<sup>1</sup>. <sup>1</sup>University of Minnesota, Minneapolis, MN, USA, <sup>2</sup>California Pacific Medical Center Research Center, San Francisco, CA, USA, <sup>3</sup>University of Pittsburgh, Pittsburgh, PA, USA, <sup>4</sup>Kaiser Permanente, Minneapolis, MN, USA, <sup>5</sup>Oregon Health Sciences Center, Portland, OR, USA.

The use of SSRIs has been associated with an increased risk of fractures in some studies, although most have been limited by inadequate control of potential confounding factors including depressive symptoms. To test the hypothesis that SSRI use in older women is associated with an increased risk of fracture, we assessed current use of SSRIs and incident fractures over a 10 year period in a cohort of 8045 older women in the Study of Osteoporotic Fractures. We verified current antidepressant use by inspection of medication containers and classified type of medication using a computerized medication dictionary. Users of other classes of antidepressants were excluded. We categorized women according to their SSRI use as users or non-users. SSRI use status was updated at each follow-up visit (average of 2.2, 4.5 and 9.3 yrs after initial assessment) using time-dependent methods. The hazard ratio (HR) and 95% CI for risk of fracture was calculated by category of SSRI use using Cox Proportional Hazards models. All results were adjusted for the following characteristics, which were updated at each follow-up visit: age, race,

weight, total hip BMD, health status, functional status, walking for exercise, cognitive function, estrogen use, bisphosphonate use, smoking, fall in previous 12 months, living situation, and depressive symptoms (measured by Geriatric Depression Scale). Average length of follow-up was 10.0±4.11 years.

Of the 8045 women, (average age 77.0 yrs at initial visit), 2682 (36%) women experienced > 1 non-spine, non-traumatic fracture during the follow-up period, including 914 (11.9%) with a hip fracture and 568 (7.1%) with a wrist fracture. 582 (7.2%) women were on an SSRI at at least one visit. Below are the age-adjusted and multivariable-adjusted HRs for risk of fracture for SSRI users vs. non-users.

	Age-adjusted HR (95% CI)	p-value	MV-adjusted HR (95% CI)	p-value
Any non-spine, non-trauma fracture	1.44 (1.18, 1.76)	0.0003	1.38 (1.12, 1.71)	0.003
Hip fracture	1.32 (0.95, 1.83)	0.09	1.04 (0.73, 1.47)	0.84
Non-spine, non-hip fracture	1.47 (1.17, 1.84)	0.0008	1.44 (1.13, 1.84)	0.003
Wrist fracture	1.38 (0.91, 2.11)	0.13	1.50 (0.97, 2.31)	0.07

Use of SSRIs in elderly women is associated with an increase in risk of non-spine fractures in age-adjusted models. The association between SSRI use and hip fracture appears to be largely explained by potential confounders, but there was a robust independent association between SSRI use and risk of non-spine, non-hip fractures.

**Disclosures:** *S. Diem, Pfizer 3; Eli Lilly 3.*

*This study received funding from: National Institutes of Health.*

## F354

**The Epidemiology of Rib Fractures in Older Men: The Osteoporotic Fractures in Men (MrOS) Study.** E. Barrett-Connor<sup>1</sup>, C. Nielsen<sup>2</sup>, E. Orwoll<sup>3</sup>, D. Bauer<sup>4</sup>, J. Cauley<sup>5</sup>. <sup>1</sup>Department of Family & Preventive Medicine, University of California, San Diego, La Jolla, CA, USA, <sup>2</sup>Bone and Mineral Unit, Oregon Health and Science University, Portland, OR, USA, <sup>3</sup>Bone and Mineral Unit, Oregon Health and Science University, Portland, OR, USA, <sup>4</sup>General Internal Medicine, University of California, San Francisco, San Francisco, CA, USA, <sup>5</sup>Department of Epidemiology, University of Pittsburgh, Pittsburgh, PA, USA.

Although rib fractures are common, they are barely mentioned in studies of osteoporotic fractures. We report here the first prospective study of validated rib fractures in ambulatory community-dwelling older men.

In MrOS we obtained demographic, lifestyle, and medical data and measured hip and spine BMD using DXA in 5995 men recruited from 6 U.S. sites; 99% responded to mailed queries about new fractures every four months for an average 5.1 year follow-up. Fractures were validated by physician review of radiographs or radiology reports; pathologic fractures were excluded. Baseline characteristics were compared between men who did or did not have an incident rib fracture. Cox proportional hazard ratios with 95% confidence intervals included all baseline variables with an age-adjusted p < 0.10.

24.1% of all incident non-spine fractures were rib fractures. At baseline the 126 men who had new rib fractures, compared to those without, were older, thinner, had lower BMD, and were significantly more likely to report a history of fracture and to report falling in the past year. Men with a history of rib fracture did not differ from men without in lifestyle, physical function, or family history of osteoporosis, but were more likely to have a history of cancer, stroke, or Parkinson's disease, and less likely to report arthritis. 48.4% had rib fractures after falling from ≤ a standing height. Only 2.3% of men had multiple rib fractures on the same date. In the final multiply adjusted Cox model (Table), age ≥ 80, BMD, history of rib/chest fracture, difficulty with 5 IADLs and statin use predicted an increased risk of rib fracture, while arthritis predicted a reduced risk. Most risk estimates were not materially changed when BMD was removed from the model except weight emerged as an independent risk factor and statin use was no longer significant.

Table. Multivariate-adjusted models of baseline risk factors for rib fracture with and without including BMD (HR [95% CI])

	Model 1: Including BMD	Model 2: Excluding BMD
Total hip BMD	1.44 (1.20-1.74)	—
Weight	NS	1.23 (1.01-1.49)
Age ≥ 80	1.55 (1.03-2.34)	1.56 (1.03-2.37)
Rib/chest/sternum fracture at any age	2.63 (1.81-3.82)	2.88 (1.99-4.19)
Arthritis	0.59 (0.41-0.85)	0.59 (0.41-0.85)
Difficulty with 5 IADLs (score)	1.13 (1.04-1.23)	1.15 (1.06-1.26)
Statin use	1.47 (1.01-2.13)	NS

Rib fractures are strongly associated with low BMD and future rib fractures, and should be considered when evaluating patients for treatment to prevent fracture.

**Disclosures:** *E. Barrett-Connor, None.*

*This study received funding from: NIAMS, NIA, NCRR and Roadmap for Medical Research under the following grant numbers: 1. U01 AR45580, U01 AR45614, U01 AR45632, U01 AR45647, U01 AR45654, U01 AR45583, U01 AG18197, U01-AG027810 and UL1 RR024140.*

## F356

**Direct Medical Costs Associated with the Treatment of Non-hip, Non-vertebral (NHNV), Hip, and Vertebral Fractures in a Managed Care Setting.** K. Foley<sup>\*1</sup>, N. Shi<sup>\*1</sup>, G. Lenhart<sup>\*1</sup>, E. Badamgarav<sup>\*2</sup>. <sup>1</sup>Thomson Healthcare, Cambridge, MA, USA, <sup>2</sup>Amgen Inc, Thousand Oaks, CA, USA.

Fracture cost burden studies in osteoporosis generally focus on hip and spine fractures. However, recent studies suggest that 60% of all fractures occur at sites other than hip and spine. Evidence characterizing the economic burden of all fractures, including NHNV, in a managed care setting is limited. This retrospective analysis examined incremental direct medical costs associated with NHNV, hip, and vertebral fractures. Fully adjudicated medical claims from a research database were used to identify patients aged  $\geq 50$  years with a closed hip, clinically evident vertebral, or NHNV fracture (distal femur, pelvic, humerus, wrist, clavicle, or leg) between 7/1/2001 and 12/2/2004. The first observed fracture became the index fracture. Patients were continuously enrolled 6 months before and 12 months after the index fracture. A 1:1 control group for each fracture category was matched on age, gender, region, and diagnostic cluster score  $\pm 3$  points. Multivariate regression modeling controlled for potential confounders. Total direct medical cost in the 12 months after the index fracture was determined. Incremental cost attributable to fractures was calculated as the difference between the costs incurred by fracture and control cohorts in the same time period. Incremental costs by fracture site and age cohorts (i.e., 50-64 and  $\geq 65$ ) were analyzed separately. Six study samples and matched controls were identified. The mean age of the 50-64-age cohort was 60 and the  $\geq 65$ -age cohort was 80. Similar to published studies, NHNV fractures were more common than hip or vertebral fractures in both age groups. The ratio of NHNV:hip fracture was 11:1 among patients aged 50-64 years and 2:1 in patients aged  $\geq 65$  years. Adjusted incremental costs and total fracture costs by fracture site and age cohort are shown in the Table.

Table: Adjusted One-Year Direct Medical Costs			
Age 50-64 yrs (N=33,233)	N	Incremental Cost (\$) (Fracture-control)	Total fracture-related cost (\$ million) (N x incremental cost)
NHNV	27,424	\$9,183	\$251.8
Hip	2,423	\$26,545	\$64.3
Vertebral	3,386	\$14,977	\$50.7
Age $\geq 65$ yrs (N=73,945)			
NHNV	40,690	\$6,106	\$248.5
Hip	21,504	\$15,196	\$326.8
Vertebral	11,751	\$6,701	\$78.7

The economic burden of all osteoporotic fractures is significant for managed care plans. Although individual NHNV fractures have a lower direct incremental cost than hip or vertebral fractures, their total cost is greater for patients aged 50-64 years because of the greater prevalence of NHNV fractures in this population.

**Disclosures:** K. Foley, Amgen 3.  
This study received funding from: Amgen Inc.

## F358

**The 10-Year Probability of Recurrent Osteoporotic Fractures After a Primary Wrist Fracture in Postmenopausal Women Enrolled in the Canadian Multicentre Osteoporosis Study (CaMOS) Cohort.** A. Hodsman<sup>1</sup>, G. Gamble<sup>\*2</sup>, R. Adachi<sup>3</sup>, G. Ioannidis<sup>3</sup>, N. Krieger<sup>4</sup>, D. Goltzman<sup>5</sup>, A. Papaioannou<sup>3</sup>, J. Prior<sup>6</sup>, T. Anastassiades<sup>7</sup>. <sup>1</sup>University of Western Ontario, London, ON, Canada, <sup>2</sup>University of Auckland, Auckland, New Zealand, <sup>3</sup>McMaster University, Hamilton, ON, Canada, <sup>4</sup>University of Toronto, Toronto, ON, Canada, <sup>5</sup>McGill University, Montreal, QC, Canada, <sup>6</sup>University of British Columbia, Vancouver, BC, Canada, <sup>7</sup>Queen's University, Kingston, ON, Canada.

**Background:** Wrist fractures are the most prevalent of the "osteoporotic" fractures in post-menopausal women, and herald future fractures; little is known of the absolute risk of recurrent (2<sup>o</sup>) fracture after a wrist fracture, when it occurs as the first (1<sup>o</sup>) fracture event in adulthood.

**Methods:** All fractures, occurring as non-trauma events after age 50, were identified among 6053 women in the CaMOS cohort, specifically at the wrist or at other sites (clinical spine, hip, pelvis or ribs). All prevalent (historical) fractures prior to enrollment (total 257, 4.2%) and incident fractures during 7 yr. follow-up (total 323, 5.2%) were included to determine the 10 yr. probability of 2<sup>o</sup> fractures following a 1<sup>o</sup> wrist fracture. Bone mineral density (BMD) measurement at the femoral neck (FN), and x-ray evidence of morphometric vertebral fractures were obtained at enrollment. From multivariable Cox proportional hazards analysis, Hazard Ratios (HR) and 95% confidence intervals (CI) were calculated.

**Results:** Within the cohort, there were a total of 580 fractures, including 265 at the wrist (46% of all identified fractures), 84 spine, 92 hip, and 158 pelvis/rib fractures. There were 247 1<sup>o</sup> wrist fractures, which occurred at mean (SD) age 65 (10) yr. Thirty two women had 2<sup>o</sup> fractures beginning at age 73 (9) yr. The 10-yr. probability of a 2<sup>o</sup> fracture was 12% (CI 7.2-16.8), but was higher for women  $> 65$  yr. (13.0%, CI 7.4-18.6) than those  $< 65$  yr. (9.0%, CI 0.5-17.5 - n.s.). Risk factors for all incident 2<sup>o</sup> fractures post-enrollment included any 1<sup>o</sup> wrist fracture (adjusted HR 3.0, CI 1.6-5.6), age at enrollment  $> 65$  yr. (HR 2.0, CI 1.3-3.2), presence of morphometric vertebral fractures, (HR 2.0, CI 1.4-3.0), and preserved FN BMD with T-score  $> -2.5$  (HR 0.4, CI 0.3-0.6) - all p-value  $< 0.001$ .

**Conclusion:** Wrist fractures are the most common of the osteoporotic fractures. Using

Canadian guidelines, (which define a high fracture risk as  $> 20\%$  probability over 10 yr.), a 1<sup>o</sup> wrist fracture may constitute only a moderate risk for future fractures, unless there are other well-defined risks for osteoporosis, including age  $> 65$ yr and osteoporotic BMD.

**Disclosures:** A. Hodsman, None.

## F361

**Improving the Diagnostic Yield of Bone Densitometry: Use of Age and Weight Thresholds in Postmenopausal Women.** J. D. McCrea, T. Hewer\*. Bone Densitometry, North Cumbria Acute Hospitals NHS Trust, Whitehaven, Cumbria CA28 8JG, United Kingdom.

Widespread dxa scanning of postmenopausal women to detect osteoporosis is not officially sanctioned in the UK while an opportunistic case finding strategy is endorsed. In 2002 we introduced a minimum age criterion of 65 years (in the absence of any other clinical risk factors) to referrals of postmenopausal women to improve the percentage of patients diagnosed with osteoporosis at any site from its then level of 30%. In 2005 we added a maximum weight criterion of 60 kg (along with a further restriction on age to 70 - 75 years) to patients referred under a special initiative. We have now compared the diagnostic yield of patients with osteoporosis in 317 postmenopausal women referred for a first scan during the year immediately prior to the introduction of the weight criterion with 325 patients referred immediately after the introduction of the criterion. 95% of the initiative patients weighed 59 kg or less (vs. 34% of controls), 93% were aged 70 or older (vs. 37% of controls) and 94% had an OST of -3 or less (vs. 22% of controls). Low trauma fractures were found in 131 initiative patients vs. 64 controls (p  $< 0.001$ ). Fracture site results for initiative vs. control patients were: 64 vs. 34 (distal forearm) p  $< 0.001$ , 34 vs. 3 (vertebral body) p  $< 0.001$ , 14 vs. 4 (hip) p  $< 0.05$  respectively. BMD results are given below:

		Routine patients (n=308) Mean ( $\pm$ SD)	Initiative patients (n=321) Mean ( $\pm$ SD)
TOTAL FEMUR	BMD (g/cm <sup>2</sup> )	0.854 ( $\pm$ 0.144)	0.759 ( $\pm$ 0.145) p $< 0.001$
	T - SCORE	- 1.2 ( $\pm$ 1.2)	- 2.0 ( $\pm$ 1.2) p $< 0.001$
FEMORAL NECK	BMD (g/cm <sup>2</sup> )	0.776 ( $\pm$ 0.139)	0.742 ( $\pm$ 0.121) p $< 0.001$
	T - SCORE	- 1.3 ( $\pm$ 1.1)	- 1.9 ( $\pm$ 1.0) p $< 0.001$

The proportion of patients found to be osteoporotic at any site was 63% in the initiative patients (vs. 35% of controls) p  $< 0.001$ . Overall, 79% of initiative patients (vs. 57% of controls) were recommended for treatment (p  $< 0.001$ ).

The raising of the minimum age requirement to 65 years only produced a marginal and non significant increase in diagnostic yield (from 30 to 35%) whereas the introduction of a maximum weight criterion had a more profound effect in identifying patients with osteoporosis who required treatment. It is clear that the important association between low body weight does not seem to be appreciated by our referring primary care physicians. We now propose to modify our bone density scanning referral criteria by adding a weight threshold. We also consider in the light of these results that serious consideration be given to the introduction of a policy of selective screening of all females who weigh 60 kg or less at age 70 and who have not had a dxa scan in the previous decade.

**Disclosures:** J.D. McCrea, Hoffmann La Roche (UK) Ltd 5.

## F363

**Percentage Body Fat and Risk of Prospective Hip Fracture in Older Men and Women: The EPIC-Norfolk Study.** A. Moayyeri, R. N. Luben\*, N. J. Wareham\*, S. Bingham\*, K. T. Khaw\*. Public Health and Primary Care, The University of Cambridge, Cambridge, United Kingdom.

The association between fat mass, an important component of total body weight, and osteoporosis is uncertain. There is particularly a paucity of data on the association of fat mass with prospective risk of fractures. We examined these associations in men and women in the European Prospective Investigation into Cancer (EPIC)-Norfolk who had measurements of both heel quantitative ultrasound (QUS) and percentage body fat (%BF) using a validated impedance technique between 1997 and 2000 and were followed for any incident fracture up to March 2007. From 14,789 participants (6,470 men) aged 42-82 years at baseline, 140 suffered a hip fracture during 114,371 person-years of follow-up (mean 7.7 ± 0.8 years). In sex-specific multivariate linear regression analyses, age-adjusted heel broadband ultrasound attenuation (BUA) measures were positively associated with %BF ( $\beta$  coefficient = 0.38 for women and 0.19 for men;  $P < 0.001$  for both). However, after inclusion of body mass index (BMI) in the model, the relation between BUA with %BF became significantly negative and remained significant after inclusion of other factors including waist-to-hip ratio, history of fracture, smoking and alcohol intake ( $\beta$  coefficient = -0.11 for women and -0.30 for men;  $P < 0.001$  for both). Women with incident hip fracture during follow-up ( $n=102$ ) had significantly lower %BF (36.1% vs. 39.8%) and BMI (25.6 vs. 26.5 kg/m<sup>2</sup>) compared to women without hip fracture ( $n=8,217$ ); however, there were no significant differences for %BF and BMI between men with ( $n=38$ ) and without fracture ( $n=6,432$ ). In sex-specific multivariate Cox proportional-hazard regression models, increasing %BF appeared significantly protective against hip fracture in women (hazard ratio [HR] for 10% increase = 0.55, 95% CI 0.39-0.78;  $P=0.001$ ) but not in men (HR = 0.70, 95% CI 0.26-1.83;  $P=0.46$ ). BMI became a significant risk factor for hip fracture in the model including %BF for women (HR for 4 kg/m<sup>2</sup> = 1.37, 95% CI 1.02-1.85;  $p=0.039$ ). In a multivariate model, a 10% increase of %BF on hip fracture risk was equivalent to about 1 standard deviation increase in BUA and about 7 years decrease in age in women. The interaction term between %BF and BMI included in the model was marginally significant ( $P$  value=0.09). The observed independent and protective effect of %BF against fractures and interaction between %BF and BMI for prediction of fractures warrant consideration. Understanding the complex relationships between different indices of obesity (such as %BF and BMI), BUA and fracture risk in men and women may help elucidate the metabolic and other underlying mechanisms involved in bone health and fracture risk.

**Disclosures:** A. Moayyeri, None.

## F365

**Factors Associated with Kyphosis Progression in Older Age.** D. M. Kado<sup>1</sup>, K. Prenovost\*, L. Palermo\*, K. Stone\*, S. R. Cummings\*. <sup>1</sup>Orthopaedics, University of California, Los Angeles, Los Angeles, CA, USA, <sup>2</sup>Medicine, University of California, Los Angeles, Los Angeles, CA, USA, <sup>3</sup>Epidemiology and Biostatistics, University of California, San Francisco, San Francisco, CA, USA, <sup>4</sup>California Pacific Medical Center, San Francisco, CA, USA.

Since only 36-38% of those with the worst thoracic hyperkyphosis have underlying vertebral fractures, there must be other important causes of age-associated thoracic postural changes. Because hyperkyphosis is associated with impaired pulmonary and physical function and increased mortality, we sought to determine other important and possibly modifiable causes. Using longitudinal data from the Study of Osteoporotic Fractures, we studied 1074 women aged 65 or older who had baseline, 3-5 year, and 15-17 year follow-up thoracic spine radiographs. From these, we calculated the Cobb angle of kyphosis (T4-T12) and measured prevalent vertebral fractures (3SD definition, from T4-L5). Participants also underwent baseline and 3.7 year follow-up calcaneal bone mineral density testing, disc height measurements (T4-T12), baseline and follow-up grip strength and walking speed testing, and answered questions regarding medical history and health behaviors. At baseline, the average kyphosis angle was 44.9 degrees (SD=12) that progressed an average of 6.7 degrees (SD= 2.5) over 15 years. Weighted multilevel models were run on Cobb angle as a function of various categories of predictors. A final combined model revealed that Cobb angle was predicted not only by age, vertebral fractures, and bone density, but also by family history of hyperkyphosis, disc height, grip strength, and walking speed. As expected, increased age, baseline and incident vertebral fractures predicted worse thoracic kyphosis. And, while low baseline heel bone density continued to predict worse kyphosis over time, the change in density did not. A family history of hyperkyphosis, decreased disc height, and low baseline grip strength predicted kyphosis progression. We also observed an interaction where a decrease in walking speed was associated with worsening kyphosis that was further accentuated in those who also experienced height loss over time. Thus, besides vertebral fractures and low bone density, a family history of hyperkyphosis, decreased disc height, low muscle strength, and decline in walking speed (indicating worse physical function) are other potential important factors that are independently associated with hyperkyphosis. Not only do predictors at a relatively early stage predict later life hyperkyphosis, some baseline effects and changes in these effects continue to affect kyphosis progression over time. Thus, development of effective treatments for thoracic hyperkyphosis should include attention to these influences.

**Disclosures:** D.M. Kado, Medtronic 2.

This study received funding from: NIH RO1 AG24246.

## F367

**Low Serum 25 Hydroxyvitamin D [25(OH)D] Is Associated with Higher Rates of Hip Bone Loss in Older Men.** K. E. Ensrud<sup>1</sup>, B. C. Taylor\*, M. L. Paudel\*, J. A. Cauley<sup>3</sup>, P. M. Cawthon<sup>4</sup>, S. R. Cummings<sup>4</sup>, H. A. Fink<sup>1</sup>, E. Barrett-Connor<sup>5</sup>, J. M. Zmuda<sup>3</sup>, J. M. Shikany\*, E. S. Orwoll<sup>7</sup>. <sup>1</sup>University of Minnesota and VAMC, Minneapolis, MN, USA, <sup>2</sup>University of Minnesota, Minneapolis, MN, USA, <sup>3</sup>University of Pittsburgh, Pittsburgh, PA, USA, <sup>4</sup>California Pacific Medical Center Research Institute, San Francisco, CA, USA, <sup>5</sup>University of California - San Diego, San Diego, CA, USA, <sup>6</sup>University of Alabama, Birmingham, AL, USA, <sup>7</sup>Oregon Health & Science University, Portland, OR, USA.

While vitamin D deficiency is common among older adults, there is inconsistent evidence to support an association between serum 25(OH)D levels and change in bone mineral density (BMD) in elderly people. To test the hypothesis that lower 25(OH)D levels are associated in a graded manner with higher rates of hip bone loss among older men, we measured total 25(OH)D (in fasting serum using LC-MS) and total hip BMD (THBMD) at baseline in a randomly selected sample of 1279 community dwelling men aged ≥65 years enrolled in the Osteoporotic Fracture in Men (MrOS) Study and followed them prospectively for an average of 4.4 years for changes in THBMD. Mean (±SD) 25(OH)D was 25.6 (±7.9) ng/mL. After adjustment for age, race, site, season, body weight, and baseline THBMD (base model), lower 25(OH)D level was associated with increasing rates of loss at the total hip ( $p$  for trend=0.009) (table). The majority of effect was observed among men in the lowest quintile (<19.2 ng/mL) who experienced a 1.5-fold increase in the rate of loss ( $p=0.003$  for Q1 vs. Q2-5); rates of loss were similar among men in higher quintiles and not different from each other ( $p>0.13$  for all comparisons). A similar pattern was observed at the hip subregions ( $p$  for trend=0.03 at trochanter and 0.08 at femoral neck). Findings were unchanged after further adjustment for additional potential confounders including health status, smoking status, alcohol intake, physical activity level, and inability to rise from a chair ( $p$  for trend at TH=0.02) (table). In conclusion, our results indicate that community-dwelling older men with low 25(OH)D levels (below 19 ng/mL) are at increased risk of hip bone loss, but suggest that rates of loss are similar among men with higher levels. These findings support the view that vitamin D deficiency, but not insufficiency, is detrimental to BMD in older men.

Mean Annualized Rate of Change in THBMD (95% CI) by Quintile of Total 25(OH)D Level		
Quintile	Base Model	Final Multivariable Model
Q1 (n=257)	-0.58 (-0.69, -0.46)	-0.56 (-0.68, -0.44)
Q2 (n=253)	-0.42 (-0.53, -0.31)	-0.41 (-0.53, -0.29)
Q3 (n=258)	-0.37 (-0.49, -0.26)	-0.38 (-0.49, -0.26)
Q4 (n=256)	-0.30 (-0.41, -0.18)	-0.30 (-0.41, -0.18)
Q5 (n=255)	-0.38 (-0.49, -0.26)	-0.39 (-0.50, -0.27)
p for trend	0.009	0.02
Quintile cutpoints: 19.2, 23.7, 27.0, 31.4 ng/mL		

**Disclosures:** K.E. Ensrud, None.

This study received funding from: NIH / NIAMS.

## F369

**Prediction of Incidental Low Trauma Limb Fractures in Older Men and Women with Quantitative CT (QCT) Variables of Bone and Muscles in Mid-Thigh: The AGES-Reykjavik Study.** G. Sigurdsson<sup>1</sup>, T. Aspelund\*, K. Siggeirsdottir\*, B. Jonsson\*, B. Mogensen\*, S. Sigurdsson\*, L. Launer\*, T. B. Harris\*, T. F. Lang\*, V. Gudnason<sup>1</sup>. <sup>1</sup>Icelandic Heart Association, Kopavogur, Iceland, <sup>2</sup>Intramural Research Program, National Institute on Aging, Bethesda, MD, USA, <sup>3</sup>University of California, San-Francisco, CA, USA.

QCT permits a direct measure of bone and muscle size and assessment of bone/muscle relationship. We have studied cross-sectional QCT variables in mid-thigh as predictors of incidental limb fractures in the AGES-Reykjavik Study, a cohort of 66-96-year-old men ( $n=2160$ ) and women ( $n=2385$ ) drawn from an established population based cohort and not taking medications affecting bone metabolism. We used a 4-detector Siemens CT system, a single axial section through the right mid-thigh (10 mm slice thickness). The variables included in the Cox's proportional hazard model were: total cross-sectional cortical area (CSA), derived cortical thickness, shaft BMD, shaft bending strength index (BSI), medullary area and buckling ratio, total cross-sectional muscle and quadriceps area and bone/muscle area ratio. All low trauma limb fractures (including proximal end of femur but excluding toes, foot, hand and finger fractures) during mean 3.5 years of follow-up were validated by medical and radiological records, altogether 170 in women and 61 in men, including 87 hip fractures.

Results; with sex as a confounding variable the most significant risk factor was the buckling ratio (ratio of bone radius to cortical thickness) with more than twofold greater risk in the top compared to the lowest tertile. This variable was >90% independent of muscle area which was however a significant protective factor independent of bone variables. Bone/muscle area ratio and BSI were not significant in multivariate analysis. The area under the ROC curve, using these QCT predictors and age, was 0.70 (CI 0.66-0.73).

We conclude that buckling ratio, a parameter which depicts the decreasing cortical thickness due to medullary expansion, is a significant risk factor for limb fractures including hip fractures in old age. Better understanding of the determinants of buckling ratio might be of importance in the prevention of these fractures in the elderly.

**Disclosures:** G. Sigurdsson, None.

This study received funding from: NIH/ N01-AG-12100.

## F371

**Loop Diuretic Use and Rates of Hip Bone Loss, and Risk of Falls and Fractures in Older Women.** L. S. Lim<sup>\*1</sup>, H. A. Fink<sup>2</sup>, T. Blackwell<sup>\*3</sup>, B. C. Taylor<sup>2</sup>, K. E. Ensrud<sup>2</sup>. <sup>1</sup>Internal and preventive medicine, Griffin Hospital, Derby, CT, USA, <sup>2</sup>VA Medical Center, Minneapolis, MN, USA, <sup>3</sup>University of California, San Francisco, San Francisco, CA, USA.

The aim of this study was to determine if loop diuretic use is associated with hip bone loss, and increased risk of falls and fractures in older women.

We conducted a prospective study of 8127 women aged 65 and older from the Study of Osteoporotic Fractures (SOF) cohort who had available medication use data at the 4<sup>th</sup> examination (V4). The following outcomes were examined (analysis cohort): 1) Change in DXA-measured hip BMD between V4 and the 6<sup>th</sup> examination (V6) (n=2980 with BMD measures at V4 and V6); 2) 2+ falls in the year after the 4<sup>th</sup> examination (n=6244); and 3) incident clinical fracture (hip, nonspine) (n=7297).

After a mean of 4.4 years (+/- 0.6) follow-up, loop diuretic users had greater loss of total hip BMD compared to nonusers (TABLE). After adjustment for multiple confounders, risk of recurrent falls was not increased among loop diuretic users compared with nonusers (multivariable OR 0.99, 95% CI 0.71-1.39). Similarly, compared with nonusers, loop diuretic users did not have an increased risk of nonspine (multivariable RR 1.04, 95% CI 0.90-1.21) or hip fracture (RR 1.03, 95% CI 0.81-1.31).

In this cohort of older women, loop diuretic use was associated with a small, but significantly higher rate of bone loss at total hip compared to nonuse. However the risk of falls or fracture did not differ between loop diuretic users and nonusers.

TABLE: Age and multivariate (MV)-adjusted mean annualized % BMD change (95% CI) from baseline as a function of loop diuretic use (bone loss cohort, n=2980)

		Loop diuretic category		P
	Model	Nonuser	User	
Total hip	Age	-0.70 (-0.75, -0.65)	-0.94 (-1.08, -0.81)	0.001
	MV†	-0.71 (-0.76, -0.66)	-0.87 (-1.01, -0.73)	0.03
Femoral neck	Age	-0.53 (-0.59, -0.47)	-0.66 (-0.82, -0.49)	0.14
	MV†	-0.53 (-0.59, -0.47)	-0.62 (-0.79, -0.44)	0.39
Trochanter	Age	-0.66 (-0.72, -0.59)	-0.86 (-1.04, -0.69)	0.03
	MV†	-0.66 (-0.73, -0.60)	-0.81 (-0.99, -0.62)	0.15

†Adjusted for age, baseline weight (kg), baseline site-specific BMD (g/cm<sup>2</sup>), impairments in instrumental activities of daily living, alcohol use (drinks/wk), total daily calcium intake (mg), physical activity (kcal/wk), self reported health status, hypertension, congestive heart failure, change in weight (kg), diabetes, smoking status, and statin use. 82 women were not included in the multivariate models due to missing covariate data.

**Disclosures:** L.S. Lim, None.

This study received funding from: NIH.

## F373

**Timed Up and Go Test and BMD as Predictors of Fracture: A 10-year Longitudinal Study.** K. Zhu<sup>1</sup>, A. Devine<sup>\*2</sup>, R. L. Prince<sup>3</sup>. <sup>1</sup>Department of Endocrinology and Diabetes, Sir Charles Gairdner Hospital, Nedlands, Australia, <sup>2</sup>School of Exercise, Biomedical and Health Science, Edith Cowan University, Perth, Australia, <sup>3</sup>School of Medicine and Pharmacology, University of Western Australia, Nedlands, Australia.

The relative importance of reduced bone structure and impaired neuromuscular function to fracture risk remains uncertain.

This study examines the association between incident osteoporotic fracture, hip DXA BMD and a standardised test of neuromuscular function, the Timed Up and Go test (TUAG), in which the patient is timed while rising from a chair, walking 3m, turning, returning to sit on the chair. The study subjects were 1500 women aged 75.2 ± 2.7 years when recruited in 1998 from the population. After finishing a five year RCT of calcium supplementation (CAIFOS), they were then recruited into a five year epidemiology study, the CARE study. The TUAG was measured at baseline and the hip DXA BMD at year one. Clinical incident osteoporotic fractures, excluding face and digits were confirmed from radiographic report, 1125 women were included in this analysis.

Baseline TUAG was 9.7 ± 2.6 seconds and one year DXA hip BMD T score was -1.1 ± 1.0. Over the study, 271 subjects had incident non-vertebral fracture, 96 subjects had incident clinical vertebral fracture and 334 subjects had at least one incident fracture at any site. Cox's proportional hazards analyses adjusted for baseline age and weight, previous fracture and calcium treatment group showed that one unit decrease in hip BMD T score was associated with 33.7%, 40.6% and 36.2% increase in the risk of non-vertebral fracture, vertebral fracture and any fracture, respectively. Whereas a 1 SD (2.6 seconds) increase in TUAG was associated with a 24.0% and 16.6% increase in the risk for non-vertebral and any fracture, respectively, it was not associated with higher risk for vertebral fracture.

	Non-vertebral fracture hazard ratio (95%CI)	Vertebral fracture hazard ratio (95%CI)	All fracture hazard ratio (95%CI)
Hip BMD (T score increase)	0.663 (0.561-0.783)	0.594 (0.445-0.794)	0.638 (0.549-0.743)
TUAG (2.6 second increase)	1.240 (1.105-1.390)	NS	1.166 (1.044-1.301)

The results confirm the independent effects of measures of neuromuscular coordination and bone structure to incident fracture risk. In addition to suggesting ways of improving fracture prediction, the data confirms the suggestion that modern fracture prevention should include assessment of both neuromuscular risk and skeletal structural risk as assessed by the TUAG and DXA hip BMD. Depending on the patients deficits, management should be directed at reducing neuromuscular risk, bone structural risk or both.

**Disclosures:** K. Zhu, None.

This study received funding from: Australian National Health and Medical Research Council.

## F376

**Percutaneous Injection of GEM OS2 (rhPDGF-BB and β Tricalcium Phosphate (βTCP)/Bovine Type I Collagen Matrix) Increases Vertebral Bone Mineral Density in Geriatric Female Baboons.** D. S. Perrien<sup>1</sup>, N. L. Fleming<sup>\*1</sup>, J. O. Hollinger<sup>\*1</sup>, C. Schmidt<sup>\*2</sup>, L. Condel<sup>\*2</sup>, D. F. Jimenez<sup>\*3</sup>, D. Dean<sup>\*3</sup>, J. Ong<sup>3</sup>, J. Li<sup>\*3</sup>, J. L. Lancaster<sup>\*3</sup>, R. Loreda<sup>\*3</sup>, G. Garcia<sup>\*3</sup>, P. Lindley<sup>\*4</sup>, A. K. Voges<sup>\*4</sup>, G. Bradica<sup>\*5</sup>, S. E. Lynch<sup>1</sup>, C. E. Hart<sup>\*1</sup>, C. S. Young<sup>1</sup>. <sup>1</sup>BioMimetic Therapeutics, Inc., Franklin, TN, USA, <sup>2</sup>Southwest Foundation for Biological Research, San Antonio, TX, USA, <sup>3</sup>UTHSCSA, San Antonio, TX, USA, <sup>4</sup>Veterinary Imaging Center, San Antonio, TX, USA, <sup>5</sup>Kensy Nash Corporation, Exton, PA, USA.

Approximately 161,000 VCFs are treated by injection of PMMA (vertebroplasty or kyphoplasty) in the U.S. each year. This treatment may increase secondary VCFs in adjacent vertebrae creating the need for local anabolic agents to prevent these secondary VCFs. To address this need, an osteoconductive βTCP/collagen matrix combined with rhPDGF-BB (GEM OS2) was created for direct injection into vertebrae as a local anabolic agent. PDGF stimulates chemotaxis and proliferation of osteoblasts, chondrocytes, fibroblasts and vascular smooth muscle cells, while synergizing with VEGF to promote neovascularization. This study was designed to assess the safety and efficacy of percutaneous injection of GEM OS2 in vertebral bodies of aged female baboons. The T12, L2, and L4 vertebrae in 6 female baboons, 17-22 yr old, were percutaneously injected with 0.5 cc of either βTCP/collagen + 1.0 mg/ml rhPDGF-BB (PDGF, n=3) or βTCP/collagen matrix + sodium acetate buffer (Matrix, n=3). The L6 vertebra in each animal was injected with sodium acetate buffer alone (Buffer). Body weights, serum chemistry, CBC, radiographs, MRI, and CT images were obtained at 1 wk pre- and post-surgery and at 1, 3, 6, and 9 mo post surgery. Volumetric bone mineral density (vBMD) was quantified from the CT images either including or excluding the needle track. All animals exhibited normal food intake, daily clinical observations, and serum chemistry markers were in or near normal limits. All radiography demonstrated that the test material was safe through 9-mo post-surgery. vBMD in the Matrix group did not change significantly through the study. In contrast, vBMD in the PDGF group at 3-mo was significantly greater than at 1 wk post-op (2.64% +/-1.16 [1-wk] vs. 5.93% +/-1.33 [3-mo]; p=0.023) and reached a peak at 6-mo and plateau at 9-mo, when the needle track was included in the analysis. A similar and significant pattern was seen when the needle track was excluded from the analysis. These data demonstrate that percutaneous injection of GEM OS2 into primate vertebral bodies is safe up to 9-mo post surgery. The QCT analysis demonstrates that direct injection of GEM OS2 containing PDGF acts as a rapid and potent anabolic agent suggesting this is a viable therapeutic for focal treatment of osteoporosis and bone augmentation.

**Disclosures:** D.S. Perrien, BioMimetic Therapeutics, Inc. 2, 5.

This study received funding from: BioMimetic Therapeutics, Inc.

## F383

**Serum Estradiol and Fracture Reduction during Treatment with Hormone Therapy: The Women's Health Initiative (WHI).** J. Cauley<sup>1</sup>, A. LaCroix<sup>2</sup>, J. Robbins<sup>3</sup>, J. Larson<sup>4</sup>, J. Wactawski-Wende<sup>4</sup>, Z. Chen<sup>5</sup>, S. Cummings<sup>6</sup>, R. Jackson<sup>7</sup>. <sup>1</sup>Univ of Pittsburgh, Pgh, PA, USA, <sup>2</sup>Fred Hutchinson Cancer Research Ctr, Seattle, WA, USA, <sup>3</sup>Univ of California at Davis Med Ctr, San Francisco, CA, USA, <sup>4</sup>Univ at Buffalo, Buffalo, NY, USA, <sup>5</sup>Univ of Arizona, Tucson, AZ, USA, <sup>6</sup>California Pacific Med Ctr, San Francisco, CA, USA, <sup>7</sup>Ohio State Univ, Columbus, OH, USA.

The WHI hormone therapy (HT) trials both demonstrated significant reductions in fractures among women randomized to either estrogen plus progestin (E+P) or Estrogen alone (E) compared to placebo. Despite these reductions in fractures, recommendations about the use of HT for the treatment of osteoporosis are cautious given the lack of overall benefits and greater risks of HT. Identification of women who are most likely to benefit could improve the overall risks/benefits ratio. We tested the hypothesis that HT reduces fracture risk to a greater degree in women with lower estrogen levels. The present study is a case-control study nested within the prospective design of the WHI-HT trials. All confirmed cases of hip (n=248) and all fracture (n=2596) were identified as potential cases. Cases were matched to controls for age, ethnicity, randomization date, fracture history, and hysterectomy status. The final set included 231 hip fracture case-control pairs and a random sample of 519 all fracture case-control pairs (Total N =1500). Of these participants, 721 were randomized to HT; 779 to placebo. Fasting baseline serum samples stored at -70° until assay were used. Serum estradiol (E2) was measured by RIA following extraction and chromatography with an intra- and inter-assay coefficient variation (CV) of 8-12%. Sex hormone binding globulin (SHBG) was measured by an immunoassay, CV, 6-13%. Logistic regression was used to evaluate the relationship between HT and the biomarkers on fractures, modeling the fracture outcome as a function of biomarker quartiles, HT, and an interaction term. The average age of the women was 65 years; 90% were Caucasian. There was no evidence that the effect of HT on fracture reduction differed by baseline level of E2, Table. Across quartiles of E2, women randomized to E+P or E alone, had about a 50% lower risk of fracture compared to placebo. For SHBG, the interaction with HT was borderline significant but there was no consistent pattern of association. We conclude that the effect of HT on fracture reduction is independent of sex steroid hormone levels.

Table 1: Odds ratio (95% confidence interval) of fracture among women randomized to HT versus placebo by levels of hormones at baseline

	All Fractures OR (95% CI) for Fracture	Interaction p-value	Hip Fractures OR (95% CI) for Fracture	Interaction p-value
Total Estradiol (pg/ml)				
≤6	0.50 (0.33, 0.75)	0.983	0.39 (0.19, 0.83)	0.793
6+ - 10	0.52 (0.35, 0.77)		0.66 (0.33, 1.36)	
10+ - 14	0.54 (0.34, 0.86)		0.47 (0.20, 1.01)	
>14	0.56 (0.36, 0.87)		0.50 (0.21, 1.20)	
Free Estradiol (pg/ml)				
≤0.16	0.49 (0.33, 0.74)	0.844	0.36 (0.17, 0.76)	0.680
0.16+ - 0.24	0.47 (0.30, 0.74)		0.55 (0.26, 1.18)	
0.24+ - 0.39	0.60 (0.39, 0.93)		0.70 (0.32, 1.50)	
>0.39	0.57 (0.37, 0.87)		0.53 (0.21, 1.34)	
Bioavailable E2 (pg/ml)				
≤4.0	0.51 (0.34, 0.75)	0.921	0.41 (0.20, 0.83)	0.720
4.0+ - 6.1	0.47 (0.29, 0.76)		0.47 (0.20, 1.06)	
6.1+ - 9.9	0.58 (0.38, 0.88)		0.74 (0.34, 1.57)	
>9.9	0.56 (0.36, 0.86)		0.50 (0.20, 1.28)	
SHBG (µg/al)				
≤30	0.58 (0.38, 0.89)	0.161	0.32 (0.11, 0.91)	0.077
30+ - 42	0.78 (0.52, 1.17)		1.10 (0.52, 2.34)	
42+ - 58	0.48 (0.32, 0.74)		0.65 (0.32, 1.31)	
>58	0.42 (0.28, 0.62)		0.32 (0.16, 0.64)	

Adjusted for age, ethnicity, randomization date, fracture history and hysterectomy status

**Disclosures:** J. Cauley, Merck & Co, Inc, Eli Lilly & Co, Pfizer, Novartis 2, 3.

This study received funding from: The WHI program is funded by the National Heart, Lung and Blood Institute, National Institutes of Health, U.S. Department of Health and Human Services.

## F389

**Strontium Ranelate Decreases Osteoblast-induced Osteoclastogenesis through the Involvement of the Calcium-Sensing Receptor.** T. C. Brennan<sup>1</sup>, M. S. Rybchyn<sup>1</sup>, A. D. Conigrave<sup>2</sup>, R. S. Mason<sup>1</sup>. <sup>1</sup>Physiology, Bosch Institute, University of Sydney, Sydney, NSW, Australia, <sup>2</sup>Molecular and Microbial Biosciences, Bosch Institute, University of Sydney, Sydney, NSW, Australia.

Strontium ranelate reduces vertebral and non-vertebral fractures in post-menopausal women. Previous studies have shown that strontium ranelate increases bone formation and decreases bone resorption. Moreover, strontium is an agonist of the calcium-sensing receptor (CaSR), a receptor involved in the strontium ranelate increase in osteoblast replication and osteoclast apoptosis. We previously showed that strontium ranelate induced replication and differentiation, as well as increasing the survival of primary human osteoblasts (HOBs) subject to stress. In the current study, we investigated the effects of strontium ranelate on osteoblast-derived osteoclastogenic signals and hypothesized that these effects could be mediated by the CaSR. After treatments as short as 24 h, strontium ranelate dose-dependently increased OPG mRNA expression (qRT-PCR), up to 1.9-fold with 2 mM strontium ranelate (p<0.001). This effect was confirmed by a strong up-

regulation of the secretion of OPG (ELISA) with 1 and 2 mM strontium ranelate (p<0.001). In parallel, RANKL mRNA expression decreased by 75% after treatment with strontium ranelate (0.1, 1 and 2 mM, p<0.01, p<0.01 and p<0.001, respectively). The expression of RANKL at the HOB surface was also strongly down-regulated after 48 h treatment with 1 mM strontium ranelate, as shown by immunoprecipitation followed by western blotting. HOBs were transfected with siRNA directed at the CaSR or scrambled sequence. Transfection occurred over 24 h and the extent of the knockdown of the CaSR in HOBs was confirmed by western blot analysis. Knocking down the CaSR had no significant effect on OPG mRNA expression in vehicle treated cells, but diminished the stimulatory effects of strontium ranelate up to 46 % (2 mM, p<0.001). In conclusion, strontium ranelate increases the production of OPG, while decreasing the production of RANKL at the osteoblast surface, thus supporting an indirect inhibitory effect on osteoclastogenesis. Previous studies have shown that the CaSR is involved in both the increase in osteoblast replication and osteoclast apoptosis induced by strontium ranelate. Our results show that the CaSR at the surface of the human osteoblasts is involved in the strontium ranelate-induced increase in OPG. This observation strengthens the proposal that the CaSR plays a key role in the dissociating effect of strontium ranelate on bone formation and bone resorption.

**Disclosures:** R.S. Mason, Servier 3.

This study received funding from: Servier.

## F391

**Injection of Mesenchymal Stem Cells Overexpressing both CXCR4 and RANK-Fc Effectively Prevented Ovariectomy-induced Bone Loss.** S. W. Cho<sup>1</sup>, H. J. Sun<sup>1</sup>, J. Y. Yang<sup>1</sup>, H. J. Choi<sup>1</sup>, D. H. Kim<sup>2</sup>, S. W. Kim<sup>1</sup>, S. Y. Kim<sup>1</sup>, C. S. Shin<sup>1</sup>. <sup>1</sup>Internal Medicine, Seoul National University College of Medicine, Seoul, Republic of Korea, <sup>2</sup>Internal Medicine, Dankook University College of Medicine, Cheonan, Republic of Korea.

Gene transfer to mesenchymal stem cell (MSC) may be a promising tool for wide variety of degenerative diseases including osteoporosis. Previously we demonstrated that intraperitoneal injection of MSCs overexpressing receptor activator of nuclear factor-κB (RANK-Fc) could prevent ovariectomy (OVX)-induced bone loss in mice. To enhance the homing efficacy of the injected cells, we introduced CXCR4 chemokine receptor 4 (CXCR4) along with the RANK-Fc to MSCs using retrovirus and studied the effects of MSC infusion in the prevention of OVX-induced bone loss. Ten weeks old adult female C57BL/6 mice were used and repeated intravenous injection of MSCs was performed as follows: (1) Sham-operated mice treated with PBS (n = 6); (2) OVX mice treated with MSCs transduced with RANK-Fc-RFP and CXCR4-GFP virus (RANK-Fc + CXCR4; n = 6); (3) OVX mice treated with MSCs transduced with RANK-Fc-RFP and GFP virus (RANK-Fc + GFP; n = 6); (4) OVX mice treated with GFP and RFP virus (GFP + RFP; n = 8); (5) OVX mice treated with PBS (OVX + PBS; n = 6). Measurement of BMD by dual energy x-ray absorptiometry (PIXImus) revealed that RANK-Fc + CXCR4 group gained significantly greater BMD compared to RANK-Fc + GFP group (2.1% vs. -0.5% at 4 weeks and 4.4% vs. -0.1% at 8 weeks, p<0.05). GFP + RFP group also showed less bone loss compared to OVX + PBS group (-1.7% vs. -6.2% at 8 weeks, p<0.05). Homing of RANK-Fc + CXCR4 cells were identified by PCR analysis of GFP DNA fragment that was co-expressed through IRES link. Serum RANK-Fc level peaked at 2 weeks post cell infusion but the level was not significantly different between RANK-Fc + CXCR4 group and RANK-Fc + GFP group. In summary, transplantation of MSCs retrovirally transduced with both RANK-Fc and CXCR4 resulted in protection of OVX-induced bone loss in mouse model. The extent of protection by RANK-Fc and CXCR4 was greater compared to RANK-Fc alone, suggesting that co-overexpression of CXCR4 could improve the efficacy of MSCs cell therapy.

**Disclosures:** S.W. Cho, None.

## F394

**Anti-Sclerostin Antibody Increases Bone Formation and Decreases Bone Resorption in Distal Tibial Metaphyseal Trabecular Bone in Ovariectomized Rats.** X. Li<sup>1</sup>, H. Y. Chen<sup>2</sup>, K. Warmington<sup>1</sup>, X. Q. Liu<sup>2</sup>, Q. T. Niu<sup>1</sup>, T. Thway<sup>1</sup>, B. Stouch<sup>1</sup>, M. Grisanti<sup>1</sup>, H. Tan<sup>1</sup>, W. S. Simonet<sup>1</sup>, C. Paszty<sup>1</sup>, W. S. S. Jee<sup>2</sup>, H. Z. Ke<sup>1</sup>. <sup>1</sup>Amgen Inc., Thousand Oaks, CA, USA, <sup>2</sup>University of Utah, Salt Lake City, UT, USA.

Sclerostin inhibition via an anti-sclerostin monoclonal antibody (Scl-Ab) increased bone formation, restored bone mass and bone strength in proximal tibial metaphysis and lumbar vertebral body of ovariectomized (OVX) rats with established osteopenia. In this study, we examined the effects of various Scl-Ab doses on bone mass, bone formation and bone resorption parameters on distal tibial metaphysis (DTM), a low bone turnover site, in adult OVX rats. Six-month-old female SD rats were sham-operated or OVX and left untreated for 5 months. OVX rats were then treated with vehicle or Scl-Ab at 2.5, 5, 10, 25 mg/kg (twice per week, s.c.) for 5 weeks. Calcein and tetracycline were injected s.c. 12 and 2 days before necropsy, respectively. Trabecular bone histomorphometric analysis was performed in the area between 0.8 mm to 2.8 mm from epiphysis using 20 µm thick longitudinal sections of DTM. Ovariectomy for more than 6 months did not induce significant changes in trabecular bone volume (BV/TV) and parameters of bone formation and bone resorption compared with sham controls in the DTM. This is in agreement with previous observation that OVX did not induce bone loss in this low bone turnover site in rats. Treatment with Scl-Ab in OVX rats increased BV/TV in all dose groups (+24, +52, +69, and +60% for 2.5, 5, 10 and 25 mg/kg groups, respectively; p < 0.05 for 10 and 25 mg/kg groups) compared with OVX controls. Significant increases were found in mineralizing surface (MS/BS, +141 to +293%), mineral apposition rate (MAR, +61 to



+110%) and bone formation rate (BFR/BS, +273 to +693%) in OVX rats treated with 5, 10 or 25 mg/kg as compared with OVX controls. In addition, MS/BS was significantly increased by 112% in OVX rats treated with 2.5 mg/kg of Scl-Ab compared to OVX controls. Eroded surface/ bone surface, a bone resorption index, was decreased in OVX rats treated with Scl-Ab at 5, 10 and 25 mg/kg groups (-22%, -28% and -44%, respectively; with  $p < 0.05$  for 25 mg/kg group) compared to OVX controls. These results reveal that treatment with a Scl-Ab in OVX rats increases bone mass by increasing bone formation and decreasing bone resorption in a low bone turnover site. Together with our previous finding, we conclude that inhibition of sclerostin via Scl-Ab stimulates bone formation and increases bone mass in both high and low bone turnover sites in OVX rat model of postmenopausal osteoporosis.

**Disclosures:** X. Li, Amgen 5.

This study received funding from: Amgen.

## F396

### One Year of Teriparatide Treatment Increases Hip Strength in Subjects with Recent History of Anti-resorptive Treatment: The OPTAMISE Study.

J. Keyak<sup>1</sup>, E. Quek<sup>\*2</sup>, P. Miller<sup>3</sup>, J. Bilezikian<sup>4</sup>, J. Stewart<sup>\*5</sup>, T. Lang<sup>2</sup>.

<sup>1</sup>Department of Orthopaedic Surgery, University of California, Irvine, CA, USA, <sup>2</sup>Department of Radiology, University of California, San Francisco, CA, USA, <sup>3</sup>Colorado Center for Bone Research, Lakewood, CO, USA, <sup>4</sup>Division of Endocrinology, Columbia University, New York, NY, USA, <sup>5</sup>Sanofi-Aventis, Laval, QC, Canada.

**Purpose:** Previous studies using QCT imaging of the hip to follow subjects being treated with teriparatide (TPTD) have shown opposing effects on cortical and trabecular bone, with loss of cortical BMD and gain in trabecular BMD. However, there is little direct information on how these compartmental changes translate to changes in strength (fracture load) of the whole proximal femur, and no information on the response of proximal femoral strength to TPTD after anti-resorptive treatment.

**Methods:** 205 subjects previously treated with alendronate (ALN, n=110) and risedronate (RIS, n=95) discontinued their bisphosphonate and were treated with TPTD (20 µg/d SQ) for 12 months. QCT images of the hip with satisfactory accuracy were obtained at baseline and 12 months. Using a previously-described method, patient-specific 3D finite element models of the hip were constructed for each time point. The mechanical properties of each element (elastic modulus and ultimate strength) were based on the BMD measured within each element. Models were evaluated under loading simulating a fall with impact on the posterolateral aspect of the greater trochanter. Percentage changes in fracture load were analyzed by ANCOVA and paired *t*-test.

**Results:** For this sample similar to the whole, analyses showed that whole-bone hip fracture load increased by  $4.3 \pm 17.5\%$ ,  $p < 0.001$  after 1 year of TPTD treatment. Percentage increase in fracture load did not differ significantly by ALN or RIS pre-treatment ( $p=0.3$ ).

**Conclusions:** One year of treatment with TPTD led to a significant increase in hip fracture load despite recent history of treatment with RIS and ALN. The extent of the increase was less than increases previously reported for vertebral strength in response to TPTD treatment. This may be explained by the opposing changes of decreasing cortical bone and increasing trabecular bone density.

**Disclosures:** J. Keyak, Sanofi-Aventis 3; Procter & Gamble 5; Merck 2.

This study received funding from: The Alliance for Better Bone Health (Procter & Gamble Pharmaceuticals and Sanofi-Aventis). ClinicalTrials.gov number: NCT00130403.

## F398

### Skeletal Plasma Clearance, as Measured by Quantitative Radionuclide Studies, Is Correlated with Bone Turnover Markers at 3 Months of Teriparatide Therapy.

A. E. B. Moore<sup>\*1</sup>, G. M. Blake<sup>1</sup>, K. Taylor<sup>2</sup>, P. Chen<sup>\*2</sup>, I. Fogelman<sup>1</sup>. <sup>1</sup>King's College London, Osteoporosis Screening and Research Unit, London, United Kingdom, <sup>2</sup>Eli Lilly, Indianapolis, IN, USA.

Teriparatide (TPTD) has profound anabolic effects on the skeleton as shown by marked increases in bone mass, bone mineral density and bone strength. TPTD increases biochemical markers of bone turnover, which may estimate clinical response to therapy. Quantitative radionuclide studies reflect bone blood flow and regional osteoblast activity and may provide a more precise measure of bone metabolism. We examined the bone metabolic response to TPTD using the radiopharmaceutical <sup>99m</sup>Tc-methylene diphosphonate (<sup>99m</sup>Tc-MDP) to quantify bone plasma clearance and correlate it with changes in bone turnover markers.

Ten postmenopausal women with osteoporosis (mean age 68 yr; mean baseline lumbar spine T-score of -3.2) had bone scans at baseline and 3 months after initiating TPTD therapy (20 µg/day sc). All women received daily calcium (1000 mg) and vitamin D (400-1200 IU) supplements. Women were injected with 600 MBq <sup>99m</sup>Tc-MDP and whole body bone scan images acquired at 10 min, 1, 2, 3 and 4 h. Multiple blood samples were taken between 5 min and 4 h and free <sup>99m</sup>Tc-MDP was measured using ultrafiltration. The Patlak plot method was used to evaluate whole skeleton <sup>99m</sup>Tc-MDP plasma clearance ( $K_{bone}$ ) as well as to derive regional values of bone clearance for the skull, spine, pelvis, arms and legs using gamma camera counts for each sub-region. At baseline and 3 months, serum concentrations of bone formation markers, amino-terminal propeptide of type I collagen (PINP) and bone-specific alkaline phosphatase (BSAP), and a bone resorption marker, urinary N-terminal telopeptide (NTX) /creatinine ratio, were measured.

From baseline to 3 months of treatment, mean whole body  $K_{bone}$  increased by 25.0% ( $P = 0.004$ ).  $K_{bone}$  was also increased at the skull (64.9%;  $P = 0.004$ ), spine (16.3%;  $P = 0.04$ ), pelvis (21.5%;  $P = 0.049$ ), arms (51.8%;  $P = 0.01$ ), and legs (36.8%;  $P = 0.02$ ). Parallel increases occurred in serum BSAP (21.8%,  $P = 0.04$ ), PINP (157.3%,  $P = 0.002$ ), and in

the urinary NTX /creatinine ratio (144.5%,  $P = 0.02$ ). Increases in these bone markers at 3 months were highly correlated with increases in  $K_{bone}$  in whole body and legs (correlation coefficients between 0.68 - 0.92).

Net plasma clearance of <sup>99m</sup>Tc-MDP to bone ( $K_{bone}$ ), a measure of osteoblastic activity, was significantly increased after 3 months of TPTD therapy. This is the first study to show a direct metabolic effect of TPTD therapy on bone blood flow kinetics at several clinically important skeletal sites. These results may provide physicians with clinical insights on the anabolic effects of TPTD as measured in bone scans.

**Disclosures:** A.E.B. Moore, None.

This study received funding from: Eli Lilly and Company

## F401

### Bone Mineral Density and Biochemical Marker Response Rates in Postmenopausal Women after Treatment with Zoledronic Acid.

P. Delmas<sup>1</sup>, I. Reid<sup>2</sup>, R. Rizzoli<sup>3</sup>, S. Adami<sup>4</sup>, P. Sambrook<sup>5</sup>, E. Eriksen<sup>6</sup>, P. Mesenbrink<sup>\*7</sup>, R. Eastell<sup>\*8</sup>. <sup>1</sup>Hôpital Edouard Herriot, Lyon, France, <sup>2</sup>University of Auckland, Auckland, New Zealand, <sup>3</sup>Geneva University Hospitals, Geneva, Switzerland, <sup>4</sup>University of Verona, Verona, Italy, <sup>5</sup>University of Sydney, Sydney, Australia, <sup>6</sup>Novartis Pharma AG, Basel, Switzerland, <sup>7</sup>Novartis Pharmaceuticals Corporation, New Jersey, NJ, USA, <sup>8</sup>University of Sheffield, Sheffield, United Kingdom.

Clinical monitoring of responses to treatment is very important, and the choice of response variable depends on the ability of that given variable to detect clinically relevant responses. In the HORIZON-Pivotal Fracture Trial, 7736 women were treated with three annual infusions of zoledronic acid 5 mg (ZOL), resulting in significant reduction of osteoporotic fractures of the spine, hip and appendicular skeleton. In this study, bone mineral density (BMD) was measured annually in all women. In a subset of women, bone turnover markers [C-telopeptides (CTX), bone alkaline phosphatase (bone ALP) (n=605) and procollagen type I intact N-terminal propeptide (PINP) (n=1248)] were measured in serum at baseline, 12, 24 and 36 months. CTX and bone ALP were also measured at 6 months. We used these measurements to assess the response rates to treatment in two ways: 1) fraction of patients showing the expected deviation from baseline and 2) fraction of patients revealing a deviation from baseline in excess of the least significant change (LSC) for the given biomarker. LSC is the least change needed to be 95% certain that a change has truly occurred. Lumbar spine BMD was more sensitive than total hip BMD exhibiting increases over baseline in 88.8%, 92.4%, 93.2%, and 94.8% of patients at 6, 12, 24, and 36 months respectively. Assuming an LSC of 3.0%, the response rates at the same time points were 50.4%, 61.9%, 83.4% and 83.6%, respectively. Among the biochemical markers serum CTX (S-CTX) was the most sensitive. The fraction of patients showing a decrease from baseline were 96.0%, 94.5%, 89%, and 86.2% at 6, 12, 24, and 36 months, respectively. Assuming an LSC for CTX of 30%, the response rates were 91.4%, 84.0%, 78.0% and 71.1%, respectively. In conclusion, assessment of S-CTX at 6 months provides excellent early monitoring of patient responses to ZOL, with 96% showing a decrease and 72.2% showing a clinically significant reduction. BMD increases in the spine were seen in 92.4% of patients at 12 and 93.2% at 24 months, while clinically significant BMD responses were seen in 61.9% at 12 months and 83.4% at 24 months. Thus, for zoledronic acid early monitoring (6-12 months) with S-CTX is more sensitive than BMD. However with increasing duration of treatment BMD becomes more sensitive.

**Disclosures:** P. Delmas, Novartis, Research Support from the Alliance for Better Bone Health 2, 3.

This study received funding from: Novartis Pharma AG, Basel, Switzerland.

## F403

**Effect of a Single Infusion of Zoledronic Acid 5 mg versus Oral Risedronate 5 mg on Bone Mineral Density at Lumbar Spine, Hip, Femoral Neck and Trochanter in Patients with Glucocorticoid-Induced Osteoporosis.** D. M. Reid<sup>1</sup>, J. Devogelaer<sup>2</sup>, K. Saag<sup>3</sup>, C. Roux<sup>4</sup>, C. S. Lau<sup>5</sup>, J. Reginster<sup>6</sup>, P. Papanastasiou<sup>7</sup>, A. Ferreira<sup>8</sup>, F. Hartl<sup>9</sup>, T. Fashola<sup>10</sup>, P. Mesenbrink<sup>9</sup>, P. Sambrook<sup>10</sup>. <sup>1</sup>Division of Applied Medicine, University of Aberdeen, Aberdeen, United Kingdom, <sup>2</sup>Saint-Luc University Hospital, Brussels, Belgium, <sup>3</sup>University of Alabama at Birmingham, Birmingham, AL, USA, <sup>4</sup>Cochin Hospital, Paris, France, <sup>5</sup>University of Dundee, Dundee, United Kingdom, <sup>6</sup>Bone and Cartilage Metabolism Unit, University of Liège, Liège, Belgium, <sup>7</sup>Novartis Pharma AG, Basel, Switzerland, <sup>8</sup>F Hoffman-LaRoche AG, Basel, Switzerland, <sup>9</sup>Novartis Pharmaceuticals Corporation, New Jersey, NJ, USA, <sup>10</sup>University of Sydney, Sydney, Australia.

The purpose of this study was to compare the safety and efficacy of intravenous zoledronic acid (ZOL) and oral risedronate (RIS) in the prevention and treatment of glucocorticoid-induced osteoporosis (GIO). A single 5 mg infusion of ZOL and oral RIS (5 mg/day) were compared in a 1-year, randomized, double-blind, double-dummy study involving 2 groups of glucocorticoid-treated patients (prevention subpopulation:  $\leq 3$  months of glucocorticoid treatment at randomization [ZOL, n=144; RIS, n=144]; treatment subpopulation:  $>3$  months of treatment at randomization [ZOL, n=272; RIS, n=273]). Within each subpopulation, the primary efficacy objective was to demonstrate non-inferiority of ZOL versus RIS, in percentage change in lumbar spine (LS) bone mineral density (BMD) between baseline and 12 months. Secondary efficacy endpoints included percentage change in LS BMD at 6 months, and in BMD of the femoral neck, total hip and trochanter at 6 and 12 months. Within each subpopulation, baseline characteristics were comparable between treatment arms.

Patients were predominantly Caucasian (94.0%) and female (68.2%). After 12 months, LS BMD had increased significantly more with ZOL than RIS in both subpopulations (treatment: ZOL, 4.1%; RIS, 2.7%;  $P=0.0001$ ; prevention: ZOL, 2.6%; RIS, 0.6%;  $P<0.0001$ ). ZOL was also significantly more effective than RIS in increasing BMD at the femoral neck, trochanter and total hip in both subpopulations at 12 months. The superior effect of ZOL on BMD was evident at 6 months (both subpopulations: LS, total hip and trochanter; prevention subpopulation only: femoral neck). In the first 3 days after treatment initiation, adverse events (AEs) were more common in ZOL-treated patients, mainly due to transient post-dose symptoms. From day 3 onwards, the 2 treatment groups had similar AE rates. Serious AE incidence was comparable between ZOL and RIS. These 1-year data indicate that a single 5 mg infusion of ZOL is significantly more effective than oral RIS (5 mg/day) in the prevention and treatment of GIO.

**Disclosures:** D.M. Reid, Novartis 1, 2, 3, 4; Amgen 1, 3, 4; Procter & Gamble 1, 4; Roche 1, 3, 4.

This study received funding from: Novartis.

## F405

**Effect of Severe Suppression of Bone Turnover on Osteocyte Viability.** C. V. Odvina<sup>1</sup>, S. Qui<sup>2</sup>, S. Palnitkar<sup>2</sup>, D. S. Rao<sup>2</sup>. <sup>1</sup>Center for Mineral Metabolism, UT Southwestern Medical Center, Dallas, TX, USA, <sup>2</sup>Bone and Mineral Research Laboratory, Henry Ford Hospital, Detroit, MI, USA.

Recently, we discovered severe suppression of bone turnover (SSBT) in some patients with osteoporosis on long-term alendronate treatment. Bone remodeling is essential for replacing dead osteocytes with new ones. However, it remains unclear about the association between SSBT and osteocyte viability.

Iliac bone biopsies were obtained from 16 postmenopausal women. Eight were patients treated with alendronate  $>5$  years and associated with very low bone turnover rate. Another 8 age-matched healthy postmenopausal women were selected for control. All subjects underwent double tetracycline labeling before biopsy. From 5  $\mu$ m sections stained with goldner trichrome, the following osteocyte related variables were measured in cancellous bone: osteocyte density [Ot.Dn/(mm<sup>2</sup>)], empty lacunar density [EL.Dn/(mm<sup>2</sup>)], total lacunar density [TL.Dn/(mm<sup>2</sup>)] and the percent empty lacunae [EL/TL(%)]. Coefficient of variation [CV (%) = SD/mean x 100] of each variable was computed from measured areas to determine the homogeneity of osteocyte and empty lacunar distribution.

Compared to the control, SSBT patients had significantly increased EL.Dn and EL/TL, and significantly decreased Ot.Dn (Table 1). CVs for Ot.Dn and TL.Dn were significantly greater in SSBT patients than in healthy control. All the subjects in control group showed double labels in the trabecular bone, and both bone formation rate and activation frequency remained in normal range. In 8 patients with alendronate treatment, 6 did not show double labels and 2 had considerably lower bone formation rate and activation frequency compared to the normal.

Bone remodeling likely targets the area with excessive osteocyte death. Consequently, a decrease in bone remodeling would result in accumulation of bone with less viable osteocytes. This study demonstrated that SSBT not only increases loss of osteocytes but also enhances heterogeneity of osteocyte distribution. Based on our previous study, increased heterogeneity of osteocyte distribution in lower remodeled cancellous bone results from the increase in trabeculae with no osteocyte. However, because of the lack of baseline biopsy, SSBT in our patients cannot be entirely attributed to the use of alendronate. The association between bisphosphonates and SSBT and decreased osteocyte viability merits further investigation.

Comparison of mean values between postmenopausal women and patients with SSBT			
	Normal	SSBT	p
N	8	8	
Age (years)	62.6 (8.43)	62.9 (9.61)	0.957
Ot.N/(mm <sup>2</sup> )	183 (26.6)	118 (38.4)	<0.001
EL.N/(mm <sup>2</sup> )	19.4 (6.85)	62.7 (7.46)	<0.001
TL.N/(mm <sup>2</sup> )	203 (24.1)	181 (34.0)	0.124
Ot/TL (%)	90.2 (3.84)	62.1 (9.61)	<0.001

**Disclosures:** C.V. Odvina, None.

## F407

**The Role of Active Site Threonine 201 in the Inhibition of Farnesyl Pyrophosphate Synthase by Nitrogen Containing Bisphosphonates.** J. E. Dunford<sup>1</sup>, E. Pilka<sup>2</sup>, A. Kwaasi<sup>1</sup>, A. Evdokimov<sup>3</sup>, B. L. Barnett<sup>4</sup>, U. Oppermann<sup>2</sup>, F. H. Ebetino<sup>5</sup>, R. G. G. Russell<sup>1</sup>, K. L. Kavanagh<sup>5</sup>. <sup>1</sup>Nuffield Department of Orthopaedic Surgery, University of Oxford, Oxford, United Kingdom, <sup>2</sup>Structural Genomics Consortium, University of Oxford, Oxford, United Kingdom, <sup>3</sup>P & G Pharmaceuticals, Cincinnati, OH, USA, <sup>4</sup>Dept. of Chemistry, University of Cincinnati, Cincinnati, OH, USA, <sup>5</sup>Dept. of Chemistry and Biochemistry, University of Texas at Austin, Austin, TX, USA.

The major molecular target of nitrogen containing bisphosphonates (N-BPs) is the mevalonate pathway enzyme Farnesyl Pyrophosphate Synthase (FPPS). However the exact mechanism of inhibition has not been determined. Recent crystallographic and kinetic studies have shown that potent N-BPs inhibit the enzyme by initially competing with one of the substrates, geranyl pyrophosphate (GPP), for a binding site, followed by a slow isomerisation of the enzyme structure to form a tightly bound complex. This complex is presumably maintained by the hydrogen bonding interactions of the bisphosphonate side chain nitrogen with a threonine hydroxyl residue and also the carbonyl oxygen of the adjacent lysine residue (Lys200/Thr201) in the active site of the enzyme. We aimed to investigate the interactions of the bisphosphonate nitrogen and these highly conserved residues. We constructed a mutant of FPPS, replacing the Thr 201 with an Ala residue (T-A Mutant). The mutant had an increased affinity (Km) for GPP with 1.5 $\mu$ M for T-A compared to 2.1  $\mu$ M in the wildtype. The Km for the second substrate, Isopentenyl Pyrophosphate was increased from 1.8 $\mu$ M in the wildtype to 17.7 $\mu$ M in the TA mutant. The maximal speed of the reaction was also reduced with Kcat of 0.34S<sup>-1</sup> for T-A compared to 0.42S<sup>-1</sup> for wildtype. The TA mutant had an increased final Ki for zoledronate, from 0.07nM to 2.17nM and also a reduced isomerisation constant (ICON), a measure of the reversibility of the inhibition, from 1224 to 37.6. Conversely, the effect of this mutation on the inhibition by risedronate was to decrease the Ki from 0.34nM to 0.16nM and increase the ICON from 237 to 1000. The inhibition of FPPS by NE58022 (Ki = 302 nM), an analogue of risedronate with no sidechain nitrogen was unchanged in the T-A mutant. Similarly, the inhibition of FPPS by ibandronate, an N-BP which is not predicted to make an interaction with Thr201 was only slightly affected with the final Ki changing from 3.6nM in the wild type to 5.5nM in the T-A mutant. We show that the interaction of the N-BP sidechain nitrogen with Thr 201 is not essential for inhibition, but can be responsible for the higher potency of many analogs. It may be that the interaction of the sidechain nitrogen with the carbonyl oxygen of Lys200 is the more important of the two possible hydrogen bonding interactions with FPPS for N-BPs.

**Disclosures:** J.E. Dunford, P & G 5.

This study received funding from: P & G Pharmaceuticals.

## F409

**Risk of Hip Fracture after Bisphosphonate Discontinuation: Implications for a Drug Holiday.** J. R. Curtis<sup>1</sup>, A. O. Westfall<sup>2</sup>, H. Cheng<sup>3</sup>, E. Delzell<sup>3</sup>, K. G. Saag<sup>1</sup>. <sup>1</sup>Center for Education and Research on Therapeutics (CERTS), University of Alabama at Birmingham, Birmingham, AL, USA, <sup>2</sup>Department of Biostatistics, University of Alabama at Birmingham, Birmingham, AL, USA, <sup>3</sup>Department of Epidemiology, University of Alabama at Birmingham, Birmingham, AL, USA.

**Purpose:** Recent data suggests that hip fracture risk was not significantly increased among women receiving 5 years of bisphosphonate therapy who were subsequently randomized to placebo. We studied older women compliant with bisphosphonates  $\geq 2$  years to evaluate the risk of hip fracture after bisphosphonate discontinuation.

**Methods:** Using administrative databases from a large U.S. healthcare organization, we identified women initiating bisphosphonate therapy who were compliant (Medication Possession Ratio, MPR  $\geq 66\%$ ) for 2 years. We examined the rate of hip fracture among women who discontinued bisphosphonates versus those who remained on therapy.

**Results:** From the original cohort, only 46% (n = 9063) of women were compliant (MPR  $\geq 66\%$ ) at 2 years and were eligible for analysis. Hip fracture incidence among women who discontinued bisphosphonates versus those who did not was 8.43 versus 4.67 per 1000 person years (p=0.016). The adjusted hazard ratio of hip fracture per 90 days following discontinuation was 1.2 (1.1-1.3). For women with higher compliance at 2 years (MPR  $\geq 80\%$ ) or compliant for 3 years, there were no significant differences in risk associated with discontinuation.

**Conclusions:** The rate of hip fracture was increased among women compliant with bisphosphonate therapy for 2 years who subsequently discontinued, suggesting that discontinuation is not advisable under these conditions. This association was attenuated with higher compliance and a longer duration of previous bisphosphonate therapy.

**Disclosures:** J.R. Curtis, Roche, UCB, Proctor & Gamble 2; Merck, Proctor & Gamble, Eli Lilly, Roche, Novartis 1; Novartis, Amgen, Merck, Proctor & Gamble, Eli Lilly, Roche 3.

This study received funding from: Novartis, PhRMA Foundation.

## F411

**Increase in Risk of Atypical Subtrochanteric Fractures with Zoledronic Acid? Results from the HORIZON-PFT.** D. M. Black<sup>1</sup>, D. C. Bauer<sup>1</sup>, P. Mesenbrink<sup>\*2</sup>, L. Palermo<sup>\*1</sup>, S. R. Cummings<sup>3</sup>, S. Boonen<sup>4</sup>, R. Eastell<sup>5</sup>. <sup>1</sup>UCSF, San Francisco, CA, USA, <sup>2</sup>Novartis Pharma, East Hanover, NJ, USA, <sup>3</sup>CPMC Research Institute & UCSF, San Francisco, CA, USA, <sup>4</sup>Leuven Univ., Leuven, Belgium, <sup>5</sup>Univ. of Sheffield, Sheffield, United Kingdom.

Two recent clinical case series studies suggested the possibility that low-trauma, subtrochanteric hip fractures may be increased in long term users of bisphosphonates. However, both of these case-series were small, uncontrolled and were derived from clinical populations: no data from population-based epidemiologic studies or randomized trials has been reported. We examined the occurrence of subtrochanteric hip and femoral shaft fractures in the Horizon Pivotal Fracture Trial, a randomized trial comparing 3 years of zoledronic acid treatment (ZOL) to placebo in 7736 patients. Self-reported fractures required central confirmation based on an x-ray report or (in some cases) review of x-rays. Confirmed hip fractures were categorized as femoral neck, intertrochanteric, subcapital, subtrochanteric or "other" (could not be classified or region uncertain). The categorization was developed prior to the study and was not specifically targeted to define the type of subtrochanteric fractures recently reported. A total of 140 women had hip fractures, of which 6 were subtrochanteric. In addition, 11 women had femoral shaft fractures. The table shows the distribution of these and femoral shaft fractures by treatment.

Type	All	ZOL	Placebo	RH (95% CI)
All hip fractures	140	52	88	0.59 (0.42, 0.83)
-Subtrochanteric hip	6	3	3	1.0 (0.2, 5.0)
Femoral shaft	11	5	6	0.84 (0.26, 2.75)

Hip fractures classified as subtrochanteric represent about 4.3% of confirmed hip fractures. While the relative hazard for subtrochanteric fractures is 1.0, the confidence interval is wide due to the low numbers. Femoral shaft fractures also did not differ by treatment.

Our analysis is limited by the small number of subtrochanteric fractures, and the short study duration (3 years) as the association may only become evident after longer term treatment. We also did not limit to those with minimal trauma. A further review to more precisely identify fractures similar to those recently reported is underway but will have limited ability to address this question due to low numbers and need to rely on x-ray reports in most cases.

Our results do not suggest an increase in risk in subtrochanteric fracture with 3 years of treatment with ZOL, but they do demonstrate the difficulty of assessing an association with such a rare outcome in a single randomized trial.

**Disclosures:** D.M. Black, Merck 1; GSK 2; Novartis, Roche 3.

This study received funding from: Novartis Pharmaceuticals

## F413

**Intravenous Ibandronate for Prevention of Early Bone Loss after Kidney Transplantation: a Prospective Study.** I. Adamsone<sup>\*1</sup>, D. Babarykin<sup>\*2</sup>, I. Folkmane<sup>\*1</sup>, D. Amerika<sup>\*1</sup>, R. Rozental<sup>\*1</sup>. <sup>1</sup>Department of Transplantation, Riga Stradin's University, Riga, Latvia, <sup>2</sup>Department of Biology, University of Lavia, Riga, Latvia.

After kidney transplantation bone mineral density (BMD) decreases dramatically (mostly during the first 6-12 months after the grafting). This is explained by the relatively high doses of glucocorticoids used immediately after operation, by a preexisting bone abnormalities caused by renal failure and by long-term increase of bone turnover probably due to persisting secondary hyperparathyroidism and calcineurin inhibitor immunosuppression. There is some evidence for a beneficial effect on BMD of antiresorptive treatments after kidney transplantation, but fracture and safety data are scarce.

Thirty eight osteopenic and osteoporotic kidney graft recipients were included in a controlled prospective intervention trial aiming to assess the effect on BMD of a 1-year treatment of quarterly infusions of ibandronate, combined with 1 g calcium and 400 U vitamin D per day. Twenty two patients with good graft function received an injection of 2 mg of ibandronate 3 weeks after transplantation and at 4, 7, and 10 mo after transplantation. Sixteen matched patients received calcium and vitamin D alone and served as controls. Primary outcome was the change in BMD after 12 mo treatment. Secondary measures included clinical fracture rate, change of body height, metabolic data (including iPTH), graft outcome (graft function, acute rejection rate).

Changes of BMD (ibandronate versus controls) were as follows: lumbar spine, +1.5±3.8% versus -2.9±4.3% ( $P<0.01$ ); femoral neck, +0.5±2.7% versus -3.6±4.7% ( $P<0.01$ ); and trochanter, +1.2±3.9% versus -2.5±4.0% ( $P<0.05$ ). There were no clinical fractures in both groups during study. Loss of body height was -1.1±1.6 cm versus -1.4±1.6 cm in control subjects ( $P=NS$ ). Graft function (serum creatinine concentration, proteinuria rate) after 1 yr was comparable. Serum iPTH concentration fell considerably in ibandronate group from 26.2±10.2 pmol/l to 14.3±11.9 pmol/l ( $P<0.05$ ) as well as in control group from 27.2±11.2 pmol/l to 10.8±9.6 pmol/l ( $P<0.01$ ), but changes did not differ ibandronate versus controls. We did not find any difference with regard to acute rejection rate between study groups. Three patients on ibandronate reported muscle pain in temporal relation to ibandronate administration while no such side effect was seen in control group ( $P<0.05$ ).

In conclusion, a 1-year prophylactic treatment with ibandronate given every 3 months to patients with existing osteopenia and osteoporosis immediately after kidney transplantation prevented further bone loss at lumbar spine and proximal femur. There were no negative effects of ibandronate on graft outcomes and bone turnover during study.

**Disclosures:** I. Adamsone, None.

## F416

**Predictors of Patient Perceived Need for Oral Bisphosphonates to Prevent Fracture: the Role of the MD-Patient Relationship.** J. T. Schousboe<sup>1</sup>, B. Dowd<sup>\*2</sup>, M. Davison<sup>\*3</sup>, P. Johnson<sup>\*4</sup>, R. L. Kane<sup>\*2</sup>. <sup>1</sup>Park Nicollet Institute; Division of Health Policy and Management, Univ of Minnesota, Minneapolis, MN, USA, <sup>2</sup>Division of Health Policy and Management, Univ of Minnesota, Minneapolis, MN, USA, <sup>3</sup>Department of Education Psychology, Univ of Minnesota, Minneapolis, MN, USA, <sup>4</sup>Carlson School of Management, Univ of Minnesota, Minneapolis, MN, USA.

**Background:** Perceived need for fracture prevention therapy is a strong predictor of persistence with oral bisphosphonate therapy. Our objective was to assess the association of self-reported medication need with patient-perceived quality of the MD-patient relationship, perceived susceptibility to and severity of fractures, personal and family history of fracture, bone mineral density (BMD), income, educational status, age, and personal & family history of fracture.

**Methods:** 1179 patients prescribed an oral bisphosphonate between 1/1/2006 & 3/31/2007 were mailed a survey to assess attitudes toward osteoporosis & medication to reduce fractures. 686 (58%) returned the survey, had complete data, and had BMD test results in their medical record. Perceived medication need, the MD-patient relationship quality (trust in physician, open communication, decision making congruence), and perceived susceptibility to & severity of fractures were assessed with Likert scales, and BMD by medical record review. The association between medication need & these predictors were assessed with ordinal logit models.

**Results:** The odds ratio for an increase of a defined unit (one quartile) of perceived medication needs for each predictor are shown in the following table.

Predictor	Medication Need, OR (95% C.I.)
MD-Patient Relationship (per SD increase)	1.64 (1.38 - 1.95)
	1 <sup>st</sup> quartile: 1.0 (reference)
	2 <sup>nd</sup> quartile: 1.53 (1.06 - 2.21)
	3 <sup>rd</sup> quartile: 2.01 (1.40 - 2.89)
	4 <sup>th</sup> quartile: 4.66 (3.30 - 6.59)
Perceived Fracture Susceptibility*Severity	
Age (per 10 year increase)	0.79 (0.69 - 0.89)
	High School: 1.0 (reference)
	Some College: 0.72 (0.55 - 1.04)
	College Graduate: 0.65 (0.44 - 0.98)
	> 4 Year College: 0.78 (0.52 - 1.17)
Education Level	
T-Score ≤ -2.5 at spine or femoral neck (vs No)	1.07 (0.81 - 1.42)
Personal History of Fracture (vs None)	1.02 (0.74 - 1.40)
Family History of Spine or Hip Fracture (vs None)	0.99 (0.71 - 1.39)

**Conclusions:** Need for medication to prevent fractures is positively influenced by the quality of the MD-patient relationship, and strongly driven by perceived susceptibility to and severity of fractures. Older patients are less likely to report need for medication, even though they are at higher risk of fractures. BMD level and fracture history are not related to perceived need for medication independent of these other predictors.

**Disclosures:** J.T. Schousboe, Roche, Inc. 2.

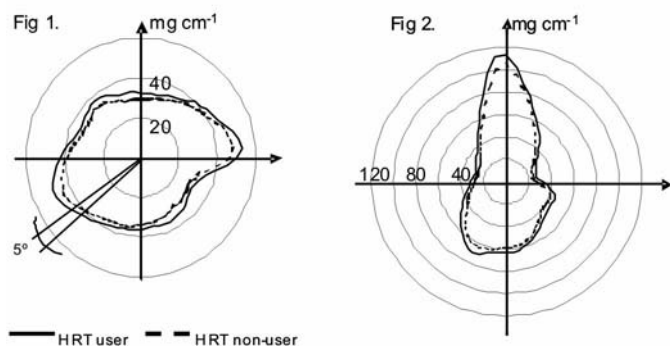
## F420

**The Influence of Long-Term Hormone Replacement Therapy on Tibia Bone Mineral Mass and Mass Distribution in Postmenopausal Women.** T. M. Mikkola<sup>\*1</sup>, A. Heinonen<sup>1</sup>, V. Kovanen<sup>\*1</sup>, S. Cheng<sup>1</sup>, U. M. Kujala<sup>\*1</sup>, H. Suominen<sup>1</sup>, M. Alén<sup>\*2</sup>, J. Puolakka<sup>\*3</sup>, P. Ronkainen<sup>\*1</sup>, M. Koskenvuo<sup>\*4</sup>, J. Kaprio<sup>\*4</sup>, T. Rantanen<sup>\*1</sup>, S. Sipilä<sup>\*1</sup>. <sup>1</sup>Department of Health Sciences, University of Jyväskylä, Jyväskylä, Finland, <sup>2</sup>Department of Medical Rehabilitation, Oulu University Hospital, Oulu, Finland, <sup>3</sup>Central Finland Central Hospital, Jyväskylä, Finland, <sup>4</sup>Department of Public Health, University of Helsinki, Helsinki, Finland.

In this study, case-control co-twin design was used to investigate the association of hormone replacement therapy (HRT) with bone mineral content (BMC), polar BMC distribution and radial volumetric bone mineral density (vBMD) distribution in tibial cross-sections.

Twenty-three (mean 62 years, range 54-72) monozygotic female twin pairs discordant for HRT participated in this study. Peripheral quantitative computed tomography (pQCT) was used to measure BMC, polar BMC distribution and radial vBMD distribution in the cross-section of distal tibia and tibial shaft.

The HRT users and non-users did not differ in body weight or physical activity. Mean duration of use of HRT was 8 years (range 1-25 years). In distal tibia, the HRT users had 10% (95% CI, 4-16%, paired sample t-test  $p=0.002$ ) and in the tibial shaft 11% (5-16%,  $p<0.001$ ) higher BMC than their non-HRT co-twins. The HRT users had significantly higher (4 to 16%) BMC on most of the 5 degree sectors around the center of mass in both distal tibia (Fig 1) and tibial shaft (Fig 2). Also, the HRT users had higher average vBMD throughout the bone from the center of mass to the bone's outer edge in distal tibia ( $p<0.001$  to  $p=0.08$ ) and throughout the cortex in tibial shaft ( $p<0.001$  to  $p=0.05$ ). Long-term HRT results in higher bone mineral mass in both epiphyseal and diaphyseal bone when controlled for genetic and shared childhood sources of variability. The gained BMC is distributed uniformly on the bone's cross-sections.



**Disclosures:** T.M. Mikkola, None.

This study received funding from: Academy of Finland, Finnish Ministry of Education, Yrjö Jahnsson Foundation.

## F426

**Influence of Body Weight on Cost-Effectiveness of Bone Densitometry and Treatment for Osteoporosis Among Older Women and Men Without Prior Fracture.** J. T. Schousboe<sup>1</sup>, B. C. Taylor<sup>2</sup>, H. A. Fink<sup>2</sup>, R. A. Adler<sup>3</sup>, M. Gourlay<sup>4</sup>, E. S. Orwoll<sup>5</sup>, E. Barrett-Connor<sup>6</sup>, S. R. Cummings<sup>7</sup>, L. J. Melton<sup>8</sup>, K. E. Ensrud<sup>2</sup>. <sup>1</sup>Park Nicollet Clinic, Division of Health Policy and Management, University of Minnesota, Minneapolis, MN, USA, <sup>2</sup>Minneapolis VAMC, University of Minnesota, Minneapolis, MN, USA, <sup>3</sup>Richmond VAMC, Richmond, VA, USA, <sup>4</sup>University of North Carolina, Chapel Hill, NC, USA, <sup>5</sup>Oregon Health & Science University, Portland, OR, USA, <sup>6</sup>University of California at San Diego, San Diego, CA, USA, <sup>7</sup>San Francisco Coordinating Center, San Francisco, CA, USA, <sup>8</sup>Mayo Clinic, Rochester, MN, USA.

**Background:** Routine DXA bone density screening is recommended for women aged 65 years and older, and by some specialty societies, for all men aged 70 and older. Both self-reported prior fracture and low body weight increase the pre-test probability of osteoporosis on DXA. Our objective was to test for body weight thresholds below which DXA followed by therapy for osteoporosis would be cost-effective for women and men without prior fracture, assuming a societal willingness to pay of \$60,000.

**Methods:** Associations between osteoporosis prevalence and self-reported prior fracture and body weight were estimated for women and men ages 65, 70, 75, 80, and 85 using data from the Study of Osteoporotic Fractures (SOF) and the Study of Osteoporotic Fractures in Men (MrOS). Participants without prior fracture at baseline were studied. Using previously published Markov models with updated (Jan 2008) fracture and treatment costs, we determined threshold body weights at which the cost per QALY gained equaled \$60,000 for DXA followed by five years of oral bisphosphonate therapy (assuming drug cost of \$500 per year) for individuals with gender-specific femoral neck T-score  $\leq -2.5$ . Using NHANES 2005-2006 data, the proportions of women and men at each age below these weight thresholds were calculated.

**Results:** Body weight thresholds below which DXA screening is cost-effective, and proportions of Men and Women Without Prior Fracture with weights below the threshold

Age	Women		Men	
	Body Weight Threshold (lbs)	Proportion	Body Weight Threshold (lbs)	Proportion
65	199.2	72.1%	171.3	22.6%
70	205.9	92.6%	183.6	36.3%
75	224.2	99.4%	204.4	67.0%
80	227.5	99.8%	211.7	92.5%
85	228.7	99.8%	216.4	94.7%

**Conclusion:** Universal bone densitometry is cost-effective for most women age 65 and older, but not for many men without prior fracture included in current osteoporosis screening guidelines. To increase cost-effectiveness, indications for DXA should consider age, prior fracture status, and body weight.

**Disclosures:** J.T. Schousboe, Roche, Inc 2.

## F433

**Cathepsin K Inhibitor, MIV-701, Suppresses Bone Resorption Markers in Healthy PMW: Results of a Phase I Clinical Trial.** D. Böttiger<sup>\*1</sup>, B. Darpo<sup>\*1</sup>, U. Grabowska<sup>\*2</sup>, M. Shiroo<sup>\*2</sup>, T. J. Chambers<sup>3</sup>, B. Samuelsson<sup>\*1</sup>. <sup>1</sup>Medivir AB, Huddinge, Sweden, <sup>2</sup>Medivir AB, Little Chesterford, United Kingdom, <sup>3</sup>St George's, University of London, London, United Kingdom.

Cathepsin K is a lysosomal cysteine protease expressed abundantly in osteoclast cells. Numerous lines of evidence support a pivotal role for cathepsin K in bone degradation and the development of cathepsin K inhibitors is being pursued by many companies. Recently cathepsin K inhibitors have demonstrated efficacy in phase II trials, as measured by increased bone mineral density (BMD), in a dose dependent manner. Studies also show that inhibition of cathepsin K can decrease bone degradation without negatively impacting bone formation, differentiating this osteoporosis treatment from currently available anti-resorptives such as bisphosphonates. A rationale for this augmentation of bone formation may arise from a new mechanism of action wherein cathepsin K inhibitors lead to the intact release of matrix-derived growth factors and/or PTH spikes. This highlights the potential for cathepsin K inhibition as a novel therapeutic approach for bone metabolism diseases such as osteoporosis.

Medivir has now developed a series of novel, highly potent, specific and non-nitrile warhead cathepsin K inhibitors. These inhibitors were additionally selected for their high potency in inhibiting bone resorption by human osteoclasts *in-vitro*. MIV-701 ( $K_i$ : Cath K = 1.7 nM; Cath L, S, B, V & H > 1500 nM; Cath F = 675 nM for the human enzymes) was selected as a candidate drug (CD) for further preclinical and clinical development.

Initially, the pharmacodynamic effect of MIV-701 was evaluated on bone markers of bone resorption, the C-terminal telopeptides of Type I collagen (CTX-I), *in vivo* in young male cynomolgus monkeys. Oral administration of MIV-701 (16 mg/kg) resulted in a rapid reduction in CTX-I levels within 2 h to a maximum of 80 % after 4-8 hours. A multiple dose study, with once daily oral administration of MIV-701, demonstrated a similar reduction of the biomarker where this suppression of CTX-I was reversible, returning to pre-treatment levels within 48 h. This quick onset and offset of suppression of bone resorption may by perturbing PTH levels give an additional advantage over other osteoporosis treatments.

MIV-701 has subsequently progressed into the clinic and in phase I studies, MIV-701 produced a dose-dependent decrease in CTX-I from baseline. In a 14 day multiple dose study in healthy males and postmenopausal women (PMW), MIV-701 was administered once daily, 300 mg, resulting in > 50 % reduction of CTX-I biomarker at trough for both males and PMW.

**Disclosures:** D. Böttiger, None.

This study received funding from: Medivir AB.

## F435

**Randomized, Placebo-Controlled, Double Blind Study on High Frequency Low Intensity Vibration in Bone Mass, Muscle Strength and Quality of Life in Children with Motor Disabilities.** M. L. Reyes<sup>1</sup>, J. Holmgren<sup>\*2</sup>, M. Hernandez<sup>\*1</sup>, E. Sanhueza<sup>\*1</sup>, J. Dixon<sup>\*3</sup>, R. Escobar<sup>\*1</sup>. <sup>1</sup>Dep of Pediatrics, Pontificia Universidad Catolica de Chile, Santiago, Chile, <sup>2</sup>Instituto de Rehabilitacion Teleton, Santiago, Chile, <sup>3</sup>Faculty of Electric Engineering, Pontificia Universidad Catolica de Chile, Santiago, Chile.

**Aim:** to determine the efficacy and safety of high frequency low intensity vibration (HFLIV) in children with motor disabilities. A randomized, placebo-controlled, double blind study, factorial design (3 treatment: placebo, 60 Hz and 90 Hz and 2 diagnosis groups: cerebral palsy (CP) and neuromuscular diseases) was conducted. Subject: children 6 to 10 yrs-old, prepubertal, sitting present, IQ > 70, otherwise healthy and with medication rather than calcium and vitamin D. Primary outcome BMD (DXA, Lunar DPX) at radii and FN, secondary outcomes: BMC and bone area; grip strengths, motor function, quality of life (PedsQL), and balance assessment. Intervention: stimulation with a placebo, 60 or 90 Hz device for 5 min on each limb, during 6 mo. All patients kept on regular physiotherapy. Baseline variables were similar between groups. Compliance (number of sessions) was 34.92±32.92%, and did not affect outcomes. No side effects were reported. Percentage of changes in BMD of Radio Ultra distal (RU), Radio 33% (R33), Area-RU and R33 were negatively correlated with initial values ( $p=0.05$ ,  $p=0.0001$ ,  $p=0.0001$  and  $p=0.001$  respectively). In a mixed model the frequency of 60 Hz affected positively the increase in BMD, BMC and area;  $p<0.0001$ ; increase in area was greater in RU ( $p<$

0.0001) and CP group ( $p=0.02$ ); and left side bones showed more increment in BMD ( $p=0.023$ ) and BMC ( $p=0.03$ ). There were no significant effects in FN. There was a positive correlation between most muscle strengths and densitometric variables. In Table are shown significant change percentages in DXA and others important variables.

Item / % of change	Placebo (n=21)	60 Hz (n=20)	90 Hz (n=16)	p
BMD-RU	0.91±5.95	31.88±135.30*	5.20±9.43	0.011
BMC-RU	-0.17±18.21	-0.91±11.78	6.42±14.32*	0.035
BMC-R33	7.33±10.99	11.58±14.78	7.10±8.14	0.060
Motor function (%)	-3.25±4.80	1.41±6.10	1.03±13.78	0.078
Tinetti test (balance)	-0.59±8.59	7.98±11.50	2.92±10.53	0.082
Muscle strength upper limbs	-19.98±49.89	165.27±164.81&	99.27±194.26	0.045
Dairy activities item PedsQL	21.18±72.28	46.52±104.39*	-17.85±51.26	0.046

\*Group 60 Hz ≠ placebo and 90 Hz. # 90 Hz ≠ 60 Hz and placebo. & 60 Hz ≠ placebo.

HFLIV was more effective than physiotherapy alone in improving bone mass, muscle strength in upper limbs. Frequency of 60 Hz is more effective than 90 Hz. Consistent with literature, trabecular bone responds better. Changes in upper limbs make these children more independent as assessed by PedsQL. Due to low cost, efficacy and safety we recommended HFLIV as a part of rehabilitation of these children. This is the first RCT on HFLIV reported in children.

**Disclosures:** M.L. Reyes, None.

This study received funding from: Government of Chile and FONIS SA05I20046.

## F439

**Deletion of FXR Leads to an Osteopenic Phenotype in Mice.** L. Y. Tang<sup>1</sup>, Y. P. Kharode<sup>1</sup>, C. Milligan<sup>\*1</sup>, J. Pirrello<sup>\*1</sup>, S. Selim<sup>\*1</sup>, M. Sharp<sup>\*1</sup>, J. A. Robinson<sup>\*1</sup>, P. Bodine<sup>1</sup>, D. Harnish<sup>\*2</sup>. <sup>1</sup>Osteoporosis in Women's Health & Musculoskeletal Biology, Wyeth Research, Collegeville, PA, USA, <sup>2</sup>Cardiovascular Metabolic Diseases Research, Wyeth Research, Collegeville, PA, USA.

Farnesoid X receptor (FXR), a member of the nuclear receptor superfamily, plays an important role in many metabolic pathways, including bile acid, lipid, and glucose metabolism via the liver and intestine. FXR is also highly expressed in the kidney and adrenal gland but its physiological or pathological importance in these organs is not understood. Renal gene profiling showed that FXR regulates genes involved in both nitric oxide production and VitD synthesis, two pathways implicated in bone mineral metabolism. This led us to investigate whether FXR signaling plays a role in the bone.

To test the hypothesis, we examined the bone mineral density (BMD) of femurs from FXR<sup>-/-</sup> and WT mice (females and males) at age of 22 weeks by pQCT. Study data showed that deletion of FXR reduced trabecular BMD by 34% ( $p<0.001$ ), cortical BMD by 5% ( $p<0.001$ ), and total BMD by 19% ( $p<0.001$ ) in female mice; and these parameters were reduced by 21% ( $p<0.02$ ), 2% ( $p<0.05$ ), and 10% ( $p<0.01$ ) respectively in male mice. Similar results were observed in FXR<sup>-/-</sup> mice at the age of 28 and 68 weeks. No significant difference in body weight was observed between FXR<sup>-/-</sup> and WT mice. To understand the skeletal change at the histological level, histomorphometric analysis was conducted in distal femoral metaphysis of female FXR<sup>-/-</sup> and WT mice at the age of 22 weeks. A moderate decrease in trabecular bone volume (BV/TV) was observed in FXR<sup>-/-</sup> mice (-27%,  $p=0.07$ ) when compared to the WT mice. Other significant findings in FXR<sup>-/-</sup> mice included increases in eroded surface (ES/BS, +27%,  $p<0.03$ ), bone turnover rate (BFR/BV, +23%,  $p<0.03$ ), bone mineral apposition rate (MAR, +22%,  $p<0.001$ ), and bone formation rate (BFR/BS, +15%,  $p=0.07$ ). No significant change in mineralized surface (MS/BS) was observed.

In summary, deletion of FXR resulted in an osteopenic phenotype in both female and male mice at ages between 22 and 68 weeks. Histomorphometric data suggests that an increase in bone turnover might contribute to the FXR deletion-induced osteopenia in female mice. Our data demonstrated that FXR is involved in bone metabolism. Whether the effect of FXR on bone was direct or indirect are under investigation.

**Disclosures:** L.Y. Tang, A full time employee of Wyeth 5.

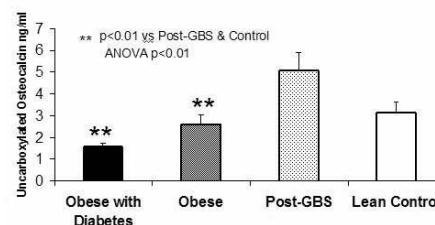
## F444

**Uncarboxylated Osteocalcin is an Endocrine Link between the Skeleton and the Glucose Metabolism: Clinical Evidences from Obese and Post Gastric By-pass Patients.** A. Spagnoli<sup>1</sup>, J. Chen<sup>\*2</sup>, Z. N. Pamuklar<sup>\*2</sup>, F. Granero-Molto<sup>\*1</sup>, A. Torquati<sup>\*2</sup>. <sup>1</sup>Pediatrics, University of North Carolina at Chapel Hill, Chapel Hill, NC, USA, <sup>2</sup>Surgery, Duke University, Durham, NC, USA.

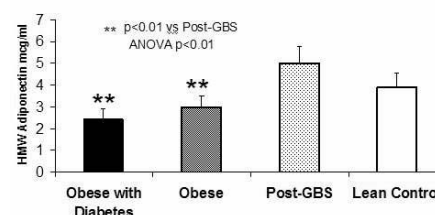
There is an increasing body of knowledge indicating that hormones that regulate fat/glucose metabolism have effects on the skeleton and vice-versa. Most recently, Karsenty's group reported that in mice, increased levels of uncarboxylated osteocalcin (uOST) protect from type 2 diabetes regulating adiponectin secretion, while lack of osteocalcin leads to insulin resistance (Lee NG et al, Cell 2007,130:458). In obese patients with diabetes, gastric bypass surgery (GBS) through unknown mechanisms, leads to ~90% resolution of type 2 diabetes before any significant weight loss occurs. Study is designed to determine: 1) uOST levels in obese patients with and without diabetes; 2) the effect of GBS on uOST; 3) the relationship of uOST with adiponectin and in turn with insulin sensitivity. We studied: 40 obese patients (BMI: 48.5±9.7 kg/m<sup>2</sup>) of which 19 had type 2 diabetes, 12 patients that had GBS 12-24 months prior to the study (post-GBS) (BMI: 29±7 kg/m<sup>2</sup>); 16 normal weight age-matched control subjects (BMI: 25±3.3 kg/m<sup>2</sup>). We evaluated fasting glucose and insulin to determine HOMA, serum total and uncarboxylated osteocalcin,

serum HMW-adiponectin by RIA or IRMA. Data are expressed as mean±SD; statistical significance is set at  $P<0.05$ . As shown in Fig. 1A, we found that uOST levels were significantly lower in obese patients with or without diabetes compared to controls, and significantly increased and normalized post-GBS. Similar results were found for HMW-adiponectin levels (Fig. 1B). GBS also normalized levels of total osteocalcin that were significantly lower than controls in obese patients with or without diabetes ( $p=0.001$ , ANOVA). When all patients were analyzed, an inverse correlation was found between uOST and HMW-adiponectin ( $r=-0.28$   $p=0.02$ ), between uOST and HOMA ( $r=-0.33$   $p=0.006$ ) and between HMW-adiponectin and HOMA ( $r=-0.32$   $p=0.008$ ). This is the first report that in obese patients, uOST levels are decreased and, normalize post-GBS. Our data provide the first clinical evidence to support the hypothesis that uOST is a bone hormone that regulates insulin sensitivity by modulating adiponectin. We postulate that normalization of uOST is a mechanism for diabetes resolution post-GBS.

**A. Serum Uncarboxylated Osteocalcin**



**B. Serum HMW Adiponectin**



**Disclosures:** A. Spagnoli, None.

This study received funding from: NIH-K23DK075907.

## F452

**Osteoblast-targeted Deletion of the Glucocorticoid Receptor has Little Impact on Peak Bone Mass but Attenuates Dexamethasone-induced Suppression of Bone Formation.** P. J. Bernard<sup>1</sup>, K. Ding<sup>\*2</sup>, C. Isaacs<sup>2</sup>, M. Hamrick<sup>3</sup>, L. J. Muglia<sup>\*4</sup>, S. L. Teitelbaum<sup>5</sup>. <sup>1</sup>Pediatrics, Medical College of Georgia, Augusta, GA, USA, <sup>2</sup>Orthopedics, Medical College of Georgia, Augusta, GA, USA, <sup>3</sup>Cell Biology and Anatomy, Medical College of Georgia, Augusta, GA, USA, <sup>4</sup>Pediatrics, Washington University, St Louis, MO, USA, <sup>5</sup>Pathology, Washington University, St Louis, MO, USA.

The pathogenesis of glucocorticoid (GC) induced osteoporosis (GIOP) is unclear. Knowing that GCs signal through the glucocorticoid receptor (GR), we generated an osteoblast specific GR knockout to define the direct effects of GCs on bone forming cells. GR was inactivated through Cre recombinase (Cre)-mediated excision of exons 1C and 2 of the GR gene. This modification deletes 50% of the mature GR protein, encompassing the translation start site and the taur1 transactivation domain, and has previously been shown to effectively disrupt GR action. Osteoblast and osteoblast precursor specific inactivation of GR was accomplished through Dermo1 promoter driven Cre expression, creating an osteoblast specific GR knockout (OB-GRKO). Once generated, 4 month old male OB-GRKO mice and control (Cre negative) littermates were randomized to receive a 14 day trial of either daily dexamethasone (Dex) (10 mg/kg) or saline IP injections. At trial completion, serum was assayed for markers of bone formation, and bones were harvested for histomorphometric, densitometric, and biomechanical analysis. In control mice, Dex exposure significantly decreased osteocalcin levels by 79% ( $p<0.001$ ,  $n=10$ ) and alkaline phosphatase levels by 30% ( $p<0.05$ ,  $n=10$ ). However, Dex treatment of OB-GRKO mice had no significant effect ( $p>0.05$ ,  $n=10$ ) on these markers. Interestingly, osteocalcin levels were 3.5 fold greater in Dex treated OB-GRKO mice than in Dex treated controls ( $p<0.05$ ,  $n=10$ ). Bone histomorphometry showed that Dex treated control mice experienced a downward, but not significant trend in mineral apposition rate (MAR) of 53% ( $p=0.07$ ,  $n=10$ ) and a significant decrease in bone formation rate/bone surface (BFR) of 80% ( $p<0.05$ ,  $n=10$ ), but Dex treated OB-GRKO mice did not. Analysis of femurs removed from untreated 4 month old (normal peak bone mass) OB-GRKO mice and control mice by PIXImus densitometry and Instron biomechanics did not reveal any significant differences. Our findings indicate disruption of GR signaling in the osteoblast reduces Dex's inhibition of bone formation at pharmacologic dosages, but does not cause abnormal bone growth when GCs are at physiologic levels. Complementing previous work that demonstrated osteoclast GR signaling modulates bone formation, we have shown that osteoblast GR signaling also plays an important role in the Dex-induced suppression of bone formation.

**Disclosures:** P.J. Bernard, None.

## F455

**Circulating DKK-1 Levels Are Reduced in Young Subjects with Low Bone Mass.** V. De Paola, L. Gennari, D. Merlotti, G. Martini, A. Avanzati\*, B. Franci\*, S. Campagna\*, B. Luciani\*, R. Nuti. Internal Medicine, Endocrine-Metabolic Sciences and Biochemistry, University of Siena, Siena, Italy.

Primary osteoporosis predominantly affects postmenopausal women and elderly men. However, low bone mineral density also occurs in middle-aged men and premenopausal women. Even though the pathogenesis of low bone mass in these individuals may be heterogeneous, several results suggest that a low bone turnover with a possible osteoblast dysfunction may be responsible of these forms of osteoporosis in both sexes. DKK-1 is an inhibitor of the Wnt/ $\beta$ -catenin signaling pathway, which is a critical signaling pathway for osteoblast differentiation. It has been recently shown that DKK-1 protein levels are detectable in the serum and elevation in DKK1 levels have been associated with decreased osteoblastic bone formation occurring in multiple myeloma or, in vitro, during glucocorticoid treatment. In order to better characterize the structural and metabolic basis of reduced bone mass in young adults, we measured circulating DKK-1 levels (DKK-1 enzyme immunoassay, Biomedica, Wien) in adult men (n=50, mean age 46.5 $\pm$ 9.6) and premenopausal women (n=23, mean age 43.4 $\pm$ 7.1) with low bone density, in subjects with senile or postmenopausal osteoporosis (n= 60, mean age 65.3 $\pm$ 8.8) as well as in young (n= 40, mean age 45.4 $\pm$ 8.2) and elderly (n= 50, mean age 68.3 $\pm$ 10.1) controls with normal bone density. The lower limit of detection was 0.38 pmol/l. The intra-assay and inter-assay coefficients of variation were 5.7% and 9.2%, respectively. All samples were run in duplicate. In controls, DKK-1 levels decreased significantly with age ( $r = -0.42$ ;  $p < 0.05$ ), and this decrease was higher in males than in females. Moreover, in normal subjects circulating DKK-1 were positively correlated with parathyroid hormone ( $r = 0.39$ ;  $p < 0.05$ ) in both sexes and negatively correlated with bone alkaline phosphatase in women ( $r = -0.30$ ;  $p < 0.05$ ). Interestingly, an unexpected decreased concentration of DKK-1 was observed in the group of premenopausal women and young adult men with low bone density with respect to age- and sex-matched controls (17.9 $\pm$ 8.9 vs. 42.9 $\pm$ 8.1;  $p < 0.001$ ), as well as to older controls (17.9 $\pm$ 8.9 vs. 35.4 $\pm$ 12.2;  $p < 0.001$ ). No statistically significant differences in DKK-1 were observed between elderly osteoporotic and non osteoporotic subjects. Longitudinal analysis in 34 of the 60 subjects showed a significant 33% decrease in DKK-1 levels during bisphosphonate treatment. In conclusion adult males aged 50 yrs or less and premenopausal females with low bone mass show an unexpected decrease in circulating DKK-1 levels, likely representing an homeostatic counteracting mechanism to limit the reduction in osteoblast activity.

**Disclosures:** V. De Paola, None.

## F458

**Low systemic BMD Increases Implant Migration in Cementless Hip Replacement.** H. T. Aro\*, N. Moritz\*, T. J. Mäkinen\*, J. J. Alm\*, P. Lankinen\*. <sup>1</sup>Department of Orthopaedic Surgery, Turku University Central Hospital, Turku, Finland, <sup>2</sup>Orthopaedic Research Unit, University of Turku, Turku, Finland.

Initial implant stability is critical in cementless total hip arthroplasty (THA). Although the surgical technique was originally developed only for patients with normal bone quality, many postmenopausal patients undergoing the procedure have been found to have unrecognized osteoporosis. We assumed that osteoporotic women might exhibit more marked femoral stem migration than those with normal bone density after cementless THA. Thirty-nine female patients with an average age 64 years (range, 41-78 years) underwent cementless THA (ABG II, Stryker) with hydroxyapatite-coated anatomically designed femoral stem equipped with tantalum markers for radiostereometric analysis. All patients had primary hip osteoarthritis and fulfilled other strict inclusion criteria (no inflammatory arthritis, no history of metabolic bone disease or any treatments with corticosteroids, bisphosphonates or calcitonin). The patients had a Type A (n=21) or Type B (n=18) bone quality according to the Dorr classification. On preoperative DXA screening (both hips, lumbar spine and distal non-dominant forearm), BMD was normal in 11 patients (28%), osteopenia was found in 22 patients (56%) and osteoporosis in 6 patients (15%). Fifteen patients (39%) had D-vitamin deficiency (S-25(OH)D < 50 nmol/l). According to the prevailing clinical practice, the patients were instructed to partial weight-bearing for a period of 6 weeks, followed by full weight-bearing as tolerated. RSA examinations were performed after surgery (within 3-7 days) and repeated at 3, 6 and 12 months. Three-dimensional migration of the femoral stem was calculated in relation to the postoperative examination. Radiostereometric analysis revealed only minor stem migration, but the degree of axial stem migration at 12 months was significantly related to the preoperative systemic BMD ( $R^2 = 0.191$ ,  $p = 0.005$ ). Axial stem migration (mean  $\pm$  SD) was  $-0.52 \pm 0.58$  mm in patients with normal BMD,  $-1.12 \pm 1.01$  mm in osteopenic patients and  $-2.09 \pm 1.37$  mm in osteoporotic patients. This study gave a proof of radiostereometric analysis that low systemic BMD may adversely affect initial stability of cementless THA. Although evidence of implant settling was observed in the majority of patients within 3 months and there has been no loosening of the implants within a 2-year follow-up, the results urge to evaluate long-term clinical consequences of increased initial migration and the efficacy of osteoporosis treatment as an intervention.

**Disclosures:** H.T. Aro, Stryker International 4.

This study received funding from: Academy of Finland, Turku University Central Hospital.

## F461

**Diffuse Osteopenia After Tibia Fracture: Benefits of Early Mobilization and Weight Bearing.** R. Zhao<sup>1</sup>, T. Z. Guo<sup>1</sup>, I. Sabsovich<sup>1</sup>, L. Wang<sup>1</sup>, T. Wei<sup>1</sup>, W. S. Kingery<sup>2</sup>. <sup>1</sup>PM&R Service (117), VAPAHCS, Palo Alto, CA, USA, <sup>2</sup>PM&R Service (117), VAPAHCS, Palo Alto, CA, and Orthopedic Surgery, Stanford University, Stanford, CA, USA.

After tibia fracture in man there is accelerated trabecular bone loss in the proximal and distal tibia and femur, peaking at 5 months post-fracture and persisting indefinitely. There is also bone loss in the spine and contralateral leg. The etiology of fracture-induced osteopenia is unknown. It has been proposed that early weight bearing may reduce this bone loss, but there is little clinical evidence supporting this hypothesis. In the current study we used microCT scanning to examine the effects of mobilization and weight bearing on bone loss induced by tibia fracture in 9-month-old rats. Fracture rats treated by 4 weeks cast immobilization (FX + cast) developed trabecular bone loss in the lumbar and thoracic spine, bilateral distal femurs, and right proximal humerus, but had no effect on cortical bone. Fracture rats treated by intramedullary nailing and casting (FX + nail + cast) for 4 weeks exhibited a similar pattern of bone loss. Fracture rats treated by intramedullary nailing alone (FX + nail) failed to develop any trabecular bone loss. Control rats that were not fractured but underwent hindlimb cast immobilization for 4 weeks (cast) developed the same pattern of trabecular bone loss as did the FX + cast treated rats. There were minimal differences between groups in serum chemistries or nutritional status. Neither chronic propranolol treatment or capsaicin lesioning of the sensory nerves had any effect on fracture-induced bone loss. Histomorphometric analysis demonstrated a reduction in bone volume and BFR with increased osteoclastogenesis and resorption activity in the FX + nail + cast and cast only groups, effects that were not observed in the FX + nail group. Collectively, these data indicate that immobilization after fracture caused increased bone resorption and decreased bone formation, leading to diffuse osteopenia. Early mobilization prevented bone loss in the tibia fracture rat model and may have similar beneficial effects in man.

**Disclosures:** R. Zhao, None.

This study received funding from: NIH.

## F465

**Vitamin D Deficiency, Osteomalacia and High Bone Turnover in Patients with Neurofibromatosis 1.** S. Seitz\*, C. Schnabel\*, H. Schmidt\*, F. T. Beil\*, V. F. Mautner\*, M. Amling<sup>1</sup>. <sup>1</sup>Center for Biomechanics, Experimental Trauma Surgery & Skeletal Biology, Hamburg, Germany, <sup>2</sup>Department of Clinical Chemistry, University Medical Center Hamburg Eppendorf, Hamburg, Germany, <sup>3</sup>Center of Orthopedics Wandsbek, Hamburg, Germany, <sup>4</sup>Department of Maxillofacial Surgery, University Medical Center Hamburg Eppendorf, Hamburg, Germany.

Neurofibromatosis 1 (NF-1) is a severe inherited disease with a wide range of clinical manifestations, including decreased bone mineral density. Although it is known, that patients with NF-1 suffer from vitamin D deficiency, which might be associated with skeletal mineralization defects, histologic and histomorphometric analysis in these patients is rare. Thus, we performed a detailed clinical evaluation including DEXA osteodensitometry and laboratory parameters, as well as a histomorphometric evaluation on non-decalcified sections of iliac crest biopsies from 14 patients that were set in direct comparison to biopsies from age- and sex-matched control individuals. Patients with NF-1 had significantly lower 25-(OH)-cholecalciferol serum levels, accompanied by secondary hyperparathyroidism and decreased bone mineral density. Histomorphometric analysis revealed a decreased bone volume and trabecular thickness in NF-1 patients, as well as a more than 3-fold increase in osteoid volume (OV/BV,  $0.96 \pm 0.77$  % vs.  $3.68 \pm 2.20$  %). Moreover, both osteoblast (NOB/BPm,  $2.17 \pm 0.69$  mm<sup>3</sup> vs.  $0.50 \pm 0.26$  mm<sup>3</sup>) and osteoclast (NOC/BPm,  $0.23 \pm 0.13$  mm<sup>-1</sup> vs.  $0.02 \pm 0.02$  mm<sup>-1</sup>) numbers were about 4-fold 10-fold increased respectively, indicating a high bone turnover. To analyze, whether normalization of vitamin D serum levels can improve the clinical outcome of the patients, we re-evaluated them by DEXA osteodensitometry and serum analysis after one year of treatment with 25-(OH)-cholecalciferol. Here we observed a normalization of serum PTH levels and a significant improvement in bone mineral density, indicated by an increase of T-Scores up to one standard deviation at the lumbar spine and hip. Taken together, our data provide the first complete histomorphometric analysis of non-decalcified biopsies from NF-1 patients. Moreover, they suggest that low Vitamin D levels significantly contribute to the skeletal defects associated with the disease.

**Disclosures:** S. Seitz, None.

## F469

**Rare Cases of X-linked Hypophosphatemic Rickets/Osteomalacia Mimicking Autosomal Recessive Hypophosphatemic Rickets/Osteomalacia.** T. Saito\*, H. Suzuki\*, N. Ito\*, T. Igarashi\*, T. Fujita\*, S. Fukumoto\*. <sup>1</sup>Department of Pediatrics, University of Tokyo Hospital, Tokyo, Japan, <sup>2</sup>Division of Nephrology & Endocrinology, Department of Medicine, University of Tokyo Hospital, Tokyo, Japan.

X-linked hypophosphatemic rickets/osteomalacia (XLH), autosomal dominant hypophosphatemic rickets/osteomalacia (ADHR) and autosomal recessive hypophosphatemic rickets/osteomalacia (ARHR) share common clinical features such as

impaired proximal tubular phosphate reabsorption and rather low serum 1,25-dihydroxyvitamin D for hypophosphatemia. Excess actions of fibroblast growth factor (FGF)23 are believed to have important roles in the development of these diseases. The responsible genes for XLH, ADHR and ARHR are *phosphate-regulating gene with homologies to endopeptidases on the X chromosome (PHEX)*, *FGF23* and *dentine matrix protein 1 (DMP1)*, respectively. However, it remains unclear whether these diseases can be clinically distinguished. The proband is a 39-year-old sister and her 37-year-old brother shows the same clinical features. They developed bowing legs and the treatment with vitamin D metabolites started with the diagnosis of hypophosphatemic rickets. When they came to our attention, they were hypophosphatemic (sister: P 1.8 mg/dL, brother: P 1.6 mg/dL) with high FGF23 levels (sister: 542 pg/mL, brother: 96 pg/mL). Because their parents are clinically normal without any features of rickets/osteomalacia, we presumed that they have ARHR. However, sequencing analysis of all the coding exons of *DMP1* and *FGF23* gene in these patients showed no mutation. Analysis of *PHEX* gene in the sister showed no point mutation, either. In contrast, exons 1 to 3 of *PHEX* gene could not be amplified using genomic DNA from the brother. Subsequent analysis revealed that there is deletion of 52,143 bp including exons 1 to 3 in *PHEX* gene of the brother. His sister was found to be a heterozygote for the same deletion indicating that they are suffering from XLH. The same deletion was detected in genomic DNA from the mother. Comparison of wild-type and mutant *PHEX* alleles by semi-quantitative PCR indicated that there is more wild-type allele and less mutant one in genomic DNA from the mother compared to that from the sister. These results suggested that the mother is a somatic mosaicism. Actually, she was found to be a heterozygote for one single nucleotide polymorphism situated in the deleted region of *PHEX* gene indicating she has two wild-type alleles. These results indicate that genetic analyses are essential for correct diagnosis of hypophosphatemic diseases caused by excess actions of FGF23.

**Disclosures:** T. Saito, None.

## F471

**The Human SLC34A3/NaPi-IIc Mutations T137M and L527del Uncouple Sodium-phosphate Co-transport.** C. Bergwitz<sup>1</sup>, G. Jaureguiberry<sup>1</sup>, B. Kremke<sup>\*2</sup>, K. Page<sup>\*3</sup>, O. Hion<sup>\*2</sup>, T. Carpenter<sup>4</sup>, K. Inosona<sup>3</sup>, S. Forman<sup>\*5</sup>, H. Jüppner<sup>1</sup>. <sup>1</sup>Endocrine Unit, Massachusetts General Hospital, Boston, MA, USA, <sup>2</sup>Pädiatrische Endokrinologie und Diabetologie, Universitätsklinikum Schleswig-Holstein, Campus Lübeck, Lübeck, Germany, <sup>3</sup>Endocrine Unit, Yale School of Medicine, New Haven, CT, USA, <sup>4</sup>Dept. of Pediatrics and Endocrine Unit, Yale School of Medicine, New Haven, CT, USA, <sup>5</sup>Dept. Anesthesiology, Massachusetts General Hospital, Boston, MA, USA.

We recently reported homozygous and compound heterozygous loss-of-function mutations in SLC34A3/NaPi-IIc as the cause for hereditary hypophosphatemic rickets with hypercalciuria (HHRH). To understand whether some of the point mutations reported by us and others (T137M, S138F, S192L, G196R, R468W, L527del, R353L, D237N and A413E) lead to renal phosphate wasting by reducing membrane expression, we generated expression plasmids encoding enhanced green-fluorescence protein (EGFP) concatenated to the N-terminus of wild-type or mutant human NaPi-IIc (EGFP-wt/NaPi-IIc or EGFP-mut/NaPi-IIc) to visualize membrane expression using confocal microscopy. Upon transient expression in Opossum kidney cells, G196R and R468W were not detected in apical patches (the renal brush border membrane equivalent of this cell line), nor were these mutants present in the plasma membranes of *Xenopus* oocytes following cRNA injection (50 ng/oocyte). For S138F, S192L, R353L, D237N and A413E oocyte membrane fluorescence was reduced to <20% compared to EGFP-wt/NaPi-IIc, as quantified by confocal microscopy. The T137M and L527del mutants were expressed in both kidney cells and oocytes, and sodium-dependent [33P]-uptake into oocytes corrected for surface expression was preserved. When further investigated, the Na:P-stoichiometry of simultaneous [33P]- and [22Na]-uptake was increased from 2.3±0.4 in wild-type to 7.1±3.6 and 23±13 for T137M and L527del, respectively. Two-electrode studies indicated that EGFP-mut/NaPi-IIc carrying these mutations remains non-electrogenic, like wild-type NaPi-IIc, but displayed a significant phosphate-independent inward-rectified sodium-leak current which appears to be insensitive to phosphonoformic acid (PFA), a known inhibitor of sodium-dependent phosphate co-transport. T137M and L527del may thus reduce the rate of phosphate uptake by uncoupling sodium-phosphate co-transport, suggesting that these amino acid residues have an important functional role in human NaPi-IIc. Interestingly, heterozygous carriers of T137M, L527del, and S138F presented with recurrent kidney stones and clinical characterization of additional heterozygous carriers may help to elucidate further the distinctive genotype-phenotype relations for these NaPi-IIc mutations.

**Disclosures:** C. Bergwitz, None.

This study received funding from: NIDDK, NKF, ASCI.

## F473

**The Synergistic Role of Npt2a and Npt2c in Inorganic Phosphate Metabolism of Mice.** H. Segawa<sup>\*1</sup>, A. Onitsuka<sup>\*1</sup>, Y. Tomoe<sup>\*1</sup>, J. Furutani<sup>\*1</sup>, I. Kaneko<sup>\*1</sup>, F. Aranami<sup>\*1</sup>, S. Kuwahara<sup>\*1</sup>, M. Li<sup>\*2</sup>, N. Amizuka<sup>2</sup>, M. Matsumoto<sup>\*3</sup>, M. Ito<sup>\*1</sup>, K. Miyamoto<sup>1</sup>. <sup>1</sup>Deptment of Molecular Nutrition, Institution of Health Biosciences, University of Tokushima Graduate School, Tokushima, Japan, <sup>2</sup>Center for Transdisciplinary Research, Niigata University, Niigata, Japan, <sup>3</sup>Division of Molecular Immunology, Institute for Enzyme Research, University of Tokushima, Tokushima, Japan.

Primary loss of inorganic phosphate (Pi) from the kidneys results in hypophosphatemia, the severity of which is directly related to the degree of secondary bone mineralization defects. While the renal type IIa sodium-dependent Pi co-transporters (NPT2a/Npt2a) play a major role in renal Pi reabsorption, Npt2a null mice (Npt2a<sup>-/-</sup>) do not exhibit rickets/osteomalacia. Type IIc sodium-dependent Pi co-transporter (NPT2c/Npt2c) is the pathogenic protein involved in hereditary hypophosphatemic rickets with hypercalciuria (HHRH). However, Npt2c null mice exhibit hypercalcemia, hypercalciuria, elevation of plasma 1,25(OH)<sub>2</sub>D<sub>3</sub> levels, and reduction of plasma fibroblast growth factor 23 (FGF23) levels, but not hypophosphatemia, hyperphosphaturia, rickets, or osteomalacia. The goal of the present study was to characterize the role of renal Pi wasting in bone disorders by studying Npt2a/Npt2c double knock-out mice (WKO mice). WKO mice showed severe hypophosphatemia, hypercalcemia, expansion of the late hypertrophic zone of the epiphyseal plate, and markedly-reduced bone mineralization (characteristics of rickets), which is the phenotype associated with HHRH. Na-dependent Pi transport activity was significantly decreased in WKO mice when compared with other mice groups. Urinary Pi and calcium excretion were further increased in the WKO mice when compared with Npt2a<sup>-/-</sup> mice (Npt2a<sup>-/-</sup>, Npt2c<sup>+/+</sup>). Severe hypophosphatemia in WKO mice may be secondary to impaired bone mineralization. In conclusion, maintenance of plasma Pi levels via Npt2a and Npt2c may be necessary for normal skeletal development in rodents.

**Disclosures:** H. Segawa, None.

## F476

**Co-Expression of p62<sup>P392L</sup> and MVNP in Osteoclasts (OCL) Precursors Increases the Formation of OCL that Express a Pagetic Phenotype.** Y. Hiruma<sup>1</sup>, N. Kurihara<sup>1</sup>, H. Zhou<sup>2</sup>, M. A. Subler<sup>\*3</sup>, D. W. Dempster<sup>2</sup>, J. J. Windle<sup>3</sup>, G. D. Roodman<sup>4</sup>. <sup>1</sup>Medicine/Hem-Onc, University of Pittsburgh, Pittsburgh, PA, USA, <sup>2</sup>Regional Bone Center, Helen Hayes Hospital, West Haverstraw, NY, USA, <sup>3</sup>Human Genetics, Virginia Commonwealth University, Richmond, VA, USA, <sup>4</sup>Medicine/Hem-Onc, University of Pittsburgh and VA Pittsburgh Healthcare System, Pittsburgh, PA, USA.

Both environmental and genetic abnormalities contribute to the development of Paget Disease (PD). We recently reported that expression of measles virus nucleocapsid protein (MVNP) in OCL in mice induces pagetic-like OCL (hyper-responsive to 1,25-(OH)<sub>2</sub>D<sub>3</sub>, hypermultinucleated, increased bone resorbing capacity/OCL) and PD-like bone lesions in 30% of mice, while expression of the p62<sup>P392L</sup> mutation, the most frequent mutation linked to PD, increases RANKL responsiveness in OCL precursors but does not induce PD in vivo. It is our hypothesis that both MVNP and p62<sup>P392L</sup> are necessary for development of PD in patients. We used the TRAP promoter to examine the effects of targeted co-expression of the MVNP gene and p62<sup>P392L</sup> in OCL precursors on the development of PD-like OCL, and their capacity to induce high levels of IL-6 as found in PD by breeding TRAP-p62<sup>P392L</sup> mice with TRAP-MVNP mice. Wild-type (WT) and TRAP-p62<sup>P392L</sup> transgenic mice were not hyper-responsive to 1,25-(OH)<sub>2</sub>D<sub>3</sub>. However, OCL precursors from both TRAP-MVNP and the double transgenic TRAPp62<sup>P392L</sup>/TRAP-MVNP mice were hyper-responsive to 1,25-(OH)<sub>2</sub>D<sub>3</sub>, and the levels of OCL formation were increased in the doubly-transgenic mice. As anticipated, TRAP-p62<sup>P392L</sup>/TRAP-MVNP-doubly-transgenic mice but not WT or TRAP-MVNP mice were hyper-responsive to RANKL. OCL formed in marrow cultures derived from both the TRAP-MVNP and the doubly-transgenic mice produced high levels of IL-6 when treated with 1,25-(OH)<sub>2</sub>D<sub>3</sub> and secreted elevated levels of IL-6 even in the absence of 1,25-(OH)<sub>2</sub>D<sub>3</sub>. In contrast, OCL precursors from TRAP-p62<sup>P392L</sup> mice did not produce increased levels of IL-6. The doubly transgenic OCL precursors appeared to secrete more IL-6 than TRAP-MVNP mice. OCL formed in vitro in marrow cultures from TRAP-MVNP/TRAP-p62<sup>P392L</sup> doubly-transgenic mice were markedly increased in size and number and have increased numbers of nuclei per OCL. These results suggest that co-expression of p62<sup>P392L</sup> with MVNP in OCL precursors should create a more robust PD phenotype in OCL in vivo.

**Disclosures:** Y. Hiruma, None.

This study received funding from: NIH/NIAMS.



## F478

**High Levels of IL-6 and Hyper-responsivity to 1,25-(OH)<sub>2</sub>D<sub>3</sub> Are Both Required for Development of Pagetic Osteoclasts (PD-OCL).** Y. Hiruma<sup>1</sup>, N. Kurihara<sup>1</sup>, H. Zhou<sup>2</sup>, M. A. Subler<sup>\*3</sup>, D. W. Dempster<sup>2</sup>, J. J. Windle<sup>3</sup>, G. D. Roodman<sup>4</sup>. <sup>1</sup>Medicine/Hem-Onc, University of Pittsburgh, Pittsburgh, PA, USA, <sup>2</sup>Regional Bone Center, Helen Hayes Hospital, West Haverstraw, NY, USA, <sup>3</sup>Human Genetics, Virginia Commonwealth University, Richmond, VA, USA, <sup>4</sup>Medicine/Hem-Onc, University of Pittsburgh and VA Pittsburgh Healthcare System, Pittsburgh, PA, USA.

Our most recent studies show that measles virus nucleocapsid protein (MVNP) can induce development of PD-OCL and pagetic lesions in vivo. MVNP induces both hyper-responsivity of OCL precursors to 1,25-(OH)<sub>2</sub>D<sub>3</sub> through increased expression of a novel VDR co-activator, TAF<sub>II</sub>-17, and high levels of IL-6 in the local bone microenvironment. Our hypothesis is that high levels of IL-6 and hyper-responsivity to 1,25-(OH)<sub>2</sub>D<sub>3</sub> are both required for development of PD-OCL. To test this hypothesis, TRAP-MVNP mice, which have MVNP targeted to the OCL lineage using the TRAP promoter and develop pagetic-like bone lesions, were mated with IL-6<sup>-/-</sup> mice to generate TRAP-MVNP/IL-6<sup>-/-</sup> mice. TRAP-TAF<sub>II</sub>-17 mice were generated to induce OCL that were hyper-responsive to 1,25-(OH)<sub>2</sub>D<sub>3</sub>. TRAP-MVNP, TRAP-MVNP/IL-6<sup>-/-</sup> and TRAP-TAF<sub>II</sub>-17 mice were then tested for their capacity to form OCL that express a pagetic phenotype in vitro. OCL precursors from TRAP-MVNP and TAF<sub>II</sub>-17 but not TRAP-MVNP/IL-6<sup>-/-</sup> mice were hyper-responsive to 1,25-(OH)<sub>2</sub>D<sub>3</sub> even though OCL precursors from MVNP/IL-6<sup>-/-</sup> mice still expressed increased levels of TAF<sub>II</sub>-17 when treated with 1,25-(OH)<sub>2</sub>D<sub>3</sub>. As expected, OCL formation in marrow cultures from both TRAP-MVNP/IL-6<sup>-/-</sup> mice, TRAP-MVNP and WT mice showed similar responses to RANKL. High levels of IL-6 were produced by OCL from TRAP-MVNP, and not by WT or TRAP-TAF<sub>II</sub>-17 mice. OCL precursors from TRAP-MVNP and TRAP-TAF<sub>II</sub>-17 mice also showed increased 24(OH)-ase activity compared to WT mice when treated with low concentrations (10<sup>-11</sup>M) of 1,25-(OH)<sub>2</sub>D<sub>3</sub>. Although OCL precursors from TRAP-TAF<sub>II</sub>-17 were hyper-responsive to 1,25-(OH)<sub>2</sub>D<sub>3</sub> and formed increased OCL numbers, they did not form PD-OCL (hyper-multinucleated, increased bone resorption capacity). In contrast, addition of high levels of IL-6 enhanced OCL formation in marrow cultures from TRAP-TAF<sub>II</sub>-17 mice, and the OCLs that formed expressed a pagetic phenotype. These data suggest that expression of TAF<sub>II</sub>-17 in the presence of IL-6 is required for hypersensitivity of OCL precursors to 1,25-(OH)<sub>2</sub>D<sub>3</sub> and that high levels of IL-6 combined with hypersensitivity of OCL precursors to 1,25-(OH)<sub>2</sub>D<sub>3</sub> may be sufficient to induce PD-OCL and pagetic bone lesions in vivo.

**Disclosures:** Y. Hiruma, None.

This study received funding from: NIH/NIAMS.

## F480

**FGF-2 Stimulates RANK Ligand Expression in Paget's Disease of Bone.** K. Sundaram<sup>1</sup>, J. Senn<sup>\*2</sup>, D. S. Rao<sup>3</sup>, S. V. Reddy<sup>1</sup>. <sup>1</sup>Charles P. Darby Children's Research Institute, Medical University of South Carolina, Charleston, SC, USA, <sup>2</sup>Bristol Myers Squibb Pharmaceuticals, Syracuse, NY, USA, <sup>3</sup>Henry Ford Hospital, Detroit, MI, USA.

RANK ligand (RANKL), a critical osteoclastogenic factor expressed in marrow stromal/preosteoblast cells is upregulated in Paget's disease of bone (PDB). We previously demonstrated that heat shock factor-2 (HSF-2) is a downstream target of fibroblast growth factor-2 (FGF-2) signaling to induce RANKL expression in bone marrow stromal/preosteoblast cells. In this study, we identified a 2.5-fold increase in serum FGF-2 levels in patients (n=8) with PDB compared to normal subjects (n=10). We showed that HSF-2 co-immunoprecipitates with heat shock protein-27 (HSP-27) and that FGF-2 stimulation significantly increased phospho-HSP-27 levels in marrow stromal cells. Confocal microscopy demonstrated HSF-2 co-localization with HSP-27 in unstimulated cells. Recent evidence indicates suppressors of cytokine signaling (SOCS) interact with and modulate FGF signaling. We therefore hypothesized that FGF-2 modulates SOCS levels to enhance RANKL expression in PDB. Interestingly, real-time PCR analysis demonstrated a significant increase in the levels of SOCS-1 (3.4-fold) and SOCS-3 (3.5-fold) mRNA expression in pagetic bone marrow mononuclear cells. Also, FGF-2 stimulation enhanced SOCS-1 and SOCS-3 mRNA expression 5.3 and 4.8-fold in stromal/preosteoblast cells respectively. We next examined if SOCS plays a role in FGF-2 signaling to modulate RANKL expression in PDB. Co-expression of SOCS-1/3 with hRANKL gene promoter-luciferase reporter plasmid in bone marrow stromal cells demonstrated a 3.0-fold increase in promoter activity without FGF-2 stimulation. Since signal transducers and activators of transcription (STAT) molecules are implicated in growth factor signaling and SOCS expression, we further examined participation of STAT in FGF signaling to enhance RANKL expression in marrow stromal/preosteoblast cells. FGF-2 stimulation significantly increased the levels of p-STAT-1/3 in these cells. Western blot analysis demonstrated that siRNA suppression of STAT-1/3 decreased (3.2-fold) RANKL expression in FGF-2 stimulated cells. Also, FGF-2 stimulated hRANKL gene promoter activity was significantly decreased by siRNA suppression of STAT-1/3. These results suggest STAT-1/3 are downstream effectors of FGF-2 signaling and that elevated levels of FGF-2 stimulates RANKL expression in PDB.

**Disclosures:** K. Sundaram, None.

This study received funding from: NIH.

## F483

**A New Long-Acting PTH/PTHrP Hybrid Analog that Binds to a Distinct PTHR Conformation has Superior Efficacy in a Rat Model of Hypoparathyroidism.** M. Shimizu<sup>\*1</sup>, F. Ichikawa<sup>\*1</sup>, H. Noda<sup>\*1</sup>, M. Okazaki<sup>1</sup>, C. Nakagawa<sup>\*1</sup>, T. Tamura<sup>\*1</sup>, T. J. Gardella<sup>2</sup>, J. T. Potts<sup>2</sup>, E. Ogata<sup>3</sup>, O. Kuromaru<sup>\*1</sup>, Y. Kawabe<sup>\*1</sup>. <sup>1</sup>Pharmaceutical Research Dept.1, Chugai Pharmaceutical Co., LTD., Gotemba, Shizuoka, Japan, <sup>2</sup>Endocrine Unit, Massachusetts General Hospital, Boston, MA, USA, <sup>3</sup>Cancer Institute Hospital, Tokyo, Japan.

Conventional therapy for hypoparathyroidism (HPT) with vitamin D analogs and calcium (Ca) is often accompanied by hypercalciuria. PTH(1-34) has been used as an alternative option, but it requires frequent injections. Thus, a long-acting PTH analog that can normalize serum Ca (sCa) levels via once-daily injection would provide more convenient and efficacious therapy for HPT than PTH. We previously reported that the modified analog, M-PTH(1-28) (M = Ala1,12,Aib3,Gln10,Har11,Trp14,Arg19) binds with greater affinity to the G-protein-uncoupled receptor conformation (R<sup>1</sup>), and produces more prolonged calcemic responses in mice than does PTH(1-34). In the present study, we evaluated a new R<sup>1</sup>-selective analog, [Ala1,3,12,Gln10,Arg11,Trp14]-PTH(1-14)/PTHrP(15-36), termed super-potent PTH, or SP-PTH, that shows even longer calcemic actions in rats than does M-PTH(1-28), as a candidate treatment for HPT. Upon single injection (i.v.) into thyroparathyroidectomized (TPTX) rats, PTH(1-34) control, at a dose-range of 1.25 - 20 nmol/kg, transiently increased sCa and decreased serum phosphorus (sPi) levels at 1 hr, but not to the normal range, as levels returned to pre-injection conditions by 6 hrs. In contrast, SP-PTH, at doses of 1.25 and 5 nmol/kg, increased sCa and decreased sPi to normal levels within 6 hrs, and these levels were maintained for 24 hrs. Blood concentrations of SP-PTH and PTH(1-34) were similar at times after injection, suggesting similar PK profiles for the two peptides. The effectiveness of SP-PTH in TPTX rats was then examined by repeated treatment. Animals were treated once-daily and for 2 weeks with either SP-PTH, via s.c. injection over a dose-range of 1 to 8 nmol/kg, or 1α(OH) vitamin D<sub>3</sub>, via oral administration over a dose-range of 0.075 to 0.2 μg/kg. Both 1α(OH) vitamin D<sub>3</sub> and SP-PTH normalized sCa in dose-dependent fashion; but, where 1α(OH) vitamin D<sub>3</sub> induced hypercalciuria, SP-PTH decreased urinary Ca excretion. Both agents ameliorated hyperphosphatemia and increased urinary phosphorus excretion. Neither SP-PTH at 1 to 4 nmol/kg, nor 1α(OH) vitamin D<sub>3</sub> caused significant increases in serum CTX or urinary DPD levels after 2-weeks of treatment. The results indicate that SP-PTH can normalize hypocalcemia in TPTX rats without causing hypercalciuria and excessive bone resorption over a certain dose range, and therefore the peptide would be a convenient and efficacious treatment option for HPT with little risk of renal complications.

**Disclosures:** M. Shimizu, None.

## F485

**PTH Increases Bone Turnover in Hypoparathyroidism.** M. R. Rubin<sup>1</sup>, S. Cremers<sup>1</sup>, D. W. Dempster<sup>2</sup>, J. Sliney<sup>\*1</sup>, D. J. McMahon<sup>1</sup>, H. Zhou<sup>2</sup>, T. Nickolas<sup>\*1</sup>, E. M. Stein<sup>1</sup>, J. P. Bilezikian<sup>1</sup>. <sup>1</sup>Columbia University, New York, NY, USA, <sup>2</sup>Helen Hayes Hospital, New York, NY, USA.

Hypoparathyroidism (HypoPT) is a disorder in which PTH is absent from the circulation. In addition to the biochemical manifestations of hypocalcemia and relative hypercalciuria, bone turnover is low. We sought to quantify bone turnover in HypoPT and to determine whether low bone turnover can be enhanced by PTH. We measured biochemical markers of bone turnover in 12 HypoPT subjects (8 women; 53 ± 9 yr) at baseline, and at monthly intervals during treatment with 100 μg of hPTH(1-84)[PTH] every other day for 2 yrs. Correlations with histomorphometric indices of bone turnover were assessed from measurements of iliac crest bone biopsy samples obtained before (n=10) and after 1 (n=3) or 2 (n=7) yrs of PTH treatment. Biochemical markers of bone turnover, measured thrice at baseline, were in the lower half of the normal reference ranges. With PTH, bone turnover markers increased significantly, peaking at 5-9 months, but fell to baseline levels by 2 yrs. Bone formation markers peaked at 6 mos with PINP (+211% from baseline to maximum level; 52 ± 127 to 162 ± 122 ng/ml; nl: 16-96); and OC (+235% from baseline to maximum level; 14 ± 41 to 47 ± 40 ng/ml; nl: 11-38); followed at 9 mos by BSAP (+47% from baseline to maximum level; 34 ± 26 to 51 ± 25 U/l; nl: 12-43). Bone resorption markers peaked at 5 mos with TRAP-5b (+84% from baseline to maximum level; 3.2 ± 3 to 6.0 ± 3 U/l; nl: 1.8-4.0); followed at 6 mos by s-CTX (+190% from baseline to maximum level; 0.4 ± 1 to 1.1 ± 1 ng/ml; nl: 0.11-1.35). Increases in bone turnover markers predicted increases in dynamic histomorphometric indices of bone remodeling: PINP predicted bone formation rate at 1 yr (R<sup>2</sup>=0.9, slope=0.01 ± 0.1, p=0.002) and at 2 yrs (R<sup>2</sup>=0.9, slope=0.01 ± 0.1, p<0.0001), osteoid perimeter at 1 yr (R<sup>2</sup>=0.9, slope=0.05 ± 0.1, p<0.0001) and mineralized perimeter at 2 yrs (R<sup>2</sup>=0.9, slope=0.04 ± 0.1, p<0.0001); BSAP predicted mineralized perimeter at 1 yr (R<sup>2</sup>=0.9, slope=0.17 ± 0.1, p<0.0001) and mineral apposition rate at 1 yr (R<sup>2</sup>=0.9, slope=0.01 ± 0.1, p=0.02); TRAP-5b predicted osteoid thickness at 1 yr (R<sup>2</sup>=0.5, slope=0.62 ± 0.2, p=0.02); s-CTX predicted mineral apposition rate at 1 yr (R<sup>2</sup>=0.9, slope=0.25 ± 0.1, p=0.04). We conclude that bone turnover is low in a state of chronic PTH deprivation and that the administration of PTH increases bone turnover in the hypoparathyroid skeleton. The dynamic changes occur within the first year of therapy, with all biochemical markers of bone remodeling returning to baseline levels by 2 yrs. Whether these changes lead to long term effects on skeletal dynamics and bone strength remains to be seen.

**Disclosures:** M.R. Rubin, None.

## F488

**Recovery from Hepatitis C-Associated Osteosclerosis (HCAO) Following Anti-viral Treatment.** R. Javier<sup>\*1</sup>, M. de Vernejoul<sup>2</sup>, N. Afif<sup>\*1</sup>, F. Habersetzer<sup>\*3</sup>, J. Kuntz<sup>\*1</sup>, J. Sibilia<sup>\*1</sup>. <sup>1</sup>Rheumatology, University Hospital, Strasbourg, France, <sup>2</sup>Inserm U606, Paris, France, <sup>3</sup>Hepatology, University Hospital, Strasbourg, France.

HCAO is characterized by a generalized increase in bone mass with a marked cortical thickening and deep bone pain and tenderness of the limbs in adults infected with hepatitis C virus (HVC). However, the pathogenesis remains imperfectly known as no direct relationship between HVC and osteosclerosis has yet been described. The purpose of this case report is to demonstrate clinically the causal relationship between HVC and bone. Case report: A 67 year-old nun was hospitalized in 1991 for ill-defined pain of the lower limbs. Compared to the normal X-rays of 1987, her radiographs revealed condensation (opacities) of all vertebrae, and thickening of femoral cortices. DEXA revealed a T-score of +7.62 at the Lumbar Spine (LS). Biochemical analysis showed: hypocalcemia 1.99 mmol/l (2.20-2.70), normal phosphorus 1.24 mmol/l and 25(OH) D 41.3 µg/l (6-30), increased PTH 177 pg/ml (10-60), increased alkaline phosphatase ALP 716 IU/l (N : 80-220), elevated γ-GT 93 U/l (11-85) with normal transaminases and negative hepatitis B, C and A serology. Undecalcified bone biopsy revealed woven bone in the trabeculae, associated with intra-cortical hyperostoidosis but with a normal mineralization rate (0.78µm/d). However, osteomalacia was evoked and vitamin D and calcium treatment was initiated. In 2000, radiographs showed an enhanced osteosclerosis, with clear thickening of cortical bones. Biochemical evaluation indicated: normal calcium, phosphorus, ALP, PTH and 25(OH) D and increased transaminases (ALAT 59 U/l and ASAT 68 U/l), positive HVC serology, weak viremia (0.28 x 105 virus particles/ml) with no co-infection with HIV. Hepatic biopsy revealed lesions of moderately active and fibrosing chronic hepatitis (Metavir index: A2 F2; Knodell score: 12). The bone marrow biopsy showed normal polymorphous marrow. DXA revealed a T-score: + 5.53 at the LS and + 15.9 at the femoral neck (FN). HCAO was diagnosed and a six-month treatment with ribavirin and interferon was undertaken, resulting in the absence of all detectable RNA following one month treatment. In June 2007, while HVC remained undetectable and transaminases normal, X-rays showed weakening of the sclerosis of the vertebrae and reduction of the width of femoral cortices. A dramatic decrease in BMD was noticed: T-score: + 0.5 at the LS and + 4.03 at the FN. Serum bone markers were in the normal range. In conclusion, we report here the first case of HCAO recovery after anti-viral treatment with clear decline in BMD and decreased trabecular and cortical radiological condensation in the absence of any specific bone treatment. This case straighten the relationship between HVC and bone sclerosis

**Disclosures:** R. Javier, None.

## F491

**Increased Proinflammatory Cytokines TNF-α and IL-6 Correlate with Pathological Bone Turnover Markers in Diabetic Patients with Acute Charcot Foot.** C. Moniz<sup>1</sup>, N. Petrova<sup>\*2</sup>, R. Musto<sup>\*1</sup>, S. Thomson<sup>\*1</sup>, T. Dew<sup>\*1</sup>, M. Edmonds<sup>\*2</sup>. <sup>1</sup>Clinical Biochemistry, Kings College Hospital, UK, United Kingdom, <sup>2</sup>Diabetes Foot Clinic, Kings College Hospital, UK, United Kingdom.

The Charcot foot is characterised by acute inflammation but its role in the pathogenesis is poorly understood. This study shows that the proinflammatory cytokines, tumour necrosis factor-α (TNF-α) and interleukin-6 (IL-6), as well as high sensitive C-reactive protein (hsCRP) - an acute phase protein, are raised in acute Charcot osteoarthropathy and are significantly associated with serum C-telopeptide of type I collagen (CTX), a marker of bone resorption. We studied 3 groups of patients: 27 presenting with acute Charcot osteoarthropathy; 14 with chronic Charcot osteoarthropathy and 24 diabetic control patients. In acute Charcot patients, there was a significant increase in the serum levels of IL-6 (3.84 ± 3.55 pg/ml) compared with chronic Charcot patients (1.73 ± 1.23 pg/ml) and diabetic controls (1.86 ± 1.52 pg/ml), p=0.025. Furthermore, there was a significant rise in serum TNF-α in acute Charcot patients (1.74 ± 0.94 pg/ml) compared with chronic Charcot patients (1.25 ± 0.38) and diabetic control patients (1.12 ± 0.38 pg/ml), p=0.008. Similarly, serum levels of hsCRP were significantly increased in acute Charcot patients (10.1 ± 13.4 mg/L) compared with chronic Charcot patients (2.6 ± 2.2 mg/L) and diabetic control patients (4.8 ± 4.3 mg/L), p=0.013. Serum CTX, a breakdown product of type I collagen, was significantly raised in patients with acute Charcot foot (0.409 ± 0.395 ng/ml), compared with patients with chronic Charcot foot (0.095 ± 0.042 ng/ml) and diabetic patients (0.107 ± 0.68 ng/ml), p=0.001. Serum bone specific alkaline phosphatase (BAP), a marker of bone formation, was also significantly raised in acute Charcot patients (18.5 ± 9.2 µg/L) compared with chronic Charcot patients (12.7 ± 4.42 µg/L) and diabetic controls (14.7 ± 5.13 µg/L), p=0.041. Serum osteoprotegerin (OPG), a cytokine that modulates bone resorption and osteoclastic activity, was significantly raised in acute Charcot patients (5.52 ± 1.74 pmol/L) compared with chronic Charcot patients (4.86 ± 1.42 pmol/L) and diabetic patients (4.37 ± 1.38 pmol/L), p=0.048. Serum IL-6 (r=0.472, p<0.001) and TNF-α levels (r=0.556, p<0.001) were significantly associated with serum CTX. Similarly, serum hsCRP levels were significantly correlated with serum CTX (r=0.561, p<0.001). This study indicates that inflammation, as reflected by the proinflammatory markers TNF-α and IL-6, and hsCRP plays an important role in the pathological bone resorption of the acute Charcot foot.

**Disclosures:** C. Moniz, None.

## F494

**Premature Aging-Like Phenotypes in Metastasis-Associated Protein 1 (Mta1) Null Mice.** S. Takiguchi<sup>\*1</sup>, M. Yaguchi<sup>\*2</sup>, K. Ogawa<sup>\*2</sup>, Y. Wada<sup>\*2</sup>, K. Matsusue<sup>\*3</sup>, T. Ito<sup>\*4</sup>, H. Hamamoto<sup>\*4</sup>, N. Akimitsu<sup>\*4</sup>, K. Sekimizu<sup>\*4</sup>, Y. Toh<sup>\*1</sup>, H. Iguchi<sup>\*5</sup>. <sup>1</sup>National Kyushu Cancer Center, Fukuoka, Japan, <sup>2</sup>Graduate School of Pharmaceutical Sciences, Kyushu University, Fukuoka, Japan, <sup>3</sup>Faculty of Pharmaceutical Sciences, Fukuoka University, Fukuoka, Japan, <sup>4</sup>Graduate School of Pharmaceutical Sciences, University of Tokyo, Tokyo, Japan, <sup>5</sup>National Shikoku Cancer Center, Matsuyama, Japan.

The metastasis-associated gene 1 (mta1) was identified initially in rat highly metastatic cancer cell lines. The expression level of human MTA1 correlates with the metastatic potential of several human cancer cell lines and tissues. MTA1 is a component of the nucleosome remodeling and deacetylation complex (NuRD), which is associated with adenosine triphosphate (ATP)-dependent chromatin remodeling and transcriptional regulation. MTA1 also interacts with estrogen receptor alpha (ER) and represses ER transcription by recruiting histone deacetylase (HDAC) to estrogen response element (ERE)-containing target gene chromatin. To study the biological effect of Mta1, we generated mice with a null mutation in the Mta1 gene. The birth rate of Mta1-deficient (Mta1KO) mice was lower and the mice were smaller than wild-type (WT) mice. Mta1KO mice had a short life span (ca. 70% of WT) and showed numerous features consistent with premature aging-like phenotypes, including lordokyphosis, muscle wasting, osteoporosis, cataract, low fertility and atrophy of the skin, testis, ovary, liver and adrenal. To examine the type of osteoporosis, computerized tomography (CT) scanning and histomorphometric analysis were performed. The density of cortical bone and substantia spongiosa from Mta1KO mice was reduced to 40-80% of that from age-matched WT mice by CT scanning. The osteoblastic and osteoclastic surface, and the number of multinuclear osteoclasts from Mta1KO mice were considerably decreased compared with that from WT mice by histomorphometric analysis. These results suggest that osteoporosis seen in Mta1KO mice is low-turnover type, which is consistent with senile osteoporosis. Mta1KO ES cells showed aberrant expression of several genes, including estrogen-regulated genes, compared to WT ES cells at the mRNA level by DNA microarray analysis. Mouse embryonic fibroblasts (MEF) from Mta1KO mice showed greater acceleration of replicative senescence than WT MEF. Several tissues from Mta1KO mice showed a higher expression of CDK inhibitors (p16INK4a, Arf, p15INK4b, p21CIP), biomarkers of aging, than tissues from WT mice at the mRNA level by real-time PCR. In conclusion, Mta1KO mice are a novel model of premature aging with aberrant estrogen-regulated pathways.

**Disclosures:** S. Takiguchi, None.

## F500

**In utero Stem Cell Therapy as Treatment for Classical Osteogenesis Imperfecta Using the Knock In Murine Model BrtlIV.** C. Panaroni<sup>\*1</sup>, R. Gioia<sup>\*1</sup>, A. Lupi<sup>\*1</sup>, A. Farina<sup>\*2</sup>, M. Casasco<sup>\*2</sup>, E. Perilli<sup>\*3</sup>, F. Baruffaldi<sup>\*1</sup>, G. Cetta<sup>\*1</sup>, S. A. Goldstein<sup>\*4</sup>, J. Kreider<sup>\*4</sup>, I. Villa<sup>\*5</sup>, A. Rossi<sup>\*1</sup>, J. C. Marini<sup>\*6</sup>, A. Frattini<sup>\*7</sup>, P. Vezzoni<sup>\*8</sup>, A. Forlino<sup>\*1</sup>. <sup>1</sup>Department of Biochemistry, University of Pavia, Pavia, Italy, <sup>2</sup>Department of Experimental Medicine, University of Pavia, Pavia, Italy, <sup>3</sup>Laboratorio di Tecnologia Medica, Istituti Ortopedici Rizzoli, Bologna, Italy, <sup>4</sup>Orthopaedic Research Laboratories, University of Michigan, Ann Arbor, MI, USA, <sup>5</sup>Bone Metabolic Unit, San Raffaele Scientific Institute, Milan, Italy, <sup>6</sup>BEMB, NICHD, NIH, Bethesda, MD, USA, <sup>7</sup>Istituto Clinico Humanitas, Rozzano, Milano, Italy, <sup>8</sup>Istituto Clinico Rozzano, Milan, Italy.

Classical Osteogenesis Imperfecta (OI) is a genetic bone disorder characterized by skeletal fragility and deformity and caused by mutations in the type I collagen genes. BrtlIV is a knock-in murine model for OI which carries the typical glycine substitution and whose phenotype models the moderately severe Type IV OI. We developed a cell therapy treatment which employs *in utero* transplantation to avoid marrow ablation for this metabolic inborn disorder. The bone marrow cells were isolated from long bones of eGFP-CD1 mice and injected into the liver of E14.5 BrtlIV and WT embryos. Mice were analyzed at 2 m, the age corresponding to the severest BrtlIV bone phenotype compared to WT. Engraftment with a characteristic patchy distribution was detected in various tissues at sacrifice by inverted microscopy. Confocal microscopy was used to directly quantify the engraftment in long bone diaphysis (3.82 ± 5.00%). The percentage of donor cells was determined by FACS, in both bone marrow (F 1.3 ± 1.8, n=18; M 0.47 ± 0.33, n=15) and spleen (F 1.48 ± 1.88, n=18; M 1.16 ± 0.83, n=16) and by Real Time PCR in different tissues. The femur length was increased in transplanted mutant mice (p<0.005). PQCT of the distal femoral metaphysis revealed increased total bone and trabecular density in treated versus untreated mutant mice. Micro CT analysis of Brtl mid-shaft femur detected improvement in Total Mineral Content, Cortical Thickness and Cortical Area. Biomechanical studies are ongoing. The analysis of the treated mice suggested that *in utero* cell therapy is a promising treatment for classical OI in spite of a relatively low engraftment.

**Disclosures:** A. Forlino, None.

This study received funding from: MIUR 2006 (Grant n. 2006050235) to A.F. (1), Fondazione Cariplo to A.F. (1,2,3), Progetto Nobel to P.V. and the European Community (FP6, LSHM-CT-2007-037471) to A.R.

## F508

**Odanacatib Increases Bone Strength and Maintains Bone Quality in Estrogen Deficient Adult Rhesus Monkeys.** K. R. Scott<sup>1</sup>, B. Pennypacker<sup>1</sup>, R. Samadfan<sup>2</sup>, S. Y. Smith<sup>\*2</sup>, D. B. Kimmel<sup>1</sup>. <sup>1</sup>Molecular Endocrinology, Merck, West Point, PA, USA, <sup>2</sup>Montreal Preclinical Services, Charles River, Montreal, QC, Canada.

Odanacatib (ODN) is a selective inhibitor of Cathepsin K (CatK) in large animals and humans. Though CatK inhibition is a promising mechanism to treat osteoporosis, more bone strength/quality data in the adult skeleton during longer treatment are needed. Rhesus monkeys (aged 13-19yrs) were ovariectomized (OVX) and given ODN (0 [N=11], 6 [N=8], or 30 [N=10] mg/kg (qd, PO)) for 21 months. Quarterly bone mineral density (BMD) measurements of spine (LV), femoral neck (FN), and total hip (H) was done. At necropsy, LV4-6 and the right femur were frozen.

The mid-point of the femur (CF) was tested in three-point bending. The femoral neck (FN) was tested in shearing. The fourth vertebral body (L4) was trimmed of endplates/processes and tested in compression. Load-deformation curves were used to calculate Ultimate Load (F.U, N), Stiffness (N/mm), Toughness (N-mm) and Ductility (mm). Peripheral quantitative computed tomography (pQCT) was done (CF and L4) to derive BMC and architectural endpoints at the site of failure.

**Results:** Baseline LVBMD differed little among the groups. Final LVBMD was 11% and 17% higher; HBMD was 10% and 16% higher and FNBMD was 11% and 12% higher than OVX+0, in the ODN groups.

CFCTh was higher (16%), as were CFFU (25-32%) and CFStiffness (23-33%) with ODN than OVX+0. FNFU was 17-19% higher and L4FU was 18% higher with ODN. Toughness and ductility (L4 only), did not differ among groups. CFFU and CFStiff correlated to CFBMC ( $r=0.95$ ;  $P<0.0001$  and  $r=0.82$ ;  $P<0.0001$ ;  $N=28$ ). LV4FU and LV4Stiff correlated to LV4BMC ( $r=0.79$ ;  $P<0.0001$  and  $r=0.46$ ;  $P<0.02$ ;  $N=27$ ). CFFU and CFStiff correlated to CFCTh ( $r=0.70$ ;  $P<0.0001$  and  $r=0.46$ ;  $P<0.02$ ;  $N=28$ ).

**Summary:** ODN-treated adult non-human primates have higher bone mass in sites of osteoporotic fracture in humans. ODN-treated animals have greater bone strength and stiffness in the central femur and trends toward better bone strength at the femoral neck and spine. The relationship of bone mass to bone strength, toughness and brittleness are normal. ODN increases bone mass and strength, while maintaining normal bone quality in adult non-human primates.

Endpoint/Group	OVX+0 (N=11)	OVX+6mg/kg ODN (N=8)	OVX+30mg/kg ODN (N=9)	ANOV A (P=)
CFCTh (mm)	1.82±0.26	2.10±0.14*	2.12±0.226**	0.022
CFFU (N)	1203±195	1507±251**	1589±203***	0.002
CF Stiffness (N/mm)	875±127	1067±248*	1157±212***	0.009
FNFU (N)	2026±444	2405±307	2379±467	0.091
L4FU (N)	3398±797	4017±1012	4017±972	0.283
L4 Ductility (mm)	0.979±0.207	0.990±0.144	0.942±0.170	0.767

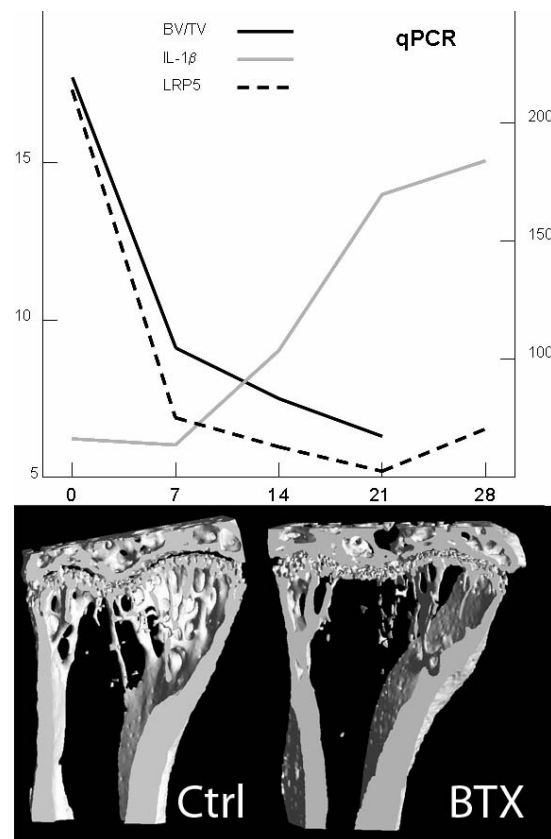
Mean±SD; \*(P<0.05); \*\*\*(P<0.001) vs. OVX (H)-hip, (LV)-spine, CF-central femur, FN-femoral neck

**Disclosures:** K.R. Scott, None.

## F516

**Disuse with a Rapid Bone Loss Affects the Expression Profile of Osteoblastic and Resorption Genes.** M. Le Drévo<sup>\*</sup>, H. Libouban<sup>\*</sup>, D. Chappard. Faculty of Medicine, INSERM U922, Angers, France.

Prolongated disuse reproduces the effects of microgravity and induces a rapid bone loss due to reduced strains. It increases the risk of irreversible damage to the skeleton. Disuse of one extremity can be induced in different ways (denervation, spinal section, tenotomy...) leading to a permanent immobilization and inducing a rapid bone loss. Nonsurgical methods (casting, bandaging, tail suspension or Botulinum toxin (BTX) injection) have become more popular. Decrease in the formation rate and increase in resorption rate have been simultaneously advocated. The aim of the present study was to elucidate the molecular events that occur in the microenvironment of immobilized bone. A single BTX injection in the quadriceps was used to induce paralysis of the right hindlimb in Swiss-Webster mice; saline injection in the left side was used as control. Bone marrows from the left and right femurs were extracted after euthanasia at 0, 7, 14, 21 and 28 days post- BTX. RNAs were extracted to perform qPCR analyses. Bone loss was measured by microCT on the tibia upper extremity. On the right side, 3D measurements showed a significant decrease in bone volume as from 7 days (-31%) associated with microarchitectural changes that intensified in time (-45.9% at 21 days). However, no significant differences in cortical thickness were observed. Expression of bone formation factors was significantly reduced as from 7 days and maintained until 28 days post-BTX; among them LRP5/6, Osteopontin, TGF- $\beta$ , Oncostatin and Runx2. At the opposite, the expression of IL-1 $\beta$ , an indicator of bone resorption, was increased as from 14 days. In conclusion, a localized disuse induces rapid modifications in the gene expression profile in the bone microenvironment leading to an early decrease of bone formation factors and an increase in bone resorption.



**Disclosures:** M. Le Drévo, None.

## F523

**The Short-Term Deleterious Skeletal Response to Hindlimb Suspension Involves Multi-Faceted Compromises in Cells of the Osteogenic Lineage.** K. M. Nicks<sup>1</sup>, T. B. Palculict<sup>\*1</sup>, N. S. Ake<sup>1\*</sup>, P. M. Savage<sup>\*1</sup>, E. E. Dupont-Versteegden<sup>\*2</sup>, L. J. Suva<sup>1</sup>, D. Gaddy<sup>1</sup>. <sup>1</sup>Physiology and Biophysics & Orthopaedic Surgery, University of Arkansas for Medical Sciences, Little Rock, AR, USA, <sup>2</sup>Rehabilitation Sciences, University of Kentucky, Lexington, KY, USA.

It is well established that musculoskeletal disuse leads to a significant loss of skeletal mass and strength in the load-bearing bones of both young and old animals and humans. Using evidence obtained from a rodent model of hindlimb suspension (HS), it has been concluded that a major component of disuse-associated bone loss is related to a decrease in bone formation. Prior studies have shown that these deleterious skeletal changes can be partly attributed to decreases in proliferation and differentiation of osteoblast (OB) progenitors. We previously demonstrated that there is an increase in adipogenesis (AD) that is associated with decreases in osteoblastogenesis after 2 weeks of HS. In this study, the time course required for this HS-induced mesenchymal marrow cell fate switch was investigated. Six month old Fisher 344/Brown-Norway male rats were subjected to HS for 24, 48 or 96 hrs. At the time of sacrifice, bone marrow cultures from femurs were established to determine the capacity of cells to be recruited into the OB/AD lineage (as determined by AP+ CFU-F), or to undergo mature OB mineralization (as determined by CFU-OB). AD cultures were initiated using insulin/hydrocortisone/IBMX (IHI) adipogenic cocktail (as measured by Oil Red O+ CFU-AD). Cell recruitment into the OB lineage (AP+ CFU-F) was unaffected within 96h of HS. However, a reciprocal increase in IHI-induced CFU-AD and decrease in CFU-OB was observed in cultures from 48-96h HS rats. This decreased OB cell fate *in vitro* was associated with compromises in both OB number and activity *in vivo*. As expected, there were no significant differences in BV/TV. However, by 48h, a significant decrease was observed in the mineralizing surface (sLPM/BPM) as measured by calcein labeling injected 48h prior to sacrifice. Dynamic changes in OB number on the bone surface at the time of sacrifice via proliferation or cell death was measured by PCNA staining and BrDU incorporation, or TdT-FragEL staining respectively. OB proliferation decreased at 24h, whereas OB apoptosis increased by 96h. Wnt pathway-specific microarrays were performed on whole femoral RNA. Wnt10b and Wnt3a were suppressed by 48h of HS, consistent with early changes in Wnt signaling leading to the mesenchymal switch from OB to AD development in response to short-term HS. Collectively, these data demonstrate that there is a rapid skeletal response to HS that involves multi-faceted compromises in proliferation, differentiation, activity and survival of cells in the osteoblastic lineage.

**Disclosures:** K.M. Nicks, None.

This study received funding from: NIH- R01-NIAMS AR053204-01A1 to EDV; NASA Arkansas Space Grant Consortium to DG.

## F527

**Load induced Changes in Trabecular and Cortical Bone are Dose Dependent in Both C57BL/6 and C3H/Hej Mice.** D. J. Webster<sup>\*1</sup>, E. Wasserman<sup>\*1</sup>, F. Weber<sup>\*2</sup>, I. Bab<sup>3</sup>, R. Mueller<sup>1</sup>. <sup>1</sup>Institute for Biomechanics, ETH Zurich Switzerland, Zurich, Switzerland, <sup>2</sup>University of Zurich, Dept. Cranio-maxillofacial Surgery, Zurich, Switzerland, <sup>3</sup>Hebrew University of Jerusalem, Bone Laboratory, Jerusalem, Israel.

Most in vivo studies addressing the skeletal responses of mice to mechanical loading have targeted cortical bone. To investigate trabecular bone responses we have developed a caudal vertebrae axial compression device (CVAD) that transmits mechanical loads to compress the fifth caudal vertebrae (C5) via stainless steel pins inserted into C4 and C6. Here we used the CVAD in C57BL/6 (B6) and C3H/Hej (C3H) mice to investigate dose-related responses of several morphometric parameters to regular bouts of mechanical stimulation. Three weeks after pinning, the 15wk-old mice were divided into 4 loading groups (N=10) for each strain, namely 0N (sham loading), 2N, 4N and 8N. Loading was applied using an acute regime of 3000 cycles at 10 Hz, 3 times weekly. The mice were sacrificed after 4-weeks of loading. Newly formed bone was double labeled with calcein administered i.p. 4 days and 1 day prior to sacrifice. Structural and functional parameters were affected only by the 8N load. Quantitative  $\mu$ CT analysis of the trabecular compartment revealed 25.9% and 14.2% increases in bone volume density in the B6 and C3H mice, respectively ( $p < 0.05$ ). In the B6 animals this increase was accompanied by 21.9% augmentation ( $p < 0.001$ ) of trabecular thickness. Histomorphometry showed respective 89.8% and 163% increases in the mineralizing perimeter (Min.Peri) ( $p < 0.05$ ), and bone formation rate (BFR) ( $p < 0.05$ ) in B6 mice and 48% ( $p < 0.05$ ) and 110% ( $p < 0.05$ ) in C3H mice. The trabecular osteoclast number was reduced by 51.7% and 77.7% in the B6 ( $p < 0.05$ ) and C3H ( $p < 0.05$ ) mice, respectively. The B6 mice showed also a nearly significant ( $P = 0.06$ ) 11% increase in cortical bone volume together with load-induced increases of 371.25% (periosteal) and 76.81% (endosteal) BFR (both at  $p < 0.05$ ). The C3H mice showed no significant cortical structural changes. However, their periosteal and endosteal BFR exhibited 371.25% and 76.81% increases, respectively. These findings demonstrate that cortical and particularly trabecular bone are mechano-sensitive in both strains in a dose dependent manner, especially in the B6 mice. The caudal vertebral loading model established here is proposed for further studies addressing load-induced changes in gene expression in both cortical and trabecular bone in addition to the effect of genetic manipulations on the response of these skeletal components to mechanical loading.

**Disclosures:** D.J. Webster, None.

This study received funding from: Swiss National Science Foundation.

## F536

**Mediation of Bone Loss with Ultrasound Induced Dynamic Mechanical Signals in an OVX Rat Model of Osteopenia.** S. Ferreri<sup>\*1</sup>, R. J. Talish<sup>\*2</sup>, T. Trandafir<sup>\*2</sup>, Y. Qin<sup>1</sup>. <sup>1</sup>Biomedical Engineering, Stony Brook University, Stony Brook, NY, USA, <sup>2</sup>Juvent Inc., Sommerset, NJ, USA.

This study tests the hypothesis that an ultrasound generated dynamic mechanical signal can inhibit bone loss in an estrogen deficient model of osteopenia. 72, 16 w.o. Sprague-Dawley rats were divided into six groups; baseline control, age-matched control, OVX control, OVX + 5 mW/cm<sup>2</sup> ultrasound (US), OVX + 30 mW/cm<sup>2</sup> US and OVX + 100 mW/cm<sup>2</sup> US. Low intensity pulsed ultrasound (LIPUS) was delivered transdermally at the L4/L5 vertebrae, using gel-coupled plane wave US transducers (Exogen, Inc.). The signal, characterized by 200 $\mu$ s pulses of 1.5 MHz sine waves repeating at 1 kHz with intensities of 5, 30 or 100mW/cm<sup>2</sup>, was applied 20 min/day, 5 days/week for 4 weeks. A 1.5 mm thick, anterior RIO containing cancellous bone, from the center of the US radiated area was imaged using  $\mu$ CT at 15  $\mu$ m and evaluated for bone volume fraction (BVf), structural model index (SMI), trabecular number (Tb.N.) and trabecular thickness (Tb.Th.). Specimen specific, voxel based, finite element (FE) models ( $E=18\text{GPa}$  &  $\nu=0.3$ ), were generated using  $\mu$ CT image data and 1% axial compressive strain was simulated using a nonlinear FE solver (ABAQUS). OVX treatment reduced BVf and compromised microstructure at 4 weeks post surgery. LIPUS treatment, however, significantly increased BVf compared to OVX controls for the 100mW/cm<sup>2</sup> treated group. Additionally, SMI, and Tb.N showed significant improvements compared with OVX for the 100mW/cm<sup>2</sup> treated group and Tb.Th was significantly improved in the 30 and 100mW/cm<sup>2</sup> treated groups. Interestingly, the 100mW/cm<sup>2</sup> treated groups showed a significant improvement over the 5mW/cm<sup>2</sup> treated group in terms of BVf, SMI and Tb.N. Improvements in bone's microstructure with 100mW/cm<sup>2</sup> US translated into significant improvements in apparent Elastic Modulus. Mean principal compressive stress demonstrated a non-significant increasing trend for the 100mW/cm<sup>2</sup> treated group, however, significant differences were observed for the same group among peak principal compressive stresses associated with the 75<sup>th</sup> percentile. These findings support the hypothesis that LIPUS can inhibit bone loss and preserve bone strength under conditions of estrogen deficient osteopenia. This study also suggests that there exists a minimum intensity threshold below which LIPUS is less effective at maintaining bone's microstructural and mechanical characteristics.

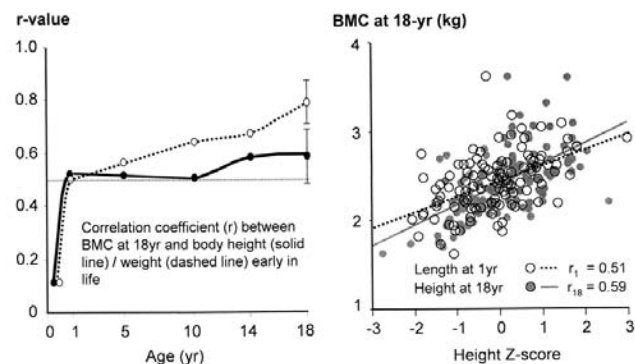
	OVX vs. Age-matched	(* = $p < 0.05$ and ** = $p < 0.02$ )		
		OVX + 5mW/cm <sup>2</sup> vs. OVX	OVX + 30mW/cm <sup>2</sup> vs. OVX	OVX + 100mW/cm <sup>2</sup> vs. OVX
BVF	-39.57 **	7.63	18.74	32.67 **
SMI	436.49 **	-0.82	-16.6	-48.41 **
Tb.N.	-16.81 **	2.45	6.45	12.27 **
Tb.Th.	-18.75 **	5.42	11.05 *	12.81 **
Apparent Elastic Modulus (MPa)	-51.11 **	-1.13	7.53	41.83 *
Mean Principal Compressive stress (MPa)	-22.87 **	-2.86	1.03	15.06
75th percentile for Principal Compressive stress (MPa)	-45.10 **	-2.47	0.65	41.47 *

**Disclosures:** S. Ferreri, None.

## F542

**Peak Bone Mass Is Determined at 1 Year-Old: Evidence from Growth Charts.** S. Cheng<sup>1</sup>, Q. Wang<sup>2</sup>, A. Lyytikäinen<sup>1</sup>, L. Xu<sup>1</sup>, F. Tylavsky<sup>3</sup>, E. Seeman<sup>2</sup>, M. Alen<sup>\*1</sup>. <sup>1</sup>Health Sciences, University of Jyväskylä, Jyväskylä, Finland, <sup>2</sup>Endocrine Centre, Austin Health, University of Melbourne, Melbourne, Australia, <sup>3</sup>Preventive Medicine, University of Tennessee, Memphis, TN, USA.

A low peak bone mass (PBM) is likely to be a risk factor for fractures in adulthood. We hypothesized that the variance in bone size and mass originates in early life and that traits track in their percentile of origin. We tested this hypothesis in 150 girls aged 18.4 (17-20) yrs, their mothers (46  $\pm$  5 yr) and fathers (50  $\pm$  6 yr). Crown-heel length (CHL) of the girls at birth, 1-, 5-, 10- 14- and 18-yrs of age was documented at birth and from growth charts while DXA was used to measure bone mass (BMC) at maturity. Gestational age, CHL and weight at birth did not correlate with BMC at 18yr. However, CHL at age 1-yr and later predicted current BMC ( $r = 0.51 - 0.58$ ) as well as height at 18 yrs did ( $r = 0.59$ ) (Fisher's z-transformation, Fig). The tracking of the ratio CHL/height in it's percentile of origin was established at 1-yr of age ( $r = 0.77-0.60$ ) and remained significant after controlling for current height (partial  $r=0.21-0.25$ ,  $p < 0.05$ ). Body weight at 1yr and later also predict current BMC ( $r = r = 0.50$ ) but current weight predicted BMC more strongly ( $r = 0.79$ , Fig).



Fathers and mothers' BMC correlated with their daughters' BMC at maturity ( $r = 0.32$  and  $0.43$ , respectively,  $p < 0.01$ ) before but not after controlling for the daughter's body length or weight at 1yr. We infer the percentile or origin of a girl's PBM in the population distribution is established as early as 1 year-old and tracks during the next two decades. Hence PBM is determined early in life, whether this has a genetic basis or is the result of intra-uterine or postnatal environmental factors is yet to be determined.

**Disclosures:** S. Cheng, None.

This study received funding from: ASBMR Bridge Funding 2006.

## F544

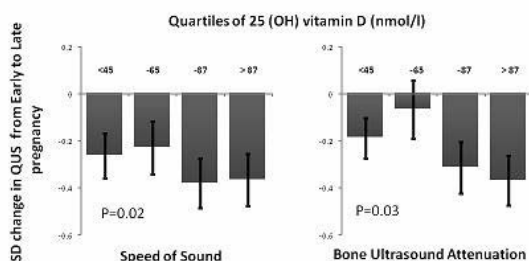
**Late Pregnancy Serum Vitamin D and Longitudinal Bone Loss During Pregnancy: The Southampton Womens Survey.** M. Javai<sup>1</sup>, I. Reading<sup>\*1</sup>, N. Harvey<sup>1</sup>, P. Taylor<sup>\*2</sup>, R. Swaminathan<sup>\*3</sup>, N. Arden<sup>1</sup>, K. Godfrey<sup>\*1</sup>, C. Cooper<sup>1</sup>.

<sup>1</sup>MRC Epidemiology Resource Centre, Southampton, United Kingdom, <sup>2</sup>Southampton University Hospitals NHS Trust, Southampton, United Kingdom, <sup>3</sup>St Thomas' Hospital, London, United Kingdom.

**Purpose:** Previously, we described a seasonality in bone loss during pregnancy. We now compare bone loss, as measured by quantitative ultrasound, with late pregnancy maternal concentrations of serum 25(OH) vitamin D (25OHD).

**Methods:** We analysed a sample of term pregnancies using an established cohort of women living in Southampton, UK. During early (11 wk) and late (34 wk) pregnancy, speed of sound (SOS) and bone ultrasound attenuation (BUA) were measured at the left calcaneus using a Hologic Sahara Quantitative Ultrasound device. Late pregnancy serum 25OHD was measured using Diasorin RIA. Linear regression models for SD change in QUS were adjusted for change in ankle width, BMI and vitamin D supplement use.

**Relationship between late pregnancy serum maternal 25(OH) vitamin D concentration and SD change in calcaneal QUS during pregnancy**



Legend: Unadjusted Mean (95% CI) shown; P values from regression models adjusted change in calcaneal width, late pregnancy adiposity, as measured by mid upper arm circumference, and vitamin D supplement use

**Results:** 416 women had paired QUS during pregnancy and serum 25OHD recorded in late pregnancy. A third of women had 25OHD  $\leq 50$  nmol/l and 4.6%  $\leq 25$  nmol/l 25OHD. 23% of mothers were taking vitamin D supplements and had significantly higher 25OHD concentrations (88.6 nmol/l) than non-supplement users (61.3 nmol/l). Season of late pregnancy accounted for 30% of variance in serum 25OHD in non-supplement users. There was a weak negative association between adiposity (mid upper arm circumference) and 25OHD ( $r = -0.12$ ,  $p = 0.04$ ).

The mean loss of SOS was 0.31 SD and BUA 0.23 SD between early and late pregnancy ( $p < 0.001$ ). There was a greater reduction in both SOS ( $p = 0.02$ ) and BUA ( $p = 0.03$ ) for women with greater vitamin D concentrations at 34 weeks gestation. (Figure). This association persisted after adjusting for adiposity, vitamin D supplement use and season.

**Conclusions:** In this observational study of healthy singleton pregnancies, women with higher concentrations of serum 25(OH)D in late pregnancy had a greater reduction calcaneal QUS measurements during pregnancy. Taken together with our previous finding that greater levels of maternal 25(OH)D are associated with increased intrauterine bone mineral accrual in the offspring, these results are consistent with the hypothesis that 25OHD facilitates mineral transfer to the foetus at the expense of the maternal skeleton.

**Disclosures:** M. Javai, None.

## F546

**Body Fatness Negatively Associated with BMD and Hip Geometry Indices in Adolescents. A Longitudinal Twin Study.** Y. Hsu<sup>1</sup>, X. Hong<sup>\*2</sup>, H. Terwedow<sup>\*3</sup>, S. Venners<sup>\*4</sup>, X. Xu<sup>\*2</sup>, X. Wang<sup>\*5</sup>. <sup>1</sup>Hebrew SeniorLife and Harvard Medical School, Boston, MA, USA, <sup>2</sup>Sch. Public Health, Univ. Illinois at Chicago, Chicago, IL, USA, <sup>3</sup>Harvard Sch Public Health, Boston, MA, USA, <sup>4</sup>Sch. Public Health, Univ. Illinois at Chicago, Chicago, IL, USA, <sup>5</sup>Children's Memorial Research Center, Northwestern Univ., Chicago, IL, USA.

In the last 30 years, a growing number of adolescents have developed overweight problems. Overweight and obesity is associated with an increased risk of cardiovascular and cerebrovascular diseases in their later life. Studies that investigated BMD in overweight teenagers have shown conflicting results. Rapid bone formation during growth influences bone strength including both bone mass and geometric properties. Therefore, we examined the effects of body fatness on bone strength in a large cohort of adolescent twins, and their genetic correlations.

Participants included 960 boys and 764 girls with age range 11-22 yrs. Body composition (g) and BMD (g/cm<sup>2</sup>) was assessed by DXA at the hip and whole body. Percentage of total body fat (%fat) was calculated. Hip structure analysis was used to determine cross-sectional area (compression strength), section modulus (bending strength) and subperiosteal width. Sex-specific mixed effect models were used to calculate means and assess regression coefficients in BMD and geometry values across %fat tertiles, adjusted for age, tanner stage, height and BMI. Sex-specific variance components analysis (M-plus) was performed to estimate genetic correlations ( $\rho_g$ ) between %fat and hip BMD and geometry indices.

Total body fat mass and %fat were significantly higher in girls than boys. No difference of the total body lean mass and hip BMD was found between girls and boys. %fat increased

with age in both boys and girls. However, hip BMD and geometry indices reached the peak values at tanner stage 3 in girls, and at tanner stage 5 in boys. Multivariable-adjusted mean hip BMD, BMC, and all three geometry indices significantly decreased from the lowest to the highest %fat tertile (table) in boys and girls, except for subperiosteal width in girls. Significant genetic correlations between %fat and bone measurements were found (-0.21 to -0.44 in girls; -0.31 to -0.44 in boys).

In summary, our study suggests that increased %fat may have a negative effect on bone growth in both boys and girls. Furthermore, the associations between body fatness and bone measurements are affected by shared genetic factors.

Outcome	FAT%	Boy (N=960)			Girl (N=764)		
		M+SD	B+SE	p	M+SD	B+SE	P
Hip BMC (g)	Low	29.4+6.0			24.4+3.7		
	Median	28.4+6.0	-1.0+0.3	<b>0.001</b>	23.9+3.4	-0.8+0.3	<b>0.003</b>
	High	27.1+5.6	-2.4+0.4	<b>&lt;0.001</b>	23.3+3.3	-1.7+0.3	<b>&lt;0.001</b>
Hip BMD (g/cm <sup>2</sup> )	Low	0.92+0.12			0.89+0.12		
	Median	0.91+0.13	-0.02+0.01	<b>0.03</b>	0.88+0.11	-0.02+0.01	0.105
	High	0.90+0.12	-0.04+0.01	<b>&lt;0.001</b>	0.88+0.10	-0.03+0.01	<b>0.003</b>
Cross-Sectional Area (mm <sup>2</sup> )	Low	140.5+27			117.9+16.8		
	Median	134.8+25.8	-5.6+1.4	<b>&lt;0.001</b>	116.4+16.2	-2.1+1.2	0.074
	High	132.1+25.2	-9.1+1.6	<b>&lt;0.001</b>	114.4+15.2	-5.2+1.3	<b>&lt;0.001</b>
Section module (mm <sup>3</sup> )	Low	570.2+149.4			421.8+79.7		
	Median	545.6+149.5	-22.3+7.9	<b>0.005</b>	414.5+76.4	-7.4+5.3	0.163
	High	532.5+140.8	-45.4+8.7	<b>&gt;0.001</b>	404.5+77.2	-19.7+6.5	<b>0.002</b>

**Disclosures:** Y. Hsu, None.

This study received funding from: NIAMS.

## F548

**Interaction Between the Skeletal Parameter Bone Mineral Density and Lifestyle Factors in 390 Adolescent Daughter-Mother Pairs.** H. Ohta, T. Kuroda\*, Y. Onoe, Y. Miyabara\*, R. Yoshikata\*, S. Orito, M. Sakai\*, Y. Haruna\*, K. Ishitani\*, H. Okano. Dpt. of Obstetrics and Gynecology, Tokyo Women's Medical University, Tokyo, Japan.

The purpose of this study was to clarify how genetic or environmental factors influence adolescent lumbar bone mineral density (L-BMD) among Japanese daughters and their mothers.

Healthy adolescent daughters and their mothers (n = 390 pairs) were enrolled in this cross-sectional study. L-BMD was measured in all subjects by using dual energy x-ray absorptiometry, as well as their height and body weight; and their current nutritional intake, physical activity patterns, birth weight and weeks, and age at menarche were also assessed by using questionnaires. Standard deviation transformation was performed for three parameters (L-BMD, height, and body weight) to exclude the influence of aging. Spearman's rank test was used to examine the parameters for correlation in each daughter and mother pair and to identify correlates for L-BMD in the daughter. Multiple regression analysis was used to estimate the association between selected parameters and L-BMD in the daughter as an endpoint.

In the pre-menarche daughter group (n = 49), L-BMD, height and nutrition intake were significantly correlated within the mother-daughter pairs ( $P < 0.05$ ). In the post-menarche daughter group (n = 339), L-BMD, birth weight, age at menarche, height, body weight, nutritional intake, physical activity patterns were significantly correlated within the mother-daughter pairs ( $P < 0.05$ ). By multiple regression analysis, L-BMD in the mother and height in the daughter were significantly associated with pre-menarche L-BMD in the daughter ( $P < 0.05$ ; model  $R^2 = 0.34$ ). L-BMD in the mother, height, body weight, age at menarche and intensity of exercise in the daughter were significantly associated with post-menarche L-BMD in the daughter ( $P < 0.05$ ; model  $R^2 = 0.37$ ).

The results suggest a strong hereditary association in L-BMD between daughter and mother and that greater age at menarche leads to low peak bone mass. Additionally, intensive physical activity and adequate body weight were found to have an important role in achieving maximal L-BMD in post-menarche daughters as interventional factors.

**Disclosures:** Y. Onoe, None.

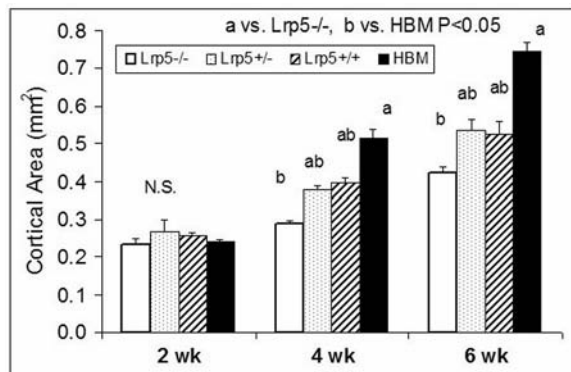
## F550

**Bone Formation in Mice with Variations in Lrp5 Expression.** S. Moen\*, B. T. Hackfort\*, G. K. Alvarez, D. M. Cullen. Osteoporosis Research Center, Creighton University, Omaha, NE, USA.

Peak bone mass in adults is determined by bone acquisition during growth where genetics may play an important role. Mutations in the low-density lipoprotein receptor-related protein 5 (LRP5) directly affect peak bone mass. Specifically, the human G171V mutation has been associated with high bone mass (HBM) and inactivation of LRP5 is associated with osteoporosis-pseudoglioma syndrome. High bone mass in humans with the G171V mutation has been observed as early as age 5, but has not been assessed in younger children. The purpose of this study is to test the hypothesis that the effects of variation in Lrp5 expression on bone mass accrual will develop in mice between 2 and 6 weeks of age. Femoral shafts from mice with increasing levels of Lrp5 expression (Lrp5<sup>+/+</sup>, Lrp5<sup>+/+</sup>, Lrp5<sup>+/+</sup> wild-type, and HBM) were examined at 2, 4 and 6 weeks of age (10/grp). Fluorochrome double labels were administered and femoral midshaft processed for histomorphometry. Measurements included area (total, marrow, cortical), moment of inertia, single and double labeled surface (LS/BS, dLS/BS), mineral apposition rate (MAR), and bone formation rate (BFR/BS) for periosteal and endocortical surfaces. Differences due to age and genotype were tested by GLM. At 2 weeks there were no differences in cortical area or bone formation rate among the four

genotypes. By 4 weeks of age there were distinct differences among the various genotypes and these differences were magnified by 6 weeks. The *Lrp5*<sup>-/-</sup> mice closely resembled the WT control throughout the study. By 6 weeks the cortical area and structural resistance to fracture (moment of inertia) of the *Lrp5*<sup>-/-</sup> mice was 19% and 26% lower than WT, respectively, and the HBM mice were 41% and 55% greater than WT. The bone formation rate increased 116% from 2 to 4 weeks for the HBM mice, while the WT and both knockout animals (*Lrp5*<sup>-/-</sup> or *Lrp5*<sup>+/-</sup>) increased less than 23%. Formation rates decreased 27-50% from 4 to 6 weeks for all genotypes. In conclusion, this study shows that the adult phenotypes seen in previous studies for the *Lrp5*<sup>-/-</sup> and HBM mice does not begins to develop until between 2 and 4 weeks of age. Furthermore, a single knockout of the *Lrp5* gene does not seem to affect cortical bone growth in size or structural resistance to fracture.

Figure: Femur cortical area at 2, 4, and 6 wks of age in *Lrp5*<sup>-/-</sup>, *Lrp5*<sup>+/-</sup>, *Lrp5*<sup>+/+</sup> and HBM mice.



**Disclosures:** D.M. Cullen, None.

This study received funding from: NIH AR051365.

## F552

**Arterial Compliance is Associated with Change in Bone Strength in Children: A 16-month Prospective Study.** J. M. Hughes<sup>1</sup>, M. A. Petit<sup>1</sup>, K. E. Reed<sup>2</sup>, H. M. Macdonald<sup>3</sup>, J. M. Cousins<sup>1</sup>, D. E. R. Warburton<sup>2</sup>, R. Z. Lewanczyk<sup>4</sup>, J. M. Scott<sup>2</sup>, J. M. McGavock<sup>4</sup>, M. J. Haykowsky<sup>4</sup>, H. A. McKay<sup>2</sup>. <sup>1</sup>School of Kinesiology, University of Minnesota, Minneapolis, MN, USA, <sup>2</sup>University of British Columbia, Vancouver, BC, Canada, <sup>3</sup>University of Calgary, Calgary, AB, Canada, <sup>4</sup>University of Alberta, Edmonton, AB, Canada.

Associations between cardiovascular disease and osteoporosis have been reported for adult populations. However, it is unclear whether these relationships exist in youth. Therefore, the purpose of this investigation was to evaluate the relationship between arterial compliance, a predictor of vascular disease, and bone strength in children. We used peripheral quantitative computed tomography (pQCT, Stratec XCT 2000) to assess bone geometry (total area, ToA, mm<sup>2</sup>), volumetric density (vBMD, mg/mm<sup>3</sup>), and indices of compressive bone strength (BSI) at the distal (8% site) tibia and bone geometry (cortical area, CoA, mm<sup>2</sup> and ToA), cortical density (CoBMD, mg/mm<sup>3</sup>), and bending strength (section modulus; Z, mm<sup>3</sup>) at the 66% site of the tibia in 84 children (45 boys; aged 9-11 years) at baseline and after 16 months. We used dual energy x-ray absorptiometry to assess lumbar spine and proximal femur bone mineral content (BMC, g). Large arterial compliance was assessed by applanation tonometry (HDI/Pulsewave CR2000) at one time point. We divided participants into 3 tertiles of arterial compliance (T1 (lo)-T3 (hi)). We used ANCOVA to compare arterial compliance with bone outcomes across tertiles. Baseline bone values were adjusted for age, tibia length and weight. Change data were adjusted for age, change in tibia length and change in weight. We noted trends (NS) for higher baseline ToA (+1.4%) and BSI (+3.4%) in those children with the highest arterial compliance (T3) compared with those in T1. For change, at the distal tibia BSI increased significantly more (+6.1%, p=0.04) in the T3 compared to the T1 group due to a greater increase in vBMD (+2.1%); there was no difference between groups for change in ToA. At the 66% site, there was a trend for bending strength (Z) to increase more in the T3 group (+4.5%, p=0.06) due to a greater increase in CoA (+3.6%) with no difference for change in CoBMD or ToA at that site. Children in T3 also had an 8.1% greater change in lumbar spine BMC compared to T1 (p=0.03). Overall, children with the highest arterial compliance at baseline showed a greater increase over 16 months for bone strength, vBMD, and spine BMC, particularly at highly trabecular sites of the distal tibia and lumbar spine. These data suggest a relationship between cardiovascular and bone health in youth that should be explored further.

**Disclosures:** J.M. Hughes, None.

## F554

**Comparison of the Effect of Puberty on Hip Structure in Boys and Girls.** A. Sayers<sup>\*</sup>, J. H. Tobias. Academic Rheumatology, University of Bristol, Bristol, United Kingdom.

Women are at greater risk of fragility fractures compared to men, the difference in risk largely reflects gender differences in hip structure that determine biomechanical competence. Puberty is a critical time for bone development, particularly in relation to gender differences in skeletal phenotype. To improve the understanding of the

pathogenesis of hip fracture, we compared how puberty influences hip structure and biomechanical strength in boys and girls. All children from the Avon Longitudinal Study of Parents and Children (ALSPAC), a large population-based birth cohort, were invited at age 13.8 years for total body and hip DXA scans using a GE-Lunar Prodigy. Following which indices of femoral neck (FN) structure were derived using GE-Lunar software. These comprised cross sectional moment of inertia (CSMI- an indicator of bone stiffness), minimum femoral neck width (FNW-an indicator of bone size), and bone cross sectional area (CSA-an indicator of cortical bone area). Relationships between pubertal stage, gender and FN structure were examined based on 3752 children with both structural data and puberty information derived from self-completed Tanner stage questionnaires. 612, 477 and 546 boys were in early (Tanner stages I and II), mid (Tanner stage III) and late (Tanner stages IV and V) puberty, compared with 348, 816 and 953 girls respectively.

Table 1: Geometric Properties of the Femoral Neck

FN structure	Puberty	Boys		Girls		Puberty sex interaction
		Mean	95% CI	Mean	95% CI	
CSMI (mm <sup>4</sup> )	Early	8041.4	[ 7852.9 , 8229.9 ]	6281.5	[ 6036.1 , 6526.8 ]	p < 0.0001
	Mid	8896.6	[ 8681.7 , 9111.5 ]	7169.5	[ 7003.7 , 7335.3 ]	
	Late	10924.1	[ 10719.8 , 11128.5 ]	7982.5	[ 7826.4 , 8138.6 ]	
CSA (mm <sup>2</sup> )	Early	131.3	[ 129.6 , 133.0 ]	118.8	[ 116.6 , 120.9 ]	p < 0.0001
	Mid	139.1	[ 137.2 , 141.0 ]	130.4	[ 128.9 , 131.9 ]	
	Late	154.3	[ 152.5 , 156.1 ]	140.5	[ 139.1 , 141.9 ]	
FNW (mm)	Early	28.9	[ 28.7 , 29.1 ]	26.9	[ 26.7 , 27.1 ]	p < 0.0001
	Mid	29.7	[ 29.5 , 29.9 ]	27.4	[ 27.2 , 27.6 ]	
	Late	31.4	[ 31.2 , 31.6 ]	27.8	[ 27.7 , 28.0 ]	

Means and 95% CI derived from OLS Regression controlling for age of scan, height and weight.

These results demonstrate that both sexes show similar proportional increases in biomechanical strength (CSMI) between early and mid puberty, but in late puberty, CSMI increases to a greater extent in boys compared to girls. Underlying these changes, periosteal expansion in late pubertal boys is evident from increases in both FNW and CSA. Although CSA also increased in late pubertal girls, there was little change in FNW, implying that gains at the endosteal surface had occurred, leading to an increase in cortical thickness, whereas there was only very limited periosteal expansion. We conclude that in late puberty, boys undergo FN periosteal expansion, whereas girls predominantly accrue bone at the endosteal surface. Since periosteal expansion influences CSMI to a greater extent than endosteal deposition, these differences result in greater improvements in biomechanical strength at the FN in late pubertal boys compared to girls, which is in turn likely to contribute to the higher fracture risk in women compared to men in later life.

**Disclosures:** A. Sayers, None.

## F557

**Suboptimal Vitamin D Status in Pregnant Adolescents is Associated with Neonatal Vitamin D Insufficiency.** K. O. O'Brien<sup>1</sup>, B. V. Essley<sup>1</sup>, E. Cooper<sup>2</sup>, A. W. McIntyre<sup>2</sup>, F. R. Witter<sup>3</sup>, Z. L. Harris<sup>3</sup>, T. Kent<sup>1</sup>, T. McNalley<sup>2</sup>. <sup>1</sup>Division of Nutritional Sciences, Cornell University, Ithaca, NY, USA, <sup>2</sup>University of Rochester School of Medicine, Rochester, NY, USA, <sup>3</sup>Johns Hopkins School of Medicine, Baltimore, MD, USA.

Pregnant adolescents may be at risk for suboptimal calcium intakes and vitamin D insufficiency. This may impact maternal and fetal bone health across pregnancy in this vulnerable age group. To assess this issue, vitamin D status was monitored in pregnant adolescents and their neonates in relation to measures of maternal and fetal bone health across gestation. Pregnant adolescents ( $\leq 18$  y of age) were recruited at or after 12 weeks of gestation and were longitudinally followed at 3 time points across pregnancy (approximately 16, 25 and 34 weeks of gestation). At each visit maternal bone health was measured using a heel ultrasound technique and data on fetal femur and humerus length were obtained by sonogram. Blood samples were collected from each adolescent at mid-gestation both maternal and cord blood were obtained in a subset of this group at parturition. To date, adolescents were  $16.9 \pm 1.1$  years of age (range 13.7 - 18.7 y, n=82) at entry into the study. Serum 25-hydroxyvitamin D (25(OH)D) concentrations were  $23.3 \pm 11.2$  ng/mL (n=82 range 5-61 ng/mL) at 25.3  $\pm$  3.5 wks gestation and these values did not statistically differ from measures obtained in a subset of these teens at delivery ( $25.1 \pm 15.7$  ng/mL; n=45, range 7-91). In this population; 48% (39/82) and 42% (19/45) of pregnant adolescents had vitamin D insufficiency (< 20 ng/mL) at mid-gestation and delivery respectively. At parturition, concentrations of 25(OH)D were significantly higher among Caucasian adolescents when compared to African American adolescents ( $31.2 \pm 18.4$  (n=17) vs.  $21.3 \pm 13.2$  (n=25), p<0.05). In the group as a whole; cord 25(OH)D concentrations ( $20.0 \pm 12.1$ , range 5-67 ng/mL) were significantly associated with maternal 25(OH)D concentrations at delivery (P<0.0001, n=45, R<sup>2</sup>=0.657). Among the neonates studied to date; 60% (24/40) had suboptimal vitamin D status (< 20 ng/mL) at birth. A net loss of bone at the calcaneus (change in BMD t-score per week) was evident across gestation ( $-0.119 \pm 0.864$ , n=27). Serum parathyroid hormone is currently being analyzed in this cohort to assess its relationship with study outcomes. Because pregnant adolescents are at high risk of vitamin D insufficiency and bone acquisition is not complete during adolescence, further studies are need to assess the impact of maternal vitamin D status on maternal and fetal bone health across pregnancy.

**Disclosures:** K.O. O'Brien, None.

This study received funding from: United States Department of Agriculture.



## F563

**Osteoprotegerin (OPG) Deficiency Mimicked by a Novel 15-Base Pair Tandem Duplication in *TNFRSF11A* Encoding RANK: Merging the Juvenile Paget's Disease and Expansile Skeletal Hyperphosphatasia Phenotypes.** S. Mumm<sup>1</sup>, C. Tau<sup>2</sup>, X. Zhang<sup>\*1</sup>, W. H. McAlister<sup>1</sup>, M. P. Whyte<sup>1</sup>.  
<sup>1</sup>Washington Univ Schl Med and Shriners Hospt Children, St. Louis, MO, USA, <sup>2</sup>Metabolismo Calcico y Oseo, Endocrinol, Hospt Pediatr J.P. Garrahan, Buenos Aires, Argentina.

Disorders of enhanced osteoclastogenesis due to genetic defects in the RANK/OPG/RANKL/NF- $\kappa$ B signaling pathway include familial expansile osteolysis (FEO), familial Paget's disease in Japan (PDB2), and expansile skeletal hyperphosphatasia (ESH) caused by 18, 27, and 15 bp tandem duplications, respectively, in exon 1 of *TNFRSF11A* (RANK). Each is an autosomal dominant trait. Juvenile Paget's disease (JPD) is an autosomal recessive disorder due to deactivating mutations in *TNFRSF11B* (OPG).

We discovered that a 5-year-old girl diagnosed with JPD carried a unique, heterozygous, 15 bp tandem duplication in exon 1 of *TNFRSF11A*. She was born to non-consanguineous Bolivian parents after an uneventful full-term pregnancy. At birth, she had a short, right femur. Subsequently, both femurs bowed. At age 1 3/4 years, she fractured a radius and cubitus. At age 2, there was bilateral deafness, but no mental retardation. Deciduous teeth were lost prematurely, with missing maxillary incisors. Radiographs at age 3 years showed cortical thickening, coarse trabeculation, and long bone widening consistent with relatively mild JPD (Fig). Some mandibular teeth, including molars, had missing roots. Vertebrae were sandwiched at age 1, but recovered. CT showed eroded cochleas with osteosclerosis. There was no ophthalmologic disease. Family history was negative for bone disease.

Markers of bone turnover were elevated, but with i.v. pamidronate they normalized except serum ALP remained elevated at 750 IU/L.

Exon 1 of *TNFRSF11A* (RANK) was amplified by PCR and sequenced in both directions, showing a heterozygous insertion/deletion in the coding sequence. The amplicons were cloned and sequenced individually to demonstrate a heterozygous, 15 bp duplication (encoding Leu-Cys-Ala-Leu-Leu) in the signal peptide of RANK. This 15 bp duplication is 3 bp displaced from the sequence repeated in the original ESH report (JBMR 17:26, 2002), but adds the same 5 amino acids. It was not detected in the mother; the father was unavailable for study. No OPG gene mutation was found.

Hence, the JPD phenotype can be recapitulated by an activating mutation in RANK, showing further "overlap" among FEO, PDB2, ESH, and JPD.



**Disclosures:** S. Mumm, None.

## F569

**Bisphosphonate-Induced Osteopetrosis: Novel Bone Modeling Defects, Metaphyseal Osteopenia, and Osteosclerosis Fractures After Drug Exposure Ceases.** M. P. Whyte<sup>1</sup>, W. H. McAlister<sup>\*2</sup>, D. V. Novack<sup>2</sup>, K. L. Clements<sup>\*1</sup>, P. L. Schoenecker<sup>\*1</sup>, D. Wenkert<sup>1</sup>. <sup>1</sup>Shriners Hospt Children, St. Louis, MO, USA, <sup>2</sup>Washington Univ Schl Med, St. Louis, MO, USA.

In 2003, we reported (NEJM 349:457) a 12-year-old boy who had developed osteopetrosis (OPT) while receiving pamidronate (PMD) for idiopathic bone pain and enigmatic elevation in serum bone alkaline phosphatase activity. Now age 17 years, he was reevaluated in 2007, 6 1/2 years after PMD exposure stopped. He described less bone pain, but further limb fractures. Growth plates were fused, yet hyperphosphatasemia persisted. Radiographs documented interval fractures of a metacarpal, an osteosclerotic distal radius, and a dense diaphyseal segment of an ulna where a "chalkstick" break was incompletely healed after 2 years. There was new L<sub>4</sub> spondylolysis, and previous L<sub>5</sub> spondylolysis had caused spondylolisthesis. Modeling disturbances of OPT persisted, but partial recovery was demonstrated by metaphyseal surfaces with a concave shape (Fig 1). Metaphyseal osteosclerosis had remodeled imperfectly to become focal areas of dense, diaphyseal bone. Newer metaphyseal bone was unexpectedly osteopenic, especially in his distal femurs where cortices were thin and a paucity of trabeculae was documented by CT. Femoral necks had become short and wide with an abnormal contour. A "bone-within-bone" configuration was now present throughout his skeleton. In vertebrae, endplates were thin and trabecular osteopenia was central and peripheral to the bands of osteosclerosis. BMD Z-scores assessed by DXA had decreased into the normal range in his spine, hip, and

whole body. Iliac crest biopsy revealed active bone formation, with much less accumulated primary spongiosa than during the PMD infusions. Osteoclasts that had been dysmorphic, round cells without polarization and off of bone surfaces were now unremarkable in number, location, and appearance (Fig 2). Hence, bisphosphonate toxicity during childhood can impair skeletal modeling and remodeling with structural changes that evolve and carry into adult life (JBMR, in press).

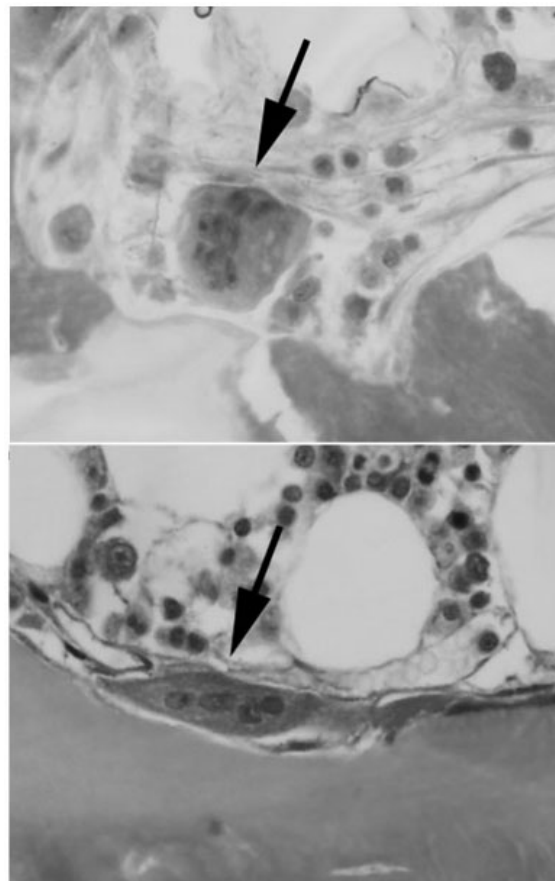


**FIGURE 2:** Osteoclasts during PMD toxicity (top, arrow) are rounded and not polarized toward bone, whereas those at followup (bottom, arrow) have a normal flat and polarized morphology.

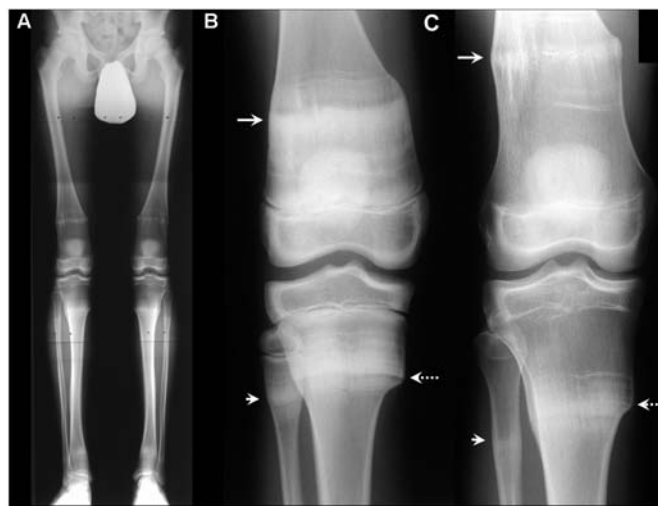


**FIGURE 3:** Modeling and remodeling abnormalities in the lower limbs in 2007 (A) include novel shaping changes and osteopenia, especially apparent in the distal femurs and proximal tibia, that developed between 2002 (B) and 2007 (C). At the right knee, metaphyseal osteosclerosis and a fracture (B) has been repaired by osteopenia and modeling failure (C) (dotted matching arrows). Some of the original osteosclerotic metaphyseal bone persists as dense metaphyseal bone (C) once again has a concave surface.

**Disclosures:** M.P. Whyte, None.

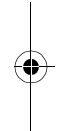


**F572**

**The Non-genomic Estrogen Receptor Gpr30 Is a Runx2 Responsive Gene that Is Required for Osteoblast Proliferation.** N. Teplyuk<sup>\*1</sup>, M. Galindo<sup>\*2</sup>, J. Pratap<sup>1</sup>, J. L. Stein<sup>1</sup>, J. B. Lian<sup>1</sup>, G. S. Stein<sup>1</sup>, A. J. van Wijnen<sup>1</sup>. <sup>1</sup>Department of Cell Biology and Cancer Center, University of Massachusetts Medical School, Worcester, MA, USA, <sup>2</sup>Program of Cellular and Molecular Biology, Institute of Biomedical Sciences (I.C.B.M.), University of Chile, Santiago, Chile.

Multiple target genes for the Runt-related transcription factor 2 (Runx2) support its biological functions in lineage-commitment, proliferation and anabolic functions of osteoblasts. Re-introduction of Runx2 into Runx2 null cells using adenoviral vectors attenuates cell proliferation. Affymetrix expression profiling of Runx2 responsive genes during growth suppression shows that Runx2 regulates groups of coordinately expressed genes involved in G-protein coupled receptor (GPCR) signaling (e.g., *Rgs2*, *Rgs4*, *Rgs5*, *Rgs16*, *Gpr23*, *Gpr30*, *Gpr54*, *Gpr64* and *Gna13*). As Runx2 activity is coupled to modulations in intracellular cAMP levels in osteoblasts, we examined the function of two genes known to work through cAMP signaling: *Gpr30*, the non-genomic estrogen receptor that activates cAMP production, and *Rgs2*, a G protein inhibitor that blocks cAMP production. We find that *Gpr30* is stimulated and *Rgs2* is down regulated by Runx2 in osteoblasts. Forced expression of *Rgs2* inhibits osteoblast proliferation as determined by a reduced number of cells in S-phase of the cell cycle as estimated at the single cell level by Ki67 immunostaining. Moreover, *Rgs2* knock-down by RNA interference stimulates S-phase entry as assessed by FACS analysis. This positive effect is more pronounced upon cAMP stimulation with forskolin, suggesting that *Rgs2* suppresses cAMP dependent stimulation of osteoblast growth. In contrast, RNA interference of *Gpr30* completely blocks proliferation of MC3T3 cells, indicating that *Gpr30* is required for osteoblast growth and could mediate mitogenic actions of estrogens in bone cells. Whether *Rgs2* interferes with *Gpr30* function directly or acts through different receptors remains to be established. However, our results clearly indicate that Runx2 sensitizes cAMP related GPCR signaling by activating *Gpr30* and repressing *Rgs2* gene expression in osteoblasts to increase responsiveness to mitogenic signals.

*Disclosures:* N. Teplyuk, None.



## SA001

**Dependence of Post Natal Osteogenic Differentiation on BMP2: Dissection of Osteogenic Lineage Commitment by Lentivirus BMP2 shRNA *ex vivo* and *in vivo*.** M. V. Bais\*, N. Wigner\*, M. Young\*, R. Toholka\*, D. Graves\*, E. F. Morgan\*, L. C. Gerstenfeld, T. A. Einhorn. Orthopaedic Research Laboratory, Department of Orthopedic Surgery, Boston University School of Medicine, Boston, MA, 02118, Boston, MA, USA.

In order to examine if autogenous BMP-2 expression is necessary for the osteogenic differentiation of marrow stromal cells, BMP-2 expression was inhibited using lentiviral transfection of a BMP2 shRNA. Inhibition of BMP2 expression decreased the expression of markers of terminal osteoblasts (osteocalcin, Runx2, osterix, APase activity, and mineral deposition), while the expression of transcription factors (Sox 9 and Msx2) that are seen in skeletal lineage progenitors were not effected. Rescue of osteogenic differentiation by the exogenous addition of either BMP7 or BMP2 recovered the levels of expression of osterix and APase and enhanced Sox9 and Msx2. However, BMP7 did not recover the expression of Runx2 and only partially recovered mineral deposition while the exogenous addition of BMP2 recovered all of these phenotypic properties. The effect of the loss of BMP2 expression on bone formation after marrow ablation lead to 80% loss of mineralized bone formation as assayed by microCT at day seven after surgery. Assay of same set of mRNAs as examined *in vitro* showed transient ~2 fold increase of Sox9 at day three after surgery in the shRNA BMP2 samples while at day seven osterix, Runx2, osteocalcin and Sox9 all showed ~50 to ~80% inhibition compared to expression in the NT (scrambled) treated samples. Interestingly, Msx2 showed ~10 fold elevation expression at seven days post surgery. Immunohistological examination of the cell populations found in the medullary space three days after surgery with antibodies for CD146 and Sox9, showed equal numbers of cells expressing these skeletal stem markers in both control and shRNA treated specimens. These results demonstrate that: 1) BMP-2 is a central morphogenetic factor for the post natal osteogenic differentiation: 2) BMP2 does not effect the initial recruitment or expansion of skeletal stem cells *in vivo*: 3) Both BMP2 and BMP7 can both induce osterix and this transcription factor can promote osteogenic differentiation: 4) Expression of Runx2 is dependent on BMP2: 5) Both osterix and Runx2 are needed to fully promote osteogenic development.



**Figure 1** MicroCt assessment of endosteal bone formation in response to surgical marrow ablation.

**Disclosures:** M.V. Bais, None.

This study received funding from: PO1-AR049920.

## SA002

See Friday Plenary number F002.

## SA003

**Clinical Application of Resorbable Polymers in Guided Bone Regeneration.** W. IP\*. Orthopaedics & Traumatology, The University of Hong Kong, Hong Kong, Hong Kong.

**INTRODUCTION:** Long segmental diaphyseal bone loss often results from high energy trauma like blast injury, osteomyelitis or wide excision of malignant conditions. Treatment of this long segmental diaphyseal defects remain a difficult clinical problem. In the literature, many authors have reported that bone loss more than 2.5 cm always require bone grafting. This is probably the critical size defect in human. Non-vascularized bone graft frequently fails if the defect is longer than 6-7 cm. 2.5 cm is probably the critical size defect in human and 7 cm is likely the critical size for non-vascularized bone graft. Various treatment methods are adopted currently to address this problem, including vascularized bone graft, distraction osteogenesis and massive allograft. However, all these methods are associated with a lot of problems.

Successful guided bone regeneration has been achieved in skull bone and jaw bone using resorbable allograft. Bone regeneration in long segmental defect and relatively small defect in tumour excision has been achieved using resorbable polylactide scaffolds.

**METHODS & MATERIALS:** 10 patients with bone defect of sizes up to 6 cm due to various causes including benign tumour, osteomyelitis & fractures were treated with resorbable polylactide scaffold impregnated with marrow blood which contains stromal cells. In cases with infection, antibiotics was also loaded into the scaffold and in this situation, the scaffold also served as a drug delivery device. The patients have assessed regularly with X rays and clinical symptoms.

**RESULTS:** Serial X ray evaluation and clinical evaluation revealed presence of bone regeneration. The limbs enjoyed satisfactory function and there was minimal donor site morbidity and major surgery can be avoided.

**DISCUSSION :** Selected cases are treated with guided bone regeneration which would be

treated otherwise by conventional technique. Vascularized bone transfer has limited supply and involves a major operation. There is always a chance of vascular complication and there is donor site morbidity. Distraction osteogenesis has a limitation of length that can be lengthened and requires a prolonged placement of external fixation. There is a high chance of traction injury to nerve and other soft tissues. Massive allograft requires a prolonged period, in terms of decades, for complete creep substitution. There is also a high incidence of disease transmission and infection. Therefore there is a constant demand for bone substitute which can bridge long segmental defect effectively with minimal morbidity and can heal in reasonable time frame. The affected limb can be rehabilitated and bear weight for functional restoration as early as possible. These early results are promising.

**Disclosures:** W. Ip, None.

## SA004

See Friday Plenary number F004.

## SA005

**CCAAT/Enhancer Binding Protein-Beta (C/EBP  $\beta$ ) Overexpression Causes Osteopenia.** S. Zanotti, A. Smerdel-Ramoya, L. Stadmeier\*, E. Canalis. Research, Saint Francis Hospital and Medical Center, Hartford, CT, USA.

C/EBPs are a family of ubiquitous transcription factors involved in cell differentiation. Six different C/EBPs are known,  $\alpha$ ,  $\beta$ ,  $\delta$ ,  $\gamma$ ,  $\epsilon$  and  $\zeta$ ; and they can form homo- and heterodimers that bind to similar sequence motifs. C/EBPs are expressed by osteoblasts and adipocytes during differentiation *in vitro*, and C/EBP  $\beta$  is required for adipogenesis. However, the role of C/EBP  $\beta$  in osteoblastogenesis is less clear, and its function in the postnatal skeleton is not known. To study the function of C/EBP  $\beta$  in osteoblasts *in vivo*, we created transgenic mice expressing C/EBP  $\beta$  under the control of the 3.8 kilobase fragment of the human osteocalcin promoter. Two transgenic lines were established in an FVB genetic background, and four week old C/EBP  $\beta$  transgenic mice were compared to wild type littermates of identical sex. Both C/EBP  $\beta$  transgenic lines exhibited osteopenia with a 30 % decrease in trabecular bone volume over tissue volume, due to a decrease in trabecular number. There was a reduction in number of osteoblasts per tissue area, although the number of osteoblasts per bone perimeter was not changed. The phenotype was the same in both male and female transgenics. To examine the mechanism leading to osteopenia, bone marrow stromal cells and calvarial osteoblasts from C/EBP  $\beta$  transgenics, and ST-2 stromal cells stably transduced with a C/EBP  $\beta$  expression construct were studied. In accordance with the results observed *in vivo*, bone marrow stromal cells from C/EBP  $\beta$  transgenics showed reduced mineralization as determined by alizarin red staining, and reduced alkaline phosphatase mRNA levels. Furthermore, calvarial osteoblasts from C/EBP  $\beta$  transgenics and ST-2 stromal cells stably expressing C/EBP  $\beta$  displayed reduced alkaline phosphatase activity. In conclusion, C/EBP  $\beta$  overexpression *in vivo* causes osteopenia, possibly by impairing osteoblastic function.

**Disclosures:** S. Zanotti, None.

This study received funding from: NIH Grant # DK42424

## SA006

See Friday Plenary number F006.

## SA007

**Use of GFP Reporter Mice for Assessing Osteoprogenitor Cell Activity in a Critical Size Calvarial Defect.** L. Wang, Y. Liu\*, P. Maye, D. W. Rowe. Dept. of Reconstructive Sciences, School of Dental Medicine, University of Connecticut Health Center, Farmington, CT, USA.

A successful repair strategy of a critical size defect in bone requires the interaction of cells from the endothelial/vascular, osteoprogenitor and hematopoietic lineages and a scaffold that is permissive or proactive to this process whether the cells are derived from host or implanted donor cells. Using a variety of GFP reporter mice that reflect the cellular activities of each tissue element and a new cryohistology for non-decalcified bone that preserves GFP signals, we have developed a calvarial defect model to assess the temporal and special events of a successful repair as a baseline for understanding why some strategies may fail. In two experimental designs, one assesses the host and donor contribution to a repair, host and donor express the same promoter driving distinguishable fluorescent proteins. Thus a defect that is closed with an acellular scaffold results in Col3.6green host cells streaming into the scaffold but never making a bone matrix as judged by the lack of xylenol orange (XO) staining or gross mineral deposition that is visible by DIC optics. However when donor cell derived from neonatal calvaria carrying the Col3.6blue reporter, a DIC positive matrix is produced that contains blue osteoblasts overlying the XO staining osteoid surface. The early woven bone present at 4 weeks begins the transition to remodeled bone observed when the repair is sampled at 8 weeks. Limited intermingling of host and donor osteoblasts can be observed at the margins, but no invasion of host osteoblasts within the scaffold is detected. However host derived osteoclastic cells are abundant in the repair and are recognized as weak Col3.6+ green cells that are not associated with the XO mineral label and are TRAP positive. The second design uses a nontransgenic host that receives donor cells carrying cell specific reporters expressing distinguishable colors. When the scaffold is inoculated with fresh bone marrow from a Col3.6green donor, no bone is formed and no donor cells survive. In contrast, when the

fresh marrow is mixed with neonatal calvarial cells carrying the Col3.6blue reporter, bone is formed with blue osteoblasts overlying the XO labeled matrix. Abundant green cells are present in the 8 week sample that have the signature of osteoclastic cells. However if marrow stromal cells that are double positive for BSP-green and DMP1-red are expanded in cultures and then used to seed the scaffold, abundant bone is formed that shows active green osteoblasts on the bone surface and red osteocytes within the bone matrix. Many permutations of this approach can be applied to assess the donor/scaffold/host variables that affect the repair of a bone defect.

**Disclosures:** L. Wang, None.

## SA008

**See Friday Plenary number F008.**

## SA009

**Bone Cell Response to Neurotransmitters and Mechanical Loading.** J. H. Kwag\*, B. G. Kim\*, H. G. Lee\*, C. H. Kim. Yonsei University, Wonju, Republic of Korea.

Mechanical loading is an important regulator of bone resorption. Also, neurotransmitters have been shown to exist in bone tissue and play a vital role in stimulating the calcium content and alkaline phosphatase level. In this study, our objective was to investigate the role of an important neurotransmitter (vasoactive intestinal peptide (VIP)) in controlling the mechanotransduction in bone cells. First, a dose study was performed. MC3T3-E1 preosteoblast cells were cultured in culture dishes with complete culture medium (CCM) for 6 days. VIP was added at either 0 (control),  $10^{-9}$ M or  $10^{-6}$ M on day 0 and day 3. mRNA was isolated on day 6 and real-time RT-PCR was performed. Second, the effect of VIP on mechanical loading was assessed. MC3T3-E1 cells were cultured in culture dishes and  $10^{-6}$ M of VIP added on day 0 and day 3. Cells were subcultured onto glass slides on day 5. Oscillatory fluid flow-induced shear stress was applied on day 6 using a custom-built loading device at 1 Pa for 1 hour. mRNA was isolated immediately after end of loading and real-time RT-PCR performed. For real time-RT-PCR, expression levels of osteoprotegerin (OPG) and receptor activator for NF- $\kappa$ B ligand (RANKL) genes were quantified. For the dose study, RANKL decreased by 40% ( $10^{-9}$ M VIP) and 60% ( $10^{-6}$ M VIP), while OPG increased by 50% ( $10^{-6}$ M VIP) compared to control. When VIP was combined with loading, RANKL decreased by over 90% and OPG increased by approximately 70% compared to control. Results suggest that VIP may have the potential to decrease osteoclastogenesis. In addition, it appears that VIP and oscillatory fluid flow-induced shear stress may have synergistic effects in controlling the bone remodeling process.

**Disclosures:** C.H. Kim, None.

*This study received funding from: Korea Science and Engineering Foundation (KOSEF).*

## SA010

**See Friday Plenary number F010.**

## SA011

**Silencing of RhoGTPases Counteract Microgravity-induced Effects on Osteoblasts.** A. Guignandon\*, C. Faure\*, M. Linossier\*, A. Rattner\*, N. Laroche\*, L. Vico. LBTO, INSERM U890, Saint Etienne, France.

Effects of space-related conditions on osteoblastic cells are characterized by a decrease in cell adhesion, disruption of cytoskeletal integrity leading to reduced differentiation potential. These effects can be mainly explained by deregulation of p21-RhoGTPases (p21), well-known regulators of actin-cytoskeleton. We exposed MG63 osteoblastic cells to 3 days of microgravity ( $\mu$ g) during Foton M3 ESA mission and compared them to ground controls (1g) kept in similar conditions except  $\mu$ g. Specific p21 activities are altered by siRNA for RhoA, Rac1, Cdc42 and compared to Scramble (SiScr). Being dependent on p21, cell migration, stress fiber number (SF), vinculin positive contacts, fibronectin matrix deposition and VEGF synthesis and immobilization into matrix are evaluated by way of RT-PCR and image analysis. We find that migration of SiScr cells increases in  $\mu$ g (+20%,  $p < 0.05$ ) as consequence of reduced adhesion (-35%,  $p < 0.01$ ) and increased polarity. SiRhoA in 1g group recapitulates most of SiScr cells  $\mu$ g-induced effects on focal adhesion area (-30%,  $p < 0.01$ ) and migration (+25%,  $p < 0.05$ ). SiRhoA does not induce major alteration in  $\mu$ g compared to  $\mu$ g SiScr and 1g SiRhoA. Interestingly, SiRac1 and SiCdc42 in 1g are not able to significantly increase SF and focal adhesion size while they increase both parameters in  $\mu$ g. SiRac cells in  $\mu$ g present an increased SF (+20%,  $p < 0.05$ ), matrix deposition (+25%,  $p < 0.01$ ) and a reduced migration (-40%,  $p < 0.01$ ). We previously showed (ASBMR 2006, #1274) that matrix-bound VEGF (VEGFm) expression is conditioned by a mechanically-increased SF. Whatever the silencing no change in basal levels of soluble (VEGFs) or VEGFm was seen in 1g. In  $\mu$ g, we observe that VEGFs/VEGFm ratio is greatly in favor of VEGFs in SiScr. SiRac1 and SiCdc42 in  $\mu$ g reduce significantly VEGFs, correcting VEGF ratio. All together SiRac1 and SiCdc42 may have activation effects on RhoA not seen in 1g leading to increased adhesion, matrix deposition and correction of VEGF alternative splicing thus counteracting  $\mu$ g-induced effects.

**Disclosures:** A. Guignandon, None.

*This study received funding from: European Space Agency (ESA) and Centre National d'Etudes Spatiales (CNES).*

## SA012

**See Friday Plenary number F012.**

## SA013

**Deciphering the Cellular Defects of Osteoblasts in Microgravity.** N. Nabavi\*. University of Toronto, Toronto, ON, Canada.

Gravity has been shown to be essential for biological events occurring in organisms on earth. It is also known that major physiological changes occur in bone during space flights, however, the intracellular changes have not been analyzed in details due to the difficult nature of these studies. The goal of this project was to understand the molecular mechanisms by which bone loss occurs during space flights using an elaborate closed culture system enabling cell proliferation. In this study, we investigated the cellular mechanism of bone loss in microgravity conditions by first determining whether osteoblasts exhibit impaired differentiation and/or function in microgravity environments compared to ground controls. Mature osteoblasts grown in microgravity environments were fixed and immunostained with antibodies. Samples were analyzed post-flight using epi- and confocal microscopy in order to determine whether the actin and microtubule (MT) cytoskeletons as well as the associating regulating proteins show differential organization and stability in osteoblast cells during spaceflight compared to ground controls. Focal adhesion proteins as well as apoptosis were examined in osteoblasts grown in microgravity versus ground control. We observe a marked impairment of cytoskeletal organization and cell adhesion which correlates with increased cell death in osteoblasts grown in space. These findings may have important relevance for astronauts participating in extended flights, as well as relevance for bone-wasting disorders, including disuse osteoporosis.

**Disclosures:** N. Nabavi, None.

*This study received funding from: The Canadian Space Agency.*

## SA014

**See Friday Plenary number F014.**

## SA015

**Microporosity In Beta-TCP Ceramics May Be Detrimental to Mesenchymal Stem Cell Survival and Osteoblastic Differentiation.** J. Isaac\*<sup>1</sup>, J. Hornez\*<sup>2</sup>, D. Jian\*<sup>3</sup>, M. Descamps\*<sup>2</sup>, C. Chauveau\*<sup>1</sup>, P. Hardouin<sup>1</sup>, D. Magne\*<sup>1</sup>. <sup>1</sup>Cellular and Molecular Biology EA2603, ULCO/Lille University, Boulogne/Mer, France, <sup>2</sup>LMP, Université de Valenciennes et du Hainaut Cambrésis, Maubeuge, France, <sup>3</sup>Orthopaedic Surgery, Shanghai Jiaotong University Sixth People Hospital, Shanghai, China.

Aims of the present study were to determine whether microporosity in beta-tricalcium phosphate (b-TCP) ceramics is beneficial or detrimental to human mesenchymal stem cells (MSCs), for the development of hybrid constructs for bone repair. MSCs, either purified or contained in bone marrow stromal cells, were seeded on ceramics with 0%, 25%, or 45% microporosity and cultured from 18 hours, 7 days, 14 days or 21 days, in an osteogenic medium consisting of DMEM with 10% FCS supplemented with  $10^{-8}$  M vitamin D3, 50  $\mu$ M ascorbic acid and 10 mM beta-glycerophosphate. Cell adhesion and viability were measured by cell counting, and with MTS and LDH assays. Osteoblastic differentiation was evaluated by measuring the activity of alkaline phosphatase (ALP) by the method of Lowry and by quantifying osteocalcin secretion by ELISA. Results indicated that whereas microporosity had no effect on cell adhesion, it increasingly inhibited cell viability in a rate and time-dependent manner. In addition, early and late osteoblastic differentiation appeared stimulated on non microporous b-TCP ceramics. Indeed, ALP activity and osteocalcin secretion were always decreased by the more microporous ceramics. Results of this in vitro study therefore reveal an unexpected negative role for microporosity in the osteoblastic differentiation of human mesenchymal stem cells.

**Disclosures:** D. Magne, None.

## SA016

**JNK Activation Is Involved in Tumor Necrosis Factor- $\alpha$ -stimulated Smurf1 Expression.** H. Lee<sup>\*1</sup>, T. Yi<sup>\*2</sup>, H. Ryoo<sup>1</sup>, K. Woo<sup>1</sup>, G. Kim<sup>\*1</sup>, J. H. Baek<sup>1</sup>. <sup>1</sup>Department of Cell and Developmental Biology, Seoul National University School of Dentistry, Seoul, Republic of Korea, <sup>2</sup>Clinical Research Center, INHA University Hospital, Incheon, Republic of Korea.

Tumor necrosis factor- $\alpha$  (TNF- $\alpha$ ) is a pro-inflammatory cytokine that induces local and systemic bone loss through the stimulation of bone resorption as well as through the inhibition of bone formation. Although previous report has shown that TNF- $\alpha$  stimulated Smurf1 expression, the signal pathways involved in TNF- $\alpha$ -induced Smurf1 transcription have not been clarified yet. Therefore, we were to examine the intracellular signaling pathways involved in TNF- $\alpha$ -mediated Smurf1 expression in C2C12 cells. As reported previously, TNF- $\alpha$  stimulated Smurf1 mRNA and protein expression in C2C12 cells. Cycloheximide treatment did not exert any effects on TNF- $\alpha$ -induced Smurf1 mRNA expression, indicating that Smurf1 induction is a direct effect. Although TNF- $\alpha$ -inhibited ALP activity was partially rescued by blocking of NF- $\kappa$ B activation as well as by c-Jun N-terminal kinase (JNK) inhibition, Smurf1 induction was suppressed only by JNK inhibition but not by NF- $\kappa$ B inhibition. This result suggests that JNK activation is involved in TNF- $\alpha$ -mediated Smurf1 induction.

**Disclosures:** J.H. Baek, None.

## SA017

See Friday Plenary number F017.

## SA018

**TGIF Regulation of Bone Mass: Impaired Osteoblast Differentiation.** M. K. Crook<sup>1</sup>, K. Mohammad<sup>1</sup>, L. Bartholin<sup>\*2</sup>, A. Carver<sup>\*3</sup>, L. Suva<sup>3</sup>, J. Chirgwin<sup>1</sup>, D. Wotton<sup>\*2</sup>, T. Guise<sup>1</sup>. <sup>1</sup>Internal Medicine, University of Virginia, Charlottesville, VA, USA, <sup>2</sup>Biochemistry and Molecular Genetics, University of Virginia, Charlottesville, VA, USA, <sup>3</sup>Orthopedics, University of Arkansas, Little Rock, AR, USA.

TG Interacting factor (TGIF) is a transcriptional corepressor of TGF-beta and retinoic acid (RA) actions. TGIF mutations occur in holoprosencephaly (HPE), a defect in craniofacial and forebrain development, also caused by mutations at three steps in the Sonic Hedgehog (SHH) pathway: SHH, Ptc-1 and Gli-2. Zebrafish lacking TGIF have low RA-activating enzyme, aldehyde dehydrogenase 1a2 (aldh1a2) and degrading enzyme cyp26a1, suggesting that TGIF may regulate RA activity gradients. Aldh1a2<sup>-/-</sup> mice have diminished SHH signaling and severe skeletal abnormalities. The SHH promoter is RA-responsive, and TGIF may act on the skeleton via altered RA activity regulating SHH expression. *Tgif*<sup>-/-</sup> mice show growth retardation, domed skulls, twisted noses, and defects in vertebrae, ribs and sternum. These mice had significantly less trabecular bone by DEXA, microCT and histomorphometry. Low bone mass was accompanied by increased osteoclast activity and reduced osteoblast number and bone formation rates. Osteoblast progenitors, CFU-OBs, were decreased in bone marrow from *Tgif*<sup>-/-</sup> compared to wild-type (WT) mice. Primary osteoblasts from *Tgif*<sup>-/-</sup> vs WT mice had increased expression of the early marker Col1a (p<0.01), and reduced expression of two late markers, osteocalcin (p<0.05) and bone sialoprotein (p<0.01), suggesting multiple effects of TGIF on the osteoblast lineage.

We previously showed that TGF-beta inhibition did not correct the low bone mass in *Tgif*<sup>-/-</sup> mice-beta. Here we focus on RA signaling. Aldh1a2 mRNA was 30% lower in *Tgif*<sup>-/-</sup> osteoblasts (p<0.05) compared to WT in an initial experiment. Cyp26a1 was increased by 30% (P<0.01), suggesting that TGIF may determine RA gradients. SHH induces osteoblastogenesis and mineralization by increasing Gli-2 expression. In one of two experiments, Gli-2 mRNA concentration was decreased in untreated *Tgif*<sup>-/-</sup> osteoblast (p=0.033) compared to WT. Diminished SHH signaling may contribute to impaired differentiation in stimulated *Tgif*<sup>-/-</sup> osteoblasts.

The actions of RA and SHH signaling are best understood during embryogenesis. The epistatic relationship of these two pathways post-developmentally and whether they act primarily on adult mesenchymal stem cell differentiation are presently unclear. TGIF may play a role in adult bone remodeling by modulating these pathways.

**Disclosures:** M.K. Crook, None.

## SA019

**Conditional Disruption of *Pkd1* in Osteoblasts Results in Osteopenia Due to Direct Impairment of Osteoblast-Mediated Bone Formation.** Z. Xiao, S. Zhang<sup>\*</sup>, L. Cao<sup>\*</sup>, R. Wu<sup>\*</sup>, L. Quarles. The Kidney Institute, Kansas University Medical Center, Kansas City, KS, USA.

Polycystin-1 (PKD1) is a highly conserved, multi-domain membrane protein widely expressed in various cell types. Mutations of human *PKD1* cause Autosomal Dominant Polycystic kidney disease, however, the biological functions of PKD1 in other tissues remain poorly defined. We recently reported that *Pkd1* is highly expressed in bone and that the *Pkd1*<sup>m1Bci</sup> mouse, which has an inactivating mutation of *Pkd1*, develops osteopenia and impaired osteoblastic differentiation. To determine whether *Pkd1* directly functions in osteoblasts to regulate bone mass, we generated mice with osteocalcin (*Oc*)-promoted selective inactivation of *Pkd1* in osteoblasts. Transgenic *Oc-Cre* mice were crossed with

*Pkd1*<sup>m1Bci/+</sup> mutant mice to create double heterozygous *Cre/+; Pkd1*<sup>m1Bci/+</sup> mice, then *Oc-Cre/+; Pkd1*<sup>m1Bci/+</sup> mice were crossed with homozygous floxed *Pkd1* (*Pkd1*<sup>lox/lox</sup>) mice to generate control mice (*Pkd1*<sup>lox/+</sup>), conditional *Pkd1* heterozygous mice (*Oc-Cre-Pkd1*<sup>lox/+</sup>), and conditional *Pkd1* null mice (*Oc-Cre-Pkd1*<sup>lox/m1Bci</sup>). Diagnostic PCR demonstrated that *Cre*-mediated recombination (*Pkd1*<sup>lox</sup>) occurred exclusively in bone, whereas non-skeletal tissues retained the floxed *Pkd1* allele (*Pkd1*<sup>lox</sup>). Compared to control mice, the conditional deletion of *Pkd1* from osteoblasts resulted in a gene-dose dependent reduction in bone mineral density (BMD; 10 versus 18%) compared to controls at 3 months-of-age. In addition,  $\mu$ CT analyses found that bone volume (BV/TV, %) and cortical thickness (Ct.Th., mm) were reduced in *Oc-Cre-Pkd1*<sup>lox/+</sup> (25.5 $\pm$ 2.5 % and 0.241 $\pm$ 0.009 mm) and *Oc-Cre-Pkd1*<sup>lox/m1Bci</sup> (18.8 $\pm$ 1.6 % and 0.211 $\pm$ 0.005 mm) compared with the age-matched control littermates (33.7 $\pm$ 2.1 % and 0.267 $\pm$ 0.005 mm). Mineral apposition rates were also reduced proportionate to *Pkd1* gene dose (1.28 $\pm$ 0.31, 0.83 $\pm$ 0.13, and 0.45 $\pm$ 0.07  $\mu$ m/day in control, *Oc-Cre-Pkd1*<sup>lox/+</sup> and *Oc-Cre-Pkd1*<sup>lox/m1Bci</sup>, respectively). Real-time RT-PCR analyses also revealed a conditional *Pkd1*-gene dosage effect on osteoblast-related genes expressions, including *Runx2-IL*, *Osteocalcin*, *Osteopontin*, and *bone sialoprotein*. Thus, the selective deletion of *Pkd1* from osteoblasts postnatally results in defective osteoblast-function and osteopenia. These findings indicate that *Pkd1* functions in osteoblasts to regulate bone formation.

**Disclosures:** Z. Xiao, None.

This study received funding from: NIAMS.

## SA020

See Friday Plenary number F020.

## SA021

**Noncanonical Wnt Signaling Is Involved mir-206 Expression in Osteoblastic Differentiation.** M. Sato<sup>\*1</sup>, M. Nashimoto<sup>\*2</sup>, D. Kanayama<sup>\*1</sup>, Y. Yawaka<sup>\*3</sup>, M. Tamura<sup>1</sup>. <sup>1</sup>Biochemisrty and Molecular Biology, Grad. Sch. Dent. Med., Hokkaido University, Sapporo, Japan, <sup>2</sup>Department of Applied Life Sciences, NUPALS, Niigata, Japan, <sup>3</sup>Dentistry for Children and Disabled Person, Grad. Sch. Dent. Med., Hokkaido University, Sapporo, Japan.

Wnt signaling plays a role in the developing skeletal system. However, the exact mechanisms by which Wnt signaling regulates bone remodeling remain to be elucidated. Our previous studies demonstrated that an interaction between  $\beta$ -catenin and Smad was crucial for Wnt-mediated regulation of BMP-2 responsive gene expression, and that BMP-2 up-regulated Wnt-induced osteoprotegerin (OPG) expression. MicroRNAs (miRNAs) are small non-coding RNAs that are emerging as important post-transcriptional gene regulators. Many miRNA are expressed in a tissue-specific manner, suggesting a role of the miRNA in the specification of the tissue during differentiation. In this study, we investigated the regulation of miRNA expression by Wnt signaling in osteoblastic differentiation. We cultured Wnt3a or Wnt5a stably over-expressing mesenchymal pluripotent C2C12 cell lines and examined levels of miR206 expression using TaqMan MicroRNA Assays. In C2C12 cells, miR-206 was expressed, while its expression was dramatically reduced in Wnt5a over-expressing C2C12 (Wnt5a-C2C12) cells. In contrast, miR-206 expression was similar in Wnt3a-C2C12 cells. These results indicated that non-canonical Wnt mediated signaling regulates miR-206 gene expression, and this is the first study linking miRNA expression to Wnt signaling. The miR-206 expression levels were also down-regulated by treatment with BMP2 in C2C12 cells. To further investigate the function of miR-206, we have examined over-expression of miR-206 or silencing of miR-206 by sgRNA (tRNaseZL-utilizing gene silencing method). Transfection of miR-206 reduced cell number in Wnt5a-C2C12 cells, indicating that miR-206 might regulate cell proliferation in these cells. RT-PCR analysis indicated that Id-1 expression was reduced by transfection of miR-206. These results show that miR-206 is a target gene for non-canonical Wnt signaling, and that its link is mediated by a novel mechanism by which miRNAs regulate cell proliferation and osteoblastic differentiation.

**Disclosures:** M. Tamura, None.

## SA022

**Accelerated Fracture Callus Remodeling and Membranous Bone Healing in STAT1 Deficient Mice.** K. Tajima<sup>\*1</sup>, H. Takaishi<sup>1</sup>, N. Ota<sup>1</sup>, N. Kosaki<sup>1</sup>, T. Tomonda<sup>\*1</sup>, M. Yoda<sup>\*2</sup>, J. Takito<sup>\*1</sup>, M. Matsumoto<sup>\*2</sup>, Y. Toyama<sup>\*1</sup>. <sup>1</sup>Department of Orthopaedic Surgery, Keio University School of Medicine, Tokyo, Japan, <sup>2</sup>Spine and Spinal Cord Disease, Keio University School of Medicine, Tokyo, Japan.

Signal transducer and activator of transcription 1 (STAT1), originally identified as a signal transducing molecule in the interferon (IFN) pathway, participates not only in immune responses but also acts directly on osteoclast precursor cells and mesenchymal cells. Bone fracture triggers a steady inflammatory cascade of bone regeneration and this reparative process consists of a variety of molecular and cellular events. Although various growth factors and cytokines that participate in fracture healing have been identified, the precise mechanism behind these processes has not been fully understood. Here, we generated a fracture model using STAT1 knock out (KO) mice to elucidate the role of STAT1 in fracture healing.

A transverse osteotomy was performed at the middle of the tibia of 8-week-old male STAT1 KO and wild type (WT) mice. The fracture site was stabilized by inserting a inner pin of a 23-gauge spinal needle intramedullary. Soft X-ray and micro CT scanning were

performed at 1, 2, 3, 4, 6, and 10 weeks after surgery. There was no difference in the rate of callus formation and bone union between STAT1 KO and WT until post-fracture-week (PFW) 4. But the cross sectional area of the fracture site after bone union significantly decreased in KO mice ( $1.48 \pm 0.39 \text{ mm}^2$  at PFD6 and  $1.35 \pm 0.32 \text{ mm}^2$  at PFW10) compared to WT ( $2.41 \pm 0.27 \text{ mm}^2$  at PFW6 and  $2.32 \pm 0.18 \text{ mm}^2$  at PFW10), suggesting the accelerated callus resorption and bone remodeling in STAT1 KO. To examine the membranous ossification in STAT1 KO mice, we next generated a cortical defect model in tibiae. Soft X-ray and histological analysis were performed at PFW1, 2, 3, and 4. STAT1 KO mice showed the rapid recovery at PFW2 and 3. The number of stromal cells existed in the defect area was the same between WT and STAT1 KO.

It is known that the skeletal phenotype in STAT1 KO mice exhibits a high bone turnover typed osteosclerosis due to accelerated RANKL-dependent osteoclastogenesis and the enhanced calcification by osteoblasts. The enhanced calcification of STAT1 KO osteoblasts is explained by the release of inhibition of Runx2 function by STAT1. Since there was no significant difference in callus formation in two groups, we assumed that the STAT1 attenuated the callus remodeling and the membranous ossification in fracture healing. Further investigation of the STAT1 signaling *in vitro* will be presented.

**Disclosures:** K. Tajima, None.

## SA023

**Characterization of Jun Activation-Domain Binding Protein (Jab1)-Interacting Motif in LIM Mineralization Protein-1.** S. Sangadala, Y. Liu, M. Viggewarapu, L. Titus, S. Boden. Orthopaedics, Atlanta VA Medical Center, Atlanta, GA, USA.

Members of the transforming growth factor  $\beta$  (TGF $\beta$ ) superfamily have important effects on osteoblast differentiation and bone formation. We have shown previously that LIM Mineralization Protein-1 (LMP-1) enhances the efficacy of BMP-2, a member of the TGF $\beta$  superfamily, in cultured mesenchymal stem cells by the association of LMP-1 with Smurf1. Additionally, we report here that LMP-1 associates with Jab1, a protein also involved in protein degradation pathways like Smurf1. We screened a bone marrow library using the yeast-2-hybrid system. Sequencing and database matching of positive clones identified Jun activation domain binding protein 1 (Jab1) as a candidate binding partner for LMP-1. Immunoprecipitations demonstrated that Jab1 was found in complexes with LMP-1.

Jab1 is also known as the 5<sup>th</sup> subunit of the COP signalosome exhibiting homology to the 26S proteasomal lid complex. Jab1 binds to Smad4, Smad5 and Smad7, key intracellular signaling molecules of the TGF $\beta$  superfamily, and results in ubiquitination and/or degradation of these Smads. We confirmed a direct interaction of Jab1 with LMP-1 using recombinantly expressed proteins in slot-blot binding assays. In these studies, we also identified interaction of Smad1 with Jab1, in addition to Smads4, 5, and 7 as reported in literature. We hypothesized that LMP-1 binding to Jab1 prevents the binding and subsequent degradation of these Smads causing increased accumulation of osteogenic Smads in cells. To test this hypothesis we overexpressed LMP-1 in cells, separated the nuclear proteins by SDS-PAGE, and probed blots with Smad4 specific antibody. We demonstrated a 2-fold increase in the amount of Smad4 detected in LMP-1 treated cells compared with untreated cells. The phosphorylated receptor Smads1, 5 or 8 oligomerize with Smad4, enter the nucleus and induce osteogenic genes in the BMP pathway. An increase in nuclear Smad4 is an indicator of enhancement of this pathway.

We identified a motif in LMP-1 that is predicted to interact with Jab1 based on the MAME/MAST sequence analysis of several cellular signaling molecules that are known to interact with Jab-1 such as p27 (a cyclin-dependent-kinase inhibitor), Leukocyte functional antigen-1, lutropin/choriogonadotropin receptor, c-jun, Smad4, p53 and psoriasins. We further mutated the potential key interacting residues in LMP-1 and showed loss of binding to Jab1 in binding assays *in vitro*. Further studies are underway to establish biological relevance of LMP-1 and Jab1 interaction in enhancing the levels of osteogenic Smads resulting in potentiation of signaling by members of the TGF $\beta$  superfamily.

**Disclosures:** S. Sangadala, None.

## SA024

**See Friday Plenary number F024.**

## SA025

**PTH/PTHrP Mediated Stimulation of Osteoblast Differentiation Involves Epac-Rap1 Dependent Processes.** N. S. Datta<sup>1</sup>, N. J. D'Silva<sup>\*2</sup>, L. K. McCauley<sup>2</sup>, A. B. Abou-Samra<sup>1</sup>. <sup>1</sup>Internal Medicine, Wayne State University, Detroit, MI, USA, <sup>2</sup>Periodontics and Oral Medicine, University of Michigan, Ann Arbor, MI, USA.

The mechanisms underlying the crosstalk between the cAMP and mitogen-activated protein kinases (MAPKs or ERKs) and the involvement of the MAPK pathway in the actions of PTH and PTHrP on osteoblast differentiation and mineralization are not completely understood. Our previous studies suggested involvement of ERK and cyclin D1 in the proliferative and differentiative actions of PTH and PTHrP; expression of cyclin D1 was dependent on ERK activity in MC3T3 osteoblastic cells. The mechanisms involved in the activation or inhibition of ERK signaling by cAMP include activation of the small G protein Ras and the protein kinase Raf-1 as well as the monomeric G protein Rap1 (GTPase Rap1) which preferentially activates B-Raf. cAMP can modulate ERKs via the Epac/Rap1/B-Raf pathway in a PKA- and Ras- independent manner. Although studies *in vivo* suggest that the anabolic actions of PTH and PTHrP are mediated by cAMP it is not known if Epac,

Rap1 and B-Raf signaling pathway is involved. To examine the involvement of Rap1 signaling pathway on the growth of MC3T3-E1 osteoblastic cells, the cells were synchronized by switching them to media without serum for 36-48h to render them quiescent and then treated with or without PTHrP (100 nM) in low serum (2%) for 30 min-5h and harvested. Differentiation was induced with ascorbic acid for 7 days; and the cells were then treated with vehicle or PTHrP for 30 min-5h before harvesting. Total cellular proteins and RNA were isolated. Using a pull-down assay, active GTP bound-Rap1 was up-regulated following SDS PAGE and Western blot analyses in differentiated MC3T3-E1 osteoblastic cells. Real-time PCR analysis demonstrated induction of Rap1B transcription ( $p < 0.01$ ) in these cells following PTHrP treatment. Ectopic ossicles, an engineered bone growth model generated with bone marrow stromal cells from C57BL6 mice implanted in nude mice, showed an increase in bone formation and increased Rap1B transcription ( $p < 0.01$ ) following 2 weeks of daily PTH treatment ( $40 \mu\text{g/kg}$ ; sc) *in vivo*. These studies show that activation of the PTH/PTHrP receptor in the osteoblastic cells increase the expression of Rap1B. The increased Rap1B provides an alternate signaling mechanism for the expression of the anabolic action of PTH and PTHrP in the differentiated osteoblasts. This work was supported by funding from NIH R03 DE018245-01.

**Disclosures:** N.S. Datta, None.

*This study received funding from: NIH.*

## SA026

**See Friday Plenary number F026.**

## SA027

**Ahnak Regulates Calcium Signaling and ATP Release in Osteoblasts in Response to Mechanical Stimulation.** Y. Shao, V. P. Fomin\*, M. C. Farach-Carson, R. L. Duncan. Biological Sciences, University of Delaware, Newark, DE, USA.

We have found that ahnak, a 700kDa scaffold protein, interacts with the auxiliary  $\beta$  subunit of the  $\text{Ca}_v1.2$  cardiac L-type voltage sensitive calcium channel (LVSCC) and appears to anchor these channels to the actin cytoskeleton. Western blot analysis and immunohistochemistry demonstrated that ahnak was primarily expressed at the plasma membrane of mouse osteoblasts, with relatively lower intracellular distribution. In addition to the structural function of ahnak, we postulate that ahnak can regulate LVSCC activity and, as a result, alter ATP release in osteoblasts in response to fluid shear. Using siRNA strategy directed at ahnak in MC3T3-E1 osteoblasts, we were able to suppress ahnak protein levels by approximately 80% of vector transfected controls. The intracellular  $\text{Ca}^{2+}$  increase in response to mechanical stimulation in MC3T3-E1 cells was significantly reduced by 70% in response to ahnak protein knockdown indicating a possible role of ahnak in the regulation of  $\text{Ca}^{2+}$  signaling. We have previously shown that this increase in  $\text{Ca}^{2+}$  through LVSCC activation was responsible for fluid shear-induced ATP release from MC3T3-E1 cells. Although ahnak protein knockdown had no effect on basal ATP release in static cells, fluid shear-induced ATP release was significantly attenuated in siRNA transfected cells ( $p < 0.01$ ). Interestingly, quinacrine staining indicated a marked accumulation of acidic vesicles (mostly ATP rich vesicles) in siRNA transfected cells in static conditions. While we have shown that shear induces polymerization of actin filaments, knockdown of ahnak protein with specific siRNA did not influence the structures of either actin filaments or microtubule cytoskeleton at static conditions. Microtubule filaments are disassembled in response to fluid shear untreated osteoblasts. However the microtubule structure was kept intact in ahnak siRNA transfected cells, suggesting that ahnak may participate in the microtubule-mediated vesicular ATP transportation and release. Collectively, our investigation revealed that ahnak functions in  $\text{Ca}^{2+}$  signal regulation in bone cells independently of the actin-based cytoskeleton. Ahnak protein was clearly involved in the ATP release induced by mechanical stimulation. Furthermore, Western analyses demonstrate that ahnak protein levels are rapidly reduced in MC3T3-E1 cells in response to fluid shear, suggesting that loss of this protein may be involved in the loss of mechanosensitivity in response to continued loading.

**Disclosures:** Y. Shao, None.

*This study received funding from: National Institute of Dental and Craniofacial Research.*

## SA028

**Integrin-associated Protein Upregulates Osteogenesis-related Transcription Factors via TGF- $\beta$  and BMP Pathways.** K. Ikeda<sup>\*1</sup>, K. Shimada<sup>1</sup>, K. Kawamoto<sup>\*1</sup>, M. Maeno<sup>2</sup>, K. Ito<sup>\*1</sup>. <sup>1</sup>Department of Periodontology, Nihon University, Tokyo, Japan, <sup>2</sup>Department of Oral Health Sciences, Nihon University, Tokyo, Japan.

To understand the mechanism of developing bone leads to open new frontiers in bone regeneration. To analyze the molecular events that occur in the developing mandible, we examined the expression of 8803 genes from samples taken at different time points during rat postnatal mandible development using cDNA microarray. We demonstrated that gene expression of Integrin-associated protein (IAP, also known as CD47) changed markedly. Transforming growth factor (TGF)- $\beta$  superfamily, including bone morphogenetic proteins (BMPs), play a specific role in developing bone. TGF- $\beta$  and BMPs induce receptor-regulated Smads (R-Smads); Smad2, 3 or Smad1, 5, 8, respectively. The R-Smads form complexes with the common-partner Smad, which is Smad4 in mammals. These complexes translocate and accumulate in the nucleus and regulate the transcription of various target genes.

To analyze the function of IAP in the TGF- $\beta$  and BMP signaling pathway, endogenous IAP was disrupted in rat osteoblastic cell line ROS 17/2.8 using a 19 nucleotide siRNA and examined its effectiveness in silencing IAP expression. The gene expression of osteogenesis-related transcription factors, including Runx2, Msx2, Dlx5 and Osterix was determined by real-time reverse-transcribed PCR. Moreover, the protein levels of Smad4, Smad1, phospho-Smad1, Smad2, phospho-Smad2 were evaluated using SDS-PAGE and Western blot analysis.

The efficiency of silencing IAP mRNA level was approximately 70%. The expression of Runx2, Msx2, Dlx5 and Osterix was markedly increased when IAP was silenced. The protein levels of Smad4, phospho-Smad1, phospho-Smad2 were increased dose dependently. Our results suggest that IAP regulates osteogenesis-related transcription factors via TGF- $\beta$  and BMP pathways.

**Disclosures:** K. Ikeda, None.

*This study received funding from: Grant from Dental Research Center, Nihon University School of Dentistry.*

## SA029

See Friday Plenary number F029.

## SA030

**Lithocholic Acid Downregulates the Effects of Vitamin D<sub>3</sub> on Primary Human Osteoblasts.** S. Ruiz-Gaspà<sup>\*1</sup>, A. Enjuanes<sup>\*1</sup>, P. Peris<sup>1</sup>, A. Martinez-Ferrer<sup>\*1</sup>, M. J. Martinez de Osaba<sup>\*1</sup>, L. Alvarez<sup>\*1</sup>, A. Monegal<sup>\*1</sup>, A. Combalia<sup>\*2</sup>, B. Gonzalez<sup>\*1</sup>, N. Guanabens<sup>1</sup>, A. Pares<sup>\*3</sup>. <sup>1</sup>Metabolic Bone Diseases Unit, Hospital Clinic, IDIBAPS, CIBEREHD, Barcelona, Spain, <sup>2</sup>Department of Orthopaedics, Hospital Clinic, IDIBAPS, CIBEREHD, Barcelona, Spain, <sup>3</sup>Liver Unit, Hospital Clinic, IDIBAPS, CIBEREHD, Barcelona, Spain.

Osteoporosis is a complication of chronic cholestasis, related to its severity and duration. Cholestasis is characterized by deficient biliary secretion of total and conjugated bilirubin and bile acids, with high circulating levels. Among bile acids, lithocholic acid has particular significance because it has potential toxic effects and on the other hand has been described as an agonist of vitamin D receptor. Therefore, this study was addressed to analyse the effect of lithocholic acid on survival and on pathways of vitamin D metabolism and cell maturation on primary human osteoblasts.

Bone cell cultures were established from trabecular bone specimens of 10 patients undergoing hip replacement for osteoarthritis. Experiments with human osteoblastic cell cultures were performed using DMEM with or without fetal bovine serum (FBS) or human albumin, and at different lithocholic acid concentrations (10<sup>-6</sup>M, 10<sup>-5</sup>M, 10<sup>-4</sup>M and 10<sup>-3</sup>M) and times (6, 24, 48 and 72 hours) with or without vitamin D<sub>3</sub> (10<sup>-7</sup>M). Cell survival was determined by cell proliferation reagent WST-1. Vitamin D 24-hydroxylase (*CYP24A*), bone gamma-carboxyglutamate protein (*BGLAP*) and osteoprotegerin (*TNFRSF11B*) gene expression were quantified by real time PCR and used as indicators of vitamin D metabolism, osteoblast maturation and osteoclast differentiation and activation, respectively.

Lithocholic acid with or without FBS or albumin at 10<sup>-3</sup>M and 10<sup>-4</sup>M, respectively had a toxic effect evidenced by a dramatic decrease in cell survival. All the following experiments were performed with lithocholic acid below these lethal concentrations. Lithocholic acid increased *CYP24A* (p=0.02) and *BGLAP* (p=0.007) mRNA expression in cell cultures with no changes on *TNFRSF11B* expression, effects which were significantly lower (*CYP24A*: - 96% and *BGLAP*: - 92%) than those observed with vitamin D<sub>3</sub>. Moreover, lithocholic acid at all time points and conditions significantly downregulated the effect of vitamin D<sub>3</sub> on *CYP24A* and *BGLAP* gene expression by -72% and -74%, respectively.

In conclusion, lithocholic acid decreases the stimulatory effect of vitamin D<sub>3</sub> on *CYP24A* and *BGLAP* expression in primary human osteoblasts. These results may explain the potential deleterious effects of retained toxic bile acids on bone formation in patients with chronic cholestasis.

**Disclosures:** S. Ruiz-Gaspà, None.

## SA031

**The Interplay Between BMP and TGF- $\beta$  Signaling in Osteoblast Differentiation.** D. J. J. de Gorter<sup>\*1</sup>, R. L. van Bezooijen<sup>\*2</sup>, C. W. G. M. Löwik<sup>\*2</sup>, P. ten Dijke<sup>\*1</sup>. <sup>1</sup>Molecular Cell Biology, Leiden University Medical Center, Leiden, Netherlands, <sup>2</sup>Endocrinology, Leiden University Medical Center, Leiden, Netherlands.

Transforming Growth Factor- $\beta$  (TGF- $\beta$ ) is a pleiotropic cytokine implicated in the control of proliferation, migration, differentiation, and survival of many different cell types. In the skeleton, TGF- $\beta$  is one of the most abundant cytokines and plays a major role in its development and maintenance by affecting both cartilage and bone metabolism. Both positive and negative effects of TGF- $\beta$  on bone formation have been reported, but the exact molecular mechanisms underlying these effects remain to be established. Among others, TGF- $\beta$  modulates signaling induced by Bone Morphogenetic Proteins (BMPs), which are required for skeletal development and maintenance of adult bone homeostasis, and play an important role in fracture healing.

Although TGF- $\beta$  is generally believed to inhibit BMP-induced osteoblast differentiation, we found that pharmacological inhibitors against the TGF- $\beta$  type I receptor ALK5 impaired BMP-induced alkaline phosphatase (ALP) activity in the murine KS483 mesenchymal and C2C12 pre-myoblast cell lines. In addition, these ALK5 inhibitors reduced BMP6 stimulated mineralization of KS483 cells. Conversely, co-stimulation with BMP6 and TGF- $\beta$ 3 further increased ALP activity and mineralization of KS483 cells compared to BMP6 alone. This was not only observed in combination with BMP6, but also with BMP2 and BMP7. In C2C12 cells, TGF- $\beta$ 3 could inhibit but also under certain conditions stimulate BMP-induced ALP activity. BMP6-induced activation of a BMP-Smad-dependent luciferase reporter was, however, always inhibited by TGF- $\beta$ 3, suggesting that the stimulatory effect of TGF- $\beta$ 3 is not due to increased BMP-Smad activity.

In conclusion, besides acting as an inhibitor, TGF- $\beta$  can also stimulate BMP-induced osteoblast differentiation. Characterization of the interplay between BMP and TGF- $\beta$  signaling and the conditions in which TGF- $\beta$  inhibits or stimulates BMP-induced osteoblastic differentiation may provide new insights into the molecular mechanisms that regulate bone formation and how this may be modulated.

**Disclosures:** D.J.J. de Gorter, None.

## SA032

See Friday Plenary number F032.

## SA033

**PTH Induces COX-2 in MC3T3-E1 Osteoblasts via cAMP-PKA and Calcium-Calcieneurin Pathways.** H. Huang<sup>\*1</sup>, D. Chikazu<sup>2</sup>, O. Voznesensky<sup>\*1</sup>, K. Dodge-Kafka<sup>\*3</sup>, H. Drissi<sup>4</sup>, C. Pilbeam<sup>1</sup>. <sup>1</sup>Department of Medicine, UCHC, Farmington, CT, USA, <sup>2</sup>Department of Oral and Maxillofacial Surgery, University of Tokyo, Tokyo, Japan, <sup>3</sup>Department of Cell Biology, UCHC, Farmington, CT, USA, <sup>4</sup>Department of Orthopedics, UCHC, Farmington, CT, USA.

Parathyroid hormone (PTH) is a major regulator of bone remodeling that is thought to have most of its effects via the cyclic adenosine monophosphate (cAMP)-protein kinase A (PKA) signaling pathway. PTH is also a potent inducer of cyclooxygenase-2 (COX-2) via the PKA pathway. The goal of this study was to identify cis-acting sites and trans-acting factors mediating the PTH induction of COX-2. We used osteoblastic MC3T3-E1 cells (MC-4 sub-clone) stably transfected with -371/+70 bp of the murine COX-2 promoter fused to a luciferase reporter. We made site-directed mutations in the promoter DNA in (1) the cAMP response element (CRE) at -57/-52 bp, (2) the activating protein-1 (AP-1) binding site at -68/-63 bp, (3) the nuclear factor of activated T-cells (NFAT) binding site at -77/-73 bp, and (4) both the AP-1 and NFAT sites (which comprise a consensus sequence for composite binding of NFAT and AP-1). Single mutation of the CRE, AP-1, or NFAT site decreased PTH-stimulated luciferase activity by about 60%, while mutation of the composite NFAT/AP-1 site reduced the PTH-stimulated activity by 90%. On electrophoretic mobility shift analysis (EMSA), PTH stimulated binding of phosphorylated CRE-binding protein (CREB) to an oligonucleotide spanning the CRE. PTH also increased binding of NFATc1, c-Fos and c-Jun to an oligonucleotide spanning the NFAT/AP-1 composite site. PTH did not increase binding of NFATc2, c3 or c4 to the composite site. EMSA competition experiments showed cooperative binding of NFATc1 and AP-1 proteins to the NFAT/AP-1 composite sequence, and the cooperativity depended more on NFAT than on AP-1 binding. Both PTH and forskolin, an activator of adenylyl cyclase, stimulated NFATc1 nuclear translocation. Phorbol myristate acetate, a protein kinase C (PKC) agonist, did not stimulate NFATc1 nuclear translocation. PKA inhibitors H-89 and KT-5720 inhibited PTH- or forskolin-stimulated COX-2 promoter activity 98 and 60%, respectively, while GF109203X, a specific PKC inhibitor, had no effect on either PTH- or forskolin-stimulated COX-2 promoter activity. Inhibition of the calcium-calcieneurin-NFAT pathway by chelation of calcium or by calcieneurin inhibitors reduced PTH- and forskolin-stimulated COX-2 promoter activity 60-80%. These results demonstrate a critical role for both the cAMP/PKA pathway and the calcium-calcieneurin pathway in NFAT activation and PTH signaling in osteoblasts and suggest that cross-talk between these two pathways may play a role in other important effects of PTH in osteoblasts.

**Disclosures:** H. Huang, None.

*This study received funding from: NIH DK48361.*

## SA034

See Friday Plenary number F034.

## SA035

**P2Y<sub>2</sub> Receptor Activation Regulates RhoA-Mediated Stress Fiber Formation in Osteoblasts.** W. D. Yang<sup>1</sup>, J. Gardinier<sup>\*2</sup>, S. Majumdar<sup>\*1</sup>, D. L. Randall<sup>1</sup>. <sup>1</sup>Biological Sciences, University of Delaware, Newark, DE, USA, <sup>2</sup>Biological Sciences, and Mechanical Engineering, University of Delaware, Newark, DE, USA.

Bone and osteoblasts rapidly lose their mechanosensitivity in response to continued loading, likely through adaption of cellular mechanism involved in the transduction of this signal. We postulate that cytoskeleton reorganization in response to load is one mechanism through which the desensitization of osteoblasts to load is incurred. Because we have shown that ATP is rapidly released from osteoblasts in response to mechanical load, we hypothesize that activation of purinergic signaling mediates the increase in actin organization. P2Y<sub>2</sub> receptor activation increases stress fibers formation in other cell types, therefore we examined the role of P2Y<sub>2</sub> in the regulation Rho-mediated stress fibers formation induced by mechanical stimulation in osteoblasts. In this study, we examined the effects of ATP and P2Y<sub>2</sub> on cytoskeleton formation, Rho activation and cell mechanical properties alterations in MC3T3-E1 cells subjected to 12 dynes/cm<sup>2</sup> fluid shear. When 100 μM ATP, ADP, BzATP or UDP were added to static cultures, ATP produced a significant change in actin stress fiber formation, mimicking the effects of shear. However, aside from a reduced effect of UDP on actin, the rest of the nucleotides tested had little effect on actin organization. Analyses of the effects of ATP and fluid shear on RhoA activation using a G-LISA kit indicated that both ATP and fluid shear increased Rho activation within minutes of stimulation, peaking at 15 min. To evaluate P2Y<sub>2</sub> function in Rho activation and stress fiber formation, MC3T3-E1 osteoblasts were transfected with P2Y<sub>2</sub> siRNA, which produced a 75% suppression of P2Y<sub>2</sub> protein 48 hours after transfection compared to vector controls. The MC3T3-E1 osteoblasts transfected with P2Y<sub>2</sub> siRNA failed to respond to ATP of fluid shear with an increase in either Rho activation or stress fiber formation. This was similar to the responses found with pretreatment of the cells with apyrase or RB-2 (P2Y<sub>2</sub> specific inhibitor). Atomic force microscopy (AFM) found that cell stiffness was significantly increased after fluid shear or ATP treatment. In contrast, P2Y<sub>2</sub> siRNA transfected cells did not increase cellular stiffness in response to these stimuli. This study suggests that P2Y<sub>2</sub> receptor activation by ATP is essential in the shear-induced, RhoA-mediated stress fiber formation, that this pathway regulates the mechanical properties of the osteoblast and that inhibition of this pathway may reduce the loss of mechanosensitivity associated with extended loads.

**Disclosures:** W.D. Yang, None.  
This study received funding from: NIH.

## SA036

**Stable Isotopic Labeling of Amino Acids in Cultured Human Bone Marrow Stem Cells: Application to BMP2 Induced Wnt/β-catenin Signaling.** J. Lee<sup>\*1</sup>, B. Kim<sup>\*1</sup>, J. Ahn<sup>\*1</sup>, H. Park<sup>\*1</sup>, E. Kim<sup>\*2</sup>, S. Park<sup>\*3</sup>, J. Kim<sup>\*1</sup>, E. Park<sup>\*4</sup>, J. Yoo<sup>\*2</sup>, J. Yates III<sup>\*3</sup>, J. Cho<sup>\*1</sup>. <sup>1</sup>Biochemistry, School of Dentistry, Kyungpook National University, Daegu, Republic of Korea, <sup>2</sup>Mass Spectrometer Development Team, Korea Basic Science Institute, Daejeon, Republic of Korea, <sup>3</sup>Cell Biology, The Scripps Research Institute, La Jolla, CA, USA, <sup>4</sup>Pathology and Regenerative Medicine, Kyungpook National University, Daegu, Republic of Korea.

Bone morphogenetic protein-2 (BMP2) is one of the most potent bone-inducing agents and promotes differentiation of osteoblasts from bone marrow stem cells (BMSC). However the potency of BMP2 varies in a species-specific manner. Especially, BMP2 induces alkaline phosphatase activity in human BMSCs is much less than rodents, although several other genes known to be steadily induced. Thus, there has been an increasing importance of discovering the unknown mechanism of BMP2 role in human BMSC. Here, we used SILAC (Stable isotope labeling with amino acids in cell culture) in combination with LTQ-FT-mass spectrometry not only to characterize the unknown mechanisms of human BMSC differentiation by BMP2 but also to find early differentiation markers. After tandem mass spectra were interpreted by SEQUEST using DTASelect2, ion chromatograms were quantified by Census program. In this analysis, 414 proteins of total 449 uniquely identified were successfully quantified with 79.21% quantification efficiency of peptides (2762 of 3487 total peptides). Of these, 12 were found to be increased more than 1.4-fold in BMP2 stimulated cells. In addition, 18 proteins were detected only in heavy-labelled cells. Nine proteins were down-regulated less than 1.4-fold by BMP2 stimulation. Interestingly, β-catenin was only detected in heavy-labelled, BMP-2 stimulated cells. BMP2-increased β-catenin level in time-dependent and dose-dependent manner. BMP-2 stimulation also increased phospho-Gsk3β levels which are known to result in the increment of β-catenin. These results suggest that up-regulation of Wnt signaling in early time could potentiate or accelerate the capability of BMP2 induced osteoblast differentiation. In conclusion, our investigation that the SILAC combined MS-based analysis could provide the basis for the understanding of human BMSC differentiation to osteoblast mechanisms upon BMP2 stimulation.

**Disclosures:** J. Lee, None.

## SA037

**High Concentrations of Hydroxytyrosol and Quercetin Antioxidants Enhance Adipogenesis and Inhibit Osteoblastogenesis in Mesenchymal Stem Cells.** A. Casado-Díaz<sup>\*1</sup>, J. Anter<sup>\*2</sup>, R. Santiago-Mora<sup>\*3</sup>, L. Luque<sup>\*4</sup>, G. Dorado<sup>\*5</sup>, J. M. Quesada<sup>3</sup>. <sup>1</sup>Dpto. I+D, SANYRES XXI (Grupo PRASA), Córdoba, Spain, <sup>2</sup>Dep. Genética, Universidad de Córdoba, Córdoba, Spain, <sup>3</sup>Unidad de Metabolismo Mineral, Hospital Universitario Reina Sofía, Córdoba, Spain, <sup>4</sup>Dep. Química Analítica, Universidad de Córdoba, Córdoba, Spain, <sup>5</sup>Dep. Bioquímica y Biología Molecular, Universidad de Córdoba, Córdoba, Spain.

The increase of age-related oxidative stress is associated with aging and major chronic aging-related diseases, such as loss of bone mineral mass and osteoporosis. Therefore, natural antioxidants may be potentially useful to reduce the impact of the oxidative stress on the organism in general and the bone in particular. We have analyzed the effect of different concentrations of plant antioxidants (hydroxytyrosol and quercetin) on the differentiation of mesenchymal stem cells (MSC). Thus, MSC were induced to differentiate to osteoblasts, in the presence of 10-8 M dexamethasone, 0.2 mM ascorbic acid and 10 mM β-glycerolphosphate, or to differentiate to adipocytes, using 5 x 10<sup>-7</sup> M dexamethasone, 0.5 mM isobutylmethylxanthine and 50 μM indometacine. The cultures were supplemented with hydroxytyrosol (10<sup>-4</sup> and 10<sup>-6</sup> M) or with quercetin (10<sup>-5</sup> and 10<sup>-7</sup> M). The expression of osteoblastogenesis and adipogenesis marker genes was analyzed by quantitative real-time PCR (QRT-PCR) after seven and 14 days of treatment. The alkaline phosphatase activity was measured on the cells induced to osteoblasts, and the formation of fat vesicles was monitored after 14 days of induction to adipocytes. We found that 10<sup>-4</sup> M hydroxytyrosol and 10<sup>-5</sup> M quercetin significantly enhanced adipogenesis, increasing the number adipocytes and the expression of adipogenic marker genes (ppar-γ2 and lpl). The other tested concentrations did not affect, or increased the adipogenesis to a lesser extent. On the other hand, the higher hydroxytyrosol and quercetin concentrations tested inhibited the studied osteoblastogenesis markers, mainly after seven days of induction. These data suggest that although low concentrations of hydroxytyrosol and quercetin may enhance the bone formation, they have the opposite effect at concentrations higher than 10<sup>-5</sup> M. Such high concentrations promote the adipogenic instead of the osteoblastogenic differentiation of MSC, which may affect negatively the bone formation.

**Disclosures:** A. Casado-Díaz, None.  
This study received funding from: P06-FQM-01515, CM0010/05 and SAF2005-05254; Grupo PAI CTS-413, Junta de Andalucía; and Sanyres (Grupo PRASA), Córdoba (Spain).

## SA038

See Friday Plenary number F038.

## SA039

**Concentration of Connective Tissue Progenitors in Autologous Cancellous Bone Graft Enhances New Bone Formation in a Canine Femoral Defect Model.** K. Kumagai<sup>\*1</sup>, J. Otonichar<sup>\*1</sup>, R. Rozic<sup>\*1</sup>, C. Boehm<sup>\*1</sup>, K. Powell<sup>\*1</sup>, A. Vasanji<sup>\*1</sup>, T. Saito<sup>\*2</sup>, G. F. Muschler<sup>1</sup>. <sup>1</sup>Orthopaedic Research Center, The Cleveland Clinic Foundation, Cleveland, OH, USA, <sup>2</sup>Department of Orthopaedic Surgery, Yokohama City University, Yokohama, Japan.

**Objective:** Osteogenic connective tissue progenitors (CTPs) in bone marrow and cancellous bone generate progeny expressing osteoblastic markers *in vitro* and contribute to new bone tissue *in vivo*. Autologous cancellous bone (ACB) is known as one of the best bone graft materials. ACB is biocompatible and provides on osteoconductive bone matrix. ACB also contains osteogenic CTPs. The purpose of this study was to define the distribution of osteogenic CTPs in ACB and the effect of impaction grafting on their delivery and efficacy in a canine femoral defect model.

**Methods:** Four identical 1.0 cm diameter and 1.0cm deep unicortical cylindrical defects for grafting were created in unilateral femur of eight mongrel dogs. After harvest of bone marrow by aspiration and cancellous bone by curetting from proximal humerus, four defects in each femur were treated with implantation of: 1) no graft, 2) bone marrow clot (BM), 3) non-compacted autologous cancellous bone (ACB1x) and 4) compacted autologous cancellous bone (3x starting volume, ACB3x) using a Latin square design. Animals were sacrificed four weeks after implantation and graft site in femur were harvested for analysis. Bone formation within defects was assessed by quantitative micro CT analysis and histological findings.

**Results:** Seventy percent of osteogenic CTPs were located on the trabecular surface. Therefore, impaction grafting concentrated CTPs by squeezing out marrow cells having lower CTP prevalence. The mean percent of bone volume (%BV) in ACB3x (12.9) was significantly greater than that in no graft (2.9) (*p* = 0.021). Although there was no statistical difference, %BV in BM (9.5) and ACB1x (9.4) was higher than that in no graft. When each defect was radially divided into three regions composed of the central third (0-1.5mm from defect center), the middle third (1.5-3mm from defect center) and the outer third (3-4.5mm from defect center), there were significant differences of %BV between ACB3x and no graft in the middle third and the outer third (*p* = 0.022, 0.027, respectively). Better bone formation was evident in the upper half of each defect.

**Conclusions:** This study demonstrated that impaction graft of autologous cancellous bone contains a higher concentration of osteogenic CTPs and results in greater new bone formation.

**Disclosures:** K. Kumagai, None.



## SA040

**Use of  $\alpha$ -smooth Muscle actin-GFP Transgene to Identify Periodontium Derived Osteoprogenitors.** S. M. San Miguel<sup>\*1</sup>, H. Li<sup>1</sup>, J. C. Igwe<sup>\*1</sup>, V. Ferrer<sup>1</sup>, H. Aguila<sup>\*2</sup>, I. Kalajzic<sup>1</sup>. <sup>1</sup>Dept. of Reconstructive Sciences, Uni. of Conn. Health Center, Farmington, CT, USA, <sup>2</sup>Dept. of Immunology, Uni. of Conn. Health Center, Farmington, CT, USA.

Cells with osteoprogenitor potential are present within the periodontal tissues during development and in postnatal life. In previous studies we identified an  $\alpha$ -SMA-GFP expressed in mesenchymal progenitor cells within the bone marrow stromal population and in adipose tissue. The purpose of this study is to define whether the  $\alpha$ -SMA promoter would direct GFP expression to osteoprogenitor cells in the dental follicle and periodontal ligament. We have utilized a transgenic mouse model approach in which GFP expression is driven by an  $\alpha$ -SMA promoter. Epifluorescence was evaluated in histological sections of mandibles derived from neonatal and 4-6 week old mice. Alpha SMAGFP expression was detected in the dental follicle, but not in mature bone. GFP+ cells were observed in apical regions of the root, the areas rich with vascularization. In addition transgene expression was evaluated in primary cultures derived from dental follicle (mDF) and periodontal ligament (mPDL). Strong expression of  $\alpha$ -SMAGFP was observed during early stages of the culture and diminished as mineralization progressed. Observation of GFP expression was complemented with analysis of osteogenic differentiation by analysis of RNA expression of bone markers, histochemical staining for alkaline phosphatase and detection of mineralized nodules by xylene orange. An intense ALP activity and the presence of mineralized nodules followed two weeks of osteogenic induction. Expression of BSP and DMP-1 increased during osteogenic differentiation. We utilized flow cytometry (FACS) to determine the proliferative potential and cellular profile of freshly isolated or cultured  $\alpha$ -SMA positive cells. FACS analysis revealed that freshly digested mDF cells expressed the mesenchymal markers Thy1 (40%) and Scal (8.79%). In vitro expansion enriched for an  $\alpha$ -SMAGFP+ population of which 60% of cells were Thy1+ and Scal+. The  $\alpha$ -SMAGFP+ population exhibited high proliferative potential, while proliferation of  $\alpha$ -SMAGFP- population was very limited. Our data suggest that the  $\alpha$ -SMA promoter has the potential to identify a population of osteoprogenitor cells residing within the dental follicle and periodontal ligament that can differentiate into mature osteoblasts.

**Disclosures:** *S.M. San Miguel, None.*

*This study received funding from: NIH DE016495-02.*

## SA041

See Friday Plenary number F041.

## SA042

**Mature Human Adipocytes differentiated from Bone Marrow Derived Mesenchymal Stem Cells.** A. C. Niemeier<sup>1</sup>, J. Prawitt<sup>\*2</sup>, M. Kassem<sup>3</sup>, U. Beisiegel<sup>\*2</sup>, J. Heeren<sup>\*2</sup>. <sup>1</sup>Orthopaedics, University Hospital Hamburg-Eppendorf, Hamburg, Germany, <sup>2</sup>IMB II: Molecular Cell Biology, University Hospital Hamburg-Eppendorf, Hamburg, Germany, <sup>3</sup>Endocrinology, University Hospital Odense, Odense, Denmark.

Bone marrow adipocytes and osteoblasts share common mesenchymal precursor cells. It is a generally accepted concept that factors exist which stimulate the differentiation process in favour of either osteoblastogenesis or adipogenesis, and that these may in part be mutually exclusive. In this context, it is likely that adipocytes and osteoblasts influence each other in a paracrine fashion. In order to identify such factors, there is a demand for suitable human cell models. Most research with regard to these questions has focused on osteoblast differentiation. Here we describe the adipogenic differentiation of a bone marrow derived telomerase-immortalized human mesenchymal stem cell line (hMSC-Tert) that maintains numerous features of terminally differentiated adipocytes even after prolonged withdrawal of the peroxisome proliferator activated receptor gamma (PPARgamma) agonist rosiglitazone. Differentiated hMSC-Tert developed the characteristic monolocular phenotype of mature adipocytes. The expression of adipocyte specific markers was highly increased during differentiation. Most importantly, the presence of the PPARgamma agonist rosiglitazone was not required for the stable expression the adipocyte markers lipoprotein lipase, adipocyte fatty acid binding protein and perilipin on mRNA and protein levels. Adiponectin expression was post-transcriptionally down-regulated in the absence of rosiglitazone. Insulin sensitivity as measured by insulin-induced phosphorylation of Akt and S6 ribosomal protein was also independent of rosiglitazone. In summary, we describe a novel model for mature human adipocytes derived from bone marrow mesenchymal stem cells. This model with its unique characteristics will be a valuable tool for the in vitro identification of secreted adipocyte-specific factors which influence osteoblastogenesis.

**Disclosures:** *A.C. Niemeier, None.*

## SA043

**Enhanced Mitochondrial Biogenesis Contributes to Wnt induced Osteogenic Differentiation of C3H10T1/2 Cells.** J. H. An<sup>\*</sup>, J. Y. Yang<sup>\*</sup>, S. W. Cho, J. Y. Jung<sup>\*</sup>, H. Y. Cho, Y. M. Cho<sup>\*</sup>, S. W. Kim, C. S. Shin. Department of Internal Medicine, Seoul National University College of Medicine, Seoul, Republic of Korea.

**Background:** Mitochondria play a key role in cell physiology including cell differentiation. We investigated the changes of mitochondrial biogenesis during Wnt induced osteogenic differentiation of murine mesenchymal C3H10T1/2 cells.

**Methods:** C3H10T1/2 cells were cultured in DMEM and osteogenic differentiation was induced by Wnt-3A conditioned medium (CM). Mitochondrial mass, mitochondrial membrane potential and intracellular reactive oxygen species were measured by flow cytometry analysis. Oxygen consumption rate was analyzed by high-resolution respirometry and mitochondrial (mt) DNA copy-number by real-time PCR.

**Results:** gnaling by Wnt-3A CM resulted in significant increase alkaline phosphatase (ALP) activities in C3H10T1/2 cells as expected. The increase in ALP activities were associated with significant increase in mitochondrial mass, mitochondrial membrane potential, intracellular reactive oxygen species, oxygen consumption rate and mtDNA copy number compared to the control group. Co-treatment with DKK-1 and WIF-1, both of which are Wnt inhibitors, abrogated the Wnt-3A-induced ALP activities as well as mitochondrial biogenesis markers. Moreover, inhibition of mitochondrial biogenesis by Zidovudine treatment resulted in significant inhibition of osteogenic differentiation as measured by ALP activities. Finally, removal of mitochondria from human osteosarcoma cell line (p<sub>3</sub> cells) by ethidium bromide treatment resulted lower ALP activity both in basal and Wnt-3A stimulated state compared to that in mitochondria-intact cells (p<sub>1</sub> cells).

**Conclusion:** Mitochondrial biogenesis is upregulated by Wnt signaling and this upregulation seems to contribute to the osteogenic differentiation of mouse mesenchymal C3H10T1/2 cells.

**Disclosures:** *J.H. An, None.*

## SA044

See Friday Plenary number F044.

## SA045

**The Comparison of the Effects of Zoledronates on the Differentiation of Human Bone Marrow and Amniotic Fluid Derived Mesenchymal Stem Cells.** J. An<sup>\*1</sup>, I. Kim<sup>\*2</sup>, Y. Kim<sup>\*2</sup>, B. Joo<sup>\*3</sup>. <sup>1</sup>Internal Medicine, Good Moonhwa Hospital, Busan, Republic of Korea, <sup>2</sup>Internal Medicine, Busan National University Hospital, Busan, Republic of Korea, <sup>3</sup>Center for Reproductive Medicine, Good Moonhwa Hospital, Busan, Republic of Korea.

**Background:** Mesenchymal stem cells (MSCs) were identified in various tissues including human bone marrow and adipose tissue. Recently it has been known that amniotic fluid is rich source of fetal MSCs. Zoledronate is the most potent amino-bisphosphonate and act primarily by inhibiting osteoclast. But many reports show that zoledronate has anabolic action by influencing osteoblast differentiation. This study was aimed to compare the effects of zoledronates on the differentiation of MSCs derived from human bone marrow and amniotic fluid into osteoblast and adipocyte.

**Method:** Amniotic fluids were collected from 5 pregnant women who underwent amniocentesis at the second trimester due to chromosomal analysis and adult male-bone marrows were obtained from 3 patients who underwent total hip arthroplasty. Zoledronate was treated to MSC derived from amniotic fluid and bone marrow to induce differentiation into osteoblast and adipocyte. Osteoblast was confirmed by alkaline phosphatase (ALP) activity assay and characteristics of adipocyte was determined by sterol regulatory element binding protein 1 (SREBP-1), fatty acid synthase (FAS), acetyl CoA carboxylase 1 (ACC1) activities.

**Result:** ALP activity tended to more prominent in MSCs derived from amniotic fluid than that of bone marrow. In osteogenic differentiation from amniotic fluid, ALP activity was positively correlated with concentration of zoledronate and it was significantly increased at 10<sup>-6</sup>M concentration of zoledronate. However, in bone marrow, ALP activity was negatively correlated with concentration of zoledronate. SREBP1 and ACC1 activities tended to be decreased but FAS activities tend to be increased in MSCs derived from both amniotic fluid and bone marrow.

**Conclusion:** These results suggest that amniotic fluid seems to be more rich source of MSCs to be differentiated into osteoblast and adipocyte than bone marrow. Zoledronates may influence differently on the differentiation of MSCs according to their origins.

**Disclosures:** *J. An, None.*

## SA046

**Overexpression of Alpha-catenin in C3H10T1/2 Cells Increases Osteoblast Differentiation.** D. Kim<sup>\*1</sup>, J. Yang<sup>\*2</sup>, J. Chung<sup>\*2</sup>, S. Cho<sup>\*2</sup>, S. Kim<sup>\*2</sup>, S. Kim<sup>\*2</sup>, C. S. Shin<sup>2</sup>. <sup>1</sup>Internal Medicine, Dankook University College of Medicine, Cheon-An, Republic of Korea, <sup>2</sup>Internal Medicine, Seoul National University College of Medicine, Seoul, Republic of Korea.

Alpha- and beta-catenin link cadherins to the actin-based cytoskeleton at adherens junctions and regulate cell-cell adhesion. Beta-catenin is also an important component of Wnt signaling pathway. Although roles of cadherins and canonical Wnt signaling in osteoblastic differentiation have been extensively studied, the role of alpha-catenin is not known. Murine embryonic mesenchymal stem cells, C3H10T1/2, were transduced with retrovirus encoding alpha-catenin (MSCV-alpha-catenin-HA-IRES-GFP). Cellular alpha-catenin expression was confirmed by western blot analysis using anti-HA antibody. In the presence of osteogenic media (10 mM beta-glycerol phosphate and 50 microgm/ml ascorbic acid) or Wnt-3A-conditioned medium, cells overexpressing alpha-catenin showed enhanced osteoblastic differentiation as measured by alkaline phosphatase (ALP) staining and ALP activity assay compared to the cells transduced with empty virus (MSCV-IRES-GFP). In addition, mRNA expression of osteocalcin and Runx2 was significantly increased compared to control cells. Cell aggregation assay revealed that alpha-catenin overexpression has significantly increased cell-cell aggregation. However, cellular beta-catenin levels (total, cytoplasmic-nuclear ratio) did not change by overexpression of alpha-catenin. Moreover, transient transfection of alpha-catenin did not increase TOPflash reporter activity nor was able to augment beta-catenin-mediated reporter activity. These results suggest that alpha-catenin overexpression increases osteoblast differentiation by increasing cell-cell adhesion rather than Wnt/beta-catenin signaling.

**Disclosures:** D. Kim, None.

## SA047

See Friday Plenary number F047.

## SA048

**Aging of Human Bone Marrow Stromal Cells: Role of WNT Pathways.** L. Shen<sup>\*</sup>, S. Zhou, J. Glowacki. Orthopedic Surgery, Brigham and Women's Hospital, Boston, MA, USA.

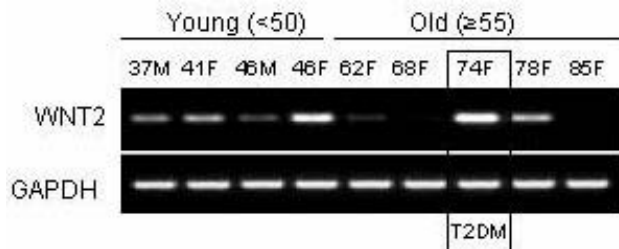
Human bone marrow stromal cells (hMSCs) include a fraction of osteoblast progenitors; we showed that there is an age-dependent decrease in their proliferation and osteoblast differentiation. In other cell types, WNT signaling maintains proliferation by stimulating cell division and inhibiting differentiation and apoptosis. Thus, we tested the hypothesis that WNT signaling may be related to aging in hMSCs. The first study tested whether there is an age related difference of WNT gene expression. The second study tested whether there is an effect of age on canonical WNT signaling in response to Parathyroid Hormone (PTH).

Bone marrow samples were obtained with IRB approval as femoral tissue discarded during total hip replacement for osteoarthritis. Low-density mononuclear cells were isolated by density centrifugation on Ficoll/Histopaque 1077(Sigma, MO). Adherent hMSCs were expanded 2-4 passages for experiments.

All Passage 2 (P2) samples of hMSCs from young subjects(<50y) expressed WNT2, a canonical WNT gene (Figure). In contrast, 3 of 4 samples from older subjects (>55y) showed no or low expression of WNT2. A notable additional sample (74 years old) with Type 2 diabetes mellitus (T2DM) as a comorbidity showed the highest expression of WNT2. All samples, including those with low or no WNT2, expressed strong signals for noncanonical WNT5a, and moderate signals for canonical WNT10b. A comparison of P2 with P4 cells showed differences attributable to *in vitro* effects: WNT 2 increased and WNT10b decreased with passage in many samples. These findings emphasize that passaging hMSCs may confound interpretation of expression profiling.

We assessed the effect of age on canonical Wnt signaling by measuring the effect of 10 nM PTH(1-34) on  $\beta$ -catenin at 6 h by Western immunoblot. In hMSCs from a 74-year-old subject, PTH did not activate  $\beta$ -catenin, compared with increased  $\beta$ -catenin (450%, 187%) in hMSCs from two younger subjects (34 and 42 years).

These pilot results indicate that 1) WNTs are expressed in hMSCs, 2) WNT2 expression is decreased with age, 3) *in vitro* passaging of cells may confound *in vivo* age differences, and 4) canonical WNT signaling in response to PTH was decreased with age. In conclusion, WNT2 may play a role in effects of aging on hMSCs.



**Disclosures:** L. Shen, None.

This study received funding from: NIH-NIA.

## SA049

**Marked Induction of Endochondral Bone Formation by Overexpression of a Constitutively Active Gli2 in Mesenchymal Stem Cells Isolated from the Healing Site.** Q. Wang<sup>\*</sup>, C. Xie<sup>\*</sup>, M. Xue<sup>\*</sup>, X. Zhang. Orthopaedics, University of Rochester Medical Center, Rochester, NY, USA.

Hedgehog/Gli2 pathway has been critically implicated in endochondral bone formation during skeletal development. The hedgehog pathway is also activated during fracture repair, indicating a potential role of the pathway in bone repair process. Using a segmental bone graft transplantation model in mice, we have succeeded in isolation of a unique population of mesenchymal stem cells from periosteum at the early stage of healing. These cells express the typical mesenchymal stem cell markers Sca-1, SSEA4, CD105, CD29 and CD140 and demonstrated marked proliferation capacity *in vitro*. They are multipotent and capable of differentiating into osteoblasts, adipocytes and chondrocytes. Among growth factors and genes examined, we found that activation of Hedgehog signaling potentially induced osteoblastic and chondrogenic differentiation of these cells *in vitro*. Furthermore, subcutaneous implantation of the isolated periosteal cells overexpressing a constitutively active Gli2 ( $\Delta$ Ngli2), the major transcriptional activator targeted by the hedgehog signaling pathway, led to marked and robust induction of endochondral bone formation *in vivo*. To further determine the mechanisms involved in Gli2 induced endochondral bone formation, we performed pellet culture using mesenchymal stem cells isolated from the healing site. We found that Gli2 overexpression increased Col2a1 and ColX gene expression by 25-fold and 18-fold respectively. Gli2 overexpression also markedly induced OSX gene expression by 5 fold and BMP-2 gene expression by 3 fold. To further determine whether chondrogenic and osteogenic differentiation induced by  $\Delta$ Ngli2 is mediated through BMP-2, we isolated mesenchymal stem cells from BMP-2<sup>fl</sup> mice. BMP-2 was eliminated by infection of an adenovirus expressing Cre recombinase. We found that elimination of BMP-2 blocked osteogenic differentiation induced by ShhN peptide and a hedgehog agonist Purmorphamine. However, BMP-2 elimination failed to block the osteogenic differentiation induced by  $\Delta$ Ngli2, suggesting additional mechanisms involved in Gli2 induced mesenchymal cell differentiation. Taken together our current data suggest that Hh/Gli2 may function as important signals for mesenchymal stem cell differentiation during repair and overexpression of Gli2 could be used in mesenchymal stem cell therapy for enhanced bone repair and regeneration.

**Disclosures:** X. Zhang, None.

This study received funding from: NIH.

## SA050

See Friday Plenary number F050.

## SA051

**Dermo1 Lineage Tracing Identifies Early Osteoprogenitor Cells in Adult Murine Bone Marrow Mesenchymal Stem Cell Cultures.** P. Maye, Y. Liu<sup>\*</sup>, L. Wang<sup>\*</sup>, M. Kronenberg<sup>\*</sup>, D. Rowe. Reconstructive Sciences, UCONN Health Center, Farmington, CT, USA.

Previous embryonic studies have shown that Twist 1 & 2 are expressed in early osteochondral progenitor cells and lie genetically upstream of Runx2 during osteogenesis. With this in mind, we hypothesized that Dermo1 (Twist 2) -Cre mice when crossed with Z/EG mice, a mouse line that ubiquitously expresses EGFP upon Cre Recombinase activity, may mark bone marrow derived osteoprogenitor cells and possibly multipotent mesenchymal stem cells in adult mice. While this approach is based on lineage tracing and results in a wide variety of mature cell types expressing EGFP, including bone cells and cartilage cells, the bone marrow compartment of F1 animals only contains a small cell population (~1%) that is EGFP positive. Preliminary attempts to FACS isolate this EGFP cell population directly from the bone marrow and test their osteogenic potential *in vitro* have proven difficult. We believe our current methodology for FACS isolation results in cell damage to the point where neither EGFP+ nor EGFP- cells attach to the culture dish. However, without FACS, standard bone marrow derived stromal cell cultures show that EGFP+ cells attach early in primary cultures. At day 3 of culture, EGFP positive cells can be observed during early colony formation. FACS isolation of EGFP positive cells from day 5 cultures reveals that these EGFP positive cells, which represent ~10% of the total cell population, when plated back into culture as a confluent spot retain very high osteogenic potential. These day 5 EGFP positive cells also have adipogenic potential and we currently are testing for their ability to differentiate into chondrocytes. To further confirm the osteogenic potential of this defined population *in vivo*, we carried out transplantation experiments where varying amounts of FACS isolated EGFP positive cells from day 5 stromal cell cultures were compared to EGFP negative cells and the matrix scaffold Helos alone in a critical size defect calvarial implant model. Quite strikingly, when 50,000 and 300,000 EGFP positive cells were loaded into the Helos scaffold, a dosage dependent increase in bone formation was observed in transplants 30 days later, while 100,000 EGFP negative cells or Helos alone resulted in no bone formation. These studies confirm that Dermo1-Cre x Z/EG leads to the identification of early osteoprogenitor cells and implicates an important role for twist genes in bone marrow derived mesenchymal stem cells.

**Disclosures:** P. Maye, None.

## SA052

**In Bone, RPTP $\mu$  Is Exclusively Expressed in Osteocytes and May Affect Bone Mass.** K. E. de Rooij<sup>1</sup>, E. Waarsing<sup>\*2</sup>, E. de Wilt<sup>\*1</sup>, I. Que<sup>\*1</sup>, M. M. L. Deckers<sup>\*1</sup>, C. W. G. M. Löwik<sup>1</sup>. <sup>1</sup>Endocrinology, LUMC, Leiden, Netherlands, <sup>2</sup>Orthopaedics, Erasmus Medical Center, Rotterdam, Netherlands.

During bone formation, some osteoblasts are embedded within the newly formed matrix, where they differentiate into osteocytes. They develop long, slender cell processes, which they use to establish a three-dimensional cellular network within the mineralized matrix, analogous to the network formed by neuronal and endothelial cells. Their position within the mineralized matrix makes them very well-positioned to act as "the nerve cells of the bone". It has now been generally accepted that osteocytes act as sensors of mechanical loading of the bone.

The receptor-like protein tyrosine phosphatase  $\mu$  (RPTP $\mu$ ) belongs a subfamily of transmembrane protein tyrosine phosphatases. RPTP $\mu$  is involved in cell-cell interactions and may play a role in the formation or maintenance of the cellular network. RPTP $\mu$  is expressed in cells in which cell-cell interactions are important, such as some types of neuronal cells, lung epithelium, cardiac muscle cells and endothelial cells. Strikingly, some of these cells also form a cellular network.

Recently, RPTP $\mu$ -knock out / LacZ knock-in mice have been described, in which the expression of the LacZ gene is controlled by the promoter of the RPTP $\mu$  gene. Long bones and calvariae of these transgenic mice were isolated and analyzed for  $\beta$ -galactosidase activity by staining with X-gal. Histological analysis showed that only osteocytes exhibit  $\beta$ -galactosidase activity. The blue staining was present throughout the cells and the cellular processes could easily be distinguished.

To investigate the possibility of generating osteocytes *in vitro*, bone marrow cells of the transgenic mice were cultured under osteogenic conditions. After 21-28 days, blue stained cells could be observed associated with nodules. Using an enzymatic LacZ assay we were able to quantify the amount of osteocytes formed. The addition of BMPs to the culture medium increased the number of LacZ positive cells. Histological analysis of these cultures revealed that all positive cells were surrounded by extracellular matrix and cellular processes could be observed. Thus, RPTP $\mu$ -knock out / LacZ knock in mice provide an excellent tool for the study of compounds on osteocyte differentiation *in vitro*.

To examine if the absence of RPTP $\mu$  gene had an effect on bone mass, we have isolated tibia of wild type and knockout mice (n=6) at 5 different age groups, up to 56 weeks for  $\mu$ CT analysis. Preliminary data of tibia from 44 weeks old mice indicate that lack of RPTP $\mu$  may result in lower bone mass. We conclude that RPTP $\mu$  could play a role osteocyte function. If absence of RPTP $\mu$  indeed results in lower bone mass, stimulating RPTP $\mu$  might increase bone mass. Therefore, RPTP $\mu$  may be a target for therapy in bone disorders.

**Disclosures:** K.E. de Rooij, None.

## SA053

**Endothelial Progenitor Cell Mobilization During Distraction Osteogenesis in Human.** D. Lee<sup>\*1</sup>, T. Cho<sup>2</sup>, H. Lee<sup>\*2</sup>, W. Yoo<sup>\*2</sup>, I. Choi<sup>\*2</sup>. <sup>1</sup>Orthopaedic surgery, Kangwon National University, Chuncheon-city, Republic of Korea, <sup>2</sup>Orthopaedic Surgery, Seoul National University, Seoul, Republic of Korea.

**Introduction:** Distraction osteogenesis (DO) is a unique postnatal bone formation process which is characterized by profuse increment of vascularization. Recently osteoblast-lineage cells (OCs) and endothelial progenitor cells (EPCs) are reported to circulate in physiologically significant numbers and contribute to bone regeneration process. We investigated OC and EPC mobilization in patients undergoing limb lengthening.

**Materials and Methods:** Blood were drawn pre-operation, pre-distraction, and 2 weeks after the start of distraction in 25 patients undergoing limb lengthening. Peripheral blood mononuclear cells (PBMNCs) were isolated and cultured under endothelial cell growth medium. After 2 weeks, the number of EPC colonies which are stained with 1,1'-dioctadecyl-3,3,3',3'-tetramethylindocarbocyanine-conjugated acetylated-low density protein and fluorescein isothiocyanate-labeled lectin was counted. In addition, we performed fluorescence-activated cell sorting (FACS) analysis of freshly isolated PBMNCs using antibodies to bone-specific alkaline phosphatase (ALP) to identify circulating OCs and antibodies to CD34 and vasculoendothelial growth factor receptor 2 (VEGFR2) to identify circulating EPCs.

**Results:** The number of EPC colonies significantly increased during distraction period. FACS analysis demonstrated that the frequency of VEGFR2 (+) cells and CD34 (+) cells, which are EPC-enriched fractions, significantly increased post-distraction while there were no differences in AC133 (+) and ALP (+) positive cells. The number of EPC colonies was correlated with the proportion of circulating CD34 (+) cells in PBMNCs.

**Conclusions:** EPCs are mobilized during distraction osteogenesis by distraction strain while OCs are not. These data suggest that EPC mobilization enhanced by distraction strain contributes to increased vascularization during DO, but bone regeneration process during DO is not associated with systemic OC mobilization.

**Disclosures:** D. Lee, None.

*This study received funding from: Seoul National University Hospital Research fund.*

## SA054

**See Friday Plenary number F054.**

## SA055

**Widespread Expression of Sclerostin in Adult and Embryonic Cartilage and Bone, Cells of the Developing Central Nervous System and Epithelia of the Embryonic Kidney and Intestine.** S. Sommer<sup>\*1</sup>, J. P. Grande<sup>\*2</sup>, R. Kumar<sup>1</sup>. <sup>1</sup>Nephrology Research, Mayo Clinic, Rochester, MN, USA, <sup>2</sup>Anatomic Pathology, Mayo Clinic, Rochester, MN, USA.

Sclerostin, an inhibitor of bone formation, is believed to be produced exclusively by osteocytes in adult tissues. We used a specific polyclonal antibody to examine expression of sclerostin in adult and embryonic mouse tissues. As previously reported, in adult bone, sclerostin immunostaining was detected in osteocytes and in the canalicular network of Haversian systems. We now show that at the growth plate, sclerostin immunostaining is present in dividing chondrocytes and osteoblasts of adult mouse bone. Less intense staining is seen in mature chondrocytes. Adult liver, spleen, and kidney exhibit no staining. Immunostaining with pre-immune serum is negative.

In the developing skeleton, sclerostin staining is noted in vertebrae and ribs, specifically in developing chondrocytes. Mature chondrocytes do not stain for sclerostin. Osteoblasts stain for sclerostin in the developing vertebral column. Similar patterns of staining are noted in ossification centers at the base of the skull. Immunostaining with pre-immune serum is negative.

Sclerostin immunostaining is noted in cells of the developing neural crest starting at day 8 p.c. Sclerostin immunostaining is observed in the developing dorsal root ganglia beginning at day 12 p.c. Sclerostin staining remains prominent in all developing bone tissues through the entire growth of the embryonic mouse. Sclerostin immunostaining is observed in scattered epithelial cells of the developing intestine and kidney starting at day 11 and disappearing by day 16 p.c. The sclerostin immunostaining in the kidney is most prominent in epithelial cells of the S-shaped tubules and epithelial cells of the intestine. No expression of sclerostin is noted in the developing heart, liver, muscle, or skin.

**Conclusion.** In adult bone, sclerostin is expressed not just in osteocytes but also in dividing chondrocytes and in osteoblasts found in the growth plate suggesting a function for sclerostin in the latter cells. In addition, sclerostin is prominently expressed in chondrocytes and osteoblasts of the developing mouse skeleton. Sclerostin is also expressed in the epithelium of the intestine and kidney suggesting an importance not only to bone development but also in epithelial development.

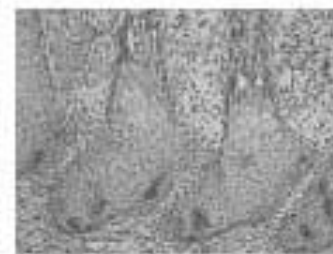


**Fig 1. Sclerostin in developing vertebral column, 15 day p.c. embryo. 200 X.**

**Disclosures:** S. Sommer, None.

*This study received funding from: NIH.*

## SA056

**Osteocytes can Modulate Osteoblastic Activity via NPY Signaling.** J. C. Igwe<sup>\*</sup>, S. M. San Miguel<sup>\*</sup>, F. Paic<sup>\*</sup>, H. T. Li<sup>\*</sup>, I. Kalajzic. Dept. of Reconstructive Sciences, Uni. of Conn. Health Center, Farmington, CT, USA.

Osteocytes are characterized by long neuronal-like cell processes, which may actively participate in the release of molecules that modulate the function of other surrounding bone cells. The location of osteocytes and their inherent inability to divide represents a major obstacle for studying osteocyte biology. We have previously shown that dentin matrix protein 1 (DMP1) is preferentially expressed in cells embedded within the bone matrix (osteocytes) or in partially embedded cells (preosteocytes). This was the key observation leading to generation of an osteocyte-specific GFP transgenic mouse (DMP1-GFP). To investigate the expression of regulatory molecules produced by osteocytes, we utilized dual transgenic mouse in which osteocytes are identified by DMP1-GFP(green), while osteoblasts are labeled by Col2.3GFP(blue). An *in vivo* gene expression analysis was generated by fluorescence activated sorting of neonatal calvarial cells derived from these dual transgenic mice. It was an intriguing observation that the osteocytes expressed neuropeptide Y (NPY), a gene whose role in the central control of bone mass has been well established. We confirmed this result by immunohistochemical detection of NPY in osteocytes. Furthermore, NPY mRNA expression was observed in DMP1GFP+ cells (osteocytes) and Col2.3GFP+ cells (osteoblasts/osteocytes) derived from fluorescent sorting of primary calvarial osteogenic cultures.

RNA analysis of the isolated osteocytes demonstrated increased levels of NPY mRNA transcripts in both DMP1GFP+ and Col2.3GFP+ populations. In addition, we investigated

the expression of NPY receptors in cultured osteoblast lineage cells. qPCR analysis of cultured calvarial osteoblasts demonstrated that mRNA of the NPY receptor subtypes Y1 and Y6 increased significantly between day 7 and day 14 of culture. We further investigated the effect of NPY at this stage of culture by in vitro treatment with NPY protein. Northern blot analysis of RNA from 1 nM NPY treated calvarial osteoblasts, showed a significant reduction of osteocalcin and bone sialoprotein expression at day 14 of culture. These results demonstrate the effect of NPY on mature osteoblasts, suggesting a novel, local regulation of osteoblast function by osteocytes via NPY signaling.

**Disclosures:** J.C. Igwe, None.

This study received funding from: NIH DE016495-02.

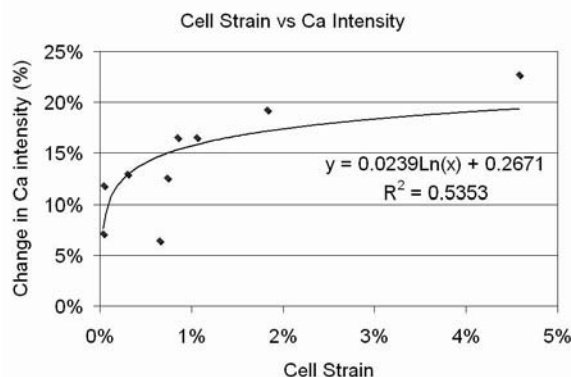
## SA057

**Direct Correlation of Osteocyte Deformation with Calcium Influx in Response to Fluid Flow Shear Stress.** A. R. Bonivitch<sup>1</sup>, L. F. Bonewald<sup>2</sup>, J. Ling<sup>\*1</sup>, J. X. Jiang<sup>3</sup>, D. P. Nicoletta<sup>1</sup>. <sup>1</sup>Southwest Research Institute, San Antonio, TX, USA, <sup>2</sup>University of Missouri at Kansas City School of Dentistry, Kansas City, MO, USA, <sup>3</sup>University of Texas Health Science Center, San Antonio, TX, USA.

Osteocytes are generally accepted to be the mechanosensors of bone regulating both resorption and formation. Calcium signaling plays an integral role in osteocyte signaling of bone formation. These cells are highly sensitive to fluid flow derived shear stress thought to occur as bone fluid passes through the osteocyte lacuno-canalicular network. However, the resulting individual cell strain has yet to be quantified and associated with any specific individual cell biological response. We have shown previously a correlation of deformation with prostaglandin production for a population of MLO-Y4 osteocyte like cells. The purpose of this study was to directly measure individual osteocyte deformation and intracellular calcium levels in response to fluid flow. The resulting deformation of each cell was then correlated to its individual biological response.

Fluo-4, AM-loaded osteocyte-like MLO-Y4 cells were exposed to uniform laminar fluid flow of 8 dynes/cm<sup>2</sup> in a closed system. The upregulation of intracellular calcium was determined from the difference in fluorescence intensity from the cell's basal level prior to exposure to fluid flow and the level immediately following the application of fluid flow. The resulting deformation of each individual osteocyte was determined using digital image correlation.

The average strain experienced by the cells was 1.12% with a standard deviation of 0.01%. The maximum and minimum strains were 4.58% and 0.03% respectively. The average upregulation of intracellular calcium in the cells was found to be 13.99% with a standard deviation of 0.05%. The maximum and minimum increases in intracellular calcium were 22.71% and 6.45% respectively. Moreover, the MLO-Y4 cells showed an increase in intracellular calcium concentration with an increase in cell strain in response to an applied fluid flow of 8 dynes/cm<sup>2</sup> (Figure 1). Osteocytes exposed to a uniform fluid flow stimulus experienced a range of strains and individual cell deformations correlated in a dose dependent manner to increases in intracellular calcium concentrations. As mechanosensing and signaling occurs at the single osteocyte level, it is important to understand how cell deformation is translated in a wide range of osteocyte responses.



**Disclosures:** A.R. Bonivitch, None.

This study received funding from: NIH.

## SA058

See Friday Plenary number F058.

## SA059

**Expression of Human Sclerostin In Heterologous Eukaryotic Insect and E. coli Expression Systems.** T. A. Craig\*, Z. Ryan\*, R. Kumar. Nephrology Research, Mayo Clinic, Rochester, MN, USA.

Sclerostin is an ~22 kDa secreted protein expressed by osteocytes which inhibits bone formation. Several sclerostin gene mutations result in a general progressive overgrowth and sclerosis of the skeleton. Sclerostin antagonizes canonical Wnt signaling pathways that control bone formation by binding to Wnt co-receptor protein, low-density lipoprotein receptor-related protein 5 and 6 (LRP5/6). High bone mass in sclerosteosis and Van Buchem disease may thus result from increased Wnt signaling due to the reduced sclerostin expression. Sclerostin mRNA has been detected in aortic tissue, in the otic vesicle and in odontoblasts suggesting that sclerostin may have functions other than bone density regulation.

In order to examine biochemical and biophysical properties of sclerostin, and its interaction with other signaling molecules, we have employed several different bacterial and insect expression systems in order to obtain soluble sclerostin. The full length cDNA for the secreted form of human sclerostin, amino acids 24-213, was expressed in the pET 28a(+) and pET 42a(+) *E. coli* expression vectors as a soluble protein with amino-terminal V5 and 6xHis tags. When sclerostin was expressed in *E. coli* using the pET 28a(+) vector nickel affinity chromatography was used for initial purification. The protein expressed in *E. coli* with the pET 42a(+) vector was a fusion protein with glutathione S-transferase (GST) and was purified using glutathione sepharose. The expression of sclerostin as a fusion protein with maltose binding protein (MBP) into the bacterial periplasmic space of BL21Star *E. coli* with the vector, pMAL-p4E, yielded, on osmotic shock of cells, some full-length 24-213 sclerostin-MBP and large amounts of MBP alone.

We used two insect expression systems for expression of sclerostin. *Trichoplusia ni* (High Five) insect cells were stably transformed with a pB/V5-His-melittin secretory signal-human 24-213 sclerostin construct. Transfected cells were selected with Blastisidin S. Secreted sclerostin was detected in the cell medium by Western blotting with anti-V5 horseradish peroxidase antibody. The cDNA for the secreted form of human sclerostin, amino acids 24-213, was also ligated in to the pTriEx-5 insect secretion vector. TriEx™ Sf9 *Spodoptera frugiperda* insect cells using GeneJuice® transfection reagent were transiently transfected in order to express sclerostin as a secreted protein.

Conclusion: Soluble sclerostin can be expressed in *E. coli* as a histidine or GST-fusion protein. Secreted, soluble sclerostin is readily expressed in insect cells using permanent and transient expression methods.

**Disclosures:** T.A. Craig, None.

## SA060

**Mechanical Perturbation of Integrin α5 with or without Association with Fibronectin Opens Connexin 43-Hemichannels in Osteocytes - a Mechanism for Release of Small Signaling Molecules in Response to Loading.** S. Burra<sup>1</sup>, A. J. Siller-Jackson<sup>\*1</sup>, M. A. Harris<sup>\*2</sup>, S. E. Harris<sup>2</sup>, G. Weber<sup>\*3</sup>, D. DeSimone<sup>\*3</sup>, L. F. Bonewald<sup>4</sup>, E. Sprague<sup>\*5</sup>, M. A. Schwartz<sup>\*6</sup>, J. X. Jiang<sup>1</sup>. <sup>1</sup>Biochemistry, University of Texas Health Science Center, San Antonio, TX, USA, <sup>2</sup>Periodontics, University of Texas Health Science Center, San Antonio, TX, USA, <sup>3</sup>Cell Biology, University of Virginia, Charlottesville, VA, USA, <sup>4</sup>Oral Biology, University of Missouri, School of Dentistry, Kansas City, MO, USA, <sup>5</sup>Radiology, University of Texas Health Science Center, San Antonio, TX, USA, <sup>6</sup>Microbiology, Biomedical Engineering and Cardiovascular Research, University of Virginia, Charlottesville, VA, USA.

Connexin 43 hemichannels are un-opposed halves of gap junctions that play a role in osteocyte viability and signaling. Mechanical stimulation in the form of fluid flow shear stress has been shown to induce the opening of hemichannels in MLO-Y4 osteocyte-like cells releasing prostaglandins, ATP and potentially other signaling molecules important for bone formation. In a search for potential mechanosensors associated with hemichannels, Cx43 was found to consistently co-localize with the α5 and β1 integrin complex on the cell but not found to co-localize with the focal adhesion proteins, vinculin or paxillin. Co-immunoprecipitation experiments validated this association between Cx43 and α5/β1 integrin.

To determine whether Cx43/integrin α5 interactions play a role in the opening of hemichannels in response to mechanical stimulation, the MLO-Y4 cell model was used. Blocking antibody to α5 integrin inhibited and α5 integrin siRNA totally abolished the opening of hemichannels and associated prostaglandin release in response to shear stress. No changes were observed in cell surface expression of Cx43. Magnetic beads coated with either anti-α5 integrin antibody or fibronectin were perturbed by a magnetic field after attachment to the cell surface. This resulted in the opening of hemichannels as visualized by dye uptake. In contrast, control beads coated with poly-lysine or anti-CD44 antibody failed to induce the opening of hemichannels when moved at the same magnitude. Similar to non-treated control, extracellular matrix substrate for α5 integrin, fibronectin, fibronectin-conjugated beads or integrin binding ligand RGD peptide did not have any effect on the opening of hemichannels by shear stress, indicating that α5 integrin, not fibronectin, is the target for opening hemichannels by shear stress. Together, these results suggest that integrin α5/β1 may serve as a mechanical tether or tensor mediating the effects of shear stress in regulating the opening of Cx43-forming hemichannels and that this novel function of integrin can be independent of its association with extracellular matrix.

**Disclosures:** J.X. Jiang, None.

This study received funding from: National Institute of Health.

## SA061

**Proteoliposomes Carrying Alkaline Phosphatase and Nucleotide Pyrophosphatase/ Phosphodiesterase-1 as Matrix Vesicle Mimetics.** P. Ciancaglini<sup>\*1</sup>, A. M. S. Simao<sup>\*1</sup>, M. C. Yadav<sup>2</sup>, S. Narisawa<sup>\*2</sup>, M. F. Hoylaerts<sup>\*3</sup>, J. L. Millan<sup>2</sup>. <sup>1</sup>Departamento de Quimica, FFCLRP-USP, Ribeirao Preto, Brazil, <sup>2</sup>Sanford Children's Health Research Center, Burnham Institute for Medical Research, La Jolla, CA, USA, <sup>3</sup>Center for Molecular and Vascular Biology, University of Leuven-Campus Gasthuisberg, Leuven, Belgium.

Experimental evidence indicates that endochondral calcification is mediated by chondroblast- and osteoblast-derived matrix vesicles (MV). The primary function of tissue-nonspecific alkaline phosphatase (TNAP) is to degrade extracellular inorganic pyrophosphate (ePPi), a potent mineralization inhibitor, which is produced ectoplasmically by the enzymatic activity of nucleotide pyrophosphatase/ phosphodiesterase-1 (NPP1), restricting the concentration of ePPi, to maintain a Pi/PPi ratio permissive for normal bone mineralization. Both these enzymes act at the level of the membrane in osteoblasts and in osteoblast-derived MVs. In this study we have used a liposome system to reconstitute proteoliposomes harboring TNAP alone, NPP1 alone, or both in combination, to study the kinetic behavior of these enzymes in a lipophilic membrane environment. TNAP and NPP1 were expressed in CHO cells, solubilized with polidocanol and inserted into dipalmitoylphosphatidylcholine (DPPC) liposomes as previously standardized. Polidocanol-solubilized detergent-free TNAP and NPP1, alone or in combination showed the ability to anchor to DPPC liposomes. The enzyme activities were measured at pH 7.4, for the substrates ATP, ADP, AMP and PPi, by measuring the amount of inorganic phosphate liberated as a function of time, as previously described. Hydrolyzed ATP nucleotide intermediates were separated and quantitated by HPLC. NPP1-liposomes exclusively hydrolyzed ATP into AMP and PPi. In contrast, TNAP-liposomes, as well as TNAP+NPP1-liposomes hydrolyzed ATP, ADP, AMP and PPi. Hence, the simultaneous presence of TNAP and NPP1 on a proteoliposome membrane enables the complementary hydrolysis of natural phospho-substrates and their intermediates, leading to very efficient phosphate accumulation in the immediate microenvironment of the phospholipid membrane surface. Therefore, we conclude that the controlled reconstitution of MV-associated phosphatases and phosphodiesterases in proteoliposome membranes generates the correct microenvironment to study phospho-substrate catalysis and PPi degradation, allowing more detailed studies of those catalytic processes that initiate skeletal calcification.

Financial Supports: FAPESP, CNPq, CAPES and DE12889 and AR47908 from NIH. I Camolezi et al., Construction of an alkaline phosphatase-liposome system: a tool for biomineralization study. *Int. J. Biochem. Cell Biol.* 34: 1091-1101 (2002).

**Disclosures:** *A.M.S. Simao, None.*  
*This study received funding from: NIH.*

## SA062

See Friday Plenary number F062.

## SA063

**Molecular Mechanisms Underlying Matrix Vesicle-induced Mineralization During Bone Formation: An Enzyme Kinetic Approach.** P. Ciancaglini<sup>\*1</sup>, A. M. S. Simao<sup>\*1</sup>, M. C. Yadav<sup>2</sup>, S. Narisawa<sup>\*2</sup>, C. Farquharson<sup>3</sup>, M. F. Hoylaerts<sup>\*4</sup>, J. L. Millan<sup>2</sup>. <sup>1</sup>Departamento de Quimica, FFCLRP-USP, Ribeirao Preto, Brazil, <sup>2</sup>Sanford Children's Health Research Center, Burnham Institute for Medical Research, La Jolla, CA, USA, <sup>3</sup>Bone Biology Group, Roslin Institute, University of Edinburgh, Edinburgh, United Kingdom, <sup>4</sup>Center for Molecular and Vascular Biology, University of Leuven-Campus Gasthuisberg, Leuven, Belgium.

Mineralization of cartilage and bone occurs by physico-chemical and biochemical processes that together facilitate the deposition of hydroxyapatite in specific areas of the extracellular matrix, mediated by chondroblast- and osteoblast-derived matrix vesicles (MVs). The primary function of tissue-nonspecific alkaline phosphatase (TNAP) is to degrade extracellular inorganic pyrophosphate (ePPi), a mineralization inhibitor, which is produced by nucleotide pyrophosphatase/phosphodiesterase-1 (NPP1), restricting the concentration of ePPi, to maintain a Pi/PPi ratio permissive for normal bone mineralization. We studied the efficiency of phospho-substrates catalysis by osteoblast-derived MVs, kinetically analyzing the hydrolysis of ATP, ADP and PPi by isolated native wild-type (WT), PHOSPHO1 null, TNAP null and NPP1 null MVs. The enzyme activities were determined at pH 7.4 by measuring the amount of inorganic phosphate liberated as a function of time, as previously described. Throughout catalysis, reaction nucleotide intermediates, during hydrolysis of ATP and ADP were monitored via separation and quantitation in HPLC. Comparison of the catalytic efficiencies measured for TNAP<sup>-/-</sup>, NPP1<sup>-/-</sup> and PHOSPHO1<sup>-/-</sup> MVs to those of native MVs identified ATP as the main substrate, hydrolyzed by WT MVs. Hydrolysis of ATP was significantly reduced in the absence of TNAP, but also of PHOSPHO1, implicating both enzymes in the processing of ATP by MVs. Also, we observed deficient PPi and ADP hydrolysis in TNAP-deficient MVs underscoring that, unlike for the hydrolysis of ATP, PPi is primarily processed by TNAP. The lack of NPP1 did not significantly affect the kinetic parameters of hydrolysis when compared to WT MVs, for any of the substrates. We conclude that the hydrolysis of phospho-substrates in MV membranes results from the concerted action of phospholipid-dependent NPP1, TNAP and PHOSPHO1, enabling hydroxyapatite mineralization under conditions of restricted PPi accumulation.

Financial Supports: FAPESP, CNPq, CAPES and DE12889, AR47908 and AR53102 from NIH. I Camolezi et al., Construction of an alkaline phosphatase-liposome system: a tool for biomineralization study. *Int. J. Biochem. Cell Biol.* 34: 1091-1101 (2002).

**Disclosures:** *M.C. Yadav, None.*  
*This study received funding from: NIH.*

## SA064

**MEPE Expression Is Regulated by BMP-2 Signaling Through the Activation of Its Downstream Transcription Factors, Dlx3, Dlx5 and Runx2.** Y. Cho, J. Park<sup>\*</sup>, W. Yoon<sup>\*</sup>, K. Woo<sup>\*</sup>, J. Baek<sup>\*</sup>, H. Ryoo<sup>\*</sup>. Department of Cell and Developmental Biology, School of Dentistry and Dental Research Institute, Seoul National University, Seoul, Republic of Korea.

MEPE (Matrix Extracellular Phosphoglycoprotein), also called OF45 (osteoblast/osteocyte factor 45), is expressed in osteoblasts, osteocytes and odontoblasts during mineralization. MEPE is a 525-amino acids extracellular matrix protein, and has osteogenic activity through its centrally located GAG- and cell-attachment motif, AC-100. On the contrary, it has mineralization inhibitory activity through its C-terminal ASARM motif (minhibin). Recent reports indicated that MEPE is a standard marker of osteocytes, however, it still remained unclear how its expression is regulated by extracellular signals. In this study, we tried to illuminate upstream signals that are regulating MEPE expression. Our previously cDNA microarray analysis indicated that mRNA level of MEPE is about 27.9 folds higher in mineralizing mouse calvarial tissue than in unmineralized suture tissue. Long-term culture of MC3T3-E1 cells in osteogenic medium showed that MEPE expression is stimulated 200,000 folds at 21 day of culture (compared to 1 day). These results implicated that MEPE expression is a mineralizing tissue-specific, especially at the late mineralization stage. Our previous reports have shown that BMP-signaling is utmost important for the mineralization of the calvarial bones. In addition, its downstream transcription factors such as Dlx3, Dlx5 and Runx2 are very important modulators of calvarial bone mineralization. Thus we have tested BMP-2 effect on MEPE expression in osteogenic cells. BMP-2 (100 ng/ml) treatment to MC3T3-E1 cells strongly increased MEPE mRNA level by 25 folds. Similarly, the overexpression of BMP-2 downstream transcription factors such as Dlx3, Dlx5, and Runx2 also up-regulated MEPE mRNA expression as well as MEPE promoter activity. Moreover, co-transfection of Dlx5 and Runx2 with MEPE reporter vector showed that there was a mild synergistic effect on the promoter activation. In contrast, knock-down of Smad1/5, Dlx3/5 or Runx2 by their siRNA treatment downregulated MEPE mRNA level even in the presence of BMP-2. With a serial MEPE promoter deletion analysis, site-directed mutagenesis experiments and electrophoretic gel mobility shift assays, we specified a couple of homeodomain and Runx2 response elements, respectively, in the proximal promoter of MEPE. Taken together, MEPE expression is specific in the late mineralization stage of in vitro cell culture, and is strongly stimulated by BMP-2 signaling through the activation of its downstream transcription factors, Dlx3, Dlx5 and Runx2.

**Disclosures:** *Y. Cho, None.*  
*This study received funding from: Basic Research Program of the Korea Science & Engineering Foundation (R01-2005-000-106650) and by the Korea Health 21 R&D Project, Ministry of Health and Welfare (Project No. A010252).*

## SA065

**TIEG1 KO Mice Display Defects in the Bone Matrix Immediately Surrounding Osteocytes.** O. Haddad<sup>1</sup>, J. R. Hawse<sup>2</sup>, M. Subramaniam<sup>2</sup>, C. Pichon<sup>3</sup>, T. C. Spelsberg<sup>2</sup>, S. F. Bensamoun<sup>1</sup>. <sup>1</sup>UMR CNRS 6600, Biomecanique et Bioingenierie, Universite de Technologie de Compiègne, Compiègne, France, <sup>2</sup>Department of Biochemistry and Molecular Biology, Mayo Clinic College of Medicine, Rochester, MN, USA, <sup>3</sup>Cnrs upr 430, Centre de Biophysique Moléculaire, Orleans, France.

Osteocytes constitute a three-dimensional network in bone and play crucial roles in cell-cell communication and mechanotransduction. Osteocytes communicate with each other, and with cells on the bone surface, via long cytoplasmic extensions referred to as canaliculi. Through the development of TGF beta Inducible Early Gene 1 (TIEG1) KO mice, we have demonstrated that TIEG1 plays an important role in osteoblast-mediated bone mineralization [1], in bone thickness and resistance to mechanical strain as well as in osteocyte density in cortical bone [2]. In order to further examine the osteocyte phenotype observed in these animals, four femurs were extracted from female TIEG1 KO and wild-type mice. Transverse cross sections were cut in the middle of the diaphysis and sections were placed in a fixative and decalcifying solution. Thin femoral cross sections (5µm) were prepared from these samples for transmission electron microscopy. Twenty osteocytes from each TIEG1 KO and wild-type (WT) femur were observed for differences in cell morphology and the structure of the bone matrix surrounding each cell. This analysis revealed differences in the unmineralized matrix surrounding osteocytes in TIEG1 KO mice relative to wild-type controls. Figure 1 highlights the unmineralized matrix (dotted line) immediately surrounding individual osteocytes. A ratio between the cell surface and the unmineralized matrix was calculated and the results indicate that significantly less (2 fold) unmineralized matrix surrounds TIEG1 KO osteocytes relative to WT controls. Currently, little is known about the role and functions of the bone matrix immediately surrounding osteocytes. However, the present study clearly reveals differences in this bone micro-environment in TIEG1 KO mice and suggests that the bone remodeling and mechanosensing properties of these cells may be compromised in the absence of TIEG1 expression. Further investigations will be performed on cellular and molecular levels to determine precisely the impact of TIEG gene invalidation on

osteocytes biology.

- [1] M. Subramaniam, et al. Mol Cell Biol 2005, 1191-1199  
[2] S.F. Bensamoun, et al. Bone 2006, 39, 1244-1251

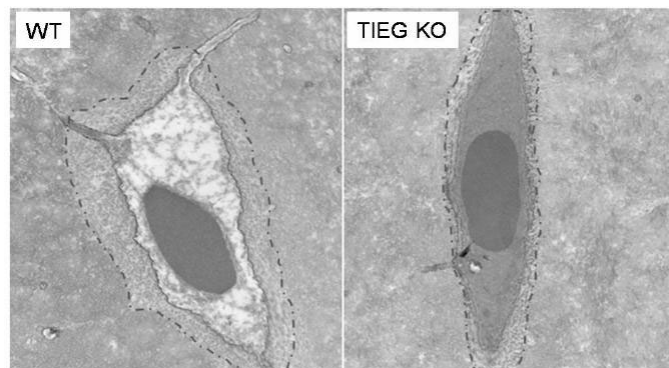


Figure 1: Electron micrographs depicting a reduced unmineralized matrix area in TIEG1 KO mice. Representative transmission electron microscopy images showing osteocytes in the cortical region of the wild-type (WT) and TIEG1 KO mouse femurs (TIEG KO). Unmineralized matrix areas are represented with dotted lines.

**Disclosures:** O. Haddad, None.

## SA066

See Friday Plenary number F066.

## SA067

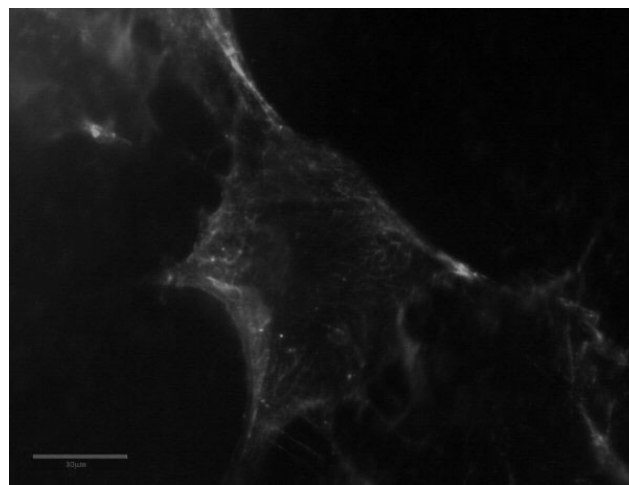
**The Response of Matrix Synthesizing MLO-A5 Cells to Fluid Shear.** H. L. Morris<sup>\*1</sup>, A. Sittichokechaiwut<sup>\*1</sup>, C. R. Jacobs<sup>\*2</sup>, J. W. Haycock<sup>\*1</sup>, G. C. Reilly<sup>1</sup>. <sup>1</sup>Engineering Materials, University of Sheffield, UK, Sheffield, United Kingdom, <sup>2</sup>Mechanical Engineering, Stanford University, Stanford, CA, USA.

Bone remodels dependent on the mechanical loading it receives. For this to occur bone must be able to sense mechanical load in order to effect changes in the tissue architecture. Osteocytes are believed to be the cell type within bone which are sensitive to mechanical stimulation [1]. The interstitial fluid around osteocytes has been shown to be displaced by bone strain. Mechanosensitivity is proposed to result from the application of shear forces from fluid movement on the osteocytes. In tissue engineered bone, osteoblasts and their precursors must directly sense and respond to mechanical forces in a less constrained environment. The aim of the current work is to investigate responses to fluid flow in the cell line MLO-A5. These cells actively and rapidly synthesize bone matrix and have been reported to represent transitional cells between osteoblasts and osteocytes, also termed 'osteoid osteocytes' [2].

Intracellular calcium release in response to fluid flow was examined using the calcium indicator fluo-4. MLO-A5 cells were grown for three days in static culture on the base of a closed parallel plate flow chamber (Ibidi Integrated BioDiagnostics, GER), cells were then loaded with the indicator and subjected to pulsatile fluid flow (0.3Pa). A transitional increase in intracellular calcium was observed a few seconds after commencement of flow. Gene expression of Collagen I and Osteopontin was analysed using RT-PCR and was seen to be upregulated two fold, 24 hours after cells were subjected to a flow of 2 Pa for 2 hours. To investigate the effects of flow on the longer term response of matrix production cells were stimulated by flow for 2 hours (2Pa) on day 3 of culture and collected on day 8. An increase in collagen production was observed in cells subjected to flow compared to no flow controls as assessed by sirius red assay.

Immunofluorescence showed that MLO-A5 cells possess both a hyaluronan (HA)-rich glycocalyx and primary cilia both putative mechanosensors of fluid shear in other bone cell types. In conclusion, we have established MLO-A5s will be a good model cell type with which to study the fluid flow responses of matrix synthesising osteoblasts.

Image showing HA glycocalyx of MLO-A5 cells, stained with HABP-FITC.



1. L. F. Bonewald. Bone 42(2008) 606-615  
2. Y. Kato. J Bone Miner Res. 16(9)(2001) 1622-33

**Disclosures:** H.L. Morris, None.

This study received funding from: EPSRC White Rose Doctoral Training Centre.

## SA068

**Notch Signaling Regulates Osteoblast Maturation Transition to Mineralization Phase.** S. Gao<sup>\*</sup>, J. Hock, P. Liu. Maine Institute for Human Genetics and Health, Brewer, ME, USA.

Notch signaling pathway is believed to control binary stem cell-fates in development. However, its precise physiological role, and temporal and spatial expression in postnatal skeletal development remains largely unknown. To address this issue, we utilized Notch GFP reporter mouse and conditionally inducible gain or loss of Notch function mouse models. To locate GFP expression as a marker for Notch activity, we used fluorescent microscopy to examine frozen bone sections from Notch GFP mice (including long bones, spines, calvarias and tails in young and adult, both sex). GFP positive cells were present on the surface of trabecular bone and within mineralized matrix. GFP expression was greatly increased in areas of high bone formation activity in the primary spongiosa underlying growth plate in young mice. To determine if this Notch expression was restricted to osteoblast lineage, mouse bone marrow stromal cells (mBMSC) from GFP mice were isolated, and induced to differentiate with osteogenic media into mature Ob. GFP expression was monitored throughout of the 21 days culture period. Although no GFP was detectable in the early stage of culture (before day 7), surprisingly strong GFP expression was observed specifically in cells at the time mineralization initiated; this expression disappeared when mineralization completed. To gain functional insight of the Notch activity in Ob lineage progression, we cultured mBMSCs from mice either with conditionally ectopic expression of active intracellular Notch domain (NICD) or mice in which Notch ligand-Jagged 1 (JAG1cKO) was knocked out. Cre was delivered to the cultures by adenovectors. Mineralization increased with increased NICD activity, but failed to occur in JAG1cKO. In the latter case, cells retained fibroblast-like morphology, and did not enter osteogenic differentiation. Collectively, these data provide new insights into the role of Notch in bone, and suggest the novel hypothesis that Notch pathway is critical in regulating progression into the mineralizing phase of Ob maturation.

**Disclosures:** S. Gao, None.

This study received funding from: Maine Institute for Human Genetics.

## SA069

See Friday Plenary number F069.

## SA070

**Enrichment of Type XI Collagen and 6b N-Terminal Domain at Sites of Mineral Nucleation Within Osteoblastic Cultures.** N. T. Huffman<sup>\*1</sup>, C. Chaoying<sup>\*2</sup>, S. V. Chittur<sup>\*3</sup>, J. T. Oxford<sup>4</sup>, J. A. Keightley<sup>\*1</sup>, R. J. Midura<sup>5</sup>, J. P. Gorski<sup>1</sup>. <sup>1</sup>Univ. of Missouri-Kansas City, Kansas City, MO, USA, <sup>2</sup>Tibet Univ. Med. College, Lhasa, China, <sup>3</sup>Univ. at Albany, Rensselaer, NY, USA, <sup>4</sup>Boise State Univ., Boise, ID, USA, <sup>5</sup>Cleveland Clinic, Cleveland, OH, USA.

Alternatively spliced 6b and 8 isoforms of type XI collagen are known to be associated with the process of embryonic bone formation. Type XI and I collagens co-exist in fibrils in bone and form hetero-dimeric complexes *in vitro* upon which type I fibrils can be built. Our goal was to determine when and where type XI RNA and protein were expressed during mineralization of UMR 106-01 osteoblastic cultures; nucleation of mineral occurs within extracellular biomineralization foci (BMF) in this model. Some cultures were treated with protease inhibitor AEBSF which blocks mineralization and activation of PCOLCE, an enhancer of BMP-1 processing of collagen. Type XI collagen expression increased 1.7-fold between 40 and 64 h after plating, just prior to when BMF are competent to mineralize. During this same period collagen I synthesis did not change suggesting that type XI may exhibit functions distinct from a role in type I fibrillogenesis. Cell layer fractions were also extracted sequentially with EDTA and then with 8 M urea/2% CHAPS; cell layer and media fractions were then subjected to western blotting. A 60 kDa N-terminal domain (NTD) was identified in EDTA and urea extracts using an antibody recognizing all type XI splice variants. NTDs were only detected in the media fraction in the absence of  $\beta$ -glycerol phosphate or with AEBSF. After AEBSF treatment, urea extracts contained elevated amounts of 60 kDa NTD. Both 6b and 8 splice variant forms were found to be expressed by UMR cells as 60 kDa and 110 kDa bands, respectively. Identification of alpha 1 chain 8 epitope was confirmed by mass spectral peptide mapping. However, neither 6b nor 8 isoforms were detected in the urea extract suggesting the 60 kDa NTD in AEBSF-treated cultures is composed of the 6a alternative splice form, which is not associated with mineralization. Finally, a 60 kDa NTD reactive with 6b splice variant specific antibodies was enriched preferentially in mineralized BMF, whereas the 8 splice form is not. These results indicate a clear distinction between the localization and distribution of up to three different alternatively spliced isoforms of type XI collagen. Based on extraction with EDTA and on direct isolation by laser capture microscopy, the 6b isoform NTD is enriched in extracellular BMF. When mineralization is blocked by AEBSF, NTDs apparently containing the 6a epitope become more tightly bound to the cell layer. The enrichment of a large NTD expressing 6b epitope only within BMF, sites of initial mineral nucleation, suggests a functional or structural role in this process.

**Disclosures:** J.P. Gorski, BoneMetrics LLC 5.  
This study received funding from: NIH AR052775 (JPG).

## SA071

**Lithium Affects Matrix Mineralization by Decreasing Tissue Non-specific Alkaline Phosphatase Levels in Osteoblasts.** J. Li<sup>\*</sup>, M. Murshed. McGill University, Montreal, QC, Canada.

Mineralization of bone extracellular matrix is achieved, at least in part, by the unique co-expression in osteoblasts of several broadly expressed genes. One of these genes *alkaline phosphatase, liver/bone/kidney (Alpl)* encodes a cell membrane-bound phosphatase, which cleaves inorganic pyrophosphate, a ubiquitously present mineralization inhibitor. We recently observed that addition of lithium ions to the cell culture medium prevented *in vitro* mineral deposition by reducing the alkaline phosphatase enzymatic activity in mouse primary osteoblasts. This reduced activity was not due to a direct inhibition of the enzyme by lithium ions as it was the case with some other magnesium-dependent phosphatases. Also, lithium treatment did not increase the release of the cell membrane-bound enzyme into the culture medium. Interestingly, we observed a decrease in alkaline phosphatase protein levels in the lithium treated cells. When added to the culture medium, recombinant bone morphogenetic protein-2 (BMP-2) reversed the effects of lithium on osteoblasts, suggesting the BMP signalling pathway a possible target for lithium action in these cells. We further investigated the mode of lithium action in pluripotent C2C12 cells stably transfected with a BMP-2 expression vector.

**Disclosures:** M. Murshed, None.  
This study received funding from: McGill University.

## SA072

**Effects of Odanacatib on Bone Mass and Turnover in Estrogen Deficient Adult Rhesus Monkeys.** T. Cusick, B. Pennypacker, D. Kimmel. Molecular Endocrinology/Bone Biology, Merck & Co, West Point, PA, USA.

Odanacatib (ODN) is a selective inhibitor of Cathepsin K (CatK) in non-human primates (NHPs) and humans. Inhibition of CatK may be a promising new mechanism for treating osteoporosis. Rhesus monkeys (aged 13-19yrs) were ovariectomized (OVX), randomized by spinal bone mineral density (LVBMD), and immediately started on ODN (0 [N=11], 6 [N=8], or 30 [N=10] mg/kg, qd, PO) in 0.5% methocel for 21 months. DXA of spine (LV), femoral neck (FN), and total hip (H) (BMD, g/cm<sup>2</sup>; BMC, bone mineral content, g) was done quarterly. Pharmacokinetic studies were used to determine ODN exposure. Dual fluorochrome labeling (tetracycline PO; 20mg/kg; 15d interval) was given just before necropsy. Left femurs and the first three lumbar vertebrae (LV1-3) were fixed in 70% ethanol.

Unstained 8m parasagittal sections of LV2 (trabecular), and 100 $\mu$ m cross-sections (cortical) at 4cm from the proximal end of the femur (PF) were prepared and evaluated for double

label, single label, and distance between labels, using fluorescent microscopy. Data collection was done on coded specimens. Cortical thickness (Ct.Th) was measured (PF). Mineralizing surface (MSBS, %), mineral apposition rate (MAR,  $\mu$ m/d), and surface-based bone formation rate (BFRBS, mm<sup>3</sup>/mm/yr) were calculated.

ODN exposure was 2.2 and 3.8  $\mu$ M-24hr. Baseline LVBMD differed little among the groups. Ending LVBMD was 11% and 17% higher than OVX+0; HBMD was 10% and 16% higher in the ODN groups. FNBMD was 11% and 12% higher than OVX+0 in the ODN groups. LVBMD was not affected by 6mg/kg/d ODN, but was ~80% lower with 30mg/kg/d ODN than OVX+0, while LVMAR was unaffected. LVBFRBS was not affected by 6mg/kg ODN, but was ~75% lower with 30mg/kg ODN than in OVX+0. PFMSBS was not affected by 6mg/kg ODN, and tended to be higher with 30mg/kg ODN than in OVX+0; PFMAR was unaffected. PFBFRBS tended to be higher with 30mg/kg ODN. Ct.Th was not affected by 6mg/kg ODN and tended to be higher with 30mg/kg ODN than in OVX+0. ODN treatment at 6 and 30mg/kg/d in NHPs causes higher bone mass in osteoporotic fracture sites in humans. ODN decreases bone formation activity in vertebral body trabecular bone only at 30mg/kg/d. These data indicate that ODN increases bone mass in adult NHPs at doses where bone formation in trabecular regions appears unaffected by histomorphometric measures. ODN treatment may also be associated with increased periosteal formation rate and cortical thickness at the hip.

Endpoint/Group	OVX+0 (N=11)	OVX+6mg/kg ODN (N=8)	OVX+30mg/kg ODN (N=9)	ANOVA (P=)
LVBMD (g/cm <sup>2</sup> )	0.665 $\pm$ 0.068	0.731 $\pm$ 0.108*	0.771 $\pm$ 0.098**	0.040
HBMD (g/cm <sup>2</sup> )	0.653 $\pm$ 0.066	0.745 $\pm$ 0.079**	0.771 $\pm$ 0.082***	0.007
LVMS/BS (%)	2.75 $\pm$ 2.26	2.21 $\pm$ 1.60	0.64 $\pm$ 0.65**	0.033
LVBFRBS (mm <sup>3</sup> /mm/yr)	9.88 $\pm$ 8.77	8.52 $\pm$ 7.00	2.20 $\pm$ 2.71*	0.057
PFMS/BS (%)	16.0 $\pm$ 12.2	16.9 $\pm$ 13.3	27.6 $\pm$ 16.2+	0.202
PFBFRBS (mm <sup>3</sup> /mm/yr)	0.125 $\pm$ 0.088	0.095 $\pm$ 0.086	0.205 $\pm$ 0.150+	0.175

Mean $\pm$ SD; +(P=0.1); \*(P<.05); \*\*\*(P<.001) vs. OVX  
H-hip, LV-spine, CF-central femur, FN-femoral neck, PF-proximal femur

**Disclosures:** T. Cusick, None.

## SA073

**Bone Effects of Odanacatib in Adult Ovariectomized Rabbits.** B. L. Pennypacker, T. E. Cusick, D. B. Kimmel. Molecular Endocrinology and Bone Biology, Merck and Co., West Point, PA, USA.

Cathepsin K (CatK), a cysteine protease highly expressed in osteoclasts, degrades type I collagen. A CatK inhibitor may be useful for treating osteoporosis. The objective was to evaluate bone mineral density (BMD) and bone turnover in surrogate osteoporotic fracture sites in ovariectomized (OVX) rabbits treated for 28 weeks with CatK inhibitor, Odanacatib (MK-0822).

New Zealand White rabbits (age 7mos) were randomized by spine BMD (DXA, Hologic QDR4500A) and body weight into five groups (N=11-13): Sham-OVX (Sh) + control diet 2031C (Harland Teklad), OVX+ control diet, OVX with 0.0016% dietary MK-0822, OVX with 0.004% dietary MK-0822, or (5) OVX + control diet, treated with alendronate (ALN, 0.3 mg/kg SC 2X/wk). ALN and special diets were started 5-7 days following OVX surgery. Pharmacokinetic studies estimated AUC at ~4 and ~9 $\mu$ m-24hr for the 0.0016% and 0.004% diets, respectively. In vivo dual calcein labeling (8 mg/kg, SC) was given on the tenth and third days before necropsy. Lumbar vertebrae (LV) 2-5 and left femurs were excised and fixed in 70% ethanol. The proximal left femur and LV3 were DXA-scanned. LV3 was embedded and sectioned parasagittally at 5 $\mu$ m and analyzed for cancellous bone volume (BV/TV), mineralizing surface, mineral apposition rate (MAR), and bone formation rate (BFR/BS). 100 $\mu$ m cross-sections of the mid-femur were analyzed for cortical thickness, endocortical (e) and periosteal (p) mineralizing surface (MS/BS), and number of double labeled Haversian systems (HS)/mm<sup>2</sup>. Significant OVX-induced BMD decline (-8.7%, p<0.05) occurred at LV3 after OVX. This BMD loss was prevented in both MK-0822 groups and by ALN. BMD was significantly higher in the total hip with MK-0822 and ALN than in OVX+0. BV/TV of LV3 was significantly higher (+13.4%, P<.05) with MK-0822 vs. OVX (P<.04). Mineralizing surface (MS/BS, %) was lower with ALN treatment vs. OVX+0, but was the same or higher than OVX with MK-0822.

These results suggest that estrogen deficiency bone loss was prevented by Cat K inhibition and ALN after seven months. However, CatK inhibition was accompanied by no suppression of bone formation, while ALN was associated with inhibition of bone formation. This may represent either transient or permanent temporal decoupling of formation from resorption in the bone remodeling process, and may differentiate the Cat K mechanism from bisphosphonates.

Variable (N)	Sham (12)	OVX (12)	OVX+4 (13)	OVX+9 (11)	OVX+ALN (10)
LV3 BMD	394.9 $\pm$ 11.9	360.3 $\pm$ 12.5†	401.3 $\pm$ 10.5*	426.6 $\pm$ 10.1**	409.1 $\pm$ 15.0*
Total Hip BMD	362.7 $\pm$ 8.7	357.4 $\pm$ 7.6	380 $\pm$ 8.9*	385.5 $\pm$ 6.2*	393.3 $\pm$ 9.0*
LV3 BV/TV	23.2 $\pm$ 1.0	21.2 $\pm$ 1.0	23.7 $\pm$ 2.1	26.3 $\pm$ 1.9*	22.4 $\pm$ 1.4
LV3 MS/BS	8.0 $\pm$ 1.8	10.0 $\pm$ 2.3	15.0 $\pm$ 2.1†	9.5 $\pm$ 1.8	5.5 $\pm$ 1.7
LV3 BFR/BS	64.3 $\pm$ 16.5	79.3 $\pm$ 18.1	120.5 $\pm$ 18.5	65.0 $\pm$ 13.1	56.8 $\pm$ 24.1
Cortical thickness	1.25 $\pm$ 0.37	1.17 $\pm$ 0.38	1.188 $\pm$ 0.35	1.30 $\pm$ 0.6	1.38 $\pm$ 0.81*
eMS/BS	11.72 $\pm$ 3.06	14.35 $\pm$ 3.38	16.82 $\pm$ 2.18	16.70 $\pm$ 1.9	5.85 $\pm$ 8.5*
DL Haversian remodeling units	0.583 $\pm$ .23	0.75 $\pm$ .25	1.31 $\pm$ .37	1.3 $\pm$ .37	0.1 $\pm$ .32

\*compared to OVX P < 0.05,

\*\* compared to OVX P < 0.001

† compared to Sham P < 0.05

**Disclosures:** B.L. Pennypacker, None.



**SA074****See Friday Plenary number F074.****SA075**

**Inhibition of MMP Activity Delays Bone Repair Whereas Inhibition of Osteoclast Function and Formation Does Not.** M. M. McDonald\*, K. Mikulec\*, L. Peacock\*, T. Lah\*, D. G. Little\*. Orthopaedic Research, The Children's Hospital Westmead, Sydney, Australia.

Osteoclasts are associated with all stages of bone repair, including the removal of the soft cartilaginous callus. It is unclear whether specific osteoclast mediated resorption or MMP secretion by osteoclasts and other cells are most important in this process. We designed a fracture healing experiment to dissociate osteoclastic and MMP functions during repair.

In a rat closed femoral fracture model MMI270, an MMP inhibitor was administered subcutaneously (s.c.) twice daily at 120mg/kg while Osteoprotegerin (OPG) at 10mg/kg, Clodronate (CLOD) at 45mg/kg, Zoledronic Acid (ZA) at 0.01mg/kg, or Saline were administered s.c. twice weekly. Dosing continued throughout the entire repair process. Outcomes were assessed at 2, 4 and 6 weeks post fracture. This study design dissociates osteoclast inhibition (the Bisphosphonates ZA and CLOD) from inhibition of osteoclastogenesis (OPG) and global MMP inhibition (MMI270).

MMI270 treatment led to decreased rates of radiographic union compared to Saline ( $p<0.01$ , Fishers exact test). MMI270 treatment produced a union rate of just 9% at 4 weeks and 30% at 6 weeks. In contrast, all other treatment groups showed equivalent union rates with 70-91% at 4 weeks and 100% union by 6 weeks.

QCT scans revealed a 26% reduction in fracture callus bone mineral content (BMC) and a 42% reduction in callus bone volume (volume) in MMI270 treated samples compared to Saline at 2 weeks ( $p<0.01$ ). At 4 weeks a 26% reduction in callus volume remained ( $p<0.05$ ), and by 6 weeks MMI270 had equivalent BMC and volume to Saline. Both ZA and OPG treatment showed increases in callus BMC (54-97%) and volume (44-66%) at 4 and 6 weeks post fracture ( $p<0.01$ ). CLOD produced smaller but significant increases in both BMC (30%) and volume (35%) over Saline at 4 weeks only ( $p<0.01$ ).

In conclusion, MMP inhibition led to delays in endochondral fracture union whereas OPG, ZA and CLOD did not. MMP inhibition also showed reduced callus BMC and volume, while OPG, ZA and CLOD treatment all produced significant increases in callus BMC and volume ( $p<0.01$ ).

These results suggest that MMP activity rather than osteoclast function may be crucial to achieving bony union in this rat fracture model. Osteoclast function and formation may therefore be redundant during initial endochondral bone repair.

**Disclosures:** *M.M. McDonald, None.*

*This study received funding from: NHMRC.*

**SA076**

**AP-1 and Mitf Interact with NFATc1 to Stimulate Cathepsin K Promoter Activity in Osteoclast Precursors.** M. Pang\*, W. Balkan\*, M. Rodriguez\*, M. Hernandez\*, B. R. Troen. Miami VAMC/GRECC and Geriatrics Institute, University of Miami Miller School of Medicine, Miami, FL, USA.

Cathepsin K (CTSK) is a secreted protease that plays an essential role in osteoclastic bone resorption and osteoporotic bone loss. We have previously shown that AP-1 stimulates CTSK promoter activity and that proximal NFATc1-binding sites play a major role in the stimulation of CTSK gene expression by receptor activator of NFkB ligand (RANKL). We undertook transfection analysis and nuclear factor binding studies to investigate AP-1, NFATc1, and microphthalmia-associated transcription factor (Mitf) cooperativity in the regulation of CTSK transcription. These experiments were carried out in RAW 264.7 cells, which can be readily differentiated to osteoclasts upon RANKL stimulation. Transfection of the individual factors with truncated CTSK promoter-luciferase plasmids significantly stimulated CTSK promoter activity. Cotransfection with combinations of two of the factors (AP-1+NFATc1, AP-1+Mitf, Mitf+NFATc1) dramatically enhanced CTSK promoter activity, with Mitf+NFATc1 producing the largest induction of CTSK promoter activity. Moreover, triple cotransfection of AP-1, NFATc1, and Mitf synergistically stimulated CTSK promoter activity well above levels observed with the double transfections. Cotransfections with dominant negative c-fos markedly inhibited both basal and stimulated CTSK promoter activity, suggesting that AP-1 plays an integral role in transcription of the CTSK gene. Deletion of the 4-bp core elements from three NFATc1 binding sites in the proximal CTSK promoter completely abrogated the response to NFATc1, but did not affect the stimulation by AP-1 or Mitf, either individually or together. Electrophoretic mobility shift assays and analysis of DNA-protein interactions using the Factor Finder system followed by western blots revealed that NFATc1, AP-1, and Mitf bind to similar regions of the CTSK promoter. While AP-1, Mitf, and NFATc1 can independently stimulate CTSK promoter activity, we now demonstrate that these factors cooperate intimately to regulate transcription of the CTSK gene by acting upon the proximal promoter region. Studies are under way to assess the direct DNA-protein interactions of the proximal promoter and thereby more fully elucidate the critical and multiple nuclear factor regulation of transcription of the CTSK gene.

**Disclosures:** *M. Pang, None.*

*This study received funding from: Department of Veterans Affairs and Indial Trail Foundation.*

**SA077**

**Identification of Osteoclast Lysosomal Proteins by Mass-Spectrometry.** H. Zhao<sup>1</sup>, R. D. LeDuc<sup>\*2</sup>, Y. Ito<sup>1</sup>, J. Chappel<sup>\*1</sup>, R. Townsend<sup>\*2</sup>, S. L. Teitelbaum<sup>1</sup>, F. P. Ross<sup>1</sup>. <sup>1</sup>Department of Pathology and Immunology, Washington University School of Medicine, St. Louis, MO, USA, <sup>2</sup>Proteomic Core Facility, Washington University School of Medicine, St. Louis, MO, USA.

Osteoclasts (OCs) secrete hydrochloric acid to dissolve bone mineral, a process that is mediated by a vacuolar-type proton pump and charge-coupled chloride channel, and release the lysosomal acidic hydrolase cathepsin K to digest the organic matrix of bone. Accumulating evidence indicates that OC secretion to the ruffled border is through regulated lysosomal exocytosis. Consistent with this notion, we have shown that Synaptotagmin VII, a calcium sensor protein that regulates exocytosis, is a key molecule regulating the fusion of lysosomes with the ruffled border membrane and osteoclast function. In order to understand better the molecular mechanisms governing OC lysosome biogenesis, trafficking, and secretion, we set out to identify the protein profile of OC lysosomes by mass-spectrometry (MS). Bone marrow macrophages were transduced with a retroviral vector expressing FLAG tagged lysosome membrane protein, LAMP-2. The cells were cultured with M-CSF and RANKL for 5 days to generate mature OCs. A lysosome-enriched fraction was collected from an iodoxanol density gradient ultracentrifugation. To achieve higher purity, lysosomes were immuno-purified with magnetic beads coated with anti-FLAG monoclonal antibody. By this method, intact vesicles (lysosomes) on the beads were isolated, as demonstrated by transmission electron microscopy. Western blots of bead elution showed that LAMP-2 and Cathepsin K were recovered, whereas the mitochondria proteins (cytochrome c), cytoskeletal proteins (actin and tubulin) and early endosomal proteins (EEA1), were removed. The proteins bound to the magnetic beads were then separated by SDS-PAGE and a total of 96 gel punches were trypsin digested and analyzed by MS. The raw data were searched with Mascot. More than 300 proteins have been identified, which belong to the families of small GTPases, vesicular/protein trafficking regulators, molecular channels, lysosomal membrane proteins and acidic hydrolases, molecular motors and cytoskeletal regulators. Importantly, several lysosomal proteins, functionally important for OCs, have also been identified, including cathepsin K, LAMP-1/2, a3 and v<sub>0</sub>d2 subunits of vacuolar ATPases, and rab 7. Thus, we have established an experimental system for proteomic analysis of protein profiles in OC lysosomes, providing the capacity to identify novel proteins regulating bone resorption. Further functional characterization of these novel proteins will provide new insights into the molecular mechanisms of OC secretion.

**Disclosures:** *H. Zhao, None.*

*This study received funding from: NIH.*

**SA078**

**Expression of NF-κB Ligand and Regulation of Osteoclastogenesis by Bone Marrow Adipocytes.** A. Hozumi\*. Orthopaedics, Nagasaki University, Nagasaki, Japan.

**Objective:** NF-κB Ligand (RANKL), Osteoprotegerin (OPG) and macrophage colony stimulating factor (M-CSF) are potent regulator of osteoclastogenesis. Adipocytes and osteoblasts share a common origin, and several studies reported adipokines have close relationship in the bone metabolism. Now we examined whether RANKL, OPG and M-CSF were secreted from adipocytes. This study examined the ability of bone marrow adipocytes to support osteoclast formation and function in vitro.

**Materials and Methods:** The bone marrow fluids were obtained from 10 individuals at prosthetic insertion. The mRNA expression of RANKL, OPG and M-CSF was measured by real time RT-PCR and examine the effect of glucocorticoid. Furthermore we examined osteoclastogenesis of osteoclastprecursor cell in co-culture system with bone marrow adipocytes. Osteoclast differentiation was assessed by expression of tartrate-resistant acid phosphatase (TRAP).

**Results:** RANKL, OPG and M-CSF messenger ribonucleic acid (mRNA) expression are confirmed in all individual. RANKL/OPG ratio was significantly increased treated by dexamethasone compared to the control group in bone marrow adipocytes. M-CSF expression was not significantly altered in both cell group. RANKL/OPG ratio was significant at  $10^{-7}$  mol/L dexamethasone in mRNA levels and it was time-dependent manner up to 24 hr. Osteoclast differentiation and maturation were undergone when cocultured with bone marrow adipocytes and significantly stimulated by dexamethasone ( $10^{-7}$ mol/l). **Conclusion:** Our studies demonstrated for the first time that primary bone marrow mature adipocytes can support osteoclasts-like cell formation and function in vitro.

**Disclosures:** *A. Hozumi, None.*

**SA079****See Friday Plenary number F079.**

## SA080

**Expression and Function of Synoviolin in Human Osteoclastogenesis.** B. Merle<sup>\*1</sup>, P. D. Delmas<sup>1</sup>, P. Miossec<sup>\*2</sup>, M. L. Toh<sup>\*2</sup>. <sup>1</sup>INSERM U831, Université de Lyon, LYON, France, <sup>2</sup>Unité Mixte Hospices Civils de Lyon-BioMérieux, LYON, France.

Synoviolin, is an anti-apoptotic E3 ubiquitin ligase implicated in Rheumatoid arthritis (RA) synovial hyperplasia, however its role in bone destruction is less well understood. Transgenic mice overexpressing synoviolin show ubiquitous expression of synoviolin in various tissues including bone. The aim of our study was to investigate if synoviolin is expressed by human osteoclasts and implicated in their function *in vitro*.

Human osteoclasts were differentiated from human peripheral blood monocytes in the presence of RANK-L and M-CSF. Osteoclast differentiation was assessed by TRAP staining and TRAP activity in conditioned media. Synoviolin expression was measured by real-time PCR, Western Blotting and immunostaining. Synoviolin inhibition was achieved by RNA interference during osteoclastogenesis. Osteoclast function was determined by analysis of pit formation and assessment of type I collagen degradation products by ELISA.

Synoviolin was expressed in human monocytes and increased during osteoclastogenesis. Synoviolin mRNA and protein expression was 2 to 3 fold higher in mature osteoclasts compared to monocyte precursors. Immunohistochemistry staining demonstrated that synoviolin was localised to the perinuclear region in pre-osteoclasts and fully differentiated osteoclasts. Synoviolin inhibition during osteoclastogenesis dramatically reduced osteoclast formation as shown by TRAP staining and activity in the cell supernatants. In parallel, resorptive activity was reduced as measured by pit formation and the release of collagen fragments in cultured medium. Finally, synoviolin expression was inhibited by IL-4 and oestrogen during osteoclast differentiation.

In conclusion, we show that synoviolin is expressed by human osteoclasts and involved in the differentiation, survival and activity of osteoclasts *in vitro*. Overall, our findings suggest that synoviolin may be involved in the inflammatory osteoclast-mediated bone resorption observed in RA, and in the alterations of bone remodeling associated with metabolic bone diseases. In addition, oestrogen may have a protective effect on bone resorption at least in part through decreasing osteoclast survival.

**Disclosures:** B. Merle, None.

## SA081

See Friday Plenary number F081.

## SA082

**A Novel Role of L-Serine for the Activation of Receptor Activator of Nuclear Factor Kappa B Ligand (RANKL)-RANK Signaling Machinery in Osteoclastogenesis *in vitro*.** T. Ogawa, T. Sakai\*, A. Bahtiar\*, N. Ishida-Kitagawa\*, T. Takeya\*. Graduate School of Biological Sciences, Nara Institute of Science and Technology, Ikoma, Nara, Japan.

The induction of two key transcription factors, c-Fos and nuclear factor of activated T cells c1 (NFATc1/NFAT2), is known to be essential for osteoclastogenesis. We previously found, using mouse macrophage cell line RAW264 cells, that culture at high cell density blocked progression to the multinucleated cell stage induced by stimulation with receptor activator of nuclear factor kappa B ligand (RANKL). This finding eventually led us to the identification of NFATc1 as a key regulator of osteoclastogenesis. We subsequently confirmed the cell density-dependent suppression of osteoclastogenesis in a bone marrow cell system, and extended the analysis further. In comparative analysis of conditioned medium from high and low cell density cultures, we noticed the indispensability of L-serine (L-Ser), one of seven non-essential amino acids in culture medium, as a pivotal factor for the expression of NFATc1 induced by RANKL. Namely, culture at high cell density caused a depletion of L-Ser in the medium. The level of NFATc1 protein was found to be correlated with the presence of L-Ser in a concentration dependent manner. In contrast, D-Ser, an enantiomer of L-Ser, showed no NFATc1-inducing activity. We further examined the effect of L-Ser depletion on the upstream events of NFATc1 induction after RANKL stimulation. It was observed that, in the absence of L-Ser, activation of MAPK pathways and c-Fos induction triggered by RANKL stimulation were also hampered. L-Ser was subsequently found to be necessary for the expression of RANK, the receptor for RANKL. In the absence of L-Ser, the expression of RANK protein was decreased to undetectable level within 8 hours. The level of *rank* mRNA was suppressed in bone marrow cells under L-Ser depleted condition, whereas downregulation of *rank* mRNA was not evident in RAW264 cells. Furthermore, forced expression of RANK as well as NFATc1 using retrovirus vectors could compensate for the depletion of L-Ser and resume the progression to the multinucleated cell stage. These results demonstrate a novel but crucial role for L-Ser that as a prerequisite factor for RANKL-induced osteoclastogenesis *in vitro*.

**Disclosures:** T. Ogawa, None.

## SA083

See Friday Plenary number F083.

## SA084

**Pyrophosphates Stimulates Osteoclast Differentiation and Bone Resorption.** S. Abdelmagid\*, A. Zajac\*, I. Salhab\*, H. Nah. Plastic and Reconstructive Surgery, Children Hospital of Philadelphia, Philadelphia, PA, USA.

Cranio metaphyseal dysplasia (CMD) is a rare disease characterized by overgrowth of facial and cranial bones and abnormal flaring of metaphyses of long bones. Although the skeletal phenotype suggests that the bone remodeling process may be dysregulated in CMD, the cellular mechanisms underlying the CMD phenotype is not known. The autosomal dominant form of CMD has recently been linked to loss of function mutations in ANKH, a transmembrane protein involved in the transport of pyrophosphate (PPi). Therefore, in this study we determined the effect of PPi on bone remodeling, using *ex vivo* murine neonatal calvarial organ and bone marrow cell cultures. Our data show that exogenous PPi (0.1-1mM) stimulates a calcium release in the media of calvarial organ cultures maintained for 3 days (p<0.05) and TRAP staining of calvarial bones (p<0.01) in a dose-dependent manner, indicating that PPi stimulates bone resorption by osteoclasts. The PPi effect on bone resorption was not inhibited by either alkaline phosphatase inhibitor (Levamisole) or Pi transport inhibitor (PFA), indicating that the effect of PPi on bone resorption is not dependent on inorganic phosphates hydrolyzed from PPi. On the other hand, PPi stimulation of calcium release was abolished by an NFkB inhibitor, indicating that the PPi effect on bone resorption is NFkB-dependent. Cell culture data show that PPi also stimulates proliferation of bone marrow-derived osteoclast precursors (p<0.01) and RAW 264.7 pre-osteoclast cell line (p<0.01) in a dose-dependent manner. Nevertheless, PPi alone was not able to induce differentiation of bone marrow-derived pre-osteoclasts. Instead, pretreatment for 48 hours with PPi (0.1-1mM) accelerated differentiation of the osteoclast precursors under a differentiation permissive condition, as measured by cell TRAP activity (p<0.01), number of TRAP positive osteoclasts (p<0.05), and nuclei fusion index (p<0.05), suggesting that PPi enhances the differentiation potential of pre-osteoclasts. Taken together, our data suggest that PPi stimulation of bone resorption in calvarial organ cultures may be mediated in part by its priming effect on pre-osteoclasts for cell differentiation.

**Disclosures:** S. Abdelmagid, None.

## SA085

See Friday Plenary number F085.

## SA086

**Inhibin Directly Targets Suppression of Isolated Human Osteoclast Precursor Development and Activity.** K. M. Nicks, N. S. Akel\*, L. J. Suva, D. Gaddy. Physiology and Biophysics & Orthopaedic Surgery, University of Arkansas for Medical Sciences, Little Rock, AR, USA.

Serum Inhibin A (InhA) is a better predictor of bone formation and resorption markers than either follicle stimulating hormone (FSH) or bioavailable E2 in premenopausal women. Regardless of changes in sex steroids or FSH, increased bone turnover markers correlate with decreased serum InhA and InhB levels in pre-, peri-, and post-menopausal women, consistent with our *in vitro* demonstration that Inh suppresses osteoblast development of hMSCs and OCL development of human peripheral blood mononuclear cells (hPBMCs). To determine if InhA suppression of osteoclastogenesis is mediated by direct effects on OCL precursors, OCL cultures of either unselected hPBMCs, or a sub-population of OCL precursor cells (purified CD14+ hPBMCs) and treated with RANKL, mCSF +/- InhA and/or FSH were initiated. In cultured CD14+ OCL precursors, FSH significantly increased RANKL-dependent OCL differentiation whereas InhA significantly suppressed OCL differentiation. However, in heterogeneous PBMCs, RANKL-dependent OCL differentiation was significantly inhibited by either InhA or FSH. The effect of InhA was significantly more potent than FSH. In both CD14+ and PBMC cultures, RANKL-induced OCL formation in response to InhA + FSH was not significantly different from InhA alone, demonstrating the dominant effect of InhA to block any FSH effect. Since InhA was found to directly target CD14+ OCL precursor development, cells were cultured on dentine slices to measure OCL activity. InhA treatment significantly decreased bone resorption and prevented OCL migration, even in the presence of FSH. The signaling receptors mediating InhA and FSH action were determined using immunofluorescence. CD14+ OCL cultures were initiated and harvested on days 1 and 7. RANK expression was observed on both days 1 and 7, unlike the FSH receptor and the Inhibin-specific receptor, betaglycan, which were not observed on day 1 of culture but were present by day 7. Also present at day 7 were Type II receptors for BMP and Activin (BMPRII, and ActRIIA, but not ActRIIB). These data suggest that isolated OCL precursor cells become capable of responding to both InhA and FSH only after RANKL initiation of OCL development. Although FSH can enhance OCL development when CD14+ precursors are cultured, InhA dominantly suppresses. In fact, InhA suppresses OCL development, migration and bone resorption in the presence or absence of FSH. Furthermore, in heterogeneous PBMC cultures, which represent a more physiological environment in which to test the integrated role of these hormones, the effect of InhA and FSH (alone or in combination) is to suppress OCL development and activity.

**Disclosures:** K. M. Nicks, None.

*This study received funding from: NIH R21-DK074024-A2 to DG; NIH F31 DK079362-01A1 to KMN.*

**SA087****See Friday Plenary number F087.****SA088**

**RANKL-mediated Osteoclast Lineage Commitment Dictates the Role of Lipopolysaccharides in Osteoclast Differentiation.** J. Liu<sup>\*1</sup>, S. M. Michalek<sup>\*2</sup>, X. Feng<sup>1</sup>. <sup>1</sup>Pathology, Univ. of Alabama at Birmingham, Birmingham, AL, USA, <sup>2</sup>Microbiology, Univ. of Alabama at Birmingham, Birmingham, AL, USA.

Lipopolysaccharides (LPS), common bacteria-derived products, are recognized as a key factor implicated in periodontal bone loss. However, the role of LPS in osteoclast (OC) formation still remains controversial. The prevailing view is that LPS stimulate OC formation, which is not only supported by various contemporaneous studies, and yet consistent with the role that LPS are presumed to play in periodontal bone loss. Two groups, however, have shown that LPS play an inhibitory role in OC formation. Here, we carried out independent and thorough studies to address the controversy. We treated primary bone marrow macrophages (BMMs) from 6-week-old mice with M-CSF (44ng/ml) and different doses of LPS (5ng/ml-10ug/ml). Our data indicate that LPS and M-CSF are unable to stimulate OC formation. Next, we determined whether LPS can promote OC formation in the presence of M-CSF (44ng/ml) and RANKL (100ng/ml). In doing so, we added LPS at the beginning of the assays. We found that LPS inhibit OC formation in a dose-dependent manner (>95% at 5ng/ml) in the presence of M-CSF (44ng/ml) and RANKL (100ng/ml). However, when we treat BMMs with M-CSF (44ng/ml) and RANKL (100ng/ml) for as short as 12 hrs, LPS promoted OC formation from these committed BMMs in the presence of M-CSF and RANKL. Moreover, we found that LPS and M-CSF, without RANKL, are sufficient to promote OC formation from the RANKL-primed BMMs. Together, these findings support that RANKL-mediated OC lineage commitment dictates the role of LPS in OC formation. To further address the issue, we treated BMMs with M-CSF (44ng/ml) and RANKL (100ng/ml) for 24hrs. We then removed RANKL and cultured the cells with M-CSF alone (44ng/ml) for 12hrs, 24hrs, 2d and 3d. At each time point, BMMs were lifted and re-plated to perform OC formation assays with M-CSF, RANKL and LPS. Even 3d after the RANKL pretreatment, BMMs are still able to form OC in response to M-CSF, RANKL and LPS, revealing that the OC lineage commitment by RANKL is long-term, not transient. Finally, given that osteoblasts are indirectly involved in LPS-mediated OC formation by producing RANKL in response to LPS, we investigated the role of LPS in OC formation in co-culture system containing osteoblasts and BMMs pretreated by RANKL (100ng/ml) for 24hrs or untreated BMMs as control. The co-cultures were treated with or without LPS (10ng/ml). While the co-cultures containing committed BMMs formed OC in response to LPS, control co-cultures failed to do so. These results further support that RANKL-mediated OC lineage commitment determines the action of LPS in OC formation.

**Disclosures:** J. Liu, None.

**SA089****See Friday Plenary number F089.****SA090**

**S100 Protein Directly and Indirectly Affects RANKL-stimulated Osteoclastogenesis.** T. Yoshida, A. Flegler<sup>\*</sup>, P. H. Stern. Department of Molecular Pharmacology and Biological Chemistry, Northwestern University Feinberg School of Medicine, Chicago, IL, USA.

Diabetic osteopenia is one of the complications associated with Diabetes Mellitus, and Advanced Glycation Endproducts (AGEs) are thought to be involved in this disease. It was also reported recently that the expression of S100A4 protein, one of the ligands for receptor of AGEs (RAGE), is regulated in the course of osteoblast differentiation and this regulation is crucial for normal differentiation. However, it is still unclear how S100 protein affects bone metabolism. We were therefore interested in determining how S100 protein affects RANKL-stimulated osteoclastogenesis, either directly or indirectly through cytokines secreted from osteoblasts.

We first determined whether there was a direct effect of S100 on osteoblast proliferation and osteoclastogenesis. Studies were carried out with MC3T3-E1 pre-osteoblastic cells and RAW 264.7 mouse monocyte/macrophage lineage cells, which differentiate into multinucleated mature osteoclasts in the presence of receptor activator of nuclear factor- $\kappa$ B ligand (RANKL). MC3T3-E1 cells were incubated for 3, 7 or 14 days and proliferation rate was determined by MTT assay. S100 significantly inhibited osteoblast proliferation at day 14 but not at the shorter time points. RAW 264.7 cells were incubated for 7 days with human soluble RANKL (sRANKL) and tartrate resistant acid phosphatase (TRAP) activity and TRAP-positive multinucleated cells were measured as markers of osteoclastic differentiation. Osteoclastic differentiation was significantly inhibited by S100. Proliferation, as assessed by MTT assay, was also decreased by S100. There was a trend towards a decrease in the number of TRAP-positive multinucleated cells, but this was not statistically significant. We then determined whether S100 protein could affect osteoclastogenesis indirectly, i.e., through altering osteoblastic secretion of a stimulator of osteoclast differentiation such as RANKL, M-CSF, or the ligand of osteoclast-associated receptor (OSCAR). MC3T3-E1 cells were incubated with or without S100 for up to 15 days. Culture medium was then changed to medium without S100 and incubated with the MC3T3-E1 cells for an additional 6h. This medium was used for treatment of the RAW

cells. Unexpectedly, media from S100 treated MC3T3-E1 cells significantly promoted the proliferation of RAW cells, but no indirect effect on differentiation was seen. Thus, osteoclastogenesis could be regulated directly and indirectly by S100, possibly secreted from osteoblasts by an autocrine process to regulate osteoclastogenesis, and this regulation might be involved in the progression of diabetic osteopenia.

**Disclosures:** T. Yoshida, None.

*This study received funding from: Manpei Suzuki Diabetes Foundation.*

**SA091****See Friday Plenary number F091.****SA092**

**Neutrophil-Like PLB-985 Cells Induce Differentiation of Human Blood Monocytic Precursors into Functional Osteoclasts via a Receptor Activator of NF $\kappa$ B ligand (RANKL)-Dependent Mechanism.** A. Chakravarti<sup>\*</sup>, P. E. Poubelle. Medicine, Université Laval, Québec, QC, Canada.

Focal bone loss in the inflammatory arthritides begins early in the disease process and can contribute to patient morbidity. This excessive bone resorption is due to increased activity of osteoclasts that require receptor activator of NF- $\kappa$ B ligand (RANKL) to function. Neutrophils are the predominant infiltrating cells at this stage. Though neutrophil presence is linked to disease severity, their role in the evolution of bony lesions is not clear. In the present study we used human myeloid cell line PLB-985, which can be induced to express a neutrophil-like phenotype, as a model for study of neutrophil-osteoclast interactions. We demonstrated that these neutrophil-like cells directly activate osteoclasts through RANKL expressed on the surface of PLB-985 cells. *In vitro* co-culture of human pre-osteoclasts, derived from circulating monocytes, with fixed PLB-985 cells induced differentiation of mononuclear osteoclast precursors into large multinucleated cells. These multinucleated cells were positive for the osteoclast specific enzymatic marker, tartrate-resistant acid phosphatase. Importantly, when co-cultures were conducted on devitalized dentine slices, well-defined bone resorption pits were observed after toluidine blue treatment. Thus, the neutrophil-like cells stimulated resorptive activity in mature osteoclasts. Gene knockdown of RANKL following nucleofection of RANKL specific siRNA in PLB-985 cells effectively diminished RANKL RNA, as seen by QRT-PCR, and surface protein expression evaluated by flowcytometric analysis. Induction of osteoclast differentiation and activity was also significantly diminished in co-culture assays of osteoclasts with transfected PLB cells, proving that PLB-derived RANKL was specifically responsible for the stimulation of osteoclasts. In conclusion, we propose that neutrophil-derived RANKL might have an important role, not only in the inflammatory component of the arthritides, but also in the early skeletal involvement that characterizes these conditions. Our work is the first to demonstrate functional interactions between the two cell types: neutrophil and the osteoclast.

**Disclosures:** A. Chakravarti, None.

*This study received funding from: CIHR/IRSC.*

**SA093****See Friday Plenary number F093.**

## SA094

**Effect of Mesenchymal Stem Cells in Coculture with Osteoclasts: A Contact Mediated and Dose-Dependent Effect?** C. Janeiro, D. Vashishth. Biomedical Engineering, Rensselaer Polytechnic Institute, Troy, NY, USA.

Osteoclasts, which are derived from stem cells, supply factors that positively influence the differentiation of osteoclast precursors to osteoclasts (OCLs) through signaling pathways [1]. However, the effect of mesenchymal stem cells (MSCs), which reside in bone marrow in close proximity to osteoclast precursors, has not been examined. To determine the mechanism, a set of experiments was devised to determine whether the effect is contact or signaling mediated.

Human adult osteoclast precursor cells and human mesenchymal stem cells (both from Cambrex Poietics™) were cocultured at varying densities (OCLs remained constant at 6000 cells/well, while MSCs were varied from 0-4200 cells/well) following supplier's instructions under standard cell culture conditions for up to 14 days, in standard 96 well plates (contact-mediated) and Transwell™ plates (signaling-mediated) alone and in the presence of bone slices. For each coculture variation, the number of differentiated OCLs and the resorption on the bone were analyzed. For each group, contact-mediated and signaling-mediated, the percent change in differentiated OCLs was calculated as a function of the positive control (OCL precursors only). Analysis of select cytokines was also examined.

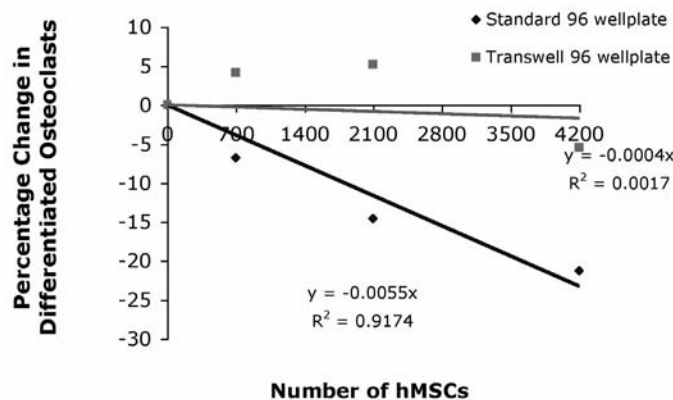
The percent change of differentiated OCLs decreased linearly with an increase in MSCs only when the cells were allowed contact (Fig 1). For the signaling mediated group, the percentage of differentiated OCLs remained steady throughout the variation of MSC number. The only cytokine that has yielded significant results was TNF- $\alpha$ , displaying a decrease in TNF- $\alpha$  with the addition of OCLs.

These results demonstrate a clear difference between contact mediated and signaling mediated cocultures of OCLs and MSCs. The increase in the number of OCLs with a decrease in MSC number suggests that the MSCs regulate the differentiation of OCLs from hematopoietic stem cells. These findings suggest the age-related decrease in MSC as a plausible mechanism of increased OCL differentiation with increased age.

1 Teitelbaum SL. Science 289:1504-8, 2000.

2 Koshihara Y *et al*, Mech Ageing Dev 123:1321-31, 1999.

3 Nishida S *et al*, J Bone Miner Metab 17:171-177, 1999.



**Disclosures:** C. Janeiro, None.

This study received funding from: NIH Grant AR049635

## SA095

**Gastric Proton Pump Inhibitors Failed to Affect Bone Resorption and Formation.** T. Nishisho\*<sup>1</sup>, L. Wang\*<sup>1</sup>, K. Hata<sup>1</sup>, M. Nakanishi\*<sup>1</sup>, N. Yasui\*<sup>2</sup>, T. Yoneda<sup>1</sup>. <sup>1</sup>Dept Biochem, Osaka Univ Grad Sch Dent, Suita, Osaka, Japan, <sup>2</sup>Dept Orthop, Univ Tokushima Grad Sch Med, Tokushima, Japan.

Osteoclasts dissolve bone minerals by releasing protons through the vacuolar type proton pump (V-ATPase), making neighboring microenvironments acidic. Inhibitors of the V-ATPase therefore could be pharmacological agents for bone diseases associated with increased osteoclastic bone resorption. On the other hand, a gastric H<sup>+</sup>, K<sup>+</sup>-ATPase, a family member of the P-ATPase, is highly expressed in parietal cells in stomach and plays central roles in gastric acid secretion. Inhibitors of H<sup>+</sup>, K<sup>+</sup>-ATPase are the most widely used drug for the treatment of gastric ulcer, duodenal ulcer and gastroesophageal reflux disease. Of note, a recent clinical study has reported that administration of gastric H<sup>+</sup>, K<sup>+</sup>-ATPase inhibitors are associated with reduced bone mass and increased fracture rate, raising the possibility that these inhibitors promote osteopenia. However, these studies remain controversial and the effects of H<sup>+</sup>, K<sup>+</sup>-ATPase inhibitors on bone have not been fully elucidated. In the present study, we investigated the effects of the gastric H<sup>+</sup>, K<sup>+</sup>-ATPase inhibitors (PPIs) on bone resorption and formation *in vitro* and *in vivo*. To study this, we tested widely-used PPI, rabeprazole and omeprazole. As control we also examined the effects of FR167356, a specific inhibitor for the  $\alpha 3$  V-ATPase. Mouse spleen cells were cultured in the presence of M-CSF (30ng/ml) and sRANKL (100ng/ml) for 6 days together with these inhibitors. Tartrate-resistant acid phosphatase-positive multinucleated osteoclast-like cell (TRAP (+) OC) formation and pit formation on dentin slices were inhibited by FR167356 (10<sup>-8</sup>M-10<sup>-6</sup>M) in a dose-dependent manner. In contrast, rabeprazole and omeprazole (10<sup>-8</sup>M-10<sup>-6</sup>M) showed no effects on TRAP (+) OC formation and bone resorption. Histological examination revealed that rabeprazole and omeprazole failed to inhibit osteoclastic bone resorption in the calvariae in the mouse model of

lipopolysaccharide-induced bone destruction. We next examined whether these inhibitors affect bone formation. Both rabeprazole and omeprazole had no effects on BMP2-induced osteoblast differentiation in C3H10T1/2 and C2C12 cells determined by alkaline phosphatase activity. Moreover, no significant effects were observed in the mineralization of primary neonatal mouse calvarial osteoblasts. In conclusion, our results show that PPIs have little direct influences on bone and suggest that yet-unknown mechanism is involved in the pathogenesis of osteopenia in PPI-treated individuals.

**Disclosures:** T. Nishisho, None.

## SA096

**Urocortin Strongly Suppresses the Formation and Function of Osteoclasts via a Novel Mechanism.** C. E. Combs\*<sup>1</sup>, K. Fuller, T. J. Chambers, K. M. Lawrence\*. Department of Histopathology, St George's Hospital Medical School, London, United Kingdom.

Urocortin (Ucn) is a 40 amino acid peptide, related to the hypothalamic corticotrophin releasing factor (CRF) family which now also includes Ucn 2 and 3. Since its discovery Ucn has been found to be widely distributed in the CNS, digestive, cardiovascular, reproductive, immune and endocrine systems. It has extremely diverse functions including reducing blood pressure in the cardiovascular system and decreasing appetite in the CNS. Recently, it has been implicated as a modulator of the immune/inflammatory system. Of particular interest, Ucn has been shown to be increased in the synovial fluid of patients with rheumatoid arthritis, and reduces inflammation and bone erosion in a mouse model of the disease. Beyond this, nothing is known of the role of Ucn in the pathobiology of bone. We therefore tested the effect of Ucn on osteoclast formation and function. Ucn showed a dose-dependent inhibition of the number of osteoclast-like cells (Ocl) formed when murine non-adherent bone marrow cells were incubated with RANKL and MCSF. We then tested the effect of Ucn on osteoclast function. To do this, *in vitro* derived Ocl were sedimented onto bone slices, and incubated with/without Ucn. We found strong suppression of bone resorption. To confirm that this was a distinct effect on osteoclastic function rather than formation, we tested the effect of Ucn on actin ring formation. Ucn similarly potently suppressed the formation of actin rings in osteoclasts, in a dose-dependent manner, with 50% inhibition of actin ring formation occurring at 5x10<sup>-9</sup>M, and almost complete inhibition at 10<sup>-7</sup>M.

It is known that activation of CRFR1 or R2 by Ucn results in elevation of either cAMP via Gs, or of IP3/diacylglycerol via Gq. We assessed expression of Ucn and its receptors in bone cells using semi-quantitative RT-PCR. We found that although osteoclasts, macrophages and osteoblasts do not express any of the known CRF receptor subtypes, osteoclasts and macrophages both express Ucn itself. The absence of known receptor types was supported by experiments in which we found that a receptor-antagonist did not block the effects of Ucn on Ocl function or formation. Furthermore, Ucn failed to generate production of either cAMP or cGMP in these cells, and selective PKA/PKC inhibitors did not suppress the anti-resorptive effect of Ucn. We did however note, using confocal microscopy, a rapid intracellular calcium transient in osteoclasts. We conclude that Ucn potently inhibits osteoclasts via a mechanism independent of known CRF receptors. Expression of Ucn by bone cells raises the possibility that it may play an autocrine/paracrine role in the pathophysiology of bone.

**Disclosures:** C.E. Combs, None.

## SA097

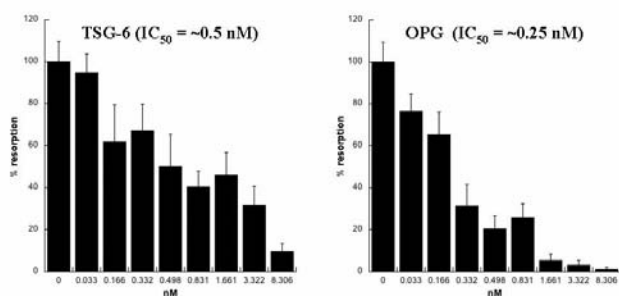
**TSG-6 Acts Synergistically with OPG to Inhibit Bone Resorption.** D. Mahoney\*<sup>1</sup>, C. M. Milner\*<sup>2</sup>, A. J. Day\*<sup>2</sup>, A. Sabokbar<sup>1</sup>. <sup>1</sup>Botnar Research Centre, University of Oxford, Oxford, United Kingdom, <sup>2</sup>Faculty of Life Sciences, University of Manchester, Manchester, United Kingdom.

TSG-6 (TNF-stimulated gene-6) is a 35-kDa protein, composed almost entirely of Link and CUB\_C domains, that is up-regulated by inflammatory mediators (e.g. TNF, IL-1). To date a wide variety of protein and glycosaminoglycan ligands (e.g. hyaluronan, heparin, bikunin, pentraxin-3 and thrombospondin-1) have been identified as associating with the Link module, whereas only fibronectin has been found to bind to the CUB\_C region. Animal models of arthritic disease have indicated that TSG-6 has anti-inflammatory and chondroprotective properties. We have recently demonstrated that recombinant TSG-6 inhibits RANKL-mediated bone resorption by osteoclasts (Mahoney *et al.*, manuscript submitted). The full-length protein had greater inhibitory activity compared to the isolated Link module and the CUB\_C domain was essentially inactive. Furthermore, binding analyses revealed that TSG-6 interacts directly with sRANKL, probably at a composite binding surface involving both the Link and CUB\_C domains. To further understand the role of TSG-6 as an inhibitor of bone resorption, we sought to (i) compare the potency of TSG-6 to that of OPG and (ii) determine whether TSG-6 can act synergistically with OPG in inhibiting RANKL-mediated osteoclastic bone resorption.

*In vitro* assays revealed that TSG-6 inhibited RANKL-induced resorption in a dose-dependent fashion, in a similar manner to that observed for OPG; the IC50 of full-length TSG-6 was 0.5nM as compared to 0.25nM for OPG. Furthermore, we have demonstrated that a combination of TSG-6 and OPG significantly inhibited the RANKL-mediated resorption compared to treatment with each protein alone.

These findings indicate that TSG-6 can act synergistically with OPG and as such TSG-6 could have therapeutic potential for the treatment of osteolytic bone disorders.

Figure 1



**Disclosures:** A. Sabokbar, None.

This study received funding from: Arthritis Rheumatism Campaign.

## SA098

See Friday Plenary number F098.

## SA099

**Proteasome Inhibitors Attenuate Osteoclastogenesis and Bone Resorption via the Modulation of RANK-mediated TRAF6, p62 and I $\kappa$ B- $\alpha$  Signaling Cascades.** E. S. Ang<sup>\*1</sup>, N. Pavlos<sup>1</sup>, T. Chai<sup>\*1</sup>, K. Yip<sup>\*1</sup>, S. Rea<sup>\*2</sup>, T. Ratajczak<sup>\*3</sup>, M. Zheng<sup>1</sup>, J. Xu<sup>1</sup>. <sup>1</sup>Centre for Orthopaedic Research, The University of Western Australia, Nedlands, WA, Australia, <sup>2</sup>Western Australia Institute for Medical Research, The University of Western Australia, Nedlands, WA, Australia, <sup>3</sup>Western Australia Institute for Medical Research, The University of Western Australia, Nedlands, WA, Australia.

Enhanced osteoclast formation and activation becomes manifest in many pathological osteolytic conditions including osteoporosis, Paget's disease and tumor metastasis to bone. Proteasome-mediated pathways regulate diverse signaling cascades that play fundamental roles in cell differentiation and apoptosis. However, the molecular mechanism(s) by which the proteasome pathway regulates osteoclast formation, bone resorption and its potential impact on RANKL-mediated signaling remains to be elucidated.

Using both primary bone marrow monocytes (BMMs) and RAW264.7 cell osteoclastogenic culture systems, we examined the effects of several proteasome inhibitors on osteoclast formation. In addition, we employed bone resorption assays and confocal microscopy to determine the effect(s) of proteasome inhibitors on the function and cytoskeletal architecture of osteoclasts. Immunoblot and immunoprecipitation analyses together with luciferase reporter gene assays and immunocytochemistry were used to dissect the molecular mechanism(s) underlying the observed effects of proteasome inhibitors on NF- $\kappa$ B, I $\kappa$ B $\alpha$ , p62 and TRAF6.

We demonstrate that proteasome inhibitors MG-132, MG-115 and Epoxomicin dose-dependently attenuate RANKL-induced osteoclastogenesis, with relative potency Epoxomicin > MG-132 > MG-115 based on the equi-molar concentrations. At high concentrations, proteasome inhibitors were found to induce cellular apoptosis and disrupt F-actin and microtubule organization in osteoclasts. Epoxomicin potently inhibited bone resorption by both BMM-derived osteoclasts and human osteoclast-like cells derived from giant cell tumors of bone. The same proteasome inhibitors were also found to effectively block RANKL-induced NF- $\kappa$ B activation, as well as prolong the proteasome-mediated degradation and targeting of I $\kappa$ B $\alpha$ , p62 and TRAF6.

Collectively, our findings demonstrate that proteasome inhibitors perturb osteoclast formation and function by influencing key RANK-mediated signaling cascades (I $\kappa$ B- $\alpha$ , p62 and TRAF6). We propose that selective proteasome inhibitors might offer potential therapeutic value for the treatment of osteoclast-mediated bone diseases.

**Disclosures:** E.S. Ang, None.

This study received funding from: National Health and Medical Research Council.

## SA100

**Resorption Mechanism of Hydroxyapatite and  $\beta$ -Tricalcium Phosphate Coating Layer.** D. Lee<sup>\*</sup>, K. Lee<sup>\*</sup>, J. Kim<sup>\*</sup>, C. Lee<sup>\*</sup>, J. Chang<sup>\*</sup>. Orthopaedic Surgery, Asan Medical Center, Seoul, Republic of Korea.

Beta-tricalcium phosphate ( $\beta$ -TCP) coating layer is known to be resorbed much faster than hydroxyapatite (HA), however, there has been no report to explain the exact reason of that to our knowledge. Therefore, we investigated whether the resorption mechanisms of these two compounds are same, if not, what is the difference. Eighty titanium discs with 12mm in diameter and 2mm in thickness were coated with HA(n=40) or  $\beta$ -TCP(n=40) by dip and spin coating method. In each group, the specimens into 2 subgroups respectively; Dissolution (D, n=20) and Osteoclast culture (C, n=20). The coated discs in D group were immersed in the cell culture media for 5 days, whereas, in C group, osteoclast-like cells ( $5 \times 10^3$  cells/500 $\mu$ l), which were isolated from human giant cell tumor, were seeded on the specimens and cultured for 5 days. Cultured cells were defined as osteoclast by the determination of osteoclast marker (tartarate-resistant acid phosphatase, TRAP). After immersion or osteoclast culture, the dissolution characteristics of coating layer surface were observed using light microscope (LM) and scanning electron microscope (SEM). In HA-C and  $\beta$ -TCP-C groups, area fraction of resorption lacunae formed by osteoclast was analysed by image analysis to evaluate the activity of osteoclastic degradation. After dissolution test,  $\beta$ -TCP coating layer showed much more cracks and denudation as compared to HA coating layer. In C group, the osteoclasts covering the coating layer were identified on LM and SEM images. Mean area fraction of resorption lacunae in HA-C group was 11.62%, which was significantly higher than that of 0.73% in  $\beta$ -TCP-C group (p=0.001). The resorption mechanisms of HA and  $\beta$ -TCP coating layers were different each other *in vitro* study. The coated  $\beta$ -TCP was degraded mainly by dissolution and separation from implant, on the other hand, the HA coating layer was resorbed by osteoclastic activity.

**Disclosures:** D. Lee, None.

## SA101

**Human OsteoProgenitor Cell Adhesion and Spreading on Functionalized Titanium Surfaces Followed by Quartz Crystal Resonators (QCM) and Confocal Laser Scanning Microscopy (CLSM).** D. Le Guillou-Buffello<sup>\*1</sup>, R. Bareille<sup>\*2</sup>, M. Gindre<sup>\*3</sup>, A. Sewing<sup>\*4</sup>, P. Laugier<sup>\*3</sup>, J. Amedee<sup>2</sup>. <sup>1</sup>CNRS UMR7623, Paris, France, <sup>2</sup>INSERM Unité 577, Bordeaux, France, <sup>3</sup>CNRS UMR 7623, Paris, France, <sup>4</sup>Biomat Deutschland GmbH, Berlin, Germany.

The surface characteristics of endosseous implant such as titanium-based biomaterials control considerably the cellular response and subsequently the quality and the quantity of new-formed bone around the implant. A variety of invasive methods exist for quantifying cell adhesion to a potential biomaterial surface (direct counting of labelled cells after fixing or enzymatic detachment, focal contact imaging by confocal microscopy or CLSM). The quartz crystal microbalance (QCM) technique is an attractive *in vitro* method for real-time characterization of initial cell adhesion with no need for destructive interventions.

The aim of this paper is to monitor cell adhesion under well defined conditions of medium without serum, on different titanium coatings (hydroxyapatite functionalized or not with RGD-containing peptides) on cell adhesion by QCM and to complete these data by using conventional methods such as immunolabelling of vinculin and actin.

Human OsteoProgenitor (HOP) cells were then seeded at a cell density of 12,500 cells/cm<sup>2</sup> and cultured on titanium surfaces, functionalized with hydroxyapatite (Ti-HA), type I collagen (Ti-Coll) or with RGD-containing for different times varying from 1 to 3h. Surfaces with adherent cells were then dedicated to quartz crystal resonator experiments. Impedance measurement is also expressed as a percentage of adherent cells to uncoated Ti quartz crystal resonator which was used as control. In parallel, we examine the intracellular distribution of F-actin and vinculin by CLSM for the imaging of focal contact formation. Data obtained by quartz crystal resonator technique revealed that RGD-containing peptides alone, increase HOP cell adhesion in early time period of culture. Moreover, association of RGD-containing peptides with either type I collagen or with HA layers induces an additive effect on HOP cell adhesion compared to Ti-Coll or Ti-HA. By CLSM, both the area of contact focal by cell unit and the cytoskeleton network organization, differed according to the surfaces. Interestingly, association of RGD-containing peptides with HA layers induces an additive effect on focal contact formation on HOP cells compared to Ti-HA alone. These data confirm that RGD peptide effect occurs in the early time of culture, provides a benefit for osteoblast to spread, differentiate and survive.

**Disclosures:** J. Amedee, None.

## SA102

**In vivo Bone Matrix Density Measurements by Water and Fat Suppressed Projection MRI (WASPI).** Y. Wu<sup>1</sup>, J. L. Ackerman<sup>\*2</sup>, H. Cao<sup>\*1</sup>, T. G. Reese<sup>\*2</sup>, M. I. Hrovat<sup>\*3</sup>, M. J. Glimcher<sup>1</sup>. <sup>1</sup>Orthopaedic Surgery, Children's Hospital, Boston, MA, USA, <sup>2</sup>Radiology, Massachusetts General Hospital, Boston, MA, USA, <sup>3</sup>Mirtech, Inc, Brockton, MA, USA.

Bone matrix density plays a significant role in the mechanical and physiological properties of bone substance, as exemplified by the critical role in defining the diagnosis of metabolic bone diseases.

Currently available X-ray based bone densitometry provides only bone mineral density. In conventional MRI, solid bone is not visible due to very short T2 relaxation time.

Water and fat suppressed proton projection MRI (WASPI) has been recently developed to suppress the dominating long T2 signal (water and fat) while preserving the short T2 signal of solid bone and other molecularly immobile substances of the matrix.

A volume transmit/receive MRI coil was built on a Teflon tube (to eliminate proton background signals) to image the ankle of pigs. A very fast crossed-diodes T/R switch and a receiver dead time of 10 micro-s were utilized to detect short T2 signal.

Yorkshire pigs 2-3 months old were scanned with WASPI and conventional gradient echo MRI in a Siemens Trio 3T system while under anesthesia, with the right rear foot inside the coil. Three polymer pellets of different densities were taped on the skin of the foot, serving as calibration phantoms. Fig. 1 shows a coronal view of conventional MRI with slice thickness 3 mm and in plane resolution 1 mm. The muscle, marrow and fat are clearly visible, while the bone is dark and the polymer pellets cannot be seen. Fig. 2 shows a coronal view of WASPI of the same portion of the foot with an isotropic resolution of 2.4 mm. The total 3D imaging time was 27 min. The cortical bone of phalanges and the polymer pellet are bright, while the muscle, marrow and fat signals are suppressed to background levels.



Fig 1. Conventional MRI of the foot of a 2-month-old pig. Solid bone matrix and polymer pellets of the calibration phantom do not yield MR signal.

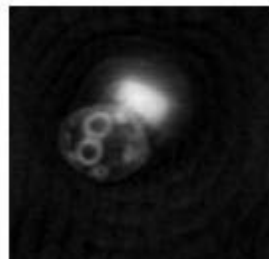


Fig 2. WASPI of the same pig. Cortical bone tissue and the polymer pellets are visualized and the soft tissue signal is suppressed.

This study demonstrates that *in vivo* WASPI measurement is feasible. We showed in a previous *in vitro* study that the WASPI intensity correlates highly with gravimetric and amino acid analysis of matrix density. We therefore anticipate that quantitative bone matrix density measurement by WASPI will be possible.

**Disclosures:** Y. Wu, None.

This study received funding from: NIH/NIBIB.

## SA103

See Friday Plenary number F103.

## SA104

**The Use of Endothelial Progenitor Cells to Promote Bone Healing: Preliminary Results from a Rat Model Study.** K. Atesok<sup>\*</sup>, R. Li<sup>\*</sup>, E. H. Schemitsch<sup>\*</sup>. Division of Orthopaedics, St. Michael's Hospital, Toronto, ON, Canada.

Vascular in growth is an essential and critical mechanism in fracture healing. Endothelial Progenitor Cells (EPCs) have been proven to contribute to repair of injured endothelium and formation of new blood vessels.

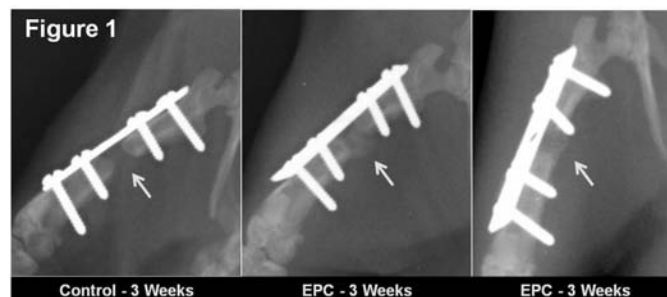
We hypothesize that local EPC therapy will enhance angiogenesis at the fracture site and this in turn will promote bone healing by increasing osteogenesis and callus formation.

The purpose of this study is to determine the role of EPCs in bone regeneration and to evaluate the effectiveness of local EPC therapy to accelerate fracture repair.

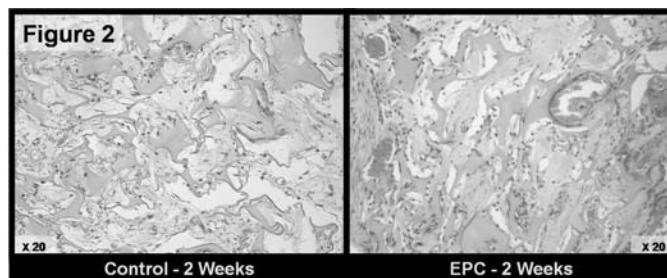
Rat bone marrow EPCs were isolated and cultured for 7 to 10 days. A segmental bone defect (4mm.) was created in rat femur diaphysis and stabilized with mini plate. A gelfoam carrier impregnated with a solution of EPCs ( $1 \times 10^6$ ) was placed into the fracture gap. Control animals were applied only gelfoam with saline but no cells. Ten rats were included in this pilot study. The rats were divided into two groups. Two control and 3 EPC treated rats were included in each group. Animals in Group 1 and Group 2 were sacrificed 2 weeks and 3 weeks after the procedure respectively. Plain radiographs of the operated femur were taken before sacrifice to verify callus formation and the specimens from the fracture gap were collected for histological evaluation.

Radiological evidence of bone regeneration was remarkable in EPC treated animals both in

2 weeks and 3 weeks compared to control animals where no signs of callus formation was observed at the osteotomy site (Fig. 1).



Histological evaluation revealed that the specimens from EPC treated animals had abundant osteoid islands contained predominantly osteoblasts and osteoclasts with more blood vessels in both groups. Conversely, the specimens from control animals were sparsely ossified with markedly less bone cells and vessels (Fig. 2).



We conclude that the preliminary data from this study encourages the further investigation of EPCs as a potential therapy to promote bone healing.

**Disclosures:** K. Atesok, None.

This study received funding from: OTC-AI0D.

## SA105

**Nanotechnological Scaffold with Combination of Prostaglandin E<sub>2</sub> Receptor EP4 Agonist and rhBMP2, Enhances Bone Repair in the Defect of Mouse Calvarium Bone.** P. Kamolratanakul<sup>\*1</sup>, A. Kawamata<sup>\*1</sup>, Y. Yamamoto<sup>\*2</sup>, Y. Ezura<sup>\*1</sup>, K. Akiyoshi<sup>\*2</sup>, T. Amagasa<sup>\*3</sup>, M. Noda<sup>1</sup>. <sup>1</sup>Tokyo Medical and Dental University, Molecular Pharmacology, Medical Research Institute, Tokyo, Japan, <sup>2</sup>Tokyo Medical and Dental University, Institute of Biomaterials and Bioengineering, Tokyo, Japan, <sup>3</sup>Tokyo Medical and Dental University, Maxillofacial surgery, Tokyo, Japan.

Prostaglandin E<sub>2</sub> (PGE<sub>2</sub>) is known as an anabolic action on bone formation both in Vivo and in Vitro studies; however, side effect of severe diarrhea in animal was reported. The alternative way to work through PGE<sub>2</sub> effect is PGE<sub>2</sub> receptors, which are identified into 4 subtypes. EP4 is the only PGE<sub>2</sub> receptor subtype that was determined in bone and reported to mediate PGE<sub>2</sub>-induced anabolic action on bone formation. Nanogel scaffold provides effective drug-trapping and releasing. This study examined whether EP4 with nanogel scaffold carrier, can be performed to be a supplemental treatment for bone reconstruction. In 36 mice, defects were created by implant drill 3.75mm in diameter at parietal bone of mouse calvariae in present or absent of scaffold reconstruction, then after 4 weeks, mice were sacrificed. Treatment with nanogel scaffold in addition with EP4 agonist (EP4A) 100µg and/or rhBMP-2 at low dose (0.5 µg), radiographic investigation and CT analysis revealed that treated with EP4A 100µg or BMP 0.5µg, bone formation areas were not significantly different from nanogel-treated group. On the other hand, combination treatment with EP4A 100µg and BMP 0.5µg, bone formation areas were significantly increased about 50% more than non-supplementary nanogel-treated group (p<0.01). This data demonstrated that nanogel scaffold-in supplement of EP4A and BMP-2 combination enhances bone formation at defect site of mouse calvariae.

**Disclosures:** P. Kamolratanakul, None.

## SA106

**Calcifications in Children with Juvenile Dermatomyositis (JDM) Contain Several Bone Formation Markers.** A. L. Urganus<sup>\*</sup>, Y. Zhao, L. M. Pachman. Cellular and Molecular Pathobiology, Children's Memorial Research Center, Chicago, IL, USA.

Previous analysis of JDM calcifications confirmed the presence of osteopontin (OPN), bone sialoprotein (BSP), and osteonectin (ON) (western blot), and Fourier Transform Infrared (FTIR) spectroscopy documented a much higher mineral to matrix ratio than bone (Pachman, 2006). We hypothesize that the mechanism of JDM calcification differs from that of bone formation. The goal of this study was to determine the presence or absence of SIBLING, bone and apoptosis markers in the pathological calcifications. This study was approved by the Children's Memorial Hospital IRB, and age appropriate informed consent

was obtained. Calcification samples surgically removed from 4 different children with JDM with a long duration of JDM symptoms ( $36.9 \pm 48.3$  months) were stained for SIBLING members: OPN (full length, N- and C-terminal fragments), BSP, ON, dentin matrix protein 1 (DMP1), the dentin phosphoprotein (DPP) domain of dentin sialophosphoprotein (DSPP), matrix extracellular phosphoglycoprotein (MEPE); bone markers: osteocalcin (OCN), core binding factor alpha 1 (Cbfa1), and alkaline phosphatase (ALP); osteoclast marker: Tartrate resistant acid phosphatase (TRAP); apoptosis marker: poly(ADP-ribose) polymerase (PARP) and mineral regulator: matrix Gla protein (MGP). The following areas of the samples were examined for these markers: the center and periphery of the mineral deposits, adjacent connective tissue and vascular endothelial cells. In all 4 samples, BSP, DPP, DMP1, OPN (full length, N- and C- terminal fragments), and ALP were present within the deposits, connective tissue, and vascular endothelial cells, while MEPE was not detected in any of the samples. OCN and ON were present within mineral deposits and endothelial cells, while Cbfa1 was present in the deposits and connective tissue. PARP was observed within vascular endothelial cells and connective tissue, indicating cell death. MGP was detected in the deposits and endothelial cells. TRAP staining identified multinucleated cells, osteoclasts, which accumulated at the periphery of calcifications. In conclusion, the osteoclastic activity at the surface of calcifications appeared to represent an attempt to resolve these pathological calcifications. Cell death may contribute to the process of calcification. The calcifications share expression of BSP, DPP, DMP1, OPN, ON, OCN, ALP and Cbfa1 with bone, indicating a possible common mechanism between bone formation and calcification in JDM, despite the higher mineral to matrix ratio found in JDM calcifications.

**Disclosures:** A.L. Urganus, None.

This study received funding from: NIH.

## SA107

See Friday Plenary number F107.

## SA108

**Novel Screening System for Bone Matrix Proteins That Control Bone Mineralization.** H. Inoue<sup>\*1</sup>, T. Nakashima<sup>\*1</sup>, A. Iwamatsu<sup>\*2</sup>, A. Suematsu<sup>\*1</sup>, A. Yamaguchi<sup>3</sup>, H. Takayanagi<sup>1</sup>. <sup>1</sup>Department of Cell Signaling, Tokyo Medical and Dental University, Tokyo, Japan, <sup>2</sup>Protein Research Network, Inc., Yokohama, Japan, <sup>3</sup>Section of Oral Pathology, Tokyo Medical and Dental University, Tokyo, Japan.

Bone consists of many kinds of matrix proteins, which are considered to be important for bone formation and mineralization by serving as crystal nucleator and regulator of crystal growth. Although many bone matrix proteins have been identified and characterized so far, the detailed molecular function of the matrix proteins in bone mineralization is still unknown. In this study, for elucidating the molecular mechanism of bone mineralization, we have developed new method for screening bone matrix proteins responsible for the mineralization. After bone marrow and connective tissues were removed from mouse tibia and femur, bone matrix proteins were extracted with acetic acid and thereafter with guanidine chloride from these bones. After the bone matrix proteins were separated with SDS-PAGE, the gel was incubated with the phosphate buffer and thereafter with the calcium buffer for the in-gel mineralization. Some matrix proteins induced calcium phosphate formation, which was detected as red band by alizarin red staining. Dissection of the band with the strongest signal and the peptide mass fingerprinting analysis revealed that this band was identical with bone sialoprotein, which was previously reported to induce the nucleation of hydroxyapatite in vitro. This result suggests that our system is very effective for screening of the nucleators or inducers of calcium phosphate formation. Molecular mechanism of mineralization based on the functions of bone matrix proteins which are under investigation will be discussed.

**Disclosures:** H. Inoue, None.

## SA109

See Friday Plenary number F109.

## SA110

**Mineralization Is Related to Collagen Cross-links in Growing Cancellous and Cortical Bone.** N. M. B. K. Willems<sup>\*1</sup>, R. A. Bank<sup>\*2</sup>, L. Mulder<sup>\*3</sup>, G. E. J. Langenbach<sup>\*3</sup>, T. Grünheid<sup>\*4</sup>, A. Zentner<sup>\*4</sup>, T. M. G. J. van Eijden<sup>\*3</sup>. <sup>1</sup>Depts. of Orthodontics and Functional Anatomy, Academic Centre for Dentistry Amsterdam (ACTA), UvA and VU, Amsterdam, Netherlands, <sup>2</sup>Dept. of Oral Cell Biology, Academic Centre for Dentistry Amsterdam (ACTA), Amsterdam/TNO Quality of Life, Leiden, Netherlands, <sup>3</sup>Dept. of Functional Anatomy, Academic Centre for Dentistry Amsterdam (ACTA), Amsterdam, Netherlands, <sup>4</sup>Dept. of Orthodontics, Academic Centre for Dentistry Amsterdam (ACTA), Amsterdam, Netherlands.

**Introduction:** An examination of the age-related changes in bone mineral and collagen including its cross-links would extend the knowledge of their concomitant development. Moreover, it might improve our understanding of the processes of modeling and remodeling. **Materials and Methods:** Thirty-five pigs, aged between 0 and 100 weeks, were used for

analysis. Cancellous and cortical bone samples were obtained from areas near the center and near the poles, respectively. The degree of mineralization of bone (DMB) was determined in cancellous and cortical bone using microcomputed tomography. The amount of collagen and its mature cross-links hydroxylslypyridinoline (HP) and lysylpyridinoline (LP) were quantified using high-performance liquid chromatography. Correlation coefficients were calculated to determine significant age-related changes. Partial correlation coefficients between collagen parameters and DMB were obtained, controlling for age.

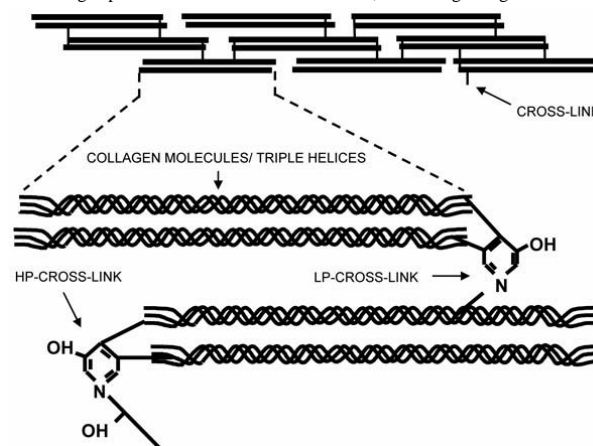


Fig.: Schematic figure of collagen molecules and their mature cross-links HP and LP.

**Results:** DMB increased with age in cancellous and cortical bone. The amount of collagen increased in cancellous bone, whereas no changes were observed in cortical bone. Moreover, the total number of the HP and LP cross-links decreased in cancellous bone only, because of the decrease found in HP. The number of LP cross-links decreased in cancellous and cortical bone after the age of 10 weeks. DMB and LP correlated significantly in cancellous and cortical bone ( $r = -0.55$  and  $-0.60$  respectively).

**Conclusions:** Bone collagen and mineralization are related during growth. The high turnover rate in cancellous bone might be responsible for the low number of the mature cross-links HP and LP. The high number of LP cross-links observed in the first weeks suggests LP plays an important role in the onset of bone mineralization.

**Disclosures:** N.M.B.K. Willems, None.

This study received funding from: Inter-University Research School of Dentistry (IOT).

## SA111

**AC-100 Promotes Cartilage Repair and Sub-Chondral Bone Healing In Surgically Induced Cartilage Defects.** C. A. Middleton-Hardie<sup>1</sup>, H. Aberman<sup>\*2</sup>, T. Simon<sup>\*2</sup>, R. C. Spiro<sup>3</sup>, B. Schnegelsberg<sup>1</sup>, D. M. Rosen<sup>1</sup>. <sup>1</sup>Research and Development, Acologix, Hayward, CA, USA, <sup>2</sup>Applied Biological Concepts, Los Alamitos, CA, USA, <sup>3</sup>RCS Consulting, Half Moon Bay, CA, USA.

AC-100 showed promising activity in two cartilage defect studies in goats to promote cartilage repair.

The sequence of AC-100 is derived from a central 23-amino acid region of the bone extracellular matrix protein MEPE and is one of the more conserved regions of the molecule. AC-100 has shown specific activity *in vivo* to promote tissue appropriate hard tissue deposition in teeth and in bone.

For the first study, an osteochondral defect (6mm diameter, 6mm deep) was made in the medial femoral condyle of Spanish goats. A cylindrical plug cut from a collagen sponge (CollaPlug; 6mm diameter, 6mm long) was implanted into the lesion site and saturated with the test article (saline; AC-100 2.5, 25mg/application). Post-operative treatments included intra-articular injections (0.5mL) of the appropriate test article into the operated knee joint at 1, 2 and 3 weeks post surgery. All animals were returned to full weight bearing activity post-surgery. The necropsy timepoints were at 3 and 6 months. The joints were evaluated by gross analysis and histology.

There was good correlation between the gross evaluation and the quantitative histological evaluation. Both showed the high dose AC-100 group had better healing outcomes than the saline and low-dose AC-100 groups at both timepoints.

In the second study a full-thickness cartilage defect was created in the medial femoral condyle. In half of the goats the defects underwent a microfracture procedure. The test articles (saline; AC-100 5, 25, 125mg/application) were administered by intra-articular injection (1.5mL) immediately after closing and 1, 2 and 3 weeks post-surgery. All animals were returned to full weight bearing activity post-surgery. In this study a short timeframe of 6 weeks was chosen to investigate early healing processes.

By gross evaluation the AC-100 treated defects showed significant improvements in the amount and quality of repair tissue with a dose-dependent effect ( $p=0.04 \rightarrow p=0.09$  vs. saline). Histological evaluation of the edge repair also showed a significant AC-100 effect ( $p=0.02 \rightarrow p=0.07$  vs. saline). The AC-100 treatment increased healing with and without microfracture.

As the defects were located in a major weight bearing site the observed improvements seen with AC-100 are very promising. Further studies are underway to investigate the long-term healing effects of AC-100 treated full thickness defects.

**Disclosures:** C.A. Middleton-Hardie, Acologix 5.

This study received funding from: Acologix.



## SA112

See Friday Plenary number F112.

## SA113

**Phosphate Induced Apoptosis in Growth Plate Chondrocytes via a Nitric Oxide and JNK-dependent Pathway.** M. Zhong\*, Z. Schwartz, B. D. Boyan. Biomedical Engineering, Georgia Institute of Technology, Atlanta, GA, USA.

Hypertrophic chondrocytes in the growth plate exit their development pathway by undergoing apoptosis, in part via the induction of high extracellular phosphate (Pi) concentration involving nitric oxide (NO) production. Recent studies show that high Pi can also initiate apoptosis in resting zone (RC) cells and NO is required. The purpose of the present study was to determine whether the c-Jun N-terminal kinase (JNK), which is associated with apoptosis in many other tissues, contributes to Pi induced apoptosis in RC cells. Rat costochondral RC cells were cultured in DMEM containing 50mM ascorbic acid and 10% FBS. Apoptosis was induced by treatment of confluent cultures with inorganic 7mM phosphate (Pi) for 24h or with the NO donor SNOG. JNK signaling was blocked by incubating the cultures with JNK inhibitor II (EMD Biosciences, Darmstadt, Germany) and NO signaling was blocked using L-NMMA. Apoptosis was assessed as a function of DNA fragmentation ([<sup>3</sup>H]-thymidine labeled DNA fragments and TUNEL staining) and cell viability using the MTT assay. NO production was determined using a DAN (2,3-diaminonaphthylene) assay. In this study, we found that Pi caused a dose-dependent increase in NO production and a corresponding increase in RC chondrocyte apoptosis, as judged by DNA fragmentation, TUNEL staining and MTT assays. Inhibition of NO production by L-NMMA blocked Pi-dependent apoptosis. Moreover, the NO donor SNOG caused a dose dependent increase in RC chondrocyte apoptosis and inhibition of JNK blocked this effect. In summary, these results show that RC chondrocytes also undergo apoptosis under the induction of Pi, and the pathway is NO-dependent and via JNK. This suggests that one mechanism for preventing premature growth plate closure may be regulation of extracellular Pi production, commensurate with low levels of alkaline phosphatase in the reserve zone.

**Disclosures:** M. Zhong, None.

This study received funding from: NSF 9731643 and Children's Healthcare of Atlanta.

## SA114

See Friday Plenary number F114.

## SA115

**Targeted Expression of SOX9 in Hypertrophic Chondrocytes Leads to Enhanced Adipogenic Activity and Spontaneous Osteoarthritis in Transgenic Mice.** B. Liang<sup>1</sup>, D. Chen<sup>\*1</sup>, B. Lee<sup>2</sup>, G. Zhou<sup>1</sup>. <sup>1</sup>Orthopaedics, Case Western Reserve University, Cleveland, OH, USA, <sup>2</sup>Molecular and Human Genetics, Baylor College of Medicine, Houston, TX, USA.

The disturbed balance in cartilage metabolism plays an important role in the pathogenesis and progression of osteoarthritis (OA). Transcription factors are key regulators of cartilage metabolism by stimulating chondrogenesis under both physiologic and pathologic conditions. Among them, SOX9 is essential for successive steps of chondrogenesis while RUNX2 is a positive regulator of chondrocytes maturation. RUNX2 also represses adipocytes differentiation and its deficiency in chondrocytes leads to increased adipogenesis. We have previously shown that SOX9 can physically interact with RUNX2 and inhibit its transcriptional activity *in vitro*. To directly investigate SOX9 effects during chondrocyte hypertrophy, a novel *Col10a1-SOX9* transgenic mouse model was generated in which *SOX9* was specifically expressed in hypertrophic chondrocytes driven by a 10kb *Col10a1* promoter. The specific transgene expression in hypertrophic chondrocyte was confirmed by RT-PCR in rib chondrocytes of 6-day-old mice and immunostaining in 10-week-old tibia samples. In monolayer culture of rib hypertrophic chondrocytes isolated from 6-day-old mice, expression of *Col10a1*, a downstream target of Runx2, was decreased by 55% in transgenic mice by quantitative RT-PCR. In comparison with wild-type mice, *Col10a1-SOX9* hypertrophic chondrocytes culture also displayed increased adipogenesis with more lipid droplets accumulation by Oil Red-O staining and higher expression levels of adipogenic genes including *C/EBPα*, *PPARγ2*, *SCD1* and *Glut4*. Additionally, mineralized areas of hypertrophic cartilage were significantly reduced in proximal tibia in 10-week-old *Col10a1-SOX9* transgenic mice. Interestingly, 11-month-old knee joints of *Col10a1-SOX9* transgenic mice but not wild-type littermates developed spontaneous severe osteoarthritis with joint space narrowing, osteophytes formation, and subchondral sclerosis. Moreover, Safranin-O histology revealed severe degradation of articular cartilage and bony outgrowth in 11-month-old transgenic mice but not in wild-type controls. Our results suggest that defective hypertrophic cartilage could contribute to the development of an adverse biomechanical environment and enhance the progression of the articular cartilage deterioration. Therefore, our study not only confirms the direct inhibitory effect of SOX9 on chondrocyte hypertrophy during cartilage formation, it also reveals a potential novel role of SOX9 in osteoarthritis pathogenesis.

**Disclosures:** G. Zhou, None.

This study received funding from: K22 DE015139 NIH/NIDCR.

## SA116

See Friday Plenary number F116.

## SA117

**Effects of Beta-D-glucopyranoside from *Phellodendron Amurense* on the Production of Inflammatory Cytokines, Growth Factors, Matrixmetalloproteinase, and on Bone Markers in Human Subchondral Osteoarthritic Osteoblasts.** D. Kim<sup>1</sup>, J. Huh<sup>\*2</sup>, Y. Baek<sup>\*3</sup>, D. Choi<sup>\*3</sup>, D. Park<sup>\*3</sup>, J. Lee<sup>\*3</sup>. <sup>1</sup>Internal Medicine, Kyung Hee University Hospital, SEOUL, Republic of Korea, <sup>2</sup>Oriental Medicine Research Center for Bone & Joint Disease, Kyung Hee University Hospital, Seoul, Republic of Korea, <sup>3</sup>Department of Acupuncture & Moxibustion, College of Oriental Medicine, Kyung Hee University Hospital, Seoul, Republic of Korea.

**Objects:** Subchondral bone sclerosis is a common feature of osteoarthritis (OA), but the mechanisms responsible for this condition remain unresolved. We investigate the effects of beta-D-glucopyranoside from *Phellodendron amurense* on the production of inflammatory cytokines (interleukin (IL)-1α, IL-6, and prostaglandin E2 (PGE<sub>2</sub>)), growth factors (vascular endothelial growth factor (VEGF) and transforming growth factor-beta (TGF-β)), matrixmetalloproteinase (MMP)/urokinase plasminogen activator (uPA) and bone markers in human subchondral OA Ob.

**Methods:** We measured the abundance of IL-1α, IL-6, PGE<sub>2</sub>, VEGF, TGF-β, MMP-1 and uPA using very sensitive ELISA in conditioned-media of human primary subchondral Ob from normal individuals and osteoarthritic patients. beta-D-glucopyranoside or selective COX-2 inhibitor (NS398) was performed to determine its effect on inflammatory cytokines, growth factors, MMP/uPA. The expression of bone cell markers was also determined.

**Results:** OA Ob produced all these factors with greater variability than normal cells. Interestingly, the production of IL-6, PGE<sub>2</sub>, VEGF and MMP-1/uPA by OA Ob separated patients into two subgroups, those whose Ob produced levels comparable to normal (low producers) and those whose Ob produced higher levels (high producers). In those cells classified as high producers, IL-6, PGE<sub>2</sub>, VEGF and MMP-1/uPA levels were increased two- to three-fold and five- to six-fold, respectively, compared with normal. In contrast, we found that IL-1α and TGF-β levels were similar in normal and all osteoarthritic Ob. beta-D-glucopyranoside significantly reduced IL-6, PGE<sub>2</sub>, VEGF and MMP-1/uPA levels in all OA Ob. In contrast, using NS398 did not reduce VEGF and MMP-1/uPA levels in either group. The evaluation of alkaline phosphatase activity, osteocalcin release and collagen type I activity increased by beta-D-glucopyranoside in OA Ob regardless to which subgroup they were assigned.

**Conclusion:** These results suggest that beta-D-glucopyranoside may contribute to bone remodeling through inhibition of inflammation and MMP/uPA system in subchondral OA Ob, ultimately leading to treatment of abnormal bone sclerosis in OA.

**Disclosures:** D. Kim, None.

This study received funding from: Grant of the Oriental Medicine R&D Project(B030008), Ministry of Health&Welfare, Republic of Korea.

## SA118

See Friday Plenary number F118.

## SA119

**Vinculin Is Involved in Hypertrophic Differentiation Through Raf/MEK/ERK Pathway in Chondrocytic ATDC5 Cells.** T. Koshimizu<sup>\*1</sup>, K. Tachikawa<sup>\*1</sup>, K. Ozono<sup>2</sup>, T. Michigami<sup>1</sup>. <sup>1</sup>Department of Bone and Mineral Research, Osaka Medical Center and Research Institute for Maternal and Child Health, Osaka, Japan, <sup>2</sup>Department of Pediatrics, Osaka University Graduate School of Medicine, Osaka, Japan.

Vinculin occurs in multimolecular complexes that function in adhesion and/or signaling between the extracellular milieu and the cell, via integrins and cadherins. Although vinculin-knockout mouse was reported to exhibit impaired limb development, the roles of vinculin in chondrogenesis remain unclear. Gene-trap mutagenesis is based on the idea that the random insertion of a trapping vector may disturb the function of inserted genes. We applied this method in ATDC5, a cell model of chondrocyte differentiation, and isolated a clone where vinculin gene is trapped. In this clone named #4-17, a truncated vinculin lacking paxillin-binding domain was produced from the trapped allele. Phosphorylation of FAK and ERK1/2 induced by adhesion to extracellular cell matrix (ECM) was markedly enhanced in #4-17 compared with parental cells, which is consistent with previous reports in vinculin-null fibroblasts. The expression of vinculin in parental ATDC5 was gradually elevated during the chondrocytic differentiation, and immunostaining for vinculin of tibial growth plates from wild-type mice demonstrated the parallel results. Thus, we investigated the roles of vinculin in chondrocyte differentiation utilizing the clone #4-17. When cultured in differentiation medium, #4-17 exhibited impaired nodule formation and less accumulation of cartilaginous matrices. The expression of *Col2a1* and *PTHrP* was detected in #4-17, but was diminished earlier than the parental ATDC5 cells. The expression of *Col10a1* was also markedly reduced in #4-17. Interestingly, the expression of SOX9 was retained. Then, we examined the effect of the trapping of vinculin gene on signal transduction during the chondrocyte differentiation. Since Raf/MEK/ERK pathway is reported to play a critical role in chondrocyte differentiation, we investigated the

phosphorylation of c-Raf and ERK1/2. In parental ATDC5 cells, phosphorylation of c-Raf and ERK1/2 was increased during the chondrocytic differentiation. On the other hand, phosphorylation of c-Raf and ERK1/2 was rather declined in #4-17 when cultured in the differentiation. The result makes a striking contrast with the enhanced phosphorylation of ERK1/2 induced by adhesion to ECM. These data suggest that vinculin plays an important role in hypertrophic differentiation of chondrocytes, and that Raf/MEK/ERK pathway might be involved in the regulation of hypertrophic differentiation by vinculin.

**Disclosures:** T. Koshimizu, None.

## SA120

**Mouse-to-Human Strategy to Identify Bone Strength QTL Genes.** C. L. Ackert-Bicknell<sup>1</sup>, B. Paigen<sup>\*1</sup>, W. G. Beamer<sup>1</sup>, C. J. Rosen<sup>1</sup>, S. Demissie<sup>\*2</sup>, L. A. Cupples<sup>\*2</sup>, Y. H. Hsu<sup>3</sup>, D. P. Kiel<sup>3</sup>, D. Karasik<sup>3</sup>. <sup>1</sup>The Jackson Laboratory, Bar Harbor, ME, USA, <sup>2</sup>Biostatistics, BU Sch Public Health, Boston, MA, USA, <sup>3</sup>IFAR, Hebrew SeniorLife, Boston, MA, USA.

Murine models have proven to be very useful for the identification of candidate genes underlying complex traits. A large number of resources are now available to allow for translatability of gene prediction in mice to human populations. We have identified QTLs for Bone Mineral Density (BMD) on proximal Chr 15 in mice in two separate F2 mapping crosses: B6xC3H (peak at 11.9 cM) and B6xNZW (peak at 17 cM). The 95% confidence interval (CI) for the B6xC3H QTL peak extended from 4.0 cM to 28.0 cM (10 Mb to 59.96 Mb) and encompassed the CI for the B6xNZW QTL peak. This region is predicted to contain greater than 270 genes. Using block haplotyping we identified 18 distinct haplotype blocks covering 12.4 Mb. In total 52 genes were found to be either completely or partially included in these haplotype blocks. Also, a QTL for BMD was reported in the literature in a B6xDBA cross with a peak at 10 cM. When DBA was added to the haplotype analysis, we were able to exclude 22 genes as candidates. The largest of these blocks was located immediately distal to the *Trps1* gene. This gene encodes a specific zinc finger protein that is a putative transcription factor. The human *TRPS1* gene has been shown to be involved in trichorhinophalangeal syndrome (also known as Langer-Giedion syndrome with exostoses). To translate the mouse finding to humans, we performed a genetic association study of polymorphisms (SNPs) in the vicinity of the *TRPS1* in a subset of unrelated individuals from the Framingham Offspring cohort. This cohort consisted of 793 women and 700 men (age 61.3 ± 9.1 yrs), for whom both DNA and bone phenotypes (DXA measurements of the hip and spine and/or heel QUS) were available. We genotyped 22 tagging SNPs in the region on chr. 8q24, covering 93% of the variance in *TRPS1* gene, using the SNPlex<sup>TM</sup> and ABI TaqMan platforms. We assessed the association between SNPs and bone phenotypes using sex-specific multiple linear regression, adjusted for age, BMI, height, smoking, and estrogen status (in women). To correct for the numerous statistical tests in our analysis, we performed permutation tests. After adjustment for multiple testing (permuted 10,000 times), 2 SNPs near the *TRPS1* were identified to be significantly associated (p values ≤ 0.0001) with the bone traits. One SNP (rs720928, associated with femoral BMD and heel QUS in men at p<0.0005) is located distal to the *TRPS1* gene and this finding corresponds to our haplotype analysis performed in mice. We are currently exploring other genes in this haplotype block. This comparative genomic approach using mouse models may be an efficient strategy to identify new candidate genes associated with bone phenotypes in humans.

**Disclosures:** D. Karasik, None.

This study received funding from: R01-AR050066, R21 AR053992.

## SA121

**Intracellular PTHR2 Alters Cell Proliferation and Pattern of Gene Expression while Antagonizing PTHR1 Signalling in Chondrocytic CFK2 Cells.** D. K. Panda<sup>\*</sup>, D. Goltzman, A. C. Karaplis. Experimental Medicine, McGill University, Montreal, QC, Canada.

TIP39 and PTHR2 are extended members of parathyroid hormone ligand and receptor family. Both the ligand (TIP39) and receptor (PTHr2) are expressed in the growth plate, the former in well differentiated hypertrophic chondrocytic cells while the latter in cells of the periaricular cartilage. This expression pattern is completely opposite to that of PTHrP and PTHR1 in the developing growth plate.

We have observed that upon TIP39 stimulation, PTHR2 expressed in CFK2 chondrocytic cells undergoes endocytosis and accumulates in the perinuclear / nuclear compartment. A bipartite nuclear localization motif is present in the C-terminal region of the receptor which also contains more than one nuclear export signature. These findings prompted us to hypothesize that PTHR2 may function intracellularly, in part at the level of the nucleus and antagonize PTHrP/PTHr1 signalling. To explore the potential for intracellular action by PTHR2, we deleted the signal sequence from the N-terminal portion of the receptor so that only the mature protein would be expressed. We then stably transfected chondrocytic CFK2 cells with this construct (ΔSSPTHr2). In the absence of TIP39, expression of ΔSSPTHr2 alone, decreased proliferation and suppressed 3H thymidine incorporation in CFK2 cells. This parallels the effects of the full length receptor on cellular proliferation following TIP39 stimulation. In addition, mRNA microarray analysis was performed to get some insight into the altered gene expression pattern between in CFK2/ΔSSPTHr2 compared to CFK2/vector cells. Expression of the transcription factor Sox9 as well as matrix proteins such as type II collagen and matrix gla protein (Mgp) were highly suppressed by ΔSSPTHr2 in CFK2 cells, as observed following treatment of full-length PTHR2 transfected CFK2 cells with TIP39. The microarray data was reconfirmed by semi-quantitative RT-PCR analysis. When 1 kb of the mouse Mgp promoter inserted in a luciferase reporter system was cotransfected with ΔSSPTHr2, the activity of the reporter plasmid was reduced three- to five-fold. Interestingly, MGP expression was up-regulated by PTHrP/PTHr1 signalling at the transcriptional level. To resolve this conundrum, we

expressed a constitutively active form of PTHR1(H410P) along with leaderless form of PTHR2. When, PTHR1(H410R) was co-expressed along with ΔSSPTHr2, Mgp expression was restored to levels comparable to vector transfected CFK2 cells. In summary our results suggest, the leaderless form of PTHR2 functioning intracellularly recapitulates the proliferative and gene expression patterns of the full length receptor following TIP39 stimulation. Moreover, PTHR1 and PTHR2 may display antagonistic signalling in chondrocytes.

**Disclosures:** D.K. Panda, None.

## SA122

See Friday Plenary number F122.

## SA123

**Hypothyroidism Is Not Deleterious to the Skeleton During Early Fetal Development.** L. P. Capelo<sup>\*1</sup>, E. H. Beber<sup>\*2</sup>, T. M. T. Zorn<sup>\*1</sup>, S. A. Huang<sup>\*3</sup>, A. C. Bianco<sup>\*4</sup>, C. H. A. Gouveia<sup>2</sup>. <sup>1</sup>Departamento de Cell and Developmental Biology, Institute of Biomedical Sciences, University of Sao Paulo, Sao Paulo, Brazil, <sup>2</sup>Departamento de Anatomy, Institute of Biomedical Sciences, University of Sao Paulo, Sao Paulo, Brazil, <sup>3</sup>Division of Endocrinology, Children's Hospital Boston, Boston, MA, USA, <sup>4</sup>Division of Endocrinology, Diabetes and Hypertension, Brigham and Woman's Hospital, Boston, MA, USA.

Thyroid hormone (TH) has a key role on post-natal bone development, while its relevance during fetal bone development is less clear. To investigate this, we induced a hypothyroid state and analyzed the skeleton during pre- and post-natal development of mice. We also examined the mRNA expression of the monocarboxylate transporter 8 (MCT8), a plasma membrane transporter that mediates the cellular influx and/or efflux of TH, and the expression of the iodothyronine deiodinases type II and III (D2 and D3). D2 is an activating enzyme that converts thyroxine (T4) into its active form, triiodothyronine (T3), while D3 inactivates T4 and T3. Hypothyroidism (HYPO) was induced pharmacologically during gestation and nursing. The fetuses and litters were harvested at embryonic days (E) 14.5, 16.5 and 18.5 and at post-natal days (P) 4, 7, 14, 21 and 35. Histological analysis of the distal epiphyseal growth plate (EGP) of the femur and vertebra showed that HYPO barely affected bone development up to E16.5. Only at E18.5, the length and area of the proliferative and hypertrophic zones, the number of chondrocytes per proliferative column and the number of hypertrophic chondrocytes were reduced in the EGPs of HYPO fetuses. Femoral D3 mRNA was detected at E14.5 and its expression decreased markedly (~10-fold) at E18.5, and even more at P14. In contrast, femoral D2 mRNA expression increased significantly by E18.5 and markedly (~2.5-fold) by P14. At E18.5, D2 activity was increased while D3 activity was diminished in the femur of HYPO fetuses (~2 fold). Like D3, the femoral mRNA expression of MCT8 decreased significantly from E14.5 to P35 (~5-fold) and was up-regulated in the femur of HYPO animals during post-natal development. In conclusion, the absence of a HYPO-induced bone phenotype during early fetal development suggests that TH signaling in bone is kept to a minimum at this stage. In addition, the reciprocal expression pattern of D2 and D3 during skeletal development suggests that these enzymes may be responsible for keeping low levels of TH in the bone for the proper early fetal bone development. However, the MCT8 expression suggests that a minimum TH influx may be necessary during the same period. In summary, D2 and D3 are likely to have an important role during pre-natal development of the skeleton, while MCT8 may be important to modulate TH effects on bone, mostly during post-natal development.

**Disclosures:** L.P. Capelo, None.

This study received funding from: FAPESP

## SA124

**Functionalization of a PLGA/PEG-PLA Composite Electrospun Scaffold with rhBMP-2 Plasmid DNA for Bone Regeneration.** X. Zhao<sup>\*1</sup>, B. Hsiao<sup>\*2</sup>, B. Chu<sup>\*2</sup>, M. Hadjiargyrou<sup>1</sup>. <sup>1</sup>Biomedical Engineering, SUNY, Stony Brook, Stony Brook, NY, USA, <sup>2</sup>Chemistry, SUNY, Stony Brook, Stony Brook, NY, USA.

Previously, our laboratory reported on the fabrication of DNA based nanofibrous and biodegradable electrospun scaffolds designed to serve as gene delivery systems for *in vivo* tissue engineering applications. In the current study, using electrospinning, we generated two scaffolds, one using a combination of 30% (w/w) poly lactide- co-glycolide (PLGA) and 3% (w/w) diblock copolymer (PEG-PLA) and by incorporating 0.025% (w/w) rhBMP2 plasmid (~1mg), and the other without any DNA. The scaffolds generated measured 15cm (width) x 30cm (length) x 100µm (thickness). Scanning electron microscopy revealed that both non-woven scaffolds looked indistinguishable and had a range of fiber diameters between 500 nm - 1.5 µm. Subsequent DNA release studies using 1.5 x 1 cm sections of the rhBMP2 DNA based scaffold showed an ~60% of DNA (in TE buffer) release in the first 24 hrs and then a steep decrease over time. Collectively, ~70% of plasmid DNA was released over 5 days, corresponding to about 2µg. Gel electrophoresis confirmed that the released plasmid was structurally intact. We are now conducting experiments in order to test the released rhBMP2 plasmid's bioactivity, by transfecting pre-osteoblastic MC3T3 cells with both the original rhBMP2 plasmid and the released DNA to see if they can enhance differentiation and mineralization. In addition, we are also carrying out *in vitro* studies with MC3T3 cells plated on top of the two types of scaffolds, again to test the effects on differentiation and mineralization. Lastly, we are now starting *in vivo* experiments using the tibial drill hole (critical size defect) model in order to assess the scaffolds capability of enhancing skeletal regeneration. Overall, we hope that the rhBMP2 plasmid DNA based scaffold will be a viable gene delivery system and have the potential to deliver therapeutic rhBMP2 plasmid DNA to stimulate tissue regeneration.

**Disclosures:** M. Hadjiargyrou, None.

This study received funding from: New York Center for Advanced Technology/STAR Inc.

## SA125

**Strong and Extensive Epistatic Interactions Affect Bone Traits in a Mouse Reciprocal Intercross of HcB/8 and HcB/23.** N. Saless<sup>1</sup>, S. J. Litscher<sup>\*1</sup>, R. S. Kattapuram<sup>\*1</sup>, M. J. Houlihan<sup>\*1</sup>, T. K. O'Neil<sup>\*1</sup>, S. Sudhakaran<sup>\*1</sup>, K. G. Abdul Raheem<sup>\*1</sup>, S. Olson<sup>\*1</sup>, P. Demant<sup>\*2</sup>, R. D. Blank<sup>1</sup>. <sup>1</sup>Medicine/Endocrinology, University of Wisconsin and Madison VAMC, Madison, WI, USA, <sup>2</sup>Genetics, Roswell Park Cancer Institute, Buffalo, NY, USA.

Linkage studies have identified quantitative trait loci (QTLs) underlying bone mineral density, bone geometry, and bone biomechanics in multiple organisms. Less progress, however, has been made in identifying the genes responsible for these QTLs. Moreover, the mapped QTLs account for only a minority of the heritable component of the measured bone properties. We hypothesize that much of the "missing" genetic contribution to bone properties arises from epistatic interactions between genes. To explore this possibility, we performed an epistasis analysis in a 603 animal, reciprocal F2 intercross of the recombinant congenic strains HcB/8 and HcB/23 that was analyzed for femoral biomechanical performance and geometry.

Animals were maintained under standard husbandry conditions and sacrificed at 17 weeks. Genotyping was done using 39 microsatellite markers spanning the approximately 300 centiMorgans over which the parental strains are known to be genetically informative. The cross includes informative regions on chromosomes 1, 2, 3, 4, 6, 9, 10, 15, 17, and 19. In single locus genome scans reported previously, we found QTLs for bone related traits on chromosomes 1, 2, 3, 4, 6, and 10. We performed the epistasis analysis with the R-QTL linkage package.

Nearly every possible pair of chromosomes yielded a significant epistatic interaction for at least 1 trait. The most striking interactions involve chromosomes 1 and 3. On chromosome 1, there are significant interactions between distinct loci on the chromosome, as well as with all the other informative chromosomes. On chromosome 3, the same pattern exists, with a significant intrachromosomal interaction as well as epistatic interactions with all the other informative chromosomes. The LOD scores for the full models, including epistasis, range from 8 to 18.

Because only approximately ¼ of the genome segregates between pairs of recombinant congenic strains, they are particularly useful for studying epistasis, as the number of potential statistical tests is reduced approximately 16-fold in comparison to an intercross between ordinary inbred strains. This increases the power to detect epistasis when present. Studying epistasis is important not only because it accounts for previously unmeasured genetic contributions to bone properties, but because interactions provide additional clues for identifying the genes underlying QTLs.

**Disclosures:** N. Saless, None.

This study received funding from: Veterans Administration.

## SA126

**A Bone Defect Model in Mouse Femur to Challenge Biomaterials, Cells and Molecules for Bone Repair.** J. Fricain<sup>\*1</sup>, L. Monfoulet<sup>\*1</sup>, B. Rabier<sup>\*1</sup>, L. Malaval<sup>\*2</sup>, J. Amedee<sup>1</sup>, O. Chassande<sup>\*1</sup>. <sup>1</sup>INSERM U577, Bordeaux, France, <sup>2</sup>INSERM U890, Bordeaux, France.

Bone loss treatment is still a challenge for orthopaedic and oral surgeons. Experimental models are useful to better understand natural bone repair and to investigate the function of therapeutic molecules in bone repair. Mice have been used for skeletal research and the defect models used have interested the femur diaphysis to study cortical reparation or metaphysis to study cancellous bone cicatrization. The aim of this study is to demonstrate the influence of the size of a mice femur metaphyseal defect on density and volume of cancellous and cortical newly bone formed and to create a critical size defect valuable to measure the effect of molecules or biomaterials on bone repair. Holes of 0.9 and 1.6 mm were performed respectively in the right and left femur of C57Bl6/J male mice (14 weeks old) and the femur were retrieved at 14, 28, 56 and 90 days, fixed in 4% paraformaldehyde for 24 hours at 4°C, then transferred into 70% ethanol and kept at 4°C. On one hand, femurs were scanned in a Explore Locus SP X-Ray microcomputerized tomography device (GE). On the other hand, femurs were decalcified in 0.5M EDTA for 3 days, then transferred in 70% ethanol, embedded in paraffin and 3 µm thick sections were stained with HES. Qualitative analysis of bone repair revealed that 14 days after surgery, fibrous tissue was mainly observed in 1.6mm defect while primary cancellous bone was present in the inner surface of 0.9mm defects. 28 days after surgery, 0.9 mm defects, were completely filled with trabecular bone while fibrous tissue was still present in 1.6 mm defects. The cortical edge of the 0.9 mm diameter defect was partially closed with dense mineralized tissue but remained completely opened in 1.6mm diameter defects. At 56 days, no marked evolution was observed in 0.9 mm defects as compared with 28 days. In 1.6 mm defects, fibrous tissue was still present in the external part of the lesion whereas trabecular like structures invaded most of the defect volume. Similar results were observed at 90 days. Quantitative analysis of cancellous bone formation showed that bone volume fraction (BVf) in the 0.9 mm defect was more important than in 1.6mm defect, due to more important trabecular number while thickness and density (BMD) were similar. At 28, 56 and 90 days no statistical difference was observed between the two size defects. For quantitative analysis of cortical bone formation, in 1.6 mm diameter defects cortical BVf was lower than in 0.9 mm defects at 28 days, and remained very low until 90 days, reflecting failure to close the perforation. In conclusion, the 1.6mm defect in mice is a cortical critical defect that could be used to test the action of molecules, cells or biomaterials on bone repair.

**Disclosures:** J. Amedee, None.

## SA127

See Friday Plenary number F127.

## SA128

**Micro-CT Abnormalities in the th3 Mouse Model of Thalassemia Start at a Young Age and Are Associated with Decreased Bone Turnover.** M. G. Vogiatzi<sup>1</sup>, J. Tsay<sup>\*1</sup>, J. Racchumi<sup>\*1</sup>, S. Rivella<sup>\*1</sup>, R. W. Grady<sup>\*1</sup>, S. B. Doty<sup>2</sup>, P. J. Giardina<sup>\*1</sup>, A. L. Bosley<sup>2</sup>. <sup>1</sup>Pediatrics, Weill Cornell Medical College, New York, NY, USA, <sup>2</sup>Hospital for Special Surgery, New York, NY, USA.

Low bone mass and fractures occur frequently in patients with beta Thalassemia Intermedia (TI), a type of congenital hemolytic anemia characterized by decreased synthesis of the beta globin chains of hemoglobin. To better understand the bone changes in TI, we studied the th3/+ mouse model of this disease. Th3/+ mice bear a heterozygous deletion of the mouse beta globin genes and, similar to humans with TI, manifest mild to moderate anemia and iron overload as well as splenomegaly.

Th3/+ mice and age-matched WT controls (6 mice per group) were studied at age 2, 4, 6 and 9 mo by micro-CT (both femurs and vertebrae) followed by mechanical testing (three-point bending). We also performed immunostaining for procollagen I and TRAP, histomorphometry for mineral apposition rate (MAR), RT-PCR for osteoprotegerin (OPG), RANKL and cathepsin K.

Compared to WT animals: i) Micro-CT of trabecular bone (L5 vertebra) showed decreased bone volume fraction, decreased number of trabeculae and increased trabecular separation in the th3/+ mouse at all ages (p<0.05). ii) Cortical bone at femur mid-diaphysis showed increased marrow area and decreased ellipticity (Imax/Imin) of the th3/+ animals (p<0.05 at all ages). iii) Micro-CT parameters in the th3/+ mice did not worsen with age. iv) Th3/+ animals exhibited decreased MAR (1.4 ± 0.3 vs. 2 ± 0.5, th3/+ vs. WT, p=0.05, age 4mo) and decreased expression of cathepsin K, OPG and RANKL (p<0.01 at all ages). The number of osteoclasts and % bone surface covered by osteoblasts were the same in both th3/+ mice and controls. iv) Biomechanics showed reduced maximum load (20 ± 3 vs. 15.5 ± 2.6, th3/+ vs. WT, p=0.01), maximum moment (35.6 ± 5 vs. 27 ± 4.5, th3/+ vs. WT, p=0.01) and structural stiffness (106 ± 19 vs. 134 ± 23 th3/+ vs. WT, p=0.05) in the th3/+ mice.

In conclusion, the th3/+ mouse model of TI manifests changes in bone micro-architecture, geometry and mechanical properties reminiscent of those in humans. Micro-CT abnormalities are present by age 2 mo and do not worsen or improve with age, suggesting problems with both bone accrual and remodeling. In fact, bone changes in this model are associated with decreased bone turnover.

**Disclosures:** M.G. Vogiatzi, None.

This study received funding from: NIH K08 HL088231.

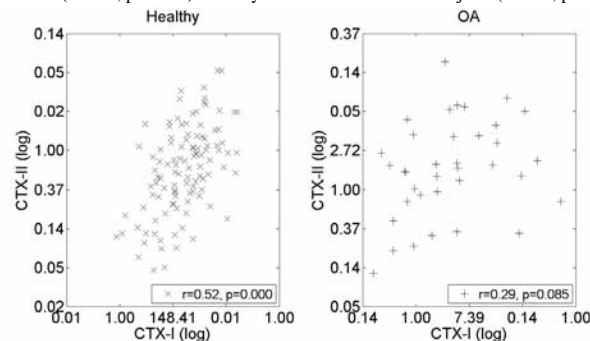
## SA129

**Longitudinal Relationships between Cartilage and Bone Turnover in Osteoarthritis.** E. B. Dam<sup>\*1</sup>, M. A. Karsdal<sup>2</sup>, I. Byrjalsen<sup>2</sup>, A. B. Jensen<sup>\*2</sup>, C. Christiansen<sup>2</sup>. <sup>1</sup>Imaging, Nordic Bioscience, Herlev, Denmark, <sup>2</sup>Nordic Bioscience, Herlev, Denmark.

**Purpose:** The pathogenesis of osteoarthritis (OA) is speculated to involve interaction patterns of bone and cartilage turnover. We investigated cross-sectional and longitudinal relationships between markers for cartilage and bone turnover in healthy subjects and subjects with OA symptoms. The focus was cartilage loss and correlations between bone and cartilage markers.

**Methods:** The 21-month study included 159 subjects prospectively selected as representative for the general population. To ensure a homogeneous population, only those over 30 years at were included, resulting in 145 subjects with age 58±13, BMI 26±4, 48% female, and 25% with OA (Kellgren and Lawrence >1). MRI scans were acquired using a Turbo 3D T1 sequence on a 0.18T Esaote scanner and total medial tibial and femoral cartilage volume was quantified automatically in a computerized framework. Bone resorption was measured by the biochemical marker serum CTX-I (C-terminal telopeptide of collagen type I) and cartilage degradation by urine CTX-II.

**Results:** At baseline (BL) CTX-I and CTX-II were linearly correlated in the healthy population ( $r=0.52$ ,  $p<0.001$ ) but only borderline for the OA subjects ( $r=0.29$ ,  $p=0.09$ ).



Inspection of the OA subjects showed that elevated CTX-II scores at BL predicted longitudinal cartilage loss. Specifically, the odds ratio (OR) for increased cartilage loss was 4.0 - comparing highest and lowest tertiles of CTX-II ( $p<0.01$ ). The same OR for CTX-I was 1.4 (not significant). There was a correlation between BL CTX-II scores and follow-up (FU) CTX-I ( $r=0.23$ ,  $p<0.01$ ). Contrarily, there was no correlation between BL CTX-I and FU CTX-II ( $r=0.08$ ,  $p=0.4$ ). All results persisted after correction for gender and age.

**Conclusion:** The results support a coupling between cartilage and bone turnover in healthy individuals that however is imbalanced in OA patients. In healthy individuals, a balanced cartilage and bone turnover may be of major importance for joint health. This emphasizes a potential need for OA treatments that restore the bone/cartilage metabolic balance. By comparison of BL and FU biomarker levels, it could be hypothesized that at least a specific stage of cartilage breakdown (elevated CTX-II at BL) is preceding bone remodeling (elevated CTX-I at FU) in OA - possibly a piece for the complex puzzle of causal relationships between cartilage and bone breakdown.

**Disclosures:** M.A. Karsdal, None.

This study received funding from: Nordic Bioscience.

## SA130

**Apc-mediated Control of  $\beta$ -catenin Is Essential for Both Chondrogenic and Osteogenic Differentiation of Skeletal Precursors.** R. L. Miclea<sup>\*1</sup>, E. C. Robanus-Maandag<sup>\*2</sup>, C. A. J. Bosch<sup>\*2</sup>, T. Kobayashi<sup>3</sup>, H. M. Kronenberg<sup>2</sup>, G. Rawadi<sup>\*4</sup>, C. W. G. M. Löwik<sup>5</sup>, R. Fodde<sup>\*6</sup>, J. M. Wit<sup>\*1</sup>, M. Karperien<sup>7</sup>. <sup>1</sup>Pediatrics, Leiden University Medical Centre, Leiden, Netherlands, <sup>2</sup>Human Genetics, Leiden University Medical Centre, Leiden, Netherlands, <sup>3</sup>Endocrine Unit, Massachusetts General Hospital, Boston, MA, USA, <sup>4</sup>Galapagos, Romainville, France, <sup>5</sup>Endocrinology, Leiden University Medical Centre, Leiden, Netherlands, <sup>6</sup>Pathology, Josephine Nefkens Institute, Erasmus MC, Rotterdam, Netherlands, <sup>7</sup>Tissue Regeneration, Institute for Biomedical Technology, Twente University, Enschede, Netherlands.

During endochondral bone formation, levels of transduced canonical Wnt/ $\beta$ -catenin signaling determine lineage commitment of skeletal precursor cells: high levels induce osteoblast differentiation, whereas low levels lead to chondrocyte differentiation. Whether Adenomatous polyposis coli (Apc), the key intracellular gate-keeper controlling  $\beta$ -catenin turnover, is involved in this process is currently unclear.

To better understand the mechanisms that modulate  $\beta$ -catenin levels in skeletal precursor cells we generated conditional knockout mice lacking functional Apc in Col2a1-expressing cells.

Conditional heterozygous and homozygous Apc mutants were monitored for the development of an abnormal phenotype. Heterozygous Col2a1-Cre-mediated Apc inactivation did not interfere with embryonic skeletal development, postnatal growth or bone mass acquisition up to 12 weeks of age. In marked contrast, conditional homozygous mutant Col2a1-Cre:Apc<sup>15lox/15lox</sup> mice died perinatally showing greatly impaired skeletogenesis. The skeletal defects were already present at E12.5. All endochondral bones

were misshaped and lacked structural integrity. Lack of functional Apc resulted in a pleiotropic skeletal cell phenotype. The vast majority of the skeletal precursor cells lacking Apc failed to differentiate and retained a mesenchymal-like spindle shape morphology. However, skeletal precursor cells in the proximal ribs were able to escape the noxious effect of functional loss of Apc resulting in formation of highly active osteoblasts.

Inactivation of Apc in chondrocytes was associated with dedifferentiation of these cells. We conclude that Apc plays a crucial role in modulating the  $\beta$ -catenin level during mouse skeletogenesis in a spatio-temporal regulated manner. In skeletal precursor cells, Apc is required for differentiation into both chondrocytes and osteoblasts. In chondrocytes, Apc is essential to maintain the chondrocytic phenotype and enable maturation.

**Disclosures:** R.L. Miclea, None.

This study received funding from: IPSEN, European Society for Pediatric Endocrinology (ESPE), Human Growth Foundation.

## SA131

See Friday Plenary number F131.

## SA132

**Differences in Femoral Bone Structure Between Juvenile Non-transgenic and Transgenic Rabbits with the WAP-hFVIII Gene Construct.** M. Martiniakova<sup>\*1</sup>, R. Omelka<sup>1</sup>, B. Grosskopf<sup>\*2</sup>, K. Dammers<sup>\*3</sup>, M. Bauerova<sup>\*1</sup>, P. Chrenek<sup>\*1</sup>. <sup>1</sup>Constantine the Philosopher University, Nitra, Slovakia, <sup>2</sup>Georg-August University, Göttingen, Germany, <sup>3</sup>Konyang University, Nonsan, Republic of Korea.

Transgenic rabbits represent an alternative way of producing recombinant human proteins and enzymes as well as serving as an appropriate animal model for different human diseases. Transgenic technology, however, can also produce possible changes in tissues other than target ones. In a previous study we identified a new type of bone tissue - fibrolamellar tissue - in 2.5 month-old transgenic rabbits carrying the WAP-hFVIII gene construct (AHE 35: 310-315, 2006). This tissue has not been identified in rabbits even in any ontogenetic stage up to date. In the present study femoral bone structure in younger (1 and 2 month-old) non-transgenic and transgenic rabbits were compared with the focus on finding the age at which the differences first appear. Altogether, 28 clinically healthy rabbits (14 transgenic and 14 non-transgenic) were analyzed. Femoral bone microstructure was evaluated in terms of qualitative and quantitative histological characteristics. In an effort to better understand the changes, concentrations of 9 bone-related mineral elements, solids and total mineral content in the femora, as well as a rate of aneuploidy in bone marrow cells were also analyzed. We identified fibrolamellar bone tissue again only in the transgenic rabbits (both 1 and 2 month-old ones). Measured values for area and perimeter of the Haversian canals and minimum diameter of the primary osteons' vascular canals were higher in the transgenic individuals ( $P<0.05$ ). On the other hand, minimum diameter of the secondary osteons was higher in non-transgenic rabbits ( $P<0.05$ ). We observed lower concentrations of Ca, P, K, solids and total mineral content in the femora of transgenic rabbits. A significant difference was observed for concentration of Ca ( $P<0.05$ ). A significantly higher rate of aneuploidy cells from bone marrow in the transgenic individuals was also identified ( $P<0.05$ ). Our results indicate evident changes in the structure of the femur in 1 and 2 month-old transgenic rabbits which result especially in a better blood supply and a slightly reduced mineralization process. For possible applications of the results, it is necessary to verify them in successive ontogenetic stages of rabbits (mainly in new-born non-transgenic and transgenic individuals) and to explain the findings on molecular level. In the future, a genetic analysis followed by a histological one in this unique model could reveal new information about the genetic contribution to the microstructure of analyzed bones. This study was supported by the grant KEGA 3/4032/06.

**Disclosures:** M. Martiniakova, None.

## SA133

**Gender-Specific Changes in Bone Microstructure of Mice Lacking Ribosomal Protein L29/HIP: An FT-IR Imaging Analysis.** L. G. Sloofman<sup>\*1</sup>, L. Spevak<sup>\*2</sup>, A. L. Boskey<sup>2</sup>, M. C. Farach-Carson<sup>1</sup>, C. B. Kirm-Safran<sup>\*1</sup>. <sup>1</sup>Biological Sciences, University of Delaware, Newark, DE, USA, <sup>2</sup>Hospital for Special Surgery, Cornell University-Weill Medical College, New York, NY, USA.

Adult HIP/RPL29-deficient mice display a short stature phenotype and were shown recently to exhibit increased bone fragility due to altered matrix protein synthesis rates (1). The purpose of this study is to provide insights into structural molecular changes that occur in HIP/RPL29-null bones versus wild type (WT) controls. To measure differences in bone properties, we examined the Fourier transform infrared (FT-IR) spectroscopic profiles of hard resin-embedded tibia sections in null mutants and WT littermates. We found that the mineral-to-matrix ratios were increased in trabecular bone and growth plate cartilage of null male tibias compared to gender-matched WT at 12 weeks. This data is consistent with previous studies performed in 24 week-old femurs that indicated that preservation of cortical thickness is associated with increased bone mineral density only in null males (1). Although female null bones did not display significant changes in their mineral-to-matrix ratios relative to gender- and aged-matched WT, their growth plate cartilage displayed a significant decrease in carbonate-to-mineral ratio. In addition, collagen maturity was severely reduced in both growth plate cartilage and trabecular bone as shown by a decrease in collagen cross-links. In contrast, our studies did not indicate significant differences in crystal growth between null and WT in either males or females. Our findings confirmed previous data that pointed to gender-specific effect of the genotype on bone material properties. We propose that in null females, ribosomal insufficiency has more pronounced consequences on the relative distribution of organic versus inorganic phases rather than absolute quantity of mineral than in null males. Ongoing work uses the HIP/RPL29 mouse model to understand the mechanisms related to protein translation that underly gender related bone fragility and fracture risk.

1. Oristian, D.S., Sloofman, L.G., Zhou, X., Wang L, Farach-Carson, M.C., and Kirm-Safran, C.B. (in press) *J. Orthop. Res.*

**Disclosures:** C.B. Kirm-Safran, None.

This study received funding from: P20 RR016458-06 and AR046121.

## SA134

**Bone Marrow Stromal Cell-derived Extracellular Matrix Promotes Mesenchymal Stem Cell Motility.** J. Ling<sup>\*1</sup>, Y. Lai<sup>\*2</sup>, C. M. Skinner<sup>\*2</sup>, X. Chen<sup>2</sup>. <sup>1</sup>Bioengineering Section, Southwest Research Institute, San Antonio, TX, USA, <sup>2</sup>Restorative Dentistry, University of Texas Health Science Center at San Antonio, San Antonio, TX, USA.

Mesenchymal stem cells (MSCs) of bone marrow have been proposed for the repair and regeneration of specific tissues such as bone, cartilage, muscle, marrow stroma, tendon, and other connective tissues. However, MSCs are rare in adult bone marrow. It has been difficult to expand MSCs without losing their stem cell properties, thereby impairing the investigation of their behavior and limiting their therapeutic potential. Recently, we have shown that the extracellular matrix (ECM) prepared from marrow stromal cells dramatically enhanced MSC proliferation and effectively retained their stem cell properties (Chen et al, JBMR. 22:1943, 2007). The mechanism of how the ECM positively affects MSC proliferation is unclear. Interestingly, it was observed that cells cultured on the ECM were evenly distributed, whereas cells maintained on plastic grouped into nodules. This finding implies that the ECM may facilitate MSC motion. To confirm this, we applied time-lapse microscopic imaging to track cell migration on the ECM versus that on an uncoated coverslip. In this experiment, human MSCs were first sorted by FACS using an antibody against SSEA-4 a surface marker for MSCs (Gang et al, Blood. 109:1743, 2007). The MSCs were then seeded onto coverslips either uncoated or coated with the ECM made by human marrow stromal cells, at 1400 cells/cm<sup>2</sup>, allowing 20-30 cells per viewing field. The motility of cells maintained on an uncoated coverslip or on the ECM was quantified by measuring the velocity, displacement, and frequency of cell-cell contact of migrating cells using a time-lapse individual cell migration assay. Time-lapse images revealed that MSCs cultured on the ECM moved along the direction of collagen fibers, whereas cells cultured on the uncoated coverslip moved randomly. The average velocity of cells on the ECM was 25.6±11.3 µm/hr, which was significantly (p < 0.001) higher than the 17.3±4.9 µm/hr on the uncoated coverslip. Interestingly, the average of uninterrupted cell displacement over 24 hrs was 123 µm on the ECM, while 62 µm on the uncoated coverslip. Moreover, time-lapse videos showed that cell-cell collisions occurred less frequently (6 in a 24-hr period) when cells were cultured on the ECM than cells cultured on the uncoated coverslip (27 in a 24-hr period). After 72 hrs of culture, the number of cells expanded on the ECM was at least 3-fold greater than that expanded on the uncoated coverslip. We conclude that the ECM promotes MSC motility, and directs the MSC migration, thereby preventing stem cell cell-to-cell contact inhibition, which in turn results in an increased number of stem cells.

**Disclosures:** X. Chen, None.

This study received funding from: NIH R21.

## SA135

See Friday Plenary number F135.

## SA136

**The Early Osteocyte Marker, E11/gp38 Is Highly Elevated in New Bone Formed in Response to Distraction as Compared to Existing Bone.** D. Pacicca<sup>1</sup>, A. Zaidi<sup>\*2</sup>, A. Shah<sup>\*3</sup>, L. Bonewald<sup>4</sup>. <sup>1</sup>Orthopaedic Surgery, Children's Mercy Hospital, Kansas City, MO, USA, <sup>2</sup>UMKC School of Medicine, Kansas City, MO, USA, <sup>3</sup>Orthopaedic Surgery, UMKC School of Medicine, Kansas City, MO, USA, <sup>4</sup>Oral Biology, University of Missouri-Kansas City, Kansas City, MO, USA.

E11/gp38 is a 40kd membrane protein expressed by cells with dendritic processes. Its expression is highly elevated in embedding osteocytes and E11 expression is also increased in response to mechanical loading. We hypothesized that E11 expression would be elevated in distraction osteogenesis due to enhanced bone formation under tension.

C57Bl/6 mice (n=20) underwent application of a distraction fixator to the right femur with midshaft osteotomy. After latency, femurs were distracted at 0.15 mm per day for 14 days. Radiographs were obtained at days 7, 14, 21 and 28. Animals were sacrificed at either 7, 14, 21 or 35 days postop and femurs were harvested. Serial frozen sections were immunostained for E11 and new bone formation in each specimen was quantified. The average number of cells expressing E11 was counted using 6-8 high power fields per section. Quantification was done for both new bone formed in the distraction site as well as the primary spongiosa. Fluorescent microscopy showed numerous E11 positive osteocytes with abundant dendritic processes in the newly formed distracted bone. In contrast, in normal trabecular bone, there were much fewer E11 positive osteocytes, and these were limited to embedding or recently embedded cells near the surface of the bone, with fewer visible dendrites. The average number of E11 positive cells per unit bone area was significantly elevated in distracted bone, compared to primary spongiosa (138±36 for distracted bone, 56±24 for primary spongiosa, p=0.0001).

These data suggest that E11 is a marker for new bone formation and for newly formed or forming osteocytes. Previously it was shown that E11 expression increases in response to mechanical stimulation *in vitro* and *vivo* (Zhang et al, 2006). Therefore, the elevated expression of E11 during distraction may be not only a reflection of the high number of embedding or recently embedded osteocytes but may also be modulated by the mechanical strains that occur within the distraction site. Further studies that compare fracture healing to distraction in mice with targeted deletion of E11 should help to determine the role of mechanical loading and E11 in new bone formation.

**Disclosures:** D. Pacicca, None.

## SA137

**TiO<sub>2</sub>-scaffolds for Use in Bone Tissue Engineering.** R. Sabetrasekh<sup>\*</sup>, G. Fostad<sup>\*</sup>, B. Hafell<sup>\*</sup>, A. Førde<sup>\*</sup>, J. Reseland, S. Lyngstadaas<sup>\*</sup>, H. Haugen<sup>\*</sup>. University of Oslo, Faculty of Dentistry, Department of Biomaterials, Oslo, Norway.

There is an increasing demand for bone repair due to bone lost cause by tumors, infections and trauma. Traditionally, autologous and allogenic bone grafts have been utilized for bone reconstructions. However, along the past decade a paradigm shift is taking place from using tissue graft to biomaterials. In this study we have chosen titanium oxide (TiO<sub>2</sub>) as scaffold's material since it has proven to fulfil many of the demands for a scaffold material. The main goal was to improve the mechanical properties of TiO<sub>2</sub> scaffolds, in terms of making stronger, bigger-load bearing devices with the desired three-dimensional geometry for bone tissue engineering.

The polymer sponge method was chosen as method making TiO<sub>2</sub> scaffolds. Fully reticulated polyester based polyurethane foams with 60 ppi were coated with solution of H<sub>2</sub>O and TiO<sub>2</sub> powder. The TiO<sub>2</sub> scaffolds were evaluated for the mechanical strength by compression test and the pore morphology was evaluated by SEM and microCT image analysis. Statistic variations were analysed by the standard deviation of four randomised scaffolds from 16 different batches. Different data groups were compared through a two-tailed ANOVA test, where the significant level was set at 0.05. Further more the TiO<sub>2</sub> scaffolds were evaluate the for bone tissue engineering by growing the murine preosteoblasts (MC-3T3-E1) on the TiO<sub>2</sub> scaffolds. Cytotoxic effect of the TiO<sub>2</sub> scaffolds on the osteoblasts was determined by lactate dehydrogenase activity in the culture medium and cell morphology was evaluated by SEM.

The scaffolds had an average pore size of 582.07µm and a porosity of 94.3% which gives us the opportunity to further coating and improvement of strength, still maintaining optimal conditions for osseointegration and vascular growth. The BET Surface Area was found to be 5.0664 m<sup>2</sup>/g. This gives a greater attachment surface for cells compared to the other commercial scaffolds. The TiO<sub>2</sub> scaffolds had compressive strength in the range of 0.6MPa to 1.2MPa after. These scaffolds had all porosity higher than 90%. The interconnectivity was also found to be high. We observed less than 5% cytotoxic effect of the TiO<sub>2</sub> scaffolds on the osteoblasts.

Study has showed that it is possible to produce TiO<sub>2</sub> scaffolds which are both mechanical loadable, have high reproducibility and low cytotoxicity. TiO<sub>2</sub> scaffolds with porosity of 90 % had compressive strength higher than 1 MPa. Since the porosity is far above what is necessary for osseointegration, reduction of porosity to reinforce the scaffolds even further is possible.

**Disclosures:** R. Sabetrasekh, None.

This study received funding from: University of Oslo, Norway.

## SA138

**Bone Marrow Stromal Cells and Osterix Contributing to Osseointegration of Dental Implants.** X. Beiyun<sup>\*1</sup>, J. Zhang<sup>\*1</sup>, E. Brewer<sup>\*1</sup>, Q. Tu<sup>1</sup>, M. Wieland<sup>\*2</sup>, J. Chen<sup>1</sup>. <sup>1</sup>General Dentistry, Tufts University, School of Dental Medicine, Boston, MA, USA, <sup>2</sup>Institute Straumann AG, Basel, Switzerland.

The purpose of this study is to identify the source and potential of cells involved in the processes of osteogenesis after implantation, and to elucidate the roles of osterix (Osx) in osteogenic differentiation at the interface between host bone and titanium dental implants. BSP9.0Luc/ACTB-EGFP mice contain a luciferase reporter gene driven by BSP promoter and an enhanced green fluorescent protein (EGFP) driven by a beta-actin promoter. Bone marrow stromal cells (BMSCs) isolated from these transgenic mice were transplanted into 4-week-old nude mice through intracardiac injection. Five weeks after transplantation, titanium implants (1.05 mm in diameter) were inserted into the femurs of these nude mice. The femurs were dissected at d7 (day7) and d21 after implantation. H&E staining and immunohistochemical (IHC) staining were performed. BSP/TVA mice, in which an avian retroviral receptor gene is hooked to a mouse BSP promoter, were divided into two groups. Titanium implants were inserted into bilateral femurs after local administration of RCAS/Osx virus or empty virus as control, respectively. The femurs were dissected for microCT, RT-PCR, H&E staining and IHC staining at d7 and d14 after implantation. In BMSCs transplanted nude mice, IHC staining showed that luciferase, BSP and GFP could be detected in the newly formed bone at d7 and d21. The ratio of luciferase positive cells to GFP positive cells detected at d7 was higher than that at d21. In BSP/TVA mice, 14 days after implantation, microCT analysis showed an increased bone mineral density at the bone-to-implant interface in RCAS/Osx group compared with the control group. As shown by semiquantitative RT-PCR analysis, levels of Osx, BSP and osteocalcin (OC) were higher in RCAS/Osx group than in the control group at d7 and d14. In both groups, levels of BSP and OC were higher at d14 than at d7 after implantation. Histomorphometrical analysis demonstrated increased percentage of bone-implant contact in RCAS/Osx group compared with control group at d7 and d14. Immunohistochemical staining revealed active expression of BSP and OC in the newly formed bone in RCAS/Osx group at d7 and d14. In conclusion, exogenous BMSCs underwent osteogenic differentiation and participated in the osseointegration after implantation. Overexpression of Osx could accelerate bone regeneration process at bone-to-implant interfaces.

**Disclosures:** X. Beiyun, Institute Straumann AG, Basel, Switzerland 3.  
This study received funding from: Institute Straumann, AG, Basel, Switzerland.

## SA139

**Regulation of Intracellular Signaling of MC3T3-E1 Osteoblasts by the Extracellular Matrix.** P. A. Jones<sup>\*</sup>, R. L. Duncan. Department of Biological Sciences, University of Delaware, Newark, DE, USA.

Osteoblast adhesion to the extracellular bone matrix (ECM) is critical to the response of these cells to hormonal and mechanical stimuli. However, the signaling mechanisms activated by attachment and growth of osteoblasts on different ECM's are poorly understood. We postulate that direct integrin attachment to different ECM proteins will result in altered calcium signaling and cell function. Early signaling responses mediated by attachment of type I collagen and fibronectin to MC3T3-E1 osteoblastic cells were investigated using atomic force microscopy (AFM) and calcium imaging. Using AFM, we determined that the average unbinding force of fibronectin to the cell was 148.3±3.3 pN, while the average unbinding force of collagen to the cell was 97.8±4.4 pN. When the fibronectin coated tip was allowed to stay in contact with the cell for 60 seconds before measuring the force of unbinding, the measured unbinding force increased two-fold. Using calcium imaging techniques, the global intracellular calcium ([Ca<sup>2+</sup>]<sub>i</sub>) response of MC3T3-E1 cells elicited by soluble ECM proteins was determined. Addition of soluble fibronectin to MC3T3-E1 cells produced a slow, sustained increase in [Ca<sup>2+</sup>]<sub>i</sub>, whereas type I collagen and the ECM associated peptide Arg-Gly-Asp-Ser (RGDS) caused a smaller, more rapid increase in intracellular calcium. The RGDS motif is contained in the sequence of fibronectin and the failure of this motif to elicit the same response as the full length fibronectin molecule indicates that other cell binding regions of fibronectin are essential to this [Ca<sup>2+</sup>]<sub>i</sub> response. The [Ca<sup>2+</sup>]<sub>i</sub> response to soluble ECM proteins was dependent on both the entry of calcium from the extracellular environment as well as the release of calcium from intracellular stores. The binding of osteoblasts to different ECM substrates also affects growth, as MC3T3-E1 cells grown on fibronectin exhibited increased proliferation as compared to the same cells grown on type I collagen. Further, this increase in proliferation on fibronectin appeared to be mediated by the L-type voltage sensitive calcium channel (L-VSCC), since the L-VSCC inhibitor, nifedipine, reduced proliferation on fibronectin coated substrates. Addition of nifedipine to osteoblasts grown on type I collagen did not have a significant effect on proliferation. Consequently, the attachment of osteoblasts to fibronectin appears to cause an increase in cell proliferation that is calcium dependent and mediated through the L-VSCC. Elucidating the signaling mechanisms in osteoblasts that are mediated by the surrounding extracellular matrix will provide important insight into the mechanisms of bone formation and maintenance.

**Disclosures:** P.A. Jones, None.  
This study received funding from: National Institutes of Health.

## SA140

**DMP1 Fragments Interact Differently with Hydroxyapatite: Insights into Mechanism of Action.** A. Boskey<sup>1</sup>, C. Qin<sup>\*2</sup>, Y. Sun<sup>\*2</sup>, W. T. Butler<sup>\*2</sup>, H. Taleb<sup>\*1</sup>, D. Redfern<sup>\*3</sup>, A. Gericke<sup>\*3</sup>. <sup>1</sup>Musculoskeletal Integrity Program, Hospital for Special Surgery, New York, NY, USA, <sup>2</sup>Department of Biomedical Sciences, Baylor College of Dentistry, Texas A & M University System Health Science Center, Dallas, TX, USA, <sup>3</sup>Department of Chemistry, Kent State University, Kent, OH, USA.

Dentin matrix protein 1 (DMP1) is an acidic noncollagenous protein critical for hydroxyapatite (HA) mineral deposition in bones and teeth. The purpose of this study was to elucidate the mechanism of action of this process. DMP1 is present in mineralized tissues as 3 fragments: the NH2-terminal (37 kDa) and COOH-terminal (57 kDa) portions and a proteoglycan fragment, DMP1-PG that is a chondroitin-sulfated 37-kDa DMP1 fragment. The effects of each of these fragments on HA formation were examined in a cell-free solution study, and the interaction of the fragments with HA determined by attenuated reflection infrared spectroscopy (ATR-FTIR). The ATR-FTIR experiment involved interaction of the peptide solution with HA or Ca<sup>2+</sup>, followed by the characterization of the resulting secondary structure changes based upon the analysis of the protein amide I band envelope. In solution, at 10, 12.5 and 25 ug/ml both the 37kDa and 57kDa fragments acted as HA formation nucleators; in contrast, DMP1-PG was an effective inhibitor at 10 ug/ml, but at higher concentrations had a lesser effect. The intact protein (full length DMP1) expressed in bovine marrow stromal cells was also an inhibitor. Conformational studies showed that the full length DMP1 in the presence of HA or Ca<sup>2+</sup> has a slightly increased  $\beta$ -sheet secondary structure content relative to the protein in the absence of HA or Ca<sup>2+</sup>. Dynamic Light Scattering experiments showed DMP1 aggregates in the presence of Ca<sup>2+</sup>. The 37 kDa fragment showed even greater aggregation. The 57 kDa fragment had increased  $\alpha$ -helical secondary structure in the presence of HA and Ca<sup>2+</sup>. In conclusion, these results suggest that in mineralizing tissues DMP1 fragments can have distinct regulatory effects on mineralization depending on their composition, via an interaction with HA. Thus, in the DMP1 KO where there is a decrease in mineral content, the absence of the nucleating fragments, appear to be important, while the DMP1-PG fragment may be more important for cell-matrix interactions.

**Disclosures:** A. Boskey, None.  
This study received funding from: NIH DE04141.

## SA141

See Friday Plenary number F141.

## SA142

**Bone Sialoprotein (BSP) Deficiency Impairs Osteoclast Differentiation and Resorption *in vitro*.** M. Boudiffa<sup>\*1</sup>, N. Wade-Gueye<sup>\*1</sup>, A. Guignandon<sup>\*1</sup>, M. Linossier<sup>\*1</sup>, A. Vanden-bossche<sup>\*1</sup>, A. Anginot<sup>2</sup>, M. Lafage-Proust<sup>1</sup>, J. Aubin<sup>3</sup>, P. Jurdic<sup>2</sup>, L. Vico<sup>1</sup>, L. Malaval<sup>1</sup>. <sup>1</sup>LBTO, INSERM 890, Saint-Etienne, France, <sup>2</sup>Umr cnrs 5161, inra 1237, ENS, Lyon, France, <sup>3</sup>Dept of Molecular Genetics, Faculty of Medicine, University of Toronto, Toronto, ON, Canada.

Like Osteopontin (OPN), Bone sialoprotein (BSP) belongs to the SIBLING (Small Integrin Binding Ligand N linked Glycoproteins) family, whose members interact with bone cells and mineral. We have previously shown that BSP knockout (KO) mice have a higher bone mass with low bone formation and reduced osteoclast (oc) surface as compared to wild type (WT) mice. Because this phenotype suggests a defect in oc recruitment and function, we studied the differentiation and activity of KO oc *in vitro*. Oc precursor-containing murine spleen cell cultures were grown in the presence of RANKL and M-CSF and analysed at day (d)2 (appearance of TRACP+ cells), d5 (onset of multinucleation) or d7 (peak number- nb- of multinucleated oc). Fixed cells and extracted RNAs were used for Tartrate Resistant Acid Phosphatase (TRACP) or immunostainings (IS) and RT-PCR, respectively. IS confirmed the strong BSP expression in WT oc and its absence in mutants. At d7, TRACP+ cell nb (1150 ± 104 vs 1486 ± 93 n=12, p<0.02) and multinucleated oc nb (≥3 nuclei) (66 ± 11 vs 447 ± 35 n=12, p<0.0001) were lower in KO than in WT. Addition of 40 nM exogenous fibronectin, 80nM BSP or >400nM recombinant OPN throughout the culture time restored multinucleated oc nb in KO to WT values. However, none of these supplements restored TRACP+ cell nb at d2 to the WT level. Thus, BSP seems to be required for oc differentiation at two levels : intracellular BSP is needed for the commitment of precursors to the oc lineage and extracellular BSP is required for multinucleation. Further, image analysis of actin-stained prefusion oc (d5) suggested a higher podosome turnover in KO with more but smaller podosomes (85 ± 51 vs 145 ± 18, n=30, p<0.05) than in WT. Oc gene expression was markedly altered in KO compared to WT cells, with expression reduced for cell adhesion genes (beta3 integrin & OPN) but increased for promigratory genes (MMP2 & 9), TRACP and cathepsin K . *In vitro* resorption assays were performed on either BSP-containing dentin slices or BSP-free mineral coated slides (Osteologic<sup>TM</sup>) in presence of RANKL and MCSF for 2 d. No difference in pit number (23 ± 4 vs 24 ± 9, n=6, p= 0.79) or pit area was seen between WT and KO on dentin slices. However, pit formation by KO oc was markedly reduced on BSP-free discs (9±1 vs 22 ± 3 , n=15, p<0.0001). In conclusion, BSP appears essential for oc formation and resorption *in vitro*, confirming our *in vivo* findings. Moreover, the down-regulation of OPN expression in KO oc suggests a physiological interplay between these two SIBLING family members which remains to be clarified.

**Disclosures:** M. Boudiffa, None.  
This study received funding from: French Ministry of Education and Research.

## SA143

**Sequestration, Proliferation and Differentiation of Osteoblasts in Hydrogels for Tissue Engineering Applications.** M. Dadsetan<sup>\*1</sup>, T. E. Hefferan<sup>1</sup>, A. Heine-Geldern<sup>\*1</sup>, M. Benedikt<sup>\*1</sup>, D. Gaustad<sup>\*1</sup>, J. Herrick<sup>\*1</sup>, T. C. Spelsberg<sup>2</sup>, L. Lu<sup>\*1</sup>, A. Maran<sup>1</sup>, M. J. Yaszemski<sup>1</sup>. <sup>1</sup>Orthopedic Surgery, Mayo Clinic, Rochester, MN, USA, <sup>2</sup>Biochemistry and Molecular Biology, Mayo Clinic, Rochester, MN, USA.

Bone is an organ that can regenerate under normal physiological conditions; however, after trauma or surgical resection for removal of bone tumors the remaining void impedes bone regeneration. In order for bone regeneration to proceed, osteoblasts must be present and functional; therefore, under these abnormal physiological conditions implementation of tissue engineering strategies to promote bone regeneration would be beneficial to provide the necessary functional cells. The osteoblasts must arrive at the site, be viable, differentiate, and eventually form bone. Therefore, our objective was to test if osteoblasts would remain viable in a hydrogel and if these cells would be able to proliferate and differentiate.

For these studies we utilized a photocrosslinkable hydrogel, oligo-(polyethylene glycol), (OPF), to encapsulate normal human osteoblasts (hFOB). The cells were cultured under static or dynamic conditions in a rotating wall vessel bioreactor (Synthecon/ RCCS-4DQ) containing DMEM/F12, 10% FBS, 1% penicillin/streptomycin and 0.6% geneticin for 3, 7 or 14 days. Rotation was set at 0 rpm for static cultures and 25 rpm for dynamic cultures. Viability of the cells was determined by uptake of calcein from a Live/Dead Kit (Molecular Probes) and proliferation was quantified by measuring DNA content using the PicoGreen Kit (Molecular Probes). Alkaline phosphatase activity was utilized as the marker of osteoblast differentiation.

The hFOB cells demonstrated calcein uptake after encapsulation in the hydrogel and during the 14 day time course, thus indicating viability throughout the experimental period. There was a significant effect of time ( $p < 0.05$ ) on the proliferation of the osteoblasts with the greatest proliferation occurring at day 3. Interestingly, there was no significant effect of culture conditions with the cells proliferating in both the static and dynamic cultures. However, there was a significant increase ( $p < 0.001$ ) in alkaline phosphatase activity for the osteoblasts grown in dynamic culture with 1.6 fold increase between days 3 and 7, and a 1.4 fold increase between days 3 and 14.

These studies have shown that osteoblasts can be successfully encapsulated in an OPF hydrogel and maintain three functions which are crucial for tissue regeneration: viability, proliferation and differentiation. Thus, OPF hydrogels can be considered as a candidate material to sequester osteoblasts and deliver these cells to sites where bone regeneration is needed.

**Disclosures:** T.E. Hefferan, None.

This study received funding from: NIH.

## SA144

**Identification of Dentin Sialoprotein-Phosphophoryn Cleavage Site.** H. H. Ritchie<sup>\*</sup>. Cariology, Restorative Sciences and Endodontics, University of Michigan School of Dentistry, Ann Arbor, MI, USA.

**Introduction:** Dentin sialoprotein (DSP) and phosphophoryn (PP) are the two noncollagenous proteins classically linked to dentin mineralization, but more recently found in bone, kidney and salivary glands. Point mutations in DSP-PP gene are linked to Dentinogenesis imperfecta. These two proteins are derived from a single copy DSP-PP gene. Because native PP has a DDPN N-terminal sequence, we hypothesized that SMQG<sup>447</sup>[D<sup>448</sup>]DPN is the specific cleavage site for generating DSP<sub>430</sub> and PP<sub>240</sub><sup>\*</sup>. To test this hypothesis, our Objective was to generate DSP-PP<sub>240</sub> containing mutated G<sup>447</sup> and follow the expression and processing of this mutated precursor protein. **Methods:** To achieve this goal, we used site-mutagenesis to generate G<sup>447</sup> mutations in DSP-PP<sub>240</sub> cDNA in pGEM7Z(+), which were subsequently subcloned into pVL1392 baculovirus vector for protein expression. **Results:** Wild type and mutated DSP-PP<sub>240</sub> precursor proteins are secreted into the extracellular space in the baculovirus expression system. Using MS, MS/MS analysis on the recombinant PP sample, the N-terminal sequence was determined to be DDPN. DSP-PP<sub>240</sub> cDNA containing G<sup>447</sup> mutant yielded a DSP-PP<sub>240</sub> precursor protein, which was not further processed into DSP<sub>430</sub> and PP<sub>240</sub><sup>\*</sup>. **Conclusion:** G<sup>447</sup>[D<sup>448</sup>] is the cleavage site for generating DSP<sub>430</sub> and PP<sub>240</sub><sup>\*</sup> from the wild type precursor molecule. This work was supported by NIH DE11442-9 to HHR.

**Disclosures:** H.H. Ritchie, None.

This study received funding from: NIDCR.

## SA145

See Friday Plenary number F145.

## SA146

**Do Type I Collagen Homotrimers Contribute to Osteoporosis by Altering Bone Remodeling?** S. Han<sup>\*1</sup>, E. Makareeva<sup>\*1</sup>, N. V. Kuznetsova<sup>\*1</sup>, A. M. DeRidder<sup>\*1</sup>, M. B. Sutter<sup>\*1</sup>, D. J. McBride<sup>\*2</sup>, C. L. Phillips<sup>\*3</sup>, U. Schwartz<sup>\*4</sup>, J. M. Pace<sup>\*4</sup>, P. H. Byers<sup>\*4</sup>, R. Visse<sup>\*5</sup>, H. Nagase<sup>\*5</sup>, S. Leikin<sup>1</sup>. <sup>1</sup>Eunice Kennedy Shriver National Institute of Child Health and Human Development, National Institutes of Health, Bethesda, MD, USA, <sup>2</sup>School of Medicine, University of Maryland, Baltimore, MD, USA, <sup>3</sup>Department of Biochemistry, University of Missouri, Columbia, MO, USA, <sup>4</sup>Department of Pathology, University of Washington, Seattle, WA, USA, <sup>5</sup>Kennedy Institute of Rheumatology, Imperial College London, London, United Kingdom.

Normal type I collagen molecules are heterotrimers of two  $\alpha 1(I)$  and one  $\alpha 2(I)$  chains, but insufficient or abnormal synthesis of the  $\alpha 2(I)$  chain can result in  $\alpha 1(I)$  homotrimers, e.g., in fetal tissues and various pathological conditions. In particular, synthesis of a small fraction of  $\alpha 1(I)$  homotrimers in individuals with a polymorphism in the SP1 binding region of COL1A1 is discussed in the literature as a factor contributing to fracture in age-related osteoporosis. It is not clear, however, how to reconcile such an effect with outcomes of complete heterotrimer replacement by  $\alpha 1(I)$  homotrimers. Severe Osteogenesis Imperfecta was reported in a patient with synthesis of nonfunctional  $\alpha 2(I)$  chains, but no dramatic bone pathology was observed in patients completely lacking the  $\alpha 2(I)$  chain synthesis. If normal bone formation is possible with the complete replacement of the heterotrimers, how can just a small fraction of the homotrimers contribute to age-related bone fragility? To address this question, we investigated murine and human  $\alpha 1(I)$  homotrimers and their mixtures with the corresponding heterotrimers. The most significant findings with potential implications to tissue pathology were: (a) the segregation of the homo- and heterotrimers at a subfibrillar level and (b) the significantly reduced susceptibility of the homotrimers to cleavage by tissue collagenases. A more detailed study with rhMMP-1 revealed that the lack of the  $\alpha 2(I)$  chain does not alter the enzyme binding but hinders opening of the triple helix necessary for presenting the unwound chains to the catalytic site. In mixtures, rhMMP-1 degraded the normal type I heterotrimers before noticeable cleavage of the homotrimers. We hypothesize that an initial deposition of  $\alpha 1(I)$  homotrimers may not reduce the bone strength. However, their subfibrillar segregation and selective proteolytic degradation of the heterotrimers may result in accumulation of defects after multiple tissue remodeling cycles, altering the bone matrix quality.

**Disclosures:** S. Leikin, None.

This study received funding from: National Institutes of Health.

## SA147

**Various Roles of Syndecan Family in Osteoblastic Cells.** T. Ikeo<sup>1</sup>, A. Kamada<sup>1</sup>, Y. Yoshikawa<sup>1</sup>, E. Domae<sup>\*1</sup>, S. Goda<sup>\*1</sup>, I. Tamura<sup>\*1</sup>, A. Kawamoto<sup>\*1</sup>, J. Okazaki<sup>\*1</sup>, Y. Komasa<sup>\*1</sup>, Y. Takaishi<sup>1</sup>, T. Miki<sup>2</sup>, T. Fujita<sup>1</sup>. <sup>1</sup>Osaka Dental University, Osaka, Japan, <sup>2</sup>Osaka City University, Osaka, Japan.

Syndecans are transmembrane heparan sulfate proteoglycans known to bind both other extracellular matrix molecules and certain growth factors, thus participating in a number of fundamental biological processes, including cell adhesion and migration, and the binding and activation of growth factors, enzymes, and inhibitors. The syndecan family in vertebrates comprises four members, syndecan-1, syndecan-2 (fibroglycan), syndecan-3 (N-syndecan), and syndecan-4 (ryudocan). Previously, we showed both protein and gene expression of syndecan-1, -2 and -4 in normal human osteoblasts. To understand the role of syndecans in osteoblasts, the effect of a bone-resorbing cytokine, IL-1 $\beta$ , and differentiation-stimulated reagent, beta-glycerophosphate (BGP), on syndecan expression were examined using human osteoblast-like cell SaOS2.

Using western blot analysis, it was found that IL-1 $\beta$  caused a marked appearance of a certain heparan sulfate proteoglycan corresponding to syndecan-4. Furthermore, the mRNA expression levels of syndecan family were measured using real-time quantitative RT-PCR technique, and demonstrated the gene expression of syndecan-1, -2 and -4 in the human osteoblast-like cells.

When cells were incubated with IL-1 $\beta$  for 24 h, there were significant decrease in mRNA levels of syndecan-1 and syndecan-2 compared with time match controls, though the expression of syndecan-4 was markedly increased. These results demonstrate that syndecan-1, -2 and -4 are synthesized in human osteoblastic cells, and syndecan-4 gene transcription is rapidly responsive to an inflammatory mediator. On the other hand, addition of BGP increased syndecan-1 and -2 expression but not syndecan-4. Hence, it is indicated that syndecan-1 and -2 may be involved with the differentiation and maturation of osteoblasts, while syndecan-4 may be important in the intracellular signal transduction.

**Disclosures:** T. Ikeo, None.



## SA148

**Immunohistochemical Localisation of Sclerostin in Human Trabecular Bone from Fragility Hip Fracture Patients.** A. Papadopoulos\*, L. Truong\*, J. S. Kuliwaba\*, N. L. Fazzalari. Bone and Joint Research Laboratory, Institute of Medical and Veterinary Science, Adelaide, South Australia, Australia.

Osteocytes, the most abundant cell type in bone, are ideally located to influence bone remodelling through their syncytial relationship with surface bone cells. The expression of osteocyte-derived factors such as sclerostin, an inhibitor of bone formation and subsequent bone mineralisation, in osteocytes imply that these bone cells may regulate mineralisation, and hence, bone material properties for bone strength. This study analysed the immuno-localisation of sclerostin in human femoral trabecular bone obtained from postmenopausal females undergoing total hip arthroplasty following a fractured neck of femur (#NOF;  $n = 10$ , mean age  $78.4 \pm 5.7$  years) and a non-fracture control (NFC) group, primary hip osteoarthritis ( $n = 8$ , mean age  $78.9 \pm 6.1$  years). Using the streptavidin biotin peroxidase method of immunohistochemistry in paraffin-embedded bone tissue, positive nuclear and cytoplasmic sclerostin immunostaining were observed specifically in the osteocytes, as well as in the canaliculi and lacunar walls, as reported in published literature. The #NOF group had significantly less bone volume fraction (BV/TV; #NOF =  $7.4 \pm 4.1\%$ , NFC =  $11.5 \pm 3.2\%$ ,  $p < 0.04$ ). No significant differences were found in the number of positive-stained and negative-stained osteocytes per bone area (N.POS.Ot/BV and N.NEG.Ot/BV, respectively), number of empty lacunae per bone area (N.Em.Lc/BV), and in the total number of lacunae per bone area (Total Lc.N/BV) observed, compared to NFC. The percentage of positive (N.POS.Ot/Total Lc.N) and negative (N.NEG.Ot/Total Lc.N) osteocytes, and percent of empty lacunae (N.Em.Lc/Total Lc.N) were similar between the two groups. Interestingly, percent positive-stained osteocytes differed significantly to negative-stained osteocytes in the #NOF group ( $28.0\%$  POS.Ot vs.  $69.3\%$  NEG.Ot,  $p < 0.009$ ), in contrast to similar percent positive-negative in the NFC group ( $47.7\%$  POS.Ot vs.  $46.3\%$  NEG.Ot). The interesting finding of decreased percent positive osteocytes in the #NOF group, compared to similar percent positive-negative osteocytes in the NFC group, may suggest bone in #NOF individuals is undermineralised, as sclerostin protein expression has been found to be expressed only in mature osteocytes in fully-mineralised bone tissue (Poole *et al.*, 2005). These results may further inform understanding the mechanism of decreased mineralisation of bone in fragility fracture patients (Sutton-Smith *et al.*, 2008). Studies of the role of osteocytes and their derived factors in normal and bone pathology will aid in furthering the understanding of the pathogenesis of fragility fractures and the efficacy of new pharmaceuticals to treat osteoporosis.

**Disclosures:** L. Truong, None.

This study received funding from: The University of Adelaide and the National Health and Medical Research Council (Australia).

## SA149

See Friday Plenary number F149.

## SA150

**Proteins Involved in Mineralization Expressions Perturbations in Bones and Teeth of Msx2 Mutant Mouse Mandibles.** A. Bolanos\*, D. Hotton\*, A. Agalliu\*, M. Molla\*, B. Castaneda\*, B. Robert\*, F. Lézo\*, A. Berdal\*. <sup>1</sup>Laboratoire de Physiologie Orale Moléculaire (Eq. 5), INSERM UMRS 872, Centre de Recherche des Cordeliers, Paris, France, <sup>2</sup>Pasteur Institute - URA 2578 CNRS, Paris, France.

Homeobox genes of Msx family are implicated in early craniofacial skeleton development. The part of these genes later in the biomineralization has been underestimated while their expressions were described in all mineralized tissues forming cells. In contrast to Msx1 null mutant (KO) mouse that died at birth, the Msx2 KO mouse survives allowing the analysis of the impact of Msx2 absence on the expression of proteins implicated in the biomineralization.

In the present study, using immuno-histochemistry, in situ hybridization and quantitative RT-PCR, expressions of calbindin-D28K, osteocalcin, osteopontin, bone sialoprotein, collagen type I, amelogenin and ameloblastin were analyzed in mandible bones and teeth comparatively between Msx2 KO, Msx2 heterozygous and wild type mice.

Results show that all protein expressions are perturbed in the Msx2 KO mouse either in intensity as osteocalcin, collagen type I and amelogenin or in pattern as calbindin-D28K. In the Msx2 heterozygous mouse, the expression levels of some proteins implicated in the mineralization are also perturbed but evidence an opposite modulation compared to Msx2 KO. Indeed, amelogenin expression is increased in the dental epithelium of Msx2 heterozygous similarly to osteocalcin, bone sialoprotein and osteopontin in bones of the mandible. In Msx2 heterozygous mouse, the most striking result is the perturbation of calbindin-D28K expression pattern with an important level observed in the dental pulp. To conclude, this study evidences that Msx2 genetic status (KO, heterozygous and wild type) has important repercussions on the expression (level and pattern) of proteins implicated in the mineralization, so on the mineralization rank itself.

**Disclosures:** A. Bolanos, None.

This study received funding from: INSERM UMRS 872.

## SA151

**Circulating Fibronectin Affects Bone Matrix.** A. Bentmann\*, N. Kawelke\*, D. Moss\*, I. Nakchbandi\*. <sup>1</sup>Max-Planck Institute for Biochemistry and University of Heidelberg, Heidelberg, Germany, <sup>2</sup>Research Center Karlsruhe (ANKA), Karlsruhe, Germany.

Targeted deletion of fibronectin production by differentiating osteoblasts affects their function, but does not result in a significant decrease in the amount of fibronectin in the bone matrix or in a change in bone matrix. The liver is a major source of fibronectin. It also produces a number of proteins that are able to infiltrate the bone such as albumin and alpha2-HS-glycoprotein. We therefore examined the role of circulating fibronectin originating from the liver in bone.

Plasma fibronectin was labeled with Oyster-500 and injected in mice intraperitoneally. Examination of bone sections revealed infiltration of labeled fibronectin throughout the bone. This was not limited to areas of active bone mineralization, determined by injecting alizarin complexone prior to injecting labeled fibronectin. We then performed matings of fibronectin floxed mice with mice carrying the Cre gene under the control of the Mx or the albumin promoters in order to delete fibronectin production by the hepatocytes. Both lines showed a decrease in circulating fibronectin by more than 95% (Circulating fibronectin in the Mx line was  $4.6 \pm 0.1$  vs.  $6.2 \pm 0.4$  mg/L in the albumin line,  $p < 0.01$ ). Fibronectin staining in the liver-specific fibronectin knockouts revealed a significant decrease in the amount of fibronectin in the bone matrix that was confirmed by Western blotting.

The deletion of fibronectin in the liver was also associated with 13% decrease in bone mineral density in the Mx-cre harboring line (conditional knockouts:  $177.9 \pm 5.4$  vs. controls:  $205.4 \pm 6.2$  mg/cm<sup>3</sup>,  $n = 24$  and  $34$ ,  $p < 0.005$ ). There were no clear changes on either dynamic or static bone histomorphometry, however. Infrared microspectroscopy was therefore performed to determine whether structural changes could be seen in the matrix itself. The ratio of mineral to matrix was significantly decreased by 12% in the conditional knockout mice compared to littermate controls (Phosphate to protein ratio in conditional knockouts:  $8.76 \pm 0.20$  vs. controls:  $9.91 \pm 0.32$ ,  $n = 6$  mice per group and 9 measurements per mouse,  $p < 0.005$ ), suggesting that the loss of fibronectin in the matrix affects its mineral content.

In summary, circulating fibronectin originating from the liver infiltrates the bone matrix, where it affects the bone mineral density and mineral content in the bone. These effects take place in the absence of clear changes in the bone forming or bone resorbing cells. Thus fibronectin originating from the liver is needed for a normal matrix mineralization. This is in contrast to the effect of the deletion of fibronectin in osteoblasts showing that its production by them is required for a normal osteoblastic function without affecting the mineralization of matrix.

**Disclosures:** A. Bentmann, None.

## SA152

**PGD2 Downregulates MMP-1 and MMP-13 Expression in Human Osteoarthritic Chondrocytes.** N. Zayed\*, H. Afif\*, N. Chabane\*, J. Martel-Pelletier\*, J. Pelletier\*, H. Fahmi\*. CHUM, Université de Montréal, Montreal, QC, Canada.

**Purpose:** Prostaglandin (PG) D<sub>2</sub>, a cyclooxygenase (COX) metabolite, has been shown to play critical roles in multiple physiological processes including inflammation. Matrix metalloproteinases (MMPs), in particular MMP-1 and MMP-13 produced by chondrocytes, are major proteases responsible for cartilage degradation during osteoarthritis. This work was designed to investigate the effects of PGD<sub>2</sub> on interleukin-1 (IL-1)-induced MMP-1 and MMP-13 expression in human chondrocytes.

**Methods:** Cultured chondrocytes were stimulated with IL-1 in the absence or presence of PGD<sub>2</sub> and MMP-1 and MMP-13 protein production was evaluated by ELISA. mRNA expression and promoter activity were analyzed by real-time RT-PCR and transient transfection experiments, respectively. The expression of PGD<sub>2</sub> receptors, DP1 and CRTH2 was investigated using RT-PCR and Western blotting.

**Results:** PGD<sub>2</sub> dose-dependently decreased IL-1-induced MMP-1 and MMP-13 protein expression. Moreover, PGD<sub>2</sub> prevented IL-1-induced MMP-1 and MMP-13 mRNA expression as well as MMP-1 and -13 promoter activation, indicating that this effect occurs at the transcriptional level. We also demonstrated that chondrocytes expressed both PGD<sub>2</sub> receptors: DP1 and CRTH2.

**Conclusions:** These data indicate that PGD<sub>2</sub> inhibits IL-1-induced MMP-1 and MMP-13 production by human chondrocytes. Therefore, PGD<sub>2</sub> may play an important role in the chondrocyte response to inflammatory stimuli and may protect cartilage integrity.

**Disclosures:** N. Zayed, None.

This study received funding from: CIHR and FRSC.

## SA153

See Friday Plenary number F153.

## SA154

**Cathepsin K Expression During Enamel Formation.** C. E. Tye, Y. Ding\*, Y. P. Li, J. D. Bartlett\*. Department of Cytokine Biology, Forsyth Institute, Boston, MA, USA.

Dental enamel is unique in that it starts forming as a soft, protein-rich substance and ends as a hard, almost protein-free mineral. It is well established that enamel matrix proteins are degraded during enamel formation and these degraded proteins are removed from the matrix to allow for the increase in mineral content. Proteolytic processing is critical for proper enamel formation as homozygous mutation of either of the resident enamel proteases, matrix metalloproteinase-20 (MMP-20) or kallikrein-4 (KLK-4), causes *Amelogenesis Imperfecta* where the enamel is hypomineralized and protein-rich. Our objective is to determine if in addition to KLK-4 and MMP-20, other proteases may be involved in enamel formation. Cathepsin K has been shown to be important in the degradation of the collagenous matrix during bone resorption and we therefore investigated if cathepsin K may play a role in the degradation of the enamel matrix. RNA from molars of 3-11 day-old mice (secretory to maturation stage) was collected and expression of cathepsin K was assessed and quantified by RT-PCR and qPCR. High levels of cathepsin K expression were observed across amelogenesis with highest expression in mature enamel organ (6.35-fold increase over secretory stage). Immunohistochemical (IHC) staining of wild-type mouse incisors confirmed cathepsin K expression by ameloblasts. Cathepsin K was found to rapidly degrade recombinant amelogenin *in vitro* indicating a possible role for cathepsin K in enamel protein degradation. Cathepsin K may degrade the enamel proteins within the lysosomes once peptides are removed from the matrix, and it is possible that cathepsin K is secreted into the matrix to degrade the proteins during the maturation stage of enamel development. Examination of incisors from cathepsin K-null mice however, showed no significant alteration to prism pattern as assessed by scanning electron microscopy. Microhardness testing of enamel from cathepsin K-null mice revealed that loss of cathepsin K expression did not significantly alter enamel hardness. Our results suggest that cathepsin K is expressed by ameloblasts and may be part of a redundant pathway necessary to degrade proteins that are resorbed from the enamel matrix.

**Disclosures:** C.E. Tye, None.

## SA155

**Identification of Dipeptidyl Peptidase I as a Potential Activator of Kallikrein-4.** C. E. Tye<sup>1</sup>, C. T. Pham<sup>\*2</sup>, J. D. Bartlett<sup>\*1</sup>. <sup>1</sup>Department of Cytokine Biology, Forsyth Institute, Boston, MA, USA, <sup>2</sup>Division of Rheumatology, Washington University School of Medicine, St. Louis, MO, USA.

Kallikrein-4 (KLK-4) is a serine protease expressed during the maturation stage of enamel development and proteolytic processing of the enamel matrix by KLK-4 has been found to be critical for proper enamel formation. Homozygous mutation of KLK-4 causes *Amelogenesis Imperfecta* where the enamel is hypomineralized and protein-rich. KLK-4 has also been found to be overexpressed in prostate and ovarian cancer. The family of KLKs are synthesized as prepro-enzymes that are proteolytically processed to secreted pro-forms via the removal of their signal peptide. The secreted inactive pro-KLKs are then activated extracellularly by specific release of their amino-terminal propeptide. Activation of the pro-forms of the family of KLKs has been well studied; however, identification of the activator of KLK-4 remains elusive. The tooth specific protease matrix metalloproteinase-20 (MMP-20) has been shown to activate KLK-4 *in vitro*; however, KLK-4 and MMP-20 expression overlap only briefly during enamel development suggesting another protease activates KLK-4 *in vivo*. Dipeptidyl peptidase I (DPP I) is an ubiquitously expressed aminopeptidase that sequentially removes two N-terminal amino acid residues from folded proteins and was demonstrated to activate proenzymes of several chymotrypsin-like serine proteases. In this study we sought to examine DPPI expression in mouse enamel organ and determine if DPPI could act as an activator of KLK-4. RNA from molars of 3-11 day-old mice (secretory to maturation stage) was collected and expression of DPPI was assessed and quantified by RT-PCR and qPCR. High levels of DPPI expression was observed across amelogenesis with highest expression in mature enamel organ (11.4-fold increase over secretory stage). Immunohistochemical (IHC) staining of wild-type mouse incisors confirmed DPPI expression by ameloblasts. Using a fluorogenic substrate specific for KLK-4, DPPI was found to activate pro-KLK-4 *in vitro*. Examination of incisors from DPPI-null mice by scanning electron microscopy showed an altered prism pattern and microhardness testing of enamel from DPPI-null mice revealed that loss of DPPI expression caused a decrease in enamel hardness. Our results demonstrate that DPPI is highly expressed by maturation stage ameloblasts and may be involved in the activation of KLK-4. Identification of the *in vivo* activator of KLK-4 is important not only for furthering the understanding of enamel formation but also has exciting potential as a therapeutic target for both ovarian and prostate cancer.

**Disclosures:** C.E. Tye, None.

## SA156

**Canonical Wnt Signaling Suppresses BMP4 Accumulation from C3H10T1/2 Cells Transfected with BMP4 Expression Vector.** K. N. Kishimoto, E. Itoi\*. Department of Orthopaedic Surgery, Tohoku University School of Medicine, Sendai, Japan.

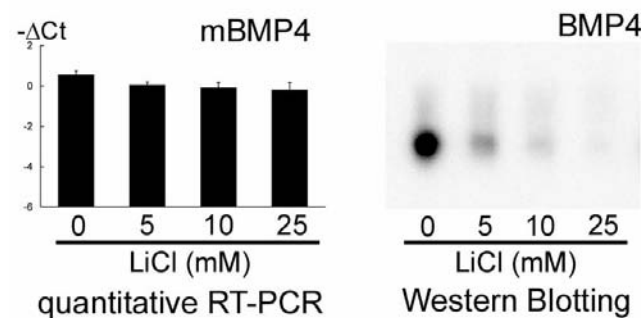
Lithium chloride is known as an inhibitor of glycogen synthase kinase-3 beta (GSK-3beta). Inhibition of GSK-3beta leads to accumulation of beta-catenin and activation of canonical Wnt signaling. The purpose of this study is to analyze the effect of canonical wnt

signal on the expression of BMP4 and other related factors during chondrogenic differentiation of C3H10T1/2 induced by BMP4 gene transfer.

C3H10T1/2 cells transfected with mouse BMP4 expressing plasmid was used for experiments. Plasmid was transferred by electroporation in the 4 mm cuvette at 500 V, 2 ms and 2 pulses using T-820 electroporator (BTX). A micromass formed with a drop of 10<sup>5</sup> transfected cells was allowed to adhere for 90 min and filled with 1 ml of medium containing 1% FBS, BSA, ascorbic acid 2 and ITS+. LiCl were added at 5, 10 and 25 mM. The effect of LiCl was confirmed by luciferase activity of wnt signaling reporter construct TOPflash. For quantitative RT-PCR, total RNA was isolated from each micromass. Real-time quantitative analyses were carried out with SYBR green I dye and ABI 7700 sequence detector. The culture medium was subjected to Western-blot analysis using anti-BMP4 antibody (SantaCruz) which react with both pro-BMP4 and BMP4. Micromass on 12-well plate were fixed with cold ethanol and immuno-staining was carried out with the same anti-BMP4 antibody and anti-mouse rabbit antibody conjugated with Alexa fluor 555 (Invitrogen).

LiCl treatment increased the luciferase activity of TOP flash reporter assay in a dose-dependent manner. The expression of BMP4 mRNA was not affected by LiCl. However, marked decrease of BMP4 protein by the addition of LiCl were seen in western blotting.(Figure) Also, immuno-staining for BMP4 on micromass showed decreased accumulation of BMP4 protein by LiCl. Under the presence of LiCl, alcian blue stainings of micromass were inhibited in a dose-dependent manner. Aggrecan, col2a1 and BMP antagonist noggin were also inhibited.

These results suggest that the activation of canonical wnt signaling by LiCl suppressed BMP4 protein synthesis or degraded BMP4 and inhibited chondrogenesis. The molecular system to explain this result has not been well understood. Cathepsin H (ctsh) which is previously reported to degrade BMP4 in the developmental stage of lung. The dose-dependent upregulation of ctsh by LiCl was also seen in our RT-PCR examination.



**Disclosures:** K.N. Kishimoto, None.

## SA157

**Coordinate Regulation of PTHrP and PTH1R in the Osteoblast Differentiation of C2C12 Cells Promoted by BMP-2.** A. R. G. Susperregui<sup>1</sup>, F. Vinals<sup>\*1</sup>, P. W. M. Ho<sup>\*2</sup>, M. T. Gillespie<sup>2</sup>, T. J. Martin<sup>2</sup>, F. Ventura<sup>\*1</sup>. <sup>1</sup>Barcelona University, Barcelona, Spain, <sup>2</sup>St. Vincent's Institute of Medical Research, Fitzroy, Australia.

PTH1R expression is enhanced during osteoblast differentiation and it is accepted as an osteoblast differentiation marker. Here we report that BMP-2 early induces PTH1R mRNA in C2C12 cells, which consequently become responsive to PTHrP in terms of cAMP production. Moreover, this induction is partially dependent on p38alpha as observed in experiments using p38alpha (-/-) MEFs. Simultaneously, BMP-2 also regulates the RANKL/OPG system strongly reducing the RANKL:OPG gene expression ratio. In our model, addition of exogenous PTHrP (1-34) does not modify BMP-2 regulation of RANKL and OPG. However, PTH1R expression and function affect osteoblast differentiation of C2C12 cells since PTHrP reduces the up-regulation of osteoblast master genes such as Runx2 and Osterix. Particularly PTHrP inhibits Osterix expression by activating the PKA pathway but not deregulating the Smad signaling pathway. C2C12 cells also modulate PTHrP expression in response to BMP-2. PTHrP mRNA expression is reduced by transcriptional regulation of PTHrP promoter but not enhancing PTHrP mRNA degradation. These data support the importance of a coordinate regulation of PTHrP and its receptor during osteoblastogenesis, and suggest that BMP-2 down-regulation of PTHrP could facilitate terminal differentiation of osteoblast.

**Disclosures:** A.R.G. Susperregui, None.

## SA158

See Friday Plenary number F158.

## SA159

**Impaired Bone Healing in a BMP2 Knockout Mouse Model of Distraction Osteogenesis.** N. Alam<sup>\*1</sup>, T. Haque<sup>\*2</sup>, M. Kotsioprifitis<sup>\*3</sup>, D. Lauzier<sup>\*2</sup>, R. St-Arnaud<sup>\*1</sup>, R. C. Hamdy<sup>2</sup>, V. Rosen<sup>\*4</sup>. <sup>1</sup>Genetics, Shriners Hospital for Children, Montreal, QC, Canada, <sup>2</sup>Orthopaedics, Shriners Hospital for Children, Montreal, QC, Canada, <sup>3</sup>Montreal Childrens Hospital, Montreal, QC, Canada, <sup>4</sup>Developmental Biology, Harvard School of Medicine, Boston, MA, USA.

Distraction osteogenesis (DO) is a surgical technique widely used for the treatment of limb length discrepancies, limb deformities, long bone non unions as well as bone loss due to trauma, infection or malignancies. One of its limitations is the long period of time required for the bone to consolidate. Bone Morphogenetic Proteins (BMPs), are essential growth factors involved in development (pre and post natal) and fracture healing. However, its specific role in DO remains to be determined. Modulating the signaling pathway of several BMPs including BMP 2, 4, 6 and 7 may be a potential strategy for accelerating bone formation during DO. The aim of the following study was to determine the significance of BMP2 during DO.

We analyzed bone formation during DO in heterozygous conditional BMP2 knockout mice. Bone samples were analyzed using MicroCT, Histology as well as Immunohistochemistry at various time intervals during the distraction and consolidation phase. Our results revealed that early bone consolidation is not impaired in mice having a 50% reduction in BMP2. MicroCT analysis showed no significant difference in bone volume, tissue volume or trabecular structure during the distraction phase and early consolidation phases. However, MicroCT images revealed poor bone healing at the end of consolidation in the mutant mice and a statistically significant reduction in trabecular number and increase in trabecular separation was apparent. Immunohistochemistry results showed that mutants had a higher upregulation of BMP2, BMP3, BMP7 BMP1b and the activin receptor compared to the control during the distraction phase. However, during early consolidation, with the exception of BMP1b, the controls had a higher expression of these genes.

In conclusion, our results indicated that in DO, BMP2 may be essential for proper bone healing at the end of consolidation but not during early consolidation. Several factors could explain these finding which include the possibility that during early bone consolidation, the function of BMP2 may be compensated for by other growth factors triggered by the process of distraction. There may also be a reserve of BMP2 within the bone, and thereby an endogenous reduction of its expression does not affect early bone healing. Further studies are being conducted in order to understand the complete role of BMP2 during DO in the molecular level.

**Disclosures:** N. Alam, None.

*This study received funding from: Shriners Grant.*

## SA160

**The Expression of BMP Antagonists During Fracture Healing.** D. B. Dean<sup>\*</sup>, H. C. Peters<sup>\*</sup>, J. T. Enders<sup>\*</sup>, W. Jin<sup>\*</sup>, J. T. Watson<sup>\*</sup>, Z. Zhang<sup>\*</sup>. Saint Louis University, St. Louis, MO, USA.

The bone morphogenetic protein (BMP) signalling cascade is "fine-tuned" by a group of BMP antagonists at almost every level of the pathway. This study investigated the temporal relationship between BMPs and their antagonists in bone formation using a normal fracture healing model.

Forty-two C57BL/6 mice (male, 7-week-old, approved by Saint Louis University Animal Care Committee) underwent controlled mid-shaft femoral fracture. Fractures were assessed with weekly radiographs, and fractures were healed in 3 weeks. Sequential sacrifice and tissue sampling of fracture callus were carried out at days 1, 3, 7, 14 and 21 for RNA isolation and immunohistochemistry. The tissue blocks were centered at the fracture line and included 2 fracture ends. Femoral bone segments from mid-shaft of the same aged unfractured mice were resected for experimental control. Real time RT-PCR was performed for the expression of BMP-2, -4, -6, -7; BMPR-1A, -2; and BMP antagonists: noggin, DAN, CHRDL, BAMBI, PRODC, SOST, SMAD6, SMAD7 CERBERUS, and Grem1.

Genes of the BMP and BMP receptors: Most noticeable trend was the upregulation of the expression of BMP-2 and 7. Both were significantly increased at day 7 (3.27 and 2.83-fold, respectively), and gradually decreased in the 2<sup>nd</sup> and 3<sup>rd</sup> weeks of fracture healing. While the expression of BMP-4 was increased with no statistical significance, BMP-6 expression decreased except at day 7, when it was virtually the same as the control. BMPR-2 was statistically unchanged at most time-points. In contrast, the expression of BMPR-1A was decreased at the most time-points.

Genes of BMP antagonists: The expression of PRDC, SOST, SMAD7, GREM1 and CERBERUS was downregulated during the course of fracture healing, except that, at day 7, CERBERUS was expressed at the control level. In contrast, noggin was significantly upregulated from day 1 through day 7 and decreased its expression at days 14 and 21. Three other genes, DAN, CHRDL and BAMBI, had increased expression only after day 7. While, the increase of expression of DAN and BAMBI continued to day 21, CHRDL was downregulated at day 21.

Using a mouse fracture model, this study demonstrated the interactions between BMPs and their antagonists during the course of normal fracture healing. The alterations of gene expression during fracture healing of each of the studied BMP antagonist are evident of the participation of BMP antagonists to bone formation. The roles of BMP antagonists in fracture healing are as diverse as BMPs. Some of them are suppressed, which may facilitate releasing and activation of BMPs. Some, which are upregulated in the late stages of fracture healing, may contribute to the bone remodelling process.

**Disclosures:** Z. Zhang, None.

*This study received funding from: Foundation for Orthopaedic Trauma.*

## SA161

**Dual Roles of Smad Proteins in the Conversion from Myoblasts to Osteoblastic Cells by BMPs.** J. Nojima<sup>1</sup>, K. Kanomata<sup>\*1</sup>, T. Fukuda<sup>1</sup>, A. Nakamura<sup>1</sup>, T. Tsukui<sup>\*2</sup>, Y. Okazaki<sup>\*3</sup>, R. Kamijo<sup>4</sup>, T. Yoda<sup>\*5</sup>, T. Katagiri<sup>1</sup>. <sup>1</sup>Division of Pathophysiology, Saitama Medical University, Research Center for Genomic Medicine, Hidaka-shi, Saitama, Japan, <sup>2</sup>Division of Experimental Animal Laboratory, Saitama Medical University, Research Center for Genomic Medicine, Hidaka-shi, Saitama, Japan, <sup>3</sup>Division of Functional Genomics & System Research, Saitama Medical University, Research Center for Genomic Medicine, Hidaka-shi, Saitama, Japan, <sup>4</sup>Department of Biochemistry, School of Dentistry, Showa University, Sinagawa-ku, Tokyo, Japan, <sup>5</sup>Department of Oral & Maxillofacial Surgery, Saitama Medical University, Moroyama, Saitama, Japan.

(Objective) BMPs induce ectopic bone formation in muscle tissue *in vivo* and convert differentiation pathway of myoblasts to differentiate into osteoblastic cells *in vitro*. At the last ASBMR Annual Meeting, we have reported that a constitutively activated mutant Smad1, Smad1(DVD), induced ALP activity and Osterix mRNA in C2C12 myoblasts. Here, we further examined the molecular mechanisms of the conversion of myoblast differentiation by BMPs.

(Method and Result) Although wild-type or Smad1(DVD) showed minimal inhibitory effect on myogenic differentiation, co-expression of Smad4 markedly reduced number of myosin heavy chain (MHC)-positive muscle cells. We found that the inhibition of myogenic differentiation was induced by nuclear Smad4 alone. The role of Smad4 in myogenic differentiation was confirmed using mouse embryonic fibroblasts (MEFs) prepared from Smad4<sup>flxed/flxed</sup> mice. The basal transcriptional activity of MyoD was increased approximately 1.4-fold in MEFs infected with Cre-expressing virus, and this increase was not suppressed by BMP-4. A deletion analysis of Smad suggested that MH2 domain may interact with other partner(s) to suppress the myogenic differentiation. We searched a protein-protein interaction (PPI) database which was constructed based on the mammalian two-hybrid method established by the RIKEN group, and found some Smad-4 binding proteins. Among them, we focused on E4F1, which contains zinc fingers and a ubiquitin E3 ligase domain. E4F1 was expressed in nuclei. The interaction between E4F1 and Smad4 was detected in nuclear Smad4 via its MH2 domain. Over-expression of wild-type E4F1 or a mutant protein lacking E3 ligase domain suppressed myogenic differentiation in the absence of BMPs. Knockdown of endogenous E4F1 reversed the inhibition of myogenic differentiation by BMP signaling.

(Conclusion) We found that Smad4 and E4F1, a novel partner of nuclear Smad4, cooperatively regulate the inhibition of myogenic differentiation by BMP signaling. Taken together, these findings suggest that the Smad signaling pathway may play dual roles in the conversion of myoblasts to osteoblastic cells induced by BMPs.

**Disclosures:** J. Nojima, None.

## SA162

**Improvement of Alveolar Bone Quality by Local bFGF Injection - Histological and Cellular Biological Analysis in a Rabbit Model.** M. Oshima<sup>\*</sup>, W. Sonoyama, M. Ono<sup>\*</sup>, K. Shimono<sup>\*</sup>, T. Hikasa<sup>\*</sup>, Y. Okamoto<sup>\*</sup>, Y. Tsuchimoto<sup>\*</sup>, Y. Matsuka<sup>\*</sup>, T. Kuboki<sup>\*</sup>. Department of Oral Rehabilitation and Regenerative Medicine, Okayama University, Okayama, Japan.

Basic fibroblast growth factor (bFGF) is known to have multiple roles in bone development and regeneration. Although it is already reported that bFGF accelerates the healing of periodontal bony defect and increases the bone quantity, its effect on local bone quality is not clarified yet. In this study, recombinant human bFGF was injected into bone marrow spaces of the rabbit mandible, then bone quantity and quality was examined histologically and bone morphometric parameters were analyzed by  $\mu$ CT. In addition, bone marrow cells were isolated, and the effects of bFGF on these cells were examined *in vitro* in terms of osteogenesis and osteoclastogenesis. Ilium and tibia was used as a control against mandible.

Four weeks after injection (100  $\mu$ g of bFGF), accelerated bone formation was observed obviously in the cancellous bone area of the mandible, but not in the tibia.  $\mu$ CT analysis revealed that several parameters (i.e. bone volume/tissue volume, trabecular thickness, and trabecular number) were significantly improved only in the mandible against control (normal saline solution injected-site). Although MTS assay revealed that cell proliferation was enhanced dose-dependently by bFGF in all osteogenic cells (isolated from bone marrow of mandible, ilium, and tibia), proliferative capacity of the mandibular osteogenic cells was significantly higher than that of the iliac and tibial cells. Under an osteogenic induction condition, the tibial osteogenic cells showed higher calcified nodule formation than the others at day-7 after osteogenic induction. Osteogenesis was suppressed by bFGF in all osteogenic cells. Osteoclastogenesis, analyzed by TRAP staining, was suppressed by high-dose ( $10^{-9}$ M) bFGF, and enhanced by low-dose ( $10^{-12}$ M) bFGF in all bone marrow cells isolated from the mandible, ilium, and tibia. However, the number of mature multinucleated osteoclasts derived from the iliac and tibial bone marrow was more than that from the mandibular bone marrow. Bone resorption activity was evaluated by pit formation assay and found to be suppressed by high-dose ( $10^{-9}$ M) bFGF. Identical to the results of TRAP staining, bone resorption area made by the iliac and tibial osteoclasts was much larger than that by the mandibular osteoclasts.

These results suggest that local bFGF injection can be one of the suitable strategies to improve alveolar bone quality, possibly due to the different nature of the mandibular bone marrow.

**Disclosures:** M. Oshima, None.

## SA163

See Friday Plenary number F163.

## SA164

**NARS Induced by Basic Fibroblast Growth Factor Regulates the Proliferation and Survival of Osteoblasts.** S. Park<sup>\*1</sup>, J. Byun<sup>\*2</sup>, H. Choi<sup>\*2</sup>, G. Jargalan<sup>\*1</sup>, Y. Rhee<sup>2</sup>, S. Lim<sup>2</sup>. <sup>1</sup>Brain Korea 21 Project for Medical Science, College of Medicine, Yonsei University, Seoul, Republic of Korea, <sup>2</sup>Division of Endocrinology and Endocrine Research Institute, Department of Internal Medicine, College of Medicine, Yonsei University, Seoul, Republic of Korea.

Basic Fibroblast growth factor (bFGF), the potent bone anabolic agent, regulates bone development, growth, remodeling and fracture healing. The intracellular signaling of bFGF leads to activation of genes involved in cell proliferation, migration, differentiation and survival. However, little is known about bFGF-regulated proteins in bone. Therefore, in this study, protein profiling in bFGF-treated MC3T3-E1 preosteoblast cells was evaluated using proteomics. Asparaginyl-tRNA synthetase (NARS) was one of the proteins that up-regulated more than ten-fold in MC3T3-E1 cells after treatment of bFGF. NARS is a member of aminoacyl-tRNA synthetases (ARSs) and is responsible for catalyzing the specific aminoacylation of tRNA with asparagines. Overexpression of NARS significantly increased the level of proliferation and conferred resistance to apoptosis induced by serum deprivation in MC3T3-E1 cells and calvarial cells. In contrast, the level of proliferation was remarkably decreased and cell death was increased in siNARS-transfected cells compared to those of control siRNA-transfected cells. In conclusion, NARS induced by growth factors could be one of highly linked enzymes to the proliferation and survival of osteoblastic cells.

Disclosures: S. Park, None.

## SA165

**Serum FGF-23 Level in Term Infants.** M. Takaiwa<sup>1</sup>, K. Aya<sup>\*2</sup>, T. Miyai<sup>\*2</sup>, B. Yuan<sup>3</sup>, M. Yokoyama<sup>\*4</sup>, M. K. Drezner<sup>3</sup>, N. Kodani<sup>\*1</sup>, T. Morishima<sup>\*2</sup>, H. Tanaka<sup>5</sup>. <sup>1</sup>Dept. of Pediatrics, Matsuyama Red Cross Hospital, Matsuyama, Japan, <sup>2</sup>Dept. of Pediatrics, Okayama University Graduate School of Medicine, Dentistry and Pharmaceutical Sciences, Okayama, Japan, <sup>3</sup>Dept. of Medicine, University of Wisconsin, Madison; GRECC, Wm F. Middleton VAMC, Madison, WI, USA, <sup>4</sup>Dept. of Obstetrics and Gynecology, Matsuyama Red Cross Hospital, Matsuyama, Japan, <sup>5</sup>Dept. of Pediatrics, Okayama Saiseikai General Hospital, Okayama, Japan.

Recent studies demonstrated that FGF-23 (fibroblast growth factor 23) is not only crucial in the pathogenesis of inherited and acquired hypophosphatemia, but also a physiological regulator of Ca and P homeostasis. Hence, serum FGF-23 level would be widely applied as a clinical marker for assessment of mineral metabolism. In our previous study on mouse FGF-23, we reported both serum level and mRNA expression of FGF-23 are elevated in pre-weaned mice than that of mature animals. From these results, we decided to establish the normal range of human serum FGF-23 level during neonatal period to utilize FGF-23 for assessment of mineral metabolisms during infancy. In this study, we examined serum FGF-23 level at 5 days after birth of normal term neonates (5 day-old infants, N=8). We also analyzed serum from umbilical vein (cord blood, N=6). As control, we tested serum of healthy adults (healthy adults, N=6). As known, Ca level in normal newborns falls rapidly within first 48 hours of life (early neonatal hypocalcemia) and consecutively, intact PTH (iPTH) and 1,25(OH)2D3 (1,25D) start elevating. Thus, we also measured serum Ca, P, iPTH and 1,25D level. All protocols were approved by the Matsuyama Red Cross hospital ethical committee. Informed consent was obtained from all participants or legal guardians. FGF-23 level was measured using FGF-23 ELISA kit (Kainos). Data are expressed as the mean  $\pm$  SEM and statistically analyzed by a 'Bonferroni' testing. A value of  $p < 0.05$  was considered significant. Serum FGF-23 level is significantly elevated in 5 day-old infants (65.8  $\pm$  10.1 pg/ml) than in healthy adults (32.0  $\pm$  8.0 pg/ml,  $p < 0.05$ ). On the other hand, serum FGF-23 level was not different from healthy adults in cord blood samples (22.6  $\pm$  4.9 pg/ml). Serum Ca, P, iPTH and 1,25D levels were compatible with previous reports. Considering P is a potent regulator of FGF-23 expression, and our previous study indicated that the elevated serum FGF-23 level in murine infants is due to increased FGF-23 mRNA expression, our present observations indicate that FGF-23 is induced in response to hyperphosphatemia commonly accompanied with early neonatal hypocalcemia. Although further investigations are required, our results suggested that regulatory mechanism of FGF-23 is already active, and may have considerable contribution in mineral metabolism during early infancy.

Disclosures: M. Takaiwa, None.

## SA166

**IL-12 Induces Apoptosis in TNF- $\alpha$ -mediated Osteoclastogenesis *in vivo*.** M. Yoshimatsu, H. Kitaura, Y. Fujimura<sup>\*</sup>, T. Eguchi<sup>\*</sup>, H. Kohara, Y. Morita<sup>\*</sup>, N. Yoshida<sup>\*</sup>. Division of Orthodontics and Dentofacial Orthopedics, Nagasaki University Graduate School of Biomedical Sciences, Nagasaki, Japan.

Recently, much importance has been placed on the relationship between cytokines and bone metabolism. We reported that IL-12 induced apoptosis in bone marrow cells treated with TNF- $\alpha$  resulted in the inhibition of osteoclastogenesis *in vitro*. This study aimed to investigate the effects of IL-12 on TNF- $\alpha$  osteoclastogenesis *in vivo*. C57BL/6J mice (8-week-old males) were classified into three groups. Each group was subjected to 5 daily supracalvarial administrations of TNF- $\alpha$  as a positive control, TNF- $\alpha$  and IL-12, or PBS as a negative control. Animals were sacrificed on day 6 and fixation and demineralization performed. Histological sections of calvariae were stained for tartrate-resistant acid phosphatase (TRAP) and TUNEL. For isolating total RNA, mice calvariae frozen in liquid nitrogen were homogenized. mRNA was isolated from homogenized samples using the TRIzol reagent. cDNA was synthesized from total RNA. The expression levels of Cathepsin K, TRAP, Fas and FasL mRNA of mice calvariae were quantified by real-time-based RT-PCR. Many osteoclasts were observed in mice administered TNF- $\alpha$ . On the other hand, the numbers of osteoclasts in mice administered TNF- $\alpha$  and IL-12 were less than those treated with TNF- $\alpha$ . The expression levels of Cathepsin K and TRAP were also reduced in mice administered TNF- $\alpha$  and IL-12 compared with mice administered TNF- $\alpha$ . The mRNA level of Fas was increased when TNF- $\alpha$  was administered and the mRNA level of FasL was increased when IL-12 was administered. The apoptotic alteration of calvarial cells in situ was recognized when TNF- $\alpha$  and IL-12 were administered. In this study, IL-12 was shown to inhibit TNF- $\alpha$ -mediated osteoclastogenesis by apoptosis *in vivo*. Apoptotic alteration might be induced by the interaction of TNF- $\alpha$ -induced Fas and IL-12-induced FasL.

Disclosures: M. Yoshimatsu, None.

## SA167

**A Model of High Body Mass: Bone Mineral Density, Bone Markers and Adipocytokine Levels in High Level Male Rugby Players.** S. Breban<sup>\*</sup>, C. Chappard, C. Benhamou. CHR Orleans, INSERM Unit 658, Orleans, France.

Rugby practice offers a chance of studying very high body mass subjects and the repercussion on BMD measurements, bone metabolism and adipocytokine concentrations. Forty six men aged between 17 and 28 years participated in this study and were divided in two groups: 20 national or international ranked rugby players (aged 21.6 $\pm$ 4.6 years; 11.9 $\pm$ 2.9 hours/week) and 26 age and sex matched controls (aged 22.7 $\pm$ 4.5 years; 2.2 $\pm$ 2.0 hours/week). BMC (g) and BMD (g/cm<sup>3</sup>) were measured by DXA (Delphi, Hologic®, Waltham, MA), at whole body (WB), lumbar spine (L1-L4) and non dominant femoral neck (FN). Height, weight and body composition (whole body lean mass (kg) and fat mass (kg)) were derived from the WB DXA measurements. Circulating levels of serum leptin (ng/mL) and adiponectin (µg/mL), serum osteocalcin (ng/mL) and C-terminal telopeptides of type I collagen (Ctx) (ng/mL) were assessed by ELISA assay. Rugby players had significantly higher BMD values at WB ( $p < 0.0001$ ), L1-L4 ( $p < 0.0001$ ) and non dominant FN ( $p < 0.0001$ ) compared to controls. These differences were maintained after adjustment to height, adipocytokine concentration and bone markers concentration, but there were no more differences when BMD values were adjusted to weight and WB lean mass. Rugby players also presented significantly higher concentrations of osteocalcin ( $p < 0.001$ ) and Ctx ( $p = 0.006$ ). Leptin concentrations were significantly lower in athletes ( $p = 0.02$ ) and this persisted after adjustment to WB fat mass. However, there was no significant difference for adiponectin concentrations between athletes and controls. No significant relationships were found between leptin concentrations and any measured BMD parameters in rugby players and controls ( $p > 0.05$ ). Male rugby players seemed to present a specific bone metabolism with very high BMD and bone turnover markers values. These BMD levels were as a majority explained by a higher WB lean mass in athletes compared to controls. Our results also suggested that, high body mass was associated with lower serum leptin levels. Finally, leptin concentrations were not directly related to BMD measurements in young adults.

Disclosures: S. Breban, None.

## SA168

See Friday Plenary number F168.

## SA169

**Mesenchymal Stem Cells Enhance Fracture Healing: Essential Role for Cytokines in Homing and Anti-Inflammatory Response.** F. Granero-Molto<sup>1</sup>, J. A. Weis<sup>\*1</sup>, B. Landis<sup>\*2</sup>, L. Longobardi<sup>\*1</sup>, M. I. Miga<sup>\*3</sup>, A. Spagnoli<sup>1</sup>. <sup>1</sup>Pediatric Endocrinology, University of North Carolina at Chapel Hill, Chapel Hill, NC, USA, <sup>2</sup>Pediatric Endocrinology, Vanderbilt University, Nashville, TN, USA, <sup>3</sup>Biomedical Engineering, Vanderbilt University, Nashville, TN, USA.

Healing failure occurs in 10-20% of the bone fractures. Limitations in adult stem cells (MSC) have been shown to be a key element in lack of healing. In this study, we determine: 1) an essential homing receptor for the migration of MSC to the fracture site; 2) the systemic anti-inflammatory effects of MSC; 3) the MSC regenerative role. MSC were

isolated from 4-6 week old syngenic FVB males mice constitutively expressing luciferase. Syngenic FVB female mice 8-10 weeks old were subjected to a three point bending stabilized fracture and injected with  $10^6$  MSC. Fractured females without transplant were used as control (NC). The anti-inflammatory effect of MSC was analyzed detecting levels of TNF $\alpha$  and IL-1 $\beta$  in the serum of MSC and NC animals at 1, 3 and 7 days post-fracture (PF). Healing was assessed by distraction biomechanical testing (BMT) at 14 days. For migration studies, MSC were selected based on the presence or absence of the surface receptor CXCR4. The *in vivo* MSC migration was detected using bioluminescence at 1, 3, 7 and 14 days PF and their influence on the callus properties analyzed by  $\mu$ CT.

BLI studies showed that MSC migrated to the fracture site and CXCR4 was essential for MSC homing. In fact, in mice transplanted with MSC lacking CXCR4, cell homing to the fracture was totally abolished. Furthermore, CXCR4 transplant produced a significant increase in the total and soft tissue volume of the callus (Fig. 1). Transplanted MSC reduced the serum levels of the pro inflammatory cytokines TNF $\alpha$  and IL-1 $\beta$  at day 1 and 3 PF.

*p<0.05 vs NC		Day 1 PF	Day 3 PF	Day 7 PF
TNF $\alpha$	NC (n=5)	89.44 $\pm$ 39.97	51.29 $\pm$ 27.19	6.69 $\pm$ 3.32
(pg/ml)	MSC (n=6)	17.68 $\pm$ 6.82*	9.57 $\pm$ 5.08*	9.13 $\pm$ 4.85
IL-1 $\beta$	NC (n=5)	84.16 $\pm$ 44.23	40.48 $\pm$ 5.03	8.25 $\pm$ 10.04
(pg/ml)	MSC (n=6)	2.88 $\pm$ 1.81*	4.62 $\pm$ 3.93*	3.58 $\pm$ 2.66

BMT analysis showed that MSC transplant improved the healing by a significant increase in the energy to failure (NC, 0.14 $\pm$ 0.05 mJ; MSC 0.49 $\pm$ 0.11 mJ, p<0.05).

In conclusion, MSC have an anti-inflammatory effect, MSC migration is dependent on CXCR4 expression and the migration is beneficial for the fracture healing process.

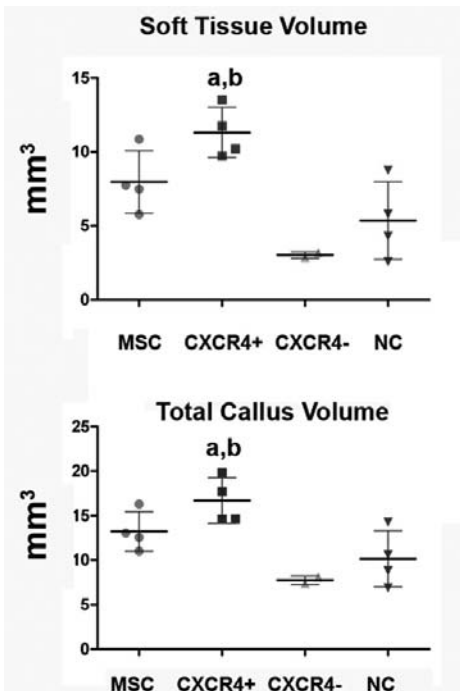


**Figure 1:  $\mu$ CT analysis of the callus 14 days after fracture shows increased amount of soft tissue and total callus volume in CXCR4+ transplanted animals. a, p<0.05 CXCR4+ vs CXCR4-; b, p<0.05 CXCR4+ vs NC.**

**Disclosures:** F. Granero-Molto, None.

This study received funding from: NIH-NIDDK.

## SA170

**Transient Expression of CXC Receptor 2 in Human Mesenchymal Stem Cells Stimulates Chemotaxis Toward CXC Ligand 8 and Increased Mineralization in the Presence of Osteogenic Medium.** D. S. Bischoff\*, N. S. Makhijani\*, D. T. Yamaguchi. Research Service, VA Greater Los Angeles Healthcare System, Los Angeles, CA, USA.

The potential role of CXC chemokines bearing the glu-leu-arg (ELR<sup>+</sup>) motif in bone differentiation was studied using a human mesenchymal stem cell (hMSC) model. Previously, we have shown that osteogenic differentiation of hMSCs increases expression of the ELR<sup>+</sup> CXC chemokine CXC Ligand 8 (CXCL8), also known as Interleukin-8 or IL-8. hMSCs from various donors were tested and in only one case did the addition of

exogenous CXCL8 (10 nM) induce the expression of the bone marker alkaline phosphatase (ALP). There are two ELR<sup>+</sup> CXC chemokines receptors, CXC Receptor 1 (CXCR1) and CXC Receptor 2 (CXCR2). CXCL8 binds equally well to CXCR1 and CXCR2 while the other ELR<sup>+</sup> CXC chemokines bind with much greater affinity to CXCR2. CXCR2 has been shown to be associated with the angiogenic function of the ELR<sup>+</sup> CXC chemokines. Since the levels of CXCR1 and CXCR2 vary among donors and seem to decrease with passage of the cells, we used the Amara Nucleofector Device to transiently transfect hMSCs with CXCR1 and CXCR2 expression plasmids or with the pTA vector as a negative control. Transfected cells were tested for the ability to migrate toward increasing levels of CXCL8 or CXCL1 (GRO $\alpha$ ) ranging from 0.1 to 100 nM using Transwell inserts. Non-transfected cells did not migrate even at the highest level of CXCL8 or CXCL1 (100 nM). Cells transfected with the negative control pTA did not migrate in response to 10 nM CXCL8. Those cells expressing CXCR1 had decreased levels of cell migration with a chemotaxis index (CI) value of 0.75 (ratio of migrating cells towards chemoattractant / migrating cells in negative control), and those expressing CXCR2 had increased levels of migration toward 10 nM CXCL8 with a CI value 1.9. Transfected hMSCs were also tested for the ability to induce mineral deposition by alizarin red staining. Cells expressing CXCR2 have larger mineralized nodules at 2 and 3 weeks post-transfection when grown in the presence of osteogenic medium (OGM) compared to cells transfected with either the pTA negative control or the CXCR1 expression plasmid. Expression of ALP mRNA was also induced at 7 days in the CXCR2-transfected cells in the presence of OGM. Transfection of pTA or the CXCR1 expression plasmid did not induce mineralization or ALP expression at 7 days in OGM. Cells grown in basal proliferation medium did not induce mineralization or ALP mRNA expression under any circumstances even in the presence of 10 nM CXCL8. Conclusion: 1) expression of CXCR2 in hMSC confers chemotactic ability of hMSC cells toward CXCL8 and 2) stimulates expression of ALP mRNA and mineralization in the presence of OGM.

**Disclosures:** D.S. Bischoff, None.

This study received funding from: VA Merit Review.

## SA171

See Friday Plenary number F171.

## SA172

**Transforming Growth Factor  $\beta$  Receptor I Kinase Inhibitor Increases Bone Mass in Normal Mice.** K. S. Mohammad<sup>1</sup>, G. Balooch<sup>2</sup>, C. Chen<sup>2</sup>, E. Stebbins<sup>3</sup>, D. Wong<sup>3</sup>, R. Derynck<sup>2</sup>, L. Suva<sup>4</sup>, T. A. Guise<sup>1</sup>, T. Alliston<sup>2</sup>.

<sup>1</sup>University of Virginia, Charlottesville, VA, USA, <sup>2</sup>University of California San Francisco, San Francisco, CA, USA, <sup>3</sup>Scios Inc., Fremont, CA, USA, <sup>4</sup>University of Arkansas for Medical Sciences, Little Rock, AR, USA.

TGF $\beta$  can promote and inhibit specific stages of osteoblast and osteoclast differentiation and function throughout development. Consequently, the net effect of altered TGF $\beta$  signaling on bone is difficult to predict, an uncertainty supported by the complicated bone phenotypes of mice with modified TGF $\beta$  signaling. Whether or not TGF $\beta$  can be modulated in a therapeutically beneficial way in bone remains unknown. Our recent findings show that partial inhibition of TGF $\beta$  signaling in genetically modified mice increases bone mass, bone matrix material properties such as elastic modulus and hardness, and fracture toughness. In addition, pharmacologic blockade of TGF $\beta$  signaling with SD-208, a specific inhibitor of the type I TGF $\beta$  receptor (T $\beta$ RI), increases bone mass in mammary tumor bearing mice. Therefore, we sought to determine the effect of pharmacologic T $\beta$ RI inhibition on the biological and mechanical properties of bone in normal mice.

C57/Bl6 mice were administered SD-208 (20 mg/kg or 60 mg/kg) or vehicle for 6 weeks (n=15/group). Bone mineral density (BMD) was assessed longitudinally by DXA and terminally by micro-CT and X-ray tomographic microscopy (XTM). T $\beta$ RI inhibitors significantly increase BMD in male and female mice at all sites (whole body, spine, tibia, femur). MicroCT analysis showed that, trabecular, but not cortical, bone volume is increased by SD-208. Histomorphometry and in vitro differentiation assays revealed that T $\beta$ RI inhibitors increase TBV by anabolic and anti-catabolic mechanisms. Osteoblast numbers and the bone formation rate are increased in SD-208-treated mice relative to vehicle treated controls, whereas osteoclast numbers are reduced. Likewise, bone marrow cultures from SD-208-treated mice have increased osteoblast colony forming activity, but a decreased capacity to form TRAP-positive multinucleated osteoclasts. Consistent with results in genetically modified mice, pharmacologic inhibition of TGF $\beta$  signaling increases the mineral concentration and elastic modulus of bone matrix, when measured by XTM and nanoindentation, respectively. Finally, vertebral bone from SD-208-treated mice exhibits an increased load to failure in unconfined compression tests. In conclusion, inhibition of TGF $\beta$  type I receptor function exerts both anabolic and anticatabolic effects on bone, causing a net increase in bone mass and vertebral bone load to failure. TGF $\beta$  inhibitors may have therapeutic value for treating diseases associated with low bone mass.

**Disclosures:** K.S. Mohammad, None.

## SA173

**IL-12 Stimulates the Osteoclast Inhibitory Peptide-1 (OIP-1) Gene Expression in CD4<sup>+</sup> T-Cells.** S. Shanmugarajan<sup>1</sup>, N. Kawanabe<sup>2</sup>, M. Koide<sup>2</sup>, J. E. Arroyo<sup>\*1</sup>, L. L. Key<sup>1</sup>, S. V. Reddy<sup>1</sup>. <sup>1</sup>Charles P. Darby Children's Research Institute, Medical University of South Carolina, Charleston, SC, USA, <sup>2</sup>Medicine-Hematology/Oncology, University of Pittsburgh, Pittsburgh, PA, USA.

Osteoclast formation and activity is regulated by local factors produced in the bone microenvironment. Immune cell products such as IFN- $\gamma$  and IL-12 are potent inhibitors of osteoclast formation. We have previously identified and characterized the human osteoclast inhibitory peptide-1 (OIP-1/hSca), a member of Ly-6 gene family. Also, demonstrated that IFN- $\gamma$  stimulates OIP-1 promoter activity and expression in osteoclast precursor cells. However, it is unknown if IL-12 regulates OIP-1 expression in the bone microenvironment. Real-time PCR analysis demonstrated that IL-12 treatment (4 hr) significantly enhanced OIP-1 mRNA expression in normal human bone marrow derived mononuclear cells. Since IL-12 induces IFN- $\gamma$  production by T-cells, we further tested if IFN- $\gamma$  participates in IL-12 stimulation of OIP-1 expression in these cells. IL-12 treatment in the presence of a neutralizing antibody against IFN- $\gamma$  significantly increased OIP-1 mRNA expression, suggesting that IL-12 directly regulates OIP-1 gene expression. Interestingly, real-time PCR analysis demonstrated that IL-12 induces OIP-1 expression (3.2-fold) in CD4 positive T-cells; however, there was no significant change in CD8 positive T-cells. Also, IL-12 (10ng/ml) treatment of Jurkat T-cells transfected with OIP-1 gene (-1 to -1988 bp) promoter-luciferase reporter plasmid demonstrated a 5-fold and 2.7-fold increase in OIP-1 gene promoter activity in the presence and absence of antibody against IFN- $\gamma$ , respectively. We previously identified a Stat binding motif (-1629 to -1639 bp position) in the OIP-1 gene promoter region. We further show that Stat-3 inhibitor peptide treatment decreased (42.8%) IL-12 stimulated OIP-1 promoter activity. In contrast, Stat-1 inhibitor has no significant effect on OIP-1 gene promoter activity. Chromatin Immunoprecipitation (ChIP) assay confirmed Stat-3, but not Stat-1 binding to the OIP-1 gene promoter element in response to IL-12 stimulation. These results suggest that IL-12 stimulates the OIP-1 gene expression through Stat-3 signaling in CD4 positive T-cells and that OIP-1 is an important autocrine/paracrine regulator of osteoclast development and bone remodeling.

**Disclosures:** S. Shanmugarajan, None.  
This study received funding from: NIH.

## SA174

See Friday Plenary number F174.

## SA175

**The Mechanism of Action of Lactoferrin's Bone Anabolic Activity.** J. Cornish, A. Chhana\*, J. M. Lin\*, K. E. Callon\*, I. R. Reid, D. Naot. Medicine, University of Auckland, Auckland, New Zealand.

Lactoferrin, an 80kDa iron-binding glycoprotein present in milk and other exocrine secretions in mammals, is anabolic to bone at physiological concentrations. Lactoferrin stimulates the proliferation, differentiation and survival of the osteoblasts, as well as potentially inhibiting osteoclastogenesis in bone marrow cultures. In vivo, local injection of lactoferrin results in substantial increases in bone formation and bone area. In a critical bone defect model in vivo, lactoferrin was also seen to promote bone growth. The mitogenic effect of lactoferrin in osteoblast-like cells is mediated mainly through LRP1, a member of the low density lipoprotein receptor-related proteins that are primarily known as endocytic receptors; however another yet unidentified receptor is responsible for the anti-apoptotic actions. Lactoferrin also induces activation of multiple pathways: p42/44 MAPK signalling as well as PI3-kinase-dependent phosphorylation of Akt in osteoblasts. Recently, we have further delineated the possible mechanisms of action of lactoferrin in bone, in both osteoclasts and osteoblasts. The mouse macrophage cell line, RAW 264.7, demonstrated that lactoferrin acts directly on osteoclasts to inhibit their development independently of osteoblasts. In addition, the receptor involved is *not* LRP1. In human osteoblasts treated with lactoferrin, we identified differentially-expressing genes, using microarray analysis then validated in real time PCR significant up-regulation of IGF1 and down-regulation of DKK1. We then extended these studies looking at earlier time points in the MC3T3-E1 osteoblastic cell-line, using real-time PCR with custom-designed microfluidic cards. The cards were used to measure the relative expression levels of 48 genes including bone-specific transcription factors, matrix and inflammatory proteins. Lactoferrin induced a rapid, dose-dependent increase in the transcription levels of IL-6, IL-11, the pro-inflammatory factor prostaglandin-endoperoxide synthase 2 (COX-2) and the transcription factor nuclear factor of activated T cells-1 (NFATc1). Subsequent real-time PCR experiments in primary rat osteoblasts confirmed that IL-6, IL-11, COX-2 and NFATc1 transcription levels increase significantly and transiently within two hours of lactoferrin treatment. The role these genes play in mediating the effects of lactoferrin in osteoblasts is currently being investigated by the use of specific inhibitors. Lactoferrin is proving to be a positive regulator of bone growth potentially having a physiological role in bone growth and healing, and a therapeutic role as an anabolic factor in osteoporosis.

**Disclosures:** J. Cornish, None.  
This study received funding from: Health Research Council of New Zealand.

## SA176

See Friday Plenary number F176.

## SA177

**Stimulation of Macrophage TNF $\alpha$  Production by Orthopaedic Wear Particles Requires Activation of the ERK1/2/Egr-1 Pathway but Is Independent of p38 and JNK.** M. A. Beidelschies\*, H. Huang\*, M. R. McMullen\*, M. V. Smith\*, A. S. Islam\*, V. M. Goldberg\*, X. Chen\*, L. E. Nagy\*, E. M. Greenfield<sup>1</sup>. <sup>1</sup>Orthopaedics, Case Western Reserve University, Cleveland, OH, USA, <sup>2</sup>Pathobiology, Cleveland Clinic Foundation, Cleveland, OH, USA.

Bone loss that causes aseptic loosening of orthopaedic implants is initiated by pro-inflammatory cytokines produced by macrophages in response to implant-derived wear particles. MAPK signaling pathways are activated by the particles; however, it is not clear which of the MAPK pathways are important for the initial response to the wear particles and which are only involved at later steps in the process, such as osteoclast differentiation. Here, we show that the ERK1/2, p38, and JNK pathways are rapidly activated by the wear particles. However, incubation of RAW264.7 cells or bone marrow-derived macrophages with specific inhibitors and their inactive analogues showed that ERK1/2 is required for the initial responses to the wear particles (TNF $\alpha$  mRNA expression and TNF $\alpha$  protein secretion). In contrast, the p38 and JNK pathways were not required for these responses. ERK1/2 activation by wear particles is also required for increased expression of the transcription factor Egr-1 as well as for Egr-1's ability to bind to the TNF $\alpha$  promoter. Measurements of luciferase activity in RAW264.7 macrophages transfected with TNF $\alpha$  promoter-luciferase constructs containing specific deletions and mutations demonstrated that Egr-1 is also required for wear particles to increase TNF $\alpha$  transcription. These results, together with our previous studies of the PI3K/Akt pathway, demonstrate that wear particles coordinately activate multiple signaling pathways and multiple transcription factors to stimulate production of pro-inflammatory cytokines, such as TNF $\alpha$ . The current study also demonstrates that the ERK1/2/Egr-1 signaling pathway is activated to a much greater extent by wear particles with adherent endotoxin than by "endotoxin-free" wear particles. These results demonstrate that the ERK1/2/Egr-1 pathway contributes to the ability of adherent endotoxin to potentiate cytokine production, osteoclast differentiation, and bone loss induced by wear particles.

**Disclosures:** M.A. Beidelschies, None.

## SA178

**Alterations in Bone Structure and Growth in Dwarf Rats with a Depressed Growth Hormone/IGF-I Axis.** A. C. F. Bassit, M. K. Altman\*, S. E. Franz\*, M. E. Leal, T. J. Wronski. Physiological Sciences, University of Florida, Gainesville, FL, USA.

Growth hormone (GH) is an important factor in the regulation of bone growth and the maintenance of adult bone. The majority of its skeletal effects appear to be mediated by insulin-like growth factor I (IGF-I). The dwarf rat is an animal model for studies of the effects of GH/IGF-I deficiency on bone structure and function. In these mutant rats, GH synthesis is selectively reduced to about 6% of normal in females, and serum IGF-I levels are about 10% of normal. Body growth is retarded, but the dwarf rats are healthy and skeletal malformations do not occur. The objective of this study was to use imaging (pQCT) and histomorphometric techniques to determine the skeletal consequences of GH/IGF-I deficiency in dwarf rats. Groups of normal Lewis rats (N=7) and dwarf rats (N=7) were maintained in the same nutritional and environmental conditions until 11 weeks of age. At the time of euthanasia, the mean body weight of the Lewis rats was 52.9% higher than the dwarf rats (187.6  $\pm$  10.9g vs. 122.7  $\pm$  5.6g, P<0.0001), and their left femurs were 14.8% longer. Not surprisingly, tibial longitudinal bone growth was three-fold greater in the Lewis rats compared to the dwarf rats (72.1  $\pm$  4.9  $\mu$ m/d vs. 24.5  $\pm$  10.7  $\mu$ m/d, P<0.0001). All the bone structural parameters evaluated by pQCT in the femur, including total mineral content, total mineral density, trabecular content, trabecular density, trabecular area, cortical density, cortical area, cortical content, cortical thickness, and periosteal circumference, were significantly greater in the Lewis rats compared with the dwarf rats. Cancellous bone histomorphometry was performed in the right proximal tibia. Cancellous bone volume was markedly lower in the dwarf rats than in the Lewis rats (1.2  $\pm$  1.4% vs. 18.9  $\pm$  3.3%, P<0.0001), and this cancellous osteopenia was associated with decreased trabecular number and width, and increased trabecular separation. Mean values for osteoclast surface, an index of bone resorption, were nearly identical in Lewis and dwarf rats. Although mean values for osteoblast and osteoid surfaces were not significantly different between the two groups, cancellous mineral apposition rate, an index of osteoblast activity, was significantly lower in dwarf rats compared with Lewis rats (0.9  $\pm$  0.2  $\mu$ m/d vs. 1.5  $\pm$  0.3  $\mu$ m/d, P<0.0005). These findings indicate that GH/IGF-I deficiency in dwarf rats has profound negative effects on bone growth, accumulation of bone mass, and osteoblast activity. In view of the contention that IGF-I may mediate the skeletal effects of bone anabolic agents, dwarf rats appear to be a promising animal model for studies of these interactions.

**Disclosures:** A.C.F. Bassit, None.  
This study received funding from: NIH Grant R37 AG09241.

## SA179

**IGF-I Secreted from Osteoblasts as a Major Chemotactic Factor for Osteoblasts.** M. Nakasaki<sup>1</sup>, K. Yoshioka<sup>\*1</sup>, H. Yoshikawa<sup>\*2</sup>, K. Itoh<sup>1</sup>. <sup>1</sup>Biology, Osaka Medical Center for Cancer and Cardiovascular Diseases, Osaka, Japan, <sup>2</sup>Orthopedic Surgery, Osaka University Medical School, Osaka, Japan.

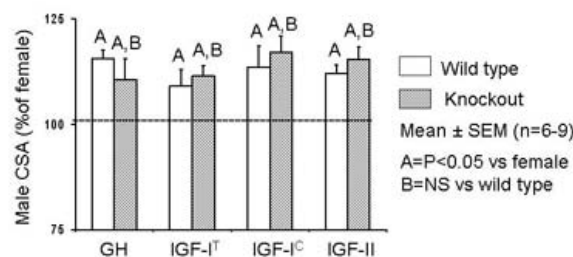
Osteoblast recruitment to the site of future bone formation is essential for skeletal development, bone remodeling and fracture healing, but the mechanism of which remains to be clarified. Here, we hypothesized that osteoblasts secrete a chemoattractant(s) for osteoblast recruitment and examined the serum-free conditioned medium of mouse osteoblast-like cell line MC3T3-E1 for its ability to induce osteoblast migration. Using a modified Boyden chamber assay, we found that the medium induced MC3T3-E1 chemotaxis in a dose-dependent manner. Employing several chromatographic procedures and liquid chromatography equipped with tandem mass spectrometry analysis, we identified insulin-like growth factor-I (IGF-I) as a potent chemotactic factor from the conditioned medium. IGF-I induced cell migration of both MC3T3-E1 cells and primary mouse osteoblasts, and checkerboard analysis revealed that IGF-I induced chemotaxis and not simply chemokinesis. By neutralization of IGF-I activity with specific anti-mouse IGF-I antibody, both osteoblast monolayer wound healing and cellular polarization were impaired, whereas human IGF-I replenishment reversed these inhibitory effects. IGF-I also promoted cell spreading on fibronectin in an integrin  $\beta$ 1-dependent manner. IGF-I induced Akt and ERK phosphorylation in MC3T3-E1 cells and a PI3K inhibitor, LY294002, but not a MEK inhibitor, PD98059, inhibited IGF-I-induced cell migration and wound healing. Together, these findings suggest that IGF-I secreted from osteoblasts regulates osteoblast migration through the activation of PI3K signaling.

**Disclosures:** M. Nakasaki, None.

## SA180

**Is Growth Hormone/IGF-I Mediated Mechanism Involved in Regulating Gender Differences in Bone Size?** S. Mohan, K. E. Govoni, J. E. Wergedal. JLP VA Medical Center and Loma Linda Univ, Loma Linda, CA, USA.

It is now generally well accepted that estrogen and testosterone exert opposite effects on periosteal bone expansion and that greater bone size in males is mediated via androgens acting through androgen receptors. However, the molecular pathway by which estrogens and androgens exert gender-specific effects on periosteal expansion remains to be fully elucidated. Based on the findings that growth hormone (GH)/IGF-I is a major regulator of postnatal skeletal growth, we and others have predicted that sex hormones interact with GH/IGF axis to regulate bone size. To evaluate this hypothesis, we compared femur cross sectional area (CSA) measured by pQCT in transgenic mice with disruption of GH/IGF axis. We predicted if gender differences in bone size are due to interaction between sex hormone and GH/IGF axis, then disruption of GH/IGF axis should eliminate gender differences in bone size. GH-deficient *lit/lit* mice with mutation in GH releasing hormone receptor, IGF-I total knockout (IGF-I<sup>-/-</sup>), lacks both endocrine and local IGF-I, osteoblast specific IGF-I conditional knockout (IGF-I<sup>-/-</sup>), lacks osteoblast produced local IGF-I and IGF-II null mice were evaluated at 3 and 8 weeks of age. Corresponding age-matched control littermate mice were used as wild types. As expected, at prepubertal age of 3-weeks, femur CSA was not different between male and female mice for any of the strains studied.



At post pubertal age of 8 weeks, femur CSA was significantly greater in the males compared to females for all four transgenic lines studied at 8 weeks of age. To our surprise, disruption of GH, IGF-I, osteoblast-derived IGF-I or IGF-II did not affect bone size differences between male and female mice at 8 weeks (Figure). However, femur CSA was decreased as previously reported by 39, 67, 31 and 21% respectively in mice lacking GH, total IGF-I, osteoblast-derived IGF-I or total IGF-II respectively, thus demonstrating the importance of GH/IGF axis in regulating bone size during postnatal growth. In conclusion, our data using the transgenic mouse models do not support the hypothesis that GH/IGF axis is a major player in contributing to gender specific effect on bone size and suggest that the greater bone size in male mice is due to GH/IGF-independent actions of androgen on bone.

**Disclosures:** S. Mohan, None.

This study received funding from: National Institutes of Health; Grant Number: AR048139 (SM).

## SA181

See Friday Plenary number F181.

## SA182

**Insulin-Like Growth Factor Binding Protein (IGFBP)-6 Is a Negative Regulator of Osteoblast Differentiation and Bone Formation.** C. A. Strohbach<sup>1</sup>, C. H. Rundle<sup>2</sup>, J. E. Wergedal<sup>\*2</sup>, T. A. Linkhart<sup>\*2</sup>, S. Mohan<sup>2</sup>, D. D. Strong<sup>\*2</sup>. <sup>1</sup>Loma Linda University, Loma Linda, CA, USA, <sup>2</sup>MDC, J.L.P. VAMC, Loma Linda, CA, USA.

We previously reported that IGFBP-6 (BP6) is a negative regulator of osteoblast (Ob) differentiation, with BP6 retroviral overexpression inhibiting MC3T3-E1 mineralization and Ob marker gene expression possibly via an IGF-independent intracellular mechanism. To further elucidate the role of BP6 in Ob differentiation, we used siRNA to knockdown BP6 mRNA and protein in MC3T3-E1 pre-Obs and less differentiated C2C12 cells and observed an increase in Osterix, Dlx5, ALP, BSP, Osteocalcin and PheX mRNAs. While our *in vitro* studies provide compelling evidence that BP6 can play an important inhibitory role in Ob differentiation, the role of BP6 in normal skeletal development and maintenance has not been established. To address this question, transgenic (Tg) mice were generated that overexpressed BP6 in Obs. The BP6 transgene was placed under the control of an Ob lineage restricted promoter that contained the proximal Col1a2 promoter and modified Runx2 enhancer sequences. Col1a2 and Runx2 are early marker genes for Ob lineage commitment and this chimeric promoter was not suppressed by BP6 transgene overexpression. Multiple founders were identified and backcrossed two generations to reduce effects of genetic background differences and establish independent Tg lines. BP6 was expressed in bones isolated from BP6 Tg mice but not in other tissues. Skeletal parameters were studied by DEXA in BP6 Tg and wild type littermate controls at 6, 12, and 24wks. Areal BMD was significantly reduced in the femurs of male (7%,  $p < 0.03$ ,  $n=8$ ) and female mice (14%,  $p < 0.002$ ,  $n=8$ ) in two independent lines of BP6 Tg mice compared to wild-type littermate controls providing evidence that BP6 is a negative regulator of bone formation *in vivo*. However, the BP6 Tg mice did not display differences in body weight or femur length, suggesting that BP6 does not influence the growth promoting effects of the IGFs that have been observed in transgenic mice expressing other IGFBPs. In conclusion, our previous and current findings demonstrate that BP6 is an important negative regulator of Ob differentiation and bone formation and that BP6 effects on Obs involve decreased expression of transcription factors and marker genes that are critical for Ob differentiation.

**Disclosures:** C.A. Strohbach, None.

This study received funding from: VA Merit Award.

## SA183

**Serum IGF-1 Is a Developmental Determinant of Bone Size.** S. Yakar<sup>1</sup>, E. Canalis<sup>2</sup>, W. Mejia<sup>\*1</sup>, H. Sun<sup>\*1</sup>, Y. Wu<sup>\*1</sup>, Y. Kawashima<sup>\*1</sup>, P. Nasser<sup>\*3</sup>, V. Williams<sup>\*3</sup>, K. J. Jepsen<sup>3</sup>. <sup>1</sup>Endocrinology, Mount Sinai School of Medicine, New York, NY, USA, <sup>2</sup>St. Francis Hospital and Medical Center, Hartford, CT, USA, <sup>3</sup>Orthopaedics, Mount Sinai School of Medicine, New York, NY, USA.

Serum insulin-like growth factor I (IGF-I) originates mainly from the liver. Liver-specific *igf1* gene deletion (LID mouse model) causes abrogated expression of IGF-I mRNA in liver, dramatic reductions (75%) in circulating IGF-I and a 3-4 fold increase in serum GH. Here we studied developmental changes in skeletal acquisition in a state of serum IGF-I deficiency. LID mice were followed from 4 to 52 weeks of age. Histomorphometry at 4, 8 and 20 weeks of age in both control and LID mice revealed no changes in bone volume fraction (%BV/TV) and a mild increase in eroded surface at 20 weeks of age (Table 1). Flow cytometry analysis of bone marrow-derived cells revealed a significant and consistent decrease in CD11b/Mac-1+ cells in LID mice, suggesting reductions in osteoclast progenitors in marrow of LID mice. Femoral microCT analyses showed reductions in total area (TtAr), marrow area (MaAr), and cortical area (CtAr) in LID relative to control mice. No differences in matrix mineralization were noted at any age. Morphological differences were apparent at 4 weeks, but were significant at 8 and 16 weeks, indicating that the reduced serum IGF-I affected bone postnatally, at the time when serum IGF-I normally peaks. The reduced serum IGF-I thus had two primary effects on bone; (1) it resulted in slender bones and (2) it impaired structural adaptation necessary to compensate for the increased slenderness (i.e. through reduced marrow expansion and/or increased matrix mineralization). These data suggest that serum IGF-I is a developmental determinant of bone size and strength, and that compensatory increases in serum GH are insufficient for gaining structural adaptations but may account for the increased resorption at later ages.

Table 1: Histomorphometry of the distal femur from control and LID mice

	4 weeks		8 weeks		20 weeks	
	Control	LID	Control	LID	Control	LID
BV/TV (%)	17.4+/-1.8	16.5+/-1.2	9.0+/-0.6	7.9+/-0.5	6.4+/-0.3	5.6+/-0.4
ES/BS (%)	12.3+/-0.4	10.7+/-1.3	8.9+/-0.5	7.9+/-0.7	12.0+/-0.6	17.2+/-1.2
TbTh (um)	14.0+/-0.9	13.1+/-0.5	13.2+/-0.4	11.7+/-0.3	12.1+/-0.5	10.5+/-0.6
Nob/Tar (/mm <sup>2</sup> )	692.9+/-111.1	696.5+/-54.4	416.8+/-14.6	412.7+/-21.2	228.8+/-20.0	246.4+/-23.4
Noc/Tar (/mm <sup>2</sup> )	74.4+/-10.7	71.8+/-11.8	28.9+/-1.8	24.3+/-2.0	59.6+/-4.7	89.6+/-10.7
TbSp (um)	67.9+/-5.3	66.7+/-4.1	137.1+/-8.1	139.8+/-8.0	178.9+/-10.9	181.2+/-14.2
TbN (/mm)	12.3+/-0.8	12.6+/-0.7	6.8+/-0.3	6.7+/-0.3	5.4+/-0.3	5.4+/-0.4
MAR (um/day)			0.4+/-0.0	0.5+/-0.0	0.1+/-0.0	
BFR (um <sup>3</sup> /um <sup>2</sup> /day)			0.024+/-0.00	0.026+/-0.00	0.004+/-0.00	0.005+/-0.00

**Disclosures:** S. Yakar, None.

This study received funding from: NIH.



## SA184

**Endocrine IGF-1 Maintains Linear Growth in the Total Absence of Tissue IGF-1.** Y. Wu\*, S. Elis\*, H. Sun\*, Y. Kawashima\*, S. Yakar. Endocrine, Mount Sinai School of Medicine, New York, NY, USA.

Insulin-like growth factor-I (IGF-I) plays a fundamental role in growth and development, and acts in an endocrine and autocrine/paracrine fashion. A daunting challenge has been to sort out which mode of IGF-I action (i.e. endocrine or autocrine/paracrine) facilitates skeletal growth. We previously generated the liver-specific IGF-I gene deletion (LID) mouse model that demonstrated a 75% reduction in circulating IGF-I levels and exhibited mild growth abnormalities, suggesting an important role for tissue IGF-I. Here we took a reversed approach and created a mouse model with total IGF-I gene-deletion (KO), that expresses Hepatic IGF-I Transgene (HIT) under the control of the transthyretin promoter. The KO-HIT mice express solely liver-derived IGF-I, show 2fold increase in serum IGF-I levels and exhibit complete absence of tissue IGF-I. Serum levels of GH and the IGF binding proteins in KO-HIT mice are similar to controls. Furthermore, body weight of KO-HIT mice was similar to controls in both males and females from 3-16 weeks of age. We reveal that in the total absence of tissue IGF-I action, endocrine IGF-I restores femoral linear growth in both males and females. These findings call into question previous concepts about the GH/IGF-I axis and have major implications for various growth disorders and therapeutic options.

**Disclosures:** S. Yakar, None.

*This study received funding from: NIH.*

## SA185

**Induction of Oxidative Stress and Diversion of  $\beta$ -catenin from TCF- to FOXO-mediated Transcription by Glucocorticoids or  $\text{TNF}\alpha$  in Osteoblastic Cells.** M. Almeida, E. Ambrogini, M. Martin-Millan, L. Han, A. Warren\*, R. S. Shelton\*, L. Plotkin, T. Bellido, C. A. O'Brien, R. L. Jilka, R. S. Weinstein, S. C. Manolagas. Center for Osteoporosis and Metabolic Bone Diseases, University of Arkansas for Medical Sciences and Central Arkansas Veterans Healthcare System, Little Rock, AR, USA.

Oxidative stress induces activation of the FoxO family of transcription factors and diverts  $\beta$ -catenin from Wnt induced TCF/Lef- transcription to FoxO-mediated transcription--thereby decreasing osteoblastogenesis. Prompted by evidence that oxidative stress is also a causal mechanism of the insulin resistance produced by glucocorticoids (GC) and the inflammatory cytokine  $\text{TNF}\alpha$  alike, we tested the hypothesis that the potent suppressive effects of GC and  $\text{TNF}\alpha$  on bone formation may be caused, at least in part, by increasing oxidative stress and antagonizing the beneficial effects of Wnt signaling on osteoblast generation and survival. We report that dexamethasone (Dex) ( $10^{-7}$  M) or  $\text{TNF}\alpha$  ( $10^{-8}$  M) increased reactive oxygen species levels in osteoblast progenitors (C2C12 cells). Moreover, Dex- or  $\text{TNF}\alpha$ -induced apoptosis in C2C12, committed osteoblasts (OB6), and osteocytes (MLO-Y4), was abolished by the antioxidant N-acetyl-L-cysteine (NAC), the glutathione peroxidase mimic ebselen, as well as catalase, the enzyme that converts  $\text{H}_2\text{O}_2$  to water. Consistent with a pro-oxidant effect, Dex or  $\text{TNF}\alpha$  increased the phosphorylation of the adapter protein  $\text{p66}^{\text{thc}}$ --a redox enzyme that generates mitochondrial  $\text{H}_2\text{O}_2$  to trigger mitochondria swelling and apoptosis. In addition,  $\text{TNF}\alpha$  or Dex, similar to  $100 \mu\text{M}$   $\text{H}_2\text{O}_2$ , increased the activity of a FoxO-luciferase reporter construct and the transcription of the pro-apoptotic gene Bim (a known FoxO target). The stimulation of  $\text{p66}^{\text{thc}}$  phosphorylation as well as the activation of FoxO-luc by Dex or  $\text{TNF}\alpha$  were abolished in cells pre-treated for 1 h with NAC. Moreover, the effect of Dex or  $\text{TNF}\alpha$  on apoptosis was prevented by a dominant negative FoxO construct. On the other hand,  $\text{TNF}\alpha$  or Dex suppressed the Wnt3a-induced activation of a TCF-reporter construct, as well as alkaline phosphatase activity. In agreement with the in vitro data, implantation of slow-release pellets containing prednisolone for 28 d in 5-month-old C57BL/6 male mice increased ROS levels in the bone marrow, as well as  $\text{p66}^{\text{thc}}$  phosphorylation and Bim gene expression in bone. All these effects were prevented by administration of NAC. We conclude that activation of FoxO transcription factors by oxidative stress represents a previously unappreciated cell-autonomous mechanism of Wnt/ $\beta$ -catenin antagonism contributing to the adverse effects of aging, GC excess and inflammatory cytokines on bone alike.

**Disclosures:** M. Almeida, None.

## SA186

See Friday Plenary number F186.

## SA187

**Monoclonal Antibody to Transforming Growth Factor  $\beta$  Inhibits Tumor Burden and Osteolysis in a Pre-clinical Model of Bone Metastasis.** S. Biswas<sup>1</sup>, C. Wilburn<sup>\*2</sup>, S. A. Munoz<sup>\*2</sup>, J. A. Sterling<sup>1</sup>, S. Lonning<sup>\*3</sup>, G. R. Mundy<sup>4</sup>. <sup>1</sup>Cancer Biology, Vanderbilt University, Nashville, TN, USA, <sup>2</sup>Vanderbilt Center for Bone Biology, Vanderbilt University, Nashville, TN, USA, <sup>3</sup>Genzyme Corporation, Framingham, MA, USA, <sup>4</sup>Vanderbilt Center for Bone Biology, Vanderbilt University, Nashville, TN, USA.

Breast cancer is the most common cancer and the second leading cause of cancer-related deaths for women in the United States. Breast cancer cells metastasize to bone with high affinity. Transforming growth factor  $\beta$  (TGF $\beta$ ), one of the most abundant cytokines

found in the bone matrix, is secreted in active form at the site of osteolytic bone resorption. By acting on both the bone microenvironment and cancer cells, TGF $\beta$  acts as a major driver of the vicious cycle of bone metastasis. Inhibiting TGF $\beta$  signaling in breast cancer cells by the use of dominant negative receptor constructs or the use of small molecular inhibitors of the receptor kinase have been shown to reduce tumor burden and bone lesions in preclinical breast cancer metastasis models. However, small molecule kinase inhibitors often show non-specific effects on unrelated kinases, and thus have potential for unwanted side effects. Therefore, we have taken a different approach, by which we block all three isoforms of TGF $\beta$  systemically using a pan-TGF $\beta$  antibody, 1D11(Genzyme). Using MDA-MB-231 human breast cancer cells in a cardiac injection model, we have investigated the efficacy of 1D11 on the following:

- (1) metastatic progression of breast cancer cells in bone and
- (2) modulation of bone lesions in tumor bearing mice.

We have demonstrated that, treatment with 1D11(10mg/ Kg, three times a week for two weeks) reduces the number of bone lesions (Control: 7.4, Treated: 2.3, P<0.005), area of bone lesions (control: 7535.5 cm<sup>2</sup>, treated: 865.5 cm<sup>2</sup>, P<0.001). Increases in the bone volume as measured by the ratio of BV/TV (Control: 0.093, Treatment: 0.198, P=.01) using micro-CT analysis of tibia. Mice were treated with either 1D11 or control antibody (13C4) i.p. three times every week for two weeks. Treatment was initiated two weeks after tumor inoculation. These results show that 1D11 effectively reduces tumor burden and bone lesions in this preclinical model of human breast cancer metastasis to bone.

**Disclosures:** S. Biswas, None.

## SA188

See Friday Plenary number F188.

## SA189

**Tissue-Engineering and Co-culture System Based Disc Regeneration Mesenchymal Stem Cell's Role.** M. Nan<sup>\*1</sup>, S. Moon<sup>2</sup>, C. Lee<sup>\*1</sup>, J. Lee<sup>\*1</sup>, E. Kwon<sup>\*1</sup>, H. Kim<sup>\*3</sup>, K. Lee<sup>\*3</sup>, H. Lee<sup>\*2</sup>, E. Moon<sup>\*2</sup>, H. Kim<sup>\*2</sup>, H. Kim<sup>\*2</sup>, I. Kwon<sup>\*1</sup>, H. Chun<sup>\*4</sup>, S. Park<sup>5</sup>. <sup>1</sup>Yonsei University College of Medicine, Seoul, Republic of Korea, <sup>2</sup>Department of Orthopedic Surgery, Yonsei University College of Medicine, Seoul, Republic of Korea, <sup>3</sup>Allgraft and Biotechnology, Korea Bone Bank Co.,Ltd, Seoul, Republic of Korea, <sup>4</sup>Kyung Hee University, Seoul, Republic of Korea, <sup>5</sup>Department of Orthopedic Surgery, Korea University, Seoul, Republic of Korea.

Intervertebral disc (IVD) degeneration is caused by loss of water content in nucleus pulposus (NP) which is resulted from proteoglycan and type II collagen reduction. To regenerate IVD, transforming growth factor-beta1 (TGF-beta1) and bone morphogenetic protein-2 (BMP-2) can be utilized. As a technique of tissue engineering, composite IVD implants are fabricated as novel materials for disc replacement. Mesenchymal stem cells (MSCs) are known to be multipotent in tissue regeneration. Hence, the object of this study was to examine MSC based co-cultured cells in atelocollagen type I scaffold under the influence of TGF-beta1 and BMP-2. NP cells and/or MSCs were cultured at the rate of 0:1, 1:1, 1:0 in type I atelocollagen scaffold. And culture media was added with 5% FBS including TGF-beta1 of 10ng/ml, BMP-2 of 100ng/ml respectively. [<sup>35</sup>S] Sulfur incorporation for proteoglycan synthesis and [<sup>3</sup>H]-thymidine incorporation for proliferation were measured. RT-PCR was performed to assess the aggrecan, collagen type I and II, osteocalcin mRNA expressions. As result, co-cultures of MSC and NP cells in scaffold showed significant decreases in proteoglycan synthesis compared to those of NP cells only (p<0.05). Co-cultures in scaffold with TGF-beta1 or BMP-2 demonstrated increased newly synthesized proteoglycan compared to simple co-cultures (p<0.05). NP cell culture in scaffold with TGF-beta1 or BMP-2 showed significant increase in proteoglycan synthesis compared to co-culture. Aggrecan and collagen type II mRNA expression were more pronounced in NP cell culture alone than co-cultures. Adding MSC to NP cells in atelocollagen type I scaffold did not result in increased matrix synthesis consequently and chondrogenic phenotype expression and MSC based tissue engineering for disc regeneration seems not to be effective.

**Disclosures:** S. Moon, None.

*This study received funding from: Brain Korea 21 project Medical Sciences Yonsei University and Grand No.R01-2006-000-10933-0 from the Basic Research Program of the Korea Science & Engineering Foundation.*

## SA190

See Friday Plenary number F190.

## SA191

**Analytical Validation of Diasorin Liaison and Roche Elecsys Methods for the Determination of Osteocalcin.** E. Cavalier\*, P. Delanaye\*, A. Carlisi\*, J. Chapelle\*. Clinical Chemistry, University Hospital of Liege, University of Liege, Liege, Belgium.

Osteocalcin (OSC) determination is not an easy task. Indeed, "intact" OSC (AA 1-49) is unstable because it is cleaved between AA 43 and 44. This generates an N-mid fragment (AA 1-43), much more stable than intact OSC. The antibodies used in the kits must thus recognize both OSC and N-mid fragment.

The aim of our study was to validate 2 automated methods (Diasorin Liaison (LIA) and Roche Elecsys (ELEC)) designed for the determination of OSC in serum.

Both methods were found to be sensible (limit of detection < 0.50 ng/mL) and reproducible (intra- and inter-assay variation respectively < 2 and < 5%).

We performed a recovery test according to the NCCLS recommendations. This showed a mean recovery of 98% for LIA and 97% for ELEC. The dilution of 3 sera containing elevated levels of OSC showed a slightly better linearity for ELEC than for LIA (mean recovery: 98 vs. 115%).

When we compared the results obtained with the 2 methods on 50 patients, the Bland-Altman test showed a mean difference of 6.9 ng/mL and a clear tendency for ELEC to give higher results than LIA in patients presenting elevated OSC levels. The results obtained with ELEC were significantly higher (31%;  $p < 0.0001$ ) than those obtained with LIA.

We studied the stability of OSC at room temperature (RT), +4°C and -20°C on 10 fresh samples. Our results showed that OSC was stable up to 3 days at RT. At 4°C, a significant ( $p < 0.05$ ) but slight increase of maximum 6% was observed after 3 days. At -20°C, we also observed a significant ( $p < 0.05$ ) increase of 8.5% after 2 days, but a decrease of 9 and 11% respectively after 15 and 30 days ( $p < 0.05$ ).

In non-menopausal women, the reference range published for ELEC is broader than LIA (< 31 ng/mL vs. < 24 ng/mL respectively) which is consistent with our observations, whereas in post-menopausal ones, LIA's reference range are surprisingly higher than ELEC (< 59 ng/mL vs. < 46 ng/mL). This discrepant observation may be attributable to the different means used by the 2 societies to establish their reference range. Indeed, Diasorin selected patients with 25-OH vitamin D levels > 20 ng/mL and estimated the higher and lower limits on a Gaussian distribution (mean  $\pm$  2 SD). On the other hand, Roche evaluated the reference range in women with no hormonal substitution treatment and took the percentiles 5 and 95 as normal limits.

In conclusion, these 2 techniques perform analytically well but they do not give comparable results. This is due, for one part, to the lack of an International standard against which the societies could calibrate their kits, and for the other part, to the possible difference in the cross reactions between the antibodies and the N-mid fragment.

**Disclosures:** E. Cavalier, None.

## SA192

**High Bone Mass Due to Increased Bone Formation in Mice Lacking the Calcitonin Receptor.** J. H. Keller\*, A. K. Huebner, P. Catala-Lehnen, T. Schinke, M. Amling. Center for Biomechanics and Skeletal Biology, Department of Trauma, Hand, and Reconstructive Surgery, University Medical Center Hamburg-Eppendorf, Hamburg, Germany.

Although the hormone calcitonin (CT) is well known for its inhibitory effect on osteoclasts, its physiologic function in bone remodelling is still not fully clarified. This is in part due to recent findings showing that the inactivation of CT in mice does not only result in increased bone resorption, but also in increased bone formation. The latter observation was especially surprising, since the calcitonin receptor (CTR) is considered not expressed by osteoblasts. Therefore, in order to analyze, how the inhibitory effect of CT on bone formation can be explained at the cellular level, we took advantage of the Cre-Lox-technology, allowing cell-specific gene deletion in mice. Since the replacement of CTR exons 6 and 7 by a neomycin resistance gene has been described to result in lethality of homozygous embryos, but in increased bone formation of heterozygous mice, we inserted loxP sites into introns 5 and 7 of the CTR gene, allowing CTR inactivation in cells expressing the *Cre-recombinase*. As a control, mice carrying two "floxed" alleles were first crossed with transgenic mice expressing *Cre* in all cell types, including germ cells, thereby leading to the generation of CTR<sup>+/+</sup> mice with a Cre-independent heterozygous deletion of exons 6 and 7. Surprisingly, when we mated these mice, we obtained living CTR<sup>-/-</sup> offspring, displaying no obvious abnormalities. To verify the success of the approach, we first confirmed the absence of functional CTR in these mice by radioligand binding assays and immunohistochemistry. Thereafter, we embarked on a complete skeletal analysis using static and dynamic histomorphometry. At the age of 3 months we already observed a significantly increased trabecular bone volume in the CTR<sup>-/-</sup> mice, accompanied by an elevated bone formation rate. The same was observed in 6 months old mice, where the differences to wildtype littermates were even more pronounced (BV/TV: 23.0  $\pm$  3.0 % vs. 12.5  $\pm$  0.6 %, BFR/BS: 230  $\pm$  31  $\mu$ m<sup>3</sup>/μm<sup>2</sup>/y vs. 101  $\pm$  6  $\mu$ m<sup>3</sup>/μm<sup>2</sup>/y). At the age of 12 months, the bone formation rate was still two-fold higher in the CTR<sup>-/-</sup> mice, but this was accompanied by cortical porosity due to increased bone resorption. Thus, since the observed phenotype resembles the one previously described for mice lacking CT, it appears that the control of bone formation is the major function of the CTR, at least in mice. In addition, having established mice with a "floxed" CTR allele should allow answering the question, whether the effect of CT on osteoblasts is mediated indirectly through CTR expression in another cell type.

**Disclosures:** J.H. Keller, None.

## SA193

**Subcutaneous Administration Of Salmon Calcitonin: Bone Protective Effect In Adjuvant Arthritis Prevention Model In Rats.** J. A. Gasser<sup>1</sup>, P. Ingold<sup>1\*</sup>, A. Venturiere<sup>\*1</sup>, B. Jost<sup>\*2</sup>, R. Loeffler<sup>\*3</sup>, J. Dawson<sup>\*2</sup>, M. Azria<sup>4</sup>.

<sup>1</sup>Musculoskeletal Research, Novartis Institutes for BioMedical Research, Basel, Switzerland, <sup>2</sup>Autoimmunity and Transplantation, Novartis Institutes for BioMedical Research, Basel, Switzerland, <sup>3</sup>Technical Research & Development, Novartis Pharma AG, Basel, Switzerland, <sup>4</sup>Calcitonin Biology & Safety, Novartis Pharma AG, Basel, Switzerland.

Skeletally mature Wistar rats were injected intradermally with a vehicle or 0.1ml of a suspension/rat containing 6mgM Tuberculosis antigen H37 RA (Difco) to induce inflammatory arthritis. Starting from day 0, rats were treated either with daily s.c injections of placebo, salmon calcitonin (sCT) at a dose of 1, 3.2 or 10μg/kg/day, or the reference compound dexamethasone given daily orally by gavage at a dose of 0.1mg/kg/day. Treatment was continued for the entire duration of the study which was 3 weeks. TRAP5b-activity in plasma and bone parameters were measured at 0, 2 and 3 weeks in the proximal tibia metaphysis by pQCT (XCT2000, Stratec Medizintechnik, Pforzheim, Germany) and cancellous microarchitecture by in vivo μCT (vivaCT40, SCANCO Medical, Bruettisellen, Switzerland).

In vehicle treated animals, inflammatory arthritis lead to rapid and continuous decrease in cancellous bone mineral density (CnBMD) of 12% at 3 weeks and a corresponding decrease in trabecular bone volume, resulting mostly from the thinning of trabecular elements. Cortical thickness (CtTh) decreased by 14% as a result of endocortical bone resorption while no significant changes in periosteal perimeter was observed. Dexamethasone administration fully prevented joint swelling and all bone changes resulting from inflammatory arthritis. Similarly, calcitonin dose dependently reduced bone loss in both, the cancellous and cortical compartment with the highest dose of 10 μg/kg/day offering full protection. Significant effects were already seen at the lowest dose of 1μg/kg/day sCT. Histomorphometric assessment of TRAP positive cells in the ankle joint confirmed the potent dose-dependent anti-osteoclastic effect sCT, which was in line with indications from plasma TRAP5b measurements. Inhibitory effects were seen in metaphyseal cancellous bone, subchondral bone in the epiphysis, as well as in the peri-articular area.

Studies should be undertaken to investigate the potential of oral formulations of sCT in animal models of inflammatory arthritis. Calcitonin is a potent inhibitor of bone degradation in the inflammatory joint and may be an interesting adjuvant therapy to anti-inflammatory drugs (NSAIDs, DMARDs).

**Disclosures:** J.A. Gasser, Employee of the Novartis Institutes for Biomedical Research 5.

## SA194

**Lack of Calcitonin Accentuates Bone Loss During Lactation by Enhanced Osteoclast Formation and Reduced Osteoblast Formation.** C. S. Kovacs<sup>1</sup>, B. J. Kirby<sup>\*1</sup>, J. P. Woodrow<sup>\*1</sup>, R. F. Gagel<sup>2</sup>, N. A. Sims<sup>3</sup>. <sup>1</sup>Memorial University, St. John's, NL, Canada, <sup>2</sup>MD Anderson Cancer Center, Houston, TX, USA, <sup>3</sup>St. Vincent's Institute, Melbourne, Australia.

Lactation in mice induces substantial reductions in bone mineral content (BMC, assessed by DXA) that are reversed rapidly after weaning. *Ctgrp*-null mice, with a global deletion of the gene encoding calcitonin and calcitonin gene-related peptide, suffer a 55% reduction in BMC during lactation (versus 25% in wild type [WT] mice) followed by complete restoration post-weaning. *Ctgrp*-null mice also demonstrate upregulated mammary gland PTHrP and serum PTH during lactation, which may increase osteoclast-mediated bone resorption during lactation even further above normal. To assess this, we performed histomorphometry in WT and *Ctgrp*-null mice during lactation and weaning. Pairs of sister WT and *Ctgrp*-null mice were sacrificed at day 7 of lactation and at weaning (day 21 after parturition) and histomorphometry was carried out on toluidine blue stained undecalcified sections of vertebrae and tibiae.

During lactation, both WT and *Ctgrp*-null mice demonstrate reduced trabecular thickness and increased trabecular separation, compared to non-pregnant mice of the same genotype, as well as high osteoclast and osteoid surfaces (OcS/BS and OS/BS). In lactating *Ctgrp*-null vertebrae and tibiae, OcS/BS was more than double that of WT (vertebrae: 13.9  $\pm$  2.2 vs 4.9  $\pm$  0.6%,  $p < 0.003$ ; tibiae: 24.5  $\pm$  4.3 vs 9.6  $\pm$  0.5,  $p < 0.01$ ). In contrast, osteoblast parameters were halved in *Ctgrp*-null vertebrae and tibiae compared to WT (vertebral osteoblast surface [ObS/BS]: 10.7  $\pm$  2.0 vs 20.4  $\pm$  2.9%,  $p < 0.03$ ; OS/BS: 11.7  $\pm$  2.3 vs 21.0  $\pm$  3.0,  $p < 0.04$ ). Large osteocytic lacunae consistent with osteocytic osteolysis were evident in both genotypes.

At weaning, the very high OcS/BS persisted in *Ctgrp*-null mice. However, between day 7 and 21 ObS/BS quadrupled in *Ctgrp*-null to 40.0  $\pm$  4.8%, and doubled in WT to 46  $\pm$  2.9%; similar changes were observed in osteoblast number and OS/BS.

Thus, we have confirmed upregulated osteoclast-mediated bone resorption and osteocytic osteolysis during normal lactation. Absence of calcitonin led to a greater increase in OcS/BS, consistent with elevated circulating PTH, but also led to a milder increase in ObS/BS vs WT. The sum of these differences may explain the more substantial bone loss in lactating *Ctgrp*-null mice. Moreover, *Ctgrp*-null mice retain the ability to upregulate osteoblast generation to a maximal level at the onset of weaning. This suggests that calcitonin normally dampens the effect of lactation on osteoclasts but not on osteocytic osteolysis, yet enhances the effect of lactation on osteoblasts, and is not required for skeletal recovery after lactation.

**Disclosures:** C.S. Kovacs, None.

This study received funding from: Canadian Institutes of Health Research.

## SA195

See Friday Plenary number F195.

## SA196

**Calcitonin Intramuscular Administration for Treating Acute Pain of Osteoporotic Vertebral Compression Fractures: A Randomized Controlled Trial.** T. Nakano\*. Orthopaedic Surgery, Tamana Central Hospital, Tamana, Japan.

Calcitonin products have an analgesic effect and vary greatly in dosage form and dose. The most common formulation of calcitonin used in the United States and European countries, etc. is a nasal spray administered on a daily basis, whereas in Japan and other East Asian countries, calcitonin therapy usually consists of intermittent intramuscular administration at relatively low doses such as 20 IU once weekly or 10 IU twice weekly. However, to date only a few clinical investigations regarding the analgesic effect of these calcitonin preparations have been conducted.

This study was designed to assess the usefulness of elcatonin, an eel calcitonin derivative, administered at 20 IU once weekly for pain relief in patients with osteoporosis who had lumbodorsal pain due to a new vertebral compression fracture. The study subjects were 78 hospitalized patients with a diagnosis of a new vertebral fracture based on MRI scan data. They were randomized either to receive elcatonin intramuscularly at 20 IU once weekly or to receive no calcitonin treatment. In these groups, other therapies included the use of a corset from the time of admission to the hospital, and also the use of non-steroidal anti-inflammatory drugs (NSAIDs) was allowed. Each patient was questioned regarding the intensity of pain at the time of getting up from a recumbent position, and the results were assessed using the visual analog scale (VAS). The inquiry to the patient using the VAS was performed by an independent member of the nursing staff who was unaware of the study being conducted.

The results of the study showed a significant reduction of the mean VAS score in patients treated with calcitonin at Week 2 of hospitalization as compared to that determined within 2 days of admission to the hospital, and the tendency remained at Weeks 3 and 4 of hospitalization. In patients with no calcitonin treatment, it was not until Week 4 that a significant decrease in the VAS score was observed; hence improvement of pain was attained earlier in the calcitonin-treated group.

The present data suggest that the therapeutic effect on pain associated with a new vertebral fracture is increased by concomitant use of elcatonin, compared to treatment with a corset and NSAIDs alone. In fact, it has been recognized that calcitonin has a mechanism of action mediated by the central serotonergic neurons, which is different from that of NSAIDs. The results of the study supported this finding.

This study has demonstrated the clinical efficacy of calcitonin intramuscularly administered at 20 IU once weekly for pain associated with osteoporosis-induced vertebral fracture, which has been widely used in the East Asia region.

**Disclosures:** T. Nakano, None.

## SA197

**The Calcitonin Receptor on Osteoclasts Plays a Physiological Role to Protect Against Hypercalcaemia in Mice.** A. G. Turner\*<sup>1</sup>, F. Tjahjono\*<sup>1</sup>, W. S. M. Chiu\*<sup>1</sup>, A. J. Moore\*<sup>2</sup>, D. M. Findlay\*<sup>3</sup>, H. A. Morris\*<sup>2</sup>, J. D. Zajac\*<sup>1</sup>, R. A. Davey\*<sup>1</sup>. <sup>1</sup>Department of Medicine, University of Melbourne, Austin Health, Heidelberg, VIC, Australia, <sup>2</sup>Hanson Institute, IMVS, Adelaide, Australia, <sup>3</sup>Orthopaedics and Trauma, University of Adelaide, Adelaide, Australia.

We have recently demonstrated using a genetically modified mouse model in which the calcitonin receptor (CTR) is globally deleted (Global CTRKO), that the CTR plays a physiological role in protecting against induced hypercalcaemia (1). The aim of the present study was to further investigate the mechanism by which the CTR exerts this protective effect. To achieve this aim, we generated mice in which the CTR is deleted specifically within osteoclasts (OCL-CTR KO) using the Cre/loxP system. At 6 weeks of age, male and female OCL-CTR KO mice were fed a low calcium diet for 2 weeks after which hypercalcaemia was induced by treatment with 0.5 µg 1,25-dihydroxyvitamin D<sub>3</sub> on 2 consecutive mornings. Total serum calcium (Ca) levels were measured immediately prior to, and 45 and 50.5 hours post-first injection. OCL-CTR KO mice display a modest bone phenotype that is currently being examined. Trabecular bone volume/tissue volume (BV/TV) in the femur of female OCL-CTRKO was decreased by 17% at 6 weeks of age compared to controls (P<0.05) while BV/TV in male OCL-CTR KO was unaffected at 6 weeks of age. Furthermore, no differences were observed in baseline serum Ca and PTH levels between control and OCL-CTR KO genotypes at baseline, consistent with our hypothesis that the CTR on osteoclasts plays a modest physiological role in regulating bone and calcium homeostasis in the basal state. Peak serum total Ca levels at 50 hours following 1,25-dihydroxyvitamin D<sub>3</sub> induced hypercalcaemia were greater in male OCL-CTR KO by 31% (0.9mM) (P<0.05) compared to controls (Table 1).

Table 1: Total serum Ca levels in OCL-CTR mice versus controls, values are mM±SEM.

		0 hrs	45 hrs	50.5 hrs
Male	Control (n=7)	1.79±/-0.06	2.62±/-0.14	2.79±/-0.24
	OCL-CTR (n=5)	1.84±/-0.03	3.23±/-0.20	3.65±/-0.10
Female	Control (n=9)	1.86±/-0.04	2.96±/-0.16	3.18±/-0.16
	OCL-CTR (n=2)	1.78±/-0.01	3.55±/-0.19	3.85±/-0.08

The data for the female OCL-CTR KO is preliminary and experiments ongoing. We are currently investigating the mechanism for this increased hypercalcaemic response by

measuring bone formation markers, osteoclast number and X-laps, as well as the renal Ca handling. In conclusion, we have demonstrated that the biological role of the CTR to protect against induced hypercalcaemia in mice is primarily mediated via its action on osteoclasts.

(1) Davey RA, Turner A et al. The Calcitonin Receptor Plays a Physiological Role to Protect Against Hypercalcaemia in Mice. JBMR In Press, Accepted 13<sup>th</sup> March, 2008.

**Disclosures:** A.G. Turner, None.

## SA198

**Low Serum Osteocalcin Predicts Carotid Plaques and Indicators of the Metabolic Syndrome.** E. Waern\*<sup>1</sup>, C. Ohlsson\*<sup>2</sup>, J. Kindblom\*<sup>2</sup>, U. Smith\*<sup>3</sup>, U. Lerner\*<sup>4</sup>, D. Mellström\*<sup>1</sup>. <sup>1</sup>Centre for Bone research at the Sahlgrenska Academy, University of Gothenburg, Gothenburg, Sweden, <sup>2</sup>Centre for Bone Research at the Sahlgrenska Academy, University of Gothenburg, Gothenburg, Sweden, <sup>3</sup>Dept of Internal Medicine at the Sahlgrenska Academy, University of Gothenburg, Gothenburg, Sweden, <sup>4</sup>Oral Cell Biology, Umea University, Umea, Sweden.

**Introduction:** The osteoblast-derived protein osteocalcin has recently been shown to affect adiposity and glucose homeostasis in mice, suggesting that the skeleton via an endocrine mechanism influences energy metabolism (Lee et al. Cell 130:456-469, 2007). The aim of the present study was to investigate the relation between serum osteocalcin and indicators of the metabolic syndrome.

**Methods and population:** 619 randomly selected 70 years old men and women participated in a longitudinal study with examinations at age 70, 76 och 86. BMD was measured in calcaneus with dual photon absorptiometry and osteocalcin was analysed by a double-antibody radioimmuno-assay. Serum was sampled after 10 hours fasting and non-smoking in the morning. Extra- and intracranial circulation was examined by means of duplex sonography and Transcranial Doppler techniques in 142 subjects at age 78.

**Results:** Osteocalcin correlated inversely to BMD and BMI in both sexes at all ages investigated (P<0.05). Osteocalcin increased by 44 percent from 70 to 86 years of age. This increase was related to, but independent of, declining kidney function (cystatin C) and increasing PTH. Serum osteocalcin (adjusted for BMI) correlated inversely to serum insulin r = -0.11 (p<0.01) and glucose r = -0.25 (p<0.0001).

A multiple regression model (diabetes excluded) with osteocalcin as dependent variable showed that glucose, (but not insulin), waist circumference and BMD were independent indirect predictors while PTH, cystatin C and ALP were independent direct predictors of osteocalcin (p<0.001).

Serum osteocalcin was inversely related to the risk of having bilateral carotid plaques (OR per SD increase in osteocalcin 0.68 (95% confidence interval 0.47-0.97)). The risk for stroke within 15 years after the age of 70 was increased in men with low serum osteocalcin (p<0.01).

Low osteocalcin increased the risk of having high waist circumference (Men > 102 cm, women > 88 cm; OR per SD increase in osteocalcin 0.77 (0.67-0.89)). In addition, low osteocalcin predicted one or more parameters of the metabolic syndrome (high waist circumference, BMI >30, high triglycerides, hypertension and diabetes; p<0.01).

**Conclusion:** Low serum osteocalcin predicts high glucose and carotid plaques and indicators of the metabolic syndrome.

**Disclosures:** E. Waern, None.

## SA199

**Oxytocin Directly Regulates Skeletal Homeostasis.** R. Tamma\*<sup>1</sup>, G. Colaiaanni\*<sup>1</sup>, L. Zhu\*<sup>2</sup>, N. Patano\*<sup>1</sup>, C. Camerino\*<sup>1</sup>, A. DiBenedetto\*<sup>1</sup>, M. Strippoli\*<sup>1</sup>, G. Greco\*<sup>1</sup>, G. Montemurro\*<sup>1</sup>, R. Vergari\*<sup>1</sup>, L. Mancini\*<sup>1</sup>, S. Colucci\*<sup>1</sup>, M. Grano\*<sup>1</sup>, R. Faccio\*<sup>1</sup>, J. Li\*<sup>2</sup>, X. Liu\*<sup>2</sup>, G. Yang\*<sup>2</sup>, J. Iqbal\*<sup>2</sup>, C. Buettner\*<sup>2</sup>, K. Nishimori\*<sup>3</sup>, L. Young\*<sup>4</sup>, I. Bab\*<sup>5</sup>, L. Sun\*<sup>2</sup>, M. Zaidi\*<sup>2</sup>, A. zallone\*<sup>1</sup>. <sup>1</sup>Department of Human Anatomy and Histology, University of Bari, Bari, Italy, <sup>2</sup>Mount Sinai Bone Program, Mount Sinai School of Medicine, New York, NY, USA, <sup>3</sup>Tohoku University Graduate School of Agricultural Science, Tohoku, Japan, <sup>4</sup>Center for Behavioral Neuroscience, Department of Psychiatry, Emory University School of Medicine, Atlanta, GA, USA, <sup>5</sup>Hadassah School of Medicine, Jerusalem, Israel.

Oxytocin, a hypothalamic neuropeptide secreted from the posterior pituitary, is indispensable for lactation. Mice lacking either oxytocin or its receptor (Oxtr) are thus unable to lactate, but deliver normally. Loss-of-function studies indicate further roles of oxytocin in the regulation of social behavior, memory, and food intake. Here, we show for the first time that oxytocin directly affects both components of bone remodeling, formation and resorption, and bone mass. Daily subcutaneous injections of oxytocin increase bone mass through a direct effect on osteoblastic bone formation, and also transiently elevate osteoclastogenesis. In contrast, oxytocin and Oxtr deficiency, including haploinsufficiency, cause a dramatic reduction in bone formation resulting in low-remodeling osteopenia. We find that the action of oxytocin is exerted directly on bone cells: preliminary studies reveal no effects of intracerebroventricular oxytocin on osteoclastogenesis or osteoblastogenesis in *ex vivo* bone marrow cell cultures. Oxytocin acts on osteoblasts to stimulate mineralization by enhancing BMP-2 expression, which, in turn, enhances Schnurri-3 causing an up-regulation of the transcription regulators *Osterix* and *ATF-4*. Oxytocin also promotes the production of the osteoclastogenic cytokine RANK-L, which consequently stimulates osteoclastogenesis indirectly. Finally, oxytocin directly stimulates osteoclast formation *via* the NF-κB and MAP kinase pathways, but paradoxically inhibits the

resorptive function of mature osteoclasts through  $\text{Ca}^{2+}$  signals that stimulate nitric oxide synthase (eNOS) to enhance NO production. We propose that oxytocin has a dominant stimulatory effect on bone formation to ensure optimal bone remodeling and appears indispensable for skeletal maintenance in both sexes. In females, the same hormone that controls parturition and lactation, we believe, facilitates the mobilization of calcium from bone, while protecting overt skeletal loss *via* a powerful bone-forming action. Finally, as oxytocin enhances bone mass, we envisage a therapeutic role for the nanopeptide in human osteoporosis.

**Disclosures:** R. Tamma, None.

## SA200

**Evidence Supporting the Necessity of UDP-N-acetyl-alpha-D-galactosamine-polypeptide N-acetylgalactosaminyl-transferase 3 (GalNac-T3) in the Processing of Fibroblast Growth Factor 23 (FGF23) in Humans.** R. I. Gafni, N. Bhattacharyya\*, J. S. Brahim\*, C. E. Dumitrescu\*, T. A. Theman\*, M. H. Kelly\*, A. A. Molinolo\*, M. T. Collins. NIDCR, National Institutes of Health, Bethesda, MD, USA.

FGF23, a protein produced primarily in bone, regulates phosphate and vitamin D homeostasis by enhancing phosphate excretion and suppressing 25-hydroxyvitamin D-1-alpha-hydroxylase in the kidney. This molecule circulates in intact and C-terminus forms, with most of the physiologic activities attributed to the intact molecule. Based on *in vitro* and animal studies, and observations in humans, the following model has evolved: 1) secretion of intact FGF23 requires O-linked glycosylation by GalNac-T3 and 2) without glycosylation, FGF23 is degraded intracellularly to the inactive C-terminus molecule by widely expressed subtilisin-like proprotein convertase(s) (PCSKs). Genetic conditions associated with increased intact FGF23 result in hypophosphatemic rickets/osteomalacia. Rarely, mesenchymal tumors produce excess FGF23 to cause tumor-induced osteomalacia (TIO). Conversely, mutations which decrease FGF23 or GalNac-T3 expression cause hyperphosphatemic tumoral calcinosis. However, direct evidence supporting the model that GalNac-T3 is present in tissues that produce both FGF23 and PCSKs in humans is lacking. We studied 8 tumors of various cell types (3 fresh frozen, 5 paraffin-embedded) from patients with TIO for the co-production of FGF23, GalNac-T3, and PCSKs. Immunohistochemistry staining was positive for both FGF23 (Immunotopics, San Clemente, CA) and GalNac-T3 (CellMab, Sweden); immunofluorescence demonstrated that FGF23 and GalNac-T3 were frequently co-expressed within the same cell. Expression of mRNA encoding FGF23, GalNac-T3 and several subtilisin-like proprotein convertases was detected by quantitative RT-PCR. Taken together, these findings suggest that the machinery necessary for post-translational modification of FGF23 is contained within these secretory tumors. The presence of GalNac-T3 in these physiologically relevant FGF23-producing tissues, and its co-expression with cells producing FGF23, support the hypothesis that GalNac-T3 is necessary for the processing of intact FGF23.

**Disclosures:** R.I. Gafni, None.

## SA201

**High Expression of the Calcium/Phosphate-Regulating Hormone Stanniocalcin 2 Is Associated with Renal Calcification in the Klotho Mutant Mice.** Y. Takei\*, H. Yamamoto, M. Masuda\*, M. Fukaya\*, T. Sato, Y. Taketani, E. Takeda. Clinical Nutrition, University of Tokushima School of Medicine, Tokushima, Japan.

Stanniocalcin (STC) has been identified firstly from the corpuscles of stannius in bony fish as calcium/phosphate-regulating hormone. Two related mammalian stanniocalcin genes, STC1 and STC2, were found to be expressed in various tissues containing intestine, kidney and bone. Klotho mutant (KL) mice as known the model of precocious aging, have hypercalcemia, hyperphosphatemia and hypervitaminosis D and exhibit ectopic calcification of vascular media, gastric wall, alveolar wall and kidney. Importantly, recent studies found that the klotho plays as the regulator of fibroblast growth factor-23 (FGF23) signaling and phosphate/calcium homeostasis. It was also previously reported that renal STC2 gene expression was increased in KL mice. However, the regulatory mechanism of STC2 expression through FGF23/Klotho signaling and the physiological role of STC2 in KL mice remains unclear. In this study, we investigated the regulation of STC2 gene expression and its localization in kidney of wild-type (WT) and KL mice. At six weeks old, Real-Time PCR analysis revealed that the mRNA levels of STC2 in kidney were significantly upregulated in KL mice compared with WT mice, while renal STC1 mRNA levels were no significant alteration. We next performed immunohistochemical analysis to clarify the localization of STC2 in kidney. The focal expression of STC2 was observed in KL mice but not WT mice. In addition, we analyzed renal calcification by von kossa stain, thus ectopic calcification of glomerulus and small artery in the renal parenchyma were detected in KL mice but not WT mice. Interestingly, high expression of STC2 was colocalized with renal calcification in KL mice. These data suggested that highly STC2 expression might be associated with renal calcification in the KL mice.

**Disclosures:** Y. Takei, None.

## SA202

See Friday Plenary number F202.

## SA203

**Fibroblast Growth Factor 23 (FGF-23) in Vitamin D Deficient Older Persons.** P. Lips<sup>1</sup>, J. E. Dijkstra<sup>\*2</sup>, N. van Schoor<sup>\*3</sup>, M. Lomecky<sup>\*2</sup>, V. Chel<sup>\*3</sup>, M. Vervloet<sup>\*4</sup>, H. Dijkstra<sup>\*2</sup>. <sup>1</sup>Department of Endocrinology, VU University Medical Center, Amsterdam, Netherlands, <sup>2</sup>Department of Clinical Chemistry, VU University Medical Center, Amsterdam, Netherlands, <sup>3</sup>EMGO Institute, VU University Medical Center, Amsterdam, Netherlands, <sup>4</sup>Department of Nephrology, VU University Medical Center, Amsterdam, Netherlands.

The phosphatonin FGF-23 promotes phosphate excretion and suppresses renal 1 $\alpha$ -hydroxylase leading to low serum 1,25(OH)2D in patients with hypophosphatemic osteomalacia. FGF-23 accumulates with renal failure. The objective of this study was to investigate whether FGF-23 plays a role in the decreased conversion of 25(OH)D into 1,25(OH)2D in older persons with vitamin D deficiency and decreased renal function. Subjects were 39 nursing home residents participating in a vitamin D supplementation study, mean age (SD) 84 years (6.3). Serum 25(OH)D and 1,25(OH)2D were measured by RIA (Diasorin and IDS). C-terminal FGF-23 was measured by ELISA (Immunotopics, San Clemente, CA) interassay CV < 10%. All data are from baseline. Results were: median (25-75<sup>th</sup>) 25(OH)D 20 nmol/l (14-34), 1,25(OH)2D 50.5 pmol/l (40.3-77.1) FGF-23 60.4 RU/ml (24.0-66.4) and mean (SD) calcium 2.33 (0.11) mmol/l, phosphate 1.01 mmol/l (0.13), albumin 33.6 g/l (3.1), creatinine 99  $\mu$ mol/l (18). Significant correlations were observed between serum 25(OH)D and 1,25(OH)2D (R = 0.59, p < 0.01), serum 25(OH)D and creatinine (R = 0.42, P < 0.01) and serum 25(OH)D and albumin (R = 0.35, P < 0.05). There was no relationship between serum FGF-23 and vitamin metabolites, phosphate or creatinine. When serum 25(OH)D was dichotomized in levels < 25 and > 25 nmol/l, there was no difference in FGF-23. The low serum 1,25(OH)2D and strong relationship between serum 25(OH)D and serum 1,25(OH)2D confirms the substrate-dependent synthesis of 1,25(OH)2D in vitamin D deficient older persons. These data do not support a role for FGF-23 in the decreased renal synthesis of 1,25(OH)2D in older persons.

**Disclosures:** P. Lips, Merck and Co 1, 2; Servier 1; Aventis 3; Procter and Gamble 3.

## SA204

**Rapid Detection of Intact FGF-23 in Tumor Tissue from Patients with Oncogenic Osteomalacia.** M. Mannstadt<sup>1</sup>, C. Lorente<sup>\*2</sup>, H. Jüppner<sup>1</sup>. <sup>1</sup>Endocrine Unit, Massachusetts General Hospital, Boston, MA, USA, <sup>2</sup>Dept. Oral & Maxillofacial Surgery, Massachusetts General Hospital and Harvard Vanguard Medical Associates, Boston, MA, USA.

Oncogenic osteomalacia (OOM) is a rare tumor-induced disease characterized by hypophosphatemia due to decreased renal threshold of phosphate reabsorption, low 1,25-dihydroxyvitamin D concentrations and osteomalacia. The localization of OOM tumors, which often produce excess amounts of the phosphaturic hormone fibroblast growth factor-23 (FGF-23), can be difficult and confirmation of successful tumor removal may require prolonged post-operative observation until normalization of serum parameters is documented. Here, we report the modification of a commercially available intact FGF-23 assay, which enabled us to rapidly document high FGF-23 content in OOM tumor extracts. The assay takes less than 30 minutes to complete and visual inspection of the test plate is sufficient to distinguish positive from negative samples, therefore allowing fast intra-operative assessment of FGF-23 content in OOM tumor extracts. Several tumors from patients with proven OOM and control tissue were studied. Simple aqueous extracts from small amounts of tumor tissue were prepared and FGF-23 content was evaluated using a commercially available two-site ELISA (Immunotopics) that detects intact FGF-23. The assay was performed according to the manufacturer's recommendations ("standard assay"), which takes about four hours, or with shortened incubation times ("rapid assay"), which takes 30 minutes. Extracts from bone and an ovarian tumor served as controls. When measured by the standard assay, extracts from OOM tumors, but not from control tissues, were shown to contain large amounts of intact FGF-23 (3,600 to >11,000 pg/ml). The rapid FGF-23 assay unequivocally documented high FGF-23 concentrations in all OOM tumor extracts. In summary, simple aqueous extracts from small portions of six different OOM-associated tumors revealed very high FGF-23 concentrations as assessed by the standard assay, which were also readily detectable by a modified rapid test that takes less than 30 minutes to complete. Similar to intraoperative PTH assays, this rapid assay could thus potentially be performed in or near the operating room, especially since visual inspection of the test plate was sufficient to detect FGF-23 in all six tumors tested. The assay may furthermore help define, intra-operatively, the disease-free margins of tumors located in areas that are difficult to access surgically.

**Disclosures:** M. Mannstadt, None.  
This study received funding from: NIH.

## SA205

See Friday Plenary number F205.

## SA206

**FGF23 and FGF2 Share a Common but Also Have Distinct Signaling Pathways for Negative Regulation of Bone Nodule Mineralization in Cultured Osteoblasts.** T. Minamizaki<sup>1</sup>, Y. Yoshiko<sup>1</sup>, S. Suzuki<sup>\*1</sup>, J. E. Aubin<sup>2</sup>, N. Maeda<sup>\*1</sup>. <sup>1</sup>Oral Growth & Developmental Biology, Hiroshima University Graduate School of Biomedical Sciences, Hiroshima, Japan, <sup>2</sup>Molecular and Medical Genetics, University of Toronto, Toronto, ON, Canada.

Fibroblast growth factor 23 (FGF23) is primarily expressed in osteoblasts/osteocytes and suppresses renal phosphate reabsorption and vitamin D metabolism via the circulation. FGF23 is also targeted to the parathyroid where it suppresses PTH production. Klotho forms a complex with FGF23-FGF receptor (FGFR), which appears to be necessary for FGF23-specific signaling in both tissues. Recently, we established that adenoviral overexpression of FGF23 in the rat calvaria (RC) cell/organ culture models inhibits osteoblast differentiation and bone formation, suggesting that FGF23 acts on bone in an autocrine/paracrine manner independently of its systemic effect on phosphate homeostasis. Similarly to adenoviral overexpression of FGF23, we found that treatment of RC osteoblasts with recombinant FGF23 (rFGF23) impaired bone nodule mineralization, and recombinant (rKlotho) was required for the rFGF23 effect under serum-deprived conditions. RC osteoblasts express only very low levels of Klotho, but Klotho (the secreted membrane isoform, sKlotho) is present in FCS. Removal of sKlotho from FCS by immunoprecipitation eliminated the rFGF23 effect. Consistent with these data, Klotho was detectable by immunofluorescence in RC osteoblasts grown under serum-deprived conditions supplemented with rFGF23 in combination with rKlotho but not without rKlotho. Moreover, FGF23 and FGFR1 were co-immunoprecipitated by anti-FGFR1 and anti-Klotho respectively, only when RC osteoblasts were co-treated with rFGF23 and rKlotho under serum-deprived conditions. These results suggest that FGF23 may act on osteoblasts when circulating sKlotho is present. Not only co-treatment with rFGF23 and rKlotho, but also treatment with rFGF2 alone suppressed matrix mineralization via FGFR1 and ERK activation, and both FGF23 and FGF2 stimulated early growth response-1 mRNA expression. However, FGF23 but not FGF2 is differentially expressed during bone nodule mineralization and is directly regulated by 1,25-dihydroxyvitamin D<sub>3</sub> (1,25(OH)<sub>2</sub>D<sub>3</sub>)-occupied vitamin D receptor at the transcriptional level. Thus, both the non-canonical FGF23 and the canonical FGF2 may act as local factors in bone at least in part via a common ERK signaling pathway. However, activity of FGF23 but not FGF2 may be regulated by circulating sKlotho and 1,25(OH)<sub>2</sub>D<sub>3</sub>, suggesting specificity of regulatory pathways of FGF family members in bone formation and mineralization.

**Disclosures:** T. Minamizaki, None.

## SA207

See Friday Plenary number F207.

## SA208

**Significance of O-linked Glycosylation of FGF23 Protein.** H. Suzuki<sup>\*</sup>, N. Ito, S. Fukumoto, T. Fujita<sup>\*</sup>. Division of Nephrology & Endocrinology, Department of Medicine, University of Tokyo Hospital, Tokyo, Japan.

FGF23 is a physiological humoral factor regulating phosphate and vitamin D metabolism. Previous studies indicated that a part of FGF23 protein is proteolytically cleaved between <sup>179</sup>Arg and <sup>180</sup>Ser into inactive fragments by an enzyme that recognize <sup>176</sup>Arg-X-X-<sup>179</sup>Arg motif. In addition, FGF23 protein has three O-glycan chains at <sup>171</sup>Thr, <sup>178</sup>Thr and <sup>200</sup>Thr. We have shown that these three O-glycans are serially attached to FGF23 protein, first at <sup>200</sup>Thr, then at <sup>171</sup>Thr and finally at <sup>178</sup>Thr. The attachment of the O-glycan chain to <sup>178</sup>Thr was shown to prevent the processing of FGF23 protein. However, the significance of O-glycan chains at <sup>171</sup>Thr and <sup>200</sup>Thr remains unclear. Therefore, we analyzed the mutant FGF23 proteins which lack O-glycan chains at <sup>171</sup>Thr and <sup>200</sup>Thr in this study. FGF23(Arg176Gln, Arg179Gln) protein is resistant to the processing. Introduction of Thr178Ala mutation into this FGF23(Arg176Gln, Arg179Gln) did not change the presence of FGF23 protein with O-glycan at <sup>171</sup>Thr analyzed by Western blotting. In contrast, the FGF23 protein with O-glycan at <sup>178</sup>Thr disappeared by the introduction of Thr171Ala mutation. Therefore, O-glycosylation at <sup>171</sup>Thr seems to be necessary for the attachment of O-glycan at <sup>178</sup>Thr and thereby preventing the processing of full-length FGF23. The introduction of Thr200Ala mutation did not modify FGF23 proteins with O-glycans at <sup>171</sup>Thr and <sup>178</sup>Thr indicating that the O-glycan at <sup>200</sup>Thr does not affect O-glycosylation at <sup>171</sup>Thr and <sup>178</sup>Thr. Therefore, we then analyzed biological activity of the mutant FGF23 protein by reporter assay of early growth response-1 (Egr-1) gene in cells expressing Klotho. FGF23 without O-glycan at <sup>200</sup>Thr showed less activity compared to that of wild-type FGF23 suggesting that O-glycosylation at <sup>200</sup>Thr enhances the receptor activation by full-length FGF23. Collectively, these results indicate that O-glycans of FGF23 protein contribute to the increased activity of FGF23 either by preventing proteolytic processing or by enhancing the ability of full-length FGF23 to induce intracellular signaling.

**Disclosures:** H. Suzuki, None.

## SA209

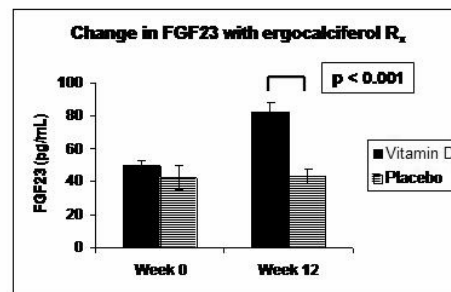
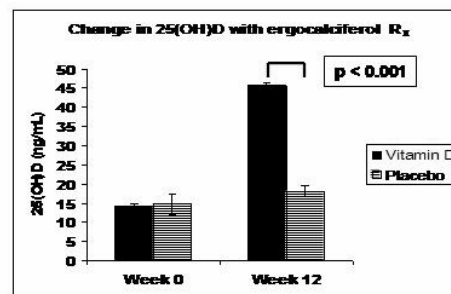
**The Effect of Treating Vitamin D Deficiency on FGF23 Levels in Humans.** S. M. Burnett-Bowie, B. Z. Leder, M. P. Henao<sup>\*</sup>, N. T. Mendoza<sup>\*</sup>, J. S. Finkelstein. Endocrine Unit, Massachusetts General Hospital, Boston, MA, USA.

**Background:** Fibroblast growth factor 23 (FGF23) is a phosphate (PO<sub>4</sub>)-regulating hormone that promotes renal PO<sub>4</sub> wasting and suppresses 1,25-dihydroxyvitamin D (1,25(OH)<sub>2</sub>D) production. Dietary PO<sub>4</sub>, serum PO<sub>4</sub>, and 1,25(OH)<sub>2</sub>D appear to regulate FGF23 secretion. Specifically, 1,25(OH)<sub>2</sub>D stimulates FGF23 production. It is not known, however, if FGF23 is regulated by 25-hydroxyvitamin D (25OHD), the more stable metabolite of vitamin D. Furthermore, the impact of treating vitamin D deficiency on circulating FGF23 is unknown.

**Methods:** 90 healthy men and women aged 18-45, with 25OHD ≤ 20 ng/mL and normal serum calcium (Ca) were randomized to ergocalciferol 50,000 international units or matching placebo (PBO) weekly for 12 weeks. Subjects consumed 1000-1500 mg of Ca daily. FGF23 (Kainos, Tokyo, Japan), 25OHD, 1,25(OH)<sub>2</sub>D, serum and urinary PO<sub>4</sub>, serum and urinary Ca, and PTH were measured at weeks 0, 4, 8 and 12. The primary endpoint was the change in FGF23 between groups. Data are presented as mean±SE in the figure and mean±SD in text.

**Results:** Subjects were well matched at baseline. 25OHD levels increased from 14±3 ng/mL at baseline to 46±17 ng/mL at week 12 with treatment but were unchanged with PBO (15±4 ng/mL at baseline to 18±10 ng/mL at week 12) (p<0.001). Urinary PO<sub>4</sub> excretion increased from 11±5 % at baseline to 13±6 % at week 12 (p=0.04) with treatment but was unchanged with PBO. Serum PO<sub>4</sub> and Ca, however, did not change with the intervention. Serum FGF23 increased significantly with treatment from 49±14 pg/mL at baseline to 83±35 pg/mL at week 12 but was unchanged with PBO (43±33 pg/mL at baseline to 43±26 pg/mL at week 12) (p<0.001). 1,25(OH)<sub>2</sub>D, PTH and urinary Ca will be presented.

**Conclusions:** Correction of vitamin D deficiency with high dose ergocalciferol significantly increases circulating serum FGF23, in the absence of any change in serum PO<sub>4</sub>. The observed increase in FGF23 is associated with an increase in urinary PO<sub>4</sub> excretion. While dietary PO<sub>4</sub> is generally well absorbed, the observed increase in urinary PO<sub>4</sub> excretion may be a result of increased dietary PO<sub>4</sub> absorption from the correction of vitamin D deficiency. Moreover, these data suggest that 25OHD, or one of its metabolites, has a direct stimulatory effect on circulating FGF23 that is independent of serum PO<sub>4</sub>. Future measurement of 1,25(OH)<sub>2</sub>D levels will help differentiate the effects of 25OHD from 1,25(OH)<sub>2</sub>D on circulating FGF23.



**Disclosures:** S.M. Burnett-Bowie, None.

This study received funding from: NIH K23-DK-073356 and M01-RR-01066.

## SA210

See Friday Plenary number F210.

## SA211

**Regulation of Renal Klotho: The Importance of ER $\alpha$ .** O. K. Oz<sup>1</sup>, A. Hajibeigi<sup>\*1</sup>, K. Korach<sup>\*2</sup>, P. Chambon<sup>\*3</sup>, J. Zerwekh<sup>4</sup>. <sup>1</sup>Radiology, UT Southwestern Medical Center at Dallas, Dallas, TX, USA, <sup>2</sup>Environmental Disease Medicine Program, NIEHS/NIH, Research Triangle Park, NC, USA, <sup>3</sup>Physiological Genetic, Inserm, U-596 / CNRS, UMR7104 / Universit  Louis Pasteur, Illkirch, Strasbourg, France, <sup>4</sup>Internal Medicine, UT Southwestern Medical Center at Dallas, Dallas, TX, USA.

The klotho gene was initially identified in mice harboring a mutation that was associated with several ageing phenotypes including shortened life span, sterility, arteriosclerosis, skin atrophy, muscle atrophy, osteoporosis and abnormal calcium re-absorption. The klotho gene encodes two forms of protein, a type I single transmembrane 130Kda glycoprotein with  $\beta$ -glycosidase activity and a splice variant lacking the transmembrane domain. Full-length klotho is predominantly expressed in tissues involved in calcium homeostasis, such as kidney, parathyroid glands and choroids plexus in the brain while the secreted form is found in the blood and cerebrospinal fluid. In a recently published study, we showed that the expression of klotho in the kidney of aromatase deficient (ArKO) mice was up-regulated both at the mRNA and protein levels when compared to wild type (WT) animals. Treatment with estradiol lowered klotho levels to WT levels. In the present study we further examined estrogen regulation of renal klotho in both in vitro and in vivo models. In vitro a mouse DCT cell line was grown in FBS or charcoal stripped FBS without or with estrogen as a model of estrogen deficiency or repletion. In vivo we used mutant mice lines (n=3-6 per group) lacking estrogen action through the AF-1 domain of the ER $\alpha$  (ERKO $\alpha$ AF-1/-) or completely lacking estrogen action through ER $\alpha$  knockout (ERKO $\alpha$ ). Finally, we compared the expression of renal klotho between male and female wild-type mice. Klotho expression in kidney homogenates or cell lysates was determined by western blot. The expression of klotho in the DCT cell lysates was increased in cells grown in 10%csFBS compared to FBS. Addition of estrogen to the csFBS decreased klotho levels. In both mutant mouse lines renal klotho expression was significantly higher than wild type. Interestingly, the male WT mice had higher klotho levels than female WT mice. In conclusion our results clearly indicate that in the kidney or a DCT cell line, estrogen down-regulates the expression of klotho. Since the complete and the AF-1 domain ER $\alpha$  knockout are estrogen replete and both show elevated klotho, the data suggest that the AF-1 domain is important for estrogen mediated down regulation of renal klotho.

**Disclosures:** O.K. Oz, None.

## SA212

**Parathyroidectomy Improves Quality of Life in Hemodialysis Patients with Severe Secondary Hyperparathyroidism.** P. G. S. Lacativa<sup>\*1</sup>, F. M. Franco<sup>\*1</sup>, C. H. Torres<sup>\*1</sup>, P. J. M. Patricio Filho<sup>\*2</sup>, M. D. C. Goncalves<sup>\*3</sup>, M. L. F. Farias<sup>1</sup>. <sup>1</sup>Endocrinology, Federal University of Rio de Janeiro, Rio de Janeiro, Brazil, <sup>2</sup>Nephrology, Federal University of Rio de Janeiro, Rio de Janeiro, Brazil, <sup>3</sup>Surgery, Federal University of Rio de Janeiro, Rio de Janeiro, Brazil.

Severe secondary hyperparathyroidism (HPT2) associated with end-stage renal disease (ESRD) leads to several complications that can affect quality of life. Total parathyroidectomy with autologous transplantation (PTX) is an alternative to revert hyperparathyroidism in those patients not submitted to renal transplantation. The aim of this study was to quantify the impact of the severe hyperparathyroidism and of PTX on quality of life. Nineteen patients with severe HPT2, age 42  $\pm$  15 years, were studied before (pre-PTX, mean serum PTH 2434  $\pm$  1821 pg/ml) and one year after parathyroidectomy (post-PTX, mean serum PTH 73  $\pm$  67 pg/ml) and compared with thirty-eight age-matched ESRD patients whose mean PTH was 108  $\pm$  86 pg/ml (control). All patients were maintained on chronic hemodialysis throughout the study. SF-36 questionnaires were used to evaluate quality of life. Pre-PTX patients had significantly lower functional status scores than control patients concerning physical function (30.8  $\pm$  28 vs. 54.6  $\pm$  26.6), physical role limitations (14.5  $\pm$  26.7 vs. 42.8  $\pm$  40), bodily pain (36.3  $\pm$  30.2 vs. 58.7  $\pm$  26.8), vitality (37.6  $\pm$  25.6 vs. 58  $\pm$  21.2) and emotional role limitations (26.3  $\pm$  41 vs. 55.3  $\pm$  44). Refractory bone pain was the only symptom related to the functional status deficits in multivariate regression analysis. Parathyroidectomy had a great impact in symptoms relief, especially bone pain, and improved all functional status deficits scores to the levels found in control patients. We conclude that severe HPT2 causes functional status deficits in daily physical activities, vitality and emotional problems, which are closely related to refractory bone pain. The surgical cure of hyperparathyroidism is effective in reverting pain and therefore has a great and positive impact in health status, allowing patients to recover the expected quality of life of ESRD individuals.

**Disclosures:** M.L.F. Farias, None.

## SA213

See Friday Plenary number F213.

## SA214

**Effects of Intermittent Human Parathyroid Hormone Administration on Bone Union with Hydroxyapatite Blocks at the Site of Cancellous Bone Osteotomy in Ovariectomized Rats.** K. Kamo, N. Miyakoshi, Y. Kasukawa, K. Nozaka<sup>\*</sup>, H. Sasaki, Y. Shimada<sup>\*</sup>. Akita University School of Medicine, Akita, Japan.

Although hydroxyapatite (HA) blocks have been widely used for reconstruction of bone defects, bone union with HA blocks is often delayed in osteoporotic patients. Intermittent administration of human parathyroid hormone (h-PHT) accelerates fracture healing by increasing callus formation at cortical bone and enhances bone union at the site of cancellous bone osteotomy in ovariectomized (OVX) rats. However, little is known about the effects of hPTH on bone union with HA blocks. The aim of this study was to evaluate whether h-PTH enhances bone union with HA blocks at the site of cancellous bone osteotomy in OVX rats. Following sham or OVX operation in 7-month-old female Sprague-Dawley rats, complete mid-sagittal osteotomy from the knee joint to the tibial diaphysis was performed. An HA block was then placed into the osteotomy site and fixed with cerclage wiring. Postoperatively, hPTH (100  $\mu$ g/kg) or vehicle only was administered subcutaneously once a week for 8 weeks (n=3-6 per group). Tibiae were harvested 1 week after last injection and bone histomorphometry at the site of osteotomy with HA blocks was performed to evaluate bone volume (BV/TV), osteoid surface (OS/BS), eroded surface (ES/BS), mineral apposition rate (MAR), bone formation rate (BFR/BS) and percentage of bone union with HA block. PTH treatment significantly increased BV/TV (107%, p<0.01), MAR (72%, p<0.01) and BFR (115%, p<0.05) in OVX rats compared to vehicle-treated controls. PTH did not significantly increase bone union with HA blocks in sham-operated rats. The percentage of bone union with HA blocks in OVX rats was increased (79%) by PTH treatment compared to vehicle-treated controls, but not significantly. Intermittent administration of hPTH stimulated bone formation and increased bone volume at the cancellous osteotomy site placed with HA blocks. Treatment with hPTH tended to stimulate bone union with HA blocks in OVX rats.

**Disclosures:** K. Kamo, None.

## SA215

See Friday Plenary number F215.

## SA216

**PTHrP Is Processed by Skin Keratinocytes and Has Immunomodulation Properties.** L. Deftos<sup>1</sup>, D. Burton<sup>1</sup>, C. Chalberg<sup>\*1</sup>, K. Smith<sup>\*1</sup>, S. Tu<sup>\*1</sup>, R. Dorschner<sup>\*2</sup>, R. Gallo<sup>\*2</sup>. <sup>1</sup>Medicine, Veterans Administration San Diego Healthcare System and University of California, San Diego, CA, USA, <sup>2</sup>Dermatology, Veterans Administration San Diego Healthcare System and University of California, San Diego, CA, USA.

Our recent appreciation of the immunomodulatory effects of PTHrP in keratinocytes sheds new light on the biology of this polypeptide. It is our overall hypothesis that the robust expression of PTHrP in keratinocytes is accompanied by processing of its three polypeptide isoforms into tissue-specific peptides with distinct biological effects that regulate the innate immune system.

In this study, we used an immortalized human keratinocyte cell line (HaCaT) to investigate the processing of PTHrP. Through size exclusion chromatography, westerns, and the use of multiple PTHrP antibodies, we showed the immunochemical and size heterogeneity of PTHrP in HaCaT keratinocytes, providing evidence for its processing in this cell. To further characterize the processed forms, we immunoprecipitated HaCaT conditioned media with N-terminal PTHrP antibody (1A5) coated beads followed by MALDI-TOF of the eluted fractions. We demonstrated several novel keratinocyte PTHrP species, consistent in masses with human PTHrP 3-30, 3-35, 9-39, and 10-36. We previously showed the biological effects of PTHrP in skin include upregulation of the antimicrobial peptide, cathelicidin, made by keratinocytes. To determine if PTHrP can act directly as an antimicrobial, we evaluated synthetic PTHrP peptides for direct antimicrobial effects on *Staphylococcus aureus* growth. While each of the peptides demonstrated some activity, PTHrP140-173 was the most potent and even more potent than the cathelicidin peptide, LL-37.

In summary, these data identify a novel role for keratinocyte-derived PTHrP in the immune defense of skin. The biological studies of PTHrP peptides and the known interactions of PTHrP with vitamin D indicate that PTHrP has a role in the innate defense system of skin against microbes and other invading agents. Our overall aim is to elucidate the molecular products and pathways of PTHrP processing and to identify the biological effects of these cellular mechanisms in keratinocyte immune function in vitro and in vivo.

**Disclosures:** D. Burton, None.

This study received funding from: VA Merit and National Institutes of Health.

## SA217

See Friday Plenary number F217.

## SA218

**At Similar Plasma 25-hydroxyvitamin D Levels, Fat Mass Influence PTH Levels in the State of Vitamin D Insufficiency.** L. Rejnmark, P. Vestergaard, L. Mosekilde. Dept. of Endocrinology and Metabolism C, Aarhus University Hospital, Aarhus, Denmark.

A relationship may exist between bone and fat metabolism. Adiposity is associated with increased PTH levels, which have been attributed to secondary hyperparathyroidism due to low plasma 25-hydroxyvitamin D (25OHD) levels. In order to further characterise this relationship, we studied PTH levels stratified by vitamin D status and body mass index (BMI).

In a cross-sectional design, we studied 1097 recent postmenopausal women recruited from the local background population. Subjects were divided into tertiles of 25OHD levels and within each vitamin D tertile we studied whether PTH levels differ according to tertiles of BMI. Results were adjusted for age, daily calcium intake, and smoking. We also determined body composition by DXA.

Within each 25OHD tertile, mean 25OHD levels did not differ according to BMI tertiles. PTH decreased with increased 25OHD levels. In the lowest vitamin D tertile (25OHD < 47nmol/l) PTH levels were significantly higher (4.3 pmol/l) than in the mid (4.0 pmol/l) and in the highest (3.7 pmol/l) 25OHD tertile. Within each vitamin D tertile, PTH levels increased significantly with increased BMI i.e., in the lowest 25OHD tertile those in the highest BMI tertile (>26kg/m<sup>2</sup>) had significantly higher PTH levels (4.3 pmol/l) than those with a BMI in the mid (4.1 pmol/l), or in the lowest (3.9 pmol/l) BMI tertile. Similarly, in the mid 25OHD tertile (25OHD 47-73nmol/l) PTH levels were 4.4, 3.9, and 3.7 pmol/l in the highest, mid and lowest BMI tertile, respectively. A similar relationship existed in the highest 25OHD tertile. However, after adjustments the significant relationship only remained within the lowest and mid 25OHD tertile, whereas BMI did not affect PTH levels in subjects with 25OHD levels above 73 nmol/l. Performing the analyses with tertiles of total fat mass instead of BMI revealed similar results, whereas lean tissue mass did not affect PTH levels. Accordingly, in vitamin D insufficiency (in this setting at 25OHD levels < 73 nM) PTH levels are - at similar 25OHD levels - influenced by the size of the total fat mass, whereas no such relationship seems to exist in the state of a sufficient vitamin D status. Further studies are needed to determine the mechanism of action by which fat tissue increases PTH levels or whether PTH by itself may increase fat mass.

**Disclosures:** L. Rejnmark, None.

## SA219

See Friday Plenary number F219.

## SA220

**Role of the Transcription Factor SOX4 in the Skeletal Response to Intermittent PTH.** D. D. Pierroz<sup>1</sup>, L. S. Nissen-Meyer<sup>2</sup>, S. L. Ferrari<sup>1</sup>. <sup>1</sup>Div of Bone Diseases, Geneva University Hospital and Faculty of Medicine, Geneva, Switzerland, <sup>2</sup>The Biotechnology Centre, University of Oslo, Oslo, Norway.

SOX4 is a transcription factor that is also expressed in the embryonic growth plate and in osteoblast-like cells. Homozygous mice die in utero from cardiac failure. We previously reported that heterozygous SOX4<sup>+/-</sup> mice have decreased BMD, cancellous and cortical microarchitecture and mineral apposition rate (1). Furthermore, bone biopsies from patients with primary hyperparathyroidism show increased SOX4 mRNA expression compared to parathyroidectomized patients, whereas PTH treatment of osteoblastic cells increases SOX4 mRNA. This led us to hypothesize that SOX4 is involved in the bone anabolic response to PTH. For this purpose, 12-week-old female wild type (WT) and Sox4<sup>+/-</sup> mice were treated with hPTH 1-34 (40 ug/kg/d) for 6 weeks or vehicle (veh) (n=9-12mice/goup). Bone mineral density and vertebral and femoral microarchitecture were evaluated by DXA and micro-CT, respectively, and bone turnover by serum biochemical markers.

In WT, PTH treatment significantly increased BMD at total body (TB) (+6.5%), spine (Sp) (+2.4%), and midshaft femur (Fem) (+8.6%) compared to veh (p<0.05). Similar BMD gains were observed in SOX4<sup>+/-</sup> mice (TB:+7.3%, Sp:+12.1%, Fem:+8.3%, p<0.05). Femur cortical thickness (CTh) and bone area (BA) were also similarly increased by PTH in WT and Sox4<sup>+/-</sup> (CTh:+7.2% and +7.6%, respectively; BA:+7.3% and +10.9%, respectively, compared to vehicle, p<0.05). Moreover, no differences were observed between WT and SOX4<sup>+/-</sup> mice on vertebral and distal femur trabecular bone volume fraction (BV/TV), connectivity-density, and trabecular thickness (TbTh) in response to PTH. PTH treatment significantly increased osteocalcin levels (+30%, p<0.006) in both genotypes, whereas CTX levels decreased similarly in SOX4<sup>+/-</sup> and WT, independent of PTH.

Thus, haploinsufficient SOX4<sup>+/-</sup> adult mice have a low bone mass and microarchitecture but responded adequately to intermittent PTH. Taken together with the evidence that PTH upregulates SOX4 expression in vivo and in vitro, these observations suggest that the level of SOX4 expression achieved in these mice was sufficient to maintain PTH activity on osteoblasts.

(1) Nissen-Meyer LS et al. J.Cell Sci. 2007, 120:2785-2795

**Disclosures:** D.D. Pierroz, None.

## SA221

See Friday Plenary number F221.

## SA222

**Dominant Tissue Accumulation of MIBI in Parathyroid Glands in Uremic Rats.** Y. Imanishi<sup>1</sup>, H. Sano<sup>\*1</sup>, H. Hasegawa<sup>\*2</sup>, Y. Funase<sup>\*2</sup>, H. Kasahara<sup>\*2</sup>, T. Minamizawa<sup>\*2</sup>, M. Inaba<sup>1</sup>, T. Miki<sup>3</sup>, Y. Nishizawa<sup>1</sup>. <sup>1</sup>Metabolism, Endocrinology and Molecular Medicine, Osaka City University Graduate School of Medicine, Osaka, Japan, <sup>2</sup>FUJIFILM RI Pharma Co., LTD., Tiba, Japan, <sup>3</sup>Geriatrics and Neurology, Osaka City University Graduate School of Medicine, Osaka, Japan.

Little is known about the mechanisms of parathyroid imaging by <sup>99m</sup>Tc sestamibi or MIBI, although MIBI is one of the most useful image analyses of enlarged parathyroid glands. MIBI accumulation in parathyroid tissue was investigated in 5/6-nephrectomized uremic rats, exhibiting secondary hyperparathyroidism. 5MBq of MIBI was administered to the rats from tail vein, followed by sacrifices of the rats and corrections the tissues such as parathyroid, thyroid, neck muscle tissues and blood in 2 hours. The <sup>99m</sup>Tc radioactivity of parathyroid glands of uremic rats was significantly 2.2-fold higher than that of sham-operated rats. The radioactivity in parathyroid glands of uremic rats was almost same as that of sham rats, when compared with the radioactivity per parathyroid gland weight, suggesting that <sup>99m</sup>Tc accumulation in parathyroid cells was not affected by uremia and secondary hyperparathyroidism. The radioactive ratio of parathyroid glands to thyroid glands increased 1.2-fold in uremic rats compared to sham rats. These finding suggested that the mechanisms of parathyroid imaging by MIBI in uremia were partly by increased parathyroid gland volume and the enhanced contrast of radioactivity to thyroid glands.

**Disclosures:** Y. Imanishi, None.

## SA223

**The C-terminal Fragment of Parathyroid Hormone-Related Protein, PTHrP (107-139), Exerts Osteogenic Features in Both Regenerating and Nonregenerating Bone in Mice with Diabetes-Related Osteopenia.** D. Lozano<sup>\*1</sup>, L. F. de Castro<sup>\*1</sup>, E. Gómez-Barrena<sup>\*2</sup>, S. Dapia<sup>\*3</sup>, F. Manzarbeitia<sup>\*4</sup>, P. Esbrit<sup>1</sup>. <sup>1</sup>Bone and Mineral Metabolism Laboratory, Fundación Jiménez Díaz, Madrid, Spain, <sup>2</sup>Dpt. of Traumatology, Fundación Jiménez Díaz, Madrid, Spain, <sup>3</sup>Trabeculae (R), S.L., Parque Tecnológico de Galicia, Orense, Spain, <sup>4</sup>Pathology Dept., Fundación Jiménez Díaz, Madrid, Spain.

Type 1 diabetes mellitus (DM) is associated with bone loss. Osteoblastic expression of parathyroid hormone-related protein (PTHrP) -an important modulator of osteoblast differentiation- decreases in age-related osteopenia. The role of C-terminal PTHrP -unrelated to PTH- on bone is currently controversial. We here examined the putative osteogenic effects of PTHrP (107-139) in a mouse model of streptozotocin (STZ)-induced diabetes. In STZ-DM and control mice, bone regeneration was induced by marrow ablation in both tibiae. The intact femurs were used as nonregenerating bone controls. Some diabetic mice were treated with PTHrP (107-139) (100 µg/Kg/every other day, s.c.) for one week before and 6 days after marrow ablation, and then sacrificed. One tibia was decalcified and included in paraffin for histological evaluation. MC3T3-E1 cells were grown in differentiation medium (a-MEM; 50 µg/ml ascorbic acid, 10 mM β-glycerolphosphate, 10% FBS), with or without high glucose (HG) (25 mM) (or mannitol, osmotic control), supplemented (or not) with 100 nM PTHrP (107-139). Gene expression was analyzed by real-time PCR after total RNA isolation. STZ-DM mice had weight loss (15%). Evaluation of femoral bone structure in these mice by µCT demonstrated a 40% decrease in trabecular number and BV/TV and a 20% increase in trabecular SMI, and no cortical changes, compared to those in control mice. This was associated with a decrease (50-80%) in the gene expression of PTHrP and vascular endothelial growth factor (VEGF), and the RANKL/OPG ratio. In the the regenerating tibia, STZ-DM mice showed a dramatic increase in adipocyte number (10-fold over control), and a 30% decrease in osteoblast number and osteoid surface at the metaphysis. This was related to a decrease (20-40%) in the expression of the aforementioned genes, and also in that of runx2, osterix, osteocalcin, and the PTH1 receptor, and an increase in PPAR-γ2. All of these effects were reversed by PTHrP (107-139) treatment at both bone sites. In vitro, either HG- or mannitol-containing medium induced similar changes in gene expression of the aforementioned factors; all which were also reversed by PTHrP (107-139) in the culture medium. In conclusion, PTHrP (107-139) can induce osteogenic effects in a mouse model of STZ-induced diabetes. These in vitro findings further support that this PTHrP fragment has potential anabolic effects in osteoblastic cells

**Disclosures:** D. Lozano, None.

## SA224

See Friday Plenary number F224.



## SA225

**Dominant-negative GCMB Mutants Causing Autosomal-Dominant Hypoparathyroidism - Protein Expression and Cellular Localization.** M. Mannstadt<sup>1</sup>, S. R. Pulusani<sup>\*1</sup>, C. Silve<sup>2</sup>, H. Jüppner<sup>1</sup>. <sup>1</sup>Endocrine Unit, Massachusetts General Hospital, Boston, MA, USA, <sup>2</sup>Inserm u561, Hôpital Saint Vincent de Paul, Université Paris 5, UFR Médicale, Paris, France.

Hypoparathyroidism (HP) is characterized by levels of parathyroid hormone (PTH) insufficient to maintain normal serum calcium concentrations. HP occurs as a sporadic disease or as a familial disorder, and may present as a familial isolated form. Autosomal dominant HP (AD-HP) can be caused by heterozygous activating mutations in the genes encoding PTH or glial cells missing B (GCMB), a transcription factor specific for the parathyroid gland. Homozygous loss-of-function mutations of GCMB in humans and null mutations in mice lead to AR-HP; heterozygous carriers appear to be healthy.

We recently identified two different heterozygous, single nucleotide deletions in GCMB in genomic DNA of the affected members of two families with AD-HP. Both mutations (mutA and mutB) are located in GCMB exon 5 and both lead to a shift in the open reading frame and replace the putative second transactivation domain located within the carboxyl-terminal region of GCMB with unrelated amino acid sequence. Consistent with the mode of inheritance, mutant proteins exhibited dominant-negative properties in luciferase assays *in vitro*, while two previously reported GCMB mutations (R47L and G63S) that are the cause of AR-HP did not affect function of wild-type (WT) GCMB.

We now generated three GCMB-specific antibodies in rabbits against peptides corresponding to residues 111-130 (N1), 225-245 (C1) and 481-500 (C2). Western blot analysis of WT GCMB expressed in fibroblast DF-1 cells using antibodies N1 and C1 revealed a protein band of the expected size of about 60 kDa. As expected, lysates from cells expressing mutA and mutB showed a protein band that was slightly larger than WT protein. Antibody C2, which is directed against the portion of the protein that is replaced in mutA and mutB, also revealed the expected protein band in lysates from cells transfected with WT, but not from cells transfected with mutA or mutB. We also generated plasmids encoding WT or mutant GCMB tagged with GFP at the amino-terminus. In transiently transfected chicken fibroblast DF-1 cells using these constructs, WT or mutant proteins demonstrated normal nuclear localization.

We conclude that the identified GCMB mutations do not impair protein expression or nuclear localization, yet exert a dominant negative effect on the WT transcription factor. The mutant GCMB proteins and the anti-GCMB antibodies will help in the analysis of GCMB functions in adult parathyroid glands.

**Disclosures:** M. Mannstadt, None.

This study received funding from: NIH.

## SA226

See Friday Plenary number F226.

## SA227

**A Possible Pathogenic Role of Aberrant Klotho Expression in Primary and Secondary Hyperparathyroidism.** T. Krajisnik<sup>1</sup>, P. Björklund<sup>\*2</sup>, G. Åkerström<sup>\*2</sup>, G. Westin<sup>\*2</sup>, T. Larsson<sup>1</sup>. <sup>1</sup>Medical Sciences, Institution of Medical Sciences, Uppsala, Sweden, <sup>2</sup>Surgical Sciences, Institution of Surgical Sciences, Uppsala, Sweden.

Klotho was recently shown to directly mediate PTH secretion in parathyroid cells in response to low extracellular calcium. In contrast, Klotho inhibits PTH secretion indirectly through the action of FGF23. Abnormal Klotho expression in parathyroid disorders remains to be determined. Herein, we explored parathyroid Klotho expression in patients with primary (pHPT) and secondary hyperparathyroidism (sHPT). Informed consent and approval by institutional ethical committee were obtained. Surgically removed parathyroid glands from patients with pHPT (n=40) and sHPT (n=25) and 4 normal parathyroid tissue specimens were analyzed for Klotho mRNA and protein levels by quantitative real-time quantitative PCR and immunohistochemistry.

In pHPT, Klotho mRNA levels were significantly decreased (n=23) or undetectable (n=17) compared to normal tissues (p<0.001). Reduced Klotho protein expression was confirmed by immunohistochemistry. Importantly, Klotho mRNA levels were significantly and inversely correlated with serum calcium (r=-0.97; p<0.0001), however, no correlation with serum PTH or adenoma weight was observed. In agreement, calcium, but not PTH, dose-dependently decreased bovine parathyroid Klotho expression *in vitro* (p<0.01). We also confirmed decreased expression of the vitamin D receptor (VDR) mRNA levels in pHPT subjects (p<0.01).

In sHPT, there was a trend of decreased Klotho mRNA expression in a majority of subjects, although not statistically significant compared to normal controls. Since all sHPT patients were on calcitriol treatment, we explored the effect of 1,25(OH)<sub>2</sub>D<sub>3</sub> on Klotho expression. Importantly, 1,25(OH)<sub>2</sub>D<sub>3</sub> dose-dependently increased Klotho expression in bovine parathyroid cells *in vitro* (p<0.01).

In conclusion, serum calcium is a major determinant of parathyroid Klotho expression, which may play a significant role in the pathogenesis of pHPT. Suppressed Klotho and VDR mRNA levels in parathyroid adenomas indicate that both FGF23/Klotho- and vitamin D/VDR-dependent inhibitory mechanisms are perturbed and unable to diminish the uncontrolled PTH secretion. Finally, since Klotho expression is induced by vitamin D treatment, the beneficial effect of vitamin D treatment in chronic kidney disease may, in part, be ascribed to enhanced FGF23/Klotho-mediated reduction of PTH secretion.

**Disclosures:** T. Krajisnik, None.

## SA228

See Friday Plenary number F228.

## SA229

**Anabolic Parathyroid Hormone Treatment Mobilizes Bone Marrow Stromal Stem Cells and Osteoprogenitors Towards Bone Surfaces: Role for the Epidermal Growth Factor Receptor Pathway.** J. Zhu, N. C. Partridge, L. Qin. Physiology and Biophysics, UMDNJ-Robert Wood Johnson Medical School, Piscataway, NJ, USA.

Intermittent injection of PTH dramatically increases bone mass and is one of the most effective treatments for osteoporosis. However, the detailed mechanisms are still largely unknown. Recently, we found that conditioned medium (CM) from PTH-treated UMR 106-01 osteoblastic cells contains factors which are chemotactic for bone marrow stromal stem cells (BMSSCs). In this assay, BMSSCs were seeded in the upper wells of chemotaxis chambers and the lower wells contained CM. We observed a 2-fold increase in the number of BMSSCs migrating toward the lower wells with PTH-treated CM compared with control CM. PTH itself has no chemotactic effect on BMSSCs. Time course experiments indicated that UMR 106-01 cells released chemoattractants within 30 min of PTH treatment and this was maximal at 4 h. Moreover, PTH stimulates MC3T3-E1 and primary calvarial osteoblastic cells to release factors chemotactic for BMSSCs. The migration of BMSSCs in these experiments is not due to random movement (chemokinesis) since there was no increase in the number of migrated cells if BMSSCs were in the upper wells in PTH-treated CM and the lower wells contained control CM. Using the protein synthesis inhibitor, cycloheximide, we demonstrated that PTH-treated osteoblastic cells must synthesize new protein(s) to exhibit chemotactic activity. Interestingly, this chemotactic activity was partially abolished by adding an epidermal growth factor receptor (EGFR) tyrosine kinase inhibitor to the chemotactic assay. Previously, we have demonstrated that the expression of amphiregulin, an EGF-like ligand that signals through the EGFR, is rapidly and transiently stimulated by PTH in osteoblastic cells. Activation of the EGFR pathway stimulates the proliferation of BMSSCs and osteoprogenitors but suppresses their differentiation into mature osteoblasts. *In vitro* assays showed that all EGF-like ligands are chemotactic for BMSSCs. *In vivo*, we found that 1 h after the last of 12 days of intermittent PTH injections of adult rats the numbers of CFU-F extractable from bone marrow were decreased. Thus, PTH appears to cause the migration of BMSSCs or osteoprogenitors from bone marrow toward bone surfaces lined with osteoblasts and therefore decreases the numbers of CFU-Fs in the flushed bone marrow. Taken together, our results suggest a novel mechanism for PTH's anabolic actions that PTH stimulates bone lining osteoblasts to produce chemotactic factors, including amphiregulin, which mobilize BMSSCs and osteoprogenitors toward bone surfaces for future proliferation and differentiation into mature osteoblasts.

**Disclosures:** J. Zhu, None.

## SA230

**Inhibition of the Mevalonate Pathway Rescues the Dexamethasone-induced Suppression of the Mineralization of Osteoblastic Cells.** I. Kanazawa, T. Yamaguchi, S. Yano, K. Hayashi<sup>\*</sup>, M. Yamauchi, T. Sugimoto. Internal Medicine 1, Shimane University Faculty of Medicine, Izumo, Japan.

AMP-activated protein kinase (AMPK) is known to be expressed ubiquitously including osteoblasts and modulate the mevalonate pathway by inhibiting HMG-CoA reductase. In this study, to clarify a physiological role of the mevalonate pathway in glucocorticoid-induced osteoporosis (GIO), we investigated the effects of 5-aminimidazole-4-carboxamide-1-β-D-ribose nucleoside (AICAR) (an AMPK activator) and fasudil hydrochloride (FH) [a specific inhibitor of Rho-kinase (ROK), downstream of HMG-CoA reductase] as well as statins (simvastatin and pitavastatin) (HMG-CoA reductase inhibitors) on dexamethasone (DEX)-induced suppression of the mineralization of osteoblastic MC3T3-E1 cells. Either AICAR (up to 0.5 mM) or FH (up to 10<sup>-4</sup> M) stimulated bone morphogenetic protein-2 (BMP-2) and osteocalcin (OC) mRNA expression by real-time PCR and mineralization by von Kossa and Alizarin red stainings until 21 days in time- and dose-dependent fashions. Simultaneous addition of either 1 mM mevalonate or 5 μM geranyl-geranyl pyrophosphate (GGPP), which also comprise the mevalonate pathway and act in the downstream of HMG-CoA reductase, antagonized BMP-2 and OC mRNA expression as well as mineralization enhanced by AICAR. On the other hand, DEX (10<sup>-8</sup> M) increased the expression of BMP-2 antagonists, Follistatin and Dan, and inhibited the mineralization of MC3T3-E1 cells. Under DEX treatments, either AICAR (0.1 mM), FH (10<sup>-5</sup> M), or statins (10<sup>-6</sup> M) still stimulated BMP-2 mRNA expression of the cells. Moreover, each agent addition reversed the DEX-induced increase in the expression of Follistatin and Dan as well as the DEX-induced suppression of mineralization of the cells. These findings showed that inhibition of the mevalonate pathway by AICAR, FH, or statins rescued the DEX-induced suppression of mineralization of osteoblastic MC3T3-E1 cells via enhancing BMP-2 expression while reducing its antagonists expression. Thus, the mevalonate pathway seems to be involved in the pathogenesis of GIO, and agents that are capable of inhibiting the pathway may be candidate drugs for the treatment of GIO by augmenting BMP-2 action.

**Disclosures:** I. Kanazawa, None.

## SA231

**Proteasome Inhibition Counteracts the Negative Effect of Glucocorticoid Treatment on Bone Metabolism by Stimulating Osteoblasts and Inhibiting Osteoclasts in Vitro.** K. Søre\*, T. L. Andersen\*, T. Lund\*, T. Plesner\*, J. Delaissé. Clinical Cell Biology and Hematology, Vejle Hospital, IRS/CSFU, Southern Denmark University, Vejle, Denmark.

We have studied if simultaneous treatment with a proteasome inhibitor may neutralize the strong side effects glucocorticoids (GC) have on bone metabolism. The proteasome inhibitor bortezomib (Bz) is used to treat multiple myeloma, and it is reported to have beneficial effects on the bone resorption/formation balance and to partly rescue ovariectomy-induced bone loss in mice. We show here in an in vitro study that combining proteasome inhibition with GC treatment overcomes the inhibitory effect of prednisolone on osteoblasts, pre-osteoblasts and human mesenchymal stem cells (hMSC), and also blocks the stimulatory effect of GC on osteoclasts.

The following osteoblast/stem cell models were used: murine calvarial osteoblast cell line (MC3T3), hMSC (Tert4) and human adipose derived stem cells (hADSC). Pre-osteoblasts were defined as hMSC or hADSC differentiated in vitro with cytokines. Endpoints were metabolic activity, alkaline phosphatase activity and Q-PCR. Osteoclasts were differentiated from CD14+ cells derived from human blood donations by culturing them with MCSF and RANKL. Endpoints were metabolic, TRACP and resorptive activity. The experimental setup was adapted to the pharmacodynamics of both prednisolone and bortezomib. We used prednisolone concentrations equivalent to a daily dose of approximately 40 to 125 mg for 24 to 72 hrs, and Bz as a 3 hrs pulse corresponding to the levels reached in patients treated with 1 to 1.3 mg/m<sup>2</sup>.

The in vitro prednisolone treatment proved toxic against osteoblasts but not against pre-osteoblasts and stem cells. However, pre-treating osteoblasts with Bz protected them from toxicity. Furthermore, Bz pre-treatment of pre-osteoblasts and osteoblasts enhanced significantly the expression of key genes such as osteocalcin, osteopontin, collagen type 1 and OPG, compared to treatment with GC alone. In osteoblasts, combined treatment also enhanced Vitamin D receptor expression. In addition, hMSC displayed a significant increase in early marker genes such as ALP activity and expression as well as the expression of osteopontin in response to the combination. Finally, prednisolone rendered osteoclast resorption more aggressive but bortezomib could completely prevent this effect. Thus, we reproduce in vitro the detrimental effects of GC on OB and OC activity and show that proteasome inhibition can overcome them. We expect therefore that a possible way to prevent the induction of GC-induced osteoporosis may be through inhibition of the proteasome or the pathways that the proteasome controls.

**Disclosures:** K. Søre, None.

## SA232

**Effect of a Dissociating Glucocorticoid Receptor Modulator on Bone Cells.** K. Nelo\*, E. Kiiskilä\*, E. Kallio\*, J. Ilvesaro\*, H. M. Surcel\*, J. Risteli\*, M. Nissinen\*, A. Nilsen\*, H. A. Järveläinen\*, T. S. Scanlan\*, J. Tuukkanen\*. <sup>1</sup>Anatomy and Cell Biology, University of Oulu, Oulu, Finland, <sup>2</sup>National Public Health Institute, Oulu, Finland, <sup>3</sup>Clinical Chemistry, University of Oulu, Oulu, Finland, <sup>4</sup>Department of Physiology and Pharmacology, Oregon Health and Science University, Portland, OR, USA, <sup>5</sup>Global Safety Assessment, Astra Zeneca R&D, Montreal, QC, Canada.

Corticosteroid therapy is known to induce side effects like bone loss and osteoporosis. Glucocorticoid receptor modulators may have the potential for a more selective anti-inflammatory profile with fewer side effects compared with traditional corticosteroids. To define the effect of a novel non-steroidal selective glucocorticoid receptor modulator (SGRM), we studied osteoblast proliferation, matrix mineralization and osteoclastogenesis.

The anti-inflammatory effect of a arylpyrazole SGRM and dexamethasone was evaluated by analyzing *in vitro* secretion of interleukin-6 (IL-6) cytokine from lipopolysaccharide (LPS) -stimulated murine macrophage-like RAW 264.7 cells and the morphological changes of the RAW cells. The dissociative effect of the SGRM on MC3T3-E1 pre-osteoblast proliferation was studied with a WST-1 assay, mineralization by using Alizarin red S staining, and type I collagen synthesis by measuring procollagen type I N-terminal propeptide. In addition, common osteoclastogenesis markers RANKL and OPG were analyzed from MC3T3-E1 cells with quantitative RT-PCR. Bone resorption was evaluated using mouse bone marrow hematopoietic stem cells.

The anti-inflammatory effect of 10<sup>-7</sup> M SGRM was 32% and 69% of the effect of dexamethasone in IL-6 secretion and in the cell size respectively. Dexamethasone decreased osteoblast proliferation on days 3, 7, 10 and 14 and mineralization on day 14, compared with a basal control, whereas the SGRM had no effect. The 10<sup>-7</sup> M SGRM was also less potent in stimulating RANKL mRNA expression and in inhibiting OPG mRNA expression than was dexamethasone in MC3T3-E1 cells (on day 10). An osteoclastogenesis assay didn't detect any differences between these two compounds. However, the effect of 10<sup>-7</sup> M SGRM on bone resorption was significantly lower when compared with the effect of dexamethasone.

Our findings indicate that a dissociation effect was detected in osteoblast proliferation and matrix mineralization and partially in osteoclast differentiation and bone resorption. The *in vitro* separation of adverse bone effects from anti-inflammatory effects suggests a possibility of developing glucocorticoids with a more selective anti-inflammatory effect.

**Disclosures:** J. Tuukkanen, None.

This study received funding from: Astra Zeneca, Lund, Sweden.

## SA233

See Friday Plenary number F233.

## SA234

**Normal Intramembranous Fracture Healing in Mice with Transgenic Osteoblast-targeted Disruption of Glucocorticoid Signalling: Analysis by Microcomputed Tomography.** A. J. Weber\*, G. Li<sup>2</sup>, R. Kalak\*, J. Street\*, C. R. Dunstan<sup>3</sup>, F. Buttgeriet\*, H. Zhou<sup>3</sup>, M. J. Seibel<sup>3</sup>. <sup>1</sup>Department of Rheumatology and Clinical Immunology, Charité University Medicine, Berlin, Germany, <sup>2</sup>Musculoskeletal Education & Research Unit, Queen's University Belfast, Belfast, United Kingdom, <sup>3</sup>Bone Research Program, ANZAC Research Institute, The University of Sydney, Sydney, Australia.

The role of endogenous glucocorticoids (GC) in osteoblast differentiation and function is not well understood. Using a transgenic (tg) mouse model of osteoblast-targeted disruption of intracellular GC signalling, we examined whether endogenous GC, or the lack thereof, affect intramembranous fracture healing.

Uncortical bone defects (Ø 0.8mm) were created in tg mice (n= 36) and their wild-type (WT) littermates (n=34) using a drill on the anteromedial aspect of the left tibia. Fracture healing was assessed by X-ray (FAXITRON) and micro-CT analysis at 1, 2, and 3 weeks post-fracture. Micro-CT images were analysed for a Region of Interest covering the immediate defect site to measure the volume of new bone and its mean density.

At week 1 post-fracture, micro-CT imaging of the fracture site demonstrated formation of mineralized bone, which increased in volume and density by week 2. At week 3, healing of the defect was nearly completed in all animals.

One week post-fracture, the amount of newly formed bone (BV/TV) was similar in WT (25%) and tg (30%) animals (p=0.28). At week 2, BV/TV was 33% in WT mice as compared to 31% in tg animals (p=0.77). Mean bone densities of the newly formed bone in the WT and tg groups did not differ significantly at week 1 and week 2.

These preliminary results suggest that disrupting endogenous GC signalling in osteoblasts does not affect direct tibia bone healing as assessed by micro-CT. However, it remains to be shown whether glucocorticoid signalling affects other aspects of fracture healing such as collagen synthesis and structure, bone composition or bone turnover and remodelling.

**Disclosures:** H. Zhou, None.

This study received funding from: NHMRC Project Grant #402462.

## SA235

**Expression of 11β-Hydroxysteroid Dehydrogenase During Murine Osteoclast Formation.** M. Yang\*, J. R. Harrison<sup>2</sup>, B. E. Kream<sup>1</sup>. <sup>1</sup>Medicine, University of Connecticut Health Center, Farmington, CT, USA, <sup>2</sup>Craniofacial Sciences, University of Connecticut Health Center, Farmington, CT, USA.

Glucocorticoids exhibit complex regulatory effects on bone remodeling, affecting cells of both the osteoblast and osteoclast lineages. Glucocorticoids have been shown to signal directly in osteoclasts to increase their longevity and suppress their activity. 11β-hydroxysteroid dehydrogenase (11β-HSD1) converts the inactive glucocorticoids cortisone and 11-dehydrocorticosterone to their biologically active forms, cortisol and corticosterone, respectively. While 11β-HSD1 is expressed by many cell types to provide a source of locally-acting glucocorticoids, only one previous study has shown 11β-HSD1 expression in osteoclasts (human). The goal of the present study was to determine whether murine osteoclast lineage cells express 11β-HSD1. Bone marrow monocytes (BMMs) were prepared from 7-week-old CD-1 mice and cultured with 30 ng/ml each of M-CSF and RANKL for 4 days to induce osteoclast formation (TRAP-positive cells with >3 nuclei). Freshly isolated BMMs expressed 11β-HSD1 mRNA as detected by real time quantitative PCR (qRT-PCR) and 11β-HSD1 protein as assessed by western blotting with a polyclonal rat 11β-HSD1 antibody (RAH113). 11β-HSD1 mRNA levels decreased more than 200-fold during osteoclast formation in BMM cultures. To assess whether the reduction of 11β-HSD1 expression occurred during the expansion of osteoclast precursors, BMMs were treated with 3 and 30 ng/ml M-CSF for up to 4 days. M-CSF caused a time- and dose-dependent reduction of 11β-HSD1 mRNA, with the greatest reduction after only one day of M-CSF treatment. To assess whether a reduction of 11β-HSD1 expression occurred during the differentiation of pre-osteoclasts to mature osteoclasts, the monocytic cell line RAW264.7 was treated with or without 30 ng/ml RANKL. 11β-HSD1 was expressed in vehicle-treated RAW264.7 cells and its expression decreased 2-fold in RANKL-induced cultures containing osteoclasts. To determine whether 11β-HSD1 was functional, BMMs were treated with M-CSF and RANKL in the presence or absence of corticosterone and its inactive metabolite 11-dehydrocorticosterone for up to 5 days. Both steroids caused a dose and time-dependent suppression of osteoclast formation, indicating that 11β-HSD1 was active. These data show that BMMs express 11β-HSD1 as a means of generating locally active glucocorticoids and that this system declines during osteoclast formation in vitro.

**Disclosures:** M. Yang, None.

This study received funding from: National Institute of Health.

## SA236

**Human Osteoblasts Synthesize VEGF In Response to ACTH.** H. C. Blair<sup>1</sup>, B. B. Yaroslavskiy<sup>\*1</sup>, L. Guo<sup>\*1</sup>, L. Liu<sup>\*1</sup>, M. Zaidi<sup>2</sup>, C. M. Isles<sup>3</sup>. <sup>1</sup>Pathology and Cell Biology, University of Pittsburgh, Pittsburgh, PA, USA, <sup>2</sup>Medicine, Mount Sinai, New York, NY, USA, <sup>3</sup>Medicine, Medical College of Georgia, Augusta, GA, USA.

High-dose glucocorticoids cause bone mineral loss and regional osteonecrosis. Osteonecrosis is an important problem in high-turnover bone such as the femoral head and calcaneus. In the adrenal, adrenocorticotrophic hormone (ACTH) maintains corticosteroid production via vascular endothelial growth factor (VEGF) production in stromal cells; a consequence of glucocorticoid treatment is reduced systemic ACTH and adrenal cortical involution. Recently, ACTH receptors were discovered in osteoblasts, and are expressed at high levels in trabecular bone. Further, VEGF is required for bone formation. There are major species differences in glucocorticoid response; rodent bone mass increases with glucocorticoids and osteonecrosis does not occur. Thus, we studied VEGF expression in human osteoblasts in vitro. We confirmed the presence of the ACTH receptor in these cells; ACTH receptors were not present in significant amounts in mesenchymal stem cells or in fibroblasts. In early mineralising human osteoblasts, real time RT-PCR showed that VEGF mRNA was present in very low levels in untreated cells. ACTH, 100 ng/ml, induced VEGF mRNA several log orders, reaching 10% of GAPDH control concentration at 3 hours. It then declined to baseline (near zero) at 18 hours. Immune precipitation showed that VEGF protein accumulates in supernatants of osteoblasts treated with ACTH with or without 100 nM dexamethasone. In all media supporting osteoblast differentiation, without added ACTH, low but detectable levels of VEGF were found in culture supernatants. In keeping with the time course of VEGF mRNA expression, withdrawing ACTH for two days reduced VEGF protein to basal levels. It is likely that ACTH is also produced within bone: its precursor, POMC, is a regulated product of macrophages. In keeping, coculture of human monocytes with osteoblasts greatly increased VEGF production in the absence of added ACTH, although twice-higher levels of VEGF occurred in supernatants with both 100 ng/ml ACTH and 100,000 CD14 cells per cm<sup>2</sup> cultured with confluent osteoblasts. Monocytes were not a significant source of VEGF. Interestingly, in monocyte-osteoblast cocultures, dexamethasone reduced VEGF nearly to levels of unstimulated osteoblasts alone, suggesting that ACTH (or possibly other VEGF-stimulating products of monocytic cells in peripheral tissues) may be inhibited by glucocorticoids, in addition to inhibiting pituitary ACTH. Our results indicate that bone pathology, including osteonecrosis, secondary to glucocorticoid administration may reflect, in major part, interference with ACTH-dependent VEGF production that promotes osteoblast growth and survival.

**Disclosures:** H.C. Blair, None.

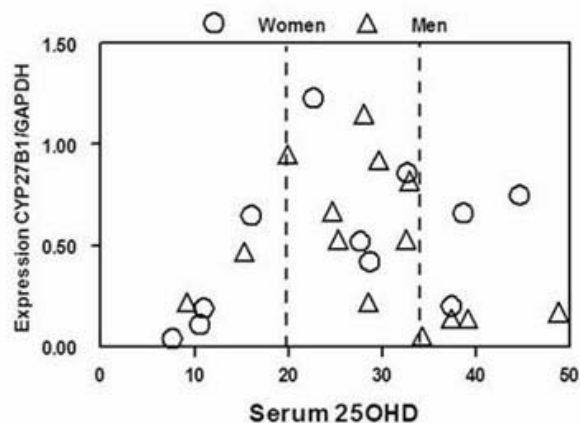
## SA237

**Expression of 1 $\alpha$ -hydroxylase (CYP27B1) in Human Marrow Stromal Cells: Correlations with Clinical Status.** J. Glowacki<sup>1</sup>, S. Zhou<sup>1</sup>, M. S. LeBoff<sup>2</sup>. <sup>1</sup>Orthopedic Surgery, Brigham and Women's Hospital, Boston, MA, USA, <sup>2</sup>Endocrinology, Brigham and Women's Hospital, Boston, MA, USA.

1,25-dihydroxyvitamin D [1,25(OH)<sub>2</sub>D] is important for bone and mineral homeostasis. Recent data show that extrarenal conversion of 25-hydroxyvitamin D (25OHD) to 1,25(OH)<sub>2</sub>D occurs in several cell types by 25OHD-1 $\alpha$  hydroxylase (CYP27B1), but little is known about its expression or regulation in bone. We examined 1) whether osteoblast differentiation in human marrow stromal cells (MSCs) responds to 25OHD; 2) whether MSCs express D-related genes; and 3) whether they are regulated. Marrow discarded during orthopedic surgery was obtained from subjects with no comorbidities/medications affecting bone metabolism; 25OHD (Diasorin RIA), 1,25(OH)<sub>2</sub>D, and PTH were obtained prior to surgery. Low-density marrow mononuclear cells were isolated by density centrifugation to enrich for undifferentiated cells including a fraction capable of adherence and osteoblastic differentiation. Adherent MSCs were cultured in osteogenic supplements  $\pm$  1,25(OH)<sub>2</sub>D or 25OHD. AlkP activity was measured colorimetrically after 6d. Gene expression was evaluated by semi-quantitative RT-PCR in MSCs obtained from 14 women (W) and 14 men (M). Level of expression was analyzed with respect to clinical parameters.

1,25(OH)<sub>2</sub>D<sub>3</sub> stimulated osteoblast differentiation in 94% samples, with peak stimulation between 1 and 10 nM. Two-thirds of the samples were also stimulated by 25OHD<sub>3</sub> (10 nM). This suggests that some marrow may synthesize 1,25(OH)<sub>2</sub>D<sub>3</sub>. In the second study, 28% of subjects were vitamin D-deficient (25OHD < 20 ng/mL); 9% had elevated PTH; and 10% had elevated 1,25(OH)<sub>2</sub>D. There was a wide range of expression of CYP27B1, with no differences between genders or with age (64.8 years  $\pm$  11.0). There was lower expression of CYP27B1 in hMSCs from subjects with serum PTH >43 pg/mL (p=0.002) and in subjects with serum 1,25(OH)<sub>2</sub>D > 50 pg/mL (p=0.0014). There were trends for lower expression of CYP27B1 in MSCs from W and M with serum 25OHD <20 ng/mL, and lower expression in M with serum 25OHD  $\geq$ 34 ng/mL (Figure). In addition, there was a negative correlation between CYP27A1 and serum 25OHD (p=0.028).

This study indicates correlations between CYP27B1 expression in human marrow stroma and serum 25OHD, 1,25(OH)<sub>2</sub>D, and PTH. These data suggest that 25OHD and local production of 1,25(OH)<sub>2</sub>D may play roles in regulation of osteoblast differentiation and function.



**Disclosures:** J. Glowacki, None.

This study received funding from: NIH-NIA

## SA238

See Friday Plenary number F238.

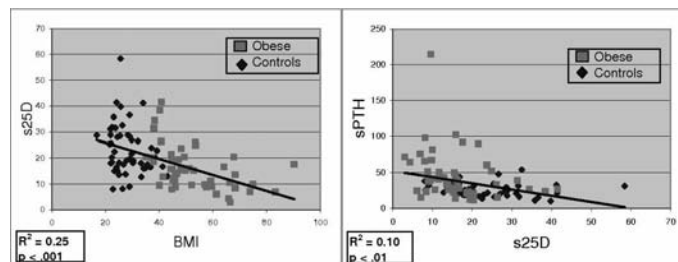
## SA239

**Vitamin D Insufficiency in Obesity.** E. R. Grethen<sup>\*1</sup>, R. V. Considine<sup>\*1</sup>, R. McClintock<sup>1</sup>, C. E. Gupta<sup>\*2</sup>, R. Jones<sup>\*2</sup>, B. M. Cacucci<sup>\*2</sup>, D. Diaz<sup>\*2</sup>, A. D. Fulford<sup>\*1</sup>, S. M. Perkins<sup>\*1</sup>, M. Peacock<sup>1</sup>. <sup>1</sup>Medicine/Endocrinology, Indiana University, Indianapolis, IN, USA, <sup>2</sup>Surgery, St. Vincent's Hospital, Carmel, IN, USA.

Obesity is a major health risk and its incidence in the USA is increasing. There are conflicting reports that serum 25-hydroxyvitamin D (s25D) levels are low in obesity. The aim of this study was to measure s25D in obese and control women and to determine if there was evidence of vitamin D insufficiency as assessed by serum PTH (sPTH). Fasting blood was obtained from obese white women prior to bariatric surgery and from healthy white women matched for age and season. Height and weight were recorded and s25D and sPTH measured by radioimmunoassay. Data were analyzed by SAS. Mean BMI and sPTH were higher and s25D was lower in obese women (Table).

		Obese women (n = 50)	Control women (n = 50)	P-value
BMI (kg/m <sup>2</sup> )	Mean (SD)	52.4 (12.4)	28.1 (5.9)	<0.001
	range	35.0- 90.2	16.7- 43.0	
s25D (ng/ml)	Mean (SD)	16.0 (8.3)	23.3 (9.8)	<0.001
	range	3.0- 41.5	8.0- 58.4	
sPTH (pg/ml)	Mean (SD)	45.2 (33.9)	25.6 (9.1)	<0.001
	range	11.5- 215*	10.2- 54.1	

\*Data were analyzed with and without the outlier PTH=215; significance was not affected. s25D was inversely related to BMI, and sPTH was inversely related to s25D (Figure).



R<sup>2</sup> of s25D vs. BMI was 0.25 (p <0.001); R<sup>2</sup> of sPTH vs. s25D was 0.10 (p <0.01). It is concluded that s25D is low in obesity and that vitamin D insufficiency is present among obese white women.

**Disclosures:** E.R. Grethen, None.

## SA240

See Friday Plenary number F240.

## SA241

**Platelet Vitamin D Receptor Levels Are Reduced in Osteoporotic Patients.**

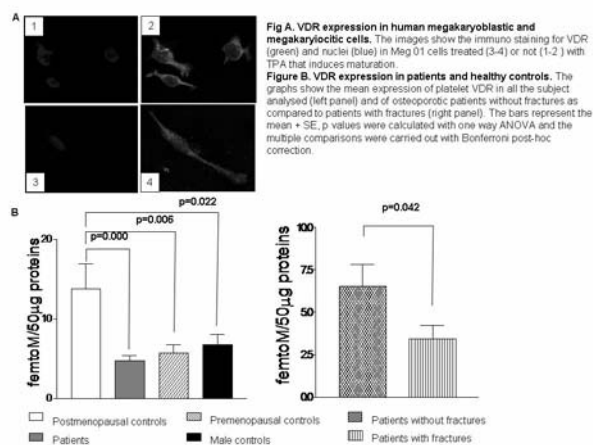
**P. D'Amelio<sup>1</sup>, M. A. Cristofaro<sup>\*1</sup>, M. Ravazzoli<sup>\*1</sup>, S. Di Bella<sup>\*1</sup>, G. P. Pescarmona<sup>\*2</sup>, G. Isaia<sup>1</sup>.** <sup>1</sup>Department of Internal Medicine, University of Torino, Torino, Italy, <sup>2</sup>Department of Biochemistry, Genetic and Biology, University of Torino, Torino, Italy.

Several findings suggest that rapid responses to the action of vitamin D are mediated by a vitamin D receptor (VDR) located in the cytosol. It has been shown that a human megakaryoblastic leukemia cell line expresses a functionally active VDR and that VDR is involved in the control of platelet (PLT) aggregation in the mouse. In the present study, we looked to see whether human PLTs express VDR, and whether its expression is different in osteoporotic as opposed to healthy subjects.

In order support to the analysis of PLT VDR we analyse the VDR expression in megakaryoblasts and megakaryocytes by immunofluorescence (Fig A). We enrolled in the study 77 women with postmenopausal osteoporosis, 33 healthy women of childbearing age, 49 healthy men, and 11 healthy women matched with patients for age and postmenopausal period. Thirty-nine patients had had one femoral fracture occurred after the age of fifty and attributable to primary osteoporosis. Bone mineral density (BMD), markers of bone metabolism and VDR levels by western blot were measured in all the subjects.

We demonstrated that VDR is expressed in the cytoplasm and the nucleus of megakaryoblasts and megakaryocytes, this lends support to the subsequent analysis of PLT VDR. After the menopause, VDR levels increase with respect to the young controls in the healthy women, but not in the osteoporotic ones. Patients with femoral fractures display fewer VDR than those without (Fig B). VDR may thus be supposed to be involved in the control of BMD and the gravity of osteoporosis. There are no marked gender-related differences in VDR expression among the healthy subjects. VDR is directly correlated with lumbar ( $r=0.4$ ,  $p=0.04$ ) and femoral ( $r=0.52$ ,  $p=0.009$ ) BMD, even after correction for age, time since menopause, BMD, PTH, 25OHvitamin D and BMI. There are no significant correlations between VDR, age and bone metabolism parameters after correction for BMD.

Our data suggest an important role for the VDR in determining bone density, the lower VDR expression in osteoporotic indicate a lower ability to react at circulating vitamin D, and could be the explanation of the increase in the PTH and decrease in the phosphorus levels in patients with respect to controls without difference in circulating vitamin D levels and in the dietary calcium intake.



**Disclosures:** P. D'Amelio, None.

## SA242

See Friday Plenary number F242.

## SA243

**Involvement of Caveolae in  $1\alpha,25(\text{OH})_2\text{D}_3$ -dependent Activation of MAPKs in Skeletal Muscle Cells.** C. Buitrago\*, R. L. Boland. Dept. Biología, Bioquímica & Farmacia, Universidad Nacional del Sur, Bahía Blanca, Argentina.

$1\alpha,25(\text{OH})_2\text{D}_3$  is a steroid hormone that induces non-transcriptional events modulating components of signal transduction pathways in various cell types. The ERK1/2 and p38 members of the MAPK family are signaling pathways which mediate rapid responses to extracellular stimuli. Although there are data indicating that  $1\alpha,25(\text{OH})_2\text{D}_3$  regulates MAPK cascades in skeletal muscle cells, the role of plasma membrane components in the fast effects of the hormone in this tissue have not been investigated. In the present work, using the skeletal muscle cell line C2C12 as experimental model, we demonstrate by Western blot analysis with phosphospecific antibodies that  $1\alpha,25(\text{OH})_2\text{D}_3$ -dependent ERK1/2 and p38 MAPK phosphorylation are suppressed by disassembling caveolae with methyl-beta cyclodextrin (M $\beta$ CD). Moreover, c-Src activation by the hormone was abolished by exposure of C2C12 cells to M $\beta$ CD. One of the main molecules of caveolae

expressed in this cellular type is caveolin-1 (cav-1). Therefore, we investigated the relationship between cav-1 and c-Src. Confocal microscopy images of immunocytochemical assays of control C2C12 cells showed that cav-1 and c-Src colocalize at the plasma membrane. Cell treatment with  $1\alpha,25(\text{OH})_2\text{D}_3$  abolished colocalization of cav-1 and c-Src. These results were corroborated by experiments showing that  $1\alpha,25(\text{OH})_2\text{D}_3$  blocks coimmunoprecipitation of cav-1 and c-Src observed under control conditions. Localization of the vitamin D receptor (VDR) in C2C12 cells was investigated. Congruent with previous results, translocation of the VDR to the plasma membrane occurs in cells treated with  $1\alpha,25(\text{OH})_2\text{D}_3$ . In cells exposed to M $\beta$ CD the VDR is present only in the nucleus. These data suggest that caveolae are involved in c-Src-dependent MAPK activation by  $1\alpha,25(\text{OH})_2\text{D}_3$  through the VDR in skeletal muscle cells.

**Disclosures:** R.L. Boland, None.

## SA244

See Friday Plenary number F244.

## SA245

**Effect of  $1\alpha,25$ -Dihydroxy Vitamin D3 on Proliferation and Differentiation of C2C12 Myoblast.**

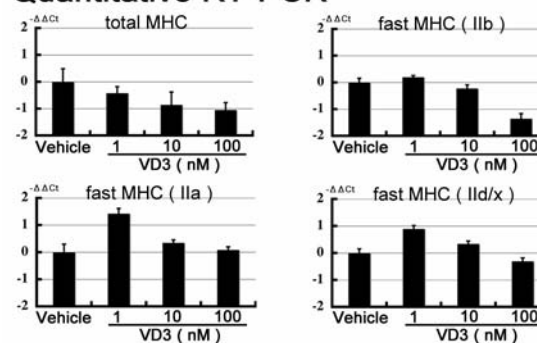
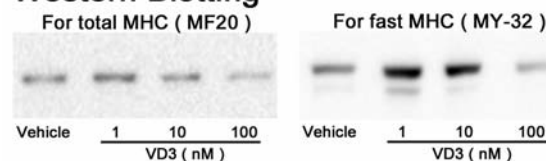
H. Okuno\*, K. N. Kishimoto, M. Hatori\*, E. Itoi\*. Department of Orthopaedic Surgery, Tohoku University School of Medicine, Sendai, Japan.

Vitamin D plays a major role in the regulation of calcium homeostasis. Recently many reports have demonstrated that  $1\alpha,25$ -dihydroxy vitamin D3 (VD3) supplementation reduced the risk of falls and osteoporosis related fractures of older individuals. An enhancement of the muscle strength and reduction of the body sway are possible mechanisms. However, in vitro effect of VD3 on skeletal muscle has not been well understood. In this study, we examined the effect of VD3 on proliferating, differentiating and differentiated phases of C2C12 myoblasts, mouse skeletal muscle cell line.

C2C12 myoblasts proliferate without fusion and differentiation when grown in 10% fetal bovine serum (FBS). Cell counting and WST-1 cell proliferation assay revealed that supplementation of VD3 under 10% FBS inhibited their proliferation and viability in a dose-dependent manner of VD3. Flow cytometric analysis showed that VD3 increased the percentage of cells in the G0/G1 phase dose-dependently. Cells cultured with VD3 exhibited larger cell size than control under the cytologic observations.

C2C12 cells start fusion and differentiation into myotubes when culture medium is changed to 2% horse serum (HS). VD3 treatment in differentiating phase was defined as starting VD3 supplementation when the medium was changed to HS. VD3 treatment in differentiated phase was defined as starting VD3 supplementation after 8 days culture in HS. VD3 treatment in differentiating phase inhibited the formation of myotube and the expression of total MHC in both mRNA and protein levels. VD3 treatment in differentiated phase did not show significant difference in amount of total MHC using western blot analysis with MF20 antibody (DSHB). However significant larger expression of fast MHC confirmed by Western blot analysis with MY-32 (Sigma) was found in the 1nM of VD3 than in the control.

Our findings indicated that VD3 inhibited proliferation of myoblasts during proliferating and differentiating phases. In the differentiated phase, 1 nM of VD3, a little higher concentration than physiological level, increased the expression of fast MHC. Our result suggested that VD3 might have anabolic effect on skeletal muscle in adequate concentration.

**Quantitative RT-PCR****Western Blotting**

**Disclosures:** H. Okuno, None.

## SA246

See Friday Plenary number F246.

## SA247

**The Spectrum of Osteogenesis Imperfecta Mutations in Sweden - A Study of 26 Families.** K. M. Lindahl\*, C. Rubin\*, A. Kindmark, Ö. Ljunggren. Medical Sciences, Uppsala, Sweden.

**Background/Aim:** Osteogenesis imperfecta (OI) is a heterogeneous disease of connective tissue with an incidence of approximately 1/15 000. More than 90% of OI is caused by a dominant mutation in the genes coding for collagen I, COL1A1 and COL1A2. The cardinal sign of OI is fragile bones with multiple fractures, but the disease can affect many other tissues with symptoms such as blue sclera, excessive bleeding, hyper mobile joints, dentinogenesis imperfecta and deafness. The severity of OI ranges from a mild disease with an average life expectancy to death perinatally. A mild phenotype is often due to a quantitative collagen defect, while patients with more severe forms generally have a mutation leading to a qualitative collagen defect.

Over 800 mutations causing OI have been described in collagen I. As COL1A1 and COL1A2 are large genes, there are still many blank spaces where no mutations have been found and positions where only a few of the possible substitutions have been reported. Approximately 80% of structurally abnormal collagen in OI is the result of a glycine mutation. At present only 11% of possible glycine substitutions in COL1A1 and 10% in COL1A2 have been described.

The mutation spectrum causing OI in Sweden has not been investigated previously. Here the collagen I genes of 26 unrelated patients with OI from all parts of Sweden were studied. Method: DNA was extracted from whole blood using a commercially available kit. Exons and flanking intron sequences of COL1A1 and COL1A2 were sequenced using standardised sequencing with ABI3130XL using 110 primer pairs.

**Results:** In 20 of the 26 families a mutation was found: 12 of these were known to cause OI while 8 were not previously reported.

12 mutations were located in COL1A1 and 8 in COL1A2. 11 patients had a glycine substitution, while 7 mutations were insertions, deletions or mutations leading to a premature stop codon. Surprisingly there were 2 non-glycine amino acid substitutions suspected to cause an OI-phenotype and 2 families were carriers of 2 separate mutations. In the latter cases only one of the mutations were of a typical OI-type.

**Conclusion:** The spectrum of mutations causing OI described in this Swedish cohort are of the expected type with the exception of 2 mutations that cause non-glycine substitutions. In 2 patients 2 separate mutations were found. It is presently unclear if both of these influence the patient's phenotype, but further investigations are planned.

Mutation type and location in cohort of Swedish OI-patients

	COL1A1	COL1A2
Mutations	12	8
Glycine substitutions	4	7
Insertions/deletions/stop codons	7	0
Non-glycine aa substitutions	1	1
> 1 mutation	1	1

**Disclosures:** K.M. Lindahl, None.

## SA248

**Dynamic Morphological Changes in the Skulls of Mice Mimicking Human Apert Syndrome Resulting From Gain-of-function Mutation of FGFR2 (P253R).** X. Du\*, X. Zhao\*, Z. Chen\*, X. Lu\*, N. Su\*, Q. Sun\*, Q. He\*, L. Zhao\*, L. Chen. Trauma Center, Daping Hospital, Chongqing, China.

The main distinctive craniofacial manifestations of Apert syndrome (AS) include shallow orbits with proptosis, and midface hypoplasia. We have generated a mouse model (Fgfr2+/P253R) mimicking human AS resulting from FGFR2 P253R mutation. Although, in general, this mouse model shows skull phenotypes similar to human AS, the detailed morphometric, especially the dynamic measurement of the skulls of this model was absent. To see if there are precise parallels between phenotypes in Fgfr2+/P253R mouse and human with AS, we measured, using EDMA approach, the skull morphology of this model and their wild-type controls (WT) at 4W and 8W stages. It was found by FDM (form difference matrix) analysis that there were significant differences in the overall skull shapes and subsets of anatomic structures between mutants and wt at both 4w and 8w of age. In both stages, compared with WT, the mutants exhibited obviously shortened skulls along the anteroposterior (AP) axis. The anterior portion of the mutant skulls was more severely shortened. In contrast, the mutant skulls were broadened along the mediolateral axis in their frontal regions, while the parietal parts were heightened. The 8w old mutants, however, showed alleviated severity of the shortened anterior portion of the skulls. Of the 351 linear distances constructed from the 27 cranial landmarks, 94% were affected in 4w old mutants, but there were only 76% linear distances showed changes in 8w old mutants. In 8w stage, the mutant skulls had more areas broadened mediolaterally. The percentage of the elongated linear distances in mutant skulls over their littermate WT was increased from 2% in 4w to 5% in 8w. The enlarged distances in 4w old mutants included height of the parietal bones, interorbital distance, maxillary width. In 8w, the width of the frontal bones, breadth of palates and zygomatic bones were also increased. GDM (growth difference matrix) analysis showed that the most significantly increased linear distances were mainly concentrated in the orbit region and anterior portion of the skulls roughly along the AP axis.

Since the skulls of Fgfr2+/P253R developed faster than that in WT mice during the stage between 4w and 8w, it's indicated that there was a "catch-up" growth in the mutant skulls, especially along the anteroposterior axis, to compensate the retarded development occurred during the early stages. Our data, from cephalometric aspect, further validate the use of the Fgfr2+/P253R mouse model to analyze the pathogenesis of human AS, and develop therapeutic measures for AS.

This study received the "973" program of China (No.2005CB522604), and the NSFC (No.30470947, 30425023).

**Disclosures:** X. Du, None.

## SA249

**See Friday Plenary number F249.**

## SA250

**Characterisation Through Computer-Assisted Microtomography of the Bone Phenotype of Mice Showing Impaired Gait and Motor Skills.** C. Martineau\*, L. Brissette\*, R. Moreau\*. Sciences Biologiques, Université du Québec à Montréal, Montréal, QC, Canada.

Osteoarthritis (OA) designates a group of diseases characterised by stiffness of the joints and ectopic calcification, ultimately leading to erosion of the articular surfaces and consequent movement impairment. Bone architecture alterations for some OA syndromes have been thoroughly documented, such as chondrocalcinosis (CC), craniometaphyseal dysplasia (CMD) and progressive ankylosis, all of which may result from a mutation of the *Ank* gene. This gene encodes a transmembrane channel carrying inorganic pyrophosphate (PPi) to the extracellular environment, preventing excessive calcification. Though CC, CMD and progressive ankylosis show similar symptoms, they are the result of modifications in the N-terminal segment of ANK protein with a gain of function, in the case of CC, and in the C-terminal portion of ANK protein, leading to a loss of function in the case of CMD and progressive ankylosis. Indeed, excessive extracellular PPi results in calcium pyrophosphate dihydrate (CPPD) deposition as seen in CC, while low extracellular PPi leads to hydroxyapatite (HA) formation as observed in the two latter syndromes. In a C57Bl/6 mice colony, 5 individuals of a 6-month-old litter of 9 mice showed abnormal stature and severe locomotor deficiency due, at a first glance, to joint stiffness. The litter was euthanised and the tibiae, femora and lumbar vertebrae were harvested for X-ray microtomography (microCT) analysis. Results confirmed that the articular stiffness was due to excessive ectopic calcification of the toes, knees and spine. Further analysis showed signs of osteoporosis with reduced trabecular tissues, as well as lower bone mineral density (BMD) in tibiae, femora and vertebrae. Alizarin Red S staining of whole mounted legs should discriminate between CPPD and HA formation in the joints, pointing to CC or CMD/progressive ankylosis respectively. Livers harvested and cryopreserved from some individuals will be used for genomic DNA analysis to establish the presence of mutations in the *Ank* gene.

**Disclosures:** C. Martineau, None.

This study received funding from: CIHR.

## SA251

**Genome-Wide Pleiotropic Associations of Bone Phenotypes: The Framingham SHARE Project.** D. Karasik<sup>1</sup>, Y. H. Hsu<sup>1</sup>, Y. Zhou<sup>\*2</sup>, L. A. Cupples<sup>\*2</sup>, D. P. Kiel<sup>1</sup>, S. Demissie<sup>\*2</sup>. <sup>1</sup>IFAR, Hebrew SeniorLife, Boston, MA, USA, <sup>2</sup>Biostatistics, BU Sch Public Health, Boston, MA, USA.

Genome-wide association studies (GWAS) using high-density genotyping platforms offer an unbiased approach to identify new candidate genes for osteoporosis. There are multiple osteoporosis-related measurements, such as DXA BMD at different skeletal sites. Previously, using a 100K SNP marker set in the Framingham Heart Study (FHS) sample, we (ASBMR 2007) reported that associations with single nucleotide polymorphisms (SNPs) were often shared among multiple bone traits. Here we report results from our FHS SHARE project, with as many as 5 times more SNPs and twice as large sample size.

We used the Affymetrix 500K+50K SNP GeneChip marker set to examine genetic associations with BMD (FN and LS), QUS (BUA and SOS), DXA-derived geometric indices of the hip, and x-ray-derived metacarpal indices, in two cohorts from the FHS. We evaluated 432,159 SNPs with genotypic call rates  $\geq 95\%$ , HWE  $p \geq 10^{-6}$ , and MAF  $\geq 1\%$  in 1554 men and 2073 women (mean age 65 yrs) with individual level call rate  $\geq 97\%$ . Linear mixed effects models (LME) were used to test associations between SNPs and multivariable-adjusted residual trait values. Variance components analysis (SOLAR) was performed to estimate genetic correlations ( $\rho_g$ ) among these traits. We compared  $\rho_g$  among each pair of traits with the proportion of SNPs associated with both of these traits. We found that at a pre-specified significance threshold  $\alpha$ , LS and FN BMD in females share only 2.5% associated SNPs at  $\alpha = 0.001$  (5.6% at 0.01 level), despite a high  $\rho_g = 0.67$  between them. Similarly, femoral neck length and width, whose  $\rho_g = 0.48$  in females, share as much as 1.1% (2.4% at 0.01 level). There are virtually no SNPs that share associations with both BMD and geometric traits (femoral neck and shaft width, neck-shaft angle, and neck length);  $\rho_g$  among these geometric traits ranges from -0.20 to +0.48.

In conclusion, GWAS offers a hypothesis-free strategy to identify new associations and may be used to examine pleiotropic relationships between osteoporosis-related traits. Despite some statistical reservations (such as unknown false-positive rate), this strategy may prove helpful to define the best combination of phenotypes to be utilized in genetic studies of pleiotropy in osteoporosis.

**Disclosures:** D. Karasik, None.

This study received funding from: R01-AR050066 and R01-AR/AG 41398.

## SA252

**Age-Associated Changes in the Material Properties of the G610C (Amish) OI Mouse Model.** E. L. H. Daley<sup>\*1</sup>, D. J. McBride<sup>2</sup>, T. E. Uveges<sup>\*3</sup>, N. V. Kuznetsova<sup>\*3</sup>, S. Leikin<sup>\*3</sup>, J. C. Marini<sup>3</sup>, S. A. Goldstein<sup>1</sup>. <sup>1</sup>University of Michigan, Ann Arbor, MI, USA, <sup>2</sup>University of Maryland, Baltimore, MD, USA, <sup>3</sup>National Institutes of Health, Bethesda, MD, USA.

The Amish OI knock-in mouse was designed to replicate a COL1A2 G610C mutation associated with OI in an Amish kindred. The mutation has been stably inherited for 6 generations, is found in over 60 individuals, and exhibits a mild, but variable phenotype. The Amish OI mouse expresses mutant type I collagen mRNA and protein. Its mean dermal collagen fibril diameter is reduced compared to WT littermates. Here, we report the first assessment of the G610C mutation on femur geometric and mechanical properties. Femurs from male 2 month old (WT=9; G610C=9) and 6 month old (WT=9; G610C=6) mice were scanned via  $\mu$ CT to quantify femur morphology and mineralization (GE Medical Systems, London, ON). Cortical regions of interest (ROI) consisted of 3 mm segments of the mid-diaphyses while trabecular ROI were chosen from volumes within the distal femoral metaphyses proximal to the growth plates. Mechanical testing of the femurs was done via 4-point bending conducted with a servo-hydraulic testing system. Predicted material properties were calculated using classical beam theory. One-way ANOVA with *post-hoc* Tukey Test was used to compare group means with a P-value  $\leq 0.05$  considered significant (SPSS, Chicago, IL).

G610C femurs were shorter, had smaller radii, and had greater volumetric cortical mineral density, but did not differ in cortical thickness compared to age-matched controls. Though cortical morphologies of the mutant genotype were not qualitatively different, voxel-by-voxel image analysis revealed divergent patterns of mineralization in the G610C. Six-month G610C trabecular thickness and mineral density were similar to 6-month controls, but trabecular number was reduced. Two-month G610C yielded and failed at lower loads than the other groups, yet by six-months G610C femurs and controls withstood similar loads. There were no significant differences in yield stress at both ages, but at 6 months failure stress was greater in G610C than control. Though G610C and age-matched controls had similar whole bone stiffness, the G610C mutants had a significantly greater Young's Modulus.

The results demonstrate that G610C has significant phenotypic alterations in bone properties compared to WT. Moreover, G610C femoral material properties appear to alter over time in a way that brings whole-bone strength on par with WT by six months of age, perhaps as part of a mechanism that compensates for the smaller size of the mutant femurs. Interestingly, this compensatory mechanism is remarkably similar to the adaptation observed in Brtl IV mice, suggesting a shared skeletal response for glycine substitutions in either type I collagen chain.

**Disclosures:** E.L.H. Daley, None.

## SA253

See Friday Plenary F253

## SA254

**Characterization of the Enthesopathy of X-linked Hypophosphatemia in the Hyp Mouse.** C. M. Macica<sup>\*1</sup>, G. Liang<sup>\*1</sup>, L. D. Katz<sup>\*2</sup>, K. L. Insogna<sup>1</sup>, T. O. Carpenter<sup>3</sup>. <sup>1</sup>Internal Medicine, Yale University, New Haven, CT, USA, <sup>2</sup>Diagnostic Radiology, Yale University, New Haven, CT, USA, <sup>3</sup>Pediatrics, Yale University, New Haven, CT, USA.

Despite the characteristic osteomalacia seen in X-linked hypophosphatemia (XLH), paradoxical calcification occurs at tendon and ligament insertion sites, as described over 20 years ago (Polisson, 1985). We confirmed a generalized enthesopathy/osteophytopathy in a clinical survey of over 30 patients affected with XLH; calcaneal spurs and Achilles enthesopathy are often affected earlier than other sites. As previously suggested, enthesopathy does not appear to be determined by phosphate/calcitriol treatment, and is likely intrinsic to the basic disease process. Nevertheless, as no studies to date have examined the progression or pathogenesis underlying mineralization of insertion sites in XLH, we examined several fibrocartilagenous insertion sites in the murine model of XLH, the Hyp (Phex deletion) mouse, including that of the Achilles tendon. Enthesis fibrocartilage (FC) was established by cellular phenotype (small, rounded cells aligned in rows between collagen fibrils) and expression of type II collagen. In contrast to aged-matched control mice (7 mos), the enthesis FC was highly cellular and dramatically thickened, extending well into both the sesamoid and calcaneal FC. The expansion of FC also extended far into the medial process of the calcaneal tuberosity. This was accompanied by a 5-fold increase in expression of type II collagen. In addition, alkaline phosphatase (AP) activity, a general marker of cartilage and bone mineralization, was minimal in the enthesis of control mice, localized only to the enthesis tide-mark. In contrast, a dramatic 20-fold increase in AP activity was observed in Hyp mice and was associated with the expanded FC. It thus appears that the Hyp mouse phenocopies the human syndrome quite precisely and will form the basis our studies characterizing the signaling molecules involved in this process.

**Disclosures:** C.M. Macica, None.

This study received funding from: R01DK62515.

## SA255

**Possible Central Function of the Calcitonin Receptor on Bone Mass.** C. B. Confavreux<sup>1</sup>, C. Settembre<sup>\*1</sup>, F. Oury<sup>\*1</sup>, R. A. Davey<sup>2</sup>, J. D. Zajac<sup>2</sup>, G. Karsenty<sup>1</sup>. <sup>1</sup>Genetics and Development Department, Columbia University, New York, NY, USA, <sup>2</sup>Department of Medicine, Austin Health, University of Melbourne, Heidelberg, Victoria, Australia.

Calcitonin, a hormone able to lower serum calcium level, mediates its signal through calcitonin receptor (Calcr), a member of the seven trans-membrane domains G protein coupled receptor family. Since *Calcr* is expressed in osteoclasts, it is generally assumed that calcitonin is a regulator of bone resorption. However, mice lacking one copy of *calcitonin receptor* displayed an increase in bone mass due to an increase in bone formation whereas bone resorption was normal. These *in vivo* data raise the hypothesis that calcitonin may be a regulator of bone formation, a function that may not be explained by the expression of *Calcr* in osteoclasts. To address this conundrum, we first analyzed *Calcr* expression pattern. Besides osteoclasts, *Calcr* is expressed in neurons of the arcuate nucleus and the paraventricular hypothalamic nucleus (PVH), two hypothalamic nuclei implicated in the control of bone mass. Interestingly, *Calcr* expression in these neurons was markedly stronger than in osteoclasts. This pattern of expression along with the phenotype of *Calcitonin receptor* deficient heterozygous mice raises the prospect that this receptor regulates bone formation through its expression in brain. In an effort to perform a thorough analysis of the function of calcitonin receptor in the different cell types where it is expressed, we used a *Cre-loxP* strategy to generate mice lacking *Calcr* in either all cells (*Calcr<sup>-/-</sup>*), osteoclasts only through the use of *CathepsinK-Cre* mice (*Calcr<sup>osc/-</sup>*) or in neurons through the use of *SynapsinI-Cre* mice (*Calcr<sup>neurons/-</sup>*). As expected, *Calcr<sup>-/-</sup>* mice displayed an increased bone mass due to an increase in osteoblast number. Remarkably there was no change in bone resorption parameters. Surprisingly, while mice lacking *Calcr* in osteoclasts only lived normally, the brain specific deletion of *Calcr* was lethal, most likely during embryogenesis. We are currently investigating the cause of death in *Calcr<sup>neurons/-</sup>* mice as well as studying the bone phenotype of the *Calcr<sup>neurons+/-</sup>* and *Calcr<sup>osc/-</sup>* mice. Results of this analysis will be presented at the meeting.

**Disclosures:** C.B. Confavreux, None.

This study received funding from: Société Française de Rhumatologie, Association pour la Recherche sur le Cancer, the Philippe Foundation, Fondation Bettencourt.

## SA256

See Friday Plenary number F256.

## SA257

**An Investigation into the Impact of Osteoarthritic Changes on Bone Mineral Density Measurements in Patients with High Bone Mass.** C. L. Gregson<sup>\*1</sup>, S. Steel<sup>\*2</sup>, K. Yoshida<sup>\*3</sup>, D. M. Reid<sup>\*3</sup>, J. H. Tobias<sup>1</sup>. <sup>1</sup>Bristol University, Bristol, United Kingdom, <sup>2</sup>Royal Infirmary, Hull, United Kingdom, <sup>3</sup>Aberdeen University, Aberdeen, United Kingdom.

High Bone Mass (HBM) is of increasing interest, but so far cases have only been reported sporadically. To identify further HBM cases, we screened 7 Dual Energy X-ray Absorptiometry (DXA) databases in the UK (5 Lunar, 2 Hologic) for T or Z score of  $\geq +4$  at the lumbar spine or hip. A problem we have met is that since osteoarthritis (OA) can artefactually raise bone mineral density (BMD), and HBM may itself be associated with OA, a method is required to identify HBM cases with or without co-morbid OA, while excluding those with OA alone. To develop this, DXA images from HBM 'cases' identified in this way were graded for OA severity using the Kellgren & Lawrence (KL) score [mild (0-2), moderate (3), severe (4)] and related to BMD results. 562 out of 197,953 scans had a T or Z score of  $\geq +4$  at the lumbar spine or hip. 77% were women. Mean age 63 years, weight 81.7kg, height 164.6cm. Mean total L1-L4 Z score was 5.09 (3.65-6.55), L1 Z score 3.40 (3.24-3.56), total hip Z score 2.11 (1.97-2.25), KL score 3.36 (3.30-3.46). Subjects with scoliosis (65), ankylosing spondylitis (9), orthopaedic metalwork (8) and other known causes of raised BMD (17) were excluded. In the remaining 463, KL score was compared with BMD using linear regression. Total L1-L4 Z score was strongly correlated with increasing KL score (1.01; 0.54, 1.48;  $p < 0.001$ ); whereas, L1 Z score was not (0.04; -0.53, 0.60;  $p = 0.89$ ). Total hip Z score was negatively correlated with KL score (-0.85; -1.33, -0.38;  $p < 0.001$ ). Total L1-L4, affected most by OA, was thus not appropriate to differentiate HBM from OA; L1 Z score was affected least, reflecting the recognized pattern of progressive OA changes seen in descending sequential lumbar vertebrae. If anything, high hip BMD was negatively associated with spondylosis. Hence a new definition of HBM was developed as a) L1 Z score of  $\geq +3.5$  plus total hip Z score  $\geq +1.2$ , or b) total hip Z score  $\geq +3.5$ . Using this definition, 179/463 (38.7%) of cases originally identified, after exclusion of other HBM causes, were defined as having HBM  $\pm$  co-morbid OA, of whom 40.2% had severe and 46.4% moderate OA. In contrast, of the remaining subjects re-classified as non-HBM, 44.8% had severe OA and 45.8% moderate OA ( $p = 0.016$ ). Furthermore, when applying this definition, HBM subjects were much heavier than non-HBM subjects (86.0 [83.4, 88.6] vs 78.2 [76.2, 80.2] kg respectively), whilst height and age were similar, providing further evidence that our revised definition was effective at distinguishing between subjects with or without HBM. In conclusion, L1 and total hip Z scores are useful in identifying HBM ( $\pm$  co-morbid OA), filtering out those with OA alone as an artefactual cause of high BMD.

**Disclosures:** C.L. Gregson, None.

This study received funding from: The Wellcome Trust, London.

## SA258

**PTHRI Mutations Associated with Ollier Disease Result in Receptor Loss of Function.** A. Couvineau<sup>\*1</sup>, V. Wouters<sup>\*2</sup>, G. Bertrand<sup>\*3</sup>, C. Rouyer<sup>\*1</sup>, B. Gérard<sup>\*3</sup>, L. Boon<sup>\*4</sup>, B. Grandchamp<sup>\*3</sup>, M. Vikkula<sup>\*2</sup>, C. Silve<sup>\*5</sup>. <sup>1</sup>Faculté Bichat, INSERM U773, Paris, France, <sup>2</sup>Université Catholique de Louvain, Laboratory of Human Molecular Genetics, Brussels, Belgium, <sup>3</sup>AP-HP, Hôpital Bichat, Service de Biochimie Hormonale et Génétique, Paris, France, <sup>4</sup>Cliniques Universitaires St Luc, Center for Vascular Anomalies, Brussels, Belgium, <sup>5</sup>AP-HP, Hôpital Bichat, INSERM U561 et Service de Biochimie Hormonale et Génétique, Paris, France.

The PTHRI signalling pathway is critical for the regulation of endochondral ossification. Thus, abnormalities in genes belonging to this pathway could potentially participate in the pathogenesis of Ollier disease / Maffucci's syndrome, two developmental disorder defined by the presence of multiple enchondromas. In agreement, a functionally deleterious mutation in PTHRI (p.R150C) was identified in enchondromas from two of six unrelated patients with enchondromatosis. However, neither the p.R150C mutation (26 tumors) nor any other mutation in the *PTHRI* gene (11 patients) could be identified in another study. To further define the role of PTHRI signalling pathway in Ollier disease and Maffucci syndrome, we have analysed the coding sequences of four genes (*PTHRI*, *IHH*, *PTHrP* and *GNAS1*) in leucocyte and/or tumor DNA from 57 and 23 patients affected with Ollier disease or Maffucci syndrome respectively. We identified three previously undescribed missense mutations in PTHRI in patients with Ollier disease at the heterozygous state. Two of these mutations (p.G121E, p.A122T) were present only in enchondromas, and one (p.R255H) in both enchondroma and leukocyte DNA. The assessment of receptor function demonstrated that these three mutations impair PTHRI function, either by reducing the affinity of the receptor for PTH or reducing receptor expression at the cell surface. These mutations have not been found in DNA from 222 control patients. The PTHRI mutations identified in Ollier disease (p.G121E, p.A122T, p.R150C) and Blomstrand chondrodysplasia (p.P132L) all lie within the structured core of the PTH-PTHrP extracellular domain complex in the crystal structure described by Pioszak and Xu (PNAS 2008), a location compatible with a functionally deleterious effect. Including our data, PTHRI functionally deleterious mutations have now been identified in 5/31 enchondromas from Ollier patients. These findings provide further support for the idea that heterozygous mutations in PTHRI that impair receptor function may participate in the pathogenesis of Ollier disease in some patients.

**Disclosures:** C. Silve, None.

This study received funding from: INSERM, AP-HP, Association Ollier Maffucci, Fédération des Maladies Orphelines, Interuniversity attraction Poles initiated by the Belgian Federal Science Policy.

## SA259

**Hypothyroidism and Autism Combined with Pseudohypoparathyroidism in the Absence of Albright's Hereditary Osteodystrophy and GNAS Imprinting Changes: A Novel Clinical Syndrome?** L. M. Ward<sup>1</sup>, T. Pinto<sup>\*1</sup>, S. Lawrence<sup>\*1</sup>, M. Lawson<sup>\*1</sup>, M. Bastepe<sup>2</sup>, H. Jüppner<sup>2</sup>, F. Rauch<sup>3</sup>. <sup>1</sup>Div. of Endocrinology, Children's Hospital of Eastern Ontario, Ottawa, ON, Canada, <sup>2</sup>Endocrine Unit, Massachusetts General Hospital, Boston, MA, USA, <sup>3</sup>Genetics Unit, Shriners Hospital for Children, Montréal, QC, Canada.

**Introduction and Aim:** Pseudohypoparathyroidism (PHP) typically arises from defects in *GNAS* (20q13.3), an imprinted gene locus with multiple transcriptional units. Recent studies have shown that the mutations responsible for the PHP-Ib form affect control elements regulating the imprinting of *GNAS*. The purpose of this report was to describe an apparently novel form of PHP-Ib in two brothers with unique clinical features.

**Clinical Report:** The male proband presented at 12 years with increasing seizure frequency and autism. Investigations suggested PHP: (Ca<sup>2+</sup> 0.9 mmol/L, N: 1.1-1.3; PO<sub>4</sub> 1.8 mmol/L, N: 1.0-1.7; PTH 54 pmol/L, N: 1.1-6.8). A PTH infusion test (Parathar 3 units/kg) demonstrated only a 6-fold increase in cAMP (N: >10-fold increase) and a 2.5% reduction in percent tubular reabsorption of phosphate (N: 5-16% reduction). A trans-iliac bone biopsy revealed increased cancellous bone volume (38% above the average) with a 4-fold elevation in bone formation rate. These results confirmed renal resistance to PTH with bone tissue responsiveness. TSH resistance was also suspected: TSH 6.7 mU/L; FT4 <5 pmol/L. TRH stimulation consistent with primary hypothyroidism, negative anti-thyroid antibodies and lack of a goiter. An older brother also manifested autism, PTH resistance and primary hypothyroidism in the absence of positive anti-thyroid antibodies; however, a large goiter was present. Southern blot analyses using gDNA from the proband and methylation sensitive restriction enzymes showed no evidence of a methylation defect in *GNAS* exon A/B. Analysis of genomic DNA from the affected children and their parents through microsatellite markers located centromeric and telomeric of *GNAS*, and through single nucleotide polymorphisms within the *GNAS* locus showed that the two affected individuals inherited different maternal and paternal alleles.

**Conclusions:** We describe two brothers with autism, primary hypothyroidism and PHP, where the genetic and epigenetic findings suggest that *GNAS* is not linked to this form of PHP-Ib. This constellation of features may represent a novel clinical syndrome.

**Disclosures:** L.M. Ward, None.

## SA260

See Friday Plenary number F260.

## SA261

**Genomic Expression Analysis of Rat Chromosome 4 for Skeletal Traits at Femoral Neck.** I. Alam<sup>1</sup>, Q. Sun<sup>1</sup>, L. Liu<sup>\*2</sup>, D. L. Koller<sup>2</sup>, Y. Liu<sup>\*3</sup>, H. J. Edenberg<sup>\*4</sup>, M. J. Econs<sup>3</sup>, T. Foroud<sup>2</sup>, C. H. Turner<sup>1</sup>. <sup>1</sup>Biomedical Engineering, Indiana University School of Medicine, Indianapolis, IN, USA, <sup>2</sup>Medical and Molecular Genetics, Indiana University School of Medicine, Indianapolis, IN, USA, <sup>3</sup>Medicine, Indiana University School of Medicine, Indianapolis, IN, USA, <sup>4</sup>Biochemistry and Molecular Biology, Indiana University School of Medicine, Indianapolis, IN, USA.

Hip fracture is the most devastating osteoporotic fracture type with significant morbidity and mortality. The primary skeletal determinants of hip fracture risk are bone mineral density, structure and strength. Several studies have demonstrated that there is a substantial genetic component to hip fragility. Thus, finding the genetic basis underlying variation in skeletal traits in femoral neck will facilitate our understanding to prevent and/or treat hip fracture successfully. Genetic linkage studies in humans and animal models identified chromosomal regions linked to hip size and bone mass. Previously, we identified that the region of 4q21-q41 on chromosome (Chr) 4 uniquely harbors multiple femoral neck quantitative trait loci (QTLs) in inbred Fischer 344 (F344) and Lewis (LEW) rats. The purpose of this study is to identify the candidate genes for femoral neck density and structure by correlating gene expression in the proximal femur with the femoral neck phenotypes linked to the QTLs on Chr 4. RNA was extracted from proximal femora of 4-week-old rats from F344, LEW and two other strains (n=4 per strain). Microarray analysis was performed using Affymetrix Rat Genome 230 2.0 arrays. A total of 104 genes in the 4q21-q41 region were differentially expressed (p<0.05) among all strains of rats with a false discovery rate (FDR) less than 10%. These 104 genes were then ranked based on the proportion of variation in femoral neck phenotypes in F2 animals homozygous for a particular strain's allele at the Chr 4 QTL explained by the expression level of the gene in that strain. A total of 37 genes, including 21 candidate genes and 16 predicted genes, were strongly correlated (r<sup>2</sup>>0.50) with different femoral neck phenotypes and prioritized for further analysis. Analysis of the related pathways among prioritized candidate genes based on their molecular function, biological process and cellular component of the gene product by Ingenuity pathway analysis revealed several direct or indirect relationships among the candidate genes related to bone metabolism including pathways related to beta-estradiol, interleukin 6, insulin growth factor 2, androgen receptor and tumor necrosis factor. This study may provide a basis for identifying the genetic determinants of skeletal traits at the hip and may lead to novel approaches to prevent and treatment of hip fracture.

**Disclosures:** I. Alam, None.

This study received funding from: NIH.

## SA262

**Recurring Mutation Causing Severe/Lethal Recessive Type VIII Osteogenesis Imperfecta in African-Americans Originated in West Africa More than 300 Years Ago.** W. A. Cabral<sup>\*1</sup>, A. M. Barnes<sup>\*1</sup>, C. N. Rotimi<sup>\*2</sup>, F. D. Porter<sup>\*3</sup>, J. Bailey-Wilson<sup>\*4</sup>, L. Brody<sup>\*5</sup>, J. C. Marini<sup>1</sup>. <sup>1</sup>Bone & Extracellular Matrix Branch/NICHD/NIH, Bethesda, MD, USA, <sup>2</sup>Inherited Disease Research Branch/NHGRI/NIH, Bethesda, MD, USA, <sup>3</sup>Heritable Disorders Branch/NICHD/NIH, Bethesda, MD, USA, <sup>4</sup>Inherited Disease Research Branch/NHGRI/NIH, Baltimore, MD, USA, <sup>5</sup>Genome Technology Branch/NHGRI/NIH, Bethesda, MD, USA.

Recessive Osteogenesis imperfecta (OI) is caused by defects in the genes encoding cartilage-associated protein (*CRTAP*) or prolyl 3-hydroxylase 1 (*LEPRE1*) and accounts for approximately 5% of OI cases in North America. Patients deficient in prolyl 3-hydroxylase 1 have severe to lethal bone dysplasia characterized by white sclerae and extreme osteopenia, with DEXA z-scores below -6. Although recessive OI accounts for only a small percentage of OI cases, we have identified a recurring mutation in the *LEPRE1* gene, IVS5+1G>T (Nat Genet 39:359-365, 2007). The common mutation occurs in a compound heterozygous or homozygous state in 6 of 9 probands (9 of 18 alleles) with recessive type VIII OI (OMIM #610915). All six probands with this mutation were born to carrier parents of West-African (Nigerian or Ghanaian) or African-American descent, suggesting the existence of a stable mutant allele in this population. In order to determine the carrier frequency of this mutation in African-Americans, we screened genomic DNA from unrelated African-American newborns from Pennsylvania (n=1429) and Washington, D.C. (n=588). We identified 5 carriers from Pennsylvania and 5 carriers from the District of Columbia, predicting a carrier frequency of 1 in 118-286 African-American newborns (0.35-0.85%). Our results predict a 1 in 55,000-330,000 rate of occurrence of lethal type VIII OI in African-Americans due to homozygosity for *LEPRE1* IVS5+1G>T. To verify the origin of the mutation, genomic DNA from 1097 contemporary West Africans was screened using a custom SNP assay, followed by PCR confirmation of positive samples. Fifteen of 1097 unrelated individuals (1.37%) from Nigeria and Ghana were heterozygous for *LEPRE1* IVS5+1G>T, two-thirds of whom are from the Yoruba or Ibo tribes of Nigeria. This high carrier frequency suggests that the incidence of recessive type VIII OI in West Africa from this founder mutation alone is 1 in 21,000 individuals, which is equivalent to the incidence of dominant OI in North America. Screening of microsatellites covering a 4.2Mb region surrounding the *LEPRE1* gene on chromosome 1p33-34.3 revealed a conserved haplotype of less than 500Kb in probands and carriers. These data support the occurrence of a common founder mutation over 300 years ago, consistent with our hypothesis that this West African allele was transported to the Americas via the colonial slave trade.

**Disclosures:** W.A. Cabral, None.

This study received funding from: NIH intramural funding.



## SA263

**Genome-Wide Association Study Reveals Genetic Variants Associated with Bone Mineral Density, Osteoporosis and Osteoporotic Fractures.** J. Richards<sup>\*1</sup>, F. Rivadeneira<sup>\*2</sup>, M. Inouye<sup>\*3</sup>, T. Pastinen<sup>\*4</sup>, N. Soranzo<sup>\*3</sup>, S. G. Wilson<sup>\*5</sup>, T. Andrew<sup>\*1</sup>, M. Falchi<sup>\*1</sup>, R. Gwilliam<sup>\*3</sup>, K. R. Ahmadi<sup>\*1</sup>, P. Arp<sup>\*2</sup>, A. M. Valdes<sup>\*1</sup>, P. Whittaker<sup>\*2</sup>, D. J. Verlaan<sup>\*6</sup>, M. Jhamai<sup>\*2</sup>, V. Kumanduri<sup>\*2</sup>, J. B. van Meurs<sup>\*2</sup>, A. Hofman<sup>\*2</sup>, H. P. Pols<sup>\*2</sup>, D. Hart<sup>\*1</sup>, G. Zhai<sup>\*1</sup>, B. H. Mullin<sup>\*5</sup>, P. Deloukas<sup>\*3</sup>, A. G. Uitterlinden<sup>\*2</sup>, T. D. Spector<sup>\*1</sup>. Twin Research Unit, King's College London, London, United Kingdom, <sup>2</sup>Erasmus MC, Rotterdam, Netherlands, <sup>3</sup>Sanger Institute, Cambridge, United Kingdom, <sup>4</sup>McGill University, Montreal, QC, Canada, <sup>5</sup>University of Western Australia, Perth, Australia, <sup>6</sup>McGill, Montreal, QC, Canada.

**Background:** Osteoporosis is diagnosed by the measurement of bone mineral density (BMD)-a highly heritable and multifactorial trait. We undertook a genome-wide association (GWA) study for BMD.

**Methods:** Using 314,075 single nucleotide polymorphisms (SNPs) we identified the most promising SNPs in 2,094 women from the United Kingdom (TwinsUK discovery cohort). These were then tested for replication in 6,463 individuals from three cohorts (the Rotterdam study, the Chingford study and TwinsUK replication cohort). We also investigated allelic expression levels in lymphoblast cell lines (LCLs). Replicated SNPs were tested for their association with osteoporotic fracture in the Chingford study (n = 718) and the Rotterdam study (n = 5921).

**Findings:** A non-synonymous SNP in the LRP5 gene was associated with decreased BMD (rs3736228: P =  $6.3 \times 10^{-12}$  for lumbar spine (LS) and  $1.9 \times 10^{-4}$  for femoral neck (FN)) and an increased risk of both osteoporotic fracture (odds ratio (OR) = 1.3, P =  $2.0 \times 10^{-3}$ ) and osteoporosis (OR = 1.3, P =  $8.0 \times 10^{-3}$ ). Three SNPs near the TNFRSF11B (osteoprotegerin) gene, were associated with decreased BMD (top SNP, rs4355801: P =  $7.6 \times 10^{-10}$ , P =  $3.3 \times 10^{-8}$  for LS and FN, respectively) and increased risk of osteoporosis (OR = 1.2, P = 0.038). The risk allele at rs4355801 was associated with a 2-fold decreased expression of TNFRSF11B in LCLs (P =  $3.0 \times 10^{-6}$ ). 22% of the entire population was at least heterozygous for both risk alleles and these alleles had a cumulative association with BMD (P for trend =  $2.5 \times 10^{-17}$ ). The presence of both risk alleles increased the risk of osteoporotic fracture (OR = 1.3, P =  $6.0 \times 10^{-3}$ ) and this effect was independent of BMD.

**Interpretation**

This first comprehensive interrogation of common genetic variants influencing BMD, in 8,557 individuals, has identified two gene variants of key biologic proteins which increase the risk of osteoporosis and osteoporotic fracture. These risk alleles, whose combined effect on fracture is similar to that of most well-replicated environmental risk factors, are present in more than one in five Caucasians.

**Disclosures:** J. Richards, None.

This study received funding from: Wellcome Trust, European Commission, CIHR, ECCEO, Genome Canada, Arthritis Research Campaign, Chronic Disease Research Foundation.

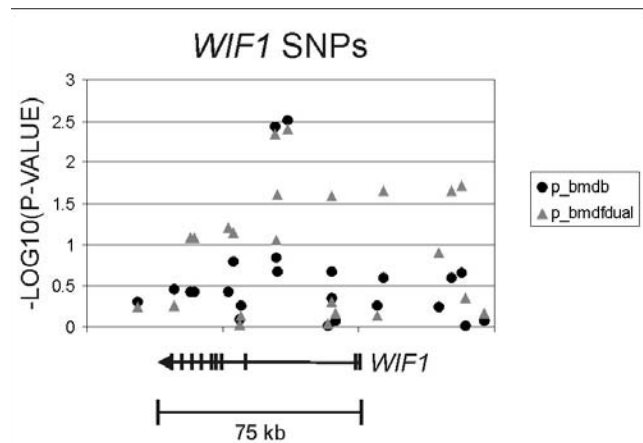
## SA264

**Polymorphisms in the Wnt Inhibitory Factor 1 Gene (WIF1) Are Associated with BMD in Elderly Swedish Women.** C. J. Rubin<sup>1</sup>, K. Michaelsson<sup>\*2</sup>, H. Melhus<sup>\*1</sup>, Ö. Ljunggren<sup>1</sup>, L. Lind<sup>\*1</sup>, A. Kindmark<sup>1</sup>. <sup>1</sup>Dept. Med. Sciences, Uppsala University, Uppsala, Sweden, <sup>2</sup>Dept. Surgical Sciences, Uppsala University, Uppsala, Sweden.

Canonical wnt-signaling promotes bone accrual and perturbations in the wnt signaling pathway can cause osteopetrosis as well as osteoporosis (LRP5 mutations). Wnt Inhibitory Factor 1 (WIF1) is a secreted protein that inhibits wnt-proteins from binding to their receptors. In prior studies of an intercross between domestic and wild-type chicken we have observed differential expression of WIF1 between chicken with high and low BMD and have also identified a Quantitative Trait Locus (QTL) for BMD in the region where WIF1 is located.

Altogether, the data from the chicken studies and the importance of wnt-signaling in bone metabolism makes WIF1 an interesting candidate gene to explore in relation to inter-individual variation in bone traits. In the present study we genotyped 24 common single nucleotide polymorphisms (SNPs) located downstream, within and upstream of the human WIF1 gene and tested if any of these were associated with bone traits. The analyzed population-based cohort (the PIVUS study) comprises 1000 men and women, phenotyped by DXA at approximately 70 years of age.

Female-specific analysis with body mass index (BMI) and age included as covariates revealed associations between BMD (total body and total hip) and genotypes of two SNPs (Figure 1). These two SNPs (rs7309476 and rs10878228) had minor allele frequencies of 0.42 and female C-allele carriers had 6% higher total hip BMD and 3% higher total body BMD compared to female A-allele homozygotes. In addition to these, several other SNPs obtained P-values < 0.05 and may also be interesting to study in follow up studies in other cohorts.



**Disclosures:** C.J. Rubin, None.

## SA265

See Friday Plenary number F265.

## SA266

**Polymorphisms in CYP24A1, the Gene Encoding 25-hydroxyvitamin D-24-hydroxylase Are Associated with BMD.** E. A. Streeten, J. Liu<sup>\*</sup>, X. Shi<sup>\*</sup>, K. Ryan<sup>\*</sup>, D. McBride<sup>\*</sup>, B. Mitchell, A. R. Shuldiner<sup>\*</sup>. Endocrinology, Diabetes and Nutrition, University of Maryland School of Medicine, Baltimore, MD, USA.

Vitamin D deficiency is an important contributor to reduced bone mineral density (BMD). We and others have found that serum level of 25(OH)D is hereditary. Since the main source of vitamin D is endogenous production, we hypothesized that variants in the genes encoding the vitamin D synthetic (*CYP2R1*, *CYP27B1*) and inactivating enzymes (*CYP24A1*) are associated with BMD. The purpose of this study was to perform association studies between SNPs of these 3 genes and BMD.

Healthy Amish participants (n=1467), including 643 men and 843 women, mean ( $\pm$ SD) age of  $55.4 \pm 14.7$  were studied at the Amish Research Clinic in Lancaster, PA. DXA was performed (Hologic 4500) of the spine (L1-4), hip (total, TH; femoral neck, FN) and distal radius (mid, MRad; total, TRad; ultradistal, UD). Lab studies included serum calcium, PTH and 25(OH)D. Association studies were done between BMD and SNPs on 500K genome-wide association (GWAS) chips for the 3 enzymes and also between BMD and 21 haplotype-tagging SNPs from *CYP24A1*.

Results showed T-scores: L1-4  $-1.13 \pm 1.38$ ; TH  $-0.24 \pm 1.07$ ; FN  $-0.54 \pm 1.15$ , and mean 25(OH)D  $22.8 \pm 7.6$ . From GWAS 500K chips, genotypes of 4 of 6 SNPs of *CYP24A1* were associated with BMD in 634 participants, best for SNP rs1570669 for TH (p=0.005). One SNP of *CYP2R1*, A2293926 was associated with UD BMD (p=0.007) and two SNPs of *CYP27B1* were associated with TRad (best p=0.024 for A 2216496). Findings in *CYP24A1* were replicated in an additional sample of 833 Amish (total n=1467). Genotyping of 21 additional SNPs to cover the *CYP24A1* gene in 634 subjects revealed significant associations between 13 SNPs and BMD, with best associations seen in those over age 50 (below). Serum 25(OH)D, PTH, and calcium (n=993) were not associated with genotype for SNPs of *CYP24A1*.

We conclude that variants of *CYP24A1*, the gene for 24-hydroxylase, which catabolizes 25(OH)D into inactive 24,25(OH)<sub>2</sub>D, are associated with BMD in men and women, most strongly in those over age 50. Only minimal association was seen in those under age 50. We speculate that with reduced endogenous skin production of D<sub>3</sub> that occurs with aging, the relative activity of the catabolic 24-hydroxylase enzyme may become more important to maintain optimal calcitriol levels and bone health.

SNP rs3787555 (left) SNP rs1570669 (from GWAS) (right)

	Spine	Tot Hip	Fem N	Tot Rad	Mid Rad	Tot Spine	Tot Hip	Fem N	Total Rad	Mid Rad
All (n=634)	0.005	0.015	0.015	0.001	0.002	0.033	0.004	0.009	0.021	0.035
Women (n=338)	0.048	0.004	0.004	0.034	0.032	0.077	0.012	0.12	0.156	0.194
Men (n=296)	0.034	0.221	0.324	0.002	0.009	0.246	0.178	0.047	0.077	0.108
Over 50 (n=400)	0.001	0.017	0.014	0.083	0.134	0.015	0.0005	0.004	0.005	0.007
≤50 (n=234)	0.55	0.417	0.593	0.082	0.114	0.033	0.053	0.021	0.09	0.101

**Disclosures:** E.A. Streeten, None.

## SA267

**Genome-wide Association Study Identified Novel Susceptibility Loci for Osteoporosis.** Y. Guo<sup>\*1</sup>, J. T. Wang<sup>\*1</sup>, T. L. Yang<sup>\*1</sup>, F. Pan<sup>\*1</sup>, F. Zhang<sup>\*1</sup>, Z. X. Zhang<sup>\*1</sup>, X. G. Liu<sup>\*1</sup>, Q. Zhou<sup>\*1</sup>, B. Drees<sup>\*2</sup>, J. Hamilton<sup>\*2</sup>, C. J. Papasian<sup>\*2</sup>, R. R. Recker<sup>3</sup>, H. W. Deng<sup>2</sup>. <sup>1</sup>School of Life Science and Technology, Xi'an Jiaotong University, Xi'an, China, <sup>2</sup>School of Medicine, University of Missouri - Kansas City, Kansas City, MO, USA, <sup>3</sup>Osteoporosis Research Center, Creighton University, Omaha, NE, USA.

Osteoporosis is a major public health problem. It is mainly characterized by low bone mineral density (BMD) and/or low-trauma osteoporotic fractures (OF), both of which have strong genetic determination, but specific genes are largely unknown. Using the Affymetrix 500K array set, we performed a case-control genome-wide association study in 700 elderly Chinese Han subjects (350 with osteoporotic hip fractures and 350 healthy matched controls). For the significant SNPs identified for OF, we further examined their relevance with hip BMD in both Chinese and Caucasian populations involving an addition 7,009 individuals. We found three novel loci highly significantly associated with OF, including rs13182402 within *ALDH7A1* ( $P = 3.09 \times 10^{-9}$ , odds ratio = 2.92), rs6711417 near *UBR3* ( $P = 4.61 \times 10^{-6}$ , odds ratio = 0.58), and rs6064822 within *PHACTR3* ( $P = 2.36 \times 10^{-5}$ , odds ratio = 0.55). Especially, these three loci were unequivocally confirmed as significantly associated with hip BMD even across ethnic boundary, in both Chinese and Caucasians (rs13182402: combined  $P = 8.18 \times 10^{-5}$ ; rs6711417: combined  $P = 3.60 \times 10^{-5}$ ; rs6064822: combined  $P = 3.80 \times 10^{-4}$ ), further attesting to their importance in osteoporosis. *ALDH7A1* gene degrades and detoxifies acetaldehyde, which inhibits the osteoblast proliferation and result in the decreased bone formation. *UBR3* encodes E3 ubiquitin ligase, which plays a specific role in osteoblast differentiation. *PHACTR3* is involved in protein phosphatase pathway regulating diverse cellular processes. Our findings provide a new insight into the pathogenesis of osteoporosis, which warrant further studies to explore generality in other populations, their biological effects and functional mechanisms.

**Disclosures:** Y. Guo, None.

## SA268

**A Common Single Nucleotide Polymorphism in the High Mobility Group AT-hook 2 (HMGA2) Gene Is Associated with Bone Mass in Men.** A. L. Kuipers<sup>1</sup>, J. A. Cauley<sup>1</sup>, K. Ensrud<sup>2</sup>, C. L. Gordon<sup>3</sup>, D. Ingilis<sup>3</sup>, V. W. Wheeler<sup>4</sup>, A. L. Patrick<sup>4</sup>, C. H. Bunker<sup>\*1</sup>, C. S. Nestlerode<sup>\*1</sup>, A. R. Hoffman<sup>\*5</sup>, E. S. Orwoll<sup>6</sup>, J. M. Zmuda<sup>1</sup>. <sup>1</sup>Epidemiology, University of Pittsburgh, Pittsburgh, PA, USA, <sup>2</sup>VA Medical Center and University of Minnesota, Minneapolis, MN, USA, <sup>3</sup>McMaster University, Hamilton, ON, Canada, <sup>4</sup>Tobago Health Studies Office, Sarborough, Trinidad and Tobago, <sup>5</sup>VA Palo Alto Health Care System and Stanford University Medical Center, Palo Alto, CA, USA, <sup>6</sup>Oregon Health and Science University, Portland, OR, USA.

*HMGA2* encodes a non-histone, chromosome protein belonging to the high mobility group (HMG) family that regulates transcription of target genes. Knockout mouse experiments and a case report of a boy with a constitutional chromosomal rearrangement suggest that *HMGA2* plays a role in growth regulation. Moreover, a recent genome-wide analysis (GWA) identified a novel association of the *HMGA2* gene with human stature. To further evaluate this gene and skeletal measures, we genotyped a C-T polymorphism in the 3' UTR of *HMGA2* identified from the GWA of short stature, and conducted genetic association analysis with body size and bone mass in an initial discovery population consisting of 1,813 men of African ancestry and in a validation sample of 979 Caucasian American men. The mean age of these men were  $58.9 \pm 10.4$  years and  $73.7 \pm 5.8$  years, respectively. Skeletal measurements were obtained with peripheral quantitative computed tomography (pQCT). Specialized segmentation and analysis software (pQCT Pro) was also used to assess apparent trabecular architecture in the African ancestry men. The minor T allele frequency was 0.34 in African and 0.49 in Caucasian men. There was no significant association with height or body weight in either ethnic group. However, there was an additive association with BMD where the T allele was associated with lower trabecular volumetric BMD at the tibia ( $P=0.002$  in Caucasians;  $P=0.007$  in Africans). For example, African ancestry men with the T/T genotype had 4% lower trabecular BMD compared to men with the C/C genotype ( $231 \pm 2$  vs  $221 \pm 3$  mg/cm<sup>3</sup>), whereas, the heterozygotes had intermediate values ( $227 \pm 2$  mg/cm<sup>3</sup>). Apparent trabecular thickness was 9% less ( $P=0.005$ ) and apparent trabecular number was 15% greater ( $P=0.01$ ) among African ancestry men with the T/T than C/C genotypes. Our analysis suggests a novel association between a common *HMGA2* genetic variant and trabecular bone mass and structure in older men.

**Disclosures:** A.L. Kuipers, None.  
This study received funding from: NIAMS.

## SA269

**Osteosclerotic Prostate Cancer Metastasis to Murine Bone: Enhanced with Increased Bone Turnover.** P. C. Buttker<sup>\*1</sup>, E. M. Paul<sup>\*1</sup>, R. A. Sikes<sup>\*2</sup>, R. R. Gomes, Jr<sup>1</sup>. <sup>1</sup>Orthopaedics and Rehabilitation, H089, Penn State College of Medicine, Hershey, PA, USA, <sup>2</sup>Biological Sciences, University of Delaware, Newark, DE, USA.

Spontaneous development of osteoblastic lesions of prostate cancer (PCa) in mice is modeled by orthotopic (prostatic) deposition of neoplastic cells followed by an extremely long latency with associated low incidence of bone metastasis. Intracardial injection results in overt bone metastases only with osteoclastic PCa cells (i.e., PC-3). Herein, we report that androgen independent osteoblastic PCa cells will readily colonize bone when it is in a high remodeling state. SCID/bg mice were subjected to periods of intermittent parathyroid hormone (PTH) exposure, followed by an intracardiac infusion of C4-2 PCa cells. Analysis of bone turnover markers in serum from mice treated intermittently with PTH revealed significant increases in osteocalcin ( $55.06 \pm 7.5$  vs  $74.01 \pm 18.5$  ng/ml) and TRACP-5b ( $3.3 \pm 0.6$  vs  $4.81 \pm 0.8$  U/L), but no change in type I collagen CTX levels relative to control mice. Subsequent MicroCT analysis of femurs revealed significant increases in bone mineral density, trabecular thickness ( $0.056 \pm 0.002$  vs  $0.062 \pm 0.001$   $\mu$ m) and porosity but significant decreases in connectivity density and trabecular number ( $5.756 \pm 0.17$  vs  $5.02 \pm 0.20$  mm<sup>-1</sup>) in mice treated with PTH relative to controls. By eight weeks post-PCa-injection 70% of mice, pre-treated with PTH, demonstrated detectable serum prostate specific antigens (PSAs). Immunohistochemical labeling of femurs for PSA and pan-Cytokeratin revealed the presence of tumor cell nests, as opposed to single cells, in marrow and trabecular spaces. These results suggest that 1) mouse bone physiology is an important factor for developing osteoblastic/sclerotic PCa bone metastases in murine hosts; 2) the establishment of osteosclerotic prostate cancer bone metastases in mice is enhanced by alterations in bone turnover, and 3) regimens of PTH administration for osteoporosis may require caution and/or enhanced monitoring of cancer patients at risk for developing bone metastases.

**Disclosures:** P.C. Buttker, None.  
This study received funding from: Pennsylvania Department of Health.

## SA270

See Friday Plenary number F270.

## SA271

**Strength Training Prevents Bone Loss at the Spine in Older Breast Cancer Survivors: Preliminary Findings from an RCT.** K. M. Winters-Stone<sup>\*1</sup>, J. A. Bennett<sup>\*1</sup>, A. Reiner<sup>\*1</sup>, J. Dobek<sup>\*1</sup>, A. Schwartz<sup>\*2</sup>, L. Nail<sup>\*1</sup>. <sup>1</sup>School of Nursing, Oregon Health & Science University, Portland, OR, USA, <sup>2</sup>School of Nursing, Arizona State University, Tempe, AZ, USA.

Approximately 85% of women who receive a first diagnosis of breast cancer are aged 50 and over, thus the combined effect of aging, menopause and breast cancer treatment may threaten bone health in these women. Yet, few studies have focused on evaluating how exercise interventions, particularly resistance training, benefit older breast cancer survivors. PURPOSE: The purpose of this report is to present preliminary findings for an on-going resistance training study in older breast cancer survivors. METHODS: We are conducting a 12-month randomized controlled trial of resistance (strength) training (STR) versus a control group of flexibility (FLEX) training in early-stage, older BCS (mean age: 63.7 yrs) who are > 1 year past radiation and/or chemotherapy. To date, 31 women (STR n=20, FLEX n=11) have completed 12 months of exercise training and interim testing. Interim findings for bone mineral density of the total hip and lumbar spine assessed by DXA are presented. Within group changes were determined by paired t-tests and between group changes were determined by repeated measures ANOVA. RESULTS: After 12 months of exercise, spine and hip BMD was maintained in STR (0.3% and -0.8%, respectively) compared to significant decreases at both sites in FLEX (-1.7% and -1.6%, respectively). Between group changes were only significant for spine BMD ( $p<.03$ ). CONCLUSIONS: These preliminary data show trends that resistance exercise maintains BMD at the spine compared to a control program of flexibility exercise in older breast cancer survivors. Definitive conclusions must await completion of the full trial.

**Disclosures:** K.M. Winters-Stone, None.  
This study received funding from: Susan G. Komen for the Cure Foundation.

## SA272

See Friday Plenary number F272.

## SA273

**TGF- $\beta$  Activates Prostate Cancer Bone Metastases, Pro-Osteolytic Gene Expression and the New TGF- $\beta$  Signaling Regulator PMEPA1.** P. G. J. Fournier, G. A. Clines, J. M. Chirgwin, T. A. Guise. Endocrinology, University of Virginia, Charlottesville, VA, USA.

Transforming growth factor- $\beta$  (TGF- $\beta$ ) increases breast cancer and melanoma bone metastases by activating pro-osteolytic genes (PTHrP, IL-11 or CTGF). We hypothesized that TGF- $\beta$  would also promote prostate cancer bone metastases.

A specific inhibitor of the TGF- $\beta$  type I receptor kinase, SD-208, decreased Smad2 phosphorylation induced by TGF- $\beta$  in PC-3 human prostate cancer cells. Osteolytic bone metastases were caused by inoculating PC-3 cells in the left cardiac ventricle of athymic mice. SD-208 (50mg/kg/d po) begun at the time of tumor inoculation decreased osteolytic bone metastases (56% decrease,  $P < 0.05$ ) and increased survival (57 to 69 days median survival,  $P < 0.05$ ). When treatment began after osteolytic lesions were detected, SD-208 decreased bone destruction (47% decrease,  $P < 0.05$ ) without significantly improving survival (51 to 55 days,  $P > 0.1$ ).

We analyzed PC-3 cells treated  $\pm$  TGF- $\beta$  (5ng/mL) by Affimetrix gene array and sqRT-PCR. Significantly up-regulated genes included PTHrP, IL-11, CTGF and ADAM19, which can increase bone resorption, as well as MMP-13 and thrombospondin-1, two activators of TGF- $\beta$ .

The most increased gene was PMEPA1 ( $>20x$ ), a protein highly expressed in breast, colon and prostate cancers. sqRT-PCR of mRNA from PC-3 cells treated  $\pm$  TGF- $\beta$  and  $\pm$  cycloheximide or  $\pm$  actinomycin-D showed that TGF- $\beta$  directly controls PMEPA1 transcription. Dual-luciferase experiments showed that a 3.7kb fragment of PMEPA1 promoter is activated by TGF- $\beta$ . This fragment contains 5 consensus Smad binding elements, but mutagenesis showed that they are not involved in TGF- $\beta$  induction. Analysis of promoter deletion constructs and overexpression of Smad2, 3 and 4 demonstrate that TGF- $\beta$  induction of PMEPA1 promoter is mediated by a 1.2kb proximal fragment through both Smad and non-Smad mechanisms.

Western blotting confirmed that TGF- $\beta$  quickly and dose-dependently increased the cytosolic isoform of PMEPA1 in PC-3 cells. PMEPA1 proteins contain 2 PPxY domains that can interact with Smurf ubiquitin ligases (which can regulate degradation of Smads and type I TGF- $\beta$  receptor) and a Smad-interaction motif (found in DNA binding co-factors that control the affinity of Smads for DNA), suggesting that PMEPA1 regulates TGF- $\beta$  signaling. shRNA knockdown of PMEPA1 significantly decreased TGF- $\beta$  activation of the Smad reporter (CAGA)<sub>3</sub>. PMEPA1 induced by bone-derived TGF- $\beta$  could potentiate TGF- $\beta$  signaling in cancer cells.

Our results show that TGF- $\beta$  can promote PC-3 bone metastases through a transcriptional program that increases bone resorption and potentiates TGF- $\beta$  signaling.

**Disclosures:** P.G.J. Fournier, None.

This study received funding from: DoD PCRP, NIH, Mellon Prostate Cancer Institute.

## SA274

**TGF- $\beta$  Blockade Inhibits Osteolytic but not Osteoblastic Prostate Cancer Metastases.** P. G. J. Fournier, K. S. Mohammad, C. R. McKenna\*, X. Peng\*, J. M. Chirgwin, T. A. Guise. Endocrinology, University of Virginia, Charlottesville, VA, USA.

Prostate cancer cells frequently metastasize to bone causing bone destruction and/or formation. Bone-derived transforming growth factor- $\beta$  (TGF- $\beta$ ) enhances osteolytic metastases. Inhibition of TGF- $\beta$  signaling with SD-208, a kinase inhibitor of the TGF- $\beta$  type I receptor, decreased osteolytic metastases in breast cancer and melanoma models. The drug also increased bone mineral density by stimulating osteoblastic bone formation and inhibiting osteoclastic bone resorption, suggesting that it might be unsuitable against osteoblastic metastases, which are common in prostate cancer. Here we report the effects of SD-208 in mouse models of osteolytic and osteoblastic prostate cancer bone metastases.

Male nude mice were inoculated in the left cardiac ventricle with osteolytic PC-3 cells ( $10^5$  cells,  $n=11-14$ /group). Immunostaining of sections of PC-3 bone metastases showed nuclear localization of phosphorylated Smad2, a marker of activated TGF- $\beta$  signaling. Mice were treated with SD-208 (50mg/kg/d po) or vehicle and followed by x-ray. SD-208 did not decrease bone metastasis number compared to vehicle (vehicle 10/11 vs SD-208 12/14) but did decrease bone lesion area measured by x-ray compared to vehicle ( $6.7 \pm 3.3 \text{ mm}^2$  vs  $15.3 \pm 2.8 \text{ mm}^2$ ,  $P < 0.05$ ) and increased mouse median survival (57 to 69 days,  $P < 0.05$ ).

In a pilot experiment, we inoculated cells from the LuCaP 23.1 human prostate cancer osteoblastic xenograft into the tibias of nude mice ( $2 \times 10^5$  cells,  $n=3-5$ /group). Nuclear immunostaining of phosphorylated Smad2 demonstrated active TGF- $\beta$  signaling in tumor cells at sites of bone metastases. However, SD-208 treatment decreased neither incidence of metastases nor skeletal tumor burden, measured by histomorphometry compared to vehicle-treated mice. New bone formation in the tibias containing tumor was not augmented by SD-208 treatment, while trabecular bone measured in vertebrae free of tumor cells was increased by SD-208 (BV/TV 270% vs vehicle,  $P < 0.01$ ).

Our results show that blockade of TGF- $\beta$  signaling with SD-208 increases bone formation, while the drug does not enhance skeletal lesions in a model of osteoblastic prostate bone metastases. SD-208 does inhibit osteolytic metastases from prostate cancer cells. Overall, TGF- $\beta$  blockade should be an efficient therapy against bone metastases with osteolytic and mixed bone responses to tumor but less so against purely osteoblastic lesions.

**Disclosures:** P.G.J. Fournier, None.

## SA275

See Friday Plenary number F275.

## SA276

**Breast Cancer Cell Conditioned Media Stimulates Osteoblastic Cells to Attract Breast Cancer Cells.** K. P. Chin-quee\*, H. J. Donahue. Department of Orthopaedics and Rehabilitation, Penn State College of Medicine, Hershey, PA, USA.

Breast cancer owes most of its mortality and morbidity to its metastasis to distant sites, especially bone. While a better understanding of what cancer cells do when they colonize bone is emerging (i.e. the "vicious cycle"), there is relatively little known as to why breast cancer cells preferentially metastasize to bone. To address this issue, we examined the hypothesis that secreted factors from breast cancer cells induce changes in osteoblastic cells, which cause them to attract metastasizing breast cancer cells. We focused on MDA-MET, a breast cancer cell line derived from MDA-MB-231, created by an *in vivo* selection process leading to a highly bone specific metastasis, and hFOB 1.19, a human fetal osteoblastic cell line. hFOB 1.19 cells were incubated for 24hr in conditioned media from MDA-MET cells (group 1), HTERT-HME1 cells (normal breast epithelial; group 2), or hFOB 1.19 cells (group 3). After this incubation, treatment media was removed from the hFOB 1.19 cells, the cells were washed with PBS and serum free media added. At the end of 12hr, this serum-free media, from all three groups was collected. The control group (group 4) consisted of serum-free media unexposed to any cells. To test the chemoattractant ability of the collected media from these four groups, we used a transwell cell migration assay, where migratory cells are placed in removable transwell inserts, the bottom of which consists of porous membranes (pore size 8 $\mu$ m), in direct contact with the test media in the lower well. The ability of media from each group to attract the MDA-MET cells, causing them to migrate to the other side of the membrane, was examined. The number of migratory cells was quantified by fluorescent labeling of the lysed cells, given in fluorescent units. Data are represented as mean fluorescence  $\pm$  SEM. We found a greater migration of breast cancer cells toward media from group 1 than toward either group 2 or group 3 ( $1533 \pm 58.2$  vs  $957 \pm 140$  vs  $983 \pm 51.4$ ), respectively;  $p < 0.01$ ), but no difference between migration towards group 2 (treated by HTERT-HME1) and group 3 (untreated) media. In addition, Group 3 media from untreated hFOB 1.19 cells caused a greater migration of cells than group 4, serum -free media alone ( $983 \pm 51.4$  vs  $653 \pm 56.1$ ;  $p < 0.01$ ). Our results suggest that factors constitutively secreted by bone cells attract breast cancer cells. More importantly, metastatic breast cancer cells (MDA-MET) but not normal breast epithelial cells (HTERT-HME1), secrete factors, which in turn increase the ability of osteoblastic cells to attract breast cancer cells.

**Disclosures:** K.P. Chin-quee, None.

## SA277

See Friday Plenary number F277.

## SA278

**Osteoclast Precursors Play a Role in Recruiting Breast Cancer Cells and Osteoblasts onto the Bone in Vitro.** Z. Shi\*, X. Feng. Pathology, Univ. of Alabama at Birmingham, Birmingham, AL, USA.

Breast cancer (BC)-induced osteolysis is not only a consequence but, more devastatingly, also a cause of BC skeletal metastasis. Three key players, osteoclasts (OC), BC cells, and osteoblasts (OB), are involved in BC-induced osteolysis. Indeed, BC cells express PTHrP, which stimulates the production of RANKL by OB. The produced RANKL promotes the differentiation of OC precursors into mature OC to resorb bone, resulting in the release and activation of TGF- $\beta$  embedded in the bone matrix. The released TGF- $\beta$  further stimulates the expression of PTHrP. As such, BC-induced osteolysis is a vicious cycle. Although this mode of the action is well documented, it is unclear how BC cells and OB are brought to the scene to act. Specifically, in tumor-induced-osteolysis, before the onset of bone resorption, OB and BC cells must be recruited to bone surface to produce RANKL, which is required for OC formation. However, based on the current models, these cells are attracted by factors released from bone matrix by OC, but how OC formed in the first place is unknown. In this study, we propose a new hypothesis that OC precursors play a key role in OB and BC recruitment to bone. We performed chemotaxis assays with the following conditioned media (CM): CM1 - from OC precursors cultured in Teflon beaker, CM2 - from the OC precursors cultured in tissue culture plates without bones slices and CM3 - from the OC precursors cultured in tissue culture plates with bones slices. CM were all prepared using MEM containing 0.2 % FBS. The control medium is MEM containing 0.2% FBS. 600ul CM was added to one well in Transwell. BC cells (MDA-MB-231) or OB ( $2 \times 10^5$ /ml) were in MEM with 0.2% FBS. Transwell were inserted into well and 100ul cells ( $2 \times 10^5$  each insert) were added to the inside compartment. Transwell were cultured for 4 hours at 37°C and 5% CO<sub>2</sub>. After 4 hours, cells were fixed for 30 seconds. Cells were stained for one hour with Crystal Blue and then counted. The results indicate that all three CM (CM 1, CM2 and CM3) exhibited chemotaxis on MDA-MB-231 cells compared with control medium. More importantly, CM3 demonstrated a higher capacity in inducing chemotaxis on MDA-MB-231 cells than CM1 and CM2. Moreover, all three CM (CM 1, CM2 and CM3) exerted higher chemotaxis on OB compared to control medium. These data indicate that OC precursors can exert chemotactic effects on BC cells and OB, suggesting that OC precursors play a key role in BC bone metastasis by recruiting OB and BC cells to the active bone remodeling sites. These studies have not only deepened our understanding of the mechanisms underlying BC cells/OB recruitment to bone but also opened new directions for future investigation of the mechanism underlying BC bone metastasis.

**Disclosures:** Z. Shi, None.

## SA279

See Friday Plenary number F279.

## SA280

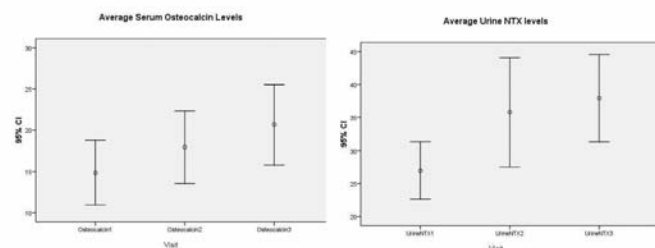
**Effects of Androgen Deprivation Therapy on Bone Health in Prostate Cancer.** A. K. McDonough<sup>1</sup>, G. G. Teng<sup>2</sup>, J. Abbott<sup>1</sup>, R. Nair<sup>1</sup>, C. Amling<sup>3</sup>, J. Colli<sup>4</sup>, J. B. Fiveash<sup>5</sup>, R. Lopez<sup>6</sup>, D. Urban<sup>3</sup>, J. R. Curtis<sup>1</sup>, K. Saag<sup>1</sup>.

<sup>1</sup>Division of Clinical Immunology and Rheumatology, University of Alabama at Birmingham, Birmingham, AL, USA, <sup>2</sup>Division of Rheumatology, National University Hospital, Singapore, Singapore, <sup>3</sup>Division of Urology, University of Alabama at Birmingham, Birmingham, AL, USA, <sup>4</sup>Birmingham VA Medical Center, Birmingham, AL, USA, <sup>5</sup>Department of Radiation Oncology, University of Alabama at Birmingham, Birmingham, AL, USA, <sup>6</sup>Department of Radiology, University of Alabama at Birmingham, Birmingham, AL, USA.

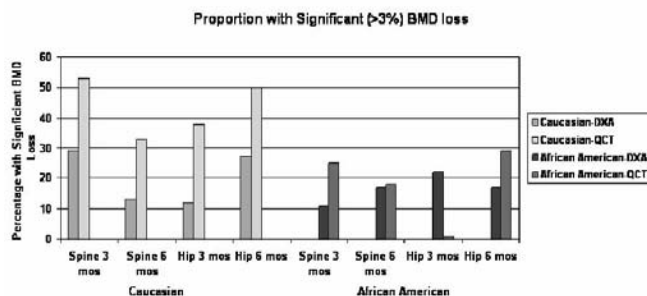
Androgen deprivation therapy (ADT) can cause bone loss in men but it is uncertain how rapidly this develops and if its bone effects differ by race/ethnicity. We examine whether short-term ADT leads to significant increases in bone turnover markers (BTM) or a decline in BMD over 6 months. We also determined the sensitivity of QCT compared with DXA for identifying early BMD change.

Men > 40 yrs with M0 prostate cancer were enrolled within 1 month of ADT initiation and seen at baseline, 3, and 6 mos. Patients with other causes of metabolic bone disease or on anti-osteoporotic meds were excluded. Descriptive analyses examined trends in osteocalcin, urine NTX, and BMD. We also analyzed factors associated with BTM change and BMD loss.

Patients (n = 30) were 40% African American (AA), had mean age 69.5 ± 8.9 yrs and mean BMI 27.6 ± 4.3. We found significant increases in BTM (p = 0.001) as early as 3 months into ADT.



Non-statistically significant trends in BMD suggest more bone loss among Caucasians by QCT and DXA. No significant association with BMD or BTM was seen with alcohol intake, smoking, BMI, testosterone levels, or caffeine. QCT and DXA BMD of the hip (r = 0.71) and spine (r = 0.87) highly correlated.



In summary, ADT significantly increased BTM within 6 months of initiating therapy. Trends in BMD decline were notable in Caucasian, but not African Americans. QCT appears more sensitive than DXA to identify need for early intervention for men who are may have accelerated ADT-associated bone loss.

**Disclosures:** A.K. McDonough, None.

This study received funding from: TAP Pharmaceutical.

## SA281

See Friday Plenary number F281.

## SA282

**Quantitative Image Analysis Method for Measuring Whole-body Tumor Burden in a Mouse Model of Breast Cancer Bone Metastasis.** R. S. Käkönen\*, J. P. Rissanen, M. I. Suominen, J. M. Halleen. Pharmatest Services Ltd, Turku, Finland.

Non-invasive fluorescence imaging is a promising new tool with several advantages over traditional radiography and histology; it is fast and allows whole-body imaging without the need of sacrificing the animals. However, the means of transforming the imaging output into descriptive and reliable quantitative data have been limited. The most commonly used output data, fluorescence emission area as an index of tumor burden does not, however, take the fluorescence signal intensity into account. Furthermore, tumor burden is conventionally measured only in histological sections of hind limbs, whereas fluorescence imaging allows whole-body imaging, but the correlation between these two methods has been poorly studied. We have validated a new image analysis method using GFP-MDA-MB-231(SA) breast cancer cells in a mouse model of breast cancer bone metastasis. Five-week-old female athymic nude mice were inoculated intracardially with MDA-MB-231(SA) breast cancer cells transfected with pTurboGFP-N vector (Evrogen JSC, Moscow, Russia). Three study groups were included (n=12/group): 1) Vehicle, 2) Doxorubicin 2.5 mg/kg, 3) Doxorubicin 5 mg/kg (all groups administered i.p. once a week). The tumor burden was assessed at day 14 and at the end of the study by measuring the total area and signal intensity emitted by GFP-MDA-MB-231(SA) cells. Osteolytic lesion area was measured on day 14 and at the end of the study by radiography. At necropsy, all macroscopic signs were recorded and tissue samples were collected for histology. Based on our earlier in vitro and in vivo studies, GFP-MDA-MB-231(SA) cells retained similar tumor growth profile and metastatic characteristics as parental cells. To measure the tumor burden by fluorescent imaging we created a value called tumor burden index which takes into account both the signal area and intensity emitted by the cancer cells transfected with GFP. The development of osteolytic lesions and tumor area was inhibited by doxorubicin at 5mg/kg. This anti-tumor effect of doxorubicin was more prominent when the tumor area was measured using the tumor burden index compared to conventional histological methods. Furthermore, the tumor burden index correlated well with histological analysis of tumor burden at the sites where histological analyses were performed. These results suggest that GFP imaging is a fast and reliable tool that can be used as quantitative method for assessment of whole-body tumor burden in a mouse model of breast cancer bone metastasis. This method negates the need to use laborious and time-consuming histology for assessing tumor burden.

**Disclosures:** R.S. Käkönen, None.

## SA283

See Friday Plenary number F283.

## SA284

**Osteoblast Differentiation Induced by Shh-expressing Prostate Cancer Cells Is Enhanced by Ascorbic Acid.** M. L. G. Lamm, S. M. Zunic\*. Pediatrics, Northwestern University Feinberg School of Medicine, Chicago, IL, USA.

Metastatic prostate carcinoma, the major cause of mortality among men with advanced prostate cancer, occurs predominantly in bone. Identification of signaling factors that mediate prostate cancer cell-bone stroma interactions is vital to our understanding of prostate cancer metastasis in bone. Sonic hedgehog (Shh), a secreted glycoprotein, is expressed in human prostate cancer tissues and several established human prostate cancer cell lines. We have previously reported that human prostate cancer cells, LNCaP, modified to overexpress Shh (LNShh cells) directly activated the hedgehog pathway in mouse pre-osteoblast MC3T3-E1 cells and induced osteoblast differentiation, a requisite process in prostate cancer metastasis in bone. LNShh-mediated initiation of early phase osteoblast differentiation in MC3T3-E1 cells occurred in the absence of exogenous ascorbic acid (AA), a factor that is routinely added to drive osteoblast differentiation in vitro. The purpose of the present study was to determine the role of exogenous AA in osteoblast differentiation induced by LNShh cells. In a novel co-culture system, MC3T3-E1 cells and control LNCaP or LNShh cells were co-cultured as mixed cell populations within the same culture well or chamber in the absence or presence of AA (50 microgram/ml). AA promoted the deposition of collagen, visualized by von Gieson staining, in the extracellular matrix of mixed co-cultures of MC3T3-E1 cells with either control LNCaP or LNShh cells. AA increased alkaline phosphatase activity and gene expression in mixed co-cultures of MC3T3-E1 and control LNCaP cells, and markedly enhanced Shh-stimulated alkaline phosphatase activity and gene expression in co-cultures of MC3T3-E1 and LNShh cells. Surprisingly, AA enhanced the expression of Shh signaling target genes Ptc1 and Gli1 in MC3T3-E1 cells co-cultured with LNShh but not with control LNCaP cells. To determine whether AA exerted a direct effect on the Shh pathway, MC3T3-E1 cells were cultured in the presence of Shh peptide (Shh-N) and/or AA for 24h. Data show that Shh-N, but not AA, increased Gli1 and Ptc1 expression, and there was no significant enhancement of gene levels by AA in Shh-N-treated cells.

Collectively, these data indicate that Shh and AA initiate early phase osteoblast differentiation via independent pathways. However, AA enhances Shh-mediated actions by indirectly activating the hedgehog pathway. Our studies demonstrate that paracrine signaling between prostate cancer cells and osteoblasts via the Shh pathway is sufficient to induce osteoblast differentiation, and this pathway can be modulated by other differentiation factors including ascorbic acid.

**Disclosures:** M.L.G. Lamm, None.

This study received funding from: National Cancer Institute, American Cancer Society.

## SA285

**Inhibition of Multiple Myeloma (MM) Growth and Preservation of Bone with Combined Radiotherapy and Anti-angiogenic Agent.** D. Jia<sup>1</sup>, R. Halakatti<sup>\*1</sup>, C. Jackson<sup>\*1</sup>, L. J. Suva<sup>2</sup>, L. Hennings<sup>\*3</sup>, X. Li<sup>4</sup>, S. Yaccoby<sup>4</sup>, P. M. Corry<sup>\*1</sup>, R. J. Griffin<sup>\*1</sup>. <sup>1</sup>Department of Radiation Oncology, U Arkansas for Medical Sciences, Little Rock, AR, USA, <sup>2</sup>Department of Orthopedics, U Arkansas for Medical Sciences, Little Rock, AR, USA, <sup>3</sup>Department of Pathology, U Arkansas for Medical Sciences, Little Rock, AR, USA, <sup>4</sup>Myeloma Institute for Research and Therapy, U Arkansas for Medical Sciences, Little Rock, AR, USA.

MM is characterized by its bone marrow preference and bone destruction. Although radiotherapy has been proven effective in cancer control in general, its use in MM treatment is less than routine except in a palliative setting. The efficacy of radiation (Rad) in MM growth control and bone protection was examined in a mouse model, wherein human MM cells expressing luciferase (Luc) were injected into bone grafts pre-implanted s.c. in SCID mice. The mice were divided into 4 groups: control, anginex (Ax), Rad, and Ax+Rad. Ax, a 33 a.a. anti-angiogenic peptide, was given 3 times a wk at 20 mg/kg/day. Rad was applied to the MM-containing bone grafts in 5 Gy fractions, once per wk, 2h after the last dose of Ax for a total 40 Gy over 8 wk. MM growth was estimated by live imaging Luc activity in bone grafts, measuring the dimensions of the grafts, and quantitating human lambda light chain in serum. Bone grafts were analyzed by histology for cellular and vascular features following radiography and microCT analyses for BMD and architecture. A 114-fold increase in Luc activity over baseline was seen in control mice by wk 8, whereas in mice receiving Ax+Rad Luc activity was reduced to 50% of the baseline. Ax or Rad alone had minimal effects. Luc activity correlated with serum MM marker as well as MM outgrowth from the bone grafts as reflected by graft volume. To evaluate MM relapse following these modalities, tumor growth was monitored for an additional 4 wk after the treatments ended. Graft volume doubled to 3652 mm<sup>3</sup> in the controls over this post-therapy period, reached 2273 mm<sup>3</sup> and 775 mm<sup>3</sup> in Ax- and Rad-treated mice, respectively, but remained small in Ax+Rad group (207 mm<sup>3</sup>). Consequently, bone grafts in the controls were mostly replaced by MM cells, and Ax or Rad alone did not prevent graft destruction. By contrast, vBMD as well as cortical and trabecular structure were preserved in grafts treated with Ax+Rad. Histological analysis showed that the number of MM loci, new blood vessels and bone resorbing osteoclasts were lower, while the number of cuboidal osteoblasts were higher in bone grafts receiving Ax+Rad, as compared with that in the other three groups ( $p < 0.05$ ). Our results demonstrate that radiotherapy, when primed by drugs such as anti-angiogenic agents, can significantly control MM growth and prevent skeletal destruction in this model, thus may have potential in MM focal lesion control.

**Disclosures:** D. Jia, None.

## SA286

See Friday Plenary number F286.

## SA287

**Role of Annexin II and Annexin II Receptor in Homing Multiple Myeloma Cells in the Bone Marrow.** D. Del Prete<sup>\*1</sup>, G. Lu<sup>1</sup>, F. Esteve<sup>\*1</sup>, Y. Shiozawa<sup>\*2</sup>, R. S. Taichman<sup>2</sup>, G. D. Roodman<sup>3</sup>. <sup>1</sup>Medicine/Hem-Onc, University of Pittsburgh, Pittsburgh, PA, USA, <sup>2</sup>School of Dentistry, University of Michigan, Ann Arbor, MI, USA, <sup>3</sup>Medicine/Hem-Onc, University of Pittsburgh and VA Pittsburgh Healthcare System, Pittsburgh, PA, USA.

Annexin II (AXII) is a multi-functional protein expressed on the surface of rejuvenating cells like fibroblasts, endothelial and epithelial cells, and involved in cell proliferation, adhesion and migration. AXII is expressed by osteoblasts (OBs) and stromal cells in the bone marrow and has been shown to play a critical role in the initial adhesion of hematopoietic stem cells (HSCs) to the marrow niche (Blood 2007; 110:82-90). AXII<sup>-/-</sup> mice have fewer HSCs and the adhesion of HSCs to OBs derived from these mice is significantly impaired compared with OBs from wild-type animals. Because myeloma (MM) cells home to the marrow in an analogous fashion to HSC, and AXII mRNA is present in MM cells, we assessed the role of AXII and its receptor (AXIIR) in MM cell interaction with the marrow microenvironment, since the homing of MM cells to the bone marrow is critical for their survival and proliferation. We previously identified an AXIIR on human stromal cells. KM101 human stromal cells and MM.1S myeloma cells as well as primary human stromal and myeloma cells were tested. RT-PCR and Western blot analysis showed that AXII and AXIIR were expressed by all the cell types tested. However, the expression levels of AXII and AXIIR differed between stromal and myeloma cells. Stromal cells expressed high levels of AXII compared with MM cells, and MM cells expressed more AXIIR than stromal cells. Further, cocultures of MM.1S cells with KM101 cells increase AXIIR expression by MM.1S cells. To further characterize the role of AXII in the interaction of MM.1S cells with stromal cells adhesion assays were performed using an AXII-blocking peptide. Adhesion of MM.1S cells to KM101 cells was dose-dependently inhibited by the AXII peptide. These results suggest a potential critical role for AXII and AXIIR in localizing MM cells to the bone marrow.

**Disclosures:** D. Del Prete, None.

## SA288

See Friday Plenary number F288.

## SA289

**Increased Signaling Through p62 in the Multiple Myeloma Microenvironment Increases Myeloma (MM) Cell Growth and Osteoclast (OCL) Formation.** Y. Hiruma, N. Kurihara, G. D. Roodman. Medicine/Hem-Onc, University of Pittsburgh, Pittsburgh, PA, USA.

The bone microenvironment plays a critical role in promoting both tumor growth and bone destruction in MM. Marrow stromal cells produce factors, which stimulate both the growth of MM cells and bone destruction and are key regulators of these processes. Marrow stromal cells produce these factors in increased amounts when they bind MM cells through adhesive interactions mediated via VCAM-1 on stromal cells and  $\beta_1$  integrins on MM cells. We examined the role of sequestosome-1 (p62), a recently described member of the NF- $\kappa$ B signaling pathway, in MM, since p62 sits at the crossroads of multiple signaling pathways potentially involved in both osteoclastogenesis and MM cell growth. Our hypothesis is that inhibiting p62 signaling will block the production of cytokines in the MM-bone microenvironment in response to the increased levels of TNF- $\alpha$  present in the MM microenvironment, decrease VCAM-1 expression on stromal cells, and markedly diminish osteolytic bone destruction and MM growth. Therefore, we isolated primary marrow stromal cells from MM patients and normals and measured p62 and PKC activation in MM marrow. PKC specifically interacts with p62 to increase its downstream signaling. Levels of phospho-PKC and VCAM-1 were significantly elevated in MM patients. We then blocked p62 activity in human stromal cells. p62 siRNA (40 nM) was transduced into normal and MM human stromal cells and p62 expression was decreased by at least 70% in these stromal cells. Stromal cells treated with p62siRNA or control siRNA were cultured with or without MM.1S cells for 3 days in separate experiments. The levels of VCAM-1 in p62siRNA transduced stromal cells were significantly lower than in control siRNA and untreated stromal cells. In addition, IL-6 production was increased when MM.1S myeloma cells were co-cultured with control siRNA treated stromal cells but not with p62siRNA treated stromal cells. Further, stromal cells lacking p62 minimally supported the growth of MM cells compared to control siRNA p62 containing stromal cells. Stromal cells lacking p62 also produced much lower levels of RANKL, and OCL formation was markedly decreased when these cells rather than control stromal cells were cocultured with normal OCL precursors. Studies of the mechanisms responsible for decreased IL-6 and RANKL production and VCAM-1 expression on MM stromal cells lacking p62 showed they resulted from decreased NF- $\kappa$ B and p38MAPK signaling. These results show that signaling through p62 plays an important role in MM cell growth and OCL formation induced by cytokines that are upregulated in the MM microenvironment.

**Disclosures:** Y. Hiruma, None.

## SA290

**Fracture Risk in Patients with Different Types of Cancer.** P. Vestergaard<sup>1</sup>, L. Rejnmark<sup>2</sup>, L. Mosekilde<sup>2</sup>. <sup>1</sup>The Osteoporosis Clinic, Aarhus Amtssygehus, Aarhus, Denmark, <sup>2</sup>Department of Endocrinology and Metabolism C, Aarhus Amtssygehus, Aarhus, Denmark.

**Background:** Few studies on the risk of fractures in patients with cancer exist, and little is known on the mechanisms of fractures in patients with cancer. We studied the risk of fracture in patients with various types of cancer.

**Subjects and methods:** Case control study. There were 124,655 fracture cases and 373,962 age and gender matched controls.

**Results:** An increased risk of fractures, primarily within the first year after diagnosis was seen in patients with primary bone cancer (OR=3.51, 95% CI: 1.54-8.01), multiple myeloma (OR=5.21, 95% CI: 2.96-9.19), metastases to the bone (OR=5.28, 95% CI: 3.58-7.79), metastases to other organs than bone (OR=1.85, 95% CI: 1.50-2.29), lung cancer (OR=1.90, 95% CI: 1.51-2.38), and cancer of the liver, gall bladder and pancreas (2.14, 95% CI: 1.39-3.31). For patients with prostate cancer an increase in the risk of fractures was seen with time. Other cancer types were not associated with an increased risk of fractures.

**Conclusions:** A high risk group regarding fractures includes cancers primarily affecting the bone (primary bone cancer, multiple myeloma, metastases to the bone, metastases to other organs than bone, lung cancer, and cancer of the liver, gall bladder and pancreas, and prostate cancer). The main increase in risk of fractures in this group was seen within the first year following diagnosis. A low risk group for fractures included all other cancer types (e.g. cancer of the breast, colon, skin etc). This may have implication for which patients should be selected for prevention against fractures.

**Disclosures:** P. Vestergaard, None.

*This study received funding from: Danish Medical Research Council.*

## SA291

See Friday Plenary number F291.

## SA292

**Influence of Imatinib on Bone Remodeling in Juvenile Mice.** J. Boehme<sup>\*1</sup>, M. Suttorp<sup>\*1</sup>, R. Fischer<sup>\*2</sup>, M. Bornhäuser<sup>\*3</sup>, J. A. Gasser<sup>\*4</sup>. <sup>1</sup>Department of Pediatrics, Division of Pediatric Hematology and Oncology, University Hospital Carl Gustav Carus, Dresden, Germany, <sup>2</sup>Institute of Pathology, University Hospital Carl Gustav Carus, Dresden, Germany, <sup>3</sup>Department of Internal Medicine I, University Hospital Carl Gustav Carus, Dresden, Germany, <sup>4</sup>Musculoskeletal Research, Novartis Institutes for BioMedical Research, Basel, Switzerland.

Imatinib (IM) is an effective treatment for chronic myeloid leukemia (CML) which inhibits the receptor tyrosine kinase BCR-ABL and other kinases like c-Kit, PDGF-R and c-FMS. The balance between bone resorption and bone formation under IM may be changed. We investigated the influence of IM on bone remodeling in growing mice.

**Methods:** At the age of 4 weeks, C3H mice were exposed to IM in drinking water for 10 weeks at doses of 80mg/kg/day (A), 110mg/kg/day (B), and 150mg/kg/day (C), resulting in serum levels of 60-674 ng/ml, 36-242 ng/ml and 51-534 ng/ml, respectively. Tibiae were analysed by pQCT, microCT and femora by histomorphometry. The plasma concentration of IM, osteocalcin, and the activity of the tartrate resistant acid phosphatase (TRAP5b) was determined.

**Results:** IM was tolerated well at all doses. At 5, but not 10 weeks, IM significantly and dose-dependently reduced the number of osteoclasts and resorption lacunae in femora of male animals from 23/field (controls) to 15 and 10, respectively. Effects were less pronounced in female mice.

Trabecular BMD was significantly increased in male mice by 8.5% and 9.9%, respectively, in groups B and C, and 5.2% in females (group C). Cortical thickness was increased in males by 6.1% and 11.2%, respectively, in group B and C and 7.5% in females (group C). Cancellous bone as assessed by microCT in males exhibited a significant increase in trabecular bone volume (BV/TV) of 19.7% and 13.2%, respectively, in groups B and C. In females a 10.6% increase was seen in group C. A significant increase in trabecular number (9.2% and 14.4%, respectively, in group B and C) in males and in females (12.8% in group C) was observed. As a result, trabecular connectivity improved significantly by 63% and 64%, respectively, in group B and C in males and by 22% and 38%, respectively, in group B and C in females. Bone biomarkers indicated a significant reduction of TRAP5b activity in groups B and C (both 5.1U/l) compared to controls (7.3U/l) and group A (6.5U/l) while osteocalcin levels remained unchanged.

**Conclusion:** In growing mice, IM reduced osteoclast number and resorption lacunae in long bones but not vertebrae. IM had a mild antiresorptive effect in cancellous bone (trabecular number), increased cortical thickness by inhibiting the expansion of the marrow cavity, and reduced TRAP5b activity. The effect was more pronounced in male mice and at younger age.

**Disclosures:** J.A. Gasser, Employee of the Novartis Institutes for Biomedical Research 3.

## SA293

See Friday Plenary number F293.

## SA294

**TGF-beta Suppresses Adipocytic Differentiation and Enhances Accumulation of Stromal Cells in Myeloma Bone Lesions.** K. Takeuchi<sup>\*1</sup>, M. Abe<sup>1</sup>, M. Hiasa<sup>\*2</sup>, O. Tanaka<sup>\*1</sup>, S. Nakamura<sup>\*1</sup>, H. Miki<sup>\*1</sup>, K. Kagawa<sup>\*1</sup>, K. Yata<sup>\*1</sup>, T. Hashimoto<sup>\*1</sup>, S. Ozaki<sup>\*1</sup>, S. Kido<sup>1</sup>, T. Matsumoto<sup>1</sup>. <sup>1</sup>Department of Medicine and Bioregulatory Sciences, University of Tokushima Graduate School of Health Biosciences, Tokushima, Japan, <sup>2</sup>Department of Orthodontics and Dentofacial Orthopedics, University of Tokushima Graduate School of Health Biosciences, Tokushima, Japan.

Multiple myeloma (MM) preferentially arises in the elderly, and develops devastating bone destruction. Although the bone marrow becomes fatty with normal aging, adipose tissue decreases and stromal cells increase in MM bone lesions. We have demonstrated that TGF-beta acts on stromal cells to inhibit their terminal differentiation into osteoblasts (OBs). TGF-beta is abundantly released and activated by enhanced bone resorption in MM bone lesions. Therefore, mesenchymal stem cell (MSC) differentiation into adipocytes may be suppressed and into stromal cells may be skewed, causing accumulation of stromal cells by enhanced TGF-beta actions in MM bone lesions. The present study was undertaken to clarify the role of bone-derived TGF-beta in MSC differentiation into adipocytes in MM. When C3H10T1/2 mesenchymal and ST2 stromal cells were cultured in an osteogenic medium with BMP-2, a considerable number of adipocytes appeared along with OBs. Addition of TGF-beta almost completely inhibited the adipocytic differentiation, without affecting Runx2 expression. TGF-beta also suppressed adipocytic differentiation of C3H10T1/2 cells facilitated by a PPARgamma ligand, ciglitazone. To simulate MM bone lesions, we co-cultured rabbit bone marrow cells with MM cells on dentine slices placed on membrane filters, and examined ciglitazone-stimulated adipocytic differentiation of C3H10T1/2 cells cultured in the lower chambers. Adipocytic differentiation by ciglitazone was potentially suppressed by TGF-beta, while blockade of TGF-beta actions by a type I receptor kinase inhibitor, SB431542, resumed adipocytic differentiation. In co-cultures without dentine slices, C3H10T1/2 cells differentiated into adipocytes. These results demonstrate that TGF-beta inhibits MSC differentiation into adipocytes while inhibiting terminal OB differentiation to create a stromal cell-rich microenvironment, and suggest that TGF-beta elaborated by enhanced bone resorption in MM bone lesions enhances accumulation of stromal cells to create "MM niche" suitable for MM expansion.

**Disclosures:** K. Takeuchi, None.

## SA295

**A New Automated Multiplex Assay for Simultaneous Measurements of 4 Serum Biochemical Markers of Bone Metabolism in Osteoporosis.** A. Claudon<sup>\*1</sup>, P. Vergnaud<sup>\*1</sup>, C. Valverde<sup>\*1</sup>, A. Mayr<sup>\*2</sup>, U. Klause<sup>\*2</sup>, P. Garnero<sup>3</sup>. <sup>1</sup>Synarc, Biochemical Markers, Lyon, France, <sup>2</sup>Roche Diagnostics, Penzberg, Germany, <sup>3</sup>Synarc, Biochemical Markers / INSERM Research Unit 664, Lyon, France.

The serum biochemical markers C-terminal crosslinked telopeptides of type I collagen (CTX) for bone resorption, N-terminal propeptide of type I collagen (PINP) and osteocalcin (OC) for bone formation and intact PTH are commonly used in epidemiological and clinical trials in osteoporosis. Each of these markers is currently measured individually by manual or automated assays requiring a significant sample volume. A fully automated protein-array based assay was developed recently for the simultaneous measurement of these 4 markers in only 20 microliters of serum. The aim of this study was to evaluate the technical and clinical performances of this novel multiplex assay in osteoporosis.

Serum CTX, PINP, OC and PTH were measured by the multiplex (Immunological Multi Parameter Chip Technology, IMPACT, Roche Diagnostics) and the corresponding single automated reference assays (Elecys, Roche) in 157 healthy premenopausal women, 74 healthy men and 56 postmenopausal osteoporotic women before and 6 months after treatment with oral ibandronate (150 mg/month).

Intra and inter assay variation of the multiplex assay was low and similar to single measurements (<10% for all markers). The lower limit of quantification (LLOQ) -which is the minimal concentration of endogenous marker that can be accurately and precisely determined- was lower for all 4 markers with the multiplex than with single assays, especially for CTX (0.023 vs 0.087 ng/ml). In premenopausal women, postmenopausal women with osteoporosis and healthy men, values determined by the multiplex technology highly correlated (r from 0.93 to 0.97, p<0.0001) with the corresponding single assays and absolute levels were comparable. After 6 months of treatment of osteoporotic women with monthly oral ibandronate, CTX, PINP and OC declined by a median of 48%, 63% and 52% (p<0.0001), decreases which were of similar magnitude as those observed with the corresponding single assays. Because of the improved sensitivity of the multiplex assay, CTX levels could be accurately and precisely determined in all samples after 6 months of ibandronate (all values above the LLOQ), whereas 28% of values were below the quantification limit of the single assay.

In conclusion, this novel fully automated protein-array assay allows the precise and sensitive measurements of serum CTX, PINP, OC and intact PTH simultaneously in a low serum volume. This assay should be useful for the investigation of bone metabolism in large clinical studies particularly when sample volume is limited.

**Disclosures:** P. Garnero, None.

## SA296

**Association of Urinary  $\gamma$ -Glutamyltransferase (GGT) and Serum FGF-23 with Prevalent Fracture: Hiroshima Cohort Study.** S. Fujiwara<sup>1</sup>, N. Masunari<sup>\*1</sup>, I. Takahashi<sup>\*1</sup>, W. Ohishi<sup>\*1</sup>, K. Ikeda<sup>2</sup>. <sup>1</sup>Clinical Studies, Radiation Effects Research Foundation, Hiroshima, Japan, <sup>2</sup>Department of Bone and Joint Disease, National Center for Geriatrics and Gerontology, Hiroshima, Japan.

We have reported that the urinary excretion of  $\gamma$ -glutamyltransferase (GGT), a recently identified bone-resorbing factor (JBC 2004, Endocrinology 2007), and the serum concentration of fibroblast growth factor (FGF)-23, an osteocyte-specific product, are associated with BMD (ASBMR 2007). The objective of the present study was to determine if urinary GGT and serum FGF-23 are associated with prevalent bone fracture in a population-based cohort. The study population consisted of 2,037 subjects (1,314 women and 723 men) aged 59 to 107 years old (average 73), followed up by biennial health examinations. A total of 252 subjects had spine fracture diagnosed by X-ray examination, and 125 had self-reported non-spine fracture. Serum FGF-23 was measured by ELISA. GGT level in the urine was determined by an autoanalyzer and corrected for creatinine concentration. BMD was measured in the spine and the hip by dual X-ray absorptiometry (QDR-4500, Hologic). Written informed consent was obtained from all participants. Multiple logistic regression was used for analysis.

Urinary GGT was significantly associated with prevalent spine fracture; when quartered (Q1-4), subjects with urinary GGT in the highest quartile (Q4) had a relative risk (RR) for spine fracture of 1.57 (95% confidence interval [CI], 1.05-2.34, p=0.03), after adjusting for age, sex and femoral neck BMD, compared with the Q2 reference group. Subjects with serum FGF-23 in the lowest quartile had RR for non-spine fracture of 1.96 (95% CI, 1.12-3.42, p=0.02). No relationship was found between GGT and non-spine fracture or between FGF-23 and spine fracture, after adjusting for age, sex and femoral neck BMD. Thus, urinary GGT and serum FGF-23 are potential markers for prediction of fracture independently of BMD.

**Disclosures:** S. Fujiwara, None.

This study received funding from: National Institute of Biomedical Innovation.

## SA297

See Friday Plenary number F297.

## SA298

**Comparison of the TRACP 5b Specificity of Two Commercial TRACP 5b Assays.** H. Ylipahkala<sup>1</sup>, K. M. Fagerlund<sup>2</sup>, A. J. Jankila<sup>3</sup>, J. M. Halleen<sup>4</sup>. <sup>1</sup>SBA Sciences Ltd, Oulu, Finland, <sup>2</sup>Anatomy, Institute of Biomedicine, University of Turku, Turku, Finland, <sup>3</sup>Medicine, Veterans Affairs Medical Center, Louisville, KY, USA, <sup>4</sup>Pharmatest Services Ltd, Turku, Finland.

Two forms of tartrate-resistant acid phosphatase (TRACP) circulate in human blood, TRACP 5a derived from macrophages and TRACP 5b derived from osteoclasts. Enzymatically active TRACP molecules constitute only 10% of circulating TRACP, while the remaining 90% circulates as fragments. We have studied the TRACP 5b specificity of commercially available BoneTRAP (IDS, Boldon, UK) and MetraTRAP5b (Quidel, San Diego, USA) assays and their clinical performance for monitoring alendronate treatment. BoneTRAP assay includes a monoclonal antibody O1A that binds both TRACP 5a and 5b, but not TRACP fragments. Bound TRACP activity is measured using pNPP as substrate at a TRACP 5b-selective pH 6.1. MetraTRAP5b assay includes two monoclonal antibodies, Trk49 that removes TRACP fragments and Trk62 that is stated to have high specificity for TRACP 5b. Bound TRACP activity is measured using CNPP as substrate at pH 6.4. Human serum TRACP 5a and 5b were separated by cation exchange chromatography and used to study TRACP 5b-specificity of the two assays. Both assays determined equal amounts of TRACP 5b activity, and the cross-reactivity to TRACP 5a was equal for both assays. When the substrate solutions were changed between the two assays, both assays still determined the same equal amounts of TRACP 5b activity as with their original substrates. Both assays determined approximately 5-fold less TRACP 5a activity with CNPP than with pNPP, indicating that CNPP is a more specific substrate for TRACP 5b. With pNPP as substrate, the antibody Trk62 bound TRACP 5a and 5b almost equally, indicating a very high cross-reactivity for TRACP 5a. The performance of the MetraTRAP5b assay is therefore mainly achieved by use of the more specific substrate CNPP, which partly compensates for the high cross-reactivity of the antibody Trk62 to TRACP 5a. We examined the clinical performance of both kits using a panel of serum samples from 137 postmenopausal women taking part in a placebo-controlled intervention trial, in which subjects received 5 mg alendronate per day. Alendronate treatment reduced TRACP 5b values by 53% when measured with the MetraTRAP5b assay, and by 42% when measured with the BoneTRAP assay. However, due to higher variability of the MetraTRAP5b assay, both assays showed similar sensitivity (80.0% vs 81.4%), signal-to-noise ratio (3.19 vs 3.14) and area under ROC curve (0.93 for both). We conclude that the BoneTRAP and MetraTRAP5b assays have equal specificity for TRACP 5b and interference by TRACP 5a, and equal clinical performance for monitoring alendronate treatment.

**Disclosures:** H. Ylipahkala, SBA Sciences Ltd 2.

## SA299

**PINP, a New Available Rat Bone Formation Marker. Usefulness in Osteopenia Studies Due to Androgen Lack and Ibandronate Treatment.** M. Montero<sup>\*1</sup>, I. Quiroga<sup>\*2</sup>, M. Rubert<sup>\*1</sup>, M. Diaz-Curiel<sup>3</sup>, F. Bausa<sup>\*4</sup>, C. De la Piedra<sup>1</sup>. <sup>1</sup>Biochemistry, Osteoarticular Pathology Laboratory, Fundacion Jimenez Diaz, Madrid, Spain, <sup>2</sup>Endocrinology, Hospital Puerta de Hierro, Madrid, Spain, <sup>3</sup>Internal Medicine, Fundacion Jimenez Diaz, Madrid, Spain, <sup>4</sup>Pharma Research Penzberg, Roche Diagnostics GmbH, Penzberg, Germany.

Ninety six Wistar rats, 9 months old, were sham operated (SHAM) or orchidectomized (OQX): untreated or treated with ibandronate (IBN) and were distributed into two studies, prevention (P) or treatment (T). P study: immediately after surgery animals were submitted to 4 groups which were administered subcutaneously for 20 weeks with either placebo (SHAM; n=12) and OQX (n=12) or with two regimens of IBN (Roche Diagnostics GmbH, Germany): 1 microg/Kg/day (OQX+IBN; n=12) or 28 microg/kg/28 days (OQX+mIBN). T study: all animals were left untreated for 6 months after surgery and subsequently submitted to 4 groups treated in a similar way than in P study: (SHAM2; n=12), (OQX2; n=12), (OQX2+IBN; n=12) and (OQX2+mIBN; n=12). After sacrifice, bone mineral density (BMD) was determined in the whole left femur by DEXA. Serum aminoterminal propeptide of collagen I (PINP, rat specific ELISA, IDS), and tartrate-resistant acid phosphatase, 5b isoenzyme (5b-TRAP ELISA, IDS) were measured. Five and 11 months after orchidectomy, OQX rats showed a decrease in PINP; 5 months after surgery OQX rats presented an increase in TRAP, that reverted 6 months later. Femoral BMD was decreased in OQX rats with respect to their SHAM groups. Both, daily or monthly treatment with IBN in P or T-studies, decreased TRAP and PINP indicating a general decrease in bone remodelling. Femoral BMD was "maintained like" or "recovered until" SHAM levels (P or T study respectively) in OQX groups treated with daily or monthly IBN. The above results suggest that PINP, a new available bone formation marker for rat experimental designs, is useful in studies about osteopenia due to androgen lack and remodelling effects of IBN treatment.

**Disclosures:** C. De la Piedra, National Institute of Health (FIS PI 06/0025) 3; Hoffman La Roche 3.

This study received funding from: National Institute of Health ( FIS 06/0025) and F Hoffmann La Roche.

## SA300

**Dickkopf-1 Predicts the Gain of Bone Mineral Density in Osteoporotic Women on Bisphosphonates.** T. Kocjan<sup>\*1</sup>, G. Hawa<sup>\*2</sup>, B. Lindner<sup>\*2</sup>, S. Maitzen<sup>\*2</sup>, J. Prezelj<sup>\*1</sup>, Z. Trošt<sup>\*3</sup>, J. Marc<sup>\*3</sup>, S. Mencej<sup>\*3</sup>. <sup>1</sup>Department of Endocrinology and Metabolic Diseases, Medical Centre Ljubljana, Ljubljana, Slovenia, <sup>2</sup>Research & Development, BIOMEDICA, Vienna, Austria, <sup>3</sup>Department of Clinical Biochemistry, Faculty of Pharmacy, Ljubljana, Slovenia.

Serum Dickkopf-1 protein (Dkk-1) is a potent inhibitor of bone formation. The aim of our study was to seek for correlation of serum Dkk-1 levels with change in bone mineral density (BMD) over a 1-year period in an osteoporotic female population treated with bisphosphonates.

51 postmenopausal women with newly diagnosed osteoporosis, who had been treated with weekly risedronate or monthly ibandronate plus calcium and vitamin D<sub>3</sub> supplements for 1 year were enrolled. The study was approved by the national medical ethics committee, and written informed consent was obtained from all participants.

Blood samples for determination of Dkk-1 and C-terminal cross linking telopeptide of type I collagen (CTX) were collected at the time of the diagnosis with first BMD measurement and after 3 months. Dkk-1 serum levels were determined by a newly developed ELISA-test. The relevance of circadian change in Dkk-1 serum levels was evaluated and found to be non significant. BMD measurement was then repeated after 1 year of treatment.

A significant negative correlation of serum Dkk-1 levels after 3 month was found with increase in spine and femoral neck BMD after 1 year of treatment.

This suggests that a single determination of serum Dkk-1 level after 3 months might be useful as an early predictor of long-term BMD gain determined by DXA after 1 year of osteoporosis treatment with bisphosphonates. Furthermore, high levels of serum Dkk-1 may identify postmenopausal women with osteoporosis who are not good candidates for bisphosphonate and might benefit more from anabolic treatment.

FUNDING: This work was supported by Grants Call CoOperate Enlarged Vienna 2005 provided by Zentrum für Innovation und Technologie, Austria and by Grants P3-0298 and P4-0127 provided by the Slovenian Research Agency.

**Disclosures:** G. Hawa, None.

## SA301

See Friday Plenary number F301.

## SA302

**Development of a Bone Specific Alkaline Phosphatase Assay on the IDS Automated Analyser 3X3™.** N. Baeyens<sup>\*</sup>, A. K. Barnes<sup>\*</sup>, G. Pirens<sup>\*</sup>, G. Sarlet<sup>\*</sup>, M. Bougoussa<sup>\*</sup>, J. V. Leblond<sup>\*</sup>, M. L. Garrity<sup>\*</sup>. Immunodiagnostic Systems (IDS) Ltd, Bolton, United Kingdom.

Circulating levels of Bone Alkaline Phosphatase (BAP) are believed to reflect the metabolic status of osteoblasts which are involved in the formation of bone. Measurement of BAP has been shown to be useful in evaluating patients with Paget's disease, osteomalacia, primary hyperparathyroidism, renal osteodystrophy, osteoporosis and metastases to bone.

BAP can be currently measured by the IDS OSTASE® ELISA. The present work was conducted to transfer the manual assay onto the IDS Automated Analyser 3X3™. Multiple types of detection are embedded on this analyser, including spectrophotometric and chemiluminescent and will allow a rapid and robust transfer from a manual assay to a fully automated version, without any major modification in reagent formulation or loss of sensitivity. The proposed product will be a colorimetric assay using magnetic particles as the solid phase.

The assay uses the spectrophotometer present on board the analyser, reading the assay at 405 nm wavelength according to a kinetic method measurement. This kinetic value is directly proportional to the BAP activity. The protocol used in the analyser is directly derived from the IDS OSTASE® BAP kit and has been adapted to the analyser, with regard to the machine constraints (e.g. volume sample, time incubation, and washing process). In summary, 75 µl of sample are incubated for 15 min in the presence of antibody linked to biotin, magnetic particles coated to streptavidin are added and incubated for a further 15 min. The BAP/Antibody-biotin complex binds to the magnetic particles. These magnetic particles are captured with magnets and washed by the washing buffer used in the analyser. After that, the magnetic particles containing BAP fixed by antibody are incubated in the presence of pNPP and the absorbance is measured during a short time (300 sec) to obtain the kinetic constant in milli optical density / min at 405 nm.

The Bone specific Alkaline Phosphatase assay on the IDS Automated Analyser 3X3™ shows a measuring range of 2.5 µg/L to 120 µg/L with a analytical sensitivity ≤ 1µg/L, a functional sensitivity close to 2.5 µg/L and a inter-assay imprecision ≤ 7%. The assay demonstrates good correlation with IDS OSTASE® ELISA (from where the reagents are derived) with Analyser = 0.88 x ELISA + 0.25 µg/L with r = 0.91 (n=46).

These results indicate that the automated BAP assay can provide a sensitive and precise immunoassay with a good correlation with the IDS OSTASE® BAP ELISA kit.\*Ostase® is a registered trademark of Hybritech Incorporated, a subsidiary of Beckman Coulter Inc.

**Disclosures:** N. Baeyens, IDS Ltd 2.



## SA303

**Development of a New N-Mid® Osteocalcin Immunoassay on the IDS Automated Analyser 3X3™.** M. Bougoussa\*, A. K. Barnes\*, G. Pirens\*, G. Sarlet\*, N. Baeyens\*, C. Hagelstein\*, M. L. Garrity\*. Immunodiagnostic Systems (IDS) Ltd, Bolton, United Kingdom.

Osteocalcin or bone Gla protein is a small 49aa protein that is rich in glutamic acid (GLA) and is a vitamin K-dependent protein that has been estimated to represent up to 20% of all non-collagenous protein in bone. A proportion of newly synthesized osteocalcin is released into the circulation, where it can be measured by immunoassay. Assays for osteocalcin are not standardised, and different antibodies clearly recognize different fragments. Antibodies that recognise both the intact and the large N-terminal mid-molecule fragment appear to provide the best clinical information.

The IDS Automated Analyser 3X3™ N-Mid® osteocalcin assay is an adaptation of the IDS Nordic ELISA assay. This assay uses two monoclonal antibodies. The biotinylated antibody is directed against residues 21-29. The second antibody recognizes residues 10-16 and is coupled to an acridinium derivative. After an incubation of 50 µl of sample with the biotinylated and second antibody, 20 µl of streptavidin magnetic particles are added to the mixture. After a second incubation, followed by a washing step, triggers are added and the measured luminescence is directly proportional to the N-Mid® osteocalcin concentration present in the sample.

A first result is available after 45min. The analytical range of the assay is 2 to 120 ng/ml. The performance was established using the CLSI protocol. The analytical sensitivity is ≤0.5 ng/ml and the functional sensitivity is < 3ng/ml. The intra-assay and inter-assay precision are respectively < 6.5 % and <11 %. The osteocalcin recovery and linearity averages 106% and 102% respectively, expressed as Observed/Expected ratios. A correlation study was performed using 72 plasma and serum samples. The assay demonstrates good correlation with the IDS Nordic ELISA kit (R=0.97) and yields the following regression equation: IDS Automated Analyser 3X3™ = 0.92 x ELISA -2.73ng/ml.

The results indicate that the IDS Automated Analyser 3X3™ N-Mid® osteocalcin assay provides a sensitive, specific and reproducible assay with good correlation with the IDS Nordic ELISA kit.

**Disclosures:** *M. Bougoussa, IDS Ltd 2.*

## SA304

**Use of Conductivity for the Correction of Urinary N-telopeptide.** S. R. Johnson, S. Carlisle\*, A. Krishnankutty\*, K. Higgs\*, K. Zak\*. R&D, SPD, Bedford, United Kingdom.

Urinary N-telopeptide (uNTx) measurements provide valuable clinical information on bone resorption and there are several assays available that can accurately measure uNTx. Measurements are normally corrected by dividing by the urine creatinine concentration to remove the influence of varying urine concentration. However, creatinine is an imperfect molecule for concentration correction because it is known to be affected by a number of variables such as muscularity, age and diet. Urine conductivity has previously been found suitable for normalising other urinary analyte concentrations, such as thromboxane B2, therefore its ability to correct uNTx measurements was examined. In particular, the influence of dietary sodium was studied as sodium ions are a major contributor of total urine conductivity.

An automated method for measurement of conductivity was developed, comprising of a biodot pump dispenser and X/Y/Z robotic arm with auto-sampler, in conjunction with a flow-through micro-conductivity cell and reader, which allowed high through put of samples. A model was built equating conductivity to creatinine using measurements from every single void of urine throughout a 24h period from 40 volunteers. This model was then applied to a study where volunteer's dietary sodium was controlled. Thirty volunteers were recruited and each spent 2 days at normal, low and high dietary sodium intake, during which they provided urine samples. Creatinine, conductivity and uNTx were measured on these samples to examine the robustness of the model.

The mean dietary sodium intake during low, normal and high sodium diets was 1.98, 3.24 and 14.89g for all volunteers. When conductivity measurements, converted using the non-linear model, were used to correct uNTx, mean concentrations for the low, normal and high dietary sodium intake were 29.27, 30.14 and 28.06 nM BCE/mM creatinine equivalent. Therefore conductivity was able to correct urine concentration under varying levels of sodium intake.

This analysis demonstrates that conductivity may be a viable alternative to creatinine for correction of uNTx. Conductivity measurements have the added benefit of being cheap, quick to perform and have low analytical variability.

**Disclosures:** *S.R. Johnson, None.*

*This study received funding from: SPD*

## SA305

**Usefulness of Alveolar Bone Density Measurement in Risk Assessment for Bisphosphonate-related Osteonecrosis of the Jaw (BRONJ).** Y. Takaishi<sup>1</sup>, A. Kamada<sup>2</sup>, T. Ikeo<sup>3</sup>, M. Nakajima<sup>4</sup>, T. Miki<sup>5</sup>, T. Fujita<sup>6</sup>. <sup>1</sup>Takaishi Dental Clinic, Himeji, Japan, <sup>2</sup>Biochemistry, Osaka Dental University, Osaka, Japan, <sup>3</sup>Osaka Dental University, Osaka, Japan, <sup>4</sup>Oral and Maxillofacial Surgery, Osaka Dental University, Osaka, Japan, <sup>5</sup>Geriatric Medicine, Osaka City University, Osaka, Japan, <sup>6</sup>Internal Medicine, Katsuragi Hospital, Osaka, Japan.

Bisphosphonate-associated osteonecrosis of the jaw (BRONJ) is becoming a serious concern in dental and medical fields. Although risk factors such as intravenous long term use of potent bisphosphonates, dental surgical procedure including dental extraction and poor oral hygiene and infection have been pointed out, it is imperative to find a reliable test method predicting the occurrence of BRONJ. Around the lesions of BRONJ, increase of alveolar bone density is frequently noted. By using dental radiography with aluminum step wedge pasted to the film to standardize X-ray exposure, density of the alveolar bone was measured at several locations around the right mandibular premolar, placing the X-ray tube parallel to the film.

By using a software (Bone Right, Dentalgraphic•Com company, Himeji), data and histogram of the alveolar bone mineral density (al - BMD) were recorded on the screen of a lap - top computer in a few minutes. This method may also be applied similarly from a panorama film covering the whole series of the teeth in an individual. The radio-opaque BRONJ lesion is surrounded by relatively radiolucent area containing bacterial flora and inflammatory granulation tissue, presenting as chronic suppurative osteomyelitis. The bone mineral density around the osteonecrosis lesions including BRONJ showed an extremely high mineral density, 168±30 (SD) in 8 measurements in 4 cases of jaw osteonecrosis including 1 case following radiation treatment. Significantly higher than the values in 24 measurement in 6 case corresponding regions without BRONJ, 130±27, (P=0.0028). In one subject in whom two extractions were simultaneously carried out, BRONJ occurred only at the location with extremely high alveolar bone density, and not on other site of dental extraction with normal bone density. Alveolar BMD measurement thus appears to predict the occurrence of BRONJ to be useful for detecting subjects at systemic or local risk for occurrence of BRONJ, in addition to low serum CTX suggested as a systemic risk factor for BRONJ.

**Disclosures:** *Y. Takaishi, None.*

## SA306

**See Friday Plenary number F306.**

## SA307

**Consistency in Measurement Assessments in Different Models of Norland DXA Scanners.** T. V. Sanchez<sup>1</sup>, D. K. Buckingham<sup>2</sup>, D. R. Purvis<sup>2</sup>, C. A. Dudzek<sup>2</sup>. <sup>1</sup>Research and Development, Norland--a CooperSurgical Company, Socorro, NM, USA, <sup>2</sup>Research and Development, Norland--a CooperSurgical Company, Fort Atkinson, WI, USA.

The consistency in the measurements made by different models of equipment is an issue in the densitometry community. To examine consistency in how Norland densitometers evaluate bone mineral density, bone mineral content and bone area we have examine scanner measurements done between 1988 and 2008 in processing measurements done on one of two AP Spine phantoms.

As part of the normal production process, at final testing Norland scanners carry out nine scans on one of two AP Spine Phantoms using standard AP Spine scan settings for the model and software being used. To examine consistency in measurements we randomly selected records from twenty-five different scanners of each model produced between January of 1988 and March of 2008. Models represented in this collection included the Norland XR-26, Eclipse, XR-36, Excell, XR-46, XR-600 and XR-800 systems. Each scanner used software current to its production date. The resulting average and standard deviation were compared for each model.

Results (%True) of Measurements on the Primary AP Spine Phantom by Different Scanner Systems Between 1988 and 2008.

	BMD	BMC	Area
XR-26	100.15±0.54	99.89±0.53	99.72±0.35
Eclipse	99.71±0.71	99.49±0.73	99.80±0.44
XR-36	99.95±0.49	99.66±0.54	99.69±0.29
Excell	100.63±0.44	101.22±0.52	100.59±0.38
XR-46	100.50±0.78	100.33±1.01	99.96±0.53
XR-600	100.12±0.24	100.68±0.41	100.56±0.34
XR-800	100.17±0.42	100.33±0.60	100.16±0.43

The results show a consistency in measured bone mineral density, bone mineral content and bone area in the various scanners. The results also demonstrate how the use of the same phantom over time can be employed to demonstrate that equipment is performing consistently over changes in hardware or software.

**Disclosures:** *T.V. Sanchez, None.*

**SA308**

See Friday Plenary number F308.

**SA309**

**The Effect of Vertebral Marrow Fat Content on the Diagnosis of Osteoporosis.** G. M. Blake<sup>1</sup>, J. F. Griffith<sup>2</sup>, D. K. W. Yeung<sup>2</sup>, P. C. Leung<sup>2</sup>, I. Fogelman<sup>1</sup>. <sup>1</sup>King's College London School of Medicine, London, United Kingdom, <sup>2</sup>Prince of Wales Hospital, Chinese University of Hong Kong, Shatin, Hong Kong.

Quantitative examination of iliac crest bone biopsies shows that as subjects become older bone and functional marrow are replaced by adipose tissue. Studies of vertebral marrow fat using nuclear magnetic resonance spectroscopy (MRS) show a highly significant relationship between spine T-score and marrow fat content. These findings suggest that the ability of dual energy x-ray absorptiometry (DXA) scans to identify patients at high risk of fracture is partly explained by the negative effect of increasing marrow fat on bone mineral density (BMD). However, care is necessary in interpreting the relationship between spine T-score and vertebral marrow fat because of a selection effect in which subjects with higher marrow fat are more likely to be found to have osteoporosis. We studied groups of elderly Hong Kong Chinese women (N = 103, mean age 73 y; range 67-84 y) and men (N = 82, mean age 73 y; range 67-101 y) who had spine DXA scans and MRS measurements of L3 marrow fat. The effect of varying marrow fat on BMD was modelled using vertebral body thicknesses measured in 50 men and women. Spine T-scores in each individual were adjusted for the measured marrow fat. Subjects were sorted into their WHO categories based on corrected T-scores, and the relationship between marrow fat and T-score status evaluated using regression analysis and analysis of variance. The average change in marrow fat per T-score unit was used to infer the proportion of the spine BMD fracture discrimination explained by marrow composition. The mean (SD) of the L1-L4 vertebral body thickness was 30.2 (2.1) mm for the Hong Kong women and 33.4 (2.5) mm for the men. When the marrow fat content measured by MRS changed from 0 to 100% the BMD change was estimated to be 0.14 g/cm<sup>3</sup> (1.3 T-score units) in women and 0.16 g/cm<sup>3</sup> (1.3 T-score units) in men. Adjustment of spine BMD for marrow fat reduced the significance of the correlation between marrow fat and T-score in both men and women compared with uncorrected data. However, there was still a trend for marrow fat to increase with decreasing T-score with a slope of  $-1.2 \pm 0.7\%$  per T-score unit ( $p = 0.078$ ) for women and  $-1.4 \pm 0.6\%$  per T-score unit ( $p = 0.023$ ) for men. When the effect of marrow composition on fracture discrimination was evaluated the results showed that 2% of the ability of spine DXA measurements to discriminate fracture risk is explained by the higher vertebral marrow fat content found in osteoporotic subjects. In conclusion, after adjustment for the selection effect patients with osteoporosis were still found to have higher vertebral marrow fat content. However, marrow composition made a negligible contribution to fracture discrimination.

Disclosures: G.M. Blake, None.

**SA310**

See Friday Plenary number F310.

**SA311**

**Correlations between Panoramic Radiomorphometric Indices and Bone Mineral Density in Postmenopausal Women.** A. F. Leite<sup>1</sup>, P. T. S. Figueiredo<sup>2</sup>, C. M. Guia<sup>3</sup>, A. P. Paula<sup>4</sup>, N. S. Melo<sup>5</sup>. <sup>1</sup>Oral Radiology, Department of Dentistry, College of Health Sciences, University of Brasília, Brasília, Brazil, <sup>2</sup>Oral Radiology, Department of Dentistry, College of Health Sciences, University of Brasília, Brasília, Brazil, <sup>3</sup>College of Health Sciences, University of Brasília, Brasília, Brazil, <sup>4</sup>Rheumatology Division, College of Health Sciences, University of Brasília, Brasília, Brazil, <sup>5</sup>Department of Dentistry, College of Health Sciences, University of Brasília, Brasília, Brazil.

The aims of this study were to correlate seven panoramic radiomorphometric indices with the BMDs of L1-L4, femoral neck and total hip, and to evaluate the accuracy of these indices in predicting densitometric diagnoses of osteoporosis, and T-Scores  $\leq -2.0$ . Three hundred and fifty one healthy postmenopausal women aged over 45 years were selected. All performed dual X-ray absorptiometries (QDR 1000, Hologic, USA) and panoramic radiographs (Rotograph Plus; Villa Medical System, Italy). Mandibular cortical indices, simple visual estimations of cortical widths, mental and antegonial indices, antegonial widths, and gonial and antegonial angles were measured. A stepwise forward logistic regression adjusted for age was performed. Significant associations were demonstrated between qualitative indices, cortical measurements and BMDs at the three bone sites ( $p < 0.001$ ). In women with severely eroded mandibular cortices, classified as C3 by the mandibular cortical index, the odds ratio (OR) was 4.82 for having osteoporosis at one of measured sites, and 10.87 for a T-Score  $\leq -2.0$ . In women with very thin mandibular cortices, determined by simple visual estimation of cortical width, the ORs were 8.02 and 5.46 for osteoporosis and T-Score  $\leq -2.0$ , respectively. In conclusion, certain qualitative indices, simpler and easier to be applied, may be considered more accurate panoramic measurements in predicting osteoporosis and T-Score  $\leq -2.0$ .

Disclosures: A.F. Leite, None.

**SA312**

See Friday Plenary number F312.

**SA313**

**6819 Analysis on Measurement of Bone Mineral Density of Phalanges by Radiographic Absorptiometry in Beijing.** J. Wang<sup>1</sup>, Z. Liu<sup>2</sup>, Z. Zhang<sup>1</sup>, P. Zhong<sup>1</sup>, Q. Wang<sup>1</sup>, X. Bi<sup>3</sup>, L. Al-Dayeh<sup>3</sup>. <sup>1</sup>Aviation Industry Center Hospital, Beijing, China, <sup>2</sup>China Osteoporosis Foundation, Beijing, China, <sup>3</sup>CompuMed, Inc., Los Angeles, CA, USA.

Osteoporosis is a very common disease in aging people in China. According to China's 2000 national census, approximately 100 million of its citizens suffer from various stages of osteoporosis. Although the T-Score based WHO criteria for osteoporosis diagnosis were derived from Bone Mineral Density (BMD) measurement of Caucasian women, they are still the mostly referenced standards in practice in China. It is very important to establish Chinese diagnostic standards for osteoporosis prevention and diagnosing. Objective: To measure phalangeal BMD of normal population in Beijing area using Radiographic Absorptiometry(RA); to establish Chinese normal reference database for RA technique and to compare BMD measurement results by RA with that of forearm by SPA. Methods: A study group consisted of 6819 healthy participants aged between 10 to 90 years old (with male 3376, female 3443) was investigated. Middle phalangeal BMD of each participant's index, middle and ring fingers in the non-dominant hand were measured using RA technique (OsteoGram2000 CompuMed, Inc, U.S.A.). The measured results were calculated and grouped according to an age interval of every 10 years. Results: The bone status of each participant was evaluated by two commonly used standards in China; which are the WHO and OCCGS. According to the WHO standard 21% of the females and 4% of the males among the investigated people had osteoporosis status. With the OCCGS standard 33% of the females and 10% of the males had osteoporosis status. Conclusion 1. A normal reference database for phalangeal BMD by RA technique has been established in China for the first time. 2. The OCCGS standard with a cutting point at  $-2.0SD$  might be more appropriate than that of the WHO standard of T-score  $= -2.5$  for Chinese population in osteoporosis disease screening and evaluation when BMD test was performed using RA. 3. The BMD results measured by RA technique are highly correlated to that of forearm by SPA in China.

Disclosures: X. Bi, None.

**SA314**

**Feasibility and Reproducibility of in-vivo Assessment of Trabecular Bone Architecture using MicroMRI-based Method at Multiple Study Centers.** N. B. Watts<sup>1</sup>, S. L. Greenspan<sup>2</sup>, R. Jackson<sup>3</sup>, M. Maricic<sup>4</sup>, W. Liu<sup>5</sup>, B. Kuzmak<sup>6</sup>, A. Grauer<sup>6</sup>, K. Driver<sup>7</sup>, T. Dufresne<sup>7</sup>, P. Chmielewski<sup>7</sup>, B. R. Gombert<sup>8</sup>, P. Seaman<sup>8</sup>, B. Borah<sup>7</sup>. <sup>1</sup>University of Cincinnati, Cincinnati, OH, USA, <sup>2</sup>University of Pittsburgh, Pittsburgh, PA, USA, <sup>3</sup>Ohio State University, Columbus, OH, USA, <sup>4</sup>Catalina Pointe Clinical Research, Tucson, AZ, USA, <sup>5</sup>UMDNJ, Newark, NJ, USA, <sup>6</sup>P & G Pharmaceuticals, Mason, OH, USA, <sup>7</sup>P&G Pharmaceuticals, Mason, OH, USA, <sup>8</sup>MicroMRI Inc., Philadelphia, PA, USA.

In-vivo imaging methods such as microMRI and peripheral quantitative CT (pQCT) allows evaluation of architectural changes in common peripheral skeletal sites that commonly fracture. The microMRI method for bone architecture measurement has been validated in a research setting. Prior to use in a longitudinal clinical study, the feasibility of the method needed further evaluation under realistic multicenter study conditions. We assessed the repeatability and reproducibility of architectural indices of the distal radius of the same 6 premenopausal females (age 29 - 42 years) at 5 study centers using a custom-made wrist coil on 1.5 Tesla GE MRI scanners. At each study center, each subject had 2 scans/day on 2 consecutive days performed by the same operator. At 1 center, 2 additional scans were obtained for each subject by a different operator. Data from 1 center was also analyzed by 2 analysts. All scans were completed within about 2 months. Bone volume fraction (BV/TV) and topological parameters (eg, surface to curve ratio and erosion index) were analyzed by MicroMRI Inc. using proprietary software. Additional conventional parameters of trabecular architecture were generated from the raw data using software package developed by Scanco Medical, Inc., available on microCT scanners. The reproducibility was assessed by root mean square coefficient of variations (RMS-CVs) and intraclass correlation coefficients (ICCs) of each of the parameters. Based on the within-site, motion-corrected, slice-matched data, the RMS-CVs for BV/TV and topological parameters ranged from 2.7 - 5.1% and 6.6 - 11.8%, respectively, and are comparable to historical data. The ICCs ( $\leq 0.75$ ) found in this study were lower than historical data ( $>0.80$ ) and may be due to small variance in structural parameters observed in the homogeneous female subjects in this study. BV/TV generated by microMRI and Scanco microCT methods compared favorably with minor differences in RMS-CV and ICC. The operator-to-operator and analyst-to-analyst variability was negligible. In conclusion, results of this study showed that the microMRI method was reproducible and repeatable at multiple study sites with multiple operators and has potential to be used in longitudinal clinical studies to assess treatment-modified changes in bone architecture.

Disclosures: N.B. Watts, Supported by funding from the Alliance for Better Bone Health 2. This study received funding from: The Alliance for Better Bone Health.

**SA315****See Friday Plenary number F315.****SA316**

**Usefulness of SpinalMouse as a Screening Tool for the Presence of Vertebral Wedge Deformity.** K. Mikawa, Y. Abe, K. Aoyagi. Public Health, Nagasaki University Graduate School of Biomedical Sciences, Nagasaki, Japan.

The purpose of this study was to evaluate the ability of a novel clinical tool, SpinalMouse®, to identify women with vertebral wedge deformities. Subjects comprised 102 women with a mean ( $\pm$ standard deviation) age of  $77.5 \pm 6.7$  years (range, 62-97 years) who visited an orthopedic outpatient clinic due to lower back pain. We measured curvature of the thoracic and lumbar spine using SpinalMouse®, and thoracic kyphotic angle and lumbar lordotic angle were calculated. Lateral spine radiography was performed and radiographic vertebral wedge deformities were assessed by quantitative morphometry. Vertebral anterior and posterior heights were measured and anterior/posterior (AP) ratio was calculated. Vertebral wedge deformity was considered present for AP ratio  $<0.8$ . Other types of vertebral deformity (i.e., central deformity and crush deformity) were not included in this study. Of the 102 subjects, 48 showed  $\geq 1$  thoracic vertebral wedge deformity and 39 had  $\geq 1$  lumbar vertebral wedge deformities. Women with thoracic vertebral wedge deformities displayed a significantly greater thoracic kyphotic angle than women without any thoracic vertebral wedge deformity. Similarly, women with lumbar vertebral wedge deformities showed significantly smaller lumbar lordotic angle than women without any lumbar vertebral wedge deformity. Receiver operating characteristic analysis showed that both thoracic kyphotic angle and lumbar lordotic angle were useful in discriminating women with wedge deformities in respective lesions. Area under the curve was 0.95 for thoracic kyphotic angle in discriminating women with thoracic vertebral wedge deformities and 0.85 for lumbar lordotic angle in discriminating women with lumbar vertebral wedge deformities. When a thoracic kyphotic angle of  $47^\circ$  was used as a cutoff, specificity and sensitivity for identifying individuals with thoracic vertebral wedge deformities were 92% and 91%, respectively. As for lumbar spine, when a lumbar lordotic angle of  $3^\circ$  was used as a cutoff, specificity and sensitivity for identifying individuals with lumbar vertebral wedge deformities were 87% and 75%, respectively. These results suggest that increased thoracic kyphosis and decreased lumbar lordosis as assessed by SpinalMouse® are significantly associated with existing vertebral wedge deformities in the respective lesions. SpinalMouse® could be useful as a screening tool to identify individuals requiring radiographic assessment for vertebral wedge deformities.

**Disclosures:** K. Mikawa, None.

**SA317****See Friday Plenary number F317.****SA318**

**Collecting Bone out of the Medial Condyle of Tibia - A New Method.** S. Jirsakova\*, V. Vyskocil<sup>2</sup>, A. Nemeckova\*, R. Pikner\*, J. Michalek\*. <sup>1</sup>Department of Bone disease, Charles University Hospital, Plzen, Czech Republic, <sup>2</sup>Metabolic Bone Disease Center, Charles University Hospital, Plzen, Czech Republic, <sup>3</sup>Department of Histology and Embryology, Charles University, Plzen, Czech Republic, <sup>4</sup>Metabolic Bone Disease Center, Charles University Hospital, Plzen, Czech Republic, <sup>5</sup>Academy of Sciences of The Czech Republic, Prague, Czech Republic.

The aim of our study was to design and develop a new osseous tissue specimen collecting method that would show advantages in comparison with methods already used. We evaluated microcracks, dynamic parameters and histomorphometry on bone biopsies from medial condyle of tibia in 35 postmenopausal women (age 60-80 yr) who had received bisphosphonate therapy for at least 9 years. We compared results with bone biopsies obtained from 10 cadavers (age 65-78 yr). Bone biopsies from medial condyle of the tibia were obtained after tetracycline double-labeling. The biopsies were taken with a mechanical bone trephine. Bone samples were bulk stained with green calcein as second fluorochrome. The microcracks and dynamic parameters were evaluated with the help of a laser confocal scanning microscope. The histomorphometry analysis of the bone samples was evaluated from semi-thick sections under light microscope. In all alendronate-treated patients the newly formed bone retains its lamellar structure, erosion cavities are shallow, osteoclasts only have few nuclei and there was no evidence of marrow fibrosis or cellular toxicity. Six women treated long-term-wise with alendronate have no visible microfractures. Among treated women, cancellous bone microcrack frequency of bone tissue was with the median crack density 0.130 microcracks/mm<sup>2</sup>, which did differ significantly from that observed in untreated group (0.085 microcracks/mm<sup>2</sup>). The mean cancellous bone microcrack length was 160  $\mu$ m among treated women and did differ significantly from that observed in untreated group (80  $\mu$ m). The mean MAR was normal in treated patients;  $0.71 \pm 0.16 \mu$ m/d. Bone remodeling was suppressed in the treated group, with the mean Ac.f. =  $0.08 \pm 0.07$  /year, MS/BS =  $0.625 \pm 0.713\%$ , BFR/BS =  $0.005 \pm 0.004 \mu$ m<sup>3</sup>/mm<sup>2</sup>/day. The authors developed and described a method for collecting and evaluating bone specimens of osseous tissue from the median condyle of the tibia. Bone specimens collected by the recommended method met the parameters required for qualitative,

quantitative histomorphometrics analysis and microfracture analysis. This method shows advantages in clinical practice in comparison with methods already used.

**Disclosures:** V. Vyskocil, None.

**SA319****See Friday Plenary number F319.****SA320**

**Morphometric Determinants of Three Dimensional Femoral Neck Structure and Strength in Older Postmenopausal Women.** R. L. Prince<sup>1</sup>, K. Zhu<sup>2</sup>, M. Pollock\*, V. H. S. Low\*. <sup>1</sup>School of Medicine and Pharmacology, University of Western Australia, Perth, Australia, <sup>2</sup>Department of Endocrinology and Diabetes, Sir Charles Gairdner Hospital, Perth, Australia, <sup>3</sup>Department of Radiology, Sir Charles Gairdner Hospital, Perth, Australia.

Both height and weight are determinants of areal BMD. However the relative importance of body mass and stature to true three dimensional bone structure and strength remains uncertain. This study examines the relationship between body mass and size to femoral neck structure measured using quantitative computed tomography (QCT) and the bone strength calculated from engineering principles.

The study subjects were 186 women aged  $73.6 \pm 8.2$  years enrolled for a dietary intervention study. Potential physical determinants were height, weight and calf girth. Bone structure was measured by QCT (Phillips Brilliance CT) with patients lying on top of the QCT Pro™ calibration phantom and analysed with Mindways QCT Pro software. Linear regression analysis of the determinants of femoral neck structure and strength variables was undertaken using the independent variables age, height, weight and calf girth.

Both height and weight accounted for some of the variance of areal femoral neck (FN) BMD ( $R^2$  Height 5.8%, Weight 5.8%,  $P < 0.01$ ) but not true volumetric FN BMD although there were strong independent correlations of height and weight with FN mass ( $R^2$  Height 15.1%, Weight 8.9%,  $P < 0.01$ ) and volume ( $R^2$  Height 13.4%, Weight 6.7%,  $P < 0.01$ ).

In multiple regression the only significant predictor of total and trabecular FN cross-sectional bone area, related to bone strength in compression, was height accounting for 16% and 7.4% of variation respectively. Regarding femoral neck section modulus, a measure of femoral neck strength in bending, both in plane and out of plane measures were related to height at 19.7% and 16.3% of variation respectively.

These results show that in elderly postmenopausal women true three dimensional volumetric FN BMD is not related to body size. This is because although both FN mass and volume are body size dependent this dependency is proportional and cancels out in the calculation of true BMD. However FN bone strength in compression and bending is related to stature presumably because of the bone size dependency of these measurements. Thus although the relationship between body size and areal FN BMD is an aberration of the method the fact that size is a predictor of strength may account for the clinical predicative value of areal bone density combining as it does both bone size and bone mass into one value.

**Disclosures:** R.L. Prince, None.

This study received funding from: Australian National Health and Medical Research Council.

**SA321****See Friday Plenary number F321.**

## SA322

**Validation of a 2D/3D Generic Mathematical Relationship Between TBS as Assessed by DXA, and BV/TV and TbTh as Assessed by Micro Computed Tomography: An Experimental Study Based on Human Cadaver Vertebrae.** L. Pothuau<sup>1</sup>, N. Barthe<sup>\*2</sup>, M. Isidore<sup>\*3</sup>, P. Carceller<sup>\*1</sup>, D. Hans<sup>4</sup>.  
<sup>1</sup>PTIB - University Hospital of Bordeaux, Med-Imaps, Pessac Cedex, France, <sup>2</sup>University Hospital of Bordeaux, Biophysics Laboratory, Bordeaux, France, <sup>3</sup>University Hospital of Bordeaux, Department of Nuclear Medicine, Bordeaux, France, <sup>4</sup>Center of Bone Disease, Department of Bone and Joint Disease, Lausanne University Hospital, Switzerland.

In a previous study [1], we have established a significant mathematical relationship between Trabecular Bone Score (TBS) as evaluated on 2D simulated projection image and 3D characteristics of bone microarchitecture: bone volume fraction (BV/TV) and trabecular thickness (TbTh). The aim of this study was to independently evaluate the accuracy of this mathematical relationship based on DXA examination of human cadaver vertebrae. 20 dried human cadaver vertebrae were measured on an iDXA densitometer (GE-Lunar) with a specific positioning system miming standard antero-posterior acquisition and immersed in 17 cm of water. A region of interest (ROI) was defined on DXA scan. The DXA image was then exported on a specific workstation for TBS calculation. 3D reconstructions of the vertebrae were obtained by  $\mu$ CT (eXplore Locus, GE). The calibrated 3D grey-level images were analyzed using MicroView-GE software with specific add-on. Auto-threshold was applied and 3D-ROI was defined enclosing complete bone microarchitecture. Standard basic parameters, BV/TV and TbTh, were evaluated in this 3D-ROI. The fit-coefficients  $\{a_{00}, a_{01}, a_{10}, a_{11}\}$  of the generic mathematical relationship  $TBS = [a_{00} + a_{01} * \ln(TbTh)] + [a_{10} + a_{11} * \ln(TbTh)] * BV/TV$  were determined following non-linear regression analysis. The accuracy of the 2D/3D mathematical relationship was evaluated by correlation coefficient and root mean square error between estimated (indirectly from  $\mu$ CT) and experimentally (from DXA image based on in house algorithm [1]) measured values of TBS. The fit-coefficients were:  $a_{00} = -0.717$ ,  $a_{01} = -0.510$  ( $p = 0.0043$ ),  $a_{10} = 0$  (not considered coefficient), and  $a_{11} = -2.028$  ( $p < 0.0001$ ). TBS value estimation was expressed as  $TBS = -0.717 - 0.510 * \ln(TbTh) - 2.028 * \ln(TbTh) * BV/TV$ , and led to a relative accuracy characterized by  $r = 0.93$  and  $RMS-SD = 0.0487$ .

In our study we have confirmed the accuracy of a generic mathematical 2D/3D relationship from DXA examination of human cadaver vertebrae. TBS as evaluated from DXA image directly represents a score of two 3D characteristics of bone microarchitecture BV/TV and TbTh.

[1] Pothuau L., Carceller P., Hans D. Correlations between grey-level variations in 2D projection images (TBS) and 3D microarchitecture: Applications in the study of human trabecular bone microarchitecture. Bone 2008 Apr;42(4):775-87.

**Disclosures:** L. Pothuau, None.

## SA323

**See Friday Plenary number F323.**

## SA324

**To Avoid Underdiagnosis of Vertebral Fracture, Recognition of True Fracture Line Including Multiple Schmorl's Node Is Necessary.** S. Okamoto<sup>1</sup>, H. Noguchi<sup>\*2</sup>, A. Itabashi<sup>3</sup>, H. Suzuki<sup>\*4</sup>, S. Okamoto<sup>5</sup>. <sup>1</sup>SORF Okamoto Clinic, Oita, Japan, <sup>2</sup>Noguchi Thyroid Clinic and Hospital Foundation, Beppu, Japan, <sup>3</sup>Saitama Center of Bone Research, Saitama, Japan, <sup>4</sup>Suzuki Orthodontic office, Nagasaki, Japan, <sup>5</sup>KS Okamoto Clinic, Shimabara, Japan.

Comparative studies between TV-X ray fluoroscopy with the 3-dimensional CT are performed. The 3-D models showed the vertebral fracture lines are rarely smooth but consist of a mixture of perforated indentations or Schmorl's nodes. To avoid underdiagnosis of vertebral fracture, recognition of true fracture line is definitely necessary. TV-X ray fluoroscopy was performed in 136 normal volunteers and 2,740 female osteoporosis patients. Also we created computerized 3-D renderings of 1280 cases. To make the X-ray pass through straight on the vertebral bodies, we asked the patients in an upright position to move their positions so that the distal and proximal edges of each vertebra would coincide. In 37 young female volunteers, the mean C/P ratios coincide with reported autopsy data of young females who died in their 20s or 30s. The mean is about 15% lower than that of reported conventional X-ray data. The widely used SQE standard stands on the image that a C/P ratio of a mild deformity, 80-75%. In fact, normal vertebrae have -15 to -20% concavity. That is, the vertebral terminal plates are not flat. For example, mean C/P ratio of L2 vertebra is 83% by the analysis of autopsy, CT or TV fluoroscopy, while that of plain X-ray assessment is 98%. That is, conventional X-ray analysis by mid-point digitization made as much as 15% error in measurement. The rim lines of vertebra almost always have remained intact and straight. These lines are readily seen on the plain X-ray. This "flat terminal plate" misconception leads to the serious misdiagnosis of vertebral fractures. The VFA method sometimes uses the rim line to measure and at other times the fractures line, caused by the vagueness of the image. As few osteoporotic fractures are symmetric, blindly taken radiographs or VFA can not avoid obliquely tilted or horizontally rotated vertebral figure. Even though the patient is going to lie down straight, vertebral bodies are tilted. Without positional adjustment, fracture lines are often mistaken for vertebral rim lines in the assessment. For osteoporotic fracture detection, only C/P ratio measurement is enough by our method. Our practical C/P standard ratios (YAM mean  $\pm$  2.5 S.D.) apparent for fractured vertebra were lower than 0.67 at T4 to T7 level, 0.69 at T8 to

T11, 0.71 at T12 to L3 or 0.74 at L4 level. 3D CT also can detect osteoporotic vertebral fractures which are often overlooked behind spinal OA. These finding suggests that vertebral fractures are included in the group of "disk herniation" into the weakened vertebral body through the perforated endplates.

**Disclosures:** S. Okamoto, None.

## SA325

**Effect of Parity on Bone Mineral Density in Premenopausal Women: JPOS Cohort Study.** J. Tamaki<sup>1</sup>, M. Iki<sup>1</sup>, A. Morita<sup>\*2</sup>, Y. Sato<sup>\*3</sup>, E. Kajita<sup>\*4</sup>, S. Kagamimori<sup>\*5</sup>, Y. Kagawa<sup>\*6</sup>, H. Yoneshima<sup>\*7</sup>. <sup>1</sup>Public Health, Kinki Univ. School of Med., Osaka-Sayama, Japan, <sup>2</sup>Nutritional Education Program, National Institute of Health and Nutrition, Tokyo, Japan, <sup>3</sup>Domestic Sciences, Jin-ai Women's College, Fukui, Japan, <sup>4</sup>Public Health & Home Nursing, Nagoya Univ. School of Health Sciences, Nagoya, Japan, <sup>5</sup>Welfare Promotion & Epidemiology, Univ. of Toyama, Toyama, Japan, <sup>6</sup>Kagawa Nutrition Univ., Tokyo, Japan, <sup>7</sup>Shuuwa General Hospital, Kasukabe, Japan.

Only cross-sectional observational or case-control studies have been available which evaluate the effect of parity on BMD. More than 15% of Japanese women between the ages of 20 and 40 are categorized in leanness, and the proportion of young women with less than standard BMI ( $22 \text{ kg/m}^2$ ) would be relatively large across Asia. Therefore, to clarify the effect between parity and body weight on BMD in women at peak bone mass, we analyzed a representative sample of Japanese women with the Japanese Population-based Osteoporosis (JPOS) Cohort Study.

We conducted a baseline survey in 1996 and follow-up surveys in 1999 and 2002. We analyzed 654 premenopausal women aged 20-44 years in 1996 cross-sectionally, and 253 women younger than 45 in 2002 longitudinally. BMD at the lumbar spine (LS), total hip (TH), and the distal 1/3 radius (DR) was examined. For sub-analyses, subjects with BMI less than  $24.2 \text{ kg/m}^2$  were analyzed cross-sectionally and longitudinally.

To clarify the effect of parity after complete recovery from delivery on BMD, multiple liner regression analysis of BMD in 1999 among 224 subjects aged less than 45 years with BMI  $< 24.2$  without delivery between baseline and 3 year follow-up was conducted, which revealed one parity was significantly associated with increased BMD at LS or DR after adjusting for age, weight, height, calcium intake, smoking habit, and exercise habit.

As results of multiple liner regression analysis predicting for change of BMD between baseline and 6 year follow-up among 160 subjects aged less than 45 years with BMI  $< 24.2$ , delivery between the first 3 years was significantly associated with increased BMD at LS, one parity at baseline was significantly associated with increased BMD at TH or DR, and delivery between the first 3 years was significantly and negatively associated with BMD at DR, in each model including age, weight, height, BMD in 1996, change of body weight in 6 years, parity in 1996, delivery during the first 3 years, and delivery during the last 3 years as dependent variables. The analysis among total 654 subjects revealed no significant effect of parity.

Our findings would suggest a positive relationship between parity and bone density at lumbar spine among premenopausal women with standard BMI or less.

**Disclosures:** J. Tamaki, Japanese Society for the Promotion of Science S.

This study received funding from: the Japan Milk Promotion Board and the Japan Dairy Council, the Japanese Society for the Promotion of Science, the Research Society for the Metabolic Bone Diseases.

## SA326

**Reimbursement for Bone Mineral Density Testing Among U.S. Medicare Beneficiaries.** J. R. Curtis<sup>1</sup>, A. Laster<sup>\*2</sup>, D. J. Becker<sup>\*3</sup>, L. Carbone<sup>4</sup>, M. Kilgore<sup>\*3</sup>, R. Matthews<sup>\*5</sup>, M. A. Morrissey<sup>\*3</sup>, K. G. Saag<sup>1</sup>, S. B. Tanner<sup>6</sup>, E. Delzell<sup>\*5</sup>. <sup>1</sup>Division of Rheumatology, University of Alabama at Birmingham, Birmingham, AL, USA, <sup>2</sup>Arthritis & Osteoporosis Consultants of the Carolinas, Charlotte, NC, USA, <sup>3</sup>Department of Health Care Organization and Policy, University of Alabama at Birmingham, Birmingham, AL, USA, <sup>4</sup>Veterans Administration Medical Center, University of Tennessee, Memphis, TN, USA, <sup>5</sup>Department of Epidemiology, University of Alabama at Birmingham, Birmingham, AL, USA, <sup>6</sup>Department of Medicine, Vanderbilt University, Nashville, TN, USA.

**Introduction:** Although the Bone Mass Measurement Act outlines the indications for central dual energy x-ray absorptiometry (DXA) testing for U.S. Medicare beneficiaries, the practical considerations regarding reimbursement are sometimes ambiguous. We evaluated the impact of gender, ICD-9 code submitted, time since previous DXA, and local Medicare carrier on whether or not the claim was reimbursed.

**Methods:** Using Medicare data from 1999-2005, we studied beneficiaries age  $\geq 65$  with part A+B, not HMO enrollees and in the 5% sample. We identified central DXA claims and evaluated the relationship between reimbursement for DXA and gender, ICD-9 code submitted for reimbursement of central DXA (CPT code 76075), interval of time since a preceding DXA, and Medicare carrier. Multivariable logistic regression was used to evaluate the independent relationship between carrier and reimbursement for DXA.

**Results:** For persons that had no DXA in 1999 or 2000 and who had one in 2001 or 2002, the percentage of DXAs claims denied was 5.3% for women and 9.1% for men. Rates of denial for repeat DXAs performed within 23 months was approximately 19% and did not differ by gender. There was substantial variability in reimbursement by ICD-9 diagnosis code submitted and varied by more than 6-fold. For DXAs repeated at  $< 23$  months, the proportion of claims denied ranged from 2% to 43%, depending on the Medicare carrier.

**Conclusion:** Reimbursement for DXA varies significantly by gender, time since previous

## ASBMR 30th Annual Meeting

DXA, ICD-9 diagnosis code submitted and local Medicare carrier. Greater guidance and transparency in coding policies is needed to improve access to DXA as a covered service for persons with Medicare.

Number of DXAs Performed and Proportion Not Paid, by Gender and Testing Interval

	Women		Men		P value*
	Number Performed	Proportion Not Paid (%)	Number Performed	Proportion Not Paid (%)	
Initial DXA	72700	5.3	6760	9.1	<0.0001
Repeat DXA< 23 months	7749	18.5	826	19.0	0.75
Repeat DXA≥ 23 months	26687	3.3	1548	4.8	0.002

**Disclosures:** J.R. Curtis, Novartis, Amgen, Merck, Procter & Gamble, Eli Lilly, Roche 3; Roche, UCB, Procter & Gamble 2; Merck, Procter and Gamble, Eli Lilly, Novartis, Roche 1.

This study received funding from: Amgen, Inc, National Institutes of Health (AR053351, AR052361), and the Arthritis Foundation (JRC).

## SA327

See Friday Plenary number F327.

## SA328

**Poor Peripheral Nerve Function Is Related to Lower BMD: The Osteoporotic Fractures in Men Study.** E. S. Strotmeyer<sup>1</sup>, K. A. Faulkner<sup>1</sup>, A. D. Juliano<sup>1</sup>, J. M. Zmuda<sup>1</sup>, A. V. Schwartz<sup>2</sup>, M. Petit<sup>3</sup>, E. Orwoll<sup>4</sup>, J. A. Cauley<sup>1</sup>. <sup>1</sup>Epidemiology, University of Pittsburgh, Pittsburgh, PA, USA, <sup>2</sup>University California, San Francisco, San Francisco, CA, USA, <sup>3</sup>University of Minnesota, Minneapolis, MN, USA, <sup>4</sup>Oregon Health & Science University, Portland, OR, USA.

Bone tissue is innervated and neurotransmitters directly affect bone remodeling. Poor motor peripheral nerve (PN) conduction was related to lower hip bone mineral density (BMD) in older adults in a dose-response manner, likely through higher bone area (Strotmeyer et al JBMR 2006). This relationship was not previously examined for sensory PN conduction. PN conduction at the sural sensory nerve (SNAP=amplitude in uV) and peroneal motor nerve (CMAP=amplitude in mV; FWL=mean F-wave latency in ms) were measured with a neurodiagnostic instrument (NC-stat®, NeuroMetrix, Inc.) in 572 community-dwelling men in the Osteoporotic Fractures in Men (MrOS) Study in Pittsburgh, PA. BMD at the total hip and femoral neck (FN), total lean mass (LM) and total fat mass (FM) were measured by DXA (QDR 4500W, Hologic Inc). Participants missing BMD, PN function or diabetes status (DM: self-report, hypoglycemic meds or fasting glucose ≥126 mg/dl) were excluded. In ANCOVA analyses with outcomes of BMD, BMC and area, PN conduction was analyzed as tertiles. Of participants (age 77.5±5.2 years; 99% white), 22% had DM. FN BMD was 4% lower in men with the worst sensory PN conduction compared to the best tertile after adjustment for age, race, diabetes, LM and FM (Table). FN area remained 1% and 3% higher with the worst motor and sensory PN conduction, respectively. Further adjustment for current smoking, drinking frequency, physical activity, calcium or vitamin D supplementation and medication use (corticosteroid, statin, thiazide, thiazolidinedione in DM, and osteoporosis medication) did not change associations. No significant differences were found for PN conduction with FN BMC or for FWL with any bone measure. Our results suggest that the lower BMD in worse sensory PN conduction may be due to an equivalent BMC in a larger hip bone area. Whether differences with worse sensory and motor PN function impact osteoporosis or fracture risk should be investigated in future studies.

FN BMD, BMC and area means by sensory and motor PN function tertile adjusted for age, race, DM, LM,

Motor PN function	Worst tertile CMAP (≤1.49 mV)	Middle tertile CMAP (1.50-3.06 mV)	Best tertile CMAP (≥3.07 mV)
FN BMD, g/cm <sup>2</sup>	0.783	0.797	0.799
FN BMC, g	4.52	4.55	4.56
FN area, cm <sup>2</sup>	5.78 <sup>†</sup>	5.71	5.72
Sensory PN function	Worst tertile SNAP (≤2.55 uV)	Middle tertile SNAP (2.56-4.99 uV)	Best tertile SNAP (≥5.0 uV)
FN BMD, g/cm <sup>2</sup>	0.769* <sup>†</sup>	0.797	0.802
FN BMC, g	4.86	4.57	4.53
FN area, cm <sup>2</sup>	5.83* <sup>†</sup>	5.74	5.66

\*p<0.05 for worst tertile vs. best tertile; <sup>†</sup>p<0.05 for worst tertile vs. best tertile at total hip, adjusted for age, race, DM, LM, and FM

**Disclosures:** E.S. Strotmeyer, None.

## SA329

**Osteoporosis in Men: Still Under-Screened and Under-Treated.** C. Anastasopoulou, S. Chandrasekaran\*, M. David\*, A. Chernoff\*. Endocrinology, Albert Einstein Medical Center, Philadelphia, PA, USA.

According to the latest National Osteoporosis Foundation recommendations men with hip fractures and all men age 70 and over should be screened for osteoporosis even in the absence of other risk factors. We conducted a retrospective chart review of men who had sustained hip fractures or were over 70. These were patients who were admitted to an urban

tertiary care medical center or were followed in the outpatient geriatric and general medicine clinics. The purpose of this study was to determine rates of screening for osteoporosis in men and to assess the impact of known risk factors for osteoporosis in this population. Data collection included demographic information (age, race, height, weight), biochemical values (calcium, creatinine, vitamin D levels) and medical information (results of DEXA bone scan, history of fractures, history of other illnesses including diabetes, thyroid and parathyroid problems, collagen diseases, seizure disorder, COPD, transplant history and the use of specific medications, including steroids, thyroid hormone, statins and antiseizure drugs).

A total of 349 charts were reviewed. There were 178 men with fracture; of these, only 1 had DEXA testing performed (0.6%). Among the men over 70, 6 had had a DEXA Scan (3.5%). Table 1 summarizes data by race.

	White	Black	Hispanic	Asian	Unknown	Total
Patient Number	175	147	12	8	7	349
Total Fracture	103	63	8	4	0	178
Weight recorded	31	30	5	2	0	68
Height recorded	25	34	4	1	0	64
Presence of Diabetes	33	36	2	0	0	71
Mean Age (SD)	74(16)	74(11)	67(20)	60(22)	78(5)	
Mean kg Weight(SD)	80(24)	82(19)	79(22)	59(8)		
Mean cm Height(SD)	157(50)	144(50)	142(55)	185		

Most of the parameters under consideration were under-recorded whether for special bloods tests like vitamin D, testosterone or intact PTH levels, or the simplest measurements such as weight, height or mobility status. Among patients that suffered bone fractures only 11 (6%) were prescribed calcium and vitamin D supplements, while none were prescribed bisphosphonates. Of the different risk factors for osteoporosis, race (p value 0.024), diabetes (p value 0.046), History of seizure disorder (p value 0.027) and the use of diuretic (p value 0.003) and antiseizure drugs (p value 0.003) were found to be statistically significant on causing bone fractures.

These observations clearly point to a lack of awareness among physicians of the guidelines for osteoporosis screening and treatment in men. More efforts will be needed to increase doctors' awareness of osteoporosis and its treatment in men so that men will be screened for osteoporosis when they have sustained a fracture, if they are over 70 years of age, or younger in the presence of risk factors.

**Disclosures:** C. Anastasopoulou, Sanofi-Aventis Pharmaceuticals 1; GlaxoSmithKline Pharmaceuticals 1; Procter & Gamble Pharmaceuticals 3.

This study received funding from: Procter & Gamble Pharmaceuticals.

## SA330

**Ten-year Change in Bone Mineral Density in a Representative Sample of Japanese Women - JPOS Cohort Study.** M. Iki<sup>1</sup>, J. Tamaki<sup>1</sup>, E. Kadowaki<sup>1</sup>, K. Kouda<sup>1</sup>, A. Yura<sup>1</sup>, Y. Ikeda<sup>2</sup>, Y. Sato<sup>3</sup>, A. Morita<sup>4</sup>, S. Kagamimori<sup>5</sup>, Y. Kagawa<sup>6</sup>, H. Yoneshima<sup>7</sup>. <sup>1</sup>Public Health, Kinki University School of Medicine, Osaka-Sayama, Japan, <sup>2</sup>University Hospital Center for Health and Safety, Kinki University School of Medicine, Osaka-Sayama, Japan, <sup>3</sup>Domestic Sciences, Jinai Women's College, Fukui, Japan, <sup>4</sup>Nutritional Education Program, National Institute of Health and Nutrition, Tokyo, Japan, <sup>5</sup>Welfare Promotion and Epidemiology, University of Toyama, Toyama, Japan, <sup>6</sup>Kagawa Nutrition University, Tokyo, Japan, <sup>7</sup>Shuuwa General Hospital, Kasukabe, Japan.

To describe the change in bone mineral density (BMD) in various ages of a representative sample of Japanese women and to examine whether a cohort effect (difference in BMD of subjects with the same age between surveys conducted in different time) exists in this population.

For 1,651 women aged 15 to 79 years at baseline selected randomly from 3 municipalities in Japan, we measured bone mineral density by DXA at the spine (LS), total hip (TH) and distal 1/3 site of the radius (DR), and body size, and obtained lifestyle factors from in-person interviews. Changes in BMD and other variables were determined 3, 6 and 10 years after the baseline.

Among the cohort from which 133 women dropped out during the 10-year follow-up because of deaths and move of residence, 1040 completed the study. 33% of the subjects were still pre-menopausal at follow-up, 42% were already post-menopausal at baseline, and 18% had entered menopause during the follow-up.

The changes in BMD varied according to ages of subjects. BMD did not show any significant change until 45 years at every skeletal site. After that, an abrupt increase in bone loss occurred at each site. Bone loss at LS decreased with increasing age, that at TH was the greatest in the group aged 75 and older, and that at DR showed a constant rate across different ages. These patterns of bone loss were similarly observed during the first 3 years of follow-up and during the last 4 years.

BMD of a particular age group at 10 years after the baseline was compared with BMD of the same age group at baseline. BMD at follow-up was significantly higher than BMD at baseline in several middle-aged and elderly groups, while no significant difference in BMD was observed in young adults. Height and weight did not differ between the subjects who completed the 10-year follow-up and those who did not. Calcium intake of the former subjects was greater than that of the latter in some age-groups. The observed cohort effect in BMD may have been biased by a healthy people effect. If this bias existed, bone health of young adults may have got worse in these 10 years.

Bone health in Japanese middle-aged and elderly women may have improved in the last decade but that in young adults may not.

**Disclosures:** M. Iki, None.

This study received funding from: Japan Society for the Promotion of Science.

## SA331

**Osteoporosis and the Acid-ash Hypothesis: Evidence Based on Bradford Hill's Criteria for Causality.** T. R. Fenton\*, A. W. Lyon\*, D. A. Hanley, S. C. Tough\*, S. Ross\*, M. Eliazziw\*. University of Calgary, Calgary, AB, Canada.

Scientists from several countries claim that the foods that make up the modern diet cause osteoporosis, due to net acid excretion under the acid-ash hypothesis. The purpose of this study was to critically evaluate the evidence in the literature regarding the acid-ash hypothesis as a potential cause of osteoporosis. A systematic review was undertaken based on Hill's criteria of causation: Temporality, Strength, Biological Gradient, Experiment, Consistency, and Biologically Plausibility. Only studies with temporal sequence were included in this review. Although the quantity of calcium excretion in response to acid loads is sufficient that over a lifetime the loss of calcium could explain the development of osteoporosis (Strength & Biological Gradient), the outcome of urinary calcium may be confounded by changes in absorption. Most studies of the hypothesis have used urinary calcium as the outcome, and Experiments of the hypothesis have failed to include the direct measures of osteoporosis. Prospective observational studies of the association between diet acid loads and changes in bone mineral density have had inconsistent results. Internal Consistency for the hypothesis is weak since there is evidence contrary to the hypothesis regarding the purported roles for phosphate (detrimental) and sodium (protective) in terms of calcium excretion, and no clear evidence for the hypothesis purported deleterious effects of grains and organic acid containing fruits on bone health. Biological Plausibility of the acid-ash hypothesis is weak based on the in-vitro studies that indicated increased bone demineralization occurs at low pHs since these studies were conducted at pHs below the physiological range. The use of Hill's criteria to evaluate the relationship between the acid-ash hypothesis and osteoporosis indicates that the evidence to support this hypothesis is weak.

**Disclosures:** T.R. Fenton, None.

This study received funding from: Canadian Foundation of Dietetic Research.

## SA332

**Glomerular Filtration Rate and Physical Function in Community-Dwelling Japanese Frail Elderlies.** J. Okuno\*, S. Tomura\*, H. Yanagi\*, N. Yabushita\*, T. Okura\*, K. Tanaka\*. Graduate school of Comprehensive Human Sciences, University of Tsukuba, Tsukuba city, Japan.

Chronic kidney disease (CKD) is becoming increasingly recognized as an important comorbid condition in elderly individuals. The risk of falling increases with aging. Falls are associated with deterioration of quality life. Vitamin D deficiency associated with falls and decreased balance. Impaired renal function with aging is detrimental for the conversion of calcidiol to calcitriol (D-hormone) and D-hormone analogue have been shown to decrease the risk of falls. The aim of this study was to assess whether estimated glomerular filtration rate (eGFR, ml/min/1.73m<sup>2</sup>) is associated with physical function in 51 community-dwelling frail elderly enrolled a three-month exercise program for nursing care prevention (76.9±5.9 yr). A longitudinal study conducted in a town near Tsukuba city (latitude 36° north) from June to September in 2006 and 2007 and November to February in 2006. The Ethics Committee of University of Tsukuba approved the study. An interview was conducted based on a questionnaire including experiences of fall or stumbling during the past one year. The serum levels of 25(OH)D, intact parathyroid hormone (iPTH) 1,25-dihydroxyvitamin D (1,25(OH)<sub>2</sub>D), calcium, and creatinine were measured. The following physical tests were measured: timed up and go (TUG), a 5-meter walk, functional reach (FR), one-legged stance with open eyes, tandem stance, tandem walk, hand grip strength, and alternate step-test. Estimated GFR was calculated using the Modification of Diet in Renal Disease (MDRD) formula (<60 versus ≥60 ml/min/1.73m<sup>2</sup>). The rate of participants with GFR<60 was 23.5%. At baseline, age, iPTH, 25(OH)D, and 1,25(OH)<sub>2</sub>D were not different between those with GFR<60 and those with GFR≥60. All physical functions were not different between two groups at baseline and at three months later. Physical functions except FR and hand grip strength improved significantly in those with GFR≥60. On the hand, many of physical functions did not improved in those with GFR<60. GFR were associated with iPTH (P<0.1), iPTH significantly correlated with 25(OH)D (P<0.05), and 25(OH)D significantly correlated with 1,25(OH)<sub>2</sub>D. Although the rate of 25(OH)D<50 nmol/L was not different between two groups, the rate of 1,25(OH)<sub>2</sub>D<42 pg/ml (lowest quartile) in the subjects with GFR<60 was higher than those with GFR≥60, but, not significant (50.0% vs 19.5%). Tandem stance, 5 chair sit to stand, and alternate step-test were significantly affected by GFR by multiple liner regression analysis (β:0.30, -0.32, -0.30, respectively). Our data suggest that eGFR is highly associated with walking ability and balance.

**Disclosures:** J. Okuno, None.

## SA333

See Friday Plenary number F333.

## SA334

**Seasonal Genetic Influence on Serum 25-hydroxyvitamin D Levels.** G. Snellman\*, H. Melhus<sup>2</sup>, R. Gedeberg<sup>3</sup>, S. Olofsson\*, A. Wolk\*, N. Pedersen\*, K. Michaëlsson<sup>1</sup>. <sup>1</sup>Department of Surgical Sciences Section of Orthopedics, Uppsala, Sweden, <sup>2</sup>Department of Medical Sciences Section of Clinical Pharmacology, Uppsala, Sweden, <sup>3</sup>Department of Surgical Sciences Section of Anaesthesiology and Intensive Care, Uppsala, Sweden, <sup>4</sup>Clinical Research Center, Uppsala, Sweden, <sup>5</sup>Division of Nutritional Epidemiology, Institute of Environmental Medicine, Stockholm, Sweden, <sup>6</sup>Department of Epidemiology and Biostatistics, Stockholm, Sweden.

Environmental factors, mainly nutrition and UV-B radiation, have been considered major determinants of vitamin D status. Nevertheless, they have only explained a modest proportion of the variation in serum 25-OH vitamin D. We aim to present the seasonal genetic impact on serum 25-OH vitamin D levels, an issue not previously resolved, and to illustrate the variability and reliability between three different 25-OH vitamin D assays.

204 same-sex twins were recruited from The Swedish Twin Registry. Serum 25-OH vitamin D was analyzed in three different laboratories, using three different techniques: high performance liquid chromatography and mass spectrometry (HPLC-MS), a radioimmunoassay (RIA), and a chemiluminescent immunoassay (CLIA). The heritability was calculated using genetic modelling techniques to estimate the relative contributions of genetic, shared and non-shared environmental factors to the variation in serum vitamin D.

Our results show high variability in 25-OH vitamin D assay results between the methods. There is a 24.9 nmol/l difference in mean 25-OH vitamin D level between the highest (HPLC-MS) and the lowest (CLIA) values. With a 50 nmol/L cut-off, only 8% of our twins are classified as vitamin D deficient with the HPLC method, 22% with the RIA method but 43% with the CLIA method. Lowest coefficient of variation was observed for the HPLC-MS method. The seasonal variation in heritability of vitamin D status is substantial. When using the HPLC-MS assay results, as much as 76% (95% CI 37-87%) of the variability in 25-OH vitamin D during the warm season (May through October) is explained by genetic factors. On the contrary, the seasonal variation in serum 25-hydroxyvitamin D is largely attributable to shared environmental influences, i.e. solar altitude. Individual environmental influences are found to only explain approximately one fourth of the variation in serum 25-OH vitamin D independent of season.

Our results indicate a strong genetic impact on serum vitamin D status during the warm season. The most likely main contributor to this genetic influence is the skin synthesis of vitamin D. Further studies are warranted to identify genes controlling vitamin D status. The high variability in results between the different serum 25-OH vitamin D assays may lead to substantial misclassification of vitamin D status.

**Disclosures:** G. Snellman, None.

## SA335

See Friday Plenary number F335.

## SA336

**Soy-based Formula Promotes Bone Growth in Neonatal Piglets by Inducing Osteo-progenitors to Differentiate into Osteoblasts via Enhanced BMP2 Signaling.** J. R. Chen\*, O. P. Lazarenko\*, M. L. Blackburn\*, T. M. Badger\*, M. J. Ronis\*. <sup>1</sup>Pharmacology & Toxicology, University of Arkansas for Medical Sciences / Arkansas Children's Nutrition Center, Little Rock, AR, USA, <sup>2</sup>Physiology, University of Arkansas for Medical Sciences / Arkansas Children's Nutrition Center, Little Rock, AR, USA.

Despite consumption of soy infant formula by 20% of infants in the United States and of soy products by children in most Asian countries, the majority of studies of soy effects on bone in both human and experimental animal models have focused on adults, particularly postmenopausal females. There have been no studies conducted on soy effects on immediate postnatal bone growth and maintenance. Moreover, the molecular mechanisms underlying soy effects have not been well elucidated. In the current study we used neonatal piglets as a model of human infants. Both male and female piglets were breast-fed (BF) or fed dairy-based formula (MF) or soy-based formula (SF) (n = 6/group) from birth until postnatal day 35. After sacrifice, blood, bone, bone marrow and other target tissues were collected for analysis. Bone quality and growth rate were assessed by peripheral quantitative computerized tomography and dynamic histomorphometry of the left tibia. Results showed that bone mineral density, content, and cortical thickness were all greater (P<0.05) in the SF group compared to the BF group. The MF group had minor effects compared to BF. Osteoblast numbers and bone formation rate were increased (P<0.05) in the SF group when compared to BF group; whereas, osteoclast numbers were decreased. Osteoblastogenesis was increased (P<0.05) in the SF group in *ex vivo* bone marrow cell cultures. Alkaline phosphatase and osteocalcin, bone formation markers in serum, were increased (P<0.05); whereas, the bone resorption marker CrossLaps was decreased in the SF group compared to BF group. Real-Time PCR results demonstrated that BMP2 was up-regulated, but RANKL was down-regulated in the SF group compared to BF group (P<0.05). Western Blots showed up-regulation of ERK, p38, Smad1/5/8 and RUNX2 from bone samples in both SF and MF groups compared to BF group (P<0.05). Treatment of C2C12 and ST2 cells with 2.5% serum from SF piglets showed increased (P<0.05) osteoblast differentiation compared to serum from BF piglets. These data indicate that SF has significant effects on promotion of bone growth, and these effects are mediated through enhancing of BMP2 signaling leading to increased osteoblast differentiation. Supported in part by USDA ARS 6251-51000-005-02S-2.

**Disclosures:** J.R. Chen, None.

**SA337****See Friday Plenary number F337.****SA338**

**Weight Reduction Is Not Deleterious for Bone Mass or Strength in Obese Women.** K. Uusi-Rasi, H. Sievänen, P. Kannus\*, M. Pasanen\*, K. Kukkonen-Harjula\*, M. Fogelholm\*. UKK Institute for Health promotion Research, Tampere, Finland.

Obesity is associated with greater bone mass. Therefore, one deleterious consequence of weight loss might be bone loss and increased bone fragility. This was a prospective 12-mo study with 3-mo weight loss following a 9-mo weight maintenance period. All 55 participants were premenopausal women with the mean age (SD) of 40 (5) years and BMI of 33.6 (4.7). All were encouraged to use VLED-products (Cambridge Diet) in reducing body mass. In addition, use of vegetables and energy-free drinks were recommended. The mean daily use of products was 2.8 (0.7) bags providing 41 (10) g of protein and 862 (216) mg of calcium per day from the products.

Body composition and bone mineral mass and strength of the right proximal femur and lumbar spine were assessed by DXA. Cortical (shaft CoD) and trabecular bone density (distal TrD) of the radius and tibia were measured with pQCT. All assessments were done at baseline and 3 and 12 months afterwards. The participants were divided into 5 equal groups (n=11; Q1-Q5) by the absolute loss of body mass during the 3-mo dieting period (Table). Analysis of variance (ANOVA) was used to find between-group difference and linearity in changes of bone characteristics during the 12-mo period.

Absolute changes in bone values were tiny and mostly not associated with weight loss (Table). The between-group differences in changes were statistically significant in CoD of the radial shaft only (p=0.020), and borderline difference was found in femoral neck BMD (p=0.063) and BMC (p=0.088). Only the mean changes in BMD of the femoral neck and trochanter showed a statistically significant linearity between weight loss groups (p=0.035 and 0.036, respectively). At the tibia or spine, there were no significant changes in bone traits in any groups. Even the greatest weight loss (group Q5) did not seem to be harmful for bone mass during a 12-mo time period. Although the Q5 showed a decline in femoral neck BMC, the change was insignificant. Simultaneously total body BMC and radial shaft CoD increased in this group.

The greater weight reduction did not seem to result in greater bone loss compared with minor weight reduction. Sufficient intake of calcium and protein were ensured during dieting, which may partly explain good maintenance of bone mass.

Weight loss groups, mean decline (kg)	Total body BMC	Lumbar spine BMC	Femoral neck BMC	Radial shaft CoD
Q1=4.1 (2.7)	-0.7 (2.9)	0.4 (3.1)	1.2 (3.0)	-0.1 (0.7)
Q2=7.3 (0.4)	-0.6 (4.0)	1.2 (3.7)	1.9 (3.3)	0.4 (0.8)
Q3=9.9 (1.0)	-1.4 (4.3)	-0.4 (3.4)	-0.4 (3.4)	-0.4 (0.7)
Q4=12.9 (0.9)	-0.9 (3.9)	-0.8 (5.9)	1.3 (2.7)	-0.03 (0.7)
Q5=16.3 (1.8)	1.1 (6.0)	-0.4 (3.7)	-1.0 (2.4)	0.8 (1.1)
P for between-group diff.	0.72	0.65	0.088	0.02
P for linearity	0.33	0.23	0.06	0.12

**Disclosures:** K. Uusi-Rasi, None.

**SA339****See Friday Plenary number F339.****SA340**

**Bone Density (BMD), Fracture and Survival in Women in Nursing/Residential Care.** M. N. Dugard\*, T. J. Jones\*, M. W. J. Davie. Charles Salt Research Centre, Robert Jones & Agnes Hunt Orthopaedic Hospital NHS Trust, Oswestry, United Kingdom.

Fractures, a common event in nursing homes (NH/RH) are often associated with low BMD. Because fractures may occur early after entry and drug treatment may take up to 18 month for effect, different strategies for fracture prevention may be required according to survival. To investigate BMD fractures and survival we restudied 156 women in NH/RH aged 56.4-98.8yr screened for fracture risk 3-8yr previously. A questionnaire was completed on all women at the first visit and distal forearm BMD (DTX 100) measured in 137. BMD was expressed as g/cm<sup>2</sup> or as a z score. Women were traced through health records, fracture details being obtained from the each woman's doctor. There were 7 <69yr, 26 70-79yr and 104 women aged >80yr at first interview.

BMD measured 1.3yr (range 0.05-9.3yr) after entry into NH/RH was low (0.317±0.084g/cm<sup>2</sup>, p<0.001). Osteoporosis (BMD<0.34 g/cm<sup>2</sup>) existed in 72.1% of women aged >80yr, compared with 33.4% less than 80yr (p<0.001). Body weight was lower in those >80yr compared with younger women (56.1±12.5 vs 62.3±16.7kg, p<0.05). Cross sectional analysis showed that BMD or body weight <6 months after entering a NH/RH (BMD 0.335±0.085g/cm<sup>2</sup>, weight 57.5±13.4kg) was similar to those >1yr after entry (BMD 0.317±0.082, 58.4±15.1kg). At follow-up 83.9% had died, 14.3% >69yr, 73.1% 70-79yr and 93.1% >80yr. Median survival time after entering a NH/RH was 4.6yr (range 0.4-15.3yr) in all subjects and 4.2yr (0.4-15.3yr) in the >80yr age group. In a Cox proportional hazards model, shortened survival in a NH/RH was associated with lower BMD z score (HR 1.42; 95% CI 1.04-1.93) in women >80yr scanned within 1yr of entry but not by age

at entry or weight. Few fractures occurred in women <70yr. Fracture analysis has been performed on 56 women >80yr (268.2 person yr). There were 22 fractures in 17 women in 4.12yr (Median: range 0.9-15.3yr), the first being 2.5yr (0.1-6.7yr) post entry. Seven women sustained fracture within 1yr of entry. Previous fracture was not a risk factor for future fracture. Post entry fracture rate was 8.2/100 person yr (1.5/100 for hip fracture). BMD was low in 3/4 women sustaining hip fracture (z score -0.474±1.089) and 9/13 women with non-hip fracture (-0.364±0.909) that occurred after entry. Most women in NH/RH have osteoporosis. In those over 80yr low BMD is associated with shorter survival. Fractures are associated with low BMD and may occur soon after entry. BMD measurement should form part of the initial entry assessment. Median survival times indicate that most women will survive long enough to benefit from bisphosphonate therapy.

**Disclosures:** M.W.J. Davie, MSD 2, 3; Procter & Gamble 4; Servier 3. This study received funding from: Bone Disease Foundation.

**SA341****See Friday Plenary number F341.****SA342**

**Effects of Obesity on Cortical Bone.** S. Ionova\*, S. H. Do\*, H. D. Barth\*, J. W. Ager\*, A. Porter\*, C. Vaisse\*, T. Alliston\*, R. O. Ritchie\*. <sup>1</sup>Material Science Division, Lawrence Berkeley National Laboratory, Berkeley, CA, USA, <sup>2</sup>University of California San Francisco, San Francisco, CA, USA, <sup>3</sup>Imperial College London, London, United Kingdom.

Obesity is associated with a host of biological and physiological changes, among which is a reduced risk of bone fracture in adults. While some studies have found obesity is associated with increased bone size and mass measures, it is still unclear whether the reduced risk stems from a change in bone quantity alone, or whether bone quality is affected as well. The objective of this study is to evaluate the changes in mechanical properties of cortical bone in response to diet-induced obesity in mice. 4 week old C57BL/6 male mice were fed a high fat diet (HFD) (N=15) or standard laboratory chow (N=15) for 16 weeks. All protocols were approved by the Institutional Animal Care and Use Committee and done according to federal guidelines for the care and use of animals in research. Blood was isolated immediately following sacrifice to evaluate serum leptin levels. Bone mass and body composition were evaluated with DEXA. The left femurs were tested in three-point bending to measure strength and bending stiffness. Right femurs were tested in notched three-point bending to measure fracture toughness (loading rate of 0.001mm/s). Bone geometry was evaluated in tomography at the Advanced Light Source and in an environmental scanning electron microscope. As expected, in the high-fat diet fed mice, body weight, fat mass, and leptin levels were significantly increased. In HFD mice, endostial and periosteal diameters, as well as cortical wall thickness increased (all p<0.015), while BMD was unchanged (p=.937). Strength, bending stiffness, and fracture toughness all were reduced in HFD (p<0.007, p=.010, p=.013, respectively). Transmission electron microscope studies point to a qualitative reduction in collagenous organization in HFD versus control group. In summary, diet-induced obesity results in increased bone size (quantity), while reducing bone strength, bending stiffness, and fracture toughness as well as other indicators of bone quality. This study indicates that bone quantity and bone quality play important, albeit counteracting, roles in determining fracture risk.

**Disclosures:** S. Ionova, None.

This study received funding from: National Institutes of Health.



## SA343

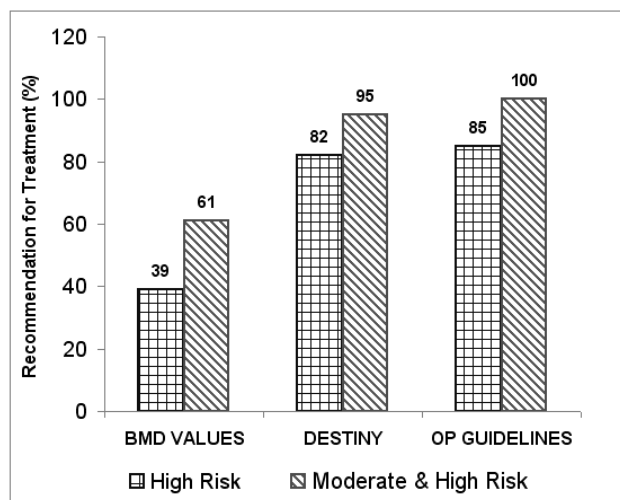
**Patients with Fragility Fracture Assessed by BMD, Bone DESTINY and Osteoporosis Canada Guidelines.** M. Larche\*, K. Beattie\*, J. D. Adachi, A. Papaioannou, W. Wong Pack\*, W. G. Bensen\*. Dept. of Medicine, McMaster University, Hamilton, ON, Canada.

**Purpose:** Fracture risk and treatment recommendations were compared in female patients with a previous fragility fracture using bone mineral density (BMD), Bone DESTINY and Osteoporosis Canada (OC) guidelines.

**Methods:** All female patients >60 years of age with a previous fragility fracture who underwent a DEXA scan between June and November 2007 were included in the analyses. Fracture risk and treatment recommendations were made based on BMD alone, Bone DESTINY and Osteoporosis Canada (OC) guidelines and results were compared. DESTINY fracture risk was an integration of BMD, age, steroid use, propensity to fall, history of falls and BMI<20 kg/m<sup>2</sup> while OC guidelines included BMD, age and steroid use. The prevalence of women in the high fracture risk group was compared between these three methods.

**Results:** 840 female patients with a previous fragility fracture were included in the analyses. BMD values resulted in treatment recommendations for 39% of patients with a T-score <-2.4 and 61% of patients at a T-score of -2 as shown in Figure 1. Bone DESTINY suggested treatment in 82% of patients with an additional 13% of patients in the moderate risk zone also seen in Figure 1. According to the OC guidelines, 85% of patients were in the high-risk zone with all patients being in the moderate and high risk zones.

**Figure 1.** Recommendations for treatment according to BMD, Bone DESTINY and OC guidelines.



**Conclusions:** Bone DESTINY suggests treatment in a much higher number of fragility fracture patients than BMD alone (82% versus 39% at -2.5), a value which is similar to OC guidelines. Based on the agreement in results between DESTINY and OC guidelines, the simplicity and ease of interpretation make DESTINY an attractive option for reporting fracture risk.

**Disclosures:** K. Beattie, None.

## SA344

**Long Term Safety of Oral Risedronate Treatment in Men with Osteoporosis as Assessed by Histomorphometry.** R. Recker<sup>1</sup>, R. Eusebio<sup>2</sup>, R. Phipps<sup>2</sup>, S. Xu<sup>2</sup>, D. Vanderschueren<sup>3</sup>, S. Boonen<sup>3</sup>. <sup>1</sup>Osteoporosis Research Center, Creighton University, Omaha, NE, USA, <sup>2</sup>Procter & Gamble, Mason, OH, USA, <sup>3</sup>University Hospital Leuven, Leuven, Belgium.

The effects of 2-4 years of 35 mg once-a-week risedronate treatment on bone quality and bone remodeling were assessed in a 2-year double-blind, placebo-controlled study in men with osteoporosis, followed by a 2-year open-label extension in a subset of subjects who all received risedronate. In the double-blind study, transiliac bone biopsies were obtained after 2-years treatment with placebo (N=7), and risedronate (N=15). During the open label study, 4 of the 7 placebo patients had a second biopsy taken after 2 years of risedronate treatment (total=19), and 9 of the 15 risedronate patients had a second biopsy taken after 4 years of risedronate treatment. There were no significant differences among groups in demographics or in any baseline characteristics including bone mineral density and bone turnover markers. Biopsies were examined for qualitative histological and quantitative histomorphometric differences. All biopsies had lamellar bone structure with no signs of osteomalacia, woven bone or bone marrow fibrosis. Tetracycline label was observed in all samples. Bone remodeling rate as expressed as mineralizing surface/bone surface was significantly lower after 2 and 4 years treatment with risedronate compared to 2 years placebo. Median eroded surface/bone surface (bone resorption parameter) was 2.8% in placebo and 1.7% after 2 years risedronate treatment (p=0.027). Median mineralizing surface/bone surface (bone formation parameter) was 3.6% after 2 years placebo, 1.2% after 2 years risedronate (p=0.0207), and 1.1% after 4 years risedronate treatment. These results indicate continued bone formation and no excessive inhibition of bone turnover with 2 and 4 years treatment with risedronate. There were no significant

differences in structural parameters with treatment. These results are concordant with previous histological studies with risedronate in postmenopausal women with osteoporosis showing that risedronate preserves normal bone structure, quality, and remodeling. This favorable long-term bone safety profile is consistent with that demonstrated in clinical trials in women with postmenopausal osteoporosis.

**Disclosures:** R. Recker, P&G 2.

This study received funding from: The Alliance for Better Bone Health (Procter & Gamble Pharmaceuticals and sanofi-aventis).

## SA345

See Friday Plenary number F345.

## SA346

**Serum Vitamin D Levels Do Not Modify the Response to an Exercise Program Following Hip Fracture: Data from the Baltimore Hip Studies.**

M. C. Hochberg<sup>1</sup>, E. Streeten<sup>1</sup>, J. Yu-Yahiro<sup>2</sup>, W. Hawkes<sup>3</sup>, R. Hebel<sup>3</sup>, R. Miller<sup>3</sup>, D. Orwig<sup>3</sup>, J. Magaziner<sup>3</sup>. <sup>1</sup>Medicine, University of Maryland, Baltimore, MD, USA, <sup>2</sup>Orthopaedic Surgery, Union Memorial Hospital, Baltimore, MD, USA, <sup>3</sup>Epidemiology and Preventive Medicine, University of Maryland, Baltimore, MD, USA.

**Background:** While older women with hip fracture often have low serum 25-hydroxyvitamin D (25[OH]D) levels, it is unknown whether recovery after hip fracture is associated with serum 25(OH)D levels.

**Objective:** To assess whether changes in BMD, muscle strength and lower extremity performance (LEGS Score) that occur in the year following hip fracture in response to a home exercise program were modified by baseline serum 25(OH)D levels.

**Methods:** We performed a post-hoc analysis of data from BHS-4, a randomized controlled trial of a home exercise program in 180 community-dwelling older women (mean [SD] age 82.3 [7.0] years) who had been hospitalized for surgical treatment of a hip fracture. Hospitalized women were recruited and baseline data were acquired within 15 days of fracture. BMD at the contralateral hip and grip strength were measured, LEGS Score was assessed and serum was collected at baseline, 2, 6 and 12 months post fracture. Serum samples stored at -70°C were analyzed for 25(OH)D levels in duplicate using DiaSorin RIA. Women were divided into two strata based on serum 25(OH)D levels either below 20 ng/ml or 20 ng/ml or above. Generalized estimating equations, with time and intervention as fixed effects, were used to examine whether 25(OH)D levels modified the effect of exercise on the outcomes.

**Results:** Baseline serum samples from 96 women were assayed for 25(OH)D levels. The mean (SD) 25(OH)D level was 22.8 (13.7) ng/ml and the median was 21.6 ng/ml with an interquartile range of 12.6 to 30.4 ng/ml; 45 (47%) women had a 25(OH)D level below 20 ng/ml. There was no evidence of seasonal variation in baseline 25(OH)D levels. There was no evidence of a significant effect of the home exercise intervention on any of the outcomes in women with 25(OH)D levels either above or below 20 ng/ml; results in Table. **Conclusion:** These data fail to demonstrate that serum 25(OH)D levels modify the effect of a home exercise program on changes in BMD, grip strength and lower extremity performance in the year following hip fracture. Results are limited by small numbers and the lack of ability to examine the potential efficacy of supplementation with vitamin D3 during the year following the fracture.

BMD, Grip Strength and LEGS Score at 2, 6 and 12 Months after Hip Fracture by Serum 25(OH)D Levels				
Outcome	Group	2 Months		12 Months
		Low 25(OH)D	Normal 25(OH)D	Low 25(OH)D
Total Hip BMD, g/cm <sup>2</sup>	Exercise	0.641 (0.025)	0.636 (0.025)	0.633 (0.024)
		0.631 (0.025)	0.619 (0.024)	0.616 (0.027)
	Control	0.651 (0.025)	0.629 (0.027)	0.635 (0.023)
		0.672 (0.026)	0.680 (0.027)	0.671 (0.031)
Grip Strength, kg	Exercise	16.8 (1.0)	16.6 (1.0)	16.7 (1.0)
		17.4 (0.8)	17.5 (0.8)	17.6 (1.0)
	Control	17.8 (1.0)	16.5 (1.0)	16.6 (0.9)
		17.9 (1.3)	16.6 (1.4)	18.1 (1.3)
LEGS Score	Exercise	22.4 (2.3)	25.3 (2.0)	31.4 (1.1)
		25.1 (1.1)	28.3 (0.8)	32.5 (0.7)
	Control	19.9 (1.9)	23.5 (2.0)	26.5 (2.0)
		25.7 (1.6)	29.5 (1.2)	33.4 (0.8)

**Disclosures:** M.C. Hochberg, None.

This study received funding from: National Institutes of Health

## SA347

See Friday Plenary number F347.

## SA348

**Excess of Post-fracture Mortality Among Men and Women: A Relative Survival Analysis.** S. A. Frost\*, N. D. Nguyen, J. R. Center, J. A. Eisman, T. V. Nguyen. Bone and Mineral Research Group, Garvan Institute of Medical Research, Sydney, Australia.

Although it is now well-established that individuals with fracture are at substantial increased risk of mortality, it is not clear how many deaths can be attributed to fracture. It can however be hypothesized that the excess deaths related to osteoporotic fracture are due to two "causes": one due to fracture and the other due to non-fracture. Therefore, if the expected background mortality rate reflects the effect of "other causes" then it is possible to estimate the excess of mortality due to osteoporotic fracture. The aims of this study were therefore (a) to estimate the "relative survival" among men and women following an osteoporotic fracture, and (b) to estimate the excess of mortality associated with specific fracture site.

The Dubbo Osteoporosis Epidemiological Study was designed as a prospective epidemiologic investigation in which men and women aged 60+ as of 1989 had been followed for 19 years. During this period incidence of atraumatic fractures ascertained by X-ray reports, and mortality was ascertained by personal report and confirmed by the New South Wales Birth, Death and Marriage Registry.

Relative survival can be illustrated by the following comparison: a 60 year-old individual died after a fracture in 2006 is considered to incur a greater loss of life than an individual with the same age died after a fracture in 1980, because the population life expectancy in 2006 is greater than that in 1980. Therefore, relative survival analysis allows a better estimate of the true effect of fracture on mortality. In this study relative survival ratio (RSR) was estimated by taking into account the age-and-sex specific expected survival in the general Australian population.

During the follow-up 585 women and 230 men sustained an incident low-trauma fracture. Death occurred in 138 (24%) women and 108 (47%) men. In men, the RSR of post-fracture mortality at 1, 5 and 10-year was 0.93 (95% CI 0.88 - 0.98), 0.83 (95% CI 0.71 - 0.96), and 0.80 (95% CI 0.56 - 1.05), respectively; in women, the corresponding estimates were: 0.99 (95% CI 0.97 - 1.01), 0.98 (95% CI 0.94 - 1.04), and 0.93 (95% CI 0.81 - 1.04). In both men and women, hip and vertebral fractures were associated with lower RSR. In comparison to forearm fracture, men and women with hip fracture had an 86% and 81%, respectively, increase in relative excess mortality. Men and women with vertebral fractures had a 23% and 96%, respectively, increase in relative excess mortality compared to forearm fractures.

In summary, relative survival analysis indicated that men had a worse outcome than women because the post-fracture risk of death in men was greater in men than in women. In both sexes the excess of mortality associated with osteoporotic fractures was mainly due hip and vertebral fractures.

**Disclosures:** S.A. Frost, None.

## SA349

See Friday Plenary number F349.

## SA350

**Performance Characteristics of a Workflow Tool for the Assessment of Vertebral Shape.** T. Ozanian\*, T. Lacey\*, G. Zubko\*, A. Brett\*, P. Steiger. Optasia Medical, Inc., Burlington, MA, USA.

The purpose of this study is to assess the performance of a new workflow tool based on statistical shape modelling for the characterization of vertebral shape.

We previously described a novel method for the computer-assisted determination of vertebral shape using 95 points representing the circumferential vertebral borders on lateral spine x-rays<sup>1</sup>. We implemented this method in a computer program that allowed an operator to annotate vertebral shapes on lateral radiographs from T4 to L4 as follows: (1) Choose image, (2) place a single point at the approximate centre of each vertebra to be analyzed, (3) using an atlas, label anatomy being analyzed and initialize automated search of vertebral contours, (4) review and correct contours. We assessed effort by measuring the time elapsed for steps 1-4. Four non-expert operators performed the analysis twice on 10 subjects after having been trained on 5 different training subjects. We then compared the results of each operator with those of a reference mark-up by measuring the average distance of all placed points (95 per vertebra, 13 vertebra per subject, 10 subjects = 12,350 points) to the curves defined by reference points. We also measured the ability to repeatedly produce accurate results (precision) by the different operators (inter-operator precision) and by the same operators (intra-operator precision).

All values mean (SD)	Effort [mins] per patient	Results	
		Accuracy [mm] per vertebra	Intra-Operator Precision [mm] per vertebra
Operator 1	8.9 (1.9)	0.92 (0.43)	0.97 (1.25)
Operator 2	7.4 (1.6)	0.85 (0.33)	0.63 (0.71)
Operator 3	6.2 (1.3)	0.85 (0.31)	0.63 (0.93)
Operator 4	6.9 (2.8)	0.91 (0.38)	0.61 (0.86)
Overall	7.4 (1.9)	0.88 (0.36)	0.71 (0.94)

Inter-operator precision was 0.91 (0.92) mm.

These results indicate that the accurate and reproducible computer assisted annotation of vertebral body shape can be accomplished within time constraints that are feasible in a point-of-care setting. The operator error was around 1 mm, which corresponds to about 3% of a vertebral height and compares favourably to the current guidelines for clinical trials,

which specify that changes of 3-4mm or 15-20% constitute vertebral fractures. Prevalent vertebral fractures are important predictors of future osteoporotic fractures in the spine and hip. This method may prove useful as a workflow tool to aid the physician to quantify vertebral shape. Further work is needed to explore how it may assist physicians in the assessment and classification of vertebral fractures. If successful, this tool could help standardize vertebral fracture assessment and make accurate quantitative assessment of vertebral shape feasible in a point-of-care setting.

<sup>1</sup>Brett et al. In Proc ASBMR, W227, Hawaii, Sept 2007.

**Disclosures:** P. Steiger, Optasia Medical, Inc. 5.

This study received funding from: Optasia Medical, Inc.

## SA351

See Friday Plenary number F351.

## SA352

**Risks and Outcomes for Hip Fractures in a Predominantly African-American Male Veteran Population.** R. U. Hashmi\*<sup>1</sup>, A. Rahman\*<sup>2</sup>, F. P. Perez\*<sup>3</sup>, S. C. Kukreja\*<sup>1</sup>, E. I. Barengolts\*<sup>3</sup>. <sup>1</sup>Medicine, University of Illinois at Chicago, Chicago, IL, USA, <sup>2</sup>Medicine, Weiss Memorial Hospital, Chicago, IL, USA, <sup>3</sup>Medicine, Jesse Brown VA Medical Center, Chicago, IL, USA.

The risks and outcomes associated with hip fractures are not well characterized in male veteran population. In this study we reviewed charts of patients admitted to VA Chicago hospital for hip fracture and for hip replacement surgery from January 2000 to December 2002. This preliminary report includes analysis of 33 age-matched subjects from each group (Table). There was no difference in smoking and alcohol abuse between the groups. DXA was done in 4 (12%) and bisphosphonates were used in 2 (6%) patients with fractures.

Table. Characteristics of cases (hip fracture) and controls (hip replacement).

Variable	Cases	Controls	P Value
Number of Subjects	33	33	x
African Americans, %	62	58	0.7
Age, years $\pm$ SD	69.8 $\pm$ 7.7	69.2 $\pm$ 6.0	0.7
<b>Outcomes</b>	<b>Cases</b>	<b>Controls</b>	<b>P Value</b>
Outcome <sup>1</sup>	1.6 $\pm$ 0.6	1.2 $\pm$ 0.4	<0.0004
Mortality in hospital, %	6.2	2.0	0.5
Mortality 1 year, %	28.1	6.5	0.02
Morbidity in hospital <sup>2</sup> , %	30.3	9.1	0.03
Co-morbid conditions, N $\pm$ SD	6.2 $\pm$ 3.2	4.2 $\pm$ 2.4	0.004
Concomitant medication, N $\pm$ SD	8.0 $\pm$ 3.7	4.3 $\pm$ 2.8	<0.0001
Hospitalization, days $\pm$ SD	7.4 $\pm$ 13.4	2.3 $\pm$ 8.6	0.07
<b>Risk Factors</b>	<b>Cases</b>	<b>Controls</b>	<b>P Value</b>
Seizure disorder, %	15.2	0.0	0.02
Stroke, %	21.2	9.1	0.17
Depression, %	21.2	9.1	0.17
COPD, %	15.2	3.0	0.08
Anti-seizure medication, %	18.2	0.0	0.01
Anti-depressants, %	33.3	9.1	0.02
Calcium supplements, %	36.4	6.1	0.003

<sup>1</sup> Outcome: 1=discharge home, 2=discharge to nursing home, 3=death

<sup>2</sup> Morbidity in the hospital included pneumonia, stroke and falls

<sup>3</sup> Hospitalization during 1 year prior to fracture

There was a high prevalence of seizure disorder, stroke and depression and in-hospital and 1 year mortality was 3-4 fold higher in patients with hip fractures than those with hip replacement. Our data suggest that patients with hip fractures have high prevalence of co-morbid, particularly neurological conditions and poor outcomes. If these data are confirmed, interventions to prevent hip fractures in high risk population with neurological disorders may be warranted.

**Disclosures:** R.U. Hashmi, None.

## SA353

**Impact of an Educational Intervention on Knowledge about Osteoporosis Following a Fragility Fracture.** L. Bessette<sup>1</sup>, S. K. Davison<sup>1</sup>, L. Ste-Marie<sup>2</sup>, S. Jean<sup>3</sup>, M. Beaulieu<sup>4</sup>, M. Baranci<sup>5</sup>, J. P. Brown<sup>1</sup>. <sup>1</sup>CHUL Research Centre, Quebec, QC, Canada, <sup>2</sup>Medicine, University of Montreal, Montreal, QC, Canada, <sup>3</sup>Institut National de Santé Publique du Québec, Quebec, QC, Canada, <sup>4</sup>Merck Frosst, Kirkland, QC, Canada, <sup>5</sup>sanofi-aventis, Laval, QC, Canada.

The objective of this analysis was to evaluate the impact of an educational intervention on general osteoporosis (OP) knowledge in women  $\geq 50$  years who recently suffered a fragility fracture.

Three educational tools were developed: a 15-minute video, written material on OP targeted to participants, and written documentation on OP targeted to physicians. Information was based on the 2002 Clinical Practice Guidelines for the Diagnosis and Management of Osteoporosis in Canada. Six to eight months after the fracture event, women with a fragility fracture were contacted by phone and offered to be randomized to one of three groups: A) the control group (no intervention); B) the documentation group (written documents for the participants and the physician); or C) the video group (a video and the written documentation for both the participants and the physician). All participants completed a phone questionnaire on OP, which included a component on OP knowledge, before the intervention. Twelve months after the intervention participants were re-contacted and the same questionnaire was administered. The current analysis was completed only for participants who were undiagnosed and untreated for OP at randomisation.

Of the 894 women with a fragility fracture, 850 (95%) accepted randomization. Of these, 546 (64%; mean age: 61.7 years) were without OP diagnosis and treatment. Ninety-six percent of these 546 women were contacted and completed the phone questionnaire 12 months after the randomization. The mean knowledge score improved significantly from baseline in both groups B and C (81.6 to 85.5% and, 79.7 to 84.4%, respectively) compared to group A for whom there was little average change (79.9% to 81.9%). As showed in the table, groups B and C improved their knowledge between baseline and 12 month follow-up more so than the group A.

A simple intervention targeting the patient increased general knowledge about OP and its consequences.

% strongly agree or agree with the statement	Groupe A Baseline/12 mo	Group B Baseline/12 mo	Group C Baseline/12 mo
I understand the possible consequences of the fracture on my health well	84.2/85.6%	83.1/92.5%	83.9/91.6%
I know OP and its consequences well	50.0/58.1%	51.1/74.1%	51.6/77.0%
I understand the relationship between OP and my fracture well	61.8/66.8%	66.6/71.9%	57.5/71.0%
I know the treatments for OP well	19.5/24.8%	19.8/38.7%	21.9/45.1%

**Disclosures:** L. Bessette, Procter & Gamble, Sanofi-Aventis 1, 3; Merck Frosst 1, 3; Amgen 1, 2, 3; Pfizer 1, 2, 3.

This study received funding from: Procter & Gamble, sanofi-aventis, Merck Frosst, Eli Lilly, Novartis.

## SA354

See Friday Plenary number F354.

## SA355

**Gender Specific Effects of TRPV4 on Osteoblast-Osteoclast Coupling and Risk of Osteoporotic Fractures.** B. C. J. van der Eerden<sup>\*1</sup>, M. Koedam<sup>\*1</sup>, F. Rivadeneira<sup>1</sup>, J. B. J. van Meurs<sup>1</sup>, J. G. J. Hoenderop<sup>\*2</sup>, H. Weinans<sup>\*3</sup>, M. Suzuki<sup>\*4</sup>, R. J. M. Bindels<sup>\*2</sup>, A. G. Uitterlinden<sup>1</sup>, J. P. T. M. van Leeuwen<sup>1</sup>.

<sup>1</sup>Internal Medicine, Erasmus MC, Rotterdam, Netherlands, <sup>2</sup>Cell Physiology, Nijmegen Centre for Molecular Life Sciences, Nijmegen, Netherlands, <sup>3</sup>Orthopedics, Erasmus MC, Rotterdam, Netherlands, <sup>4</sup>Molecular Pharmacology, Jichi Medical School, Tochigi, Japan.

TRPV4 is a member of the transient receptor potential (TRP) superfamily and responds to an array of stimuli, including osmolarity, heat, pH, temperature and pressure. Recent findings showing that TRPV4 deficiency leads to reduced sensing of mechanical stimuli led us to explore the role of TRPV4 in bone.

Using real-time PCR, TRPV4 mRNA was abundantly expressed in both osteoblasts and osteoclasts. Femoral cortical and trabecular bone mass (thickness and volume) as assessed by microcomputed tomography was higher in male but not female TRPV4 knockout mice compared to wild type mice.

Next, osteoclast and osteoblast differentiation and function was studied by bone marrow cultures from wildtype and TRPV4 knockout mice. Osteoclast numbers (TRAP staining) as well as the formation of resorption pits (coomassie brilliant blue staining) were significantly reduced in cultures of TRPV4 knockout mice compared to wildtype littermates. In contrast, osteoblast differentiation at day 9 of culture (alkaline phosphatase activity) and matrix mineralization at day 21 (alizarin red) was significantly increased in TRPV4 knockout bone marrow cultures. These data implicate osteoblast-osteoclast uncoupling and support the observed increase in bone mass in male TRPV4 deficient mice. To assess the possible impact of TRPV4 function on osteoporotic outcome in humans, we extracted data from a recently performed genome-wide association study (Illumina 550K SNP array) within the Rotterdam Study ( $\pm 7,500$  individuals, 55 years and older). Two

single nucleotide polymorphisms (SNPs) in the TRPV4 gene showed strong associations with osteoporotic fracture risk (Hazard Ratio 1.79; Confidence Intervals 1.19-2.69), fragility fracture risk (HR 2.58; CI 1.36-4.87) and hip fracture risk (HR 2.75; CI 1.31-5.75) in men, but not in women. This was not affected after adjusting for height, weight, age and bone mineral density (BMD). No associations were found for femoral neck or lumbar spine BMD in either sex.

In conclusion, TRPV4 plays an important role in male but not female bone biology. TRPV4 deficiency results in a male-specific increase in bone mass implicating a negative role for TRPV4 in male bone metabolism. In line with this male specificity, variations in the TRPV4 gene are predicting fracture risk in men but not in women.

**Disclosures:** B.C.J. van der Eerden, None.

## SA356

See Friday Plenary number F356.

## SA357

**Disability in Patients with Osteoporotic Pertrocantheric Hip Fracture: A Prospective Study.** E. Casado, M. Larrosa\*, C. Galisteo\*, A. Gómez, P. Lisbona\*, E. Graell\*, N. Navarro\*, M. Moreno\*, J. Gratacós\*. Rheumatology, Hospital Sabadell, Sabadell, Spain.

**Background:** Hip fracture in elderly is an important health problem, but the short-medium term disability associated, is not commonly assessed.

**Purpose:** To study the short-medium term (6 months) disability associated to the stable osteoporotic pertrocantheric hip fracture.

**Methods:** Prospective study, with inclusion, during a two-year period (March 2002 - December 2003), of all patients older than 65 years with stable osteoporotic pertrocantheric hip fracture (Kyle I-III) who were attended in a 400-bed hospital in Spain. Patients with a moderate-severe disability (impossible to walk by themselves or Barthel <60) prior to hip fracture were excluded. Functional status was evaluated at inclusion (retrospective measurement of disability prior to fracture), and during follow-up (1,3 and 6 months) using: Barthel Index (0-100), the Activities of Daily Living index (ADL, 0-6), and the evaluation of the Walking Ability (WA) by a validated method that gather the need for walking aids.

**Results:** 82 patients (90% women) with a mean age of  $83 \pm 7$  years were included. The functional status at inclusion was: Barthel index  $61 \pm 22.6$ ; and 44% and 68% of the patients were independent according to ADL and WA scales respectively (table 1). Disability clearly improved during the follow up, but still remained very important after 6 months (table 1). At six months 37 patients (45%) were lost.

**Table:**

	Baseline	1 month	3 months	6 months
Barthel Index	88,3 $\pm$ 10,8	61 $\pm$ 22,6 75	75,9 $\pm$ 22,4	85,4 $\pm$ 15,7
ADL scale*	44%	3,5%	18%	26,5%
WA scale**	68%	0%	9%	21%

\*Independent patients for the 6 basic ADL. \*\*Independent patients for walk

**Conclusion:** Hip fracture, even the most stable type, produces an important disability at medium term that is not always taken into account in these patients.

**Disclosures:** E. Casado, None.

## SA358

See Friday Plenary number F358.

## SA359

**Family Physician Characteristics that Predict Appropriate X-ray Ordering: Canadian Quality Circle (CQC) National Project.** A. Papaioannou<sup>1</sup>, G. Ioannidis<sup>1</sup>, B. Kvern<sup>\*2</sup>, A. Hodsman<sup>3</sup>, L. Thabane<sup>\*1</sup>, A. Gafni<sup>\*1</sup>, A. Walsh<sup>\*4</sup>, F. Jiwa<sup>5</sup>, J. D. Adachi<sup>1</sup>. <sup>1</sup>McMaster University, Hamilton, ON, Canada, <sup>2</sup>University of Manitoba, Winnipeg, MB, Canada, <sup>3</sup>University of Western Ontario, London, ON, Canada, <sup>4</sup>Procter and Gamble Pharmaceuticals, Toronto, ON, Canada, <sup>5</sup>Osteoporosis Canada, Toronto, ON, Canada.

The project is an integrated disease management study designed to improve family physicians' (FPs) adherence with the Osteoporosis Canada 2002 guidelines. This analysis examined the association between appropriate x-ray ordering and FPs characteristics. The guidelines recommend that x-rays should be ordered in all patients with kyphosis or height loss. A total of 225 FPs from across Canada completed the physician characteristics questionnaire, which captured 13 physician characteristics including sex; year of graduation from medical school; country of medical school; does the physician have a full or part-time practice, has hospital privileges, provide house calls, or has after hours call coverage for a defined group of patients; does the physician work in a solo or group practice, work in a teaching practice, is involved with an interdisciplinary team on site, uses electronic health records, or mainly uses fee-for-service billings; and is the physician a current member of the college of family physicians of Canada. During the course of the study, FPs examined a total of 13970 patients who were randomly selected from their practices. The generalized estimating equations (GEE) technique was used to examine the

association between appropriate x-ray ordering and physician characteristics. Odds ratios (OR) and 95% confidence intervals (CI) were calculated. Results indicated that 52% (117/225) of FPs were women, 61% (132/216) provided house calls, 71.5% (156/218) provided after hour call coverage, 30% (67/223) worked in a teaching practice, 32% (73/223) worked within an interdisciplinary team, and 85% (192/225) used fee-for-service billings. Patients were younger in practices of women FPs (56.6% versus 66.4% of patients over the age of 65 years) as compared with men FPs. The likelihood of appropriate x-ray ordering was lower if the physician was a woman (OR: 0.76; 95% CI: 0.63, 0.92), provide house calls (OR: 0.71; 95% CI: 0.59, 0.85), worked within an interdisciplinary team (OR: 0.70; 95% CI: 0.56, 0.88), or used fee-for-service billings (OR: 0.66; 95% CI: 0.51, 0.85). The likelihood of appropriate x-ray ordering was higher if the physician provided after hour call coverage (OR: 1.87; 95% CI: 1.46, 2.38) or worked in a teaching practice (OR: 1.29; 95% CI: 1.06, 1.58). In conclusion, physician characteristics may influence x-ray ordering and that appropriate x-ray ordering may result in a greater number of vertebral fractures detected.

**Disclosures:** A. Papaioannou, Amgen, Eli Lilly, Merck Frosst, Novartis, Procter and Gamble Pharmaceuticals, sanofi-aventis, Servier 2.

This study received funding from: Procter & Gamble Pharmaceuticals Canada Inc, sanofi-aventis Pharma Inc., and from the Ontario College of Family Physicians

## SA360

**Failure to Perceive Increased Risk of Fracture in Women  $\geq 55$  Years. The Global Longitudinal Registry of Osteoporosis in Women.** E. S. Siris<sup>1</sup>, A. Diez-Perez<sup>2</sup>, S. Boonen<sup>\*3</sup>, C. Cooper<sup>4</sup>, A. LaCroix<sup>5</sup>, N. B. Watts<sup>6</sup>, K. G. Saag<sup>7</sup>, S. Silverman<sup>8</sup>, R. Dedrick<sup>\*9</sup>, S. L. Greenspan<sup>\*10</sup>. <sup>1</sup>Department of Medicine, Columbia University College of Physicians and Surgeons, New York, NY, USA, <sup>2</sup>Hospital del Mar, Barcelona, Spain, <sup>3</sup>Leuven University Center for Metabolic Bone Diseases, Leuven, Belgium, <sup>4</sup>Southampton General Hospital, Southampton, United Kingdom, <sup>5</sup>Fred Hutchinson Cancer Research Center, Seattle, WA, USA, <sup>6</sup>University of Cincinnati, Cincinnati, OH, USA, <sup>7</sup>University of Alabama-Birmingham, Birmingham, AL, USA, <sup>8</sup>David Geffen School of Medicine, Los Angeles, CA, USA, <sup>9</sup>UMASS Medical School, Worcester, MA, USA, <sup>10</sup>University of Pittsburgh, Pittsburgh, PA, USA.

The purpose of the study was to compare self-perceived risk of osteoporotic fracture among women  $\geq 55$  years of age with reported risk factors.

The Global Longitudinal registry of Osteoporosis in Women is an observational follow-up study of women  $\geq 55$  years of age recruited by 540 primary physician practices (17 sites, 10 countries). Practices typical of each region were identified by primary care networks organized for administrative, research or educational purposes. All non-institutionalized patients visiting the practice within the prior 2 years were eligible. Self-administered questionnaires were mailed, with 2:1 over-sampling of women  $\geq 65$  years of age. Data collected included information on demographics; medical history; risk factors for osteoporosis-related fracture; fracture occurrence; and self-report of prevention, diagnosis and treatment of osteoporosis. Respondents rated their perceived risk of fracture vs women of the same age using a 5-point scale from "much lower" to "much higher."

Of the women with no risk factors, 90% believed their risk was the same as or lower than that of women of the same age, whereas the majority of women with risk factors failed to appreciate their increased risk of fracture (Table). Among women diagnosed with osteoporosis, 56% believed they were not at increased risk. One quarter of the 15,163 women with a FRACTURE Index  $\geq 5$  perceived themselves at higher risk.

**Table.** Perceived Risk of Fracture Compared with Women of Same Age

Risk factor	N	Perceived risk of fracture	
		Lower	Higher
No risk factor	20,943	41%	10%
History of fracture	11,544	21%	35%
Maternal hip fracture	5972	28%	26%
Parental hip fracture	7397	28%	25%
Weight <125 lb (57 kg)	7705	32%	26%
Smoker	4391	31%	19%
Alcohol >14 units/week	1604	38%	15%
Current steroid use	1484	22%	39%
Rheumatoid arthritis	5196	25%	28%
FRACTURE Index $\geq 5$	15,163	31%	25%
<b>Diagnosis</b>			
Osteoporosis	9353	18%	44%
Osteopenia	8195	27%	25%
Normal	30,166	42%	8%

Most women at elevated likelihood of osteoporotic fracture do not perceive themselves to be at increased risk.

**Disclosures:** E.S. Siris, Lilly, Merck, Procter & Gamble, sanofi-aventis, Novartis 1.

This study received funding from: The Alliance for Better Bone Health (Procter & Gamble Pharmaceuticals and sanofi-aventis).

## SA361

See Friday Plenary number F361.

## SA362

**Risk Factors for Fragility Fracture in a Multiracial Cohort of US Women.**

**The Global Longitudinal Registry of Osteoporosis in Women.** S. Silverman<sup>1</sup>, J. Adachi<sup>2</sup>, S. Gehlbach<sup>\*3</sup>, S. L. Greenspan<sup>\*4</sup>, F. Hooven<sup>\*3</sup>, A. LaCroix<sup>5</sup>, R. Lindsay<sup>\*6</sup>, K. G. Saag<sup>\*7</sup>, E. S. Siris<sup>8</sup>, A. Wyman<sup>\*3</sup>, N. B. Watts<sup>9</sup>.

<sup>1</sup>David Geffen School of Medicine, Los Angeles, CA, USA, <sup>2</sup>St. Joseph's Hospital, Hamilton, ON, Canada, <sup>3</sup>UMASS Medical School, Worcester, MA, USA, <sup>4</sup>University of Pittsburgh, Pittsburgh, PA, USA, <sup>5</sup>Fred Hutchinson Cancer Research Center, Seattle, WA, USA, <sup>6</sup>Helen Hayes Hospital, New York, NY, USA, <sup>7</sup>University of Alabama-Birmingham, Birmingham, AL, USA, <sup>8</sup>Columbia University Medical Center, New York, NY, USA, <sup>9</sup>University of Cincinnati, Cincinnati, OH, USA.

The purpose of the study was to identify risk factors for fragility fracture in a multiracial cohort of women from the USA.

GLOW is a prospective, multinational, observational study. Seventeen sites in 10 countries in North America, Australia and Europe are participating. Practices typical of each region were identified through primary care networks. The present report is limited to data collected from US White, Black and Asian women. All non-institutionalized women  $\geq 55$  years of age who visited the practices within the previous 2 years were eligible. Self-administered questionnaires were mailed (2:1 over-sampling of women aged  $\geq 65$  years).

In a population of 20,888 women from 6 physician practices, 18,613 were White, 1932 were Black and 343 were Asian. Risk factors for fracture (established from studies of primarily White populations) varied among the 3 groups (Table). White women had the highest prevalence of personal history of fracture, parental fracture, alcohol and steroid use. Black women reported higher rates of smoking, use of arms in rising, rheumatoid arthritis and secondary osteoporosis. Asians had the highest prevalence of weight <125 lb. White women reported higher rates of prior fracture than Black women, which varied from 4.8 times higher for rib to 1.1 times higher for ankle fractures. Both Black and Asian women had hip fracture rates similar to those for White women.

**Table.** Age-standardized patient risk factors for fracture, by race

Risk factor (%)	White (n=18,613)	Black (n=1932)	Asian (n=343)
Arms used to assist from sitting	35.7	55.3	24.3
Steroid use	34.9	23.5	19.9
Personal history of fracture	24.2	14.4	18.4
Parental fracture	17.5	7.0	11.3
Secondary osteoporosis	16.0	25.3	17.1
Weight <125 lb (57 kg)	15.6	4.7	47.6
Rheumatoid arthritis	8.0	21.4	11.8
Current smoker	7.3	11.5	2.4
Alcoholic drinks (>14 per week)	2.6	0.3	0.3

Racial differences for prevalent fractures and clinical risk factors for fragility fracture were observed in this US cohort. The prevalence of prior fractures among both Black and Asian women, although less than that of White women, is substantial, and places them at risk for future fracture.

**Disclosures:** S. Silverman, Wyeth, Lilly, Novartis, Alliance 3; Lilly, Novartis, Pfizer, Procter & Gamble 1; Lilly, Argen, Wyeth, Merck, Roche, Novartis 2.

This study received funding from: The Alliance for Better Bone Health (Procter & Gamble Pharmaceuticals and sanofi-aventis).

## SA363

See Friday Plenary number F363.

## SA364

**Association Between BMD Change, Use of Antiresorptive Agents and Fragility Fracture in Women and Men.** C. Berger<sup>\*1</sup>, L. Langsetmo<sup>\*1</sup>, L. Joseph<sup>\*1</sup>, D. A. Hanley<sup>2</sup>, K. S. Davison<sup>3</sup>, R. Josse<sup>4</sup>, N. Kreiger<sup>\*4</sup>, A. Tenenhouse<sup>\*1</sup>, D. Goltzman<sup>1</sup>. <sup>1</sup>McGill University, Montreal, QC, Canada, <sup>2</sup>University of Calgary, Calgary, AB, Canada, <sup>3</sup>Laval University, Quebec city, QC, Canada, <sup>4</sup>University of Toronto, Toronto, ON, Canada.

Our objective was to determine the relationship between baseline BMD, longitudinal change in BMD, and fragility fractures in men and women, taking or not taking antiresorptive agents (bisphosphonates, estrogen). We studied 3635 women and 1417 men aged 50 to 85 years old from the CaMos cohort with at least two BMD measurements in the first five years, with fracture information in the first seven years, and without long-term glucocorticoid use. Multiple logistic regression models were used to assess the relationship between baseline BMD (lumbar spine, femoral neck, total hip and trochanter), BMD change and fragility fractures (any, main, forearm/wrist, ribs and hip) in users and non-users of antiresorptive agents. All models are adjusted for age, height, BMI, previous fracture, diabetes, osteoarthritis and rheumatoid arthritis. Among antiresorptive non-users, a higher rate of total hip BMD loss is associated with a greater risk of fragility fracture with an odds ratio (OR) of 1.19 (95% CI: 0.94; 1.51) for each 0.01g/cm<sup>2</sup> per year in women, and an OR of 1.60 (95% CI: 1.20; 2.14) for each 0.01g/cm<sup>2</sup> per year in men. Furthermore, the association was even stronger for women with the lowest baseline BMD (first tertile) with an OR of 1.62 (95% CI: 1.12; 2.34) and with the highest loss of BMD with an OR of 1.93 (95% CI: 1.28; 2.90). In men, the association was stronger in those with the lowest baseline BMD with an OR of 1.85 (95% CI: 1.17; 2.93) and in osteopenic men with an OR of 1.73 (95% CI: 1.20; 2.49). In women, the risk of forearm/wrist fragility fracture for a decrease of 0.01g/cm<sup>2</sup> in baseline total hip is 1.04 (95% CI: 1.00; 1.07) in non-users and 1.06 (95% CI: 1.03; 1.08) in users. The risk of forearm/wrist fragility fracture for a decrease of 0.01g/cm<sup>2</sup> per year at the total hip is 1.50 (95% CI: 1.07; 2.11) in non-users compared to 1.03 (95% CI: 0.78; 1.35) in users. The results show that there is an association between the rapidity of bone loss and fragility fractures in non-users, although stronger in non-user men, suggesting that rate of change is an independent risk factor from baseline BMD. Rapid bone loss is an important risk factor for fragility fractures in subgroups of the population such as those who lose bone faster or those with osteopenia. The inconclusive results between rate of BMD loss and risk of fractures in antiresorptive users support the position that prevention of BMD loss is not the only mechanism for fracture protection with antiresorptives.

**Disclosures:** C. Berger, None.

## SA365

**See Friday Plenary number F365.**

## SA366

**Positive Celiac Disease Serology and Bone Mineral Density in Adult Women.** W. D. Leslie, D. Duerksen<sup>\*</sup>. Department of Medicine, University of Manitoba, Winnipeg, MB, Canada.

Celiac disease (CD) is associated with decreased BMD. Seropositivity with tissue transglutaminase antibody (TTG) and/or endomysial antibody (EMA) is highly specific for CD, while antigliadin antibody (AGA) has lower specificity. We investigated the relationship between BMD and CD serology in a clinical cohort of adult women to determine the role of seropositivity as a risk factor for decreased BMD. The Manitoba BMD Database (1990-2007) was linked to a provincial database of CD serology (1996-2007) to identify all women in Manitoba over age 20 with BMD results preceding CD serology by 6 m or less (mean interval 3 m). In women with multiple CD serologies only the first was used. CD seropositivity was defined from high specificity assays (CD-HS: TTG or EMA) or low specificity assays (CD-LS: AGA). ANCOVA models (age, height, weight-adjusted) were used to assess the effect of CD seropositivity on BMD at multiple measurement sites (total hip, lumbar spine L1-4, trochanter and femoral neck). There were 377 matches between the 2 databases (31 CD-HS seropositive, 71 CD-LS seropositive, 296 CD seronegative for both). Mean age was 62 (SD 13) y, and mean Z-scores ranged from -0.30 (SD 1.07) at the femoral neck to -0.86 (SD 1.57) at L1-4. HS-CD seropositivity was associated with lower BMD at all sites, and LS-CD seropositivity was associated with lower BMD at 3 sites (see Table). When HS-CD and LS-CD serology were discordant there was a significant effect of HS-CD seropositivity on BMD ( $P < .05$  for lower BMD at the total hip, trochanter, L1-4) whereas in those with LS-CD seropositivity (with HS-CD negative) BMD was no different from CD seronegative women.

Table: Least-squares mean T-scores ( $\pm$ SE) from ANCOVA models (age, height, weight-adjusted).

	CD-HS Seronegative	CD-HS Seropositive	CD-LS Seronegative	CD-LS Seropositive
Total hip	-1.34 $\pm$ 0.06 *	-1.92 $\pm$ 0.20	-1.30 $\pm$ 0.06 *	-1.65 $\pm$ 0.13
L1-4	-1.96 $\pm$ 0.07 *	-2.59 $\pm$ 0.24	-1.93 $\pm$ 0.09	-2.25 $\pm$ 0.17
Femoral neck	-1.66 $\pm$ 0.05 *	-2.03 $\pm$ 0.16	-1.63 $\pm$ 0.05 *	-1.88 $\pm$ 0.10
Trochanter	-1.62 $\pm$ 0.06 *	-2.29 $\pm$ 0.19	-1.59 $\pm$ 0.06 *	-1.97 $\pm$ 0.13

\*  $P < .05$ , Seronegative vs Seropositive

In conclusion, we found a significantly lower BMD in CD seropositive women compared with seronegative women. This effect was only seen with high specificity CD antibodies (TTG or EMA), and not with low specificity CD antibodies (AGA).

**Disclosures:** W.D. Leslie, None.

## SA367

**See Friday Plenary number F367.**

## SA368

**Predictors of Osteoporosis Management Among Residents Living in Long-Term Care.** L. M. Giangregorio<sup>1</sup>, A. Papaioannou<sup>2</sup>, J. Hirides<sup>\*3</sup>, C. J. Maxwell<sup>\*4</sup>, M. Jantzi<sup>\*3</sup>, J. W. Poss<sup>\*3</sup>. <sup>1</sup>Kinesiology, University of Waterloo, Waterloo, ON, Canada, <sup>2</sup>Medicine, McMaster University, Hamilton, ON, Canada, <sup>3</sup>Health Studies and Gerontology, University of Waterloo, Waterloo, ON, Canada, <sup>4</sup>Community Health Sciences & Medicine, University of Calgary, Calgary, AB, Canada.

The present study describes the extent to which individuals living in long-term care (LTC) with a recent fracture or diagnosed osteoporosis are receiving osteoporosis management, and identifies factors associated with management.

The sample included 1910 LTC residents living in Ontario and Manitoba, Canada. Data were obtained using the Resident Assessment Instrument Minimum Data Set 2.0. Osteoporosis management was assessed among residents with a diagnosis of osteoporosis or recent fracture. Sociodemographic, clinical and functional characteristics were assessed as correlates of pharmacological osteoporosis management in multivariable logistic regression analyses.

Individuals who had sustained a recent fracture or who had a history of hip fracture or documented osteoporosis represented 27.5% (n = 525) of the sample; use of any osteoporosis medication was reported in 40% of these individuals (from here called the osteoporosis group). Twenty-seven percent (n=140) of residents in the osteoporosis group were documented to be taking both calcium and vitamin D supplementation, 6.5% (n=34) were documented to be taking calcium supplements only, 3.6% (n=19) were taking vitamin D only, and multivitamin use was reported in 19% (n=100) of residents. 54 (10.3%) of residents in the osteoporosis group were taking a bisphosphonate and were not taking vitamin D or a multivitamin. The odds of individuals in the osteoporosis group receiving pharmacological therapy were lower if they had six or more co-morbid conditions, if they used a wheelchair as their primary mode of mobility, if they had depression (DRS 3+), if they had health instability, or if they resided in a facility in Manitoba. Female sex and prescription of ten or more medications were variables positively associated with current use of osteoporosis therapy.

The current study reveals that osteoporosis management is not optimal among individuals at risk of fracture living in LTC facilities, and identifies predictors of osteoporosis management. It may be necessary to incorporate an initiative for health care providers, facility staff, residents and their families to educate them about the importance of fracture prevention strategies in LTC.

**Disclosures:** L.M. Giangregorio, None.

This study received funding from: Ontario Ministry of Health and Long Term Care

## SA369

**See Friday Plenary number F369.**

## SA370

**The Relationship Between Focal Erosions and Generalized Osteoporosis in Postmenopausal Women with Rheumatoid Arthritis: The Osteoporosis in Rheumatoid Arthritis (OPiRA) Cohort Study.** D. H. Solomon<sup>1</sup>, J. S. Finkelstein<sup>2</sup>, N. Shadick<sup>\*1</sup>, M. S. LeBoff<sup>3</sup>, C. Winalski<sup>\*4</sup>, M. Stedman<sup>\*5</sup>, R. Glass<sup>\*1</sup>, M. A. Brookhart<sup>\*5</sup>, M. E. Weinblatt<sup>\*1</sup>, E. M. Gravallese<sup>\*6</sup>.

<sup>1</sup>Rheumatology, Brigham and Women's Hospital, Boston, MA, USA,

<sup>2</sup>Endocrinology, Massachusetts General Hospital, Boston, MA, USA,

<sup>3</sup>Endocrinology, Brigham and Women's Hospital, Boston, MA, USA,

<sup>4</sup>Radiology, Cleveland Clinic Foundation, Cleveland, OH, USA,

<sup>5</sup>Pharmacoepidemiology, Brigham and Women's Hospital, Boston, MA, USA,

<sup>6</sup>Rheumatology, University of Massachusetts Medical Center, Worcester, MA, USA.

After 10 years of rheumatoid arthritis (RA), half of all patients have focal erosions and the risk of fracture is doubled. However, little information exists about the relationship between focal erosions and bone mineral density (BMD). We enrolled postmenopausal women with RA who were not current users (but could be past users) of any osteoporosis medications. Participants underwent DXA testing at the hip and spine. A single radiologist blinded to the DXA results and other data read all the hand films and scored them using the Sharp method. We examined the relationship between BMD and erosions using correlation coefficients and adjusted linear regression models.

Sharp scores and DXA results (hip or spine) were examined for 163 women, mean age was 62.4 years ( $\pm$  9) with an average duration of RA of 13.7 years. Almost all patients were currently using a disease modifying antirheumatic drug. 63% were rheumatoid factor (RF) positive, the median Health Assessment Questionnaire score was 0.7, and the average DAS-28 was 3.8 ( $\pm$  1.6). The erosion score was significantly correlated with the total hip BMD (Spearman R = -0.33,  $p < 0.0001$ ) but not with the lumbar spine BMD (Spearman R = -0.09,  $p = 0.27$ ). Hip BMD was significantly lower in RF positive women (0.83 g/cm<sup>2</sup>) versus RF negative (0.89 g/cm<sup>2</sup>,  $p = 0.02$ ). In multivariable models that included age, BMI, and cumulative oral glucocorticoid dosage, neither total hip nor spine BMD were



significantly associated with focal erosions. The relationship between total hip BMD and erosions appears different in patients with: fewer years of disease ( $<5$  versus  $\geq 5$  years), higher BMI ( $< 28$  versus  $\geq 28$  kg/m<sup>2</sup>), less cumulative oral steroid use ( $< 960$  versus  $\geq 960$ mg), and lower 25-OH vitamin D levels ( $< 20$  versus  $\geq 20$  ng/dl). These results suggest that total hip BMD, but not lumbar spine BMD, is associated with focal erosions among postmenopausal women with RA, but this association disappeared after adjustment. Positive RF is associated with a reduced BMD. This study is limited by the fact that most patients had long-standing well-controlled RA. While BMD and erosions may be correlated bone manifestations of RA, their relationship is influenced by other disease-related factors and anatomic sites.

**Disclosures:** D.H. Solomon, Millenium 3; Biogen/Idec 3.

This study received funding from: NIH-NIA.

## SA371

See Friday Plenary number F371.

## SA372

**Homocysteine Levels in Relation to Physical Performance.** N. M. Van Schoor<sup>\*1</sup>, S. M. F. Pluijm<sup>\*2</sup>, M. Visser<sup>\*1</sup>, S. Simsek<sup>\*3</sup>, Y. Smulders<sup>\*3</sup>, P. Lips<sup>3</sup>.  
<sup>1</sup>EMGO Institute, VU University Medical Center, Amsterdam, Netherlands, <sup>2</sup>Public Health, Erasmus MC, Rotterdam, Netherlands, <sup>3</sup>Internal Medicine, VU University Medical Center, Amsterdam, Netherlands.

Elevated homocysteine concentrations are associated with osteoporotic fractures, but the pathophysiologic pathway is not clear. Elevated homocysteine levels might lead to osteoporosis and/or increased fall risk. There is some evidence that elevated homocysteine levels may lead to decreased physical performance. In this study, the relationship between homocysteine levels and physical performance will be examined.

The study was performed using data of the Longitudinal Aging Study Amsterdam, an ongoing multidisciplinary cohort study that started in 1992/93. The current study was performed in persons who participated in the medical interview in 1995/96, and were born in or before 1930 (aged 65 years and older as of January 1, 1996) (n=1509). Data on homocysteine, physical performance and potential confounders were available for 1212 persons. EDTA plasma samples were obtained in the morning, after subjects had eaten a light breakfast. Total homocysteine levels were measured with the use of a fluorescence polarization immunoassay on an IMx analyzer (Abbott Laboratories). Physical performance was assessed in 1995/96 using three tests: the chair stand, the walking test and the tandem stand (total score 0-12). The data were analyzed with homocysteine levels in quartiles (with the lowest quartile as the reference group) using multiple regression analyses.

In total, 589 men and 623 women were included with a mean age of 75.4 years (standard deviation=6.5). No interaction with age was found. The interaction with sex was significant (p=0.076 for the fourth quartile). Therefore, further analyses were stratified on sex. Both in men and women, physical performance decreased with increasing quartiles of total homocysteine in the univariate analyses. After adjustment for age, years of education, region, body mass index, alcohol use, smoking, cognition, heart disease, peripheral arterial disease, stroke, serum 25-hydroxyvitamin D and creatinine, homocysteine was no longer significantly associated with physical performance in men. In women, the second quartile (beta= -0.512, p=0.076) and third quartile (beta= -0.450, p=0.151) were no longer statistically significant. However, the fourth quartile remained significantly associated with decreased physical performance as compared to the lowest quartile (beta= -0.898, p=0.013).

In conclusion, elevated homocysteine levels were associated with decreased physical performance in elderly women.

**Disclosures:** N.M. Van Schoor, None.

This study received funding from: Ministry of Health, Welfare, and Sports of The Netherlands.

## SA373

See Friday Plenary number F373.

## SA374

**Risk Factors for Bone Loss in the Hip in 70-Year-Old Women: A Nine-Year Follow-up.** G. Sigurdsson<sup>1</sup>, S. L. Gudmundsdottir<sup>\*1</sup>, D. Oskarsdottir<sup>\*2</sup>, O. S. Indridason<sup>\*1</sup>, L. Franzson<sup>\*3</sup>. <sup>1</sup>Department of Medicine, Landspítali - University Hospital, Reykjavik, Iceland, <sup>2</sup>University of Iceland, Reykjavik, Iceland, <sup>3</sup>Genetic and Molecular Medicine, Landspítali - University Hospital, Reykjavik, Iceland.

The purpose of this study was to examine risk factors for longitudinal bone loss in the hip of 70-year-old women.

Bone mineral density (BMD, g/cm<sup>3</sup>) was measured in the femoral neck, trochanter and total hip using dual X-ray absorptiometry (DXA) at five year intervals, in 1997-1998, 2003-2004 and 2007. At each visit, the women also underwent extensive blood test and answered lifestyle questionnaire. Changes in BMD from baseline and its relationship with baseline BMD, weight, lean and fat mass, markers of bone remodeling, hormones, vitamins and lifestyle according to questionnaire as well as weight changes during follow-

up were examined. The relationship between 2003-2004 measurements and subsequent bone loss was also studied.

Of 308 women initially studied, 162 returned for the final visit. Mean follow-up time was 9.12 years. Mean 9-year bone loss was -0.83%/year in the femoral neck, -0.47%/year in the trochanter (p<0.01 compared to femoral neck), and -0.53%/year in the total hip (p<0.01/0.05 compared to femoral neck/trochanter). Lower baseline (1997) S-25(OH)D correlated with increased bone loss in the femoral neck (r=0.21, p<0.01) and baseline trochanter BMD correlated inversely with trochanter BMD loss (r=-0.41, p<0.01). We found no significant relationship between other baseline measurements and hip BMD change. Based on 2003-2004 measurements, significant risk factors for subsequent bone loss were high serum calcium and low number of leisure walks per week for the femoral neck, lower anabolic index (AI= osteocalcin/crosslaps) and lower estradiol for the trochanter and lower AI for total hip. Bone loss in the femoral neck, trochanter and hip was -9.8%, -7.5% and -8.7% in women experiencing weight loss >5% during follow-up but in women who had stable or increased weight the bone loss was -6.4%, -2.6% and -2.9% respectively (p<0.01 for all sites). Weight loss in the first part of follow-up was not related to bone loss in the latter part of follow up.

This study suggest that high 25(OH)D may reduce longitudinal cortical bone loss. Also, it lends further support to the role of physical activity and weight maintenance as important preventive factors for bone loss in the elderly. Moreover, it shows that the anabolic index, which theoretically gives a ratio of bone formation to bone resorption may predict bone loss and this needs to be studied in more detail.

**Disclosures:** S.L. Gudmundsdottir, None.

## SA375

**Teriparatide Improves Trabecular Architecture as Measured by  $\mu$ CT at Simulated *in vivo* Resolution in the Femoral Neck of Ovariectomized Monkeys.** P. Chen<sup>\*1</sup>, B. Gomberg<sup>\*2</sup>, M. S. Westmore<sup>\*1</sup>, K. Krohn<sup>1</sup>, M. Sato<sup>\*1</sup>.  
<sup>1</sup>Eli Lilly, Indianapolis, IN, USA, <sup>2</sup>MicroMRI Inc, Philadelphia, PA, USA.

Teriparatide (TPTD) has been shown to improve bone mass, spatial architecture and bone strength in ovariectomized monkeys. Recently, techniques were developed to further characterize architectural features of trabecular bone at *in vivo* resolution beyond bone volume fraction and conventional histomorphometry. Digital topological analyses (DTA) were developed initially for high-resolution MRI, it is not clear whether it can also be applied to high-resolution images obtained with  $\mu$ CT. We tested the hypothesis that TPTD can improve trabecular bone micro-architecture in the primate femoral neck (FN), as quantified by DTA at simulated *in vivo* resolution. Ovariectomized monkeys were administered 0 (OVX vehicle, n=20), 1.0 (TPTD1, n=19) or 5.0  $\mu$ g/kg/day (TPTD5, n=20) TPTD for 18 months. At necropsy, L4-6 and proximal femora were excised and adjacent or contralateral bones were processed for histomorphometry and biomechanical analyses for each monkey.  $\mu$ CT images of the FN were acquired *ex vivo* at 15  $\mu$ m isotropic voxel size. Conventional histomorphometry analyses were published previously (Sato et al. 2004). Images were resampled to 75  $\mu$ m isotropic to simulate *in vivo* resolution, and then analyzed by DTA, which comprises thresholding, thinning, and topological classification. The analysis identifies surfaces, profiles, curves, and their mutual junctions representing trabecular variations of plates, rods, and their junctions after thinning, and the DTA parameters reflect the micro-architectural integrity of the trabecular network. TPTD significantly improved trabecular architecture measured at *in vivo* resolution by both histomorphometric and DTA endpoints relative to OVX. Additionally, *in vivo* resolution DTA endpoints correlated significantly with bone strength in both lumbar vertebra and FN. These results show that TPTD improves the trabecular architecture in the FN of primates using DTA analysis at *in vivo* data resolution. The data also demonstrate that DTA parameters correlate well with measures of trabecular bone strength at the vertebra and FN. Further clinical studies are needed to confirm the simulated results shown here.

Architecture Parameters†	OVX	TPTD1	TPTD5	Correlation Coefficient	
				Vertebral Strength	Femoral Neck Strength
Histomorphometric parameters					
Trabecular bone volume	0.23±0.05	0.36±0.09*	0.41±0.05*	0.70**	0.64**
Trabecular number	1.43±0.39	2.01±0.50*	2.03±0.42*	0.59**	0.48**
Trabecular separation	0.58±0.18	0.35±0.13*	0.30±0.08*	0.66**	0.56**
Trabecular thickness	0.17±0.02	0.18±0.03*	0.21±0.04*	0.28**	0.29**
Topological parameters					
Topological skeleton density	0.11±0.03	0.16±0.04*	0.17±0.03*	0.65**	0.56**
All surface voxel density (10 <sup>2</sup> )	10.48±2.93	15.44±4.02*	16.02±3.20*	0.65**	0.56**
All curve voxel density (10 <sup>2</sup> )	1.01±0.98	0.53±0.50	0.42±0.25*	-0.41**	-0.31**
All junction voxel density (10 <sup>2</sup> )	0.78±0.38	1.81±0.79*	2.39±0.67*	0.67**	0.59**
Surface to curve ratio (10 <sup>3</sup> )	2.78±4.02	6.25±5.85*	5.73±3.80*	0.52**	0.42**
Topological erosion index	0.32±0.11	0.31±0.06	0.27±0.04*	-0.26**	-0.36**

†Data were expressed as mean ± SD. \* P<0.05 compared to OVX; \*\*P<0.05 for correlation coefficients.

**Disclosures:** P. Chen, Eli Lilly 5.

## SA376

See Friday Plenary number F376.

## SA377

**Dietary Strontium (Sr) in a Model of Established Osteopenic Rats Reduce the Levels of 25hydroxyvitamin D.** M. M. S. Gonzales Chaves<sup>\*1</sup>, C. Marotte<sup>\*1</sup>, G. G. Pellegrini<sup>\*2</sup>, S. M. Friedman<sup>\*3</sup>, A. Pighin<sup>\*4</sup>, M. C. de Landeta<sup>\*5</sup>, S. N. Zeni<sup>1</sup>. <sup>1</sup>Sección Osteopatías Médicas, Hospital de Clínicas, Universidad de Buenos Aires, Buenos Aires, Argentina, <sup>2</sup>Bioquímica General y Bucal, Facultad de Odontología, UBA, Buenos Aires, Argentina, <sup>3</sup>Bioquímica General y Bucal., Facultad de Odontología, UBA, Buenos Aires, Argentina, <sup>4</sup>Cs.Básicas. Analítica, Universidad Nacional de Luján, Buenos Aires, Argentina, <sup>5</sup>Cs.Básicas.Analítica, Universidad Nacional de Luján, Buenos Aires, Argentina.

Previously we found that vitamin D (vitD) status (i.e.normal or insufficient) interferes with bone mass recovery from bisphosphonate therapy in a model of OVX rats with established osteopenia (Bone 39: 837,2006). Using this model we investigated bone recovery from SrRanelate (SrRa) therapy. After 15 days post surgery and during 45 days, 20 OVX rats fed a diet containing 200IU% D (+D) and 20 a diet lacking vitD (-D) to obtain osteopenic/vitD depleted or depleted groups. Thereafter, 10 -D and 10 +D OVX rats were treated with vehicle (-RaSr) or RaSr (900mg/kg/d) (+RaSr) for 45 days to obtain 4 subgroups (table). A SHAM group was run as control. At 0, 60 and 105 days total skeleton BMD and BMC(teBMC) were assessed by DXA, 25OHD by RIA (Diasorin) and serum Ca and phosphorus (P) by atomic absorption spectrophotometry (AAS) and colorimetric methods, respectively. At day 105, rats were sacrificed and tibia total bone volume (BV/TV) and Sr in bone were determined by histology and AAS, respectively. Results (mean±SE)

Different letter indicates a p<0.05. There were no differences in teBMC, bony Sr and BV/TV between +SrRa treated -D or +D groups. BV/BT in +RaSr was 50% higher than in -SrRa groups but only represented a 10% of SHAM level. The 25OHD levels were significantly lower in +D+RaSr than in +D-RaSr rats. Conclusions: under our experimental conditions Sr may be incorporated into the formed bone independently of vitamin D status. We surprisingly found a diminution in serum 25OHD in +D+SrRa treated rats compared to +D-RaSr groups suggesting, as previously found in chicks (this effect on rats was not previously reported), an inhibition of vitD metabolism to its functional metabolite of nutritional status, 25OHD. (J Biol Chem 247: 5520, 1972).

**Disclosures:** M.M.S. Gonzales Chaves, None.

This study received funding from: Grant PIP 6483, CONICET.

## SA378

**Aging Dependent and Independent Effects of b2 Adrenergic Receptor Signaling on Bone Formation Induced by Intermittent PTH Treatment in Female Mice.** R. Hanyu<sup>1</sup>, Y. Saita<sup>\*1</sup>, J. Nagata<sup>1</sup>, Y. Izu<sup>1</sup>, H. Hemmi<sup>1</sup>, S. Takade<sup>2</sup>, Y. Ezura<sup>1</sup>, H. Kurosawa<sup>\*3</sup>, M. Noda<sup>1</sup>. <sup>1</sup>Dept Molecular Pharmacology Medical Research Institute Tokyo Medical and Dental University, Tokyo, Japan, <sup>2</sup>Department of Orthopedics, Tokyo Medical and Dental University, Tokyo, Japan, <sup>3</sup>Department of Orthopedics, Juntendo University school of Medicine, Tokyo, Japan.

Intermittent administration of PTH enhances bone mass levels in postmenopausal osteoporosis patients. This enhancement by PTH on bone mass is modulated by the sympathetic tone through its action on b2 adrenergic receptor. However, whether aging could affect such action of PTH in the presence or absence of sympathetic tone has not been known. We therefore examined the effects of the presence and absence of b2 adrenergic receptor on the anabolic action of intermittent PTH treatment in young adult mice(9w) and compared the results to those in aged adult mice(54w). Cancellous bone mass was enhanced by the treatment with PTH in aged mice, however there was only a trend for the increase in young adult mice. Base line levels of such fraction of bone mass in cancellous bone were about 15% in young while they were about 5% for the aged animal. Interestingly, the enhancement of PTH was approximately 80% in aged mice, but such modulation was only about 30% in young adult mice. In the absence of b2 adrenergic receptor the basal levels of fraction of bone volume were higher than wild type, and in contrast to wild type, PTH no longer enhanced the bone mass levels in both young and aged adult mice. Analysis of the axial bone (vertebrae) also revealed similar trend. However, in this case young adult wild type animals responded to PTH (p< 0.05). Such trend was observed but not statistically significant in aged adult mice. In the absence of b2 adrenergic receptor base line levels were higher than wild type aged mice but such difference was less in young adult mice. Intermittent PTH treatment in the absence of b2 adrenergic receptor was no longer observed in both young and aged adult mice. In contrast to the cancellous bone, cortical bone volume as well as the bone mineral density, which mostly represent the cortical compartment, were similar regardless of the age on the treatment with PTH in the absence or presence of b2 adrenergic receptor. Mean cortical bone thickness was similar. However in terms of cortical bone volume, aged KO mice tended to exhibit higher bone mass levels compared to the young adult KO or WT mice. In conclusion, our data indicated that there were the age dependent and independent effects of the presence or absence of b2 adrenergic receptor signaling on intermittent PTH treatment for its anabolic action.

**Disclosures:** R. Hanyu, None.

## SA379

**Prior Treatment with Vitamin K<sub>2</sub> Significantly Improves the Efficacy of Risedronate.** Y. Mikuni-Takagaki<sup>1</sup>, Y. Matsumoto<sup>\*2</sup>, Y. Kozai<sup>\*2</sup>, K. Miyagawa<sup>\*1</sup>, K. Naruse<sup>\*3</sup>, H. Wakao<sup>\*2</sup>, R. Kawamata<sup>\*2</sup>, I. Kashima<sup>\*2</sup>, T. Sakurai<sup>\*1</sup>. <sup>1</sup>Functional Biology, Kanagawa Dental College, Yokosuka, Japan, <sup>2</sup>Maxillofacial Diagnostic Science, Kanagawa Dental College, Yokosuka, Japan, <sup>3</sup>Orthopedic Surgery, Kitasato University School of Medicine, Sagami-hara, Japan.

The objective of this study was to determine the best combinatory administration method of bisphosphonate (risedronate) with vitamin K<sub>2</sub> (MK-4) to improve the strength of osteoporotic bone.

Female 9-week ICR mice were given ovariectomy or sham operation. Thirty days later, they were divided into treatment groups (n=8), based on the 16-week daily administration of risedronate (R) and/or MK-4 (K). Ovariectomized (OVX) and sham operated (sham) mice groups and the groups of ovariectomized mice given the treatments were: daily concomitant administration of R and K throughout (2RK), alternate-day administration throughout (R→K), 8 weeks of R followed by 8 weeks of K (R→K), K followed by R (K→R), or given R and then withdrawn (R→w/dr), K and then withdrawn (K→w/dr), concomitant administration and then withdrawn (RK→w/dr). Mice were terminated after 8- or 16-week treatment. Femurs were subjected to analyses of bone mineral density (BMD) and structure by peripheral quantitative computed tomography (pQCT) and micro focus X-ray tube computed tomography (μCT). Quality of bone was also examined by confocal laser Raman spectroscopic measurements. The serum levels of metabolic markers were measured at 0 (before the treatments), 8, 12, and 16 weeks. Three point bending and compression tests were carried out to assess the mechanical properties of femoral diaphyses and distal metaphyses.

At the 8th week mid point, the trend of improved bone strength was suggested in groups treated with risedronate or MK-4 alone. Quality of bone, judged from the increased matrix-to-mineral ratio and posttranslational processing of collagenous protein, was significantly improved by treating mice with MK-4 alone. Concomitant administration, RK, did not provide equivalent parameters. At the 16th week, cortical BMD in K→R and R→w/dr group femoral diaphyses showed significantly higher values than in the control OVX group. Trabecular structure of K→R and K→w/dr femurs was significantly improved in comparison to the OVX controls. Mechanical tests showed significant improvement of femur strength only in K→R in both diaphyses and metaphyses. Risedronate treatment after MK-4 (K→R) seems to have prevented the CTx rise, which was observed after the withdrawal of MK-4 in K→w/dr.

In conclusion, sequential administration (K→R) was superior to other combinations in treating osteoporotic model mice. Prior treatment with vitamin K<sub>2</sub> significantly improved the efficacy of risedronate by improving the quality of bone matrix.

**Disclosures:** Y. Mikuni-Takagaki, None.

## SA380

**Withdrawn**

## SA381

**Toremifene Inhibits Osteoclast Activity in vitro and Prevents Orchiectomy-induced Bone Resorption in Male Rats.** S. Raghoebari<sup>1</sup>, J. T. Dalton<sup>\*1</sup>, N. Doyle<sup>2</sup>, J. Jolette<sup>2</sup>, S. Y. Smith<sup>2</sup>, K. A. Veverka<sup>1</sup>, R. Narayanan<sup>\*1</sup>. <sup>1</sup>Preclinical Research, GTx, Inc, Memphis, TN, USA, <sup>2</sup>Preclinical Research, CRL, Montreal, QC, Canada.

Recent clinical trials in men undergoing androgen deprivation therapy (ADT) for prostate cancer indicated that toremifene (TOR), a SERM, elicited anti-osteoporotic effects. However, the mechanism for this bone protective effect of TOR in males undergoing ADT is not clear. Using orchiectomy-induced bone resorption in adult male rats and rat bone marrow cell culture in the presence of M-CSF and RANKL, we evaluated the mechanism of TOR action in bone. Estradiol was used in vitro for comparison. For the in vivo study, ~9 mo old male rats were randomly assigned to each of five groups containing 10 animals each: baseline, Sham, ORX control and ORX groups treated with TOR at 10 or 30 mg/kg/day. TOR was administered once daily by gavage for 12 months starting one day post-ORX. Biochemical markers of bone resorption (urinary DPD and serum CTx) were evaluated. Cortical (tibia diaphysis) and cancellous (L2 and tibia metaphysis) bone regions were analyzed by histomorphometry. In vitro, TOR at 10<sup>-6</sup> to 10<sup>-8</sup> M significantly inhibited osteoclastogenesis (p<0.05 vs. vehicle control) as evidenced by lower number of TRAP-positive multinucleated osteoclasts in bone marrow cultures. In rats, ORX-induced bone turnover as evidenced by increases in CTx and decreases in DPD was suppressed by treatment with TOR at 10 and 30 mg/kg/day. Histomorphometric evaluations of cancellous bone in Sham animals revealed decreases in fractional bone volume (BV/TV) relative to baseline, with further decreases in ORX rats, primarily due to decreases in trabecular number (Tr.N) and separation (Tr.S). These structural changes were associated with marked increases in bone formation rates (BFR) and mineralizing surfaces (MS/BS) consistent with accelerated bone turnover. TOR at 10 and 30 mg/kg consistently reduced Oc.S/BS at both tested sites, demonstrating its bone antiresorptive effects. At the tibia diaphysis, ORX animals showed decreased cortical bone area (Ct.Ar) and width (Ct.Wi) compared to aged Sham males principally due to an increased medullary cavity area (Me.Ar). ORX increased endocortical labeled surface (Ec.L.Pm/Ec.Pm) and BFR but reduced the periosteal labeled surface (Ps.L.Pm/Ps.Pm) significantly (p<0.05). TOR treatment canceled the ORX-induced effects on the periosteal and endocortical surfaces, consistent with reduced bone turnover. In summary, toremifene inhibited



osteoclastogenesis in vitro and showed antiresorptive activity in the bones of orchidectomized male rats, providing a mechanistic basis for its bone sparing effects in men on ADT.

**Disclosures:** S. Raghoebar, *GTxInc 3*.  
This study received funding from: *GTx*.

## SA382

**Raloxifene Ameliorates Detrimental Collagen Cross-link Formation in Bone from an Ovariectomized Rabbits With or Without Hyperhomocysteinemia.** M. Saito, K. Marumo\*, Y. Kida\*, C. Ushiku\*, S. Soshi\*, A. Shinohara\*. Orthopaedic Surgery, Jikei University School of Medicine, Tokyo, Japan.

Collagen cross-links are a determinant of bone quality. Cross-links involve two different types; enzymatic divalent immature and trivalent mature cross-links and glycation induced crosslinking (AGEs; pentosidine). We first reported in a human study that hyperhomocysteinemia (HHCY) in patients with an osteoporotic fracture might lead to detrimental crosslinking in bone. Interestingly, homocysteine interferes with normal collagen cross-link formation. Raloxifene (RLX) is thought to ameliorate poor bone quality in osteoporosis. However, there is presently no evidence to demonstrate whether RLX alters the collagen cross-link formation in estrogen-deficiency either with or without HHCY. In order to clarify this issue, we established a rabbit model in which collagen abnormalities were induced by an ovariectomy (OVX) with or without a HHCY and investigated the effects of RLX on collagen cross-link formation in the bone. We divided mature New Zealand white rabbits into the following 6 groups (n=6-9 per group): 1) sham operation, 2) sham+ 1% methionine (Met) diet, 3) OVX only, 4) OVX+ RLX (10mg/kg/day) treated group, 5) OVX+ 1% Met diet, 6) OVX+1% Met diet +RLX. RLX or vehicle was administered by oral gavage for 16 weeks after an initial 16 weeks of OVX or OVX+ 1% Met diet. The femur, vertebra, urine, and blood were collected. We measured cross-link contents in bone by our established HPLC method. Homocysteine levels in the Met diet groups were significantly higher (p<0.001) than the normal diet groups. Met diet without OVX resulted in a significant reduction in enzymatic cross-link content (79-85%, p<0.01) and a marked increase in the pentosidine content (120-179%, p<0.05). The OVX group without the Met diet showed a significant reduction in enzymatic cross-links to the same extent as the Met diet group, whereas the increase in pentosidine was weaker than Met diet group. The OVX+Met diet group showed the most severe detrimental cross-link patterns in the bone. Enzymatic cross-link formation in the OVX +RLX group and the OVX+Met diet +RLX group was restored to the same level as that of the sham group. Pentosidine content in the bone from the RLX treated groups with OVX showed no significant difference in comparison to the sham group. These findings suggest that 1) not only OVX, but also HHCY induced collagen cross-link abnormalities as well as human osteoporosis, as reported previously, and 2) RLX may increase enzymatic cross-links, while reducing either the glycation or oxidation induced pentosidine in both OVX and HHCY in the OVX rabbit model. In conclusion, RLX may improve bone quality via the alteration of enzymatic and glycation induced cross-links of collagen.

**Disclosures:** M. Saito, *None*.

## SA383

See Friday Plenary number F383.

## SA384

**Effect of Raloxifene and Alfacalcidol on Bone and Joint Pain Assessed by Fall of Skin Impedance (Electroalgometry).** T. Fujita<sup>1</sup>, M. Ohue<sup>2</sup>, Y. Fujii<sup>3</sup>, Y. Takagi<sup>3</sup>. <sup>1</sup>Medicine, Calcium Research Institute, Kishiwada, Japan, <sup>2</sup>Orthopedic Surgery, Katsuragi Hospital, Kishiwada, Japan, <sup>3</sup>Medicine, National Hospital System Hyogo Chuo Hospital, Sanda, Japan.

By measuring fall of skin impedance in response to exercise loading using an electroalga - meter (EAM), attempts were made to assess the effect of raloxifene and alfacalcidol on back or knee pain in postmenopausal patients with osteoporosis and/or osteoarthritis against alfacalcidol alone. Subjective pain was simultaneously recorded on a visual rating scale (VRS) dividing the distance between severe and unbearable pain at 100 and no pain at 0. Patients consulting Osteoporosis and Osteoarthritis Clinic of Katsuragi Hospital giving consent to the study after a full explanation on the purpose, method and possible risk of the study were asked to join Group EA to be given 60mg raloxifene and 1µg alfacalcidol or Group A to be given only 1µg alfacalcidol daily in chronological sequence. Exercise loading consisted of standing from a sitting position on a chair and knee bending mainly for knee loading (ST), walking about 30 steps on a flat corridor, climbing up about 10 stairs and down about 10 stairs for combined knee and spine loading (WK), and lying flat on an examining table and standing up again mainly for spine loading (LY). On average of all exercise loading, EAM showed significantly superior analgesic effect in EA than A (p=0.0239), but subjective assessment by VRS failed to do so (p=0.0739). On standing up, EA significantly more efficiently decreased pain (p=0.0017) than A according to VRS, but less clear difference was noted by EAM (p=0.0531). On WK, on the contrary, significant improvement in EA than A was noted by EAM (p=0.110), but only a tendency of improvement was noted on VRS. On climbing up stairs, only EAM revealed a significant improvement in Group EA, but not in A. On LY, only EAM detected significantly better analgesic effect of EA over A (p=0.048). Instead of the complete dependence of pain evaluation on subjective judgement, additional assessment by using an objective and quantitative electroalgometry apparently made it possible to analyze the mechanism of

pain sensation and action of analgesic agents in more detail. Electroalgometry appearing to be especially sensitive to measure pain on walking confirmed the analgesic effect of raloxifene with alfacalcidol on pain associated with osteoporosis and osteoarthritis.

**Disclosures:** T. Fujita, *None*.

## SA385

**Bazedoxifene (BZA) in Combination with Conjugated Estrogens (CE) Improves Bone Mass and Strength in the Ovariectomized (OVX) Rat.** E. Viassero<sup>1</sup>, S. Y. Smith<sup>1</sup>, L. Chouinard<sup>1</sup>, R. Samadfam<sup>1</sup>, C. H. Turner<sup>2</sup>, D. Minck<sup>3</sup>, B. Komm<sup>3</sup>. <sup>1</sup>Charles River Laboratories, Montreal, QC, Canada, <sup>2</sup>Indiana University, Indianapolis, IN, USA, <sup>3</sup>Wyeth Research, Collegeville, PA, USA.

Estrogen replacement therapy reduces accelerated bone remodelling, prevents bone loss and increases bone mass (particularly at cancellous bone sites), but is also associated with limiting uterotrophic effects. SERM's bind to estrogen receptors and are intended to prevent OVX-induced bone loss with a favourable influence on lipid profile and an absence of uterotrophic effects. In this study, the combined effects of co-administration of the SERM BZA with CE were evaluated. BZA/CE was administered by oral gavage to OVX Sprague-Dawley rats (24/group) once daily for 52 weeks. BZA was dosed at 0.1, 0.3, or 1.0 mg/kg/day and 2.5 mg/kg/day CE. Additional groups received BZA (0.3 mg/kg/day) or CE alone. OVX and Sham control groups received vehicle. Clinical serum chemistries were measured and bone turnover was monitored using biochemical markers and dynamic histomorphometry (animals were injected with two fluorochrome labels prior to bone harvesting). Bone densitometry (DXA and pQCT) was measured at the lumbar spine, femur and tibia. Histomorphometry was performed on the tibial diaphysis, L1 and L2 vertebra. Destructive testing was performed by 3-point bending of the femur diaphysis, shearing of the femur neck, and compression of lumbar vertebral specimens. Microscopic evaluations were performed on reproductive tissues. BZA/CE prevented OVX-induced increases in serum cholesterol and at 0.3/2.5 and 1.0/2.5 mg/kg/day partially inhibited the uterotrophic effect observed with CE alone. At all dose levels BZA/CE decreased bone turnover, completely prevented bone loss due to OVX and preserved bone mass and strength to at least Sham control levels. The high dose combination was associated with increases in biochemical markers of bone formation consistent with preservation of bone mass and slight increases in trabecular bone mass compared to Shams, suggesting this combination may have a superior effect on bone. There were trends that biomechanical competency was also improved at the lumbar spine and femur diaphysis. Overall, protective effects on bone were observed at both appendicular (tibia, femur) and axial (lumbar spine) sites in cancellous and cortical bone. No deleterious microscopic effects (bone quality and/or mineralization) were noted after daily treatment at doses up to BZA/CE 1.0/2.5 mg/kg/day. Combination treatment with BZA and CE may be an effective clinical treatment to prevent the effects of estrogen depletion and maintain bone mass and strength, while reducing serum lipid levels and the uterotrophic effects associated with estrogen treatment alone.

**Disclosures:** B. Komm, *Wyeth Research employee 5*.  
This study received funding from: *Wyeth Research*.

## SA386

**IC162, a New Flavonoid, Preserves Bone Mass and Microarchitecture without Affecting Uterine Weight in Ovariectomized (OVX) Rats.** H. Xie\*, E. Liao\*. Institute of Endocrinology & Metabolism, The Second Xiangya Hospital of Central South University, Changsha, China.

Flavonoids including genistein have structural similarity to estrogen and have been reported to prevent bone loss caused by estrogen deficiency. IC162 is a new flavonoid compound isolated from vegetable sources. The present study was undertaken to investigate the effects of IC162 on bone and uterus under conditions of estrogen deficiency caused by ovariectomy (OVX). Female Sprague-Dawley rats were randomly divided into six groups: (I) sham operation + vehicle treatment (sham, n = 8); (II) OVX + vehicle treatment (V, n = 9); (III) OVX + 10 µg/kg/d 17β-estradiol treatment (E<sub>2</sub>, n = 8); (IV) OVX + 50mg/kg/d genistein treatment (Gen, n = 7); (V) OVX + 33 µg/kg/d IC162 treatment (TL, n = 10); (VI) OVX + 330 µg/kg/d IC162 treatment (TH, n = 8). At 8 months of age, the rats were either sham-operated or OVX, and then treated daily by intraperitoneal injection of vehicle, E<sub>2</sub>, genistein, or IC162. After 8 weeks of treatment, bone mineral density (BMD) and bone mineral content (BMC) of the vertebrae and femur were determined by Dual-energy X-ray absorptiometry (DEXA) and microcomputed tomography (µCT), and uterine weight was measured. Vehicle-treated OVX rats showed significant decreases in BMD, BMC, trabecular bone volume (Tb.BVf), trabecular thickness (Tb.Th) and cortical thickness (Cr.Th), and a significant increase in trabecular separation (Tb.Sp) compared to sham controls. These alterations were prevented by treatment of OVX rats with IC162 or E<sub>2</sub>. Genistein treatment had the weakest effect on improving these parameters. In addition, treatment with E<sub>2</sub> increased uterine weight to the value of sham controls in OVX rats. Treatment with genistein partially restored uterine weight in OVX rats. However, IC162 had no effect on uterine weight. We conclude that IC162 is efficacious for the preservation of bone mass but does not adversely affect uterine. Hence, our data strongly suggest that IC162 merits investigation as a potential therapeutic alternative to hormone replacement for osteoporosis.

**Disclosures:** H. Xie, *None*.

## SA387

**A Juvenile Murine Model of Ovariectomy-induced Trabecular and Cortical Osteoporosis.** L. Oste<sup>\*1</sup>, P. L. Salmon<sup>2</sup>, G. Kerckhofs<sup>\*3</sup>, L. Van Rompaey<sup>\*1</sup>, G. Dixon<sup>1</sup>. <sup>1</sup>Galapagos plc, Mechelen, Belgium, <sup>2</sup>SkyScan N.V., Kontich, Belgium, <sup>3</sup>Department of Metallurgy and Materials Engineering, Catholic University of Leuven, Leuven, Belgium.

**Introduction.** The ovariectomised mouse is routinely used as a model of osteoporosis, and commonly a mature adult age such as 4 months at surgery is used. Here we validate a murine ovariectomy model in young (6 week) growing mice in three strains, evaluating trabecular and cortical osteopenia by micro-computed tomography (micro-CT) bone morphometry.

**Materials and Methods.** Mice from the BALBc, C3H and C57BL/6 strains were either ovariectomised or sham operated at 6 weeks age, and femurs and tibias were harvested from them five weeks later. Micro-CT morphometric analysis of these bones was carried out on the distal femur and proximal tibia.

**Results.** All three strains showed substantial trabecular bone loss due to ovariectomy, slightly less in BALBc than in the C3H or C57BL/6 strains. Architectural parameters such as Trabecular pattern factor and fractal dimension showed profound structural change in the C3H and C57BL/6 strains but less change in BALBc. All three strains showed significant cortical osteopenia in the ovariectomised groups but with a different pattern between strains: while the cortex expanded in BALBc and C3H mice both periosteally and endosteally, in the C57BL/6 mice the periosteum contracted slightly. Cortical porosity showed a large ovariectomy-related increase in the BALBc and C3H strains but less change in C57BL/6.

**Conclusions.** Comparing the results to published data for the more mature mouse OVX model, OVX-related osteopenia in both trabecular and cortical bone is much more pronounced and significant in the younger mice. Older mouse bone morphometry is compromised by sparse trabecular bone. The growing mouse OVX model is justified by evidence that the changes seen are directly linked to withdrawal of estrogen, not an epiphenomenon of growth, and that, architecturally, these changes are generally similar in young and old age. Specific cortical OVX-related changes namely thinning, periosteal and endosteal expansion, endocortical trabecularisation and increased porosity, all associated with human perimenopausal femoral osteoporosis, were all seen in this growing mouse OVX model. Thus a growing mouse OVX model may be useful in studying effects of estrogen on bone throughout female adulthood.

**Disclosures:** *P.L. Salmon, SkyScan N.V. 3.*  
*This study received funding from: SkyScan.*

## SA388

**Skeletal Effects of a Fibroblast Growth Factor Agonist (F2A) in Ovariectomized Rats.** S. E. Franz<sup>\*1</sup>, M. K. Altman<sup>\*1</sup>, J. N. Stabley<sup>\*2</sup>, J. I. Aguirre<sup>1</sup>, M. E. Leal<sup>1</sup>, X. Lin<sup>\*3</sup>, P. O. Zamora<sup>\*3</sup>, T. J. Wronski<sup>1</sup>. <sup>1</sup>Physiological Sciences, University of Florida, Gainesville, FL, USA, <sup>2</sup>Applied Physiology and Kinesiology, University of Florida, Gainesville, FL, USA, <sup>3</sup>BioSurface Engineering Technologies, Inc, Rockville, MD, USA.

F2A is a synthetic peptide designed as an agonist for FGF2. It binds with high affinity to FGF receptor 1. A previous study showed that F2A, when applied locally, accelerated bone repair in a rabbit experimental model of tibial fractures. The purpose of the current study was to determine if systemically-administered F2A had skeletal effects in ovariectomized (OVX) rats and adverse side effects in non-skeletal tissues. Groups of sham-operated and OVX rats were maintained untreated for six weeks postovariectomy to allow for cancellous bone loss to occur in the latter animals. These groups (N=6) were then treated IP with vehicle or varying doses of F2A (0.3, 1.0, or 3.0 mg/kg) for 14 consecutive days. All rats were injected SC with declomycin and calcein 10 and 3 days prior to necropsy, respectively, in order to measure surface-referent, bone formation rate. At necropsy, hematocrit was found to be normal in all F2A-treated OVX rats. Histological samples of the liver, kidney, lung, and heart showed no significant abnormalities in these animals. The proximal tibial metaphyses of vehicle-treated OVX rats were characterized by cancellous osteopenia and increased bone turnover compared with vehicle-treated control rats. F2A did not increase tibial cancellous bone or osteoid volume at any dose tested, but OVX rats treated with 1 mg/kg did exhibit a significant 25% increase in osteoclast surface, an index for bone resorption. Normal fluorochrome labeling of bone occurred, which indicates that mineralization of osteoid was not impaired by F2A, as was previously observed in FGF2-treated OVX rats. Furthermore, all 3 doses of F2A induced a modest increase in cancellous bone formation rate. In contrast, periosteal bone formation in the tibial diaphysis was unaffected by F2A treatment. Based on our past studies with systemically-administered FGF2, the skeletal effects of F2A are more subtle than those of FGF2. F2A appears to induce a modest increase in both bone resorption and formation, but these skeletal processes are in balance so that cancellous bone mass is not increased in F2A-treated OVX rats. However, F2A did not induce the anemia and impaired bone mineralization seen with FGF2. The increase in cancellous bone formation and the lack of side effects is supportive of F2A for local bone fracture applications. Therefore, locally-delivered F2A appears to have a favorable pharmacokinetic profile, and yet has minimal side effects even if the peptide circulates systemically.

**Disclosures:** *S.E. Franz, None.*  
*This study received funding from: Biosurface Engineering Technologies, Inc.*

## SA389

**See Friday Plenary number F389.**

## SA390

**The Use of Alternative Medicine for Treating Osteoporosis in Korea.** S. Han<sup>\*</sup>, J. Park<sup>\*</sup>, Y. Park<sup>\*</sup>, E. Bae<sup>\*</sup>, Y. Kim<sup>\*</sup>. Department of Family Medicine, Dong-A University Hospital, Pusan, Republic of Korea.

As life expectancy increases, the interest in osteoporosis is now an international trend. People in Korea are becoming more and more interested in osteoporosis, but many patients still prefer alternative medicines such as health foods than going to the hospital. The authors of this study aimed at surveying what the Korean patients select as a treatment for osteoporosis and wanted to offer the information to doctors.

The study took place in 3 cities of Korea from June, 2007 to December, 2007. The objectives were 1,524 randomly selected postmenopause women between the age of 50 and 70, and a questionnaire was performed.

74% of the objectives had bone mineral densitometry(BMD) tests. 36% of them were diagnosed with osteoporosis, and 64% had been diagnosed with osteopenia.

Among them, 83% had experienced one or more alternative medicine such as health foods. Safflower seed(64%), glucosamine(43%), calcium complex food(41%), chlorella(29%), vitamin D enriched food(25%), herb medicine(21%), ginseng steamed red(19%), plant estrogen(18%), soybean protein food(15%), acupuncture(6%), physical therapy such as cupping(5%) were included in the descending order.

The mean term they took the medications was 7.5 months.

The satisfaction on the alternative medicines was the highest in safflower seed (53%), and calcium complex food(42%), ginseng steamed red(41%), plant estrogen(35%), herb medicine(28%) followed. The satisfaction on alternative medicine itself (42%) was slightly higher than treatment from doctors(38%).

Many patients use alternative medicine for the treatment of osteoporosis, and they are highly satisfied with it. It would be very helpful if the doctors take interest in alternative medicine in treating osteoporosis and provide the patients with accurate information.

**Disclosures:** *S. Han, None.*

## SA391

**See Friday Plenary number F391.**

## SA392

**Strontium Ranelate and Teriparatid (PTH 1-34) Enhance Fracture Healing in Osteoporotic Sprague Dawley - Rats.** B. Habermann<sup>\*1</sup>, G. Olender<sup>\*2</sup>, C. Eberhardt<sup>\*1</sup>, P. Augat<sup>\*2</sup>, A. A. Kurth<sup>\*1</sup>. <sup>1</sup>Orthopedic Hospital Frankfurt, Frankfurt, Germany, <sup>2</sup>Biomechanical Research Laboratory Murnau, Murnau, Germany.

Strontium ranelate and PTH 1-34 both result in an increased formation of bone when given to patients with osteoporosis. The purpose of the study was to elaborate if strontium ranelate and PTH 1-34 affect fracture healing when given the first time after an osteoporotic fracture and if they show any benefit in stability of the callus.

45 Sprague Dawley rats were ovariectomized at the age of 12 weeks. After 12 weeks, an osteopenia was diagnosed using Dual x-ray energy (DXA). Then, a standardized closed mid-diaphyseal fracture of the femur stabilized by a K-wire was produced. Afterwards, the animals were randomly put into three groups. The first group was substituted with 0.9% NaCl s.c., the second received 20 µg PTH 1-34 3x/week s.c. and the last group was treated with 600 mg strontium ranelate per kg body weight orally. After 28 days the bones were excised. The samples were subsequently scanned using MicroCT and, afterwards, torsion testing on the bones was done.

Strontium ranelate and PTH 1-34 both showed a significant increase in bone volume of the callus. (strontium ranelate +46.4%, p<0.05; PTH 1-34 +31.9%, p<0.05) though difference among them was not significant. This was also expressed in callus tissue volume (strontium ranelate +32.4%, p<0.05, PTH 1-34 +6%, p>0.05) while the increase under substitution with strontium was significantly higher (+ 24.8%, p<0.05). Torsion to bone fracture was significant higher under substitution with strontium ranelate while substitution with PTH 1-34 showed no difference.

Strontium ranelate and PTH 1-34 are both considered to be anabolic when given to patients with osteoporosis. Intermittent substitution of PTH 1-34 causes an increase in bone mineral density by an enhancement of osteoblast proliferation. Strontium ranelate does not only increase collagen synthesis and enhance the activity of osteoblasts by activating the calcium sensing receptor but also causes a downregulation of osteoclast activity by reducing preosteoclast differentiation. There is evidence that it also modifies the OPG/RANK(L) system.

Our results support that both strontium ranelate and PTH 1-34 may enhance fracture healing with an increase in callus tissue and bone volume. Callus in strontium substituted animals seems to be more resistant to torsion in comparison to sham-treated animals or animals being treated with PTH 1-34. Strontium had significant better results in torsion testing to the fracture point. This may be an effect from a higher callus volume and callus bone volume / tissue volume.

The animal experiments were approved by the Regierungspräsidium Darmstadt, Germany (F-119/04). This study was supported by the Elsbeth Bonhoff Stiftung.

**Disclosures:** *B. Habermann, None.*  
*This study received funding from: Elsbeth Bonhoff Stiftung.*

## SA393

**QUS, BMD and QCT in Women with Established Osteoporosis Treated with Teriparatide.** C. Cepollaro<sup>1</sup>, R. Monaco<sup>\*1</sup>, F. Cioppi<sup>\*1</sup>, L. Masi<sup>1</sup>, A. Falchetti<sup>1</sup>, G. Marcucci<sup>\*1</sup>, G. Caracchini<sup>\*2</sup>, G. D'Elia<sup>\*2</sup>, A. Tanini<sup>\*1</sup>, M. Brandi<sup>1</sup>.

<sup>1</sup>Department of Internal Medicine, University of Florence, Florence, Italy, <sup>2</sup>SOD Radiodiagnostica 1 CTO, Azienda Ospedaliero-Universitaria Careggi, Florence, Italy.

This study was aimed to evaluate the effect of a 18-month teriparatide treatment on bone mineral density (BMD), quantitative ultrasound (QUS) and quantitative computed tomography (QCT) in women with established osteoporosis. We studied 31 women with established osteoporosis previously treated with antiresorptive drugs. They were given teriparatide (Forsteo, Eli Lilly) by subcutaneous injection, at the dose of 20 µg once daily, plus calcium and Vitamin D. In all subjects BMD at lumbar spine (BMD-LS), femoral neck (BMD-FN) and total femur BMD (BMD-T) was assessed at baseline, and every 6 months for 18 months. At the same time we also performed QUS at phalanges, by Bone Profiler-IGEA (amplitude dependent speed of sound: AD-SoS, ultrasound bone profile index: UBPI, bone transmission time: BTT). At baseline and after 18 months vertebral QCT scans of the first, second and third lumbar vertebrae were obtained using a specific software (OSTEO) to quantify the volumetric mineral density (vBMD) of somatic trabecular bone.

Teriparatide significantly ( $p<0.001$ ) increased BMD-LS; no significant variation in femoral subregions was found during the study period even though BMD-T tended to increase with the duration of PTH treatment and BMD-FN showed a reduction at month 6 with a progressively return to basal values. No significant changes were observed also for UBPI and AD-SoS, even if the last decreased at month 6 and thereafter it tended to increase. BTT significantly decreased at all time points ( $p<0.05$ ). Teriparatide induced an important and significant ( $p<0.001$ ) increase in vBMD at lumbar spine, as assessed by QCT. Our study shows that in women with established osteoporosis teriparatide determined the expected increase in BMD and vBMD at lumbar spine, with a less strong or negative effect at skeletal sites mainly composed by cortical bone. Further studies in larger population would be necessary to define the clinical role of QUS parameters in patients treated with teriparatide.

**Disclosures:** C. Cepollaro, None.

## SA394

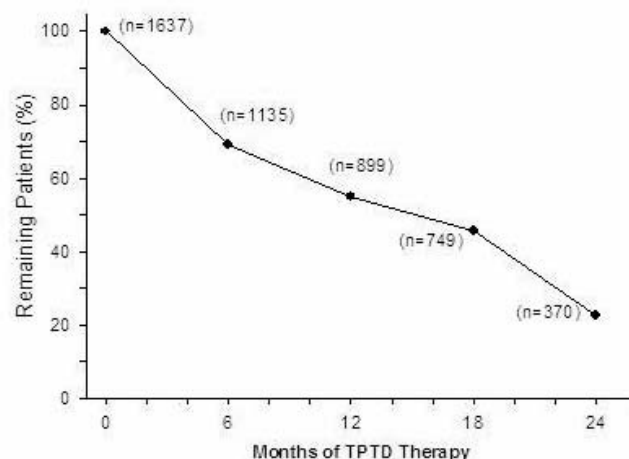
See Friday Plenary number F394.

## SA395

**Teriparatide Therapy in a Community Setting: Persistence and Use of Other Osteoporosis Medications in DANCE.** K. Taylor<sup>1</sup>, D. T. Gold<sup>2</sup>, P. Miller<sup>3</sup>, P. Chen<sup>\*1</sup>, M. Wong<sup>1</sup>, K. Krohn<sup>1</sup>. <sup>1</sup>Eli Lilly, Indianapolis, IN, USA, <sup>2</sup>Duke University, Durham, NC, USA, <sup>3</sup>Colorado Center for Bone Research, Lakewood, CO, USA.

The Direct Assessment of Non-vertebral Fracture in Community Experience (DANCE) observational study completed enrollment of 4106 patients on Dec 3 2007. Study investigators prescribe TPTD 20 µg/d for up to 24 months to patients, and follow them for another 24 months. As this cohort matures, more robust "real world" observations may be derived from patients' experience with teriparatide (TPTD) in a community setting. Poor persistence to osteoporosis therapy can reduce therapeutic benefit, despite the fracture risk reductions shown in clinical trials [Mayo Clin Proc 2006;81:1013-22]. Overall 1-yr persistence with osteoporosis therapies was found to be between 25-45% [Maturitas 2004;48:271-87, Arch Int Med 2005;165:2414-9]. This updated analysis from DANCE shows the persistency to therapy in 1637 patients with data on their first and last dose of TPTD (Figure). The percentage of patients remaining at 6, 12, 18, and 24 months was 69%, 55%, 45%, and 23%, respectively.

Of the 256 patients (16%) who reported concomitant use of  $\geq 1$  other bone-active agent during the TPTD treatment phase, 214 (84%) had initiated these other agents prior to starting TPTD. Estrogen was most often used ( $n=111$ ), followed by alendronate ( $n=57$ ), raloxifene ( $n=45$ ), risendronate ( $n=32$ ), and calcitonin ( $n=25$ ). After cessation of TPTD therapy, 747 patients (45.6%) reported using  $\geq 1$  other bone-active agent in the follow-up phase, and of these patients, 220 reported having used  $\geq 1$  other bone-active agent concomitantly during the TPTD treatment phase. Bisphosphonates, such as alendronate ( $n=244$ ), ibandronate ( $n=226$ ), risendronate ( $n=152$ ), and zoledronic acid ( $n=23$ ), were most commonly used in the follow-up phase. Estrogen ( $n=104$ ) and raloxifene ( $n=76$ ) were also used. In summary, the present analysis shows that 1) about half of patients who started TPTD persist with therapy at 1 year; 2) patients who took other bone-active agents concomitantly with TPTD had initiated use of these agents prior to starting TPTD; and 3) about half of patients take other bone-active agents after stopping TPTD therapy. Continued analysis of the DANCE cohort may provide insight on factors affecting persistence to TPTD therapy, on how TPTD is used among a spectrum of osteoporosis medications, and offer new approaches to optimize TPTD use in the community.



**Disclosures:** K. Taylor, Eli Lilly 5.

This study received funding from: Eli Lilly and Company.

## SA396

See Friday Plenary number F396.

## SA397

**Repetitive Rapid Delivery of Pharmacologically-Active hPTH 1-34 Across Human Skin Without Injection.** S. Ish Shalom<sup>1</sup>, Y. Kenan<sup>\*2</sup>, T. Matsumoto<sup>\*3</sup>, R. Neer<sup>4</sup>. <sup>1</sup>Metabolic Bone Diseases Unit, Rambam Medical Center, Haifa, Israel, <sup>2</sup>TransPharma Medical Ltd, Lod, Israel, <sup>3</sup>Department of Medicine and Bioregulatory Sciences, University of Tokushima Graduate School of Medical Sciences, Tokushima, Japan, <sup>4</sup>Endocrine Unit, Massachusetts General Hospital, Boston, MA, USA.

TransPharma has developed a system for transdermal delivery of hPTH 1-34 (TD) to alleviate the discomfort of injections (SC) and improve patient acceptance of and compliance with hPTH 1-34 therapy. The system utilizes RF ablation to create MicroChannels in the upper skin, allowing rapid diffusion of peptide from a subsequently-applied drug patch into the inner skin and systemic circulation. We compared the safety, tolerability, pharmacokinetics (PK), and type I procollagen N-terminal propeptide (PINP) based pharmacodynamic (PD) profile of TD vs. SC hPTH 1-34 administered once-daily for 7 days. 48 healthy post-menopausal women, age  $65 \pm 4$  years, were randomly allocated in 3 blocks of 16 to a daily TD dose of 50, 70, or 90 µg or a daily SC dose of 20 µg (FORTEO®). On days 1 and 7 we measured fasting serum PINP 1 hour before dosing (after which participants ate breakfast), and measured serum hPTH 1-34 15 minutes before and 0.25, 0.5, 1, 1.5, 2, 2.5, 3, 4, 6, 8, 10, 14 and 24 hours after TD or SC administration of the peptide. To minimize assay-related bias, all sera for a woman were measured in the same hPTH 1-34 or PINP assay. In each treatment group the mean PK profile on day 7 (presented in the Table below) did not differ significantly from that on day 1, indicating reproducible peptide delivery and no peptide accumulation.

Treatment	Cmax (pg/ml) mean $\pm$ SD	Tmax (h) mean $\pm$ SD (range)	AUC <sub>0-1</sub> (hr*pg/ml) mean $\pm$ SD	PINP absolute change from baseline (µg/L) (% Change) mean $\pm$ SD
TD 50 µg (n = 12)	53 $\pm$ 16	2.0 $\pm$ 0.5 (1.5-2.5)	135 $\pm$ 48	13 $\pm$ 7 (28 $\pm$ 15)
TD 70 µg (n = 12)	68 $\pm$ 28	2.3 $\pm$ 0.3 (1.5-2.5)	162 $\pm$ 73	13 $\pm$ 9 (26 $\pm$ 15)
TD 90 µg (n = 12)	90 $\pm$ 37	2.5 $\pm$ 0.6 (1.5-4.0)	250 $\pm$ 116	12 $\pm$ 9 (22 $\pm$ 15)
SC 20 µg (n = 10-12)	72 $\pm$ 21	0.6 $\pm$ 0.4 (0.25-1.0)	117 $\pm$ 45	8 $\pm$ 17 (20 $\pm$ 29)

Cmax occurred approximately 2 hours after TD application and 0.6 h after SC injection. Serum hPTH 1-34 was quantifiable 1.5-3.5 hours longer after TD dosing than after 20µg SC dosing. The bioavailability of TD hPTH 1-34, calculated from the area under the time-concentration curves, was ~40% of SC injection. Following 6 days of hPTH 1-34 treatment, serum PINP increased significantly in each treatment group by paired t-test ( $p^* < 0.0001 - 0.05$ ). Transdermal therapy was well-tolerated; application sites showed only very minor and transient erythema and edema, and no infections. These safety, tolerability, PK and early PD data demonstrate that TD hPTH 1-34 is a promising alternative to the currently-marketed injections.

\* P values are based on percent changes

**Disclosures:** S. Ish Shalom, TransPharma Medical Ltd. 2.

This study received funding from: TransPharma Medical Ltd.

## SA398

See Friday Plenary number F398.

## SA399

**A Phase 1, Randomized, Double-Blind, Placebo Controlled Trial of the PK/PD Effect and Safety of ZT-031, a hPTH Analog, in Healthy Elderly Women.** C. L. Barclay\*, R. Anderson\*, D. Krause, B. MacDonald. Zelos Therapeutics, Inc, West Conshohocken, PA, USA.

Parathyroid hormone (PTH) mediates its anabolic effect on bone via transient stimulation of PTH receptors (PTHr) on osteoblasts, leading to adenyl cyclase (AC) activation, cyclic AMP production and increased bone formation. AC activation in renal tubular cells results in renal Ca retention and increased PO<sub>4</sub> excretion. ZT-031 is a novel, 31 a cyclic analog of human PTH, currently in late clinical development for the treatment of post-menopausal osteoporosis.

The purpose of this study was to evaluate the safety, PK, and PD effect of ZT-031 in healthy elderly women.

20 healthy adult women  $\geq 65$  years of age (mean 69 y) were randomized to 7 days of treatment with 20, 30, or 40  $\mu$ g of ZT-031 or placebo, given by daily SC injection. PD markers included urine cAMP on Days (D) 1 and 7 pre- and 2h post-dose. PK parameters were evaluated using a validated ELISA. Safety parameters included adverse events (AEs), EKGs and serum Ca as well as urinary Ca and PO<sub>4</sub>.

Urine cAMP increased in dose-proportional fashion 2h after dosing on D1 and 7; increases are shown in the Table.

Dose	20 $\mu$ g n=7	30 $\mu$ g n=4	40 $\mu$ g n=6	Placebo n=3
Day 1 Urine cAMP <sup>1,2</sup>	542.7	728.4	1941.3	-15.2
Day 7 Urine cAMP <sup>1,2</sup>	394.3	1026.0	1375.8	28.7

<sup>1</sup>  $\mu$ mol/mmol Cr<sup>2</sup>p < 0.01

By 8 h post-dose, mean urine cAMP returned to baseline (BL) for all groups. Subsequent to the increase in urine cAMP a sequence of reduced urinary Ca and increased urinary PO<sub>4</sub> excretion followed by the converse changes in serum were observed. All changes in Ca and PO<sub>4</sub> profile returned to BL by 8-12 h post dose. PK parameters were similar on Days 1 and 7. C<sub>max</sub> and AUC(0-4h) were approximately dose proportional whereas T<sub>1/2</sub> (average 1.12h for all time points/doses), clearance and volume of distribution were dose-independent. A total of 72 AEs was reported by 17 subjects reported; none was severe or serious. The frequency of AEs did not vary by dose. Headache was the most common AE. Three Ca values > ULN (2.55 mmol/L) were observed, 1 in a 30  $\mu$ g subject and 2 in 40  $\mu$ g group. None was symptomatic, persistent or exceeded 2.61 mmol/L. No subject withdrew due to a treatment-emergent AE. A dose-dependent effect on resting heart rate was observed.

ZT-031 was well tolerated and exhibited dose proportional PD and PK responses in healthy elderly women. The effect on serum and urinary Ca/PO<sub>4</sub> profiles indicated that cAMP generation was secondary to activation of PTHr. The observed PK/PD profiles are appropriate for the intermittent stimulation of PTHr required for the anabolic effects of a PTH analog.

**Disclosures:** D. Krause, Employee of Zelos Therapeutics 5.

This study received funding from: Zelos Therapeutics, Inc.

## SA400

**Bone Mineral Density and Vertebral Fracture in Women with Breast Cancer and Antiaromatase Therapy.** E. Hoppe\*, B. Bouvard\*, C. Lassalle\*, R. Levasseur\*, M. Audran\*, D. Chappard\*, E. Legrand\*.

<sup>1</sup>Rheumatology and Inserm U 922, Centre Hospitalier Universitaire, Angers, France, <sup>2</sup>Inserm U 922, Centre Hospitalier Universitaire, Angers, France.

**Background:** Recovery from breast cancer in women has been achieved using chemotherapy, radiotherapy that can affect bone tissue. Furthermore, aromatase inhibitors therapy can accelerate bone loss and increase the fracture risk.

**Objectives:** Prospective and longitudinal study to evaluate bone mineral density and fractures in 515 women with treated breast cancer, before and after one year of aromatase inhibitors therapy.

**Methods:** Medical history, clinical risk factors for osteoporosis, non spine fractures, hip and spine Bone Mineral Density (BMD) were checked at baseline and after one year of antiaromatase therapy. Bone remodelling was evaluated by serum levels of C-telopeptide (CTX), osteocalcin and bone specific alkaline phosphatase (BSAP). Spinal X-ray films were analyzed independently by two trained investigators who were unaware of the patient status. Vertebral fracture was defined as a reduction of at least 20 percent in the anterior, middle or posterior vertebral height

**Results:** At baseline, 44.2% of women had a BMD T-score <-1 (on spine or hip) and 21.6% had a T-score <-2. Spinal radiographs revealed that 21.7% women had at least one vertebral fracture and 13 (6.8%) had 2 or more vertebral fracture. 13.7% of women reported non spine fractures. Logistic regression analysis showed that age (+5 years : OR=1.46, CI 95% 1.15-1.85), weight (-1 kg : OR =1.14, CI 95% 1.08-1.19), self-reported non spine fracture (OR = 4.17, CI 95% 1.80-9.63) and radiographic vertebral fractures (OR = 6.12, CI 95% 2.42-15.71) were associated with the presence of low BMD (T-score <-2 on spine or hip). Women with osteoporosis (25% of the initial cohort) received risendronate (35 mg weekly) and were investigated after one year of antiaromatase therapy : the mean BMD was increased by 1.77% on spine and by 0.78% on hip. We observed that 5.4% of these women have a new fracture but only 3.6% had a new vertebral fracture.

Women with normal BMD or osteopenia (75% of the initial cohort) didn't received any anti osteoporotic therapy and were investigated after one year: the mean BMD was reduced by

1.25% on spine and by 1.75% on hip. We observed that 5.8% of these women have a new fracture but only 1.5% had a new vertebral fracture.

**Conclusion:** These results strongly suggest that (1) 20 to 25% of women with treated breast cancer have low BMD or osteoporotic fractures before starting antiaromatase therapy (2) these women should benefit from clinical evaluation, BMD measurement and specific bone therapy, (3) in women with normal BMD or osteopenia, the rate of bone loss and the incidence of fractures (after one year) is quite similar that expected for postmenopausal women.

**Disclosures:** E. Legrand, None.

## SA401

See Friday Plenary number F401.

## SA402

**Renal Safety Across a Wide Range of Dosing Regimens of Risedronate.** P. Miller<sup>1</sup>, R. Miday\*, A. Klemes\*, D. Ramsey\*. <sup>1</sup>Colorado Center for Bone Research, Lakewood, CO, USA, <sup>2</sup>Procter & Gamble Pharmaceuticals, Mason, OH, USA.

The incidence of both osteoporosis and renal insufficiency increases with age; thus, the effect of osteoporosis treatments on renal function is a clinical concern. This retrospective analysis was conducted to study the influence of multiple dosing regimens of risedronate on the renal function of postmenopausal women with osteoporosis or osteoarthritis.

Combined data from over 14,000 patients in the Risedronate phase III clinical trials of post-menopausal osteoporosis (PMO) and osteoarthritis were analyzed across multiple dose regimens; 5 and 15 mg daily, 35 and 50 mg weekly, 75 mg on 2 consecutive days monthly or 150 mg monthly, or placebo. Median treatment duration was 2 years. Subgroups with baseline renal function impairment or renal risk factors were also examined. Serum creatinine (SCr), estimated serum creatinine clearance (CrCl - Cockcroft-Gault) and renal function related adverse events (AEs) were analyzed.

94% of subjects were female, with a mean age of 70 years. The frequency distributions of changes in CrCl from baseline to endpoint value were not different between placebo and risedronate groups or between different dose/regimen groups, for each of the populations examined. Also, there was a similar frequency of patients who developed abnormal SCr or who developed SCr increases > 0.5 mg/ml from baseline, within each of the active treatment group and placebo comparisons (Table 1). Patients with baseline renal impairment (CrCl  $\leq$  50 ml/min) or baseline renal risk factors (diabetes mellitus, hypertension, ACE inhibitor or NSAID treatment) also did not show treatment group differences. Renal function-related adverse events were not different across groups, all  $\leq$  2%. While risedronate serum C<sub>max</sub> levels for 75 mg and 150 mg are approximately 11 and 29-fold greater than for 5 mg, there is no indication of adverse renal effects from these higher doses.

Risedronate demonstrates a favorable renal safety profile across a wide range of doses, regimens and patient populations with no evidence of effect on renal function parameters.

Table 1 Renal Safety Endpoints in Risedronate Post-Menopausal Osteoporosis Studies						
Parameter	5 mg Daily		75 mg Two Consecutive Days (Monthly)		150 mg Once a Month	
	Placebo %	5 mg Daily %	5 mg Daily %	75 mg/2cd %	5 mg Daily %	150 mg Monthly %
Serum Cr - Treatment Emergent Abnormal <sup>1</sup>	8.0	8.4	1.7	1.4	1.7	0.8
Serum Cr - 7 from Baseline > 0.5 mg/dL at Endpoint	0.7	0.7	0.3	0.2	0.0	0.3
Renal Function Adverse Events	1.9	1.5	1.1	0.6	0.5	0.5
	Mean(SD)	Mean (SD)	Mean (SD)	Mean (SD)	Mean (SD)	Mean (SD)
CrCl - 7 from Baseline to Endpoint	-0.62 (10.14)	-0.42 (9.56)	-3.62 (11.13)	-4.12 (10.94)	-1.14 (7.59)	-1.45 (8.06)
CrCl - 7 from Baseline to Endpoint (Baseline CRCL $\geq$ 50)	0.95 (6.36)	0.85 (6.40)	0.97 (8.51)	-0.26 (5.44)	-0.35 (4.79)	0.73 (5.96)

<sup>1</sup>Treatment emergent abnormal serum creatinine are patients with a normal baseline creatinine and 1 or more abnormal values after dosing. Number of patients varies depending on analysis but numbers of patients treated are the following: 5 mg Daily Studies (4878 placebo and 4846 5 mg daily), Two Consecutive Days (613 5 mg daily and 616 75 mg/2CD), and Once a Month (642 5 mg daily and 650 150 mg monthly).

**Disclosures:** P. Miller, P&G 2.

This study received funding from: The Alliance for Better Bone Health (Procter & Gamble Pharmaceuticals and sanofi-aventis).

## SA403

See Friday Plenary number F403.

## SA404

**Fracture Reduction During Two Years of Treatment with Risedronate or Alendronate, a Retrospective Cohort Study.** P. Delmas<sup>1</sup>, J. Lange<sup>2</sup>, S. Silverman<sup>3</sup>, N. Watts<sup>4</sup>, R. Lindsay<sup>5</sup>. <sup>1</sup>INSERM Research Unit 831, Lyon, France, <sup>2</sup>P&G Pharmaceuticals, Mason, OH, USA, <sup>3</sup>Cedars Sinai Medical Center, Los Angeles, CA, USA, <sup>4</sup>Bone Health and Osteoporosis Center, Cincinnati, OH, USA, <sup>5</sup>Helen Hayes Hospital, West Haverstraw, NY, USA.

In the published REAL cohort study,<sup>1</sup> we observed in the first year of treatment that patients using risedronate had a lower incidence of hip and nonvertebral fractures than patients using alendronate. We now have additional data that extends these observations into a second year of therapy. For the current analysis, we used patients with a single bisphosphonate prescription as a referent cohort.

The original study population of women over age 65 included new users of once-a-week dosing of risedronate (n = 12,215) or alendronate (n = 21,615) who initiated treatment between July 2002 and June 2004 within records of health services utilization. This population is followed through June 2006 or until no longer therapy adherent. As a referent cohort, we selected patients who filled only a single prescription of alendronate or risedronate during the observation period (n = 5,390). Proportional hazard modeling was used to compare the incidence of hip and nonvertebral fractures between cohorts, adjusting for potential differences in baseline fracture risk.

Based on history of clinical fractures and age upon study entry, the cohort at highest baseline fracture risk was the referent cohort, followed by the risedronate cohort, then the alendronate cohort. At the end of two years of observation for the referent cohort, the cumulative incidence of hip fractures was 1.9% and of nonvertebral fractures was 6.3%. Compared to the referent cohort, patients on risedronate had an approximately 40% lower incidence of hip fractures at 6, 12, 18, and 24 months of therapy. For patients on alendronate, a similar lower incidence of hip fractures was observed at 18 and 24 months of therapy but not at 6 or 12 months. Results for the hip and nonvertebral fracture outcomes were similar.

In summary, the results of this observational study indicate 1) the real-world effectiveness of risedronate and alendronate through two years of treatment are consistent with results of randomized controlled trials; 2) the reduction of hip and nonvertebral fractures, relative to the referent cohort, occurs earlier after initiation of therapy with risedronate than with alendronate. Given the low adherence to therapy for chronic medications, the consequence of our observation may impact the cost/effectiveness perspective of each bisphosphonate.<sup>1</sup> Silverman et al. Osteoporosis Int. 18:25-34 (2007)

**Disclosures:** P. Delmas, P&G 2.

*This study received funding from: The Alliance for Better Bone Health (Procter & Gamble Pharmaceuticals and sanofi-aventis).*

## SA405

See Friday Plenary number F405.

## SA406

**Homocystinuria Associated Bone Disease: Effect of Long Term Bisphosphonate Treatment.** M. D'Amours<sup>\*</sup>, A. Răkel<sup>\*</sup>, L. G. Ste-Marie. Endocrinology, Hôpital Saint-Luc, CHUM, University of Montreal, Montreal, QC, Canada.

Homocystinuria is an autosomal recessive disease classically associated with dislocation of the eye lens, mental retardation, hyperhomocysteinemia and skeleton abnormalities such as deformities, vertebral fractures and osteoporosis. The mainstream of treatment consists of dietary amino acids and vitamin supplementation. There is little data in the literature about the effects of bone active agents such as bisphosphonates in this population. Here we report the cases of 2 brothers diagnosed with homocystinuria in childhood (one at age 5 years and the other at 4 months) who were addressed initially for decreased bone density. They were treated with betain, folic acid, vitamin B12 and calcium. Both had a normal development and growth without fractures or deformities except for a moderate scoliosis in the eldest. The biochemical work-up did not show any abnormality of the phosphocalcic metabolism including PTH and 25(OH)vitaminD. Both presented a slightly elevated level of urinary hydroxyproline suggesting increased bone resorption. Their initial bone mineral density (BMD) showed osteopenia affecting lumbar spine (L2-L4: 0.850 and 0.931 g/cm<sup>2</sup> respectively) and femoral neck (0.965 and 1.055g/cm<sup>2</sup> respectively). Alendronate (ALN) was introduced in 1996 in both patients (then aged 23 and 18 year old). Treatment was continued for the next 10 years without any incident fracture. Sequential lumbar spine BMD was unreliable in the eldest because of progressive scoliosis whereas it increased by 18% in the youngest (1.128 g/cm<sup>2</sup> in 2007). Femoral neck BMD remained stable (2007 values: 0.961 g/cm<sup>2</sup> and 1.047 g/cm<sup>2</sup>, respectively). Bone turnover markers, serum osteocalcin (14 and 12ng/ml respectively) and serum C-telopeptide (0.122 and 0.086 ng/ml respectively) were suppressed in these young men. Long term bisphosphonate treatment was associated with the prevention of bone loss and osteoporotic fractures in two patients with homocystinuria. The addition of bisphosphonates to the therapeutic armamentarium for homocystinuria should be considered for fracture prevention.

**Disclosures:** M. D'Amours, None.

## SA407

See Friday Plenary number F407.

## SA408

**Patients Desire of Administration Form and Dose Interval in Bisphosphonate Therapy of Osteoporosis.** C. Günther, A. Kapner<sup>\*</sup>, C. Spanier<sup>\*</sup>, L. Erich<sup>\*</sup>, V. Schäfer<sup>\*</sup>. Fachklinik Johannesbad, Bad Füssing, Germany.

**Introduction:** A drug can only work, if you take it in. This platitude is worth on oral bisphosphonate too and the compliance is according to Hadji@al (ECCEO 2005) in daily taken alendronate 27.8% and in weekly taken alendronate 46.5% after 1 year. This cannot satisfy. Before the back ground of a futural available yearly zoledronate intravenous infusion (meanwhile registered as "Aclasta") we were therefore interested which administration form patients would prefer.

**Material and methods:** From 19.10.2005 to 05.07.2007 we asked 100 patients with osteoporosis (t-score < -2.5), 91 women (Ø 70,7 years old) and 9 men (Ø 69,5 years old), if they would prefer a daily, a weekly or monthly oral bisphosphonate. After this we began the treatment with the wished oral bisphosphonate under basic therapy with calcium and vitamin D. In addition to the first question we asked the patients if they would prefer a yearly intravenous bisphosphonate infusion if it would be available.

**Results:** From the 100 patients nobody wanted a daily oral bisphosphonate, 11 patients wanted a weekly drug and 89 patients a monthly. According to the additional question 57 % of the patients would prefer a yearly intravenous zoledronate infusion in comparison to the 43% which would prefer an oral administration.

**Discussion:** The results show that the majority of patients (89%) prefer the monthly intake of an oral bisphosphonate and only 11% a weekly administration.

If the complete package "Actonel plus Calcium D" - meanwhile available in Germany - can change this relation will be investigated in the next weeks.

Theoretically in the patients who would prefer the yearly zoledronate infusion (57%) could be reached a compliance of 100 % in comparison to the 43% of patients with wished oral administration.

If the "infusion patients" - after registration of "Aclasta" in Germany - switched to infusion indeed will be presented later.

But both application forms - oral and intravenous - will be only effective if a sufficient substitution with vitamin D and calcium is guaranteed. Therefore "Actonel plus Calcium D" in Germany is a good innovation to improve the compliance of patients with osteoporosis.

**Disclosures:** C. Günther, None.

## SA409

See Friday Plenary number F409.

## SA410

**Does Alendronate Use Prevent Kyphosis Progression in Older Women?** D. M. Kado<sup>1</sup>, M. H. Huang<sup>\*2</sup>, E. Barrett-Connor<sup>3</sup>, K. Ensrud<sup>4</sup>, A. La Croix<sup>\*5</sup>, S. R. Cummings<sup>6</sup>. <sup>1</sup>Orthopaedic Surgery, University of California, Los Angeles, Los Angeles, CA, USA, <sup>2</sup>University of California, Los Angeles, Los Angeles, CA, USA, <sup>3</sup>University of California, San Diego, La Jolla, CA, USA, <sup>4</sup>University of Minnesota, Minneapolis, MN, USA, <sup>5</sup>University of Washington, Seattle, WA, USA, <sup>6</sup>California Pacific Medical Center, San Francisco, CA, USA.

Hyperkyphosis, or increased thoracic curvature, is commonly observed in older persons. While it is well established that alendronate use decreases the incidence of vertebral fractures and prevents height loss, it is not known whether alendronate use reduces progression of kyphosis. Given that many older women are concerned about the cosmetic deformity known commonly as the dowager's hump, it is of interest to know whether alendronate actually helps mitigate the progression of age-related kyphosis, especially since a substantial number of the most severely affected women have no evidence of underlying vertebral fractures. Therefore, we compared the effects of alendronate to placebo on the progression of kyphosis in 6,459 women aged 55-81 with low bone mass (femoral neck T-score < 0.68 g/cm<sup>2</sup>) using data from the Fracture Intervention Trial (FIT), a randomized blinded trial of alendronate. The kyphosis angle was measured using the Debrunner kyphometer at baseline and closeout in 98% of the participants after an average of 4.2 years.

There were no significant baseline differences between the alendronate and placebo groups in terms of demographic, physical measures, health status, bone mineral density, prevalent vertebral fractures, or kyphosis angle. The mean kyphosis angle was 47.6 degrees (SD = 11.9) and the mean change was an increase of 3.9 (SD = 9.3). For women who did not have baseline vertebral fracture, the average change of kyphosis was 3.9 degrees for both treatment and placebo groups (mean difference = -0.20 degrees, 95% CI: -0.69 - 0.28; p = 0.42). For women who had a baseline vertebral fracture, average changes of kyphosis for the treatment and placebo groups were 4.1 and 4.3 degrees, respectively (mean difference = -0.54, 95% CI: -1.36 - 0.28; p = 0.20). Our data do not demonstrate that kyphosis progression is slowed by alendronate treatment; however, 5% of the participants had changes in kyphosis of greater magnitude (>20 degrees) than would be expected over 4 years, given data from prospective cohort studies. As suggested by findings from prior observational studies, these results support the theory that age-related kyphosis is not primarily caused by underlying spinal osteoporosis, and that its progression may mainly be due to other factors besides vertebral fractures and low bone density.

**Disclosures:** D.M. Kado, Medtronic 4.

**SA411**

See Friday Plenary number F411.

**SA412**

**Bisphosphonate-associated Osteonecrosis of the Jaw cases in South Korea.** Y. Chung<sup>1</sup>, Y. Kwon<sup>2</sup>, J. Lee<sup>3</sup>, D. Kim<sup>4</sup>, S. Lee<sup>5</sup>, B. Lee<sup>6</sup>. <sup>1</sup>Endocrinology and Metabolism, Ajou University Hospital, Suwon, Republic of Korea, <sup>2</sup>Oral and Maxillofacial Surgery, Kyung Hee University Hospital, Seoul, Republic of Korea, <sup>3</sup>Dentistry, Ajou University Hospital, Suwon, Republic of Korea, <sup>4</sup>Nuclear Medicine, Kyung Hee University Hospital, Seoul, Republic of Korea, <sup>5</sup>Biochemistry and Internal Medicine, Eulji University School of Medicine, Daejeon, Republic of Korea, <sup>6</sup>Obstetrics and Gynecology, Inha University Hospital, Incheon, Republic of Korea.

**Introduction:** Bisphosphonate-associated osteonecrosis of the jaw (ONJ) is a rare but serious side effect of bisphosphonate therapy. Case reports of ONJ had been reported in many Western countries but relatively few from Asian countries. Recently, we had experienced five cases of ONJ in South Korea. Three of them were related with osteoporosis and two of them were associated with malignancy.

**Case 1:** A 74-year-old woman had been treated with weekly oral alendronate for osteoporosis for 5 years. ONJ of the left mandible precipitated by teeth (1<sup>st</sup> and 2<sup>nd</sup> molars) extraction. The patient had multiple systemic risk factors including old age and diabetes mellitus.

**Case 2:** A 72-year-old woman had been treated with weekly oral alendronate for osteoporosis for 3 years. ONJ of the right mandible and left maxilla area precipitated by teeth extraction. The patient had multiple systemic risk factors including old age, diabetes mellitus, rheumatoid arthritis, and glucocorticoid therapy.

**Case 3:** A 76-year-old woman had been treated with oral alendronate for osteoporosis for 7 years. ONJ of the right mandible precipitated by teeth (canine and premolar) extraction. The patient had multiple systemic risk factors including old age and diabetes mellitus.

**Case 4:** A 56-year-old man who had been diagnosed as Waldenström's macroglobulinemia has been treated with chemotherapeutic agents. Concomitantly, 45mg of pamidronate was injected monthly for 2 years. There was pain and pus drainage in left mandible 1<sup>st</sup> molar tooth area after spontaneous foliation. The patient had multiple systemic risk factors including chemotherapy and glucocorticoid for malignancy.

**Case 5:** A 50-year-old man had been diagnosed as multiple myeloma (non-secretory type). He has been treated with chemotherapeutic agents. Concomitantly, 45mg of pamidronate was injected monthly for 3 years. There was pain and pus drainage in right mandible 1<sup>st</sup> molar tooth area after extraction. The patient had multiple systemic risk factors including chemotherapy and glucocorticoid for malignancy.

**Conclusion:** Bisphosphonate-associated ONJ both in osteoporosis and malignancy might be an emerging issue in Asian countries as well as Western countries.

**Disclosures:** Y. Chung, Eli Lilly, GSK 1; MSD, Sanofi-Aventis 1, 2, 3, 4; Novartis 1, 4; Hanlim, Yuyu 1, 2, 3.

**SA413**

See Friday Plenary number F413.

**SA414**

**Treatment Discontinuation Due to Gastrointestinal Adverse Events and Decreased Bone Mineral Density in Patients Switched from Branded Alendronate to Generic Alendronate.** D. Grima<sup>1</sup>, G. Ioannidis<sup>2</sup>, A. Papaioannou<sup>3</sup>, J. D. Adachi<sup>3</sup>. <sup>1</sup>Center for Osteoporosis and Arthritis Research and Education, Oakville, ON, Canada, <sup>2</sup>McMaster University, Hamilton, ON, Canada, <sup>3</sup>Medicine, St. Joseph's Healthcare - McMaster University, Hamilton, ON, Canada.

**Introduction:** Generic alendronate was introduced in Canada in July 2005 and within 2 months the conversion from brand to generic alendronate was almost complete. The generic has a different dissolution profile compared to brand alendronate which may impact gastrointestinal (GI) adverse events (AE).

**Methods:** A chart review study was conducted of postmenopausal women 50 years of age and older who were on brand alendronate prior to July 2005 from a single clinic that specialized in treating patients with osteoporosis. Data collected included GI AEs, bone mineral density (BMD), osteoporosis therapies used, discontinuation, reason for discontinuation and concomitant use of NSAIDs, PPIs and H2 blockers.

**Results:** A total of 199 women were identified as starting alendronate prior to the introduction of generic alendronate in July 2005 and having visits after this date. Of these 18 switched therapy before July 2005. Of the remaining 181, 53 patients (29%) discontinued alendronate after July 2005, due to GI AEs (27/181) and declining BMD (26/181).

**Discussion:** Generic alendronate may not be as well tolerated as brand alendronate and should not be considered equivalent in all individuals. This may have implications for treatment adherence and effectiveness, as well as the preferential reimbursement of generic alendronate.

**Disclosures:** D. Grima, Procter & Gamble Pharmaceuticals 2, 3, 4; sanofi-aventis 2, 3, 4.

This study received funding from: Procter & Gamble Pharmaceuticals.

**SA415**

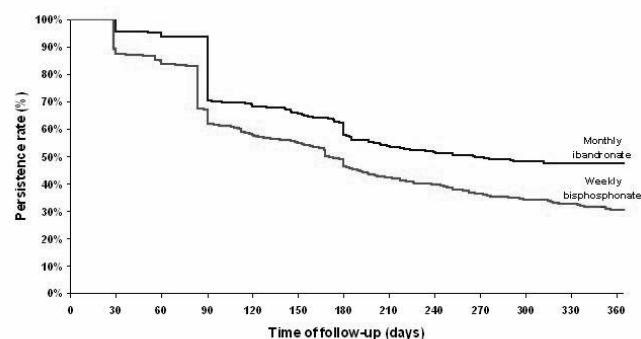
**1-Year Analysis of Adherence with Bisphosphonate Treatments in Osteoporotic Patients: Monthly versus Weekly Formulation.** C. Roux<sup>\*1</sup>, E. Côté<sup>2</sup>, F. Mercier<sup>\*3</sup>, A. F. Gaudin<sup>2</sup>. <sup>1</sup>Department of Rheumatology, Paris Descartes University, Paris, France, <sup>2</sup>Economic & Health Outcomes, GlaxoSmithKline France, Marly le Roi, France, <sup>3</sup>StatProcess, Port-Mort, France.

**Purpose:** To assess medication adherence encompassing both compliance and persistence among women newly receiving monthly ibandronate or weekly bisphosphonates (BPs) in general practice.

**Method:** Patient data were retrospectively analysed from a computerized database representative of the French GPs prescriptions (1.6 million patients cover). Eligible women were all patients aged at least 45 years with first prescription of BPs (12 months of prior wash-out) from ibandronate availability in France to the end of the follow-up (Jan.2007-Jan.2008). Two cohorts were formed consisting of patients treated with monthly ibandronate and weekly BPs. Compliance was assessed by medication possession ratio (MPR) calculated by dividing the duration of all filled prescriptions by the follow-up period. Persistence was measured by the time to discontinuation therapy (permissible gap in refills were 45 days for monthly and 30 days for weekly regimen due to a two-week difference in dosing window). Treatment survival analyses were completed in both cohorts and analysed by log-rank test. A backward procedure was used to adjust for confounders.

**Results:** A total of 2,990 women were prescribed for the first time a bisphosphonate treatment: 1,001 received monthly ibandronate and 1,989 received weekly BPs. On average, women were significantly younger in the first cohort than in the second one (68.8 SD:10.3 and 70.4 SD:10.3 years old respectively; p<.001). The mean MPR was higher with monthly than with weekly dosing (84.5% vs 79.5%; p<.001). Kaplan-Meier curves showed that the proportion of women still persistent at 1-year with monthly ibandronate was 17 percentage points higher than those persisting on weekly BPs (47.5% vs 30.5%; p<.0001). This difference was also significant using similar permissible gaps in both cohorts (p<.0001). After adjustment for age, history of fracture, co-treatments, comorbidities and DXA scan, monthly users were 37% (hazard ratio = 0.630 SD:0.0613; P<.0001) less likely to discontinue therapy vs weekly users

**Conclusion:** These results demonstrate that monthly ibandronate improved adherence (i.e.



compliance and persistence) of osteoporotic patients compared with weekly bisphosphonates.

**Disclosures:** F.E. Côté, GlaxoSmithKline 2, 3.

This study received funding from: GlaxoSmithKline.

**SA416**

See Friday Plenary number F416.

**SA417**

**Development, Reliability, and Validity of a New Preference Satisfaction Questionnaire (PSQ).** D. T. Gold, R. Horne<sup>\*</sup>, C. Hill<sup>\*</sup>, J. Borenstein<sup>\*</sup>, S. Varon<sup>\*</sup>, D. Macarios<sup>\*</sup>. Amgen Inc., Thousand Oaks, CA, USA.

We developed a questionnaire that assesses preference, satisfaction, and bother with a weekly pill versus a 6-monthly, subcutaneous injection for the treatment of postmenopausal osteoporosis.

Thirty-four questions were developed based on literature review and expert input. For nine items, subjects choose one of: the pill, the injection, or neither, with respect to preference, satisfaction, and bother. For 20 items, subjects specify the degree of bother or satisfaction on a 5 point Likert scale for treatment separately (no comparison between treatments). For the remaining five items, subjects select the degree of agreement/disagreement (5 point Likert) with one treatment being favorable over the other on various domains. Two separate, in-depth group interviews were conducted with subjects to evaluate item comprehension, questionnaire length, and identify additional constructs. The PSQ was revised after the first group interviews. Women currently taking or who had previously taken ( $\leq 3$  years) weekly bisphosphonate therapy for osteoporosis were eligible for interviews. Reliability and validity were assessed in a separate study, by incorporating the PSQ into a phase 3 randomized clinical study comparing 60 mg denosumab every 6 month

injection and 70 mg alendronate weekly pill.

Twenty-four subjects participated in initial cognitive interviews. Participants understood the PSQ and did not feel the questions were confusing or contained irrelevant information. 1100 subjects completed the PSQ as part of the clinical study. The construct validity of the PSQ items was investigated through inter-item correlations and correlations between the PSQ items and the EQ-5D. Inter-item correlations supported convergent validity and were for preference items (range 0.62 to 0.97), pill satisfaction items (range 0.23 to 0.90), and injection satisfaction items (range 0.13 to 0.91). Correlations with the EQ-5D were low (range 0.00 to 0.09) supporting divergent validity. The proportion of correlations achieving coefficients of 0.40 or greater among items within the same domain (150/178, 84.3%) is larger than the proportion of coefficients 0.40 or greater among items across domains (122/383, 31.9%), supporting both convergent and divergent validity. Items were retained based on strong inter-item correlations, strong factor loading, and feedback from cognitive interviews. At the scale level, the Cronbach's alpha reliability values for satisfaction, pill-bother and injection-bother were 0.90, 0.85, and 0.62, respectively. The PSQ was refined and formatted appropriately based on the cognitive interview. Results from a large phase 3 trial show good reliability and validity of the preliminary PSQ.

**Disclosures:** D.T. Gold, Amgen Inc. 1, 2; P&G / Sanofi-Aventis 1, 2, 4; Eli Lilly 1, 2, 4; Merck / Novartis 1, 4.

This study received funding from: Amgen Inc.

## SA418

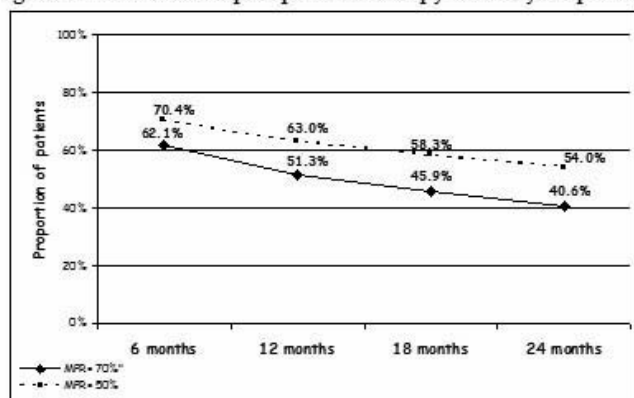
**Patient Persistence with Weekly Bisphosphonates for Two Years after Initiation of Therapy: A Retrospective Cohort Study.** D. Gold<sup>1</sup>, N. Borisov<sup>2</sup>, R. Sheer<sup>2</sup>. <sup>1</sup>Duke University Medical Center, Durham, NC, USA, <sup>2</sup>Procter & Gamble Pharmaceuticals, Mason, OH, USA.

Therapy persistence is important for a patient to maximize efficacy benefit of medications. The study objective was to assess patient persistence with bisphosphonates during two years of therapy using two integrated administrative medical claims databases (Ingenix Lab/Rx<sup>TM</sup> and Medstat MarketScan<sup>®</sup>).

The study included women 50+ years with a new prescription fill for weekly bisphosphonate (risedronate 35mg or alendronate 35/70 mg) between January 1, 2003 and June 30, 2005. To qualify for the study, patients were required to be continuously enrolled for 6 months prior to and 24 months following the index date (the first script date). The 6-month history was used as a wash-out period and to assess baseline clinical characteristics. During follow-up patient's adherence was defined as a medical possession ratio (MPR) of at least 70%. Proportion of patients with MPR  $\geq$  70% was assessed at 6, 12, 18, and 24 months of therapy. Patients with MPR < 70%, were examined further to assess proportion of patients who reinitiated and remained on the therapy for at least 6 months at any time during follow up. Sensitivity analysis was conducted using different levels of MPR.

We identified 134,032 women with a new prescription for bisphosphonate therapy; mean age was 65 years (SD = 11). Just over half (51%) were persistent with therapy at 12 months, and 41% were still persistent at 24 months after initiation of therapy (Figure 1). Overall, 59% (79,630) of women had MPR < 70% during the follow-up, however, 20% (15,632) of them were persistent with therapy for at least another 6 months, and 8% (6,483) for at least 1 year at some point during follow up. The study demonstrated a decline in patient persistence to approximately 40% over 24 months of bisphosphonate therapy. Although about 60% of women were not persistent with therapy during the follow up, 20% (12% overall) reinitiated and stayed on therapy for at least 6 months. Thus, studies that include efficacy inputs (e.g., cost-effectiveness) should not ignore this cohort of re-starters that attains efficacy for at least another 6 months.

Figure 1 Patients on bisphosphonate therapy over 2-year period



**Disclosures:** D. Gold, P&G 2.

This study received funding from: The Alliance for Better Bone Health (Procter & Gamble Pharmaceuticals and sanofi-aventis)

## SA419

**Hip Structure Analysis for Raloxifene Treatment in Japanese Women with Osteoporosis.** J. Takada<sup>1</sup>, T. J. Beck<sup>2</sup>, T. Miki<sup>3</sup>, Y. Imanishi<sup>4</sup>, K. Nakatsuka<sup>5</sup>, H. Wada<sup>6</sup>, H. Naka<sup>3</sup>, K. Iba<sup>1</sup>, T. Yoshizaki<sup>7</sup>, T. Yamashita<sup>\*1</sup>. <sup>1</sup>Orthopedic Surgery, Sapporo Medical University, Sapporo, Japan, <sup>2</sup>Radiology, The Johns Hopkins University, Baltimore, MD, USA, <sup>3</sup>Geriatrics, Osaka City University, Osaka, Japan, <sup>4</sup>Metabolism, Endocrinology, and Molecular Medicine, Osaka City University, Osaka, Japan, <sup>5</sup>Inoue Hospital, Suita, Japan, <sup>6</sup>Wada Obstetrics and Gynecology Clinic, Asahikawa, Japan, <sup>7</sup>Kitago Orthopedic Clinic, Sapporo, Japan.

Hip Structure Analysis (HSA) was used to measure proximal femur geometry using conventional DXA scans. This study is the first analysis of HSA data in Japanese osteoporotic women treated with raloxifene (60 mg).

198 Japanese osteoporotic women aged between 47 and 83 years of age were treated with raloxifene for at least 6 months. DXA scans were acquired at baseline and every 6-12 months of follow-up. Geometry and BMD were measured at the narrowest point of the neck (NN), intertrochanteric region (IT), and proximal shaft (PS). Measurements included BMD, cortical thickness, cross-sectional area (CSA), section modulus, and buckling ratio. Section modulus is calculated cross-sectional moment of inertia divided by the maximum distance from the bone edge to the centroid ( $d_{max}$ ), and represents the index of bending and torsional strength. Buckling ratio is an index of cortical stability under compressive loads, and calculated as the ratio of  $d_{max}$  to the estimated mean cortical thickness.

The percent changes of BMD between baseline and year 1 at NN, IT, and PS regions were 0.47 %, 2.73 %, and 1.77 %, respectively. Section moduli were 2.53 %, 4.62 %, and 2.56 %, respectively. Buckling ratios were 0.47 %, -2.36 %, and -1.26 %, respectively. Section modulus has a positive relationship with BMD ( $r = 0.535 - 0.794$ ,  $p < 0.001$ ), cortical thickness ( $r = 0.561 - 0.785$ ,  $p < 0.001$ ), and CSA ( $r = 0.797 - 0.879$ ,  $p < 0.001$ ), but a negative relationship with buckling ratio ( $r = -0.361 - -0.648$ ,  $p < 0.001$ ) at three measured regions.

In conclusion, raloxifene treatment in Japanese women with osteoporosis increased BMD and improved structure strength in the femur.

**Disclosures:** J. Takada, None.

## SA420

See Friday Plenary number F420.

## SA421

**Arzoxifene in Postmenopausal Women with Normal or Low Bone Mass.** M. Bolognese<sup>1</sup>, J. Krege<sup>2</sup>, W. H. Utian<sup>\*3</sup>, R. Feldman<sup>4</sup>, S. Brody<sup>5</sup>, J. Alam<sup>\*2</sup>, D. L. Meats<sup>\*2</sup>, M. Lakshmanan<sup>2</sup>, L. Plouffe<sup>\*2</sup>, M. Omizo<sup>6</sup>. <sup>1</sup>Bethesda Health Research Center, Bethesda, MD, USA, <sup>2</sup>Lilly Research Laboratories, Indianapolis, IN, USA, <sup>3</sup>North American Menopause Society, Mayfield, OH, USA, <sup>4</sup>Miami Research Associates, Miami, FL, USA, <sup>5</sup>Illinois Bone and Joint Institute, Morton Grove, IL, USA, <sup>6</sup>Oregon Osteoporosis Center, Portland, OR, USA.

Arzoxifene is a benzothiophene estrogen agonist/antagonist that is more potent and bioavailable than raloxifene (Palkowitz et al. 1997). The study was a 24-month, Phase 3, double-blind, multicenter trial of postmenopausal women with femoral neck or lumbar spine bone mineral density (BMD) T-score between -2.5 and 0 randomized to arzoxifene 20 mg/day (N=172) or to placebo (N=159). Elemental calcium 500 mg/day was provided. Primary endpoints were lumbar spine and total hip BMD change and endometrial safety. At baseline, subjects were well matched (Caucasian 83%, mean age 55 years, mean body mass index 28 kg/m<sup>2</sup>, mean lumbar spine BMD 0.95 g/cm<sup>2</sup>, total hip BMD 0.89 g/cm<sup>2</sup>, median CTX 0.58 ng/L, and median PINP 52 mcg/L). At 6 months and at subsequent assessments, BMD increases at all skeletal sites were significant ( $p < 0.05$ ) in the arzoxifene vs placebo group. At 24 months, BMD increases in the arzoxifene vs placebo group were lumbar spine 3.2%, total hip 2.3%, femoral neck 2.1%, and trochanter 3.0% ( $p < 0.001$  for all comparisons). In the arzoxifene vs placebo group, Lumbar spine BMD (2.9%,  $p < 0.001$ ) and total hip BMD (2.2%,  $p < 0.001$ ) increased from baseline to last-observation-carried-forward endpoint. No significant subgroup treatment effect at any skeletal site was observed (years postmenopausal [ $\geq 2$  and  $< 5$  vs  $\geq 5$  years], age [ $< 55$  vs  $\geq 55$  years], and ethnicity [Caucasian vs non-Caucasian]; all  $p > 0.1$ ). At 3 months and at subsequent assessments, CTX and PINP displayed a significant decrease in the arzoxifene vs placebo group ( $p < 0.001$ ), and at 24 months, CTX was decreased by 30% ( $p < 0.001$ ) and PINP was decreased by 31% ( $p < 0.001$ ) in the arzoxifene vs placebo group. There were no significant between-group differences in the incidence of endometrial hyperplasia or cancer as assessed by serial endometrial biopsy (placebo 2, arzoxifene 0) or in endometrial thickness assessed by transvaginal ultrasound. Adverse event monitoring showed no significant increase in adverse events in the arzoxifene group except for the MedDRA term "vulvovaginal mycotic infection" (placebo 0%, arzoxifene 4%,  $p = 0.02$ ). New or worsening hot flashes were not significantly different between the groups (placebo 11%, arzoxifene 12%,  $p = 0.87$ ). There were no deaths or venous thromboembolic events. In postmenopausal women with normal to low bone mass, arzoxifene 20 mg/day demonstrated significant skeletal efficacy and was well tolerated.

**Disclosures:** M. Bolognese, Eli Lilly and Company 1.

This study received funding from: Lilly Research Laboratories.



## SA422

### Excess Medical Cost after a Fragility Fracture during 3-year Follow-up: Medicare Perspective. D. Brixner<sup>\*1</sup>, N. Borisov<sup>\*2</sup>, C. Purple<sup>2</sup>. <sup>1</sup>University of Utah, Utah, UT, USA, <sup>2</sup>Procter & Gamble Pharmaceuticals, Mason, OH, USA.

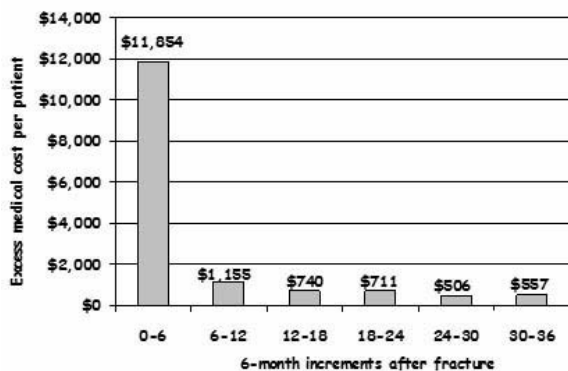
The medical costs of a fragility fracture are high in the year following the fracture (Ohsfeldt, 2006). This study estimated long-term fracture-related excess medical cost incurred during 3 years following fragility fracture compared to the cost incurred before the fracture.

Using medical claims database (Medstat MarketScan<sup>®</sup>), we conducted a retrospective cohort study among women 65+ years with a new Medicare claim for a closed non-traumatic fracture (index) at any of 7 anatomical sites: hip, leg, humerus, clavicle, pelvis, wrist, or spine between July 1, 2000 and June 30, 2005. Women with a claim for malignant neoplasm, radiation oncology or chemotherapy were excluded. The cohort was followed in 6-month increments over 3-year follow up period. To estimate fracture excess cost each post-fracture time increment was compared to the 6-month before the fracture. The excess cost was examined by place of service, fracture site, and subsequent fractures and reported in 2007 US dollars.

Out of 1,665,837 eligible women 65+ in the database during the study period, we identified 31,758 (3%) women with a Medicare claim for the specified fragility fractures. The total fracture excess medical cost was \$15,522 per patient during 3-year follow-up. Most (76%) of the excess cost was incurred during the first 6 months after the fracture (Figure 1) with costs in inpatient hospital and long term care contributing 55% and 28%, respectively. The excess prescription cost (\$590/patient) contributed 4% to the total excess cost. Nonvertebral fractures accounted for 85% of all fractures (vertebral and nonvertebral) and for 87% (\$13,469/patient) of the total excess cost. Wrist, hip, humerus, and clavicle fractures incurred excess medical costs continuously over each 6 month period of the follow-up; whereas leg, spine and pelvic fractures did not have excess costs beyond 24 months. About 14% (4,419) of women experienced a subsequent fracture during the follow-up with a total \$28,021 in excess medical cost per patient during the entire 3-year period after the index fracture.

Although most of the excess medical cost attributable to fragility fractures occurred in the first 6 months, the cost did not return to the baseline over the 3-year follow-up. This demonstrates the long-term nature of the fragility fracture costs.

Figure 1. Fracture-related excess medical cost



Disclosures: D. Brixner, P&G 2.

This study received funding from: The Alliance for Better Bone Health (Procter & Gamble Pharmaceuticals and sanofi-aventis).

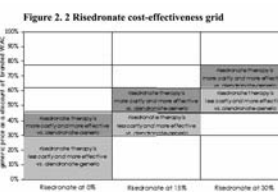
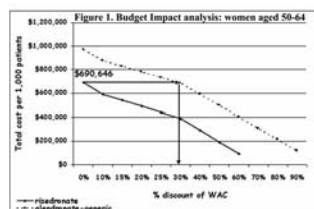
## SA423

### Cost-Effectiveness of Risedronate vs. Generic Alendronate: 1-year Analysis among Women 50-64 Years Old. D. Grima<sup>\*1</sup>, N. Borisov<sup>2</sup>. <sup>1</sup>Cornerstone Research Group Inc, Burlington, ON, USA, <sup>2</sup>Procter & Gamble Pharmaceuticals, Mason, OH, USA.

Generic alendronate to treat osteoporosis was introduced to the US market in February, 2008, at price discounts of 10% to 44% of branded alendronate. A lower price of generic may introduce some savings to a managed care (MC) budget, however, to measure the true cost, therapy's copayments, rebate discounts, and efficacy should be considered. We used a model of postmenopausal osteoporosis to compare the budget impact of risedronate to generic alendronate at a range of generic wholesale acquisition cost (WAC).

The analysis included women 50-64 years, with T-scores <-2.5, under a 1-year time horizon from MC perspective. Fracture rates and costs were derived from US sources. Vertebral and nonvertebral risk reductions were 59% and 47%, respectively, for alendronate and 65% and 74%, respectively, for risedronate. The budget impact analysis included (1) Net Drug Cost (NDC), WAC adjusted for copayment and rebate discount, and, (2) Fracture-related Cost. The discounts on both products were varied independently from 0% to 90%. Annual WAC (before adjustment) and copayment were \$1,001.39 and \$390 for risedronate and \$947.50 and \$130 for branded alendronate, respectively.

The results found risedronate's NDC below generic's NDC at every level of WAC discount due to a higher annual copayment. The difference in copayment and fracture efficacy, resulted in price equivalence of risedronate with no discount to generic alendronate at 30% discount (Figure 1). The efficacy advantage of risedronate translated into cost savings or cost-effectiveness in a wide number of rebate discount scenarios (Figure 2)



. Given current generic alendronate price discount (10%, 19%, 44% of the branded WAC by Watson, Barr, and Teva, respectively), risedronate is more effective and cost-saving without any discounts compared to the Watson and Barr generics and more effective and cost-effective compared to the Teva generic. In case of generics reducing their prices further (up to 61% of branded WAC), risedronate would remain cost-effective at 15% rebate.

Disclosures: D. Grima, P&G 5.

This study received funding from: The Alliance for Better Bone Health (Procter & Gamble Pharmaceuticals and sanofi-aventis).

## SA424

### Cost-Effectiveness of Risedronate versus Ibandronate at One Year: The Case of the United Kingdom. D. Farquhar<sup>\*</sup>, M. Pasquale<sup>\*</sup>. Procter & Gamble, Mason, OH, USA.

**Background/Objectives:** A recent observational cohort study directly comparing risedronate to ibandronate showed that women initiating treatment with risedronate had a lower incidence of hip fractures than women initiating treatment with ibandronate (Ringe, 2008). The incidence of hip fracture during the first year of therapy was 0.37% for risedronate and 0.81% for ibandronate (adjusted relative risk for risedronate vs. ibandronate: 0.51 (95% CI 0.30 - 0.87)). Despite limitations in interpretation of observational cohort studies due to the non-randomized nature of the study design, the objective of this analysis was to determine the cost-effectiveness of risedronate compared to ibandronate using these effectiveness data for the case of patients with confirmed osteoporosis in the United Kingdom (UK).

**Methods:** A validated Markov model of osteoporosis (Tosteson, 2001) was used to estimate the impact of therapy on hip fractures and costs. The model simulated a cohort of 1,000 women aged 65+, with BMD ≤ -2.5 and a previous fracture, treated with once-a-week dosing of risedronate or ibandronate over one year. UK data included annual drug cost (risedronate £264.60/year; ibandronate £257.40/year) and one-year fracture costs.

**Results:** In a cohort of 1,000 women treated with risedronate versus ibandronate, the model predicted 11 fewer fractures and a cost savings in total medical costs (drug plus fracture treatment) of £148,160. Risedronate dominates ibandronate in cost-effectiveness. Cost savings by age are specified in Table 1.

Extrapolating this result to the population of women aged 65+ in the UK initiating osteoporosis therapy suggests that risedronate would prevent an additional 1,340 hip fractures in the first 12 months of therapy and a cost savings of over £18 million, compared to ibandronate.

Table 1. Total Medical Cost Savings with Risedronate vs. Ibandronate (Cohort of 1,000)

Age Group	Number of Hip Fractures	Difference in Hip Fractures	Total Medical Cost (Drug + Fracture Treatment)	Cost Savings with Risedronate vs. Ibandronate
65-74	Ris: 4.47 Iban: 7.21	2.74	Ris: £177,848 Iban: 205,569	£27,721
75-84	Ris: 7.27 Iban: 11.73	4.46	Ris: £150,759 Iban: £218,551	£52,647
85+	Ris: 6.44 Iban: 10.39	3.95	Ris: £150,759 Iban: £218,551	£67,792
Total	Ris: 18.18 Iban: 29.33	11.15	Ris: £513,461 Iban: £661,621	£148,160

Disclosures: D. Farquhar, P&G 2.

This study received funding from: The Alliance for Better Bone Health (Procter & Gamble Pharmaceuticals and sanofi-aventis).

## SA425

### Cost-Effectiveness of Risedronate versus Ibandronate at One Year: The Case of Germany. J. Brecht<sup>\*1</sup>, M. Pasquale<sup>2</sup>, W. Moehrke<sup>3</sup>, H. Kruse<sup>\*4</sup>. <sup>1</sup>InForMed – Outcomes Research and Health Economics, Ingolstadt, Germany, <sup>2</sup>Procter & Gamble Pharmaceuticals, Mason, OH, USA, <sup>3</sup>Procter & Gamble Pharmaceuticals, Schwalbach, Germany, <sup>4</sup>Universitätsklinikum Hamburg-Eppendorf, Hamburg, Germany.

**Background/Objectives:** Recently an observational cohort study directly comparing risedronate to ibandronate showed that women initiating treatment with risedronate had a lower incidence of hip fractures than women initiating treatment with ibandronate (Ringe, 2008). The incidence of hip fracture during the first year of therapy was 0.37% for risedronate and 0.81% for ibandronate. Statistically, relative to ibandronate patients, the adjusted relative rate of hip fracture for risedronate patients was 0.51 (95% CI 0.30 - 0.87). The objective of this analysis was to determine the cost-effectiveness of risedronate compared to ibandronate using these effectiveness data for the case of osteoporotic women in Germany.

**Methods:** A validated Markov model of osteoporosis (Tosteson, 2001) was used to estimate the impact of therapy on hip fractures and costs. The model simulated a cohort of 1,000 women aged 65+, with BMD $\leq$ -2.5 and a previous fracture, treated with once-a-week dosing of risedronate or ibandronate over one year. German data included annual drug cost (risedronate €468.32/year; ibandronate €571.20/year) and one-year hip fracture costs €23,895 (Brecht, 2003).

**Results:** In a cohort of 1,000 women aged 65+ treated with risedronate versus ibandronate, the model predicted 6 fewer hip fractures and a cost savings in total medical costs (drug plus fracture treatment) of €282,520, for patients treated with risedronate versus ibandronate (Table 1). Risedronate dominates ibandronate in cost-effectiveness. Extrapolating this result to the population of women aged 65+ in Germany initiating bisphosphonate therapy suggests that risedronate would prevent an additional 1,899 hip fractures in the first 12 months of therapy at a cost savings of over €89 million, compared to ibandronate.

**Conclusions:** Based on "real world" observational data, this analysis of post-menopausal women in Germany aged 65+ suggests risedronate provides more fractures averted at a lower total medical cost, resulting in substantial cost savings compared to treatment with ibandronate.

Table 1. Fracture and Medical Cost Savings with Risedronate vs. Ibandronate (Cohort of 1,000)

Age Group	Fractures Averted with Risedronate vs. Ibandronate	Total Medical Cost (Drug + Fracture Treatment Cost)	Cost Savings with Risedronate vs. Ibandronate
65-69	3	Ris. €593,247Iban. €774,583	€181,336
70-74	4	Ris. €628,297Iban. €831,512	€203,215
75-79	9	Ris. €808,609Iban. €1,123,067	€314,215
80+	10	Ris. €842,505Iban. €1,179,303	€336,798

**Disclosures:** J. Brecht, P&G 2.

This study received funding from: The Alliance for Better Bone Health (Procter & Gamble Pharmaceuticals and sanofi-aventis).

## SA426

See Friday Plenary number F426.

## SA427

**Modeled Cost-Effectiveness of Risedronate versus Ibandronate: The Case of Italy.** S. Maggi<sup>\*1</sup>, M. Pasquale<sup>2</sup>, O. Bouin<sup>\*3</sup>. <sup>1</sup>CNR Aging Branch, University of Padua, Padua, Italy, <sup>2</sup>Procter & Gamble Pharmaceuticals, Mason, OH, USA, <sup>3</sup>sanofi-aventis, Paris, France.

**OBJECTIVE:** Recently an observational cohort study directly comparing risedronate to ibandronate showed that women initiating treatment with risedronate had a lower incidence of hip fractures than women initiating treatment with ibandronate (Ringe, 2008). The incidence of hip fracture during the first year of therapy was 0.37% for risedronate and 0.81% for ibandronate (adjusted relative risk 0.51, CI: 0.30-0.87). The objective of this analysis was to determine the cost-effectiveness of risedronate compared to ibandronate using these effectiveness data for the case of patients with confirmed osteoporosis in Italy.

**MATERIAL AND METHODS:** A validated Markov model of osteoporosis (Tosteson, 2001) was used to estimate the impact of therapy on hip fractures and costs from the Italian National Health System (NHS) perspective. The analysis included 75 year-old women treated with risedronate or ibandronate for 1 year. The model further simulated downstream costs for an additional 5 years. Country-specific data included general population hip fracture incidence rates and mortality, hip fracture costs (€11,571 in the first year, and €1,320 in subsequent years per fracture, Piscitelli, 2006), and annual drug costs (risedronate €36.34 per box and ibandronate €43.7 per box). Costs and outcomes were discounted at 3%. A differential relative risk reduction of 49% was applied to risedronate vs. ibandronate (Ringe, 2008).

**RESULTS:** In a cohort of 1,000 post-menopausal osteoporotic women with 1 year of treatment the model predicted 8 fewer hip fractures, 7 more QALYs, and a cost savings of €187,407 for risedronate compared to ibandronate. If extrapolated to a population of Italian osteoporotic women aged 70-79, this analysis suggests that 648 additional hip fractures can be avoided and over €14.6 million saved by treating patients with risedronate rather than ibandronate. Sensitivity analysis on the cost of hip fracture confirmed dominance of risedronate versus ibandronate in this patient population.

**CONCLUSIONS:** Based on Italian epidemiological data and "real world" observational effectiveness data, this analysis of post-menopausal women in Italy suggests risedronate provides more fractures averted at a lower total medical cost, resulting in substantial cost savings compared to treatment with ibandronate.

**Disclosures:** S. Maggi, P&G 2.

This study received funding from: The Alliance for Better Bone Health (Procter & Gamble Pharmaceuticals and sanofi-aventis).

## SA428

**Physician Practices in Bone Density Testing among Medicare Patients.** J. M. Neuner<sup>1</sup>, X. Zhang<sup>\*2</sup>, R. Sparapani<sup>\*2</sup>, P. W. Laud<sup>\*1</sup>, A. B. Nattinger<sup>\*1</sup>.

<sup>1</sup>Medicine, Medical College of Wisconsin, Milwaukee, WI, USA,

<sup>2</sup>Biostatistics, Medical College of Wisconsin, Milwaukee, WI, USA.

**Purpose** Medicare has recently added bone density testing of women 65 and older to its pay-for-performance program, but little is known about current testing. We sought to determine the rate of testing among physician practice panels and the contribution of both

physician and physicians' practice variables to BMD testing.

**Methods:** Women aged  $\geq$  65 enrolled in Medicare between 1999-2003 in CA, FL, IL, or NY were identified using Medicare administrative data. Physicians from these states were identified as "plurality of care" physicians if they saw subjects at least twice over a two-year period, and more than any other general internal medicine, obstetrician/gynecologist (GYN), family medicine, or general practice physician. Logistic regression models of factors associated with subject receipt of  $\geq$ 1 bone density test (ultrasound, central or peripheral DXA) in 2002-2003 was developed with the physician and his/her patient panel as the units of analysis.

**Results:** The 27,882 physicians (51% internal medicine, 32% family medicine, 10% GYN, 6% general practice) were plurality of care physicians for a median of 52 subjects. The median proportion of subjects in a physician panel with bone density tests in 2002-2003 was 27% (interquartile range 16-45%). In a regression model including only physician factors and state (table), the strongest individual predictor of bone density testing was GYN specialty. When patient panel variables were added to the model, specialty effects were reduced for gynecologists (OR 2.59 95% CI 2.53, 2.64) but increased for other specialties. The effects of other physician characteristics on testing were all slightly reduced in the larger model. Higher patient panel age, income, visit number, and percentage of black or Hispanic patients, and lower percentage of Medicaid recipients were all associated with more testing.

**Conclusions** Physician characteristics are strongly associated with bone density testing, but these associations are somewhat attenuated by physician's patient panel characteristics. Given previously described age and racial/ethnic testing disparities and limited data regarding patient preferences, pay-for-performance initiatives may need to emphasize improvements in addition to performance thresholds.

Association of Physician Characteristics with Bone Density Testing			
Physician Characteristics		Odds Ratio	95% CI
Specialty	GYN	3.38	{3.31, 3.44}
	Internal Med	1.49	{1.47, 1.52}
	Family Med	1.23	{1.21, 1.25}
	General Practice	reference	
Female Sex		1.28	{1.27, 1.29}
Panel size >median		1.30	{1.29, 1.31}
Years in Practice>median		0.84	{0.83, 0.84}

**Disclosures:** J.M. Neuner, None.

This study received funding from: National Institute on Aging.

## SA429

**Cost-Effectiveness of Ibandronate Therapy for Women with Postmenopausal Osteoporosis with Respect to Nonvertebral Fracture Efficacy.** J. A. Sunycz<sup>\*1</sup>, C. Silberman<sup>2</sup>, S. Poston<sup>\*3</sup>, S. Earnshaw<sup>\*4</sup>. <sup>1</sup>Laurel Highlands Ob/Gyn, Hopwood, PA, USA, <sup>2</sup>Roche, Nutley, NJ, USA, <sup>3</sup>GlaxoSmithKline, Research Triangle Park, NC, USA, <sup>4</sup>RTI, Research Triangle Park, NC, USA.

Bisphosphonate trials in osteoporosis are typically powered to examine change in bone mineral density and/or vertebral fracture incidence. Efficacy against nonvertebral fractures, which are less frequent, is more difficult to demonstrate. A pooled analysis of ibandronate clinical trials has been performed in which the impact of ibandronate therapy on nonvertebral fractures was estimated. In this analysis, we developed a Markov model to examine cost-effectiveness of ibandronate in postmenopausal women with established osteoporosis (vertebral fracture and bone mineral density T-score  $\leq$ -2.5; mean age 78 years) while considering nonvertebral fracture efficacy. The model, based on 5 years of therapy and a lifetime time horizon, compared cost-effectiveness of ibandronate and other bisphosphonates versus no bisphosphonate therapy. Bisphosphonate efficacy was obtained from published meta-analyses. Fracture risks, mortality, resource use, costs, and utilities were obtained from the literature. Persistence rates at 3, 6, 9, and 12 months for patients on monthly bisphosphonate therapy were derived retrospectively from managed care claims. For modeling purposes, other bisphosphonate regimens were assumed to have similar persistence rates to monthly ibandronate. Persistence was extrapolated to a maximum of 5 years. Following discontinuation, treatment benefit declined linearly and proportionally to the duration of active treatment. Yearly drug cost was referenced to wholesale acquisition cost and assumed to be the same for all bisphosphonates. Costs and outcomes were discounted 3% annually. All costs were reported in 2007 US\$. Bisphosphonate therapy conferred improvements in quality-adjusted life years (QALYs) versus no bisphosphonate therapy; ibandronate patients had greater QALY increases than patients on other bisphosphonates (0.0233 vs 0.0197). Fracture care costs were less per patient with ibandronate (\$7,652 vs. \$8,308) or other bisphosphonates (\$7,816 vs. \$8,308) than without any bisphosphonate therapy. Drug costs per patient were similar between ibandronate and other bisphosphonates--\$855 per year. Incremental cost/QALY gained (vs. no therapy) was lower with ibandronate (\$8,512) than with other bisphosphonate therapy (\$18,431). Ibandronate treatment thus resulted in cost-savings compared with other bisphosphonates. Our Markov model predicts that reduced incidence of key nonvertebral fractures with ibandronate may reduce fracture care costs for improved cost-effectiveness in comparison to other bisphosphonates.

**Disclosures:** J.A. Sunycz, GlaxoSmithKline, Roche 1.

This study received funding from: Roche and GlaxoSmithKline.

## SA430

**Falls Predict Higher Medical Costs among Osteoporosis Patients in Community Setting.** A. I. Wertheimer<sup>\*1</sup>, T. Fan<sup>\*2</sup>, S. S. Sen<sup>\*2</sup>, S. Rajagopalan<sup>\*3</sup>. <sup>1</sup>School of Pharmacy, Temple University, Philadelphia, PA, USA, <sup>2</sup>Global Outcomes Research, Merck & Co., Inc, Whitehouse Station, NJ, USA, <sup>3</sup>Med Data Analytics, Inc., New York, NY, USA.

**OBJECTIVE:** To estimate the direct medical costs of falls in a population of community-dwelling patients with osteoporosis.

**METHODS:** Data from a sample of 462 community-dwelling patients with self-reported diagnosis of osteoporosis from the 2004 Medical Expenditure Panel Survey were included to estimate their fall-associated medical expenses. The results were projected to the entire population of civilian, non-institutionalized elderly in the United States.

**RESULTS:** In 2004, among patients with osteoporosis, 13.6% of the non-institutionalized elderly osteoporotic patients in the United States reported medical conditions related to falls. The estimated total direct medical cost of these conditions was \$1.00 billion - 1.43 billion in 2004 dollars. The mean cost per person who had fallen was \$2,974 in 2004 dollars. Inpatient hospitalizations accounted for 45.6% of total costs, followed by office-based medical visits and home health care, each accounting for about 10% of total direct medical costs, and hospital outpatient visits for 7.6%. About 48.1% of fall-related costs were reimbursed by Medicare. In general linear regression models, a history of fall was a significant predictor of medical expenditures for osteoporosis patients, after adjusting for age, gender, race, education level and geographic region ( $t=-3.13$ ,  $P=0.0019$ ).

**CONCLUSION:** Fall-related medical conditions affect a substantial number of community-dwelling patients with osteoporosis and result in an enormous economic burden in the United States. Actual burden of falls may be significantly higher when nonmedical and indirect costs were included. The results of this study highlighted the importance of research about strategies to prevent falls among patients with osteoporosis.

**Disclosures:** T. Fan, Merck & Co., Inc 5.

## SA431

**Effects of Acanthopanax Senticosus Extract on Bone Metabolism In Korean Postmenopausal Women.** H. Chung<sup>1</sup>, E. Kim<sup>2</sup>, S. Yoon<sup>\*3</sup>, I. Jeong<sup>\*1</sup>, K. Ahn<sup>\*1</sup>, M. Kwon<sup>\*1</sup>, S. Chon<sup>\*1</sup>, S. Oh<sup>\*1</sup>, J. Woo<sup>\*1</sup>, S. Kim<sup>\*1</sup>, J. Kim<sup>\*1</sup>, Y. Kim<sup>\*1</sup>. <sup>1</sup>Medicine, Kyung Hee University, Seoul, Republic of Korea, <sup>2</sup>Medicine, Fatima Hospital, Daegu, Republic of Korea, <sup>3</sup>Food and Nutrition, Yonsei University, Seoul, Republic of Korea.

Acanthopanax senticosus is a traditional herbal medicine for reducing inflammation, enhancing liver function and musculoskeletal system. In preliminary study, Acanthopanax senticosus extract has shown increased osteoblastic cell proliferation, differentiation and bone nodule formation. The purpose of this study was to determine the safety and effect of Acanthopanax senticosus extract as an alternative medicine on bone metabolism in Korean postmenopausal women. The subjects were 81 healthy female with postmenopausal osteopenia and osteoporosis. The subjects were randomly assigned into treatment and control group. Treatment group received Acanthopanax senticosus extract (3g/d) and all subjects were received calcium and vitamin D for 6 months. DXA of spine and hip were obtained at baseline and at 6 months. Level of serum C-telopeptide and osteocalcin were also measured as bone markers. Safety was assessed by recording of all adverse events and regular monitoring of blood biochemical tests. In the treatment group, bone mineral density did not increased at spine and femur compared with the control group. At 6 months, however, levels of serum osteocalcin significantly increased in the treatment group. There are no significant differences of adverse events and biochemical blood tests between the groups. This study suggest that Acanthopanax senticosus extract is safe as an alternative herbal medicine and may have a role in bone metabolism. However, further study for longer period to see BMD changes should be performed.

**Disclosures:** H. Chung, None.

This study received funding from: Korea Health Industry Development Institute.

## SA432

**The Effect of a One Year Exercise Program on Markers of Bone Metabolism after Hip Fracture.** J. Yu-Yahiro<sup>1</sup>, E. Streeten<sup>2</sup>, M. Hochberg<sup>2</sup>, D. Orwig<sup>\*2</sup>, J. Magaziner<sup>2</sup>. <sup>1</sup>Department of Orthopaedics, Union Memorial Hospital, Baltimore, MD, USA, <sup>2</sup>Epidemiology and Preventive Medicine, University of Maryland School of Medicine, Baltimore, MD, USA.

A study has been conducted to evaluate the impact of home-based exercise over one year in minimizing losses in bone and muscle. This project compared markers of bone metabolism in hip fracture patients randomized exercise or usual care.

Community dwelling women, with fresh femur fractures were randomized to exercise and usual care groups (N=75 each). Exercisers began the intervention at the end of the usual post-acute physical therapy (mean 72 ± 4.5 days). Exercise was five, 45 minute sessions per week, 3 aerobic and 2 strength training, including a maximum of 56 trainer-supervised sessions decreasing in frequency from the beginning to the end of program.

Serum was collected at baseline (within 15 days of fracture), and 60, 180, and 360 days post fracture. Samples were processed and stored at -70C and analyzed for bone specific alkaline phosphatase (BAP) by immunoradiometric assay, and C-terminal propeptide of type 1 collagen (CICP) and carboxyterminal cross-linked telopeptide of type 1 collagen (CTX) by ELISA. The intention-to-treat principle was followed and generalized estimating equations were used to perform repeated measures analyses with time and intervention as fixed effects.

Of exercisers, 81% were actively followed by a trainer and 18% refused participation after being enrollment. Participants received an average of 44 (78%) of the prescribed visits by the exercise trainer.

Although markers of osteoblastic activity, BAP and CICP appeared to decline over time in both exercisers and controls, there were no significant differences in levels of either marker over time (Table 1). Likewise, there were no differences between the two groups at 2, 6, or 12 months. CTx levels were similar in controls and exercisers at all points with no differences found overtime in either group.

In conclusion, compared to a group receiving usual care post fracture, participation in a year long program of exercise after hip fracture did not cause changes in osteoblastic or osteoclastic activity as evidenced by measurement of three markers of bone metabolism.

Table 1: Serum Markers of Bone Metabolism and Exercise Intervention

Group	2 months mean (SE) n	6 months mean (SE) n	12 months mean (SE) n	Between Group Differences
Control	18.42 (1.65) 56	14.65 (1.42) 57	11.93 (1.03) 53	
BAP				
Exercise	17.84 (2.11) 51	13.35 (0.93) 60	10.97 (0.87) 55	p=0.91
Control	108.9 (8.3) 56	98.1 (6.8) 57	77.5 (5.7) 53	
CICP				
Exercise	116.9 (11.9) 51	89.9 (5.8) 60	81.6 (5.4) 55	p=0.16
Control	0.74 (0.05) 56	0.64 (0.05) 57	0.52 (0.04) 53	
CTX				
Exercise	0.74 (0.05) 51	0.55 (0.03) 60	0.54 (0.04) 55	p=0.103

All time specific differences n.s. at the .05 level.

Note: all post-randomization values (2 months to 12 months) were adjusted for baseline (pre-randomization) values.

**Disclosures:** J. Yu-Yahiro, None.

This study received funding from: National Institute on Aging.

## SA433

See Friday Plenary number F433.

## SA434

**Male Perspectives on Osteoporosis Suggest that Continuous Followup and Tailored Groups for Patient Education Are Important Issues - Focus Group Interviews.** D. S. Nielsen<sup>1</sup>, K. Brixen<sup>2</sup>, L. Huniche<sup>\*3</sup>. <sup>1</sup>Endocrinology, Odense University Hospital, Odense, Denmark, <sup>2</sup>Institute of Clinical Research, University of Southern Denmark, Odense, Denmark, <sup>3</sup>Health, Man & Society, Institute of Public Health, University of Southern Denmark, Odense, Denmark.

Several studies have confirmed that osteoporotic fractures in men are an increasing public health problem. Male osteoporosis, however, is underdiagnosed and undertreated. The purpose of this study was to gain insight into how men experience being diagnosed with osteoporosis and how they handle osteoporosis in their everyday lives. In particular focus was directed on information, patient education, and patients' acceptance of treatment.

**Methods:** Data were collected from 4 focus groups with a total of 16 men aged 52-82 years diagnosed with osteoporosis. Data analysis aimed to elicit knowledge derived from the men's everyday lives and experiences. A thematic analysis approach was used. The analysis was discussed with other researchers, in order to develop analytical categories and interpretations.

**Results:** The interviews illustrated that information, patient education, and acceptance of treatment are of varying importance and utilised in different ways in the everyday lives of men with osteoporosis.

Problem	Impact on everyday life
Difficult to tell friends, family and colleagues about having osteoporosis - osteoporosis is considered a female's disease	Barrier to implement lifestyle changes and abstain from heavy lifting and strenuous jobs - It is important for most men to appear as strong and masculine.
In health promotion campaigns are often used.	Professionals should have a concerned and empathetic approach to patients - Important to patient's motivation, and to how patients handle osteoporosis in the every day life.
The health care system is offering mainly individual consultations.	Most of the men suggested group-based patient education programs. Some preferred being together with women due to women's way of being open about feelings. Others preferred men-only groups to enhance the sharing of experiences.
At times, participants felt it difficult to take the medication.	Motivation fades out with time. A continuous follow up (e.g. once a year) at the doctor or osteoporosis specialist nurse was considered as very important.

**Conclusion:** The study underscores the importance of working with the everyday context and perspective of the patient in the health care system. A better understanding of how osteoporosis affects men may help to develop specific preventive strategies as well as enhancing patients' acceptance of treatment.

**Disclosures:** D.S. Nielsen, None.

## SA435

See Friday Plenary number F435.

## SA436

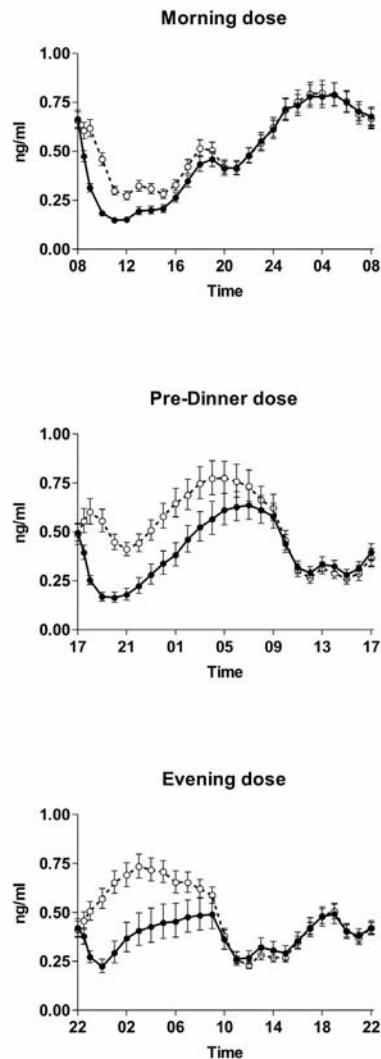
**Exploring the Effect of Food Intake On Bone Resorption for Optimal Drug Delivery and Efficacy in Osteoporosis with Oral Calcitonin.** M. A. Karsdal, I. Byrjalsen, B. J. Riis\*, C. Christiansen. Nordic Bioscience, Herlev, Denmark.

Bone resorption displays marked diurnal variation. Completely reversible inhibition of bone resorption may result in best possible efficacy when bone resorption peaks, i.e. during the night. The aim of the study was to assess the pharmacokinetic (PK) and pharmacodynamic (PD) profiles of 0.8 mg of oral salmon calcitonin (sCT) and the effect of timing of drug intake in healthy postmenopausal women.

The study was a randomized, double-blind, double-dummy, placebo-controlled, crossover phase I study to assess the pharmacokinetic (PK) and pharmacodynamic (PD) profiles of 0.8 mg of oral sCT in healthy postmenopausal women. 81 subjects were included. Morning dose was given at 8:00 ( $n=42$ ), a pre-dinner dose given at 17:00 ( $n=20$ ) and evening dose given at 22:00 ( $n=19$ ). Blood sampling occurred before drug intake, and at 5, 10, 15, 30, 45 minutes, 1, 1½, 2, 2½, 3 hours, and every hour until 24 hours after dosing. The absorption of calcitonin was assessed by measurement of plasma sCT concentrations, and bone resorption by the biochemical marker serum CTX-1.

Morning and pre-dinner dosing led to comparable concentrations of sCT (45 pg/ml), whereas there was a tendency towards lower  $C_{max}$  for the evening dosing having a mean of 24 pg/ml. Overall, dosing with oral sCT resulted in significant suppression of serum CTX irrespective of dosing time, although with different pharmacodynamic parameters (Figure 1). The morning dose of oral sCT resulted in a placebo-corrected  $AUC_{0-24hrs}$  of serum CTX of -232 (% x hrs) corresponding to a permanent overall suppression of bone resorption by 10%. The pre-dinner dose was twice as effective in suppression of serum CTX giving a mean  $AUC_{0-24hrs}$  of -603 (% x hours) equal to an overall suppression of 25%. The  $AUC_{0-24hrs}$  of the evening dose was at the same level of magnitude at -538 (% x hrs) although there seemed to be a higher inter-individual variation in the response associated with this dosing time.

**Conclusion:** The study suggests that orally administered 0.8 mg of salmon calcitonin was effective in suppression of serum CTX over 24h irrespective of time of dosing. The pre-dinner dosing at 17:00 resulted in optimum efficacy response corresponding to an overall suppression of bone resorption by 25%. In the optimization of efficacy of completely reversible anti-resorptive drugs, the physiological timing of drug dosage is important to optimise drug efficacy.



**Disclosures:** M.A. Karsdal, None.

## SA437

**Osteoporosis in the Old Old: Review of the Evidence.** C. A. Inderjeeth, A. Foo\*, M. Lai\*. Rehabilitation and Aged Care, Sir Charles Gairdner Hospital, Nedlands, Australia.

Women  $\geq 80$  years of age comprise approximately 8% of the post-menopausal population but contribute  $> 30\%$  of all fragility fractures and 60% of hip fractures because of the high prevalence of osteoporosis and high incidence of falls in this age group. However there is limited data in this age group for treatment.

**Objectives of this review:** To review the published literature on the clinical efficacy and safety of specific anti osteoporosis treatments in the reduction in fracture risk in females in the old old (greater than 80 years of age). The following major endpoints were used in this review:

1. Vertebral fracture reduction at 1 year and 3 years
2. Non-vertebral fracture reduction at 1 year and 3 years
3. Hip fracture reduction at 1 year and 3 years.
4. Safety data with these agents in the old old.

Studies had to be randomised placebo or active comparator control trials of at least 1-year duration including post-menopausal females. Pooled analysis and published sub-group analysis, specifying the sub-group 80 years or older were also included.

**Results:** The only publications that specifically reported data in patients from 80 - 100 years old were pooled analysis of the SOTI and the TROPOS study by Seeman et al and the pooled analysis of VERT MN, VERT NA and HIP study by Boonen *et al*. These results are summarised in table 1.

**Table 1. Fracture Efficacy In Randomised Patients 80-100 Years**

Fracture Risk	STRONTIUM RANELATE STUDIES				RISERDRONATE 5mg STUDIES			
	Placebo	Strontium Ranelate	Relative Risk Reduction (p value)	ARR NNT	Placebo	Risedronate	Relative Risk Reduction (P Value)	ARR NNT
Vertebral Fracture 1 Year	8.3%	3.5%	59% (p=0.002)	4.8% 21	10.9%	2.5%	81% (p < 0.001)	8.4% 12
-3 Years	26.5%	19.1%	32% (p=0.013)	7.4% 14	24.6%	18.2%	44% (p= 0.003)	6.4% 16
Non Vertebral Fracture 1 Year	6.8%	4.0%	41% (p=0.027)	2.8% 36	NA	NA	NA (p=0.66)	NA (NS)
3 Years	19.7%	14.2%	31% (p=0.011)	5.5% 18	16.2%	14.0%	NS 2.2% (NS)	- (NS)
Hip Fracture 3 Years	7.4%	5.2%	41% (NS) (p=0.112)	2.2% (NS)	5.1%	4.2%	NS* (p=0.35)	0.9% (NS)

\* Includes Hip study patients only - selected on the basis of non-skeletal risk factors for hip fractures rather than established osteoporosis.

**Conclusion:** This literature review reinforces the irony that we have the least evidence for fragility fracture reduction in the group at greatest risk who are likely to sustain the greatest potential harm with the greatest risk of disability and mortality and at potentially the greatest cost to society. This calls for better randomised controlled trials to provide better evidence for treatment of this patient group who are likely to place increasing demands on limited per-capita health care resources in future decades.

**Disclosures:** C.A. Inderjeeth, Servier 1, 2, 3; Sanofi Aventis 1, 2, 3, 4; MSD 1, 3; Eli Lilly 1, 4.

## SA438

**Weight and Body Mass Index Predict Bone Mineral Density and Fractures in Women 40 to 59 years.** S. N. Morin<sup>1</sup>, J. F. Tsang<sup>\*2</sup>, W. D. Leslie<sup>2</sup>.<sup>1</sup>Medicine, McGill University, Montreal, QC, Canada, <sup>2</sup>Medicine, University of Manitoba, Winnipeg, MB, Canada.

Risk factors for the prediction of osteoporosis and fractures have not been extensively characterized in younger women. We evaluated the associations between weight, body mass index (BMI), Osteoporosis Self-Assessment Tool (OST), bone mineral density (BMD) and fracture risk in women aged 40 to 59 years.

Using administrative databases, we conducted a retrospective cohort study in 8,254 women age 40-59 years who had baseline BMD testing. Cox proportional hazards models were created to examine the associations with weight, BMI, OST, BMD and subsequent non-traumatic fractures during 3.3 years of follow up.

Body weight, BMI and OST had similar overall performance in their ability to classify women with femoral neck T-score  $\leq -2.5$  (area under the ROC curve 0.76; 95% CI: 0.73-0.78, 0.72; 95% CI: 0.70-0.75, 0.77; 95% CI: 0.75-0.79, respectively). During 27,256 person-years of observation, 225 women (2.7 %) experienced one or more incident fractures. After adjustment for age, prevalent fractures and use of systemic corticosteroids, each standard deviation decrease in weight was associated with a 19% increase in the risk of incident fracture (95% CI: 1.01-1.35). Femoral neck BMD and the presence of prevalent fractures were also positively associated with the risk of incident fractures.

Low weight and BMI predict osteoporosis and are associated with an increase in the risk of fractures in younger women. The negative impact of low body weight on bone health should be more widely recognized.

Table Risk of Incident Fractures

	Univariate HR (95% CI)	Multivariate HR (95% CI) without BMD	Multivariate HR (95% CI) with BMD
<b>Model 1</b>			
Weight per SD decrease	1.17 (1.01-1.35)	1.19 (1.03-1.37)	0.97 (0.84-1.14)
Age per decade increase	--	1.07 (0.94-1.22)	0.98 (0.85-1.12)
Prevalent osteoporotic fracture	--	3.28 (2.36-4.57)	2.68 (1.91-3.76)
Systemic corticosteroid use	--	1.24 (0.75-2.04)	0.97 (0.59-1.61)
Femoral neck BMD per SD decrease	--	--	1.61 (1.37-1.89)
<b>Model 2</b>			
BMI per SD decrease	1.17 (1.01-1.35)	1.18 (1.02-1.37)	1.00 (0.86-1.17)
Age per decade increase	--	1.07 (0.94-1.22)	0.98 (0.86-1.12)
Prevalent osteoporotic fracture	--	3.26 (2.35-4.54)	2.70 (1.93-3.78)
Systemic corticosteroid use	--	1.25 (0.76-2.06)	0.98 (0.59-1.63)
Femoral neck BMD per SD decrease	--	--	1.59 (1.36-1.86)
<b>Model 3</b>			
OST per SD decrease	1.19 (1.03-1.38)	1.20 (1.04-1.39)	0.98 (0.83-1.14)
Prevalent osteoporotic fracture	--	3.29 (2.36-4.57)	2.68 (1.91-3.75)
Systemic corticosteroid use	--	1.24 (0.75-2.03)	0.97 (0.59-1.62)
Femoral neck BMD per SD decrease	--	--	1.60 (1.37-1.88)

**Disclosures:** S.N. Morin, Merck 1; Amgen 4; Novartis 1, 4; Alliance Better Bone Health 1, 4.

## SA439

See Friday Plenary number F439.

## SA440

**Obesity and Bone Architecture in Men - Can We Apportion the Metabolic and the Mechanical Effect?** P. Szulc, S. Boutroy<sup>\*</sup>, P. D. Delmas. INSERM 831, Hopital E. Herriot, Lyon, France.

Obesity is associated with higher areal bone mineral density (aBMD), but architectural basis and pathophysiological mechanisms underlying this association at the weight-bearing and the non-weight-bearing sites are not fully understood. High resolution peripheral quantitative computed tomography was carried out in 1128 men aged 20 to 88 years at the distal radius and distal tibia by using the XtremeCT device (Scanco Medical AG). Architectural parameters were compared in three groups of men according to their body mass index (BMI): normal weight ( $\leq 25$  kg/m<sup>2</sup>, n=349, mean age - 56 years), overweight ( $25 < \text{BMI} \leq 30$  kg/m<sup>2</sup>, n=555, mean age - 65 years) and obesity ( $> 30$  kg/m<sup>2</sup>, n=224, mean age - 68 years). For the comparisons between the skeletal sites, all the investigated variables were transformed into Z-score using the parameters of the normal weight men as the reference group. At the radius and tibia, total cross-sectional area did not differed across the groups. After adjustment for age, overweight and obese men had significantly higher cortical area and thickness, higher total and trabecular (but not cortical) volumetric BMD (vBMD), higher trabecular number (but not the estimated trabecular thickness) and more homogeneously distributed trabeculae (lower variability of the trabecular separation in an individual). In the overweight and obese men, total, trabecular and outer (subendocortical) trabecular vBMD were similarly increased at the radius (0.25 to 0.39 SD,  $p < 0.005$ -0.0001) and at the tibia (0.31 to 0.45 SD,  $p < 0.001$ -0.0001) compared with the

normal men. In the overweight and obese men, trabecular separation and its variability were similarly reduced at the radius (0.27 to 0.50 SD,  $p < 0.005$ -0.0001) and the tibia (0.23 to 0.58 SD,  $p < 0.01$ -0.0001). By contrast, in comparison with the normal weight men, some parameters were more increased in the obese men at the tibia than at the radius: cortical area (0.61 vs 0.39 SD,  $p < 0.02$ ), trabecular number (0.84 vs 0.62 SD,  $p < 0.03$ ) and the central (inner) trabecular vBMD (0.42 vs 0.26 SD,  $p < 0.03$ ).

Thus, in these predominantly trabecular skeletal sites, obesity was associated with a similar increase in certain parameters at the weight-bearing distal tibia and at the non-weight-bearing distal radius suggesting that they may depend mainly on the metabolic changes related to the obesity e.g., higher peripheral estrogen synthesis. By contrast, in the obese men, the cortical area, the trabecular number and the inner trabecular vBMD were more increased at the weight-bearing distal tibia compared with the non-weight-bearing distal radius suggesting that, in men, the mechanical load may be a significant determinant of these architectural parameters.

**Disclosures:** P. Szulc, None.

## SA441

**A High-fat Diet Negatively Regulates Bone Development in Growing Mice.**

L. Wang<sup>\*1</sup>, S. Yan<sup>\*2</sup>, C. Li<sup>\*1</sup>, J. Zhao<sup>\*3</sup>, K. Ding<sup>\*4</sup>, M. Wang<sup>\*5</sup>, J. Xu<sup>\*1</sup>, L. Zhou<sup>\*6</sup>, M. Hamrick<sup>7</sup>, C. Isaacs<sup>4</sup>, Q. Mi<sup>6</sup>. <sup>1</sup>Center for Biotechnology and Genomic Medicine, Medical College of Georgia, Augusta, GA, USA, <sup>2</sup>Dept. of Medicine, The Medical School Hospital of Qingdao University, Qingdao, China, <sup>3</sup>Dept. of Medicine, Shangdong University Medical School, Jinan, China, <sup>4</sup>Dept. of Medicine, Medical College of Georgia, Augusta, GA, USA, <sup>5</sup>Dept. of Physiology, Medical College of Georgia, Augusta, GA, USA, <sup>6</sup>Dept. of Pathology, Medical College of Georgia, Augusta, GA, USA, <sup>7</sup>Dept. of Cellular Biology, Medical College of Georgia, Augusta, GA, USA.

High fat diet (HFD) results in obesity, which is well known to affect both bone density and quality in adults. However, it is unclear how HFD affects the bone development during childhood. The purpose of this study was to determine the effect of HFD on bone structure and mechanics in young adult mice. Female CD1 mice were fed with either HFD or normal fat diet (NFD) starting at 4-weeks of age for 10 weeks. The HFD contained 36% fat (15.2% saturated, 20.8% unsaturated) and NFD 4.4% fat (2.5% saturated, 1.9% unsaturated). The bone mineral content (BMC), bone mineral density (BMD), fat and lean mass were examined in 14-week old mice using dual-energy X-ray absorptiometry, and bone biomechanical properties were also evaluated using three-point bending test. The body weight and fat mass in HFD-treated mice increased almost 2-5 fold compared to that in NFD-treated mice, respectively. The whole body BMD, BMC, bone area and lean mass in HFD-treated mice were slightly higher than that in NFD mice ( $P > 0.05$ ). However, the spine BMC and bone area in HFD mice were significantly lower than that in NFD mice ( $P < 0.01$ ), while femoral BMD ( $P < 0.01$ ), BMC ( $P < 0.01$ ) and bone area ( $P < 0.05$ ) in HFD mice were significantly greater than that in NFD mice. But, there was no statistically different in bone biomechanical values between the two groups. When these results were adjusted based on body weight or fat mass, the body BMD, BMC, bone area, and femur BMD and BMC tended to be lower in HFD-treated mice in comparison to NFD mice although the difference was not statistically significant. Our preliminary data suggest that the vertebral bone is more sensitive to HFD-induced bone loss compared to the long bones in young, growing animals. Considering that childhood and adolescence are crucial periods to acquire nearly half of the peak bone mass, high-fat diet in young adult might be one reason for the increasing prevalence of osteoporosis during adult and aging.

**Disclosures:** Q. Mi, None.

This study received funding from: JDRF and CNSF.

## SA442

**Effects of Diacylglycerol Oil on Body Composition, Bone Mineral Density and Bone Strength in Mice.** H. Choi<sup>\*1</sup>, W. Jung<sup>\*2</sup>, Y. Rhee<sup>1</sup>, S. Kim<sup>\*3</sup>, J. Y. Jeon<sup>\*4</sup>, I. Paik<sup>\*2</sup>, E. Lee<sup>\*1</sup>, S. Lim<sup>1</sup>.

<sup>1</sup>Department of Internal Medicine, Yonsei University College of Medicine, Seoul, Republic of Korea, <sup>2</sup>Department of Physical Education, Yonsei University, Seoul, Republic of Korea, <sup>3</sup>Department of Internal Medicine, Kwandong University College of Medicine, Goyang, Republic of Korea, <sup>4</sup>Department of Sports and Leisure Studies, Yonsei University, Seoul, Republic of Korea.

Background: A high fat diet (HFD) is known to promote obesity and insulin resistance, causing metabolically deleterious effects on the body. Total fat intake, especially saturated fat intake, has been reported to be associated with a higher risk of osteoporotic fractures. Meanwhile, consuming a diet rich in diacylglycerol (DAG) oil instead of triacylglycerol (TAG) has been reported to have metabolically beneficial effects such as reduction in body weight and abdominal fat and improvement in lipid profile. However, there has been no study investigating the effects of DAG on bone mineral density (BMD) and strength in mice.

Methods: Four-week-old male 38 C57BL/6J mice were divided into 4 groups: the chow diet group (n=10), HFD group (n=9), HFD with high DAG group (n=10), and HFD with exercise group (n=9). After 17 weeks of treatment, body composition and BMD were measured using DXA, and bone strength of the femur was measured by a 3-point bending test.

Results: Body weight was significantly lower in the HFD with high DAG ( $38.3 \pm 2.0$  g) and HFD with exercise ( $36.2 \pm 2.8$  g) groups than the HFD group ( $46.2 \pm 2.3$  g). Percent fat mass was significantly lower in the HFD with exercise group ( $32.7 \pm 5.6\%$ ) than the HFD

group ( $42.7 \pm 3.3\%$ ). The HFD with high DAG ( $0.0668 \pm 0.0041 \text{ g/cm}^2$ ) and HFD with exercise ( $0.0684 \pm 0.0053 \text{ g/cm}^2$ ) groups had significantly higher femur BMD than the HFD group ( $0.0611 \pm 0.0032 \text{ g/cm}^2$ ), although such differences were not found in the 3-point bending test.

Conclusions: DAG may have beneficial effects on BMD. Further studies are needed to elucidate the effects of DAG on the skeleton.

**Disclosures:** H. Choi, None.

## SA443

**Vitamin K Treatment for One Year Does Not Alter Femur Geometry in Postmenopausal Women.** N. Vallarta-Ast<sup>1</sup>, D. Krueger<sup>1</sup>, J. W. Suttie<sup>2</sup>, N. Binkley<sup>1</sup>. <sup>1</sup>Osteoporosis Clinical Research Program, University of Wisconsin, Madison, WI, USA, <sup>2</sup>University of Wisconsin, Madison, WI, USA.

A potential role of vitamin K in reducing osteoporotic fracture risk remains controversial. Recently, it has been reported that vitamin K supplementation favorably alters femur geometric parameters. Such effects could lead to a reduction in fracture risk but not be appreciated by bone mineral density as measured by dual energy x-ray absorptiometry (DXA). To investigate this possibility, we re-analyzed femur DXA scans from a prospective randomized clinical study of healthy postmenopausal women without osteoporosis. Briefly, in this study, 381 postmenopausal women were randomly assigned to receive phylloquinone (K1) 1,000 mcg daily, menatetrenone (MK4) 45 mg daily, or placebo for one year. Subjects were [mean ( $\pm$  SE)]  $62.3 (\pm 0.4)$  years and had a mean BMI of  $28.5 (\pm 0.3) \text{ kg/m}^2$ . All participants received daily calcium with vitamin D. DXA scans were performed using a GE Lunar DPX-IQ at baseline and after 6 and 12 months. For this report, the baseline and 12 month femur scans were re-analyzed with software version 4.7. Hip geometric parameters were obtained using the software auto-analysis feature and include femur neck and total femur area, femur neck width, hip axis length (HAL), femur neck cross-sectional area (CSA), femur neck cross-sectional moment of inertia (CSMI) and the GE proprietary femur strength index (FSI).

No change in any of the measured femur geometric parameters was observed in the placebo group and no differences in any parameter were observed with either K1 or MK4 treatment compared with placebo (Table).

Table: Selected femur DXA parameters

Group	N	FN BMC (g)		FN Width (mm)		CSA (mm <sup>2</sup> )		FSI	
		Base	12m	Base	12m	Base	12m	Base	12m
Placebo	124	4.342 (.059)	4.343 (.060)	31.28 (.24)	31.39 (.23)	154.2 (2.2)	153.7 (2.2)	1.29 (.03)	1.31 (.03)
K1	115	4.464 (.062)	4.445 (.062)	31.57 (.21)	31.51 (.21)	159.6 (2.3)	159.4 (2.2)	1.43 (.04)	1.45 (.04)
MK4	119	4.432 (.063)	4.407 (.062)	31.72 (.22)	31.72 (.22)	157.8 (2.3)	157.3 (2.3)	1.40 (.03)	1.39 (.03)

Data presented as mean  $\pm$  SE.

In conclusion, no effect of one-year treatment with vitamins K1 or MK4 on DXA-measured parameters of femur geometry was observed. It remains possible that longer duration studies could identify vitamin K-related changes.

**Disclosures:** N. Vallarta-Ast, None.

## SA444

See Friday Plenary number F444.

## SA445

**Goettingen Minipigs - A Model for Ca/Vit D-Deficiency Osteomalacia and Steroid-induced Osteoporosis.** K. E. Scholz-Ahrens<sup>1</sup>, C. C. Glüer<sup>2</sup>, W. Timm<sup>3</sup>, Y. Açı<sup>1</sup>, W. Yan-Clasen<sup>1</sup>, J. Schrezenmeier<sup>1</sup>. <sup>1</sup>Physiologie und Biochemie, Max-Rubner-Institut, Kiel und Karlsruhe, Germany, <sup>2</sup>Medizinische Physik, Klinik für Diagnostische Radiologie, Universitätsklinikum Schleswig-Holstein - Campus Kiel, Kiel, Germany, <sup>3</sup>Klinik für Mund-, Kiefer- und Gesichtschirurgie, Universitätsklinikum Schleswig-Holstein - Campus Kiel, Kiel, Germany.

Ca and Vit D intake of the elderly in Western societies is often inadequate and their Vit D synthesis and renal Ca reabsorption tend to be diminished. To study this condition, we developed a minipig model for osteomalacia by evaluating the effect of Vit D and Ca deficiency in comparison with a model for osteoporosis induced by glucocorticoids. Three diet groups, each made up of ten 30 month-old minipigs, were studied: 1) 0.6% Ca, 6500 IU Vit D/kg diet (control group), 2) 0.2% Ca, no Vit D (osteomalacia); 3) 0.6% Ca, 6500 IU Vit D/kg diet and a daily dose of 1mg/kg BW prednisolone for 8 wks, thereafter 0.5mg/kg BW (osteoporosis). After 15 months, the Ca balance (mg/7d) had decreased in both experimental groups, by 6175 mg ( $\pm$ 2355) in the osteomalacia group ( $p < 0.05$ ), and by 3411 ( $\pm$ 2023) mg in the osteoporosis group ( $p > 0.05$ ), while there was only a small decrease of 388 ( $\pm$ 1146) mg in the control group. The decrease in bone mineral density (BMD, mg/cm<sup>3</sup>) in vivo was similar in both experimental groups ( $51.2 \pm 14.7$  and  $56.7 \pm 8.3$ , respectively), and significantly different from the marginal decline in the control group ( $2.3 \pm 11.8$ ). In the osteomalacia group, plasma concentrations of 25(OH)-Vit D were lower ( $p < 0.05$ ) and of 1,25(OH)<sub>2</sub>-Vit D higher ( $p < 0.05$ ) than in the osteoporosis and control group. Bone alkaline phosphatase levels tended to be higher in the osteomalacia group, compared to the control, and were significantly higher most of the time than in the

osteoporosis group. Bone resorption, evaluated by deoxypyridinoline-crosslinks, was unchanged and not different between groups. Because bone density loss was similar in both conditions, but differed with regard to osteoblast activity and Vit D metabolism, the minipig seems to be a valid model to study Ca/Vit D-deficiency osteomalacia and steroid-induced osteoporosis.

**Disclosures:** K.E. Scholz-Ahrens, None.

This study received funding from: Deutsche Forschungsgemeinschaft.

## SA446

**Effects of Potassium Bicarbonate on Calcium- and Bone Metabolism during High Salt Intake.** P. Frings-Meuthen<sup>\*</sup>, J. Buehlmeier<sup>\*</sup>, N. Baecker<sup>\*</sup>, M. Heer. Institute of Aerospace Medicine, German Aerospace Center, Cologne, Germany.

We have recently shown that high salt intake led to decreases in blood pH and bicarbonate concentration accompanied by increases in bone resorption markers (Frings-Meuthen et al. J Bone Miner Res 2008; 23:517-524). Since pH decrease is a mandatory condition to activate osteoclasts, we hypothesize that the increased bone resorption is initiated by a low-grade metabolic acidosis. Administration of an alkali salt may counteract the acidosis and thereby decrease the bone resorption induced by a high salt intake. In a metabolic ward study with 8 healthy male test subjects (mean age:  $25.8 \pm 3.9$  years; body weight (BW)  $75.4 \pm 3.6$  kg) we examined the ability of KHCO<sub>3</sub> to prevent salt-induced bone loss. 4 days of adaptation with a normal salt intake (2.8 mmol/kgBW/d) were followed by 10 days of high salt intake (7.7 mmol/kgBW/d) combined in one trial with a supplementation of  $3 \times 30$  mmol KHCO<sub>3</sub> per day in a cross-over design. Urinary calcium (UCA) excretion and bone resorption markers (C- and N-terminal telopeptide of type I collagen (CTX, NTX)) were analyzed in all 24-hour urine collections. Fasting morning blood was analyzed for the bone formation markers, bone specific alkaline phosphatase (bAP), and N-terminal of propeptide of type I procollagen (PINP). Postprandial parathyroid hormone (ppPTH) measurements were used to provide an insight into the involvement of PTH in salt-induced bone loss. KHCO<sub>3</sub> supplementation was able to reduce salt-induced calciuria by only 12 % ( $p = 0.04$ ) and NTX excretion by only 8 % ( $p = 0.04$ ); no significant decrease was observed in the bone resorption marker CTX ( $p = 0.18$ ). Bone formation marker PINP ( $p = 0.92$ ) and bAP ( $p = 0.95$ ) remained unchanged. However, ppPTH levels were twofold higher 25 minutes after KHCO<sub>3</sub> supplementation ( $p < 0.001$ ). High salt intake itself did not affect ppPTH. The KHCO<sub>3</sub>-induced PTH increase might play an important role in the attenuated effectiveness of potassium bicarbonate to reduce salt-induced bone loss.

**Disclosures:** P. Frings-Meuthen, None.

## SA447

**Ovariectomy-Induced Hyperphagia Does Not Modulate Bone Mineral or Bone Strength in Female Sprague-Dawley Rats.** J. M. Y. Jiang<sup>\*</sup>, S. M. Sacco<sup>\*</sup>, W. E. Ward. Nutritional Sciences, University of Toronto, Toronto, ON, Canada.

Osteoporosis is a skeletal disorder characterized by compromised bone strength, leading to an increased susceptibility to fragility fractures. The adult ovariectomized (OVX) rat is the FDA-recommended model for postmenopausal osteoporosis and plays a crucial role in the development of prevention and treatment strategies. While ovariectomy closely mimics the postmenopausal skeleton, it also induces secondary effects of hyperphagia, increased weight gain, and adiposity. Increased body weight is associated with protective effects on bone, and thus may be a confounder in preclinical studies investigating the effects of interventions on bone health. For this reason, pair-feeding is commonly used to control food intake and prevent hyperphagia-associated weight gain. However, the effects of hyperphagia on bone and the importance of pair-feeding have not been elucidated. The objective of this study was to determine whether the type of feeding, pair versus *ad libitum*, modulates bone mineral and bone strength using the OVX rat model of postmenopausal osteoporosis. Three-month old female Sprague-Dawley rats ( $n=14$ /group) were randomized to 1) sham-operated control (SHAM); 2) ovariectomized pair-fed (OVX-PF); or 3) ovariectomized *ad libitum* (OVX-AL). All rats were fed a standard pelleted diet (AIN93M). Pair-feeding involved matching the food intake of OVX-PF rats to the average amount of food eaten by the SHAM group the day before. At the end of 14 weeks, lean mass and fat mass were measured by dual energy x-ray absorptiometry (DEXA). Bone mineral density (BMD) and biomechanical bone strength were assessed at the femur and the lumbar vertebrae (LV). OVX-AL rats consumed more food ( $P < 0.05$ ) than both the SHAM and OVX-PF during the first 5 weeks of study, but hyperphagia disappeared by 7 weeks. Final body weight ( $P < 0.01$ ), weight gain ( $P < 0.01$ ), and fat mass ( $P < 0.05$ ) were higher among OVX-AL rats than both SHAM and OVX-PF rats, while no differences were observed between the SHAM and OVX-PF groups. SHAM rats had higher femur ( $P < 0.001$ ) and LV1-3 BMD ( $P < 0.001$ ) than both the ovariectomized groups. The peak load of LV4 was also significantly higher ( $P < 0.01$ ) among the SHAM rats compared to the ovariectomized groups. No differences in bone outcomes were observed between OVX-PF and OVX-AL groups. In summary, ovariectomy-induced hyperphagia and weight gain do not modulate BMD or biomechanical bone strength at 14 weeks post-ovariectomy. Pair-feeding is not necessary to prevent excess weight gain and adiposity from confounding bone outcomes in this model.

**Disclosures:** J.M.Y. Jiang, None.

This study received funding from: Discovery Grant from the Natural Sciences and Engineering Research Council of Canada to W. Ward.

## SA448

**High-fat Diet Facilitated Decreases in BMD of Ovariectomized Mice and Suppressed the Anabolic Effects of PTH on Bone.** S. Tanaka<sup>1</sup>, A. Sakai<sup>1</sup>, T. Tanigawa<sup>2</sup>, H. Hirasawa<sup>1</sup>, Y. Katae<sup>1</sup>, K. Tanaka<sup>1</sup>, T. Nakamura<sup>1</sup>. <sup>1</sup>Orthopaedic Surgery, University of Occupational and Environmental Health, Kitakyushu, Japan, <sup>2</sup>1st medicine, University of Occupational and Environmental Health, Kitakyushu, Japan.

The post-menopausal osteoporosis is caused by decreases in estrogen activity and sequential increases in bone turnover. High-fat diets also decreased bone volume, what we clearly demonstrated in our recent study using mouse given high-fat diet due to increases in bone resorption and decrease in bone formation. We hypothesized that decreases in BMD of estrogen deficient women is facilitated by high-fat diet.

We tested the effects of high-fat diet to the ovariectomized (OVX) mice on bone metabolism and of intermittent administration of PTH on recovery from decreased bone. Seven weeks old, female, C57BL/6J mice were purchased and subjected to 6 groups, sham operated mice given standard chow, OVX mice given standard chow, sham given high-fat diet, OVX given high-fat (OH), sham given high-fat diet and intermittent PTH injection, and OVX given high-fat and PTH, after 1 week acclimatization and operated. Feeding started from 8 weeks age and 3 times per one week PTH injection were performed from 14-week (6 weeks after operation) until the end of the experiment.

Decreases in BMD were observed in the lumbar spine of OVX mice and what was more apparent in OVX mice given high-fat diet, while the lumbar BMD did not decreased in sham operated mice given high-fat diet. The PTH injection partially recovered lumbar BMD up to the OVX mice given standard chow level. In femur, although BMD in OVX mice given standard chow or sham operated mice given high-fat diet did not decrease, BMD in OVX mice given high-fat diet decreased apparently. PTH injection recovered the femoral BMD in OVX mice given high-fat diet to the levels of sham operated or OVX mice given standard chow.

High-fat diet facilitated decreases in BMD of OVX mice and suppressed the anabolic effects of PTH on bone especially in non-weighted site.

**Disclosures:** S. Tanaka, None.

## SA449

**Treadmill Exercise Provides Only Short-Term Protection Against Cancellous Bone Loss with Reduced Dietary Energy Intake: Endocrine Mechanisms.** S. N. Swift<sup>1</sup>, K. Baek<sup>1</sup>, M. J. De Souza<sup>2</sup>, S. A. Bloomfield<sup>1</sup>. <sup>1</sup>Intercollegiate Faculty of Nutrition, Health & Kinesiology, Texas A&M University, College Station, TX, USA, <sup>2</sup>Kinesiology, Pennsylvania State University, University Park, PA, USA.

Dietary energy deficits leading to weight loss can induce loss of cancellous bone. We sought to elucidate whether endurance exercise maintains cancellous bone mass in female rats subjected to a 40% energy deficit. Forty Sprague-Dawley virgin female rats 5-mo-old were acclimated to AIN-93M purified diet for 8 wks. For the next 12 wks, the control groups (ADLIB-EX & ADLIB-SED) were fed AIN-93M *ad lib*. Energy restriction with exercise group (ER-EX) and sedentary energy-restriction (ER-SED) groups were fed modified AIN93M diet with 30% and 40% less energy, respectively, with 100% of all other nutrients provided. Exercising rats performed treadmill running 4 d/wk, 90-100 min/d (~60% V<sub>O2</sub> max) to increase weekly energy expenditure by 10%. At day 0, wk 4, and wk 12, urine & serum were collected for ELISA assays on IGF-1, estrogen glucuronide (E1G), leptin, C-terminal telopeptides of type I collagen (CTX) and N-terminal propeptides of type I collagen (PINP). At the same time points, peripheral quantitative tomography (pQCT) scans were performed at the proximal tibia metaphysis (PTM) for cancellous volumetric bone mineral density (vBMD). Body weights for all *ad lib* fed animals increased by 12 wk (+9%) while all ER rats lost weight (-16%), with no effect of exercise in either energy status group. ER decreased cancellous vBMD (-17%) by 12 wk in sedentary animals. Exercise increased cancellous vBMD by 4 wk regardless of energy status (+12%), but did not protect against losses by 12 wk in ER-EX (-9%). Bone turnover appears to be suppressed in both ER groups, with decreases in PINP (-43%) and CTX (-4%) by 12 wk, but not in ADLIB-EX. Serum leptin declines significantly in EX-ER by 4 wk (-75%) and in SED-ER at 12 wk (-96%). Trends were observed for suppression of serum IGF-1 in both ER groups that were significant in ER-EX (-33%) by 12 wk. Uterine weight was significantly lower in ER-EX at 12 wks (-48% vs. ADLIB-EX). In summary, endurance training in energy-replete rats increased cancellous vBMD and protected against bone loss in rats experiencing energy deficits at 4 wk, but not when restriction was maintained for 12 wk. Estrogen status (estimated by uterine weight) and endocrine markers of energy status were maintained in ADLIB-EX rats, but declined over time in all energy-restricted rats (SED and EX). Energy deficit-induced changes in estrogen status, leptin and IGF-1 may contribute to this loss of cancellous bone.

**Disclosures:** S.N. Swift, None.

This study received funding from: Department of Defense #WSIXWH-06-1-0479.

## SA450

**Prevention of Glucocorticoid-induced Osteoporosis with Alendronate or Alfacalcidol in Patients with Ophthalmologic Diseases.** T. Ikeda<sup>1</sup>, C. Hamanishi<sup>1</sup>, S. Souen<sup>2</sup>. <sup>1</sup>Orthopaedic Surgery, Kinki Univ. School of Medicine, Osaka, Japan, <sup>2</sup>Orthopaedic Surgery and Rheumatology, Kinki Univ. Nara Hospital, Nara, Japan.

Glucocorticoid (GC)-induced osteoporosis is a major public health problem for patients taking GC therapy. To clarify the drug therapy strategy for the increased risk fracture, we studied the changes in bone mineral density (BMD) by dual energy X-ray absorptiometry after initiating high dose GC treatment over 12 months in patients with ophthalmologic diseases. Alendronate or alfacalcidol treatment was started concurrently with GC treatment. We studied 36 Japanese patients (12 male and 24 female) suffering from ophthalmologic diseases who required long-term (>3 months) treatment with oral GC at an average daily dose of at least 10 mg prednisolone.

The mean BMD in alfacalcidol group were continuously lower than it's baseline during 12 months treatment. The lowest mean changes of BMD were observed at 9 months in both alendronate group (-1.14%) and for alfacalcidol group (-5.01%).

In male subjects, the mean changes of BMD for alendronate group were greater than for alfacalcidol group at 3 months and 6 months after treatment. In female alfacalcidol group, significant BMD reductions from baseline were observed in comparison to female alendronate group at both 3 and 6 months. In addition, we checked urinary excretion of type I collagen cross-linked N-telopeptides corrected for creatinine (NTx/Cr) data as a marker for bone turnover. For alendronate group, the mean percentage changes from baseline were -41.7% and -42.3% at 3 and 6 months after treatment, respectively. For alfacalcidol group, the mean percentage changes from baseline were 11.3% and -4.4% at 3 and 6 months after treatment, respectively. In alendronate group, the mean decrements of NTx/Cr were statistically greater in comparison to alfacalcidol group.

In conclusion, we have investigated the preventive effect of alendronate or alfacalcidol for GC-induced osteoporosis in patients with ophthalmologic field diseases. Alendronate is efficacious in preventing bone mass at the lumbar spine in above populations. In addition, alfacalcidol might be efficacious in the restricted population such as male subjects as a second-line anti-osteoporotic agents.

In this study, the enrolled population includes relative young female population and also includes male patients, and the comparison between postmenopausal patients and premenopausal patients might be important, therefore, we should design further studies to solve these points.

**Disclosures:** T. Ikeda, None.

## SA451

**Effects of Intermediate Doses of Glucocorticoids on Bone Turnover and Circulating Dkk-1, MIF, sRANKL and OPG in Patients with Interstitial Lung Disease. A Three-Month Longitudinal Study.** A. Dovio<sup>\*</sup>, E. Palmas<sup>\*</sup>, L. Saba<sup>\*</sup>, A. Termine<sup>\*</sup>, E. Bianco<sup>\*</sup>, L. Mercante<sup>\*</sup>, C. Albero<sup>\*</sup>, A. Angeli. Dept. of Clinical and Biological Sciences, University of Turin, Orbassano - Torino, Italy.

High-dose glucocorticoid (GC) administration causes early and transient increase of bone resorption. Whether such an increase occurs also for intermediate and low doses is unknown. Dynamics over time of this effect, relationships to routes of administration and schedules of tapering down doses, and underlying mechanisms are unclear. We have performed a longitudinal study lasting a 3-month span in patients diagnosed as having interstitial lung disease responsive to GCs and starting treatment with intermediate doses. Fourteen patients (M/F 8/6; age 54, 34-77 yr (median, range)) suffering from sarcoidosis (n=10), nonspecific interstitial pneumonia (n=2), usual interstitial pneumonia (n=1), desquamate interstitial pneumonia (n=1) were included. All patients did not take drugs affecting bone, including GCs, in the previous 6 months. Serum osteocalcin (OC), C-telopeptide of type I collagen (CTX), Dickkopf-1 (Dkk-1), osteoprotegerin (OPG), total soluble RANKL (sRANKL), and macrophage migration inhibitory factor (MIF) were measured by commercially available ELISAs at baseline, after 3 days and after 1, 2, 4, 8, 12 weeks of treatment. The starting dose was 25 (n=3) - 50 mg (n=11) of prednisone; the dose at week 12 was 12.5 (5-25) mg; cumulative dose and average daily dose were 1925 (1225-2975) mg and 23 (15-35) mg, respectively. With this regimen, GCs caused a rapid decrease of serum OC (P<0.001 by multiple measures ANOVA - at day 3 median -34%, P<0.001 vs baseline by Dunnett's test), persistent up to week 2, with a subsequent progressive raise until week 12; levels comparable to baseline, however, were not attained. CTX showed a marginally significant trend to an early increase (P=0.10 by ANOVA), peaking at day 7 (median +28%, P=0.02 vs baseline by Dunnett's test) and declining thereafter. Consistently, OC/CTX ratio showed a rapid, marked and sustained decrease (P<0.001). Serum OPG showed an early and persistent decrease (P<0.01 by ANOVA - at day 7 median -19%, P=0.03 vs baseline by Dunnett's test). No significant effect of GC therapy was noticed on serum sRANKL, MIF and Dkk-1. Our data indicate that also a regimen of intermediate doses of GCs with rapid tapering down is able to alter in a few days the balance between bone resorption and formation. They lend support to the preventive use of antiresorptive drugs in patients starting such regimens. Less availability of OPG in the bone microenvironment deserves attention among mechanisms accounting for the early increase of bone resorption.

**Disclosures:** A. Dovio, Procter & Gamble 2; Stroder 5; Novartis 5; Eli-Lilly 5.

## SA452

See Friday Plenary number F452.



## SA453

**Impaired Angiogenesis and Compromised Fluid Volume Accompanies Increased Osteoblast and Osteocyte Apoptosis with Glucocorticoid Excess: Interconnected Pathogenetic Changes Responsible for the Loss of Bone Strength.** Q. Liu<sup>\*1</sup>, C. Wan<sup>1</sup>, Y. Wang<sup>1</sup>, E. A. Hogan<sup>\*2</sup>, S. B. Berryhill<sup>\*2</sup>, S. C. Manolagas<sup>2</sup>, T. L. Clemens<sup>1</sup>, R. S. Weinstein<sup>2</sup>. <sup>1</sup>Department of Pathology, University of Alabama at Birmingham, Birmingham, AL, USA, <sup>2</sup>Center for Osteoporosis and Metabolic Bone Diseases, University of Arkansas for Medical Sciences and Central Arkansas Veterans Healthcare System, Little Rock, AR, USA.

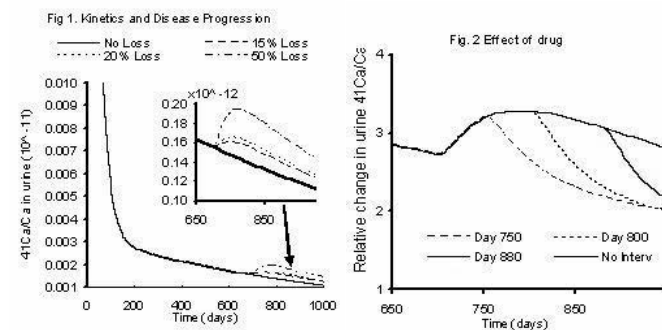
Glucocorticoid (GC) excess causes a decline in bone strength that is greater than the loss of bone mass, but the mechanisms behind these phenomena remain unknown. Based on evidence that glucocorticoids may affect blood flow as well as the vasculature itself, we have undertaken in vivo and in vitro studies to elucidate the effects of GCs on bone fluid and vasculature in the mouse and the cellular and molecular mechanism responsible for such effects. After 28 days of administration of prednisolone to 8-month-old C57Bl/6 mice, vertebral and femoral BMD decreased by 4.5-6.6% ( $p < 0.003$ ), osteoblast and osteocyte apoptosis increased by 160-250% ( $p < 0.01$ ), while vertebral compression strength and femoral 3-point bending decreased by 25% ( $p < 0.04$ ). These changes were associated with a striking decrease in interstitial fluid, as determined by 2-dimensional fluorescent imaging of the osteocyte-lacunar-canalicular system using Procion Red-a metabolically inert tracer. Further, prednisolone decreased vertebral vessel volume and surface area by 79-74% ( $p < 0.05$ ), as determined by 3-dimensional microCT imaging following lead chromate perfusion. The changes in fluid and vasculature volume were associated with diminished immunostaining for the endothelial markers CD34 and von Willebrand factor-factor VIII complex in cancellous bone sections. In agreement with the in vivo data, dexamethasone (DEX) (1, 10, 100 nM) impaired endothelial sprouting as assessed by CD31 immunostaining in fetal metatarsals from both wild type mice and mice overexpressing VEGF. Likewise, DEX dose dependently (1 nM-1  $\mu$ M) impaired tube-like structure formation of cultured human umbilical vein endothelial cells (HUVECs). At higher doses (1  $\mu$ M), DEX induced HUVEC apoptosis as determined by increased caspase 3/7 activity ( $p < 0.05$ ). At 10 and 100 nM, DEX decreased BrdU positive cell numbers, while at a low dose (1 nM), modestly increased BrdU positive cell numbers. Collectively, these results strongly suggest that decreased osteocyte-lacunar-canalicular fluid volume, diminished bone vasculature, increased osteoblast and osteocyte apoptosis, and impaired angiogenesis represent interconnected pathogenetic changes that are responsible for the disproportional loss of bone strength over bone mass with glucocorticoid excess.

**Disclosures:** C. Wan, None.

## SA454

**Development of Empirical Model Using <sup>41</sup>Ca for the Study of Bone Remodeling in Human.** M. Sharma<sup>\*</sup>, S. K. Hui. Department. of Therapeutic Radiology, University of Minnesota, Minneapolis, MN, USA.

Osteoporotic fractures are a significant public health problem, resulting in substantial morbidity and mortality. Initial studies show that the <sup>41</sup>Ca assay may become useful diagnostic tool for monitoring metabolic bone disease and its treatment management (1, 2). There is lack of empirical model to study the effect of bone loss and antiresorptive therapy on <sup>41</sup>Ca based bone turnover assay. The purpose of this study is to (a) develop a general empirical model that can describe <sup>41</sup>Ca tracer kinetics in human; (b) study its feasibility to monitor metabolic bone disease and (c) monitor response to preventive drugs. A mathematical model has been developed using the Berkeley software to study calcium kinetics and investigate bone turnover. Difference in the contributions of oral and intravenous drug is also taken into account. The rate of bone loss has been parameterized to detect percent change in bone turnover with the severity of disease. The change in <sup>41</sup>Ca/Ca from steady state during metabolic bone disease causing bone loss is calculated over time. Bone dynamics after bisphosphonate drug intervention is simulated and verified. Our model based on four compartments fits well with the available experimental data (1,2). Figure 1 and its inset reflects the bone loss due to severity of disease by urine calcium ratio increase over time compared to the steady state. The relative effect of bisphosphonate intervention at 15% bone loss is shown in Figure 2. Early intervention (day 750) with drug shows early recovery of bone remodeling compared to late intervention (day 880).



The present <sup>41</sup>Ca tracer kinetics model will be a useful tool to understand how <sup>41</sup>Ca assay monitor bone remodeling is affected by disease progression and drug intervention. This may allow better treatment management to prevent bone fracture and will be a useful guide in the use of <sup>41</sup>Ca assay for clinical scenarios.

## References:

1. E. Denk et al., J. Bone Miner. Res. 22(10):1518, 2007 and references therein.
2. S.K. Hui et. al., Nucl. Inst. and Methd. in Phys. Res. B 259(1):796, 2007 and references therein.

**Disclosures:** M. Sharma, None.

This study received funding from: NIH/NIAMS (RO3-AR055333-01).

## SA455

See Friday Plenary number F455.

## SA456

**Impact of Physical Inactivity (10 Days Bed Rest) on Markers of Bone Turnover in Young Men with Low and Normal Birth Weight.** K. Karnik<sup>1</sup>, D. Talbot<sup>\*1</sup>, J. Dick<sup>\*1</sup>, M. Sonne<sup>\*2</sup>, L. Højbjerg<sup>\*2</sup>, A. Alibegovic<sup>\*3</sup>, B. Stallknecht<sup>\*2</sup>, F. Dela<sup>\*2</sup>, A. Vaag<sup>\*3</sup>. <sup>1</sup>Corporate Research, Unilever plc, Bedfordshire, United Kingdom, <sup>2</sup>University of Copenhagen, Copenhagen, Denmark, <sup>3</sup>Steno Diabetes Centre, Copenhagen, Denmark.

Physical activity plays an important role in maintaining skeletal integrity throughout life. Reduced skeletal loading, as often seen in the elderly as a result of long term bed rest and reduced mobility, has been shown to result in bone loss. It has been proposed that low birth weight is associated with changes in adult body composition including low bone mineral content. In this study, we compare the effect of bed rest for 10 days on the bone turnover markers in young men with low and normal birth weight.

40 healthy men aged 21-28 yrs were recruited in the study, 20 of which were low birth weight (LBW) individuals born at term and 20 were normal birth weight (NBW) individuals born at term. Participants were confined to a hospital bed for 10 days and consumed a standardised diet. At the end of the intervention period, all the participants underwent 4-weeks of rehabilitation training programme under supervision.

At the end of the intervention, serum carboxy-terminal collagen crosslink (CTX) increased by 31.6% in the entire group, which was statistically significant ( $p < 0.0001$ ). The mean percent increase from baseline for serum CTX for the LBW group was 37% and for NBW group was 28%. Although, the differences between LBW and NBW groups for percent change in CTX did not reach the level of statistical significance, there was a trend for higher bone resorption as a result of bed rest in the LBW group. At the end of bed rest period, serum parathyroid hormone decreased significantly ( $p < 0.001$ ) in the entire group. The mean percent decrease was 24% in the LBW group and 23% in NBW group. The difference between the groups was not statistically significant. There was no difference in the levels of serum osteocalcin as a result of bed rest.

These results confirm the detrimental effect of bed rest on the skeletal health as evident by the increase in serum CTX. Our findings also suggest a trend for greater loss of skeleton in the LBW group as a result of bed rest. This particular finding needs to be investigated further with larger number of participants.

**Disclosures:** K. Karnik, Unilever plc 5.



## SA457

**Influence of Markers of Bone Turnover on Calcaneal Quantitative Ultrasound: Results from the European Male Ageing Study (EMAS).** S. R. Pye<sup>\*1</sup>, T. W. O'Neill<sup>1</sup>, H. Borghs<sup>\*2</sup>, D. Vanderschueren<sup>2</sup>, J. E. Adams<sup>3</sup>, K. A. Ward<sup>3</sup>, G. Bartfai<sup>\*4</sup>, F. Casanueva<sup>\*5</sup>, J. D. Finn<sup>\*6</sup>, G. Forti<sup>\*7</sup>, A. Giwercman<sup>\*8</sup>, I. T. Huhtaniemi<sup>\*9</sup>, K. Kula<sup>\*10</sup>, M. Punab<sup>\*11</sup>, A. J. Silman<sup>\*1</sup>, F. C. Wu<sup>\*6</sup>, S. Boonen<sup>2</sup>. <sup>1</sup>ARC Epidemiology Unit, The University of Manchester, Manchester, United Kingdom, <sup>2</sup>Katholieke Universiteit Leuven, Leuven, Belgium, <sup>3</sup>Department of Imaging Science and Biomedical Engineering, The University of Manchester, Manchester, United Kingdom, <sup>4</sup>University of Szeged, Szeged, Hungary, <sup>5</sup>University of Santiago de Compostela, Santiago de Compostela, Spain, <sup>6</sup>Department of Endocrinology, The University of Manchester, Manchester, United Kingdom, <sup>7</sup>University of Florence, Florence, Italy, <sup>8</sup>Lund University, Malmö, Sweden, <sup>9</sup>Imperial College, London, United Kingdom, <sup>10</sup>University of Lodz, Lodz, Poland, <sup>11</sup>University of Tartu, Tartu, Estonia.

The majority of studies on biochemical measurements of bone turnover have focused on women with fewer data in middle aged and elderly men. The aim of this analysis was to characterize the influence of bone markers on calcaneal ultrasound measurements in middle aged and elderly European men. Men aged between 40 & 79 years were recruited from population registers in 8 European centres. Subjects were invited to attend for quantitative ultrasound (QUS) of the calcaneus (Hologic - SAHARA) and a fasting blood sample from which the bone markers serum N-terminal propeptide of type I procollagen (PINP) and crosslinks (-Ctx) were measured. In three of the recruitment centres, osteocalcin (OC) and serum C-terminal telopeptide of type I collagen (ICTP) were also measured. Height and weight were assessed in all subjects. The relationships between QUS parameters (broadband ultrasound attenuation [BUA] and speed of sound [SOS]) and bone markers were assessed using linear regression with adjustments made for age, height, weight and centre. 3136 men, mean age 60.0 years (standard deviation [SD]=11.0) were included in the analysis. Mean BUA was 80.1 dB/MHz (SD=19.0) and SOS 1550.6 m/s (SD=34.1). Mean PINP was 41.6 ng/ml (SD=17.6), OC 22.1 ng/ml (SD=7.1), -Ctx 353.6 pg/ml (SD=181.8) and ICTP 3.2 ng/ml (SD=0.9). There was a significant decrease in OC levels with age ( $\beta = -0.066$ ;  $p < 0.01$ ) and an increase in ICTP ( $\beta = 0.024$ ;  $p < 0.001$ ). PINP and -Ctx were unrelated to age. Higher -Ctx levels were associated with lower BUA ( $\beta = -0.006$ ; 95% CI -0.010, -0.003) and SOS ( $\beta = -0.016$ ; 95% CI -0.022, -0.009). Higher OC levels were associated with lower BUA ( $\beta = -0.159$ ; 95% CI -0.304, -0.014) while higher PINP levels were associated with lower SOS ( $\beta = -0.114$ ; 95% CI -0.180, -0.048). ICTP levels were not associated with either QUS parameter. In this population survey of middle aged and elderly European men, higher levels of bone turnover markers were associated with lower QUS parameters.

**Disclosures:** S.R. Pye, None.

This study received funding from: Commission of the European Communities.

## SA458

See Friday Plenary number F458.

## SA459

**Bone Loss With Smoke Exposure and Lrp5 Expression.** G. K. Alvarez, B. T. Hackfort<sup>\*</sup>, M. P. Akhter, J. A. Yee, D. M. Cullen. Osteoporosis Research Center, Creighton University, Omaha, NE, USA.

Smoking is a risk for osteoporosis associated with low bone mass and poor fracture healing, but the mechanism for these effects is unknown. This study examined the interaction of Lrp5 receptor (low density lipoprotein like receptor protein) and smoke exposure on bone. Lrp5 is a Wnt co-receptor and the G171V mutation in LRP5 (HBM) is a gain of function mutation with greater WNT/ $\beta$  catenin signaling that results in high bone mass.

We examined bones after 12 wks of smoke exposure in WT (C57Bl6), Lrp5<sup>+/-</sup>, and HBM female (5.3  $\pm$  0.5mo) and male mice. Mice were randomly assigned to control or smoke exposure (3 hrs/d 5 d/wk at 129 $\pm$ 38 mg/mm<sup>3</sup>TSP). Female femora (15/grp) were processed for cortical and cancellous histomorphometry. Measurements included area (total, marrow, bone volume -BV/TV), mineralizing surface (MS/BS), mineral apposition rate (MAR), and bone formation rate (BFR/BS). Male tibiae (8/grp) were cleaned, frozen at -80C, mRNA extracted, and mRNA quantified relative to control (ABI 7500, control GAPDH). Differences due to smoke and genotypes were analyzed by GLM. There were no differences in initial body weight (25  $\pm$  3 g), but controls gained more weight than treated mice by 12 wks. In cortical bone there was no difference due smoke exposure in total area, but marrow area was greater in Wt and HBM mice than control mice (table). Exposure to smoke increased periosteal BFR in the Lrp5<sup>+/-</sup> mice, but not in WT and HBM mice. There were no effects on endocortical BFR. Cancellous BV/TV was significantly lower in HBM mice after smoke exposure, but not in WT or Lrp5<sup>+/-</sup> mice where initial BV/TV was <3%. MS/BS was depressed in WT mice and tended downward in the other genotypes. Osteoclast surface was lower in the HBM animals than the other genotypes, but there was no smoking effect. Analysis of WNT responsive genes showed that Cyclin D1, associated with cell proliferation, was suppressed with smoke exposure in Wt (0.6  $\pm$  0.1) and Lrp5<sup>+/-</sup> (0.7 $\pm$ 0.1) mice, but not HBM mice (1.0  $\pm$  0.1). PTGS2 was elevated in response to smoke exposure in HBM (3.2  $\pm$  1.2), but not in Lrp5<sup>+/-</sup> (1.8  $\pm$  0.8) or WT (0.5  $\pm$  0.1) mice.

Smoke exposure resulted in cortical and cancellous bone loss especially in HBM mice, but HBM cancellous BV/TV remained 10 fold greater than in WT and Lrp5<sup>+/-</sup> bone. Bone turnover reached a steady state after 12 wks of treatment. While the HBM gain of function mutation maintained or increased gene expression for the WNT responsive genes tested, this did not prevent bone loss. \

Treatments	Cortical Midshaft Femur			Cancellous Distal Femur		
	Mar Area (mm <sup>2</sup> )	P-BFR ( $\mu$ m/yr)	E-BFR ( $\mu$ m/yr)	BV/TV (%)	MS/BS (%)	OcS/BS (%)
Lrp5 <sup>+/-</sup> con	0.77 (0.06)	28 (17)	98 (63)	1.6 (1.2)	23 (9)	6.8 (3.7)
smoke	0.80 (0.05)	48 (25) <sup>a</sup>	113 (41)	1.2 (2.0)	20 (8)	7.5 (5.0)
Wt con	0.80 (0.07)	49 (18)	127 (43)	2.7 (1.0)	27 (6)	8.7 (5.2)
smoke	0.87 (0.06) <sup>a</sup>	34 (16)	101 (40)	1.1 (0.7)	20 (8) <sup>a</sup>	8.5 (4.9)
HBM con	0.76 (0.11)	44 (22)	101 (32)	22 (8)	25 (8)	4.6 (3.4)
smoke	0.87 (0.10) <sup>a</sup>	30 (15)	86 (23)	14 (6) <sup>a</sup>	24 (7)	4.2 (3.7)
Int (Gene x Trt)	ns	0.004	ns	0.003	ns	ns

Mean (S.D.) <sup>a</sup> smoke effect  $P < 0.05$

**Disclosures:** G.K. Alvarez, None.

This study received funding from: Nebraska Department of Health and Human Services.

## SA460

**Profile Analysis of Rodent Metaphyseal Trabecular Bone Reveals a Biphasic Dose-Dependent Response To Administered Bone Active Agents.** A. Pitsillides<sup>1</sup>, P. L. Salmon<sup>2</sup>, A. Tivesten<sup>3</sup>, S. Moverare-Skrtic<sup>3</sup>, C. Ohlsson<sup>3</sup>, L. Oste<sup>4</sup>, G. Dixon<sup>4</sup>, A. Idris<sup>5</sup>, R. Van T'Hof<sup>6</sup>. <sup>1</sup>Royal Veterinary College, London, United Kingdom, <sup>2</sup>SkyScan, Kontich, Belgium, <sup>3</sup>Sahlgrenska Institute, Goteborg, Sweden, <sup>4</sup>Galapagos plc, Mechelen, Belgium, <sup>5</sup>Molecular Medicine Centre, Edinburgh University, Edinburgh, United Kingdom.

The rodent bones in the vicinity of the knee - the proximal tibia and distal femur - are standard sites for bone morphometric analysis for disease models such as ovariectomy-induced osteoporosis. There are two ways in which the amount of metaphyseal trabecular bone can change: either by a change to the balance of formation and resorption at the surface of the trabecular bone throughout the metaphysis, or, in young rodents, by a change to the rate of output of secondary trabecular bone from the growth plate and primary spongiosa.

Here we review three rodent OVX studies involving ovariectomy and drug treatment of (initially) 2-3 month old rodents, all employing micro-CT imaging. The 3D images of the whole metaphyses are reanalysed to assess the profile of trabecular percent crosssectional area (BA/TA) with increasing distance from the growth plate - the "metaphyseal profile" - in order to elucidate the relative roles of these two above mechanisms in bringing about change in metaphyseal trabecular volume. These studies include treatment with the sex steroids estrogen and testosterone, the bisphosphonate alendronate, PTH and the novel antiresorptive ABD365.

The results suggest a biphasic dose-dependent effect of treatment. Where trabecular volume in OVX rodents is restored by administered treatment to levels similar to or just above sham control levels, the first mechanism is predominant, the alteration of remodeling balance throughout the metaphysis, causing uniform elevation of the metaphyseal profile but no change to its slope. However where a treatment causes trabecular volume to be elevated to a level substantially above sham control levels, an upturn in the metaphyseal profile occurs in the metaphyseal region closest to the growth plate, implicating the additional effect of a second mechanism, that of an increased rate of new trabecular bone output at the growth plate.

Sex steroids and alendronate are both demonstrated to elevate trabecular volume to well above the sham level in a manner involving this latter mechanism. This indicates that even generally anti-resorptive compounds such as the bisphosphonate alendronate, at high enough dose levels, can stimulate increased growth plate formation of trabecular bone.

**Disclosures:** P.L. Salmon, SkyScan 3.

This study received funding from: SkyScan.

## SA461

See Friday Plenary number F461.



## SA462

**Trabecular Bone Loss in Response to Transient Muscle Paralysis Is Not Gender Dependent.** T. S. Gross, S. Srinivasan, B. J. Ausk\*, S. L. Poliachik\*, S. D. Bain. Orthopaedics and Sports Medicine, University of Washington, Seattle, WA, USA.

Whether gender provides systemic influences that significantly impact disuse induced bone loss remains controversial. In general, however, the female skeleton is thought to be more sensitive than the male skeleton to bone loss observed in models such as hindlimb suspension. In this study, we sought to clarify this relation in an in vivo model in which focal osteoclastogenesis is induced by transient muscle paralysis. High resolution (11 micron) microCT images of the proximal tibia metaphysis and lower resolution images of the entire lower limb (21 micron) were obtained for 7 female and 7 male C57B6 mice (16 wk) immediately prior to injection of Botox into the calf muscle group (2U/100 g, d 0). In vivo scans of all mice were also obtained by d 7 and d 15 post post induction of muscle paralysis. Standard image analysis procedures were used to determine trabecular bone parameters within the proximal tibia, while the lower resolution imaging was used to assess soft tissue volume changes. All data were assessed by comparison with time zero data. Lower limb soft tissue volume was significantly decreased by 7 d (F:  $-11.8 \pm 3.5\%$ , M:  $-11.5 \pm 1.9\%$ ) and further decreased by 15 d (F:  $-24.2 \pm 7.3\%$ , M:  $-21.8 \pm 3.5\%$ ; all  $p < 0.01$ ), with no gender based differences. Within 7 d, proximal tibia BV/TV was significantly diminished in both female ( $-61.7 \pm 10.2\%$ ,  $p=0.02$ ) and male mice ( $-44.4 \pm 6.4\%$ ,  $p=0.02$ ). The loss of BV/TV in female mice was significantly greater than that of male mice ( $p=0.03$ ). Further BV/TV degradation was observed by 15 d but the magnitude of bone loss was equal across gender (F:  $-70.2 \pm 9.3\%$ ; M:  $-70.6 \pm 6.9\%$ , both  $p<0.01$ ). At both time points, degraded BV/TV was associated with a significant erosion of trabecular thickness, decreased trabecular number, and increased trabecular spacing. No gender based statistical differences were identified for any of these morphological parameters. In summary, we found that female mice demonstrated a more rapid loss of BV/TV within the first 7 d than male mice, but the extent of bone trabecular degradation was equivalent across gender by 15 d. Whether this transient difference arose due to gender associated levels of basal bone turnover will require further clarification. In our view, the equivalent degradation of muscle volume across gender and equivalent deterioration of trabecular architecture within 15 d suggests that the signaling pathway responsible for rapidly initiating osteoclastogenesis following transient muscle paralysis is the same in females and males. These results also suggest that gender based differences previously observed in other disuse models may be associated with acute osteoblastic responses identified in those models.

**Disclosures:** T.S. Gross, None.

## SA463

**Brain-derived Serotonin Positively Regulates Bone Mass Accrual.** V. K. Yadav\*, F. Oury\*, J. Ryu\*, N. Suda\*, P. Ducy\*, G. Karsenty. Genetics and Development, Columbia University, New York, NY, USA.

Serotonin (5-hydroxytryptamine) is a biogenic amine that functions both as a neurotransmitter in mammalian central nervous system and as a hormone in the periphery where most of (~95%) it is produced. Remarkably serotonin does not cross the blood-brain barrier thus it has potentially two different functions depending on its site of synthesis. Serotonin synthesis is initiated following tryptophan hydroxylation by an enzyme called tryptophan hydroxylase (Tph). Brain-derived serotonin synthesis is initiated by Tph2 and peripheral-derived serotonin is initiated by Tph1. To analyse the spatio-temporal pattern of serotonin expression and the function of brain-derived serotonin on bone mass, we introduced a LacZ allele in the mouse *Tph2* locus by homologous recombination in embryonic stem cells. LacZ staining during embryonic development and postnatally delineated serotonergic neurons in the mouse brain and showed that in the adult, Tph2 neurons are clustered in to six groups in the brain stem, those neuronal groups are known as dorsal, ventral and caudal raphe nuclei. Furthermore, histological analysis of the vertebrae and long bones revealed that *Tph2*-deficient mouse develop a severe low bone mass phenotype early during adult life thus identifying serotonin as the first bona fide neuropeptide regulating bone mass. Histomorphometric analysis revealed that this is due to a decrease in bone formation and an increase in bone resorption. We have also identified through genetic means one of the 14 serotonin receptor that is responsible for the regulation of bone mass. We will present at the meeting the signaling pathway in which brain-derived serotonin acts.

**Disclosures:** V.K. Yadav, None.

## SA464

**Kenney-Caffey Syndrome in a Caucasian Man.** P. Tondapu\*, C. V. Odvina<sup>2</sup>. <sup>1</sup>Mineral Metabolism, UT Southwestern Medical Center, Dallas, TX, USA, <sup>2</sup>Charles and Jane Pak Center for Mineral Metabolism, UT Southwestern Medical Center, Dallas, TX, USA.

29 year old white man presented to our Mineral Metabolism Clinic with history of hypocalcemia, hypomagnesemia, short stature and hypoparathyroidism. He was born full term by spontaneous vaginal delivery, weighing 6 lb 11oz. There is no family history of consanguinity. He developed generalized tonic clonic seizures about 1 week after birth and was found to have hypocalcemia. Initial diagnosis was pseudohypoparathyroidism and he was managed with calcium supplements. Subsequent evaluation revealed papilledema. Cranial sutures fused at age 4. At age 12 years and 10 months, he had a bone age of a 14 year old and at age 13 1/2 years; he was -3.14 SD (29kg) for weight and -3.22 SD (134 cm)

for height. Additional work up showed low calcium, magnesium and PTH but normal somatomedin C and IGFBP 3 which ruled out growth hormone deficiency. He has poor vision all his life and is legally blind without glasses but has no hearing problem. When he was seen at our clinic, it was noticed that he has short stature (135 cm), brachydactyly and facial dysmorphism with microcephaly, micrognathia, deep set eyes, hypotelorism, beaked nose and poor dentition with malformed tooth. He has had multiple fractures related to trauma and poor union in one of them. He has not been taking calcium regularly and has had multiple admissions for hypocalcemia. Work up showed normal serum magnesium, low calcium and PTH. Fractional excretion of magnesium was 2.7%, which ruled out renal magnesium wasting as the cause of hypomagnesemia. DEXA scan showed high Z score (+3.2) at the spine and slightly low Z scores at the hip(-0.5) and distal 1/3 of the radius (-1.7). Karyotype is normal male (46XY). Because of the clinical findings, we suspected Kenney-Caffey syndrome and DNA was sent for genetic testing to confirm the diagnosis. Kenney-Caffey syndrome is an extremely rare hereditary skeletal disorder characterized by osteosclerotic bone dysplasia with associated hypocalcemia, dental caries and ocular abnormalities. Kenney-Caffey and related disorder HRD map to 1q42-q43 and are due to mutations in the tubulin specific chaperone E (TBCE) gene, a protein involved in tubulin folding. Most of the cases that had been described in the literature were of Arab decent. To the best of our knowledge, there is only one reported case of this syndrome in a Caucasian patient.

**Disclosures:** P. Tondapu, None.

## SA465

See Friday Plenary number F465.

## SA466

**Bony Symptoms and Vertebral Fractures in Gaucher Disease Type 1. Data from the 105 Patients of the French Observatoire on Gaucher Disease.** R. Javier\*, R. Jaussaud\*, C. Rose\*, P. Chérin\*, E. Noël\*, C. de Roux Serratrice\*, D. Dobbelaere\*, A. Hartmann\*, E. Hachulla\*, B. Grosbois\*, C. Roux\*. <sup>1</sup>Rheumatology, University Hospital, Strasbourg, France, <sup>2</sup>Internal Medicine, Hôpital Robert Debré, Reims, France, <sup>3</sup>Haematology, Hôpital St Vincent de Paul, Lille, France, <sup>4</sup>Internal Medicine, Pitié-Salpêtrière, Paris, France, <sup>5</sup>Internal Medicine, University Hospital, Strasbourg, France, <sup>6</sup>Internal Medicine, Hôpital St Joseph, Marseille, France, <sup>7</sup>Paediatrics, University Hospital, Lille, France, <sup>8</sup>Neurology, Hôpital Pitié-Salpêtrière, Paris, France, <sup>9</sup>Internal Medicine, Hôpital Claude Huriez, Lille, France, <sup>10</sup>Internal Medicine, Hôpital Sud, Rennes, France, <sup>11</sup>Rheumatology, Hôpital Cochin, Paris, France.

**Background/objectives:** Gaucher disease type1 (GD1) is a rare disease with a heterogeneous clinical presentation. A French national prospective registry was implemented to describe the clinical features of adult GD1 patients with focus on bone symptoms and their impact on patients' quality of life.

**Methods:** Clinical data were collected during a routine visit. No additional tests were performed. A specific case report form was designed to guide the physicians.

**Results:** From March 2005 to September 2006, 105 patients were included and represent about one third of the French GD1 population. Mean age (SD) was 45 (14) years (54% female). Early diagnosis (< 1 year after the first signs) was less frequent when first signs are skeletal manifestations (25% vs 47%). 85% of patients had a history of bony symptoms including osteonecrosis in 30 % and 17% of patients had undergone joint replacement at a mean age (SD) of 40 (10) years. Other manifestations are bone infarction 28 %, bone crisis 21 %, peripheral fracture 18 % and vertebral fractures (VF) 15% (to be compared to 9-11% in the literature). Almost all vertebrae can be involved, from T3 to L5, and many patients have 2 to 4 concomitant VF. Most of these VF, even those of grade 3 according to Genant classification, occurred spontaneously or for minimal trauma at a mean age of 43 years (min-max: 29-61). Chronic back pain remained in half of these patients. Of the 64 patients with bone mineral density data available, 44% had osteopenia and 18% had osteoporosis. **Conclusion:** These results illustrate the high frequency of bone fragility in GD1 patients and the frequency of VF. Bone disease remains a major issue in GD1 patients and a multidisciplinary team approach including bone evaluation and specific bone fragility treatment seems essential for optimizing patients' care.

**Disclosures:** R. Javier, None.

This study received funding from: Actelion.

## SA467

**Age-Related Changes in Bone Mineral Density, Cross-Sectional Area and the Strength of Rat Femur; an Involvement of Suppression of Growth Hormone-IGF-1 Signaling.** M. Tomita<sup>1</sup>, S. Motokawa<sup>\*2</sup>, H. Shindo<sup>\*1</sup>, K. Kumagai<sup>\*1</sup>, I. Shimokawa<sup>\*3</sup>. <sup>1</sup>Orthopedic Surgery, Nagasaki University Graduate School of Medicine, Nagasaki, Japan, <sup>2</sup>Orthopedic Surgery, National Nagasaki Medical Center, Ohmura, Japan, <sup>3</sup>Investigative Pathology, Nagasaki University Graduate School of Medicine, Nagasaki, Japan.

In order to investigate aging-related changes in the bone structure and strength and an involvement of the growth hormone (GH)-insulin-like growth factor (IGF)-1 axis, we examined bone mineral density (BMD), cross-sectional area (Area), and bone strength strain index (SSI) of rat femoral bone by peripheral quantitative computed tomography (pQCT).

**Materials and Methods:** We used wild type (WT) male Wistar rats and the transgenic rat strain (mini), in which GH secretion was suppressed by overexpression of anti-sense GH gene. F1 hybrid rats (F1), which showed intermediate phenotypes in the GH-IGF-1 level and body weight between WT and mini rats, were also used. Rats were sacrificed at 6, 15, and 24 months of age (mo). The cancellous bone parameters of BMD, Area, and SSI were measured at 12mm proximal side from growth plate of distal femur by pQCT.

**Results:** 1) WT showed the highest BMD of total, subcortical bone, and cancellous bone at 6, 15, and 24 mo. F1 showed the intermediate values of BMD between WT and mini rats at 6, 15, and 24 mo. Cancellous bone showed the most apparent age-dependent decrease in all groups.

2) Areas of total, subcortical bone, and cancellous bone at 6, 15, and 24 mo were highest in WT. And F1 showed the intermediate value of those three groups at 6, 15, 24 mo. Area continued to increase between 6 and 24 mo in WT, but in F1 and mini Area it increased from between 6 and 15 mo, but not thereafter.

3) All SSI's (X-, Y-, and polar-) showed almost same age-dependent change as was in Area. WT showed the highest values of SSI in 6, 15, and 24 mo. In WT, SSI continued to increase between 6 and 24 mo, but in F1 and mini, SSI increased between 6 and 15 mo, but decreased thereafter.

**Discussion:** Age-dependent changes were the most obvious in cancellous bone BMD in all groups. Area and SSI showed almost same age dependent-changes but those were different from those of BMD. These data suggested that bone strength correlated not only to BMD, but also Area. Senile bone frailty might cause the changes of bone morphology. Suppression of GH secretion decreased all of BMD, Area, and SSI. GH secretion level plays a role in maintenance of the bone quality during the aging.

**Disclosures:** M. Tomita, None.

## SA468

**Adult Hypophosphatasia Treatment with Teriparatide.** P. M. Camacho<sup>1</sup>, A. M. Mazhari<sup>\*1</sup>, R. Kadanoff<sup>\*2</sup>. <sup>1</sup>Endocrinology, Loyola University Medical Center, Maywood, IL, USA, <sup>2</sup>Rheumatology, Loyola University Medical Center, Maywood, IL, USA.

Hypophosphatasia is a rare inherited metabolic bone disorder that is characterized by defective bone mineralization due to a deficiency of tissue-nonspecific alkaline phosphatase (TNSALP), which results from a deactivating gene mutation. Inorganic phosphate accumulates extracellularly impairing bone mineralization.

A 68-year-old African-American female was evaluated at the Loyola University Osteoporosis and Metabolic Bone Disease Center in April 2006 for low bone mass and low serum total alkaline phosphatase (AP). She reported a femur fracture at age 27 after a fall and a metatarsal fracture in her 50's. She was treated with prednisone since 2002 (ranging from 10-60 mg/day) for her dermatomyositis. She had a maternal history of fractures. Other medical illnesses included hypertension, Reynaud's, reflux disease and pulmonary fibrosis. The patient was on esomeprazole, ranitidine, methotrexate, tacrolimus (for dermatomyositis), furosemide and calcium carbonate. She had been on ergocalciferol 50,000 international units/wk and oral ibandronate 150 mg for 6 months prior to her initial visit.

The diagnosis of hypophosphatasia was based on the following biochemical findings and clinical history: persistently low AP ranging from 11-20 U/L (30-110 U/L), low bone specific alkaline phosphatase (BSAP) ranging from 2.9-3.4 ug/L (7-22 ug/L), high pyridoxal 5'-phosphate (PLP) 95 ng/mL (5-30 ng/mL) and history of low-trauma fractures. Her baseline urinary N-telopeptide on ibandronate was 32 nm BCE/mm creat (26 - 124). She had a normal serum creatinine, ionized calcium, phosphorus, intact PTH and 25 OH-Vitamin D and 24-urine calcium. Mutation analysis for TNSALP gene is pending.

Her DXA scan in 2005 showed lumbar spine bone mineral density (BMD) of 1.006 gm/cm<sup>2</sup>, T-score -1.6, Z-score -1.4; mean femoral neck BMD of 0.693 gm/cm<sup>2</sup>, T-score -2.9 and Z-score -2.8. There was a significant decline of 14% in the hip and 13% in the spine and compared to the 2003 DXA.

In May 2006, ibandronate was discontinued and four months later, BSAP remained low at 2.9 ug/L. Teriparatide 20 ug subcutaneously was given. BSAP subsequently increased to 5 U/L at 7 months. After 13 months of teriparatide therapy, BSAP increased to 7 U/L, AP increased from 14 to 26 IU/L and PLP decreased from 95 to 78 ng/mL.

Her follow up DXA in October of 2007 (spine BMD 1.012 gm/cm<sup>2</sup>, T-score -1.6 and mean femoral neck BMD 0.714 gm/cm<sup>2</sup>, T-score -2.3) showed stable BMD of the lumbar and femoral neck regions. She did not report any fractures during the treatment period.

Our results showed beneficial effects of teriparatide on adult hypophosphatasia which is similar to two previously reported cases. Teriparatide is a promising agent for this metabolic bone disease.

**Disclosures:** R. Kadanoff, None.

## SA469

See Friday Plenary number F469.

## SA470

**Clinical Usefulness of Measurement of Fibroblast Growth Factor 23 (FGF23) in Hypophosphatemic Patients-Proposal of Diagnostic Criteria using FGF23 Measurement.** I. Endo<sup>1</sup>, S. Fukumoto<sup>2</sup>, K. Ozono<sup>3</sup>, N. Namba<sup>3</sup>, H. Tanaka<sup>4</sup>, D. Inoue<sup>5</sup>, M. Minagawa<sup>6</sup>, T. Sugimoto<sup>7</sup>, M. Yamauchi<sup>7</sup>, T. Michigami<sup>8</sup>, T. Matsumoto<sup>1</sup>. <sup>1</sup>Medicine and Bioregulatory Sciences, University of Tokushima Graduate School of Medical Sciences, Tokushima, Japan, <sup>2</sup>Division of Nephrology & Endocrinology, Medicine, University of Tokyo Hospital, Tokyo, Japan, <sup>3</sup>Department of Pediatrics, Osaka University Graduate School of Medicine, Osaka, Japan, <sup>4</sup>Pediatrics, Okayama Saiseikai-Sogo Hospital, Okayama, Japan, <sup>5</sup>Third department of Medicine, Teikyo University School of Medicine, Chiba, Japan, <sup>6</sup>Pediatrics, Chiba University Graduate School of Medicine, Chiba, Japan, <sup>7</sup>Endocrinology/Metabolism and Hematology/Oncology, Shimane University School of Medicine, Shimane, Japan, <sup>8</sup>Bone and Mineral Research, Osaka Medical Center for Maternal and Child Health, Osaka, Japan.

Fibroblast growth factor 23 (FGF23) plays central roles in the development of hypophosphatemic diseases such as tumor-induced osteomalacia (TIO) and X-linked hypophosphatemic rickets/osteomalacia (XLH). However, clinical usefulness of FGF23 measurement has not been established. The objective of this study is to validate FGF23 measurement and establish diagnostic criteria for these diseases. In this cross-sectional study, we examined serum intact-FGF23 concentrations by two-site IRMA (Kainos, Japan) and other biochemical parameters of phosphate metabolism in 32 patients with TIO, 28 patients with XLH and 16 hypophosphatemic patients with other causes including vitamin D deficiency, Fanconi's syndrome and Cushing's syndrome. These patients were recruited by questionnaires to members supported by grants from Research on Measures for Intractable Diseases by Japanese Ministry of Health, Labor and Welfare. In patients with TIO, serum phosphate was 1.67 +/- 0.08 mg/dl with severely suppressed TmP/GFR (1.24 +/- 0.08) and high FGF23 (1149 +/- 541 pg/ml). In patients with XLH, basically the same findings were observed with serum FGF23 being 155 +/- 30 pg/ml. FGF23 was above the upper limit of the reference range in most patients even under medical treatment with active vitamin D3 and/or phosphate. The lowest FGF23 in these patients was 38.0 pg/ml. In contrast, FGF23 in hypophosphatemic patients with other causes was undetectable in 12 out of 16 patients and the highest FGF23 in this group was 23.9 pg/ml. These results clearly indicate that FGF23 measurement is useful for the differential diagnosis of hypophosphatemic diseases caused by excess FGF23 actions and other etiologies. We propose that the intact FGF23 of more than 30 pg/ml in hypophosphatemic patients indicates the presence of diseases caused by FGF23.

**Disclosures:** I. Endo, None.

## SA471

See Friday Plenary number F471.

## SA472

**Vitamin D Deficiency in Inner City Infants: Impact of DBP Genotype.** T. O. Carpenter<sup>1</sup>, J. H. Zhang<sup>\*2</sup>, F. Herreros<sup>\*1</sup>, E. Torrealba-Fox<sup>\*1</sup>, C. Simpson<sup>\*3</sup>, M. Savoye<sup>\*1</sup>, N. Held<sup>\*1</sup>, B. Ellis<sup>\*1</sup>, D. E. C. Cole<sup>4</sup>. <sup>1</sup>Pediatrics (Endocrinology), Yale University School of Medicine, New Haven, CT, USA, <sup>2</sup>The Cooperative Studies Program Coordinating Center, VA Connecticut Healthcare System, West Haven, CT, USA, <sup>3</sup>Internal Medicine, Yale University School of Medicine, New Haven, CT, USA, <sup>4</sup>Laboratory Medicine and Pathobiology, Medicine, and Genetics, University of Toronto, Toronto, ON, Canada.

The prevalence of nutritional rickets is not known but is thought to occur more frequently in northern latitudes and in urban settings. Biochemical abnormalities are detectable before overt skeletal disease is seen. To ascertain risk for development of nutritional rickets in a northern latitude urban environment, we sampled over 500 healthy infants (6 mos - 3 yrs old) during well-child visits to neighborhood clinics in our area. Demographics and detailed diet histories (3 separate 24-hr recall interviews) were obtained. Serum Ca (10.1 ± 0.5 mg/dl), P (5.4 ± 1.7 mg/dl), alkaline phosphatase (AP, 322 ± 453 IU/L), PTH 22 ± 19 nEq/ml, 25-OHD (25D, 27 ± 6 ng/ml), and 1,25(OH)2D (1,25D, 66 ± 24 pg/ml) were measured and genotypes for VDR, TRPV6, and DBP were analyzed. Average daily intakes of calcium (745 ± 299 mg), phosphate (772 ± 280 mg), and protein (39 ± 15 g) were calculated (NDS, U. Minn.).

Prevalences of hypovitaminosis D (25D < 20 ng/ml), hyperparathyroidism, and elevated AP were 12.9%, 24.4%, and 12.6 % respectively. 3.5% of subjects had elevations in both PTH and AP. 25D correlated negatively with PTH (R = -0.098, P = 0.02), but not significantly with AP. In patients with normal PTH, 25D was 27 ± 6 ng/ml. In a preliminary genetic analysis, DBP D432E genotype correlated closely with both 25D (levels lowest in DD genotype, which was less than DE, which was less than EE, P = 0.003) and 1,25D (highest in DD, which was greater than DE and EE, P = 0.02). T436K also correlated with 25D (levels in TT greater than TK and KK, P = 0.018) and 1,25D (TT greater than TK,



which was greater than KK,  $P = 0.037$ ). Multivariate regression adjusting for age and season indicates that both DBP loci are significant ( $P < 0.002$ ) predictors of 1,25D, while D432E is the stronger predictor ( $P = 0.02$ ) of 25D. Analysis of VDR and TRPV6 genotypes were unrevealing.

This study suggests a lower than expected "risk" for rickets based on the limited number of combined biochemical abnormalities observed. These data provide useful population reference data for 25-OHD levels in the pediatric population where vitamin D deficiency is often suspected, and for which age-specific normative data is rarely provided for interpretation. Finally there is a significant dependence of both 25D and 1,25D levels on DBP genotype. DBP genotype may impact the interpretation of 25D level as an index of total body vitamin D stores in this population.

**Disclosures:** T.O. Carpenter, None.

This study received funding from: Gerber Foundation.

## SA473

See Friday Plenary number F473.

## SA474

**A Novel Hypothesis Explains the Syndrome of Chronic Musculoskeletal Pain and Comorbid Painful Healed Fracture Sites in Vitamin D Deficiency.** T. R. Roesel. Deployment Health Clinical Center, Walter Reed Army Medical Center, Washington, DC, USA.

Vitamin D deficiency was found in 93% of 150 patients from the general population with chronic musculoskeletal pain (Plotnikoff, Mayo Clin Proc. 2003; 78:1463). A retrospective chart review revealed vitamin D deficiency in nearly half (49%) of 61 service members with chronic pain who returned from Iraq and Afghanistan (Roesel, J Occ Environ Med. 2008, in press). Service members were referred over an 18 month period from March 2005 until September 2006 to a program for graded exercise and cognitive behavior therapy, and were screened for vitamin D deficiency. Referral was for treatment of post traumatic stress disorder or multiple unexplained physical symptoms. Vitamin D deficiency was defined as  $<20$  ng/ml. Five of these veterans with chronic musculoskeletal pain and vitamin D deficiency had healed, but still painful, deployment-related fracture sites. Holick (Mayo Clin Proc. 2003 Dec; 78(12):1457) has proposed that vitamin D deficiency associated bone and muscle pain is generated by inadequate mineralization of the endosteal and periosteal bone matrix leading to matrix swelling that stimulates periosteal nerve pain fibers. Since service members also revealed concomitant chronic widespread musculoskeletal pain beyond the localized bone injury, a new alternative and augmentative hypothesis is hereby proposed to explain the phenomenon of chronic pain in the presence of vitamin D deficiency. Recent identification of vitamin D receptors in the hypothalamus and amygdala by Eyles et al. (J Chem Neuroanat. 2005; 29:21), suggests that vitamin D deficiency may impair known descending pain inhibitory pathways that regulate the peri-aqueductal grey matter, which in turn controls ascending pain signals travelling through the spinothalamic tract. Thus, the localized chronic bone pain at the fracture site, as well as the co-morbid chronic musculoskeletal pain beyond the fracture site, can be explained through vitamin D deficiency through these two mechanisms, one at the healed fracture site, and the other within the central nervous system. Anecdotal improvement in generalized and local pain seen with supplementation suggests that further studies are needed to determine to what extent vitamin D supplementation prevents or ameliorates chronic generalized musculoskeletal pain and localized pain at healed fracture sites in this newly defined syndrome.

**Disclosures:** T.R. Roesel, None.

## SA475

**Large Collaborative Study on Geographic Variation of SQSTM1 Mutations in Paget's Disease of Bone in Italy.** L. Gennari<sup>1</sup>, F. Gianfrancesco<sup>\*2</sup>, M. Di Stefano<sup>\*3</sup>, D. Rendina<sup>\*4</sup>, D. Merlotti<sup>1</sup>, T. Esposito<sup>\*2</sup>, V. De Paola<sup>1</sup>, A. Aloia<sup>\*2</sup>, G. Martini<sup>1</sup>, M. Mazzetti<sup>\*3</sup>, S. Gallone<sup>\*5</sup>, I. Rainero<sup>\*5</sup>, L. Pinessi<sup>\*5</sup>, G. Isaia<sup>3</sup>, P. Strazzullo<sup>\*4</sup>, R. Nuti<sup>1</sup>, G. Mossetti<sup>\*4</sup>. <sup>1</sup>Internal Medicine, Endocrine-Metabolic Sciences and Biochemistry, University of Siena, Siena, Italy, <sup>2</sup>Institute of Genetics and Biophysics, CNR, Naples, Italy, <sup>3</sup>Internal Medicine, University of Turin, Turin, Italy, <sup>4</sup>Clinical and Experimental Medicine, Federico II University of Naples, Naples, Italy, <sup>5</sup>Neuroscience, University of Turin, Turin, Italy.

Paget disease of bone (PDB) is a chronic disease of the skeleton with a consistent genetic component. The geographic distribution of PDB is not uniform, with a higher prevalence of the disease in populations of British descent. Moreover increased prevalence areas have been described in different Countries. We recently characterized an area of increased prevalence of PDB in the region of Campania, in Southern Italy. Patients from this region also showed increased severity of disease with peculiar phenotypic characteristics and an increased number of familial cases. In this study we examined the clinical characteristics, and the prevalence and type of SQSTM1 mutations in a large sample of 542 unrelated PDB subjects from several regions including 164 patients from Campania. Nine different mutations in SQSTM1 gene were observed in 35.2% and 11.3% of familial and sporadic PDB cases, respectively (equivalent to 15.6% of the overall cohort). Five of these mutations, M401V, A427D, G425E, Y383X and 1224-1226 insT leading to E396X were novel and have not been previously described. The other mutations, P387L, P392L, M404V and G425R have been previously described. An higher prevalence

of SQSTM1 mutations was observed in polyostotic than monostotic cases (7% vs 22%;  $p < 0.005$ ). The distribution of mutations in this sample was more heterogeneous than in other countries, with a significantly increased prevalence of the M404V. In keeping with previous studies, the P392L was however the most common observed mutation in both sporadic and familial cases. Genotype-phenotype analysis confirmed an increased severity of disease and an earlier age of onset in mutations that insert a stop codon. Interestingly, in PDB subjects from Campania a different distribution and a significantly reduced prevalence of mutations was observed with respect to the other regions, despite an increase in disease severity and the higher prevalence of familial cases. In particular, in this region less than 20% of familial PDB had SQSTM1 mutation, as compared to 36-50% in the other regions. This might imply the presence of mutations in different genes as well an increased persistence of a possible environmental trigger, or both these conditions.

**Disclosures:** L. Gennari, None.

## SA476

See Friday Plenary number F476.

## SA477

**Archaeological Skeletons Support a North-West European Origin for Paget's Disease of Bone.** S. Mays. English Heritage, Portsmouth, United Kingdom.

Although the aetiology of Paget's disease of bone (PDB) remains incompletely understood, it seems clear that there is a strong genetic predisposition. This, coupled with the marked geographic variation in prevalence of PDB, with high prevalences in populations of British origin, has led to the suggestion that the disease originated in Britain and was spread around the world by migration and admixture of British populations(1). The aim of the current work is to investigate this suggestion using the geographical distribution of PDB cases in skeletons excavated from archaeological sites.

The methodology for the study is meta-analysis of the world literature on PDB in archaeological skeletons published from 1889 to the present. Re-evaluation of published work indicates that many dubious archaeological cases of PDB have entered the literature, and have been treated in previous reviews as though they were good data. For diagnosis of PDB in archaeological cases to be reliable it needs to be based on currently acceptable radiographic and/or histological criteria. Published examples, and unpublished cases known to the author, that met these criteria were included in the current study.

Using these criteria, 109 archaeological cases of PDB were identified (table 1). The sex ratio was 2.4: 1 in favour of males. The earliest known cases date from the time of the Roman Empire (1<sup>st</sup>-4<sup>th</sup> cent. AD). No cases were identified outside western Europe. Ninety-four percent of cases came from England. The British cases show no particular geographical distribution; the largest numbers of cases come from London but this simply reflects the large number of archaeological skeletons excavated there.

Country	Males	Archaeological cases of PDB		TOTAL
		Females	Unstated sex	
France	1	1	0	2
Germany	0	0	3	3
Portugal	1	0	0	1
England	49	20	34	103
TOTAL	51	21	37	109

The results indicate that PDB has existed in western Europe for at least 2000 years. The concentration of archaeological cases of PDB in western Europe, and in Britain in particular, supports the hypothesis that PDB originated in that geographical area.

References

1. Cundy T. et al. 1999. Paget's disease in New Zealand: is it changing? Bone 24 (5): 7S-9S.

**Disclosures:** S. Mays, None.

## SA478

See Friday Plenary number F478.

## SA479

**Efficacy and Safety of Intravenous Zoledronic Acid in the Treatment of Patients with Resistant Paget's Disease of Bone.** J. R. Tucci, Medicine, Roger Williams Medical Center, Providence, RI, USA.

Though responses have been seen in many of our patients with Paget's disease (PD) treated with several potent bisphosphonates, not infrequently, remissions and especially sustained remissions have not been induced. Two recent reports have described greater efficacy and more sustained remissions following zoledronic acid (ZA) as compared with risedronate. Objectives of this study were to determine 1) the efficacy of ZA in patients with PD who had not had a remission or had had a relapse within a year of therapy with other bisphosphonates, 2) the duration of remissions, and 3) the safety of ZA. Inclusion criteria include serum alkaline phosphatase (AP) at least 50% greater than the upper limit of normal and creatinine clearance of  $\geq 35$  ml/min. Six females and 6 males, mean age 78 years, were studied. At baseline, blood chemistry profile, serum 25-OHD, and urine NTx/creatinine (NTx) were obtained. Patients were supplemented with up to 1.5 g of Ca and at least 600 units of vitamin D daily. Patients received an infusion of 5 mg of ZA. 9 to 11 days later, serum Ca levels were measured. AP and NTx were measured at 1, 3, 6, 9, and 12 months and subsequently at 4 monthly intervals. Results: At baseline, serum Ca, phosphate, and 25-OHD levels were within normal limits. Mean creatinine clearance was  $64 \pm 3$  ml/min. Following therapy, 3 patients had mild flu-like symptoms. Nine to 11 days after therapy, mean serum Ca fell from  $9.5 \pm 1.1$  to  $8.9 \pm 1.2$  mg/dl. Two patients developed asymptomatic hypocalcemia with serum Ca of 8 mg/dl and 8.3 mg/dl. Excess AP levels fell by 72-100% in the 12 patients. AP normalization occurred in 11 patients and in all but one patient within 1 to 6 months. Normalization of NTx was evident in these 11 patients and in 10 within 1 month. The following data in 11 patients in remission (mean  $\pm$  SE):

	preRx	1 mo	3 mos	6 mos	9 mos	12 mos	16 mos	Normal Range
AP	321 $\pm$ 65	166 $\pm$ 21	92 $\pm$ 7	80 $\pm$ 7	77 $\pm$ 7	81 $\pm$ 6	84 $\pm$ 8	25-100
NTx	247 $\pm$ 47	32 $\pm$ 8	37 $\pm$ 10	32 $\pm$ 7	37 $\pm$ 9	33 $\pm$ 5	46 $\pm$ 12	19-66

At 16 months, AP and NTx remain normal in 9 patients. At baseline and 6 months, serum 25-OHD levels were  $34 \pm 0.9$  ng/ml and  $33 \pm 1.5$  ng/ml, respectively, and at baseline and 12 months, creatinine clearances were  $64 \pm 3.4$  ml/min and  $68 \pm 5.5$  ml/min, respectively. In summary, in 12 patients with suboptimal responses to previous bisphosphonate therapy, ZA induced a response in all 12 patients with remissions in 11 patients that are continuing at 16 months in 9 patients. Adverse effects were flu-like symptoms in 3 patients and asymptomatic hypocalcemia in 2 patients. These observations in a selected group of patients with resistant PD treated with ZA demonstrate early suppression of pagetic activity, a continuing remission at 16 months in 9 of 12 responders, good tolerability and renal safety.

**Disclosures:** J.R. Tucci, GlaxoSmithKline 1, 3; Novartis 1, 2, 3; Merck 1; P&G Pharmaceuticals, Inc. 1, 2.

This study received funding from: Novartis Pharmaceutical Company.

## SA480

See Friday Plenary number F480.

## SA481

**Comparison of Intravenous and Intramuscular Neridronate Regimens for the Treatment of Paget's Disease of Bone.** D. Merlotti<sup>1</sup>, D. Rendina<sup>\*2</sup>, G. Mossetti<sup>\*2</sup>, L. Gennari<sup>1</sup>, V. De Paola<sup>1</sup>, G. De Filippo<sup>\*2</sup>, G. Martini<sup>1</sup>, A. Avanzati<sup>\*1</sup>, P. Strazzullo<sup>\*2</sup>, R. Nuti<sup>1</sup>. Internal Medicine, Endocrine-Metabolic Clinics and Biochemistry, University of Siena, Siena, Italy, <sup>2</sup>Department of Clinical and Experimental Medicine, Federico II University of Naples, Naples, Italy.

Aminobisphosphonates represent the most common treatment for Paget's disease of bone (PDB), with the potential for sustained remission. Intravenous regimens with different compounds demonstrated improved efficacy and compliance with respect to oral regimens. In a recent study we demonstrated that either zoledronate (4 mg) and neridronate (200 mg) given as a single intravenous infusion showed a similar efficacy in achieving biochemical remission at 6 and 12 months in up to 90% of patients non-responders to pamidronate. In this study we compared the effects of a same neridronate dose (200 mg) given as intravenous (i.v.) (100 mg infusion over a 2-hours period for 2 consecutive days) or intramuscular (i.m.) (25 mg once a week for 1 month) regimen in 56 patients with active PDB. Randomization was stratified according to baseline total alkaline phosphatase (ALP) levels and previous bisphosphonate treatment. All patients were advised to receive calcium plus vitamin D supplementation throughout the study period (1 g of calcium and 800 UI colecalciferol per day). Blood samples were collected at baseline and after 3, 6, and 12 months. The primary efficacy end-point was the rate of therapeutic response at 6 months, defined as normalization of ALP levels or a reduction of at least 75% in total ALP excess. Serum levels of bone ALP, C-terminal telopeptides of Type I collagen, and 25-hydroxyvitamin D (25 OH-D) were also measured. A significant 40-50% decrease in ALP levels was observed with both regimens after 3 months. At 6 months, 92% and 96% of patients receiving i.v. and i.m. neridronate, respectively had a therapeutic response. Normalization of ALP levels at 6 months was achieved in 89% of patients in i.v. group and in 93% of patients in i.m. group. Interestingly, the response to treatment was significantly correlated with baseline ALP and 25 OH-D levels at 6 months. The decrease in ALP levels was highest in patients with higher baseline total or bone specific ALP levels and with higher 25 OH-D levels at 6 months. Normalization in ALP levels was maintained at 12

months in 22/27 (81.5%) and 24/29 (83%) of patients, in i.v. and i.m. neridronate groups, respectively. Both regimens were well tolerated. The only side effect was an acute phase response, occurring in 11-13% of the patients. In conclusion, both i.m. and i.v. neridronate regimens (at a cumulative dosage of 200 mg in 12 months) showed a similar efficacy in achieving biochemical remission in up to 90% of patients with active PDB.

**Disclosures:** D. Merlotti, None.

## SA482

**Usefulness of *HRPT2* Gene and Parafibromin Studies in Two Patients with Primary Hyperparathyroidism and Uncertain Pathological Assessment.** C. Marcocci<sup>1</sup>, E. Pardi<sup>\*1</sup>, E. Ambrogini<sup>\*1</sup>, C. Banti<sup>\*1</sup>, S. Borsari<sup>\*1</sup>, P. Viacava<sup>\*2</sup>, A. Pinchera<sup>\*1</sup>, F. Cetani<sup>\*1</sup>. <sup>1</sup>Endocrinology, University of Pisa, Pisa, Italy, <sup>2</sup>Oncology, University of Pisa, Pisa, Italy.

*HRPT2* and parafibromin studies improved the diagnostic accuracy in two patients with primary hyperparathyroidism (PHPT) referred to us after parathyroidectomy, in whom the clinical data were at variance with the pathological diagnosis of adenoma and carcinoma, respectively. Patient #1 had had a 1.5-cm tumor easily removed with a histological diagnosis of parathyroid carcinoma and normocalcemia for 2 years. Re-examination of the histology showed no cardinal signs of parathyroid cancer. Patient #2, with severe PHPT, had had the removal of a 3.5-cm tumor described histologically as adenoma. Ten years later PHPT recurred and persisted despite removal of two parathyroid glands that were normal by routine histological examination. Re-review of the initial histology showed a trabecular pattern, fibrous bands, and atypical mitoses, suggesting an atypical adenoma. Because of the suspicion that case #1 could be an atypical adenoma and case #2 a carcinoma further molecular studies were performed. No *HRPT2* and parafibromin abnormalities were identified in patient #1, strongly indicating a benign lesion. In patient #2, an *HRPT2* germline mutation was found (E115X in exon 4) and associated with no parafibromin staining. These data, together with the clinical features, supported the suspicion of a parathyroid carcinoma that was confirmed by histological examination of further slides of the tumor, showing capsular and vascular invasion. A lung 1.5-cm nodule detected by CT was excised. Histology showed a metastasis of parathyroid carcinoma. *HRPT2* gene studies may be of clinical utility in the management of patients with parathyroid tumors of uncertain pathology.

**Disclosures:** C. Marcocci, None.

## SA483

See Friday Plenary number F483.

## SA484

**Low Density Lipoprotein-Cholesterol Levels Affect Vertebral Fracture Risk in Female Patients with Primary Hyperparathyroidism (pHPT).** H. Kaji<sup>1</sup>, I. Hisa<sup>\*1</sup>, Y. Inoue<sup>\*1</sup>, T. Sugimoto<sup>2</sup>. <sup>1</sup>Kobe University Graduate School of Medicine, Kobe, Japan, <sup>2</sup>Shimane University Faculty of Medicine, Izumo, Japan.

Patients with pHPT have reduced bone mineral density (BMD) with enhanced bone turnover. The risk of vertebral and forearm fractures are increased in pHPT patients. Although several reports indicated that increased arterial stiffness and dyslipidemia were observed in pHPT patients, it still remains unclear about the relationships between lipid and bone metabolism in pHPT patients, especially about fracture risk. The present study was performed to examine the relationship between lipid metabolism parameters including body composition and bone metabolism in 116 female patients with pHPT and 116 age-matched control subjects. BMD and body composition were measured by dual-energy x-ray absorptiometry. Serum levels of total cholesterol (T-Chol) and high density lipoprotein-cholesterol (HDL-Chol) as well as albumin (Alb) were significantly lower in pHPT group, compared with those of control group. Fat mass (FM) and lean body mass (LBM) as well as % fat were similar in both groups. Serum levels of all parameters (T-Chol, LDL-Chol, TG and HDL-Chol) were not significantly related to serum levels of calcium and PTH as well as bone metabolic indices. As for BMD parameters, only serum LDL-Chol levels were significantly and negatively related to z-score of BMD at femoral neck, but not those of BMD at lumbar spine and radius. FM was positively related to Z-score of BMD at lumbar spine and femoral neck. On the other hand, LBM was negatively related to serum levels of PTH and bone resorption indices and positively to Z-scores of BMD at all. Serum levels of T-Chol and LDL-Chol were significantly lower in the group with vertebral fractures, compared with the group without vertebral fractures, in only pHPT patients. Serum levels of HDL-Chol, TG and Alb as well as body composition parameters were not significantly different between the groups with and without vertebral fractures in both control and pHPT groups. In a univariate logistic regression analysis, age, height, BMD at lumbar spine and radius, serum levels of creatinine, T-Chol and LDL-Chol were selected for the predictors of vertebral fracture risk. Multiple logistic regression analyses suggest that the relationship between LDL-Chol and vertebral fractures was independent of these parameters. In conclusion, the present study demonstrated that lower serum LDL-Chol levels were related to vertebral fracture risk independently of renal function, age, body size index, BMD, bone turnover and serum levels of Ca, PTH, Alb in pHPT women. Increased LBM seemed to be protective for osteopenia induced by pHPT.

**Disclosures:** H. Kaji, None.

## SA485

See Friday Plenary number F485.

## SA486

**Normocalcemic Primary Hyperparathyroidism: Update on a New Clinical Phenotype.** H. Lowe\*, D. J. McMahon, M. D. Walker, M. Rubin, J. P. Bilezikian, S. J. Silverberg. College of Physicians & Surgeons, Columbia University, New York, NY, USA.

Patients with elevated parathyroid hormone (PTH) and consistently normal serum calcium levels in whom secondary causes of high PTH have been excluded may represent the earliest presentation of primary hyperparathyroidism (PHPT). We update data on 37 patients (mean age 59 yrs, range 32-78; 95% female) with normal corrected serum calcium ( $9.6 \pm 0.1$  mg/dl; nl: 8.6-10.4) and elevated PTH ( $93 \pm 5$  pg/ml; nl: 10-65) levels. All patients had 25(OH)vitamin D levels  $>20$  ng/dl, 24 hr urinary calcium (Uca)  $<350$  mg/d, normal renal, hepatic, and thyroid function, and no malabsorption. Classical features of PHPT included a history of kidney stones in 5 (14%), and fragility fractures in 4 (11%). In 11 subjects (30%), 1,25(OH)<sub>2</sub>D levels were elevated, while 7 (18%) had high Uca. BMD did not show evidence of preferential bone loss at the more cortical distal 1/3 radius (LS T-Score:  $-2.03 \pm 0.25$ ; FN T:  $-1.84 \pm 0.18$ ; RAD T:  $-1.74 \pm 0.22$ ). Osteoporosis (OP; found in 59%, n=22 patients) was more common at the LS (38%) and FN (41%) than at the RAD (22%).

Patients were followed for  $4 \pm 0.3$  yrs (1-9 yrs), during which 8 subjects (22%) became frankly hypercalcemic. Those who developed hypercalcemia were older ( $64 \pm 2$  vs.  $57 \pm 2$ ,  $P=0.02$ ) and had higher baseline serum calcium levels ( $9.9 \pm 0.2$  mg/dl vs.  $9.5 \pm 0.1$ ,  $P<0.001$ ). Seven patients (5 normocalcemic) developed NIH surgical criteria for hypercalcemic PHPT: marked hypercalciuria in 3; recurrent kidney stone in 1; traumatic fracture in 1; new OP in 4. Repeat BMD testing (n=33) demonstrated that 51% lost  $\geq 5\%$  and 33% lost  $\geq 10\%$  BMD at  $\geq 1$  skeletal sites, with similar declines seen at all sites. Osteoporosis at baseline did not predict who would lose  $\geq 10\%$  BMD (with OP: 7/22, 32%; no OP: 4/15, 27%). Significant bone loss, new OP or new kidney stone developed in 15/37 (40%).

Sestamibi scans were positive in 13/21 cases. Ten patients had successful PTX: 5 hypercalcemic and 5 normocalcemic patients with NIH surgical criteria: kidney stones (n=1), OP (n=4). Pathology in normocalcemic patients showed adenoma (n=2) and hyperplasia (n=3), while hypercalcemic patients had single adenoma (n=3), double adenoma (n=1) or hyperplasia (n=1). One yr post-PTX BMD rose 5% at LS, but was unchanged at FN and RAD.

In summary, these patients with normocalcemic PHPT do not have the typical profile of hypercalcemic PHPT. They present with more signs and symptoms, and develop more complications over time. Despite this,  $>75\%$  of patients remain normocalcemic. There are no predictors of the timing or onset of hypercalcemia. We conclude that these patients do not represent emerging asymptomatic PHPT. Instead they may be an early presentation of a more symptomatic variant of PHPT, some of whom may never become hypercalcemic.

**Disclosures:** H. Lowe, None.

*This study received funding from: NIH.*

## SA487

**Antioxydants (Phytoestrogens and Quercetin) Are Potentials Agents Against Rheumatoid Arthritis.** I. Henry-Desailly\*<sup>1</sup>, E. Flipo\*<sup>2</sup>, P. Lefauveau\*<sup>1</sup>, D. Ursu\*<sup>1</sup>, C. Benneteau-Pelissero\*<sup>3</sup>, S. Kamel\*<sup>4</sup>, M. Brazier\*<sup>4</sup>, P. Fardellone\*<sup>2</sup>. <sup>1</sup>Rheumatology, University Hospital, Amiens, France, <sup>2</sup>Rheumatology - Inserm Eri12, University Hospital, Amiens, France, <sup>3</sup>ENITA, Bordeaux, France, <sup>4</sup>Inserm eri12, Faculty of Pharmacy, Amiens, France.

**Objective:** To estimate the influence of alimentary phytoestrogens and quercetin alimentary intake on rheumatoid arthritis (RA).

**Methods:** We performed a case control study comparing 30 women having Rheumatoid Arthritis with 30 controls women matched on BMI and age, (between 45 to 65). The flavonoids exposure was assessed by biological dosages in plasma (pl) and urines (u) by an ELISA immuno-assay (genistein, daidzein, equol) and by liquid chromatography-mass spectrometry (quercetin).

Some patients were excluded if under medical condition (like pregnancy or hormonal dependent cancers,) or treatments (oral contraceptive, hormonal replacement for menopause) which could influence their hormonal status.

We compared the means of phytoestrogens concentration in plasma and urines of the two groups, using matched controls "t" test after log-transformation.

**Results:** Phytoestrogens and quercetin concentrations according to the two groups are shown in the table.

Phytoestrogens and Quercetine (ng/ml)	RA Mean (SD)	Controls Mean (SD)	P
Genistein (u)	225.0 (582.0)	178 (501,4)	0.135
Genistein (pl)	20.9 (83.8)	70,3 (262,3)	0.778
Daidzein (u)	677.7 (1619.7)	359 (786,6)	0.144
Daidzein (pl)	16,4 (57.6)	31.5 (112,2)	0.752
Equol cor (u)	10.7 (33.8)	48,2 (108,4)	<b>0.029</b>
Equol cor (pl)	0.83 (3.7)	0.87 (3,4)	0.991
Quercetine (u)	19,02 (2,05)	18,2 (2,9)	0.530
Quercetine (p)	7,2 (3,2)	10,8 (4,2)	<b>0.038</b>

Equol in urines and quercetin in plasma are the only flavonoids for which we observed a significant difference between the two groups Equol u ( $p=0.029$ ) and Quercetin pl ( $p=0.038$ ).

Equol is chemically unique among the isoflavone, it is the major metabolite of the phytoestrogen daidzein. This phytoestrogen has one of the strongest estrogen activity and could interact with the immunologic system.

Quercetin, flavonol widely distributed in plants has antioxidant properties with antiproliferative, anti-inflammatory and immunosuppressive activities.

**Conclusion:** Our results suggest that equol and quercetin have a protective effect toward the onset of Rheumatoid Arthritis, thanks to their antioxidants and anti-inflammatory properties.

**Disclosures:** E. Flipo, None.

*This study received funding from: Hospital university of Amiens.*

## SA488

See Friday Plenary number F488.

## SA489

**The Association Between Several Factors Affecting Aortic Calcification and Bone Mineral Density In Postmenopausal Women.** W. H. Choi, H. Han\*, S. M. Hong\*, Y. H. Ahn\*. Endocrinology, Hanyang University, Seoul, Republic of Korea.

**Background:** Aortic calcification increases with age and several epidemiologic studies shows that it is linked to cardiovascular mortality such as myocardial infarction and stroke. Elderly person whose degree of aortic calcification increases greater tends to lose more bone than those whose gain for aortic calcification is minimal. Osteoclastic potential is greater in preosteoclasts from bone marrow in hyperlipidemic compared with normal mice. Therefore we are to evaluate the factors that contributes to vascular calcium accumulation and the association between Lipid profile and bone mineral density(BMD)

**Methods:** Postmenopausal women who visited the health promotion center at Hanyang Univ. hospital from Jan 2003 to Sep 2007 have taken baseline checkup including history taking, physical examination, and blood sampling. Lumbar spinal and femoral BMD was measured by dual energy X-ray absorptiometry(DXA). The presence of aortic calcification was identified by Abdominal CT. According to the extent of sum of aortic calcification observed in all cross sectional area, all patients were divided to 3 groups: None(No calcification), Mild to moderate( $0-180^\circ$ ), Severe( $180-360^\circ$ )

**Results:** Patients with aortic calcification had significantly lower BMD than those without aortic calcification. High triglyceride and low HDL cholesterol was significantly associated with aortic calcification. Diabetic patients had a higher incidence of aortic calcification than non-diabetic patients(83% vs 49%;  $P$  value $<0.01$ ), and they had significantly higher triglyceride and lower HDL cholesterol levels than non-diabetic patients. As the degree of aortic calcification increases, BMD especially femoral BMD tends to decreases. However, none of the lipid profiles was significantly correlated with BMD.

**Conclusion:** There is a reciprocal relationship between degree of aortic calcification and bone mineral density. Among other cardiovascular risk factors, DM is a potent risk factor for aortic calcification. In addition to metabolic stress induced by hyperglycemia, Dyslipidemia may contribute to vascular calcium accumulation. Although dyslipidemia including high TG and low HDL is significantly associated with aortic calcification, there is no meaningful correlation between serum lipid level and BMD.

**Disclosures:** W.H. Choi, None.





## SA490

### Elevated Serum Ionic Fluoride Levels in Post-menopausal Women is Due to the Enhanced Release of Fluoride from Bone. K. Itai<sup>\*1</sup>, M. Ohsawa<sup>\*1</sup>, K. Tanno<sup>1</sup>, T. Onoda<sup>\*1</sup>, T. Sato<sup>\*1</sup>, T. Kuribayashi<sup>\*1</sup>, K. Sakata<sup>\*1</sup>, A. Okayama<sup>\*2</sup>.

<sup>1</sup>Hygiene and Preventive Medicine, Iwate Medical University, Morioka, Japan, <sup>2</sup>The First Institute of Health Service, Anti-Tuberculosis Association, Tokyo, Japan.

Serum ionic fluoride (SIF) levels may reflect changes in bone metabolism along with osteoporosis, especially in the middle-aged and elderly post-menopausal women. However, useful references of age-specific SIF levels and the confounding factors significantly associated with SIF levels have not been fully elucidated in a general population. The purpose of this study is to determine sex- and age-specific mean levels of SIF and to estimate confounding factors associated with SIF levels. A total of 332 participants (167 men and 165 women) were enrolled. Fasting blood samples were collected from all participants. SIF levels were measured by the flow injection method with an ion selective electrode as a detector. A multiple regression analysis was performed to determine confounding factors associated with SIF levels. Participants were divided into sex- and age-specific groups and multivariate-adjusted SIF levels were compared between the groups using ANCOVA after adjustment for the associated factors separately by sex. The crude means of SIF levels ( $\mu\text{mol/l}$ ) were 0.495 in men and 0.457 in women, respectively. Crude SIF levels were positively associated with age in both sexes (see table). Estimated glomerular filtration rate (eGFR) and plasma glucose (FPG) levels were independently associated with SIF levels in both sexes. Menopause status was independently associated with SIF levels in women. Crude and adjusted SIF levels in post-menopausal women were significantly higher than those in pre-menopausal women. Decreased glomerular filtration rate was the most powerful factor that increases SIF levels in men. Elevated SIF levels in post-menopausal women indicate that the enhanced fluoride release from bone exists accompanied with the accelerated bone resorption after menopause.

Crude and adjusted serum ionic fluoride levels stratified by sex and age classes				
Age classes (years)	40-49	50-59	60-69	trend P
Male subjects (n)	55	53	59	-
Crude, $\mu\text{mol/l}$	$0.454 \pm 0.158$	$0.509 \pm 0.159$	$0.519 \pm 0.185$	0.045
Adjusted (95% CI), $\mu\text{mol/l}$	0.463 (0.463-0.506)	0.513 (0.420-0.557)	0.508 (0.469-0.550)	0.143
Female subjects (n)	53	57	55	-
Crude, $\mu\text{mol/l}$	$0.383 \pm 0.135$	$0.470 \pm 0.166$	$0.516 \pm 0.151$	<0.001
Adjusted (95% CI), $\mu\text{mol/l}$	0.439 (0.439-0.489)	0.461 (0.388-0.500)	0.471 (0.423-0.514)	0.418

**Disclosures:** K. Itai, None.

## SA491

See Friday Plenary number F491.

## SA492

### Improved Forearm Bone Mineral Density after Treatment with Vitamin D<sub>3</sub> in a Patient 30 Years after Bariatric Surgery. S. E. Williams<sup>1</sup>, A. A. Licata<sup>2</sup>.

<sup>1</sup>Center for Nutrition and Metabolic Medicine, Greene Memorial Hospital, GMH Health Center, Xenia, OH, USA, <sup>2</sup>Metabolic Bone Center, Cleveland Clinic Foundation, Cleveland, OH, USA.

Our purpose is to report a case of severe secondary metabolic bone disease in which a statistically significant increase in forearm bone mineral density occurred as a result of vitamin D<sub>3</sub> supplementation.

A 76-year-old nonambulatory woman who underwent jejunum-ileal bypass (JIB) bariatric surgery in 1974 presented to our metabolic bone center with hypocalcemia, hypovitaminosis D, hyperparathyroidism, proximal weakness, and debilitating bone pain. The DXA T-scores for total hip and forearm were -5.0 and -6.5 standard deviations, respectively. Oral cholecalciferol and calcium were prescribed, and dose adjustments were made in an effort to promote adequate absorption in response to periodic laboratory tests. Our patient required 100,000 IU cholecalciferol and 1800 mg calcium citrate on a daily basis due to iatrogenic malabsorption.

The 25-hydroxyvitamin D level, undetectable at first presentation, returned to normal limits during an 8-month period of aggressive oral supplementation. Lab data are noted in Table 1. During this period the distal forearm bone mineral density increased by 17.9%; there was no significant change in the left total hip.

**Table 1**  
**Data Before and After Supplementation with Cholecalciferol<sup>1</sup>**

Serum Factor	Ref Range	Baseline	After
Albumin (g/dL)	3.4 - 4.7	2.8	3.8
Creatinine (mg/dL)	0.7 - 1.4	1.2	1.4
Total Calcium (mg/dL)	8.5 - 10.5	7.4	8.7
Alkaline Phosphatase (U/L)	40 - 150	456	333
Parathyroid Hormone (pg/mL)	10 - 60	488	190
25-hydroxyvitamin D (ng/mL)	31 - 80	< 7.0	37

<sup>1</sup> First three months: 50,000 IU cholecalciferol twice weekly, patient stopped calcium supplement due to dyspepsia; 4<sup>th</sup> month: 600 mg calcium carbonate tid with meals plus 50,000 IU cholecalciferol daily; 5<sup>th</sup> month: increased cholecalciferol to 100,000 IU daily, and changed to calcium citrate.

We conclude that supplementation with vitamin D<sub>3</sub> and calcium alone can improve forearm bone density in certain skeletal problems and that clinicians must carefully interpret abnormal DXA data, since it may not always reflect primary osteoporosis.

**Disclosures:** S.E. Williams, None.

## SA493

### (22-52) Adrenomedullin Prevents Systemic Bone Loss Related to Inflammation in Mice. C. Asensio<sup>\*1</sup>, M. Ah-Kioon<sup>\*1</sup>, H. Ea<sup>\*1</sup>, B. Uzan<sup>\*1</sup>, A. Kadri<sup>\*1</sup>, C. Bazille<sup>\*1</sup>, C. Marty<sup>\*1</sup>, C. Collet<sup>\*1</sup>, J. Launay<sup>\*2</sup>, F. Liote<sup>\*1</sup>, M. E. Cohen-Solal<sup>1</sup>. <sup>1</sup>Hôpital Lariboisière, INSERM U606, Paris, France, <sup>2</sup>Hôpital Lariboisière, Laboratoire de Biochimie, Paris, France.

Rheumatoid arthritis is associated with focal and systemic bone loss involving many inflammatory factors. Among them, adrenomedullin (ADM) reduces inflammation in collagen-induced arthritis (CIA) mice model. Moreover, ADM exerts *in vivo* anabolic effects on bone along with *in vitro* anti-apoptotic effects on osteoblast cells. (22-52)ADM, a fragment peptide which binds to ADM receptor, might act as an antagonist of ADM *in vitro* but its *in vivo* effects are unknown. We evaluated the action of ADM and (22-52)ADM, on systemic bone loss in a CIA mice model. DBA/1 mice were immunized with bovine type II collagen and treated with ADM or (22-52)ADM (1.2  $\mu\text{g/g}$  for both) or saline. Total body and vertebral bone mineral densities (BMD) were measured at baseline and at sacrifice (D45), and expressed as Delta BMD. Arthritic scores were evaluated in a blinded manner and histological studies of joints and bone were performed at sacrifice. Histomorphometric parameters were evaluated at the lumbar vertebrae. Bone resorption was quantified using the urinary deoxypyridinoline assay. At 45 days after disease onset, ADM and (22-52)ADM decreased arthritic score compared to saline ( $6.8 \pm 1.6$  and  $5.8 \pm 2$  vs  $11 \pm 3$ , respectively). Moreover, total histological score (inflammation, pannus and cartilage) was decreased with ADM compared to controls ( $1.30 \pm 0.07$  vs  $3.78 \pm 0.26$ ) and further decreased with (22-52)ADM ( $0.56 \pm 0.04$  vs  $3.78 \pm 0.26$ ,  $p < 0.05$ ). Furthermore, CIA induced systemic bone loss, as evidenced by Delta BMD, compared to the naive group (total body (TB):  $17.9 \pm 2.7\%$  vs  $25.5 \pm 0.2\%$ ; vertebrae (V):  $16.8 \pm 2.8\%$  vs  $29.4 \pm 7.7\%$ ). Compared to CIA mice treated with saline, ADM partly prevented CIA-induced bone loss ( $23.6 \pm 2.3\%$  vs  $17.9 \pm 2.7\%$  at TB and  $20.0 \pm 2.8\%$  vs  $16.8 \pm 2.8\%$  at V,  $p = \text{NS}$ ). Moreover, (22-52)ADM also increased BMD ( $25.7 \pm 2.6\%$  vs  $17.9 \pm 2.7\%$  at TB and  $33.2 \pm 3.6\%$  vs  $16.8 \pm 2.8\%$  at V,  $p < 0.05$ ). Indeed, (22-52)ADM increased trabecular bone volume ( $12 \pm 0.6$  vs  $10 \pm 0.5\%$ ,  $p < 0.05$ ) as well as trabecular thickness ( $28.3 \pm 0.8$  vs  $25.2 \pm 0.8 \mu\text{m}$ ,  $p < 0.05$ ) suggesting an effect on bone formation. Urinary deoxypyridinoline levels were increased in CIA compared to naives ( $14.09 \pm 0.92$  vs  $8.22 \pm 0.47$ ,  $p < 0.05$ ) but were unchanged with ADM and (22-52)ADM. In conclusion, both ADM and (22-52)ADM prevented bone loss in CIA mice. (22-52)ADM could prevent bone loss by maintaining osteoblast activity. Although the mechanism of action of each peptide remains to be determined, these molecules might represent a potential interest for the prevention of inflammatory-related bone loss.

**Disclosures:** C. Asensio, None.

This study received funding from: Rhumatisme et Travail.

## SA494

See Friday Plenary number F494.

## SA495

Withdrawn

## SA496

### Vitamin D Status and Bone Remodeling Marker CTx-I in Patients with Early Rheumatoid Arthritis (RA): Association with Disease Activity and Joint Damage. M. L. Gonzalez-Casaús<sup>\*1</sup>, P. Aguado<sup>\*2</sup>, M. C. Ordoñez<sup>\*2</sup>, A. Cabezon<sup>\*3</sup>, D. Pascual-Salcedo<sup>\*3</sup>, A. Balsa<sup>\*2</sup>, E. Martín-Mola<sup>\*2</sup>.

<sup>1</sup>Biochemistry, Hospital Central de la Defensa, Madrid, Spain, <sup>2</sup>Rheumatology, Hospital Universitario La Paz, Madrid, Spain, <sup>3</sup>Immunology, Hospital Universitario La Paz, Madrid, Spain.

**Background:** Vitamin D (VD) is a potent regulator of calcium homeostasis and musculoskeletal function and may also have immunomodulatory effects. The influence of VD on RA is not well defined. The type I collagen C-telopeptide bone breakdown product (CTX-I) has been related with joint damage in chronic persistent arthritis

**Objectives:** To study the association of baseline 25 (OH) D3 serum level with disease activity and with functional scores in patients with early RA, and to investigate the relationship between baseline CTX-I and radiographic joint damage

**Methods:** Patients attending an early arthritis clinic and showing signs of probable RA were studied. Disease activity was recorded at initial evaluation and every 6 months thereafter, taking into account pain, patient and physician assessment, articular indices, acute phase reactants and functional capacity (HAQ). In addition, rheumatoid factor (RF) and cyclic citrullinated peptide antibody levels (anti-CCP) were determined. X-Rays of hands and feet were taken at initial evaluation and every 12 months. Basal levels of serum



calcidiol (SC) and CTX-I were determined by electrochemiluminescence (ECLIA) using an Elecsys analyser (Roche). X-Rays were evaluated by the Sharp-van der Heijde method, following a chronological order and by pairs. Patients were treated according to physician's criteria and biological agents were not used. Results were compared by t test, ANOVA (Scheffe), and correlation studies (Pearson and Spearman), as required

**Results:** 165 patients with RA were studied; 75.8% were female, mean age was  $53 \pm 17$  years and disease duration,  $16 \pm 10$  weeks. 161 (97%) patients fulfilled ACR criteria for RA during follow-up. At baseline, mean SC was  $25.6 \pm 10.7$ . SC levels were not related to RF or anti-CCP antibodies. Eighty-two percent of patients had a vitamin D insufficiency ( $<30$  ng/ml). Basal SC was inversely correlated with patient global disease assessment ( $r = -0.4$ ,  $p=0.05$ ), and with the number of painful joints, both at entry and during the first 2 years ( $r = -0.23$ ,  $p=0.04$ ). Basal CTX-I levels were correlated with radiological damage at all time points; at entry ( $r=0.46$ ;  $p=0.006$ ), at one year ( $r=0.41$ ;  $p=0.03$ ) and at 2 years ( $r=0.38$ ,  $p=0.05$ )

**Disclosures:** M.L. Gonzalez-Casaús, None.

## SA497

### Application of a Treatment Algorithm to Avoid BMD Loss and Limit Bisphosphonate Use after Kidney and Kidney Pancreas Transplantation.

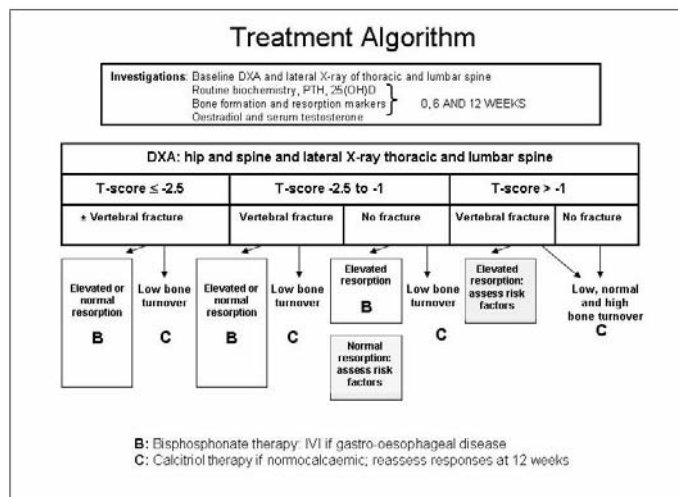
R. Mainra<sup>\*1</sup>, G. J. Elder<sup>2</sup>. <sup>1</sup>Division of Nephrology, St. Paul's Hospital, Saskatoon, SK, Canada, <sup>2</sup>Centre for Transplant and Renal Research, Westmead Millenium Institute, Sydney, Australia.

Despite reduction of glucocorticoid exposure in current immunosuppressive regimens, BMD levels often fall after kidney (K) and kidney pancreas (KP) transplantation and the incidence of post-transplant fractures is high. In meta-analysis, bisphosphonates and vitamin D reduce loss of BMD at the spine and hip but both have potential adverse effects. We studied the consequences of allocating patients to bisphosphonate and calcitriol therapy using a treatment algorithm.

In this prospective study, 155 transplant recipients (K: 92 and KP: 63) were followed for 12 months. Kidney recipients differed from KP recipients by age ( $48 \pm 12$  vs.  $38 \pm 7$  years,  $p<0.0001$ ), dialysis vintage ( $37 \pm 5$  vs.  $17 \pm 2$  months;  $p<0.01$ ) and haemo. vs. peritoneal dialysis (65% vs. 44%,  $p<0.01$ ). Transplant recipients were assessed with bone turnover markers (serum osteocalcin and urinary deoxypyridinoline/creatinine), levels of iPTH, vitamin D and sex hormones 4-6 weeks after transplant. BMD by DXA and lateral spine X-ray were performed. Patients were allocated to bisphosphonate or calcitriol according to an algorithm based on these results and assessment of standard risk factors. Patients with 25OHD levels  $<60$  nmol/L received cholecalciferol.

Using the algorithm, 56% of patients received bisphosphonates. Age was similar between treatment groups as was gender and transplant type. More patients allocated to bisphosphonates were on haemodialysis pre-transplant (66% vs. 43%;  $p=0.02$ ) and were of longer dialysis vintage ( $32 \pm 4$  vs.  $22 \pm 6$  months;  $p=0.006$ ). Patients receiving bisphosphonates had lower baseline BMD at the lumbar spine and femoral neck ( $p<0.0001$  for each). At 12 months, BMD increased in bisphosphonate treated patients at the lumbar spine and femoral neck ( $p=0.0012$  and  $p=0.002$  respectively). BMD in non-bisphosphonate treated patients did not change significantly at any site.

When patients with chronic kidney disease are transplanted, post-transplant laboratory and BMD data may be difficult to interpret due to pre-existing renal osteodystrophy. Targeting therapy using this algorithm resulted in reduced bisphosphonate exposure and potential drug-related risks, while maintaining or improving BMD at all sites.



**Disclosures:** R. Mainra, None.

## SA498

### Change of Pathological Bone Lesion in Recipients with Renal Osteopathy after Renal Transplantation.

T. Tokumoto<sup>\*1</sup>, T. Nozaki<sup>\*1</sup>, K. Yoshida<sup>\*1</sup>, H. Suzuki<sup>\*1</sup>, T. Akiba<sup>2</sup>, K. Tanabe<sup>\*2</sup>. <sup>1</sup>Kidney Center, Dept. of Urology, Toda Central General Hospital, Saitama, Japan, <sup>2</sup>Kidney Center, Tokyo Women's Medical University, Tokyo, Japan.

**OBJECTIVES:** We expect if chronic renal failure (CRF) is improved after renal transplantation (RTx), dialysis osteopathy is also recover to normal in bone lesion. Nevertheless, it is controversial whether bone lesion is really improved after RTx. In this study, we evaluated whether dialysis osteopathy was pathologically improved after RTx.

**MATERIALS AND METHODS:** Forty-one cases that underwent living related RTx at Toda central general hospital from January, 2004 were enrolled in this 28 males and 13 females. The periods of hemodialysis (HD) were an average of 40.2 months. The immunosuppression was basically triple drug therapy such as FK, MMF and Steroid. The parameter of Ca, P, whole PTH (w-PTH) and metabolic bone marker and bone density (DXA) were examined with relation to dialysis osteopathy in before RTx, and 1 year after RTx. In addition, bone biopsy was performed after having made osteal labeling twice in principle before bone biopsy.

**RESULTS:** All cases are survival and the renal grafts are functioning well in all cases. The mean level of Ca and P before RTx were 9.4mg/dl and 5.5mg/dl, respectively. The mean level of w-PTH was 73.4 pg/ml before RTx. The mean level of ALP was 262.1 U/l before RTx. The mean level of BAP was 29.6 U/l before RTx. The mean of bone volume (BV/TV) before RTx was 18.0%. The mean of osteoid volume (OV/TV) before RTx was 3.6%. The mean of fibrosis volume (Fb.V/TV) before RTx was 0%. The mean of bone formation rate (BFR/BV) before RTx was 25.5 %/year. Both of BV/TV and BFR/BV after RTx were increased pathologically. On the other hand, Fb.V/TV and OV/TV were also remarkably increased. Out of 41 cases, 30 cases (73.2%) were pathologically diagnosed as renal osteodystrophy, 7 cases (17.1%) were aplastic osteopathy, 2 cases (4.9%) were renal osteodystrophy or aplastic osteopathy, one case (2.4%) was osteitis fibrosa and one case (2.4%) was osteomalacia by bone biopsy at RTx. Six cases were already underwent the bone biopsy at 1 year after RTx. Out of these cases, 3 cases were renal osteodystrophy, 2 cases were aplastic osteopathy, and one case was renal osteodystrophy or aplastic osteopathy at RTx. Of 6 cases, 2 cases were pathologically diagnosed as renal osteodystrophy, 2 cases were mixed type, and 2 cases were osteomalacia at 1 year after RTx.

**CONCLUSIONS:** The bone metabolism was greatly improved at one year after RTx, but bone lesion in recipients with renal osteopathy did not seem to be recover pathologically. In particular, the tendency strongly resisted in case of aplastic osteopathy. The further examination by metabolic bone marker and bone biopsy will be needed in future.

**Disclosures:** T. Tokumoto, None.

## SA499

### Bone Metabolism in Long-term Kidney Transplantation Recipients.

A. Suzuki<sup>1</sup>, H. Sasaki<sup>\*2</sup>, S. Yamamoto<sup>\*1</sup>, S. Sekiguchi<sup>1</sup>, M. Shibata<sup>1</sup>, S. Asano<sup>1</sup>, K. Hoshinaga<sup>\*2</sup>, M. Itoh<sup>\*1</sup>. <sup>1</sup>Division of Endocrinology, Department of Internal Medicine, Fujita Health University, Aichi, Japan, <sup>2</sup>Department of Urology, Fujita Health University, Aichi, Japan.

Recent pharmacological advances in immunosuppressive therapy and transplant techniques have been improving long-term survival of graft recipients. Post-transplantation bone diseases negatively affect quality of life of solid organ recipients, because osteoporosis is prevalent in more than half of them. Bone loss during the first year after transplantation is most pronounced, but bone density development in long-term transplant recipients is still controversial. In the present study, we conducted cross-sectional study for bone metabolism in long-term survivors after kidney transplantation. Subjects were post-renal transplantation recipients ( $n=31$ , M/F=15/16, age  $54.8 \pm 8.9$ ). Mean duration of hemodialysis was  $116 \pm 83.7$  months. Mean duration after renal transplantation was  $14 \pm 3$  years (9-20 years). All the patients were prescribed methylprednisolone ( $4.07 \pm 0.84$  mg/day) with various immunosuppressive agents (cyclosporin, 28/31; mizoribine, 13/31; tacrolimus hydrate, 3/31; mycophenolate mofetil, 5/31). Mean concentrations of serum corrected calcium, phosphate and creatinine were  $9.8 \pm 0.6$  mg/dl,  $2.9 \pm 0.4$  mg/dl and  $1.19 \pm 0.46$  mg/dl, respectively. Mean serum 25-hydroxyvitamin D level was  $20.3 \pm 4.3$  ng/ml, while serum 1,25-dihydroxyvitamin D3 was  $48.5 \pm 15.7$  pg/ml. Mean concentration of intact parathyroid hormone (iPTH) ( $142.8 \pm 74.3$  pg/ml) was about three times higher than that of whole parathyroid hormone (wPTH) ( $54.3 \pm 34.3$  pg/ml). Serum iPTH and wPTH levels were negatively associated with the duration after kidney transplantation, but not with the duration for hemodialysis. In summary, these findings suggest us that long-term survivors after kidney transplantation have less persistent hyperparathyroidism, and that there is huge difference between serum iPTH and wPTH concentrations in post-kidney transplantation recipients.

**Disclosures:** A. Suzuki, None.

## SA500

See Friday Plenary number F500.

## SA501

**Marked Vitamin D Deficiency in Recent Heart and Liver Transplant Recipients.** E. M. Stein<sup>1</sup>, A. Cohen<sup>2</sup>, M. Freeby<sup>\*2</sup>, S. Kokolus<sup>\*2</sup>, D. Mancini<sup>\*2</sup>, S. Restaino<sup>\*2</sup>, R. Brown<sup>\*2</sup>, D. J. McMahon<sup>2</sup>, E. Shane<sup>2</sup>. <sup>1</sup>Columbia University, New York, NY, USA, <sup>2</sup>Medicine, Columbia University College of Physicians and Surgeons, New York, NY, USA.

Vitamin D deficiency is an increasingly recognized condition with many serious sequelae. Several factors place patients with end-stage organ failure at particular risk for vitamin D deficiency, including limited sunlight exposure and hepatic dysfunction, resulting from intrinsic liver disease or in heart failure patients, hepatic congestion. Subjects were recruited as part of a randomized trial comparing two bisphosphonates for prevention of bone loss after transplantation. Serum 25-hydroxy vitamin D (25OHD: DiaSorin Chemiluminescent assay) was measured immediately after heart or liver transplantation, and before bisphosphonate therapy. Of 65 subjects studied (mean age: 53 ± 11 years), 44 (68%) received heart and 21 (32%) received liver transplants. Subjects were ethnically diverse, 57% Caucasian, 14% African American, 20% Hispanic, 2% Asian and 8% of other ethnicity. Vitamin D levels did not differ by ethnicity. The distribution of serum 25OHD is shown in the table:

Serum 25OHD (ng/ml)	Study Population (n=65)	Heart Transplant (n=44)	Liver Transplant (n=21)
Mean ± SD	17.1 ± 9.3	19.2 ± 9.4	12.7 ± 7.2
<10	12 (18%)	4 (9%)	8 (38%)
10-20	36 (55%)	26 (59%)	10 (48%)
20-30	12 (18%)	10 (23%)	2 (10%)
≥30	5 (8%)	4 (9%)	1 (5%)

Low 25OHD levels were nearly ubiquitous; 92% had levels below 30 ng/ml, the threshold commonly used to denote sufficiency. Six had levels below 7 ng/ml, the lower limit of detection of the 25OHD assay. The distribution of vitamin D levels was significantly lower among liver than heart transplant recipients ( $p=0.01$ ). Severe vitamin D deficiency was particularly widespread in liver transplant recipients; 8 (38%) had levels <10 ng/ml and of these, 5 (24%) had undetectable levels.

Severe vitamin D deficiency is extremely prevalent among heart and liver transplant recipients. Patients with end-stage liver disease are at exceptionally high risk, likely because of disease related factors such as malabsorption, and impaired hepatic 25-hydroxylation of vitamin D. Patients with severe vitamin D deficiency are at risk for hypocalcemia and tetany after treatment with intravenous bisphosphonates. It is imperative to assess vitamin D status and correct vitamin D deficiency in all patients presenting for transplantation, particularly if intravenous bisphosphonates are prescribed to prevent transplant-related bone loss.

**Disclosures:** E.M. Stein, None.  
This study received funding from: Novartis.

## SA502

**A Retrospective Study Evaluating the Relationship of Vitamin D 25 OH and Free Testosterone Levels with Changes in Hip Bone Density after Liver Transplantation.** R. K. Bhattacharya<sup>1</sup>, M. Hagan<sup>\*1</sup>, R. Krebill<sup>\*2</sup>, B. Lukert<sup>1</sup>, L. Graves<sup>1</sup>. <sup>1</sup>Endocrinology, University of Kansas, Kansas City, KS, USA, <sup>2</sup>Biostatistics, University of Kansas, Kansas City, KS, USA.

Osteoporosis and increased fracture risk are common complications following orthotopic liver transplantation (OLT). Pre-transplant markers have not been clearly identified to predict post-transplant changes in bone density.

**Aims of this study:** 1. To evaluate changes in BMD post transplantation and to correlate these changes with baseline Vitamin D 25 OH and free testosterone (in males) levels; 2. To explore the relationship between BMD changes and free testosterone levels pre and post transplantation. **Methods:** This retrospective study evaluated the baseline characteristics of 32 individuals (17 men, 15 women) prior to liver transplantation. The individuals were followed for an average of 425 days post-transplantation and the BMD of the spine and hip, free testosterone (men only) and Vitamin D 25 OH were measured. A paired t-test was used to contrast pre-post changes in BMDs after liver transplantation. Spearman's correlation was used to determine the correlations between several parameters.

**Results:** There was a significant decrease in hip BMD after transplantation (4.29%,  $p<.001$ ). Pre-transplant free testosterone positively correlated with percent change in hip BMD in males ( $r = .5827$ ,  $p=.028$ ). Despite having only 12 males with testosterone measurements done post-transplantation, there was a positive correlation with hip BMD ( $r = .77273$ ,  $p=.0053$ ). Pre-transplant free testosterone also correlated positively with post-transplant free testosterone ( $r = .7135$ ,  $p=.0092$ ).

In the entire population the study found no significant change in spine BMD after transplantation. The pre-transplant and post-transplant levels of Vitamin D 25 OH had a significant correlation on the percent change of spine BMD after transplantation (pre-transplant levels:  $r = .5495$ ,  $p=.003$ , post-transplant levels:  $r = .559$ ,  $p=.0104$ ).

**Conclusion:** This study is consistent with other studies demonstrating bone loss following organ transplantation in the first year. Our findings revealed a correlation between 25-OH D and changes in bone density following liver transplantation. In men, free testosterone also correlated with the change in bone density of the hip after transplantation. This study is limited by the small patient numbers. Further studies are needed to confirm these results and to evaluate a true cause and effect. Future studies should be undertaken to evaluate the potential effect of correcting vitamin D and testosterone deficiency to affect BMD changes.

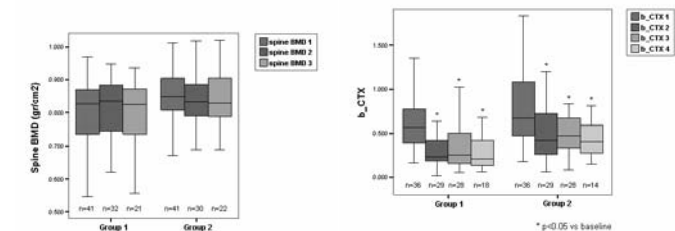
**Disclosures:** R.K. Bhattacharya, Solvay 3.  
This study received funding from: Solvay.

## SA503

**Effect of Risedronate in Liver Transplantation Patients with Low Bone Mass.** S. Guadaluix<sup>\*</sup>, G. Martinez<sup>\*</sup>, B. Cobaleda<sup>\*</sup>, C. Vargas<sup>\*</sup>, D. Lora<sup>\*</sup>, E. Jódar<sup>\*</sup>, J. Meneu<sup>\*</sup>, E. Moreno<sup>\*</sup>, F. Hawkins. University Hospital 12 de Octubre, Madrid, Spain.

Osteoporosis is found in up to 50% of transplant recipients, but the most appropriate preventive measures are not clearly established. The purpose of this study is to analyze the preventive effect of oral risedronate on bone loss in patients with low bone mass detected after liver transplantation (LTx).

**Patients and Methods:** This is a randomized open-label single center prospective study. Eighty-three LTx patients (64 males, 19 females; age  $54.8 \pm 10.6$  years) with lumbar and/or femoral T-score <-1 have been included. After transplantation (mean time  $34 \pm 21$  days) patients were randomly assigned to one of two treatment arms: Group 1 (n=41) received oral risedronate (35 mg once weekly) plus calcium (1000 mg/day) and vitamin D (800 IU); Group 2 (n=42) received calcium and vitamin D at same doses. Primary endpoint was bone mineral density (BMD) change at lumbar spine (L1-L4) and femoral regions (measured at baseline, 6 and 12 months after LTx with an Hologic QDR 4500w densitometer); secondary endpoints include changes in serum  $\beta$ -CTX and PINP. **Results:** No differences were found in baseline characteristics between groups. Forty-three patients (21/22) have completed 12 months of treatment so far. No significant changes in BMD were observed in any group, neither at spine or hip. In Group 1, serum  $\beta$ -CTX decreased after 3 months ( $p=0.008$ ), 6 months ( $p<0.05$ ) and 12 months ( $p=0.008$ ). In Group 2, a significant decrease in  $\beta$ -CTX was also observed. Serum PINP increased in Group 2 after 3, 6 and 12 months of treatment ( $p<0.05$ ). At baseline, 90% of patients had 25-OH vitamin D<sub>3</sub> below 30 ng/ml. In both groups 25-OH vitamin D<sub>3</sub> levels increased at three months ( $p<0.001$ ), maintaining this level throughout the study. Treatment was well tolerated in both groups. **Conclusions:** Preliminary data of our study suggest: 1) risedronate effectively decreases bone resorption after LTx, and 2) LTx patients have low baseline vitamin D levels.



**Disclosures:** G. Martinez, None.  
This study received funding from: Fundación Mutua Madrileña (project number 2005/072).

## SA504

**12 Months of Teriparatide Therapy Increases Ultradistal Radius Bone Strength in Severely Osteoporotic Postmenopausal Women.** H. M. Macdonald<sup>1</sup>, D. A. Hanley<sup>\*2</sup>, S. K. Boyd<sup>1</sup>. <sup>1</sup>Mechanical & Manufacturing Engineering, University of Calgary, Calgary, AB, Canada, <sup>2</sup>Medicine, University of Calgary, Calgary, AB, Canada.

Teriparatide, the amino terminal fragment of parathyroid hormone [PTH (1-34), Forteo<sup>TM</sup>], is an established anabolic therapy for osteoporosis treatment. To date, one study has used non-invasive high-resolution pQCT (HR-pQCT) to quantify changes in bone microarchitecture following PTH administration (JBMR 2007 22:S24). However, PTH-mediated changes in estimated bone strength have not been investigated using novel, subject-specific finite element (FE) analysis with HR-pQCT scans. Thus, we aimed to determine the effects of PTH-therapy on estimated bone strength (ultimate failure load) at the ultradistal (UD) radius in severely osteoporotic postmenopausal women. We used HR-pQCT (Scanco Medical, Switzerland) and FE analysis (Bone 2007 41:129-37) to evaluate changes in estimated UD radius bone strength in 16 women (mean age  $66 \pm 14$  yrs) diagnosed as severely osteoporotic (BMD T-score < -3.5 SD). All women had received bisphosphonate therapy prior to starting on PTH (1-34). We acquired HR-pQCT scans at baseline and 6- and 12-months after initiation of 20 ug/day of PTH (1-34). We analyzed 6-month data for all subjects and 12-month data for 7 of 16 subjects (remaining scans to be analyzed by August 2008). In addition to FE analysis we performed a standard microarchitectural morphological analysis. We used the Wilcoxon Signed Ranks test to compare outcomes before and after treatment. None of the women sustained a fracture during the study. After 6 months, we observed a decrease in bone strength (-5.9%, Table) despite a small increase in trabecular bone volume/total volume (BV/TV). Six months of PTH therapy was also associated with a decrease in cortical density (Dcort) and thickness (C.Th). In contrast, after 12 months we observed a trend for a small increase (+4.3%) in bone strength together with trends for increases in BV/TV, trabecular number (TbN) and thickness (Tb.Th) and continued decreases in Dcort and C.Th. These preliminary data suggest that 12 months of teriparatide therapy may increase UD radius bone strength in severely osteoporotic women, primarily through positive effects on cancellous bone morphology. Further study is needed to determine the influence of the apparent treatment-related increase in cortical porosity (evidenced by the decrease in Dcort) on radius bone strength.

## ASBMR 30th Annual Meeting

Variable	6- and 12-month Percent Change in HR-pQCT outcomes			
	6-Month %Change Median [Interquartile Range (IQR)] (n=16)	p-value	12-month %Change [Median (IQR)] (n=7)	p-value
Estimated Failure Load	-5.9 (-7.9 - (-0.2))	0.02	4.3 (0.5 - 10.4)	0.2
BV/TV	1.9 (0.35 - 4)	0.03	3.8 (-2.3 - 6.7)	0.3
TbN	2.4 (-3.7 - 4.6)	0.4	4.3 (-7.2 - 7)	0.9
Tb.Th	1.5 (-2.8 - 8)	0.4	2.2 (-4.4 - 5.3)	0.9
Dcort	-9.2 (-11.7 - (-1.5))	0.02	-2.2 (-2.8 - 0.2)	0.2
C.Th	-1.7 (-5.2 - 0.8)	0.2	-2.9 (-7.5 - 1)	0.3

**Disclosures:** H.M. Macdonald, None.

## SA505

**Effect of Risedronate on Bone Strength and Work to Failure Determined by Finite Element Analysis and Simulation of Clinically-Measured Bone Loss and Mineralization Changes.** H. Hong\*, G. J. Gross\*, T. E. Dufresne\*, P. A. Chmielewski\*, R. J. Phipps, B. Borah. Procter & Gamble Pharmaceuticals, Mason, OH, USA.

The reduction in relative fracture risk by risedronate is largely due to the reduction of bone remodeling resulting in the prevention of bone loss, preservation of architecture and increase in mineralization. These factors contribute to the relative difference in bone strength in patients with and without treatment. We performed bone loss simulations and FEA on iliac biopsies to assess bone strength in patients treated with risedronate or placebo. Changes in bone volume and mineralization were simulated to match 3 year results as measured originally by 3D micro-CT (Bone, 2004, 34:736-46; Bone, 2005, 37:1-9). We used 12 baseline biopsy images (4 placebo; 8 risedronate) with varying trabecular bone volumes (11-29%). A uniform volume (3.5 mm<sup>3</sup>, 34 microns resolution) was used to normalize for structural variability in the biopsies. A custom program simulated bone loss through random surface erosion of bone using a 3D Euclidian distance map. The 3D images before and after simulation were directly converted into finite element models for analysis of mechanical properties by compression loading using a non-linear ABAQUS analysis. Simulation of a 26% bone volume loss to match the 3 year placebo-treated group produced deterioration of trabecular architecture that closely matched clinical results. It resulted in ~65% reduction in the apparent properties (stiffness, strength and work to failure) compared to baseline. Reducing bone volume by 26% also reduces mineral density by 26%. Reducing density alone by 26% by simulating loss of tissue mineralization (at constant bone volume) reduced strength by only ~25%, suggesting that bone architecture is a more important determinant of bone strength. To simulate the effect of risedronate treatment, mineralization levels were increased 5% to match the change observed in clinical samples. This resulted in increases in stiffness and strength of 3-4%, and no significant change in work to failure. Thus, simulation of the risedronate and placebo treatment effects on trabecular bone resulted in bone strength ~70% higher for risedronate compared to placebo. In conclusion, the preservation of bone architecture is significantly more important than the increase in mineralization for preserving bone strength with risedronate treatment.

Parameter	% Change vs baseline after 26% reduction in volume Mean (SD)	% Change vs baseline after 26% reduction in density Mean (SD)	% Change vs baseline after 5% increase in density Mean (SD)
Stiffness	-64.9 (8.2)	-25.8 (5.8)	3.8 (1.6)
Strength	-66.5 (6.7)	-25.4 (0.3)	3.5 (0.3)
Work to Failure	-65.2 (2.3)	-26.4 (0.9)	1.7 (1.6)

**Disclosures:** H. Hong, Procter & Gamble 5.

## SA506

**Oral Strontium Ranelate Treatment Markedly Improves Implant Osseointegration.** L. Maimoun\*, R. Rizzoli\*, P. Ammann\*. Department of Rehabilitation and Geriatrics, University Hospital, Geneva, Switzerland.

The employment of metallic implantation into bone is frequently used in orthopaedics and dentistry all the more with the aging population. The process of implant osseointegration begins with a phase of bone resorption around the implant, with bleeding and inflammation, and is followed by a phase of bone formation. However, the incidence of implant failure is high due to alteration of bone turnover and tissue quality. Strontium ranelate (SR), efficacious in the treatment of osteoporosis, was shown to inhibit bone resorption, to increase bone formation and to improve bone material quality. Whether SR treatment improves implant osseointegration is not known. We measured the resistance to pull-out of 1 mm diameter titanium rods implanted into the proximal tibia of 6 month-old female rats. The implants, sandblasted and acid-etched along the surface of non threaded part, were inserted into both tibias and the rats received SR (625 mg/kg, 5/7 days, n=15), alendronate (ALN) (18 microg/kg/d, 2/7 days, n=15, positive control) or vehicles (n=15) for 8 weeks. The tibias were then removed for microtomographic histomorphometry and resistance to pull-out was tested by recording the maximal force necessary to completely loosen the implant. Nanoindentation (intrinsic bone tissue quality in the vicinity of the implant) and histomorphometry were performed (in a subgroup of n=7). Results are expressed as means±SEM. Significance of differences were evaluated by analysis of variance (\* p<0.05 vs control).

	Control	Strontium ranelate	Alendronate
Pull out Force (N)	32.52±3.79	43.54±3.03*	48.40±3.05*
Hardness (mPa) trabecular bone	624.8±21.6	721.7±27.6*	654.8±23.3
Hardness (mPa) cortical bone	837.3±24.5	918.5±30.54*	822.8±25.6

Both SR and ALN improved pull-out force compared to the controls, i.e. implant osseointegration. Whereas both treatments positively influenced microarchitecture, one of the determinants of pull-out force, intrinsic bone tissue quality was improved in rats treated with SR but not in rats treated with ALN. Furthermore, dynamic histomorphometry demonstrated tetracycline labelling along the implant in rats treated with SR, but not in rats treated with ALN, compatible with the hypothesis that SR may induce bony ingrowths into the surfaces of the implants. The dose of SR of 625 mg/kg correlates to human therapeutic exposure. In conclusion, whilst both treatments induce a similar pull-out force, only strontium ranelate improves implant osseointegration by positively altering formation of bone and the intrinsic bone material quality in the vicinity of the implant.

**Disclosures:** P. Ammann, None.

This study received funding from: Servier.

## SA507

**Hip Structural Analysis Based on DXA Data in Women with Postmenopausal Osteoporosis Receiving Once-Monthly Oral Ibandronate for 12 Months.** E. M. Lewiecki<sup>\*1</sup>, H. K. Genant<sup>\*2</sup>, K. Engelke<sup>\*3</sup>, T. Fuerst<sup>\*4</sup>, M. Fries<sup>\*5</sup>, M. Enslin<sup>\*5</sup>, L. A. Fitzpatrick<sup>\*5</sup>, A. Kivitz<sup>\*6</sup>. <sup>1</sup>New Mexico Clinical Research & Osteoporosis Center, Albuquerque, NM, USA, <sup>2</sup>University of California, San Francisco, and Synarc, Inc, San Francisco, CA, USA, <sup>3</sup>Synarc, Inc, Hamburg, Germany, <sup>4</sup>Synarc, Inc., San Francisco, CA, USA, <sup>5</sup>GlaxoSmithKline, King of Prussia, PA, USA, <sup>6</sup>Altoona Arthritis & Osteoporosis Center, Duncansville, PA, USA.

Bone quality, strength, and geometry contribute to fracture resistance. This 12-month randomized, double-blind, parallel-group, multicenter study determined effects of once-monthly oral ibandronate or placebo on bone quality and strength measured by volumetric quantitative computed tomography (QCT), finite element analysis, and dual-energy x-ray absorptiometry (DXA) in 93 postmenopausal women with BMD T-scores of ≤-2.0 to ≥-5.0. The primary endpoint was total hip volumetric BMD assessed by QCT. Hip structural analysis (HSA) parameters were a secondary endpoint. Femoral DXA was performed at baseline and Month 12. HSA assessed cross-sectional geometry of the intertrochanter region, narrow neck, and femoral shaft. All analyses were exploratory. HSA changes from baseline were evaluable in 42 of 47 ibandronate patients and 37 of 46 placebo patients. Ibandronate induced greater mean percentage increases than placebo in total hip BMD by DXA (1.7% ± 2.8% vs -0.6% ± 2.5%; treatment difference 2.0% [95% CI 0.7% to 3.3%]). Cross sectional moments of inertia improved with ibandronate versus placebo at the shaft (1.9% ± 5.1% vs -0.6% ± 4.5%; treatment difference 2.0% [95% CI -0.2% to 4.2%]) and narrow neck (4.1% ± 9.4% vs -0.7% ± 7.3%; treatment difference 4.0% [95% CI -0.04% to 8.1%]) denoting increased resistance to bending and torsional loading; corresponding intertrochanter data were 4.1% ± 7.5% vs 1.2% ± 8.9%, treatment difference 2.4% (95% CI -1.4% to 6.2%). Average cortical thickness of the narrow neck, a parameter associated with hip fracture resistance, decreased with placebo (-2.1% ± 5.4%) but was maintained with ibandronate (0.3% ± 6.2%); treatment difference 2.2% (95% CI -0.6% to 5.0%). In other regions, average cortical thickness increased with ibandronate and was maintained with placebo (shaft: 2.0% ± 5.2% vs 0.2% ± 5.1%, treatment difference 0.7% [95% CI -1.6% to 3.0%]; intertrochanter: 3.3% ± 6.0% vs 1.4% ± 5.8%, treatment difference 1.3 [95% CI, -1.4% to 4.0%]). Ibandronate treatment for 12 months was associated with trends toward improvement in hip geometry relative to placebo as measured by HSA.

**Disclosures:** E.M. Lewiecki, New Mexico Clinical Research & Osteoporosis Center; Merck, Eli Lilly, Novartis, Sanofi-Aventis, Amgen, Pfizer, Wyeth, Roche, GSK, Procter & Gamble 3; Merck, Eli Lilly, Novartis, Procter & Gamble, Sanofi-Aventis, Roche, GSK 1; Merck, Eli Lilly, Novartis, Procter & Gamble, Sanofi-Aventis, Roche, GSK, Wyeth, Servier, Amgen, Upsher-Smith 4; Board of Directors: International Society for Clinical Densitometry 5.

This study received funding from: Roche and GlaxoSmithKline.

## SA508

See Friday Plenary number F508.

## SA509

**QCT and FEA Assessment of Proximal Femur Bone Quality and Strength in Women with Postmenopausal Osteoporosis Receiving Once-Monthly Oral Ibandronate for 12 Months.** A. Kivitz<sup>\*1</sup>, T. M. Keaveny<sup>\*2</sup>, H. K. Genant<sup>\*3</sup>, K. Engelke<sup>\*4</sup>, T. Fuerst<sup>\*5</sup>, D. Kopperdahl<sup>\*6</sup>, M. Fries<sup>\*7</sup>, G. Dasic<sup>\*7</sup>, L. A. Fitzpatrick<sup>\*7</sup>, E. M. Lewiecki<sup>\*8</sup>. <sup>1</sup>Altoona Arthritis & Osteoporosis Center, Duncansville, PA, USA, <sup>2</sup>University of California, Berkeley, and O.N. Diagnostics, Berkeley, CA, USA, <sup>3</sup>University of California, San Francisco, and Synarc, Inc, San Francisco, CA, USA, <sup>4</sup>Synarc, Inc., Hamburg, Germany, <sup>5</sup>Synarc, Inc., San Francisco, CA, USA, <sup>6</sup>O.N. Diagnostics, LLC., Berkeley, CA, USA, <sup>7</sup>GlaxoSmithKline, King of Prussia, PA, USA, <sup>8</sup>New Mexico Clinical Research & Osteoporosis Center, Albuquerque, NM, USA.

Decreased femoral bone mineral density (BMD) and cortical thinning are associated with osteoporotic hip fracture risk. We examined effects of once-monthly oral ibandronate on measures of bone strength and quality in a 12-month randomized, double-blind, placebo-controlled study. Postmenopausal women (N=97) aged 55-80 years with BMD T-scores  $\leq -2.0$  and  $\geq -5.0$  received oral ibandronate (150 mg/mo) or placebo. The primary endpoint was assessment of integral (cortical plus trabecular compartments) total hip volumetric BMD by quantitative computed tomography (QCT) after 12 months' ibandronate or placebo treatment in the intent-to-treat population (n=93); secondary analyses included other proximal femur sites and finite element analysis (FEA). All analyses were exploratory. *P*-values were generated post-hoc for descriptive purposes only and were not corrected for multiple comparisons. Integral and trabecular volumetric BMD increased more over 12 months' treatment with ibandronate than placebo in the total hip (integral,  $1.5\% \pm 3.4\%$  vs  $-1.0\% \pm 2.5\%$ ; trabecular,  $2.6\% \pm 8.0\%$  vs  $-2.9\% \pm 5.1\%$ ), trochanter (integral,  $2.5\% \pm 4.2\%$  vs  $-1.0\% \pm 3.4\%$ ), and femoral neck (integral,  $0.8\% \pm 3.2\%$  vs  $-1.4\% \pm 2.5\%$ ). Cortical volumetric BMD changes from baseline in these regions were similar between the groups. The treatment difference in the primary endpoint, integral BMD of the total hip (least-squares means and 95% confidence intervals (CI), ibandronate minus placebo,  $2.2\%$  [0.7%-3.7%],  $P = 0.005$ ) showed a clinically meaningful ibandronate effect. FEA modeling of femoral strength under falling load showed that ibandronate improved strength of the whole proximal femur (treatment difference,  $5.9\%$ ; 95% CI,  $2.7\%$ - $9.0\%$ ,  $P = 0.0004$ ) and the pericortical (treatment difference,  $2.5\%$ ; 95% CI,  $0.6\%$ - $4.5\%$ ,  $P = 0.0113$ ) and trabecular (treatment difference,  $3.5\%$ ; 95% CI,  $1.3\%$ - $5.7\%$ ,  $P = 0.0025$ ) compartments. Once-monthly oral ibandronate for 12 months resulted in integral and trabecular volumetric BMD gains in the proximal femur. FEA modeling demonstrated that ibandronate also improved femoral strength with an increase in pericortical as well as trabecular compartment strength.

**Disclosures:** A. Kivitz, Roche, GlaxoSmithKline 1.  
This study received funding from: Roche, GlaxoSmithKline.

## SA510

**Bone Tissue Quality Is Differently Altered by PTH, Bisphosphonates and SERMs.** T. C. Brennan<sup>\*</sup>, R. Rizzoli, P. Ammann. Faculty of Medicine, Division of Bone Diseases, Geneva University Hospital, Genève, Switzerland.

Bone strength, a determinant of resistance to fracture, depends on bone mineral density, bone geometry, microarchitecture, bone turnover rate and intrinsic bone tissue quality. Despite comparable antifracture efficacy, bone resorption inhibitors and bone anabolic agents are likely to modify the various determinants of bone strength in different ways. To address this hypothesis, we treated 8-month old osteoporotic ovariectomized (OVX) rats with pamidronate (APD, 0.6mg/kg 5 days/month s.c.), PTH(1-34) (10 ug/day, s.c.), raloxifene (3 mg/kg 5/7 days) or vehicle for 16 weeks, and measured maximal load and other biomechanical properties with an axial compression test, areal BMD, microarchitecture by microCT, and intrinsic bone quality by nanoindentation. Markers of bone turnover, deoxypyridinoline (Dpd) and osteocalcin, were also determined. Results are Means  $\pm$  SEM, with significances tested by ANOVA.

Vertebral body	Sham	OVX	APD/OVX	PTH (1-34)/OVX	Raloxifene /OVX
Maximal Load (N)	303.5 $\pm$ 27.3**	215.8 $\pm$ 11.3	321.1 $\pm$ 18.1***	404.9 $\pm$ 25.0***	261.9 $\pm$ 21.7
BV/TV (%)	28.4 $\pm$ 1.25***	18.3 $\pm$ 0.87	23.3 $\pm$ 1.13**	36.4 $\pm$ 1.77***	22.1 $\pm$ 1.06
Total Energy (mN*mm)	4265.2 $\pm$ 84.8*	3891.7 $\pm$ 68.4	4160.6 $\pm$ 136.0	3578.4 $\pm$ 49.0***	4283.2 $\pm$ 62.9*
Osteocalcin (ng/ml)	11.1 $\pm$ 0.68	14.9 $\pm$ 1.30	8.23 $\pm$ 0.05***	23.4 $\pm$ 1.21***	12.3 $\pm$ 1.71

(\*\*\* $p < 0.001$ , \*\* $p < 0.01$  and \* $p < 0.05$  compared to OVX vehicle or \*\*\* $p < 0.001$  compared to Sham) All treatments improved maximal load compared to OVX animals, although the difference was not significant in raloxifene-treated rats. The PTH-induced increase in maximal load was associated with improved microarchitecture, including marked increases in trabecular bone volume and connectivity, leading to values higher than in sham. APD corrected the effects of OVX on trabecular bone volume. Raloxifene had no effect. All treatments increased areal BMD, with potency: PTH>APD>raloxifene. PTH was ineffective in correcting the steep decreases in tissue hardness and working energy caused by OVX. In contrast, APD normalized bone strength, together with a reduced bone turnover and increased hardness. Raloxifene also improved hardness, elastic modulus and markedly enhanced working energy, with low levels of bone turnover markers.

These results demonstrate that inhibitors of bone resorption and stimulators of bone formation reduce fracture risk through different mechanisms. PTH markedly improved bone mass and microarchitecture yet lead to poor trabecular bone quality and increased bone turnover. APD and raloxifene improved bone mass and positively influenced intrinsic bone tissue quality. Through a reduced bone turnover these agents prevented further degradation of mechanical properties.

**Disclosures:** T.C. Brennan, None.

## SA511

**Development of An Animal Model of Bisphosphonate-Induced Severe Suppression of Bone Turnover.** J. E. Zerwekh<sup>1</sup>, W. Geng<sup>\*1</sup>, C. T. Skurla<sup>\*2</sup>, C. V. Odvina<sup>1</sup>. <sup>1</sup>Center for Mineral Metabolism and Clinical Research, University of Texas Southwestern Medical Center at Dallas, Dallas, TX, USA, <sup>2</sup>Department of Mechanical Engineering, Baylor University, Waco, TX, USA.

There is a growing body of clinical evidence supporting the development of bisphosphonate-induced severe suppression of bone turnover (SSBT) in some patients taking bisphosphonates singly or in combination with other antiresorptive agents. We undertook the development of an animal model of SSBT that recapitulated the histological, biochemical, and biomechanical findings in humans. Twelve ovariectomized adult female Sprague-Dawley rats were allowed to acclimatize to their housing. After 2 weeks, rats were placed in individual metabolic cages and urine collected for 3 subsequent days. Under anesthesia, BMD was assessed by Hologic DEXA, and a blood sample obtained. One-half of the rats then received weekly i.p. injections of alendronate at a dose of 35ug/kg for four months, a dosing regimen calculated to expose the skeleton to the same amount of alendronate obtained from weekly 70 mg oral dosing for a total of 10 years. Control rats received saline. At the end of 4 months, all baseline procedures were repeated. Two animals in the control group died following baseline examination. At sacrifice, one femur was obtained for dynamic histomorphometry and determination of osteocyte density. The contralateral femur was procured for biomechanical testing. Compared to control rats, alendronate-treated rats demonstrated a greater increase in spine BMD ( $30.3 \pm 5.2$  SEM vs  $12.7 \pm 3.6\%$ ,  $p=0.028$ ) and significant reductions in bone turnover as determined from histomorphometry. The most striking finding was the total lack of any identifiable tetracycline double label in cancellous bone compared to controls ( $4.5 \pm 2.1\%$ ). In addition, alendronate-treated rats had significantly lower viable osteocyte number and an increased number of empty lacunae compared to controls ( $238 \pm 29$  vs  $85 \pm 16/\text{mm}^2$ ,  $p=0.004$ ). Biomechanical testing of femurs demonstrated no significant differences between groups for stiffness or maximum flexural strength. However, alendronate-treated rats demonstrated a significant decline in yield strength of the femur compared to controls ( $69 \pm 9$  vs  $53 \pm 11$  MPa,  $p=0.040$ ). Taken together, these findings are consistent with an alendronate-induced suppression of bone turnover characterized by a lack of bone formation, an increase in the number of empty cortical and cancellous osteocytic lacunae, and reduced biomechanical competence as shown by a significant reduction in the yield point. This animal model of bisphosphonate-induced SSBT will be useful to begin to unravel the complex effects of long-term bisphosphonate use on bone cells and biomechanical integrity.

**Disclosures:** J.E. Zerwekh, None.

This study received funding from: Discretionary funds from the Center for Mineral Metabolism.

## SA512

**Effects of Resorption Cavities on Strength of Trabecular Bone.** S. K. Easley<sup>\*1</sup>, D. Shindich<sup>\*1</sup>, C. J. Hernandez<sup>2</sup>, T. M. Keaveny<sup>1</sup>. <sup>1</sup>Mechanical Engineering, University of California, Berkeley, Berkeley, CA, USA, <sup>2</sup>Mechanical and Aerospace Engineering, Case Western Reserve University, Cleveland, OH, USA.

Understanding the relation between bone strength and presence of microcavities should provide insight into how osteoporosis and treatments might alter bone quality. While it has been shown that simulated suppression of microcavities in low-density vertebral bone can in theory improve bone quality, commensurate improvements in bone quality have not been observed due to antiresorptive therapy when applied to high-density canine bone. To understand this discrepancy, we sought to quantify the effect of adding cavities to both low-density and high-density bone on strength after accounting for differences in bone volume fraction (BV/TV). Trabecular bone from the human femoral neck (n=14, age:  $70.4 \pm 10.1$ , BV/TV:  $22.5 \pm 5.9\%$ ) and the vertebral body (n=16, age:  $72.9 \pm 11.7$ , BV/TV:  $11.2 \pm 3.7\%$ ) were scanned with micro-CT at 22-micron voxel size. Each image was converted into three finite element (FE) models, using the original image of bone or using images in which cavities (44 microns deep) were digitally added to the bone surface either at random (non-targeted) or in regions of greatest maximum principal strain (targeted). FE analysis was used to compute the compressive strength of each specimen, in its intact and altered states. Results indicated that the presence of cavities deleteriously altered the strength-density relationship as compared to models without cavities ( $p < .001$ ). Strength change per unit percent change in BV/TV due to the addition of non-targeted cavities ( $1.87 \pm 0.23$  MPa/%BV/TV) was two times larger than expected from changes in BV/TV alone ( $0.91$  MPa/%BV/TV). The dependency of percent reduction in strength associated with introducing non-targeted cavities ( $17.1 \pm 2.25$ ) on BV/TV was negligible for the pooled data, while strength reduction associated with targeted cavities was negatively correlated with BV/TV ( $p=.0012$ ), such that at high densities, there was a smaller difference between non-targeted and targeted models. This study indicates that remodeling cavities can have a disproportionate biomechanical effect in high-density bone as well as low-density bone. However, our prior work on high-dose risedronate treatment of dogs (Eswaran, JBMR 2006) revealed no change in the strength-BV/TV relation compared to untreated controls, using the same type of FE analysis techniques as used here on the unmodified micro-CT scans. We conclude that further research is required to determine the conditions (cavity size, drug treatment, skeletal region), if any, under which alteration of the remodeling space might alter bone strength.

**Disclosures:** S.K. Easley, None.

This study received funding from: NIH AR43784, NIH AR54448.

## SA513

**Alteration of Trabecular Bone Architecture Following Sciatic Denervation and Subsequent Reinnervation in Rat Proximal Tibiae.** H. Tamaki<sup>1</sup>, K. Yotani<sup>1</sup>, A. Yuki<sup>1</sup>, I. Sakashita<sup>1</sup>, K. Kitada<sup>2</sup>, H. Kirimoto<sup>3</sup>, F. Ogita<sup>1</sup>, H. Takekura<sup>1</sup>. <sup>1</sup>Department of Physiological Sciences, National Institute of Fitness and Sports, Kanoya, Japan, <sup>2</sup>Ishikawa National College of Technology, Kanazawa, Japan, <sup>3</sup>Niigata University of Health and Welfare, Niigata, Japan.

Disused rat hindlimb caused by sciatic denervation is characterized by osteopenia accompanying alterations in trabecular bone architecture. We studied the effects of short-term denervation followed by reinnervation on the 2-dimensional architecture of trabecular bone using a unilateral sciatic nerve freezing model rat of temporary disuse. Male Fischer-344 rats aged 11-weeks underwent unilateral hind-limb denervation by either sciatic neurectomy (SN) or nerve freezing (NF) by contact with a stainless steel rod cooled in liquid nitrogen, while control rats were sham-operated. Right and left tibiae of denervated and control rats were obtained at 0, 1, 2, 3, 4 and 5 weeks after surgery. After fixation with a mixture of 1% glutaraldehyde, 1% formaldehyde and 0.05%  $\text{CaCl}_2$  in 0.1M sodium cacodylate buffer (pH. 7.3), the tibiae were demineralized in 0.1M disodium ethylenediaminetetraacetic acid (pH 7.3) for 6 weeks at 4°C, dehydrated through a graded ethanol series, and then embedded in paraffin. Histomorphometric analyses were performed on longitudinal sections of proximal tibial metaphyseal secondary spongiosa. Sciatic denervation by SN or NF resulted in a marked loss of trabecular bone, mostly within first 2 weeks after denervation. Trabecular bone area decreased and gradually recovered with the breaking point at 3 weeks, returning to approximately 55% of basal-control levels (at 0 weeks) by 5 weeks after NF. Both the thickness and length of trabecular bone were significantly decreased after denervation. Trabecular thickness at 5 weeks after NF was significantly greater compared to that at 3 weeks after NF and at 5 weeks after SN, while decreased trabecular length after NF did not during the experimental period. These findings suggest that 1) sciatic nerve freezing results in marked loss of trabecular bone, mostly within the first 2 weeks after surgery; 2) temporary denervation and subsequent reinnervation reversibly affects trabecular bone architecture, particularly trabecular thickness.

**Disclosures:** H. Tamaki, None.

*This study received funding from: Japan Society for the Promotion of Science.*

## SA514

**Beta-Adrenergic Receptor Agonist Administration During Hindlimb Unloading Effectively Mitigates Reductions in Cancellous Bone Formation.** J. M. Swift<sup>1</sup>, S. N. Swift<sup>2</sup>, S. A. Bloomfield<sup>2</sup>. <sup>1</sup>Health and Kinesiology, Texas A&M University, College Station, TX, USA, <sup>2</sup>Health and Kinesiology, Intercollegiate Faculty of Nutrition, Texas A&M University, College Station, TX, USA.

Significant losses in bone mass during extended duration spaceflight pose a major challenge to manned exploration. One ground-based technique for effectively modeling cardiovascular and skeletal effects of spaceflight is rodent hindlimb unloading (HU). HU significantly decreases bone formation rate (BFR/BS) at the proximal tibia metaphysis (PTM) and blood flow to long bone metaphyses. In addition, our lab has demonstrated that dobutamine (DOB), a beta-adrenergic receptor agonist (ADRB), prevents significant declines in PTM total volumetric bone mineral density (vBMD) during HU. The purpose of this study was to assess the effectiveness of DOB in attenuating HU-associated decrements in static and dynamic histomorphometric properties at the PTM. Six-month-old male Sprague-Dawley rats were randomly assigned to cage control (CC) or HU groups (n=24/group). Half of each group was given one daily injection (4 mg/kg BW/d) of DOB (n=12) or an equal volume of saline (VEH; n=12). Two and nine days prior to sacrifice, animals were given subcutaneous doses of calcein (25 mg/kg). After 28 days of HU, undemineralized proximal tibiae were processed for histomorphometric analyses. The 4µm sections (Von Kossa and tetrachrome counter-stained) were analyzed for metaphyseal bone volume (BV/TV), osteoblast surface (Ob.S/BS), osteoclast surface (Oc.S/BS), and trabecular thickness, number and separation (Tb.Th, Tb.N, Tb.S). Unstained 8µm sections quantified mineralizing surface (MS/BS), mineral apposition rate (MAR), and bone formation rate (BFR/BS). At the PTM, HU resulted in no significant changes in BV/TV, Ob.S/BS, Oc.S/BS, Tb.Th, Tb.N, and Tb.Sp. HU did result in significant reductions of MS/BS (-46%), MAR (-25%), and BFR/BS (-58%; p<0.01). However, HU animals treated with DOB had significantly higher MS/BS (105%), MAR (35%), and BFR (168%) than their VEH-treated counterparts (p<0.01). No significant differences were detected for these values in the CC rats given DOB vs. CC-VEH (p>0.05). These results, in combination with previous *in vivo* peripheral quantitative computed tomography data, suggest that DOB administration during HU prevents significant declines in total vBMD at PTM by mitigating associated decrements in BFR/BS. Future work will determine if these positive effects of ADRB administration are due to enhanced blood flow to the unweighted limbs.

**Disclosures:** J.M. Swift, None.

*This study received funding from: The National Space Biomedical Research Institute through NASA NCC 9-58.*

## SA515

**Significant Trabecular Bone Degradation Occurs within Five Days of Muscle Paralysis.** S. L. Poliachik\*, S. D. Bain, S. Srinivasan, B. J. Ausk\*, D. Threer\*, P. Huber\*, T. S. Gross. Orthopaedics and Sports Medicine, University of Washington, Seattle, WA, USA.

Previously, we have shown that transient muscle paralysis induced by Botox leads to significant bone loss within 3 wk. Furthermore, we have shown that electrical stimulation of the paralyzed muscle fails to prevent this bone loss. The inability of electrical stimulation to prevent this bone loss led us to hypothesize that muscle paralysis leads to an irreversible activation of osteoclastogenesis that cannot be overcome by electrical stimulation intervention. To investigate this hypothesis, we utilized high-resolution microCT to assess the longitudinal changes in trabecular bone of the proximal tibia following transient calf paralysis.

Experimentally, high-resolution microCT images spanning a 2 mm section of the proximal tibia metaphysis were obtained for 28 female C57BL/6 mice (16 wk) immediately prior to injection of Botox into the calf muscle group (2U/100g, d 0). During the course of the study, groups of mice (n = 4) were scanned every other day, beginning d 3 after Botox injection, and ending on d 17 (maximum of 3 live scans per mouse, interim scans separated by 8 d; each total scan time lasting less than 35 min). All mice were sacrificed and a final scan was performed on d 21. Standard image analysis procedures were used to determine trabecular bone parameters for each scan, while ANOVA with multiple comparisons was used to define temporal differences across groups.

Profound degradation of BV/TV was evident within 5 d (-58.1%, p<0.001) after calf paralysis and a maximum loss of BV/TV was observed at d 11 (-75.3%, p<0.001). While the greatest trabecular bone loss occurred in the proximal tibia metaphysis by d 11, some recovery of BV/TV was evident by d 21 (+23.8% vs. d 11; -51.5% vs. d 0). Maximal decrease in trabecular thickness (-20.03%, p=0.018) was observed at d 11 and trabecular number (-22.4%, p=0.007) at d 15, with upturn evident by d 21 (+13.1% vs. d 11; +12.7% vs. d 15, respectively).

The magnitude and rapidity of trabecular bone loss observed in this study was surprising, and is similar in magnitude and time course to pathological bone resorption that is induced by pharmacological doses of Vitamin D or PTH. The rapid nature of the skeleton's response to muscle paralysis may also explain, at least in part, the relative ineffectiveness of external muscle stimulation in the treatment of spinal cord injury patients. Further investigations in this model will provide a critical context from which to explore activating mechanisms of osteoclastogenesis, and the apparent role of normal muscle function as an active mediator of skeletal homeostasis.

**Disclosures:** S.L. Poliachik, None.

*This study received funding from: The Christopher and Dana Reeve Foundation; Sigvard T. Hansen, Jr. Endowed Chair.*

## SA516

See Friday Plenary number F516.

## SA517

**Musculoskeletal Disuse Worsens the Acute Detrimental Effects of Heavy Particle Radiation on Osteoblastogenesis.** K. Yumoto\*, R. Mojarrab\*, J. Arakaki\*, A. Wang\*, D. Hilton\*, E. A. C. Almeida\*, C. Limoli\*, N. D. Searby\*, R. K. Globus<sup>1</sup>. <sup>1</sup>NASA Ames Research Center, Moffett Field, CA, USA, <sup>2</sup>Radiation Oncology, University of California Irvine, Irvine, CA, USA.

Space presents many challenges to human health, including radiation exposure and musculoskeletal disuse. Astronauts lose bone in long duration missions and recovery after return to earth occurs slowly. Although the detrimental effects of disuse on bone are clear, we do not know how the cells needed for skeletal recovery from spaceflight are affected by space-relevant radiation either alone or in combination with musculoskeletal disuse. To test this, 16 week old, male C57BL/6 mice were either continuously hind limb unloaded (HU) or normally loaded (NL), then irradiated (IR) four days later with Fe-56 (1GeV at 0, 0.1, 0.5 or 2.0 Gy) at the NASA Space Radiation Laboratory (Brookhaven National Laboratory). Tissues were harvested after three more days (total time of HU was 7 days). Bone marrow cells (BMCs) were flushed from femora, counted, plated at constant density, and grown *ex vivo* with osteogenic or osteoclastogenic additives. Cultures were analyzed for osteoblastogenesis (alkaline phosphatase, ALP- positive colonies and enzymatic activity, DNA content as surrogate for cell number) or for osteoclastogenesis (count of multinucleated TRAP-positive cells). Proximal tibiae were analyzed by microcomputed tomography to assess cancellous structure. IR dose-dependently reduced the numbers of marrow cells freshly harvested from bone but HU had no effect. All the groups demonstrated comparable osteoclastogenesis. IR of NL mice had no effect on growth of osteogenic cells *ex vivo* but did inhibit osteoblastogenesis (74, 80 and 53% relative to controls with 0.1, 0.5 and 2 Gy, respectively). HU alone also inhibited osteoblastogenesis (75% of controls). Together, IR and HU had a greater effect than either treatment alone; HU plus 0.5 Gy IR showed the lowest ALP activity (41% of controls). Despite the short duration of this study, IR with only 0.1 Gy caused a 16% reduction in cancellous bone volume fraction and 21% decrease in connectivity compared to control. HU did not have an additional effect on the acute bone loss caused by IR. In sum, low doses of heavy particle radiation caused a rapid decline in cancellous bone volume fraction and inhibited osteoblastogenesis while musculoskeletal disuse worsened the inhibitory effects of radiation on osteoblastogenesis. We hypothesize musculoskeletal disuse sensitizes bone marrow osteoprogenitors to radiation and speculate that radiation exposure in microgravity can impair skeletal recovery from disuse.

**Disclosures:** K. Yumoto, None.

*This study received funding from: NASA Grant #NNH04ZU0005N/RAD2004-0000-0110.*

## SA518

**Effects of Running Exercise on Bone Quality After Immobilization.** Z. Peng<sup>1</sup>, H. K. Väänänen<sup>2</sup>. <sup>1</sup>Pharmatest Services Ltd, Turku, Finland, <sup>2</sup>Department of Anatomy, Institute of Biomedicine, University of Turku, Turku, Finland.

Previous studies have shown that exercise improves mechanical properties of bone in growing rats. The aim of the present study was to investigate whether running exercise can improve bone quality after immobilization. Sixty-seven 10-week-old Sprague-Dawley male rats were used in this experiment. The right hind legs of 59 animals were immobilized with plaster cast in plantar flexion for 3 weeks. After removing the casts, the animals were divided into free activity and treadmill running groups (10 m/min for 30 min/day, 5 days/week). Tetracycline and calcein were injected 6 and 2 days before sacrifice, respectively. Bone samples were collected from the immobilized legs and the non-immobilized control legs of each animal, and analyzed at 0, 3, 5, 7 and 11 weeks with peripheral quantitative computed tomography (pQCT), histomorphometry and mechanical testing. Immobilization inhibited longitudinal growth of the femur and decreased cortical bone mineral density (BMD), trabecular bone volume (TBV) and tibia ash weight. Running exercise helped to restore the cortical BMD and TBV of the immobilized leg to the level of the non-immobilized control leg. Exercise also increased the growth rate of the immobilized leg and the length of its femur. Three weeks immobilization decreased cantilever bending strength of the femoral neck (FN), but not the three point bending strength of the tibial diaphysis (TD). However, after removing the casts, the strength of the TD was significantly lower in the immobilized leg compared with the control leg. The running exercise was not able to improve the strengths of the FN and TD. Alterations of the cross sectional moment of inertia resulted in different bending strengths of TD between the two legs, and suggested that the alteration of the bone structural properties were related to the pressure of muscles on the bone tissues. Although running exercise significantly increased bone formation rate in the immobilized legs compared with the control legs at the end of the experiment, changes in stress-strain of the tibia revealed that immobilization decreased plastic properties of the bone material. These results demonstrate that running exercise can accelerate the restoration of bone after immobilization, and that a longer than 3-week immobilization may induce irreversible functional decreases in bone quality.

**Disclosures:** Z. Peng, None.

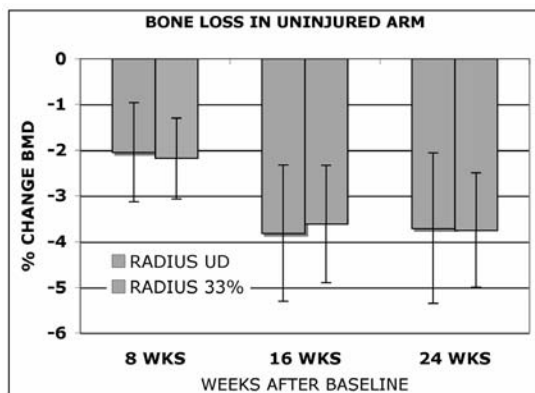
## SA519

**Bilateral Bone Density Loss after Unilateral Disuse in the Forearm.** J. A. Spadaro, W. H. Short\*, P. R. Shee\*, R. M. Hickman\*. Orthopedic Surgery, Upstate Medical University, Syracuse, NY, USA.

An opportunity arose to determine if changes occurred in the contralateral forearm of subjects with BMD losses due to injury-initiated disuse in one forearm in data from the e-Bone study. We, like many others, assumed that the "normal" forearm would either remain unchanged or perhaps experience a slight BMD increase due to some increased use. The e-Bone study was a randomized, double blind, sham controlled trial approved by the IRBPHS at SUNY Upstate Medical University (ASBMR 2007 T430). Entry (baseline) was 6-8 weeks after a distal radius fracture or carpal surgery and 99 subjects were randomized to wear a distal forearm PEMF transducer or sham device, 1-4 hours per day for 8 weeks on their involved forearm. Bone mineral density (BMD) and geometry at several sites in both forearms were measured by DXA and peripheral CT at baseline, 8, 16, and 24 weeks. Complete data was available in 82 subjects. Bone formation marker (BSAP) was unchanged on average at 8 weeks vs. baseline, while the resorption marker (CTX) was decreased. In the immobilized forearm, BMD losses by DXA were 5-7 % in the ultra-distal region and 3-4% in the midshaft (p<0.005). Since no detectable changes were observed with PEMF, we analyzed the entire group of subjects for changes in the contralateral forearm.

Results showed a statistically significant and substantial BMD loss in the contralateral forearm on average, despite inter-subject variability. The loss tended to increase over the observation period to 24 weeks after baseline, as has been typically observed for an injured extremity (Fig. 1). The magnitude of loss was about half of that in the injured side at the ultra-distal site (2-4%), but similar to the injured side at the radial shaft site (2-4%).

We hypothesize that this contralateral loss is due to either: (a) systemic hyper-resorptive effects from the injury and/or 'disuse' of the injured side, or (b) may be related to a generalized lower activity level after a forearm injury. This phenomenon needs further exploration and suggests caution in using the uninjured limb as control when studying unilateral BMD changes. (Supported by NIH, NIAMS.)



**Disclosures:** J.A. Spadaro, None.

## SA520

**Immediate Abnormalities at the Chondro-Osseous Junction due to Severe Spinal Cord Injury in Growing Rats.** L. R. Morse\*, B. Solomon\*, P. Stashenko\*, R. A. Battaglin\*. <sup>1</sup>Physical Medicine and Rehabilitation, Harvard Medical School, Boston, MA, USA, <sup>2</sup>Cytokine Biology, Forsyth Institute, Boston, MA, USA.

Spinal cord injury is associated with rapid bone loss and arrested long bone growth by a mechanism that is poorly understood. In this study we sought to determine the effects of severe T10 contusion spinal cord injury (SCI) on the chondro-osseous junction in adolescent rats. A severe lower thoracic (vertebral T10) spinal cord injury was generated by weight drop contusion (10g x 50mm). Severely injured and body weight-matched naïve (no surgery, n=4) male Sprague-Dawley (SD) rats were studied. At 2 days post-injury, hindlimb functional deficits, bone mineral density assessment by PIXImus scan, histological analysis of the distal femoral metaphysis, and immunohistochemical staining for Substance P were performed. At 2 days post-injury, we observed severe hindlimb functional deficits typical of this model. We detected an increase in trabecular osteoclast activation, a decrease in hypertrophic chondrocytes per column of growth plate, a reduction in growth plate width, and an increase in bone levels of Substance P in the injured animals. We demonstrated a rapid activation of trabecular osteoclasts and growth plate arrest due to loss of hypertrophic chondrocytes following contusion spinal cord injury in rodents. These changes are associated with increased substance P expression suggesting that this neurotransmitter may be involved in the mechanism of bone loss and long bone growth arrest following spinal cord injury. If confirmed, Substance P is a potential therapeutic target to alleviate the bony sequelae of spinal cord injury in humans.

**Disclosures:** R.A. Battaglin, None.

## SA521

**Effects of Simulated Resistive Exercise on Cortical Bone in the Tibia Mid-Diaphysis of Hindlimb Unloaded Rats.** H. A. Hogan<sup>1</sup>, J. M. Swift<sup>2</sup>, M. I. Nilsson\*, S. A. Bloomfield<sup>2</sup>. <sup>1</sup>Mechanical Engineering, Texas A&M University, College Station, TX, USA, <sup>2</sup>Health and Kinesiology, Texas A&M University, College Station, TX, USA.

The objective of this study was to characterize the effects of controlled electrical muscle stimulation on cortical bone in the tibia mid-diaphysis of hindlimb unloaded (HU) adult male rats. This same general muscle stimulation procedure has been used successfully previously as a countermeasure, but the focus has been on cancellous bone in the proximal tibia metaphysis (PTM). Previous studies showed dramatic anabolic effects in the PTM using eccentric muscle contractions of either 500ms or 1000ms duration. In order to more closely simulate actual resistive exercise in the current study, the protocol used a combination of 1000ms of isometric contraction followed by 1000ms of eccentric contraction. Six-mo. male Sprague-Dawley rats were randomly assigned to cage control (CC; n=12), hindlimb unloading plus muscle stimulation (HU+STIM; n=10), or HU plus anesthesia as another control (HU+AN; n=6) groups. The HU+STIM animals were anesthetized and subjected to muscle stimulation every other day (4 sets of 5 reps) for the 28 days of HU, while HU+AN animals were anesthetized without stimulation following the same schedule. In vivo peripheral quantitative computed tomography (pQCT) scans were taken at the tibial mid-diaphysis on anesthetized animals on days 0 and 28 to assess bone properties. Simulated exercise had a beneficial effect on both BMC and vBMD. The pre-to-post change for HU+STIM animals was +9% for BMC and +5% for vBMD, which are similar to results from the 500ms and 1000ms protocols in previous studies. There was no change for HU+AN, and an 8% increase for CC animals. In addition, tibiae were excised post-sacrifice for determination of mechanical properties at the mid-diaphysis using 3-point bending. Surprisingly, simulated exercise had little effect on mechanical properties. Comparing endpoint values (28d) between HU+STIM and HU+AN, the ultimate load was essentially the same, and there was a trend (non-significant) toward lower stiffness, elastic modulus, and yield stress (~5%). The only dramatic difference was for the total energy absorbed, or work-to-fracture, which was 34% higher for HU+STIM. We speculate that the lack of a beneficial effect on most mechanical properties may be due to differences in the organic matrix, perhaps less mature due to cross-sectional remodeling. Another possible reason may be the relatively low number of animals for biomechanics.

**Disclosures:** H.A. Hogan, NSBRI 3.

This study received funding from: NSBRI NASA NCC 9-58.

## SA522

**Mechanical Strain Prevents Adipogenesis in Mesenchymal Stem Cells By Stimulating a Durable  $\beta$ -Catenin Signal.** B. Sen\*, Z. Xie\*, N. Case<sup>1</sup>, M. Ma\*, C. Rubin<sup>2</sup>, J. Rubin<sup>1</sup>. <sup>1</sup>Medicine, UNC-CH, Chapel Hill, NC, USA, <sup>2</sup>Biomedical Engineering, SUNY, Stony Brook, NY, USA.

The ability of exercise to decrease fat mass and increase bone mass may arise through mechanical biasing of mesenchymal stem cell (MSC) commitment towards osteoblastogenesis and away from adipogenesis. To study the effect of mechanical strain on lineage selection we ascertained that C3H10T1/2 MSC cultured in a highly adipogenic "A" medium contained lipid at 3 days, and nearly all cells stained for oil-red-O after 5 days. PPAR $\gamma$  and adiponectin mRNA (RT-PCR) and protein (Western) was present at 3d and continued to rise at 5d. Active and total  $\beta$ -catenin levels fell sharply over the 5 d of adipogenesis. Application of strain daily (3600 cycles, 2%) inhibited adipocyte differentiation as measured by decreased cellular lipid droplets at 3 and 5d. Strain as well inhibited expression of PPAR $\gamma$  mRNA by nearly 50%, and



adiponectin by 75%, changes were confirmed by Western. The decrease in  $\beta$ -catenin seen during adipogenesis was entirely prevented by daily application of strain. Cyclin D1 expression reflected the change in  $\beta$ -catenin: cyclin D1 mRNA fell to  $51 \pm 5\%$  after 5 d in A medium compared to cells in growth medium. Mechanical challenge increased cyclin D1 mRNA to  $195 \pm 23\%$  at 3d, and nearly 3-fold at 5d ( $p < 0.01$ ) compared to unstrained cells in A medium. Expression of second  $\beta$ -catenin response gene, WISP1, paralleled that of cyclin D1: WISP1 dropped to  $21 \pm 1\%$  by 5d in A medium ( $p < 0.05$ ), and increased with mechanical strain to  $245 \pm 46\%$  and  $611 \pm 116\%$  after 3d and 5d respectively ( $p < 0.05$  for both). LiCl similarly prevented adipogenesis, implicating  $\beta$ -catenin in strain's ability to inhibit adipogenesis. Mechanical strain activated AKT followed by inactivation of GSK3 $\beta$ , demonstrated by increase in phospho-forms of both kinases after strain, suggesting a possible pathway for mechanical control of  $\beta$ -catenin activity. Finally, in cultures subjected to mechanical strain, there was enhanced potential for entry into the osteoblast lineage: cells were cultured in A medium  $\pm$  strain for 3 d, followed by 2 d of BMP2 treatment to induce osteoblast differentiation. In unstrained cultures, Runx2 and osterix did not rise in response to BMP2, but in cultures subjected to mechanical strain, BMP2 increased expression of Runx2 by 40% and osterix by 68%. These results indicate that MSC commitment to adipogenic lineage can be suppressed by mechanical signals even during highly adipogenic conditions, and implicate  $\beta$ -catenin activation as a mechanism. Further, by preserving  $\beta$ -catenin levels, mechanical strain allows MSC to be more responsive to osteogenic factors. Our work suggests that exercise should have positive effects for both osteoporosis and obesity by affecting MSC lineage allocation.

**Disclosures:** J. Rubin, None.

This study received funding from: NIAMS.

## SA523

See Friday Plenary number F523

## SA524

**The Effects of Electrical Stimulation on Nitric Oxide Expression and Osteocyte Viability in Ovariectomized Rats.** A. P. R. Lirani-Galvao<sup>\*1</sup>, P. Chavassieux<sup>2</sup>, N. Portero-Muzy<sup>\*2</sup>, O. L. Silva<sup>\*3</sup>, C. Bergamaschi<sup>\*1</sup>, M. Lazaretti-Castro<sup>1</sup>, P. D. Delmas<sup>2</sup>. <sup>1</sup>Departamento de Medicina, Universidade Federal de Sao Paulo, Sao Paulo, Brazil, <sup>2</sup>INSERM Unit 831, Université de Lyon, Lyon, France, <sup>3</sup>Bioengenharia, Universidade de Sao Paulo, Sao Paulo, Brazil.

We have previously shown in rats that electrical stimulation (ES) may prevent the increased bone turnover, microarchitecture deterioration and bone loss induced by ovariectomy (OVX) (J. Bone Miner. Res. 22 Suppl1:S447, 2007). Osteocytes have been hypothesized to mediate this effect by releasing biochemical signals such as nitric oxide (NO). The aim of the present study was to investigate the potential role of NO in the response to ES on the osteocyte viability in OVX rats. Sixty rats (200-220g) were divided into 6 groups: SHAM; SHAM treated with 6mg/d of L-NAME, an inhibitor of NO synthase (SHAM-L); ovariectomized (OVX); OVX treated with L-NAME (OVX-L) or subjected to an electrical stimulation (OVX-ES) or both (OVX-L-ES) for 12 weeks.

The expressions of endothelial NO synthase (eNOS) and inducible NOS (iNOS) and osteocyte apoptosis (caspase-3 and TUNEL) were assessed by immunostaining. eNOS and iNOS were similarly expressed in subperiosteal regions of the cortices of metaphysis and diaphysis of tibiae in SHAM group, but they were not detected in OVX and L-NAME treated groups. In OVX-ES group, similar expressions of eNOS and iNOS were detected in cortical bone of tibial diaphysis as in SHAM. When compared to SHAM, OVX significantly increased the percentage of apoptotic cells and empty lacunae ( $p < 0.05$ ) but this effect was prevented by ES. SHAM-L and OVX-L showed a diminished percentage of apoptotic osteocytes when compared to SHAM and OVX, respectively. Interestingly, this difference was not observed between OVX-L-ES and OVX-ES.

In conclusion, ES may counteract the effects of OVX on bone tissue in rats through the activation of iNOS and eNOS, preserving the osteocyte viability and secondary acting on bone remodelling to maintain the bone structure and architecture. It was not possible, however, to identify if L-NAME blocks the effects of ES on osteocytes, since their effects on these cells are similar. Regarding osteocyte viability it seems that the effects of ES and L-NAME are similar. We hypothesized that the decreased percentage of apoptotic osteocytes in groups under L-NAME may be due to bone mechanical stimulation caused by high blood pressure levels induced by NO blockage (Turner et al., Bone 1997, 21:487-90). However, the other results cited above suggest that NO may mediate the effects of ES on bone tissue.

**Disclosures:** A.P.R. Lirani-Galvao, None.

This study received funding from: CAPES, CNPQ.

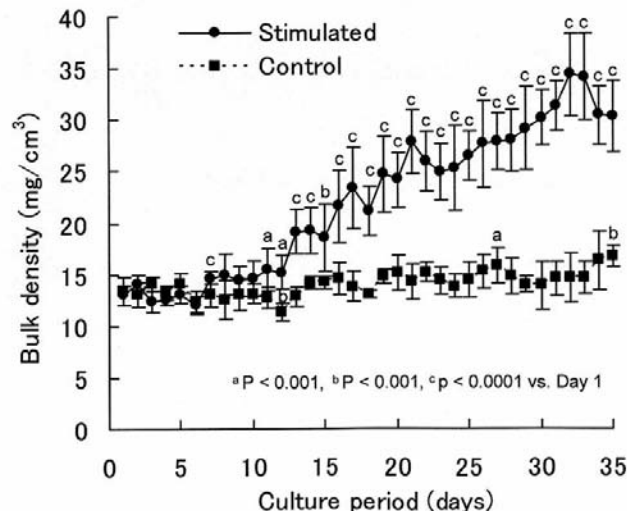
## SA525

**Strain-Induced Fluid Flow in a Three-Dimensional Porous Matrix Promotes Osteoblastic Calcification *in vitro*.** S. M. Tanaka<sup>1</sup>, M. Kakio<sup>\*2</sup>, K. Yamakoshi<sup>\*2</sup>. <sup>1</sup>Institute of Nature and Environmental Technology, Kanazawa University, Kanazawa, Ishikawa, Japan, <sup>2</sup>Graduate School of Natural and Science Technology, Kanazawa University, Kanazawa, Ishikawa, Japan.

Bone strain generated by external loading force induces fluid flow in bone matrix, which creates fluid shear stress on bone cells. Strain-induced fluid flow is known to play a dominant role in the regulation of stress-sensitive genes in osteoblasts *in vitro*, compared to substrate strain alone [1]. The purpose of this study is to investigate the capability of strain-induced fluid flow to promote osteoblastic calcification *in vitro*. Osteoblasts differentiated

from mesenchymal stem cells in rat bone marrow were seeded into a porous scaffold made of type I collagen (16 mm in length x 20 mm in width x 2 mm in thickness, pore size: about 100  $\mu$ m) at a cell number of  $0.7 \times 10^6$  with an osteogenic medium containing 50  $\mu$ g/ml L-ascorbic acid, 10 mM  $\beta$ -glycerolphosphate, and  $10^{-8}$ M dexamethasone. A sinusoidal mechanical load with a magnitude of 2000  $\mu$ strain was applied to the scaffold at 0.8 Hz for 3 minutes per day for 35 days using a piezoelectric mechanical stimulator to give cyclic strain-induced fluid flow to the cells in the porous scaffold [1]. The degree of osteoblastic calcification in a scaffold was monitored non-destructively once a day using an optical sensing unit composed of four light emitting diodes (LED) and a photodiode (PD) placed under a culture chamber. The LEDs irradiate a scaffold with near-infrared light at 850 nm increasing its intensity ( $I_0$ ) and the intensity of diffuse reflectance light ( $I$ ) from the scaffold is measured by the PD. Using the slope of  $I_0$ - $I$  curve, the degree of calcification is evaluated as bulk density ( $\text{mg}/\text{cm}^3$ ). In the scaffolds stimulated by strain-induced fluid flow, bulk density started to increase after day 10 and reached finally to about  $30 \text{ mg}/\text{cm}^3$ . On the other hand, the controls without the stimulation did not represent a remarkable increase in bulk density. The results indicated that strain-induced fluid flow could be a potent enhancer for osteogenesis *in vitro*.

1. S.M. Tanaka, et al., Calcif. Tissue Int., 76(4):261-271, 2005.



**Disclosures:** S.M. Tanaka, None.

This study received funding from: The Japanese Ministry of Education, Science, Sports and Culture.

## SA526

**Mechanical Loading Upregulates Expression of the Transcription Factor EGR2/Krox-20 by a COX2-mediated Mechanism.** G. Zaman<sup>\*</sup>, L. K. Saxon, B. Javaheri<sup>\*</sup>, A. Sunters<sup>\*</sup>, J. S. Price, L. E. Lanyon. Basic Sciences, The Royal Veterinary College, London, United Kingdom.

Microarray analysis of mRNA extracted from the tibiae of 8 female C57BL/6 mice showed differential regulation of 621 genes between bones that had been subjected *in vivo* to a single period of dynamic axial loading (2 Hz for 30 seconds) capable of stimulating osteogenesis, compared with unloaded contra-lateral bones. At 3 hours after loading one of the genes showing substantial (1.9 fold) differential up-regulation was EGR2/Krox-20. Expression levels were restored to those in controls by 8 hours after loading. These results were confirmed by quantitative real-time PCR (qRT-PCR).

*In vitro*, monolayer cultures of primary osteoblast-like cells prepared from C57BL/6 mouse long bones and UMR106 cells, when subjected to a single period of mechanical strain (peak strain 3400 microstrain, 1 Hz, 600 cycles), showed a maximal 2 and 3 fold increase respectively in EGR2 mRNA levels (by qRT-PCR) 1 hour after exposure to strain. This strain-related increase in EGR2 mRNA levels was abolished by the COX2 inhibitor NS398 (1  $\mu$ M) and imitated (2.6 fold increase) by exogenous prostaglandin (PG) E2 (5  $\mu$ M). The PGE2-induced increase in EGR2 expression was abolished by blocking the EP1 & EP2 PG receptors (30  $\mu$ M AH6809), whereas inhibiting the EP4 receptor inhibitor (30  $\mu$ M AH23848) only partially lowered expression (by 29%). The PKC agonist PMA (500 nM) caused a significant increase in EGR2 mRNA expression whereas exogenous dibutyryl-cyclic AMP (100  $\mu$ M), which activates PKA signaling, caused a significant decrease. Consistent with this finding, pretreatment with the PKA antagonist H89 (1  $\mu$ M) significantly increased PGE2-induced EGR2 expression.

That bone cells respond to mechanical strain by COX2 mediated release of prostanoids has been recognized for some time. The immediate downstream consequences of this PG release have been unclear. The data reported here suggest that one of these downstream targets is EP receptor-mediated increase in the expression of EGR2, a zinc finger transcription factor belonging to the Early Growth Response (EGR) family. EGR2 has previously been reported to be involved in osteoblast differentiation and to act as a pro-survival factor. Suppression of EGR2 expression has been implicated in glucocorticoid-induced osteoporosis and EGR2 mutant mice have defective bone formation. To our knowledge EGR2 has never before been implicated in bone cells' responses to mechanical loading.

**Disclosures:** G. Zaman, None.

This study received funding from: The Wellcome Trust.

**SA527**

See Friday Plenary number F527.

**SA528**

**Integrin Mediated Mechanical Forces Stimulate Differentiation of Mesenchymal Stem Cells.** P. Müller\*, A. Kasten\*, C. Bergemann\*, J. Rychly. Laboratory for Cell Biology, University of Rostock, Rostock, Germany.

Mesenchymal stem cells are multipotent and differentiate into different phenotypes including osteoblasts in dependence on the environment. Mechanical forces play a significant physiological role in the control of cells. Although evidence exists that mechanical forces are a significant factor to drive mesenchymal stem cells towards the osteogenic differentiation, little is known how physical forces contribute to the decision for a defined differentiation pathway. Concerning the mechanisms, how cells sense mechanical forces, adhesion receptors like integrins function as mechanotransducers and mediate applied forces from the extracellular matrix to the cytoskeleton in the cell interior. Therefore we applied a technique to mechanically stress integrin receptors on the apical surface of adherent cells, using antibody coating magnetic beads.  $\beta 1$ -integrin receptors of human bone marrow derived mesenchymal stem cells were mechanically stressed for 15 min with 1 Hz. Scanning electron microscopy revealed that stressing the receptors induced a slight distortion of the cell surface in the vicinity of a bead but had no effect on the global cell shape. Mechanical stress to the integrin receptor induced a signal transduction which was detected by activation of the MAP-kinases ERK 1/2 and the signaling protein Akt. To test the effect of mechanical integrin stress on the differentiation of mesenchymal stem cells, we analysed the expression of characteristic marker proteins for osteogenic and adipogenic differentiation using real-time PCR and Western blot. Mechanical stress induced an increased expression of the transcription factor Runx2 as well as VEGF, collagen I and ALP on the mRNA level within 1 hour after the applied stress. This indicated that integrin mediated mechanical forces induced the osteogenic differentiation of mesenchymal stem cells. Analyses of the expression of PPAR $\gamma$ , a marker for the adipogenic differentiation pathway, revealed a pronounced increase of the mRNA due to mechanical stress after 24 h. Together, the results demonstrated that mechanical integrin stress drives mesenchymal stem cells both to the osteoblastic and adipogenic differentiation. It appeared that expression of osteogenic markers occurred faster, whereas proteins related to the adipogenic pathway are stimulated later by mechanical forces. We conclude that mechanical forces mediated by integrin receptors are able to stimulate the differentiation of mesenchymal stem cells into different directions and the final cellular phenotype will be determined in the context with different other environmental factors.

**Disclosures:** J. Rychly, None.

This study received funding from: DFG.

**SA529**

**Effect of MKP-1 Deletion on the Fluid Shear Stress Induction of COX-2 Expression in Osteoblasts.** L. Ma<sup>\*1</sup>, M. Mehrotra<sup>\*2</sup>, S. Choudhary<sup>1</sup>, L. Raisz<sup>1</sup>, C. Pilbeam<sup>1</sup>. <sup>1</sup>Department of Medicine, University of Connecticut Health Center, Farmington, CT, USA, <sup>2</sup>Department of Pathology and Laboratory Medicine, Medical University of South Carolina, Charleston, SC, USA.

Mitogen activated protein (MAP) kinase phosphatase-1 (MKP-1) can dephosphorylate and inactivate MAP kinases, including extracellular signal-regulated kinase (ERK). ERK activation has been shown to be important for the fluid shear stress (FSS) induction of cyclooxygenase-2 (COX-2), the major enzyme regulating prostaglandin production, in osteoblasts. The goal of this study was to evaluate the role of MKP-1 in the FSS regulation of COX-2. We applied 30 min of FSS (pulsatile, 10 dynes/cm<sup>2</sup>) to MC3T3-E1 cells or calvarial osteoblasts, followed by static culture for up to 4 h. Calvarial osteoblasts were sequentially digested from neonatal calvariae of MKP-1 wild type (WT) and knockout (KO) mice, and populations 2-5 were pooled, grown to confluence and replated for experiments. mRNA and protein expression was measured by real-time PCR and Western blot, respectively. In MC3T3-E1 cells, FSS stimulated a 6-fold induction of MKP-1 mRNA and an 8-fold induction of COX-2 mRNA. The induction of both MKP-1 and COX-2 peaked 30 min after cells were returned to static culture (post-FSS). The FSS induction of ERK phosphorylation in MC3T3-E1 cells was biphasic, peaking at 30 min of FSS and decreasing at 30 min to 1 h in post-FSS culture before increasing again at 2-4 h. Treatment with a specific ERK inhibitor PD98059 (50  $\mu$ M) significantly decreased COX-2 induction. In calvarial osteoblasts from MKP-1 WT and KO mice, the temporal patterns of FSS-stimulated ERK phosphorylation and COX-2 mRNA expression were similar to those seen in MC3T3-E1 cells. However, the FSS-stimulated phosphorylation of ERK was increased in MKP-1 KO osteoblasts at all time points compared to WT osteoblasts. FSS-stimulated COX-2 mRNA expression was also increased in MKP-1 KO osteoblasts compared to WT osteoblasts. These data suggest that FSS-stimulated MKP-1 expression limits the FSS stimulation of both ERK phosphorylation and COX-2 expression. We conclude that FSS-stimulated MKP-1 expression may be important for regulating responses to mechanical loading of bone.

**Disclosures:** S. Choudhary, None.

This study received funding from: NIH AR47673.

**SA531**

**Interfacial Tissue Response is Influenced by Local Strain Created During Implant Micromotion.** R. M. Wazen<sup>\*1</sup>, J. B. Brunski<sup>\*2</sup>, J. A. Currey<sup>\*2</sup>, J. A. Helms<sup>\*3</sup>, P. Leucht<sup>\*3</sup>, A. Nanci<sup>\*1</sup>. <sup>1</sup>Faculty of Dentistry, Université de Montréal, Montréal, QC, Canada, <sup>2</sup>Rensselaer Polytechnic Institute, Troy, NY, USA, <sup>3</sup>Stanford University, Stanford, CA, USA.

During healing of an implant in bone, loading can create implant micromotion at the bone-implant interface. Mechanical conditions and interfacial strain associated with implant micromotion also contribute to the regulation of cell and tissue healing response. Excessive implant micromotion can lead to fibrous encapsulation and implant loosening. The objective of this study was to characterize the influence of interfacial strain in the environment of an implant on bone healing in a mouse. The micromotion system consisted of a miniature device in which pin or screw-shaped implants were installed through a hole drilled in one cortex of the tibia. These implants were placed in holes of different sizes to produce interfaces with (1) no initial contact between implant and bone, and (2) a direct bone-implant contact. Implants were subjected to a displacement of 150  $\mu$ m at ~1 cycle/sec for 60 cycles/day for a 7 day period. Control implants in both types of interfaces were stabilized throughout the 7-day healing period. Undecalcified tissue sections of control and strained interfaces at 7 days were prepared and stained with Goldner to evaluate tissue reaction in relation to higher strain regions present at the ridges and base of the pin implants, and lower strain regions on the smooth sides of the pins. Experimental strain analyses and finite element simulations were used to characterize interfacial strain fields. In stable implants, normal bone formation occurs consistently around the implants. In implants subjected to micromotion, bone regeneration was disrupted in areas of high strain concentrations (e.g., greater than 30%), whereas lower strain values contributed to bone formation. These results suggest that in the early healing period, high principal tensile and/or compressive strains interfered with normal bone regeneration. It is concluded that implant micromotion as well as interfacial strain field contribute to regulating the interfacial mechanobiology at healing bone-implant interfaces.

**Disclosures:** R.M. Wazen, None.

This study received funding from: NIH EB00504-04.

**SA532**

**Bone Resorption and Articular Cartilage Degenerative Changes Following Performance of High Repetition High Force Tasks Are Attenuated by Secondary Ibuprofen Treatment.** M. F. Barbe<sup>1</sup>, M. Amin<sup>\*2</sup>, M. Harris<sup>\*2</sup>, J. B. Driban<sup>\*3</sup>, F. F. Safadi<sup>4</sup>, A. E. Barr<sup>\*5</sup>. <sup>1</sup>Physical Therapy; Anat & Cell Biology, Temple University, Philadelphia, PA, USA, <sup>2</sup>Physical Therapy, Temple University, Philadelphia, PA, USA, <sup>3</sup>Kinesiology, Temple University, Philadelphia, PA, USA, <sup>4</sup>Anat & Cell Biology, Temple Medical School, Philadelphia, PA, USA, <sup>5</sup>Physical Therapy, Thomas Jefferson University, Philadelphia, PA, USA.

Using our rat model of voluntary repetitive and forceful reaching, we have shown that high repetition low force tasks result in increased osteoclasts and macrophages in forelimb musculoskeletal tissues. Here, our purpose was to determine if high demand repetitive tasks lead to bone resorption, cartilage damage and increased serum biomarkers of bone and cartilage turnover, and if the mechanism has an inflammatory component. 54 young adult, female Sprague-Dawley rats were trained to perform an upper extremity high force lever pulling task (60% max. force) at high reach rates (12 reaches/min) (HRHF) for 12 weeks; 21 were treated with ibuprofen (oral; 45 mg/kg body weight/day) from the end of wk 4 to wk 12 while continuing to perform the task. Results were compared to 12 normal and 9 ibuprofen treated age- and weight-matched controls. After perfusion fixation, micro-CT analysis was used to examine distal forelimb bones from 3 rats/gp. We observed decreased trabecular number and increased trabecular separation in 12 wk HRHF rats (Tb N/mm: 1.75  $\pm$  0.19 and Tb Sp (um): 0.36  $\pm$  0.03) compared to controls (Tb N/mm: 2.33  $\pm$  0.21 and Tb Sp): 0.26  $\pm$  0.006), changes ameliorated by ibuprofen (Tb N/mm: 2.22  $\pm$  0.39 and Tb Sp: 0.32  $\pm$  0.06) ( $p < 0.01$ ). Forelimb bones ( $n = 6$ /gp) were embedded, sectioned, stained immunostained and osteoclasts counted. Osteoclasts increased in distal radius and ulna at the periosteal-bone interface and trabecular surfaces in 12 wk HRHF rats ( $p < 0.001$ ). Bones were also stained with Safranin O to examine wrist joint surfaces for cartilage changes. Safranin O losses were observed in the articular cartilages of 12 wk HRHF rats only. Serum from all rats was assessed using ELISA for bone turnover markers ( $n = 6$ -9/gp). Serum C12C, CTX1 and TRAP5b were significantly increased in the 12 wk HRHF rats (1.5 fold, 1.79 fold and 1.28 fold increases, respectively). Ibuprofen treatment did not ameliorate TRAP5b increases, but reduced C12C, CTX 1 and the ratio of CTX/TRAP5b levels back to control levels ( $p = 0.04$ ,  $p < 0.001$ ,  $p < 0.01$ , respectively). Thus, performance of the HRHF task for 12 weeks resulted in increased osteoclast numbers and activity, and bone resorption in forelimb bones. These changes were attenuated by secondary intervention with ibuprofen, thus suggesting that these changes are at least partially induced by inflammatory processes.

**Disclosures:** M.F. Barbe, None.

This study received funding from: NIAMS grant to AEB.

## SA533

**Targeted Exercise against Hip Fragility.** R. Nikander<sup>1</sup>, P. Kannus<sup>\*1</sup>, P. Dastidar<sup>\*2</sup>, M. Hannula<sup>\*3</sup>, L. Harrison<sup>\*2</sup>, T. Cervinka<sup>\*3</sup>, N. G. Narra<sup>\*3</sup>, R. Aktour<sup>\*3</sup>, T. Arola<sup>\*3</sup>, H. Eskola<sup>\*3</sup>, S. Soimakallio<sup>\*4</sup>, A. Heinonen<sup>5</sup>, J. Hyttinen<sup>\*3</sup>, H. Sievänen<sup>1</sup>. <sup>1</sup>UKK Institute, Tampere, Finland, <sup>2</sup>Radiology, Regional Medical Imaging Center, Tampere University Hospital, Tampere, Finland, <sup>3</sup>Biomedical Engineering, Tampere University of Technology, Tampere, Finland, <sup>4</sup>Radiology, Regional Imaging Center, Tampere University Hospital, Tampere, Finland, <sup>5</sup>Health Sciences, University of Jyväskylä, Jyväskylä, Finland.

**Objectives** To investigate whether sports involving either high-magnitude vertical impacts (triplejumping and high-jumping), moderate-magnitude impacts from rapidly varying and odd directions (soccer and squash-playing), high-magnitude muscle forces (power-lifting), low-magnitude impacts at high repetition rate (endurance running), or non-weight bearing muscle activity at high repetition rates (swimming) would strengthen the cortical bone at the proximal femur, and if so, to what extent and at which anatomic regions of the femoral neck.

**Design** Cross-sectional study

**Setting** The UKK Institute for Health Promotion Research and Tampere University Hospital, Finland in 2007-2008

**Participants** 91 adult female athletes, with ~10 years of intense sport-specific training on average and competing actively at the national or international level, and 20 non-athletic female referents

**Main outcome measures** Segmental cortical thickness at the femoral neck and trochanteric region of the proximal femur as assessed by three-dimensional magnetic resonance imaging of the whole proximal femur.

**Results** At the inferior segment, only the high-impact group differed significantly (~55%,  $p=0.012$ ) from the reference group, while at anterior segment, the cortical thickness in both the high-impact and odd-impact group differed from the reference group (~20%,  $p=0.042$  and  $p=0.044$ , respectively). Similarly, the posterior cortical wall was ~20% thicker ( $p=0.014$  and  $p=0.006$ , respectively) in these two groups. At the superior segment, the cortical thicknesses did not significantly differ between the groups.

**Conclusion** Long-term high-impact and odd-impact exercise-loading has similar ability to strengthen the femoral neck cortical bone - not only at the primary weight-bearing inferior segment but also at the lateral segments of the femoral neck, considered critical in terms of hip fragility. Since odd-impact exercises are mechanically less demanding to joints, muscles, and bones than vertical high-impact exercises, this type of training, comprising moderate-magnitude impacts from odd directions, is recommended as a feasible basis for devising targeted exercises against hip fragility.

**Disclosures:** R. Nikander, None.

This study received funding from: The Medical Fund of the Pirkanmaa Hospital District, Finnish Ministry of Education, The Päivikki and Sakari Sohlberg Foundation.

## SA534

**Bone Density Comparisons in Young Male Rock Climbers, Weight Lifters and Sedentary Controls.** V. D. Sherk, M. G. Bembem\*, D. A. Bembem. Health and Exercise Science, University of Oklahoma, Norman, OK, USA.

Technical free rock climbing is a physically demanding activity that has gained popularity in recent years, but it is unclear how climbing affects bone health. The combination of impact loading received on the body when taking a lead or bouldering fall and the dynamic movements required for climbing often mimic calisthenic, resistance training or plyometric exercises, therefore, this recreational activity may have bone loading effects. The purpose of this study was to compare bone density of the total body, AP lumbar spine, dual proximal femur and forearm in advanced rock climbers (RC), resistance trained men (RT), and untrained controls (CTR), ages 18-35 years. Fifteen advanced rock climbers, 16 resistance-trained men, and 16 untrained men volunteers were recruited for the study. Areal bone mineral density (aBMD) and bone mineral content (BMC) were assessed using DXA (GE Lunar Prodigy, enCORE 2006 version 10.50.086). Body composition variables (% body fat, fat mass, bone free lean body mass) were obtained from the total body scan analysis. Subjects also completed questionnaires to assess physical activity (Baecke) and daily calcium intake. No significant ( $p > 0.05$ ) group differences in calcium intake, body weight, or bone free lean body mass were observed. RT ( $22.3 \pm 0.5$  yrs) was significantly ( $p < 0.05$ ) younger than other two groups (RC  $25.9 \pm 1.4$  years; CTR  $26.7 \pm 1.3$  years). RC reported being more physically active than RT and CTR, and they had a significantly ( $p < 0.05$ ) lower % body fat ( $14.5 \pm 4.8\%$ ) and fat mass ( $10.9 \pm 1.2$  kg) than RT ( $19.4 \pm 2.2\%$  and  $10.9 \pm 1.2$  kg) and CTR ( $27.3 \pm 2.3\%$  and  $23.2 \pm 2.6$  kg). One-way ANOVA showed that RT had significantly ( $p < 0.05$ ) greater aBMD at the L1-L4 spine and femoral neck than RC and CTR, and RC had significantly lower aBMD at the 33% radius than CTR. After adjusting for fat mass, RT also had significantly ( $p < 0.05$ ) total body BMD than CTR. In conclusion, rock climbers exhibited similar BMD values as controls for the spine and hip sites, however, their mean forearm BMD was approximately 10% lower than controls.

Table 1. Areal Bone Mineral Density Values for Rock Climber (RC), Resistance Trained (RT), and Control (CTR) Subjects. (Means  $\pm$  SE)

aBMD site (g/cm <sup>3</sup> )	RC (n=15)	RT (n=16)	CTR (n=16)
Total Body	1.246 $\pm$ 0.024	1.319 $\pm$ 0.020	1.268 $\pm$ 0.019
L1-L4 AP Spine	1.203 $\pm$ 0.031	1.341 $\pm$ 0.031 <sup>a</sup>	1.217 $\pm$ 0.020
Total Hip	1.111 $\pm$ 0.033	1.215 $\pm$ 0.027	1.142 $\pm$ 0.032
Femoral Neck	1.092 $\pm$ 0.032	1.267 $\pm$ 0.034 <sup>a</sup>	1.129 $\pm$ 0.035
Trochanter	0.907 $\pm$ 0.026	0.966 $\pm$ 0.023	0.920 $\pm$ 0.035
33% Radius	0.882 $\pm$ 0.030 <sup>b</sup>	0.954 $\pm$ 0.023	0.979 $\pm$ 0.018

<sup>a</sup> Significantly greater than RC and CTR,  $p < 0.05$ ; <sup>b</sup> Significantly lower than CTR,  $p < 0.05$ .

**Disclosures:** V.D. Sherk, None.

## SA535

**Jumping Mechanography Safely Evaluates Muscle Performance in Older Adults.** B. Buehring, S. Valentine\*, A. Woods\*, M. Checovich, D. Krueger, N. Binkley. Osteoporosis Clinical Research Program, University of Wisconsin, Madison, WI, USA.

Neuromuscular function declines with advancing age and is strongly associated with increased risk for falls, hip fractures and decreased quality of life. A variety of tests, e.g., chair-rise or timed-up-and-go, assess muscle function. However, a need exists for more sensitive tools to evaluate interventions designed to enhance neuromuscular performance. Jumping mechanography quantitatively measures an individual's ability to generate power and correlates with the methods noted above. However, only limited data evaluating the safety of older adults performing maximal countermovement jumps (CJ) on a force platform exists. As such, this study investigated safety and utility of jumping mechanography in 40 (20 men/20 women), community-dwelling adults over age 60. At baseline, jumping mechanography of two-leg CJ was performed on a force platform (Leonardo, Novotec, Pforzheim, Germany). All participants completed three maximal CJ; maximal jump height [cm] and specific power [W/kg] were calculated. Main outcomes were worsening pain and new vertebral fracture. Pain was assessed using a visual analog pain scale before and immediately after jumping and 7 days later. Bone mineral density (BMD) and vertebral fracture assessment (VFA) were performed using a Lunar iDXA densitometer (GE Healthcare, Madison, WI) prior to CJ and VFA was repeated in 7 days. Stadiometer measured height was obtained at baseline and day 7. Data were analyzed using linear regression and t-test. Age [mean ( $\pm$  SD, range)] and BMI were  $77 (\pm 9, 63-91)$  years and  $25.5 (\pm 3.6, 19.4-34.1)$  kg/m<sup>2</sup> respectively. Mean lowest T-score of the L1-4 spine, total femur or femur neck was  $-1.43 (\pm 1.1; \text{range } 2.4 \text{ to } -3.1)$ . At baseline, 6 participants had prevalent fractures; 4 had multiple fractures. Power and jump height were lower in older volunteers and did not differ by gender. Mean jump height in women was  $14.4 \text{ cm} \pm 5.8$  and  $16.4 \text{ cm} \pm 6.8$  in men. Mean power in women was  $19.2 \text{ W/kg} \pm 5.6$  and  $21.1 \text{ W/kg} \pm 6.3$  in men. Pain was low at baseline and follow-ups, ranging from 0 to 5. Pain was reported by 8 individuals before jumping; after jumping, 4 reported a pain change of 1, two noted new pain, one worsened and one improved. A week later, compared to baseline, 6 reported worsening pain and 6 improved. No height or vertebral fracture status change was observed after jumping. In summary, jumping mechanography demonstrates lower jump height and generated power with advancing age. Additionally, it is safe with no substantial increase in pain or worsening of vertebral fracture status in older adults, including those with low BMD and prevalent vertebral fracture. Further evaluation of this methodology as a tool to evaluate change in neuromuscular performance of older adults is indicated.

**Disclosures:** B. Buehring, None.

## SA536

See Friday Plenary number F536.

## SA537

**The Influence of Muscle Size and Strength on Changes in Bone Mass and Size During Growth and in Response to Exercise: A Longitudinal Study.** G. Ducher<sup>1</sup>, R. Daly<sup>2</sup>, J. Black<sup>\*3</sup>, C. Turner<sup>\*4</sup>, S. Bass<sup>1</sup>. <sup>1</sup>Centre for Physical Activity and Nutrition Research, Deakin University, Burwood, Australia, <sup>2</sup>Department of Medicine, Western Hospital, The University of Melbourne, Melbourne, Australia, <sup>3</sup>Musculoskeletal Research Centre, La Trobe University, Heidelberg, Australia, <sup>4</sup>Biomedical Engineering, Indiana University-Purdue University, Indianapolis, IN, USA.

The objective of the study was to investigate the influence of growth and exercise-related changes in muscle size and strength on the changes in bone mass and geometry. Fifty-two competitive tennis players (26 boys), mean age 13.7 yrs (range 6.7-16.5 yrs), had their dominant and non-dominant humeri scanned by MRI at baseline and 12 months. Total bone and muscle cross-sectional areas (BCSA and MCSA) were determined from the mid (40-50%) and distal humerus (60-70%). Humeral bone mass (BMC) was derived from the whole body DXA scan and grip strength was assessed using a dynamometer. Annual changes ( $\Delta$ ) were calculated for height and all the aforementioned parameters. Pubertal status was self-assessed using Tanner stages.

Growth effect (nondominant humerus):  $\Delta$ BMC,  $\Delta$ BCSA,  $\Delta$ MCSA and  $\Delta$  grip strength were closely related to the increase in height ( $r=0.35-0.71$ ,  $p<0.05-0.0001$ ). Baseline pubertal status was a significant predictor of  $\Delta$ BMC and  $\Delta$ BCSA only after adjustment for  $\Delta$  height ( $r=0.26-0.40$ ,  $p<0.01-0.07$ ). Although  $\Delta$ BMC and  $\Delta$ BCSA correlated with  $\Delta$ MCSA ( $r=0.30-0.55$ ,  $p<0.005$ ) and  $\Delta$  grip strength ( $r=0.33-0.40$ ,  $p<0.05$ ), hierarchical regression showed that  $\Delta$  height and baseline pubertal status explained 36-55% of the variance for the  $\Delta$ BMC and  $\Delta$ BCSA ( $p<0.05$ ) and neither  $\Delta$ MCSA nor  $\Delta$  grip strength contributed to the model. Exercise effect: The dominant humerus, which was submitted to repetitive loading through tennis playing, showed 44-66% greater  $\Delta$ BMC and  $\Delta$ BCSA than the nondominant humerus ( $p<0.0001$ ). The difference in  $\Delta$ BMC between both humeri remained significant after adjustment for  $\Delta$ MCSA or  $\Delta$  grip strength ( $p<0.01$ ). This suggests that non-muscular factors contributed to the exercise-induced increase in bone mass and bone size. The average training volume throughout the year (hours/wk) was a significant predictor of  $\Delta$ BMC and  $\Delta$ BCSA ( $r=0.28-0.41$ ,  $p<0.05$ ), even after adjustment for  $\Delta$ MCSA. The largest proportion of the variance in  $\Delta$ BMC was explained by  $\Delta$  height and baseline pubertal status (33%,  $p<0.0001$ ) with an extra 9% explained by the average training volume ( $p=0.009$ ).

Changes in body size affect both muscle and bone tissues, largely explaining the strong associations between changes in bone mass or size and muscle size. Additional loading (tennis playing) stimulates bone accrual independently of changes in muscle size or muscle strength, possibly through repetitive impacts.

**Disclosures:** G. Ducher, None.

This study received funding from: National Health and Medical Research Council, Australia.

## SA538

**HSA and Physical Activity in Boys and Girls During Puberty.** G. Y. Rochefort<sup>\*1</sup>, R. El Hage<sup>\*2</sup>, D. Courteix<sup>\*1</sup>, E. Lespessailles<sup>1</sup>, C. L. Benhamou<sup>1</sup>, C. Jacob<sup>\*2</sup>, C. Jaffre<sup>\*1</sup>. <sup>1</sup>Rheumatology, INSERM U658, IPROS, CHR Orleans, Orleans, France, <sup>2</sup>Faculty of Arts and Sound Sciences, Physical Education Division, Tripoli, Libyan Arab Jamahiriya.

**Introduction:** Physical loading increases bone mass, bone mineral density and bone strength during puberty. During adolescence, sexual dimorphism in bone, lean and fat mass increases, giving rise to greater size and strength of the male skeleton. However, little is known about the gender differences in femoral neck geometry in adolescent athletes.

**Methods:** 12 adolescent boys and 8 adolescent girls participated in this study (mean age 15.25 +/- 1.07 years). They were all athletes practicing impact sports (mean 8h/week). Body composition, total body, lumbar spine and femoral neck bone mineral content (BMC) and bone mineral density (BMD) were measured by dual-energy X-ray absorptiometry (DXA). Hip Structure Analysis (HSA) software was used to analyze bone densitometry scans. HSA was derived from images acquired from bone mineral scanners at femoral necks. The main structural parameters derived by HSA are the bone cross-sectional area (CSA), the section modulus (Z) and the cross-sectional moment of inertia (CSMI). A bone Strength Index (SI = Z/height) and two related bone strength (RBS\_lean and RBS\_weight) were calculated to express bone morphology based on known relationships. Physical activity and daily calcium intake were calculated using questionnaires.

**Results:** Results are presented in table below. Height, weight, lean mass and calcium intake were significantly greater in boys compared to girls. BMC measurements were also greater in boys than in girls. After adjustment by anthropometric parameters all differences disappeared. Cross-sectional area (CSA), section modulus (Z) the cross-sectional moment of inertia (CSMI) and the SI were greater in boys compared to girls. In contrast, SI normalized to lean mass or weight (RBS\_lean and RBS\_weight) did not differ between the two groups.

**Conclusion:** These data suggest that the differences between girls and boys at this age seem only bound to anthropometric differences and that the physical activity does not seem to have a sex-specific action on the bone parameters analyzed in this study.

(Mean +/- SD)	Boys (n=12)	Girls (n=8)
BMC (g)	2.57 +/- 0.42	2.02 +/- 0.23
BMD (g/cm <sup>2</sup> )	1.20 +/- 0.13	1.11 +/- 0.06
CSA (cm <sup>2</sup> )	4.27 +/- 0.64	3.37 +/- 0.30
CSMI	4.23 +/- 0.76	2.63 +/- 0.41
Z (cm <sup>3</sup> )	2.34 +/- 0.37	1.66 +/- 0.18
SI (Z/height)	7.39 +/- 2.05	7.05 +/- 0.92
RBS_lean	0.025 +/- 0.003	0.026 +/- 0.002
RBS_weight	0.021 +/- 0.002	0.020 +/- 0.002

**Disclosures:** G.Y. Rochefort, None.

## SA539

**Bone Volumetric Density, Geometry and Strength in Male and Female Collegiate Runners.** A. J. Thieschafer<sup>\*1</sup>, J. M. Hughes<sup>\*1</sup>, K. L. Popp<sup>\*1</sup>, B. Kaufman<sup>\*1</sup>, R. J. Wetzsteon<sup>2</sup>, S. D. Stovitz<sup>\*3</sup>, M. A. Petit<sup>1</sup>. <sup>1</sup>School of Kinesiology Laboratory of Musculoskeletal Health, University of Minnesota, Minneapolis, MN, USA, <sup>2</sup>Children's Hospital of Philadelphia, Philadelphia, PA, USA, <sup>3</sup>Department of Medicine, University of Minnesota, Minneapolis, MN, USA.

Given the characteristics of the mechanical loads on bone during running, this activity should theoretically have a positive effect on bone strength. However several studies suggest runners have low or normal areal bone mineral density (aBMD, g/cm<sup>2</sup>) compared to non-running controls. Bone geometry can adapt in ways that improve bone strength with no change in bone density or mass. The purpose of this study was to explore differences in tibial bone geometry, volumetric density (vBMD, mg/mm<sup>3</sup>), and estimates of bone strength in runners and healthy, inactive controls. We used peripheral quantitative computed tomography (pQCT, Orthometrix XCT 3000) to assess tibial bone properties in male (n = 21) and female (n = 38) runners and inactive age-matched healthy controls (n = 17 males, 32 females) aged 18-35 (mean 22.6±3.3yrs). We measured vBMD, bone area (ToA, mm<sup>2</sup>) and an index of compressive bone strength (bone strength index; BSI, mg<sup>2</sup>/mm<sup>4</sup>= ToA \* ToD<sup>2</sup>) at the distal (4%) tibia. At the midshaft sites (50 and 66% tibia) ToA and cortical (CoA, mm<sup>2</sup>) bone area, cortical density (CoD, mg/cm<sup>3</sup>), cortical thickness (CoTh, mm), estimated bending strength (strength strain index; SSIp, mm<sup>3</sup>) and muscle cross-sectional area (MCSA) were assessed. We used analysis of covariance (ANCOVA) adjusting bone outcomes for age, tibia length and body weight. At the distal (4%) tibia, female runners had significantly greater BSI (+19%, p < 0.05) due to a larger ToA (+11%, p < 0.05), but no difference in vBMD compared to controls. At the proximal sites, female runners also had significantly greater bone strength (SSIp +17-19%, p < 0.001) due to a greater ToA (+14%), CoA (+15%), and CTh (+8-9%) but no difference in vBMD compared to female controls. Male runners, compared to controls had significantly greater CTh (+8-14%, p < 0.05) at both proximal sites as well as a greater CoA (+11%, p < 0.009) at the 66% site, but no differences in bone strength or vBMD. Greater bone strength in female runners was attributable to greater bone area rather than density. In contrast, there was no difference in bone strength between male groups; however male runners had favorable bone geometric properties. These data suggest that running may optimize bone geometry resulting in increased bone strength in females.

**Disclosures:** A.J. Thieschafer, None.

## SA540

**Bone Geometry, Strength, and Muscle Mass in Female Distance Runners with a History of Stress Fracture.** K. L. Popp<sup>\*1</sup>, J. M. Hughes<sup>\*1</sup>, A. J. Thieschafer<sup>\*1</sup>, S. A. Novotny<sup>\*1</sup>, S. D. Stovitz<sup>\*2</sup>, S. Koehler<sup>\*3</sup>, M. A. Petit<sup>1</sup>. <sup>1</sup>Kinesiology, University of Minnesota, Minneapolis, MN, USA, <sup>2</sup>Medicine, University of Minnesota, Minneapolis, MN, USA, <sup>3</sup>Allina Clinics, Northfield, MN, USA.

Stress fractures are common among distance runners. While stress fractures are associated with low areal bone mineral density, little is known about the correlation of lower extremity stress fractures with both bone structure and muscle mass. The purpose of this study was to determine differences in bone geometry, estimates of bone strength, and muscle size in female runners with and without a history of stress fractures. A total of 39 competitive female distance runners aged 18-35, with (SFX, n = 19) or without (NSFX, n = 20) a history of lower limb stress fracture were recruited for this cross-sectional study. Peripheral Quantitative Computed Tomography (pQCT, Orthometrix XCT 3000) was used to assess volumetric bone mineral density (vBMD, mm<sup>3</sup>), bone area (ToA, mm<sup>2</sup>), and estimated compressive bone strength (bone strength index; BSI= ToA \* ToD<sup>2</sup> (bone density)) at the distal tibia (4%). Total (ToA, mm<sup>2</sup>) and cortical (CoA, mm<sup>2</sup>= ToA \* ToD<sup>2</sup>) bone area, cortical density, and estimated bone bending strength (stress strain index; SSIp, mm<sup>3</sup>) were measured at the 15%, 25%, 33%, 45%, 50% and 66% sites. Muscle cross sectional area (MCSA) was measured at the 50% and 66% sites. Questionnaires were used to assess health and training history. There were no significant differences in age, BMI, years of training, miles run per week, or age of menarche between groups. Women with a history of SFX had significantly smaller (7 - 8%) CoA at the 45%, 50%, and 66% sites in both the right and left legs (p < 0.05 for all). SSIp was significantly lower (9 - 10%) at the 50% and 66% sites. Runners with a history of stress fracture also had smaller MCSA (7 - 8%) at the 66% site in both the legs. The remaining bone parameters, including vBMD were not significantly different between groups. After adjusting for MCSA there were no differences between groups for any measured bone outcomes. These findings suggest that bone CoA, strength and MCSA are all lower in runners with a history of stress fracture. However, the lower bone CoA and strength were adapted to the lower muscle size, suggesting interventions to reduce stress fracture risk might be aimed at improving muscle size and strength.

**Disclosures:** K.L. Popp, None.

## SA541

**Previous Sport Activity During Childhood and Adolescence Is Associated with Bone Geometry in Young Adult Men.** M. Nilsson<sup>\*</sup>, C. Ohlsson<sup>\*</sup>, D. Mellström<sup>\*</sup>, M. Lorentzon<sup>\*</sup>. Center for Bone Research at the Sahlgrenska Academy, University of Gothenburg, Gothenburg, Sweden.

Physical activity (PA) during growth has been associated with altered cortical bone geometry, but it remains uncertain if the PA induced increments in cortical bone size remain when the level of PA is diminished or ceased. The aim of this study was to investigate if PA during growth is associated with areal bone mineral density (aBMD) and cortical bone geometry parameters in currently inactive men at the age of peak bone mass (PBM).

In this population-based study, 367 currently physically inactive men, 19.0 ± 0.6 (mean±SD) years old, were included. DXA was used to assess aBMD at several bone sites, whereas cortical bone geometry and trabecular vBMD at the tibia and radius were measured using pQCT. A standardized questionnaire was used to collect information about previous sport activity (SA).

Regression analysis (including covariates age, height, weight, calcium intake, smoking, and duration of inactivity) revealed that previous SA was independently associated with aBMD, at weight-bearing sites, and with cortical bone size of the tibia (cross sectional area (CSA), periosteal circumference (PC)). Previous SA explained 7.9% of the total variation in cortical CSA. Subjects, who ceased their sport activity for up to 6.5 years previously, still had greater cortical PC and CSA of the tibia, at the age of PBM, than ever inactive subjects.

In conclusion we demonstrate that SA during childhood and adolescence is associated with aBMD and bone geometry in currently physically inactive Swedish men at the age of PBM, suggesting that SA during growth confers positive effects on bone geometry even though SA is ceased.

**Disclosures:** M. Nilsson, None.

## SA542

**See Friday Plenary number F542.**

## SA543

**Path Analysis (Structural Equation Modeling) and Covariation of Bone Traits following Delayed Puberty.** V. R. Yingling. Kinesiology and Anatomy and Cell Biology, Temple University, Philadelphia, PA, USA.

Functional interactions among morphological and tissue-quality bone traits are hypothesized to be part of a biological paradigm that results in multiple paths to achieve organ-level functionality. This focus on relationships between bone traits and not individual bone trait differences may elucidate new mechanisms of bone adaptation.

Therefore, the purpose was to illustrate that functional relationships between bone traits and body weight were altered by a delay in puberty using path analysis. Twenty-three day old female rats were randomly assigned into a control group and experimental groups that received injections of Gonadotropin releasing hormone antagonists. Femora were embedded for histomorphometric analyses. A path model was constructed to test the hypothesis that variability in bone size (T.Ar/Length) and body size (Body Weight) is related to variability in relative cortical area (Ct.Ar/T.Ar) and % ash content. The model for the control groups (Figure 1) had excellent "goodness of fit" indicators. The chi-square was non significant ( $p = 0.493$ ). The CFI (Comparative Fit Index) was 1.0; greater than 0.9 indicates a good fit. The RMSEA (Root Mean Square Error of Approximation) was 0.00; less than 0.05 indicates a good model fit. The model indicates that 56% of the variation of Ct.Ar/T.Ar is explained by Body Weight and bone size. Similar results were found in mice. Percent ash content was not affected by body weight or (Ct.Ar/T.Ar). In summary, control animals alter their relative cortical area by a direct relationship with body weight. A negative relationship was found between bone size (T.Ar/Length) and relative cortical area. Comparing these results to the model for the delayed puberty group (Figure 2) indicates that these relationships are no longer valid. Following a delay in pubertal timing only 9% of the variation in Ct.Ar/T.Ar was explained by body weight and bone size. To sum up, the path analysis suggests that (for these data sets) there is an effect of delayed puberty on the relationship between body weight, bone size and relative cortical area.

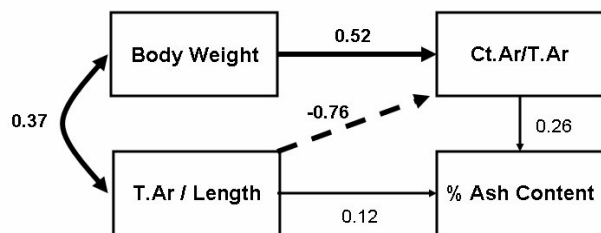


**Figure 1:**  
 $\text{Ct.Ar/T.Ar} = 0.52\text{BodyWeight} - 0.76\text{T.Ar/Length}$ ,  $R^2=0.56$   
 Chi-square = 0.471, df=1, p-value=0.493  
 CFI=1.0, RMSEA=0.00

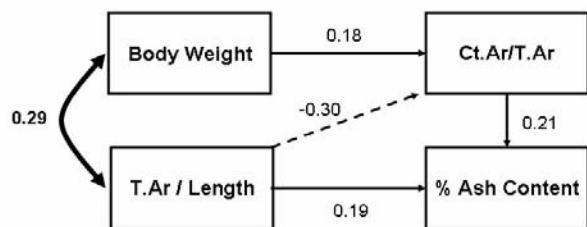


**Figure 2:**  
 $\text{Ct.Ar/T.Ar} = 0.18\text{BodyWeight} - 0.30\text{T.Ar/Length}$ ,  $R^2=0.09$   
 Chi-square = 3.430, df=1, p-value=0.064  
 CFI=0.46, RMSEA=0.289

**Disclosures:** V.R. Yingling, None.

## SA544

See Friday Plenary number F544.

## SA545

**Effect of Particle Size of Calcium Carbonate Supplement on Calcium Retention in Adolescent Girls.** A. E. Elble<sup>\*1</sup>, K. M. Hill<sup>2</sup>, C. Y. Park<sup>\*2</sup>, B. R. Martin<sup>2</sup>, C. M. Weaver<sup>2</sup>. <sup>1</sup>Foods & Nutrition and Public Health, Purdue University, West Lafayette, IN, USA, <sup>2</sup>Foods & Nutrition, Purdue University, West Lafayette, IN, USA.

Previously we reported that substituting small for large (commercial standard) particle sized calcium (Ca) carbonate in diets of growing female rats resulted in higher calcium absorption and retention (JBMR 21: S184, Abst SA 368, 2006). Here we assessed the effect of large versus small calcium carbonate particle size and small particle Ca carbonate versus placebo on Ca retention in adolescent girls. Twenty-eight adolescent girls ( $13.1 \pm 1.7$ y) participated in two 3-wk controlled feeding trials separated by a 1-wk washout period. During both sessions, the subjects consumed a diet identical in nutrient profile tailored to their individual energy needs containing 650 mg Ca/d. Using a cross-over design, one group (n=18) received an additional 650mg/d Ca via supplementation delivered twice a day in a 325mg Ca dose as either an average of 18 micron sized Ca carbonate (large) or 13 micron sized Ca carbonate (small). A second group (n=10) received the small particle sized Ca carbonate or placebo. All 24-h urine and feces were collected throughout the study and analyzed for calcium content by Inductively Coupled Plasma Spectrophotometry (ICP). The overall balance results (Balance = Ca intake - urine Ca -

fecal Ca) indicated that the small particle size supplement resulted in greater calcium retention compared to placebo ( $p<0.05$ ). However, there was no significant difference ( $p = 0.39$ ) in Ca retention due to particle size of the supplement. Thus, the rat model did not predict the effect of particle size on Ca retention in humans. Unlike the rat study which started the treatment diet during weanling and continued throughout adolescence, the human subjects received the treatment during peak skeletal acquisition. Perhaps the overwhelming effects of growth during puberty overpowered the more subtle effect of Ca particle size treatment.

**Disclosures:** A.E. Elble, Delavau 3.

This study received funding from: Delavau.

## SA546

See Friday Plenary number F546.

## SA547

**The Effects of Growth Hormone on Bone Micro-Architecture by In Vivo Micro-CT.** E. Kristensen<sup>\*1</sup>, B. Hallgrímsson<sup>2</sup>, D. W. Morck<sup>\*3</sup>, S. K. Boyd<sup>1</sup>.

<sup>1</sup>Mechanical and Manufacturing Engineering, University of Calgary, Calgary, AB, Canada, <sup>2</sup>Cell Biology and Anatomy, University of Calgary, Calgary, AB, Canada, <sup>3</sup>Faculty of Veterinary Medicine, Faculty of Science, University of Calgary, Calgary, AB, Canada.

Children deficient in growth hormone (GH) are typically treated with injections of GH to attain normal body size. Dosage, duration of treatment, and age of onset of treatment all contribute to body shape and size. Untreated GH deficiency during puberty leads to low lumbar spine bone mineral density (BMD) when compared to age-matched healthy controls. Also, increasing the duration and decreasing the age of onset of treatment contribute to improved BMD [1]. BMD is the current gold-standard parameter to assess efficacy of GH treatment on bone. Presently, the effect of GH treatment on bone micro-architecture has not been investigated, as micro-architecture cannot be derived from BMD measurements.

The study's purpose was to perform a longitudinal assessment of the onset of GH treatment on bone micro-architecture using micro-computed tomography (micro-CT). Ghrhr homozygous 'little' mice have reduced GH synthesis and release, although injection of exogenous GH can stimulate growth. Heterozygous mice have normal GH synthesis and release. A total of six experimental groups were studied. Two groups of homozygous mice received daily injections of GH starting at 21 days of age (early treatment group; ETG), or at 35 days of age (late treatment group; LTG). Two additional homozygous groups included vehicle controls (daily saline injections) and untreated controls. All injections ended at age 60 days. Two heterozygous groups were examined: a group receiving no treatment and a radiation control group. Micro-CT scans of the fourth lumbar vertebra were obtained for all groups (except radiation control) at age 21, 27, 35, 45, and 60 days (vivaCT 40, Scanco Medical AG). The radiation control group was scanned at days 21 and 60 only. Bone architectural parameters were calculated (IPL v. 4.29d, Scanco) and statistical tests determined treatment effects ( $p<0.05$ ).

Relative to heterozygotes, there is a significant reduction in trabecular bone thickness in the untreated 'little' mice. There is no change in micro-architecture in the ETG as compared to the untreated homozygous mice. In the LTG relative to the untreated GH deficient mice, there is a trend towards increased bone quality, however these results are non-significant, likely due to small sample sizes (n=4 to n=8) at the current stage of study. Additional animals are being added to each group to increase statistical power. The data suggests support for the hypothesis that there is a benefit to late treatment, but no gains in bone quality when GH treatment is administered early.

[1] Mukherjee, A. et al. *Med Pediatr Oncol*, 2003. 41:235-42

**Disclosures:** E. Kristensen, None.

## SA548

See Friday Plenary number F548.

## SA549

**Prevalence and Incidence of Viral Infections among Musculoskeletal Tissue Donors and First-Time Blood Donors.** F. Yao\*, M. Zheng, D. Wood\*. Centre for Orthopaedic Research, University of Western Australia, Nedlands WA, Australia.

Musculoskeletal tissue is second only to blood as the most frequently transplanted human tissue, and there continues to be an enormous demand for these allografts throughout the world. Little information is known about the risks associated with musculoskeletal tissue donation.

Our objective was to define the prevalence and incidence of viral markers of human immunodeficiency virus (HIV), hepatitis B virus (HBV), hepatitis C virus (HCV), and human T-cell lymphotropic virus (HTLV) in musculoskeletal tissue donors in Australia, and to compare the results with recently published data on rates of viral infection among tissue donors from Canada, Scotland, and the United States.

We studied blood serum samples from 12,415 consecutive musculoskeletal tissue donors from 3 large musculoskeletal tissue banks in Australia from 1993 through 2004. We defined prevalence as the number of donors with confirmed positive test results divided by the total number of donors tested. We estimated the incidence of new infections among donors by using a method similar to that of Zou and colleagues (1). We then compared the serologic data with those of first-time blood donors obtained during the same period.

The prevalence of viral markers in Australian musculoskeletal tissue donors was much higher than in Australian first time blood donors, by factors of about 10 for HIV, 3 for HBV, 2.5 for HCV, and 35 for HTLV ( $P < 0.05$ ). The prevalence of viral markers was greater in tissue donors than blood donors in all countries, except for anti-HIV antibody in Scottish tissue donors (Table 1). The prevalence of viral markers was higher in tissue donors in Australia than in Canada and Scotland. Estimated incidence rates of viral infections were also higher among tissue donors than first-time blood donors in Australia, Canada, and the United States.

We believe these findings have important implications. Monitoring viral prevalence and incidence among tissue donations is a vital tool for evaluating the safety of the tissue supply and provides important information with which to implement appropriate public health measures and policies.

<sup>1</sup> Zou S, Dodd RY, Stramer SL et al. Probability of viremia with HBV, HCV, HIV and HTLV among tissue donors in the United States. *N Eng J Med*. 2004; 351: 751-9.

<sup>2</sup> Zahariadis G, Plitt SS, O'Brien S, et al. Prevalence and estimated incidence of blood-borne viral pathogen infection in organ and tissue donors from Northern Alberta. *Am J Transplant*. 2007; 7: 226-34.

<sup>3</sup> Galea G, Dow BC. Comparison of prevalence rates of microbiological markers between bone/tissue donations and new blood donors in Scotland. *Vox Sang*. 2006; 91: 28-33.

**Disclosures:** F. Yao, None.

## SA550

See Friday Plenary number F550.

## SA551

**Born Small Is Not Bad for Bone.** Q. Wang<sup>1</sup>, A. Iyytikainen<sup>2</sup>, M. Alen<sup>3</sup>, E. Tylavsky<sup>4</sup>, E. Seeman<sup>1</sup>, S. Cheng<sup>2</sup>. <sup>1</sup>ECE, Repatriation Hospital/Austin Health, The University of Melbourne, Heidelberg West, VIC 3081, Australia, <sup>2</sup>Health Sciences, The University of Jyväskylä, Jyväskylä, Finland, <sup>3</sup>The University of Oulu, Oulu, Finland, <sup>4</sup>Department of Preventive Medicine, The University of Tennessee Health Science Center, Knoxville, TN, USA.

Intrauterine growth is believed to be important in development of peak bone mass (PBM). We tested the hypothesis that born small adversely affects bone mineral content (BMC) at maturity. Crown-heel length (CHL) at birth and 1 year were documented from growth charts while BMC and areal bone mineral density (aBMD) of total body and sub-regions were assessed by dual-energy X-ray absorptiometry (GE Lunar) at 18.3 ± 1.0 yrs in 150 Finnish girls. Gestational age at birth ranged from 33 to 43 weeks (40 ± 1.5 weeks). Contrary to our hypothesis, BMC or aBMD of any site at 18 yrs was not predicted by CHL or birth weight (all NS). Growth rate in the first year of life did not track; 23% of girls increased their trait percentile and 23% decreased their trait percentile by > 1 quartile of their CHL despite no difference in their gestational age at birth (39.4 ± 1.2 vs. 40.4 ± 1.1 weeks,  $p = 0.084$ ). Girls with catch-up growth were shorter at birth than those with slowdown grow (48.6 ± 1.0 vs. 50.9 ± 1.2,  $p < 0.01$ ), but longer (77.1 ± 1.7 vs. 73.4 ± 1.4 cm) at 1yr and taller at 18 yrs (168.1 ± 4.5 vs. 163.7 ± 4.4,  $p < 0.01$ ). Although being born smaller, BMC of total body and sub-regions at 18 yrs of age was 12.4% to 17.4% more in girls with catch-up growth than those with slowdown growth ( $p < 0.01$ ). This difference in BMC at 18 yrs between the two groups was independent of CHL and weight at birth, but not independent of CHL and weight at 1yr or 18 yrs. Being born small is not a risk factor of suboptimal PBM, perhaps due to programming that facilitates expression of the phenotype during the first year of life.

**Disclosures:** Q. Wang, None.

## SA552

See Friday Plenary number F552.

## SA553

**Relationship between Physical Fitness and Bone and Physical Activity and Calcium Retention in Adolescent Girls.** K. M. Hill, A. E. Elble\*, C. Y. Park\*, B. R. Martin, S. L. Mobley\*, C. M. Weaver. Foods and Nutrition, Purdue University, West Lafayette, IN, USA.

Adolescence is a crucial period for bone growth as half of the adult skeletal mass is accrued during this time. Physical activity has been associated with beneficial effects on bone mass in adolescents. However, the influence of physical activity on calcium (Ca) retention in adolescents is unknown. The purpose of this study was to determine the relationships between physical fitness scores and bone parameters and between Ca retention and physical activity (PA). Secondary data analysis from a 6-wk Ca metabolic balance study in adolescent girls ( $n = 48$ ; ages 11-14 y) was performed. As a part of the metabolic study, subjects consumed a controlled diet and 24-hour urine and feces were collected. Ca retention was determined by dietary Ca intake minus urinary and fecal Ca. PA was assessed over four days during each 3-wk session by hip-worn omnidirectional accelerometers. Physical fitness was assessed by three fitness tests: push-ups, sit-ups, and sit-and-reach. Dual-energy x-ray absorptiometry (DXA), peripheral quantitative computed tomography (pQCT), and ultrasound (QUS) were used to determine bone parameters. Body composition was determined by DXA. Relationships among variables were analyzed by Pearson correlations; Paired t-tests were used to assess the influence of PA on Ca retention. Push-up fitness scores were positively associated with several bone parameters including radius total BMD and cortical BMD ( $r = 0.37, 0.36$ , respectively,  $p < 0.01$ ) from pQCT and heel BMD ( $r = 0.34, p < 0.05$ ) from QUS. Push-up fitness scores were also associated with percent fat mass ( $r = -.37, p = 0.01$ ) and percent lean mass ( $r = 0.38, p = 0.01$ ). PA assessed by accelerometry was not significantly related to Ca retention. PA may influence Ca retention if a broad range of PA were studied in contrast to our summer camp setting. Push-up fitness scores may best reflect habitual PA that influences bone mass at the forearm in adolescent girls.

**Disclosures:** K.M. Hill, Delavau LLC 3.

This study received funding from: Delavau LLC.

## SA554

See Friday Plenary number F554.

## SA555

**The Effect of 12 Months Gymnastics Participation on Bone Mass Accrual in 4 to 7 Year Olds.** M. C. Erlandson\*, A. D. G. Baxter-Jones. College of Kinesiology, University of Saskatchewan, Saskatoon, SK, Canada.

Studies of postpubertal gymnasts have constantly shown them to have greater bone mineral content (BMC) than age and maturity matched controls. However, it is unknown if this increased mineralization is the result of training or due to a genetic predisposition. The aim of this study was to assess the effect of 12 months gymnastics participation on BMC accrual in young prepubertal children. Gymnasts and controls were measured at baseline and after 12 months. Age, height, weight and dual-energy X-ray absorptiometry (DXA) of the whole body (WB), total hip (TH) and lumbar spine (LS) BMC were measured annually. Data were analyzed using analysis of variance (ANOVA) and covariance (ANCOVA; covariates, age, initial bone values, and changes in height and weight). Data are presented as mean ± SD. Three groups were identified: Gymnasts (Gym,  $n=54$ , age=5.6 ± 1.1), Gymnast who left the sport (Nongym,  $n=31$ , age=6.2 ± 1.2) and controls (Cont,  $n=75$ , age=5.9 ± 1.1). At study entry no significant differences ( $p > 0.05$ ) were found between the groups for age, height, weight or any BMC measures. At 12 months the mean adjusted BMC values for Gym, Nongym and Cont were 774.1 ± 8.7, 791.3 ± 9.9, 765.5 ± 7.2 g for WB, 9.5 ± 0.3, 9.7 ± 0.3, 9.2 ± 0.2 g for TH and 17.6 ± 0.2, 17.6 ± 0.3, 17.1 ± 0.2 g for LS (means adjusted for age, baseline BMC, change ht, change wt). No group differences were found at any site ( $p > 0.05$ ). The results from this study indicate that the effects of gymnastics training consistently reported in postpubertal adolescent samples were not present in this cohort at this young age, either a study entry or after 12 months of participation. To answer the question as to whether positive changes in bone mass accrual observed in adolescent gymnasts are due to prolonged training this cohort requires further follow-up measures spanning the pubertal period.

**Disclosures:** M.C. Erlandson, None.

## SA556

**Valproate: A Model for Adverse Psychoactive Drug Effects on Bone Mineral Density.** B. L. Gracious<sup>1</sup>, D. Heyer<sup>\*2</sup>, M. Parkhurst<sup>\*3</sup>, S. Messing<sup>\*4</sup>, J. Puzas<sup>5</sup>. <sup>1</sup>Psychiatry and Pediatrics, University of Rochester Medical Center, Rochester, NY, USA, <sup>2</sup>Neurology, University of Rochester Medical Center, Rochester, NY, USA, <sup>3</sup>Psychiatry, University of Rochester Medical Center, Rochester, NY, USA, <sup>4</sup>Biostatistics, University of Rochester Medical Center, Rochester, NY, USA, <sup>5</sup>Orthopedics, University of Rochester Medical Center, Rochester, NY, USA.

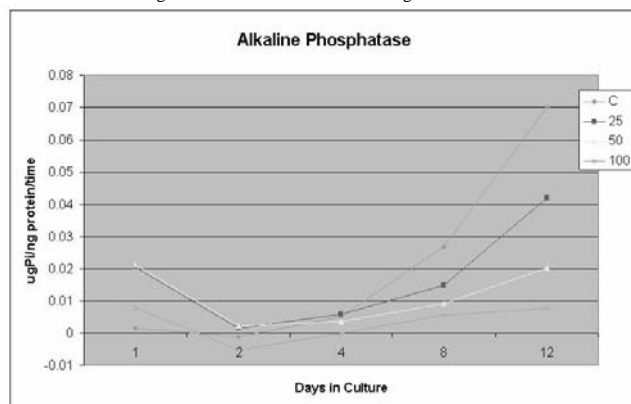
**Purpose:** To implement controlled translational experiments at cellular and human levels using valproic acid (VPA) as a model drug that may adversely affect BMD.

**Aim I:** Determine alkaline phosphatase (AP), Type I collagen, and osteocalcin production in osteoblasts exposed to VPA; **Aim II:** Compare BMD, bone biomarkers, and cortisol as potential mediators in teen girls with bipolar disorder treated with VPA.

**Methods:** AIM I: Primary rat osteoblasts (PROs) were exposed to control vs. VPA media, at human sub-, supra-, and therapeutic concentrations in culture. Protein was extracted across time points up to 18 days. Total protein and AP were measured via photospectroscopy, staining, and ELISA to examine changes in expression across time and conditions. AIM II: A cross-sectional matched study of teen girls taking VPA for Bipolar I disorder compared BMD via DXA and bone biomarkers with girls with BP I disorder not taking VPA and healthy controls.

**Results:** There is a differential effect of VPA on osteoblast AP production related to time and dose, with high therapeutic doses initially stimulating but then suppressing AP production. Interim analysis of DXA and biomarkers in bipolar teen girls exposed to VPA versus controls does not yet show separation between groups, however, salivary cortisol and BSAP trended higher in the VPA group.

**Conclusions:** VPA directly affects primary rat osteoblasts, altering alkaline phosphatase production, which at higher therapeutic doses may result clinically in decreased bone formation. VPA-induced elevations of cortisol in humans may also play a role in adverse effects on BMD. There are likely multiple mechanisms by which VPA affects bone mineral metabolism. Clinical implications include that VPA dose and serum level necessary to treat patients may largely determine effect on BMD. Effects may also be different between cancellous and trabecular bone at different serum levels. Further basic and clinical prospective study of bone formation and resorption in response to VPA levels and sustained release dosing versus immediate release dosing is warranted.



**Disclosures:** B.L. Gracious, None.

This study received funding from: NCRR 1 KL2 RR024136-1.

## SA557

See Friday Plenary number F557.

## SA558

**BMD Changes Over Time Associated with Illness and Recovery in Young Women with Anorexia Nervosa.** E. J. Waugh<sup>1</sup>, B. Woodside<sup>\*2</sup>, P. Cote<sup>\*3</sup>, D. E. Beaton<sup>\*4</sup>, G. A. Hawker<sup>1</sup>. <sup>1</sup>Osteoporosis, Women's College Hospital, Toronto, ON, Canada, <sup>2</sup>Psychiatry, University Health Network, Toronto, ON, Canada, <sup>3</sup>Rehabilitation Solutions, University Health Network, Toronto, ON, Canada, <sup>4</sup>Mobility Program, St. Michael's Hospital, Toronto, ON, Canada.

We examined the effect of duration of illness and recovery of anorexia nervosa (AN) on BMD in a retrospective cohort study of patients aged 17-40 yrs who had received inpatient treatment for AN over a 12-yr time period. A detailed illness history was obtained by a Life History Calendar semi-structured interview. BMD at the lumbar spine L1-L4 (LSP), femoral neck (FN) and total body (TB) was measured by DXA. Low BMD was defined as a Z-score value  $\leq -1.5$  at one more sites.

We recruited 190 participants from two centers. At interview, mean age was  $27.2 \pm 5.6$  yrs and mean BMI was  $19.4 \pm 3.4$  ( $11.1 - 35.5$ )  $\text{kg/m}^2$ . Age at AN onset was  $18.2 \pm 4.2$  ( $10-32$ ) yrs, duration of illness was  $5.9 \pm 4.6$  ( $1 - 25$ ) yrs and lowest lifetime BMI was  $13.9 \pm 2.3$  ( $7.2 - 18.0$ )  $\text{kg/m}^2$ . Eighty-three participants were recovered (achieved a BMI  $\geq 18.5$   $\text{kg/m}^2$  and resumed menstruation); duration of recovery was  $4.8 \pm 3.9$  ( $0.8 - 26$ ) yrs. Linear regression was used to estimate the rate of change in BMD Z-score values per year of illness and recovery, adjusted for weight.

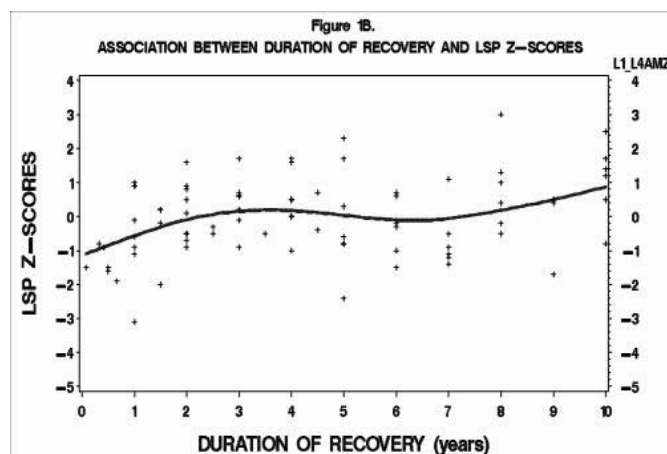
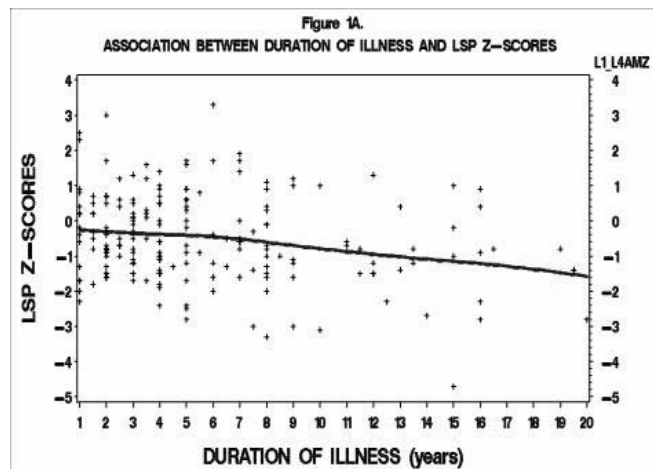


Figure 1 shows the relationships between durations of illness and recovery and LSP z-scores. Similar relationships were observed at the FN and TB (data not shown). A gradual and linear loss of BMD was associated with duration of illness ( $\beta = -0.05/\text{yr}$ , 95% CI -0.09, -0.009). The decline in LSP z-scores commenced immediately after onset of AN: 26.7% of participants ill for 1 yr had low BMD. In contrast, a rapid increase in BMD was associated with the first 3 yrs of recovery ( $\beta = 0.59/\text{yr}$ , 95% CI 0.23, 0.95) followed by stabilization of BMD after 3 yrs ( $\beta = 0.02/\text{yr}$ , 95% CI -0.7, 0.12). Low BMD was observed in 67% of those recovered for  $< 1$  yr but only persisted in 25% of those recovered for 1 yr and 10% of those recovered for  $\geq 2$  yrs.

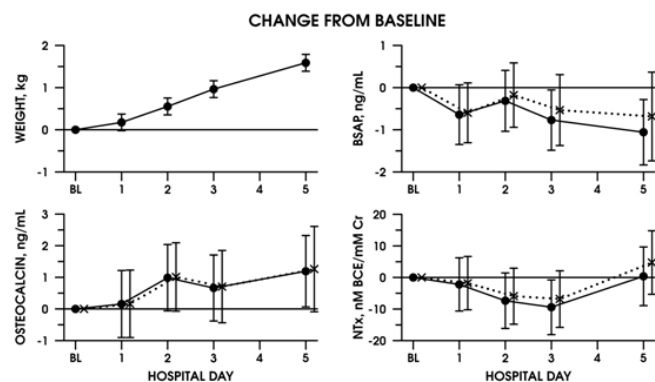
**Disclosures:** E.J. Waugh, None.



## SA559

**The Effect of Bed Rest on Bone Turnover in Adolescents Hospitalized for Anorexia Nervosa.** A. D. DiVasta<sup>\*1</sup>, H. A. Feldman<sup>\*2</sup>, A. Quach<sup>\*1</sup>, C. M. Gordon<sup>1</sup>. <sup>1</sup>Adolescent Medicine, Children's Hospital Boston, Boston, MA, USA, <sup>2</sup>Clinical Research Program, Children's Hospital Boston, Boston, MA, USA.

Bone loss is a well-established medical complication of anorexia nervosa (AN). At highest risk for skeletal insults may be those adolescents who become so malnourished that they require medical hospitalization to manage their illness and low weight. Current clinical standards often require bed rest for the duration of hospital stay. However, studies of healthy adults demonstrate that even short-term immobilization leads to disruptions in normal patterns of bone turnover. Our study aimed to determine the effect of short-term bed rest and relative immobilization on bone turnover in adolescents hospitalized for AN. In this observational study, 28 female adolescents (mean age=16.7 ± 2.3 y) were prospectively enrolled upon hospitalization. Eligible patients met DSM-IV diagnostic criteria for AN, and had no other co-morbid conditions or medication use known to affect bone health. As per standard care, all patients were placed on bed rest and graded nutritional therapy. Weight was measured daily, in a standard fashion. Markers of bone formation [bone-specific alkaline phosphatase (BSAP) and osteocalcin (OC)] and bone resorption [urinary N-telopeptides (NTx)] were measured in a fasting state at baseline and days 1, 2, 3, and 5 of hospitalization. Results are presented as adjusted trend estimates from repeated-measures regression analysis. During the 5 days of hospitalization, mean weight increased by 0.33 kg/day (p<0.001). BSAP declined by 0.18 ± 0.07 ng/mL/day (p=0.01). Serum OC, interestingly, increased by 0.24 ± 0.1 ng/mL/day (p=0.02). Urine NTx reached a nadir on day 3, declining -7.0 ± 2.7 nM BCE/mM Cr (p=0.01), but then returned to baseline levels by day 5 (p>0.05; Figure 1). After controlling for weight gain, as well as age, baseline percentage of ideal weight, duration of amenorrhea, hours of weekly exercise, and family history of osteoporosis, the effect of time on BSAP was no longer significant (p=0.24).



Limitation of physical activity during hospitalization for patients with AN leads to a suppression of both bone formation and resorption, and a potential imbalance of bone turnover. Future interventional studies involving mechanical stimulation and/or weight-bearing activity are needed to determine whether medical protocols prescribing strict bed rest are appropriate.

**Disclosures:** A.D. DiVasta, None.

## SA560

**The Effect of Vitamin D<sub>2</sub> and Vitamin D<sub>3</sub> on Intestinal Calcium Absorption in Nigerian Children with Rickets.** T. D. Thacher<sup>1</sup>, M. O. Obadofin<sup>\*2</sup>, K. O'Brien<sup>3</sup>, S. A. Abrams<sup>\*4</sup>. <sup>1</sup>Family Medicine, Mayo Clinic, Rochester, MN, USA, <sup>2</sup>Family Medicine, Jos University Teaching Hospital, Jos, Nigeria, <sup>3</sup>Division of Nutritional Sciences, Cornell University, Ithaca, NY, USA, <sup>4</sup>USDA/ARS Children's Nutrition Research Center, Baylor College of Medicine, Houston, TX, USA.

Children with nutritional rickets due to calcium deficiency have high serum 1,25(OH)<sub>2</sub>D values. We examined if additional vitamin D increased calcium absorption. We randomly assigned 17 Nigerian children with rickets, ages 2-10 years, to either vitamin D<sub>3</sub> (cholecalciferol; n=8) or vitamin D<sub>2</sub> (ergocalciferol; n=9) 1.25 mg given orally. Using stable isotope methods, fractional calcium absorption was determined at baseline and 3 days after vitamin D administration. Mean daily dietary calcium intakes were 182±73 mg, and mean baseline 25(OH)D concentrations were 20 ng/mL (range 5-31 ng/mL). Three days after oral vitamin D, the increase in serum vitamin D<sub>3</sub> (52±22 ng/mL) in the cholecalciferol group and vitamin D<sub>2</sub> (48±18 ng/mL) in the ergocalciferol group demonstrated equivalent drug absorption. The increase in 25(OH)D was equivalent with cholecalciferol (29±10 ng/mL) and ergocalciferol (29±17 ng/mL). Mean 1,25(OH)<sub>2</sub>D values increased from 143±76 pg/mL to 243±102 pg/mL (P=0.001), and the increase in 1,25(OH)<sub>2</sub>D did not differ between ergocalciferol and cholecalciferol (107±110 and 91±102 ng/mL, respectively). The rise in 1,25(OH)<sub>2</sub>D was explained almost entirely by the baseline 25(OH)D concentration (r<sup>2</sup>=0.72; P<0.001). The increase in serum calcium was similar with cholecalciferol (0.29±0.34 mg/dL) and ergocalciferol (0.41±0.51 mg/dL; P=0.57) and significantly greater than baseline values (P=0.004). 24-hour urinary calcium excretion did not differ before

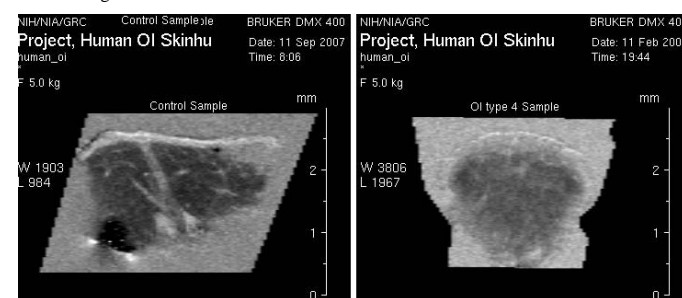
(1.4±1.9 mg) or after (1.4±1.7 mg) vitamin D administration. Mean fractional calcium absorption did not differ before (52.6±21.4%) or after (53.2±23.5%) vitamin D administration, and there was no significant difference between the effect of ergocalciferol and cholecalciferol on calcium absorption. Fractional absorption of calcium was not closely related to concentrations of 25(OH)D (r=0.01, P=0.93) or 1,25(OH)<sub>2</sub>D (r=0.21, P=0.24). The effect of vitamin D on calcium absorption did not vary with baseline 25(OH)D values or with the absolute increase in 25(OH)D or 1,25(OH)<sub>2</sub>D values. Despite the marked rise in 1,25(OH)<sub>2</sub>D in response to oral vitamin D, consistent with vitamin D inadequacy, no augmentation of fractional absorption of calcium absorption occurred. Ergocalciferol and cholecalciferol appear to be bioequivalent.

**Disclosures:** T.D. Thacher, None.

## SA561

**Identification of Skin Abnormalities in Osteogenesis Imperfecta Patients by Magnetic Resonance Imaging-A Pilot Study.** C. L. Raggio<sup>\*1</sup>, K. W. Fishbein<sup>\*2</sup>, E. M. Carter<sup>\*3</sup>, M. Kim<sup>\*4</sup>, N. Pleshko<sup>5</sup>, R. G. Spencer<sup>\*6</sup>. <sup>1</sup>Orthopaedic Surgery, Hospital for Special Surgery, New York, NY, USA, <sup>2</sup>National Institutes on Aging, National Institutes of Health, Baltimore, MD, USA, <sup>3</sup>Kathryn O. and Alan C. Greenberg Center for Skeletal Dysplasias, Hospital for Special Surgery, New York, NY, USA, <sup>4</sup>Mineralized Tissue Laboratory, Hospital for Special Surgery, New York, NY, USA, <sup>5</sup>Biomechanics, Exponent, Philadelphia, PA, USA, <sup>6</sup>Nuclear Magnetic Resonance Unit, National Institute on Aging, National Institutes of Health, Baltimore, MD, USA.

Osteogenesis imperfecta (OI) is a genetic disorder characterized by bone fragility and frequent fractures. Diagnosis is based on clinical and radiological criteria, which can be nonspecific in mild-to-moderate cases, and increasingly by genetic testing, which is time-consuming. We tested the hypothesis that magnetic resonance imaging (MRI) can detect skin abnormalities that correlate with OI genotype and phenotype. Our primary research objectives were to determine: 1. whether MRI can differentiate between skin from OI and control subjects; 2. whether nondestructive MRI analysis is supported by invasive but highly specific Fourier transform infrared spectroscopic imaging (FT-IRIS); and 3. whether there is a relationship between type I collagen genotype, skeletal phenotype, and skin phenotype across patients of all ages. MRI analysis of 3-mm full-thickness forearm skin biopsies from OI (n=6) and non-OI control (n=2) subjects was performed, followed by FT-IRIS. MRI parameters, including T1, T2, and magnetization transfer (MT), were compared to FT-IRIS parameters characterizing dermal collagen. Initial findings showed clear differences in both MRI and FT-IRIS parameters between patients with OI and controls. Findings within the OI group correlated with the severity of clinical phenotype; epidermal and dermal layers were thinner in OI patients compared to controls (See attached T2 image) with the degree of thinning correlating with the severity of OI phenotype. MRI revealed fat deposits within the dermis of OI skin only. FT-IRIS revealed differences in collagen orientation in the dermis of OI skin compared to controls. We conclude that MRI is sensitive to presence and severity of OI in human skin, as confirmed by FT-IRIS analysis. This supports the potential for developing an MRI approach for rapid non-invasive diagnosis of children with OI.



**Disclosures:** C.L. Raggio, None.

## SA562

**Autosomal Recessive Hypophosphatasia Manifesting in Utero with Long Bone Deformity but Showing Spontaneous Postnatal Improvement.** D. A. Stevenson<sup>\*1</sup>, J. C. Carey<sup>\*1</sup>, S. P. Coburn<sup>\*2</sup>, K. L. Ericson<sup>\*2</sup>, J. L. B. Byrne<sup>\*3</sup>, S. Mumm<sup>4</sup>, M. P. Whyte<sup>4</sup>. <sup>1</sup>Division of Medical Genetics, Dept Pediatr, Univ Utah; Shriners Hospt Children, Salt Lake City, UT, USA, <sup>2</sup>Dept Chemistry, Indiana Univ-Purdue Univ, Fort Wayne, IN, USA, <sup>3</sup>Div Maternal-Fetal Medicine, Dept ObGyn, Univ Utah, Salt Lake City, UT, USA, <sup>4</sup>Washington Univ Schl Med; Shriners Hospt Children, St. Louis, MO, USA.

Hypophosphatasia (HPP) is the heritable metabolic disorder of the skeleton and dentition featuring highly variable expressivity conditioned primarily by gene dosage effect and the variety of loss-of-function mutations in the tissue nonspecific alkaline phosphatase gene (*TNSALP*). Extracellular accumulation of the *TNSALP* substrate inorganic pyrophosphate, an inhibitor of skeletal mineralization, accounts for the accompanying rickets or osteomalacia. Four principal forms have been characterized based on age at diagnosis of underlying skeletal disease: perinatal, infantile, childhood, and adult

HPP. Patient age when skeletal problems first manifest generally predicts the clinical course, with autosomal recessive perinatal HPP causing bone disease *in utero* that is obvious at birth and typically lethal soon after. Milder forms may be due to autosomal dominant or autosomal recessive inheritance.

We describe a boy with HPP detected prenatally by sonography showing long bone deformity (Figure) which spontaneously improved *in utero* and after birth. His older brother has the childhood form of HPP without clinical findings until after infancy. Both boys are compound heterozygotes for the same *TNSALP* missense mutations (c.526G>A, p.Ala176Thr in exon 6, and c.814C>T, p.Arg272Cys in exon 8), documenting autosomal recessive inheritance for their HPP. The parents are carriers for HPP, but are clinically unaffected (Table).

Our findings show that prenatal detection of HPP by sonography because of bowing of long bones caused by autosomal recessive inheritance does not necessarily predict lethality, but can represent variable expressivity or the effects of modifiers on the *TNSALP* defects.

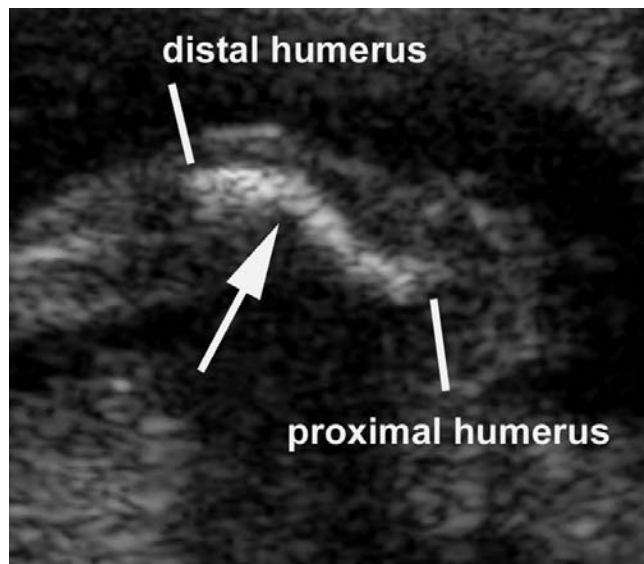


FIGURE. The patient had sharp, mid-diaphyseal angulation (arrow) of his right humerus at 20 weeks gestation.

TABLE Biochemical Studies Indicating Hypophosphatasia

Test	Patient (Sib #1)	Father	Mother	Sister (Sib #2)	Brother (Sib #3)	Normal Range*	
Age (years)**	3	29	28	4	2.5	6	Pediatric Adult
Serum ALP (IU/L)	47	55	32	308	36	63	133-347 30-114
Bone Specific ALP† (IU/L)	29	21	11	144	30	36	47-181 3-38
Plasma PLP (nmol/L)	3,505	191	258	117	1,332	4,034	5-107

\* Normal ranges ( $\pm 2$  SD mean) for were constructed from data from fasting blood specimens obtained from 20 children ages 4.6 – 12.9 years with ad libitum diets and assayed at Shriners Hospital for Children, St. Louis, MO, USA in 1997. ALP = alkaline phosphatase. The range for plasma pyridoxal-5'-phosphate (PLP) concentration is appropriate for both children and adults. (Whyte et al, JBMR 18:624, 2003)

\*\* Age when samples for biochemical studies were obtained.

† Metra Biosystems, Inc., Mountain View, CA, U.S.A.

Disclosures: M.P. Whyte, None.

## SA563

See Friday Plenary number F563.

## SA564

**Prevalence of Transient Hyperphosphatasemia among Healthy Infants and Toddlers.** S. Y. Huh\*, H. A. Feldman\*, C. M. Gordon. Children's Hospital, Boston, MA, USA.

Transient hyperphosphatasemia (TH) is a condition characterized by a temporary elevation of serum alkaline phosphatase in the absence of bone or liver disease. The epidemiology and etiology of TH are not well-understood. Our study goal was to describe the prevalence and clinical characteristics of TH in a cohort of healthy infants and toddlers. We performed a secondary data analysis of 364 children, aged 8 to 24 months, enrolled in a study examining the epidemiology of vitamin D deficiency. After obtaining parental consent, children were enrolled at well-child visits conducted from October 2005 to June 2007 in an urban primary care pediatric clinic. Children with a chronic disease or using medications known to affect bone metabolism were excluded. At enrollment, we collected data regarding child age, gender, height, and weight; maternal race/ethnicity; and season (fall/winter, October to March, or spring/summer, April to September). We measured serum levels of alkaline phosphatase (AP), 25-hydroxyvitamin D [25(OH)D], parathyroid hormone, calcium, and magnesium. We defined TH as an AP > 1000 U/L at enrollment. We examined simple associations and used multiple logistic regression to evaluate the association between clinical characteristics and TH.

Nine of 364 children (2.5%) had an AP > 1000 U/L (mean 2165 U/L, range 1006 to 4293 U/L). Twenty-four children had a high AP that did not meet the definition for TH (mean 546 U/L, range 423 to 835 U/L). Three hundred thirty-two children had a normal AP (mean 261 U/L, range 100 to 400 U/L). Among the 9 children with TH, mean age was 11.8 months (range 9.0 to 19.0 months) and 5 children (56%) had mothers of black race. Fifty-six percent of children with TH were enrolled during the winter, compared with 50% of children with a normal AP. Compared to the 332 children with a normal AP, children with TH had similar mean serum levels of 25(OH)D (32.3 vs. 34.9 ng/mL), PTH (30.0 vs. 27.6 pg/mL), calcium (10.6 vs. 10.4 mg/dL), and magnesium (2.3 vs. 2.3 mg/dL); mean weight-for-length Z-score (0.23 vs. 0.31 SD) and length-for-age Z-score (-0.09 vs -0.06 SD) were also similar. Child age, gender, weight-for-length Z-score, length-for-age Z-score, and serum 25(OH)D levels were not associated with TH in a multivariable model. In conclusion, the 2.5% prevalence found within this study suggests that TH is not a rare condition among healthy infants and toddlers. In this small sample, TH was not associated with anthropometric measures, vitamin D deficiency, or biomarkers of bone turnover. Recognition of this benign condition is important to avoid unnecessary investigations.

Disclosures: C.M. Gordon, None.

This study received funding from: Allen Foundation Inc.

## SA565

**Pediatric Crohn Disease Is Associated with Negative Calcium Balance and Increased Renal Losses of Calcium.** F. A. Sylvester<sup>1</sup>, M. Lincoln<sup>\*1</sup>, L. T. Fourman<sup>\*2</sup>, K. O. O'Brien<sup>\*2</sup>. <sup>1</sup>Pediatric Gastroenterology, Connecticut Children's Medical Center, Hartford, CT, USA, <sup>2</sup>Division of Nutr Sciences, Cornell University, Ithaca, NY, USA.

Pediatric Crohn disease (CD) is associated with significant deficits in bone mass, but the responsible mechanisms are not clear. The purpose of this study was to examine calcium balance in children with CD in remission using stable isotopes of calcium. We excluded subjects exposed to glucocorticoids in the previous 3 months. We enrolled 9 subjects (mean  $12.9 \pm 2.6$  [9.1-15.4] y, 7 M). We measured BMD by DXA (GE Lunar Prodigy Advanced). Subjects received  $972 \pm 47$   $\mu$ g/kg  $^{45}$ Ca IV over 5 min and  $3777 \pm 117$   $\mu$ g/kg  $^{44}$ Ca in milk as part of a meal. We recorded their food intake for subsequent dietary analysis. During a 1-day inpatient stay, we collected timed samples of blood, a 24-h urine collection, and all stools. As outpatients, subjects collected 3 spot urine samples/day and all stools for 5 days. Calcium was extracted from each sample for analysis by mass spectrometry (Thermoquest Triton TI Magnetic Sector Thermal Ionization Mass Spectrometer) and atomic absorption spectrometry. We determined fractional absorption of calcium and endogenous fecal losses. In addition, we performed sum-of-exponential and multi-compartmental modeling of the time-dependent disappearance of intravenous tracer from plasma with the Simulation, Analysis, and Modeling computer program. Data were compared to published normative age- and sex-matched data. We used two-tailed paired t-tests to determine significance between CD and healthy subjects, and two-tailed unpaired t-tests when data was not available to match each subject to an appropriate healthy counterpart. We compared the two groups in terms of Ca intake, intestinal absorption, bone deposition, bone resorption, urinary calcium excretion, endogenous fecal excretion, and calcium balance. Mean BMI Z-score was  $-0.61 \pm 0.79$  kg/m<sup>2</sup>. Lumbar spine BMD Z-score was <-1 in 4/9 subjects with CD (mean  $-0.70 \pm 1$ ). Average calcium intake was  $1257 \pm 446$  mg/d. Mean bone Ca deposition was lower than expected in relation to normative data in healthy children ( $1.98 \pm 0.34$  g/day;  $p = 0.013$ ), whereas fractional absorption of calcium was normal. Calcium balance was significantly lower in combined Tanner stages 3 and 4 subjects with CD ( $37 \pm 25$  mg/day;  $p = 0.029$ ). Urinary calcium excretion exceeded values in healthy counterparts by  $104 \pm 127$  mg/day ( $p = 0.040$ ). Fecal excretion was not significantly different than in controls. In summary, children with CD in remission are in a state of negative calcium balance, especially in late puberty, characterized by excessive urinary losses of calcium. Based on these data, we predict an annual loss of 1.6% of skeletal calcium, which may affect the achievement of peak bone mass.

Disclosures: F.A. Sylvester, None.

## SA566

**c.1250A>G, p.N417S is a Common American *TNSALP* Mutation Involved in all Clinical Forms of Hypophosphatasia (HPP), Including Pseudo-HPP.**

D. Wenkert<sup>1</sup>, W. H. McAlister<sup>2</sup>, S. Mumm<sup>2</sup>, M. P. Whyte<sup>2</sup>. <sup>1</sup>Shriners Hospt for Children, St. Louis, MO, USA, <sup>2</sup>Washington Univ Schl of Medicine, St. Louis, MO, USA.

Hypophosphatasia (HPP) is an inborn error of metabolism caused by loss-of-function mutation(s) in the gene encoding the tissue nonspecific isoenzyme of alkaline phosphatase (*TNSALP*). HPP is highly variable in severity, ranging from tooth manifestations only, to death in utero from profound skeletal hypomineralization. The 7 clinical forms are perinatal, infantile (lethal in 50% of patients), childhood (rickets, +/- short stature, and delayed fracture healing), adult (fractures from osteomalacia), odonto-HPP (early loss of 1° dentition), "benign prenatal" (in utero bowing with improvement ex utero), and pseudo-HPP (infantile HPP phenotype, but normal serum alkaline phosphatase (ALP) activity in clinical laboratories).

We describe 19 individuals with a p.N417S mutation near the active site of *TNSALP*. Of the ~170 patients with HPP followed at our research center, 12 carried this c.1250A>G mutation (representing 7 families) and were studied with fasting serum, 24 hour urine collections, and radiologic studies. Serum and DNA were obtained from 7 additional unrelated patients. None was receiving multivitamins. All manifested *TNSALP* substrate accumulation. The average pyridoxal 5'-phosphate (PLP) and inorganic pyrophosphate (PPi) accumulation in compound heterozygotes was 3x greater than that in individuals with a single *TNSALP* c.1250A>G allele.

5 patients with c.1250A>G were compound heterozygotes, and presented with benign prenatal, infantile, childhood, and pseudo-HPP. Perinatal HPP in a compound heterozygote has been previously reported for the c.1250A>G *TNSALP* mutation. The 14 individuals who carry c.1250A>G as a single mutation of *TNSALP* represented carriers (6), odonto (4), mild childhood (1), adult (2), and benign prenatal (1). Thus, the c.1250A>G is a common, "mild," *TNSALP* mutation that may be susceptible to other genetic or environmental factors, and occurs in all forms of HPP, including pseudo-HPP.

**Disclosures:** M.P. Whyte, None.

## SA567

**Dysosteosclerosis in a 2-Year-Old Girl: Investigation of a Rare, Sclerosing Bone Disorder.**

D. Wenkert<sup>1</sup>, W. H. McAlister<sup>2</sup>, S. Mumm<sup>2</sup>, M. P. Whyte<sup>1</sup>. <sup>1</sup>Shriners Hospt Children, St. Louis, MO, USA, <sup>2</sup>Wash U Sch Med, St. Louis, MO, USA.

Dysosteosclerosis (OMIM # 224300) is an extremely rare, sclerosing bone disorder. Pts typically acquire short stature, optic atrophy, and blindness. Some develop cranial nerve palsies, developmental or dental problems, and frequent fractures. Bone histology suggests disrupted osteoclast function.

We investigated a 23 mo girl of Turkish descent whose episodic joint pain prompted a skeletal survey at age 7 mos. She was the 3<sup>rd</sup> child of unrelated parents in their 30's, and was 6-lb, 19", and 38-wks gestation at birth. At age 5 mo, CT for rapidly increasing head size showed prominent ventricles, sulci, and subarachnoid spaces. Tooth eruption and development were normal. She had recurrent ENT and skin infections. Between our evaluations at ages 11 and 23 mos, weight was ~30%, but length fell to -2.4 SD, and head circumference was +4 SD with frontal bossing, flattened nasal bridge, low-set ears, white sclera, 9 normal teeth, genu valgum, and normal joints.

Family history was negative for bone disease. Her mother, 5'1", had cholesteatomas with residual deafness. Her father was healthy. Their radiographs were unremarkable.

Pt x-rays showed progressive metaphyseal widening and sclerosis of all long bones, medial clavicular expansion, orbital and facial sclerosis, basilar thickening, "bone-in-bone" in the pelvis, 10 rib and one femur fracture, flattened and beaked vertebrae in keeping with dysosteosclerosis (Fig). With generous dietary calcium, she had slight hypercalcemia, intermittent hypercalciuria, and normal serum PTH and phosphorus. Alkaline phosphatase and osteocalcin seemed low. Heavy metal screening was negative. The significant elevations in serum LDH or the brain isoform of creatine kinase, seen in osteopetrosis (OPT), were absent. Hemogram suggested no bone marrow suppression. Commercial mutation analysis of the chloride channel 7 (*CLCN7*), T-cell immune regulator 1 (*TCIRG1*), and OPT-associated transmembrane protein 1 (*OSTM1*) genes revealed a heterozygous transition in *CLCN7* (T181M) thought not to be pathogenic because this amino acid is not conserved across species, and occurred in her father. We showed no defects in the RANK (exon 1) or OPG genes, but an unreported heterozygous change in *TNFSF11* (RANKL, c.107C>G, p.P36R).

Our patient's findings suggest that dysosteosclerosis is a form of OPT, but without the serologic hallmarks or mutations in established OPT genes.



**Disclosures:** M.P. Whyte, None.

## SA568

**First Clinical Application of Electric Stimulation on Human Distracted Bone.**

Y. Nabil<sup>\*1</sup>, H. Selim<sup>\*2</sup>, O. Hegge<sup>\*3</sup>, M. D'Angelo<sup>4</sup>, A. A. Selim<sup>\*5</sup>. <sup>1</sup>Dental Surgery Department, Military Hospital, Cairo, Egypt, <sup>2</sup>Maxillary Oral Surgery, Ain Shams University Dental School, Cairo, Egypt, <sup>3</sup>Rehabilitation and Rheumatology Department, Ain Shams University School of Medicine, Cairo, Egypt, <sup>4</sup>Anatomy and Cell Biology, Philadelphia College of Osteopathic Medicine, Philadelphia, PA, USA, <sup>5</sup>College of Science, Biomedical research group, KFUPM, Dhahran, Saudi Arabia.

Skeletal tissue is subjected to several biological and physiological forces that modulate its regenerative responses. Management of skeletal deformities in the maxillofacial region has presented a challenge to clinicians. Successful animal model applications of distraction osteogenesis (DO), also refer to as osteodistraction, in the maxillofacial complex has been extensively reported. DO is a surgical technique that uses the body's own repairing mechanisms as allies for optimal tissue reconstruction and this method has joined the conventional techniques for comprehensive treatment of patients with skeletal insufficiencies. Distraction osteogenesis is known to produce mechanical strains that are transformed by bone cells into electrical signals. In accordance with that, several animal studies suggested that the application of electric current may stimulate bone cells to form new bone. In this study, we report the first clinical application of electric stimulation on human distracted bone. Six adult patients underwent segment transfer distraction osteogenesis of mandibular defects combined with the application of direct electric current. We hypothesized that osteodistraction accompanied with electrical stimulation, will make higher speed feasible without compromising bone quality. Direct current of 10  $\mu$ A was started at 7 days postoperatively and continued throughout activation and consolidation periods with a rate of distraction at 2mm per day. The distracted and control non-distracted sides were compared during latency, activation and consolidation periods at 1, 3, 6 and 12 month post operatively. Clinical examination, ultrasonography, digital plain radiographs, bone densitometry and computed tomography demonstrated marked increase in bone density of the distracted bone during the distraction process, at the end of consolidation period and surprisingly the distracted bone demonstrated higher densities compared to control. In conclusion, electric stimulation was an effective method to enhance bone formation in mandibular osteodistraction cases. These data suggests that electric stimulation during osteodistraction may be a good modality to shorten the time needed for distraction osteogenesis and to insure high bone quality during distraction process.

**Disclosures:** A.A. Selim, None.

## SA569

See Friday Plenary number F569.

## SA570

**Alfacalcidol Prevents Aromatase Inhibitor (Letrozole) Induced Bone Mineral Loss in Young Growing Female Rats.** M. H. Idris\*, X. Q. Liu, J. K. Yeh. Metabolism Lab., Winthrop Univeristy Hospital, Mineola, NY, USA.

Long-term aromatase inhibitors use causes bone loss and increase fracture risk secondary to induced estrogen deficiency. We postulated that alfacalcidol (vitamin D3 analog) could prevent the letrozole induced bone mineral loss. Fifty intact 1 month old female rats were randomly divided into five groups with 10 rat each; basal group (B) was sacrificed at start of the experiment; age matched control group (C); letrozole group (L) oral administration of 2 mg/kg per day; alfacalcidol group (A): oral administration of 0.1 ug/kg per day; group L+A: letrozole 2 mg/kg + Alfacalcidol 0.1 ug/kg per day for a period of 8 weeks. When animal sacrificed, serum estrone (E1), estradiol (E2), testosterone (T), LH, FSH, IGF-1 were measured and femoral bone mineral density were scanned by DEXA. Data was analyzed by One-Way ANOVA with group comparison. Eight weeks administration of Letrozole resulted in a significant increase in body weight, tibial and femoral bone length and a significant decrease in the ovary+utrus horn weight as compared to the non-treated groups with or without alfacalcidol. Letrozole administration increased serum T, LH, FSH, IGF-1 and suppressed E1 and E2 significantly. None of those parameters were affected by Alfacalcidol treatment. The result of DEXA shows that Letrozole increased femoral bone area ( $1.8 \pm 0.09 \text{ cm}^2$  vs C;  $1.64 \pm 0.07 \text{ cm}^2$  (mean  $\pm$  S.D.),  $P < 0.05$ ) without a significant effect on the bone mineral content ( $0.39 \pm 0.02 \text{ g}$  vs C;  $0.38 \pm 0.02 \text{ g}$ ). Therefore, the BMD ( $217.8 \pm 4.4 \text{ mg/cm}^2$ ) was significantly lower than that of the control group ( $229.8 \pm 4.9 \text{ mg/cm}^2$ ,  $P < 0.05$ ). Alfacalcidol increased the bone area ( $1.78 \pm 0.07 \text{ cm}^2$ ,  $P < 0.05$ ), bone mineral content ( $0.44 \pm 0.03 \text{ g}$ ,  $P < 0.05$ ) and BMD ( $249.8 \pm 5.9 \text{ mg/cm}^2$ ,  $P < 0.05$ ) as compared to the C group. L+A combine intervention resulted in a significant increase in the bone area ( $1.91 \pm 0.09 \text{ cm}^2$ ,  $P < 0.05$  vs C, L and A groups), bone mineral content ( $0.46 \pm 0.03 \text{ g}$ ,  $P < 0.05$  vs C and L groups) and BMD ( $236.8 \pm 8.0 \text{ mg/cm}^2$ ,  $P < 0.05$  vs C and L groups). This study demonstrates that Letrozole treatment to the young growing female rats enhances body weight and bone elongation due to elevation of both T and IGF-1 with the suppression of E1 and E2. However, the bone density decreased significantly. We believe that Letrozole induced reduction in BMD was secondary to increase bone volume without corresponding increase in mineral deposition. Increased mineral deposition to the growing bone by Alfacalcidol demonstrates that it has therapeutical value in preventing Letrozole induced bone osteopenia.

**Disclosures:** M.H. Idris, None.

## SA571

**The Effects of Long-term Administration of High-dose Growth Hormone on Body Composition and Bone Mineralization.** L. K. Branski\*<sup>1</sup>, D. N. Herndon\*<sup>2</sup>, G. Kulp\*<sup>2</sup>, M. G. Jeschke\*<sup>2</sup>, W. B. Norbury\*<sup>2</sup>, K. E. Naylor\*<sup>3</sup>, R. Eastell\*<sup>3</sup>, G. L. Klein\*<sup>4</sup>. <sup>1</sup>Surgery, Shriners Burns Hospital and University of Texas Medical Branch, Galveston, TX, USA, <sup>2</sup>Surgery, University of Texas Medical Branch and Shriners Burns Hospital, Galveston, TX, USA, <sup>3</sup>Academic Unit of Bone Metabolism, University of Sheffield, Sheffield, United Kingdom, <sup>4</sup>Pediatrics, University of Texas Medical Branch and Shriners Burns Hospital, Galveston, TX, USA.

Recovery from massive burn injury is marked by persisting catabolism for up to one year. Treatment with recombinant human growth hormone (rhGH) is reported safe and effective in promoting an anabolic response following burn. The aim of this study was to assess the effects of long-term (one year) treatment with high doses of rhGH on body composition and bone metabolism. 161 pediatric patients with burns >40% total body surface area were studied from 2000-2006. They were prospectively randomized to receive either placebo (control group, n=93) rhGH at a daily dose of 0.1 mg/kg (0.1 group, n=46), or 0.2 mg/kg (0.2 group, n=22) for one year after discharge. Patients were followed from discharge at 6,9,12, and 24 mo post-burn (intent to treat study design). Weight, lean body mass (LBM), total body bone mineral content (BMC) and % total body fat (FAT) were measured at each time point. IGF-1, IGFBP3, PTH, osteocalcin, and serum total calcium were also measured at admission. Urinary NTx was measured at 12 mo. Statistical analysis was performed using Tukey's t-test or repeated measures ANOVA followed by Bonferroni's t-test. In each case %change of each parameter from discharge was compared vs controls. Significance was accepted at  $p < 0.05$ . LBM increased at 9,12, and 24 mo in the 0.1 group ( $p < 0.04$ ) and in the 0.2 group beginning at 6 mo ( $p < 0.02$ ). FAT decrease was seen in the 0.1 group (6,9,12,24 mo,  $p < 0.03$ ) and in the 0.2 group ( $p < 0.04$ ). IGF-1 levels were elevated in both treatment groups compared to control ( $p < 0.05$ ). BMC fell in the 0.2 group at 9 and 12 mo ( $p < 0.02$ ) with elevated osteocalcin ( $p < 0.002$ ) and decreased PTH ( $p < 0.01$ ) at 9 and 12 mo postburn. Urine N-Tx trended toward increase at 12 mo ( $p = 0.06$ ). We conclude that high dose rhGH increases LBM in burned children but with an accompanying decrease in total body BMC and increased bone resorption in the 0.2 mg/kg/d dose at 12 mo post-burn. Data are insufficient at present to determine whether BMC recovers at 24 mo but if as in the GH-associated bone resorption of GH-deficient children at 12 mo it takes another year of administration to show an increase in BMC, cost vs benefit of treatment must be determined to see if any additional therapy is worthwhile.

**Disclosures:** G.L. Klein, None.

This study received funding from: National Institutes of Health.

## SA572

See Friday Plenary number F572

## SU001

**Continuous Local Infusion of Alendronate Prevents Osteopenia of the Lengthened Segment During Distraction Osteogenesis.** A. Abbaspour\*<sup>1</sup>, T. Baghdadi\*<sup>1</sup>, R. Espandar\*<sup>1</sup>, S. Saberi\*<sup>1</sup>, P. Heidari\*<sup>1</sup>, S. Takata\*<sup>2</sup>, N. Yasui\*<sup>2</sup>. <sup>1</sup>Orthopedics, Tehran University/ medical science, Tehran, Iran, Islamic Republic of, <sup>2</sup>Orthopedics, Health Bioscience, Tokushima, Japan.

Distraction osteogenesis is a well-established method for bone lengthening with widespread clinical application. However to achieve extensive bone regeneration, the external fixator must be applied for a long period, which may result stress-shielding osteopenia. In this study we performed the ability of continuous local injection of alendronate to the lengthened segment of distraction osteogenesis for prevention of osteopenia.

Seventy-two male rabbits had subperiosteal osteotomy of the left tibia and an external fixator was applied anteromedially. There was a lag phase for one week, a distraction phase for two weeks, and a consolidation phase for five weeks. At the beginning of consolidation phase, alendronate was injected continuously at a rate of  $7.14 \mu\text{g/kg/day}$  into the lengthened segment through a needle and catheter connected to a subcutaneously implanted osmotic pump. Control group received purified buffer solution (PBS-) using the same osmotic pump. The bone formation of lengthening segment evaluated through radiograph measurement, weekly. The bone mineral content (BMC) and bone mineral density (BMD) of lengthened segment, surrounding segment of operated and contra-lateral tibiae measured by DXA weekly. Rabbits were sacrificed at 4, 6, and 8 weeks after operation for examination by pQCT and three-point bend test.

Radiographic evaluation indicated osteopenia significantly prevented in alendronate treated group compared with the PBS- treated group. The BMC of the lengthened segment was 7 times higher in alendronate treated group at 8 weeks ( $P < 0.0001$ ). The mean areal BMD ( $\text{g/cm}^2$ ) at 8 weeks in the lengthened 83% ( $p < 0.0001$ ), in the proximal to the lengthened segment 37% ( $p < 0.001$ ), and the distal to the lengthened segment 43% ( $p < 0.001$ ) were higher in alendronate treated group. The mean volumetric density (BMD) in the lengthened segment at 4 weeks 12% ( $p = 0.35$ ), 6 weeks 89% ( $p < 0.003$ ), and 8 weeks 94% ( $p < 0.001$ ) higher in alendronate treated group. In the proximal and the distal to the lengthened segment at 6 and 8 weeks were significantly higher in alendronate treated group ( $p < 0.001$ ). Three-point bending test demonstrated that alendronate treated bone at 6 and 8 weeks were significantly stronger than PBS- treated group.

This study has demonstrated that continuous local injection of alendronate into the lengthened segment can prevent osteopenia during distraction osteogenesis.

**Disclosures:** A. Abbaspour, None.

## SU002

**Dried Plum Polyphenols Increase Insulin-like Growth Factor I (IGF-I) Production in Osteoblast-like Cells.** S. Hooshmand\*, S. C. Chai\*, B. H. Arjmandi\*. Nutrition, Food and Exercise Sciences, Florida State University, Tallahassee, FL, USA.

Osteoblast-like cells (MC3T3-E1) secrete several growth regulating factors include insulin like growth factor I (IGF-I), transforming growth factor beta (TGF- $\beta$ ) and IGF-II in descending order of abundance. It has been shown that these growth factors produced by MC3T3-E1 have autocrine actions on these cells. Amarnani et al. showed that exogenous addition of IGF-I and IGF-II stimulates MC3T3-E1 cell proliferation; however, TGF- $\beta$  inhibited osteoblast proliferation. IGF-I not only causes osteoblast proliferation but also enhances bone

matrix proteins synthesis in these cells. Our earlier clinical study showed that consumption of dried plum increase IGF-I level in serum of osteopenic postmenopausal women. To investigate the mechanism of action of this observation, we treated MC3T3-E1 cells with 0, 10, 100 and 1000  $\mu\text{g/ml}$  dried plum extract for 3, 6, 9, 12 and 15 days. Media were collected every three day to measure alkaline phosphatase (ALP) activity and IGF-I. At the end of 15 day period, RNA was extracted to further measure the mRNA expressions of ALP and collagen. Dried plum extract was able to increase IGF-I significantly in dose of 1000  $\mu\text{g/ml}$  in days of 12 and 15 compare to control group. ALP increased numerically in dose of 1000  $\mu\text{g/ml}$  in day 15. However, this increase in ALP was not significant. Changes in mRNA levels of ALP and collagen will be reported at the time of poster presentation. The findings of this study suggest that polyphenols in dried plum play important role in bone formation.

**Disclosures:** B.H. Arjmandi, None.

## SU003

**Inhibition of Major Bone Catabolic Mediators in Human Subchondral Bone Osteoblasts upon EphB4 Receptor Activation by Ephrin-B2 Ligand: A New Specific Target against Subchondral Bone Resorption in Osteoarthritis.** S. Kwan Tat<sup>\*1</sup>, J. Pelletier<sup>\*1</sup>, N. Amiable<sup>\*1</sup>, C. Boileau<sup>\*1</sup>, N. Duval<sup>\*2</sup>, J. Martel-Pelletier<sup>\*1</sup>. <sup>1</sup>Osteoarthritis Research Unit, University of Montreal Hospital Centre, Notre-Dame Hospital, Montreal, QC, Canada, <sup>2</sup>Centre de Convalescence Pavillon des Charmilles, Montreal, QC, Canada.

Abnormal subchondral bone (SB) metabolism is involved during osteoarthritis (OA). Recently, ephrin-B2 and its specific receptor EphB4 were suggested to be involved in bone homeostasis. We previously reported that human OA SB osteoblasts could be discriminated into two subpopulations: L-OA osteoblasts, which have pro-bone resorption properties, and H-OA osteoblasts, which have pro-formation properties. We investigated, in human OA SB, the importance of the ephrin system during OA. Gene expression was determined using real-time PCR and the intracellular signaling factors determined by specific ELISA. EphB4 expression was significantly elevated in L-OA osteoblasts compared to normal ( $p < 0.002$ ) and H-OA ( $p < 0.0007$ ), whereas there was no difference when normal was compared to H-OA. In L-OA osteoblasts  $PGE_2$  and IL-17 significantly increased the EphB4 level ( $p < 0.04$ ), whereas IL-1 $\beta$ , TNF- $\alpha$ , and IL-6 had no effect. Ephrin-B2 activation of the EphB4 receptor significantly inhibited IL-1 $\beta$ , IL-6, MMP-1, MMP-13, MMP-9 and RANKL levels, whereas MMP-2 and OPG were unaffected. Interestingly, and well in line with the previous data, factors that activated or upregulated EphB4 including ephrin-B2,  $PGE_2$  and IL-17 markedly inhibited bone resorption. Activation of EphB4 resulted in a significant reduction in PI3K/Akt phosphorylation. Data revealed, for the first time, that activation of the EphB4 receptor on L-OA osteoblasts may trigger a switch towards reduced bone resorption, suggesting that ephrin-B2 could act as a specific therapeutic approach to reduce remodeling activity in the human SB osteoblasts.

**Disclosures:** S. Kwan Tat, None.

## SU004

**Overexpression of the Transcriptional Cofactor Lbh Impairs Angiogenesis and Endochondral Bone Formation During Fetal Bone Development in Chickens.** K. L. Conen<sup>1</sup>, S. Nishimori<sup>\*1</sup>, S. Provot<sup>\*2</sup>, H. M. Kronenberg<sup>1</sup>. <sup>1</sup>Endocrine Unit, Massachusetts General Hospital, Boston, MA, USA, <sup>2</sup>Department of Anatomy, University of California, San Francisco, CA, USA.

Limb-bud and heart (Lbh) is thought to act as a transcriptional coactivator and is highly conserved among species. We previously showed that Lbh is expressed in proliferative chondrocytes, hypertrophic chondrocytes and the primary spongiosa (PS) of growth plates in mice and chicken. However, its role in endochondral bone formation is still uncharacterized. We hypothesized that Lbh might regulate chondrocyte maturation and PS-formation. To test this hypothesis, we used the avian Replication-Competent ASLV long terminal repeat with Splice acceptor (RCAS) retroviral vector strategy that increases Lbh expression in the developing chicken limb by forced expression of retroviral-encoded Lbh. We found that Lbh overexpression results in mildly shortened skeletal elements with a shortened zone of mineralization in Alcian Blue and Alizarin Red skeletal preparations. Examination of the growth plates between E10 and E11.5, when hypertrophic chondrocytes and the bone collar are seen normally, revealed a delay in vascular invasion and bone collar formation, resulting in a delayed appearance of endochondral ossification centers (OC). TRAP staining of trabecular and cortical bone showed fewer TRAP positive cells in the Lbh-overexpressing bones, demonstrating a delay in cartilage resorption. We also found a reduction in CD31 positive cells within the nascent OC of Lbh-overexpressing wings. Moreover, there was reduced apoptosis and a delay in DNA synthesis within the nascent OC. In situ hybridization analysis showed that the expression of osteopontin mRNA, a typical indication of terminal hypertrophic differentiation in chick fetal growth plates, was markedly decreased, despite relative preservation of the expression of type X collagen mRNA in the adjacent region. Finally, we found a dramatic suppression of Runx2 and VEGF mRNAs in chondrocytes and osteoblasts in Lbh overexpressing bones. These results were confirmed by quantitative RT-PCR analysis using cDNA from both infected and uninfected wings. Taken together, these results suggest that Lbh, normally expressed both in chicken chondrocytes and osteoblasts, may negatively regulate vascular invasion and formation of the early OC. Our data also suggest that Lbh regulates this process at least in part by interfering with VEGF and/or Runx2 expression.

**Disclosures:** K.L. Conen, None.

## SU005

**Selective Retention of Bone Marrow Cells in Repair of Canine Femoral Defect with Polycaprolactone-tricalcium Phosphate Scaffolds.** K. Kumagai<sup>\*1</sup>, J. Otonichar<sup>\*1</sup>, J. Wright<sup>\*2</sup>, L. Griffith<sup>\*2</sup>, C. Boehm<sup>\*1</sup>, R. Rozic<sup>\*1</sup>, K. Powell<sup>\*1</sup>, A. Vasanji<sup>\*1</sup>, T. Saito<sup>\*3</sup>, G. F. Muschler<sup>1</sup>. <sup>1</sup>Orthopaedic Research Center, The Cleveland Clinic Foundation, Cleveland, OH, USA, <sup>2</sup>Department of Biological Engineering, Massachusetts Institute of Technology, Cambridge, MA, USA, <sup>3</sup>Department of Orthopaedic Surgery, Yokohama City University, Yokohama, Japan.

**Introduction:** Bone marrow-derived connective tissue progenitors (CTPs) can be rapidly concentrated into the osteoconductive scaffold when passed through a porous matrix. This clinically useful method called selective cell retention (SCR) technique delivers more progenitor cells and fewer competing cells into a graft site. This study was designed to test the hypothesis that the 3D-structured osteoconductive scaffold matrix in combination with osteogenic cells enhances bone formation in an in vivo bone grafting model.

**Methods:** Four identical 1.0 cm diameter and 1.0cm deep unicortical cylindrical defects were created in the lateral femur of eight dogs. Bone marrow was harvested by aspiration and was heparinized. Non-heparinized bone marrow cells were separately harvested. Three dimensional scaffolds composed of polycaprolactone and tricalcium phosphate were used as the graft matrices after loading of bone marrow cells using SCR system. Four defects were treated with implantation of: 1) scaffold alone, 2) scaffold loaded with 4x volume of bone marrow (4x), 3) scaffold with 1x volume of bone marrow clot (Clot) and 4) scaffold loaded with 4x volume of bone marrow and 1x volume of bone marrow clot (4x+Clot). Bone formation was assessed by quantitative micro CT analysis four weeks after implantation.

**Results:** New bone formation tended to begin at the outer surface contacting the marrow space and to migrate into the scaffold matrix. The better bone formation could be seen in the outer region compared to the center region. The 4x loading graft indicated that the bone ingrowth front migrated to the middle region whereas the bone formation in the scaffold alone grafting stopped at the outer-third region. Although the difference in the mean values of %BV was not significant among the different levels of the grafts, 4x grafting showed greater bone formation compared to the scaffold alone grafting. Then the effect of grafts on the bone formation was evaluated with the radially located regions. An all pairwise multiple comparison test indicated the significant bone formation in the outer region.

**Conclusion:** The bone migration to the inside matrix was moderate in the scaffold alone grafting because of limited delivery of osteogenic CTPs. When the CTPs were retained in the graft matrix, bone ingrowth front moved toward the center region. The SCR system for CTP concentration in 3-D scaffold matrix appears to be effective in bone grafting.

**Disclosures:** K. Kumagai, None.

## SU006

**Regulation of Dickkopf-1 and Dickkopf-2 is Needed for Osteoblast Terminal Differentiation on Microstructured Titanium Surfaces.** R. Olivares-Navarrete<sup>\*1</sup>, S. Hyzy<sup>\*1</sup>, M. Wieland<sup>\*2</sup>, B. D. Boyan<sup>1</sup>, Z. Schwartz<sup>1</sup>. <sup>1</sup>Georgia Institute of Technology, Atlanta, GA, USA, <sup>2</sup>Institut Straumann, Basel, Switzerland.

Wnt/beta-catenin-signaling plays an important role in wound healing, osteoblast differentiation and bone formation, suggesting that enhanced peri-implant osteogenesis associated with microstructured hydrophilic titanium surfaces in vivo involves specific modulation of this pathway. Expression of Dkk proteins upstream of Wnt-signaling has been shown to inhibit osteogenesis, but Dkk expression after Wnt-signaling induces a terminal osteoblast phenotype. In this study we hypothesized that the microtopography and hydrophilicity of the substrate affect Dkk1 and Dkk2 expression and signaling in osteoblasts and downregulation of Wnt-beta-catenin signaling is necessary for surface-dependent osteoblast differentiation. MG63 cells were grown for 6 days on tissue culture polystyrene (TCPS) and microstructured titanium substrates (PT [Ra<0.2 $\mu$ m], SLA [Ra=4 $\mu$ m], modSLA [hydrophilic-SLA]). Changes in mRNA levels were measured by an RNA-microarray and confirmed by real time PCR. Surface effects on Dkk1 and Dkk2 protein were measured by ELISA. MG63 cells were transduced with lentivirus particles containing the Dkk2-siRNA template and selected with puromycin. MG63 and Dkk2-silenced cells were cultured on the test surfaces +/- exogenous Dkk1 and Dkk2 protein. Alkaline phosphatase specific activity (ALP), OCN, OPG, TGF- $\beta$ 1, VEGF and Dkk2 protein levels were analyzed. Dkk1 and Dkk2 expression and protein content based on RNA-microarray, real time PCR, and direct measurement of Dkk1 and Dkk2 protein were increased on SLA and modSLA. Dkk2 was reduced in siRNA-Dkk2 cells by more than 70%. These cells had significantly lower levels of ALP, OCN, OPG, VEGF and TGF- $\beta$ 1 than MG63 cells on each test surface. Effects of Dkk2 knock-down were comparable on SLA and modSLA. Dkk2 but not Dkk1 protein treatment partially rescued the osteoblast differentiation phenotype in Dkk2-silenced cells, and this effect was dose-dependent. These results indicate a major role for Dkk2 in late-stage osteoblastic differentiation on microstructured and hydrophilic surfaces, and suggest the importance of Wnt/beta-catenin-signaling and Dkk2 during implant osteointegration in vivo.

**Disclosures:** R. Olivares-Navarrete, None.

This study received funding from: ITI FOUNDATION.

## SU007

**Angiotensin II Type 2 Receptor Blockade Increases Bone Mass.** Y. Izu<sup>\*1</sup>, T. Hayata<sup>1</sup>, F. Mizoguchi<sup>\*2</sup>, A. Kawamata<sup>\*3</sup>, T. Nakamoto<sup>1</sup>, Y. Ezura<sup>1</sup>, M. Noda<sup>1</sup>.

<sup>1</sup>Department of Molecular Pharmacology, Medical Research Institute, Tokyo Medical and Dental University, Tokyo, Japan, <sup>2</sup>Department of Medicine and Rheumatology, Tokyo Medical and Dental University, Tokyo, Japan, <sup>3</sup>Department of Maxillofacial Surgery, Tokyo Medical and Dental University, Tokyo, Japan.

Renin angiotensin system (RAS) regulates circulating blood volume and blood pressure systemically while RAS also plays a role in local milieu. Previous *in vitro* studies suggested that RAS may be involved in the regulation of bone cells. However, it was not known whether molecules involved in RAS are present in bone *in vivo*. In this paper, we examined the presence of RAS components in adult bone and the effects of angiotensin II type 2 (AT2) receptor blocker on bone mass. Immunohistochemistry revealed that AT2 receptor protein was expressed in both osteoblasts and osteoclasts. In addition, renin and angiotensin II converting enzyme (ACE) were expressed in bone microenvironment. Treatment with AT2 receptor blocker significantly enhanced the levels of bone mass and this effect was based on the enhancement of osteoblastic activity as well as the suppression of osteoclastic activity *in vivo*. These results indicate that RAS components are present in adult bone and that blockade of AT2 receptor results in alteration in bone mass.

**Disclosures:** T. Hayata, None.

## SU008

Withdrawn

## SU009

**RANKL/OPG in Primary Cultures of Osteoblasts from Patients with Osteoporotic Hip Fractures.** M. J. Montoya<sup>\*1</sup>, M. Giner<sup>\*2</sup>, M. J. Ríos<sup>\*1</sup>, M. A. Vazquez<sup>\*1</sup>, L. Naji<sup>\*1</sup>, R. Pérez-Cano<sup>\*3</sup>. <sup>1</sup>University of Seville, Seville, Spain, <sup>2</sup>University Hospital " Virgen Macarena", Seville, Spain, <sup>3</sup>University of Seville and University Hospital, Seville, Spain.

The OPG/RANKL/RANK system is very important in the balance between bone formation and resorption. There are very few papers that evaluate the OPG/RANKL system in osteoporotic patients and they use cell pools as an experimental model and not isolated OBs, without conclusive results.

M&M: Primary hOB cells were isolated from bone fragments of patients subjected to hip arthrodesis, 21 hOB cultures from osteoporotic (OP) patients and 18 osteoarthritis (OA), (63-92 years). We quantified OPG and RANKL protein levels (ELISA) and the mRNA of OPG, RANKL by semi-quantitative RT-PCR in basal conditions and after adding 17- $\beta$ -estradiol (E2) 10-7M; 1,25(OH)<sub>2</sub>vitaminD (1,25D) 10-8M and E2+1,25D (10-7M and 10-8M).

Results: The hOB cultures from OP patients grow more slowly, during the 1st stage, than OA (31 $\pm$ 2 and 20.4 $\pm$ 1 days respectively, p<0.05). The OP group, secret OPG protein levels significantly higher to OA (7.7 $\pm$ 1 and 4.1 $\pm$ 0.7 pmol/L respectively, p<0.05). The OPG and RANKL mRNA expression is comparable between both groups in basal conditions and after adding E2. The 1,25D and 1,25D+E2 induce an increase in RANKL and RANKL/OPG mRNA expression in OP patients above 200% (p<0.05). None of these increases were significant in cultures from OA patients.

Conclusions: The hOB proceeding from hip OP, initially grow more slowly, but after reaching the first cellular confluence, the growth time is equal to that of OB proceeding from patients with OA. Moreover, the hOB from the OP group present a higher protein secretion of OPG and a higher RANKL gene expression and RANKL/OPG ratio in response to stimuli that increase bone resorption, so making these patients more inclined to a greater bone loss.

**Disclosures:** M.J. Montoya, None.

## SU010

**Protein Hydrolyzate Directly Modulates the Expression of Glucose-dependent Insulinotropic Peptide by Osteoprogenitor Cells.** Q. Zhong<sup>\*1</sup>, S. Sridhar<sup>\*1</sup>, K. Ding<sup>\*1</sup>, X. Shi<sup>2</sup>, M. Hamrick<sup>3</sup>, B. Kang<sup>\*4</sup>, W. B. Bollag<sup>\*1</sup>, N. Chutkan<sup>\*4</sup>, K. Insogna<sup>5</sup>, C. M. Isles<sup>4</sup>. <sup>1</sup>Medicine, Medical College of Georgia, Augusta, GA, USA, <sup>2</sup>Pathology, Medical College of Georgia, Augusta, GA, USA, <sup>3</sup>Cellular Biology, Medical College of Georgia, Augusta, GA, USA, <sup>4</sup>Orthopaedic Surgery, Medical College of Georgia, Augusta, GA, USA, <sup>5</sup>Medicine, Yale University School of Medicine, New Haven, CT, USA.

Glucose-dependent insulinotropic peptide (GIP) is an incretin hormone released from intestinal endocrine cells in response to nutrient (carbohydrates and fat) ingestion. We have previously shown both *in vitro* and *in vivo* that GIP promotes bone formation both by inhibiting osteoclasts and stimulating the differentiation of bone marrow stromal cells (BMSCs) into mature osteoblasts. We sought to further define the cellular basis for this latter observation. Since GIP has not only been reported to act as a hormone but also as an autocrine/paracrine factor, we examined osteoprogenitor BMSCs for GIP expression. Bone marrow was harvested from C57BL6 mice and enriched for BMSCs using negative and positive selection. BMSCs were analyzed for GIP mRNA expression using real time RT-PCR. Changes in GIP mRNA expression in direct response to nutrient addition to the culture

medium was also examined. BMSCs were grown to 80% confluence and placed in Krebs-Ringer bicarbonate buffer with FBS (0.5%) for 3 hours. The appropriate agonists were then added for 6 hours and mRNA extracted. Protein (in the form of 0.3-2% meat hydrolyzate) significantly and dose-dependently stimulated GIP expression by greater than 20-fold. In contrast, glucose, fat, methylpyruvate and glyceraldehyde (metabolites that bypass glycolysis) had not effect on GIP expression. GIP protein expression, as assessed by immunocytochemistry, was significantly increased only by addition of amino-acids (1.6x vs. control). Notably, as the BMSCs differentiated to osteoblasts GIP expression was lost. Several signaling pathways were evaluated as mediators of protein-stimulated GIP expression. We found that amino acids (but not carbohydrates or fat) stimulated GIP expression through the MAPK pathway, increasing ERK phosphorylation within 1 minute of stimulation, with peak phosphorylation at 10 minutes. Consistent with this finding, the MAPK inhibitor PD98059 (1  $\mu$ M) completely inhibited amino-acid stimulated GIP expression.

In conclusion we have demonstrated the existence of a potential autocrine/paracrine pathway in BMSCs where nutrients (amino-acids) activate the MAPK pathway, increasing GIP expression and ultimately inducing osteoblastogenesis. These data suggest a dual pathway where specific nutrients (carbohydrates and fat) are primarily antiresorptive while other nutrients (protein) are primarily anabolic.

**Disclosures:** C.M. Isles, None.

## SU011

**Neuropeptide Y Effect on Osteoblast Cells.** L. Teixeira<sup>\*1</sup>, A. Nunes<sup>\*2</sup>, M. Sousa<sup>\*2</sup>, M. Lamghari<sup>1</sup>. <sup>1</sup>Laboratório de Biomateriais, INEB - Instituto de Engenharia Biomédica, Porto, Portugal, <sup>2</sup>Molecular Neurobiology, IBMC - Instituto de Biologia Molecular e Celular, Porto, Portugal.

NPY neuronal pathway has been correlated to several physiological processes. Its involvement in bone physiology is currently the focus of much recent area of research.

Recent studies suggested that Neuropeptide Y (NPY) may be involved in the regulation of bone homeostasis and that osteoblasts are under NPY neuronal control. In fact, it has been demonstrated that mice lacking NPY-Y1 and Y2 receptor genes show an increased bone mass. However, the mechanisms behind the biological functions involving NPY receptors are not yet understood. Hence, we investigated, *in vitro*, the expression of Y1 and Y2 receptors, in the osteoblastic lineage and analyzed the osteoblasts response to NPY. We were able to detect Y2 receptor gene expression by osteoblasts only upon continuous stimulation by NPY or Y2 receptor agonist (PYY2-36). We also show that Y1 receptor mRNA expression was down regulated when cells were exposed to NPY or Y2 receptor agonist.

Functional analysis showed that NPY stimulated osteoblast proliferation. However, this effect was not mediated by the Y2 receptor. NPY appeared to promote osteoprogenitor cell differentiation to osteoblasts. The pharmacological stimulation/blockade of Y2 receptor revealed its involvement in this process. In contrast, NPY inhibited calcium deposition in osteoblast extracellular matrix. This effect was not mediated by the Y2 receptor. Lastly, NPY acted on osteoblasts also by modulating RANKL promoter responsiveness.

**Disclosures:** L. Teixeira, None.

This study received funding from: INEB.

## SU012

**Evaluation of Two Novel Bone Growth Factors to Enhance Fracture Healing.** I. Arango-Hisijara<sup>1</sup>, K. Buck<sup>\*1</sup>, F. Del Carpio-Cano<sup>\*1</sup>, S. Rehman<sup>\*2</sup>, W. G. DeLong<sup>\*2</sup>, S. N. Popoff<sup>1</sup>, F. F. Safadi<sup>1</sup>. <sup>1</sup>Department of Anatomy and Cell Biology, Temple University School of Medicine, Philadelphia, PA, USA, <sup>2</sup>Department of Orthopaedic Surgery and Sports Medicine, Temple University Hospital, Philadelphia, PA, USA.

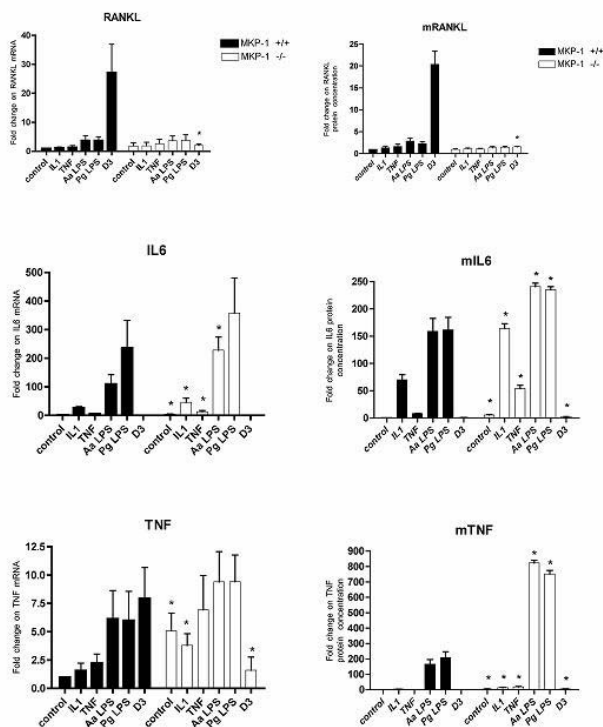
Osteoactivin (OA) and connective tissue growth factor (CTGF) are two novel proteins that have been shown to be anabolic agents in bone. *In vitro* and *in vivo* studies have shown that both CTGF and OA play an important role in osteoblast differentiation and bone formation. In previous studies, we have shown that recombinant CTGF has an osteoinductive effect when injected into the distal femoral marrow cavity of rats, and a peptide derived from the C-terminal domain of OA (OA-P) has osteogenic effects that are similar to the full-length OA protein. In this study, we evaluated the role of CTGF and the OA-peptide using a rat model of femoral fracture. A standard closed femoral fracture was performed on ten week old male Sprague-Dawley rats and the rats were separated into three groups: 1) PBS (negative control); 2) OA-P; 3) adenovirus-CTGF (AV-CTGF). Rats were injected with either PBS, OA-P (100 $\mu$ g) or AV-CTGF at 1, 7 and 14 days post-surgery and followed for 7, 14 or 21 days post-fracture. Radiographs were taken on a weekly basis. Rats were injected with calcein at 7 and 2 days prior to being euthanized at each time point; skeletal tissues were collected and processed for analysis. Radiographic examination of the fracture callus demonstrated greater bony consolidation in the OA-P or AV-CTGF groups compared to control group. Histological analysis of the fracture callus demonstrated greater amounts of periosteal (intramembranous) and endochondral bone formation occurring in the OA-P or AV-CTGF compared to control rats. Calcein labeling demonstrated a significant increase in bone formation rates in the OA-P or AV-CTGF injected rats, providing direct evidence that OA-P or AV-CTGF can increase bone formation at the fracture site. Micro-CT analysis showed a dramatic increase in bone volume in OA-P and AV-CTGF injected rats compared to control group. Overall, animals treated with OA-P or AV-CTGF demonstrated an increase in periosteal and endochondral bone formation at the fracture site, demonstrating OA and CTGF function as anabolic agents to enhance fracture healing. Future studies are underway to examine differential gene expression of the effect of OA-P and AV-CTGF on fracture healing.

**Disclosures:** I. Arango-Hisijara, None.

## SU013

**MKP-1 Is an Endogenous Negative Regulator of Pro-Inflammatory Cytokines in Bone Marrow Stromal Cells.** C. Rossa<sup>\*1</sup>, M. Liu<sup>\*2</sup>, K. L. Kirkwood<sup>1</sup>. <sup>1</sup>Stomatology, Medical University of South Carolina, Charleston, SC, USA, <sup>2</sup>Periodontics and Oral Medicine, University of Michigan, Ann Arbor, MI, USA.

Activation of p38 MAPK by stress, inflammatory and infectious stimuli plays a fundamental role for the expression of cytokines that affect bone turnover, such as IL-6, TNF- $\alpha$  and RANKL. Dual-specificity MAP kinase phosphatase-1 (MKP-1) is an inducible, endogenous negative regulator MAP kinase activation that is localized in the cell nucleus and targets preferentially p38 MAPK. The aim of this study was to determine the role of MKP-1 on the expression of IL-6, TNF- $\alpha$  and RANKL induced by different stimuli in bone marrow stromal cells. Bone marrow stromal cells were collected from MKP-1 knockout C57/Bl6 mice by flushing the marrow cavities of the femur and tibia with cell culture medium. Cells harvested from marrow cavities of wild-type C57/Bl6 mice were used as controls. These cells were stimulated in culture by IL-1 $\beta$ , TNF- $\alpha$ , LPS from *A. actinomycetemcomitans*, LPS from *P. gingivalis* and 1,25 di(OH)vitamin D<sub>3</sub> for 18 hours. The role of MKP-1 was assessed by comparing the levels of cytokine expression by BMSC from knockout and wild-type animals using RT-qPCR and ELISA assays. Cell culture supernatants were used for determination of cytokines by ELISA (n=5). Total RNA was harvested by guanidine isothiocyanate method, reverse transcribed into cDNA and used to assess mRNA level of the cytokines by qPCR (n=5). The results indicated that MKP-1 has an important role on both cytokine- and LPS-induced expression of IL-6 and TNF- $\alpha$ , but not RANKL. Interestingly, MKP-1 is required for the induction of RANKL expression by 1,25 di(OH)vitamin D<sub>3</sub> in BMSC (see figure, \*p<0.05 by unpaired t-test in comparison to the same treatment in WT BMSCs). In conclusion, these results show that MKP-1 plays an important role as an endogenous negative regulatory mechanism for IL-6 and TNF- $\alpha$  expression after inflammatory and infectious stimuli.



**Disclosures:** K.L. Kirkwood, None.

This study received funding from: 1R01DE018290.

## SU014

**Modulation of Skeletal Modeling by Silica-Based Nanoparticles.** G. R. Beck<sup>1</sup>, S. Ha<sup>\*2</sup>, C. E. Camalier<sup>\*1</sup>, B. Hood<sup>\*3</sup>, T. P. Conrads<sup>\*3</sup>, J. Lee<sup>\*2</sup>, M. N. Weitzmann<sup>1</sup>. <sup>1</sup>Endocrinology, Metabolism and Lipids, Emory University School of Medicine, Atlanta, GA, USA, <sup>2</sup>School of Chemistry, Seoul National University, Seoul, Republic of Korea, <sup>3</sup>Clinical Pharmacology, University of Pittsburgh, Pittsburgh, PA, USA.

Nanotechnology is a multidisciplinary field involving the development of engineered "devices", including particles, at the nanometer size (typically 1-100 nm). Recent advances in nanotechnology have raised exciting possibilities for use of nanoparticles as therapeutic interventions and disease imaging. Silica based nanoparticles appear to have good biocompatibility as they are generally thought to be non-toxic in vivo, and consequently are good candidates for use in biomedical applications. We have recently developed a novel 50 nm silica-based fluorescent nanoparticle (designated herein as NP1) for purposes of targeted drug delivery to bone cells. While evaluating the biochemical properties of NP1 relating to toxicity, cell growth and differentiation on a number of different cell types, we were intrigued to discover that NP1 is endowed with potent stimulatory activity on the differentiation and mineralization of osteoblasts in vitro, while concomitantly inhibiting in vitro differentiation of osteoclasts. Preliminary studies in vivo suggest that NP1 is indeed capable of increasing bone mineral density, as assessed by DEXA and  $\mu$ CT.

In order to assess the likely safety profile of these nanoparticles in vivo and to understand potential toxic or non-specific side-effects on skeletal and non-skeletal cells we have begun to define the molecular mechanisms by which they regulate cellular processes. Our studies suggest that one mechanism by which NP1 achieves its stimulatory effects on osteoblasts, and inhibitory effects on osteoclasts, is by suppressing activation of the Nuclear Factor Kappa B (NF- $\kappa$ B), a transcription factor known to repress osteoblast commitment and differentiation, and to be critical for osteoclast differentiation.

The idea that certain nanoparticles themselves might possess intrinsic cell regulatory functions that may be exploitable as pharmaceutical agents is a novel concept and a shift from current attempts to use nanoparticles simply as drug delivery vehicles. In summary, these engineered nanoparticles represent a potentially powerful dual anticatabolic and proanabolic agent for the treatment of numerous skeletal diseases related to bone remodeling without the need for additional drug delivery.

**Disclosures:** G.R. Beck, None.

This study received funding from: Emory University.

## SU015

**Nuclear Factor I Transcription Factors Regulate IGF Binding Protein 5 Gene Transcription In Human Osteoblasts.** L. A. Pérez, X. Wang<sup>\*</sup>, K. Howard<sup>\*</sup>, D. Strong, T. Linkhart. Musculoskeletal Disease Center, Loma Linda VA Medical Center, Loma Linda, CA, USA.

Insulin-like growth factor binding protein 5 (IGFBP5) is expressed in many cell types including osteoblasts and modulates IGF activities. IGFBP5 may affect osteoblasts and bone formation, in part by mechanisms independent of binding IGFs. The highly conserved IGFBP5 proximal promoter contains functional cis regulatory elements for C/EBP, Myb and AP-2. We report evidence for a functional Nuclear Factor I (NFI) cis element that mediates activation or repression of IGFBP5 transcription by members of the NFI gene family. All four NFI genes were expressed in human osteoblast cultures and osteosarcoma cell lines. Co-transfection with human IGFBP5 promoter luciferase reporter and murine Nfi expression vectors showed that Nfib was the most active in stimulating transcription. Nfix was less active and Nfia and Nfic were inhibitory. Co-transfection of human NFIB3 (lacking transactivation domain) with Nfib2 isoform dose dependently increased IGFBP5 transcription. Knockdown of NFIB and NFIC expression using siRNA decreased and increased IGFBP5 expression, respectively. Effects of NFIB knockdown on IGFBP5 promoter activity were reversed by overexpressing mouse Nfib. Analysis of IGFBP5 promoter deletion and mutation reporter constructs identified a functional NFI cis element overlapping the AP2 binding site. All four NFI proteins bound the NFI site in electrophoretic mobility shift experiments and NFI-B bound in Chromatin Immunoprecipitation assays. Results suggest that NFI proteins are important regulators of IGFBP5 expression in human osteoblasts and thus in modulating IGFBP5 functions in bone.

**Disclosures:** L.A. Pérez, None.

This study received funding from: Department of VA Medical Research grants to TAL and DDS. LAP was supported by a predoctoral fellowship from LLU-NIH IMSD R25 GM060507 and a NIAMS predoctoral fellowship 1F31AR054722.



## SU016

**Effect of Strontium on PTHrP, OPG and RANKL mRNA Expression in Osteoblastic Like Cells UMR 106.1.** N. Nijs-Dewolf<sup>\*1</sup>, R. Karmali<sup>\*2</sup>, L. Beyer<sup>\*3</sup>, P. J. M. Bergmann<sup>4</sup>. <sup>1</sup>Laboratory of Experimental Medicine, CHU Brugmann (ULB), Brussels, Belgium, <sup>2</sup>Internal Medicine, CHU Brugmann (ULB), Brussels, Belgium, <sup>3</sup>Geriatrics, CHU Brugmann (ULB), Brussels, Belgium, <sup>4</sup>Nuclear Medicine, CHU Brugmann (ULB), Brussels, Belgium.

**AIM:** Sr<sup>2+</sup> increases bone mass by increasing formation and decreasing resorption (Bone 2007;40S1:S5). PTHrP production by osteoblastic cells could regulate bone formation (J Clin Invest 2005;115:2402). Sr<sup>2+</sup> could decrease resorption by regulating the OPG/RANK-L balance (Calcif Tissue Int 2006;78 S1:129). Here we investigated the effect of Sr<sup>2+</sup> on PTHrP, OPG and RANKL expression in osteoblast like cells.

**METHOD:** UMR 106.1 cells were cultivated in EMEM medium with 1 % FCS and 50 ng/mL ascorbic acid. At confluence the cells were placed for 24h in a medium without Ca. SrCl<sub>2</sub> was then added (0.5 - 2 mM) during 1 - 6 hours. Sr<sup>2+</sup> effect was also investigated with 1.25 mM Ca<sup>2+</sup>. Total RNA was reverse transcribed and analyzed by real-time PCR. Hprt1 and ubiquitin C were used as housekeeping genes. Cells incubated without Sr<sup>2+</sup> were used as reference. A gravid uterus and UMR 106.1 cells cultivated in  $\alpha$  MEM -10%FCS were used as positive controls for PTHrP mRNA and for OPG and RANKL mRNA respectively. Water and samples without RT were used as negative controls. The results were expressed as 2 <sup>$\Delta\Delta C_t$</sup>  between cells incubated with and without Sr<sup>2+</sup> in the same incubation.

**RESULTS:** In the absence of Ca<sup>2+</sup>, the expression of PTHrP was significantly increased by Sr<sup>2+</sup> (2 <sup>$\Delta\Delta C_t$</sup> =1.22 (1.07-1.37), p<0.01, n=72). The increase was significant at 1 h., with a maximum for a [Sr<sup>2+</sup>] between 1 and 1.5mM (2 <sup>$\Delta\Delta C_t$</sup> =1.47 (1.09-1.86), p=0.025 at 1mM; 1.37 (1.01-1.74), p=0.047 at 1.5mM, n=6). The expression of OPG mRNA was significantly increased by Sr<sup>2+</sup> (2 <sup>$\Delta\Delta C_t$</sup> =1.18 (1.06-1.31), p<0.01, n=72). The increase was significant after an incubation of 6h, and maximal for a [Sr<sup>2+</sup>] of 2mM (2 <sup>$\Delta\Delta C_t$</sup> =1.66 (1.28-2.05), p<0.01, n=6). In the presence of Ca<sup>2+</sup> 1.25mM, the expression of PTHrP was significantly increased only at 6h (2 <sup>$\Delta\Delta C_t$</sup> =1.29 (1.11-1.45), p<0.001, n=24), with a maximum for [Sr<sup>2+</sup>] 0.5mM, and a decreasing dose-action curve at higher concentrations. Above 1.5mM, there was no significant effect. The expression of OPG was significantly decreased after 3h incubation with Sr<sup>2+</sup> in the presence of Ca<sup>2+</sup>. There was no significant effect of Sr<sup>2+</sup> on the RANKL expression.

**CONCLUSION:** Incubation of OB like cells with Sr<sup>2+</sup> increases PTHrP mRNA expression independently of the presence of calcium in the incubation medium. An increased local production of PTHrP could contribute to increase formation in patients treated with Sr<sup>2+</sup>. OPG expression is only increased by Sr<sup>2+</sup> when cells are incubated without Ca<sup>2+</sup>. There is no effect of Sr<sup>2+</sup> on RANKL in this culture system.

**Disclosures:** N. Nijs-Dewolf, None.

## SU017

**Global Transcriptome Analysis in Mouse Osteoblasts Identifies a Mechanosensing Osteoblast Gene Signature.** A. Rufo<sup>\*</sup>, M. Capulli<sup>\*</sup>, A. Teti, N. Rucci. Department of Experimental Medicine, University of L'Aquila, L'Aquila, Italy.

Mechanical unloading is detrimental for the skeleton, but the underlying molecular mechanisms are not at all elucidated. Global transcriptome analysis of mouse calvarial osteoblasts grown for 5 days at unit gravity (1xg) or under modeled microgravity (0.008xg) in the NASA-developed Rotating Wall Vessel (RWV) bioreactor revealed 45 genes up-regulated and 88 down-regulated in modeled microgravity, with a cut-off >2 and <0.5 respectively and a p value <0.05. We validated a subset of genes by real time RT-PCR and/or protein analysis, thus confirming reliability of microarray data. Degree of modulation of these genes correlated with intensity of gravitational force. Among the regulated genes some were involved in osteoblast differentiation and function, such as Runx2, Sfrp2, osteomodulin, osteoglycin, fibronectin 1 and Ctgf. Interestingly, our results also showed the regulation of some genes whose involvement in bone homeostasis had not yet been recognized, such as the most up-regulated gene, Lcn2 (Lipocalin 2), and the most down-regulated gene, Penk1 (preproenkephalin 1). We also examined potential regulation of genes involved in osteoblast-osteoclast cross-talk, such as RankL and Opg, which were increased and reduced at 0.008xg respectively, leading to a significant increase of the RankL/Opg ratio, confirmed both at mRNA and protein level. This result is consistent with the observation that conditioned media from osteoblasts grown in microgravity stimulated osteoclast formation in mouse bone marrow cell cultures. Another interesting gene up-regulated was IL-6, which has a dual role in bone tissue, as it stimulates osteoclastogenesis and impairs osteoblast differentiation. Transcriptional and protein up-regulation of IL-6 was confirmed, along with its ability to reduce osteoblast proliferation, differentiation and matrix mineralization. Clustering the significantly modulated genes by the GOTM (gene ontology tree machine) software showed up-regulation of genes involved in apoptosis, in the response to stress and in the activity of selected growth factors. Other molecular functions, such as extracellular matrix components, glycosaminoglycan/heparin binding activity and other growth factor activity, were consistently down-regulated. We finally matched our results with other public global gene profiles obtained in loading and unloading conditions and identified a more selected cluster of commonly regulated genes, which could represent a "mechanosensing osteoblast gene signature". We believe that our transcriptome analysis could contribute to recognize novel mechanisms affecting bone mass in unloading conditions and identify new targetable molecules to prevent and/or cure bone pathologies.

**Disclosures:** A. Rufo, None.

## SU018

**T-box 3 Negatively Regulates Osteoblast Differentiation by Inhibiting Expression of Osterix and Runx2.** K. E. Govoni, G. Linares, S. Chen<sup>\*</sup>, S. Pourteymoor<sup>\*</sup>, S. Mohan. JLP VAMC and Loma Linda Univ, Loma Linda, CA, USA.

T-box (Tbx)3, a known transcriptional repressor, is a member of a family of transcription factors which contain a highly homologous DNA binding domain known as the Tbx domain. Mutation of Tbx3 gene results in limb malformation. We recently reported that Tbx3 is required for osteoblast (Ob) proliferation and that growth hormone, an important regulator of skeletal growth, stimulates Tbx3 expression in vitro and in vivo. Based on these findings and that Tbx3 expression increases during Ob differentiation, we predicted that Tbx3 is an important regulator of Ob cell functions. To determine the role of Tbx3 in Obs, we evaluated the consequence of transgenic overexpression of Tbx3, using a retroviral vector, on Ob differentiation. Retroviral overexpression increased Tbx3 expression > 100-fold compared with control (P < 0.01) as determined by real-time RT-PCR. In addition, a significant increase in Tbx3 protein was observed by western immunoblot. To determine the role of Tbx3 in Ob differentiation, MC3T3-E1 cells were plated in media to induce differentiation and mineralized nodule formation. Alizarin Red staining of cells 24 days after addition of differentiation media demonstrated little to no mineralization of Tbx3 overexpressing cells (28  $\pm$  8 vs. 7  $\pm$  1 %). In support of these data, alkaline phosphatase (ALP) activity was reduced 33 to 70% (P < 0.05) in both MC3T3-E1 cells and primary calvaria Obs overexpressing Tbx3. Furthermore, Tbx3 effect on ALP activity was dose dependent. Consistent with reduced differentiation, the increased expression of key Ob marker genes ALP, bone sialoprotein (BSP), and osteocalcin (Oc) within 6 days after addition of differentiation media in control cells (59, 35, and 3-fold; P  $\leq$  0.01, respectively), was not observed in cells overexpressing Tbx3 (ALP 3-fold increase, P < 0.01; BSP 4-fold decrease, P < 0.01; and no change in Oc, P = 0.83). Based on our findings that osterix and runx2 contain Tbx binding site in the regulatory region, we considered the possibility that the negative effect of Tbx3 on Ob differentiation could be mediated via its effects on expression of transcription factors that are critical for Ob differentiation. Accordingly, we found Tbx3 overexpression abolished increased osterix and runx2 expression (12- and 3-fold increase, respectively in controls) observed during normal Ob differentiation. However, expression of Msx2, a transcription factor that does not contain the Tbx binding site, did not differ in expression between control and Tbx3 overexpressing cells over time. Based on these data and our previous findings, we conclude that Tbx3 promotes proliferation and suppresses differentiation of Obs by binding to Tbx binding sites in the regulatory regions of osterix and runx2 to suppress their expression.

**Disclosures:** K.E. Govoni, None.

This study received funding from: National Institutes of Health Grant Number: AR048139 (SM).

## SU019

**PBX1 Interaction with HOXA10 Regulates Timing and Expression of Phenotypic Bone Genes During Osteoblastogenesis.** J. A. R. Gordon, M. Q. Hassan, S. Saini<sup>\*</sup>, A. J. van Wijnen, J. L. Stein, G. S. Stein, J. B. Lian. Department of Cell Biology and Cancer Center, University of Massachusetts Medical School, Worcester, MA, USA.

We have recently demonstrated a novel role for the *Abdominal B* class homeobox protein HOXA10 in regulating phenotypic bone genes (Hassan et al. *Mol Cell Biol* 27:3337 2007). HOX factors frequently form multimeric complexes combining with distinct three amino acid loop extension (TALE) class homeodomain proteins to regulate specific transcriptional functions. Here we establish a role for the TALE class protein PBX1 in regulating HOXA10 activity and contributing to the timed expression of bone related genes during osteoblastic differentiation. Exogenous expression of PBX1 in mesenchymal progenitor cells represses the BMP2-induced expression of osteoblast-related genes including RUNX2, osteocalcin and bone sialoprotein. Conversely, disruption of normal PBX1 function by expression of targeted shRNA or alteration of PBX1-DNA binding consensus sequence resulted in increased osteoblast-related gene expression and promoter activity. This regulatory role of PBX1 is further demonstrated by chromatin immunoprecipitation and co-immunoprecipitation experiments showing that HOXA10 and PBX1 interact on osteoblast-related promoters while cells committed to the osteoblast lineage are actively proliferating. This repression complex is also associated with negative modulators of chromatin remodeling, including several histone deacetylases. At the onset of osteocalcin and bone sialoprotein gene expression, the association of HOXA10 and PBX1 is functionally replaced with an activation complex containing HOXA10 and RUNX2. The dissociation of PBX1 from osteoblast-related promoters is coincident with increased histone acetylation and methylation at lysine residues frequently associated with gene activation including H3K4 and H3K36. These HOXA10 co-regulatory protein interactions are consistent with repression and activation of osteoblastic genes during differentiation and identifies a mechanism for the severe skeletal abnormalities observed in PBX-null mice (Selleri et al *Development* 128:3543, 2001). Given our findings we propose that PBX1 plays a central role in the attenuation of HOXA10 as a transcriptional activator of osteoblast-related genes, establishing proper timing of gene expression during osteogenesis.

**Disclosures:** J.A.R. Gordon, None.

## SU020

**Transcription Factor NFATp Regulates BMP-Induced Chondrocyte Differentiation in a Tissue-Specific Manner.** J. G. Yost\*, Q. Lu\*, B. M. Gardner\*, M. Rodova\*, J. Wang. Orthopedic Surgery, University of Kansas Medical Center, Kansas City, KS, USA.

Bone morphogenetic protein (BMP) plays an important role in skeletal development and postnatal bone repair. NFATp (NFAT1/NFATc2) is a member of the NFAT (nuclear factor of activated T cells) family of transcription factors originally identified to be critical in regulating gene transcription in immune response. Previous studies suggested that NFATp also acted as a repressor of chondrogenesis in adult mice. This study was designed to determine if NFATp affects chondrocyte differentiation during BMP-induced endochondral ossification. Recombinant human BMP-7 (rhBMP-7) with type-I collagen as a carrier was implanted into 5-mm cranial bone defects and thoracic subcutaneous pouches created in NFATp<sup>-/-</sup> or wild type (WT) mice. Cellular responses to the implanted material were evaluated by histochemical and immunohistochemical analyses. The expression levels of chondrocyte or osteoblast marker genes were detected by quantitative real-time PCR (qPCR) at days 2, 5, 8, 12, and 21. The results showed that implantation of rhBMP-7 into cranial defects induced bone formation primarily via an intramembranous pathway in the areas close to the dura accompanied by chondrocyte differentiation and endochondral ossification near the skin flap in both NFATp<sup>-/-</sup> and WT mice. Type-X collagen expression peaked at day 8 in both NFATp<sup>-/-</sup> and WT groups, although it remained relatively higher in WT mice at day 12. In contrast, implantation of rhBMP-7 into thoracic subcutaneous tissues first induced differentiation of local mesenchymal stem cells into chondrocytes at day 5, both in WT and NFATp<sup>-/-</sup> mice. However, newly formed chondrocytes differentiated into type-X collagen-expressing hypertrophic chondrocytes with mineralization of cartilage matrix at day 8 in NFATp<sup>-/-</sup> mice, while this process was not evident until days 11-12 in WT mice. BMP-induced cartilage eventually underwent endochondral bone formation in both NFATp<sup>-/-</sup> and WT mice. Further analysis revealed that the expression levels of several proposed positive regulators of chondrocyte terminal differentiation such as Runx2 and Indian hedgehog were significantly higher in cranial bone and surrounding tissues than in subcutaneous tissues. Taken together, our results suggest that the absence of NFATp facilitates terminal differentiation of chondrocytes in a tissue-specific manner during BMP-induced endochondral ossification. This is due, at least in part, to a higher expression of positive regulators of chondrocyte terminal differentiation in the cranial bone environment, resulting in specific patterns of chondrocyte differentiation in the cranial and subcutaneous implants.

**Disclosures:** J. Wang, None.

## SU021

**Post-translational Regulation of Mx2 Protein.** W. Yoon\*, Y. Cho<sup>1</sup>, J. Cho\*, J. Baek\*, K. Woo\*, H. Ryoo\*. <sup>1</sup>Department of Cell and Developmental Biology, School of Dentistry and DRI, Seoul National University, Korea, Seoul, Republic of Korea, <sup>2</sup>Department of Biochemistry, School of Dentistry, Kyungpook National University, Korea, Daegu, Republic of Korea.

Mx2 is not only essential for epithelial organogenesis or bone formation in early embryonic development of vertebrates, but also a target gene of bone-related cytokines, such as BMP2 and bFGF. Post-translational regulation of protein is fundamental processes in biological control system and little is known about post-translational modifications of Mx2 protein. Here, we investigated the importance of FGF2-induced post-translation processing of Mx2 protein, which is regulated through protein-protein interaction. We identified that Mx2 protein is stabilized in the presence of FGF2. Immunoblot assay of transiently transfected Mx2 in C2C12 cell-line showed that the FGF2 treatment significantly increases the level of Mx2 protein. Blocking JNK activity dramatically decreases the level of Mx2 protein increased by FGF2, while other kinases had no effect on Mx2 level. These results implicate JNK-mediated phosphorylation driven by FGF signal upregulates the stability of Mx2 protein. We also identified that the stability of Mx2 protein requires acetyltransferase activity of p300. Transient cotransfection of Mx2 with p300 showed increased level of Mx2 as well as acetylation of Mx2 protein through Mx2-p300 interaction by immunoprecipitation and immunoblot assays. Increased protein level of Mx2 by p300 reduced ubiquitylation of Mx2 protein, implicating that acetyltransferase activity of p300 prevents Mx2 from ubiquitin-dependent degradation. Additionally, FGF2 treatment strongly increased Mx2-p300 interaction as well as Mx2 protein level. These indicate that FGF2 signal stimulates Mx2 stability via protein acetylation and the same lysine residue(s) of Mx2 can be substrate(s) for both acetylation and ubiquitylation. Finally, we challenged proteomic approach to identify Mx2-binding proteins by using a LC-MS/MS and identified Dlxin-1 among numerous candidates, which is known as a stimulator of Dlx5 transcription activity as well as a target molecule of Prra1, E3 ligase. Co-transfection of Mx2 with Dlxin-1 showed that Dlxin-1 is essential for the Mx2 degradation through the enhancement of binding between Mx2-Prra1, thereby it increases ubiquitylation of Mx2 protein. In summary, we found that intracellular Mx2 protein level is controlled by a balance between ubiquitylation (degradation) and acetylation (stabilization), and FGF2-induced JNK activation makes the balance to the protein acetylation that consequently stabilizes Mx2 protein.

**Disclosures:** W. Yoon, None.

## SU022

**Mab21 Suppresses the Osteogenic Markers by Recruiting Sin3A and Stimulates Osteoclast by Up-regulation of IL-6 and LIF.** S. Heo\*, E. Cho\*, Y. Jang\*, K. Seul\*, H. Ryoo<sup>2</sup>, J. Kim<sup>1</sup>, J. Cho\*. <sup>1</sup>Biochemistry, Kyungpook National University, Daegu, Republic of Korea, <sup>2</sup>Cell and Developmental Biology, Seoul National University, Seoul, Republic of Korea.

In a previous study, we have shown that the expression of Myeloid Elf-1 like factor (MEF), also known as ELF4, suppresses the osteogenic differentiation by suppressing Runx2 transcriptional activity through directly interacting with it. Also, we found that MEF stimulates the transcription of Mab21L1. To understand the inhibitory mechanism of MEF in osteoblast differentiation, we investigated the role of Mab21 on the osteogenic markers. Mab21L1 suppressed not only the transcriptional activity of IL-6 and osteopontin (OP) but also, of 83bp region of osteocalcin (OC) promoter. The transcriptional repressive activity of Mab21 on those promoters was maintained when the C-terminal of Mab21 is deleted up to N-terminal 114 aa remained. In addition, we found that Mab21 physically interacts with Sin3A, a co-repressor, and the binding was also remained for the N-terminal 114aa of Mab21. Our data suggest that the suppressive effect of MEF might be, in part, accomplished by activating a transcriptional repressor Mab21. Also, the 114aa N-terminus of Mab21 suppresses the OP and OC osteogenic markers by recruiting Sin3A. In addition, our data showed that MEF-transduced osteoblast cells up-regulate the expression of IL-6 and LIF, pro-resorptive and calciotropic factors to osteoclast.

**Disclosures:** S. Heo, None.

## SU023

**PPARγ2-mediated Proteolytic Degradation of b-catenin Determines an Anti-osteoblastic Effect of Anti-diabetic TZDs.** S. Rahman\*, P. Czernik\*, B. Lecka-Czernik. Department of Orthopaedic Surgery, Center for Diabetes and Endocrine Disease, University of Toledo Medical Center, Toledo, OH, USA.

The transcription factor PPARγ2 is a key regulator of marrow mesenchymal stem cells (MSCs) differentiation. It positively regulates adipocyte and suppresses osteoblast differentiation. Anti-diabetic drugs thiazolidinediones (TZDs), which specifically activate PPARγ protein, upregulate fat production in the bone marrow and cause bone loss in animals and humans. In order to understand the mechanisms of TZD-induced bone loss, we performed microarray analysis of gene expression changes in a cellular model of PPARγ2-controlled MSC differentiation, U-337/2 cells. Cells were treated with a TZD rosiglitazone (R) for 2, 24, and 72h and gene expression was analyzed using Affymetrix platform representing 45,000 gene transcripts. Among the early responders to R were the proteins involved in Wnt signaling pathway, which is essential for MSC differentiation towards osteoblast and bone formation. The expression of two members of Wnt pathway, WISP-1 and Tle3, was significantly altered within 2h post treatment followed by the suppressive effect on the expression of multiple members of this pathway including Fzd receptors, Dkk1, Sfrp1, and Wif1 modulators, and Tcf3 and Tcf4 transcriptional effectors. Cellular silencing of WISP-1 and Tle3 using siRNA suggested that they are not the major mediators of R-induced suppression of osteoblast phenotype. Therefore, we tested whether R affects activity of b-catenin, a key mediator of Wnt signaling activity. We found that R-activated PPARγ2 induced proteolytic degradation of more than 90% of cytoplasmic (active) form of b-catenin as early as within 1 hr post treatment, not affecting a pool of protein bound (inactive) b-catenin. Consistent with this finding, R suppressed transcriptional activity of b-catenin, measured by the activity of TOP-FLASH construct in a luciferase gene reporter assay. Moreover, R suppressed alkaline phosphatase activity even in the presence of LiCl, which stabilizes an active form of b-catenin. To test whether b-catenin degradation is responsible for R anti-osteoblastic effects we modified PPARγ2 protein domains responsible for b-catenin degradation. Using transfected marrow MSC with mutated PPARγ2 constructs, we are currently testing the hypothesis that a lack of PPARγ2 proteolytic activity for b-catenin protects Wnt pathway gene expression and osteoblast phenotype against the negative effects of anti-diabetic TZDs.

**Disclosures:** B. Lecka-Czernik, None.

## SU024

**Identification of IRX3 a Novel Transcription Factor During BMP2 Mediated Osteoblast Differentiation.** Y. Bae\*, B. C. Dawson\*, T. Bertin\*, E. Munivez\*, B. Lee. Molecular and Human Genetics, Baylor College of Medicine, Houston, TX, USA.

Mesenchymal stem cells have a potential to differentiate to various cell types including osteoblasts, chondrocytes, adipocytes, myoblasts and fibroblasts, depending on the signaling pathway activated during the initial phase of differentiation. These signaling cascades are likely to regulate specific set of early response genes that would govern the final fate of the differentiation process. Osteoblast differentiation can be induced by various stimuli and the most potent inducer are bone morphogenetic proteins (BMPs). Upon the BMP2 treatment, murine premyoblast cell line C2C12 can differentiate into osteoblasts. This *in vitro* biological model allows identifying novel potential regulators involved in osteoblast differentiation. Here, we have examined genes expression during early phase of osteoblast differentiation from C2C12 by 8 hours BMP2 treatment. Gene expression was analyzed by using Mouse Genome 430 2.0 Affymetrix microarray. Real-time quantitative RT-PCR analysis was performed to validate BMP2 mediated osteoblast marker expression from C2C12 cells. A total of 226 genes were differentially regulated after BMP2 treatment. The immediate BMP2 target genes, *Id5*, were highly up-regulated after BMP2 treatment. *Sp7 (Osterix)*, key regulator of osteoblast differentiation, and early

response genes such as *Prrx2*, *Klf10*, *Snai1*, and *Tcf7* were up-regulated upon BMP2 treatment. Interestingly, we have identified a novel transcription factor, Iroquois Homeobox 3 (IRX3), according to its induction upon BMP2 treatment. The expression of *Irx3* was further validated by quantitative RT-PCR along with other early response genes. Consistent with previous report, *in situ* hybridization analysis showed *Irx3* expression at the proximal region of the limb buds of E 11.5 embryo. *Iroquois* homeobox genes are found in all multicellular organisms, and have essential roles in governing various developmental patterning.

In our study, IRX3 protein was identified as a novel transcription factor during early-phase of BMP2 mediated osteoblast differentiation. IRX3 may play a role in the limb development as suggested by its expression pattern. However, the underlying molecular mechanism of IRX3 remains to be elucidated to understand its function during limb development.

**Disclosures:** Y. Bae, None.

## SU025

**Functional Association of MAP Kinase and Runx2 on Osteoblast Chromatin.** Y. Li\*, Q. Yang\*, C. Ge\*, R. T. Franceschi. Periodontics and Oral Medicine, University of Michigan, Ann Arbor, MI, USA.

As previously shown by this laboratory, integrin-mediated osteoblast-ECM interactions are critical for osteoblast differentiation. This response is explained by activation of the Erk-MAP kinase pathway that phosphorylates Runx2 on specific serine residues in the C-terminal proline/serine/threonine-rich domain. In this study, we explore interactions between Runx2 and phospho-Erk on osteoblast chromatin using ChIP analysis. MC3T3-E1 clone 4 cells were cultivated in growth medium (GM = MEM alpha/10% FBS) or differentiation medium (DM = GM+50 ug/mL ascorbate) and chromatin was isolated for ChIP analysis using Runx2 and P-Erk specific antibodies and PCR primers to specific regions of *Ocn*. Runx2 was associated with 2 previously defined *Ocn* promoter binding sites, OSE2a and OSE2b, and this association was not affected by growth in GM or DM. Interestingly, P-Erk was also associated with OSE2a and OSE2b-containing chromatin regions and this interaction was stimulated by DM, a condition known to increase Erk phosphorylation and *Ocn* transcription. This interaction was specific in that it required intact Runx2 binding sites and was blocked by the specific MAPK inhibitor, U0126. Furthermore, neither Runx2 nor P-Erk was detected in association with a distal transcribed region of *Ocn* approx. 500 bp downstream from OSE2a. Taken together, this work shows that Runx2 and P-Erk are physically associated with a bone-related gene in chromatin where they can directly regulate osteoblast-specific transcription.

**Disclosures:** Y. Li, None.

This study received funding from: NIH DE11723.

## SU026

**Cloning and Functional Expression of the Full Length Mouse GIP Receptor and the Regulation of its Expression in Osteoblasts by the Sp1 Transcription Factor.** B. Kang<sup>1</sup>, J. Xu<sup>\*2</sup>, R. J. Bollag<sup>\*2</sup>, W. B. Bollag<sup>\*3</sup>, N. Chutkan<sup>\*1</sup>, C. M. Isales<sup>1</sup>. <sup>1</sup>Orthopaedic Surgery, Medical College of Georgia, Augusta, GA, USA, <sup>2</sup>Pathology, Medical College of Georgia, Augusta, GA, USA, <sup>3</sup>Medicine, Medical College of Georgia, Augusta, GA, USA.

Glucose-dependent insulintropic peptide (GIP) is an incretin hormone secreted from the endocrine cells in the intestine in response to meals. The GIP receptor (GIPR) belongs to the Gprotein-coupled seven transmembrane domain family of receptors that also includes such bone-active hormones as calcitonin and PTH/PTHrP. The GIPR is widely distributed in the body including in the pancreatic islets, brain, intestine and vasculature. Our group was the first to report GIPR expression in osteoblasts and osteoclasts as well as the fact that GIP stimulates bone formation and inhibits bone breakdown. The expression, regulation and signaling characteristics of pancreatic islet GIPR has been reported and splicing variants of the receptor are known to exist but little characterization of the GIPR present in bone cells has been performed previously.

We cloned the mouse GIP receptor (GIPR) complete cDNA by RT-PCR in combination with 5' and 3' RACE using mouse gut total RNA as template. The primers were based on NCBI sequence XM\_884678.2. First, we used primers to clone the coding sequence, and then used 5' RACE to determine the transcription start site; finally 3' RACE was used to decide where transcription ended. We found that our cloned GIPR was 14 bp longer in the 5' end and 121 bp shorter in the 3' end in comparison with the predicted sequence. To characterize the cloned mouse GIPR, we isolated GIPR-expressing stable cell lines after transfecting CHO cells with a plasmid in which the cloned GIPR was inserted into pcDNA3.1 under the control of the CMV promoter. We tested its functionality using [<sup>125</sup>I]-GIP for binding studies and measuring known GIP signaling pathways: intracellular calcium, cAMP and ERK phosphorylation after GIP stimulation. Signaling characteristics of the mouse GIPR were similar to those previously reported for rat and human GIPR, with significant stimulation of all three signaling pathways. To determine how GIPR transcription is regulated in MC3T3 cells (a mouse osteoblastic cell line), we generated a series of GIPR promoter-luciferase reporter constructs. Our data demonstrate that SP1 is a powerful positive regulator while a series of repressive elements are located more upstream. Our data would suggest that osteoblastic GIPR is regulated in a similar fashion to the GIPR present in other tissues in the body.

**Disclosures:** C.M. Isales, None.

## SU027

**Protein Kinase D Regulates Histone Deacetylase 7 Localization and Interaction with Runx2 During Bone Morphogenic Protein 2-Stimulated Osteogenesis.** E. D. Jensen<sup>\*1</sup>, R. Gopalakrishnan<sup>1</sup>, J. J. Westendorf<sup>2</sup>. <sup>1</sup>Oral and Maxillofacial Pathology, University of Minnesota School of Dentistry, Minneapolis, MN, USA, <sup>2</sup>Department of Orthopedics, The Mayo Clinic, Rochester, MN, USA.

The transcriptional activity of Runx2 in osteoblasts is determined by associations with co-repressors including histone deacetylase 7 (HDAC7). We previously found that HDAC7 suppression increases the expression of osteoblast maturation genes in bone morphogenic protein 2 (BMP2) stimulated cells. We also found that BMP2 induces export of HDAC7 from the nucleus of osteoblasts and osteoblast progenitors. In this study we demonstrate that BMP2 specifically stimulates redistribution of HDAC7 but not HDAC 4, 5 or 6. We found that HDAC7 subcellular redistribution requires Crm-1 mediated nuclear export, is associated with increased HDAC7 serine phosphorylation, and requires conserved serines in the HDAC7 amino-terminus. To understand the molecular mechanisms of BMP2-induced export of HDAC7, we tested a variety of kinase inhibitors. Only two inhibitors had measurable effects. A CaMK inhibitor (KN93) enhanced basal localization of HDAC7 to the nucleus but did not inhibit export of HDAC7 from the nucleus. In contrast, the PKD inhibitor Gö6976 blocked both basal and BMP2-directed HDAC7 nuclear export. In accord, a constitutively active form of PKD1 stimulated nuclear export of wildtype HDAC7, but not of a mutant HDAC7 protein lacking four serines within consensus PKD phosphorylation sites. Protein Kinase D1 (PKD1) associated with HDAC7 in a BMP2-enhanced manner. Further, constitutively active PKD1 inhibited repression of Runx2-mediated transcription by HDAC7. Inhibition of PKD by Gö6976 severely impaired BMP2 induced osteoblast gene expression. Suppression of HDAC7 did not rescue BMP2 induction of osteoblast marker genes in Gö6976-treated cells, suggesting that PKD-dependent factors beyond attenuation of HDAC7 repressive activity are required for osteoblast differentiation. These results establish a novel pathway by which BMP2 signaling regulates Runx2 activity and gene expression in osseous cells via PKD-dependent inhibition of HDAC7 transcriptional repression.

**Disclosures:** E.D. Jensen, None.

## SU028

**Engineering Mice with Multiple BAC Fluorescent Protein Reporter Gene Elements.** P. Maye, M. L. Stover\*, Y. Liu\*, D. Rowe, A. Lichtler. Reconstructive Sciences, UCONN Health Center, Farmington, CT, USA.

Reporter gene mice are valuable animal models for biological research providing a gene expression readout that can contribute to cellular identity within the context of a developmental process. With the advancement of bacterial recombination techniques to engineer reporter gene constructs from BAC genomic clones and the generation of optically distinguishable fluorescent protein reporter genes, there is an unprecedented capability to engineer more informative transgenic reporter mouse models relative to what has been traditionally carried out. We present here the development of a three stage bacterial recombination strategy to physically link multiple genes together with their respective fluorescent protein (FP) reporters in one DNA fragment for the generation of animal models with two to three reporter gene readouts. To test this concept, we have linked two genomic fragments together, one of which contains the TRAP gene and the other DNA fragment contains the genes DMP1 and IBSP. TRAP, DMP1, and IBSP drive the expression of ECFP, mCherry, and Topaz fluorescent protein reporter genes, respectively. We have successfully generated transgenic reporter mice that retain two to three gene readouts. While we continue to characterize these transgenic lines, our analysis suggests that in most mouse lines fluorescent protein reporters from the DMP1-IBSP genomic fragment are strongly expressed in a predictable fashion, while expression of TRAP-ECFP can be more difficult to detect being expressed at lower levels and is best visualized in younger animals. However, the accuracy of TRAP-ECFP expression shows excellent correspondence with histological staining for endogenous TRAP activity. Calvaria and stromal cell cultures derived from these transgenic mouse lines allow easy detection of IBSP and DMP1 expression thereby allowing the visualization and study of osteoblasts and osteocytes *in vitro*. Moreover, these animal models have proven to be an excellent tool for assessing the osteogenic potential of progenitor cells in transplantation studies. Details of the methodology and characterization of different transgenic lines will be presented.

**Disclosures:** P. Maye, None.

## SU029

**Twist1 Haploinsufficiency Is Associated with Reduced IGF1 Levels and an Osteoporotic Phenotype.** J. Connerney<sup>\*1</sup>, V. Andreeva<sup>\*1</sup>, K. Dowell<sup>\*1</sup>, W. G. Beamer<sup>2</sup>, C. J. Rosen<sup>1</sup>, D. B. Spicer<sup>1</sup>. <sup>1</sup>Center for Molecular Medicine, Maine Medical Center Research Institute, Scarborough, ME, USA, <sup>2</sup>The Jackson Laboratory, Bar Harbor, ME, USA.

Haploinsufficiency of the basic-Helix-Loop-Helix (bHLH) transcription factor Twist1 is associated with Saethre-Chotzen syndrome, which is characterized by premature fusion of the calvaria sutures, termed craniosynostosis. Craniosynostosis occurs around birth, and hence the vast majority of studies have focused on the role of Twist1 during embryonic development and infancy, with very few studies being done in the adult in either mice or humans. Here we have investigated whether *Twist1* haploinsufficiency affects the phenotype of the bones in adult mice. Femurs of wild type and Twist1<sup>+/−</sup> mice were analyzed at 5, 8, and 16 weeks old. At all time points the Twist1<sup>+/−</sup> mice had less body weight than wild type mice, and this was most significant at 16 weeks (p value=.0003). MicroCT analysis of femurs at 5 weeks indicated that Twist1<sup>+/−</sup> mice had significantly less total trabecular volume (p value=.048), trabecular number (p value=.043), mid-shaft cross-sectional area (p value=.025), mid-shaft cortical area (p value=.041), and mid-shaft marrow area (p value=.05) than wild type mice. Bone mineral density (BMD) and percent marrow fat were determined in 8 week and 16 week old mice using a DEXA scan (PIXIMUS). Bones were also analyzed by magnetic resonance imaging (MRI) with transversal measurements of cortical bone and percent marrow fat. Twist1<sup>+/−</sup> mice had lower BMD than wild type mice at 8 weeks, although it was not quite significant, and by 16 weeks it was significantly lower (p value=.0047). The percent marrow fat was not different from wild type mice at 8 weeks, however there was a significant decrease in the Twist1<sup>+/−</sup> mice at 16 weeks (p value=.0017). The decrease in marrow fat was also observed by MRI. Twist1 has been implicated in regulating TNF $\alpha$  expression, however levels of TNF $\alpha$  were similar in Twist1<sup>+/−</sup> and wild type mice. In contrast, serum IGF1 levels were significantly lower in the Twist1<sup>+/−</sup> mice (p value=.0049), which may at least partially account for the bone phenotype in these mice. The effect on both BMD and marrow fat suggests that Twist1 function is required for correct specification and/or differentiation of the bone marrow mesenchymal stem cells.

**Disclosures:** D.B. Spicer, None.  
This study received funding from: NIH.

## SU030

**The Atypical Antipsychotic Clozapine Reduces Rat Osteoblast Proliferation and Osteoclastogenesis at Therapeutic Levels.** J. L. Costa<sup>1</sup>, G. Smith<sup>\*2</sup>, K. Callon<sup>\*1</sup>, J. M. Lin<sup>\*1</sup>, M. Watson<sup>\*1</sup>, P. Shepherd<sup>\*2</sup>, J. Cornish<sup>1</sup>. <sup>1</sup>Medicine, University of Auckland, Auckland, New Zealand, <sup>2</sup>Molecular Medicine and Pathology, University of Auckland, Auckland, New Zealand.

Atypical antipsychotic drugs (AADs) such as clozapine are now widely used in the treatment of schizophrenia, which affects >1% of the world population and has been associated with an increased risk of fracture. Serotonergic signalling has been implicated in regulation of bone mass, so AADs, which are anti-serotonergic, may adversely affect bone mass. In this study, we assessed the skeletal effects of clozapine *in vivo* and *in vitro*, and the effects of haloperidol and quetiapine *in vivo*. Adolescent rats received daily subcutaneous injections of clozapine (10mg/kg), haloperidol (0.25mg/kg), quetiapine (10mg/kg) or vehicle for 28 days, yielding circulating levels similar to therapeutic levels found in human serum. Only haloperidol and clozapine treatment reduced body weight; neither haloperidol nor quetiapine treatment affected bone mass. Compared to vehicle treated controls, however, clozapine significantly reduced bone mineral content (2.03 g  $\pm$  0.06 vs 2.19  $\pm$  0.004, p<0.05) and whole body bone density (0.13 g/cm<sup>2</sup>  $\pm$  0.001 vs 0.14 g/cm<sup>2</sup>  $\pm$  0.002, p<0.01) as measured by DXA. The skeletal effects of clozapine may be in part mediated by indirect endocrine mechanisms, as serum corticosterone levels were higher (371 ng/ml  $\pm$  48 vs 224 ng/ml  $\pm$  18, p<0.001) and testosterone levels were lower (192 pg/ml  $\pm$  50 vs 630  $\pm$  136, p<0.01) after 7 daily injections with clozapine, compared to control animals. However, clozapine may also act directly on bone. We found that clozapine (0.1 $\mu$ M- 10 $\mu$ M) dose-dependently reduced proliferation of primary rat osteoblasts (ROb), by up to 88%. In preliminary experiments, these doses of clozapine also increased apoptosis of ROB, and reduced osteoclastogenesis in murine bone marrow cultures. Taken together, these data suggest that clozapine exerts adverse skeletal effects by both indirect and direct mechanisms in rodents, the latter potentially by its anti-serotonergic actions. Long-term clozapine treatment for schizophrenia in humans may therefore have detrimental effects on bone health.

**Disclosures:** J.L. Costa, None.

## SU031

**Prostaglandins Enhance Extracellular Matrix Mineralization Through the Enhancement of Both Na-dependent Phosphate Transport Activity and ALP Activity in Osteoblast-like Cells.** S. Asano, S. Sekiguchi, M. Shibata, A. Yokoyama\*, K. Inagaki\*, H. Kakizawa\*, N. Hayakawa\*, N. Oda\*, A. Suzuki, M. Itoh\*. Department of Internal Medicine, Fujita Health University, Aichi, Japan.

Prostaglandins (PGs) are important regulators of bone formation and resorption. Among them, PGD<sub>2</sub> and PGF<sub>2 $\alpha$</sub>  have been reported to be released from osteoblastic cells, and to stimulate the proliferation of these cells. Inorganic phosphate (Pi) transport probably represents an important function of bone forming cells in relation to extracellular matrix mineralization. We have previously reported that both PGD<sub>2</sub> and PGF<sub>2 $\alpha$</sub>  stimulate Na-

dependent Pi transport in MC3T3-E1 osteoblast-like cells. In the present study, we additionally investigated the effect of these PGs on Pi transport in osteoblast-like MC3T3-E1 cells and their effects on their extracellular mineralization. Both PGD<sub>2</sub> and PGF<sub>2 $\alpha$</sub>  stimulated Na-dependent Pi transport dose-dependently in the range between 10<sup>-10</sup> M and 10<sup>-6</sup> M in MC3T3-E1 cells. The effect of PGF<sub>2 $\alpha$</sub>  was time-dependent up to 24 h, but the effect of PGD<sub>2</sub> showed its peak at 6 h, and then decreased to base line at additional 24 h. The long-term treatment with PGF<sub>2 $\alpha$</sub>  and PGD<sub>2</sub> stimulated the calcification of MC3T3-E1 cells in the range between 10<sup>-10</sup> M and 10<sup>-6</sup> M. Phosphonoformic acid, an inhibitor for Pit-1, attenuated the mineralization by PGs. These PGs stimulated proliferation and suppressed alkaline phosphatase (ALP) activity during proliferative phase, but enhanced ALP activity in the phase of differentiation.

In summary, these results suggest that PGD<sub>2</sub> and PGF<sub>2 $\alpha$</sub>  stimulate the proliferation of osteoblast-like cells, and enhance the extracellular matrix mineralization through the enhancement of both Na-dependent phosphate transport activity and ALP activity.

**Disclosures:** S. Asano, None.

## SU032

**Substance P Stimulates Bone Marrow Stromal Cell Osteogenic Activity and Osteoclast Differentiation and Function *in vitro*.** L. Wang, R. Zhao, X. Shi\*, W. S. Kingery. PM&R Service (117), VAPAHCS, Palo Alto, CA, USA.

Substance P (SP) is a neuropeptide richly distributed in the sensory nerve fibers innervating the medullar tissues of bone as well as the periosteum. It has been proposed that this sensory neuron-osseal network is involved in modulating bone remodeling. Our previous studies demonstrated that inhibition of neuropeptide signaling after capsaicin treatment or chronic administration of a SP receptor antagonist resulted in a loss of bone mass and a reduction in bone strength in mature rat limbs. We therefore hypothesized that SP plays an important role in maintaining bone integrity through regulating osteogenesis and osteoclastogenesis. To test this hypothesis, primary bone marrow stromal cells (BMSC) and macrophages (BMM) were cultured from the long bones of the 6 week-old C57BL/6 mice. Immunocytochemical staining and RT-PCR demonstrated that NK1, a SP preferred receptor, localized on the plasma membrane and in the cytoplasm of primary mouse osteoblasts and osteoclasts. SP treatment stimulated BMSC proliferation on BrdU incorporation in a dose-dependent manner. The osteogenic effects of continuous exposure to SP (10<sup>-8</sup>-10<sup>-12</sup>M) were examined after 7, 14, and 21 days of BMSC culture. The 10<sup>-12</sup>M concentration of SP had the greatest stimulatory effect on BMSC differentiation by significantly increasing alkaline phosphatase (ALP) activity and stimulating ALP and osteocalcin gene expression after 14 and 21 days. The effect of SP on osteoclast differentiation and function was also studied. SP dose-dependently increased tartrate-resistant acid phosphatase (TRAP)-positive multinucleated cells and increased total pit erosion area on dentine discs in the BMM culture in the presence of M-CSF and RANKL. Furthermore, SP stimulated protein production of RANKL in the BMM culture in a dose dependent manner. In conclusion, NK1 receptors are expressed by primary osteoblasts and osteoclast precursors. SP stimulated osteoblast and osteoclast differentiation and function *in vitro*. SP neurotransmitter release from sensory neurons could potentially regulate local bone turnover *in vivo*.

**Disclosures:** L. Wang, None.

## SU033

**Calcitonin-Gen Related Peptide (CGRP) Stimulates Osteogenesis and Inhibits Osteoclastogenesis *in vitro*.** L. Wang, X. Shi\*, R. Zhao, W. S. Kingery. PM&R Service (117), VAPAHCS, Palo Alto, CA, USA.

CGRP is a neuropeptide richly distributed in sensory nerve fibers innervating the medullar tissues of bone as well as the periosteum. It has been proposed that this sensory neuron-osseal network is involved in modulating bone remodeling. Previously we observed that inhibition of neuropeptide signaling after capsaicin treatment or sciatic nerve section resulted in a reduction of trabecular bone mass and hypothesized that CGRP plays an important role in maintaining bone integrity. To better understand the effects of CGRP signaling at the cellular level we examined the effects of CGRP on osteogenesis and osteoclastogenesis *in vitro*. Bone marrow stromal cells (BMSC) and macrophages (BMM) were cultured from mouse long bones. Immunocytochemical staining and real time PCR demonstrated expression of the CGRP receptor calcitonin receptor-like receptor (CRLR) and its chaperone receptor activity modifying protein (RAMP1), co-localized on the plasma membrane and in the cytoplasm of primary osteoblasts and osteoclasts. CGRP treatment stimulated BMSC proliferation on the BrdU assay and increased alkaline phosphatase (ALP) activity, at day 14 to day 21 of cell culture, in a dose-dependent manner. CGRP treatment also upregulated the expression of ALP, osteocalcin, collagen type I, and RUNX2 mRNA in the BMSC at day 7 and 14. Furthermore, CGRP treatment dose-dependently inhibited the generation of functional osteoclasts from BMM cultures. CGRP significantly decreased tartrate-resistant acid phosphatase (TRAP)-positive multinucleated cells and decreased bone resorption activity. In addition, levels of osteoclastic genes like TRAP and Cathepsin K mRNA were significantly down-regulated by CGRP. Collectively, these data confirm that CGRP has the potential to maintain a positive bone mass by directly stimulating BMSC proliferation and osteoprogenitor cell differentiation and inhibiting osteoclastogenesis by decreasing osteoclast number and resorption activity.

**Disclosures:** L. Wang, None.

## SU034

**Menaquinone-4 Derived from Phylloquinone Regulates Osteoblast Function.** K. Nakagawa\*, N. Sawada\*, Y. Suhara\*, T. Okano. Hygienic Sciences, Kobe Pharmaceutical University, Kobe, Japan.

Vitamin K serves as a coenzyme for vitamin K-dependent carboxylase (gamma-glutamyl carboxylase : GGCX). GGCX converts glutamate residues into gamma-carboxyglutamate (Gla) residues in vitamin K-dependent proteins, such as blood coagulation factors (prothrombin, factors IX and X) and bone formation factors (osteocalcin and matrix Gla protein). Thus, vitamin K may exert beneficial effects on bone formation and remodeling. There are two forms of naturally occurring vitamin K, phylloquinone (PK) and menaquinones (MK-n). Moreover, menadiolone or vitamin K3 (K3) is a synthetic compound lacking a side chain. Clinically, MK-4 the most common form of vitamin K, has been shown to prevent bone fractures. This osteoprotective effect is more pronounced in MK-4 than in PK, and hence MK-4 has been used to treat osteoporotic patients in Japan. MK-4 has been shown to act as a ligand for the steroid and xenobiotic receptor (SXR) in human osteoblastic cells. It transcriptionally regulates gene expression and represents a new pathway of vitamin K action. Recently, we demonstrated that deuterium labeled-PK (PK-d7) and deuterium labeled-K3 (K3-d8) administration resulted in the accumulation of MK-4-d7 in tissues [J.Biol.Chem. 283, 11270-11279, (2008)], particularly in liver, brain and bone. Moreover, K3-d8 was converted into MK-4-d7 in human osteoblast-like MG-63 cells. This is the first direct evidence using deuterium labeled compounds and LC-APCI-MS/MS analysis demonstrating that PK and K3 are converted into MK-4 in bone, especially by osteoblasts. To clarify the role of MK-4 biosynthesis in osteoblasts, we examined the biological activity of MK-4 and other vitamin K derivatives in MG-63 cells. We constructed SXR-GAL4 expression vectors containing full-length human SXR and GAL4 DNA-binding site using hybrid luciferase assay system. As a result, MK-4 was shown to be most active in terms of SXR-mediated transcriptional activity. GGCX activity and calcification-inducing activity in MG-63 cells. In LC-APCI-MS/MS analysis, K3 was converted into MK-4 in a dose-dependent fashion in MG-63 cells. The cells treated with K3-d8 significantly increased transcriptional activity in SXR-GAL4 hybrid luciferase assay. These results suggest that MK-4 derived from K3, functions as a ligand of SXR and as a cofactor of GGCX for bone formation by osteoblasts. Our results indicate that MK-4 is a true physiologically active form of vitamin K for bone formation and originated from dietary vitamin K.

**Disclosures:** K. Nakagawa, None.

## SU035

**Angiopietin-1 Enhanced Bone Morphogenetic Protein-2 Induced Osteoblast Differentiation.** I. Bae\*, B. Jeong\*, Y. Kim\*, R. T. Franceschi<sup>2</sup>, G. Koh\*, J. Koh<sup>1</sup>. <sup>1</sup>Pharmacology and Dental Therapeutics, Dental Science Research Institution and Brain Korea 21 Project, Chonnam National University Dental School, Gwangju, Republic of Korea, <sup>2</sup>Periodontics and Oral Medicine, University of Michigan Dental School, Ann Arbor, MI, USA, <sup>3</sup>Korea Advanced Institute of Science and Technology, Daejeon, Republic of Korea.

In process of bone development and fracture healing, vascular formation (angiogenesis) preceded bone formation. However, roles of angiogenic factors in bone formation are not fully determined. This study was designed to examine whether angiopietin-1 (Ang-1), an important modulator of vascular homeostasis and angiogenesis, is involved in bone morphogenetic protein (BMP)-2 induced osteoblast differentiation using a soluble, stable, and potent Ang-1 variant, replacing the N-terminal portion of Ang-1 with short coiled-coil domain of cartilage oligomeric matrix protein (COMP). In osteoblast-like cell lines and primary calvarial cells, expression of Ang-1 and its Tie-2 receptor mRNA was screened by RT-PCR analysis, and was also monitored during osteoblast differentiation induced by BMP-2 and/or ascorbic acid (AA) and  $\beta$ -glycerolphosphate (GP). C3H10T1/2 and C2C12 cells showed strong expression of Tie-2 mRNA. Under the presence of BMP-2 and/or AA and b-GP, expression of Ang-1 and Tie-2 mRNA increased with induction of alkaline phosphatase (ALP) and osteocalcin (OC) mRNA in C3H10T1/2 and primary mouse calvarial cells. Overexpression of Comp-Ang-1 using adenoviral vectors significantly enhanced BMP2-induced ALP activity and OC production, as well as formation of mineralized nodules. Promoter study also revealed that Comp-Ang-1 stimulated the BMP-2 transactivation of OG2 and 6xOSE promoter genes. In Western blot analysis, Comp-Ang-1 enhanced BMP-2 induction of p38 MAPK and Akt phosphorylation in C3H10T1/2 cells. These results suggest that Ang-1 can enhance BMP-2 induced osteoblast differentiation through MAPK and Akt pathways. The study was supported by BK21 project for school of dentistry funded by the Korea government.

**Disclosures:** I. Bae, None.

## SU036

**SOST Blocks GSK3-beta Inhibitor-Induced Alkaline Phosphatase Activity.** T. Grabenstaetter\*, Y. Sakane\*, C. Jacobi\*, C. Lu\*, A. Bauer\*, C. Fernandez\*, P. Ramage\*, L. Hartmann\*, O. Leupin<sup>1</sup>, M. Kneissel<sup>1</sup>, C. Halleux<sup>1</sup>. <sup>1</sup>Novartis Institutes for BioMedical Research, Basel, Switzerland, <sup>2</sup>Novartis Institutes for BioMedical Research, Sanghai, China, <sup>3</sup>Cellzome AG, Heidelberg, Germany.

SOST is a selective, potent osteocyte secreted negative regulator of bone formation. It was initially thought to act in adult bone as a BMP antagonist. Subsequently, SOST was found to bind to LRP5/6 *in vitro* and to antagonize canonical Wnt signaling downstream of BMP signaling. The rationale that SOST might impact adult bone formation by inhibition of canonical Wnt signaling is supported by the phenotypic overlap in human bone overgrowth disorders related to loss-of-function mutations in *SOST* and gain-of-function mutations in *LRP5*. In the present study, we examined how SOST exerts its inhibitory effect on alkaline phosphatase (ALP) and mineralization in UMR106 and MC3T3-E1-1b osteoblastic cell lines. We found that SOST potently inhibited Wnt1-induced Supertopflash reporter activity in UMR106 cells. It inhibited mineralization in this cell line in absence of exogenous BMP or Wnt. Likewise, SOST inhibited BMP2-induced mineralization in MC3T3 cells. Furthermore, SOST inhibited BMP2- and Wnt3a-induced ALP activity. The BMP antagonist noggin blocked BMP-2-induced but not Wnt3a-induced ALP activity. SOST decreased Wnt3a-induced ALP activity in the presence of noggin confirming its action downstream of BMP receptors. LRP5/6 antagonist Dkk1 and SOST additively decreased BMP2- and Wnt3a-induced ALP activity. An LRP5/6 antibody partially decreased Wnt3a-induced ALP, confirming that LRP5/6 are, at least partially, implicated in Wnt3a-induced ALP activation. However, we found that SOST is still fully inhibitory when ALP activity was induced downstream of LRP5/6 by blocking GSK3-beta with lithium chloride or GSK3-inhibitor IX. Interestingly, we found ALP to be a putative interaction partner for SOST in addition to LRP5/6 in a proteomic approach consisting of the purification of expressed TAP tagged SOST in UMR106 cells. In line with this notion, we observed in a biochemical ALP assay, that SOST weakly inhibited ALP activity. In conclusion, we corroborate that SOST can inhibit Wnt signaling induction of ALP downstream of BMP signaling. However, we also find that SOST is able to inhibit ALP activity downstream or independently of GSK3-beta. Our data raise the possibility that SOST may bind ligands beyond LRP5/6 to exert its action in bone. Such a hypothesis is supported by our observation that SOST, aside from a disulphide-linked core, is largely unstructured according to NMR based studies, a characteristic that is frequently observed in proteins involved in protein-protein interactions and would therefore suggest SOST binding to one or more different proteins.

**Disclosures:** C. Halleux, None.

## SU037

**Neuroendocrine Activation of AMP-activated Protein Kinase (AMPK) in Osteoblasts.** M. Shah\*, B. Kola\*, A. Suters\*, M. Korbonits\*, C. C. Chen<sup>1</sup>. <sup>1</sup>VBS, Royal Veterinary College, London, United Kingdom, <sup>2</sup>Department of Endocrinology, Queen Mary's School of Medicine and Dentistry, London, United Kingdom.

Adenosine 5'-monophosphate-activated protein kinase (AMPK), a regulator of energy homeostasis, has a central role in mediating the appetite-modulating and metabolic effects of many hormones and neuromodulators, including leptin, ghrelin, and noradrenalin, as well as the antidiabetic drugs metformin and glitazones. Since all these compounds also regulate bone mass, we tested whether AMPK is activated in osteoblasts in response to these hormones and antidiabetic drugs and whether stimulation of AMPK activity in osteoblasts plays a role their function. Two osteoblastic cell lines UMR106 and ROS 17/2.8 rat osteosarcoma cell lines, as well as osteoblasts isolated from new-born rat calvaria, were cultured in the presence of various hormones and neuromodulators. AMPK activity in cell lysates was measured by a functional kinase assay using SAMS, a synthetic peptide substrate of AMPK, as well as by western blotting using an antibody recognizing AMPK $\alpha$  phosphorylated at Thr-172. Osteoblast cell proliferation was determined by cell counting using the "In Cyto" system, while osteoblast differentiation was evaluated by alkaline phosphatase activity. We first showed that treatment of osteoblastic cell lines for 1 hour with AICAR, a cell-permeable analogue of natural activator AMP, stimulates Thr-172 phosphorylation of AMPK and dose-dependently increases its activity. Both propranolol (a non-specific beta-adrenergic antagonist) and ghrelin (a growth hormone secretagogue and orexigenic hormone) dose-dependently stimulated AMPK activity in osteoblastic cells. In contrast, we did not show any effect of estrogens or dexamethasone on AMPK activity in osteoblasts. Stimulation of AMPK activity in osteoblasts was associated with decreased proliferation but increased differentiation. The antidiabetic drug metformin also dose-dependently stimulated AMPK activity and osteoblast differentiation. Interestingly, AMPK phosphorylation and activity were upregulated in osteoblasts when subjected to mechanical loading *in vitro*. Our preliminary results in primary osteoblasts derived from rat calvaria suggest that the effects of propranolol and ghrelin effects on AMPK activation may be dependent on the state of osteoblast differentiation. Our results confirm the existence of a hormonal link between bone mass and energy metabolism and are consistent with AMPK playing a role in osteoblast function. Further studies will determine the role of AMPK in skeletal physiology.

**Disclosures:** M. Shah, None.

## SU038

### Synergistic Activation of Osteogenesis in Multi-Lineage Progenitor Cells by Oxysterols. W. Huang, R. Jarrahy\*, G. H. Rudkin\*, D. T. Yamaguchi, T. A. Miller\*. VA Greater LA Healthcare Systems, Los Angeles, CA, USA.

Oxysterols are naturally occurring cholesterol oxidation products capable of inducing osteogenic differentiation. The purpose of this study is to examine the effect of oxysterols on osteogenic differentiation of Multi-lineage Progenitor cells (MLPC), a cell line that is isolated from post-partum human umbilical cord blood and capable of differentiating into various tissue types. We also compared the effect of oxysterols on MLPCs cultured on two- and three-dimensional systems.

MLPCs (BioE, Inc) were cultured in alpha-MEM medium containing 20% FBS. One day after cells were seeded onto PLGA films or scaffolds, osteogenic differentiation medium was added to induce differentiation. Cells were pulse-treated with 10  $\mu$ m of various oxysterols or their equal ratio mixture for a period of 3 days. Cells were then harvested at day 1, 3, 7, 10, and 14 for total RNA preparation. Real-time RT-PCR assay was performed to examine expression of osteogenic marker genes. At day 14, some cultures were histologically processed and stained with Alizarin Red for Mineralization.

When MLPCs grown on PLGA films were treated with individual isomers of oxysterols (20S, 22S, and 22R), there were modest increases (2-4-fold) in expression of osteoblastic marker genes, including Cbfa-1, alkaline phosphatase (ALP), bone sialoprotein (BSP) and osteocalcin (OCN). The increases were 2-3 fold greater when cells were grown in 3-D PLGA scaffolds. Strikingly, when both 2-D and 3-D cultured cells were treated with an equal ratio mixture of three oxysterol isomers, there was an additional 10-20-fold increase on top of the increase induced by individual isomers. In addition, the oxysterol mixture induced robust mineralization of MLPC cells grown both on 2-D and 3-D cultures in comparison to modest mineralization caused by individual isomers. The synergistic effect of the oxysterol mixture is partially mediated by ERK MAP kinase.

Collectively, our data indicate that oxysterols, especially their equal-ratio mixtures, have a great potential to healing bony defect. The potent osteo-inductive activity of oxysterols on 3-D cultured MLPC makes them ideal candidates for creating a clinically useful bone graft substitute.

**Disclosures:** W. Huang, None.

*This study received funding from: VA Merit Review.*

## SU039

### The Role of Cell Surface ATP Synthase in Fluid Shear Stress Induced ATP Release in Osteoblasts. S. Majumdar, K. Czymbek\*, M. Malik\*, R. L. Duncan. Biological sciences, University of Delaware, Newark, DE, USA.

Bone formation is tightly controlled by the mechanical environment of the skeleton and is mediated through activation of osteoblasts. One of its initial osteoblastic responses to fluid shear stress (FSS) is the vesicular release of ATP from the cell and data from our lab, as well as numerous others, indicate that binding of this nucleotide to purinergic receptors is essential for mechanotransduction in bone. While these data highlight the importance of ATP signaling in the mechanosensitivity of bone, the mechanism of ATP release remains elusive. Caveolin 1 is a membrane protein present in lipid rafts and intracellular vesicles that has been implicated in several signaling functions in osteoblasts. The recent discovery of ATP synthase on the cell surface of many cell types has led us to postulate that ATP synthase on the membrane of osteoblasts is scaffolded by caveolin 1 and is critical for vesicular ATP release into the extracellular milieu as well as in the formation of ATP filled vesicles in preparation for release. Using both immunofluorescence and western analyses, we found ATP synthase to be present on the cell membrane of MC3T3-E1 osteoblasts. Co-immunoprecipitation and imaging studies demonstrated that ATP synthase and caveolin 1 co-immunoprecipitate and that ATP synthase appears to be closely associated with lipid rafts on the cell surface. Transmission electron microscopy demonstrated that caveolin 1 was on both the surface and cytoplasmic vesicles in static cells and that subjecting MC3T3-E1 cells to 12 dynes/cm<sup>2</sup> FSS increased the number of vesicles in the cell, suggesting that FSS may increase recycling of caveolin 1 scaffolds. Quinacrine staining of acidic vesicles, denoting the presence of ATP loaded vesicles indicated that FSS rapidly depletes these vesicles in osteoblasts, but addition of methyl  $\beta$ -cyclodextrin, a cholesterol chelating agent which disrupts lipid rafts, greatly enhanced the number and the size of these ATP filled vesicles. These data suggest that dissociating ATP synthase from lipid rafts on the membrane causes more caveolin 1-ATP synthase (CAS) vesicles to accumulate in the cytoplasm and increase the amount of ATP loaded into each individual vesicle. This mechanism may be central to ATP packaging into CAS vesicles for shear challenge and subsequent activation of purinergic signaling to elicit an anabolic response of the bone as a result

**Disclosures:** S. Majumdar, None.

*This study received funding from: R01AR043222.*

## SU040

### P2X<sub>7</sub> Receptor Activation Mediates PKC $\alpha$ Translocation in Osteoblasts Through Alteration in Actin Cytoskeletal Organization. V. P. Fomin, P. Timothee\*, K. Czymbek\*, R. L. Duncan. Biological Sciences, University of Delaware, Newark, DE, USA.

Osteoblasts respond to mechanical load with a rapid increase in intracellular calcium concentration ([Ca<sup>2+</sup>]<sub>i</sub>) that is essential for load-induced bone formation. This increase in Ca<sup>2+</sup><sub>i</sub> induces vesicular release of ATP that, in turn, stimulates bone cells in an autocrine/paracrine manner through activation of purinergic receptors, P2X or P2Y. P2X receptors

are ligand-gated channels while P2Y receptors are G-protein coupled receptors. While we have shown that the P2X<sub>7</sub> receptors are essential for the response of the skeleton to mechanical loads, activation of second messenger systems, such as protein kinases A and C (PKA and PKC), are also necessary for the complete response of osteoblasts to load. Since activation of PKC and PKA is dependent on activation of G-protein coupled receptors, we predicted that P2Y receptors would be responsible for the mechanically-induced activation of PKC in osteoblasts. To test whether stimulation of purinergic receptors causes activation and translocation of PKC, primarily PKC $\alpha$ , in osteoblasts we infected MC3T3-E1 preosteoblastic cells with an adenoviral cDNA construct for PKC $\alpha$ -GFP to monitor the kinase in live osteoblasts. The PKC $\alpha$ -GFP infected osteoblasts were also loaded with Ca<sup>2+</sup> fluorescent indicator, Fura Red, to allow simultaneous imaging of PKC $\alpha$  translocation and [Ca<sup>2+</sup>]<sub>i</sub>. When 0.5mM ATP was added to infected MC3T3-E1 osteoblasts, a rapid increase in [Ca<sup>2+</sup>]<sub>i</sub> was observed with no change in PKC $\alpha$  distribution within the cell. However, addition of 0.5mM BzATP, a specific agonist for P2X<sub>7</sub> receptors, produced rapid increase in [Ca<sup>2+</sup>]<sub>i</sub> followed by translocation of PKC $\alpha$  to the cell periphery. This effect of BzATP on PKC $\alpha$  translocation was abrogated by addition of the Rho kinase (ROCK) inhibitor, Y27632, suggesting an involvement of the actin cytoskeleton in the regulation of PKC $\alpha$  translocation. While these findings are contradictory to our hypothesis that a G-protein coupled purinergic receptor must be involved in PKC activation in the osteoblast, these data are supportive of the role of P2X<sub>7</sub> in the regulation of the cellular response to mechanical loading. However, the translocation of PKC $\alpha$  may be an indirect response of changes in the actin cytoskeleton, possibly through activation of myosin light chain kinase, to increase the cellular tension.

**Disclosures:** V.P. Fomin, None.

*This study received funding from: NIH DK058246.*

## SU041

### Characterization of Osteoblastic Properties of 7F2 and UMR-106 Cultures after Acclimation to Reduced Levels of Fetal Bovine Serum. S. Ganguly\*, L. A. Ashley\*, G. C. Howard\*, R. D. Grey\*, C. M. Pendleton\*, L. D. Castle\*, M. E. Fultz\*, D. K. Peyton\*, D. L. DeMoss. Biological Sciences, Morehead State University, Morehead, KY, USA.

Estrogen plays an important role in skeletal physiology by maintaining a remodeling balance between the activity of osteoblasts and osteoclasts. In an attempt to decipher the mechanism through which estrogen elicits its action on osteoblasts, experimentation necessitated the development of a culturing environment reduced in estrogenic compounds. The selected media (OPTI-MEM) is enriched to sustain cultures under reduced fetal bovine serum (FBS) conditions and is devoid of the pH indicator phenol red, a suspected estrogenic agent. This protocol reduced the concentration of FBS supplementation to 0% through successive, 24-hour incubations with diminishing amounts of total FBS (1%, 0.1%, and 0%) and incorporated the use of charcoal filtered FBS for comparative purposes. The protocol does not appear to alter the viability, cell morphology or osteoblast-like phenotype of 7F2 and UMR-106 cell lines when compared to control cells grown in various concentrations of FBS. Although the rate of mitotic divisions declined, the 7F2 and UMR-106 cultures continued to express osteoblast specific markers and exhibited estrogen responsiveness. Osteoblasts should express characteristic phenotypic markers. Utilizing a variety of techniques, 7F2 and UMR-106 cultures exposed to media devoid of FBS maintained the ability to express the following markers: alkaline phosphatase, osteopontin, receptor activator of nuclear factor (NF)- $\kappa$ B ligand, parathyroid hormone receptor 1, procollagen type I  $\alpha$ 1, runt-related transcription factor 2 and osteocalcin. Cells cultured using this protocol retained the ability to express the specific osteoblastic markers examined and some markers exhibited  $\beta$  estradiol responsiveness. Hence, the cell culture protocol developed allowed cultures to proliferate while maintaining their osteoblastic phenotype and provides an alternative avenue to study the anti-resorptive role of estrogen on skeletal turnover.

**Disclosures:** D.L. DeMoss, None.

## SU042

### Reciprocal Relation Between MR Measures of Marrow Adiposity and Cortical Bone in the Appendicular Skeleton of Healthy Adults. P. P. Campbell\*, D. Lee, S. Bluml\*, T. Wren, V. Gilsanz. Radiology, Childrens Hospital Los Angeles, Los Angeles, CA, USA.

Considerable data indicate that mesenchymal stem cells (MSC) in the bone marrow differentiate into osteoblasts or adipocytes through alternative activation of mutually exclusive transcriptional programs.

Using the three-point Dixon (3PD) magnetic resonance (MR) technique, which provides measures of fat content in any tissue, we examined the relations between marrow adiposity and bone accumulation in the appendicular skeleton. MR measures of percent marrow fat (MF) and cortical bone area (CBA) at the mid-third of the femurs were obtained in 20 healthy white adults (10 females and 10 males), 18-68 years of age.

There were strong negative correlations between values for MF and CBA throughout the MR images at the mid-third of the femurs. This was true for each femur in all subjects;  $r$ 's ranged from -0.6 to -0.9; all  $p$ 's  $\leq$  0.01. When subjects were grouped by gender, the means for the associations between MF and CBA were strongly negative ( $r$  = -0.80 and -0.75 for females and males, respectively; both  $p$ 's  $\leq$  0.001) (see table below). Similar findings were observed when the means for the associations of all males and females were combined, and when the right and left femurs were analyzed independently.

We conclude that the amount of cortical bone in the appendicular skeleton is inversely related to marrow adiposity. These results provide support for the growing body of

evidence indicating an inversely coupled relationship between osteogenesis and adipogenesis in the skeleton.

	Correlations Between MF and CBA		
	Females (n = 10)	Males (n = 10)	Combined (n = 20)
Mean $\pm$ SD	-0.80 $\pm$ 0.12	-0.75 $\pm$ 0.14	-0.76 $\pm$ 0.13
(range)	(-0.55 - -0.97)	(-0.48 - -0.95)	(-0.48 - -0.97)

**Disclosures:** V. Gilsanz, None.

## SU043

**bFGF Induces the Expression of a Subset of Bcl-2 Family Genes to Inhibit the Apoptosis of ATDC5 Chondroprogenitor Cells.** J. Choi<sup>\*1</sup>, H. Kim<sup>\*1</sup>, Y. Kim<sup>\*2</sup>. <sup>1</sup>Biochemistry, Chungbuk National University, Cheong-Ju, Republic of Korea, <sup>2</sup>Orthopaedic, Chungbuk National University, Cheong-Ju, Republic of Korea.

In response to proper extracellular stimuli, chondroprogenitor cell lines such as ATDC5 can be induced either for chondrogenic differentiation or for cellular proliferation. Although Fibroblast Growth factors (FGFs) including basic Fibroblast Growth factor (bFGF) have been known for their pleiotropic effect on the cell survival and apoptosis, the underlying mechanism during this process remains poorly characterized. Through this study using Ribonuclease Protection Assay, Real-Time PCR, FACS and other molecular biology techniques, we attempted to investigate molecular mechanism by which bFGF influenced on a cell physiology of ATDC5 chondroprogenitor cells and induced differential gene expression. A subset of Bcl-2 family genes was found to be up-regulated at the transcription level by bFGF in a NFkB dependent manner. Treatment of siRNAs against these genes attenuates the bFGF mediated protection of ATDC5 cells from apoptosis as assessed by FACS analysis of PI or Annexin-V stained cells. These data suggest a protective role of bFGF in the ATDC5 cell survival through induction of prosurvival Bcl2 family genes. Our findings may provide a therapeutic basis for bFGF in promoting chondrogenic cell survival in inflammatory disease including osteoarthritis.

**Disclosures:** J. Choi, None.

This study received funding from: GRRC Project of Gyeonggi Provincial Government, Korea.

## SU044

**TNF-alpha and IL-1beta Stimulate ALP Activity and Mineralization but Decreases RUNX2 Expression and Osteocalcin Secretion in Human Mesenchymal Stem Cells.** D. Jian<sup>\*1</sup>, O. Broux<sup>\*2</sup>, P. Lencel<sup>\*2</sup>, O. Ghali<sup>\*2</sup>, C. Chauveau<sup>\*2</sup>, J. Devedjian<sup>\*2</sup>, P. Hardouin<sup>2</sup>, D. Magne<sup>\*2</sup>. <sup>1</sup>Orthopaedic Surgery, Shanghai Jiaotong University Sixth People Hospital, Shanghai, China, <sup>2</sup>Cellular and Molecular Biology EA2603, ULCO/Lille University, Boulogne/Mer, France.

Effects of inflammation on osteoblast differentiation appear contradictory. Indeed, joint inflammation leads to bone erosions in rheumatoid arthritis whereas it induces syndesmophytes and new bone formation in ankylosing spondylitis. Aims of the present study were to clarify the effects of TNF-alpha and IL-1beta on osteoblast differentiation and calcification in human mesenchymal stem cells (MSCs) and bone marrow stromal cells (BMSCs), and to determine whether these cytokines are redundant or not. Cell differentiation was assessed by quantitative PCR, ELISA, measure of alkaline phosphatase (ALP) activity by the method of Lowry and mineralization by Alizarin red staining. Results indicated that in both cultures TNF-alpha (from 0.1 to 10 ng/ml) and IL-1beta (from 0.1 to 1 ng/ml) stimulated calcification, which was not due to cell death but was linked to a stimulation of ALP expression and activity. Addition of 50 ng/ml IL-1 receptor antagonist in TNF-alpha-treated cultures revealed that whereas IL-1 was responsible for TNF-alpha-stimulated RANKL secretion, it was unnecessary for TNF-alpha-increased ALP activity. In addition, both TNF-alpha and IL-1beta decreased RUNX2 expression and osteocalcin secretion suggesting that RUNX2 is not involved in calcification. To check this hypothesis, dominant negative RUNX2 was overexpressed in osteosarcoma SaOS-2 cells. In transfected cells, ALP expression and activity were not reduced in absence of functional RUNX2, suggesting that RUNX2 plays no role in ALP activity and mineralization in differentiated osteoblasts. Finally, the finding that TNF-alpha and IL-1beta decrease expression of alpha1(I) collagen in MSCs and BMSCs might explain why inflammation decreases bone formation whereas it induces syndesmophyte formation in collagen-rich entheses.

**Disclosures:** D. Magne, None.

## SU045

**Regulation of Osteogenesis by Wnt Signaling in Rat Mesenchymal and Human Adipose-Derived Stem Cells.** A. Regmi<sup>\*</sup>, X. Yang<sup>\*</sup>, R. J. Galvin, A. G. Geiser. Musculoskeletal Research, Eli Lilly and Company, Indianapolis, IN, USA.

Stimulation of new bone formation is a goal for treating conditions such as osteoporosis where decreased bone formation or the balance between formation and resorption leads to weakened bones and the risk of fractures. Bone formation may be stimulated by favoring the differentiation of progenitor cells towards the osteoblast lineage. This study evaluated the relative role of wnt in sensitizing either rat marrow mesenchyme (RMM) or human adipose derived stem cells (ASC) to osteogenic signals. ASC cells were cultured in WNT3A-conditioned media (WNT3A) for 1-7 days and osteogenic genes (i.e., alkaline phosphatase (ALPL), osteomodulin (OMD), plasminogen activator inhibitor 2 (SERPINB2)) or wnt-pathway regulated genes (Dickkopf 2 (DKK2) and AXIN2) were measured by real-time PCR. These genes were robustly regulated by WNT3A within 1-day. Osteogenesis was confirmed in both cell types by accumulation of calcified mineral matrix detected by labeling with calcein or alizarin red. Pretreatment of both cell types by WNT3A for 24-hrs followed by removal of WNT3A and subsequent induction of mineralization by osteogenic cocktail (10 mM b-glycerolphosphate, 1 mM ascorbate and 100 nM corticosteroid) showed significant increases in fluorescent calcein by 4 days (ASC) or 7 days (RMM). When both cell types were co-incubated for 14-days in the presence of both mineralizing cocktail and WNT3A, the ASC but not the RMM showed significant increases in the mineral matrix. These data suggest that both cell types have the capacity to respond to WNT3A stimulation. However, lack of increased mineralization with continuous WNT-signaling in the rat cell population indicates that the marrow derived cells are different in response compared to ASCs. This difference could be due to heterogeneity of the marrow cell population. These findings indicate that both populations of progenitor cells are driven to osteogenic differentiation by wnt signaling, but they differ in response to wnt signaling when other osteogenic stimuli are present.

**Disclosures:** A. Regmi, None.

This study received funding from: Eli Lilly and Company.

## SU046

**Blockade of Ephrin/EphB4 Signaling within the Osteoblast Lineage Reduces Osteoblast Differentiation and Mineralization.** E. H. Allan<sup>\*1</sup>, S. Pompolo<sup>\*1</sup>, J. H. Gooi<sup>\*1</sup>, M. T. Gillespie<sup>1</sup>, N. A. Sims<sup>1</sup>, V. Krasnopetrov<sup>\*2</sup>, T. J. Martin<sup>1</sup>. <sup>1</sup>St Vincent's Institute, Melbourne, Australia, <sup>2</sup>Vasgene Therapeutics, Inc, Los Angeles, CA, USA.

Members of the ephrin and Eph family are local mediators of cell function acting largely through contact-dependent processes in physiological development and maturity. Osteoclast-derived ephrinB2 has been shown previously to act upon the receptor tyrosine kinase, EphB4 in osteoblasts through a contact-dependent mechanism to favour bone formation. The aim of the present study was to investigate the consequences of interaction of the ligand, ephrinB2, produced by osteoblasts, with its receptor, EphB4, within the same cell lineage. PTH and PTHrP enhanced ephrinB2 mRNA and protein levels up to 6-fold in murine osteoblastic cell lines, primary murine calvarial osteoblasts and UMR106 rat osteogenic sarcoma cells, but did not affect the levels of EphB4 or any of several other ephrin and Eph products in these cells. In order to block ephrinB2/EphB4 interaction within the osteoblast population, we used either a synthetic peptide antagonist of ephrinB2/EphB4 receptor interaction (Koople *et al.*, 2005 J Biol Chem 280:17301), or recombinant soluble extracellular domain of EphB4 (sEphB4), an antagonist of both forward and reverse EphB4 signaling (Kertesz *et al.*, 2006 Blood 107:2330). In murine mesenchymal cells (Kusa 4b10) grown under osteoblast differentiating conditions, the effect of both agents on osteoblast gene expression (real time RT-PCR) and on mineralization (Alizarin staining) were measured when cultures were differentiated in the presence of ascorbate and beta glycerolphosphate (for mineralization). Osteoblast genes expressed late in differentiation, DMP-1, and interferon induced transmembrane protein 5 (Ifitm5) were significantly down-regulated (2 fold in both cases) by both agents and mineralization was significantly inhibited in a dose-dependent manner by the peptide receptor antagonist and sEphB4. Immunohistochemistry of sections of paraffin-embedded 3 week old male rat femur revealed differential ephrinB2 expression, with groups of osteoblasts on mature trabecular bone positive for ephrinB2, while immature (woven) bone osteoblasts were negative suggesting the action may be most relevant in mature bone. Osteoclasts also stained positively for ephrinB2, as previously reported.

Thus the functional consequence of blocking ephrinB2/EphB4 signaling in osteoblasts in this study was to inhibit mineralization and the expression of several osteoblast genes involved late in osteoblast differentiation. This is consistent with ephrinB2/EphB4 signaling within the osteoblast lineage having a paracrine role in osteoblast differentiation, in addition to the proposed role of osteoclast-derived ephrinB2.

**Disclosures:** E.H. Allan, None.



## SU047

**Hormonal Control of RANKL Expression Is Independent of Runx Family Proteins: Evidence That Commitment to the Osteoblast Lineage Is Not a Requirement for the Stromal Cells That Support Osteoclast Differentiation.** C. Galli<sup>1</sup>, Q. Fu<sup>\*1</sup>, W. Wang<sup>\*2</sup>, B. R. Olsen<sup>\*2</sup>, R. L. Jilka<sup>1</sup>, S. C. Manolagas<sup>1</sup>, C. A. O'Brien<sup>1</sup>. <sup>1</sup>Endo/Metab, Center for Osteoporosis & Metabolic Bone Diseases, Central Arkansas Veterans Healthcare System, Univ. Arkansas for Med. Sciences, Little Rock, AR, USA, <sup>2</sup>Department of Cell Biology, Harvard Medical School, Boston, MA, USA.

Differentiation of bone resorbing osteoclasts from hematopoietic precursors depends upon expression of RANKL by stromal cells, which some evidence suggests are precursors of osteoblasts. It has been shown previously that hormonal-responsiveness of the murine RANKL gene is mediated in part by a distal enhancer, designated the Distal Control Region (DCR). In addition, the DCR binds Runx2, a transcription factor required for commitment to the osteoblast lineage, supporting the idea that osteoclast-supporting stromal cells may be osteoblast progenitors. However, dibutyl-*l*-cAMP is able to stimulate RANKL mRNA expression to the same extent in mouse embryonic fibroblasts (MEFs) from both wild-type and Runx2-deficient mice. MEFs express significant levels of Runx1 and Runx3, which can bind to the same DNA sequence as Runx2, raising the possibility that these other members of the Runx family may compensate for the lack of Runx2. Consistent with this possibility, we found that Runx1 was able to bind to the Runx2 binding sequence in the DCR in electrophoretic mobility shift assays. To determine whether any member of the Runx family is required for the expression of RANKL, we silenced CBF $\beta$ , an essential cofactor required for the transcriptional activity of all Runx proteins, in a stromal/osteoblastic cell line using short hairpin RNAs introduced via lentiviral transduction. Basal and PTH-stimulated RANKL mRNA levels were not altered by the suppression of CBF $\beta$ , while mRNAs for known Runx2 target genes, such as osteocalcin, bone sialoprotein, and osterix were dramatically reduced. Similar results were obtained when CBF $\beta$  was silenced in MEFs or primary osteoblastic cells obtained from mouse calvaria. Lastly, we investigated whether Runx proteins were required for the transcriptional activity of the DCR. Silencing of CBF $\beta$  in stromal/osteoblastic cells stably transfected with a chimeric reporter construct, consisting of the DCR inserted upstream from a minimal RANKL promoter, did not block the ability of PTH or dibutyl-*l*-cAMP to stimulate the reporter construct. These results demonstrate that Runx family proteins are not required for RANKL expression or DCR activity in stromal/osteoblastic cells or primary fibroblasts. Moreover, they suggest that commitment to the osteoblast lineage is not a requirement for stromal cells that support osteoclast differentiation.

**Disclosures:** C.A. O'Brien, None.

## SU048

**BMP-6 Stimulated Osteogenesis of HOB Cultures Is Associated with Suppression of PYK2.** L. Buckbinder<sup>1</sup>, W. Grasser<sup>\*2</sup>, P. Bonnette<sup>\*1</sup>, A. Baumann<sup>\*2</sup>, K. Riccardi<sup>\*2</sup>, B. Robinson<sup>\*2</sup>, V. Paralkar<sup>2</sup>. <sup>1</sup>CVMED Exploratory Biology, Pfizer Inc., Groton, CT, USA, <sup>2</sup>Healthy Ageing Translational Pharmacology, Pfizer Inc., Groton, CT, USA.

We recently identified the PYK2 tyrosine kinase as a negative regulator of bone formation *in vivo* and during the osteogenic differentiation of hMSC cultures (PNAS 2007, **104**, 10619-24). In this report we characterize the expression of PYK2 during osteogenesis of human osteoblast cultures (HOBs). As we observed in hMSC cultures, adenovirus mediated down regulation of PYK2 with shRNA yielded enhanced osteogenesis. In time course experiments, we find that PYK2 protein levels increase during the differentiation of HOBs, with a peak that coincides at the time of high alkaline phosphatase activity. PYK2 levels then decrease as the cells progress to mineralization. We find that BMP6, which stimulates osteogenesis in HOB cultures (Int. Ortho. 2007, **31**, 759-765), leads to both a reduction of active PYK2, as well as total PYK2 protein levels across all time points. Quantitative PCR analysis demonstrates that PYK2 is regulated at the RNA level throughout differentiation in response to BMP6 treatment. In addition, we find that the phosphorylation state of a PYK2 substrate, paxillin pY31, mirrors the levels of active PYK2, and is reduced in response to BMP6 treatment. Furthermore, active forms of FAK and Src, proteins often associated with PYK2 signaling pathways, were found to undergo only relatively minor changes during differentiation or in response to BMP6 treatment. Thus we find: 1) that PYK2, a negative regulator of osteogenesis, is itself regulated at the RNA level during osteogenic differentiation of HOBs, and 2) that pro-osteogenic BMP-6 treatment down-modulates the expression of PYK2. These data suggest that PYK2 induction serves in a feed back loop to limit osteogenesis and that BMP6 acts on this inhibitor by repressing its expression at the RNA level.

**Disclosures:** L. Buckbinder, None.

## SU049

**Isolation and Characterization of Osteoblasts from Alveolar Bones of Aged Donors.** M. Aino<sup>\*1</sup>, M. Saito<sup>\*2</sup>, A. Umezawa<sup>\*3</sup>, T. Noguti<sup>\*1</sup>, T. Yoneda<sup>2</sup>. <sup>1</sup>Dept Periodont, Aichi-gakuin Univ, Nagoya,Aichi, Japan, <sup>2</sup>Dept Mol Cell Biochem, Osaka Univ Grad Sch Dent, Suita,Osaka, Japan, <sup>3</sup>Dept Reprod Biol Pathol, Natl Res Inst Child Hlth Develop, Tokyo, Japan.

Establishment of human osteoblasts that retain bone-forming capacity is one of the prerequisites for successful bone regeneration therapy. Since the demand for bone

regeneration considerably increases in elderly, use of osteoblasts derived from these aged individuals should significantly facilitate bone regeneration therapy. However, isolation of osteoblasts from elderly is difficult mainly due to a limited proliferative capacity of these osteoblasts with conventional culture techniques. Here we show a novel culture technique of human osteoblasts isolated from jaw/alveolar bones of elderly donor. We also characterized the phenotype of these osteoblasts *in vitro* and *in vivo*. We attempted to isolate osteoblasts using alveolar bones of 27-, 52-, 53- and 66-year-old donors. Those bones, which were readily obtainable during the course of tooth extraction, were sequentially digested by collagenase and primary human alveolar bone osteoblasts (HAOBs) were isolated. HAOBs from all of the individuals were successfully expanded and continually grow more than 60 population doublings (PDs) in a defined medium. HAOBs exhibited high alkaline phosphatase activity and mineralized nodule formation and expressed osteoblast marker genes such as *runx2*, *osterix*, *osteocalcin* and *bone sialoprotein* upon treatment with rhBMP-2. These characteristics of HAOBs remained unchanged until 16 PDs but were significantly lost after 29 PDs. Affimetrix HG-U133 Gene Chip analysis using HAOBs at 6 PDs and 35 PDs showed that osteocalcin mRNA expression was down-regulated in HAOBs at 35 PDs compared with 6PDs, suggesting that osteogenic phenotype was decreased with increasing cell divisions. To examine bone forming capacity of HAOBs *in vivo*, HAOBs at 6 PDs were subcutaneously transplanted into the dorsal skin in severe combined immunodeficiency (SCID) mice. Histological examination revealed that the transplanted HAOBs formed bone tissues with human vimentin expression 4 weeks after the transplantation, showing that these bones were formed by HAOBs. RT-PCR analysis also showed that these bones expressed human bone sialoprotein and osteocalcin mRNA. In conclusion, our results show that the culture technique used here allows us to successfully grow human osteoblasts of aged donors. They also suggest that HAOBs are a useful cell source for future application to cell based bone regeneration therapy for local bone diseases such as periodontal diseases.

**Disclosures:** M. Aino, None.

## SU050

**Adipose Tissue Derived Mesenchymal Stem Cells: Differentiation into Osteoblastic Phenotype and Interaction with Nanostructured Titanium Alloys.** S. Sorace<sup>\*1</sup>, I. Tognarini<sup>\*1</sup>, R. Zonefrati<sup>\*1</sup>, G. Galli<sup>\*1</sup>, G. D. Zappoli Thyron<sup>\*1</sup>, A. M. Carossino<sup>\*1</sup>, F. Marini<sup>\*1</sup>, S. Ciuffi<sup>\*1</sup>, A. Facchini<sup>\*2</sup>, E. Sbaiz<sup>\*2</sup>, A. Tanini<sup>1</sup>, M. L. Brandi<sup>1</sup>. <sup>1</sup>Department of Internal Medicine, University of Florence, Florence, Italy, <sup>2</sup>Lima-Lto spa Medical System, Villanova di San Daniele Del Friuli, Udine, Italy.

The purpose of the present work is to examine the effect of different nanostructured Titanium alloys on osteogenic differentiation of adipose tissue mesenchymal stem cells (AMSCs). Previous work in this laboratory has demonstrated that AMSCs have the same ability to produce bone matrix as bone marrow derived stem cells (BMMSCs) and that Ti6Al4V surfaces exhibit an osteoinductive action on AMSCs, promoting their differentiation into functional osteoblasts and increasing bone formation. In this study *in vitro* tests were used to assay the ability of nanostructured Ti6Al4V and Ti13Nb13Zr to promote and to maintain the osteogenic differentiation on three primary cultures of AMSCs, using polystyrene (PS) and normal human osteoblast cells (NHost) for comparison.

AMSCs were seeded onto Titanium alloys or PS and cultured for up to 40 days. Cell morphology, adhesion, proliferation and differentiation were evaluated by Laser Scanning Confocal Microscopy analysis, cell counting and alkaline phosphatase (ALP) activity evaluation.

Significant differences were observed in term of cell morphology and adhesion when cells were seeded on the three substrates. Morphological analysis revealed that after 4 days of culture both Nhost and AMSCs on nanostructured alloys were less spread, but formed a higher number of focal contacts than on PS. Moreover AMSCs on Ti6Al4V and Ti13Nb13Zr, when compared to cells cultured on PS, displayed a lower proliferation and a greater level of differentiation towards an osteoblastic phenotype, as demonstrated by an increased ALP activity and a higher expression of osteopontin, osteocalcin and collagen type I.

In conclusion our preliminary results confirm that the nanonization of the Titanium alloys promotes cellular adhesion and suggest that the nanostructured surfaces may have an osteoinductive action on AMSCs, leading to interesting alternatives in the design of efficient prostheses.

**Disclosures:** S. Sorace, None.

## SU051

**Osteoformin Increases the Levels of Intracellular Calcium of Human Preosteoblast Cells in Culture.** L. X. Bi<sup>1</sup>, E. G. Mainous<sup>1</sup>, Y. Zeng<sup>\*2</sup>, Z. Gugala<sup>\*2</sup>, W. J. Buford<sup>\*2</sup>. <sup>1</sup>Dept. of Surgery, University of Texas Medical Branch, Galveston, TX, USA, <sup>2</sup>Dept. of Orthopaedics & Rehabilitation, University of Texas Medical Branch, Galveston, TX, USA.

Our previous studies have shown that Osteoformin (negatively charged polypeptide) increases activity of alkaline phosphatase, expression of type-I collagen and BMP-7 and bone mineralization (Bi LX et al, JBMR 18: S212 Suppl. 2, 2003), and activities of intercellular gap junctional communication of human preosteoblast cells in culture (Bi LX et al, JBMR 22: S142-143, Suppl. 1, 2007). To investigate an early response of preosteoblast cells to osteoformin, we examined the levels of intracellular calcium concentration using Laser scanning confocal microscope. Human preosteoblast cells were cultured in a-minimum essential medium [a-MEM] and 10% fetal bovine serum with or without osteoformin (5ug/ml) for 3 and 5 days. The cells were loaded with 5  $\mu$ M fluo-4

AM (Molecular Probes, USA). After 30 min of dye loading at 37°C in the dark, the coverslips were placed in a stainless steel chamber (Attofluor, 2 ml volume, Molecular probes) that was mounted on a thermostatically controlled stage (37°C) of an inverted confocal laser scanning microscope (AXIOVERT, LSM PASCAL, Zeiss, Germany). The cells were washed with DPBS free Calcium at pH 7.4 and observed using a Zeiss 40× water lens. For imaging of the Ca2+-sensitive fluo-4 fluorescence, excitation wavelength of 488 nm was provided by an argon laser. Fluorescence signals were filtered at 505 nm long-pass and recorded using a photomultiplier of the LSM Pascal. Osteoformin enhanced levels of intercellular calcium concentration by 41% and 22% (P<0.01), respectively, compared to that of the control group. We conclude that osteoformin significantly enhances intracellular calcium concentration which is associated with gene expression and osteoblast differentiation in vitro. It might be an important regulator of bone formation by accelerating fracture and bone defect healing, and controlling bone diseases.

**Disclosures:** L.X. Bi, None.

## SU052

**Development of Pharmacological HIF Activators for Fracture Healing.** S. R. Gilbert<sup>\*1</sup>, X. Shen<sup>\*1</sup>, C. Wan<sup>\*2</sup>, M. Sweetwyne<sup>\*3</sup>, J. E. Murphy-Ullrich<sup>\*2</sup>, T. Clemens<sup>2</sup>. <sup>1</sup>Surgery, U. Alabama Birmingham, Birmingham, AL, USA, <sup>2</sup>Pathology, U. Alabama Birmingham, Birmingham, AL, USA, <sup>3</sup>Cell Biology, U. Alabama Birmingham, Birmingham, AL, USA.

Delayed or failed bone healing is a significant clinical problem resulting in a high burden of disease to individuals and society. Current biologic approaches to aid healing predominantly involve growth factors which can be prohibitively expensive. We have recently identified the hypoxia inducible factor (HIF) pathway as a key transcriptional activator of angiogenesis which is required for skeletal repair. In this study, we investigated the utility of prolyl hydroxylase inhibitors, which elevate HIFs as a means to activate angiogenesis in a mouse model of long bone fracture. Several small molecules including desferrioxamine (DFO), L-mimosine (L-mim) and dimethyloxallyl glycine (DMOG) robustly activated a HIF-responsive reporter gene, and increased HIF-1 $\alpha$  and VEGF expression in mesenchymal stromal cells in vitro. We next tested these agents in a functional angiogenesis assay. Capillary sprouting from explanted mouse embryo metatarsals was evaluated by CD31 staining after exposure to DFO and DMOG, and was found to be robust. These agents only slightly inhibited collagen processing as assessed by Western blotting for both secreted and intracellular collagen I. We then evaluated DFO application after midshaft femur fracture stabilized by intramedullary fixation. DFO or saline was directly injected at the fracture site every other day for five doses. At two weeks post-fracture, mice were sacrificed and perfused with a silicone lead contrast agent for angiography. DFO treatment dramatically increased vascularity as assessed by microCT angiography. Vessel volume/tissue volume and vessel number in the region of interest surrounding the fracture site were elevated 4 fold. The enhanced vascularity was associated with complete radiographic union by 4 weeks. We conclude that HIF activation using a small molecule prolyl hydroxylase inhibitor increases angiogenesis in the setting of healing long bone fractures. The agent tested in this study is relatively inexpensive and has been in clinical use for some time as an iron chelator. This finding may have implications for the treatment of clinical non-unions which are frequently associated with hypovascularity.

**Disclosures:** S.R. Gilbert, None.

*This study received funding from: NIH.*

## SU053

**Use of GFP Reporters to Map the Progression of Multipotential Progenitor Cells into the Osteoblast Lineage.** Y. H. Wang, X. Jiang<sup>\*</sup>, L. Wang<sup>\*</sup>, I. Kalajzic, D. W. Rowe. Univ Connecticut Health Center, Farmington, CT, USA.

Mapping lineage progression, especially a lineage branch point, is a major challenge to our understanding of the molecular events that determine lineage specification. The pericyte is emerging as the cell within a wide variety of adult tissues with potential for differentiation into numerous elements of the musculoskeletal system. We have shown that the smooth muscle alpha actin promoter reporter (SMAA-GFP) identifies a heterogeneous population of cells, some of which appear to be progenitor cells for bone, fat and vascular smooth muscle by in vitro differentiation and in vivo transplantation. The present study was designed to develop evidence for the direct transition of this cell type into an osteoblast. Mice double transgenic for SMAA-GFP (green) and Col3.6-CFP (blue) were bred and subjected to a tibial fracture protocol. In this model, weak blue preosteoblasts have developed by day 4 on the periosteal surface distal to the fracture site. These cells progressed toward the fracture site and by day 7 they became strong blue and began to deposit a woven mineralized bone matrix. Activation of SMAA (green) was observed by day 2-3 at the leading edge of the blue preosteoblasts. At the junction of the two colors, double positive cells were visible. While the source of these cells was still conjecture, SMAA green cells were abundant around small blood vessel whose walls have a ragged appearance. To determine if this green to blue cell progression can be observed in primary osteogenic cultures, calvarial cultures from the double transgenic mice were examined for GFP expression during the initial expansion phase of the culture. By day 3, numerous green cells and occasional blue or blue/green were present in the sparsely populated culture. However by day 6, the culture was highly confluent with a preponderance of blue/green and blue cells. The visual progression was confirmed by fluorescent activated cell sorting (FACS) analysis in which a large population of GFP-negative cells at day 3 have progressed to blue/green or green cells by day 6. However, when calvarial cultures derived from SMAA-GFP(green)/Col2.3-CFP(blue) double transgenic were examined, green cells were the predominant cell at day 7 while the proportion of blue only cells have increased by day 14. FACS analysis demonstrated two distinct populations of green or blue cells that

developed at the expense of the other with very few double positive cells. Thus the visual reporters suggest a progression of SMAA(-) => SMAA(+) => SMAA(+)/Col3.6(+) => Col3.6(+)/Col2.3(+). This strategy should be useful in defining a lineage branch point when applied to reporters for the osteogenic and adipogenic lineages.

**Disclosures:** Y.H. Wang, None.

## SU054

**Osteogenic Potential of Periodontal Ligament Cells in vivo.** T. Hiraga<sup>1</sup>, T. Ninomiya<sup>\*2</sup>, A. Hosoya<sup>\*1</sup>, H. Nakamura<sup>1</sup>. <sup>1</sup>Histology and Cell Biology, Matsumoto Dental University, Nagano, Japan, <sup>2</sup>Institute for Oral Science, Matsumoto Dental University, Nagano, Japan.

Periodontal disease characterized by destruction of periodontal tissues is a major cause of tooth loss in adults and represents a substantial public health burden. However, predictable regeneration is not always achieved by the currently-available techniques. Periodontal ligament (PDL) is a unique connective tissue that not only connects cementum and alveolar bone to support teeth but also plays an important role in reconstructing periodontal tissues. Several lines of evidence suggest that PDL cells have osteoblast-like properties; however, their bone-forming activity has not been extensively studied yet. Thus, in the present study, we examined osteogenic potential of PDL cells in vivo. PDL cells were isolated from rat molars by enzymatic digestion. The PDL cells exhibited substantial alkaline phosphatase activity and induced mineralization at levels equivalent to primary calvarial osteoblastic cells in vitro. RT-PCR analyses showed that the PDL cells expressed the osteoblast markers, Runx2, osterix, and osteocalcin. These results suggest that PDL cells share similar phenotypes with osteoblasts. In support of the notion that PDL cells contain multipotent mesenchymal cells, a small population of the PDL cells showed the differentiation to oil red O-positive adipocytic cells. To examine the osteogenic activity of PDL cells in vivo, PDL cells isolated from green fluorescent protein (GFP)-transgenic rats were implanted with hydroxyapatite (HA) disks into wild-type rats. Five weeks after the implantation, the pores in HA disks were occupied by GFP-positive cells. Mineralized matrix formation was also found on the surface of HA pores. At 12 weeks, some of the pores were filled with bone-like mineralized matrices (BLMM). Immunohistochemical studies showed that the BLMM were positive for the bone matrix proteins, osteopontin, bone sialoprotein, and osteocalcin. Of note, they also revealed that most of osteoblast-like and osteocyte-like cells on and in the BLMM were GFP-positive, suggesting that the BLMM were directly formed by the inoculated PDL cells. The existence of cement lines and multinucleated TRAP-positive osteoclasts indicates that the BLMM experienced remodeling. On the pore surfaces, we found that Sharpey's fiber-like structures were embedded in cementum-like mineralized layers. Thus, it is likely that the PDL cells also have a potency to differentiate to other periodontal cells, including cementoblasts. In conclusion, these results suggest that PDL cells possess the osteogenic potential in vivo. PDL cells could be a useful source for regenerative therapies of periodontal diseases.

**Disclosures:** T. Hiraga, None.

## SU055

**Different Osteogenic Properties of Human Bone Marrow Stromal Cells from Different Skeletal Site Origin.** H. Park<sup>\*</sup>, J. Lee<sup>\*</sup>, D. Kwon<sup>\*</sup>, J. Kim<sup>\*</sup>, J. Cho. Biochemistry, School of Dentistry, Kyungpook National University, Daegu, Republic of Korea.

There are reports regarding skeletal site-related differences, such as the affects on anatomic skeletal site-specific differences in autologous graft and skeletal site-related phenotypic and functional properties. Also, in recent proteomic analysis (our unpublished observation) some chondrogenic factors were up-regulated in the long bone origin hBMSCs (by the 3 day-treatment of BMP2) implicating their different bone formation process compared to that of flat bones. These evidences suggest that there are differences in bone metabolism dependent on their skeletal sites. In this study, we investigated skeletal site-related differences in human bone metabolism in multipotent mandible (orofacial) - and iliac crest (axial) - derived human bone marrow stromal cells (hBMSCs). First, we established hBMSCs selecting by single colonies among adherent cells exhibiting a typical fibroblast-like morphology. Isolated putative hBMSCs were shown individual colony-forming ability and mesenchymal lineage differentiation potential. Second, we investigated the gene expression pattern of osteogenic and chondrogenic-related representative transcription factors and marker genes along osteogenic differentiation of both human mandible- and iliac crest- derived BMSCs by means of Real-Time PCR analysis based on their different developmental bone formation process. In an osteogenic medium, the mRNA expression pattern of osteogenic- and chondrogenic-related genes revealed overall higher mRNA levels in mandible-derived hBMSCs (MandBMSCs) compared to those of iliac crest-derived hBMSCs (IliacBMSCs). Interestingly, the maximum of expression of runx2, osteonectin, osteopontin in IliacBMSCs were shown retarded pattern, three- or four-day intervals, compared to those in MandBMSCs. Type 11 collagen was maximally expressed on day 7 of differentiation in both MandBMSCs and IliacBMSCs with similar pattern. Aggrecan was expressed higher in MandBMSCs than in IliacBMSCs at the beginning of osteogenic differentiation, and was dramatically decreased on day 7. In IliacBMSCs, however, although expression level was low, it peaked twice in its expression; day 2 and day 7. These results indicate that MandBMSCs differentiate into osteoblast earlier than IliacBMSCs by expressing osteogenic markers earlier and probably not inducing the chondrogenic markers significantly in osteogenic stimulation.

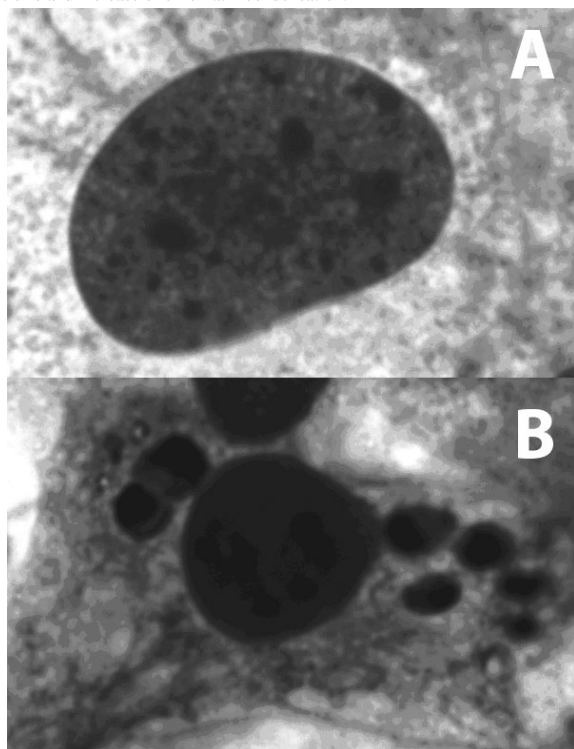
**Disclosures:** H. Park, None.

## SU056

**Thiazolidinediones Modify Nuclear Heterochromatin Architecture.** M. Moreau<sup>\*1</sup>, H. Libouban<sup>\*1</sup>, M. J. Y. Audran<sup>2</sup>, D. Chappard<sup>1</sup>. <sup>1</sup>Faculty of Medicine, INSERM U922, Angers, France, <sup>2</sup>Rheumatology, University Hospital, Angers, France.

Thiazolidinediones (TZDs) are an adjunctive therapy for diabetes mellitus. TZDs act by binding to PPAR $\gamma$  (peroxisome proliferator-activated receptors- $\gamma$ ). PPAR $\gamma$  is a key element for the differentiation of Mesenchymal stem cells (MSCs) into adipocytes when osterix and runx2 differentiate into osteoblasts. In vitro TZDs induce storage of cytoplasmic droplets lipids, but nuclear chromatin has been not very studied in this process. The murine Pluripotent Mesenchymal Cell line C3H10T1/2 was cultured in DMEM medium in presence of Pioglitazone (PGZ) [5 $\mu$ M] or rosiglitazone (RGZ) [0.5 $\mu$ M] during 5-6-7-8 days. Cells were fixed with 10% formaldehyde and stained with Oil red O. Nuclei were stained with Harris Hematoxyline. Cells cultured without TZDs (fig.A) and adipocytes with perceptible lipids droplets (fig.B), were photographed at x1000 magnification and pictures were standardized and analysed with the MAZDA texture analysis logiciel (Institute of Electronics, Lodz, Poland). The Nucleus area and Run length parameters have been calculated. N-area decrease suddenly at J5 for RGZ and J6 for PGZ. SRE-short run emphasis, expected to be large for fine texture, decrease. LRE-long run emphasis, expected to be large for coarse structure texture, increase at J7 for PGZ and RGZ with apparition of large dark run with compact texture. GLN-gray level nonuniformity measures the similarity of gray level values throughout the image, decrease with the decrease of clear run of euchromatin. RLN-run length nonuniformity measures the similarity of the length of the runs throughout the image, decrease with the decrease of clear run euchromatin and the increase of dark run heterochromatin (but less than the clear runs). RP-run percentage measures the homogeneity and the distribution of runs of an image in a specific direction, decrease.

Conclusion: TZDs modify the cellular metabolism when the C3H10T1/2 cells differentiate into adipocyte and probably induce inactivation of some genes who induce decrease of nucleus size and increase of chromatin condensation.



**Disclosures:** D. Chappard, None.

## SU057

**Tracking Adipose Differentiation in Vitro with aP2-GFP Reporters and Flow Cytometry: Lipid Staining and Macrophage Mimicry.** J. R. Harrison<sup>1</sup>, M. S. Kronenberg<sup>\*2</sup>, D. W. Rowe<sup>2</sup>. <sup>1</sup>Craniofacial Sciences, University of Connecticut Health Center, Farmington, CT, USA, <sup>2</sup>Reconstructive Sciences, University of Connecticut Health Center, Farmington, CT, USA.

Cell culture of whole bone marrow leads to the appearance of bone marrow stromal cells (BMSC), which can be induced to differentiate into osteoblasts, adipocytes, chondrocytes and myoblasts. In studies designed to simultaneously track osteoblast and adipose differentiation, we have used transgenic mice that express GFP under the control of the FABP4 (aP2) promoter. Cells of the adipose lineage selectively express this marker in vivo and in vitro. However, aP2 is also expressed in macrophages, leading us to more closely examine the identity of the presumptive adipocytes in BMSC cultures. Bone marrow was flushed from femurs and tibiae of mice carrying either aP2/GFP(topaz) or aP2/GFP(cyan) transgenes to establish BMSC cultures. After 10-11 days, cultures were

either left untreated or given an adipogenic treatment (ADP; 0.5  $\mu$ M rosiglitazone, 1  $\mu$ M insulin). Cultures were stained with LipidTOX, a fluorescent dye that selectively binds neutral lipids, scanned by fluorescence microscopy, and harvested for analysis on an LSRII flow cytometer after staining with fluorochrome-conjugated antibodies against the macrophage cell surface markers CD11b and F4/80.

Surprisingly, flow cytometry indicated that 50% or more of the cells in BMSC cultures were derived from the myeloid lineage, staining positive for CD11b and F4/80. Microscopy and flow cytometry both revealed expression of the GFP transgene within 48 h of ADP. Typically, 7-8% of the total cells were positive for GFP at 48 h, decreasing slightly to around 5% by day 7. Flow cytometry revealed that approximately half of all GFP-positive cells in BMSC cultures were positive for CD11b and F4/80, identifying them as macrophages. LipidTOX fluorescence, which lagged slightly behind transgene expression, was also equally distributed between macrophage and non-macrophage (adipocyte) compartments, and was closely associated with transgene expression. Thus, it was not possible to distinguish these cell types based on their ability to take up and store fat. Staining of terminal cultures with Oil Red O showed parallel results with the vital LipidTOX dye. A similar macrophage profile has been observed in cultures derived from the adipose stromal-vascular compartment.

These results indicate that macrophages are a significant component of BMSC cultures that persist, differentiate and accumulate fat following ADP treatment. Therefore, studies on adipogenesis in BMSC cultures using conventional fat staining techniques may be confounded by the presence of lipid-containing macrophages.

**Disclosures:** J.R. Harrison, None.

## SU058

**SATB2 Overexpression Promotes Osteoblast Differentiation and Enhances Regeneration of Bone Defects.** E. Brewer<sup>\*</sup>, J. Zhang<sup>\*</sup>, Q. Tu, J. Tang<sup>\*</sup>, J. Chen. General Dentistry, Tufts University School of Dental Medicine, Boston, MA, USA.

SATB2, a gene expressed in branchial arches and in cells of osteoblast lineage, is identified as responsible for preventing craniofacial abnormalities and defects in osteoblast differentiation and function. In knockout experiments, mice lacking SATB2 were found to exhibit craniofacial abnormalities and defects in osteoblast differentiation and function. These knockout embryos displayed delayed bone formation and defects in extracellular matrix deposition, causing craniofacial abnormalities such as cleft palate. To investigate the role of SATB2 overexpression in enhancing bone regeneration, we transduced murine bone marrow stromal cells (BMSCs) isolated from 6-week-old BSP9.0Luc/ACTB-EGFP mice to achieve SATB2 overexpression in these cells. These mice were generated by cross-breeding a male ACTB-EGFP mouse with a homozygote mBSP9.0Luc female mouse. Luciferase expression is driven by BSP promoter, while GFP expression is driven by beta-actin promoter and cytomegalovirus enhancer. GFP staining was used to track the fate and migration of BMSCs, whereas luciferase staining served as a marker for osteogenic differentiation of the transplanted BMSCs. Cells transduced with empty vector served as controls. Real-time RT-PCR was performed to determine the expression levels of BSP, Osx, and Runx2. In addition, cell migration assays were performed to investigate the role of SATB2 in promoting engraftment of adult stem cells during wound regeneration. The SATB2 overexpressing BMSCs were implanted into the mandibular and femoral bone defects of 10-week-old B6D2F1 mice, a species from which mBSP9.0Luc mice are derived. In addition to histomorphometric analysis, the expressions of luciferase, GFP and BSP were determined using immunohistochemical staining, and real-time RT-PCR. SATB2 overexpression in BMSCs induced increased expression of bone matrix proteins and osteogenic transcription factors such as BSP, Osx, and Runx2 in these cells. Migration rate was also increased in SATB2 overexpressing BMSCs. These results are significant because cellular migration is a central process in development as well as tissue regeneration. Immunohistochemical staining and real-time RT-PCR analysis demonstrated that luciferase expression, which indicated transplanted BMSCs undergoing osteogenic differentiation, was higher in SATB2 overexpressing group compared to the control group. As a result, transplantation of SATB2 overexpressing BMSCs promotes bone tissue regeneration. These findings suggest that SATB2 may play an important role in the regeneration of tissues to a normal, pre-disease state.

**Disclosures:** E. Brewer, None.

This study received funding from: NIH grants DE13745 and DE16710 to JC.

## SU059

**The Effect of Resveratrol and Flax Oil on MC3T3-L1 Pre-Adipocyte and ST2 Bone Marrow Stromal Stem Cell Proliferation and Differentiation.** O. J. Kelly, Y. Kim<sup>\*</sup>, P. Liu, H. Shin, C. C. Douglas<sup>\*</sup>, J. Ilich. Nutrition, Food and Exercise Sciences, Florida State University, Tallahassee, FL, USA.

Osteoporosis and obesity may be linked as both are caused by an imbalance in bone marrow stem cell metabolism. Resveratrol, a phytoestrogen found in grape skin, used primarily in cancer research for its anti-proliferative and anti-inflammatory properties may have applications in osteoporosis and obesity by regulating differentiation of stem cells into osteoblast or adipocyte lineage. Flax oil, a source of the essential n-3 fatty acid, alpha-linolenic acid, and lignans, also is employed in cancer research. The aim of this study is to investigate if resveratrol and/or flax oil have dual functions (anti-adipogenic and pro-osteoblastogenic) in the bone microenvironment. Experiments were carried out in standard tissue culture conditions (96 well plates) for a duration of 6 days; 48 hours after seeding, cells were dosed with resveratrol and/or flax oil and the media was changed every two days. ST2 cells were allowed to differentiate into osteoblasts using ascorbic acid and glycerophosphate. Cell numbers (proliferation) were assessed using the cell counting kit (Dojindo, Japan). Resveratrol treatment (96 hours) significantly (P<0.001) inhibited

MC3T3-L1 proliferation at 12.5, 25 and 50 microM, however, there was no significant difference between the concentrations tested. Flax seed oil at 10, 20, 40 and 80 microL/mL did not have any significant effect on the proliferation of MC3T3-L1 cells compared to control; however there was a tendency for high lignan flax oil to reduce proliferation. In ST2 cells, resveratrol (96 hours) at 25, 50 and 100 microM significantly ( $P<0.001$ ) inhibited cell proliferation with the higher doses having the greater effects. Flax oil, dissolved in ethanol (1microL/mL) as a vehicle, significantly increased ST2 cell proliferation at 5 ( $P<0.001$ ) and 10 microL/mL ( $P<0.05$ ) however ethanol alone, also increased proliferation of ST2 cells ( $P<0.001$ ). Neither resveratrol nor flax oil (including high lignan) had a significant effect on differentiating ST2 cells however, there was a propensity for resveratrol and flax seed oil combined to increase cell proliferation in differentiating ST2 cells. Results from this preliminary research suggest that resveratrol at low doses (12.5 microM) inhibits pre-adipocyte proliferation as well as the ST2 proliferation at higher concentrations ( $>25$  microM). Flax oil did not affect pre-adipocytes, but increased proliferation of ST2 cells; however the ethanol (flax vehicle) may be the driving force for this outcome. The effects of resveratrol and flax oil need to be examined in more detail to derive some practical applications.

**Disclosures:** O.J. Kelly, None.

*This study received funding from: Florida State University.*

## SU060

**Distinct Modes of Osteoblastic Differentiation from Bone Marrow Stromal and Vascular Smooth Muscle Cells: Induction by BMP-2 and PKA and Suppression by Vitamin D Derivatives.** D. Inoue, R. Okazaki. Third Department of Internal Medicine, Teikyo University School of Medicine, Ichihara-shi, Chiba, Japan.

Epidemiological evidence has suggested a link between vascular calcification and osteopenia. Although vascular smooth muscle cells (VSMCs) have been shown to express osteoblastic phenotype under certain conditions, regulatory mechanisms of VSMC differentiation into osteoblast-like cells are not completely understood. In the present study, we attempted to establish an in vitro model of BMP-2 induced osteoblastic differentiation from VSMCs using a mouse VSMC cell line, p53LMAC01 (MACO), and to compare its mode of differentiation with that of a mouse bone marrow stromal cell line, ST-2. Treatment with BMP-2 induced ALP activity and mRNA expression within 3 days in MACO, although to a weaker extent than ST-2. Only 1hr treatment with BMP-2 was sufficient to induce ALP after 3 days in ST-2, while 24hr treatment was necessary for MACO to differentiate. In ST-2, Runx2, Msx2 and Osterix were constitutively expressed, and the expression was slightly up-regulated by BMP-2 after 24 hrs and maintained thereafter. In MACO, only Runx2 was induced by BMP-2 within 24 hrs, and Msx2 and Osterix was unchanged. As previously reported, forskolin slightly enhanced BMP-2 induced ALP in ST-2, and both basal and induced ALP activities were strongly suppressed by a PKA inhibitor, H89. In MACO, effect of H89 on the basal ALP activity was marginal, but forskolin induced ALP to a much larger extent, which was completely blocked by H89. These results indicate a critical role of PKA in osteoblastic differentiation and a lower basal activity of PKA in MACO compared to ST-2. We also found that calcitriol inhibited BMP-2-induced ALP in a dose-dependent manner with a significant effect from 0.3 nM in ST-2 but that this effect was a hundred times weaker in MACO even though VDR mRNA was expressed at a comparable level. 22-oxacalcitriol (OCT), a non-calcemic analogue of vitamin D, was 10 times more potent than calcitriol. The inhibitory effect vitamin D could not be explained by alterations in the expression level of Runx2, Msx2 or osterix. Interestingly, inhibitory effect of calcitriol on ALP induction required 24hr pretreatment before exposure to BMP-2, suggesting that transcriptional induction of an unknown factor is necessary. In summary, we have established an in vitro culture system of early osteoblastic differentiation of VSMCs and demonstrated a distinct mode of regulation from marrow stromal cells. Our results suggest that escape from the inhibitory effect of vitamin D contributes to pathological vascular calcification and further implicate a requirement of PKA-stimulating factors in addition to BMP-2.

**Disclosures:** D. Inoue, None.

## SU061

**Osteogenic Cell Lineages Show Differential Responsiveness to Angiogenic Signals.** J. L. Fitch<sup>1</sup>, D. N. Kotton<sup>\*2</sup>, L. C. Gerstenfeld<sup>1</sup>, T. A. Einhorn<sup>1</sup>. <sup>1</sup>Orthopaedic Surgery, Boston University School of Medicine, Boston, MA, USA, <sup>2</sup>Pulmonary Center, Boston University School of Medicine, Boston, MA, USA.

Both osteogenesis and angiogenesis are essential for skeletal development and bone repair. Previous studies have suggested that osteogenic cells express and respond to angiogenic signals, including VEGF. The expression of VEGF ligands and receptors, and cellular responses to VEGF(s) was assessed during osteogenic differentiation of primary murine marrow stromal cultures (MSC). Fluorescence-activated cell sorting (FACS) analysis of the cells present in control cultures at day 6 indicates that while there are hematopoietic (CD45+, CD31-) and mesenchymal (CD45-, CD31+) populations present in these cultures, there was an almost complete absence of cells of the endothelial (CD45-, CD31+) lineage. During osteogenic differentiation of MSCs, increased expression of the genes encoding VEGFs A and C was observed but expression of the genes encoding their receptors VEGFR1 (flt1), 2 (flt1) and 3 (flt4) decreased. Enhancement of osteogenic differentiation via addition of exogenous rhBMP2 or 7 did not result in significant increases in expression of either VEGF ligands or receptors. Addition of exogenous rhVEGFA-162, which is recognized by both VEGFRs 1 and 2 did not cause observable changes in expression of genes encoding matrix factors produced by differentiated osteogenic cells (bone sialoprotein (bsp) and osteocalcin (oc)). VEGFA-162 did, however, result in increased expression of factors indicative of angiogenic progression, including VEGFRs 2 and 3. Therefore, rhVEGFd, which is specific for VEGFR3 was

exogenously added to our MSC cultures. Treatment with VEGFd resulted in down-regulation of matrix factors osteopontin (opn) and bsp early in the time course of differentiation. At 21 days, however, the expression of opn, bsp and oc returned to levels observed in control (no treatment) cultures. These results suggest that osteogenic cells selectively respond to VEGFd through the VEGFR3. They also suggest that VEGFa has very little direct autocrine activity within osteogenic cells; rather, they are responsive to secondary paracrine signaling mediated by feedback from vascular or lymphatic endothelial cells which produce VEGFd. These data further suggest that the promotion of osteogenic differentiation *in vivo* occurs as a result of interactions with angiogenic cells through paracrine effects or as a consequence of increased oxygenation or nutrition resulting from angiogenesis.

**Disclosures:** J.L. Fitch, None.

*This study received funding from: NIH P01AR049920.*

## SU062

**Induction of Runx2 and Osterix by Bisphosphonate Promote Osteogenic Differentiation.** N. Saoji<sup>\*1</sup>, S. Sittitavornwong<sup>\*1</sup>, N. Said-Al-Naiet<sup>\*1</sup>, H. Chen<sup>1</sup>, H. F. Thomas<sup>\*1</sup>, S. E. Gutierrez<sup>\*2</sup>, A. Javed<sup>1</sup>. <sup>1</sup>Oral & Maxillofacial Surgery, University of Alabama, School of Dentistry, Birmingham, AL, USA, <sup>2</sup>Biología Molecular, Universidad de Concepción, Concepción, Chile.

Bisphosphonate is widely used as an effective treatment to prevent bone loss associated with osteoporosis and bone metastasis. Bisphosphonate treatment however is linked with osteonecrosis of the jaws but its effects on the mesenchymal cells of the jaw and teeth remains unknown. To test this, we isolated Pulp and PDL tissue from non-infected, impacted third molars of healthy individuals. Primary mesenchymal cells from pulp and PDL were cultured in various concentrations of bisphosphonate to evaluate their viability, growth, and differentiation properties. Pulp cells exhibited a 10-fold increased sensitivity to oral forms of bisphosphonate and an early susceptibility to the IV form of bisphosphonate when compared to PDL cells. Proliferation of both PDL and pulp cells was inhibited by bisphosphonate. When cultured in osteogenic media, PDL and pulp cells differentiated to osteoblast with a progressive increase in ALP activity, matrix synthesis and mineral deposition. Surprisingly, bisphosphonate treatment resulted in enhanced osteoblast differentiation of PDL and pulp cells. For a molecular understanding of how bisphosphonate stimulated osteoblast differentiation, we analyzed profile of gene expression. At earlier time points, expression of Runx2 and Osterix, the two essential regulators of osteoblast differentiation was increased two fold. This coincided with an increased expression of ALP, osteopontin, and osteocalcin. Immunofluorescence studies demonstrated that bisphosphonate treatment enhances nuclear accumulation of Runx2 but did not alter its association with splicing factor SC35. These results provide evidence that in tooth derived mesenchymal cells, bisphosphonate target Runx2 to activate program of osteoblast differentiation.

**Disclosures:** A. Javed, None.

*This study received funding from: NIH/NIA.*

## SU063

**R-spondin 2 Is a Novel Osteogenic Factor Required for Wnt11 Mediated Osteoblast Differentiation.** M. S. Friedman<sup>\*1</sup>, S. M. Owersman<sup>\*1</sup>, W. Luo<sup>\*2</sup>, K. D. Hankenson<sup>3</sup>. <sup>1</sup>Thermogenesis Corporation, Rancho Cordova, CA, USA, <sup>2</sup>University of Michigan, Ann Arbor, MI, USA, <sup>3</sup>Animal Biology, University of Pennsylvania, Philadelphia, PA, USA.

The four members of the R-spondin family share structural features including two conserved cysteine rich domains and a thrombospondin type I repeat. R-spondins interact with Frizzled and LRP family members and enhance Wnt signaling. We previously reported that Wnt11 increases osteoblast differentiation and activates Rspo2 expression in MC3T3 E1.14 pre-osteoblasts. We hypothesized that Rspo2 may be involved in Wnt11-induced osteoblast differentiation. Rspo2 was retrovirally overexpressed in MC3T3 E1.14 pre-osteoblasts. We observed that Rspo2 potentially synergized BMP-induced alkaline phosphatase expression and matrix mineralization (Alizarin red S). We examined osteoblast-specific gene expression in Rspo2 overexpressing cells relative to Wnt11 overexpressing and GFP control cells, with and without BMP treatment. BMP-treated Rspo2 cells show statistically significant higher levels of osterix, Bsp, Dmp1, and Phex expression relative to BMP treated Wnt11 and GFP control cells. To evaluate if Rspo2-mediated gene expression was dependent on Tcf/beta-catenin signaling, we retrovirally overexpressed dominant/negative Tcf4 in Rspo2 overexpressing cells. dnTcf4 expression in Rspo2 cells significantly decreases osterix expression to levels comparable to GFP control cells. Phex expression is also decreased in Rspo2-dnTcf4 cells relative to Rspo2 cells, but remains higher than Wnt11 overexpressing cells. To determine if Rspo2 expression was necessary for Wnt11-enhanced osteoblast differentiation, we used retroviral-based micro RNAi to knock-down expression of Rspo2. GFP cells were infected with a control LacZ miRNAi retrovirus, while Wnt11 cells were infected with either a LacZ control miRNAi retrovirus or the Rspo2 miRNAi retrovirus. Knock-down of Rspo2 expression in Wnt11 cells decreases Wnt11-enhanced alkaline phosphatase induction to near control levels. Importantly, knock-down of Rspo2 expression resulted in a nearly complete blockade of mineralization. We also evaluated levels of osteoblast associated gene expression in Wnt11 expressing/Rspo2 knockdown cells. By quantitative PCR, Rspo2 expression in knock-down cells was reduced by 99% relative to the Wnt11-LacZ miRNA control cells. Knockdown of Rspo2 in untreated Wnt11 cells significantly decreased expression of Otoraplin/Cdrap, Bsp, and Phex. BMP treated Wnt11-Rspo2 knockdown cells also demonstrate significantly reduced expression of BSP and Phex. We conclude that Rspo2 expression is both necessary and sufficient to mediate the effects of Wnt11-enhanced osteoblast differentiation.

**Disclosures:** M.S. Friedman, None.

*This study received funding from: NIH.*

## SU064

**Dock5 an Essential Rac Exchange Factor in Osteoclasts that Controls Adhesion Structure Organization and Bone Resorbing Activity.** A. Blangy<sup>1</sup>, H. Brazier<sup>\*1</sup>, V. Vives<sup>\*1</sup>, J. Toubol<sup>\*1</sup>, G. Pawlak<sup>\*2</sup>, M. Laurin<sup>\*3</sup>, J. F. Cote<sup>\*3</sup>.

<sup>1</sup>RhoGTPases in osteoclast biology, CNRS UMR5237, Montpellier, France, <sup>2</sup>CRI U823/UJF, Grenoble, France, <sup>3</sup>Clinical Research Institute of Montreal, Montréal, QC, Canada.

RhoGTPase signaling pathways have essential functions in osteoclast biology. Dock5 belongs to the Dock/CZH family of exchange factors, a group of proteins that activate RhoGTPases. It is the closest homolog to Dock180. We reported previously that the expression of Dock5 increased during RANKL-induced osteoclast differentiation and that its suppression was not compatible with cell survival during osteoclastogenesis (Brazier et al, JBMR, 2006, 21(9), 1387). We further studied Dock5 to identify its functions in osteoclasts.

We showed by quantitative reverse PCR that Dock5 mRNA was predominantly expressed in osteoclasts and to a lesser extent in placenta. Its level of expression was very low in all other mouse tissues tested including mammary gland and total bone marrow. By GTP-trapping assays, we also showed that Dock5 was an activator of Rac. As its closest homolog Dock180, Dock5 guanine nucleotide exchange activity was inhibited by its amino-terminal SH3 domain and could be activated through its binding to the adaptor protein Elmo.

In osteoclasts, we found that endogenous and overexpressed Dock5 localized to adhesion structures: the podosome belt and the sealing zone. Using small interfering RNAs, we performed a partial silencing of Dock5, reducing the protein levels by 70%. This was compatible with osteoclast survival and differentiation and it did not affect the fusion index. Interestingly, Dock5 deficient osteoclasts presented very few podosomes and they were unable to assemble a podosome belt. When plated on mineralized substrates, the osteoclasts failed to contract and to organize a sealing zone. Consequently, reduction of Dock5 expression in osteoclasts impaired mineralized matrix resorption. Lower Dock5 expression also resulted in strong reduction of the level of active Rac in osteoclasts. The influence of Dock5 on mouse bone density in vivo is under investigation. Dock5 expression was deleted and micro-computed tomography analyses of the mice will be discussed.

These observations suggest that Dock5 is a major activator of Rac in osteoclasts and that the exchange factor plays an essential role for adhesion structure organization and then mineralized matrix resorption. As a Rac activator predominantly expressed in osteoclasts, Dock5 represents an interesting new candidate for antiresorptive therapy.

**Disclosures:** A. Blangy, None.

This study received funding from: Centre National de la Recherche Scientifique, Association pour la Recherche sur le Cancer, Association de Recherches sur la Polyarthrite.

## SU065

**Identification of the Regulatory Mechanism(s) of Protein Tyrosine Phosphatase (PTP-PEST) Associating with the Sealing Ring Formation and Bone Resorption in Osteoclasts.** M. A. Chellaiiah<sup>1</sup>, M. D. Schaller<sup>\*2</sup>.

<sup>1</sup>Department of Biomedical Sciences, Dental School, University of Maryland, Baltimore, MD, USA, <sup>2</sup>Department of Cell & Developmental Biology, University of North Carolina, North Carolina, NC, USA.

Sealing ring formation is a prerequisite for efficient bone resorption by osteoclasts. Although the role of WASP, Src, and the phosphatase PTP-PEST in actin-rich sealing ring formation has been identified, the potential regulatory mechanism(s) mediated by PTP-PEST is poorly understood. In order to determine the role of PTP-PEST in sealing ring formation, osteoclasts (OCs) were transfected with PTP-PEST, constitutively active-Src (CA-Src mutated at Y527F), and dominant negative-Src (DN-Src mutated at K297R and Y527F) constructs by adenoviral delivery. Some cultures transfected as above were either treated with a phosphatase inhibitor, phenyl arsine oxide (PAO) or bisphosphonates (BPs; alendronate or pamidronate). Untreated but transfected as well as untransfected OCs were used as controls. We observed an increase in the phosphorylation of cortactin at Y421, WASP at Y294 (Y294, corresponding to Y291 in human) and Src at Y418 in OCs transfected with PTP-PEST and CA-Src as compared with control untransfected and DN-Src transfected OCs. Additionally, a decrease in the phosphorylation of Src at Y527 was observed in OCs expressing PTP-PEST. Colocalization of c-Src/WASP, c-Src/cortactin, WASP/cortactin, c-Src/PTP-PEST, and WASP/PTP-PEST was observed in the sealing ring of OCs expressing CA-Src and PTP-PEST constructs. However, these cells failed to display colocalization of cortactin/PTP-PEST in the sealing ring. An increase in the number of OCs displaying sealing ring was observed. This corresponded well with the increase in bone resorption activity of these OCs. OCs treated with BPs and PAO inhibited the processes listed above, although at various levels, in OCs expressing PTP-PEST construct. BPs have been shown to inhibit phosphatases that modulate dephosphorylation of Src at Y527. Inhibition of PTP-PEST activity by BPs reduces the dephosphorylation state of c-Src at Y527 and activity of c-Src as well. Consequently, this may have caused a decrease in the phosphorylation state of cortactin and WASP, formation of ternary complex (WASP•cortactin•Arp2/3 complex), sealing ring formation, and bone resorption. We suggest that BPs affect the function of OCs via inhibiting downstream signaling pathways mediated by PTP-PEST and c-Src. PAO and BPs did not reduce the above-mentioned processes in OCs expressing CA-Src construct because of the mutation at Y527F. Taken together, our observations indeed have demonstrated that PTP-PEST has a regulatory role in the dephosphorylation of c-Src at Y527 and activates it.

**Disclosures:** M.A. Chellaiiah, None.

This study received funding from: NIH-NIAMS R01-AR46292 to MAC.

## SU066

**TRIP6 Regulates Osteoclast Formation, Adhesion, and Resorptive Capacity.** B. K. McMichael, B. S. Lee. Physiology and Cell Biology, The Ohio State University, Columbus, OH, USA.

Members of the LIM domain-containing zyxin family of proteins shuttle between the nucleus, where they are involved in transcriptional regulation, and the cytoplasm, where they localize to focal adhesions. TRIP6 (Thyroid Hormone Receptor-interacting Protein 6), like other members of the zyxin family, contains transcriptional transactivation domains and LIM domains. In the nucleus of non-bone cells, TRIP6 has been shown to activate AP1 sites, coactivate transcription with v-Rel, and be involved in activation of NFκB and ERK pathways. In fibroblasts, it was shown that Src phosphorylation of TRIP6 in the cytoplasm enhances migration. Because NFκB and Src signaling pathways play vital roles in osteoclast formation and function, we have begun to examine how TRIP6 activity may affect osteoclast motility and resorptive capacity.

A role for TRIP6 in osteoclast function was first indicated by its direct binding to tropomyosin-4, an actin-binding protein that we previously showed to play a role in regulating osteoclast adhesion complexes (i.e. podosomes and the sealing zone). Immunocytochemistry of osteoclasts on glass and bone demonstrated TRIP6 to reside primarily in the nuclei, but with some presence in podosomes and the sealing zone. Suppression of TRIP6 by RNA interference resulted in increased cell fusion of both RAW264.7 and marrow-derived precursors. When plated on glass, TRIP6-suppressed cells also demonstrated increased spreading and enhanced podosome numbers at the cell periphery. On bone, these cells exhibited increased spreading, and altered sealing zone dimensions, pit formation, and overall resorptive capacity.

Stable overexpression of wild-type TRIP6 in cells on bone led to altered sealing zone dimensions while causing a dramatic increase in total resorption. To define the role of Src-mediated phosphorylation of TRIP6 in osteoclasts, either wild-type TRIP6 or TRIP6 mutated at Tyr-55 were transiently expressed in mature osteoclasts. Inhibition of Src-mediated TRIP6 phosphorylation by a Tyr-Phe substitution in cells on bone enhanced nuclear localization of TRIP6, and suppressed sealing zone formation and resorptive capacity. In contrast, the phosphomimetic Tyr-Glu substitution resulted in increased formation of sealing zones and actin patches, and enhanced resorption. These data suggest TRIP6 regulates osteoclast fusion and function in part through a Src-dependent pathway to regulate sealing zone formation, and thus resorption.

**Disclosures:** B.K. McMichael, None.

This study received funding from: NIH RO1 AR051515.

## SU067

**The Role of Alpha Gene Tropomyosins in Osteoclast Function.** P. Kotadiya<sup>\*</sup>, B. S. Lee. Physiology and Cell Biology, The Ohio State University, Columbus, OH, USA.

Tropomyosins (Tms) are actin-binding proteins that stabilize microfilaments and inhibit or recruit binding of other actin-associated proteins. In nonmuscle cells, over twenty alternately spliced isoforms are expressed from four distinct genes, namely the alpha, beta, gamma, and delta genes. Recent studies have indicated that individual Tm isoforms are distributed to different intracellular locations where they regulate specific actin pools. The goal of this work is to determine the roles of alpha gene tropomyosin isoforms in mature osteoclast activity.

Four alpha gene, non-muscle Tms are expressed in osteoclasts, namely Tm-2, -3, -5a, and -5b. Tm-2 and -3 are closely related high molecular weight tropomyosins that differ from the low molecular weight Tm-5a and -5b only by alternately spliced exons that encode the amino termini. However, this difference of 80 amino acid residues mediates markedly different patterns of expression, subcellular distribution, and function for these Tms. The high molecular weight Tm-2/3 are not expressed in the monocytic lineage precursors of osteoclasts, but are strongly upregulated late in osteoclastogenesis. In contrast, low molecular weight Tms are present in monocytic precursors and are modestly upregulated early during osteoclast formation. Further, Tm-5a/b are strongly enriched in adhesion complexes of osteoclasts, while Tm-2/3 are distributed internally throughout the cells, and are not strongly associated with these actin-rich adhesion structures. RNAi-mediated suppression of Tm-2/3 causes increased spreading and flattening of the cells, while overexpression causes decreased spreading and induction of actin patches or stress-fiber like actin filaments. These results demonstrate that Tm-2/3 are expressed in fusing osteoclasts to regulate the cytoskeletal scaffolding of these large multinucleated cells. In contrast, suppression of Tm-5a/b causes clustering and thickening of adhesion complexes when cells are plated on glass, and a thinning of the complexes when cells are plated on bone, demonstrating the role of these Tms in regulation of cell adhesion. Therefore, the alternately spliced exons that form the N-termini and upstream sequences in the alpha gene mediate differential patterns of expression, subcellular location, and function in osteoclasts.

**Disclosures:** P. Kotadiya, None.

This study received funding from: NIH RO1 AR051515.

## SU068

**Formation of Podosome Belts by Osteoclasts on Plastic Correlates with Resorptive Activity.** J. L. Ross\*, K. Fuller, T. J. Chambers. Department of Histopathology, St George's Hospital Medical School, London, United Kingdom.

Resorption of bone by osteoclasts is accompanied by the formation of characteristic actin rings in the bone-apposed pole of the cell. It is considered that these actin rings reflect the formation of peripheral sealing zones of close adhesion to the bone surface, within the confines of which the cell secretes protons and hydrolytic enzymes. It seems likely that in vivo, osteoclasts undertake resorptive activity (secretion of protons and hydrolytic enzymes) only on bone surfaces. The characteristics of the bone surface that induce resorptive activity in osteoclasts are unknown.

When osteoclasts are incubated on plastic or glass substrates they can form belts of podosomes that resemble the actin rings formed by osteoclasts during bone resorption. However, the relationship between podosome belts and actin rings is controversial. We therefore decided to analyse this relationship by comparing makers of resorptive behaviour in osteoclasts expressing actin rings and podosome belts.

We have previously found that secretion of tartrate-resistant acid phosphatase (TRAP) by osteoclasts on bone correlates with bone resorption. Therefore, we tested the correlation between podosome belts, actin rings and TRAP release by osteoclasts on plastic and bone. To do this, osteoclasts were generated in vitro from non-adherent murine bone marrow cells by incubation in RANKL and M-CSF for 5 days. The osteoclasts were then lifted into suspension and sedimented onto slices of devitalized bovine bone, or onto plastic coverslips previously coated with vitronectin, collagen or fibronectin.

Both vitronectin and collagen stimulated TRAP release from osteoclasts on plastic. TRAP release was up to ten times greater on vitronectin-coated than uncoated plastic, and was over three times greater than on bone. TRAP release on collagen was biphasic, rising to twice the level induced by bone before falling at higher collagen densities. The proportion of osteoclasts exhibiting podosome belts on plastic correlated with TRAP release for both vitronectin- and collagen-coated plastic. In contrast, osteoclasts on coverslips coated with fibronectin neither released TRAP nor formed podosome belts.

These results suggest that vitronectin- and collagen-coating of plastic induces resorptive behavior in osteoclasts, and that, despite the difference in appearance, podosome belts, like actin rings, signify actively resorbing cells.

**Disclosures:** T.J. Chambers, None.

## SU069

**The Extracellular Matrix Protein Fibronectin Positively Regulates the Osteoclast Function.** A. Gramoun\*, D. P. Trebec<sup>2</sup>, N. Azizi\*, J. Sodek\*, M. F. Manolson<sup>1</sup>. <sup>1</sup>Dentistry, University of Toronto, Toronto, ON, Canada, <sup>2</sup>Department of Biochemistry, University of Toronto, Toronto, ON, Canada.

The extracellular matrix (ECM) proteins and their fragments play critical and controversial roles in connective tissue homeostasis. Osteoclasts (OCs), the bone resorbing multinucleated cells, are formed by fusion of mononuclear precursors. The ECM proteins, vitronectin (VN), fibronectin (FN) and osteopontin (OPN), all implicated in arthritis, interact with OCs through the surface receptors known as integrins. To determine the effects of VN, FN and OPN on OC formation and resorptive activity RAW 264.7 cells were plated and differentiated (using 100 ng/ml RANKL) on dishes or Osteologic™ slides precoated with 0.01-20 µg/ml FN, VN, and OPN; concentrations shown not to affect cell proliferation. After 96 hours of differentiation, dose response experiments showed that OC number on VN and FN remained significantly lower than those on OPN and the uncoated controls. Furthermore, the number of mononuclear TRAP+ cells (preOCs) at 48 hours and large OCs (> 10 nuclei) at 96 hours showed that while FN did not affect preOC number, it significantly decreased OC multinucleation compared to the uncoated control. OPN conversely had the opposite effect. When 20 µg/ml of FN was added to cultures plated on OPN on day 0 or on day 2 of differentiation, OC number was reduced by 40% indicating that FN was able to inhibit OPN's stimulatory effect on OC formation by preventing preOC fusion. Resorption studies revealed that both FN and OPN increased the total area of resorption and resorptive activity/OC by 40% compared to VN and the uncoated control groups. Further, FN increased the released TRAP5b/OC in cultures. Sealing zone formation (assessed by counting the number of actin rings) was 70% higher on FN than on any of the other experimental groups. Nitric oxide (NO) levels (as measured by Griess reagent) were significantly elevated by FN but not in any of the other groups. This increase in NO levels was associated with an increase in interleukin 1β (IL1β). IL1β levels were reduced in the presence of the NO-synthase inhibitor L-N<sup>G</sup>-monomethyl Arginine in a dose dependant manner. Functionally blocking the OC attachment formed on FN using anti-αvβ3 antibody did not interfere with their attachment. While the anti-α5β1 antibody significantly inhibited OC adhesion to FN. In conclusion, despite its inhibitory effect on preOC fusion and OC formation, FN significantly enhanced resorption/OC and due to an increase of the activity of the formed OCs. FN's induction of NO and IL1β, could both explain the increased OC activity. This study has identified a new role for FN as a key player in the regulation of bone metabolism and a positive modulator of OC activity.

**Disclosures:** A. Gramoun, None.

## SU070

**1,25-dihydroxyvitamin D<sub>3</sub> Can Directly Induce Osteoclast Formation in Osteoclast Precursors in the Absence of RANKL.** N. Kurihara<sup>1</sup>, Y. Hiruma<sup>1</sup>, J. A. Lorenzo<sup>2</sup>, G. D. Roodman<sup>3</sup>. <sup>1</sup>Medicine/Hem-Onc, University of Pittsburgh, Pittsburgh, PA, USA, <sup>2</sup>Medicine/Endocrinology, University of Connecticut, Farmington, CT, USA, <sup>3</sup>Medicine/Hem-Onc, University of Pittsburgh and VA Pittsburgh Healthcare System, Pittsburgh, PA, USA.

1,25-(OH)<sub>2</sub>D<sub>3</sub> can induce osteoclast (OCL) formation indirectly by increasing the expression of RANKL and decreasing the expression of osteoprotegerin (OPG) in marrow stromal cells and osteoblasts. Consistent with this observation, RANKL or RANK receptor knockout mice are profoundly osteopetrotic. This result could reflect that 1,25-(OH)<sub>2</sub>D<sub>3</sub> exclusively induces OCL formation via RANKL or that normal OCL precursors, which express VDR, can only directly form OCL in response to supra-physiologic levels of 1,25-(OH)<sub>2</sub>D<sub>3</sub> (10<sup>-9</sup> to 10<sup>-8</sup>M), which are used in vitro but are not produced in vivo. To test this hypothesis, normal human marrow cultures were treated with 10<sup>-11</sup> to 10<sup>-7</sup>M 1,25-(OH)<sub>2</sub>D<sub>3</sub> or 50 ng/ml RANKL and with or without 50 ng/ml OPG. OPG completely inhibited OCL formation induced by RANKL. OPG also inhibited OCL formation induced by (10<sup>-8</sup>M) 1,25-(OH)<sub>2</sub>D<sub>3</sub> by approximately 40% in normal marrow cultures. Normal marrow cultures only formed OCL in the presence of high levels (10<sup>-9</sup> to 10<sup>-8</sup>M) of 1,25-(OH)<sub>2</sub>D<sub>3</sub>. The OCL that formed with 1,25-(OH)<sub>2</sub>D<sub>3</sub> in the absence of RANKL, resorbed dentine. RANKL levels were 177±5 pg/ml in normal marrow cultures treated with 1,25-(OH)<sub>2</sub>D<sub>3</sub> (10<sup>-8</sup>M). In contrast, OPG did not inhibit OCL formation in cultures of highly purified early human OCL precursors (CFU-GM) treated with 10<sup>-11</sup> to 10<sup>-7</sup>M 1,25-(OH)<sub>2</sub>D<sub>3</sub>, but totally blocked the effects of RANKL on these cells. RANKL was undetectable in cultures of highly purified human OCL precursors treated with 10<sup>-8</sup>M 1,25-(OH)<sub>2</sub>D<sub>3</sub>, consistent with the absence of stromal cells in these cultures. Importantly, CFU-GM derived from RANK<sup>-/-</sup> or wild type (WT) mouse spleen cells formed OCL when treated with 10<sup>-8</sup>M 1,25-(OH)<sub>2</sub>D<sub>3</sub>, but only WT CFU-GM formed OCL in the presence of 50 ng/ml RANKL plus 30 ng/ml M-CSF. OCL formation by RANK<sup>-/-</sup> cells was significantly decreased compared to WT cells, but the OCL that formed resorbed dentine. These results demonstrate that supra-physiologic concentrations of 1,25-(OH)<sub>2</sub>D<sub>3</sub> stimulate OCL formation by both direct (RANKL-independent) and indirect (RANKL-dependent) mechanisms.

**Disclosures:** N. Kurihara, None.

This study received funding from: NIH.

## SU071

**Modulation of Osteoclastogenesis by Fatty Acids.** G. A. Williams\*, J. Lin\*, A. McGibbon\*, M. Watson\*, K. E. Callon\*, J. E. Dunford\*, A. B. Grey\*, D. Naoi\*, J. Cornish\*, I. R. Reid<sup>1</sup>. <sup>1</sup>Medicine, University of Auckland, Auckland, New Zealand, <sup>2</sup>Fonterra Research Centre, Palmerston North, New Zealand, <sup>3</sup>Botnar Research Centre, University of Oxford, Oxford, United Kingdom.

Clinical studies have shown that total body fat mass is related to both bone density and fracture risk, and that fat ingestion reduces bone turnover. These effects are at least partially mediated by endocrine mechanisms, but it is also possible that lipids might act directly on bone. Because milk is a rich source of lipids in mammals, we initially assessed the effects of broad fractions of milk lipids in primary cultures of osteoblasts, bone marrow and neonatal mouse calvariae. Inhibition of osteoclastogenesis in murine bone marrow cultures was apparent with several milk fractions and their hydrolysates, so we proceeded to assess the effects of free fatty acids in this model. Saturated fatty acids (0.1-10 µg/mL) inhibited osteoclastogenesis in bone marrow cultures. This effect was maximal for C14:0 (28% inhibition, p<0.01), C16:0 (50% inhibition, p<0.05) and C18:0 (29% inhibition, p<0.01) at 10µg/mL. Similar effects were observed in RAW 264 cells, suggesting that the fatty acids act directly on osteoclast precursors to inhibit differentiation. The introduction of >1 double bond abrogated this effect, and even led to its reversal. ω3 and ω6 fatty acids had comparable low activity. Osteoblast proliferation was modestly increased (29% and 24% for C16:0 and C18:0 respectively, at 1µg/ml (P<0.01), ruling out a non-specific toxic effect. Fatty acids that inhibited osteoclastogenesis did not change expression of RANKL or osteoprotegerin in osteoblastic cells nor did they affect the activity of key enzymes in the mevalonate pathway. However, members of a family of G protein coupled receptors known to bind medium and long-chain fatty acids were found to be expressed in osteoblastic (GPR120) and osteoclastic (GPR40, 41, 43, 120) cells. These findings suggest a novel link between lipid and bone metabolism which might contribute to the positive relationship between adiposity and bone density, as well as providing novel targets for pharmaceutical and nutraceutical development.

**Disclosures:** G.A. Williams, None.

This study received funding from: Lactopharma Consortium and the Health Research Council of New Zealand.



## SU072

**Carboxyl-terminal Parathyroid Hormone (CPTH); Prediction of Novel Functions, Structural Features and Potential Receptor.** A. A. Selim<sup>\*1</sup>, R. Bringhurst<sup>2</sup>. <sup>1</sup>Biomedical Technology Research Group, KFUPM, Dhahran, Saudi Arabia, <sup>2</sup>Harvard Medical School, Endocrine Unit, MGH, Boston, MA, USA.

**Background:** Parathyroid hormone (PTH) is the major physiological regulator of blood calcium and phosphate, and it exerts potent effects upon cells in bone, cartilage, and kidney. The PTH1 receptor (PTH1R) recognizes the highly conserved amino (NH2)-terminal domain of PTH (and the homologous NH2 terminus of PTHrP) and thus is fully activated by both PTH-(1-34) and the intact hormone, PTH-(1-84). Carboxyl (C) fragments of intact PTH-(1-84), such as PTH-(39-84) or PTH-(53-84), do not bind or activate the PTH1R. A possible physiological role for this region of the hormone is suggested by observations that the amino acid sequence of the COOH-terminal domain is highly homologous across species. Furthermore, direct physical evidence of a putative receptor, i.e., a carboxyl-terminal PTH receptor (CPTHR) with binding specificity for COOH-terminal PTH sequences, was obtained by cross-linking of 125I-[Tyr34]-hPTH-(19-84) (which does not bind to the PTH1R) to 40-kDa and 90-kDa proteins in the ROS 17/2.8 rat osteosarcoma cell line.

**Objectives:**

To characterize CPTH functional and structural features using bioinformatic analytical tools. The premise is that such characterization would allow for future experimental examinations on the pathophysiology of diseases involving significant changes in CPTH expression levels or mode of function.

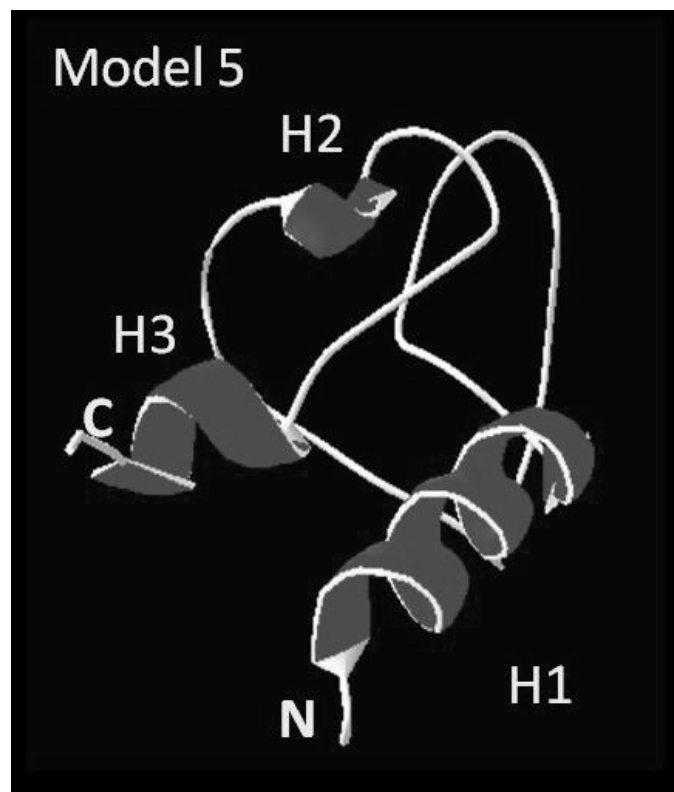
**Methods:** Several bioinformatic tools were utilized including Pfam, ELM, ProFun, PFP, Consensus Secondary Structure Prediction server and I-TASSER.

**Results:**

1- ELM predicted N-Arg dibasic convertase cleavage site at position 40-42, Casien Kinase II (CK2) phosphorylation site (71-74), Protein kinase C phosphorylation site (53-55).

2- Function prediction analysis suggested that CPTH may play a role in the following biological processes; cell proliferation (growth factor), cAMP metabolism, cell-cell signaling, calcium ion homeostasis, GTPase activity and GTP binding.

3-Secondary and Tertiary structure predictions suggested that CPTH has two helical domains on its termini at positions (23-35) and (74-83) as well as coils and sheets regions in the middle (36-73).



**Conclusions:** CPTH bioinformatic analysis data provide useful resources for researchers to understand and manipulate CPTH functions and to predict potential CPTH receptor(s).

**Disclosures:** A.A. Selim, None.

## SU073

**Relationship between Serum Levels of Inflammatory Cytokines and Bone Turnover Markers in the Year Following Hip Fracture.** J. A. Chan<sup>\*1</sup>, R. R. Miller<sup>\*1</sup>, J. A. Yu-Yahiro<sup>2</sup>, W. G. Hawkes<sup>\*1</sup>, J. R. Hebel<sup>\*1</sup>, M. D. Shardell<sup>\*1</sup>, G. E. Hicks<sup>\*1</sup>, M. C. Hochberg<sup>1</sup>, E. A. Streeten<sup>1</sup>, J. Magaziner<sup>1</sup>, D. Orwig<sup>1</sup>. <sup>1</sup>Epidemiology and Preventive Medicine, University of Maryland Baltimore, Baltimore, MD, USA, <sup>2</sup>Department of Orthopaedics, Union Memorial Hospital, Baltimore, MD, USA.

The purpose of this study was to examine the relationship between serum levels of inflammatory cytokines and markers of bone turnover in the year following hip fracture. Women who sustain a hip fracture have increased rates of bone loss (decline in BMD) as well as continually elevated serum levels of inflammatory cytokines up to one year post-fracture. Several proinflammatory cytokines have been associated with bone remodeling; however with inconsistent results. Furthermore, little is known about a potential relationship after hip fracture.

The Baltimore Hip Studies (BHS4) cohort was a randomized clinical trial in which participants were assigned to either a home-based exercise program or standard of care group. Women age 65 years and older (mean 82 years  $\pm$  6.8) were enrolled within 15 days after fracture (n=180).

Serum samples were analyzed for sTNF- $\alpha$ R1, IL-6, bone alkaline phosphatase (BAP), C-terminal telopeptide of type I collagen (CTX), and C-terminal propeptides of type I procollagen (CICP) at baseline and 2-, 6-, and 12-months after fracture. Generalized estimating equations were used to model the association of sTNF- $\alpha$ R1 and IL-6 levels with markers of bone turnover over time adjusting for age, BMI, type of fracture and intervention group.

The analysis included 88, 95, 107, and 91 participants at baseline, 2-, 6-, and 12-months after fracture respectively. Higher levels of sTNF- $\alpha$ R1 were associated with higher levels of CTX during the year after fracture (p<0.0001). For each ng/ml increase in sTNF- $\alpha$ R1, CTX was 0.16 (95% CI: 0.10, 0.22), 0.14 (95% CI: 0.05, 0.22), 0.12 (95% CI: 0.04, 0.20), and 0.09 (95% CI: 0.02, 0.16) ng/ml higher at baseline, 2-, 6-, and 12-months. Serum IL-6 levels were also positively associated with CTX levels during the year post-fracture (p<0.0001). There was no evidence of association between sTNF- $\alpha$ R1 and IL-6 with either BAP or CICP (p>0.10).

These data demonstrate that serum levels of sTNF- $\alpha$ R1 and IL-6 are positively associated with increased bone turnover. The results suggest that inflammation leads to increased bone resorption, contributing to the excess decline in bone mineral density in the year following hip fracture.

Mean difference in CTX (ng/ml) per ng/ml of sTNF- $\alpha$ R1 and per 10 pg/ml of IL-6 (higher vs lower)

	sTNF- $\alpha$ R1 (ng/ml) CTX ng/ml (95% CI)	P-value	IL-6 (10 pg/ml) CTX ng/ml (95% CI)	P-value
<b>Baseline</b>	0.16 (0.10, 0.22)	<.0001	0.03 (0.005, 0.06)	0.0222
<b>2 month</b>	0.14 (0.05, 0.22)	0.0028	0.03 (-0.02, 0.07)	0.19
<b>6 month</b>	0.12 (0.04, 0.20)	0.0043	0.01 (-0.04, 0.07)	0.66
<b>12 month</b>	0.09 (0.02, 0.16)	0.0073	0.07 (0.05, 0.09)	<.0001

**Disclosures:** J.A. Chan, None.

This study received funding from: National Institute on Aging.

## SU074

**The Tyrosine Kinase Inhibitor Dasatinib Decreases Osteoclast Formation and Activity *in vitro*.** K. Vandyke<sup>\*</sup>, A. L. Dewar<sup>\*</sup>, A. N. Davis<sup>\*</sup>, S. Fitter<sup>\*</sup>, T. P. Hughes<sup>\*</sup>, L. B. To<sup>\*</sup>, A. C. W. Zannettino<sup>\*</sup>. Division of Haematology, The Hanson Institute, The Institute of Medical and Veterinary Science, Adelaide, Australia.

We have previously shown that the tyrosine kinase inhibitor imatinib mesylate potently inhibits osteoclast formation and activity due, in part, to its specificity for the macrophage colony stimulating factor (M-CSF) receptor, c-fms. We have also shown that imatinib therapy is associated with altered bone remodelling and an increase in trabecular bone volume in chronic myeloid leukaemia patients. In the present study, we examined whether a second-generation tyrosine kinase inhibitor, dasatinib, could similarly inhibit c-fms activation and osteoclastogenesis. Initially, we assessed whether dasatinib could affect c-fms phosphorylation in human peripheral blood CD14<sup>+</sup> mononuclear cells (PBMNC) and mouse bone marrow monocytes (mBM) using Western blotting. We next examined the effects of dasatinib treatment on cell proliferation/survival in M-CSF-dependent (FDC-fms and mBM) and -independent (RAW-264.7) cells. Additionally, we investigated if dasatinib affected osteoclast formation and activity in PBMNC, mBM and RAW-264.7 cells.

Our studies show that dasatinib inhibits the activation of c-fms by M-CSF at pharmacologically-relevant concentrations (5 nM) in PBMNC and mBM. Furthermore, dasatinib treatment dose-dependently decreased cell numbers in FDC-fms (IC<sub>50</sub> = 57.8 nM) and mBM (IC<sub>50</sub> = 5.0 nM) cultured with M-CSF. In contrast, cell numbers were not significantly altered by dasatinib-treatment in M-CSF-independent RAW-264.7 cells (p = 0.4894) or in FDC-fms cells cultured in IL-3 (p = 0.2008). In PBMNC and mBM cultures stimulated with RANKL and M-CSF, the number of TRAP-positive, multinucleated osteoclasts was significantly reduced in the presence of 20 nM dasatinib in PBMNC (p < 0.001; IC<sub>50</sub> = 10.5) and 10 nM dasatinib in mBM (p < 0.01; IC<sub>50</sub> = 8.0 nM), relative to vehicle controls. In addition, there was a dose-dependent decrease in bone resorption by osteoclasts at 2.5 nM dasatinib and higher (p < 0.05; IC<sub>50</sub> = 2.4 nM [PBMNC] and 3.5 nM [mBM]). In RAW-264.7 cells cultured with RANKL alone, osteoclast numbers were significantly decreased at 20 nM dasatinib and higher (p < 0.05) relative to vehicle.

These studies show for the first time that dasatinib treatment is associated with a decrease



in osteoclast formation and activity in both human and murine systems *in vitro*. This decrease can partly be attributed to an inhibition of signal transduction through c-fms. These data suggest that decreased bone resorption may be a potential side-effect of dasatinib therapy and these *in vitro* findings warrant further investigation *in vivo*.

**Disclosures:** K. Vandyke, None.

## SU075

**Angiogenic Potential of Osteoclasts.** F. C. Cackowski<sup>\*1</sup>, R. J. Choksi<sup>\*1</sup>, J. J. Windle<sup>\*2</sup>, D. Roodman<sup>3</sup>. <sup>1</sup>Medicine/Hem-Onc, University of Pittsburgh, Pittsburgh, PA, USA, <sup>2</sup>Human Genetics, Virginia Commonwealth University, Richmond, VA, USA, <sup>3</sup>Medicine/Hem-Onc, University of Pittsburgh and VA Pittsburgh Healthcare System, Pittsburgh, PA, USA.

It is our hypothesis that in diseases associated with increased osteoclast (OCL) activity, OCL secrete, or release from matrix, factors that stimulate angiogenesis either directly or by induction of angiogenic factor secretion by other cell types. Further, agents such as bisphosphonates may in part suppress angiogenesis through their effects on osteoclast activity. In support of this hypothesis, we demonstrated that human OCL secrete numerous pro-angiogenic factors including angiopoietin-1, angiopoietin-4, IL-8, osteopontin, and MCP-1, and that conditioned media (CM) from cultures of highly purified human OCL formed *in vitro* from normal bone marrow stimulated angiogenesis in co-cultures of fibroblasts and endothelial cells. OCL CM induced angiogenesis to a greater extent than CM from macrophages on a per cell basis. To determine if OCL stimulated angiogenesis in a bone microenvironment, we used the fetal mouse metatarsal angiogenesis assay to determine if the OCLs present in these bones contribute to their angiogenic potential. This assay employs bone explants from fetal mice, which contain OCLs, osteoblasts, fibroblasts and endothelial cells, to permit testing modulators of OCL activity for their effects on angiogenesis in a bone microenvironment. The OCL inhibitor osteoprotegerin (OPG) reproducibly inhibited basal angiogenesis in this assay even though metatarsals treated with OPG remained responsive to VEGF. Thus, OPG did not directly suppress the angiogenic capacity of endothelial cells. Further, activity of tartrate resistant alkaline phosphatase, a measure of OCL activity, was significantly reduced in the metatarsals at concentrations of OPG that inhibited angiogenesis. These data support the hypothesis that suppression of OCL activity can decrease angiogenesis in the bone microenvironment and that increased OCL activity in conditions such as inflammatory arthritis and bone metastasis may contribute to the increased angiogenesis found in these conditions.

**Disclosures:** D. Roodman, Novartis 1, 2; Amgen 2; Millenium 2.  
This study received funding from: Novartis.

## SU076

**Recovery of Bone Architecture after RANKL Administration in Rats Is Characterized by Increased Bone Mass on Existing Trabeculae Assessed by *in vivo* Micro-CT.** G. M. Campbell<sup>1</sup>, M. S. Ominsky<sup>\*2</sup>, S. K. Boyd<sup>1</sup>. <sup>1</sup>University of Calgary, Calgary, AB, Canada, <sup>2</sup>Amgen Inc, Thousand Oaks, CA, USA.

Receptor activator of nuclear factor NF- $\kappa$ B ligand (RANKL) is required for osteoclast production and survival. Excess RANKL expression has been linked to post-menopausal bone loss. We have employed a model that introduces an excess-RANKL state in order to mimic osteoporotic bone loss and potential recovery. The purpose of this study was to determine (1) if changes in the trabecular architecture of rats injected with soluble RANKL follow the same patterns as the ovariectomized (OVX) rat and (2) the architectural patterns during recovery following withdrawal of RANKL injections.

Female retired breeder Wistar rats aged 7-9 months were assigned to one of four groups: high-dose RANKL (0.25mg/kg s.c. 5dy/wk), low-dose RANKL (0.05mg/kg s.c. 5dy/wk), vehicle or OVX (N = 8/gp). RANKL injections began at the time of surgery, and were stopped at wk 6. The right proximal tibial metaphysis was micro-CT scanned *in vivo* (vivaCT 40, Scanco Medical, Switzerland) at a voxel size of 12.5  $\mu$ m every two weeks from wk 0 to wk 12 and every four weeks from wk 12 to wk 20 (9 scans/rat). Bone volume ratio (BV/TV), trabecular thickness (Tb.Th), separation (Tb.Sp), number (Tb.N), connectivity density (Conn.D), structure model index (SMI) and cortical thickness (Ct.Th) were determined. Paired t-tests were used to detect changes from week to week and from baseline values.

The patterns of bone loss during the injection period were similar in the OVX and RANKL groups; however the rate and magnitude differed. At wk 2, the mean BV/TV in the high group was significantly reduced to 52% of the baseline value and was further reduced to 39% at wk 4. Significant changes in BV/TV of the low group were first observed at wk 6 (94% of baseline). BV/TV in the OVX group was reduced to 90% of baseline at wk 2, and 77% at wk 6. Throughout the injection period, significant changes were observed in the high RANKL and OVX group for all parameters, and in the low RANKL group for all parameters except Tb.N. After stopping injections, full recovery of Tb.Th and Ct.Th and partial recovery of BV/TV (55% of baseline) and SMI (1.34 to 0.89 above baseline) occurred in the high dose group. In the low dose group, BV/TV, SMI and Tb.Th recovered fully. Conn.D and Tb.N showed no improvement after withdrawal of RANKL in either group. RANKL treatment had a dose-dependent effect on the tibia of the rat and appeared to affect the architecture in a similar manner to OVX. Changes to BV/TV, Tb.Th, SMI and Ct.Th due to RANKL injection appear to be reversible, while changes to Conn.D and Tb.N do not. Direct observation by registration of the micro-CT data showed thin trabeculae that became thicker following RANKL withdrawal.

**Disclosures:** G.M. Campbell, None.

## SU077

**Comparison of Direct Osteoclastogenic Potential on Osteoclast Precursor Cells Among Proinflammatory Cytokines.** S. Park<sup>\*</sup>, J. Ju<sup>\*</sup>, J. Park<sup>\*</sup>, H. Oh<sup>\*</sup>, H. Kim<sup>\*</sup>. Internal Medicine, Division of Rheumatology, College of Medicine, The Catholic University of Korea, Seoul, Republic of Korea.

Various cytokines play an important role in the pathogenesis of autoimmune disease such as rheumatoid arthritis. Bone destruction which comes from cytokine-associated inflammation finally results in joint dysfunction. This study was performed to examine the direct influences of these cytokines on osteoclast precursor cells during the osteoclastogenesis and to compare the osteoclastogenic potentials among TNF $\alpha$ , IL-1, IL-6, IL-17, and IL-23. Monocytes which were derived from mice bone marrow were prepared for progenitor cells of osteoclasts. Precursor cells were incubated in the presence of M-CSF (30 ng/ml) for the first 2 days and then IL-1 (0.1 ng/ml~10 ng/ml), IL-6 (0.1 ng/ml~10 ng/ml), IL-17 (0.1 ng/ml~10 ng/ml), IL-23 (0.1 ng/ml~10 ng/ml), and TNF (0.1 ng/ml~10 ng/ml) in the presence of M-CSF for a further 7 days. Every culture condition was treated with various concentration of RANKL (1, 5, 10, 50, and 100 ng/ml). Permissive level of RANKL was essential for osteoclastogenesis in every condition. IL-1 and TNF $\alpha$  enhanced osteoclastogenesis, but IL-6 inhibited osteoclastogenesis on the contrary. IL-1 showed most powerful potential for osteoclastogenesis in dose dependent manner. Interestingly, during the later time of osteoclastogenesis, TNF $\alpha$  enhanced osteoclastogenesis in the moderate dose of RANKL 50ng/ml, but dose-dependently inhibited osteoclastogenesis in concentration of 100ng/ml RANKL. IL-1 was universally pro-osteoclastogenic, and IL-6 was universally anti-osteoclastogenic. TNF $\alpha$  had the various effects on osteoclast precursor according to treatment time and RANKL concentration. It was interesting to compare osteoclastogenic potential of various proinflammatory cytokines in the same condition and would be more interesting to elucidate the difference of intracellular signaling in the cytokine-associated osteoclastogenesis.

**Disclosures:** J. Ju, None.

## SU078

**TGF- $\beta$ 1 Induces Human Osteoclast Apoptosis.** N. Houde<sup>\*</sup>, E. Chamoux, M. Bisson<sup>\*</sup>, S. Roux. Rheumatology, Faculty of Medicine, University of Sherbrooke, Sherbrooke, QC, Canada.

Transforming growth factor- $\beta$ 1 (TGF- $\beta$ 1) is the most abundant TGF- $\beta$  isoform detected in bone. TGF- $\beta$ 1 is stored in the bone matrix and may be released and activated during osteoclastic bone resorption. The effects of TGF- $\beta$ 1 on bone cells are complex and may depend on cell differentiation stage, TGF- $\beta$ 1 concentration and *in vitro* culture conditions. We previously showed that TGF- $\beta$ 1 induces apoptosis in human osteoclasts, however the mechanisms involved in these cells are not known, and the aim of the present study was to evaluate the apoptotic intracellular pathways activated by TGF- $\beta$ 1 in human osteoclasts. We used cord blood monocytes as osteoclast precursors. In long term cultures in the presence of MCSF and RANKL, multinucleated cells (MNCs) that express osteoclast markers form and are able to resorb bone. By immunocytochemistry we showed that these MNCs express both type I and II TGF- $\beta$ 1 receptors. Apoptosis was evaluated using a TUNEL-derived method, and in the presence of 1 ng/ml of TGF- $\beta$ 1, apoptosis was significantly increased to 48.8 $\pm$ 3% of the MNCs compared to 33.6 $\pm$ 3% in control cultures (p<0.01). In these cultures, the rate of TGF- $\beta$ 1-induced apoptosis significantly decreased in the presence of a caspase 9 inhibitor (36.6 $\pm$ 4% vs 44.3 $\pm$ 2.3% in control cultures, p<0.05) but not with an inhibitor of caspase 8. In addition, the expression of activated caspase-9 evaluated by immunocytochemistry was significantly increased (52 $\pm$ 1.8% vs 39.5 $\pm$ 2.6%, p<0.05). In various cells, TGF- $\beta$ 1 signaling involves primarily Smad proteins, but also interferes with intracellular modulators of apoptosis such as JNK, p38, Akt, NF- $\kappa$ B and Bcl2 family members. Using Western blot analysis to evaluate the expression of phosphorylated (activated) MAPKs and Smad2, we showed that upon TGF- $\beta$ 1 stimulation, activation of p38 occurred after 15 min (1.86 fold higher at 15 min vs non-treated cells, p<0.01), followed by a slight activation of JNK between 15 and 30 min. Moreover, the main activation was observed for Smad2 with a high level of phosphorylation after 60 min (up to 7 fold increase compared to non-treated cells). In contrast, the phosphorylation of ERK1/2 was not increased upon TGF- $\beta$ 1 stimulation. Our results suggest that TGF- $\beta$ 1 induces human osteoclast apoptosis, a process involving Smad signaling as well as Stress-Activated Protein Kinase (p38, JNK) activation. These signaling cascades may modulate the intrinsic pathway of apoptosis in osteoclasts, reflected by caspase 9 activation. This may represent a regulatory mechanism involved in the inhibition of osteoclast activity by TGF- $\beta$ 1 during bone resorption.

**Disclosures:** N. Houde, None.

## SU079

**Elevated Serum Levels of CXCL12 Is Associated with Increased Osteoclast Activity and Osteolytic Bone Disease in Multiple Myeloma Patients.** P. Diamond<sup>\*1</sup>, A. Labrinidis<sup>\*1</sup>, S. K. Martin<sup>\*1</sup>, S. Gronthos<sup>1</sup>, L. To<sup>\*1</sup>, N. Fujii<sup>\*2</sup>, P. O'Loughlin<sup>\*1</sup>, A. Evdokiou<sup>\*1</sup>, A. C. W. Zannettino<sup>\*1</sup>. <sup>1</sup>Department of Haematology, Institute of Medical and Veterinary Science, Adelaide, Australia, <sup>2</sup>Department of Bioorganic Medicinal Chemistry, Graduate School of Pharmaceutical Sciences, Kyoto University, Kyoto, Japan.

Multiple myeloma (MM) is an incurable plasma cell (PC) malignancy able to mediate massive destruction of the axial and craniofacial skeleton. The aim of this study was to investigate the role of the potent chemokine, CXCL12 (also termed stromal derived factor 1, SDF-1) in the recruitment of OC precursors to the bone marrow (BM). Our studies show that MM PC produce significant levels of CXCL12 protein and exhibit elevated plasma levels of CXCL12 when compared with normal, age-matched subjects. The level of CXCL12 positively correlated with the presence of multiple radiological bone lesions in individuals with MM, suggesting a potential role for CXCL12 in OC precursor recruitment and activation. To examine these findings further, PB-derived CD14<sup>+</sup> OC precursors were cultured in an *in vitro* OC-potentiating culture system in the presence of recombinant human CXCL12. Whilst failing to stimulate an increase in TRAP<sup>+</sup>, multinucleated OC formation, CXCL12 mediated a dramatic increase in both the number and the size of the resorption lacunae formed. The increased OC motility and activation in response to CXCL12 was associated with an increase in the expression of a number of bone resorption-related genes including, RANKL, TRAP, matrix metalloproteinase-9 (MMP-9), Carbonic Anhydrase II (CA-II), and Cathepsin K. These findings are further supported by our recent *in vivo* studies where the human MM PC line, RPMI-8226, or genetically modified RPMI-8226 over-expressing CXCL12, were directly injected into the intra-tibial space of athymic nude mice, mimicking MM PC infiltration. The osteoclast activating potential of MM PC-derived CXCL12 was assessed by micro-CT, histological analyses and serum markers of bone loss. While implantation of RPMI-8226 into the tibiae resulted in a 5% decrease in bone volume (BV; compared with vehicle control), RPMI-8226 over-expressing CXCL12 mediated a 13% decrease in BV and a concomitant increase in osteolytic lesions and serum collagen I breakdown products. Furthermore, MM PC mediated osteolysis was significantly inhibited in animals receiving the CXCL12/CXCR4 antagonist, T140. These studies show that synthesis of high levels of CXCL12 by MM PC may contribute to the development of osteolytic lesions seen in patients with MM, by recruiting OC precursors to local sites within the BM and enhancing their motility and bone resorbing activity. Therefore, inhibition of CXCL12-CXCR4 may be an effective modality to inhibit osteolysis in MM patients.

**Disclosures:** P. Diamond, None.

## SU080

**CXCL12 Expression Is Regulated by HIF-2 $\alpha$  in Multiple Myeloma Plasma Cells.** S. K. Martin<sup>\*1</sup>, P. Diamond<sup>\*1</sup>, L. B. To<sup>\*1</sup>, D. Peet<sup>\*2</sup>, S. Gronthos<sup>1</sup>, A. C. W. Zannettino<sup>\*1</sup>. <sup>1</sup>Department of Haematology, Institute of Medical and Veterinary Science, Adelaide, Australia, <sup>2</sup>School of Molecular and Biomedical Science, University of Adelaide, Adelaide, Australia.

Multiple myeloma (MM) is an incurable haematological malignancy characterised by increased bone marrow (BM) angiogenesis and extensive lytic bone disease. Previous studies from our laboratory show that MM plasma cells represent an abundant source of the chemokine CXCL12, which serves to recruit both osteoclastic and vascular endothelial cells proximal to the MM plasma cells, thereby facilitating disease progression (Zannettino *et al.* 2005, Martin *et al.* 2006). Given the role of hypoxia-inducible factor-1 (HIF-1 $\alpha$ ) in inducing CXCL12 expression in other systems (Ceradini *et al.* 2004), we examined whether hypoxia could stimulate MM PC expression of CXCL12. Using the MM PC line, LP-1, our studies show that exposure to hypoxia induces a time dependent expression of CXCL12 mRNA and protein. By examining the hypoxia-induced expression profiles of CXCL12, HIF-1 $\alpha$  and HIF-2 $\alpha$  in the MM PC line LP-1, our results suggest that HIF-2 $\alpha$  is the primary regulator of CXCL12 expression under hypoxia. To examine this further, we engineered MM cells to express constitutive, high levels of HIF-1 $\alpha$  or HIF-2 $\alpha$ . Over-expression studies in MM cells show that HIF-1 $\alpha$  had little effect on CXCL12 expression, while HIF-2 $\alpha$  over-expression resulted in a 7.6 fold increase of CXCL12 mRNA and a 1.6 fold increase of CXCL12 protein. HIF-2 $\alpha$  regulation of CXCL12 was further examined using lentiviral expression constructs expressing shRNA for HIF-2 $\alpha$ . HIF-2 $\alpha$  knockdown in LP-1 cells resulted in a significant (p=0.01) decrease in CXCL12 expression. Finally, binding of HIF-2 $\alpha$  to the CXCL12 promoter was confirmed using CXCL12 promoter luciferase assay reporter gene studies, electrophoretic mobility shift and chromatin immunoprecipitation assays. These studies demonstrate, for the first time, that hypoxia regulates CXCL12 expression in MM PCs and occurs predominantly via activation of HIF-2 $\alpha$ .

1) Zannettino AC *et al.* (2005). Elevated serum levels of stromal-derived factor-1 $\alpha$  are associated with increased osteoclast activity and osteolytic bone disease in multiple myeloma patients. *Cancer Res.* 2005;65:1700-1709.

2) Martin, SK *et al.* (2006). "Tumor angiogenesis is associated with plasma levels of stromal-derived factor-1 $\alpha$  in patients with multiple myeloma." *Clin Cancer Res* 12(23): 6973-7.

3) Ceradini, DJ *et al.* (2004). "Progenitor cell trafficking is regulated by hypoxic gradients through HIF-1 induction of SDF-1." *Nat Med* 10(8): 858-64.

**Disclosures:** P. Diamond, None.

## SU081

**The Effects of IL-27 on Regulation of Osteoclastogenesis by Way of T Cells.** S. Kamiya<sup>\*1</sup>, T. Fukawa<sup>\*1</sup>, C. Nakamura<sup>\*2</sup>, T. Yoshimoto<sup>\*3</sup>, S. Wada<sup>1</sup>. <sup>1</sup>Clinical Sciences, Josai International University, Chiba, Japan, <sup>2</sup>Bio-analytical Chemistry, Josai International University, Chiba, Japan, <sup>3</sup>Intractable Immune System Disease Research Center, Tokyo Medical University, Tokyo, Japan.

A number of evidence has shown that bone remodeling process was affected by host immune reactions. Above all, cytokines that could modulate T cell functions were much focused in this area. Interleukin (IL) -27, a member of the IL-6/IL-12 family, has been shown to initiate type 1 helper T (Th1) cell responses and, however, to suppress excessive immune responses. Here, we examined the effects of this cytokine on osteoclast (OC) formation induced by M-CSF/RANKL in the presence of T cells.

Mouse bone marrow macrophage like cells (BMMs) were prepared from bone marrow cells with M-CSF, and were cocultured with activated T cells which were partially purified from isolated splenocytes by adhesion properties and were stimulated by anti-CD3 antibody.

When T cells were activated by 0.2  $\mu$ g/ml anti-CD3 antibody and cocultured with BMMs in the presence of M-CSF/sRANKL, the number of OC was reduced compared with that of co-cultures with innate T cells. The addition of IL-27 in this culture much strongly and significantly inhibited OC formation. To understand this phenomenon more precisely, we explored possible factors which could be produced by the activated T cells and modulate OC formation. Although the production of TNF $\alpha$ , IL-4, and IFN $\gamma$ , detected by ELISA, was not changed in T cells treated with IL-27, the production of IL-10 was increased by ~200% in T cells treated with IL-27. In this process, we found that treatment with IL-27 also significantly reduced sRANKL production in activated T cells. This effect of IL-27 on sRANKL production was observed in Th1 and Th2 cell subsets. Furthermore, FACS analysis revealed that treatment with IL-27 suppressed the expression of membrane-bound RANKL on the Th1 and Th2 cells, but not on osteoblasts stimulated by IL-6. The effects of IL-27 on RANKL expression of Th17 cells are under investigation.

In this study, we found that IL-27 inhibited OC formation when cocultured with activated T cells. The effects of IL-27 would be associated with modified cytokine-expression profile of the T cells. The findings observed in this study would suggest that IL-27 may play crucial roles for OC formation in autoimmune-related skeletal diseases.

**Disclosures:** S. Kamiya, None.

## SU082

**Establishment of a Murine Model of Hypercalcemia by Overexpression of sRANKL Using an Adenovirus Vector.** H. Yasuda<sup>1</sup>, Y. Furuya<sup>\*1</sup>, Y. Tomimori<sup>\*1</sup>, K. Mori<sup>\*1</sup>, J. Miyazaki<sup>\*2</sup>, T. Enomoto<sup>\*1</sup>. <sup>1</sup>Nagahama Institute for Biochemical Science, Oriental Yeast Co., Ltd., Shiga, Japan, <sup>2</sup>Graduated School of Medicine, Osaka University, Osaka, Japan.

Hypercalcemia is a significant complication of certain human malignancies, and is primarily caused by release of calcium from bone due to marked bone resorption by osteoclast activation. Animal models with hypercalcemia are useful tools for drug development and basic researches. In this study, we tried to generate a murine model overexpressing soluble receptor activator of NF-kappa B ligand (sRANKL) using an adenoviral vector. Adenoviral vector encoding sRANKL gene was injected i.p. to male C57BL/6 mice. As a negative control, adenoviral vector encoding LacZ gene was injected. Sera were collected at days 0, 7, and 14 for measurements of biochemical markers of bone turnover and sRANKL. Food and water intakes and body weights were measured every 3 or 4 days. All the mice were sacrificed 2 weeks after injection and their femurs were collected for measurements of bone mineral density (BMD). Serum sRANKL levels dramatically increased on day 7. Serum calcium levels increased peaking on day 7 and eventually returned to baseline levels on day 14. Food intakes and body weights significantly declined on day 7. These results indicated that the mice exhibited hypophagia that was one of symptoms of hypercalcemia. Increases in bone resorption and formation markers with a decrease in BMD were observed on day 14. The results reflect an acceleration of bone formation following activation of osteoclasts, namely coupling. In conclusion, we established a hypercalcemia model by overexpression of sRANKL. This model would be useful for researches of hypercalcemia and coupling between bone resorption and bone formation.

**Disclosures:** H. Yasuda, Oriental Yeast Co., Ltd. 1.

This study received funding from: Oriental Yeast Co., Ltd.

## SU083

**Lipopolysaccharide Suppresses RANK Gene Through the Down-Regulation of PU.1 and MITF.** R. Kitazawa<sup>1</sup>, J. Ishii<sup>\*1</sup>, T. Kondo<sup>1</sup>, K. Mori<sup>1</sup>, K. P. McHugh<sup>2</sup>, S. Kitazawa<sup>1</sup>. <sup>1</sup>Department of Pathology, Kobe University, Graduate School of Medicine, Kobe, Japan, <sup>2</sup>Orthopaedic Research, Beth Israel Deaconess Medical Center, Boston, MA, USA.

Receptor Activator of NF-kB (RANK) expressed on osteoclasts and their precursors is a receptor for RANKL, and signals transduced by RANK-RANKL interaction are prerequisite for the differentiation and activation of osteoclasts. We cloned and characterized a 6-kb fragment containing the 5'-flanking region of the mouse RANK gene. A fragment of 1-kb from the transcription start sites containing four Sp-1 sites and putative binding sites for MITF, CRE/AP-1 and PU.1 was ligated to the pGL3-basic vector, as pGL3-WT, and the promoter activity was confirmed by transfection studies using RAW

264.7 cells. By EMSA, the oligonucleotide spanning the PU.1 (-497/-463) showed a specific DNA protein binding that was washed out with excess amounts of the cold competitor containing the consensus PU.1 binding sequence. Moreover, the oligonucleotide spanning the proximal MTF binding site (-114/-93) showed a specific DNA protein binding that was block-shifted with an anti-MTF antibody. Co-transfection studies with MTF- and PU.1- expression vectors revealed that MTF and PU.1 increased RANK promoter activity 3- and 2-fold, respectively, and 6-fold synergistically. Mutagenesis of the PU.1 site, generated as pGL3-PU.1m, diminished the inducible effect of the PU.1-expression vector on the promoter activity; mutagenesis of the MTF site, generated as pGL3-MTFm, nullified the effect of the MTF-expression vector. Taken together, these results show that RANK transcription is positively regulated by both PU.1 and MTF. The effect of lipopolysaccharide (LPS) on RANK gene expression, analyzed by in situ hybridization using mouse bone tissue, showed that intra-peritoneal injection of LPS remarkably decreased RANK transcripts of both precursor and mature osteoclasts. Furthermore, assessed by quantitative real-time PCR, LPS treatment of RAW.264.7 cells decreased their RANK mRNA expression by 70%, mirroring the decrease of PU.1 and MTF mRNA. Transfection studies using the pGL3-RANK constructs revealed that short-term treatment of LPS decreased the promoter activity of pGL3-WT by 70%, but not that of pGL3-PU.1m or pGL3-MTFm. Although LPS has been reported to promote osteoclastogenesis in chronic and local pyogenic inflammation such as periodontitis by the indirect actions of other cytokines including the up-regulation of RANKL in odontoblast or osteoblastic cells, we speculate that LPS per se may directly suppress RANK expression on the osteoclast cell lineage, at least in part, by down-regulating the expression of PU.1 and MTF genes in acute and systemic severe endotoxemia, such as in septic shock.

**Disclosures:** R. Kitazawa, None.

This study received funding from: Ministry of Education, Sports and Culture, Japan.

## SU084

**Rheumatoid Synoviocytes Are Stimulated with IL-23 to Enhance Osteoclastogenesis Through Upregulation of RANKL Expression.** J. Min\*. Rheumatism Research Center, Catholic University of Korea, Seoul, Republic of Korea.

Purpose of this study is to delineate the osteoclastogenic effect of IL-23 via the fibroblast like synoviocyte (FLS). FLSs were separated from synovia of patients with rheumatoid arthritis (RA) and osteoarthritis (OA), and they were stimulated with IL-23. Receptor activator of nuclear factor kappa B ligand (RANKL) expression was measured by real time PCR and immunostaining. Osteoclast precursor cells were cocultured with IL-23-stimulated RA and OA FLS, respectively, and subsequently stained with mature osteoclast markers. In this study, we found that IL-23 upregulates RANKL expression on FLS and thus contributes to osteoclastogenesis. This indirect pathway is NF- $\kappa$ B and STAT3-mediated. We also discovered that RA FLS was more responsive to IL-23 in RANKL expression than OA FLS or normal FLS. We propose that IL-23-enhanced osteoclastogenesis of RA is mediated not only by IL-23-induced RANKL expression but also by the higher responsiveness of RA FLS to IL-23. Based on the results of this study, IL-23 might be a promising therapeutic target for the treatment of RA-associated bone destruction.

**Disclosures:** J. Min, None.

## SU085

**Mechanism of BMP-2 Enhancement of PGE<sub>2</sub> Stimulated Osteoclastogenesis.** K. A. Blackwell<sup>1</sup>, P. Hortschansky<sup>2</sup>, S. Sanovic<sup>1</sup>, C. Alander<sup>1</sup>, L. Raisz<sup>1</sup>, C. Pilbeam<sup>1</sup>. <sup>1</sup>New England Musculoskeletal Institute, University of Connecticut Health Center, Farmington, CT, USA, <sup>2</sup>Leibniz Institute for Natural Product Research and Infection Biology, Hans-Knöll-Institute (HKI), Jena, Germany.

Bone morphogenetic protein-2 (BMP-2) at high doses can enhance bone repair in animals. Combination therapy with other osteoinductive agents may be a strategy to decrease the dose of BMP-2 required and increase cost effectiveness. Preclinical models have suggested that prostaglandin E<sub>2</sub> (PGE<sub>2</sub>) or prostaglandin receptor agonists may increase the anabolic effects of BMP-2. However, PGE<sub>2</sub> is also a potent stimulator of osteoclastogenesis and the effect of the combination of BMP-2 and PGE<sub>2</sub> on osteoclast formation, which may oppose the anabolic response, has not been explored. To study osteoclastogenesis in the presence of osteoblastic cells, we cultured whole bone marrow from femora and tibiae of CD1 mice. Cells were plated at 1 $\times$ 10<sup>6</sup> cells/cm<sup>2</sup> and treated with BMP-2 (100 ng/ml), PGE<sub>2</sub> (1  $\mu$ M), or the combination for up to 8 days. Cultures were stained for tartrate-resistant acid phosphatase (TRAP) activity and osteoclasts were defined as TRAP positive multinucleated cells (MNCs) with 3 or more nuclei. mRNA levels of receptor activator of NF- $\kappa$ B ligand (RANKL) and osteoprotegerin (OPG) were measured by quantitative RT-PCR. To study the direct effects on osteoclast precursors, we cultured spleen cells with macrophage colony stimulating factor (30 ng/ml) and RANKL (30 ng/ml) for 7 to 8 days and measured TRAP+ MNCs.

In marrow cultures, BMP-2 treatment alone did not increase osteoclast number compared with control at any time point. PGE<sub>2</sub> increased osteoclast numbers on days 5-7 of culture. BMP-2 + PGE<sub>2</sub> increased osteoclast number 2-3-fold compared with PGE<sub>2</sub> alone. In spleen cultures, BMP-2 and PGE<sub>2</sub> treatment did not increase osteoclast formation compared with control. In marrow cultures, PGE<sub>2</sub> increased RANKL mRNA levels 6- to 13-fold. BMP-2 alone, or in the presence of PGE<sub>2</sub>, had no effect on RANKL mRNA expression. Either BMP-2 or PGE<sub>2</sub> alone decreased OPG mRNA levels by 34-40%. BMP-2 + PGE<sub>2</sub> further suppressed OPG compared with PGE<sub>2</sub> or BMP-2 alone to 43-54%. PGE<sub>2</sub> increased the RANKL:OPG ratio, which was further increased in the presence of BMP-2. Our results

suggest that BMP-2 enhances PGE<sub>2</sub> stimulated osteoclast formation by increasing the RANKL:OPG ratio, primarily by decreasing OPG.

**Disclosures:** K.A. Blackwell, None.

This study received funding from: NIH DK048361.

## SU086

**Roles of Cxcl2 in Osteoclast Precursor Cells.** J. Ha\*, H. Kim. Cell and Developmental Biology, Dental Research, Seoul, Republic of Korea.

Recently, some chemokines were shown to be expressed in bone cells and regulate the activity of osteoblasts and osteoclasts. But many chemokines remain to be elucidated for their role in bone microenvironment. We have shown that osteoclast precursors, bone marrow macrophages (BMMs), have CXCR2 chemokine receptor. BMMs highly expressed CXCR2 and decreased during osteoclastogenesis. The ligand of CXCR2, CXCL2, is known to be induced by endotoxin in macrophages. But we first found that osteoclastogenic cytokines (M-CSF and RANKL) can induce CXCL2 expression. CXCL2 was up-regulated in osteoclastic culture condition as determined by RT-PCR, Westernblot, and ELISA analysis. RANKL could induce CXCL2 expression and M-CSF addition elicited synergy in the RANKL induced CXCL2 expression. Up-regulation of CXCL2 by RANKL was through JNK and p38 dependent pathway. To specifically assess the role of CXCL2 in BMMs, we studied the effect of recombinant CXCL2 on BMMs. CXCL2 potently increased osteoclastogenesis dose dependent manner. TRAP positive multinucleated cells significantly increased with treatment of recombinant cxcl2 at BMM and pOC stage of differentiation. CXCL2 secreted by RANKL could stimulate the adhesion and migration of BMMs. Neutralization of CXCL2 with CXCL2 specific antibody at pOC stage potently inhibited osteoclastogenesis. However, in the presence of CXCL2 specific antibody, BMMs could not survive. Therefore, we checked the effect of CXCL2 on proliferation of BMMs. CXCL2 alone could not induce proliferation of BMMs but CXCL2 enhanced proliferation of BMMs in a dose dependent manner with low dose of M-CSF. Using siRNA system, BMMs treated with CXCL2 siRNA cultured with M-CSF and RANKL could not proliferate comparing with scrambled siRNA-treated cells. In summary, CXCL2 induced by RANKL can increase the adhesion, migration, and proliferation of osteoclast precursors and ultimately enhance osteoclastogenesis. These events may contribute to the recruitment of osteoclast precursors to bone lesion and inflammatory regions in vivo under pathological conditions.

**Disclosures:** J. Ha, None.

## SU087

**Real Time Oscillations in TNF-induced Gene Expression MAP Kinase Phosphorylation and Promoter Binding.** J. Iqbal\*, L. Sun, L. Zhu\*, G. Yang\*, M. Zaidi. Medicine, Mount Sinai School of Medicine, New York, NY, USA.

With only few exceptions that include Hes-1 p53, and I $\kappa$ B, the expression of genes has never been shown to be oscillatory. Here, we show that TNF triggers oscillations in >5000 genes. Microarrays performed at 30-minute intervals revealed that 15% of genes in the murine genome underwent a >3-fold increase in expression, with 89% oscillating at frequencies as low as every 50 minutes. Analysis of two sub-clusters by qPCR revealed continuous oscillations. Such oscillations, but with unique induction profiles, were also triggered by the related cytokines RANK-L. Further analysis showed that multiple signaling components downstream of the TNF receptor, such as TRAF-1, also underwent oscillations. TNF likewise triggered oscillations in the phosphorylation of three MAP kinases, as well as p65. An NF- $\kappa$ B super-repressor altered oscillation amplitude and frequency, attesting to a role for NF- $\kappa$ B as a modulator of such cyclical activation. Finally, we studied how these oscillations can combine in a ligand-specific manner at the level of the promoter to initiate gene transcription. For this, we utilized the late onset gene CD38, since TNF, but not the related cytokine RANK-L, induces its expression. Quantitative ChIP analysis revealed that TNF induced oscillations in p65 and p50 recruitment to the CD38 promoter, which correlated with MAP kinase-induced AP-1 recruitment. Through re-ChIP analysis, we determined the formation of a unique transcriptional complex on the promoter at 3 hours post-TNF addition, which corresponded to the onset of CD38 transcription. RANK-L, in contrast, was unable to combinatorially recruit AP-1 and NF- $\kappa$ B transcription factors to the CD38 promoter, despite inducing the activation of both signaling pathways. These results constitute a new paradigm through which cells dynamically coordinate time-resolved gene transcription by the formation of novel time-specific transcriptional complexes. Considering this dynamism, timed analyses of gene transcription, MAP kinase phosphorylation and promoter binding should become the experimental norm.

**Disclosures:** J. Iqbal, None.

## SU088

**Differential Contribution of Osteoclast- and Osteoblast-Lineage Cells to Lipopolysaccharide Modulation of Osteoclastogenesis.** V. Alshits\*, Z. Bar-Shavit. Experimental Medicine and Cancer Research, Hebrew University, Jerusalem, Israel.

Bacterial infections cause pathological bone loss by accelerating differentiation and activation of the osteoclast. A variety of bacteria-derived molecules have been shown to enhance osteoclast differentiation via activation of Toll-like receptors (TLRs). Lipopolysaccharide (LPS), activating TLR4, is the most studied bacterial-derived molecule in this regard. The interactions of LPS with TLR4 in both osteoclast- and osteoblast-lineage cells contribute to its osteoclastogenic effect. Here we examine the relative contribution of each of the lineages to LPS osteoclastogenic effect. To answer this question we chose to employ the co-culture system. To this end we used C3H/HeN (wt) and C3H/HeJ (mut) mice expressing a functional and a non-functional mutant TLR4, respectively. We performed our analyses in mixed co-cultures of osteoclast precursors (OCPs) and osteoblasts (OBs) containing all 4 possible combinations (OCPs.wt/OBs.wt, OCPs.mut/OBs.mut, OCPs.wt/OBs.mut and OCPs.mut/OBs.wt). This approach enables us to examine LPS modulation of one lineage (wt-derived) in the presence of the other (mut-derived). We first confirmed that both osteoclast- and osteoblast-lineage cells derived from C3H/HeJ do not respond to LPS. We found that LPS increased osteoclastogenesis in OCPs.wt/OBs.wt and did not affect osteoclastogenesis in OCPs.mut/OBs.mut. In the 2 mixed co-cultures there was a reduction in the LPS ability to affect osteoclast differentiation. The LPS osteoclastogenic activities in OCPs.wt/OBs.mut and in OCPs.mut/OBs.wt were 57% and 22% of the activity in OCPs.wt/OBs.wt, respectively. LPS induced TNF-alpha expression in OCPs.wt/OBs.wt, but not in OCPs.mut/OBs.mut. This activity was impaired in the mixed co-cultures; the inhibition was more prominent in OCPs.mut/OBs.wt. Our data are consistent with the dependence of LPS-induced osteoclastogenesis on TLR4 on both, OCPs and OBs and show that the activation of TLR4 in OCPs is more crucial to induction of osteoclastogenesis than activation of the osteoblastic TLR4. Our data also indicate that OCPs-derived TNF-alpha modulates the activity of the OBs and OBs-derived TNF-alpha modulates the activity of the OCPs.

**Disclosures:** V. Alshits, None.

## SU089

**The Matrix PRoline/arginine-rich End Leucine-rich Repeat Protein (PRELP) Interferes with the NF-kappaB Pathway and Impairs Osteoclast Formation and Activity.** N. Rucci<sup>1</sup>, A. Rufo<sup>\*1</sup>, M. Alamanou<sup>\*1</sup>, M. Capulli<sup>\*1</sup>, A. Del Fattore<sup>\*1</sup>, D. Heinegard<sup>\*2</sup>, A. Teti<sup>1</sup>. <sup>1</sup>Department of Experimental Medicine, University of L'Aquila, L'Aquila, Italy, <sup>2</sup>Department of Experimental Medical Science, University of Lund, Lund, Sweden.

PRELP is a heparin binding anchor protein, highly expressed in cartilage and developing bone. We found that a peptide corresponding to its heparin-binding domain (hbdPRELP) irreversibly impaired osteoclastogenesis of non-fractionated mouse bone marrow cultures or purified bone marrow macrophages, and inhibited bone resorption and mature osteoclast adhesion. hbdPRELP specifically affected late pre-fusion osteoclasts with a mechanism dependent on chondroitin sulfate cell surface proteoglycans, while not on heparan sulfate. Tagged hbdPRELP co-localized with cell surface chondroitin sulfate, was internalized in endosomes and transferred to the nucleus with a mechanism dependent on cell activity and abolished by chondroitinase treatment of cells. Internalization also required annexin II, which co-localized with cell surface chondroitin sulfate and tagged hbdPRELP, with which it formed a complex, revealed by immunoprecipitation. hbdPRELP translocated to the nucleus, bound p65 NF-kappaB subunit and inhibited its DNA binding by 50%, leading to a significant reduction of the downstream osteoclast-specific genes cathepsin K, calcitonin receptor, metalloproteinase 9, RANK, TRAcP, DC-STAMP and CD44. Consistently, in hbdPRELP-treated pre-fusion osteoclasts no nuclear localization was found for the transcriptional factor NFATc1. hbdPRELP did not prevent RANKL-induced MAPK phosphorylation, nor did it trigger apoptosis, as showed by normal nuclear morphology and lack of modulation of caspase 3 and Bax/Bcl-2 protein expression. Finally, effects of hbdPRELP appeared osteoclast-specific, as the peptide failed to affect mouse calvarial osteoblast differentiation, function, gene expression and transcription of osteoclastogenic cytokines. In conclusion, the heparin binding domain of PRELP is a novel direct negative regulator of osteoclast formation blocking NF-kappaB signaling in late pre-fusion osteoclast precursors with no effect on osteoblasts. We believe that these data could allow a deeper understanding of osteoclast biology as well as the direct involvement of matrix molecules in bone remodeling.

**Disclosures:** N. Rucci, None.

## SU090

**IFN-beta Is a Key Molecule in Inhibition of Human Osteoclast Differentiation by 1alpha, 25-dihydroxyvitamin D<sub>3</sub>.** S. Sakai<sup>\*1</sup>, H. Takaishi<sup>2</sup>, K. Matsuzaki<sup>\*2</sup>, H. Kaneko<sup>\*2</sup>, M. Furukawa<sup>2</sup>, A. Shiraishi<sup>\*1</sup>, T. Suda<sup>\*3</sup>, T. Miyamoto<sup>4</sup>, Y. Toyama<sup>\*2</sup>. <sup>1</sup>Product Research Department, Chugai Pharmaceutical CO., LTD, Gotemba, Japan, <sup>2</sup>Department of Orthopedic Surgery, Keio University, Tokyo, Japan, <sup>3</sup>Department of Cell Differentiation, Keio University, Tokyo, Japan, <sup>4</sup>Department of Orthopedic Surgery, Department of Musculoskeletal Reconstruction and Regeneration, Department of Cell Differentiation, Keio University, Tokyo, Japan.

Vitamin D plays a critical role in calcium and bone metabolism. In cocultures of the bone marrow and osteoblastic cells, 1 $\alpha$ ,25(OH)<sub>2</sub>D<sub>3</sub>, an active form of vitamin D<sub>3</sub>, induces the expression of RANKL in osteoblastic cells and thereby stimulating osteoclastogenesis. This fact leads to the widespread belief that active vitamin D<sub>3</sub> is a bone-resorbing hormone. On the other hand, active vitamin D<sub>3</sub> treatment reduces bone resorption and bone fracture risks in osteoporotic patients, however, the molecular mechanisms how active vitamin D<sub>3</sub> inhibits bone resorption are largely unknown. In this study, we revealed that 1 $\alpha$ ,25(OH)<sub>2</sub>D<sub>3</sub> directly inhibits human osteoclastogenesis through IFN- $\beta$  and NFATc1 axis. CFU-GM cells generated from human bone marrow cells were used for this study as osteoclast progenitor cells. CFU-GM cells were stimulated with 30 ng/mL M-CSF and 30 ng/mL RANKL for 6 days to generate multinucleated (n>3) osteoclasts (OCLs). 1 $\alpha$ ,25(OH)<sub>2</sub>D<sub>3</sub> significantly inhibited OCLs formation in a dose-dependent manner. Vitamin D receptor (VDR) was detected in CFU-GM cells indicating that 1 $\alpha$ ,25(OH)<sub>2</sub>D<sub>3</sub> may inhibit osteoclastogenesis directly through VDR. The expression of IFN- $\beta$ , a strong inhibitor of osteoclastogenesis, was significantly upregulated by 1 $\alpha$ ,25(OH)<sub>2</sub>D<sub>3</sub> treatment. To elucidate the role for IFN- $\beta$  in the inhibitory effect of 1 $\alpha$ ,25(OH)<sub>2</sub>D<sub>3</sub> on osteoclastogenesis, we added the neutralizing antibody against IFN- $\beta$  into the culture medium. The expression of NFATc1, a downstream molecule of RANKL-RANK signaling, and osteoclast differentiation were significantly restored by treatment with anti IFN- $\beta$  antibody. Taken together, our data suggest a novel mechanism that 1 $\alpha$ ,25(OH)<sub>2</sub>D<sub>3</sub> inhibits osteoclastogenesis through the upregulation of IFN- $\beta$ , which downregulates NFATc1 expression in osteoclast progenitor cells in an autocrine/paracrine manner.

**Disclosures:** S. Sakai, None.

## SU091

**In vitro Aging of Young Bone Enhances Osteoclastogenesis.** D. J. Leeming, I. Byrjalsen, K. Henriksen, M. G. Sørensen, P. Qvist, C. Christiansen\*, M. A. Karsdal. Nordic Bioscience, Herlev, Denmark.

**Purpose:** Bone remodeling is essential for maintaining the quality of bone. Preliminary data have suggested that osteoclasts prefer to resorb aged bone compared to that of young bone by in vitro culturing of human osteoclasts. To further elucidate this mechanism we biochemically increased the age of young bones, by in-vitro incubation, and investigated the effect of bone age on the differentiation and activity of osteoclast precursors cultured on bone slices.

**Methods:** Cortical bone slices from a 9-month-old calf and an 8-year-old cow were incubated for 0, ½, 1, 2½, or 7 months at 37°C in 70% EtOH. The bone slices from each incubation step were stored at -80°C until use. The age of the bone slices were measured as the ratio between newly synthesized non-isomerized ( $\alpha$ CTX) and isomerized ( $\beta$ CTX) C-telopeptide of type I collagen, a ratio that reflects the age of collagen type I. CD14 positive monocytes were isolated from human peripheral blood, seeded on bone slices, and cultured in 1% serum for 30 days in the presence of 25ng/ml of M-CSF and RANKL to follow osteoclastogenesis. Osteoclastic resorption was assayed using the resorption markers  $\alpha$ CTX and  $\beta$ CTX, as well as hydroxyproline, in the conditioned medium collected during culture. Osteoclast number was investigated by measurement of TRAcP activity in conditioned medium. Total cell viability was assessed by the metabolic dye Alamar Blue.

**Results:** The  $\alpha/\beta$  CTX ratio measured in bone slices revealed that young bone was aged by incubation at 37° C. The  $\alpha/\beta$  CTX ratio in young bone decreased with increased time of incubation reaching the lowest level after 2½ month of incubation. In contrast the ratio in aged bone remained virtually unchanged during the in-vitro incubation.

Osteoclasts cultured on the in-vitro aged young bone slices released higher amounts of  $\alpha$ CTX,  $\beta$ CTX and hydroxyproline in an age-dependent manner (2-fold and 700-fold increased at 7 months, p<0.001). On the eight-year-old bone there was minute change in the release of resorption markers with increased in-vitro age. Total cell viability was higher on bone slices from the in-vitro aged young bone (p<0.001) as compared with the initial young bone. On the aged bone, the cell viability was relatively constant with increasing in-vitro age.

**Conclusions:** These data indicate that the osteoclastogenesis, number and activity of osteoclasts precursors are enhanced on aged bone compared to young bone. We speculate that that a biochemical change of the bone matrix accumulates during aging, which promote osteoclastogenesis and thereby results in increased numbers of mature resorbing osteoclasts on old bone.

**Disclosures:** D.J. Leeming, Employee of Nordic Bioscience 5.

## SU092

**Transactivation of RANKL by C/EBP $\beta$  and C/EBP $\delta$  in Adipocyte Lineage Cells.** S. Takeshita, T. Fumoto\*, K. Ikeda. Bone and Joint Disease, National Center for Geriatrics and Gerontology, Obu, Japan.

Although RANKL expression has been studied in osteoblastic/stromal cells, the cell types in the bone microenvironment which actually express RANKL *in vivo* remain unknown. We reported that adipogenic cultures of mouse whole bone marrow cells induced robust formation of extremely long-lived osteoclasts in the absence of any exogenous osteotropic hormones or RANKL, and that the expression of RANKL was induced in such cultures (ASBMR 2007). Further, when the bone marrow stromal cell lines ST2 and MC3T3-G2/PA6 were stimulated to adipogenic differentiation, RANKL was transiently induced with concomitant down-regulation of OPG, suggesting that pre-adipocytes express RANKL and support osteoclastogenesis. In the present study, we examined the molecular mechanism by which RANKL gene expression is induced during adipocytic differentiation. When an NIH3T3 fibroblastic cell line was transduced with retroviral vectors encoding adipogenic transcription factors, C/EBP $\beta$  and C/EBP $\delta$  induced RANKL expression, while PPAR $\gamma$  did not. In transient transfection into NIH3T3 cells and luciferase reporter assays, C/EBP $\beta$  stimulated RANKL promoter activity, while mutations in the binding sites of C/EBP $\beta$  abrogated the Luc activity. Chromatin immunoprecipitation assays revealed that C/EBP $\beta$  and C/EBP $\delta$  bind to RANKL promoter *in vivo*, suggesting that RANKL is a direct target of these adipogenic transcription factors. The pre-adipocyte capacity to express RANKL and support osteoclastogenesis may contribute to the accelerated osteoclastogenesis which develops with aging under the influence of the adipose tissue-rich microenvironment in bone marrow.

**Disclosures:** S. Takeshita, None.

## SU093

**Grape Seed Extract (GSE) Suppresses IL-23/Th17 Inflammatory Pathways and Bone Destruction in Collagen Induced Arthritis.** J. Min\*. Rheumatism Research Center, Catholic University of Korea, Seoul, Republic of Korea.

**Objective :** Rheumatoid arthritis (RA) is a chronic inflammatory disease that a hallmark is a persistent inflammation of the synovium of the joints, leading to destruction of the surrounding bone and cartilage and ultimately joint deformities. we have investigated therapeutic effect of GSE, antioxidant compounds containing Procyanidins from Vitis vinifera seeds, on Type II collagen-induced arthritis (CIA) in mice

**Methods :** After GSE or saline administration, animals were monitored for 10 weeks. The progression of CIA (incidence, severity) was evaluated by arthritis scoring of paws. Histopathologic changes (cartilage destruction and pannus formation) and expression of inflammatory cytokines (IL-1b, TNF $\alpha$ , IL-17) within the knee joints were evaluated by immunohistochemistry. CII-specific IgG1 and IgG2a levels in serum and IL-23, IL-17, TNF- $\alpha$  and IL-4 concentrations in cultured supernatants were measured by ELISA and FACS. Osteoclasts were measured by tartrate-resistant acid phosphatase (TRAP) staining assay on RANKL and M-CSF induced osteoclast formation system. The number of TRAP positive multinucleated cells in cultures was counted.

**Results :** GSE treated arthritis mice suppressed bone erosion and destruction with an decrease in TRAP-positive osteoclasts. Treatment with GSE significantly reduced bone erosion and destruction with an decrease in TRAP-positive osteoclasts and the severity of osteolysis in CIA mice. In vitro examinations using bone marrow cultures containing M-CSF plus RANKL indicated that the osteoclast development was suppressed by GSE treatment. Histological analysis shows that cell infiltration and cartilage destruction was dramatically reduced and expression of IL-1b, TNF $\alpha$ , IL-23, IL-17 in the arthritic joint after treatment with GSE. Treatment of mice with GSE also decreased the amounts of CII-specific IgG2a and led to significant reduction of IL-17 and TNF- $\alpha$  production in cultured supernatant compared to saline-treated mice.

**Conclusion :** This study revealed GSE may be new effective agents for attenuating the joint destruction in RA.

**Disclosures:** J. Min, None.

## SU094

**Increased Osteoclast Differentiation and Bone Resorption During Spaceflight.** A. Di Benedetto\*, C. Camerino\*, R. Tamma\*, G. Colaianni\*, G. Greco\*, M. Strippoli\*, R. Vergari\*, A. Grano\*, L. Mancini\*, A. Zallone. Human Anatomy and Histology, University of Bari, Bari, Italy.

Serious effects on human health are experienced after long duration space missions. Prolonged exposure to microgravity seems to affect several physiological systems. Bone loss is considerable, with losses of 1-2% of bone mass per month in flight, occurring predominantly in the load bearing regions of the legs and lumbar spine. Microgravity induces an uncoupling of bone remodeling between bone formation and resorption that could lead to bone loss. Both processes are probably involved, but their relative importance and how they are orchestrated remain unclear. In order to fully understand the mechanisms underlying this bone loss we participated to the FOTON M3 mission launched on September 2007 that carried three experiments OSTEO, OCLAST and PITS developed by our team. We studied for the first time the *in vitro* effect of microgravity on osteoclasts (OCs) and our preliminary results indicate that OCs are directly affected. The OSTEO experiment was performed within a perfusion system of bioreactors, where the differentiation of precursors cells in mature OCs was tested on a synthetic 3D bone-like biomaterial, *skelite*, that partially reproduces the chemical composition and physical structure of natural bone. The aim was to analyze the gene expression pattern of osteoclasts differentiation in microgravity, compared with ground controls. RNA extracted from the cells was examined by RT-PCR. The preliminary results indicate that genes involved in osteoclast final maturation and activity, as integrin beta3, cathepsin K, MMP9 are upregulated in microgravity compared to ground control, while other genes were substantially at the same level. In OCLAST and PITS experiments, bone resorption by mature OCs was studied and the cells were cultured on bovine bone slices. The experiments, started in orbit, lasted 4 days. After landing the amount of collagen telopeptides, as index of bone resorption, was measured in OCLAST samples, while, for a genetic screening RNA was obtained from PITS samples. We found an increase in bone resorption after 4 days of space flight, indicated by higher telopeptide concentration and upregulation of genes related to osteoclast activity. These results are consistent with an increased osteoclastogenesis observed by our group in simulated microgravity conditions, and indicate osteoclasts precursors as direct target of microgravity.

**Disclosures:** A. Di Benedetto, None.

## SU095

**Implication of Prostaglandin D<sub>2</sub> in the Birth and Death of Human Osteoclasts.** M. A. Gallant\*, M. Durand\*, A. J. de Brum-Fernandes. Division of Rheumatology, Université de Sherbrooke, Sherbrooke, QC, Canada.

Bone resorption depends on osteoclastogenesis, individual osteoclast activity and on osteoclast apoptosis. The lifespan of osteoclasts is tightly regulated by many growth factors and survival signals. We recently demonstrated that human osteoclasts produce prostaglandins in resting conditions (Hackett et al, J of Rheum July 2006), and that prostaglandin D<sub>2</sub> (PGD<sub>2</sub>) can decrease osteoclasts differentiation and bone resorption (Durand et al, JBMR July 2008).

The objectives of the present study were to determine the effects of PGD<sub>2</sub> on osteoclastogenesis and on osteoclast apoptosis. CD14+ cells were purified from human peripheral blood and cultured for 7, 14 and 21 days in presence of RANKL and M-CSF to induce osteoclast differentiation. PGD<sub>2</sub> or specific PGD<sub>2</sub> receptors agonists were added to study the effects of DP and CRTH2 receptor activation. The expression of NFAT-C1 and PU.1, two transcription factors implicated in osteoclast differentiation, and of TRAP5b and Cathepsin K, mature osteoclasts markers, was determined using real-time quantitative PCR. Osteoclasts apoptosis was quantified using the TACS Blue kit from R&D Systems. Results show that NFATC-1 gene expression is decreased by half, while PU.1 gene expression was brought down to 75% upon PGD<sub>2</sub> stimulation. The use of specific agonists indicated that both PGD<sub>2</sub> receptors were implicated in this effect. The Cathepsin K gene was also downregulated by 75% by PGD<sub>2</sub> during the differentiation course, while TRAP gene expression was transiently decreased by 50% during the 14 first days of differentiation by PGD<sub>2</sub> receptor CRTH2 only. To study the role of PGD<sub>2</sub> in osteoclasts apoptosis, mature differentiated osteoclasts were stimulated with PGD<sub>2</sub> and apoptosis was evaluated. Results demonstrate that PGD<sub>2</sub> doubles human osteoclasts apoptosis compared to the basal apoptosis in the control conditions.

In conclusion, this study indicates that PGD<sub>2</sub> is controlling human osteoclasts differentiation at the molecular level, by decreasing the expression of essential transcription factors, what is corroborated by a decrease in the expression of mature osteoclast markers. PGD<sub>2</sub> also increases osteoclasts apoptosis. These results indicate that activation of PGD<sub>2</sub> receptors could inhibit bone resorption.

**Disclosures:** M.A. Gallant, None.

## SU096

**Simvastatin Induces Wnt Signaling and Reduces CSF-1 Secretion and RANKL/OPG Ratio to Block Osteoclast Differentiation.** C. C. Mandal<sup>1</sup>, N. Ghosh-Choudhury<sup>2</sup>. <sup>1</sup>Pathology, University of Texas Health Science Center at San Antonio, San Antonio, TX, USA, <sup>2</sup>Pathology, University of Texas Health Science Center at San Antonio and South Texas Veterans Health Care System, San Antonio, TX, USA.

An improper balance in bone remodeling, caused by increased osteoclast (OC) function, leads to debilitating diseases like osteoporosis and multiple myeloma. OC activities critically depend on osteoblast (OB)-derived factors. Colony stimulating factor-1 (CSF-1) and receptor activator of NFκB ligand (RANKL) are positive regulators of OC formation while osteoprotegerin (OPG), a soluble decoy for RANKL, balances the activity of RANKL during OC differentiation. We have shown recently that statins stimulate OB differentiation. Since statins suppress bone resorption we evaluated the clinical potential of simvastatin (Sim) in treating diseases originating from increased OC activity. We determined the effect of simvastatin on OC formation in a coculture assay using 2T3 osteoblasts and mouse spleen derived OC precursor cells. 5 μM Sim completely blocked OPG-induced formation of TRAP positive multinucleated (MNC) osteoclasts with significant reduction in TRAP enzyme activity. To elucidate the mechanism, we examined the effect of Sim on osteoclastogenic CSF-1 expression. Sim dose-dependently inhibited CSF-1 mRNA expression as determined by Northern blotting and real time qRT-PCR, resulting from reduced transcriptional activity of CSF-1 promoter. This translated into significant reduction in CSF-1 protein secretion as judged by ELISA. Real time qRT-PCR and transcriptional assays showed significant attenuation of osteoclastogenic RANKL expression upon Sim treatment. At the same time, Sim increased OPG expression resulting in reduction of RANKL/OPG ratio. Activation of Wnt signaling is reported to inhibit OC differentiation. To understand the signaling mechanism underlying statin-induced inhibition in expression of OB-derived OC differentiation factors, we tested the involvement of Wnt signaling pathway. Activation of Wnt signal transduction stimulates β-catenin translocation to the nucleus. We found that Sim induced translocation of β-catenin into the nucleus as determined by the immunoblotting of the nuclear fractions from 2T3 osteoblasts. Nuclear β-catenin increases transcription of Wnt-responsive genes. We used the reporter construct TOP-flash, which contains the Wnt-sensitive TCF/Lef1-responsive DNA element. Sim dose-dependently increased the TCF/Lef1 responsive reporter activity. Together these data for the first time show reduction of CSF-1 secretion and RANKL/OPG ratio in osteoblasts treated with Sim together with activation of Wnt signaling. Thus we provide a novel mechanism for reduced OC differentiation in response to Sim.

**Disclosures:** C.C. Mandal, None.

This study received funding from: NIAMS RO1 and VA MERIT Review.

## SU097

**Vimentin Binds c-Fms in an M-CSF Dependent Manner and Regulates Osteoclast Differentiation.** Y. Ito, H. Zhao, J. Chappel, S. L. Teitelbaum, F. P. Ross. Department of Pathology and Immunology, Washington University, St. Louis, MO, USA.

M-CSF is central to the differentiation, proliferation and survival of osteoclasts and their precursors. We previously reported that M-CSF regulates osteoclast differentiation and macrophage proliferation via the phosphoinositide 3-kinase (PI3K)/Akt pathway. Specific signals downstream of Akt that regulate the cytoskeleton remain incompletely defined. To identify novel Akt targets we treated BMMs with M-CSF and blotted lysates with a rabbit monoclonal antibody (PAS) that recognizes peptides or proteins containing R-X-R-X-X-phospho-(Ser/Thr). We found that many proteins are phosphorylated in response to M-CSF in a time-dependent manner. To investigate the Akt substrates which interact with c-Fms, the M-CSF receptor, total cell lysates of M-CSF-treated cells were immunoprecipitated with anti-c-Fms Ab and then immuno-blotted with anti-PAS. We found a single 57kDa-protein which we subjected to mass spectrometry and identified the molecule as vimentin, an intermediate filament protein. Using reciprocal immuno-precipitation/ western blot analysis we confirmed the M-CSF dependent interaction between c-Fms and vimentin. In addition, pre-treatment of BMMs with Ly294002, a PI3K inhibitor blocks binding of the receptor and intermediate filament protein. We next examined whether Akt can phosphorylate vimentin directly by *in vitro* kinase assay. Recombinant vimentin and Akt or p70S6 kinase (S6K), a Ser/Thr kinase which acts downstream of PI3K and the target of rapamycin (mTOR), were incubated in the presence or absence of ATP. Samples were immuno-blotted with anti-PAS Ab. S6K, but not Akt, phosphorylates vimentin ATP-dependently. Consistent with this observation, rapamycin, an inhibitor of mTOR, blocks the interaction between c-Fms and vimentin in response to M-CSF. To address the role of vimentin in osteoclast biology, we depleted vimentin by transducing BMMs with vimentin-specific shRNA lentiviral vector. Vimentin depletion suppresses but does not eliminate osteoclast differentiation. Brd U incorporation into M-CSF treated vimentin knockdown BMMs is significantly decreased. The levels of phospho-JNK, ERK and Akt are all decreased significantly in vimentin knockdown BMMs in response to M-CSF, as compared control cells. Therefore, we have identified vimentin is a novel M-CSF/c-Fms downstream signaling molecule regulating macrophage proliferation and osteoclast differentiation.

**Disclosures:** Y. Ito, None.

## SU098

**Cell Cycle-Arrested Quiescent Osteoclast Precursors (QOP) Are Cells Committed to the Osteoclast Lineage.** A. Arai<sup>1</sup>, T. Mizoguchi<sup>1</sup>, A. Muto<sup>1</sup>, Y. Kobayashi<sup>1</sup>, I. Kawahara<sup>1</sup>, K. Yamada<sup>2</sup>, N. Udagawa<sup>3</sup>, N. Takahashi<sup>1</sup>.

<sup>1</sup>Institute for Oral Science, Matsumoto Dental University, Shiojiri, Nagano, Japan, <sup>2</sup>Department of Orthodontics, Matsumoto Dental University, Shiojiri, Nagano, Japan, <sup>3</sup>Department of Biochemistry, Matsumoto Dental University, Shiojiri, Nagano, Japan.

We have identified QOP as the direct precursors of osteoclasts (JBMR 22 Suppl 1: S082, 2007). *In vivo* studies have shown that osteoblasts prepare the osteoclast niche, in which QOP are maintained for a long period under the undifferentiated state. QOP in the osteoclast niche expressed both RANK and c-Fms (RANK<sup>+</sup>/c-Fms<sup>+</sup>) and differentiated into osteoclasts without cell proliferation. Here, we examined functional properties of QOP in comparison with those of bone marrow-derived macrophages (BMMφ), osteoclast progenitor cells. (1) Flow cytometric analysis showed that 0.2% of mononuclear cells in the total mouse bone marrow cells expressed both RANK and c-Fms. RANK<sup>+</sup>/c-Fms<sup>+</sup> cells isolated by magnetic cell sorting differentiated into osteoclasts even in the presence of hydroxyurea, an inhibitor of DNA synthesis, in the presence of RANKL and M-CSF. BMMφ were obtained by culturing mouse bone marrow cells with M-CSF. BMMφ failed to differentiate into osteoclasts in the presence of hydroxyurea. (2) F4/80 is a marker of mature macrophages. Immunocytochemical studies showed that BMMφ strongly expressed F4/80, but most of RANK<sup>+</sup>/c-Fms<sup>+</sup> cells failed to express F4/80. Double staining of tibial sections with anti-F4/80 and -RANK antibodies showed that RANK-positive cells failed to express F4/80. (3) In phagocytosis experiments using latex beads, BMMφ showed potent phagocytic activity. In contrast, most of RANK<sup>+</sup>/c-Fms<sup>+</sup> cells failed to incorporate latex beads. (4) Dendritic cells and osteoclasts are differentiated from the common precursors. BMMφ and RANK<sup>+</sup>/c-Fms<sup>+</sup> cells were cultured with GM-CSF, followed by LPS, to induce dendritic cell differentiation. BMMφ could differentiate into CD11c and CD86 double-positive dendritic cells under the culture condition, but RANK<sup>+</sup>/c-Fms<sup>+</sup> cells could not. These results suggest (1) that QOP are non-proliferating cells committed to the osteoclast lineage, and (2) that these characteristics of QOP make it possible for QOP to promptly differentiate into osteoclasts in response to bone-resorbing stimuli in the osteoclast niche.

**Disclosures:** A. Arai, None.

## SU099

**Identification, Characterization and Isolation of Peripheral Osteoclast Progenitors.** C. Jacome-Galarza<sup>1</sup>, K. Lamothe<sup>1</sup>, J. Lorenzo<sup>2</sup>, H. L. Aguila<sup>1</sup>.

<sup>1</sup>Immunology, University of Connecticut Health Center, Farmington, CT, USA, <sup>2</sup>Medicine, University of Connecticut Health Center, Farmington, CT, USA.

Osteoclasts are cells of hematopoietic origin derived from monocyte progenitors that develop in the bone marrow. Using flow cytometry, we have characterized the phenotype of bone marrow progenitors and isolated cells with clonal ability to generate osteoclasts in *in vitro* readout assays. These cells have the phenotype B220<sup>+</sup> CD3<sup>+</sup> CD11b<sup>lo</sup> CD115<sup>+</sup> CD117<sup>+</sup>, and also generate macrophages and dendritic cells when cultured in media containing differential cytokines. Cells with osteoclastogenic potential are also found in periphery and it has been proposed that they can contribute to pathologies associated to bone destruction in inflammatory processes. To test if the fate of these cells is regulated by microenvironmental influences we need to have strict ways to identify them. Using similar approaches to the ones used to study bone marrow precursors we have dissected cell populations from blood and spleen. We have found that the phenotype of peripheral osteoclast progenitors is different to the ones in bone marrow. They are negative for lymphoid markers (CD3 and B220), and the majority is positive for the myeloid marker CD11b. Further dissection of these populations, using anti CD115/c-fms antibodies, showed that positive and negative fractions can generate osteoclasts. The negative fraction seems to contain a population of progenitors that develop rapidly into osteoclasts at a low frequency, while the CD115 positive population develops osteoclasts at high frequency. Lineage relationships between these populations and further dissection using Gr-1, F4.80 and CD11c markers are being considered. CD117 is poorly expressed in osteoclastogenic precursors in the periphery.

In these studies we isolate progenitors from mice expressing GFP under the control of the col3.6 promoter. We reported that this promoter is active in hematopoietic cells, preferentially in the osteoclast lineage. Even when an explanation for this apparently anomalous behavior is not known, we have taken advantage of the system to visualize osteoclastogenesis in real time. This allows us to compare the kinetics of osteoclast formation between different putative progenitors, including fusion between different populations. Also it allows us to track the fate of progenitors *in vivo* after adoptive transfer. We have detected GFP/TRAP positive cells associated to endosteal areas shortly after transplanting hematopoietic stem cells from these mice into lethally irradiated recipients. Our findings will be important to identify equivalent populations in human peripheral blood to study their correlation with pathologies associated to bone resorption.

**Disclosures:** C. Jacome-Galarza, None.

## SU100

**The Pacemaker Channel, HCN, Controls Functions of Osteoclasts.** T. Notomi<sup>\*1</sup>, M. Kuno<sup>1</sup>, H. Amano<sup>2</sup>, T. M. Skerry<sup>3</sup>. <sup>1</sup>Molecular and Cellular Physiology, Graduate School of Medicine, Osaka City University, Osaka, Japan, <sup>2</sup>Department of Pharmacology, School of Dentistry, Showa University, Tokyo, Japan, <sup>3</sup>Academic Unit of Bone Biology, School of Medicine & Biomedical Sciences, University of Sheffield, Sheffield, United Kingdom.

Hyperpolarization-activated cyclic nucleotide (HCN) modulated channels plays fundamental roles as the pacemaker in excitable cells including those in the central nervous system and heart. Previously we reported that an HCN subtypes (HCN2) influences bone mass and strength. Since the role of other HCN subtypes in bone remains unknown, we investigated their functions.

The mRNA and protein for all four HCN subtypes, HCN1-4, were identified in mouse bone (C57/BL6, 4wk-old) by RT-PCR and immunoblotting. Localization of HCNs revealed site specific expression of different subtypes. HCN1 and HCN4 were both expressed in bone resorbing osteoclasts. HCN1 immunoreactivity was abundant in the sealing zone and ruffled border that is responsible for acid secretion. HCN2 and HCN3 were expressed in bone marrow cells and osteoblasts respectively. Patch clamp recordings from RAW cell showed the characteristic inward currents (I<sub>h</sub>) generated by HCN, and further that acidic condition accelerated the activation of I<sub>h</sub>. Following acute acidosis of osteoclasts loaded with a pH sensitive-dye, we showed that proton extrusion was inhibited by HCN antagonist (ZD7288) with a similar potency to the proton pump blocker (Bafilomycin). The differentiation of osteoclast from bone marrow cells was also inhibited by ZD7288.

Our findings suggested that HCNs have the key roles in the skeleton and particularly that HCN1 is important in osteoclast function. The regulation of HCN function by pH at sealing zone and ruffled border sites suggests that the role of the channels involves local proton homeostasis in the resorption lacuna.

**Disclosures:** T. Notomi, None.

*This study received funding from: BBSRC (UK) and JSPS (Japan).*

## SU101

**Endocytotic Processes Underlying Calcium-induced Inhibition of Plasma Membrane Vacuolar-type H<sup>+</sup>-ATPase in Murine Osteoclasts.** H. Sakai, T. Notomi<sup>\*</sup>, Y. Moriura<sup>\*</sup>, J. Kawawaki<sup>\*</sup>, M. Kuno. Osaka City Univ. Grad. Sch. Med., Osaka, Japan.

Vacuolar-type H<sup>+</sup>-ATPases (V-ATPases) are widely distributed from yeast to mammals and could transport H<sup>+</sup> across membranes against negative pH gradients. They acidify intracellular vesicles and generate proton-motive force. In osteoclasts, V-ATPases are rich at the ruffled membrane facing to the bone surface and plays an important role in acid secretion into the resorption pit. Acids demineralize bone tissue and Ca<sup>2+</sup> is accumulated in the closed extracellular compartment. The elevated Ca<sup>2+</sup> in turn inhibits osteoclast functions, thus serving as a negative feedback signal for bone resorption. As the V-ATPase is an electrogenic H<sup>+</sup> pump, electrophysiological recordings provide a most direct and quantitative method to evaluate the activity of functional V-ATPases. We recently succeeded to record proton currents of the plasma membrane V-ATPase in RAW264-derived osteoclast-like cells using the conventional whole-cell clamp technique, and revealed that the pump activity was inhibited by increased extracellular Ca<sup>2+</sup> (Sakai et al., 2006). V-ATPases are recruited to the plasma membrane by exocytotic fusion of lysosomal membranes. In this study, we investigated whether endocytotic/exocytotic processes were involved in the Ca<sup>2+</sup>-induced inhibition of the V-ATPase monitoring the cell capacitance (C<sub>m</sub>), a parameter parallel to surface area. The C<sub>m</sub> was calculated from capacitive currents evoked by depolarization pulses. Extracellular Ca<sup>2+</sup> (5-40 mM) decreased the H<sup>+</sup> current and the C<sub>m</sub> with similar time courses. Ca<sup>2+</sup>-induced inhibition was dose-dependent and was mimicked by Mg<sup>2+</sup>. The decrease in the C<sub>m</sub> by 40 mM Ca<sup>2+</sup> was ~15 pF, corresponding to ~10% of the control C<sub>m</sub> (~150 pF). An endocytotic inhibitor, bafilomycin A<sub>1</sub>, inhibited the Ca<sup>2+</sup>-induced decrease in the C<sub>m</sub>. Bafilomycin A<sub>1</sub>, however, did not decrease the C<sub>m</sub> further when the C<sub>m</sub> had been diminished already by high Ca<sup>2+</sup>. Thus Ca<sup>2+</sup> and bafilomycin may share the same mechanism in the inhibition. These data suggest that extracellular Ca<sup>2+</sup> triggers internalization of the V-ATPase through endocytosis, which may decrease the pump activity.

**Disclosures:** H. Sakai, None.

## SU102

**IL-27/WSX-1 Signaling Inhibits RANKL-induced Osteoclastogenesis through STAT1 Activation: A Possible Involvement in TLR4/MyD88-mediated Inflammatory Arthritis.** M. Furukawa, H. Takaishi, M. Yoda<sup>\*</sup>, T. Tohmonda<sup>\*</sup>, J. Takito<sup>\*</sup>, S. Sakai, M. Matsumoto<sup>\*</sup>, Y. Toyama<sup>\*</sup>. Orthopaedic, Keio university, Tokyo, Japan.

IL-27, a novel IL-12 family member of cytokines, has a role in limiting the intensity and duration of adaptive immune responses in controlling the early Th1 initiation and IFN- $\gamma$  production in naive CD4<sup>+</sup> T cells. Even though osteoclastogenic helper T cell subset links T cell activation and bone destruction, further clarification of the paradigms of early Th1 commitment step would provide approaches to therapeutic intervention. To elucidate a role of IL-27 in the regulation of inflammatory bone destruction, we examined a direct effect of IL-27 on human and mouse osteoclast precursors and analyzed the downstream signaling pathways of IL-27. 1) Mononuclear cells were isolated from bone marrow obtained through prosthetic joint replacement surgery by light density separation using MethoCult culture system. Recombinant IL-27 strongly inhibited RANKL-induced osteoclastogenesis from human colony-forming units granulocyte-macrophage (CFU-GM) cells. 2) IL-27 induced the phosphorylation of STAT1 and STAT3. IL-27 increased STAT1 mRNA by 20-fold in human CFU-GM cells. 3) IL-27-induced suppression of osteoclastogenesis was rescued by Fludarabine, STAT1 inhibitor. 4) IL-27 downregulated c-Fos protein and its transcriptional target NFATc1 mRNA in human CFU-GM cells. Confocal microscopy detected little nuclear NFATc1 in the multinucleated and mononucleated cells treated with IL-27. 5) IL-27 did not change the level of IFN- $\gamma$  and IL-10, anti-osteoclastogenic cytokine, in human CFU-GM cells. 6) Expression of p28 and EBI3 was increased by LPS stimulation. WSX-1-Fc chimera partially rescued the inhibition of osteoclastogenesis induced by LPS. 7) IL-27 weakly inhibited RANKL and M-CSF induced osteoclastogenesis from mouse bone marrow macrophages (BMM $\Phi$ ) through STAT1 activation. IL-27 induced IL-12 receptor mRNA expression in BMM $\Phi$ . 8) Escherichia coli-primed WSX-1 (a component of IL-27 receptor) KO mice after intraarticular challenge with LPS were more susceptible to reactive arthritis due to increased proinflammatory cytokine production. Taken together, IL-27/WSX-1 signaling inhibits RANKL-induced osteoclastogenesis through STAT1 activation. Recent study showed that IL-27 negatively regulates the development of Th17 during chronic inflammation, and neutralization of the p28 subunit exerts an anti-inflammatory effect. Therefore, IL-27/WSX-1 signal is a therapeutic target for suppressing inflammatory bone destruction in TLR4/MyD88-mediated arthritis.

**Disclosures:** M. Furukawa, None.

## SU103

**MEK5/ERK5 Signal Regulates RANKL-induced Osteoclastogenesis.** S. Uchikawa<sup>1</sup>, H. Takaishi<sup>1</sup>, T. Hikata<sup>1</sup>, A. Hakozaiki<sup>1</sup>, M. Furukawa<sup>1</sup>, S. Tomita<sup>\*1</sup>, T. Tohmonda<sup>\*1</sup>, M. Yoda<sup>\*1</sup>, J. Takito<sup>1</sup>, M. Matsumoto<sup>\*2</sup>, Y. Toyama<sup>1</sup>. <sup>1</sup>Orthopaedic Surgery, Keio University, Tokyo, Japan, <sup>2</sup>Spine and Spinal Cord Disease, Keio University, Tokyo, Japan.

ERK5 belongs to an evolutionally conserved subfamily of mitogen-activated protein kinases (MAPKs) including extracellular-regulated protein kinase 1 and 2 (ERK1/2), c-Jun NH2-terminal protein kinases (JNKs), and p38 MAPKs. ERK5 activity is activated by growth factors, oxidative stress and serum stimulation via its TEY motif by MEK5. At present, details of the regulatory mechanism and a physiological function of the MEK5/ERK5 signaling in bone metabolism are unexplored. We aimed to clarify the role of the signaling in osteoclast differentiation. Western blots and RT-PCR revealed the expression of endogenous MEK5 and ERK5 in the bone marrow macrophages derived from ddY mouse and RAW264.7 cells. The activity of MEK5 and ERK5 was examined by measuring the luciferase reporter activity using pAP-1 luc and c-fos promoter luc in Cos7 cells. Cotransfection of a constitutive-active form of MEK5 with ERK5 increased the AP-1 luc activity by 200-fold and raised the c-fos promoter activity by 20-fold. But cotransfection of wild type or inactive form of MEK5 with ERK5 into Cos7 cells had no effects on the reporter activities. We used siRNA technology to examine the role of MEK5 in osteoclastogenesis. RAW264.7 cells were seeded at 5 x 10<sup>3</sup> cells/48-well. Next day, 30  $\mu$ M MEK5 siRNA or control siRNA was added to the medium. Osteoclast differentiation was induced by 50 ng/ml RANKL and the number of TRAP positive multinuclear cells was counted. MEK5 siRNA decreased the endogenous MEK5 mRNA to 10 % and attenuated the formation of TRAP positive multinuclear cells to 30% of control. From these results, we concluded that MEK5/ERK5 pathway probably regulated the transcriptional activity of c-fos and that the MEK5/ERK5 signaling acted as a positive regulator in RANKL-mediated osteoclastogenesis. We are currently exploring the upstream and downstream molecules of the MEK5/ERK5 signaling in osteoclastogenesis. Moreover, the analysis of physiological role of MEK5 *in vivo* is under investigation in our laboratory.

**Disclosures:** S. Uchikawa, None.



## SU104

### A Novel Role for Thrombopoietin in Regulating Osteoclast Development.

A. F. Taylor<sup>\*1</sup>, C. L. T. Barnes<sup>\*2</sup>, M. C. Horowitz<sup>3</sup>, M. A. Kacena<sup>1</sup>.  
<sup>1</sup>Orthopaedic Surgery, Indiana University School of Medicine, Indianapolis, IN, USA, <sup>2</sup>Mallinckrodt Institute of Radiology, Barnes-Jewish Hospital, Washington University School of Medicine, St. Louis, MO, USA, <sup>3</sup>Orthopaedics and Rehabilitation, Yale University School of Medicine, New Haven, CT, USA.

Recent studies suggest that megakaryocytes (MKs) may play a significant role in skeletal homeostasis, as evident by the fact that multiple MK related diseases result in osteoclastogenesis. We have previously demonstrated that MKs have a pleiotropic effect on osteoblasts (OBs) and osteoclasts (OCs). Briefly, culturing OBs in contact with MKs increases OB proliferation, while co-culturing OC precursors with MKs or MK conditioned media results in an inhibition of OC formation. As OCs and MKs are derived from the same hematopoietic precursor, in these studies we sought to examine the potential role of the major MK growth factor, thrombopoietin (TPO), on osteoclastogenesis.

Using real-time PCR, Western blotting and immunocytochemistry we have identified c-mpl, the TPO receptor, in both primary (bone marrow macrophages from C57BL/6 mice (BMMs)) and clonal OC progenitors. Moreover, we also detected in these cells Ink, an important protein regulator of TPO induced intracellular signaling. Western blotting demonstrates that treating BMMs with 100 ng/ml of TPO activates a variety of intracellular signaling mechanisms, including phosphorylating members of the MAPK, and STAT signaling pathways. Western blotting also illustrated that AKT is not phosphorylated in BMMs treated with TPO.

To study the role of TPO in osteoclastogenesis, BMMs ( $1 \times 10^5$  cells/ml), were cultured with M-CSF (30 ng/ml) and RANKL (50 ng/ml) to induce OC formation. TPO (0.1-1000 ng/ml) was titrated into these cultures and OCs were identified as tartrate resistant acid phosphatase positive (TRAP<sup>+</sup>) giant cells with >3 nuclei. TPO treatment significantly enhanced OC formation up to six-fold ( $p < 0.01$ ). Interestingly, these data are dramatically different from the ten-fold decrease ( $p < 0.001$ ) we previously observed when we co-cultured BMMs with MKs.

These data also illustrate dramatic differences between the direct and indirect effect of TPO on osteoclastogenesis. Indirectly, TPO inhibits OC formation through the stimulation of MKs, while direct TPO application enhances osteoclastogenesis. Given that TPO is secreted by bone marrow stromal cells, and thus could act directly on OC precursors in vivo, these data highlight a novel and potentially therapeutic role for TPO in regulating osteoclastogenesis.

**Disclosures:** M.A. Kacena, None.

## SU105

### Lysophosphatidic Acid Regulates Osteoclast Survival and Retraction.

D. M. Lapierre<sup>\*</sup>, M. M. Leblanc<sup>\*</sup>, A. Pereverzev<sup>\*</sup>, S. J. Dixon, S. M. Sims<sup>\*</sup>.  
 Physiology and Pharmacology, The University of Western Ontario, London, ON, Canada.

Lysophosphatidic acid (LPA) is a bioactive phospholipid consisting of a phosphoglycerol backbone with one fatty acyl chain. The functions of LPA are mediated primarily through five receptors (LPA1-5), which couple to multiple G proteins. In several cell types, LPA induces diverse responses, including differentiation, chemotaxis, migration, survival. LPA is released by activated platelets and is thought to play roles in wound healing and tumor progression. We have recently shown that osteoblasts also produce LPA, raising the possibility that LPA may mediate local signaling in bone between osteoblasts and osteoclasts. However, nothing is known about possible actions of LPA on osteoclasts. The aim of this study was to investigate the responses of osteoclasts to LPA. Osteoclasts were isolated from the long bones of neonatal rats and cytosolic free calcium concentration was measured using the calcium-sensitive dye fura-2. Focal application of LPA (5  $\mu$ M) elicited acute, transient increases in cytosolic calcium to peak amplitude of  $207 \pm 35$  nM above basal levels (mean  $\pm$  SEM). This response was concentration-dependent, with half maximal effects observed at 3  $\mu$ M LPA, and was blocked by the LPA1/3 receptor antagonist VPC-32183. In contrast to the effect of LPA, the inactive control compound oleoyl glycerol (3  $\mu$ M) did not evoke a rise of cytosolic calcium. Predominant expression of LPA1 (Edg2) was revealed by real-time RT-PCR analysis of purified osteoclasts generated in cultures of murine bone marrow cells. Digital time-lapse microscopy revealed that LPA (5  $\mu$ M) induced acute retraction of osteoclasts (planar area of osteoclasts was reduced to  $52 \pm 3\%$  of initial area). Cell counting and assessment of nuclear morphology were used to quantify osteoclast survival and apoptosis. LPA (5  $\mu$ M) enhanced survival of rat osteoclasts over a period of 18 hours from  $18 \pm 5\%$  to  $35 \pm 7\%$  ( $P < 0.001$ ). This effect was blocked by VPC-32183. At 6 hours, LPA (5  $\mu$ M) reduced the percentage of osteoclasts undergoing apoptosis from  $55 \pm 2\%$  to  $38 \pm 2\%$  ( $P < 0.001$ ), consistent with the effects of LPA on survival. This effect was also blocked by VPC-32183. This study reveals that osteoclasts express LPA1 and respond directly to LPA with elevation of cytosolic calcium and cellular retraction. Moreover, LPA reduces osteoclast apoptosis, enhancing survival. Thus, LPA may mediate intercellular signaling between osteoblasts and osteoclasts, a novel signaling axis in bone.

**Disclosures:** D.M. Lapierre, None.

This study received funding from: Canadian Institutes of Health Research.

## SU106

### VEGF Induction Provides Evidence for Different Signaling Pathway Activation by Large and Small Osteoclasts.

D. P. Trebec<sup>1</sup>, J. N. M. Heersche<sup>\*2</sup>, M. F. Manolson<sup>2</sup>. <sup>1</sup>Dept. of Biochemistry, University of Toronto, Toronto, ON, Canada, <sup>2</sup>Faculty of Dentistry, University of Toronto, Toronto, ON, Canada.

Increased bone resorption in several bone diseases (e.g. rheumatoid arthritis) is associated with increased osteoclast (OC) size in the affected areas, suggesting this increase in OC size is related to pathological resorptive activity. We have previously shown that large OCs ( $\geq 10$  nuclei) were more active and resorbed more bone and more frequently than smaller OCs (2-5 nuclei) (Lees et al, 2001). In addition, we found that large OCs express higher levels of activating receptors than small OCs (Trebec et al, 2007). We hypothesized that large and small OCs activate different signaling pathways in response to activating factors such as IL-1 $\beta$  and RANKL. Consequently, we performed a signaling pathway microarray using RNA isolated from large and small OCs differentiated from RAW 264.7-cells in the presence of RANKL to identify any differences in common signaling pathways. RNA was also isolated from large and small OCs exposed to IL-1 $\beta$  for 3 hours and compared to unstimulated OCs to identify early pathway activation events. Arrays demonstrated that overall a greater number of pathway target genes were activated in large OCs than in small OCs and at higher levels. There was also differential activation of vascular endothelial growth factors (VEGF). Small OCs expressed VEGF-C while large OCs expressed little VEGF-C resulting in 2.5-fold higher expression in small OCs compared to large. In response to IL-1 $\beta$  the difference between large and small OCs increased to 10-fold. In contrast, VEGF-A was expressed by large OCs but little induction was seen in small OCs resulting in 11-fold higher expression in large OCs compared to small OCs. However, VEGF-A expression in large OCs decreased in response to IL-1 $\beta$  and only a 4.5-fold difference in expression was seen in large OCs compared to small OCs treated with IL-1 $\beta$ . Furthermore, inhibitor studies suggested that the induction of VEGF-C and VEGF-A are mediated by different pathways and not solely through NF- $\kappa$ B signaling. In summary, these results suggest that large and small OCs use different signaling pathways. We currently hypothesize that the VEGFs in large and small OCs are induced by pathways other than the NF- $\kappa$ B pathway. This could provide information regarding their differential activation in response to activating factors under pathological conditions. The variations in VEGF expression could, in turn, result in different downstream activities of these OCs. Establishing mechanistic differences between large and small OCs could be exploited to stop pathological bone loss, or could be used as a marker for pathological bone loss in diseased versus normal tissue.

**Disclosures:** D.P. Trebec, None.

## SU107

### RANKL Induces Calcium Channel Activation in Human Osteoclasts.

E. Chamoux<sup>1</sup>, M. Bisson<sup>\*2</sup>, M. Payet<sup>\*3</sup>, S. Roux<sup>2</sup>. <sup>1</sup>Rheumatology, Faculty of Medicine, University of Sherbrooke & Bishop's University, Sherbrooke, QC, Canada, <sup>2</sup>Rheumatology, Faculty of Medicine, University of Sherbrooke, Sherbrooke, QC, Canada, <sup>3</sup>Physiology - Biophysics, Faculty of Medicine, University of Sherbrooke, Sherbrooke, QC, Canada.

Most of the signaling effectors downstream RANK activation are calcium sensitive. However, early signaling events after RANKL binding remain scarcely understood, particularly for intracellular calcium mobilization in human osteoclasts. Using a model of primary human osteoclasts, our aim was to determine the characteristics of calcium response after RANKL binding. Cord blood monocytes were incubated for 18 days in presence of RANKL and M-CSF, thus leading to fully matured osteoclasts. Prior to experimentation, osteoclasts were loaded with Fura2-AM for 30 min, washed and up to 30 cells were selected for computation. Cells were sequentially excited with 340 and 380nm rays and optical densities of Fura2-emitted 510 nm rays were recorded. A ratio of calcium-bound (excited at 340 nm) to calcium-free (excited at 340 nm) Fura-2 light emission was thus generated. As Fura-2 is only found intracellularly, an increased ratio corresponds to an elevation of calcium ions in the cytosol. After a short equilibration period (stabilized ratio), cells were stimulated with various doses of RANKL. All doses varying from 10 to 200ng/ml of RANKL induced a rapid and significant increase in intracellular calcium. In order to better characterize the origin of this calcium spark, EGTA was added to the medium and lead to an almost complete reversal. Similarly, no calcium spark was observed when stimulations were conducted in calcium-free medium. We then depleted intracellular calcium stores by incubating cells overnight with Thapsigargin before RANKL stimulations. This did not affect the intracellular calcium increase, suggesting that the ion is brought from the extracellular medium. To further confirm these results, which differ from what has been described in rodent osteoclasts, we pre-incubated cells with a phospholipase C inhibitor (U73122) for 10 min before stimulation, in order to prevent intracellular store mobilization from inositol phosphate release. This condition again did not affect the RANKL-induced calcium spark. In contrast, the depolarization of membranes with KCl (200mM) induced an intracellular calcium increase similar to the one observed with RANKL, suggesting that a voltage-dependant calcium channel is present on human osteoclasts. Overall, our results showed that RANKL induces a strong elevation of intracellular calcium. Our experiments also strongly suggest an extracellular origin for this RANKL-induced calcium increase, likely due to the opening of calcium channels, which we have not identified yet, at the surface of human osteoclasts.

**Disclosures:** E. Chamoux, None.

## SU108

**AG490, A Jak2 Specific Inhibitor, Induces Osteoclast Survival by Activating Akt and ERK Signaling Pathway.** H. Kwak\*<sup>1</sup>, H. Sun\*<sup>2</sup>, H. Kim\*<sup>2</sup>, J. Lee\*<sup>2</sup>, H. Ha\*<sup>2</sup>, Z. Lee\*<sup>2</sup>. <sup>1</sup>Anatomy, School of Medicine, Wonkwang University, Iksan, Republic of Korea, <sup>2</sup>Cell & Developmental Biology, College of Dentistry, Seoul National University, Seoul, Republic of Korea.

Osteoclasts are multinucleated cells with the unique ability to resorb bone. Elevated activity of these cells under pathological conditions leads to the progression of bone erosion, such as osteoporosis, periodontal disease, and rheumatoid arthritis. Thus, the regulation of osteoclast apoptosis is important for bone homeostasis. In this study, we examined the effects of the Janus tyrosine kinases (JAK) 2 specific inhibitor AG490 on osteoclast apoptosis. We showed that AG490 greatly inhibited osteoclast apoptosis under conditions of survival factors deprivation and that suppressed the cleavage of pro-caspase-9 and -3 to its active forms. AG490 stimulated the phosphorylation of Akt and ERK. Adenovirus-mediated expression of dominant negative (DN)-Akt and DN-Ras in osteoclasts inhibited the survival of osteoclast despite the presence of AG490. Cytochrome c release during osteoclast apoptosis was inhibited by AG490 treatment, which was inhibited in the presence of LY294002 or U0126. AG490 suppressed pro-apoptotic proteins Bad and Bim, which was inhibited in osteoclasts infected with DN-Akt and DN-Ras adenovirus. In addition, constitutive active (CA)-MEK and (myristoylate) Myr-Akt adenovirus suppressed the cleavage of pro-caspase-9 and -3 and inhibited osteoclast apoptosis induced by etoposide. Taken together, our results suggest that AG490 inhibited cytochrome c release into cytosol at least partly by inhibiting pro-apoptotic proteins Bad and Bim and in turn suppressed caspase-9 and -3 activation, thereby inhibiting osteoclast apoptosis.

**Disclosures:** H. Kwak, None.

## SU109

**Proteomic Identification and Characterization of the Small GTPase Rab18 in Human Osteoclasts.** A. Taylor\*, M. Rogers, F. Coxon\*. University of Aberdeen, Aberdeen, United Kingdom.

Rabs are a large family (>70 members) of small GTPases that play a crucial role in the regulation of intracellular vesicular trafficking. The correct subcellular localisation, and therefore function, of these proteins is dependent on prenylation, which involves the attachment of isoprenoid groups to C-terminal cysteine residues. We have found that anti-resorptive phosphonocarbonylate drugs specifically inhibit Rab prenylation, highlighting the critical role of these GTPases for osteoclast function. However, the expression profile and role of specific Rab GTPases in osteoclasts remains poorly understood. We have therefore employed a proteomic approach to identify the Rab GTPases that are highly expressed in osteoclasts. PBMCs were isolated from whole blood of healthy volunteers and osteoclasts generated by culturing with M-CSF and RANKL. These mature osteoclasts were then lysed in buffer containing triton X114, which enabled enrichment of the Rab GTPases following fractionation into aqueous and detergent-rich phases, since the prenylated Rab proteins partition into the latter. Enriched proteins were then separated by 2D SDS-PAGE and prenylated Rabs identified by overlaying with an identical gel from lysates of cells in which prenylated Rabs had been metabolically labelled using [<sup>14</sup>C]mevalonate. Selected spots were trypsin-digested and proteins identified by peptide analysis using MALDI-ToF. An alternative approach was also used, in which proteins enriched as above were separated by 1D SDS-PAGE, then spots corresponding to the molecular weight of Rabs (21-28kDa) were picked for analysis by LC-MS/MS. Using these two approaches we have identified 19 Rabs in human osteoclasts (all 19 by LC-MS/MS, but only 8 using MALDI-TOF), as well as Rap1, a prenylated GTPase that we previously showed to be highly expressed in osteoclasts. The Rabs identified include several that have been previously described in osteoclasts, including Rab7, Rab3D, Rab6 and Rab11 but also several that have not previously been described in osteoclasts. These include Rab18, for which there is no known role in any cell type, although it has been shown to localise to lipid droplets in several cell types. Using western blotting and immunostaining, we have confirmed that Rab18 is expressed in vesicular structures in osteoclasts, although its abundance is unaltered during RANKL-induced osteoclast differentiation. Moreover, EGFP-Rab18 clearly localised to the surface of lipid containing vesicles (particularly when formation of these vesicles was stimulated by incubation of the osteoclasts with oleic acid), but did not localise to endosomal vesicles. We are now analysing the function of Rab18 in osteoclasts using adenoviral delivery of a dominant-negative form and knockdown of expression using siRNA.

**Disclosures:** A. Taylor, None.

## SU110

**Adiponectin Inhibits Osteoclast Formation via AKT Signaling Pathway.** Q. Tu, J. Zhang\*, B. Xu\*, E. Brewer\*, J. Chen. Department of General Dentistry, Tufts University School of Dental Medicine, Boston, MA, USA.

Adiponectin is an adipose tissue-derived hormone that has important functions in the regulation of lipid and glucose metabolism, immunity, cancer and bone formation. A link between adiponectin and bone homeostasis has been documented. A recent study revealed that adiponectin is able to inhibit RANKL-induced osteoclast differentiation. However, the signaling mechanisms responsible for the action of adiponectin remain largely unknown. The current study aimed to determine the signaling pathways in adiponectin-mediated inhibitory effects in osteoclast differentiation. We characterized molecules of the RANKL-stimulated NFATc1 signaling using RAW264.7 cells stably transfected with a luciferase reporter driven by an osteoclast specific cathepsin K (CtSK) promoter. We also determined the transduction pathway of kinase AKT in regulating apoptosis of osteoclasts and NFATc1 level in nuclei by

fluorescence peptide substrate-based assay, homogeneous caspase assays (Promega) and gene expression quantification. The results showed that recombinant globular adiponectin strongly inhibited CtSK promoter activity in a dose- and time-dependent manner in RAW264.7 cells cultured in the presence of RANKL, which was consistent with our observation that the expressions of RANKL-induced NFATc1 and other osteoclastic differentiation markers such as cathepsin K or TRACP were reduced significantly. MTT survival assay demonstrated that adiponectin decreased RAW264.7 cell proliferation during RANKL-mediated differentiation. Caspase activity assays also showed that the activity levels of apoptosis executioner caspases-3 and initiator caspases-8 and -9 were much higher in RAW264.7 cells treated with adiponectin and RANKL than in those treated with RANKL alone for 3 days. Moreover, RAW264.7 cells treated with adiponectin exhibited decreased activation of AKT signaling, an anti-cell apoptosis and pro-NFATc1 activation pathway signaled by RANKL. Furthermore, overexpression of APPL1, a key adaptor protein mediating adiponectin signaling and coordinating different pathways, reduced AKT-mediated downstream events. Taken together, our findings for the first time indicate that adiponectin negatively regulate RANKL-mediated osteoclast formation by decreasing osteoclastogenesis and osteoclast survival, and increasing osteoclast apoptosis via suppressing AKT pathway. APPL1 may act as a critical regulator of the crosstalk between adiponectin signaling and RANKL signaling pathways.

**Disclosures:** Q. Tu, None.

This study received funding from: NIH grants DE13745 and DE16710 to JC.

## SU111

**Investigations into the Role of Focal Adhesion Kinase (FAK) in Bone Marrow-Derived Osteoclasts.** B. J. Ray\*, A. H. Bouton\*. Microbiology, University of Virginia, Charlottesville, VA, USA.

The focal adhesion kinase (FAK) family of protein tyrosine kinases contains two members, FAK and proline-rich tyrosine kinase 2 (Pyk2), which are both expressed in osteoclasts. Pyk2<sup>-/-</sup> mice are mildly osteopetrotic and display defects in sealing zone formation and bone resorption. FAK is also thought to be involved in bone resorption; however a global FAK knockout is embryonic lethal in mice, making it difficult to evaluate the role of FAK in bone and other tissues. Our lab has developed a mouse model in which FAK is conditionally deleted in cells of the myeloid lineage, which includes osteoclasts. Five-week old mice with this conditional knockout contained equivalent numbers of osteoclast progenitor cells in bone marrow compared to control mice. Differentiation of bone marrow cells into preosteoclasts and multinucleated osteoclasts does not appear to be impaired in FAK<sup>-/-</sup> cells compared to their wildtype counterparts. However, FAK<sup>-/-</sup> osteoclasts display defects in bone resorption marked by a decrease in the area of degradation pits that form on bone discs. This coincides with potential abnormalities in podosome and sealing zone structure. Preliminary data using total internal reflection fluorescence (TIRF) microscopy indicate that cortactin, which is a major plaque protein that is present in these structures, may be mislocalized in FAK<sup>-/-</sup> osteoclasts. These data show for the first time that, in addition to Pyk2, FAK also plays a critical role in osteoclast function. Future studies will focus on identifying common and unique functions of FAK and Pyk2 within this cell population and on determining whether FAK expression in osteoclasts impacts bone density.

**Disclosures:** B.J. Ray, None.

## SU112

**The Ubiquitin-Like Domain of IKK $\beta$  Is Critical for Osteoclastogenesis.** J. Otero\*<sup>1</sup>, Y. Zhang\*<sup>2</sup>, M. Kuziez\*<sup>2</sup>, S. Dai\*<sup>2</sup>, Y. Abu-Amer\*<sup>2</sup>. <sup>1</sup>Orthopedic Surgery and DBBS, Washington University School of Medicine, Saint Louis, MO, USA, <sup>2</sup>Orthopedic Surgery and Cell Biology & Physiology, Washington University School of Medicine, Saint Louis, MO, USA.

Nuclear Factor kappa B (NF- $\kappa$ B) is a family of transcription factors with conserved structural and functional characteristics that regulates various cellular and pathological processes such as immune system development, cell survival, and inflammatory signaling. NF- $\kappa$ B is considered an immune-modulator of rheumatoid arthritis and inflammatory osteolysis. NF- $\kappa$ B is also essential for osteoclast development and survival, evidenced by the osteopetrotic phenotype displayed by mice doubly deficient in subunits NF- $\kappa$ B1 and NF- $\kappa$ B2. Under normal and naïve conditions, NF- $\kappa$ B proteins are bound to inhibitory proteins and reside inactive in the cytoplasm. A wide range of cellular stimuli prompt activation of NF- $\kappa$ B. This activation is controlled by the upstream I $\kappa$ B kinase (IKK) complex which contains, among other proteins, IKK $\alpha$ , IKK $\beta$ , and IKK $\gamma$ . The role of IKK $\alpha$  and IKK $\beta$  in the skeletal development and inflammatory osteolysis has been described. However, the precise molecular mechanisms underlying IKK regulation of osteoclasts remains enigmatic. Since mice lacking IKK $\beta$  in osteoclast precursors suffer from osteopetrosis due to a defect in osteoclastogenesis, it is critical to functionally identify the domains of IKK $\beta$  which are required for its function in the setting of osteoclast differentiation. Prior studies have shown that the NEMO-binding domain of IKK $\beta$  regulates osteoclastogenesis and inflammatory osteolysis. Another candidate domain which has been shown to be absolutely required for IKK $\beta$  function is the Ubiquitin-Like Domain (ULD). Using retroviral delivery system compatible with osteoclast precursors, we demonstrate that IKK $\beta$  which lacks the ULD (IKK $\beta$  dULD) fails to rescue osteoclastogenesis in osteoclast precursors deficient in endogenous IKK $\beta$  compared with successful rescue using the wild type IKK $\beta$  form. Furthermore, IKK $\beta$  lacking the ULD domain (dULD) inhibits osteoclastogenesis in wild-type osteoclast precursors, and this inhibition correlates with a defect in p65 nuclear translocation and NF- $\kappa$ B DNA binding activity in response to RANKL. IKK $\beta$  dULD is also capable of inhibiting NF- $\kappa$ B activity in response to overexpression of wild-type IKK $\beta$  in IKK $\beta$ -deficient mouse embryonic fibroblasts, indicating that it possesses dominant negative activity. Our studies suggest that the ubiquitin-like domain of IKK $\beta$  may be a useful target for the treatment of osteoclast mediated diseases.

**Disclosures:** J. Otero, None.

## SU113

### Efficient and Stable Gene Expression into Human Osteoclasts Using an HIV-1 Based Lentiviral Vector. K. Chu<sup>1</sup>, K. G. Cornetta<sup>\*2</sup>, M. J. Econs<sup>1</sup>.

<sup>1</sup>Medicine, Indiana University School of Medicine, Indianapolis, IN, USA, <sup>2</sup>Medical and Molecular Genetics, Indiana University School of Medicine, Indianapolis, IN, USA.

**Introduction:** Since osteoclasts are terminally differentiated cells without proliferating activity, efficient and stable gene expression into these cells remains a difficulty. In the current study, we investigate gene transduction into human pre-osteoclasts by a replication defective lentivirus-based vector containing a modified HIV-1 genome.

**Methods:** Human pre-osteoclasts (differentiating osteoclasts) were transduced with lentiviruses bearing an enhanced green fluorescence protein reporter gene. Transduction efficiencies were measured by flow cytometry for EGFP protein expression. Sorted human transduced pre-osteoclasts were re-plated and differentiated under hM-CSF and hRANKL. Mature osteoclasts were then analyzed by the cell viability assay, TRACP assay, and pit formation assay.

**Results:** Efficient gene transduction was obtained at multiplicity of infection of 10 and gene expression lasted for over 4 weeks using our protocol. Lentiviral transduction did not affect osteoclast survival, formation, or function.

**Conclusions:** These results establish an efficient method for gene transduction into human pre-osteoclasts using a lentiviral vector. Importantly, these transduced pre-osteoclasts could differentiate into mature osteoclasts without a negative impact from the lentiviruses. This protocol provides a new tool for studies of osteoclast biology. Further work in this area may open new avenues for the study of osteoclast gene signaling and gene therapy of disorders of osteoclast function.

**Disclosures:** K. Chu, None.

This study received funding from: International Osteopetrosis Association.

## SU114

### Suppression of TREM-2 Expression and TREM-2-mediated Costimulation of RANK Signaling by Cytokines that Inhibit Human Osteoclast Differentiation. K. Park-Min<sup>\*1</sup>, M. Humphrey<sup>\*2</sup>, M. Nakamura<sup>\*3</sup>, L. B. Ivashkiv<sup>\*1</sup>.

<sup>1</sup>Hospital for Special Surgery, New York, NY, USA, <sup>2</sup>Department of Medicine and Microbiology and Immunology, VA Medical Center and University of Oklahoma Health Science Center, Oklahoma City, OK, USA, <sup>3</sup>Department of Medicine, VA Medical Center, University of California, San Francisco, CA, USA.

TREM-2 (triggering receptor expressed on myeloid cells 2) is an ITAM-associated immunoreceptor that plays an important role in bone resorption and osteoclastogenesis in humans by providing costimulation for signaling by RANK (Receptor Activator of Nuclear Factor  $\kappa$  B), a key receptor required for osteoclast differentiation. We found that TREM-2 expression is induced in parallel with RANK expression during generation of human osteoclast precursors and in synovial macrophages in rheumatoid arthritis. In contrast to RANK, TREM-2 expression was not dependent on M-CSF and was inhibited by interferons (IFNs) and interleukin-10 (IL-10), potent inhibitors of human osteoclastogenesis. IL-10 inhibited TREM-2 expression by a transcriptional mechanism and suppressed costimulation of RANK signaling, leading to the attenuation of calcium oscillations, NFATc1 expression, and inhibition of a newly described CaMKII-MEK-ERK calcium-dependent signaling pathway downstream of RANK. These findings provide a new mechanism of inhibition of human osteoclast differentiation and implicate regulation of TREM-2 expression as an important component of human osteoclast differentiation that can be effectively targeted for inhibition.

**Disclosures:** K. Park-Min, None.

This study received funding from: NIH.

## SU115

### Breast Cancer Derived Factors Synergize with TGF $\beta$ to Induce Phosphorylation of ERK1/2 and to Stimulate Osteoclastogenesis. K. Tiedemann<sup>\*1</sup>, O. Hussein<sup>\*1</sup>, E. Gusev<sup>\*1</sup>, P. M. Siegel<sup>\*2</sup>, S. V. Komarova<sup>1</sup>.

<sup>1</sup>Faculty of Dentistry, McGill University, Montreal, QC, Canada, <sup>2</sup>Departments of Biochemistry and Medicine, McGill University, Montreal, QC, Canada.

**Background:** Breast cancer metastasizes to bone, giving rise to osteolytic lesions. Tumor cells cannot resorb bone but act by stimulating osteoblasts to produce osteoclastogenic cytokine RANKL, which subsequently stimulates osteoclast formation. We have recently found that soluble factors secreted from human breast carcinoma cells (MDA-MB-231), also can directly stimulate osteoclast formation from RANKL-primed precursors. The objective of this study was to examine signaling events induced in osteoclast precursors by breast cancer-derived factors.

**Method:** Osteoclast precursors, RAW 264.7 murine monocytic cells were primed with RANKL for 2 days, after which the cells were either cultured without addition, or were treated with RANKL or conditioned medium (CM) from MDA-MB-231 cells. Protein was extracted from parallel samples after 15 min - 2 h of treatment. To study calcium dynamics, osteoclast precursors were loaded with calcium sensitive dye fura-2 and examined using microspectrofluorimetry.

**Results:** MDA-MB-231 CM strongly induced sustained phosphorylation of ERK1/2, which was evident for at least 1 h after initiation of the treatment. In contrast, no significant

ERK1/2 phosphorylation was observed in RANKL-treated or untreated osteoclast precursors. Treatment of MDA-MB-231 CM with a neutralizing antibody for TGF $\beta$  did not affect ERK1/2 phosphorylation at early time points (30 min), but inhibited it at later times (1 h). Similar to the effects of anti-TGF $\beta$ , inhibition of MEK1/2 with PD98059 prevented ERK1/2 phosphorylation at 1 h. Since it was recently shown that PKC $\alpha$  may directly phosphorylate ERK1/2, we assessed its role using PKC inhibitor Go6976. Inhibition of PKC prevented ERK1/2 phosphorylation at all times. Since PKC $\alpha$  is a calcium-dependent isoform, we assessed if MDA-MB-231 CM affects calcium levels in osteoclast precursors. We have found that both in untreated RAW 264.7 cells and in osteoclast precursors primed with RANKL for 2 days, MDA-MB-231 CM (but not control media conditioned by normal breast cells MCF10A) induced elevation in cytosolic free calcium, resulting in calcium oscillations in some cells.

**Conclusion:** We have found that calcium/PKC pathway synergizes with TGF $\beta$ /MAPK pathway at the level of ERK1/2 phosphorylation, likely contributing to RANKL-primed osteoclast precursors' ability to respond to breast cancer-derived factors. Supported by CIHR, CRC and NSERC

**Disclosures:** S. V. Komarova, None.

This study received funding from: CIHR, CRC and NSERC.

## SU116

### Histone Deacetylase Inhibitors Suppress Interleukin-1 $\beta$ -induced Nitric Oxide and Prostaglandin E<sub>2</sub> Production In Human Chondrocytes. N. Chabane<sup>\*</sup>, N. Zayed<sup>\*</sup>, H. Afif<sup>\*</sup>, J. Martel-Pelletier<sup>\*</sup>, J. P. Pelletier<sup>\*</sup>, H. Fahmi<sup>\*</sup>.

CHUM, Université de Montréal, Montreal, QC, Canada.

**Objective:** Overproduction of nitric oxide (NO) and prostaglandin (PG) E<sub>2</sub> plays an important role in the pathogenesis of osteoarthritis (OA). In the present study, we determined the effect of trichostatin A (TSA) and butyric acid (BA), two histone deacetylase (HDAC) inhibitors, on NO and PGE<sub>2</sub> synthesis, inducible NO synthase (iNOS) and cyclooxygenase (COX)-2 expression, and NF- $\kappa$ B DNA-binding activity, in interleukin-1 $\beta$  (IL-1)-stimulated human OA chondrocytes, and on IL-1-induced proteoglycan degradation in cartilage explants.

**Methods:** Chondrocytes were stimulated with IL-1 in the absence or presence of increasing concentrations of TSA or BA. The production of NO and PGE<sub>2</sub> was evaluated using Griess reagent and an enzyme immunoassay, respectively. The expression of iNOS and COX-2 proteins and mRNAs were evaluated using Western blotting and real-time reverse transcriptase-polymerase chain reaction (RT-PCR), respectively. Proteoglycan degradation was measured with dimethylmethylene blue assay. Electrophoretic mobility shift assay (EMSA) was utilized to analyze the DNA binding activity of NF- $\kappa$ B.

**Results:** HDAC inhibition with TSA or BA resulted in a dose-dependent inhibition of IL-1-induced NO and PGE<sub>2</sub> production. IL-17- and tumor necrosis factor- $\alpha$  (F- $\alpha$ )-induced NO and PGE<sub>2</sub> production was also inhibited by TSA and BA. This inhibition correlated with the suppression of iNOS and COX-2 protein and mRNA expression. TSA and BA also prevented IL-1-induced proteoglycan release from cartilage explants. Finally, we demonstrate that the DNA-binding activity of NF- $\kappa$ B, was induced by IL-1, but was not affected by treatment with HDAC inhibitors.

**Conclusions:** These data indicate that HDAC inhibitors suppressed IL-1-induced NO and PGE<sub>2</sub> synthesis, iNOS and COX-2 expression, as well as proteoglycan degradation. The suppressive effect of HDAC inhibitors is not due to impaired DNA-binding activity of NF- $\kappa$ B. These findings also suggest that HDAC inhibitors may be of potential therapeutic value in the treatment of OA.

**Disclosures:** N. Chabane, None.

This study received funding from: CIHR and FRSQ.

## SU117

### Latexin Is a Novel Effector Of BMP-2 Signaling in Modulation of Chondrocyte Differentiation. I. Kadouchi<sup>\*1</sup>, K. Sakamoto<sup>\*2</sup>, T. Murakami<sup>\*3</sup>,

E. Kobayashi<sup>\*3</sup>, Y. Hoshino<sup>\*1</sup>, A. Yamaguchi<sup>2</sup>. <sup>1</sup>Department of Orthopaedic Surgery, Jichi Medical University, Tochigi, Japan, <sup>2</sup>Section of Oral Pathology, Tokyo Medical and Dental University, Tokyo, Japan, <sup>3</sup>Division of Organ Replacement Research, Center of Molecular Medicine, Jichi Medical University, Tochigi, Japan.

We identified latexin (Lxn), a unique inhibitor of endogenous carboxypeptidase A, as a downstream target of BMP-2 signaling in mesenchymal cell lines by microarray analysis using Runx2-deficient cells with or without BMP-2 treatment. Lxn expression was also significantly upregulated in MC3T3-E1 and C2C12 cells with BMP-2 treatment. In situ hybridization and immunohistochemical staining revealed that Lxn was expressed in chondrocytes and perichondrium in day 13.5 embryo, and in the mesenchymal cells and chondrocytes at the site of bone regeneration in adult mice. Lxn expression was increased in parallel with the chondrogenic differentiation of C3H10T1/2 cells cultured under a high-density micromass condition with BMP-2 treatment. We generated C3H10T1/2 cells that stably overexpressed Lxn using a retroviral vector. In the Lxn-overexpressing C3H10T1/2 cells, chondrogenic potential was significantly increased compared with the original C3H10T1/2 cells, as demonstrated by the alcian blue staining and the expression of *type II collagen*, *type X collagen* and *aggrecan*. Our data indicates that Lxn is a downstream factor of BMP-2 signaling and may play an important role in modulating the chondrogenic differentiation.

**Disclosures:** I. Kadouchi, None.

## SU118

**DHCR24 Gene Is Mandatory for the Proper Growth of Long Bone.** R. Mirza<sup>\*1</sup>, T. Miyamoto<sup>2</sup>, T. Kaji<sup>\*3</sup>, Y. Murata<sup>\*4</sup>, H. Seo<sup>\*1</sup>. <sup>1</sup>Biomedical Science, College of Life and Health Sciences, Chubu University, Kasugai, Japan, <sup>2</sup>Department of Orthopedic Surgery, Keio University School of Medicine, Tokyo, Japan, <sup>3</sup>Pharmaceutical Research Unit, Research and Development division, Mitsubishi Pharma Corporation, Yokohama, Japan, <sup>4</sup>Department of Genetics, Research Institute of Environmental Medicine, Nagoya University, Nagoya, Japan.

DHCR24 gene encodes an enzyme catalyzing conversion of desmosterol to cholesterol. Desmosterolosis is an autosomal recessive disease due to mutations in DHCR24 gene, with severe developmental abnormalities including limb anomalies and short stature. To find out the mechanisms involved in these abnormalities, we utilized DHCR24 knockout mice in our study. It is known that DHCR24 can protect cells from oxidative stress in some cell lines, but its function on bone growth has not been studied yet. As the DHCR24<sup>-/-</sup>(KO) mice die soon after birth, we investigated the growth of metatarsal bone in culture obtained from newborn KO mice. The longitudinal growth of bone was retarded and the rate of bone growth started to decrease significantly after one week of culture. The metatarsal bone of one week culture showed less proliferating chondrocytes in the growth plate. At the same time, abnormal hypertrophy of the chondrocytes in the prehypertrophic zone was observed in the bone from KO mice. It is recently reported that oxidative stress could induce chondrocyte hypertrophy. We demonstrated that DHCR24 acts as potent ROS scavenger. These observations led us to treat the bone from KO mice with an antioxidant, NAC (N-acetyl L cysteine). The treatment could recover the hypertrophy of chondrocyte and could restore the proliferating zone after one week of culture. Since hydrogen peroxide (H<sub>2</sub>O<sub>2</sub>) treatment for 48 hrs has been shown to induce the genes for the chondrocyte hypertrophy such as mmp13, collagen type X and Runx2 in the ATDC5 cells. We infected the ATDC5 cells with adenovirus expressing DHCR24. As expected, the expression of the above mentioned genes was significantly decreased in the adenovirus infected cells after H<sub>2</sub>O<sub>2</sub> treatment. Thus DHCR24 gene can protect chondrocytes from H<sub>2</sub>O<sub>2</sub> induced hypertrophy. This is the first demonstration that expression of DHCR24 gene is mandatory for proper bone growth.

**Disclosures:** R. Mirza, None.

This study received funding from: Japan Society for Promotion of Science.

## SU119

**Protein Sulfation Is Required to Prevent Chondrocytes Autophagy and Growth Factor Signaling During Endochondral Ossification.** C. Settembre<sup>\*1</sup>, E. Artega<sup>\*1</sup>, M. D. McKee<sup>\*2</sup>, A. Ballabio<sup>\*3</sup>, G. Karsenty<sup>\*1</sup>. <sup>1</sup>Columbia University, NY, NY, USA, <sup>2</sup>McGill University, Montreal, QC, Canada, <sup>3</sup>Tigem, Napoli, Italy.

Growth plate extracellular matrix is mainly composed of collagen fiber and proteoglycans. Proteoglycans consists of a core protein decorated by highly sulfated sugar chains, known as glycosaminoglycans (GAGs). Although the extent of proteoglycan sulfation regulates many developmental processes its role during endochondral ossification has not been systematically analyzed. The extent of sulfation of the GAGs moiety of proteoglycans is regulated by a group of enzymes called sulfatases whose activity is regulated by Sulfatase Modifying Factor 1 (Sumf1). Sumf1 is highly expressed in proliferating chondrocytes and osteoblasts and its inactivation in humans results in severe and complex skeletal abnormalities. Thus to address the importance of protein sulfation during endochondral ossification we generated and analyzed Sumf1<sup>-/-</sup> mice. This analysis showed that the extent of protein sulfation affects profoundly chondrocytes survival. Indeed, in absence of Sumf1 proliferating chondrocytes die through autophagy and produce less extracellular matrix. Remarkably none of these cellular abnormalities are observed in osteoblasts. Additionally proteoglycan sulfation regulates chondrocytes maturation. Preliminary results suggest that this latter function of Sumf1 relates to the importance of proteoglycan sulfation in transducing appropriately FGF signaling in the growth plate. Together these results establish that extracellular matrix through the extent of GAG sulfation affects endochondral ossification by acting on chondrocytes in several ways: it prevents chondrocytes autophagy, promotes ECM production and favours growth factor signaling.

**Disclosures:** C. Settembre, None.

## SU120

**Reduced Cell Proliferation and Chondrodysplasia in Mice Lacking the Mitotic Protein NuSAP.** A. Vanden Bosch<sup>\*1</sup>, S. Torrekens<sup>\*1</sup>, M. Van Camp<sup>\*1</sup>, R. Bouillon<sup>1</sup>, P. Carmeliet<sup>\*2</sup>, G. Carmeliet<sup>1</sup>. <sup>1</sup>Experimental Medicine, KULeuven, Leuven, Belgium, <sup>2</sup>VIB Vesalius Research Center, KULeuven, Leuven, Belgium.

During endochondral ossification, chondrocyte proliferation and differentiation within the cartilage growth plate are the driving forces behind longitudinal bone growth. Proliferation is strictly controlled by several cell cycle checkpoints including the spindle checkpoint, however, their role in bone development is largely unknown. NuSAP is a spindle-associated protein, expressed in proliferating cells and essential for normal mitosis of cultured cells and developing mouse embryos. To investigate whether triggering mitotic defects would activate cell cycle control mechanisms during bone development, we generated chondrocyte-specific NuSAP null mice by crossing *Nusap*<sup>fl/fl</sup> mice with mice expressing the Cre recombinase driven by the collagen 2 promoter (*Nusap*<sup>chm/-</sup>). *Nusap*<sup>chm/-</sup> mice were born at a normal frequency and were comparable in size and weight to control (*Nusap*<sup>chm+/+</sup>) mice. However, mutant mice died at birth, due to asphyxia, for their ribs were splayed and their sternum was shorter, resulting in a narrow, bell-shaped thoracic cage.

The long bones of *Nusap*<sup>chm/-</sup> pups at embryonic day 18.5 (E18.5) were shorter than those of control littermates (tibias: 3.5 mm compared to 4.1 mm for controls; p=0.003). Furthermore, H&E staining revealed that NuSAP inactivation lead to a chondrodysplasia characterized by smaller growth plates, disturbed columnar organization of the flat chondrocytes and a manifest disorganization of the hypertrophic zone. The number of hypertrophic chondrocytes was decreased, their size was highly variable and empty lacunae were present between cells. As expected, proliferation, assessed by BrdU incorporation, was significantly decreased, and almost absent in the region of the flat chondrocytes of *Nusap*<sup>chm/-</sup> growth plates. Apoptosis on the other hand, was increased and present at abnormal sites, as shown by TUNEL labeling. The mechanism responsible for induction of apoptosis was investigated. In primary chondrocyte cultures derived from E18.5 *Nusap*<sup>chm/-</sup> embryos, p53 levels were three-fold increased compared to controls. Concomitantly, the expression of the cell cycle inhibitor p21 and of the pro-apoptotic protein Bax was markedly increased.

In summary, our results demonstrate that mitotic defects in chondrocytes, induced by NuSAP deficiency, lead to p53-dependent apoptosis. NuSAP is thus essential for chondrocyte proliferation and for maintaining normal growth plate architecture and function.

**Disclosures:** A. Vanden Bosch, None.

## SU121

**Role of Wdr5 in Endochondral Bone Formation During Chicken Limb Development.** S. Zhu<sup>1</sup>, E. Zhu<sup>\*1</sup>, S. Provot<sup>2</sup>, F. Gori<sup>1</sup>. <sup>1</sup>Endocrine Unit, Massachusetts General Hospital, Harvard Medical School, Boston, MA, USA, <sup>2</sup>Department of Anatomy, UCSF, San Francisco, CA, USA.

Wdr5 is expressed in chondrocytes and osteoblasts in vitro and in vivo. While in vitro stable expression of Wdr5 dramatically accelerates osteoblast differentiation, silencing of Wdr5 markedly inhibits osteoblast differentiation. Targeted expression of Wdr5 to osteoblasts, using the 2.3-kb fragment of the mouse  $\alpha(1)$  I collagen promoter results in accelerated osteoblast differentiation during mouse embryonic development. To address whether Wdr5 is required for endochondral bone formation in vivo, a Replication Competent Avian No Splicer (RCAN) system delivering Wdr5 short hairpin RNA (shRNA) was utilized to silence Wdr5 expression throughout the developing chicken limb. High-titer RCAN-shWdr5 and RCAN-scrambled retroviral inoculates were injected into the right limb bud of chick embryos at Hamburger&Hamilton (HH) stage 18-20 (E3-3.5), when mesenchyme condensation begins. Embryos were harvested at HH stage 35 (E8.5), 36 (E10.5) and 38 (E12.5) to evaluate chondrocyte and osteoblast differentiation. The uninfected left wings served as controls. Alcian Blue and Alizarin Red staining of whole mount skeletons showed that RCAN-shWdr5 infected wings were shorter and displayed reduced mineralized bone compared to uninfected left wings at all time points. Histological analyses showed that RCAN-shWdr5 infected wings displayed a smaller hypertrophic chondrocyte layer and a delay in vascular invasion compared to uninfected left wings. Histological analyses were confirmed by in situ hybridization. While, the uninfected left wings displayed a normal pattern of chondrocyte and osteoblast maturation, RCAN-shWdr5 infected wings displayed higher expression of Sox9 and reduced type X collagen, and osteopontin expression compared to uninfected left wings, suggesting that silencing of Wdr5 resulted in delay of chondrocyte differentiation. RCAN-shWdr5 infected wings displayed also reduced type I collagen expression and mineral deposition as shown by Von Kossa staining, suggesting that silencing of Wdr5 also resulted in impaired osteoblast differentiation. Some of RCAN-shWdr5 infected wings exhibited a more severe phenotype. These wings displayed considerably shorter and thicker skeletal elements of the zeugopod and stylopod and absence of mineralized bone relative to the uninfected left wings. Proximal elements of the autopod, such as the carpo-metacarpus, were significantly shorter and phalanges 3 and 4 were missing, suggesting that Wdr5 is required for proper limb patterning and outgrowth. Taken together, these findings demonstrate that Wdr5 is required for proper endochondral bone formation and suggest that Wdr5 may play a role in limb patterning and outgrowth.

**Disclosures:** S. Zhu, None.

## SU122

**TGF $\beta$  and Smad3-dependent Repression of Runx2 Function in ATDC5 Chondrocytes.** E. N. Chin\*, T. Alliston. Orthopaedic Surgery, University of California, San Francisco, San Francisco, CA, USA.

Transforming growth factor- $\beta$  (TGF $\beta$ ) is an essential anabolic cytokine for articular chondrocytes. TGF $\beta$  induces the expression of extracellular matrix proteins such as aggrecan and collagen II, and inhibits resting articular chondrocytes from undergoing hypertrophic differentiation. The mechanisms by which TGF $\beta$  inhibits terminal chondrocyte differentiation remain unclear. Previously, we demonstrated that TGF $\beta$  inhibits terminal osteoblast differentiation by repressing the expression and function of Runx2. Specifically, TGF $\beta$  inhibits Runx2 function through Smad3-mediated recruitment of class II histone deacetylases to Runx2-binding promoter elements. In chondrocytes, Runx2 drives terminal differentiation, hypertrophy, and the expression of hypertrophy of late-stage differentiation markers, including collagen X and matrix metalloproteinase-13 (MMP-13). TGF $\beta$  can inhibit the expression of both collagen X and MMP-13. Thus, we seek to determine if TGF $\beta$  represses Runx2 function in chondrocytes to inhibit the expression of late-stage differentiation markers and the progression of hypertrophic chondrocyte differentiation. Here we test the hypothesis that TGF $\beta$  represses Runx2 through a Smad3-dependent mechanism.

Murine ATDC5 chondroprogenitor cells were transiently transfected with a synthetic Runx2-responsive promoter reporter construct, pOSE2-Luciferase. Reporter activity was normalized to  $\beta$ -galactosidase expression from a cotransfected control plasmid. Consistent with previous reports, overexpression of Runx2 increased relative luciferase activity. However, treatment with TGF $\beta$ 1 repressed the activity of this Runx2 reporter plasmid in a dose dependent manner. Cotransfection of a constitutively active TGF $\beta$  type I receptor construct also repressed pOSE2-Luc reporter activity. To determine if TGF $\beta$  repression of pOSE2-Luc reporter activity was Smad3-dependent, ATDC5 cells were cotransfected with a Smad3 expression construct. Overexpression of Smad3 conferred even greater TGF $\beta$ -dependent repression of pOSE2-Luc activity. TGF $\beta$ /Smad3 dependent repression of pOSE2-Luc activity in chondrocytes was comparable to that observed in osteoblasts and mesenchymal cells. Using a combination of quantitative reverse-transcription PCR and additional promoter-reporter constructs, we are currently investigating the extent to which TGF $\beta$  and Smad3 repress Runx2 function to regulate the transcription of chondrocyte genes. In conclusion, TGF $\beta$  and Smad3 repress the transcriptional activity of Runx2 in chondrocytes and may play a role in the regulation of endogenous chondrocyte gene expression and chondrocyte differentiation.

**Disclosures:** E.N. Chin, None.

This study received funding from: Arthritis Foundation.

## SU123

**Chondrocyte Differentiation Is Differentially Affected by Cyclooxygenase-2 and 5-Lipoxygenase during Fracture Healing.** J. A. Cottrell\*, J. P. O'Connor. Biochemistry & Molecular Biology, UMDNJ-New Jersey Medical School, Newark, NJ, USA.

Bone regeneration following a fracture is critically regulated by arachidonic acid (ArA) metabolism. Following release from membrane stores, ArA is converted into prostaglandins or leukotrienes via cyclooxygenase-2 (COX-2) or 5-lipoxygenase (5-LO) activity. Using radiographic, histomorphometric, and mechanical testing analyses, we have demonstrated that COX-2 and 5-LO have diametric effects on bone regeneration. Whereas fracture healing is impaired in COX-2 knockout mice, fracture healing is dramatically accelerated and enhanced in 5-LO knockout mice. Similarly, fracture healing is impaired in rats treated with a COX-2 inhibitor (celecoxib) but is accelerated in rats treated with a 5-LO inhibitor (AA-861). To elucidate the mechanism by which COX-2 and 5-LO regulates fracture healing, cell proliferation and gene expression were analyzed during femur fracture healing in female Sprague-Dawley rats treated with oral doses of celecoxib, AA-861, or vehicle (1% methylcellulose). Following fracture, cell proliferation analysis showed that callus cell proliferation peaked at day 2 after fracture in rats treated with AA-861 as compared to day 4 in vehicle-treated rats. Celecoxib treatment significantly reduced callus cell proliferation even though the 4-day calluses from the celecoxib-treated rats had the highest number of cells. RT-qPCR analysis of chondrocyte differentiation markers revealed that Type II collagen expression was significantly elevated in celecoxib and AA-861 treated rat fracture calluses. However, only AA-861 treatment significantly increased Type X collagen expression. These data indicate that COX-2 and 5-LO regulate chondrocyte differentiation during fracture healing endochondral ossification. COX-2 appears to be necessary for the progressive differentiation of chondrocytes whereas 5-LO activity appears to normally limit this progression. By altering chondrocyte differentiation during fracture healing, loss or inhibition of COX-2 delays healing while loss or inhibition of 5-LO accelerates healing.

**Disclosures:** J.P. O'Connor, Accelalox Inc. 3, 5; Medtronic 3; Biomimetics 3; Celgene 2.

This study received funding from: New Jersey Commission on Science and Technology.

## SU124

**Phosphate Regulates Chondrocyte Differentiation, Proliferation and Apoptosis in a Model of Embryonic Endochondral Bone Formation.** A. A. Zalutskaya, M. B. Demay. Endocrine Unit, Massachusetts General Hospital, Harvard Medical School, Boston, MA, USA.

Phosphate is required for terminal differentiation of hypertrophic chondrocytes during postnatal growth plate maturation. To investigate whether extracellular phosphate plays a role during embryonic endochondral bone formation, we performed investigations in the mouse metatarsal culture model. This model recapitulates *in vivo* bone development in culture and circumvents the homeostatic changes that occur in the intact animal. Metatarsals were isolated from day 15.5 C57BL/6J embryos and cultured in phosphate-free high glucose DMEM (1% Pen/Strep, 0.05mg/ml ascorbic acid and 0.25% heat-inactivated FBS) for 4, 8 and 12 days (37°C, 5% CO<sub>2</sub>) with 1.25 mM (control) and 7 mM phosphate (high). The length of each metatarsal was measured at the time of isolation, as well as at the end of the 12 day culture period. Frozen sections were obtained to permit histology, immunohistochemistry, TUNEL and *in situ* hybridization analyses with digoxigenin-UTP labeled probes. Metatarsals cultured with 7 mM phosphate showed a decrease in growth and proliferation compared to 1.25 mM phosphate. Histologic analysis and *in situ* hybridization with Collagen II, Collagen X and Osteopontin revealed an early enhancement of hypertrophic chondrocyte differentiation in metatarsals cultured with 7 mM phosphate (4 days), followed by a decrease in osteopontin expression (8 and 12 days), compared to 1.25 mM phosphate. In contrast to the control, Von Kossa staining showed no mineralization in metatarsals cultured with 7 mM phosphate. TUNEL assays revealed a dramatic increase in apoptosis of hypertrophic chondrocytes in metatarsals cultured with high phosphate. Immunohistochemistry with anti-cleaved caspase-9 antibody showed an increase in activated caspase-9 in hypertrophic chondrocytes of metatarsals cultured with 7 mM phosphate compared to 1.25 mM. Treatment of metatarsals with 20  $\mu$ M Z-LEHD-FMK caspase-9 inhibitor inhibited apoptosis and partially reversed the growth inhibition observed with 7 mM phosphate. Thus, our studies demonstrate that embryonic hypertrophic chondrocytes are susceptible to phosphate mediated apoptosis by activation of the caspase-9-mediated mitochondrial pathway in the metatarsal culture system.

**Disclosures:** A.A. Zalutskaya, None.

## SU125

**A Novel Model System for Drug Discovery in Osteoarthritis: Monitoring Whole Tissue Turnover in Murine Femur Heads.** K. Henriksen, S. H. Madsen\*, N. Schultz\*, G. Thomsen\*, A. V. Neutzsky-Wulff, M. A. Karsdal. Pharmacology, Nordic Bioscience A/S, Herlev, Denmark.

Osteoarthritis (OA) is a complicated disease of the whole joint. The pathology is a characterized by chondrocyte hypertrophy and cartilage degradation, but also subchondral changes in osteoclastic bone resorption and osteoblastic bone formation. No *ex vivo* models allowing investigation of turnover in the whole joint exist. We developed a femur head model, and characterized the response to both catabolic and anabolic stimulation with respect to changes in whole tissue turnover, monitored using a panel of biochemical markers of bone and cartilage turnover.

Femur heads from three week old mice were isolated and cultured for 10 days in DMEM containing either IL-1 $\alpha$  [10 ng/ml], PTH [100ng/mL], or the general MMP inhibitor GM6001 [10  $\mu$ M]. The conditioned medium was kept for analysis of biochemical markers of bone and cartilage turnover, including CTX-I (bone resorption), ALP activity (Bone formation), CTX-II (cartilage degradation), PIINP (cartilage formation), TRACP (osteoclast number), aggrecanase activity (Bachem substrate cleavage and 374ARGS-fragment release), MMP activity (Bachem substrate cleavage and 342FFGV-fragment release), and GAG release (cartilage turnover). Overall cell numbers were monitored using the dye Alamar Blue. Passive release from metabolically inactive femur heads was measured as background.

Stimulation of the femur heads with IL-1 $\alpha$  led to a two-fold increase in CTX-I release, which was abrogated by addition of GM6001. IL-1 $\alpha$  induced a three-fold increase in sGAG release, which was unaffected by GM6001. CTX-II release was abrogated by IL-1 $\alpha$ , as well as GM6001. The osteoclast marker TRACP increased by 50%. PIINP release was reduced by 50% in the presence of IL-1 $\alpha$ , whereas GM6001 did not affect it. PTH on the other hand augmented cartilage formation measured by PIINP, but did not affect sGAG release.

We have developed a whole tissue model to monitor both cartilage and bone in one single system, which is highly responsive to both catabolic and anabolic stimulation. This is useful to investigate the interaction between cartilage and bone cell types. This model may be more representative for screening and testing potential novel treatments for OA, than traditional single cell culture systems.

**Disclosures:** K. Henriksen, None.

## SU126

**Trps1 Represses Runx2 During Endochondral Bone Formation.** D. Napierala<sup>1</sup>, K. Choudhry<sup>\*1</sup>, E. Munivez<sup>\*1</sup>, T. Bertin<sup>\*1</sup>, B. Lee<sup>2</sup>. <sup>1</sup>Baylor College of Medicine, Houston, TX, USA, <sup>2</sup>Baylor College of Medicine, Howard Hughes Medical Institute, Houston, TX, USA.

Runx2 is a transcription factor that specifies osteoblast cell fate commitment and chondrocyte maturation. Runx2 is also expressed early in mesenchymal condensations. However, in mesenchyme destined for chondrogenic lineages Runx2 is down-regulated. Also later, during endochondral ossification Runx2 is attenuated in prehypertrophic

chondrocytes where the balance of cellular proliferation versus terminal hypertrophy is maintained. Here we present evidence that the Trps1 transcriptional repressor physically interacts with Runx2 and inhibits Runx2-mediated trans-activation. Interestingly, during skeletal development, Trps1 is highly expressed in chondrogenic mesenchyme and prehypertrophic chondrocytes, where Runx2 is attenuated. Moreover, Trps1 mutant mice demonstrate increased Runx2 expression in growth plate chondrocytes and perichondrial cells, accompanied by elevated expression of Runx2 target genes: Ihh and collagen type X, and advanced mineralization of perichondrium. These molecular in vitro studies and analyses of growth plate abnormalities in Trps1 mutant mice demonstrate that Trps1 is a novel Runx2 repressor in developing endochondral bones.

**Disclosures:** D. Napierala, None.

*This study received funding from: NIH grants DE016990 and HD22657, and the Bone Diseases Program of Texas.*

## SU127

**The Regulation of Chondrogenesis and Bone Development by Neogenin via BMP Pathway.** Z. Zhou, D. Lee\*, J. Xie\*, L. Zhou\*, Y. Liu\*, L. Mei\*, W. Xiong. Medical College of Georgia, Augusta, GA, USA.

Neogenin, an immunoglobulin family transmembrane receptor, is implicated in axon guidance, neuronal differentiation, morphogenesis, and apoptosis. It is widely expressed in different tissues, including bones. However, the role of neogenin in bone development is unknown. We here characterized the skeletal phenotypes of mice lacking neogenin. Neogenin mutant mice showed defect in limb development at embryonic stage, and reduced endochondral ossification and angiogenesis at the early postnatal stage. Bone size and bone volumes were decreased in p30 neogenin mutant mice. Cultured osteoblast from neogenin mutant mice exhibited defective osteoblast differentiation and bone formation, in vitro. The epiphyseal cartilage and cultured osteoblasts from neogenin mutant mice also showed impaired BMPs signaling. Together, we speculated that neogenin appears to be involved in the regulation of chondrogenesis and bone development through BMP signaling pathways. The underlying molecular mechanism is under further characterizing.

**Disclosures:** Z. Zhou, None.

*This study received funding from: NIH.*

## SU128

**Study of Growth Hormone (hGH) and Insulin-like Growth Factor (IGF) Type 1 Receptors in the Human Fetal Femoral Growth Plate.** M. Edwards<sup>1</sup>, C. G. Goodyer<sup>2</sup>. <sup>1</sup>Experimental Medicine, McGill University, Montreal, QC, Canada, <sup>2</sup>Pediatrics, Experimental Medicine, McGill University, Montreal, QC, Canada.

**Introduction:** hGH plays an essential role in human postnatal growth. The long bones of the skeletal system are major targets for hGH, where it is thought to affect final adult height by promoting chondrocyte proliferation and differentiation within the growth plate and bone mineral density by regulating osteoblast activities. The effectiveness of hGH depends on the availability of its receptor (hGHR) on target cells. GHR expression has been demonstrated in long bone chondrocytes and osteoblasts of the bovine, mouse and rat; however, comparable studies in the human have not been reported and there is a general lack of information concerning hGH effects on human long bone development in the fetus. Dysfunctional bone development can underlie abnormal growth patterns, osteoporosis and bone cancers. Approximately 50% of pediatric endocrine clinic patients have abnormal growth patterns for which there is no known medical explanation. In adults, especially women and the elderly, osteoporosis is an even greater problem, affecting more than 75 million people in North America, Europe and Japan alone. Osteosarcomas, the most common type of malignant pediatric bone cancers in North America, have one of the highest mortality rates of pediatric cancers. We have, therefore, begun a systematic analysis of the hGH/hGHR/IGF axis in human fetal long bones. Here we report immunohistochemical data on hGHR and IGF-1R expression in human (n=3, 14-16 week fetal age) femur growth plates.

**Results:** The femurs were fixed in 4% paraformaldehyde, decalcified, paraffin embedded and sectioned at 5µm. Sections underwent a citrate-buffer antigen retrieval step followed by incubation with either a mouse anti-hGHR monoclonal primary antibody (mAb263)/goat anti-mouse IgG Alexa Fluor 488 conjugated secondary antibody or rabbit anti-IGF-1R polyclonal primary antibody/goat anti-rabbit IgG Alexa Fluor 594 conjugated secondary antibody. The growth plate distribution of hGHR- and IGF-1R-expressing chondrocytes in the resting, proliferating and hypertrophic zones was compared with markers for specific chondrocyte subpopulations (parathyroid hormone receptor 1 [proliferating], collagen X [hypertrophic]). Both hGHR and IGF-1R were expressed in all chondrocytes of the femoral growth plate at this stage in fetal long bone development, demonstrating punctate as well as general cytoplasmic staining, with variable intensities in cells of the different zones.

**Conclusion:** These findings demonstrate expression of hGHR and IGF-1R in human fetal long bone chondrocytes prior to midgestation and suggest a role for hGH and IGF function in early stages of normal human bone development.

**Disclosures:** M. Edwards, None.

*This study received funding from: Canadian Institutes of Health Research.*

## SU129

**Overcoming the Zone of Chondrocyte Death Associated with Osteochondral Harvest by Sequential Treatment with Collagenase and IGF-1.** A. J. McGregor<sup>\*1</sup>, B. A. Amsden<sup>\*1</sup>, S. D. Waldman<sup>\*2</sup>. <sup>1</sup>Chemical Engineering, Queen's University, Kingston, ON, Canada, <sup>2</sup>Mechanical Engineering, Chemical Engineering, Queen's University, Kingston, ON, Canada.

Osteochondral harvesting has been shown to induce a zone of chondrocyte death (ZCD) which has been implicated in the poor cartilaginous integration of the graft with the surrounding host tissue after implantation. This zone originates from the cut surface and can extend up to 400 µm into the tissue, limiting the ability of chondrocytes to migrate through the dense extracellular matrix (ECM) to the wound edge. The aim of the current study is to determine if the ZCD can be reduced by disrupting the ECM using collagenase and treating the tissue with IGF-1 as a means of inducing a chemotactic and/or proliferation response on the chondrocytes. Bovine articular cartilage explants were harvested and a ZCD was induced using the OATS osteochondral harvesting tool. Explants were either treated for 10 minutes with 0.15% collagenase or left untreated. After enzymatic disruption of the ECM, samples were cultured in serum-free media supplemented with or without IGF-1 (25 ng/mL). Cultures were harvested weekly (at 7, 15, 21 days) and stained with calcein AM and ethidium homodimer to assess cell viability. The ZCD was measured using confocal microscopy and statistically compared amongst the different treatment groups. Results indicated that there was a significant effect of the various culture conditions on the ZCD ( $p < 0.001$ ). Collagenase treatment reduced the ZCD by approximately 40% compared to control (control:  $140 \pm 17 \mu\text{m}$ ; collagenase:  $241 \pm 21 \mu\text{m}$ ). Although IGF-1 supplementation alone had no discernable effect on the ZCD, IGF-1 supplementation after pre-treatment with collagenase significantly reduced the ZCD by 80% compared to control (IGF-1:  $255 \pm 13 \mu\text{m}$ ; collagenase + IGF-1:  $48 \pm 13 \mu\text{m}$ ). In addition, there appeared to be a linear trend in the collagenase + IGF group whereby the ZCD decreased over time (Day 7:  $65 \pm 18 \mu\text{m}$ ; Day 21:  $34 \pm 9 \mu\text{m}$ ). Thus, treating osteochondral grafts with collagenase and IGF-1 induces chondrocyte repopulation of the ZCD generated by osteochondral graft harvesting. This effect should allow for an increased number of chondrocytes near the graft edge to promote cartilaginous integration with surrounding native cartilage after implantation.

**Disclosures:** A.J. McGregor, None.

## SU130

**Over-expression of CNP Enhances the Formation of Long Bone Exostoses in Ext1<sup>+/+</sup> Mice.** H. Bukulmez<sup>\*1</sup>, F. Khan<sup>\*1</sup>, C. Fernando<sup>\*2</sup>, J. S. Grewal<sup>\*1</sup>, A. Bilgin<sup>\*1</sup>, J. D. Esko<sup>\*3</sup>, M. L. Warman<sup>4</sup>. <sup>1</sup>Genetics/Pediatrics, CWRU/NEOUCOM, Cleveland/Akron, OH, USA, <sup>2</sup>Otolaryngology, CWRU, Cleveland, OH, USA, <sup>3</sup>Cellular and Molecular Medicine, UCSD, La Jolla, CA, USA, <sup>4</sup>Orthopaedics and Genetics, Children's Hospital Boston, Harvard Medical School, Boston, MA, USA.

Multiple hereditary exostoses (MHE) is an autosomal dominant skeletal disorder caused by heterozygous loss-of-function mutations in either EXT1 or EXT2, which encode enzymes involved in heparan sulfate biosynthesis. Although exostoses in patients with EXT mutations can occur at diverse skeletal sites and can undergo malignant degeneration, the exostoses in Ext1 heterozygous (Ext1<sup>+/+</sup>) mice predominantly affect the ribs and do not become malignant.

In this study we bred Ext1<sup>+/+</sup> mice to transgenic mice that over-express C-type natriuretic peptide under the control of the type II collagen promoter/enhancer (CNP<sup>col2aITG</sup>). The purpose of this study was to determine whether CNP over expression would enhance the Ext1<sup>+/+</sup> phenotype. By itself, CNP over-expression causes skeletal overgrowth, but does not produce exostoses. Ext1<sup>+/+</sup> and CNP<sup>col2aITG</sup> mice were mated and 27 offspring were followed for up to 8 months. Non-rib exostoses were detected clinically and/or radiographically, and they were examined histologically following sacrifice.

Eight of the 27 offspring developed non-rib exostoses (2 vertebral, 2 femoral head, 1 distal femur, 1 proximal tibia, 1 distal radius, and 1 ischial bone) and these 8 offspring were both Ext1<sup>+/+</sup> and CNP<sup>col2aITG</sup>. Of the remaining 19 mice in which we did not observe long bone or vertebral exostoses, 9 were Ext1<sup>+/+</sup> and CNP<sup>col2aITG</sup>, 4 were Ext1<sup>+/+</sup> and non-transgenic for CNP, and 6 were entirely wild-type. The histologic appearance of each exostosis was similar to that of human exostotic lesions.

We find that CNP over-expression can enhance the exostoses phenotype in Ext1<sup>+/+</sup> mice. At present, we do not know whether CNP enhances the phenotype indirectly by increasing chondrocyte proliferation or directly by activating a signaling pathway that depends upon Ext1.

**Disclosures:** H. Bukulmez, None.

*This study received funding from: NIH/NIAMS, NIH/NIGMS, HHMI.*

## SU131

**Continuous Culture of Tissue Engineered Cartilage.** A. A. Khan<sup>\*1</sup>, J. M. Suits<sup>\*1</sup>, R. A. Kandel<sup>\*2</sup>, S. D. Waldman<sup>\*3</sup>. <sup>1</sup>Chemical Engineering, Human Mobility Research Centre, Kingston General Hospital, Queen's University, Kingston, ON, Canada, <sup>2</sup>Department of Pathology and Laboratory Medicine, Mount Sinai Hospital, Toronto, ON, Canada, <sup>3</sup>Chemical Engineering, Mechanical and Materials Engineering, Human Mobility Research Centre, Kingston General Hospital, Queen's University, Kingston, ON, Canada.

The use of bioreactors for cartilage tissue engineering has become increasingly important as traditional batch-fed culture is not optimal for tissue growth *in vitro*. Most tissue engineering bioreactors rely on convection as the primary means to provide mass transfer; however, convective transport of nutrients can also impart potentially unwanted or uncontrollable mechanical stimuli to the cells resident in the construct. The reliance on diffusive transport may not necessarily be ineffectual as previous studies have observed improved tissue growth when the constructs were cultured in elevated volumes of media. In this study, to approximate an infinite reservoir of media, we investigated the effect of continuous culture on cartilaginous tissue growth *in vitro*. Isolated bovine articular chondrocytes were seeded on Millicell™ filters and after two weeks of pre-culture, the constructs were cultivated under continuous media flow (5 to 10 µL/min) for a period of one week. Tissue engineered cartilage constructs cultivated in the continuous flow bioreactor significantly accumulated more collagen and proteoglycans (between 50-70%). These changes were similar in magnitude to the reported effect of through-thickness perfusion without the need for large volumetric flow rates. In addition, tissues cultivated in the reactor appeared to adopt an appearance closer to the characteristic structure of native articular cartilage. Tissues grown in the reactor displayed some evidence of the stratified morphology of native cartilage as well as containing stores of intracellular glycogen. Future studies will investigate the effect of long-term culture in the reactor in terms of ECM accumulation and subsequent changes in mechanical function.

**Disclosures:** A.A. Khan, None.

## SU132

**Identification And Characterization of 3.6 Col I Positive Cells from Mouse Temporomandibular Joint.** J. Chen<sup>\*1</sup>, Y. Bi<sup>\*2</sup>, M. F. Young<sup>2</sup>, S. Wadhwa<sup>\*1</sup>. <sup>1</sup>Craniofacial sciences, University of Connecticut Health Center, Farmington, CT, USA, <sup>2</sup>Craniofacial and Skeletal Diseases Branch, National Institute of Dental and Craniofacial Research, US National Institutes of Health, Bethesda, MD, USA.

The mandibular condylar cartilage (MCC) is unique from other articular cartilages in that it is derived from periosteum and composed of fibrocartilage. Little is known about the exact stages of MCC cell differentiation. Due to its periosteal origin, we hypothesized that the early osteoblast differentiation marker (3.6 kb fragment of the rat collagen type I promoter (3.6 Col I)) would be an early marker for MCC cell differentiation. To test the hypothesis, transgenic mice containing the 3.6 Col I fused to a Topaz-fluorescent protein (3.6 Col I-GFP), the 3.6 Col I fused to CRE recombinase (3.6 Col I-CRE), the collagen type II promoter fused to a Cyan-fluorescent protein (Col II-GFP), and Rosa26-LacZ mice (containing floxed beta-galactosidase gene) were used in this study. In addition, primary cells obtained from digesting MCC from 3.6 Col I-GFP mice were cultured for colony-forming units (CFUs).

The mandibular condylar cartilage is organized into 4 zones -1. articular zone, 2. polymorphic zone (contains the precursor cells), 3. flattened zone (Col II expression), and 4. hypertrophic zone (Col X expression). Using histology, we found that the 3.6 Col I-GFP expression is localized in the polymorphic zone and distinct from Col II-GFP expression, which is localized in the flattened zone of the MCC. Cell fate mapping experiments, by the breeding of 3.6 Col I-CRE mice with the Rosa26-LacZ, revealed that beta-galactosidase expression was not only in the polymorphic, but also in the flattened and hypertrophic zones of the MCC. In vitro studies further showed that the CFUs from the MCC were not 3.6 Col I positive but were able to differentiate to fat (oil red staining), bone (alizarin red staining) and cartilage (alcian blue staining).

Our results indicate that 3.6 Col I expression is an early marker of MCC cell maturation. In our current working model we believe that MCC differentiation proceeds by the initial formation of precursor/progenitor cells that are negative for 3.6 Col I expression. Later stages progress to be 3.6 Col I positive, followed by Col II and then to Col X expression. This is the first report showing the expression of 3.6 Col I promoter and the identification of mesenchymal precursors in the mouse MCC. These data provide an important foundation for future work further defining regenerative therapies of the TMJ.

**Disclosures:** J. Chen, None.

This study received funding from: NIH, American Association of Orthodontists Foundation.

## SU133

**Nicotine Induces Chondrogenesis via Calcineurin/NFAT.** H. Ho<sup>\*</sup>, X. Lu<sup>\*</sup>, D. Hoak<sup>\*</sup>, J. E. Puzas, R. J. O'Keefe, M. J. Zuscik. Orthopaedics, University of Rochester, Rochester, NY, USA.

Cigarette smoking is documented to have deleterious effects on skeletal healing based on human data and animal studies. While numerous compounds present in smoke likely contribute to its influence on healing, little is known about the key effectors or their underlying mechanisms of action. One important bioactive molecule in smoke is nicotine,

which can impact effects on cells that express nicotinic acetylcholine receptors (nAChRs). In previous work studying the influence of nicotine on skeletal repair, we found that i) mesenchymal stem cells (MSCs) express the nAChR, ii) activation of the receptor leads to initiation of its calcium channel function, and iii) cartilage deposition *in vitro* and *in vivo* is enhanced following exposure to nicotine. To study the signaling mechanisms that are activated and their contribution to nicotine's chondrogenic effect, we have examined the activation of calcineurin and subsequent nuclear translocation of NFATc1. We have also assessed the role of this pathway in nicotine's phenotypic effects. C3H10T1/2 cells were plated in monolayer and NFAT signaling was assessed using a luciferase-based reporter (NFAT-luc), western blotting, and NFATc1 cell localization studies. Then, pharmacologic blockade of calcineurin was employed to evaluate the dependence of nicotine on this pathway to enhance chondrogenesis in limb bud MSCs. Regarding signaling, nicotine evoked a dose-dependent activation of NFAT-luc that was 5-fold at the 5 microM dose. Western blotting corroborated this finding by revealing a 10-fold increase in nuclear NFATc1 that was coupled with a 60% reduction of its cytoplasmic pool following a 6 hr treatment with 5 microM nicotine. Fluorescence studies also demonstrated strong localization of eGFP-NFATc1 in the nucleus of cells following 120 min treatment with 10 microM nicotine. These results implicate the calcineurin/NFAT pathway in nicotine's effects on MSCs. To confirm this, limb bud MSCs were cultured in micromass and the ability of nicotine to accelerate chondrogenesis was examined in the presence and absence of cyclosporine A (CSA), an inhibitor of calcineurin. Similar to positive control treatment with BMP-2, nicotine enhanced cartilage nodule formation by 7 days relative to untreated cultures. This positive effect of nicotine was lost in cells treated with 0.2 microg/ml CSA during the 7 day culture period. Overall, nicotine was not only found to induce NFAT signaling in MSCs, but activation of this pathway was found to be required for the positive effect of nicotine on chondrogenesis. This is consistent with the known function of NFAT as an inducer of chondrogenesis and identifies a potential mechanism underlying the influence of cigarette smoke/nicotine on repair processes that rely on an endochondral phase of healing.

**Disclosures:** H. Ho, None.

This study received funding from: DOD, NIH.

## SU134

**Regulation of Autophagy in the Epiphyseal Growth Plate by AMPK and mTOR Requires HIF-1.** J. Bohensky<sup>\*</sup>, I. M. Srinivas, V. Srinivas<sup>\*</sup>. Orthopaedic Surgery, Thomas Jefferson University, Philadelphia, PA, USA.

During maturation chondrocytes experience ER stress and increase their intracellular calcium levels. It has been proposed that this sensitizes the cells to apoptogens. Increased calcium levels also activate the energy sensor, AMPK. We have previously shown that another energy sensor, HIF-1 induced autophagy as an intermediate step in the maturation of the chondrocyte, allowing the chondrocyte to reach the terminally differentiated state in its stressful microenvironment. The goal of the study is to examine the role of sensor molecules, mTOR and AMPK in regulating chondrocyte survival and autophagy in the growth plate in relationship to HIF-1. We showed that chondrocytes expressed the energy sensor AMPK $\alpha$ 1 and that activation of this protein is dependent on HIF-1. Furthermore its activation by thapsigargin, an ER stressor is also dependent on HIF-1. This activation was shown to promote autophagy and correlates with determinants of chondrocyte energy metabolism. Using serum-starved AMPK silenced cells, we show that AMPK is required for the induction of the autophagic response. We also note that there is a change in chondrocyte sensitivity to apoptogens, due to alterations in levels of bound Bcl-2, activation of caspase-8 and cleavage of BID. To test the hypothesis that AMPK signaling directly promotes autophagy we inhibited AMPK activity in mTOR silenced cells and showed that while mTOR suppression induced autophagy, AMPK inhibition did not block this activity. Based on this finding, it is concluded that activation of autophagy is due to AMPK's regulatory effects on mTOR and regulated by HIF-1.

In conclusion it is suggested that the maturation-dependent decrease in the chondrocyte energy status activates AMPK. As this protein promotes autophagy, the post-mitotic chondrocytes remain viable and can complete their life cycle. Once terminally differentiated, these late autophagic cells are sensitized to local apoptogens. Activation of apoptosis serves to delete hypertrophic chondrocytes from the plate thereby permitting osteoblast invasion and metaphyseal bone formation.

**Disclosures:** V. Srinivas, None.

## SU135

**Osteogenesis Effect of Human Ligamentum Flavum, Myoblast, Osteoblast and Mesenchymal Stem Cell by DBM and BMP-2.** J. Lee<sup>\*1</sup>, H. Kim<sup>\*1</sup>, U. Kwon<sup>\*1</sup>, C. Lee<sup>\*1</sup>, M. Nan<sup>\*1</sup>, K. Lee<sup>\*1</sup>, H. Kim<sup>\*1</sup>, I. Kwon<sup>\*2</sup>, H. Chun<sup>\*3</sup>, E. Moon<sup>\*1</sup>, H. Lee<sup>\*1</sup>, S. Moon<sup>\*1</sup>. <sup>1</sup>Orthopaedic surgery, Yon-sei University, Seoul, Republic of Korea, <sup>2</sup>Kyung Hee University, Seoul, Republic of Korea, <sup>3</sup>Mechanical Engineering, Yon-sei University, Seoul, Republic of Korea.

Demineralized bone matrix (DBM) derived from human tissues and Bone morphogenetic protein-2(BMP-2) induces bone formation and spinal fusion. Ligamentum flavum (LF) and mesenchymal stem cell (MSC) was reported to have osteogenic potential with stimulation of BMP-2. It can be hypothesized that LF, MSC, Osteoblast and Myoblast treated with BMP-2, DBM and mixture of BMP-2 and DBM can be a substitute for autogenous bone graft in spinal fusion. Therefore, we cultured all cells with BMP-2, DBM and mixture of BMP-2 and DBM. They were analyzed osteogenic differentiation. LF from stenotic lumbar spine, Osteoblast, Myoblast and MSC were harvested and cultured. Then all cells were treated with BMP-2, DBM and mixture of BMP-2 and DBM for 0 and 7day. Cellular proliferation was assessed by alamarblue assay. Reverse transcription-polymerase chain reaction (RT-PCR) for osteocalcin and collagen type I was performed. Alkaline phosphatase activity and Von-kossa staining was done. All cells showed increased



proliferation rate without cytotoxicity compared to control group. Human LF cells with DBM, BMP-2, mixture of BMP-2 and DBM demonstrated two times more upregulation of Collagen type I compared to control group in RT-PCR. Also MSC and Osteoblast cells with BMP-2 group demonstrated upregulation of Osteocalcin in RT-PCR. Furthermore all cells cultured with DBM, BMP-2, mixture of BMP-2 and DBM showed positive alkaline phosphatase activity and Von-kossa staining. In conclusion, All groups of all cells showed increase in proliferation rate and upregulation of osteogenic phenotypes. Furthermore all cells showed positive ALP activity and Von-kossa staining. Given osteogenic potential of human LF, MSC and Osteoblast with all tissues with DBM and/or BMP-2 can be used for bone graft substitute in spinal surgery.

**Disclosures:** S. Moon, None.

*This study received funding from: the Brain Korea21 project for Medical Sciences Yonsei University and grant No.R01-2006-000-10933-0 from the Basic Research Program of the Korea Science & Engineering Foundation.*

## SU136

**Biological Activation of Biomaterials by Recombinant Adeno-Associated Virus Vector.** H. Ito<sup>1</sup>, T. Nasu<sup>\*1</sup>, R. Tsutsumi<sup>\*1</sup>, T. Kitaori<sup>\*1</sup>, E. M. Schwarz<sup>2</sup>, T. Nakamura<sup>\*1</sup>. <sup>1</sup>Orthopaedic Surgery, Kyoto University Graduate School, Kyoto, Japan, <sup>2</sup>The Center for Musculoskeletal Research, University of Rochester, Rochester, NY, USA.

**Introduction:** Recently many kinds of biomaterials have been used in reconstructive surgery. The common problem of all biomaterials is that they are less capable of activating recipient tissues biologically. In order to add the property of biological activity to biomaterials, administration of growth factors or mesenchymal stem cells is also considered but has not been established. We examined if rAAV vectors on biomaterials could effectively induce gene transduction.

**Material & methods:** On hydroxyapatite,  $\beta$ -tricalcium phosphate ( $\beta$ -TCP) and titanium alloy plates, rAAV vectors were immobilized by lyophilization. The activities of  $\beta$ -galactosidase ( $\beta$ -gal) were assayed with the Luminescent  $\beta$ -gal assay kit. The lyophilized hydroxyapatite disc with rAAV-LacZ or -BMP-2 was inserted into the dorsal muscle of adult Wistar rat operatively under sterile condition. The extraction of the materials was performed 2, 4, and 8 weeks after operation. The frozen sections were stained with  $\beta$ -gal and nuclear fast red. Fixed discs with rAAV-BMP were treated into paraffin sections and stained with hematoxylin and eosin.

**Results:** *Lyophilized rAAV on biomaterials:* The respective  $\beta$ -gal activity of rAAV-treated fibroblasts on each material was significantly higher than that of control.

*In vivo transduction:* At 4 weeks, almost all pores of implants in each group were filled with fibrous tissues, but the AAV-treated sample showed a remarkable staining of the cells compared with control. At 8 weeks, the pores were almost completely filled with fibrous tissues. The evaluation of  $\beta$ -gal activity demonstrated that the activity in rAAV group was higher than those in control group at each time point, and the statistical significances were detected at 4 and 8 weeks.

*Hydroxyapatite with lyophilized rAAV-BMP:* At 4 and 8 weeks, mature bone formation started to be seen only on BMP-treated hydroxyapatite blocks, but only immature bone was observed on control.

**Discussion:** In recent reports of rAAV as a gene transducer, vectors were injected locally or systemically. In this experiment rAAV vectors were lyophilized on biomaterials without injection. The present result shows that the major bone-related materials can be used combined with rAAV, and that rAAV-BMP can, indeed, induce de novo bone formation in rat back muscles. Not only hydroxyapatite with rAAV-BMP but another biomaterial or rAAV with another gene may be epochal material in clinical occasions in the future.

**Disclosures:** H. Ito, None.

## SU137

**Catecholamines Accelerate BMP-induced Osteoblastic Differentiation and Bone Formation.** T. Uemura<sup>\*</sup>, Y. Ohta<sup>\*</sup>, Y. Nakao<sup>\*</sup>, Y. Hashimoto<sup>\*</sup>, K. Takaoka. Orthopaedic Surgery, Osaka City University Graduate School of Medicine, Osaka, Japan.

It has recently been reported that the sympathetic nervous system is involved in regulation of osteoblastic function mainly through  $\beta$ -type adrenergic receptors on the cell surface. The stimulatory effects of the sympathetic nervous system are mediated by catecholamines, such as adrenaline, noradrenaline and dopamine, which elevate the intracellular cyclic adenosine 3', 5'-monophosphate (cAMP) level through the Gs-coupled receptors. In a previous study, we showed that intracellular cAMP accumulation consistently enhanced bone morphogenetic protein (BMP)-induced osteoblastic differentiation, predominantly via the protein kinase A (PKA) signaling pathway. This study was designed to substantiate the potential of these catecholamines to enhance BMP-induced bone formation.

To confirm the action of the catecholamines in elevating the intracellular cAMP level in osteoblastic cell lines, changes of cAMP levels in these cells after addition of catecholamines (adrenaline, noradrenaline and dopamine) were assayed in time sequence. Intracellular cAMP levels increased significantly within 15 minutes by addition of the respective catecholamine. Changes of alkaline phosphates (ALP) levels in osteoblastic cell lines by BMP with or without catecholamine treatment were assayed after 3 days incubation. The ALP levels were consistently elevated by rhBMP-2(100 ng/ml) and the elevation of ALP levels were further enhanced by treatment with each catecholamine (adrenaline;  $10^{-7}$ ,  $10^{-8}$ M, noradrenaline;  $10^{-8}$ M, and dopamine;  $10^{-8}$ M).

To investigate the ability of these catecholamines to augment the bone-inducing action of BMP under *in vivo* condition, 30 mg of polymer discs (poly-D, L-lactic acid-p-dioxanone-polyethylene glycol block copolymer; PLA-DX-PEG) containing rhBMP-2(5  $\mu$ g) with or

without catecholamines (10, 20, 40  $\mu$ g) were implanted into the dorsal muscle pouch of mice. All ossicles induced by BMP were harvested 3 weeks later and examined by radiological and histological analyses. On soft X-ray radiogram, all of the ossicles revealed a trabecular network encased within a shell-shaped bone and the ossicles induced by rhBMP-2 when used in conjunction with each catecholamine (adrenaline; 10, 20, 40  $\mu$ g, noradrenaline; 40  $\mu$ g, and dopamine; 10, 20, 40  $\mu$ g) were significantly larger in size and higher in bone mineral content (BMC) on dual-energy X-ray absorptiometry (DXA) compared with those induced by rhBMP-2 alone.

In this study, we showed that catecholamines accelerate BMP-induced osteoblastic differentiation and bone formation probably by increasing cAMP via the PKA signaling pathway.

**Disclosures:** T. Uemura, None.

## SU138

**Wnt Pathway Regulation by Demineralized Bone Requires TGFbeta/BMP Signaling.** S. Zhou, J. Glowacki. Orthopedic Surgery, Brigham and Women's Hospital, Boston, MA, USA.

Allogeneic demineralized bone is used extensively as a clinical material because it has osteoinductive and osteoconductive properties. Demineralized bone powder (DBP) induces chondrogenic differentiation of human dermal fibroblasts (hDFs), but the initiating mechanisms have not been characterized. BMPs have been isolated from DBP, but it is not known whether BMPs recapitulate all the events induced by DBP in target cells. We had previously reported that DBP and BMP-2 regulate common and distinct pathways, and, further, that DBP stimulates the two distinct Smad pathways responsive to either TGF/activin or BMP. In this study, we tested the hypothesis that DBP, BMP-2, and TGF- $\beta$ 1 would similarly affect expression of Wnt signaling genes. A three-dimensional collagen scaffold was used in which hDFs were cultured with and without 3 mg DBP in a 3-D porous collagen sponge or with 10 ng/ml TGF- $\beta$ 1 or 100 ng/ml rhBMP-2. Total RNA was isolated after 3 days of culture, a time that precedes differentiation. Effects of DBP, BMP-2, and TGF- $\beta$ 1 on Wnts in hDFs were compared by microarray, RT-PCR, and Western blot analysis. Of the canonical Wnts, Wnts 2 and 10b were upregulated by all three agents; only DBP and TGF- $\beta$ 1 stimulated Wnt 7b and 16b and downregulated Wnt 2b; only DBP stimulated Wnt 3a; only BMP-2 induced Wnt 1. Of non-canonical Wnt/Ca<sup>2+</sup> members, Wnt 4, 5a, and 11 were upregulated by only DBP and TGF- $\beta$ 1. DBP and TGF- $\beta$ 1 stimulated  $\beta$ -catenin, but BMP-2 did so only weakly and inconsistently. LiCl and Wnt-agonist SB216763 mimicked DBP stimulation of Runx2 and SOX9. Stimulation of  $\beta$ -catenin and Wnts by DBP was attenuated by SB413542, an inhibitor of TGF- $\beta$ 1 activin receptor-like kinases. Thus, DBP's stimulation of Wnt genes and of  $\beta$ -catenin partially requires TGF- $\beta$ /activin signaling. In sum, BMP-2 does not, but TGF- $\beta$  does recapitulate many of DBP's effects on Wnt pathways in human target cells. DBP stimulation of  $\beta$ -catenin and Wnts involves TGF- $\beta$ 1 activin receptor-like kinases.

Thus, there are many effects of DBP that are not shared with BMP-2, which is the putative active component of DBP. DBP contains substantial amounts of TGF- $\beta$  and other factors that can contribute to DBP's effects *in vivo*.

**Disclosures:** S. Zhou, None.

*This study received funding from: Musculoskeletal Transplant Foundation and NIH.*

## SU139

**Interferon- $\gamma$  Attenuates BMP-2 Signaling Via Stat-1 Binding Of Smad4 In The Cytoplasm.** F. A. Sylvester<sup>1</sup>, N. Wyzga<sup>\*2</sup>. <sup>1</sup>Pediatric Gastroenterology, Connecticut Children's Medical Center, Hartford, CT, USA, <sup>2</sup>Research, Saint Francis Hospital & Medical Center, Hartford, CT, USA.

Activated T lymphocytes can affect osteoblast formation. We have previously shown that interferon- $\gamma$  (INF- $\gamma$ ), the prototypical Th1 cytokine, inhibits osteoblast development *in vitro*. We hypothesized that this effect is due to the blockade of BMP-2 signaling, a key osteogenic factor. To test this hypothesis, we treated ST-2 cells, a mouse clonal stromal cell line, with BMP-2  $\pm$  INF- $\gamma$  under osteogenic conditions at different time points. We found that treatment with INF- $\gamma$  significantly decreased the transactivation of the reporter construct 12X-SBE-Luc, under the control of a minimal osteocalcin promoter, suggesting that INF- $\gamma$  blocks the Smad-dependent BMP-2 pathway. We then investigated if the concentration of each of the different molecules involved in the canonical BMP-2 pathway was affected by treatment with INF- $\gamma$ . In ST-2 cells treated with BMP-2  $\pm$  INF- $\gamma$ , we did not detect differences in Western blot band density of the following factors: inactive or phosphorylated R-Smads 1, 5, 8; Smad 4, or the inhibitory Smad 6 or Smad 7. We also did not see differences in the concentration of the E-ubiquitin ligases Smurfs 1 and 2. Blockade of the proteasome with several inhibitors did not rescue the effect of INF- $\gamma$ . We repeated these experiments in the pre-osteoblastic cell line MC3T3 cells with identical results. These data suggested that treatment of stromal cells or pre-osteoblasts with INF- $\gamma$  did not alter the concentration of the components of the BMP-2 pathway, and that these factors are not degraded by ubiquitination. We then explored the possibility that the complex formed by Smad4 and R-Smads 1,5,8 was sequestered in the cytoplasm under the influence of INF- $\gamma$ . Using confocal microscopy, we observed that Smad4 accumulated in the cytoplasm of ST-2 cells treated with BMP-2 + INF- $\gamma$ . Co-immunoprecipitation experiments revealed that Smad4 bound to Stat-1 in cells treated with INF- $\gamma$ . Phosphorylated (activated) Stat-1 did not immunoprecipitate with Smad4. ST-2 cells treated with BMP-2 upregulated the expression of Stat-1, which was further increased by adding INF- $\gamma$ . In summary, INF- $\gamma$  blocks BMP-2 signaling by binding of Stat1 to Smad4 in the cytoplasm of osteogenic cells, preventing its nuclear localization. This provides a novel mechanism by which an inflammatory cytokine may affect bone formation.

**Disclosures:** F.A. Sylvester, None.

## SU140

Withdrawn

## SU141

**Bone Morphogenetic Protein-6 (BMP-6) from Bone Regulates Serum Glucose via IGF-1 Released from Pancreas.** P. Simic<sup>\*1</sup>, L. Grgurevic<sup>\*1</sup>, I. Orlic<sup>\*1</sup>, M. Zuvic<sup>\*2</sup>, S. Vukicevic<sup>1</sup>. <sup>1</sup>Laboratory for Mineralized Tissues, Zagreb Medical School, Zagreb, Croatia, <sup>2</sup>Department of Oncology and Nuclear Medicine, Clinical Hospital Centre Zagreb, Zagreb, Croatia.

Systemic administration of BMP-6 restores the bone volume (BV) in osteoporotic rats (Simic et al, J Biol Chem, 2006) and lowers the blood glucose in *Bmp-6*<sup>-/-</sup> and non obese diabetic mice (Orlic et al, Calc Tiss Int, 2007). We hypothesized that BMP-6 released from the bone might mediate the endocrine function of the pancreas. We therefore revisited the phenotype of the *Bmp-6*<sup>-/-</sup> mouse and found that the loss of *Bmp-6* function exerts both an abnormal bone development and the reduced pancreatic function. Although long bones of the wild type (WT) and *Bmp-6*<sup>-/-</sup> littermates are of a similar size and shape, BV is reduced up to 120% and 80% at embryonic day 15 and 17, respectively. Apart from the abnormal bone development, *Bmp-6*<sup>-/-</sup> born mice have a reduced number of Langerhans islands with a lower serum insulin and a subsequent increase of the serum glucose levels. Exogenously injected BMP-6 (60 µg/kg/3xweek) reduced the blood glucose in 2h and at 3 weeks of therapy increased the BV of *Bmp-6*<sup>-/-</sup> mice to normal. To test whether the endogenous BMP-6 deposited in the bone matrix could be released into the circulation and affect the serum glucose level we treated *Bmp-6*<sup>-/-</sup> and WT mice with 3 injections of phosphate (0.6 mg/kg i.v.) to stimulate the bone resorption. This resulted in the identification of BMP-6 in plasma of WT mice by liquid chromatography - tandem mass spectrometry and immuno blot analysis. WT mice exposed to the glucose tolerance test at days 3, 5 and 7 following the phosphate overload resulted in a reduction of glycemia in animals with measurable bone serum level of BMP-6 as compared to control WT mice (P<0.01). Molecular analyses of tissue samples revealed that BMP-6 released from bone inhibited the hepatic glucose production and increased the expression of IGF-1 in the pancreas, and elevated the serum concentration of IGF-1. In addition, co-administration of an IGF-1 neutralizing antibody to these mice reduced the BMP-6 glucose lowering effect. These results suggest that BMP-6 has a unique developmental role both in the bone and pancreas, while in the post natal life BMP-6 released from the bone regulates the glucose homeostasis via releasing IGF-1 from the pancreas.

**Disclosures:** P. Simic, None.

## SU142

**Circulating BMP-1 Isoforms: Novel Diagnostic and Therapeutic Challenges for Bone Fracture Repair.** L. Grgurevic<sup>\*1</sup>, B. Macek<sup>\*2</sup>, M. Mann<sup>\*2</sup>, S. Vukicevic<sup>1</sup>. <sup>1</sup>Laboratory for Mineralized Tissues, Zagreb Medical School, Zagreb, Croatia, <sup>2</sup>Department of Proteomics and Signal Transduction, Max-Planck-Institute for Biochemistry, Martinsried, Germany.

We hypothesized that bone, kidney and liver injury results in the release of different endogenous bone morphogenetic proteins (BMPs) into circulation reflecting the success of regeneration. Plasma (50 ml) from normal individuals (16) and from patients with a long bone fracture (6), chronic renal failure (8) and liver cirrhosis (7) were collected, purified by heparin beads and all protein bands from SDS gel electrophoresis have been analyzed by liquid chromatography - tandem mass spectrometry (LC-MS) and immuno blots. While only mature BMP-6 was detected in plasma of healthy individuals, surprisingly BMP1-3 isoform of the BMP-1 gene, a procollagen C-protease, was found in serum of healthy individuals and in patients with CRF. BMP-1-3 has not been previously detected at the protein level, while BMP-1-1, originally isolated with other BMPs from the bone matrix, did not circulate. As there was no information available on the function of BMP-1-3 isoform we cloned, expressed and purified the protein and raised specific polyclonal neutralizing antibodies for in vitro and in vivo experiments. BMP-1-3 isolated from the plasma of normal individuals lacked the prodomain and was active in processing procollagen I in vitro. As BMP1-3 was not found in the plasma of patients with a single fracture we administered intravenously I<sup>125</sup> labeled BMP-1-3 to rats with a fractured femur and found by microradiography that it accumulated in the bone callus. Moreover, when rats with a fracture were injected intravenously (iv) with recombinant human BMP-1-3 (25 g/kg 5 x weekly for two weeks) the femurs healed significantly faster than in control animals. To check whether the amount of BMP-1-3 in the serum was physiologically relevant the BMP-1-3 circulating in the plasma was neutralized with an iv injected BMP-1-3 neutralizing antibody (12 g/kg 2x weekly for two weeks). Subsequently, the femurs were fractured in the same rats and it was found that the bone healing was significantly delayed suggesting that the presence of BMP-1-3 in blood was important for bone regeneration. Next, we tested the potential mechanism of action of BMP1-3 in the rat calvariae assay and found that BMP-1-3 added to the culture medium supported the release of BMP-6 and -7, which then stimulated the synthesis of extracellular matrix, in particular procollagen I and III. In conclusion, we discovered for the first time that BMP1-3 isoform, and not BMPs, circulates in the human and rat serum, significantly enhancing bone regeneration, providing thus a diagnostic and therapeutic challenge.

**Disclosures:** S. Vukicevic, None.

## SU143

**Bmp3-Null Aged Mice Display Increased Trabecular Bone Volume and Reduced Cross Sectional Area at the Mid-Femoral Diaphysis.** R. Raz<sup>1</sup>, L. Huang<sup>1</sup>, D. A. Panus<sup>\*2</sup>, Y. Xue<sup>\*1</sup>, D. M. Valenzuela<sup>\*1</sup>, G. D. Yancopoulos<sup>\*1</sup>, A. Murphy<sup>\*1</sup>, M. Bouxsein<sup>\*2</sup>, V. Rosen<sup>3</sup>, A. N. Economides<sup>1</sup>. <sup>1</sup>Regeneron Pharmaceuticals, Tarrytown, NY, USA, <sup>2</sup>Beth Israel Deaconess Medical Center, Boston, MA, USA, <sup>3</sup>Harvard School of Dental Medicine, Boston, MA, USA.

BMP3 was originally purified from bovine bone matrix as osteogenin, an activity with osteogenic function. However, it has later been identified as an inhibitor of osteogenic BMPs and a negative regulator of bone density in mice. Using VelociGene® technology, we have generated *Bmp3* homozygous-null (KO) mice where the first exon (encoding the N-terminal part of the precursor region) was replaced in frame with the LacZ reporter. We used micro-computed tomography to evaluate trabecular bone microarchitecture in the distal femur and the vertebral body, as well as cortical bone morphology in the mid-femoral diaphysis. We found that in aged animals (36 to 44 wks), trabecular bone volume in the distal femur and vertebral body was significantly higher in KO compared to wild type littermate controls (30% to 70%) primarily due to increased trabecular number. At the mid-femoral diaphysis, the relative cortical bone area fraction and cortical thickness was unchanged, but the total cross-sectional area, bone area and medullary area were smaller in KO than in controls, correlating with a reduction in body weight. The results of this study confirm that BMP3 is a negative modulator of bone density *in vivo* and uncover a role for BMP3 in the regulation of body mass.

**Disclosures:** R. Raz, Regeneron Pharmaceuticals.

This study received funding from: Regeneron Pharmaceuticals.

## SU144

**Negative Regulation of Tcf/Lef-dependent Transcription by the BMP/Smad4 Signaling Axis.** V. S. Salazar, G. Mbalaviele, R. Civitelli. Internal Medicine, Washington University Medical School, Saint Louis, MO, USA.

β-catenin and BMP signaling are critical regulators of osteogenesis. To understand how these pathways interact during osteoblastogenesis, and to determine the biologic importance of such interactions, we used the mouse embryonic fibroblasts (C3H10T1/2) to characterize how BMP signals affect canonical β-catenin/Tcf/Lef activity. We previously reported that phosphorylation of β-catenin at S33/S37/T41 dramatically decreases after 5 min of BMP-2 exposure, coinciding with β-catenin/Smad4 co-immunoprecipitation. Immunoblot of fractionated cell proteins or expression of chimeric EGFP-β-catenin protein indicates that BMP-2 promotes nuclear accumulation of β-catenin. Intriguingly however, a Tcf/Lef-dependent luciferase reporter is not stimulated by 24hr of BMP-2. EMSA on nuclear fractions from BMP-2 treated cells reveals that BMP-2 causes β-catenin and Smad4 to assemble a nucleoprotein complex at consensus Smad4-binding DNA sequences. We concordantly find that expression of a transcriptionally-defective β-catenin mutant blocks BMP-2 stimulation of a Smad-dependent luciferase reporter. The collective data lead us to hypothesize that BMP signals can act through Smad4 to regulate β-catenin activity thus antagonizing Tcf/Lef-dependent transcription. To test this hypothesis, we manipulated Smad4 expression levels using either Smad4 siRNA or a Smad4 expression plasmid. As expected, activation of a Smad-dependent luciferase reporter is dose-dependently decreased by Smad4 knockdown and enhanced by Smad4 overexpression. Conversely, Tcf/Lef reporter activity is dose-dependently decreased by Smad4 overexpression and is enhanced by silencing of Smad4. We also find that Smad4 abundance is inversely proportional to Tcf/Lef activity at the human *Cyclin-D1* promoter, as well as to endogenous gene expression of murine *Cyclin-D1*, a canonical Wnt gene target. And in fact, knockdown of Smad4 synergistically enhances the ability of Wnt3a or activated β-catenin to induce *Cyclin-D1* transcription (>6 and >17-fold, respectively). Our results provide evidence that BMP signals can act through Smad4 to interact with β-catenin in a manner that antagonizes canonical Wnt activity at the level of Tcf/Lef-dependent transcription. This novel signaling mechanism may impact osteoblast cell number or cell fate.

**Disclosures:** V.S. Salazar, None.

This study received funding from: NIAMS AR041255 and Bridge Grants from Endocrine Society and ASBMR.

## SU145

**BMPR2 Is Dispensable for Formation of the Limb Skeleton.** L. Gamer<sup>\*1</sup>, K. Tsuji<sup>\*1</sup>, K. Cox<sup>\*1</sup>, E. Gagarin<sup>\*1</sup>, H. Beppu<sup>\*2</sup>, V. Rosen<sup>1</sup>. <sup>1</sup>Developmental Biology, Harvard School of Dental Medicine, Boston, MA, USA, <sup>2</sup>Cardiovascular Research Center, Massachusetts General Hospital, Boston, MA, USA.

In vivo studies examining the role of BMPs in skeletal development have established a requirement for BMP signaling during endochondral ossification and identified specific functions for individual type I BMP receptors. Initiation of BMP signaling is dependent on activation of the type I BMP receptor by the constitutively active type II BMP receptor after ligand binding occurs. In this study, we focus on the regulatory role of the type II BMP receptor in endochondral ossification. Of the 3 type II BMP receptors identified, ActRIIA and ActRIIB are multifunctional, serving as type II receptors for BMPs and also for activin-like ligands while BMPRII (BMPRII) only functions as a BMP receptor. Based on the specificity of BMPRII and the fact that loss of either ActRIIA or ActRIIB is not associated with deficits in limb development, we hypothesized that BMPRII is essential for BMP signaling during embryonic skeletal development. Using a conditional deletion

approach, we removed BMPR2 from early limb mesoderm prior the onset of skeletogenesis by crossing Bmpr2 floxed mice with mice carrying the Prx1cre transgene and analyzed Bmpr2Prx1cre mice at E16, P0, and weeks 1-6 after birth. At each of these times, mice lacking limb expression of BMPR2 appeared to have normal skeletons and could not be distinguished from control littermates. No anomalies in limb skeletal patterning or joint morphogenesis were observed in the absence of BMPR2. Detailed analysis of limb skeletons from newborn Bmpr2Prx1cre mice showed no changes in the expression of markers for chondrogenesis (Col2, Col10, Ihh) or osteogenesis (Runx2, OPN, OCN) and X-rays taken of Bmpr2Prx1cre limbs weekly for the first 6 weeks after birth showed no spontaneous fractures or appearance of osteopenia conditions that are associated with reduced BMP signaling. From these data we conclude that BMPR2 is not required for endochondral ossification in the limb and that loss of BMPR2 is compensated for through the use of ActRIIA and/or ActRIIB as type II BMP receptors.

**Disclosures:** L. Gamer, None.

## SU146

**Efficacy of Single-Level Instrumented Posterolateral (Intertransverse) Lumbar Spinal Fusion (PLF) in Baboons with BMP-7 Putty.** A. Pierce<sup>1</sup>, M. Goad<sup>1</sup>, M. H. Alaoui-Ishmaili<sup>2</sup>, D. Schrier<sup>1</sup>. <sup>1</sup>Preclinical Development, Stryker Biotech, Hopkinton, MA, USA, <sup>2</sup>Biology, Stryker Biotech, Hopkinton, MA, USA.

BMP-7 putty is indicated for use as an alternative to autograft in revision PLF. BMP-7 putty consist of 3.5 mg bone morphogenetic protein-7 (BMP-7) with 1 g type I collagen particles and 200 mg carboxymethylcellulose (CMC) as a handling excipient. This baboon study assessed safety and efficacy of BMP-7 putty in an instrumented model of PLF. Twenty-four adult male baboons (26 ± 4.7kg) were used in this IACUC-approved study. Surgery consisted of single level lumbar vertebral (L4-L5) fusion with pedicle screw and rod fixation along with the BMP-7 putty (n=20) or iliac crest autograft (n=4). BMP-7 putty treated animals had 0.5 mL of putty implanted subcutaneously as a distant site control. Fusion was assessed by radiograph and biomechanical testing. BMP-7 groups were 0 (collagen and CMC, only), 0.33, 1, 2, and 4 mg of BMP-7/mL putty. Total volume of BMP-7 putty was 12 mL per level. Safety assessment included clinical observations, clinical pathology (hematology, serum chemistry), body weights, organ weights, necropsy, and histology of selected tissues. Serum BMP-7 concentrations and anti-BMP-7 antibodies were analyzed.

None of the animals had any evidence of altered clinical or necropsy parameters: clinical pathology, organ weights, body weights, macroscopic, or microscopic findings in tissues other than the vertebral fusion site, were within the range of normal. A separate subcutaneous implant site had no evidence of the BMP-7 putty grossly or microscopically (i.e. no bone or inflammation) by 16 weeks. The new bone formed had normal cortical and cancellous bone with central bone marrow. Anti-BMP-7 antibodies were measured in the serum of half the autograft and 0 mg/mL BMP-7 putty animals. Three of four animals treated with 0.33 mg/mL BMP-7 putty and all animals treated with 1, 2, or 4 mg/mL BMP-7 putty exhibited antibodies against BMP-7. However, robust fusion was noted in all BMP-7 treated animals except one animal in the 0.33 mg/mL BMP-7 putty group. No animals in the 0 mg/mL putty group fused and all autograft animals fused.

The results of this study provide evidence of a BMP-7 dose-response in instrumented PLF in a non-human primate with radiographical and biomechanical parameters similar to or better than autograft. No adverse or abnormal findings were seen associated with BMP-7 putty implantation in a baboon model of instrumented PLF.

**Disclosures:** A. Pierce, Stryker Biotech 5.

*This study received funding from: Stryker Biotech.*

## SU147

**Congenic Mouse Models Provide Novel Evidence of Caveolae-1 alpha Domain Regulation of Osteoblast Differentiation.** B. Bragdon<sup>1</sup>, J. Bonor<sup>1</sup>, A. St. Jeanos<sup>1</sup>, K. L. Shultz<sup>2</sup>, W. G. Beamer<sup>2</sup>, A. Nohe<sup>1</sup>. <sup>1</sup>Dept. of Chem. and Bio. Engineering, University of Maine, Orono, ME, USA, <sup>2</sup>The Jackson Laboratory, Bar Harbor, ME, USA.

Osteoblasts and osteoclasts must communicate and differentiate correctly for proper bone development and maintenance. With the use of congenic mouse models, C57BL/6J (B6) and B6.C3H-1-12 (1-12), to define mechanisms for altered bone mineral density (BMD), it reasons the communication and signaling is altered as well. An early initiating signal to differentiate into osteoblasts is bone morphogenetic proteins (BMPs). Involved with the onset of BMP signal are plasma membrane domains resembling flask-shaped invaginations called caveolae. There are two isoforms of caveolae-1 (Cav-1), alpha and beta, currently evidence is absent on the role of Cav-1 isoforms possess on osteoblast differentiation; although there is evidence that support caveolae are involved with osteoblast differentiation. Our current model of BMP-2 signaling links BMP receptor (BMPR) dynamics to those of Cav-1 alpha and beta. The interaction of Cav-1 beta to that of the constitutively active BMPR complex silences its signal. Upon activation, this receptor redistributes to Cav-1 alpha beta or alpha alone where it is no longer silenced, however evidence for this is lacking.

We advanced this model of receptor dynamics with control mice, B6, and a Chromosome 1 congenic mouse strain, 1-12, with an increased peak BMD. To determine the signaling differences due to altered caveolae domains, we did an assessment of B6 and 1-12 bone marrow stromal cells by confocal microscopy with state of the art family image correlation spectroscopy (FICS), novel approaches with atomic force microscopy (AFM), and gene activation with reporter gene assays. The results illustrated that 1-12 cells exhibited a repressed BMP-2 signal compared to that of B6 cells. By AFM and FICS measurements the membrane of 1-12 cells showed a reduced recruitment of Cav-1 beta into Cav-1 alpha and the rearrangement

of BMPR Ia to Cav-1 alpha was not observed. Due to the lack of membrane domain rearrangements, enhanced signaling of BMP-2 did not occur. Although 1-12 does have the increase peak BMD, we hypothesize these cells are further along development and therefore additional BMP-2 activation for early differentiation is not required. The signaling differences between the congenic mouse models have furthered the signaling model. This provides new evidence to support that Cav-1 alpha are located independent of Cav-1 beta. This data supports that the different isoforms have adverse effects on osteoblast differentiation. In addition, further therapies will develop from identifying the mechanisms of early osteoblast differentiation of mice models with a higher peak BMD.

**Disclosures:** B. Bragdon, None.

## SU148

**BMP7 Is not Required for Fracture Healing.** K. Tsuji<sup>1</sup>, D. Graf<sup>2</sup>, K. Cox<sup>3</sup>, A. Economides<sup>3</sup>, V. Rosen<sup>1</sup>. <sup>1</sup>Developmental Biology, Harvard School of Dental Medicine, Boston, MA, USA, <sup>2</sup>Institute of Immunology, Biomedical Sciences Research Center 'Al. Fleming', Hellas, Greece, <sup>3</sup>Regeneron Pharmaceuticals, Inc, Tarrytown, NY, USA.

Sequential changes in expression of individual BMPs occur during fracture healing in mice. Increased BMP2 levels are observed within the first 24 hours after fracture and this spike in BMP2 expression activates periosteal cells to begin the repair process. In contrast to BMP2 expression, a spike in BMP7 expression is observed between days 14 to 21 post fracture at the time of cartilaginous callus replacement by bone. Based on this expression pattern, we hypothesized that BMP7 regulates osteogenesis during the late stages of fracture healing. To examine this hypothesis, we established mice in which BMP7 is removed from limb mesenchyme prior to the onset of skeletogenesis by crossing mice carrying floxed BMP7 alleles with mice carrying cre recombinase driven by the Prx1 promoter (*Bmp7<sup>flx</sup>;Prx1::cre*). *Bmp7<sup>flx</sup>;Prx1::cre* mice form limb skeletal elements in the absence of BMP7 and no BMP7 is present in extracellular matrix of these limb bones. We monitored *Bmp7<sup>flx</sup>;Prx1::cre* mice through 14 weeks of age by X-ray and found no change in postnatal bone morphology. To determine if BMP7 is required for fracture repair, we made transverse femur fractures in 10 week-old *Bmp7<sup>flx</sup>;Prx1::cre* and control littermates and monitored the fracture healing process by X-ray and histology. As predicted, loss of BMP7 did not affect the activation of periosteal cell proliferation early in fracture repair. We also observed bridging callus formation at day 10 post fracture in the absence of BMP7 and bony union after 20 days in *Bmp7<sup>flx</sup>;Prx1::cre* mice by X-ray. These results show that the spike in BMP7 production in late stages of fracture healing is not required for completion of the repair process and allow us to conclude that BMP7 is not necessary for fracture healing.

**Disclosures:** K. Tsuji, None.

*This study received funding from: Musculoskeletal Transplant Foundation.*

## SU149

**Safety and Efficacy of BMP-7 Putty in a Rabbit Model of Posterolateral Vertebral Lumbar Fusion.** M. Goad<sup>1</sup>, A. Pierce<sup>1</sup>, M. H. Alaoui-Ishmaili<sup>2</sup>, D. Schrier<sup>1</sup>. <sup>1</sup>Preclinical Development, Stryker Biotech, Hopkinton, MA, USA, <sup>2</sup>Biology, Stryker Biotech, Hopkinton, MA, USA.

The efficacy, safety and pharmacokinetics of BMP-7 putty (BMP-7 with collagen and carboxymethylcellulose) were evaluated in a surgical model of posterolateral vertebral transverse process fusion (PLF) in male and female New Zealand White (NZW) rabbits. Five treatment groups (3/sex/group) included a sham surgery control, 3 BMP-7 putty groups and a group injected IV with BMP-7 (for PK analysis). During surgery, 1.5mL of the BMP-7 putty was placed on each side of the vertebrae between transverse processes L4 and L5. The IV group was injected with 1mg/kg of 6mg/mL BMP-7 on Day 0. Animals were monitored for clinical observations, body weights, and food consumption. PK serum samples were collected on Day 0, 14, and 35. Serum for anti-BMP-7 antibodies were collected before surgery and on Days 14 and 35. Clinical pathology (hematology, serum chemistry, coagulation, and urinalysis) was assessed pre-dose and before euthanasia. On Day 35, animals were euthanized and selected tissues were evaluated microscopically. BMP-7 putty-treated rabbits had bone formed based on radiographs and macroscopic fusion assessments. BMP-7 putty treated animals had new bone at the site of BMP-7 putty placement; this new cortical and cancellous bone had medullary cavities. Low but persistent BMP-7 serum concentrations were seen in the implanted groups suggesting that it is released slowly from the putty. Anti-BMP-7 antibodies were not detected in the sham control or IV-treated groups; all BMP-7 putty-implanted rabbits had detectable anti-BMP-7 antibodies on Days 14 and 35. No BMP-7 related adverse effects were seen in the putty-treated animals compared with sham controls. Animals in all surgical groups had mild to moderate chronic focal inflammation along the surgical/incision site as expected with a surgical procedure.

In conclusion, BMP-7 was effective and safe in a rabbit model of vertebral transverse process fusion. No evidence of toxicity was seen at any BMP-7 dose. The PK analysis was consistent with slow release of BMP-7 from the implant site. Although anti-BMP-7 antibodies were noted in BMP-7 treated animals 14 days after implant, these antibodies had no apparent effect on efficacy or safety. Moreover, an immune response is expected in animals treated with a xenogeneic protein. The No Observed Adverse Effect Level (NOAEL) for BMP-7 putty (surgically-dosed) and BMP-7 (IV-dosed) in NZW rabbits are greater than 12 mg BMP-7 (in 3mL BMP-7 putty) and 1 mg/kg BMP-7 IV. These results are consistent with clinical data that indicate that BMP-7 putty is safe and effective.

**Disclosures:** M. Goad, Stryker Biotech 5.

*This study received funding from: Stryker Biotech.*

## SU150

**Regulation of the Bmp2 Distant Osteoblast Enhancer by Fibroblast Growth Factor 2.** R. L. Chandler<sup>\*1</sup>, R. L. Ostroff<sup>\*1</sup>, S. Jiang<sup>\*2</sup>, M. B. Rogers<sup>\*2</sup>, D. P. Mortlock<sup>1</sup>. <sup>1</sup>Molecular Physiology & Biophysics, Vanderbilt, Nashville, TN, USA, <sup>2</sup>Biochemistry and Molecular Biology, UMDNJ New Jersey Medical School, Newark, NJ, USA.

Factors that induce Bmp2 expression are of particular interest as they may indicate pathways components controlling bone formation. We have previously identified a distant 3' enhancer for Bmp2, ~156 kilobases downstream of its dual promoters, that controls its expression in pre-osteoblasts. FGF (Fibroblast Growth Factor) signaling is critical for proper development of osteoblasts in intramembranous and long bones, and FGF2 can induce Bmp2 expression in cultured mouse calvaria and MC3T3-E1 cells. We transfected Bmp2-LacZ BAC (Bacterial Artificial Chromosome) constructs into MC3T3-E1 cells to determine their response to FGF2. This revealed that Bmp2 BACs could be induced by FGF2 treatment in culture only when the BAC insert extended into the distant 3' flanking region. We have established transgenic mice carrying an Hsp68LacZ reporter minigene linked to the +156 kilobase enhancer, and this confers *in vivo* expression specific to differentiating osteoblasts. Explanted long bones from fetal transgenic mice were cultured *in vitro* and found to maintain LacZ expression for at least four days. When cultured in presence of ascorbate and beta-glycerophosphate for 7-10 days, osteogenic cells migrated into the dish and produced alizarin-red-staining matrix. The area of new matrix was preceded by a wave front of LacZ-positive cells. Primary cell cultures were also established from transgenic explants. These cultures failed to maintain robust LacZ expression, but LacZ could be strongly re-induced following 24 hours of FGF2 treatment. Finally, we examined effects of FGF2 on the +156 kilobase enhancer in the context of Bmp2 promoter constructs. Bmp2 transcripts initiate at either of two sites (termed distal and proximal promoters) separated by approximately 700 bases. When transfected into MC3T3-E1 cells under unstimulated conditions, the enhancer had little or modest ability (less than 2-fold) to enhance expression of Bmp2 fragments spanning the distal, or both promoters. However, FGF2 treatment resulted in an almost 8-fold enhancer-dependent and dose-dependent induction of the distal promoter fragment. FGF2 had no effect on promoter constructs lacking the enhancer. Surprisingly, FGF2 also had no effect on the enhancer in the context of a fragment spanning both the distal and proximal start sites, suggesting a repressor exists between the promoters. Taken together, these data further indicate that FGF signaling regulates Bmp2 in developing osteoblasts, and that this effect is mediated by interactions between the distant 3' enhancer and sequences near the promoter(s).

**Disclosures:** D.P. Mortlock, None.

## SU151

Withdrawn

## SU152

**IFN- $\gamma$  Inhibits TNF- $\alpha$ -induced Osteoclastogenesis *in vitro* and *in vivo*.** H. Kohara, H. Kitaura, Y. Fujimura<sup>\*</sup>, M. Yoshimatsu, T. Eguchi<sup>\*</sup>, Y. Morita<sup>\*</sup>, N. Yoshida<sup>\*</sup>. Division of Orthodontics and Dentofacial Orthopedics, Nagasaki University Graduate School of Biomedical Sciences, Nagasaki, Japan.

It has been reported that RANKL expressed by osteoblasts is essential for inducing osteoclastic differentiation. Recently, it has been found that osteoclastic differentiation is also induced by the inflammatory cytokine TNF- $\alpha$ . IFN- $\gamma$  has an important role in host defense at inflammatory sites. Many reports show that IFN- $\gamma$  inhibits RANKL-induced osteoclastogenesis. However, there are few reports of the effects of IFN- $\gamma$  on TNF- $\alpha$ -induced osteoclastogenesis. In this study, we investigated the effect of IFN- $\gamma$  to TNF- $\alpha$ -induced osteoclastogenesis *in vitro* and *in vivo*. Bone marrow cells were collected from 5-week-old C57BL/6 mice. Bone marrow cells and macrophages were cultured with M-CSF, TNF- $\alpha$  and various concentrations of IFN- $\gamma$  (0.1~100ng/ml). The cultured cells were then stained with TRAP. We subcutaneously injected TNF- $\alpha$  with or without IFN- $\gamma$  into supra-calvariae of mice for 5 consecutive days. Mice were sacrificed on day 6. Histological sections of calvariae taken from each mouse were stained with TRAP. IFN- $\gamma$  inhibited TNF- $\alpha$ -induced osteoclastogenesis in a dose-dependent manner *in vitro*. IFN- $\gamma$  also blocked the generation of osteoclasts in response to TNF- $\alpha$  *in vivo*. Furthermore, we found that IFN- $\gamma$  inhibited M-CSF-induced cell proliferation in a dose dependent manner. We analyzed the expression of CDK inhibitor p16, which is known to inhibit cell proliferation, by RT-PCR. IFN- $\gamma$  increased the expression of p16. The mechanism of inhibition was postulated as being that p16 was induced by the IFN- $\gamma$  inhibited interaction of CDK and cyclin D, which induced cell proliferation. These results indicated that IFN- $\gamma$  inhibits the effects of the cytokines such as RANKL, TNF- $\alpha$  and M-CSF involved in osteoclastogenesis. IFN- $\gamma$  may control not only the host defense but also osteoclastogenesis at an inflammatory site.

**Disclosures:** H. Kohara, None.

## SU153

**Myostatin (GDF-8) Regulates the Secretion of Growth Factors Localized to the Muscle-Bone Interface.** S. Patterson<sup>\*</sup>, W. Hill<sup>\*</sup>, P. McNeill<sup>\*</sup>, C. M. Isaacs, M. Hamrick. Medical College of Georgia, Augusta, GA, USA.

A close functional association between muscle and bone is indicated by the coupling of muscle and bone anabolism and catabolism during growth, development and aging. The

traditional explanation for this coupling is that a muscle-bone mechanostat exists in which bone adapts to the strains placed on it by muscles. The cellular and molecular mechanisms that link muscle and bone anabolism are, however, poorly understood. It is known that muscle flaps accelerate fracture healing, suggesting that muscle tissue itself can provide a direct anabolic stimulus to bone by not only providing a vascular supply but also by serving as a local source of growth factors. We sought to test this hypothesis by determining first whether IGF-1 and TGF $\beta$ 1, two factors known to regulate bone formation, were present at the muscle bone interface *in vivo* and second, whether the secretion of these factors from myotubes was altered with myostatin treatment *in vitro*. Immunohistochemistry shows that both IGF-1 and TGF $\beta$ 1 are abundant at the interface between periosteum and muscle along the radius and ulna in the mouse forelimb. Mouse C2C12 myotubes were cultured in differentiating medium and treated with myostatin (0.1-1.0  $\mu$ g/ml), and conditioned medium collected at 4, 8 and 10 days for ELISA assays of secreted IGF-1 and TGF $\beta$ 1. Results show that TGF $\beta$ 1 is significantly (10-fold) more abundant in medium than IGF-1 at 4 days of differentiation, and remains more abundant at 10 days (+50%). Myostatin treatment (1.0  $\mu$ g/ml) significantly (~35%) decreases IGF-1 secretion by 8 days of culture, whereas myostatin (0.1  $\mu$ g/ml) significantly (~15%) increases TGF $\beta$ 1 secretion at 10 days. These findings suggest that muscle itself is a source of secreted growth factors, and that regulation of muscle growth and development by myostatin may in turn influence the local abundance of growth factors available for osteoprogenitor cells in the periosteum.

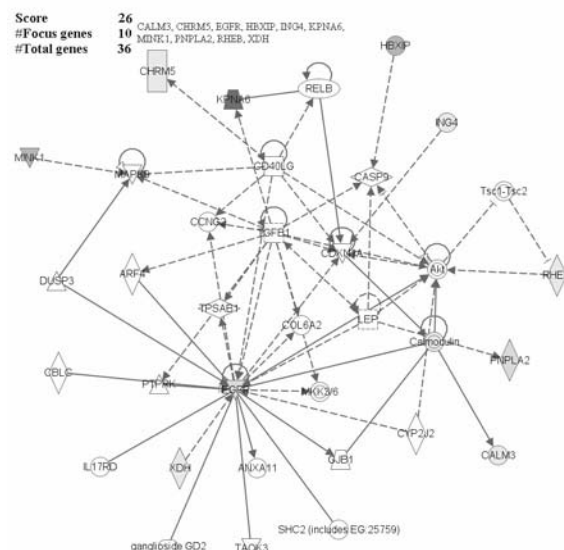
Funding for this research was provided by the National Institutes of Health (AR049717).

**Disclosures:** M. Hamrick, None.

## SU154

***In vivo* Differential Expression Profiling Study on Human Circulating B Cells Suggested a Novel EGFR and CALM3 Network Underlying Smoking and BMD.** P. Xiao<sup>1</sup>, X. D. Chen<sup>\*1</sup>, Y. Chen<sup>\*1</sup>, F. Pan<sup>\*1</sup>, H. Jiang<sup>\*1</sup>, B. Y. Sha<sup>\*1</sup>, R. R. Recker<sup>1</sup>, H. W. Deng<sup>\*2</sup>. <sup>1</sup>Osteoporosis Research Center, Creighton University Medical Center, Omaha, NE, USA, <sup>2</sup>Departments of Orthopedic Surgery and Basic Medical Sciences, University of Missouri-Kansas City, Kansas City, MO, USA.

B lymphocytes play important roles in bone homeostasis. Studies showed that B cells may participate in osteoclastogenesis via expression of osteoclast-related factors, such as transforming growth factor beta (TGF $\beta$ ) and osteoprotegerin (OPG). Our recent genome-wide expression study on human B cells also suggested a novel ER- $\alpha$  and MAPK3 network for postmenopausal osteoporosis. Smoking is an important risk factor for low BMD and related with the apoptosis of B cells. In this study, we aimed to explore important genes that may underlie the mechanism of smoking-related osteoporosis using functional genomic approach. We recruited 40 unrelated postmenopausal Caucasian women aged 54-60, 20 with high BMD (spine or hip Z-score > 0.84) and 20 with low BMD (spine or hip Z-score < -0.84). Each BMD group consisted of 10 smoking and 10 non-smoking subjects. Total RNA from circulating B cells for each subject was extracted and hybridized to an Affymetrix HG-U133A GeneChip<sup>®</sup> array. Significant genes underlying both smoking and BMD were tested by two-way ANOVA and the raw p values were adjusted with Bonferroni procedure for multiple testing. Seventeen significant genes were identified. In particular, network analysis (www.ingenuity.com) showed an interesting gene network centered by epidermal growth factor receptor (EGFR) and calmodulin 3 (CALM3) genes. EGFR gene is important for both osteoclasts and osteoblasts. CALM3 is a critical regulator of osteoclastic differentiation, function and survival. It was also found that CALM3 regulated intracellular trafficking of EGFR and MAPK signaling pathway. This is the first *in vivo* genome-wide expression study on human B cells for smoking-related osteoporosis. Our results suggested that a novel network including EGFR and CALM3 genes may involve in smoking-related bone metabolism.





## SU158

**CCR2 Receptor Signaling Is Involved in Bone Mass Regulation and Mediates the Response to Anabolic but not Catabolic Regimens of PTH(1-34).** E. A. Smith, N. A. Hanson\*, D. T. Crawford\*, T. A. Brown, L. Buckbinder. Pfizer Global R&D, Groton, CT, USA.

Chemokine signaling through CCR2 and the CCR2-ligand MCP1 have been implicated in both osteoclastogenesis and osteoblast function. This study first aimed to evaluate the role of CCR2-mediated signaling on bone mass using CCR2 knockout mice. It has also recently been demonstrated that MCP-1 is upregulated after intermittent but not continuous treatment with PTH(1-34) (X Li, et al. JBC 282: 33098, 2007). This study also examined the role of CCR2 signaling in the bone response to both intermittent and continuous PTH(1-34). Female CCR2<sup>-/-</sup> mice at 18 weeks have increased aBMD of the lumbar spine measured by pDXA between 12 and 18 weeks of age (+6-10%, p<0.05), yet lumbar vertebral trabecular BV/TV is decreased by 25% (p<0.0001) measured by  $\mu$ CT. This suggests that the increase in aBMD is due to changes in cortical bone. The femoral diaphysis in CCR2<sup>-/-</sup> mice has an increased polar moment of inertia (+24%, p=0.0001) with decreased cortical thickness (-10%, p<0.0001) and increased marrow volume (+23%, p<0.0001), suggesting that the cortical bone phenotype is due to periosteal expansion. Serum CTx (RatLAPS, Nordic Biosciences Diagnostics) was decreased in CCR2<sup>-/-</sup> compared to WT mice at 18 weeks (-39.8%, p<0.001) while serum osteocalcin (RIA, Alpco, Windham, NH) was unchanged. CCR2<sup>-/-</sup> and WT mice were then administered intermittent (40ug/kg/day, SC) PTH(1-34) (iPTH) or continuous (40ug/kg/day, Alzet osmotic pump) PTH(1-34) (cPTH) for 6 weeks beginning at 12 weeks. iPTH increased lumbar trabecular BV/TV by 30% in WT mice (p<0.0001), while BV/TV only increased 15% in CCR2<sup>-/-</sup> mice (p=0.005). Two-way ANOVA revealed a significant interaction of genotype x treatment (p=0.004). iPTH also increased cortical thickness of the femoral mid-diaphysis by 8.8% in WT mice (p=0.001) but by only 3.7% in CCR2<sup>-/-</sup> mice (p=0.037). Again, the interaction of genotype x treatment was significant by two-way ANOVA (p=0.046). In contrast, cPTH did not affect trabecular BV/TV in the lumbar spine or distal femur in WT or CCR2<sup>-/-</sup> mice. CPTH decreased cortical thickness in both WT (-5.6%, p=0.06) and CCR2<sup>-/-</sup> mice (-6%, p=0.002) (genotype x treatment not significant by 2-way ANOVA). In summary, CCR2<sup>-/-</sup> mice have a high bone mass phenotype in the cortical envelope but a low bone mass phenotype in the trabecular compartment. CCR2<sup>-/-</sup> mice exhibited a blunted anabolic response to iPTH but an equivalent catabolic response to cPTH compared to WT mice. Taken together, these data suggest that chemokine signaling through CCR2 regulates trabecular and cortical bone mass and in part mediates the anabolic response to intermittent but not the catabolic response to continuous PTH(1-34).

**Disclosures:** E.A. Smith, None.

## SU159

**Histamine H4 Receptor (H4R) Is Expressed By Both Osteoarthritic (OA) And Rheumatoid Arthritis (RA) Human Tissues.** C. Manacu\*<sup>1</sup>, M. Dion\*<sup>1</sup>, L. H. Attalah\*<sup>1</sup>, R. Renous\*<sup>2</sup>, M. Frohn\*<sup>3</sup>, G. Y. Ng\*<sup>3</sup>, F. Moldovan<sup>2</sup>. <sup>1</sup>Université de Montréal, Montreal, QC, Canada, <sup>2</sup>Centre de Recherche CHU Sainte-Justine, Montreal, QC, Canada, <sup>3</sup>AMGEN inc., Thousand Oaks, CA, USA.

The objective of this study was to determine whether the H4R is pharmacologically expressed in normal, OA and RA human tissues, and the types of cells expressing this receptor. Human synovial tissues from OA and RA patients were investigated using RT-PCR, immunohistochemistry and by competitive radiolabeled antagonist binding assays. To determine the phenotype of the cells expressing H4R, mast cells were revealed using anti-tryptase and c-kit antibodies. Dendritic cells, macrophage and endothelial cells were revealed using S100, CD68 and the Von Willebrand factor respectively. CD4 was used as a marker for mature helper T cells, and CD8 as a marker for mature Cytotoxic T cells. The H4 receptor was detected at RNA and protein levels in both OA and RA synovial tissues, with a significantly greater number of cells staining positive in inflammatory RA tissues. In synovial membranes from patients with RA, H4 receptor was detected in mast and dendritic cells as well as in the macrophage-like type B synoviocytes infiltrating within the vascular wall, in the diffuse cellular infiltrate and in the superficial lining cell layer and in the pannus. When vessels from rheumatoid synovial membranes or OA showed features of vasculitis, a positive signal for H4 receptor was detected within the media and adventitia of the vascular wall but not in the internal tunic endothelial cells (intima, which stains positive for the von Willebrand factor). In contrast, fibroblast-like synovial cells, follicular aggregates and CD8 positive cells were all negative for H4R. In newly dissociated and cultured human OA synoviocytes, specific [3H] radiolabeled antagonist binding was displaced by the selective H4R antagonist JNJ 7777120 and Thioperamide. This study shows the *in situ* localization of H4R in human OA and RA tissues in both infiltrating immune cells and synoviocytes associated with disease pathogenesis. We provide also first pharmacological evidence of H4R expression by radiolabeled binding. Hence, H4R may be an attractive target in the development of new approaches for therapeutic treatment of OA and RA and possibly other diseases where histamine plays a crucial event in mediating leukocyte trafficking and tissue degradation.

**Disclosures:** M. Dion, None.

This study received funding from: AMGEN Inc.

## SU160

**Decreased Bone Formation, Increased Bone Resorption, and Osteopenia in Mice Lacking Substance P.** S. Hou<sup>1</sup>, L. Wang<sup>1</sup>, I. Sabsovich<sup>2</sup>, R. Zhao<sup>2</sup>, T. Wei\*<sup>2</sup>, W. S. Kingery<sup>1</sup>. <sup>1</sup>Physical Medicine and Rehabilitation Service, Veterans Affairs Palo Alto Health Care System, Palo Alto, CA. Department of Orthopedics, Stanford University School of Medicine, Stanford, CA, USA, <sup>2</sup>Physical Medicine and Rehabilitation Service, Veterans Affairs Palo Alto Health Care System, Palo Alto, CA, USA.

Substance P (SP) is a neuropeptide which is extensively distributed in the sensory neurons innervating bone. There is evidence that SP can regulate bone cell function in vitro, but it is unclear whether SP can modulate bone modeling or remodeling in vivo. To answer this question we characterized the bone phenotype of mutant mice with a targeted deletion of the Tac1 gene expressing SP. Immunocytochemical staining and RT-PCR were used to demonstrate the expression of the SP NK1 receptor on MC3T3-E1 osteoblastic cells and Raw 264.7 osteoclastic cells. The phenotype of 2-month-old and 5-month-old Tac1<sup>-/-</sup> mice and their corresponding wild-type controls were characterized using microCT imaging, static and dynamic bone histomorphometry, and by measuring urinary collagen degradation products. No differences were observed between the Tac1<sup>-/-</sup> mice and their wild-type controls in body weight, rotarod testing, femur and tibia bone length, and gastrocnemius and soleus muscle weights. By 5 months of age both the wild-type and Tac1<sup>-/-</sup> mice had developed trabecular osteopenia, but relative to the wild-type mice, SP deficient mice had significantly greater cortical and trabecular bone loss. The 5-month-old Tac1<sup>-/-</sup> mice also exhibited decreased bone formation rates, increased osteoclast number per bone surface, and increased urinary levels of deoxypyridinoline cross-links. In conclusion, these in vivo data suggest that SP signaling does not contribute to bone modeling, but has a positive effect on age-related bone remodeling that may be due to a direct neural-osseal stimulatory effect on osteoblast function.

**Disclosures:** S. Hou, None.

## SU161

**Hedgehog Signaling Regulates Growth Plate Chondrocyte Proliferation and Growth Factor Expression.** J. A. Horton\*, B. S. Margulies, M. J. Allen, T. A. Damron. Orthopedic Surgery, SUNY Upstate Medical University, Syracuse, NY, USA.

Growth plate chondrocyte proliferation and differentiation are governed by a feedback loop involving Indian hedgehog (Ihh) and parathyroid hormone-related peptide (PTHrP). PTHrP is understood to act as a negative regulator of chondrocyte maturation. The precise role of Ihh-signaling in this loop is unclear, though it has been proposed that Ihh may promote chondrocyte proliferation, in part by regulating PTHrP and/or IGF2 expression. Modulation of Smoothened (Smo) activity by the agonist purmorphamine (PUR) or the antagonist cyclopamine (CYC) has been demonstrated to alter hedgehog pathway signal transduction in several cell types. The purpose of this study was to evaluate the response of growth plate chondrocytes to manipulation of the hedgehog signaling pathway using these agents. We hypothesized that cells exposed to PUR would exhibit increased proliferation, Gli-mediated transcription and up-regulated expression of specific factors including PTHrP and IGF2, while treatment with CYC would have the opposite effect. Primary rat costal chondrocytes were exposed 10  $\mu$ M PUR or CYC, and data were normalized to control cells treated with 0.5% DMSO vehicle. Changes in cell viability were determined by MTT assay. Flow cytometry was used to assess agent induced alterations in cell cycle kinetics. Gli-mediated transcription was assessed using a Gli-luciferase reporter plasmid, and sub-cellular localization of Gli2 was observed by immunocytochemistry. Expression of PTHrP, IGF2, and their respective receptors, and key cell cycle regulators were assayed by RT-PCR, immunoblotting and/or immunocytochemistry. Chondrocytes exposed to PUR for 72 hours showed a 26.3% increase in viable cell number, while CYC-treated cells were reduced up to 20.1%. Cell cycle analysis showed that PUR treatment reduced the S-phase fraction and increased the G2/M population phase. CYC treated cells accumulated in S-phase and showed reduced nuclear localization of PCNA and cyclin D1. Gli-luciferase reporter activity was increased 3-fold by PUR exposure, and was accompanied by nuclear translocation of Gli2. Gli2 was largely excluded from the nuclei of CYC treated cells, however reporter activity was not affected by CYC. PUR treated cells showed up-regulation of PTHrP and IGF2 at the protein and mRNA levels, while CYC down-regulated factors. Neither agent affected the expression or localization of the respective transmembrane receptors, PTHR1 and IGF1R, Smo or Ihh. Taken together, our results demonstrate that hedgehog signaling, downstream of Smo, participate in the regulation of growth plate chondrocyte proliferation and cell cycle progression, as well as inducing the expression of several pro-mitotic gene products, including PTHrP and IGF2.

**Disclosures:** J.A. Horton, None.

## SU162

**The Distinct Biological Activity of Interleukin 8 Isoforms.** K. M. Nicks, N. S. Akel\*, D. Gaddy, L. J. Suva. Physiology and Biophysics & Orthopaedic Surgery, UAMS, Little Rock, AR, USA.

Previous studies have shown that the chemokine interleukin 8 (IL-8) is able to directly stimulate human osteoclast formation independent of RANKL expression and that human breast cancer and ovarian cell lines secrete distinct IL-8 isoforms (IL-8 (1-77) and (6-77)).



In this study, the role of the two tumor-secreted IL-8 isoforms was examined *in vitro*. Both isoforms were tested for their ability to bind to the specific IL-8 receptors CXCR1 and CXCR2, to recruit human neutrophils and to promote human osteoclastogenesis. The IL-8 isoforms specifically bound both human CXCR1 and CXCR2. Interestingly, the binding affinity of IL-8 (1-77) to CXCR1 (the primary IL-8 receptor) was significantly greater than IL-8 (6-77) ( $IC_{50}$   $5 \times 10^{-9}$  M vs.  $10^{-6}$  M), whereas there was no difference in affinity for CXCR2. Human neutrophils (expressing CXCR1 and 2) were isolated from peripheral blood and chemotaxis assessed using standard 24-well microchemotaxis chambers covered with polyethylene terephthalate membranes. The lower wells were filled with various concentrations of either IL-8 (1-77), (6-77) or medium without IL-8 peptide. The neutrophils rapidly passed through the membranes toward the wells of the lower chamber containing either IL-8 peptide. No significant differences in chemotaxis were observed with either IL-8 peptide (50% migration at  $5 \times 10^{-8}$  M). In contrast, human osteoclastogenesis was significantly greater when human osteoclast precursors isolated from peripheral blood were stimulated with IL-8 (1-77) than with (6-77). The difference in osteoclastogenic potency was related to the binding affinity of the peptides to CXCR1, the only receptor expressed on osteoclasts and their precursors. In addition, the osteoclastogenic potential of IL-8 was completely inhibited by the CXCR1-specific antagonist (reperitaxin) demonstrating receptor specificity. The activity of RANKL was unaffected by the addition of reperitaxin. To confirm the potency of the IL-8 peptides, purified CD14+ human osteoclast precursors were treated with (1-77) and (6-77). Similar differences in IL-8 peptide potencies were observed, with IL-8 (1-77) inducing significantly more TRAP positive osteoclasts than (6-77), demonstrating a selectivity difference between the response of human neutrophils and osteoclasts to IL-8 isoforms. Collectively, these data demonstrate that tumor-derived IL-8 isoforms have significant distinct effects on osteoclastogenesis that require further investigation.

**Disclosures:** K.M. Nicks, None.

This study received funding from: Carl L. Nelson Chair of Orthopaedic Surgery.

## SU163

**Gene Expression in Blast-Injured Muscle: Insights into the Mechanism of Heterotopic Ossification.** A. B. Aragon<sup>\*1</sup>, W. M. Jackson<sup>\*2</sup>, J. Onodera<sup>\*2</sup>, R. S. Tuan<sup>\*2</sup>, L. J. Nesti<sup>1</sup>. <sup>1</sup>Department of Orthopaedics and Rehabilitation, Walter Reed Army Medical Center, Washington, DC, USA, <sup>2</sup>Cartilage Biology and Orthopaedics Branch, National Institute of Arthritis and Musculoskeletal and Skin Diseases, Bethesda, MD, USA.

Post-traumatic heterotopic ossification (HO) occurs at a high frequency in time-of-war extremity injuries; however the etiology of HO is poorly understood. We have previously identified a population of multipotent mesenchymal progenitor cells (MPCs) within traumatized muscle. Dysregulation of traumatic and wound healing factors could signal these MPCs to become osteoprogenitors and initiate ectopic bone formation. Therefore, the hypothesis of this study was that osteogenic cytokines are up-regulated in traumatically injured muscle tissue. Our specific aims were (1) to identify the cytokines that are up regulated in the injured muscle, (2) to verify the expression of these cytokines in the tissue, and (3) to localize these cytokines within the traumatized muscle relative to the populating cells. Debrided muscle samples were obtained during serial washouts of traumatic extremity wounds, and untraumatized muscle was obtained from elective orthopaedic reconstructions. Cytokine expression was assayed by homogenizing the tissue samples in the TRIzol reagent to extract mRNA and protein. mRNA was analyzed with real-time RT-PCR for cytokines associated with HO (i.e., BMP-4, gremlin, etc) and with a SuperArray RT2Profiler array containing primers for 84 cytokines and cytokine receptors. Cytokine and cellular localization was assayed using immunohistochemistry on tissue samples that were fixed, paraffin embedded and sectioned. We identified a cytokine gene expression profile associated with the traumatized muscle, which included up-regulation of cytokines associated with osteogenic induction (i.e., IL-6, GDF-5, BMP-1). There was no significant up-regulation of the cytokines typically involved in HO formation (i.e., BMP-4, as occurs in the genetic disorder Fibrodysplasia ossificans progressiva). The expression of the up-regulated cytokines in the traumatized muscle tissue was verified by western blotting. In addition, the immunohistochemistry demonstrated that these traumatic cytokines were expressed in a region-specific distribution. This study further characterizes interactions at the cellular and tissue levels that participate in the etiology of HO. Through a greater understanding of how traumatic cytokines are regulated and localized in injured muscle, we hope to better define the key events that contribute to this pathological process and identify novel targets for prophylactic or therapeutic interventions.

**Disclosures:** A.B. Aragon, None.

## SU164

**Central and Peripheral Leptin Treatment Produce Similar Increase in Cortical and Trabecular Bone Mass in ob/ob Mice.** S. M. Bartell<sup>\*1</sup>, D. R. Gaddam<sup>\*1</sup>, S. Ambati<sup>\*1</sup>, S. Rayalam<sup>\*1</sup>, D. L. Hartzell<sup>\*1</sup>, M. Hamrick<sup>\*2</sup>, J. She<sup>\*3</sup>, M. A. Della-Fera<sup>\*1</sup>, C. A. Baile<sup>1</sup>. <sup>1</sup>Dept of Animal & Dairy Science, University of Georgia, Athens, GA, USA, <sup>2</sup>Dept of Cellular Biology & Anatomy, Medical College of Georgia, Augusta, GA, USA, <sup>3</sup>Dept of Pathology, Medical College of Georgia, Augusta, GA, USA.

Central or peripheral leptin administration reduces body weight, food intake, & body fat in leptin deficient ob/ob mice. However, opposing reports dominate when assessing the effects of leptin on cortical & trabecular bone mass in rodents. This study's objective was to determine effects of central & peripheral administration of leptin on bone metabolism in cortical & trabecular bone in ob/ob mice (15 wk old, init. BW=61.3g). Leptin was continuously delivered intracerebroventricularly (ICV, 0 or 1.5µg/d) or subcutaneously

(SQ, 0 or 10µg/d) via osmotic pumps for 12 days (n=10). Mice were injected intraperitoneally with calcein, a fluorochrome label, to measure bone formation during the experimental period. There were no significant differences in bone parameters between the modes of leptin administration. Regardless of mode of administration, leptin increased whole body bone mineral density (BMD; 0.0565 vs 0.0542 vs 0.0503g/cm<sup>2</sup>, p=0.0003; mean of ICV vs SQ leptin treatments vs controls), & bone mineral content (BMC; 0.518 vs 0.483 vs 0.397g, p=0.001), lumbar BMD (0.0943 vs 0.0891 vs 0.0723g/cm<sup>2</sup>, p=0.0002) & BMC (0.034 vs 0.031 vs 0.024g, p<0.0001), proximal femoral BMD (0.0995 vs 0.0973 vs 0.0732g/cm<sup>2</sup>, p=0.0002) & BMC (0.051 vs 0.052 vs 0.039g, p=0.0006), distal tibial BMD (0.0856 vs 0.0825 vs 0.0675g/cm<sup>2</sup>, p=0.0009), cortical (4.74 vs 5.29 vs 2.64microns/d, p<0.0001) & trabecular (5.26 vs 6.12 vs 2.65microns/d, p<0.0001) mineral apposition rate, serum osteocalcin (96.408 vs 123.481 vs 35.493ng/mL, p<0.0001), pyridinoline (PYD) (2.577 vs 2.447 vs 0.831nmol/L, p=0.04), & RANK-L (145.51 vs 186.93 vs 111.21pg/mL, p<0.001) concentrations. These observed increases in BMD, BMC, bone formation & bone marker concentrations indicate that both SQ & ICV (1/7th the SQ dose) leptin administration increased cortical & trabecular bone equally in ob/ob mice.

**Disclosures:** S.M. Bartell, None.

This study received funding from: the Georgia Research Alliance (GRA) Eminent Scholar endowment (CAB) & a GRA Challenge Grant (CAB & JXS).

## SU165

**Chemerin and CMKLR1 Expression and Function in Human Bone Marrow Mesenchymal Stem Cell Adipogenesis.** A. A. Roman<sup>\*</sup>, C. J. Sinal. Pharmacology, Dalhousie University, Halifax, NS, Canada.

Osteoporosis is a progressive skeletal disorder characterized by low bone mass and microarchitectural deterioration of bone tissue that ultimately leads to an increase in bone fragility and susceptibility to fracture. A hallmark characteristic of osteoporotic bone is an increase in fatty marrow that develops as a consequence of an increase in the number of marrow adipocytes. Recent findings demonstrate that this increase in marrow adipocytes is directly related to bone loss, as adipocytes share a common mesenchymal stem cell (MSC) precursor with bone forming osteoblasts. As marrow adipogenesis is attributable to alterations in bone marrow MSC differentiation, and not to adipocyte infiltration from tissues outside the bone, manipulation of the physiological milieu of MSCs to favour osteoblast formation over adipocyte formation may offer a novel target for the treatment of osteoporosis. In the bone marrow, many factors influence the fate of MSCs including secreted signalling molecules, such as cytokines and nutritional factors, such as Vitamin D. Recently, our laboratory identified chemerin as a signaling molecule released from adipocytes that regulates adipogenesis by activation of chemokine like receptor-1(CMKLR1). The purpose of this study was to characterize the expression and function of chemerin and CMKLR1 in the adipogenic differentiation of human bone marrow derived MSCs. Chemerin and CMKLR1 mRNA and protein expression were evaluated using quantitative real time PCR and western blotting, respectively. We have identified that chemerin and CMKLR1 are expressed in human bone marrow derived MSCs and that the expression of chemerin and CMKLR1 are increased during adipogenesis, *in vitro*. We have also demonstrated that treatment of adipocyte precursors with Vitamin D *in vitro* caused a significant induction in chemerin expression, therefore providing support for one mechanism whereby chemerin may be directly regulated to affect bone formation.

**Disclosures:** A.A. Roman, None.

## SU166

**The Effects of Exercise and Estrogen on Osteoprotegerin in Premenopausal Women.** S. L. West<sup>\*1</sup>, J. L. Scheid<sup>\*1</sup>, S. Awidishu<sup>\*1</sup>, M. J. De Souza<sup>2</sup>. <sup>1</sup>University of Toronto, Toronto, ON, Canada, <sup>2</sup>Penn State University, University Park, PA, USA.

The benefits of exercise are widely recognized, however physically active women can develop exercise associated menstrual cycle disturbances such as amenorrhea (i.e., estrogen deficiency) secondary to a chronic energy deficiency. The purpose of this cross-sectional observational study was to assess the effects of exercise status and estrogen deficiency on osteoprotegerin (OPG) and its relationship to bone turnover in premenopausal women. Serum OPG, urinary c-telopeptides (uCTX), urinary estrone 3-glucuronide (E1G), urinary pregnanediol 3-glucuronide (PdG) and bone mineral density (BMD) by DXA were measured repeatedly in 67 women. Volunteers were retrospectively grouped: 1) Sedentary menstruating group (SedMen n=8), 2) Exercising menstruating group (ExMen, n=36), 3) Exercising amenorrheic group (ExAmen, n=23). One-way ANOVAs were performed, and LSD post-hoc tests were performed when differences were detected. Subjects were similar with respect to age (24.2±1.0 yrs), weight (57.8±1.7 kg), height (164.3±1.3 cm), and BMI (21.5±0.6 kg/m<sup>2</sup>) (p>0.05). ExMen and ExAmen groups were more aerobically fit than the SedMen group (p=0.003). E1G mean (p<0.001), E1G AUC (p<0.001), and PdG AUC (p=0.018) were lower in the ExAmen group vs. the SedMen and ExMen groups. uCTX was elevated (p=0.033) in the ExAmen group (281.8±40.3 ug/L/mmCr), compared with the SedMen and ExMen groups (184.5±22.4, 197.2±14.7 ug/L/mmCr, respectively). OPG was concomitantly suppressed (p=0.005) in the ExAmen group (4.6±0.2 pmol/L) vs. ExMen group (5.2±0.2 pmol/L), and OPG was also lower in the SedMen group (4.1±0.3 pmol/L) compared with the ExMen group. Findings were translated to BMD; the ExAmen group had suppressed total body BMD (p=0.014) and L2-L4 BMD (p=0.015) vs. the ExMen group. Our results suggest that OPG responds to the bone loading effect of exercise, and that suppressed OPG may play a role in the etiology of increased bone resorption observed in exercising women with hypothalamic amenorrhea.

**Disclosures:** S.L. West, None.

This study received funding from: US DoD (PR054531), and CIHR.



## SU167

### Increased Circulating Dickkopf-1 in Acute Coronary Syndrome - Association with Platelet Release and Endothelial Inflammatory Response.

T. Ueland\*, K. Otterdal\*, T. Lekva\*, W. Sandberg\*, B. Halvorsen\*, J. Bollerslev, E. Oie\*, L. Gullestad\*, P. Aukrust\*. Rikshospitalet-Radiumhospitalet Medical Center, oslo, Norway.

**Purpose:** Increasing evidence indicates a pathological link between atherogenesis and osteoporosis. The Wnt signaling pathway plays an important role in regulating bone remodeling and we sought to investigate the role of Dickkopf (DKK)-1 in atherogenesis and plaque destabilization. **Methods:** We investigated this by different experimental approaches including studies in patients with stable (n = 40) and unstable angina (n = 40) and healthy control subjects (n = 20). **Results:** The following was discovered: 1) patients with stable, and particularly those with unstable, angina had markedly raised serum levels of DKK-1 compared with control subjects. 2) Platelets are a rich source of DKK-1 and release large amounts upon activation. This release was inhibited by preincubation with PGE1, suggesting that DKK-1 is secreted from alpha-granules during activation. 3) DKK-1 protein was detected in atherosclerotic plaques and coronary thrombi. 4) endothelial cells produce DKK-1 upon stimulation with CD40L in vitro. 5) siRNA-mediated knocking down of DKK-1 in endothelial cells decreased the production of IL-8 suggesting that DKK-1 may enhance endothelial inflammatory response. 6) Aspirin reduced the SFLRN-stimulated release of DKK-1 from platelets, and when administered to healthy control subjects for 7 days, it reduced circulating DKK-1. **Conclusion:** The data may suggest a pathogenic role for DKK-1 in atherogenesis involving modulation of platelet-induced inflammatory responses in endothelial cells.

**Disclosures:** T. Ueland, None.

## SU168

### FGF-23 and Post -Transplant Hypophosphatemia: Evidence for a Causative Link.

A. Trombetti<sup>1</sup>, L. Richert<sup>\*1</sup>, K. Hadaya<sup>\*2</sup>, J. D. Graf<sup>\*3</sup>, P. Y. Martin<sup>\*2</sup>, R. Rizzoli<sup>1</sup>. <sup>1</sup>Department of Rehabilitation and Geriatrics, University Hospital of Geneva, Geneva 14, Switzerland, <sup>2</sup>Nephrology Service, University Hospital of Geneva, Geneva 14, Switzerland, <sup>3</sup>Central Laboratory, University Hospital of Geneva, Geneva 14, Switzerland.

**Objective:** Hypophosphatemia is frequent in the early post-transplant period. Fibroblast growth factor-23 (FGF-23) may be involved in hypophosphatemia pathogenesis. Other factors could modulate serum phosphate level such as increased parathyroid hormone (PTH) level, renal function and dietary phosphorus intake. Therefore, we tested the hypothesis that FGF-23 level is associated with decreased serum phosphate levels and renal phosphate threshold (TmPi/GFR) independently of renal and parathyroid function, and of dietary phosphate intake in renal transplant recipients.

**Methods:** We investigated 48 recipients of kidney transplant. Plasma PTH, calcitriol, FGF-23 (intact FGF-23, Kainos Laboratories, Inc., Tokyo, Japan, and C-terminal FGF-23 fragments, Immotopics, San Clemente CA, USA) were measured 11 days [95% CI, 9.1-15.9] after renal transplantation. Fasting plasma and urinary calcium, phosphate and creatinine were also measured simultaneously and renal tubular reabsorption of phosphate was calculated as well as renal function, using the Cockcroft and Gault formula. Hypophosphatemic and patients with normal phosphate level were compared by a non-parametric test. Correlations between serum phosphate levels, renal phosphate threshold and recorded variables were determined by simple or multiple linear regression analyses.

**Results:** Hypophosphatemia, defined as a serum phosphate level  $\leq 0.8$  mmol/l, was observed in 26 (54%) of the patients in the early post transplant period. Patient with hypophosphatemia had a significantly higher level of both intact and C-terminal FGF23 ( $238 \pm 215$  vs  $99 \pm 125$  ng/l for the intact,  $p < 0.05$ ;  $486 \pm 520$  vs  $275 \pm 460$  U/ml for the C-terminal assay,  $p < 0.01$ ). In univariate analysis, intact FGF-23 was inversely correlated with plasma phosphate ( $r^2 = 0.16$ ,  $p < 0.03$ ) and renal tubular reabsorption of phosphate ( $r^2 = 0.19$ ,  $p < 0.03$ ). The association between C-terminal form and plasma phosphate was of borderline significance ( $r^2 = 0.06$ ,  $p < 0.1$ ), while the inverse association was significant for renal phosphate threshold ( $r^2 = 0.13$ ,  $p < 0.02$ ).

When PTH levels, renal function and dietary phosphate intake were included in a multivariate model, PTH and FGF-23 remained independently associated with renal phosphate threshold. These variables explained 46% of the variance of TmPi/GFR (p value for the model  $< 0.001$ ).

**Conclusion:** Our study strongly suggest that FGF-23 may be a causative factor for the developpement of hypophosphatemia in conjunction with increased levels of PTH in the early post-transplant period.

**Disclosures:** A. Trombetti, None.

## SU169

### Effects of hPTH(1-34) Infusion on Circulating Serum Phosphate, 1,25-dihydroxyvitamin D and FGF-23 Levels in Healthy Men.

S. M. Burnett-Bowie, M. P. Henao\*, M. E. Dere\*, H. Lee\*, B. Z. Leder. Endocrine Unit, Massachusetts General Hospital, Boston, MA, USA.

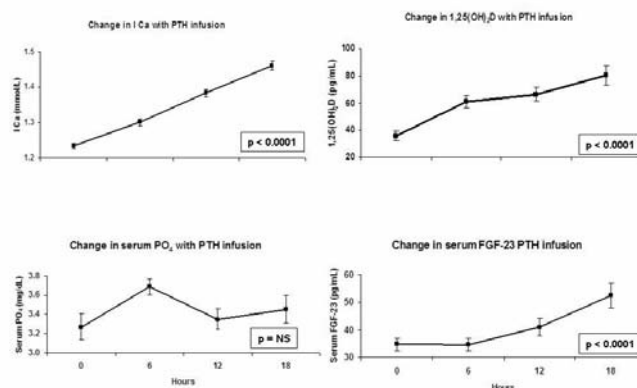
**Introduction:** Fibroblast growth factor 23 (FGF23) is a phosphate ( $PO_4$ )-regulating hormone that promotes renal  $PO_4$  wasting and suppresses 1,25-dihydroxyvitamin D ( $1,25(OH)_2D$ ) production. PTH also promotes renal  $PO_4$  wasting but, in contrast to FGF23, stimulates  $1,25(OH)_2D$  production. While studies suggest that dietary  $PO_4$ , serum  $PO_4$ , and  $1,25(OH)_2D$  stimulate FGF23 secretion, the relationship between FGF23 and PTH is

unclear. Furthermore, the acute effect of a pharmacologic dose of PTH on FGF23 secretion is unknown.

**Methods:** 20 healthy men, aged 20-45, with normal serum calcium,  $PO_4$  and renal function were treated with human parathyroid hormone (1-34) (hPTH(1-34)) at a dose of 44ng /kg/ hour for 24 hours. Blood ionized calcium levels were monitored regularly and the infusion discontinued if ionized calcium exceeded 1.5 mmol/L. ANOVA was performed to determine if our primary endpoints (serum  $PO_4$  and FGF23) or secondary endpoints ( $1,25(OH)_2D$ , ionized calcium and serum N-telopeptide) changed over time. If such a change were detected, paired t-tests were performed to compare hour 6, 12, or 18 data to baseline.

**Results:** Compared to baseline, serum FGF23,  $1,25(OH)_2D$ , ionized calcium and N-telopeptide increased significantly over the 18-hour hPTH(1-34) infusion ( $p < 0.0001$ ), while serum  $PO_4$  did not change. Specifically, serum FGF23 increased from  $35 \pm 10$  pg/mL at baseline to  $53 \pm 20$  pg/mL at 18 hours ( $p = 0.0002$ );  $1,25(OH)_2D$  increased from  $36 \pm 16$  pg/mL at baseline to  $80 \pm 33$  pg/mL at 18 hours ( $p < 0.0001$ ); ionized calcium increased from  $1.23 \pm 0.03$  mmol/L at baseline to  $1.46 \pm 0.05$  mmol/L at hour 18 ( $p < 0.0001$ ); and serum N-telopeptide increased from  $17 \pm 4$  nM BCE at baseline to  $28 \pm 8$  nM BCE at peak ( $p < 0.0001$ ). Serum  $PO_4$  was  $3.3 \pm 0.6$  mg/dL at baseline, transiently rose to  $3.7 \pm 0.4$  mg/dL at hour 6 ( $p = 0.0016$ ), and then returned to  $3.4 \pm 0.5$  mg/dL at hour 12 ( $p = 0.651$ ).

**Conclusions:** hPTH(1-34) infusion significantly increases endogenous  $1,25(OH)_2D$  and FGF23 levels within 18 hours in healthy men. Additionally, we observed a transient rise in serum  $PO_4$  that is likely due to PTH mediated bone resorption. Prior animal and *in vitro* data suggest that neither PTH nor calcium stimulate FGF23 secretion, but that serum  $PO_4$  and  $1,25(OH)_2D$  do. Our data support the assertion that  $1,25(OH)_2D$  is a potent physiologic stimulator of FGF23 secretion, and that serum  $PO_4$  may be a stimulator of FGF23 secretion.



**Disclosures:** S.M. Burnett-Bowie, None.

This study received funding from: NIH K23-DK-073356, K23-RR-161310, and M01-RR-01066.

## SU170

### Development of Nephrotic In Transgenic Rats Over Expressing TypeIII Na-Dependent Phosphate Transporter.

S. Sekiguchi, S. Asano, M. Shibata, A. Yokoyama\*, K. Inagaki\*, H. Kakizawa\*, N. Hayakawa\*, N. Oda\*, A. Suzuki, M. Itoh\*. Division of Endocrinology, Fujita Health University, Toyoake Aichi, Japan.

Phosphate uptake at the cellular membrane is essential to maintain the cell activity because phosphate has to be supplied for ATP synthesis. On the contrary, accumulating evidence suggests that phosphate overload from the extracellular milieu would be stressful for the cells, resulting in the apoptosis of the cells. We have previously reported that the overexpression of a type III Pi transporter (Pit-1) in rats induces the phosphate-dependent cellular stress, which results in the damage of the filtration at glomerulus without affecting renal function itself. In the present study, we further investigate the effect of over expression of Pit-1 on the kidney in Pit-1 transgenic (Tg) rats, and analyzed the mechanism of the development of nephrotic syndrome.

On day 10 after birth, when its glomerulus achieved development, there was no difference of glomerulus between wild type (WT) and Tg rats under electron microscope (EM). However, glomerulus in Tg rats progressively exhibits diffuse loss of processes of visceral epithelial cells (podocytes) and thickened basement membrane under EM after 8 weeks old. At 8 months old, when Tg rats were going to die because of cachexia, glomerulus in Tg rats had thickened basement membrane, increased mesangial matrix, and were sclerosed and hyalinized. In order to further explore the mechanism of the development of nephrotic syndrome in Pit-1 Tg rats, we next examined the effect of extracellular phosphate on primary cultured podocyte from both WT and Tg rats. A two fold increase of Pi transport activity was recorded in primary cultured podocyte from Tg rats compared with WT littermates. More apoptosis of podocytes by high phosphate in extracellular milieu was found in Tg rats than in WT by TUNEL method.

In conclusion, our findings suggest us that cell stress by extracellular Pi induces apoptosis of podocyte, and continuous stress on podocytes by Pit-1 overexpression at least in part explains the progress of glomerulus damage, which results in the nephrotic syndrome.

**Disclosures:** S. Sekiguchi, None.

## SUI171

**A Homozygous Threonine to Methionine Substitution in FGF23 Gene Is Associated with Tumoral Calcinosis in a 12 Year-old Girl.** N. S. Dunbar<sup>1</sup>, C. Nelson-Williams<sup>2</sup>, R. L. Lifton<sup>2</sup>, T. O. Carpenter<sup>1</sup>. <sup>1</sup>Pediatrics, Yale University, New Haven, CT, USA, <sup>2</sup>Genetics, Yale University, New Haven, CT, USA.

Familial tumoral calcinosis (FTC) is a rare disorder of phosphate metabolism characterized by ectopic calcified masses as well as vascular calcifications. Patients are hyperphosphatemic with elevated or inappropriately normal circulating 1, 25 dihydroxyvitamin D (1,25D). The calcified lesions can cause pain, decreased mobility, loss of function and disfigurement. Inactivating mutations of fibroblast growth factor 23 (FGF23), GalNAc transferase 3 (GALNT3), and Klotho (KL) have been identified in patients with autosomal recessive FTC.

A previously healthy 12 year old Caucasian girl noted tenderness and swelling over the back of her neck. A large, well-defined, multilocal calcific mass was identified sonographically in the posteriolateral aspect of the left neck, extending from the posterior arch of the first cervical vertebra to the thoracic inlet. A chalky, non-purulent slurry periodically drained from the site of an open biopsy. Circulating phosphorus levels ranged from 4.8 to 5.1 mg/dl (high normal to slightly elevated), serum calcium levels ranged from 9.2 to 9.6 mg/dl (normal), and circulating 1,25D was 71 pg/ml (increased). Circulating PTH was normal (20 nleq/ml). The threshold maximum for renal tubular phosphate reabsorption (TMP/GFR) was 5.2 mg/dl. Serum FGF23 using an assay detecting the intact molecule (Kainos, Japan) was 24 pg/ml but no immunoreactive species was detected using an assay directed toward the C-terminus of the molecule (Immutopics). Surgical debulking was performed.

Mutational analysis was performed employing direct sequencing of the FGF23, KLOTHO and GALNT3 genes on DNA derived from peripheral leukocytes. A homozygous G->A transition was identified in the FGF23 gene indicating a T239M substitution in the protein. This missense mutation replaces a noncharged, polar, hydrophilic residue with a non-polar, hydrophobic one, suggesting a potential functional consequence of this mutation. The discordance in results when employing two different assays is not clear at this time, but may represent an effect of the mutation on interaction with antibodies used in FGF23 assays.

**Disclosures:** *N.S. Dunbar, None.*

## SUI172

**Signaling of Extracellular Inorganic Phosphate Mediated via Sodium-Phosphate Co-transporters Influences FGF23 Signaling in Renal Tubular Cells.** M. Yamazaki<sup>1</sup>, T. Okada<sup>1</sup>, K. Tachikawa<sup>1</sup>, K. Ozono<sup>2</sup>, T. Michigami<sup>1</sup>. <sup>1</sup>Department of Bone and Mineral Research, Osaka Medical Center and Research Institute for Maternal and Child Health, Osaka, Japan, <sup>2</sup>Department of Pediatrics, Osaka University Graduate School of Medicine, Osaka, Japan.

FGF23 increases renal phosphate excretion by binding FGF receptor and membrane-bound form of klotho. However, the impact of serum levels of inorganic phosphate (Pi) on the effect of FGF23 remains uninvestigated. Thus, we have examined the effects of extracellular Pi on FGF23 signaling utilizing renal tubular cell line HEK293. Real-time PCR for klotho demonstrated its low expression in HEK293 cells. HEK293 cells were capable of responding to treatment with recombinant FGF23[R179Q], a constitutively active form of FGF23, based on the phosphorylation of ERK1/2 and the expression of early growth response-1 (Egr-1), and over-expression of klotho markedly enhanced the response in HEK293 as previously reported. Then, we examined the effects of increased extracellular Pi on phosphorylation of ERK1/2 and expression of Egr-1. Interestingly, treatment with increased Pi (4 mM) resulted in phosphorylation of ERK1/2. The time course of phosphorylation of ERK1/2 induced by increased extracellular Pi was similar to that induced by FGF23[R179Q]. In addition, increased extracellular Pi induced the expression of Egr-1 within 30 min., and simultaneous treatment with increased Pi and FGF23[R179Q] exerted additive effects, suggesting the commonality between FGF23 and extracellular Pi in terms of the downstream signaling networks. Increased extracellular Pi induced the phosphorylation of c-Raf as well, indicating the activation of Raf/MEK/ERK pathway. Since the increase in extracellular Pi failed to induce phosphorylation of FRSS2α (FGF receptor substrate 2α), the cascade upstream of ERK1/2 in Pi-induced signaling is likely to be different from that in FGF23-induced signaling. Treatment with phosphonoformic acid (PFA), an inhibitor of Na<sup>+</sup>/Pi co-transporters, abolished the effects of increased extracellular Pi on phosphorylation of ERK1/2 and induction of Egr-1 expression. Real-time PCR for Na<sup>+</sup>/Pi co-transporters revealed the dominant expression of type III co-transporter PiT-1 and the marginal expression of type IIa and IIc co-transporters in HEK293 cells. The knockdown of PiT-1 utilizing siRNA reduced the Pi-induced phosphorylation of ERK1/2. Over-expression of type IIa co-transporter enhanced the phosphorylation of ERK1/2 and the up-regulation of Egr-1. These results suggest that increased extracellular Pi exerts an influence on FGF23-signaling by the interaction with ERK1/2 pathway, depending on Na<sup>+</sup>/Pi co-transporters.

**Disclosures:** *M. Yamazaki, None.*

## SUI173

**c-Fos Is Associated with Renal FGF23-Mediated Signaling: Effect of the Hyp Mutation.** E. Farrow<sup>1</sup>, L. Summers<sup>1</sup>, S. Davis<sup>1</sup>, S. Schiavi<sup>2</sup>, K. White<sup>1</sup>. <sup>1</sup>Medical and Molecular Genetics, Indiana University, Indianapolis, IN, USA, <sup>2</sup>Genzyme Corporation, Framingham, MA, USA.

Fibroblast growth factor-23 (FGF23) is a key regulator of phosphate metabolism, and requires a heteromeric complex of Klotho (KL) and a canonical FGF receptor (FGFR) to initiate MAPK signaling in the kidney. The mRNA levels for the transcription factor, Early growth response gene-1 (EGR1) can be used as an index for FGF23 bioactivity. The Hyp mouse, a model of X-linked hypophosphatemic rickets (XLH), is characterized by hypophosphatemia associated with significantly increased serum FGF23 concentrations, however the relative level of FGF23 activity in the kidney in these animals is unknown. The goals of the present studies were to identify new genes within FGF23-mediated signaling pathways, and to further understand FGF23 activity in the Hyp mouse. FGF23-regulated genes were identified via array technology using kidney RNA isolated from wild type mice injected with 10 µg FGF23 and sacrificed after 1 h. Using qPCR on kidney RNA, c-Fos was found to be elevated by 13-fold compared to control animals (p<0.05). The positive control, EGR1, showed a 70-fold increase (p<0.01) at the same time point. To confirm these results, HEK293 cells stably expressing membrane Klotho (mKL) were treated with 100 pg/mL of FGF23 for 30 and 60 minutes. qPCR analyses showed time dependent increases of 3- and 6-fold for c-Fos mRNA at 30 and 60 minutes when compared to vehicle treated cells. As expected, EGR1 mRNA increased 5- and 15-fold at 30 and 60 minutes, respectively. Hyp mice are known to manifest increased FGF23 levels, similar to most patients with XLH. At six weeks of age, male Hyp mice had over a 12-fold elevation in serum FGF23 concentrations when compared to wild type mice (1275 vs 92 pg/ml; p<0.05). However, in contrast to the substantial increases in c-Fos and EGR1 RNA observed in the FGF23-injected mice, expression of these genes was only 2-fold elevated in Hyp mice kidneys compared to sex- and age-matched wild type littermates (p<0.05). These results suggest that FGF23 signaling may be altered in Hyp mice given their significantly elevated serum FGF23 levels. Consistent with the apparent reduction of FGF23 signaling in Hyp, KL mRNA was reduced by 60% in these mice compared to wild type littermates. In summary, we have identified c-Fos as an FGF23-responsive gene in vivo and in vitro, and have determined that Hyp mice have low, but measurable signaling in the kidney in the face of markedly elevated FGF23 concentrations. Taken together, our results indicate that FGF23 signaling involving c-Fos and EGR1 is down regulated in the Hyp mouse despite elevated serum FGF23 concentrations, and the mechanisms for this reduced activity likely involve suppressed KL mRNA.

**Disclosures:** *E. Farrow, None.*

## SUI174

**Role of Fibroblast Growth Factor-23 (FGF-23) in the Early Response to the PTH Analogue; Teriparatide.** M. Sridharan<sup>1</sup>, P. Manghat<sup>1</sup>, D. MacDonald<sup>2</sup>, I. Fogelman<sup>2</sup>, A. S. Wierzbicki<sup>3</sup>, W. D. Fraser<sup>3</sup>, G. Hampson<sup>1</sup>. <sup>1</sup>Chemical Pathology, St Thomas Hospital, London, United Kingdom, <sup>2</sup>Nuclear Medicine, Guy's Hospital, London, United Kingdom, <sup>3</sup>Clinical Chemistry, Royal Liverpool University Hospital, London, United Kingdom.

The importance of FGF-23 in phosphate metabolism is well established. FGF-23 is produced by osteoblasts and osteocytes. Recent studies indicate that it may be implicated in bone formation and is regulated by PTH. Intermittent PTH administration has anabolic effects on bone. The aim of our study was therefore to investigate firstly the early effect of intermittent PTH on circulating FGF-23 and secondly the relationship between FGF-23 and bone and mineral metabolism following intermittent PTH.

We studied 26 women aged (mean [SD] :75.8 [5.4] years) treated with the recombinant PTH analogue 1-34 (Teriparatide) for established postmenopausal osteoporosis. We investigated their early response following treatment with Teriparatide for 6-9 months. Bone mineral density (BMD) was measured by DXA at the lumbar spine (LS) and Total Hip (TH) at baseline and at 6-9 months. Biochemical markers of bone turnover; PINP, Bone alkaline phosphatase (BALP), osteocalcin (OC) and urine CTX were measured at baseline, 1-3 months and 6-9 months. Circulating FGF-23 was determined at the same time-points using the Immuntopics C-terminal FGF-23 ELISA. BMD at the LS increased significantly (mean [SEM] 6.6% [0.9]). No significant change was seen at the TH. Significant increases in the bone turnover markers were observed at 1-3 months with further increases at 6-9 months (PINP ug/L baseline 41.8 [5.4], 6-9 months 147.7 [18.6]; BALP ug/L 16.4 [2.1], 27.0 [2.8]; OC ug/L 8.8 [1.4], 13.2 [1.9]; uCTX ug/mmol creatinine 188.0 [27.4], 579.0 [113.1] p<0.05). Serum albumin adjusted calcium (mmol/L) increased significantly from baseline (mean [SD] baseline 2.37 [0.09], 6-9 months 2.46 [0.12] (p<0.05). This was accompanied by a significant reduction in PTH ng/L (baseline 40.4 [4.8], 6-9 months 34.4 [5.1] p<0.01). No significant change in serum phosphate was seen. Baseline FGF-23 ranged from 1 to 847 U/ml. There was a significant correlation between FGF-23 and PTH at baseline (r=0.618, p=0.0048). FGF-23 increased significantly at 6-9 months (median [range] baseline 39 [1-847], 6-9 months 55 [3-1457] p=0.017). Early changes in serum calcium were associated with changes in FGF-23 at 6-9 months (r=0.47, p=0.026). A significant correlation was seen between the changes in FGF-23 and PINP at 6-9 months (r=0.78 and p<0.001). In conclusion, the data suggest that intermittent PTH regulates circulating FGF-23 and this factor may be implicated in bone and mineral metabolism following PTH administration for post-menopausal osteoporosis.

**Disclosures:** *M. Sridharan, None.*

## SUI175

Withdrawn

## SUI176

**Phosphatonins and Liver Resection-Related Hypophosphatemia.** O. Nafidi<sup>\*1</sup>, R. W. Lapointe<sup>\*1</sup>, R. Lepage<sup>\*1</sup>, J. H. Brossard<sup>1</sup>, R. Kumar<sup>\*2</sup>, P. D'Amour<sup>1</sup>. <sup>1</sup>CHUM - Hôpital Saint-Luc, Departments of Medicine, Biochemistry and Surgery, Université de Montréal, Montréal, QC, Canada, <sup>2</sup>Departments of Internal Medicine, Biochemistry and Molecular Biology, Mayo Clinic, Rochester, MN, USA.

Post-hepatectomy hypophosphatemia (HP) is believed to be the result of metabolic demands by the regenerating liver. However, we and others have reported excessive fractional urinary phosphate excretion ( $F_{\text{e}}\text{PO}_4$ ) early after hepatectomy in possible association with hypocalcemia and increased circulating levels of Intact PTH. In this study we explored the role of three phosphatonins comparatively to PTH in post-hepatectomy HP. Serum phosphate (Pi), ionized calcium ( $\text{Ca}^{2+}$ ),  $\text{HCO}_3^-$ , pH and  $F_{\text{e}}\text{PO}_4$  (24 hour collection) were measured before and serially on postoperative (po) days 1, 2, 3, 5 and 7 in 18 patients undergoing successful liver resection. At identical time-points, we quantified I-PTH and carboxyterminal (C) and intact (I) fibroblast growth factor-23 (FGF-23), FGF-7 and frizzled related-protein-4 (FRP-4). pH decreased to  $7.32 \pm 0.01$  on po day 1 and the acidosis was resolved by po day 2 without respiratory alkalosis.  $\text{Ca}^{2+}$  declined (N:  $1.16-1.29$ ) to  $1.10 \pm 0.01$  mmol/L ( $p < 0.01$ ) while I-PTH (N:  $1.4-6.8$  pmol/L) peaked to  $8.8 \pm 0.9$  ( $p < 0.001$ ). Pi (N:  $0.7-1.3$  mmol/L) fell on the first 2 po days to  $0.66 \pm 0.03$  mmol/L ( $p < 0.001$ ) during which  $F_{\text{e}}\text{PO}_4$  (N: 10-15%) peaked to  $25.1 \pm 2.3\%$  ( $p < 0.05$ ). The I-PTH peak on po day 1 was correlated both with the latter ( $r = 0.65$ ,  $p = 0.006$ ) and with po day 1 serum  $\text{Ca}^{2+}$  ( $r = -0.62$ ,  $p = 0.016$ ). I-FGF-23 dropped to  $7.8 \pm 6.9$  pmol/L on po day 3 ( $p < 0.001$ ) with parallel kinetics to Pi. C-FGF-23 (N < 100 RU/ml) increased to  $70.1 \pm 28.8$  RU/ml in po day 2 (NS). I-FGF-23 and C-FGF-23 were not correlated and both were not associated with  $F_{\text{e}}\text{PO}_4$ . FGF-7 rose continually to  $52.4 \pm 8.9$  pg/ml (NS) on po day 7 while FRP-4 increased slightly to  $104.8 \pm 17.4$  ng/ml on po day 1 (NS). Both FGF-7 and FRP-4 kinetics were not associated with Pi and  $F_{\text{e}}\text{PO}_4$ . HP and hyperphosphaturia were constant postoperative findings after hepatectomy. Decreased po I-FGF-23 may have resulted from a low Pi negative feedback. The I-FGF-23 decline coincided with the peak  $F_{\text{e}}\text{PO}_4$  itself associated with the I-PTH level at the start of the urine collection. FGF-7 and FRP-4 did not play a phosphaturic role after hepatectomy in the group of patients as a whole, but may have in some individuals. More investigations are needed to explore the mechanism of post-hepatectomy HP.

**Disclosures:** P. D'Amour, None.

## SUI177

**FGF-23 and Parameters of Calcium and Bone Metabolism Are Positively Influenced by GH Replacement in Adult Growth Hormone Deficiency Patients from the KIMS Survey.** W. J. Fassbender<sup>1</sup>, S. Schmitz<sup>\*1</sup>, P. Kann<sup>2</sup>, U. C. Stumpf<sup>3</sup>. <sup>1</sup>Internal Medicine - Endocrinology, Hospital zum Heiligen Geist, Kempen, Germany, <sup>2</sup>Internal Medicine - Endocrinology, Diabeteology, University Hospital Philipps University Marburg, Marburg, Germany, <sup>3</sup>Traumatology and Handsurgery, University Hospital Heinrich Heine University Duesseldorf, Duesseldorf, Germany.

**Introduction:** Growth hormone deficiency leads to reduction in bone turnover, mainly due to alterations in PTH circadian rhythmicity as well as to a lack of sensitivity of the kidney and bone to the effects of PTH. These mechanisms may be responsible for the reduction in bone turnover and the development of osteoporosis. Patients with GHD show abnormalities of renal phosphate metabolism, which may also contribute to the pathogenesis of bone loss in these patients. GH treatment leads to restoration of renal tubular reabsorption and sensitivity of target organs to PTH and bone turnover and to improvement of BMD under ongoing GH replacement therapy. **Materials and Methods:** The aim of our study was to investigate the role of the phosphatonine FGF-23 in this complex process. We measured the relationship between the parameters of calcium metabolism such as Calcium, Phosphate, Creatinine and PTH and their correlation to the phosphatonine FGF-23 and 25-OH VitaminD levels in GDH patients before, after six and twelve months therapy with growth hormone. **Results:** EDTA-Plasma (due to better stability than serum samples) of 15 patients was investigated. Arithmetic means for intact FGF-23 before therapy were 17.3 pg/ml, after 6 months therapy 15.3 pg/ml and 23 pg/ml at 12 months (all  $p < 0.001$ ). C-terminal FGF-23 initial was 58 U/ml, at 6 months 47 U/ml and at month 12 108.6 U/ml (all  $p < 0.001$ ). Calcium values were 2.38, 2.44 and 2.43 mmol/l. Corresponding phosphate levels were 3.04, 3.39 and 3.08 mg/dl (all  $p < 0.001$ ). As expected, FGF-23 was inversely correlated to serum phosphate.

**Discussion:** The results suggest that GH supplementation in GHD patients leads to normalization of tubular reabsorption of phosphate due to regulation by FGF-23 and reverses the GHD-induced relative phosphate-deficient state. Restoration of physiological regulation of phosphate metabolism emphasizes the beneficial effect of GH supplementation of GHD patients on bone remodeling.

**Disclosures:** W.J. Fassbender, None.

## SUI178

**Altered Regulation and Expression of FGF23 in the Adenine-induced Uremic Rat Model.** D. Cuerrrier<sup>\*</sup>, C. Helvig<sup>\*</sup>, A. Kharebov<sup>\*</sup>, K. Ryder<sup>\*</sup>, J. Kim<sup>\*</sup>, B. Ireland<sup>\*</sup>, M. Petkovich. Cytochroma Inc., Markham, ON, Canada.

FGF23 is a systemic hormone involved in phosphate homeostasis. Circulating FGF23 is produced primarily in bone and is independently regulated by circulating  $1,25-(\text{OH})_2\text{D}_3$  and elevated serum phosphorus levels. In addition, circulating FGF23 can limit intestinal absorption of phosphate by suppressing renal expression of CYP27B1, thereby limiting production of  $1,25-(\text{OH})_2\text{D}_3$  and decreasing renal phosphate reabsorption leading to a decrease in circulating phosphorus levels. Recently, FGF23 was proposed to upregulate renal CYP24 expression which could lead to further decrease  $1,25-(\text{OH})_2\text{D}_3$  levels and intestinal absorption of phosphate. Hyperphosphatemic patients with chronic kidney disease (CKD) show significant elevation of circulating FGF23 levels, exacerbating a deficiency in renal  $1,25-(\text{OH})_2\text{D}_3$  production. In this study, we have examined the profile of FGF23 expression in the adenine-induced uremic rat model. Circulating FGF23 levels was found to be upregulated 50-fold in the plasma of uremic rats relative to normal rats.  $1,25-(\text{OH})_2\text{D}_3$  treatment resulted in an additional 6-fold increase. Interestingly, tissue profiling of FGF23 revealed upregulation of its expression by 50-fold in the kidney of uremic rats relative to normal rats. Moreover, renal FGF23 expression in the adenine model was unaffected by  $1,25-(\text{OH})_2\text{D}_3$  treatment, indicating a different mode of regulation compared to bone FGF23. These results suggest a possible role of FGF23 in a paracrine or autocrine regulation of CYP27B1 and CYP24 in the kidney with relevance to vitamin D deficiency observed in CKD.

**Disclosures:** D. Cuerrrier, None.

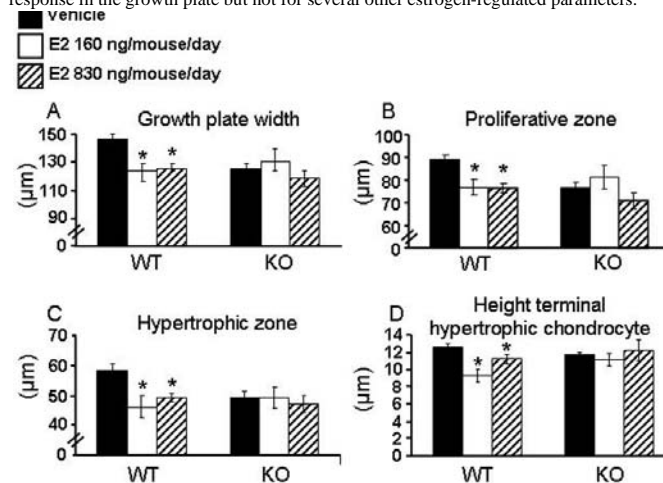
## SUI179

**The Role of the G Protein-coupled Receptor GPR30 in Effects of Estrogen in Ovariectomized Mice.** S. H. Windahl<sup>1</sup>, N. Andersson<sup>1</sup>, A. Chagin<sup>\*2</sup>, U. E. Mårtensson<sup>\*3</sup>, H. Carlsten<sup>\*1</sup>, B. Olde<sup>\*3</sup>, L. M. F. Leeb-Lundberg<sup>\*3</sup>, C. Swanson<sup>\*1</sup>, L. Sälvendahl<sup>\*2</sup>, M. K. Lagerquist<sup>1</sup>, C. Ohlsson<sup>1</sup>. <sup>1</sup>Department of Medicine, Center for Bone Research, Sahlgrenska Academy, Gothenburg, Sweden, <sup>2</sup>Department of Woman and Child Health, Pediatric Endocrinology Unit, Karolinska Institute, Stockholm, Sweden, <sup>3</sup>Department of Experimental Medical Science, Unit of Drug Target Discovery, Lund University, Lund, Sweden.

Estrogen exerts a variety of important physiological effects, which have been suggested to be mainly mediated via the two known nuclear estrogen receptors (ERs)  $\alpha$  and  $\beta$ . *In vitro* studies suggest that the G protein-coupled receptor GPR30 is also a functional estrogen receptor. The aim of the present study was to determine the *in vivo* role of GPR30 for several well-known estrogen-regulated parameters.

Three-month-old ovariectomized (ovx) GPR30<sup>-/-</sup> and WT mice were treated with either placebo or different doses of estradiol (0, 30, 70, 160 or 830 ng/mouse/day) (E2). The estrogenic responses on most investigated parameters including increase in bone parameters (total body BMD, trabecular bone mineral density and cortical bone mineral content), increase in uterine weight, thymus atrophy, fat mass reduction and increase in bone marrow cellularity were for all investigated E2 doses similar in WT and GPR30<sup>-/-</sup> mice. However, the inhibitory effect of E2 on longitudinal bone growth, reflected by reduced femur length and distal femur growth plate width, seen in the adult ovx WT mice was not seen in the ovx GPR30<sup>-/-</sup> mice.

These *in vivo* findings demonstrate that GPR30 is required for a normal estrogenic response in the growth plate but not for several other estrogen-regulated parameters.



**Disclosures:** S.H. Windahl, None.

## SU180

**Cell Type Specific Regulation of Transcription by Estrogen.** S. A. Krum<sup>1</sup>, M. Brown<sup>\*2</sup>. <sup>1</sup>Orthopaedic Surgery, UCLA, Los Angeles, CA, USA, <sup>2</sup>Medical Oncology, Dana-Farber Cancer Institute, Boston, MA, USA.

Estrogen is an important regulator of female development, and also plays a role in the bone, among other tissues. The effects of estrogen are mediated by two nuclear receptors: estrogen receptor alpha (ER $\alpha$ ) and estrogen receptor beta (ER $\beta$ ). ER $\alpha$  and ER $\beta$  are both expressed in many cell types, but at lower levels than those found in reproductive tissues. The mechanism by which estrogen exerts tissue-specific effects, remains to be explained. We have compared the global gene expression profile of the MCF7 breast cancer cell line with that of the osteoblast-like cell line U2OS-ER $\alpha$  by expression microarrays. We find that fewer than 10% of the estrogen-regulated genes are common to both cell types. We have validated many of these genes in primary calvarial osteoblasts. To dissect the mechanism underlying the cell-type specific estrogen regulation of gene expression in MCF7 and U2OS-ER $\alpha$  cells, we compared the ER $\alpha$  binding sites in the two cell types obtained by performing chromatin immunoprecipitation (ChIP) on genomic tiling arrays (ChIP-on-chip). ER $\alpha$  binding in U2OS-ER $\alpha$  cells best correlates with genes up-regulated in U2OS-ER $\alpha$  cells, and not with down-regulated genes or genes up-regulated in MCF7 cells. Furthermore, we discovered a correlation between the number of ER $\alpha$  binding sites and gene induction. More specifically, ER $\alpha$  is recruited to multiple enhancers near genes that are induced by estrogen. Interestingly, while the forkhead factor FoxA1 plays a critical role in defining the ER $\alpha$  binding sites in MCF7 cells, it is not expressed in U2OS-ER $\alpha$  cells and forkhead motifs are not enriched in the ER $\alpha$  binding sites in these cells. Finally, the ER $\alpha$  binding sites are correlated with cell-type specific epigenetic histone modifications. These results support a model for the cell-type specific action of estrogen being driven primarily through cell-type specific ER $\alpha$  occupancy of epigenetically marked cis-regulatory regions of target genes.

**Disclosures:** S.A. Krum, None.

This study received funding from: Susan G. Komen for the Cure.

## SU181

**Altered TNSALP Expression and Phosphate Regulation Contribute to Reduced Mineralization in Mice Lacking Androgen Receptor.** H. Kang<sup>\*</sup>, C. Huang<sup>\*</sup>, K. Huang. Graduate Institute of Clinical Medical Sciences, Chang Gung University, Kaohsiung, Taiwan.

While androgen receptor (AR)-deficient mice developed osteopenia in endochondral bones due to the high bone turnover with increased bone resorption by osteoclasts, little is known about the mechanism of intramembranous bone loss contributed by AR in osteoblasts. Here we discovered a dramatic decrease in the area of calcification, new bone, and the number of osteocytes in calvaria from AR-deficient mice related to a reduction in mineralization caused, in part, by the diminished activity of AR-deficient osteoblasts. Enforced AR expression in differentiated osteoblasts boosts mineralization while knockdown of AR expression prevents androgen-induced mineralization. We identified the tissue-nonspecific alkaline phosphatase (TNSALP) and several members of small integrin binding ligand N-linked glycoprotein (SIBLING) gene family as androgen target genes required for AR-mediated bone formation. We show that inorganic phosphate (Pi) levels and TNSALP activity increased in response to androgen/AR and Pi signals increase the expression and translocation of AR. The ectopic expression of TNSALP or Pi partially rescued the bone loss due to AR deficiency. Thus, androgen/AR signaling plays an essential role in bone formation by coordinating the expression of genes associated with phosphate regulation.

**Disclosures:** H. Kang, None.

## SU182

**Ethanol Alters Estrogen Receptor Signaling and Activates Senescence Pathways in Osteoblasts While Estradiol Attenuates Ethanol Effects.** J. R. Chen<sup>\*1</sup>, O. P. Lazarenko<sup>\*2</sup>, R. L. Haley<sup>\*3</sup>, T. M. Badger<sup>\*2</sup>, M. J. Ronis<sup>\*1</sup>. <sup>1</sup>Pharmacology & Toxicology, University of Arkansas for Medical Sciences / Arkansas Children's Nutrition Center, Little Rock, AR, USA, <sup>2</sup>Physiology, University of Arkansas for Medical Sciences / Arkansas Children's Nutrition Center, Little Rock, AR, USA, <sup>3</sup>Physical Medicine and Rehabilitation, University of Arkansas for Medical Sciences / Arkansas Children's Nutrition Center, Little Rock, AR, USA.

Epidemiological and animal studies suggest that chronic alcohol consumption increases the risk of osteoporosis. However, the mechanisms underlying alcohol-induced bone loss are largely unknown. Using bone from chronic ethanol (EtOH) infused cycling female rats and osteoblastic cells *in vitro*, we have been able to determine the direct effects of ethanol (EtOH) and the interaction with estrogen signaling pathways in osteoblasts. We found that EtOH increased (P<0.05) estrogen receptor alpha (ER $\alpha$ ) and beta (ER $\beta$ ) RNA and encoded ER $\alpha$  protein levels in bone *in vivo* and in osteoblasts *in vitro* when analyzed by real-time RT-PCR and Western blotting. Treatment with 17 $\beta$ -estradiol (E2) subcutaneously, *in vivo*, or pre-treatment of osteoblasts with E2, *in vitro*, antagonized all the effects of EtOH on ER expression in bone and osteoblastic cells (P<0.05). ER $\alpha$  agonist propylpyrazoletriol (PPT) and ER $\beta$  agonist diarylpropionitrile (DPN) attenuated (P<0.05) EtOH-induced ER $\alpha$  and ER $\beta$  gene over expression, respectively, indicating non-ER specific actions of EtOH on osteoblasts. In addition E2 attenuated EtOH-induced activation of p53 and p21 in bone tissue *in vivo* and osteoblasts *in vitro*. UMR-106 osteoblastic cells were transiently

transfected with ER $\alpha$ -ECFP for ER $\alpha$  translocation analysis, and transiently transfected with ERE-TK-Luc or p21 promoter pGL2-p21-Luc reporter plasmids with or without co-transfection of ER $\alpha$  for expression analysis using luciferase assays. Similar to estrogen receptor antagonist ICI 182,780, EtOH blocked nuclear translocation of ER $\alpha$ -ECFP in the presence of E2. EtOH down-regulated (P<0.05) the ERE-luc reporter activity, however, E2 blocked this EtOH effect in osteoblasts. On the other hand, EtOH transactivated the luciferase activity of the p21 promoter region independent of additional exogenous ER $\alpha$ . EtOH activated (P<0.05) senescence-associated beta-galactosidase activity in rat stromal osteoblasts, while E2 attenuated this EtOH action. We conclude that inhibitory cross-talk between EtOH and E2 in osteoblasts on ERs, p53/p21 and cell senescence provides a pathophysiologic mechanism underlying bone loss and the protective effects of estrogens in alcohol-exposed females. *Supported in part by R01 AA12928 (M.J.R.).*

**Disclosures:** J.R. Chen, None.

## SU183

**Genetic Variations in Sex Steroid-Related Genes as Predictors of Serum Estrogen Levels in Men.** A. Eriksson<sup>1</sup>, M. Lorentzon<sup>1</sup>, L. Vandenput<sup>1</sup>, E. Labrie<sup>\*2</sup>, M. Lindersson<sup>\*3</sup>, A. Syvänen<sup>\*3</sup>, E. S. Orwoll<sup>4</sup>, S. R. Cummings<sup>5</sup>, J. S. Lee<sup>\*6</sup>, J. M. Zmuda<sup>\*7</sup>, Ö. Ljunggren<sup>\*3</sup>, M. K. Karlsson<sup>\*8</sup>, D. Mellström<sup>1</sup>, C. Ohlsson<sup>1</sup>. <sup>1</sup>Center for Bone Research at the Sahlgrenska Academy, Göteborg University, Göteborg, Sweden, <sup>2</sup>Laboratory of Molecular Endocrinology and Oncology, Laval University Hospital Research Center and Laval University, Québec, QC, Canada, <sup>3</sup>Department of Medical Sciences, Uppsala University, Uppsala, Sweden, <sup>4</sup>Oregon Health and Science University, Portland, OR, USA, <sup>5</sup>CPMC Research Institute, UC San Francisco, San Francisco, CA, USA, <sup>6</sup>Department of Internal Medicine, University of California Davis, Sacramento, CA, USA, <sup>7</sup>Department of Epidemiology, University of Pittsburgh, Pittsburgh, PA, USA, <sup>8</sup>Department of Clinical Sciences, Lund University, Lund, Sweden.

Epidemiological studies have reported that many conditions including osteoporosis are associated with serum levels of sex steroids. Sex steroid levels are believed to be influenced by genetic factors, but there is no reported genetic variation, which in a reproducible manner predicts estradiol (E2) or testosterone (T) levels in men. The aim of this study was to identify genetic variations in sex steroid-related genes which are associated with serum E2 and/or T in men. Single nucleotide polymorphism (SNP) markers (n= 604) with minor allele frequencies of  $\geq 5\%$  in 50 major sex-steroid related genes were selected from HapMapData Rel 21a/phaseII using a pairwise correlation method ( $r^2 \geq 0.80$ ), including 10 kb upstream and 5 kb downstream of each gene. Genotyping of these markers was performed on the Illumina Bead Station system in the GOOD study (n=1041 men, 18.9 $\pm$ 0.6 yr). Replications of significant associations were performed in the MrOS Sweden study (n=2568 men, 75.5  $\pm$  3.2 yr) and in the MrOS US study (n=1922 men, 73.5  $\pm$  5.8 yr). Serum E2, T and estrone (E1) levels (n=5531) were analyzed using gas chromatography/mass spectrometry (GC-MS). The screening in the GOOD cohort identified the SNP rs2470152 in intron 1 of the CYP19 gene, which codes for aromatase, responsible for the final step of biosynthesis of E2 and E1, to be most significantly associated with E2 levels (p = 2  $\times$  10<sup>-6</sup>). This association was confirmed both in the MrOS Sweden study (p = 9  $\times$  10<sup>-7</sup>) and in the MrOS US study (p = 1  $\times$  10<sup>-4</sup>). When analyzed in all subjects (n=5531) rs2470152 was clearly associated with both E2 (p = 2  $\times$  10<sup>-14</sup>) and E1 (p = 8  $\times$  10<sup>-19</sup>) levels. Subjects with the GG genotype had 8-13 % higher E2 and 10-16 % higher E1 levels, depending on cohort, than subjects with the AA genotype. AG subjects had intermediate levels. In conclusion, the SNP rs2470152 of the CYP19 gene is clearly associated with serum E2 and E1 levels in men. Further studies are needed to determine the impact of this SNP for sex-steroid-related disorders such as osteoporosis, and fractures.

**Disclosures:** A. Eriksson, None.

## SUI84

**Increased Caloric Intake in Energy Deficient Exercising with Functional Hypothalamic Amenorrhea Women Is Associated with Decreased Ghrelin and Increased Bone Formation: Preliminary Data from an RCT to Reverse Exercise-Associated Menstrual Disturbances.** J. L. Scheid<sup>\*1</sup>, N. I. Williams<sup>2</sup>, S. L. West<sup>\*1</sup>, S. Awdishu<sup>\*1</sup>, M. J. De Souza<sup>2</sup>. <sup>1</sup>University of Toronto, Toronto, ON, Canada, <sup>2</sup>Penn State University, University Park, PA, USA.

Exercise-associated menstrual disturbances (EAMD), such as amenorrhea, are observed secondary to a chronic energy deficiency and are associated with low bone mass. We report data from an ongoing 12 month randomized controlled trial to determine the effectiveness of increased caloric intake to reverse amenorrhea, and improve bone health. Subjects were categorized by menstrual and ovulatory status into either an ovulatory control (OvCon, n=13), EAMD + calories (EAMD+Cal, n= 5) group, or an EAMD control group (n= 2). Subjects in the EAMD+Cal group were required to increase daily caloric intake (20-30%) above their baseline energy needs. Resting energy expenditure (REE), dietary energy intake, daily energy expenditure, body composition, serum markers of bone formation (PINP) and resorption (sCTX), fasting ghrelin and triiodothyronine (TT3), and daily urinary ovarian steroids (E1G and PdG) were assessed during the study. Statistical analysis includes t-tests to determine baseline differences, repeated measures ANOVA to determine longitudinal differences between baseline and intervention, and correlations to identify significant associations. Presented are preliminary data for 13 OvCon and 5 EAMD+Cal participants who have completed 2 of 12 months of intervention. Groups were similar for age (25.1±1.6 y), weight (58.7±1.9 kg) and history of exercise (605±143 min/week). The EAMD+Cal group experienced a mean increase in body weight of 0.4kg and an increased energy prescription of 536±69 kcal/day above baseline energy status. A significant time x group interaction was observed for change in caloric intake (p=0.020), body fat percentage (p=0.024), and ghrelin (p=0.040). Body fat was increased and ghrelin was decreased over time in the EAMD+Cal compared to the OvCon group. No changes were observed in REE, TT3, PINP, or sCTX. Decreases in ghrelin were associated with a higher caloric prescription ( $r=-0.18$ ,  $p=0.006$ ) and decreases in ghrelin were associated with increased bone formation ( $r=0.956$ ,  $p=0.011$ ) in the EAMD+Cal group. Increased caloric intake and or weight gain was associated with 3/5 and 4/5 subjects resuming menses within 4 and 6 months, respectively. Our preliminary results suggest that increased caloric intake and related weight gain were associated with the resumption of menses in exercising amenorrheic women. Increased caloric intake was associated with reductions in ghrelin, and increased bone formation.

**Disclosures:** J.L. Scheid, None.

This study received funding from: US DoD (PR054531) and CIHR.

## SUI85

**The Antiapoptotic Action of 17 $\beta$ -Estradiol in Skeletal Muscle Cells Involves ERK 1/2, p38 MAPK, ASK-1 and HSP27.** A. C. Ronda\*, N. Zanetti\*, A. Vasconsuelo\*, L. Milanese\*, A. Russo de Boland\*, R. L. Boland. Dept. Biología, Bioquímica & Farmacia, Universidad Nacional del Sur, Bahía Blanca, Argentina.

Estrogens exert antiapoptotic effects in various cell types, e.g. vascular endothelial, smooth muscle and breast cancer cells. We have previously reported that 17 $\beta$ -estradiol inhibits apoptosis through estrogen receptors with non-nuclear localization, e.g. mitochondria and endoplasmic reticulum, in the mouse skeletal muscle C2C12 cell line. The steroid hormone abrogates DNA damage, PARP cleavage and cytochrome c release induced by H<sub>2</sub>O<sub>2</sub> or etoposide. This mechanism involves fast activation of the PI3K/Akt/Bad pathway. It was demonstrated that the estrogen also triggers rapid phosphorylation of ERK 1/2 and p38 MAPK. Using specific inhibitors it was shown that both MAPKs mediate the effects of estradiol on Akt and Bad phosphorylation, cytochrome c and Smac/Diablo release, caspase 3 and PARP cleavage, and morphological changes of the cells. Interestingly, we found that ERK1/2 activated by 17 $\beta$ -estradiol is located mainly in mitochondria. Parallel studies showed that the interaction between proapoptotic kinase ASK-1 with phospho-Akt increases in presence of estrogen. This fact suggests another possible point of negative regulation of the apoptotic cascade by Akt. Furthermore, evidence was obtained that 17 $\beta$ -estradiol at longer exposure times increases the expression of HSP27. Assays under apoptotic conditions linked this chaperone to the protective action of the hormone, specifically regulating caspase-3 activity. Immunocytochemistry and co-immunoprecipitation assays revealed interaction of HSP27 and ER  $\beta$  in mitochondria. Altogether, these data imply that ERK 1/2, p38 MAPK, ASK-1 and HSP27 play a role in the mechanism underlying the antiapoptotic action of 17 $\beta$ -estradiol in skeletal muscle cells.

**Disclosures:** R.L. Boland, None.

## SUI86

**Multinuclear Expression of ER $\alpha$  in Mature Osteoclasts.** M. Youn\*, I. Takada\*, S. Kondou\*, Y. Imai, S. Kato. Institute of Molecular and Cellular Biosciences, University of Tokyo, Tokyo, Japan.

Osteoclasts became multinucleate during processes of maturation that are governed by a number of regulators including transcription factors. Although osteoclasts, as multinucleate cells, are unique among bone cells, little is still known about gene regulation network between multiple nuclei in the mature osteoclast. To address this point, we tested if gene expression occurs in a limited number or all of the osteoclastic nuclei. For this

purpose, the expressions of estrogen receptor alpha (ER $\alpha$ ) transcript and protein were measured in mature osteoclasts since we recently provided genetic evidence that the osteoprotective estrogen action was mediated by the osteoclastic ER $\alpha$ . In multinucleated osteoclasts differentiated from RAW264 cells or bone marrow cells by stimulation with receptor activator of nuclear factor-kappaB (RANKL) / Macrophage colony-stimulating factor (M-CSF), levels of ER $\alpha$  mRNA and protein were measured by real-time RT-PCR and immunocytochemistry, respectively. Notably, ER $\alpha$  was expressed in all multiple nuclei in osteoclasts of both origins. Additionally, to understand molecular mechanisms of the osteoprotective estrogen action, the expression levels of some osteoclast-specific genes were examined. When mature osteoclasts were treated with estrogens, the expressions of Cathepsin K (CtsK) and tartrate-resistant acid phosphatase (TRAP) were reduced at both the mRNA and protein levels. However, estrogen treatment did not affect the size of multinucleated osteoclasts or the number of nuclei in a mature osteoclast. These results indicate that in mature osteoclasts, estrogens inhibit the expression of osteoclast-specific genes through ER $\alpha$  present in all of multiple nuclei. Functional competence of the receptor was further confirmed by detection of Ser167-phosphorylated ER $\alpha$  in all nuclei of a single osteoclastic cell, suggesting that ER $\alpha$  protein is functional in mature osteoclasts in similar fashion as in other ER $\alpha$ -expressing cells like female reproductive cells, for example. Thus, these findings suggest that the osteoprotective estrogen action in mature osteoclasts is mediated by ER $\alpha$  in all of the cell multiple nuclei.

**Disclosures:** M. Youn, None.

This study received funding from: ERATO, Japan Science and Technology Agency.

## SUI87

**Carborane BE360, One of the Carbon-Containing Polyhedral Boron-Cluster Compounds, Is a New Type of Selective Estrogen Receptor Modulator.** M. Inada<sup>1</sup>, T. Tominari<sup>\*1</sup>, M. Hirata<sup>1</sup>, C. Matsumoto<sup>\*1</sup>, M. Takita<sup>1</sup>, Y. Endo<sup>\*2</sup>, C. Miyaura<sup>1</sup>. <sup>1</sup>Department of Biotechnology and Life Science, Tokyo University of Agriculture and Technology, Tokyo, Japan, <sup>2</sup>Division of Organic and Medicinal Chemistry, Tohoku Pharmaceutical University, Sendai, Japan.

Carboranes (dicarba-closo-dodecaboranes) are a class of carbon-containing polyhedral boron-cluster compounds having exceptional hydrophobicity, interacts hormone receptors in the result of computer docking simulation. We designed carborane compounds with an affinity for estrogen receptor (ER) and synthesized these compounds to search for effective agents to treat osteoporosis. Among several carborane compounds, we noted two compounds, BE120 and BE360. BE120 has a carborane structure with one phenol and is the most potent compound bearing a carborane cage exhibiting a binding affinity for ER. Its binding affinity with ER $\alpha$  is 10-fold greater than that of 17 $\beta$ -estradiol (E2). BE360 has a carborane structure with two phenols, and its ER binding affinities are 1.6-fold to ER $\alpha$  and 0.15-fold to ER $\beta$  compared with E2. To examine the estrogenic activity of these compounds in bone, ovariectomized (OVX) mice were given BE120, BE360 or E2 subcutaneously for 4 weeks using a miniosmotic pump. Reduced uterine weight in OVX mice was completely restored by not only E2 but also BE120. However, 1000-fold higher doses of BE360 did not increase the uterine weight of OVX mice. Histological analysis also showed that BE360 did not exhibit any estrogenic activity in the uterus. In OVX mice, the trabecular bone volume of the femoral distal metaphysis was reduced markedly, when measured by DEXA and histological analysis. Treatment with BE120 at 1-30 ng/head/day markedly prevented bone loss in OVX mice, and its effective doses in bone and uterus were similar to those of E2. BE360 at 1-30  $\mu$ g/head/day dose-dependently restored bone loss in OVX mice to a sham level without estrogenic action in the uterus. Therefore, 1000-fold higher doses of BE360 were needed to prevent bone loss in OVX mice compared with that of E2 and BE120. These results indicate that BE360 binds to ERs and exhibits estrogenic action in bone to prevent bone loss without inducing estrogenic action in the uterus, suggesting its possible application to osteoporosis as a new type of selective estrogen receptor modulator (SERM). To examine the effects of BE360 in androgen deficiency, male mice were sham-operated or orchidectomized (ORX) and a subgroup of ORX mice was treated with BE360. Treatment with BE360 at 1-30  $\mu$ g/head/day prevented bone loss in ORX mice without androgenic action on the sex organs. We currently tested anti-androgenic carboranes in ORX mice to clarify androgenic action in male bone metabolisms, which may be a new candidate of selective androgen receptor modulator (SARM).

**Disclosures:** C. Miyaura, None.

## SUI88

**Genetic Variation of the SHBG Gene, SHBG Levels and Bone Parameters.** L. Stolk<sup>\*1</sup>, F. Rivadeneira<sup>1</sup>, J. B. J. van Meurs<sup>1</sup>, P. Arp<sup>\*1</sup>, M. Jhamai<sup>\*1</sup>, M. C. Zillikens<sup>\*1</sup>, A. Hofman<sup>\*2</sup>, F. H. de Jong<sup>\*1</sup>, H. A. P. Pols<sup>\*1</sup>, A. G. Uitterlinden<sup>1</sup>. <sup>1</sup>Internal Medicine, Erasmus MC, Rotterdam, Netherlands, <sup>2</sup>Epidemiology, Erasmus MC, Rotterdam, Netherlands.

Sex hormone-binding globulin (SHBG) binds testosterone (T) and estradiol (E2), thereby regulating their access to target tissue. Several studies showed that elderly men and women with high SHBG levels had higher risk for fractures (fx) and lower lumbar spine bone mineral density (LS-BMD) and found SHBG polymorphisms to be associated with SHBG levels in men and women, and hip BMD in men. In elderly men and women of the Rotterdam study we investigated the effect of SHBG levels (determined by direct immunoassays) on both BMD and fx risk, and also studied the association of 24 SNPs in a 154kb region surrounding the SHBG-gene with SHBG levels, estradiol levels and BMD and fx risk. Correlation of SHBG-levels, LS and femoral neck (FN) BMD was calculated using linear regression. The effect of quartiles (Q1 - Q4) of plasma SHBG on fx was

calculated using logistic regression. In 5974 subjects Illumina 550K SNP genotypes were available while 2 additional SNPs were genotyped using Taqman. Association of 24 SNPs (MAF >5%) with plasma SHBG (n=1339 subjects with data (swd)) and E2 levels (n=1133 swd), LS-BMD (n=4757 swd), FN-BMD (n=4758 swd) and vertebral (n=2914 swd) and non-vertebral (n=5596 swd) fx risk were calculated using a X2 test. Associations were significant if  $p < 2.08 \times 10^{-3}$  (Bonferroni corrected). SHBG levels correlated with LS-BMD  $r = -0.25$ ,  $p = 4 \times 10^{-19}$  (0.03 g/cm<sup>2</sup> (0.17SD) difference for Q1 vs. Q4 of SHBG), and with FN-BMD  $r = -0.30$ ,  $p = 7 \times 10^{-29}$  (0.026 g/cm<sup>2</sup> (0.2SD) difference for Q1 vs. Q4 of SHBG) in 1280 subjects. Plasma SHBG levels were 3.5 nmol/L (9%) higher in subjects with vertebral fx (n=795 swd,  $p=0.03$ ), and 5.2 nmol/L (13%) higher in subjects with non vertebral fx (n=1435 swd,  $p=1.4 \times 10^{-6}$ ). 9 out of the 24 SNPs were associated with plasma SHBG levels ( $P < 2.08 \times 10^{-3}$ ) with an allele-dose effect varying between 4.2 (10.5%) and 2.1 (5%) nmol/L per allele. All 9 SNPs are located in or 5' of the SHBG gene, with the two SNPs with the highest effect size within 5 kb in the 5' region. For LS and FN BMD and for fractures none of the SNPs were associated. In this study we confirmed the correlation of plasma SHBG-levels with LS and FN BMD, and with fracture risk. We found 9 SNPs 5' or in the SHBG gene to be associated with plasma SHBG-levels, with 8.4 nmol/L (21%) difference between extreme genotypes. From this and the SHBG levels studies we then expect a 0.008 g/cm<sup>2</sup> difference (0.04 SD) in BMD, while we only had power to detect a 0.085 SD difference. Thus, larger studies are required to confirm a genetic effect while also other loci than SHBG might contribute to explain variance in SHBG levels, and thus with BMD and/or fx risk.

**Disclosures:** L. Stolk, None.

## SU189

**Estrogens Reverse a Potentiating Effect of the Unliganded Estrogen Receptor on BMP-induced Transcription and Osteoblastogenesis by Promoting ERK-dependent Smad1 Phosphorylation at the Linker Region.** M. Martin-Millan, L. Han, E. Ambrogini, A. Warren\*, M. Almeida, S. C. Manolagas. Center for Osteoporosis and Metabolic Bone Diseases, University of Arkansas for Medical Sciences and Central Arkansas Veterans Healthcare System, Little Rock, AR, USA.

Estrogens attenuate osteoclastogenesis and osteoblastogenesis, and maintain focal balance between resorption and formation by stimulating osteoclast and attenuating osteoblast apoptosis. But, it is unclear whether some or all of these effects are mediated via *cis* or *trans* interactions of the estrogen receptor (ER $\alpha$  or  $\beta$ ) with DNA or kinase-mediated extranuclear actions of the ERs. Based on evidence that estrogens suppresses BMP-induced osteoblastogenesis, and that Smad1/5/8 phosphorylation at the linker region by kinases such as ERK, JNK, and p38 promotes Smad proteasomal degradation, we have explored the possibility that estrogens inhibit osteoblastogenesis through a kinase-mediated action. We report that inducible expression of the ER $\alpha$  in the human osteoblast-like cell line U2OS, or transfection of C2C12 cells with increasing amounts of plasmids encoding the ER $\alpha$  or the ER $\beta$ , dose-dependently increased BMP-induced transcription, as measured by a Smad6-luciferase reporter construct and promoted the expression of BMP2-induced genes like Mx2, alkaline phosphatase and Smad 6. On the other hand, silencing the ER $\alpha$  by shRNA in C2C12, the pre-osteoblasts 2T3, or primary cultures of murine bone marrow, attenuated the effect of BMP on osteoblastogenesis and BMP-induced transcription, as did ICI182,780 ( $10^{-7}$  M), the ER antagonist that promotes its degradation. ER $\alpha$  was co-immunoprecipitated with Smad1 and Smad4 in all these cell models. Moreover, 17 $\beta$ -estradiol (E<sub>2</sub>) at  $10^{-7}$  M abrogated BMP-2 induced phosphorylation of Smad1/5/8 at the C-terminal region as well as BMP2-induced Smad6 transcription. Furthermore, E<sub>2</sub> as well as FGF, used as a positive control, phosphorylated Smad1 at the linker region, as determined by an antibody specific for phospho-Smad1<sup>MAPK</sup> (p-serine 214), generously provided by Dr. De Robertis (Howard Hughes Medical Institute, Los Angeles, CA). And, the effects of E<sub>2</sub> on BMP-2 induced Smad1/5/8 phosphorylation at the C terminus and Smad6 transcription were completely reversed by the specific MEK antagonist PD98059. Consistent with this, E<sub>2</sub> inhibited BMP-2 induced differentiation in calvaria derived osteoblasts from knock-in mice in which classical ER $\alpha$  signaling through ERE sites has been selectively eliminated while preserving non-classical signaling (ER $\alpha$ <sup>NERKL</sup>). These results provide a molecular mechanism of the suppressive effect of estrogens on osteoblastogenesis and support the notion that this effect is exerted via an extranuclear action of the ER.

**Disclosures:** M. Martin-Millan, None.

## SU190

**Low Serum IGF-I Alters the Cortical Bone Response to Estrogen Deficiency.** J. C. Fritton\*, K. B. Emerton\*, H. Sun\*, Y. Kawashima\*, A. Sinofsky\*, W. Mejia\*, Y. Wu\*, M. B. Schaffler\*, M. Bouxsein\*, C. J. Rosen\*, S. Yakar\*. <sup>1</sup>Orthopaedics and Endocrine Divisions, Mount Sinai School of Medicine, New York, NY, USA, <sup>2</sup>Orthopedic Biomechanics Laboratory, Beth Israel Deaconess Medical Center, Harvard Medical School, Boston, MA, USA, <sup>3</sup>Maine Medical Center Research Institute, Scarborough, ME, USA.

Postmenopausal women with low circulating IGF-I levels have accelerated loss of BMD by DEXA. However, the contribution of cortical bone has not been teased out. In animal models, abrupt estrogen loss is associated with aggressive endosteal bone erosion that rapidly leads to degradation of mechanical function because of a high rate of marrow expansion. We hypothesized that the cortical response to ovariectomy-induced bone loss would be altered with low circulating IGF-I. To test our hypothesis we employed 12-week-old, liver IGF-I deficient (LID) mice that were generated previously using the

Cre-loxP system. LID mice exhibit 75% reductions in circulating IGF-I levels and 3-4fold increases in serum GH levels that are maintained 12 weeks after ovariectomy. Both 4 and 8 weeks after ovariectomy dampened resorption was revealed on the endosteal surface in LID versus control mice. Furthermore, maintenance of cortical bone area was found in LID mice (Figure 1, Table 1). We speculate that this altered adaptation represents a lag in osteoclastic response to ovariectomy, possibly due to increased serum GH, which remains elevated in LID female mice even 12 weeks post OVX. Further work is required to determine the mechanisms behind this cortical bone maintenance after abrupt estrogen loss. N.B. The first two authors contributed equally to this study.

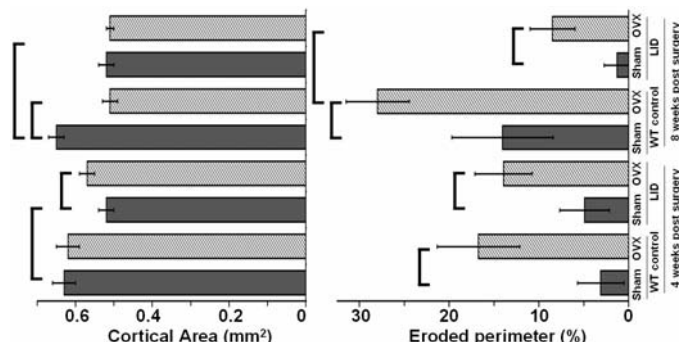


**Table 1. Histomorphometry of cortical bone at the endosteal surface of tibial midshaft 4 and 8 weeks post ovariectomy (OVX).**  
a,  $p < 0.05$  vs control sham, b,  $p < 0.05$  vs LID sham, c,  $p < 0.05$  vs control OVX.

	Control Sham	Control OVX	LID Sham	LID OVX
<b>4 Weeks</b>				
Tt.Ar (mm <sup>2</sup> )	0.79 (0.03)	0.86 (0.02)	0.65 (0.02)	0.71 (0.02)
Ma.Ar (%)	21 (1.5)	28.6 (2.4) <sup>a</sup>	19.5 (0.6)	19.6 (0.9) <sup>c</sup>
BFR (mm/d*100)	42.2 (5.1)	40.6 (4.2) <sup>a</sup>	39.1 (7.6)	51.1 (3.2)
<b>8 Weeks</b>				
Tt.Ar (mm <sup>2</sup> )	0.89 (0.01)	0.76 (0.01) <sup>a</sup>	0.74 (0.05) <sup>a</sup>	0.67 (0.01) <sup>c</sup>
Ma.Ar (%)	26.9 (1.9)	32.8 (2.0) <sup>a</sup>	29.3 (2.0)	23.7 (0.6) <sup>b,c</sup>
BFR (mm/d*100)	nd	5.7 (2.4) <sup>a</sup>	1.5 (1.6) <sup>b</sup>	11.6 (5.1)

**Disclosures:** J.C. Fritton, None.

This study received funding from: NIH (HS, MBS, MB, CJR, SY) & The Charles H. Revson Foundation (Fellowship to JCF).

## SU191

**Elevated Androgens Are Associated with Increased Bone Formation in Premenopausal Exercising Oligomenorrheic Women.** S. Awdishu\*, S. L. West\*, J. L. Scheid\*, M. J. De Souza\*. <sup>1</sup>Exercise Science, University of Toronto, Toronto, ON, Canada, <sup>2</sup>Kinesiology, Penn State University, State College, PA, USA.

Androgens have multiple actions on the skeleton, specifically, hyperandrogenism may promote osteoblast function. Oligomenorrhea (i.e., menses occurring at intervals of 36-90 days) in exercising women may be associated with hyperandrogenism. The purpose of this cross-sectional observational study was to evaluate the relationship between androgen status and bone formation in premenopausal exercising women. Serum procollagen type 1 propeptide (PINP), calculated free testosterone (cFreeT), calculated bioavailable testosterone (cbioT), free androgen index (FAI), sex-hormone binding globulin (SHBG), urinary estrone 3-glucuronide (E1G), and urinary pregnanediol 3-glucuronide (PdG) were measured repeatedly in 29 women. Volunteers were retrospectively grouped: 1) Exercising ovulatory group (ExOvul n=20), and 2) Exercising oligomenorrheic group (ExOligo, n=9). Independent t-tests and correlations to detect significant associations were performed. Subjects were similar with respect to age ( $24.0 \pm 1.44$  yrs), weight ( $57.8 \pm 1.3$  kg), height ( $163.5 \pm 1.0$  cm), and BMI ( $21.4 \pm 0.5$  kg/m<sup>2</sup>) ( $p > 0.05$ ). The ExOligo group had suppressed PdG AUC ( $p = 0.003$ ), and similar E1G AUC ( $p > 0.05$ ) to the ExOvul group. cFreeT ( $p = 0.003$ ), cbioT ( $p = 0.003$ ), and FAI ( $p = 0.006$ ) were elevated, while SHBG ( $p = 0.039$ ) was suppressed in the ExOligo group compared to the ExOvul group. Bone formation, as indicated by PINP, was elevated ( $p = 0.011$ ) in the ExOligo group compared with the ExOvul group ( $141.6 \pm 25.1$  and  $78.7 \pm 10.4$  ug/L, respectively). PINP was positively correlated with cFreeT ( $p = 0.031$ ,  $r = 0.451$ ), and with cbioT ( $p = 0.030$ ,  $r = 0.452$ ). The results of this study demonstrate that oligomenorrhea in premenopausal exercising women is associated with hyperandrogenism, and elevated androgen levels may be contributing to the etiology of increased bone formation in these women.

**Disclosures:** S. Awdishu, None.

This study received funding from: US DoD (PR054531), and CIHR.



## SU192

**Overexpression of Androgen Receptor in Mature Osteoblasts and Osteocytes Inhibits Osteoblast Differentiation.** X. Zhang, K. Wiren. VA Medical Center, Oregon Health & Science Univ, Portland, OR, USA.

Mature osteoblasts/osteocytes are important mediators of androgen action in the skeleton. The direct mechanisms by which androgens influence bone cells are not fully understood. In these initial studies, we have focused on AR2.3-transgenic cultures with overexpression in mature osteoblasts/osteocytes. To assess the direct effects of androgen signaling during osteoblast differentiation, we are studying the effects of DHT on cell differentiation in primary calvarial cultures (mOB) derived from AR2.3-transgenic fetal mice. Osteoblast function is assessed by determining cell growth, alkaline phosphatase activity, and mineral deposition. Osteoblastic cells were isolated after collagenase digestion from neonatal calvaria from both wild-type (wt) and AR2.3-transgenic (AR2.3-tg) mice. Beginning at day 7, cultures were switched to differentiation medium containing 50µg/ml ascorbic acid. From day 14 on, 5 mM  $\beta$ -glycerophosphate was added to the differentiation media. The mineralization was assessed by alizarin red assay. AR2.3 stable cells were established by co-transfecting with col2.3AR and pRSVneo plasmid DNA in MC3T3-E1 cells under G418 selection. Changes in gene expression (type I collagen and osteocalcin) were determined with qRT-PCR analysis. We first determined the level of AR abundance in both wt and AR2.3-tg cultures by Western analysis, with polyclonal rabbit AR antibodies (ARN-20). As expected, AR levels increase during differentiation in both cultures. The highest level of AR overexpression noted after day 21 in AR2.3-tg cultures. We then assessed growth characteristics of wt and AR2.3-tg cultures without hormone treatment. Osteoblastic cells from both transgenic and wild-type mice display similar growth kinetics. We also determined mineralization capacity, and observed no significant difference between AR2.3-tg versus wt cultures without hormone addition. To assess the consequences of androgen signaling, cultures were treated continuously with vehicle or  $10^{-8}$ M DHT (a nonaromatizable androgen) in charcoal-stripped serum. We characterized DHT action on osteoblast differentiation by determination of alkaline phosphatase (an osteoblast marker activity) and gene expression. Cultures treated with DHT for 14 days showed significant inhibition in alkaline phosphatase activity, with the most robust inhibition observed in AR2.3-tg cultures. Consistent with these results, analysis of gene expression after DHT treatment in stably transfected MC3T3 cultures employing the same promoter showed significant inhibition of both collagen and osteocalcin gene expression. These results are consistent with a reduction in osteoblast differentiation and may reflect the reduced osteoblast vigor observed in AR2.3-tg mice.

**Disclosures:** K. Wiren, None.

## SU193

**DHT Administration Is Effective for the Prevention of Hypogonadal Bone Loss.** A. A. Semirale, K. M. Wiren. Behavioral Neuroscience, Oregon Health & Science University, Portland, OR, USA.

Generally characterized as anabolic hormones, androgens have pervasive effects on many tissues including bone. Since low bone density and osteoporosis are often coupled with a hypogonadal state in both men and women, sex steroids are implicated in the maintenance of skeletal health. However, the specific effects of androgens on skeletal homeostasis remain poorly characterized and understudied. To gain better insight into the cell types important for mediating the effects of androgens on bone, we constructed and compared two distinct transgenic lines of mice employing different  $\alpha 1(I)$ -collagen promoter fragments to control skeletally-targeted AR overexpression. The col3.6 AR-transgenic (AR3.6-tg) mice demonstrate AR overexpression throughout the osteoblast lineage including the periosteum, while col2.3 (AR2.3-tg) mice have more restricted overexpression in mature osteoblasts and osteocytes. To assess the effect of the non-aromatizable androgen DHT on bone mineral, we compared a treatment versus prevention experimental paradigm in a rodent model of hypogonadal bone loss. AR-transgenic mice and wild-type B6D2F2 littermates were gonadectomized or sham operated, receiving subcutaneous DHT pellet implants either at the time of surgery or after a two month delay. Following six weeks of DHT administration, bone mineral was assessed by whole body DXA. In the treatment model, after two months in a hypogonadal state, wild type mice of both genders lose significant BMD and BMC. In this setting, six weeks of DHT treatment was effective at partially restoring lost bone mineral. In contrast, while both AR2.3-tg and AR3.6-tg male and female mice similarly lost BMD and BMC, they were resistant to the effects of DHT treatment over the same time frame. In the prevention model, during a high bone turnover state, both male and female wild type mice were protected from bone mineral loss when DHT was present compared to placebo controls. AR3.6-tg and AR2.3-tg male mice were also protected from bone loss following gonadectomy and AR3.6-tg males even gained BMD and BMC with six weeks of DHT administration. In contrast, female AR2.3-tg and AR3.6-tg mice did not benefit and continued to lose bone mineral in the presence of DHT. In summary androgen therapy may be beneficial for the prevention of hypogonadal bone loss, but is less effective at restoring lost bone.

**Disclosures:** A.A. Semirale, None.

## SU194

**Is Vitamin D Deficiency More Common in Children with Cerebral Palsy than in Healthy Children?** S. Yigit<sup>1</sup>, B. McKinney<sup>2</sup>, J. Pedersen<sup>\*1</sup>, B. Draheim<sup>\*2</sup>, F. Sylvester<sup>3</sup>. <sup>1</sup>Pediatric Endocrinology, Connecticut Children's Medical Center, Hartford, CT, USA, <sup>2</sup>Special Kids Support Center, Connecticut Children's Medical Center, Hartford, CT, USA, <sup>3</sup>Pediatric Gastroenterology and Nutrition, Connecticut Children's Medical Center, Hartford, CT, USA.

Children with cerebral palsy (CP) may be at higher risk for vitamin D (vit D) deficiency because of limited exposure to unfiltered sunlight, impaired nutrition because of swallowing dysfunction and use of anticonvulsants that increase vit D breakdown. In addition, vit D deficiency is more prevalent in Northern latitudes, even among healthy children. Therefore, we hypothesized that children with CP have a higher prevalence of vit D deficiency than their unaffected siblings. To test this hypothesis, we measured serum 25 (OH) vit D (RIA, Immunodiagnostic Systems Ltd, Fountain Hills, AZ) levels in children with CP and their unaffected, healthy siblings living in the same household. Seasonal differences were examined. Vit D deficiency was defined as serum level  $\leq 15$  ng/ml and vit D insufficiency as serum level  $\leq 20$  ng/mL based on previously published pediatric studies. 31 children with CP and 31 healthy siblings as controls between ages of 6-18 years were enrolled. 12.9 % of children with CP were vit D deficient while 29 % of the siblings were deficient. Vit D insufficiency was found in 29 % of children with CP and 38.7 % of healthy siblings. Only 20 % of the children with CP and 13 % of healthy siblings had 25 (OH) vit D level of more than 30 ng/ml, a level considered as optimal. While the mean 25 (OH) vit D levels were low on both groups, healthy siblings had a significantly lower 25 (OH) vit D levels compared to the children with CP (mean 25 (OH) vit D level for children with CP  $24.5 \pm 12.9$ , healthy siblings  $19.6 \pm 8.4$ ,  $p=0.04$ ). Low vit D levels were more prevalent in healthy siblings during winter season (mean 25 (OH) vit D level for children with CP  $33.2 \pm 16.5$ , healthy siblings  $19.8 \pm 8.8$ ,  $p=0.01$ ). 80 % of the healthy siblings were consuming  $\leq 1$  serving of milk per day. 58.8 % of the children with CP who had sufficient vit D levels were on supplemental tube feedings. Only one CP patient with vit D deficiency was on tube feedings but was on a ketogenic diet. None of the healthy siblings were taking vit D supplements while only 2 children with CP were on multivitamin supplements. Vit D deficiency/ insufficiency appear to be a prevalent public health care problem in both children with CP and healthy children. Although children with CP have higher risk factors, healthy siblings seem to have a higher prevalence of vit D deficiency/ insufficiency. Children with CP who are on tube feedings are less likely to develop vit D deficiency/ insufficiency. Healthy children may need counseling for prevention.

**Disclosures:** S. Yigit, None.

## SU195

**Vitamin D Toxicity Due to a Commonly Available Remedy From the Dominican Republic.** H. Lowe<sup>\*1</sup>, N. Binkley<sup>2</sup>, W. S. Blaner<sup>\*1</sup>, L. A. Plum<sup>\*2</sup>, J. P. Bilezikian<sup>1</sup>. <sup>1</sup>College of Physicians & Surgeons, Columbia University, New York, NY, USA, <sup>2</sup>University of Wisconsin-Madison, Madison, WI, USA.

Vitamin D toxicity is a known cause of hypercalcemia. We report a series of 8 patients presenting with hypercalcemia and found to be vitamin D toxic due to recently ingesting Soladek<sup>®</sup>, a supplement manufactured in the Dominican Republic and readily available over the counter in New York City (NYC). All patients were ambulatory with normal previous serum calcium levels, despite harboring, in many cases, a disorder that can be associated with hypercalcemia (squamous cell cancer (n=1), lymphoma (n=1), hyperthyroidism (n=2), mycobacterial or pneumocystis infection (n=2)). Cases presented with hypercalcemia (range: 10.8-17.2 mg/dl, nl: 8.4-9.8), suppressed PTH (range: <3 to 11 pg/ml), elevated 25(OH)Vitamin D (25OHD, range: 94-525 ng/ml, nl: 20-57) and in some cases elevated 1,25(OH)<sub>2</sub>Vitamin D (1,25OHD, range: 39 to >200 pg/ml, nl: 15-75) levels. All patients were treated with aggressive hydration, and all but 2 received a bisphosphonate and/or glucocorticoid, with subsequent normalization of serum calcium and a substantial decrease in vitamin D levels over weeks to months. Soladek is commonly used in the Dominican Republic for prevention and treatment of the common cold or any general illness. According to the manufacturer's label, each 5mL vial contains Vitamin D (600,000 IU), Vitamin A (120,000 IU), and Vitamin E (5 mg). Instructions are for biweekly to monthly dosing, or as directed by a physician. We purchased 2 vials of the product from the same lot, at a Dominican market in NYC. Laboratory analysis by HPLC revealed that the vial of supplement (5 mL) contains Vitamin D3 (864,000 IU) and Vitamin A (predominantly retinyl palmitate 123,500 IU). These amounts are, respectively, >400X and 5X the safe daily upper limits of Vitamins D and A as recommended by the Food and Nutrition Board of the Institute of Medicine. The circulating 25OHD was solely due to endogenous conversion of vitamin D because there was no 25OHD in the preparation itself as assayed by reverse phase HPLC. This report calls attention to a preparation readily available in the Dominican Republic (and therefore also in many parts of the United States) that contains toxic amounts of vitamins D and A, and can be associated with hypercalcemia. In most of these patients, there was another potential cause of hypercalcemia in addition to the use of Soladek. Elevated levels of 25OHD, to concentrations that are often associated with hypercalcemia, were most likely due to exogenous intake from the vitamin supplement. Although hypercalcemia due to exogenous use of vitamin D is unusual, it is important to consider it in the differential diagnosis particularly among individuals who have access to Soladek.

**Disclosures:** H. Lowe, None.



## SU196

**Improved Motor Performance in Vitamin D Deficient Mice with VDRMs.** L. Porras\*, Q. Zeng\*, R. L. Cain\*, K. Stayrook\*, L. Burris\*, M. Carson\*, J. Dodge\*, J. Andrews\*, H. U. Bryant, M. Sato, Y. L. Ma. Eli Lilly and Company, Indianapolis, IN, USA.

Vitamin D receptors are found expressed in the muscle, brain and the spinal cord, the areas involved in the regulation of motor function and behavior. In humans, vitamin D deficiency is often accompanied by muscle pain, weakness and other neuromuscular disorders. In vitamin D receptor knock out mice, neurological and behavioral disorders have been observed; therefore vitamin D receptors are known to play an important role in neuromuscular function. The goals for our study were to examine whether neuromuscular coordination was impaired in mice maintained on a vitamin D deficient diet and how vitamin D receptor ligands would affect motor performance. Female Balb/C mice were maintained on either a vitamin D deficient (D-) or normal diet from the embryo gestation stage, or weanling stage until 6 weeks of age, or older. Serum calcium levels were not significantly altered in mice fed D- from the weanling stage, but were slightly decreased in mice maintained on D- from the embryo gestation stage. Body weight of D- mice tended to be slightly heavier than normal diet fed mice, which was due to increased whole body fat to lean mass ratio, as accessed by quantitative magnetic resonance (Echo systems). Although muscle wet weight and grip strength were not significantly different, inverted screen testing revealed a 20-50% impairment in the mobility of mice fed D- when compared to normal diet fed mice. Non-hypercalcemic doses of 1, 25(OH)<sub>2</sub>D<sub>3</sub> and our orally active, tissue selective, non-secosteroidal, VDRM dose-dependently improved inverted screen performance of D- fed mice. Fiber cross sectional area analyses showed a trend towards bigger gastrocnemius muscles of 1,25(OH)<sub>2</sub>D<sub>3</sub> and VDRM-treated mice. Our data indicate that 1,25(OH)<sub>2</sub>D<sub>3</sub> and VDRMs have positive effects in regulating motor performance in mice maintained on a vitamin D deficient diet.

**Disclosures:** Y.L. Ma, Eli Lilly 3.

## SU197

**Measurements of Vitamin D Do Not Necessarily Reflect What You Give to Your Patients.** E. Cavalier<sup>1</sup>, C. Cormier<sup>2</sup>, J. Souberbielle<sup>3</sup>. <sup>1</sup>Clinical Chemistry, University Hospital of Liege, University of Liege, Liege, Belgium, <sup>2</sup>Rheumatology, University Paris-V, Hôpital Cochin, AP-HP, Paris, France, <sup>3</sup>Clinical Chemistry, University Paris Descartes, Inserm U845, and, Hôpital Necker, Service d'Explorations Fonctionnelles, AP-HP, Paris, France.

A Laboratory error is defined by ISO 22369 Standard as « Any error, from analyses prescription to the final report of the results, bad interpretation of these ones and inappropriate reaction in front of them ». We present here what might thus be considered as a laboratory error in a 25-hydroxyvitamin D (25VTD) determination. Indeed, we report the case of a 60 yo woman diagnosed as having a VTD deficiency (serum 25VTD measured with the automated Roche Elecsys method at 12 ng/mL) who was given a single 60000IU VTD2 dose. Two weeks later, the serum 25VTD measured with the same assay did not change and was still at 11 ng/mL. She was then referred to our unit for extensive laboratory testing. All the tests that we performed 3 month later were normal, including 25VTD (50 ng/mL with the Diasorin RIA). In order to explain the discrepant results between the Roche and Diasorin methods, we studied in 11 healthy subjects (5 men, 6 women aged 21-62) the elevation of 25VTD after a single 60000IU VTD2 dose. Samples were drawn before (D0), 7 (D7) and 28 days (D28) after the supplementation and we used a third method (HPLC), which separates 25VTD2 and 25VTD3, as a reference. At D0, the mean 25VTD concentration±SD of our volunteers was similar with the RIA (29.3±6.8 ng/mL) and the Elecsys (30.2±6.0 ng/mL) but slightly higher (p<0.001) with HPLC (33.1±8.1 ng/mL). Five, 6 and 8 subjects had a 25VTD concentration >30 ng/mL on D0 with RIA, Elecsys, and HPLC respectively. At D7, 25VTD increased only with the RIA and HPLC assays. This increase was due solely to an increase in 25VTD2, as indicated by the HPLC data. All the subjects had a 25VTD concentration >30 ng/mL with the RIA and HPLC assay, whereas this was the case in only two subjects when the Elecsys assay was used. At D28, 25VTD remained >30 ng/mL in all subjects with RIA and HPLC, whereas the level was <30 ng/mL in all subjects with the Elecsys assay. Although skin exposure to UVB produces VTD3 and food sources of VTD contain mainly VTD3, supplementation is often made with VTD2, especially in the USA. As long as VTD2 is available, it is mandatory to measure 25VTD with a method that recognizes both 25VTD2 and 25VTD3. The case briefly described above shows that measuring 25VTD with an assay exclusively specific for 25VTD3, like Roche Elecsys, may underestimate VTD status and thus potentially lead to overtreatment, and to expensive and stressful explorations.

**Disclosures:** E. Cavalier, None.

## SU198

**Cooperativity between VDR and Liver Enriched Inhibitory Protein (LIP) in the Regulation of TRPV6 Identifies a Novel Function for LIP as a Transcriptional Activator.** B. S. Benn<sup>\*1</sup>, M. B. Meyer<sup>\*2</sup>, J. W. Pike<sup>2</sup>, S. Christakos<sup>1</sup>. <sup>1</sup>Biochemistry and Molecular Biology, UMDNJ- New Jersey Medical School, Newark, NJ, USA, <sup>2</sup>Biochemistry, University of Wisconsin, Madison, WI, USA.

1,25-Dihydroxyvitamin D<sub>3</sub> (1,25(OH)<sub>2</sub>D<sub>3</sub>) is known to increase the rate of calcium entry into the intestinal cell. Recently the apical calcium channel TRPV6, which is co-localized with calbindin and is induced by 1,25(OH)<sub>2</sub>D<sub>3</sub> in intestine, has been identified, suggesting a calcium entry mechanism. Previous studies have shown that vitamin D response elements (VDREs) located at -1.2, -2.1 and -4.3 kb in the human TRPV6 promoter are required for the full transcriptional response to 1,25(OH)<sub>2</sub>D<sub>3</sub> and that the VDREs at -2.1 and -4.3 appear to be most significant for 1,25(OH)<sub>2</sub>D<sub>3</sub> mediated transcriptional activation. C/EBPβ has been shown previously to enhance 1,25(OH)<sub>2</sub>D<sub>3</sub> mediated 24(OH)ase promoter activation. To determine if the C/EBPβ isoforms LIP and LAP are involved in 1,25(OH)<sub>2</sub>D<sub>3</sub> mediated hTRPV6 transcription, Caco-2 cells were transfected with the hTRPV6 promoter (-7000/+160) and increasing concentrations of LIP or LAP in the presence or absence of 10<sup>-8</sup>M 1,25(OH)<sub>2</sub>D<sub>3</sub>. Increasing concentrations of LIP, which has been reported to repress LAP induced transcription, was consistently found to result in a significant potentiation of 1,25(OH)<sub>2</sub>D<sub>3</sub> induced hTRPV6 transcription (2-4 fold; p<0.05 compared to 1,25(OH)<sub>2</sub>D<sub>3</sub> treatment alone; maximal 1,25(OH)<sub>2</sub>D<sub>3</sub> induced transcription in the presence of LIP was 20-25 fold). LIP alone had no effect on hTRPV6 transcription. Increasing concentrations of LAP, C/EBPα or C/EBPδ in the presence or absence of 1,25(OH)<sub>2</sub>D<sub>3</sub> also had no effect on hTRPV6 transcription. In COS-7 cells LIP enhancement of VDR mediated hTRPV6 transcription was not observed, suggesting cell type specificity. LIP enhancement of 1,25(OH)<sub>2</sub>D<sub>3</sub> induced transcription was also observed using a hTRPV6 promoter construct with a mutation in the -2.1 VDRE but with a functional -4.3 VDRE. No effect of LIP was observed using a hTRPV6 promoter construct with the -4.3 and -2.1 VDREs mutated. Caco-2 cells were transfected with an ~200bp construct containing the -4.3 VDRE upstream of the minimal thymidine kinase (tk) promoter. Results of these experiments yielded a similar enhancement with LIP. Further, co-immunoprecipitation experiments indicated that VDR and LIP interact. ChIP/re-ChIP experiments indicated that VDR and LIP can bind simultaneously to the hTRPV6 promoter at the -4.3 VDRE. These findings suggest a novel function for LIP where LIP acts as a transcriptional activator in the 1,25(OH)<sub>2</sub>D<sub>3</sub> mediated regulation of TRPV6.

**Disclosures:** B.S. Benn, None.

## SU199

**25-OH-D<sub>3</sub>-24-hydroxylase (CYP24A1): Mutagenesis and Activity Studies Reveal Important Residues Involved in Regioselectivity and Substrate Access.** M. Kaufmann\*, D. E. Prosser\*, B. O'Leary\*, V. Byford\*, G. Jones. Biochemistry, Queen's University, Kingston, ON, Canada.

CYP24A1 catalyzes the multi-step catabolism of 1α,25-(OH)<sub>2</sub>D<sub>3</sub> via alternative C24 or C23 hydroxylation pathways ending in either calcitroic acid or 1α,25-(OH)<sub>2</sub>D<sub>3</sub>-26,23-lactone. We set out to test the relative importance of A326, M416 & M252 in regioselectivity and catalytic efficiency using homology modeling, sequence alignment and mutagenesis of hCYP24A1 at residues of predicted structural & functional importance. Metabolism of 1α,25-(OH)<sub>2</sub>D<sub>3</sub> was studied in transfected V79-4 cells & products were analyzed by HPLC coupled- PDA, <sup>3</sup>H-detection or LC-MS. Previous research revealed that residues 326 in hCYP24A1 (PNAS 104:12673-8) and 416 in rCYP24A1 (Mol Pharmacol 70:120-8) are important determinants of regioselectivity. The substitution A326G in hCYP24A1, which catalyzes mainly C24-hydroxylation, resulted in a shift in preference to C23 hydroxylation, similar to the G326-containing opossum CYP24A1. The mutation T416M, in rCYP24A1, as it is in the human, also increased preference for C23-hydroxylation. In order to study which of these two residues is a more important determinant of regioselectivity in hCYP24A1, we created a A326G/M416T double mutant. The activity of the double mutant was characterized by mainly 1α,25-(OH)<sub>2</sub>D<sub>3</sub>-26,23-lactone production, similar to A326G, without any formation of tetranor-1α,25-(OH)<sub>2</sub>D<sub>3</sub>, which was the major C24-hydroxylation product formed by M416T. This suggested that A326 is a more important determinant of regioselectivity than M416 in hCYP24A1. Studies of M252T revealed a dramatic reduction in activity, and an apparent metabolic block in the C24-hydroxylation pathway. At μM substrate, CYP24A1 is characterized by the production of proximal pathway intermediates whereas nM substrate results in primarily terminal pathway products, tetranor-1α,23-(OH)<sub>2</sub>D<sub>3</sub> and calcitroic acid. At μM substrate, the M252T metabolic profile is dominated by 1α,24,25-(OH)<sub>3</sub>D<sub>3</sub>, with smaller amounts of 1α,23,25-(OH)<sub>3</sub>D<sub>3</sub>, and arrest of the 24-hydroxylation pathway occurring at the level of 24-oxo-1α,23,25-(OH)<sub>3</sub>D<sub>3</sub>. Unlike hCYP24A1, this profile remains unchanged as the substrate is decreased. These data suggest that substrate and initial product access to the active site is impeded by M252T, and that further metabolism towards calcitroic acid is blocked. Highly conserved Met252 is located near the end of the F-helix in a putative substrate access channel and could potentially interact with the substrate A-ring. In summary, we have identified two residues critical to CYP24A1 function, that enhance our knowledge of how 1α,25-(OH)<sub>2</sub>D<sub>3</sub> gains access to and is held within the active site.

**Disclosures:** M. Kaufmann, None.

## SU200

**A New 25-Hydroxy Vitamin D Assay on the IDS Automated Analyser 3x3™.** L. A. Mudford\*, A. A. Tang\*, S. Middlemist\*, C. J. Fox\*, C. M. Roffe\*, M. J. Gardner\*, D. Laurie\*, A. K. Barnes\*, M. L. Garrity\*. Immunodiagnostic Systems (IDS Ltd), Boldon, United Kingdom.

The importance of measuring 25-Hydroxy Vitamin D (25-OH D) to determine a patient's vitamin D status is becoming more widely recognised as part of a panel of tests for a variety of conditions including bone diseases, muscle function, diabetes, immune disorders, heart and circulatory disease, cancer and nervous system disorders. The 25-OH D assay will be part of a comprehensive panel of bone and growth tests on the new IDS Automated Analyser 3X3™. The purpose of this study was to develop and evaluate an assay for the determination of 25-OH D using this new fully automated, random access analyser. This analyser will enable clinical laboratories to determine 25-OH D, PTH, Calcium and Phosphorus from a single specimen tube. The IDS Automated Analyser 3X3™ contains integrated measurement modules for concurrent analysis of different types of diagnostic test, to include immunochemistry, biochemistry and coagulation. The 25-OH D assay uses the immunochemistry module of the IDS Automated Analyser 3X3™ and is performed as a chemiluminescent immunoassay. This utilises an acridinium labelled antibody, which emits light upon treatment with hydrogen peroxide and sodium hydroxide. This light is measured as relative light units (RLU) and quantified by a luminometer. The 25-OH D assay is a competitive immunoassay which comprises of an automated sample pre-treatment step, followed by the addition of a neutralising and displacing solution and the acridinium labelled antibody. After an incubation step magnetic particles labelled with 25-OH D are added to the assay mixture, which compete with the sample 25-OH D for the acridinium labelled antibody. Therefore the signal produced is inversely proportional to the concentration of 25-OH D in the sample. The analytical sensitivity of this assay has been determined as 1.2ng/mL and the functional sensitivity has been determined as less than 3.2ng/mL. The assay range is 0-200ng/mL with patient sample correlation to IDS 25-OH D RIA (n=78) of  $r = 0.93$  with an intercept of -0.66 and slope of 1.11 (linear regression). Linearity performed by diluting a high sample in a low sample gave a mean observed/expected value of 93.0% and recovery performed by spiking 25-OH D into samples gave a mean recovery of 103.6%. This automated 25-OH D assay is co-specific for both 25-OH D<sub>2</sub> and 25-OH D<sub>3</sub>. The assay shows the potential to be an excellent addition to the new bone panel on the IDS Automated Analyser 3X3™ essential for the measurement of a patients vitamin D status, with good correlation and sensitivity that will provide an accurate and rapid measurement of 25-OH D in the clinical laboratory.

**Disclosures:** L.A. Mudford, IDS Ltd 2.

## SU201

**Vitamin D Status in Severely Obese Individuals Can Be Predicted By Demographic and Lifestyle Factors.** E. M. Stein<sup>1</sup>, N. Sinha<sup>2</sup>, D. Ortiz<sup>2</sup>, G. Strain<sup>3</sup>, A. Pomp<sup>3</sup>, G. Dakin<sup>3</sup>, D. J. McMahon<sup>1</sup>, R. Bockman<sup>1</sup>, S. J. Silverberg<sup>1</sup>. <sup>1</sup>Medicine/ Endocrinology, Columbia University College of Physicians and Surgeons, New York, NY, USA, <sup>2</sup>Medicine/ Endocrinology, Weill Cornell Medical College, New York, NY, USA, <sup>3</sup>Surgery, Weill Cornell Medical College, New York, NY, USA, <sup>4</sup>Medicine/ Endocrinology, Weill Cornell Medical College and Hospital for Special Surgery, New York, NY, USA.

The factors governing vitamin D insufficiency in severe obesity are not well understood. The purpose of this study was to assess vitamin D status and whether factors important in normal weight populations influence vitamin D levels in severely obese individuals.

56 obese (BMI>35kg/m<sup>2</sup>) men and women (20-64 years) awaiting bariatric surgery were enrolled in this cross-sectional investigation. Study measurements included dietary calcium and vitamin D intake, sun exposure, intact parathyroid hormone (PTH) and 25-hydroxyvitamin D (25OHD).

Serum 25OHD was below 30 ng/ml in 85% of subjects, and was inversely associated with BMI ( $r = -0.36$ ;  $p < 0.01$ ). Seventy-five percent of individuals had secondary hyperparathyroidism (mean PTH  $72 \pm 34$  pg/ml). African American (AA) race was independently associated with 25OHD level ( $r = -0.35$ ;  $p < 0.01$ ), and levels below 20 ng/ml were found in 90% of AA subjects (vs. 51% of non-AA). Sun exposure was directly associated with 25OHD ( $r = 0.33$ ;  $p = 0.02$ ), and 25OHD levels were highest in the summer (summer:  $22.8 \pm 6.5$  ng/ml vs. non-summer:  $16.5 \pm 9.0$  ng/ml;  $p = 0.02$ ). The association between 25OHD and dietary/supplement vitamin D was not significant. In a stepwise regression model, BMI, sun exposure, African American race, and PTH predicted 40% of the variance in 25OHD levels ( $p$ -value  $< 0.0001$  overall model). When PTH was taken out of the model, BMI was the strongest predictor of 25OHD level; each increase in BMI of 1 kg/m<sup>2</sup> was associated with a decrease of 0.5 ng/ml in 25OHD level ( $p < 0.01$ ).

In conclusion, severely obese individuals share many risk factors for vitamin D deficiency with the general population; those who are most overweight, African American, and have limited sunlight exposure are at greatest risk. Although many of these risk factors are not easily modifiable, they can be utilized to identify the patients at greatest risk for vitamin D deficiency, and to foster crucial repletion prior to bariatric surgery.

**Disclosures:** E.M. Stein, None.

## SU202

**Low Plasma 25-Hydroxyvitamin D and Vitamin D Receptor Polymorphisms Are Associated with Increased Breast Cancer Risk.** K. D. Crew<sup>\*1</sup>, M. D. Gammon<sup>\*2</sup>, D. L. Hershman<sup>\*1</sup>, S. Cremers<sup>3</sup>, E. Dworakowski<sup>\*3</sup>, E. Shane<sup>3</sup>, M. Kappil<sup>\*4</sup>, M. Terry<sup>\*5</sup>, A. I. Neugut<sup>\*1</sup>, R. M. Santella<sup>\*4</sup>. <sup>1</sup>Medicine and Epidemiology, Columbia University, New York, NY, USA, <sup>2</sup>Epidemiology, University of North Carolina, Chapel Hill, NC, USA, <sup>3</sup>Medicine, Columbia University, New York, NY, USA, <sup>4</sup>Environmental Health Sciences, Columbia University, New York, NY, USA, <sup>5</sup>Epidemiology, Columbia University, New York, NY, USA.

Vitamin D has been associated with decreased risk of several cancers, including breast cancer. In experimental studies, vitamin D has been shown to inhibit cell proliferation and induce differentiation and apoptosis in normal and malignant breast cells. Using a population-based case-control study on Long Island, NY, we examined associations of breast cancer with plasma 25-hydroxyvitamin D [25-OHD] levels, a measure of body stores of vitamin D, and vitamin D receptor (VDR) polymorphisms (*FokI*, *Apal*, *BsmI*, and *TaqI*). In-person interviews and blood specimens were obtained from 1,026 incident breast cancer cases diagnosed in 1996-1997 and 1,075 population-based controls. Median age was 57.3 years (range 20-95); 93.4% of the study population was white and 67% postmenopausal. Plasma 25-OHD was measured in batched, archived specimens by Diasorin radioimmunoassay. The mean (SD) plasma 25-OHD concentration was 27.1 (13.0) and 29.7 (15.1) ng/ml in the cases and controls, respectively ( $P < 0.0001$ ). Plasma 25-OHD was inversely associated with breast cancer risk in a concentration-dependent fashion. Compared to women with vitamin D deficiency (25-OHD  $< 20$  ng/ml), plasma 25-OHD  $\geq 40$  ng/ml was associated with reduced breast cancer risk (OR = 0.58, 95% CI = 0.38-0.90). A greater protective effect was observed in postmenopausal compared to premenopausal women, and the effect did not vary according to tumor hormone receptor status. Additionally, the presence of at least one variant allele in *TaqI* (*Tt* or *tt*) was associated with a modest decrease in breast cancer risk (OR = 0.83, 95% CI = 0.69-0.99). Among women with vitamin D deficiency, the *FokI* *ff* genotype correlated with reduced risk of breast cancer (OR = 0.49, 95% CI = 0.29-0.81). No significant associations were noted with *Apal* and *BsmI* genotypes and breast cancer risk. In summary, these results add to a growing body of evidence that adequate vitamin D stores may prevent breast cancer development. Whereas circulating 25-OHD levels of  $> 32$  ng/ml are associated with normal mineral metabolism, our data suggest that the optimal level for breast cancer prevention is  $\geq 40$  ng/ml. Well-designed clinical trials are urgently needed to determine whether vitamin D supplementation is effective for breast cancer chemoprevention.

**Disclosures:** K.D. Crew, None.

This study received funding from: UL1 RR024156.

## SU203

**Vitamin D Status in Young Women Is Strongly Negatively Related to Body Weight, Body Mass Index and Body Fat, but Is Not Associated to Bone Mass.** R. Kremer<sup>1</sup>, P. Campbell<sup>\*2</sup>, T. Reinhardt<sup>3</sup>, V. Gilsanz<sup>2</sup>. <sup>1</sup>Medicine, McGill University, Montreal, QC, Canada, <sup>2</sup>Radiology, University of Southern California, Los Angeles, CA, USA, <sup>3</sup>Metabolic Diseases/Immunology, National Animal Disease Center, Ames, IA, USA.

Available data in elderly adults suggest that circulating 25-hydroxyvitamin D (25OHD) concentrations are positively correlated with bone mineral density (BMD) and inversely associated with obesity. To characterize whether these relations are also present at the time of peak bone mass, we examined the associations between serum 25OHD measures using a radioimmunoassay and values for weight (wt) and body mass index (BMI), and bone and fat determinations obtained by dual energy x-ray absorptiometry (DXA) and computed tomography (CT) in 90 white females, ages 16-22 years, who had achieved sexual and skeletal maturity. Significant negative relations were present between serum 25OHD and weight, BMI and all imaging measures of body fat (see Table). Values for PTH were also inversely correlated to 25OHD. In contrast, no relation was observed between circulating 25OHD and CT or DXA measurements in the appendicular or axial skeleton. Similar relations were seen in the 53 (59%) women with vitamin D deficiency/insufficiency ( $\leq 29$  ng/ml), but were not present in the 37 (41%) with  $\geq 30$  ng/ml vitamin D levels. In conclusion, we found strong negative relations between vitamin D values and measures of weight, BMI and body adiposity, but no relation with bone mass in young women.

	Deficient/Insufficient (n = 53)	Sufficient* (n = 37)	All Women (n = 90)
Weight	-0.28 (0.05)	-0.14	-0.28 (0.007)
BMI	-0.33 (0.02)	-0.18	-0.34 (0.001)
Trunk DXA Fat	-0.35 (0.01)	-0.16	-0.37 (0.0004)
Mean Leg DXA Fat	-0.33 (0.02)	-0.16	-0.29 (0.006)
Total DXA Fat	-0.32 (0.02)	-0.18	-0.32 (0.002)
CT Visceral Fat	-0.30 (0.03)	-0.05	-0.28 (0.007)
CT Subcutaneous Fat	-0.32 (0.02)	-0.19	-0.36 (0.001)

Values represent  $r$ 's (P's); \*Correlations are NS

**Disclosures:** R. Kremer, None.

This study received funding from: CIHR, NSERC, NIH.

## SU204

**Decreasing Calcidiol (25-OHD3) In Serum Is Related to Impaired Function and Increased Mortality in The Elderly.** E. Waern<sup>\*1</sup>, C. Christiansen<sup>2</sup>, E. Haug<sup>\*3</sup>, E. Rothenberg<sup>\*4</sup>, D. Mellström<sup>1</sup>. <sup>1</sup>Centre for Bone Research at the Sahlgrenska Academy, University of Gothenburg, Gothenburg, Sweden, <sup>2</sup>Center for Clinical and Basic Research, Ballerup, Denmark, <sup>3</sup>Hormone Laboratory, Aker University Hospital, Oslo, Norway, <sup>4</sup>Dept of Clinical Nutrition, Sahlgrenska University Hospital, Gothenburg, Sweden.

**Introduction:** The main target organs for vitamin D are the small intestine, the kidneys and the skeleton, tissues related to calcium metabolism. However, recent years investigations have discovered vitamin D receptors in many other tissues and vitamin D deficiency may increase the risk of many common chronic diseases and have effects on function and mortality.

**Population and Method:** A representative sample of 70 years old were invited to participate in a prospective study of ageing. 806 subjects were invited, 619 accepted to participate (317 women, 302 men). 405 participants were re-examined at 76 years of age. In 377 men and women serum levels of calcidiol (25-hydroxyvitamin D) were followed longitudinally.

The study included an interview as well as a thorough medical and laboratory examination. Venous sample were obtained at 7.30-8.00 am after 10 hours fast.

The serum levels were related to several variables known to affect the vitamin-D levels such as dietary intake and out-door activities. The correlation between vitamin D levels and muscle-strength, pulmonary-function, walking, daily intake of vitamin D, number of daily activities and mortality were studied.

**Results:** In the 377 individuals followed longitudinally the mean serum concentrations of 25-OHD3 were 73.7 nmol/L at 70 years of age and 62.9 nmol/L at the age of 76 years, not significantly different from the total group examined at 70

and 76 years of age. A decrease with 12 % in men and 17 % in women.

Men had a slightly, but significantly, higher 25-OHD concentrations than women. Both men and women decreased in weight and height with increasing age but there were no correlation to vitamin D-levels. The daily intake of vitamin D were lower in 76 years of age compared to 70 years of age (5.8 - 4.5 µg) and was below the daily recommended intake in Sweden (10 µg). The daily intake were correlated to the serum concentrations of calcidiol ( $r=0.28$ ,  $p=0.005$ ).

Serum levels of vitamin-D were related to muscle-strength ( $r=0.21$ ,  $p=0.0001$ ), pulmonary-function ( $r=0.15$ ,  $p=0.001$ ), walking ( $r=0.22$ ,  $p=0.0001$ ) and daily activities ( $r=0.21$ ,  $p=0.0001$ ). Low vitamin D levels were related to increased mortality.

**Conclusion:** The serum levels of calcidiol decreases with increasing age and correlates to the daily intake.

Low vitamin-D levels is correlated to impaired muscle-strength and pulmonary function and increased mortality.

**Disclosures:** E. Waern, None.

## SU205

**Prevalence of Vitamin D Deficiency Among Surgical Orthopedic Patients: A Single Center Analysis.** L. Bogunovic<sup>\*1</sup>, L. Shindle<sup>\*1</sup>, J. Virbalas<sup>\*1</sup>, B. Beamer<sup>\*1</sup>, N. Karkare<sup>\*1</sup>, J. Nguyen<sup>\*2</sup>, J. M. Lane<sup>3</sup>. <sup>1</sup>Metabolic Bone Disease, Hospital for Special Surgery, New York, NY, USA, <sup>2</sup>Research, Hospital for Special Surgery, New York, NY, USA, <sup>3</sup>Metabolic Bone Disease, Orthopedic Trauma, Hospital for Special Surgery, New York, NY, USA.

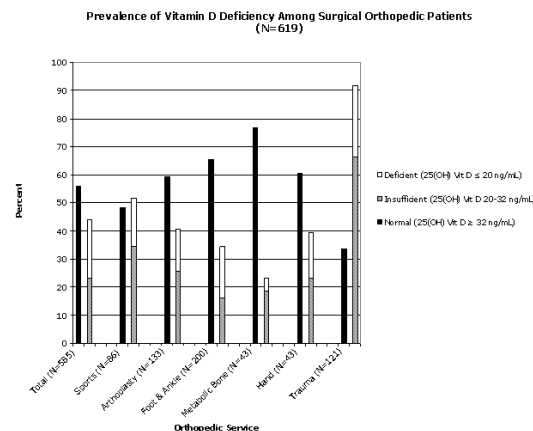
The purpose of this study was to determine the prevalence of 25-hydroxy vitamin D deficiency ( $\leq 20$  ng/mL) among surgical orthopedic patients at our institution.

Six hundred and nineteen adults, ages 18-98, underwent pre-operative measurement of 25-hydroxy vitamin D (25OHD). Surgical candidates from the following six services were included in the study: Sports Medicine, Arthroplasty, Orthopedic Trauma, Foot and Ankle, Hand, and Metabolic Bone Disease. On the following four services 25OHD was assessed in patients with a specific diagnosis and/or intervention: Sports Medicine (meniscal and anterior cruciate ligament repair), Arthroplasty (total knee and total hip replacement), Hand (colles' fracture), and Metabolic Bone Disease (vertebral compression fracture). In both the Foot and Ankle and the Orthopedic Trauma services, 25OHD status was assessed in all surgical candidates. Patient 25OHD status was categorized as being normal ( $\geq 32$  ng/mL), insufficient (20-32 ng/mL), or deficient ( $\leq 20$  ng/mL). Additional variables included the following: age, sex, race, and body mass index (BMI kg/m<sup>2</sup>).

At our institution, 44% of patients were found to have abnormal levels of 25OHD ( $< 32$  ng/mL). The highest rates of deficiency were seen in the trauma population where the risk of vitamin D deficiency was three times that seen on the other services ( $p<0.05$ ) (fig. 1). Race also appears to be a factor. Average vitamin D in the obese group (BMI  $> 30$ ) was found to be 37.5 ng/mL and 21.8 ng/mL in the black population, a difference which is significant ( $p<0.001$ ). There appears to be a significant difference in the vitamin D levels between the BMI groups ( $p=0.0001$ ). Mean vitamin D level in the obese group (BMI  $> 30$ ) is statistically lower when compared to the two other BMI groups, normal (BMI=18.5-24.9) and overweight (BMI=25-29.9) ( $p<0.001$  and  $p=0.018$  respectively).

The results of this study give an overview of vitamin D status among the surgical orthopedic population at our institution. Given the importance of vitamin D on bone and muscle health, pre-operative assessment of 25OHD status appears to be valuable.

**Disclosures:** L. Bogunovic, None.



## SU206

**Evaluation of Automated Methods for Quantifying Serum 25-Hydroxyvitamin D.** H. E. C. Hanwell<sup>\*</sup>, D. Wagner<sup>\*</sup>, R. Vieth. Nutritional Sciences, University of Toronto, Toronto, ON, Canada.

The accepted biomarker of vitamin D nutritional status is serum 25-hydroxyvitamin D [25(OH)D]. However, a clear understanding of vitamin D research is confounded by the variability among assays used for measuring 25(OH)D.

The purpose of this study was to compare two new automated assays with the well-established reference method, the DiaSorin radioimmunoassay (RIA) for serum 25(OH)D quantification.

The 25(OH)D from human sera (n=160) was quantified using the RIA and two automated non-radioactive immunoassays: DiaSorin Liaison Total 25(OH)D and Roche Elecsys 25-OH. Correlation was assessed with the Pearson test and agreement with the Bland-Altman method.

The RIA and Liaison correlated well ( $r = 0.919$ ) with negligible bias (bias  $\pm$  95% limits of agreement =  $-0.72 \pm 16.01$  nmol/L). The Roche correlated similarly with both the RIA and Liaison but with higher bias versus the RIA ( $r = 0.871$ ; bias =  $-2.55 \pm 21.06$  nmol/L) than the Liaison ( $r = 0.861$ ; bias =  $-1.72 \pm 21.34$  nmol/L). Imprecision (CV%) within-run for the RIA, Liaison and Roche was 9.66%, 6.29%, and 4.52%, and between-run was 10.8%, 6.67%, and 9.13%, respectively.

In conclusion, the Liaison Total 25(OH)D demonstrated a stronger correlation and better agreement with the reference method (DiaSorin RIA) than the Roche Elecsys 25-OH for quantification of serum 25(OH)D.

**Disclosures:** H.E.C. Hanwell, Donation of Analytical Kits (Roche, DiaSorin) 5. This study received funding from: Multiple Sclerosis Society of Canada.

## SU207

**Effect of 1,25-Dihydroxyvitamin D<sub>3</sub> and 25-Hydroxyvitamin D<sub>3</sub> on Osteoblastogenesis and Bone Strength in Vitamin D Sufficient Growing Mice.** L. Rossdeutsch<sup>\*1</sup>, D. C. Huang<sup>1</sup>, X. F. Yang<sup>1</sup>, F. T. Marino<sup>\*2</sup>, J. Barralet<sup>\*2</sup>, R. Kremer<sup>1</sup>. <sup>1</sup>Department of Medicine and Center for Bone and Periodontal Research, McGill University, Montreal, QC, Canada, <sup>2</sup>Faculty of Dentistry, McGill University, Montreal, QC, Canada.

Vitamin D and its active metabolites have been shown to exert a positive effect on bone in human and animal models of osteoporosis. However, the beneficial effect of vitamin D on peak bone mass is controversial. In this study, we analyzed 4-week old vitamin D-replete female FVB mice treated with a continuous infusion of either 1,25(OH)<sub>2</sub>D<sub>3</sub> (12 pM/24h and 24 pM/24h), 25-OHD<sub>3</sub> (2000 pM/24h) or vehicle for eight weeks using Alzet osmotic minipumps. In this model peak bone mass is achieved around twelve weeks. At sacrifice, ex-vivo cultures of bone marrow mesenchymal stem cells (BM-MSC) were prepared and induced to differentiate with an osteogenic medium. BM-MSC obtained from mice treated with 1,25(OH)<sub>2</sub>D<sub>3</sub> demonstrated a significant (2.5 fold) increase of CFU-OB stained with alkaline phosphatase or alizarin red as compared to controls. In contrast, no effect was observed in BM-MSC obtained from mice treated with 25-OHD<sub>3</sub>. In the 1,25(OH)<sub>2</sub>D<sub>3</sub>-treated groups blood calcium levels remained within the normal range in the low dose group but increased in the hypercalcemic range in the high dose group. In 25-OHD<sub>3</sub>-treated animals 25-OHD<sub>3</sub> levels increased by two fold but blood calcium levels did not differ significantly from controls. We next analyzed in detail the skeletal phenotype by mineral bone density (BMD), 3D micro-CT, histomorphometry and three-point bending test. BMD, microarchitectural parameters and mechanical strength remained unchanged in both the low dose 1,25(OH)<sub>2</sub>D<sub>3</sub> and 25-OHD<sub>3</sub>-treated groups as compared to controls. In contrast, BMD and bone strength decreased significantly in the high dose 1,25(OH)<sub>2</sub>D<sub>3</sub>-treated group. Histomorphometric analysis indicated a significant increase in the number of osteoblasts in the 1,25(OH)<sub>2</sub>D<sub>3</sub>-treated groups but not in the 25-OHD<sub>3</sub>-treated group as compared to controls. In summary our data indicate that 1,25(OH)<sub>2</sub>D<sub>3</sub> stimulate osteoblastogenesis and does not affect bone strength at low dose but decreases bone strength at high dose. In contrast 25-OHD<sub>3</sub> has no effect on either osteoblastogenesis or bone strength. Our data do not support a beneficial effect of either 1,25(OH)<sub>2</sub>D<sub>3</sub> or its inactive precursor on peak bone mass in vitamin D-replete female growing mice.

**Disclosures:** L. Rossdeutsch, None.

## SU208

**1,25(OH)<sub>2</sub>D<sub>3</sub> Regulates Collagen Maturation in Osteoblastic Cell Culture System.** H. Nagaoka\*, Y. Mochida, P. Atsawasuwan\*, M. Kaku\*, M. Yamauchi. Dental Research Center, University of North Carolina, Chapel Hill, NC, USA.

The biologically active form of vitamin D<sub>3</sub>, 1,25(OH)<sub>2</sub>D<sub>3</sub> (1,25VD), has a broad range of physiological effects, however, little is known about its effect on collagen quality in bone. The objectives of this study were to investigate the effects of 1,25VD on gene expression of enzymes critical for collagen cross-linking and collagen post-translational modifications using an osteoblastic cell culture system. MC3T3-E1 (MC) cells were cultured and treated with ethanol (E), cholecalciferol (VD) or 1,25VD. The former two served as controls. Total RNA was isolated at four time points (12, 24, 48 and 72 hours), mRNA expression of Cbfa1/Runx2, type I collagen alpha 2 chain (Col1a2), lysyl hydroxylase isoforms (LH1-3), lysyl oxidase isoforms (LOX, LOXL1-4) and GAPDH (internal control) was analyzed by real-time PCR and the relative gene expression was calculated. In another set of experiments, MC cells were cultured under the same condition for 2 weeks, cell/matrix layer was collected, reduced with standardized NaBH<sub>4</sub>, hydrolyzed with 6N HCl and subjected to quantitative amino acid and cross-link analyses. The analyses were performed in triplicate. The results of two control groups (E and VD) were essentially identical to each other for both experiments. Of the mRNA expression examined, LH2 in the 1,25 VD treated group showed a 3.5 fold increase at 12 hr and 5-7 fold increases at 48-72 hr compared to controls. LH1 expression also showed 2-4 fold increases by the treatment at all time points analyzed. LOXL2 expression in the treated group showed a 12 fold increase at 12 hr and a 40 fold increase at 48hr. Other isoforms did not show significant differences. Cbfa1/Runx2 expression was decreased with the 1,25 VD treatment. The biochemical analysis demonstrated that the extent of lysine hydroxylation of collagen was significantly higher (~45%) in the 1,25VD treated group than that of controls. The major collagen cross-links in all groups were dihydroxylysinoxonolucine (DHLNL), hydroxylysinoxonolucine (HLNL) and pyridinoline (Pyr). Of those, DHLNL and Pyr were significantly higher in the 1,25VD treated group (1.85 and 5 folds, respectively) than those of controls while HLNL was comparable to control groups. Hydroxylysine aldehyde, as its reduced form, was detected only in the 1,25 VD treated group. These findings indicate that 1,25VD upregulates the gene expression of specific LH and LOX isoforms in osteoblastic cells resulting in higher levels of lysine hydroxylation, hydroxylysine aldehyde-derived cross-links and a total number of cross-links. Thus, 1,25VD may control the stability and maturation of collagen in bone.

**Disclosures:** H. Nagaoka, None.

## SU209

**Increased Osteoclasts in Brlt Mouse Model for Osteogenesis Imperfecta Are Independent of Decreased Osteoblast Matrix Production and RANKL/OPG Ratio, but Are Associated with Increased Osteoclast Precursors in Marrow.** P. Collin-Osdoby\*, T. E. Uveges<sup>2</sup>, W. A. Cabral\*, L. Goldberg\*, G. A. Gronowicz\*, P. Osdoby<sup>1</sup>, J. C. Marini<sup>2</sup>. <sup>1</sup>Department of Biology and Division of Bone and Mineral Metabolism, Washington University, St. Louis, MO, USA, <sup>2</sup>Bone & Extracellular Matrix Branch/NICHD/NIH, Bethesda, MD, USA, <sup>3</sup>Department of Orthopaedic Surgery, University of Connecticut Health Center, Farmington, CT, USA.

The Brlt mouse, a knock-in model for moderately severe osteogenesis imperfecta, has a glycine substitution (G349C) in half of type I collagen  $\alpha 1(I)$  chains and a 45% reduction in cortical and trabecular bone volume. We examined the cellular contribution to Brlt bone phenotype in 2 and 6 month old mice using static and dynamic histomorphometry, quantitative immunohistochemistry and real-time RT-PCR. Brlt Obs/BS is comparable to wild-type before and after puberty; also, both genotypes have equivalent numbers of CFU, showing that marrow can replenish osteoblasts equally. However, osteoblast matrix production (MAR) decreases to half of wild-type values after puberty, suggesting that production of matrix by individual Brlt osteoblasts declines after puberty. In contrast, Brlt OcS/BS is increased 36-45% at 2 and 6 months compared to wild-type, as are the number of TRAP positive cells, 57% and 47%, respectively. Furthermore, the greater size and staining intensity of TRAP positive cells in Brlt suggests that the activity of individual osteoclasts may be increased. In total RNA from Brlt femora, TRAP expression was almost double WT levels. As a result of this cellular uncoupling, Brlt BFR declines from a normal level at 2 months to half of wild-type at 6 months. The combination of increased osteoclast activity and decreased osteoblast matrix production causes the weak Brlt femoral geometry. Quantitative immunohistochemistry and real time RT-PCR examination of the basis of the Brlt cellular imbalance revealed increased RANK, RANKL and OPG levels in Brlt, although Brlt's RANKL/OPG ratio was comparable to wild-type. Alternatively, the elevation of Brlt RANK transcripts suggests that more osteoclast precursors may be present. Marrow cultured from 2 month old mice in the presence of MCSF and RANKL yielded a 7-fold increase in the number of TRAP positive cells in Brlt vs wild-type mice. Although the genetic cause of classical OI is structurally defective type I collagen in bone matrix, this work shows that cellular asynchrony is a crucial contributor to the tissue-level mechanism of decreased bone volume in Brlt. The elevated osteoclast number and function in Brlt is mediated by non-RANK/RANKL pathway(s) which increase the number of RANK-expressing osteoclast precursors. Defining these pathways may lead to novel therapeutic approaches for OI.

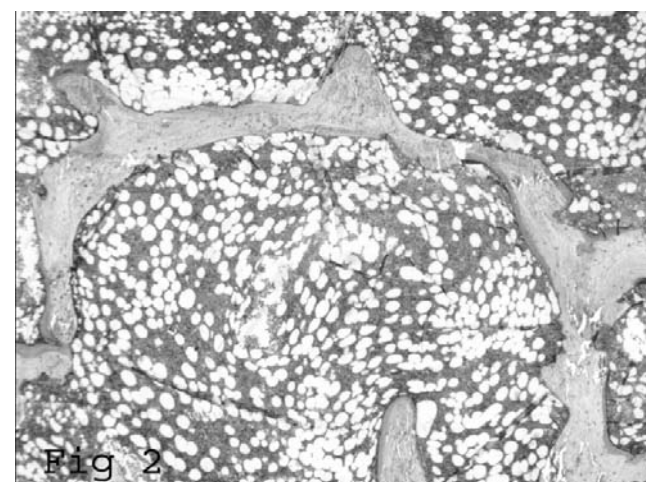
**Disclosures:** P. Collin-Osdoby, None.

This study received funding from: NIH intramural funding, Grant#1R21AR05449701A1.

## SU210

**Hyperphosphatasia: A Unique Type Without Mutations in *TNFRSF11A* (RANK), *TNFRSF11B* (OPG), or *SQSTM1* (Sequestosome 1).** S. Minisola<sup>1</sup>, A. Scillitani<sup>2</sup>, V. Guarnieri<sup>2</sup>, G. Guglielmi<sup>2</sup>, C. Battista<sup>2</sup>, M. L. Mascia<sup>1</sup>, P. Ballanti<sup>1</sup>, E. Romagnoli<sup>1</sup>, X. Zhang<sup>3</sup>, S. Mumm<sup>3</sup>, M. P. Whyte<sup>3</sup>. <sup>1</sup>Univ Rome "Sapienza", Rome, Italy, <sup>2</sup>S. Giovanni Rotondo Hospt, Foggia, Italy, <sup>3</sup>Shriners Hospt for Children and Washington Univ Schl Med, St Louis, MO, USA.

We report a 49-year-old man with a seemingly unique type of hyperphosphatasia. His mother carried a presumptive diagnosis of Paget's disease of bone (PDB). At age 27 years, he developed widespread skeletal pain. Serum total alkaline phosphatase (ALP) activity was elevated almost 10-fold, while liver function testing and principal parameters of calcium homeostasis were normal. There was no mental retardation. Since 1997, several hospitalizations occurred for bone pain unresponsive to non-steroidal anti-inflammatory drugs. Calcitonin for two years transiently relieved his discomfort; bisphosphonates led to brief normalization of serum ALP only after i. v. pamidronate and zoledronate. Sequential Tc-99m methylene diphosphonate bone scans showed progressive involvement, including newly affected bones. Distinctive radiographic features were multiple osteolytic areas of the skull, enlargement of the first and second lumbar vertebrae, selective sclerotic lesions of the long bones together with normal epiphyses, and non-progressive, indistinctly margined, osteolytic lesions (Fig 1). Histopathologic, histomorphometric, and ultrastructural analysis of affected bone revealed some similarities with PDB (increased trabecular remodeling and paramyxovirus-like structures in osteoclast nuclei). However, in contrast to advanced PDB, trabecular bone volume was decreased and trabeculae were disconnected (Fig 2). Moreover, osteoclasts were not "hypernucleated". Mutation analysis of the *TNFRSF11A* (exon 1), *TNFRSF11B*, and *SQSTM1* genes did not reveal a mutation in RANK, OPG, or Sequestosome 1, respectively. Thus, our patient's clinical, radiographic, and histopathological features appear unique. This disorder, perhaps familial and genetically based, should be added to the hyperphosphatasia syndromes.



**Disclosures:** S. Minisola, None.

## SU211

**A Polyostotic Form of Fibrous Dysplasia in a 13 years Old Colombian Girl Exhibiting Clinical and Biochemical Response to Neridronate Intravenous Therapy.** A. Falchetti, E. Parra Prada\*, L. Masi, S. Ciuffi\*, F. Marini\*, F. Franceschelli\*, D. Strigoli\*, A. Tanini, M. Brandi. Internal Medicine, University of Florence, Florence, Italy.

Fibrous Dysplasia (FD), a rare skeletal disorder due to activating mutations of *GNAS1* gene, is characterized by impaired proliferation of the medullary fibrous tissue, abnormal bone matrix, focal areas of woven bone and osteolytic areas. The clinical consequences are represented by bone deformities and increased skeletal fragility. FD rarely occur as an isolated monostotic or polyostotic form, and more frequently is a component of the McCune-Albright Syndrome (MAS) in which bone deformities are associated to precocious puberty, endocrinopathies and coffee-milk spotty skin. Similarly to the Paget's disease of bone, FD exhibits increase of the bone alkaline phosphatase (BAP) and other bone turnover markers (BTMs). Symptoms consist of bone pain, long or facial bones deformities and pathological fractures. We describe a case of a 13 years old Colombian girl resident in Italy since from 2006. Familial history is negative for bone metabolic disorders. In 2003, due to strong pain of the face, with a tumefaction on the right side, a diagnosis of FD by CT has been made. Moreover, she had coffee-milk spots in the limbs and at gluteus level. Clinical examination evidenced pain at the level of the right humer, ulna, left femur, right tibia and a moderate impaired deambulation. BAP and deoxypyridinoline (DPD), were increased. Biopsy of the affected maxillary bone showed features of a dysplasia. Skeletal scintigraphy evidenced a polyostotic form: skull, left humer distal epiphysis, left ulnar diaphysis, medial arch of the sixth left rib, right femur proximal epiphysis, and right tibia distal diaphysis. Clinical and biochemical assessments were not suggestive for MAS. In order to differentially diagnosed this FD with Paget-like syndromes, mutational analysis of the exon 1 of *TNFRSF11A* gene has been made with a negative result. Currently, mutational analysis of *GNAS1* gene has been performing. On October 2007, we decided to treat this case by intravenous infusion of neridronate, an amino-bisphosphonate (a-BP) already used in children affected by Osteogenesis Imperfecta, 2 mg/kg of body weight every three months. A daily supplementation with calcium carbonate, 1 g/day, and cholecalciferol, 800 UI/day, has been also associated. Since from the third month of therapy, bone pain disappeared, BAP and DPD resulted within the normal ranges and at the control X-rays an improvement of bone mineralization has been observed. Up to date no side effects has been reported. We suggest that neridronate is able to improve both clinical and biochemical features of FD and it could be added to the therapeutical harmamentarium.

**Disclosures:** A. Falchetti, None.

## SU212

**Additional Clinical Features of Idiopathic Multicentric Osteolysis with Nephropathy (OMIM %166300).** D. Wenkert<sup>1</sup>, W. H. McAlister<sup>2</sup>, M. P. Whyte<sup>1</sup>. <sup>1</sup>Shriners Hospt for Children, St. Louis, MO, USA, <sup>2</sup>Washington Univ Schl of Medicine, St. Louis, MO, USA.

Idiopathic multicentric osteolysis with nephropathy (IMON) presents in early childhood with carpal-tarsal destruction followed by nephropathy causing renal failure. The genetic basis is unknown. In 3 sporadic cases, we excluded mutation of the matrix metalloproteinase 2 (MMP2) gene (CORR 462:80, 2007) known to cause nodulosis-arthropathy-osteolysis, Winchester, and Torg syndromes. Here, we report further clinical features shared among these 3 boys, and an additional boy and 3 girls with IMON. Each patient (ages 3 to 21 yrs) had carpal, tarsal, and elbow osteolysis. 5 had knee swelling and contraction, and all but one (age 3 years) had proteinuria (onset 2 months to 12 yrs). Skin: 5 had one or more skin lesions: plantar foot nodules (3), neck "lumps" (2), axillary piloleiomyoma (1), and keloids (1). Temporal Mandibular Joint: 6 pts had small oral apertures (4), and/or retrognathia (5). 1 panorex (age 3 yrs) showed TMJ destruction. Growth varied from 15-90% in height. All patients were slender (~90% ideal body weight (4)), some had poor wt gain (79%-84% IBW (3)). Faces: All had a similar micrognathia, retrognathia, maxillary hypoplasia, prominent eyes (all previously reported) as well as a long narrow nose, flat profile, and remarkably long, dark eyelashes. Headaches were common. Platybasia affected 3 of 4 pts. MRI (1 pt) revealed a Chiari I malformation with obstructive hydrocephalus. 1 pt was hypothyroid. Ophthalmologic: There was delayed visual maturation, retino-choroidal colobomas and corneal opacities (1) and uveitis thought to be due to gold therapy (1), as well as significant visual loss from corneal clouding (1) and strabismus (1). Bone Density: L<sub>1-4</sub> BMD z score (prior to bisphosphonate) seemed bimodal: -1.8 to -2.5 in 3 pts; the other 4 had z-scores of -0.6 to 0.1. TNF inhibitor Rx: ESR was occasionally elevated (20's - 30's). Remarkable symptomatic improvement occurring in 2 pts receiving etanercept waned over 6 months without cessation of osteolysis. The distinct facial appearance of IMON may lead to early recognition and guide clinicians to avoid nephrotoxic agents. The pattern of osteolysis (carpal-tarsal, sucked candy appearance of proximal metacarpals, without widening of metacarpals and metatarsals or interphalangeal arthropathy) is distinct from the MMP-2 associated disorders, but osteoporosis, and skin nodules can not distinguish between the disorders. We suggest that all pts with possible IMO be monitored for proteinuria, signs of Chiari malformation, hypothyroidism, ophthalmologic difficulties, and TMJ disease. These features of IMON may be clues to the pathogenesis and guide candidate gene analysis.

**Disclosures:** M.P. Whyte, None.

## SU213

**Effect of Hypercalciuria and Diet on Bone in Genetic Hypercalciuric Stone-forming Rats.** M. Grynpas<sup>1</sup>, S. Waldman<sup>\*1</sup>, D. Holmyard<sup>\*1</sup>, D. Bushinsky<sup>2</sup>. <sup>1</sup>Pathology, University of Toronto, Toronto, ON, Canada, <sup>2</sup>Medicine, University of Rochester, Rochester, NY, USA.

Hypercalciuria is the most common metabolic abnormality in patients with Ca containing kidney stones. Patients with hypercalciuria often excrete more Ca than they absorb, indicating a net loss of total body Ca, almost certainly derived from bone. Studies have shown a decrease in bone mineral density (BMD) and an increase in fractures in hypercalciuric stone formers compared to controls. However, in human stone formers it is difficult to determine if the reduction in BMD is due to a primary bone disorder or to any number of dietary factors, such as sodium, Ca and protein, which may be altered in stone formers over their lifetime. To study the independent effects of hypercalciuria on bone, we utilized the genetic hypercalciuric stone-forming (GHS) rats which were established by successively inbreeding the most hypercalciuric progeny of hypercalciuric Sprague-Dawley rats. 46th generation female GHS and control (Ctl) rats were placed in metabolic cages and fed a similar amount of either a low Ca (0.02% Ca, LCD) or a high Ca (1.2% Ca, HCD) diet for 6 weeks, and then their femurs, tibiae, humeri and lumbar spines were studied for BMD, histomorphometry, degree of mineralization and mechanical properties. All comparisons are to Ctl rats, n=8 in each group. Urine Ca was significantly greater in the GHS rats on both diets. GHS fed HCD had reduced cortical (humerus) and trabecular (L1-L5 vertebrae) BMD while GHS rats fed LCD had a reduction in BMD that did not differ from Ctl. Histomorphometric analysis demonstrated that GHS rats fed HCD had a significant decrease in trabecular volume and thickness while LCD led to a ~20 fold increase in both osteoid surface and volume. GHS rats fed HCD had no change in vertebral strength (failure stress), ductility (failure strain), stiffness (modulus) or toughness while in the humerus there was a reduction in ductility and toughness and an increase in modulus indicating that the defect in mechanical properties in GHS rats is mainly manifested in cortical, rather than trabecular bone. GHS rat cortical bone is more mineralized than trabecular bone and LCD led to a decrease in the mineralization profile. Thus the GHS rats, fed an ample Ca diet, have reduced bone mineral density with reduced trabecular volume, mineralized volume and thickness and their bones are more brittle and fracture prone, indicating that hypercalciuric stone-forming rats have an intrinsic bone disorder that is not secondary to diet. It is unclear whether therapy to reduce stone formation in the GHS rats will restore the mechanical properties of their bone.

**Disclosures:** D. Bushinsky, None.

## SU214

**ANKH Mutation Causing Craniometaphyseal Dysplasia Inhibits Osteoclast Differentiation.** N. Park\*, Y. Jung\*, H. Kim\*, S. Kim, E. Park, J. Choi\*. Biochemistry & Cell Biology, Skeletal Diseases Genome Research Center, Kyungpook Natl. Univ. School of Medicine, Daegu, Republic of Korea.

*ANKH* is responsible gene for craniometaphyseal dysplasia (CMD), a childhood disease characterized by sclerosis of the skull and abnormal modeling of the long bones. The mechanism of skeletal abnormality, however, has not been determined in CMD patients. Previously, *ANKH* was identified as one of upregulated membrane proteins during osteoclastogenesis (Ha BG et al., Proteomics, in press). In this study, we identified and characterized a novel *ANKH* mutation causing CMD with changing amino acids 290-295 of *ANKH* (YGWLTE) into *ANKH* (QG). After cloning of mutant construct (*ANKH290QG*) with full length context, we characterized *ANKH290QG* with respect to the protein localization, and bone cell functions particularly during osteoclastogenesis. In transient transfection assay, *ANKH290QG* mutant protein was localized in membrane as wild type *ANKH*. During osteoclastogenesis, *ANKH290QG* stable cells showed the inhibition of osteoclastogenesis, which was confirmed by TRAP staining and expression of osteoclast markers by RT-PCR. Probenecid, *ANKH* inhibitor, suppressed *RANKL* mediated osteoclast differentiation. Collectively, these results indicate that skeletal abnormality in CMD patients is due in part to the inhibition of osteoclast differentiation by *ANKH* mutation.

**Disclosures:** J. Choi, None.

## SU215

**A Hotspot Splicing Mutation in *LEPRE1* Affects Prolyl 3-hydroxylation and Causes Recessive Osteogenesis Imperfecta.** A. Willaert<sup>\*1</sup>, S. Symoens<sup>\*1</sup>, F. Malfait<sup>\*1</sup>, K. Gevaert<sup>\*2</sup>, P. Coucke<sup>\*1</sup>, A. De Paepe<sup>\*1</sup>. <sup>1</sup>Department of Medical Genetics, Ghent University, Ghent, Belgium, <sup>2</sup>Department of Medical Protein Research, VIB/Department of Biochemistry, Ghent University, Ghent, Belgium.

Recently, it has been shown that recessive forms of Osteogenesis Imperfecta (OI) can be caused by the absence of 3-hydroxylation of Pro986 in the  $\alpha 1(I)$ -collagen chain, resulting from mutations in prolyl 3-hydroxylase 1 (P3H1) or cartilage-associated protein (CRTAP), which, together with cyclophilin B (CyPB) are constituents of the prolyl 3-hydroxylation complex. We screened *LEPRE1* (encoding P3H1), *CRTAP* and *CyPB* by complete cDNA and/or genomic DNA sequencing in a European/Middle East cohort of lethal/severe OI patients without a type I collagen mutation.

While no mutations were found in *CRTAP* and *CyPB*, novel homozygous and compound heterozygous mutations were identified in *LEPRE1* in 5 patients. Patient 1 is homozygous for a frameshift mutation (c.1365\_1366delAGinsC) in exon 9, resulting in a premature termination codon in the same exon. Patient 2 and 3, which are sibs, are homozygous for a nonsense mutation (c.628C>T) in exon 3. Patient 4 carries a heterozygous nonsense mutation (c.1102C>T) in exon 6. Finally, a recurrent splice site mutation (c.2055+18G>A) was identified in patients 4 and 5, respectively in heterozygous and homozygous state. As expected from the different ethnicity of patients 4 and 5, haplotype analysis suggests that c.2055+18G>A is a hotspot mutation. As confirmed by RT-PCR, the latter mutation converts a suboptimal into an optimal donor splice site in intron 14, resulting in a full switch in donor splice site utilization. Consequently, this mutation results in the absence of the only splice form of P3H1 which contains the endoplasmic reticulum (ER) retention signal KDEL and which is therefore putatively responsible for the prolyl 3-hydroxylation function of P3H1 in the ER. While western blotting of fibroblast protein extracts shows absence of P3H1 protein in patients compared to controls, tandem mass spectrometry and SDS-PAGE analysis indicate respectively a severe reduction of  $\alpha 1(I)$ Pro986 3-hydroxylation and a resulting overmodification of type I (pro)collagen chains in all patients. In conclusion, we identified 4 novel *LEPRE1* mutations in lethal/severe OI patients of European/Middle East descent with one hotspot splice site mutation, specifically affecting the P3H1 splice form responsible for  $\alpha 1(I)$ Pro986 3-hydroxylation. Other splice forms of P3H1 can not rescue this function and could be responsible for the other presumed functions of P3H1, which include a role as growth suppressor and a role as the extracellular matrix proteoglycan, leprecan.

**Disclosures:** A. Willaert, None.

## SU216

**Two Novels SQSTM1 Mutations in American Patients with Paget's disease of Bone.** L. Michou<sup>\*1</sup>, J. Morissette<sup>\*1</sup>, A. Marquis<sup>\*1</sup>, E. R. Brochu<sup>\*1</sup>, J. P. Brown<sup>1</sup>, E. S. Siris<sup>\*2</sup>. <sup>1</sup>CHUL Research Centre, Quebec, QC, Canada, <sup>2</sup>Columbia-Presbyterian Medical Centre, New York, NY, USA.

Since 2002, 14 mutations of SQSTM1 gene have been reported in familial and sporadic patients affected by Paget's disease of bone in different populations.

We performed a systematic screening for SQSTM1 mutations in 52 consecutively evaluated patients with Paget's disease of bone living in the US. Those patients have a typical phenotype of Paget's disease of bone. They live in the New York City area and have a heterogeneous ethnic background. DNA was isolated from whole blood, and sequencing of exon 7 and 8 was performed. Of the 52, two were sisters, but the remainder were unrelated.

Five of the unrelated patients (10%) have SQSTM1 mutations and no mutation was detected in the 2 sisters. Three patients carried a 1215C>T (P392L) mutation, of whom only one had a positive family history. Two patients carried novel SQSTM1 mutations also located in the exon 8 coding for the ubiquitin-binding associated domain. One carried a 1290T>A (L417Q) mutation and the other had a 1209C>T (A390V) mutation. Both patients with novel SQSTM1 mutations have polyostotic Paget's disease with elevated alkaline phosphatase at diagnosis. The patient who carried the A390V mutation had a family history of Paget's disease of bone in the mother and in a sister. The SQSTM1 mutation rate in those unrelated American patients is similar to that reported in European populations.

Our results differ from those of a recently published study on SQSTM1 mutation in patients with Paget's disease of bone from Texas and California where the authors found no SQSTM1 mutation in 73 unrelated patients, whereas eight SQSTM1 mutations were found in the 39 patients with a family history of Paget's disease of bone. Five of them had a P392L mutation; one carried a 1215delC (L394X) mutation, one carried a 1210delT (394X) mutation, and one a P387L mutation. No novel SQSTM1 mutation was reported in this population. We report here preliminary results of a mutation screening in 52 patients with Paget's disease from the US. Five patients carried SQSTM1 mutations. Two novel SQSTM1 mutations were reported; L417Q and A390V, and three patients carried a P392L mutation.

**Disclosures:** L. Michou, Novartis France 3.

## SU217

**Bone Mineral Density in Children and Adolescents with Sickle Cell Disease: A Descriptive Analysis.** L. J. Chambers<sup>\*1</sup>, L. Hillman<sup>2</sup>. <sup>1</sup>Pediatrics, Scott and White Hospital, Temple, TX, USA, <sup>2</sup>Child Health, University of Missouri - Columbia, Columbia, MO, USA.

**Objective:** Stallings has reported low serum 25-hydroxy vitamin D (25-OHD) in children with Sickle Cell Disease (SCD) in Philadelphia. We wished to assess the frequency of low serum 25-OHD in a more southern location and evaluate its' effects on mineral metabolism and bone mineralization.

**Methods:** Fourteen children with SCD were assessed for serum 25-OHD, Ca, PTH, bone alkaline phosphatase (BAP), urine free pyridinoline (PYD) and DXA of whole body, spine and femur.

**Results:** Two clearly vitamin D deficient children were found. A 17-year old male had a 25-OHD of 5 ng/ml and a Ca of 8.9mg/dl however PTH, BAP and PYD were normal. Whole body and femur DXA were within normal range, >2 SD but spine was low, <2 SD. An 11-year old female had a 25-OHD of 11 ng/ml with a Ca of 8.5 mg/dl, PTH of 145 pg/ml and BAP of 150 u/L. However all DXA scans were within normal range. Mean 25-OHD for the entire group was 20±7ng/ml, with 8 of 14 below 20 ng/ml and all but one below 30 ng/ml. These values are below that seen in local Caucasian children (35±13 ng/ml), however African-American controls are needed. Nine of 14 children had at least one low DXA and 3 had two low DXAs, defined as a BMD < 2SD below the mean for age. Four of 14 had low whole body, 6/14 low lumbar and 7/14 low femur. Excluding the above vitamin D deficient child, PTH was appropriate at 31±18 pg/ml. BAP at 94±36u/L and PYD/Cr at 69±92nmol/mmol were also appropriate for growing children. Correlations between vitamin D status and DXA were not seen. Liver function tests were normal and hip x-rays showed infarcts in only one child. DXA did not correlate with hemoglobin.

**Conclusion:** The data supports that, even in Missouri, African-American SCD patients have unacceptably low 25-OHD levels and unacceptably poor bone mineralization. The inability to correlate 25-OHD and DXA probably relates to 25-OHD being a relatively acute measure and DXA being a chronic measure. Oral supplementation with at least 1,000 IU D/d should be given to all SCD patients. Correction of vitamin D deficiency will probably not eliminate low DXA because of the complexity of SCD, however we were not able to identify specific confounding factors related to Sickle Cell Disease.

**Disclosures:** L.J. Chambers, None.

This study received funding from: Sear Foundation.

## SU218

**Bi-allelic Loss of *Nf1* in Osteoblasts Delays Bone Fracture Healing.** W. Wang<sup>\*1</sup>, J. S. Nyman<sup>2</sup>, B. Livesay<sup>\*1</sup>, F. Elefteriou<sup>1</sup>. <sup>1</sup>Vanderbilt Center for Bone Biology, Department of Medicine, Vanderbilt University Medical Center, Nashville, TN, USA, <sup>2</sup>Vanderbilt Center for Bone Biology, Department of Orthopaedics, Vanderbilt University Medical Center, Nashville, TN, USA.

The etiopathology of Neurofibromatosis (NF1) bone pseudoarthrosis (PA) is unclear. As a result, this bone fracture healing defect cannot be prevented, and even with modern orthopaedic techniques a complete and durable union is difficult to achieve, leading to lifelong disability and amputation in the most severe cases. The congenital, localized, unilateral and non-systematic nature of the lesion strongly suggests that *Nf1* loss-of-heterozygosity (LOH) is necessary for pseudoarthrosis to occur. However, the cellular complexity of the bone marrow environment coupled with the difficulty of identifying *Nf1* mutations has hampered the characterization of the mechanism(s) whereby NF1 pseudoarthrosis develops. In an effort to address this question, we have generated a mouse model (the *Nf1<sub>ob</sub><sup>-/-</sup>* mice) characterized by bi-allelic *Nf1* deletion specifically in osteoblasts, the bone forming cell, with the hypothesis that *Nf1* LOH in the mesenchymal osteoprogenitor lineage causes the bone quality and healing defects characteristic of NF1 PA. Using this mouse model, we previously found that *Nf1* regulates normal bone remodeling by inhibiting collagen synthesis and mineralization by osteoblasts and the formation of osteoclasts, via a signaling pathway involving Ras, ERK, RSK2 and the transcription factor ATF4. In this study, we used a tibia fracture model to determine whether lack of *Nf1*'s function in osteoblasts causes the NF1 bone healing defects. Our results, based on 3D-microtomography and histomorphometric measurements indicate that the formation of the fracture callus is delayed in *Nf1<sub>ob</sub><sup>-/-</sup>* mice: 21 days post-fracture, the callus of *Nf1<sub>ob</sub><sup>-/-</sup>* mice is bigger and less calcified than the one of WT littermates, still displays cartilaginous remnants, and is also characterized by bone surfaces covered with a thick osteoid surface, which is reminiscent of what is observed in human NF1 PA lesions. *In vitro*, *Nf1<sup>-/-</sup>* osteoblasts are characterized by constitutive Ras and ERK activation, which can be inhibited by the inhibitory effect of lovastatin on Ras prenylation. Based on this proof-of-concept result and previous data, we propose that lovastatin may have multiple beneficial actions on the NF1 skeletal defects: not only may it improve the low bone mineral density of NF1 patients in general, it may also prevent NF1 pseudoarthrosis. The *Nf1<sub>ob</sub><sup>-/-</sup>* mice is a valuable pre-clinical model to test this hypothesis.

**Disclosures:** W. Wang, None.

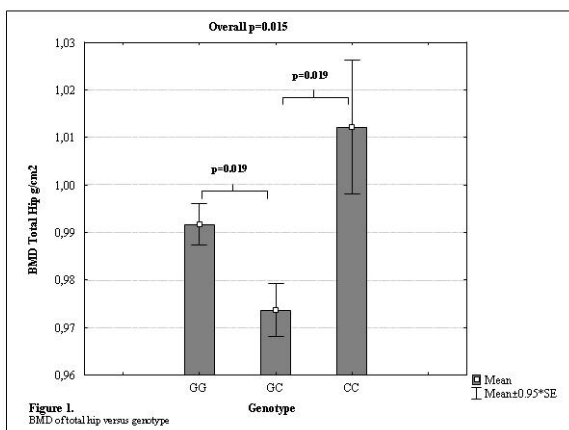
## SU219

**The Functional Polymorphism in COL1A2 (Ala459Pro) that is Associated with Intracranial Aneurysms, Shows Heterozygous Disadvantage Concerning Bone Mineral Density and Stroke in Elderly Men - MrOS Sweden.** K. M. Lindahl<sup>\*1</sup>, H. Brändström<sup>\*1</sup>, M. K. Karlsson<sup>\*2</sup>, A. H. Holmberg<sup>\*2</sup>, C. Ohlsson<sup>\*3</sup>, D. Mellström<sup>\*3</sup>, E. Orwoll<sup>\*4</sup>, H. Mallmin<sup>\*5</sup>, A. Kindmark<sup>1</sup>, Ö. Ljunggren<sup>1</sup>. <sup>1</sup>Medical Sciences, Uppsala, Sweden, <sup>2</sup>Clinical Sciences, Malmö, Sweden, <sup>3</sup>Clinical Sciences, Gothenburg, Sweden, <sup>4</sup>Oregon Health and Science University, Portland, OR, USA, <sup>5</sup>Surgical Sciences, Uppsala, Sweden.

Genetics play an important role in the development of osteoporosis and a prime candidate gene is the collagen alpha 2 (I) gene (COL1A2). A coding polymorphism of COL1A2 (Ala459Pro) has previously been associated with intracranial aneurysms. Here the significance of this polymorphism in relation to bone phenotype and incidence of stroke and myocardial infarction (MI) has been studied.

The polymorphic site Ala459Pro (rs42524) was studied by fluorescence polarization detection technique in part of the Swedish MrOs cohort (n=2004). At inclusion bone mineral density (BMD) was measured by Dual energy X-ray Absorptiometry (DXA) and the participants were interviewed using a structured questionnaire concerning previous and current health issues.

A significant association measured by overall *p* was found between the heterozygous genotype and lower BMD at total hip (*p*=0.015) (figure 1), femoral neck (*p*=0.036) and trochanter (*p*=0.010). When comparing both homozygotes to heterozygotes (GG and CC vs. GC) a significant association was established between lower BMD at total hip (2.0%; *p*=0.0098), femoral neck (1.7%; *p*=0.027) and trochanter (2.1%; *p*=0.0096) and heterozygous genotype. This genotype also increased the risk for stroke (OR 1.4; *p*=0.0498). There was a trend for association between heterozygous genotype and decreased BMD of total body (0.7%; *p*=0.089) and increased risk of MI (OR 1.3; *p*=0.065). There was no association between the genotype and BMD of lumbar spine.



This study indicates that the genotype "GC" leads to a heterozygous disadvantage, compared to both the more favorable homozygous variants, affecting BMD and risk of suffering a stroke.

P-value for different genotypes versus bone and vascular phenotype				
Characteristic	GC vs. GG	GC vs. CC	GC vs. GG+CC	Overall p
BMD femoral neck	0.048	0.026	0.027	0.036
BMD total hip	0.019	0.019	0.0098	0.015
BMD trochanter	0.021	0.011	0.0096	0.010
BMD total body	0.089	0.51	0.089	0.23
BMD L1-L4	0.14	0.88	0.16	0.32
Stroke	0.050	0.53	0.0498	0.14
Myocardial Infarction	0.079	0.27	0.065	0.17

**Disclosures:** K.M. Lindahl, None.

This study received funding from: Swedish research council, project nr: 2007-2946.

## SU220

**Polymorphisms of the ALOX12 Gene Are Associated with Increased Risk of Osteoporotic Fracture.** T. Harsløf<sup>\*</sup>, L. Husted<sup>\*</sup>, M. Carstens<sup>\*</sup>, L. Stenkaer<sup>\*</sup>, B. Langdahl. Department of Endocrinology and Metabolism, Aarhus University Hospital, Aarhus C, Denmark.

Osteoporosis is a common disorder with a multifactorial pathogenesis. Stimulation of the PPAR $\gamma$ -receptor with ligands produced by the ALOX enzymes forces mesenchymal stem cells to develop in the adipocyte direction at the expense of osteoblasts leading to decreased osteoblast number and BMD. Previously, polymorphisms of the ALOX12 gene have been associated with osteoporosis.

The aim of this study was to examine the effect of ALOX12 polymorphisms on BMD and the risk of vertebral fractures. On the basis of patterns of linkage disequilibrium between SNPs throughout the gene we chose 10 polymorphisms for investigation.

The polymorphisms were investigated in a case-control study comprising 462 osteoporotic patients and 336 controls. Polymorphisms were examined using Taqman assays and BMD was examined by DXA.

Rs3840880, rs9897850 and rs1126667 were significantly associated with vertebral fractures in women (*P*<0.05 for all). The increased fracture risk was found in individuals heterozygous for the polymorphisms. The frequencies of heterozygosity were higher in patients with osteoporotic fractures than in normal controls: rs3840880: 53.9 % vs. 42.5 %, *P*=0.014 rs9897850: 54.8 % vs. 42.9 %, *P*=0.011 and rs1126667: 53.5 % vs. 42.5 %, *P*=0.019. Furthermore, lumbar spine (Ls) BMD was significantly lower in individuals heterozygous at these three polymorphic loci and at the rs2292350 locus (*P*<0.05 for all). None of the other polymorphisms were associated with BMD or fracture risk.

The four polymorphisms were in strong linkage disequilibrium (LD) (*D'*=1.0, *r*<sup>2</sup> = 0.47 - 0.98) and rs1126667 was in complete LD with rs1042357. Rs1126667 is situated in exon 6 and causes a change of amino acid 261 from arg to gln whereas rs3840880 and rs9897850 are located in the promoter region and rs2292350 lies in intron 2.

Molecular heterosis is the term for the phenomenon that heterozygosity for a given genotype influences a certain trait, and it has previously been described in a number of human conditions including osteoporosis (PLOD1 and PPAR $\gamma$  genes). In a such case classic haplotype analysis does not make sense since only one allele is considered and both alleles need being taken into account, however, the two most common haplotypes were exactly opposite to each other and we were therefore able to show that individuals possessing one copy of each and, thus being heterozygous at all 4 loci, had an increased risk of fracture compared to those being homozygous at all loci (*P*=0.025).

Based on the observations above we suggest that polymorphisms of the ALOX12 gene are associated with increased risk of osteoporotic fractures and decreased LsBMD through molecular heterosis.

**Disclosures:** T. Harsløf, None.

## SU221

**The RsaI Polymorphism in ESR2 Is Associated with Postmenopausal Fracture Risk.** N. Gonzalez-Bofill<sup>1</sup>, L. Husted<sup>1</sup>, P. Vestergaard<sup>2</sup>, C. Tofteng<sup>\*2</sup>, P. Eiken<sup>\*3</sup>, K. Brixen<sup>4</sup>, B. Langdahl<sup>1</sup>. <sup>1</sup>Endocrinology and Metabolism, Århus Hospital, Århus, Denmark, <sup>2</sup>Endocrinology and Metabolism, Hvidovre Hospital, Copenhagen, Denmark, <sup>3</sup>Endocrinology and Metabolism, Hillerød Hospital, Hillerød, Denmark, <sup>4</sup>Endocrinology and Metabolism, Odense Hospital, Odense, Denmark.

Estrogen participates in the acquisition and maintenance of BMD by binding to its receptors, ER $\alpha$  and ER $\beta$ . Polymorphisms in the genes encoding these receptors, ESR1 and ESR2 have previously been associated with bone health outcomes. We and others have previously found that the AluI polymorphism in the 3'UTR of ESR2 and a haplotype including this polymorphism are associated with fracture risk in elderly populations. In the present study we wanted to investigate the effect of four polymorphisms in ESR2: a polymorphism in intron 2 (rs1256031), a synonymous RsaI polymorphism in exon 5 (rs1256049), a CA-repeat polymorphism (D14S1026) in intron 5 and an AluI polymorphism in the 3'UTR (rs4986938) on BMD and risk of fractures in 1717 perimenopausal women. We also wanted to examine the effect on postmenopausal bone loss and response to HRT. Genotyping for the SNPs was performed by TaqMan assays and the number of CA-repeats was determined by capillary electrophoresis. BMD was measured by DXA.

The four studied polymorphisms were in Hardy-Weinberg equilibrium with the following allele frequencies: rs1256031 A/G 0.52/0.48; RsaI C/T 0.97/0.03; AluI C/T 0.65/0.35. The CA-repeat polymorphism was classified in low-high number of repeats with a cut-point of 21 repeats. The allele frequencies for this polymorphism were L/H 0.23/0.77. The RsaI and the CA-repeat polymorphisms were in linkage disequilibrium, as were the rs1256031 and the AluI polymorphisms, and haplotypes could therefore be estimated.

We found no convincing effect of any of the four polymorphisms or haplotypes on perimenopausal BMD, postmenopausal bone loss or response to HRT. However, we found that in the group of women not treated with HRT, those carrying the T-allele of the RsaI polymorphism or 1 or 2 copies of haplotype RsaI-CA (T-L) had lower fracture incidence ten years after menopause (7.4% vs. 16.9% in non-carriers and 7.4% vs.17.0% in non-carriers, respectively, *p*=0.02).

Conclusion: The RsaI polymorphism in ESR2 and a haplotype containing this polymorphism are associated with risk of fractures, despite not being associated with perimenopausal bone mass, postmenopausal bone loss or response to HRT. None of the other polymorphisms or haplotypes are associated with fracture risk, perimenopausal bone mass, postmenopausal bone loss or response to HRT.

**Disclosures:** N. Gonzalez-Bofill, None.



## SU222

**Prediction of Fracture Risk by LRP5 Gene Haplotype.** B. H. Tran, N. D. Nguyen, J. R. Center, J. A. Eisman, T. V. Nguyen. Bone and Mineral Research Program, Garvan Institute of Medical Research, Sydney, Australia.

Polymorphisms of the low density lipoprotein receptor related protein 5 (LRP5) gene have been shown to be linked to or associated with bone mineral density (BMD), but their association with fracture risk is not known. The present study sought to assess the association between LRP5 gene polymorphisms and fracture risk in women by using haplotype analysis.

Haplotype tagging single nucleotide polymorphisms (in order rs314776, rs3736228, rs4988320, rs4988321, rs556442, rs587808 and rs660925) of LRP5 gene was determined in a sample of 1286 (821 women) participants from a population-based cohort. Bone mineral density (BMD) was measured at baseline. During the follow-up period of 1989-2006, 125 men and 338 women sustained at least one fracture.

There were no statistically significant association between any single SNP and BMD or fracture risk. The seven SNPs were in tight linkage disequilibrium which were ultimately used to construct a haplotype block. Using bioinformatic tools (haplo.assoc and haplo.ccs program), 7 haplotypes accounted for ~90% of the sample. Further haplotype analysis showed that three haplotypes [CCAGAAGC (3% in the population), CCGGAGA (3%) and TCGGGAG (2%)] were associated with variation in BMD. Furthermore, carriers of haplotype CTGGGGA (6% in the population) had an increased risk of fracture (RR: 1.4, 95% CI: 1.1-3.0), hip fracture (2.2, 1.0-4.9) and wrist fracture (2.4, 1.1-4.9), after adjusting for age and BMD. There was no significant association between any haplotype and BMD or fracture risk in men. The proportion of fracture cases that is attributable to the haplotype was 2.3%.

These results suggest that common genetic variation at the LRP5 gene was modestly associated with fracture risk in women independent of its association with BMD. The present study also suggests that a haplotype-based analysis is more powerful than a SNP-based analysis in the detection of association.

**Disclosures:** B.H. Tran, None.

This study received funding from: NHMRC.

## SU223

**Single Nucleotide Polymorphisms in the P2X7 Receptor Gene Are Associated with Increased Postmenopausal Bone Loss and Fracture Incidence.** N. R. Jorgensen<sup>1</sup>, L. B. Husted<sup>2</sup>, P. Schwarz<sup>3</sup>, C. L. Tofteng<sup>4</sup>, J. B. Jensen<sup>5</sup>, N. Nissen<sup>6</sup>, P. Eiken<sup>6</sup>, L. Ødum<sup>1</sup>, B. L. Langdahl<sup>2</sup>. <sup>1</sup>Dep. of Clinical Biochemistry, Roskilde University Hospital, Roskilde, Denmark, <sup>2</sup>Dep. of Endocrinology and Metabolism, Aarhus University Hospital, Aarhus, Denmark, <sup>3</sup>Research Center for Ageing and Osteoporosis, Glostrup University Hospital, Glostrup, Denmark, <sup>4</sup>Dep. of Endocrinology, Copenhagen University Hospital Hvidovre, Hvidovre, Denmark, <sup>5</sup>Dep. of Endocrinology, Odense University Hospital, Odense, Denmark, <sup>6</sup>Dep. of Endocrinology, Hilleroed Hospital, Hilleroed, Denmark.

The purpose of the study was to examine the association of single nucleotides polymorphisms (SNP) in the purinergic P2X7 receptor to bone mass and vertebral fracture incidence in a cohort of post-menopausal women.

Two thousand and sixteen early postmenopausal women were included in the DOPS study and followed for 10 years. 1093 did not receive any HRT while 135 were treated continuously with HRT. Genotyping was performed on DNA from 1710 participants using TaqMan assays. Genotyping was done for five non-synonymous SNP placed in exons (Gly150Arg, His155Tyr, Arg307Gln, Ala348Thr, and Thr357Ser) and for one placed in an intron-splicing site (151+1: G-T).

The following allele frequencies were found: 151+1:GT (G/T: 0.99/0.01), Gly150Arg (G/A: 0.98/0.02), His155Tyr (C/T: 0.57/0.43), Arg307Gln (G/A: 0.99/0.01), Ala348Thr (G/A: 0.61/0.39), and Thr357Ser (C/G: 0.91/0.09). For all SNP Hardy-Weinberg equilibrium was found. Firstly, association of SNP to bone mineral density (BMD) right after menopause was examined. No association was found for any of the SNP with respect to BMD in hip or at the lumbar spine. Next, the association to BMD five and ten years after menopause was examined as well as rate of bone loss during the first five and ten post-menopausal years. We found a significant association between the Arg307Gln SNP with the highest rate of bone loss in the femoral neck in individuals and the GA genotype at both five and ten years (5/10 years: -2.0/-0.9 % per year) compared to the GG genotype (5/10 years: -1.2/-1.4 % per year) ( $p$ -value=0.009/0.004). The same was found for bone loss in total hip. Next, we examined the association between P2X7 genotype and fracture incidence ten years after menopause. Interestingly, we found a significant association between the Ala348Thr SNP and fracture incidence with the following incidences for individuals carrying the three genotypes: GG: 0.13, GA: 0.10, AA: 0.04 ( $p$ -value=0.035). No significant associations to any of the other SNP could be detected.

In conclusion, SNP in the P2X7 receptor gene are associated with bone loss after menopause as well as susceptibility to vertebral fractures in women. Further studies are needed to consolidate these findings.

**Disclosures:** N.R. Jorgensen, None.

## SU224

**Loss of Function Polymorphisms in The P2X<sub>7</sub> Receptor Gene Are Associated with Accelerated Lumbar Spine Bone Loss in Postmenopausal Women.** A. Gartland<sup>1</sup>, K. K. Skarratt<sup>2</sup>, L. J. Hocking<sup>3</sup>, L. Stokes<sup>2</sup>, R. Clifton-Bligh<sup>2</sup>, C. Parsons<sup>3</sup>, W. D. Fraser<sup>4</sup>, D. M. Reid<sup>3</sup>, J. S. Wiley<sup>2</sup>, J. A. Gallagher<sup>4</sup>. <sup>1</sup>Academic Unit of Bone Biology, The University of Sheffield, Sheffield, United Kingdom, <sup>2</sup>Department of Medicine, University of Sydney at Nepean Hospital, Sydney, Australia, <sup>3</sup>Division of Applied Medicine, University of Aberdeen, Aberdeen, United Kingdom, <sup>4</sup>The University of Liverpool, Liverpool, United Kingdom.

The gene for the P2X<sub>7</sub> receptor (P2RX7) is highly polymorphic with at least six known loss of function (LOF) single nucleotide polymorphisms (SNP) (151+1, c.474G>A, c.946C>A, c.1096C>G, c.1513A>C, and c.1729T>A). Two SNPs have previously been shown to be associated with an increased 10-year fracture risk in elderly postmenopausal Danish women. In addition, we recently reported association of c.946A with low lumbar spine (LS) bone mineral density (BMD), a key determinant of fracture risk, in younger postmenopausal women. The purpose of this study was to determine if other functional P2RX7 SNPs are associated with loss of BMD. We genotyped 508 postmenopausal women from the Aberdeen Prospective Osteoporosis Screening Study (APOSS) for six known functional P2RX7 SNPs. Females were recruited randomly from among the general population in the North East of Scotland from 1990-94 when aged 45-54y. Lumbar spine (LS) BMD was measured at baseline and at 6-7 year follow up when blood samples were collected for DNA extraction. P2RX7 genotyping was performed by homogeneous mass extension. Allelic frequencies for all P2RX7 SNPs were in Hardy-Weinberg equilibrium ( $p$ -values 0.2-1.0). We found association of c.946A with lower LS-BMD at baseline ( $p$ =0.006,  $\beta$ =-0.12) and follow-up ( $p$ =0.004,  $\beta$ =-0.13). Further analysis showed that the rate of loss of LS-BMD in a combined group of subjects who have a single LOF SNP at either 151+1, c.474, c.946, c.1096, and c.1729 ( $n$ =109) was five fold greater than subjects who were wild type at all known LOF positions ( $n$ =77) (rate of loss = 0.0064g/cm<sup>2</sup>/year and 0.0012g/cm<sup>2</sup>/year respectively,  $p$ =0.011, unpaired t-test). The significant difference in rate of LS-BMD loss disappears if subjects with the c.1513C allele are included in the combined group. A possible explanation is that although c.1513A>C SNP results in defective pore formation, the ATP-operated P2X<sub>7</sub> receptor channel remains intact. In contrast, the combined SNPs affect both channel and pore functionality. This analysis suggests that not only is the c.946A LOF SNP associated with low LS-BMD, but that other LOF SNPs, which result in similar pathophysiology of the P2X<sub>7</sub> receptor, are associated with accelerated bone loss at this site. The effect of the LOF SNPs on loss of BMD were not evident at the femoral neck, emphasising a site-specific effect of P2RX7 SNPs on BMD.

**Disclosures:** A. Gartland, None.

## SU225

**Variation in the Osteocalcin Gene: Association Study of BMD, Fracture and Changes in Body Fat Mass in Elderly Women.** F. McGuigan<sup>1</sup>, K. Ivaska<sup>1</sup>, P. Gerdhem<sup>2</sup>, H. Luthman<sup>1</sup>, K. Åkesson<sup>1</sup>. <sup>1</sup>Lund University, Malmö, Sweden, <sup>2</sup>Karolinska Institute, Stockholm, Sweden.

Limited information exists on variation in the Osteocalcin (OC) gene and bone phenotypes in various populations. The aim of this study was to determine the relationship between variation in OC, a marker of bone remodelling, and bone density and fracture in elderly women. In view of recent findings linking OC to energy metabolism, we are also evaluating the relationship with body fat parameters.

The study was performed in the Malmö Osteoporosis Prospective Risk Assessment study (OPRA) cohort, consisting of 1044 elderly women, all 75-yrs old at baseline which has been followed for up to 9 years. With respect to measures of adiposity, bone density and fracture, we analysed genotypes and derived haplotypes of 4 SNPs around the OC locus on chromosome 1, including rs18002487 located in the promoter. Only haplotypes with a >95% probability were used in the analysis.

Four of the 7 haplotypes observed in the population accounted for 85% of the alleles at the OC locus (Hap1 28%; Hap2 21%; Hap4 17%; Hap5 19%).

Individually, SNPs rs1800247 and rs2842880 were associated with percentage body fat ( $p$ =0.045 and 0.009 respectively) which was highest in the variant homozygotes.

Differences in the 5 year percentage change in fat mass were observed for rs1800247 ( $p$ =0.004), rs2842880 ( $p$ =0.012) and rs933489 ( $p$ =0.003). Variant homozygotes of rs1800247 and rs2842880 lost body fat whereas rs933489 variant homozygotes increased in adiposity. Haplotype analyses revealed only Hap1 to be related with body composition (total body fat mass at 5 years,  $p$ =0.028).

Individually, only rs2842880 was associated with BMD (FN,  $p$ =0.026). At baseline, Hap2 was associated with LS ( $p$ =0.03) and TB BMD ( $p$ =0.037). Bone mass increased incrementally with the number of haplotype alleles carried.

At 5 year follow-up Hap1 was associated with LS ( $p$ =0.038) and TB BMD ( $p$ =0.033). BMD decreased as haplotype allele number increased. Hap2 carriers exhibited similar trends at the LS ( $p$ =0.019).

We found no association with fracture sustained during lifetime, however for fractures sustained after the age of 50, Chi2 analysis identified differences associated with carriers of Hap1 ( $p$ =0.042) and Hap2 ( $p$ =0.045). Regression analysis identified Hap1 as a predictor of fracture ( $p$ =0.008) independent of BMD and body composition.

Our findings suggest that variation in the OC gene is linked to BMD and fracture in elderly caucasian women. Furthermore, and interestingly we can not exclude an independent influence on changes in fat mass, not previously recognized.

**Disclosures:** F. McGuigan, None.

## SU226

**Association Study of the TF and IGFBP3 Gene Polymorphisms with an Osteonecrosis of Femoral Head in Korean Population.** J. Hong<sup>\*1</sup>, T. Kim<sup>\*1</sup>, E. Park<sup>2</sup>, S. Kim<sup>3</sup>. <sup>1</sup>Skeletal Diseases Genome Research Center, Kyungpook National University Hospital, Daegu, Republic of Korea, <sup>2</sup>Department of Pathology and Regenerative Medicine, School of Dentistry, Kyungpook National University, Daegu, Republic of Korea, <sup>3</sup>Department of Orthopedic Surgery, Kyungpook National University Hospital, Daegu, Republic of Korea.

Osteonecrosis of the femoral head (ONFH) is devastating disease that frequently leads to the progressive collapse of the femoral head. The pathophysiology of ONFH is not completely elucidated, but it has been suggested that common pathogenesis involves the interruption of blood supply to femoral head. The disruption of the blood supply to the bone often caused hypoxia, which is the first stimulus for angiogenesis. Therefore, we hypothesized that angiogenesis regulated by hypoxia may play an important role in development or progression of osteonecrosis.

Transferrin (TF) and IGF-Binding Proteins 3 (IGFBP3) plays an important role in angiogenesis induced by hypoxia. TF is essential for iron regulation and acts as an angiogenesis factor produced by hypertrophic cartilage during endochondral bone formation. IGFBP3 is the most abundant in the circulation. It increases the bone resorption and reduces bone formation. Also, TF as an IGFBP-3 binding protein could enhance the modulation of cell proliferation and apoptosis. TF specifically might modulate IGFBP-3 activity by binding IGFBP-3.

To examine the associations between the TF/IGFBP3 gene polymorphisms and ONFH in Korean population, we selected several polymorphic sites of TF/IGFBP3 from public databases, and genotyped in 460 ONFH patients and 300 control subjects. We classified the patients according to etiology: alcohol-induced, steroid-induced, and idiopathic ONFH subgroup. Three SNPs (rs1880669, rs2692695 and rs2718806) in TF gene and two SNPs (rs2453839 and rs3110697) in IGFBP3 gene were associated with increased risk of ONFH. The stratified analysis by etiology revealed that two SNPs (rs1880669 and rs2692695) of TF gene and rs2453839 of IGFBP3 were significantly associated with increased risk of ONFH in idiopathic patients ( $P=0.0008$ - $0.0204$ , OR 1.38-2.37 in TF gene,  $P=0.0066$ , 8.67 in IGFBP3 gene). Our results suggest that TF and IGFBP3, hypoxia induced angiogenesis gene, are related to non-traumatic ONFH in Korean population. Defining the genetic susceptible factors for development of ONFH may provide more effective therapeutic implications and early diagnosis for disease.

**Disclosures:** S. Kim, None.

## SU227

**Effect of Tamoxifen and Aromatase Inhibitors on the Risk of Fractures in Women with Breast Cancer.** P. Vestergaard<sup>1</sup>, L. Rejnmark<sup>2</sup>, L. Mosekilde<sup>2</sup>.

<sup>1</sup>The Osteoporosis Clinic, Aarhus Amtssygehus, Aarhus, Denmark,

<sup>2</sup>Department of Endocrinology and Metabolism C, Aarhus Amtssygehus, Aarhus, Denmark.

One prior study has pointed at an increased risk of hip fractures in users of tamoxifen among women with breast cancer compared to non-users. We studied the risk of fractures among women who had used tamoxifen or aromatase inhibitors compared to non-users.

**Subjects and methods:** Case control study in women. There were 64,548 fracture cases and 193,641 age and gender matched controls.

**Results:** Use of tamoxifen in general was not associated with any significant change in the risk of any fracture, wrist fractures, and spine fractures. A significantly decreasing relative risk of fractures was seen with increasing dose although the risk never declined statistically significantly below that in non-users. An increased risk of hip fractures was seen, but the increase was limited to patients who had used low average doses (<20 mg of tamoxifen per day) and were prior users (i.e. had not used tamoxifen within the last year). Aromatase inhibitors were associated with a significant increase in overall risk of fractures and in the risk of hip fractures.

**Conclusions:** Tamoxifen does not seem to be bone protective in such a degree that the risk of fractures decreases below that of non-users. Tamoxifen per se does not seem to increase the risk of fractures. Aromatase inhibitors were associated with a significant increase in the risk of fractures. In women at high risk of fractures, supplementary measures i.e. bisphosphonates may be considered.

**Disclosures:** P. Vestergaard, None.

This study received funding from: Danish Medical Research Council.

## SU228

**Platelets Contribute to Circulating Levels of Dickkopf-1 (Dkk-1): Clinical Implications in Multiple Myeloma.** N. Voorzanger-Rousselot<sup>\*1</sup>, D. Goehrig<sup>\*2</sup>, P. Clézardin<sup>2</sup>, T. Facon<sup>\*3</sup>, P. Garnero<sup>4</sup>. <sup>1</sup>Molecular Markers, Synarc, Lyon, France, <sup>2</sup>INSERM U664, Lyon, France, <sup>3</sup>Services des Maladies du Sang, Hôpital Huriez, CHRU Lille, Lille, France, <sup>4</sup>Molecular Markers, SYNARC and INSERM U664, Lyon, France.

The Wnt signaling pathway plays an important role in regulating bone metabolism. Levels of Dickkopf-1 (Dkk-1) -a soluble inhibitor of Wnt- measured in the bone marrow aspirates of patients with multiple myeloma (MM) have shown to be associated with radiological bone lesions. The clinical value of circulating Dkk-1 measurements is currently unclear. The aim of the study was to evaluate circulating levels of Dkk-1 in

patients with MM and investigate whether platelets contribute to its level.

Dkk-1 was measured by ELISA in serum (activation of platelets during the clotting phase) and paired plasma (no platelet activation) samples of 30 patients with MM stage II or III (mean age: 59 years from 44 to 72 years) and 33 healthy age-matched controls. To assess platelet contribution to circulating Dkk-1 levels, platelet-rich plasma was obtained from 5 healthy individuals and platelets were activated with thrombin receptor activator peptide 6 (TRAP-6) (from 0 to 6μM) or native collagen (0 to 10μg/ml). Expression and localization of Dkk-1 by platelets, was analyzed by RT-PCR and immunogold electron microscopy, respectively.

As shown on the table, serum levels of Dkk-1 were significantly higher than in paired plasma samples both in patients with MM and in controls, suggesting a release of Dkk-1 from platelets during the clotting phase. Plasma- but not serum- levels of Dkk-1 were significantly increased (+205 %  $p=0.0002$ ) in patients with MM compared to healthy controls. Both TRAP-6 and collagen induced a dose dependent release of Dkk-1 by platelets. Electron microscopy revealed the presence of Dkk-1 protein within the  $\alpha$ -granules of platelets, although RT-PCR failed to show mRNA expression. This suggests that the origin of platelet Dkk-1 is endocytosis of circulating Dkk-1 rather than endogenous synthesis.

Subjects	Dkk-1 levels (mean $\pm$ SD), ng/ml	
	Serum	Plasma
Multiple Myeloma (n=30)	7.00 $\pm$ 1.49*	4.47 $\pm$ 0.81#
Controls (n=33)	4.13 $\pm$ 2.58**	1.47 $\pm$ 0.18

\* $p<0.05$  \*\* $p<0.001$  vs paired plasma samples

#  $p<0.0001$  vs controls

In conclusion platelets contribute significantly to circulating levels of Dkk-1. Measurement of Dkk-1 in plasma, rather than in serum is recommended to limit the interference of platelet contribution, and improve the sensitivity to detect alterations of the Wnt signaling pathway in multiple myeloma.

**Disclosures:** P. Garnero, None.

## SU229

**Notch Pathway Is Activated In Osteosarcoma and Inhibitors of  $\gamma$ -secretase Inhibit Osteosarcoma Growth By Cell Cycle Regulation.** M. Tanaka<sup>\*</sup>, T. Setoguchi, M. Hirotsu<sup>\*</sup>, H. Sasaki<sup>\*</sup>, S. Komiya. Department of Orthopaedic Surgery, Kagoshima University, Kagoshima City, Japan.

**Purpose:** The Notch signaling pathway functions as an organizer in embryonic development. Recent studies have shown constitutive activation of the Notch pathway in various types of malignancies. However, it remains unclear whether Notch pathway is activated in human osteosarcoma. In an attempt to better understand osteosarcoma pathogenesis, we investigated the expression and activation of Notch proteins in osteosarcoma and examined the effect of  $\gamma$ -secretase inhibitor (GSI) to osteosarcoma growth. GSI are considered pan-Notch inhibitors. And also, we examined the molecular mechanism of osteosarcoma growth inhibition by GSI.

**Materials and Methods:** RT-PCR and immunohistochemistry was performed using human osteosarcoma cell lines and human osteosarcoma samples. Cells were treated with various GSIs to inhibit Notch activation. RBP-jk siRNA was used to confirm the effect of Notch signal inhibition. Nude mice were injected with osteosarcoma cells intradermally. Cell cycle was analyzed by flowcytometry. The expression of the components of cell cycle machinery was analyzed by quantitative RT-PCR and western blot.

**Results:** RT-PCR revealed high levels expression of Notch related genes in all of osteosarcomas cell lines. And also, 7 osteosarcoma human samples also showed high levels expression of Notch related genes. In addition, immunohistochemistry showed high expression of NIC in nucleus of osteosarcoma cell lines and human osteosarcoma samples. And also, expression of Jagged1 and Hes1 was observed in human osteosarcoma samples. These data suggest that notch signaling pathways are activated in osteosarcoma. MTT assay showed that GSI and RBP-jk siRNA suppressed the growth of the osteosarcoma cell lines in vitro. Intraperitoneally GSI administration dramatically inhibited the osteosarcoma xenografts growth in vivo. Kaplan-Meier analysis showed that GSI administration confers statically significant survival benefit. When osteosarcoma cell were cultured without GSI, 39.8 % cells were in G1 phase. On the other hand, when cultured with GSI, 53.3 % cells were in G1 phase. These data suggest that GSI promoted G1 arrest. Real time RT-PCR revealed that GSI suppressed transcription of cyclin D1, D3, cyclin E1, E2, and Skp2. Western blot revealed GSI promoted suppression of cyclin D1, D3, cyclin E1, E2, c-Myc, and Skp2 proteins. On the other hand, P21<sup>cip1</sup> protein was upregulated by GSI treatment. These data suggest that GSI suppressed osteosarcoma growth and promoted G1 arrest by regulation of cell cycle regulators expression.

**Discussion:** These data suggest that inactivation of Notch may be a therapeutic approach for treating patients suffering from osteosarcoma.

**Disclosures:** M. Tanaka, None.

## SU230

**Zoledronic Acid Inhibits the Capacity of Myeloid-Immune Suppressor Cells in Myeloma to Form Osteoclasts.** J. Zhuang, C. M. Edwards, J. Zhang, S. T. Lwin\*, G. R. Mundy. Vanderbilt Center for Bone Biology, Nashville, TN, USA.

Bisphosphonates accumulate in the bone matrix and cause direct inhibition of osteoclasts (OCs) by their effect on mature multinucleated bone resorbing cells. Powerful nitrogen-containing bisphosphonates such as zoledronic acid are taken up under the ruffled border of multinucleated OCs and inhibit enzymes important in mevalonic acid synthesis, causing loss of osteoclast polarity and apoptosis (Coxon et al. Bone 2005). Little is known of the effects, if any, on osteoclast precursors, which are not polarized or developed ruffled borders. We have found that a subset of primitive hematopoietic precursor cells called myeloid immune suppressor cells (MISCs), which are Gr-1 and CD11b positive, accumulate significantly in bone marrow and spleen during myeloma progression, and promote myeloma growth. We have also found that MISCs in myeloma-bearing mice are osteoclast precursors and have increased capacity to form OCs. We hypothesized that bisphosphonates have inhibitory effects on MISCs, as well as on mature OCs. Results: We used the well-characterized 5TGM1 murine model of myeloma. 5TGM1-GFP tagged myeloma cells were inoculated via tail vein. Zoledronic acid (ZA) 100ug/kg was injected subcutaneously 2/week from time of tumor inoculation (n=8). We found that ZA reduces the proportion of spleen MISCs by 30% as well as OC number in myeloma bearing mice by histology ( $6.13 \pm 2.34$  vs  $0.88 \pm 0.16$ /mm bone surface). MISCs were sorted from these mice by magnetic beads. After 14 day culture with M-CSF (25ng/ml) and RANKL (50ng/ml) in vitro, ZA treatment of mice impairs the capacity of harvested MISCs to form OCs (OC number/x100 field  $42.4 \pm 4.0$  vs  $25.6 \pm 3.5$ ,  $p < 0.01$ ). To identify the potential of MISCs to form dendritic cells (DCs), we cultured MISCs from myeloma-bearing mice with GM-CSF (20ng/ml) for 8 days and determined the CD11c+ cells by flow cytometry. ZA reduced the proportion of CD11c+ (from 60% to 44%), indicating the capacity of MISCs to form DCs is also suppressed. We did not find inhibition of prenylation of small GTPases, namely Rap1A and Rab6 in MISCs from myeloma-bearing mice treated with ZA. This suggests that the effect of ZA on MISCs is not mediated by effects on the mevalonate pathway, and thus may be indirect. We have also found that after co-culture with MISCs for 96h, the inhibition of CD4+ T cell proliferation by tumor MISCs was reversed in the ZA treated group ( $52.9 \pm 12.1\%$  vs  $78.2 \pm 8.7\%$  viable cells compared with control MISCs,  $P < 0.05$ ). Thus we conclude that when myeloma-bearing mice are treated with ZA, MISCs are reduced, and the residual MISCs have reduced capacity to form not only OCs, but also DCs. Our conclusions are that ZA inhibits precursors of OCs, and this effect is likely indirect and independent of effects of ZA on GTPase prenylation in OCs.

**Disclosures:** J. Zhuang, None.

## SU231

**Transcriptional Silencing of Frzb/sFRP3 by Promoter Methylation in Osteogenic Sarcoma.** T. Tsuchiya\*, K. L. Shogren\*, E. Mahlum\*, A. Maran\*, M. Yaszemski\*, G. Sarkar\*. <sup>1</sup>Orthopedic Department, Yamagata University, Yamagata, Japan, <sup>2</sup>Orthopedic Department, Mayo clinic, Rochester, MN, USA.

Frzb/sFRP3 is an antagonist of the transmembrane frizzled receptor, a component of the Wnt signaling pathway, and has been suggested to be a candidate tumor suppressor in several human malignancies. Frzb/sFRP3 belongs to a family of five genes that includes sFRP1, sFRP2, sFRP4, and sFRP5. These last four genes were reported to be inactivated by promoter hypermethylation in some cancers. Frzb/sFRP3 has also been reported to be inactivated in some cancers, but it is not known whether the inactivation is due to promoter methylation. Consequently, the mechanism underlying inactivation of sFRP3 remains unknown. We previously demonstrated severe suppression of Frzb/sFRP3 mRNA expression in osteogenic sarcoma (OGS). In this report, we have tested the hypothesis that the inactivation of Frzb/sFRP3 mRNA expression was due to promoter methylation. Our investigation shows that demethylation treatment restored the expression of Frzb/sFRP3 mRNA in 4 osteogenic sarcoma cell lines. Bisulfite treated-DNA sequencing confirmed methylation of the Frzb/sFRP3 promoter in all 4 OGS cell lines. In addition, we screened 9 other OGS cell lines, through bisulfite treated DNA sequencing, which showed methylation at some CpG-residues in the Frzb/sFRP3 promoter in 6 of these 9 OGS cell lines. Thus our findings demonstrate that 10 (77%) out of 13 OGS cell lines show at least partial methylation in the Frzb/sFRP3 promoter. This is the first report providing a correlation between inactivation of Frzb/sFRP3 mRNA expression with methylation of the cognate promoter.

**Disclosures:** T. Tsuchiya, None.

## SU232

**EphB4 Expression in Osteoblasts is Regulated by Myeloma Cells and the Wnt Signaling Pathway.** A. L. Bates\*, S. T. Lwin\*, G. R. Mundy, C. M. Edwards. Vanderbilt Center for Bone Biology, Vanderbilt University, Nashville, TN, USA.

Multiple myeloma (MM) is associated with a destructive osteolytic bone disease, characterized by an increase in osteoclastic bone resorption and a reduction in osteoblastic bone formation. The coupling between osteoblasts and osteoclasts during normal bone homeostasis may be due to bidirectional signaling between the ligand ephrinB2 on osteoclasts, and its receptor EphB4 on osteoblasts. Reverse signaling through ephrinB2 inhibits osteoclast activity whereas forward signaling through EphB4 stimulates osteoblast differentiation. Since the normal coupling of bone resorption to formation is dysregulated in MM, we hypothesized this may be mediated by modifications in the EphB4/ephrinB2 receptor/ligand interaction. Our previous studies have suggested that myeloma cells release a soluble factor which mediates a decrease in EphB4 expression by osteoblasts. The aim of the present study was to further study the regulation of EphB4 expression in osteoblasts, focusing on regulation by (i) myeloma cells and (ii) the Wnt signaling pathway. Although conditioned media from 5TGM1 myeloma cells significantly decreased EphB4 expression in osteoblasts, it had no effect on ephrinB2 protein or mRNA expression, suggesting that the effect of myeloma cells is specific for EphB4. 2T3 osteoblasts were cultured for 48h in the presence or absence of 5TGM1 myeloma cells. Following coculture, myeloma cells were separated by differential trypsinization, and a purity of >95% confirmed by flow cytometry. Real-time PCR demonstrated an 85% decrease in EphB4 expression by osteoblasts following direct culture with myeloma cells, as compared with osteoblasts cultured alone. In contrast, no change in expression of alkaline phosphatase, collagen 1 or Runx2 was found by PCR, suggesting that the decrease in EphB4 expression is not related to osteoblast differentiation. MM bone disease is associated with inhibition of Wnt signaling in osteoblasts. Transfection of C2C12 osteoblasts with constitutively active beta-catenin resulted in a significant increase in EphB4 promoter activity, whereas dominant-negative TCF4 significantly reduced EphB4 promoter activity. Treatment of either C2C12 or 2T3 osteoblasts with 20mM LiCl, which acts to inhibit GSK-3beta and increase Wnt signaling, increased both EphB4 promoter expression and EphB4 mRNA expression. This suggests that EphB4 in osteoblasts is a target of beta-catenin. Taken together, our studies suggest that MM cells decrease EphB4 expression by osteoblasts, and implicate the Wnt signaling pathway in the regulation of EphB4. Therefore, down-regulation of EphB4 by MM cells may disrupt the normal coupling of bone formation to resorption and contribute to MM bone disease.

**Disclosures:** A.L. Bates, None.

## SU233

**Melanoma-Induced Bone Loss is Mediated by the Rapid Recruitment of Osteoclasts.** J. R. Edwards, L. C. Dumitrescu\*, J. A. Sterling, S. T. Lwin\*, G. R. Mundy. Center for Bone Biology, Vanderbilt University Medical Center, Nashville, TN, USA.

Dramatic bone destruction is a common feature of tumor-bone metastasis, resulting in extensive bone loss, chronic pain and often represents the terminal phase of disease. Despite the common consensus that osteoclasts remain the sole bone-resorbing cell of the body, recent studies have suggested that melanoma-associated bone loss is not mediated by osteoclasts (Sanchez-Sweetman *et al*, 1997; Jones *et al*, 2006). Since we have been unable to find convincing evidence that bone osteolysis in any cancer occurs independent of osteoclasts, we studied melanoma-osteoclast interactions using the identical bone metastasis model employed above. *In vivo* bone mass was assessed by uCT and histomorphometry, and direct evidence of osteoclast involvement determined by TRAP and vitronectin receptor (VNR) staining, and by examining urinary markers of resorption. *In vitro* resorption assays and molecular studies were used to identify potential mechanisms of melanoma-osteoclast interactions. C57Bl6 mice inoculated with B16F10 melanoma cells or PBS by intra-cardiac injection were sacrificed at day 18 or 24, upon which the tumor burden was clearly obvious by a blackened marrow cavity. This corresponded with a significant decrease in bone volume in both groups, and interestingly DPD analysis indicated a higher level of resorptive activity at the earlier time point. This corresponded with a greater increase in osteoclast surface/bone surface ratio at day 18 (59%) than that seen at day 24 (28%), compared to control animals. Treatment of normal marrow cells with media conditioned by B16F10 or Mel A melanoma cells showed a significant dose-dependent increase in TRAP+, VNR+ osteoclast formation and correlated with increased resorption on dentine discs. RT-PCR analysis identified expression of the osteolytic factors PTHrP and MIP-1α in both cell lines. These studies demonstrate a clear osteoclast-related bone loss associated with melanoma metastasis and identify factors capable of stimulating osteoclast activity. These findings are consistent with a central role for osteoclasts in the extensive osteolysis observed in melanoma bone metastases.

**Disclosures:** J.R. Edwards, None.

## SU234

**Alpha-Calcium/Calmodulin Dependent Kinase II Controls Osteosarcoma Cell Migration.** K. Yuan\*, M. Zayzafoon. Pathology, University of Alabama at Birmingham, Birmingham, AL, USA.

Calcium/Calmodulin dependent kinase II (CaMKII) is a multifunctional serine/threonine kinase that is highly expressed in neuronal cells, but is also expressed in other cells. We have previously shown that alpha-CaMKII controls the growth of osteosarcoma through regulating p21<sup>CIP/KIP</sup> expression. CaMKII has also been implicated in the modulation of cell migration. The purpose of this study was to determine the role of CaMKII in regulation of osteosarcoma cell migration. First immunohistochemistry staining for phosphorylated alpha-CaMKII was performed on osteosarcoma tissue microarray slides. Results of the immunophenotypic evaluation of tissue microarray showed that 65% of patients were positive staining for phosphorylated alpha-CaMKII. We used a lentivirus to deliver designed human alpha-CaMKII-targeted short hairpin RNAs (shRNA) into MG63 human osteosarcoma cell lines and examined shRNA inhibition ability. The gene expression and protein level of alpha-CaMKII decreased 81% in stable alpha-CaMKII shRNA expression cells, when compared to scramble shRNA expression cells. A wound-healing assay revealed that alpha-CaMKII knock-down cells are unable to migrate efficiently into in vitro wound space, the cells moved in original wound space decreased 40% as compared to scramble shRNA expression cells. Results from a transwell migration assay also showed that alpha-CaMKII knock down MG63 cells decreased their migration ability, suppression of the alpha-CaMKII caused a 49% reduction in the number of cells that traversed the membrane versus nonsilencing control. F-Actin staining results showed that the number of both filopodia and lamellipodia formed in alpha-CaMKII knock-down cells was decreased 75% and 79%, respectively, compared to scramble shRNA expression cells, suggesting the low motility ability of alpha-CaMKII knock-down cells. Furthermore, scramble shRNA expression cells have an asymmetrical focal adhesions distribution; comparatively, alpha-CaMKII knock-down cells exhibit more peripherally distributed focal adhesions along the entire basal surface of the cell. These results suggest that alpha-CaMKII controls the migration of osteosarcoma cells by regulating filopodia and lamellipodia formation and is implicated in the modulation of osteosarcoma metastasis.

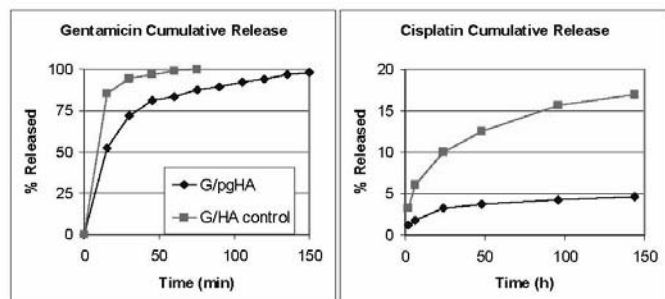
**Disclosures:** K. Yuan, None.

## SU235

**Controlled Drug Release from Calcium Phosphate-Based Orthopaedic Implants.** G. Zhu\*, M. Saadia\*, S. J. Lippard\*, L. D. Silverman\*. <sup>1</sup>Chemistry, MIT, Cambridge, MA, USA, <sup>2</sup>Chemistry, Yeshiva University, New York, NY, USA.

A route to making novel controlled-drug release coatings on porous calcium phosphate-based orthopaedic implants was explored by binding lifesaving drugs, including the antibiotic gentamicin (G) and chemotherapeutic agent cisplatin (cis-[Pt(NH<sub>3</sub>)<sub>2</sub>Cl<sub>2</sub>], cDDP), to poly-L-glutamic acid (pg) adsorbed on implant surfaces. pg adsorbed onto hydroxyapatite powder (HA) was used to test the concept. G was adsorbed onto the coated powder to make a 0.83% G drug release product (G/pgHA), with controls made by impregnation of non-coated HA at equal drug loading (G/HA). In vitro release rates were measured in PBS buffer (4.0 mg/mL, pH 7.4, 37°C), with sequential removal/replacement of buffer in some experiments. Samples reached equilibrium with buffer in < 1 h, with less G released by G/pgHA (53%) than by G/HA (71%). Fig 1A shows slower drug release for G/pgHA vs. G/HA with sequential buffer replacement.

cDDP was loaded on pgHA and HA controls by overnight mixing and filtration, to make 5.3% and 5.7% cPT products, respectively. Drug release was measured in simulated body fluid (4.5 mg/mL, pH 7.4, room temperature) via centrifugation and AA analyses. Release of cDDP with buffer exchange (Fig 1B) shows slower drug release from cDDP/pgHA vs. cDDP/HA over 6 days.



The drug loading in G/pgHA is sufficient to kill staphylococci in 500 cc of tissue from 1 g of powder. The G/pgHA data represents a series of sequential equilibria, analogous to chromatographic migration that would occur in a large piece of coated porous implant material in vivo. The experiment demonstrates that: (1) G is bound to pgHA in clinically significant quantities, (2) it is released more slowly than the control, and (3) it is completely removed under the sequential sampling conditions, which is important for prevention of breeding antibiotic resistant bacteria. We anticipate that G release will be significantly slower in a larger porous implant sample in the presence of clotted blood in a surgical site in vivo (J Orthopaedic Res (2007) 25:23-9).

The cDDP/pgHA loading is sufficient to kill cancer cells in 3.5 kg of tissue per g cDDP/pgHA. The release rate of cDDP is greatly reduced from pgHA vs. HA. We conclude that

pgHA and acidic polypeptide coated calcium phosphate implants in general represent promising materials for local delivery of a variety of drugs, including gentamicin and cisplatin.

**Disclosures:** L.D. Silverman, None.

## SU236

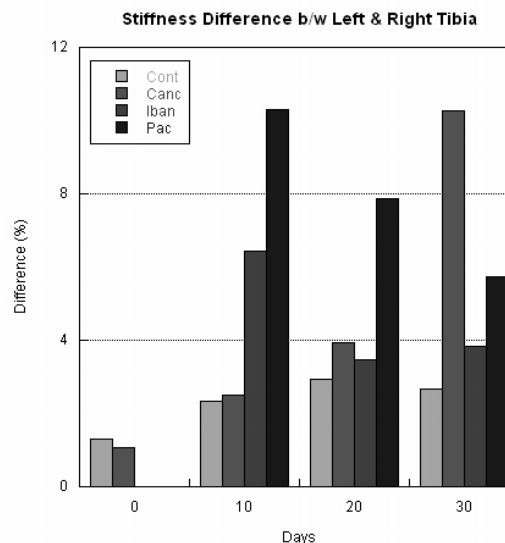
**Biomechanical and Geometrical Property Changes in Rat Tibias with Tumor-Induced Osteolysis after Anti-Resorptive or Anti-Cancer Treatments.** T. Lee<sup>1</sup>, R. C. Soong<sup>2</sup>, Y. H. Chan<sup>3</sup>, S. Das De<sup>4</sup>, J. C. Goh<sup>4</sup>. <sup>1</sup>Division of Bioengineering, National University of Singapore, Singapore, <sup>2</sup>Department of Pathology, National University of Singapore, Singapore, <sup>3</sup>School of Medicine, National University Hospital, Singapore, Singapore, <sup>4</sup>Department of Orthopaedic Surgery, National University Hospital, Singapore, Singapore.

The study investigates the efficacy of anti-cancer (Paclitaxel) and anti-resorptive (Ibandronate) in treating tumor-induced osteolysis by assessing changes in geometrical and mechanical properties of the affected bone. A rat tibia model for tumor-induced osteolysis using W256 malignant breast cancer cells was used. Of the 30 rats implanted with cancer cells, 12 were injected cancer cells only (Canc), 9 received ibandronate (Iban), 9 received paclitaxel (Pac) and 12 underwent a sham operation (Cont). At 10-days intervals up to 30-days, the paired-tibias were assessed by  $\mu$ CT scans to quantify the geometrical parameters. The paired-bones were also assessed by a 3-point bending test using a custom-made jig for their mechanical property.

The total BV was significantly smaller in the tumor-induced compared to the contra-lateral tibia in the Canc group. While the geometric parameters were markedly lower for both Iban and Pac groups, the Iban group seems more successful, with a further 5.5% reduction in total BV difference, in comparison to Pac group. This pattern is repeated in CSA of cortical bones at 25% of the distal femur length.

Higher Tb.Th, Tb.N, BV/TV, and BS/BV of the tumor-implanted femurs were noted in both Iban or Pac groups compared to those in Canc group. With the exception in Tb.N, Iban group was better than Pac group in maintaining the trabecular properties.

The paired-difference in stiffness in the Iban group was lowered to 3.8% at 30-days, whereas the Pac group had a stiffness lowered to 5.7%. The results suggest that both Iban and Pac treatments in tumor osteolysis have the potential to preserve the structural integrity of the affected bones, and improve the mechanical property. While ibandronate results in less reduction imprint the in bone geometry, paclitaxel seems more effective in maintaining its stiffness.



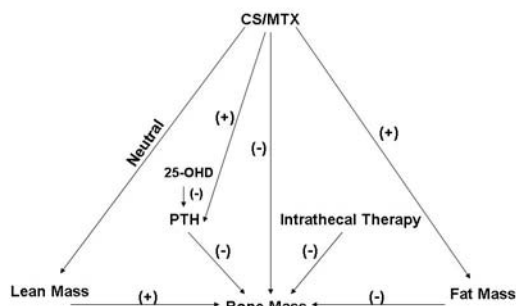
**Disclosures:** T. Lee, None.

This study received funding from: NMRC (R397-000-059-213).

## SU237

**Modeling Pathways for Bone Loss in Childhood Malignancies: A Prospective Study.** G. El-Hajj Fuleihan<sup>1</sup>, S. Muwakkit<sup>2</sup>, A. Arabi<sup>1</sup>, L. El-Onsi<sup>1</sup>, J. Chaiban<sup>1</sup>, M. Abboud<sup>2</sup>. <sup>1</sup>Calcium Metabolism and Osteoporosis Program, American University of Beirut-Medical Center, Internal Medicine, Beirut, Lebanon, <sup>2</sup>Children Cancer Center, American University of Beirut-Medical Center, Pediatrics, Beirut, Lebanon.

Our group and others have shown that children treated for malignancies have low bone mass due to poor nutrition, direct effects of chemotherapy on bone, as well as effects of chemotherapy and radiation therapy on growth, and gonadal status. We currently report on follow-up of the same cohort investigating predictors of bone mass changes over time. 31 children (N=29 with ALL), mean age 9±2.8 years, 21 still receiving therapy for 80±2.8 weeks, 9 having finished 40±22 weeks prior, and 32 age and gender-matched controls, were followed over 14 months. Age at diagnosis, calcium intake, exercise activity, doses of corticosteroids (CS) and Methotrexate (MTX) received within the follow-up period, and intrathecal MTX-CS therapy were assessed. Blood was obtained for routine chemistries, parathyroid hormone (PTH), 25 hydroxy vitamin D (25-OHD) levels, osteocalcin and crosslaps at baseline and follow-up. Bone mass and body composition were measured at baseline and follow-up. Univariate and multivariate analyses were conducted to evaluate predictors of changes in bone mass. At follow-up, 22/31 remained at Tanner stage 1. Patients had a lower calcium intake, exercise activity, serum calcium, albumin and bone markers levels, and higher PTH levels than controls. They also had higher fat mass and lower bone mass at the spine and hip, and lower increments in bone mass at the total body compared to controls. Predictors of bone mass changes on univariate analyses were: age at diagnosis (R= -0.49 to -0.39, p<0.05), MTX/CS doses (R= -0.54 to -0.37, p<0.05), intrathecal therapy (p<0.03), % changes in lean mass (R=0.38 to 0.54, p<0.04), fat mass and % changes in fat mass (R= -0.46 to -0.41, p<0.02), 25-OHD levels (R=0.38 to 0.41, p<0.04), and PTH levels (R= -0.45 to -0.37, p<0.04). The predictive effect of vitamin D disappeared when adjusting for PTH levels and that of PTH disappeared when adjusting for MTX/CS dose. On multivariate analyses predictors of changes in bone mass, depending on the skeletal site, were: age at diagnosis, fat mass, lean mass, MTX/CS, and intrathecal therapy. Based on our results we propose the following paradigm to outline pathophysiological mechanisms for bone loss in children on therapy for malignancies.



**Disclosures:** G. El-Hajj Fuleihan, None.

This study received funding from: Novartis Pharmaceuticals.

## SU238

**Microstructural Changes at the Ultradistal Radius in Monoclonal Gammopathy of Undetermined Significance.** N. Charatcharoenwittaya<sup>1</sup>, S. Kumar<sup>2</sup>, S. V. Rajkumar<sup>2</sup>, R. A. Kyle<sup>2</sup>, S. J. Achenbach<sup>3</sup>, M. F. Holets<sup>1</sup>, L. K. McCready<sup>1</sup>, S. Amin<sup>4</sup>, M. T. Drake<sup>1</sup>. <sup>1</sup>Endocrinology, Mayo Clinic, Rochester, MN, USA, <sup>2</sup>Hematology/Oncology, Mayo Clinic, Rochester, MN, USA, <sup>3</sup>Biostatistics, Mayo Clinic, Rochester, MN, USA, <sup>4</sup>Rheumatology, Mayo Clinic, Rochester, MN, USA.

Recent population-based studies have demonstrated that the risk for fractures is increased in patients with monoclonal gammopathy of undetermined significance (MGUS), a premalignant condition with an approximately one percent annual risk of progression to multiple myeloma. While MGUS has been consistently associated with elevated bone resorption and/or reduced bone formation markers, DXA-based studies evaluating whether areal bone mineral density (aBMD) is reduced in patients with MGUS have yielded conflicting results. Further, although DXA provides quantitative information about bone mass, the microstructural properties of the measured bone which are critical determinants of bone quality and strength, are not measured. To better understand the effect of MGUS on skeletal health, we performed both standard aBMD measurements by DXA, and high resolution 3D-pQCT (XtremeCT, Scanco AG, voxel size ~82 microns) measurements at the ultradistal radius to evaluate bone microstructural parameters, in 25 subjects with MGUS (8 F and 17 M; mean age 71.2 ± 9.5 years). Study subjects were age-, sex-, and BMI-matched (1:2) with control subjects (16 F and 34 M; mean age 71.2 ± 9.8 years) from the local community. Comparison of the MGUS cohort to the control subjects revealed no significant differences in DXA aBMD measurements at the femur, lumbar spine, total spine, forearm, or total body. Trabecular microstructure (bone volume, trabecular number, thickness, or separation) also did not differ in the MGUS compared to control subjects. In contrast, we found that cortical volumetric BMD (vBMD) was significantly decreased (P < 0.02) at the ultradistal radius in subjects with MGUS. Further, endocortical area (P = 0.07) and total bone

area (P = 0.08) demonstrated a trend towards an increase in patients with MGUS, suggesting increased endocortical bone resorption, with perhaps a compensatory increase in periosteal apposition. In summary, these data represent the first assessment of *in vivo* bone microstructure in subjects with MGUS, and demonstrate that (1) the increased incidence of fractures previously found to occur in patients with MGUS may not be reflected in DXA aBMD measurements, which were not different between patients with MGUS and matched controls; and (2) patients with MGUS have reduced cortical vBMD, at least at the distal radius. Further prospective studies are needed to test whether the observed losses of cortical bone predict progression to myeloma.

**Disclosures:** M.T. Drake, None.

This study received funding from: Mayo Clinic.

## SU239

**Preclinical Validation of a Novel Dkk-1 Neutralizing Antibody for the Treatment of Multiple Myeloma Related Bone Disease.** S. Pozzi<sup>1</sup>, H. Yan<sup>2</sup>, S. Vallet<sup>1</sup>, N. Vaghela<sup>1</sup>, D. Cirstea<sup>3</sup>, L. Santo<sup>3</sup>, S. Mukherjee<sup>2</sup>, T. Hideshima<sup>3</sup>, L. Schirtzinger<sup>4</sup>, S. Kuhstoss<sup>4</sup>, K. C. Anderson<sup>3</sup>, D. Scadden<sup>2</sup>, N. Raju<sup>1</sup>. <sup>1</sup>Massachusetts General Hospital-Dana Farber Cancer Institute-Harvard Medical School, Boston, MA, USA, <sup>2</sup>Massachusetts General Hospital-Harvard Medical School, Boston, MA, USA, <sup>3</sup>Medical Oncology, Dana Farber Cancer Institute-Harvard Medical School, Boston, MA, USA, <sup>4</sup>Eli Lilly and Company, Indianapolis, IN, USA.

Multiple myeloma (MM) is a plasma cell dyscrasia characterized by osteolytic bone lesions in 80% of patients. Bisphosphonates reduce skeletal related events, without impacting bone healing. Increased expression of Dkk1 in a subset of MM patients and its association with lytic bone disease makes it a potential new target for the treatment of myeloma bone disease. Dkk1, an inhibitor of the wingless int (wnt) pathway, is important in osteoblastogenesis. The aim of this study was to test the effect of a Dkk-1 neutralizing chimeric antibody (Mab B3) on osteoblasts (OB), osteoclasts (OC) and MM cells in the context of the bone microenvironment. First, we tested the expression of Dkk1 in plasma and bone marrow of 16 MM patients and 10 MM cell lines. Dkk1 levels were >18 ng/mL in 2 out of 16 patients; levels were comparable in blood and bone marrow plasma. In contrast, very little Dkk1 (2-9 ng/ml) was produced by bone marrow stromal cells (BMSC). One out of 10 MM cell lines (INA-6) expressed low concentrations of Dkk1 in the supernatant. Second, we tested the effect of Mab B3 on MM cell lines, in the presence or absence of BMSC, and on OB and OC from MM patient derived bone marrow. The effects on OC were evaluated by TRAP staining and pit formation. Effects on OB were assayed by alkaline phosphatase staining and alizarin red assays for calcium deposition. Our data demonstrates no direct cytotoxic effects on MM cell lines negative for Dkk1 using Mab B3. Mab B3, however, enhanced OB differentiation and calcium deposition in a dose dependent manner and inhibited OC differentiation and function, as evidenced by a decrease in number of multinucleated TRAP+ cells and a decrease in pit formation. Ongoing studies are addressing the effect of Mab B3 on MM cells in the context of OC and OB. In conclusion our preliminary data suggests that Mab B3 functions as an anabolic agent; a corresponding human monoclonal antibody may be useful for the treatment of MM related bone disease. Future studies will evaluate the effect of Mab B3 in an *in vivo* mouse model of multiple myeloma, alone and in combination with bisphosphonates.

**Disclosures:** S. Pozzi, None.

This study received funding from: Eli Lilly and Company, Indianapolis.

## SU240

**2-Methoxyestradiol Alters eIF4E Activity and Causes Protein Synthesis Inhibition in Osteosarcoma Cells.** K. L. Shogren<sup>1</sup>, E. W. Mahlum<sup>1</sup>, M. J. Yaszemski<sup>1</sup>, A. Maran<sup>1</sup>. Orthopedic Research, Mayo Clinic, Rochester, MN, USA.

Regulation of protein synthesis plays an important role in the control of malignancy. Majority of the regulation of protein synthesis takes place at the level of translation initiation involving eIF4F protein complex, which consists of three proteins: eIF4E, eIF4A and eIF4B. The eIF4E, which serves as a rate-limiting factor of the eIF4F complex, binds to 7-methyl guanosine triphosphate cap present in most mRNAs, and thereby globally regulates cap-dependent protein synthesis. Previous studies in several systems demonstrate the involvement of eIF4E in malignant transformation and progression.

Osteosarcoma is the most common primary malignant bone tumor that affects children and young adults. Current treatment of osteosarcoma relies on a combination of surgery and chemotherapy. Although this has led to improved survival rate, a definite therapy is yet to be determined in most cases. We have demonstrated that 2-Methoxyestradiol (2-ME), a metabolite of 17beta-estradiol, induces apoptosis and exerts anti-tumor effects in osteosarcoma cells. The molecular mechanism of action of 2-ME on osteosarcoma cells is not well understood, but appears to involve RNA-dependent protein kinase (PKR) signaling.

To further understand the mechanism of 2-ME-induced cell death, we have studied the regulation of translation initiation factor eIF4E in 2-ME-treated osteosarcoma cells by affinity chromatography, co-immunoprecipitation and western blot analysis. Our results show that 2-ME-treatment modulates both eIF4E and eIF4E-binding protein (4EBP1) in MG63 human osteosarcoma cells. 2-ME treatment resulted in a decrease in binding of eIF4E to cap. In addition, analysis of cap-binding complexes showed that 2-ME treatment reduced the association of eIF4E with the eIF4G subunit, and at the same time, its association with eIF4E-BP1 increased. Also, MG63 cells, stably transfected with a cDNA for a "loss of function mutant" RNA-dependent protein kinase (PKR) protein, were resistant to 2-ME-induced regulation of eIF4E. These findings show that 2-ME treatment

results in modifications of the eIF4F complex, which is further supported by the inhibition of protein synthesis in 2-ME-treated cells. Thus, our study suggests that translational regulation plays an important role in 2-ME-mediated control of osteosarcoma cells.

**Disclosures:** A. Maran, None.

*This study received funding from: Mayo Clinic.*

## SU241

**Hedgehog Pathway Is Activated in Osteosarcoma and Cyclopamine Prevents Osteosarcoma Growth by Cell Cycle Regulation.** M. Hirotsu\*, T. Setoguchi, H. Sasaki\*, S. Komiya\*. Orthopaedic Surgery, Kagoshima University, Kagoshima, Japan.

Hedgehog proteins are essential morphogens and hedgehog signaling pathway plays an important role in embryonic development. Recent studies have shown constitutive activation of hedgehog signaling promote various types of malignancies. However, it remains unclear whether hedgehog pathway is activated in human osteosarcoma. In an attempt to better understand osteosarcoma pathogenesis, we investigated the expression and activation of hedgehog related proteins in osteosarcoma and examined the effect of cyclopamine to osteosarcoma growth. And also, we examined the molecular mechanism of osteosarcoma growth inhibition by cyclopamine. RT-PCR revealed high expression of hedgehog related genes in both osteosarcoma cell lines and human specimens. Immunohistochemistry showed high expression of hedgehog related proteins in both osteosarcoma cell lines and human specimens. Next, we investigated the effects of hedgehog pathway inhibition on osteosarcoma growth. MTT assay showed that cyclopamine and Gli2 siRNA suppressed the growth of the osteosarcoma cell lines in vitro. Cell proliferation assay showed that cyclopamine suppressed the osteosarcoma cell proliferation. Next we performed cell cycle analysis by flow cytometry. As a result, cyclopamine promoted G1 arrest. Next we examined the transcription of the cell cycle related genes which transcription was regulated in cell cycle. Real time RT-PCR and western blot revealed that cyclopamine suppressed transcription of cyclin D1, cyclin E1, Skp2, phosphorlated Rb. And also, P21<sup>cip1</sup> protein was upregulated by cyclopamine treatment. These data suggest that cyclopamine suppressed osteosarcoma growth and promoted G1 arrest by regulation of cell cycle regulators expression. We found that the components of hedgehog pathway were overexpressed in human osteosarcoma. And to explore how hedgehog pathway activation contributes to osteosarcoma growth, we blocked hedgehog pathway. Treatment of osteosarcoma cells with cyclopamine or Gli2 siRNA prevented osteosarcoma growth in vitro. Moreover, flow cytometry for cell cycle analysis showed that cyclopamine promote cell cycle arrest in osteosarcoma in vitro. In addition, we found that expression of cell cycle regulators was regulated by hedgehog signal inhibition with cyclopamine treatment.

These data suggest that inactivation of hedgehog signaling may be a therapeutic approach for the treatment of patients with osteosarcoma.

**Disclosures:** M. Hirotsu, None.

## SU242

**Bone Marrow Stromal Cells Up-regulate M-CSF Receptor in Monocytes to Disrupt Dendritic Cell Differentiation While Facilitating Osteoclastogenesis in Myeloma.** M. Abe<sup>1</sup>, M. Hiasa<sup>2</sup>, A. Oda<sup>1</sup>, H. Amou<sup>1</sup>, K. Takeuchi<sup>1</sup>, O. Tanaka<sup>1</sup>, S. Nakamura<sup>1</sup>, H. Miki<sup>1</sup>, K. Kagawa<sup>1</sup>, K. Yata<sup>1</sup>, S. Ozaki<sup>1</sup>, S. Kido<sup>1</sup>, T. Matsumoto<sup>1</sup>. <sup>1</sup>Department of Medicine and Bioregulatory Sciences, University of Tokushima Graduate School of Medicine, Tokushima, Japan, <sup>2</sup>Department of Orthodontics and Dentofacial Orthopedics, University of Tokushima Graduate School of Medicine, Tokushima, Japan.

Interaction of myeloma (MM) cells with bone marrow stromal cells facilitates osteoclastogenesis and tumor expansion in MM. In contrast to osteoclastogenesis, the number and function of dendritic cells (DCs) are reduced in MM bone lesions, causing immune escape of tumor cells and susceptibility to infection in MM. Because monocytes are a common precursor of both osteoclasts (OCs) and DCs, there is a possibility that monocytic differentiation may be deregulated in MM. In the present study, we therefore explored whether an interaction between MM cells and bone marrow stromal cells plays any role in lineage commitment of monocytic differentiation in MM. Induction of CD1a-positive DCs from monocytes by GM-CSF and IL-4 (25 ng/ml each) was strongly inhibited when co-cultured with human primary bone marrow stromal cells or murine MC3T3-E1 pre-osteoblasts. Interestingly, cell surface M-CSF receptor (M-CSFR) on monocytes was robustly up-regulated when co-cultured with primary stromal cells as well as MC3T3-E1 cells. The up-regulation of M-CSFR in monocytes by stromal cells was further enhanced in the presence of MM cells, while MM cells themselves were without effect. Disruption of M-CSF binding to M-CSFR by a soluble M-CSF-Fc fusion protein abrogated osteoclastogenesis enhanced by co-cultures of U266 cells with rabbit bone cells, and antagonized the suppression of GM-CSF and IL-4-mediated DC differentiation in the presence of stromal cells. These results demonstrate that bone marrow stromal cells are responsible for triggering monocytic differentiation into OC lineage while reciprocally suppressing its DC differentiation in an M-CSF-dependent manner, and that up-regulation of M-CSFR in monocytes by stromal cell-MM interaction at least in part contributes to the M-CSF-mediated up-regulation of OC and down-regulation of DC differentiation. It is suggested that a stromal cell-rich microenvironment created by impaired osteoblast differentiation in "MM niche" plays a critical role in the deregulation of monocytic differentiation to cause bone destruction and immunodeficiency, contributing to the development of the characteristic features of MM.

**Disclosures:** M. Abe, None.

## SU243

**Wnt/bCatenin/TCF Is a Constitutive Repressor Pathway Interfering with Foxo3-mediated Induction of Syndecan-2, a Tumor Suppressor in Osteosarcoma Cells.** F. Dieudonné\*, A. Marion\*, E. Haÿ, P. J. Marie, D. Modrowski. Unit 606, INSERM, Paris, France.

Syndecan-2 (synd2) acts as a tumor suppressor in osteosarcoma cells. We previously showed defective synd2 expression and induction in osteosarcoma tissues as compared to normal bone. Our current hypothesis is that this defect contributes to resistance to chemotherapeutic agents. We therefore investigated the mechanisms involved in the control of synd2 expression in basal conditions and after induction by Doxorubicin in human osteosarcoma cells. Using Genomatix software tools we analyzed in silico the 5' region upstream the synd2 gene and identified features for a promoter region and binding sites for members of the TCF/LEF family and forkhead factors. Chromatin immunoprecipitation assays were performed to determine whether these factors bind to these sites. A 3.6 Kb sequence of the 5' region upstream the synd2 gene was cloned in a reporter gene system to perform transactivation assays. Expression of synd2 was also determined by RT-qPCR. Overexpression of TCF4, constitutively active b-catenin or both using transient transfection induced a strong inhibition of basal reporter gene transactivation and of synd2 expression whereas repression of LEF-1 expression by siRNA resulted in increased basal synd2 expression. Treatment with recombinant Wnt3a also reduced synd2 mRNA and this effect was inhibited by DKK1. These results indicate that canonical Wnt signaling is involved in the repression of synd2. In contrast, we found that Doxorubicin increased transactivation of the reporter gene and synd2 expression. The effect of Doxorubicin is in part mediated by Foxo factors. Indeed, Doxorubicin induced the translocation of Foxo3 into the nucleus and siRNA inhibiting Foxo3 expression reduced the inductive effect of Doxorubicin on synd2 expression. Furthermore, overexpression of Foxo3 or a constitutively active form of this factor, Foxo3(A3) resulted in increased synd2 mRNA level. Foxo3 factors are known to compete with TCF/LEF to interact with b-catenin. Western blot analysis showed that Doxorubicin promoted the interaction between b-catenin and Foxo3 in U2OS cells. Additionally, overexpression of TCF4 or active b-catenin or both counteracted the induction of synd2 by Doxorubicin. This suggests that the Wnt pathway actually competes with the induction of synd2 by Doxorubicin. Overall, our data indicate that Wnt/b-catenin/TCF is a constitutive repressor pathway of synd2 expression in osteosarcoma cells. Doxorubicin increases synd2 expression in part through Foxo3 factors that may directly activate transcription and also could act by "hijacking" b-catenin and inhibiting formation of the b-catenin/TCF repressor complexes.

**Disclosures:** F. Dieudonné, None.

*This study received funding from: ARC and LIGUE contre le cancer.*

## SU244

**Characterisation of an Antigen Found in Giant Cell Tumour and Osteosarcoma Cells.** V. J. Green\*, P. W. Wilson\*, A. A. Walsh\*, J. A. Gallagher. Human Anatomy and Cell Biology, University of Liverpool, UK, Liverpool, United Kingdom.

Screening of a panel of monoclonal antibodies has identified a protein abundantly expressed in osteoclasts of giant cell tumour and at lower levels in human osteosarcoma cell lines, SaOS-2, TE-85 and MG63. It has also been seen at low levels in the culture medium from MG63 cells and less frequently in that from TE85 cells, those which represent the earlier stages of differentiation.

Co-localisation studies were performed with confocal microscopy using markers of intracellular organelles including the nucleus, endoplasmic reticulum, endocytic pathway, mitochondria and the golgi apparatus. Live fluorescent imaging was used to monitor the expression of the antigen over a one week period. Purified antibody was directly labelled with Alexa 488 dye, and mixed with the vector Chariot, to facilitate antibody uptake into the cell. MG63 cells were seeded at 30% confluence. Time lapse imaging was performed for the initial three hours to monitor uptake of the antibody, followed up by still image collection at 24 hour intervals for the following 7 days until cells reached confluence.

Immunoprecipitation using Dynal beads was performed and run on 1D gels and stained with Simply Blue Safe Stain, Silver Quest staining and Western blotted using the X cell Surelock mini-cell system.

Co-localisation studies show the antigen co-localises with the Golgi apparatus and not the nucleus, endoplasmic reticulum, endocytic pathway or mitochondria. It appears to remain here through to cell confluence.

Immunoprecipitation reveals a band at 90kDa visible by Western blotting but not by Simply Blue Safe Stain or Silver Quest staining.

It is necessary to eliminate more abundant proteins prior to immunoprecipitation to allow for a scaling up of antigen yield to a level visible with Simply Blue Safe Stain. 2D gel electrophoresis may provide better separation of proteins and clearer isolation of our antigen.

The presence of antigen in the culture medium of MG63 and TE85 cells suggests it may have a role in extracellular signalling.

Screening of an array of cancer tissues including breast, prostate, liver and colo-rectal cancer compared to case matched controls may identify a possible biomarker of disease or disease progression and provide further insights into therapeutic targets useful in the treatment of neoplastic disease.

**Disclosures:** V.J. Green, None.

## SU245

**BAMBI Gene Is Epigenetically Silenced in a Subset of High-grade Bladder Cancer.** S. Kitazawa, S. Sanda Khin\*, K. Mori, T. Kondo, R. Kitazawa. Department of Pathology, Kobe University Graduate School of Medicine, Kobe, Japan.

The BMP and activin membrane-bound inhibitor (BAMBI) is a transmembrane pseudoreceptor, preserved from *Xenopus* to *Homo sapiens*, and antagonizes TGF- $\beta$ /BMP signaling by interacting with TGFRII/BMPRII. In the current study, to evaluate the role of BAMBI in carcinogenesis and cancer progression in human bladder cancer from the viewpoint of both etiological and molecular backgrounds, we first screened the expression pattern of BAMBI protein by immunohistochemistry and the methylation status of the BAMBI gene promoter by the use of clinical specimens, and then the functional aspects of the BAMBI gene by forced-expression and knock-down in cancer cell lines *in vitro*. In the normal or reactive urothelium, BAMBI expression was mostly overlapped with that of BMPRI. A similar colocalization pattern of BAMBI and BMPRI was noted in noninvasive low-grade papillary cancers. In high-grade and invasive cancers, however, two reciprocal immunohistochemical expression patterns were observed: BAMBI-low and BMPRI-high, and BAMBI-high and BMPRI-low, indicating that BAMBI expression is controlled such that it does not interfere cellular demand for TGF- $\beta$ /BMP signaling defined by the level of TGF- $\beta$ /BMP receptors. On the other hand, methylation of one or more genes, especially of sFRP2 and BAMBI, was frequent in high-grade invasive tumors. Moreover, methylation of the BAMBI gene correlated with negative BAMBI expression in primary bladder tumors. Treatment of three bladder cancer cell lines with 5-aza-dC for 7 days restored the expression of BAMBI mRNA in T24 and HTB9. In KU1, where no BAMBI promoter methylation was detected, no significant difference was observed in the expression of the mRNA transcript. Transfection of BAMBI siRNA effectively suppressed BAMBI mRNA expression by at least 60% compared with that of its control, as determined by RT-PCR. Although a slight decrease in the apoptotic count by siRNA transfection was observed in HTB9, BAMBI knockdown did not have much effect on the apoptosis. Cell motility assay, on the other hand, revealed that after 24h treatment with TGF- $\beta$ 1, T24 and HTB9 cells showed a drastic increase in the number of migrated cells which decreased significantly through the forced expression of BAMBI by the transfection of the pEGFP-N3-hBAMBI expression vector in T24 and HTB9. In contrast, TGF- $\beta$ 1 had no effect on the motility of KU1 cells. Since certain subsets of aggressive tumors often promote cell motility, vascular invasion and survival, by inducing epithelial-to-mesenchymal transition by TGF- $\beta$ /BMP in an autocrine and paracrine manner, hypermethylation of the BAMBI gene promoter that leads to BAMBI gene suppression may be one of the indicators of the aggressiveness or the poor prognosis of bladder cancers.

**Disclosures:** S. Kitazawa, None.

This study received funding from: Ministry of Education, Sports and Culture, Japan.

## SU246

**Medullar Carcinoma of the Thyroid and Anomalies of the Calcium Metabolism: Case Report.** C. Poiana\*, M. Carsote\*, C. Chirita\*, D. Hortopan\*, D. Ioachim\*, A. Goldstein\*. <sup>1</sup>Endocrinology, Carol Davila University of Medicine and Pharmacy, Bucharest, Romania, <sup>2</sup>Endocrinology, C.I. Parhon Institute of Endocrinology, Bucharest, Romania.

**Introduction.** Medullar carcinoma is a rare form of thyroid cancer, sporadic or hereditary. Most of the cases are aggressive and limited therapeutic options are available once the tumor is spread.

**Aim.** We present a case of sporadic medullar thyroid carcinoma diagnosed almost a decade after a surgical approach of the thyroid. At that moment multiple metastasis were seen together with oncogenic osteomalacia and hypercalcaemia.

**Case Report.** On admission, a 66 years old female patient had progressive neck masses for the last 4 years. The medical history is the following: 11 years ago total thyroidectomy for endemic polinodular goiter was performed. Since the last 4 years she suffered for chronic diarrhea and she was followed up for the progressive enlargement of both thyroid lobes. She refused fine needle aspiration biopsy (FNAB). At this moment, ultrasound showed cervical remnants on the right lobe of 1 by 1 by 2.5 cm and on the left of 3.2 by 3 by 2.6 cm going retrosternal. Also left supraclavicular adenopathy of 4.1 by 3.3 by 4.1cm and left laterocervical adenopathy of 4.5 cm were revealed. The computed tomography showed that the neck mass was spread up to the superior mediastin, and osteolytic lesions were seen on the third dorsal vertebra as well as multiple hepatic metastases. The FNAB suggested medullar carcinoma. The serum parameters showed: hypercalcemia (10.6 mg/dl), normal levels of phosphorus (3.7 mg/dl), normal PTH levels (16 pg/ml) but very low levels of 25-OH vitamin D (11.33 ng/ml). The plasma calcitonin was extremely high (> 2000 ng/ml). The lumbar DXA exam showed low BMD (0.846g/cm<sup>2</sup>), T-Score of -2.9 and Z-Score -1.8. Based on this, medullar carcinoma with multiple metastasis was diagnosed, associated with osteomalacia. The high levels of calcium were suggestive for neoplastic hypercalcemia, marking the terminal disease. The patient suffered 2 months later a fragility fracture on the right arm and she died 10 months later by sepsis due to perineal metastasis.

**Conclusion.** The medullar carcinoma can be a very aggressive form of thyroid cancer that may be associated during the last phase of evolution with endocrine paraneoplastic signs as hypercalcemia, regarded as the most frequent endocrine anomaly on cancer. In this situation, the serum levels of calcium are high even the patient has osteomalacia, possible by tumorigenic cause.

**Disclosures:** C. Poiana, None.

## SU247

**CXC Chemokine Ligand-13 Stimulates RANK Ligand Expression in Squamous Cell Carcinoma.** S. Yuvaraj<sup>1</sup>, K. Sundaram<sup>1</sup>, W. L. Ries<sup>2</sup>, S. V. Reddy<sup>1</sup>. <sup>1</sup>Charles P. Darby Children's Research Institute, Medical University of South Carolina, Charleston, SC, USA, <sup>2</sup>College of Dental Medicine, Medical University of South Carolina, Charleston, SC, USA.

Head and neck squamous cell carcinoma (SCC) is the most common malignant neoplasm estimated to be more than 40,000 cases per year in the US. These malignant tumors are known to have a potent activity for local bone invasion; however the molecular mechanisms of SCC associated osteolysis is unknown. We showed subcutaneous injection of SCC 14a cells onto the surface of calvaria in NCr-nu/nu athymic mice develop tumors in 4-5 weeks. Histochemical staining demonstrated tumor cell invasion/osteolysis with a significant increase in the numbers of multinucleated TRAP positive osteoclasts at the tumor/bone interface. We identified high levels of chemokine ligand, CXCL13 and RANK ligand (RANKL), a critical osteoclastogenic factor, expression in SCC derived cell lines. Real-time PCR analysis demonstrated that recombinant hCXCL13 treatment (0-25 ng/ml) to SCC 14a cells for 48 hr increases (4-fold) RANKL expression in a dose dependent manner. Interestingly, CXCL13 also induced (2.4-fold) CXCR5 receptor expression in these cells. Western blot analysis further demonstrated that anti-CXCR5 receptor antibody inhibits CXCL13 stimulated RANKL and CXCR5 expression in SCC 14a cells. These results indicate an autocrine regulatory function for CXCL13 in SCC tumor cell invasion/osteolysis. We further examined the molecular mechanism by which CXCL13 regulates RANKL expression. CXCL13 stimulation of SCC14a cells transfected with hRANKL gene promoter-luciferase reporter plasmid demonstrated a significant increase (3.0-fold) in RANKL gene promoter activity. Transcription factors array (super array) screening by real-time PCR identified a 3.2-fold increase in c-Jun mRNA expression in CXCL13 stimulated SCC 14a cells. Also, CXCL13 significantly increased phospho-c-Jun levels in these cells. We further show that JNK (c-Jun N-terminal Kinase) inhibitor suppressed CXCL13 stimulated RANKL expression. These results suggest CXCL13 signaling stimulates RANKL expression and implicates a potential therapeutic target to prevent osteolysis associated with SCC *in vivo*.

**Disclosures:** S. Yuvaraj, None.

## SU248

**Osteoporosis In Elderly Fallers - Underdiagnosed and Undertreated.** E. Segal\*, N. Mative\*, L. Dvorkin\*, S. Ish-Shalom<sup>1</sup>. <sup>1</sup>Metabolic Bone Diseases Unit, Ramabam Health Care Campus, Haifa, Israel, <sup>2</sup>Department of Gerontology, Western Galilee Hospital, Nahariya, Israel.

Falls are a major risk factor for osteoporotic fractures in the elderly. The use of diagnostic and therapeutic modalities in elderly fallers in Israel has not been assessed.

**Aims:** to assess the use of bone densitometry (DXA) and osteoporosis (OP) treatment in elderly women with propensity to fall; to detect factors interfering with implementation of diagnostic and therapeutic procedures in this population.

**Patients:** 242 community dwelling women, aged 65-91, that were hospitalized in the Western Galilee hospital after a fall.

**Methods:** At hospitalization the patients (pts) were interviewed regarding medical history, previous fractures, nutritional status, DXA and the use of treatment for OP. Three months after hospital discharge a phone interview was performed with all participants. The pts were asked about diagnostic and therapeutic procedures for OP after hospital discharge.

**Results:** 50 pts (20.6%) were diagnosed with OP before hospitalization (group A); 192 pts (79.4%) were not (group B), 164 (85%) of them received a written recommendation to perform DXA examination (group B1); 28 (15%) had not (group B2).

	Group A	Group B	Significance
Age, mean $\pm$ SD	78.4 $\pm$ 8.7	78.4 $\pm$ 9.8	NS
Previous falls	30 (60%)	90 (46.9%)	NS
Previous fractures	11 (22%)	26 (16.5%)	NS
Lack of sun exposure	9 (18%)	41 (21.3%)	NS
Medication Use			
Calcium + D	43 (86%)	57 (14%)	< 0.0001
Alendronate	39 (78%)	0	
Risedronate	4 (8%)	0	

There was no significant difference between the groups in socio-economic and nutritional status, health insurance and use of medications

157 (95) of group B1 pts underwent post hospital discharge phone interview: 46 (24%) performed DXA, 24 (52%) were diagnosed with OP, 6 (13%) with osteopenia.

Of 24 OP pts 14 (58%) were treated with calcium + D before the diagnosis of OP, and all of them after diagnosis. After diagnosis 14 pts (58%) were treated with alendronate, 10 (42%) with risedronate. Of 6 osteopenic pts, 3 (50%) received calcium + D, none was treated for OP although two (30%) had previous OP fractures and according to WHO criteria had severe OP.

Of group B2 one pt (3.5%) performed DXA and was diagnosed with OP; 8 (28.5%) pts received calcium + D. Reasons for not performing DXA: 50 (26%) pts didn't ask, 24 (12.5%) not referred after asking, 28 (14.1%) refused: 13 (6.8%) due to poor health, 13 (6.8%) due to distance, 2 (1%) due to economic problems.

**Conclusion:** In spite of high rate of OP and increased fracture risk, the disease in elderly fallers is underdiagnosed and undertreated. Recommendation in hospital discharge letter may improve the rate of diagnosis and promote treatment initiation.

**Disclosures:** E. Segal, None.



## SU249

**Bone Strength Measurement: New Approach.** A. Bazarra-Fernandez\*. ObGyn, Juan Canalejo University Hospital Trust, La Corunna, Spain.

The bone is a physical structure having an irregular shape anisotropy. Precise in vivo measurement of trabecular bone mechanical properties is very important. A method for assessing bone mass and anisotropy is essential at all scales of measurement between the greatest and the smallest scale and over all with trabecular. Compact bone properties constitute another system with microsystems, isotropy and anisotropy and variety of cross-section. The measurement of bone mineral density by dual energy X-ray absorptiometry (DXA) has served as a fit surrogate for the measurement of bone strength. By reason of the two-dimensional nature of DXA, assumptions must be made regarding the tridimensional nature of the bones, dealing with an inference problem from a set of measurements. Therefore, it is tried to regain some information about the third dimension by building a model of the bone, which assumes axial symmetry and asymmetry. By using a model, to be arranged the parameter of this model in such a way that they best fit the data, so it is only gained information about how good the model can explain the data, but it is not gotten any information of how good this model actually is, and maybe there is a much better model. It is very difficult to make good inference of the bone strength. But there are anisotropic problems too, and therefore we will make different inferences. Therefore it is deduced, that this method seems to be very sensitive to error, and it is necessary to know how to deal with these errors, especially with the systematic errors introduced by using a parameterized model.

So, a mathematical, physical and physiological 5-dimensional model must be developed in order to gauge bone properties including geometry (2-dimensional DXA), space, time, motion and stress with a portable-computer-device

**Disclosures:** A. Bazarra-Fernandez, None.

## SU250

**Quantitative MicroCT Imaging of Adipocyte Volume in Bone Marrow of Mice with High and Low Bone Mass.** D. J. Adams, R. Rydzik\*, V. Diaz-Doran\*, J. Xi\*, C. Ushiku\*. Orthopaedic Surgery, New England Musculoskeletal Institute, University of Connecticut Health Center, Farmington, CT, USA.

The relationship between bone density and marrow fat has been of increasing interest due to observations that marrow stromal cells can differentiate either to adipocytes or osteoblasts. Although histology can allow visualization of fat using lipid stains such as oil red O and osmium tetroxide (OsO<sub>4</sub>), adipocytes may be few in number and irregularly distributed, limiting quantitative precision. To remedy this, we have developed a technique for volumetric quantitation of marrow adipocytes in excised whole bones using lipophilic OsO<sub>4</sub> staining and X-ray computed microtomography imaging (μCT). Here, the technique was applied to 10 wk old "high" C3H/HeJ (C3H) and "low" C57Bl/6J (B6) bone density mice to survey marrow fat distribution and potential correlates to site-, strain-, and gender-specific bone mass. Fluorochromes were administered 7 and 2 days prior to sacrifice to confirm site-specific differences in bone formation (C3H > B6). DXA confirmed ~12% higher whole body BMD and fat in C3H vs B6. The femora, tibiae, humeri, L3-4 vertebrae, and sternum were fixed in 10% formalin, with analysis of double labels from contralateral specimens. Morphometry was quantified at 6 μm resolution (Scanco μCT40) prior to decalcifying in 14% EDTA and staining in 2% OsO<sub>4</sub>. Whole bones were imaged again using μCT, providing 3D image arrays of the high contrast spherical adipocytes. Quantitation of fat volume, density, and distribution throughout the marrow was registered to relatively low contrast (decalcified) bone. Complete staining of adipocytes was verified histologically.

Adipocytes were very few in number within the vertebra, humerus, and sternum. In femurs, adipocytes were nearly absent at mid-diaphysis of B6, but well populated in C3H, lining the anterior endocortical border, and 5-fold greater in male vs female. At the distal femur metaphysis, fat volume was similar in C3H vs B6 females, but 8-fold higher in C3H vs B6 males. Metaphyseal fat was similar for C3H male vs female, but 5-fold higher in B6 females vs males. In tibiae, adipocytes spanned the posterior diaphysis and in greater number medially within the proximal metaphysis, where fat volume was 3-fold higher in females vs males and 2-fold higher for C3H vs B6.

C3H maintain higher osteoblast activity and lower apoptosis vs B6, as well as higher mineralization, bone formation rate, and serum IGF-I, but accompanied with relatively lower response to exogenous mechanical stimuli. These genetic differences are often specific to skeletal site and gender. For example, trabecular density at the femur metaphysis is higher in C3H vs B6 for females and equal for males, whereas marrow fat content at the same site follows the opposite relationship.

**Disclosures:** D.J. Adams, None.

## SU251

**Assessment of Fracture Risk and Treatment of Osteoporosis in Postmenopausal Women: Bone Density vs. Bone Destiny.** K. Beattie\*<sup>1</sup>, W. Bensen\*<sup>1</sup>, M. Larche\*<sup>1</sup>, A. Papaioannou<sup>1</sup>, W. Wong Pack\*<sup>1</sup>, J. D. Adachi<sup>2</sup>.

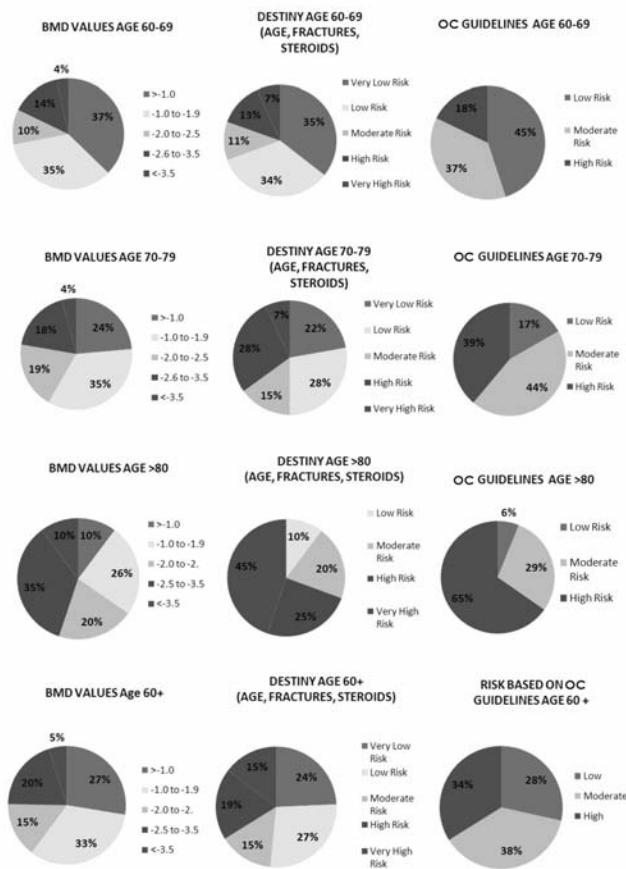
<sup>1</sup>Dept. of Medicine, McMaster University, Hamilton, ON, Canada, <sup>2</sup>Dept. of Medicine, St. Joseph's Healthcare - McMaster University, Hamilton, ON, Canada.

**Purpose:** The objective of this study was to compare the prevalence of high risk fracture patients identified as such by bone mineral density (BMD) alone, by Bone DESTINY and by Osteoporosis Canada (OC) guidelines.

**Methods:** All post-menopausal women > 60 years of age who had undergone their first ever DEXA scan during the period of June to November 2007 were included in the analyses. Based on bone density alone, women were assessed as being at high risk for fracture if they had a bone density in the osteoporotic range (T score < -2.4). These same women were also assessed for fracture risk using Osteoporosis Canada (OC) guidelines and Bone DESTINY, both of which take into account BMD, age, current glucocorticoid use > 3 months and previous fragility fracture. Colour codes were used to identify fracture risk where purple=very high risk, red=high risk, orange=moderate risk, yellow=low and green= very low. The prevalence of women in each of these groups was compared between these three differing criteria. In the BMD and Bone DESTINY data, the high risk and very high risk groups were combined to compare against the OC guideline high risk group.

**Results:** A computer database of all patients who had visited the bone density clinic within the designated time period was searched. Of those searched, 239 were post-menopausal women > 60 years old who visited the clinic for the first time; 118 (49%) were 60-69 years, 72 (30%) were 70-79 years and 49 (21%) were 80 years or older. For each age group, 3 graphs are shown comparing the distribution of females in each fracture risk group according to BMD, Bone DESTINY and OC. BMD alone typically demonstrated the lowest prevalence of women at high risk for fracture compared to DESTINY and OC guidelines which were relatively close. See graphs in Figure 1.

**Figure 1.** Prevalence of fracture risk groups as defined by BMD alone, Bone DESTINY and OC guidelines.



**Conclusions:** These results emphasize the difference between the number of women who are identified as being at high risk for fracture according to BMD alone as compared to Bone DESTINY and OC guidelines. Bone DESTINY results are easily read and interpreted and are consistent with OC guidelines.

**Disclosures:** K. Beattie, None.

## SU252

**Validation of Bone Mineral Measurements on the New Norland Model XR-600 and XR-800 Using the BMIL QA/QC Phantom.** T. V. Sanchez<sup>1</sup>, G. Ekker<sup>2</sup>, D. K. Buckingham<sup>3</sup>, D. R. Purvis<sup>3</sup>, K. M. Dudzek<sup>3</sup>. <sup>1</sup>Research and Development, Norland--a CooperSurgical Company, Socorro, NM, USA, <sup>2</sup>Engineering and Development, Norland--a CooperSurgical Company, Fort Atkinson, WI, USA, <sup>3</sup>Research and Development, Norland--a CooperSurgical Company, Fort Atkinson, WI, USA.

The current study evaluated DXA-based measurements of bone mineral content in the BMIL QA/QC Phantom using the newly released Norland XR-600 and XR-800 scanners. The XR-600 and XR-800 measurements made over the wide range of samples available in the BMIL QA/QC Phantom were compared to measurements seen in the earlier Norland XR-46 scanner.

The commercially available BMIL QA/QC Phantom was evaluated on the three Norland scanners using AP Spine Software at 1.5 x 1.5 mm and scan speeds of 130mm/s (standard) or 65mm/s and both Research and Small Subject Software at 1.0 x 1.0 mm with a scan speed of 15mm/s. The Phantom was scanned 25 times on each setting and operator set regions of interest analyzed bone mineral for the L1, L2, L3 and L4 regions.

When analyzed the studies of L1, L2, L3 and L4 done using AP Spine at 130mm/s on the XR-46 resulted in BMC of 4.557, 15.325, 28.878 and 46.324 g/cm, respectively. Regression analysis between AP Spine mode at 130mm/s on the XR-46 and results on the XR-600 ( $y=1.0223x-0.269$ ;  $r=0.999$ ) and XR-800 ( $y=1.0328x-0.3217$ ;  $r=0.999$ ) indicated strong relationships. Regressions between AP Spine at 65mm/s on the XR-46 and results on the XR-600 ( $y=1.0019x-0.124$ ;  $r=0.999$ ) and XR-800 ( $y=1.0244x-0.0352$ ;  $r=0.999$ ) also indicated strong relationships. Similar finding were seen in regressions between Research Scan Software using the XR-46 and results on the XR-600 ( $y=1.0231x-0.1624$ ;  $r=0.999$ ) and XR-800 ( $y=1.0184x-0.0906$ ;  $r=1.000$ ) and in regression studies when using Small Subject Software on the XR-46 and the XR-600 ( $y=1.0227x-0.1486$ ;  $r=1.000$ ) or XR-800 ( $y=1.0437x-0.3808$ ;  $r=0.999$ ).

Results using the BMIL QA/QC Phantom show that, although fitted with different hardware, the Norland XR-46 and the newer Norland XR-600 and XR-800 systems measure bone mineral content similarly over the wide range found in the phantom. The study also shows the similarity continues using different scanning and analysis softwares. The study also demonstrates the value of the BMIL QA/QC Phantom in evaluating densitometry hardware and software systems.

**Disclosures:** T.V. Sanchez, None.

## SU253

**Ten-Year Fracture Risk Assessment in Norland-based Equipment in a Chinese Population.** J. Wang<sup>1</sup>, Y. Y. Zhen<sup>2</sup>, Y. Liu<sup>3</sup>, W. Y. Shi<sup>4</sup>, T. V. Sanchez<sup>5</sup>. <sup>1</sup>Research and Development, Norland--a CooperSurgical Company, Beijing, China, <sup>2</sup>Surgical Department, Beijing Haidian Hospital, Beijing, China, <sup>3</sup>Peking University Third Hospital, Beijing, China, <sup>4</sup>Research and Development, Beijing Vigor Medical Equipment Company, Beijing, China, <sup>5</sup>Research and Development, Norland--a CooperSurgical Company, Socorro, NM, USA.

Until recently the clinical interpretation of an initial DXA-based assessment involved a review of the patient T-score. More recently, however, the literature suggests complementing the T-score based assessment with a Ten-Year Fracture Risk Assessment when reviewing the need for therapy. This study examines the use of the Norland based Femur Neck T-score and a Ten-Year Fracture Risk Assessment in a population of Chinese subjects.

A total of 440 subjects who had gone to Haidian Hospital or Peking University Third Hospital in Beijing for clinical evaluation or for routine "Health Checkup" were evaluated on Norland scanners. All subjects underwent a Hip Scan and an extensive clinical history. The clinical history and the Femur Neck T-score allowed us to carry out a Ten-Year Hip Fracture Risk Assessment using the Chinese Database in the FRAX<sup>TM</sup> WHO Fracture Risk Assessment Tool. These results were then evaluated to estimate the relative impact on clinical assessments made on the basis of a T-score alone, a T-score and Ten-Year Fracture Risk Assessment or a Ten-Year Fracture Risk Assessment alone.

With regards to clinical assessment a T-score value that falls below -2.5 or a Fracture Risk Value greater than 3% would trigger consideration of aggressive therapy. Of the subjects evaluated in this study--352 subjects (80%) would not trigger to aggressive therapy based on result from both the T-score and Fracture Risk Value, 8 subjects (2%) would trigger to aggressive therapy on the T-score but not the Fracture Risk Value, 53 subjects (12%) would trigger aggressive therapy on the Fracture Risk Value but not the T-score and 27 subjects (6%) would trigger to aggressive therapy based on both the T-score and the Fracture Risk Value.

The study has demonstrated an ability to complement the T-score clinical assessment so that an additional twelve percent of subject may be identified for aggressive therapy. The study suggests that the Ten-Year Fracture Risk Assessment was useful to the clinicians trying to determine a clinical course.

**Disclosures:** J. Wang, None.

## SU254

**Densitometric Vertebral Fracture Assessment in Postmenopausal Women: A Systematic Review.** O. Gajic-Veljanoski<sup>1</sup>, D. A. Butt<sup>2</sup>, D. S. Feig<sup>2</sup>, A. M. Cheung<sup>1</sup>. <sup>1</sup>University Health Network, University of Toronto, Toronto, ON, Canada, <sup>2</sup>University of Toronto, Toronto, ON, Canada.

Vertebral fractures (VFs) are the most common osteoporotic fractures, occurring in 35-50% of women 50 years and older, however, two thirds are asymptomatic. Densitometric Vertebral Fracture Assessment (DXA-VFA) is a new technology for detecting VFs and is a promising clinical alternative to lateral spine radiography because of its low radiation dose, standardized patient positioning, digital single image acquisition and semi-automated analysis.

We performed a systematic review of the literature to examine the diagnostic accuracy of DXA-VFA using lateral spine radiography as the gold standard. We systematically searched Medline, EMBASE and the Cochrane Database of Systematic Reviews (1950-April 2008), and bibliographies, and included original English-language studies assessing the detection of VFs with both DXA-VFA and spine radiography in postmenopausal women. Two reviewers independently assessed studies using validated diagnostic quality criteria. For each study, we analyzed sensitivity and specificity of DXA-VFA for detecting grade I-III VFs (per-subject and per-vertebrae) and calculated likelihood ratios (LRs).

Of 91 identified articles, 11 studies satisfied the eligibility criteria. Eight studies were considered "good" or "fair" quality, with a total study population of 1736 postmenopausal women (mean age > 64 years, body mass index: 25-27 kg/m<sup>2</sup>). The prevalence of VFs was 1.6-11% in low-risk and 14.7-98% in high-risk (osteoporotic) postmenopausal populations. For detecting grade II and III VFs in women without scoliosis, DXA-VFA showed excellent performance with sensitivities 74.4-95% and specificities 93.3-99.5% (positive LRs >13.1 using per-subject analysis). The kappa( $\kappa$ ) agreement between DXA-VFA and gold standard was 0.64-0.97. Only one study reported DXA-VFA sensitivity (50%) and specificity (96.2%) for detecting grade I VFs. Two studies included patients with scoliosis and found moderate performance for detecting any VFs (positive LRs = 4.6-5.5). Inter-observer reliability depended on the method of interpretation of VF severity ( $\kappa=0.51-0.73$  for the semi-quantitative Genant method and 0.60-0.86 for the ABQ, Melton, Eastell, McCloskey methods). The percentage of unreadable vertebrae was substantially higher in DXA scans compared to spine radiographies (5-19.5% vs. 0.5-1.5%).

Our systematic review suggests excellent diagnostic accuracy of DXA-VFA for identifying grade II and III VFs in non-obese postmenopausal women without scoliosis. More research is needed to determine the performance of DXA-VFA for detecting mild VFs in general postmenopausal populations and for detecting any VFs in scoliosis or obese populations.

**Disclosures:** O. Gajic-Veljanoski, None.

## SU255

**Lack of Correlation between Glycemic Control and Bone Mineral Density in Type 2 Diabetic Women.** B. Manwani<sup>\*</sup>, M. S. Leboff, M. Pendergrass<sup>\*</sup>, R. Garg<sup>\*</sup>. Brigham and Women's Hospital, Boston, MA, USA.

Women with type 2 diabetes mellitus (T2DM) have higher bone mineral density (BMD) compared to non-diabetic controls. In spite of that, they have a higher risk of fractures. We hypothesized that poorly controlled T2DM is associated with lower BMD after adjusting for obesity. Medical records of 1397 patients who got a dual-energy x-ray absorptiometry (DXA) scan done in the year 2006 and 2007 at the Brigham and Women's Hospital were studied. After excluding men, patients with type 1 diabetes, coexistent medical conditions like hyperparathyroidism, hyperthyroidism, multiple myeloma, history of organ transplant or chronic steroid use and other disorders affecting bone, 315 women were included in the final analysis. Characteristics of the included women are shown in table 1. On linear regression analysis there was a significant correlation between BMI and BMD parameters. However, there was no correlation between HbA1C and any of the BMD parameters (table 2). Inclusion of BMI into the linear regression model did not make a difference. These results demonstrate no significant effect of glycemic control on BMD in T2DM. However, it confirms that BMI is significantly associated with the BMD at both total hip and spine in patients with T2DM. We speculate that bone structure may be defective in patients with T2DM, thus making them more prone to fractures.

Table 1. Characteristics of patients included in the study.

Age (mean $\pm$ SD) (years)	66.8 $\pm$ 9.8
BMI (kg/sq.m)	32.2 $\pm$ 7.1
HbA1C (%)	7.2 $\pm$ 1.4
Serum Creatinine (mg/dl)	0.96 $\pm$ 0.47
Smokers (n and %)	94 (29.84%)

Table 2. Pearson's correlation between BMD parameters Vs BMI and HbA1C.

	Vs BMI		Vs A1C	
	r	p	r	p
BMD spine	0.361	<0.01	0.103	NS
T score spine	0.375	<0.01	0.040	NS
Z score spine	0.292	<0.01	-0.004	NS
BMD hip	0.459	<0.01	0.067	NS
T score hip	0.454	<0.01	0.015	NS
Z score hip	0.391	<0.01	-0.057	NS

**Disclosures:** B. Manwani, None.

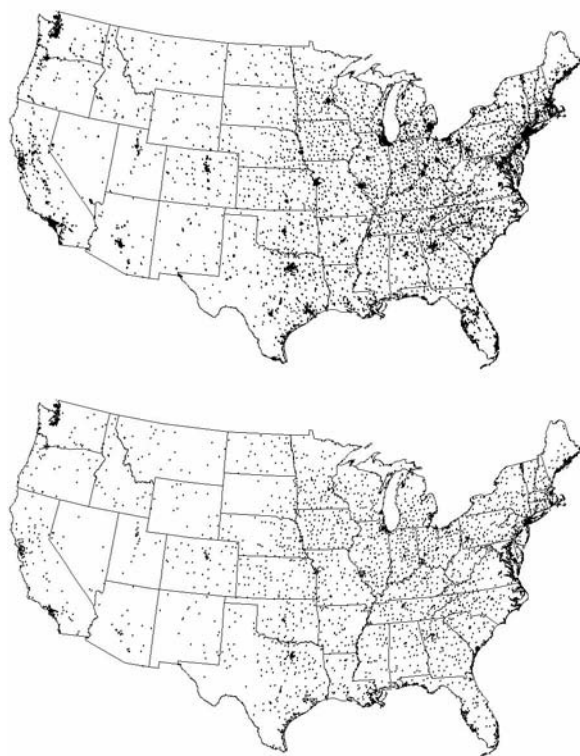
## SU256

**What Happens to the Availability of DXA if Physicians Stop Performing Them in Their Offices?** J. R. Curtis<sup>1</sup>, A. Laster<sup>\*2</sup>, D. J. Becker<sup>\*3</sup>, L. Carbone<sup>4</sup>, M. Kilgore<sup>\*3</sup>, R. Matthews<sup>\*5</sup>, M. A. Morrissey<sup>\*3</sup>, K. G. Saag<sup>1</sup>, S. B. Tanner<sup>6</sup>, E. Delzell<sup>\*5</sup>. <sup>1</sup>Division of Rheumatology, University of Alabama at Birmingham, Birmingham, AL, USA, <sup>2</sup>Arthritis & Osteoporosis Consultants of the Carolinas, Charlotte, NC, USA, <sup>3</sup>Department of Health Care Organization and Policy, University of Alabama at Birmingham, Birmingham, AL, USA, <sup>4</sup>Veterans Administration Medical Center, University of Tennessee, Memphis, TN, USA, <sup>5</sup>Department of Epidemiology, University of Alabama at Birmingham, Birmingham, AL, USA, <sup>6</sup>Department of Medicine, Vanderbilt University, Nashville, TN, USA.

**Introduction:** Reimbursement for central dual-energy x-ray absorptiometry (DXA) performed in non-facility settings (e.g. physician offices) substantially declined for Medicare beneficiaries in 2007 but was stable for DXAs performed in facilities (e.g. hospitals). The effect on the geographic availability of DXA if physicians stopped performing them in non-facility settings because of low reimbursement is unclear.

**Methods:** Using Medicare administrative claims from 1999-2006, we identified DXAs performed in non-facility and facility settings. We evaluated trends in the number of DXA tests performed and the change in the number of non-facility and facility DXA providers for each year. We then used provider zip codes to map the geographic availability of DXAs in 2006 for both types of DXA providers. We then mapped a hypothetical scenario if non-facility DXA providers stopped performing DXAs and only facility DXA providers remained.

**Results:** There were an estimated 2.88 million central DXAs performed in 2006, a 103% increase since 1999. In 2006, 69% of DXAs were performed in non-facility settings, which accounted for 77% of the sites performing DXAs. Over 1999 to 2006, there was an 106% increase in the number of non-facility DXA providers and a 53% increase in the number of facility DXA providers. The location of all DXA providers in 2006 is shown in the Figure, top panel. DXA availability if non-facility DXA providers stopped performing DXAs is shown in the Figure, bottom panel.



**Conclusion:** The majority of DXAs performed in 2006 were performed in non-facility settings (e.g. physician offices). Since 1999, the number of new non-facility providers was more than double the number of new facility providers. Ongoing analyses are evaluating the importance of the current and future geographic availability of DXA on receipt of this service.

**Disclosures:** J.R. Curtis, Novartis, Amgen, Merck, Proctor & Gamble, Eli Lilly, Roche 3; Merck, Proctor & Gamble, Eli Lilly, Roche, Novartis 1; Roche, UCB, Proctor & Gamble 2. This study received funding from: Amgen, Inc, National Institutes of Health (AR053351, AR052361), and the Arthritis Foundation (JRC).

## SU257

**Impact of Varying BMD Resources on Prediction of Hip Fracture using FRAX<sup>TM</sup>.** E. McCloskey, H. Johansson\*, A. Oden\*, J. A. Kanis. WHO Collaborating Centre for Metabolic Bone Diseases, Sheffield, United Kingdom.

In many healthcare systems, including the National Health Service in the UK, widespread use of DXA is not possible and case-finding strategies are promoted. The aim of the present study was to examine the effects of the use of clinical risk factors (CRFs), BMD or the combination using the FRAX<sup>TM</sup> tool for the detection of women at risk of hip fracture.

Data from 10 prospective population based cohorts, in which BMD and CRFs were documented, were used to compute the 10-year probabilities of hip fracture calibrated to the fracture and death hazards of the UK using the FRAX<sup>TM</sup> tool. The base case examined the effects in women at the age of 65 years. Simulation samples of 1000 women were derived with BMD measurements undertaken in none, all or intermediate proportions of the population in order to identify women in whom the probability of hip fracture lay above the 10-year probability of hip fracture at which treatment became cost-effective using data previously published for the UK. For the strategies with limited use of BMD tests, the tests were targeted to those lying nearest the intervention threshold in order to maximise the positive predictive value (PPV) and hence the NNT to prevent 1 hip fracture. When women aged 65 years were assessed with CRFs, increasing the number of BMD tests, from zero up to 100% of women, increased progressively the number of women categorised at high risk and decreased the NNT. The change in NNT was non-linear. NNT was 54 with the use of CRFs alone and fell to 43 when BMD was used in 10-30% of women. When BMD tests were undertaken in all women, the NNT decreased to 33. NNT with the use of BMD alone was 47.

The combined use of BMD and CRFs outperforms the use of BMD or CRFs alone. The input of BMD as part of a FRAX<sup>TM</sup> assessment increases, therefore, the performance characteristics of fracture risk assessment. Whereas the optimal use of the FRAX<sup>TM</sup> tool is with the concurrent use of BMD tests, where resources are limited, the use of BMD tests are optimally targeted to 10-30% of women that lie closest to the intervention threshold.

**Disclosures:** E. McCloskey, None.

## SU258

**Do Different Densitometers, or Use of T-score vs. Z-score, Affect Fracture Risk Estimation?** A. Woods<sup>\*1</sup>, D. Krueger<sup>1</sup>, P. D. Miller<sup>2</sup>, S. Baim<sup>2</sup>, E. M. Lewiecki<sup>3</sup>, N. Binkley<sup>1</sup>. <sup>1</sup>Osteoporosis Clinical Research Program, University of Wisconsin, Madison, WI, USA, <sup>2</sup>Colorado Center for Bone Research, Lakewood, CO, USA, <sup>3</sup>New Mexico Clinical Research & Osteoporosis Center, Albuquerque, NM, USA.

The WHO fracture risk assessment tool (FRAX<sup>TM</sup>) allows input of either the BMD T- or Z-score without regard to the manufacturer of the DXA instrument used. While the White female NHANES database is the international reference standard for femur neck (FN) T-score derivation, manufacturer specific reference databases are used to derive Z-scores and GE Lunar allows for weight adjustment. Whether women receive the same fracture probability result when scanned on different manufacturer's densitometers, and whether use of T- or Z-score alters fracture risk estimation, is not known. This study compared calculated 10-year fracture probability for women imaged on 2 different manufacturer's densitometers and evaluated the impact of T- or Z-score use on fracture risk estimation and subsequent treatment recommendation.

Femur BMD was measured in 60 postmenopausal women; mean (SD) age 62 (9.1) years and weight 142 (29.3) pounds on both Hologic (HOL) Delphi and GE Lunar Prodigy densitometers at 2 centers. Scans were performed in 2003, but analyzed with current software (GE v 11.4, HOL v 12.4), with race entered as White. T- and Z-score agreement was evaluated by linear regression. Age, height, weight, FN or total femur (TF) T-score, Z-score (with and without weight-adjustment for GE) were entered into FRAX<sup>TM</sup> to obtain 10-year fracture probability; no additional clinical risk factors were entered. Treatment was deemed appropriate if the major fracture probability was  $\geq 20\%$  or hip fracture  $\geq 3\%$ .

There is good agreement between HOL and GE for mean FN and TF T- and Z-scores. Additionally, linear regression analysis finds good agreement between HOL and GE,  $r^2$  range 0.69 - 0.95. Similar agreement is present in classifying women as appropriate for therapy regardless of whether GE or HOL T- or Z-score was used ( $p < 0.0001$ ). The same 10 women were identified as appropriate for drug therapy using FN T- and Z-scores; however, one additional woman was identified using the HOL T-score. Eight of these 10 were also identified as appropriate for therapy using the TF scores. However, using GE non-weight-adjusted Z-score 11 and 8 women were identified at the FN and TF respectively.

In conclusion, there is good between-manufacturer agreement in FN and TF T- and Z-scores in white postmenopausal women. As such, the FRAX-calculated 10-year fracture probability and subsequent treatment recommendations are similar whether a woman is imaged on a HOL or GE Lunar densitometer. Whether similar results are obtained in women of different races and in men should be evaluated.

**Disclosures:** A. Woods, None.

## SU259

**Height Loss, Vertebral Fractures and Misclassification of Osteoporosis.** W. Xu<sup>1</sup>, D. L. Medich<sup>1</sup>, G. Enright<sup>1</sup>, M. Ferchak<sup>1</sup>, B. Lane<sup>1</sup>, S. Perera<sup>2</sup>, S. L. Greenspan<sup>1</sup>. <sup>1</sup>Department of Medicine, University of Pittsburgh, Pittsburgh, PA, USA, <sup>2</sup>Department of Biostatistics, University of Pittsburgh, Pittsburgh, PA, USA.

The presence of a vertebral fracture (VF) identifies a patient who has clinical osteoporosis. However, 2/3 to 3/4 of VFs are asymptomatic. Vertebral Fracture Assessment (VFA), a DXA-derived method, assesses VFs. The objectives of this study were 1) to determine the degree of height loss in older men and women that predicts a VF, and 2) to determine if knowledge of VF will alter the classification of osteoporosis based on bone mineral density (BMD) alone. 197 men and women over the age of 65, with no previous history of osteoporosis or use of osteoporosis medications were recruited from the Claude D. Pepper Aging Registry, Benedum Geriatric Center and local advertising. Patients underwent a DXA scan of their spine (including BMD and VFA) and hip, measurement of their height by stadiometer, and a questionnaire regarding young adult peak height. BMD classification for osteoporosis was based on the World Health Organization guidelines of T-score  $\leq -2.5$  SD. The mean age of our population was 75 years old with 45% female. There was a significant association between height loss and one or more VFs (Table;  $p=0.0098$ ), but not between BMD and VFs. 37% of patients with low bone mass (osteopenia, T-score between -2.5 and -1.0 SD) and 43% of patients with normal BMD (T-score  $\geq -1.0$  SD) had one or more VFs. 34% of total participants were osteoporotic, but would have been misclassified by BMD criteria alone. We conclude height loss is an indicator for the presence of VFs. BMD criteria alone may miss older patients who have osteoporosis. VFA and presence of a VF increases the sensitivity of osteoporosis diagnosis in men and women compared to BMD criteria alone.

Table: Height Loss and Risk of Vertebral Fracture

Height Loss (inches)	Odds Ratio	95% Confidence Interval
.5	1.18	1.04-1.34
1.0	1.38	1.09-1.78
1.5	1.63	1.13-2.38
2.0	1.91	1.18-3.18
2.5	2.25	1.23-4.25
3.0	2.65	1.29-5.68

Logistic Regression Model for Risk of 1+ VF Using Height Loss as Predictor

**Disclosures:** S.L. Greenspan, None.

This study received funding from: NIH K24 award to Dr. Greenspan; University of Pittsburgh School of Medicine Dean's Summer Research Program; NIH-sponsored T35 training grant (DK065521).

## SU260

**Regional Differences of Femoral BMD Changes after One Year Once-Monthly Ibandronate as Measured by 3D QCT.** K. Engelke<sup>1</sup>, T. Fuerst<sup>2</sup>, M. Enslin<sup>3</sup>, R. Y. Davis<sup>3</sup>, L. A. Fitzpatrick<sup>3</sup>, D. Ethgen<sup>3</sup>, H. K. Genant<sup>4</sup>. <sup>1</sup>Institute of Medical Physics, University of Erlangen, Erlangen, Germany, <sup>2</sup>Synarc, San Francisco, CA, USA, <sup>3</sup>GlaxoSmithKline, King of Prussia, PA, USA, <sup>4</sup>University of California, San Francisco, CA, USA.

**Objective:** To evaluate local BMD changes in the proximal femur as measured by 3D QCT in postmenopausal osteoporotic women after one year of oral ibandronate.

**Methods:** 93 women (age  $64 \pm 7$ ) were randomized 1:1 to receive oral once-monthly ibandronate ( $n=47$ ; 150 mg) or placebo ( $n=46$ ); all women received calcium 1000 mg/day and vitamin D 400 mg/day. 3D QCT of the proximal femur was performed at baseline and after 12 months. In the 3D QCT analysis (MIAF-Femur) cortical, subcortical and trabecular compartments of the neck, trochanter, intertrochanter and total VOIs were investigated. Extended cortical (trabecular) compartments combined subcortical and cortical (trabecular) VOIs.

Mean percentage change from baseline to month 12 was calculated in placebo and ibandronate groups, with treatment differences and 95% CIs determined by ANOVA adjusting for center and baseline value. Analyses were exploratory; post hoc  $p$  values were generated for descriptive purposes only and were not adjusted for multiple comparisons. **Results:** scans from 39 (32) subjects in the ibandronate (placebo) group were evaluable at both visits. Integral, trabecular, and cortical %BMD treatment differences (95% CI) of the total hip were 2.2% (0.7, 3.7), 4.4% (0.8, 8.0), and 0.5% (-1.2, 2.2), respectively. In contrast to cortical results, the subcortical treatment difference of 3.7% was significant as indicated by a 95% CI that does not include zero (0.96, 6.4). Apart from the femoral neck, 95% CIs of the treatment differences for extended VOIs also indicated significance (see table).

Extended VOI	% BMD changes $\pm$ SD from baseline after 12 month <sup>a</sup>	Placebo Ibandronate	% BMD Treatment Diff (95% CI) <sup>a</sup>	p
Cortical femoral neck	-0.88 (4.13)	0.52 (3.82)	1.14 (-0.50, 2.79)	0.170
Cortical total hip	-0.76 (2.81)	1.24 (3.50)	1.51 (0.02, 3.00)	0.047
Cortical trochanter	-0.64 (3.37)	2.38 (3.93)	2.41 (0.54, 4.28)	0.012
Trabecular femoral neck	-2.38 (3.95)	1.03 (5.58)	2.94 (0.12, 5.77)	0.041
Trabecular total hip	-2.53 (3.84)	2.27 (6.14)	3.98 (1.24, 6.73)	0.005
Trabecular trochanter	-2.81 (4.38)	3.87 (8.79)	5.15 (1.46, 8.85)	0.007

<sup>a</sup>unadjusted means, <sup>a</sup>adjusted for center and baseline value

**Conclusions:** Once-monthly ibandronate increases integral and trabecular BMD of the

proximal femur. This preliminary analysis indicates that BMD changes also occur in the subcortical VOI suggesting that regional differences in the hip may be responsible for increase in bone strength noted on FEA analysis.

**Disclosures:** K. Engelke, Synarc 5.

This study received funding from: GSK.

## SU261

**Prevalence of Vertebral Compression Fracture Deformity by X-ray Absorptiometry in Patients Selected According to Simple Clinical Tests.** Z. Killinger<sup>\*</sup>, D. Cierny<sup>\*</sup>, L. Baqi<sup>\*</sup>, M. Krizko<sup>\*</sup>, J. Payer<sup>\*</sup>. 5th Department of Internal Medicine, University Hospital In Bratislava, Bratislava, Slovakia.

**Introduction:** Vertebral fracture is a severe complication of osteoporosis because of back pain, impaired quality of life and increased mortality. Despite its common severity and its value to predict further osteoporotic fractures, vertebral fractures are currently underdiagnosed. Performing spine radiographs in all patients screened for osteoporosis may be costly and time consuming. To overcome this issue lateral spine scan could be to obtain using dual energy X-ray absorptiometry (DXA), with a vertebral fracture assessment (VFA). This technique may facilitate detection of vertebral fractures, but in clinical practice is important to select appropriate patients for VFA.

**Aim of the study** was to assess the differences in vertebral fracture prevalence between patients referred for BMD testing according to standard ISCD criteria for bone densitometry (group I - so-called standard group) and a group of patients selected according to simple clinical criteria (group II or so-called high risk group).

**Methods:** Single-energy 20 s morphometry scans were performed using the Hologic Discovery densitometer. Fracture evaluation was performed semiquantitatively using the Genant classification by severity as mild, moderate or severe.

**Characteristic of patients:** We report a study of 277 patients referred for BMD testing. In group I we recruited 147 consecutive postmenopausal women (mean age 75.3 y.) and in group II 130 women (mean age 77.3 y.) selected according to following criteria: height loss of 3 cm or more or thoracic kyphosis or rib-pelvis distance less than 2 fingers or wall-occiput distance greater than 0 cm or weight less than 51kg.

**Results:** Among 147 patients from group I 32% had at least one vertebral fracture, 6% had multiple fractures. 84% of fractures in group I were classified as mild, 10% as moderate and only 6% as severe.

In group II 67% of patients had at least one vertebral fracture, 57% of patients had multiple fractures. 56% of fractures were mild, 30% moderate and 14 % severe.

In both groups together 21,7% of patients with vertebral deformities had osteopenia by WHO criteria and without VFA these high risk patients may not be offered pharmacological therapy.

**Conclusion:** Selection of patients according to described simple clinical parameters seems to be sensitive and it may be reasonable to perform VFA at least in this group of patients. Because of the need for pharmacological intervention in patients with osteopenia and asymptomatic vertebral fractures, we recommend to perform to the scan in patients with selected risk factors.

**Disclosures:** J. Payer, None.

## SU262

**Low Calcaneal Bone Mineral Density Estimated by a Periferal DXA Heel Scanner Is Associated with a High Risk to Have Had a Distal Radius Fracture.** I. Atroshi<sup>1</sup>, F. Ahlander<sup>1</sup>, M. Billsten<sup>1</sup>, D. Mellstrom<sup>2</sup>, C. Ohlsson<sup>2</sup>, O. Ljunggren<sup>3</sup>, H. G. Ahlberg<sup>4</sup>, M. K. Karlsson<sup>4</sup>. <sup>1</sup>Hässelholm Hospital, Department of Orthopaedics, Hässelholm, Sweden, <sup>2</sup>Sahlgrenska University Hospital, Departments of Internal Medicine and Geriatrics, Gothenburg, Sweden, <sup>3</sup>Academic University Hospital, Departments of Medical Science, Uppsala, Sweden, <sup>4</sup>Department of Clinical Science, Malmö University Hospital, Clinical and Molecular Osteoporosis Unit, Malmö, Sweden.

Portable DXA heel scanners have gained interest despite that they are less evaluated than total body scanners. The purpose of this study was to characterize the association between calcaneal BMD and distal forearm fracture risk in elderly women and men. Patients aged 20-80 years with a distal forearm fracture during two consecutive years, were invited to a calcaneal BMD measurement. Of 421 eligible patients, 333 participated; 270 women with a mean age of  $63 \pm 12$  years (mean  $\pm$  SD) and 64 men with a mean age of  $54 \pm 15$  years. A Calscan DXL<sup>®</sup> heel scanner estimated BMD ( $\text{g/cm}^2$ ) and T-scores. 153 women with a mean age of  $58 \pm 13$  years and 305 men with a mean age of  $74 \pm 5$  years, all population based, served as controls. As the controls included women 40-80 years and men 60-80 years, the comparison between fracture cases and controls involved these ages. The prevalence of osteoporosis was determined as well as the ability of calcaneus BMD to discriminate between the distal forearm fracture and the population-based normative cohort by receiver operating characteristic (ROC) analysis. The prevalence of osteoporosis in women aged 40-80 years with a distal forearm fracture was 32% compared with 16% in the controls (age-adjusted prevalence ratio 1.46, 95% CI 1.01-2.11,  $p=0.046$ ). The corresponding proportion in men aged 60-80 years was 44% and 6%, (age-adjusted prevalence ratio 10.5, 5.9-18.7,  $p<0.001$ ). The fracture cohort had lower age-adjusted BMD than the normative cohort, a mean difference in women of  $0.11 \text{ g/cm}^2$  (95% CI 0.10-0.13,  $p<0.001$ ) and in men of  $0.13 \text{ g/cm}^2$  (0.09-0.18,  $p<0.001$ ). One standard deviation (SD) lower BMD was associated with an odds ratio for having a distal forearm fracture of 1.8 (95% CI 1.4-2.3) in women and of 2.3 (1.6-3.3) in men. The area under the curve (AUC) in the ROC analyses was in women 0.63 (95% CI 0.57-0.69,  $p<0.001$ ) and in men 0.77 (95% CI 0.67-0.87,  $p<0.001$ ). The prevalence of osteoporosis is higher in individuals

with a distal forearm fracture than in a normative cohort. Impairment in calcaneal BMD by one SD is associated with an around doubled risk of having had a distal forearm fracture.

**Disclosures:** I. Atroshi, None.

## SU263

**Role of the Lean Muscle and Fat Mass in Hip Fractures Production.** L. del Rio, S. Di Gregorio\*, C. Sole\*, E. Bonel\*, M. Garcia\*, J. Rosales\*. Bone densitometry, CETIR.Centre Medic, Barcelona, Spain.

Low lean mass, has been associated with reduced muscle strength and lower functioning in elders. Also, the fat mass surrounding the proximal femur may help to absorb the energy generated by fall. Both variables can be accurately measured by dual-energy x-ray absorptiometry (DXA) technology.

**Subjects:** 109 female and male patients were divided into two groups, Cases group: 42 hip fracture patients (35 women and 7 men, mean age 63,2 years, mean BMI 78,5) with 29 cervical and 17 trochanter fractures) were selected by a history of low energy hip fracture in the previous six months (mean 3,4  $\pm$ 2,5 month). Control group: 67 patients (54 women and 13 men, mean age 61,9 years, mean BMI 84,1) without hip fracture or history of any condition associated with soft-tissue asymmetry in the lower extremities.

**Method:** Femur and total body DXA scans were performed using a whole body DXA model (GE-Lunar Prodigy) on all patients. BMD (g/cm<sup>2</sup>), BMC (g) and "R" value were evaluated for every femur scan. The "R" value is the ratio between low and high-energy absorptiometry coefficients, has a linear relationship with fat mass and was automatic taken in gluteus and peri-trochanteric area surrounding the hip. In total body scan, fat mass (g), lean mass (g) and bone mass (g), were evaluated from trunk, legs, hips, and whole body.

**Statistics:** Mean and standard deviation of all variables from both groups were compared by T-test, multivariable linear regression model. The results were divided in quartiles and chi-square and odds ratios were obtained from crosstab.

**Results:** Significant differences were found in legs lean mass (p=0,004), total lean mass (p=0,007) and femoral BMD (p<0,0001). Fat mass around the proximal femur did show a protective value against trochanteric hip fractures, especially in patients with a lower bone density in trochanter (p=0,027), but regional fat mass did not have a significant protective effect in femur neck fracture. The odds ratios in the lowest quartile for predicting any hip fracture were: regional fat mass 3,01; legs lean mass 2,65; total femur BMD 2,67; femoral neck BMD 3,46; and trochanter BMD 2,40.

**Conclusion:** A lower proportion of lean mass in legs is related with higher hip fracture risk, even after adjusting for BMD and this may reflect a lower muscle mass probably due to minor physical activity, which in turn leads to a higher risk of fall and subsequent fracture. Also, a lower risk fracture appeared when the proximal femur of the patients were found to be surrounded by larger amount of fat mass, with this having a protective effect against trochanteric hip fractures. In this regards the additional value of body composition capabilities of DXA may enhance the fracture risk calculation in individual patients.

**Disclosures:** L. del Rio, None.

## SU264

**FRAX™ and the Assessment of Ten-Year Fracture Probability in Hong Kong Southern Chinese According to Age and BMD Femoral Neck T-Scores.** S. W. Y. Tsang\*, A. W. C. Kung<sup>1</sup>, J. A. Kanis<sup>2</sup>, H. Johansson<sup>2</sup>, A. Oden<sup>2</sup>. <sup>1</sup>Medicine, The University of Hong Kong, Hong Kong, China, <sup>2</sup>Centre for Metabolic Bone Diseases (WHO Collaborating Centre), University of Sheffield Medical School, Sheffield, United Kingdom.

At present, studies using Asian subjects to estimate the probability of osteoporotic fracture remain sparse. Although the WHO algorithms (FRAX™) risk assessment tool has data for Chinese population, the absolute fracture risk estimated for Chinese living in mainland China may not be applicable to southern Chinese in Hong Kong because of differences in lifestyle habits and subject characteristics. The objective of this study was to estimate the 10-year probability of osteoporotic fracture in Hong Kong southern Chinese according to age and BMD T-score at the femoral neck based on the methodology of FRAX™ risk assessment tool calibrated to the epidemiology of Hong Kong. Fracture data was obtained from the Clinical Data Analysis Reporting System (CDAS) of the Hospital Authority of Hong Kong while population size and death rates were taken from the Hong Kong Government Census and Statistics Department. Fracture probability was calculated using the cut-off values for T-scores derived from the NHANES III data for Caucasian women aged 20-29 years for BMD at the femoral neck.

We found that the 10-year probability of osteoporotic fracture in Hong Kong southern Chinese men and women increased markedly with increasing age and decreasing femoral neck BMD T-score. Furthermore, the results showed that the 10-year absolute fracture risk for Hong Kong southern Chinese was substantially higher than the mainland Chinese and was comparable to Caucasians in other developed countries like USA and UK. Based on this evidence and until we have Hong Kong southern Chinese population-specific information, we recommend the application of the Caucasian risk profile to calculate the absolute fracture risk for Hong Kong southern Chinese subjects.

**Disclosures:** S.W.Y. Tsang, None.

## SU265

**Bone Mineral Density (BMD) Measurement: an Independent Risk Factor of Breast Cancer Recurrence?** A. Sassi\*, F. Liebens\*, B. Carly\*, S. Rozenberg<sup>1</sup>, M. Tondeur<sup>2</sup>. <sup>1</sup>Department of Obstetrics and Gynaecology, CHU Saint-Pierre, Université Libre de Bruxelles, Brussels, Belgium, <sup>2</sup>Department of Nuclear Medicine, CHU Saint-Pierre, Université Libre de Bruxelles, Brussels, Belgium.

**Background :** Bone mineral density (BMD) may be seen as a marker of lifetime estrogen exposure and high BMD has been associated with an increased breast cancer risk. On the other hand, it is debated whether estrogen induced breast cancer is associated with a favourable prognosis.

**Aim :** We evaluated whether bone mineral density (BMD) measurements are associated with a higher risk of breast cancer recurrence.

**Design :** Retrospective case control matched study.

**Patients & methods:** Review of women diagnosed with breast cancer and followed since 1992. A data bank was constituted of breast cancer patients who had their vertebral or femur BMD measured. Data included prognostic indicators (TNM stage, grading, estrogen and progesterone receptor, HER2/neu, KI67) and osteoporosis risk factors. We included only patients who had their BMD measured at the time of diagnosis. Cases were defined as women with a proven breast cancer recurrence (n=22 mean age  $\pm$  SEM 54.04  $\pm$ 2.9). The controls were chosen out of a series of 254 controls. Each case was matched with two breast cancer patients without recurrence with similar age, prognostic indicators and period of follow-up (n=44, mean age  $\pm$  SEM 53.64  $\pm$ 1.9), while the BMD results and the names of the patients were blinded.

**Statistical analysis :** We calculated the mean BMD between the two controls and tested whether differences between the mean control and the case were not different from zero using paired t-test (p<0.05).

**Results & conclusions:** There were no significant differences in vertebral or femur BMD measurements between cases and controls (respectively mean  $\pm$  SEM : BMDL 1.03  $\pm$  0.02 vs 1.02  $\pm$  0.02; BMD femur 0.893  $\pm$  0.02 vs 0.873  $\pm$  0.02 g/cm<sup>2</sup>).

**Conclusions:** Although this study was only powered to detect a difference of about 7% between pairs, it is unlikely that BMD is an independent risk factor of breast cancer recurrence.

**Disclosures:** S. Rozenberg, None.

This study received funding from: IRIS Foundation.

## SU266

**Evaluation of Tibial Bone Density Surrounding Tantalum Tibial Implants in TKA.** C. Simonelli<sup>1</sup>, T. J. Gioe<sup>2</sup>, S. J. Penny<sup>3</sup>, M. C. Schoeller<sup>1</sup>, A. Harrison<sup>4</sup>. <sup>1</sup>Osteoporosis Services, HealthEast Clinics, Woodbury, MN, USA, <sup>2</sup>Orthopedic Service, Veteran's Administration, Minneapolis, MN, USA, <sup>3</sup>Medical Research, HealthEast, St. Paul, MN, USA, <sup>4</sup>Orthopedics, University of Minnesota, Minneapolis, MN, USA.

Total knee arthroplasty (TKA) with conventional metal-backed tibial implants subjects the tibial metaphysis to stress shielding, with resultant loss of bone density. The biomaterial properties of tantalum closely match that of bone. We hypothesized that tibial bone mineral density (BMD) in patients with porous tantalum (trabecular metal, TM) tibial baseplates would be maintained better than in conventional historic controls, and would more closely parallel tibial BMD in the nonoperative control limb. Forty patients (35 M/ 5 F)  $\leq$  60 years underwent TKA with uncemented TM tibial components (Zimmer NexGen®, Warsaw, IN). All perioperative and postoperative treatments were identical, and patients were allowed immediate weight-bearing. In addition to routine clinical followup with radiographs and validated scoring instruments, patients underwent dual-energy x-ray absorptiometry (DEXA) scans of the bilateral proximal tibiae with designated precision knee software (GE Lunar Prodigy Advance®, v.10.5) preoperatively, and at 2 months, 1 year and 2 years postoperatively. Three selected regions of interest (ROI) (Zone 1=between the pegs; Zone 2= beneath the pegs; Zone 3=directly below entire baseplate) were chosen to evaluate BMD using a standardized protocol. Additional ROI were used to help align the composite template on the non-operated knee. Lumbar spine and hip BMD values were also obtained preoperatively and at two years. Precision analysis revealed precision error  $\leq$  4% for each of the ROI indicating adequate power to detect BMD changes of  $\geq$  8% in an individual patient. BMD was not significantly different between the operative and nonoperative knees in any ROI at any time period. BMD decreased significantly in all ROI in the nonoperative knee at the one-and two-year evaluations (p =.004 to p=.01). Only in Zone 3 (immediately below the baseplate) did the BMD decrease significantly at 2 months (p=.03) and 2 years (p=.05) in the operative knee. This is the first report of BMD measurement surrounding a TM tibial implant utilizing the contralateral non-operative limb as a control. Although BMD decreases immediately below the baseplate at 2 months and 2 years in TM implants, similar changes occur in the nonoperative limb. Trabecular metal implants appear to maintain tibial BMD in a parallel fashion to the nonoperative limb in this population.

**Disclosures:** C. Simonelli, Eli Lilly 1, 2, 3; Roche 1, 2, 3; GSK 1; Novartis 3. This study received funding from: Zimmer, Inc.

## SU267

**Areal BMD by DXA May Predict Similar Risk of Fracture in Elderly Women and Men due to Offsetting Effects of Bone Size and True Volumetric BMD.** B. Srinivasan<sup>1</sup>, S. Amin<sup>2</sup>, B. L. Riggs<sup>1</sup>, E. J. Atkinson<sup>3</sup>, L. J. McDaniel<sup>4</sup>, L. J. Melton<sup>4</sup>, S. Khosla<sup>1</sup>. <sup>1</sup>Endocrinology, Mayo Clinic, Rochester, MN, USA, <sup>2</sup>Rheumatology, Mayo Clinic, Rochester, MN, USA, <sup>3</sup>Biostatistics, Mayo Clinic, Rochester, MN, USA, <sup>4</sup>Epidemiology, Mayo Clinic, Rochester, MN, USA.

While the current practice in the US is to define osteopenia and osteoporosis in women and men using gender-specific T-scores, the actual areal BMD (aBMD) value by DXA seems to predict equivalent fracture risk in both sexes (Johnell et al., JBM 20:1185, 2005). Since bone size and structure differ considerably between women and men, the reason(s) why absolute aBMD by DXA has equivalent predictive ability for fracture outcomes in both sexes is somewhat unclear. To address this issue, we assessed femur neck (FN) aBMD by DXA and true volumetric BMD (vBMD) and geometry by QCT at the same site in a population-based sample of older (age  $\geq 50$  years) women (n = 157) and men (n = 68). From these subjects, we matched 58 women and 51 men for FN aBMD by DXA.

Table: Data are mean  $\pm$  SEM, p-values are adjusted for age and aBMD

	Older women	Older men	P value
Age, yrs	65.1 $\pm$ 1.3	73.3 $\pm$ 1.4	<0.001
DXA FN areal BMD, gm/cm <sup>2</sup>	0.93 $\pm$ 0.02	0.94 $\pm$ 0.02	--
FN QCT parameters			
Area, cm <sup>2</sup>	6.8 $\pm$ 0.1	9.6 $\pm$ 0.2	<0.001
Total vBMD, mg/cm <sup>3</sup>	331.0 $\pm$ 9.5	286.1 $\pm$ 7.8	<0.001
Cortical vBMD, mg/cm <sup>3</sup>	604.2 $\pm$ 13	587.0 $\pm$ 10	0.470
Trabecular vBMD, mg/cm <sup>3</sup>	202.9 $\pm$ 7.2	176.2 $\pm$ 6.0	<0.001

As shown in the Table, matching for FN aBMD resulted in the men being  $\sim 8$  yrs older than the women. As compared to the women, the men matched for FN aBMD had significantly larger bone area but lower total and trabecular FN vBMD, with similar cortical vBMD. Since both bone size and vBMD contribute to bone strength, and bigger bones have higher aBMD values by DXA due to the intrinsic artifact of this technique, our findings provide a potential explanation for the apparently fortuitous ability of absolute aBMD by DXA to predict equivalent levels of absolute fracture risk (and presumably, bone strength) in women and men: the bone strength gains due to larger bone size in the men matched for aBMD to women are offset by losses in strength due to lower true vBMD values. Additional studies using finite element modeling are needed to further define the relative contributions of bone size and vBMD to bone strength in women vs. men.

**Disclosures:** B. Srinivasan, None.

This study received funding from: NIH/NIA - AR27065.

## SU268

**Prevalence of Osteoporosis in Indolent Systemic Mastocytosis.** E. van der Veer<sup>1</sup>, W. E. van der Goot<sup>2</sup>, J. G. R. de Monchy<sup>2</sup>, J. C. Kluin-Nelemans<sup>3</sup>, J. J. van Doormaal<sup>2</sup>. <sup>1</sup>Laboratory Medicine, University Medical Center Groningen, Groningen, Netherlands, <sup>2</sup>Allergy, University Medical Center Groningen, Groningen, Netherlands, <sup>3</sup>Hematology, University Medical Center Groningen, Groningen, Netherlands.

**Introduction:** Indolent Systemic Mastocytosis (ISM) is characterized by an accumulation of pathological mast cells in bone marrow. Release of histamine, tryptase, heparin and other mast cells mediators might cause bone destruction.

**Aim:** To establish the prevalence of osteoporosis in ISM-patients, and investigate whether osteoporosis in ISM-patients is accompanied by higher levels of serum tryptase and urinary histamine metabolites.

**Methods:** All patients visiting the multidisciplinary Mastocytosis Outpatient Clinic with ISM according to the WHO criteria (48 men; 66 women) were included. Bone Mineral Density (BMD) of radius, lumbar spine, and femoral neck was measured by Dual-Energy X-ray Absorptiometry. Serum tryptase and urinary methylhistamine (MH) and methylimidazole acetic acid (MIMA) were analyzed. Descriptive statistics were used to define the groups of patients that developed osteoporosis. ROC curves were made to examine the predictive value of tryptase, MH and MIMA for osteoporosis.

**Results:** Analyses were performed on 111 BMD measurements. Three patients were excluded due to lack of adequate BMD data. Osteoporosis (BMD of lumbar spine- or hip-T-score  $\leq -2.5$ SD) was detected in 24% (7/29) and 29% (5/17) of the male patients, younger respectively older than 50 years. If the radius BMD was included this percentage increased to 34% (10/29) for the younger men. For women these percentages were 12% (4/34) and 26% (8/31) respectively, and 12% and 29% if the radius BMD was included. The median ages of the older male and female ISM-group were 57 and 58 years, respectively. Only 2 men and 4 women were  $>65$  years old. Age related prevalence for osteoporosis in the Dutch population (Rotterdam-study) is 0.5% till 5% for men and 3% till 16% for women of the age-groups 55-65 years, respectively. ROC curves of female patients showed a significant test accuracy of MH (AUC=0.718; p=0.002), MIMA (AUC=0.713; p=0.003), and tryptase (AUC=0.646; p=0.049) with a BMD lumbar spine, hip or radius T-score = -2.5 SD as cut-off point. ROC curves of men showed no significance.

**Conclusions:** The prevalence of osteoporosis in ISM-patients under the age of 65 years is high, especially in men  $<50$  years. Elevated levels of MH and MIMA and to a lesser extent tryptase signal this higher risk in women, with a test accuracy of 72%, 71% and 65%, respectively, but not in men. Routine measurement of BMD should be considered in patients with indolent systemic mastocytosis in order to detect and treat osteoporosis.

**Disclosures:** E. van der Veer, None.

## SU269

**Biomechanical Impact of Chronic Haemodialysis (CHD) on Bones and Muscles. A pQCT Study.** S. Feldman\*, I. Grappiolo\*, R. F. Capozza\*, G. Inchauspe\*, B. Radice\*, P. S. Reina\*, S. Castellini\*, G. Nicola\*, F. Acosta\*, J. L. Ferretti, G. R. Cointry\*. CEMFoC, Faculty of Medicine, National University of Rosario, Rosario, Argentina.

This paper aims to describe the impact of CHD on the musculoskeletal system in men and women following biomechanical criteria. Tomographic (pQCT) indicators of bone mass (trabecular and cortical BMC -TbC, CtC-; trabecular vBMD -TbD-; cortical CSA -CtA-), tissue mineralization (cortical vBMD corrected from the partial-volume effect -CtD-), cross-sectional design (endosteal perimeter -EoPm-; cortical thickness -CtTh-; bending and torsion moments of inertia -CSMI's-) and strength (Bone Strength Indices -BSI's-; Stress-Strain Index -SSI-), and of muscle strength (height-adjusted muscle CSA, -mCSA-) were determined in tibial (4, 14, 38, and 66% sites) and radial (4 and 66% sites) scans of 21 men and 14 women aged 15-66 years under CHD. Z-scores of these data were calculated with reference to 260 healthy adults (60 men, 80 pre-MP women, 120 post-MP women) of comparable age. The pQCT data were correlated with serum PTH activity and time on dialysis (TOD).

Both CHD men and women showed significant impairments of TbC and TbD and less intense reductions of CtC, CtA, CtTh, BSI's and SSI. Bone mass loss was generally greater in women than men. EoPm was generally increased. A relatively mild impairment in CSMI's was observed, only significant in women. No changes were induced in CtD. The natural, hyperbolic relationships observed between CSMI's (y) and CtD (x) ("distribution/quality" curves, regarded as descriptive of the functional status of the bone *mechanostat* in the cortices) showed lower ordinates than normal only in the women. The mCSA was generally reduced, especially in the women. Bone mass (but not CSMI's) per unit of mCSA decayed, more severely in the women. The biomechanical changes in bone-muscle interactions were significant only in the tibial, not radial scans. All the described changes correlated significantly with both serum PTH and time on dialysis. The CHD-induced osteopenia was more severe in metaphyseal regions with thin cortices than in diaphyses, and predominantly so in the women. As long as the cortical loss seemed to have resulted predominantly from endosteal resorption, its impact on the CSMI's was relatively mild, and cortical mineralization was rather kept unaltered. The mechanical orientation of bone modeling by bone *mechanostat* as a function of mechanical usage (CSMI/CtD ratio) was affected only in women, reflecting a metabolic (not mechanical) disturbance. Bone loss was associated to PTH activity and TOD in all patients, also suggesting a metabolic disturbance. Predominance of effects in the legs may be associated with stroll-related (i.e. mechanical) problems.

**Disclosures:** J.L. Ferretti, None.

## SU270

**Hip Structure Analysis (HSA) in Women - a Population Based Study.** M. F. Nielsen<sup>1</sup>, J. Ryg<sup>1</sup>, R. Barkmann<sup>2</sup>, C. C. Glüer<sup>2</sup>, K. T. Brixen<sup>1</sup>. <sup>1</sup>Endocrinology, Odense University Hospital, Odense, Denmark, <sup>2</sup>Klinik für Diagnostische Radiologie, Christian-Albrechts-Universität, Kiel, Germany.

Bone mineral density (BMD) is closely related to fracture risk (1), however, several studies have suggested that hip geometry or hip structural analysis (HSA) (2,3) may also predict fracture risk or even improve such prediction. In this study, we aimed at describing age-related changes in HSA in women.

Women aged 20-40 and 55-80 years selected at random from the population listing of Funen County, Denmark, were invited by direct mailing to participate and a total of 453 women were included in the study. Patients with prior bilateral calcaneal fractures, bilateral hip prostheses, cognitive impairment or pregnancy were excluded.

HSA was performed using a Hologic Discovery A densitometer and the recently developed APEX software (version 2.0). Comparisons were performed using T-test.

Results regarding HSA of the narrow neck in pre- and post-menopausal women are shown in table 1. Also, BMD, cross sectional area, cross sectional moment of inertia, width, section modulus correlated directly and significantly (p<0.01) with body weight (controlling for age). In contrast, buckling ratio correlated inversely and significantly (p<0.01) with body weight.

Parameter	Pre-menopausal n = 138	Post-menopausal n = 315	P	Diff. (z-score)
Age	30 [20-40]	59 [55-79]	NA	
BMD (g/cm <sup>3</sup> )	1.04 $\pm$ 0.14	0.88 $\pm$ 0.13	<0.001	-1.14
Cross sectional area (cm)	3.10 $\pm$ 0.47	2.71 $\pm$ 0.40	<0.001	-0.83
Cross sectional moment of inertia (cm <sup>2</sup> ) <sup>2</sup>	2.57 $\pm$ 0.62	2.48 $\pm$ 0.49	NS	-0.15
Width (cm)	3.13 $\pm$ 0.21	3.26 $\pm$ 0.19	<0.001	0.62
Section modulus	1.53 $\pm$ 0.30	1.35 $\pm$ 0.22	<0.001	-0.6
Buckling ratio	8.44 $\pm$ 1.55	11.17 $\pm$ 2.26	<0.001	1.76

We conclude that both BMD, cross sectional area and section modulus are significantly lower in post-menopausal compared with pre-menopausal women while width and buckling ratio of the narrow neck are significantly higher after the menopause.

1) Marshall D et al. BMJ 1996; 312:1254

2) Faulkner KG et al. JBM 1993; 8:1211

3) Rivadeneira F et al. JBM 2007; 22:1781

**Disclosures:** M.F. Nielsen, None.

This study received funding from: European Union / Interreg 3.

## SU271

**A Clinical Prediction Rule to Identify Women for Bone Mineral Density Testing at Menopause.** G. A. Hawker, M. Lam\*, P. S. Akhavan\*, E. J. Waugh, S. Jamal, J. Susan, D. A. Sutton\*. Osteoporosis Research Program, Women's College Hospital, Toronto, ON, Canada.

Guidelines to facilitate decision making regarding BMD testing in healthy women around the time of menopause do not currently exist. The objective of this study was to develop a clinical prediction rule for BMD testing in healthy women approaching menopause (aged 40-60 years), suitable for use in primary care. Participants were healthy women aged 40-60 years, referred for a first-ever BMD test at a large urban hospital. Risk factors for low BMD were assessed by a structured self-administered questionnaire. BMD at the lumbar spine, femoral neck and total hip were assessed with DXA. DXA was performed blind to risk assessment. Predictors of low BMD (T-score  $\leq -2.0$  at any site) were determined by multivariate regression. Several algorithms were compared to identify one with the highest sensitivity and acceptable specificity, to discriminate women with/without low BMD. Among 628 participants, 69 (12.6%) had low BMD. The algorithm that recommended testing women who had 1 or more of the following risk factors: weight  $\leq 65$  kg, low trauma fracture after age 40, age at menarche  $> 15$  years, or physical inactivity during adolescence, had a sensitivity of 88.7% and a specificity of 41.3%. Using this algorithm as the decision rule, 38.4% of participants would not have been recommended for testing; among those not recommended, the likelihood of low BMD was 2.9%. A clinical prediction rule to assist in determining the need for initial BMD assessment in healthy perimenopausal women was developed. The rule recommends BMD testing in women who have 1 or more of the following risk factors: weight  $\leq 65$  kg, low trauma fracture after age 40, age at menarche  $> 15$  years, or physical inactivity during adolescence.

**Disclosures:** G.A. Hawker, None.

This study received funding from: Ontario Ministry of Health and Long Term Care.

## SU272

**Osteoporosis: Evaluation of Screening Patterns Primary Care Group Practice.** K. Cohen\*, D. Maier\*. New West Physicians, Golden, CO, USA.

**Background:** An estimated half of all women over age 50 will have an osteoporosis-related fracture in their lifetime. National osteoporosis clinical guidelines for screening recommend measurement of bone mineral density in average-risk women beginning at age 65. Little data is available regarding compliance with this recommendation.

**Purpose:** To evaluate osteoporosis screening rates in a random sample of women, age 66 or older, in a large multi-site primary care group practice.

**Methods:** The study was conducted in a primary care group practice serving over 180,000 patients in the Denver metropolitan area. Medical records of a random sample of 833 female patients aged 66 years or older were reviewed retrospectively. Patients were seen at one of 13 practice locations, by one of 34 physicians, who practiced either family medicine or internal medicine. Main Outcome Measure: The frequency of osteoporosis screening was calculated. Accepted methods of screening include peripheral bone density measurement by ultrasound or DXA, or central DXA.

**Results:** The physician-specific osteoporosis screening rates varied widely, ranging from 19% to 97%. The practice-specific osteoporosis screening rates ranged from 26% to 91%. Overall, the mean rate of osteoporosis screening among all physicians was 56%.

**Conclusions:** Despite improvements in osteoporosis screening, there continues to be a gap in the quality of care provided compared to national recommended guidelines. Policy changes, performance improvement measures and interventions are needed to improve screening rates in primary care practices.

**Disclosures:** K. Cohen, Novartis Pharmaceuticals Corporation 3.

This study received funding from: Novartis Pharmaceuticals Corporation

## SU273

**Bone Mineral Density Is Associated with Lean Mass and not Fat Mass.** B. H. Arjmandi, S. Hooshmand, R. L. Saadat\*, S. C. Chai\*. Nutrition, Food and Exercise Sciences, Florida State University, Tallahassee, FL, USA.

Obese individuals hold an increased risk of several chronic and degenerative diseases such as cardiovascular disease (CVD). We have shown earlier that body mass index (BMI;  $\text{kg}/\text{m}^2$ ) values can be used as predictor of CVD risk factors. Elsewhere, we reported that a relationship exist between BMI and indices of CVD risk factors including lipid profiles and fasting blood glucose levels in postmenopausal women. To further investigate the relationship between BMI and chronic diseases, we measured C-reactive protein (CRP) level, a marker of inflammation, in 122 osteopenic, otherwise healthy postmenopausal women. These participants were divided into three groups based on their BMI values: 1) normal (18.5-24.9); 2) overweight (25-29.9); and 3) obese ( $\geq 30$ ). BMI was positively correlated with CRP ( $r=0.355$ ;  $P<0.0001$ ) in this population. In addition, overweight and obese individuals had higher serum levels of CRP compared to individuals with normal BMI (Table 1). In contrast to existing relationship between higher BMI and higher incidence of chronic diseases, epidemiological studies have shown that osteoporosis is the only chronic disease that has negative correlation with BMI. To further investigate this relation, we evaluated the correlation between BMI and bone mineral density (BMD) in this osteopenic postmenopausal population.

**Table 1:** Pearson correlation coefficients among BMI values, CRP levels and BMD; and Pearson correlation coefficients among BMD and components of body composition in osteopenic postmenopausal women

	Body Mass Index ( $\text{kg}/\text{m}^2$ )			ANOVA	
	18.5-24.9	25-29.9	$>30$	r	p
C-reactive protein (mg/dL)	1.405 $\pm$ 0.12 <sup>a</sup>	2.286 $\pm$ 0.28 <sup>b</sup>	3.156 $\pm$ 0.42 <sup>b</sup>	0.3547	$<0.0001$
BMD ( $\text{g}/\text{cm}^2$ )	1.077 $\pm$ 0.01	1.087 $\pm$ 0.01	1.119 $\pm$ 0.02	0.222	0.2
	Bone Mineral Density ( $\text{g}/\text{cm}^2$ )			ANOVA	
	18.5-24.9	25-29.9	$>30$	r	p
BMI ( $\text{Kg}/\text{m}^2$ )	18.5-24.9	25-29.9	$>30$	-	0.001
Fat (Kg)	21.367 $\pm$ 0.49	30.993.1 $\pm$ 0.701	42.110 $\pm$ 1.392	-	0.001
Lean (Kg)	35.828 $\pm$ 0.428 <sup>a</sup>	38.315 $\pm$ 0.790 <sup>b</sup>	44.084 $\pm$ 1.155 <sup>c</sup>	0.306	0.0001

Values are means  $\pm$  SEM; N=122

<sup>a,b,c</sup> Values that do not share the same superscript letters are significantly ( $P < 0.05$ ) different from each other

As expected, BMI was positively correlated with BMD (Table 1) which means a negative correlation with osteoporosis; however, when we examined the correlation between BMD and components of body composition including fat mass and lean mass; BMD was highly correlated with lean mass ( $r=0.306$ ;  $P=0.0006$ ) but not with fat mass ( $P=0.94$ ; Table 1). Although these data supports the notion that individuals with higher BMI have lower risk of osteoporosis, break down of body composition clearly demonstrate that the credit for this correlation should be given to lean mass and not fat mass.

**Disclosures:** B.H. Arjmandi, None.

## SU274

**Hip Fracture Patients with Vertebral Fractures Have More Severe Osteoporosis and Are Candidates for more Active Treatment Including PTH.** J. Browne\*, N. Maher\*, M. Healy\*, E. McGovern\*, M. C. Casey\*, J. B. Walsh. Medicine for the Elderly, St James Hospital, Dublin, Ireland.

Patients with hip fracture are at increased risk for further fracture, however prior to having a hip fracture, these patients may demonstrate additional evidence of osteoporosis and be asymptomatic. Vertebral fractures may indicate higher risk of further fracture and should be targeted for optimum fracture prevention.

This was a retrospective review of patients admitted with acute hip fracture who underwent DXA and lateral vertebral assessment (LVA). LVA is performed on all patients that present for DXA in St James Hospital. There was also a retrospective review of bone markers, PTH, vitamin D, and GFR.

Between June 2003 to October 2007, 643 patients were admitted to St James with acute hip fracture. 413 patients subsequently had a DXA scan performed. Of these patients, 9.7% had a previous hip fracture on the opposite side. 34.6% of hip fracture patients had evidence of at least one vertebral fracture, with 22.1% having at least 2 or more vertebral fractures. 55% of vertebral fractures occurred in the thoracic region.

	Differences in patients with only hip fractures and patients with both hip and vertebral fracture	
	Hip and Vertebral Fracture (n=143)	Hip Fracture only (n=270)
Age (yrs)	78.71 (+/- 9.25)	76.87 (+/- 10.56)
Spine BMD ( $\text{g}/\text{cm}^2$ )	0.853 (0.212)	0.929 (+/- 0.215)
Hip BMD ( $\text{g}/\text{cm}^2$ )	0.655 (0.142)	0.739 (+/- 0.165)
CTx (ng/ml)	0.525 (0.067)	0.516 (+/- 0.315)
Osteocalcin (ng/ml)	29.67 (+/- 29.99)	26.03 (+/- 27.1)
PTH (pg/ml)	56.47 (+/- 47.85)	48.59 (+/- 37.81)
Weight (kg)	56.79 (+/- 11.51)	60.97 (+/- 13.56)

In conclusion, over a third of patients with hip fracture have a concurrent vertebral fracture. All patients who have a hip fracture should have their vertebrae assessed. These patients were older and were significantly osteoporotic both in their remaining unfractured hip and vertebrae. PTH level tended to be raised in the vertebral fracture group however there was no difference in bone markers or vitamin D levels. Hip fracture patients who have vertebral fractures appear to be at higher risk of subsequent fracture, highlighting the need for active treatment and should be considered as potential cases for PTH therapy.

**Disclosures:** J. Browne, None.



## SU275

**Breaking an Egg-Shell; Regional Thinning of the Femoral Neck Cortex with Advancing Age Predisposes to Hip Fracture.** K. E. S. Poole<sup>1</sup>, P. M. Mayhew<sup>\*1</sup>, C. M. Rose<sup>\*1</sup>, K. Brown<sup>\*2</sup>, S. K. Kaptoge<sup>\*1</sup>, P. Bearcroft<sup>\*3</sup>, N. Loveridge<sup>\*1</sup>, J. Reeve<sup>1</sup>. <sup>1</sup>Department of Medicine, University of Cambridge, CB2 2QQ, United Kingdom, <sup>2</sup>Mindways Software Inc, Austin, TX, USA, <sup>3</sup>Department of Radiology, University of Cambridge, CB2 2QQ, United Kingdom.

**Purpose:** DXA measurements of the hip are moderately predictive of fracture but 3D measurements have the potential to predict better. This would allow clinicians to target preventive therapies to the majority of current cases who have T-scores > -2.5. In biopsy specimens, ageing was associated with thinning of the supero-posterior (SP) cortex while in intracapsular hip fracture specimens, inferior thinning was also identified. These regions are subjected to a high applied force during sideways falling. The 100 Women Study is a cross-sectional study investigating cortical thickness (C.Th) in life from 20-90 years using multi-slice CT.

**Methods:** 100 healthy women were recruited, stratified by decade from age 20 to 90 (IQR 38-72). Participants consented to an extension of a routine clinical pelvic CT scan (Siemens 64) to include both hips (1mm slice thickness, 0.59 mm voxel size). The starting position for cross sections was a 1mm thick mid-femoral neck slice at an eccentricity (max/min ratio) of 1.4, since this location along the neck axis was highly reproducible and unaffected by age (mean 51% distal, SE 0.016%), being unaffected by age. 5 parallel 1mm slices were evaluated towards the midline. Age effects on regional C.Th were evaluated using linear regression in anatomical quadrants using a fixed threshold of 450mg/cm<sup>3</sup> and Mindways Software (BIT-2). Existing measurements of post-mortem femurs using pQCT and clinical CT were used to validate BIT-2.

**Results:** There was a marked decline in estimated C.Th in the supero-posterior quadrant, from 2.0 mm at age 25 to 0.4mm aged 85 (C.Th =  $2.6 - 0.026 \times \text{Age}$ ,  $r^2 = 0.51$ ,  $p < 0.0001$ ). In contrast, age had no effect on infero-anterior C.Th ( $p = 0.79$ ). Age explained 51%, 31%, and 28% of the variance in SP, SA, and IP C.Th respectively ( $p < 0.0001$ ). Weight had a positive association with IP C.Th ( $p < 0.001$ ) that was age-independent.

**Conclusion:** The thinning of the supero-posterior femoral neck cortex, which can become egg-shell thin by the eighth decade can be estimated in-vivo. Such changes are a cause of the exponentially increased hip fracture susceptibility observed in elderly fallers. Future clinical studies of hip fracture should include measurements of cortical thickness in the proximal femur.

**Disclosures:** K.E.S. Poole, None.

## SU276

**In Vivo Assessment of 3-Dimensional Bone Micro Architecture with HR-pQCT in Patients With and Without Fractures.** H. Radspieler<sup>1</sup>, I. Frieling<sup>2</sup>, M. A. Dambacher<sup>3</sup>, M. Neff<sup>4</sup>. <sup>1</sup>Osteoporosezentrum München, München, Germany, <sup>2</sup>Osteoporosezentrum Hamburg Neuer Wall, Hamburg, Germany, <sup>3</sup>ZORG International, Zollikerberg, Switzerland, <sup>4</sup>Osteoporosezentrum Zürich, Zürich, Switzerland.

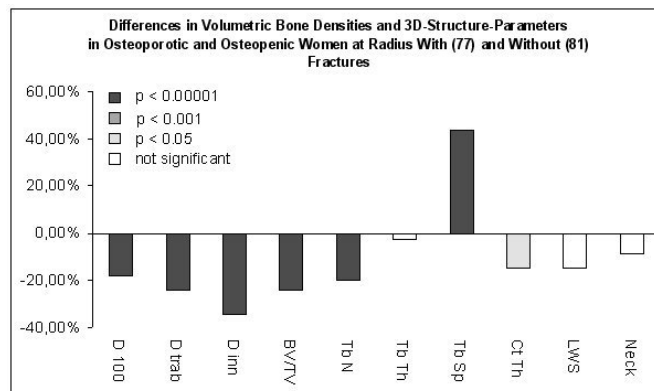
Measurement of areal bone mineral density (BMD/DXA) with derived T-scores may not be sufficient to evaluate the individual fracture risk. HR-pQCT reveals volumetric cortical and trabecular bone density and structural parameters as BV/TV, trabecular thickness and separation and cortical thickness.

We examined more than 200 women in the centres of osteoporosis in Hamburg and Munich with normal (T-Score > -1SD), osteopenic (-2.5 SD > T-score < -1.0 SD) or osteoporotic (T-score < -2.5 SD) BMD measured with DXA. In all patients volumetric BMD and trabecular architecture of the radius and tibia were measured by HR-pQCT (XtremeCT<sup>®</sup>, SCANCO Medical AG).

Women with and without fractures showed no significant differences in height and weight but in age (68 vs. 63 y). The median T-scores from DXA measurements in women with and without fractures showed no significant differences (lumbar spine: -2.2 and -2.1, total hip: -2.2 and -2.2, neck: -2.0 and -1.8, respectively).

However, selective and region specific trabecular densities as well as structure parameters measured by HRpQCT differed significantly in osteopenic and osteoporotic women with and without fractures. The mean total density was lower in women with fracture than in women without fractures (D100, 247 vs. 291 mg/ml,  $p < 0.001$ ), as well as the mean trabecular density (Dtrab, 94 vs. 123 mg/ml,  $p < 0.001$ ) and the mean inner trabecular density (Dinn, 49 vs. 75 mg/ml,  $p < 0.001$ ). Furthermore structure parameters in patients with fractures showed significantly increased trabecular separation (TbSp, 678 vs. 548  $\mu\text{m}$ ,  $p < 0.001$ ) and significantly decreased trabecular number (TbN, 1.3 vs. 1.6/mm,  $p < 0.001$ ) as well as BV/TV (7.8 vs. 10.3%,  $p < 0.001$ ) and significantly decreased cortical thickness (CtTh, 623 vs. 735  $\mu\text{m}$ ,  $p < 0.05$ ) with visible inhomogeneity of trabecular structure.

In conclusion, high-resolution peripheral computed tomography might help to predict fracture risk in osteopenic and osteoporotic patients. Especially in patients with osteopenia (according WHO-definition), the T-score seems to underestimate the fracture risk.



**Disclosures:** H. Radspieler, None.

## SU277

**Grayscale MR Image Based Finite Element Mechanical Modeling of Trabecular Bone at In Vivo Resolution.** J. F. Magland<sup>\*1</sup>, C. S. Rajapakse<sup>\*1</sup>, M. J. Wald<sup>\*1</sup>, B. Vasilic<sup>\*1</sup>, X. E. Guo<sup>\*2</sup>, X. H. Zhang<sup>\*2</sup>, F. W. Wehrli<sup>1</sup>. <sup>1</sup>Radiology, University of Pennsylvania, Philadelphia, PA, USA, <sup>2</sup>Biomedical Engineering, Columbia University, New York City, NY, USA.

In addition to bone volume fraction (BV/TV), trabecular network architecture is known to significantly impact overall bone strength. Advances in imaging technology now allow images to be acquired at isotropic resolution. The purpose of this work was to explore the association of finite-element (FE)-derived compressive modulus with parameters of scale and topology. MRI of 30 distal tibia specimens from 15 donors (ages 55-85 years) were obtained with a 3D spin-echo sequence after marrow substitution with gadolinium-doped water at 1.5T field strength (128 slices at 160x160x160  $\mu\text{m}^3$ ). The data was subjected to virtual bone biopsy (VBB) processing for structural and mechanical analysis. The entire trabecular bone region was manually selected (excluding the cortex) involving the center 64 slices. FE simulations were performed on the basis of inverted grayscale bone volume fraction maps, with intensities representing fractional voxel occupancy by bone. Each voxel with greater than 20% bone volume was modeled as a single hexahedral element assuming a Young's modulus (YM) of 13 GPa and Poisson's ratio of 0.3 for pure bone. Each element's YM was chosen proportional to BV/TV. Compression in the longitudinal direction was simulated with a piecewise tri-linear equilibrium displacement function using custom-designed software, resulting in solving a sparse system of 3N linear equations in 3N variables (N = number of vertices of elements in the structure, ~2 million on average). These were solved using a preconditioned conjugate gradient algorithm programmed in C++ and run on a Linux workstation with dual quad core Xeon CPUs (3.16 GHz) and 28 GB RAM. For efficiency, four simulations ran simultaneously on separate CPUs of the same machine. Finally, the intrinsic modulus of each structure was obtained by computing surface forces from the displacement function. Each FE simulation completed in around 1 hour. Fig. 1 shows BV/TV and strain maps and association between compressive modulus and structural parameters. Of note is the significant independent contribution of the topological surface-to-curve (S/C) ratio to overall mechanical behavior showing BV/TV and S/C to explain over 90% of the variation in the elastic modulus.

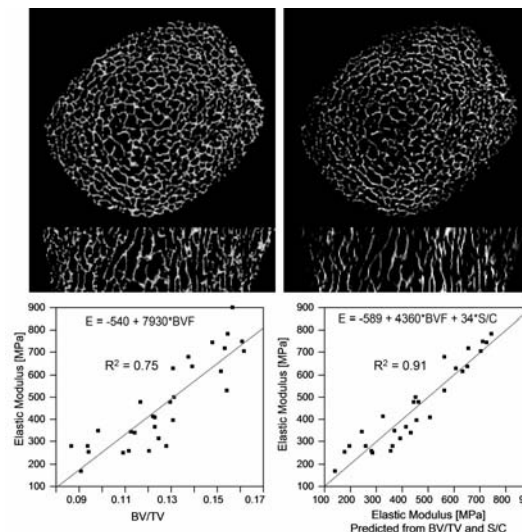


**Fig. 1:** Top left: TB/TV, top right: corresponding strain maps; bottom left: Elastic modulus (MPa) versus BV/TV; bottom right: FE-computed versus predicted modulus using 2-parameter model.

**Disclosures:** J.F. Magland, None.  
This study received funding from: NIH.

## SU278

**Validating pQCT Muscle Cross-Sectional Area Measurement.** S. Kontulainen<sup>1</sup>, A. Lorbergs<sup>\*1</sup>, J. Johnston<sup>\*2</sup>. <sup>1</sup>University of Saskatchewan, Saskatoon, SK, Canada, <sup>2</sup>University of British Columbia, Vancouver, BC, Canada.

Measurement of muscle cross-sectional area (MCSA) by peripheral QCT (pQCT) is valuable when assessing musculoskeletal adaptation to exercise, inactivity, growth or aging in healthy and clinical populations. There are several acquisition and analysis options available for MCSA but little is known about the validity of these protocols. Our aim was to compare an authenticated MCSA measure (gained using a custom-made, scans-specific (SSp) analysis protocol employing manual correction) with XCT-derived MSCA measures obtained using the recommended manufacturer protocol and modified protocols with and without selected muscle filters.

Twelve healthy volunteers (mean age 28 yrs) participated in the study. Non-dominant leg was scanned at 66% of the distance from the medial malleolus to the medial condyle of the tibia with pQCT (Stratec XCT2000). Images were obtained with recommended muscle scanning (voxel=0.8 mm, scan speed=20 mm/s) and enhanced resolution (0.4 mm and 20 mm/s) protocols. The SSp analysis protocol defined individual thresholds for fat/muscle and muscle/bone boundaries using a custom-written algorithm (Matlab 2007a). SSp MCSA was determined using commercial software (Analyze 6.0). Enhancement of the fat/muscle boundary was accomplished using an edge retaining smoothing filter (ITK Binary Min/Max Curvature Flow Filter). SSp MSCA was obtained using a region growing segmentation technique with scan-specific threshold values, followed by manual correction using a stylus and interactive touch-screen tablet (Cintiq 21UX) to ensure smooth and consistent anatomical representations. XCT6.0 software measures of MSCA were obtained using manufacturer's recommended and modified (using thresholds from SSp analysis) protocols with and without XCT muscle filters (CO1, CO2, CO4). Differences between XCT-derived MCSA values were compared to the SSp MCSA using GLM repeated measures adjusted for multiple comparisons (SPSS15.0). SSp MSCA and XCT-derived MCSA values (mean) and comparisons to the SSp (mean, % diff.) are shown in Table 1.

When using XCT2000 for MCSA analysis filtering the image was required for accurate representation of MCSA with both 0.8mm and 0.4 resolutions. These results are limited for XCT2000, used protocols and healthy young individuals. Similar comparisons are warranted for forearm muscle measurements and other populations.

Table 1.

Voxel size 0.4	MCSA mm <sup>2</sup>	Diff.	%-diff.	Sig.*
Scan-Specific	7643.4			
C1 <sup>a</sup> _40 <sup>b</sup> _280 <sup>c</sup>	9830.8	2187.4	28.6	0.003
C1_31_280	9888.1	2244.7	29.4	0.002
FILTERC01_C1_40_280	8686.6	1043.2	13.6	0.041
FILTERC01_C1_31_280	9177.4	1534.1	20.1	0.016
FILTERC02_C1_40_280	7593.8	-49.6	-0.6	1.000
FILTERC02_C1_31_280	8124.6	481.2	6.3	0.090
FILTERC04_C1_40_280	7441.2	-202.1	-2.6	0.683
FILTERC04_C1_31_280	7848.8	205.4	2.7	0.665
Voxel size 0.8				
Scan-specific	7526.6			
C3_40_280	7139.8	-386.8	-5.1	0.001
C1_40_280	8612.4	1085.8	14.4	0.016
FILTERC01_C1_40_280	7459.6	-67.0	-0.9	0.004
FILTERC01_C1_33_280	7559.6	32.9	0.4	0.283
FILTERC02_C1_40_280	7429.6	-96.9	-1.3	0.000
FILTERC02_C1_33_280	7534.1	7.5	0.1	1.000
FILTERC04_C1_40_280	7446.4	-80.2	-1.1	0.002
FILTERC04_C1_33_280	7549.3	22.72	0.3	0.921

\*Adjustment for multiple comparisons: Sidak.

a=Contour mode

b= threshold for fat/muscle boundary

c=threshold for muscle/bone boundary

**Disclosures:** S. Kontulainen, None.

This study received funding from: SHRF.

## SU279

**Precision of pQCT Measurements of Bone and Muscle Area in the Forearm and Lower Limb.** A. Lorbergs<sup>\*1</sup>, S. Jackowski<sup>\*1</sup>, C. Bennett<sup>\*1</sup>, J. Johnston<sup>\*2</sup>, S. Kontulainen<sup>1</sup>. <sup>1</sup>University of Saskatchewan, Saskatoon, SK, Canada, <sup>2</sup>University of British Columbia, Vancouver, BC, Canada.

Precise measures of bone and muscle cross-sectional areas (BCSA and MCSA) are essential in longitudinal studies assessing musculoskeletal changes. Thus, our primary objective was to assess precision of both BCSA and MCSA at forearm and lower leg with two scanning resolutions. Our secondary aim was to investigate whether precision is related to the number of scans recently trained operators have performed.

Healthy adult volunteers (28 women and 10 men, mean age 28.3 yrs, range 18-77 yrs) participated in the study. Two measurements (one day apart) of the non-dominant leg (66% of the distance from the medial malleolus to the medial condyle of the tibia) and forearm (65% of the length from the proximal head the distal margin of the styloid process of the radius) were scanned using pQCT (Stratec XCT2000). Three trained students performed

the scanning.

Recommended muscle scanning (voxel size=0.8 mm, scan speed=20 mm/s) and enhanced resolution (voxel=0.4mm) protocols were used for data acquisition. BCSA (of radius and ulna; tibia and fibula) and MCSA (forearm; lower leg) were analyzed with XCT6.0 software using contour mode 1 with a thresholds of 40 mm/cm<sup>3</sup> to separate fat from muscle and a threshold of 280 mg/cm<sup>3</sup> to separate muscle from bone. Muscle filter CO2 was used at both measured sites. Precision (CV%) was assessed for each operator and mean CVrms (%) was calculated for the each outcome according to Gluer et al (Osteoporosis Int 1995). Spearman rank correlation was used to assess relationship between order of scan and operator's precision (SPSS16.0).

In the forearm, precision of radius and ulna BCSA was 3.7 and 9.2% and precision of MCSA was 1.7% and 1.8%, when measured with the recommended and enhanced resolutions, respectively. In the lower leg, precision of tibia and fibula BCSA was 5.1 and 8.7%, and precision of MCSA was 2.9 and 3.7% with the lower and higher resolutions, respectively. Number of performed scans was only related to the BCSA precision at the forearm when measured with 0.4mm voxels size ( $r = -0.37$ ,  $p=0.02$ ).

Lower resolution seemed to provide more precise MCSA and BCSA measures. Repeatability of BCSA may be enhanced if bones were analyzed separately with another protocol. Additional scans are required to assess the number of practice scans needed to optimize precision when graduate students are trained for the pQCT measurements.

**Disclosures:** S. Kontulainen, None.

## SU280

**Implications of Resolution Isotropy on Apparent Topology of Trabecular Bone Architecture in MR Images.** M. J. Wald<sup>\*1</sup>, J. F. Magland<sup>\*1</sup>, C. S. Rajapakse<sup>\*1</sup>, X. H. Zhang<sup>\*2</sup>, E. Guo<sup>2</sup>, F. W. Wehrli<sup>1</sup>. <sup>1</sup>Department of Radiology, University of Pennsylvania, Philadelphia, PA, USA, <sup>2</sup>Department of Biomedical Engineering, Columbia University, New York, NY, USA.

Digital topological parameters related to the plate-strut architecture of trabecular bone (TB) derived from in vivo MR images have been shown to be sensitive to disease progression and treatment effects. Signal-to-noise limitations in micro-magnetic resonance imaging (μMRI) usually call for reduced resolution along the loading direction which can potentially compromise the sensitivity of topological parameters to microstructural changes since transversely oriented trabeculae and perforations of plate-like elements may not be detectable. Here we explore the effect of anisotropic voxel size on the digital topological parameters, in particular plates (surfaces) and rods (curves). Fifteen sets of demineralized tibia specimens (from right and left legs) were immersed in water doped with 1 mM gadolinium-DTPA and 10% formalin resulting in a medium closely matching the MRI properties of fatty marrow. The specimens were imaged using a two-channel phased-array ankle coil on a 1.5T Siemens Sonata system. A 3D fast large angle spin echo (FLASE) pulse sequence was used to acquire a 80x50x20 mm<sup>3</sup> volume at an isotropic voxel size of 160μm<sup>3</sup>. Each TB region was manually masked to remove the cortex and any trapped air inclusions. Each dataset was down-sampled along the longitudinal direction to produce datasets with 160x160x480 μm<sup>3</sup> effective resolution. These data were intensity normalized, bone volume fraction (BVf) mapped, skeletonized, and processed using digital topological analysis. The topological parameters were compared at the two resolutions. An average increase in apparent surface density of 7% was observed while the average curve density was reduced by 37% commensurate with a loss of transversely oriented trabeculae (rods). The increase in apparent surface voxels and decrease in curve voxels resulted in an increase in surface-to-curve ratio by 70% and a decrease in erosion index by 30%. The TB cores in Figures 1 b) and c) illustrate preservation of plate-like topology and rod-like trabeculae are either unresolved or become more plate-like at a reduced slice resolution. In conclusion, isotropic resolution is preferred for 3D structural analysis of TB using μMRI in order to detect changes (for example, due to osteoporosis) in rod-like trabeculae.

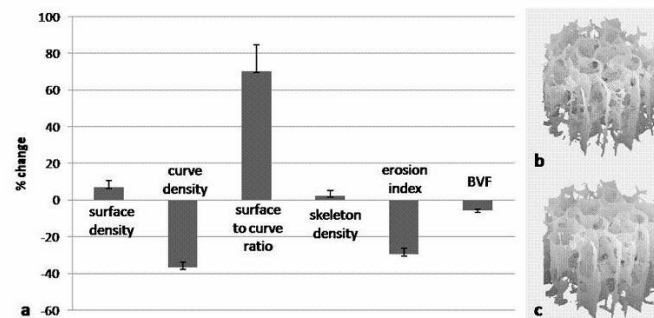


Figure 1. a) Mean change and standard deviation (%) of topological parameters derived from 30 specimen images due to lowering longitudinal resolution from 160 to 480μm; b, c) virtual cores at 160 and 480 μm longitudinal resolution. Plate perforations visible in b) are not seen in c).

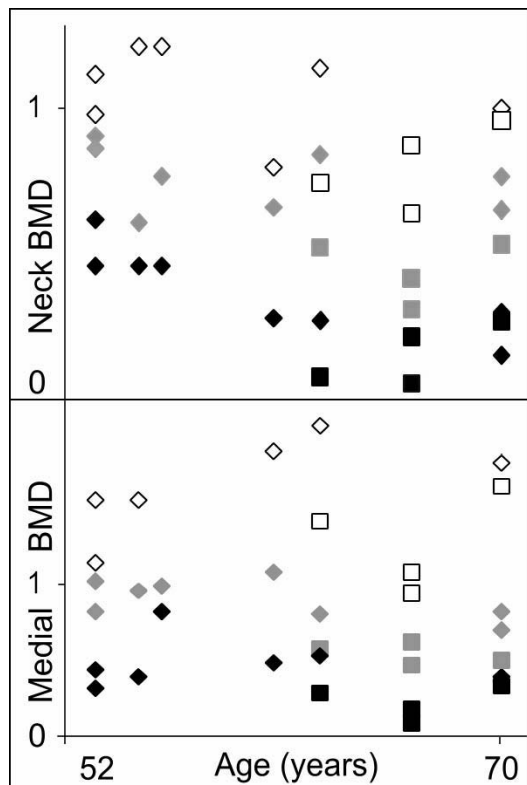
**Disclosures:** M.J. Wald, None.

This study received funding from: F31 EB007448-01A1/R01-AR-053156.

## SU281

**New Link Between Trabecular Properties and T-score at the Human Femur.** M. Ascenzi<sup>1</sup>, N. Hetzer<sup>\*1</sup>, A. Mac<sup>\*1</sup>, A. Lomovtsev<sup>\*1</sup>, R. Rude<sup>2</sup>, A. Nattiv<sup>\*1</sup>, A. Favia<sup>\*3</sup>. <sup>1</sup>Orthopaedic Surgery, UCLA, Los Angeles, CA, USA, <sup>2</sup>Department of Medicine, University of Southern California and Orthopaedic Hospital, Los Angeles, CA, USA, <sup>3</sup>Department of Human Anatomy, University of Bari, Bari, Italy.

The cancellous microstructure in the human femur was investigated to identify parameters relevant to assessment of fracture risk. Preliminary data on independence of trabecular thickness from trabecular density by site prompted the study. The femora of twelve postmenopausal Caucasian female donors, aged 52 to 70, free from metabolic pathologies and medical therapies that can affect the bone tissue, except for postmenopausal osteoporosis, provided the material. A novel analysis of (1) trabeculae by morphometry and (2) bone mineral density (BMD) by dual energy x-ray absorptiometry (DXA), was conducted regionally. First, each proximal femur was DXA-scanned and classified by age and T-score. Second, the distal femur was scanned at the lateral, medial and central regions. Each femur was then sectioned longitudinally to expose the trabeculae, which were labeled manually and measured automatically. The mean trabecular thickness and trabecular density were calculated on a sub-division of the conventional DXA template, consistent with the trabecular patterns that span the proximal femur, and at the medial, central and lateral regions of the distal femur. At each age, the two parameters were found to vary independently from each other and dependently on both region and T-score ( $p < 0.01$  at proximal and  $p < 0.03$  at distal). A pattern of variability emerged in terms of age. Further, the two trabecular parameters allowed computation of lower bound (black in Figure that shows two regions as examples - BMD in  $\text{g/cm}^2$ ) and upper bound (white) for DXA's BMD (grey) for normal T-score (triangle) and below normal T-score (square) by age. Trabeculae at the more mechanically-stimulated sites are here conjectured to degrade more slowly with age under normal conditions, while degradation would accelerate degradation at such sites of the below normal T-score group, consistently with increased fracture risk. Application in clinical imaging technology of the newly proposed femoral template that identifies regions of relatively homogeneous microstructure, is hypothesized to provide information on the trabecular changes due to aging with presence or absence of osteoporosis. Such information offers the prospect of improved assessment of fracture risk.



**Disclosures:** M. Ascenzi, Procter & Gamble Pharmaceuticals 3.  
This study received funding from: Procter & Gamble Pharmaceuticals.

## SU282

**Reduction of Magnetic Resonance Image Processing Time for Assessment of Trabecular Bone Microarchitecture.** J. J. Smith, J. T. Kirby<sup>\*</sup>, M. M. Morrissey<sup>\*</sup>, J. T. Edger<sup>\*</sup>, C. M. Modlesky. Health Nutrition and Exercise Sciences, University of Delaware, Newcastle, DE, USA.

High resolution magnetic resonance imaging (MRI) can be used to assess trabecular bone microarchitecture in vivo. Because image processing can be labor intensive, identifying strategies that limit processing time is desirable. The purpose of this study was

to determine if processing a fewer number of magnetic resonance images yields acceptable estimates of trabecular bone microarchitecture in the distal femur of children. Twenty-six high-resolution axial magnetic resonance images were collected from the distal femur of 27 children (6 to 12 y) using a GE 1.5 T MRI (3D fast gradient echo sequence, reconstructed spatial resolution =  $175 \times 175 \times 700 \mu\text{m}^3$ ). The 20 most central images were analyzed for measures of trabecular bone microarchitecture [i.e., apparent trabecular bone volume to total volume (appBV/TV), trabecular number (appTb.N), trabecular thickness (appTb.Th) and trabecular spacing (appTb.Sp)] in the lateral aspect of the distal femur using a program created with Interactive Data Language (Research Systems, Inc). The average values for appBV/TV, appTb.N, appTb.Th and appTb.Sp for the entire set of images (20IM) were compared against values taken from a single image located at the middle of the image set (1IM), average values from 5 images (5IM; every fourth image), and average values from 10 images (10IM; every other image). Paired t-tests and linear regression analysis were used to assess the agreement between trabecular bone microarchitecture measures from 20IM and the other approaches in which fewer images were processed. The 10IM approach provided the best estimates of trabecular bone microarchitecture from 20IM, with no group differences ( $p > 0.05$ ) and a high proportion of the variance explained in appBV/TV ( $r^2 = 0.973$ ) appTb.N ( $r^2 = 0.97$ ), appTb.Th ( $r^2 = 0.98$ ) or appTb.Sp ( $r^2 = 0.97$ ). The 5IM approach also provided good estimates of trabecular bone microarchitecture from 20IM with no group differences ( $p > 0.05$ ) and a high degree of explained variance in appBV/TV ( $r^2 = 0.95$ ), appTb.N ( $r^2 = 0.96$ ), appTb.Th ( $r^2 = 0.95$ ) and appTb.Sp ( $r^2 = 0.96$ ). The 1IM approach provided the worst estimates of trabecular bone microarchitecture. Although there were no group differences ( $p > 0.05$ ), 1IM explained substantially less variance in BV/TV ( $r^2 = 0.740$ ), appTb.N ( $r^2 = 0.725$ ), appTb.Th ( $r^2 = 0.79$ ) and appTb.Sp ( $r^2 = 0.71$ ) from 20IM than the other approaches. The findings suggest that analyzing as few as one fourth of the magnetic resonance images collected can yield accurate estimates of trabecular bone microarchitecture from the entire image set while substantially reducing processing time.

**Disclosures:** J.J. Smith, None.

This study received funding from: National Institutes of Health

## SU283

**The Association of Urine Measures of Diet-derived Acid Excretion with Bone Loss and Fractures: The CaMos Study.** T. R. Fenton<sup>\*</sup>, D. A. Hanley, M. Eliasziw<sup>\*</sup>, S. C. Tough<sup>\*</sup>, S. Ross<sup>\*</sup>, A. W. Lyon<sup>\*</sup>. University of Calgary, Calgary, AB, Canada.

The modern diet has been purported to induce osteoporosis due to diet acid-ash, net acid excretion, altered acid-base balance which has been assumed to cause bone demineralization.

The purpose of this study was to examine the associations between urine measures of dietary acid load (pH, sodium, potassium, calcium, magnesium, phosphate, chloride, and sulfate, measured, and organic acids, calculated, in fasting morning urine samples ( $n = 795$ ) with the bone outcomes: changes in bone mineral density (BMD) (femoral neck, lumbar spine, and total hip) and fractures.

Fasting urine samples and DEXA BMD were measured at baseline and at 5-years among the Canadian Multicentre Osteoporosis Study A prospective population-based cohort study. Analyses were undertaken (multiple linear regression for changes in BMD, and logistic regression for the incidence of fractures), controlling for potential confounders eg: age, gender, family history of osteoporosis, physical activity, smoking, calcium intake, vitamin D status, hormonal status, medications, renal function, urine creatinine, change of body mass index.

There was no association between urine pH and either the change of BMD over 5-years or the incidence of fractures over 7 years. Among 11 measured associations between urine measures of dietary acid load and BMD at different sites and fragility fractures, only low urine potassium was associated with increased BMD in the lumbar spine over 5-years, percent explained variance = 4%. Urine potassium was not associated with change at the other bone sites. The finding of only one weak association between urine potassium and the change of spine BMD provided little support for the acid-ash hypothesis. It is unknown if this limited evidence was due to the absence of an association or the limitation of fasting urine samples to be assessed for diet acid load.

**Disclosures:** T.R. Fenton, None.

This study received funding from: Canadian Foundation for Dietetic Research.

## SU284

**Compartment Specific Genetic Analysis of Trabecular and Cortical Volumetric BMD in Men.** L. Yerges<sup>1</sup>, J. Cauley<sup>1</sup>, S. Moffett<sup>1</sup>, C. Nestlerode<sup>\*1</sup>, K. Ensrud<sup>2</sup>, C. Kammerer<sup>\*1</sup>, L. Marshall<sup>\*3</sup>, A. Hoffman<sup>\*4</sup>, T. Lang<sup>\*5</sup>, R. Ferrell<sup>\*1</sup>, E. Orwoll<sup>3</sup>, J. Zmuda<sup>1</sup>. <sup>1</sup>University of Pittsburgh, Pittsburgh, PA, USA, <sup>2</sup>University of Minnesota, Minneapolis, MN, USA, <sup>3</sup>Oregon Health & Science University, Portland, OR, USA, <sup>4</sup>Stanford University, Palo Alto, CA, USA, <sup>5</sup>University of California, San Francisco, CA, USA.

Quantitative computed tomography (QCT) provides a 3-dimensional measure of volumetric bone mineral density (vBMD) that can resolve both trabecular and cortical bone. Little is known about the genetic determinants of compartment specific vBMD in humans.

To investigate the genetic determinants of cortical (cBMD) and trabecular vBMD (tBMD) at the femoral neck, we systematically screened candidate genes for bone metabolism in 882 Caucasian men aged  $\geq 65$  in the Osteoporotic Fractures in Men Study (MrOS). Tag SNPs from Phase I of the HapMap project, potentially functional SNPs that were either non-synonymous coding SNPs, predicted to alter transcription factor binding or within an

exon splice enhancer site were genotyped.

4108 SNPs in 371 genes were genotyped using the Illumina GoldenGate assay, met quality control criteria, and were analyzed for their association with vBMD. Analyses assumed a recessive and additive model of inheritance and adjusted for participant age and clinic. Principal components eigenanalysis was used to account for population substructure.

10 SNPs across 9 genes were associated with cBMD and 7 SNPs across 7 genes were associated with tBMD at  $p < 0.001$ . None of the SNPs associated with one bone compartment were associated with the other bone compartment at  $p < 0.001$ . For example, the most promising SNP for cBMD was an intronic SNP located in ENPP1, a gene involved in regulating bone mineralization. Specifically, a 4.8% lower cBMD was observed in those with the less common genotype compared to those with the common genotype ( $p = 0.0001$ ). However, no association with trabecular vBMD was observed ( $+0.7$ ,  $p = 0.71$ ). This SNP is associated with cBMD at the femoral shaft, but not with tBMD at the spine. Furthermore, two other SNPs in ENPP1 were associated with cortical vBMD at a less stringent significance level ( $p < 0.01$ ), but neither of these were associated with trabecular vBMD at the femoral neck. Although these findings are preliminary, these data suggest that there may be some genetic factors regulating vBMD that are compartment specific and that QCT may be a useful tool for dissecting the complex genetic architecture of the "BMD phenotype".

**Disclosures:** L. Yerges, None.

This study received funding from: National Institute of Arthritis and Musculoskeletal and Skin Diseases (NIAMS).

## SU285

### Lactose Intolerance Does Not Have Effect on Bone Status in Adolescence.

S. Yamamoto<sup>1</sup>, T. Yamaura<sup>\*1</sup>, M. Kodama<sup>\*1</sup>, K. Nawata<sup>1</sup>, H. Ishida<sup>1</sup>, K. Uenishi<sup>1</sup>, M. Konishi<sup>\*2</sup>, Q. Zhou<sup>\*2</sup>. <sup>1</sup>Kagawa Nutrition University, Saitama, Japan, <sup>2</sup>GE Healthcare, Madison, WI, USA.

Adequate calcium ingestion during adolescence is necessary for developing peak bone mass and preventing osteoporosis in the future. However, a decline of lactase activity at about the beginning of Japanese adolescence and increase in associated symptoms of lactose intolerance may lead to avoidance of milk consumption. Our study aimed to examine the effect of self-diagnosed lactose intolerance on milk and calcium intake, as well as on bone status in Japanese late adolescence. A total of 2132 subjects (1369 boys and 763 girls) aged 17 or 18 years were divided into 5 groups (0, ~100, ~200, ~400 and 400~ ml/day) according to milk consumption level. All subjects completed questionnaires about milk intake, milk tolerance, and food frequency. Bone status was measured using a calcaneus quantitative ultrasound device (GE Healthcare Lunar, Achilles Insight<sup>TM</sup>). Stiffness Index (SI) was the primary result variable. Milk consumption was positively related to calcium intake in both boys ( $r = 0.656$ ,  $p < 0.001$ ) and girls ( $r = 0.531$ ,  $p < 0.001$ ). Results showed that higher milk intake was associated with higher SI, even after adjusted for exercise level. Lactose Intolerant subjects (306 boys (22.4 %) and 119 girls (15.6 %)) had lower milk and Ca intakes than tolerant subjects. However, there was no significant difference in SI between two groups in both sexes. These results imply that there may be some adaptive mechanism protecting bone in subjects with lower calcium intake level due to low milk consumption among lactose intolerant subjects.

**Disclosures:** S. Yamamoto, None.

## SU286

### Deformity of the Distal Radius Fractures Resulting From Falls in Japanese Women Over 50 Years of Age Is Closely Associated with Bone Mineral Density of the Lumbar Spine.

A. Sakai<sup>1</sup>, T. Oshige<sup>\*1</sup>, Y. Zenke<sup>\*2</sup>, M. Suzuki<sup>\*1</sup>, Y. Yamanaka<sup>\*1</sup>, T. Nakamura<sup>1</sup>. <sup>1</sup>Department of Orthopaedic Surgery, University of Occupational and Environmental Health, Kitakyushu, Japan, <sup>2</sup>Department of Orthopaedic Surgery, Kagawa Rosai Hospital, Marugame, Japan.

**Purpose:** To clarify whether the degree of radiographic pre-treatment distal radius deformity resulting from falls is associated with the degree of bone mineral density (BMD) of the lumbar spine in Japanese women over 50 years of age.

**Methods:** The subjects were 125 consecutive Japanese female patients aged over 50 years with Colles' type (type A and C of AO classification) dorsally angulated distal radius fractures caused by falls. Fractures due to high-energy injuries such as traffic accidents were excluded. The degree of radius deformity was assessed on antero-posterior and lateral radiographs by measuring ulnar variance, radial inclination, and dorsal angulation at initial examination before manual repositioning of the fractured bone. BMD of the lumbar spine was measured by dual energy X-ray absorptiometry.

**Results:** There were significant differences in the respective values of ulnar variance, radial inclination, and dorsal angulation between patients with BMD values less than 70% of the mean value of young adults and those with BMD values of 70% and over. Radius deformity was significantly greater for all three parameters in the former group relative to the latter. The respective values of increased ulnar variance, decreased radial inclination, and increased dorsal angulation significantly correlated with lower BMD. Stepwise regression analysis of data of all subjects revealed that ulnar variance was significantly associated with dorsal angulation, BMD, and radial inclination. The addition of body height, body weight, body mass index, and urinary type I collagen cross-linked N-telopeptides to the regression analysis of data of a subset of patients confirmed that ulnar variance was significantly associated with BMD.

**Conclusions:** There is a significant association between BMD of the lumbar spine and radiographic radius deformity seen in low-energy distal radius fractures resulting from falls in Japanese women over 50 years of age.

**Disclosures:** A. Sakai, None.

This study received funding from: a Health and Labour Sciences Research Grant (Comprehensive Research on Aging and Health, project registered No. 031) from the Japan Ministry of Health, Labour and Welfare.

## SU287

### Regional Differences in the Management of Osteoporosis. The Global Longitudinal Registry of Osteoporosis In Women.

R. Lindsay<sup>\*1</sup>, P. Delmas<sup>2</sup>, S. Boonen<sup>\*3</sup>, A. Diez-Perez<sup>4</sup>, R. Dedrick<sup>\*5</sup>, K. G. Saag<sup>\*6</sup>, <sup>1</sup>Helen Hayes Hospital, New York, NY, USA, <sup>2</sup>Hôpital Edouard Herriot, Lyon, France, <sup>3</sup>Leuven University Center for Metabolic Bone Diseases, Leuven, Belgium, <sup>4</sup>Hospital del Mar, Barcelona, Spain, <sup>5</sup>UMASS Medical School, Worcester, MA, USA, <sup>6</sup>University of Alabama-Birmingham, Birmingham, AL, USA.

The purpose of the study is to compare use of diagnostic technology and osteoporosis medication in women  $\geq 55$  years of age in four geographic regions.

The Global Longitudinal registry of Osteoporosis in Women (GLOW) is an observational follow-up study of women  $\geq 55$  years recruited by 540 primary physician practices (17 sites, 10 countries). Practices typical of each region were identified by primary care networks. All non-institutionalized patients visiting the practice within the prior 2 years were eligible. Self-administered questionnaires were mailed, with a 2:1 over-sampling of women aged  $\geq 65$  years. Data collected included information on demographics; medical history; risk factors for osteoporosis-related fracture; fracture occurrence; self-report of diagnosis including bone mineral density testing and treatment with a bone medication (risedronate, etidronate, alendronate, ibandronate, pamidronate, zoledronate, raloxifene, teriparatide, tibolone, calcitonin, strontium ranelate).

Overall, 67% of the 50,226 women in the population reported having had a bone density test; frequency of testing ranged from 51% (Europe) to 85% (Canada). Reported current use of bone medications averaged 27% (range 20% in Europe to 34% in USA). Current use increased with age, and increased with clinical risk: 36% of women with FRACTURE Index<sup>®</sup> scores  $\geq 5$  (indicating a 5-year risk of non-vertebral fracture of 26%) reported taking bone-related medication. Frequencies ranged from 28% in Europe to 43% in Australia. When use was assessed by self-reported diagnosis of osteoporosis or osteopenia, frequency was 68% and 44%, respectively, with 8.7% of women without either diagnosis reporting current use.

**Table.** Bone-density testing and bone medication by region.

	Bone-density test (%)				Bone medication (%)			
	Australia	Canada	Europe	USA	Australia	Canada	Europe	USA
All women	74	85	51	78	28	31	20	34
Age >65 years	78	85	51	79	34	36	22	39
Age >75 years	74	80	44	74	42	41	24	42
Increased risk of fracture								
-Fracture history	85	87	60	80	49	46	33	47
-FRACTURE Index $\geq 5$	77	82	51	75	43	42	28	42
Self-reported diagnosis								
-Normal	63	77	37	66	11	8.9	6.7	11
-Osteoporosis	92	96	82	92	70	70	58	77
-Osteopenia	95	98	84	96	38	46	27	53

Management of osteoporosis in this population is not entirely consistent between Europe and other regions involved in GLOW. Use of bone-density testing and bone medications is lower in Europe than in other regions. Even in women with high FRACTURE Index scores, Europe appears to be more conservative than other regions in using medications.

**Disclosures:** R. Lindsay, The Alliance for Better Bone Health (Procter & Gamble Pharmaceuticals and sanofi-aventis) 4.

This study received funding from: The Alliance for Better Bone Health (Procter & Gamble Pharmaceuticals and sanofi-aventis).



## SU288

**Bone Fragility Beyond Bone Mineral Density: A French Prospective Experience.** M. Rancier<sup>\*1</sup>, T. Maire<sup>\*1</sup>, V. Pascal-Vigneron<sup>\*1</sup>, L. Fiorani<sup>\*1</sup>, A. Bellou<sup>\*2</sup>, D. Mainard<sup>\*3</sup>, H. Coudane<sup>\*4</sup>, D. Mole<sup>\*5</sup>, G. Weryha<sup>1</sup>.

<sup>1</sup>Endocrinology, CHU Nancy-Brabois, Vandoeuvre, France, <sup>2</sup>Primary Care Department, Sau-Chu, Nancy, France, <sup>3</sup>Cot Chu, Nancy, France, <sup>4</sup>Atol Chu, Nancy, France, <sup>5</sup>CTO Clinique de Traumatologie, Nancy, France.

Osteoporosis is commonly discovered through fragility fractures. Strategic diagnosis sites are primary care units. During one year we have recorded all low energy fractures in patients attending the primary care department of the University Hospital of Nancy (France). Patients are 45 years old and over.

**Population:** 929 women (73.8 years  $\pm$  13.5), 365 men (65.4 years  $\pm$  14.3).

Complete exploration of osteoporosis was performed in 170 women and 72 men.

**Fractures:**

Women: 150 wrist; 283 femoral neck; 52 vertebra; 120 humerus; 19 pelvis; 302 other.

Men: 32 wrist; 99 femoral neck; 20 vertebra; 46 humerus; 14 pelvis; 133 other.

Fourteen double fractures; 2 triple fractures. 72% of patients experienced their first osteoporotic fracture.

**WHO classification status:** Data are summarized in table 1. 70 to 85% of patients don't have radiological osteoporosis according to the 1994 WHO definition, especially men. Data in table 2 show no influence of past fracture events. Sex difference exist at femoral site only.

**Fracture sites:** Patients with a femoral fracture have significantly lower Bone Mineral Density than those with a wrist or other fracture. In the subgroup of the previously fractured patients, no difference persists. In the subgroup with no past fracture, BMD at the femoral neck is significantly lower in femoral fractures than in all other sites. At lumbar spine, femoral and humeral fractures are associated with lower BMD (only significant for femur).

**Conclusion:** About one fourth of the patients over 45 years old treated for a low energy fracture have under a T-score under the -2.5SD threshold. Thus the imputability of bone mineral density in fragility fracture seems to be fewer than previously believed.

Table 1: WHO status according to sex and BMD site

WHO Status	Women Spine	Women Femoral	Men Spine	Men Femoral
Normal	24,1%	28,8%	34,7%	49,3%
Osteopaenia	46,5%	47,8%	41,7%	35,2%
Osteoporosis	29,4%	23,2%	23,6%	15,5%

Tables 2: WHO status repartition according to BMD site and past fractures

BMD site	Past fracture events	Normal	Osteopaenia	Osteoporosis
Spine	No	51 (30,2%)	77 (45,6%)	41 (24,2%)
Spine	Yes	15 (20,6%)	32 (43,8%)	26 (35,6%)
Femoral	No	60 (36,6%)	72 (43,9%)	32 (19,5%)
Femoral	Yes	22 (31,4%)	31 (44,3%)	17 (24,3%)

Khi Square non significant (spine and femoral)

**Disclosures:** M. Rancier, None.

## SU289

**A Composite Bone Score with QCT Bone Measurements and Fracture History.** N. Rianon<sup>1</sup>, T. Lang<sup>2</sup>, G. Sigurdsson<sup>3</sup>, K. Siggeirsdottir<sup>\*4</sup>, G. Eiriksdottir<sup>\*5</sup>, S. Sigurdsson<sup>\*5</sup>, B. Jonsson<sup>\*6</sup>, V. Gudnason<sup>7</sup>, T. Harris<sup>\*1</sup>.

<sup>1</sup>LEDB, NIA, Bethesda, MD, USA, <sup>2</sup>Radiology, UCSF, San Francisco, CA, USA, <sup>3</sup>Medicine/Endocrinology & Metabolism, University of Iceland, Reykjavik, Iceland, <sup>4</sup>Development, Icelandic Heart Association, Kopavogur, Iceland, <sup>5</sup>Icelandic Heart Association, Kopavogur, Iceland, <sup>6</sup>Orthopedics, University Hospital, Malmo, Sweden, <sup>7</sup>Cardiovascular Genetics, University of Iceland, Reykjavik, Iceland.

The distributions of quantitative computerized tomography (QCT) measures of cortical and trabecular density, bone volume and cross-sectional area with age, gender and fracture history have been reported. How these measures aggregate and correlate with a standard BMD measure is unknown. We examined the gender-specific relationship of each QCT measures and a combined score with prevalent fractures for participants in the Age, Gene/Environment Susceptibility-Reykjavik Study (AGES-R) (mean age=77  $\pm$  6 for 2438 men & 3326 women). We contrasted the QCT measures with the relationship of QCT-derived DEXA-like BMD of total hip (TOBD) and fracture history.

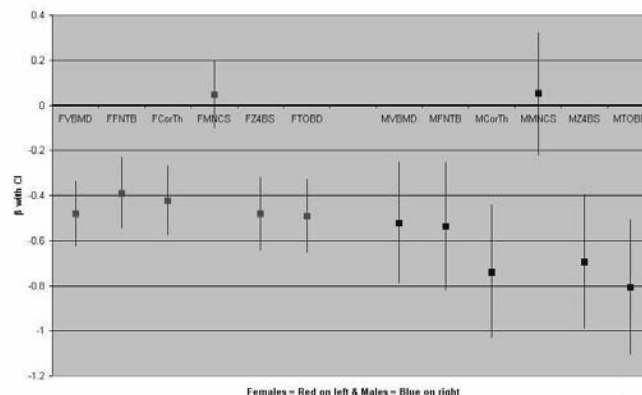
Four QCT measures (standardized using gender specific Z-scores) were included in a composite score (Z4BS): vertebral trabecular BMD (VBMD); minimal cross sectional area of femur neck (MNCS); femur neck cortical thickness (volume/femur neck integral volume) (CorTh); and femur neck trabecular BMD (FNTB). Sum of the four Z scores of these measures was divided into quartiles. The lowest quartile indicated poor bone health; the middle two were combined together as moderate bone health; and the highest quartile indicated good bone health and this variable was used in age-adjusted logistic regression models. Fracture history was based on report of vertebral or wrist fracture at age 65 or older or hip fractures.

Mean BMI, height and weight were (respectively) 27  $\pm$  4, 1.8 meters  $\pm$  6, and 83 kg  $\pm$  13 in men; and 27  $\pm$  5, 1.6 meters  $\pm$  6, and 70 kg  $\pm$  13 in women. Fracture history demonstrated a negative association with Z4BS (p < 0.001 for both genders) as did all QCT measures (p < 0.001 both genders) except MNCS. However, except for MNCS, the QCT measures did

not differ significantly from each other in relation to fracture history.

The combined QCT measure was not a stronger correlate of fracture than TOBD and fracture. MNCS was not related to fracture history and had minimal impact on the Z score composite measure.

$\beta$  of Fracture History and QCT Bone Measurements (Males and Females)



**Disclosures:** N. Rianon, None.

## SU290

**Lean Body Mass is a Better Predictor of Bone Mineral Density than Leg Power or Grip Strength in Healthy Caucasian Adults--The Rancho Bernardo Study.** A. Afghani<sup>\*1</sup>, E. Barrett-Connor<sup>2</sup>. <sup>1</sup>Health Sciences, TUI University, Cypress, CA, USA, <sup>2</sup>Family & Preventive Medicine, University of California, San Diego, La Jolla, CA, USA.

Our aim was to investigate the associations between bone mineral density (BMD) and specific markers of muscular fitness (lean mass, leg power, and grip strength) in healthy Caucasian adults. 380 women and 284 men aged 46-80 years participated in this community-based study. Lean body mass (LBM) and BMD of the lumbar spine (L1-L4), total hip, and total body were measured using dual energy x-ray absorptiometry. Leg extensor power of each leg was measured 3 times by the Nottingham Power Rig; the mean of the dominant side was used in this study. Grip strength was measured in each hand by isometric dynamometry. Leg power (102 versus 191 watts, p<0.0001) and grip strength (22.5 versus 40 kg, p<0.0001) were lower in women than in men. Using Spearman correlations, in women, leg power and grip strength were associated with BMD at all sites (r=-0.20-0.35; p<0.001). In men, leg power (r=0.28; p<0.0001) and grip strength (r=0.19; p<0.005) were associated with hip BMD but not with spine BMD (r=0.10, p=0.09). Total body BMD in men was correlated with leg power (r=0.27; p<0.0001) and grip strength (r=0.23; p<0.0001). In stepwise multiple linear regression models adjusted for age, fat mass, leg power, and grip strength, LBM emerged as the strongest predictor of total body BMD, explaining 13% and 31% of the variance in women and men, respectively. Thus, leg extensor power and grip strength are significantly associated with hip and total body BMD but LBM was a better predictor of BMD than measured leg power or grip strength in both sexes.

**Disclosures:** A. Afghani, None.

This study received funding from: National Institute of Aging and the National Institute of Diabetes and Digestive and Kidney Diseases.

## SU291

**Relationship Between the Metabolic Syndrome and Bone Mineral Density in Korean Middle-Aged Women.** H. Choi<sup>1</sup>, Y. Lee<sup>\*2</sup>, I. Joo<sup>\*3</sup>, S. Kim<sup>\*1</sup>, H. Oh<sup>\*3</sup>.

<sup>1</sup>Department of Family Medicine, Eulji University School of Medicine, Daejeon, Republic of Korea, <sup>2</sup>Department of Internal Medicine, Eulji University School of Medicine, Daejeon, Republic of Korea, <sup>3</sup>Department of Family Medicine, Kwandong University College of Medicine, Cheil General Hospital, Seoul, Republic of Korea.

**Background:** Bone mineral density (BMD) increases with body fat mass and obesity has a protective effect against osteoporosis. However, obesity-induced chronic inflammation is a key component in the pathogenesis of insulin resistance and the metabolic syndrome. It has been suggested that proinflammatory cytokines and low-grade systemic inflammation activate bone resorption and may lead to reduced bone mineral density (BMD). The objective of the current study was to determine the relationship between the metabolic syndrome and BMD.

**Methods:** This was a cross-sectional study of 510 premenopausal women and 788 postmenopausal women age of 40-78 years who had visited Health Promotion Center, Eulji University Hospital from March 2004 to May 2006. Medical history and lifestyle data were collected by a questionnaire and history taking. Basic physical examination and laboratory tests were performed after at least 12 hours of fasting. Spinal BMD was measured by dual-energy X-ray absorptiometry. The modified National Cholesterol Education Program Adult Treatment Panel III (NCEP-ATP III) and the American Diabetes Association (ADA) criteria were used for the definition of the metabolic syndrome.

Analyses were adjusted for relevant covariates.

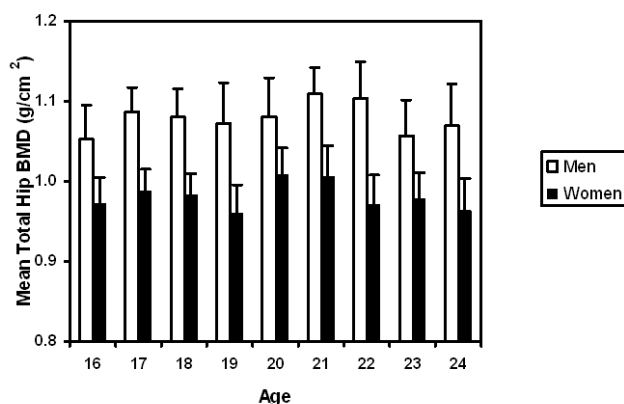
Results: Among 1,298 women, 453 (34.9%) had the metabolic syndrome. Women with the metabolic syndrome were significantly older ( $56.4 \pm 7.7$  vs.  $51.1 \pm 8.1$  years old respectively,  $P < 0.001$ ) and suffer from more of osteoporosis (24.3% vs. 18.2% respectively,  $P = 0.002$ ) than women without the metabolic syndrome. After adjusting for age, menopause status, smoking, alcohol and exercise, spine BMD was significantly lower among women with the metabolic syndrome ( $0.878 \pm 0.171$  vs.  $0.910 \pm 0.160$  g/cm<sup>2</sup> respectively,  $P = 0.007$ ). Adjusted spine BMD decreased with additional components of the metabolic syndrome, but women with all components (abdominal obesity, high blood pressure, high fasting glucose, high triglyceride, low high density lipoprotein) had higher spine BMD than women with two components. Conclusion: In middle-aged Korean women, the metabolic syndrome may be associated with reduced spine BMD.

**Disclosures:** H. Choi, None.

## SU292

**Normative Z-scores from the Canadian Multicentre Osteoporosis Study Youth Cohort.** W. Zhou<sup>\*1</sup>, C. Berger<sup>\*1</sup>, J. D. Adachi<sup>2</sup>, A. Papaioannou<sup>2</sup>, G. Ioannidis<sup>2</sup>, C. Webber<sup>2</sup>, S. Atkinson<sup>2</sup>, W. P. Olszynski<sup>3</sup>, J. P. Brown<sup>4</sup>, D. A. Hanley<sup>5</sup>, R. Josse<sup>6</sup>, N. Kreiger<sup>\*6</sup>, J. Prior<sup>7</sup>, S. Kaiser<sup>8</sup>, S. Kirkland<sup>8</sup>, D. Goltzman<sup>1</sup>, K. S. Davison<sup>4</sup>. <sup>1</sup>McGill Univ., Montreal, QC, Canada, <sup>2</sup>McMaster Univ., Hamilton, ON, Canada, <sup>3</sup>Univ. of Saskatchewan, Saskatoon, SK, Canada, <sup>4</sup>Laval Univ., Ste-Foy, QC, Canada, <sup>5</sup>Univ. of Calgary, Calgary, AB, Canada, <sup>6</sup>Univ. of Toronto, Toronto, ON, Canada, <sup>7</sup>Univ. of British Columbia, Vancouver, BC, Canada, <sup>8</sup>Dalhousie Univ., Halifax, NS, Canada.

The development of normative bone mineral density (BMD) data allows for the comparison of an individual's BMD to the healthy-population average. The International Society of Clinical Densitometry recommends the use of Z-scores, which are age- and sex-specific, when interpreting DXA results in children and adolescents. Therefore, the purpose of this study was to establish Z-scores for the Canadian population between the ages of 16-24 years. In the Canadian Multicentre Osteoporosis Study (CaMos) a cohort of 1001 males and females between the ages of 16-24 years were recruited to describe the natural history of bone development in this age group. Of the 1001 participants, 877 were white and 375 had previously experienced a fracture, of which 114 were classified as minimal trauma fractures. Further, more than 111 participants used inhaled glucocorticoids. There were no differences between the mean BMD of all white participants and the mean BMD in the minimal fracture or inhaled glucocorticoid user subgroups, so these groups were integrated and means and standard deviations (SD) of all white participants were used as our reference data to construct Canadian youth BMD Z-scores. Z-scores were derived for five skeletal sites using CaMos reference data by sex and for each age year. Since the majority of the data was normally distributed (85 of 90 groups; age by gender by site), z-score was defined as follows: (measured BMD - matched mean BMD)/matched SD. The figure presents the mean BMD values in the total hip BMD by sex, along with the upper bound of the 95% confidence interval. The mean (SD) total hip z-score by centre varied in young men from -0.42 (0.96) in Toronto to 0.29 (0.90) in Kingston and in women from -0.36 (1.00) in Vancouver to 0.33 (0.93) in Saskatoon.



In this study normal BMD data for the Canadian population between the ages of 16-24 years was established. This information will be valuable in helping to identify those individuals with very low BMD.

**Disclosures:** W. Zhou, None.

## SU293

**Socioeconomic Status, Bone Mineral Density Testing and Hip Fracture Rates in a Universal Health-care System.** O. S. Donescu<sup>1</sup>, D. Thiruchelvam<sup>\*2</sup>, G. A. Hawker<sup>3</sup>, S. B. Jaglal<sup>4</sup>. <sup>1</sup>Toronto Rehabilitation Institute at University of Toronto, Toronto, ON, Canada, <sup>2</sup>Institute for Clinical Evaluative Sciences, Toronto, ON, Canada, <sup>3</sup>Division of Rheumatology, Department of Medicine, Women's College Hospital, Toronto, ON, Canada, <sup>4</sup>Department of Physical Therapy, University of Toronto, Toronto Rehabilitation Institute at University of Toronto, Toronto, ON, Canada.

The purpose of the study was to describe rates of hip fracture and BMD test utilization, by socioeconomic status (SES). This retrospective, observational cohort study used linked population-based administrative data from Ontario, Canada and SES geographical indicators from the 2001 Canadian Census. Individuals' postal codes determined residential neighborhoods average household income. The geographically based SES indicators based on median SES of all residents of a postal code were used as a proxy for individual SES. The Ontario population was divided into five groups of income ranges (quintiles) with 1 being the lowest and 5 being the highest.

Study subjects were individuals 40 years of age and older who had a hip fracture or underwent to BMD testing between April 1st, 2005 and March 31st, 2006 in Ontario. The study population included approximately 6 million individuals.

Analyses were stratified by age (40-64; 65-84 and 85-105 years old) and gender. There was a general trend of lower hip fracture rates in individuals with higher income, except in women 85 years and older (RR=1.14, 95% CI: 1.00-1.29). All trends were statistically significant ( $p < 0.01$ ), with the exception of that in men over 85 years old ( $p = 0.64$ ). Relative rates for individuals of highest SES ranged from 0.47 in men and women 40-64 years of age (95% CI: 0.30-0.64, and 0.31-0.62, respectively), to 0.91, 95% CI: 0.68-1.14 in men 85-105 years of age. A trend of higher rates of BMD test utilization was found among individuals of higher SES compared to individuals of lower SES in all age strata ( $p < 0.0001$ ). RR for individuals of highest SES ranged from 1.08 in men 40-64 years of age, 95% CI: 1.04-1.13 to 1.46 in men 85-105 years of age, 95% CI: 1.26-1.65.

Individuals of higher SES experience in general lower hip fracture rates and higher diagnostic testing rates, suggesting an inequality in access to care in a universal health-care system.

**Disclosures:** O.S. Donescu, None.

## SU294

**Prevalence of Osteoporosis and Osteopenia in Men and Women According to the Fragility Fracture Type: A Nationwide Swiss Survey.** O. Lamy<sup>1</sup>, N. Suhm<sup>\*2</sup>, K. Lippuner<sup>3</sup>. <sup>1</sup>Department of Internal Medicine, University Hospital, Lausanne, Switzerland, <sup>2</sup>Treatment Center for Musculoskeletal Diseases, University Hospital, Basel, Switzerland, <sup>3</sup>Osteoporosis Policlinic, University Hospital, Bern, Switzerland.

**Background:** The prevalence of a low BMD (T-score  $\leq -1$  SD) in postmenopausal women with a fragility fracture may vary from 70% to less than 50%. In one study (Siris ES. Arch Intern Med 2004; 164:1108-1112), the prevalence of osteoporosis was very low at 6.4%. The corresponding values in men are more rarely reported.

**Methods:** In a nationwide Swiss survey, all consecutive patients aged 50+ presenting with one or more fractures to the emergency ward, were recruited by 8 participating hospitals between 2004 and 2006. Diagnostic workup was collected for descriptive analysis.

**Results:** 3667 consecutive patients with a fragility fracture, 2797 women (73.8 $\pm$ 11.6 years) and 870 men (70.0 $\pm$ 12.1 years), were included. DXA measurement was performed in 1152 (44%) patients. The mean of the lowest T-score values was -2.34 SD in women and -2.16 SD in men. In the 908 women, the prevalence of osteoporosis and osteopenia according to the fracture type was: sacrum (100%, 0%), rib (100%, 0%), thoracic vertebral (78%, 22%), femur trochanter (67%, 26%), pelvis (66%, 32%), lumbar vertebral (63%, 28%), femoral neck (53%, 34%), femur shaft (50%, 50%), proximal humerus (50%, 34%), distal forearm (41%, 45%), tibia proximal (41%, 31%), malleolar lateral (28%, 46%), malleolar median (13%, 47%). The corresponding percentages in the 244 men were: distal forearm (70%, 19%), rib (63%, 11%), pelvis (60%, 20%), malleolar median (60%, 32%), femur trochanter (48%, 31%), thoracic vertebral (47%, 53%), lumbar vertebral (43%, 36%), proximal humerus (40%, 43%), femoral neck (28%, 55%), tibia proximal (26%, 36%), malleolar lateral (18%, 56%).

**Conclusion:** The probability of underlying osteoporosis or osteopenia in men and women aged 50+ who experienced a fragility fracture was beyond 75% in fractures of the sacrum, pelvis, spine, femur, proximal humerus and distal forearm. The medial and lateral malleolar fractures had the lowest predictive value in women, not in men.

**Disclosures:** O. Lamy, None.

## SU295

**Linkage and Association Study of Chromosome 1p36 with Bone Mineral Density in Southern Chinese.** H. Li\*, Q. Huang, A. Kung. The University of Hong Kong, Hong Kong, Hong Kong.

Chromosome 1p36 is a region that has previously shown good evidence of linkage to bone mineral density (BMD) in multiple studies. We aim to determine if 1p36 is linked to BMD variation in southern Chinese population by linkage analysis and to evaluate the association of the candidate genes at 1p36 with BMD by a gene-wide and tag SNP-based association study. Seven microsatellite markers with average inter-marker distance 4.3cM in 1p36 were genotyped in 1459 subjects from 306 southern Chinese families, which were ascertained through a proband with BMD Z-score  $\leq -1.28$  at either the lumbar spine or total hip. Multi-point linkage analysis was performed using the regression-based method implemented in the Merlin package. In the entire study population and female subjects, modest evidence of linkage to total hip BMD was observed at 18.04 cM (LOD = 1.762) and 17.07 cM (LOD = 1.83) respectively. Sub-group analysis in the 678 pre-menopausal women showed suggestive evidence of linkage to total hip BMD at 16.57 cM (LOD=2.93). Twenty-three tag SNPs (tSNPs) of four candidate genes (TNFRSF1B, PLOD, CNR2, and MTHFR) at 1p36 were genotyped in 1243 unrelated Chinese case-control subjects using the high-throughput Sequenom platform. The cases were individuals with low BMD (Z-scores  $\leq -1.28$ ) while the controls had high BMD (Z-score  $\geq +1.0$ ) at either the L1-4 lumbar spine or femoral neck. Allelic and genotypic associations were evaluated by Haploview and binary logistic regression implemented in SPSS respectively. Potential epistasis was tested by multifactor dimensionality reduction (MDR) and validated by conditional logistic regression. The PLOD rs7529452 (C385T; F98F) and MTHFR rs1801133 (C677T; A429E) showed significant genotypic and allelic associations with BMD at all skeletal sites measured ( $p = 0.04$ - $0.001$ ), and a promising two-locus gene-gene interaction for femoral neck BMD ( $p = 0.0013$ ; cross-validation consistency = 20/20; testing accuracy = 59.18%). The CNR2 rs2501431 (A592G; G155G) showed nominally significant allelic associations with trochanter BMD and hip BMD. Our results suggest that 1p36 is linked to BMD, and multiple genes at 1p36, individually or in combination, contribute to osteoporosis susceptibility in Chinese.

**Disclosures:** H. Li, None.

This study received funding from: Hong Kong Research Grant Council (HKU7514/06M) and CRCG Grant, The University of Hong Kong.

## SU296

**BMD Measurement by DXA after a Fragility Fracture Increases the Likelihood of Subsequent Osteoporosis Treatment.** A. W. Popp<sup>1</sup>, C. Semm<sup>\*1</sup>, N. Suhm<sup>\*2</sup>, O. Lamy<sup>3</sup>, K. Lippuner<sup>1</sup>. <sup>1</sup>Osteoporosis Polyclinic, University Hospital and University of Bern, Bern, Switzerland, <sup>2</sup>Treatment Centre for Musculoskeletal Diseases, University Hospital of Basel, Basel, Switzerland, <sup>3</sup>Department of Internal Medicine, University Hospital of Lausanne, Lausanne, Switzerland.

DXA is the reference method for the determination of BMD and the diagnosis of osteoporosis. Whether DXA measurement increases the likelihood of subsequent osteoporosis treatment is unknown.

In a nationwide Swiss survey, patients aged 50+ presenting with one or more fractures to the emergency ward, were recruited by 8 participating hospitals between 2004 and 2006, diagnostic workup and treatment patterns of underlying osteoporosis were collected for descriptive analysis.

In total, 4'966 consecutive male (N=1'368, mean age 69.0 yrs) and female (N=3'598, mean age 73.9 yrs) patients presented with a clinical fracture at one of the emergency wards. Of these patients, 3'667 were considered as having a fragility fracture and included in the survey.

According to predefined categories, 30.7% of the acute fractures occurred at the upper limbs (distal forearm or proximal humerus), 19.5% at the axial skeleton (spine including sacrum and ribs or pelvis), 26.4% at the lower limbs (femur or tibia) and 23.4% at another localization (including malleolar fractures).

Diagnostic workup data were available for 2615 (71.3%) patients. DXA measurement was performed in only 1152 (44.0%) of these patients. Forty-six percent of the patients had severe osteoporosis (BMD T-score  $\leq -2.5$  SD and one or more fragility fractures), 35.1% had osteopenia (T-score -1 to -2.5 SD), 14.4% were normal (T-score  $> -1$  SD), and 4.5% no available value.

The rate of subsequent treatment with a bone active substance (bisphosphonate, SERM, PTH, HRT, or calcitonin) alone or in combination with a calcium and/or vitamin D supplement was significantly higher in patients with compared to those without BMD measurement, i.e. 51.0% (463/ 908) vs. 10.8% (204/ 1889) in women, and 41.4% (101/ 244) vs. 3.2% (20/ 626) in men, respectively ( $p < 0.001$  by chi-square test).

BMD measurement by DXA vs. no BMD measurement lead to a fivefold increase in treatment with a bone active substance in women and to a more than tenfold increase in men, who presented with a fragility fracture.

The infrequent usage of BMD measurements by DXA in the routine diagnostic workup of fracture patients may contribute to explain underdiagnosis and undertreatment of osteoporosis in Switzerland, even in the high risk group of patients aged 50+ presenting with an acute fragility fracture.

**Disclosures:** A.W. Popp, None.

This study received funding from: MSD-Chibret Switzerland AG.

## SU297

**Rate of Bone Loss is Greater in Young Adult Men than Women.** J. R. Shaffer<sup>1</sup>, C. M. Kammerer<sup>1</sup>, J. M. Bruder<sup>2</sup>, R. L. Bauer<sup>\*2</sup>, B. D. Mitchell<sup>3</sup>. <sup>1</sup>Department of Human Genetics, University of Pittsburgh, Pittsburgh, PA, USA, <sup>2</sup>University of Texas Health Science Center, San Antonio, TX, USA, <sup>3</sup>Division of Endocrinology, Diabetes and Nutrition, University of Maryland School of Medicine, Baltimore, MD, USA.

Differences between sexes in rate and onset of bone loss, leading to differences in risk for osteoporosis, are well established in older populations. Bone loss in women is commonly thought to occur more rapidly and begin earlier (at menopause) than in men. However, recent studies have shown that substantial bone loss, particularly in trabecular bone, occurs in young adults of both sexes, but possible sex differences have not been well characterized. We examined percent change in bone mineral density (BMD) at several skeletal sites in participants of the San Antonio Family Osteoporosis Study.

Annual percent change in BMD of the femoral neck, total hip, lumbar spine, 1/3 radius, and ultradistal radius was calculated from DXA measurements taken at two time points, 5.6 years apart, in 327 young adult Mexican Americans (116 men, 211 women, ages 25-45 years at baseline). Because this sample contains related individuals, analyses were performed using maximum likelihood methods while conditioning on the familial dependence among participants. We tested whether percent change in BMD differed from zero in each sex, and whether percent change differed between men and women.

Young adult men lost BMD at the femoral neck, lumbar spine, and ultradistal radius (-0.47, -0.40, and -0.91 %/year, respectively;  $p < 10^{-4}$  for all) and gained BMD at the total hip and 1/3 radius (+0.23 and +0.28 %/yr, respectively;  $p < 0.02$  for both). Young women also gained BMD at the total hip and 1/3 radius (+0.69 and +0.68 %/yr;  $p < 10^{-10}$  for both), lost BMD at the ultradistal radius (-0.30 %/yr,  $p < 10^{-4}$ ), but had no change in femoral neck or lumbar spine BMD. However, at all skeletal sites, men experienced greater loss or smaller gain in BMD than women ( $p < 0.001$  for all). This sex difference in BMD change was also present after adjusting for age, interim menopause, body mass index (BMI), and interim change in BMI ( $p < 0.02$ ).

The loss of BMD at skeletal sites comprised of a substantial proportion of trabecular bone (femoral neck, lumbar spine, ultradistal radius) but not at sites that contain mostly cortical bone (1/3 radius) is consistent with other studies indicating that trabecular bone is lost from early adulthood, whereas cortical bone is lost later in life, and may be gained in young adults. The greater bone loss observed in young men versus young women challenges conventional wisdom regarding the sex-dependency of bone loss and subsequent risk of osteoporosis.

**Disclosures:** J.R. Shaffer, None.

## SU298

**Relationship between BMD of the Lumbar Spine and Knee Osteoarthritis in South Korean.** I. Park<sup>1</sup>, S. Cheon<sup>\*2</sup>. <sup>1</sup>Orthopedic Surgery, Kyungpook University Hospital, Daegu, Republic of Korea, <sup>2</sup>Orthopedic Surgery, 16th Korean Airforce Division, Yaecheon, Republic of Korea.

This is a post hoc analysis of prospective, nation-wide 13 multi-center study named "Risk Factors of Knee Osteoarthritis(OA) in Korean". Authors reviewed the relationship between BMD of the lumbar spine and knee OA in South Korean. One-hundred ninety South Korean from 40 to 64 year were evaluated by matching the age by 5 year interval. Over 65 year-old was excluded to rule out possibilities of natural aging process of knee OA. Knee OA group has 96 (male 14, female 82) persons, and control has 94 (male 24, female 70). Knee osteoarthritis was defined by both a clinical interview using OA scales of WOMAC TM 3.01 and Kellgren-Lawrence grade III or IV using bilateral posteroanterior, lateral, and tangential knee radiography. Erythrocyte sedimentation rate(ESR), cross-reacting protein(CRP), and RA factor were checked to exclude other arthritis. BMD of the lumbar spine was measured by DXA with consideration of precision error at each center. After correcting gender and age difference, there is a statistical inverse difference between the BMD of L3 spine and knee osteoarthritis by t-test ( $p=0.048$ ), and no statistical difference between whole L1-L4 spines and knee OA. But, there is a tendency that knee OA patients showed higher lumbar spine BMD than control group ( $p=0.067$ ). Knee OA group showed very strong statistical difference of higher ( $p=0.001$ ) BMI(body mass index) than control group and this may affect the tendency of higher BMD of lumbar spines in knee OA patients. Other factors also have impact the inverse relationship between BMD of lumbar spine and knee OA by other studies.

**Disclosures:** I. Park, None.



## SU299

**Determinants of Trabecular and Cortical Volumetric Bone Mineral Density Differ in Men of African Ancestry.** Y. Sheu<sup>1</sup>, J. A. Cauley<sup>1</sup>, C. H. Bunker<sup>\*1</sup>, A. L. Patrick<sup>\*2</sup>, V. W. Wheeler<sup>\*2</sup>, C. L. Gordon<sup>\*3</sup>, C. M. Kammerer<sup>\*4</sup>, J. M. Zmuda<sup>1</sup>. <sup>1</sup>Epidemiology, Graduate School of Public Health, University of Pittsburgh, Pittsburgh, PA, USA, <sup>2</sup>The Tobago Health Studies Office, Scarborough, Trinidad and Tobago, <sup>3</sup>Radiology, McMaster University, Hamilton, ON, Canada, <sup>4</sup>Human Genetics, Graduate School of Public Health, University of Pittsburgh, Pittsburgh, PA, USA.

Quantitative computed tomography (QCT) is a 3-dimensional imaging technique that distinguishes trabecular (TRAB) from cortical (CRT) bone and provides a measure of volumetric bone mineral density (vBMD). Few studies have examined the factors related to vBMD in men, especially in men of African ancestry. We evaluated comprehensively the relationship of TRAB and CRT vBMD (measured at the radius and tibia skeletal sites) with age, anthropometric, medical and behavioral factors in a large cohort of Afro-Caribbean men (n=1,901) aged 40 years and above from the Tobago Bone Health Study. Cross-sectionally, mean TRAB vBMD at both sites decreased significantly before age 50 (4-9%, p=0.01) and then remained constant or decreased slightly thereafter. In contrast, mean CRT vBMD decreased steadily with advancing age. In general, multiple linear regression analyses identified advanced age, smoking, and prostate cancer as major correlates of lower vBMD. Men with type 2 diabetes had higher vBMD, but the effect was much larger for TRAB versus CRT bone. Other relationships with covariates also differed between CRT and TRAB vBMD, and between skeletal sites. For example, body weight was positively correlated with TRAB vBMD but negatively correlated with CRT vBMD. Identified correlates for each site explained approximately 6-10% variation in TRAB vBMD and 13-16% variation in CRT vBMD. Our findings suggest that there are different age patterns and correlates for TRAB and CRT vBMD in men of African ancestry emphasizing the importance of examining the type of bone separately.

**Disclosures:** Y. Sheu, None.

## SU300

**Cortical Bone Mass and Structure in Older Afro-Caribbean and Caucasian Men.** Y. Sheu<sup>1</sup>, J. A. Cauley<sup>1</sup>, V. W. Wheeler<sup>\*2</sup>, M. Petit<sup>\*3</sup>, K. E. Ensrud<sup>3</sup>, A. L. Patrick<sup>\*2</sup>, C. H. Bunker<sup>\*1</sup>, C. L. Gordon<sup>\*4</sup>, L. M. Marshall<sup>5</sup>, E. S. Orwoll<sup>5</sup>, J. M. Zmuda<sup>1</sup>. <sup>1</sup>Epidemiology, Graduate School of Public Health, University of Pittsburgh, Pittsburgh, PA, USA, <sup>2</sup>The Tobago Health Studies Office, Scarborough, Trinidad and Tobago, <sup>3</sup>VA Medical Center & University of Minnesota, Minneapolis, MN, USA, <sup>4</sup>Radiology, McMaster University, Hamilton, ON, Canada, <sup>5</sup>Oregon Health & Sciences University, Portland, OR, USA.

In contrast to dual-energy x-ray absorptiometry (DXA), peripheral quantitative computed tomography (pQCT) measures cortical volumetric BMD (vBMD) and bone structure. Little is known about racial differences in pQCT measures of cortical bone mass and structure in men. We tested the hypothesis that racial differences in cortical bone mass and structure would be independent of differences in body size and composition by investigating data from 1150 Caucasian American men in the Osteoporotic Fractures in Men Study and 452 Afro-Caribbean men in the Tobago Bone Health Study. All men were aged 65 years and older. Cortical vBMD, cortical bone mineral content (BMC), total cross-sectional area (CSA), cortical thickness (THK), and section modulus (SM) at the radius and tibia were measured by pQCT (Stratec XCT-2000). Body fat and non-bone lean mass were measured by DXA (Hologic QDR 4500). Age, height, body fat and tibia length were higher in Caucasian than Afro-Caribbean men whereas radius length and prevalence of diabetes, smoking and physical activity were lower in Caucasians (all p<0.003). However, whole body lean mass did not differ between the two groups. After adjusting for these variables, cortical vBMD, BMC, SM and total CSA were significantly greater at both the radius and tibia in Afro-Caribbean than Caucasian men (Table). Cortical THK was greater in Caucasian men only at the tibia. However, racial differences were most apparent in SM and were relatively greater in Afro-Caribbean men at the weight-bearing tibia (+17%) than at the radius (+10%). Thus, compared with Caucasians, men of African ancestry have greater cortical bone mass which does not appear to be explained by differences in body size, composition, or physical activity. In addition, bone mass is distributed further from the central axis of the long bones leading to more favorable bone geometry in Afro-Caribbean men. Further studies are needed to identify the factors contributing to racial differences in measures of cortical bone structure in men.

	Radius		Tibia	
	Caucasian	Afro-Caribbean	Caucasian	Afro-Caribbean
vBMD(mg/cm <sup>3</sup> )	1159±32	1194±24	1136±31	1162±26
BMC(mg/mm)	123±20	131±18	365±46	385±53
CSA(mm <sup>2</sup> )	147±20	152±23	459±52	514±69
THK(mm)	3.3±0.5*	3.4±0.4*	5.6±0.7	5.2±0.8
SM(mm <sup>3</sup> )	360±67	396±83	2064±331	2414±436

Values are adjusted means ± SD; \*p=0.11; all other differences p<0.0005

**Disclosures:** Y. Sheu, None.

## SU301

**Effects of Exercise and Milk Intake on Bone in Adolescents.** K. Nawata<sup>\*1</sup>, M. Kodama<sup>\*1</sup>, T. Yamaura<sup>\*1</sup>, S. Yamamoto<sup>1</sup>, H. Ishida<sup>1</sup>, K. Uenishi<sup>1</sup>, M. Konishi<sup>2</sup>, Q. Zhou<sup>2</sup>. <sup>1</sup>Kagawa Nutrition University, Saitama, Japan, <sup>2</sup>GE Healthcare, Madison, WI, USA.

Adolescence is an important period for achieving adequate bone mass. The study was aimed at assessing how exercise and milk intake effected bone status in adolescents longitudinal observations. We measured bone status at the os calcis using quantitative ultrasound (QUS, GE Healthcare Achilles Insight TM) and assessed diet and other lifestyle factors using questionnaires annually for 5 years. All subjects (aged 12.6 ±0.6years) attending the first years were recruited for this study and follow-up to the after five years. In total, 226 boys and 180 girls students were observed every year. In boys, mean stiffness index (SI) was 82.0 at the first years and 114.5 at the after five years(increased 40.3±19.8%). Multiple regression analyses revealed that SI increased in boys significant positive related with the mean frequency of exercise in a week and mean daily milk intake during the 5 years (p<0.05); In girls, on the other hand, mean SI was 85.9 at the first year and 104.2 at the after 5 years (increased 22.6±18.9%). Multiple regression analyses revealed that the increase in SI in girls significant positive correlated with the mean frequency of exercise (p<0.05), but no significant correlation with mean daily milk intake (p>0.05). For the girls, analysis results revealed that, in those students who had SI below 78.0 (25 %) in the first year, their SI increased during following 5-year period had no significant relationship with the frequency of exercise, although there is a significant positive correlation with the frequency of milk intake. This longitudinal study indicate that frequent of exercise is important for bone growth in all adolescent boys and girls; Daily milk intake is important for adolescent boys and especially for low SI adolescent girls.

**Disclosures:** K. Nawata, None.

## SU302

**Volumetric Bone Parameters in Relation to Fracture History in Healthy Men at the Age of Peak Bone Mass.** H. Zmierzczak<sup>1</sup>, B. Lapauw<sup>\*2</sup>, Y. Taes<sup>\*2</sup>, S. Goemaere<sup>1</sup>, J. Kaufman<sup>2</sup>. <sup>1</sup>Unit for Osteoporosis and Metabolic Bone Diseases, Ghent University Hospital, Ghent, Belgium, <sup>2</sup>Endocrinology, Ghent University Hospital, Ghent, Belgium.

The present cross-sectional, population-based study investigates volumetric bone mineral density (vBMD) and bone geometry in relation to prevalent self-reported clinical fractures in a sib-pair setting of young healthy male subjects (n = 677) at the age of peak bone mass (25-45 yr).

Cortical bone parameters of the radius and tibia at the 66% site (2/3 of bone length from distal) of the dominant limbs were assessed using peripheral quantitative computed tomography (XCT2000, Stratec GmbH). Trabecular bone parameters of the radius at the non-dominant limb were assessed at the 4% site. Fracture history was obtained from patient recall. Differences in volumetric bone parameters between participants with an without prevalent fractures were investigated using linear mixed-effects modeling analyses, accounting for the interdependence of measurements within siblings. Subjects with diseases or clinical conditions, including hormonal and other laboratory parameters, known to affect bone metabolism, were excluded.

Thirty three % of the participants reported one or more fracture, of which 16% sustained wrist, 5% shoulder, 4% humerus, 7% lower limb and 1% rib fracture. Four participants reported a hip fracture (0.6%) after major trauma. Finger, toe and cranial fractures were excluded from the analysis. No differences in weight, height or age between participants with or without previous fracture were observed (all P > 0.35). Descriptives of volumetric bone parameters are given in the table below.

		With fracture (n=226)	Without fracture (n=451)	p
Radius	Trabecular vBMD (mg/cm <sup>3</sup> )	223 ± 39	231 ± 40	0.019
	Cortical vBMD (mg/cm <sup>3</sup> )	1095 ± 36	1103 ± 35	0.009
	Cortical thickness (mm)	2.47 ± 0.31	2.55 ± 0.32	0.001
	Periosteal circumference (mm)	48.3 ± 3.8	48.1 ± 3.7	0.324
Tibia	Cortical vBMD (mg/cm <sup>3</sup> )	1109 ± 24	1114 ± 24	0.022
	Cortical thickness (mm)	4.47 ± 0.60	4.55 ± 0.54	0.194
	Periosteal circumference (mm)	94.9 ± 5.5	94.7 ± 6.2	0.557

In conclusion, we found that healthy men with a history of fractures presented with lower trabecular and cortical vBMD, as well as with smaller cortical thickness at the radius. No differences in periosteal bone circumference were observed. The lower level of mineralization is associated with fracture history independently of bone size and might contribute to a greater future fracture risk. As diseases or clinical conditions affecting bone metabolism were excluded, the degree of mineralization is presumed to be determined by subclinical or genetic factors.

**Disclosures:** H. Zmierzczak, None.

*This study received funding from: Flemish Fund for Scientific Research.*

## SU303

**Baseline Assessment of Osteoporosis Risk in Oklahoma Native American Women.** B. J. Smith<sup>1</sup>, M. Leyva<sup>\*2</sup>, C. E. Aston<sup>\*2</sup>, L. D. Stephens<sup>\*2</sup>, M. Z. Baker<sup>\*3</sup>. <sup>1</sup>Department of Nutritional Sciences, Oklahoma State University, Stillwater, OK, USA, <sup>2</sup>General Clinical Research Center, University of Oklahoma Health Sciences Center, Oklahoma City, OK, USA, <sup>3</sup>Department of Medicine, University of Oklahoma Health Sciences Center, Oklahoma City, OK, USA.

Osteoporosis is estimated to afflict 1 out of 2 women over the age of 50 y. These estimates are based primarily on Caucasian populations with limited information on Native Americans. Native American women may be considered high risk for osteoporosis-related fractures due to lifestyle factors (e.g. physical activity, dietary calcium and vitamin D intake) in conjunction with the incidence of diabetes. This study was designed to begin to examine the prevalence of osteoporosis in Native American women and to assess various lifestyle factors and medical conditions that influence the rate of bone loss and consequent risk for osteoporosis. Native American women aged, 50+ years, who were eligible for services at Indian Health Clinics in the Oklahoma City area were recruited for the study. Participants underwent a baseline osteoporosis risk assessment (i.e. medical history, whole body, hip, spine and forearm DXA scans, anthropometrics and calcium intake assessment). Baseline demographic data (n=77) were: age (62 ± 9), BMI (29 ± 5), waist:hip ratio (0.9 ± 0.1), and years postmenopausal (15.0 ± 3.8). Self-reported osteoporosis was 14.3%, previous vertebral fractures (3.8%), hip fracture (3.8%), and wrist fractures (3.8%). Additionally, 28.6% of the study participants reported a previous history of type II diabetes and 46.8% of hypertension. Similar to other ethnic groups, increasing BMI appeared to be protective of BMD for the total hip, femoral neck and lumbar spine while women with a BMI < 24 were at greater risk of osteopenia and/or osteoporosis. Several weight related measures, such as BMI, were significantly positively correlated with BMD measures of the lumbar spine, femoral neck, and total hip, with waist circumference showing the largest correlations. Total hip T-scores appear to decline with age at a similar rate as Caucasian women and dietary calcium intake did not appear to influence this decline in BMD. Interestingly, protection of total hip BMD appeared to be afforded to individuals with hypertension and/or the combination of hypertension and type II diabetes over and above that afforded by increasing BMI. Based on these very preliminary results it appears that the risk for osteoporosis is very similar in Native American women compared to their Caucasian counterparts.

**Disclosures:** B.J. Smith, None.

## SU304

**Negative Association between the Metabolic Syndrome and Bone Mineral Density in Korean Adults.** H. Y. Kim<sup>1</sup>, S. H. Lee<sup>\*2</sup>, H. K. Kim<sup>\*2</sup>, J. M. Koh<sup>2</sup>, G. S. Kim<sup>2</sup>. <sup>1</sup>Division of Endocrinology and Metabolism, University of Wonkwang College of Medicine, Sanbon Medica Center, Gunpo, Republic of Korea, <sup>2</sup>Division of Endocrinology and Metabolism, University of Ulsan College of Medicine, Asan Medical Center, Seoul, Republic of Korea.

**Background:** Recently many studies suggested the relationship between osteoporosis and cardiovascular disease. The association between different diseases might have been attributable to common risk factors. Metabolic syndrome (MS) was composed of major risk factors of cardiovascular disease. There had been many contradictory reports about the association between each component of metabolic syndrome and bone mineral density (BMD). However, the combined effects of the metabolic syndrome on BMD had been reported rarely. The aim of this study was to determine the association between metabolic syndrome and bone mineral density in Korean adults.

**Methods:** We examined the association between metabolic syndrome and BMD in Korean men (n=1241) and postmenopausal women (n=1109). BMD was measured at the femoral neck and lumbar spine using dual energy X-ray absorptiometry. We made cross-sectional analysis of BMD for subjects with and without metabolic syndrome defined by NCEP-ATP III criteria.

**Results:** The prevalence of metabolic syndrome was 13.0% in men and 17.3% in women. After adjusting for age and BMI, femur neck BMD (FN-BMD) was lower among subjects with MS (0.801 ± 0.010 g/cm<sup>2</sup>; 0.692 ± 0.009 g/cm<sup>2</sup>) than those without (0.826 ± 0.004 g/cm<sup>2</sup>; 0.724 ± 0.004 g/cm<sup>2</sup>) in both men and women (P=0.019; P=0.001). No significant association was seen between MS and BMD at lumbar spine. In multiple regression analysis between each MS component and FN-BMD, waist circumference and glucose were associated with BMD. We found significantly lower FN-BMD in subgroups of abdominal obesity (P<0.001). With the presence of increasing component of MS, there was a significant trend toward lower FN-BMD (P=0.001). The adjusted log-transformed hsCRP level increased with more components. (P=0.002)

**Conclusions:** In Korean men and postmenopausal women, the metabolic syndrome was associated with lower FN-BMD. Among MS component, there was a significant negative association between FN-BMD and abdominal obesity. This association suggested the possibility that increased inflammation induced by visceral fat, somewhat different from total fat mass, might lead to reduced BMD.

**Disclosures:** H.Y. Kim, None.

## SU305

**Impact of Dietary Protein on Calcium Homeostasis and Nitrogen Excretion in the Presence and Absence of Potassium Bicarbonate.** L. Ceglia<sup>1</sup>, S. S. Harris<sup>1</sup>, S. A. Abrams<sup>2</sup>, H. M. Rasmussen<sup>\*1</sup>, G. Dallal<sup>\*1</sup>, B. Dawson-Hughes<sup>1</sup>. <sup>1</sup>Jean Mayer USDA Human Nutrition Research Center on Aging at Tufts University, Boston, MA, USA, <sup>2</sup>USDA Children's Nutrition Research Center, Houston, TX, USA.

There are conflicting data on whether dietary protein stimulates calcium absorption and few data on whether giving an alkaline salt to reduce the acid load that accompanies protein would alter the impact of dietary protein on calcium handling and muscle breakdown. In this study we determine the effect of dietary protein on calcium absorption, urinary calcium excretion (UCa), and urinary nitrogen excretion (UNi), and evaluate whether any effects seen are modulated by neutralizing the diet with potassium bicarbonate (KHCO<sub>3</sub>).

20 subjects age 54-82 were randomized to take KHCO<sub>3</sub> (up to 90 mmol/d, n=9) or placebo (n=11) for 41 days. All subjects gave written informed consent. After 2 weeks on treatment, all subjects went through 2 successive 10-d metabolic diet periods containing either low (0.5 g/kg) or high (1.5 g/kg) protein in random order, with a 5-d wash-out period between diets. Calcium intake throughout was 1200 mg/d. After each diet cycle, UCa, UNi, and net acid excretion (NAE) were collected over a 24-hr period, and fractional calcium absorption was measured using dual stable isotopes.

Table. UCa, UNi, and fractional calcium absorption after each diet in the 2 groups

	Placebo		KHCO <sub>3</sub>	
	Low Protein	High Protein	Low Protein	High Protein
UCa (mg)	105.2±42.1	154.7±83.0 <sup>a</sup>	99.0±38.7	134.5±70.3 <sup>a</sup>
UNi (mg)	4.3±0.8	13.6±2.4 <sup>a</sup>	5.6±2.5	12.1±3.5 <sup>a</sup>
Fractional Calcium Absorption (%)	16.6±7.2 <sup>b</sup>	17.2±5.8 <sup>c</sup>	23.7±6.3	23.5±10.0

Diet effect: <sup>a</sup> differs within group from low protein diet at P<0.05.

Treatment effect: differs within diet at <sup>b</sup> P<0.05, <sup>c</sup> P=0.099 (trend)

After each diet cycle, NAE levels revealed full neutralization by KHCO<sub>3</sub> (Placebo group: low protein 10.9±22.4 mmol/L, high protein 19.6±11.7 mmol/L; KHCO<sub>3</sub> group: low protein -20.6±7.8 mmol/L, high protein -12.7±9.0 mmol/L). These results in healthy older subjects confirm increases in calcium and nitrogen excretion with increasing protein in the diet, but do not confirm the previous observation that protein increases calcium absorption (1). These findings also suggest that KHCO<sub>3</sub> may enhance intestinal calcium absorption.

1. Kerstetter JE, O'Brien KO, Caseria DM, Wall DE, Insogna KL (2005) The impact of dietary protein on calcium absorption and kinetic measures of bone turnover in women. J Clin Endocrinol Metab 90:26-31.

**Disclosures:** L. Ceglia, None.

This study received funding from: Unilever Corporate Research.

## SU306

**Air Pollution Might Be a Neglected Risk-Factor of Hypovitaminosis D.** D. H. Manicourt<sup>\*</sup>, J. P. Devogelaer. Rheumatology Unit, St-Luc University Hospital, Brussels, Belgium.

By absorbing sunlight UVB, ozone, a common urban pollutant, might reduce cutaneous vitamin D photosynthesis. Therefore, we conducted a cross-sectional study that established the characteristics and percentage of subjects with serum 25-hydroxyvitamin D [25(OH)D] levels<30 ng/ml among postmenopausal housewives having outdoors activities either in Brussels city or in the countryside and consulting for low back pain. Parameters included dietary intakes, sun exposure index (SEI), levels of PTH, and femoral neck (FN) T-score. Among 249 women consulting for low back pain in June and July, 121 were free of conditions/drugs affecting bone/calcium metabolism, and were selected. Brussels-dwellers (n=52) and rural-dwellers (n=69) had similar mean age (65-67 year), body mass index (24 kg/m<sup>2</sup>) and vitamin D intakes (191-200 IU/day), but differed in mean SEI (113 versus 87;p<0.001) and prevalence of 25(OH)D <30 and <20 ng/ml (83% vs 42% and 46% vs 9%, respectively). In each group, SEI correlated positively with 25(OH)D, but ozone levels were 4-times greater in Brussels than in countryside. After adjusting for SEI, 25(OH)D was 2-times higher in rural-dwellers, and after adjusting for 25(OH)D, SEI was 3-times higher in Brussels-dwellers. In subjects with 25(OH)D<30 ng/ml, but not in subjects with higher 25(OH)D levels, the mean PTH was higher in those with a calcium intake 700 mg/day. FN T-score correlated positively with 25(OH)D and negatively with PTH.

It is concluded that air pollution is a neglected risk-factor of hypovitaminosis D known to compromise several health outcomes. As long as 25(OH)D is >30 ng/ml, calcium intake>700 mg/day is not mandatory for preventing high PTH levels.

**Disclosures:** J.P. Devogelaer, None.

## SU307

**Effect of Low Dose Vitamin K2 (MK-4) Supplementation on Bio-indices in Postmenopausal Japanese Women.** N. Koitaya<sup>\*1</sup>, J. Ezaki<sup>\*1</sup>, M. Nishimuta<sup>\*1</sup>, J. Yamauchi<sup>\*1</sup>, E. Hashizume<sup>\*2</sup>, K. Morishita<sup>\*2</sup>, S. Sasaki<sup>\*1</sup>, Y. Ishimi<sup>1</sup>.  
<sup>1</sup>Nutritional Epidemiology Program, National Institute of Health and Nutrition, Tokyo, Japan, <sup>2</sup>Healthcare Products Development Center, Kyowa Hakko Kogyo Co., LTD, Tsukuba, Japan.

It is well known that vitamin K is responsible for  $\gamma$ -carboxylation of peptide-bound glutamate (Glu) residues to produce  $\gamma$ -carboxyglutamate (Gla) in target proteins that are synthesized in limited number of tissues such as bone and vascular tissues.

Dietary vitamin K exists in 2 major forms: phyloquinone (PK) and menaquinones (MK-1 ~ MK-14). The adequate intake (AI) of vitamin K for women aged 30 years and more was set at 65  $\mu$ g/day in the Dietary Reference Intakes (DRIs) for Japanese, 2005. However, epidemiological studies reported that daily intake of vitamin K less than 109  $\mu$ g/day increased the risk of hip fracture in peri- and postmenopausal women. Furthermore, higher circulating vitamin K concentrations are required for OC  $\gamma$ -carboxylation in elderly people compared with younger people. In Japan, 45mg/day of MK-4 has been used for treatment of the patients with osteoporosis. On the other hand, it is not well known whether supplementation of low doses of MK-4 benefits bone metabolism in healthy postmenopausal women at a high risk of bone loss. Thus, the aim of this study is to examine the effects of an additional intake of 1.5mg/day MK-4 on bone metabolism and other indices in healthy postmenopausal women.

The study was performed as a randomized double blind placebo-controlled trial, participants aged 53-65 years randomly assigned to 2 groups, and supplemented with 1.5mg/day MK-4 or placebo in 2 soft capsules for 4 weeks (n=20 for each group). The serum concentrations of lipids, vitamin K, vitamin D, intact  $\gamma$ -carboxylated, and undercarboxylated serum osteocalcin (iOC, GlaOC and uOC, respectively); and urinary bone resorption markers were assessed at the baseline, 2 and 4 weeks. Intake of Natto which is fermented soybean containing MK-7 was restricted during the study period. The study was carried out according to the guidelines of the Declaration of Helsinki. The most marked effects of MK-4 intake were observed on serum OC concentrations. Serum GlaOC increased, and the uOC and the uOC/iOC ratio that indicates the degree of OC  $\gamma$ -carboxylation decreased significantly at 2 weeks compared with that at baseline in the MK-4 group. The serum uOC and uOC/iOC ratio in the MK-4 group were significantly lower than those in the placebo group at 4 weeks. These results suggest that supplementation with 1.5mg/day MK-4 accelerated the degree of OC  $\gamma$ -carboxylation. Thus, the additional daily intake of low dose MK-4 might be beneficial in the maintenance of bone health in postmenopausal women.

**Disclosures:** Y. Ishimi, None.

## SU308

**Calcium Intake and Serum Bone Formation Markers Are Associated with the Functional Single Nucleotide Polymorphism in the Tissue-Nonspecific Alkaline Phosphatase Gene.** M. Goseki-Sone<sup>1</sup>, N. Sogabe<sup>\*1</sup>, N. Tsugawa<sup>\*2</sup>, R. Maruyama<sup>\*1</sup>, M. Kamao<sup>\*2</sup>, T. Okano<sup>2</sup>, T. Hosoi<sup>3</sup>. <sup>1</sup>Food and Nutrition, Japan Women's University, Tokyo, Japan, <sup>2</sup>Department of Hygienic Sciences, Kobe Pharmaceutical University, Kobe, Japan, <sup>3</sup>Department of Advanced Medicine, National Center of Gerontology and Geriatrics, Aichi, Japan.

Osteoporosis is characterized by a low bone mass, the micro architectural deterioration of bone tissue, and an increasing risk of fracture in the elderly. The disease results from complex interactions between genetic and environmental factors such as nutrition. It seems to be important to maximize peak bone mass during youth, and so nutritional education targeted at accelerating and maintaining bone health is indispensable for young people. Tissue-nonspecific alkaline phosphatase (TNSALP) is suggested to be essential for bone mineralization. Recently, we identified polymorphisms of the *TNSALP* gene 787T>C (Y246H) associated with BMD among 501 postmenopausal women (JBMR, 20:773-782, 2005). In the present study, we attempted to examine the nutritional effects of the *TNSALP* genotype on serum markers of bone metabolism. The subjects were 60 healthy young male volunteers. Dietary nutrient intakes were determined by food records kept for 3 consecutive days. Serum concentrations of bone-specific ALP (BAP), ALP, intact osteocalcin (OC), 25(OH)<sub>2</sub>D<sub>3</sub>, 1 $\alpha$ , 25(OH)<sub>2</sub>D<sub>3</sub> were measured. All subjects were genotyped for the presence of the polymorphism (Y246H). There were no significant correlations between the levels of serum BAP, ALP, intact OC, 25(OH)<sub>2</sub>D<sub>3</sub>, 1 $\alpha$ , 25(OH)<sub>2</sub>D<sub>3</sub>, calcium and vitamin D intakes among genotypes. In all subjects, there was a significant positive correlation between the levels of BAP and 1 $\alpha$ , 25(OH)<sub>2</sub>D<sub>3</sub> (p<0.001). Interestingly, calcium intake was significantly correlated with the level of serum BAP or intact OC in 787T>C homozygotes (CC-type) (p<0.01), but not in heterozygotes (TC-type), nor in 787T homozygotes (TT-type). Our findings indicate the possibility that the osteoporosis-susceptibility gene *TNSALP* has nutritional effects on serum bone formation markers, and that gene-nutritional factor-related interactions potentially modulate the risk of osteoporosis.

**Disclosures:** M. Goseki-Sone, None.

## SU309

**Dietary Patterns in Canadian Men and Women Ages 25 and Older: Relationship to Body Mass Index and Bone Mineral Density.** L. Langsetmo<sup>1</sup>, S. Poliquin<sup>\*1</sup>, D. Hanley<sup>2</sup>, J. Prior<sup>3</sup>, S. Barr<sup>\*3</sup>, T. Anastassiades<sup>4</sup>, T. Towheed<sup>4</sup>, D. Goltzman<sup>5</sup>, N. Krieger<sup>\*6</sup>. <sup>1</sup>CaMos, Montreal, QC, Canada, <sup>2</sup>University of Calgary, Calgary, AB, Canada, <sup>3</sup>University of British Columbia, Vancouver, BC, Canada, <sup>4</sup>Queen's University, Kingston, ON, Canada, <sup>5</sup>McGill University, Montreal, QC, Canada, <sup>6</sup>University of Toronto, Toronto, ON, Canada.

Previous research has shown that underlying dietary patterns are related to the risk of many different adverse health outcomes, but the relationship of these underlying patterns to skeletal fragility is not well understood. The objective of the study was to determine whether dietary patterns in men (ages 25-49, 50+) and women (pre-menopause, post-menopause) are related to bone mineral density (BMD) independently of other associated lifestyle variables and how this relationship is mediated by body mass index. This cohort study included 1928 men and 4611 women participants in the Canadian Multicentre Osteoporosis Study, a randomly selected population-based longitudinal cohort. Dietary patterns were assessed at year 2 and based on self-administered food frequency questionnaire. BMD was measured at year 5 by dual x-ray absorptiometry and calibrated using a phantom. We identified two underlying dietary patterns using factor analysis and then derived factor scores. The first factor score (nutrient dense or "Prudent") was most strongly associated with intake of fruits, vegetables, and whole grains. The second factor score (energy dense or "Western") was most strongly associated with intake of soft drinks, potato chips and French fries, certain meats (hamburger, hot dog, lunch meat, bacon, and sausage), and certain desserts (doughnuts, chocolate, ice cream). The energy dense factor score was associated with higher body mass index independently of other demographic and lifestyle factors. Body mass index was a strong independent predictor of BMD. For a fixed body mass index, each standard deviation increase in the energy dense score was associated with a BMD decrease of 0.009 (95% CI: 0.002, 0.016) g/cm<sup>2</sup> for men 50+ years old and 0.004 (95% CI: 0.000, 0.008) g/cm<sup>2</sup> for postmenopausal women, whereas there was no significant association in either group without the adjustment for body mass index. For a fixed body mass index, each standard deviation increase in the nutrient dense score was associated with a BMD increase of 0.012 (95% CI: 0.002, 0.022) g/cm<sup>2</sup> for men 25-49 years old. There was a positive association between an energy dense diet and higher body mass index, but this did not translate to positive association between an energy dense diet and BMD. Therefore, diet is related to BMD through multiple causal pathways.

**Disclosures:** L. Langsetmo, None.

## SU310

**Relationship among Nutritional Status, Oxidative Stress and Bone Density in Institutionalized Elderly.** V. Mocanu<sup>\*1</sup>, O. Voroniu<sup>\*2</sup>, R. Haliga<sup>\*1</sup>, T. Oboroceanu<sup>\*1</sup>, R. Costan<sup>\*3</sup>, V. Luca<sup>\*1</sup>, C. Galesanu<sup>\*3</sup>. <sup>1</sup>Pathophysiology, University of Medicine and Pharmacy, Iasi, Romania, <sup>2</sup>Hygiene, University of Medicine and Pharmacy, Iasi, Romania, <sup>3</sup>Endocrinology, University of Medicine and Pharmacy, Iasi, Romania.

**OBJECTIVE:** Nutrition plays a role in health promotion and well-being, but there is still a lack of knowledge about nutrition-related risk factors in aging. The purpose of this project was to evaluate the link between nutritional status, pro/antioxidant balance and bone status in elderly subjects residing in a nursing home. **METHODS:** The subjects were 50 elderly people (36 females and 14 males aged 72.6 $\pm$ 7 years, mean  $\pm$  standard deviation SD, range 63-93). Their nutritional status was assessed by weight, height, albumin, transthyretin (prealbumin), C-reactive protein, 25OHvitamin D, glucose, cholesterol, total proteins, lymphocytes and count of CD4 and CD8, a 10 day food record combined with a food-frequency questionnaire; the MNA nutritional screening. Plasma malondialdehyde and erythrocyte reduced glutathione, catalase and superoxide dismutase were evaluated in elderly people as indices of the oxidative balance. Femoral neck and lumbar bone mineral density (BMD) were measured by DXA scan. **RESULTS:** The mean vitamin and mineral intake for participants met the RDAs except for calcium and vitamin D. The MNA scores have been found to be significantly correlated to nutritional intake (p < 0.01 for energy, carbohydrates, calcium, vitamin D), anthropometric and biological nutritional parameters (p < 0.01 for albumin, transthyretin, cholesterol, 25OHvitamin D). An MNA score between 17 and 23.5 can identify those persons with mild malnutrition in which nutrition intervention may be effective. A significant negative correlation (p < 0.05) between dietary intake of vitamin D and malondialdehyde and between dietary 25OH vitamin D and low bone density (p < 0.01) was observed. **CONCLUSION:** The results of the present study showed the potential impact of nutritional factors and oxidative stress on bone health in older adults.

**Disclosures:** V. Mocanu, None.

*This study received funding from: Romanian Academy of Sciences.*

## SU311

**Increasing the Number of Steps Taken per Day Leads to a Greater Weight Loss and More Favorable Body Composition in Overweight Postmenopausal Women.** C. C. Douglas<sup>\*1</sup>, P. Liu<sup>1</sup>, H. Shin<sup>1</sup>, A. P. Crombie<sup>\*1</sup>, K. Humphrey<sup>\*1</sup>, O. J. Kelly<sup>1</sup>, G. R. Dutton<sup>\*2</sup>, J. Z. Ilich<sup>1</sup>. <sup>1</sup>Nutrition, Food and Exercise Sciences, Florida State University, Tallahassee, FL, USA, <sup>2</sup>Medical Humanities and Social Sciences, College of Medicine, Florida State University, Tallahassee, FL, USA.

Pedometers are inexpensive and simple tools that provide a specific and measurable assessment of the number of steps taken, or distance walked. Some clinical studies have demonstrated that pedometers could be used to assess activity of participants and relate it to various outcomes. Our purpose was to examine the relationship between pedometer-assessed activity and body composition in Caucasian overweight and obese postmenopausal women enrolled in a weight loss study for a period of 3 months. Participants at baseline included 45 early postmenopausal (from 2-10y) women, aged 56.0±3.2 y, with a BMI of 32.9±6.7 kg/m<sup>2</sup> (mean±SD). After enrollment, baseline measurements were recorded, and participants were assigned a low energy diet plan (consisting of a normal ratio of macronutrients), and were encouraged to increase number of steps/day. Each participant received a pedometer (Optimal Health Products) and was instructed how to use it and record the steps/day over a 7-day period. Analysis for the 3 months follow-up included only those participants who completed all baseline and 3-month measurements (n=32). Number of steps/day was recorded over seven days at baseline and 3 months. At baseline, the average number of steps/day was 6,941±3,468; only six (13.3%) participants exceeded the recommended 10,000 steps/day. Results showed significant negative correlation (Pearson's r ranging from -0.3 to -0.5) between number of steps/day and iDXA-analyzed trunk, android (abdominal), gynoid (hip) and total fat, all p's <0.05. ANCOVA, with age and energy intake (kcal) as the covariates, revealed significant difference in trunk fat and android fat, and BMI between participants divided in groups below and above mean number of steps/day, resulting in lower values in the group exceeding the mean number of steps/day (p's <0.05). After 3 months, the number of steps increased by 823±2855 steps/day; a 24% increase in activity from baseline. There was a 3.3±4.2 kg loss in body weight, representing a 3.9±5.3% weight loss for the group. Participants who lost 5 kg or more (n=11) of body weight demonstrated a significant increase in steps/day (vs. baseline) compared to those who lost <5 kg (p=0.05), even though energy consumption was similar between groups. We conclude that increasing the number of steps/day (even if the recommended level has not been reached) could help in weight loss and contribute to a more favorable body composition in this population.

**Disclosures:** J.Z. Ilich, None.

This study received funding from: USDA/CSREES/NRI #2004-05287.

## SU312

**Designing a Latino Osteoporosis Awareness Campaign.** K. Cody<sup>\*1</sup>, B. Tracewell<sup>\*1</sup>, A. Focil<sup>2</sup>, V. Lujan<sup>\*3</sup>, K. Campbell<sup>\*4</sup>, M. Wang<sup>\*5</sup>. <sup>1</sup>Foundation for Osteoporosis Research and Education, Oakland, CA, USA, <sup>2</sup>California Hispanic Osteoporosis Foundation, Oxnard, CA, USA, <sup>3</sup>La Clínica de la Raza, Concord, CA, USA, <sup>4</sup>Procter & Gamble, Irvine, CA, USA, <sup>5</sup>UC Berkeley Center for Weight and Health, Berkeley, CA, USA.

Hip fractures have doubled among California Latinos since 1983, while remaining unchanged or declining in other ethnic groups[1]. Despite prevention efforts, Latinos as a group do not take recommended actions to protect themselves from bone loss, osteoporosis and fractures.

In 2007, a partnership[2] formed to design and test effective messages and strategies for an osteoporosis awareness campaign for Latinos. These experts examined existing literature, identified education tools and dissemination strategies and tested them in focus group settings with 63 Latinos (56% females) ranging in age from 23 to 89 with a mean age of 58.

Literature shows that among Latinos there is a general fear of health testing ("fatalismo") that runs counter to preventive health care, making them particularly vulnerable to asymptomatic diseases. Good communication and experience with health care providers is critical.

Focus groups revealed a wide range of knowledge about osteoporosis, from those who have never heard the word "osteoporosis" to those who have been diagnosed with osteoporosis. Familiarity was usually due to family members or friends suffering with osteoporosis.

Focus groups reported that messages should be simple, positive, familial, hopeful and delivered in Spanish. Colored illustrations and graphics drew the most attention. Participants favored doctors as the first choice for delivering messages, followed by promotores, nurses or other clinic staff.

Preferred methods for message delivery were varied and included local Spanish-language radio and television programs, short videos with testimonials, "stories" with families about what to eat, and how to incorporate daily exercise. Other effective media was printed materials with illustrations, appealing graphics, and "bulletins" or colorful, "newsy" mailings to adults over 50.

Focus on the family was prevalent throughout the focus groups. Having someone in the family with osteoporosis and learning more about it raised interest in prevention.

[1] Zingmond D, Melton LJ III, Silverman SL. Increasing hip fracture incidence in California Hispanics, 1983-2000. *Osteoporosis International*. 2004. DOI 10.1007/s00198-004-1592-7.

[2] Partners included the Foundation for Osteoporosis Research and Education, La Clínica de la Raza, California Hispanic Osteoporosis Foundation; UC Berkeley Center for Weight and Health; and Procter & Gamble Pharmaceuticals.

**Disclosures:** K. Cody, None.

This study received funding from: John Muir Community Health Fund.

## SU313

**Interventions to Prevent Falls in the Community-Dwelling Elderly: A Systematic Review.** D. A. Butt<sup>1</sup>, O. Gajic-Veljanoski<sup>\*2</sup>, A. Cheung<sup>2</sup>. <sup>1</sup>Family & Community Medicine, University of Toronto, Toronto, ON, Canada, <sup>2</sup>Osteoporosis, University Health Network, Toronto, ON, Canada.

The evidence for interventions to prevent falls in elderly has undergone much change with the publication of several recent trials. Our study assessed the effectiveness of various interventions in preventing falls in community-dwelling elderly by reviewing published randomized controlled trials, systematic reviews and meta-analyses.

We conducted a systematic search of Medline, EMBASE and all Evidence-Based Medicine Reviews (1950-January 2008). The bibliographies of relevant articles were also searched. The search words were: "community-dwelling", "elderly", "accidental falls" and "falls". All English-language articles in the elderly (age ≥ 65 years), living at home that provided the number of falls, number of fallers or fall-related injuries were included. Two independent reviewers extracted data on participants, interventions and falls outcomes, and rated the studies for quality based on established criteria.

We identified 546 abstracts and 27 studies met eligibility criteria for inclusion into our systematic review. These studies include 1 systematic review on interventions, 2 studies on multifactorial interventions (1 meta-analysis, 1 trial), 12 trials on exercise, 3 studies on withdrawal of drugs (2 meta-analyses, 1 trial), 4 studies on vitamin D (1 meta-analysis, 3 trials), 1 trial on cognitive-behavioural learning, 2 trials on correction of visual impairment and 2 studies on assistive devices (1 systematic review, 1 trial). Interventions that reduce falls in community-dwelling elderly include exercises (tai chi, relative risk (RR) 0.45-0.67), muscle strengthening (RR 0.77-0.80), gait and balance training (RR 0.54-0.69); home hazard assessment and modification in elderly at risk of falls (RR 0.59-0.66); gradual withdrawal of psychotropic drugs (RR 0.34); vitamin D supplementation in women (odds ratio (OR) 0.54-0.78); cognitive-behavioural learning in elderly at risk of falls (RR 0.69) and correction of cataracts via phacoemulsification in women (RR 0.66). There was insufficient evidence to support the use of multifactorial interventions and external hip protectors to reduce falls and the number of fallers in community-dwelling elderly. Exercise in visually impaired and older persons transitioning to frailty, and correction of visual impairment in elderly not at risk of falls increased the incidence of falls (RR 1.15-1.57) and fractures (RR 1.15-1.74).

Based on current evidence, there are a number of effective interventions for the prevention of falls in community-dwelling elderly. Health care professionals need to be better informed so that these interventions can be integrated into routine care to prevent falls and injuries in the elderly.

**Disclosures:** D.A. Butt, None.

## SU314

**Prevention of the Metabolic Syndrome together with Osteoporosis in Young Men: 4 Months Trial by Improvement of Diet and Physical Activity with Milk Intake.** T. Hirota<sup>1</sup>, I. Kawasaki<sup>\*1</sup>, H. Ikeda<sup>\*1</sup>, T. Aoe<sup>\*1</sup>, K. Hirota<sup>\*2</sup>. <sup>1</sup>Research Laboratory, Tsuji Academy of Nutrition, Osaka-city, Japan, <sup>2</sup>Obstetrics & Gynecology, Nissay Hospital, Osaka-city, Japan.

To assess strategy for prevention of not only osteoporosis but also the metabolic syndrome (MetS) in young men by increasing calcium intake with milk.

Thirty five male students (21±4 yr, BMI: 21.8±2.5) who voluntarily attended 4-mo study to decrease fat and increase muscle mass and bone mineral density (BMD) were randomly assigned to either an obligatory milk intake of 200 ml/day (milk group, n=19) or not (control group, n=16). All subjects had been educated for proper diet and physical activity and the diaries of meals and sports written by themselves had been constantly followed by dietitians. Body fat, lean mass, and bone mineral by dual energy x-ray absorptiometry and risk factors of MetS including blood pressure, fasting glucose, lipids and waist circumference were measured. Calcium intake by 3-day dietary record, vitamin D status by 25(OH)D (RIA), and intact PTH as serum calcium regulating hormone were determined.

Baseline calcium intake in the subjects was as low as 468 mg/day which were quite similar to the National Health and Nutrition Survey in Japanese young men. Total number of risk factors of MetS at baseline was 11 in control and 18 in milk groups. These risk factors were decreased to 10 and 8, respectively after 4-mo trial, however, such significant changes were observed only in milk group. Mean blood pressure was decreased and HDL-cholesterol and femoral neck BMD were increased significantly only in milk group, while their body weight, fat and lean mass were changed a little after 4-mo. Four subjects (1 in control and 3 in milk groups) out of 6 (2 in control and 4 in milk groups) who had two or more of MetS risk factors at baseline, became to the normal range of these risk factors after 4-mo.

Increased intake of milk which is the best source of calcium should help not only to increase BMD but also to decrease risks of MetS in young Japanese men whose calcium intake is much lower than Europeans and Americans.

**Disclosures:** T. Hirota, None.

This study received funding from: Japan Dairy Association.

## SU315

**Rosiglitazone-induced Change in Bone Mineral Density among African Americans with Type 2 Diabetes Mellitus or Impaired Glucose Tolerance.** S. W. Ing<sup>1</sup>, K. Osei<sup>\*1</sup>, T. Gaillard<sup>\*1</sup>, L. T. Sinnott<sup>\*2</sup>, R. D. Jackson<sup>1</sup>. <sup>1</sup>Internal Medicine, Ohio State University, Columbus, OH, USA, <sup>2</sup>Optometry, Ohio State University, Columbus, OH, USA.

**Purpose:** This was an exploratory study to assess BMD changes among African Americans with type 2 diabetes mellitus (T2DM) or impaired glucose tolerance (IGT) treated with rosiglitazone.

**Methods:** We retrospectively evaluated data from a cohort of African American subjects with T2DM or IGT treated with rosiglitazone 8 mg daily for 12 weeks. Body composition DXA scans (Lunar DPX) at baseline and 12 weeks were performed at the total body including subregions: arm, leg, trunk, pelvis, and spine. Serum total adiponectin concentrations at baseline and 12 weeks were also measured. For each subject, change in BMD and adiponectin levels over the 12 weeks was computed. An ordinary least squares regression was performed for each BMD location, with change in BMD as outcome and change in adiponectin level as predictor. We controlled for gender, age, baseline BMI, and group (T2DM or IGT) in these analyses.

**Results:** The study cohort consisted of 24 women and 4 men, mean age 50.1 years, 17 with T2DM and 11 with IGT, and mean BMI of 37 kg/m<sup>2</sup>. Short term precision using root mean square coefficient of variation by site was: total body 0.5%, arm 2.9%, leg 1.6%, trunk 1.6%, pelvis 3.4%, and spine 3.8%. Change in BMD (SD) by site was: arm +1.4% (4.6), leg +0.6% (3.6), trunk +0.5% (4.3), pelvis +0.2% (5.1), spine +2.4% (9.8) and total body +0.2% (2.0). All were statistically nonsignificant. Adiponectin significantly increased from baseline 7.7 mcg/ml (SD 4.3) to 15.5 (8.4). Baseline adiponectin correlated with baseline BMD at the leg ( $r = -0.49$ ,  $p < 0.05$ ). Regression analyses between adiponectin change (mcg/ml) and BMD change (mg/cm<sup>2</sup>) were nonsignificant, but point estimates of the regression parameters were negative at the arm (-1.3), trunk (-1.6), pelvis (-2.4), and spine (-3.5). After multiplying these estimates by the mean adiponectin increase (7.7 mcg/ml), mean (and percent) changes in BMD by body site were: arm -9.8 (-1.1%), trunk -12.4 (-1.2%), pelvis -18.6 (-1.4%), and spine -26.7 (-2.3%) mg/cm<sup>2</sup>, respectively.

**Conclusion:** Rosiglitazone therapy in middle aged African Americans with T2DM or IGT may not lead to short term decreases in BMD. Serum adiponectin concentration doubled and correlations between increase in adiponectin and change in BMD were nonsignificant, but the direction of this relationship was negative, suggesting that increasing adiponectin may be associated with bone loss in this population.

**Disclosures:** S.W. Ing, None.

## SU316

**Bone Is More Susceptible to Vitamin K Deficiency than Liver.** A. Kuwabara<sup>\*1</sup>, K. Tanaka<sup>1</sup>, N. Tsugawa<sup>\*2</sup>, M. Kamao<sup>\*2</sup>, M. Himeno<sup>\*1</sup>, Y. Ogawa<sup>\*1</sup>, M. Kishimoto<sup>\*1</sup>, M. Fukuda<sup>\*1</sup>, S. Kido<sup>\*1</sup>, T. Okano<sup>1</sup>. <sup>1</sup>Kyoto Women's University, Kyoto, Japan, <sup>2</sup>Kobe Pharmaceutical University, Kobe, Japan.

**Aim:** In most countries including Japan,  $\gamma$ -carboxylation of blood coagulation factors in the liver has been the basis for determining adequate intake (AI) for vitamin K. Recently, vitamin K is known to be an essential nutrient for preventing fracture. In this study, relative susceptibility of liver and bone to vitamin K deficiency was investigated in two study models.

**Study (1) Methods:** Elderly institutionalized subjects were evaluated for vitamin K status by measuring serum PIVKA (protein induced by vitamin K absence) -II and uOC (undercarboxylated osteocalcin) levels, as the sensitive markers for hepatic and skeletal vitamin K deficiency, respectively. Cut-off values were 28mAU/ml for PIVKA-II and 4.5ng/ml for uOC. **Results:** Serum PIVKA-II and uOC levels were 20.8 $\pm$ 5.9mAU/ml and 4.8 $\pm$ 3.3ng/ml, respectively. Serum PIVKA-II and uOC concentration exceeded the cut-off value in 8% and 47% of subjects, respectively. Median vitamin K intake was approximately 200 $\mu$ g, which more than 2.5 times higher than current Japanese AI.

**Study (2) Methods:** Patients with inflammatory bowel disease (IBD; 50 Crohn's disease; CD, 65 ulcerative colitis; UC) were evaluated for their BMD, urinary bone resorption marker (NTx), plasma vitamin D and K levels, serum parathyroid hormone (PTH), PIVKA-II and uOC levels, and their food intake. **Results:** BMD were generally decreased, most notably at radius. Urinary NTx excretion was elevated in most patients. CD patients had significantly lower vitamin D and K levels, significantly higher serum PTH, uOC and PIVKA-II concentrations than UC patients. Serum PIVKA-II and uOC levels were elevated in 18% and 80% of patients respectively, suggesting that bone is more vitamin K-deficient than liver. Plasma vitamin D and K levels correlated with fat intake, but not with their intake of these vitamins. Decreased plasma vitamin D and K concentrations were risk factors for radial low BMD by multiple regression analysis.

**Discussion:** In these two study models, the prevalence of elevated PIVKA-II was much higher than that of elevated uOC levels, suggesting that bone is much more susceptible to vitamin K deficiency. These differences are likely to arise from the anatomical reason such that vitamin K absorbed from the intestine is first delivered and utilized in the liver, then to extra-hepatic tissues including bone (first pass effect). These facts should be taken into account in determining the AI for vitamin K.

**Disclosures:** K. Tanaka, None.

## SU317

**Impaired Methylation Capacity Is Associated with Low Bone Mineral Density.** J. van Meurs<sup>1</sup>, N. Yazdanpanah<sup>\*1</sup>, C. Zillikens<sup>\*1</sup>, R. de Jonge<sup>\*2</sup>, F. Rivadeneira<sup>1</sup>, A. Hofman<sup>\*3</sup>, J. Lindemans<sup>\*2</sup>, H. Pols<sup>1</sup>, A. Uitterlinden<sup>1</sup>. <sup>1</sup>Internal Medicine, Erasmus Medical Center, Rotterdam, Netherlands, <sup>2</sup>Clinical Chemistry, Erasmus Medical Center, Rotterdam, Netherlands, <sup>3</sup>Epidemiology, Erasmus Medical Center, Rotterdam, Netherlands.

**OBJECTIVE:** A mildly elevated circulating homocysteine (Hcy) level is a new and potentially modifiable risk factor for osteoporotic fractures. It is not clear whether the Hcy toxicity effects are direct or if they are caused by disturbed levels of associated metabolites. One such associated factor might be aberrant methylation patterns, through which epigenetic control of gene transcription occurs. Dietary methionine is converted to S-adenosylmethionine (SAM). SAM serves as the major intracellular methyl donor in many transmethylation reactions in the cell. The demethylated product of the transmethylation reaction is S-adenosylhomocysteine (SAH), which is further converted to homocysteine. Chronic elevation in Hcy levels is associated with a parallel decreased SAM/SAH ratio, which leads to decreased methylation of DNA. This suggests that elevated Hcy levels may be an indirect indicator of decreased SAM/SAH ratio and compromised cellular methylation capacity. The aim of the current study was to examine the relation between methylation capacity as measured by circulating SAM/SAH ratio and bone parameters.

**METHODS:** We measured circulating homocysteine, SAM and SAH levels in serum of 500 women aged 65-75 years from the prospective population-based Rotterdam study. Association analysis was done between SAM/SAH ratios and femoral neck bone mineral density and fracture incidence.

**RESULTS:** Low SAM/SAH ratios were significantly correlated with high homocysteine levels, ( $r=0.21$ ,  $p<0.001$ ) and age ( $r=0.16$ ,  $p<0.001$ ), but not with height and weight.

Multiple linear regression analysis showed that low SAM/SAH ratios were associated with low BMD (standardized B=0.13,  $p=0.006$ ), independent of age and homocysteine levels. Quartile specific analysis showed that women with a SAM/SAH ratio in the highest quartile had a 0.3SD higher BMD compared to women in the lowest quartile. Similar analysis for Hcys levels showed no relation between BMD and hcy levels. In addition, fracture incidence was higher in women with SAM/SAH ratio in the lowest 3 quartiles compared to the highest quartile with borderline significance (1.6% vs 6%, Chi-square  $p=0.055$ , HR 3.6[0.9-15.3]). This increased fracture risk was independent of age, Hcys levels, and BMD. **CONCLUSION:** Low methylation capacity (SAM/SAH ratio) is associated to low BMD, independent of age and homocysteine levels. In addition, low SAM/SAH ratio show a strong trend towards a higher fracture risk independent of homocysteine levels, but this needs to be confirmed in a larger study.

**Disclosures:** J. van Meurs, None.

This study received funding from: European Commission.

## SU318

**Does Adiposity Affect Bone Strength Indices in Young Adult Black Females?** N. K. Pollock<sup>1</sup>, E. M. Laing<sup>1</sup>, M. W. Hamrick<sup>2</sup>, C. A. Baile<sup>1</sup>, R. D. Lewis<sup>1</sup>. <sup>1</sup>Foods and Nutrition, The University of Georgia, Athens, GA, USA, <sup>2</sup>Cellular Biology and Anatomy, The Medical College of Georgia, Augusta, GA, USA.

Some studies suggest that obesity may have a negative impact on bone health. Since obesity rates have been increasing among young adult black females, it is important to ascertain the impact of adiposity on bone in this racial group. To date, the relationship between adiposity and indices of bone strength in young adult black females has not been investigated. The purpose of this study was to compare tibial and radial bone measurements between two groups defined as having normal and high levels of body fat, while taking into consideration the muscle and bone relationship. Black females (N=44, aged 19.2 $\pm$ 1.2 years) participated in this cross-sectional study. Participants were divided into 2 groups on the basis of their percent body fat: normal-fat (less than 32% fat; n=29) and high-fat (greater than 32% fat; n=15). These classifications were selected based on levels of body fat associated with cardiovascular risk factors. Fat-free soft tissue, fat mass and % fat were measured using DXA. Tibial and radial bone measurements were assessed by peripheral quantitative computed tomography (pQCT) at the 4%, 20% and 66% sites from the distal metaphyses, which reflect trabecular bone, cortical bone and muscle cross-sectional area (MCSA), respectively. Data were analyzed using independent samples t-tests and ANCOVA. Unadjusted bone measures were not different between groups. After controlling for MCSA, the high- vs. normal-fat group had lower bone measures at the 20% site of the tibia (periosteal circumference and polar strength-strain index;  $P<0.05$ ). No differences were found at the adjusted radial bone measurements. Traditionally, excess adiposity is presumed to be advantageous for the skeleton. However, in this study, excess weight in the form of fat mass does not seem to provide additional benefits to cortical bone at a weight-loaded site in young adult black females.

**Disclosures:** N.K. Pollock, None.

## SU319

**Does Dietary Protein reduce Hip Fracture Risk in Elderly Men and Women? The Framingham Study.** D. Misra<sup>\*1</sup>, S. D. Berry<sup>1</sup>, K. E. Broe<sup>1</sup>, K. L. Tucker<sup>2</sup>, L. A. Cupples<sup>3</sup>, D. P. Kiel<sup>1</sup>, M. T. Hannan<sup>1</sup>. <sup>1</sup>IFAR, HSL, Boston, MA, USA, <sup>2</sup>Tufts Univ, Boston, MA, USA, <sup>3</sup>Boston Univ, Boston, MA, USA.

Although higher protein intake has been associated with higher bone mineral density (BMD), the effect of protein intake on fracture risk remains unclear. A few large studies have revealed an inverse relation between dietary protein intake and hip fracture risk in younger persons (<70y) but the relation between protein and hip fracture risk is unclear in individuals >70y. Thus, we examined the relation between protein intake and hip fracture among older men and women in the Framingham Study.

Our subjects included persons who attended Framingham exam 1988-89 and provided information on protein intake by 126-item Willett's Food Frequency Questionnaire (FFQ). Participant with missing or implausible FFQ energy intake (<600 and >4000 kcal) and those with prior hip fracture were excluded. Total protein intake (g/d) was energy-adjusted. Information was collected at baseline on the following covariates: age (y), sex, weight (lb) & height (cm) to calculate body mass index (BMI) and total energy intake (kcal). Femoral neck BMD (g/cm<sup>2</sup>) was also obtained with Lunar Dual photon absorptiometry using standard technique.

Hip fractures were ascertained and confirmed through interview and review of medical records through 12/31/05. Incidence rates were calculated for each protein quartile. Cox proportional hazard regression was used to examine the risk of hip fracture associated with energy-adjusted protein intake (in continuous and quartile forms) adjusting for age, sex, BMI and total energy intake.

Of the 946 participants (576 women and 370 men), mean age 75y, 100 incident fractures (80 women, 20 men) were identified over the 17-year follow-up. There was no reduction in risk of hip fracture per gram of energy-adjusted total protein intake (HR= 0.995, 95%CI 0.98-1.01). Reduction in risk of hip fracture across quartiles showed a protective trend but result was only borderline statistically significant (p=0.07), see table.

Energy-adjusted Protein Quartiles(mean.g/d)	Hazard Ratios	95% CI
Q1 46.5± 7.29	1	
Q2 59.6± 2.24	0.70	0.41-1.19
Q3 67.7± 2.43	0.56	0.32-1.0
Q4 82.7± 10.27	0.63	0.37-1.09

Hazard ratios were similar when femoral neck BMD was added to the model.

We found that high dietary protein may be associated with reduced risk of hip fracture in elderly men and women, but our study had limited power. Larger studies are needed to confirm this finding in elders.

**Disclosures:** D. Misra, None.

This study received funding from: NIH (RO1 AR 053205)/HRSA (5 T32 GM12453-03).

## SU320

**Costs Associated with Non-hip, Non-vertebral (NHNV) Fractures in a Managed Care Setting.** K. Foley<sup>\*1</sup>, N. Shi<sup>\*1</sup>, G. Lenhart<sup>\*1</sup>, E. Badamgarav<sup>\*2</sup>.

<sup>1</sup>Thomson Healthcare, Cambridge, MA, USA, <sup>2</sup>Global Health Economics, Amgen Inc., Thousand Oaks, CA, USA.

NHNV fractures are the most common fractures, occurring 11 times more frequently in patients aged 50-64 yrs than in those aged ≥ 65 yrs. NHNV fractures are often followed by subsequent fractures at the same or new skeletal sites. To determine the economic and clinical burden associated with NHNV fractures, a retrospective claims analysis was conducted to evaluate rates of subsequent fractures following an initial NHNV fracture and associated incremental costs in a managed care setting.

Fully adjudicated medical claims from a research database were used to identify patients aged ≥ 50 yrs with a closed hip, vertebral, or NHNV fracture (including distal femur, pelvic, humerus, wrist, clavicle, and leg) between 07/01/2001 and 12/02/2004. The first observed fracture was the index fracture. Patients were continuously enrolled 6 mos before and 12 mos after the index fracture. A 1:1 control group was selected for each fracture category by matching on age, gender, region, and diagnostic cluster score ± 3 points. Subsequent new-site fractures were identified by ICD-9 codes; subsequent same-site fractures were identified by 2 consecutive fracture claims with same diagnosis ≥ 180 days apart. Multivariate regression modeling controlled for potential residual confounding factors. Incremental direct medical costs of NHNV fractures (fracture group minus control) in the 12 mos after the index fracture were estimated.

NHNV fractures occurred in 27,424 of 33,233 fracture patients aged 50-64 yrs and 40,690 of 73,945 fracture patients aged ≥ 65 yrs. Mean (SD) ages were 58.7 (4.0) yrs and 79.9 (7.5) yrs, respectively. The average adjusted incremental per-fracture cost associated with individual NHNV fractures was \$9,183 for patients aged 50-64 years and \$6,106 for patients aged ≥ 65 yrs. Overall, 31.3% of patients aged 50-64 yrs and 34.9% of patients aged ≥ 65 yrs had subsequent fractures within 12 mos of the index fracture. Subsequent fractures were associated with a 3-fold increase in incremental annual costs compared with initial fractures (Table).

Annual Incremental Cost of NHNV Fracture Treatment				
	Patients Aged 50-64 Years (N=27,424)		Patients Aged 65+ Years (N=40,690)	
	N	Incremental Cost	N	Incremental Cost
Annual cost of single NHNV fracture without a subsequent fracture	18,847	\$5,654	26,622	\$3,479
Annual cost of NHNV fracture with subsequent fractures	8,577	\$16,919	14,068	\$11,008

NHNV fractures are prevalent and can pose a substantial economic burden for managed care plans. NHNV fractures occur early in disease progression and more frequently in younger patients. This analysis suggests that avoiding initial fractures may be a factor in decreasing the rate of subsequent fractures and associated costs.

**Disclosures:** K. Foley, Amgen Inc. 3.

This study received funding from: Amgen Inc.

## SU321

**"Pathologic" Fractures: To Include or Exclude?** J. R. Curtis<sup>1</sup>, D. J. Becker<sup>\*2</sup>, M. Kilgore<sup>\*2</sup>, L. C. Gary<sup>\*2</sup>, R. Matthews<sup>\*3</sup>, M. A. Morrissey<sup>\*2</sup>, N. Patkar<sup>\*1</sup>, K. G. Saag<sup>1</sup>, A. H. Warriner<sup>\*4</sup>, E. Delzell<sup>\*3</sup>. <sup>1</sup>Division of Rheumatology, University of Alabama at Birmingham, Birmingham, AL, USA, <sup>2</sup>Department of Health Care Organization and Policy, University of Alabama at Birmingham, Birmingham, AL, USA, <sup>3</sup>Department of Epidemiology, University of Alabama at Birmingham, Birmingham, AL, USA, <sup>4</sup>Division of Endocrinology, Diabetes and Metabolism, University of Alabama at Birmingham, Birmingham, AL, USA.

**Introduction:** Analyses of osteoporosis-related fractures that use administrative claims data often exclude pathologic fractures (ICD-9 code 733.1x) due of concern that these are caused by a malignancy. We examined pathologic fracture diagnoses of the vertebrae and hip to evaluate their impact on fracture incidence estimates and to determine whether there was evidence for a malignancy.

**Methods:** We studied U.S. Medicare beneficiaries age ≥ 65 with part Medicare A+B and not HMO coverage with new fractures following a 12-month "clean" period with no fracture diagnoses. The ICD-9 diagnosis codes used were 733.13 (pathologic vert) and 805.2, 805.4 and 805.8 (non-pathologic vert); and 733.14 (pathologic hip) and 820.0, 820.2 and 820.8 (non-pathologic hip). We further examined the proportions of people with ≥ 1 inpatient or physician diagnosis of a malignancy in the prior year or 1 month following the fracture.

**Results:** We identified 69,867 individuals with a vertebral fracture diagnosis. Median age was 78 years; 77% women, 95% white. The proportion of persons with pathologic fracture diagnoses only, non-pathologic diagnoses only, and both are shown (Table). Each of these three groups constituted approximately one-third of fracture cases; the proportion with evidence for malignancy was approximately equal.

There were 90,039 persons with a hip fracture; median age was 80 years; 78% women, 93% white. Persons with pathologic fracture diagnoses accounted only for 1% of all hip fractures; the proportion of these with evidence for a malignancy was higher (51%) than for people with only non-pathologic hip fracture diagnoses (26%).

**Conclusion:** Among U.S. Medicare beneficiaries, only one-third to one-half of people with a pathologic fracture diagnosis of the vertebrae or hip had evidence for a malignancy. Particularly for vertebral fractures, excluding persons with pathologic fractures in epidemiologic analyses that utilize administrative claims data substantially underestimates the burden of fractures due to osteoporosis.

	Pathologic Diagnoses Only	Non-pathologic Diagnoses Only	Both Diagnoses
Spine (% of total spine fractures)	30	38	32
Proportion of these persons with ≥ 1 claim for malignancy	32	28	32
Hip (% of total hip fractures)	1	95	4
Proportion of these persons with ≥ 1 claim for malignancy	51	26	44

**Disclosures:** J.R. Curtis, Roche, UCB, Proctor & Gamble 2; Merck, Proctor & Gamble, Eli Lilly, Roche, Novartis 1; Novartis, Amgen, Merck, Proctor & Gamble, Eli Lilly, Roche 3.

This study received funding from: Amgen, Inc, National Institutes of Health (AR053351, AR052361), and the Arthritis Foundation (JRC).

## SU322

**Prevalence of Vertebral Fractures in Aging Women Suffering from Hip Fracture.** M. Sosa<sup>1</sup>, Working Group on Osteoporosis<sup>\*2</sup>. <sup>1</sup>Medicine, University of Las Palmas de GC and Hospital University Insular, Las Palmas de Gran Canaria, Spain, <sup>2</sup>Osteoporosis Working Group, Sociedad Española de Medicina Interna, Spain.

**Background.** Fractures are the clinical complication of osteoporosis. There are no previous studies that describe the prevalence of vertebral fractures (VF) in patients admitted into a hospital due to a hip fracture (HF).

**Objective.** To study the prevalence of vertebral fractures in elderly women in the moment of their admission to the hospital due to a hip fracture.

**Method.** This is a cooperative, multicentric, case control study, performed in 21 different hospitals of Spain by the Working Group on Osteoporosis of the Spanish Society of Internal Medicine. A total of 143 elderly women with hip fractures comprised the case group. The control group consists of 138 elderly women admitted into other wards of the hospital due to other diseases with no relationship with osteoporosis. A questionnaire was administered and a lateral thoracic and lumbar X-ray was performed to assess vertebral fractures applying Genant's criteria.

**Results.** The mean age of the patients with HF was 79.8 ± 6.9 years and the mean age of the controls was 77.7 ± 8.9 years. Patients suffering from HF had less weight than controls (BMI: 25.9 ± 4.4 g/m<sup>2</sup> vs 27.7 ± 5.2 kg/m<sup>2</sup>, p = 0.002). Prevalence of VF was 62.6% in patients with HF, and 50% in controls (p = 0.039).

## ASBMR 30th Annual Meeting

Basal characteristics of the population studied			
	Hip fracture n= 143	Controls n= 129	p value
Age (years)	79.8 (6.9)	77.7 (8.9)	0.03
Weight (Kg)	63.5 (12.1)	67.0 (12.9)	0.02
Height (cm)	156.4(8.1)	155.5 (7.3)	0.33
BMI (Kg/m <sup>2</sup> )	25.9 (4.4)	27.8 (5.2)	0.002
Arm span (cm)	150.1 (16.0)	151.0 (10.4)	0.586

Comparison of some risk factors between hip fracture and controls				
	Hip fracture	Controls	p value	OR (95% CI)
Actual tobacco use	6.3%	7.2%	0.763	0.866 (0.341; 2.201)
Actual alcohol consumption	5%	5.8%	0.769	0.855 (0.302; 2.426)
Use of statins	18.9%	28.1%	0.081	0.597 (0.334; 1.068)
Use of hypnotics	42.3%	29.7%	0.029	1.731 (1.056; 2.837)
Previous falls	42.4%	38.8%	0.540	1.163 (0.717; 1.886)
Maternal history of Hip fracture	6.6%	5.6%	0.732	0.195 (0.431; 3.310)
Prevalence of vertebral fractures	62.6%	50.0%	0.039	1.673 (1.025; 2.731)

Conclusions. Elderly women admitted to a hospital due to hip fracture have a very high prevalence of previously undiagnosed VF. Indeed, elderly women admitted into the hospital because of other diseases also have a high prevalence of VF. These facts must be taken into account due to the morbidity and mortality of VF, that increases the HF morbidity and mortality.

**Disclosures:** M. Sosa, None.

## SU323

**Poor Peripheral Sensorimotor Nerve Function Is Associated with High Fall Risk.** K. A. Faulkner<sup>1</sup>, E. S. Strotmeyer<sup>1</sup>, S. Zivkovic<sup>\*2</sup>, J. Verghese<sup>\*3</sup>, J. Van Swearingen<sup>\*2</sup>, S. Studenski<sup>\*2</sup>, J. A. Cauley<sup>1</sup>. <sup>1</sup>Epidemiology, University of Pittsburgh, Pittsburgh, PA, USA, <sup>2</sup>University of Pittsburgh, Pittsburgh, PA, USA, <sup>3</sup>Albert Einstein College of Medicine, Bronx, NY, USA.

It is not known whether poor subclinical peripheral nerve function predicts falls. Participants were 377 community-dwelling men (mean age=76.8 years, SD=4.9), who were enrolled in the Osteoporotic Fractures in Men Study at the Pittsburgh clinic. Subclinical was defined as meeting electrodiagnostic criteria without clinical signs or symptoms. Electrophysiologically-detected peripheral nerve conduction was measured at the non-dominant sural sensory nerve (SNAP=amplitude in uV and DSL=distal sensory latency in ms) and bilaterally at the deep peroneal motor nerve (CMAP=amplitude in mV and DML=distal motor latency in ms) using the NC-stat® (NeuroMetrix, Inc.). DSL was available in 305 men with valid SNAP. Clinical signs, including loss of 10g monofilament detection on the worse toe and open sores, and 3 symptoms of peripheral neuropathy were assessed. Number of falls in two subsequent years were self-reported in postcard mailings every 4 months. Multivariate-adjusted (see footnote) Relative Risks of falling (RR) were calculated using Poisson regression models. The average fall rate during the study was 50.8/100 man-years. Fall rates were 113-486% higher among men in the middle and worst tertiles of non-dominant side DML compared to men in the best tertile (Table). Middle and worst tertiles of dominant-side DML were associated with 11-41% higher fall rates compared to men in the best tertile. Fall rates were 41% higher among men in the middle tertile of DSL compared to men in the best tertile. Among 210 men without clinical signs or symptoms, associations of poor dominant and non-dominant side DML and fall rates remained. Middle and worst tertiles non-dominant-side DML RRs were 5.69 (95% CI:3.40-9.53) and 2.13 (95% CI:1.23-3.72) and middle and worst tertiles dominant-side DML tertiles were 2.07 (95% CI:1.31-3.28) and 2.84 (95% CI:1.76-4.61), respectively (data not shown).

Table. Relative risks of falls (95%CI)\* according to tertile of peripheral nerve conduction, N=377.

	Best Tertile	Middle Tertile	Worst Tertile	P-Value
CMAP amplitude, non-dominant side	1.00 (Referent)	0.94 (0.73-1.21)	0.86 (0.66-1.12)	0.55
CMAP amplitude, dominant side	1.00 (Referent)	1.33 (1.01-1.77)	1.10 (0.83-1.47)	0.10
DML, non-dominant side	1.00 (Referent)	5.68 (3.40-9.53)	2.13 (1.23-3.72)	<.001
DML, dominant side	1.00 (Referent)	1.11 (0.84-1.48)	1.41 (1.08-1.84)	0.03
SNAP amplitude, non-dominant side	1.00 (Referent)	1.16 (0.87-1.55)	1.27 (0.95-1.70)	0.26
DSL, non-dominant side	1.00 (Referent)	1.40 (1.04-1.88)	1.04 (0.76-1.42)	0.05

\* Adjusted for age, height, muscle area, fat mass, diabetes, depressive symptoms, visual acuity, cognitive function (Teng 3MS), physical activity, use of anti-anxiety & antidepressant medications, use of anticonvulsants, dizziness, smoking, and alcohol consumption

Poor peripheral nerve function, particularly motor, is associated with high fall risk in older community-dwelling men, even in men without signs or symptoms of peripheral neuropathy. Electrodiagnostic evidence of poor peripheral nerve function may help us to identify older men at high fall risk.

**Disclosures:** K.A. Faulkner, None.

This study received funding from: Neurometrix, Inc.

## SU324

**8 year Fracture & Mortality Outcomes of the Fracture Liaison Service That Provides Systematic Assessment for Prevention of Secondary Fractures to All Patients Age 50+ With New Low-trauma Fractures.** A. R. McLellan, M. Fraser<sup>\*</sup>. Medical Sciences, Western Infirmary, Glasgow, United Kingdom.

This study reports secondary fracture incidence & mortality in patients who, after presenting with a new fracture, were routinely offered assessment to reduce the incidence of

secondary fractures, during the first 8yr of the Fracture Liaison Service (FLS).

Cox proportional hazards was used to calculate hazard ratios & 95% CI for risk factors for occurrence of secondary fractures & mortality. 7505 women, age (mean(SD)) 73.3(12)yr & 2180 men, age 68.8(11.7)yr, with 11096 consecutive new low-trauma fracture presentations were assessed; index fractures were of radius/ulna, hip, humerus, ankle, hand/foot & 'other sites' in 29%, 24%, 13%, 9%, 10% & 15% resp. All were offered post-fracture assessment; 88% underwent assessment but 12% were too unwell or refused. 31% were treated with bisphosphonate (& calcium/vitD), 24% with calcium/vitD, 4% with other treatments & 41% received no treatment (incl. those who were unwell or refused).

11% sustained ≥1 further fracture: of these, 21% occurred within 6months(mo.) of the index fracture, and 35% & 58% occurred within 12 & 24mo. After adjustment for gender, cumulative fracture history, socioeconomic status, alcohol intake, femoral neck (FN) T-score & site of index fracture, treatment with bisphosphonates was associated with reduced HR for secondary fracture (0.64 (0.51 to 0.80)); this was not seen for other treatment groups. Occurrence of secondary fractures was associated with greater cumulative fracture history e.g. 1, 2 or 4 fractures were associated with HR (95%CI) of 2.24 (1.02 to 4.91), 3.05 (1.35 to 6.90) & 3.70 (1.37 to 11.49), with alcohol excess (1.84 (1.42 to 2.39)), socioeconomic deprivation (most v least deprived) (1.40 (1.13 to 1.74)), site of original fracture - in particular, the group of 'other sites' (1.33(1.03 to 1.72)) & FN T-score (0.68 (0.61 to 0.74)).

20% of patients died: 41% of these died within first 12mo. of index fracture. Male gender was associated with doubling of mortality risk (2.03 (1.66 to 2.48)). Mortality risk was also associated with age (1.07(1.06 to 1.08)), FN T-score (0.77 (0.70 to 0.84)), smoking (1.67 (1.38 to 2.03)), alcohol excess (1.61 (1.22 to 2.11)), socioeconomic deprivation (most v least deprived) (1.43 (1.14 to 1.80)) & whether the index fracture was managed as an inpatient (v outpatient) (1.26 (1.06 to 1.50)).

A systems-based approach, such as our FLS, can achieve delivery of routine post-fracture assessment for fracture secondary prevention in 88% of patients with new fractures. Use of bisphosphonates protects against secondary fractures. Groups at greater risk of secondary fractures & mortality have been identified; the remaining challenge is how their outcomes can be improved.

**Disclosures:** A.R. McLellan, None.

## SU325

**Trauma Type of Non-hip, Non-vertebral Fractures in Postmenopausal Women Being Treated for Osteoporosis in Europe.** C. Roux<sup>1</sup>, C. Cooper<sup>2</sup>, S. Ortolani<sup>3</sup>, A. Díez-Pérez<sup>\*4</sup>, R. Horne<sup>\*5</sup>, N. Franchimont<sup>6</sup>, V. Easton<sup>\*7</sup>, N. Freemantle<sup>\*8</sup>. <sup>1</sup>Département de Rhumatologie B, Hospital Cochin, Paris, France, <sup>2</sup>MRC Epidemiology Resource Centre, University of Southampton, Southampton, United Kingdom, <sup>3</sup>Istituto Auxologico Italiano, Milan, Italy, <sup>4</sup>Dept. de Medicina, Hospital del Mar, Barcelona, Spain, <sup>5</sup>Practice & Policy, The School of Pharmacy, University of London, London, United Kingdom, <sup>6</sup>Amgen (Europe) GmbH, Zug, Switzerland, <sup>7</sup>Biostatistics, Amgen Ltd, Cambridge, United Kingdom, <sup>8</sup>University of Birmingham, West Midlands, United Kingdom.

Recent evidence challenged the notion that fractures due to high trauma are not osteoporotic fractures (JAMA 2007;298(20):2381). We examined this assertion by analyzing fracture history data from 2117 European women being treated with active osteoporosis treatments who are enrolled in an ongoing study. The Prospective Observational Scientific Study Investigating Bone Loss Experience in Europe (POSSIBLE EU<sup>®</sup>) is being conducted in primary care centers in France, Germany, Italy, Spain and the United Kingdom. Fracture history data were collected at study start. Physicians coded all fractures according to 22 different locations (or Other and Unknown). Fractures, excluding those of the face, skull, fingers or toes, are described and characterized by location (hip, vertebral, and nonhip/nonvertebral [NHNV]), type of trauma according to physician (major: falling off ladder to car accident; minor: no to mild trauma), and timing of fracture relative to reported age at menopause (pre- vs post-menopausal). These women had a median age of 69 years (median time since menopause, 20 years). Of 859 women who had experienced fractures, 577 (67%) and 281 (33%) had 1 and ≥ 2 fractures, respectively. Of 1291 reported fractures, most (71%) were NHNV, versus 22% vertebral and 7% hip; most occurred after menopause (Table). 25-39% of postmenopausal fractures occurred after major trauma (Table).

Table. Summary of Fracture Type by Trauma Type

Fracture Type	Trauma Type According to Physician	Number of Premenopausal Fractures	Number of Postmenopausal Fractures
Hip	Minor	2	48
	Major	1	29
Spine	Minor	1	166
	Major	6	54
NHNV	Minor	76	414
	Major	61	254

Note: 105 fractures had missing data related to date of menopause, trauma type or location

In summary, based on interim results from this study of postmenopausal women receiving active osteoporosis treatment, NHNV fractures are common, but occur more frequently after menopause. Actual relatedness of fractures to trauma may be questioned, especially as perception of trauma may be affected by patient age. These results suggest that the notion of attributing fracture to a trauma type may be non-essential in the osteoporosis population.

**Disclosures:** C. Roux, Amgen Ltd 4.

This study received funding from: Amgen Ltd.



## SU326

**High Mortality in Male Nursing Home Residents with Hip Fracture.** S. D. Berry, E. J. Samelson, M. Bordes\*, K. E. Broe, D. P. Kiel. Heb SenLife, Boston, MA, USA.

Prior studies have demonstrated mortality following a hip fracture is greater in men compared to women. It remains unclear whether this gender difference is independent of pre-fracture characteristics or peri-operative and post-fracture complications, especially among frail elders. Therefore, our study is the first to compare all-cause mortality in male and female nursing home residents with a hip fracture. We also examined whether specific peri-operative and post-fracture complications predict mortality in this frail population. Participants included 196 residents (154 women, 42 men) of Hebrew Rehabilitation Center, a 725-bed long-term care facility in Boston, MA, who experienced a hip fracture between 1999-2006 and were followed until death, relocation, or June 30, 2007. Hip fractures were identified by federally mandated incident reports, and vital status was determined from an administrative database. Fractures and deaths were confirmed by medical records. Pre-fracture characteristics including age, sex, functional status (ADL short scale), dementia (Cognitive Performance Scale), co-morbidities (anemia, arrhythmia, coronary disease, congestive heart failure (CHF), cancer, diabetes, emphysema) and BMI (kg/m<sup>2</sup>) were collected from the Minimum Data Set, a federally mandated assessment of nursing home residents. Peri-operative complications (Acute Myocardial Infarction, CHF, delirium, and infection) and 6-month post-operative complications (delirium, pressure ulcer, pneumonia, and UTI) were determined from physician notes. We examined the bivariate association between each peri-operative and post-fracture complication and mortality individually using Cox proportional hazards models. Variables that were significant at  $p \leq 0.1$  and pre-fracture characteristics were included in multivariate models. The mean age of participants was 89.0 yrs ( $\pm 6.3$  yrs). During a median follow-up of 1.3 yrs, 146 participants (112 women, 34 men) died. In multivariate models, male residents were twice as likely to die compared to females (HR=1.9, 95% CI 1.2, 3.0). Post-operative complications of pressure ulcer and pneumonia were associated with a 70% increase in mortality in men and women (combined results: pressure ulcer, HR=1.7, 95%CI 1.2, 2.6; pneumonia, HR=1.7, 95% CI 1.1, 2.7). Individual peri-operative complications were not associated with mortality, nor were the 6-month complications of delirium and UTI. In conclusion, male nursing home residents with a hip fracture had greater mortality compared to females, even after accounting for pre-fracture status, peri-operative complications, and post-fracture complications. Post-fracture prevention of pressure ulcers and timely treatment of pneumonia may help to reduce mortality in this frail population.

**Disclosures:** S.D. Berry, None.

## SU327

**Incidence and Costs of Proximal Humerus and Wrist Fractures in Women in France.** M. Maravic\*<sup>1</sup>, P. Taupin\*<sup>2</sup>, P. Landais\*<sup>2</sup>, C. Roux<sup>3</sup>. <sup>1</sup>DIM, Hôpital Léopold Bellan, Paris, France, <sup>2</sup>SBIM, Hôpital Necker, Paris, France, <sup>3</sup>Rheumatology, Hôpital Cochin, Paris, France.

Fracture of the proximal humerus (PHF) is one of the most frequent fractures related to osteoporosis, with substantial morbidity. An increased risk of mortality has been described in the year following this fracture. The aim of this study was to describe the hospital incidence rate of PH fracture, the inpatient costs, and the outcome of these patients, as compared to patients suffering from wrist fracture (WF).

**Patients and methods:** Data are from the French National hospital database; in this database, all patients hospitalized in the country for fractures are registered. We selected in years 2002 and 2006 female patients hospitalized for medical or surgical treatment of upper humerus fracture, or distal radius fracture, and excluded patients with a concomitant diagnosis for cancer. We described the number of hospitalizations, the incidence, the type of entry and exit of hospital, and the inpatients costs in 2006.

**Results:** The data were reported in the following table.

	PHF	WF
Number of hospitalizations in 2002/2006	10 888 / 11432	30 772 / 30 889
Incidence in 2002 / 2006 *	568 / 597	1 580 / 1 613
Increase with age-group 2001 / 2006 °		
30-49	66 / 60	347 / 318
50-69	395 / 435	1 640 / 1 780
> 69 years	1 825 / 1 906	3 960 / 3 960
Entry from home (2006)	95%	97%
Outcomes (2006)		
Home	66%	90%
Rehabilitation	25%	7%
Other care	6%	2%
Living in institution	2%	1%
Death	1%	0%
Inpatients costs (euros 2006)	42 739 508	69 162 264

\*Incidence per million, °  $p < 0.0001$

**Conclusion:** In contrast to the reported data about the decrease of hip fractures incidence, the incidence of PHF and WF did not decrease in France between 2002 and 2006 in women. Whatever the type of fractures or the year studied, the incidence increased with age, stressing the role of the underlying osteoporosis. The inpatient cost was higher for PHF than for WF.

**Disclosures:** M. Maravic, None.

## SU328

**Proximal Humerus Fractures in Men. Epidemiology and Costs.** M. Maravic\*<sup>1</sup>, P. Taupin\*<sup>2</sup>, P. Landais\*<sup>2</sup>, C. Roux<sup>3</sup>. <sup>1</sup>DIM, Hôpital Léopold Bellan, Paris, France, <sup>2</sup>SBIM, Hôpital Necker, Paris, France, <sup>3</sup>Rheumatology, Hôpital Cochin, Paris, France.

In contrast to intensive research into hip and vertebral fractures, little is known about proximal humerus (PH) fractures in men. The aim of this study was to describe the incidence and cost of these fractures and short-term outcome of men with PH fractures.

**Patients and methods:** Data are from the French National hospital database; in this database, all patients hospitalized in the country for fractures are registered. We selected in years 2002 and 2006 male patients ( $\geq 30$  years) hospitalized for medical or surgical treatment of upper humerus fracture, and excluded patients with a concomitant diagnosis of cancer. We described the number of hospitalizations, the incidence in 3 aged-groups, the number of associated diagnoses, the type of entry and exit of hospital, and the inpatients cost in 2006.

**Results:** 3 689 and 3 805 fractures were registered in 2002 and 2006. The incidence rate was 216 and 223 per million in 2002 and 2006 respectively. In 2006, the incidence rate was 110, 233 and 553 in age-group 30-49, 50-69 and  $>69$  years, respectively. This incidence increased significantly with age ( $p < 10^{-4}$ ). The mean of associated diagnoses were  $1.33 \pm 1.92$ ,  $1.69 \pm 2.14$  and  $2.18 \pm 2.53$  in the 3 aged-group, respectively ( $p < 10^{-4}$ ). In 2006, 96% of patients came from home; however, only 74% returned home directly, 17% were transferred to rehabilitation centre, 7% to other type of care, 1% in institution and 1% died. The inpatients costs in 2006 was 14 564 849 euros.

**Conclusion:** The incidence of PH in men did not decrease between 2002 and 2006. The increase with age, especially in the age group upper 69 years, outlined the role of underlying osteoporosis. This increased incidence had consequences in terms of inpatients costs.

**Disclosures:** M. Maravic, None.

## SU329

**Clinical Outcome in Elderly with Proximal Femur or Humerus Fractures in an Orthogeriatric Rehabilitation Unit.** G. A. Carmona\*, R. Rizzoli, P. Ammann. Division of Bone Disease, WHO Collaborating Centre, Dpt of Rehabilitation and Geriatrics, Geneva University Hospitals/Faculty of Medicine, Switzerland.

Benefits of orthogeriatric intervention in recovery following a fracture of the proximal femur in the elderly are well documented. Whilst fractures of the proximal humerus are associated with a marked decrease in functional independence, the influence of orthogeriatric intervention in elderly who have sustained a proximal humerus fracture is still poorly documented. We performed a retrospective observational study in patients admitted to an orthogeriatric unit between 2002 and 2006, for a hip fracture (HIP#, n=291) or proximal humerus fracture (HUM#, n=73). The rehabilitation program, administered by an interdisciplinary team, integrated walking/balance exercises, muscle strengthening and daily life-training activities. Functional capacity during rehabilitation was evaluated by the Functional Independence Measure (FIM) score at admission (median: 11 days after fracture), after two weeks, and just prior to discharge (median: 33 days observation time). To further evaluate functional outcomes, we separated the functional motor items (MOTOR FIM) into upper and lower limb items (UPPER and LOWER FIM). Values are means  $\pm$  SD and differences were tested using Students' t-test. At admission, age and all motor functional independence scores were significantly higher in patients with HIP# vs. HUM# (83.3  $\pm$  7 vs. 81.5  $\pm$  7 yrs,  $p=0.04$ ; MOTOR FIM: 38.2  $\pm$  11 vs. 33.6  $\pm$  11,  $p=0.002$ ; UPPER FIM: 18.9  $\pm$  4 vs. 12.8  $\pm$  4,  $p<0.0001$  and LOWER FIM: 16.6  $\pm$  6 vs. 12.9  $\pm$  4,  $p<0.0001$ ). At discharge, there was a significant overall gain with HIP# and HUM# (FIM: 24.1  $\pm$  16 vs. 25.9  $\pm$  13,  $p=0.4$ ; MOTOR FIM: 20.6  $\pm$  12 vs. 23.3  $\pm$  11,  $p=0.12$ ; UPPER FIM: 5.3  $\pm$  5 vs. 8.7  $\pm$  5,  $p<0.0001$  and LOWER FIM: 6.5  $\pm$  5 vs. 9  $\pm$  5,  $p<0.0001$ ). For upper and lower limbs the gain was significantly higher for HUM#. The kinetics of MOTOR FIM increases differed between the groups; in the HIP# the functional gain was significantly higher during the first two weeks, while those in HUM# group improved constantly throughout the observation period. Similar trends were observed for the other parameters tested. A functional performance gain was observed for both types of fracture independently of cognitive status (Mini-Mental State score of less or more than 24). This study indicates that an orthogeriatric rehabilitation program improves the functional performance of elderly who have sustained hip or humerus fractures independently of cognitive level. The kinetics of these positive effects differ in the second half of the recovery period with an increase significantly higher in humerus fractured patients.

**Disclosures:** G.A. Carmona, None.

## SU330

**Evaluation of Bone Mineral Density Following an Education Intervention on Osteoporosis Offered to Women after a Fragility Fracture.** L. Bessette<sup>1</sup>, J. P. Brown<sup>1</sup>, S. Jean<sup>\*2</sup>, S. K. Davison<sup>1</sup>, M. Beaulieu<sup>\*3</sup>, M. Baranci<sup>\*4</sup>, L. Ste-Marie<sup>5</sup>. <sup>1</sup>CHUL Research Centre, Quebec, QC, Canada, <sup>2</sup>Institut national de santé publique du Québec, Quebec, QC, Canada, <sup>3</sup>Merck Frosst, Kirkland, QC, Canada, <sup>4</sup>sanofi-aventis, Laval, QC, Canada, <sup>5</sup>University of Montreal, Montreal, QC, Canada.

The objective of this analysis was to evaluate the rate of bone mineral density (BMD) testing by dual-energy x-ray absorptiometry (DXA) 12 months following an osteoporosis (OP) education intervention offered to women  $\geq 50$  years who suffered a fragility fracture within the past year.

Three educational tools were developed: a 15-minute video, written material on OP targeted to the participants, and written documentation on OP targeted to physicians. Information was based on the 2002 Clinical Practice Guidelines for the Diagnosis and Management of Osteoporosis in Canada. Six to eight months after the fracture event, women who suffered a fragility fracture were contacted by phone and offered to be randomized into one of three educational groups: A) The control group (no intervention); B) the documentation group (written documents for the participants and the physician); or C) the video group (both the video and the documentation for the participants and the physician). Women randomized into groups B and C were invited to consult their treating physician with the written documentation. The BMD testing rate was evaluated during a phone interview 12 months after the intervention. The current analysis was completed only with participants who had no diagnosis and treatment for OP at randomisation.

Of 894 women, 850 (95%) accepted to be randomized. Of these, 546 (64%) (mean age: 61.7 years) were without OP diagnosis and treatment. Ninety-six percent of these 546 women were contacted and completed the phone questionnaire 12 months after randomization. In group B, 84% read the document and 58% gave the document to their physician. In group C, 87% read the document and/or saw the video and 61% transmitted the document to their physician. The BMD testing rates 12 months after the intervention were 24% in group A compared to 32% in both groups B and C. For the women randomized to one groups B and C, 60% consulted their physicians with the Osteoporosis Canada Guidelines for the Diagnosis, Prevention and Treatment of Osteoporosis. When isolating those participants randomized to both groups B and C and who consulted their treating physician with the documents, the BMD testing rate increased to 40%.

An intervention targeting the patient increased the rate of BMD testing in the group of participants who provided this documentation to their doctors.

**Disclosures:** L. Bessette, Procter & Gamble, Sanofi-Aventis 1, 3; Merck Frosst 1, 3; Amgen 1, 2, 3; Pfizer 1, 2, 3.

This study received funding from: Merck Frosst, Procter & Gamble, sanofi-aventis, Eli Lilly, Novartis.

## SU331

**Genome-wide Association Study Identified RTP3 as a Novel Gene for Bone Strength.** L. Zhao<sup>1</sup>, X. Liu<sup>\*2</sup>, Y. Liu<sup>\*2</sup>, L. Wang<sup>\*3</sup>, Y. Liu<sup>\*2</sup>, H. Yan<sup>\*3</sup>, J. Liu<sup>\*2</sup>, D. Xiong<sup>\*1</sup>, F. Pan<sup>\*3</sup>, Z. Tang<sup>\*4</sup>, T. Yang<sup>\*3</sup>, X. Chen<sup>\*4</sup>, Y. Guo<sup>\*3</sup>, S. Lei<sup>\*4</sup>, R. R. Recker<sup>1</sup>, H. Deng<sup>2</sup>. <sup>1</sup>Osteoporosis Research Center, Creighton University Medical Center, Omaha, NE, USA, <sup>2</sup>School of Medicine, University of Missouri - Kansas City, Kansas City, MO, USA, <sup>3</sup>School of Life Science and Technology, Xi'an Jiaotong University, Xi'an, China, <sup>4</sup>Laboratory of Molecular and Statistical Genetics, College of Life Sciences, Hunan Normal University, Changsha, China.

Femoral bone geometry is an important determinant of bone strength and predictor of hip fracture, the most severe osteoporotic fracture. Genome-wide association has been approved to be an efficient and feasible approach to identify genetic factors for complex disorders. Here we report the first genome-wide association study on femoral bone geometry, examining ~500,000 SNPs in 1,000 Caucasians. A common variant rs7430431 in the RTP3 (receptor transporting protein 3) gene was identified in strong association with BR (buckling ratio) ( $P=1.61E-07$ ), an index for bone structural instability, and CT (cortical thickness) ( $P=1.92E-06$ ). Haplotype analysis indicated that the block containing rs7430431 had highly suggestive association with BR ( $P=5.76E-05$ ). Subjects carrying the C allele of rs7430431 had, on average, 9.8% higher BR than those carrying the alternative T allele ( $P=3.00E-05$ ), thus suffering higher hip fracture risk. In addition, most SNPs of the RTP3 gene achieved highly suggestive association with both BR and CT ( $P \leq 0.001$ ). To verify our findings in another ethnic group and to assess the relevance of the RTP3 gene to hip fracture risk, we tested the association of the SNPs of the RTP3 gene with osteoporotic hip fracture in a Chinese sample composed of 360 hip fracture patients and 340 healthy controls. Significant association ( $P=0.001$  and  $P=0.003$ ) between two SNPs (rs10514713 and rs883739) of the gene and hip fracture was found and hence substantiated the importance of RTP3 to bone strength. These observations, combined with potential functional relevance of RTP3 to bone development, suggest that RTP3 is a novel candidate gene for bone strength.

**Disclosures:** L. Zhao, None.

## SU332

**Recognition and Treatment of Male Osteoporosis is Low.** J. LaFleur<sup>\*1</sup>, C. McAdam-Marx<sup>\*1</sup>, S. Pickard<sup>\*2</sup>, J. Nebeker<sup>\*2</sup>. <sup>1</sup>Department of Pharmacotherapy, University of Utah, Salt Lake City, UT, USA, <sup>2</sup>Division of Clinical Epidemiology, University of Utah, Salt Lake City, UT, USA.

**Background:** The prevalence of osteoporosis among males over age 50 in the US ranges from 3% of Hispanics and 4% of Blacks to 7% of White and Asian men. The expected rate of fragility fractures for males over age 50 is 25% in their remaining lifetimes. In secondary osteoporosis, bisphosphonates have been shown to reduce the risk of these fractures by 67-81%.

**Purpose:** The purpose of this analysis was to characterize the disease burden of osteoporosis and fragility fractures, treatment rates, and the prevalence of risk factors in male veterans.

**Methods:** We used Veterans Health Administration clinical datasets for veterans treated in the US rocky mountain region to create a cohort of males over the age of 49 who received care during the calendar years of 2005 and 2006. We identified the proportions of patients with documented osteoporosis or fragility fracture and, of those, the proportions who were treated and untreated. The prevalence of well-known clinical risk factors and their associated fracture rates were also documented.

**Results:** 115,012 males age 50 and over received care. The mean age of the cohort was 67.1 (SD 10.6). Among the 38% with recorded race information, 92.7% were Caucasian. Among the 74% with recorded body mass index (BMI), 3.6% were underweight and 30.6% were normal weight. An osteoporosis diagnosis was reported in only 1.9% of patients. The prevalence of fragility fracture during the two-year period was 1.3%. Among those that had a fragility fracture, only 6.3% had a prescription for an oral bisphosphonate, compared to 74.0% of patients with a documented osteoporosis diagnosis.

Overall, the incidence of fracture over a median follow-up of 2.8 years was 2.1/1000 person-years (PY). The incidence was increased significantly in patients with a prior vertebral fracture (83.0/1000 PY,  $p<0.001$ ), hip fracture (76.1/1000 PY,  $p<0.001$ ), or wrist fracture (59.7/1000 PY,  $p<0.001$ ). The incidence was lower in patients being treated with a bisphosphonate (7.3/1000 PY) compared to patients with untreated osteoporosis (43.7/1000 PY,  $p=0.048$ ).

**Conclusions:** In the rocky mountain region, the proportion of male veterans diagnosed with osteoporosis is less than a third of the national rate, suggesting low levels of recognition. Moreover, only a small fraction of veterans with fragility fractures appear to be receiving oral bisphosphonates, the current standard of care for men.

**Disclosures:** J. LaFleur, NPS Pharmaceuticals 3; Sanofi Aventis 2.

## SU333

**Changes in Histomorphometric Parameters after Menopause: A Prospective Study.** L. A. G. Armas, J. M. Lappe, R. R. Recker. Osteoporosis Research Center, Creighton University, Omaha, NE, USA.

Menopause is the event in women's lives most closely linked to bone loss and subsequent risk of osteoporosis and attendant fractures late in life. This study was designed to determine bone tissue- and cell- level changes in bone remodeling that occur with rapid bone loss at menopause.

Fifty healthy premenopausal white women (mean age  $49.4 \pm 1.9$  yrs) had a transilial bone biopsy after tetracycline labeling on entry into study and returned for a 2<sup>nd</sup> biopsy 12 months after their last menses. The biopsy specimens were fixed, embedded, sectioned, and evaluated. Measured and calculated variables in trabecular bone histomorphometry used here are described by Parfitt.

Analysis of within-subject change in variables in the 50 women who experienced normal menopause was done by paired t-test. Structural variables were not significantly different between pre and post menopausal females except osteoid volume was significantly higher in the postmenopausal females. Most of the surface based data (eroding surface (ES/BS), osteoclast surface (OcS/BS), osteoblast surface (ObS/BS), mineralizing surface (MS/BS), and mineral apposition rate (MAR)) were significantly higher in the postmenopausal women.

The dynamic variables were calculated based on perimeter measurements that included double label plus half the single label. The bone formation rate and activation frequency (AcF) were higher in postmenopausal females. The formation period (FP), remodeling period (RmP), mineralization lag time (Mlt), and off time (OfT) was shorter for postmenopausal women.

The changes in dynamic variables seen by histomorphometry during menopause reflect the increased rate of bone remodeling during estrogen deficiency.

Table 1 Dynamic data (based on double label plus half single label surface)

Variable	N	Premenopausal Median CI)	Postmenopausal Median CI)	Paired T test P value
BFR/BV %/yr	48	6.6 (0.84 - 23.6)	13.4 (3.2 - 39.5)	0.0001
FP yr	48	0.76 (0.16 - 6.3)	0.37 (0.17 - 1.6)	0.001
RP yr	48	0.14 (0.02 - 1.7)	0.14 (0.04 - 0.64)	NS
RmP yr	48	0.92 (0.26 - 6.8)	0.53 (0.22 - 2.2)	0.002
Mlt days	48	48.6 (6.4 - 213.2)	26.2 (10.8 - 89.1)	0.001
OfT days	48	-19.5 (-309.1 - - 2.3)	-13.1 (-95.5 - -2.8)	0.013
AcF /yr	48	0.13 (0.02 - 0.46)	0.24 (0.04 - 0.73)	0.0001

**Disclosures:** L.A.G. Armas, None.

This study received funding from: NIH grant AR 39221.

## SU334

**Predictive Capacity of Biochemical Markers of Bone Turnover and Endogenous Hormones for Osteoporosis in Men: Ten-year Follow-up of a Japanese Cohort.** N. Yoshimura<sup>1</sup>, H. Oka<sup>\*1</sup>, S. Muraki<sup>2</sup>, T. Akune<sup>\*2</sup>, H. Kawaguchi<sup>3</sup>, K. Nakamura<sup>3</sup>. <sup>1</sup>Dept of Joint Disease Research, 22nd Century Medical and Research Center, the University of Tokyo, Tokyo, Japan, <sup>2</sup>Dept of Clinical Motor System Medicine, 22nd Century Medical and Research Center, the University of Tokyo, Tokyo, Japan, <sup>3</sup>Dept of Orthopaedic Surgery, the University of Tokyo, Tokyo, Japan.

Although social and economic impacts of male osteoporosis (OP) are increasing worldwide, there is little understanding of the etiology or epidemiology due to the lack of longitudinal data on this disorder. This study aimed at exploration of the incidence and evaluation of the predictive capacity of biochemical markers of bone turnover (BTMs) and endogenous hormones for the male OP in residents of a rural population in Japan followed for 10 years. Two-hundred subjects aged 40-79 years with 50 men in each generation (40-49, 50-59, 60-69 and 70-79) were randomly selected in 1992 from the full list of residents born in 1913-1952. Baseline BMD of the lumbar spine and proximal femur was measured by DXA in 1993, 1996, 2000 and 2003. Serum intact OC, total OC, ALP, BAP, PICP, PINP, ICTP, serum and urinary CTX, NTX, urinary PYR, DPD, serum free testosterone (FT), estradiol and intact parathyroid hormone were measured in the initial survey. One-hundred and fifty-three out of 200 men (76.5%) who had been initially recruited completed a 10-year follow-up. Rates of change of BMD at lumbar spine and femoral neck were 0.26%/y and 0.16%/y over the first three years, and those over 10 years were 0.08%/y and -0.03%/y, respectively. Incidence of OP at the lumbar spine and femoral neck over 10 years were 23.8/10,000 person years and 17.1/10,000 person years, respectively. According to multivariate regression analysis utilizing the rate of change of BMD as an objective factor, and each BTM and endogenous hormone as an explanatory factor after adjusting for age and body mass index (BMI), the mean values of PYR and FT were significantly related to the rate of change of BMD during the first three years (PYR and BMD at lumbar spine; beta 0.20, R<sup>2</sup> 0.05, P<0.01, FT and BMD at femoral neck; beta 0.21, R<sup>2</sup> 0.05, P<0.01), while none of the values of BTMs or endogenous hormones could predict the bone loss during 10 years. Then, after the analysis of Cox proportional hazards model adjusted for age and BMI, serum levels of PINP correlated with incidence of OP at lumbar spine and FT was significantly related to incidence of OP at femoral neck (PINP vs. +1 standard deviation (SD); hazard ratio (HR) 1.86, 95% confidence interval (CI) 1.13-3.07; FT vs. +1SD; HR 0.25, 95%CI 0.08-0.80). We conclude that the serum levels of PYR and FT could be the useful predictor for bone loss within three years and PINP and FT for future occurrence of the male OP.

**Disclosures:** N. Yoshimura, None.

## SU335

**Influence of Sex Hormones on Bone Mineral Density in Middle Aged and Elderly Men.** S. R. Pye<sup>\*1</sup>, S. Boonen<sup>2</sup>, H. Borghs<sup>\*2</sup>, D. Vanderschueren<sup>2</sup>, J. E. Adams<sup>3</sup>, K. A. Ward<sup>3</sup>, G. Bartfai<sup>\*4</sup>, F. Casanueva<sup>\*5</sup>, J. D. Finn<sup>\*6</sup>, G. Forti<sup>\*7</sup>, A. Giwercman<sup>\*8</sup>, I. T. Huhtaniemi<sup>\*9</sup>, K. Kula<sup>\*10</sup>, M. Punab<sup>\*11</sup>, A. J. Silman<sup>\*1</sup>, E. C. Wu<sup>\*6</sup>, T. W. O'Neill<sup>1</sup>. <sup>1</sup>ARC Epidemiology Unit, The University of Manchester, Manchester, United Kingdom, <sup>2</sup>Katholieke Universiteit Leuven, Leuven, Belgium, <sup>3</sup>Department of Imaging Science and Biomedical Engineering, The University of Manchester, Manchester, United Kingdom, <sup>4</sup>University of Szeged, Szeged, Hungary, <sup>5</sup>University of Santiago de Compostela, Santiago de Compostela, Spain, <sup>6</sup>Department of Endocrinology, The University of Manchester, Manchester, United Kingdom, <sup>7</sup>University of Florence, Florence, Italy, <sup>8</sup>Lund University, Malmö, Sweden, <sup>9</sup>Imperial College, London, United Kingdom, <sup>10</sup>University of Lodz, Lodz, Poland, <sup>11</sup>University of Tartu, Tartu, Estonia.

Serum sex hormones particularly estrogen are known to be associated with bone mass in men. Most studies have been in cohorts of elderly men with fewer data including middle age subjects. Moreover the relative role of age related changes in total versus free or bioavailable fractions of sex hormones on bone health remains unclear. The aim of this study was to determine the influence of sex hormones on bone mineral density (BMD) in middle aged & elderly European men.

Men aged between 40 & 79 years were recruited from population registers in two European centres (Manchester, UK; Leuven, Belgium). 400 subjects (100 in each of the four decades of interest) from each centre were invited to attend for dual energy X-ray absorptiometry (DXA) of the hip & spine (Hologic QDR 4500 & Discovery). Fasting blood samples were assayed for serum testosterone (T), estradiol (E2) & sex-hormone binding globulin (SHBG) by electrochemoluminescence immunoassays (Roche Diagnostics, Germany). Free & bioavailable (bio) T & E2 levels were derived using mass action equations & association constants. Height & weight were measured in all subjects. Associations between BMD at the spine and hip and sex hormones were assessed using linear regression with adjustments for age, height, weight & centre.

753 men, mean age 60.1 years (SD=10.9) were included in the analysis. Higher levels of total E2 were associated with increased BMD at the total hip ( $\beta$  per 10 pmol/l change = 0.004; 95% CI 0.001, 0.007) & lumbar spine ( $\beta$  per 10 pmol/l change = 0.006; 95% CI 0.001, 0.010). Similar associations were observed with free & bio E2. Total T was unrelated to BMD, but higher levels of free & bio T were associated with increased BMD at the total hip ( $\beta$  per 10 pmol/l change in free T = 0.001; 95% CI 0.000, 0.003 &  $\beta$  per nmol/l change in bio T = 0.005; 95% CI 0.000, 0.010 respectively). SHBG was unrelated to BMD at any site.

In this population survey of middle aged and elderly European men, higher levels of E2 and free T were associated with increased bone mass at the hip and spine.

**Disclosures:** S.R. Pye, None.

This study received funding from: Commission of the European Communities.

## SU336

**Menopausal and Postmenopausal Women Have Significantly Higher Bone Resorption and Oxidative Stress Parameters than Premenopausal Women.**

E. S. Mackinnon<sup>\*1</sup>, A. V. Rao<sup>\*2</sup>, R. G. Josse<sup>\*1</sup>, L. G. Rao<sup>1</sup>. <sup>1</sup>Department of Medicine, St. Michael's Hospital, Toronto, ON, Canada, <sup>2</sup>Department of Nutritional Sciences, University of Toronto, Toronto, ON, Canada.

We have previously shown that oxidative stress is associated with an increased risk of osteoporosis (Osteoporos Int., 2007;18(1):109-15). Based on these results, we extended our cross-sectional study to include premenopausal, menopausal and postmenopausal women in order to confirm whether oxidative stress correlates with bone resorption and predicts the risk for osteoporosis in these women. A total of 108 women, aged 25-70, were recruited (Research Ethics Board approved, St. Michael's Hospital, Toronto). None of the participants were on medications for diabetes, high blood pressure or osteoporosis. Fasting blood samples, dietary records from the preceding seven days and the following information was collected: age, menopausal status, height, weight and blood pressure. Fasting blood samples were assayed for the bone resorption marker cross-linked aminoterminal N-telopeptide (NTx), lipid peroxidation (TBARS) and protein oxidation (where low protein thiols indicates higher oxidation). Participants were stratified into three groups: premenopausal (n=27), menopausal (n=27), and postmenopausal (n=54) women. One-way ANOVA and the Bonferroni Multiple Comparison test were used to determine differences in bone resorption and oxidative stress parameters between groups. Within groups, Pearson Correlation was used to determine whether bone resorption was associated with oxidative stress. As shown in the table below, bone resorption and oxidative stress parameters were significantly higher in menopausal and postmenopausal women than those in premenopausal women. Furthermore, a high bone resorption was significantly correlated with a lower protein thiols (higher protein oxidation) in both menopausal ( $r = -0.2711$ ,  $p < 0.05$ ) and postmenopausal women ( $r = -0.4202$ ,  $p < 0.05$ ). In conclusion, our results provide further confirmation that oxidative stress is important in the development of osteoporosis. Therapeutic agents such as the antioxidant lycopene, which can inhibit oxidative stress, may be beneficial for the prevention of osteoporosis.

Parameters	Mean $\pm$ SEM (p value vs. PR)		
	Premenopausal women (PR)	Menopausal women (M)	Postmenopausal women (PM)
NTx (nM BCE)	16.3 $\pm$ 1.0	23.8 $\pm$ 1.5 (p<0.001)	20.8 $\pm$ 1.0 (p<0.05)
Protein Thiols* ( $\mu$ M)	537.8 $\pm$ 12.3	456.2 $\pm$ 18.9 (p<0.05)	459.8 $\pm$ 15.6 (p<0.01)
TBARS (nmol/ml)	4.8 $\pm$ 0.2	7.8 $\pm$ 0.6 (p<0.001)	8.9 $\pm$ 0.3 (p<0.001)

\*low protein thiols = high protein oxidation

**Disclosures:** E.S. Mackinnon, None.

## SU337

**Bone Mineral Density and Body Composition in Postmenopausal Women with Psoriasis and Psoriatic Arthritis.** P. G. Pedreira<sup>\*</sup>, M. M. Pinheiro<sup>\*</sup>, V. L. Szejnfeld<sup>\*</sup>. Reumatology, São Paulo University, São Paulo, Brazil.

**BACKGROUND:** Patients with psoriatic arthritis (PsA) have local and systemic bone loss. Besides, they may have low lean mass related to chronic inflammation, immobilization and joint impairment. Psoriasis (Ps) can affect joints in 5 to 8%, with increased concentrations of TNF- $\alpha$  and IL-6 which enhance bone resorption. However, it is not known if osteoporosis or sarcopenia is more frequent in PsA or Ps patients.

**OBJECTIVE:** To compare bone mineral density (BMD) and body composition (BC) measurements in Ps and PsA patients.

**METHODS:** This a cross-sectional study in 47 Ps postmenopausal women and 39 PsA postmenopausal women. All patients performed dual X-ray absorptiometry (DXA) at lumbar spine, total femur and total body (GE-lunar DPX, MD+). Besides, the patients performed cutaneous and articular evaluation with specific instruments (PASI, HAQ and DAS28) as well answered a questionnaire that included details about lifestyle, habits, gynecological factors, previous fracture, concomitant diseases and medications. Spine fractures were evaluated using lumbar and thoracic spine X-ray. Secondary osteoporosis and patients using mobility devices were excluded.

**RESULTS:** Age, body mass index (BMI) and BMD at lumbar spine, total femur and total body were similar in Ps and PsA patients. However, vertebral and femoral osteoporosis was significantly more frequent in PsA than Ps patients. PsA patients had significantly total lean mass lower than Ps patients. Moreover, sarcopenia was three times more frequent in PsA than Ps patients. PsA patients presented higher total fat mass than Ps patients, but fatty distribution (android shape) was not different between the groups. Our results are listed in table below.



	PsA (N = 39)	Ps (N = 47)	P
Age (years)	61 ± 8	61 ± 9	NS
BMI (kg/m <sup>2</sup> )	29.03 ± 3.72	28.9 ± 5.48	NS
Lumbar Spine BMD (g/cm <sup>2</sup> )	1.060 ± 0.2	1.050 ± 0.1	NS
Total Femur BMD (g/cm <sup>2</sup> )	0.940 ± 0.1	0.920 ± 0.1	NS
Total Body BMD (g/cm <sup>2</sup> )	1.120 ± 0.1	1.110 ± 0.1	NS
Spine			
Osteopenia (%)	30.8	29.8	NS
Osteoporosis (%)	17.9	12.8	<0.05
Femur			
Osteopenia (%)	35.9	46.8	<0.05
Osteoporosis (%)	7.7	4.2	<0.05
Total Lean Mass (kg)	35.34 ± 3.96	37.46 ± 5.00	0.01
Android Shape (%)	61.5	61.7	NS
Fat Mass (%)	45.9	43.4	0.02

BMI: Body Mass Index; BMD: Bone Mineral Density; PsA: Psoriatic Arthritis; Ps: Psoriasis

**CONCLUSIONS:** Although Ps and PsA patients present high prevalence of low bone mass, there was no significant difference between them. PsA patients had lower lean mass and higher fat mass than Ps patients. These findings in PsA patients may be related to more risk to disability, osteoporotic fractures, metabolic syndrome and cardiovascular diseases.

**Disclosures:** P.G. Pedreira, None.

## SU338

**Self Reported Weight At Birth Predicts Measures of Femoral Size but Not Volumetric BMD in Elderly Men: MrOS.** M. Javai<sup>1</sup>, L. Lui<sup>2</sup>, P. Cawthon<sup>2</sup>, T. Lang<sup>3</sup>, N. Lane<sup>3</sup>, E. Orwoll<sup>4</sup>, E. Barrett-Conner<sup>5</sup>, M. Nevitt<sup>3</sup>, C. Cooper<sup>1</sup>, S. Cummings<sup>2</sup>. <sup>1</sup>The Botnar Research Centre, Oxford, United Kingdom, <sup>2</sup>CPMC, San Francisco, CA, USA, <sup>3</sup>UCSF, San Francisco, CA, USA, <sup>4</sup>OHSU, Portland, OR, USA, <sup>5</sup>UCSD, San Diego, CA, USA.

**Purpose:** The mechanism for poor intrauterine growth leading to adult hip fracture is unclear. We report the association between birthweight and hip geometry and bone density in community-dwelling elderly men.

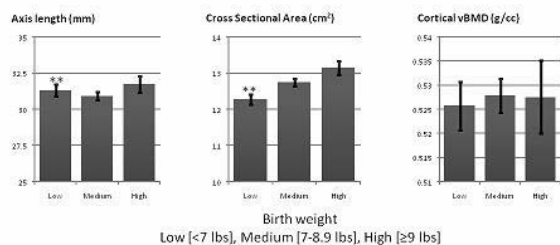
**Methods:** Of baseline recorded data, we used self-reported birthweight, measured height, weight and quantitative computed tomography (QCT) measurements of femoral neck axis length, cross sectional area (CSA) and volumetric BMD (vBMD) among the participants in the Osteoporotic Fractures in Men (MrOS), a cohort study of US men ages 65 years and older. Neck axis length was measured as the distance between the minimum (femoral neck [FN]) and maximum CSA. CSA was derived from the area within the periosteal boundary. The neck shaft angle was calculated from the FN and shaft angles. Of the 3786 men with QCT data, 1831 (48.3%) reported birth weight. We compared men with birthweight < 7 pounds (low birthweight (LBW); n=501) and ≥ 9 pounds (high birthweight (HBW); n=262) with those weighing 7-8.9 pounds (medium birthweight, referent group; n= 1,068) using linear regression models adjusting for current age, height and BMI.

**Results:** The mean age of the 1831 men with both birthweight and QCT measurements was 73 yrs (SD 5.9).

The HBW men had a longer femoral neck and this remained statistically significant after adjusting for adult BMI but was of borderline significance (p=0.06) after also adjusting for adult height. LBW men also had a longer neck than the referent group after adjusting for current height and BMI (p=0.009). FN cross sectional area was reduced in LBW men by 0.25 SD (p<0.001) and this remained significant after adjusting for both current height and BMI. Neck shaft angle was not predicted (p>0.1) by birth weight. Neither cortical nor trabecular vBMD at the femoral neck were associated with birth weight.

**Conclusions:** These findings support the hypothesis that the skeletal envelope, but not density, is set, in part, at birth. LBW men have a longer femoral neck than expected for their cross sectional area. Additional research describing the relationship between the early developmental factors and lifetime fracture risk should be pursued; such research may inform primary preventative strategies for fracture prevention

**Relationship between reported birth weight and QCT measures of bone strength in cohort elderly men**



Legend: Unadjusted Mean (95% CI) shown; P values from regression models adjusted for age, height and BMI with referent medium birth weight group (\* p<0.05, \*\* p< 0.01)

**Disclosures:** M. Javai, None.

## SU339

**Casual Decomposition of Risk Factors in Osteoporosis Burden.** Z. Hamidi<sup>1</sup>, R. Majdzadeh<sup>2</sup>, A. Soltani<sup>3</sup>, B. Larijani<sup>4</sup>. <sup>1</sup>Endocrinology and Metabolism Research Centre of Tehran University of Medical Sciences, Tehran, Iran, Islamic Republic of, <sup>2</sup>Public Health School of Tehran University of Medical Sciences, Tehran, Iran, Islamic Republic of.

Osteoporosis is an extending problem in the world and priority setting of prevention efforts and researches about it, is necessary.

In our study we calculated the Generalized Impact Fraction (GIF) index and avoidable burden of Osteoporosis related to "low calcium intake, smoking, reduced sun Exposure, low physical activity, low BMI and systemic glucocorticoid therapy. These risk factors, all can be intervened. Data about prevalence, casual effect and counterfactual prevalence of any of above risk factors obtained from different Iranian (and if needed Non-Iranian) studies that contained best qualified evidences that was attainable.

When counterfactual prevalence considered 0% (theoretical minimum risk), GIFs of smoking, low calcium intake, reduced sun Exposure, low physical activity, low BMI and systemic glucocorticoid therapy, was 0.038, 0.038, 0.110, 0.290, 0.211 and 0.020, respectively. When appropriate feasible minimum risk was considered as counterfactual prevalence, GIF of smoking, low calcium intake, low physical activity, and systemic glucocorticoid therapy, was 0.019, 0.010, 0.290 and 0.007.

Interventions that reduce low physical activity are at the priority of osteoporosis prevention strategies. Of course cost-effectiveness and practicality of any intervention must be appreciated.

**Disclosures:** Z. Hamidi, None.

## SU340

**Fragility Fractures and Health Status in a Multinational Cohort. The Global Longitudinal Registry of Osteoporosis in Women.** C. Cooper<sup>1</sup>, J. Adachi<sup>2</sup>, F. A. Anderson<sup>3</sup>, J. Compston<sup>4</sup>, J. C. Netelenbos<sup>5</sup>, J. Pfeilschifter<sup>6</sup>, S. Silverman<sup>7</sup>, R. Dedrick<sup>8</sup>, S. Adami<sup>8</sup>. <sup>1</sup>Southampton General Hospital, Southampton, United Kingdom, <sup>2</sup>St. Joseph's Hospital, Hamilton, ON, USA, <sup>3</sup>UMASS Medical School, Worcester, MA, USA, <sup>4</sup>University of Cambridge School of Clinical Medicine, Cambridge, United Kingdom, <sup>5</sup>VU University Medical Center, Amsterdam, Netherlands, <sup>6</sup>Medizinische Klinik I, Lutherhaus, Essen, Germany, <sup>7</sup>David Geffen School of Medicine, Los Angeles, CA, USA, <sup>8</sup>University of Verona, Verona, Italy.

The purpose of this study was to examine baseline self-rated health among women with and without prevalent fractures.

The Global Longitudinal registry of Osteoporosis in Women (GLOW) is an observational follow-up study of women aged ≥55 years recruited by 540 primary physician practices (17 sites, 10 countries). Practices typical of each region were identified through primary care networks organized for administrative, research or educational purposes. All non-institutionalized women visiting the practice within the prior 2 years were eligible. Self-administered questionnaires were mailed, with a 2:1 over-sampling of women ≥65 years. Data on occurrence of prior fractures since age 45 at any of 10 bone locations were collected. Respondents rated their overall health on a 5-point scale, from "excellent" to "poor," and completed EQ-5D, a generic instrument that captures 5 dimensions of health status (mobility, self-care, usual activities, pain/discomfort, anxiety/depression).

Among 47,786 women, 23% reported ≥1 fracture since age 45. Site-specific prevalence varied from 5.8% (wrist) to 0.4% (pelvis). Prevalence of "fair" or "poor" self-rated health was 21% for women without fractures vs 41% for those with multiple fractures (range 24% for wrist to 42% for spinal fracture). Mean EQ-5D scores were significantly higher in women without fractures (0.78 vs 0.74 or 0.65 of a possible score of 1.00), and tended to indicate greater impairment for those who had had fractures to spine, hip, and clavicle. All mean scores for those with fractures were significantly different from means for subjects without fractures (P<0.0001).

Table. Overall self-rated health status and fracture history (age standardized). \*P<0.05

	No fracture 77%	Any 1 fracture 17%	Multiple fractures 6%
Subjects			
EQ-5D: "Any problems"			
Mobility	27%	33%	50%
Self care	6%	9%	18%
Usual activities	26%	32%	50%
Pain	68%	74%	83%
Anxiety	40%	44%	53%
EQ-5D, mean (standard deviation)	0.78 (0.21)	0.74 (0.24)	0.65 (0.29)
SF-36: "Any limitations"			
Vigorous activity	79%	83%	89%
Moderate activity	39%	48%	63%
Bathe or dress self	11%	15%	25%
Health "fair" or "poor"	21%*	27%	41%

Women who have sustained fractures after age 45 reported poorer health status than contemporaries without fractures, particularly women with fractures of the spine, hip and pelvis.

**Disclosures:** C. Cooper, The Alliance for Better Bone Health (Procter & Gamble Pharmaceuticals and sanofi-aventis) 4; Novartis, Servier, Lilly, MSD 4.

This study received funding from: The Alliance for Better Bone Health (Procter & Gamble Pharmaceuticals and sanofi-aventis).

## SU341

### Risk Factors for Low BMD in Healthy Men Age 50 Years or Older: A Systematic Review. C. C. Kennedy<sup>1</sup>, A. Papaioannou<sup>1</sup>, A. Cranney<sup>2</sup>, G. Hawker<sup>3</sup>, J. P. Brown<sup>4</sup>, S. M. Kaiser<sup>5</sup>, W. D. Leslie<sup>6</sup>, C. J. M. O'Brien<sup>\*7</sup>.

<sup>1</sup>Medicine, McMaster University, Hamilton, ON, Canada, <sup>2</sup>Medicine & Clinical Epidemiology, University of Ottawa, Ottawa, ON, Canada, <sup>3</sup>Medicine and Health Policy, Management and Evaluation, University of Toronto, Toronto, ON, Canada, <sup>4</sup>Medicine, Université Laval, Quebec, QC, Canada, <sup>5</sup>Medicine, Dalhousie University, Halifax, NS, Canada, <sup>6</sup>Medicine & Radiology, University of Manitoba, Winnipeg, MB, Canada, <sup>7</sup>Radiology, Brantford General Hospital, Brantford, ON, Canada.

Research to date has largely focused on the diagnosis and management of osteoporosis in postmenopausal women. The objective of this systematic review was to evaluate the evidence regarding risk factors for low bone mineral density (BMD) and bone loss in healthy men age 50 years or older.

Our population of interest was men age 50 years or older. The search was carried out on several databases via the OVID search interface between January 1990 and January 2006. The three main search concepts were bone density, densitometry and risk factors. Only observational studies that used dual energy x-ray absorptiometry (lumbar spine or proximal femur) were included. We were interested in factors that could be assessed in primary practice via clinical history; Studies investigating osteoporosis associated with diseases or medications were excluded. Trained reviewers assessed methodological quality and an individual grade ('Good', 'Fair', 'Poor') was assigned to each study based on the United States Preventive Services Task Force (USPSTF) rating system. Studies assigned a grade of 'Poor' were excluded.

The search strategy identified 642 relevant abstracts. In total, 25 articles from 18 different studies met both the inclusion and quality criteria. Sample sizes ranged from 137 to 5995 with a median of 458. Consistent risk factors were: age, smoking, low weight, physical/functional limitations and previous fracture. In longitudinal studies, physical activity and alcohol were not predictive of bone loss; in cross-sectional studies, there was inconsistent evidence. The evidence was inconsistent or weak for: calcium, muscle strength, family history of fracture/osteoporosis, and height/height loss.

This systematic review highlights several easily assessed risk factors for low BMD and bone loss in healthy men. This data will assist policy makers and primary care physicians in assessing which men over age 50 should be referred for bone densitometry.

On behalf of the Male BMD Guidelines Committee of Osteoporosis Canada

**Disclosures:** C.C. Kennedy, None.

This study received funding from: Ontario Ministry of Health and Long-Term Care, Ontario Osteoporosis Strategy.

## SU342

### Distribution of Risk Factors for Fracture in Women With and Without a Fracture History: A Regional Comparison. The Global Longitudinal Registry of Osteoporosis in Women. J. D. Adachi<sup>1</sup>, P. Sambrook<sup>2</sup>, A. Diez-Perez<sup>3</sup>, J. Compston<sup>\*4</sup>, F. Hooven<sup>\*5</sup>, J. C. Netelenbos<sup>5</sup>, N. B. Watts<sup>7</sup>, R. Dedrick<sup>\*8</sup>, C. Roux<sup>\*8</sup>.

<sup>1</sup>Medicine, St. Joseph's Hospital - McMaster University, Hamilton, ON, USA, <sup>2</sup>University of Sydney-Royal North Shore Hospital, Sydney, Australia, <sup>3</sup>Hospital del Mar, Barcelona, Spain, <sup>4</sup>University of Cambridge School of Clinical Medicine, Cambridge, United Kingdom, <sup>5</sup>UMASS Medical School, Worcester, MA, USA, <sup>6</sup>VU University Medical Center, Amsterdam, Netherlands, <sup>7</sup>University of Cincinnati, Cincinnati, OH, USA, <sup>8</sup>Hopital Cochin, Paris, France.

The aim of this study was to compare the prevalence of risk factors for fracture in 3 regions in women with and without report of prior fracture, in a large cohort of women aged  $\geq 55$  years.

The Global Longitudinal registry of Osteoporosis in Women (GLOW) is an observational follow-up study of 50,226 women aged  $\geq 55$  recruited through 540 primary physician practices (17 sites, 10 countries). Practices typical of each region were identified. All non-institutionalized patients visiting the practice within the prior 2 years were eligible. Self-administered questionnaires were mailed, with 2:1 over-sampling of those aged  $\geq 65$ . Reminder postcards and second surveys were sent to enhance participation; in some sites patients were followed-up by telephone. Follow-up questionnaires will be sent at 12-month intervals for 5 years.

Among women who reported a history of fracture after age 45, 41% required their arms to rise from sitting versus 32% of those without a history of fracture. Overall, 28% of women with a history of fracture reported cortisone use vs 23% in those without a fracture history. Women in the US with a fracture history were more likely to report being on cortisone (39%) than European women with a fracture history (18%) (Table). Of the women in Australia and Canada without a fracture history, 5.6% reported drinking  $>14$  alcoholic drinks/week vs 3.4% of European women and 2.4% of US women. When comparing the 3 regions, all variables were highly significantly different ( $P < 0.0001$ ) except for weight  $< 125$  lb in women with a fracture history ( $P < 0.05$ ).

Table. Age-standardized prevalence of risk factors for fracture.

Risk factor (%)	History of fracture (n=11,893)			No history of fracture (n=38,333)		
	Can/Aust (n=1448)	Europe (n=5494)	USA (n=4951)	Can/Aust (n=4936)	Europe (n=16,965)	USA (n=16,432)
Maternal hip fracture	15	13	16	12	11	12
Weight $< 125$ lbs (57 kg)	18	19	15	15	18	14
Current smoker	7.8	11	9.2	8.6	10	7.6
Arms used to assist from sitting	41	38	46	32	29	34
Parental fracture	18	17	20	15	13	15
Cortisone (ever taken)	28	18	39	24	13	32
Alcoholic drinks ( $> 14$ /week)	6.4	3.3	2.1	5.6	3.4	2.4
Rheumatoid arthritis	12	15	11	9.0	12	8.8

In this international "real-world" population of women, self-reported risk factors for fracture varied widely by both geographic region and by history (vs no history) of fracture.

**Disclosures:** J.D. Adachi, Amgen, Eli Lilly, GSK, Merck, Novartis, Pfizer, Procter & Gamble, Roche 3; Amgen, Astra Zeneca, Eli Lilly, GSK, Merck, Novartis, Pfizer, Procter & Gamble, Roche, sanofi-aventis, Servier 1; Amgen, Astra Zeneca, Eli Lilly, GSK, Merck, Novartis, Pfizer, Procter & Gamble, Roche, sanofi-aventis, Servier 2. This study received funding from: The Alliance for Better Bone Health (Procter & Gamble Pharmaceuticals and sanofi-aventis).

## SU343

### The Development of a Point-of-care Clinical Decision Support Tool for Osteoporosis Disease Management. M. Kastner<sup>\*1</sup>, D. Lottridge<sup>\*2</sup>, J. Li<sup>\*2</sup>, S. E. Straus<sup>\*3</sup>.

<sup>1</sup>Health Policy, Management and Evaluation, University of Toronto, Toronto, ON, Canada, <sup>2</sup>Mechanical and Industrial Engineering, University of Toronto, Toronto, ON, Canada, <sup>3</sup>Medicine, University of Calgary, Calgary, AB, Canada.

**Purpose:** To develop a prototype tool that can support clinical decision making in osteoporosis disease management (OP-DM) at the point of care.

**Methods:** Key findings from a systematic review of randomized trials assessing OP-DM interventions were used to develop a conceptual design of the tool. We then conducted a qualitative study of focus groups with family physicians and general internists to develop a working prototype of the tool. The goal of the focus groups was to assess which features, functions, format, and evidence are important to include in the tool; and to discuss barriers to using such a tool in clinical practice. Focus groups were audiotaped and transcribed verbatim. 2 reviewers independently coded data using a combination of grounded theory methodology and verbal protocol analysis.

**Results:** 4 focus groups (n=17) were needed to achieve saturation of themes (mean age range 47-55 years, 76% men). Using an iterative model, the OP-DM tool was modified from analysis of the first focus group, which informed changes to the tool for subsequent focus groups. Barriers identified were related to the accuracy and feasibility of extracting BMD test results and medications from the risk assessment questionnaire, and the need to include well-balanced information in the patient education sheet. Suggestions for modifying the prototype included the addition of a percentile graph showing patients' 10-year absolute risk for fractures, and ensuring that the tool takes no more than 5 minutes to complete. The resulting working prototype is multi-targeted (patients, physicians, and clinic nurses), and includes 3 components: 1) an osteoporosis risk assessment questionnaire filled out by eligible patients on a Tablet PC in the examination room while waiting for their physician; 2) a one-page sheet outlining appropriate OP-DM recommendations according to guidelines made available for physicians at the point of care in print or via an EMR system; 3) a customized educational sheet given to patients soon after they complete the questionnaire, which includes their 10-year absolute risk for fractures, and tailored osteoporosis information about their diagnosis and treatment recommendations.

**Conclusions:** We developed a comprehensive OP-DM prototype that may aid physicians in their clinical decision making at the point of care. Next steps include conducting usability testing with all end users of the tool, and a pilot study to evaluate the tool in 3 family practice settings.

**Disclosures:** M. Kastner, None.

This study received funding from: CIHR.



## SU344

**Multinational Comparison of Bone Health in Women 55 Years of Age and Older. The Global Longitudinal Registry of Osteoporosis in Women.** P. Delmas<sup>1</sup>, S. Adams<sup>2\*</sup>, F. A. Anderson<sup>3</sup>, S. Gehlbach<sup>3</sup>, J. Pfeilschifter<sup>4</sup>, P. Sambrook<sup>5</sup>, S. Silverman<sup>6</sup>, R. Dedrick<sup>3</sup>, C. Roux<sup>7</sup>, R. Lindsay<sup>8</sup>. <sup>1</sup>Hôpital Edouard Herriot, Lyon, France, <sup>2</sup>University of Verona, Verona, Italy, <sup>3</sup>UMASS Medical School, Worcester, MA, USA, <sup>4</sup>Lutherhaus, Essen, Germany, <sup>5</sup>University of Sydney-Royal North Shore Hospital, Sydney, Australia, <sup>6</sup>David Geffen School of Medicine, Los Angeles, CA, USA, <sup>7</sup>Hopital Cochin, Paris, France, <sup>8</sup>Helen Hayes Hospital, New York, NY, USA.

The purpose of this study was to compare bone health among women ≥55 years of age from 3 geographic regions.

Practices typical of each region were identified through primary care networks organized for administrative, research or educational purposes. All non-institutionalized patients visiting each practice within the prior 2 years were eligible. Self-administered questionnaires were mailed, with 2:1 over-sampling of women ≥65 years of age. Follow-up questionnaires will be sent at 12-month intervals for 5 years.

The study population comprises 50,187 women from 716 physician practices in Europe, USA and Canada/Australia. Twenty-four percent of women reported at least 1 fracture occurring after age 45: 18% had a single fracture and 6.0% had 2 or more. The most frequently reported fracture was of the wrist (8.8%) followed by the ankle (6.3%; Table). Overall, 10.9% of fractures affected weight-bearing bones of the lower body, which are associated with greater levels of disability. Twelve percent of women said that their mothers had sustained a hip fracture. Across study sites, age-adjusted prevalence of previous fractures ranged from 22% in the USA to 25% in Europe. Wrist fractures were reported by 10% of women in Europe but only 7.1% of US women; hip fracture reports were highest in Europe (2.1%) and lowest in Canada/Australia (1.4%).

Table. Women reporting fracture by geographic region (age-adjusted)

Fracture site (%)	Europe N=22,459	USA N=21,344	Canada/Australia N=6384
Clavicle	1.6	1.2	1.4
Arm	3.2	2.9	2.6
Wrist	10	7.1	8.7
Spine	2.9	1.8	2.0
Rib	4.6	3.9	4.1
Hip	2.1	2.0	1.4
Pelvis	1.0	1.2	0.8
Ankle	5.7	6.9	6.1
Upper leg	1.0	1.1	0.6
Lower leg	2.5	2.6	2.2
Upper body	18	14	16
Lower body	11	12	9.9

Fracture incidence data gathered in subsequent years of the GLOW study will provide a better assessment of whether there is significant variation in the incidence of certain fracture types between regions. This study will also provide the opportunity to assess variation in quality-of-life outcomes according to type of fracture and region.

**Disclosures:** P. Delmas, Procter & Gamble 3; Procter & Gamble; sanofi-aventis 2, 4. This study received funding from: The Alliance for Better Bone Health (Procter & Gamble Pharmaceuticals and sanofi-aventis).

## SU345

**Comparison between Logistic Regression and Artificial Neural Networks for Vertebral Fracture Risk Assessment: Analysis from GISMO Lombardia Database.** M. Bevilacqua<sup>1</sup>, E. Grossi<sup>2\*</sup>, G. Gandolini<sup>3</sup>, M. Massarotti<sup>4</sup>, I. Chiodini<sup>5</sup>, M. Longhi<sup>6</sup>, L. Pietrogrande<sup>7</sup>, I. Santi<sup>8</sup>. <sup>1</sup>Endocrinology Unit, Sacco Hospital, Milan, Italy, <sup>2</sup>Centro Diagnostico Italiano, Milan, Italy, <sup>3</sup>Rheumatology Unit, IRCCS Don Gnocchi, Milan, Italy, <sup>4</sup>Rheumatology Unit, IRCCS Humanitas, Rozzano (Milan), Italy, <sup>5</sup>Endocrinology and Diabetology Unit, IRCCS Policlinico, Milan, Italy, <sup>6</sup>Rheumatology Unit, IRCCS Galeazzi, Milan, Italy, <sup>7</sup>San Paolo Hospital, University of Milan, Milan, Italy, <sup>8</sup>Pio Albergo Trivulzio Geriatrics Institute, Milan, Italy.

**Background** -Artificial neural networks (ANNs) are computer algorithms inspired by the highly interactive processing of the human brain. When exposed to complex data sets ANNs can learn the underlying laws that associate different variables to a definite outcome.

**Aims** - A cooperative Italian database of 490 osteoporotic women described by 39 variables was analysed to evaluate the capacity of ANNs to recognise patients with (VF<sup>+</sup>, n= 214) or without (VF, n= 276) vertebral fracture on the basis of classical bone osteoporotic risk factors, and other common clinical information

**Method** - The performance of ANN and LR (logistic regression) were assessed by calculating the percentage of correct identifications of VF<sup>+</sup> and VF patients (sensitivity and specificity, respectively) and the prediction accuracy (arithmetic mean between sensitivity and specificity) using a rigorous and homogeneous training and testing protocol typically employed with ANNs.

**Results** - The results showed that ANNs can be trained to identify VF<sup>+</sup> and VF subjects

more accurately than logistic regression. Using all information available, the prediction accuracies of the ANNs and LR providing the best results were 49.57 % and 53.96%, respectively. When the ANNs were allowed to choose the relevant input data automatically (TWIST system-Semeion), 27 variables were selected among 39. Using this set of variables as input data, the performance of the ANNs in the classification task reached an overall prediction accuracy of 75% (Table 1).

Age, BMI, menopause age, smoking, alcohol use, schooling, hypertension, milk and yogurt intake resulted to be the most relevant variables for the best performing model.

**Conclusions** - ANNs technology is highly promising in the development of accurate diagnostic tools designed to recognize patients at high risk of vertebral fracture.

**Table 1** - Summary of model classifications performances

Model	Sensitivity	Specificity	Overall accuracy
LR	44.26%	54.88%	49.57%
ANNs	63.70%	44.21%	53.96%
ANNs (selected var)	75.00%	75.00%	75.00%

**Disclosures:** M. Bevilacqua, None.

## SU346

**Is the Association between Hypertension and Bone Osteoporotic Fracture Expressing a Real Interdependence? Clues from GISMO Lombardia Database.** G. Gandolini<sup>1</sup>, E. Grossi<sup>2\*</sup>, M. Bevilacqua<sup>3</sup>, M. Massarotti<sup>4</sup>, I. Chiodini<sup>5</sup>, M. Longhi<sup>6</sup>, L. Pietrogrande<sup>7</sup>, I. Santi<sup>8</sup>. <sup>1</sup>Rheumatology Unit, IRCCS Don Gnocchi, Milan, Italy, <sup>2</sup>Centro Diagnostico Italiano, Milan, Italy, <sup>3</sup>Endocrinology Unit, Sacco Hospital, Milan, Italy, <sup>4</sup>Rheumatology Unit, IRCCS Humanitas, Rozzano (Milan), Italy, <sup>5</sup>Endocrinology and Diabetology Unit, IRCCS Ospedale Maggiore Policlinico, Milan, Italy, <sup>6</sup>Rheumatology Unit, IRCCS Galeazzi, Milan, Italy, <sup>7</sup>San Paolo Hospital, University of Milan, Milan, Italy, <sup>8</sup>Pio Albergo Trivulzio Geriatrics Institute, Milan, Italy.

**Background** - The interaction between osteoporosis (OP) and arterial hypertension (AH) is a controversial issue in clinical epidemiology. Various alterations of calcium metabolism have been described in AH; such alterations can cause decreased bone mass, the principal determinant of fracture. On the other hand patients with AH are frequently treated with beta-blockers, thiazides or angiotensin converting enzyme inhibitors which have a beneficial effect on bone mass. This is currently considered one of the possible explanation about the lower incidence of bone fracture in AH in some clinical trials.

**Aim** - To assess the association between AH and vertebral bone fracture (VF) with a novel statistical approach based on non linear mapping in addition to traditional statistics.

**Methods** - We have addressed this issue carrying out a data mining procedure on a cooperative Italian database, composed by of 490 OP women described by 39 variables (214 with VF and 276 without VF). We studied the association between AH and VF with two approaches: Principal Component Analysis (PCA), a linear statistical analysis, and a new non linear mapping method (PST, Semeion Institute).This algorithm is able to perform a multidimensional scaling of variables finding out their optimal spatial distribution in bidimensional space, and identifying emerging natural clusters.

**Results** - Prevalence of AH in the whole group was 35.7%. The prevalence of AH was higher in the subgroup with VF: 41.1% (C.I 95% = 34.52% - 47.69%) than in the subgroup without VF: 31.5% (C.I 95%= 26.02% - 36.98%). In the overall study group as in the subgroup with VF the mean T-score of AH subjects resulted almost equal to that of non-AH subjects. A natural clustering of AH and VF was observed with PCA (at least in 1<sup>st</sup> and 2<sup>nd</sup> component projection) and with PST algorithm as well. With PST algorithm the association among these variables was unquestionable and remained unaffected by increasing progressively the number of clusters, pointing out the existence of a real interdependence among these two conditions.

**Conclusions** - Further work is required to explain the possible mechanisms of the interdependence between AH and OP, given the complexity of variables associations.

**Disclosures:** M. Bevilacqua, None.

## SU347

**Prospective Observational Study of Osteoporosis Medication Use in Postmenopausal Women in the European Union (POSSIBLE EU®): Characteristics, Health Status and Quality of Life at Baseline.** N. Freemantle<sup>\*1</sup>, C. Cooper<sup>2</sup>, R. Horne<sup>\*3</sup>, S. Kakad<sup>\*4</sup>, V. Easton<sup>\*5</sup>, L. Martinez<sup>\*6</sup>.  
<sup>1</sup>Health Care Evaluation Group, University of Birmingham, Birmingham, United Kingdom, <sup>2</sup>MRC Epidemiology Resource Centre, University of Southampton, Southampton, United Kingdom, <sup>3</sup>Practice & Policy, University of London, London, United Kingdom, <sup>4</sup>Amgen Ltd, Uxbridge, United Kingdom, <sup>5</sup>Amgen Ltd, Cambridge, United Kingdom, <sup>6</sup>Société Française de Médecine Générale, Issy les Moulineaux, France.

POSSIBLE EU® is an ongoing, observational cohort study that describes the characteristics of postmenopausal (PMO) women being treated for osteoporosis by primary care physicians (PCPs), their behaviors, and attitudes towards treatment. 196 primary care centers in France, Germany, Italy, Spain and the United Kingdom are involved. During routine visits, eligible women who gave consent were enrolled into 1 of 3 cohorts based on osteoporosis therapy status: Inception (initiate therapy at enrolment); Switch (change to alternative therapy at enrolment); or Established (continue on same therapy as prior 12 months). PCPs and patients provide data at enrolment and at quarterly intervals for 12 months. For this interim analysis, complete baseline (BL) data are available for 2117 women; 1432 had BL patient-reported outcome data (Table). Of 1432 patients, 29% currently smoke or are exsmokers; >50% report drinking alcohol; 15% report falling in the past month; and 74% had a family history of fracture. Only 14 women reported living in assisted care facilities; the rest live alone or with spouse, family, or others. These women represent a severely osteoporotic population based on T-score and fracture history (Table). QOL measured by EuroQol - 5 dimensions (EQ-5D) and Osteoporosis Assessment Questionnaire - short Version (OPAQ-SV) are lower than observed previously for the age group and population in clinical trials of fracture prevention (Arthr Rheum. 2001;44:2611; JBMR. 2000;15:1384) (Table). Most patients reported moderate to severe pain (Table). 84% of patients on treatment at BL report taking bisphosphonates. Overall, data from this interim analysis indicate PMO women in Europe being treated with osteoporosis medication live in the community and report severe osteoporotic disease, pain and low QOL. Future data from this study should provide insight into the "real world" management of osteoporosis in Europe, outside of the clinical trial setting.

	All Patients (N=2117)	Inception (N=1120)	Established (N=654)	Switch (N=343)
Age (years), median (25 <sup>th</sup> , 75 <sup>th</sup> quartiles)	69.0 (61.0, 76.0)	69.0 (60.0, 76.0)	70.0 (62.0, 76.0)	70.0 (63.0, 78.0)
Diagnosis of osteopenia/osteoporosis, %/%	30.6% / 68.0%	36.3% / 62.3%	21.9% / 76.9%	29.1% / 69.2%
History of any fracture before baseline, %	41.2%	38.0%	44.6%	45.2%
Minimum T-score <sup>a,b</sup> at diagnosis, median (25 <sup>th</sup> , 75 <sup>th</sup> quartiles)	-2.7 (-3.3, -2.2)	-2.7 (-3.2, -2.2)	-2.8 (-3.4, -2.4)	-2.7 (-3.3, -2.2)
% reporting any pain (%moderate or severe) <sup>c</sup>	89.4% (54.8%)	90.5% (61.7%)	88.5% (56.1%)	87.5% (54.5%)
EQ-5D (index score) median (25 <sup>th</sup> , 75 <sup>th</sup> quartiles) <sup>c</sup>	0.73 (0.59, 0.80)	0.73 (0.52, 0.80)	0.73 (0.62, 0.80)	0.73 (0.60, 0.80)
OPAQ-SV (physical function dimension) median (25 <sup>th</sup> , 75 <sup>th</sup> quartiles) <sup>c</sup>	76.3 (58.3, 90.3)	74.3 (57.9, 86.8)	78.9 (60.5, 93.4)	81.6 (61.8, 92.4)

<sup>a</sup> n=1049, 564, 313, and 172, respectively

<sup>b</sup> Minimum T-score is defined as the minimum T-score value between location femoral neck, hip, and lumbar spine.

<sup>c</sup> n=1432, 750, 451, and 231, respectively

**Disclosures:** N. Freemantle, Amgen 4.  
 This study received funding from: Amgen Ltd.

## SU348

**Assessment of The 10-Year Risk of Fracture in Italian Postmenopausal Women Using BMD and Clinical Risk Factors: A Multicenter Study.** M. Pedrazzoni<sup>1</sup>, A. Giusti<sup>2</sup>, A. Barone<sup>\*2</sup>, G. Girasole<sup>\*3</sup>, G. Pioli<sup>4</sup>, G. Passeri<sup>\*1</sup>, E. Palummen<sup>\*2</sup>, G. Bianchi<sup>\*3</sup>. <sup>1</sup>Internal Medicine, University of Parma, Parma, Italy, <sup>2</sup>Gerontology, Galliera Hospital, Genoa, Italy, <sup>3</sup>Rheumatology, Colletta Hospital, Arenzano, Italy, <sup>4</sup>Gerontology, Santa Maria Hospital, Reggio Emilia, Italy.

The aim of this study was to estimate the absolute risk of fracture in a cohort of postmenopausal women using the Italian FRAX™ charts recently published (<http://www.shef.ac.uk/FRAX/chart.htm>) based on femoral neck BMD and 3 internationally validated clinical risk factors (CRFs: prior history of fragility fracture, family history of fracture, current smoking). Postmenopausal women from 3 osteoporosis centers of Northern Italy (Arenzano, Genoa, Parma) answered a standardized questionnaire to assess smoking habits, history of fragility fractures and fractures in first-degree relatives. Glucocorticoid treated subjects were excluded since, according to Italian guidelines, the management of these subjects depends only on dosage and duration of steroid use. BMD measurements at the femoral neck were

obtained by DXA; T-scores were calculated based on NHANES reference values. The 10-year risk of fracture was computed by linear interpolation of the FRAX™ charts as a function of age, femoral T-score and number of CRFs.

The overall population consisted of 9280 women (mean age 64; range: 50-90). The mean femoral neck T-score was -1.7 (range: from -4.0 to +1.0). The proportion of women with 0, 1, 2 and 3 prevalent CRFs was 69.7%, 27.0%, 3.3% and 0.1%, respectively. The median 10-year risk was 8.8% for osteoporotic fracture (clinical spine, hip, forearm and humerus) and 2.4% for hip fracture. 25% of subjects had a 10-year risk greater or equal to 13.6% for osteoporotic fracture and 5.5% for hip fracture. In women younger than 65 years the median 10-year risk of osteoporotic fracture was 5.9% (range: from 2.7% to 45%); in contrast, in older women the median 10-year risk was 13.6% (range: from 4.3% to 60.2%). The respective figures for hip fracture were 1.1% (0.01-30.6%) and 5.5% (0.3-51.2%). The addition of CRFs greatly amplified risk stratification as compared to age and BMD: from 8.8% the median risk increased to 12.6%, 17.6% and 33.3% with 1, 2 and 3 CRFs, respectively. The integration of CRFs, age and BMD using the FRAX™ charts enhances the assessment of fracture risk. Further prospective studies are needed for validation.

**Disclosures:** A. Giusti, None.

## SU349

**Smoking is an Independent Predictor of Low Bone Mineral Density, Prevalent Vertebral Fractures and Incident Fractures in Elderly Men.** Mr OS Sweden. H. Jutberger<sup>\*1</sup>, M. Lorentzon<sup>1</sup>, Ö. Ljunggren<sup>2</sup>, M. Karlsson<sup>3</sup>, E. Orwoll<sup>4</sup>, C. Ohlsson<sup>1</sup>, D. Mellström<sup>1</sup>. <sup>1</sup>Centre for Bone Research at the Sahlgrenska Academy, University of Göteborg, Sweden, Göteborg, Sweden, <sup>2</sup>Dep of Medical Sciences, University of Uppsala, Sweden, Uppsala, Sweden, <sup>3</sup>Dep of Ortopaedics, Malmö University Hospital, Sweden, Malmö, Sweden, <sup>4</sup>Bone and Mineral Research Unit, Oregon Health and Sciences University, Portland, OR, USA, Portland, OR, USA.

Smoking is considered to be a risk factor for osteoporosis and fractures in women, but is unclear in men. The aim of this study was to examine the effect of smoking for bone mineral density, prevalent vertebral fractures and incident fractures in elderly men.

We studied 3014 men, aged 69 - 80 years, in the Swedish part of Mr OS (centres in Göteborg, Malmö and Uppsala). The international Mr OS questionnaire was used. Standardized BMD was measured with calibrated scanners (Lunar Prodigy and Hologic 4500 A). In the two centres Göteborg and Malmö 1395 men had an X-ray of the thoracic and lumbar spine at baseline.

9 per cent were current smokers, 54 per cent were ex-smokers and 37 per cent were never-smokers. 226 men (17 per cent) had one or more X-ray verified vertebral fracture. Current smoking was an independent negative predictor of standardized BMD in total hip, femoral neck, trochanter and lumbar spine when using linear regression models. Prevalent fractures among smokers are presented in fig.1. Risk for vertebral fractures among smokers: OR 1.77 (1.172-2.686). Adjusted for lumbar-BMD, ( $p < 0.05$ ). During the three first years after baseline 209 X-ray verified fractures occurred. Fracture risk in smokers was calculated with Cox proportional hazard ratio and is presented in table 1.

We conclude that tobacco smoking in elderly men is an important predictor for low bone mineral density, prevalent vertebral fractures and incident fractures, especially vertebral fractures and hip fractures.

**Fig 1. Prevalent vertebral fractures (%)**

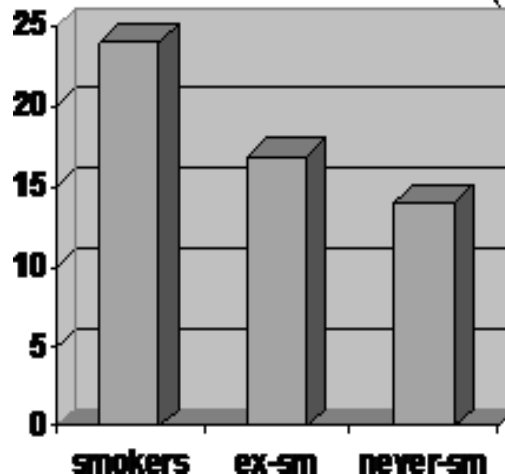


**Table 1. Risk for incident fracture. Cox prop. HR**

Fracture (N=209)	HR 1.76 (1.171-2.642)
Non-vertebral osteoporotic fracture (N=83)	HR 2.16 (1.191-3.909)
Vertebral fracture Clin. & X-ray verified (N=67)	HR 2.72 (1.482-5.001)
Hip fracture (N=38)	HR 3.27 (1.491-7.158)

**Disclosures:** H. Jutberger, None.



## SU350

**The Association of Stiffness Index and Cross-Linked N-Telopeptides of Type I Collagen (NTx) with Any Clinical Fractures Differs with Age and Gender.** A. Yasuyo, K. Aoyagi. Department of Public Health, Nagasaki University Graduate School of Biomedical Sciences, Nagasaki, Japan.

The purpose of this cross-sectional study was to evaluate associations of calcaneal stiffness index and cross-linked N-telopeptides of type I collagen (NTx) with fractures among Japanese community-dwelling people  $\geq 40$  years old. Subjects comprised 453 men with a mean ( $\pm$ standard deviation (SD)) age of  $66.8 \pm 10.0$  years (range, 40-91 years) and 897 women with a mean age of  $65.9 \pm 9.8$  (range, 40-87 years). Calcaneal stiffness index was obtained using quantitative ultrasound measurements. Urinary NTx divided by creatinine was measured for 263 men and 534 women for whom urine samples were available. Information on previous fractures after 45 years old (due to minor or moderate trauma) was obtained by questionnaire. Stiffness index showed significant negative correlations with age and urinary NTx in both genders. When adjusted for age, Pearson's partial correlation coefficient between stiffness index and urinary NTx was -0.27 ( $p < 0.001$ ) for men and -0.19 ( $p < 0.001$ ) for women. Among all subjects, 39 men (8.6%) and 147 women (16.4%) reported at least one clinical fracture. Among women, fracture prevalence significantly increased with age ( $p < 0.001$ ), while no significant association was observed between age and fracture prevalence among men. Associations of stiffness index and urinary NTx with fractures were examined using logistic regression analysis, adjusting for age. Among younger women ( $< 65$  years), urinary NTx was significantly associated with fracture, whereas stiffness index was not. Age-adjusted odds ratios (ORs) for fracture were 0.70 (95% confidence interval (CI), 0.45-1.10) for stiffness index (per 1 SD decrease) and 1.66 (95%CI, 1.04-2.65) for urinary NTx (per 1 SD increase). In contrast, among older women ( $\geq 65$  years), stiffness index was significantly associated with fracture, whereas urinary NTx was not. Age-adjusted ORs were 1.32 (95%CI, 1.04-1.67) for stiffness index and 0.94 (95%CI, 0.71-1.24) for urinary NTx. However, neither stiffness index nor urinary NTx was significantly associated with fracture among men in both age groups. These results suggest that increased bone turnover appears to be an important risk factor for fracture among younger women, while bone mass appears important among older women. Although stiffness index significantly correlated with urinary NTx in both men and women, the impact of stiffness index and urinary NTx on risk of fracture may differ substantially with age and gender. When assessing fracture risk, age- and gender-specific approaches for interpreting and applying bone mass measurements or bone turnover markers to individuals would be desirable.

**Disclosures:** A. Yasuyo, None.

This study received funding from: The Japan Society for the Promotion of Science.

## SU351

**Fractures of the Spine and Hip Increase the Risk of Death in Canadians.** G. Ioannidis<sup>1</sup>, A. Papaioannou<sup>1</sup>, N. Akhtar-Danesh<sup>\*1</sup>, W. M. Hopman<sup>\*2</sup>, T. Anastassiades<sup>3</sup>, J. C. Prior<sup>4</sup>, L. Pickard<sup>1</sup>, K. S. Davison<sup>4</sup>, C. C. Kennedy<sup>4</sup>, W. P. Olszynski<sup>5</sup>, D. Goltzman<sup>6</sup>, E. Papadimitropoulos<sup>7</sup>, J. P. Brown<sup>4</sup>, L. Thabane<sup>\*1</sup>, A. Gafni<sup>\*1</sup>, R. G. Josse<sup>8</sup>, D. A. Hanley<sup>9</sup>, J. D. Adachi<sup>1</sup>. <sup>1</sup>McMaster University, Hamilton, ON, Canada, <sup>2</sup>Queen's University, Kingston, ON, Canada, <sup>3</sup>University of British Columbia, Vancouver, BC, Canada, <sup>4</sup>Laval University, Ste-Foy, QC, Canada, <sup>5</sup>University of Saskatchewan, Saskatoon, SK, Canada, <sup>6</sup>McGill University, Montreal, QC, Canada, <sup>7</sup>Eli Lilly and Company, Toronto, ON, Canada, <sup>8</sup>Toronto University, Toronto, ON, Canada, <sup>9</sup>Calgary University, Calgary, AB, Canada.

Utilizing data from the Canadian Multicentre Osteoporosis Study (CaMos) we evaluated the association between new fractures and mortality over a 5-year period in a cohort of women and men from across Canada. A total of 7753 participants, 2187 men and 5566 women over the age of 50 years participated in this prospective study. New fractures were based on self-reports and included hip, vertebral, rib, forearm, pelvic, and others. The fracture groups were subdivided based on timing of the fracture: during the 1st, 2nd, 3rd or 4th/5th year; those without incident fracture were the reference. Multivariable Cox proportional hazards analyses were conducted to examine the association between the time to incident fracture and time to death. Hazard ratios and 95% confidence intervals (CI) were calculated. During the 5-years of follow-up, 636 (8.3%) participants died. Of these, 239 (11.1%) were men and 397 (7.2%) were women. For men, the adjusted results showed that the hazard ratio was 6.1 (95% CI: 1.4, 26.9) indicating a higher hazard for death in men with hip fracture during the 1st year compared with men without hip fractures. For women, the hazard ratio was 2.9 (95% CI: 1.0, 8.2) showing higher mortality for those with a hip fracture during the 1st year of follow-up as compared with women without these fractures. Also for women with vertebral fractures, the hazard ratios were 3.5 (95% CI: 1.1, 11.4) and 3.8 (95% CI: 1.5, 9.5) for those occurring during the 1st and 2nd year of follow-up, respectively. In conclusion, hip and vertebral fractures contribute importantly to deaths in Canadians. Thus, interventions that reduce fracture rates should be implemented to decrease mortality.

**Disclosures:** G. Ioannidis, None.

## SU352

**Very High Frequency of Poor Vitamin D Status in French Women with Bone Fragility.** F. E. Levy-Weil<sup>\*1</sup>, D. Sitruk-Khalfon<sup>\*2</sup>, S. Djennane<sup>\*1</sup>, C. Rosenberg<sup>\*1</sup>, Y. Nourmamod<sup>\*2</sup>, C. Cormier<sup>3</sup>, J. C. Souberbielle<sup>\*4</sup>. <sup>1</sup>Rheumatology Department, Centre Hospitalier Victor Dupouy, Argenteuil, France, <sup>2</sup>Biochemistry Laboratory, Centre Hospitalier Victor Dupouy, Argenteuil, France, <sup>3</sup>Rheumatology Department, Hopital Cochin APHP Université Paris-Descartes, Paris, France, <sup>4</sup>Physiology Laboratory, Hopital Necker-Enfants Malades, Paris, France.

Vitamin D is an important determinant of bone health. Inadequate vitamin D status might raise the risk of osteoporotic fracture by increasing bone loss from secondary hyperparathyroidism and by its direct effect on muscle strength.

The aim of this study was to determine and to compare the prevalence of vitamin D deficiency and its level of severity in post-menopausal osteopenic or osteoporotic French women with and without any fracture.

We measured serum 25-hydroxyvitamin D (25OHD) concentration in 261 women with a low bone density and/or a prevalent low trauma fracture seen consecutively in our unit from January 2006 to March 2008. History of secondary osteoporosis was excluded. 129 patients had at least one prevalent fracture while 132 had no prevalent fracture. As described among the recent literature, regarding its optimal benefit on multiple health outcomes, we used 30 ng/mL (75nmol/mL) as the cut-off point defining vitamin D inadequacy. Vitamin D status was categorised in four groups: normal (25OHD $>30$ ng/mL), moderate insufficiency (20ng/mL $<25$ OHD $<30$ ng/mL), severe insufficiency (10ng/mL $<25$ OHD $<20$ ng/mL) and deficiency (25OHD $<10$ ng/mL). Data are presented as median (interquartile range) for continuous variables, and as % (n/total) for nominal variables.

Women with prevalent fracture were significantly older than those without fracture [68 years (59-75) versus 62 years (57-70);  $p < 0.001$ ] and had a moderately, but significantly lower 25OHD serum level [15 ng/mL (9-22) versus 18.4 ng/mL (11.0-24.9);  $p < 0.01$ ]. Only 5 patients in each group had a 25OHD level above 30ng/mL. The proportion of women with a 25OHD concentration  $< 10$  ng/mL was not different in both groups [27.9% (36/129) in women with fracture versus 19.7% (26/132) in those without fracture] but more women with a previous fracture had a 25OHD level  $< 20$  ng/mL [67.4% (87/129) versus 53.8% (71/132);  $p < 0.05$ ]. There was no correlation between age and 25OHD neither in the whole population nor in each separate group.

This study confirms that vitamin D inadequacy is highly prevalent in French women with bone fragility. Adequate vitamin D supplementation may thus significantly improve bone health in this population.

**Disclosures:** F.E. Levy-Weil, None.

## SU353

**Femoral Neck and Trochanteric Fractures and Vitamin D.** M. J. Davis<sup>\*</sup>, F. H. N. Budden. Medicine, St. Joseph's Health Centre, Toronto, ON, Canada.

The relevance of the femoral neck and trochanteric fracture is reviewed in relation to age, sex, serum calcium, albumin, and 25OH vitamin D3 in patients with a "fractured hip". The charts and laboratory results of 127 in-patients, admitted to an orthopaedic unit in a community hospital in 2007, were reviewed electronically.

Mean age was 80.56 years, median age 82 years and range 51-98 years. 94, 74% were women and 33, 26% were men. 37, 29% had femoral neck fractures and 90, 71% had trochanteric fractures. 29 women, 78% and 8 men, 22% had femoral neck fractures. 65 women, 73% and 25 men, 27% had trochanteric fractures.

Not all of the patients had blood work done. Blood work was done post-operatively. 112 patient had serum calcium and albumin measured. Mean serum calcium was 2.16 mmol/L, median 2.17 mmol/L and range 1.82-2.44 mmol/L. Normal range is 2.20-2.60 mmol/L. No patient was hypercalcemic. Serum albumin mean was 29.7 g/L, median 30.5 g/L, and range 15-41 g/L. Normal range is 35-50 g/L. 70 patients had 25OH vitamin D3 measured with the mean 36.39 nmol/L, median 32 nmol/L and range  $< 12$ -92 nmol/L. 25OH vitamin D3 deficiency is less than 25 nmol/L, insufficiency is 25-75 nmol/L and an adequate level is above 75 nmol/L. 5 patients had a 25OH vitamin D3 level greater than 75 nmol/L. The lowest monthly average 25OH vitamin D3 was 22.2 nmol/L in March.

These patients were old which is a risk for any fracture, particularly the "fractured hip". Women had femoral neck and trochanteric fractures three times more often than men. The femoral neck fracture is considered the paradigm of osteoporotic fractures while the trochanteric fracture is rarely mentioned. A trochanteric fracture was three times more frequent than a femoral neck fracture. The trochanter is large and strong relative to the femoral neck. In the orthopaedic literature, trochanteric fractures are associated with poorer functional outcome and higher morbidity and mortality than the femoral neck. The low serum albumin may reflect their poor nutritional status pre-operatively but also is decreased by trauma and the surgical procedure. Except for 5 patients, all were either 25OH vitaminD3 deficient or insufficient. This reflects their low vitamin D3 state pre-admission but the vitamin D3 level drops post-operatively due to a decrease in the D binding protein. The few younger men had lower vitamin D3 levels than the older men, possibly caused by poor nutrition. The patients with femoral neck fractures had lower vitamin D3 levels than the trochanteric fractures.

This was a retrospective study fraught with problems: a small number of subjects with incomplete laboratory investigations. This study raised more questions to be answered Question: "Is the femoral neck fracture associated more with vitamin D3 deficiency while the trochanteric fracture is related more to "pure" osteoporosis?"

**Disclosures:** F.H.N. Budden, None.

## SU354

### Questionnaire-based Osteoporosis Risk Assessment in a Rural Area Primary Care Setting. H. Schober<sup>1</sup>, M. Lüder<sup>2\*</sup>, K. Biebler<sup>3</sup>, R. Andresen<sup>4</sup>.

<sup>1</sup>Internal Medicine, City Hospital Südstadt Rostock, Teaching Hospital of University of Rostock, Rostock, Germany, <sup>2</sup>General Practice Wolgast, Wolgast, Germany, <sup>3</sup>Biometry Center, Ernst Moritz Arndt University Greifswald, Greifswald, Germany, <sup>4</sup>Department of Radiology, Hospital Güstrow, Teaching Hospital of University of Rostock, Güstrow, Germany.

Osteoporosis represents a major health problem. Major risk factors include age and diminished bone density. Recommendations for bone mass measurement are based on the patients' history. The aim of the present study was to evaluate the proportion of patients at risk of osteoporosis as identified by a questionnaire in a primary care setting.

Patients (n=1500) presenting to a general practitioner in a rural area were offered a questionnaire, resulting in 737 complete data sets (508 females/229 males) for analysis. Questions were related to estrogen deficiency (menarche, menopause, amenorrhoe, pregnancy), increased fracture susceptibility (fractures at age > 40 ys), parental fractures, specific diseases (asthma, rheumatoid arthritis, hyperthyroidism), drug therapy (heparin, coumarin, steroid), diet, and physical activity. Results for every question were scored in increments of ten (maximal score 2,325 points). Points were not assigned to patient's age. Patients suffering from overt osteoporosis were used as control group.

Scores varied between 15 and 822. Females demonstrated significantly higher scores compared to males (p<0.04). Among controls with established osteoporosis, 61.3 % achieved scores exceeding 200 points, and 43.4 % more than 250 points. Using the latter criterion as risk threshold, 13.5 % (66 females/28 males) of the study population was identified. Part of these patients underwent bone density measurement (QCT) which revealed osteoporosis in 54 % and osteopenia in 25 %, respectively. This investigation established an overall proportion of questionnaire-based patients with osteoporosis to 10.3 %. All of these patients were older than 64 years.

Using a questionnaire, 13.5 % of patients presenting to a general practitioner in a rural area could be identified of being at risk for osteoporosis. After bone density analysis, this number was corrected to 10.3 %. A questionnaire-based approach to osteoporosis risk assessment is a simple and potentially useful tool in detecting patients at risk for osteoporosis.

**Disclosures:** H. Schober, Procter & Gamble Pharmaceuticals Germany 3.

This study received funding from: Procter & Gamble Pharmaceuticals Germany.

## SU355

### The Relationship Between Clinical Risk Factors for Osteoporosis and BMD in Women Aged Less than 50 Years. M. S. Surdhar\*, I. Fogelman, G. M. Blake, M. L. Frost. Osteoporosis Screening & Research Unit, King's College London, London, United Kingdom.

Currently there are no clear guidelines on how to identify, diagnose or treat premenopausal women who may be at risk of osteoporosis or early bone loss. The aim of this study was to investigate the relationship between clinical risk factors for osteoporosis and BMD in a large group of women aged less than 50 years to identify which risk factors have the greatest impact on BMD. This will provide important information to facilitate DXA referral decisions in the premenopausal population. The study population consisted of 552 women aged less than 50 years. 432 were found to have one or more of the following risk factors (i) a history of atraumatic fracture; (ii) a BMI less than 20kg/m<sup>2</sup>; (iii) X-ray osteopenia; (iv) a medical condition known to influence bone metabolism; (v) current use of therapy known to influence bone metabolism; (vi) a family history of osteoporosis; (vii) Premature menopause before age of 45 years; (viii) Amenorrhoea greater than 6 months duration. BMD was measured at the lumbar spine (LS), femoral neck (FN) and total hip (THIP) using DXA. Multivariate regression analysis was used to calculate the Z-score decrements associated with each of the eight clinical risk factors. A significant difference in LS, FN and THIP BMD between those with and without risk factors was observed (p<0.001). Fifteen percent of women with clinical risk factors had a T-score equal to or less than -2.5 compared to 1% of those without risk factors. Z-score decrements associated with each risk factor are shown in the table.

Table: Z-score decrements associated with each clinical risk factor

	LS BMD	FN BMD	THIP BMD
History of fracture	-0.61 (0.15)**	-0.62 (0.14)**	-0.57 (0.12)**
BMI less than 20	-0.63 (0.15)**	-0.79 (0.13)**	-0.79 (0.12)**
X-ray osteopenia	-0.56 (0.40)	-0.05 (0.36)	-0.06 (0.31)
Medical condition	-0.09 (0.15)	-0.08 (0.13)	-0.05 (0.11)
Therapy	-0.20 (0.12)	-0.18 (0.11)	-0.10 (0.09)
Family history	-0.13 (0.11)	-0.12 (0.10)	-0.09 (0.09)
Early menopause	-0.22 (0.12)	-0.03 (0.11)	-0.04 (0.10)
Amenorrhoea	-0.43 (0.13)**	-0.29 (0.11)*	-0.26 (0.10)*
No risk factors	0.19 (0.09)	0.17 (0.08)	0.13 (0.07)

\* p = <0.05 vs. no risk factors; \*\* p = <0.001 vs. no risk factors.

The lowest Z-scores were found in those women with history of an atraumatic fracture, a BMI less than 20 and a history of amenorrhoea for both spine and hip BMD. This study may aid in the identification of younger women aged less than 50 years who should be referred for osteoporosis screening using DXA.

**Disclosures:** M.L. Frost, None.

## SU356

### No Fracture Is a Poor Predictor of Fracture Risk. A. Hoiseth. Sentrum Rtg., Oslo, Norway.

Fractures are reported to be an independent risk factors for new fractures. However, as early as in 1994 a group of experts (WHO technical report on osteoporosis) commented that many first fractures occur too late in life to be useful as risk predictors. We address the associations between earlier in life fractures and fractures occurring in age group 66-75 and age >75. Fracture data (age at fracture, fracture types and fracture sequela) were recorded in two cohorts of women (N=5138 and 8731) at routine bone densitometry (DXA). Results were considered "significant" when the two cohorts agreed. Results are presented as pooled for the two cohorts. Fractures were grouped as number of fractures and fracture types. More than 3 fractures were recorded as 3 fractures. The fractures were classified as: 'Femoral', at least a femoral fracture; 'Vertebral', at least a vertebral fracture but no femoral fractures and 'Other', one or more fractures but no femoral or vertebral fractures (results not presented). Age at first fracture was classified as 'Early', before age 50; 'Middle-age', between age 50 and 65 and 'Late', after age 65. **Results** There was an increasing frequency of cases with first fractures with increasing age: Of those aged 66-75, respectively 30.0%, 39.7% and 30.3% had an Early, Middle-age and Late first fracture. For cases >75 the values were 18.2%, 23.8% and 57.9%. Those with Late first fracture reported the smallest number of fractures: In age group 66-75, 40.0% with an Early first fracture had suffered one fracture only as compared to 70.3% for those with a Late first fracture. The respective values for cases aged >75 were 29.1% and 62.7%. The fractures were somewhat more severe in those with a late first fracture: In age group 66-75, 9.6% of the cases with an Early first fracture suffered a Femoral fracture and 13.3% a Vertebral fracture, with a Middle-age first fracture the values were respectively 15.3% and 8.8% and with a Late first fracture 23.5% and 10.6%. The respective values for cases aged >75 were 18.8% and 13.6%; 13.0% and 14.4%; 22.6% and 16.0%. Cases with a late in life first fracture reported a higher frequency of sequela: In age group 66-75 10.0% with an Early first fracture reported a sequela as compared to 19.8% in those with a Late first fracture. In cases >75 the values were 17.3% and 25.2%. **Conclusion** Our results support the view held by the WHO-report from 1994. A large proportion of first fractures occur too late in life for using previous fractures as a predictor for later fractures; having had no fracture early in life does not imply low late in life fracture risk. Although those with early fractures had the largest number of life-time fractures, those with late in life first fractures suffered the most severe fractures. Excluding cases with no "previous" fractures for further fracture risk assessment, for example by DXA, may substantially underestimate real fracture risk.

**Disclosures:** A. Hoiseth, None.

## SU357

### Reduced Renal Function Is Associated with Increased Rates of Bone Loss At The Hip And Spine: The Canadian Multicentre Osteoporosis Study. S. A. Jamal<sup>1</sup>, D. A. Hanley<sup>2</sup>, J. Prior<sup>3</sup>, A. Papaioannou<sup>4</sup>, R. G. Josse<sup>1</sup>, D. Goltzman<sup>5</sup>. <sup>1</sup>Medicine, University of Toronto, Toronto, ON, Canada, <sup>2</sup>Medicine, University of Calgary, Calgary, AB, Canada, <sup>3</sup>Medicine, University of British Columbia, Vancouver, BC, Canada, <sup>4</sup>Medicine, McMaster University, Hamilton, ON, Canada, <sup>5</sup>Medicine, McGill University, Montreal, QC, Canada.

The relationship between renal function and rates of bone loss is unclear.

We determined the association between changes in BMD at the total hip, femoral neck and lumbar spine over 5 years and estimated glomerular filtration rate (eGFR) among men and women aged 50 and older participating in CaMos.

We restricted our analyses to men and women aged 50 and older in whom serum creatinine was measured at baseline. We calculated the eGFR using the Cockcroft-Gault formula. We calculated the percent change in BMD at the total hip, femoral neck and lumbar spine over 5 years. We used linear regression to determine the annualized percent change in BMD per 10 mL/min/1.73m<sup>2</sup> of eGFR. Results are stratified by gender, and adjusted for baseline BMD, and creatinine.

Data on 191 men and 444 women was available for analysis. The mean age of women was 58.7 (±11.7) years, the mean body weight 64.4 kg (±12.9) kg and the creatinine at study entry was 74.3 (±13.3) mmol/L. Men were slightly older 57.7 (±13.0) years, weighed more: 77.9 (±12.3) kg and had a higher creatinine at baseline: 92.8(±16.6) mmol/L. Among women, for each 10 mL/min/1.73m<sup>2</sup> decrease in eGFR femoral neck BMD decreased by 1.6% (95% Confidence Interval: 0.76 to 2.42), total hip BMD decreased by 1.7% (95% CI: 0.84 to 2.5) and spine BMD decreased by 1.3 (95% CI: 0.44 to 2.1). In contrast among men, there was no significant decrease in femoral neck BMD 0.54% (95% CI: -0.9 to 1.98), total hip BMD (0.5%; 95% CI: -0.95 to 1.94), or lumbar spine BMD 0.4% (95% CI: -0.94 to 1.84).

Our findings indicate that among women, but not men, there is a strong and consistent decrease in BMD at the hip and spine with worsening renal function based on the eGFR. One potential explanation for the lack of relationship between bone loss and eGFR in men is the small sample size and the small change in BMD over time. Our findings, together with those of others, highlight the importance of renal function as a risk factor for bone loss and fracture.

**Disclosures:** S.A. Jamal, None.

## SU358

**Are There Any Ethnic Differences in Bone Mineral Density in a Lupus Cohort?** A. Costinescu\*<sup>1</sup>, I. Moldovan\*<sup>2</sup>. <sup>1</sup>University of Medicine and Pharmacy, Bucharest, Romania, <sup>2</sup>Loma Linda University, Loma Linda, CA, USA.

The purpose of this study is to determine if there are any differences in bone mineral density (BMD) between Hispanic and Caucasian patients in a lupus cohort. The charts of one hundred Hispanic and fifty Caucasian patients with SLE (systemic lupus erythematosus) were reviewed. Twenty Hispanic (previously presented in an abstract) and nine Caucasian women that had their BMD assessed by dual X-ray absorptiometry (DXA) were identified. The patients were divided into pre- and post menopausal status and the Hispanics were compared to the Caucasians within the two groups. Statistical analysis was performed using the student t-test. Clinical determinants of BMD that were recorded included age, height, weight, body mass index (BMI), duration of disease, SLE disease activity index (SLEDAI) at the time of the DXA scan, SLE damage index (SLICC), steroid treatment as well as use of immunosuppressive and osteoporosis medications. There was no statistically significant difference between the Hispanic and Caucasian pre- and postmenopausal groups in terms of age, average BMI, duration of SLE, average SLEDAI score and average prednisone dose. BMI results for Hispanic women were in the range of overweight as opposed to the Caucasian patients, who had BMI within normal range. Four Hispanic premenopausal and five postmenopausal patients were obese, as opposed to one Caucasian obese patient in each group. The Hispanic premenopausal women had statistically significant ( $P=0.001$ ) more damage from lupus by SLICC score. Overall, seventeen Hispanic patients (85%) were taking glucocorticoids, but only five (25%) were taking medications for osteoporosis, including bisphosphonates, calcium and vitamin D. In the Caucasian population, six patients (67%) were on glucocorticoids, and five (55%) out of nine patients were on medications for osteoporosis. Our analysis showed that the postmenopausal Caucasian women were found to have a statistically significant lower BMD at the hip, as compared to the Hispanic ones. Neither the spine, nor the femoral neck sites examined showed any significant difference for Hispanics versus Caucasians within the respective groups. However, 15% of the Hispanic patients were found to be osteoporotic and 30% were osteopenic as opposed to 33% and respectively 55% of the Caucasians. In conclusion, this small study suggests that the Caucasian lupus women are more prone to osteopenia and osteoporosis, especially after menopause, when compared to the Hispanic patients. The role of higher BMI observed in our Hispanic patients, in preserving bone mass is yet to be determined. Larger studies are needed to better define the distinct characteristics of the two ethnic populations that are affected by lupus.

**Disclosures:** A. Costinescu, None.

## SU359

**Carotid Plaque Causes Low Spinal Bone Mineral Density in Korean Postmenopausal Women with Diabetes.** D. Byun, J. Kim\*, M. Roh\*, J. Mok\*, Y. Kim\*, H. Park\*, C. Kim\*, S. Kim\*, K. Suh\*, M. Yoo\*. Endocrinology, Soonchunhyang University Hospital, Seoul, Republic of Korea.

**Background:** Recent studies suggest a possible pathogenic linkage between the osteoporosis and atherosclerosis which closely related with diabetes. Both atherosclerosis and osteoporosis are independent predictors of cardiovascular disease (CVD) events, and may share common regulatory mechanisms. In this study we want to show the relationship between bone mineral density (BMD) and atherosclerotic parameters in Korean postmenopausal women with diabetes.

**Methods:** Total 60 postmenopausal women with diabetes were enrolled in the study. We measured pulse wave velocity (PWV), carotid intima-media thickness (IMT) and carotid plaque as a atherosclerotic parameters. We also checked anthropometric and serologic including HbA1C, C-peptide, lipid profiles and bone markers. The lumbar spine, femur neck and total hip BMD was measured using dual-energy X-ray absorptiometry (DXA).

**Results:** From multiple linear regression analyses of all the study subjects, lumbar spine, femur neck and total hip BMD were significantly decreased according to age ( $r^2 = -0.288$ ,  $p=0.028$ ,  $r^2 = -0.358$ ,  $p=0.003$ ,  $r^2 = -0.297$ ,  $p=0.023$  respectively). Serum calcium, aortic PWV, and mean IMT were significantly increased according to increase of age ( $r^2 = 0.386$ ,  $p=0.012$ ,  $r^2 = 0.396$ ,  $p=0.002$ ,  $r^2 = 0.297$ ,  $p=0.024$  respectively). From bivariate analyses, the lumbar spine, femur neck and total hip BMD showed a negative correlation with duration of diabetes ( $r^2 = -0.307$ ,  $p=0.019$ ,  $r^2 = -0.284$ ,  $p=0.03$ ,  $r^2 = -0.259$ ,  $p=0.05$  respectively). Lipid profile, IMT, PWV were not correlated with BMD. The prevalence of carotid plaque in our study was 30%. Only the patients with presence of plaque showed significantly decreased lumbar spine BMD compare to those with absence of plaque ( $p=0.048$ ). Patients with presence of carotid plaque also showed significant relationship with increased duration of DM ( $p=0.033$ ) and aortic PWV ( $p=0.001$ ) compare to patients with absence of carotid plaque.

**Conclusion:** Out of many atherosclerotic risk factors, carotid plaque causes low spinal BMD and has significant relationship with high serum calcium level, increased aortic PWV and increased duration of DM.

**Disclosures:** D. Byun, None.

This study received funding from: SOonchynhyang University.

## SU360

**Vertebral Fracture in Men: Level of Trauma, Bone Mineral Density and Lean Body Mass.** S. F. Evans\*, C. A. Sharp\*, M. W. J. Davie. Charles Salt Research Centre, Robert Jones & Agnes Hunt Orthopaedic Hospital NHS Trust, Oswestry, United Kingdom.

Low trauma vertebral fracture (LTVF) in men is associated with low lean body mass (ALMI) and low bone density (BMD). Recent data suggest that men with high trauma fracture also have low BMD. We have investigated whether men with high trauma vertebral fracture (HTVF) have low ALMI and low BMD.

Men with clinical vertebral fracture (referred with symptoms) were categorised as having low trauma (fall from no more than standing height or no discernible trauma;  $n=59$ ; age  $63 \pm 13$ yr) or high trauma (fall from more than standing height  $n=30$ ; age  $60 \pm 12$ yr). Control subjects ( $n=180$ ; aged 16-84yr) with no fracture and no significant medical history were taken from a larger study of osteoporosis in men. BMD (L2-4=LS; Femoral neck=FN) and ALMI  $\{=(\text{sum of lean in all four limbs})/\text{Ht}^2\}$  were measured by DXA (Hologic QDR4500). T scores were established from control men aged 20-39yr and Z scores from appropriate age groups. Differences were established by Chi square or by the Binomial test. The study was approved by the local research ethics committee.

Results are shown in the Table.

	Low trauma VF			High traumatic VF		
	LS-BMD	FN-BMD	ALMI	LS-BMD	FN-BMD	ALMI
<b>T score</b>	-1.36	-1.83	-0.69	-0.98	-1.58	-0.27
% with < T-2.5	15	28	2	7	17	0
<b>Z score</b>	-1.28	-1.15	-0.51	-0.93	-0.90	-0.14
% Z score < ZERO	91	88	66	77	87	52

The proportion of patients with BMD T score less than -2.5 did not differ between groups. In both groups there were significantly more men with BMD Z score values below zero at both FN and LS sites (Binomial test,  $p<0.01$ ), deficits at both sites being similar for both LTVF and HTVF. ALMI was significantly low in LTVF but not HTVF. Men with vertebral fracture have low BMD irrespective of degree of trauma but low ALMI is a feature of low trauma VF only. This suggests that ALMI may influence the risk of minor trauma in leading to a vertebral fracture.

**Disclosures:** M.W.J. Davie, MSD 2, 3; Procter & Gamble 4; Servier 3.

This study received funding from: Bone Disease Foundation.

## SU361

**A Computer-based Measure Using Normalized Heights Predicts Vertebral Fracture Independent of BMD in Post-menopausal Women.** A. Ghosh\*<sup>1</sup>, M. Bruijine\*<sup>2</sup>, P. Pettersen\*<sup>3</sup>, M. Karsdal\*<sup>1</sup>, D. Leeming\*<sup>1</sup>, C. Christiansen\*<sup>1</sup>, M. Nielsen\*<sup>2</sup>. <sup>1</sup>Nordic Bioscience, Herlev, Denmark, <sup>2</sup>University of Copenhagen, Copenhagen, Denmark, <sup>3</sup>Center for Clinical and Basic Research, Ballerup, Denmark.

Baseline deformity in the vertebral shape plays an important role in spine fracture risk assessment for post-menopausal women. Since they are discrete, most of these measures can not be used in progressive monitoring of fracture risk. Building on these methods a novel computer based continuous vertebral fracture risk measure is proposed. The most deformed (maximum difference in heights) one among T12-L5 vertebrae for each of the individuals in the study was chosen. To adjust for the variation due to the physical size of the subjects, the three vertebral heights (anterior, posterior and middle) were normalized to unit average. The risk for an individual to sustain a fracture was computed using a probability measure derived from a quadratic classifier based on the minimum and the maximum of the normalized heights.

There were 72 healthy elderly women in the study, of which 36 maintained skeletal integrity (Group 1) and 36 sustained at least one fracture in the lumbar spine over a 7.5-year study period (Group 2). The two groups were carefully matched for age ( $65.8 \pm 1$  vs.  $64.6 \pm 1.3$ ), BMI ( $25.1 \pm 0.63$  vs.  $24.8 \pm 0.63$ ), spine BMD ( $0.83 \pm 0.02$  vs.  $0.83 \pm 0.03$ ), smoking habits (8 vs. 7), and physical activity at baseline. The quadratic classifier to compute the continuous measure of the fracture risk was built using the subjects at baseline and to separate test from training, the fracture risks for the baseline subjects were calculated in a leave-one-out fashion.

Separating the future fractures based on baseline measurements, the area under the ROC curve was 0.76. At baseline, the means of the fracture risk for Group 2 and Group 1 were significantly different ( $0.6 \pm 0.03$  vs.  $0.4 \pm 0.04$ ,  $p < 10^{-3}$ ). A fracture further increased the risk measure ( $0.9 \pm 0.03$  vs.  $0.6 \pm 0.03$ ,  $p < 10^{-7}$ ) in Group 2, whereas no statistically significant change was detectable in Group 1 between baseline and follow up ( $0.4 \pm 0.04$  vs.  $0.5 \pm 0.04$ ,  $p=0.06$ ). The increase in the risk in Group 1 from baseline to follow up was consistent with the clinical findings that the fracture risk increases with age. Defining high/low risks as above/below the median measurements the proposed method yields significantly larger odds ratio compared to the traditional height ratios (7 vs. 3.3), justifying the choice. The continuous nature of the measure also enables us to assess the severity of risk.

We envisage that the method will lead to efficient prediction of vertebral fracture facilitating: (a) early diagnosis, (b) decrease in the required sample size for studies, and (c) easier assessment of the efficacy of fracture preventing drugs.

**Disclosures:** A. Ghosh, None.

This study received funding from: Nordic Bioscience A/S.

## SU362

**Muscle Power and Tibial Bone Strength in Older Women.** M. C. Ashe, T. Y. L. Liu-Ambrose\*, D. M. L. Cooper\*, K. M. Khan, H. A. McKay. Centre for Hip Health, Vancouver, BC, Canada.

Previous literature has highlighted the importance of strength training on bone outcomes in older women. However, to our knowledge, there are no reports that investigated the relation between muscle power and bone strength for this age group. Therefore, the purpose of this study was to assess the association between muscle power and tibial bone strength in older women aged 65-75 years. Seventy-four community-dwelling healthy older women aged 65-75 years were recruited. Muscle power and strength (one repetition maximum; 1RM) of bilateral leg extension was measured using Keiser air-pressure resistance equipment (Keiser Sports Health Equipment, Fresno, California). Participants were asked to wear a waist-mounted ActiGraph (GT1M ActiGraph, LLC, Fort Walton Beach, FL) accelerometer to objectively record physical activity for 7 days. In addition, participants were asked to recall physical activity in the previous 7 days using the Physical Activity Scale for the Elderly (PASE) self-report questionnaire. Peripheral quantitative computed tomography (pQCT) was used to measure tibial mid-shaft (50% site) bone strength (strength-strain index, section modulus). We used Pearson correlations and multi-level linear regression to investigate the associations between muscle performance and bone strength. Muscle power contributed 6.6% ( $p=0.007$ ) of the variance for bone strength-strain index and 8.9% ( $p=0.001$ ) of the variance of section modulus in older women after accounting for age, height, weight and self-report physical activity (PASE). Moderate-vigorous physical activity (MVPA) as recorded by accelerometry was significantly related to muscle power in the lower extremity ( $r=0.260$ ;  $p=0.041$ ). There were no significant associations between muscle strength (1RM) in the lower extremity and bone strength or MVPA. In this cross-sectional investigation, muscle power significantly contributed to estimated bone strength and was associated with MVPA in healthy community dwelling older women. Further investigation is necessary to determine whether power training will prove to be a more effective stimulus for bone strength than conventional strength training.

**Disclosures:** M.C. Ashe, None.

This study received funding from: Canadian Institutes of Health Research, British Columbia Medical Services Foundation, Michael Smith Foundation for Health Research.

## SU363

**High Sex Hormone Binding Globulin (SHBG) Levels in Older Patients with Acute Hip Fracture Are Correlated with Worse Function and Increased Bone Resorption.** A. Egli<sup>\*1</sup>, B. Dawson-Hughes<sup>2</sup>, R. Theiler<sup>\*3</sup>, H. Staehelin<sup>\*4</sup>, J. Henschkowski<sup>\*1</sup>, H. A. Bischoff-Ferrari<sup>1</sup>. <sup>1</sup>Rheumatology, University of Zurich, Zurich, Switzerland, <sup>2</sup>Tufts University, Boston, MA, USA, <sup>3</sup>Rheumatology, Triemli StadtSpital, Zurich, Switzerland, <sup>4</sup>Geriatrics, University of Basel, Basel, Switzerland.

**Background:** Previous studies suggested that higher SHBG levels are associated with an increased hip fracture risk and that higher testosterone levels may reduce the odds of falling among men and women age 65 and older. **Aim:** To study the correlation of serum testosterone and SHBG with function (timed up & go test) and bone resorption (urinary deoxypyridinolin = DPD) within 1 to 2 weeks after hip fracture surgery. **Results:** Mean age was 86 year ( $\pm 6.9$ ), 79% women, and 69% admitted from home. These are baseline data from the ongoing Zurich hip fracture trial with vitamin D including 173 patients with acute hip fracture. Total testosterone serum levels were above the laboratory detection threshold ( $> 0.1$  nmol/l) in 33 of 36 men and in 57 of 135 women. Mean total testosterone levels were  $5.16 (\pm 4.51)$  nmol/l in men and  $0.60 (\pm 0.41)$  nmol/l in women. We did not find significant univariate correlations between total testosterone and function or DPD in men or women. Mean serum SHBG levels were  $47.9 (\pm 17.4)$  nmol/l in men and  $58.4 (\pm 20.0)$  nmol/l in women. Among men and women, higher SHBG levels correlated with slower performance in the timed up&go test (men:  $r = 0.49$ ,  $p = 0.01$ ; women:  $r = 0.35$ ,  $p < 0.0001$ ). Similarly, higher SHBG levels were correlated with higher urinary DPD excretion in men ( $r = 0.37$ ,  $p = 0.03$ ) and women ( $r = 0.18$ ,  $p = 0.02$ ). In the multivariate model, a higher SHBG level was significantly associated with slower performance in the timed up&go test ( $p = 0.001$ ) independent of age, gender, type of dwelling, serum 25(OH)D level, and body mass index. Apart from SHBG level, only female gender was associated with slower test performance (0.03). Furthermore, in the second multivariate model, a higher SHBG level was significantly associated with higher DPD excretion ( $p = 0.03$ ) independent of age, gender, type of dwelling, serum 25(OH)D level, and body mass index. Adding testosterone to both multivariate models did not change significance of SHBG and testosterone had no independent effect. **Conclusion:** Higher SHBG levels in patients with acute hip fracture are independently associated with worse function and increased bone resorption during acute care after hip fracture surgery. Total testosterone levels were low in men with acute hip fracture, and did not correlate with function or DPD excretion in men or women early after hip fracture surgery.

**Disclosures:** H.A. Bischoff-Ferrari, None.

This study received funding from: Swiss National Foundations.

## SU364

**Effects of Neurological Impairment and Functional Mobility on Bone Mineral Density Following Stroke: A Pilot Study.** N. M. Wysocki\*, S. H. Saxon\*, P. Supanwanid\*, Y. Wang\*, R. L. Harvey\*, E. J. Roth\*, T. J. Schnitzer. Physical Medicine and Rehabilitation, Northwestern University Feinberg School of Medicine, Chicago, IL, USA.

Stroke patients have a 2-4 fold increased risk of hip fracture compared to the general population, primarily on the paretic side. Decreased bone mineral density (BMD) on the paretic side may be an important risk factor. However, the relationship between BMD and stroke related motor impairment and functional mobility is not known. The purpose of this study was to investigate the relationship between bone mineral density (BMD), neurological impairment, and functional limitations in stroke patients and to identify risk factors for osteoporosis in this population. A cross-sectional study design was used; a convenience sample of 33 stroke patients was recruited from an outpatient rehabilitation clinic. Descriptive data including demographics and clinical history were collected. Patients answered a questionnaire regarding functional status, and motor function was assessed by trained physicians using the motor components (questions 4-7) of the NIH stroke scale (NIHSS), (possible score 0 - 21). BMD was measured using dual energy X-ray absorptiometry (DEXA). ANOVA was used to compare BMD between patients with differing walking ability and neurological impairment. Paired t-test was used to compare BMD between the paretic and non-paretic hip. The patients' mean age was  $58.4 \pm 14.5$  years; there were 19 male and 14 female patients; time post-stroke was  $6.3 \pm 6.3$  years. Patients with more severe neurological impairment (higher sum NIHSS) had lower BMD at the paretic total hip ( $r = -0.396$ ,  $p = 0.027$ ) and non-paretic total hip ( $r = -0.469$ ,  $p = 0.007$ ). Patients with limited walking ability had lower BMD and Z-score at both the paretic and non-paretic total hip ( $p = 0.014$  and  $p = 0.035$ , respectively). BMD and Z-score were significantly decreased in the paretic vs. non-paretic limb at the hip ( $t = 3.31$ ;  $p = 0.002$ ). The majority of patients (73%) had decreased BMD at the paretic hip compared to age matched normals (average z-score,  $-1.22$  at paretic hip). Of note, most patients in this study were not being treated for low bone mass or osteoporosis. Only 3% of patients were being treated with a bisphosphonate, 12% with vitamin D supplements, and 15% with calcium supplementation. In conclusion, this study suggests that severe neurological impairment and reduced walking ability are associated with low BMD following stroke and that the BMD in the paretic lower limb is more affected than the nonparetic leg. This study highlights the effect that disuse and function can have on BMD and reinforces the importance of addressing bone health and osteoporosis risk in stroke patients.

**Disclosures:** N.M. Wysocki, None.

This study received funding from: Proctor and Gamble.

## SU365

**Genetic Variation in IL6 and LRP5 Is Associated with Osteoporosis in the Marshfield Clinic Personalized Medicine Project: Evidence for Interaction with Smoking.** P. Giampietro<sup>1</sup>, C. McCarty<sup>\*2</sup>, B. Mukesh<sup>\*2</sup>, F. McKiernan<sup>1</sup>, D. Wilson<sup>1</sup>, A. Shuldiner<sup>\*3</sup>, J. Levasseur<sup>\*3</sup>, L. Ivacic<sup>\*2</sup>, T. Kitchner<sup>\*2</sup>, N. Ghebranious<sup>\*2</sup>. <sup>1</sup>Marshfield Clinic, Marshfield, WI, USA, <sup>2</sup>Marshfield Clinic Research Foundation, Marshfield, WI, USA, <sup>3</sup>University of Maryland School of Medicine, Baltimore, MD, USA.

Osteoporosis is a complex disease mediated by genetic and environmental factors. A nested case-control study within the Marshfield Clinic Personalized Medicine Research Project was performed to assess the relative impact of cigarette smoking, statin use, genetic polymorphisms, and one-way interaction of these factors on the development of osteoporosis in post-menopausal women. Genotyping of 14 SNP alleles corresponding to VDR, ESRI, COL1A1, IL-6, TGF- $\beta$ , ApoE and LRP5 genes, was performed on 309 postmenopausal Caucasian females with osteoporosis (DXA T-scores  $\leq -2.5$  (spine, femur or radius) or history of low energy fracture) and 293 matched controls without osteoporosis (T-scores  $> -2.5$ ). The ethnic composition of the sub population studied was 99.7% Caucasian with predominant German ancestry. Cases differed from controls with respect to BMI (cases:  $32.9 \pm 6.7$  vs. controls:  $26.9 \pm 5.0$ ;  $p < 0.001$ ), mean age ( $70.4 \pm 9.4$  vs.  $61.6 \pm 8$  years,  $p < 0.001$ ) and smoking (70.2% cases 'never smoked' vs. 60.1% controls;  $p = 0.02$ ) but not statin use. SNPs were chosen based upon known function consequences or prior evidence for association in other studies and were genotyped using MALDI-TOF. The IL6-C634G (rs1800796) C allele of the promoter region was found to be associated with osteoporosis (odds ratio (OR) for CC + CG = 2.51 (95% CI=1.33, 4.75;  $p = 0.0047$ ), independent of statin use or smoking status.) This finding replicates the association of rs1800796 with osteoporosis reported by Ota et al. (J Hum Genet 2001; 46: 267-272) in a Japanese population. However, we found the opposite allele associated with osteoporosis suggesting the causative variant may be on a different haplotype in the two populations. On stratification for smoking, an association with LRP5 (C135242T) and osteoporosis emerged (OR 2.8 in smokers with the A/G allele (95% CI= 1.1, 7.0  $p = 0.03$ ), suggesting a role for an environmental interaction in this association. In conclusion, we provide evidence for a role of genetic variation in IL6 and LRP5 in osteoporosis risk in Caucasian women, the latter manifest only in smokers.

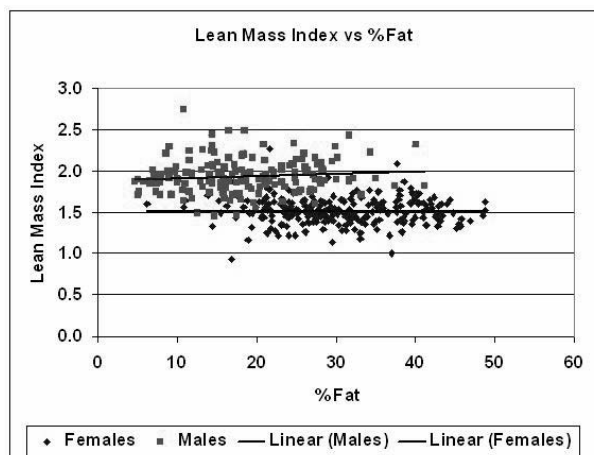
**Disclosures:** P. Giampietro, None.

This study received funding from: Marshfield Clinic Research Foundation.

## SU366

**Establishing Healthy Body Composition Values with DXA.** M. K. Oates<sup>\*1</sup>, D. W. Oates<sup>\*1</sup>, H. S. Barden<sup>2</sup>, D. Ergun<sup>2</sup>. <sup>1</sup>Mary Oates M.D. Inc, Santa Maria, CA, USA, <sup>2</sup>GE Healthcare, Madison, WI, USA.

There is considerable interest for body composition reference data for healthy adults. Protocols for collecting reference data should be restricted to subjects with few, if any, medical conditions affecting general health and body composition, and should encompass a wide variety of body shapes and sizes. We are collecting male and female reference data of healthy subjects following a protocol that excludes subjects who have or have had medical conditions including, but not restricted to: coronary heart disease, diabetes, kidney disease, liver disease, HIV, cancer, eating disorders, hypertension under 50 years of age, surgical procedures for obesity, BMI less than 18 or greater than 40, and surgical implants. In addition, we excluded subjects who were dieting, did not exercise at least 3x a week, consumed >2 alcohol drinks/day, had smoked within the past 6 mo., or were professional athletes. We are reporting preliminary body composition results (age 18-59 years) measured with dual-energy X-ray absorptiometry (DXA) using Lunar iDXA or Lunar Prodigy (GE Healthcare). Average female and male age, height, weight, and BMI were 40.7 and 31.9 years, 164.5 and 179.4 cm, 63.8 and 82.6 kg, and 23.8 and 25.6 kg/m<sup>2</sup>, respectively. 117 women and 85 men were measured on the iDXA; 118 different women and 79 different men in a separate study were measured on the Prodigy. Mean %fat values by decade for iDXA and Prodigy were not significantly different between densitometers, except for male values that differed for age 18-29, due to more younger subjects measured with Prodigy. Lean Mass Index (LMI), defined as lean mass/height<sup>2</sup> may be useful to compare and identify muscular density of individuals of similar body BMI or %fat (Figure).



Age (yrs)	Male and Female %Fat by Age			
	Female iDXA %Fat Mean (sd)	Female Prodigy %Fat Mean (sd)	Male iDXA %Fat Mean (sd)	Male Prodigy %Fat Mean (sd)
18-29	28.3 (6.6)	27.4 (8.5)	19.8 (5.5)	13.2 (7.6)*
30-39	31.8 (8.1)	29.6 (10.0)	22.3 (6.1)	21.8 (7.4)
40-49	30.6 (7.6)	31.9 (9.6)	20.8 (6.1)	18.6 (9.3)
50-59	31.0 (7.4)	33.6 (7.3)	20.1 (5.2)	23.1 (7.9)

\* p<0.001

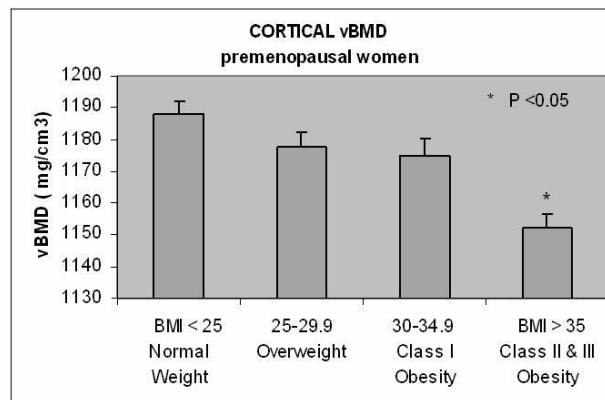
**Disclosures:** M.K. Oates, GE Healthcare 2.  
This study received funding from: GE Healthcare.

## SU367

**Hormonal Influences on Volumetric Bone Density and Geometric Properties in Obesity.** D. Sukumar<sup>\*1</sup>, Y. Schluskel<sup>\*1</sup>, H. Ambia-Sobhan<sup>\*1</sup>, C. Gordon<sup>2</sup>, T. Stahl<sup>\*3</sup>, S. Schneider<sup>\*3</sup>, S. A. Shapses<sup>1</sup>. <sup>1</sup>Nutritional Sciences, Rutgers University, New Brunswick, NJ, USA, <sup>2</sup>McMaster University, Hamilton, ON, Canada, <sup>3</sup>University Medicine & Dentistry of NJ, New Brunswick, NJ, USA.

Obesity is associated with an altered hormonal milieu and a higher bone density. We examined how body mass index (BMI) influences trabecular and cortical bone in women by examining hormones such as parathyroid hormone (PTH), estradiol (E2), vitamin D (25 OH D) and bone markers. We measured trabecular and cortical bone parameters including volumetric bone mineral density (vBMD), bone mineral content (BMC), geometric properties, polar moment of inertia (Ip) and stress strain index (SSI). We examined 174 women (ages 24-70 years) with extreme differences in BMI (18-57 kg/m<sup>2</sup>). Data was categorized by the four definitions of BMI (Figure) and assessed by analysis of variance in the pre- and post-menopausal women. Not surprisingly, all women with a BMI >35 kg/m<sup>2</sup> had higher trabecular BMC, vBMD, cortical BMC, area and thickness, periosteal circumference, Ip and SSI in comparison with normal weight women. Interestingly, premenopausal women with a high BMI (> 35 kg/m<sup>2</sup>) showed a lower cortical vBMD (p <

0.05) than leaner women (Figure) that may be explained by the higher serum PTH (R = 0.60, p<0.0001) and urinary pyridinoline (R = 0.38, p< 0.01). In contrast, BMI did not influence cortical BMD in postmenopausal women, but this may be due to the positive association between serum estrogen and PTH (R = 0.51, p < 0.01) that was analyzed in a subset of the postmenopausal women (n=56). Estrogen associated with obesity in postmenopausal women (R= 0.61, p < 0.001) may be preventing a catabolic effect of PTH on bone. An altered hormonal milieu associated with obesity may influence cortical bone although the role of other adipokines and hormones remain to be investigated.



**Disclosures:** D. Sukumar, None.

This study received funding from: NIH AG12161

## SU368

**Radiation-Induced Bone Loss: Description of Dose, Time Course, Age, Strain and Sex Variables.** L. C. Bowman<sup>\*1</sup>, E. W. Livingston<sup>\*1</sup>, J. S. Willey<sup>1</sup>, M. E. Robbins<sup>\*2</sup>, J. D. Bourland<sup>\*2</sup>, T. A. Bateman<sup>1</sup>. <sup>1</sup>Bioengineering, Clemson University, Clemson, SC, USA, <sup>2</sup>Radiation Oncology, Wake Forest University School of Medicine, Winston-Salem, NC, USA.

Cancer patients have an increased fracture risk resulting from atrophy after radiotherapy. Factors contributing to bone loss are poorly understood. The aim of these studies was to characterize a murine model of radiation-induced bone loss. Our goal was to describe how absorbed dose; animal age, strain, and sex; and time course early after exposure can influence trabecular bone parameters. Dose: 10-wk old female C57BL/6 (B6) mice received 2, 4, or 6 Gy X-rays (140 kVp)(n=5/group). Lower bone volume fraction (BV/TV; microCT analysis; proximal tibia) was observed 2-wks post-irradiation in all groups vs. non-irradiated control (2 Gy, -42%; 4 Gy, -39%; 6 Gy, -44%)(P<0.05). Deterioration of trabecular microarchitecture was also indicated by lower trabecular number and connectivity (P<0.05). No differences were observed between doses. 2 Gy was the lowest dose to produce bone loss without an effect on body mass. This dose was thus used in subsequent studies. Time Course: 20-wk-old female B6 mice were irradiated (n=12/group) and euthanized after either 7 or 14 days. Lower BV/TV (day 7, -32%; day 14, -42%) was observed at both time points (P<0.05). Based on these data, 2-wks after irradiation was used for subsequent studies. Age: Skeletally immature (9-wk old) and mature (19-wk old) female B6 mice were irradiated (n=6/group). BV/TV was lower in both immature and mature mice (9 wk, -42%; 19 wk, -35%) compared with age-matched controls (P<0.001). Strain 1: 19-wk old female B6 and BALBc mice were irradiated (2 Gy) and compared to strain-matched, non-irradiated controls (n=6/group). Irradiated B6 mice had lower BV/TV (-38%) vs. control (P<0.001). BALBc mice exhibited a non-significant decline in BV/TV (-17%, P=0.07). Strain 2: 13-wk-old female B6 and DBA/2 (DBA) mice were irradiated and compared with strain-matched, non-irradiated controls (n=6/group). BV/TV was lower for irradiated mice (B6, -35%; DBA, -29%)(P<0.01). Sex: 14-wk old male and female B6 mice were irradiated (n=6/group). Irradiated mice had lower BV/TV (male, -35%, P<0.05; female, -28%, P<0.01) vs. sex-matched, non-irradiated controls. In these murine studies, bone loss occurred early after exposure to moderate doses of X-rays across a broad range of conditions, including strain, age, sex, and absorbed dose. These changes occurred without a change in body mass. The consistent early skeletal response to radiation across murine strains and conditions facilitates the development of a robust animal model to study the cellular and molecular cause of atrophy after irradiation.

**Disclosures:** L.C. Bowman, None.

This study received funding from: NIH and NSBRI/NASA.

## SU369

**Obesity Is Associated with Higher BMD, Lower Bone Resorption and Slower Hip Bone Loss: Are these Associations Mediated by Adipokines?** J. Finigan, F. Gossiel\*, D. M. Greenfield\*, R. A. Hannon, R. Eastell. University of Sheffield, Sheffield, United Kingdom.

It is known that obesity is associated with a reduced risk of spine and hip fractures, higher BMD, lower bone turnover markers and slower rates of bone loss. It has also been observed that adipocyte-derived hormones, or adipokines, are altered in obesity: leptin is increased and adiponectin is decreased. The aim of this study was to investigate whether the bone differences associated with obesity are mediated by adipokines.

A population-based cohort of women 50-85 years old took part in a 10-year observational study with visits at 0, 2, 5, 7 and 10 years. Height, weight, fasting blood and urine samples, and BMD by DXA at the lumbar spine (LS), total hip (TH) and total body (TB) were measured at the 5-year visit. The annual percentage rate of change in BMD at TH was calculated for each subject from the regression line through all their available BMD results over a period of 5, 7 or 10 years. We identified 67 women with normal body mass index (BMI 18-25) and 34 obese women (BMI >30), excluding any subjects who were diabetic or taking HRT. We measured markers of bone resorption S-CTX (Elecsys, Roche; n=98) and U-NTX (Vitros Eci, Orthoclinical Diagnostics; corrected for creatinine, n=85), and also adiponectin (n=88) and leptin (n=87) (ELISA, R&D Systems), with log-transformation of the results.

There was no difference in age between obese and normal subjects, but in obese subjects BMD was higher at all sites ( $p<0.001$ ), CTX was lower ( $0.333 \pm 0.469$  ng/ml,  $p=0.016$ ) although NTX was no different ( $p>0.9$ ), and TH bone loss was slower ( $0.38 \pm 0.71$  %/yr,  $p=0.032$ ) compared to normal subjects. The obese women also had higher leptin ( $294.9 \pm 84.1$  pg/mL,  $p<0.001$ ) and lower adiponectin ( $124.6 \pm 162.7$  ng/mL,  $p=0.023$ ) than the normal subjects.

Leptin and adiponectin were associated, directly and inversely respectively, with TH BMD ( $p=0.006$ ,  $p=0.045$ ). Higher leptin was also associated with a lower rate of TH bone loss ( $p=0.024$ ). These associations were independent of BMI group and CTX, and for leptin, of NTX. There was no significant correlation between leptin or adiponectin and either resorption marker, even when adjusted for BMI group, although within the normal group only, leptin correlated with CTX ( $r=0.3$ ,  $p=0.031$ ).

We conclude that obesity is associated with higher BMD, lower bone resorption and slower rates of bone loss. Although the altered adipokine levels in obese women are associated with high BMD, they are not strongly associated with bone turnover or rates of hip bone loss and so are unlikely to mediate the effects of obesity on bone.

**Disclosures:** J. Finigan, None.

This study received funding from: Arthritis Research Campaign.

## SU370

**Baseline Characteristics of Women Taking Part in an Osteoporosis Intervention: the Primary Care Osteoporosis Risk of Fracture Screening (POROS).** D. Schneider\*, K. Worley\*, K. Campbell\*, M. Steinbuch\*. <sup>1</sup>La Jolla, La Jolla, CA, USA, <sup>2</sup>Procter & Gamble Pharmaceuticals, Mason, OH, USA.

In clinical practice, perimenopausal and early postmenopausal women are not systematically assessed for fracture risk. The Primary Care Osteoporosis Risk of Fracture Screening (POROS) study is a prospective 24-month observational study designed to examine the impact of a 3-step osteoporosis/osteoporosis screening program in the primary care setting within a large, diverse patient population of women 50-64 years of age.

The screening consisted of 3 sequential steps: Step 1: Fracture risk assessment questionnaire. Subjects with no risk factors were assigned to receive usual care, and subjects with  $\geq 1$  risk factor for fracture were randomized to intervention or non-intervention with 4:1 allocation. Step 2: Urine NTx test for intervention group. Step 3: If NTx result was  $>50$ , hip and spine DXA were done. Subjects' physicians received results and submitted a baseline case report form (CRF) to document intention for prevention and disease management strategies. The subjects will be observed through self-administered questionnaires at baseline, 1, 6, 12, and 24 months to assess health behaviors, treatment initiation, fractures, and resource utilization.

This report summarizes the baseline demographics and fracture risk factors of 2919 women enrolled in the study from 7 medical groups in the Western United States. A total of 1025 women had no risk factors. The intervention group consisted of 1514 women and the non-intervention 380. The mean age for all groups was 56 years and approximately 70% were White. Approximately 80% were postmenopausal and 35% had previously used hormone therapy. There were significantly more Hispanic women (28%) in the no risk factors group compared to both the intervention (23%) and the non-intervention groups (22%). The subjects were educated with 73% having at least some college.

Of the 8 risk factors assessed, BMI  $< 24$  kg/m<sup>2</sup> was most frequent at 42%. Others included previous fracture (15%), mother or father with hip fracture (20%), weight  $\leq 125$  pounds (19%), current smoker (11%), need arms to assist self in standing up from chair (37%), drinks 3+ alcoholic beverages per day (7%), rheumatoid arthritis (17%), and recent corticosteroid use (3%).

POROS will provide data on the effectiveness of utilizing a sequential screening program to identify younger women at high risk of fracture in a primary care setting.

**Disclosures:** D. Schneider, P&G 3.

This study received funding from: The Alliance for Better Bone Health (Procter & Gamble Pharmaceuticals and sanofi-aventis).

## SU371

**Fracture Risk in Young Patients with Chronic Diseases.** M. L. Bianchi<sup>1</sup>, M. Biggioggero<sup>\*1</sup>, C. Limonta<sup>\*1</sup>, C. Colombo<sup>\*2</sup>, L. Ghio<sup>\*2</sup>, A. Edefonti<sup>\*2</sup>, F. Corona<sup>\*2</sup>, G. Nebbia<sup>\*2</sup>, L. Morandi<sup>\*3</sup>. <sup>1</sup>Bone Metabolism Unit, Istituto Auxologico Italiano IRCCS, Milano, Italy, <sup>2</sup>Clinica Pediatrica, Università di Milano, Milano, Italy, <sup>3</sup>Istituto Neurologico Besta, Milano, Italy.

To estimate the risk of fragility fractures is important in the decision about implementing preventive treatment strategies in patients with bone metabolism problems and low bone mass. There is strong evidence to consider BMD an independent predictor of the risk of fragility fractures in adults with osteoporosis. Accordingly, we did a prospective 5-year study to evaluate if BMD could be used to estimate the risk of fractures also in children affected by chronic diseases potentially affecting bone.

Our total study sample includes 1,000 children/adolescents (508 F, 492 M, age 2-19 years) affected by different chronic diseases (renal diseases, systemic connective diseases, cystic fibrosis, liver diseases, Duchenne Muscular Dystrophy). In this sample, 71% of the subjects sustaining at least one low-trauma fracture had a vertebral BMD Z-score of  $-2$  or less.

We recently completed a 5-year follow-up of 579 of these patients (277 F, 302 M, age 3-18 years). In all patients, vertebral and total body (TB) BMC and BMD were measured with DXA (Hologic); vertebral BMD was adjusted for bone size to calculate BMAD.

During the follow-up, 126 (21.8%) patients had one or more fractures for minor trauma. The average vertebral Z-score was  $-2.6 \pm 1.7$ ; in 83 cases (65.9%), the Z-score was  $<-2$  and in the remaining 43 (34.1%) between  $-2$  and  $-0.9$ .

A Z-score  $<-2$  at baseline was significantly associated with an increased risk of fractures in the following 5 years ( $p<0.001$ ). For each 1 SD decrease in TB-BMD there was a 2.1-fold increase in the risk of a limb (mainly forearm) fracture; and for each 1 SD decrease in vertebral BMAD, there was a 2.8-fold increase in the risk of a vertebral fracture.

We also observed that a previous fracture was independently associated with an increased risk (1.8-fold) of a new fracture. The use of steroids, independently of the cumulative dose, doubled the risk of fractures in subjects with a Z-score  $<-1.5$ .

Contrary to the previous reports that, among healthy children and adolescents, boys had more fractures than girls, we did not find any gender differences for fragility fractures in chronically ill children. Also, while in healthy subjects the higher incidence of fractures was observed during adolescence, age and puberty were not associated with an increased risk of fractures in our sample.

In conclusion, our study shows that in young patients affected by chronic diseases, BMD, previous fractures and steroid use are independently related to an increased risk of fractures over 5 years.

**Disclosures:** M.L. Bianchi, None.

## SU372

**The Bone-Building Effects of the Oral Calcium-Sensing Receptor Antagonist, Ronacaleret, in Ovariectomized Rats.** S. J. Hoffman\*, C. A. Capriotti\*, J. A. Vasko\*, X. Liang\*, G. B. Stroup\*, L. N. Casillas\*, R. W. Marquis\*, S. Kumar. GlaxoSmithKline, Collegeville, PA, USA.

Short-term antagonism of calcium-sensing receptors (CaR) on parathyroid cells transiently releases endogenous parathyroid hormone (PTH(1-84)), which stimulates bone formation. This study investigated the bone-building effects of ronacaleret (SB-751689), a CaR antagonist under investigation as an oral treatment for osteoporosis, in ovariectomized (OVX) rats.

Sprague Dawley virgin female rats aged 10.5 months were divided into 8 groups of 9 or 10 animals: 2 groups underwent ovariectomy or sham surgery and were euthanized 6 weeks after surgery to provide baseline data; 2 control groups (OVX or sham) received oral vehicle (1% methylcellulose); 3 OVX groups received oral ronacaleret, 30, 60 or 120 mg/kg; and the final OVX group received PTH(1-34) subcutaneously at  $1 \mu\text{g/kg}$  (a dose previously shown to be comparable to PTH(1-84) release after oral administration of ronacaleret). All treatments were given once daily for 8 weeks from day 43 post-surgery.

Peak plasma levels ( $C_{\text{max}}$ ) of ronacaleret increased dose dependently after oral administration during week 8 (858, 1338 and 3259 ng/ml, for the 30, 60 and 120 mg/kg doses, respectively). However, the effect of ronacaleret on PTH(1-84) release was less dose dependent ( $C_{\text{max}}$  33, 66 and 68 pM, respectively). In comparison, the  $C_{\text{max}}$  of PTH(1-34) was 27 pM. At 2 h postdose, the 2 highest doses of ronacaleret dose dependently and significantly ( $p<0.05$ ) increased plasma ionized calcium levels compared with baseline measurement.

Ovariectomy induced significant bone loss in the lumbar spine and the proximal tibia. Only PTH(1-34) significantly reduced bone loss in the lumbar spine as measured by dual-energy X-ray absorptiometry (DXA) ( $p<0.05$  compared with OVX controls at week 10), although DXA is unable to discriminate between trabecular and cortical bone. In contrast, histological analysis revealed significant increases in bone formation rates and osteoid perimeter at the lumbar spine with ronacaleret, 120 mg/kg ( $p<0.01$ ). At the proximal tibia, loss of trabecular bone mineral density was reduced by the 2 highest doses of ronacaleret and PTH(1-34) ( $p<0.01$ ). For the distal tibia, treatment outcome varied when different analyses were applied, but overall cortical bone loss was reduced with ronacaleret. Ovariectomy significantly increased the markers of bone turnover, urinary deoxypyridinoline and plasma osteocalcin, but treatment with ronacaleret and PTH(1-34) did not significantly decrease their levels.

Thus, oral administration of ronacaleret in OVX rats stimulates PTH(1-84) release which leads to reduced trabecular and cortical bone loss.

**Disclosures:** S.J. Hoffman, GlaxoSmithKline, Collegeville, PA, USA 5.

This study received funding from: GlaxoSmithKline, Collegeville, PA, USA.

## SU373

**The Anabolic Skeletal Effects of a Growth Hormone-Derived Peptide (AOD9604) in the Ovariectomized Rat Model of Osteoporosis.** I. Kamikowski<sup>\*1</sup>, R. Renlund<sup>\*2</sup>, M. D. Grynpas<sup>3</sup>. <sup>1</sup>Institute of Biomaterials and Biomedical Engineering, University of Toronto, Toronto, ON, Canada, <sup>2</sup>Department of Laboratory Medicine and Pathobiology, University of Toronto, Toronto, ON, Canada, <sup>3</sup>Samuel Lunenfeld Research Institute, Mount Sinai Hospital, Toronto, ON, Canada.

A synthetic human Growth Hormone (hGH) 16-AA C-terminus peptide, AOD9604 (AOD, Tyr-hGH171191), has been shown to modulate fat metabolism and is currently being developed as a novel weight-loss drug. However, hGH is known to affect both adipocytes and osteoblasts, which suggests that AOD may also affect bone. Previously, it has been shown that AOD can prevent OVX-induced bone loss and fragility. This study focuses on the ability of AOD to rebuild the bone lost during ovariectomy (OVX) in a rat model of osteoporosis. Nine month-old female rats were ovariectomized and left without treatment for 12 weeks in order to lose bone. The OVX rats were divided into an untreated control group (N=13) and three groups treated with increasing doses of AOD (0.01 mg/kg/day [N=13], 0.03 mg/kg/day [N=14], 0.25 mg/kg/day [N=14]) administered orally by gavage for 12 weeks. An additional sham-OVX operated group (N=15) served as a negative control. The two control groups were given vehicles by gavage as per the AOD treated groups. Following sacrifice, dual energy x-ray absorptiometry (DXA) was used to determine femoral and vertebral Bone Mineral Density (BMD). Three-point bending, torsion, femoral neck fracture and vertebrae compression tests were used to evaluate femoral and vertebral mechanical properties. DXA results showed no significant increase in BMD following AOD administration. However, vertebral compression showed a dose-dependent increase in ultimate stress and elastic modulus. In three-point bending, the highest dose of AOD (0.25 mg/kg/day) caused a significant ( $p<0.05$ ) decrease in ultimate stress while the lowest dose of AOD (0.01 mg/kg/day) caused a significant ( $p<0.05$ ) increase in shear stress following torsion testing. Future work includes assessing mineralization changes, through back-scattered electron imaging and microhardness testing, and structure and remodelling changes, through static and dynamic histomorphometry. In conclusions, our results suggest that AOD had differential effects on cortical and trabecular bone and, despite the lack of AOD effect seen with DXA, mechanical tests indicate AOD administration resulted in a dose dependent restoration of vertebral bone strength.

**Disclosures:** I. Kamikowski, None.

This study received funding from: Metabolic Pharmaceuticals.

## SU374

**Inhibition of PPAR $\gamma$ 2 by BADGE and Vitamin D in Male Mice Increases Osteoblastogenesis and Inhibits Bone Matrix Mineralization Leading to Osteomalacia.** G. Duque<sup>1</sup>, D. Rivas<sup>2</sup>, J. Ong<sup>\*2</sup>, W. Lee<sup>\*3</sup>, J. E. Henderson<sup>3</sup>. <sup>1</sup>Nepean Clinical School-University of Sydney, Penrith, Australia, <sup>2</sup>Lady Davis Institute-McGill University, Montreal, QC, Canada, <sup>3</sup>JTN Wong Laboratories-McGill University, Montreal, QC, Canada.

Bone marrow fat infiltration is a prevalent feature in people with age-related bone loss, which correlates inversely with bone formation and positively with high expression levels of peroxisomal proliferator-activated receptor gamma 2 (PPAR $\gamma$ 2). Inhibition of PPAR $\gamma$ 2 thus represents a potential therapeutic approach for age-related bone loss. In this study, we examined the effect of PPAR $\gamma$ 2 inhibition on bone in skeletally mature C57BL/6J male mice. Four-month-old mice were treated with a PPAR $\gamma$ 2 antagonist, bisphenol-A-diglycidyl ether (BADGE) (30 mg/Kg/day, IP) alone or in combination with 1,25(OH)2D3 (18 pmol/24 h, SC) for 6 wk. Micro computed tomography and bone histomorphometry indicated that mice treated with both BADGE + 1,25(OH)2D3 had significantly increased bone volume and improved bone quality compared with mice treated with either BADGE or 1,25(OH)2D3 alone ( $p<0.001$ ). This phenotype occurred in the absence of alterations in osteoclast numbers or eroded surfaces. The BADGE-treated mice exhibited classic signs of osteomalacia including increased osteoid length and width in association with broad, diffuse tetracycline bands with low fluorescence intensity. All of the treated groups showed a significant increase in circulating levels of bone formation markers without changes in bone resorption markers ( $p<0.001$ ) and parathyroid hormone (PTH), Ca+ and P+ remained normal. The effects were more pronounced in mice treated with BADGE + 1,25(OH)2D3. Ex-vivo cultures of bone marrow cells from treated mice showed significantly higher level of osteoblastogenesis, reduced adipogenesis and a reduction in fat volume ( $p<0.01$ ). These changes were accompanied by increased expression of osteocalcin and Runx2 protein and a decrease in PPAR $\gamma$ 2 nuclear activation complex. Taken together, these observations demonstrate that inhibition of PPAR $\gamma$ 2 in adult male mice decreased marrow fat and enhanced bone formation. The presence of osteomalacia in the absence of high levels of PTH or low levels of either calcium or vitamin D, suggests that BADGE may influence bone mineralization by an alternate pathway.

**Disclosures:** G. Duque, None.

This study received funding from: University of Sydney Medical Foundation and Canadian Institutes for Health Research.

## SU375

**Cannabinoid Receptor Ligands Rescue Bone Loss and Stimulate Fracture Healing.** O. Ofek<sup>\*1</sup>, A. Bajayo<sup>\*1</sup>, E. Melamed<sup>\*1</sup>, Y. Gabet<sup>\*1</sup>, E. Shohami<sup>\*2</sup>, R. Mechoulam<sup>\*3</sup>, I. Bab<sup>1</sup>. <sup>1</sup>Bone Laboratory, The Hebrew University of Jerusalem, Jerusalem, Israel, <sup>2</sup>Pharmacology, The Hebrew University of Jerusalem, Jerusalem, Israel, <sup>3</sup>Medicinal Chemistry and Natural Products, The Hebrew University of Jerusalem, Jerusalem, Israel.

A number of studies have recently demonstrated the presence of cannabinoid receptors in osteoblasts, osteoclasts and skeletal sympathetic nerve terminals. Cannabinoid receptor null mice have a low bone mass phenotype and cannabinoid ligands, which activate the Gi-protein coupled receptors CB1 and CB2, are capable of attenuating ovariectomy (OVX)-induced bone loss. CB1 is mainly neuronal whereas CB2 is preferentially expressed in peripheral tissues. Using models for testing the reversal of OVX-induced bone loss and stimulation of fracture healing we show here that cannabinoid receptor agonists have a net bone anabolic activity. In the OVX model, mice were left untreated for 6 weeks postoperatively. Combined  $\mu$ CT/histomorphometric analysis indicated that during this time the trabecular bone volume density (BV/TV) in the lumbar vertebrae and distal femoral metaphyses stabilized at respective 25% and 40% lower levels compared to sham-OVX controls. This was followed by a 6-week i.p. administration of the CB2-specific agonist HU-308, at 20 mg/Kg/day. This treatment resulted in a 35% rescue of the OVX-induced bone loss, mainly by stimulating bone formation and augmenting the trabecular thickness. The magnitude of this effect is comparable to that of PTH(1-34) in a similar experimental setting. To assess the effect of cannabis abuse on fracture healing, adult male rats were treated chronically with a mixture of tetrahydrocannabinol (THC) and cannabidiol, the most abundant constituents of marijuana and hashish. Administration of these cannabinoids, each at 5 mg/Kg/day, commenced immediately after standardized femoral pinning and mid-diaphyseal fracturing.  $\mu$ CT assessment carried out after 2 weeks showed 37% increase in the BV/TV of the newly formed mineralized callus, accompanied by 32% increase in trabecular number and, particularly important, 52% stimulation of the trabecular connectivity density. Additional experiments in MC3T3 E1 and primary osteoblast cultures suggest that the effects of CB1/CB2 agonists like THC and of CB2 specific agonists like HU-308 and AM1241 are mediated by a Gi-protein - Erk1/2 pathway, but not p38. Together, these results portray cannabinoid receptor agonists as potent bone anabolic agents. Further studies characterizing the skeletal activity of selective CB2 agonists are advocated for the rescue of skeletal deficits, since this receptor is not involved in the well established cannabinoid psychotropic effects and control of energy metabolism.

**Disclosures:** O. Ofek, None.

This study received funding from: Israel Anti-drug Authority.

## SU376

**A Soluble Activin Receptor Type IIA Fusion Protein, ACE-011, Increases Bone Mass by Stimulating Bone Formation and Inhibiting Bone Resorption in Cynomolgus Monkeys.** S. Lotinun<sup>1</sup>, R. J. Fajardo<sup>\*2</sup>, R. S. Pearsall<sup>3</sup>, M. L. Boussein<sup>2</sup>, R. Baron<sup>1</sup>. <sup>1</sup>Harvard School of Dental Medicine and Harvard Medical School, Boston, MA, USA, <sup>2</sup>Beth Israel Deaconess Medical Center and Harvard Medical School, Boston, MA, USA, <sup>3</sup>Accelaron Pharma, Cambridge, MA, USA.

Activin A, a member of the TGF- $\beta$  superfamily, has been shown to inhibit osteoblast differentiation and stimulate osteoclastogenesis *in vitro*. An antagonist to activin, a soluble form of extracellular domain of the activin receptor type IIA (ActRIIA) fused to the Fc domain of murine IgG has been shown to have an anabolic effect on bone in mice. The present study was designed to test human ActRIIA-IgG-Fc (ACE-011) in non-human primates to determine if the increased bone mass was due to an increase in bone formation, a decrease in bone resorption or both. Young, female Cynomolgus monkeys were injected subcutaneously with either 10 mg/kg ACE-011 or vehicle biweekly for 3 months. PIXImus, pQCT and micro-CT analysis demonstrated that ACE-011 improved bone density and microarchitecture in the axial and appendicular skeleton. Mechanical testing indicated a higher vertebral compressive strength in ACE-011-treated monkeys compared to vehicle-treated controls. To further characterize the mechanism by which ACE-011 increased bone mass and strength, histomorphometry analysis of distal femur, femoral midshaft, femoral neck and 12<sup>th</sup> thoracic vertebrae was evaluated. Compared to vehicle, ACE-011 significantly increased cancellous bone volume (87%,  $p<0.001$ ) with a 36% ( $p<0.05$ ) increase in trabecular thickness, 40% ( $p<0.01$ ) increase in trabecular number and 50% ( $p<0.05$ ) decrease in trabecular separation at distal femur. Interestingly, ACE-011 induced a 154% ( $p<0.01$ ) increase in bone formation rate, 75% ( $p<0.05$ ) increase in mineralizing surface and 43% ( $p<0.05$ ) increase in mineral apposition rate. Monkeys treated with ACE-011 had greater osteoblast surface and a decrease in osteoclast surface, with only modest changes in bone biochemical marker data. No differences were observed in parameters of cortical bone at the midshaft of the femur. Similar to distal femur, ACE-011 treatment led to an increase in cancellous bone volume, bone formation rate and osteoblast surface at the femoral neck. Similar trends were observed in thoracic vertebrae with an increase in cancellous bone volume (32%,  $p=0.09$ ), bone formation rate (77%,  $p=0.12$ ) and osteoblast surface (49%,  $p=0.19$ ) and significantly decreased osteoclast surface (72%,  $p<0.05$ ). These data demonstrate that ACE-011 is a dual anabolic-antiresorptive compound, improving cancellous bone volume by promoting bone formation and inhibiting bone resorption. Thus, soluble ActRIIA fusion protein may be useful in the prevention and/or treatment of skeletal fragility.

**Disclosures:** S. Lotinun, None.

This study received funding from: Accelaron Pharma.



## SU377

**Inhibition of Bone Loss and Muscle Atrophy by Dihydrotestosterone in a Mouse Hindlimb Disuse Model.** Y. Qin<sup>1</sup>, A. Ali<sup>\*1</sup>, S. Judex<sup>1</sup>, Q. Zeng<sup>\*2</sup>, V. Krishnan<sup>\*2</sup>, Y. L. Ma<sup>2</sup>. <sup>1</sup>Biomedical Engineering, SUNY Stony Brook, Stony Brook, NY, USA, <sup>2</sup>Eli Lilly Research Laboratories, Indianapolis, IN, USA.

Musculoskeletal adaptations to microgravity and functional disuse have significant physiological effects leading to skeletal complications, i.e., bone loss and muscle atrophy. Generally hormone is considered to be a key regulator of skeletal formation and/or inhibition of loss, e.g., androgen hormone is essential for increasing and maintaining muscle mass during functional disuse. The objective of the study was to investigate the role of androgen on bone and muscle during a course of hindlimb suspension in the presence of Dihydrotestosterone (DHT), an active form of testosterone. 34 adult female BALB mice were randomly separated to 4 groups: 1) control vehicle, no suspension, 2) control vehicle, hind limb suspension (HLS), 3) DHT 2mg/kg/d sc, hind limb suspension, 4) baseline control, for 3 weeks. Whole body and wet muscle weight were measured. Bone mass was assessed by pDEXA. Longitudinal body weight data showed significant reduction in body weight in the HLS control group, while DHT treatment attenuated the body weight loss in HLS mice in the first week and completely restored the body weight to the non suspension group by end of the study. Suspension decreased hind limb muscle mass in soleus (-34%), gastrocnemius (-23%), and quadriceps muscles (-26%) ( $p < 0.05$ ), while the DHT group protected the muscle wet weight loss with an increasing trend in all muscle groups ranging from 3% to 12%. HLS reduced BMD and BMC in whole femur (-20%, -21%,  $p < 0.01$ ), mid-diaphysis (-11%, -9%,  $p < 0.05$ ), and distal femoral regions, (-25%, -25%,  $p < 0.01$ ). DHT treatments partially protected BMD and BMC in whole femur (+14%), mid-diaphyseal femur (+7%), and distal femur (21%, 25%) when compared to HLS control. Our data suggested that Dihydrotestosterone protected against the muscle atrophy and bone loss in the functionally disused model of hindlimb suspension.

**Disclosures:** Y. Qin, Eli Lilly Research Laboratories 5.  
This study received funding from: NIH (AR052379) and Eli Lilly Research Laboratories.

## SU378

**Effects of Statins on eNOS and BMP2 in Osteoblasts.** M. M. Moore, J. R. Edwards, G. E. Gutierrez, G. R. Mundy. Center for Bone Biology, Vanderbilt University Medical Center, Nashville, TN, USA.

Statins stimulate osteoblast differentiation, bone formation, and enhance fracture healing. Although they have been shown to increase BMP2 transcription, the mechanism by which they do this is unclear. We hypothesize that the activation of endothelial nitric oxide synthase (eNOS) in osteoblasts may be responsible, since statins have been shown to increase eNOS expression in endothelial cells, and eNOS null mice have a bone phenotype that is the mirror image of statin-treated mice (Armour et al, 2001). To determine if statins increase eNOS mRNA expressed in bone cells, a pre-osteoblastic cell line, 2T3, was incubated with osteoblastic medium in the presence or absence of 5µM lovastatin. Lovastatin caused a maximal 3-fold increase in eNOS mRNA after 19 days of culture, although there was a steady significant increase after day 5. In the same cells, BMP2 mRNA was increased 25-fold after 19 days in culture, with a steady and significant increase after day 2. Lovastatin also increased mineralized bone nodule formation and alkaline phosphatase activity after 11 days in culture. Although control cultures also demonstrated an increase in BMP2 and eNOS mRNAs, and an increase in mineralized bone nodule formation and alkaline phosphatase activity, this occurred more rapidly in the lovastatin-treated osteoblasts, and to a greater extent. In the untreated cultures, these effects were not seen before 10 days of culture. We conclude that lovastatin hastens osteoblast differentiation in 2T3 osteoblastic cells, as evidenced by more rapid expression of eNOS mRNA, BMP2 mRNA, alkaline phosphatase activity and mineralized bone nodule formation, and causes increases in each of these parameters compared with osteoblasts cultured in control media for the same time period. These data are consistent with effects of statins to sequentially increase BMP2 and eNOS expression in osteoblasts.

**Disclosures:** M.M. Moore, None.

## SU379

**Rapid Optical Imaging of Bone Formation Responses in the Rodent Skeleton.** K. Petrosky\*, M. Pegurri\*, A. Studer\*, M. Merdes\*, R. Kneuer\*, H. Gremlich\*, M. Kneissel. Musculoskeletal Disease Area, Novartis Institutes for BioMedical Research, Basel, Switzerland.

Changes in bone formation are monitored by biomarker or histomorphometric readouts. Biomarker readouts are rapid, but do not provide information about changes in local bone turnover. Histomorphometry allows for detailed analyses in regions of interest, but is time consuming. In the present studies we monitored rapidly local bone forming activity by near-infrared fluorescence (NIRF) imaging, using a NIRF bisphosphonate derivative homing to bone and binding to hydroxyapatite. First 6-month-old female OF1 mice ( $n = 6$  / group) were administered twice daily 33, 100, or 300 nM hPTH(1-34) sc. onto the calvaria to induce local bone formation. Animals received either alizarin and calcein on day 5 and 12 respectively for classical histomorphometry or 0.1 mg/kg of Cy5.5 labeled pamidronate at day 7 and 8. A time-domain small animal optical imager (GE eXplore Optix) was used for *in vivo* detection of NIRF signal in their calvaria 4 hours after the second application of the NIRF probe. We observed a dose-related increase in fluorescent signal in PTH treated calvarias which reached significance at the 100 nM dose. Histomorphometric evaluation revealed that bone formation rates were increased at the calvaria surface, but not in the underlying marrow cavities. Pooled bone formation rates of the two compartments corresponded to NIRF signal changes

observed in PTH treated calvarias. Histology confirmed presence of the NIRF probe at mineralizing fronts. We proceeded to systemic PTH treatment of 11-month-old female OF1 mice and 9-month-old female Wistar rats ( $n = 8$  / group). Animals received daily sc. 6 (rats only), 25 or 100 microg/kg of hPTH(1-34) or vehicle for 14 days. Animals were administered iv. 0.1 mg/kg of the bisphosphonate derivative on day 13 and 14. The animals were sacrificed 6 hours after the second application for excision of hind limbs and lumbar spine. *Ex vivo* measurements demonstrated a dose-related increase in NIRF signal in the distal femur and the proximal tibia of PTH treated mice. Increases were significant and reached about two-fold in animals treated with the highest dose. A similar increase was observed in the lumbar spine. In rats significant increases in NIRF signal were observed from 25 microg/kg onwards in the proximal tibia, while in the spine a significant increase was already detectable in animals treated with 6 microg/kg PTH. In summary we were able to monitor bone formation responses triggered by local or systemic anabolic treatment at various skeletal sites in rodents. The results suggest that bone formation responses can be quantified rapidly *in vivo* by the use of this optical imaging technology.

**Disclosures:** M. Kneissel, None.

## SU380

**Intermittent PTH Administration Increases Bone Mass and Strength in Aged Mice by Antagonizing Oxidative Stress-induced Osteoblast Apoptosis via ERK-mediated Attenuation of p66<sup>shc</sup> Phosphorylation.** R. L. Jilka, M. Almeida, L. Han, R. S. Weinstein, S. C. Manolagas. Center for Osteoporosis and Metabolic Bone Diseases, Central Arkansas Veterans Healthcare System, University of Arkansas for Medical Sciences, Little Rock, AR, USA.

The cellular and molecular mechanisms of the anabolic effect of intermittent PTH in animal models have been largely investigated at peak adult bone mass. However, it is unknown whether similar mechanisms underlie the effectiveness of PTH in young and old subjects. C57BL/6 mice lose bone mass and strength with advancing age and these changes are associated with increased oxidative stress and increased osteoblast apoptosis. Based on this and extensive evidence that oxidative stress induces osteoblast apoptosis in a cell autonomous manner, we compared the effects of intermittent PTH administration on bone mass, strength, and prevalence of osteoblast apoptosis in 6 versus 26 month old female C57BL/6 mice; and also examined the effects of PTH on H<sub>2</sub>O<sub>2</sub>-induced apoptosis of osteoblastic cells *in vitro*. Prior to treatment, old mice exhibited the expected reductions in vertebral and femoral bone mass, and cancellous bone volume, as compared to young mice as determined by DEXA and microCT. These changes were associated with reduced vertebral and femoral strength. Moreover, the prevalence of osteoblast apoptosis in vertebral cancellous bone was 30% in old mice, as compared to 9% in young mice. Daily injections of 100 ng/g PTH(1-34) for 28 days increased femoral and vertebral BMD, vertebral bone volume, femoral cortical thickness, and indices of bone strength in both young and old mice; and in the latter reversed all these parameters to levels that approached or exceeded those seen in the untreated young ones. More important, PTH reduced the prevalence of apoptotic osteoblasts in cancellous vertebral bone by 2- and 3-fold in young and old animals respectively; in the latter to the level of the untreated young animals. Consistent with the *in vivo* findings, 1 h pretreatment of murine calvaria cells or the osteoblastic cell line OB-6 with 50 nM PTH prevented apoptosis induced by H<sub>2</sub>O<sub>2</sub>. The anti-apoptotic effect of the hormone was associated with a striking attenuation of the H<sub>2</sub>O<sub>2</sub>-induced phosphorylation of p66<sup>shc</sup>, a redox enzyme that generates mitochondrial H<sub>2</sub>O<sub>2</sub> to trigger mitochondria swelling and apoptosis. The reduction in H<sub>2</sub>O<sub>2</sub>-induced p66<sup>shc</sup> phosphorylation was reproduced by dibutyl-1-cAMP (100 µM) and was abrogated by the MAP kinase inhibitor PD98059. Collectively, these results demonstrate that PTH can reverse age-related bone loss, in part, by a previously unappreciated action of the hormone that involves ERK-mediated attenuation of p66<sup>shc</sup> phosphorylation, which counteracts the apoptotic effects of oxidative stress on osteoblasts.

**Disclosures:** R.L. Jilka, None.

## SU381

**Combination of Flaxseed and Estrogen Benefits Bone Health in the Ovariectomized Rat Model of Postmenopausal Osteoporosis.** S. M. Sacco\*, J. M. Jiang\*, S. Reza-Lopez\*, D. W. Ma\*, W. E. Ward<sup>1</sup>. <sup>1</sup>Nutritional Sciences, University of Toronto, Toronto, ON, Canada, <sup>2</sup>Department of Human Health and Nutritional Sciences, University of Guelph, Guelph, ON, Canada.

The unanticipated increase in risk of stroke reported by the Women's Health Initiative stimulated interest in newer formulations of estrogen therapy (ET) that contain lower-than-standard doses and alternative modes of delivery. Moreover, many postmenopausal women are consuming natural health products such as flaxseed (FS) to relieve menopausal-like symptoms and to improve overall health. FS is an oilseed rich in lignans and n-3 polyunsaturated fatty acids (PUFA) that may modulate bone metabolism through their estrogen-like or anti-inflammatory properties, respectively. Whether FS enhances or interferes with ET is unknown. This study determined the effect of 10% FS, standard dose (SD) ET, low dose (LD) ET, and their combination on bone mineral and biomechanical bone strength in ovariectomized (ovx) rats. Ovx rats were treated for 12 weeks with 1) basal diet (negative control); 2) 10% FS diet; 3) SD ET implant (25 µg, 90 day release); 4) LD ET implant (13 µg, 90 day release); 5) FS + SD; 6) FS + LD. A sham-operated group was included as a positive control. Femurs and lumbar vertebrae (LV) were analyzed for bone mineral density (BMD) by densitometry and biomechanical strength testing using a material testing system. Total fatty acid composition of tibias and LV3 were measured to determine if n-3 PUFA from FS are incorporated into bone. FS + LD and FS + SD resulted in higher BMD ( $p < 0.05$ ) and peak load ( $p < 0.05$ ) in the LV compared to the negative control while FS alone was neither beneficial nor detrimental to bone mineral and strength. SD ET and LD ET were

intermediate to negative control and combination groups. No effects on bone mineral or strength in femurs were observed. FS feeding resulted in higher relative levels of n-3 PUFA ( $p < 0.05$ ) including  $\alpha$ -linolenic acid and eicosapentaenoic acid, and lower relative levels of n-6 PUFA including linoleic acid and arachidonic acid in tibias and LV compared to all other groups. Linoleic acid in LV3 tended to be inversely associated with LV bone mineral content ( $r = -0.323$ ,  $p = 0.063$ ) indicating that the altered fatty acid composition by FS may not be the primary modulator of bone metabolism in ovx rats. In summary, FS combined with LD ET provided the greatest protection against ovariectomy-induced bone loss, and this benefit is site-specific to vertebrae with no benefit to long bones. FS feeding resulted in higher incorporation of n-3 PUFAs in both tibias and LV but the lack of association between fatty acid composition and bone outcomes suggest that the lignans may be primarily responsible for positive outcomes of combined ET and FS intervention.

**Disclosures:** S.M. Sacco, None.

This study received funding from: Discovery Grant from the Natural Sciences and Engineering Research Council of Canada to Dr. Wendy E. Ward.

## SU382

**Short-term Effect of Zoledronic Acid on the Superficial Vascularisation of Membranous Bone Sites: An Intravital Study on Rat Calvarium.** J. Paccou<sup>\*1</sup>, M. Vieillard<sup>\*1</sup>, G. Penel<sup>\*2</sup>, B. Duquesnoy<sup>\*1</sup>, B. Cortet<sup>1</sup>. <sup>1</sup>Hopital Roger Salengro, Lille, France, <sup>2</sup>Faculté de Chirurgie Dentaire, EA 4032., Lille, France.

**Introduction:** The superficial vascularisation is of great importance in membranous bone healing process. A new rat calvarium intravital model was developed to study the short-term effect of a single high-dose zoledronic acid infusion on the superficial angiogenesis.

**Materials and methods:** Eighteen adult Sprague Dawley male rats were used. Optical bone chambers were implanted under general anaesthesia, with an optical window in contact with the bone tissue surface. A digital camera was used for the acquisition of photographs of the vascular network. Photographs were analysed using Aphelion<sup>®</sup> software to determine vascular density (VD). This was defined as the ratio of blood vessel pixels to all other pixels in the region of interest. The rats were randomly distributed between two groups. Nine rats were injected with 400  $\mu$ g/kg of zoledronic acid (Z) (ZOMETA<sup>®</sup>, Novartis, Switzerland) and nine other rats were injected with physiologic saline solution (PSS). Photographs were taken just before the infusion (T0), 2 hours after the start of infusion (T120), and then at days 2, 3 and 5.

**Results:** During the fifteen days prior to infusion, a decrease in vascular density was observed in both groups, corresponding to the bone healing process. No statistical difference was observed between the two groups at T0 just before infusion ( $p = 0.38$ ). An early dissociation between the PSS group and the Z group was observed after infusion. A decrease in vascular density was observed in the Z group until the fifth day. No statistical differences were observed at T120 and day 2. Statistical differences were observed between Z and PSS groups at day 3 ( $p = 0.009$ ) and day 5 ( $p = 0.0005$ ).

**Discussion:** A rat calvarium intravital model was used to study the effect of a slow infusion of zoledronic acid on vascular density during the bone healing process. A decrease in vascular density was observed during the five-day follow up when compared to the infusion of physiologic saline solution. The decrease in vascular density was probably due to a vasoconstrictor effect. As our model was a static model with no hemodynamic measurements, extrapolation of these results is difficult. The exact mechanism accounting for the hemodynamic effect of zoledronic acid has yet to be elucidated. A better understanding of the molecular mechanisms underlying the actions of zoledronic acid on blood vessels is necessary.

**Conclusion:** For the first time, this study demonstrates a short-term effect of a zoledronic acid infusion on vascular density at a membranous bone site. The observed decrease in vascular density is presumably linked to a vasoconstriction mechanism. Larger and longer trials are required to assess this hypothesis.

**Disclosures:** J. Paccou, None.

This study received funding from: Société Française de Rhumatologie (SFR).

## SU383

**Changes of Bone Metabolism in Immunosuppressant, FK506 Treated Rats.** H. Wakabayashi<sup>1</sup>, J. Kanda<sup>1</sup>, E. Katayanagi<sup>\*1</sup>, A. Takahashi<sup>\*2</sup>, K. Onodera<sup>\*3</sup>. <sup>1</sup>Clinical Pharmacotherapy, Niigata University of Pharmacy and Applied Life Sciences, Niigata, Japan, <sup>2</sup>Clinics of Dentistry for the Disabled, Tohoku University Dental Hospital, Sendai, Japan, <sup>3</sup>Pharmacotherapy, Yokohama College of Pharmacy, Yokohama, Japan.

Immunosuppressant drugs like FK506 (tacrolimus), cyclosporine are widely used for solid organ transplantation. However, immunosuppressant drugs also have severe side effects. One of prominent side effects is an induction of osteoporosis. In the present study, we investigated the effects of short-term administration of immunosuppressant drug, FK506 (tacrolimus) on bone metabolism (bone mineral density, bone vitamin K analogs, serum osteocalcin and calcium, and serum tartrate-resistant acid phosphatase). Male Wistar rats (6 week-old) were administered orally with the dose of FK506 (6 mg/kg) every day for 2 weeks. For the control group of rats, physiological saline was administered in the same manner. FK506-treated group showed the significant decreases in bone mineral density (BMD) and bone vitamin K analog (MK-4) in compared with the control group. Whereas these significant decreases were prevented by the injection of sodium risedronate hydrate (5 mg/kg).

**Disclosures:** H. Wakabayashi, None.

## SU384

**Efficacy and Safety of Monthly Oral Ibandronate in Postmenopausal Women with Low Bone Density.** M. A. Bolognese<sup>1</sup>, M. R. McClung<sup>\*2</sup>, F. Sedarati<sup>\*3</sup>, R. R. Recker<sup>\*4</sup>, P. D. Miller<sup>\*5</sup>. <sup>1</sup>Bethesda Health Research, Bethesda, MD, USA, <sup>2</sup>Oregon Osteoporosis Center, Portland, OR, USA, <sup>3</sup>Roche, Nutley, NJ, USA, <sup>4</sup>Osteoporosis Research Center, Omaha, NE, USA, <sup>5</sup>Colorado Center for Bone Research, Lakewood, CO, USA.

Monthly oral ibandronate has been shown to increase bone mineral density (BMD) and reduce bone turnover in clinical trials of women with postmenopausal osteoporosis. For some patients, bisphosphonate therapy may be useful to prevent the progression of low bone density (osteopenia) to osteoporosis. This study investigated the efficacy and safety of treatment with monthly oral ibandronate (150 mg) in postmenopausal women with low bone density. PREVENTION was a 1-year, double-blind, placebo-controlled, randomized study, which enrolled ambulatory postmenopausal women aged 45-60 years with baseline lumbar spine (LS) BMD T-score  $< -1.0$  and  $> -2.5$  and baseline proximal femur BMD T-score  $> -2.5$ . The relative change from baseline (%) in mean LS BMD at 1 year was the primary endpoint (intent-to-treat population). Treatment groups were compared using a two-way ANOVA model, which adjusted for independent factors including baseline LS BMD T-score, and time since menopause. Changes in proximal femur and serum C-terminal telopeptide of type 1 collagen (sCTX) were assessed as secondary endpoints. Adverse events and safety laboratory parameters were monitored continuously. Calcium and vitamin D supplements were provided to all participants. This study enrolled a total of 160 women; 77 received monthly ibandronate and 83 received placebo. Participants treated with ibandronate achieved larger increases in LS BMD after 1 year compared with patients receiving placebo (3.7% vs -0.4% [difference of 4.1%,  $P < 0.0001$ ], after adjustment for baseline LS BMD T-score, and time since menopause). The mean relative change in total hip BMD was 1.5% for women receiving ibandronate and -0.9% in women receiving placebo. After 3 months, median sCTX levels were reduced by over 55% in the ibandronate group compared with ~4% in the placebo group. Monthly ibandronate was well tolerated and the incidence of adverse events was similar between treatment groups. The most common treatment-related adverse events in patients receiving ibandronate were dyspepsia (5.2%), myalgia (5.2%), and influenza-like illness (5.2%). Treatment of appropriate patients with monthly ibandronate therapy may prevent bone loss in women with low bone density.

**Disclosures:** M.A. Bolognese, Astra-Zeneca, GlaxoSmithKline, Lilly, Roche, I.

This study received funding from: Roche and GlaxoSmithKline.

## SU385

**Effects of Vitamin K2 and Risedronate on Bone Formation and Resorption, Osteocyte Lacunar System and Porosity in the Cortical Bone of Glucocorticoid-Treated Rats.** J. Iwamoto<sup>1</sup>, H. Matsumoto<sup>\*1</sup>, T. Takeda<sup>\*1</sup>, X. Liu<sup>\*2</sup>, J. K. Yeh<sup>2</sup>. <sup>1</sup>Department of Sports Medicine, Keio University School of Medicine, Tokyo, Japan, <sup>2</sup>Department of Medicine, Winthrop-University Hospital, Mineola, NY, USA.

The purpose of the present study was to examine the effects of vitamin K2 and risedronate on bone formation and resorption, the osteocyte lacunar system and porosity in the cortical bone of glucocorticoid (GC)-treated rats. Forty-nine female Sprague-Dawley rats, 3 months of age, were randomized into five groups according to the following treatment schedule: age-matched control, GC administration, and GC administration with concomitant administration of vitamin K2, risedronate, or vitamin K2 + risedronate. At the end of the 8-week experiment, classical bone histomorphometric analysis was performed and the osteocyte lacunar system and porosity were evaluated on the cortical bone of the tibial diaphysis. GC administration decreased percent cortical bone area and increased percent marrow area as a result of decreased periosteal bone formation and increased endocortical bone erosion, and increased cortical porosity. Vitamin K2 prevented a reduction in periosteal bone formation, but did not affect percent cortical bone and marrow areas. Risedronate prevented a reduction in periosteal bone formation and an increase in endocortical bone erosion, resulting in prevention of alterations in percent cortical bone and marrow areas. Both vitamin K2 and risedronate increased viable osteocyte density and lacunar occupancy, and prevented a GC-induced increase in cortical porosity. Vitamin K2 and risedronate had additive effects on viable osteocyte density and lacunar occupancy and a synergistic effect on cortical porosity. The present study showed the efficacy of vitamin K2 and risedronate for bone formation and resorption, the osteocyte lacunar system and porosity in the cortical bone of GC-treated rats.

**Disclosures:** J. Iwamoto, None.

## SU386

**The Bisphosphonate, Pamidronate, Suppresses the Pro-inflammatory Response in a Mouse Model of Osteogenesis Imperfecta (OI) as Well as Normal (NL) Littermates.** A. I. Leet<sup>1</sup>, Y. Ni<sup>\*2</sup>, T. Kazarian<sup>\*1</sup>, A. Jain<sup>\*2</sup>, N. S. Fedarko<sup>\*2</sup>. <sup>1</sup>Orthopedic Surgery, Johns Hopkins University, Baltimore, MD, USA, <sup>2</sup>Geriatrics, Johns Hopkins University, Baltimore, MD, USA.

Historically, OI patients have had a history of massive blood loss during surgery, but in a recent clinical study, we found no evidence of this increased blood loss during femoral surgery. Many children in our study were being treated with bisphosphonates and we hypothesized that bisphosphonates had an anti-inflammatory effect. We used an animal model of OI to test whether pamidronate (Aredia) could suppress cytokine release.

OIM, carrier and NL mice were used to measure pro-inflammatory cytokines including IL- $\beta$ , TNF $\alpha$ , INF $\gamma$ , and IL-6, IL-8, IL-10, & IL-12. A tibia fracture model was used to study the differences in pro-inflammatory response between OIM and NL mice at 15, 30, 60, 120, & 480 min. from fracture.

OIM (OI) and normal (NL) mice were treated with no drug (0) or Aredia (Novartis) at 0.12mg/kg x 4 doses (LD). A high dose group (HD) was given 10 x this dose, which proved highly toxic over the treatment course; thus, only baseline data could be obtained. Fractures were created using a closed model with a 3-point bend applied to the tibia. At a planned time point after the fracture, 1 ml of blood per animal were collected via facial bleeding and the blood was spun to separate out the serum layer used for assay. Assays of the pro-inflammatory markers were performed via ELISA using a 96 well, 7 chamber multiplex plate (MSD Inc.).

Baseline means in pg/ml for cytokines are shown in the table below. Pamidronate suppressed the pro-inflammatory response in all pro-inflammatory markers. The underlined values all had  $p < .05$  on ANOVA non-parametric analysis comparing the means within each genotype.

	NL 0	NL LD	NL HD	OI 0	OI LD	OI HD
IL-1 beta	19.4	16.6	16.7	<u>23.4</u>	<u>5.2</u>	<u>2.6</u>
IL- 6	18.1	9.2	10.9	30.9	15.9	12.0
IL- 8	<u>94.8</u>	<u>27.6</u>	<u>36.8</u>	98.1	53.9	46.3
IL- 10	<u>38.1</u>	<u>14.8</u>	<u>17.3</u>	49.5	27.1	20.5
IL- 12	<u>55.1</u>	<u>9.7</u>	<u>0</u>	84.3	75.6	0
INFgamma	0.9	0.6	0.1	<u>3.7</u>	<u>2.5</u>	<u>1.3</u>
TNF	<u>4.0</u>	<u>1.40</u>	<u>1.3</u>	<u>9.2</u>	<u>1.1</u>	<u>2.8</u>

The fracture data also showed that pamidronate suppressed the pro-inflammatory markers over the first 8 hours from a fracture. The suppressive effect seemed greater in OI than in NL mouse serum.

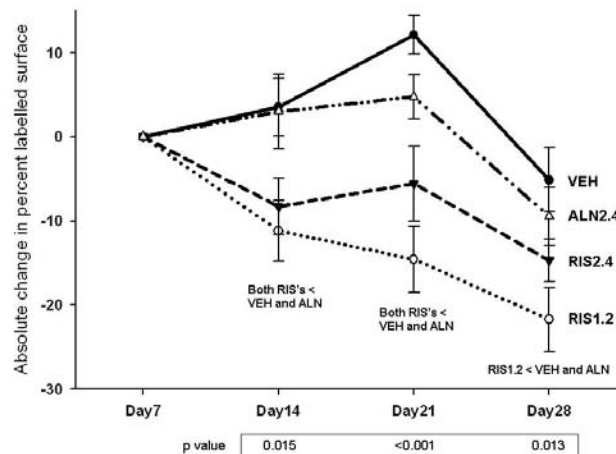
The bisphosphonate, pamidronate, seems to have an anti-inflammatory effect in both NL and OI mice. This may explain why patients have less blood loss after fracture or surgery than historically reported. More study is necessary as to when bisphosphonates should be given after fractures or osteotomies to avoid interference with bone healing.

**Disclosures:** A.I. Leet, None.

## SU387

**Risedronate Has a More Rapid Onset of Remodeling Suppression than Alendronate in Rabbit Vertebral Trabecular Bone.** M. R. Allen<sup>1</sup>, R. J. Phipps<sup>2</sup>, A. S. Koivuniemi<sup>\*1</sup>, M. C. Koivuniemi<sup>\*1</sup>, D. B. Burr<sup>1</sup>. <sup>1</sup>Anatomy & Cell Biology, Indiana University School of Medicine, Indianapolis, IN, USA, <sup>2</sup>Procter and Gamble Pharmaceuticals, Mason, OH, USA.

In a retrospective observational study, risedronate-treated patients had significantly lower incidence of hip and non-vertebral fractures in the first year on therapy than alendronate-treated patients [Silverman et al. 2007]. The goal of this study was to test the hypothesis that risedronate suppresses bone remodeling significantly more quickly than alendronate after the initiation of drug treatment. Four month old female rabbits (n = 32) were divided into four groups and treated with vehicle (VEH), low or high dose risedronate (RIS, 1.2 or 2.4  $\mu$ g/kg), or alendronate (ALN, 2.4  $\mu$ g/kg) subcutaneously 3x/week for 5 weeks. The lower RIS dose and the ALN dose were consistent, on a mg/kg basis, with those used for treatment of post menopausal osteoporosis; the higher RIS dose served as a mg equivalent to the ALN dose. Rabbits received weekly injections of fluorochromes to label actively forming bone surfaces according to the following schedule: tetracycline (week 1), alizarin (week 2), calcein (week 3) and xylenol orange (week 4). Rabbits were euthanized five days after the final label and the fourth lumbar vertebra was processed for histological assessment. The percentage of trabecular bone surface covered with each of the fluorochrome labels was measured to determine the level of active bone formation over time. The amount of labeled bone surface at week 1 was not significantly different among groups. Relative to the amount of labeled surface at week 1, there was significantly less percent labeled surface at weeks 2 and 3 in RIS1.2 (-8%) and RIS2.4 (-11%) groups compared to both VEH and ALN; there was no difference between VEH and ALN. At week 4 only the RIS1.2 group was significantly different from VEH and ALN. These results show that at doses equivalent to those used clinically for treatment of postmenopausal osteoporosis, risedronate exerts a more rapid onset of remodeling suppression compared to alendronate in vertebral trabecular bone.



**Disclosures:** M.R. Allen, The Alliance for Better Bone Health 3; Amgen 3; Eli Lilly and Co. 2.

This study received funding from: The Alliance for Better Bone Health.

## SU388

**Monthly Intravenous Zoledronate Suppresses Tissue-Level Remodeling Significantly More Than Daily Oral Alendronate in the Mandible and Rib of Skeletally Mature Female Dogs.** M. R. Allen, D. J. Kubek<sup>\*</sup>, D. B. Burr. Anatomy & Cell Biology, Indiana University School of Medicine, Indianapolis, IN, USA.

Bisphosphonate treatment significantly reduces bone loss and skeletal metastases in cancer patients partly through its suppression of bone remodeling. The bisphosphonate doses currently used for cancer treatment greatly exceed those used for post-menopausal osteoporosis and while these different regimens produce similar levels of remodeling suppression when measured using systemic biomarkers, there are no data concerning their effects on regional bone remodeling. The goal of this study was to use histology to compare tissue-level remodeling suppression at various bone sites between the most commonly used cancer and osteoporosis treatment regimens. One-year-old intact female beagles were treated for 3 months with vehicle (VEH), alendronate (ALN; 0.2 mg/kg/day) or zoledronic acid (ZOL; 0.06 mg/kg/month). ALN was administered orally each day while VEH and ZOL were administered intravenously every 4 weeks via a 15 minute infusion. These doses and treatment regimens are consistent, on a mg/kg basis, with those used for the treatment of post-menopausal osteoporosis (ALN) and cancer (ZOL). Animals were sacrificed 4 weeks following the last infusion of ZOL. The extent of intracortical bone remodeling in the mandible (subdivided into alveolar and non-alveolar regions), rib, and tibia was quantified as the number of labeled osteons normalized to bone area. Compared to VEH, intracortical bone remodeling was significantly reduced in ZOL-treated animals within the alveolar bone of the mandible (-92%), the non-alveolar bone of the mandible (-83%) and the rib (-85%). These reductions of remodeling in ZOL-treated animals also were significantly lower than ALN-treated animals at each of these three analysis sites (-56%, -55%, and -57%, respectively). Levels of intracortical remodeling were not significantly different between ALN and VEH at any of the sites and there was no difference in the number of labeled osteons among any of the treatment groups in the tibia. Comparing these data to previous experiments in our laboratory shows that the level of remodeling suppression in animals treated with three-months of ZOL was 50% greater in mandibular alveolar bone compared to animals treated for three years with oral alendronate. Based on these results, we conclude that monthly intravenous zoledronate, at doses consistent with those used for cancer treatment, reduces tissue-level intracortical bone remodeling in the mandible and rib significantly more than oral alendronate at doses used for osteoporosis.

**Disclosures:** M.R. Allen, The Alliance for Better Bone Health 3; Amgen 3; Eli Lilly and Co. 2.

This study received funding from: Amgen.

## SU389

**Sites of Femoral Fractures in the Fracture Intervention Trial (FIT) of Alendronate and Its Long-term Extension (FLEX).** D. C. Bauer<sup>\*1</sup>, D. M. Black<sup>\*1</sup>, H. Genant<sup>\*1</sup>, A. de Papp<sup>2</sup>, A. Santora<sup>\*3</sup>, E. Rosenberg<sup>\*2</sup>, K. Ensrud<sup>\*4</sup>, S. R. Cummings<sup>\*5</sup>. <sup>1</sup>UCSF, San Francisco, CA, USA, <sup>2</sup>Merck & Co., Inc., North Wales, PA, USA, <sup>3</sup>Merck & Co., Inc., Rahway, NJ, USA, <sup>4</sup>University of Minnesota, Minneapolis, MN, USA, <sup>5</sup>CPMC, San Francisco, CA, USA.

Recent reports suggest subtrochanteric or proximal diaphyseal fractures of the femur may occur in patients receiving oral bisphosphonates, but the epidemiology of these fractures is less well understood compared to other femur fractures. No placebo controlled studies have specifically investigated the relationship between such fractures and use of bisphosphonates. The Fracture Intervention Trial (FIT, n=6459) and the FIT Long-term Extension (FLEX, n=1099) were randomized, placebo-controlled, double-blind studies of

alendronate (ALN) in postmenopausal women. FIT examined 5-10 mg ALN or placebo (PBO) daily in women with low BMD, in cohorts with or without vertebral fractures, for 3-4.5 years. In FLEX, ALN-treated women from FIT were re-randomized to 5 mg ALN, 10 mg ALN, or PBO daily for an additional 5 years to examine the effects of ALN discontinuation on BMD. Femur fractures were centrally adjudicated and categorized by the UCSF Coordinating Center as femoral neck, intertrochanteric, hip:other, or femoral shaft based on review of X-ray reports or radiographs. Subtrochanteric fractures were not specifically noted. Time to first hip or femoral shaft fracture in the ALN and PBO groups was analyzed using Cox models (Table). In FIT, hip fracture risk was lower in the ALN group (0.9% vs. 1.4%). Most hip fractures were coded as femoral neck or intertrochanteric, but 2 hip fractures were captured as hip:other (both PBO), and 5 femoral shaft fractures without further sub-categorization were recorded. In FLEX, hip fracture risk was similar among ALN and PBO groups (3.0% in both); 1 hip fracture was captured as hip:other (PBO) and 3 femoral shaft fractures in 2 women (ALN) were recorded. A blinded review of available source documents to more precisely identify atypical hip and shaft fractures is underway, but our analysis is limited by the small number of events and wide CI. Large epidemiologic studies and meta-analysis of treatment trials will be required to better describe the epidemiology of non-hip femoral fractures in osteoporotic patients and to determine the potential relationship with long-term bisphosphonate treatment.

Table. Patients with hip and femoral shaft fracture events.

Fracture Site	FIT			FLEX		
	ALN (n=3236)	PBO (n=3223)	RH (95% CI)	ALN* (n=662)	PBO (n=437)	RH (95% CI)
Any Hip	30	46	0.6 (0.4, 1.0)	20	13	1.0 (0.5, 2.1)
Femoral neck	16	31	0.5 (0.3, 0.9)	10	7	0.9 (0.4, 2.5)
Intertrochanteric	14	13	1.1 (0.5, 2.3)	10	5	1.3 (0.5, 3.9)
Other	0	2	NA	0	1	NA
Femoral shaft	3	2	1.5 (0.3, 9.1)	2	0	NA

RH=relative hazard, NA=too few events to estimate RH

\* Pooled 5 mg and 10 mg doses

**Disclosures:** E. Rosenberg, Employee of Merck & Co., Inc., the sponsor of the study. 5. This study received funding from: Merck & Co., Inc.

## SU390

**The Prevalence of Subtrochanteric Fractures in Patients Older than 50 Years Presenting with a Clinical Vertebral or Non-vertebral Fracture.** A. Boonen<sup>\*1</sup>, D. Wakefield<sup>\*2</sup>, K. Huntjens<sup>\*3</sup>, S. van Helden<sup>\*4</sup>, P. Geusens<sup>1</sup>. <sup>1</sup>Internal Medicine/Rheumatology, University Maastricht, Maastricht, Netherlands, <sup>2</sup>University Aberdeen, Aberdeen, United Kingdom, <sup>3</sup>University Maastricht, Maastricht, Netherlands, <sup>4</sup>Surgery, University Maastricht, Maastricht, Netherlands.

Several case series have suggested a link between bisphosphonate (BP) therapy and atypical fractures of the femoral diaphysis. However, in none of the studies the prevalence of these fractures nor the total number of screened patients were documented. Only one study mentioned the proportion of patients on alendronate. We carried out a review of all consecutive patients older than 50 years presenting with a clinical fracture in the context of the osteoporosis and fracture clinic of the hospital.

In total, 3412 patients presented with a clinical vertebral or non-vertebral fracture over a period of 3 years, of whom 2520 consulted the fracture nurse and 892 did not participate in the fracture prevention program. X-rays of all femur fractures (n=558) were reviewed and 31 cases of subtrochanteric fractures were identified. Of the 29 in whom medication intake at the time of fracture could be verified, 2 (7%) were on treatment with BPs at the time of fracture. One patient on daily alendronate since 18 months had a spiral fracture, one patient on generic alendronate since unknown time had a transverse fracture (of 45°). The only patient with a horizontal transverse fracture (of 0°) had a history of metastatic breast carcinoma without radiographic evidence of bone metastasis at the fracture site and had no previous treatment with BPs. Eight of the 57 patients with a hip prosthesis for osteoarthritis had a periprosthetic femur fracture, of whom one patient used BP at the time of fracture. Of patients who participated in the program, 111 (4%) reported to have BP treatment at the time of fracture (odds ratio for subtrochanteric fracture when on BP compared to not on BP: 1.6; 95% confidence interval: 0.4-6.9). Most subtrochanteric fractures (75%) were the result of a simple fall. We conclude that subtrochanteric fractures represent <1% of all clinical vertebral and non-vertebral fractures in patients older than 50 years presenting with a clinical fracture. More >90% of subtrochanteric fractures were found in patients not taking BPs at the time of fracture, indicating that in most patients with a subtrochanteric fracture other mechanisms than low bone turnover associated with intake of BPs are needed to explain their presence.

**Disclosures:** P. Geusens, None.

## SU391

**Comparison of the Effects of Ibandronate Alone with Ibandronate in Combination with SNAC on Bone Density and Bone Strength in Ovariectomized Rats.** R. Samadfam<sup>1</sup>, S. Y. Smith<sup>1</sup>, A. Varela<sup>1</sup>, T. Pfister<sup>2</sup>, F. Bauss<sup>3</sup>. <sup>1</sup>Bone Research, Charles River Laboratories, Senneville, QC, Canada, <sup>2</sup>F. Hoffmann-La Roche Ltd, Basel, Switzerland, <sup>3</sup>Roche Diagnostics GmbH, Penzberg, Germany.

Oral bioavailability of bisphosphonates is low (~1%). Increasing bioavailability would allow either a lower dose than currently used, or keeping the dose while increasing the dosing-free interval. The purpose of this study was to compare the effects of two different dose formulations of Ibandronate (IBN) with or without an absorption enhancer, sodium N-[8-(2-hydroxybenzoyl)amino]caprylate (SNAC), on bone parameters. Seven week old Sprague-Dawley CD rats were assigned to 10 groups of 10 females/group. All animals were ovariectomized (OVX), with the exception of one group which underwent sham surgery. One day after surgery, animals were given a weekly dose of vehicle, IBN or IBN+SNAC by gavage for 10 weeks. Doses for IBN alone treated animals were 1, 3, 10, and 30 mg/kg/dose. In SNAC+IBN treated animals, doses for IBN were 0.2, 0.6, 2 and 6 mg/kg/dose. The doses of IBN for IBN+SNAC groups were based on the expectation that SNAC increases AUC and Cmax by about 2 and 4-5 fold respectively. Ratio IBN:SNAC was 1:30. Bone mass, architecture and strength were analyzed by means of bone mineral density, biomechanical analyses, and histomorphometry.

In lumbar vertebrae, IBN alone or in combination with SNAC increased bone mass dose-dependently compared to controls, however, group mean comparisons indicated that IBN/SNAC treated animals had lower BMD compared to their corresponding IBN alone groups. These increases correlated with increases in vertebral bone strength parameters obtained from compression analyses. Femoral BMD was also dose-dependently increased however this did not translate into increases in bone strength parameters for the 3-point bending due to the effect of IBN on bone geometry in young growing rats.

Both formulations of IBN (with or without SNAC) resulted in dose-dependent increases in BV/TV, Md.V/TV, Tb.Th, Tb.N and osteoclast surface and decrease in Tb.Sp at the proximal tibia metaphysis. The effects of IBN alone on the evaluated histomorphometric parameters were generally superior to those of IBN/SNAC when compared to their corresponding IBN dose groups. Relative potency estimation analyses based on a linear model revealed an approx. 2-fold increase in the pharmacodynamic efficacy of oral IBN by SNAC. However, it remains to be determined whether bioavailability and renal excretion of IBN are similar throughout the tested dose range, and whether non-linear calculations including these parameters would justify translation into clinical use.

**Disclosures:** R. Samadfam, Charles River Laboratories 3.

## SU392

**Alendronate Affects Cross-talk of Osteoclasts and Osteoblasts *in vivo*.** E. Shimizu<sup>1</sup>, J. Tamasi<sup>\*2</sup>, N. C. Partridge<sup>1</sup>. <sup>1</sup>Physiology and Biophysics, UMDNJ-Robert Wood Johnson Medical School, Piscataway, NJ, USA, <sup>2</sup>Clinical Discovery Technologies, Bristol-Myers Squibb Pharmaceutical Research Institute, Princeton, NJ, USA.

Bisphosphonates are potent inhibitors of osteoclastic bone resorption and are valuable therapeutic agents in the treatment of postmenopausal osteoporosis, osteitis deformans, and bone metastasis with or without hypercalcemia. Although it has recently been discovered that bisphosphonates are associated with osteonecrosis of the jaw (ONJ), the pathophysiological mechanism of ONJ is not clear. Since bisphosphonates inhibit the functions of osteoclasts, osteoclast feedback to osteoblasts may also be ablated, and thus inhibit normal physiological bone remodeling and turnover resulting in ONJ. Our hypothesis is that bisphosphonates indirectly regulate the functioning of osteoblasts via feedback from osteoclasts to osteoblasts. To investigate this, adult mice were injected with alendronate (10 ug/100 g/week) for 8-weeks. We found that alendronate significantly stimulated BMD and inhibited osteoclast marker genes such as TRAP, cathepsin K and NFAT2 in femurs. We also found that alendronate increased osteoprotegerin (OPG) gene expression and decreased the ratio of receptor activator of nuclear factor-kB ligand (RANKL) to OPG. Thus, alendronate also indirectly suppressed osteoclast differentiation via the osteoblast. Alendronate may also affect ligands produced by osteoclasts which act on receptors on osteoblasts. We investigated ephrin ligands and eph receptors, and found that alendronate increased ephrin B1, and Eph B1, B3, B6 in femurs. Next, we examined if alendronate affected osteoblastic function. Alendronate suppressed expression of bone sialoprotein (BSP) and osteonectin (ON) in both femurs and bone marrow osteoblastic cells from mice which had received alendronate. In addition, the same cells had increased Eph B1 and B3. We investigated if alendronate directly affected osteoblastic differentiation using primary cultures of osteoblasts. Alendronate at a high concentration (10 uM) suppressed bone mineral nodule formation and osteocalcin gene expression but did not affect other genes. Thus, alendronate, through its effects on the osteoclast, appears to regulate expression of ephrin B1 which may then regulate and act through the Eph B1, B3, B6 receptors on the osteoblast to suppress osteoblast differentiation.

**Disclosures:** E. Shimizu, None.

## SU393

**Improved Bone Mass After Co-administration of Strontium Ranelate and Risedronate in a Rat Model of Osteoporosis using “in-vivo” Micro-CT.** M. R. Doschak, C. T. Lee\*, M. D. Jones\*, G. Li\*, J. Foster\*, M. J. M. Duke\*. Pharmacy & Pharmaceutical Science, University of Alberta, Edmonton, AB, Canada.

Antiresorptive therapy is often initiated retrospectively, after the significant loss of both bone mass and trabecular connectivity. Despite slowing further bone loss, antiresorptive agents have limited capacity for increasing bone mass. Furthermore, increases in bone mass can only occur where pre-existing trabecular connections remain. Thus, we tested if prospective combination antiresorptive-anabolic drug therapy would improve bone mass and trabecular connectivity in a rat model of osteoporosis.

Twenty 6-month old female rats were randomly assigned to one of five groups (n=4/group): 1) Ovariectomized (OVX) untreated controls, 2) Strontium ranelate (Protos™) treated (STR; 308 mg/kg qd p.o.), 3) Risedronate-treated (RIS; 0.06 mg/kg q3.5d s.c.), 4) Combined STR-RIS, and 5) Sham-operated (SHAM). Each rat was imaged at baseline using “in-vivo” micro-CT to assess bone mass and bone mineral density (BMD). Antiresorptive drug interventions (either STR or RIS) were also initiated at time-zero and continued to the same endpoint of 5 months post-OVX, and assessed longitudinally with “in-vivo” micro-CT at monthly intervals. At the experimental endpoint, rat tibiae were dissected free of soft tissues and tested for mechanical strength to failure in 3-point flexural analyses, then incinerated in a muffle-furnace and the ash used to assess calcium and strontium content by Instrumental Neutron Activation Analysis (INAA).

Results confirmed significant loss of bone mass in OVX rats as measured with “in-vivo” micro-CT, particularly during the first 2 months. Both RIS dosed groups significantly slowed the further loss of bone mass over untreated OVX controls, however, only the combined STR-RIS group resulted in a significant increase in bone mass compared to all groups (bar the sham-operated controls). Micro-CT based histomorphometric analyses of trabecular bone was significantly correlated with bone strength measurements from mechanical testing. INAA accurately measured bone strontium content, and the relationship with BMD positive bias was explored.

We conclude that the co-administration of bone antiresorptive and anabolic drugs in a prospective regimen during the pathogenesis of Osteoporosis significantly improved bone mass over either agent alone as a monotherapy.

**Disclosures:** M.R. Doschak, None.

This study received funding from: Faculty of Pharmacy & Pharmaceutical Sciences, University of Alberta, Canada.

## SU394

**Alfacalcidol Ameliorates Bone Dynamics in Senescence-accelerated SAMP6 Mice and in Fracture Repair Rat Model.** A. Shiraishi\*, S. Sakai\*, M. Mihara\*. Product Research Dept., Chugai Pharmaceutical Co., Ltd., Gotemba, Japan.

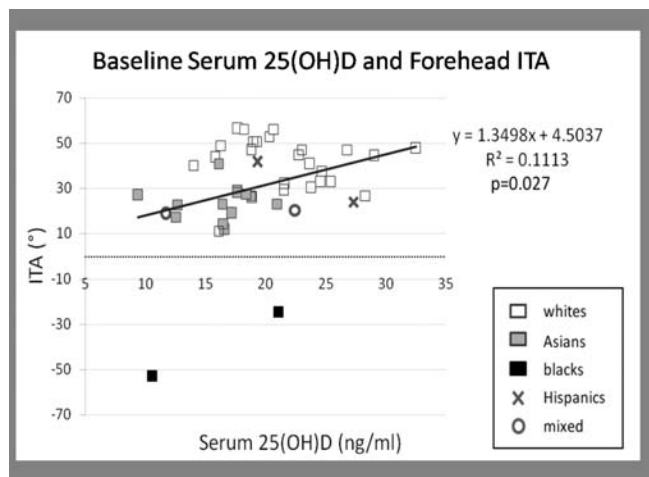
Alfacalcidol (1 $\alpha$ (OH)D<sub>3</sub>: ALF), the prodrug of calcitriol, is an inhibitor of bone resorption in estrogen-deficient high-turnover osteoporosis rat model. In this study, we assessed the effects of ALF on the bone loss in low-turnover osteoporosis using senescence-accelerated SAMP6 mice and on the processes of fracture repair using rat model. <Exp.1> Four month-old male SAMP6 mice were received ALF (0.1 or 0.2 $\mu$ g/kg, p.o. 5 times/week) administration for 6 weeks. Micro-CT analysis revealed that ALF treatment dose-dependently increased the bone volume (BV/TV), trabecular number (Tb.N) and connectivity density (Conn.D) at trabecular region of proximal tibia and the bone area of cortical tibia. Histomorphometrical analysis indicated that, in trabecular and endocortical bone, ALF markedly suppressed bone resorption parameters such as ES/BS and N.Oc/BS. <Exp.2> Wistar rats at three months of age were either sham operated or ovariectomized (OVX) and divided into three groups: SHAM control, OVX control, ALF (0.1 $\mu$ g/kg, p.o. 5 times/week) groups. Treatment began immediately after the surgery. Three weeks after ovariectomy, bilateral osteotomies were performed on the femoral midshaft and fixed with intramedullary wires. Fracture calluses were excised at twelve weeks after fracture. Callus sizes were not different among all groups. ALF treatment did not show significant effect on the progression of fracture repair. The ratio of lamellar to woven bone in ALF-treated group was similar to sham control group. In ALF-treated group, BMD at fracture region was significantly higher than vehicle control group. Moreover, the mechanical properties at fracture site in ALF-treated group were higher than those in vehicle control group (max load: 149.7 vs. 119.5 N, stiffness: 260.3 vs. 166.5 N/mm, respectively). Histomorphometrical analysis revealed that ALF increased bone formation (BFR/BS) at fracture site, while suppressed bone resorption (ES/BS) at normal site of femoral midshaft. In conclusion, ALF ameliorated bone dynamics in senescence-accelerated SAMP6 mice and in fracture repair rat model.

**Disclosures:** A. Shiraishi, None.

## SU395

**Effect of Skin Color and Oral Vitamin D Supplementation on Serum 25(OH) Vitamin D in Adolescent Girls.** C. Y. Park\*<sup>1</sup>, K. M. Hill\*<sup>1</sup>, A. E. Elble\*<sup>1</sup>, B. R. Martin\*<sup>1</sup>, M. Peacock\*<sup>2</sup>, C. M. Weaver\*<sup>1</sup>. <sup>1</sup>Dept of Foods and Nutrition, Purdue University, West Lafayette, IN, USA, <sup>2</sup>Dept of Medicine, Indiana University School of Medicine, Indianapolis, IN, USA.

Sunlight exposure and skin pigmentation are important determinants of serum 25(OH) vitamin D (s25D) levels. We investigated these relationships while minimizing UVB exposure and controlling diet in adolescent girls in Indiana. Forty-four girls (25 white, 13 Asian, 2 black, 2 Hispanic, 2 mixed) aged 11-14y participating in a metabolic balance study during the summer were monitored for skin color and s25D for 7 weeks. Skin color was measured by reflectance (Minolta CM-2600d) and these values were used to calculate individual typology angle (ITA), a measurement of skin pigmentation. The forehead and forearm were measured for facultative skin color (color of skin where light-induced pigmentation occur), and the upper inner arm for constitutive skin color (photo-protected skin color). S25D was assessed by RIA. Subjects were provided with sunscreen (sun protection factor  $\geq 15$ ) and 200 IU/d vitamin D in a controlled diet. During the last 4 weeks, 14 girls were given 1000 IU/d vitamin D<sub>3</sub>. At baseline, higher ITA (less pigmentation) predicted higher levels of s25D in the forehead (Figure). At 7 weeks, ITA decreased from baseline in the upper arm only. S25D increased in all subjects, but the increase in vitamin D supplemented girls was significantly greater than non-supplemented girls (p<0.01). Although facultative skin color predicted s25D levels at baseline, changes in skin color were not associated with change of s25D levels, regardless of vitamin D supplementation.



**Disclosures:** C.Y. Park, Delavau LLC 3.

This study received funding from: Delavau LLC.

## SU396

**Vitamin D Concentrations of Healthy Children Living in the Calgary Health Region.** C. A. Stoian\*, J. K. Mah\*, R. G. Cox\*, D. K. Stephure, M. Lyon\*. University of Calgary, Calgary, AB, Canada.

Vitamin D deficiency results in rickets in children and osteomalacia in adults. The purpose of our study was to examine the vitamin D status among healthy children aged 2 to 13 years living in Southern Alberta, Canada.

The data in this study was collected prospectively from healthy children 2 to 13 years of age who presented consecutively at the Alberta Children's Hospital for elective surgery from December 2005 to December 2006. Data collected from children eligible to enter the study and for whom informed consent was obtained included child's weight, height, age, gender, ethnicity, use of vitamin supplements, physical activity, time spent outdoors, and medications used on a regular basis. Each child's dietary intake was assessed using the Harvard Service Food Frequency Questionnaire. Measurements of blood concentrations were performed according to manufacturer's specifications: serum 25 hydroxyvitamin D (25(OH) D) and parathyroid hormone (DiaSorin); total calcium, phosphate, albumin and creatinine (Ortho Clinical Diagnostics), and alkaline phosphatase (Rosche). Demographic data were available for 1862 subjects. Serum 25(OH) D concentrations were available for 1442 subjects, of whom 862 (59.78%) were boys and 580 (40.22%) were girls. The mean age of subjects for whom serum 25(OH) D concentrations were known was 6.09 years (SD = 2.85 years). There was no statistical difference for age or sex between the study group and the group without laboratory data. Seventy five children (5.2%) were found to be vitamin D deficient, defined as serum 25(OH)D concentrations  $\leq 37.5$  nmol/L. Suboptimal vitamin D (serum 25(OH)D concentrations  $\leq 80$  nmol/L) was determined in 689 subjects (47.78%). Only 22 subjects (1.53%) were found to have severe vitamin D deficiency (serum 25(OH) D concentrations  $\leq 20$  nmol/L). More subjects were vitamin D deficient in the older age group (9 to 13 years) compared to the younger age groups (2 to 4.99 years and 5 to 8.99 years): 11.24%, 3.93% and 3.83%, respectively. There was no statistical difference between boys and girls with respect to vitamin D deficiency status. Children in the vitamin D deficient group spent significantly less hours outdoor compared to those whose serum 25(OH)D concentrations were greater than 37.5 nmol/L (p value = 0.005). During winter the mean  $\pm$  standard deviation of serum 25(OH) D

concentrations were significantly lower ( $77.98 \pm 37.34$  nmol/L) when compared with values obtained during summer ( $96.42 \pm 37.50$  nmol/L).

In our study vitamin D deficiency was less prevalent than reported by other authors. Children who do not participate in outdoor activities regularly throughout the year or those who do not have sufficient vitamin D intake from dietary sources should receive appropriate vitamin D supplementation to ensure optimal bone health.

**Disclosures:** C.A. Stoian, None.

This study received funding from: Alberta Children's Hospital Foundations, DiaSorin, Ortho Clinical Diagnostics.

## SU397

### The Comparative Antifracture Efficacy of N-containing Bisphosphonates.

M. C. Hochberg, Medicine, University of Maryland, Baltimore, MD, USA.

**Background:** Four N-containing bisphosphonates (BPs), alendronate (ALN), ibandronate (IBAN), risedronate (RIS) and zoledronic acid (ZOL), are approved for the treatment of women with postmenopausal osteoporosis (PMO). While several head-to-head studies have compared the efficacy of some of these BPs using surrogate outcomes (changes in bone mineral density and bone turnover markers), no head-to-head trials have been designed to compare antifracture efficacy.

**Objective:** To estimate the comparative antifracture efficacy of N-containing BPs.

**Methods:** Data on the antifracture efficacy of the N-containing BPs in women with PMO were abstracted from several sources: the updated 2008 Cochrane systematic reviews by Wells and colleagues provided data on radiographic vertebral (VFX), non-vertebral (non-VFX) and hip fracture reduction for ALN and RIS; the pivotal phase III trial and individual patient meta-analysis by Harris and colleagues provided data for VFX and non-VFX reduction for IBAN, respectively; and the pivotal phase III trial provided data for VFX, non-VFX and hip fracture reduction for ZOL. For both ALN and RIS, the analysis was limited to results of secondary prevention (treatment) trials that used the daily doses of 10 mg and 5 mg, respectively. For IBAN, data on VFX for the daily dose of 2.5 mg and non-VFX reduction for the high-dose cumulative exposure group of 150 mg monthly or 3 mg IV every 3 months, respectively, were used in the analysis. The method of adjusted indirect comparisons (Bucher et al: J Clin Epidemiol 1997;50:683-91) was used to calculate the estimated relative risk (RR) and 95% confidence intervals (CI) for hypothetical head-to-head studies; statistical significance is inferred if the CI does not include unity.

**Results (Table):** There were no significant differences in estimated antifracture efficacy between ALN, RIS and IBAN for either VFX or non-VFX; between ALN, RIS and ZOL for non-VFX including hip fractures; or between IBAN and ZOL for non-VFX. ZOL appeared to be more efficacious for reduction in VFX than ALN, RIS and IBAN.

**Conclusions:** These data, derived using the method of adjusted indirect comparisons (Level 2A evidence), suggest that ZOL may be more efficacious than other N-containing BPs for reduction in risk of new radiographic VFX. Head-to-head RCTs would be needed to confirm this finding. There were no significant differences, however, in estimated efficacy for reduction in either non-VFX or hip fractures.

Relative Risk (95% Confidence Intervals) for Incident Fractures: Adjusted Indirect Comparisons			
Drug Comparison	Vertebral Fracture	Non-vertebral Fracture	Hip Fracture
ALN vs RIS	0.90 (0.66, 1.24)	0.96 (0.78, 1.19)	0.63 (0.34, 1.20)
ALN vs IBAN	1.14 (0.72, 1.83)	1.17 (0.77, 1.77)	N/A
ALN vs ZOL	1.83 (1.28, 2.55)	1.04 (0.82, 1.31)	0.80 (0.40, 1.58)
RIS vs IBAN	1.27 (0.80, 2.00)	1.21 (0.82, 1.80)	N/A
RIS vs ZOL	2.04 (1.49, 2.77)	1.08 (0.90, 1.30)	1.25 (0.83, 1.89)
IBAN vs ZOL	1.60 (1.01, 2.55)	0.89 (0.59, 1.34)	N/A

**Disclosures:** M.C. Hochberg, Merck & Co., Inc. 2, 4; Roche Pharmaceutical Co. 2; Proctor & Gamble Pharmaceutical Co. 5; Novartis Pharma AG 2, 5.

## SU398

**Zoledronic Acid Treatment of Osteoporosis: Effects in Men.** D. A. Johnson<sup>\*1</sup>, M. I. Williams<sup>\*1</sup>, J. LaFleur<sup>\*2</sup>, R. A. Adler<sup>1</sup>. <sup>1</sup>Endocrinology, McGuire VAMC, Richmond, VA, USA, <sup>2</sup>University of Utah College of Pharmacy, Salt Lake City, UT, USA.

Although clinical trials of zoledronic acid have shown excellent bone mineral density increases and fracture risk reductions, there is always concern that results cannot be generalized to other populations. We have used zoledronic acid 4 mg infusions off-label for patients intolerant to or non-adherent to oral bisphosphonate therapy for osteoporosis. We previously reported that routine laboratory measurements of the bone resorption marker NTx found that NTx was often suppressed for > 12 months. We have experience with treatment of a heterogeneous group of approximately 100 patients and report here the results in 41 men who have had bone density measurements before and after at least one infusion.

Bone mineral density was measured by a Hologic Discovery densitometer and changes in spine, total hip, and total forearm were determined. All patients had monitoring of renal function, serum calcium, and 25-hydroxyvitamin D levels. Vitamin D was replaced in all subjects before infusion.

In this group, the number of infusions varied from 1 to 4, but the average was two. The average time between bone density measurements was 3.1 years. Patients did not receive additional infusions until the NTx level returned to the low normal range. Thus, the interval between infusions was usually more than one year.

In the spine, the average increase of BMD was 3.99%, and the average increase in the total hip was 1.77%. The total forearm is the default setting on the Hologic densitometer. Thus, the average change in the forearm was a decrease of 0.74%, although some men showed an

increase in the forearm.

When the data are expressed per year, the increase in the spine was 1.47% and the increase in the hip was 0.59%. Overall, 82% of men demonstrated an increase in the spine, 71% an increase in the total hip and 42% an increase in the forearm. In our population, 66% of patients had been prescribed oral bisphosphonates or intravenous pamidronate before receiving zoledronic acid. As might be expected, larger increases in spine (5.5% naive group v. 1.4% bisphosphonate exposed group) occurred in the bisphosphonate naive patients.

Thus, in a real world setting of a heterogeneous group of men with osteoporosis, there was a change in bone density similar to what has been reported in men receiving oral bisphosphonates. Further studies are underway to analyze suppression of NTx with change in BMD.

**Disclosures:** R.A. Adler, Novartis 2, 3, 4.

## SU399

**Atypical Osteoclast Phenotype after Long-Term Alendronate Therapy for Osteoporosis: A Paired Bone Biopsies Report.** N. Dion, J. L. Petit\*, L. G. Ste-Marie. Saint-Luc Hospital, Research Centre of the Centre Hospitalier de l'Université de Montréal (CRCHUM), Montréal, QC, Canada.

Bisphosphonates (BPs) have been the preferred agents for the treatment of osteoporosis for almost 10 years. The paradigm for the last years was that by decreasing bone resorption and promoting osteoclast apoptosis, BP treatment reduces bone turnover and allows more complete secondary mineralization leading to a lower risk of fractures. We present the cases of 4 patients (1 woman and 3 men) with osteoporosis treated for 6 or 8 years with alendronate (ALN). As expected, ALN treatment increased significantly bone mineral density which gradually led to a plateau after 3 to 4 years of treatment. To evaluate bone turnover at the tissue level, we compared bone histomorphometric results of trans-iliac bone biopsies (Bx) performed in each patient before (pre-ALN) and after 6 or 8 years of ALN (ALN+). Before ALN treatment, all patients had moderate to high turnover osteoporosis characterized by low trabecular bone volume (BV/TV) with normal or high bone formation activity and normal or high bone resorption surfaces (ES/BS). After ALN therapy, BV/TV increased or remained unchanged whereas matrix synthesis was drastically reduced as shown by the suppression of the bone formation rate (BFR/BS) when compared to pre-ALN Bx. No significant difference for ES/BS and for the number of osteoclast per bone perimeter (N.Oc/B.Pm) was observed in ALN+ Bx comparing to the pre-ALN Bx (cf table). As reported recently by Weinstein R.S. et al., and Dempster D.W. et al., (ASBMR 2007, abstract 1058 and 1096, respectively) in Bx of patients on ALN therapy, we observed, in all ALN+ Bx, giant multinucleated osteoclasts which were occasionally detached from bone surfaces and/or adjacent to shallow Howship's lacunae. Surprisingly, most of the osteoclasts observed in ALN+ Bx, showed an intense positive reaction to tartrate resistant acid phosphatase (N.OcTRACP+/B.Pm =  $0.39 \pm 0.09$  / mm). Our results emphasize that long-term ALN therapy does not induce a decrease in the number of osteoclasts as an increased apoptosis would suggest (if not compensated by an increase in osteoclastogenesis). The development of a new phenotype of giant osteoclasts positively active for TRACP could involve an unknown compensatory mechanism to BP treatment. Further studies are needed to better explain this phenomenon and explore its relevance to clinical response to BP treatment.

	Pre-ALN	ALN+	P-value (paired t-test)
BFR/BS ( $\mu\text{m}^3/\mu\text{m}^2/\text{y}$ )	47.8 $\pm$ 8.7*	6.2 $\pm$ 3.2	0.01
ES/BS (%)	8.0 $\pm$ 1.2	7.4 $\pm$ 1.7	0.85
N.Oc/B.Pm (/mm)	0.30 $\pm$ 0.04	0.32 $\pm$ 0.07	0.78
% of giant Oc	>1	13 $\pm$ 3.5	0.04

\*mean $\pm$ SEM

**Disclosures:** N. Dion, None.

## SU400

**Reduced Osteoclastogenesis and RANKL Expression in Marrow from Women Taking Alendronate.** B. Eslami<sup>\*1</sup>, S. Zhou<sup>1</sup>, M. S. LeBoff<sup>2</sup>, J. Glowacki<sup>1</sup>. <sup>1</sup>Orthopedic Surgery, Brigham and Women Hospital, Boston, MA, USA, <sup>2</sup>Division of Endocrinology, Brigham and Women Hospital, Boston, MA, USA.

Osteoporosis is a major public health problem and bisphosphonates such as Alendronate (AL) are commonly used for prevention of fracture and treatment of osteoporosis. Little is known about the effects of AL on human marrow cells and regulation of osteoclast differentiation. The first study tested the hypothesis that marrow from women taking AL generates fewer osteoclasts and expresses less RANKL compared with women not taking AL. The second study tested the hypothesis that treatment of the stromal fraction of marrow with AL would alter expression of genes that regulate osteoclastogenesis.

Marrow was obtained as discarded tissue during total hip replacement for osteoarthritis in postmenopausal women. For the first study, low-density immature bone marrow cells (LDBMC) from 4 subjects taking AL at the time of surgery (+AL) were matched with LDBMC from 5 untreated subjects (-AL) and cultured  $\pm$  25 ng/ml M-CSF to stimulate osteoclast differentiation. After two weeks, expression of CAT-K, RANKL, OPG and M-CSF was evaluated relative to expression of a housekeeping gene. For the second study, adherent marrow stromal cells (MSCs) from 10 subjects (-AL) were treated with AL ( $10^{-5}$ ,  $10^{-7}$  and  $10^{-9}$  M) and 25 ng/ml M-CSF. Expression of OPG and MCSF was assessed at 1, 3, and 5 days.

In the first study with unfractionated LDBMC, the +AL samples showed lower basal expression of the osteoclast marker gene Cat-K (8%,  $P=0.015$ ) and the pro-osteoclastogenic regulatory gene RANKL (17%,  $P=0.027$ ) than the -AL samples. As expected, M-CSF significantly increased Cat-K in both +AL (8.8 fold,  $P=0.028$ ) and -AL (2.9 fold,  $P=0.028$ ); nevertheless, Cat-K expression remained lower in cells from +AL subjects (24%,  $P=0.015$ ) than from -AL. There were no significant differences in expression of OPG and M-CSF.

In the second study with adherent MSCs, AL ( $10^{-9}$  M) upregulated OPG expression in a subset 4 of 10 samples ( $P=0.009$ ), by an average of  $52\% \pm 34$ . The responsive cells differed from the non-responsive ones in that they showed a constitutive increase in M-CSF production, perhaps reflecting different states of differentiation or genetic features. These results indicate that in addition to AL's inhibition of osteoclastic bone resorption, AL may directly inhibit osteoclastogenesis by affecting the key regulatory genes in stromal cells. Furthermore, these studies affirm the usefulness of human marrow cultures to explore the clinical effects of therapeutic interventions at the cellular level.

**Disclosures:** B. Eslami, None.

This study received funding from: NIH-NIA.

## SU401

**Do Physicians Who Practice Together Provide Similar Osteoporosis Care?**

J. R. Curtis<sup>1</sup>, J. Xi<sup>\*1</sup>, T. Arora<sup>\*1</sup>, A. G. Silver<sup>\*2</sup>, C. Colon-Emeric<sup>\*3</sup>, A. O. Westfall<sup>\*4</sup>, E. Delzell<sup>\*5</sup>, K. G. Saag<sup>1</sup>. <sup>1</sup>Division of Rheumatology, University of Alabama at Birmingham, Birmingham, AL, USA, <sup>2</sup>The Carolinas Center for Medical Excellence, Cary, NC, USA, <sup>3</sup>Department of Medicine, Duke University, Durham, NC, USA, <sup>4</sup>Department of Biostatistics, University of Alabama at Birmingham, Birmingham, AL, USA, <sup>5</sup>Department of Epidemiology, University of Alabama at Birmingham, Birmingham, AL, USA.

**Introduction:** Patients' receipt of prescription osteoporosis therapies (OP Rx) is likely to be influenced by their physician's prescribing patterns. Additionally, if physicians in contiguous practices influence one another's prescribing, successful quality improvement interventions need to target at the practice level rather than at individual physicians.

**Methods:** To address this issue in two high risk populations we examined receipt of OP Rx in: 1) long term glucocorticoid (GC) users in a large U.S. healthcare organization and 2) nursing home (NH) residents with prior fracture or osteoporosis. A common practice setting was defined as doctors who practiced at the same address or in the same nursing home. Hierarchical linear modeling (HLM) and alternating logistic regression (ALR) evaluated the relationship between OP Rx and the common practice setting and the individual physician and are reported as cluster-specific odds ratios and intra-class correlation coefficients (ICCs).

**Results:** Among 6281 long term GC users treated by 2096 doctors in 1295 practices, the proportion receiving OP Rx was 24%. Among 1447 NH residents in 350 nursing homes treated by 67 physicians, the proportion receiving OP Rx was 33%. The relationship between OP Rx and clustering at the physician practice and individual physician level is shown in the Table. There was no significant relationship between receipt of OP Rx and physician practice or nursing home after accounting for the significant effect of the individual physician.

**Conclusion:** In long term glucocorticoid users and NH residents with prior fracture, physicians practicing together were not more likely to prescribe osteoporosis prescription medications than those who did not. Osteoporosis quality improvement interventions can likely ignore the effect of physician groups and common practice settings and maximize power by targeting individual physicians.

Relationship Between OP Rx & Clustering at the Practice Setting and Individual Physician

	Cluster OR (95% CI)	Adjusted* Cluster OR (95% CI)	Adjusted* ICC
<b>Glucocorticoid users</b>			
Physician group practice effect	1.22 (0.88 - 1.69)	1.16 (0.86 - 1.57)	0.03
Individual Physician effect	1.56 (1.34 - 1.82)	1.53 (1.32 - 1.77)	0.08
<b>Nursing home residents</b>			
Nursing home effect	1.06 (0.94 - 1.20)	1.07 (0.94 - 1.22)	0.02
Individual Physician effect	1.22 (1.00 - 1.49)	1.24 (1.02 - 1.51)	0.05

OR = odds ratio; ICC = intra-class correlation;

\* adjusted for patient factors (e.g. age, gender)

**Disclosures:** J.R. Curtis, Novartis, Amgen, Merck, Procter & Gamble, Eli Lilly, Roche 3; Roche, UCB, Procter & Gamble 1; Merck, Procter and Gamble, Eli Lilly, Novartis, Roche 1.

This study received funding from: Arthritis Foundation, PhRMA Foundation Research Grant in Health Outcomes.

## SU402

**Effect of 10-Year Fracture Risk Tool Results on Likelihood of Bisphosphonate Prescribing.** B. Ettinger<sup>1</sup>, K. Cody<sup>\*2</sup>, C. Gross<sup>3</sup>. <sup>1</sup>University of California, San Francisco, CA, USA, <sup>2</sup>Foundation for Osteoporosis and Education (FORE), Oakland, CA, USA, <sup>3</sup>AVIYA Clinical Res and Dev, Orinda, CA, USA.

Previous research has shown that likelihood of prescribing osteoporosis drugs was affected by the way clinical data were presented.\* Several fracture risk assessment tools have recently been posted on web sites. To evaluate the effect of fracture data presentation from one of these tools (FRC®; [www://riskcalculator.fore.org](http://www.riskcalculator.fore.org)), we designed a comparison study among attendees of two national scientific meetings.

In September-October 2007, 213 surveys were completed by attendees at the annual meetings of the North American Menopause Society (NAMS), non-osteoporosis experts, largely OB/GYN practitioners, and of the American Society for Bone and Mineral Research (ASBMR), osteoporosis experts. Respondents all reported prescribing bisphosphonates (BP) and being familiar with bone densitometry. Enthusiasm for prescribing BP was rated for each of 3 postmenopausal women (70% or more likelihood of prescribing was set as the threshold). By random assignment, half of those surveyed were provided with only case descriptions (including T-scores) while half were also given a fracture risk assessment graphic and numerical display of fracture risk. Three hypothetical cases were presented: patient A with established osteoporosis; patient B, an osteopenic, younger woman at low fracture risk; patient C, older, but not obviously osteoporotic, with several clinical risk factors that led to high fracture risk. Our hypotheses related to cases B and C; that FRC would reduce prescribing in Case B and would increase prescribing in Case C.

BP treatment for Case A was universally chosen as likely (90-100%), regardless of the type of report (case information only 96.3%; FRC 92.3%). In Case B, the likelihood of prescribing BP fell 60% (from 11.9% to 4.8%) when the FRC was provided. In Case C, the likelihood of prescribing BP increased 21% (from 57.8% to 70.2%) when FRC was provided. Responses of those surveyed at ASBMR differed from those surveyed at NAMS in regard to Case B; NAMS respondents markedly reduced likelihood of BP prescribing (from 22% to 4%;  $p=.004$ ) when fracture risk was provided while ASBMR respondents voted very low (0-6%) likelihood whether or not the fracture risk was provided.

Enthusiasm for treating postmenopausal women with BP varies depending on clinical risk profile and can be further modified by addition of fracture risk information. The FRC tool yielded greatest effect in reducing likelihood of prescribing BP to a younger osteopenic woman by practitioners who were generalists (OB/GYN largely) and less effect was found among bone experts.

\* Ettinger BH, Hillier TA, Pressman AR, Che M, Hanley DA. Computer model for calculating fracture risk. J Women's Health 2005;14:158-72.

**Disclosures:** B. Ettinger, Foundation for Osteoporosis Research and Education 2; Procter&Gamble 4; Duramed-Barr 2, 4; Organon 2.

This study received funding from: Procter & Gamble.

## SU403

**Once-A-Month (OAM) Risedronate 150 mg Reduced Vertebral Fracture Risk at One Year in a Historical Control Analysis.** N. Watts<sup>1</sup>, A. Klemes<sup>2</sup>, L. Wagner<sup>\*2</sup>, J. Brown<sup>3</sup>.

<sup>1</sup>University of Cincinnati Bone Health & Osteoporosis Center, Cincinnati, OH, USA, <sup>2</sup>Procter & Gamble Pharmaceuticals, Mason, OH, USA, <sup>3</sup>Rheumatology and Bone Diseases Research Group, Sainte-Foy, QC, Canada.

The anti-fracture efficacy of new osteoporosis therapies is evaluated in randomized placebo controlled trials. The inclusion of a placebo arm in subsequent studies of other dosing regimens may be limited by practical or ethical considerations. In these cases, an historical control group can be a viable alternative. In a recent active-controlled study, OAM risedronate 150 mg demonstrated increases in bone mineral density (BMD) that are non-inferior to those seen with the risedronate 5 mg daily dose, which has proven anti-fracture efficacy.

To assess the anti-fracture efficacy of this new regimen, fracture data collected in the active controlled study of 150 mg of risedronate was analyzed using matched historical control data from previous placebo-controlled trials with identical baseline characteristics. Women in the OAM study were matched with placebo patients in the Vertebral Efficacy of



Risedronate Therapy (VERT) trials for age, years since menopause, BMD, and prevalent vertebral fractures. An historical active treatment group was also constructed from the 5 mg daily arm of the VERT trials for comparison with the 5 mg daily and 150 mg OAM treatment groups in the OAM study.

Over one year new vertebral fractures occurred in 1.4% of the risedronate 5 mg daily group from the OAM study (n = 642) and 1.4% of the 150 mg OAM group (n = 650), in 5% of the historical placebo patients (n = 101, matched from 988) and 2% of the risedronate 5 mg daily patients (n = 99 matched from 979) in the VERT studies. New vertebral fracture risk at 12 months was reduced by 72% in the 150 mg OAM group compared with the historical placebo group (RR 0.27; 95% CI, 0.08 to 1.07, P = 0.032), similar to the 1-year risk reduction observed in the VERT trials of risedronate 5 mg daily (61-65%). OAM risedronate appears as effective as the 5 mg daily dose in reducing the risk of new vertebral fractures in the first year of treatment when a historical placebo control group is used. The use of appropriate historical control data is an alternative to assess fracture effects in osteoporosis trials for which placebo-controlled data are not available.

**Disclosures:** N. Watts, P&G 2.

This study received funding from: The Alliance for Better Bone Health (Procter & Gamble Pharmaceuticals and sanofi-aventis).

## SU404

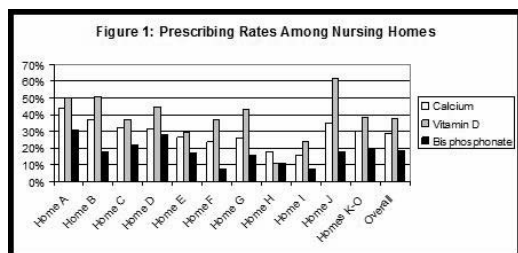
**Treating Osteoporosis in the Elderly: An Environmental Scan of Nursing Home Prescribing in Ontario, Canada.** A. Papaioannou<sup>1</sup>, C. C. Kennedy<sup>1</sup>, G. Campbell<sup>2</sup>, L. M. Giangregorio<sup>3</sup>, J. Ma<sup>4</sup>, J. D. Adachi<sup>1</sup>. <sup>1</sup>Medicine, McMaster University, Hamilton, ON, Canada, <sup>2</sup>Medical Pharmacies Group, Hamilton, ON, Canada, <sup>3</sup>Kinesiology, University of Waterloo, Waterloo, ON, Canada, <sup>4</sup>Mathematics and Statistics, McMaster University, Hamilton, ON, Canada.

In 2005, the provincial health ministry in Ontario, Canada launched the Osteoporosis Strategy as a comprehensive approach to preventing and managing osteoporosis. For the Long Term Care (LTC) component, the major objective is to develop and deliver knowledge translation tools aimed at improving care processes to reduce falls and fragility fractures in elderly LTC residents. To understand the current level of treatment for osteoporosis in LTC, we partnered with a large pharmacy provider that delivers pharmacy care to over 35,000 residents in long term care homes across Ontario, Canada.

In this analysis, we examined 15 LTC homes (N=3,132 residents) from across the province. Means (standard deviation, SD) and proportions were computed as appropriate. The impact of age and gender on prescribing rates were examined in linear regression analysis.

The mean age of the study sample was 83 years; approximately 66% were women. The overall rate of prescribing was 29% for calcium, 38% for vitamin D, and 18% for bisphosphonates (alendronate, risedronate, or etidronate). Of residents prescribed calcium, the mean daily dose was 922 mg (SD 438). Of residents prescribed vitamin D, the mean daily dose (including multi-vitamins) was 923 IU (SD 773). As displayed in Figure 1, there was considerable prescribing variation between homes. Bisphosphonate use ranged from 7-31%; vitamin D use from 11-62%; and calcium use from 16-44%. Age and gender did not significantly impact the prescribing rates amongst the homes.

The variation in prescribing rates between homes likely represents the previous lack of standardized guidelines and academic detailing for prescribing in nursing homes. The aim of the provincial-wide Osteoporosis strategy in Long Term Care, is to educate physicians and front-line staff and deliver tailored knowledge translation tools to all LTC homes in Ontario. It is hoped this initiative will increase appropriate use of calcium, vitamin D, and bisphosphonates for all elderly residents, irrespective of region.



**Disclosures:** C.C. Kennedy, None.

This study received funding from: Ontario Ministry of Health and Long Term Care

## SU405

**Effect of Once-Yearly Zoledronic Acid on Integral Bone Mineral Density of the Spine: Quantitative Computed Tomography Results of HORIZON-PFT.** R. Eastell<sup>1</sup>, T. Lang<sup>2</sup>, S. Boonen<sup>3</sup>, S. R. Cummings<sup>4</sup>, P. D. Delmas<sup>5</sup>, J. A. Cauley<sup>6</sup>, Z. Horowitz<sup>7</sup>, E. Kerzberg<sup>8</sup>, G. Bianchi<sup>9</sup>, D. Kendler<sup>10</sup>, P. Leung<sup>11</sup>, Z. Man<sup>12</sup>, P. Mesenbrink<sup>13</sup>, E. F. Eriksen<sup>14</sup>, D. M. Black<sup>2</sup>. <sup>1</sup>Univ. of Sheffield, Sheffield, United Kingdom, <sup>2</sup>UCSF, San Francisco, CA, USA, <sup>3</sup>Katholieke Univ. Leuven, Leuven, Belgium, <sup>4</sup>CPMC Res Institute & UCSF, San Francisco, CA, USA, <sup>5</sup>Hôpital Edouard Herriot Pavillon, Lyon, France, <sup>6</sup>Univ. of Pittsburgh, Pittsburgh, PA, USA, <sup>7</sup>Savient Pharmaceuticals, East Brunswick, NJ, USA, <sup>8</sup>Hospital Ramos Mejía, Buenos Aires, Argentina, <sup>9</sup>La Colletta Hospital, Genova, Italy, <sup>10</sup>Osteoporosis Research Centre, Vancouver, BC, Canada, <sup>11</sup>Chinese Univ. of Hong Kong, Prince of Wales Hospital, Shatin NT/Hong Kong SAR, China, <sup>12</sup>Centro TIEMPO, Buenos Aires, Argentina, <sup>13</sup>Novartis Pharmaceuticals, East Hanover, NJ, USA, <sup>14</sup>Novartis Pharma AG, Basel, Switzerland.

We have reported that lumbar spine (LS) bone mineral density (BMD) increases by 6.7% after 3 yrs of zoledronic acid 5 mg (ZOL) given as a 15-minute infusion annually to women with postmenopausal osteoporosis (Black et al, NEJM 2007). Such increases not only reflect an increase in the density of the lumbar vertebral bodies but also any change in the calcification of the aorta or density of the posterior processes of the vertebrae, neither of which are likely to contribute to the strength of the vertebral body. Changes in the vertebral body alone can be studied by quantitative computed tomography (QCT). We planned a substudy of HORIZON-PFT, a 3 yr, double-blind, placebo-controlled trial of women with postmenopausal osteoporosis randomized to a 15-minute infusion of ZOL or placebo at baseline, 12 and 24 months. This substudy included 233 women (mean age 74 yrs) who had QCT of the LS at baseline; 180 had evaluable LS QCT data at 36 months. LS BMD (L1-4) was measured by DXA at baseline, Months 6, 12, 24 and 36 and by QCT (L1-2) at baseline and Month 36 using a bone mineral reference phantom of hydroxyapatite. LS QCT was analyzed to give similar regions of interest to DXA, namely total integral AP- and lateral-BMD estimates. Between-group difference for change in LS BMD by DXA was intermediate between that for spinal BMD anteroposterior (AP) and lateral views DXA-like (Table). Neither % change in spine BMD AP nor lateral-BMD decreased with placebo (Table). In conclusion, once-yearly ZOL increases BMD of the vertebra as measured by DXA and vertebral body as measured by QCT by similar amounts compared to placebo.

Variable	Least square mean ( $\pm$ SD) ZOL	Least square mean ( $\pm$ SD) Placebo	% change from baseline P-value
BMD (DXA)	8.81 $\pm$ 5.63 (n=67)	1.83 $\pm$ 6.75 (n=68)	<0.0001
BMD AP view DXA-like	5.98 $\pm$ 6.51 (n=92)	0.31 $\pm$ 7.77 (n=88)	<0.0001
BMD lateral view DXA-like	9.80 $\pm$ 12.03 (n=92)	1.44 $\pm$ 11.22 (n=88)	<0.0001

**Disclosures:** R. Eastell, Novartis Pharmaceuticals 2, 3, 5.

This study received funding from: Novartis Pharma AG

## SU406

**The Premenopausal Reference Ranges of Bone Turnover Markers and the Effect of Bisphosphonates in Korean Postmenopausal Women.** D. Chung, J. Chung\*, D. Cho\*, M. Chung\*. Internal Medicine, Chonnam National University Medical School, Gwangju City, Republic of Korea.

High bone turnover after menopause or in various conditions is related to increased bone loss and risk of osteoporotic fracture. Bisphosphonates rapidly reduce the bone turnover rate and significantly decrease fragility fracture. However, although it is clinically very rare, oversuppression of bone turnover can cause mineralization defect and atypical fracture. Therefore, adequate suppression of bone turnover is very important to maintain normal bone quality and to prevent fracture. Many clinical trials report that bisphosphonates decrease the bone turnover rate to premenopausal range without oversuppression. In this study, we investigated the reference levels of bone turnover markers in Korean premenopausal women (N=160) without any disease or drug history affecting bone metabolism. Serum CTX and osteocalcin levels in this group are 0.277 $\pm$ 0.135 ng/ml and 16.87 $\pm$ 5.74 ng/ml, respectively. In postmenopausal women (N=269), the levels are significantly increased to 0.518 $\pm$ 0.312 ng/ml (p=0.000 vs premenopausal women) and 25.57 $\pm$ 10.89 ng/ml (p=0.000 vs premenopausal women), respectively. In postmenopausal osteoporotic women using bisphosphonates (10 mg/day or 70 mg/week for alendronate and 35 mg/week for risedronate) at least more than 6 months (N=51), serum CTX level was significantly lower (0.124 $\pm$ 0.090, p=0.000) than premenopausal reference range. However, osteocalcin level (17.59 $\pm$ 11.31, p=N.S.) was similar to that of premenopausal women. These results indicate that bone resorption marker, CTX, is more significantly suppressed than usual premenopausal level in Korean postmenopausal women with bisphosphonates. The meaning of this kind of change of bone turnover should be interpreted with caution, and due to small number of cases of bisphosphonate users in this trial, further studies would be needed to clarify or define more appropriate suppression ranges of bone turnover rate.

**Disclosures:** D. Chung, None.

## SU407

**Effect of Risedronate on Bone Density in Hematopoietic Stem Cell Transplant Patients: A Prospective, Randomized, Double-Blind Placebo-Controlled Trial.** K. Baek<sup>\*1</sup>, G. Kim<sup>\*1</sup>, M. Kim<sup>\*1</sup>, D. Lim<sup>\*1</sup>, S. Lee<sup>\*1</sup>, J. Han<sup>1</sup>, H. Kim<sup>\*1</sup>, K. Oh<sup>\*2</sup>, M. Kang<sup>\*1</sup>. <sup>1</sup>Department of Internal Medicine, College of Medicine, The Catholic University of Korea, Seoul, Republic of Korea, <sup>2</sup>Department of Endocrinology and Metabolism, Sungkyunkwan University School of Medicine, Seoul, Republic of Korea.

**Background:** Osteoporosis is a relatively common complication after hematopoietic stem cell transplantation (HSCT). To our current knowledge, there has been no randomized controlled study on the effect of oral bisphosphonates on bone mineral density (BMD) after HSCT.

**Subjects and Methods:** We conducted a double-blind, randomized controlled trial comparing risedronate (35 mg/week) with placebo in patients receiving HSCT at the Catholic Hematopoietic Stem Cell Transplantation Center. 121 patients were enrolled prior to HSCT from September 2005 until February 2008. All received combined calcium and vitamin D supplementation and were followed for 12 months. Primary outcome variables were BMD changes at the spine and total hip at the end of the follow-up period. Secondary variables were the changes of bone turnover markers.

**Results:** Data from 55 patients who were enrolled until March 2007 were analyzed. 36 patients (65.45%) completed the study until March 2008. The risedronate group and the placebo group consisted of 16 and 20 patients, respectively. The major causes of dropout were infection and disease relapse (n=10), loss to follow-up (n=4), and patient withdrawal due to gastrointestinal discomfort (n=2). Patients treated with risedronate demonstrated significantly less bone loss at the lumbar spine (-0.7 vs. -6.46%, P=0.05) during a 1-yr longitudinal follow-up. Notably, serum 1-CTP levels showed a significant decrease in the risedronate-treated patients (P<0.001).

**Conclusion:** Risedronate significantly attenuated bone loss in HSCT patients. This effect was most prominent in the lumbar spine.

**Disclosures:** K. Baek, None.

## SU408

**Fracture Risk with Once-Monthly Oral Ibandronate Compared with Weekly Bisphosphonates: Primary and Sensitivity Analyses from the eValuation of Ibandronate Efficacy (VIBE) Database Fracture Study.** S. T. Harris<sup>1</sup>, W. A. Blumentals<sup>\*2</sup>, S. A. Poston<sup>\*3</sup>, S. L. Silverman<sup>4</sup>. <sup>1</sup>University of California, San Francisco, San Francisco, CA, USA, <sup>2</sup>Roche, Nutley, NJ, USA, <sup>3</sup>GlaxoSmithKline, Research Triangle Park, NC, USA, <sup>4</sup>Cedars-Sinai Medical Center/UCLA, Beverly Hills, CA, USA.

The VIBE study compared fracture risk between patients treated with once-monthly and weekly oral bisphosphonates (BPs).

Women ≥45 years old, newly prescribed once-monthly oral ibandronate or weekly oral alendronate or risedronate, adherent for ≥90 days, and without malignancy or Paget's disease were included. Data were censored at fracture, 12 months after BP initiation, end of health plan enrollment, BP brand switch, regimen switch, or treatment discontinuation. Fracture risk was compared using Cox regression models and adjusted for potential confounding factors. The analysis was repeated for weekly alendronate or risedronate patients separately compared with ibandronate patients. Sensitivity analyses were conducted excluding patients with codes in the pre-index period for each of the following: estrogen or non-estrogen osteoporosis medications, glucocorticoids, fractures, GI medications, and glucocorticoids and/or osteopenia. Additional analyses varied the requirement for adherence to treatment.

The primary analysis included 7,354 patients receiving once-monthly ibandronate and 56,837 patients receiving weekly BPs (alendronate 35,865, risedronate 20,972). Mean age was 60.14 years for ibandronate patients and 60.54 years for weekly BP patients. The risks of hip fracture, nonvertebral fracture (NVF) and all fractures were not significantly different between groups (rate of all fractures 1.51% for weekly BPs, 1.40% for ibandronate, adjusted hazard ratio [HR] 0.82, p=0.052), but the risk of vertebral fracture was statistically lower in the ibandronate group (0.24% vs 0.11%, adjusted HR 0.36, p=0.006). Similarly, the risks of hip fracture or NVF were not significantly different between ibandronate and alendronate or risedronate, but the risk of vertebral fracture was significantly lower for ibandronate than either weekly BP (alendronate p=0.004, risedronate p=0.014). In all sensitivity analyses, there were no significant differences between groups in the risks of hip fracture or NVF. The risk of vertebral fracture was statistically lower in the ibandronate group, except when non-adherent patients were included in the analysis.

In this study, patients treated with oral once-monthly ibandronate or weekly BPs had a similar risk of hip fracture or NVF during the first year of treatment. The risk of vertebral fracture was lower for ibandronate patients, though the clinical implications of these findings require further exploration and validation.

**Disclosures:** S.T. Harris, Amgen, Eli Lilly, GlaxoSmithKline, Merck, 2; Eli Lilly, GlaxoSmithKline, Merck, Novartis, 1.

This study received funding from: Roche and GlaxoSmithKline.

## SU409

**Quarterly Intravenous Ibandronic Acid in the Community Setting in England - Cost-effective Healthcare Delivery for Osteoporosis Patients.** S. Venkatachalam<sup>1</sup>, R. Suchitra<sup>\*1</sup>, C. Molloy<sup>\*2</sup>, J. McPeake<sup>\*2</sup>, S. Darrington<sup>\*2</sup>, D. Lloyd<sup>\*2</sup>, T. Price<sup>1</sup>. <sup>1</sup>Rheumatology, Cannock Chase Hospital, Cannock, United Kingdom, <sup>2</sup>South Staffordshire Primary Care Trust, Cannock, United Kingdom.

Oral bisphosphonates are the mainstay in the treatment of osteoporosis. Intolerance due to upper gastrointestinal side-effects and their complex administration regime do not help patient compliance. They are inappropriate for patients with cognitive impairment or dysphagia. Intravenous (IV) Disodium Pamidronate in hospital, is an option for these patients, but unlicensed. IV Ibandronic acid is a licensed alternative and lends itself for delivery in the community.

We provide Rheumatology and Osteoporosis services for a population of 500,000 over 5 sites. We had 200 patients receiving IV Disodium Pamidronate quarterly as day cases at the base hospital. Each infusion lasted over an hour and cost \$600. Patients from outreach clinics had to travel far. In contrast, IV Ibandronic acid injection takes less than a minute, costs only \$300, enables rapid turnover of patients and allows more time for education. The annual cost of IV Ibandronic acid for 200 patients delivered by the community team is \$240,000 compared to \$500,000 for IV Disodium Pamidronate in hospital. Community delivery of IV Ibandronic acid has resulted in considerable savings.

We have treated 250 patients with quarterly IV Ibandronic acid in the community over a year. We had very few adverse events which include acute phase reaction, phlebitis and dyspepsia in about 2% of our patients. We have performed about 50 injections at home for patients with difficulties in access. The strength of the service is in delivering care by community nurses and clinicians working together.

IV Ibandronic acid is a safe treatment in the community and ensures compliance. Our innovative service enables effective treatment closer to the patient's home and saves considerable resources for the local health economy.

**Disclosures:** S. Venkatachalam, None.

## SU410

**Measurement Equivalence of Osteoporosis-Specific and General Quality of Life Instruments in Aboriginal and Non-aboriginal Women.** L. M. Li<sup>\*1</sup>, C. Metge<sup>\*2</sup>, W. D. Leslie<sup>3</sup>. <sup>1</sup>Community Health Sciences, University of Manitoba, Winnipeg, MB, Canada, <sup>2</sup>Pharmacy, University of Manitoba, Winnipeg, MB, Canada, <sup>3</sup>Medicine, University of Manitoba, Winnipeg, MB, Canada.

This study assessed the psychometric equivalence of osteoporosis-specific and general health-related quality of life (HRQOL) instruments in two ethnic groups. The assessment of HRQOL is challenging because individuals with different cultural or socio-demographic characteristics may not interpret questions about their well-being or functional status in the same way.

A total of 258 Aboriginal and 181 non-Aboriginal women were recruited to the First Nations Bone Health Study from rural and urban sites in the province of Manitoba, Canada. The mini-Osteoporosis Quality of Life Questionnaire (mini-OQLQ) and the Medical Outcomes Study Short Form 36 (SF-36) instrument were administered to study participants by trained interviewers. Confirmatory factor analysis (CFA) techniques were used to test different forms of measurement equivalence in the two groups using likelihood ratio tests and other goodness of fit indices. The analyses were conducted using LISREL software.

The CFA results showed that the weakest forms of measurement invariance, configural and metric invariance, were satisfied for the mini-OQLQ instrument, indicating that Aboriginal and non-Aboriginal women have the same conceptualization of osteoporotic quality of life and the concepts have equivalent meaning in the two groups. However, two more stringent forms of equivalence, scalar and complete measurement invariance, were not satisfied. For the SF-36, all forms of measurement invariance were satisfied.

Evidence of measurement invariance is necessary to make valid comparisons between groups on HRQOL measures. This study concluded that measurement equivalence was not demonstrated for the disease-specific quality of life measure but was supported for the general quality of life measure. Ethnicity appears to influence responses about the effect of osteoporosis on one's life. The cross-cultural validation methodology adopted in this study could be applied to data from other HRQOL instruments, other ethnic groups, or groups defined by differences on other characteristics such as age, sex, or type of disease.

**Disclosures:** W.D. Leslie, None.

This study received funding from: Canadian Institutes of Health Research; Manitoba Health Research Council.

## SU411

**Rehabilitation after Clinically-diagnosed Osteoporotic Vertebral Fracture: Results of a Pilot Study.** K. M. Shipp, E. Hegedus<sup>\*</sup>, C. F. Pieper<sup>\*</sup>, H. White<sup>\*</sup>, J. K. Richardson<sup>\*</sup>, T. J. Weber, H. Hoening<sup>\*</sup>. Duke University, Durham, NC, USA.

The objectives of this pilot study were 1) to assess feasibility and safety and 2) to derive estimates of treatment effects for the outcomes of a physical-therapist delivered mobility training intervention designed to control pain and maintain function during recovery from a new vertebral fracture (VF). Participants were 6 independently-living, cognitively robust older women with back pain ≥ 4 on visual analog scale and diagnosis of new osteoporotic

vertebral fracture (confirmed by MRI indicating edema in the vertebral body or new fracture, in comparison with previous radiographs, within one spinal level of the area of back pain). Recruitment occurred via referral by geriatricians and endocrinologists at a tertiary medical center. The women were randomly allocated to usual care (UC, n=2) or the rehabilitation intervention (INT, n=4). The intervention included up to 7 1-hour individual, in-home visits over 1 month focused on finding and maintaining neutral spine alignment during transitional movements (sit to stand, bed mobility) and functional activities (brushing teeth, lifting, getting in and out of a car, walking). In addition, subjects were provided with a four-wheeled walker and instructed to push down on the handles with their arms while walking to assist in keeping the trunk upright. Baseline, 1-month and 3-month follow-up measures of pain, osteoporosis-specific quality of life, and physical function were assessed. Differences between groups were analyzed using an exact permutation test on ranked change scores. The mean age was 84.5 years, with mean number of vertebral fractures 3.2 and mean number of medical problems 5. All subjects completed the study. No falls, fractures (including radiographically-identified VF), or serious adverse events occurred in either arm during the study. Compared to the UC subjects, the INT subjects displayed a trend (p=0.067) toward improvement in pain (81% decrease INT vs. 4% increase UC), the symptom scale (119% increase INT vs. 35% increase UC -- higher score is better) and combined physical and activities of daily living scales (65% increase INT vs. 18% increase UC -- higher score is better) of the Osteoporosis Quality of Life Questionnaire. Physical performance did not change in either group. The trends in pain reduction and better self-reported physical function indicate that this mobility training rehabilitation intervention is worthy of further study and can be adequately powered with a small sample size.

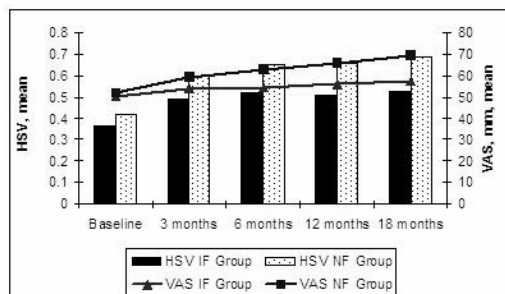
**Disclosures:** K.M. Shipp, None.

This study received funding from: Foundation for Physical Therapy and NICHD (K12HD04344603).

## SU412

**Women with Severe Osteoporosis Treated with rhPTH(1-34) (teriparatide) Improve Quality of Life Regardless of Incident Fractures: 18 Month Results from the European Forsteo® Observational Study (EFOS).** B. Langdahl<sup>1</sup>, Ö. Ljunggren<sup>2</sup>, W. Lems<sup>3</sup>, J. B. Walsh<sup>4</sup>, C. Barker<sup>5</sup>, A. Fahrleitner-Pammer<sup>6</sup>, D. Karras<sup>7</sup>, G. Rajzbaum<sup>8</sup>, F. Jakob<sup>9</sup>, A. Kutahov<sup>5</sup>, F. Marin<sup>5</sup>. <sup>1</sup>Univ Hosp, Århus, Denmark, <sup>2</sup>Univ Hosp, Uppsala, Sweden, <sup>3</sup>VU Univ Hosp, Amsterdam, Netherlands, <sup>4</sup>St James's Hosp Trinity College, Dublin, Ireland, <sup>5</sup>Lilly Res Ctr, Windlesham, United Kingdom, <sup>6</sup>Med Univ, Graz, Austria, <sup>7</sup>Veterans Admin Hosp, Athens, Greece, <sup>8</sup>St Joseph Hosp, Paris, France, <sup>9</sup>Julius-Maximilians-Univ, Würzburg, Germany.

**AIM:** To describe the influence of incident fractures in changes in health related quality of life (HRQoL) in postmenopausal women with osteoporosis treated with teriparatide for 18 months in the European Forsteo® Observational Study (EFOS). **PATIENTS AND METHODS:** Prospective, observational study in female patients with osteoporosis from 8 European countries. Treatment with teriparatide was for up to 18 months. Clinical vertebral and non-vertebral fragility fractures were recorded at follow-up visits. HRQoL was measured using EQ-5D. **RESULTS:** 1648 women were enrolled for a total of 1924.7 women-years follow-up. 138 women (8.8%) sustained a total of 168 incident fractures (38.7% clinical vertebral, 61.3% non-vertebral) over 18 months (821 fractures /10,000 women-years). Median duration of treatment was 540 and 533 days in Incident Fracture (IF) and No Fracture (NF) groups, respectively. Mean EQ-5D Health State Values (HSV) and Visual Analogue Scale (VAS) showed significant increase in both groups (NF and IF) from baseline to 18 months (HSV p values = < 0.001; VAS p values = < 0.001). After 18 months the HSV in the NF group exceeded the values in the IF group (p = 0.053). Over the duration of treatment women in NF group had a higher increase in VAS than those with IF (p<0.001) (Figure). Women in NF group compared to IF group more frequently reported "no problems" across all domains of EQ-5D. The largest improvement was reported in the EQ-5D sub-domains of usual activities and pain/discomfort. **CONCLUSION:** Women being prescribed teriparatide in the EFOS cohort suffer from severe osteoporosis with significant impact on their HRQoL. Women in EFOS showed clinically significant improvement in HRQoL regardless of fracture during treatment.



**Disclosures:** B. Langdahl, Eli Lilly 4.

This study received funding from: Eli Lilly and Company.

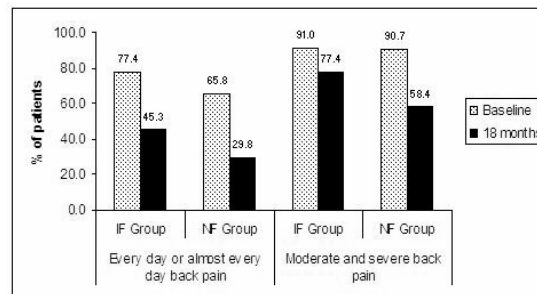
## SU413

**Back Pain is Reduced in Postmenopausal Women with Severe Osteoporosis Treated with rhPTH(1-34) (teriparatide) Regardless of Incident Fractures: 18 Month Results from the European Forsteo® Observational Study (EFOS).** Ö. Ljunggren<sup>1</sup>, A. Fahrleitner-Pammer<sup>2</sup>, A. Kutahov<sup>3</sup>, J. B. Walsh<sup>4</sup>, B. Langdahl<sup>5</sup>, F. Jakob<sup>6</sup>, W. Lems<sup>7</sup>, G. Rajzbaum<sup>8</sup>, C. Barker<sup>3</sup>, D. Karras<sup>9</sup>, F. Marin<sup>3</sup>. <sup>1</sup>Univ Hosp, Uppsala, Sweden, <sup>2</sup>Med Univ, Graz, Austria, <sup>3</sup>Lilly Res Ctr, Windlesham, United Kingdom, <sup>4</sup>St James's Hosp Trinity College, Dublin, Ireland, <sup>5</sup>Univ Hosp, Århus, Denmark, <sup>6</sup>Julius-Maximilians-Univ, Würzburg, Germany, <sup>7</sup>VU Univ Hosp, Amsterdam, Netherlands, <sup>8</sup>St Joseph Hosp, Paris, France, <sup>9</sup>Veterans Admin Hosp, Athens, Greece.

**AIM:** To describe the differences in back pain (BP) in postmenopausal women with osteoporosis with or without incident fracture treated with teriparatide for 18 months in the European Forsteo® Observational Study (EFOS). **PATIENTS AND METHODS:** Prospective, observational study in women with osteoporosis from 8 European countries. Treatment with teriparatide was for up to 18 months. Clinical vertebral and non-vertebral fragility fractures were recorded at follow-up visits. BP was measured using a 100 mm Visual Analogue Scale (VAS) ranging from no BP (0) to worst possible BP (100), and a BP questionnaire. **RESULTS:** 1648 women were enrolled for a total of 1924.7 women-years follow-up. 138 women (8.8%) sustained a total of 168 incident fractures (38.7% clinical vertebral, 61.3% non-vertebral) over 18 months (821 fractures /10,000 women-years). A reduction of BP was observed in both groups - with and without incident fracture - after 18 months (p values < 0.001). Patients in the No Fracture (NF) group had a greater decrease (improvement) in back pain VAS (-27 mm) than those in the Incident Fracture (IF) group (-18.5 mm) (p<0.001) (Table). A reduction of frequency and severity of back pain in the NF group exceeded the values in the IF group (Figure). **CONCLUSION:** Patients being prescribed teriparatide in the EFOS cohort suffer from severe osteoporosis with frequent and severe back pain. Patients in EFOS showed clinically significant reduction in frequency and severity of back pain regardless of fracture during treatment.

Back pain VAS in patients with back pain, mean±SD		
Back Pain VAS (mm)	IF Group	NF Group
Baseline	59.3 ± 25.0	57.6 ± 26.8
3 months	46.3 ± 23.5	42.5 ± 25.2
6 months	44.0 ± 22.9	37.6 ± 25.5
12 months	40.6 ± 25.0	33.9 ± 25.7
18 months	40.8 ± 23.7	30.6 ± 25.6

### Frequency and severity of back pain



**Disclosures:** Ö. Ljunggren, Eli Lilly 4.

This study received funding from: Eli Lilly and Company.

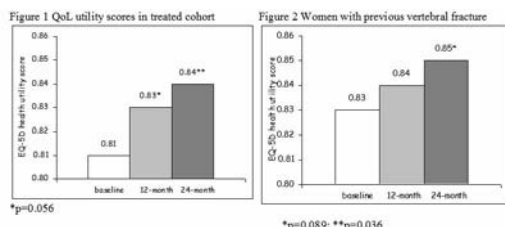
## SU414

**Improvement in Quality of Life among Women Treated with Risedronate: Experience from a 2-Year Randomized Controlled Study.** D. Gold<sup>1</sup>, N. Borisov<sup>2</sup>, M. Steinbuch<sup>\*2</sup>, D. Brixner<sup>\*3</sup>. <sup>1</sup>Duke University Medical Center, Durham, NC, USA, <sup>2</sup>Procter & Gamble Pharmaceuticals, Mason, OH, USA, <sup>3</sup>University of Utah, Salt Lake City, UT, USA.

Well-proven fracture prevention of bisphosphonate treatment should result in improved quality of life (QoL) for patients on therapy. This study assessed QoL utilities as measured by 5-dimensional EuroQol (EQ-5D) questionnaire among postmenopausal osteoporotic (PMO) women at baseline and throughout 2-year risedronate treatment and compared follow-up data to baseline measures.

The sample included PMO women with or without prevalent vertebral fracture who were treated for 2 years with risedronate either 5mg daily or 75 mg on 2 consecutive days per month. For the purpose of this study, both treatment arms were combined in a single treatment cohort. EQ-5D (US scoring) was collected at baseline, 12 and 24 months of treatment. The baseline QoL utility values were compared to 12-month and 24-month values by age groups and fracture history. Each dimension of EQ-5D (mobility, self-care, usual activities, pain, and anxiety) was also explored among selected groups.

Of 1,229 treated women in the study, 1,213 (99%) completed the EQ-5D questionnaire during the study period and were included in the analysis. Mean (SD) age of the study subjects was 65 (8). The mean (SD) baseline utility was reported at 0.83 (0.15); this utility is consistent with US average for females in the same age group (Fryback, 2007). Mean baseline utility decreased with age (0.84 vs. 0.83,  $p=0.06$ , <65 vs. 65-74; 0.84 vs. 0.82,  $p=0.08$ , <65 vs. ≥75), history of vertebral fracture (0.81 vs. 0.84,  $p=0.001$ ), and BMI ≥30 (0.77 vs. 0.84,  $p<0.001$ ). Overall, mean QoL utility showed improvement over the course of the treatment (Figure 1). Women with prevalent vertebral fracture reported significantly higher level of utility at 24-month of treatment vs. baseline (Figure 2) and improvements in all 5 dimensions of the EQ-5D. Two-year treatment with risedronate significantly improved QoL as measured by the overall utility score and 5 dimensions of EQ-5D among PMO women. The greatest impact on QoL was observed among women with previous vertebral fracture.



**Disclosures:** D. Gold, P&G 2.

This study received funding from: The Alliance for Better Bone Health (Procter & Gamble Pharmaceuticals and sanofi-aventis).

## SU415

**In Osteoporotic Other than in Healthy Bone, Thoracolumbar Fractures Spare the Adjacent Discs.** T. R. Blatter<sup>\*</sup>, C. Josten<sup>\*</sup>. Trauma & Reconstructive Surgery, Leipzig University, Leipzig, Germany.

**Introduction:** In fractures of the thoracolumbar spine, adjacent discs typically are disrupted. It is uncertain, however, whether this pathomechanism is true as well for patients with generalized osteoporosis. As a theoretical alternative, fractures in the osteoporotic spine might spare the adjacent discs (due to minor set off-trauma?, preexistent sclerosis of discs?). Cognition of the true mechanism will have immediate impact on the surgical technique, as an undisrupted disc does not have to be addressed by discectomy and thus an anterior reconstruction will be dispensable.

**Method:** We compared 2 groups of patients. Inclusion criteria for the first group were: age ≤40, adequate trauma, thoracolumbar vertebral body fracture types A3 acc. to Magerl (1). Initially, posterior short segment instrumentation was performed. Patients were readmitted 5-7 weeks later for secondary anterior reconstruction (disc-/corpectomy, cage-interposition). Prior to anterior reconstruction, native X-rays and CT-scans were performed to screen for radiographic signs of posttraumatic disc alterations. Inclusion criteria for the second group were: age ≥60, osteoporosis (t-score ≤-2.5; DEXA), adequate trauma, thoracolumbar vertebral body fractures of the above types. After posterior short segment instrumentation (Sextant, Medtronic) with cement-augmentation of pedicle screws and balloon-kypheoplasty (Kyphon) of the fractured vertebra, native X-rays and CT-scans were performed 5-7 weeks after trauma. These again were screened for radiographic signs of posttraumatic disc alterations.

**Results:** In group 1, 8 patients (average age 34) with traumatic burst fractures (Th8-L3) were included. In group 2, 20 patients (average age 74) with traumatic burst fractures (Th10-L5) were included. In contrast to group 1, the latter patients suffered from osteoporosis (average t-score 2.9). Prior to anterior reconstruction, all 8 patients of group 1 clearly showed signs of vacuum-phenomena in the affected discs at 5-7 weeks after trauma. In contrast, none of the 20 patients in group 2 showed radiographic signs of secondary disc alteration.

**Conclusion:** In generalized osteoporosis, adjacent discs to burst fractures do not show radiographic signs of posttraumatic alterations. This finding has immediate impact on the surgical procedure; with this subgroup - other than in the healthy young - an anterior reconstruction with disc-/corpectomy is not necessary. For these cases, we favor posterior short segment instrumentation with cement-augmentation of pedicle screws in combination with balloon-kypheoplasty of the fractured vertebra.

**Literature:** (1) Magerl et al. (1994) A comprehensive classification of thoracic and lumbar injuries. Eur Spine J 3:184-201

**Disclosures:** T.R. Blatter, Dr. Blatter is a consultant to Kyphon Europe. 5.

## SU416

**Electronic Medical Record Based "ALERT System" improved Diagnosis and Treatment of Osteoporosis in Orthopaedic Out-Patient Clinic.** C. Lee<sup>\*1</sup>, S. Moon<sup>1</sup>, N. Sul<sup>\*1</sup>, K. Yang<sup>\*1</sup>, J. Lee<sup>\*1</sup>, E. Moon<sup>\*1</sup>, S. Park<sup>\*1</sup>, H. Kim<sup>\*1</sup>, J. Jahng<sup>\*1</sup>, H. Lee<sup>\*1</sup>, H. Chun<sup>\*2</sup>, I. Kwon<sup>\*3</sup>. <sup>1</sup>Orthopaedic Surgery, Yonsei University, Seoul, Republic of Korea, <sup>2</sup>Mechanical Engineering, Yonsei University, Seoul, Republic of Korea, <sup>3</sup>School of Dentistry, Kyung Hee University, Seoul, Republic of Korea.

Under-diagnosis and under-treatment of osteoporosis is world wide phenomenon, especially in orthopaedic practice. Various interventions resulted in less dramatic improvement in diagnosis and treatment of osteoporosis. Electronic medical record (EMR) proved to be an efficient tool for medical practice. In this study, EMR based reminder for bone mineral density (BMD) measurement "ALERT" in orthopaedic out patient clinic (OPC) was tested prospectively. Rate of diagnosis and treatment of osteoporosis was compared before and after "ALERT". All patients in OPC (age above 50 years) were included from 1 month before and after ALERT program initiation. Before ALERT, 599 patients visited while 659 patients visited to OPC after ALERT. ALERT criteria were set according to National Osteoporosis Diagnosis Guideline. Rates of BMD measurement and prescription of osteoporotic medication were assessed. Before ALERT only 29% of female patients from whom were eligible for BMD screening, underwent BMD. After ALERT reminder 61% of those were screened with BMD. Only 11% of male patients from whom were eligible for BMD, underwent BMD before ALERT. After ALERT reminder, 58% of those were screened with BMD. In female and male patient combined, BMD screening increased from 23% to 60% after ALERT reminder in EMR. Also proportion of the patients who underwent medical treatment of osteoporosis increased from 9% to 31% after ALERT reminder. EMR based ALERT system definitely increased diagnosis and treatment of osteoporosis in orthopaedic OPC. Therefore EMR based ALERT system can be best solution for world wide under-diagnosis and under-treatment of osteoporosis in orthopaedic field.

**Disclosures:** S. Moon, None.

This study received funding from: the Brain Korea 21 Project for Medical Science, Yonsei University and grand No. R01-2006-000-10933-0 from the Basic Research Program of the Korea Science & Engineering Foundation.

## SU417

**Gastrointestinal Side Effects in Postmenopausal U.S. Women on Osteoporosis Therapies: 6-month Findings from the POSSIBLE US<sup>TM</sup> Study.** C. Woo<sup>1</sup>, G. Gao<sup>\*1</sup>, S. Wade<sup>\*2</sup>, M. Hochberg<sup>3</sup>. <sup>1</sup>Amgen Inc., South San Francisco, CA, USA, <sup>2</sup>Wade Outcomes Research and Consulting, Salt Lake City, UT, USA, <sup>3</sup>University of Maryland, Baltimore, MD, USA.

Gastrointestinal (GI) side effects have been observed among osteoporosis (OP) patients receiving therapy, which may lead them to switch or discontinue treatment. The impact of GI side effects on treatment satisfaction and health-related quality of life (HRQOL) is not well-known.

In the Prospective Observational Scientific Study Investigating Bone Loss Experience (POSSIBLE US<sup>TM</sup>), women on osteoporosis therapies are followed for 2 to 3 years, with data collected every 6 months by self-administered questionnaire. To understand the impact of GI side effects on women new to (n=1483) or stable on (n=1861) pharmacologic OP therapy, we examined patient report of GI side effects overall and by drug class (bisphosphonate users vs non-bisphosphonate users), and the association between GI side effect reporting and treatment satisfaction and HRQOL.

About 20% of new or stable patients reported ≥ 1 GI side effect over 6 months of follow-up (TABLE). Overall, bisphosphonate users were more likely to report any GI side effect than non-bisphosphonate users at entry [age adj. OR (95% CI) 2.0 (1.66, 2.40)] and month 6 [1.4 (1.18, 1.62)]. Adjusting for age at entry, drug class, number of comorbidities and concomitant medications, women who reported any GI side effect at entry were 8% (23% vs 15%) more likely to discontinue or switch agents by month 6 than women who reported no GI side effects at entry (adj OR = 1.71, 95% CI: 1.33, 2.21). Of women continuing on the same agent at month 6, 44% reported taking antacids, H2 blockers, or proton pump inhibitors. Women new to OP therapy and with GI side effects at entry reported lower mean treatment satisfaction scores (Treatment Satisfaction Questionnaire for Medication Global dimension: 55.0 vs 64.1,  $p=0.002$ ) and lower mean HRQOL (EQ-5D Current Health State: 78.3 vs. 82.2,  $p=0.054$ ) at month 6, than those who did not report GI side effects at entry.

Among postmenopausal U.S. women on OP therapies, GI side effects are common and associated with lower HRQOL, lower treatment satisfaction, and higher rates of discontinuation of or switching pharmacologic OP agents

GI side effects at entry & month 6 in patients new to & stable on pharmacologic OP therapies				
	New Entry n = 1483 %	New Month 6 n = 1127 %	Stable Entry n = 1861 %	Stable Month 6 n = 1608 %
Any GI side effect*	20.0	30.6	21.6	25.8
Heartburn	6.1	11.2	8.6	10.7
Nausea	4.3	5.4	3.3	3.4
Painful swallowing	1.1	1.9	1.7	1.6
Stomachache	4.3	4.2	2.5	2.8
Constipation	6.8	12.4	8.5	9.7

\*Also includes upper or lower abdominal pain, diarrhea

**Disclosures:** C. Woo, Amgen 5.

This study received funding from: Amgen Inc.

## SU418

**Functionality Outcomes Including Brisk Walking Speed Are Associated with Bone Mineral Density in Postmenopausal Women.** K. Humphrey\*, P. Liu, H. Shin, C. C. Douglas\*, A. P. Crombie\*, O. J. Kelly, L. B. Panton\*, J. Z. Ilich. Nutrition, Food and Exercise Sciences, Florida State University, Tallahassee, FL, USA.

Functionality is the measurement of one's ability to perform simulated daily tasks and can be assessed by measuring strength, endurance, flexibility, agility and balance. Functionality outcomes may be related to an individual's overall health status and physical conditioning. Our purpose was to examine the relationship between various aspects of functionality and bone mineral density (BMD) in Caucasian overweight and obese postmenopausal women. BMD of the total body, femur (neck, Ward's triangle, trochanter, shaft, total) and forearm (radius and ulna at ultradistal and 1/3 distance) were measured by iDXA (GE Medical Systems, Madison, WI). Participants included 37 early postmenopausal (from 2-10 y) women, aged 54.7±3.8 y, with a body mass index (BMI) of 31.3±4.8 kg/m<sup>2</sup> (mean±SD). Participants completed functionality tests including: 8 meter normal and brisk walks, normal and brisk step length, handgrip strength assessment, and the chair-stand test. In multiple regression models containing age, and BMI, brisk walk speed was significantly associated with BMD of all femoral sites (except the trochanter), and total body (adjusted R<sup>2</sup> range, 16%-25%; P<0.05). Normal walk speed and step length were not related to the BMD of any skeletal site of the femur or total body. Handgrip strength was significantly associated with forearm BMD at most of the sites (adjusted R<sup>2</sup> range=13-21%, P less than or equal to 0.05). Trends for associations were observed between the chair stand and femoral BMD (significant for shaft only; adjusted R<sup>2</sup> range=12-14%). We conclude that functionality performance is related to BMD of various skeletal sites. Conditioning with regard to these functionality measures may be beneficial in osteoporosis prevention.

**Disclosures:** J.Z. Ilich, None.

This study received funding from: USDA/CSREES/NRI #2004-05287.

## SU419

**Quality of Life in Mexican Hip Fractures Patients Using EUROQOL (EQ-5) After Discharge from Hip Fracture and 6 Months of Followup.** P. Clark<sup>1</sup>, F. Carlos<sup>\*1</sup>, E. Ramirez<sup>\*2</sup>, A. Camacho<sup>\*1</sup>, F. Franco-Marina<sup>\*2</sup>. <sup>1</sup>Clinical Epidemiology Unit, IMSS-Faculty of Medicine UNAM, Mexico City, Mexico, <sup>2</sup>Epidemiología y Socio-medicina, Instituto Nacional de Rehabilitación, Mexico City, Mexico.

**Objective:** To identify trajectories in Health related quality of life (HRQOL) observed between months 1 and 6 after initial discharge in treated and surviving hip fracture Mexican patients.

**Methods:** Hip fracture patients attending 5 Mexico City public and private hospitals were identified and observed between months 1 and 6 after initial discharge.

The Euroqol questionnaire was applied to each individual to gather information on their HRQOL during the first, third and sixth month after initial hip fracture discharge from the hospital. In 72% of the individuals this assessment was retrospective and performed during the sixth month after initial discharge.

Eq5d score valuations were obtained for each time period using the UK values assigned to each health state. Five EUROQOL trajectories in these patients were visually identified: a) Continuous HRQOL improvement during the 6 month observation period, b) EarlyHRQOL improvement concentrated on the first 3 months after discharge, c) Delayed HRQOL improvement mainly occurring between the third and the sixth month after discharge, d) Same HRQOL over the observation period and e) HRQOL worsening over the study period.

Predictors related to these trajectories included: age, gender, marital status, Eq5d score at the first month, type of surgery, co-morbidities and hospital readmissions. Data were analyzed through a multinomial logistic regression model which also included a term indicating whether the HRQOL assessment was either prospective or retrospective.

**Results:** 136 treated and surviving hip fracture patients were analyzed. Of them 78.6% showed an improvement in their Eq5d scores over the observation period (38.9% a continuous improvement and 37.5% an early improvement). Only 8.1% showed a worsening in their HRQOL over the observation period and 12.5% maintained during the observation the same HRQOL. Statistically significant results that follow come from the final multivariate model. Prospective interviews were more frequent in the trajectories showing continuous improvement or worsening HRQOL. Persons showing the same or worsening trajectory over the observation period had an older average age than those showing any of the three improving trajectories. Persons with worsening or delayed improvement trajectories had a better Eq5d score at the start of observation. Patients treated by partial or total hip replacement tended to show more frequently the same or worse HRQOL over the study period, whereas those receiving an open or closed hip screw tended to show more frequently a continuous or early improvement.

**Disclosures:** P. Clark, None.

## SU420

**The Association Between Falls and Health-Related Quality of Life (HRQoL).** J. McFetridge<sup>\*1</sup>, E. Barrett-Connor<sup>2</sup>, S. G. Sajjan<sup>\*3</sup>, T. Fan<sup>\*3</sup>, P. D. Miller<sup>4</sup>, S. S. Sen<sup>\*3</sup>, E. S. Siris<sup>5</sup>. <sup>1</sup>Lehigh University, Bethlehem, PA, USA, <sup>2</sup>University of California, San Diego, La Jolla, CA, USA, <sup>3</sup>Merck & Co., Inc, Whitehouse Station, NJ, USA, <sup>4</sup>Colorado Center for Bone Research, Lakewood, CO, USA, <sup>5</sup>Columbia University Medical Center, New York, NY, USA.

To assess the association between falls and HRQoL in women age 50 - 99 who participated in the National Osteoporosis Risk Assessment (NORA) Survey, 152,065 women completed the baseline and one-year follow-up NORA surveys. HRQoL was assessed by SF-12 Physical (PCS) and Mental Component Summary (MCS) scores. Information on self-reported falls and associated medical care for the 12 months prior to 1st follow-up survey was collected. Three groups were formed: falls not resulting in medical care (doctor's visit, emergency room) and/or fracture (Group I), falls resulting in medical care without fracture (Group II), and falls resulting in fracture (Group III). Group least squares means of PCS and MCS at the one-year follow-up survey were adjusted for key factors (age, ethnicity, BMD T-score, education, BMI, fractures prior to baseline and baseline health status). Differences by fall status for the entire cohort, as well as by age group (50-64 yrs vs. 65-99 yrs) were determined. Statistical significance of the interaction effect of age and fall status on PCS and MCS was also examined. A total of 28,887 patients [group I (n=19,303), group II (n=6,407), group III (n=3,177)] reported having a fall during the one year between surveys. For both age groups, with all fall types, women with fall had poorer PCS than those who had not fallen with a general pattern of PCS worsening with increasing fall severity (see table). The interaction between age group and fall status was not significant. A significant association was also found between MCS and falls (data not shown), but it was inconsistent and of a lesser magnitude. Falls even in absence of resultant fracture was associated with a lower HRQoL. The association between recent fall in the past year and HRQoL was similar for older and younger postmenopausal women. These findings highlight the importance of falls in postmenopausal women of all ages.

Fall group	Differences of Least Squares Means for PCS		
	All patients	50-64 yrs	65-99 yrs
Group I	-1.8469*	-1.7145*	-1.9792*
Group II	-3.8959*	-3.9813*	-3.8104*
Group III	-4.4390*	-4.3454*	-4.5327*

\* Differences of least squares means versus the no fall group: p < 0.0001

**Disclosures:** J. McFetridge, Merck & Co., Inc 5.

## SU421

**Superiority of Alfacalcidol over Plain Vitamin D in Men with Osteoporosis: A Prospective, Observational, Single Center, Two Year Trial on 214 Patients.** J. D. Ringe<sup>1</sup>, P. Farahmand<sup>\*1</sup>, E. Schacht<sup>2</sup>. <sup>1</sup>Medical Clinic 4, Klinikum Leverkusen (Univ. of Cologne), Leverkusen, Germany, <sup>2</sup>ZORG (Zurich Osteoporosis Research Group), Zollikerberg, Switzerland.

**Background:** Due to pleiotropic actions on bone, gut, muscle and other target tissues alfacalcidol is an interesting drug for treating osteoporosis and preventing falls. Within studies on glucocorticoid-induced osteoporosis always men have been treated with this active D-hormone prodrug, but there is no pure male study in the literature. Therefore we conducted a study to compare the efficacy of alfacalcidol versus plain vitamin D in patients with established male osteoporosis.

**Methods:** For ethical reasons and to simulate practical conditions we selected in a pair-wise manner 107 patients with established male osteoporosis and prevalent vert. fxs (group A) and 107 patients without prevalent vert. fxs (group B). Group A we treated with 1mcg alfacalcidol + 500 mg calcium daily and group B with 1000 I.U. vitamin D + 1000 mg calcium daily for two years.

With this design we are comparing two groups with a different risk at onset. Due to the prevalent vert. fxs and lower average BMD values there is a higher risk for incident fractures in group A. The scientific question is whether despite these differences the therapeutic results in group A are not inferior or even superior. BMD was measured at the lumbar spine and at the femoral neck with dual energy x-ray absorptiometry (LUNAR) and lateral x-rays of the spine were taken, both annually and observer blind.

**Results:** After 2 years we found significantly higher increases for LS-BMD (+3.2 vs. +0.8%) and TH-BMD (+1.9 vs. -0.9%) in group A and B resp. 18 incident falls were reported in the alfacalcidol group and 38 in the group treated with plain vitamin (p = 0.04). There were significantly lower rates of patients with new vert. and non-vert.-fxs in group A than in group B (-48% for each type of fractures; p = 0.035 and p = 0.004 resp.) Concerning the incidence of new non-vert fxs we found out that there was a relation to renal function in the two groups. The advantage for alfacalcidol was mainly due to a higher non-vert, fall-related fxs reducing potency in patients with a creatinine-clearance below 60ml/min. (Odds ratio: 5.652; p = 0.002). There were no SAE and no deterioration of renal function in both groups.

**Conclusion:** Despite the higher risk profile of the patients in the alfacalcidol group at onset alfacalcidol showed a higher therapeutic efficacy in terms of BMD, falls and fractures. One important advantage of alfacalcidol may be that it works in vitamin D deplete and replete patients and also in those with mild to moderate deterioration of renal function.

**Disclosures:** J.D. Ringe, TEVA Pharmaceuticals Ltd. 3.

This study received funding from: TEVA Pharmaceuticals Ltd.

## SU422

**Vitamin D<sub>3</sub> Treatment of Elderly People - Twice a Day or Every Four Months? A Comparative Study of Efficacy and Safety of Two Oral Dosages with Same Annual Dose of 292000 Units.** V. V. Välimäki<sup>1</sup>, T. Pekkarinen<sup>2</sup>, S. Aarum<sup>1</sup>, U. Turpeinen<sup>3</sup>, E. Hämäläinen<sup>3</sup>, E. Löyttyniemi<sup>4</sup>, M. J. Välimäki<sup>1</sup>.

<sup>1</sup>Department of Medicine, Division of Endocrinology, Helsinki University Central Hospital, Helsinki, Finland, <sup>2</sup>Department of Internal Medicine, Helsinki University Central Hospital, Vantaa, Finland, <sup>3</sup>Department of Clinical Chemistry, Helsinki University Central Hospital, Helsinki, Finland, <sup>4</sup>Department of Statistics, University of Turku, Turku, Finland.

This randomized, double blind two-arm parallel vitamin D<sub>3</sub> supplementation trial compared efficacy and safety of two oral dosages of vitamin D<sub>3</sub> resulting in equal annual dose of 292,000 IU.

Forty women aged 69.3-78.8 years were randomly assigned to either vitamin D<sub>3</sub> 400 IU twice daily (Daily) or vitamin D<sub>3</sub> oil 97333 IU every four months (Every 4 months) for one year. All received one gram calcium supplementation daily. Serum 25OHD<sub>3</sub> in relation to the target levels of 50-75 nmol/l, serum PTH, and serum type I procollagen aminoterminal propeptide (PINP) were followed as efficacy parameters and serum and urine calcium and different measures of renal function as safety parameters.

The 25OHD<sub>3</sub> concentration differed between the study groups over time (P<0.0001), and increased more in the Daily group than in the Every 4 months group with the increases in mean values from baseline to 12 months being 16.4 nmol/l (P<0.0001) and 3.9 nmol/l (P=0.142), respectively. One hundred percent and 47% in the Daily group and 67% and 28% in the Every 4 months group had 25OHD<sub>3</sub> concentration above 50 nmol/l and 75 nmol/l at the end of the study, respectively. PTH levels did not show any seasonal perturbation in either group. Serum PINP levels declined similarly in both groups over time (P<0.0001). Serum ionized calcium levels remained stable and did not differ between the groups. 24-hour urinary calcium excretion rose (P<0.0001 for time) similarly in the study groups, the increases in mean values from baseline to 12 months being 1.21 mmol (P<0.0001) in the Daily group and 0.58 mmol in the Every 4 months group (P=0.040). Renal function fluctuated (P<0.0001) but did not worsen over time in either group in terms of serum creatinine, cystatin C, or creatinine clearance.

In terms of serum 25OHD<sub>3</sub> concentrations daily treatment was more efficient than four monthly treatment, but to increase adherence to supplementation the latter is still worth developing e.g. by shortening the dosing interval to 3 months. Both treatments increased urinary excretion of calcium, but did not worsen renal function.

**Disclosures:** V.V. Välimäki, None.

This study received funding from: Helsinki University Central Hospital (Erityisvaltionosuu), Recip AB, Eli Lilly Finland, Paulo Foundation and Päivikki and Sakari Sohlberg Foundation.

## SU423

**Anti-fall Efficacy of Oral Supplemental Vitamin D and Active Vitamin D.** J. Henschkowski<sup>1</sup>, B. Dawson-Hughes<sup>2</sup>, H. B. Staehelin<sup>3</sup>, A. E. Stuck<sup>4</sup>, J. E. Orav<sup>5</sup>, A. Egli<sup>1</sup>, H. A. Bischoff-Ferrari<sup>1</sup>.

<sup>1</sup>Rheumatology, University of Zurich, Zurich, Switzerland, <sup>2</sup>Jean Mayer USDA HNRCA, Tufts University, Boston, MA, USA, <sup>3</sup>Geriatrics, University of Basel, Basel, Switzerland, <sup>4</sup>Geriatrics, University of Bern, Bern, Switzerland, <sup>5</sup>Biostatistics, Harvard School of Public Health, Boston, MA, USA.

**Background:** Results from fall prevention trials with supplemental vitamin D have been mixed and trials varied by dose, type of vitamin D (D<sub>3</sub> = cholecalciferol or D<sub>2</sub> = ergocalciferol), and quality of fall assessment. A possible differential benefit of supplemental versus alpha-hydroxylated vitamin D (active D) has not been established.

**Aim:** We performed a meta-analysis on the efficacy of supplemental vitamin D in preventing falls among older individuals (age 65+) and compared the pooled effects from supplemental and active vitamin D trials.

**Studies included:** The primary analysis included double-blind RCTs with prospective fall assessment of oral vitamin D with or without calcium supplementation compared to calcium or placebo.

**Results:** Supplemental vitamin D: 8 RCTs (n=2426) met our inclusion criteria. For supplemental vitamin D, heterogeneity was observed for dose of vitamin D (low-dose: 200-600 IU / day versus higher dose: 700 IU + / day; p -value 0.017) and achieved 25-hydroxyvitamin D level (< 60 nmol/l versus ≥ 60 nmol/l; p-value = 0.003). Higher dose supplemental vitamin D reduced the relative risk (RR) of a fall by 19% (pooled RR=0.81; 95% CI, 0.71-0.92; n = 1921 from seven trials) and effects were most pronounced (26%) with D<sub>3</sub> (pooled RR = 0.74; 95% CI, 0.58-0.93; n= 946). Falls were not reduced by low dose supplemental vitamin D (pooled RR = 1.10, 95% CI, 0.89-1.35) or by achieved serum 25-hydroxyvitamin D concentrations less than 60 nmol/l (pooled RR = 1.34, 95% CI, 0.98-1.84).

Active vitamin D: 2 RCTs, (n= 624) met our inclusion criteria. Active vitamin D in a dose of 1µg 1αCalcidiol or 0.5 µg Calcitriol per day reduced fall risk by 22% (pooled RR = 0.78; 95% CI, 0.64-0.94).

**Conclusion:** Supplemental vitamin D in a higher dose of at least 700 IU reduced the risk of falling among older individuals by at least 19% and to a similar degree as active D. Low dose supplemental vitamin D of 600 IU or less, or supplementation resulting in serum 25-hydroxyvitamin D concentrations of less than 60 nmol/l may not reduce the risk of falling among older individuals.

**Disclosures:** H.A. Bischoff-Ferrari, None.

This study received funding from: Robert Bosch Foundation and Swiss National Foundation Professorship Grant.

## SU424

**Vitamin D Deficiency Is Associated with Diminished Quality of Life Based on Qualeffo-41 Questionnaire Analysis.** P. M. Camacho<sup>1</sup>, A. M. Mazhari<sup>1</sup>, B. Sexton<sup>1</sup>, P. Sapountzi<sup>1</sup>, J. Sinacore<sup>2</sup>.

<sup>1</sup>Endocrinology, Loyola University Medical Center, Maywood, IL, USA, <sup>2</sup>Preventive Medicine, Loyola University Medical Center, Maywood, IL, USA.

Vitamin D deficiency leads to bone loss, fractures, bone pain and muscle weakness. Vitamin D deficient individuals frequently report an improvement in pain, muscle strength, mood and sense of well-being when treated with vitamin D, translating to a better quality of life. We describe the partial results of an ongoing prospective study that aims to determine the effect of vitamin D deficiency on health-related quality of life.

The Qualeffo-41 questionnaire is a quality of life survey validated for patients with osteoporosis. It contains questions in five domains: pain, physical function, social function, general health perception and mental function. The scores are expressed on a 100-point scale, with 0 corresponding to the best and 100 being the worst health related quality of life.

Individuals evaluated at Loyola Osteoporosis and Metabolic Bone Disease Center for osteopenia and osteoporosis were screened for vitamin D deficiency. Patients with 25 OH Vitamin D (25OHD) level <20 ng/ml were enrolled in the vitamin D deficient group (VDG) and those with 25 OHD > 20 ng/ml were enrolled in the control group (CG). When the study was initiated in 2004, vitamin D deficiency was defined as 25 OHD < 20 ng/ml. 36 patients (6 male and 30 female) were enrolled in the VDG and 24 patients (all female) in the CG. The mean age in years for the VDG was 58 +/- 13 versus 60 +/- 11 in the CG (p=0.406). The mean 25 OHD in the VDG was 14.78 +/- 4.47 versus 38.04 +/- 12.08 in the CG (p<0.0005). Intact PTH was 61.90 +/- 33.31 in the VDG versus 36.30 +/- 13.24 in the CG (p=0.001). Spine BMD in the VDG was 1.105 gm/cm2 +/- 0.229 versus 0.915 +/- 0.271 in the control group (p=0.012) and mean T scores were -.85 +/- 1.93 and -1.55 +/- .338, respectively, (p=0.19). Femoral neck BMD and T scores were not statistically different.

The mean total score was significantly higher in the VDG at 34.5 +/- 15.9 versus 22.4 +/- 12.3 in the CG (p=0.003). 4 out of 5 domains showed significantly higher scores in the VDG compared to the CG; general health perception (p<0.0005), physical function (p=0.005), pain (p=0.020) and social function (p=0.012). Mental function was not significantly different between the 2 groups. There was an inverse correlation between the total score and vitamin D levels r=-.371 (p=0.004), when corrected for age. There was no correlation between the total score and LS and FN BMD and T scores.

Our study clearly shows that vitamin D deficient individuals suffer from diminished quality of life, independent of the severity of bone loss. Future results of this ongoing study will determine if correction of the deficiency will lead to a significant improvement.

**Disclosures:** A.M. Mazhari, None.

## SU425

**Effect of Vitamin D<sub>2</sub> or Vitamin D<sub>3</sub> Supplementation on Serum 25(OH)D.**

N. Binkley, D. Gemar, A. Woods\*, J. Engelke\*, R. Ramamurthy, D. Krueger, M. K. Drezner. Osteoporosis Clinical Research Program, University of Wisconsin-Madison, Madison, WI, USA.

Ergocalciferol (D<sub>2</sub>) has been assumed less effective than cholecalciferol (D<sub>3</sub>) in maintaining serum 25-hydroxyvitamin D [25(OH)D]. However, data supporting this are limited and a recent report challenges this assumption. The effect of oral vitamin D dosing on circulating 25(OH)D concentration depends on absorption, subsequent metabolism, and the impact on pre-existing circulating 25(OH)D<sub>3</sub> concentration. However, data evaluating the effect of vitamin D<sub>2</sub> administration on circulating 25(OH)D<sub>3</sub> concentration are limited and existing studies of short duration. This study investigates the effects of long-term administration of vitamin D<sub>2</sub> or vitamin D<sub>3</sub> on circulating levels of 25(OH)D<sub>2</sub>, 25(OH)D<sub>3</sub> and total 25(OH)D. In this year-long randomized, double-blind trial, community-dwelling adults age 65+ were randomly assigned to receive daily (1,600 IU) or once-monthly (50,000 IU) vitamin D<sub>2</sub> or vitamin D<sub>3</sub>. Serum for 25(OH)D measurement by HPLC was obtained at baseline and immediately before monthly dosing at months 1, 2, 3, 6, 9 and 12. All 25(OH)D measurements for each individual were performed in a single HPLC run to minimize assay variability. Study enrollment (total n = 64) was completed in summer 2007; preliminary data for the first 17 study completers (13 women/4 men) are reported here. Baseline mean (± SD) age, BMI and 25(OH)D were 73.5 (4.7) years, 24.9 (4.7) kg/m<sup>2</sup> and 28.8 (11.2) ng/ml respectively. At one year, a greater increase in mean total 25(OH)D was observed with vitamin D<sub>3</sub> than with vitamin D<sub>2</sub> whether dosed daily (16.2 vs. 8.6 ng/ml) or monthly (7.9 vs -0.9 ng/ml). As expected, the increase in total 25(OH)D, seen with vitamin D<sub>3</sub> dosing, reflects an increase (p < 0.05) in 25(OH)D<sub>3</sub>; 19.4 and 8.6 ng/ml for daily and monthly dosing respectively. Similarly, vitamin D<sub>2</sub> administration raises 25(OH)D<sub>2</sub>; 19.6 and 18.7 ng/ml for daily and monthly dosing respectively. However, with vitamin D<sub>2</sub> dosing, a reciprocal decrease (p < 0.01) in 25(OH)D<sub>3</sub> of approximately the same magnitude as the increase in 25(OH)D<sub>2</sub>, results in minimal or no increase in total 25(OH)D. Substantial between-individual variability exists in 25(OH)D response to identical vitamin D<sub>2</sub> and vitamin D<sub>3</sub> doses. Serum and 24-hour urinary calcium concentrations were unchanged over 12 months for all groups.

These preliminary results suggest that, over the course of one year, the long-term effects of vitamin D<sub>2</sub> administration on total 25(OH)D are largely negated by a reduction in the circulating 25(OH)D<sub>3</sub> concentration. Thus, vitamin D<sub>3</sub> appears a more effective treatment than vitamin D<sub>2</sub> to increase serum 25(OH)D.

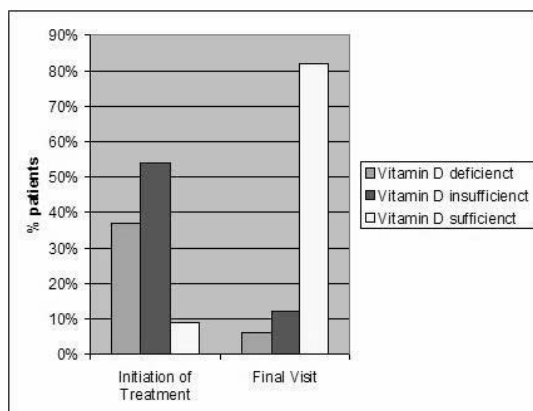
**Disclosures:** N. Binkley, None.

This study received funding from: GSK/Roche.

## SU426

**The Effects of 50,000 IU of Vitamin D<sub>2</sub> Twice per Month on Circulating 25-Hydroxyvitamin D and Calcium Levels.** S. M. Pietras\*, B. K. Obayan\*, M. H. Cai\*, M. F. Holick. Vitamin D, Skin and Bone Research Laboratory, Endocrine Section, Department of Medicine, Boston University School of Medicine, Boston Medical Center, Boston, MA, USA.

**Purpose:** Knowledge about the many physiologic functions of vitamin D is growing. Vitamin D is important for muscle and skeletal health and may have a role in reducing the risk of malignancies, autoimmune and cardiovascular diseases. To date there have been no long-term studies using pharmacologic dosing to maintain vitamin D sufficiency. Here we report our experience treating patients with 50,000 IU of vitamin D<sub>2</sub> twice a month for up to six years. **Methods:** Retrospective chart review of patients seen in a specialty bone clinic. Data collected included serum 25(OH) D values, calcium (Ca) and parathyroid hormone (PTH) levels. **Results:** 90 patients qualified. We found a significant improvement in 25(OH) D values with a mean value prior to treatment of 23.1 +/- 9.5 ng/mL, compared to 46.4 +/- 18.0 ng/mL at the final visit during the review period (p<0.001). 9% of patients were vitamin D sufficient (25(OH) D ≥ 30 ng/mL) at the initiation of treatment, compared with 82% at the final visit (p<0.001). After an initial improvement during the first 6 months (serum 25(OH) D levels increased to approximately 35 ng/mL) levels remained stable over time. 43 patients were initially treated with 50,000 IU of vitamin D<sub>2</sub> weekly for 8 weeks prior to starting maintenance therapy with twice monthly vitamin D. Mean values for Ca and PTH did not significantly change. 13 patients with primary or tertiary hyperparathyroidism were included in the review, and when analyzed separately the Ca levels in these patients did not significantly change (mean initial value 10.3 +/- 0.9 mg/dL, mean final value 10.2 +/- 0.7 mg/dL, p=0.89), nor did the PTH values (mean initial value 176.7 +/- 263.5 pg/mL, final value 168.5 +/- 120.3 pg/mL, p=0.88). **Conclusion:** Treating patients with 50,000 IU of vitamin D<sub>2</sub> twice per month is an effective method to prevent the recurrence of vitamin D deficiency and maintain serum levels in what is now considered to be the preferred range for health.



**Graph 1: Status of Vitamin D Sufficiency: Initiation of Treatment vs. Final Visit**  
 Vitamin D deficiency: 25(OH) D levels <20 ng/mL. Vitamin D insufficiency: 25(OH) D levels 20-29.9 ng/mL. Vitamin D sufficiency: 25(OH) D levels ≥ 30 ng/mL.

**Disclosures:** *S.M. Pietras, None.*

## SU427

**What Is Your Patient's Vitamin D Status? Clinical Consideration of Variability in a 25(OH)D Measurement.** N. Binkley, D. Krueger, J. Engelke\*, M. K. Drezner. Osteoporosis Clinical Research Program, University of Wisconsin-Madison, Madison, WI, USA.

Clinicians are increasingly obtaining 25(OH)D measurements and using this value to recommend vitamin D supplementation. However, a 25(OH)D measurement, like all laboratory tests, is impacted by assay and biologic variability. An additional source of variability for many laboratory tests, including 25(OH)D, is lack of standard calibrators. Finally, it is logical that assaying 25(OH)D<sub>2</sub> and 25(OH)D<sub>3</sub> separately to determine total 25(OH)D increases measurement error. Despite the above, it is our impression that clinicians may not consider 25(OH)D measurement variability when prescribing high-dose vitamin D treatment. The purpose of this report is to raise clinician awareness to potential variability in 25(OH)D measurement and suggest how to confront this reality. 25(OH)D assay variability was investigated using 3 serum controls, containing differing amounts of 25(OH)D<sub>2</sub> and 25(OH)D<sub>3</sub>, measured 49 times over 14 months for routine quality assurance. Between-lab variability was explored (data previously reported) by sending 16 specimens to 2 clinical laboratories for 25(OH)D measurement. Biologic variability is reported for 3 volunteers in whom blood was obtained weekly for 16 weeks following substantial sun exposure. Finally, the possibility that specimens containing both 25(OH)D<sub>2</sub> and 25(OH)D<sub>3</sub> produce greater variability in total 25(OH)D was explored. Two samples with total 25(OH)D near 30 ng/ml, one comprised of only 25(OH)D<sub>3</sub>, the other with nearly equal amounts of 25(OH)D<sub>2</sub> and 25(OH)D<sub>3</sub>, are being measured weekly. In the 3 QC sera, 25(OH)D<sub>2</sub> and 25(OH)D<sub>3</sub> were evaluated separately; the mean values ranged from 15.1 to 91.1 ng/ml with 95% confidence intervals from +/-1.9 to 4.7%.

Between-laboratory bias for the 2 clinical labs was 4.4 ng/ml (~15% at 30 ng/ml). Combining these sources of variability, a single 25(OH)D result may vary by ~20%. As such, a single value of "30 ng/ml" is between 24 and 36 ng/ml. Similarly, a value of "25 ng/ml" may be 31 ng/ml, while a value of 33 ng/ml may be 27 ng/ml. Day-to-day biologic variability appears minimal, although seasonal variability was observed with a decline in 25(OH)D of 15-30% over 16 weeks in the fall/winter.

In conclusion, based on assay and between-lab variability, a single reported 25(OH)D result is likely within 20% of the "true" value. It is possible that serum containing both 25(OH)D<sub>2</sub> and 25(OH)D<sub>3</sub> will have even greater variability. Clinicians are well advised to consider this variability when applying any cutpoint approach, e.g., 30 ng/ml, to define optimal vitamin D status. In patients with borderline vitamin D status, e.g., 25-35 ng/ml, a conservative approach to vitamin D repletion, rather than prescription of high-dose vitamin D<sub>2</sub>, seems appropriate.

**Disclosures:** *N. Binkley, None.*

## SU428

**A Randomised Controlled Trial of the Effects of Vitamin D Supplementation upon Muscle Function in Adolescent Girls.** K. A. Ward<sup>1</sup>, G. Das<sup>2\*</sup>, J. L. Berry<sup>3</sup>, S. A. Roberts<sup>4\*</sup>, J. E. Adams<sup>1</sup>, Z. Mughal<sup>5</sup>. <sup>1</sup>Clinical Radiology, University of Manchester, Manchester, United Kingdom, <sup>2</sup>Paediatrics, Central Manchester Primary Care Trust, Manchester, United Kingdom, <sup>3</sup>Medicine, University of Manchester, Manchester, United Kingdom, <sup>4</sup>Health Methodology Research Group, University of Manchester, Manchester, United Kingdom, <sup>5</sup>Paediatric Medicine, Central Manchester and Manchester Childrens University Hospitals NHS Trust, Manchester, United Kingdom.

Myopathy is the major clinical symptom of hypovitaminosis D. As part of a double blind, randomised controlled trial of vitamin D supplementation we measured muscle power and force at baseline and follow-up. We hypothesised that after 12 months vitamin D supplementation muscle power would increase more in the supplemented group than in the placebo group.

73 of the original 99 girls screened for the trial had 25(OH)D levels < 15ng/ml. All girls had baseline muscle measurements using jumping mechanography and hand-held dynamometry. Muscle measurements were repeated after 12 months vitamin D supplementation (4 doses 150 000IU Ergocalciferol). A single two legged jump (2LJ), multiple one leg jumps (1LJ) and grip strength measurements were performed.

69 girls (94%) completed the trial; reasons for loss to follow up are leaving school (n=3) and starting treatment for clinical symptoms of 25(OH)D deficiency. Differences between groups were tested using ANCOVA adjusting for baseline weight, log baseline 25(OH)D and baseline measurement. Exploratory analyses of whether vitamin D level affected response to supplementation was performed after splitting baseline 25(OH)D level into tertiles (< 5.5ng/ml, 5.51 - 6.95 ng/ml, >6.95 ng/ml); ANOVA tested difference between groups.

At follow up 25(OH)D status was 22.4ng/ml (SD 3.6, range 13.8 to 29.2) in the active group and 6.3 ng/ml (SD 2.6, range 2.4 to 13.2) in controls. There were no significant differences between the vitamin D treated group and controls for any of the parameters studied in the lower or upper limb. Muscle power, but not force, increased in the supplementation group with lowest baseline 25(OH)D levels (p = 0.057).

There were no overall differences in muscle power between the treated group and controls despite improvements in 25(OH)D status. There were no changes in force, perhaps reflecting that these girls had completed growth prior to the study. The improvement in power in girls taking supplementation in the lowest tertile of baseline 25(OH)D was through increased jumping velocity (p = 0.012). These data support the clinical observation of loss of proximal muscle function at the very lowest levels of 25(OH)D. The implications of this loss of function upon skeletal growth and development remain to be determined.

**Disclosures:** *K.A. Ward, None.*

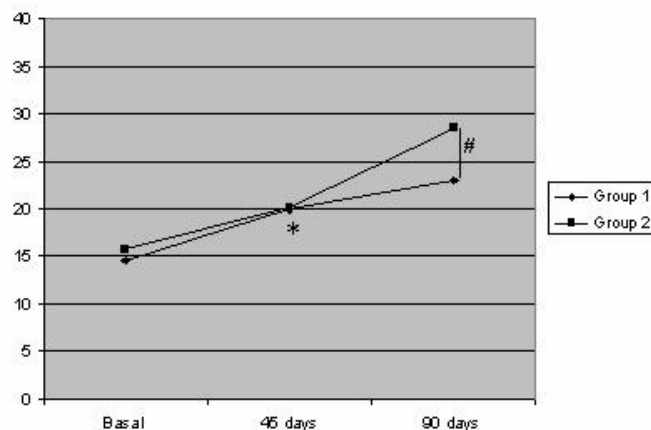
*This study received funding from: Central Manchester and Manchester Childrens University Hospitals NHS Trust.*



## SU429

**Which is the Best Oral High-Dose Vitamin D<sub>3</sub> Regimen for Postmenopausal Women with Hypovitaminosis D?** S. R. Mastaglia\*, M. Seijo\*, A. Bagur, J. Somoza\*, B. Oliveri. Sección Osteopatías Médicas, Hospital de Clínica. Universidad de Buenos Aires, Buenos Aires, Argentina.

Hypovitaminosis D is a common problem in postmenopausal and elderly people. Intermittent administration of vitamin D is being studied as a means to ensure compliance with the supplementation regimen and to ensure adequate levels. The aim of this study was to assess the effectiveness and safety of two high-dose oral intermittent vitamin D<sub>3</sub> regimens. Sixteen healthy postmenopausal women aged 58.4±5.0 years (X±SD), with 25OHD <20ng/ml, not receiving any treatment known to affect bone metabolism were recruited. They were randomly assigned to one of two groups: Group 1 receiving a single 100,000IU dose of cholecalciferol (D<sub>3</sub>) and Group 2 receiving an additional similar dose on day 45. Serum calcium, phosphorus, bone alkaline phosphatase, iPTH and urinary Calcium/creatinine were measured at baseline (previous to D<sub>3</sub> administration), and at 45 and 90 days. Average 25OHD levels rose from 14.5±4.3 ng/ml at baseline to 20.1±3.0 ng/ml at day 45 (p<0.004), and to 24.7±5 at day 90 (p<0.001 vs. baseline) in all the patients. When divided according to regimen both groups had similar values at 45 days (G1=20.0±4 and G2:20.2 ± 2ng/ml) Group 1 maintained vitamin D levels between day 45 and 90 (23.0±4 ng/ml; ns); only 9% reached 25OHD levels ≥30ng/ml. Group 2 showed a significant increase in 25OHD levels between day 45 and 90 (28.5±3 ng/ml; p<0.04). Forty percent of women had 25OHD levels ≥30ng/ml. No significant differences in the remaining biochemical parameters were observed between groups at any time point and all the values were within the reference range for postmenopausal women. A single oral 100,000IU dose of cholecalciferol is safe but not sufficient. A second similar dose administered at 45 days improves 25OHD levels but is still not enough for healthy postmenopausal women with hypovitaminosis D to reach adequate 25OHD levels.



\* Group 2: baseline vs. 45 days; p<0.01  
# Group 1 vs. Group 2 at 90 days; p<0.003

**Disclosures:** S.R. Mastaglia, None.

## SU430

**A Single Dose of 100,000IU D<sub>3</sub> Appears to be Insufficient to Achieve Desirable Levels of 25OHD in Patients with Hypovitaminosis D.** A. Bagur<sup>1</sup>, M. V. Ferro<sup>\*1</sup>, D. González<sup>\*2</sup>, M. C. Fernández<sup>\*1</sup>, B. Oliveri<sup>1</sup>, M. S. Parisi<sup>1</sup>. <sup>1</sup>Sección Osteopatías Médicas, Hospital de Clínicas, Universidad de Buenos Aires, Buenos Aires, Argentina, <sup>2</sup>Sección Osteopatías Médicas, Centro de Osteopatías Médicas, Buenos Aires, Argentina.

Hypovitaminosis D is a major worldwide public problem. Correction of vitamin D is important for prevention of osteoporosis since bone loss and fractures have been linked with vitamin D deficiency. The aim of the study was to evaluate the response and safety to a unique vitamin D<sub>3</sub> dose (100,000 IU) in patients with low 25OHD levels. Ninety three clinical records from patients who received this unique dose of vitamin D<sub>3</sub> for hypovitaminosis D were reviewed. Inclusion criteria were: 25OHD levels below 32 ng/ml, 25OHD determinations at baseline and after 1 to 3 months of treatment, performed at the same laboratory, and normal serum calcium. Thirty eight out 90 had the inclusion/exclusion criteria defined, and all of them were women. We excluded 55 clinical records, 34 due to uncompleted data, 3 because the samples were made in different laboratories and 15 did not have 25OHD determinations after the first dose of vitamin D<sub>3</sub>. The mean age ± 1SD was 63.3 ± 9.6 years, 35 of them were postmenopausal and 3 premenopausal women. Laboratory tests were: serum calcium, phosphate, 25OHD, bone alkaline phosphatase, CTX, iPTH and urine 24hs calcium at baseline and post treatment. Subjects were divided in three groups according to baseline 25OHD: 0-10, 11-20 and 21-31 ng/ml. At baseline 2 patients (5.3%) had values between 0 to 10, 19 (50%) between 11 to 20 ng/ml and 17 (44.7%) between 21 to 31 ng/ml. The 25OHD levels post 1 to 3 months dose of vitamin D were: nobody had values under 10 ng/ml, 2 (5.3%) were between 11 to 20 ng/ml, 17 (44.7%) between 21 to 31 ng/ml and 19 (50%) had 25 OHD levels above 32

ng/ml.

There were not cases of hypercalcemia or hypercalciuria after treatment.

One or two new doses of vitamin D were prescribed in patients who did not reach optimal levels of vitamin D with the first treatment (this analysis was pending to complete all the data).

**Conclusion:** A unique dose of 100,000 IU D<sub>3</sub> was safe but insufficient since only 50% of patients reached the recommended 25OHD levels at the first 3 months of treatment. Additional doses have to be recommended to obtain normal levels in patients who continued with hypovitaminosis D.

**Disclosures:** M.S. Parisi, None.

This study received funding from: Fundación de Osteoporosis y Enfermedades Metabólicas Óseas.

## SU431

**Efficacy of the Vitamin D Supplementation in Patients with Hypovitaminosis D and Secondary Hyperparathyroidism.** E. Casado, M. Larrosa<sup>\*</sup>, I. Vázquez<sup>\*</sup>, C. Orellana<sup>\*</sup>, M. García-Manrique<sup>\*</sup>, J. Gratacós<sup>\*</sup>. Rheumatology, Hospital Sabadell, Sabadell, Spain.

**Purpose:** To analyze which proportion of patients with hypovitaminosis D and secondary hyperparathyroidism normalize PTH levels after on month of treatment with calcidiol. To analyze if the chronic treatment with vitamin D (calcidiol or cholecalciferol) is useful to maintain compensated the hyperparathyroidism of these patients.

**Methods:** Prospective, open-label study, with systematic inclusion of all patients with hypovitaminosis D (25(OH)D<sub>3</sub> < 25 ng/ml) and secondary hyperparathyroidism (PTH < 65 pg/ml), who were attended in the Rheumatology out-patient clinic during a two-year period. Patients with a suspected primary hyperparathyroidism or with renal failure were excluded. All the included patients were treated with calcidiol (16000 IU/week) during the first month (64000 IU). During the follow up the patients were randomized in two groups of treatment: calcidiol (16000 IU/3 weeks) or cholecalciferol (800 IU/day). 25(OH)D<sub>3</sub> and PTH levels were analysed after the first month of treatment with calcidiol, and after 3 months of the two-branch treatment.

**Results:** 61 patients with hypovitaminosis D and secondary hyperparathyroidism were included (53 female, 8 male). Mean age 74.5±7.8 years (45.5-88). The mean 25(OH)D<sub>3</sub> levels were 16.9±5.5 ng/ml and the PTH 101.6±44.5 pg/ml. After the first month of treatment with 64000 IU of calcidiol 61/61 (100%) of the patients normalized the 25(OH)D<sub>3</sub> levels (mean 88.9±26.1 ng/ml), although only 32/61 (52.5%) patients compensated the secondary hyperparathyroidism, with a mean of PTH 67.1±33 pg/ml (44.9±11.5 in the group who normalized the PTH levels vs 92.5±31.3 in the group who didn't). After 3 months of treatment with vitamin D we observed a decrease in the 25(OH)D<sub>3</sub> levels (61.8±24.4 ng/ml) and increase in the PTH levels (71.7±30.2 pg/ml), with 58% of patients with secondary hyperparathyroidism. Of the 32 patients that normalized PTH levels after the first month of treatment 39% had a high PTH after 3 months of treatment with vitamin D. We didn't find any difference between calcidiol or cholecalciferol respecting their efficacy to maintain PTH levels in the normal range after 3 months of treatment (40% and 38.5% of the patients treated with calcidiol and cholecalciferol failed to maintain normal PTH levels). **Conclusions:** The induction treatment with calcidiol 64000 IU/month is useful to normalize vitamin D levels in patients with hypovitaminosis D, but it seems insufficient to compensate the secondary hyperparathyroidism that have some of these patients. The long-treatment with vitamin D seems to be also unsuccessful to maintain PTH levels in the normal range in this population. <!--presmeth-->

**Disclosures:** E. Casado, None.

## SU432

**Red Flags Are Missed in the Prevention of Hip Fractures: Baseline Results of the Zurich Hip Fracture Trial.** H. A. Bischoff-Ferrari<sup>1</sup>, H. B. Staehelin<sup>\*2</sup>, B. Dawson-Hughes<sup>3</sup>, A. Platz<sup>\*4</sup>, U. Can<sup>\*4</sup>, S. Looser<sup>\*1</sup>, B. Bretschner<sup>\*5</sup>, R. Theiler<sup>\*5</sup>. <sup>1</sup>Rheumatology, University of Zurich, Zurich, Switzerland, <sup>2</sup>Geriatrics, University of Basel, Basel, Switzerland, <sup>3</sup>Tufts University, Boston, MA, USA, <sup>4</sup>Traumatology, Triemli StadtSpital, Zurich, Switzerland, <sup>5</sup>Rheumatology, Triemli StadtSpital, Zurich, Switzerland.

**Background:** From 1-2005 to 12-2007, we recruited 173 patients age 65 and older with acute hip fracture and a Folstein mini mental score of at least 15 into an ongoing double-blind RCT with vitamin D. 69% of hip fracture patients were admitted from home and 31% from institutions, 79% were women. Mean age was 86 year (± 6.9).

**Aim:** We present results from 3 self-reported "red flag" questions answered 3 to 7 days after the acute hip fracture that should have triggered vitamin D supplementation prior to the hip fracture event.

**Results:** Upon admission to acute care, only 12% of hip fracture patients enrolled had any dose of vitamin D including multivitamin formulations. Mean 25(OH)D was 31.3 nmol/l (± 19) in hip fracture patients admitted from home and 33.3 nmol/l (± 23) in those from institutionalized care. 51% of hip fracture patients admitted from home and 54% admitted from institutions had severe vitamin D deficiency (25(OH)D of less than 30 nmol/l). 48% of hip fracture patients admitted from home and 51% of those admitted from institutions reported that they had a previous fracture outside the hip prior to the acute hip fracture event. Of those admitted from home, 29% reported that they had fallen rarely and 20% that they had fallen repeatedly in the last 6 month prior to the acute hip fracture event. Similarly, of those admitted from institutions, 27% reported that they had fallen rarely and 34% that they had fallen repeatedly in the last 6 month prior to the acute hip fracture event. Furthermore, 33% of those admitted from home and 24% from institutions reported that

they felt weakness in their legs 6 months prior to their acute hip fracture event.

**Conclusion:** Vitamin D supplementation for the prevention of falls and fractures is recommended in several guidelines, however, according to our data collected between 2005 and 2007, guideline practice is still low. The positive report of red flags including previous fractures, previous falls, and muscle weakness is common in patients with acute hip fracture and may help increase guideline practice in older individuals.

**Disclosures:** H.A. Bischoff-Ferrari, None.

This study received funding from: Swiss National Foundations.

## SU433

### Wintertime Vitamin D Supplementation Inhibits Seasonal Variation of Calcitropic Hormones and Maintains Bone Turnover In Healthy Men. H. T. Viljakainen<sup>\*1</sup>, M. Väisänen<sup>\*1</sup>, V. Kemi<sup>\*1</sup>, T. Rikkinen<sup>2</sup>, H. Kröger<sup>3</sup>, E. K. A. Laitinen<sup>\*4</sup>, C. Lamberg-Allardt<sup>1</sup>.

<sup>1</sup>Department of Applied Chemistry and Microbiology, division Nutrition, University of Helsinki, Helsinki, Finland, <sup>2</sup>Bone and Cartilage Research Unit, University of Kuopio, Kuopio, Finland, <sup>3</sup>Department of Surgery, Kuopio University Hospital, Kuopio, Finland, <sup>4</sup>Department of Obstetrics and Gynaecology, Helsinki University Central Hospital, Helsinki, Finland.

Vitamin D is suggested to have a role in the coupling of bone resorption and formation. The association between bone mineral density (BMD) and vitamin D status is evident among men. Compared with women, men are believed to have more stable bone turnover, and thus, are considered less susceptible to the seasonal variation of calcitropic hormones. We examined whether seasonal variation exists in calcitropic hormones, bone remodelling markers and BMD in healthy men. Furthermore, we determined which vitamin D intake is required to prevent this variation.

Subjects (N=54) comprised healthy Caucasian men aged 21-49 years, with a mean (SD) habitual dietary intake of vitamin D of 6.6 (5.1) µg/d. This was a 6-month double-blinded vitamin D intervention study, in which subjects were allocated to three groups of 20 µg (800 IU), 10 µg (400 IU), or placebo. Randomization was performed (by age, weight, initial S-25-OHD status and dietary intake of vitamin D) into three groups. The trial lasted from November to April, altogether 26 weeks. Fasting blood samplings were collected six times for analyses of serum 25-OHD, PTH, BALP and TRACP. Radial volumetric BMD was measured at the beginning and end of the study with pQCT.

Wintertime variation was noted in S-25-OHD, PTH and TRACP (p<0.001, p=0.012 and p<0.05, respectively), but not in BALP or vBMD in the placebo group. Until the 20-week time point, vitamin D supplementation increased the S-25-OHD concentration dose-dependently, the mean dose-response being 1.55 (1.24) nmol/l/µg. Supplementation inhibited the winter elevation of PTH (p=0.035), decreased the BALP concentration (p=0.044), but did not affect TRACP.

Healthy men are exposed to wintertime decrease in vitamin D status that impacts PTH concentration. Ratio of TRACP/BALP and their correlation illustrate the coupling of bone remodelling in a robust way. The coupling was maintained in vitamin D supplemented groups, but not in the placebo group. Although the results concerning radial vBMD hardly showed a tendency towards benefit, our study supports the prevailing data of the benefits of vitamin D. A total intake of 17 µg of vitamin D is required to prevent season-related changes both in calcitropic hormones and in bone turnover among healthy men.

**Disclosures:** H.T. Viljakainen, None.

This study received funding from: The Juho Vainio Foundation.

## SU434

### The Efficacy and Safety of Short Term Treatment with Different Doses of Cholecalciferol on 25-Hydroxy Vitamin D Levels in Postmenopausal Females with Osteoporosis. H. C. Hoeck<sup>\*1</sup>, B. Li<sup>\*2</sup>, P. Qvist<sup>\*2</sup>. <sup>1</sup>CCBR, Aalborg, Denmark, <sup>2</sup>Nordic Bioscience, Herlev, Denmark.

The study was performed on the baseline data from a cohort of 433 ambulatory postmenopausal females (mean age 68.5 y) screened between March 2007 and March 2008 for participation in an osteoporosis study. Main inclusion criteria was a DEXA-scanning demonstrating osteoporosis as defined by a T-score below - 2.5 SD or between - 1.0 and - 2.5 SD and at least one osteoporotic fracture. An amendment included a new FDA guideline to change the lower acceptable limit of 25-hydroxy vitamin D (25(OH)D) for inclusion to 60 nmol/L. Subjects with a 25(OH)D < 60 nmol/L were allowed to be substituted with vitamin D and the biochemistry retested. This study reports on the efficacy and safety of oral treatment with 25 µg (N=22; mean age: 70.6 y), 50 µg (N=19; mean age: 66.7 y), 75 µg (N=19; mean age: 68.7 y), 100 µg (N=41; mean age: 70.0 y) or 200 µg (N=30; mean age: 66.9 y) of cholecalciferol daily for 10 days. In the group of subjects treated with 25 µg of cholecalciferol daily 25(OH)D increased significantly from 32.4±2.7 nmol/L (mean±SEM) to 50.8±2.9 nmol/L. In the groups treated with 50 µg, 75 µg, 100 µg and 200 µg of vitamin D3 daily 25(OH)D concentrations increased significantly from 46.7±2.8 nmol/L to 65.8±2.6 nmol/L, from 41.6±2.7 nmol/L to 67.4±2.9 nmol/L, from 46.7±1.4 nmol/L to 64.4±2.2 nmol/L and from 42.1 ± 2.0 nmol/L to 71.2 ± 2.8 nmol/L respectively (P < 0.001 for all groups). Seventy-one, 37, 37, 40 and 27 %, respectively, had a 25(OH)D level below 60 nmol/L in response to the five different doses of cholecalciferol. In the 25 µg, 100 µg and 200 µg group s-calcium increased within the reference range (P<0.006) whereas PTH only decreased in the 25 µg group (P=0.004). Apart from a significant increase in alkaline phosphatase (AP) in the 50 µg group (P=0.003) and in creatinine in the 200 µg group (P=0.023) no changes in AP or creatinine was observed in any of the other groups (P>0.1). No adverse events were observed during treatment with any dose of vitamin D. In conclusion, 10 days of treatment with 25 µg, 50 µg, 75 µg, 100 µg or 200 µg of vitamin D3 was safe and increased 25(OH)D levels significantly although

responses were variable. In order to increase in 25(OH)D levels above 60 nmol/L in all subjects our data indicate that the treatment period should be extended beyond 10 days rather than to increase the daily dose of vitamin D3 further. Future strategies for correction of vitamin D insufficiency on a short term basis should take this information in to consideration.

**Disclosures:** H.C. Hoeck, Hans Chr. Hoeck is employed by CCBR a private company engaged in contract research 3, 5.

## SU435

### Male and Female Cynomolgus Monkey Models of Osteoporosis: Comparative In Vivo Data. N. Doyle<sup>\*1</sup>, S. Y. Smith<sup>1</sup>, K. A. Veverka<sup>2</sup>, <sup>1</sup>Charles River Laboratories, Senneville, QC, Canada, <sup>2</sup>GTx, Inc, Memphis, TN, USA.

Osteoporosis in women is often a consequence of menopause while in men it can be associated with hypogonadism or a consequence of androgen deprivation therapy for patients with prostate cancer. Ovariectomized (OVX) and orchidectomized (ORX) aged non-human primates are proposed surgically-induced models to evaluate drugs for the treatment or prevention of osteoporosis. Data from Sham and gonadectomized (OVX and ORX) animals were derived using the same instruments and assays and compared. The effects of OVX/ORX were monitored *in vivo* for 16 months using DXA, pQCT and biochemical markers of bone turnover. Cynomolgus monkeys aged ≥ 9 years old from both sexes (13 to 15 females/group [previously reported in Bone 2003, 32:45-55] and 20 males/group) were obtained from established colonies in the USA or Mauritius and assigned to two groups by whole body bone mineral content for each gender. The effects of OVX and ORX were evident for all *in vivo* parameters measured as early as 4 months following gonadectomy when compared to Sham controls and baseline values. Relative to controls, decreases were obtained in lumbar spine DXA BMD of 10 and 9%, and 11% and 16% at the femoral neck, for females and males, respectively. Decreases in trabecular BMD measured by pQCT at the proximal tibia were also similar (-17 to 20%) for both sexes. Over the study period, endosteal circumference was increased for both OVX and ORX animals compared to Sham whereas the changes in periosteal circumference (and total slice area) were minimal. Increased endosteal resorption for gonadectomized animals resulted in decreases in cortical thickness of the tibial diaphysis of 5 to 6%. Biochemical markers were elevated with maximal levels noted after 4 to 8 months for males (up to 6 X higher) and 8 to 12 months for females (up to 3 X higher). Body weights for females were unaffected by OVX, however for males body weight decreased by 20% in the first 4 months following ORX and then stabilized. This was associated with a decrease in muscle area measured by pQCT of -18% compared to baseline. In conclusion, both OVX and ORX were associated with bone activation as evidenced by increases in biochemical markers of bone turnover and loss of bone mass measured by densitometry techniques. Tibial cortical thinning attributed to endosteal expansion was observed in both sexes. In males, bone loss may be secondary to the loss of muscle mass following ORX. These data support the use of both genders as models of osteoporosis in the preclinical evaluation of potential bone anabolic or anti-catabolic agents.

**Disclosures:** N. Doyle, Charles River Laboratories 3.

## SU436

### Osteoporosis in the Aging Males after Hip Fracture. W. Misiorowski<sup>\*</sup>, M. Rabijewski<sup>\*</sup>, W. Zgliczynski<sup>\*</sup>. Endocrinology Dept., Medical Centre for Postgraduate Education, Warsaw, Poland.

While most studies of osteoporosis have focused on postmenopausal women, older men are also at increased risk of fragility fractures. However, yet even with a comprehensive evaluation, approximately 40% of men with osteoporosis have no identifiable risk factor or cause.

**Objective:** The aim of the study was to determine risk factors or cause of osteoporosis in males after hip fracture.

**Material and methods:** We studied 97 men, aged 69 to 89 years old, recently after low-trauma hip fracture. Bone mineral density (BMD) of nonfractured hip was measured using DXA. The serum calcium, PTH-intact, 25-OHD3, LH, FSH, testosterone and estradiol levels were measured.

**Results:** 53 men (59.5%) were current smokers, next twelve had smoked previously. 9% reported no alcohol intake, while 15 men had a history of alcohol abuse. Previous nontraumatic vertebral fracture was reported by 15 men. Nearly all of the men were categorized as osteoporotic at the nonfractured hip defined as BMD Tscore -2.5 or less. 51.7% of the subjects had hypovitaminosis D (25-OHD < 20 ng/ml). Testosterone deficiency (< 3.5 ng/ml) was found in 42 hip fracture men (47.2%). In next thirteen serum testosterone was in low normal limits (3.5 to 4.0 ng/ml), however T/LH index was below 1.0.

**Conclusions:** Gonadal deficiency appears to be an important and heretofore understudied risk factor for hip fracture in men. Other important risk factors are smoking and hypovitaminosis D. Prevention of hip fractures in men may involve early recognition and treatment of testosterone deficiency.

**Disclosures:** W. Misiorowski, None.

This study received funding from: CMKP 501-2-08-57/05 grant.

## SU437

**Acute Change in Serum Ionized Calcium Directly Affects Bone Formation Independent of PTH Action During Hemodialysis.** S. Yano<sup>1</sup>, T. Yamaguchi<sup>1</sup>, K. Suzuki<sup>2</sup>, M. Sumi<sup>3</sup>, Y. Himeno<sup>3</sup>, T. Sugimoto<sup>1</sup>. <sup>1</sup>Department of Internal Medicine 1, Shimane University Faculty of Medicine, Izumo, Japan, <sup>2</sup>Otsuka Clinic, Izumo, Japan, <sup>3</sup>Himeno Clinic, Izumo, Japan.

Serum ionized calcium (iCa) and parathyroid hormone (PTH) levels are known to be dynamically changed during hemodialysis (HD) session. However, little is known about the effects of their acute changes on bone metabolism during HD. In this study, we addressed effects of changes in serum Ca and PTH on bone formation during HD session. In 100 patients undergoing maintenance HD therapy, blood samples were obtained before and after 4hr HD session to measure serum iCa, whole (w) and total (t) PTH, and procollagen type-1 amino-terminal propeptide (PINP, a bone formation marker). Ca concentration in dialysate was 3.0 mEq/l in 50 patients and 2.5 mEq/l in the rest patients. wPTH and tPTH levels were significantly increased after HD session (183 to 211 pg/ml and 289 to 314 pg/ml, respectively,  $p < 0.0001$ ) with concomitant elevation in serum iCa level (2.57 to 2.76 mEq/l). On the other hand, serum PINP levels were significantly decreased during HD session (416 to 355 ng/ml). Simple regression analysis showed that change in serum iCa ( $\Delta$ iCa) was negatively and significantly correlated with change in wPTH ( $\Delta$ wPTH) ( $r = -0.566$ ,  $p < 0.0001$ ) and with change in tPTH ( $\Delta$ tPTH) ( $r = -0.550$ ,  $p < 0.0001$ ) during HD session, and that % change in PINP was positively and significantly correlated with  $\Delta$ iCa ( $r = 0.298$ ,  $p < 0.0001$ ), and negatively and significantly with  $\Delta$ wPTH ( $r = -0.337$ ,  $p = 0.0006$ ). When multiple regression analysis was performed with  $\Delta$ iCa and  $\Delta$ wPTH as independent variables and % change in PINP as a dependent variable,  $\Delta$ iCa, but not  $\Delta$ wPTH, was selected as an index affecting % change in PINP ( $p < 0.0001$ ). The present study suggests that during HD session, although acute change in serum iCa negatively correlates with that in PTH, increase in iCa itself might directly augment bone formation independent of PTH action.

**Disclosures:** S. Yano, None.

## SU438

**Hemodialysis Patients Rapidly Lose Their Bone Minerals After 60 Years of Age.** M. Ohsawa<sup>1</sup>, K. Itai<sup>1</sup>, K. Tanno<sup>1</sup>, K. Kato<sup>2</sup>, Y. Fujishima<sup>2</sup>, R. Konda<sup>2</sup>, T. Fujioka<sup>2</sup>, T. Onoda<sup>1</sup>, K. Sakata<sup>1</sup>, F. Yamauchi<sup>3</sup>, M. Fujishima<sup>4</sup>. <sup>1</sup>Hygiene and Preventive Medicine, Iwate Medical University, Morioka, Japan, <sup>2</sup>Department of Urology, Iwate Medical University, Morioka, Japan, <sup>3</sup>Division of Internal Medicine, San-ai Hospital, Morioka, Japan, <sup>4</sup>Division of Urology, San-ai Hospital, Morioka, Japan.

End-stage renal disease is commonly accompanied by abnormal mineral metabolism and abnormal bone metabolism. The purpose of this study is to determine age-specific mean levels of bone mineral density (BMD) and annual changes in BMD among adult Japanese hemodialysis patients. A total of 84 hemodialysis patients (66 men and 18 women) were enrolled. BMD was re-measured in each patient at least six months after initial examination. Densitometry of radial bone was evaluated using dual-energy X-ray absorptiometry (DXA) with DCS-600EX (Aloka Japan). Patients were divided into 4 age-specific groups (20-49, 50-59, 60-69, 70 years or older). Annual percent change in BMD was estimated in each patient. Mean levels of the latest BMD, the latest T score (expressed as percent of YAM), and annual percent changes in BMD were determined in each age group. Mean levels of BMD, T score, and % changes in BMD in each group were shown in the Table. Mean levels of BMD, and T score were low among hemodialysis patients aged 60 years or older. Annual changes of their BMD were -2.1% in 20-50's and -2.8% in 60's and -5.9% in 70's or older. These data suggest that hemodialysis patients rapidly lose their bone minerals after 60 years of age.

Mean levels of BMD, percent of YAM, and annual change of BMD				
Age-group	(subjects)	BMD (g/cm <sup>2</sup> )	% of YAM	Change of BMD (%/year)
20-49	(n=11)	0.657 $\pm$ 0.127	87.5 $\pm$ 14.8	-2.0
50-59	(n=18)	0.719 $\pm$ 0.069	94.0 $\pm$ 8.6	-2.1
60-69	(n=27)	0.572 $\pm$ 0.134	76.7 $\pm$ 14.4	-2.8
$\geq 70$	(n=28)	0.551 $\pm$ 0.164	73.6 $\pm$ 18.8	-5.9

**Disclosures:** M. Ohsawa, None.

## SU439

**Kidney Dysfunction Disturbs Collagen Maturation in Adynamic Bone Disease as Assessed by Confocal Laser Raman Spectroscopy.** Y. Iwasaki<sup>1</sup>, H. Yamato<sup>2</sup>, M. Fukagawa<sup>3</sup>. <sup>1</sup>Health Sciences, Oita University of Nursing and Health Sciences, Oita, Japan, <sup>2</sup>Development, Kureha Special Laboratory Co, Ltd., Fikushima, Japan, <sup>3</sup>Nephrology & Dialysis center, Kobe University, Kobe, Japan.

Adynamic bone disease (ABD), which is a major type of renal osteodystrophy, is highly prevalent in chronic kidney disease. ABD has lowered bone formation and is associated with increased fracture rates, and brittle calcium control. However, it still remains unknown why fracture rates increases in ABD. On the other hand, we have already established an ABD model in rats. In addition, we reported that the low turnover bone was induced by uremic toxin which accumulated in blood associated with reducing renal function, because of the toxic effect of uremic toxin to osteoblast. In the present study,

evaluating the bone quality of ABD, we evaluated the mineral-matrix ratio and a couple of matrix-related parameters by confocal laser raman spectroscopy. As for the ABD model, after male SD rats underwent thyroparathyroidectomy (TPTx), they underwent 5/6 nephrectomy (Nx) or sham operations. These rats were continuously infused with rat PTH and injected with L-thyroxine subcutaneously to maintain physiological levels. Therefore TPTx-Nx rats can simulate ABD, because of their low turnover bone associated with the suppression of renal function. Groups were ABD (TPTx-Nx) and control (TPTx-sham). Recently, it has become easier to obtain spectroscopic properties from bone with a laser raman spectroscopy system (Nicolet Almega XR, Thermo Fisher Scientific Co.). We can get much information about the matrix in bone and we can also evaluate local change of bone contents by this system. Concerning As the results, mineral-matrix [PO4/Amid I] ratio, hydroxyl proline-proline [Hypro/pro] ratio, and a parameter of collagen crosslink in ABD revealed lower values compared with control. Particularly, Hypro/pro and collagen crosslink in ABD were 12% and 21% to control respectively. From the histomorphometry, the osteoblast surface and mineral apposition rate were decreased in ABD. The bone formation rate in ABD reduced to 8% of control. The bone mineral density of tibial metaphysis and diaphysis were not significantly different between the two groups. These results suggest that kidney dysfunction inhibits collagen maturation and suppressed bone turnover. Those matrix changes affect bone fragility and could lead to increase fracture risk without bone loss.

**Disclosures:** Y. Iwasaki, None.

## SU440

**Serum Ionic Fluoride Levels among Hemodialysis Patients are Positively Associated with Levels of Serum Phosphate and Intact PTH.** K. Tanno<sup>1</sup>, M. Ohsawa<sup>1</sup>, K. Itai<sup>1</sup>, T. Onoda<sup>1</sup>, K. Sakata<sup>1</sup>, K. Kato<sup>2</sup>, Y. Fujishima<sup>2</sup>, R. Konda<sup>2</sup>, T. Fujioka<sup>2</sup>, F. Yamauchi<sup>3</sup>, M. Fujishima<sup>3</sup>, A. Okayama<sup>4</sup>. <sup>1</sup>Department of Hygiene and Preventive Medicine, Iwate Medical University, Morioka, Japan, <sup>2</sup>Department of Urology, Iwate Medical University, Morioka, Japan, <sup>3</sup>San-ai Hospital, Morioka, Japan, <sup>4</sup>The First Institute of Health Service, Japan Anti-Tuberculosis Association, Tokyo, Japan.

We previously reported that serum ionic fluoride (SIF) levels were extremely higher in adult hemodialysis patients than in normal controls. The aim of this study is to clarify whether excess levels of serum fluoride in hemodialysis patients are associated with abnormal bone and mineral metabolism. A total of 83 hemodialysis patients (65 men and 18 women) were enrolled. Bone mineral density (BMD) in the radius was evaluated using dual-energy X-ray absorptiometry (DXA) with DCS-600EX (Aloka Japan). Blood sampling was performed at the beginning of the dialysis session. Serum calcium (Ca) and phosphate (P) levels were determined by enzymatic assays. Levels of intact parathyroid hormone (iPTH) were determined by Electrostatic Controlled Linear Inchworm Actuator (ECLIA). SIF levels were determined by the flow injection method with an ion selective electrode. Patients were divided into tertile groups according to SIF levels. Sex- and age-adjusted mean levels of Ca (mg/dL), logarithm transformed P (geometric mean, mg/dL), logarithm transformed iPTH (geometric mean, pg/mL) and BMD (g/cm<sup>2</sup>) were calculated in each group. Mean age of patients was 65.8 years. Crude mean SIF level was 60.9  $\mu$ g/L. SIF levels were positively related to serum P levels and iPTH levels after sex and age adjustment. However, SIF levels were not related to serum Ca levels and BMD. (See table) These findings suggest that elevated SIF levels reflect activated bone mineral metabolism due to hyperphosphatemia and hyperparathyroidism.

	Sex- and age-adjusted mean level (95% CI) of each variable by the tertile groups according to SIF			trend P
	T1	T2	T3	
Range of SIF, $\mu$ g/L	30.3-47.7	48.0-58.2	59.1-487.8	
Subjects, n (% male subjects)	27 (81.5)	28 (78.6)	28 (75.0)	
Ca, mg/dL	8.7 (8.5, 9.0)	8.8 (8.6, 9.1)	8.7 (8.5, 9.0)	0.947
P (geometric mean), mg/dL	4.7 (4.3, 5.1)	5.4 (4.9, 5.9)	5.8 (5.3, 6.4)	0.001
iPTH (geometric mean), pg/mL	131.4 (99.3, 173.9)	170.5 (129.4, 224.6)	208.3 (157.3, 275.8)	0.019
BMD (g/m <sup>2</sup> )	0.659 (0.619, 0.699)	0.657 (0.617, 0.697)	0.650 (0.610, 0.690)	0.749

**Disclosures:** K. Tanno, None.

## SU441

**Kidney Disease is Associated with Abnormal Cortical Geometry Independent of Age and Gender.** T. L. Nickolas<sup>1</sup>, E. A. Stein<sup>1</sup>, V. Thomas<sup>1</sup>, H. F. Eisenberg<sup>1</sup>, D. J. McMahon<sup>1</sup>, M. B. Leonard<sup>2</sup>, E. Shane<sup>1</sup>. <sup>1</sup>Medicine, Columbia University, New York, NY, USA, <sup>2</sup>Pediatrics, Children's Hospital of Philadelphia, Philadelphia, PA, USA.

Chronic kidney disease (CKD) and osteoporosis (OP) are highly co-prevalent in the elderly. Although both CKD and OP result in increased fracture risk, the mechanisms of bone fragility may differ. Both CKD and aging are associated with secondary hyperparathyroidism, which has catabolic effects on cortical (Ct) bone. Estrogen deficiency, which affects both postmenopausal women and, to a lesser extent, older men, may have a greater impact on trabecular (Tb) bone. High resolution quantitative CT (HRpQCT) (XtremeCT, Scanco Medical AG, resolution 82  $\mu$ m) provides discrete measures of Ct and Tb microarchitecture in vivo. To assess the effects of CKD on Ct and Tb bone, we are conducting a cross-sectional study in older adults across a spectrum of kidney function. We hypothesized that Ct bone abnormalities

would predominate in patients with more advanced CKD.

To date, we have evaluated 76 subjects (33 women), ages 50-88. The MDRD formula was used to estimate GFR (eGFR), based upon serum creatinine, age, gender and race. 19 subjects were on dialysis and 27 had an eGFR > 60 mL/min. Among the rest, the median eGFR was 31 mL/min (range, 15-58). Univariate analyses demonstrated that abnormal Tb microstructure (low density, bone volume fraction, Tb number, thickness and increased separation) were significantly associated with female gender. Decreased Ct thickness and density were significantly associated with lower eGFR and older age. Multiple linear regression was used to determine the relationship between HRpQCT microarchitectural parameters and eGFR, adjusted for age and gender. Both Ct density and thickness were correlated with eGFR and age. Tb microarchitecture parameters remained associated with female gender (Table 1).

HR-pQCT Measurements	MDRD $\beta$ -coefficient	se	p-value	Age $\beta$ -coefficient	Se	p-value	Gender (female) $\beta$ -coefficient	se	p-value
Cortical Density (mg HA/cm <sup>3</sup> )	0.0013	0.0004	0.003	-0.0046	0.001	0.001	-0.0232	0.03	0.3
Cortical Thickness ( $\mu$ m)	0.0033	0.001	0.01	-0.0112	0.004	0.01	-0.2149	0.08	0.01
Trabecular Density (mg HA/cm <sup>3</sup> )	-0.0004	0.002	0.8	-0.0055	0.005	0.2	-0.3035	0.09	0.002
Trabecular Volume (%)	-0.0004	0.002	0.8	-0.0056	0.005	0.2	-0.3026	0.09	0.002
Trabecular Number (n/mm)	-0.0005	0.001	0.6	-0.0021	0.003	0.5	-0.1690	0.07	0.01
Trabecular Thickness ( $\mu$ m)	0.0001	0.001	0.9	-0.0033	0.003	0.2	-0.1320	0.05	0.02
Trabecular Separation ( $\mu$ m)	0.0006	0.001	0.6	0.0029	0.004	0.5	0.2080	0.07	0.01
Trabecular Separation Standard Deviation ( $\mu$ m)	0.0007	0.002	0.7	0.0054	0.007	0.4	0.3581	0.1	0.01

These data confirm that low kidney function is associated with lower Ct thickness and density, independent of age and gender. The data also confirm that female gender is associated with alterations in Tb microarchitecture and lower Ct density, independent of kidney function and age. Alterations in both Ct and Tb structure likely contribute to the increased risk of fragility fracture observed in patients with CKD and end stage kidney disease. Further studies are required to elucidate the pathogenesis of these microarchitectural abnormalities and their relationship to bone strength.

**Disclosures:** T.L. Nickolas, None.

## SU442

**Albuminuria, 25-Hydroxyvitamin D, 1,25-Dihydroxyvitamin D, and intact Parathyroid Hormone in Older Adults: The Rancho Bernardo Study.** S. K. Jassal<sup>\*1</sup>, M. Chonchol<sup>\*2</sup>, D. von Muhlen<sup>\*3</sup>, E. Barrett-Connor<sup>3</sup>. <sup>1</sup>Medicine, UCSD & VASDHS, San Diego, CA, USA, <sup>2</sup>Medicine, UCHSC, Denver, CO, USA, <sup>3</sup>Family & Preventive Medicine, UCSD, La Jolla, CA, USA.

**Purpose:** Mild declines in estimated glomerular filtration rate (eGFR < 60mL/min/1.73m<sup>2</sup>) are associated with decreased serum levels of 25-hydroxyvitamin D (25(OH)D) and 1,25-dihydroxyvitamin D (1,25(OH)<sub>2</sub>D) and increased intact parathyroid hormone (iPTH); treatment with 1,25(OH)<sub>2</sub>D reduces albuminuria. However, the association between albuminuria, an earlier marker of kidney dysfunction, and these three mineral metabolites has not been investigated.

**Methods:** A cross-sectional study of community dwelling, older adults (411 men and 662 women) from Southern California evaluated in 1997-1999. Serum levels of 25(OH)D, 1,25(OH)<sub>2</sub>D and iPTH and urine albumin and creatinine were measured on morning specimens.

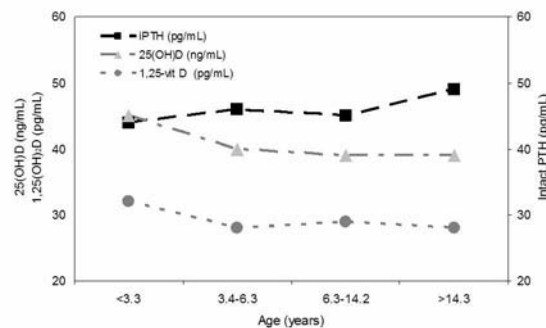
**Results:** Mean age was 75 years; mean eGFR 74mL/min/m<sup>2</sup>, and median urine albumin/creatinine ratio (ACR) 6mg/g. Median serum levels of 25(OH)D, 1,25(OH)<sub>2</sub>D, and iPTH were 40ng/mL, 29pg/mL, and 46pg/mL, respectively and median serum levels by ACR quartile are shown in the Figure. In unadjusted analyses, there was a significant inverse association between increasing quartile of urine ACR and 25(OH)D (p for trend=0.001) and direct association with iPTH (p=0.004), but not 1,25(OH)<sub>2</sub>D (p=0.295). After adjusting for age alone, or multiple covariates including age, sex, body mass index, eGFR, systolic blood pressure, and fasting plasma glucose (Table), only iPTH continued to be significantly associated with urine ACR quartiles (age only, p = 0.04; all covariates p= 0.028). In a subset of 893 participants without diabetes, there was no significant association between any marker of mineral metabolism and ACR quartile.

**Conclusions:** ACR was independently associated with iPTH but not 25(OH)D or 1,25(OH)<sub>2</sub>D, in community dwelling older participants in Southern California. This association was not found in those without diabetes.

Adjusted mean levels of 25(OH)D, 1,25(OH) <sub>2</sub> D and iPTH by quartile of ACR					
Adjusted* mean by ACR quartile (mg/g)	1 ≤3.3	2 3.4-6.3	3 6.3-14.2	4 ≥14.3	p for trend
25(OH)D (ng/mL)	41 (39-42)	43 (41-44)	40 (38-41)	40 (38-41)	0.115
1,25(OH) <sub>2</sub> (pg/mL)	30 (28-33)	31 (29-33)	32 (30-35)	31 (29-33)	0.776
iPTH (pg/mL)	50 (47-53)	50 (47-54)	50 (47-54)	55 (52-58)	0.028

\*Adjusted for age, sex, body mass index, eGFR, systolic blood pressure, and fasting plasma glucose

Median Serum 25(OH)D, 1,25(OH)<sub>2</sub>D, and Intact PTH by ACR Quartile



**Disclosures:** S.K. Jassal, The Alliance for Better Bone Health: Procter & Gamble Pharmaceuticals and Sanofi-Aventis Pharmaceuticals 5.

This study received funding from: The Alliance for Better Bone Health: Procter & Gamble Pharmaceuticals and Sanofi-Aventis Pharmaceuticals.

## SU443

**Postprandial Hyperphosphatemia Is a Novel Risk Factor for Cardiovascular Disease by Involving Endothelial Dysfunction.** E. Shuto<sup>\*1</sup>, Y. Taketani<sup>1</sup>, R. Tanaka<sup>\*1</sup>, A. Tanimura<sup>\*1</sup>, T. Uebanso<sup>\*1</sup>, M. Isshiki<sup>\*2</sup>, N. Harada<sup>\*3</sup>, H. Yamamoto<sup>1</sup>, Y. Nakaya<sup>\*3</sup>, E. Takeda<sup>1</sup>. <sup>1</sup>Department of Clinical Nutrition, University of Tokushima Graduate School, Tokushima, Japan, <sup>2</sup>Department of Nephrology and Endocrinology, University of Tokyo, Tokyo, Japan, <sup>3</sup>Department of Nutrition and Metabolism, University of Tokushima Graduate School, Tokushima, Japan.

Hyperphosphatemia is closely associated with progress of cardiovascular disease and mortality in end-stage renal disease patients. It has been well known that hyperphosphatemia causes vascular calcification. Furthermore, recently overintake of phosphorus (P) has been speculated a risk of cardiovascular disease (CVD) in healthy persons as well as chronic kidney disease patients. We have hypothesized that hyperphosphatemia may also contribute to the progress of atherosclerosis on early-stage chronic kidney disease by involving endothelial dysfunction. Previously, we reported that high P-loading increased production of reactive oxidative species and decrease nitric oxide (NO) availability in endothelial cells. In this study, we investigated the effect of dietary P-loading on endothelial function in healthy male volunteers. Eleven healthy male volunteers were alternately served either P400 meal (400mg P/meal) or P1200 meal (1200mg P/meal), and measured biochemical markers in the blood and flow-mediated dilation (%FMD) of brachial artery before and at 2h after the meal ingestion (double-blinded crossover study). While serum P level significantly increased at 2h after P1200 meal ingestion, %FMD significantly decreased (P<0.001), but not after P400 meal ingestion. Negative correlation was detected between %FMD and serum P. All other biomarkers were within normal range in the preprandial and postprandial status, and above changes were dependent on serum P level. Additionally, we investigated the effect of high P-loading on the endothelium-dependent vasodilation by using rat aortic ring. Correspondingly high P-loading significantly decreased endothelium-dependent vasodilation in the rat aortic ring. These results suggest that dietary P-loading can cause endothelial dysfunction in human as well as animal model. This may offer an additional explanation of the relationship between higher serum P level and CVD risk or mortality as epidemiologically observed. This study was approved by Ethics Committee of our university hospital and by Animal Experimentation Committee of our university.

**Disclosures:** E. Shuto, None.

## SU444

**A Therapy with Alfacalcidol Leads to a Significant Increase in Muscle Power and Balance.** L. C. Dukas<sup>\*1</sup>, E. Schacht<sup>2</sup>, M. Runge<sup>\*3</sup>. <sup>1</sup>Acute Geriatric University Clinic, Kantonsspital Basel, Basel, Switzerland, <sup>2</sup>ZORG Zurich Osteoporosis Research Group, Zurich, Switzerland, <sup>3</sup>Aerpah Klinik, Esslingen, Germany.

In an open prospective study we investigated the effect of Alfacalcidol (Bondiol®) on muscle power and balance in German patients with a Creatinine Clearance of <65ml/min., diagnosed to be at an increased risk of falls. Therefore patients underwent 3 monthly, different muscle power and balance tests for 6 months. Here we present the results for the Timed-Up and Go test (TUG).

The performance in the TUG was assessed as follows: the ability to successfully perform the TUG (<12sec.) (A), non successful performance in the TUG (>12sec.) (B), and the inability to perform the TUG (C), a non successful performance of the TUG being associated with an increased risk of falls. 261 patients (17.6% men and 82.4% women / mean age: 75.9 years / mean BMI: 26.3kg/m<sup>2</sup>) participated in this study.

Controlled for age, gender and BMI, a treatment with Alfacalcidol was associated with a significantly increased performance in the TUG (p<.0001): after 6 months the number of patients who successfully performed the TUG was significantly increased from 29.9% of the population to 51.7% (from N=78 to 135), a significant 73% increase. Also in group C we observed a significant improvement, corresponding to 12.8% decrease in the number of patients who at baseline were not able at all to perform the TUG. The mean time for the TUG performance was significantly diminished by 2.0sec. from 16.1sec at baseline to 14.1sec after 6 months.

We conclude therefore that a treatment with Alfacalcidol increases muscle power and balance as measured with the TUG. The number of patients who at baseline did not successfully perform the TUG and were therefore at an increased risk of falls, was diminished considerably under the treatment with Alfacalcidol.

For the practitioner the TUG is a validated test to monitor the risk of falls under the treatment with Alfacalcidol and therefore to document the therapeutic success of the treatment with Alfacalcidol.

Significant Improvement in TUG Performance under a 6 month therapy with Alfacalcidol			
TUG performance	at baseline	after 3 month	after 6 month
unable (N)	47	46	41
>12sec./not successful (N)	136	102	85
<12sec./successful (N)	78	113	135
p<.0001			

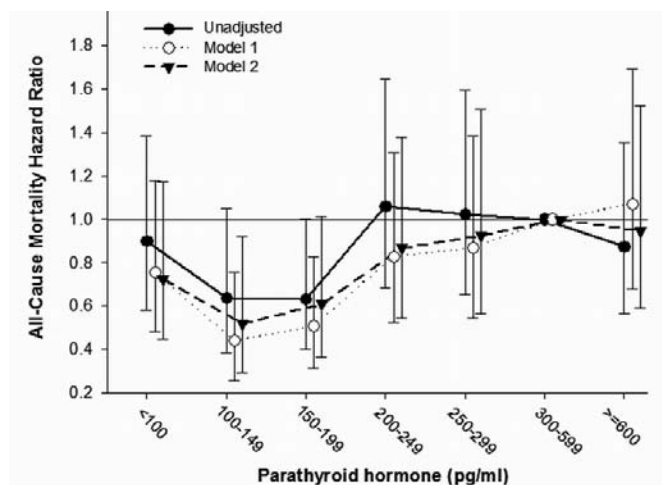
**Disclosures:** L.C. Dukas, TEVA Pharmaceuticals Industries 3.  
This study received funding from: TEVA Pharmaceuticals Industries.

## SU445

**Serum Intact PTH of 100 to 150 pg/ml Is Associated with Greatest Survival in Maintenance Hemodialysis Patients.** M. Rambod<sup>\*1</sup>, S. Sprague<sup>2</sup>, K. Kalantar-Zadeh<sup>\*1</sup>. <sup>1</sup>Nephrology and Hypertension, Los Angeles BioMedical Research Institute, Torrance, CA, USA, <sup>2</sup>Nephrology and Hypertension, Northwestern University Feinberg School of Medicine, Chicago, IL, USA.

**Background:** The Kidney Disease Outcome Quality Initiative (KDOQI) guidelines recommended intact (i) PTH of 150 to 300 pg/ml as the target range for maintenance hemodialysis (MHD) patients (pts) is higher than the normal iPTH (<65 pg/ml). We hypothesized that lower than the KDOQI recommended iPTH range is associated with greatest survival in MHD pts. **Methods:** We examined the 5-yr (10/01-1/07) mortality-predictability of iPTH in 748 MHD pts after multivariate adjustment for case-mix (Model 1) and also for serum albumin, phosphorus and interleukin-6 levels (Model 2). **Results:** Pts, 54±15 yrs old, including 45% women, 32% Blacks and 55% diabetics, with median dialysis vintage of 20 months, had a median iPTH of 247 pg/ml (inter-quartile range: 159-408 pg/ml). During the 5-yr follow-up, 228 pts died. Cox proportional regression calculated hazard ratio (HR) and 95% confidence intervals for all-cause mortality across increments of serum PTH were lowest for iPTH between 100 and 150 pg/ml (Table & Figure).

Death Hazard Ratio (Ref: iPTH 300-600 pg/ml)				
Death hazard ratio (95% CI)	<100 pg/ml	100-149 pg/ml	150-199 pg/ml	200-249 pg/ml
Model 1	0.75 (0.48-1.18)	0.44 (0.26-0.75)	0.51 (0.31-0.83)	0.83 (0.53-1.31)
Model 2	0.72 (0.45-1.17)	0.52 (0.29-0.92)	0.61 (0.37-1.01)	0.87 (0.55-1.38)



**Conclusion:** Serum PTH level below the KDOQI range appears associated with the greatest survival in MHD patients even after controlling for case-mix, nutritional status and inflammation.

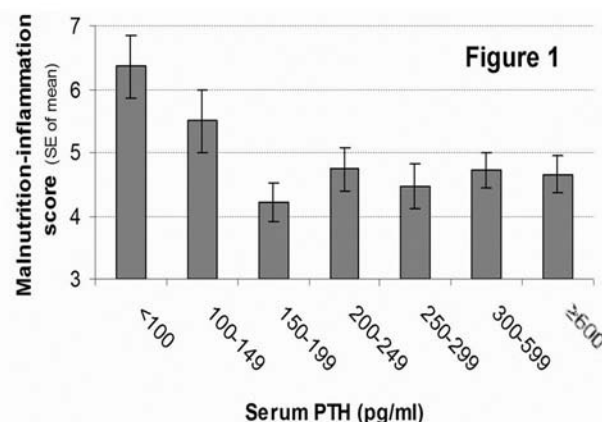
**Disclosures:** M. Rambod, None.

This study received funding from: NIH / NIDDK.

## SU446

**Association of the Marker of Adynamic Bone Disease with Malnutrition-Inflammation Complex in Hemodialysis Patients.** M. Rambod<sup>\*1</sup>, S. Sprague<sup>2</sup>, K. Kalantar-Zadeh<sup>\*1</sup>. <sup>1</sup>Medicine/Nephrology, Harbor-UCLA, Torrance, CA, USA, <sup>2</sup>Medicine/Nephrology, Northwestern Univ. Feinberg School of Medicine, Chicago, IL, USA.

**Background:** In maintenance hemodialysis (MHD) patients, the adynamic bone disease, which is associated with adverse outcomes, is believed to be more likely when serum intact PTH (iPTH) level is below 150 pg/ml (as compared to the recommended target range of 150-300 pg/ml). We hypothesized that serum iPTH<150 pg/ml is associated with higher risk of malnutrition and inflammation in MHD patients. **Methods:** In 748 MHD patients of a 5-year cohort (10/01-12/06) we examined the association of serum iPTH with pro-inflammatory markers and the "malnutrition-inflammation score" (MIS), which is a score between 0 [normal] and 30 [most abnormal], consisting of 7 components of the Subjective Global Assessment of nutrition, and serum albumin, transferrin and body mass index (Am J Kidney Dis 2001; 38:1251-63). **Results:** Patients were 54±15 yrs (mean±SD) old and included 45% women, 32% Blacks and 55% diabetics, with a median dialysis vintage of 20 months. The mean, median, and inter-quartile (IQ) range of 4 relevant variables were: MIS: 4.9 [median: 4, IQ: 2-6]; interleukin-6 (IL-6): 17.5 [7.4, 4.1-14.3] ng/ml, C-reactive protein (CRP): 5.8 [3.7, 1.5-7.6] mg/L, and tumor-necrosis factor-α (TNF-α): 9.1 [6.0, 4.1-9.2] ng/ml. The MIS was higher (worse) in patients with lower serum iPTH (p=0.003) (Figure 1).



High levels of pro-inflammatory markers were associated with iPTH <150 pg/ml (compared to 150-300 pg/ml) (Figure 2 & Table).

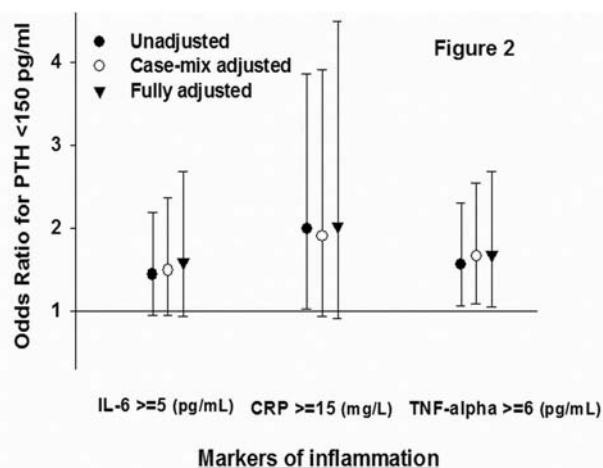


Table - Odd Ratios of PTH<150 pg/ml in 460 pts with PTH<300 pg/ml

	IL-6>=5 (pg/ml)	CRP>=15 (mg/L)	TNF-alpha >=6 (pg/ml)
Unadjusted	1.44 (0.95-2.18)	1.99 (1.03-3.86)	1.56 (1.06-2.30)
Case-mix adjusted	1.49 (0.94-2.36)	1.91 (0.93-3.90)	1.66 (1.08-2.54)
Fully adjusted	1.58 (0.93-2.69)	2.01 (0.90-4.49)	1.68 (1.05-2.67)

**Conclusion:** Low serum iPTH<150 pg/ml, the presumed marker of adynamic bone disease, may be another facet of the malnutrition-inflammation-complex syndrome in MHD patients.

**Disclosures:** M. Rambod, None.

This study received funding from: NIH / NIDDK.

## SU447

**Osteopenia in Chronic Kidney Disease: Effects of Phosphate Overload.** E. G. Gracioli\*, L. M. dos Reis\*, D. G. Batista\*, R. M. A. Moysés\*, V. Jorgetti, K. R. Neves\*. Nephrology, University of São Paulo, São Paulo, Brazil.

Calcium, phosphate (P), parathormone (PTH) and calcitriol metabolism disturbances are commonly seen in chronic kidney disease (CKD) and are involved in the pathogenesis of renal osteodystrophy. It is difficult to understand the role of each one separately, since small serum variations are capable of triggering compensatory mechanisms that try to re-establish their normal concentrations. We evaluated the isolated effect of P on bone of CKD rats, kept on a fixed PTH infusion, altering the P content in their diet. Fifty-five male wistar rats were submitted to parathyroidectomy and 5/6 nephrectomy (Nx). PTH activity was restored by an osmotic minipump in continuous infusion of 1-34 rat PTH (0.022µg/100g/hour-PTHn or 0.11µg/100g/hour-PTHh) or were sham-operated and received vehicle. P content (low P- LP= 0.2%; high P- HP= 1.2%) differentiated diets. We divided the groups as follow: sham; shamLP; PTHnNxLP; PTHhNxLP; shamHP; PTHnNxHP; PTHhNxHP. After 2 months, biochemistry and bone histomorphometry were analyzed. The Nx groups that were fed a P-rich diet presented higher P levels, as well as lower levels of calcium than those that were fed a diet poor in P. Histomorphometric analysis revealed that the rats were fed a P-rich diet (shamHP; PTHnNxHP; PTHhNxHP) presented lower trabecular volume (BV/TV) than their counterparts. This effect was minimized in the animals that received a high PTH infusion. **CONCLUSIONS:** P overload was associated with a decrease in trabecular bone volume. In those animals that received a high PTH infusion, this effect was minimized. Our findings demonstrated that P overload is hazardous to bone architecture and that uremia requires higher PTH levels to keep the bone integrity. The molecular basis of the effect of P overload on bone should be elucidated in further studies.

N.Ob/B.Pm:osteoblastic/B.Pm;N.Oc/B.Pm:osteoclast/B.Pm; ° vs all; \*vs PTHh; +vs PTHhLP; #vs PTHhHP

	BV/TV (%)	N.Ob/B.Pm (/mm)	N.Oc/B.Pm (/mm)	BFR/BS (m³/m²/day)
Sham	22.8±1.8	1.7±0.3	1±0.3+	0.02±0.002#
Sham LP	26.8±1.7	2.9±0.5*	1.3±1.2	0.02±0.005#
Sham HP	17±1.7	3.3±1.2*	1.4±0.2	0.03±0.008
PTHnNx LP	24.7±2.4	4.6±0.1*	1.4±0.3	0.05±0.006
PTHnNx HP	16.7±1.5	5.8±1.9*	1.2±0.2+	0.07±0.02
PTHhNx LP	39.3±3.3°	29.8±1.7	2.6±0.2	0.04±0.01
PTHhNx HP	25.6±2.2	16.7±3.5	1.9±0.3	0.05±0.01

**Disclosures:** V. Jorgetti, Genzyme Co 3, 4; Amgen Co 3.

This study received funding from: FAPESP.

## SU448

**Comparison of 1,25-dihydroxyvitamin D<sub>2</sub> and Calcitriol Effects in an Adenine-induced Model of CKD Reveals Differential Control Over Serum Calcium and Phosphate.** C. Helvig\*, D. Cuerrier\*, A. Kharebov\*, B. Ireland\*, J. Kim\*, K. Ryder\*, M. Petkovich. Cytochroma Inc., Markham, ON, Canada.

Calcitriol and related synthetic analogs have been used extensively in the clinic to control secondary hyperparathyroidism (SHPT) associated with chronic kidney disease (CKD) with the goal of minimizing the impact of disturbances of mineral metabolism and chronic elevation of parathyroid hormone levels on bone. Replacement therapy using active hormone can alter mineral balance leading to hypercalcemia and phosphatemia resulting in soft tissue mineralization. With the goal of identifying compounds with reduced toxicity, we have identified 1,25-dihydroxyvitamin D<sub>2</sub> (1,25-(OH)<sub>2</sub>D<sub>2</sub>) as a promising therapeutic candidate with efficacy equal to that of calcitriol, but without the same level of toxicity.

For the testing of different vitamin D compounds, we established a model of experimental CKD based on feeding rats a diet containing 0.75% adenine for 4 weeks.

This is the first time that this model has been used to compare the effects of 1,25-(OH)<sub>2</sub>D<sub>2</sub> and calcitriol, a drug currently used in the treatment of CKD to control PTH levels, on plasma PTH, serum alkaline phosphatase, serum calcium and phosphorus and gene regulation in order to find potential differences between these two vitamin D compounds. Moreover, metabolism and the effect on gene regulation such as intestinal alkaline phosphatase (IAP) of 1,25-(OH)<sub>2</sub>D<sub>2</sub> and calcitriol was investigated *in vitro*.

We have shown that 1,25-(OH)<sub>2</sub>D<sub>2</sub> is as potent as calcitriol in decreasing plasma PTH levels. Serum calcium and phosphorus were elevated after treatment with both compounds, however 1,25-(OH)<sub>2</sub>D<sub>2</sub> required higher doses than calcitriol to reach significant elevation of serum calcium and phosphorus. In general, as shown by the animal weight gain and survival, 1,25-(OH)<sub>2</sub>D<sub>2</sub> was found to be less toxic than calcitriol. Using human intestinal microsomes, 1,25-(OH)<sub>2</sub>D<sub>2</sub> was more susceptible than calcitriol to metabolism. In Caco-2 cells, 1,25-(OH)<sub>2</sub>D<sub>2</sub> differentially regulated IAP and CYP24. These studies implicate metabolism as an important mechanism to differentiate 1,25-(OH)<sub>2</sub>D<sub>2</sub> from calcitriol. Thus, we have shown that 1,25-(OH)<sub>2</sub>D<sub>2</sub> is equally potent compared to calcitriol to decrease plasma PTH levels *in vivo*. However, 1,25-(OH)<sub>2</sub>D<sub>2</sub> was shown to be less toxic than calcitriol possibly due to greater instability in the intestine. This study demonstrates that 1,25-(OH)<sub>2</sub>D<sub>2</sub> could offer an advantage over calcitriol for the treatment of SHPT associated with CKD.

**Disclosures:** C. Helvig, None.

## SU449

**Osteopenia in Chronic Kidney Disease: Effects of Calcium Overload.** L. M. dos Reis\*, D. G. Batista\*, E. G. Gracioli\*, A. O. Magalhães\*, V. C. N. Gouveia\*, K. R. Neves\*, R. M. A. Moysés\*, V. Jorgetti. Nephrology, University of São Paulo, São Paulo, Brazil.

The use of calcium (Ca) salts to control phosphorus (P) retention has long been recognized as a key component in the clinical management of chronic kidney disease (CKD). However, some concerns had arisen because Ca salts were linked to PTH over suppression and vascular calcification. In addition, the direct effects of Ca on bone were rarely evaluated because Ca use is always associated with a decrease in PTH and in P. We studied the isolated role of Ca in bone tissue of CKD animals, maintained on a fixed PTH infusion, fed with different Ca content in their diet. Thirty four male Wistar rats were submitted to parathyroidectomy (PTX) and 5/6 nephrectomy (Nx). PTH activity was restored by an osmotic minipump in continuous infusion of 1-34 rat PTH (0.022µg/100g/hour) or were sham-operated and received vehicle. Ca content was differentiated in diets (low Ca-LCa = 0.02%; high Ca-HCa = 1.2%). We divided the groups as follows: Sham, ShamLCa, ShamHCa, NxLCa and NxHCa. After 2 months, biochemical and bone histomorphometry were performed. Animals in ShamLCa group presented higher PTH levels as well as lower Ca than their counterparts. Nx groups that were fed a high Ca diet presented higher Ca levels, as well as lower P than those fed with low Ca. Histomorphometric analysis showed that Ca restriction was associated with a mineralization defect whereas Ca overload was associated with a decrease in bone trabecular volume.

In conclusion, despite a better control of serum P and a maintained PTH level, Ca overload presented an osteopenic effect, suggesting that it should be used with caution, either in CKD or in the general population.

\*vs ShamLP, HCa, NxHCa; #vs ShamLCa, NxHCa; +vs all; °vs Sham, HCa, NxHCa; \*\*vs ShamHCa, NxHCa;

	BV/TV(%)	Tb.N(/mm)	OV/BV(%)	OS/BS(%)
Sham	22.8±1.8*	3.4±0.2#	0.2±0.04	3.9±0.7
ShamLCa	14.3±2.1	1.9±0.3	2.7±1.3	29.7±9.7**
ShamHCa	13.4±2.2	2.6±0.1	0.6±0.2	10.1±2.7
NxLCa	17.7±2.3	3±0.3	6.4±2.2+	27.1±5.2°
NxHCa	11.7±1.5	1.9±0.2	0.5±0.2	9.3±1.7

**Disclosures:** V. Jorgetti, Genzyme Co 3, 4; Amgen Co 3.

This study received funding from: FAPESP.

## SU450

**The Protective Actions of Vitamin D Analogs in the Vascular Calcification of Chronic Kidney Disease (CKD).** S. Mathew\*, F. Strebeck\*, K. A. Hruska. Pediatrics, Washington University, St. Louis, MO, USA.

Careful analysis of the scientific literature leads to the strong conclusion that the dose response curve for vitamin D receptor activation (VDRA) is biphasic. Vitamin D intoxication, a well-known clinical situation, involves dermal calcification by VDRA. However, VDRA is required for normal physiology as demonstrated by genetic studies in mice rendered deficient of  $1\alpha$ -hydroxylase or the vitamin D receptor. Furthermore, correction of calcitriol deficiency has been shown to have efficacy in clinical medicine. The importance of the biphasic dose response curve for vitamin D receptor activators is called into focus by recent observational studies that suggest exposure to VDRA, paricalcitol and hectorol, improve survival and cardiovascular outcomes in dialysis patients. In examining vascular calcification, an important component of cardiovascular morbidity and mortality in ESKD, several studies suggest that VDRA stimulates vascular calcification. Here we report that lower doses of the VDRA are protective in atherosclerotic vascular calcification stimulated by CKD in high fat fed mice due to the effects of the VDR to inhibit osteoblastic gene expression, including inhibition of aortic RUNX2, MSX2 and osterix expression. Studies in vitro demonstrate that low dose VDRA inhibit calcifying vascular smooth muscle cell cultures by decreasing osteoblastic gene transcription whereas higher doses fail to do so, thereby becoming permissive for the actions of oxidant injury. Furthermore, in mice with high levels of vascular calcification, VDRA stimulates bone formation rates, and in vitro, stimulate, not inhibit, osteoblastic function of bone marrow derived progenitors. The basis of these differential actions of VDRA in vascular versus skeletal osteoblastic cells lies in the cell fate step in differentiation to the contractile vascular smooth muscle cell. The mechanism of the actions of low-dose VDRA are shown in the studies reported here. Through activation of vascular smooth muscle cell differentiation, osteoblastic differentiation is repressed and vascular calcification is inhibited. We conclude that at low appropriate doses VDRA is protective against cardiovascular calcification in CKD.

**Disclosures:** K.A. Hruska, Genzyme 3, 4; Abbott 3.  
This study received funding from: NIH, Genzyme, Abbott.

## SU451

**Reduction of Bone Mineral Density in the Patients with Rheumatoid Arthritis Is More Remarkable at Proximal Femur than at Lumbar Spine.** N. Hisanori\*, F. Hagiwara\*, S. Tohma\*. Department of Rheumatology, Sagami-hara National Hospital, Sagami-hara, Kanagawa, Japan.

**Objective:** Rheumatoid arthritis (RA) patients have different rates of bone mass loss at different bone sites during RA progression, with different mechanisms operating at each site. Here, we measured the bone mineral density (BMD) of the lumbar spine and proximal femur in RA patients to determine which site is more affected by RA prevalence. **Methods:** We recruited 675 Japanese RA patients and 156 gender-matched non-RA patients with connective tissue disease (CTD) as controls. BMD in the lumbar spine and proximal femur were measured by dual energy X-ray absorptiometry. These measurements were performed before treatment with a bone antiresorptive agent; either a bisphosphonate or estrogen. **Results:** BMD Z scores in the proximal femur were significantly lower in RA patients than in non-RA/CTD patients, while those for the lumbar spine did not differ significantly between the two groups of patients. The RA patients were divided into four groups based on Steinbrocker's disease stage and functional classification, and the differences between the mean BMD Z scores in the femur were statistically significant among these groups ( $p < 0.001$ ), decreasing progressively as disease stage and functional class increased from 1 to 4. In contrast, the lumbar spine BMD Z score did not show a significant difference among these groups. Disease duration of RA showed a significantly stronger correlation with BMD Z scores in the femur than those for the lumbar spine, while CRP, ESR and anti-agalactosyl (AG) IgG antibody levels exhibited significant correlations with the proximal femur BMD Z score, but not with that of the lumbar spine. Furthermore, multiple regression analysis confirmed a significant and independent association of RA stage, class, CRP and anti-AG IgG antibody levels with the BMD T score in the femoral neck, but not that in the lumbar spine. **Conclusion:** Our results suggest that BMD reduction is preferentially observed in the proximal femur in RA patients through an RA-associated mechanism.

**Disclosures:** N. Hisanori, None.

## SU452

**Relationship between Low Bone Mass and Aortic Valve Sclerosis in Korean Men and Women.** H. Choi\*<sup>1</sup>, Y. Rhee\*<sup>1</sup>, S. Kim\*<sup>2</sup>, N. Chung\*<sup>1</sup>, E. Lee\*<sup>1</sup>, S. Lim\*<sup>1</sup>. <sup>1</sup>Department of Internal Medicine, Yonsei University College of Medicine, Seoul, Republic of Korea, <sup>2</sup>Department of Internal Medicine, Kwandong University College of Medicine, Goyang, Republic of Korea.

**Background:** Aortic valve sclerosis and low bone mass are both diseases of old age. Many studies have reported that osteoporosis or low bone mass is related to cardiovascular disease or vascular calcification. The aim of this study was to assess the relationship between aortic valve sclerosis and low bone mass in Korean men and women.

**Methods:** A total of 165 men and 97 women who visited Severance Hospital for medical checkups were included in this study. Each subject's bone mineral density (BMD) was measured by dual energy X-ray absorptiometry, and aortic valve sclerosis was assessed using transthoracic echocardiography.

**Results:** Among the 262 subjects, 61 had aortic valve sclerosis. The mean age of participants with and without aortic valve sclerosis was  $62.9 \pm 6.8$  yr and  $52.8 \pm 7.6$  yr, respectively. The prevalence of osteopenia and osteoporosis was higher in participants with aortic valve sclerosis (52.5% in subjects with aortic valve sclerosis, 36.8% in subjects without aortic valve sclerosis). Inversely, the prevalence of aortic valve sclerosis increased as BMD T-scores decreased. Based on logistic regression analysis of cardiovascular risk factors including age, male gender, BMI, smoking, hypertension, hypercholesterolemia, diabetes, and BMD T-score  $< -1.5$ , the independent predictors of aortic valve sclerosis were age (OR 1.23, 95% CI 1.14 - 1.30;  $p < 0.001$ ), male gender (OR 3.06, 95% CI 1.20 - 7.82;  $p = 0.019$ ), hypertension (OR 3.09, 95% CI 1.43 - 6.68;  $p = 0.004$ ), and BMD T-score  $< -1.5$  (OR 3.24, 95% CI 1.02 - 10.30;  $p = 0.046$ ).

**Conclusions:** Low bone mass might have an additional role to age, male gender, and hypertension in calcification of the aortic valve. Patients with low bone mass should be further evaluated for the presence of aortic valve sclerosis and related cardiovascular diseases.

**Disclosures:** H. Choi, None.

## SU453

**Association between Vascular Calcification and Low Total Femur Bone Mineral Density in Elderly People Community-Dwelling.** C. F. Danilevicius\*<sup>1</sup>, J. B. Lopes\*<sup>1</sup>, L. Takayama\*<sup>1</sup>, V. F. Caparbo\*<sup>1</sup>, I. R. S. Oliveira\*<sup>2</sup>, M. E. Kuroishi\*<sup>2</sup>, P. R. Menezes\*<sup>3</sup>, M. Scazufca\*<sup>3</sup>, E. Bonfa\*<sup>1</sup>, R. M. R. Pereira\*<sup>1</sup>. <sup>1</sup>Rheumatology Division, University of São Paulo, São Paulo, Brazil, <sup>2</sup>Radiology, University of São Paulo, São Paulo, Brazil, <sup>3</sup>Preventive Medicine, University of São Paulo, São Paulo, Brazil.

The aim of this study was to determine the possible association of aortic abdominal calcification and bone mineral density (BMD) in elderly people community-dwelling. One thousand and forty-one subjects ( $\geq 65$  years-old) were selected in a well established elderly community in the São Paulo city. Lateral lumbar X-rays were analyzed for the presence of abdominal aortic wall calcification in the region corresponding to the first through fourth lumbar vertebrae. The severity of the anterior and posterior aortic calcification was graded individually on a 0-3 scale for each lumbar segment (total: 0-24). BMD were evaluated using DXA-HOLOGIC. Spearman's correlations were used to analyze the presence of aortic calcification ( $\geq 5$  score) with the following variables: anthropometric and clinical parameters, BMD and laboratorial biochemical data. Logistic regression analysis was done with the variables that show significance in the Spearman's correlation. Sixty hundred and eighty-one patients (65.41%) presented any calcification and the mean score was  $7.67 \pm 5.94$ . Of these patients, 61.23% had five or more aortic abdominal calcification score. Spearman analysis showed a significant correlation between the presence of aortic abdominal calcification (score  $\geq 5$ ) and the following parameters: age ( $r = 0.236$ ,  $p < 0.001$ ), height ( $r = -0.100$ ,  $p = 0.001$ ), weight ( $r = -0.093$ ,  $p = 0.003$ ), current and previous tobacco ( $r = 0.123$ ,  $p < 0.001$ ), falls ( $r = 0.069$ ,  $p = 0.026$ ), fragility fracture ( $r = 0.103$ ,  $p = 0.001$ ), diabetes mellitus ( $r = 0.093$ ,  $p = 0.003$ ), arterial hypertension ( $r = 0.118$ ,  $p < 0.001$ ), cardiovascular event ( $r = 0.093$ ,  $p = 0.003$ ), phosphorus ( $r = 0.131$ ,  $p < 0.001$ ), PTH ( $r = 0.083$ ,  $p = 0.01$ ), femoral neck BMD ( $r = -0.132$ ,  $p < 0.001$ ), total femur BMD ( $r = -0.148$ ,  $p < 0.001$ ), total body BMD ( $r = -0.130$ ,  $p < 0.001$ ) and lean mass ( $r = -0.141$ ,  $p < 0.001$ ). Logistic regression analysis revealed that the presence of aortic abdominal calcification was positively associated with age (OR=1.086, CI= 1.058-1.114,  $p < 0.001$ ) and negatively associated with total femur BMD in elderly people community-dwelling (OR=0.149, CI= 0.062-0.357,  $p < 0.001$ ). The demonstration of a positive correlation between low bone mineral density in total femur and advanced aortic calcification in a large elderly people community-dwelling reinforces previous hypothesis of a common physiopathological mechanisms underlying these two conditions.

**Disclosures:** R.M.R. Pereira, None.

This study received funding from: Fapesp #03/09313-0, CNPQ #305691/2006-6, FAPESP #04/12694-8.



## SU454

**Influence of Hip Flexor or Knee Extensor Muscle Strength on Spinal Sagittal Alignment or Falls.** Y. Kasukawa, N. Miyakoshi, M. Hongo, H. Noguchi, K. Kamo, H. Sasaki, Y. Shimada\*. Department of Orthopedic Surgery, Akita University, Akita, Japan.

We have previously reported that decreased back extensor strength, decreased mobility of lumbar spine, and increased spinal inclination could represent risk factors for falls in patients with osteoporosis. However, muscle strength of lower extremity, which is hip flexor or knee extensor muscle, may influence the spinal sagittal alignment and mobility or the incidence of falls. The purpose of this study was to evaluate whether hip flexor or knee extensor muscle strength may influence the sagittal alignment or mobility of spine or the incidence of falls. Subjects comprised 26 elderly people (mean age, 73 years; range, 60-82 years, 11 male and 15 female) participated in physical check-up. Angles of thoracic or lumbar kyphosis and mobility of the thoracic or lumbar spine were measured in the upright position and at maximum flexion/extension using a computer-assisted device (SpinalMouse). Spinal inclination reflecting spinal sagittal alignment was also evaluated using SpinalMouse. Bilateral grip strengths were measured using a handgrip dynamometer. The bilateral hip flexor or knee extensor muscle strength was measured using portable dynamometer (PowerTrackII). Correlation of the muscle strength of lower extremity and the sagittal alignment or mobility of spine was analyzed. Then subjects were divided into 2 groups: subjects with a history of falls, fear of falling, or need for support when walking (Fall group, n=13; 5 men, 8 women); and subjects with no such history (Non-fall group, n=13; 6 men, 7 women). There was no significant correlation of hip flexor or knee extensor muscle strength and thoracic, lumbar, thoracic+lumbar spinal alignment or mobility. The hip flexor or knee extensor muscle strength also did not show significant correlation with spinal inclination or its mobility. Mean grip strength and mean knee extensor muscle strength, but not hip flexor muscle strength, were 43% (p<0.01) and 10% (p<0.05) lower in the Fall group than in the Non-fall group. These results of this study suggest that hip flexor and knee extensor muscle strength had no significant effect on spinal sagittal alignment and mobility. The muscle strength of lower extremity was decreased in the elderly patients with history of falls in the present study.

**Disclosures:** Y. Kasukawa, None.

## SU455

**Determinants of low BMD in HIV infected postmenopausal women.** M. T. Yin<sup>1</sup>, D. Ferris<sup>2</sup>, D. McMahon<sup>1</sup>, S. Cabral<sup>1</sup>, H. Eisenberg<sup>3</sup>, J. Laurence<sup>3</sup>, V. K. Thomas<sup>3</sup>, S. Creemers<sup>3</sup>, E. Shane<sup>1</sup>. <sup>1</sup>Columbia University, NY, NY, USA, <sup>2</sup>Bronx Lebanon Hospital Center, NY, NY, USA, <sup>3</sup>Weill Medical College, NY, NY, USA.

Several studies have reported low BMD and abnormal mineral metabolism in association with HIV infection and its therapy. Although postmenopausal (PM) minority women constitute a growing segment of the HIV+ population in the US and may be at higher risk for osteoporosis and fracture than younger HIV+ men and women, little is known about their skeletal status. We therefore measured BMD by DXA in 101 HIV+ and 102 HIV- PM women from New York. Serum levels of pro-resorptive cytokines (TNF- $\alpha$ , RANKL, IL-6), 25OHD, parathyroid hormone (PTH), estrone (E), bone alkaline phosphatase (BAP) and N-telopeptide (NTX) were also measured. HIV+ women were younger (57 $\pm$ 6 vs 61 $\pm$ 6 yrs, p<0.0001) and had lower BMI (27.5 $\pm$ 5.9 vs 30.2 $\pm$ 5.8 kg/m<sup>2</sup>, p=0.001) but were of similar race/ethnicity (66% Hispanic, 34% African American) as HIV- women. Mean CD4 count was 509 $\pm$ 309 cells/mm<sup>3</sup> and 78% were on antiretrovirals (ARVs). T scores were lower in HIV+ than HIV- women at the lumbar spine (LS; -1.82 $\pm$ 0.1 vs -1.26 $\pm$ 0.1, p=0.0008), total hip (TH; -0.95 $\pm$ 0.1 vs -0.49 $\pm$ 0.1, p=0.0008) and femoral neck (FN; -1.30 $\pm$ 0.1 vs -0.9 $\pm$ 0.1, p=0.007). More HIV+ women had T scores <-1.0 at the LS (75% vs 60%, p=0.03), FN (63% vs 44%, p=0.006) and TH (48% vs 28%, p=0.003). Prevalence of osteoporosis (T score <-2.5) in HIV+ and HIV- at the LS (25% vs 18%, p=0.22), TH (5% vs 1%, p=0.10), and FN (12% vs 7%, p=0.22) and self-reported fracture at any site (10% vs 7%, p=0.51) were similar between groups. In a multivariate model, HIV+ status remained negatively associated with LS T score (partial correlations r=-0.17, p=0.02) and TH T score (partial correlations r=-0.15, p=0.03) after adjustment for age, weight, and other predictors such as alcohol, calcium and multivitamin supplementation. Serum BAP, NTX and TNF- $\alpha$  were higher and PTH and E lower in HIV+ women than controls (Table), while serum 25OHD and IL-6 were similar. Cytokine levels did not correlate with BMD at any site, but estrone was positively associated with FN, TH and 1/3 radius even after adjustment for BMI. Among the HIV+ women, BMD did not correlate with ARV exposure. In conclusion, BMD is significantly lower and prevalence of osteopenia is higher in PM HIV+ than HIV- women. Although HIV status is an independent predictor of BMD, it appears not to be mediated by upregulation of pro-resorptive cytokines or ARV exposure.

	HIV+ (N=100)	HIV- (N=102)	P value
Osteocalcin (ng/ml)	6.6 $\pm$ 0.3	6.0 $\pm$ 0.2	0.09
BAP (U/L)	38.2 $\pm$ 1.8	30.6 $\pm$ 1.2	0.0008
NTX (nmol/BCE/L)	21.3 $\pm$ 1.1	16.5 $\pm$ 0.6	0.0001
IL-6 (ng/ml)	2.6 $\pm$ 0.3	2.3 $\pm$ 0.3	0.45
TNF- (pg/ml)	40.4 $\pm$ 2.6	30.1 $\pm$ 1.5	0.0008
RANKL (nmol/L)	57.3 $\pm$ 1.8	58.7 $\pm$ 2.5	0.65
Intact PTH (pg/ml)	34.8 $\pm$ 1.7	42.9 $\pm$ 1.9	0.002
Estrone	24.7 $\pm$ 1.1	30.8 $\pm$ 1.8	0.004

**Disclosures:** M.T. Yin, None.

*This study received funding from: NIH K23AI059884 (MTY), R01AI065200 (ES).*

## SU456

**Type 1 Diabetes Is Associated with Lower Bone Mineral Density in Premenopausal Women But Not in Middle-aged Men - DIOS-Study.** T. Neumann<sup>1</sup>, A. Sämann<sup>2</sup>, S. Lodes<sup>1</sup>, M. Kiehnopf<sup>3</sup>, S. Franke<sup>1</sup>, C. Hemmelmann<sup>4</sup>, U. Müller<sup>5</sup>, G. Hein<sup>1</sup>, G. Wolf<sup>2</sup>. <sup>1</sup>Internal Medicine III, Rheumatology/ Osteology, Friedrich-Schiller-University, Jena, Germany, <sup>2</sup>Internal Medicine III, Nephrology, Friedrich-Schiller-University, Jena, Germany, <sup>3</sup>Institute of Clinical Chemistry and Laboratory Diagnostics, Friedrich-Schiller-University, Jena, Germany, <sup>4</sup>Institute of Medical Statistics, Computer Sciences and Documentation, Friedrich-Schiller-University, Jena, Germany, <sup>5</sup>Internal Medicine III, Endocrinology, Friedrich-Schiller-University, Jena, Germany.

It is assumed that type 1 diabetes mellitus (T1DM) is associated with an increased fractures risk. The aim of this study was to investigate the association between T1DM and bone mineral density (BMD) in comparison with non-diabetic healthy controls. A single-centre, cross sectional study of men and premenopausal women with T1DM was designed. Age, gender and body-mass index (BMI) were matched in the healthy control group. Investigation of BMD (lumbar spine, total hip, femoral neck and whole body), parameters of bone metabolism and bone-related clinical data were performed.

A total of 128 patients with T1DM and 77 non-diabetic controls were studied. BMD was significantly lower in females with T1DM compared with female healthy controls (total hip 0.999g/cm<sup>2</sup> vs. 1.077g/cm<sup>2</sup>, P<0.05; femoral neck 0.945g/cm<sup>2</sup> vs. 0.999g/cm<sup>2</sup>, P<0.05; total body 1.154g/cm<sup>2</sup> vs. 1.191g/cm<sup>2</sup>, P<0.05). However, BMD was not different in male patients compared to healthy men. C-terminal telopeptide of type I collagen (CTX), osteocalcin, parathormone, 25-hydroxyvitamin D and 1.25-dihydroxyvitamin D were significantly lower in male with T1DM compared to healthy controls. Females with T1DM had significantly lower osteocalcin and 25-hydroxyvitamin D but higher alkaline phosphatase compared with healthy women.

In multiple linear regression models for female participants, BMI was the strongest predictor of BMD. T1DM, reported fractures and CTX were inversely associated with BMD. Diabetes-related complications as neuropathy, nephropathy and retinopathy did not predict BMD. Participants with T1DM of all investigated ages reported more fractures but this did not reach statistical significans.

Our data suggest, that bone loss associated with T1DM is more pronounced in women than in man. Bone turn-over was lower in T1DM but did not explain differences in BMD. BMI and history of fractures were strong predictors of BMD and should be considered in risk estimation.

**Disclosures:** T. Neumann, None.

## SU457

**Histomorphometric Evaluation in an Experimental Model of Hepatic Osteodystrophy.** F. A. Pereira, I. Facincani\*, L. N. Z. Ramalho\*, L. M. dos Reis\*, V. Jorgetti. Internal Medicine, School of Medicine of Ribeirão Preto, University of São Paulo, Ribeirão Preto, Brazil.

Hepatic Osteodystrophy is an important co-morbidity of chronic liver disease. Conflicting results have been previously obtained about the predominating bone disease in this situation. Some data indicating that it is osteomalacia and others osteoporosis with different degrees of bone remodeling activity. The aim of this study was to evaluate bone remodeling. Twenty-nine Wistar rats were divided into two groups: Sham Group (SG n=15) and Hepatic Cholestasis Group (HCG n=14). HCG animals were submitted to bile-duct obstruction for induction of hepatic cholestasis. Thirty days after surgery the animals were sacrificed and blood samples, fragments of liver tissue and the right tibia were collected. The data of histomorphometric analysis showed that trabecular volume (BV/TV) was significantly smaller in HCG compared to SG: (HCG = 16.8  $\pm$  5.2 vs SG = 26.4  $\pm$  4.1 % p = 0.0001). The trabecular thickness (Tb.Th) and number of trabeculae (Tb.N) were significantly lower in HCG compared to SG. (Tb.Th: HCG = 33.5  $\pm$  4.6 vs SG=44.9  $\pm$  18.6  $\mu$  m p=0.01; Tb.N: HCG = 4.9  $\pm$  1.0 vs SG = 6.3  $\pm$  1.3 /mm p = 0.004). Trabecular separation (Tb.Sp) was significantly greater in HCG compared to SG. (Tb.Sp: HCG= 181.5  $\pm$  72.0 vs SG=124.7  $\pm$  34.4  $\mu$  m p=0.002). Dynamic histomorphometric parameters that express bone mineralization such as mineral apposition rate (MAR) and adjusted appositional rate of bone mineralization rate (Aj.AR) were significantly lower in HCG compared to SG: (MAR: HCG = 0.5  $\pm$  0.2 vs SG = 0.7  $\pm$  0.3  $\mu$  m/d p = 0.01; Aj.AR: HCG = 0.13  $\pm$  0.12 vs SG = 0.06  $\pm$  0.02  $\mu$  m/d p = 0.006). The mineralization lag time (Mit) as significantly longer in HCG compared to SG. (HCG = 78.7  $\pm$  64.4 vs GC = 41.6  $\pm$  27.0 days p = 0.02). The present results suggest that, in addition to a bone mass reduction, hepatic cholestasis is associated with a disorder of bone mineralization in rats. The definition of the pattern of osteometabolic disease in hepatic cirrhosis is fundamental for an appropriate treatment planning.

**Disclosures:** F.A. Pereira, None.

## SU458

**Cortical and Trabecular Microarchitecture in HIV-Infected Postmenopausal Women.** A. D. Shu<sup>1</sup>, M. T. Yin<sup>1</sup>, D. Ferris<sup>\*2</sup>, D. J. McMahon<sup>1</sup>, H. Eisenberg<sup>\*1</sup>, V. K. Thomas<sup>\*1</sup>, S. Cabral<sup>\*1</sup>, E. S. Shane<sup>1</sup>.<sup>1</sup>Columbia University Medical Center, New York, NY, USA, <sup>2</sup>Bronx-Lebanon Hospital, Bronx, NY, USA.

Several studies have reported low BMD in association with HIV infection and its therapy. Although postmenopausal (PM) minority women are a growing segment of the HIV positive (HIV+) population in the United States, and may be at higher risk for osteoporosis and fracture than younger men and women with HIV/AIDS, little is known about their skeletal status. We measured BMD by DXA in 101 HIV+ and 102 HIV- PM Hispanic and African American women residing in New York and in a subset (39 HIV+ and 57 HIV-), we assessed cortical (Ct) and trabecular (Tb) microarchitecture by HRpQCT (Xtreme CT; Scanco Medical AG; resolution 82 µm) at the radius (RAD) and tibia (TIB). We excluded women with known osteoporosis, metabolic bone disease and serum Cr > 2.5 mg/dL.

HIV+ subjects were younger ( $56 \pm 6$  vs  $60 \pm 7$  yrs,  $p = 0.009$ ), had lower BMI ( $29 \pm 6$  vs  $31 \pm 7$ ,  $p = 0.006$ ), but were similar with regard to race/ethnicity, history of fracture (15% vs 11%,  $p = 0.48$ ), use of glucocorticoids, estrogen and anti-epileptic drugs. Of HIV+ subjects, 77% were on antiretroviral therapy (ARV).

Despite their younger age, HIV+ women (Table) had lower BMD at the total hip (TH) and femoral neck (FN) than HIV- women. By HRpQCT, when compared to premenopausal (PreM) women, both groups of PM women had lower Ct thickness, and Tb bone density, bone volume and number, and higher Tb separation and standard deviation of Tb separation reflecting inhomogeneity of the Tb network. However, the HIV+ and HIV- PM women did not differ from each other by any HRpQCT measure at the RAD or TIB (data not shown). When we limited the analysis to subjects with low BMD (T-score < -2), the HIV+ and HIV- groups (N = 21 and 23) remained similar.

In summary, despite their younger age, HIV+ PM women had lower hip BMD than HIV- PM women. When compared to premenopausal controls, Ct and Tb microstructural deterioration was similar in HIV+ and HIV- PM women, even though the HIV+ was younger than the HIV- group. These results suggest earlier deterioration of bone microarchitecture in PM HIV+ women.

**Table:** DXA and Radius HRpQCT for HIV+ and HIV- PM women (mean  $\pm$  SD) along with PreM reference values

	Our study			PreM reference
	HIV+ N = 39	HIV- N = 57	p-value	N = 26
DXA lumbar spine BMD, T-score	-2.0 (1.1)	-1.6 (1.4)	0.15	0.4 (0.8)
DXA total hip BMD, T-score	-1.0 (1.0)	-0.5 (0.9)	0.015	0.3 (0.7)
DXA femoral neck BMD, T-score	-1.4 (0.9)	-0.9 (1.2)	0.037	0.1 (0.7)
Cortical thickness, µm	754 (168)	747 (218)	0.87	847 (161)
Tb density, mg HA/ccm	115 (36)	118 (40)	0.77	161 (25)
Tb bone volume, %	9.6 (3.0)	9.8 (3.3)	0.77	13.3 (2.1)
Tb number, 1/mm	1.6 (0.3)	1.6 (0.4)	0.84	2.1 (0.2)
Tb separation, µm	579 (156)	616 (217)	0.41	436 (63)
Tb separation standard deviation, µm	305 (203)	362 (334)	0.31	436 (63)

**Disclosures:** A.D. Shu, None.

This study received funding from: NIH K23AI059884 (MTY), R01AI065200 (ES).

## SU459

**Plasma Osteocalcin is Inversely Related to Fat Mass and Plasma Glucose in Elderly Swedish Men.** J. M. Kindblom<sup>1</sup>, C. Ohlsson<sup>1</sup>, O. Ljunggren<sup>\*2</sup>, M. K. Karlsson<sup>\*3</sup>, A. Tivesten<sup>\*1</sup>, U. Smith<sup>\*1</sup>, D. Mellstrom<sup>1</sup>.

<sup>1</sup>Internal Medicine, Sahlgrenska Academy, Gothenburg, Sweden, <sup>2</sup>Uppsala University, Department of Medical Sciences, Gothenburg, Sweden, <sup>3</sup>Department of Clinical Sciences, Clinical and Molecular Osteoporosis Research Unit, Lund and Malmö, Sweden.

The osteoblast-derived protein osteocalcin has recently been shown to affect adiposity and glucose homeostasis in mice, suggesting that the skeleton via an endocrine mechanism influences energy metabolism. The aim with the present study was to investigate the relationship between plasma osteocalcin and parameters reflecting fat mass and glucose homeostasis in humans.

Fasting levels of plasma osteocalcin, plasma glucose, serum insulin and lipids were analysed in elderly men ( $75.3 \pm 3.2$  years) in the Gothenburg part (all subjects n = 1010, non-diabetic n = 857 and diabetic n = 153) of the MrOS Sweden study. Fat mass and lean mass were analysed using dual energy X-ray absorptiometry.

Diabetic subjects had lower plasma osteocalcin (-21.7 %,  $p < 0.001$ ) than non-diabetic subjects. For both all subjects and non-diabetic subjects, plasma osteocalcin was clearly inversely related to BMI, fat mass and plasma glucose ( $p < 0.001$ ), while it was not associated with height or lean mass. Plasma osteocalcin explained a substantial part (6.3%) of the variance in plasma glucose while it associated moderately with serum insulin. Multiple linear regression models adjusting for serum insulin and fat mass demonstrated that plasma osteocalcin was an independent negative predictor of plasma glucose ( $p < 0.001$ ).

We herein, for the first time in humans, demonstrate that plasma osteocalcin is inversely related to fat mass and plasma glucose. Although one should be cautious with mechanistic interpretations of cross-sectional association studies, our human data support recently published experimental studies, revealing endocrine functions of osteoblast-derived osteocalcin on glucose and fat homeostasis.

**Disclosures:** C. Ohlsson, None.

This study received funding from: the Swedish Research Council, the Swedish Foundation for Strategic Research, European Commission Grant QLK4-CT-2002-02528, the ALF/LUA research grant in Gothenburg, the Lundberg Foundation, the Emil and Vera Cornell Foundation.

## SU460

**A Possible Role for the T<sub>H</sub>17 System in a Mouse Model of Ankylosing Spondylitis.** G. Thomas<sup>1</sup>, T. Glant<sup>\*2</sup>, M. Brown<sup>1</sup>.

<sup>1</sup>Dimanatina Institute, University of Queensland, Woolloongabba, Australia, <sup>2</sup>Rush University Medical Center, Chicago, IL, USA.

Ankylosing spondylitis (AS) is a common inflammatory arthritis with an incidence similar to that of rheumatoid arthritis (RA)(0.5%). Characteristic clinical features are inflammatory back pain, asymmetric peripheral arthritis, enthesitis, and anterior uveitis. The condition primarily affects the spine and sacroiliac joints of the pelvis, causing pain and stiffness and eventual fusion. Unlike 'seropositive' forms of arthritis like RA in which inflammation leads to bone and joint erosion, in AS initial erosion is followed by relentless new bone formation leading to joint fusion. This process is very poorly understood. Although anti-TNF drugs produce improvements in acute inflammation in AS, there are no treatments which induce remission or retard the progressive joint fusion that inevitably occurs in the disease. Thus there is an urgent need for new effective therapies.

AS is a highly heritable condition and our group has recently demonstrated a genetic association between the *IL23r* gene and AS. IL23R is the specific subunit of the receptor complex for the cytokine IL-23 which has been shown to be a key regulatory factor in the development of the recently discovered T<sub>H</sub>17 effector T-cell subset. T<sub>H</sub>17 cells are characterised by production of the pro-inflammatory cytokine interleukin 17 (IL-17), which has been shown to play a key role in a number of mouse models of autoimmune diseases such as multiple sclerosis, colitis, arthritis and psoriasis.

We have established the proteoglycan induced spondylitis (PGISp) mouse model of AS in our laboratory. Inflammation is induced in BALB/c mice by 3 injections of a human cartilage crude proteoglycan extract which initially induces peripheral inflammation but is then followed by sacroiliitis and vertebral inflammation, disc destruction and eventual ankylosis. Mice were stopped 12 weeks after the initial proteoglycan injection and spines and peripheral joints collected for histological and RNA analysis. Spleens were also collected to measure immune cell responses. Significant peripheral inflammation was seen in >90% of the mice analysed. Similarly almost 100% penetrance of axial inflammation was seen with massive disc destruction in the vertebrae. The potential role of T<sub>H</sub>17 cells was assessed by determining the proportion of T<sub>H</sub>17 and T<sub>H</sub>1 cells in the spleen by measuring IL-17 and interferon gamma (IFNγ). PGISp-affected mice showed significant increases in the numbers of IL-17+ve T<sub>H</sub>17 cells with a corresponding decrease in IFNγ+ve T<sub>H</sub>1 cells resulting in a 3-fold increase in the T<sub>H</sub>17/T<sub>H</sub>1 cell ratio.

Thus we have demonstrated altered T<sub>H</sub>17 activity in a mouse AS model supporting our genetic findings. Further studies will elucidate the potential of anti-T<sub>H</sub>17 therapies in AS.

**Disclosures:** G. Thomas, None.

## SU461

**Reduced Serum Osteocalcin and Sex Hormone Binding Globulin in Men with Type II Diabetes.** N. D. Nguyen, J. R. Center, J. A. Eisman, T. V. Nguyen.

Bone and Mineral Research Program, Garvan Institute of Medical Research, Sydney, Australia.

Serum osteocalcin (OC), a 49-amino acid bone matrix protein, has recently been shown to be associated with diabetes in mice. However, it is unknown whether the association is present in men. Therefore, this study sought to examine the contribution of OC to the susceptibility of type II diabetes in men.

Serum OC, sex hormone binding globulin (SHBG), 25(OH)D, and PTH were measured by radioimmunoassay in 443 men aged 60+ at baseline (1989) in the Dubbo Osteoporosis Epidemiology Study. The men's health status, including fracture and diabetes, had been monitored between 1989 and 2007. Bone mineral density (BMD), clinical risk factors, and lifestyle factors had also been obtained at baseline and subsequent biannual visits.

During the follow-up, 41 men (or 9%) reported to have type II diabetes. Although the two groups of men were similar in age ( $69 \pm 7$  years, mean  $\pm$  SD) men with diabetes had greater body mass index (BMI,  $27 \pm 4$  vs  $26 \pm 3$ ), greater weight ( $83 \pm 13$  vs  $78 \pm 12$ ), 22% lower in log OC ( $1.46 \pm 0.59$  vs  $1.71 \pm 0.52$ ) and 15% lower in log SHBG ( $3.72 \pm 0.56$  vs  $3.89 \pm 0.40$ ), with p-values < 0.05. There was no significant difference in log estradiol ( $4.13 \pm 0.72$  vs  $4.21 \pm 0.55$ ) or log of 25(OH)D ( $4.24 \pm 0.30$  vs  $4.25 \pm 0.32$ ) between the men with and without diabetes. In multivariable analysis, after adjusting for BMI and smoking, the risk of diabetes was increased with each SD lower in osteocalcin (OR 1.52, 1.10-2.09) and SHBG (1.37, 1.00-1.87). Approximately 15% of the liability to diabetes was accounted for by osteocalcin and 13% by SHBG.

Thus, these data suggest that lower osteocalcin and SHBG were associated with an increased risk of type 2 diabetes in men. The use of serum OC and SHBG may help improve the prognostic accuracy of type II diabetes in men.

**Disclosures:** N.D. Nguyen, None.

This study received funding from: National Health and Medical Research Council, Australia.

## SU462

**Bone Histomorphometry in Patients with Crohn's Disease.** A. Oostlander<sup>\*1</sup>, N. Bravenboer<sup>1</sup>, P. Holzmann<sup>\*1</sup>, J. van der Woude<sup>\*2</sup>, G. Dijkstra<sup>\*3</sup>, A. van Bodegraven<sup>\*4</sup>, P. Lips<sup>1</sup>. <sup>1</sup>Endocrinology, VU University Medical Center, Amsterdam, Netherlands, <sup>2</sup>Gastroenterology and Hepatology, Erasmus Medical Center, Rotterdam; on behalf of the ICC, Netherlands, <sup>3</sup>Gastroenterology and Hepatology, University Medical Center Groningen, Groningen; on behalf of the ICC, Netherlands, <sup>4</sup>Gastroenterology, VU University Medical Center, Amsterdam; on behalf of the ICC, Netherlands.

Inflammatory bowel disease (IBD) is associated with an increased prevalence of osteoporosis. Etiopathogenesis of bone loss in IBD-patients is complex, multifactorial and partly unclear. In this study we evaluated bone mass and structure by histomorphometry in iliac crest bone obtained from patients with Crohn's disease.

A subset of 14 patients with quiescent Crohn's disease (CD) from a randomized, double blind, placebo-controlled trial were analyzed in this study. The group comprised 9 women and 5 men, aged 23-56 years (mean 39 years). All had a lumbar spine and/or total hip bone mineral density with a T-score of -1 to -2.5 SD. Patients with current corticosteroid treatment and metabolic bone diseases were excluded. Disease activity (CDAI), C-reactive protein (CRP) and Alkaline Phosphatase (ALPase) levels were determined. Transiliac bone biopsies were obtained at baseline. Five micrometer undecalcified sections were stained with Goldner's Trichrome and Tartrate-resistant Acid Phosphatase (TRAP). Bone histomorphometry was performed automatically using NIS-Elements and according to the ASBMR nomenclature.

Total CDAI ranged from 0 to 194 (mean 83), CRP levels varied from 1 to 15 mg/L (mean 5 mg/L), and ALPase levels were between 52 and 88 U/L (mean 67 U/L). Histomorphometric analysis of bone biopsies of 14 patients with quiescent CD showed a mean bone volume of 19.8% (95% CI: 8.6-30.9). Trabecular thickness was 117.3 µm (69.4-165.3), trabecular number 1.7/mm (0.9-2.5), and trabecular separation 499.0 µm (233.1-764.9). Relative osteoid volume was 1.3% (0.0-3.6) and osteoid thickness 6.5 µm (3.6-9.5). The number of TRAP positive osteoclasts was 0.4/mm<sup>2</sup> (0.0-0.8). Trabecular bone volume correlated well with femoral neck BMD (p=0.025). Correlation with clinical and biochemical parameters of Crohn's disease showed a borderline positive association between osteoclast number and disease activity (p=0.074).

Comparison of our data to histomorphometric data from obduction material of age-matched men reveals similar structural parameters<sup>1</sup>. However, osteoid volume as well as thickness tend to be lower in patients with CD. We conclude that bone mass and structure in patients with quiescent Crohn's disease is quite normal, whereas bone formation is slightly impaired. Furthermore, bone resorption seems to be associated with disease activity.

<sup>1</sup>N. Bravenboer *et al.* Bone (1996) 18:551-557

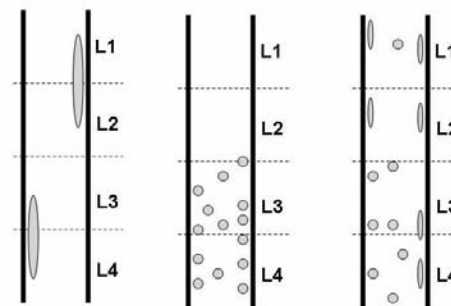
**Disclosures:** A. Oostlander, None.

This study received funding from: Aventis.

## SU463

**Morphological Atherosclerosis Calcification Distribution (MACD) Index is a Strong Predictor of Cardio-Vascular Death and Include the Predictive Power of BMD.** C. Christiansen<sup>1</sup>, M. Karsdal<sup>1</sup>, M. Ganz<sup>\*2</sup>, E. Dam<sup>\*1</sup>, M. Nielsen<sup>\*2</sup>. <sup>1</sup>Nordic Bioscience, Herlev, Denmark, <sup>2</sup>Department of Computer Science, University of Copenhagen, Copenhagen, Denmark.

Aortic calcification is a major risk factor for cardiovascular disease (CVD) related deaths. We investigated the relation between mortality and aspects of number, size, morphology and distribution of calcified plaques in the lumbar aorta and BMD of postmenopausal women. 308 women aged 48 to 76 were followed for 8.3±0.3 years and CVD deaths were recorded. BMD and several aortic calcification markers were computed: number, morphology, distribution, from outlines of the calcified plaques in lumbar X-rays. These markers were compared to BMD, SCORE card, Framingham score, and the Aortic Calcification Severity score - AC24. AC24 adjusted by age, waist circumference, and triglyceride levels (ATW) predicted mortality in postmenopausal women (CVD p=0.03, All-cause p=0.006). The SCORE card and the Framingham score resulted in mortality odds ratios (MOR) of 5.0 and 5.2 - defining high risk as ≥6 and ≥18, respectively. BMD and BMD adjusted for ATW was lower in the group of deceased than in survivors (p<0.001) and negatively correlated to calcification markers in survivors (R<sup>2</sup> = 0.27, p<0.001). All scores based on the calcification geometry provided highly significant predictions. The number of calcified deposits (NCD) was a significant predictor even after adjustment by the AC24 score (p=0.002). The AC24 score adjusted by NCD had no predictive value (p=0.53). The high risk patients (NCD ≥ 13) had MOR 12. The morphological atherosclerosis calcification distribution (MACD) index provided MOR 20 which was significantly higher than AC24 and any single or multivariate metabolic/physical marker. BMD correlates with AC24 among CVD dead patients (p=0.03) unlike MACD (p=0.43). The recent MACD-index provides a unique combination of morphology and distribution of aortic calcifications, factors that in a combination increase the biological relevance of the index by emphasizing that smaller plaques with a spread elongated morphology have a larger growth potential and thereby subsequent rupture potential. It includes the predictive power of BMD unlike the AC24 index. Thereby, in the current cohort with a long term follow-up the MACD-index is a convincingly strong predictor of CVD mortality, with an odds ratio of 20, of postmenopausal death related to CVD events



AC24	8	8	8
NCD	2	14	14
MACD	1	2	4

**Disclosures:** C. Christiansen, None.

This study received funding from: Nordic Bioscience A/S.

## SU464

**Bone Quality in Chinese American and Caucasian Women.** M. D. Walker<sup>1</sup>, C. Go<sup>\*1</sup>, J. Udesky<sup>\*1</sup>, D. J. McMahon<sup>\*1</sup>, G. Liu<sup>\*2</sup>, J. P. Bilezikian<sup>1</sup>. <sup>1</sup>Medicine, College of Physicians and Surgeons, Columbia University, New York, NY, USA, <sup>2</sup>Medicine, New York Downtown Hospital, New York, NY, USA.

Chinese Americans have low rates of hip fracture (fx) despite lower areal bone density (aBMD) by dual x-ray absorptiometry (DXA) compared to other racial groups. Aspects of bone quality, other than aBMD, may influence fx risk. These include bone size, volumetric bone density (vBMD), microarchitecture, mineralization density, crystallinity, & bone turnover. Data regarding these indicators of bone quality in Chinese American (CH) women could be helpful in understanding their low rates of hip fx. The goal of this study is to compare vBMD, bone size, as well as microarchitectural, structural & remodeling features of bone in CH and Caucasian (CA) women using DXA, central quantitative computed tomography (cQCT), high resolution peripheral QCT (HRpQCT), calciotropic hormones, bone turnover markers, & analysis of bone biopsies.

Data are presented for the first 15 women. The CH (n=7) and CA (n=8) groups did not differ in age (33 ± 3 vs. 34 ± 4 yrs; p=0.4), BMI (22 ± 2 vs. 24 ± 7 kg/m<sup>2</sup>; p=0.4), tobacco or alcohol use, family history of osteoporosis, oral contraceptive use, daily calcium (732 ± 197 vs. 1094 ± 635 mg; p=0.2) or vitamin D intake (295 ± 135 vs. 555 ± 435 IU; p=0.2). Serum 25-hydroxy vitamin D levels were lower in the CH group (29 ± 7 vs. 42 ± 13 ng/dl; p=0.03), but there was no difference in PTH levels (32 ± 11 vs. 31 ± 15 pg/ml; p=0.8). CH women tended to be less physically active (Baecke index 1.1 ± 0.5 vs. 1.5 ± 0.5; p=0.07) & spent less time outside (time outside score 2.2 ± 0.4 vs. 3.0 ± 1.1 p=0.06).

In the subset of women who have completed all tests (n = 7), aBMD did not differ for the lumbar spine (1.079 ± 0.05 vs. 1.065 ± 0.121 g/cm<sup>2</sup>; p=0.9), total hip (0.898 ± 0.047 vs. 0.977 ± 0.231 g/cm<sup>2</sup>; p=0.6), femoral neck (0.786 ± 0.059 vs. 0.844 ± 0.173 g/cm<sup>2</sup>; p=0.6) or 1/3 radius (0.666 ± 0.032 vs. 0.684 ± 0.045; p=0.6). There were no differences in HRpQCT indices at the radius. At the tibia, however, there was significantly greater trabecular thickness (Tb.Th) (0.098 ± 0.00 vs. 0.079 ± 0.01 mm; p=0.002) & a trend toward greater average total vBMD in the CH (382 ± 8 vs. 316 ± 47 mgHA/cm<sup>3</sup>; p=0.07) versus the CA group. There was no difference in cortical bone density, cortical thickness, trabecular bone density, trabecular bone volume/tissue volume, trabecular # or trabecular spacing.

Despite lower vitamin D levels, CH women did not differ from CA women of similar weight in aBMD, Tb.Th & average vBMD at the tibia, but not the radius, were greater in CH than CA women. The greater Tb.Th among CH women is of unclear clinical significance as this is a calculated variable. These data may provide insight into differences between Chinese Americans and Caucasians in a loaded bone, which could be important in understanding disparities in risk of hip fx.

**Disclosures:** M.D. Walker, None.

## SU465

**Fluoride Effects on Bone Formation, Mineralization and Mechanical Properties Are Influenced by Genetics.** M. Mousny<sup>\*1</sup>, S. Omelon<sup>\*2</sup>, L. Wise<sup>\*2</sup>, E. T. Everett<sup>3</sup>, M. Dumitriu<sup>\*2</sup>, D. P. Holmyard<sup>\*2</sup>, X. Banse<sup>\*1</sup>, J. P. Devogelaer<sup>4</sup>, M. D. Grynpas<sup>2</sup>. <sup>1</sup>Orthopaedic Research Laboratory, Catholic University of Louvain, Brussels, Belgium, <sup>2</sup>Samuel Lunenfeld Research Institute, Mount Sinai Hospital, Toronto, ON, Canada, <sup>3</sup>Department of Pediatric Dentistry and The Carolina Center for Genome Sciences, University of North Carolina, Chapel Hill, NC, USA, <sup>4</sup>Arthritis Unit, Catholic University of Louvain, Brussels, Belgium.

**Introduction:** The purpose of this study was to assess the effect of increasing fluoride (F<sup>-</sup>) doses on bone properties in inbred mouse strains in order to study the influence of genetic background.

**Materials and Methods:** Three inbred mouse strains with different susceptibilities to developing dental fluorosis (A/J a "susceptible" strain, SWR/J an "intermediate" strain, 129P3/J a "resistant" strain) were studied. Bone F<sup>-</sup> concentrations were determined. Bone mineral density (BMD) was evaluated through DEXA. Mechanical properties of cortical and trabecular bone were determined. Bone microarchitecture was quantified with microcomputed tomography and strut analysis. Bone formation was evaluated by static histomorphometry. Bone mineralization was quantified with Back Scattered Electron imaging (BSE) and powder X-ray diffraction. Microhardness measurements were taken from cortical and trabecular bone.

**Results:** Concordant with increasing F<sup>-</sup> dose were significant increases of F<sup>-</sup> bone concentration in all 3 strains. F<sup>-</sup> treatment had little effect on BMD. Mechanical testing showed significant alterations in "bone quality" in A/J, moderate alterations in SWR/J and no effect in 129P3/J. F<sup>-</sup> treatment had no significant effect on bone microarchitecture. Each strain demonstrated a significant increase in osteoid formation. The bone mineralization profiles showed a non-significant increase towards higher mineralization with increasing F<sup>-</sup> dose. Powder X-ray diffraction showed significantly smaller crystals for 129P3/J, and increased crystal width with increasing F<sup>-</sup> dose for all strains. There was no effect on bone microhardness.

**Conclusion:** Genetic factors may contribute to the variation in bone response to fluoride exposure. The increased crystal cross-section with increasing F<sup>-</sup> dose correlates with most of the decreased mechanical properties. An increase in bone F<sup>-</sup> might affect the mineral-organic interfacial bonding and/or bone matrix proteins. The smaller bone crystallites of the resistant strain may indicate a stronger organic/inorganic interface, reducing crystallite growth rate and increasing interfacial mechanical strength.

**Disclosures:** M. Mousny, None.

*This study received funding from: Willy and Marcy De Vooght Foundation.*

## SU466

**Correlation of Hip Geometry and Bone Density with Fragility Fracture in Japanese Postmenopausal Women.** M. Ito<sup>1</sup>, M. Uetani<sup>\*1</sup>, N. Wakao<sup>\*2</sup>, A. Harada<sup>\*3</sup>. <sup>1</sup>Radiology, Nagasaki University, Nagasaki, Japan, <sup>2</sup>Orthopaedic Surgery, Nagoya University, Nagoya, Japan, <sup>3</sup>Restorative Medicine, National Center for Geriatrics & Gerontology (NCGG), Oobu, Japan.

We investigated the characteristics of three-dimensional hip geometry and bone mineral density (BMD) in Japanese women in relation to fragility fracture using clinical CT. We also investigated structural factors relating to femoral neck (NECK) vs. trochanteric (TRO) fractures. Age-related changes in BMD and geometry of the proximal hip were studied in 208 postmenopausal women. The fracture study included 37 women with hip fracture (mean age: 75.9 years old) and 49 age-matched control women (79.4 years). We compared 20 women with NECK fracture (83.0 years) and age-matched 19 with TRO fracture (85.6 years). CT scanners used were Aquilion 16 (Toshiba) and Somatom 64 (Siemens) at Nagasaki University Hospital (NU) and NCGG, respectively. The reference phantom was B-MAS200 (Fjirebio Inc, Japan) containing hydroxyapatite at 0, 50, 100, 150 and 200 mg/cm<sup>3</sup>. The scanning condition are adjusted as much as possible; 120kV, 250mA, reconstruction thickness 0.5 mm at both institutes, and spatial resolution 0.625x0.625 mm at NCGG and 0.652x0.652 mm at NG. QCT PRO software (Mindways, USA) was used to analyze data for BMD, bone mass and areas in total, cortical and trabecular regions, and cortical thickness (CoTh), curvature, distance to center of bone mass (dist to CM), perimeter in cross-sectional femoral neck (CSFN). Hip axis length (HAL), neck shaft angle (NSA) and neck width, and biomechanical parameters such as cross-sectional moment of inertia (CSMI) and buckling ratio (BR) were also obtained. The shape of CSFN changed with aging; CoTh in superior, but not in inferior, region decreased significantly, maximal dist to CM increased, and curvature decreased. Women with hip fracture had a significantly lower total and cortical BMD, smaller cortical area and larger total and trabecular areas than those without hip fracture. Women with hip fracture had a significantly larger NSA, longer HAL, smaller curvature, lower CSMI and higher BR than those without fracture. The results of multiple regression analysis revealed that neck BMD was the strongest predictor of hip fracture among single parameters (coefficient of determination (CD)=26.4%), and adding geometrical parameters to neck BMD increased CD (43.0%). We also found that women with TRO fracture had a significantly lower cortical BMD, larger trabecular area, smaller NSA and lower BR than those with NECK fracture. We conclude that important parameters related to fragility fracture can be detected using clinical CT, that neck BMD is the strongest predictor of hip fracture, and that combination of BMD and geometrical data is useful for fracture risk assessment.

**Disclosures:** M. Ito, None.

## SU467

**Prediction of Trabecular Level Microdamage and Bone Fracture Through Local Strain.** P. J. Thurner<sup>\*1</sup>, R. Jungmann<sup>\*2</sup>, R. Tang<sup>\*3</sup>, G. Schitter<sup>\*2</sup>, D. Vashishth<sup>\*3</sup>, P. K. Hansma<sup>\*2</sup>. <sup>1</sup>School of Engineering Sciences, University of Southampton, Southampton, United Kingdom, <sup>2</sup>University of California Santa Barbara, Santa Barbara, CA, USA, <sup>3</sup>Rensselaer Polytechnic Institute, Troy, NY, USA.

The diagnosis of bone fracture risk in individuals is still mostly based on measurements of bone mineral density (BMD). Since diagnosis from BMD alone can carry large errors, additional parameters are necessary to reliably diagnose bone quality. One route to achieve this is the simulated mechanical evaluation of trabecular bone structures using finite element analyses (FEA) on acquired 3D data sets. To ensure meaningful results, such approaches need to include valid damage models predicting the occurrence of microdamage and fracture at certain thresholds, which weaken the structure. Here we present the results of a key experiment providing a first damage model by linking whitening in bone, seen during loading, to microdamage and involved local strains at the level of a single trabecula.

Rod-like trabeculae were excised from a proximal bovine femur and imprinted with a point grid using an ink jet printer. The trabeculae were tested in three-point bending, capturing force-displacement data and high-speed video images. Local strain fields on the sample surfaces were calculated using a custom digital image correlation algorithm. The average elastic modulus of (1.9±0.9) GPa was obtained from force-displacement data using the Euler-Bernoulli equation. For validation, experimental local strain patterns were compared to ones from a linear elastic FEA. After testing, trabeculae were subjected to basic fuchsin labeling, embedded and sectioned for microdamage analysis.

Whitening initiated on the tension side on loaded trabeculae in the form of a growing ellipsoid zone and faded upon formation of a macro-crack. At this point a whitened zone in front of the propagating crack tip appeared. Using basic fuchsin labeling, we find that whitening and microdamage occurrence are highly correlated, and that the size of cracks range from sub-μm to the μm range. Of the experimentally determined local strains, the tensile strain in x-direction, along the long axis of the samples, correlated best with the detected ellipsoidal whitening zone. The average tensile strain in x-direction at whitening onset was determined to be (1.9±0.1)% and the highest tensile strain just prior to failure was determined to be (12±6)%. Qualitatively, experimentally determined local strains agreed well with FEA. Quantitative values from experiments were generally lower due to the nonlinear properties of bone.

Based on our results and comparison to previous reports, we propose a brittle damage model for trabecular bone, asymmetric in tension and compression, with microdamage originating at tensile strains of 1.9%.

**Disclosures:** P.J. Thurner, None.

## SU468

**Thermoreversible Pluronic F108 Gel as a Universal Tissue Immobilization Material for Micro-Computed Tomography Analyses.** E. Atti<sup>\*1</sup>, S. Tetradis<sup>1</sup>, C. E. Magyar<sup>\*2</sup>, J. K. Armstrong<sup>\*3</sup>. <sup>1</sup>UCLA School of Dentistry, Los Angeles, CA, USA, <sup>2</sup>David Geffen School of Medicine at UCLA, Los Angeles, CA, USA, <sup>3</sup>Keck School of Medicine, USC, Los Angeles, CA, USA.

Micro-computed tomography (μCT) provides high-resolution 3-D images and quantitative architectural and density data for whole animal and tissue specimens. Despite remarkable developments in μCT technology, facilitating its commonplace use today, little attention is paid to the development of a reliable method for single and multiple sample immobilization for an individual acquisition run. Pluronic F108 is a water-soluble 14 kDa block copolymer that forms a thermoreversible gel in aqueous solution at a concentration >20% (w/w). A 30% solution of Pluronic F108 in water has a gelation temperature of 17 °C, below which it is a free-flowing viscous fluid, and at room temperature is a firm, optically-clear gel. In this study, the use of a 30% solution of Pluronic F108 (polymer) in water was compared to two common techniques for sample immobilization for μCT analyses: polyethylene spacer (PE) and wet gauze in ethanol. Mice tibiae were excised, fixed in buffered formalin and stored in 70% ethanol. Tibiae were immobilized using polymer by half-filling a scanning tube with cold polymer liquid, allowing the polymer to gel at room temperature and inserting the tibiae into the gel in the desired orientation. The tube was then filled with cold polymer liquid and allowed to gel. The same tibiae were also immobilized using PE or wet gauze in ethanol. Tibiae were scanned using a Scanco-40 scanner with a voxel-isotropic resolution of 12 μm and an X-ray energy of 55 KVP and 72 UA. Background homogeneity was qualitatively assessed using the scout view. For the same anatomical site between the three methods, quantitative architectural and density parameters measured were total volume, bone volume and volume fraction, trabecular number, thickness and spacing, connectivity density, degree of anisotropy, structure model index and bone mineral density. In the scout view, a homogeneous background was observed for polymer, whereas heterogeneous backgrounds were observed for PE and gauze (air bubbles). For architectural and density parameters measured, comparable values for each parameter were obtained with all three immobilization techniques. The advantages of Pluronic F108 gel were the ease of sample orientation, homogeneous medium, clarity of scout views, absence of air bubbles and lack of pressure on the specimen. The use of Pluronic F108 gel provides a rapid and simple technique to reliably immobilize excised bone samples in the desired orientation that does not interfere with quantitative measurements, and may be applicable to immobilize any hard or soft tissue samples for μCT and other analytical techniques.

**Disclosures:** J.K. Armstrong, None.

## SU469

**Changes in Volumetric Bone Density and Bone Strength at the Tibial Midshaft in Boys and Girls 12-17 Years of Age.** Y. Ahamed<sup>\*1</sup>, D. M. L. Cooper<sup>\*2</sup>, M. Burrows<sup>\*1</sup>, S. Braid<sup>\*1</sup>, H. A. McKay<sup>1</sup>. <sup>1</sup>Orthopaedics, Family Practice, Centre for Hip Health and Musculoskeletal Research, University of British Columbia, Vancouver Coastal Health Research Institute, Vancouver, BC, Canada, <sup>2</sup>Anatomy and Cell Biology, University of Saskatchewan, Saskatoon, SK, Canada.

The greater incidence of fragility fractures in older women compared to men may be related to sex-specific patterns of bone strength development during growth. We recently compared adaptation at the periosteal and endosteal surfaces of the tibial midshaft in boys and girls during puberty. Although all children increased bone size through periosteal apposition, boys had substantially larger bones than girls ( $p < 0.001$ ). Similarly, the magnitude of endosteal apposition during adolescence was greater for girls ( $p < 0.001$ ). Given the greater contribution of geometry, as compared with density to bone strength, in theory, men would better resist structural failure as they have significantly larger but less dense bones, on average. Bone density, bone mineral content, bone size, and shape all contribute to bone strength but their relative contribution to bone strength in boys versus girls is largely unknown. Thus, our objective was to compare a) how volumetric bone density (vBMD) at the tibial midshaft is accrued in boys and girls across 6 years of growth and b) to compare sex differences in bone strength accrual. We hypothesized that girls would exhibit greater gains in vBMD compared with boys across adolescence; whereas, boys would exhibit greater gains in bone strength. Participants were 89 girls and 93 boys followed for 6 years as part of the longitudinal Healthy Bones Study. Participants were 12.0 years ( $\pm 0.55$ ) at baseline (2001) and 17.7 years ( $\pm 0.58$ ) at follow-up (2007). Peripheral QCT (Stratec XCT 2000) was utilised to acquire a 2.5 mm mid-diaphyseal slice of the left tibia at both time points. Stratec XCT 5.50 program with a threshold of 480 mg/cm<sup>3</sup> was used to process the grayscale pQCT images to determine cortical density (CoD, mg/cm<sup>3</sup>) and strength strain index (SSI, mm<sup>3</sup>). We utilized a mixed linear model to compare the rate of change of the selected bone outcomes between the sexes. Sex-specific comparisons showed no significant differences for change in CoD ( $p = 0.904$ ) across the years of adolescent growth and significantly greater differences for change in SSI for boys ( $p < 0.001$ ). The magnitude of these differences was 1.3% for CoD and 54.7% for SSI. Between the sexes, girls demonstrated significantly greater gains in CoD as compared with boys ( $p < 0.001$ ) whereas boys demonstrated significantly greater gains in SSI ( $p < 0.001$ ). Thus, although both boys and girls enhance their bone strength as they mature, the specific adaptation favors bone strength in boys.

**Disclosures:** Y. Ahamed, None.

This study received funding from: MSFHR.

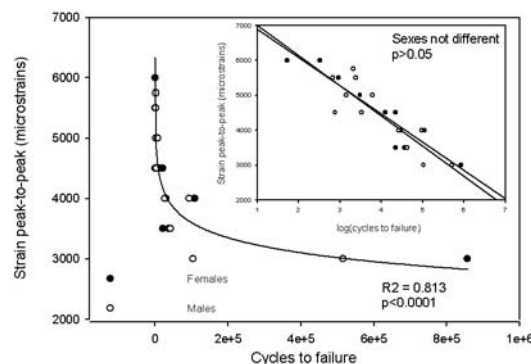
## SU470

**An Investigation of the Fatigue Behaviour of Rabbit Tibiae: Effects of Sex and Age.** T. L. Willett<sup>1</sup>, J. Wang<sup>\*2</sup>, M. D. Grynpas<sup>1</sup>. <sup>1</sup>Samuel Lunenfeld Research Institute, Mount Sinai Hospital, Toronto, ON, Canada, <sup>2</sup>Faculty of Dentistry, University of Toronto, Toronto, ON, Canada.

Stress fractures in bone are the result of cyclic loading during intensive exercise but do not result solely from fatigue of the bone material. Stress fractures are most prevalent in athletes and army recruits and are more common in females and younger adults. Investigations in animal models have been done using rats and rabbits but age and sex have received little attention. The objective of this study is to investigate sex differences in the fatigue behaviour of tibiae from pubescent (4 months) and mature (12 months) rabbits ex vivo, establishing baseline material fatigue behaviour for a new rabbit model.

To date, tibiae from six male and seven female New Zealand White rabbits (age 4 months) have been tested. Prior to fatigue testing, the bones were scanned with both DEXA and CT scans to measure diaphyseal bone mineral density (BMD) and cross-sectional geometry respectively. The tibiae were loaded in 3-point bending using an Instron 8511 mechanical testing machine. The load was applied at the mid-diaphysis on the posterior-medial surface. Tests were performed under load control at 2Hz with load levels corresponding to initial peak-to-peak strain levels ranging from 3000 to 6000 microstrains with a strain at minimum load of approximately 500 microstrain. Tensile strain due to bending was accurately measured using a strain gauge bound to the anterior-lateral surface of the mid-diaphysis. During the testing, load, displacement, strain, time and cycle count (N) were acquired using a HBM Spider8 data acquisition system.

Diaphyseal BMD was not detectably different between the sexes. As a first comparison of the fatigue behaviour, peak-to-peak strain (S) versus log transformed number of cycles to failure (log(N)) curves were compared between the sexes using linear regression techniques at the 95% confidence level. The S-log(N) curves for the males (n=12) and females (n=12) at 4 months of age were not detectably different ( $p > 0.05$ ). A sex difference in the S-log(N) curves was not detected, perhaps, because the 4-month old rabbits had not yet completed skeletal maturation and any sex differences had not yet fully developed or due to variability between animals. Further analysis of the fatigue behaviour will be presented. Based on the literature, we expect that mature animals will display differences from both the younger group and between the sexes.



**Disclosures:** T.L. Willett, None.

## SU471

**Subject-specific Mechanical Properties of Trabecular Bone Using a Low-dose Imaging.** E. Sapin<sup>\*1</sup>, K. Briot<sup>2</sup>, S. Kolta<sup>2</sup>, C. Roux<sup>2</sup>, W. Skalli<sup>\*1</sup>, D. Mitton<sup>\*1</sup>. <sup>1</sup>Biomechanics Laboratory, ENSAM - Arts et Métiers ParisTech, Paris, France, <sup>2</sup>Rheumatology Department, Paris-Descartes University, Cochin Hospital, Paris, France.

Subject-specific finite-element models to predict failure load are based on quantitative computed tomography (QCT). Relationships between the Young's modulus (E) of vertebral trabecular bone and bone mineral density (BMD) assessed by QCT have been proposed in order to evaluate subject-specific vertebral stiffness. However, QCT is not adapted to analyse the whole spine for osteoporotic patients' follow-up because of the important radiation dose. Towards further in vivo applications, this study aims at evaluating the mechanical properties of the vertebral trabecular bone using a low-dose X-ray device.

Nineteen vertebrae (from T10 to T12; 7 females and 12 males;  $69 \pm 13$  years old) were considered. Biplanar X-rays were obtained using the EOS® system (the radiation dose is ten times lower than a conventional X-rays [2]) with a dual-energy modality to evaluate antero-posterior BMD (AP-BMD in g.cm<sup>-2</sup>) and lateral BMD related to the vertebral width (LAT-BMD in g.cm<sup>-3</sup>). A cylindrical sample was extracted from each vertebral body and tested in axial compression until failure to assess the Young's modulus (E) and the ultimate stress ( $\sigma_{max}$ ).

E was significantly related to AP- and LAT- BMDs ( $r^2 = 0.68$  - SEE=107.7MPa and  $r^2 = 0.53$  - SEE=125.6 MPa respectively;  $p < 0.01$ ). Significant relationships with  $\sigma_{max}$  were also found (AP-BMD:  $r^2 = 0.50$  - SEE=1.24 MPa; LAT-BMD:  $r^2 = 0.64$  - SEE=1.15 MPa;  $p < 0.01$ ).

These values are consistent with BMD assessed using QCT [1] and even better than previous study considering BMDs evaluated using dual X-ray absorptiometry [3]. This study showed that subject-specific mechanical properties of cancellous bone can be predicted from low-dose imaging. It is a first step towards subject-specific models using low-dose imaging to predict vertebral strength of osteoporotic patients.

1 D. L. Kopperdahl, E. F. Morgan and T. M. Keaveny. (2002) Journal of orthopaedic Research. 20, 801-805

2 J. Dubousset, G. Charpak, I. Dorion, et al. (2005) Bulletin de l'Académie nationale de médecine. 189, 287-97

3 E. Cendré, D. Mitton, M. E. Arlot, et al. (1999) Osteoporosis International. 10, 353-360

**Disclosures:** E. Sapin, None.

## SU472

**Peripheral Quantitative Computed Tomography (pQCT) Predicts Vertebral Fractures in Osteoporotic Postmenopausal Women.** K. D. Stathopoulos<sup>\*1</sup>, E. Metania<sup>\*1</sup>, P. Katsimbri<sup>\*1</sup>, T. Kaplanoglou<sup>\*1</sup>, N. Kordalis<sup>\*1</sup>, E. Efsthopoulos<sup>\*2</sup>, P. N. Soucacos<sup>\*1</sup>, G. Skarantavos<sup>1</sup>. <sup>1</sup>Department of Bone Metabolic Diseases, 1st Orthopedic clinic, University of Athens, "Attikon" University Hospital, Athens, Greece, <sup>2</sup>2nd Department of Radiology, University of Athens, "Attikon" University Hospital, Athens, Greece.

**Purpose** was to compare results of tibial pQCT measurements, in order to estimate differences in volumetric densities and geometric properties of the bone, between osteoporotic postmenopausal women with vertebral fractures of the thoracic spine and postmenopausal osteoporotic women without such fractures.

**For material and methods**, we examined retrospectively medical records of 50 osteoporotic postmenopausal women from a total of 1246 treated as outpatients in our department. Patients were separated in 2 groups: Group A (n=24, mean age 72.0y) had  $\geq 1$  osteoporotic fractures of the thoracic spine and Group B (n= 26, mean 68.6y) had no such fractures. Inclusion criteria: 1) age > 50y, 2) postmenopausal status > 2 years 3) DEXA (Spine or Hip) T-scores < -2.5 SD to define osteoporosis, 4) positive (Group A)/negative (Group B) x-rays for vertebral fracture (loss of anterior/central height of > 30% of the vertebral body) and 5) no previous use of bone anabolic agents (estrogens, teriparatide, parathormone). Exclusion criteria: secondary osteoporosis' conditions (glucocorticoid-induced or other), bone metabolic diseases, high-energy vertebral fractures, previous tibia fracture and malignancy. We compared tibial pQCT measurements at the 4%, 14% and 38% of tibia length sites between the 2 groups and performed statistical analysis of our results (t-test, ANOVA).

**Results:** there were no statistical differences between the 2 groups concerning age (p=0.197), time of menarche (p=0.729) or menopause (p=0.196), and tibia length (p=0.102). Trabecular density at the 4% site was significantly lower (p=0.016) in the fracture group (mean 146.521) than in the non-fracture group (mean 166.803). Subcortical density at the 14% site was lower in the fracture group (mean 658.83 vs 695.23 in the non-fracture group) but the results were not statistically significant (p=0.343). Patients with  $\geq 2$  vertebral fractures had lower trabecular densities than patients without fracture (p=0.020) or patients with 1 vertebral fracture (p=0.284). Finally, patients with vertebral fractures had lower total area (p=0.097), trabecular area (p=0.098) and cortical area (p=0.075) and lower cortical thickness (p=0.047) at the 4% site.

Our **conclusion** was that trabecular density on tibial pQCT was significantly lower in osteoporotic women with vertebral fractures than in non-fractured ones. pQCT technology may be helpful in recognizing women of high risk for osteoporotic vertebral fractures.

**Disclosures:** K.D. Stathopoulos, None.

## SU473

**Effects of a High G Environment on Bone Mineral Density in UK Fast-Jet Trainee Pilots.** D. Pearson<sup>\*1</sup>, J. P. Greeves<sup>2</sup>, S. E. Day<sup>\*2</sup>, J. Adams<sup>3</sup>, B. Horton<sup>\*1</sup>, D. Green<sup>\*1</sup>, D. Hosking<sup>1</sup>. <sup>1</sup>Nottingham University Hospitals NHS Trust, Nottingham, United Kingdom, <sup>2</sup>QinetiQ Ltd, Farnborough, United Kingdom, <sup>3</sup>Manchester University, Manchester, United Kingdom.

Pilots ejecting from fast-jet aircraft are susceptible to vertebral fractures, particularly at T12/L1. Reduced bone mineral density (BMD) is a risk factor for vertebral fracture. Pilots training on the Hawk T1 aircraft experience G forces ranging between -4 and +8 G, in different axes, that might confer potential positive effects on vertebral BMD. The purpose of this study was to examine the effect of high G training on lumbar spine BMD in fast-jet trainee pilots.

Twenty-five male fast-jet trainee pilots (mean (1SD) age 25.4 (3.1) y; height (1.80 (0.07) m; body mass 79.7 (8.0) kg) starting Advanced Flying Training (AFT) on the Hawk T1 trainer volunteered to take part. BMD at the lumbar spine (L1-L4), total hip, femoral neck and the whole body, and body composition were measured at the start (baseline) and during the final week (follow-up) of AFT. The duration of training ranged between 2.7 and 4.7 months, and pilots flew 60 (20) h. Lumbar spine, total hip and femoral neck BMD was also measured in 12 size-matched male controls (age 27.3 (6.9) y; height 1.80 (0.06) m; body mass 80.7 (8.7) kg) on two occasions, six months apart. Scans were performed using a Hologic® QDR 4500.

Pilots were significantly younger than controls (P<0.01), but no significant differences in lumbar spine, total hip or femoral neck BMD were shown at baseline between the two groups (P>0.05). Lumbar BMD did not change between baseline and follow-up in pilots (1.107 (0.115) vs 1.102 (0.114) g·cm<sup>2</sup>) or in controls (1.138 (0.141) vs 1.149 (0.157) g·cm<sup>2</sup>) (P>0.05). A significant decrease in total hip BMD between baseline and follow-up was observed in pilots (1.121 (0.132) vs 1.110 (0.131) g·cm<sup>2</sup>; P<0.05) but not in controls (P>0.05). No significant change occurred in femoral neck BMD in either group (P>0.05), or in whole body BMD and body composition in pilots.

These findings suggest that exposure to high G training does not alter mineralisation at the lumbar spine, and, therefore, may not offer protective effects against vertebral fracture in pilots ejecting from fast-jet aircraft. The effect of longer-term G exposure on BMD should be investigated. The mechanism for the significant reduction in BMD detected at the hip in pilots is uncertain, but might be explained by reduced levels of leisure time physical activity during AFT.

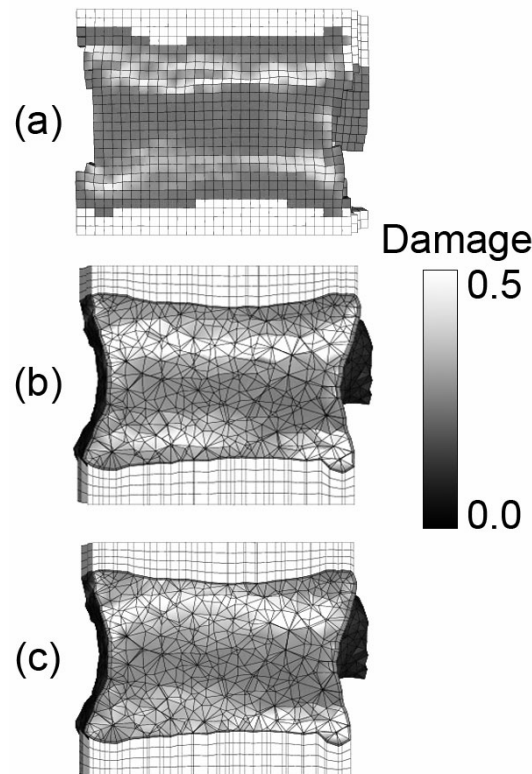
**Disclosures:** J.P. Greeves, None.

This study received funding from: UK Ministry of Defence.

## SU474

**Comparison of Voxel-Based and Smooth Finite Element Models to Predict Damage Accumulation in Vertebral Bodies.** Y. Chevalier<sup>\*</sup>, D. Pahr<sup>\*</sup>, P. K. Zysset. Institute of Lightweight Design and Structural Biomechanics, Vienna University of Technology, Vienna, Austria.

**Slipped Discs** are a common cause of low back pain. The aim of this study was to compare the results of two different modeling approaches to predict damage accumulation in vertebral bodies. A voxel-based finite element model (FEM) and a smooth FEM were used to simulate the mechanical behavior of a vertebral body under compression. The results of the two models were compared in terms of damage accumulation. The voxel-based FEM showed higher damage accumulation than the smooth FEM. This is due to the fact that the voxel-based FEM takes into account the local geometry of the vertebral body, while the smooth FEM uses a simplified geometry. The results of this study show that the voxel-based FEM is more accurate in predicting damage accumulation in vertebral bodies.



**Indication** of the model results is shown in the figure. The results of the two models are compared in terms of damage accumulation. The voxel-based FEM shows higher damage accumulation than the smooth FEM. This is due to the fact that the voxel-based FEM takes into account the local geometry of the vertebral body, while the smooth FEM uses a simplified geometry. The results of this study show that the voxel-based FEM is more accurate in predicting damage accumulation in vertebral bodies.

**Disclosures:** Y. Chevalier, None.

This study received funding from: Lilly Deutschland GmbH.

## SU475

**Changes in Chemical, Mechanical, and Structural Properties of Lamellar Bone during Young Adulthood.** V. Bornikolas<sup>\*1</sup>, M. Ruppel<sup>\*1</sup>, L. Miller<sup>2</sup>, S. Judex<sup>1</sup>. <sup>1</sup>Biomedical Engineering, Stony Brook University, Stony Brook, NY, USA, <sup>2</sup>Brookhaven National Laboratories, Upton, NY, USA.

Despite clear evidence that factors pertaining to the quality of a bone may greatly influence its mechanical behavior, the precise identity of the underlying matrix components is unclear. Here, using the young adult rat skeleton, relations between chemical, mechanical, and structural properties were determined. Femurs of female Sprague-Dawley rats were harvested at 2mo, 4mo, and 5mo of age (n=4 each) and subjected to in situ chemical Fourier transform infrared microspectroscopy (FTIRM) analysis, static and dynamic nano-indentation, as well micro- and nano-computed tomography. All measurements were performed at anterior, posterior, medial, and lateral strips of the middiaphysis that spanned the entire cortex between the endocortical and periosteal surfaces. Preliminary data showed that the degree of mineralization, as indicated by the phosphate to protein ratio, increased between 2mo and 5mo of age. Interestingly, this increase was spatially highly-site specific and focal in nature (Fig. 1). Spatial correlations were performed site-specifically between the chemical, mechanical, and structural measurements. Together, these data indicate a great degree of site-specificity by which the diaphyseal rat femur alters its matrix properties, a characteristic that can be exploited for identifying chemical and structural components that modulate bone's mechanical behavior.

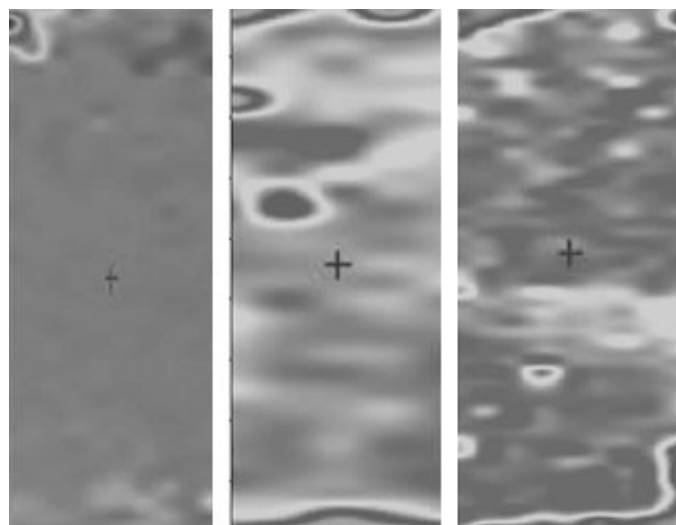


Figure 1: Map of the phosphate to protein ratio imaged at the posterior aspect of 2m old (left), 4m old (middle), and 5m old (right) rat femur. Brighter areas indicate higher levels of mineralization.

**Disclosures:** V. Bornikolas, None.

This study received funding from: NIAMS.

## SU476

**Neonatal Exposure to Soy Isoflavones Attenuates Deterioration of Bone Tissue in Female but Not Male Mice After Cessation of Sex Steroid Production.** J. Kaludjerovic\*, W. E. Ward. Nutritional Sciences, University of Toronto, Toronto, ON, Canada.

Isoflavones, abundant in soy foods such as soy protein-based infant formula, are structurally similar to estrogen and thus, may have the potential to elicit estrogen-like activity. Infants consuming soy protein-based infant formulas are exposed to substantial levels of soy isoflavones during developmental stages of life that are sensitive to environmental disturbances. Previous investigation from our laboratory has demonstrated that neonatal exposure to soy isoflavones, at levels similar to that of infants consuming soy protein-based infant formula, results in higher bone mineral density (BMD) and greater bone strength in female CD-1 mice at young adulthood. The primary objective of this study was to determine if the higher BMD and greater bone strength observed at 4 months of age from early exposure to soy isoflavones provides protection against the deterioration of bone tissue that occurs after the withdrawal of endogenous sex steroid production. Male and female mice (n=8-12 pups/group/gender) were randomized to subcutaneous injections of daidzein (DAI, 2 µg/d), genistein (GEN, 5 µg/d), DAI+ GEN (7 µg/d), diethylstilbestrol (DES, positive control, 2 µg/d), or corn oil (CON) from postnatal day one to five. At 4 months of age, mice were either ovariectomized (females) or orchidectomized (males) and were followed to 8 months of age. BMD and biomechanical bone strength were assessed at the femur and lumbar vertebrae to determine the effects of early isoflavone exposure on skeletal sites that differ in the proportion of cortical and trabecular bone. Females treated with DAI, GEN, DAI+GEN or DES had higher (p<0.05) lumbar vertebrae (LV1-LV3) bone mineral content (BMC) and BMD compared to the CON group. These improvements resulted in stronger vertebrae that were more resistant to fracture, as the peak load of LV2 was higher (p<0.05) in the DAI and DAI+GEN groups compared to CON. Similar trends were observed at the femur with DAI and DAI+GEN providing the greatest protection against the deterioration of bone tissue that occurs after the decline of endogenous sex steroid production. Among males, the effects of early exposure to isoflavones on bone metabolism were not significantly different from the CON group. In conclusion, short-term neonatal exposure to isoflavones provides protection against the deterioration of bone tissue postovariectomy in females but not postorchidectomy in males. The greatest protection resulted from treatment with DAI, either alone or in combination with GEN. Future research is required to elucidate the mechanisms by which early exposure to soy isoflavones modulates bone metabolism.

**Disclosures:** J. Kaludjerovic, None.

This study received funding from: International Life Sciences Institute North America, Future Leader Award to W. Ward.

## SU477

**Bone Size, Volumetric Bone Density in relation to Fat Mass in Healthy Young Men at age of Peak Bone Mass.** Y. E. Taes\*, B. Lapauw\*, S. Goemaere\*, H. Zmierzak\*, J. Kaufman\*. <sup>1</sup>Endocrinology, Ghent University Hospital, Ghent, Belgium, <sup>2</sup>Unit for Osteoporosis and Metabolic Bone Diseases, Ghent University Hospital, Ghent, Belgium.

This study was performed to assess the individual contribution of lean and fat mass on volumetric trabecular and cortical bone parameters.

We recruited 677 healthy male siblings at the age of peak bone mass (25-45 yrs) in a cross-sectional, population-based study. Trabecular and cortical bone parameters of the radius and cortical bone parameters of the tibia were assessed using peripheral quantitative computed tomography (pQCT). Lean and fat mass were determined using DXA. Cross-sectional associations between cortical, trabecular bone parameters and fat or lean mass were investigated using linear mixed-effects modeling analyses to account for family structure.

Positive univariate associations between height, body weight, lean or fat mass and bone size as determined by pQCT are observed. After controlling for age, weight and height, lean mass remains a strong positive determinant of cortical bone area, as well as cortical thickness and periosteal circumference, both at the radius ( $\beta = 0.26-0.91$ ;  $P < 0.003$  to  $0.0001$ ) and the tibia ( $\beta = 0.58-0.93$ ;  $P < 0.0001$ ). At the radius trabecular area ( $\beta = 0.70$ ;  $P < 0.0001$ ) and density ( $\beta = 0.19$ ;  $P = 0.03$ ) relate positively with lean mass. Fat mass is negatively associated with cortical bone area, cortical thickness and periosteal circumference, both at the radius ( $\beta = -0.33$  to  $-0.88$ ;  $P \leq 0.0001$ ) and the tibia ( $\beta = -0.59$  to  $-0.93$ ;  $P < 0.0001$ ) as well as with trabecular area ( $\beta = -0.65$ ;  $P < 0.0001$ ) at the radius, after correction for age, height and weight/lean mass. Cortical density is positively associated with fat mass ( $\beta = 0.18$  to  $0.20$ ;  $P = 0.01$  to  $0.03$ ) and inversely with lean mass ( $\beta = -0.25$  to  $-0.28$ ;  $P = 0.001$  to  $0.006$ ).

In conclusion, we found that lean mass is as expected a strong positive determinant of bone size at both the radius and tibia in healthy men at the age of peak bone mass, consistent with the model of bone adaptation to applied muscle force. After controlling for age, weight or lean mass and height, fat mass is negatively associated with cortical and trabecular bone size and positively with cortical density. Though no conclusion about the underlying mechanism can be drawn from this study, these findings could be explained through the mechanostat model of bone adaptation, programming of the mesenchymal stem cell or adipocyte-related factors.

**Disclosures:** Y.E. Taes, None.

## SU478

**Non-Enzymatic Glycation Alters Collagen Fibrillar Structure and Energy Dissipation Characteristics.** A. A. Poundarik\*, D. Vashishth. Biomedical Engg., Rensselaer Polytechnic Institute, Troy, NY, USA.

The ability of bone to resist fracture is determined not only by bone mineral density and architecture but also by the quality of its extracellular matrix (ECM) [1]. Post translational modifications including non enzymatic glycation (NEG), resulting from the formation of advanced glycation endproducts (AGEs), have been shown to alter the bone's ECM including collagen [2]. Because collagen is the principal structural protein in bone providing ductility, the accumulation of AGEs in collagen may increase bone fragility by altering its ultrastructure and energy dissipation characteristics.

Here we used atomic force microscopy (AFM) to study the effect of glycation on the fibrillar structure of collagen and on interfibrillar energy dissipation characteristics. Acid solubilized rat tail collagen was precipitated in vitro and incubated to obtain fibrils with 67nm D-periodicity. A 1.5M ribose solution was used to glycate [3] the collagen. Control (C) and glycated (G) collagen were imaged for topography using AC 160 cantilevers ( $k=40N/m$ ,  $f_c=300kHz$ ). Fibril diameter (D) was measured using section analysis (N=8). Force measurements on these samples (pulling rate of 5µm/sec) were carried out in PBS under ambient conditions using Olympus Biolever ( $k=0.025N/m$ ). As a measure of energy dissipation during deformation of collagen, area under the force-distance curves (A) was quantified (N=5). Data was assessed using non-parametric Mann-Whitney Rank Sum Tests. Fluorescence based AGE content was measured using established protocol [3]. AGEs increased three fold in the glycated samples with values being in the physiological range (p<0.05). Compared to the control sample, fibril diameter ( $D_c=363\pm40.4nm$ ) of glycated collagen showed a significant (p<0.001) reduction ( $D_g = 88.3\pm13.5nm$ ). Area under curve (energy dissipation) comparison between the two groups was also statistically significant (p=0.022) with the mean dissipation value for the glycated fibrils ( $A_g=4.216E-15\pm4.059E-15Nm$ ) being about an order of magnitude smaller than that of the control ( $A_c=3.014E-14\pm2.014E-14Nm$ ).

In conclusion, non-enzymatic glycation alters collagen fibrillar structure and reduces energy dissipation. Collagen in bone is responsible for providing ductility and absorbing energy thereby reducing fracture propensity. Known accumulation of AGEs due to diabetes and aging may consequently manifest as a degradation of bone matrix properties and an increased risk of fracture. Further studies are needed to investigate the molecular origin of these changes.

**References:**

- [1]: Vashishth. Critical Reviews in Eukaryotic Gene Expression. (2005)
- [2]: Viguet-Carrin et al. Osteoporos. Int. (2006)
- [3]: Vashishth et al. Bone. (2001)

**Disclosures:** A.A. Poundarik, None.

This study received funding from: NIH Grant AG 20618,



## SU479

**Transmenopausal Changes In the Trabecular Bone Intrinsic Properties.** B. J. Polly<sup>\*1</sup>, J. A. Turner<sup>\*1</sup>, M. P. Akhter<sup>2</sup>, R. R. Recker<sup>2</sup>. <sup>1</sup>Engineering Mechanics, University of Nebraska, Lincoln, NE, USA, <sup>2</sup>Medicine, Creighton University, Omaha, NE, USA.

Bone fragility related to post-menopausal osteoporosis in women leads to atraumatic fractures of skeletal sites. Three-dimensional bone architecture has been reported previously. However, little is known about the intrinsic material strength changes during the transmenopausal period. The general hypothesis for this work is that measured variables describing trabecular bone intrinsic material properties are affected by change in hormonal status at menopause soon after final menses, such that indentation modulus and hardness will decline. Minimal data exist describing intrinsic material properties in human transilial bone biopsies representing transmenopausal period. Paired transilial biopsies specimens (n= 6 pairs) were used from a previously reported study in which bone biopsies were obtained from women on entry (pre-menopausal and >age 46), and at 12 months past the last menstrual period. Trabecular bone intrinsic properties were obtained using the nanoindentation technique (Hysitron, MN). Embedded bone biopsies were prepared with a flat and smooth surface by grinding with 600, 800, and 1200 grit sand papers and then polished with 1 micron and 0.25 micron diamond slurry (Buehler, IL). At least 20 indents per biopsy were made on trabecular sites using a Berkovich indenter tip. Indentation modulus was determined from the load displacement diagram using the Oliver-Pharr method. The loading and unloading sections were each 10 seconds, with loading rates of 600  $\mu\text{N/s}$  and -600  $\mu\text{N/s}$  respectively. The hold section was 10 seconds at the maximum force of 6,000  $\mu\text{N}$ . Paired t-tests were used to compare pre- and post-menopausal trabecular bone intrinsic properties. BV/TV (published micro-CT data, Table) decreased during transmenopausal period. There is no significant change between pre- and post menopausal bone specimens in their indentation modulus and hardness. Data from additional paired bone biopsies will allow us to document differences in trabecular bone intrinsic material properties. One limitation of this study is that the previously used bone biopsies were embedded in Methyl methacrylate, which may influence the measured intrinsic properties of bone. We expect that intrinsic material properties will be different in unembedded bone biopsies thus reflecting any true decline in skeletal quality during the transmenopausal period.

Mean $\pm$ SD	Pre	Post
BV/TV % (3D micro-CT)	28.3 $\pm$ 7.1	24.9 $\pm$ 7.4 <sup>a</sup>
Indentation modulus (GPa)	16.8 $\pm$ 2.0	17.1 $\pm$ 3.7
Indentation Hardness (GPa)	0.60 $\pm$ 0.06	0.64 $\pm$ 0.12

<sup>a</sup> P < 0.05; as compared to Pre by paired student's t test

**Disclosures:** B.J. Polly, None.

## SU480

**Non-invasive In Vivo Raman Spectroscopy in Mice.** K. A. Dooley<sup>\*1</sup>, M. V. Schulmerich<sup>\*1</sup>, J. M. Kreider<sup>\*2</sup>, J. H. Cole<sup>1</sup>, S. A. Goldstein<sup>2</sup>, M. D. Morris<sup>1</sup>. <sup>1</sup>Chemistry, University of Michigan, Ann Arbor, MI, USA, <sup>2</sup>Orthopaedic Surgery, University of Michigan, Ann Arbor, MI, USA.

Bone fragility is associated with changes in composition that are metrics of bone quality. Currently, no *in vivo* techniques are available for assessing the composition contributions to bone quality in animals used in the laboratory for studying disease states. We have developed a non-invasive Raman spectroscopic fiber optic probe to acquire bone spectra through the skin of mice and other small animals. The objective of this study was to investigate our ability to measure bone composition parameters non-invasively in mice. Strains of mice were selected to mimic the variation seen in a healthy human population. For all transcutaneous measurements, an approved protocol was followed. Mice were anesthetized, and hair was removed using a depilatory agent. Glycerol was applied to increase skin transparency. Plastic wrap was then placed over the limb, and water irrigation was used to prevent thermal damage. Multiple spectra were acquired on each tibia. The small size of the mouse limbs required great care in positioning the fiber optic probe to obtain valid results. Following transcutaneous measurements, the mice were sacrificed, overlying tissues were removed, and spectra of the exposed bone were collected for validation. Bone spectra were separated from spectra of overlying tissue using multivariate methods. The mineral/matrix ratio and mineral crystallinity, metrics of bone quality, were subsequently calculated. Both measures of mineral content and matrix content obtained transcutaneously were in good agreement with the values obtained from exposed bone. Our results demonstrate that important composition contributions to bone quality can be determined via transcutaneous measurements in mice. Preliminary measurements on rat and canine limbs demonstrate that this approach to *in vivo* spectroscopic measurement of bone quality is easily adapted to these larger animals with only minor changes in the placement and spacing of optical fibers.

**Disclosures:** K.A. Dooley, None.

## SU481

**Estimation of Relative Stiffness Contributions of Cortical and Trabecular Compartments by MRI-based Finite Element Analysis.** C. S. Rajapakse<sup>\*1</sup>, J. F. Magland<sup>\*1</sup>, M. J. Wald<sup>\*1</sup>, B. Vasilic<sup>\*1</sup>, X. H. Zhang<sup>\*2</sup>, X. E. Guo<sup>2</sup>, F. W. Wehrli<sup>1</sup>. <sup>1</sup>University of Pennsylvania, Philadelphia, PA, USA, <sup>2</sup>Columbia University, New York, NY, USA.

Whole bone stiffness has contributions from both cortical and trabecular bone (TB). The relative stiffness contribution of the two compartments can be estimated using finite element (FE) analysis. However, such estimations have been impractical due to the computational complexity. To estimate overall stiffness, a fast, custom-designed FE algorithm was developed. MR images of 30 whole cross-section distal tibia specimens of approx. 20mm length from 15 donors (ages 55-85 years) were obtained with 3D FLASE (spin-echo) pulse sequence in a 1.5T whole-body scanner, with 128 slices acquired at 160  $\mu\text{m}^3$  isotropic voxel size. Cortical, TB, and combined regions were manually selected to generate three data sets for each specimen. The FE analysis was then performed on the basis of inverted grayscale bone volume fraction (BVF) maps. The tissue properties were assumed to be linear elastic and isotropic with Poisson's ratio 0.3 and Young's modulus 13GPa, and the Young's modulus of each bone voxel was weighted by the corresponding BVF value. Simulated compression was applied along the principal loading (i.e. the bone's longitudinal) direction, and the stiffness was obtained by comparing the surface forces to the applied compression. Total computation time was around 75 hours for all 90 simulations on a dual quad-core system with 28GB of RAM. Figure 1a shows the relative stiffness contributions from cortex and TB for 15 specimens. The trabecular compartment was found to contribute 32 $\pm$ 12% to overall stiffness. Also noted from Figure 1a is the greater strength of the whole bone relative to the sum computed for each compartment. Such a relationship is also evident from Figure 1b in which whole-bone stiffness is plotted versus the sum from each compartment. The data show that whole-bone FE now is possible and can provide new insight into compartmental contributions to overall mechanical behavior in practical computation times on dedicated laboratory computer systems.

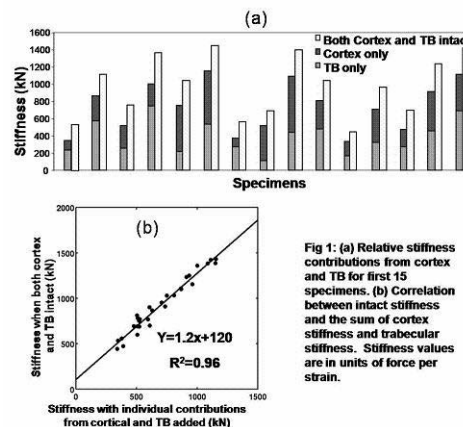


Fig 1: (a) Relative stiffness contributions from cortex and TB for first 15 specimens. (b) Correlation between intact stiffness and the sum of cortex stiffness and trabecular stiffness. Stiffness values are in units of force per strain.

**Disclosures:** C.S. Rajapakse, None.

This study received funding from: NIH.

## SU482

**Vitamin D Insufficiency: Seasonal Variation in Healthy 6-12 year old African American and Caucasian Children.** K. Rajakumar<sup>1</sup>, M. F. Holick<sup>2</sup>, K. Jeong<sup>\*3</sup>, Y. Lin<sup>\*4</sup>, T. C. Chen<sup>2</sup>, F. Olabopo<sup>\*5</sup>, M. Haralam<sup>\*5</sup>, A. Nucci<sup>\*5</sup>, S. B. Thomas<sup>\*6</sup>, S. L. Greenspan<sup>7</sup>. <sup>1</sup>Pediatrics, University of Pittsburgh School of Medicine, Pittsburgh, PA, USA, <sup>2</sup>Medicine, Boston University School of Medicine, Boston, MA, USA, <sup>3</sup>Biostatistics, University of Pittsburgh, Pittsburgh, PA, USA, <sup>4</sup>Medicine & Biostatistics, University of Pittsburgh, Pittsburgh, PA, USA, <sup>5</sup>Children's Hospital of Pittsburgh, Pittsburgh, PA, USA, <sup>6</sup>Center for Minority Health, University of Pittsburgh, Pittsburgh, PA, USA, <sup>7</sup>Medicine, University of Pittsburgh School of Medicine, Pittsburgh, PA, USA.

**Background:** Data characterizing the vitamin D (Vit D) status of healthy young school age children in the United States are limited.

**Objective:** To estimate the seasonal variation of vit D insufficiency in healthy 6-12 year old pre- and early adolescent African American (AA) and Caucasian (C) children residing in Pittsburgh, PA (latitude: 40.4N) and examine risk factors for vit D insufficiency.

**Design:** Serum 25-hydroxyvitamin D (25(OH)D), parathyroid hormone (PTH), calcium (Ca), phosphorus, albumin, and dietary intake of vit D and calcium were assessed during summer (June through September) and/or winter (December through March). Vit D deficiency was defined as serum 25(OH)D <20 ng/mL and insufficiency as 20 - <30 ng/mL. Serum 25(OH)D was measured by liquid chromatography tandem mass spectrometry (LC-MS/MS).

**Results:** A total of 123 children (mean age (yrs): 9.1 $\pm$ 1.7 [SD], AA: 93 [75%], C: 30 [25%], male: 72 [58%]) were enrolled during August, 2006 through September, 2007 and assessed during summer (N=116) and winter (N=72).

	Summer		Winter	
	AA (N=87)	C (N=29)	AA (N=57)	C (N=15)
Vit D Insufficient†	17(20%)	2(7%)	21(37%)	0(0%)*
BMI (Kg/M <sup>2</sup> )	19.4±3.9	17.1±2.1*	19.2±3.5	16.9±1.8*
Diet Vit D (IU/day)	308±178	410±193*	330±158	322±230
Diet Ca (mg/day)	1303±665	1321±457	1405±658	1221±454
25(OH)D (ng/mL)	39±11.4	48.8±14.7*	35.4±11.4	42.1±10.9*
PTH (pg/mL)	38.2±22.3	26.7±26.5*	36.6±20.2	23.3±8.9*

\*p<0.05, †: 2 subjects with vit D deficiency during summer and winter are included as vit D insufficient.

In a multivariate model, race (AA) and season (winter) were significant predictors of low serum 25(OH)D levels and low dietary intake of vitamin D was a predictor of higher PTH levels. AA children were 8 times more likely than C children to be vit D insufficient, odds ratio (CI): 8.4 (1.71, 41.3).

**Conclusion:** Vit D insufficiency was significantly greater during winter among pre-and early adolescent AA children compared to C children residing in the Northeast. Compared to C children, AA children had lower 25(OH)D and higher PTH in summer and winter. The benefits of optimizing the vitamin D status of young school age children need to be explored further.

**Disclosures:** K. Rajakumar, None.

This study received funding from: R03HD053479 (NICHD), K23HD052550 (NICHD) & UL1 RR024153-01 (PCTRC grant).

## SU483

**Advanced Vertebral Compression at Diagnosis among Children with Acute Lymphoblastic Leukemia.** L. M. Ward<sup>1</sup>, M. Matzinger<sup>\*1</sup>, N. Alos<sup>2</sup>, S. Atkinson<sup>3</sup>, C. Clarson<sup>\*4</sup>, R. Couch<sup>\*5</sup>, E. Cummings<sup>\*6</sup>, F. H. Glorieux<sup>7</sup>, R. Grant<sup>\*8</sup>, J. Halton<sup>\*1</sup>, B. Lentle<sup>\*9</sup>, H. Nadel<sup>9</sup>, C. Rodd<sup>7</sup>, K. Siminoski<sup>\*5</sup>, D. Stephure<sup>\*10</sup>, S. Taback<sup>\*11</sup>, N. Shenouda<sup>\*1</sup>, F. Rauch<sup>7</sup>, and the Canadian STOPP Consortium<sup>\*12</sup>. <sup>1</sup>Univ of Ottawa, Ottawa, ON, Canada, <sup>2</sup>Univ de Montréal, Montréal, QC, Canada, <sup>3</sup>McMaster Univ, Hamilton, ON, Canada, <sup>4</sup>Univ of Western Ontario, London, ON, Canada, <sup>5</sup>Univ of Alberta, Edmonton, AB, Canada, <sup>6</sup>Dalhousie Univ, Halifax, NS, Canada, <sup>7</sup>McGill Univ, Montréal, QC, Canada, <sup>8</sup>Univ of Toronto, Toronto, ON, Canada, <sup>9</sup>Univ of British Columbia, Vancouver, BC, Canada, <sup>10</sup>Univ of Calgary, Calgary, AB, Canada, <sup>11</sup>University of Manitoba, Winnipeg, MB, Canada, <sup>12</sup>Canadian Pediatric Bone Health Working Group, Ottawa, ON, Canada.

Vertebral compression is a serious complication of childhood acute lymphoblastic leukemia (ALL). The frequency and pattern of vertebral fractures, as well as their relationship to bone mineral density and other clinical indices, have not been systematically studied. We evaluated spine health in 186 newly diagnosed children (age (mean±SD) 6.6±4.1 years; 108 boys) with ALL (precursor B cell: N=167; T cell: N=19), who were enrolled in a national bone health research program. Patients were assessed within 30 days of diagnosis, including lateral thoracolumbar spine x-ray and bone densitometry. Vertebral morphometry was carried out by the Genant semi-quantitative method. Thirty-seven patients (20%) had a total of 118 grade 1 or more prevalent vertebral compression fractures (80 thoracic, 68%; 38 lumbar); back pain occurred in 18/37 (49%). The frequency of spine fractures per patient was as follows: 1 to 2 fractures, 22/37 patients (59%); 3 to 7 fractures, 8 patients (22%); 8 or more fractures, 7 patients (19%). The T6/T7 and T12/L1 vertebrae were most commonly affected (21 and 17% of fractures, respectively). Seventy-nine percent (93/118) of fractures were mild (grade 1), 18 (15%) moderate (grade 2) and 7 (6%) severe (grade 3). Minimal vertebral changes (15-20% loss in height, grade 0.5) were noted in an additional 17 patients. Children with grade 1 or more vertebral compression had reduced lumbar spine areal bone mineral density (LS aBMD) z scores compared to those without (mean±SD, -1.7±1.4 vs. -0.8±1.2; P < 0.001). Among the clinical indices including age, gender, height, body mass index, leukemia sub-diagnosis and risk, white blood count, calcium/vitamin D intake, physical activity and LS aBMD z score, only spine BMD was associated with vertebral compression. For every 1 standard deviation reduction in LS aBMD z score, the odds for fracture increased 2.1-fold (95% CI 1.5, 3.0). Whether the children with vertebral fractures in this study will undergo rebuilding of the vertebral bodies and restitution of bone mass with ALL treatment remains under study.

**Disclosures:** L.M. Ward, None.

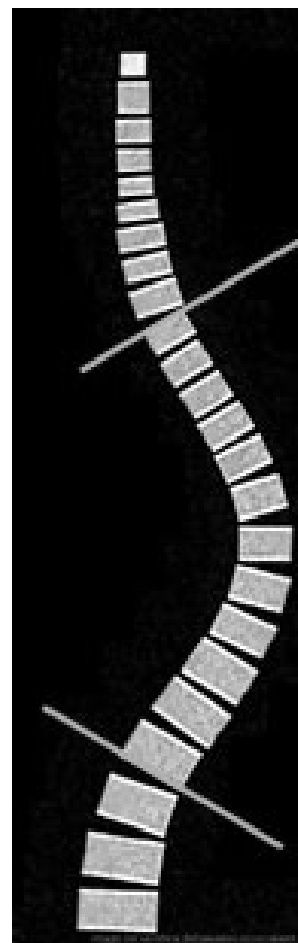
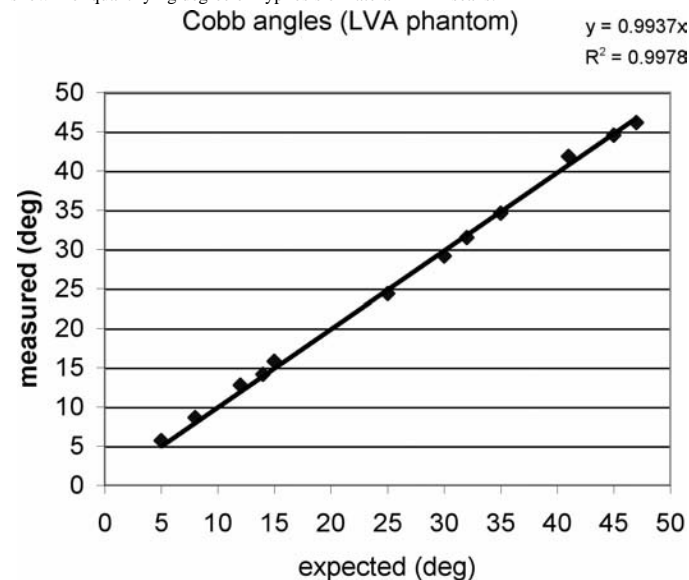
This study received funding from: Canadian Institutes for Health Research.

## SU484

**Accuracy of Cobb Angle Measurement with iDXA.** P. Markwardt\*, H. S. Barden, D. Ergun. GE Healthcare, Madison, WI, USA.

The diagnosis and monitoring of scoliosis, a medical condition characterized by lateral curvature of the spine, relies on accurate measurement of spinal curvature. The Cobb angle, the standard method of quantifying this curvature, is generally measured by hand from anteroposterior (AP) spine radiographs. The angle is determined by first locating the vertebra (apex vertebra) that is laterally displaced furthest from the centerline of the spine, and then locating the vertebrae at either end of the curve with the least lateral displacement from the center line and maximum end plate tilt. The Cobb angle is defined as the angle between the intersection of two lines, or lines perpendicular to them, drawn parallel to the superior endplate of the end vertebra above and the inferior endplate of the end vertebra below the apex vertebra.

AP images of an aluminum spine phantom were acquired with iDXA (GE Healthcare - Lunar) and analyzed with version 12.0 software. The spine geometry option was used to calculate Cobb angles for all combinations of vertebral ROIs from C1 to L5. ROIs were manually positioned over the C1 superior endplate and the C2-L5 inferior endplates. iDXA software automatically calculated the Cobb angle for each set of endplates. A protractor (Starrett No. 12) was used to measure phantom end-plate angles. iDXA values were compared to measured values. Results showed a very close relationship ( $R^2 = 0.998$ ) between iDXA-measured and protractor-measured Cobb angles, with slope of the regression not significantly different from identity. The mean difference and absolute mean difference between expected and measured angle was -0.01 degree and 0.53 degree, respectively. We conclude that Cobb angles measured from vertebral end plates on an aluminum spine phantom were measured accurately with iDXA. Similar results were shown for quantifying degree of kyphosis on lateral iDXA scans.



**Disclosures:** H.S. Barden, GE Healthcare 5.  
This study received funding from: GE Healthcare.

## SU485

**25-HydroxyVitamin D Levels in Children with Chronic Kidney Disease (CKD) as Measured by Tandem Mass Spectrometry.** H. E. Price\*, C. B. Langman, F. Ali\*, E. R. Brooks\*, F. B. Vicente\*. Division of Kidney Diseases, Children's Memorial Hospital, Chicago, IL, USA.

Vitamin D is one of 3 hormones regulating calcium, phosphorus and bone homeostases. Human biology allows two forms: vitamin D3 (cholecalciferol) and vitamin D2 (ergocalciferol) to be used. Vitamin D3 is produced in the skin, while dietary vitamin D is derived from animal sources (D3) and from plant sterols (D2). In the liver, cyp2R1 produces 25(OH)D from either form, and both are subsequently converted to 1,25(OH)<sub>2</sub>D in the kidney. Circulating [25(OH)D] is the most sensitive measure of vitamin D nutritional status, since it has a half-life of ~3 weeks. Hypovitaminosis D is a common problem in individuals with chronic kidney disease (CKD), and is manifested by calcium malabsorption, 2<sup>o</sup> hyperparathyroidism, muscle weakness, and osteomalacia. Evidence-based medicine (EBM) guidelines have provided rationale for its supplementation in advancing CKD. In this study, we measured 25(OH)D in 97 children (7-19 years) with CKD and in 39 of their healthy siblings (6-21 years) utilizing Tandem Mass Spectrometry (TMS) methodology. 25(OH)D was subdivided into measured 25(OH)D2 and 25(OH)D3. Results are reported in ng/mL. 25(OH)D in children with CKD ranged from 6.7 to 114 (mean = 40.1, SD=20.3). These values differed from, and were greater than, their siblings group which ranged from 8.8 to 49.9 (X= 22.0, SD=8.7, p<0.001). Further in CKD, 25(OH)D2 (X= 5.8) was higher than in siblings who had no measurable 25(OH)D2 (p<0.001). In CKD, 25(OH)D3 was greater (X=34.2) compared to siblings (X=22.0, p<0.001). 19/97 children with CKD were receiving oral D2 and 8 were receiving oral D3 supplementation. Comparisons of mean 25(OH)D in CKD without supplementation as compared to the siblings showed that the CKD group were higher (30.4 vs. 22.0, respectively, p<0.001). In conclusion, and differently than we have reported for the decade prior to EBM recommendations for vitamin D supplementation, children with CKD were 25(OH)D sufficient while their healthy siblings were not. Many of the CKD children were receiving supplementation with oral D2 or D3, and the TMS methodology allowed for measurement of both these forms of 25(OH)D. Therefore, due to the accuracy of measuring 25(OH)D2 and D3 using TMS, we found that children with CKD may have normal levels of 25(OH)D, likely due to supplementation, while healthy children continue to remain below the recommended levels of nutritional vitamin D adequacy. Attention should be paid to the entire family of patients with CKD for adequacy of vitamin D nutrition. Further study is now needed to determine if there are additional factors, perhaps an increase in cyp2R1, which may regulate 25(OH)D levels in children with CKD.

**Disclosures:** H.E. Price, None.

## SU486

**Bone Status Evaluation in Pre-Pubertal Children with Cystic Fibrosis.** N. Haddad\*<sup>1</sup>, M. Howenstine\*<sup>1</sup>, M. Peacock\*<sup>2</sup>, L. A. DiMeglio\*<sup>1</sup>. <sup>1</sup>Pediatrics, Indiana School of Medicine, Indianapolis, IN, USA, <sup>2</sup>Medicine, Indiana School of Medicine, Indianapolis, IN, USA.

**Background:** Osteoporosis is a sequela of cystic fibrosis (CF) and is multi-factorial. No study has comprehensively assessed bone metabolism in young children with CF. Yet identification of factors contributing to early osteoporosis onset would permit development of prophylactic interventions.

**Objective:** To characterize bone mineral density (BMD) & bone metabolism in a group of pre-pubertal children with CF. Unaffected pre-pubertal siblings (sibs) were enrolled as controls.

**Methods:** Heights, weights, & pubertal assessments were done. Fracture & steroid history was collected by questionnaire. Serum calcium, phosphorus, PTH, 25-vitamin D, & markers of bone turnover & resorption were measured after an overnight fast. BMD & % body fat were measured using dual X-ray absorptiometry (DXA, Prodigy GE). Bone age radiographs were obtained.

**Results:** 20 CF patients (pts) & 20 unaffected sibs (45% males) were enrolled. 39 pts had genetic analyses. Nine CF pts were homozygous for Δ508 mutations, 10 had other mutations or were compound heterozygotes for Δ508 mutations. 12 sibs were heterozygous for Δ508 mutations, 3 were heterozygous for other mutations, & 5 had no mutation detected. Mean age was 6.9 ± 1.8 yr (range 4.2-10.1). Pts & sibs had comparable ages, bone ages, & gender distributions. CF pts had normal bone ages. 2 CF pts & 1 sib had a prior fracture. Five CF pts & 2 sibs had received a course of steroids during the prior year. CF pts had lower total body less head BMD Z-scores than sibs (-0.53±0.78 vs 0.32±1.48, p<0.05). CF pts also had lower % body fat, height, weight, sitting height & BMI than sibs (all p<0.05). One CF pt & her sib had BMD Z-scores < -2.0. BMD z-scores were not lower in older children. There were no differences in Ca, Phos, PTH, vitamin D, bone resorption (NTX/Cr, DPD/Cr) or formation (alkaline phosphatase (AP), bone AP, osteocalcin) between groups. CF pts homozygous for Δ508 mutations had significantly lower BMD Z-scores, shorter sitting heights, & lower % body fat and had lower AP & bone AP. Sibs heterozygous for Δ508 mutations did not differ from other unaffected sibs.

**Conclusions:** Young CF pts have normal calcium & vitamin D status & no evidence of increased bone resorption or decreased bone formation. They do have lower BMD compared to sib controls but this appears due to smaller body size. However, CF pts homozygous for Δ508 mutations did have some suggestion of worse bone status. Since CF pts were smaller than their sibs, & had lower BMD for age, optimizing nutrition will be an important component of their future bone health. Particular attention to strategies directed toward optimizing bone health (improved nutrition, physical activity) may be warranted for CF children homozygous for Δ508 mutations.

**Disclosures:** N. Haddad, None.

## SU487

**Is it Time to Update Normative Values for Ionized Calcium and Urine Calcium:Creatinine Ratios in Healthy Canadian Infants?** S. Gallo\*<sup>1</sup>, H. Weiler\*<sup>1</sup>, K. Trussler\*<sup>1</sup>, C. Vanstone\*<sup>1</sup>, A. Sharma\*<sup>2</sup>, J. Mitchell\*<sup>2</sup>, A. Khamessan\*<sup>3</sup>, M. L'Abbe\*<sup>4</sup>, C. Rodd\*<sup>2</sup>. <sup>1</sup>Dietetics and Human Nutrition, McGill University, Montreal, QC, Canada, <sup>2</sup>Montreal Children's Hospital, McGill University Health Center, Montreal, QC, Canada, <sup>3</sup>Euro-Pharm International Canada Inc., Montreal, QC, Canada, <sup>4</sup>Bureau of Nutritional Sciences, Health Canada, Ottawa, ON, Canada.

There is a paucity of information on normal plasma ionized calcium (iCa) and urine calcium:creatinine ratios (Ca:Cr) in Canadian infants. Both changing technology and a lack of appropriate reference data in healthy infants complicate the interpretation of critical laboratory values, even as physicians are being asked to assess asymptomatic infants with hypercalcemia. We measured iCa and urine Ca:Cr ratios as part of a clinical trial to assess vitamin D<sub>3</sub> dose response in healthy, term, breastfed infants randomized to 4 vitamin D<sub>3</sub> treatment groups (400, 800, 1200 and 1600 IU). Infants (30 boys, 24 girls) were recruited at their 2 week paediatrician visit from clinics located in the Montreal area. Study visits were conducted between 1 and 12 months of age at the Mary Emily Clinical Nutrition Research Unit of McGill University. Blood and urine samples from each visit were analyzed in the clinical laboratory of the Montreal Children's Hospital for iCa (Radiometer Analyzer, Radiometer, Copenhagen, DE) and urine Ca:Cr (Beckman CXI Analyzer, Beckman Instruments, Fullerton, CA). The effects of gender, vitamin D dose, and time were assessed by repeated measures ANOVA. Data are presented up to 3 months of age. Neither gender nor vitamin D dose were significant predictors of iCa. A significant time effect was noted (p<0.02) with a decline in iCa with age (Table 1), localized by post-hoc testing to the comparison of 1 and 3 month mean values. Neither gender, vitamin D dose, nor time were significant predictors of urine Ca:Cr. Adding iCa values to the model as a predictor revealed no further relationship between urine Ca:Cr and iCa levels. For those infants with persistently elevated levels, there were no ECG changes (n=5) or renal ultrasound changes (n=6) consistent with hypercalcemia/hypercalciuria. These data represent reference values for healthy term Canadian infants and suggests that it may be time to re-examine normative calcium values in such children.

Table 1: Mean ± SE [Range]. Ionized calcium and urine calcium:creatinine ratio from 1-3 months of life.

Time Point	Ionized Ca++ (mmol/L)	Urine Ca:Cr (mmol/mmol)
1 mo (n=54)	1.40 ± 5.0 × 10 <sup>-3</sup> [1.29, 1.52]	1.79 ± 0.14 [0.24, 4.23]
2 mo (n=46)	1.40 ± 6.0 × 10 <sup>-3</sup> [1.32, 1.48]	1.84 ± 0.19 [0.31, 5.07]
3 mo (n=40)	1.39 ± 6.0 × 10 <sup>-3</sup> [1.31, 1.46]	1.83 ± 0.14 [0.90, 4.02]

**Disclosures:** S. Gallo, None.

## SU488

**Use of Bone Biomarkers as an Endpoint in a Pediatric Study of Alendronate.** E. von Scheven\*<sup>1</sup>, C. M. Gordon\*<sup>2</sup>, D. Wypij\*<sup>2</sup>, M. Chagomerana\*<sup>2</sup>, J. Shepherd\*<sup>3</sup>, M. Wertz\*<sup>1</sup>, L. Bachrach\*<sup>4</sup>. <sup>1</sup>Pediatrics, UCSF, San Francisco, CA, USA, <sup>2</sup>Pediatrics, Harvard University, Boston, MA, USA, <sup>3</sup>Radiology, UCSF, San Francisco, CA, USA, <sup>4</sup>Pediatrics, Stanford University, Stanford, CA, USA.

We previously demonstrated significant gains in bone mineral density (BMD) in an alendronate trial for children with inflammatory diseases receiving glucocorticoid (GC) therapy. In this substudy we aimed to identify correlations between bone turnover markers and the observed densitometric gains in BMD.

We completed a randomized, placebo-controlled, double-blind multi-center trial of weekly alendronate (N=12) versus placebo (N=11) in children (83% female, mixed ethnicity, age 8-18 yrs with Lupus, vasculitis, juvenile dermatomyositis, Crohn's disease, and juvenile idiopathic arthritis). All subjects received calcium carbonate and vitamin D supplements for 18 months. Treated subjects demonstrated greater improvement of spinal BMD Z-score, spinal BMD, and bone mineral apparent density by dual energy x-ray absorptiometry. Markers of bone formation (serum bone alkaline phosphatase [ALP, chemiluminescent immunoassay] and osteocalcin [OC, radioimmunoassay]) and bone resorption (urine N-telopeptide/creatinine ratio [NTX, competitive inhibition ELISA]) were determined at baseline and 18 months. All assays were performed at Esoterix, Inc. T-tests, Wilcoxon rank sum tests and multi-variable linear regression models were utilized to compare groups.

At baseline, groups were matched for age, gender, Tanner stage, ethnicity, height, underlying disease, disease severity, concurrent medications, and vitamin D level. There were no significant group differences at baseline for ALP, OC, NTX or the ALP/NTX ratio. However the OC/NTX ratio was greater for subjects randomized to alendronate than placebo (0.04 ± 0.02 vs 0.02 ± 0.01, p=0.03). The percent change of ALP, OC, NTX, ALP/NTX ratio and OC/NTX ratio at 18 months was variable, and ranged from -61.3% to 534.8% for ALP, -73.6% to 882.7% for OC, -73.6% to 882.7% for NTX, -82.4% to 1168.1% for OC/NTX, and -35.4% to 151.6% for ALP/NTX ratio. Subjects receiving placebo demonstrated greater percent increases in ALP (28.9 ± 127.6% vs 26.17 ± 205.8%) which approached significance (p=0.07). No other treatment group differences were observed, even after controlling for age, gender, gains in height and weight, or GC dose. The observed change of BMD did not correlate with bone biomarkers, even after controlling for confounders.

In contrast to results from studies in adults, we found ALP, OC and urine NTX to be poor predictors of response to therapy among children with inflammatory diseases receiving alendronate. Efforts to identify alternative surrogate markers of skeletal response in this pediatric population are warranted.

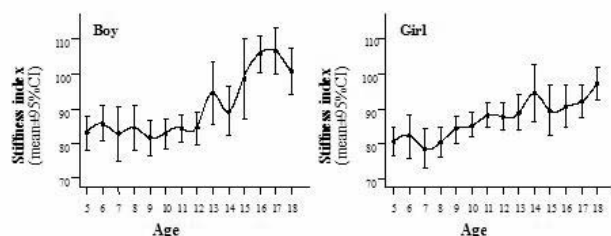
**Disclosures:** E. von Scheven, None.

This study received funding from: Merck and Co.

## SU489

**Normal Reference Values for Quantitative Ultrasound Bone Densitometry of the Calcaneus in Chinese Children and Adolescents.** H. Xu<sup>1</sup>, J. Li<sup>1\*</sup>, Q. Wu<sup>2</sup>, J. XIANG<sup>3</sup>, H. S. Barden<sup>4</sup>, Q. Zhou<sup>5</sup>. <sup>1</sup>Department of Nuclear Medicine, The First Affiliated Hospital, Jinan University, Guangzhou, China, <sup>2</sup>Medical College, Jinan University, Guangzhou, China, <sup>3</sup>Jiaxing 1st Hospital, Jiaxing, China, <sup>4</sup>GE Healthcare, Madison, WI, USA, <sup>5</sup>GE Healthcare, Shanghai, China.

Bone mass accumulated during childhood and adolescence is a primary determinant of fracture risk and osteoporosis in late adulthood. Due to quantitative ultrasound (QUS) densitometry's radiation-free, low-cost, simple, and portable advantages, it is adaptable to large-scale surveys. Normal calcaneal QUS of Chinese adults has already been determined and used in screening for osteoporosis and for evaluation of fracture risk. In China, pediatric QUS utility is currently limited, due to lack of reference data. Thus, an ethnicity-matched pediatric reference database needs to be established for use in Chinese children. A total of 1048 healthy children and adolescents (512 boys, 536 girls) from Guangzhou (n = 605) and Jiaxing (n = 443) aged from 5-18 years were examined with a Achilles densitometer (GE Healthcare, Lunar). Measurements on the left heel included speed of sound (SOS), broadband ultrasound attenuation (BUA), and a calculated stiffness index (SI). The Achilles densitometer has been shown to provide good precision for SI (1.8%), SOS (0.4%) and BUA (2.9%). Our results found that there were no significant differences for SI between males and females, except in the age range of 16 to 17 years. A steady increase of BUA, SOS, and SI was seen with increasing age, body height and weight in both sexes. In conclusion, our data can be used as normal reference values for children and adolescents in China. Further studies in children with disorders influencing bone metabolism are anticipated.



**Disclosures:** H. Xu, None.

## SU490

**Differences in Bone Mineral Content at the Lumbar Spine and Proximal Femur in SA Children of different Ethnic groups.** L. K. Micklesfield<sup>1</sup>, S. A. Norris<sup>1</sup>, L. van der Merwe<sup>2\*</sup>, E. V. Lambert<sup>3</sup>, J. Pettifor<sup>1</sup>. <sup>1</sup>Department of Paediatrics, University of Witwatersrand, Johannesburg, South Africa, <sup>2</sup>Biostatistics Unit, Medical Research Council, Cape Town, South Africa, <sup>3</sup>Department of Human Biology, University of Cape Town, Cape Town, South Africa.

We have shown despite differences in size and age, whole body BMC is greater in SA children of mixed ancestral origin than in black and white US and SA children. To further investigate differences between ethnic groups within SA, we compared lumbar spine (LSBMC), proximal femur (PFBMC) and femoral neck (FNBMC) BMC in black (SAB; n=263) and white (SAW; n=73) children from Johannesburg, and in children of mixed ancestral origin (SAM; n=64) from Cape Town. SAW and SAB groups were slightly older (SAW: 9.5 ± 0.3; SAB: 9.6 ± 0.3; SAM: 9.3 ± 0.6 years) and heavier than the SAM group. There was no significant difference in mean body weight between the girls, however SAM boys were lighter than the other two groups. In what follows, "adjusted" indicates that comparisons between means were adjusted for age and height. Unadjusted LSBMC was lower in SAM boys compared to SAW boys, however this difference was not significant after adjustment. Unadjusted LSBMC was significantly lower in SAW girls compared to SAM girls, and remained so after adjustment. After adjustment, the following pattern was significant for LSBMC between the girls: SAM>SAB>SAW. The same pattern was significant for unadjusted and adjusted FNBMC in the girls, as well as in the boys after adjustment. Unadjusted PFBMC was not different between the boys in the three groups, however SAM girls had significantly higher PFBMC than SAW and SAB girls. After adjustment, SAM boys and girls had significantly higher PFBMC than their SAB and SAW counterparts. In addition, PFBMC was significantly higher in SAB boys than SAW boys. There was no difference between SAW and SAB girls for unadjusted or adjusted PFBMC. Best predictors were selected for BMC at the 3 sites from linear models containing the following: gender, height, weight, age, birth weight and ethnic group. Linear models containing the best predictors accounted for 40-59% of the variance at these sites. Birth weight contributed significantly to the models for LSBMC and PFBMC. Ethnicity, height and weight were significant contributors to BMC at all 3 sites. It is well established that black South African adults and children have higher FNBMD than SA whites, but the finding of higher BMC in children of mixed ancestral origin is of interest, as this ethnic group has not been studied previously.

**Disclosures:** L.K. Micklesfield, None.

## SU491

**Infantile Hypercalcemia: Relationship of Dietary Intake of Calcium and Vitamin D to Serum and Urine Levels.** E. Assor<sup>\*</sup>, C. Grasemann<sup>\*</sup>, K. T. Parker<sup>\*</sup>, E. B. Sochett. Hospital for Sick Children, Toronto, ON, Canada.

Mild hypercalcemia in infants is a common diagnostic problem seen in the calcium bone clinic at HSC. A specific cause is infrequently found and most children are designated as having idiopathic hypercalcemia of infancy. As close to referral as practicable, a formal dietary assessment focusing on intake of calcium and vitamin D is obtained by a registered dietitian (RD). We have reviewed this experience to establish whether there is a relationship between dietary intake of calcium and vitamin D (expressed as a percentage of DRI for age) and their respective serum and urinary levels. Nineteen patients with a mean age of 13.8 month (range 0.6 - 40 months) have been evaluated over the last 2-3 years. A specific cause for the hypercalcemia was identified in only four (2 Williams syndrome, 2 Subcutaneous fat necrosis). All patients were formally assessed by the same RD. Average duration between the patients first clinic visit to dietary assessment was 3.8 months (range -3 - 25 months). Assessment was based on food records completed by the family and reviewed with the RD. At time of assessment, 3 patients were receiving vitamin D and 1 patient received a multivitamin containing both calcium and vitamin D. Nine patients (47%) were consuming a regular infant/toddler diet, 5 patients (26%) were on solids and formula, 2 (11%) were on formula and breast fed and 2 (11%) were on formula only. One patient (5%) was on solids and breast fed. Mean dietary calcium was 152 % of DRI for age (range 14% - 322 %). Mean dietary vitamin D was 270 IU (135% of DRI for age, range 0% - 350%). Mean ± SD for serum calcium, 25 OH vitamin D, PTH and urinary Ca/creatinine ratio were 2.75 ± 0.14 mmol/l, 65 ± 16 nmol/l, 23.5 ± 15 ng/l and 1.35 ± 1.23 respectively. There was no correlation between dietary calcium and serum calcium, between dietary calcium and urinary calcium/creatinine ratio nor between dietary vitamin D intake and 25 OH vitamin D levels. Despite increased intakes, neither dietary calcium nor vitamin D appears to play a causative role in mild hypercalcemia of infancy. DRI for vitamin D in infants need to be revised.

**Disclosures:** E. Assor, None.

## SU492

**Forearm pQCT Measurements in Males with Duchenne Muscular Dystrophy.** J. Landoll<sup>1\*</sup>, W. King<sup>2\*</sup>, J. Kissel<sup>2\*</sup>, V. Matkovic<sup>1</sup>. <sup>1</sup>Bone and Mineral Metabolism Laboratory, Ohio State Univ., Columbus, OH, USA, <sup>2</sup>Department of Neurology, Ohio State Univ., Columbus, OH, USA.

Duchenne Muscular Dystrophy (DMD) is the most common childhood muscular dystrophy. Studies using dual energy x-ray absorptiometry (DXA) have shown that patients with DMD have low areal bone mineral density (BMD) as compared to the general population of the same age and that the deviation from normal increases with age. There is a question of whether these patients require bone modifying medications (e.g., bisphosphonates) to mitigate this apparently decreased bone mineral density. However whether the deviation from normal reflects a true deficit in bone mineral density or may be related to geometric parameters (due to the relatively small size of DMD patients) inherent in areal bone density analyses, is unclear. This ongoing study examines the volumetric bone mineral density of DMD boys (n=23, age 7-17 y., average 11.4 y.) using pQCT of the forearm. Volumetric bone mineral density measurements of the non-dominant radius at the distal (4%) and proximal sites (33%) were performed using a pQCT (Stratec XCT-2000) densitometer. Preliminary results are compared to a population of healthy male individuals (n=189, age 7-17 y., average 11.7 y.). The average total cross-sectional area of the distal site (177 ± 50 mm<sup>2</sup>) is significantly lower than that for the control group (294 ± 75 mm<sup>2</sup>; p<0.001). The average total bone mineral density and trabecular bone mineral density at the distal site for the DMD group (254 ± 65, 127 ± 34 mg/cm<sup>3</sup>, respectively) is significantly lower than the control group (300 ± 34, 214 ± 32 mg/cm<sup>3</sup>, respectively; p<0.002). The average cortical area at the proximal site is significantly lower than the controls (40 ± 7 vs. 63 ± 17 mm<sup>2</sup>, respectively; p<0.001); however, the average cortical density is significantly higher than that of the control population (1147 ± 67 vs. 1092 ± 33 mg/cm<sup>3</sup>, p<0.002). These data show that boys with DMD do have smaller bones. They suggest that there is a real deficit in volumetric bone mineral density at the distal forearm site which is rich in trabecular bone whereas the bone mineral density at the proximal site (cortical bone) is normal. This information may determine the risk for bone fragility fractures in DMD patients and may influence prevention programs.

**Disclosures:** J. Landoll, None.

This study received funding from: Muscular Dystrophy Association.

## SU493

**Age at Menarche Associated with Bone Strength in Girls: An X-treme CT Study.** M. Burrows<sup>1</sup>, D. Liu<sup>\*1</sup>, Y. Ahamed<sup>\*1</sup>, S. Braid<sup>1</sup>, H. A. McKay<sup>2</sup>. <sup>1</sup>Dept of Orthopaedics, University of British Columbia, Vancouver, BC, Canada, <sup>2</sup>Dept of Orthopaedics and Family Practice, University of British Columbia, Vancouver, BC, Canada.

Late menarche is a determinant of low bone mineral density in women and a strong risk factor for fracture (1). This could be due to either; 1) years of exposure to estrogen (women experiencing early menarche have higher years of exposure to estrogen); or 2) body habitus associated with early menarche (higher body mass index) (2). Our aim was to assess the influence of age at menarche on bone strength in girls. Participants were 77 girls; Age  $16.2 \pm 1.3$  yrs; Height  $161.2 \pm 6.5$  cm; Weight  $55.2 \pm 8.6$  kg; Age at menarche  $12.3 \pm 1.4$  yrs. They were assessed for physical activity using the physical activity questionnaire (PAQ), and total calcium intake using a food frequency questionnaire. We assessed maximal force production (Fmax, N/kg) using the Leonardo force platform (Novotech, Medical). We utilised X-tremeCT (Scanco Medical, 110 slices, 82µm) to assess bone strength at the 8% site of the non dominant distal tibia. Images were segmented using Image Processing Language (IPL, Scanco Medical) as per the manufacturer's *in-vivo* protocol. We assessed total area (ToA, mm<sup>2</sup>) and total bone mineral density (ToD, mg/cm<sup>3</sup>) and calculated bone strength index as ToA x ToD<sup>2</sup> (BSI, mg<sup>2</sup>/mm<sup>4</sup>) (3), which served as our dependent variable (DV). We developed a linear regression model based on relationships between the DV and the predictor variables (PV) and on association between DV and selected predictors using bivariate correlation. Our model included age at menarche as PV and age, height, weight, Fmax, physical activity and calcium intake as control variables (SPSS, v15.0). The age at menarche model (p=0.013) explained 33% of variance in BSI (Table 1), with ToD rather than ToA underpinning the relation between BSI and age at menarche. Although our findings suggest that timing of maturity may relate to bone strength longitudinal data are required to more adequately assess this relationship.

1. Silman AJ. Osteo Int 14: 213-218; 2003.

2. Eastell R. Clin Sci 83: 375-382; 2005.

3. Martin RB. J Biomech 24: 79-88; 1991.

**Table 1. Regression Model for Bone Strength Index at the Distal Tibia**

DV	IV	(SE)	R <sup>2</sup>	P value
Bone strength index	Age	241.5 (106.9)	.24	.052
	Age at menarche	-247.2(105)	.33	.013

DV = Dependant variable. IV = Independent variable. = estimated regression coefficient; SE = standard error. Other variables entered into the model were age, height, weight, physical activity score, total calcium intake and maximal force production.

**Disclosures:** M. Burrows, None.

## SU494

**Three Unrelated Patients with a Unique Spondylo-Epi-Metaphyseal Dysplasia.** M. B. Bober<sup>1</sup>, W. Mackenzie<sup>\*2</sup>, L. Nicholson<sup>\*1</sup>, C. I. Scott<sup>\*1</sup>. <sup>1</sup>Division of Genetics, AI duPont Hospital for Children, Wilmington, DE, USA, <sup>2</sup>Department of Orthopedics, AI duPont Hospital for Children, Wilmington, DE, USA.

We present three males currently ages 5 (Patient 1), 17 (Patient 2) and 23 years (Patient 3) with disproportionate short stature of short limbed type with rhizomelia. Radiographic evaluations demonstrate mild spinal involvement with thoracic platyspondyly, anterior notching of the lower thoracic vertebrae and lumbar lordosis. There is absent lumbar interpediculate widening. The lower extremities demonstrate metaphyseal widening of the long bones most notably at the distal femora. The epiphyses were small and irregular throughout. The iliac wings showed a wide lateral flare and the acetabulum was mildly dysplastic. The hands were brachydactylic with phalangeal shortening more distally than proximally. The metacarpals are short and broad. Ossification is age appropriate. No cervical spine instability or rib changes were noted. Clinically, the children have a strikingly similar facial appearance with outgoing and pleasant personalities. The scalp hair is of normal texture and distribution with a blonde color. Upper eyelid fullness is present and the iridae are blue. The nose is relatively short with a tall broad philtrum. The lower lip is full. The external ears had normal structure and position. The mandible was not prognathic, but appeared prominent in the AP view with a pointed chin. The teeth are all within normal limits. The children have mild pectus carinatum. Ligamentous laxity was present in all children. All three children had significant patellar instability with spontaneous subluxation. Patients 1 and 2 both underwent surgery to correct this abnormality. Patient 2 had a cleft palate and bifid uvula. Patient 2 and 3 have significant learning abnormalities with FSIQ (WISC-III) of Patient 2 49 and Patient 3 58.

**Disclosures:** M.B. Bober, None.

## SU495

**Newborn Infant Bone Mineralization is Affected by Their Umbilical Cord Length.** G. M. Chan, D. Wright\*. Pediatrics, University of Utah, Salt Lake City, UT, USA.

Activity has been demonstrated in promoting bone mass in infants and adults. The effect of activity on the fetal bone mass has not been studied. One of the major restrictions to fetal activity may be the length of the umbilical cord. We hypothesized that the newborn with a shortened umbilical cord may have low bone mineralization because of decreased fetal movement or activity. We investigated seven healthy newborn term infants with shorten umbilical cords and 15 control term infants. Mothers with pre-eclampsia or hypertension, chorioamnionitis or prolonged ruptured of membranes were excluded from the study. Mother's age, parity, infants' gender and birth and placenta weights were recorded. The umbilical cord length and diameter were measured as well as the newborn's tibial speed of sound (SOS). Speed of sound measurements (Sunlight Omnisense 7000P instrument) were obtained at the tibial midshaft and reflected the tibial cortical thickness and bone mineral density. Measurement reproducibility was  $0.8 \pm 0.6\%$  (mean  $\pm$  SD) for repeat speed of sound measures in the same (n = 20). There were no differences between the two groups in mother's age ( $24.6 \pm 5.8$  v  $25.8 \pm 3.3$  years), parity ( $2 \pm 1$  v  $2 \pm 1$ ), infant's gender (29% females v. 47% females), birth weights ( $3320 \pm 451$  v  $3409 \pm 452$  g) or placental weights ( $521 \pm 69$  v  $588 \pm 105$  g). Umbilical cord diameters were also similar,  $1.1 \pm 0.3$  v  $1.1 \pm 0.2$  cm. However, there was a difference in the cord length between the two groups,  $46 \pm 2$  v  $57 \pm 4$  cm (Mann Whitney, P<0.001). The newborn infants with the shorter umbilical cord also had lower tibial SOS compared to controls,  $3006 \pm 96$  v  $3235 \pm 304$  m/sec (Mann Whitney, P<0.05). Tibial SOS was related to the infant's umbilical cord length (r = 0.57, P<0.01) but not to infant's birth weight, gender, umbilical cord diameter, maternal age, or placenta weight. In conclusion, newborn infants with a short umbilical cord length have lower bone mineralization.

**Disclosures:** G.M. Chan, None.

## SU496

**Randomized Dose Comparison of Pamidronate in Children with Types III and IV Osteogenesis Imperfecta: 3 vs 6 Month Cycles.** J. C. Marini<sup>1</sup>, M. K. Abukhaled<sup>\*1</sup>, H. L. Cintas<sup>\*2</sup>, A. A. Obafemi<sup>\*1</sup>, J. F. Troendle<sup>\*3</sup>, A. D. Letocha<sup>\*1</sup>, J. C. Reynolds<sup>\*4</sup>, S. Paul<sup>\*2</sup>. <sup>1</sup>Bone and Extracellular Matrix Branch, National Institute of Health. National Institute of Child Health & Human Development., Bethesda, MD, USA, <sup>2</sup>Rehabilitation Medicine, National Institute of Health. Clinical Center, Bethesda, MD, USA, <sup>3</sup>Biometry and Mathematical Statistics Branch, National Institute of Health. National Institute of Child Health & Human Development., Bethesda, MD, USA, <sup>4</sup>Nuclear Medicine, National Institute of Health. Clinical Center, Bethesda, MD, USA.

Controlled trials of bisphosphonates in children with osteogenesis imperfecta (OI) demonstrated significant increases in vertebral BMD, height and area, while effect on fracture rate is controversial. However, high cumulative doses of pamidronate in children are associated with significant side effects such as impaired bone modelling, delayed fracture healing, and decline in bone material quality. The purpose of this study was to determine whether the vertebral benefits of q3m infusion cycles could be attained on q6m cycles, with a lower cumulative dose. Twenty-seven children with types III and IV OI were randomly assigned to receive 1mg/kg/3d IV pamidronate in q3 or q6 month cycles. All patients had serial spine radiographs, L1-L4 DXA, and musculoskeletal and function testing. L1-L4 DEXA increased significantly after 1 year of q3m cycles, with average change in z-score = +1.41 SD, but did not improve significantly with further treatment. In the q6m group, the average change in DEXA was not significant. Repeated measures analysis of DEXA z-scores yielded a z-score rate change of 0.064 SD/m for q3 vs 0.036 SD/m for q6 group (p=0.13). T12-L4 vertebral area and percent central compression were determined from radiographs. On repeated measures analysis, there was significant improvement of q6m group average L1-L4 and T12-L2 vertebral height (p=0.05, 0.01) and area (p=0.002, 0.006). The rate of improvement of the q3 group did not differ from the q6m for L1-L4 area or height (p=0.52, 0.86) or T12-L2 area or height (p=0.28, 0.77). Neither group of OI children had significant improvement in fracture incidence, manual muscle testing or BAMF motor scores after two years. It is noteworthy that the response to treatment was highly variable in each treatment group. For individual OI children, the improvement in vertebral area did not correlate with change in DEXA z-score. We concluded that equivalent gains in vertebral height and area are obtained with q6m and q3m pamidronate cycles. Both cycle interval and total number of cycles should be limited to minimize cumulative bisphosphonate dose in pediatric OI bone.

**Disclosures:** J.C. Marini, None.

This study received funding from: NICHD Intramural Fund.

## SU497

### Large Osteoclasts in Pediatric Osteogenesis Imperfecta Patients Receiving Intravenous Pamidronate. M. Cheung\*, F. H. Glorieux, F. Rauch. Shriners Hospital for Children, Montreal, QC, Canada.

Intravenous pamidronate is widely used to treat children with moderate to severe osteogenesis imperfecta (OI). Changes in the appearance of osteoclasts have previously been noted in children receiving pamidronate and have been interpreted as signs of toxicity. In the present study we analyzed osteoclast parameters in paired iliac bone specimens before and after two to four years of cyclical intravenous pamidronate therapy in 44 pediatric OI patients (age range: 1.4 to 17.5 years; 21 girls). During pamidronate treatment, average osteoclast diameter and the mean number of nuclei present per osteoclast increased by 18% ( $P = 0.02$ ) and 43% ( $P = 0.001$ ), respectively. The percentage of osteoclasts with no visible attachment to a bone surface was similar before (2%) and after (3%) pamidronate treatment ( $P = 0.30$ ). The number of samples containing large osteoclasts (LOC, diameter more than 50  $\mu\text{m}$ ) increased from 6 (14%) before treatment to 23 (52%) after pamidronate therapy ( $P < 0.001$  by chi square test). Post-treatment samples containing LOC had a greater core width ( $P = 0.04$ ) and higher cancellous bone volume per tissue volume ( $P < 0.001$ ), because cancellous bone volume had increased more during pamidronate treatment ( $P < 0.001$ ). Osteoclast number and surface were higher in samples with LOC, but there was no difference in cancellous bone formation parameters. The presence of LOC was independent of OI type, type of collagen type I mutation, lumbar spine bone mineral density and other clinical or biochemical measures. Thus, the presence of LOC may indicate greater sensitivity to bisphosphonates leading to greater core width and increased bone volume per tissue volume. No evidence was found that the presence of LOC is associated with adverse clinical events.

**Disclosures:** F. Rauch, Novartis 4.

This study received funding from: Shriners of North America.

## SU498

### Effect of Bone Marrow Transplantation (BMT) in a Child with Malignant Infantile Osteopetrosis. C. Tau<sup>1</sup>, M. Bondue<sup>1,2</sup>, C. Mautalen<sup>3</sup>, C. Casco<sup>3</sup>, E. Fradinger<sup>4</sup>, E. Pellisa<sup>4</sup>, R. Staciuk<sup>2</sup>, C. Figueroa<sup>2</sup>. <sup>1</sup>Metabolismo Cálculo y Óseo, Endocrinología, Hospital de Pediatría Garrahan, Buenos Aires, Argentina, <sup>2</sup>Trasplante de Medula Ósea, Hospital de Pediatría Garrahan, Buenos Aires, Argentina, <sup>3</sup>Centro de Osteopatías Médicas, Buenos Aires, Argentina, <sup>4</sup>Instituto de Investigaciones Metabólicas, Buenos Aires, Argentina.

Infantile osteopetrosis (IO) is an hereditary sclerosing bone disease caused by osteoclast dysfunction, defective bone resorption and modeling. Hematopoietic stem cell transplantation (HSCT) is the only curative therapy. A girl with IO was seen at 4.5 months of age. She was born at term from consanguineous parents. At 1 month she had upper respiratory tract infection and required a blood transfusion for anemia. Height was -2.7 (z-score), she had protruding eyes, bilateral nystagmus, hepatosplenomegaly, audio and visual evoke response were absent. Bone marrow biopsy showed myelofibrosis and osteosclerosis. X-rays showed dense bones, generalized sclerosis, lack of corticomedullary differentiation, rickets, flaring of metaphyses of long bones, sclerosis of skull base. Since 2 months of age she was treated with methylprednisone 1 mg/kg/day and vitamin D 1000 IU/day was added at month 5 of life. Biochemical studies showed hypocalcemia (SCa) 8.1 mg/dl, hypophosphatemia (SP) 2.8 mg/dl, elevated bone alkaline phosphatase (BAP) 787 IU/L and PTH 173 pg/ml, low serum 25OHD (8 ng/ml), low hemoglobin (9.4 g/dl), uCa/uCr was 0.22 mg/mg, urinary CrossLaps (uCTX) and D-pyridoline (D-pyr) were low (590 ug/mmolCr and 16 nmol/mmolCr respectively). At the age of 5 months, she underwent an identical sibling BMT. Busulfan (16 mg/kg) and cyclophosphamide (200 mg/kg) were used as conditioning. She received  $8.93 \times 10^8/\text{kg}$  nucleated cells. Neutrophils count was  $>500/\text{mm}^3$  on day 20 and platelet count was  $>50,000/\text{mm}^3$  on day 47. The evolution after the BMT was uneventful. Forty months after the transplantation, a sustained hematological and immunological recovery was observed. SCa and SP normalized by day 19. SCa and SP increased by day 30 (10.8 mg/dl and 6.5 mg/dl respectively) but were asymptomatic. An impressive increment of uCTX and D-pyr was observed (uCTX was 4733 by day 15 and 8716 ug/mmolCr by day 42. D-pyr was 87 by day 42, 68 by month 6, 32 by month 9 and 24 nmol/mmolCr one year after BMT). Serum 25OHD was normal 2 months after BMT (39 ng/ml). BAP decreased to 520 by month 2, to 455 by month 6 and 163 IU/L 2 years after BMT. X-rays taken 6 months after BMT showed normal bones. Growth and hearing improved but no her visual acuity. We conclude, that BMT performed in this child with IO improved bone markers, radiological signs of rickets and bone sclerosis. Early referral for consideration of HSCT is mandatory in IO to reverse neurological damage.

**Disclosures:** C. Tau, None.

## SU499

### Teriparatide Treatment in a Young Man with Idiopathic Juvenile Osteoporosis Diagnosis. M. S. Parisi, A. Bagur, B. Oliveri. Sección Osteopatías Médicas, Hospital de Clínicas, Universidad de Buenos Aires, Buenos Aires, Argentina.

Idiopathic Juvenile Osteoporosis (IJO) diagnosis is based on the exclusion of other diseases causing severe demineralization and fractures in childhood. A 27y old man, diagnosed with IJO, was treated with Teriparatide 18m. He was healthy until 14y old, when knees and ankle pain developed, and suffered femoral and humerus fractures. On presentation (18y) he uses crutches because of lumbar, knees, and ankle pain.

Rx: compression fractures of all vertebral bodies, genu varum, and aseptic necrosis of right femoral neck. L2L4BMD (DXA) Z-score was -7.3. Bone scan was unspecific with multiple areas of hypercaptation. Lab tests were normal, except for high bone alkaline phosphatase (BALP). Bone biopsy showed osteoporosis features, histomorphometry evidenced reduced osteoblast (Ob) and erosion surfaces, and negative double label tetracycline (TC).

He received calcium (Ca) and vit D 12m, and bisphosphonates for 2 y, that were suspended when he suffered a humeral fracture, and bone biopsy showed an increase in osteoid surface, still reduced bone volume and osteoblast surface, and without double label TC. However, bone pain diminished and BMD increased. Thereafter he continued on Ca/vit D 5y. Teriparatide (20ug/d), vit D2 (800IU/d), and Ca (0.5g/d) treatment was indicated based on the evidence of reduced Ob activity. The patient signed an informed consent approved by the Hospital Ethical Committee. Follow up: serum Ca, phosphate, BALP, iPTH, 25OHD, cross laps (CTX), osteocalcin (BGP), creatinine, uric acid, hemogram, hepatogram; and urinary Ca and creatinine at 0, 1, and every 3m. BMD and Rx every 6m; and bone biopsy and bone scan at 0, and 18m.

At baseline bone volume, osteoid surface, and osteoid thickness were in the normal range, with a low % single label TC; Ob surface persisted reduced. With Teriparatide, bone pain disappeared. Lab tests were normal, except for BALP (table 1). L2L4 BMD increased 19.9%, from 0.592 to 0.710g/cm<sup>2</sup>. Bone scan areas of hypercaptation disappeared. Bone biopsy results are pending. A caryotype informed a Robertsonian translocation (13.14). Molecular studies in progress.

Teriparatide produced clinical, densitometric and centellographic improvement. The response to treatment could sustain the hypothesis of an Ob defect. The abnormal caryotype suggests the possibility of an existing gene mutation.

Table 1

	CTX (ng/L)	BGP (ng/ml)	BALP (IU/L)
Normal Values	14-450	24-70	31-95
Months 0	278	35	111
6	357	42	84
12	283	54	96
18	334	60	100

**Disclosures:** M.S. Parisi, None.

This study received funding from: Fundación de Osteoporosis y Enfermedades Metabólicas Óseas.

## SU500

### Vitamin D Supplementation in Breast Fed Infants: A Prospective Trial-Recruitment Problem Encountered Along the Way. T. Ponnappakkam, E. Bradford\*, R. C. Gensure. Pediatrics, Ochsner Clinic Foundation, New Orleans, LA, USA.

Exclusive breast feeding of newborns is more common because of the well documented benefits to mother and baby; however, there are concerns if the breast milk has sufficient vitamin D to prevent rickets. Anticipating this, the American Academy of Pediatrics (AAP) recommends universal vitamin D supplementation (200 IU/day) from 2 months of age, but there are few studies to support these recommendations. We are therefore conducting a study to compare vitamin D supplementation with placebo control in breastfed children. After obtaining approval from the Ochsner Institution Review Board (2006-186A) normal newborns (breast milk intake  $>50$  percent of total) were randomized into three study groups: no supplementation, 200 IU per day from 2 months, and 200 IU per day from birth. Blood samples and questionnaires are collected at birth, two, four, and six months of age. Our goal was to recruit 450 patients in 2 years; however, after one year only 42 patients were recruited (6 patients have completed the study). We screened 757 infants from July 2007-December 2007. 408 (53%) were breastfed post partum. 94% of these mothers were approached, only 5% agreed to participate in our study. The major reasons given for not wanting to participate are: not interested in a research study (26.5%), not willing to give a daily medication (10.3%); not breastfeeding at least 50% of the time (8.6%), and not wanting blood tests (5.9%). Retention among the recruited patients was also very low, with 66% dropping out in the first 2 months. The most common reason for dropping out of the study was cessation of breastfeeding. The blood samples collected so far in our study were analyzed for calcium, phosphorus, parathyroid hormone, 25-hydroxyvitamin D, alkaline phosphatase, and osteocalcin (cord blood at birth). There was no apparent difference in the levels of any of these measurements between the placebo and vitamin D treated groups at any time point; however, we do not yet have sufficient power in the study to support a negative conclusion. One case of rickets and one case of hypervitaminosis D has been reported by the pediatric endocrinologist at Ochsner, neither patient was enrolled in the study. A retrospective chart review of pediatric practices at Ochsner revealed that only 5% of breastfed infants receive vitamin D supplementation, revealing that there is poor compliance with the AAP recommendations. We recommend that the health care professionals should educate mothers of the importance of vitamin D and inform them of the current recommendations until future research can determine whether or not vitamin D supplementation is required to prevent rickets.

**Disclosures:** T. Ponnappakkam, None.

This study received funding from: The Gerber Foundation.

## SU501

**Differential Effects of Growth Hormone and 1 Alfa Calcidiol on Cancellous and Cortical Bone in Hypophysectomized Rats.** A. A. Chaudhry<sup>\*1</sup>, M. Castro-Magana<sup>\*1</sup>, X. Q. Liu<sup>2</sup>, J. F. Aloia<sup>3</sup>, J. K. Yeh<sup>2</sup>. <sup>1</sup>Pediatric Endocrinology, Winthrop University Hospital, Mineola, NY, USA, <sup>2</sup>Metabolism laboratory, Winthrop University Hospital, Mineola, NY, USA, <sup>3</sup>Endocrinology, Winthrop University Hospital, Mineola, NY, USA.

Growth hormone deficiency in children causes severe growth retardation, Vitamin D deficiency and osteopenia. We investigated whether 1 alfa calcidiol alone or in combination with growth hormone can improve bone formation. Forty hypophysectomized Sprague-Dawley female rats (HX) at the age of 8 weeks (body weight in the range of 190-220 gm) were divided into 4 groups; HX, HX+ alfa calcidiol (oral 0.1 ug/kg daily), HX+GH (0.66 mg/0.2 ml SC daily), HX + GH + alfa calcidiol. Ten intact rats were used as controls. Total duration of treatment was 4 weeks. All rats received calcein (10 mg/kg) subcutaneously at day 19 and day 26 to label new bone formation. Data was analyzed using one-way ANOVA with group comparison and two-way ANOVA for treatment interactions. Results showed that GH increased body weight, femoral bone length, bone area, bone mineral content and bone density while alfa calcidiol only increased bone mineral content and bone density. In cortical bone, GH increased both periosteal and endocortical bone formation rate (BFR) resulting in a significant increase in cortical area (85.4±1.89 % vs HX 81.5±1.81 %, mean±SD, P<0.05). While alfa calcidiol suppressed endocortical eroded surface % without a significant effect on either periosteal or endocortical BFR resulting in a non-significant increase in cortical area (83.1±1.61%, ns). In cancellous bone both GH (7.97±1.95%) and alfa calcidiol (9.29±3.65%) increased cancellous bone area % (P<0.05) as compared to the HX group (4.55±1.33%). However GH effect was primarily due to increase in BFR while alfa calcidiol effect was primarily due to suppression of cancellous bone turnover in the HX rats. The combination of GH and alfa calcidiol had no additive effect on cancellous bone area (9.32±3.11%, interaction F value = 2.11, P = 0.155), but a negative interaction was observed on the cortical area (84.1±1.50%, interaction F value = -6.89, P<0.013). In conclusion, the increase in cortical and cancellous area percentage by GH is due to increase in BFR whereas alfacalcidol increased cortical and cancellous bone area percentage by primarily suppressing bone turnover. Hence, there is a differential anabolic effect of GH and alfa calcidiol on cortical and cancellous bone in HX rats.

Cortical and cancellous bone group comparison				
Group	Cortical Area %	periosteal BFR (mcm/d)	Cancellous Area %	Cancellous BFR (mcm/d)
HX	81.47±1.81	9.71±6.56	4.55±1.33	49.0±12.6
HX+Alfa	83.07±1.61	6.79±6.16	9.29±3.65	20.6±6.1
HX+GH	85.35±1.89	288±64.5	7.97±1.96	74.1±11.8
HX+Alfa+GH	84.11±1.50	269±59.5	9.32±3.11	48.9±10.5
Intact	82.26±1.77	210±29.3	26.5±4.37	36.4±7.9

**Disclosures:** A.A. Chaudhry, None.

## SU502

**Interaction of Combined Intervention of Parathyroid Hormone and Growth Hormone on Trabecular and Cortical Bone Formation and Resorption in the Hypophysectomized Rats.** M. N. Guevarra<sup>\*1</sup>, M. Castro-Magana<sup>\*1</sup>, X. Q. Liu<sup>2</sup>, J. F. Aloia<sup>3</sup>, J. K. Yeh<sup>2</sup>. <sup>1</sup>Pediatric Endocrinology, Winthrop University Hospital, Mineola, NY, USA, <sup>2</sup>Metabolism Laboratory, Winthrop University Hospital, Mineola, NY, USA, <sup>3</sup>Endocrinology, Winthrop University Hospital, Mineola, NY, USA.

Growth hormone deficiency in pediatrics results in short stature and osteopenia. We postulated that growth hormone (GH) and parathyroid hormone (PTH) combination would result in an improvement of the bone formation. Forty hypophysectomized Sprague Dawley female rats (HX) at age 8 weeks were divided into four groups; HX, HX+PTH (62.5 ug/kg, SC daily), HX+GH (0.66mg/0.2ml, SC daily), and HX+PTH+GH. Ten intact rats were used as control. The total duration of the experiment was 4 weeks. Data was analyzed using One-way ANOVA with group comparison and Two-way ANOVA for treatment interaction. Results showed that GH increased body weight, femoral bone length, bone area, bone mineral content (BMC) and the bone density (BMD) whereas, PTH increased BMC and BMD without a significant increase in the body weight, femoral bone length, and bone area. The F value of the Two-way ANOVA showed that the combined treatment of GH and PTH had a synergistic effect on increasing BMD (F = 4.85, P<0.05). In cortical bone GH increased cortical area (85.5±1.89%, mean ± SD) significantly as compared to the HX (81.5±1.81%, P<0.05). The increase is primarily due to increased periosteal bone formation rate (BFR) without a significant effect on the endocortical BFR and the eroded surface %. PTH administration resulted in non-significant increase in cortical area (83.7± 2.05%, P = 0.087) since PTH increased only endocortical BFR without a significant effect on the endocortical eroded surface% nor the periosteal BFR as compared to the HX group. The result of combined intervention showed no additive effect in the cortical area (85.3±1.83%), in periosteal BFR and endocortical BFR. However, it showed a synergistic effect on suppression of endocortical eroded surface % (F value = 4.67, P = 0.037). In trabecular bone GH increased BFR with a statistic non-significant increase in the trabecular area (7.97±1.96% vs HX 4.55±1.33, P = 0.079) whereas PTH increased trabecular BFR with a significant increase in the trabecular area (15.98±5.68, P<0.05) as compared to the HX. The result of combined intervention shows an additive effect on increasing the trabecular area (24.03±5.56%). In conclusion, either PTH or GH treatment alone is able to enhance cortical and trabecular bone formation and bone density in the hypophysectomized rats. The combination treatment of PTH and GH has synergistic effect on increasing bone density and additive effect on increasing trabecular bone mass.

**Disclosures:** M.N. Guevarra, None.

## SU503

**Bone Health Impairment in Children with Chronic Calcium and Vitamin D Deficiency due to Nutritional Allergies.** C. Grasemann<sup>\*</sup>, K. T. Parker<sup>\*</sup>, E. Assor<sup>\*</sup>, E. B. Sochett. Hospital for Sick Children, Toronto, ON, Canada.

Environmental allergies are a known but infrequently reported cause of nutritional rickets in children. We present here four children (3 boys, 1 girl, 5.3 - 13.6 yrs) with severe environmental allergies referred to the calcium bone clinic at HSC for further evaluation of rickets. Referrals were made based on abnormal x-rays in all cases. X-rays had been taken for: femur fracture, planned dental surgery, knee pain and work up of short stature. At presentation, three of the children had several clinical stigmata of rickets and had been symptomatic from leg deformities and bone pain for a period of 0.6 - 3 yrs. Biochemical evaluation at time of diagnoses showed:

	Calcium (mmol/L)	Phosphorus (mmol/L)	25-Hydroxy Vit.D (nmol/l)	PTH (ng/L)	Total Alkaline Phosp. (U/L)
Mean	1.92	1.18	14	468	1060
range	1.25 - 2.35	0.85 - 1.12	<10 - 32	49 - 948	191 - 2957

3 patients showed radiological characteristics of rickets and one decreased bone mineralization. Z-scores for Bone Mineral Density were - 2.7 and -2.9 in the two older children. Nutritional allergies included a wide variety of foods including milk, fish, nuts and beans. Dietary intakes were severely restricted by the families based on anxiety about allergic reactions. None of the three patients with rickets had been seen by a recognized allergy specialist. None were receiving supplementation with calcium or vitamin D. Clinic treatment recommendations included 4000 - 8000 UI of Vitamin D, 0.6 - 2mcg of Calcitriol and 750 - 1200 mg of Calcium per day. Biochemical evaluation after 6 months of treatment showed:

	Calcium (mmol/L)	Ca/Crea Ratio (Urin)	25-Hydroxy Vit.D (nmol/l)	PTH (ng/L)	Total Alkaline Phosp. (U/L)
Mean	2.42	0.074	55.5	101	438.5
range	2.33 - 2.48	0.05 - 0.09	32 - 84	26 - 241	164 - 1110

In conclusion, children with severe environmental allergies are at an increased risk for bone health impairment if not treated with adequate vitamin D and calcium supplements. Given, the high degree of self management in these families and fear of allergic reactions, there seems to be an under-recognized subgroup of patients at risk of rickets/osteomalacia. On treatment, the repair process is prolonged, whether due to compliance or due to the severity of the demineralization. Physicians taking care of these patients need to encourage and monitor calcium and vitamin D supplementation.

**Disclosures:** C. Grasemann, None.

## SU504

**BONE DESTINY - A One Step Fracture Risk Predictor for Clinicians.** W. G. Bensen<sup>1</sup>, W. Bensen<sup>\*2</sup>, K. A. Beattie<sup>\*1</sup>, A. Papaioannou<sup>\*1</sup>, W. Wong Pack<sup>\*1</sup>, M. Larche<sup>\*1</sup>, J. D. Adachi<sup>3</sup>. <sup>1</sup>Dept. of Medicine, McMaster University, Hamilton, ON, Canada, <sup>2</sup>None, Hamilton, ON, Canada, <sup>3</sup>Dept. of Medicine, St. Joseph's Healthcare - McMaster University, Hamilton, ON, Canada.

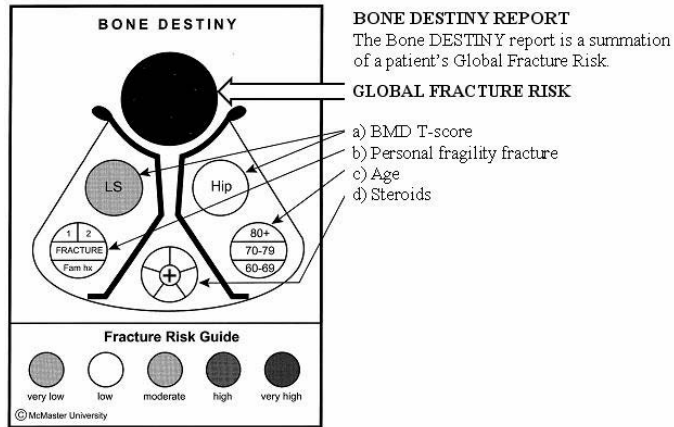
**Purpose:** To create a simple fracture risk predictor tool for clinicians that combines bone mineral density (BMD) with other risk factors for fracture in a way that is simple, easy to interpret and meaningful to patients.

**Methods:** BMD alone is an inadequate predictor of overall fracture risk and results expressed in T-scores often do not synapse a treatment response. In addition, T- scores often do not activate patients or doctors to initiate or adhere to therapy. Because BMD values do not take into account other risk factors for fracture, including previous fragility fracture and steroid use, many patients with significant fracture risk are not on treatment to prevent future fractures. Thus, "DESTINY" was created as an integrated model; a one-step fracture risk predictor that expresses BMD and overall fracture risk after taking into account age, BMD, previous fragility fracture and steroid use. This model uses 5 treatment specific colour zones which are easily recognizable and treatment-impelling to health care professionals.

**Results:** Destiny was designed over a two-year period as a cost-neutral, one-step program that integrates data input to a hand-held computer with BMD from a DEXA scanner to expresses fracture risk.



**Figure 1.** Bone DESTINY report



1. Technicians, while conducting DEXA scanning, input previous fragility fracture, steroid use, age and BMD into a hand-held computer model that is uploaded into a software program that produces a diagrammatic (DESTINY) report.2. The DESTINY report is colour coded by fracture risk where green=very low risk, yellow=low risk, orange=moderate risk, red=high risk and purple = very high risk (Figure 1).3. The reporter sees both BMD and DESTINY while dictating.4. DESTINY reports are easily understood by family physicians and other clinicians who arrange follow-up appointments guided by treatment zones.5. The report can also be shown to a patient to express their actual fracture risk. **Conclusion:** Bone DESTINY, a one-step fracture risk predictor tool, has been used successfully in over 10,000 patients in the greater Hamilton area. DESTINY reports conveying integrated fracture risk results through a colour-coded diagram are simple to interpret and explain to patients and have been positively received within the medical community.

**Disclosures:** K.A. Beattie, None.

## M001

**Anti-myeloma Effects of Osteoblasts Is Mediated Through Production of Small Leucine-rich Proteoglycans.** X. Li\*, A. Pennisi\*, S. Yaccoby. Myeloma Institute for Research and Therapy, University of Arkansas for Medical Sciences, Little Rock, AR, USA.

We have previously demonstrated that while osteoclasts support multiple myeloma (MM) growth, osteoblasts have negative impact on growth of MM cells from a subset of patients, indicating that MM bone disease drives tumor progression. Main small leucine-rich proteoglycans SLRPs such as decorin and lumican which are essential for proper bone remodeling have been shown to inhibit growth of various tumors and their expression level is inversely correlated with tumor progression. The aim of the study was to investigate the role of decorin in the anti-MM effects of osteoblasts. We confirmed at the molecular and protein levels that in contrast to mesenchymal stem cells (MSCs) and osteoclasts, osteoblasts express and produce high level of decorin. We also found that normal but not MM plasma cells express decorin and that decorin expression tends to be lower in patient's osteoblasts than in donors' osteoblasts. Recombinant decorin was rapidly internalized by MM cells, directly induced upregulation of p21<sup>waf</sup> and apoptosis in primary MM cells. In co-culture with osteoclasts recombinant decorin inhibited growth of primary MM cells in 6 of 9 experiments by 47±10% (p<0.007). Co-culture of MM cells with osteoclasts in the presence of osteoblast's conditioned media resulted in reduced MM cell survival (n=5, p<0.002), an effect that was partially but significantly attenuated by decorin neutralizing antibody (5 µg/ml, n=5, p<0.01). Down-regulation of decorin by lentiviral-containing decorin siRNA in osteoblasts resulted in increased survival of MM cells in MM-osteoblast co-cultures (p<0.03). In contrast, overexpression of decorin in MSCs reduced MSCs-induced MM cell survival by (p<0.04). We also demonstrated that decorin significantly attenuated MM-induced tube formation by HUVECs in a matrigel assay (p<0.001), and effectively inhibited differentiation of human osteoclasts (p<0.01). Immunohistochemical analysis revealed reduced decorin level in myelomatous bones engrafted with primary MM cells and marked increased levels following treatment with osteoblast activating agents such as bortezomib, PTH and anti-DKK1, providing a possible molecular mechanism for anti-MM efficacy of these agents. We conclude that mature osteoblasts express high level of decorin which exerts the anti-MM effects directly and indirectly through inhibition of angiogenesis and osteoclastogenesis. Increasing endogenous or exogenous SLRPs in myelomatous bones are safe approaches to control MM and its associated bone disease.

**Disclosures:** X. Li, None.

This study received funding from: NCI and MMRF.

## M002

**An Impaired Oxidative Stress Defense Mechanism May Reduce Bone Stiffness in Diabetic Charcot Neuroarthropathy.** K. A. Witzke<sup>1</sup>, A. I. Vinik<sup>2</sup>, H. K. Parsons<sup>2</sup>, G. Pittenger<sup>2</sup>. <sup>1</sup>Kinesiology, California State University, San Marcos, CA, USA, <sup>2</sup>Internal Medicine, Eastern Virginia Medical School, Norfolk, VA, USA.

**BACKGROUND:** Charcot neuroarthropathy is a serious consequence of prolonged neuropathy causing low-trauma foot fractures in up to 3% of diabetics. Charcot may be related to the overexpression of the cytokine receptor activator of NFκB ligand (RANKL)/osteoprotegerin (OPG) pathway, central to the processes regulating bone turnover. The advanced glycation end-product (AGE)/RAGE pathway may activate RANK and oxidative stress known pathogens in diabetic neuropathy. AGEs accumulating in diabetic collagen may also promote osteoblast apoptosis contributing to deficient bone formation. This study evaluated differences between type 2 diabetics with and without Charcot, and controls, with respect to: 1) bone remodeling, 2) RANKL/OPG, 3) RAGE, and 4) bone stiffness. **METHODS:** 80 males (aged 55.3±9.0y) [30 healthy controls (C), 30 type 2 diabetics with peripheral neuropathy (DN), and 20 age-matched type 2 diabetics with Charcot arthropathy (CA)] provided fasting blood samples evaluated for sRANKL, OPG, sRAGE, cross-linked N-telopeptides of type I collagen (NTx), and osteocalcin. Calcaneal bone stiffness was measured using quantitative ultrasound (QUS). **RESULTS:** sRANKL was similar between groups, but OPG was higher for DN (p=0.017) and somewhat higher for CA (p=0.067) compared to C, suggesting OPG is more related to diabetes/neuropathy than to Charcot specifically. NTx was similar but osteocalcin was much higher for CA than either DN or Controls. Protective sRAGE levels decreased with worse neuropathy, where DN levels were 54% lower, and CA levels were 86% lower than C (Table 1). sRAGE was positively correlated with calcaneal bone stiffness, where those with lowest sRAGE also had the lowest bone stiffness and resistance to fracture (r=0.35, p<0.006). **CONCLUSION:** These data suggest DN patients have impaired oxidative stress defense mechanisms and this capacity is markedly worse in CA. CA may indeed experience AGE-mediated osteoblast apoptosis, thereby limiting bone repair, which may be independent of the RANKL/OPG pathway. Administration of exogenous sRAGE may be a viable therapy for those at risk for Charcot.

**Table 1. Inflammation, oxidative stress, bone biomarkers, and bone stiffness**

	sRANKL (pg/ml)	OPG (pmol/L)	sRAGE (ng/L)	NTX (nmol)	Osteocalcin (ng/ml)	QUS (stiffness index)
Control (n=30)	0.03±0.03	5.5±0.39	1140±471	13.6±5.5	1.29±0.96	105.2±14.0
Diabetic (n=30)	0.01±0.003	7.4±0.54*	522±660*	11.4±5.7	1.23±0.68	103.3±18.6
Charcot (n=20)	0.02±0.01	7.2±0.59	162±67**	13.8±8.2	2.29±2.57**	77.1±26.2**

\*p<0.001 DN different than C

\*\*p<0.001 CA different than DN, C

**Disclosures:** K.A. Witzke, None.

This study received funding from: Commonwealth Health Research Board of Virginia.

## M003

**Fat Suppresses Osteoblast Differentiation by Soluble Factors That Induce Apoptosis.** S. Urs<sup>1</sup>, S. A. Bornstein<sup>1</sup>, M. Kawai<sup>1</sup>, M. C. Horowitz<sup>2</sup>, G. Duque<sup>3</sup>, A. C. Brown<sup>4</sup>, D. Roopenian<sup>5</sup>, C. J. Rosen<sup>1</sup>. <sup>1</sup>Research Institute, Maine Medical Center, Scarborough, ME, USA, <sup>2</sup>Yale University, New Haven, CT, USA, <sup>3</sup>University of Sydney, Penrith, Australia, <sup>4</sup>Bar Harbor Biotechnology, Trenton, ME, USA, <sup>5</sup>The Jackson Laboratory, Bar Harbor, ME, USA.

Low bone mass, reduced IGF-I, and increased marrow fat are noted with aging, caloric restriction, steroid and TZD use. In this study, we hypothesized that adipocytes secrete factors that influence IGF-I and inhibit osteoblast (OB) differentiation, potentiating the reciprocal relationship between marrow fat and BV/TV. To test that, we cultured marrow stromal cells (MSCs) from Swiss Webster mice in the lower part of a 2 chamber system separated by an insert that allowed only soluble factors from an upper chamber containing 500 mg fat isolated from peri-renal and visceral depots (PRVF), minced then rinsed in PBS and plated with MEMα. Fat was changed every 3 days (d) and CM assayed for IGF-I, osteocalcin, adiponectin and leptin. MSCs were grown for 7d in 10% FCS, switched to βGP and ascorbic acid for an additional 11 d in the lower chamber. Cells were stained at d10 and d14 for alkaline phosphatase (ALP). With PRVF in the upper chamber, the # of ALP+ colonies in the lower chamber was reduced by 60% vs MSCs without fat at both days (p<0.0003). Osteocalcin from MSCs co-cultured with PRVF was suppressed by 80% vs MSCs with no fat; but adiponectin, leptin and IGF-I in CM did not differ. Co-culture of fat and MSCs without an insert produced identical results: i.e. reduced ALP+ cells. To understand the failure of OB differentiation, we did qRT-PCR using a 384 well array to examine differentially regulated genes induced by PRVF. Runx2, BMP2, DMP1, Osterix and Osteocalcin were suppressed by 5 fold when MSCs were co-cultured with PRVF (p<0.0001). PTH1R was reduced 50 fold by PRVF (p<1.0 x 10<sup>-6</sup>) and IGF-I was reduced 30 fold (p<0.002). In contrast, TNF, VEGFα, IL-6 and IL-11 were up-regulated 10 fold (p<0.01). TNF, IL-1, IL-6 and VEGFα were also increased in the CM. TUNEL staining revealed an increase in MSC apoptosis. qRT-PCR for apoptosis genes revealed *Igf1* was the most highly suppressed gene (i.e. 24-40 fold at both days, p<0.002) and *Igf1bp3* the most highly expressed (30 fold, p<0.0001). Two pro-apoptotic genes (*Bnip*, *Unc5b*) were up regulated (p<0.05), while one anti-apoptosis gene, *Pawr*, was suppressed 10 fold at d10 and 14 (p<0.007). Thus, intra-abdominal fat produces a soluble factor that inhibits OB differentiation by activation of an apoptosis program involving *Igf1* and *Igf1bp3*. We conclude that age-related changes in bone mass and marrow fat may be due to release of adipokines or fatty acids within or outside the marrow milieu. Low IGF-I may be a permissive factor for enhancing marrow adipogenesis, but future studies are needed to define the function of marrow fat.

**Disclosures:** C.J. Rosen, None.

This study received funding from: NIH AR 54604.

## M004

**Brief Pulsing Electromagnetic Field Exposure Differentially Effects Cell Cycle in Proliferating and Confluent Osteoblasts.** B. S. Margulies<sup>1</sup>, J. A. Spadaro<sup>2</sup>. <sup>1</sup>Animal Biology, University of Pennsylvania School of Veterinary Medicine, Philadelphia, PA, USA, <sup>2</sup>Orthopedic Surgery, S.U.N.Y. Upstate Medical University, Syracuse, NY, USA.

**Introduction:** Making electromagnetic stimulation of bone cells into a more reliable clinical agent will require understanding the mechanism by which these responses occur. The objective of this experiment was to examine the cell cycle phase distribution and metabolic activity in MC3T3-E1 osteoblast-like cells after treatment with either a nitric oxide synthase inhibitor (NOSi) or calmodulin inhibitor (CAMi) prior to a single PEMF exposure in both low density and ~confluent cultures with treatment. Our hypothesis was that a brief PEMF exposure would alter the relative distribution of cells in different phases of the cell cycle and metabolic activity, and that the NOSi and CAMi would alter the PEMF effects. **Methods:** MC3T3-E1 mouse osteoblasts (ATCC) were seeded in 24 well plates at 2x10<sup>4</sup> cells/well (low density) and 2.5 x 10<sup>5</sup> cells/well (~confluent). A single PEMF or sham control treatment was applied for 30 minutes. The magnetic waveform was similar to that used clinically and consisted of bursts of short, asymmetric pulses repeated at 15 Hz, with peak amplitudes of 2 mT. Cultures were supplemented with the general NOSi LMMNA or the CAMi calmidazolium 1 hour prior to treatment. Cell cycle phases were assayed with flow cytometry while metabolic activity was assayed with the reduced-mitotracker dye (Invitrogen). **Results:** Results showed that in confluent cultures, PEMF appeared to reduce the transition from G<sub>0</sub>/G<sub>1</sub> to S and G<sub>2</sub>/M phase (p<0.05). In the low-

density cultures the PEMF exposure appeared to promote the transition from S-phase to G<sub>2</sub>/M by 10% (p<0.05). In both cases CAMi and NOSi altered these effects. PEMF also transiently decreased mitotracker staining, while NOSi and CAMi shifted the mitotracker staining. The sham-treated cells were identical in distribution to incubator control cultures and viability was not affected. **Discussion:** These findings suggest that PEMF may have effects on the pathways controlling the cell cycle. Previous studies have speculated that calcium signaling is responsible for transmitting the PEMF effect. A number of reports have suggested that calcium signaling may play an important role in the cell cycle through the following: The stimulation of  $\beta$ -catenin and calmodulin inhibition resulting in increased p21 and cells remaining in G<sub>0</sub>/G<sub>1</sub>. The current work would seem to support a similar mechanism, however, though this remains to be confirmed.

**Disclosures:** B.S. Margulies, None.

*This study received funding from: NASA grant to the Central New York Biotechnology Research Center.*

## M005

**Osteoblasts Apoptosis Is Mediated Through Glycogen Synthase Kinase 3 $\beta$ .** S. Yun<sup>\*1</sup>, H. Yoon<sup>\*1</sup>, S. Yi<sup>\*1</sup>, S. Jeong<sup>\*2</sup>, Y. Chung<sup>1</sup>. <sup>1</sup>Endocrinology and Metabolism, Ajou University School of Medicine, Suwon, Republic of Korea, <sup>2</sup>Medical Genetics, Ajou University School of Medicine, Suwon, Republic of Korea.

Mechanisms controlling the survival of osteoblast cells are critical during bone development and diseases.

In osteoblasts, glycogen synthase kinase-3 (GSK3) is a bone mass regulator in Wnt signaling pathway, which alters markers of osteogenesis, chondrogenesis, and adipogenesis. In this study, we found that genotoxic stress promoted apoptotic signaling through GSK3 $\beta$  in osteoblast cell line (CH310T1/2 cells) derived from mouse embryonic mesenchymal stem cells. Etoposide induced genotoxic stress and apoptosis. The protein expression of phosphorylation on serine-9 in GSK3 $\beta$  was decreased time-dependently that meant activation of GSK3  $\beta$ . To investigate the apoptosis by etoposide, we examined the caspase-3 activity, the key apoptosis mediator of apoptosis, and the protein expression of cleaved PARP, the caspase-3 substrate. Both of them were markedly increased. However, LiCl, a specific GSK3 inhibitor antagonized those effects dose-dependently. Moreover, the plant extract, which had protective effects in osteoblasts apoptosis was also related with GSK3 $\beta$  activity.

These data suggest that genotoxic stress may be able to enhance the osteoblasts survival by inhibition of GSK3, which maybe involved in osteoblasts function by regulation of apoptosis.

This research was supported by the "GRRC" Project of Gyeonggi Provincial Government, Republic of Korea.

**Disclosures:** Y. Chung, Eli Lilly, GSK 1; MSD, Sanofi-Aventis 1, 2, 3, 4; Novartis 1, 4; Hanlim, Yuyu 1, 2, 3.

*This study received funding from: "GRRC" Project of Gyeonggi Provincial Government, Republic of Korea.*

## M006

**Functional Role of Odd-Skipped Related 2 in Preosteoblastic Cells.** S. Kawai, M. Yamauchi, A. Amano\*. Department of Oral Frontier Biology, Osaka University Graduate School of Dentistry, Suita-Osaka, Japan.

Zinc-finger transcription factor Odd-skipped related 2 (Osr2) is one of the regulators in osteoblast proliferation and bone formation. We previously reported its regulatory role using dominant-negative Osr2 transgenic mice. The transgenic mice revealed the characteristic features, including 1) delayed mineralization in calvarial and cortical bone tissues, 2) distinctly increased radiolucency in soft X-ray analysis, 3) reduced staining intensities with alcian blue and alizarin red in the skull and skeletal elements, and 4) markedly thinner parietal and cortical bones. Differentiation and proliferation of alveolar osteoblasts of transgenic mice were also found to be highly attenuated. In addition, Osr2-deficient mice revalidated that Osr2 play a critical role in the secondary palate development. In this study, we further analyzed the functional role of Osr2 in preosteoblastic cells in detail. At first, we analyzed an epigenetic regulation on Osr2 expression by multipotent mesenchymal C3H10T1/2 cells. Osr2 expression was remarkably upregulated by serum starvation as well as confluent culture, whereas the expression was downregulated to basal level following the serum re-addition. DNA methylation of Osr2 promoter was analyzed with the sodium bisulfite sequencing method. Consequently, the Osr2 promoter was demethylated in serum starvation as well as confluent growth arrest. Moreover, histone acetylation on Osr2 promoter was also analyzed with the chromatin immunoprecipitation. The histones on Osr2 promoter was acetylated in serum starvation as well as confluent culture. Secondly, we analyzed downstream target genes of Osr2 with microarray profiling. Osr2 overexpressing adenovirus was constructed and infected to C3H10T1/2 cells. Total RNAs were prepared and analyzed with Affymetrix mouse genome 430 2.0 arrays. As a result of array classification analysis of downstream genes, the genes in Wnt signaling pathway were regulated by Osr2. Our study indicates that Osr2 expression is regulated by epigenetic modification of DNA and histones. These findings demonstrate that Osr2 play an important role in cell cycle regulation through Wnt signaling pathway.

**Disclosures:** S. Kawai, None.

## M007

**Strontium Ranelate Protects Osteoblasts from Apoptosis Independently of the Calcium Sensing Receptor.** O. Fromiguet, A. Barbara\*, E. Hay\*, P. J. Marie\*. Osteoblast biology and pathology laboratory, Inserm U606 & University Paris, 7, Hôpital Lariboisiere, Paris Cedex 10, France.

Several clinical trials have established that strontium ranelate is a new treatment for postmenopausal osteoporosis. We previously showed that strontium ranelate promotes murine osteoblastic cell proliferation in part through activation of the calcium sensing receptor (CaSR). Recent studies have shown that bone formation is controlled by osteoblast survival. Moreover, osteoblast apoptosis was found to be increased in osteoporosis. In this study, we hypothesized that strontium ranelate may have a beneficial effect on osteoblast survival through activation of the CaSR. To test this hypothesis, primary mouse calvaria pre-osteoblasts were isolated from wild type (CaSR<sup>+/+</sup>) and CaSR null (CaSR<sup>-/-</sup>) mice by collagenase digestion. Cell cultures were used for determination of apoptosis using the Apopercut assay using a dye that is selectively imported by cells undergoing apoptosis. We tested the effect of strontium ranelate on apoptosis induced by IL-1  $\beta$  and TNF $\alpha$  which are pro-inflammatory cytokines that are known to induce osteoblast apoptosis. Treatment with IL-1 $\beta$  or TNF $\alpha$  (5 ng/ml, 24 hrs) increased apoptosis in both CaSR<sup>+/+</sup> and CaSR<sup>-/-</sup> murine calvaria osteoblasts. Strikingly, the addition of strontium ranelate (1-5 mM) blunted apoptosis induced by IL-1 $\beta$  or TNF $\alpha$ , and this effect occurred in both CaSR<sup>+/+</sup> and CaSR<sup>-/-</sup> osteoblasts. Furthermore, we showed that strontium ranelate (3, 5 and 10 mM) blunted osteoblast apoptosis induced by serum deprivation (0.5 %). Western blot analysis showed that strontium ranelate increased phospho-P13K and phospho-Akt levels in CaSR<sup>+/+</sup> and CaSR<sup>-/-</sup> osteoblasts, suggesting the involvement of these pro-survival signaling cascade in the observed anti-apoptotic effect. These results indicate that 1) strontium ranelate protects primary osteoblasts from apoptosis induced by inflammatory cytokines or serum deprivation in mouse calvaria osteoblasts, 2) The CaSR is not essential for the anti-apoptotic effect of strontium ranelate in osteoblasts and 3) The protective effect of strontium ranelate on osteoblast apoptosis involves activation of PI3K/Akt signaling in osteoblasts. These data indicate that strontium ranelate protects osteoblasts from apoptosis and that this protective effect of strontium ranelate on osteoblast apoptosis could involve additional receptor in addition to the calcium sensing receptor.

**Disclosures:** O. Fromiguet, None.

*[This study received funding from: Servier.]*

## M008

**Importance of Melastatin-like Transient Receptor Potential 7 and Magnesium in the Stimulation of Osteoblast Proliferation and Migration by Platelet-Derived Growth Factor.** E. Abed\*, R. Moreau\*. Sciences biologiques, Université du Québec à Montréal, Montréal, QC, Canada.

Bone is a dynamic tissue continuously being remodeled throughout life. Bone tissue is removed from the skeleton by osteoclasts and a novel bone matrix is added by osteoblasts. Normally, both resorption and formation processes are in balance and maintain skeletal strength and integrity. In this regard, adequate osteoblast proliferation, migration, differentiation and secretory function are essential both for adequate formation and for resorption processes, and thereby for the maintenance of bone remodeling equilibrium. Disturbances of this equilibrium may lead to decreased bone mass with associated increase in bone fragility and susceptibility to fracture (osteoporosis). Epidemiological studies have mentioned a link associating insufficient dietary magnesium intake in humans with low bone mass and osteoporosis. Here, we have investigated the importance of magnesium and melastatin-like transient receptor potential 7 (TRPM7), a calcium and magnesium channel, in the stimulation of osteoblast proliferation and migration by platelet-derived growth factor (PDGF), a known factor for the regulation of bone remodeling. We observed that the stimulation by PDGF of cell proliferation and migration was significantly reduced under culture conditions of low extracellular magnesium concentrations. The gene expression of TRPM7 by osteoblasts was increased by PDGF in a time-dependent manner. The reduction of TRPM7 expression by specific interfering RNA prevented the stimulation of proliferation and migration by PDGF. Our results indicate that extracellular magnesium and TRPM7 are important for PDGF-induced human osteoblast proliferation and migration which suggests that magnesium deficiency, a common condition among the general population, may lead to inadequate bone formation resulting in the development of osteoporosis.

**Disclosures:** E. Abed, None.

*This study received funding from: NSERC.*

**M009**

**Lentiviral Short Hairpin RNA Mediated Inhibition of Glutaredoxin 5 Expression Induces Apoptosis via a Mechanism Involving Increased ROS and Cardiolipin Oxidation, and Reduced Superoxide Dismutase Activity.** G. R. Linares, W. Xing, K. Govoni, S. Mohan. JLP VAMC and LLU, Loma Linda, CA, USA.

Oxidative stress poses detrimental effects on bone by depleting antioxidants, activating osteoclasts, and inhibiting osteoblast (Ob) cell functions. Therefore, it is important to understand components of defense mechanisms to combat oxidative stress in bone. We recently found that Glutaredoxin 5 (Grx5), a member of an antioxidant enzyme family, which functions to maintain cellular redox homeostasis, is highly expressed in bone, induced by growth hormone and modulates Ob apoptosis and ROS production in MC3T3-E1 cells. In the present study, we sought to determine the molecular mechanism by which Grx5 protects against oxidative stress induced apoptosis by utilizing short hairpin RNA (shRNA) and to examine the effect of long term inhibition of Grx5 on Ob apoptosis. Lentiviral Grx5 shRNA infection of MC3T3-E1 cells reduced Grx5 expression by 72 % ( $P < 0.01$ ) in comparison to non-target shRNA control. Cytotoxicity induced by TNF- $\alpha$ , a known inducer of ROS, increased by 3.5-fold ( $P < 0.05$ ) in Grx5 shRNA treated cultures in comparison to shRNA control. Since caspase dependent apoptosis is a major mechanism by which TNF- $\alpha$  and  $H_2O_2$  induce apoptosis, we examined the consequence of Grx5 inhibition on caspase activity induced by these agents. In the presence of  $H_2O_2$  and TNF- $\alpha$ , caspase activity of Grx5 shRNA cells increased by 3.6-fold ( $P < 0.05$ ) and 2.3-fold ( $P < 0.05$ ) in comparison to shRNA control cells, respectively. We next evaluated the effects of ROS on oxidation of cardiolipin since it is known to modulate cytochrome c dependent activation of caspase. In the presence of  $H_2O_2$ , cardiolipin oxidation was significantly higher (2-fold increase,  $P < 0.001$ ) in Grx5 shRNA cells compared to shRNA control cells. Grx5 deficiency reduces formation of Fe-S cluster and thereby increases levels of free iron, a competitive inhibitor of manganese superoxide dismutase (Mn-SOD), which is a key mitochondrial ROS scavenger. Accordingly we found that Mn-SOD activity was reduced in Grx5-deficient Obs. If the increased caspase activity caused by ROS-induced cardiolipin oxidation is caused by reduced Mn-SOD activity, excess Mn should reverse the effect of Grx5 deficiency on Ob apoptosis by rescuing Mn-SOD activity. Accordingly, we found that 200  $\mu$ M  $MnCl_2$  rescued the increased caspase activity by  $H_2O_2$  in Grx5 shRNA treated Ob cultures ( $2504 \pm 44.9$  vs.  $3940 \pm 102.2$  RLU;  $P < 0.001$ ). Our findings are consistent with the hypothesis that Grx5 is an important determinant of Ob cell functions and acts via a molecular pathway that involves regulation of ROS production, cardiolipin oxidation, caspase activity, Fe-S cluster formation, and Mn-SOD activity.

**Disclosures:** G.R. Linares, None.

**M010**

**$\beta$ -Catenin Protects Osteoblasts from Oxidative Stress by Co-activating the Expression of Pro-survival, but not Pro-apoptotic, Target Genes of the FoxO Transcription Factors.** M. Almeida, L. Han, E. Ambrogini, M. Martin-Millan, A. Warren\*, S. C. Manolagas. Center for Osteoporosis and Metabolic Bone Diseases, University of Arkansas for Medical Sciences and Central Arkansas Veterans Healthcare System, Little Rock, AR, USA.

Progressive loss of bone mass and strength with age in mice is associated with increased oxidative stress and expression of target genes of the FoxO transcription factors, as well as increased osteoblast and osteocyte apoptosis. In support of a mechanistic link among these phenomena,  $H_2O_2$  promotes the translocation of FoxOs into the nucleus and the transcriptional activation of pro-apoptotic genes. Albeit, FoxOs also activates the transcription of antioxidant enzymes like MnSOD and catalase, thereby mounting a defense against oxidative stress. Heretofore, the factor(s) influencing the balance between the pro-apoptotic versus pro-survival gene program activation by FoxOs remain unknown. Based on evidence that  $H_2O_2$  stimulates FoxO-mediated transcription in osteoblastic cells and induces the association of FoxOs with  $\beta$ -catenin, we investigated the relevance of the FoxO/ $\beta$ -catenin partnership to the lifespan of osteoblastic cells. Similar to the addition of  $H_2O_2$  into the culture medium, overexpression of FoxO3a in C2C12 cells increased apoptosis, as determined by the number of cells with altered nuclear morphology. A dominant negative FoxO mutant abolished the effect of  $H_2O_2$  on apoptosis; and both  $H_2O_2$  and FoxO3a increased the transcription of the pro-apoptotic gene Bim as measured by a Bim-luciferase reporter construct. Furthermore, mutation of the FoxO binding site on the Bim gene promoter abolished the effect of  $H_2O_2$  or FoxO3a, confirming the essential role of FoxO-stimulated transcription of pro-apoptotic genes in  $H_2O_2$ -induced apoptosis. Strikingly, the pro-apoptotic effect of either  $H_2O_2$  or FoxO3a was abolished in cells co-transfected with a mutant form of  $\beta$ -catenin (S33Y), which cannot be targeted for degradation. The S33Y  $\beta$ -catenin mutant also antagonized the stimulatory effect of  $H_2O_2$  or FoxO3a on Bim expression. Albeit,  $H_2O_2$  or FoxO3a also stimulated MnSOD gene expression as measured by a MnSOD-luciferase reporter construct. More strikingly,  $\beta$ -catenin S33Y upregulated the effects of  $H_2O_2$  and FoxO3a on MnSOD. Conversely, the  $\beta$ -catenin antagonist DKK-1 inhibited both basal MnSOD expression as well as the upregulation of MnSOD produced by  $H_2O_2$  or FoxO3a. We conclude that the level of active  $\beta$ -catenin in osteoblastic (and perhaps other cell types) is an important determinant of their fate by tilting the balance of FoxO-mediated transcription towards a pro-survival, as opposed to a pro-apoptotic, gene program.

**Disclosures:** M. Almeida, None.

**M011**

**Glucose-dependent Insulinotropic Peptide Inhibits Glucose-induced Apoptosis of Bone Cells.** S. Sridhar\*<sup>1</sup>, M. Marrero\*<sup>2</sup>, X. Shi\*<sup>3</sup>, S. Sridhar\*<sup>1</sup>, Q. Mi\*<sup>3</sup>, W. B. Bollag\*<sup>1</sup>, N. Chutkan\*<sup>4</sup>, C. M. Isles\*<sup>4</sup>. <sup>1</sup>Medicine, Medical College of Georgia, Augusta, GA, USA, <sup>2</sup>Pharmacology, Medical College of Georgia, Augusta, GA, USA, <sup>3</sup>Pathology, Medical College of Georgia, Augusta, GA, USA, <sup>4</sup>Orthopaedic Surgery, Medical College of Georgia, Augusta, GA, USA.

We have previously demonstrated that Glucose-dependent insulinotropic peptide (GIP) receptors are present in a variety of bone cells including osteoblasts and bone marrow derived osteoprogenitor or stromal cells (BMSC). We have proposed that GIP is the hormonal link between nutrient intake and dietary-induced stimulation of bone formation. We have also shown that BMSC not only express GIP receptors but that GIP also promotes osteoblast differentiation. To further define the mechanism responsible for GIP's anabolic effect on bone we examined whether GIP might also affect apoptosis of osteoblasts and BMSC. Specifically, hyperglycemia (Diabetes Mellitus) is known to negatively impact bone formation and result in a higher number of fractures. Thus, we used high glucose as an apoptotic signal. For these experiments we used primary calvarial osteoblasts and BMSCs harvested from C57BL6 mice bone marrow and enriched for stem cells by using negative and positive selection. Cells were grown in 60 mm dishes to confluence and placed in either normal glucose (5.5 mM) or high glucose medium (25 mM) with or without increasing concentrations of GIP (0.1-10 M). Cell protein was extracted and analyzed by Western blot (n=3). We found GIP dose-dependently and very significantly inhibited high-glucose induced apoptosis as assessed by caspase 3 cleavage or Akt phosphorylation. Since GIP levels are known to decrease in diabetes mellitus we propose that loss of the anti-apoptotic effects of these hormone could contribute at least in part to diabetes related bone loss.

**Disclosures:** C.M. Isles, None.

**M012**

**Butyrate Stimulates Mineralized Nodule Formation and Osteoprotegerin Expression by Osteoblasts.** T. Kawato\*<sup>1</sup>, T. Katono\*<sup>1</sup>, N. Tanabe\*<sup>1</sup>, N. Suzuki\*<sup>2</sup>, T. Iida\*<sup>1</sup>, K. Ochiai\*<sup>3</sup>, M. Maeno\*<sup>1</sup>. <sup>1</sup>Oral Health Sciences, Nihon University School of Dentistry, Tokyo, Japan, <sup>2</sup>Biochemistry, Nihon University School of Dentistry, Tokyo, Japan, <sup>3</sup>Microbiology, Nihon University School of Dentistry, Tokyo, Japan.

**Objective:** Butyric acid (sodium butyrate; BA) is a major metabolic by-product of main periodontopathic bacteria present in subgingival plaque. In the present study, we examined the effects of BA on cell proliferation, alkaline phosphatase (ALPase) activity, mineralized nodule formation, extracellular matrix protein expression, macrophage colony-stimulating factor (M-CSF), and osteoprotegerin (OPG) in normal human osteoblasts.

**Methods:** The cells were cultured with 0,  $10^{-8}$ ,  $10^{-6}$  or  $10^{-4}$  M BA for up to 12 days. Mineralized nodule formation was detected by alizarin red staining, and the calcium content in mineralized nodules was determined using a calcium assay kit. The gene and protein expression levels for type I collagen, bone sialoprotein (BSP), osteopontin (OPN), M-CSF, and OPG were examined using real-time PCR and ELISA, respectively.

**Results:** Mineralized nodule formation and the calcium content of mineralized nodules were increased by BA in a dose-dependent manner. Cell proliferation and ALPase activity were not affected by the addition of BA. Following the addition of  $10^{-4}$  M BA, the expression levels of BSP, OPN, and OPG increased, whereas the expression levels of type I collagen and M-CSF were not markedly affected.

**Conclusion:** These results suggest that BA stimulates bone formation by increasing the production of BSP and OPN, whereas it suppresses osteoclast differentiation by increasing the production of OPG by human osteoblasts.

**Disclosures:** T. Kawato, None.

## M013

**OPG Serum Levels in Shaft Fractures Healing and Non-union.** C. F. Corradini<sup>\*1</sup>, D. Marchelli<sup>\*2</sup>, L. Parravicini<sup>\*1</sup>, C. Crapanzano<sup>\*3</sup>, F. M. Ulivieri<sup>\*2</sup>, C. A. Verdoia<sup>\*4</sup>. <sup>1</sup>Orthopaedic and Traumatologic Clinic, Studies University of Milan c/o G. Pini Institute, Milan, Italy, <sup>2</sup>Nuclear Medicine Unit, IRCSS Fondazione Policlinico Mangiagalli, Milan, Italy, <sup>3</sup>Clinical Pathology Unit, G. Pini Institute, Milan, Italy, <sup>4</sup>Orthopaedic and Traumatologic Clinic, Studies University of Milan c/o G.Pini Institute, Milan, Italy.

In normal bone healing, osteoblastic formation follows osteoclastic bone resorption along rhymes fracture. In non-unions no callus formation is radiologically evident. In the last years OPG/RANKL/RANK system has been recognized to play a key role in the cross-talk between osteoblasts and osteoclasts. In particular OPG has been involved in the bone repair process following fracture. But in animal model OPG treatment impairs the normal remodeling and consolidation.

The aim of this study was to verify OPG serum levels in shaft fractures healing and non-union in male adults.

To be eligible for the study, a patient with single closed shaft fracture of lower limbs had to be aged between 20 and 39 years and not under treatment with drugs interfering with bone metabolism. Patients with local or systemic severe diseases or with previous same limb segment fractures or non-union were excluded.

Sixteen male patients with atrophic non-union fractures and nineteen age-matched male with healing fractures were enrolled. Two orthopaedic surgeons reviewed all medical records pertaining to the patients and independently verified the correct synthesis and diagnosed the atrophic non-union fractures due to non infective causes.

Serum OPG, RANKL, bone alkaline phosphatase (BAP) and osteocalcin(OC) were determined.

The mean age was 28.1±5.9 for non-unions group and 29.7±6.0 for healing group. OPG was significantly higher in non-unions group (0.558±0.114 ng/ml) compared to healing group (0.425±0.110 ng/ml; p=0.0014). In the two groups RANKL was not significantly decreased even if a difference of 15% was detected. For the other bone turn-over markers mean serum levels were within normal references range and not significantly different. OC was negative correlated to OPG.

Significant high OPG serum levels in shaft fracture non-unions vs healing suggests an altered bone remodeling. The reason of no proportional OPG/RANKL balancing is unknown. Further studies are necessary to explain if OPG could be directly involved in the pathogenesis of shaft fractures non union and consequently used as predictive marker in clinical practice.

**Disclosures:** C.F. Corradini, None.

## M014

**Cardiotrophin-1 Is an Osteoclast-derived Coupling Factor Required for Normal Bone Remodeling.** E. C. Walker<sup>\*</sup>, N. E. McGregor<sup>\*</sup>, I. J. Poulton<sup>\*</sup>, S. Pompolo, E. H. Allan<sup>\*</sup>, J. M. W. Quinn, M. T. Gillespie, T. J. Martin, N. A. Sims. St. Vincent's Institute, Melbourne, Australia.

Cardiotrophin-1 (CT-1) is a cytokine that signals through gp130 and the LIF receptor (LIFR). Both receptors are expressed in osteoblasts but not in osteoclasts and deletion of either receptor results in neonatal lethality, dwarfism and osteopenia indicating a critical role in bone metabolism. We investigated the role of CT-1 in bone by immunohistochemistry, which revealed positive staining for CT-1 in active osteoclasts in mouse bone, suggesting a role in local regulation of bone metabolism. Administration of recombinant CT-1 to cultured mouse stromal cells and by calvarial injection in vivo increased osteoblast activity and mineralization. CT-1 also stimulated STAT, Erk and ATF4 phosphorylation and runx2 activation in mouse stromal cells in vitro, confirming a direct effect on osteoblast activity. In addition, CT-1 stimulated osteoclast formation from mouse bone marrow, but only in the presence of osteoblasts. Surprisingly, administration of CT-1 to mouse stromal cells did not enhance RANKL mRNA expression, but rapidly upregulated IL-6 mRNA ~8 fold, providing a putative mechanism for the pro-osteoclastogenic effect.

To determine the importance of CT-1 in vivo, we examined the phenotype of neonate CT-1 ligand null (CT-1 KO) mice, which had no survival defect and no reduction in neonatal bone size. These neonates did demonstrate a 75% reduction in BV/TV, associated with a 60% reduction in ObS/BS, and a doubling in OcS/BS. Furthermore, CT-1 KO osteoclasts were double the size of wild type osteoclasts. Despite this, the percentage of cartilage within the trabecular bone of CT-1 KO mice was doubled, suggesting impaired resorption. The similarity with the receptor knockout phenotypes suggests that CT-1 is the critical gp130:LIFR signaling cytokine required for normal trabecular development, but is not the cytokine required for normal bone size. Cultured bone marrow (BM) from CT-1 KO mice generated many oversized osteoclasts and BM mesenchymal precursors mineralized poorly when cultured under osteoblastic conditions compared to wild type BM, consistent with the in vivo phenotype. As the CT-1 KO mice aged, reduced osteoblast surface (ObS/BS) was no longer detected but impaired bone resorption continued resulting in normalization of BV/TV at 4 weeks, and an osteopetrotic phenotype in male and female mice at 10 and 26 weeks of age indicating different requirements for CT-1 during bone development and remodeling.

Taken together, these data indicate that CT-1 may now be classed as an essential osteoclast-derived coupling factor, capable of stimulating both bone formation and resorption through direct actions on the osteoblast.

**Disclosures:** N.A. Sims, None.

This study received funding from: NHMRC (Australia).

## M015

**Primary Bone Cells of Pregnant Mice Exposed to Oscillatory Fluid Flow.** H. G. Lee<sup>\*</sup>, B. G. Kim<sup>\*</sup>, J. H. Kwag<sup>\*</sup>, C. H. Kim. Yonsei University, Wonju, Republic of Korea.

Mechanical loading and pregnancy are conditions that can affect the balance of bone remodeling. However, the relationship between pregnancy and loading-induced bone remodeling has not been well studied. Therefore, the aim of this study was to investigate whether bone during pregnancy responded differently to mechanical loading compared to bone during non-pregnant conditions. Bone cells were isolated from 11 week old ICR mice. The mice were either non-pregnant, 10-day pregnant, or 18-day pregnant. The long bones were harvested and removed of bone marrow and surface cells. The bones were cut in small pieces and bone cells were allowed to migrate out of the bone pieces into a culture dish. 48 hours prior to mechanical loading, cells were seeded on glass slides and treated with vitamin D3 for expression of receptor activator of NF- $\kappa$ B ligand (RANKL). Oscillatory fluid flow-induced shear stress was applied to cells at 1 Pa for 1 hr. Control cells received no flow. Immediately after end of loading, mRNA was extracted. Real-time RT-PCR was performed to quantify the following genes: core binding factor  $\alpha$ 1 (cbfa1), osteopontin (OPN), collagen I, osteoprotegerin (OPG) and RANKL. Alkaline phosphatase protein level was quantified by kinetic reaction method. Results for RANKL and OPG of non-pregnant and 18-day pregnant mice have been quantified thus far. Comparing 18-day pregnant mice to non-pregnant mice, OPG expression was significantly increased by 10-fold due to pregnancy. This resulted in a significant decrease in RANKL/OPG ratio in pregnant mice. Effects of loading was also compared in both non-pregnant and 18-day pregnant groups. Compared to the respective non-loading group, RANKL expression decreased by 40% in the non-pregnant loading group and by 60% in the 18-day pregnant loading group. OPG expression showed no difference in the non-pregnant group, but significantly increased by 2-fold when loading was applied to the 18-day pregnant group. Results suggest that pregnancy may hinder bone resorption by decreasing the RANKL/OPG ratio through significant increases in OPG level. Also, bone cells during the third trimester of pregnancy (corresponding to 18-day pregnancy) appear to be more sensitive to mechanical loading than bone cells during non-pregnant conditions. This may help pregnant women in their third trimester to effectively prevent significant bone loss through minimal exercise.

**Disclosures:** C.H. Kim, None.

This study received funding from: Korea Science and Engineering Foundation and Korea Institute of Oriental Medicine.

## M016

**Msx1 Homeogene Specific and Non-redundant Function in Oral Bones.** F. Méary<sup>\*</sup>, J. Nefussi<sup>\*</sup>, A. Marchadier<sup>\*</sup>, A. Berdal<sup>\*</sup>, S. Babajko<sup>\*</sup>. Centre de Recherche des Cordeliers, INSERM, Paris, France.

Msx (1 and 2) homeogenes are transcriptional regulators involved in skeleton patterning. Even if both of them are expressed during embryonic development in the craniofacial mesenchyme and in limbs, the phenotypes of Msx1 and Msx2 knock-out mice are different suggesting a non-redundant function. We have already shown that in adults, Msx1 is expressed in the dental bone and that Msx2 is involved in osteo-dental growth. In order to answer the question concerning the specific role of Msx1, we have explored Msx1 -/- mouse oral phenotype (Houzelstein et al., 1997 Mech Dev, 65, 123-133). As these mice die before birth, osteo-chondrogenic patterning was investigated by analysing gene expression by RT-Q-PCR on E18 fetal mice. Our results showed a clear and strong decrease of Msx2 expression in the mandible and maxillary bones of Msx1 -/- mice but no difference in limbs, suggesting a link between Msx1 and Msx2 in oral bones only. Moreover, osteo-chondrogenic marker expression was similar in -/- and +/- animals suggesting that Msx1 is involved in bone morphogenesis but probably not in differentiation.

We also explored Msx1 +/- adult mouse oral phenotype by scanning their heads using a 1072 Skyscan® micro CT. 3D-skyscan analysis illustrated a distinct morphological maxillar alveolar bone process in Msx1 heterozygous mice compared to control animals. The vestibular ridge appeared to be larger in its crestal part (339 ± 47 vs 269 ± 36 p<0.005) but smaller in length (117 ± 6 vs 128 ± 9 p<0.01). This dysmorphology was coincident with areas of Msx1-expressing cells evidenced by beta-galactosidase histochemistry. It was the first time that a clear phenotype was evidenced in adult Msx1 heterozygous mice which is in accordance with the situation in humans where (heterozygous) Msx1 mutations lead to oral anomalies.

In conclusion, this study showed a link between Msx1 and Msx2 specifically in maxillary and mandible bones thus explaining, at least in part, a phenotype of Msx1 -/- mice restricted to oral bones only, even if Msx1 is also expressed in limbs. Msx1 could be considered as a bone morphogenetic factor, not involved in differentiation. Moreover, the role of Msx1 homeogene in the adult dental bone morphology might contribute to the specific dental bone physiology which diverges from the rest of the skeleton.

**Disclosures:** F. Méary, None.

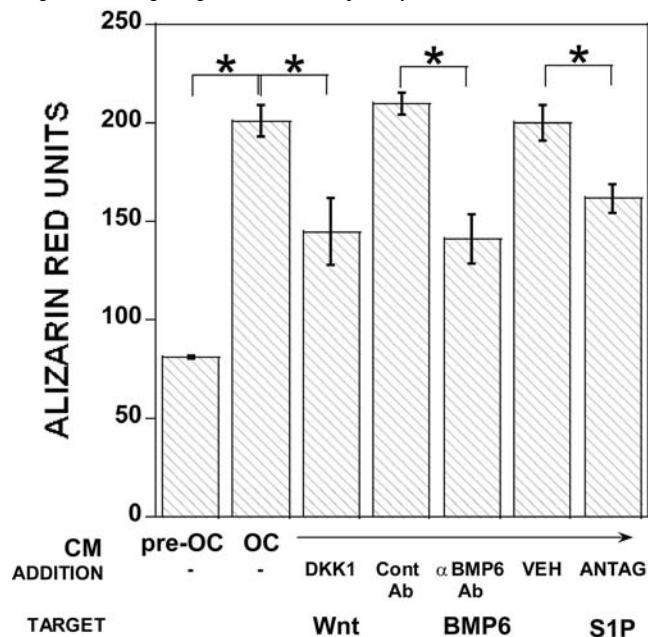
This study received funding from: ANR, INSERM and Université Paris 7.

## M017

**Regulation of Bone Formation by Osteoclasts Involves Wnt/Bmp Signaling and the Chemokine Sphingosine-1-Phosphate.** L. Pederson<sup>\*1</sup>, M. Ruan<sup>\*1</sup>, J. J. Westendorf<sup>2</sup>, S. Khosla<sup>1</sup>, M. Oursler<sup>1</sup>. <sup>1</sup>Endocrine Research Unit, Mayo Clinic, Rochester, MN, USA, <sup>2</sup>Orthopedic Research Unit, Mayo Clinic, Rochester, MN, USA.

Under most conditions, resorbed bone is nearly precisely replaced in location and amount by new bone. Thus, it has long been recognized that bone loss through osteoclast-mediated bone resorption, and bone replacement through osteoblast-mediated bone formation, are tightly coupled processes. Abundant data conclusively demonstrate that osteoblasts direct osteoclast differentiation. Key questions remain, however, as to how osteoblasts are recruited to the resorption site, and how the amount of bone laid down is so precisely controlled. This has led to further consideration of the role(s) that osteoclasts and/or their activity play in the promotion of bone formation.

We examined osteoclasts for influences on osteoblasts and found that conditioned medium (CM) from both primary osteoclasts and RANKL-induced RAW 264.7 cell-derived osteoclasts stimulate human mesenchymal stem (hMS) cell migration and differentiation. We sought to identify candidate osteoclast-derived coupling factors using the unbiased approach of Affymetrix microarray. Comparing pre-osteoclasts to mature osteoclasts, we observed 4-fold induction of sphingosine kinase 1 (SPHK1), which catalyzes the phosphorylation of sphingosine to form sphingosine 1-phosphate (S1P). S1P induces osteoblast precursor recruitment and promotes mature cell survival. There was also increased expression of Wnt10b (by 4-fold) and BMP6 (by 5-fold) as osteoclasts matured. As shown in the Figure, CM from mature osteoclasts (differentiated from RAW cells) increased mineralized nodule formation of hMS cells as compared to CM from RAW pre-osteoclasts. The stimulation of hMS cell nodule formation by the osteoclast CM could be at least partially inhibited by the Wnt antagonist, Dkk1, a BMP-6 neutralizing Ab, and by a S1P antagonist, demonstrating a role for Wnt/BMP signaling and S1P in osteoclast-mediated stimulation of bone formation. Further, during osteoclast differentiation, expression of Sclerostin, an inhibitor of Wnt-induced osteoblast precursor responses, was suppressed. In summary, our findings indicate that osteoclasts may recruit osteoprogenitors to the site of bone remodeling through the chemokine, S1P, and stimulate bone formation through increased signaling via the Wnt/BMP pathways.



Disclosures: M. Oursler, None.

This study received funding from: Mayo Clinic.

## M018

**Proteinase-Activated Receptor (PAR)-2 Activation Induces Bone Resorption via RANKL Upregulation in Human Osteoarthritic Subchondral Bone Osteoblasts.** N. Amiable<sup>\*1</sup>, J. Martel-Pelletier<sup>\*1</sup>, S. Kwan Tat<sup>\*1</sup>, F. Mineau<sup>\*1</sup>, N. Duval<sup>\*2</sup>, J. Pelletier<sup>\*1</sup>, C. Boileau<sup>\*1</sup>. <sup>1</sup>Osteoarthritis Research Unit, University of Montreal Hospital Centre, Notre-Dame Hospital Centre, Montreal, QC, Canada, <sup>2</sup>Centre de Convalescence Pavillon des Charmilles, Vimont, QC, Canada.

In osteoarthritis (OA), subchondral bone remodelling is closely related to cartilage degradation. The former tissue has shown a remodelling process involving factors synthesized by human osteoblasts (Ob) including the OPG/RANKL system. Moreover, these factors are produced in abnormal levels by OA subchondral bone Ob. Recently our group showed that PAR-2 was implicated in catabolic and pro-inflammatory processes in human OA cartilage. Here, we investigated the presence, production, and role of PAR-2 in human OA subchondral bone Ob.

PAR-2 expression was determined by real-time PCR, PAR-2 protein by Western blot, membranous RANKL protein by flow cytometry, and OPG, MMP-9 and intracellular signalling pathways by specific ELISA assays. Bone resorption activity was measured by using a co-culture model of human PBMC and human OA subchondral bone Ob. PAR-2 expression and protein levels were markedly increased in OA Ob compared to normal (p<0.05). On OA Ob, activation of PAR-2 with a specific agonist induced a significant upregulation of the membranous RANKL (p<0.006) without affecting OPG production. Interestingly, MMP-9 levels were also significantly increased (p<0.03), as was the bone resorption activity (p<0.05). The PAR-2 effect was mediated by the activation of the MAP kinases ERK1/2 and JNK (p<0.05).

This study demonstrated, for the first time, that PAR-2 plays a role in bone resorption via an upregulation of a major bone remodelling factor, RANKL, in human OA subchondral bone Ob. These data strongly reinforce the suggestion that PAR-2 could be a potential therapeutic target for the treatment of OA, as this factor acts on catabolic processes of both cartilage and subchondral bone.

Disclosures: N. Amiable, None.

## M019

**LPS-induced Inhibition of Osteogenesis Is TNF-α Dependent.** N. Tomomatsu<sup>\*1</sup>, K. Aoki<sup>2</sup>, M. A. Hussain<sup>\*2</sup>, N. Alles<sup>\*2</sup>, H. Shimokawa<sup>2</sup>, T. Amagasa<sup>\*1</sup>, K. Ohya<sup>2</sup>. <sup>1</sup>Maxillofacial surgery, Tokyo Medical and Dental University, Bunkyo-ku Tokyo, Japan, <sup>2</sup>Hard Tissue Engineering (Pharmacology), Tokyo Medical and Dental University, Bunkyo-ku Tokyo, Japan.

**[Introduction]** Several lines of evidence show the inhibition of osteoblast differentiation by TNF-α *in vitro*. However, there are almost no reports showing the inhibitory role of TNF-α in osteogenesis *in vivo*. The purpose of this study is to investigate whether the LPS-induced inhibition of osteogenesis is TNF-α dependent or not by using tooth extraction model.

**[Materials & Methods]** Ten mg/kg LPS (Re595) was injected subcutaneously on calvariae in either wild type (WT) or TNF-α deficient (KO) mice, and the left incisor was extracted 4 days after LPS injections. Mice were sacrificed 3 days, 1 week and 3 weeks after the extraction. TNF-α and osteocalcin levels in serum were measured by ELISA. The measuring area of BMD by pQCT and histomorphometry was set in the incisor tooth socket under the mesial root of the first molar as shown in the attached figure. The mRNA levels of bone formation marker in the tooth socket of the mandibular bone on day 3 were measured using real-time RT-PCR.

**[Results]** We confirmed the significant increase of TNF-α level in serum in the LPS-injected group (LPS-G) compared to the vehicle-injected group (Vh-G). At 3 weeks after the extraction, the significant decrease of trabecular BMD and the bone volume (BV/TV) was observed in LPS-G compared to Vh-G in WT mice (P<0.05). The significant decrease of bone formation parameters (MS/BS, MAR) was appeared in LPS-G compared to Vh-G at 1 week in WT mice. The osteocalcin level in serum and the mRNA level in the mandible were significantly decreased by LPS in WT mice compared to Vh-G. However, those differences by LPS were not observed in TNF-KO mice. Since almost no osteoclasts were observed in the measuring area, LPS-induced inhibition of bone volume in WT mice would be occurred by the inhibition of bone formation, not by the increase of bone resorption.

**[Conclusions]** The present data clearly showed LPS-induced inhibition of osteogenesis was TNF-α dependent. The neutralization of TNF-α might be a useful therapeutic strategy to accelerate bone formation after the tooth extraction or the distraction in the patients suffering from inflammatory diseases.



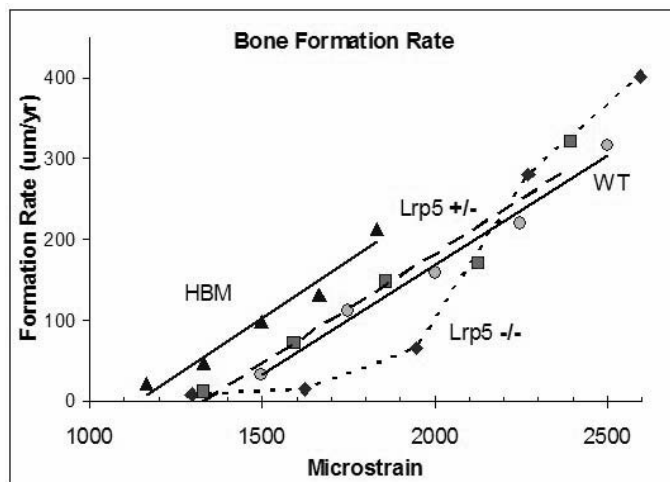
Disclosures: N. Tomomatsu, None.

## M020

**Bone Response to Mechanical Loads and Lrp5 Genotype.** B. T. Hackfort<sup>\*</sup>, D. A. Knierim<sup>\*</sup>, G. K. Alvarez, D. M. Cullen, M. P. Akhter. Osteoporosis Research Center, Creighton University, Omaha, NE, USA.

Genetic variations in Lrp5 (low density lipoprotein like receptor protein) are associated with bone mass variations. Lrp5 is a Wnt co-receptor and when Wnt binds it activates β-catenin translocation into the nucleus and up-regulation of Wnt response genes. The Lrp5 G171V (HBM) mutation causes a gain of function in Wnt signaling and high bone mass. The Wnt pathway is important for bone adaptation to mechanical loads and data suggests that variations in Lrp5 alter bone sensitivity to loads. This study examined the dose response curve of cortical bone to loading in mice with variation in Lrp5 expression. The genotypes tested were Lrp5<sup>-/-</sup>, Lrp5<sup>+/-</sup>, WT (C57Bl6), and HBM. Right tibiae were loaded in tibial compression at 100 cycles, 2 Hz, 3d/wk, 10 sessions. The left tibiae served as a contralateral control. Adult virgin female mice within each genotype were randomized to 5

load groups ranging from 4 to 11 N to overlap strains among genotypes. Strains were calculated based upon load and average cortical area. Strains ranged from 1300 to 2600  $\mu\epsilon$  (Figure). Tibia sections 1-3 mm proximal to the TFJ were measured by histomorphometry for area (total, marrow, cortical), mineralizing surface (MS/BS), mineral apposition rate (MAR), and bone formation rate (BFR/BS). Less than 3% of the tibiae had woven bone and the majority was seen in Lrp5<sup>-/-</sup> at the highest loads. Differences were significant at  $P < 0.05$ . In nonloaded legs, all genotypes were different from each other for total area and cortical area. The Lrp5<sup>-/-</sup> mice had the smallest marrow area, but there were no other difference among genotypes. There were no differences in either periosteal or endocortical bone formation rate. However, WT tibiae had the greatest endocortical MAR which tended to increase endocortical BFR ( $P=0.07$ ). The load effect was calculated as Loaded-nonLoaded within each animal. All genotypes demonstrated a dose response to loading for periosteal BFR (Figure). The periosteal bone response to increasing strain was linear in all groups except Lrp5<sup>-/-</sup>. The homozygote KO mice did not respond to strains  $<1600\mu\epsilon$  and showed a rapid response above 2000 $\mu\epsilon$ . The threshold for response was lowest in HBM mice at 1330 $\mu\epsilon$ . Endocortical BFR was not different due to strain in Lrp5<sup>+/-</sup> tibiae, but was significant in all other groups. In conclusion, gain of function in Lrp5 increases bone sensitivity to loads and total loss of Lrp5 function suppresses the bone response, but does not eliminate it.



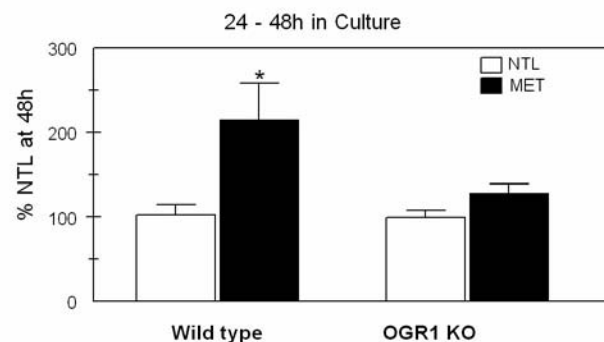
Disclosures: D.M. Cullen, None.

This study received funding from: NIH AR051365.

## M021

**Acid-induced Stimulation of Bone Resorption Is Decreased in OGR1 Knockout Mouse Calvariae.** N. S. Krieger, A. C. Michalenka\*, D. A. Bushinsky. Medicine, University of Rochester, Rochester, NY, USA.

Chronic metabolic acidosis, a systemic increase in proton concentration [ $H^+$ ], stimulates net calcium (Ca) efflux from bone. This net efflux is mediated primarily through increased osteoblastic cyclooxygenase 2, leading to prostaglandin  $E_2$ -induced up-regulation of RANKL and increased osteoclastic bone resorption. We have recently found that perfusion of calvarial osteoblasts with medium simulating metabolic acidosis induces a marked, rapid, flow-independent, transient increase in intracellular Ca ( $Ca_i$ ) in individual cells. We and others have demonstrated that osteoblasts express the recently characterized  $H^+$ -sensing G-protein coupled receptor, OGR1. As activation of OGR1 results in increased inositol trisphosphate mediated  $Ca_i$  signaling, our findings suggest that OGR1 may be the  $H^+$  sensor that detects the increase in acidity during metabolic acidosis and initiates the increase in  $Ca_i$  signaling. To test the hypothesis that OGR1 is the functioning  $H^+$  sensor in osteoblasts leading to increased bone resorption, we measured net Ca efflux, as an index of bone resorption, in calvariae from mice with a genetic null mutation in OGR1 (kindly provided by Klaus Seuwen, Novartis). Neonatal mouse calvariae from OGR1 knockout (KO, -/-) or wild type (+/+) mice were incubated for 48h in physiological neutral (NTL, pH=7.41,  $HCO_3^-$ =25 mM,  $Pco_2$ =39 mmHg) or acidic (MET, pH=7.19,  $HCO_3^-$ =15 mM,  $Pco_2$ =39 mmHg) medium that was changed at 24h. At 24h, when Ca efflux occurs primarily by physicochemical dissolution, incubation in MET induces a similar, significant increase in net Ca efflux from both wild type ( $153 \pm 7\%$  increase vs wild type, NTL,  $p < 0.01$ ) and OGR1 KO calvariae ( $161 \pm 12\%$  increase vs OGR1 KO, NTL,  $p < 0.01$ ). However at 48h, when cell-mediated Ca efflux predominates, there is a significant increase in net Ca efflux in response to MET only in wild type calvariae ( $p < 0.01$ ) but not in OGR1 KO calvariae (Figure) indicating that loss of the  $H^+$  sensing receptor OGR1 eliminates acid-induced bone resorption. Thus, our results are consistent with OGR1 being the primary osteoblast  $H^+$  sensor that detects the increase in  $H^+$  during metabolic acidosis and initiates the Ca signaling cascade which results in increased acid-induced, cell-mediated bone resorption.



Disclosures: N.S. Krieger, None.

## M022

**Secretomic Analysis of Calcium Supplement-Mediated Bone Remodeling.** G. G. Xiao, Y. Zhao\*, R. Cao\*, J. Xiao\*, J. Lappe, R. Heaney, R. Recker. Osteoporosis Research Center-Medicine, Creighton University, Omaha, NE, USA.

**Introduction:** Calcium is essential for bone health. Calcium intakes in the U.S. are much lower than recommended levels. In a recent efficacy study of milk mineral in human bone health, the results suggest that calcium supplement and milk drink can improve bone quality. To understand the mechanism of the calcium supplement intake on bone remodeling, we further analyzed proteome profile in serum samples from participating postmenopausal female subjects.

**Methods and Materials:** Sample preparation: To minimize the interference with our proteomics analysis, high abundance proteins in serum samples from postmenopausal female subjects, placebo group (17), milk drink group (28), and calcium supplement intake group (30), were depleted by using YM-30 filtration with molecular cutoff 30kDa. Then, about 5  $\mu$ g of depleted serum protein was further cleaned up using C8 magnetic beads in ClinProt robot. Cleaned samples were premixed with CHCA matrix and directly spotted onto 384-well plate.

Protein pattern discovery using direct mass spectrometry (dMS): Protein profiling was carried out by using MALDI-TOF mass spectrometry with the laser power 25%-45%. Comprehensive statistical protocols were used for selection of differentially expressed protein peaks, which were identified by MALDI-TOF/TOF mass spectrometry.

**Results**

To understand the mechanism of calcium supplement intake on bone remodeling, we aim to compare secretome profiles between calcium supplement intake and milk drink in postmenopausal female subjects using functional proteomics approach. We found that intake of calcium supplement can regulate proteome expression profile in a different fashion from that milk drink does. After 6-month designated diet-stimulation, postmenopausal female subjects have shown different proteome profiles. Milk drink can suppress protein peak at 6068 m/z ( $p < 0.000001$ ) while this peak was suppressed marginally in calcium supplement group. Further identification of this peak at 6068 m/z using Ultraflex III direct TOF/TOF mass spectrometry is subject to be alpha-methylacyl-CoA racemase (AMACR). On the other hand, milk can stimulate over-expression of proteins at 3504 m/z (3-hydroxyisobutyryl-coenzyme A hydrolase,  $p < 0.0008$ ), 3768 m/z (Sal-like 4,  $p < 0.000214$ ) and 4788 m/z (F-box protein FBL5,  $p < 0.0009$ ), while these proteins seem to be suppressed by calcium induction as demonstrated in calcium supplement group. In additions, calcium supplement intake can also suppress over-expression of a protein at 5005 m/z, which is cysteine-rich motor neuron 2 protein (CRIM-2). As expected, there is no significant difference between before and after treatment in protein expression in placebo group.

Disclosures: G.G. Xiao, None.

This study received funding from: State of Nebraska LB 692.



## M023

### Chemical Composition and Nanoscale Structure of Risedronate-treated Mineralizing MC3T3-E1 Cells. M. E. Ruppel<sup>1</sup>, R. Phipps<sup>2</sup>, L. M. Miller<sup>3</sup>.

<sup>1</sup>Biomedical Engineering, Stony Brook University, Stony Brook, NY, USA, <sup>2</sup>Procter and Gamble Pharmaceuticals, Mason, OH, USA, <sup>3</sup>National Synchrotron Light Source, Brookhaven National Laboratory, Upton, NY, USA.

Prevention of bone loss by inhibition of osteoclast-mediated bone resorption appears to be the major mechanism for fracture risk reduction seen with bisphosphonates (BPs) in osteoporosis. Recent examination into the effects of BPs has demonstrated that under certain conditions BPs may stimulate osteoblasts or prevent osteoblast and osteocyte apoptosis, but whether they have direct effects on the quality and/or structure of newly forming bone matrix is unknown. The goal of the present study was to determine if BP-treatment alters the quality and nanostructure of newly formed tissue. 2H-risedronate-treated and untreated MC3T3-E1 mouse osteoblasts were mineralized in culture for 0, 4, 11, 21, and 28 days. 2H-risedronate was used so that the binding and distribution of the drug within the mineralized culture could be visualized using Fourier transform infrared imaging (FTIRI) since the deuterated drug has absorption features in a spectral region different from those of bone. FTIRI was used to study the chemical composition of the cells, including level of mineralization, crystallinity, collagen cross-linking, carbonate uptake and BP binding as a function of time and drug concentration. Nano-transmission x-ray microscopy was used to probe the nanoscale structure and organization of the collagen and mineral produced by the cells. Quantification of collagen production and mineral formation were measured via hydroxyproline and osteocalcin production, respectively. Thus, these studies provide an understanding of how BPs directly affect the nanostructure and composition of mineral production by osteoblasts, which will help to evaluate the long-term effects of bisphosphonate treatment on bone quality.

**Disclosures:** M.E. Ruppel, None.

*This study received funding from: The Alliance for Better Bone Health.*

## M024

### Transgenic Mice Over-expressing TIEG in Osteoblasts Display a Gender Specific Bone Phenotype. M. Subramaniam<sup>1</sup>, J. R. Hawse<sup>1</sup>, F. A. Syed<sup>2</sup>, D. G. Monroe<sup>1</sup>, K. D. Peters<sup>\*1</sup>, T. C. Spelsberg<sup>1</sup>. <sup>1</sup>Biochemistry and Molecular Biology, Mayo Clinic & Foundation, Rochester, MN, USA, <sup>2</sup>Endocrine Research Unit, Mayo Clinic & Foundation, Rochester, MN, USA.

TGF $\beta$  inducible early gene (TIEG) is a member of the zinc finger containing Kruppel-like transcription factor family which was originally cloned from human osteoblasts. TIEG plays an important role in TGF $\beta$  mediated osteoblast growth and differentiation. TIEG over-expression in human osteoblasts mimics TGF $\beta$  action by regulating the expression of osteoblast specific marker genes. Further, we and others have demonstrated that TIEG plays an important role in TGF $\beta$  mediated Smad signaling in various cell types. In order to further define the role of TIEG in bone, we developed a transgenic mouse model that over-expresses TIEG in osteoblasts under the control of the Col 3.6 promoter. Characterization of osteoblasts isolated from transgenic mice revealed a significant increase in TIEG expression. To determine if TIEG over-expression in osteoblasts has an effect on the skeleton, we analyzed the tibias of young (1 month), adult (3 months) and aging (12 months) male and female mice by pQCT. Analysis of the femoral metaphysis revealed a trabecular osteopenic phenotype in all age groups of male mice relative to wild-type controls. This phenotype was not observed in the female transgenic mice. pQCT analysis of the femoral diaphysis revealed that male adult and aging transgenic mice display significant reductions in total and cortical vBMD. Interestingly, aging females maintained cortical and total vBMD at this site compared to their wild-type littermates. Taken together, our results suggest that over-expressing TIEG in osteoblasts has distinct effects on male and female trabecular and cortical bone, with TIEG over-expression resulting in trabecular and cortical osteopenia in male mice as a function of age, whereas female mice maintain bone densities at these sites.

**Disclosures:** M. Subramaniam, None.

*This study received funding from: NIH.*

## M025

### Bril (Bone Restricted Ifitm-Like) Localization in Mouse and Rat Bones. P. Moffatt<sup>1</sup>, R. Wazen<sup>\*2</sup>, G. P. Thomas<sup>3</sup>, A. Nanci<sup>\*2</sup>. <sup>1</sup>Genetics Unit, Shriners Hospital for Children, Montreal, QC, Canada, <sup>2</sup>Stomatologie, Université de Montreal, Montreal, QC, Canada, <sup>3</sup>Musculoskeletal Genetics Group, Diamantina Institute for Cancer, Immunology & Metabolic Medicine, University of Queensland, Woolloongabba, Australia.

Bril is a novel osteoblast-specific membrane protein that we originally discovered in UMR106 cells. The gene encoding Bril had been previously named interferon inducible transmembrane protein (ifitm) 5, but no localization or functional studies had been undertaken on this gene. Bril encodes a 134 amino acid protein with two transmembrane domains. Our initial characterization of Bril showed it to be present in mouse and human osteoblastic cell lines, and its expression coincides with the onset of matrix formation and mineralization. Functional evidence for Bril in mineralization was demonstrated by overexpression and shRNA knockdown increasing or inhibiting mineralization respectively in vitro. The purpose of this study was to map the distribution of Bril by immunoperoxidase labeling in embryonic and adult rodent tissues. In developing mouse embryonic E14.5 bones, Bril localized exclusively to osteoblasts of both endochondral

(clavicle, mandible, calvaria) and intramembranous (humerus, vertebra, ribs) skeletal elements. Only osteoblasts forming the bony collar of the long bones and vertebrae stained highly positive for Bril. The developing growth plate chondrocytes showed no labeling. In adult rat tissues, osteoblasts on actively forming bone surfaces were positive for Bril, especially in the mandible and tibia. Osteoclasts and osteocytes were not immunoreactive. No other tissues showed appreciable expression of Bril, except for discrete portion of the gingiva. Bril localization was also examined during repair of bony defects drilled in rat mandibles. At 3 days post-surgery, new bone deposition was not yet evident and there was no obvious Bril staining in the defects. By day 5, foci of bone formation were found throughout the defects and osteoblasts covering the actively forming bone surfaces were immunostained. In summary, the data presented indicate Bril is associated with osteoblasts in regions of active bone formation and its expression is activated during repair. Therefore, Bril represents an attractive target of intervention for modulating bone formation and repair.

**Disclosures:** P. Moffatt, None.

## M026

### Deficiency of NCK1, an Actin Cytoskeletal Modulator with SH2/SH3 Motifs, Induces Bone Loss via Suppression of Bone Formation and Induction of Biochemical High Bone Turnover State. K. Miyai<sup>1</sup>, Y. Izu<sup>1</sup>, H. Hemmi<sup>\*1</sup>, T. Hayata<sup>1</sup>, T. Nakamoto<sup>1</sup>, Y. Ezura<sup>1</sup>, T. Pawson<sup>\*2</sup>, S. Mizutani<sup>\*3</sup>, M. Noda<sup>1</sup>. <sup>1</sup>Molecular Pharmacology, Medical Research Institute, Tokyo Medical and Dental University, Tokyo, Japan, <sup>2</sup>Department of Medical Genetics and Microbiology, University of Toronto, Toronto, ON, Canada, <sup>3</sup>Department of Pediatrics and Developmental Biology, Tokyo Medical and Dental University, Tokyo, Japan.

NCK proteins are adapter molecules which contain a SH2 domain at C-terminal portion and three tandem repeat of SH3 domains at N-terminal portion. SH2 domain binds to phosphorylated tyrosines and SH3 domain binds to proteins which are involved in the regulation of actin cytoskeleton. Among the NCK family members, NCK1 single knockout mice have not been regarded to show any phenotype, though NCK1 function has been observed based on the defects in foot processes in podocytes as well as neurites formation in compound knockouts. To understand the role of the actin cytoskeletal modulator protein in bone, we examined the mice deficient for NCK1. In contrast to previous observations where single knockout did not show any major phenotypes, NCK1 single knockout mice did show reduction in trabecular bone volume based on 3D micro CT analysis. The deficiency of NCK1 resulted in the impairment of osteoblastic activities, which were revealed by the analyses of bone formation rate. This was due to the influence on the individual osteoblastic function as mineral apposition rate was reduced by the deficiency of NCK1. In contrast to the reduction in the histomorphometrical parameters of bone formation, bone resorption parameters such as osteoclast number, osteoclast surface as well as in vitro development of TRAP positive multinucleated cells in the cultures of bone marrow cells did not show any major alterations by the deficiency of NCK1. However, surprisingly urinary deoxypyridinoline levels were increased in KO mice. Serum alkaline phosphatase levels were enhanced in NCK1 deficient mice indicating high turnover state based on the analyses of biochemical markers. We further examined the effect of NCK1 deficiency on the cell autonomous functions of osteoblasts. The expression levels of bone phenotypic markers such as alkaline phosphatase and osteocalcin were increased in wild type cells. In contrast, NCK1 deficiency suppressed such increase in the expression of osteoblastic phenotype marker genes in the culture of the cells. In conclusion, we found that single NCK1 deficiency resulted in reduction in bone mass indicating the role of this SH2/SH3 adapter protein in the regulation of bone metabolism.

**Disclosures:** K. Miyai, None.

## M027

### High Bone Mass Phenotype in the Bone Specific Dlx3 Knock Out mice. M. S. Islam<sup>\*1</sup>, I. Chen<sup>\*2</sup>, D. Adams<sup>2</sup>, J. Xi<sup>2</sup>, H. Li<sup>2</sup>, M. Kronenberg<sup>2</sup>, M. Duffin<sup>\*2</sup>, M. Morasso<sup>\*3</sup>, E. Reichenberger<sup>\*2</sup>, A. C. Lichtler<sup>2</sup>. <sup>1</sup>University of Minnesota, Minneapolis, MN, USA, <sup>2</sup>University of Connecticut, Farmington, CT, USA, <sup>3</sup>National Institute of Health, Bethesda, MD, USA.

A major goal of our research is to understand the role of *Dlx3* in bone formation and metabolism. In a previous abstract we reported our initial results using the Cre-LoxP system to generate bone specific *Dlx3* knock out mice. We used a 3.6 kb type I collagen fragment to drive *CreERT2* expression in bone and rearrange the floxed *Dlx3* gene (*FDlx3*). The bone specific *Dlx3* knock out mice were homozygous for *FDlx3* and carried one copy of *Cre* transgene (*F/F; Cre+*). A skeletal phenotype was not detectable by whole mount skeletal staining of knock out and age and sex matched control mice. However, repeated studies at multiple ages, involving quantitative measurement of long bone, vertebrae and calvaria using microCT and static histomorphometry, and Von Kossa staining of undecalcified bone sections confirmed a significant increase in bone mass in the conditional knock out mice compared to the control group. The conditional knock out mice had lower numbers of osteoblasts that was statistically significant in male knock out mice. Osteoclast surface was significantly higher in females but not males. Analysis of serum markers Trap5b and CTX were done to measure osteoclast differentiation and function respectively. No difference was observed in these studies, suggesting osteoclast differentiation and function were not affected in these mice. Bone formation rate and mineral apposition rate were not significantly different, however serum PINP, a measure of osteoblast function, was higher in 10 week old males. Gene expression was studied using RNA from cultured calvarial osteoblasts by quantitative PCR and showed changes in the

expression pattern of other *Dlx* genes and bone expressed genes including osteocalcin, bone sialoprotein, Collagen I (*Coll1a1*) and alkaline phosphatase. Von Kossa staining did not show obvious differences between wild type and knockout cells. Our results show that lack of *Dlx3* results in a higher bone mass and that *Dlx3* may be required for completely normal osteoblast function but not for mineralization.

**Disclosures:** M.S. Islam, None.

This study received funding from: NIH.

## M028

**Towards Development of a Porous Silicon-Based Hybrid Biomaterial with Osteoconductivity and Osteoinductivity.** T. Sheu<sup>1</sup>, W. Sun<sup>\*2</sup>, X. Liu<sup>\*2</sup>, M. Chen<sup>1</sup>, P. M. Faucher<sup>\*2</sup>, E. J. Puzas<sup>1</sup>. <sup>1</sup>Orthopaedics, U of Rochester, Rochester, NY, USA, <sup>2</sup>Biomedical Engineering, U of Rochester, Rochester, NY, USA.

An ideal material for orthopaedic tissue engineering should be biocompatible, biodegradable, osteoconductive, mechanically stable, and widely available. Porous silicon (PSi), a silicon-based material fulfills these criteria. It is biocompatible and biodegradable, and supports hydroxyapatite nucleation. The micro/nano-architecture of porous silicon can regulate cell behavior. The surface chemistry of PSi is flexible so that the interfacial properties between this material and living cells can be tailored easily by chemical modifications. In our previous work, we have demonstrated that PSi can support and promote primary osteoblast growth, protein matrix synthesis, and mineralization *in vitro*. The osteoconductivity of porous silicon can be controlled by altering the micro/nano architecture of the porous interface. Macro-scale porous silicon (MacPSi), with pore openings of approximately 1  $\mu\text{m}$ , has the highest osteoconductive potential *in vitro*. In the present work, we have further developed a hybrid biomaterial by coating MacPSi with recombinant adenovirus vectors encoding bone morphogenetic proteins, and thus making the material osteoinductive both *in vitro* and *in vivo*. With this material, we are closer to an osteoconductive and osteoinductive medical device with drug delivery functions. The knowledge obtained in this study on the interaction between living cells and a semiconductor material will also be the foundation for further development of electronic and optoelectronic biointerfaced devices.

**Disclosures:** T. Sheu, None.

This study received funding from: NIH.

## M029

**VEGF and PTEN Regulate Bone Homeostasis via Control of Osteoblastogenesis, Osteoclastogenesis and Adipocyte Differentiation.** Y. Liu<sup>\*</sup>, B. R. Olsen<sup>\*</sup>. Developmental Biology, Harvard School of Dental Medicine, Boston, MA, USA.

We have found that conditional loss of VEGF in osteoblasts results in osteoporosis in mice. In a recent study, it was reported that mice deficient in PTEN in osteoblasts/osteocytes exhibited high bone mass because of Akt activation. To test the hypothesis that loss of PTEN in osteoblasts rescues the bone loss of VEGF conditional knockout mice, we generated VEGF /PTEN double conditional knockout mice by crossing VEGF and PTEN floxed mice with Osterix-Cre mice. The double mutant mice look normal at birth, but they are getting smaller with age compared with control littermates. Surprisingly, the double mutants had dramatically reduced bone density compared with VEGF conditional knockout mice at 2.5 months of age. Loss of PTEN in the osteoblasts therefore does not rescue the bone loss caused by loss of VEGF, but instead aggravates the bone loss. H&E of 6 weeks old double knockout mice showed abnormal amounts of woven bone in the cortices of long limb bones and a dramatic increase in adipocytes in the bone marrow. To further elucidate the underlying mechanisms, bone marrow cells from 8-12 weeks old double knockout mice and control littermates were isolated for osteoclastogenesis assay, CFU-F and CFU-A assays to determine whether the bone loss is caused by increased osteoclastogenesis, reduced osteoblastogenesis or increased adipocyte differentiation. Osteoclastogenesis assay showed a dramatic increase in osteoclast formation with bone marrow cells of double mutants compared with cells from control littermates. CFU-F and CFU-A assays showed a decreased number of osteoblast progenitors and a large increase in adipocyte formation with bone marrow cells isolated from double mutant mice. These data suggests that the reduced bone density in mice due to loss of VEGF and PTEN in osteoblasts results from decreased osteoblastogenesis and excessive osteoclastic bone resorption as well as increased adipocyte differentiation in bone marrow. Taken together, the findings demonstrate a critical role of VEGF and PTEN in regulating bone homeostasis via control of osteoblastogenesis, osteoclastogenesis and adipocyte differentiation.

**Disclosures:** Y. Liu, None.

## M030

**Enamel Matrix Derivative (Emdogain) Enhance Osteoblast Differentiation on Titanium Surfaces.** R. Miron<sup>\*1</sup>, M. Wieland<sup>\*2</sup>, D. Hamilton<sup>\*1</sup>. <sup>1</sup>Anatomy and Cell Biology, University of Western Ontario, London, ON, Canada, <sup>2</sup>Institut Straumann, Zurich, Switzerland.

Osseointegration represents a dynamic structural and functional connection between living bone and the surface of a titanium implant and is critically important for the long-term success of bone-contacting devices, including titanium dental implants. Attempts to improve this functional connection between the implant and host bone tissue have focused mainly on altering the topography of the titanium implant surface. However, incorporation of bioactive proteins could also facilitate the healing of the bone around the titanium implant. Emdogain® - enamel matrix proteins derived from developing porcine teeth - has been shown to promote regeneration of the periodontal ligament *in vitro* and *in vivo*. There are few studies of the influence of Emdogain® on bone healing, but *in vivo* data suggest that Emdogain® speeds the healing of trabecular bone. The influence of Emdogain® on bone formation adjacent to titanium implants has yet to be investigated. The aim of the present study was to evaluate the effect of Emdogain® on the differentiation of osteoblasts on titanium surfaces *in vitro*. Polished titanium discs were coated with or without Emdogain®. MC3T3-E1 osteoblast-like cells were then cultured on these substrates for 0 to 4 weeks. Differentiation was assessed by staining for alkaline phosphatase activity and by quantifying osteoblast marker expression using real-time RT-PCR. At time points ranging from 0 to 4 weeks of culture, alkaline phosphatase activity was significantly increased on Emdogain®-coated titanium compared with titanium alone. Furthermore, there were significant increases in expression of bone sialoprotein, osteocalcin, osterix and collagen I in osteoblasts cultured on Emdogain®-coated titanium surfaces. We conclude that coating of titanium with Emdogain® enhances the differentiation of osteoblasts. Thus, Emdogain® may increase the speed and quality of osseointegration around bone contacting implants *in vivo*.

**Disclosures:** R. Miron, None.

This study received funding from: Emerging Materials Knowledge (EMK) Network of the Ontario Centres of Excellence (OCE) and Insitut Straumann.

## M031

**Transcriptional Activation of Osteocalcin by Runx2 During Osteoblast Development Is Controlled at the Post-Translational Level.** S. Pregizer<sup>\*1</sup>, S. K. Baniwal<sup>1</sup>, X. Yan<sup>\*2</sup>, D. P. Mortlock<sup>\*3</sup>, B. Frenkel<sup>4</sup>. <sup>1</sup>Department of Biochemistry & Molecular Biology, Keck School of Medicine, University of Southern California, Los Angeles, CA, USA, <sup>2</sup>Department of Biological Sciences, College of Letters, Arts, & Sciences, University of Southern California, Los Angeles, CA, USA, <sup>3</sup>Department of Molecular Physiology & Biophysics, Vanderbilt University School of Medicine, Nashville, TN, USA, <sup>4</sup>Department of Orthopaedic Surgery, Keck School of Medicine, University of Southern California, Los Angeles, CA, USA.

Runx2 is a potent transcriptional regulatory factor in osteoblasts and is itself subject to transcriptional, as well as post-transcriptional and post-translational regulatory mechanisms. The purpose of this study was to ascertain whether these mechanisms play a role in the stimulation of Osteocalcin (OC), a classic Runx2 target gene, during osteoblast development. OC expression increases robustly in differentiating MC3T3-E1 cells, making this a convenient system for studying the dynamics of its regulation by Runx2. We monitored Runx2 mRNA and protein levels, as well as OC promoter occupancy in this system from confluence until the time at which OC expression peaks, approximately 2 weeks later. Each type of measurement was performed on samples collected in parallel from cells plated on the same day, thus permitting a meaningful comparison between them. Surprisingly, Runx2 mRNA and protein levels both declined as the cells matured and OC expression increased. This paradoxical inverse relationship is a novel discovery that raises the interesting question of how Runx2 can stimulate OC expression under these circumstances. Accordingly, we discovered that in contrast to its expression, Runx2 occupancy of the OC promoter increased in parallel with OC mRNA levels. Thus, activation of OC by Runx2 is attributable to enhanced promoter occupancy. The discrepancy between expression levels and occupancy may reflect post-translational regulatory control of Runx2 and its critical role in the stimulation of OC expression during osteoblast differentiation. Having identified conditions under which Runx2 is maximally recruited to the OC promoter, we then searched for novel Runx2 genomic targets by ChIP-Chip, using the NimbleGen platform. We identified a total of 64 occupied sites along mouse chromosome 3, many of which were close to transcribed sequences. Thus, we identified a novel mechanism of Runx2 regulation, occurring at the level of promoter occupancy. Moreover, we employed cells in which this mechanism is maximally operative to discover novel Runx2 target genes, some of which may mediate the well-established but poorly understood role of Runx2 in osteoblast differentiation and bone formation.

**Disclosures:** S. Pregizer, None.

## M032

**RANKL Suppression by Small Interfering RNAs in Rat Primary Osteoblasts.** F. Pei, K. Gao, Y. Hao, H. Zhang, M. Zongyu. West China Hospital of Sichuan University, Chengdu, China.

**Purpose:** The receptor activator of nuclear factor- $\kappa$ B ligand (RANKL)/RANK/osteoprotegerin(OPG) system is a crucial factor in osteoclastogenesis. RNA interference (RNAi) has promising therapeutic potential. Our studies were designed to explore the preliminary possibility of using siRNA targeting RANKL as a novel therapeutic strategy. **Experimental Design:** Four small interfering RNA (siRNA) were designed and the most effective siRNA were selected via real time RT-PCR. At a serial time points post-transfection, the RANKL/OPG protein expression was examined by Western blotting and the function of osteoblasts were investigated through cell proliferation rate and alkaline phosphatase activity.

**Results:** siRNA targeting RANKL could specifically inhibit the expression of RANKL without affecting that of OPG, but the decrease of RANKL gradually restored. Both cell proliferation rate and alkaline phosphatase activity weren't influenced by RANKL-siRNA. **Conclusions:** Through there are many obstacles to clinic application of siRNAs, these results provide strong evidence that RANKL siRNA is a promising method for osteolytic diseases.

**Disclosures:** F. Pei, None.

## M033

**Mitogen Activated Protein Kinase-dependent Inhibition of Osteocalcin Gene Expression by Transforming Growth Factor-beta.** S. Kwok<sup>\*1</sup>, N. C. Partridge<sup>1</sup>, N. Srinivasan<sup>\*2</sup>, S. K. Nair<sup>\*3</sup>, N. Selvamurugan<sup>3</sup>. <sup>1</sup>UMDNJ-Robert Wood Johnson Medical School, Piscataway, NJ, USA, <sup>2</sup>University of Madras, Chennai, India, <sup>3</sup>Centre for Nanosciences, Amrita Institute of Medical Sciences, Kochi, India.

TGF- $\beta$  (transforming growth factor-beta) plays a key role in osteoblast differentiation and bone development. While the ability of TGF- $\beta$  to inhibit the expression of osteoblast differentiation genes has been well documented, the mechanism of this inhibition is not yet completely characterized. Runx2, a transcription factor necessary for expression of osteoblast differentiation genes is a central target of inhibition by TGF- $\beta$ . In this study, we found that TGF- $\beta$ 1 inhibits expression of osteoblast differentiation genes (osteocalcin) without altering expression of Runx2. Transient transfection experiments determined that TGF- $\beta$ 1 inhibited osteocalcin promoter activity and this effect is mediated through Runx2. We further identified by Western blot, Immunofluorescence and Chromatin immunoprecipitation (ChIP) techniques that there was no change in protein expression, cellular localization, or DNA binding affinity of Runx2 after TGF- $\beta$ 1-treatment of osteoblasts. This suggested that Runx2 undergoes post-translational modifications following TGF- $\beta$ 1 treatment. Co-immunoprecipitation experiments identified increased phosphorylation of Runx2 when differentiating osteoblasts were treated with TGF- $\beta$ 1. Mitogen activated protein kinase (MAPK) inhibitors abolished Runx2 phosphorylation at threonine amino acids and relieved the TGF- $\beta$ 1-inhibitory effect on Runx2-mediated osteocalcin promoter activity. ChIP and reChIP experiments identified that there was recruitment of histone deacetylases-4 and -5 (HDAC-4, -5; co-repressors) by Runx2 on the osteocalcin promoter upon TGF- $\beta$ 1-treatment in rat differentiating osteoblasts. Thus, our results suggest that TGF- $\beta$ 1-inhibition of osteocalcin gene expression is dependent on the MAPK pathway and this effect is most likely mediated by Runx2 phosphorylation, followed by recruitment of HDACs.

**Disclosures:** N. Selvamurugan, None.

## M034

**Identification and Analysis of Human LMP Gene Promoter Region.** Y. Liu, M. Vigneswarapu, S. Sangadala, M. Bargouti<sup>\*</sup>, L. Titus, S. D. Boden. Orthopaedics, Atlanta VA Medical Center, Atlanta, GA, USA.

LIM mineralization protein (LMP) is an intracellular protein that is ubiquitously expressed in tissues. It belongs to the PDZ-LIM family of proteins that are associated with the cytoskeleton. These proteins possess an N-terminal PDZ domain and one or three C-terminal LIM domains. LMP has a PDZ domain, three LIM domains and a unique region. These domains endow LMP with a variety of functions. LMP has at least 3 alternatively spliced functional isoforms which have different bone-inducing activities. Forced expression of LMP-1 induces bone formation in vitro and in vivo in rats, rabbits and non-human primates. Further studies indicate that LMP-1 is both necessary and sufficient for induction of bone formation. Thus, we are interested in understanding regulation of the expression of this important bone inducing factor.

The genomic sequence of human LMP is localized on chromosome 5. We determined that the LMP gene contains at least 14 exons and 13 introns by comparing genomic sequence of the human LMP gene with its cDNA sequence. We cloned a putative 3.0 kb promoter fragment from a human genomic DNA PAC clone by restriction digestion. Primer extension analysis and 5'-RACE indicate a single transcription start site without a TATA box. This suggests that the various isoforms of LMP are splice variants of a single transcript. Sequence analysis revealed several putative AP-1, Egr-1, C/EBP $\alpha$ , and SP-1 binding sites within this region. Deletion mutants of the promoter were prepared in order to study the importance of these transcription factor binding sites. RD (human rhabdomyosarcoma) or TE-85 (human osteoblast) cells were transfected with the LMP promoter or its deletion fragments ligated to the luciferase reporter gene. Except for the shortest 37 bp fragment, all fragments showed significant luciferase activity. Mutation

studies demonstrated that the C/EBP $\alpha$  and Egr-1 sites within the -246 to -170 fragment are critical for full promoter activity. Promoter reporter constructs with mutated C/EBP $\alpha$  or Egr-1 site showed 37% and 61% reductions in promoter activity respectively compared with the native construct. Electrophoretic Mobility Shift Assays (EMSA) confirmed that mutated C/EBP $\alpha$  and Egr-1 sites within the -246 to -170 fragment lost their binding capacities with the corresponding nuclear binding proteins.

Our results suggest that the human LMP gene is constitutively expressed but the possibility remains that there may be cell and/or tissue specific regulation.

**Disclosures:** Y. Liu, None.

## M035

**DNA Methylation Analysis of Osteogenic Gene Promoter Regions in Mouse Bone Marrow Stromal Cells.** H. Egusa<sup>\*</sup>, S. Ashida<sup>\*</sup>, M. Kobayashi<sup>\*</sup>, Y. Akashi<sup>\*</sup>, H. Yatani<sup>\*</sup>. Department of Fixed Prosthodontics, Osaka University Graduate School of Dentistry, Suita-city, Osaka, Japan.

Early studies proposed that DNA methylation might regulate gene expression during stem cell differentiation. However, little is known about DNA methylation during osteogenic differentiation of mesenchymal stem cells. **Objectives:** To analyze the methylation status of osteocalcin and osteopontin promoter regions in genomes of bone marrow-derived stromal cells (BMSCs) before and after osteogenic differentiation. **Methods:** Clonal cultures of C57BL/6J mouse BMSCs were established. Genomic DNA and total RNA were extracted from uninduced or osteogenically induced BMSCs, gingival fibroblasts, brain, calvaria, and C2C12 myoblasts. DNA was treated with bisulfite conversion and amplified by PCR using primer sets for osteocalcin and osteopontin promoter regions (amplified regions contained 6 and 4 CpG sites, respectively). Subsequently, PCR products were sequenced and the methylation status of the CpG sites was analyzed. Relative expression levels were determined by RT-PCR. **Results:** The overall methylation pattern in the BMSC osteocalcin promoter region did not significantly change after osteogenic differentiation. However, the fourth CpG site was methylated less frequently (<15%) in osteogenic BMSCs, C2C12, and calvaria, all of which highly expressed osteocalcin mRNA. In contrast, the frequency of methylation at this site was high (>60%) in fibroblasts and brain, which did not express osteocalcin transcripts. In the BMSC osteopontin promoter region, the frequency of methylation at the fourth CpG site was specifically decreased after osteogenic differentiation. In addition, this CpG site was hypomethylated (<30%) in osteogenic BMSCs, fibroblasts, C2C12, and calvaria, all of which highly expressed osteopontin mRNA, and hypermethylated (>60%) in uninduced BMSCs and brain, which expressed osteopontin at lower levels. **Conclusion:** These results suggest that the methylation status of specific CpG loci in mouse osteocalcin and osteopontin promoter regions vary depending on cell type and differentiation stage, and may thus be involved in the regulation of gene expression.

**Disclosures:** H. Egusa, None.

*This study received funding from: Grant-in-Aid for Scientific Research (B) from Japan Society for the Promotion of Science (16390554).*

## M036

**Possible Physiological Function of Menin Protein as Transcriptional Factor that Modulates microRNA Expression During Osteogenesis.** E. Luzi<sup>\*</sup>, F. Marini<sup>\*</sup>, I. Tognarini<sup>\*</sup>, G. Galli<sup>\*</sup>, A. Falchetti, M. Brandi. Internal Medicine, University of Florence, Florence, Italy.

In mesenchymal stem cells that have not been yet committed to the osteoblastic lineage, menin interacts with Smad1 and Smad5, two crucial mediators of BMP-2 signaling. The disruption of this menin-Smad1/5 interaction, due to menin inactivation, antagonizes the transcriptional activity of Smad1 and Smad5, resulting in inhibition of osteoblastic differentiation.

MicroRNAs (miRNAs) are a family of naturally occurring, evolutionary conserved, small (approximately 19-23 nucleotides), non-protein-coding RNA molecules that negatively regulate post-transcriptional gene expression. miRNAs are estimated to account for >3% of all human genes and to control expression of thousands of target mRNAs, with multiple miRNAs targeting for a single mRNA.

Using osteoblast precursors obtained by subcutaneous human adipose tissue we had previously demonstrated that miR-26a level increased in differentiating osteoblasts and that miR-26a inhibition by 2'-O-methyl-antisense RNA, increased protein levels of Smad1 transcription factor in treated osteoblasts, up-regulating bone marker genes and, thus, enhancing osteoblast differentiation.

Recently, we found that siRNA silencing of *MEN1* mRNA, in human osteoblast precursors from Human Adipose Tissue-Derived Stem cells, induces a downregulation of miR-26a and thus an up-regulation of Smad1 protein. These results suggest a possible physiological function of menin protein as transcriptional factor that modulates miRNA expression during osteogenesis.

**Disclosures:** A. Falchetti, None.

**M037**

**Retinoblastoma Binding Protein-1 Is Critical For Runx2 Expression, Transcriptional Activity and Nodule Formation in Osteoblasts.** D. G. Monroe<sup>1</sup>, J. R. Hawse<sup>1</sup>, M. Subramaniam<sup>1</sup>, J. B. Lian<sup>2</sup>, G. S. Stein<sup>2</sup>, A. J. van Wijnen<sup>2</sup>, T. C. Spelsberg<sup>1</sup>. <sup>1</sup>Biochemistry and Molecular Biology, Mayo Clinic, Rochester, MN, USA, <sup>2</sup>Cell Biology and Cancer Center, University of Massachusetts Medical School, Worcester, MA, USA.

The retinoblastoma binding protein-1 (RBP1) is a broadly expressed transcription factor involved in the suppression of cell proliferation mediated through the retinoblastoma protein (pRb), a major pathway implicated in the pathogenesis of numerous cancers including osteosarcoma. We have previously demonstrated an estrogen receptor- $\alpha$ -specific induction of RBP1 in osteoblasts, suggesting a role for RBP1 in osteoblast function. To further characterize the importance of RBP1 in the transcriptional regulation of bone marker genes, we utilized shRNAs to reduce RBP1 expression in a mouse calvarial osteoblast model. Depletion of RBP1 resulted in significant inhibition of important osteogenic regulators (Runx2, Osterix, TIEG, BMP2) and bone phenotypic genes (osteocalcin and osteopontin) as well as significantly delayed the appearance of Alizarin Red-stained bone nodules. We present evidence that RBP1 is also involved in both Runx2 expression and Runx2-dependent transcriptional activation of target genes. Therefore, RBP1 may cooperate with Runx2 to establish and sustain the osteoblast phenotype during skeletal development. Overexpression of RBP1 in U2OS osteosarcoma cells significantly enhances Runx2-dependent activation of the Runx2-dependent osteocalcin gene. This coactivation appears to be independent of pRb, as mutation of the RBP1 LxCxE motif essential for pRb binding, retains the potent co-activation of the Runx2-dependent osteocalcin promoter. Deletion analysis demonstrates that the N-terminal domain (1-235) of RBP1 is sufficient to synergize with Runx2. Furthermore, deletion analysis of the Runx2 protein demonstrates that amino acids 391-432, encompassing the Smad interaction domain (SMID) and a subnuclear targeting signal (NMTS), are critical for maximal RBP1-mediated Runx2 coactivation of the osteocalcin gene. These results suggest that RBP1 is a critical regulator of osteoblast growth and differentiation by modulating Runx2-dependent transcriptional activation.

**Disclosures:** D.G. Monroe, None.

**M038**

**Depletion of the Chromosome Remodeling Subunit BRM Accelerates Differentiation of Osteoblast Precursors.** S. Flowers<sup>\*1</sup>, N. G. Nagl<sup>\*2</sup>, G. R. Beck<sup>3</sup>, E. Moran<sup>1</sup>. <sup>1</sup>Dept. of Orthopaedics and NJMS-UH Cancer Center, University of Medicine and Dentistry of New Jersey, Newark, NJ, USA, <sup>2</sup>Fels Institute for Cancer and Molecular Biology, Temple University School of Medicine, Philadelphia, PA, USA, <sup>3</sup>Division of Endocrinology, Metabolism and Lipids, Emory University School of Medicine, Atlanta, GA, USA.

ATPase-dependent chromatin-remodeling complexes such as the SWI/SNF complex are strongly conserved throughout evolution, and play coordinating roles during programmatic changes in gene expression. Mammalian cells have evolved to contain alternative versions of two subunits of this complex. These variations in complex configuration permit fine-tuned control of gene expression, and offer the possibility of selectively manipulating entire programs of gene expression. The alternative subunits include two versions of the core ATPase, either BRG1 or BRM. We have studied the individual roles of these subunits in osteoblast differentiation, using siRNA technology to deplete them selectively in an MC3T3-E1 pre-osteoblast model. This study revealed that the alternative complexes play opposing roles in the differentiation of these cells. Depletion of BRG1 leaves the cells unable to differentiate, but depletion of BRM accelerates progression to the osteoblast phenotype indicating that BRM-containing complexes play a specific role in restraining osteoblast differentiation. Multiple osteoblast differentiation markers, including the tightly regulated osteocalcin gene, are expressed constitutively in BRM-depleted cells. Chromatin immunoprecipitation (ChIP) analysis of the osteocalcin promoter shows BRM complexes present exclusively on the repressed promoter, and required for association of the transcriptional co-repressor HDAC1. Comparison with early stage markers shows that BRM complexes dissociate sequentially from these promoters, concordant with their order of activation. BRM is an attractive target for accelerating osteoblast differentiation in applications such as bone healing because it has a fundamental role in the coordination of events, and because its biological activity is enzyme-based.

**Disclosures:** E. Moran, None.

This study received funding from: NIH: NIGMS.

**M039**

**Wdr5 is Required for Chromatin Modifications at the Runx-2 Promoter.** F. Gori, M. B. Demay. Endocrine Unit, Massachusetts General Hospital, Harvard Medical School, Boston, MA, USA.

Wdr5 is developmentally expressed in osteoblasts and accelerates osteoblast differentiation in vitro and in vivo. Wdr5 is a critical component of the Set/Ash histone methyltransferase complex and is essential for histone H3 lysine 4 (H3K4) trimethylation. Posttranslational methylation, acetylation, phosphorylation and ubiquitination of histones are known to alter chromatin conformation, thereby activating/repressing gene transcription. Histone methylation at lysine 4 of H3 and acetylation of H3 are histone modifications associated with transcriptional activation of genes. Silencing of Wdr5, using plasmid-based small interfering RNAs (siRNAs), dramatically impairs the differentiation of MC3T3-E1 cells as evidenced by a significant decrease in Runx-2 and osteocalcin mRNAs and absence of mineralized matrix formation. Wdr5 suppression resulted in a significant reduction in global acetylation of H3 lysine 9-14 (H3K9ac14ac) and trimethylation of H3K4 (H3K4me3), suggesting that posttranslational acetylation and methylation are closely linked and that Wdr5 is required for these modifications. These findings also point to a critical role for Wdr5 in regulating chromatin modifications at the promoters of genes involved in osteoblast differentiation. To test this hypothesis, the effect of suppression of Wdr5 expression on H3 acetylation and methylation at the Runx-2 promoter was examined. Chromatin immunoprecipitation (ChIP) analyses were performed using chromatin isolated from cells in which Wdr5 expression was suppressed or cells stably expressing a scrambled siRNA (siRNA-S). Real time PCR was used to quantitate the presence of Wdr5, H3K9ac14ac and H3K4me3 at the Runx-2 promoter. These analyses demonstrated that Wdr5 associates with the Runx-2 promoter (-123 to +123) and that Wdr5 occupancy of the Runx-2 promoter decreased by 2.3-fold in cells with Wdr5 knockdown compared to the siRNA-S cells. A concomitant 2.4-fold reduction in H3K9ac14ac and a 3.3-fold reduction in H3K4me3 occupancy at the Runx-2 promoter were observed in the cells with Wdr5 knockdown, relative to the siRNA-S cells. These data demonstrate that reduction of a key component of the methylation complex (Wdr5) alters these histone marks at the Runx-2 promoter and correlates with a 3-fold reduction in Runx-2 mRNA levels in the cells in which Wdr5 expression is suppressed. These findings link H3K4me3, H3K9ac14ac with Wdr5 occupancy at the Runx-2 promoter and suggest that suppression of Wdr5 expression impairs the dynamic chromatin changes that accompany expression of Runx-2 as MC3T3E1 cells recapitulate the program of osteoblast differentiation.

**Disclosures:** F. Gori, None.

**M040**

**Expression Profiles of Wnt Signaling Pathway Components in Response to cAMP Stimulation at Different Stages of Osteoblast Maturation.** R. S. Kao, W. Lu<sup>\*</sup>, A. Louie<sup>\*</sup>, R. A. Nissenson. Endocrine Unit, VA Medical Center and University of California, San Francisco, CA, USA.

Parathyroid hormone (PTH) can exert both anabolic and catabolic effects on bone depending on the pattern and duration of circulating levels of PTH. The cAMP pathway is one of the key effector pathways mediating PTH signaling. We postulate that the paradoxical effects of PTH on bone results from cAMP signaling having different effects on osteoblasts depending on the stage of cell maturation. Since the Wnt signaling pathway has been shown to play an important role in bone cell differentiation, proliferation, and apoptosis, we sought to determine whether cAMP signaling in osteoblasts controls bone formation by regulating Wnt signaling differently at different stages of osteoblast differentiation. Utilizing a real time RT-PCR based gene expression array (SuperArray), expression of 84 genes related to Wnt-mediated signal transduction was examined in 10-day (immature) and 23-day (mature) bone marrow derived murine osteoblast cultures. Cells were exposed to cAMP treatment for either a 3- or 24-hour duration at both differentiation time points to assess immediate-early and late gene regulation by cAMP. Very little change in the expression of Wnt signaling genes was detected after 3-hours of cAMP treatment in 10-day and 23-day cultures. Treatment with cAMP for 24 hours induced changes in the expression of several Wnt signaling genes in both immature and mature osteoblasts. 24 hours of cAMP treatment down-regulated Wnt1 and Wnt11 expression by more than two-fold. Up-regulation of Wnt9a was only detected in 10-day cells, while down-regulation of Wnt2 and Wnt16 and up-regulation of Wnt4 were uniquely observed in the 23-day osteoblasts. Expression of a negative modulator of Wnt signaling, Sfrp4, was up-regulated by cAMP in 23-day osteoblasts. This gene has been implicated to be an important negative regulator of bone mass in humans. Additionally, we compared gene expression profiles of Wnt signaling components of 10-day and 23-day untreated osteoblasts to assess changes in Wnt signaling as cells differentiate. Dramatic changes in gene expression profiles were detected. Significant among these genes were Sfrp4, Wnt16, Wnt7b, and Wif1, which were up-regulated in mature cells. These results indicate that differentiation of osteoblasts is associated with increased potential to regulate Wnt signaling. The expression levels of several secreted modulators of Wnt signaling are altered as osteoblasts differentiate. On the other hand, relatively few Wnt-related genes appear to be subject to acute regulation by cAMP. Mature osteoblasts may represent an essential control point for the paracrine regulation of Wnt signaling in the bone marrow microenvironment.

**Disclosures:** R.S. Kao, None.

**M041**

**A Runx2 Threshold for the Cleidocranial Dysplasia Phenotype.** Y. Lou\*, A. Javed\*, S. Hussain\*, J. Colby\*, D. Frederick\*, J. Pratap\*, R. Xie\*, T. Gaur\*, A. J. van Wijnen, S. N. Jones\*, G. S. Stein, J. B. Lian, J. L. Stein. Department of Cell Biology and Cancer Center, University of Massachusetts Medical School, Worcester, MA, USA.

Cleidocranial dysplasia (CCD) in humans is an autosomal dominant skeletal disease which results from mutations in bone specific transcriptional factor Runx2/Cbfa1/AML3. However, several studies have reported that there is no obvious relationship between the type of Runx2 mutations and the severity of the human CCD phenotypes which have a broad range from craniofacial to limb abnormalities. Here, we used gene targeting to generate a novel, hypomorphic Runx2 mutant allele through insertion of a neomycin(*neo*) cassette into Intron 7 (Runx2<sup>neo7</sup>) that allowed us to establish the minimum requirement of functional Runx2 levels for normal bone development. In the resulting mice, the normal splicing of Runx2 was disrupted, thus permitting expression of both wild-type Runx2 and an alternative Runx2-*neo* chimeric mRNA which encodes a truncated subnuclear defective Runx2 protein. In the homozygous Runx2<sup>neo7</sup> mice, splicing of the chimeric transcripts reduces the levels of full length Runx2 mRNA to a mean value of 62% with 38% representing the non-functional mutant Runx2. The Runx2<sup>neo7</sup> mice have grossly normal skeletons, but exhibit developmental defects in calvaria and clavicle that persist through post-natal growth. These phenotypes are somewhat similar to those of the heterozygotes of Runx2 null (Mundlos et al., 1997; Komori et al., 1997) and Runx2ΔC (Choi et al., 2001) mouse model. Our hypomorphic mice have altered bone volume parameters, as observed by histology and microCT imaging. A reduction in the expression of osteoblast marker genes, Alkaline Phosphate, Osteocalcin and Osterix were found with the decreased bone volume measurement. Only in new-born mice, we observed an enhanced proliferation with increase Histone gene expression. *Ex vivo* studies of the calvarial osteoblast from the hypomorphic mouse provided an additional evidence for these changes. In the heterozygotes with 21% of total Runx2 present as a truncated Runx2 protein, a normal bone phenotype was found. The results show that there is a critical gene dosage requirement of Runx2 for normal formation of intramembranous bone tissues during embryogenesis, and that the functional Runx2 activity levels are related to extent of the CCD-like phenotype in the mouse. These findings also indicate that the bone phenotype of CCD patients is directly attributable to a reduction in the quantitative levels of Runx2 gene expression.

**Disclosures:** Y. Lou, None.

**M042**

**Parathyroid Hormone Regulation of Osterix Transcription in Osteoblasts.** S. H. H. Hong\*<sup>1</sup>, M. S. Nanes\*<sup>2</sup>, J. Mitchell<sup>1</sup>. <sup>1</sup>Pharmacology and Toxicology, University of Toronto, Toronto, ON, Canada, <sup>2</sup>Department of Medicine, Emory University, Atlanta, GA, USA.

The aim of this study was to examine parathyroid hormone (PTH) regulation of the zinc finger transcription factor osterix (osx) in osteoblasts. Intermittent administration of PTH is anabolic to bone while continuous exposure of PTH is catabolic to bone indicating that a better understanding of the mechanism of PTH regulation in osteoblasts is important. Runt-related transcription factor 2 (runx2) and osx are transcription factors essential for osteoblast differentiation and bone formation. Runx2 is regulated by PTH where short term treatment enhances runx2 transactivational activity and long term treatment promotes proteosomal degradation of runx2. However, it is not clear if PTH regulates osx. As runx2 is upstream of osx and the osx promoter contains runx2 binding sites, we hypothesized that short term PTH treatment would increase osx levels and long term PTH treatment would decrease osx expression. Real-time PCR and western blotting were used to quantify osx mRNA and protein levels in rat UMR106-01 cells, E18.5 and PN4-5 mouse primary calvaria treated with PTH for various times. Signaling inhibitors and activators were used to determine signaling pathways. DRB and cycloheximide were used to determine the half-life of osx mRNA and the requirement for *de novo* protein synthesis for the effect of PTH respectively. Luciferase assays were performed to examine PTH stimulation of runx2 activity and transcriptional regulation of the osx promoter. In UMR cells, 3-24 hr of 10<sup>-8</sup>M PTH suppressed 50±7 % osx mRNA level and 6-24 hr of 10<sup>-8</sup>M PTH suppressed 55±10 % osx protein expression. In primary calvaria, 4-24 hr of 10<sup>-7</sup>M PTH suppressed 65±5 % osx mRNA level. In comparison, runx2 mRNA levels were not regulated by PTH but runx2 activity was stimulated by PTH in luciferase assays. PTH-mediated suppression of osx mRNA could be mimicked by cAMP analogues and forskolin suggesting involvement of cAMP- or PKA- dependent pathways. PTH did not alter osx mRNA stability and osx mRNA suppression did not require new protein synthesis. Luciferase assays suggested that PTH regulated osx expression by acting at the 5' flanking region 304bp to 119bp upstream from the initiation start site of osx promoter. In summary, PTH suppressed osx mRNA and protein by regulating the 5' flanking region of osx promoter. As osx is involved in bone formation, PTH-mediated suppression of osx expression probably results in a catabolic effect on bone. Although osx is characterized as downstream target for runx2, PTH regulation of osx expression occurs more rapidly than the effect of PTH on runx2 indicating a runx2-independent process in regulating osx expression.

**Disclosures:** S.H.H. Hong, None.

**M043**

**Runx2 and Canonical Wnt Signaling Cooperatively Regulate BMP-Induced Differentiation Pathways of Adult Dural Cells into Osteoblasts or Chondrocytes.** M. Rodova\*, B. M. Gardner\*, Q. Lu\*, J. G. Yost\*, J. Wang. Orthopedic Surgery, University of Kansas Medical Center, Kansas City, KS, USA.

While the roles of transcription factor Runx2 and canonical Wnt signaling in embryonic skeletal development have been extensively studied, their regulatory functions in postnatal skeletal regeneration remain unclear. Implantation of bone morphogenetic protein (BMP) or its raw material, demineralized bone matrix (DBM), into soft tissue sites first induces chondrocyte differentiation followed by an endochondral sequence of ossification. Interestingly, our previous studies showed that BMP/DBM-induced repair of adult rat/mouse cranial defects occurred initially by the proliferation and differentiation of dura-derived progenitor cells directly to osteoblasts that synthesized bone tissue, which was spatially distinct from the formation of cartilage near the skin flap covering the cranial defect. This study was designed to elucidate why BMP induces direct osteoblast differentiation at the dural site. Normal 3-5 months old BALB/C mice were used for analysis in this study. We isolated total RNA from the dura mater, subcutaneous tissue covering the cranial defect, and thoracic subcutaneous tissue for gene expression analysis. Genes for the potential regulators of chondrocyte and osteoblast differentiation in these tissues were detected by quantitative real-time PCR (qPCR). The expression levels of Runx2, Wnt-1, -7a, -9a, and β-catenin were significantly higher (p < 0.01) in dural cells than in cranial or thoracic subcutaneous tissue cells. In contrast, expression levels of Sox9 and AP-2α were significantly lower in dura than in cranial or thoracic subcutaneous tissues (p < 0.001). The differences in expression levels of Msx2 and Twist1 between these tissues were not statistically significant. To explore if Runx2 and/or Wnt/β-catenin signaling is the determinant for controlling the BMP-induced dural cell differentiation pathways, we conducted a loss of function experiment using Runx2 and β-catenin short interfering RNA (siRNA) delivered with lentiviral vectors in primary dural cell cultures. The results revealed that transfection with Runx2 siRNA or β-catenin siRNA alone decreased the expression of osteoblast markers, but did not increase the expression of chondrocyte markers in rhBMP-7-treated dural cell cultures, while the combination of Runx2 siRNA and β-catenin siRNA did significantly increase the expression of chondrocyte markers with a decrease in osteoblast markers. These results suggest that higher expression levels of Runx2 and Wnt/β-catenin cooperatively suppress the chondrogenic potential of BMP-treated adult dural cells, which can be reversed by knockdown of Runx2 and Wnt/β-catenin expression.

**Disclosures:** J. Wang, None.

**M044**

**Interaction of Ciz, a Nucleo-cytoplasmic Shuttling Transcription Factor with C-propeptides of Type I Collagen.** T. Hayata, T. Nakamoto, Y. Ezura, M. Noda. Medical Research Institute, Tokyo Medical & Dental University, Tokyo, Japan.

Ciz is a zinc finger transcription factor with nucleocytoplasmic shuttling activity. We previously showed that Ciz-deficient mice show high bone mass phenotype. As a first step to address how Ciz suppresses bone formation, we examined the binding proteins of Ciz based on a yeast two-hybrid screening. While Ciz is an intracellular protein, 47% of the positive clones were genes encoding extracellular matrix proteins, including Colla1, Colla2, Fbln2, and Rpsa. Since type I collagen is a major protein in bone tissue, we focused on type I collagen. In vitro co-immunoprecipitation experiments using in vitro translated proteins revealed direct binding of Ciz-Delta ZF (zinc finger) to C-propeptides of Colla1 and Colla2. In vivo association of the transfected Ciz and C-propeptide of Colla1 was observed in COS-7 cells based on immunoprecipitation experiments. In terms of intracellular localization, C-propeptides of Coll1 and Ciz overexpressed in MC3T3-E1 and COS-7 cells were co-localized in nuclei. These results revealed that Ciz interacts with C-propeptides of type I collagen and this association takes place in nuclei.

**Disclosures:** T. Hayata, None.

## M045

**Osteotropic Peptides: Anabolic and Osteogenic Effects.** V. Madhu\*, G. Beck\*, D. Huang\*, G. Balian. Orthopedic Research Laboratories, Dept of Orthop Surg and Biochem & Molec Genetics, University of Virginia, Charlottesville, VA, USA.

The objective of this study is to establish the molecular targets of bone targeting peptides that were identified from a phage display library. These peptides promote the differentiation of mesenchymal cells *in vitro* and potentiate bone repair in uncortical defects *in vivo*. Identification of the molecular targets for these osteotropic peptides will help us understand the mechanism of peptide mediated bone regeneration. Our studies demonstrated that two of the peptides, designated R1 and L7, stimulate bone regeneration *in vivo*. The two peptides have unique sequences and showed distinct properties. R1 binds to marrow mesenchymal cells *in vitro* and promotes cortical bone and marrow *in vivo*. By contrast, L7 potentiates bone repair but without marrow regeneration at 12 weeks. The differentiation of mesenchymal cells *in vitro* was shown by measuring increases in alkaline phosphatase activity and gene expression for osteocalcin, bone sialoprotein, osterix and Runx2. In addition, the OPG/RANKL ratio is greater than the RANKL/OPG ratio, which suggest that the peptides may have a direct effect on osteoblasts and regulate bone resorption. OPG expression is regulated by Wnt/ $\beta$ -catenin signaling in osteoblasts, which is the same pathway that regulates osteoblastic bone formation. Bone mass is determined by the combined influence of osteoblasts and osteoclasts, and is regulated in osteoblasts by two major signaling pathways: RANKL/RANK and Wnt/ $\beta$ -catenin. To further elucidate the signaling pathway, we have analyzed the Wnt pathway genes. The two bone tropic peptides increased the expression of Wnt receptor LRP6,  $\beta$ -catenin, Wnt10b and Wnt7a and decreased the expression of Wnt5a and Wnt antagonist DKK1. These results suggest that the peptides act through the canonical Wnt signaling pathway. We have also identified the molecular targets for these peptides in mesenchymal cells, including elongation factor, vimentin and myosin, and certain pathways in bone metabolism through which the peptides exert their osteogenic effects. Synthetic peptides may have advantages over larger molecules such as speed of preparation, molecular stability, long shelf lives and potentially therapeutic applications. Significant progress has been made in attempts to modulate bone loss and regeneration by controlling cytokines and growth factors. These osteotropic peptides may offer attractive alternatives to existing therapies that stimulate bone anabolism and bone regeneration.

**Disclosures:** G. Balian, None.

## M046

**The Proinflammatory Cytokine TWEAK Induces Sclerostin Expression in Human Immature Osteoblasts in a MAPK Dependent Fashion.** G. J. Atkins<sup>1</sup>, C. Vincent<sup>1</sup>, A. R. Wijenayaka<sup>1</sup>, K. J. Welldon<sup>1</sup>, D. R. Haynes<sup>2</sup>, T. S. Zheng<sup>3</sup>, A. Evdokiou<sup>1</sup>, D. M. Findlay<sup>1</sup>. <sup>1</sup>Discipline of Orthopaedics and Trauma, University of Adelaide, Adelaide, Australia, <sup>2</sup>Discipline of Pathology, University of Adelaide, Adelaide, Australia, <sup>3</sup>Biogen Idec, Boston, MA, USA.

We recently showed that TNF-like weak inducer of apoptosis (TWEAK), a member of the TNF superfamily is a novel mediator in a mouse model of inflammatory bone destruction.<sup>[1]</sup> We sought to investigate a role for TWEAK in human osteoblast biology, and how TWEAK might interact with TNF in this context. Human primary osteoblasts (NHBC) were found to express TWEAK and its receptor, Fn14. Both TWEAK and TNF were mitogenic for NHBC, regulated by extracellular signal-regulated kinase (ERK)1/2 phosphorylation. TWEAK dose- and time-dependently suppressed the transcription of the master osteoblast transcription factor, RUNX2. Consistent with this, TWEAK inhibited *in vitro* mineralisation, whereas TNF had a positive effect. Notably, TWEAK, alone and in conjunction with TNF, induced the expression in proliferating and therefore phenotypically immature cells, of the osteoblast differentiation inhibitor, sclerostin, in a c-Jun N-terminal kinase (JNK) and Erk1/2-dependent manner. Sclerostin expression was observed at both the mRNA and protein levels. TWEAK induction of sclerostin was sensitive to cycloheximide, implying the requirement for new protein synthesis in the sclerostin response. Exposure of NHBC to exogenous sclerostin mimicked the TWEAK and TWEAK/TNF effects on RUNX2 and osteocalcin expression. Our results suggest that TWEAK acts in part by promoting sclerostin expression, which in turn regulates the expression of key osteoblast transcription factors. Our results suggest that the persistent presence of TWEAK may be anti-anabolic, and that TWEAK and TNF need to be considered together in the aetiology of inflammatory bone remodelling. Our results also demonstrate for the first time that sclerostin, hitherto described as a product of mature osteocytes embedded in mineral, may be induced under inflammatory conditions in osteoblasts at earlier stages of their differentiation.

1. Perper S, et al. (2006) TWEAK is a novel arthritogenic mediator. *J Immunol* 177:2610-2620.

**Disclosures:** G.J. Atkins, None.

## M047

**Gene Expression Analysis of *In vitro*-Aged and Immortalized Human Mesenchymal Stem Cells.** P. Benisch<sup>\*1</sup>, T. Schilling<sup>\*1</sup>, L. Klein-Hitpass<sup>\*2</sup>, M. Kassem<sup>\*3</sup>, F. Jakob<sup>1</sup>, R. Ebert<sup>1</sup>. <sup>1</sup>Orthopedic Center for Musculoskeletal Research, University of Wuerzburg, Wuerzburg, Germany, <sup>2</sup>Institute of Cell Biology, University of Duisburg-Essen, Essen, Germany, <sup>3</sup>Department of Endocrinology, University of Southern Denmark, Odense, Denmark.

Differentiation of human mesenchymal stem cells (hMSC) into osteoblasts is a major step for maintaining bone homeostasis, which is disordered in patients with osteoporosis and impaired during aging. Human MSC obtained from the bone marrow stop proliferation and enter replicative senescence *in vitro* after several months in culture. Thereby they lose their potential for multilineage differentiation and self-renewal. In contrast, telomerase-immortalized hMSC (hMSC-TERT) do not age *in vitro* and were handled as a model for rejuvenation in this study.

We investigated the gene expression pattern of hMSC of early passages, senescent hMSC and hMSC-TERT to reveal new insights into the *in vitro* aging process and possibly age-related bone loss. Therefore, cultures of human hMSC from 9 different donors were maintained until cells stopped proliferation. RNA samples of the first 2 passages (n=5) and the last passages (n=5) as well as hMSC-TERT (n=3) were extracted and analysed by microarray chip hybridization. The transcribed genome of senescent hMSC and hMSC-TERT was statistically evaluated and compared to the gene expression pattern of hMSC of early passages by SAM (Significance Analysis of Microarrays) calculations.

Using SAM analysis we found reproducible differences in the gene expression patterns of our 3 groups of hMSC. In comparison to early-passage cultures of hMSC, 1515 gene products showed more than two-fold up or down regulation of gene expression in senescent hMSC and/or hMSC-TERT. One third of these mRNA species was reciprocally expressed in aged and immortalised cells. Surprisingly, compared to hMSC of early passages, about 400 gene products showed parallel expression changes in aged hMSC and hMSC-TERT with 93 up regulated and 306 down regulated gene products in both groups. This finding was unexpected, but indicates that ageing and rejuvenation might have at least some common attitudes. In addition, we found approximately 200 gene products, which are exclusively expressed in hMSC of the first passages and could not be detected in aged cells or hMSC-TERT by SAM analysis. We conclude that these gene clusters could play a major role in maintaining the characteristics of early-passage hMSC and will therefore be examined further. Functional analysis of differentially expressed genes in aged versus telomerase-immortalized cells will also give hints for molecular mechanisms involved in cellular aging and rejuvenation *in vitro*.

**Disclosures:** P. Benisch, None.

## M048

**FHL2 Mediates Dexamethasone-Induced Mesenchymal Stem Cell Osteogenic Differentiation by Activating Wnt/ $\beta$ -Catenin Signaling and Runx2 Expression.** Z. Hamidouche<sup>\*1</sup>, E. Hay<sup>1</sup>, P. Vaudin<sup>\*2</sup>, P. Charbord<sup>\*3</sup>, P. J. Marie<sup>1</sup>, O. Fromiguet<sup>1</sup>. <sup>1</sup>Inserm U606 and University Paris 7, Paris cedex 10, France, <sup>2</sup>University François Rabelais, Tours, France, <sup>3</sup>Inserm-ESPRI, Tours, France.

The differentiation of bone marrow mesenchymal stem cells (MSCs) into osteoblasts is a crucial step in bone formation. However, the mechanisms involved in the early stages of MSC osteogenic differentiation are not well understood. In this study, we identified FHL2, a member of the LIM-only subclass of the LIM protein superfamily, as a key factor involved in dexamethasone-induced osteogenic differentiation in MSCs. We found that FHL2 was up-regulated during early osteoblast differentiation induced by dexamethasone in murine C3H10T1/2 pluripotent MSCs, bone marrow derived osteogenic BMC10 cells and primary human bone marrow derived MSCs. Forced FHL2 expression using lentiviral vector (LV-FHL2) promoted the expression of Runx2, alkaline phosphatase, type I collagen as well as *in vitro* extracellular matrix mineralization in both murine and human MSCs. Knocking down FHL2 using sh-RNA reduced basal and dexamethasone-induced osteoblast marker gene expression as well as *in vitro* mineralization. Immunocytochemical analysis showed that FHL2 overexpression induced  $\beta$ -catenin translocation to the nucleus where the two proteins were found to be co-localized. Furthermore, a specific sh-FHL2 partially blunted  $\beta$ -catenin nuclear translocation induced by Wnt3a. Immunoprecipitation analysis confirmed that FHL2 promoted  $\beta$ -catenin nuclear translocation which was blocked by a specific sh-FHL2. We further showed that LV-FHL2 transduction led to increase TCF/LEF-dependent reporter gene activity and potentiated Wnt3a-induced TCF/LEF transactivation. Blocking Wnt/ $\beta$ -catenin signaling using DKK1 overexpression abolished the stimulatory effect of Wnt3a and FHL2 overexpression on ALP activity and Runx2 expression. Finally, transfection with a Runx2 mutant bearing a Ser191Asn mutation in the runt domain that impairs DNA binding abolished the stimulatory effect of FHL2 on ALP expression. Altogether, the present study shows that 1) the transcription cofactor FHL2 acts as an endogenous osteogenic activator in MSCs and is involved in dexamethasone-induced mesenchymal cell differentiation into osteoblasts and 2) FHL2 interaction with  $\beta$ -catenin results in increased  $\beta$ -catenin nuclear translocation which in turn potentiates TCF/LEF dependent transcription, increased Runx2 expression and osteogenic differentiation in MSCs. These findings provide evidence that FHL2 is an important mediator of osteogenic differentiation in MSCs via activation of Wnt/ $\beta$ -catenin signaling.

**Disclosures:** P.J. Marie, None.

**M049**

**GILZ (Glucocorticoid Induced Leucine Zipper) Promotes Osteoblast Development and Modulates RANKL/OPG Levels.** T. Lekva<sup>\*1</sup>, C. Kristo<sup>\*1</sup>, T. Ueland<sup>\*1</sup>, O. K. Olstad<sup>\*2</sup>, J. Bollerslev<sup>1</sup>, R. Jemtland<sup>\*1</sup>. <sup>1</sup>Rikshospitalet University Hospital, Oslo, Norway, <sup>2</sup>Ullevaal University Hospital, Oslo, Norway.

Glucocorticoid (GC)-induced bone loss is a frequent and serious complication in patients with endogenous Cushing's syndrome (CS). However, the exact mechanism(s) by which GC influences bone metabolism is still not completely understood. To identify candidate genes with putative roles in GC-induced osteoporosis (GIO), we used global profiling of bone biopsies from CS patients (n=9), before and 3 months after surgery, to screen for changes in gene expression. Out of several hundred differentially expressed genes (p<0.05), the gene encoding GC-induced leucine zipper (GILZ) was selected to further characterize its regulated expression in (proliferating and differentiated) cultured human fetal osteoblast (hFOB 1.19), with or without exposure to dexamethasone (Dex). A putative functional role of GILZ in hFOB was assessed by means of small interfering RNA (siRNA) technology in relation to changes in mRNA levels of typical osteoblastic phenotypic markers and cytokines known to influence bone resorption. Following surgery, normalization of serum cortisol was accompanied by a significant increase in serum markers of bone turnover, 11-fold (p=0.018) for osteocalcin (OC) and 2.2-fold (p=0.018) for CrossLaps (CTX). Moreover, our microarray data demonstrated a fall in levels of GILZ mRNA in bone biopsies 3 months after surgery vs. baseline (p=0.028), whereas levels for Type I collagen and OC increased (also validated using quantitative real-time RT-PCR). We further demonstrate that GILZ is expressed in cultured hFOB osteoblastic cells *in vitro*, and that it is regulated by Dex in a dose- and time-dependent fashion, with a half-maximal effective concentration (EC50) of approx. 10<sup>-9</sup> M and maximum effect of 8.9-fold at 10<sup>-8</sup> M after 4h. Silencing experiments revealed that a reduction in GILZ mRNA levels of more than 75% was associated with reduction in levels of several skeletogenic mRNAs such as ALP, OC and RUNX2, consistent with a role for GILZ in normal osteoblast development. A similar effect of siGILZ on skeletogenic mRNAs was observed also in Dex-treated hFOB. Dex (10<sup>-8</sup> M) has reciprocal effects on OPG (decreased) and RANKL (increased) in hFOB already by 6h. OPG mRNA and protein is further reduced in siGILZ-treated vs. control cells, both in the presence or absence of Dex. However, siGILZ has little or no effect on RANKL mRNA in untreated (i.e. -Dex) osteoblasts, whereas Dex-elicited augmentation of RANKL is largely blunted in siGILZ osteoblasts. Taken together, these results suggest a positive (anabolic) role for GILZ in osteoblast development, and indirectly on bone remodeling, by influencing the balance between bone resorptive and protective cytokines.

**Disclosures:** T. Lekva, None.

**M050**

**Both the Smad and ERK MAP Kinase Pathway Play Critical Roles in BMP-2-induced Osteogenic Transcription Factors Expression.** J. Park, K. M. Woo\*, J. H. Baek\*, H. M. Ryoo\*. Seoul National University, Seoul, Republic of Korea.

Bone morphogenetic protein-2 (BMP-2) is one of the strongest osteogenic signaling molecules. The osteogenic activity induced by BMP-2 is mediated both by canonical Smad signaling and by MAP kinase activation. The canonical Smad signaling is initiated by ligand-receptor binding, subsequent heterotetramerization of BMPRII and BMPRI receptors, receptor Ser/Thr kinase activation and finally BMP specific R-Smads activation. These BMPRI-activated Smads mediates the transcriptional activation of osteogenic transcription factors, Dlx5, Runx2 and Osx. On the other hand, activation of MAP kinases also is critical for the BMP-2-induced osteogenesis. Unfortunately, however, there were a few reports that comprehensively explain both canonical Smad pathway and MAP kinases pathway. In this study, we tried to explain cross-talk between these two signaling pathway. Our previous reports indicate that Dlx5 is one of the critical target of BMP-signaling and plays a pivotal role in stimulating downstream osteogenic master transcription factor Runx2. Its expression by BMP signaling is mainly regulated by Smad-mediated canonical BMP signaling pathway. We found that BMP-2-induced osteogenic differentiation of C2C12 cell is blocked by ERK MAP kinases. ERK MAP kinase activation by BMP-2 occurred 15-30 min after BMP-2 treatment. Moreover, ERK MAP kinase blocker strongly suppressed BMP-2-induced Dlx5 mRNA level, and overexpression of constitutive active form of MEK1/2 stimulated Dlx5 mRNA level even in the absence of BMP-2 treatment. As Dlx5 expression is stimulated both by canonical Smad signaling and ERK MAP kinase signaling, we can assume that BMP specific R-Smads could be the site of both of the BMP-2 downstream signals converge.

**Disclosures:** J. Park, None.

**M051**

**LMP1, Positive Regulator in Osteolineage Differentiation of Human PDL Fibroblasts.** Z. Lin\*, Q. Jin\*, J. V. Sugai\*, W. V. Giannobile\*. Department of Periodontics and Oral Medicine, University of Michigan, School of Dentistry, Ann Arbor, MI, USA.

LMP-1, a recently discovered intracellular LIM domain protein, strongly induces osteolineage differentiation in bone marrow stromal cells and accelerates posterior thoracic and lumbar spine fusion. However, little is known about the role of LMP1 in periodontal ligament (PDL) cell differentiation and alveolar bone regeneration. This study sought to determine whether LMP1 is a positive regulator in the differentiation of PDL cells *in vitro*.

Primary culture of PDL cells were observed over 10 d via inducing and in non-inducing conditions to determine expression of LMP-1 and osteoblastic-related gene expression. Full-length cDNA of human LMP1 was acquired by RT-PCR from MG-63 cells, and cloned into a pQCXIN retroviral vector and production of retrovirus via 293T cells. PDL cells were transfected by pQC-hLMP1 or control retrovirus. After Geneticin selection for 10 d, survival cells were pooled and induced to osteolineage differentiation. qRT-PCR was utilized to detect the expression of bone-specific marker genes over time. Alizarin Red staining was used to evaluate the mineralization over a course of 3w. Our result showed that LMP1 was highly expressed in the early stages of mineralization induced by PDL cells *in vitro*. LMP1 was stably overexpressed in PDL cells via retroviral transduction. LMP1-engineered stable cells possessed elevated baseline levels of BMP2 expression, compared to controls. At 7 d osteolineage promotion conditions resulted in potent increased expression (~20 fold) for osteix, an early marker of osteoblast differentiation in pQC-hLMP1 cells compared to controls, as well as other osteogenesis associated genes including osteopontin and osteocalcin. At 2w, Alizarin red staining demonstrated more mineralization nodules were found in pQC-hLMP1 cells compared to controls. The conclusion is LMP1 is involved in the osteolineage differentiation of PDL cells leading to mineralization *in vitro*. Furthermore, PDL cells driven by LMP1 over-expression displayed enhanced osteo-lineage differentiation, which may be associated with elevated BMP2 expression. These studies suggest LMP-1 may play an important role in regulating periodontal tissue homeostasis and repair.

**Disclosures:** Z. Lin, None.

This study received funding from: NIH/NIDCR DE13397 and ITI Foundation.

**M052**

**TIEG: A Key Regulator of Runx2 and Osterix Gene Expression and Osteoblast Differentiation.** J. R. Hawse<sup>1</sup>, M. Subramaniam<sup>1</sup>, D. G. Monroe<sup>1</sup>, E. A. Syed<sup>2</sup>, U. T. Iwaniec<sup>\*3</sup>, M. J. Oursler<sup>2</sup>, J. B. Lian<sup>4</sup>, G. S. Stein<sup>4</sup>, A. J. van Wijnen<sup>4</sup>, H. Drissi<sup>5</sup>, R. T. Turner<sup>\*3</sup>, T. C. Spelsberg<sup>1</sup>. <sup>1</sup>Biochemistry and Molecular Biology, Mayo Clinic, Rochester, MN, USA, <sup>2</sup>Endocrine Research Unit, Mayo Clinic, Rochester, MN, USA, <sup>3</sup>Department of Nutrition and Exercise Sciences, Oregon State University, Corvallis, OR, USA, <sup>4</sup>Department of Cell Biology, University of Massachusetts, Worcester, MA, USA, <sup>5</sup>Department of Orthopedics, University of Connecticut Health Center, Farmington, CT, USA.

TGFβ Inducible Early Gene-1 (TIEG/KLF10) is a highly expressed member of the Kruppel-like family of transcription factors that regulates a multitude of genes in osteoblasts (OB). We have generated TIEG-null mice that display a severe gender-specific osteopenic phenotype revealing a critical role for TIEG in bone. Female TIEG<sup>-/-</sup> mice have significant reductions in multiple bone parameters and exhibit nearly a 60% reduction in the osteoblast perimeter/bone perimeter resulting in a 42% reduction in bone formation rate. To elucidate the basis for this bone phenotype, we assessed if the loss of TIEG expression affected the commitment of mesenchymal progenitors to the OB lineage, the differentiation and mineralization of committed cells, or both. Methylene blue staining of marrow stromal cells isolated from 2-month old female TIEG<sup>-/-</sup> (n=9) and WT (n=10) mice revealed a modest, but insignificant increase in the number of colony forming units-fibroblast (CFU-F) between the two genotypes (an avg. of 17.8 vs. 14.2 per mouse respectively) suggesting that TIEG does not regulate the number of mesenchymal cells that have the potential to become OBs. However, a significant decrease in the number of CFU-OBs in marrow cultures isolated from TIEG<sup>-/-</sup> mice as determined by alizarin red staining (an avg. of 5.1 vs. 10.5 per mouse respectively) was observed. Additionally, calvarial OBs isolated from TIEG<sup>-/-</sup> mice exhibit significant defects in mineralization relative to WT controls and exhibit reduced expression levels of Runx2 and Osterix. Complementing these studies, over-expression of TIEG in U2OS cells results in increased Runx2 and Osterix expression while depletion of TIEG, using siRNA in primary calvarial OBs, reduces the levels of Runx2 and Osterix mRNA. Transient transfection and ChIP assays reveal that TIEG directly binds to, and activates, the Runx2 and Osterix promoters. Collectively, these data demonstrate that loss of TIEG expression results in decreased expression of Runx2 and Osterix and reduces the ability of marrow stromal cells to fully differentiate into mature OBs. This defect leads to a significant reduction in the number of mature OBs lining the bone surface of TIEG<sup>-/-</sup> mice contributing to the observed osteopenic phenotype.

**Disclosures:** J.R. Hawse, None.

This study received funding from: NIH.

**M053**

**Serine Protease Inhibitor AEBSF Blocks Transcription of Phex by Osteoblasts.** J. P. Gorski<sup>1</sup>, N. T. Huffman<sup>\*1</sup>, S. V. Chittur<sup>\*2</sup>, S. Liu<sup>\*3</sup>, L. D. Quarles<sup>3</sup>, R. J. Midura<sup>4</sup>, N. G. Seidah<sup>\*5</sup>. <sup>1</sup>Univ. of Missouri-Kansas City, Kansas City, MO, USA, <sup>2</sup>Univ. at Albany, Rensselaer, NY, USA, <sup>3</sup>Univ. of Kansas Med. Ctr., Kansas City, KS, USA, <sup>4</sup>Cleveland Clin. and Fdn., Cleveland, OH, USA, <sup>5</sup>IRCM, Montreal, QC, Canada.

Bone mineralization has been shown to be under local osteoblastic control. We have recently demonstrated that AEBSF specifically blocks mineral nucleation within extracellular biomineralization foci (BMF) and inhibits cleavage of biomarker proteins BSP and BAG-75 in BMF isolated by laser capture microscopy. The purpose of this study was to clarify the inhibitory action(s) of AEBSF. UMR 106-01 osteoblastic cells were grown under standard conditions and cultures harvested at different times after addition of β-glycerolphosphate (BGP). Initial studies indicated that UMR 106-01 osteoblastic cells



express proprotein convertase SKI-1 (S1P) which demonstrated a well-known susceptibility to AEBSF. Specifically, assays using a non-permeant, fluorescent peptide substrate showed that intracellular SKI-1 activity became expressed extracellularly reaching a peak at the same time when mineral crystal nucleation in BMF begins. Since proprotein convertases are known to play role in proteolytic activation of transcription factors, e.g., SREBP-1 and SREBP-2, we also investigated whether exposure to a minimum dose of AEBSF had an effect on transcription by UMR osteoblastic cells. PolyA+ RNA was prepared from cultures incubated for 12 h with added  $\beta$ -glycerolphosphate with or without added AEBSF. Triplicate specimens of each condition were subjected to microarray analysis using whole genome 2.30 rat Affymetrix genechips. Interestingly, expression of *Phex* was reduced 1.7-fold by AEBSF along with about 180 other genes. In order to confirm this finding, we transfected UMR 106-01 osteoblasts with a luciferase reporter construct representing 2736 bp of the 5' flanking region of the mouse *Phex* promoter 20-24 h after plating. The 2.7 kb murine *Phex* promoter contains a consensus SREBP response element. Some cultures were also treated with  $1 \times 10^{-7}$  M dexamethasone, a known inducer of *Phex*. Following addition of BGP and AEBSF, cultures were lysed 6-12 h later and luciferase activity determined using a fluorimetric assay. As expected, dexamethasone increased *Phex* expression by several fold compared with control cultures. However, AEBSF was found to significantly reduce *Phex* promoter activity by about 50-60% in all conditions. Alizarin red S staining of parallel cultures confirmed that AEBSF blocked mineralization in these cultures. Our results demonstrate that *Phex* RNA expression can be inhibited by short-term treatment with AEBSF. A hypothetical mechanism involving proteolytic activation of transcription factors by SKI-1 is presently under investigation.

**Disclosures:** J.P. Gorski, BoneMetrics LLC 5.

This study received funding from: NIH AR052775 (JPG).

## M054

**Dlx5 Overexpression Stimulates Odontoblast Differentiation and Function.** V. L. S. Ferrer<sup>1</sup>, Y. Kawano<sup>\*2</sup>, H. Chin<sup>\*1</sup>, L. Wang<sup>\*3</sup>, H. Li<sup>\*1</sup>, A. Lichtler<sup>1</sup>. <sup>1</sup>Reconstructive Sciences and Genetics and Developmental Biology, University of Connecticut Health Center, Farmington, CT, USA, <sup>2</sup>Division of Oral Anatomy, Niigata University, Niigata University, Japan, <sup>3</sup>Institute of Molecular Biology, Academia Sinica, Taipei, Taiwan.

Our lab and others have shown that Dlx5 promotes differentiation in several cell types, including osteoblasts and chondrocytes. Based on similarities between osteoblasts and odontoblasts, we hypothesize that Dlx5 also promotes odontoblast differentiation. We have previously shown by histology that 3.6 kb type I collagen promoter driven Dlx5 overexpressing (Col3.6 Dlx5) mouse incisor odontoblasts differentiate closer to the apical loop than the wild type (WT); microCT showed that mineralized enamel is initiated closer to the apical loop as well. This is consistent with our hypothesis: Dlx5 overexpression early in the odontoblast lineage results in early odontoblast and ameloblast differentiation and early dentin and enamel secretion. Our current studies involving electron probe microanalysis have validated our microCT data. Dual fluorescent dye labeling using calcein as a 1st label and alizarin as a 2nd label at 5-day interval showed that the initiation of both 1st and 2nd labels are closer to the apical alveolar bone in the transgenic mice (TG) than in the WT, further confirming early mineralization in the TG. Double labeling also revealed that the distance between the initiation of the 1st and 2nd labels is shorter in the TG, suggesting a decrease in the growth rate. Direct measurement of the incisors showed a decrease in the eruption rate in the TG. The decrease in growth and eruption rates may alternatively explain the early odontoblast polarization observed in our TG, especially since the transgene is also expressed in the periodontal ligament (PDL). Published studies of other labs involving defective PDL function using mechanical and genetic techniques showed a decreased eruption rate. In particular, the models exhibited wavy odontoblast and ameloblast layers that are positioned closer to the apical loop but secreted buckled matrices. This is in contrast to our Col3.6 Dlx5 incisor: although the eruption rate was decreased, the odontoblasts and ameloblast layers were not wavy and secreted regular, unfolded dentin and enamel at the apical end. A proliferation study using BrdU showed a dramatic decrease in proliferative cells in the apical mesenchyme and apical loop of the TG incisor. We speculate that a significant number of progenitor cells have entered differentiation thus reducing the number of available progenitor cells to proliferate. Overall, our findings suggest that Col3.6 overexpression of Dlx5 directly stimulates odontoblast differentiation and function independent of any transgene effects in the PDL.

**Disclosures:** V.L.S. Ferrer, None.

This study received funding from: NIAMS.

## M055

**Regulation of RUNX2 at the Nuclear Lamina.** P. M. Fonseca<sup>1</sup>, T. Yang<sup>\*1</sup>, T. Bertin<sup>\*1</sup>, B. Dawson<sup>\*1</sup>, Y. Chen<sup>\*1</sup>, G. Zhou<sup>2</sup>, B. Lee<sup>1</sup>. <sup>1</sup>Molecular Human Genetics, Baylor College of Medicine, Houston, TX, USA, <sup>2</sup>Department of Orthopedics, Case Western Reserve University, Cleveland, OH, USA.

RUNX2 is a member of the RUNT family of transcription factors that is essential for osteoblast formation and chondrocyte maturation. Loss-of-function mutations result in cleidocranial dysplasia (CCD). RIP (RUNX2-Interacting Protein) was isolated in a screen of a human osteosarcoma cDNA library using a yeast 2-hybrid approach. Two families with rearrangements involving chromosome 8q - where RIP maps - have been reported to have a CCD-like phenotype. In transient transfection experiments, RIP down-regulated the transactivation by RUNX2 in a dose-dependent manner in both 10T1/2 and ROS17/2 cells. RIP localizes in the inner nuclear membrane and it has been identified as a component of the nuclear envelope in proteomic screens. Its major components are lamins, which have

an important role in nuclear organization, cell division, apoptosis and transcriptional regulation. Mutations in A-type lamins and associated proteins result in several laminopathies. Mandibuloacral dysplasia (MAD) phenocopies CCD and includes other clinical features such as acroosteolysis and early fractures. RUNX2 function can be regulated at both transcriptional and post-translational level, but it can also be determined by its subnuclear localization. We hypothesize that the skeletal defects observed in MAD patients are due to the disruption of lamin interactions with transcriptional regulators relevant in bone formation such as RUNX2 and RIP.

GST pull-down assays showed an interaction between lamin and RIP, as well as the RUNT domain, through the tail domain, which is mutated in MAD patients. Lamin repressed RUNX2 transactivation of a reporter gene in COS7 cells. Lamin versions carrying MAD mutations seem to lose their repressive action and have altered binding properties but show similar nuclear localization as the wild-type protein. Lamin is capable of inhibiting RUNX2 binding to a double-stranded ColX probe in EMSA. RUNX2 partially co-localizes at the nuclear rim in both ROS17/2 cells and in cultured calvarial osteoblasts from mouse. Lamin is required for terminal differentiation of C2C12 cells into osteoblasts. Knockdown experiments in ROS17/2 cells down-regulate both *Runx2* and *Osterix* genes as well as downstream targets. The up-regulation of RIP in transgenic mice causes severe osteopenia. To elucidate the potential effect of lamin in osteoblast differentiation, we are currently analyzing transgenic mice over-expressing both wild-type and MAD mutant forms. Overall, these data suggest a novel mechanism for transcription regulation of skeletogenesis involving sequestration of a RUNX2 complex at the nuclear lamina.

**Disclosures:** P.M. Fonseca, None.

This study received funding from: Portuguese Foundation for Science and Technology.

## M056

**Comparison of Gene Expression in Osteocytes versus Osteoblasts.** E. Paic<sup>\*1</sup>, H. Wang<sup>\*2</sup>, M. S. Kronenberg<sup>\*1</sup>, L. Kuo<sup>\*3</sup>, D. Shin<sup>\*2</sup>, S. E. Harris<sup>4</sup>, I. Kalajzic<sup>\*1</sup>. <sup>1</sup>Dept. of Reconstructive Sciences, Uni. of Conn. Health Center, Farmington, CT, USA, <sup>2</sup>Dept. of Comp. Science, Uni. of Conn., Storrs, CT, USA, <sup>3</sup>Dept. of Statistics, Uni. of Conn, Storrs, CT, USA, <sup>4</sup>Dept. of Perio., Uni. of Texas, San Antonio, TX, USA.

Osteocytes represent the most abundant cellular component of mammalian bones with important function in its remodeling and turnover. However, little is known about the osteoblast-to-osteocyte transition process. We utilized visual markers to selectively identify osteocytes and osteoblasts. This was achieved by development of dual GFP reporter mice in which osteocytes are expressing GFP(green) directed by the DMP-1 promoter, while osteoblasts are identified by expression of GFP(blue) driven by 2.3kb of the Col1a1 promoter. Histological analysis of 5-day-old neonatal calvaria revealed the expression of DMP1 in osteocytes and Col2.3 in osteoblasts and osteocytes. To isolate distinct populations of cells we utilized fluorescent activated cell sorting (FACS). Cells expressing GFPgreen were sorted as osteocytes and cells expressing only GFPblue were collected as osteoblasts. Cells suspensions were subjected to RNA extraction, in vitro transcription and labeling of cDNA. Gene expression was analyzed using Illumina WG-6v1 BeadChip.

Following normalization and statistical analysis (SAM, LIMMA), 30% of genes covered with microarray oligonucleotide probes were called present. We selected 380 genes with statistically significant changes in expression from osteocytes versus osteoblasts. Among them, 230 had higher expression ( $\geq 2$  fold), and 150 genes were expressed at lower level ( $\leq 0.5$  fold) in osteocytes vs. osteoblasts. We utilized gene ontology databases to arrange related groups according to known biological functions. As expected, among genes clustered to osteogenesis and skeletal development, *Bmp3*, *Bmp4*, *Bmp8a*, *Dmp1*, *Enpp1*, *Phex* and *Ank* were highly expressed in osteocytes. Interestingly, five of six differentially expressed genes involved in Wnt signaling pathway were downregulated (*Fzd1*, *Wnt10a*, *Wnt9a*, *Sfrp2*, *Dkk3*) with an increase in *Dkk1* expression. Muscle proteins or related molecules were all (38) upregulated. Most of the transcription factors that are significantly changed were upregulated in osteocytes, including *Notch3*, *Dlx3*, *Sox11* and *Crem* while most of extracellular matrix proteins were downregulated (12/26). We also found that most of the cytoskeletal protein (38/7), genes involved in cell differentiation (25/16) cell organization and biogenesis (25/10), cell migration (12/0) and localization (11/0) were upregulated. Therefore, utilization of isolation of osteocytes and osteoblasts allowed us to identify a number or genes and pathways with potential role in osteoprogenitor lineage differentiation and function.

**Disclosures:** F. Paic, None.

This study received funding from: NIH R03AR053275.

**M057**

**Normal Human Osteoblasts Internalize Urate Crystals by Phagocytosis and Autophagy.** I. Allaey\*, A. Marceau\*, P. E. Poubelle. Medicine, Université Laval, Québec, QC, Canada.

Chronic gouty arthritis can be associated with major tissue destruction of cartilage and bone directly related to the presence of monosodium urate monohydrate crystals (MSUM). Tissue destruction associated with MSUM can be located in joint cartilage and bone structure adjacent to and far from the joints. Since osteoblasts (OB), which orchestrate bone remodeling via soluble factors and cell-to-cell interactions, have been described in contact with microcrystals, particularly in uratic foci of gout, we hypothesized that OB have the capacity to phagocytose MSUM. This phagocytosis could result in alteration of osteoblastic functions. We first determined that OB had the capacity to phagocytose MSUM. We observed in OB, after 24h incubation with MSUM, formation of multiple and large vacuoles still present after 10 days of culture. MSUM did not affect OB viability (measured by propidium iodide incorporation), but dramatically reduced OB proliferation in a dose-dependent manner. We showed that MSUM phagocytosis was dependent on PKC, Syk, ERK and PI3K. We also found by QRT-PCR that OB gene expression was modified by MSUM stimulation. Collagen I, OPG and RANKL mRNA expression was significantly modified after 48h stimulation. Furthermore, MSUM induced an autophagic response in OB. Autophagy is an intracellular bulk degradation system, through which a portion of the cytoplasm is delivered to lysosomes to be degraded. Microtubule-associated protein light chain 3 (LC3) has been used as a specific marker to monitor autophagy, and we found that MSUM dose- and time-dependently induced the cleavage of LC3-I into LC3-II. Those results suggest that human trabecular OB can ingest MSUM with major alterations of osteoblastic functions. These modifications could be associated with decrease of bone formation and could play a role in bone loss observed in chronic gouty arthritis.

**Disclosures:** I. Allaey, None.

*This study received funding from: NIH.*

**M058**

**Tcf Is Required For Wnt11 Mediated Osteoblast Differentiation.** M. S. Friedman\*<sup>1</sup>, W. Luo\*<sup>2</sup>, S. M. Oyersman\*<sup>1</sup>, K. D. Hankenson<sup>3</sup>. <sup>1</sup>Thermogenesis Corporation, Ranch Cordova, CA, USA, <sup>2</sup>University of Michigan, Ann Arbor, MI, USA, <sup>3</sup>Animal Biology, University of Pennsylvania, Philadelphia, PA, USA.

Wnt proteins are traditionally divided into two subclasses, Wnt-1 (canonical) and Wnt5a (Wnt4, Wnt5a, Wnt11 - non-canonical). Depending on the developmental stage, Wnt11 can activate either the non-canonical or the canonical pathway involving beta-catenin. We previously reported that Wnt11 overexpression in pre-osteoblasts (MC3T3 E1.14) activated beta-catenin and enhanced BMP-mediated osteoblast differentiation. For the current studies, we performed microarray analysis of Wnt11 and BMP induced gene expression to determine the transcriptional targets of Wnt11 and how Wnt11 and BMP signaling coordinate to synergistically increase osteoblast differentiation. Wnt11 and GFP control cells were cultured in osteoinductive media (BGP and ascorbate), with or without BMP2. The cells were harvested for RNA at days 3, 6, and 9 post-induction and gene expression analyzed on an Affymetrix 420A 2.0 microarray chip. A number of genes were differentially expressed in both Wnt11 and BMP treated Wnt11 cells relative to GFP and BMP treated GFP controls. We performed qPCR-based validation on a select set of those genes. The extracellular matrix proteins dentin matrix protein 1 (Dmp1) and Cdrap/Otoraplin showed elevated expression in Wnt11 cells. Sprouty 1 (Spry1), an Fgf antagonist, and Rspo2, an activator of Beta-catenin, also showed elevated expression in Wnt11 cells. Interestingly, by microarray analysis Tcf7 expression showed no difference with Wnt11 overexpression, but was increased in BMP treated cells. By western blot, Tcf7 showed increased expression and nuclear localization in BMP treated cells. To evaluate if Tcf activity was required for enhanced osteoblast differentiation by Wnt11, we overexpressed a dominant/negative form of Tcf4 (dnTcf) in Wnt11 and GFP control cells. dnTcf expression inhibited mineralization in both GFP and Wnt11 overexpressing cells. We used qPCR to examine gene expression in dnTcf cells relative to controls. Expression of Rspo2, Osterix, Dmp1, Bsp, and Phex were significantly reduced in BMP treated Wnt11-dnTcf cells relative to BMP treated Wnt11 cells. However, dnTcf had no effect on gene expression in BMP-induced control cells. We conclude that BMP increases expression and nuclear localization of Tcf7. Wnt11, in turn, activates beta-catenin, resulting in nuclear accumulation. Tcf7 and beta-catenin may complex to cooperatively activate transcription of target genes, such as Dmp1, Phex, Osterix, Bsp, and Rspo2, resulting in enhanced osteoblast differentiation. Future studies will focus on the role of these target genes in Wnt11 enhanced osteoblast differentiation.

**Disclosures:** M.S. Friedman, None.

*This study received funding from: NIH.*

**M059**

**Osteocalcin Is a Stress Hormone: Interaction with the Sympathetic Nervous System.** P. E. Patterson-Buckendahl<sup>1</sup>, A. Vitenzon\*<sup>1</sup>, A. Shah\*<sup>1</sup>, M. Shahid\*<sup>1</sup>, R. Kvetnansky\*<sup>2</sup>. <sup>1</sup>Center of Alcohol Studies, Rutgers University, Piscataway, NJ, USA, <sup>2</sup>Institute of Experimental Endocrinology, Slovak Academy of Sciences, Bratislava, Slovakia.

Interaction of the sympathetic nervous system (SNS) and bone has received increasing attention, with adrenergic as well as neuropeptide receptors identified on both osteoblasts and osteoclasts. SNS activation by emotional and physical stressors is also well known, and affects circulating levels of human, monkey and rodent osteocalcin (pOC) in ways that are stressor specific. Most dramatic is the rapid, hormone-like elevation during acute fight/flight response. A target for influence of OC was suggested by immuno-detection of OC in rat dorsal root ganglia (DRG) in cells of nociceptive and proprioceptive neurons. We previously reported altered sensory and stress responses in OC null mutant (KO) mice. We have extended those observations by subjecting male wildtype (WT) and KO mice to foot restraint immobilization (Immo) for up to 2 hours with and without supplementation with OC or synthetic uncarboxylated OC (uOC). We evaluated stress responsive hormones in plasma, adrenal gene expression for enzymes of the catecholamine synthetic pathway and NPY, a neuropeptide decreased by Immo, and localization of OC in DRG. We measured glucose, insulin, adiponectin and leptin in blood taken from 12 KO mice before and 5 and 30 min after i.p. injection of saline or 150 ng native mouse OC/g BW (6 each) and immediate Immo. As expected, glucose increased ( $p < 0.001$ ) and insulin decreased ( $p < 0.05$ ) in all mice. There was a trend for decreased adiponectin and increased leptin, but no effect of OC supplementation, suggesting that stress-induced energy needs over-ride the published effects of OC on this axis. We compared adrenal gene expression for TH, DBH, PNMT and NPY in 6 WT and 6 KO unstressed controls with 4 groups (6 each: WT and KO injected with saline, KO injected with 300 ng/g BW OC or uOC) subjected to 2 hr Immo followed by 3 hr recovery. Native, fully carboxylated OC significantly increased ( $p < 0.01$  or less) TH, DBH, and PNMT mRNA in Immo KO compared to both WT and KO controls, whereas it decreased NPY after Immo, consistent with observations in other models. By comparison, uOC administration had lesser or non-significant effects. To determine further involvement of SNS, we dissected DRG from unstressed paraformaldehyde-perfused mice. Frozen sections (8  $\mu$ m) were reacted with goat anti-mouse OC and visualized with FITC conjugated donkey anti-goat serum. OC positive staining was seen in heterozygous DRG and limb bone, but not in KO confirming presence of OC in DRG. The data confirm that OC has a hormonal influence on the adrenal possibly via uptake by DRG innervating the adrenal. Further study of both OC and uOC in stressed and non-stressed animals is warranted.

**Disclosures:** P.E. Patterson-Buckendahl, None.

*This study received funding from: NIH/NIAAA; NSF.*

**M060**

**Regulatory Signaling Pathways in BMP Mediated Osteogenesis of Adult Human Mesenchymal Stem Cell Cultures.** K. Zdunek\*<sup>1</sup>, A. Wojtowicz\*<sup>1</sup>, J. Skarzynska\*<sup>1</sup>, L. Skrzypek\*<sup>1</sup>, M. Damulewicz\*<sup>1</sup>, P. S. Leboy<sup>2</sup>, A. M. Osyczka\*<sup>1</sup>. <sup>1</sup>Cytology and Histology, Jagiellonian University, Faculty of Biology and Earth Sciences, Krakow, Poland, <sup>2</sup>Biochemistry, University of Pennsylvania, School of Dental Medicine, Philadelphia, PA, USA.

We previously reported that BMP-mediated osteogenesis of adult human MSC (ahMSC) was negatively regulated by ERK signaling and required insulin- or IGF-activated PI3-K [Endocrinology 2005, 146:3428-37]. These studies have now been extended 1) to identify which of the downstream mediators of insulin/IGF signaling are required for BMP-stimulated osteogenesis of ahMSC cultures, and 2) to define the mechanism involved in ERK inhibition of BMP stimulation.

We blocked insulin/IGF signaling using chemical inhibitors of AKT/PKB, GSK3, PKC, and p70S6K, and examined the effects on BMP-mediated osteoblast differentiation in ahMSC cultured under serum-free conditions. The PKC inhibitor GF 109 203X decreased ALP activity in BMP-treated cultures, and decreased mRNA expression of ALP, osteopontin, and osteocalcin. PKC inhibition also reduced Msx2 expression, thus demonstrating a direct effect on BMP-stimulated Smad transcriptional activity. Inhibiting AKT/PKB with ML-9 (15-30  $\mu$ M) or triciribine (10  $\mu$ M), or inhibiting p70/S6K with rapamycin also decreased BMP-stimulated ALP activity. However, the GSK3 inhibitor SB 21673 at concentrations up to 30  $\mu$ M significantly increased BMP-induced ALP activity. These results suggest that the insulin/IGF-I requirement for BMP-stimulated Smad transcriptional activity involves PKC signaling, perhaps via PKC activation of p70S6K. In contrast, GSK3 appears to negatively regulate BMP-mediated osteogenesis in adult human mesenchymal stem cells.

The negative role of ERK on BMP signaling was examined by altering the linker region of Smad1 and over-expressing the construct in ahMSC. Because serine residues within SMAD linker regions are putative ERK phosphorylation sites and ERK phosphorylation of SMADs is reported to modulate SMAD signaling, we prepared three adenoviral constructs carrying either unmodified human Smad1, Smad1 mutated in the linker region to preclude ERK phosphorylation, and control vector carrying LacZ. Non-mutant Smad1 overexpression caused only modest increases in ALP activity compared to control LacZ-infected cells, whereas expression of Smad1 mutated in the linker region markedly increased BMP stimulation of ALP. This demonstrates that phosphorylation of SMADs in the linker region is an important regulatory mechanism in BMP-mediated ahMSC osteogenesis.

**Disclosures:** A.M. Osyczka, None.

*This study received funding from: European Community 6FP Grant MIRG-CT-2007-046479.*

## M061

**Inactivation of the Integrin-Linked Kinase (ILK) in Osteoblasts Increases Mineralization.** J. El-Hoss<sup>\*1</sup>, A. Arabian<sup>1</sup>, S. Dedhar<sup>\*2</sup>, R. St-Arnaud<sup>1</sup>. <sup>1</sup>Genetics Unit, Shriners Hospital for Children, Montreal, QC, Canada, <sup>2</sup>BC Cancer Research Centre, Vancouver, BC, Canada.

Following engagement with the extracellular matrix (ECM), integrin receptors signal via multiple downstream effectors, including the Integrin-Linked Kinase (ILK). The net effect of stimulating ILK is to modulate gene transcription: ILK-dependent phosphorylation of the cJun transcriptional coactivator,  $\alpha$ NAC, induces its nuclear accumulation and potentiates c-Jun-dependent transcription. To determine the role of ILK in osteoblasts, we inactivated ILK using siRNA in osteoblastic cells. In parallel, we engineered mice with specific ablation of ILK in osteoblasts and analyzed the phenotype of the mutant animals, as well as the behavior of primary cultures of ILK-deficient osteoblasts. MC3T3-E1 cells were stably transfected with expression vectors encoding specific ILK siRNAs or a control siRNA. ILK protein expression was inhibited in the ILK siRNA-transfected cells. ILK knockdown led to cytoplasmic retention of  $\alpha$ NAC and increased expression of the osteoblastic differentiation markers type I collagen and bone sialoprotein. ILK-deficient osteoblasts showed dramatically increased mineralization. Bone was harvested at intervals from mice with ILK-deficient osteoblasts (Col-1-Cre;ILK<sup>-/-</sup>) and analyzed using histomorphometry. Surprisingly, we did not measure any significant changes in static or dynamic histomorphometric parameter. Marker gene expression was unchanged between control and mutant mice, with the exception of reduced ILK expression in bone tissue. These results prompted us to study primary osteoblasts isolated from the osteoblast-specific ILK deficient mice. When placed in culture, ILK-deficient primary osteoblasts showed increased expression of osteoblastic differentiation markers and increased mineralization, similar to the ILK-knockdown osteoblasts. These data suggest that in vivo, redundancy of function could account for the absence of an obvious osteoblast phenotype. The main difference between the in vivo and ex vivo conditions involves the ECM, and thus we cultured the ILK-knockdown cells on either plastic or the ECM component, type I collagen. Culture on collagen reduced the exuberant mineralization of ILK-deficient osteoblasts, and this was accompanied by increased phosphorylation of Focal Adhesion Kinase (FAK). Taken together, our data suggest that the ILK cascade normally inhibits osteoblastic activity. We propose that in vivo, other signaling pathways operating downstream of ECM-engaged integrins, such as signaling through FAK, are able to compensate for the loss of ILK activity, leading to the absence of an obvious phenotype in osteoblast-specific ILK-deficient mice.

**Disclosures:** R. St-Arnaud, None.

This study received funding from: Shriners of North America.

## M062

**In Vivo Demonstration that PTH Acts on Early Osteoprogenitor Cells to Enhance Bone Formation During Repair of Critical-Size Calvarial Defects.** Y. H. Wang, L. Wang<sup>\*</sup>, X. Jiang<sup>\*</sup>, S. Hong<sup>\*</sup>, D. W. Rowe. Univ Connecticut Health Center, Farmington, CT, USA.

Cellular targets within the osteogenic lineage responsible for the anabolic effect of intermittent parathyroid hormone (PTH) on bone formation are unclear. Our previous work suggests that progenitor cells prior to the preosteoblast stage of the lineage are sensitive to intermittent PTH exposure. Those studies are done on primary osteoblast cultures from either a bone marrow or calvarial source. When the early cultures are treated with PTH for 2h per day from day 3 to 7 after which no further PTH is given, a higher proportion of the progeny of these cells commit to the osteogenic lineage and acquire a higher level of differentiation than untreated cultures. To test if this in vitro anabolic effect can also be observed as enhanced bone formation in vivo, calvarial cultures from mice transgenic for pOBCol3.6-GFP (green) or pOBCol3.6-CFP (blue) were subjected to either the intermittent PTH or control protocol and subsequently used to seed a scaffold that was transplanted into critical-size calvarial defects of wild-type host. Two 3-mm diameter parietal defects per recipient were transplanted with 50%/50% mixture of cell from the green and blue culture in which one of the two colors was exposed to PTH or both were from control condition. These fluorescent reporters identify osteoblasts in vivo by their strong fluorescent intensity, relative to low intensity in fibroblastic cells, and their close association with a newly deposited mineralized matrix which is stained with xylenol orange (XO). By mixing the two colors of cells from the calvarial cultures prior to scaffold seeding and scoring the resulting repair for the percentage of XO labeled bone surface that is occupied by either the green or blue cells, the contribution from each population to bone formation can be assessed. Four weeks after transplantation, there was more bone formation in transplantation in the sites in which one cellular source had received PTH treatment. In transplant containing PTH-treated cells, the percentage of osteoblasts (either GFP or CFP) lining the XO labeled surface was greater than the transplant from untreated cells. We also observed that transplants formed from PTH-treated cells have less residual apatite-containing scaffold which is a reflection of the resorption and new bone formation associated with bone remodeling. This result is consistent with PTH having a deterministic effect on a progenitor population, long after the PTH has been discontinued, to have enhanced properties for bone formation and potentially bone remodeling. This conditioning protocol may be a useful adjunct for bioengineering an osseous lesion.

**Disclosures:** Y.H. Wang, None.

## M063

**Traf2 Regulates BMP Signaling Pathway in Osteoblastic Cells.** K. Shimada<sup>1</sup>, K. Ikeda<sup>\*1</sup>, K. Ando<sup>\*1</sup>, M. Maeno<sup>2</sup>, K. Ito<sup>\*1</sup>. <sup>1</sup>Department of Periodontology, Nihon University School of Dentistry, Tokyo, Japan, <sup>2</sup>Department of Oral Health Sciences, Nihon University School of Dentistry, Tokyo, Japan.

Bone morphogenetic proteins (BMPs) play a specific role in osteoblastic differentiation and maturation. BMPs induce receptor-regulated Smads (R-Smads). The R-Smads form complexes with the common-partner Smad, which is Smad4 in mammals. These complexes translocate and accumulate in the nucleus and regulate the transcription of various target genes. However, the function of Smad4 remains unclear. Here, we performed a yeast two-hybrid screen using Smad4 as bait and a cDNA library from human bone marrow to identify the proteins interacting with Smad4. For this screen, full-length human Smad4 was cloned in pGBKT7 vector to express it as a fusion with the GAL4-binding domain, and the cDNA library was screened. Two cDNA clones of full-length Traf2 were identified. This interaction was confirmed with GST pull-down assay in *E. coli*. To analyze the function of Traf2 in the BMP signaling pathway, endogenous Traf2 was disrupted in human osteoblastic cell line Saos-2 or rat osteoblastic cell line ROS 17/2.8 using siRNA and examined its effectiveness in silencing Traf2 expression. The expression levels of BMP-induced transcription factor genes including Runx2, Dlx5, Msx2, and Osterix, and Smad4, Smad1 and phospho-Smad1 were examined using real-time reverse-transcribed PCR or Western blotting. The efficiency of silencing Traf2 mRNA level was more than 80%. The expression of Runx2, Dlx5, Msx2, and Osterix mRNA was markedly increased when Traf2 was silenced. The protein levels of Smad4 and phospho-Smad1 increased by siRNA for Traf2. In conclusion, it is suggested that Traf2, which is related to TNF- $\alpha$  signaling pathway, might regulate negatively BMP signaling pathway because the gene expression of the transcription factors and the protein level of phospho-Smad1 increase by siRNA for Traf2.

**Disclosures:** K. Shimada, None.

This study received funding from: Uemura Fund, Nihon University School of Dentistry.

## M064

**Conversion of Vitamin K Analogues to Menaquinone-4 in Osteoblastic Cells.** Y. Suhara, M. Kamao<sup>\*</sup>, K. Nakagawa<sup>\*</sup>, N. Tsugawa<sup>\*</sup>, T. Okano. Department of Hygienic Sciences, Kobe Pharmaceutical University, Kobe, Japan.

Vitamin K (VK) is an essential nutrient and a cofactor for the carboxylation of specific glutamyl residues of proteins to  $\gamma$ -glutamyl residues, which activates osteocalcin related to bone formation. Among its homologues, menaquinone-4 (MK-4) shows most potent biological activities, and up-regulates gene expression of bone markers, and thus has been clinically used in the treatment of osteoporosis in Japan. Recently, we confirmed MK-4 was biosynthesized from dietary phyloquinone (PK), and then accumulated in various tissues in a high concentration. This system should play an important role for biological functions including bone formation, however, the biosynthetic pathway of MK-4 remains unclear. Therefore, we studied the biosynthetic mechanism of MK-4 with chemical technique using deuterated VK analogues.

The proposed mechanism of MK-4 synthesis is that a side chain moiety of dietary PK is cleaved and resulting intermediate vitamin K<sub>3</sub> (menadione) is subsequently converted to MK-4 with geranylgeranylpyrophosphate (GGPP) derived from mevalonate pathway. In this study, we investigated whether MK-4 was biosynthesized by way of vitamin K<sub>3</sub> (VK<sub>3</sub>), and whether MK-4 was produced from VK<sub>3</sub> and GGPP. Deuterated VK compounds were used *in vitro* study to distinguish from native vitamin K analogues in cells. To investigate production of deuterated MK-4 (MK-4-d<sub>n</sub>), we added chemically synthesized deuterated vitamin K<sub>3</sub> (VK<sub>3</sub>-d<sub>8</sub>) and deuterated geranylgeranylpyrophosphate (GGPP-d<sub>8</sub>) to MG-63 cell culture medium. After incubation for 24 h, the concentration of MK-4-d<sub>8</sub> in cells was measured with LC-APCI-MS/MS. As a result, the amount of biosynthesized MK-4-d<sub>8</sub> increased in a dose-dependent manner. These results indicate that MK-4 was biosynthesized from VK<sub>3</sub> and GGPP in osteoblastic cells.

We further examined whether MK-4 was biosynthesized through VK hydroquinone derivative. In the process of biosynthesis route of MK-4, a side chain part would be removed after reduction of VK quinone part. However, novel evidences have not been reported so far. We therefore chemically synthesized several hydroquinone derivatives of VK<sub>3</sub>, which could be a substrate of biosynthesis of MK-4, and investigated whether geranylgeranyl side chain bind to VK<sub>3</sub> derivatives. Based on the experiment, it was revealed that a hydroxyl group of C-4 position is most important to form MK-4. A more detailed examination is currently undergoing based on these findings using other synthetic compounds.

**Disclosures:** Y. Suhara, None.

## M065

### Activation of P2X7 Nucleotide Receptors Increases Metabolic Acid Production by Osteoblastic Cells. M. W. Grol<sup>1</sup>, I. Zelnier<sup>2</sup>, S. J. Dixon<sup>2</sup>.

<sup>1</sup>Anatomy and Cell Biology, The University of Western Ontario, London, ON, Canada, <sup>2</sup>Physiology and Pharmacology, The University of Western Ontario, London, ON, Canada.

Nucleotides such as ATP are released from cells in response to mechanical stimulation and may mediate mechanotransduction in bone. The P2X7 receptor is expressed by cells of the osteoblast lineage and forms calcium-permeable channels when stimulated with high concentrations of extracellular ATP. Targeted disruption of *P2rx7* results in decreased periosteal bone formation and impaired response to mechanical stimulation. Previous studies from our laboratory have shown that activation of P2X7 promotes osteoblast differentiation and bone formation, though the mechanisms remain to be resolved. It is known that osteoblastogenesis coincides with an elevation in aerobic respiration. Thus, the purpose of this study was to characterize the effects of P2X7 receptor activation on osteoblast metabolism. For these experiments, we employed the MC3T3-E1 osteoblast-like cell line. The P2X7 agonist 2',3'-O-(4-benzoylbenzoyl)-ATP (BzATP, 300  $\mu$ M) induced membrane blebbing and transient elevation in the concentration of cytosolic free calcium, consistent with the expression of functional P2X7 receptors. Using a Cytosensor microphysiometer to monitor metabolic acid production, we found that BzATP (300  $\mu$ M) induced a sustained increase in acid production ~75% above basal. This increase persisted for at least 60 min following removal of BzATP. Moreover, repeated applications of BzATP elicited dramatic increases in acid production reaching levels 300% above basal. High concentrations of extracellular ATP (1 mM, sufficient to activate P2X7) mimicked the effect of BzATP, whereas agonists for other P2 receptors did not. To examine the role of mitochondrial activity in this phenomenon, we used the fluorescent probe JC-1, a vital dye sensitive to mitochondrial membrane potential. BzATP induced mitochondrial hyperpolarization, consistent with increased aerobic respiration. We conclude that activation of P2X7 receptors stimulates metabolism in osteoblast-like cells through a mechanism that involves increased mitochondrial activity. Stimulation of bone formation by P2X7 receptors may be due in part to their ability to enhance osteoblast metabolism.

**Disclosures:** M.W. Grol, None.

This study received funding from: Canadian Institutes of Health Research (CIHR).

## M066

### Induction of CTGF by TGF- $\beta$ 1 in Osteoblasts: Independent Effects of Src and Erk on Smad Signaling. X. Zhang<sup>1</sup>, J. A. Arnott<sup>2</sup>, S. Rehman<sup>3</sup>, W. G. DeLong<sup>3</sup>, A. Sanjay<sup>1</sup>, F. F. Safadi<sup>1</sup>, S. N. Popoff<sup>1</sup>. <sup>1</sup>Anatomy and Cell Biology, Temple University School of Medicine, Philadelphia, PA, USA, <sup>2</sup>Basic Sciences, The Commonwealth Medical College, Scranton, PA, USA, <sup>3</sup>Orthopaedics and Sports Medicine, Temple University School of Medicine, Philadelphia, PA, USA.

Connective tissue growth factor (CTGF/CCN2) is a cysteine rich, extracellular matrix protein that acts as an anabolic growth factor to regulate osteoblast differentiation and function. In osteoblasts, CTGF is induced by transforming growth factor beta 1 (TGF- $\beta$ 1) where it acts as a downstream mediator of TGF- $\beta$ 1 induced matrix production. The molecular mechanisms that control CTGF induction by TGF- $\beta$ 1 in osteoblasts are not understood. We have previously demonstrated the requirement of Src, Erk and Smad signaling for CTGF induction by TGF- $\beta$ 1 in osteoblasts. However, the potential interaction among these signaling pathways in osteoblasts has not been examined. In this study we demonstrate that TGF- $\beta$ 1 activates Src kinase in osteoblasts (primary rat and rat osteosarcoma cell line) and that treatment with the Src family kinase inhibitor, PP2, or two independent Src kinase mutants (kinase-dead; kinase-dead and open) prevented Src activation and CTGF induction by TGF- $\beta$ 1. The inhibition of Src kinase activity prevented TGF- $\beta$ 1 induced Smad 2 & 3 activation and Smad nuclear translocation in osteoblasts as determined by immunofluorescent and Western blot analyses. In addition, inhibiting Src prevented Erk activation. MAPKs such as Erk can modulate the Smad pathway through directly mediating the phosphorylation of Smads or indirectly through activation/inactivation of required nuclear co-activators that mediate Smad DNA binding. When we treated osteoblasts with the Erk inhibitor, PD98059, it inhibited TGF- $\beta$ 1-induced CTGF promoter activity and protein expression but had no effect on Smad activation or Smad nuclear translocation. Using electro-mobility shift assays we found that treatment with PD98059 impaired transcriptional complex formation on the Smad binding element (SBE) of the CTGF promoter, demonstrating that Erk activation was required for SBE transactivation. Taken together these data demonstrate that Src is an essential upstream signaling partner of both Erk and Smads for TGF- $\beta$ 1 induction of CTGF in osteoblasts, and that Src and Erk have independent effects on Smad signaling required for the formation of a transcriptionally active complex that regulates CTGF promoter activity and expression. Future studies will focus on examining whether these interactions are unique to osteoblasts compared to other non-osteoblast cells or lines. Evaluation of the regulation of CTGF expression in osteoblasts is important to understand its effects on osteoblast differentiation and function.

**Disclosures:** S.N. Popoff, None.

This study received funding from: NIAMS AR047432.

## M067

### Effects of G $\alpha$ 11 Overexpression on Osteoblast Signaling and Function in Transgenic Mice. M. Mattocks<sup>\*</sup>, J. Mitchell. Pharmacology, University of Toronto, Toronto, ON, Canada.

We have created an osteoblast-specific G $\alpha$ <sub>11</sub> transgenic mouse strain in order to examine the effects of increased osteoblastic G $\alpha$ <sub>11</sub> on parathyroid hormone receptor (PTHr) signaling in bone. Our group has previously shown that dexamethasone, a potent glucocorticoid, can alter parathyroid hormone (PTH) signaling through the parathyroid hormone receptor (PTHr) in osteoblasts, by extending the half-life of the G $\alpha$  subunit G $\alpha$ <sub>11</sub>. Since overexpression of G $\alpha$ <sub>11</sub> in osteoblastic cells increases PTH signaling through the phospholipase C pathway and activation of MMP-13 this effect may contribute to glucocorticoid-induced osteoporosis.

We examined the effects of increased levels of osteoblastic G $\alpha$ <sub>11</sub> in vivo by generating a transgenic mouse model overexpressing G $\alpha$ <sub>11</sub> driven by the 3.6kb rat Col1A1 promoter fragment. This promoter fragment drives osteoblast and fibroblast specific expression of genes under its control. The effects of this increased G $\alpha$ <sub>11</sub> expression in the bones of these mice have been assayed by histomorphometry and micro CT. We have also examined the effect of the transgene in vitro, in stably transfected UMR106-01 and ROS 17/2.8 osteosarcoma lines, as well as primary transgenic osteoblast cultures, in order to understand the effects of increased PTHr signaling through G $\alpha$ <sub>11</sub> on downstream gene regulation.

Results osteoblasts in vitro show that our transgenic model increases the extent of PTH-mediated induction in MMP-13 mRNA expression, suggesting that the PTHr signaling in transgenic G $\alpha$ <sub>11</sub> overexpressing osteoblasts is more catabolic.

**Disclosures:** M. Mattocks, None.

## M068

### Stable Expression of Constitutively Active G $\alpha$ 12 in Osteoblastic Cells Promotes Matrix Protein Expression and Alkaline Phosphatase Activity. J. Wang, T. Yoshida, P. H. Stern. Department of Mol Pharm & Biol Chem, Northwestern University, Chicago, IL, USA.

Heterotrimeric ( $\alpha\beta\gamma$ ) G proteins mediate signaling from cell surface G protein-coupled receptors (GPCRs) to downstream effector molecules. G proteins are classified into four subfamilies, based on the  $\alpha$  subunit: G $\alpha$ s, G $\alpha$ q/11, G $\alpha$ i and G $\alpha$ 12/13. The G $\alpha$ s, G $\alpha$ q/11 and G $\alpha$ i subfamilies have been associated with differentiation and signaling responses in osteoblastic cells, whereas the role of the G $\alpha$ 12/13 class in bone has not been well defined. In other cells, G $\alpha$ 12/13-mediated effects are generated largely through RhoA small G proteins and affect cytoskeletal structures and cell migration, tumor cell invasion, and cell proliferation and survival. We have found that disruption of RhoA signaling in osteoblastic cells results in loss of actin cytoskeletal elements. In order to obtain more insight into the potential role of G $\alpha$ 12/13 signaling in osteoblasts, we stably transfected UMR-106 cells with constitutively active G $\alpha$ 12Q226L (CA-G $\alpha$ 12). Genes related to osteoblast differentiation and alkaline phosphatase activity were compared in cells transfected with either CA-G $\alpha$ 12 or empty vector (pcDNA). RT-PCR revealed that in the CA-G $\alpha$ 12 cells the expression of the matrix proteins osteopontin and decorin was more than doubled, compared to cells transfected with empty vector, whereas type I collagen, Runx2, BMP2 and alkaline phosphatase gene expression were not significantly affected. However, alkaline phosphatase activity was approximately twice as high in the CA-G $\alpha$ 12 cells, compared to cells transfected with the empty vector. The results represent novel findings regarding the role of this class of G proteins and suggest that osteoblast responses mediated through G $\alpha$ 12/13 affect bone matrix proteins and may also be involved in mineralization.

**Disclosures:** J. Wang, Procter & Gamble 5.

## M069

### Gut-derived Serotonin Is an Inhibitor of Bone Formation. V. K. Yadav<sup>\*</sup>, J. Ryu<sup>\*</sup>, N. Suda<sup>\*</sup>, P. Ducy<sup>\*</sup>, G. Karsenty. Genetics and Development, Columbia University, New York, NY, USA.

The role, if any, of serotonin in the regulation of bone remodeling has not been studied systematically. This is a matter of great importance given the impact of serotonin reuptake inhibitors on bone health. Serotonin produced in the gut accounts for ~95% of total serotonin in the body, and does not cross the blood-brain barrier thus its function must be different from the one synthesized in the brain. The synthesis of gut-derived serotonin (GDS) is initiated by the enzyme Tph1. To determine the influence, if any, of GDS on bone remodeling we generated various mice harboring cell-specific deletion of *Tph1*. Mice lacking *Tph1* in the duodenum developed a high bone mass phenotype while *Tph1* deletion in osteoblasts does not affect bone mass. This high bone mass phenotype was secondary to an increase in osteoblast numbers and bone formation rates while bone resorption parameters were not affected. These results identify gut-derived serotonin as a bona fide hormone regulating bone formation. Serotonin mediates its action through its binding to one of the 14 receptors present on the target cells. We could detect the expression of 3 serotonin receptors in osteoblasts, Htr1b, Htr2a and Htr2b. We are currently analyzing mice lacking each of these receptors to determine which one mediates the effect of serotonin on osteoblasts. Results of this investigation will be presented at the meeting.

**Disclosures:** V.K. Yadav, None.

**M070**

**Inhibition of Lamin A/C Attenuates Osteoblast Differentiation and Stimulates Osteoclastogenesis Through Enhanced RANKL Signaling.** M. Rauner<sup>\*1</sup>, U. Hempel<sup>\*1</sup>, W. Sipos<sup>\*2</sup>, A. Wutzl<sup>\*3</sup>, R. Foisner<sup>\*3</sup>, P. Pietschmann<sup>3</sup>, L. C. Hofbauer<sup>1</sup>. <sup>1</sup>Technical University of Dresden, Dresden, Germany, <sup>2</sup>University of Veterinary Medicine, Vienna, Austria, <sup>3</sup>Medical University of Vienna, Vienna, Austria.

Osteoporosis in the elderly is a condition of low bone mass and poor bone quality due to impaired osteoblastogenesis and decreased bone formation. However, the underlying molecular mechanisms are poorly defined. Recently, the Hutchinson-Gilford progeria syndrome (HGPS), a disease of accelerated aging and premature osteoporosis, has been linked to mutations in the lamin A/C gene. We tested the hypothesis that the loss of lamin A/C in osteoblasts leads to impaired osteoblast differentiation and enhanced osteoclastogenesis. Endogenous protein levels of lamin A/C were assessed in human mesenchymal stem cells undergoing osteogenic differentiation. We found that the expression of lamin A/C increased with osteoblast maturity. Next, lamin A/C was knocked-down continuously with small interfering RNAs in human mesenchymal stem cells differentiating towards osteoblasts. Lamin A/C knock-down led to an inhibition of osteoblast proliferation by 26% ( $p < 0.001$ ), and impaired osteoblast differentiation by 48% ( $p < 0.05$ ) based on mineralized matrix formation assessed with alizarin red S staining. Expression levels of runx2 and osteocalcin mRNA assessed by quantitative RT-PCR were decreased in mature lamin A/C-knock-down osteoblasts by 44% and 78% ( $p < 0.05$ ), respectively. Furthermore, Western blot analysis showed that osteoblasts with diminished levels of lamin A/C also produced less osteocalcin. The RANKL/OPG ratio was increased at the mRNA and protein level by two-fold, resulting in an increased ability to support osteoclastogenesis based on the number of TRAP-positive multinucleated cells (+34%,  $p < 0.05$ ). Our data indicate that lamin A/C is essential for proper osteoblastogenesis. Moreover, lack of lamin A/C favors enhanced osteoclastogenesis. These data provide evidence for a link between loss-of-function of lamin A/C and impaired osteoblast differentiation, as present in the progeroid syndrome HGPS.

**Disclosures:** M. Rauner, None.

**M071**

**Chemerin and CMKLR1 Targeted Gene Delivery Identifies A Novel Molecular Switch in the Treatment of Osteoporosis.** S. Muruganandan<sup>\*</sup>, A. Roman<sup>\*</sup>, C. Sinal. Pharmacology, Dalhousie, Halifax, NS, Canada.

A common feature in the development of osteoporosis is the enhanced differentiation of adipocytes versus osteoblasts in bone marrow. Both of these cell types originate from a common mesenchymal progenitor stem cell type. Our laboratory has identified chemerin as a novel adipokine that is secreted by mature adipocytes and acts in a paracrine fashion to further drive the differentiation of immature preadipocytes into the adipocytic lineage. The interaction of secreted chemerin with its cognate receptor, CMKLR1 was also found to be essential to the adipocyte differentiation processes. Based on these earlier findings, we hypothesized that chemerin and CMKLR1 are essential for the development of adipocytes in bone marrow. In our first set of experiments we found that chemerin is secreted during adipocyte differentiation of both mouse bone marrow mesenchymal stem cell progenitors and 7F2 preosteoblast cells. To disrupt chemerin/CMKLR1 signalling in these cells, we used short hairpin loop RNAs (shRNA) targeting chemerin or CMKLR1 mRNA and delivered these using adenoviral vectors. Consistent with our previous work, chemerin and CMKLR1 knockdown abrogated both preadipocyte clonal expansion and subsequent adipocyte differentiation (arrested lipid accumulation, decreased expression of adipocyte marker genes and transcriptional factors). Interestingly, this was also associated with up regulation of osteoblast transcriptional factors. Phenotypical characterization of the knockdown cells revealed enhanced osteoblastic marker gene expression and an increased mineralization with subsequent addition of mineralization media. All these studies mark a novel therapeutic strategy for osteoporosis that 1) arrests preadipocyte clonal expansion, 2) abrogates adipocyte differentiation, and 3) drives the cells to osteoblast differentiation.

**Disclosures:** S. Muruganandan, None.

**M072**

**Pulse Treatment with Zoledronic Acid Causes Sustained Commitment of Bone Marrow Derived Mesenchymal Stem Cells for Osteogenic Differentiation.** R. Ebert, S. Zeck<sup>\*</sup>, R. Krug<sup>\*</sup>, J. Meissner-Weigl<sup>\*</sup>, D. Schneider<sup>\*</sup>, L. Seefried<sup>\*</sup>, J. Eulert<sup>\*</sup>, F. Jakob<sup>\*</sup>. Orthopedic Center for Musculoskeletal Research, University of Wuerzburg, Wuerzburg, Germany.

The aminobisphosphonate zoledronic acid (ZA) is a bone-seeking specific inhibitor of the enzyme farnesyl pyrophosphate synthase, which causes inhibition of osteoclast function and apoptosis. It is widely used as an osteoclast targeted antiresorptive treatment of metastatic bone disease, Paget's disease and osteoporosis. Mesenchymal stem cells and osteoblast precursors can also be targets of bisphosphonates, but the clinical relevance of these effects is under debate.

We investigated the influence of  $\mu\text{M}$  ZA concentrations on the proliferation and apoptosis capacity of human mesenchymal stem cells (hMSC) after 24, 48 and 72 h stimulation. Additionally, we treated hMSC with  $\mu\text{M}$  concentrations of ZA for 3 and 6 h prior to a 2 to 4 weeks period of osteogenic culture. The expression of osteogenic markers as alkaline phosphatase (ALP), osteocalcin (OC), osteopontin (OP), collagen 1A2 (Col1A2) and the wnt signaling inhibitor dickkopf 1 (Dkk1) were analyzed by RT-PCR after 2 weeks, the mineralization degree was quantified after alizarin red and alkaline phosphatase staining after 4 weeks.

ZA in vitro causes inhibition of proliferation and induction of apoptosis in hMSC, when applied in concentrations of 20 and 50  $\mu\text{M}$  for more than 24 h. However, pulse stimulation for 3 and 6 h with the same concentrations and subsequent culturing for up to 2 weeks under osteogenic conditions exerts sustained regulation of osteogenic marker genes in hMSC. The effect on gene regulation translates into marked enhancement of mineralization, as shown by alizarin red and alkaline phosphatase staining after 4 weeks of osteogenic culture.

ZA, when applied as a pulse stimulus in  $\mu\text{M}$  concentrations, might therefore also stimulate osteogenic differentiation in vivo, since  $\mu\text{M}$  plasma concentrations can be achieved by intravenous application of 5 mg in patients. These data set the stage for the future dissection of the effects of ZA and other aminobisphosphonates on cells beyond osteoclasts, with respect to cell differentiation in benign metabolic and to antitumor efficacy in metastatic bone diseases, as well as adverse events due to putative substance accumulation in bone during long-term treatment.

**Disclosures:** R. Ebert, None.

This study received funding from: Novartis.

**M073**

**The Deletion of ADAM15 Decreases Osteoblast Differentiation and Bone Formation in vitro.** F. Kolb<sup>\*</sup>, B. Thuring<sup>\*</sup>, S. Barbieri<sup>\*</sup>, F. Morvan<sup>\*</sup>.

<sup>1</sup>Expertise Protease Platform, Novartis Institutes for Biomedical Research, Basel, Switzerland, <sup>2</sup>Musculoskeletal Disease Area, Novartis Institutes for Biomedical Research, Basel, Switzerland.

Bone formation involves the development of multiple cell-cell contacts and cell-matrix interactions. These interactions are mediated by proteins such as cadherins which ensure cell-cell adhesion, connexins which are involved in cell-cell communication through gap-junction and integrins involved in cell-matrix adhesion. These complex cell-cell and cell-matrix interactions are required for osteoblast adhesion, communication, and gene expression during all stages of cell differentiation. ADAM15 (named for a disintegrating and metalloprotease 15 or metargidin) is a membrane-anchored glycoprotein that has been implicated in the cleavage of cell-matrix or cell-cell interactions such as N-Cadherin. ADAM15 is widely expressed, including robust expression in the vasculature, brain and bone of mice. Mice carrying a null mutation in ADAM15 are viable and fertile without any evident pathological phenotype, probably due to redundancy of the function of the ADAMs family members. The goal of the present study was to investigate the role of ADAM15 during osteoblastogenesis. To this end we isolated cells from the calvaria of ADAM15 deficient or control mice and performed a 21 day osteoblastic differentiation assay using an osteogenic cocktail. At various time points, RNA was extracted and quantitative real time PCR was performed to verify the expression of key osteogenic genes such as Runx2. Alkaline phosphatase (ALP) expression was determined at day 5 and its activity was measured at day 14 and 21 of culture. Furthermore calcium deposition was measured at day 14 and 21 and mineralized nodules were visualized by alizarin red staining. In ADAM15 deficient osteoblastic cells, the expression of ALP was down regulated by 4-fold compared to control littermate osteoblasts at day 5. Likewise ALP activity was reduced 4-fold at day 14 and 21. Consistent with this observation Runx2, bone sialoprotein, and osteocalcin expression level were reduced 2- to 5-fold at day 14 and 21. Calcium deposition was reduced by 5-fold at day 21 compared to control cultures, whereas at day 14 no statistical difference was observed. Nodule formation by ADAM15 deficient osteoblasts appeared decreased at day 14 and 21 post-osteogenic treatment. Taken together these data suggest a novel role for ADAM15 in the regulation of osteoblastogenesis in vitro presumably by regulating osteoblast adhesion and cell-cell communication.

**Disclosures:** F. Morvan, None.

## M074

**Cortical Bone Acquisition in the Appendicular Skeleton of Healthy Young Females is Reciprocally Related to Marrow Adiposity.** N. Di Iorgi<sup>1</sup>, P. P. Campbell<sup>1</sup>, M. Rosol<sup>1</sup>, G. Adams<sup>2</sup>, V. Gilsanz<sup>1</sup>. <sup>1</sup>Radiology, Childrens Hospital Los Angeles, Los Angeles, CA, USA, <sup>2</sup>Center for Stem Cell and Regenerative Medicine, Keck School of Medicine, Los Angeles, CA, USA.

Osteoblasts and adipocytes share a common progenitor cell in the bone marrow capable of mutually exclusive differentiation into the cell lineages responsible for bone and fat formation. We examined whether bone acquisition in healthy young women is inversely related to changes in marrow adiposity.

Computed tomography (CT) measurements of femoral cortical bone area (CBA), cross sectional area (CSA) and fat density (FD) in the marrow, and dual energy x-ray absorptiometry (DXA) measurements of total body fat (BF) and lean mass (LM) were obtained in 39 healthy females (15-20 years of age) at baseline and 18 to 24 months later. Marrow FD was inversely related to CBA at baseline and at follow-up ( $r$ 's = 0.39 and 0.33;  $P$ 's = .015 and 0.039, respectively), but was not associated to CSA ( $r$ 's = 0.19 and 0.17;  $P$ 's = .24 and 0.32, respectively). The reciprocal association between FD and CBA persisted even after controlling for age, BMI, DXA values for BF and LM and femoral CSA (see table below).

	BASELINE		FOLLOW-UP	
	$\beta$	$P$	$\beta$	$P$
Age	-0.013	0.60	-.034	0.12
BMI	0.011	0.64	-0.005	0.79
DXA Total Body Fat	-8.794E-6	0.51	1.957E-6	0.80
DXA Total Lean Fat	7.489E-6	0.55	2.700E-6	0.79
Femoral CSA	0.516	<0.0001	0.570	<0.0001
Marrow Fat Density	3.089	0.02	2.909	0.03
$R^2$ adjusted	0.68		0.77	

Gains in CBA during the course of the study were inversely related to decreases in marrow fat ( $R^2 = 0.15$ ;  $P = .009$ ); a relation that persisted even after accounting for changes in body mass, bone size and body composition (see table below). Marrow FD was not associated to weight, BMI, or DXA values of BF.

Regression analyses for the prediction of femoral CBA gains			
Univariate Regression Analyses			
Percent changes of:	$\beta$	$P$	$R^2$
Weight	0.021	0.84	-
Height	-0.806	0.58	-
BMI	0.26	0.24	-
DXA BF	-0.007	0.88	-
DXA LM	0.215	0.15	0.04
Femoral CSA	0.853	0.001	0.47
CT Marrow FD	-1.053	0.009	0.15
Multiple Regression Analyses			
Femoral CSA	0.738	<0.0001	0.52
CT Marrow FD	-0.524	0.03	

We conclude that bone acquisition in the appendicular skeleton of healthy young females is inversely related to changes in marrow adiposity. Deciphering the mechanisms that influence the inseparable reciprocal transformation of MSCs into osteoblasts or adipocytes could lead to the development of strategies to maximize bone mass and to prevent osteoporosis.

**Disclosures:** N. Di Iorgi, None.

## M075

**Fibroblast Growth Factor 1 Inhibits Adipogenic Differentiation and Transdifferentiation of Human Mesenchymal Stem Cells.** N. Schuetze<sup>1</sup>, S. Jatzke<sup>1</sup>, R. Kueffner<sup>2</sup>, L. Klein-Hitpass<sup>3</sup>, R. Zimmer<sup>2</sup>, F. Jakob<sup>1</sup>, T. Schilling<sup>1</sup>. <sup>1</sup>Orthopedic Center for Musculoskeletal Research, University of Wuerzburg, Wuerzburg, Germany, <sup>2</sup>Institute of Informatics, University of Munich, Munich, Germany, <sup>3</sup>Institute of Cell Biology, University of Duisburg-Essen, Essen, Germany.

The age-related gain of fatty tissue in human bone marrow and the simultaneous loss of bone mass could contribute to diseases like osteopenia. Acceleration of adipogenesis of mesenchymal stem cells (MSCs) or transdifferentiation of pre-osteoblasts may contribute to this degeneration. The dissection of the hitherto unknown molecular basis is a prerequisite to uncover novel targets for therapeutic interventions that inhibit adipogenesis and enhance osteogenesis. Previously, we established a cell culture system of human MSCs to monitor transdifferentiation from osteoblasts into adipocytes and vice versa. Here, we aim to identify gene products differentially regulated during transdifferentiation that could initiate this process.

To examine adipogenic transdifferentiation of committed osteoblasts as well as osteogenic transdifferentiation of adipocytes, RNA was isolated 3 h and 24 h after initiation of transdifferentiation and subjected to Affymetrix microarray analyses in duplicates. Signal log ratios and change p-values allowed for evaluation of reproducibility and distinct regulation as well as reciprocity of gene regulation between both transdifferentiation

directions. Gene regulations were confirmed by RT-PCR, adipogenesis and osteogenesis was assessed by marker analyses.

414 and 922 gene products were reproducibly regulated in adipogenic and osteogenic transdifferentiation, respectively; many showed reciprocal regulation. Further bioinformatic analyses integrated reproducibility, degree of regulation and distinct reciprocity into a new scoring scheme that ranked genes due to their potential relevance. Some of the highly ranked genes are components of signaling pathways like Wnt/ $\beta$ -catenin, IGF or FGF signaling. Functional examination of FGF1 as one of the highly ranked potential key factors confirmed its largely inhibitory effect on adipogenic differentiation and transdifferentiation of MSCs.

Our findings serve as a prerequisite for further functional examinations of promising candidates that could provoke transdifferentiation or even act as switches between the adipogenic and osteogenic lineage. The identification of FGF1 as an inhibitor of adipogenic differentiation and transdifferentiation confirmed the array data provides a proof of principle for the gene ranking procedure. Therapeutic interventions based on our findings could counteract age-related bone loss by specific enhancement of osteogenesis and inhibition of adipogenesis.

**Disclosures:** N. Schuetze, None.

This study received funding from: German Research Society.

## M076

**OPG and Bisphosphonates Had Differential Effects on Osteoclast Numbers, Bone Marrow Fibrosis and Cortical Porosity in a Mouse Model of Constitutive Activation of the PTH/PTHrP Receptor.** M. Ohishi<sup>1</sup>, R. Chiusaroli<sup>1</sup>, F. Asuncion<sup>2</sup>, M. Ominsky<sup>2</sup>, P. Kostenuik<sup>2</sup>, E. Schipani<sup>1</sup>. <sup>1</sup>Endocrine unit, Massachusetts General Hospital, Boston, MA, USA, <sup>2</sup>Metabolic Disorders, Amgen Inc., Thousand Oaks, CA, USA.

Transgenic mice expressing constitutively active PTH/PTHrP receptors in cells of the osteoblast lineage (PPR\*Tg) display augmented trabecular bone, bone marrow (BM) fibrosis, increased number of osteoclasts and severe cortical porosity. In this model, cortical porosity is characterized by the presence of stromal cells, blood vessels and osteoclasts, and it is thus similar to the histological picture of BM fibrosis in the trabecular bone areas. These phenotypes are also typical of severe hyperparathyroidism and fibrous dysplasia. We investigated whether the presence or activity of osteoclasts influences porosity or fibrosis in PPR\*Tg mice. Three-month-old wild type (WT) and PPR\*Tg mice were injected s.c. with either vehicle (Veh), the RANKL inhibitor OPG-Fc (3mg/kg, 3/week), alendronate (ALN, 500µg/kg, once/week) or zoledronate (ZOL, 100µg/kg, once/week) for 3 months. Femurs were assessed by  $\mu$ CT and tibia were assessed by histomorphometry. PPR\*Tg mouse tibiae had 2.5-fold more trabecular osteoclasts per bone area than WT controls. OPG treatment of PPR\*Tg mice reduced osteoclast numbers by 80%, whereas ALN and ZOL treatment caused no reductions. Despite differential effects on osteoclast numbers, all treatments caused similar (~2-fold) increases in trabecular bone volume, which suggests similar suppression of trabecular osteoclast activity. Veh-treated PPR\*Tg mice showed severe BM fibrosis ( $8.17 \pm 2.12\%$  of marrow volume), while no fibrosis was observed in Veh-treated WT mice. BM fibrosis was completely abrogated by OPG-Fc treatment, whereas treatment with ALN or ZOL reduced fibrosis by 54% and 55%, respectively (both  $p < 0.01$  vs Veh). MicroCT of femur diaphysis revealed a 10-fold increase in cortical porosity in PPR\*Tg mice ( $p < 0.01$  vs WT controls), and OPG-Fc treatment of PPR\*Tg mice fully prevented this cortical porosity. ALN reduced cortical porosity by 39% ( $p < 0.05$  vs Veh), while ZOL caused no significant reduction in porosity. These data suggest that BM fibrosis and cortical porosity in PPR\*Tg mice were related to both the presence and the activity of osteoclasts. While all treatments appeared to cause similar reductions in trabecular bone resorption, only OPG caused marked reductions in osteoclast numbers and total abrogation of both marrow fibrosis and cortical porosity. It will now be important to identify the molecular mechanisms underlying this dichotomy.

**Disclosures:** M. Ohishi, Amgen Inc. 3.

This study received funding from: Amgen Inc.

## M077

**Use of GFP Reporters to Assess Cell Lineage in a Murine Model of Tibial Fracture Repair.** C. Ushiku<sup>1</sup>, J. Xi<sup>2</sup>, L. Wang<sup>2</sup>, D. J. Adams<sup>1</sup>, D. W. Rowe<sup>2</sup>. <sup>1</sup>Orthopaedic Surgery, University of Connecticut Health Center, Farmington, CT, USA, <sup>2</sup>Reconstructive Sciences, University of Connecticut Health Center, Farmington, CT, USA.

Successful repair of a fracture requires the coordinated action of cells from a variety of the mesodermal lineage, including hematopoietic, endothelial, pericytes/vascular smooth muscular, osteogenic, chondrogenic and potentially skeletal muscle. A variety of GFP reporter mice and a new cryohistology technique for non-decalcified bone were used to identify the temporal and spatial appearance of cells within each lineage. The Col3.6GFP reporter, which identifies preosteoblast-early osteoblast cells, provided a template for interpreting the expression of other reporters. Initially, Col3.6 is weakly expressed 4 days after fracture on the periosteum at sites distant from the fracture. As this initial callus expands toward the fracture site, strongly expressed Col3.6+ cells form its base and extend over the bridging domain. The cells are followed by a zone of mineralization and subsequently by the appearance of osteocalcin (OC-GFP) positive cells. By three weeks after the fracture, most of the Col3.6+ cells have been replaced by OC+ cells. This pattern of expression reflects the initial deposition of woven bone and its eventual remodeling to lamellar bone. To characterize the initial cellular events that occur distant to the fracture site, the smooth muscle alpha actin reporter (SMAA-GFP) was combined with Col3.6.

This reporter identifies an early progenitor population with multi-lineage potential, including bone and fat. In the advancing healing cascade, the SMAA+ cells appeared at the leading front of cells, with a gradient of cells in their wake that were double positive, followed by cells that were Col3.6+ only and associated with mineralization. The SMAA+ cells were most abundant in association with small vessels, and appeared to extend into the leading edge of the advancing callus base, suggesting regions of angiogenic-osteogenic coupling. The progression and remodeling of the cartilage component of the callus was assessed by combining a Col2A1 reporter with Col3.6. Four patterns of reporter expression were observed in chondrocytic shaped cells: no GFP; Col2A1+, Col3.6+, and rarely double positive cells. Other markers of lineage and repair are being mapped to this pattern of early osteogenic, chondrogenic, and angiogenic differentiation by introducing additional reporters, immunostaining, and fluorescent in situ hybridization. These techniques are robust in cryohistology, providing an avenue for identifying which cells generate specific molecular signals that control processes of differentiation during fracture repair.

**Disclosures:** C. Ushiku, None.

## M078

**Osteogenic Potential of Human Bone Marrow and Circulating Stro-1+/CD45<sup>low</sup> Cells.** A. H. Undale, B. Srinivasan, S. Khosla. Endocrinology, Mayo Clinic, Rochester, MN, USA.

It has been established that bone marrow contains plastic adherent cells that have osteogenic potential. Although the identification of bone marrow stromal cells based on plastic adherence has become synonymous with the bone marrow stem cell population, there is increasing evidence that non-adherent bone marrow cells also have osteogenic potential. These cells could circulate in peripheral blood due to their non-adherent properties. We have identified circulating cells in peripheral blood expressing osteogenic markers and these circulating osteogenic cells potentially could play a role in bone repair. Following *in vitro* culture, bone marrow mesenchymal stem cells (MSCs) have been shown to be CD34 and CD45 negative (CD34- and CD45-), whereas hematopoietic stem cells (HSCs) are typically CD34 and CD45 positive (CD34+ CD45+). Although *in vivo* data regarding the expression of hematopoietic markers such as CD34 and CD45 on freshly harvested, uncultured MSCs is not very clear, studies done by Deschaseaux et al, showed that freshly isolated human bone marrow mesenchymal cells were CD49a+ and had a CD45<sup>med,low</sup> phenotype (Deschaseaux et al, 2003, *Br J Haematol*). We examined the coexpression of CD45 on the Stro-1+ (mesenchymal stromal cell marker) cells by flow cytometry analysis of freshly isolated bone marrow mononuclear cells (BMMNCs) obtained from healthy human volunteers. Fluorescent-labeled anti-human Stro-1 monoclonal antibody and an anti-human CD45 monoclonal antibody were used to identify surface expression of CD45 on the Stro-1+ BMMNCs. Our data indicates that freshly isolated human bone marrow and peripheral blood cells that are Stro-1+ also express the hematopoietic marker CD45. Based on the intensity of CD45, we identified two populations of the Stro-1+ BMMNCs: CD45<sup>low</sup> and CD45<sup>hi</sup>. Moreover, the Stro-1+/CD45<sup>low</sup> BMMNCs formed mineralized nodules under osteoblastic conditions *in vitro*; by contrast, Stro-1+/CD45<sup>high</sup> cells formed rare mineralized nodules, and Stro-1+/CD45- cells were virtually all positive for the erythroid marker, glycophorin A, and did not form nodules. In summary, we have identified a novel osteoprogenitor population contained within the Stro-1+/CD45<sup>low</sup> fraction of BMMNCs and our data provide a potentially important tool for identifying bone marrow and circulating osteoprogenitors.

**Disclosures:** A.H. Undale, None.

## M079

**Role of ATF4 in Osteoblast Proliferation and Survival.** X. Zhang<sup>\*1</sup>, S. Yu<sup>1</sup>, D. L. Galson<sup>1</sup>, M. Luo<sup>\*1</sup>, J. Fan<sup>\*2</sup>, J. Zhang<sup>1</sup>, Y. Guan<sup>\*3</sup>, G. Xiao<sup>1</sup>. <sup>1</sup>Medicine, University of Pittsburgh, Pittsburgh, PA, USA, <sup>2</sup>Surgery, University of Pittsburgh, Pittsburgh, PA, USA, <sup>3</sup>Department of Physiology and Pathophysiology, Peking (Beijing) University Health Science Center, Beijing, China.

ATF4 (activating transcription factor 4) is essential for bone formation. However, the mechanism of its actions in bone is poorly understood. The present study examined the role for ATF4 in the regulation of proliferation and survival of primary mouse bone marrow stromal cells (BMSCs) and osteoblasts. Results showed that Atf4<sup>-/-</sup> cells display a severe proliferative defect as measured by multiple cell proliferation assays. Cell cycle progression of Atf4<sup>-/-</sup> BMSCs was largely delayed with a significant G1 arrest. Expression of cyclins A1, D1, and D3 was dramatically decreased both at the mRNA and protein level. A similar proliferation defect was observed in Atf4<sup>-/-</sup> calvarial periosteal osteoblasts *in vivo*. Knocking down Atf4 mRNA by small interfering RNA in MC3T3-E1 subclone 4 preosteoblasts markedly reduced expression of the cyclins and cell proliferation. In contrast, overexpression of ATF4 increased cyclin D1 expression as well as cell proliferation. In addition, apoptosis was significantly increased in cultured Atf4<sup>-/-</sup> BMSCs and calvarial periosteal osteoblasts *in vivo* relative to wt controls. Taken together, this study demonstrates that ATF4 is a critical regulator of proliferation and survival in primary BMSCs and osteoblasts.

**Disclosures:** G. Xiao, None.

This study received funding from: NIH and DoD.

## M080

**The Small G-Protein Rap1 Promotes Osteoblast Differentiation.** A. Ueda<sup>1</sup>, T. Hiraga<sup>\*2</sup>, T. Yoneda<sup>1</sup>. <sup>1</sup>Biochem, Osaka Univ Grad Sch of Dent, Osaka, Japan, <sup>2</sup>Histol and Cell Biol, Matsumoto Dental Univ, Nagano, Japan.

The Small G-Protein Rap1 is a family member of Ras with high homology to Ras. Previous studies reported that Ras regulated osteoblast and osteoclast differentiation. On the other hand, the role of Rap1 in bone is still unclear. To study this, we analyzed bones of mice deficient in SPA-1, a GTPase-activating protein which selectively inactivates Rap1. Histomorphometrical examination showed significant increase in trabecular bone volume, mineral apposition rate and bone formation rate in SPA-1-deficient (SPA-1<sup>-/-</sup>) mice compared with wild-type (WT) mice. Ral-GDS pull-down assay showed that Rap1 was markedly activated in primary osteoblasts isolated from the SPA-1<sup>-/-</sup> mice. To further examine the role of Rap1 in osteoblastogenesis, we introduced a constitutive-active (Rap1V12) or a dominant-negative (Rap1N17) mutant of Rap1 into the murine multipotent mesenchymal stem cell line C3H10T1/2 using the adenovirus system. Overexpression of Rap1V12 enhanced BMP2-induced osteoblast differentiation as determined by alkaline phosphatase (ALP) activity, whereas Rap1N17 suppressed it. Moreover, osteoblast differentiation induced by constitutive-active BMPRIIs (ALK3QD and ALK6QD) was enhanced by Rap1V12. Quantitative RT-PCR analysis showed that Rap1V12 increased BMP2-induced mRNA expression of ALP, osteocalcin and bone sialoprotein. Next, we examined the relationship between Rap1 and BMP2-Smad1-Runx2/Osterix pathway. Western blot analysis showed that Rap1V12 had no effect on BMP2-induced Smad1 phosphorylation. ALP staining showed that Rap1V12 could not rescue the osteoblastogenesis suppressed by Smad6, an inhibitory Smad in the BMP2 signaling pathway. Rap1V12 enhanced Runx2-induced osteoblast differentiation. Quantitative RT-PCR analysis showed that Rap1V12 increased Runx2 mRNA expression. On the other hand, Rap1V12 had no effect on osterix-induced osteoblast differentiation despite that Rap1V12 augmented osterix mRNA expression. Finally, we examined the relationship between the BMP2 signaling pathway and Rap1 activation. Ral-GDS pull-down assay showed that Rap1 was activated by BMP2, ALK3QD and ALK6QD. Smad6 showed no effects on Rap1 activation. Western blot analysis showed that Rap1V12 enhanced ERK phosphorylation induced by BMP2, whereas Rap1N17 suppressed it. A MEK inhibitor, U0126, suppressed BMP2-induced osteoblast differentiation. Rap1V12 could not rescue osteoblastogenesis suppressed by U0126. In conclusion, our results suggest that Rap1 plays a critical role in osteoblastogenesis through an enhancement of BMP2-induced osteoblast differentiation via MEK-ERK pathway.

**Disclosures:** A. Ueda, None.

## M081

**Oleuropein from Olive Stimulates the Differentiation and Mineralization of Cultured Osteoblasts and Inhibits the Formation of Osteoclasts in Culture.** K. Hagiwara<sup>\*1</sup>, T. Goto<sup>\*2</sup>, H. Hagiwara<sup>2</sup>. <sup>1</sup>Dept. of Bioscience and Biotechnology, Tokyo Institute of Technology, Yokohama, Japan, <sup>2</sup>Dept. of Biomedical Engineering, Tooin University of Yokohama, Yokohama, Japan.

The polyphenol displays antioxidant and anti-inflammatory properties. In our efforts to identify factors that might cause, prevent, or treat bone metabolic diseases, we screened a numerous polyphenol for the ability to regulate the proliferation, differentiation, and mineralization of osteoblasts, and the formation of osteoclasts. To date, we reported that curcumin, which is an important constituent of rhizomes of the plant *Curcuma longa* Linn, and quercetin, which is one of the major flavonoids in onion, inhibited the proliferation and mineralization of osteoblastic cells and the formation of osteoclasts. Furthermore, both compounds inhibited ovariectomy-stimulated bone resorption in mouse. The present study was designed to evaluate the effects of oleuropein, a main polyphenol of olive, on the formation of bone using cultured osteoblasts and osteoclasts. Oleuropein did not affect the proliferation of MC3T3-E1 cells until 10<sup>-5</sup> M and showed 50% inhibition of vehicle at 10<sup>-4</sup> M with MTT assay. Oleuropein at 10<sup>-5</sup> to 10<sup>-4</sup> M also stimulated the activity of alkaline phosphatase (day 14) and the deposition of calcium (day 18) in a dose-dependent manner at the post-proliferation. By contrast, oleuropein at 10<sup>-5</sup> to 10<sup>-4</sup> M inhibited the formation of multinucleated osteoclasts in a dose-dependent manner. Osteoclasts were formed from splenic cells of 6-week old male mouse by the addition of sRANKL and M-CSF.

Our results indicate that oleuropein might accelerate the formation of bone by stimulation of the proliferation and mineralization of osteoblastic cells and inhibition of the formation of osteoclastic cells. Furthermore, our preliminary examination indicates that this compound slightly inhibits ovariectomy-stimulated bone resorption in mouse. Oleuropein can prevent bone metabolic diseases.

**Disclosures:** H. Hagiwara, None.



## M082

**Development of High-throughput Screening System for Osteogenic Drugs Using Cell-based Sensor.** H. Hojo<sup>\*1</sup>, K. Igawa<sup>1</sup>, S. Ohba<sup>1</sup>, F. Yano<sup>1</sup>, K. Nakajima<sup>\*1</sup>, Y. Komiyama<sup>\*1</sup>, T. Yonezawa<sup>\*1</sup>, J. T. Woo<sup>\*1</sup>, A. C. Lichtler<sup>\*2</sup>, D. W. Rowe<sup>\*2</sup>, T. Ikeda<sup>3</sup>, K. Nakamura<sup>3</sup>, H. Kawaguchi<sup>3</sup>, U. Chung<sup>1</sup>. The Center for Disease Biology and Integrative Medicine, University of Tokyo, Tokyo, Japan, <sup>2</sup>Department of Genetics and Developmental Biology, and Department of Orthopedics, University of Connecticut Health Center, Farmington, CT, USA, <sup>3</sup>Department of Sensory and Motor System Medicine, University of Tokyo, Tokyo, Japan.

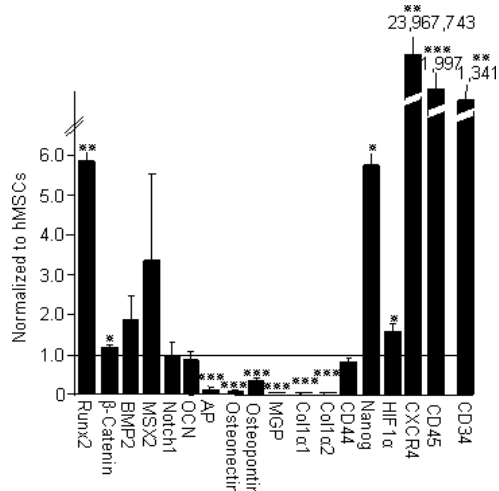
To effectively treat osteoporosis and other bone defects, there is a need for the development of small chemical compounds that potently induces bone formation. The present study initially attempted to establish a monitoring system that could detect osteogenic differentiation in a convenient, reliable, and real-time manner. For this purpose, we established several lines of pre-osteoblastic MC3T3E1 cells stably transfected with GFP reporter gene driven by the 2.3 kb fragment of rat type I collagen promoter (Col1a1GFP-MC3T3E1). Among them, we selected a clone that fluoresced upon osteogenic stimulation by BMP-2. This cell line was confirmed to show an increase in alkaline phosphatase (ALP) staining and osteocalcin (OC) mRNA level in a dose-dependent manner. Using this system, we screened natural and synthetic compound libraries and identified an isoflavone derivative, glabrisoflavone (GI). GI induced GFP fluorescence at 7 days. Treatment with different concentration of GI revealed that GI upregulated the OC mRNA level in a dose-dependent manner; ALP staining concurred with the osteocalcin expression. We next examined the involvement of major osteogenic pathways in GI's action using luciferase reporter plasmids driven by BMP-responsive elements (12XGCCG), Runx2-responsive elements (6XOSE2), and canonical-Wnt-responsive elements (TOPFLASH). GI did not significantly alter these signaling pathways. The mRNA expression level of Id1, Runx2, and Tcf1 were also not altered by GI treatment. In conclusion, we established a high-throughput screening system for osteogenic drugs using Col1a1GFP-MC3T3E1 cells. This system may be useful for identifying novel osteogenic drugs.

**Disclosures:** H. Hojo, None.

## M083

**Expression of Bone-Related Genes by Peripheral Blood CD34 Cells.** U. I. L. Moedder, M. Gössl<sup>\*</sup>, A. Lerman<sup>\*</sup>, S. Khosla. Mayo Clinic, Rochester, MN, USA.

Peripheral blood CD34+ cells, an endothelial/hematopoietic progenitor-enriched cell population, may be involved in the repair of vascular injury. In addition, these cells have been shown to possess osteogenic potential and to express osteocalcin (OCN), suggesting that they may also initiate or modulate vascular calcification. We hypothesized that increases in local calcium (Ca<sup>2+</sup>) concentrations, perhaps related to tissue injury, may induce expression of osteogenic genes by these cells. Thus, we used MACS to isolate CD34+ cells from peripheral blood of 6 normal donors and examined expression of bone-related genes in these cells compared to undifferentiated human mesenchymal stromal cells (hMSCs). We also cultured the CD34+ cells for 5 days in the presence of Ca<sup>2+</sup> (5 mM) followed by an additional 7 days in osteoblast differentiation medium. As shown in the figure, CD34+ cells expressed significantly higher levels of RUNX2 and  $\beta$ -catenin than hMSCs; additional bone-related genes (BMP-2, MSX2, Notch, and OCN) were expressed at levels similar to hMSCs. AP, osteonectin, osteopontin (OPN), MGP, Col1 $\alpha$ 1 and Col1 $\alpha$ 2 were expressed by CD34+ cells at low levels. The stem cell marker, Nanog, was expressed at significantly higher levels in CD34+ compared to hMSCs, whereas CD44, another stem cell marker, was expressed at similar levels. HIF-1 $\alpha$  and the chemokine receptor, CXCR4, both which are involved in homing of cells to ischemic tissues, were expressed at very high levels in the CD34+ cells. CD34+ cells also expressed mRNAs for CD34 and CD45.



Following culture, mRNA expression of CD34 virtually disappeared, and CD45 mRNA

was significantly decreased. Expression of OPN, a non-collagenous bone matrix protein which is known to have chemoattractant properties, increased dramatically (by 35,800-fold) following culture. Of the 6 CD34+ cell samples, the 3 with the highest expression of OCN prior to culture significantly (by 600 fold) upregulated Col1 $\alpha$ 1 expression, whereas the 3 with low OCN mRNA levels did not.

Our data indicate that human circulating CD34+ cells express a spectrum of bone-related genes. Exposure to high Ca<sup>2+</sup> concentrations and osteogenic conditions dramatically upregulates expression of the chemoattractant, OPN, to potentially recruit additional cells for tissue repair. Moreover, the level of OCN expression by CD34+ cells may be a predictor of the ability of these cells to develop an osteogenic phenotype.

**Disclosures:** U.I.L. Moedder, None.

## M084

**Mineralization Potential and Orientational Aspects of Osteogenic Cell Cultures by Raman Spectroscopy.** G. S. Mandair<sup>1</sup>, P. Steenhuis<sup>\*2</sup>, M. D. Morris<sup>1</sup>. <sup>1</sup>Department of Chemistry, University of Michigan, Ann Arbor, MI, USA, <sup>2</sup>Department of Orthodontics and Pediatric Dentistry, University of Michigan School of Dentistry, Ann Arbor, MI, USA.

The aim of this study is to determine, using Raman spectroscopy, whether mineralized bone nodules formed in osteogenic cell cultures is relevant to normal bone. It is known that culturing cells with  $\beta$ -glycerophosphate ( $\beta$ GP) can lead to formation of abiotic mineral as well as normal bone mineral. Spectroscopic procedures were devised to distinguish between bone mineral and suspected abiotic mineral. Osteoprogenitor cells obtained from fetal day 18.5 (FD18.5) mouse calvaria were plated onto fused-silica slides. Confluent cells were cultured in standard osteogenic media containing 10 mM  $\beta$ GP and 1  $\mu$ M dexamethasone for 35 days. The physicochemical composition of the mineralizing cell cultures were assessed using unpolarized Raman spectroscopy. Known spectroscopic markers for mineralization (P-O stretch/collagen amide I band area ratio), carbonation (C-O stretch/P-O stretch band area ratio), and crystallinity (P-O stretch band width) were estimated with standard deviations. Estimates for FD18.5 calvaria and 6-month old mouse tibia were also obtained. Polarized Raman spectroscopy was used to test for orientation of mineralizing bone nodules parallel to the collagen fibril axis. When 10 mM  $\beta$ GP was used, abiotic mineral appeared early in the cell cultures and that apatitic mineral formed in the collagen scaffold later. For example, mineralized bone nodules that first appeared at day 8 were found by unpolarized Raman to be highly carbonated with levels comparable to 6-month old mouse tibia (0.12  $\pm$  0.01). Similar trends were also noted for mineralization, whereas crystallinity at day 28 (17.1  $\pm$  2.1 cm<sup>-1</sup>) was lower compared to FD18.5 calvaria (13.8  $\pm$  0.2 cm<sup>-1</sup>, p  $\leq$  0.001). These results show that carbonated apatite mineral formed during the early stages of the culture period maybe abiotic. Apatitic mineral formed during the later stages appeared to resemble normal bone. However, polarized Raman spectroscopy revealed a mixture of both bone mineral and abiotic mineral phases. Collagen amide I orientation in small spherical nodules was sensitive to polarized Raman scatter and thus was found to be structurally similar to normal bone mineral, whereas collagen orientation in large irregular-shaped nodules was reduced. In conclusion, we demonstrated the feasibility of using polarized and unpolarized Raman spectroscopy to potentially classify mineralized bone nodules formed in osteogenic cell cultures as either normal or abiotic, thus enabling more detailed study of the time course of bone mineralization.

**Disclosures:** G.S. Mandair, None.

This study received funding from: RO1 AR047969.

## M085

**Sirtuin 1 (SIRT1) Is a Regulator of Mesenchymal Stem Cell Lineage Allocation.** E. Cohen-Kfir<sup>\*</sup>, A. Levin<sup>\*</sup>, E. Abramovitz<sup>\*</sup>, J. Lavi<sup>\*</sup>, G. Hamdani<sup>\*</sup>, R. Dresner-Pollak. Endocrinology and Metabolism, Medicine, Hadassah-Hebrew University Medical Center, Jerusalem, Israel.

Osteoblasts originate from progenitor mesenchymal stem cells (MSCs) which can differentiate into several distinct lineages including osteoblasts and adipocytes. Lineage commitment is determined by cell-specific master transcription factors, RUNX2 in osteoblasts and PPARGamma in adipocytes. The regulatory mechanisms of these transcriptional factors are still unknown. Sirtuin 1 (SIRT1), the mammalian ortholog of yeast Sir2 (silent information regulator 2), a key NAD<sup>+</sup> dependent protein deacetylase in aging, is a PPARGamma repressor and inhibits adipogenesis in adipose tissue.

We aimed to investigate whether SIRT1 is a regulator of osteoblastogenesis and adipogenesis from their common progenitor MSC. A murine marrow-derived mesenchymal stem cell line and primary marrow stromal cell cultures obtained from SIRT1-deficient mice were used for *in-vitro* studies. Bone mass and architecture were determined in SIRT1 deficient mice.

SIRT1 in C3HT101/2 cells was modified through retroviral infection with pBABE-SIRT1 for overexpression, and a SIRT1 dominant negative mutant (SIRT1 H355Y) for downregulation. This mutation abolishes deacetylase activity. Cells were induced to differentiate into either osteoblasts or adipocytes using an osteogenic medium or an adipogenic medium, respectively. Primary bone marrow cultures were obtained from SIRT1 haploinsufficient (HET) and wild type (WT) mice. Femurs of 3-month-old female SIRT1 knock-out (KO), HET and WT were analyzed by microCT.

mRNA expression of RUNX2 and osterix was increased by 10 and 20 fold respectively in SIRT1 overexpressing cells compared to C3HT101/2 cells. In cells expressing the mutant SIRT1 a 3 and 4 fold reduction in RUNX2 and alkaline phosphatase mRNA expression compared to SIRT1 overexpressing cells was found. Increased triglyceride accumulation determined by Oil red O staining was observed in mutant SIRT1-transfected cells compared to SIRT1 overexpressing cells. RUNX2 and Osterix mRNA expression was reduced by 50% and PPARGamma was increased by 30% in primary marrow cultures

obtained from SIRT1 HET compared to WT mice. SIRT1-deficient mice were smaller than their HET and WT counterparts, which were similar in size. Trabecular BV/TV was lower by 45% and 34% in KO and HET mice respectively compared to WT mice. Trabecular thickness was reduced by 32% in KO compared to WT, and cortical thickness was reduced in KO and HET by 30% and 25% respectively. SIRT1 plays a regulatory role in osteoblastogenesis, plausibly by affecting the relationship between osteoblastogenesis and adipogenesis from their common progenitor MSC, and may be an important linkage between aging and osteoporosis.

**Disclosures:** R. Dresner-Pollak, MSD 1, 4; Novartis 4; Sanofi Aventis 1. This study received funding from: Israel Science Foundation.

## M086

**Ghrelin Inhibits Early Osteogenic Differentiation of C3H10T1/2 Cells by Suppressing Runx2 Expression and Enhancing PPAR $\gamma$  and C/EBP $\alpha$  Expression.** S. Kim<sup>1</sup>, O. Choi<sup>\*2</sup>, J. Yang<sup>\*3</sup>, S. Cho<sup>\*1</sup>, C. Shin<sup>1</sup>, K. Park<sup>\*1</sup>, S. Kim<sup>\*1</sup>. <sup>1</sup>Department of Internal Medicine, Seoul National University College of Medicine, Seoul, Republic of Korea, <sup>2</sup>Department of Internal Medicine, Seoul National University Boramae Hospital, Seoul, Republic of Korea, <sup>3</sup>Clinical Research Institute, Seoul National University Hospital, Seoul, Republic of Korea.

Ghrelin is a 28-residue peptide identified in the stomach as an endogenous ligand of the growth hormone secretagogue receptor that is expressed in a variety of peripheral tissues, as well as in the brain. In previous studies, ghrelin has been shown to stimulate both adipogenic differentiation from preadipocyte and osteogenic differentiation from preosteoblasts or primary osteoblasts. This study was undertaken to investigate the direct effect of ghrelin on the lineage allocation of mesenchymal stem cells (MSCs). We identified ghrelin receptor mRNA in C3H10T1/2 cells, and we found the levels of this mRNA to be attenuated during osteogenic differentiation. Treatment of cells with ghrelin resulted in both proliferation and inhibition of caspase-3 activity. In addition, ghrelin-treated cells showed an increase in bcl-2 expression and a reduction in cytochrome c release. Moreover, ghrelin inhibited early osteogenic differentiation, as shown by alkaline phosphatase activity and staining, and inhibited osteoblast-specific gene expression by altering Runx2, PPAR $\gamma$ , and C/EBP $\alpha$  protein expression.

**Disclosures:** S. Kim, None. This study received funding from: Seoul National University Hospital (#04-2003-010-0).

## M087

**The Regulation of Osteoblast Differentiation by MicroRNA.** H. Inose, A. Kimura\*, M. Iwasaki\*, K. Shinomiya\*, S. Takeda. Orthopaedic Surgery, Tokyo Medical and Dental University, Tokyo, Japan.

Osteoblastic differentiation from mesenchymal stem cell is a multistep process regulated by several factors including cytokines and hormones. Central to this regulation is the control of gene expression by transcription factors. Recent identification of non-coding small RNAs, i.e., microRNA (miRNA), revealed a novel and important regulatory mechanisms for gene expression and cell differentiation. Therefore, we tried to elucidate the role of miRNAs in osteoblastic differentiation. miRNAs that are differentially expressed upon BMP2 treatment in C2C12 cells were comprehensively analyzed by using microarray. Of the many downregulated miRNAs, we focused on microRNA 206 (miR-206). In line with its expression profile in C2C12 cells, miR-206 expression was gradually decreased along with the osteoblastic differentiation of mouse primary osteoblasts. To address the functional role of miR-206, we overexpressed miR-206 in C2C12 cells or mouse primary osteoblasts and observed a marked inhibition of osteoblastic differentiation as evident by diminished alkaline phosphatase activity and mineralization. Conversely, knockdown of miR206 by siRNA specific for miR206 resulted in an increase in osteoblastic differentiation. Successively, searching potential targets for miR-206 using the Targetscan program revealed Connexin43 (Cx43), a gap junction protein implicated in osteoblast differentiation previously, as one highly probable target. Indeed, miR-206 bound to the 3'UTR of Cx43 genome and inhibited the translation of Cx43 protein. Finally and most importantly, Cx43 overexpression rescued the inhibition of osteoblastic differentiation by miR-206. These results demonstrated that miR-206 regulates osteoblast differentiation physiologically through the modulation of Cx43 expression.

**Disclosures:** H. Inose, None.

## M088

**Activation of FGF Receptors Is a Novel Mechanism by which Extracellular Calcium Stimulates the Proliferation of Osteoblasts.** J. Caverzasio. Service of Bone Diseases, Dept of Rehabilitation and Geriatrics, University of Geneva, Geneva, Switzerland.

Extracellular calcium concentration ([Ca<sup>2+</sup>]<sub>e</sub>) can regulate bone remodelling by acting on osteoclasts and osteoblasts and local changes in [Ca<sup>2+</sup>]<sub>e</sub> may serve as a key coupling factor between bone resorption and formation. The mechanisms by which osteoblasts sense [Ca<sup>2+</sup>]<sub>e</sub> are still unclear. Controversy exist concerning a role of the calcium-sensing receptor (CaR) in mediating changes in osteoblast chemotaxis and proliferation. Beside CaR, effects through autocrine growth factors have been reported but incompletely investigated.

In this study, analysis of transduction pathways involved in cell replication induced by [Ca<sup>2+</sup>]<sub>e</sub> was performed in MC3T3-E1 cells having a high replicative response to this cation. In these cells, CaCl<sub>2</sub> (3-5 mM) induced a 14-16 fold increase in 3H-thymidine uptake and a 2-3 fold increase in cell number. To assess the potential role of transduction pathways activated by growth factor receptors in cell replication induced by CaCl<sub>2</sub>, we investigated the effect of different selective receptor tyrosine kinase (RTK) inhibitors. Of several RTK (FGFR, EGFR, VEGFR, PDGFR) inhibitors tested, only the selective FGFR inhibitor, PD173074, dose-dependently and completely (0.2-1.0  $\mu$ M) blunted cell replication induced by CaCl<sub>2</sub> without influencing basal cell replication. Associated with this effect, CaCl<sub>2</sub> markedly activated FGF2 signaling pathways such as FRS2, PLC $\gamma$ , SHP2, Akt, PKC, PKD, ERK1,2 and p38 MAP kinase. Activation of these pathways by CaCl<sub>2</sub> was already maximal after 2 min incubation and were completely blunted by PD173074. Effects on cell proliferation and activation of FGF2 signaling pathways were also obtained with 0.1 mM gadolinium suggesting the implication of a cation-sensitive like mechanism. Increased cell replication induced by CaCl<sub>2</sub> and FGF2 was associated with decreased alkaline phosphatase activity (ALP), a response also completely prevented by PD173074 but not by other RTK inhibitors. Lower concentrations of CaCl<sub>2</sub> was required to reduce ALP activity compared with those for inducing cell replication suggesting different signaling pathways involved in these responses. Similar effects of the FGFR inhibitor on cell replication and ALP activity induced by CaCl<sub>2</sub> were also observed in C3H10T1/2 pluripotent mesenchymal cells.

In conclusion, results presented in this study indicate that activation of FGFRs mediates cell replication induced by [Ca<sup>2+</sup>]<sub>e</sub> in osteoblast-like cells. The molecular mechanism by which this cation stimulates FGFR signaling remains to be investigated. These data reveal a new mechanism by which [Ca<sup>2+</sup>]<sub>e</sub> may influence the activity of osteoblastic cells.

**Disclosures:** J. Caverzasio, Servier (Courbevoie, France) 3.

## M089

**Icariin Induces Osteogenic Differentiation *in vitro* in a BMP- and Runx2-Dependent Manner and Bone Regeneration *in vivo*.** J. Zhao<sup>\*1</sup>, S. Ohba<sup>\*2</sup>, Y. Komiyama<sup>\*2</sup>, U. Chung<sup>3</sup>, T. Nagamune<sup>\*1</sup>. <sup>1</sup>Department of Chemistry and Biotechnology, School of Engineering, University of Tokyo, Tokyo, Japan, <sup>2</sup>Center for Disease Biology and Integrated Medicine, School of Medicine, University of Tokyo, Tokyo, Japan, <sup>3</sup>Department of Bioengineering, School of Engineering, University of Tokyo, Tokyo, Japan.

To effectively treat bone diseases using bone regenerative medicine, there is an urgent need to develop safe and cheap drugs that can potently induce bone formation. Here, we demonstrate the osteogenic effect of icariin, the main active compound of *Epimedium pubescens*. Icariin induced osteogenic differentiation in pre-osteoblastic MC3T3-E1 cells and mouse primary osteoblasts. Icariin upregulated the mRNA expression levels of the osteoblast marker genes (including osteocalcin, bone sialoprotein and alkaline phosphatase), runt-related transcription factor 2 (Runx2) and inhibitor of DNA-binding 1 (Id-1). The osteogenic effect was inhibited by the introduction of Smad6 or dominant-negative Runx2, as well as Noggin treatment. Furthermore, icariin induced mRNA expression of bone morphogenetic protein (BMP)-4. These data suggest that icariin exerts its potent osteogenic effect through induction of Runx2 expression, production of BMP-4 and activation of BMP signaling. The osteogenic effect of icariin was also confirmed in mouse calvarial bone defect model. Eight-week-old male C57BL/6N mice were transplanted with icariin-calcium phosphate cement (CPC) tablets or CPC only (n=5) and bone regeneration was evaluated at 4, 6 and 8 weeks after the operation. Significant new bone formation was observed in icariin-CPC group at 4w and thickness of new bone increased at 6w and 8w. Obvious blood vessel invasion also occurred in icariin-induced new bone. We are now evaluating the effect of icariin on age-related osteoporosis. The extremely low cost of icariin and its high abundance make it appealing for bone regenerative medicine.

**Disclosures:** J. Zhao, None.

## M090

**A Program of MicroRNAs Control BMP2 Induced Bone Phenotype Development.** Z. Li<sup>\*1</sup>, M. Q. Hassan<sup>1</sup>, A. J. van Wijnen<sup>1</sup>, J. L. Stein<sup>\*1</sup>, C. M. Croce<sup>\*2</sup>, J. B. Lian<sup>1</sup>, G. S. Stein<sup>1</sup>. <sup>1</sup>Department of Cell Biology and Cancer Center, University of Massachusetts Medical School, Worcester, MA, USA, <sup>2</sup>Department of Molecular Virology, Immunology and Medical Genetics and Comprehensive Cancer Center, Ohio State University, Columbus, OH, USA.

BMPs are potent morphogens that activate transcriptional programs for lineage-specific differentiation. How BMP induction of a phenotype is coordinated with microRNAs (miRNAs) that inhibit biological pathways to control cellular processes, remains unknown. Here we show by profiling miRNAs during BMP2 induced osteogenesis of C2C12 mesenchymal cells, that 22 miRNAs (from an array of 318 miRNAs) were downregulated in response to BMP2. These miRNAs were all predicted to target osteogenic signals, including mediators of the Wnt, BMP and FGF signaling pathways (ligands and their receptors), signal transduction cascades (JAK/STAT, MAPK), as well as transcriptional regulators of osteogenesis (including Runx2, Msx2, Dlx3, Smads, TCF/Lef). Thus, BMP2 inhibition of these miRNAs resulted in induced protein levels of osteogenic factors. Two miRNAs representative of these osteogenic pathways were characterized, identifying miR-133 directly targeting *Runx2*, an early BMP response gene essential for bone formation and miR-135 directly targeting *Smad5*, a key transducer of the BMP2 osteogenic signal, controlled through their 3'UTR sequences. Both these miRNAs functionally inhibit differentiation of preosteoblasts by attenuating the Runx2 and Smad5 osteogenic pathways that synergistically contribute to bone formation. In addition our studies reveal that miR-133 which is established as essential for promoting MEF2 dependent myogenesis and proliferation of C2C12 cells, has a second complementary function by inhibiting Runx2 mediated osteogenesis. Our studies show that BMP2 controls bone cell determination by also inducing miRNAs that target muscle genes to suppress C2C12 cell myogenesis. Thus, a novel function for morphogens, as BMP2, is established to promote cell lineage determination by both suppressing alternative phenotypes but mainly by releasing from miRNA inhibition a program of target genes required for differentiation of a tissue-specific phenotype.

**Disclosures:** J.B. Lian, None.

## M091

**The Role of FIP200 in Osteoblast Differentiation.** F. Liu<sup>1</sup>, B. Gan<sup>\*2</sup>, J. Guan<sup>\*3</sup>. <sup>1</sup>BMS department, University of Michigan, Dental School, Ann Arbor, MI, USA, <sup>2</sup>Department of Medical Oncology, Dana-Farber Cancer Institute, Harvard Medical School, Boston, MA, USA, <sup>3</sup>Division of Molecular Medicine and Genetics, Department of Internal Medicine, University of Michigan, Medical School, Ann Arbor, MI, USA.

FAK-family interacting protein of 200kDa (FIP200) is a key signaling node to coordinately regulate various cellular processes. Our previous work identified FIP200 as a novel protein inhibitor for both Pyk2 and FAK. We showed that targeted deletion of FIP200 in the mouse led to embryonic death. It was reported that FIP200 expresses in musculoskeletal system and is critical for myoblast differentiation. To determine whether FIP200 plays a role in the osteoblast differentiation, bone marrow stromal cells were isolated from the femurs of 2 month old FIP200 F/F mice. The cells were treated with the recombinant adenovirus encoding Cre (Ad-Cre) to inactivate FIP200 or a control adenovirus (Ad-lacZ) along with addition of the osteogenic inducers at day 7 of culture. Ad-Cre treatment resulted in an approximately 50% of reduction in the expression of FIP200 as assessed by real time PCR. Osteoblast differentiation was then assessed by the expression of osteoblast differentiation markers (ALP, BSP, OCN) and Alizarin red staining. The expression of above osteoblast differentiation markers was decreased by about 50% in Ad-Cre treated group compared to Ad-LacZ treated group after 7 days osteogenic culture. The Alizarin red staining was decreased by over 75% in Ad-Cre treated cells at day 21. The expression of two critical osteoblast differentiation transcription factors, Runx2 and Osx, was moderately decreased in Ad-Cre treated cells. In the control cells treated with Ad-lacZ, in agreement with other report, the expression of Wnt7b, an endogenous canonical Wnt that plays important role in osteoblast differentiation, was increased at the early differentiation stage and the Dkk2, a Wnt antagonist, which may also suppress the Wnt7b expression, was not significantly upregulated before the Wnt7b expression peaked. Interestingly, in the cells treated with Ad-Cre, Dkk2 mRNA expression was 4-6 folds higher compared with the control group throughout the culture. Conversely, the Wnt7b expression was 4-6 folds lower in these cells. We further determined the role of FIP200 in Wnt signaling utilizing the mouse MEF cells. We found that the Dkk2 mRNA expression level in FIP200<sup>-/-</sup> MEF cells was increased over 20 folds compared to FIP200<sup>+/+</sup> MEF cells. Furthermore, infection of FIP200<sup>-/-</sup> MEF cells with adenovirus encoding FIP200 greatly decreased Dkk2 expression. In conclusion, our data suggests that FIP200 may play a role in osteoblast differentiation by regulating canonical Wnt signaling through the control of Dkk2 expression.

**Disclosures:** F. Liu, None.  
This study received funding from: NIH

## M092

**Effect of a Novel Splice-site Mutation of PHEX Gene During Osteoblast Differentiation.** L. Masi<sup>1</sup>, A. Gozzini<sup>\*1</sup>, S. Sorace<sup>\*1</sup>, I. Tognarini<sup>\*1</sup>, G. Galli<sup>\*1</sup>, S. Parrini<sup>\*1</sup>, I. Pela<sup>\*2</sup>, A. Tanini<sup>\*1</sup>, M. L. Brandi<sup>1</sup>. <sup>1</sup>Internal Medicine, University of Florence, Florence, Italy, <sup>2</sup>Pediatric, University of Florence, Florence, Italy.

X-linked hypophosphatemia (XLH), is a dominantly inherited rickets, characterized by renal phosphate wasting, abnormal vitamin D and PTH metabolism, and defective bone mineralization. The disease is caused by mutations in the PHEX gene (phosphate-regulating gene with homologies to endopeptidases on the X-chromosome), which is located at Xp22.1 and encodes a 749-amino acid protein. PHEX is expressed in various tissues, including bones, and its pivotal role is to cleave and to inactivate phosphatonins. The absence of functional PHEX could lead to the accumulation of phosphaturic factors and/or mineralization inhibitors. We found a novel hemizygous splice-site mutation of PHEX gene in 3 years old female children referring to our Center, affected by XLH and with a negative familial history.

The aim of this study is to evaluate the effect of this kind of mutation on osteogenic differentiation of human mesenchymal stem cells obtained from this patient in order to characterize the molecular mechanisms underlying this nucleotide substitution. Two primary cultures of Human adipose tissue-derived mesenchymal stem cells (PA4 and PA9 cells) were obtained respectively from the patient carrying the mutation and from a healthy child of the same age (control). These cells were used to evaluate the role of PHEX in osteoblastogenesis. PA4 and PA9 cells were isolated from subcutaneous adipose tissue biopsies, characterized by the expression of stem cell surface markers (CD45 and CD105) and induced into the osteoblastic phenotype. After 14 days from induction ALP activity (cytochemical staining), mineralization (light microscopy and calcein staining), and the synthesis and distribution of extracellular matrix proteins (osteopontin, osteocalcin and type I collagen) were monitored. PA4 and PA9 induced cells were highly positive for ALP staining (83% and 85% of positive cells, respectively), with the capability to deposit mineralized matrix. Nevertheless, an impaired mineralization was observed in PA4 cells that compared with PA9 cells deposited an altered calcified matrix not organized into compact nodules and not adhering to the cells. LSCM analysis showed that the osteogenic induction stimulated the synthesis of extracellular type I collagen fibrils at similar level in both primary cell lines. Osteogenic induction was accompanied by an increase of osteopontin expression and by a synthesis ex novo of osteocalcin only in PA9 cells. These results indicate that alterations in the PHEX gene control bone matrix mineralization and this can happen through the regulation of bone proteins' synthesis and deposition.

**Disclosures:** A. Gozzini, None.

## M093

**Permanent FGFR2 Activation Promotes Osteoblast Differentiation in Mesenchymal Stem Cells Through Activation of PKC Signaling.** H. Miraoui<sup>\*1</sup>, C. Dufour<sup>\*1</sup>, Y. Tanimoto<sup>\*2</sup>, K. Moriyama<sup>2</sup>, P. J. Marie<sup>1</sup>. <sup>1</sup>Inserm U606 and University Paris 7, Paris cedex 10, France, <sup>2</sup>Department of Maxillofacial Reconstruction and Function, Tokyo Medical and Dental University, Tokyo, Japan.

One important challenge in skeletal biology is to identify factors and pathways that may be used to increase mesenchymal stem cells (MSC) differentiation into mature osteoblasts. We previously showed that Fibroblast Growth Factor Receptor 2 (FGFR2) activating mutations increase osteoblast differentiation in human Apert craniosynostosis. We therefore hypothesized that permanent activation of FGFR2 may promote MSC osteogenic differentiation. To test this hypothesis, murine C3H10T1/2 cells were stably transfected with wild type (WT-FGFR2) FGFR2, a constitutively activating S252W mutation in FGFR2 (MT-FGFR2) or empty vector (EV). Western blot analysis showed that both constructs increased FGFR2 levels. However, only MT-FGFR2 increased tyrosine phosphorylated FGFR2, indicating sustained activation of the receptor. WT-FGFR2 and MT-FGFR2 slightly increased MSC proliferation but had no effect on cell survival in basal or serum-deprived conditions. WT-FGFR2 and MT-FGFR2 increased by 3-4 fold Runx2 mRNA expression, and increased by 2-fold alkaline phosphatase (ALP), type I collagen (Col1A1) and osteocalcin (Oc) expression, as shown by quantitative PCR analysis. However, MT-FGFR2 induced a more rapid increase in Runx2, ALP and Oc expression than WT-FGFR2. Consistently, MT-FGFR2 induced a greater and sooner increase in ALP staining and in vitro matrix mineralization compared to WT-FGFR2. Both WT-FGFR2 and MT-FGFR2 decreased early or late adipocyte differentiation markers (PPARgamma2, C/EBPalpha, LPL) but had no effect on adipogenesis evaluated by oil red staining at 14 days in the presence or absence of the PPARgamma agonist linoleic acid. Both WT-FGFR2 and MT-FGFR2 decreased Sox9 whereas type X collagen was increased by WT-FGFR2 but not by MT-FGFR2. Western blot analysis showed that both WT-FGFR2 and MT-FGFR2 induced sustained ERK1/2 MAPK phosphorylation, whereas JNK, PI3K or Akt signaling was not affected. Pharmacological inhibition of ERK1/2 decreased MSC proliferation induced by either WT-FGFR2 or MT-FGFR2. However, inhibition of ERK1/2 decreased Runx2, ALP and Oc mRNA expression in WT-FGFR2 but not in MT-FGFR2-transfected cells. Conversely, inhibition of protein kinase C (PKC) reduced Runx2, ALP and Col1A1 mRNA levels in MT-FGFR2, but not in WT-FGFR2 transfected cells. These results provide evidence that sustained FGFR2 activation effectively induces osteogenic differentiation in MSCs which is mainly mediated by PKC signal transduction, thus providing a new mechanism involved in osteogenic differentiation of mesenchymal stem cells.

**Disclosures:** P.J. Marie, None.

## M094

**Heparan Sulfate Proteoglycans Modulate Osteogenic Differentiation through Heparan Sulfate Chains.** A. Kamada<sup>1</sup>, T. Ikeo<sup>1</sup>, Y. Yoshikawa<sup>1</sup>, E. Domae<sup>\*1</sup>, S. Goda<sup>\*1</sup>, I. Tamura<sup>\*1</sup>, A. Kawamoto<sup>\*1</sup>, J. Okazaki<sup>\*1</sup>, Y. Komasa<sup>\*1</sup>, Y. Takaishi<sup>1</sup>, T. Miki<sup>2</sup>, T. Fujita<sup>3</sup>. <sup>1</sup>Osaka Dental University, Osaka, Japan, <sup>2</sup>Osaka City University, Osaka, Japan, <sup>3</sup>Katsuragi Hospital, Osaka, Japan.

Bone cells are regulated by interaction with growth factors and components of the extracellular matrix. Cell surface heparan sulfate proteoglycans (HSPGs), syndecan family and glypican family, are known to bind both other extracellular matrix molecules and certain growth factors, such as fibroblast growth factor (FGF), transforming growth factor (TGF) and bone morphogenetic protein (BMP), thus playing a unique role as a regulator of growth factor behavior. In this study, we investigated the role of HSPG in osteogenic differentiation of murine pro-osteoblastic cell line MC3T3-E1 cells using the HS-degrading endoglycosidase, heparitinase.

Cells were pretreatment with heparitinase or chondroitinase ABC, and were stimulated by ascorbic acid (VC) and beta-glycerophosphate (BGP) to induce osteoblastic differentiation. Mineralization of the cell cultures was detected by von Kossa stain and by Alizarin Red. The mRNA expression level was measured using real-time quantitative RT-PCR.

Enzymatic depletion of the HS chains by heparitinase treatment enhanced the mineralization induced by VC and BGP. VC and BGP-dependent induction of osteocalcin increased significantly by heparitinase treatment compared with non-digested controls ( $p < 0.01$ ).

Heparitinase treatment also enhanced the expression of bone-specific transcription factor Runx2 induced by BMP-2 addition, but not the BMP-2 expression.

These results demonstrate that cell surface HSPGs suppress the mineralization in osteoblasts through HS side chain-mediated binding to BMP-2. Hence the control of cell surface HSPGs may be useful for modulate osteogenic differentiation of osteoblasts.

**Disclosures:** A. Kamada, None.

## M095

**Enhanced Osteogenic Potential of Alveolar vs. Long Bone Derived Marrow Stromal Cells.** T. Aghaloo, O. Bezouglaia<sup>\*</sup>, N. Chaichanasakul<sup>\*</sup>, B. Kang<sup>\*</sup>, R. Franco<sup>\*</sup>, E. Atti<sup>\*</sup>, S. Tetradis. UCLA School of Dentistry, LA, CA, USA.

Systemic and local factors and associated signaling cascades have distinct effects in craniofacial vs. appendicular skeleton, while conditions such as bisphosphonate related osteonecrosis of the jaws (BRONJ), affect only maxillofacial bones. Although substantial evidence suggests differences in homeostasis between alveolar vs. appendicular bone, much of our knowledge concerning alveolar bone (AB) cell function is extrapolated using cells from other skeletal sites. Here, we have established a protocol to reproducibly isolate and culture AB MSCs from the rat mandible and compared them to long bone (LB) MSCs from the same animal.

A needle was inserted into the mandibular alveolar ridge to collect the marrow. Cells were expanded to confluence and passaged for experiments. For control, tibia marrow from the same animals was handled identically. In osteogenic media, both AB and LB MSCs stained for alkaline phosphatase (ALP) and mineralized after 2-3 weeks. To confirm absence of dental pulp/odontoblast contamination, dentin sialophosphoprotein (DSPP) expression was tested, using rat incisor pulp as positive control. Pulp tissue expressed DSPP levels 42,000 fold greater than AB and LB MSC cultures, suggesting that pulp cell contamination of AB MSCs, if any, is minimal. Interestingly, ALP staining was stronger in AB MSCs from the beginning of the culture and continued for the duration of the experiment. Von Kossa staining and [<sup>45</sup>Ca] assays showed increased mineral deposition in AB vs. LB MSCs. Furthermore, AB MSCs demonstrated an 8 fold higher ALP, almost 2 fold higher Cbfa-1 and a slightly higher osteocalcin mRNA expression. Collectively, these data demonstrate that AB MSCs possess a higher osteogenic potential compared to their LB counterparts.

To examine the direct effects of the potent bisphosphonate (BP) zoledronate (ZA) on MSC differentiation, cells were grown in the presence of various ZA doses. ZA similarly affected AB and LB MSCs, where 10<sup>-5</sup> M ZA induced cell death and decreased ALP staining, while 10<sup>-6</sup>-10<sup>-9</sup> M ZA had no effect. MSC response to ZA does not appear to be the determining factor underlying jaw sensitivity to BRONJ. Surprisingly, AB MSCs expressed lower RANKL mRNA levels and a lower RANKL/OPG ratio than LB MSCs, suggesting a decreased osteoclastogenic potential of the AB marrow.

In summary, we have established a reliable and reproducible model for AB MSC isolation and culture. Our results demonstrate that AB MSCs have an increased osteogenic potential compared to their LB counterparts. Moreover, decreased baseline RANKL expression and RANKL/OPG ratio in AB MSCs, suggest lower osteoclastogenic potential. This model provides a useful tool to investigate molecular mechanisms underlying alveolar bone homeostatic mechanisms.

**Disclosures:** T. Aghaloo, None.

This study received funding from: NIH K08 DE 015800 and NIH R01 DE13316.

## M096

**The Age-Related Impairment of IGF-I Receptor Activation Is Associated with Changes in Integrin and SHP-2 Expression.** F. Lima<sup>\*1</sup>, P. Kurimoto<sup>\*2</sup>, B. Boudignon<sup>2</sup>, B. P. Halloran<sup>1</sup>. <sup>1</sup>Endocrine Unit, VA Medical Center, University of California San Francisco, San Francisco, CA, USA, <sup>2</sup>Endocrine Unit, VA Medical Center, San Francisco, CA, USA.

The loss of bone with aging is associated with declines in osteoblast number and in the rate of bone formation. These changes are attributed, in part, to alterations in recruitment, proliferation and differentiation of osteoprogenitors. Insulin-like growth factor-I (IGF-I) promotes osteoprogenitor formation, proliferation, osteoblast formation and survival, and stimulates bone formation. With aging, the anabolic response of bone to IGF-I diminishes. We have shown that the loss of responsiveness is linked to disruption of ligand-induced receptor activation. The level of receptor phosphorylation depends on integrin function and tyrosine phosphatase SHP-2 activity. Loss of function of  $\alpha\beta3$  and  $\beta1$  induced by disintegrins and disruption of SHP-2 activity impair receptor activation and downstream IGF-I signaling. To determine the roles that the integrins and SHP-2 play in the age-related loss of IGF-I receptor responsiveness to ligand we measured expression ( $\alpha\beta3$ ,  $\beta1$  and SHP-2) and association (immunoprecipitation) of the receptor with SHP-2 in bone marrow stromal cells (day 10) from 6-week- (young), 6-month (adult), and 24-month (old) mice. With aging IGF-I receptor expression increased while receptor activation, as judged by degree of phosphorylation, decreased. Expression of mRNA and protein for  $\alpha\beta3$  was lower in cells from older animals by 30-50% while  $\beta1$  expression showed little change. SHP2 expression (+40%) and the association of SHP-2 with the IGF-I receptor (+400%) increased with age. The augmented increase in SHP-2 association would be expected to increase the rate of receptor dephosphorylation and reduce the level of receptor activation. The decrease in integrin expression and the increase in both expression and association of SHP-2 with the receptor (which depends on integrin activation), suggest that the age-related loss of IGF-I receptor responsiveness may be linked to changes in integrin function directly and indirectly through regulation of SHP-2.

**Disclosures:** F. Lima, None.

## M097

**Mapping the Interrelationship of the Adipogenic and Osteogenic Lineage with Visual Reporters.** M. S. Kronenberg<sup>\*1</sup>, J. R. Harrison<sup>2</sup>, D. W. Rowe<sup>1</sup>. <sup>1</sup>Reconstructive Sciences, University of Connecticut Health Center, Farmington, CT, USA, <sup>2</sup>Craniofacial Sciences, University of Connecticut Health Center, Farmington, CT, USA.

The adipocyte and osteoblast lineages are closely related, but the branch point at which these lineages diverge from a common progenitor remains undefined. Previously we developed a series of GFP reporter mice to map osteogenic maturation from preosteoblast (Col3.6weak) to early osteoblast (Col3.6strong) to mature osteoblast (Col2.3 and OC) to osteocyte (DMP1). Here we describe a strategy to monitor the progression of the adipocyte lineage using the FABP4 (aP2) promoter driving GFP. When bone marrow stromal cells from dual Col3.6-Cyan x aP2-Topaz mice were expanded in  $\alpha$ MEM+FCS for 10 days, 17% of the cells were Cyan-positive by flow cytometry. This increased to 38% by day 17 in untreated cultures, suggesting a default differentiation toward the osteoblast lineage. In contrast, adipogenic treatment at day 10 (ADP; 0.5  $\mu$ M rosiglitazone, 1  $\mu$ M insulin) arrested the Col3.6-Cyan population (18%). Following ADP, aP2-Topaz cells appeared within 48 h, scattered between Col3.6-Cyan positive nodules. These cells developed multiple lipid vacuoles that stained with LipidTOX, a vital fluorescent dye. The aP2-Topaz population (7% of total) was equally comprised of both adipocytes and macrophages, the latter identified by CD11b or F4/80 staining. About 10% of the total macrophage population also expressed Col3.6-Cyan. However, there was no evidence for co-expression of Col3.6-Cyan and aP2-Topaz, even as early as 48 hours post-ADP, suggesting that Col3.6-Cyan cells are not adipose progenitors. To assess trans-differentiation, cultures were developed under either osteogenic or adipogenic conditions, then switched at day 17. At this time, scanning fluorescence microscopy of osteogenic cultures showed multiple Col3.6-Cyan colonies with few aP2-Topaz cells while the ADP cultures showed numerous Topaz-positive clusters with smaller interspersed Cyan colonies. When switched to ADP, osteogenic cultures supported a robust induction of aP2-Topaz cells. Cyan-positive colonies failed to expand further, but persisted and mineralized. In contrast, when the ADP culture was switched to osteogenesis, aP2-Topaz colonies faded while the Cyan-positive nodules expanded in size and mineralized. Under both condition, aP2-Topaz and 3.6-Cyan cells were distinct with no evidence of co-expression or trans-differentiation. These data suggest that our cultures support commitment of osteoblast and adipocyte progenitor cells that require additional signals for terminal differentiation. Development of reporters that focus on genes upstream of the Col3.6 and aP2 activation stages is currently underway.

**Disclosures:** M.S. Kronenberg, None.

## M098

**BMP/Wnt Antagonists Are Upregulated by Dexamethasone in Osteoblasts and Reversed by Alendronate and PTH: Potential Therapeutic Targets for Glucocorticoid-Induced Osteoporosis.** T. Yamaguchi, K. Hayashi\*, S. Yano, M. Yamauchi, M. Yamamoto\*, T. Sugimoto. Internal Medicine 1, Shimane University Faculty of Medicine, Izumo-shi, Shimane, Japan.

Glucocorticoid-induced osteoporosis (GIO) is known to be caused by suppression of osteoblast-mediated osteogenesis, and to be effectively treated by bisphosphonate and parathyroid hormone (PTH). However, the exact mechanisms by which glucocorticoid suppresses osteoblast function, or alendronate and PTH alleviate GIO are still unclear. We used osteoblastic MC3T3-E1 cells in order to clarify these mechanisms. Dexamethasone (Dex) (10<sup>-7</sup>M) significantly inhibited cell growth and proliferation, which were shown by cell counting and BrdU incorporation, respectively. Dex (10<sup>-9</sup>-10<sup>-7</sup> M) also strongly and dose-dependently suppressed mineralization of the cells. Dex (10<sup>-7</sup> M) reduced mRNA expression of type I collagen and osteocalcin. On the other hand, Dex (10<sup>-7</sup> M) increased mRNA expression of bone morphogenetic protein (BMP) antagonists, follistatin and Dan, and mRNA expression of a Wnt antagonist, secreted frizzled-related protein (sFRP) and a Wnt signal inhibitor, axin-2, while concomitantly decreased mRNA expression of Runx2, downstream of the BMP signal pathway. Moreover, pretreatments with alendronate (10<sup>-8</sup> M) or human PTH (1-34) (10<sup>-8</sup> M) totally or partially antagonized not only the Dex-induced enhancement in mRNA expression of follistatin/Dan and sFRP/axin-2 but also the Dex-induced reduction in Runx2 mRNA expression and mineralization. The present study shows that Dex suppresses the Wnt and BMP pathways by enhancing the expression of BMP and Wnt antagonists, suggesting that glucocorticoids can modify osteoblastic differentiation and activity through these pathways. The effect of bisphosphonate and PTH on the cancellation of these processes may partly explain their anti-GIO pharmacologic efficacy.

**Disclosures:** T. Yamaguchi, Merck & Co. 3.

## M099

**Regulation of Runx2 Function in Osteoblasts by Sex Steroid Receptors.** S. K. Baniwal<sup>1</sup>, O. Khalid<sup>\*2</sup>, D. Purcell<sup>\*2</sup>, N. LeClerc<sup>\*1</sup>, Y. Gabet<sup>\*1</sup>, M. Stallcup<sup>\*2</sup>, G. Coetzee<sup>\*2</sup>, B. Frenkel<sup>1</sup>. <sup>1</sup>Institute of Genetic Medicine at Keck School of Medicine, Los Angeles, CA, USA, <sup>2</sup>Norris Cancer Center, Los Angeles, CA, USA.

Osteoblasts from either gender harbor receptors for estrogens (ER) and androgens (AR) through which sex steroids manifest their protective effects on the skeleton. We hypothesize that these beneficial effects are mediated, at least in part by directly influencing the function of Runx2, a master regulator of osteoblast differentiation. Fluorescence microscopy and co-IP experiments revealed hormone-dependent ER $\alpha$ -Runx2 and AR-Runx2 complexes in the Osteoblastic MC3T3-E1 cells. Runx2 binding was mapped to more than one domain in the ER $\alpha$  and AR by GST pull-down assays. As GST fusion baits, the DNA or ligand binding domains (LBD) of either AR or ER $\alpha$  bound *in vitro* translated Runx2; binding to LBD were correspondingly ligand dependent. Furthermore, deletion analyses of Runx2 indicated multiple contact points (in regions aa 176-303; 408-596) to bind DNA binding domains of ER $\alpha$  and AR.

As a consequence of these interactions the transactivational property of Runx2 was strongly repressed by both ER $\alpha$  and AR in transiently transfected COS7 cells and in MC3T3-E1 cells expressing them endogenously. Interestingly, in MC3T3-E1 cells the repression was only detectable during late developmental stages, when the expression of osteocalcin, a known Runx2 target gene, otherwise peaks. On the other hand, ER $\beta$  did not repress Runx2 activity despite being as active as ER $\alpha$  in transient transactivation assays. Additionally, transcriptionally inactive mutants of ER $\alpha$  and AR fully repressed Runx2 activity, indicating that the repression was not caused by proteins whose expression is ER $\alpha$  or AR dependent. Our results, and the fact that Runx2 over-expression in mice causes high-turnover osteoporosis, suggest that bone loss after sex steroid withdrawal is attributable to the unleashing of otherwise restrained Runx2 activity. Consistent with this notion, a selective estrogen receptor modulator (SERM), tamoxifen partially mimicked E2-mediated Runx2 inhibition, while a selective estrogen receptor down-regulator (SERD) ICI-182780 had the opposite effect, possibly explaining their respective influences on bone. Given the central role of ER $\alpha$ , AR and Runx proteins in osteogenesis and in cancer biology, present investigation will improve our understanding and set the stage for novel drug development to treat osteoporosis and sex hormone-driven cancers.

**Disclosures:** S.K. Baniwal, None.

This study received funding from: DK071122 to BF and CA109147 to GAC from the National Institutes of Health; W81XWH-05-1-0025 to BF and W81XWH-04-1-0823 and W81XWH-07-1-0067 to GAC from the Department of Defense; and by awards from the Prostate Cancer Foundation to GAC.

## M100

**The Challenge of Continuous Exogenous Glucocorticoid Administration in Mice.** M. Herrmann<sup>\*1</sup>, H. Henneicke<sup>\*1</sup>, J. Street<sup>\*1</sup>, J. Modzelewski<sup>\*1</sup>, F. Buttgerit<sup>\*2</sup>, C. R. Dunstan<sup>1</sup>, H. Zhou<sup>1</sup>, M. J. Seibel<sup>1</sup>. <sup>1</sup>Bone Research Program, ANZAC Research Institute, Concord, Australia, <sup>2</sup>Charite Universitätsmedizin, Berlin, Germany.

Experimental investigation of the effects of glucocorticosteroids on bone often requires continuous exogenous dosing to animals. However, administering steroid hormones at a constant delivery rate and thus attaining and maintaining elevated hormone levels over time can be a challenge. This study compares the efficacy of three different methods of continuous glucocorticosteroid administration in achieving sufficient and constant drug delivery. Corticosterone (CS) was administered to CD1 Swiss White mice by (i) subcutaneous injection, (ii) subcutaneous implantation of slow-release pellets (Innovative Research, nominally 21 day release), and (iii) subcutaneous implantation of micro-osmotic slow-release pumps (Alzet). Serial blood samples were taken to determine changes in plasma CS and serum osteocalcin (OC) levels; the latter are known to readily decrease in response to supra-physiological levels of CS. A single subcutaneous injection of CS at a dose of 10 mg/kg resulted in peak plasma CS levels of 1800  $\pm$  800 ng/mL after 1h. Plasma CS levels returned to baseline at 4h, while serum OC levels became suppressed within 1h and remained so for  $\geq$  12 h. In contrast, a single subcutaneous injection of 2 mg/kg had no effect on circulating CS or OC levels. The implantation of slow-release pellets (10 mg/pellet) induced a significant rise in circulating CS within 24 h. However, plasma CS levels returned to baseline within 7 days. Serum OC levels fell rapidly on day 1 and remained suppressed for the next 7 days. Replacement of pellets after 7 and 14 days restored elevated CS plasma levels and maintained suppressed serum OC concentrations. Delivery of CS through micro-osmotic pumps had no significantly effect on CS or OC plasma levels, indicating insufficient drug delivery, independent of the carrier solution (ethanol, polyethanolglycol or dimethylsulfoxide). We conclude that slow-release pellets, at a dose of 10 mg/pellet, achieve medium-term CS delivery in mice although replacement is required after 7 days to maintain elevated CS levels. None of the methods tested provided CS delivery at a constant rate and results need to be interpreted against the background of continually varying blood levels.

**Disclosures:** M. Herrmann, None.

## M101

**Effects of Alendronate and Raloxifene on the RANKL/OPG System in Primary Cultures of Human Osteoblasts.** M. Giner<sup>\*1</sup>, M. J. Rios<sup>\*2</sup>, M. J. Montoya<sup>\*2</sup>, M. A. Vazquez<sup>\*2</sup>, L. Najj<sup>\*1</sup>, R. Pérez-Cano<sup>\*3</sup>. <sup>1</sup>Medical., University Hospital Virgen Macarena, Seville, Spain, <sup>2</sup>Medical., University Seville, Seville, Spain, <sup>3</sup>Medical., University Hospital Virgen Macarena and University Seville, Seville, Spain.

The OPG/RANKL system is considered as one of the effector ways of communication between osteoblasts (OB) and osteoclasts, modulating the process of bone remodeling. Hormones such as estrogens and vitamin D influence bone remodeling by acting through receptors in the OB.

Alendronate (ALE) and Raloxifene (RX) are anti-reabsorptive drugs which have been demonstrated to be efficient in reducing the risk of osteoporotic fractures. It is known that they reduce the activity of bone remodeling and increase BMD. However, it is not known if they can exert a direct effect in hOB on the RANKL/OPG system.

**Objective:** To evaluate the effect of ALE and RX on OPG production as well as OPG and RANKL expression in primary cultures of human osteoblasts (hOB), comparing osteoporotic patients with a control group of patients affected by arthrosis.

**M & M:** Cell cultures of hOB were obtained from bone biopsies of 33 patients who had had an arthroplasty, 17 were due to osteoporotic hip fracture (OP) and 16 due to arthrosis (AR). The levels of OPG secretion (ELISA) and OPG and RANKL expression (RT-PCR) were quantified in basal conditions, and after incubation with ALE (10<sup>-6</sup>M), RX (10<sup>-7</sup>M) or 17-beta estradiol (E) (10<sup>-7</sup>M), for 24h. The statistical significances were determined by Student's *t*-test and ANOVA.

**Results:** OPG secretion in hOB cultures was higher in patients with OP (7.5  $\pm$  5 pmol/L) than those with AR (4.1  $\pm$  3.1 pmol/L), and remained significantly higher in all conditions of the study (*p*<0.05). The treatment with E, ALE or RX did not change the secretion levels of OPG in either of the two groups studied.

The OP group was more sensitive to treatment, in this group we observed an increase in the OPG expression after being treated with RX (34%  $\pm$  18; *p* = 0.038) and E (37%  $\pm$  19; *p* = 0.019) respect basal condition and also we found an increase in the expression of RANKL with RX about 60% (*p* = 0.013) and with ALE about 118% (*p* = 0.05) respect basal condition. No significant differences were found between OP and AR group in the expression of RANKL.

The RANKL/OPG mRNA ratio was higher in OP than AR patients under all conditions studied and become significantly higher after treatment with RX (*p* = 0.02). In the OP group, the ratio RANKL/OPG was increased significantly after treatment with ALE (112%, *p* = 0.048) and after treatment with RX (60%, *p* = 0.017).

**CONCLUSIONS:** These results indicate a direct action of alendronate and raloxifene, to the concentrations used on primary hOB cultures isolated from osteoporotic patients, and said drugs are able to modulate the OPG/RANKL system. This fact can have repercussions in patients' bone remodeling.

**Disclosures:** M. Giner, None.

## M102

**Glucocorticoid-Induced Bone Loss in Mice Is Dependent on Beta 2-adrenergic Signaling.** Y. Ma<sup>\*1</sup>, J. Nyman<sup>2</sup>, F. Elefteriou<sup>1</sup>. <sup>1</sup>Vanderbilt Center for Bone Biology, Dpt of Medicine, Vanderbilt University, Nashville, TN, USA, <sup>2</sup>Vanderbilt Center for Bone Biology, Dpt of Orthopaedics, Vanderbilt University, Nashville, TN, USA.

High dose glucocorticoids used as anti-inflammatory and immunosuppressive agents cause bone loss by promoting osteoclastogenesis and bone resorption and by inhibiting bone formation. Beta 2-adrenergic receptor ( $\beta$ 2AR) stimulation by norepinephrine released by nerve terminals and the non-selective  $\beta$ 1/ $\beta$ 2AR agonist isoproterenol leads to a similar outcome, i.e. increased bone resorption and decreased bone formation. Based on this observation, we hypothesized that glucocorticoid receptor and  $\beta$ 2AR signaling may share a common pathway. Using mouse calvaria primary osteoblasts, we found that dexamethasone induces a significant increase in *Adrb2* mRNA expression,  $\beta$ 2AR protein expression and isoproterenol-induced cAMP accumulation, demonstrating that dexamethasone promotes  $\beta$ 2AR signaling in osteoblasts in vitro. These findings and our previous studies thus led us to hypothesize that glucocorticoids induce bone loss by increasing the responsiveness of osteoblasts to the anti-osteogenic action of the sympathetic nervous system in vivo. If this hypothesis is correct, we reasoned that mice lacking  $\beta$ 2AR should be resistant to glucocorticoid-induced bone loss. Two month-old  $\beta$ 2AR-deficient mice and wildtype (WT) littermates were thus treated with control or prednisolone pellets (2.1 mg/kg/day) for two months and their skeletons analyzed by 3D-microtomography and histomorphometry. In this model of genetic  $\beta$ 2AR blockade, prednisolone treatment had no significant effect on bone mass, while in WT mice it induced a significant decrease in bone volume over tissue volume. These results suggest that glucocorticoid-induced bone loss is dependent on  $\beta$ 2AR signaling, and that pharmacological blockade of  $\beta$ 2AR signaling may have a protective effect on bone mass in patients taking high dose glucocorticoids.

**Disclosures:** Y. Ma, None.

## M103

**Cis-Regulatory Motifs and Computationally-Derived Transcriptional Networks Predict Dynamic Motions for Osteocytes.** A. K. Dean<sup>\*1</sup>, W. Yang<sup>2</sup>, M. A. Harris<sup>2</sup>, J. Gluhak-Heinrich<sup>\*3</sup>, L. F. Bonewald<sup>4</sup>, D. W. Rowe<sup>5</sup>, I. Kalajzic<sup>6</sup>, J. Ruan<sup>\*1</sup>, S. E. Harris<sup>2</sup>. <sup>1</sup>Computer Science, University of Texas at San Antonio, San Antonio, TX, USA, <sup>2</sup>Periodontics, University of Texas Health Science Center, San Antonio, TX, USA, <sup>3</sup>Orthodontics, University of Texas Health Science Center, San Antonio, TX, USA, <sup>4</sup>Oral Biology, University of Missouri at Kansas City, Kansas City, MO, USA, <sup>5</sup>University of Connecticut Health Center, Farmington, CT, USA, <sup>6</sup>University of Connecticut Health Center, Farmington, CT, USA.

Osteocytes are thought to regulate load induced new bone formation. Gene expression profiles were obtained from osteocytes purified from calvariae of 5 day mice expressing 8kbDMP1 promoter driving GFP. Comparison of the GFP+ve osteocytes with the GFP-ve cells show osteocytes express genes and transcription factors (TFs) known to control muscle differentiation. Over 12 myosin related genes are enriched in the GFP+ve osteocytes, as well as TFs, myogenin, Mef2c, and Myf5. Enrichment for muscle and contractile related genes had a  $P < 0.05$ . We determined evolutionarily conserved and enriched TF binding sites in 5Kb flanking the transcription start site of 505 genes in the GFP+ve dataset. Within this dataset, 18 TF binding sites were enriched ( $p < 0.005$ ) including muscle related cis-motifs, Ets, Smad3, and FoxO1/4 sites. Using the Q-cut clustering algorithm, 15 gene clusters were formed from 290 of the 505 genes based on presence of enriched TF binding sites. These data were used to construct a gene network of the 290 genes and their cis-regulatory motifs. Many of the muscle and contractile related genes have conserved Mef2 and myogenin/MyoD cis-motifs, as also seen in muscle regulated genes.

As Dentin Matrix Protein1/DMP1 is highly expressed in osteocytes and Sost/sclerostin is a marker for late osteocytes and as both are regulated by mechanical load (Dmp1 is increased and Sost is decreased), a focused analysis of their cis-regulatory 5Kb regions was undertaken. The DMP1 gene has a cluster of 5 CREB binding sites related to PKA signaling. Within 200bp of these CREB sites, clusters of Mef2 and MyoD, Ets and FoxO1/4 cis-elements are located in the DMP1 5Kb region. (Similar conserved Mef2, MyoD and Ets cis-element modules are in Spp1 also.) In the 5kb region of the Sost gene, a muscle related cis-element pattern was also noted. One module at the -170 to 360 region contains 5 Mef2 and 1 MyoD conserved cis-elements, and another at -1650 to -1240 contains 1 Mef2 and 4 myogenin cis-elements. This highly conserved clustering of muscle related cis-regulatory elements in osteocyte selective/specific genes support the concept that a muscle related gene network is important in osteocyte biology and may play a role in contractility and dynamic movements of the osteocyte.

**Disclosures:** A.K. Dean, None.

This study received funding from: NIH P01 AR46798

## M104

**Analysis of CXCR7-Deficient Mice Reveals CXCR7 Expression in Osteocytes But No Apparent Bone Phenotype.** H. Gerrits<sup>\*</sup>, K. J. Decherer<sup>\*</sup>, N. E. C. Bakker<sup>\*</sup>, D. S. Ingen Schenau<sup>\*</sup>, M. A. M. Krajnc-Franken<sup>\*</sup>, J. A. Gossen<sup>\*</sup>. N.V. Organon, part of Schering-Plough Corporation, Oss, Netherlands.

CXCR7 is a G-protein coupled receptor that was recently de-orphanized and shown to have SDF1 and I-TAC as high affinity ligands. Microarray analysis of BMP2 induced osteogenesis in C2C12 cells revealed CXCR7 upregulation during osteoblast differentiation. Here we describe the characterization of CXCR7-deficient mice that were generated to further investigate the function of this receptor in vivo. Expression analysis using a LacZ reporter knockin revealed that postnatally *Cxcr7* was specifically expressed in osteocytes of the bone, cardiomyocytes, vascular endothelial cells of the lung and heart, and in the cerebral cortex. Adult tissues revealed high expression in osteocytes and cardiomyocytes. The observation that 70% of the *Cxcr7*<sup>-/-</sup> mice died in the first week after birth coincides with expression of *Cxcr7* in vascular endothelial cells and in cardiomyocytes. An important role of CXCR7 in the cardiovascular system was further supported by the observation that hearts of the *Cxcr7*<sup>-/-</sup> mice were enlarged, showed myocardial degeneration and fibrosis of postnatal origin, and hyperplasia of embryonic origin. Despite high expression in osteocytes no apparent bone phenotype was observed, neither in combination with ovariectomy nor orchidectomy. Although it can not be excluded that the function of CXCR7 in osteocytes is prone to redundancy or masked by compensatory mechanisms, our data indicate that CXCR7 does not seem to play an important role in bone.

**Disclosures:** H. Gerrits, None.

## M105

**SDF-1 is Expressed in Osteocytes and Periosteal Cells in Response to Mechanical Loading.** A. B. Castillo<sup>1</sup>, P. Leucht<sup>\*2</sup>, J. Tang<sup>\*3</sup>, J. A. Helms<sup>\*2</sup>, C. R. Jacobs<sup>1</sup>. <sup>1</sup>Mechanical Engineering, Stanford University, Stanford, CA, USA, <sup>2</sup>Department of Surgery, Stanford University, Stanford, CA, USA, <sup>3</sup>Bone and Joint Research and Rehabilitation Center, Veterans Affairs Medical Center, Palo Alto, CA, USA.

Bone's response to mechanical loading involves activation of bone-lining cells at the periosteal and endosteal surfaces and recruitment of multipotent mesenchymal stem cells (MSCs) in the marrow. The mechanisms by which bone cell progenitors sense and respond to mechanical loading remain largely unknown. Stromal cell-derived factor-1 (SDF-1) and its receptor, CXCR4, are important signaling molecules in MSC survival, migration and proliferation, and have been shown to play important roles in hematopoiesis, angiogenesis and stem cell mobilization. SDF-1 is a soluble factor produced by stromal cells, osteocytes and osteoblasts. CXCR4 is a seven-pass membrane bound receptor expressed in MSCs, hematopoietic stem cells, osteoblasts and osteoclasts. SDF-1 may play a role in recruitment of progenitor cells to regions of active bone remodeling in response to mechanical loading. Right ulnae in 20-wk-old C57BL/6 mice were subjected to compressive axial loading (120 cycles, 2 Hz, 3N) while left ulnae served as internal controls. Animals were sacrificed 24h post-loading, and ulnae were processed for in situ hybridization using DIG-labeled SDF-1 and CXCR4 antisense RNA probes. In addition, multipotent C3H10T1/2 cells were grown in monolayer and subjected to either oscillatory fluid flow (OFF) (10 dynes/cm<sup>2</sup>, 1 Hz) or static conditions for either 1h or 3h, and SDF-1 and CXCR4 message was quantified by qRT-PCR. In vivo mechanical loading resulted in more broadly expressed SDF-1 in the periosteum and cortical osteocytes (Fig. 1). Three hours of OFF resulted in a 20-fold increase in CXCR4 mRNA expression ( $p = 0.05$ ) in C3H10T1/2 cells by one-way ANOVA; SDF-1 mRNA expression was not significantly affected after 1h and 3h of OFF. Taken together, these data suggest that mechanical loading of bone can result in activation of the SDF-1/CXCR4 pathway, which may ultimately play a role in progenitor recruitment.

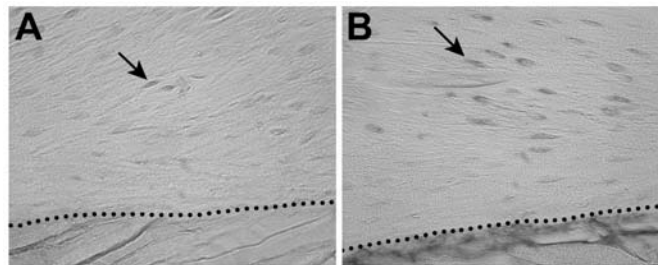


Fig. 1. In situ hybridization analysis of SDF-1 in 20-wk-old mouse ulnar cortical bone at midshaft. (A) Non-loaded control ulna showing cortical osteocytes (arrow) and the periosteal surface (dotted line). (B) Loaded ulna showing SDF-1 positive cortical osteocytes (arrow) and prominent expression in periosteal cells (purple).

**Disclosures:** A.B. Castillo, None.

This study received funding from: NIH AR045989, Air Force FA9550-04-1-0075.

## M106

**Molecular Phenotyping of Osteoblastic and Osteocytic Cell Fractions Isolated from Mouse Calvaria.** G. Guiglia\*, I. Kramer\*, M. Kneissel, C. Halleux. Novartis Institutes for BioMedical Research, Basel, Switzerland.

Osteocytes are the terminally differentiated cells of the osteoblastic lineage embedded within the mineralized bone matrix and interconnected with each other and with cells on the bone surface via an extensive canalicular network. They have been identified as critical regulators of mineral homeostasis and are thought to be the key players in mechanotransduction. Furthermore they appear to have a central role in the mediation of bone anabolism, since they secrete the potent bone formation inhibitor *Sost*. Yet, their cellular and molecular functions are poorly characterized because of the technical hurdles to isolate these cells. In the present study, we aimed at establishing a protocol for isolation of mouse primary osteocytes. To this end calvariae were isolated from 6 day-old C57BL/6J pups and subjected to sequential digestion with 0.2% collagenase type IV and 5 mM EDTA. Seven fractions were obtained and the cell number was determined in each fraction. The cell number decreased from  $1-2 \times 10^6$  cells in fraction 1 and 2 and  $3.5 \times 10^6$  cells in fraction 3 to  $2-3 \times 10^5$  cells in fraction 5 and 6. Based on the relative cell size observed during cell counting, different types of cells were found to be enriched in different digestion fractions. Fraction 1 consisted mainly of cells with a relatively small cell size, potentially fibroblastic cells, whereas larger-sized cells, putative osteoblastic and osteocytic cells, were present in later fractions. Total RNA was isolated from each fraction using TRIzol reagent (Invitrogen). Real-time PCR was performed to quantitatively determine mRNA levels for selected osteoblastic and osteocytic marker genes. The osteoblastic marker genes *bone sialoprotein*, *osteocalcin* and *procollagen type I* were highest in fraction 2 with 9-, 5-, and 2-fold increase in expression compared to fraction 1, respectively. Expression of these osteoblastic markers gradually decreased in further fractions and was at least 2-fold higher in fraction 2 than in fraction 5. Expression of the osteocytic markers *Dmp1*, *Mepe*, *PheX* and *Sost* peaked in fraction 5 with 20-, 14-, 12- and 16-fold increase in expression compared to fraction 1, respectively. In summary, different bone cell types can be isolated from mouse calvariae by sequential digestion. Cell size and osteoblast/osteocyte marker gene expression suggest that fraction 2 is highly osteoblast and fraction 5 osteocyte enriched. This simple isolation protocol allows hence for further studies of the differential gene expression profile of osteoblastic and osteocytic cells.

**Disclosures:** C. Halleux, None.

## M107

**Estrogen Deficiency Alters the Localized Material Properties of the Peri-Lacunar Bone Matrix in Old Rats.** D. P. Nicoletta<sup>1</sup>, W. Yao<sup>2</sup>, N. Lane<sup>2</sup>. <sup>1</sup>Materials Engineering, Southwest Research Institute, San Antonio, TX, USA, <sup>2</sup>Aging Center, Medicine and Rheumatology, University of California at Davis Medical Center, Sacramento, CA, USA.

Loading of the skeleton increases bone mass and decreases bone turnover while unloading increases bone turnover and reduces bone mass. Also, estrogen deficiency and aging increases the activation of new remodeling units, resulting in a reduction in trabecular architecture and bone mass such that bone fractures with very little trauma. Osteocytes are ideally situated to sense mechanical strain (or a lack of strain) and to translate mechanical signals into biochemical signals that regulate bone turnover. Macroscopic bone strains are amplified at the level of the osteocyte due to the strain concentrating effect of the osteocyte lacuna and the surrounding extracellular matrix [1]. The osteocyte can modify its local peri-lacunar matrix environment as a function of hormone treatment [2] and skeletal loading [3]. We have shown that the amount of mechanical strain acting on osteocytes is a function of the properties of the peri-lacunar bone matrix; decreased peri-lacunar bone matrix modulus results in increased lacuna strain while an increase in peri-lacunar bone matrix modulus results in a decrease in lacuna strain [4]. We measured the the peri-lacunar bone matrix elastic modulus associated with osteocytes within trabecular bone from 10 month old OVXed rats (110 days post-ovx, n=3) and sham-operated controls (n=3) using a nano-indenter (Triboscope, Hysitron, Inc.) operating in the modulus mapping mode (3 lacuna/rat). Using this method, an imaged derived from the mechanical properties of the bone matrix surface was generated and microstructural spatial differences in bone tissue elastic modulus were quantified in an ROI of 20 microns around the osteocyte lacunae. Elastic modulus in OVXed rats 2-3 microns from the osteocyte lacuna ( $36.0 \pm 2.8$  GPa) was increased by 35% compared to matrix more than 10 microns from the lacunae ( $26.7 \pm 1.7$  GPa) ( $p < 0.05$ ). There was no increase in the peri-lacunar bone tissue stiffness in sham operated animals ( $24.2 \pm 3.02$  vs.  $23.8 \pm 3.75$  GPa). Based on our previous work [4], this suggests that this stiff peri-lacunar bone tissue attenuates the strain signal acting on embedded osteocytes. Thus, given equal skeletal forces, osteocytes in the OVXed animals would experience less mechanical strain than osteocytes in sham operated animals, which may lead to increased bone turnover and decreased bone mass. Additional studies are needed to determine if the mechanical strain at the osteocyte is altered after treatment with bone active agents. 1. Nicoletta et al., J. Biomech., 39:9, 2006. 2. Lane et al., JBMR, 21:3, 2006. 3. Rubin et al., J. Orthop. Res., 17:3, 1999. 4. Bonivitch et al., J. Biomech., 40:10, 2007.

**Disclosures:** D.P. Nicoletta, None.

This study received funding from: NIH: NIAMS, NIA.

## M108

**Kinase Activation and Osteocyte Survival Promoted by Mechanical Stimulation Require LRP5/6 Signaling and Beta-catenin Accumulation, but not beta-catenin/TCF-Dependent Transcription.** M. Martin-Millan, L. I. Plotkin, K. Vyas\*, G. Frera\*, A. R. Gortazar\*, M. Almeida, S. C. Manolagas, T. M. Bellido. Department of Internal Medicine, University of Arkansas for Medical Sciences, Little Rock, AR, USA.

Osteocyte viability is a critical determinant of bone strength and it is promoted by both mechanical stimulation and activation of the Wnt signaling pathway. Thus mechanical stimulation inhibits apoptosis of osteocytes *in vitro*. Conversely, skeletal unloading increases osteocyte apoptosis in mice. Moreover, genetic models of increased Wnt signaling (mice deficient in the Wnt antagonist secreted frizzled related protein-1 or expressing the high bone mass LRP5 mutant G171V) exhibit decreased osteocyte apoptosis; and Wnts inhibit osteoblastic cell apoptosis *in vitro*. Furthermore, activation of T-cell factor (TCF), the main transcription factor induced by Wnt/beta-catenin, in osteocytes is one of the early responses of bone to loading. Based on evidence that both mechanical stimulation and activation of the Wnt signaling pathway promote osteocyte survival by a mechanism that requires activation of ERKs, we explored here the possibility that Wnt/beta-catenin signaling is required for the transduction of mechanical forces into survival kinase signaling and anti-apoptosis in osteocytic cells. Biaxial stretching of MLO-Y4 cells at 5% elongation for 10 min (Flexercell Strain Unit FX4000) induced activation and nuclear accumulation of ERKs and prevented glucocorticoid-induced apoptosis. Stretching also induced phosphorylation, and thereby inactivation, of GSK3beta and the consequent accumulation of beta-catenin, as detected by Western blot analysis. Furthermore, overexpression of DKK1, an antagonist that blocks Wnt activation by binding to LRP5/6 Wnt co-receptors, or overexpression of axin2, a molecule that induces beta-catenin proteasomal degradation, abolished ERK nuclear translocation as well as the anti-apoptotic effect of stretching. Remarkably, however, and in contrast to Wnt-induced anti-apoptosis, overexpression of a dominant negative mutant of TCF did not alter the response to mechanical stimulation. We conclude that LRP5/6 activation and beta-catenin accumulation are essential components of the mechanotransduction apparatus that leads to ERK activation and osteocyte survival, albeit beta-catenin/TCF-mediated transcription is not required.

**Disclosures:** M. Martin-Millan, None.

This study received funding from: NIH.

## M109

**Low Intensity Pulsed Ultrasound Synergistically Modulates SOST and OPG/RANKL Ratio in MLO-Y4 Osteocytes *in vitro*.** D. Liu. Orthodontics, Marquette University, Milwaukee, WI, USA.

Low intensity pulsed ultrasound (LIPUS) has been applied to enhance angiogenesis, growth and healing of bone, however its mechanisms are still unclear, especially the effect of LIPUS on osteocytes - the most abundant cells in bone. Recent studies show that osteocytes exclusively express sclerostin (SOST) protein negatively regulating bone formation, as well as produce OPG and RANKL modulating bone remodeling. We hypothesize that LIPUS induces anabolic responses in osteocytes, in turn modulates the remodeling of bone. To testify this, MLO-Y4 osteocytes were seeded on Ø35 mm Petri dishes. Upon 80% confluence, the cells were serum starved for 24 hours, then subjected to LIPUS (30mW/cm<sup>2</sup>, 1.5MHz frequency, 1kHz repetition) for either 10 minutes to test ERK1/2 activation, or 20 minutes followed by 6 hours of post-incubation to examine protein production of cyclooxygenase-2 (COX-2), sclerostin (SOST), osteoprotegerin (OPG) and receptor activator of NF- $\kappa$ B ligand (RANKL). The "LIPUS+cells" system was maintained at 37°C with 95% air-5% CO<sub>2</sub>. Controls were set under identical conditions without LIPUS application. After LIPUS application, the cells were lysed, 50 microgram of cell lysates were resolved through 5-10% SDS-PAGE, immunoblotted with the 1st antibodies against pERK1/2, ERK1/2; COX-2, SOST, OPG and RANKL. As results, 10 minutes of exposure to LIPUS significantly activated ERK1/2 (n=6, p<0.05). When the cells were subjected to LIPUS for 20 minutes followed by a post-incubation of 6 hours, COX-2 production was slightly increased but not significantly (n=4, p>0.05). SOST protein was significantly increased (n=3, p<0.05), while the OPG/RANKL ratio was significantly decreased (n=3, p<0.05). In contrast to our previous data showing that fluid shear stress reduced the level of RANKL in MLO-Y4 cells, the increased SOST and decreased OPG/RANKL ratio exhibited a catabolic (not anabolic as we expected) change in MLO-Y4 cells when subjected to LIPUS. It could be possible that LIPUS's effects in enhancing bone formation as a long process as in bone healing may be through a temporary "resorptive phase" as its initial step. Our data also suggest that the nature of action of LIPUS exerting on osteocytes is different from that of fluid shear stress; ERK1/2 activation may possibly play a common role leading to different down-stream events; the synergistic changes of SOST and OPG/RANKL ratio lead us to speculate a possible cross-talk between SOST modulation and OPG/RANKL changes in osteocytes during bone remodeling.

**Disclosures:** D. Liu, None.



**M110**

**Osteocytic Perilacunar Remodeling as a Significant Source of Calcium During Lactation.** H. Qing<sup>\*1</sup>, L. Ardeshipour<sup>\*2</sup>, V. Dusevich<sup>\*1</sup>, M. Dallas<sup>\*1</sup>, J. J. Wysolmerski<sup>\*2</sup>, L. F. Bonewald<sup>1</sup>. <sup>1</sup>Oral Biology UMKC Dental School, University of Missouri-Kansas City, Kansas City, MO, USA, <sup>2</sup>Yale University School of Medicine, New Haven, CT, USA.

Osteoclastic resorption of bone is thought to be the major source of calcium for milk production. Maternal bone mineral density is reduced by 30% during lactation, but this cannot be accounted for by reduced bone volume, which only declines by 20-25%. Furthermore, while treatment of lactating mice with pamidronate effectively prevents the increase in osteoclast activity, it only blunts the decline in BMD by 60%. Since the osteocyte lacuno-canalicular surface area is extensive, we hypothesized that this internal bone surface area could be a source of additional calcium during lactation. Twelve-wk-old, CD1 mice were allowed to become pregnant, deliver and lactate. Pups were removed to induce the weaning response on the 12th day of lactation. Mice were sacrificed on the 12th day of lactation (n=5) or the 7th day after weaning (n=6). Age-matched, virgin CD1 mice were used as controls (n=4). Tibiae were embedded in methyl-methacrylate, sectioned, polished, and imaged using backscatter SEM. Osteocyte lacunar area,  $\mu\text{m}^2$ , significantly increased ( $p<0.05$ ) in cortical bone during lactation ( $42.93\pm2.35^*$ ) as compared to virgin ( $38.67\pm1.23$ ) or 7 days post-lactation ( $38.36\pm3.52$ ). A similar increase was seen in trabecular bone during lactation. The same samples were acid etched and SEM was used to measure canalicular diameter. A significant increase in canalicular width was observed in lactating animals in cortical bone (virgin  $0.26\pm0.04\ \mu\text{m}$ , lactating  $0.31\pm0.04^*$ ,  $p<0.054$ ) and in trabecular bone (virgin  $0.24\pm0.03$ , lactating  $0.36\pm0.02^*$ ;  $p<0.001$ ). These data demonstrate a reversible change in lacunar and canalicular size associated with the reproductive cycle, suggesting that the osteocyte can remove mineral from its perilacunar and pericanalicular matrix during lactation. Consistent with this idea, osteocytes in bone from lactating mice expressed significant acid phosphatase activity, which was rapidly lost after weaning. This study shows that osteocytes can remove and replace their perilacunar matrix and may play a role in providing calcium to the breast for milk synthesis during lactation.

**Disclosures:** H. Qing, None.

This study received funding from: NIHAR46798.

**M111**

**Primary Human Bone Marrow Adipocytes Stimulate Osteoclast Differentiation.** H. Goto<sup>\*</sup>, M. Osaki<sup>\*</sup>, K. Sakamoto<sup>\*</sup>, A. Hozumi<sup>\*</sup>, H. Shindo<sup>\*</sup>. Orthopaedic Surgery, Nagasaki University School of Medicine, Nagasaki, Japan.

[Introduction] In late years it becomes clear that the subcutaneous fat and the visceral fat are not a simple spacer and energy storehouse and secrete physiologically active substance named adipokines, which is associated with hypertension or metabolic syndrome. Also, adipokines act on osteoclasts and osteoblasts and are associated with bone metabolism. On the other hand, the functions of marrow fat cells, existing in large quantities in the marrow which is a choke space, are not well known. We examined the relations between human marrow adipocytes and the bone metabolism.

[Materials and methods] We divided marrow fat cells by collagenase treatment from marrow liquid obtained at operations of total hip arthroplasty and conducted primary adipocytes culture. We examined gene expressions of the RANKL, OPG and M-CSF in human adipocytes by using Real Time RT-PCR. We also examined the gene expression changes after 24 hours treated by glucocorticoids, TNF- $\alpha$  and VitD3. We conducted co-culture of marrow adipocytes and human osteoclast progenitor cells, and examined TRAP staining.

[Results] Primary human adipocytes expressed RANKL, OPG, and M-CSF genes. The RANKL/OPG ratio was elevated with time course. The RANKL gene expressions significantly increased by glucocorticoids, TNF- $\alpha$  and VitD3 treatments. In co-culture system with marrow adipocytes and human osteoclast progenitor cells, the onset of the TRAP positive human osteoclast progenitor cells which were poly-nuclear and had ability of bone resorption, by glucocorticoids, TNF- $\alpha$  and VitD3 treatments.

[Discussion] RANKL is essential molecules for the osteoclast differentiation which is presented by osteoblasts and marrow stem cells. In this study, we demonstrated that the expressions of RANKL gene and are increases by the stimulation such as activated VitD3 or PTH. Similar to osteoblasts and other RANKL expressing cells, the human bone marrow adipocytes have ability to promote the osteoclast differentiation and activities. These results demonstrate the importance of human bone marrow adipocytes in the bone metabolism and possible participation in bone resorption induced by steroid administration, rheumatoid arthritis, and other disorders.

**Disclosures:** H. Goto, None.

**M112**

**Recombinant Mouse M-CSF Receptor C-fms Inhibits TNF- $\alpha$ -induced Osteoclastogenesis.** H. Kitaura, Y. Fujimura<sup>\*</sup>, M. Yoshimatsu, T. Eguchi<sup>\*</sup>, H. Kohara, Y. Morita<sup>\*</sup>, N. Yoshida<sup>\*</sup>. Division of Orthodontics and Dentofacial Orthopedics, Nagasaki University Graduate School of Biomedical Sciences, Nagasaki, Japan.

It is reported that TNF- $\alpha$  can induce osteoclastogenesis and has a pivotal role in many forms of inflammatory osteolysis. Understanding the mechanism by which TNF- $\alpha$  induces osteoclastogenesis is pivotal to the design of drugs to prevent such disorders. M-CSF is also essential for osteoclastogenesis. We have reported that administration of the M-CSF receptor c-fms antibody completely blocked osteoclastogenesis and bone erosion induced by TNF- $\alpha$  administration or inflammatory arthritis. The results suggested that anti-c-fms antibody is a candidate for an inhibitor of osteolysis at inflammatory sites. However, there is the problem that the cost of this antibody is high for most therapies. This study aimed to analyze the effect of recombinant mouse c-fms on TNF- $\alpha$ -induced osteoclastogenesis. Whole bone marrow cells were collected from C57/BL6 mice. Bone marrow macrophages generated from whole bone marrow cells were cultured in a medium containing M-CSF for 3 days. Total cDNA was generated from M-CSF-stimulated bone marrow macrophages. The c-fms gene was taken from total cDNA macrophages by PCR. The expression vector of c-fms was constructed from the c-fms gene. Recombinant of c-fms was expressed in *E. coli* and purified. Whole bone marrow cells collected from C57/BL6 mice were cultured in a medium containing M-CSF and TNF- $\alpha$  with or without recombinant c-fms. When bone marrow cells were cultured in the medium without recombinant c-fms, osteoclasts were formed. On the other hand, when they were cultured with recombinant c-fms, the number of osteoclast was less than in the culture without recombinant c-fms. The results suggested recombinant c-fms could inhibit TNF- $\alpha$ -induced osteoclastogenesis. In summary, we generated murine recombinant c-fms and recombinant c-fms had the ability to block osteoclast generated by TNF- $\alpha$ . It was postulated that recombinant c-fms was a candidate for a neutralizing therapy of osteolysis related to TNF- $\alpha$  at inflammatory sites.

**Disclosures:** H. Kitaura, None.

**M113**

**Multi-Walled Carbon Nanotubes Inhibit Osteoclast Differentiation by Inhibiting Nuclear Translocation of NFATc1.** N. Narita<sup>\*1</sup>, Y. Kobayashi<sup>\*2</sup>, H. Nakamura<sup>2</sup>, K. Maeda<sup>\*2</sup>, T. Mizoguchi<sup>\*2</sup>, H. Kato<sup>\*1</sup>, H. Ozawa<sup>\*2</sup>, N. Udagawa<sup>2</sup>, M. Endo<sup>\*3</sup>, N. Takahashi<sup>2</sup>, N. Saito<sup>\*4</sup>. <sup>1</sup>Department of Orthopaedic surgery, Shinshu University, Matsumoto, Japan, <sup>2</sup>Institute of Oral Science, Department of Biochemistry, Department of Oral Histology, Matsumoto Dental University, Shiojiri, Japan, <sup>3</sup>Faculty of Engineering, Shinshu University, Nagano, Japan, <sup>4</sup>Department of Applied Physical Therapy, Shinshu University, Matsumoto, Japan.

Attention has been focused on carbon nanotubes (CNTs) as new biocompatible materials for bone substitutes due to their high mechanical strength. We previously showed that implanted multi-walled CNTs (MWCNTs) exhibited high compatibility with bone tissues and accelerated bone formation. However, implanted MWCNTs never induced bone resorption in vivo. Here, we examined effects of MWCNTs on differentiation of osteoclasts in culture, in comparison with those of carbon black (CB). (1) MWCNTs but not CB added at 5  $\mu\text{g}/\text{ml}$  to the coculture of mouse osteoblasts and bone marrow cells strongly inhibited osteoclast formation induced by  $1\alpha,25(\text{OH})_2\text{D}_3$ . Expression of RANKL, OPG and M-CSF mRNAs in osteoblasts was not affected by MWCNTs or CB, suggesting that MWCNTs act on osteoclast precursors. (2) Unexpectedly, MWCNTs failed to inhibit osteoclast formation in mouse bone marrow macrophage (BMM $\phi$ ) culture, when added simultaneously with RANKL. However, pretreatment of BMM $\phi$  with MWCNTs but not CB for 24 hours strongly inhibited RANKL-induced their differentiation into osteoclasts. Electron microscopic analysis confirmed that MWCNTs and CB were similarly incorporated into BMM $\phi$  during the pre-incubation for 24 hours. These results suggest that MWCNTs incorporated into BMM $\phi$  specifically inhibit their differentiation into osteoclasts. (3) Neither MWCNTs nor CB suppressed RANKL-induced degradation of I $\kappa$ B $\alpha$ , phosphorylation of p38 MAPK and induction of NFATc1 in BMM $\phi$ . RANKL also stimulated nuclear translocation of NFATc1 in BMM $\phi$ . MWCNTs but not CB strongly suppressed the RANKL-induced nuclear translocation of NFATc1. Treatment of BMM $\phi$  with RANKL similarly induced nuclear translocation of NF- $\kappa$ B p65, which was not affected by MWCNTs at all. These results suggest that CNTs act as a specific modulator of a certain transcription factor such as NFATc1. In conclusion, our experiments provide a new inhibitory mechanism of CNTs for bone resorption when implanted into bone. MWCNTs but not CB possess many wholes in their structures, and may specifically trap NFATc1 in the cytosol of osteoclast precursors.

**Disclosures:** N. Narita, None.

**M114**

**Modeled Microgravity Sensitizes Osteoclast Precursors to RANKL Mediated Osteoclastogenesis by Increasing DAP12.** R. Saxena<sup>\*1</sup>, G. Pan<sup>\*2</sup>, J. M. McDonald<sup>2</sup>. <sup>1</sup>Department of Cell Biology, University of Alabama at Birmingham, Birmingham, AL, USA, <sup>2</sup>Department of Pathology, University of Alabama at Birmingham, Birmingham, AL, USA.

Mechanical forces are essential to maintain skeletal integrity, and microgravity exposure leads to bone loss. It has been well documented that the microgravity induced bone loss is due to both a decrease in osteoblastic bone formation and an increase in the osteoclastic bone resorption. However, the underlying molecular mechanisms leading to these changes remain to be fully elucidated especially the mechanisms responsible for osteoclast-mediated bone loss. Due to the infrequency of spaceflights and payload constraints, establishing *in vitro* systems that mimic microgravity conditions becomes necessary for understanding the microgravity induced bone loss. Our lab has been successful in establishing a simulated microgravity (modeled microgravity, MMG) system to study the changes induced in osteoclast precursors and to determine the molecular mechanisms responsible for increased osteoclastogenesis. We have observed that 24h of MMG incubation of RAW264.7 cells and mouse bone marrow macrophages leads to activation of ERK, p38 and c-fos. MMG was not able to induce osteoclastogenesis on its own in osteoclast precursors, however, when MMG-incubated cells were subsequently stimulated with 10ng/ml RANKL and/or M-CSF in gravity for 3-4 days, the formation of TRAP positive multinucleated osteoclasts was enhanced as compared to those formed in gravity. Specifically the number of very large osteoclasts with greater than 30 nuclei was increased nearly three fold in the osteoclasts formed from mouse bone marrow macrophages. This was accompanied by a RANKL mediated upregulation of osteoclast marker genes- TRAP and Cathepsin K. Although MMG did not induce the mRNA expression of RANK in the precursor cells, it was found that DAP12 (an ITAM-motif bearing adaptor molecule) mRNA expression was increased two fold as a result of 24h incubation in MMG. It is known that DAP12 plays a key role in the formation of multinucleated osteoclasts. Thus, MMG increases the sensitivity of osteoclast precursor cells to RANKL treatment possibly via an increase in DAP12 expression leading to increased osteoclastogenesis that contributes to bone loss.

**Disclosures:** R. Saxena, None.

This study received funding from: NIH.

**M115**

**Duffy Antigen Receptor for Chemokines (DARC) Regulates Osteoclast Differentiation via Modulating Chemokine Effects on Migration/Fusion of Osteoclast Precursors.** B. Edderkaoui<sup>\*1</sup>, N. Popa<sup>\*2</sup>, S. Mohan<sup>1</sup>. <sup>1</sup>JLP VAMC and Loma Linda Univ, Loma Linda, CA, USA, <sup>2</sup>JLP VAMC, Loma Linda, CA, USA.

We recently showed that variations in DARC gene, a BMD QTL gene in chromosome 1, contribute to peak BMD differences between high BMD CAST and low BMD C57BL/6 strains by influencing endosteal bone resorption. Bone marrow cells (BMCs) isolated from DARC-knockout mice showed significant reduction in numbers of TRAP-positive multinucleated cells (MNCs) after treatment with RANKL and M-CSF compared to cells isolated from wild type mice. Furthermore, neutralizing DARC with its specific antibody (Ab) altered the formation TRAP-positive MNCs. To investigate the mechanism by which DARC regulates osteoclast formation, we proposed, based on the known function of DARC in regulating chemokine mediated neutrophils trafficking, the hypothesis that DARC interacts with chemokines to regulate trafficking and subsequent fusion of osteoclast precursor cells. We found that neutralization of DARC action with DARC-Ab caused a >40% reduction (P<0.01) in the number of nuclei per osteoclast in differentiating cultures of M-CSF-dependent BMCs and RAW264.7 cells compared to IgG control. Furthermore, MCP-1 and RANTES, ligands for DARC protein, have been shown to be involved in the recruitment and fusion of osteoclast precursors and, thereby facilitate RANKL-induced osteoclastogenesis. We, therefore, determined the consequence of neutralizing DARC action on the migration of RAW264.7 cells towards chemokines. We found that RANTES and MIP-1 induced chemotaxis of RAW264.7 cells using an established transmigration chamber assay which was reduced by >50% (P<0.01) upon treatment with DARC-Ab compared to control IgG. Based on our finding that the migration of Raw264.7 cells towards chemokines is dependent on DARC, we next determined if neutralization of DARC action resulted in decreased expression of cell fusion and differentiation markers. Accordingly, we found that treatment of Raw264.7 cells with RANKL led to a significant increase in the expression of CD47 and DC-Stamp, while neutralization of DARC protein led to 79 and 92% reduction (P<0.01) in the expression levels of CD47 and DC-Stamp, respectively. To determine the molecular pathway by which DARC-chemokine interaction regulates chemotaxis, we tested if MAPK pathway is activated in RAW264.7 cells based on the findings that addition of MEK inhibitor to peripheral blood mononuclear cells inhibited their fusion. We found that chemokine induced ERK1/2 phosphorylation was reduced in RAW264.7 cells upon treatment with DARC-Ab. In conclusion, our findings provide the first experimental evidence that the DARC-chemokine interaction is involved in regulating trafficking and fusion of osteoclast precursors.

**Disclosures:** B. Edderkaoui, None.

This study received funding from: US Army.

**M116**

**Brain-type Creatine Kinase Is Required for RANKL-induced Osteoclastogenesis.** H. Wu<sup>\*1</sup>, J. Chen<sup>\*1</sup>, M. Wang<sup>\*1</sup>, Y. Chen<sup>2</sup>. <sup>1</sup>Pediatric Dentistry, University of Alabama at Birmingham, Birmingham, AL, USA, <sup>2</sup>Pathology, University of Alabama at Birmingham, Birmingham, AL, USA.

We compared the protein expression profile between mature osteoclasts derived from primary bone marrow macrophages (BMMs) in the presence of RANKL and M-CSF with the osteoclast precursors in the presence of M-CSF and identified a 43kDa protein that is highly expressed in the mature osteoclasts. This molecule was further identified as brain-type creatine kinase (CKb) by Mass Spectrometry. The presence of CKb in patient sera is a hallmark of osteopetrosis among sclerosing bone disorders. Elevated serum acid phosphatase activity and the appearance of circulating CKb can be used to indicate osteoclast failure. However it is unknown how the CKb is associated with osteoclast function. We found that the expression of CKb mRNA was increased by 40 fold in mature osteoclasts as determined by quantitative real-time PCR. Western blot analysis confirmed an increase in CKb proteins. By contrast, other isoenzymes of creatine kinases were not detected during osteoclastogenesis, suggesting RANKL and M-CSF uniquely induced the production of CKb during osteoclastogenesis. Cyclocreatine, a creatine analog and an inhibitor of CKb, at non-toxic concentrations, inhibited osteoclastogenesis in both BMMs and RAW cells. Furthermore, knockdown of ckb by ckb-specific shRNA delivered with lentivirus vectors inhibited osteoclastogenesis as well, whereas non-specific shRNA control did not affect osteoclastogenesis. Western blot analysis revealed that inhibition of Ckb function by CCr inhibitor or knockdown Ckb by shRNA severely impaired RANKL-mediated activation of JNK and ERK, but not NFkB, p38-MAPK. Ckb knockdown significantly inhibited NFATc1 expression and reduced intracellular calcium mobilization, concurrently with decreased ATP level and increased ADP/ATP ratio in response to RANKL. Interestingly CKb knockdown did not affect the small GTPase RhoA function. Taken together, we conclude that the CKb is required for osteoclastogenesis via its influence on Calcium-NFATc1 axis and ATP production. Further characterization of molecular mechanism involved in CKb-regulated osteoclastogenesis may shed light on new therapeutic target for osteoclast function. This work was supported by NIH P30 AR046031.

**Disclosures:** H. Wu, None.

This study received funding from: NIH.

**M117**

**All-trans-retinoic Acid (Vitamin A) Increases Expression of MafB and Inhibits Osteoclast Formation by Interfering with Differentiation of Osteoclast Progenitor Cells.** E. Persson<sup>1</sup>, H. H. Conaway<sup>2</sup>, M. Halén<sup>\*1</sup>, S. Granholm<sup>\*1</sup>, O. Svensson<sup>3</sup>, U. Pettersson<sup>4</sup>, A. Lie<sup>\*1</sup>, U. H. Lerner<sup>1</sup>. <sup>1</sup>Dept of Oral Cell Biology, Umea University, UMEÅ, Sweden, <sup>2</sup>Dept of Physiology and Biophysics, University of Arkansas for Medical Sciences, Little Rock, AR, USA, <sup>3</sup>Dept of Orthopedic Surgery, Umea University, Umea, Sweden, <sup>4</sup>Dept of Clinical Pharmacology, Umea University, Umea, Sweden.

Effects of vitamin A (retinol) derivatives are mediated by two families of nuclear receptors, the retinoic acid receptors (RARs) and the retinoid X receptors (RXRs). Each receptor family is made up of three isoforms ( $\alpha$ ,  $\beta$  and  $\gamma$ ), produced by separate genes. An isomer of retinoic acid, all-trans-retinoic acid (ATRA), is thought to mediate the physiological retinol signal by binding RAR partners of RAR/RXR heterodimers. Activated RAR/RXR heterodimers function as transcription factors, activating specific retinoic acid response elements (RAREs) for transcriptional regulation. In the present study, the effects by ATRA on osteoclast formation have been assessed in cultures of crude mouse bone marrow cells (BMC), mouse spleen cells and mouse bone marrow macrophages (BMM). ATRA inhibited osteoclast formation in 1,25(OH)<sub>2</sub>-vitamin D<sub>3</sub> and PTH stimulated BMC cultures without affecting D<sub>3</sub> or PTH induced RANKL mRNA. ATRA also inhibited osteoclast formation in RANKL stimulated spleen cell cultures and in RANKL stimulated BMM. Inhibition was observed at and above 0.1 nM of ATRA with no signs of cytotoxicity (studies on morphology, MTT) or increased apoptosis (expression of Bax, Bcl-2). Pit formation on ivory slices caused by RANKL stimulated BMM was abolished by ATRA. Inhibition of osteoclast formation was associated with decreased mRNA expression of calcitonin receptor, cathepsin K and TRAP. In BMM, ATRA inhibited RANKL induced increase of c-Fos mRNA and protein and Fra-2 mRNA, without affecting Fra-1, JunB or JunD mRNA and slightly increasing c-Jun mRNA. The increase of NFAT2 mRNA and protein caused by RANKL in BMM was abolished by ATRA. In contrast, ATRA did not affect NF- $\kappa$ B activity. Most interestingly, ATRA reversed RANKL induced decrease of MafB, a recently described negative regulator of osteoclastogenesis. Most of the BMM expressed RAR $\alpha$  and RAR $\beta$  at both mRNA and protein level, but very few expressed RAR $\gamma$ . These data show that vitamin A has the capacity to inhibit the differentiation of early osteoclast progenitor cells, an effect involving both decreased expression of the pro-osteoclastogenic transcription factors c-Fos and NFAT2, as well as increased expression of the anti-osteoclastogenic factor MafB.

**Disclosures:** E. Persson, None.

## M118

**Isoform-Specific Expression of Peroxisome Proliferator-Activated Receptors (PPARs) and Gene Regulation during Osteoclastogenesis in RAW/C4 Cells.** J. Fidalgo<sup>\*1</sup>, D. Ovchinnikov<sup>\*1</sup>, B. Fletcher<sup>\*1</sup>, G. Muscat<sup>\*2</sup>, A. I. Cassidy<sup>1</sup>. <sup>1</sup>Institute for Molecular Bioscience; Co-operative Research Centre for Chronic Inflammatory Diseases, University of Queensland, The University of Queensland, Brisbane, Australia, <sup>2</sup>Institute for Molecular Bioscience, University of Queensland, The University of Queensland, Brisbane, Australia.

Peroxisome Proliferator-Activated Receptors (PPARs) are nuclear steroid hormone receptors and have three isoforms: PPAR $\alpha$ , PPAR $\gamma$  and PPAR $\delta$ , with characteristic patterns of tissue distribution and specific roles. PPARs have been demonstrated to have a role in regulating bone biology. The PPAR $\delta$  agonist, carbaprostacyclin, stimulates osteoclast (OCL) activity whereas the PPAR agonists bezafibrate, fenofibrate and the specific PPAR $\delta$  agonist L165041, repress human OCL differentiation *in vitro*. We have sought to understand the role of PPAR $\delta$  in osteoclast biology.

In this study, we investigated the expression and role of PPAR isoforms and those of its heterodimeric partner, RXR, during the differentiation of the osteoclastogenic RAW/C4 sub-clone of the RAW264.7 murine macrophage cell line. PPAR $\delta$  is the prevailing isoform in RAW/C4-derived OCL and its expression is markedly upregulated during OCL differentiation whereas expression of the other isoforms decreases. The specific PPAR $\delta$  agonist, GW501516, induces elevated expression of the typical OCL markers tartrate-resistant acid phosphatase (TRAP), cathepsin K and calcitonin receptor (CTR) but further decreases the levels of expression of all PPAR isoforms during OCL differentiation. Stable over-expression of PPAR $\delta$  in RAW/C4 cells also upregulates the expression of these genes and this effect is further stimulated by the presence of GW501516.

The expression of PPAR-responsive element (PPRE)-containing reporter gene constructs was induced by co-expression of PPAR $\delta$  in transiently transfected RAW/C4 cells. PPRE-reporter gene expression was further induced by co-expression of the transcriptional co-activator PGC-1. The PPAR $\delta$  agonist GW501516 stimulated expression of these constructs. The expression of RXR isoforms was differentially regulated during RAW/C4 osteoclastogenesis, such that the expression of RXR $\alpha$  and RXR $\gamma$  was repressed while RXR $\beta$  was induced, showing a similar expression profile to PPAR $\delta$  itself.

PPAR $\delta$  has been shown to regulate gene expression during murine osteoclast differentiation and therefore we propose that it has a significant role in bone biology.

**Disclosures:** A.I. Cassidy, None.

## M119

**Downregulation of Connexin 43 Expression and Osteoclastogenesis by a Bioceramic Bone Graft Substitute.** Z. Mladenovic<sup>\*</sup>, B. Andersson<sup>\*</sup>, M. Ransjö. Odontology/Oral Cell Biology, Umeå University, Umeå, Sweden.

Biomaterials are becoming more frequent as bone graft substitutes when treating patients with bone defects. Integration of bone graft substitutes and surrounding tissues are crucial in bone reconstruction therapies. Increased knowledge of biomaterial and bone cell interactions are of importance. Gap junctional intercellular communication (GJIC) is important in osteoblast proliferation, differentiation and extra cellular matrix mineralization. Connexin 43(Cx43) is the most widely expressed Cx protein in the osteoblasts (Stains et al., 2005). Furthermore, Cx43 mRNA has been demonstrated in osteoclasts (Ransjö et al., 2003). We have also demonstrated that GJIC and Cx43 are crucial in the fusion and formation of osteoclasts (Matemba et al., 2006). One interesting group of synthetic biomaterials is the bioactive glass ceramics, containing calcium, phosphate and silica ions. It is suggested that osteoblast proliferation and differentiation is promoted when exposed to soluble ionic constituents released from bioactive glasses (Hench LL, 2006). There are a few published very interesting studies on effects of biomaterials on gap junction communication. Our aim is to investigate effects of 45S5 Bioglass on osteoclastogenesis and Cx43 expression. We used mouse bone marrow cultures and RAW 264.7 cells for this study. Bioglass dissolution medium and particles caused time and dose dependent significant inhibition in the number of TRAP positive multinucleated cells. Real-time PCR analysis supported these findings by showing decreased osteoclast phenotypic markers. Both Bioglass dissolution medium and particles dose dependently significantly decreased Cx43 mRNA expression in RANKL-stimulated RAW cells. In conclusion this study demonstrates an inhibitory action of 45S5 Bioglass on osteoclastogenesis and Cx43 expression.

**Disclosures:** Z. Mladenovic, None.

## M120

**A Novel Selective P2X<sub>7</sub> Receptor Antagonist Inhibits Human Osteoclast Formation *in vitro*.** A. Gartland<sup>\*1</sup>, K. A. Buckley<sup>\*2</sup>, K. Bowers<sup>\*3</sup>, A. Gaw<sup>\*3</sup>, M. Furber<sup>\*4</sup>, J. A. Gallagher<sup>2</sup>. <sup>1</sup>Academic Unit of Bone Biology, The University of Sheffield, Sheffield, United Kingdom, <sup>2</sup>Human Anatomy and Cell Biology, The University of Liverpool, Liverpool, United Kingdom, <sup>3</sup>Discovery BioScience, AstraZeneca R&D Charnwood, Loughborough, United Kingdom, <sup>4</sup>Medicinal Chemistry, AstraZeneca R&D Charnwood, Loughborough, United Kingdom.

The P2X<sub>7</sub> receptor (P2X<sub>7</sub>R), a unique receptor that can form pores in the cell membrane, has been implicated in the process of multinucleation and cell fusion. We have previously demonstrated that osteoclast precursors and mature osteoclasts express functional P2X<sub>7</sub>R and that blockade of P2X<sub>7</sub>R using a monoclonal antibody or oxidised ATP inhibited formation of multinucleated osteoclasts *in vitro*. Here we provide further evidence for the role of the P2X<sub>7</sub>R in the formation of functional multinucleated human osteoclasts using a small-molecule antagonist from a distinct chemical series of cyclic imides, which are potent and highly selective for the P2X<sub>7</sub>R. When added to human blood monocytes cultured in the presence of recombinant RANKL and M-CSF, compound 15d, in a concentration-dependent manner, decreased the formation of multinucleated TRAP-positive osteoclasts, the number of actively resorbing osteoclasts, and the overall area of resorption excavated on dentine discs by these cells. These data support the argument that the P2X<sub>7</sub>R is indeed directly involved in osteoclast fusion and the utility of P2X<sub>7</sub>R antagonists in the management of diseases where bone metabolism is disturbed such as rheumatoid arthritis, Pagets disease or osteoporosis.

**Disclosures:** A. Gartland, None.

This study received funding from: AstraZeneca R&D Charnwood.

## M121

**Nanogel Cross-linking Hydrogel as a Drug Delivery System for Tumor Necrosis Factor-alpha Antagonist.** N. Alles<sup>\*1</sup>, N. S. Soysa<sup>\*1</sup>, A. Mian<sup>\*1</sup>, N. Tomamatsu<sup>\*1</sup>, N. Morimoto<sup>\*2</sup>, U. Hasegawa<sup>\*2</sup>, S. Sawada<sup>\*2</sup>, Y. Tada<sup>\*2</sup>, K. Akiyoshi<sup>\*2</sup>, K. Ohya<sup>1</sup>, K. Aoki<sup>1</sup>. <sup>1</sup>Section of Pharmacology, Department of Hard Tissue Engineering, Tokyo Medical and Dental University, Tokyo, Japan, <sup>2</sup>Organic Biomaterials, Institute of Biomaterials and Bioengineering, Tokyo Medical and Dental University, Tokyo, Japan.

Our previous studies have already shown that a TNF antagonist peptide (WP9QY/W9) is effectively inhibits RANKL-induced bone resorption in many bone resorption models (J Clin Invest. 116:1525-1534, 2006, Arthritis Rheum. 56:1164-74, 2007). Easy degradation in serum is a major drawback towards clinical application of this peptide. We have shown previously that the W9 peptide could bind with cholesterol-bearing pullulan (CHP) nanogels in preventing bone resorption in a mouse model of low Ca diet. The objective of this study is to find out the most efficient control release system for W9 peptide. In this study we used two kinds of systems namely, the injection type of CHP nanogel and the implant type of CHP nanogel cross-linking (CHP-PEG hybrid nanogels). Five week old, male C57BL/6J mice on low Ca diet were injected with vehicle (veh), CHP-nanogel, W9 or the CHP-W9 complex (W9- 24mg x2/kg/day) twice a day for 7 days. In the case of hydrogel, CHP-hydrogel-W9 (W9- 10.28mg/kg/day) was implanted on the first day of the experiment. At the end of the experiment mice were sacrificed and the long bones were subjected to bone mineral density (BMD) measurements. The BMD of low Ca group was significantly reduced compared to normal Ca-veh group (p<0.01). CHP-W9 complexes prevented the reduction in BMD compared to low Ca-veh (p< 0.01) in both types. The BMD data was further confirmed by histomorphometry and microCT data. Twice a day CHP-W9 injection and CHP-hydrogel-W9 implantation prevented the increase of number of osteoclasts significantly (p<0.001). Both CHP nanogel and CHP-hydrogel by themselves do not have any bone resorption or bone formation effects. Taken together, the implant type of nanogel cross-linking hydrogel inhibited bone resorption by a low Ca feeding at a lower dose of W9 (10.28 mg/kg/day) compared to the injection type of CHP nanogel (48 mg/kg/day), and these results suggested that the nanogel cross-linking hydrogel could be used as an effective carrier to deliver the W9 peptide.

**Disclosures:** N. Alles, None.

## M122

**Acidosis Augments the Resorptive Capacity of Human Osteoclasts by Increasing Lysosomal Acidification.** K. Henriksen, V. K. Jensen\*, M. G. Sorensen\*, M. A. Karsdal. Pharmacology, Nordic Bioscience A/S, Herlev, Denmark.

Metabolic acidosis results in detrimental effects on bone health, and local acidosis as seen in metastatic bone disease leads to localized bone destruction. The mechanism underlying the increased resorption involves a combination of upregulation of RANKL expression by osteoblasts, and upregulation of the resorptive activity by the osteoclasts. To further clarify the mechanism underlying the increased resorption, we investigated the effect of acidosis on cultures of human osteoclasts.

We used CD14+ sorted monocytes cultured in the presence of RANKL and M-CSF to generate mature human osteoclasts. We seeded the mature osteoclasts on bone slices and exposed them to medium with pH values ranging from 6.5 to 8.0 and investigated bone resorption by measurement of calcium release and osteoclast number by TRACP activity after 5 days of culture. We then measured lysosomal acidification using both the acid influx assay in membranes isolated from osteoclasts exposed to pH 6.8 and 7.5, and finally we quantified lysosomal acidification in osteoclasts using acridine orange. In addition, we measured V-ATPase activity in the membrane preparations.

We found that osteoclasts exposed to low pH values resorbed 200% of the level observed in control osteoclasts at normal pH values. Furthermore, we found that the TRACP activity increased, but that the increase did not fully explain the increase in resorption. Finally, we found the low pH treatment increased acid influx by 40% and V-ATPase activity in the membrane fractions. Finally, we found that the lysosomal pH was reduced mildly by the low pH when incubating the cells at low pH for 24 hours, but not 45 minutes.

In conclusion, we found that lowering pH leads to an increase in osteoclastic resorption via increased V-ATPase activity leading to increased acidification of the lysosomes. These data for the first time show that human osteoclasts are activated by low pH, which correlates well with the findings in disorders involving both systemic and local acidosis.

**Disclosures:** K. Henriksen, None.

## M123

**The Chloride Channel CIC-7 Mediates Acidification of the Resorption Lacuna in Osteoclasts.** K. Henriksen<sup>1</sup>, A. V. Neutsky-Wulff<sup>1</sup>, V. K. Jensen\*<sup>1</sup>, J. Bollerslev<sup>\*2</sup>, J. Gram<sup>\*3</sup>, M. A. Karsdal<sup>1</sup>. <sup>1</sup>Pharmacology, Nordic Bioscience A/S, Herlev, Denmark, <sup>2</sup>Section of Endocrinology, Dept. of Medicine, National University Hospital, Oslo, Norway, <sup>3</sup>Department of Endocrinology, Ribe County Hospital, Esbjerg, Denmark.

The chloride channel CIC-7 has been speculated to be involved in acidification of the lysosomes and the resorption lacunae in osteoclasts, however neither direct measurements of chloride transport nor acidification have been performed.

Human osteoclasts harboring a dominant negative mutation in CIC-7 (G215R) or CIC-7 deficient murine osteoclasts were isolated, and used to investigate bone resorption measured by CTX-I, calcium release and pit scoring. CIC-7 enriched membranes from the osteoclasts were isolated, and used to test acidification rates in the presence of a V-ATPase and a chloride channel inhibitor, using a H<sup>+</sup> and Cl<sup>-</sup> driven approach. Finally, acidification rates in CIC-7 enriched membranes from ADOII osteoclasts and CIC-7 deficient bones, and their corresponding controls were compared.

Resorption by the G215R osteoclasts was reduced by 60% when measured by both CTX-I, calcium release, and pit area when comparing to age and sex matched controls. In the mouse model bone resorption was completely abrogated. Furthermore, V-ATPase and chloride channel inhibitors completely abrogated the H<sup>+</sup> and Cl<sup>-</sup> driven acidification. Finally, the acid influx was reduced by maximally 50% in the ADOII membrane fractions when comparing to controls, and completely eliminated in CIC-7 deficient bone membrane vesicles.

These data for the first time demonstrate that CIC-7 is essential for bone resorption, via its role in acidification of the lysosomes and resorption lacunae in osteoclasts.

**Disclosures:** K. Henriksen, None.

## M124

**Protein Kinase Cδ Is Important for Acidification of the Lysosomes and Resorption Lacuna in Osteoclasts.** M. G. Sorensen, K. Henriksen, M. A. Karsdal. Nordic Bioscience A/S, Herlev, Denmark.

Bone resorption is initiated by the osteoclastic acidification of the resorption lacunae. This process is mediated by secretion of protons through the V-ATPase and chloride through the chloride channel CIC-7. Since little is known about the intracellular machinery controlling extracellular acidification, we utilized a panel of kinase inhibitors to investigate the intracellular control of lysosomal acidification in human osteoclasts and osteoclastic bone resorption.

Human osteoclasts were generated from CD14+ monocytes cultured with 25ng/ml M-CSF and RANKL. The effect of different kinase inhibitors on lysosomal acidification in human osteoclasts seeded on plastic was investigated using the dye acridine orange for different incubation times (45min, 4 hours and 24 hours). The PKC inhibitors were tested in the acridine orange based acid influx assay using membranes isolated from osteoclasts. We seeded the mature osteoclasts on bone slices and investigated bone resorption by measurement of calcium release and CTX-I into the supernatants. Cell number was measured using the AlamarBlue dye.

The PKC inhibitor, GF 109203X, inhibited both the lysosomal acidification in osteoclasts

and the acid influx in membranes from osteoclasts (IC50=0.06μM), whereas the PKC inhibitors Hypericin and Ro 31-8220 only inhibited the acid influx with IC50 values of 1.8μM and 5.8μM, respectively. All three compounds inhibited bone resorption with IC50 values of 0.8μM, 0.7μM and 3.6μM, respectively. Hypericin and Ro 31-8220 showed low levels of toxicity with IC50 values of 6.9μM and 7.2μM, respectively, whereas GF 109203X was not toxic to the osteoclasts at the tested concentrations.

Rottlerin, an inhibitor of PKCδ, inhibited lysosomal acidification in human osteoclasts. The effect was not seen after short time incubation (45 minutes) but first after long time incubations (4 hours and 24 hours). Furthermore, Rottlerin inhibited the acid influx potently with an IC50 value of 0.08μM. Moreover, Rottlerin inhibited bone resorption with an IC50 value of 1.8μM, and showed low levels of toxicity (IC50=7.3μM). However, the two PKC inhibitors Sphingosine and Palmitoyl-DL-carnitine Cl did not inhibit acidification and bone resorption, potentially due to low potency in osteoclasts. Finally, HBDDE, which inhibits the PKCα and PKCγ isozymes, did not inhibit acidification and bone resorption.

In conclusion, PKC, and especially the PKCδ isoform, appears to play a role in the acidification in human osteoclasts, and through this in bone resorption. On the other hand the PKCα and PKCγ isozymes do not appear to play a role in acidification in osteoclasts, showing that this process is specifically regulated in the osteoclasts.

**Disclosures:** M.G. Sorensen, None.

## M125

**Microarchitecture and Tissue Age Influence In Vivo Bone Resorption.** C. Janeiro, D. Vashishth. Biomedical Engineering, Rensselaer Polytechnic Institute, Troy, NY, USA.

Previously we have demonstrated that both microarchitecture and tissue age influence and direct *in vitro* bone resorption [1]. Because bone resorption *in vivo* can be influenced by osteocytes [2], here we report results of an *in vivo* study in which osteocytes can influence bone resorption and alter the interaction between tissue age, microarchitecture, and bone resorption.

Proximal sections of 16 cadaveric human tibiae (Ages 34-89, M & F) containing naturally occurring resorption pits were obtained, stained in toluidine blue and imaged. Each resorption pit was measured, and classified as Type I, II or III based on its interaction with the microarchitecture, particularly the cement line. Type I resorption pits encountered but did not cross the cement line. Type II resorption pits encountered and breached the cement line. Type III resorption pits did not interact with the cement line. The second classification of resorption pits dealt with tissue age. Each resorption pit was classified based upon its location on the bone surface as either interstitial (I) or osteonal (O).

The number of Type III resorption pits was significantly ( $p < 0.001$ ) higher than the number of Type I and II resorption pits (I = 0.0017; II = 0.0004; III = 0.0265 #/mm<sup>2</sup>). No significant difference between the number of Type I and II interactions was seen. There were also no significant differences between the average areas of the type I, II or III resorption pits (I = 88.9; II = 125.1; III = 75.1 μm<sup>2</sup>). The number of interstitial resorption pits was significantly ( $p < 0.01$ ) higher than the number of osteonal resorption pits (I = 0.029; O = 0.001 #/mm<sup>2</sup>), while no significant difference in resorption pit size was seen (I = 77.3; O = 46.6 μm<sup>2</sup>).

In conclusion this study demonstrates that both microarchitecture and tissue age influence bone resorption *in vivo*. In particular, resorption activity is localized in regions containing interstitial bone and devoid of cement lines. These results are similar to a previous *in vitro* study, showing the same trends for tissue age as well as the increases and decreases of size, number and types of resorption pits [1]. Thus the presence of osteocytes in bone does not mitigate the role of microstructure and tissue age in directing bone resorption. These findings may help explain bone turnover induced changes with aging and disease, and with the use of antiresorptive drugs and anabolic treatments [3].

1 Vashishth D, Janeiro C, ASBMR 2006.

2 van Oers RF *et al*, Bone 42:250-9, 2008.

3 Finkelstein JS *et al*, NEJM 349:1216-1226, 2003.

**Disclosures:** C. Janeiro, None.

This study received funding from: NIH Grant AR049635.

## M126

**Losartan® (Cozaar) Increases Appendicular Bone Formation by Inhibiting Osteoclastogenesis.** T. Sibai\*, T. Yang\*, D. Napierala, B. Dawson\*, S. Chen\*, J. Black\*, Y. Chen\*, B. Lee. Baylor College of Medicine, Houston, TX, USA.

Losartan® (Cozaar), an FDA approved angiotensin II type 1 receptor blocker (AT1 antagonist or ARB) is primarily indicated as an antihypertensive agent. It has been found to inhibit TGF-β1 in mouse models of chronic renal insufficiency and in aortic aneurysms of Marfan mouse models. TGF-β1 plays a fundamental and complex role in bone formation. We hypothesized that Losartan can affect bone homeostasis by antagonizing TGF-β1. Histologic femoral bone analysis at 6 weeks, micro CT analysis and Von Kossa staining for femurs and lumbar vertebrae, histomorphometry for osteoclast (OC) and osteoblast (OB) parameters on toluidine blue and tartrate resistant acid phosphatase (TRAP) stained distal femoral sections were performed in C57B6 mice treated with Losartan vs. non-treated controls. In vitro splenocyte to osteoclast differentiation assays at different doses of Losartan (+/- angiotensin II) were also performed. Six-week and 3-3.5 month old postnatally treated mice were 6% heavier ( $p=0.03$ ). Micro CT analysis showed a 9% increase in femoral cortical thickness and a 29-98% improvement in trabecular bone parameters (BV/TV, trabecular thickness, number and separation) ( $p<0.01$ ). Trabecular bone formation at the L3 and L4 vertebrae and micro CT showed a similar trend that did not reach statistical significance. Von Kossa staining confirmed the trabecular phenotype in

the femurs and lumbar spine ( $p < 0.01$ ). Histomorphometric analysis revealed a decrease in OC parameters ( $p = 0.02$ ) but no difference in OB parameters. Losartan inhibited in vitro OC differentiation assays while angiotensin II increased OC counts compared to controls. The mechanism for the enhanced appendicular bone effect and the relationship between the AT1 receptor and TGF- $\beta 1$  remains to be elucidated. Antagonism of the AT1 receptor can act as a potential target in the treatment of osteoporosis and low bone mass states.

**Disclosures:** T. Sibai, None.

## M127

**Effects of the Cathepsin K Inhibitor Odanacatib on Osteoclast-Mediated Bone Resorption.** P. Leung<sup>\*1</sup>, Y. Zhou<sup>\*1</sup>, P. Masarachia<sup>\*1</sup>, G. A. Wesolowski<sup>1</sup>, M. Pickarski<sup>1</sup>, J. Y. Gauthier<sup>\*2</sup>, D. Percival<sup>\*2</sup>, W. C. Black<sup>\*2</sup>, L. T. Duong<sup>1</sup>. <sup>1</sup>Merck & Co., Inc, West Point, PA, USA, <sup>2</sup>Merck & Co., Inc, Montreal, QC, Canada.

Cathepsin K (Cat K) is the major collagenase responsible for degradation of demineralized matrix proteins during osteoclastic bone resorption. Odanacatib (ODN) is a selective, potent and reversible inhibitor of Cat K that has demonstrated effective inhibition of bone loss in animal models and osteoporotic women. The objectives of this study were to characterize the cellular effects of ODN in blocking bone resorption. First, localization of Cat K in osteoclasts was confirmed using electron microscopy immunolabeling in thin sections of mouse femur. Cat K is found within lysosomes, late endosomes, ruffled border and resorption lacunae. It is not detected in osteoblasts or other bone marrow cells. In vitro studies with ODN (hCat K IC<sub>50</sub> = 0.2nM) in human osteoclasts, cultured on dentin or plastic, demonstrated no effect on formation or survival of multinucleated TRAP(+) cells at 100 nM. Similarly, equivalent numbers of multinucleated osteoclasts were generated from bone marrow isolated from CatK knockout versus wild type mice. ODN dose-dependently reduced bone resorption, as evidenced by reduction in CTx (IC<sub>50</sub> = 9.4nM) and resorption area (IC<sub>50</sub> = 6.5nM), without affecting pit number. In contrast, alendronate at 5  $\mu$ M reduced TRAP(+) cell number and abolished resorption pit formation. Characterization of pit morphology by lectin-labeled peroxidase staining revealed that untreated purified human osteoclasts generate typical trail-like resorption lacunae. In contrast, cells treated with ODN form small discrete pits with intense staining and ambiguous borders, suggesting shallow pits with undigested demineralized bone matrix proteins. Lastly, a BODIPY<sup>®</sup>-labeled analog of ODN was developed as a probe for detecting the active form of Cat K. While confocal microscopy with anti-Cat K antibody confirmed expression in all osteoclasts on bone, the fluorescence probe detected active enzyme in only a subgroup of resorbing cells, in which Cat K was found to be localized to intracellular vesicles and ruffled border, suggesting another mechanism involved in regulation of Cat K activation during resorption. Probe binding to active Cat K was readily overcome by unlabeled Cat K inhibitor (100nM), confirming accessibility and reversibility of Cat K inhibition. Staining of actin rings revealed that pharmacological inhibition of Cat K had an insignificant effect on sealing zone formation in actively-resorbing osteoclasts. Taken together, our data supports a mechanism for ODN inhibition of osteoclast mediated bone resorption that includes reduction of matrix degradation without affecting osteoclast formation, survival or polarization.

**Disclosures:** P. Leung, Merck & Co., Inc 3.

## M128

**Effect of Luteolin on Bone Loss, Microarchitecture and Bone Resorption in Ovariectomized Mice.** J. Jung<sup>\*1</sup>, J. Hong<sup>\*1</sup>, T. Kim<sup>\*1</sup>, S. Lee<sup>\*1</sup>, M. Ha<sup>\*1</sup>, H. Kim<sup>\*1</sup>, E. Park<sup>2</sup>, S. Kim<sup>3</sup>. <sup>1</sup>Skeletal Diseases Genome Research Center, Kyungpook National University Hospital, Daegu, Republic of Korea, <sup>2</sup>School of Dentistry, Department of Pathology and Regenerative Medicine, Kyungpook National University, Daegu, Republic of Korea, <sup>3</sup>Department of Orthopedic Surgery, Kyungpook National University Hospital, Daegu, Republic of Korea.

Phenolic compounds including flavonoids have been implicated in suppression of osteoclast differentiation/function and prevention of bone diseases. The flavonoid luteolin has anti-inflammatory properties both in vivo and in vitro. It has been demonstrated that luteolin has an anabolic effect in osteoblastic cells. However, the impact of luteolin on experimental models of bone and osteoclastic cell remains to be elucidated. We therefore investigated the effects of luteolin on bone metabolism in an ovariectomized (OVX) mouse model, and also osteoclast differentiation and function.

C57BL/6 mice ( $n = 32$ ) were OVX or sham-operated at 9 weeks, and luteolin treatment with different concentrations (5mg and 20 mg/kg) was started immediately after surgery. The effect of luteolin on bone of the OVX mice was evaluated by  $\mu$ CT bone morphometric analysis. Data were analyzed by One-way ANOVA test. In this study, we found that luteolin markedly decreased the differentiation of both murine bone marrow mononuclear (BMM) culture models and Raw264.7 cells into osteoclasts in dose dependent manner. Also, luteolin had increased bone mineral density (BMD), bone mineral content (BMC), tissue mineral density (TMD), bone volume fraction, trabecular number, trabecular separation, cortical BMD, and cortical BMC of the distal femur compared with control OVX mice. These results suggest that the effect of luteolin is mediated by its inhibitory effects on RANKL-induced osteoclast formation, and prevent bone loss in OVX mice. Luteolin may provide more effective therapeutic implication by progressive bone loss including osteoporosis.

**Disclosures:** S. Kim, None.

## M129

**Are All Anti-resorptive Treatments the Same? Lessons Learned From Inhibition of Human Osteoclastic Bone Resorption by Alternative Pathways - Inhibition of Proteolysis vs. Inhibition of Acidification.** A. V. Neutzsky-Wulff<sup>1</sup>, M. G. Sorensen, M. A. Karsdal, K. Henriksen. Nordic Bioscience, Herlev, Denmark.

Inhibition of osteoclastic bone resorption is the primary objective by anti-resorptive treatments for osteoporosis. However, the effect on human osteoclast phenotype and subsequently the effect of bone phenotype, that may be related to bone quality, remain to be carefully investigated.

Osteoclasts are responsible for degradation of both the organic and inorganic part of the bone matrix. The degradation takes place in the resorption lacuna, where acidification is responsible for dissolution of the inorganic phase. The organic phase is dissolved by proteolysis, mainly by Cathepsin K, however MMPs might play a role as a compensatory mechanism. We investigated the effect of inhibition of proteolysis and acidification on human osteoclast phenotype and bone resorption.

Human monocytes were isolated from blood and differentiated into mature osteoclasts by treatment with M-CSF and RANKL. Cells were seeded on cortical bone slices and treated with an inhibitor of proteolysis (E64) or inhibitors of acidification (bafilomycin and ethoxylzolamide). Resorption of the different types of bone matrix was measured by Ca<sup>2+</sup> (inorganic), CTX-I (organic, Cathepsin K generated) and ICTP (organic, MMP generated). Resorbed area was scored by pit staining.

Inhibitors of acidification gave rise to very similar IC<sub>50</sub> values for degradation of the organic and the inorganic bone matrix. On the contrary, the inhibitor of proteolysis, E64, did effectively inhibit resorption of the organic bone matrix (IC<sub>50</sub> < 1 $\mu$ M), whereas inhibition of dissolution of the inorganic bone matrix was not observed. Scoring of pit area, showed a massive reduction when inhibiting acidification (>80%), whereas inhibiting proteolysis did not lead to reduced pit area compared to control. In addition, ICTP release was highly increased with inhibition of proteolysis, which was not seen with inhibition of acidification.

In conclusion, inhibition of proteolysis with E64 leads to increased release of MMP generated fragments, pointing towards a compensatory resorptive activity by MMPs. The discrepancies in the IC<sub>50</sub> values of organic vs. inorganic resorption for inhibition of proteolysis, may in addition explain the somewhat lower efficacy on BMD compared to that of biochemical markers, recently observed in osteoporosis studies with Cathepsin K inhibitors. Interestingly, inhibition of osteoclastic resorption by acidification inhibitors did not display discrepancies between the IC<sub>50</sub> values.

**Disclosures:** A.V. Neutzsky-Wulff, None.

## M130

**The Fungal Secondary Metabolites Beauvericin and Enniatin Inhibit Osteoclast Differentiation and Bone Resorption.** S. Forsdahl<sup>\*1</sup>, F. Tedjiosop-Feudjio<sup>\*2</sup>, J. Nguemo<sup>\*2</sup>, R. Lemmens-Gruber<sup>\*2</sup>, O. Hoffmann<sup>2</sup>.

<sup>1</sup>Institutt for farmasi det medisinske fakultet, Universitetet i Tromsø, Tromsø, Norway, <sup>2</sup>Pharmacology and Toxicology, University of Vienna, Vienna, Austria.

Beauvericin and enniatins are structurally related cyclohexadepsipeptides, that are produced by several strains of the fungi genus *Fusarium*, *Beauveria*, *Polyporus* and *Paecilomyces* that are known to contaminate food and feed. They are known ionophores capable of boring holes into cell membranes, allowing for the exchange of cations in cells. We have evidence that these fungal compounds may influence development and activity of osteoclasts (OC) and thus, may be useful therapeutics. To evaluate their effects on OCs, we used the following: 1.) coculture murine bone marrow cells with primary calvarial osteoblasts (OBs) to generate OC for the assessment of OC differentiation using TRAP staining, OC bone resorption on bovine bone slices, and stained cytoskeleton with phalloidin-rhodamine, 2.) OC precursor cell line RAW 264.7 for the evaluation of cell survival and viability, and 3.) RANKL-stimulated RAW 264.7 cells were used as an OC-model to study the effect of the fungal products on MAP kinase signal transduction pathways. Beauvericin and enniatin inhibited OCs in a dose-dependent fashion in all assays tested at a range between 0.1  $\mu$ M and 10  $\mu$ M. At 10  $\mu$ M, beauvericin and enniatin completely inhibited OC bone resorption, disrupted actin rings and caused apoptosis. Moreover, both influenced OC differentiation via the MAP kinase pathway. Phosphorylation of MAPKp44/42 was reduced within 15 min of treatment and stimulated after 1 - 2 h. Beauvericin and enniatin inhibited OC differentiation and function, and induced apoptosis in OCs. These fungal products inhibit motility and resorption, and increase cytotoxicity. Beauvericin is more potent than enniatin. These data suggest that beauvericin and enniatin may be a novel class of clinically relevant compounds for the treatment of osteoporosis and bone tumours.

**Disclosures:** O. Hoffmann, None.

This study received funding from: Hochschuljubilaumsstiftung of the City of Vienna.

## M131

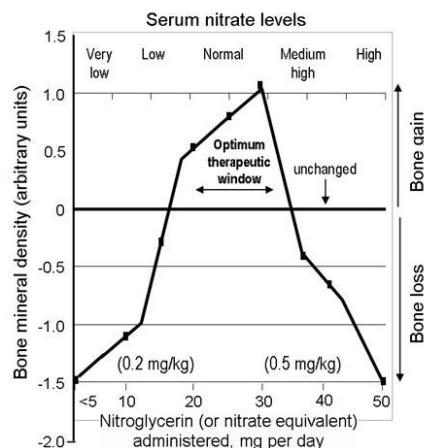
**Nitric Oxide Has a Powerful Effect of Osteoclast Cells.** S. J. Wimalawansa\*. Endocrinology - Medicine, Robert Wood Johnson Medical School, New Brunswick, NJ, USA.

Relative over-activation of osteoclast cells has been shown as one of the causes of age-associated as well as postmenopausal osteoporosis. Hence, in most cases, anti-osteoclastic agents have beneficial effects on improving bone mineral density (BMD), bone quality, as well as fracture reduction.

Others and we have demonstrated the effects of nitric oxide (NO) donor therapy as well as inhibition of NO synthase (NOS) enzymes with NOS inhibitors *in vitro* as well as *in vivo* animal studies. Here we demonstrate a dose-dependant effect of NO donor therapy as well as inhibition of NO/cGMP on the osteoclastic bone resorption activity *in vitro* cell culture system.

At very low doses or suppression of NOS activities with NOS inhibitors in culture over-activated osteoclast cells (i.e., increased bone resorption as indicated with the number of pits formed as well as the surface area/depth of pits. Whereas, adding NO donor therapies into the culture medium up to a certain levels suppressed the osteoclast-induced bone resorption and higher doses enhanced pit resorption capacity of osteoclasts. Data confirmed the previous *in vivo* data in rats that the effects of NO-cGMP on osteoclasts are biphasic and the therapeutic margin is narrow.

Our previous studies also suggested that NO donor agents (at appropriate doses have biphasic effects of the osteoblasts including cell proliferation/apoptosis as well as their activities. Figure demonstrates the proposed overall *in vivo* biphasic effects of NO donors on bone. It is important to notice that the therapeutic margin is narrow and the correct dose is necessary to obtain beneficial effects from this therapy in animals as well as in humans. Conclusion: taken together *in vitro* and *in vivo* studies suggests that at correct dose-exposure, NO donor therapies have highly beneficial effects on bone cells and hence protective effect on the skeleton in general.



**Disclosures:** S.J. Wimalawansa, None.

## M132

**Over-expression of RAGE Prevents Ovariectomy-mediated Bone Loss in CD1 Mice.** C. Li<sup>\*1</sup>, K. Ding<sup>\*2</sup>, S. Yan<sup>\*3</sup>, B. Lee<sup>\*1</sup>, D. Meng<sup>\*1</sup>, J. Xu<sup>\*1</sup>, L. Zhou<sup>\*4</sup>, M. Hamrick<sup>\*5</sup>, C. Isales<sup>6</sup>, Q. Mi<sup>4</sup>. <sup>1</sup>Center for Biotechnology and Genomic Medicine, Medical College of Georgia, Augusta, GA, USA, <sup>2</sup>Dept. of Medicine, Medical College of Georgia, Augusta, GA, USA, <sup>3</sup>Dept. of Medicine, The Medical School Hospital of Qingdao University, Qingdao, China, <sup>4</sup>Dept. of Pathology, Medical College of Georgia, Augusta, GA, USA, <sup>5</sup>Dept. of Cellular Biology, Medical College of Georgia, Augusta, GA, USA, <sup>6</sup>Dept. of Orthopedic Surgery, Medical College of Georgia, Augusta, GA, USA.

It has been reported that the advanced glycation endproducts (AGEs) and receptor for AGEs (RAGEs) are involved in diabetic complications. We recently reported that RAGE knockout mice in B6 genetic background have a significantly increased bone mass and bone biomechanical strength and a decreased number of osteoclasts compared to wild-type mice in B6 genetic background. These data therefore indicate that RAGE serves as a positive factor to regulate the osteoclast formation, and document that the over-expression of RAGE may account for diabetes-associated bone loss. To further test this, we used RAGE transgenic mice in CD1 genetic background. The bone mineral content (BMC), bone mineral density (BMD), fat and lean mass were examined using dual-energy X-ray absorptiometry, and bone biomechanical properties were also evaluated using three-point bending test. Interestingly, over-expression of RAGE did not reduce bone density or bone biomechanical properties at 18-week old age. Surprisingly, over-expression of RAGE significantly inhibited bone marrow macrophage (BMM) differentiation to osteoclasts and reduced bone resorption function compared to wild-type CD1 mice. To further test the function of RAGE over-expression *in vivo*, we ovariectomized mice at 18-week old age. Strikingly, over-expression of RAGE prevented ovariectomy-mediated bone loss. Our data suggest that RAGE negatively regulates osteoclast development modulated by ovariectomy in CD1 mice, and indicate that RAGE has dual functions to regulate

osteoclast development based on the different genetic backgrounds. Our data strongly argue that AGE/RAGE pathway in osteoclast development is very complex, which may complicate the design of novel therapies targeting this pathway.

**Disclosures:** Q. Mi, None.

This study received funding from: JDRF and CNSF.

## M133

**TGF $\beta$  Inducible Early Gene-1 Knockout Mice Display Defects in the Molecular Structure of Tendon Fibers.** L. Gumez<sup>1</sup>, C. Pichon<sup>\*2</sup>, J. R. Hawse<sup>3</sup>, M. Subramaniam<sup>3</sup>, J. Doucet<sup>\*4</sup>, T. C. Spelsberg<sup>3</sup>, S. Bensamoun<sup>1</sup>.

<sup>1</sup>Biomécanique et Bioingénierie UMR CNRS 6600, Université de Technologie de Compiègne, Compiègne, France, <sup>2</sup>Centre de Biophysique Moléculaire CNRS UPR 4301, Université d'Orléans, Orléans, France, <sup>3</sup>Department of Biochemistry and Molecular Biology, Mayo Clinic, Rochester, MN, USA, <sup>4</sup>Laboratoire de Physique des Solides UMR 8502, Université Paris-Sud, Orsay, France.

TGF $\beta$  inducible early gene-1 (TIEG1) is a member of the Krüppel-like family of transcription factors and plays an important role in Smad signaling. TIEG has also been shown to play an important role in the morphological and mechanical properties of tendons.

The purpose of this study was to characterize the effect of TIEG on the molecular structure of collagen (triple helix, intra and inter fiber structure) in tendon fibers.

Three month old female C57Black6/129 wild-type (WT) and TIEG KO mice were used. Approximately 3-4 tendon fibers were extracted from the WT and TIEG KO tails. Synchrotron X-ray microdiffraction experiments were carried out using a 13 KeV monochromatic beam (2 $\mu$ m in diameter). Each single tendon fiber (WT = 9 and TIEG\_KO = 8) was inserted into a capillary (diameter = 0.7mm) and placed vertically in the X-ray beam. Diffraction data arising from the internal supramolecular architecture of the tendon fiber were collected on a 2D detector. An X-ray pattern was obtained by scanning the fiber along the radial direction (160  $\mu$ m). The X-ray intensity along the meridional direction (fiber axis) was extracted for detailed analysis of the molecular packing.

The same patterns were observed within each of the fiber samples isolated from the same genotype (TIEG KO and WT). The X-ray diffraction patterns from TIEG KO mice revealed differences in the organization of fibril structure compared to WT controls. Figure 1 illustrates the intensity profiles along the meridian. WT tendon fibers displayed a sixth order maximal intensity peak while TIEG KO fibers were maximal at the fifth order.

These preliminary data demonstrate that the organization of tendon fiber structure is different in TIEG KO mice relative to WT mice. These results suggest that lack of TIEG expression results in a disorganization of the internal structure of tendon fibers. Further characterization of tendon fibers will allow us to better understand the influence of TIEG on the structure of the musculoskeletal system.

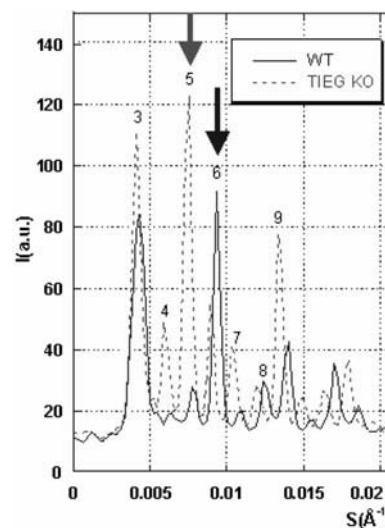


Figure 1: Meridional X-ray profile of WT and TIEG KO tendon fiber

**Disclosures:** L. Gumez, None.

## M134

**Biomarker Discovery for Bone and Cartilage Based on Metabolic Reconstruction Bioinformatics.** E. Selkov<sup>\*1</sup>, G. Hawa<sup>2</sup>, R. Datema<sup>\*1</sup>, W. Woloszczuk<sup>2</sup>. <sup>1</sup>encyclopedia Genomica GmbH, Linz, Austria, <sup>2</sup>Research & Development, Biomedica, Vienna, Austria.

In recent years the palette of biomarkers to study the biological processes leading to severe bone and cartilage diseases like osteoporosis, osteoarthritis, rheumatoid arthritis has increased significantly. Recently the focus was drawn to several regulation molecules either influencing osteoclast or osteoblast proliferation. Especially the importance of molecules involved in the Wnt signalling pathway in the progression of osteoarthritis

gained much attention. Despite that progress in understanding the biology of bone turnover, more biomarkers are needed for basic research and clinical studies on bone and cartilage disease to yield a full picture.

Therefore we developed procedures for the mining of public databases containing information about gene expression in human tissues. Transcriptomes of tissues represented in databases are deemed to be of sufficient quality for analysis of tissue-selective expression of genes, if enzymes and protein isoforms are well represented in twenty metabolic domains (examples in the table). The tool used, MPW Analyzer, is a bioinformatics mining tool that uses symbols to connect entries in protein databases with gene transcripts. Protein-coding transcripts occurring with high selectivity in bone and cartilage could thus be identified, and were further ranked based on occurrence of a gene product in body fluids, occurrence of veterinary homologues, disease association, low number of interactions with ECM-proteins, and protein features considered undesirable for future assay development. Of these selected proteins, seven represent hypothetical proteins ("unknowns"), 13 are highly selective for bone, 17 for cartilage, and three for the vasculature. Of the selected proteins, nine are expressed intracellularly; the remainder are secreted and are minor components of the ECM. Some of these proteins can be characterized by circulating peptides derived from them. We present the first sets of potential new marker molecules generated by this approach.

	H. sapiens				M. musculus		
	all tissues	bone tissue	connective tissue	vascular tissue	all tissues	bone tissue	connective tissue
Genes Expressed	29718	11741	13924	8707	36292	7370	5377
Expressed EC Numbers	1079	856	938	719	1026	640	570
ECs asserted in pathways	979	746	819	596	900	537	451
<b>Asserted Complete Pathways</b>	<b>3819</b>	<b>3277</b>	<b>3411</b>	<b>2945</b>	<b>3706</b>	<b>2888</b>	<b>2711</b>
Amino acid Metabolism	342	239	243	210	325	173	136
Aromatic compound metabolism	11	8	10	8	15	12	12
One-carbon Metabolism	11	10	10	7	11	9	1
Carbohydrate Metabolism	492	355	417	269	461	297	305
Coenzymes and Vitamins	77	58	68	53	80	43	41
Electron Transport	48	44	42	36	48	35	31
Enzyme metabolism	31	23	21	21	28	7	5
Exogenous Compounds	38	36	32	26	35	27	17
other pathways	29	12	12	12	20	14	14
Lipid Metabolism	690	592	601	497	656	442	433
Membrane transport	207	201	204	203	207	197	194
Nucleic acid Metabolism	306	294	301	284	301	260	248
Oxygen Metabolism	45	40	40	40	40	35	40
Phosphorus Metabolism	14	14	14	6	14	14	14
Protein Metabolism	643	551	584	527	636	570	476
Purine Metabolism	194	173	177	138	191	167	137
Pyrimidine Metabolism	110	107	111	89	108	101	82
Signal transduction	523	512	515	510	532	523	519
Sulfur Metabolism	9	8	9	9	9	6	6

**Disclosures:** G. Hawa, None.

This study received funding from: Österreichische Forschungsförderungsgesellschaft (FFG).

## M135

**Human Skeletal Muscle Cells Undergo Matrix Mineralization in an Osteogenic Pellet Culture Assay.** K. A. Corsi<sup>\*1</sup>, A. Usas<sup>\*1</sup>, T. R. Payne<sup>\*2</sup>, R. J. Jankowski<sup>\*2</sup>, J. Huard<sup>1</sup>. <sup>1</sup>Department of Orthopaedic Surgery, University of Pittsburgh, Pittsburgh, PA, USA, <sup>2</sup>Cook MyoSite, Inc., Pittsburgh, PA, USA.

Previous studies indicate that murine skeletal muscle cells undergo osteogenic differentiation in the presence of bone morphogenetic protein (BMP), and that this process occurs more rapidly in cells obtained from male mice than from female mice.<sup>1</sup> The ability of human skeletal muscle-derived cells (hMDCs) to undergo osteogenesis is not as widely reported. In this study, we investigated the osteogenic differentiation of male and female hMDCs in an in vitro osteogenic pellet culture assay. Cells were isolated from the skeletal muscle of 4 female (ages 22-25) and 4 male (ages 20-31) human donors. Their expression of the cell surface marker CD56 (myogenic marker) was determined by flow cytometry. For osteogenic differentiation, hMDCs were cultured as pellets in osteogenic medium (OSM) for 28 days and analyzed by  $\mu$ CT at 7, 14, 21 and 28 days for bone volume (BV) and density (BD). Gene expression for collagen type I (*Col1*) was determined by quantitative RT-PCR after 28 days in OSM. Matrix mineralization was evident in 6 of the 8 populations as early as 7 days after initiation of cultures. The female and male cell population with the lowest percentage of CD56 on their surface began displaying calcified tissue only after 14 days in culture. The mean BV and BD increased over time in all cell populations. No sex-related differences were observed at all time points tested for both BV and BD. *Col1* gene expression was increased for both male and female hMDCs after 28 days of culture in OSM, and this was significant for female hMDCs. These results suggest that by combining the pellet culture method with microCT analysis, we were able to observe the same pellet over time and determine the rate of mineralization for each cell population tested. It was shown that all hMDCs in this study undergo osteogenic differentiation as evidenced by mineralization and the expression of osteogenic genes. Unlike murine muscle cells, hMDCs underwent mineralization in OSM that did not contain BMP. As well, hMDCs did not display a significant difference between cells obtained from male and female donors, although the current study was done with a small sample size. Nevertheless, this osteogenic assay allowed us to determine that hMDCs with low CD56 expression did not mineralize as quickly as those expressing higher levels, suggesting that CD56 may be a possible marker for the osteogenic potential of hMDCs. In conclusion, hMDCs warrant further investigation, as they represent a potential cellular candidate for bone tissue engineering applications.

**Disclosures:** A. Usas, None.

## M136

**Quantification of Non-mineralized Tissue via  $\mu$ CT as a Readout for Glucocorticoid Effects on Rat Growth Plate.** F. Chen<sup>\*</sup>, S. Riley<sup>\*</sup>, D. H. Euler<sup>\*</sup>, J. E. Fisher<sup>\*</sup>, P. E. Brandish<sup>\*</sup>, J. C. Hershey<sup>\*</sup>. Molecular Endocrinology, Merck Research Laboratories, West Point, PA, USA.

Glucocorticoids (GCs) inhibit chondrocyte proliferation and increase apoptosis that result in reduction of non-mineralized tissue in growth plate (GP) and thinning of GP. This study focuses on establishing a quick and reliable method to quantify GP changes related to GC treatment in rats.

Sixteen week old intact female SD rats (N=10-12/grp) were treated for 7 d with 0.1 mpk dexamethasone (DEX) (sc, qd), 1.5 mpk 6 $\alpha$ -methyl prednisolone (6-MP) or vehicle (po, bid). In a second study, SD rats were ovariectomized (OVX) at age 12 weeks, and 6-MP (0.1, 0.3, 1 and 3 mpk, po, bid) treatment was started at age 18 weeks and continued for 28 d. Left tibias were collected and stored in 70% ethanol. The proximal tibia was scanned (SCANCO microcomputed X-ray tomography ( $\mu$ CT) 40) at 20  $\mu$ m resolution. Non-mineralized area (NMA) within GP in a fixed region (2.5x2.5 mm<sup>2</sup>) located in the center of the GP was quantified via 2D analysis at a threshold of 250 on 20 consecutive  $\mu$ CT slices. The NMA (mean of 20 slices, mm<sup>2</sup>) was calculated for each bone. Average GP thickness (GPT, mm) was also obtained by hand contouring the GP area within the above fixed region on the 1<sup>st</sup> and the 20<sup>th</sup> slices and dividing each area by 1/2 of the corresponding perimeter of the contouring line.

In the 7d experiment, both DEX and 6-MP significantly reduced the NMA (mm<sup>2</sup>) with DEX 0.148  $\pm$  0.015<sup>\*\*\*</sup>, 0.204  $\pm$  0.020<sup>\*\*\*</sup> for 6-MP vs. vehicle 0.358  $\pm$  0.031. Similarly, both DEX and 6-MP also reduced GPT (mm) with DEX 0.074  $\pm$  0.004<sup>\*\*\*</sup> and 6-MP 0.093  $\pm$  0.007<sup>\*</sup> vs. 0.120  $\pm$  0.008 for vehicle. Data from the second study also showed that 0.1 mpk of 6-MP reduced the NMA from OVX vehicle 0.234  $\pm$  0.018 to 0.155  $\pm$  0.009<sup>\*\*\*</sup>. Higher doses of 6-MP further reduced the NMAs to 0.114  $\pm$  0.015<sup>\*\*\*</sup> for 0.3 mpk, 0.066  $\pm$  0.003<sup>\*\*\*</sup> for 1 mpk and 0.066  $\pm$  0.007<sup>\*\*\*</sup> for 3 mpk. GPTs also revealed a dose dependent reduction ranging from 0.106  $\pm$  0.004, 0.083  $\pm$  0.006<sup>\*\*</sup>, 0.072  $\pm$  0.004<sup>\*\*\*</sup>, 0.060  $\pm$  0.004<sup>\*\*\*</sup> to 0.059  $\pm$  0.002<sup>\*\*\*</sup> corresponding to vehicle and low to high doses of 6-MP. Correlation study between NMA and GPT from both studies showed that NMA is significantly correlated to GPT with R<sup>2</sup> ~ 0.71 (P<0.001).

In conclusion, measurement of non-mineralized tissue via  $\mu$ CT as a readout of GC effects on rat GP is a quick, reliable and user friendly approach. It generates qualitatively similar data to those obtained by measuring GPT. The method can quantify growth plate changes induced by DEX and 6-MP after 7 d treatment in 16 week old rats. It can also reveal GC-related growth plate changes in OVX rats after 28 d treatment.

<sup>\*</sup>P<0.05, <sup>\*\*</sup>P<0.01, <sup>\*\*\*</sup>P<0.001 vs. vehicle

**Disclosures:** F. Chen, None.

## M137

**Bone Turnover Evaluated by a Combined Calcium Balance and <sup>45</sup>Calcium Kinetic Study, and Dynamic Histomorphometry: Effect of Ovariectomy and Sub-optimal Dietary Calcium in Rats.** M. Shahnazari<sup>\*1</sup>, W. Lee<sup>\*2</sup>, B. R. Martin<sup>\*2</sup>, C. M. Weaver<sup>2</sup>. <sup>1</sup>UC Davis Medical Center, Sacramento, CA, USA, <sup>2</sup>Purdue University, West Lafayette, IN, USA.

The gold standard approach for evaluating bone turnover responses to an intervention is dynamic histomorphometry. This is a laborious approach that is typically restricted to animal models because of the difficulties associated with taking iliac crest biopsies in humans. Calcium (Ca) tracer kinetic studies can be used to determine bone formation and bone resorption rates. The objective of this study was to validate isotopic approaches, in a rat model, against dynamic histomorphometry for establishing rapid detection methods for evaluating the effectiveness of treatments. The interventions used in our experiments included ovariectomy and sub-optimal level of dietary Ca.

Kinetic studies involved oral and intravenous administration of radioactive <sup>45</sup>Ca and monitoring of the tracer in blood, urine, feces, and bone over a 4-d period. Complete Ca balance including dietary intake as well as urinary and fecal excretion was also measured during this time. Histomorphometric indices of mineral apposition rate, mineralizing surface, and bone formation rate were obtained from tibia.

Ca tracer kinetic data showed a significant difference (p<0.001) in skeletal resorption and formation rates in response to ovariectomy (27.6 vs 13.8 mg/d for bone resorption and 42.7 vs 28 mg/d for bone formation in ovariectomized and sham rats, respectively). Highly significant correlations were found between bone deposition evaluated by kinetic data (organ level) and histomorphometric index of bone formation rate in cortical and trabecular bone (r = 0.63 and 0.76, p<0.001). Significant correlations were also demonstrated between bone resorption and formation rates at the organ level (r = 0.91, p<0.001) using Ca balance and <sup>45</sup>Ca kinetic data. Kinetic studies also showed that bone formation and bone balance were significantly lower when dietary Ca level was reduced from 0.4% to 0.2% (25.5 vs 19.7 mg/d and 11.3 vs 4.2 mg/d, respectively, p<0.001).

Our study suggested that Ca tracer kinetic data can be used reliably to rapidly detect changes in bone in response to interventions and can lower the sample size in studies by allowing a sequential testing of treatments in the same animals.

**Disclosures:** M. Shahnazari, None.



**M138**

**Dynamic Histomorphometry of Mineralized Tissue Using Cryosections of Murine Bone and Teeth.** X. Jiang\*, C. Ushiku\*, H. Li\*, D. W. Rowe. Dept. of Reconstructive Sciences, School of Dental Medicine, University of Connecticut Health Center, Farmington, CT, USA.

Dynamic histomorphometry requires the preservation of trabecular architecture and cellular detail, detection of fluorescent mineralization dyes and maintenance of enzymatic and immunoreactivity. Traditionally, embedding in plastic matrices has been employed to maintain structural integrity but at the expense of reduced biological activities. Previously we have implemented a tape transfer protocol for quality sections of frozen decalcified sections of murine bone that preserves GFP expression and immunoreactivity. Here we demonstrate a new tape protocol that provides excellent integrity of cryosections from mineralized tissues and preserves biological activities for histological detection. The mineralized matrix is detected by DIC optics. Because fluorescent reporters provide excellent signal discrimination, we have developed our histology to employ fluorescent signals that can be mapped back to the DIC image and the GFP reporters that identify specific cell types within bone. Examples of immunostaining for surface antigens (CD31, F/480), enzymatic staining for AP and TRAP, and in situ identification for BSP or Cbfa1 will show the low background and strong fluorescent signal strength that can be produced. However the most useful application of this histology may be the fluorescent mineralization labels to measure osteoid deposition. Five different colors can be detected to demonstrate the sequential deposition and removal of mineral from which the dynamic nature of a skeletal structure can be appreciated. For example the elongation rate of the dental incisor can be measured while the rapid turnover rate of trabecular bone relative to cortical bone can be observed. Not only can a matrix apposition rate be calculated, a label loss rate can be measured. We are exploring the potential of using this histology as a new standard for dynamic histomorphometry in which cells within the osteoblast lineage are identified by AP activity while their place within the lineage is identified by their association with a mineralization label. Similarly, cells within the osteoclast lineage are identified by their TRAP activity. A protocol to register the stained sections to the original DIC images has been developed so that the cellular activities can be expressed as a percentage of trabecular bone surface, an essential measurement of dynamic histomorphometry. Because the histology sections can be produced in a shorter period of time than plastic embedding/sectioning and the information obtained from the same section is extremely rich, we believe that it could become a very valuable tool for phenotyping murine models of bone disease.

**Disclosures:** X. Jiang, None.

**M139**

**Automatic Estimation of Body Composition Using Micro-CT and a Gaussian Mixture Model.** F. J. Ayres\*, G. M. Campbell, S. K. Boyd. Mechanical and Manufacturing Engineering, University of Calgary, Calgary, AB, Canada.

The use of micro-computed tomography (micro-CT) may present an alternative method for the measurement of body composition in mice, particularly when dual-energy X-ray absorptiometry (DXA) [1] is not practical. Body composition measurement with DXA has been validated in rats and provides a basis for which to compare micro-CT based composition measurements.

The standard procedure for the estimation of body fat ratio from micro-CT images consists of determining the percentage of voxels whose CT values fall within a predetermined range, typically associated with the density of fat. This method is prone to errors since the actual CT value of a voxel within a fatty region is better modeled as a random variable, whose distribution may extend beyond the typical range of CT values for fat tissue, with decreasing probability. The same reasoning applies to other tissues: a voxel within a lean mass region may exhibit a value that is typically associated with fat tissue due to the stochastic nature of the CT values and to the occurrence of partial volume effects.

In the present work we propose a method that does not require segmentation of the micro-CT data. A Gaussian mixture model (GMM) was applied to estimate the fractional contribution of fat, lean tissue, and bone, to the body composition of rats, while accounting for the random nature of CT values within each tissue category. The GMM represents the probability distribution of CT values in the body as a weighted sum of Gaussian distributions, each Gaussian representing the probability distribution of CT values associated with each tissue. The weights in the GMM provide the fractional composition of the body in terms of the various tissue types. The weights and the statistical parameters (mean and standard deviation) of each Gaussian in the GMM are determined such that the difference between the GMM and the observed probability distribution of values in the CT volume (given by the normalized histogram) is minimized. A genetic algorithm is used to automatically fit the GMM parameters.

Validation was conducted with skeletally mature rats subjected to ovariectomy (n = 10) or sham (n = 10) surgeries that were scanned using micro-CT and DXA. The histogram of the CT values in each volume was obtained, and a GMM was fit to the histogram data. It was observed that the correlation between GMM and DXA was high ( $r^2 = 0.93$ ), with a linear coefficient of 0.87. This is an improvement over traditional segmentation methods, especially when resolution is low, in terms of determination of body composition and computational effort. Future work will improve the GMM fitting procedure by incorporation of a filtering step prior to obtaining the histogram.

**Disclosures:** F.J. Ayres, None.

*This study received funding from: Alberta Breast Cancer.*

**M140**

**Rapid EDTA Microwave Decalcification of Rabbit Osteochondral Samples Preserves Enzyme Activity and Antigen Epitopes.** V. Lascau-Coman\*, M. D. Buschmann\*, C. D. Hoemann\*. Chemical Engineering, Ecole Polytechnique, Montreal, QC, Canada.

Decalcifying rabbit osteochondral samples with EDTA solution protects proteins from acid hydrolysis, however this is a lengthy procedure requiring 3 months to fully demineralize. It was previously shown that microwave decalcification of bone, using 10% EDTA/2% paraformaldehyde, could shorten the decalcification time. Here we report that rapid microwave decalcification of osteochondral samples with 10% EDTA/0.1% paraformaldehyde at 37°C preserves antigen epitopes and enzyme activity in osteoclasts. The goal of current study was to optimize a microwave decalcification method to conserve tartrate-resistant acid phosphatase (TRAP) activity, immunodetection of collagen II and I, and glycosaminoglycan (GAG) staining in osteochondral cryosections and paraffin sections.

Femurs from 3.5 month old rabbits were fixed in 4% paraformaldehyde/1% glutaraldehyde/0.1M sodium cacodylate for 5 days at 4°C. As our laboratory uses the rabbit knee trochlea as a cartilage repair model, each trochlea was trimmed to 12 mm length with a diamond saw and decalcified in 10% EDTA/0.1% paraformaldehyde in a Milestone microwave oven. For 6 consecutive days, samples were irradiated 9 hours per day using 3 hour cycles of 20 min/500W and 15 min/150W all at 37°C, and left each night at RT in EDTA. After decalcification, blocks were cut in half with a razor: the proximal half was embedded in OCT compound and the distal half in paraffin. 6 µm thick sections were immunostained for collagen I, and II. TRAP was detected by enzymatic stain and GAG by histostaining with Safranin O.

Complete decalcification in EDTA was obtained in 6 days using the microwave procedure versus 3 months in standard procedures. TRAP enzyme activity and immunoreactive antigens were preserved in both paraffin sections and cryosections. This method is a significant improvement over traditional methods due to the relatively short processing time and high quality of cartilage chondrocyte morphology and preservation of bone marrow.

**Disclosures:** C.D. Hoemann, None.

*This study received funding from: Canadian Institutes of Health Research (CIHR).*

**M141**

**Effects of Platinum Group Metals Treatment on the Bone of Developing Chick Embryos.** I. E. Pavel<sup>1</sup>, Z. E. Gagnon<sup>\*2</sup>, J. Cawley<sup>\*2</sup>, D. Reens<sup>\*2</sup>.

<sup>1</sup>Department of Chemistry, Wright State University, Dayton, OH, USA, <sup>2</sup>School of Science, Marist College, Poughkeepsie, NY, USA.

Recent studies showed that platinum group metals (PGMs) such platinum (Pt), palladium (Pd), and rhodium (Rh) from automobile catalytic converters, accumulate in the tissues of a variety living organisms. However, the effect of PGMs on bone microarchitecture and development is unknown. To examine these aspects, developing chick embryos were injected at the 7<sup>th</sup> and 14<sup>th</sup> day of incubation with either 0.1, 1.0, 5, or 10 ppm solutions of Pt (<sup>IV</sup>), Rh (<sup>III</sup>), Pd (<sup>II</sup>) or with a PGMs mixture (containing an equal amount of each metal) in saline solutions. Chick organs and tibiotarsus were harvested at the 20<sup>th</sup> day of incubation and examined. 1) Treatments with PGMs concentration above 1 ppm resulted in a bone weight loss accompanied by a decrease in the bone length and diameter directly proportional to the metal concentration (in comparison with the control samples). 2) The PGMs accumulation in soft tissue and bone was followed and quantified by graphite furnace atomic absorption spectrometry (GFAAS) on finely ground powder. The highest metal bioaccumulation was recorded for Pt. It ranged from ~0.012 mg/g of liver tissue to ~0.028 mg/g of brain tissue for metal treatments of 0.1 ppm, and showed a nonlinear increase with the metal treatment concentration. Similar PGM values were found in bone samples. X-ray fluorescence (XRF) and micro-Raman spectroscopy imaging were then used to examine the microspatial distribution of PGMs and the bone demineralization in paraffin embedded bone cross-sections of 4 µm thickness. 3) Pathological changes were observed for all PGM treatments above 1ppm. The most significant changes were noticed for the Pt treatments of 5 and 10 ppm, for which the threshold level of toxicity and the embryo mortality, respectively, were reached. At the Pt exposure level of 10 ppm, apoptotic neurons were detected, eosinophilic inclusion bodies were present in the liver, and the visual appearance of the organs indicated diseased tissue. The first brain cell edemas were noticed at the lowest concentration of 0.1 ppm. Calcium deposits were detected in the brain tissue treated with Rh at a concentration of 5 ppm (Von Kossa staining). This work demonstrated for the first time the accumulation and effects of PGMs in the bone tissues of developing chick embryos.

**Disclosures:** I.E. Pavel, None.

*This study received funding from: Wright State University - Dayton, OH and Marist College - Poughkeepsie, NY.*

## M142

**Specific Inhibitors of TNAP's Pyrophosphatase Activity Suppress Medial Arterial Calcification.** W. C. O'Neill<sup>\*1</sup>, K. A. Lomashvili<sup>\*1</sup>, S. Narisawa<sup>\*2</sup>, M. C. Yadav<sup>2</sup>, R. Dahl<sup>\*3</sup>, Y. Su<sup>\*3</sup>, M. F. Hoylaerts<sup>\*4</sup>, J. L. Millan<sup>2</sup>. <sup>1</sup>Renal Division, Emory University, Atlanta, GA, USA, <sup>2</sup>Sanford Children's Health Research Center, Burnham Institute for Medical Research, La Jolla, CA, USA, <sup>3</sup>San Diego Center for Chemical Genomics, Burnham Institute for Medical Research, La Jolla, CA, USA, <sup>4</sup>Center for Molecular and Vascular Biology, University of Leuven-Campus Gasthuisberg, Leuven, Belgium.

Humans and mice with low levels of extracellular inorganic pyrophosphate (ePPi), due either to deficient production (NPP1-deficiency) or transport (ANK-deficiency) develop soft-tissue calcification abnormalities, such as severe "idiopathic infantile arterial calcification" (IIAC), ectopic ossification in spinal ligaments, ankylosis and osteoarthritis. Calcification of the medial lamina of blood vessels occurs in IIAC, renal failure, obesity, diabetes, and aging, where it is thought to increase mortality through decreased arterial compliance. Using cultures of vascular smooth muscle cells (VSMC), we have established that VSMCs from Enpp1<sup>-/-</sup> and ank/ank mutant mice upregulate TNAP expression and calcify more than control cells. We have also found that TNAP is upregulated in the aortas of uremic rats. Our working model is that upregulated TNAP activity in the vasculature leads to reductions in ePPi concentrations to levels that no longer suppress calcification. In order to test the hypothesis that inhibition of TNAP's pyrophosphatase activity will prevent/reverse medial calcification we first need to develop potent, specific TNAP inhibitors. An initial screen of 53,280 compounds identified 3 novel inhibitors of TNAP's pyrophosphatase activity. We validated their usefulness kinetically, their ability to prevent calcification in primary cultures of osteoblasts and Enpp1<sup>-/-</sup> VSMCs, and their inhibition of TNAP's pyrophosphatase activity in whole rat aortas ex vivo. More recently, a screening of 66,000 additional compounds resulted in the identification of 4 new scaffolds. At present we have tested two new TNAP inhibitors active in the low  $\mu$ M range, that demonstrate good inhibition of calcification by Enpp1<sup>-/-</sup> VSMCs in vitro and also reduction of the amount of calcium deposited in ex vivo rat aortas. This increased efficiency correlates with improved docking in the TNAP active site. Initial absorption, distribution, metabolism and elimination parameters were established. Both MLS-0010847 and MLS-0038949 show good microsomal and plasma stability and high membrane permeability. We have identified MLS-0038949 as the best candidate to test in vivo and have performed initial pharmacokinetic and biodistribution studies to test the validity of using TNAP as a therapeutic target for vascular calcification.

**Disclosures:** J.L. Millan, None.

This study received funding from: NIH.

## M143

**Role of Pyrophosphate and Inorganic Phosphate in PKA-Mediated Osteoblastic Differentiation and Mineralization of Primary Murine Aortic Cells.** A. P. Sage<sup>\*</sup>, M. S. Huang<sup>\*</sup>, J. Lu<sup>\*</sup>, L. L. Demer, Y. Tintut. Cardiology (Medicine), UCLA, Los Angeles, CA, USA.

Vascular calcification is associated with increased cardiovascular morbidity and mortality. In vitro evidence suggests that vascular calcification occurs by osteo/chondrogenic differentiation of smooth muscle cells. We have previously found that the inflammatory cytokine, TNF-alpha, induces osteogenic differentiation of smooth muscle cell via activation of the PKA pathway. Recent studies have highlighted the importance of phosphate transport and pyrophosphates in osteoblastic differentiation and mineralization. Therefore, we investigated the role of phosphate transport in PKA-induced osteoblastic differentiation and mineralization of vascular cells isolated from murine aorta. Treatment of primary murine aortic cells with forskolin, which activates adenylate cyclase and downstream PKA signaling, significantly accelerated osteoblastic differentiation, as evidenced by the increased expression of osteoblastic differentiation markers - alkaline phosphatase (ALP), bone sialoprotein and osteocalcin. Forskolin also induced expression of ectonucleotide pyrophosphatase/phosphodiesterase-1 (Enpp-1) and pyrophosphate transporter, Ank, but did not induce the expression of sodium phosphate cotransporter, Pit-1. In the presence of 5 mM beta-glycerophosphate, mineralization was significantly induced by forskolin. Levamisole (an ALP inhibitor) and phosphonoformic acid (PFA; Pit-1 inhibitor) completely abrogated mineralization but did not attenuate expression of the osteoblastic differentiation markers. Inorganic phosphate also induced mineralization of these cells but did not induce expression of the osteoblastic differentiation markers. Phosphate-induced mineralization was inhibited by PFA but not by levamisole. Probenecid (ANK inhibitor) also inhibited mineralization, but further increased forskolin-induced expression of the osteoblastic differentiation markers. These results suggest that phosphate transport and pyrophosphate are needed for mineralization of vascular cells. Pyrophosphate also modulates osteoblastic differentiation. Interestingly, phosphate transport inhibition can completely block mineralization without affecting forskolin-induced markers of osteoblastic differentiation.

**Disclosures:** A.P. Sage, None.

This study received funding from: NIH.

## M144

**Abnormality of Bone Formation in Transgenic Mice Expressing Odd-Skipped Related 1.** M. Yamauchi<sup>1</sup>, S. Kawai<sup>2</sup>, A. Amano<sup>\*2</sup>, T. Ooshima<sup>\*1</sup>. <sup>1</sup>Department of Pediatric dentistry, Osaka university Graduate School of Dentistry, Suita-Osaka, Japan, <sup>2</sup>Department of Oral Frontier Biology, Osaka university Graduate School of Dentistry, Suita-Osaka, Japan.

Odd-skipped gene is one of the pair-rule genes which contribute to Drosophila somite formation. Two mammalian homologues, Odd-skipped related 1 (Osr1) and Osr2, are expressed in limb, branchial arches, kidney, eye, and dermis. Previous study on Osr1 deficient mice shows that Osr1 plays a critical role in the heart and urogenital development. We previously reported that Osr2 regulated osteoblast proliferation and bone formation using dominant-negative Osr2 transgenic mice, suggesting that Osr1 is involved in bone formation and osteoblast proliferation. However, the functional role of Osr1 in osteogenesis remains to be elucidated. In this study, we thus generated Osr1 transgenic mice (Osr1 Tg) which expressed full length of Osr1 gene driven by a 2.7 kb mouse Osr1 gene promoter. Genotype was determined by PCR of tail genome using transgene-specific primers. Consequently, the body length and body weight of Osr1 Tg were significantly decreased compared with those of wild type mice. RT-PCR analysis from 5 weeks old wild type mice tissues revealed endogenous Osr1 mRNA expressed in calvarial bone, femur, and tibia. Higher level of Osr1 mRNA expression was detected in those tissues of Osr1 Tg. At 5 weeks and 6 months after birth, soft X-ray analysis of Osr1 Tg revealed an increased radiolucency in cranial bone, compared with those of the wild type mice, and Osr1 Tg also had gibbosity and more round skull shape than those of wild type mice. In addition, we found that the long bones of Osr1 Tg were slightly shorter. Morphologically, calvaria, femur, and tibia of Osr1 Tg were composed of markedly thinner parietal and cortical bones, indicating delayed intramembranous ossification. Osr1 Tg newborn mice skeletons stained with alcian blue and alizarin red showed that calvarial sutural space was wider than that of wild type mice. Our data indicate that Osr1 gene has a role in osteogenesis, especially craniofacial and crural development. The abnormalities such as gibbosity and round skull were found at 5 weeks old Tg mice, however these abnormalities were not seen at newborn Tg mice. The shape of the skull may be dependent on the rate of cranial bone growth and on the timing of suture closure through postnatal growth. We previously reported that Osr1 gene expression was suppressed by Runx2 which is known as an indispensable factor in bone formation. We are investigating whether the role of Osr1 in bone formation is dependent on Runx2 with primary osteoblastic cells from Osr1 Tg and Runx2 deficient mice.

**Disclosures:** M. Yamauchi, None.

## M145

**Quantitation of Bone Marrow Fat in Long Bones of Mice Using MRI or  $\mu$ CT.** D. J. Adams<sup>1</sup>, I. Pinz<sup>\*2</sup>, M. Praeda<sup>\*2</sup>, E. Canalis<sup>3</sup>, N. Troiano<sup>\*4</sup>, M. C. Horowitz<sup>4</sup>, C. Rosen<sup>2</sup>. <sup>1</sup>UCONN Hlth Ctr, Farmington, CT, USA, <sup>2</sup>Maine Med Ctr Res Instit, Scarborough, ME, USA, <sup>3</sup>St. Francis Hospital, Hartford, CT, USA, <sup>4</sup>Yale Univ, New Haven, CT, USA.

Bone marrow fat can be assessed histologically, but has often been considered incidental. Recent reports have noted an inverse correlation between the length of the T1 weighted signal in vertebral marrow and bone density in humans. But the developmental sequence of marrow fat in mice has not been reported. In this study we used two techniques to image and quantitate marrow fat in mice: 1) in vivo MRI of the distal femur of C57BL/6J (B6), and two mutants, Alox5<sup>-/-</sup> (Lipoxygenase 5) and *small*, which carries a mutation in the IRS-1 gene; 2) ex vivo  $\mu$ CT with osmium staining. Longitudinal MRI was performed using images acquired with a RARE pulse sequence (TR 1500 ms, TE 10.39 ms, slice thickness 0.5 mm, FOV 3.5 cm, matrix 256x256, averages 20, and total scan time 16.49 min). Localized <sup>1</sup>H MR spectroscopy was performed using PRESS (point resolved spectroscopy, TR 2000 ms, TE21.44 ms, averages 800, total scan time 26.4 min) in a 1x7x1 mm voxel positioned over the marrow. B6 females were scanned at 8, 12, 26 and 30 wks. By spectroscopy marrow fat was highest in B6 at 8 wks, lower but similar at 12, 26 and 30 wks. In Alox 5<sup>-/-</sup>, marrow fat was assessed at 8, 26 and 36 wks. At 8 wks, Alox 5<sup>-/-</sup> had greater cortical thickness (cort th) vs B6 (0.045  $\pm$  0.001 mm vs. 0.035  $\pm$  0.004 mm, p<0.05), but 40% lower marrow fat. At 26 wks, cort th was higher in B6 than Alox 5<sup>-/-</sup> (0.054  $\pm$  0.004 mm vs 0.047  $\pm$  0.002 mm, p<0.05), but Alox 5<sup>-/-</sup> had 30% higher marrow fat than B6. By 36 wks, cort th in B6 had doubled (0.063 mm  $\pm$  0.003 mm) whereas Alox 5<sup>-/-</sup> showed a slight increase to 0.051  $\pm$  0.001 mm. However, marrow fat did not change between 26 and 36 wks in either strain. In *small* mice there was near total absence of marrow fat by MRI but very low BV/TV and cort th; this was confirmed by histology. An alternative approach to MRI is osmium tetroxide (OT), which specifically stains fat and we have demonstrated that OT staining can visualize and enumerate adipocytes in nondecalcified, plastic embedded bone sections. However, this approach is time consuming and limited by the field of the section. Because OT is radiopaque to X-ray, stained adipocytes can be imaged using  $\mu$ CT. Femora from Ebf1<sup>-/-</sup> mice (high marrow fat and high BV/TV) and littermate controls were fixed, decalcified, stained with OT, and imaged using  $\mu$ CT. Adipocyte density was greatest in the epiphysis and metaphysis of the distal femur, extending proximally a few millimeters in an anterolateral cluster. Adipocyte volume in Ebf1<sup>-/-</sup> mice showed a 16-fold increase vs control bone. Thus, we believe use of MRI and  $\mu$ CT to quantitate fat in bone is a major technological advance, and facilitates developmental analysis of the relationship between osteoblastogenesis and adipogenesis.

**Disclosures:** M.C. Horowitz, None.

## M146

**The Effect of Lead on Bone Mineral Properties from Female Adult C57/BL6 Mice.** A. Monir<sup>\*1</sup>, S. Yagerman<sup>\*2</sup>, M. C. H. van der Meulen<sup>2</sup>, C. M. Gundberg<sup>3</sup>, A. Boskey<sup>4</sup>, T. Dowd<sup>1</sup>. <sup>1</sup>Department of Chemistry, Brooklyn College of the City University of New York, New York, NY, USA, <sup>2</sup>Mechanical and Aerospace Engineering, Cornell University, Ithaca, NY, USA, <sup>3</sup>Department of Orthopedics, Yale University School of Medicine, New Haven, CT, USA, <sup>4</sup>Musculoskeletal Integrity Program, Hospital for Special Surgery, New York, NY, USA.

Lead toxicity continues to be a major problem in the U.S. with elevated blood lead levels being highest among very young children and older adults  $\geq 50$  years old. Bone is the major reservoir of body lead and accounts for 75% in children and 90% in adults. We investigated the effect of lead accumulation on the femora from adult, 6 month old female C57/BL6 mice ( $n=10$ /group) who were administered lead in the drinking water (250 ppm, blood lead 35 $\mu$ g/dl at sacrifice) for 4 months. Bone mineral properties were examined using Fourier Transform Infrared Microscopy (FTIRM), quantitative microcomputed tomography (microCT) and biomechanical measurements. Lead significantly decreased the bone mineral density in the cortical and proximal trabecular bone, increased the marrow area in the cortical bone and increased the bone volume fraction in proximal bone with microCT. Whole bone three-point bending showed a trend of decreased maximum and failure moments in the lead treated bones compared to controls. Lead significantly decreased the mineral/matrix ratio, collagen maturity and crystallinity in the trabecular bone as measured by FTIRM. In the cortical bone lead significantly decreased collagen maturity and produced a trend showing an increased carbonate/mineral ratio by FTIRM. In contrast to cell culture studies, lead significantly increased serum osteocalcin levels ( $71 \pm 3.5$  vs.  $46 \pm 3.3$ ,  $p<.001$ ) suggesting increased bone turnover. These data show a weakening of cortical bone with lead in adult, female mice and suggest that lead may exacerbate bone loss and osteoporosis in the elderly.

**Disclosures:** T. Dowd, None.

This study received funding from: NIH ES009032 & AR046121.

## M147

**Betulin Down Regulates Interleukin-1 $\alpha$ -stimulated Aggrecanases and Matrix Metalloproteinases Gene Expression in Human Chondrocytes.** J. Huh<sup>\*</sup>, Y. Baek<sup>\*</sup>, D. Kim<sup>\*</sup>, D. Choi<sup>\*</sup>, J. Lee<sup>\*</sup>, D. Park<sup>\*</sup>. <sup>1</sup>Oriental Medicine Research Institute for Bone and Joint disease, KyungHee University, Seoul, Republic of Korea, <sup>2</sup>Department of Acupuncture & Moxibustion, College of Oriental Medicine, KyungHee University, Seoul, Republic of Korea, <sup>3</sup>Department of Nuclear Medicine, College of Medicine, KyungHee University, Seoul, Republic of Korea.

**Objects:** Interleukin-1 $\alpha$ (IL-1 $\alpha$ ) is a pro-inflammatory cytokine that causes anti-anabolic and catabolic effects on articular chondrocytes via four major signaling pathways. In this study, we investigated the role of betulin, a triterpenoid agent, on these pathways for the repression of aggrecan and type II collagen, and induction of aggrecanases and matrix metalloproteinases in human osteoarthritic chondrocytes.

**Methods:** Chondrocytes were pretreated with various dose of betulin for 24 h, followed by IL-1 $\alpha$  for 1 h. Reverse transcription-polymerase chain reaction was performed to determine mRNA levels of type II collagen and aggrecan, matrix metalloproteinases (MMP-1,13), aggrecanases (-1, -2). Activity of mitogen-activating protein kinases (MAPK) was assayed by Western blot.

**Results:** Betulin enhance the synthesis of aggrecan and type II collagen and reduce the aggrecanase-1, -2 and MMP-1, -13 synthesis. In addition, betulin effectively inhibit the IL-1 $\alpha$ -activated extracellular signal-regulated kinases (ERK1/2), c-Jun NH<sub>2</sub>-terminal kinase (JNK) and p38-MAPK activation, and the binding of NF-kappaB and AP-1 transcription factors, two key factors involved in the expression of several pro-inflammatory genes in chondrocytes.

**Conclusion:** These results suggest that use of betulin or triterpenoid compounds derived from it may be of potential benefit in inhibiting signaling events associated with cartilage degradation in osteoarthritis.

**Acknowledgement:** This study was supported by a grant of the Oriental Medicine R&D Project, Ministry of Health & Welfare, Republic of Korea (B030008).

**Disclosures:** J. Huh, None.

## M148

**OAH19, an Ethanol Extract from Combined Two Herbs, Inhibits Interleukin-1 Alpha-induced Expression of Matrix Metalloproteinase-1 and -13 in Osteoarthritic Human Cartilage and Synovial Fibroblast.** Y. Baek<sup>\*1</sup>, J. Huh<sup>\*2</sup>, J. Lee<sup>\*1</sup>, D. Choi<sup>\*1</sup>, D. Kim<sup>3</sup>, D. Park<sup>\*1</sup>. <sup>1</sup>Department of Acupuncture & Moxibustion, College of Oriental Medicine, KyungHee University, Seoul, Republic of Korea, <sup>2</sup>Oriental Medicine Research Center for Bone & Joint Disease, KyungHee University, Seoul, Republic of Korea, <sup>3</sup>Department of Nuclear Medicine, College of Medicine, KyungHee University, Seoul, Republic of Korea.

**Objects:** Subchondral bone sclerosis is a common feature of osteoarthritis (OA), but the mechanisms responsible for this condition remain unresolved. we investigate the effects of beta-D-glucopyranoside from *Phellodendron amurense* on the production of

inflammatory cytokines (interleukin (IL)-1 $\alpha$ , IL-6, and prostaglandin E2 (PGE<sub>2</sub>)), growth factors (vascular endothelial growth factor (VEGF) and transforming growth factor-beta (TGF- $\beta$ )), matrixmetalloproteinase (MMP)/urokinase plasminogen activator (uPA) and bone markers in human subchondral OA Ob.

**Methods:** We measured the abundance of IL-1 $\alpha$ , IL-6, PGE<sub>2</sub>, VEGF, TGF- $\beta$ , MMP-1 and uPA using very sensitive ELISA in conditioned-media of human primary subchondral Ob from normal individuals and osteoarthritic patients. beta-D-glucopyranoside or selective COX-2 inhibitor (NS398) was performed to determine its effect on inflammatory cytokines, growth factors, MMP/uPA. The expression of bone cell markers was also determined.

**Results:** OA Ob produced all these factors with greater variability than normal cells. Interestingly, the production of IL-6, PGE<sub>2</sub>, VEGF and MMP-1/uPA by OA Ob separated patients into two subgroups, those whose Ob produced levels comparable to normal (low producers) and those whose Ob produced higher levels (high producers). In those cells classified as high producers, IL-6, PGE<sub>2</sub>, VEGF and MMP-1/uPA levels were increased two- to three-fold and five- to six-fold, respectively, compared with normal. In contrast, we found that IL-1 $\alpha$  and TGF- $\beta$  levels were similar in normal and all osteoarthritic Ob. beta-D-glucopyranoside significantly reduced IL-6, PGE<sub>2</sub>, VEGF and MMP-1/uPA levels in all OA Ob. In contrast, using NS398 did not reduce VEGF and MMP-1/uPA levels in either group. The evaluation of alkaline phosphatase activity, osteocalcin release and collagen type I activity increased by beta-D-glucopyranoside in OA Ob regardless to which subgroup they were assigned.

**Conclusion:** These results suggest that beta-D-glucopyranoside may contribute to bone remodeling through inhibition of inflammation and MMP/uPA system in subchondral OA Ob, ultimately leading to treatment of abnormal bone sclerosis in OA.

**Disclosures:** Y. Baek, None.

This study received funding from: a grant of the Oriental Medicine R&D Project (B030008), Ministry of Health & Welfare, Republic of Korea.

## M149

**Effect of Bisphosphonate Treatment of Osteoarthritis in a Guinea Pig Model.** A. Brüel, T. S. Straarup<sup>\*</sup>, C. C. Danielsen<sup>\*</sup>, H. Oxlund<sup>\*</sup>, J. S. Thomsen. Institute of Anatomy, University of Aarhus, Aarhus, Denmark.

Dunkin Hartley guinea pigs spontaneously develop osteoarthritis (OA) at approximately 3 months of age. The effect of bisphosphonate (Risedronate, BP) on the development of OA in Dunkin Hartley guinea pigs was investigated. Our hypothesis is that treatment with BP would decrease bone turnover and thereby reduce formation of new subchondral bone resulting in a reduced load on the articular cartilage, thus arresting the development of OA.

Fifty-six 3-month-old male Dunkin Hartley guinea pigs were randomized into 7 groups. Three groups received Risedronate (30  $\mu$ g/kg) injections s.c. 5 times a week for 6, 12, or 24 weeks. The remaining four groups served as either baseline or controls receiving vehicle. The left hind limb was removed from the anesthetized animals before they were perfusion fixed. The right knee was embedded undecalcified in MMA and 7- $\mu$ m-thick frontal sections were cut through the central part of the condyles, where the articular cartilage is not covered by meniscus. The sections were stained with Safranin O, TRAP, or von Kossa. The OA was scored with the Osteoarthritis Research Society International (OARSI) score. The articular surface of the left proximal tibia was stained with Indian ink, and the area of the articular cartilage lesion was determined from digital images of the medial tibial plateau. Using TRAP sections, osteoclast covered surfaces were counted in the medial epiphysis with CAST grid software. Digital images of the von Kossa stained sections were obtained and combined trabecular and cortical bone volume fraction (bone density) and subchondral plate thickness were determined using custom software.

The OARSI score did not differ between the BP-treated and the control animals at any time-point. The area of the articular cartilage lesions of the BP-treated animals was significantly higher after 6 weeks, but did not differ at the later time-points. The combined OARSI and area score did not differ at any time-point. The bone density was higher for the BP-treated animals, but significant only at 6 and 12 weeks. The OARSI score was significantly correlated with the bone density when all animals were pooled. The subchondral plate was significantly thicker in BP-treated animals than in control animals at all time-points. The BP treatment significantly suppressed the fraction of osteoclast covered surfaces at all time-points.

In conclusion, treatment with Risedronate did not influence the development of OA in Dunkin Hartley guinea pigs.

**Disclosures:** A. Brüel, None.

## M150

**Impact of Calpain Inhibition on Chondrocyte Development.** A. Kashiwagi<sup>\*1</sup>, E. Schipani<sup>1</sup>, P. A. Greer<sup>\*2</sup>, A. P. McMahon<sup>\*3</sup>, M. Shimada<sup>1</sup>.

<sup>1</sup>Endocrine Unit, Massachusetts General Hospital and Harvard Medical School, Boston, MA, USA, <sup>2</sup>Queen's University Cancer Research Institute, Kingston, ON, Canada, <sup>3</sup>Department of Molecular and Cellular Biology, Harvard University, Cambridge, MA, USA.

We have previously demonstrated that the calpain small subunit directly binds the intracellular C-terminal tail of the PTH/PTHrP receptor (PPR) and modifies its cellular functions *in vitro*. To investigate a role of *capn4* in cells of osteoblast lineage *in vivo*, we established osteoblast-specific *capn4* knockout mice by mating mice homogenous for floxed *capn4* alleles (*Capn4*<sup>fl/fl</sup>) with mice expressing *Cre* under the control of osterix promoter (*Osx-Cre*<sup>+/+</sup>). As previously reported, *Osx-Cre*<sup>+/+</sup>*Capn4*<sup>fl/fl</sup> (mutant) mice had smaller bodies with shorter limbs, reduced trabecular bone, and decreased osteoblast number, at least in part, due to reduced proliferation of cells of the osteoblast lineage.

Interestingly, in *Osx-Cre<sup>+/+</sup>* transgenic mice, *Cre* recombinase is expressed not only in early cells of the osteoblast lineage but also in late proliferating chondrocytes. We, thus, hypothesize that the smaller size of the skeleton of mutant mouse at E14.5 and birth could be caused by abnormal growth plate development secondary to genetic ablation of *capn4* in chondrocytes. Routine histology and *in situ* hybridization analysis were performed on histological sections of hind limbs isolated from E14.5, E15.5 and E18.5 embryos, respectively. At E14.5, the expression patterns of type II collagen, *PPR*, and type X collagen (*ColX*) mRNAs were similar in *Osx-Cre<sup>+/+</sup>Capn4<sup>fl/-</sup>* (control) and mutant mice. Conversely, the domain of *OP* mRNA expression was markedly reduced and *MMP13* mRNA was virtually undetectable in mutants vs. controls. A spatially restricted expression of both *ColX* and *OP*, and a severe decrease of the *MMP13* mRNA levels were also observed in E15.5 mutants vs. controls. Thus, these data suggest that terminal differentiation of chondrocytes was delayed in mutant embryos. Consistent with this developmental delay, mutant mice displayed a shorter bone collar as indicated by von Kossa staining. Blood vessel invasion and formation of the primary ossification center were also delayed in mutant embryos as shown by histology and *in situ* hybridization analysis of type I collagen mRNA expression. We further tested calpain's role in chondrocyte proliferation and differentiation using chondrogenic progenitor cells, ATDC5. ATDC5 cells treated with calpain-specific inhibitor, ALLM, showed significantly reduced both cell mitosis and cyclin D protein accumulation, and mRNA expression of chondrocyte differentiation markers such as *ALP*, *PPR*, *ColX*, and *MMP13*. Collectively, these results suggest that calpain plays a critical role in chondrocyte proliferation and differentiation.

**Disclosures:** A. Kashiwagi, None.

This study received funding from: NIH/NIDDK.

## M151

**Essential Hox Gene Function in Limb Skeletal and Synovial Joint Formation.** E. Koyama<sup>\*1</sup>, T. Ochiai<sup>\*1</sup>, D. Wellik<sup>\*2</sup>, M. Pacifici<sup>1</sup>. <sup>1</sup>Department of Orthopaedic Surgery, Thomas Jefferson University, Philadelphia, PA, USA, <sup>2</sup>Department of Internal Medicine, University of Michigan, Ann Arbor, MI, USA.

*Hox* genes are key regulators of early limb skeletal patterning, but their subsequent roles in cartilaginous anlage and synovial joint development remain largely unclear. Here we analyzed mice lacking *Hoxa10/Hoxc10/Hoxd10* or *Hoxa11/Hoxc11/Hoxd11* paralogues and focused on their hindlimbs. Newborn *Hox10* compound mutants contained a drastically shortened and abnormally shaped femoral cartilaginous anlage, while the *Hox11* mutants contained abnormal tibial and fibula anlagen. Interestingly, the latter mutant anlagen closely resembled each other, implying that the normal significant morphological difference between tibia and fibula was lost. The chondrocytes within the prospective metaphyseal and diaphyseal regions of all affected skeletal elements failed to organize in growth plates, displayed a small size and expressed markedly lower levels of genes normally associated with their maturation and hypertrophy, including Indian hedgehog and collagen X. Not surprisingly, primary spongiosa and intramembranous bone collar formation were severely delayed compared to age-matched wild type mice. Behavior and function of epiphyseal joint-associated chondrocytes were deranged as well. Normally, the knee joint involves articulation of distal femoral epiphysis with proximal tibial epiphysis without the participation of fibula. In the mutants, however, the knee joints were mis-shaped and both tibia and fibula epiphyses articulated with an enlarged femoral epiphysis, thus creating an ectopic fibula-femoral joint. In addition, articular cartilage tissue was disorganized, and the ectopic fibula-femoral joint was associated with ectopic expression of joint-associated genes such as lubricin. In sum, *Hox* genes not only direct early skeletal patterning, but have essential roles in continuation of long bone development and in synovial joint formation. Presence of an ectopic fibula-femoral joint in addition to a tibial-femoral joint indicates that fibula and tibia anlagen lose their identity and developmental distinction in the absence of *Hox10* or *Hox11* function.

**Disclosures:** E. Koyama, None.

## M152

**BT-201, a Butanol Extract of *Panax notoginseng* Inhibits Progression of Joint Degeneration in a Rat Model of Osteoarthritis.** S. Chang<sup>\*1</sup>, J. Han<sup>\*1</sup>, J. Park<sup>\*1</sup>, M. Son<sup>\*1</sup>, D. Jung<sup>\*2</sup>, B. Lee<sup>\*2</sup>, S. Shim<sup>\*2</sup>, S. Kim<sup>1</sup>, J. Ko<sup>1</sup>, K. Kim<sup>\*1</sup>. <sup>1</sup>Dept. of Pharmacology and Mechanism, Oscotec Inc., Cheonan, Republic of Korea, <sup>2</sup>Dept. of Botanical Medicine, Oscotec Inc., Cheonan, Republic of Korea.

Osteoarthritis (OA) is a degenerative joint disease in which proinflammatory cytokines such as IL-1 $\beta$  and TNF- $\alpha$  stimulate cartilage destruction. From the screening of various herbal extracts, we found that BT-201, an n-butanol extract of *Panax notoginseng* (Burk.) F. H. Chen (*P. notoginseng*) has the ability to inhibit TNF- $\alpha$  secretion and protect from the degradation of cartilage matrix. The purpose of this study has been to evaluate potential therapeutic effects of BT-201 on osteoarthritis. The cartilage protective effects of BT-201 were evaluated by measuring the production of matrix metalloproteinase (MMP-2), matrix metalloproteinase-13 (MMP-13), tissue inhibitor of matrix metalloproteinase-3 (TIMP-3) and glycosaminoglycan (GAG). BT-201 significantly inhibited the production of MMP-13 and GAG in a dose-dependent manner, but not MMP-2 *in vitro*. And BT-201 increased the production of TIMP-3 from osteosarcoma cells. In addition, oral administration of BT-201 (15 mg/kg, once a day for 21 days) to OA rat significantly reduced cartilage destruction. These results suggest that BT-201 may be used as a promising botanical drug for the treatment of osteoarthritis.

**Disclosures:** S. Chang, None.

## M153

**Overexpression of CCN2/CTGF in Cartilage Shows Prolonged Bone Length Resulting from Stimulation of Chondrogenesis, Chondrocyte Growth, Apoptosis, and Bone Mineralization During Endochondral Ossification.** N. Tomita<sup>\*1</sup>, T. Hattori<sup>\*1</sup>, S. Ito<sup>\*1</sup>, E. Aoyama<sup>\*1</sup>, M. Yao<sup>\*1</sup>, T. Yamashiro<sup>\*2</sup>, M. Takigawa<sup>1</sup>. <sup>1</sup>Biochemistry and Molecular Dentistry, Okayama University Graduate School of Medicine, Dentistry, and Pharmaceutical Sciences, Okayama City, Japan, <sup>2</sup>Orthodontics, Okayama University Graduate School of Medicine, Dentistry, and Pharmaceutical Sciences, Okayama City, Japan.

CCN2/CTGF is highly expressed in prehypertrophic chondrocytes. Our previous studies using cultured chondrocytes and the analysis of *ccn2*-deficient mice show CCN2 promotes proliferation, differentiation, and maturation of growth plate chondrocytes. However, there is no direct evidence showing that it promotes cartilage development and growth *in vivo*. Here we generated transgenic mice (tg) overexpressing the *ccn2* gene in cartilage under the control of the type II collagen (*col2a1*) promoter and show for the first time that this overexpression of CCN2 causes extended bone length. To overexpress CCN2 in cartilage, *ccn2* cDNA was inserted to downstream of the 6 kb-*Col2a1*-enhancer/promoter followed by *IRES-LacZ*. Whole mount X-gal staining showed transgene expression in all cartilage, overexpressed *ccn2* mRNA and CCN2 protein were detected in tg cartilage. Tg mice showed increased body size resulting from prolonged bones. Immunohistochemical analysis of tibia showed accumulation of proteoglycans and type II collagen in cartilage, while hypertrophic zone was shortened. The length of tibia was prolonged depending on the overexpression level of *ccn2* mRNA. Cell proliferation was accelerated in the resting zone in addition to the growth plate. TUNEL assay showed accelerated apoptosis in cartilage-bone transition. Bone density of cancellous bone and thickness of cortical bone were increased in tg mice by peripheral quantitative computed tomography (pQCT) analysis. Cultured chondrocytes isolated from tg mice showed enhanced expression of *col2a1*, *col10a1* and *aggrecan* mRNA and accumulation of proteoglycans. Furthermore, expression of vascular invasion factors such as *vegf* and *mmp9* mRNA was also enhanced. Micromass culture of limb buds from 11.5E tg embryos showed accelerated chondrogenesis.

Our findings indicate that CCN2 promotes chondrogenesis and accelerates growth of cartilage, chondrocyte death, and bone mineralization during endochondral ossification, resulting in prolonged long bones.

**Disclosures:** N. Tomita, None.

This study received funding from: Grants-in-Aid for Scientific Research from Japan Society for the Promotion of Science.

## M154

**Development of Osteoarthritis and Its Relationship to Meniscal Ossification in Dunkin Hartley Guinea Pigs.** J. S. Thomsen, T. S. Straarup<sup>\*</sup>, C. C. Danielsen<sup>\*</sup>, H. Oxlund<sup>\*</sup>, A. Br  l. Institute of Anatomy, University of Aarhus, Aarhus, Denmark.

Dunkin Hartley guinea pigs is a well established animal model of spontaneous development of osteoarthritis (OA). It has been observed that the menisci of these rodents ossify at a very early age and well before the OA develops. Our hypothesis is that this meniscal ossification may play a role in the pathogenesis of OA in these animals. Ten male Dunkin Hartley guinea pigs to each of the ages 2, 6, 9, and 12 months were anaesthetized and the left hind limb was removed before the animals were perfusion fixed. The meniscus of the left tibia was dissected free and embedded in MMA. Horizontal 7- $\mu$ m-thick sections were cut at every 140  $\mu$ m through the entire meniscus and stained with Goldner trichrome. For all sections the amount of fibrous cartilage, hyaline cartilage, and bone was determined using CAST grid software. The articular surface of the left proximal tibia was stained with Indian ink and the areas of the articular cartilage lesions were determined from digital images of the tibial plateaus. The right knee was embedded in MMA and 7- $\mu$ m-thick frontal sections were cut through the central part of the condyles, where the articular cartilage is not covered by meniscus, and stained with Safranin O. The degree of OA was scored using the Osteoarthritis Research Society International (OARSI) score.

At the medial condyle, no articular cartilage lesions were found in the 2-month-old animals, whereas the older animals showed increasing OA score. At the lateral condyle, early stage OA was found in five 12-month-old animals, whereas no cartilage lesions were found in the younger animals. The meniscal bone volume/total meniscal volume (ossified meniscus fraction) increased with age from 26% to 38% (medial), and from 16% to 28% (lateral). The severity of the articular lesions were significantly correlated to the medial ossified meniscus fraction ( $r^2 = 0.6$ ,  $p < 0.0001$ ).

In conclusion, the present study showed that ossification of the medial meniscus is correlated to the development and progression of OA in Dunkin Hartley guinea pigs. However, additional factors may also play a role in the pathogenesis of OA. Nevertheless, these findings may question whether the OA developed in this animal model is comparable to human primary OA, where ossification of the meniscus rarely occurs.

**Disclosures:** J.S. Thomsen, None.

**M155**

**PTH has Direct Anabolic Effects on Osteoarthritic Articular Cartilage *in Vitro* and *in Vivo*: Is PTH a New Treatment for Osteoarthritis?** B. C. Sondergaard<sup>\*1</sup>, S. H. Madsen<sup>\*1</sup>, A. B. Jensen<sup>\*1</sup>, N. A. Sims<sup>2</sup>, J. Gooi<sup>\*2</sup>, M. A. Karsdal<sup>1</sup>. <sup>1</sup>Pharmacology, Nordic Bioscience, Herlev, Denmark, <sup>2</sup>St. Vincent's Institute, Fitzroy, Australia.

The pathogenesis of osteoarthritis (OA) involves major changes in both the bone and cartilage compartments of the affected joints. It is well-known that PTH is bone anabolic. One signaling pathway of the PTH G-coupled receptor on osteoblasts is through cAMP. cAMP has recently shown to be of major importance for chondrocyte phenotype. We investigated whether chondrocytes, which originate from the same mesenchymal stem cell type as osteoblasts, responded anabolically to PTH treatment, and thereby whether PTH may represent a novel possible treatment opportunity for OA. We used validated human OA cartilage models and a pre-clinical model of accelerated cartilage loss for our investigations.

*In vitro*: Human chondrocytes were isolated and maintained serum-free for 1h in the presence of 100µM IBMX (PDE inhibitor), and subsequently stimulated with PTH 1nM-100nM + IBMX and the cAMP levels were quantified by ELISA. Articular cartilage explants were cultured in 6 replicates for 17 days, with or without 10nM PTH treatment, and 5µCi <sup>35</sup>Sulphate was added for the last 24h. Soluble proteoglycans were released by 4M GuHCl and incorporated sulphate was measured. Neo-epitopes of pro-peptides of collagen type II (PIINP) were quantified as a measure of formation in the conditioned medium. *In vivo*: Forty 5-month old female rats were subjected to either sham or ovariectomy (OVX), and administered either vehicle or hPTH(1-34) 30µg/kg by s.c. injection for 5 weeks, n=10. Serum samples were evaluated by osteocalcin, CTX and CTX-II ELISAs.

Accumulated intracellular cAMP levels increased dose-dependently from 1nM PTH, p=0.003, with a maximum 23-time increase at 100nM PTH, p<0.0001. In cultures of OA articular cartilage explants PIINP levels increased over 100% after PTH stimulation compared to non-stimulated cartilage explants. Additionally, 10nM PTH increased incorporation of <sup>35</sup>Sulphate by 40%, p=0.002. In the OVX animals the osteocalcin levels were significantly elevated after PTH treatment compared to sham and vehicle treated, p<0.001. Cartilage degradation measured by CTX-II in serum was decreased by 60% as well, p<0.01.

An increasing amount of attention is directed to potential treatments for OA with positive effect on calcium metabolism. The current data strongly suggest that PTH also has direct anabolic effects on chondrocytes. Furthermore, in a pre-clinical model of OA, PTH decreased cartilage degradation significantly. These data warrant further investigation of PTH as a potential as treatment for OA.

**Disclosures:** B.C. Sondergaard, None.

**M156**

**Gene Expression Profiling within Murine Growth Plates Using DNA Microarrays.** S. Nishimori, T. Kobayashi, H. M. Kronenberg. Endocrine Unit, Massachusetts General Hospital / Harvard Medical School, Boston, MA, USA.

To investigate gene expression profiling in the murine growth plates comprehensively, we took a systems-biological approach based on a high density oligonucleotide probe array (Affymetrix GeneChip<sup>®</sup>), using total RNA obtained from three anatomically and functionally distinct chondrocyte types (round cell layer (RL), flat cell layer (FL), and hypertrophic cell layer (HL)). We chose manual microdissection of fresh-frozen newborn proximal tibiae rather than Laser Capture Microdissection to obtain as much total RNA as possible, to avoid possible distortion of gene expression by multiple rounds of RNA amplification. We assessed chondrocyte layers with biological triplicate RNA samples, using Mouse Genome 430 2.0 Arrays. RT-PCR and *in situ* hybridization were used with a subset of genes to validate the microarray data.

We judged expression of a probe set positive, when Affymetrix GeneChip<sup>®</sup> Operating Software called it as "present" for all three chips from the same layer. Out of 45,037 probe sets, 18,763 (42 %), 17,749 (39 %), and 18,772 probe sets (42 %) were expressed in RL, FL, and HL, respectively. 15,744 probe sets (35 %) were expressed in all three layers, and 23,846 (53 %) were not expressed in any layer. 1281 (2.8%), 460 (1.0 %), and 1101 (2.4 %) probe sets were expressed only in RL, FL, and HL, respectively.

To analyze differentially expressed genes, we used Rosetta Resolver<sup>®</sup> software. We imported the triplicate data from 21,191 probe sets (=45,037-23,846) into Rosetta Resolver<sup>®</sup>, which then defined one normalized value for each probe. After filtering by "fold ratio≥2" in at least one ratio (R vs. F, F vs. H, H vs. R), we identified 2,683 probe sets that correspond to genes expressed differentially in various layers. Cluster analysis was then used to group these 2,683 probe sets into 9 groups with similar patterns of expression across the three types of chondrocytes.

Out of these groups, we focused on 163 probe sets that are differentially expressed in the flat cell layer (F/R≥2 and F/H≥2), because few genes have been described as unique to the flat cell layer. Interestingly, we found 60 genes identified as "muscle" genes by the Gene Ontology Database in this group. Though manual dissection might have led to muscle contamination of these chondrocytes, several genes highly expressed in muscle were not found in this group, making contamination as unlikely explanation. Since the transcription factor, MEF2C, regulates gene expression in the growth plate, we are exploring the possible roles of muscle transcription factors as potential regulators of these genes.

**Disclosures:** S. Nishimori, None.

**M157**

**Thyroid Hormone Activates Wnt Signaling Pathways in Rat Growth Plate Chondrocytes.** L. Wang<sup>\*1</sup>, Y. Y. Shao<sup>\*1</sup>, R. T. Ballock<sup>2</sup>. <sup>1</sup>Biomedical Engineering, The Cleveland Clinic Foundation, Cleveland, OH, USA, <sup>2</sup>Orthopaedic Surgery and Biomedical Engineering, The Cleveland Clinic Foundation, Cleveland, OH, USA.

Both thyroid hormone signaling and Wnt signaling pathways are involved in the regulation of skeletal maturation in the growth plate. Previously we demonstrated that thyroid hormone promotes canonical Wnt/beta-catenin signaling and terminal differentiation of growth plate chondrocytes by upregulating Wnt-4 expression, increasing the intracellular accumulation of beta-catenin, enhancing TCF/LEF transcriptional activity, and activating transcription of the Wnt target gene Runx2.

There are at least nineteen Wnt genes, ten Wnt receptor Frizzled genes, and five Wnt antagonist secreted frizzled related receptors (sFRPs) in the mouse and human genome. To increase our understanding of the interactions between thyroid hormone and Wnt signaling, we examined the expression of Wnt pathway components in the growth plate, including Wnt, Frizzled and sFRP genes, and analyzed their expression in response to thyroid hormone treatment.

RT-PCR analysis revealed that Wnt-4, Wnt-5a, Wnt-5b, Wnt-9a, and Wnt-11 genes are expressed in the rat growth plate. Likewise, Frizzled-1, Frizzled-2, Frizzled-5, and Frizzled-7 expression was detectable, as well as sFRP-1, sFRP-2, sFRP-3 and sFRP-4.

Expression of these genes was then analyzed in T3-treated cells using quantitative real-time PCR. Growth plate chondrocytes were collected from the resting zone of the distal femurs of 2-day old rats. The cells were cultured in pellets and incubated in serum-free medium. T3 was added at a concentration of 100 ng/ml. RNA was extracted at day 2, day 5 and day 7 of treatment.

The results showed that T3 increased the expression of Wnt-4, Wnt-5b, and Wnt-11 as early as day 2 of treatment, and increasing at day 5 and day 7. Wnt-9a was expressed at relatively lower levels; however, Wnt-9a was also upregulated by T3 at day 5 and day 7. All four Wnt receptors (Frizzled-1, -2, -5, and -7) were not significantly regulated by T3 treatment. Administration of sFRP1, -2 and -3 recombinant proteins all resulted in an inhibition of T3-mediated terminal differentiation, as shown by the decreases in both Col10a1 mRNA expression and alkaline phosphatase activity. sFRP1 and sFRP2 expression was down-regulated by T3 at day 2, day 5 and day 7, while sFRP3 was decreased at day 2 and day 7 only. In contrast, sFRP4 was significantly upregulated by T3 treatment from day 2 to day 7.

Together these data suggest that thyroid hormone promotes Wnt signaling in growth plate chondrocytes by activating expression of both canonical and non-canonical Wnt ligands while downregulating the expression of several Wnt antagonists.

**Disclosures:** L. Wang, None.

This study received funding from: NIH.

**M158**

**Regulation of Hypertrophic Chondrocyte Apoptosis.** S. U. Miedlich<sup>\*</sup>, M. B. Demay. Endocrine Unit, MGH, Boston, MA, USA.

*In vivo* studies in genetically modified (Npt2a knockout, VDR knockout and hyp) and dietary manipulated mouse models have demonstrated that hypophosphatemia leads to impaired apoptosis of hypertrophic chondrocytes in the growth plate. Treatment of wild type C57BL/6 mice with caspase 9-inhibitors prevents apoptosis of hypertrophic growth plate chondrocytes demonstrating a critical role for the mitochondrial apoptotic pathway in hypertrophic chondrocytes. Because proliferative chondrocytes are not susceptible to phosphate-mediated apoptosis we hypothesized that during maturation hypertrophic chondrocytes either increase their phosphate transport or increase their susceptibility to phosphate-induced apoptosis. Recent studies suggest a decrease in the mitochondrial membrane potential during chondrocyte maturation as a possible prerequisite to apoptosis in chicken chondrocytes.

The clonal chondrocytic cell line (RCJ3.1C5.18) recapitulates the program of chondrocytic differentiation in culture, including acquisition of markers of hypertrophic differentiation and formation of mineralized matrix nodules. These cells were used as an *in vitro* model of chondrocyte maturation and phosphate-induced apoptosis. Collagen X, a marker of hypertrophic chondrocyte differentiation, was observed in RCJ3.1C5.18 cells after 7-10 days of culture in the presence of ascorbic acid. Annexin V-PE was employed to measure plasma membrane changes associated with apoptosis. Quantification of the mitochondrial membrane potential was performed by FACS analysis of JC-1 and/or Mitotracker Orange, dyes which are used to evaluate mitochondrial depolarization. Treatment of hypertrophic chondrocytes with phosphate (7 mM) resulted in a significant increase in apoptosis within 24h of treatment and was partially (50%) inhibited by alendronate, an inhibitor of phosphate transport. In addition, a progressive decrease in the mitochondrial membrane potential was observed during chondrocyte maturation.

These findings were confirmed in primary chondrocytes isolated from costal cartilage of newborn C57BL6 mice. Treatment of hypertrophic chondrocytes with 7 mM phosphate resulted in caspase 9 activation and a significant increase in apoptotic cells within 24h. A differentiation-dependent decrease in mitochondrial membrane potential was also observed.

Characterization of the mechanisms underlying the susceptibility of hypertrophic chondrocytes to phosphate-induced apoptosis in hypertrophic chondrocytes will not only further our understanding of the development of rickets but may also provide insights into the regulation of growth plate maturation and apoptosis.

**Disclosures:** S.U. Miedlich, None.

## M159

**Proinflammatory Mediators Downregulate Peroxisome Proliferator-Activated Receptor gamma1 Expression and Activity In Osteoarthritic Synovial Fibroblasts.** H. Afif\*, N. Chabane\*, N. Zayed\*, J. Martel-Pelletier\*, J. P. Pelletier\*, H. Fahmi\*. CHUM, Université de Montréal, Montreal, QC, Canada.

**Introduction:** Peroxisome proliferator-activated receptor gamma (PPAR $\gamma$ ) is a nuclear receptor involved in the regulation of many cellular processes including inflammation. We and other have previously shown that PPAR $\gamma$  activators inhibit several inflammatory and catabolic responses in synovial fibroblasts and to be protective in animal models of osteoarthritis. PPAR $\gamma$  has two isoforms, PPAR $\gamma$ 1 and PPAR $\gamma$ 2 generated by alternative promoters and differential splicing. So far, little is known about the factors and the mechanisms that regulate PPAR $\gamma$ 1 and PPAR $\gamma$ 2 expression in synovial fibroblasts.

**Aim:** In this study we investigated the effect of IL-1 $\beta$ , TNF- $\alpha$ , IL-17 and PGE2, on the expression and activity of PPAR $\gamma$ 1  $\alpha$ 8  $\gamma$ 2 in osteoarthritic synovial fibroblasts.

**Methods:** Synovial fibroblasts were treated with increasing concentrations of IL-1 $\beta$ , TNF-1, IL-17 or PGE2 for different time periods. PPAR $\gamma$ 1 and  $\gamma$ 2 mRNA and protein levels were evaluated by real-time PCR and western-blotting analysis, respectively. PPAR $\gamma$ 1 promoter activity and PPAR $\gamma$ 1 transcriptional activity were analyzed in transient transfection experiments.

**Results:** Quantification of PPAR $\gamma$ 1 and PPAR $\gamma$ 2 mRNAs revealed that PPAR $\gamma$ 1 mRNA levels were 20-fold higher than PPAR $\gamma$ 2 mRNA levels. IL-1 $\beta$ , TNF- $\alpha$ , IL-17 and PGE2 reduced the expression of PPAR $\gamma$ 1 protein in a dose-dependent manner. Similarly, these factors dose- and time-dependently inhibited the expression of PPAR $\gamma$ 1 mRNA as well as PPAR $\gamma$ 1 promoter activity, suggesting that these effects occurred at the transcriptional levels. Finally, we demonstrated that IL-1 $\beta$ , TNF- $\alpha$ , IL-17 and PGE2 dose-dependently suppressed PPAR $\gamma$ 1 transcriptional activity.

**Conclusion:** These results suggest that OA synovial fibroblasts express predominantly PPAR $\gamma$ 1 isoform, and that IL-1 $\beta$ , TNF- $\alpha$ , IL-17 and PGE2 might contribute to the pathogenesis of arthritis by downregulating the expression and activity of PPAR $\gamma$ 1.

**Disclosures:** H. Afif, None.

This study received funding from: CIHR and FRSQ.

## M160

**Reconstruction of Massive Skeletal Defects due to Osteomyelitis by Distraction Osteogenesis.** D. Peng\*<sup>1</sup>, Z. Li\*<sup>2</sup>, X. Zhang\*<sup>2</sup>, D. Liqun\*<sup>3</sup>.

<sup>1</sup>Department of Orthopaedics, The Second Xingyia Hospital of Central South University, Changsha, China, <sup>2</sup>Orthopaedics, The Second Xiangya Hospital of Central South University, Changsha, China, <sup>3</sup>Orthopaedics, Anhui Provincial Hospital, Hefei, China.

Reconstruction of large skeletal defects secondary to osteomyelitis is a challenging clinical problem. To evaluate the effectiveness of distraction osteogenesis in the treatment of massive skeletal defects following osteomyelitis, we used a combination of an intramedullary nail and a monolateral external fixator in 17 patients (11 male and 6 female, 17 to 32 years old, average age 24 years old) with massive skeletal defects of femur resulting from osteomyelitis. After a diaphyseal osteotomy of the femur, an intramedullary nail was inserted into the femur, and a monolateral external fixator was placed with a half-pin laterally to the nail. The femur lengthening was started on the seventh postoperative day at a rate of 1 mm per day. When the docking site achieved solid bone union, the monolateral external fixator was removed while the intramedullary nail remained for bone consolidation until it was completely reconstructed. The outcome was assessed clinically and radiographically at a mean of 70.3 months postoperatively. The results show that at an averaged of 70.3 months follow-up, ranging from 24 months to 8 years, the skeletal defects were filled by new bone, bone union at the docking site was achieved in the absence of bone graft, and the leg length discrepancy (LLD) was less than 2.5 cm in all 17 patients. The average gain in length was 12.9 cm (from 10.5 to 18.0 cm). According to Paley's evaluation criteria, the bone results were graded as ten excellent, five good, one fair and one poor; the functional results were graded as twelve excellent, four good, and one fair. The mean external fixation index was 18.1 days/cm, and the mean consolidation index was 35.7 days/cm. Although ten out of 17 patients had pin site infection and one patient had a recurrent deep infection, none of the patients developed neurological or vascular complications. We conclude that the distraction osteogenesis technique using the combination of an intramedullary nail and a monolateral external fixator is a reliable method for reconstruction of massive skeletal defects resulting from osteomyelitis.

**Disclosures:** D. Peng, None.

## M161

**Comparison of Cyclic Parathyroid Hormone (cPTH) 1-31 to PTH 1-34 in the Enhancement of Experimental Fracture Healing.** M. L. Young\*<sup>1</sup>, R. Fontaine\*<sup>2</sup>, Z. Mason\*<sup>2</sup>, G. Bishop\*<sup>1</sup>, L. C. Gerstenfeld<sup>1</sup>, E. F. Morgan<sup>2</sup>, T. A. Einhorn<sup>1</sup>. <sup>1</sup>Orthopaedic Surgery, Boston University Medical Center, Boston, MA, USA, <sup>2</sup>Biomedical Engineering, Boston University, Boston, MA, USA.

The purpose of this study was to compare the effects of PTH 1-34 and two doses of cPTH 1-31 on the structural and mechanical integrity of bone during experimental fracture healing. Standard closed femoral fractures were performed on 192 male Sprague Dawley rats, and each animal was randomly assigned to one of four experimental groups: control, PTH 1-34 (30 $\mu$ g/kg), or cPTH 1-31 (30 or 45  $\mu$ g/kg). Daily subcutaneous injections of

saline (control) or drug were administered for 21 or 35 days after the fracture. Following euthanasia the fractured bones and contralateral femurs were harvested and subjected to microquantitative computed tomography and mechanical torsion testing. Analysis of variance determined if treatment, time, or the cross of treatment and time had a significant effect on the outcome variables ( $p < 0.05$ ), and the Tukey method identified differences between the groups. By 21 days, all of the calluses from the active treatment animals had a significantly increased bone volume fraction (BV/TV) compared to controls ( $p < 0.0097$ ), and this effect was sustained after 35 days of fracture healing. At 35 days, the cPTH 1-31 groups demonstrated a higher BV/TV than the PTH 1-34 group, but these values did not reach statistical significance. The effect of PTH treatment alone significantly increased the BMC compared to controls ( $p < 0.0087$ ). No differences were observed between the groups across time with respect to bone mineral density (BMD), bone mineral content (BMC), and stiffness. Only the cPTH 1-31 (30 $\mu$ g/kg) group showed greater torque strength and work to failure compared to controls ( $p < 0.0245$ ) at 35 days. Evaluation of the contralateral femurs revealed a positive effect of treatment on torque strength with the high dose cPTH 1-31 group showing significant improvements over controls ( $p < 0.003$ ).

Summary of Bone Densitometry and Biomechanical Testing				
Day 21 Fractures	BV/TV	BMC (mg/line)	Max Torque (Nm)	Stiffness (Nmm <sup>2</sup> /rad)
Control	0.56 $\pm$ 0.06	314.5 $\pm$ 58.1	0.20 $\pm$ 0.07	33831 $\pm$ 20085
PTH 1-34 (30mg/kg)	0.69 $\pm$ 0.07	360.0 $\pm$ 45.8	0.21 $\pm$ 0.08	34746 $\pm$ 20786
PTH 1-31 (30mg/kg)	0.69 $\pm$ 0.07	353.0 $\pm$ 85.9	0.20 $\pm$ 0.09	32591 $\pm$ 16379
PTH 1-31 (45mg/kg)	0.65 $\pm$ 0.07	334.9 $\pm$ 69.1	0.18 $\pm$ 0.45	24853 $\pm$ 11486
Day 35 Fractures				
Control	0.59 $\pm$ 0.05	269.5 $\pm$ 60.9	0.37 $\pm$ 0.09	57651 $\pm$ 16600
PTH 1-34 (30mg/kg)	0.72 $\pm$ 0.05	315.2 $\pm$ 81.2	0.46 $\pm$ 0.15	61444 $\pm$ 26740
PTH 1-31 (30mg/kg)	0.75 $\pm$ 0.04	314.5 $\pm$ 70.8	0.53 $\pm$ 0.17	63659 $\pm$ 16893
PTH 1-31 (45mg/kg)	0.76 $\pm$ 0.06	336.2 $\pm$ 68.7	0.45 $\pm$ 0.15	62398 $\pm$ 19719

Daily systemic administration of cPTH 1-31 is equivalent to PTH 1-34 in enhancing fracture healing by increasing percentage of bone volume and mineral content within the callus tissue and by improving torque strength. The trends suggest treatment with cPTH 1-31 may be superior to PTH 1-34 with respect to BV/TV, BMC and torque strength during the remodeling phase as well as the torsional strength of the entire skeleton.

**Disclosures:** M.L. Young, Zelos Therapeutics 3.

This study received funding from: Zelos Therapeutics.

## M162

**Role of Galectin-3 in Osteoarthritis.** C. Boileau\*<sup>1</sup>, A. Janelle-Montcalm\*<sup>2</sup>, J. Pelletier\*<sup>2</sup>, J. Martel-Pelletier\*<sup>2</sup>, P. Reboul<sup>2</sup>. <sup>1</sup>Pharmacology, University of Montreal, Montreal, QC, Canada, <sup>2</sup>Medicine, University of Montreal, Montreal, QC, Canada.

Osteoarthritis (OA) is a chronic disease linked to aging and characterized by cartilage destruction and subchondral bone modifications. More specifically, subchondral bone presents a sclerosis and a perturbation of its mineralization in OA. During OA, some synovial membrane inflammation occurs, leading to a structure named pannus, which covers cartilage and subchondral bone. Macrophages present in the pannus can directly secrete catabolic factors (interleukin-1 $\beta$ ) as well as other proteins involved in inflammation such as galectin-3 (gal-3).

Based on results obtained by Ohshima(2003), demonstrating that gal-3 was over expressed in inflamed synovial membrane during OA, our work focused on gal-3 which, when present extracellularly, induces deleterious effects in both cartilage and subchondral bone (Janelle-Montcalm 2007). In brief, our data showed that gal-3 decreases the expression of osteocalcin in human OA subchondral bone osteoblasts whereas a truncated form of gal-3 (Trc-gal-3) although having similar binding properties as gal-3 but unable to activate second messengers, had no effect.

We have since cloned the 850 bp osteocalcin promoter into a pBasicGL3 vector and transfected human OA osteoblasts. Human OA osteoblasts were transfected with a firefly luciferase vector driven by 850 bp of the proximal osteocalcin promoter (p850-OCN-GL3) or with a vector not driven by a promoter (i.e. pBasicGL3). Without Vit D3, the p850-OCN-GL3 gave a background value equivalent to pBasicGL3. As expected, the addition of Vit D3 increased the activity of p850-OCN-GL3 (sixfold) but had no effect on pBasicGL3. When cells were incubated with both Vit D3 and gal-3, the promoter activity decreased by 40% ( $p < 0.02$ ,  $n = 8$ ) compared to Vit D3 alone. In contrast, Trc-gal-3 had no effect. These data indicate that this regulation takes place in the osteocalcin promoter.

In addition to inducing, in human OA chondrocytes, the expression of two major enzymes cleaving aggrecan, we now have results showing that extracellular gal-3 stimulates type X collagen expression twofold ( $p = 0.04$ ,  $n = 5$ ). This collagen is typically found in growth plates but also abnormally re-expressed in OA. Therefore, it is tempting to postulate that gal-3 could be involved in this process. In an in vivo model, new results show that the intra-articular injection of Trc-gal-3 does not induce OA-like lesions in WT mice, unlike gal-3.

Finally, we are able to measure gal-3 in media of synovial membrane. The incubation of synovial membrane with LPS (1  $\mu$ g/ml) increases significantly gal-3 concentration in media ( $p = 0.005$ ,  $n = 6$ ).

All of these data corroborate the concept of a deleterious effect of gal-3 when it is secreted into the joint during phases of inflammation.

**Disclosures:** P. Reboul, None.

This study received funding from: CIHR, Canadian Arthritis Society, Chaire en Arthrose.

## M163

**Identification and Characterization of Angiogenesis-inducing Secretory Molecules from Osteogenically Differentiated Mesenchymal Stem Cell.** J. Kim\*, J. Kim\*, Y. Kim\*, J. Choi\*, S. Ryu\*, P. Suh\*. Postech, Pohang, Republic of Korea.

The relationship between osteogenesis and angiogenesis has been examined for a long time. Despite of its importance, much of cellular and molecular communications between them have been unknown. Fracture repair process is complex step including proliferation, migration, differentiation and activation of many different cells, such as endothelial cell, osteoblast, and osteoclast. Since bone fracture is accompanied with disruption of blood vessels, the interaction between bone forming-osteoblast and vessel forming-endothelial cell is essential to bone fracture healing process. In this process, communicators between osteoblast and endothelial cell are needed. In this point of view, focusing the secretory molecules from osteoblast, we identified several molecules to modulate angiogenesis of endothelial cell. First, we conducted differentiation of human bone marrow derived-mesenchymal stem cell (MSC) into the mature osteoblast and collected conditioned medium from differentiated osteoblast and undifferentiated MSC. And then, we checked the effect of conditioned medium on endothelial cell angiogenesis including cell proliferation, migration and tube formation. As a result, conditioned medium from differentiated osteoblast showed highly increasing effect on endothelial cell migration when compared with the effect of conditioned medium from undifferentiated MSC. To identify the secretory molecules with migration-inducing activity, we used reverse phase-high performance liquid chromatography and selected fractions of chromatography with increasing activity for endothelial cell migration. We used ESI-LC-MS/MS analysis for fractions with activity and could find out several candidate proteins and peptides especially increased in differentiated osteoblast. Based on this study, identification of new molecules they have endothelial cell migration-inducing activity and elucidation of signal transduction pathways associated with that molecules will be helpful for understanding of the communications between osteoblast and endothelial cell. Furthermore, understanding of these communications can be applied to regulation of bone fracture repair process, bone development and disease treatments.

**Disclosures:** J. Kim, None.

## M164

**Bone Tether Formation in Femoral and Basicranial Growth Plates Have Similar Responses to Growth Disruptions Due to Nuclear Vitamin D Receptor Genotype and Mineral Homeostasis.** C. S. D. Lee\*<sup>1</sup>, J. Chen\*<sup>2</sup>, Y. Wang\*<sup>1</sup>, J. K. Williams\*<sup>3</sup>, R. E. Guldberg\*<sup>1</sup>, Z. Schwartz\*<sup>1</sup>, B. D. Boyan\*<sup>1</sup>. <sup>1</sup>Institute of Bioengineering and Bioscience, Georgia Institute of Technology, Atlanta, GA, USA, <sup>2</sup>Chongqing University, Chongqing, China, <sup>3</sup>Children's Healthcare of Atlanta, Atlanta, GA, USA.

Mutations in  $1\alpha,25(\text{OH})_2\text{D}_3$  mediated signaling can cause mechanical instability in limbs and craniofacial deformities. We have shown that micro-CT imaging of distal femoral growth plates of mice can be used to quantify an accumulation of mineralized struts called "tethers" during normal growth plate closure and decreased tether formation is highly correlated with growth disruption in long bone growth plates of mice lacking functional nuclear vitamin D receptors (nVDR). Our results suggest that growth plate tethers facilitate overall skeletal structural stability during rapid bone growth, however tether formation in growth plates in other bones are currently uncharacterized and the mechanism causing tether formation is still unknown. Therefore, our goals were to verify that growth disruption is associated with tether formation in basicranial growth plates (BGP) and that tether formation in these growth plates and the femoral growth plate (FGP) is dependent on normal mineral homeostasis. FGPs in right distal femurs and BGPs next to the occipital and basisphenoid were isolated from micro-CT scans of 10 week old male and female nVDR<sup>-/-</sup> and nVDR<sup>+/+</sup> mouse littermates. Treatments included regular diet, rescue diet (includes 20% lactose, 2% Ca, 1.25% P) and rescue diet +200IU Vitamin D<sub>3</sub>/kg. Parameters of average growth plate thickness and tether volume fraction (tether volume/growth plate volume) were determined with standard morphometric software. Knocking out the nVDR increased growth plate thicknesses and decreased tether formation and rescue diets partially restored normal morphologies in both FGPs and BGPs. Tether volume fraction in nVDR<sup>-/-</sup> growth plates was 0.2-0.4% of those in nVDR<sup>+/+</sup> mice. Average growth plate thickness increased by 7.8-10 fold in nVDR<sup>-/-</sup> mice on regular diet. Rescue diets decreased nVDR<sup>-/-</sup> growth plate thicknesses by 24-27% in FGPs and BGPs and also increased tether volume fraction by ~35 fold in FGPs and by ~150 fold in BGPs. Rescue diets with or without vitamin D<sub>3</sub> were not statistically different with respect to affecting measured parameters. There was no significant difference between male and female samples with respect to diet or genotype except for nVDR<sup>+/+</sup> mice treated with a rescue diet with vitamin D. These results suggest that tether formation is conserved in growth plates throughout the skeletal system and that their development is strongly dependent on serum calcium and phosphorous concentration levels but not the nuclear effects of  $1\alpha,25(\text{OH})_2\text{D}_3$ .

**Disclosures:** C.S.D. Lee, None.

## M165

**Reconstituting Marrow-derived Extracellular Matrix *Ex Vivo*: An Optimal Niche for Retaining the Properties of Human Mesenchymal Stem Cells.** Y. Lai\*, C. M. Skinner\*, Y. Sun\*, X. Chen. Restorative Dentistry, University of Texas Health Science Center at San Antonio, San Antonio, TX, USA.

Mesenchymal stem cells (MSCs) show great potential in cell and gene therapy applications for multiple tissue repair and regeneration in age-related diseases. However, one of the major bottlenecks in the use of MSCs has been their limited number to achieve a clinical successful result, because MSCs are extremely rare in the primary tissue and are very difficult to expand *ex vivo* without losing their properties. Recently, we reported that extracellular matrix (ECM) prepared from mouse marrow stromal cells dramatically enhanced mouse MSC proliferation, and preserved their stemness (Chen et al, JBMR. 22:1943, 2007). Encouraged by these findings in the mouse model, we attempt to study the properties of ECM to support *human* MSC behavior using a similar approach. In this study, we prepared a cell-free ECM made by human marrow stromal cells. Consistent with the mouse model, cultured human marrow stromal cells elaborated a fibrillar ECM with ~12  $\mu\text{m}$  thickness, containing at least collagen type I, fibronectin, and biglycan. Human marrow stromal cells were cultured on the ECM, or 2D culture systems comprising plastic, or plastic coated with fibronectin or type I collagen, in  $\alpha$ -MEM/15%FCS for 14 days. The proportion of human MSCs present in the cultures after 3, 7 10 and 14 days was determined by using flow cytometry to quantify SSEA-4<sup>+</sup> cells [a surface marker for MSCs (Gang et al, Blood. 109:1743, 2007)]. The results showed that the percentage of SSEA-4<sup>+</sup> cells progressively decreased (from ~60% to ~18%) during 14 days of culture maintained on the 2D culture systems. In contrast, the ECM retained 70-82% of SSEA-4<sup>+</sup> cells during the entire 14 days of culture. The number of cells in culture maintained on the 2D culture systems reached a plateau at day 10. In contrast, the number of cells in culture maintained on the ECM continued to increase during 14 days of culture. More important, the increase in the number of SSEA-4<sup>+</sup> cells was ~7-fold more when cells were cultured on the ECM than on the other substrata. Strikingly, the intracellular level of reactive oxygen species (ROS) was at least 3-fold lower in cells maintained on the ECM than in cells maintained on the other substrata. In hematopoietic stem cells, it has been reported that a high level of ROS is associated with loss of stem cell characteristics and increased differentiation as well as apoptosis (Tothova et al, Cell. 128: 325, 2007). We conclude that culture of human bone marrow cells on such ECM may produce massively amount of MSCs without needing extensively subculturing or passaging of the cells for the purpose of enriching their population.

**Disclosures:** Y. Lai, None.

This study received funding from: NIHR21.

## M166

**Studies on the Deposition of Ochronotic Pigment in Alkaptonuria Reveal Tyrosine Metabolism in Human Chondrocytes.** A. M. Taylor\*<sup>1</sup>, P. J. M. Wilson\*<sup>1</sup>, W. D. Fraser\*<sup>2</sup>, L. R. Ranganath\*<sup>2</sup>, J. A. Gallagher\*<sup>1</sup>. <sup>1</sup>Human Anatomy & Cell Biology, University of Liverpool, Liverpool, United Kingdom, <sup>2</sup>Clinical Chemistry, University of Liverpool, Liverpool, United Kingdom.

Alkaptonuria (AKU) is a genetic disorder resulting from the absence of homogentisate dioxygenase (HGO), an important enzyme in tyrosine metabolism. The lack of HGO results in a failure to breakdown homogentisic acid (HGA), which is deposited as ochronotic pigment in connective tissue, especially cartilage, and leads to severe and early onset arthropathies. Using electron microscopy, we have recently identified specific binding of ochronotic pigment to collagen fibrils *in vivo* and *in vitro*, but the mechanisms underlying the deposition of pigment has not been elucidated. It has previously been suggested that enzymatic activity, possibly by polyphenol oxidases (PPOs), is required for the polymerization of HGA and subsequent pigment formation. In this study, we have looked for the expression of candidate enzymes and we report for the first time, the detection of enzymes involved in tyrosine metabolism in primary human chondrocytes and the chondrocytic cell line C20-A4. We designed primers to tyrosinase (TYR), tyrosine hydroxylase (TH) and HGO. Using reverse transcription PCR positive signals have been identified for TYR, TH and HGO in the C20-A4 cell line. TH has also been detected in all primary cells from alkaptonuric bone, cartilage and capsule tissue. Initial experiments on the osteoblastic cells lines, SaOS-2 and MG63, were negative but the technique used may not be sensitive enough to detect low levels of expression. HGO has been previously reported only in liver and kidney, where the majority of tyrosine metabolism takes place. Our investigations point towards the presence of TYR and TH, previously not known to be present in chondrocytes, as possible candidates for polyphenol oxidases involved in ochronotic pigment formation in AKU. In the liver and kidneys, these enzymes act on their preferential substrates, such as tyrosine or L-DOPA. However, in AKU cartilage, the presence of HGA, and other environmental factors affecting substrate specificity may result in the PPOs polymerising HGA as an alternative substrate. The specific localization of pigment in tissues may depend upon the local PPO-like activity. A better understanding of the mechanism of pigment formation and deposition including a clarification of the role of the PPO-like enzymes may allow specific targets for therapy in AKU to be identified. These results also raise the more general issue of why chondrocytes express enzymes involved in tyrosine metabolism.

**Disclosures:** A.M. Taylor, None.



**M167**

**(Ala-Gly)<sub>n</sub> Sequences Configured Silk Protein Scaffold Induces Osteoblast Differentiation and Bone Formation via Increased Cbfa1 and Osterix Expression.** M. Hirata, M. Kobayashi\*, A. Yoshida\*, C. Miyaura, T. Asakura\*, M. Inada. Department of Life Science and Biotechnology, Tokyo University of Agriculture and Technology, Tokyo, Japan.

**Bone formation induced by growth factors is well characterized, the ligand bind to osteoblast leads to up regulate specific transcriptional factors.** Several genes are implicated for bone formation, cbfa1 (runx2) and osterix (osx) mainly regulate activation of osteoblast functions. The other potential factors controlling osteoblast functions are the scaffolds for osteoblast. Type I collagen, a major bone ECM acts as scaffold that is consisting multiple (Gly-X-Y)<sub>n</sub> and (Arg-Gly-Asp; RGD) sequences, activation of osteoblast functions through direct or indirect manners. The other aspects of type I collagen, to form fibrous scaffold enclose osteoblasts with three-dimensional network that assumed to activate cell functions. Here we investigated osteoblast differentiation and function using silk protein scaffold configured multiple (Ala-Gly)<sub>n</sub> simple sequences. We developed silk film sheet from silkworms dissolved in 9 M LiBr solution was dialyzed in lyophilized water, and regenerated silk fibroin sheet. The experiments were performed maintaining osteoblasts on silk scaffold film (SF) or control plastic plate (PP) within the same culture well, silk scaffold film attached into center of culture well plate, comparing bone nodule formation. To quantify osteoblastic gene expression in culture, mRNA was extracted from SF or PP individually then used for RT-PCR analysis. On day 1, both runx2 and osx expression was dramatically increased in osteoblasts cultured on SF compared to PP. Type I collagen, coll1 $\alpha$ 1 expression also increased in SF about 2 times fold than PP, suggesting the transcriptional stream of runx2, osx and its target gene coll1 $\alpha$ 1 was enhanced functionally in early phase of osteoblasts culture. In long term culture of 4 weeks, expression of osteocalcin was detected, and the expression level was 2 times higher in SF than PP. To determine calcified bone nodule formation, alizarin red staining was performed. After 4 weeks, alizarin red positive calcified bone nodules were only found in SF. At 6 weeks, the area of bone nodule was expanded, and the thickness was enhanced at twice. These results clearly indicated that silk protein scaffold induced osteoblast specific genes in both early and later phase of bone formation. Multiple (Ala-Gly)<sub>n</sub> sequences formed simple structured  $\beta$ -sheet protein may apply as a supportive carrier for tissue regeneration of bone in various clinical cases.

**Disclosures:** M. Inada, None.

**M168**

**Histologic and Radiographic Analysis of Osteopromotive Property of Demineralized Allogenic Dentin Matrix in Parietal Bone Defects in Rabbit.** N. Bakhshalian\*, H. Azimi\*, T. Jalaier\*, B. H. Arjmandi<sup>1</sup>. <sup>1</sup>Nutrition, Food and Exercise Sciences, Florida State University, Tallahassee, FL, USA, <sup>2</sup>Oral and Maxillofacial Surgery, Shahed Dental School, Tehran, Iran, Islamic Republic of, <sup>3</sup>Oral and Maxillofacial Radiology, Shahed Dental School, Tehran, Iran, Islamic Republic of.

The aim of this study was to evaluate the bone forming ability of demineralized allogenic dentin matrix (DADM) using rabbit model of experimental surgical bone defect. The DADM specimens were obtained from the mandibular incisors of rabbits. DADM specimens were cut into small pieces (less than 3 mm<sup>3</sup>) and then mixed in order to make them homogenous. Surgical bone defects (6 mm in diameter) were created on the skull of 6 New Zealand white rabbits (two defects in each rabbit). Experimental defects were filled with DADM applying the guided bone regeneration technique (GBR.) with the use of Paraguide collagen membrane while control defects' inner and outer surfaces were covered by Paraguide membrane with no material in between. The rabbits were sacrificed after 15, 30, 45, 60, 75 and 90 days (one rabbit at a time) and the defects were examined radiographically and histologically. Histological data indicated that bone mass and the rate of bone formation were significantly greater in the experimental defects in comparison to control defects. Additionally, bone formation in experimental defects was seen in both center and border of the defects. By comparison, bone formation was not observed in the center of control defects. Radiographic examination showed that the experimental defects achieved radiopacity more quickly than the control defects. DADM pieces served as nuclei facilitating bone growth in and around them resulting in complete closure of bone defects with normal bone. No infection and inflammatory reaction were detected at the tissue level.

Post Surgery Period (Days)	Experimental Defects (% Osteogenesis)	Control Defects (% Osteogenesis)
15	2%	0%
30	38%	11.50%
45	19%	24.50%
60	31%	10%
75	43%	18%
90	54%	31%

**Disclosures:** B.H. Arjmandi, None.

**M169**

**A Novel Modification of Bone Grafts Inhibits Bacterial Colonization.** C. Ketonis\*, A. Ayer\*, I. M. Shapiro<sup>1</sup>, C. S. Adams<sup>1</sup>, N. J. Hickok\*, J. Parvizi\*. <sup>1</sup>Thomas Jefferson University, Philadelphia, PA, USA, <sup>2</sup>Rothman Institute, Philadelphia, PA, USA.

Infection is the most devastating complication associated with use of allograft bone due to bacterial colonization of its surface. We developed a new method for covalently modifying allografts with an antibiotic and demonstrated long term, stable bactericidal activity with no adverse effects.

Morselized human bone was coupled with aminoethoxyethoxyacetate (AEEA) linkers (2X) and vancomycin (VAN). Surface-bound VAN was visualized by confocal laser microscopy after incubation with rabbit anti-VAN IgG (4°C, 12h) and AlexaFluor 488-coupled goat anti-rabbit IgG. To test bacterial colonization, equal dry weights of sterile control and VAN-modified bone (VAN-bone) were incubated with *S. aureus* (C=10<sup>4</sup> cfu) in trypticase soy broth (TSB), 37°C, for 2, 5, 8 and 12 hrs. Non-adherent bacteria were removed by washing and adherent bacteria stained with the Live/Dead BacLight Kit and visualized by confocal microscopy. In parallel, adherent bacteria were suspended by sonication in 0.3% Tween-80 followed by serial dilutions and plating. To determine elution kinetics, bone was modified with fluorescent dansyl-glycine modified VAN (dVAN-bone) or dVAN was adsorbed onto control unmodified bone. The adsorbed and dVAN-bone were incubated in PBS, 37°C for up to 3 weeks and eluted dVAN measured daily. Biocompatibility of the VAN-bone was assessed by seeding Human Fetal Osteoblasts (hFOB) on sterile VAN-modified and control cortical bone squares and performing a BCECF AM assay at 3 days to measure cellular attachment, and proliferation; LDH was measured to assess toxicity. Finally, adherent hFOBs were visualized using confocal microscopy and SEM.

Using anti-VAN antibodies, VAN-bone displayed a uniform, bright signal with only background fluorescence on controls, indicating good VAN coverage. By confocal microscopy, few fluorescent bacteria were observed at any time (2-12hrs) on VAN-bone, whereas abundant fluorescence was present on control bone. These observations were confirmed by direct bacterial counts. dVAN elution after adsorption to control bone occurred mainly within the first 4 days; dVAN-bone showed minimal if any release of dVAN. After 17 days, when challenged with *S. aureus*, dVAN-bone resisted bacterial colonization whereas dVAN-adsorbed bone was highly colonized. hFOBS readily proliferated on VAN-bone with similar cell numbers, toxicity and morphology to unmodified controls.

We have described a novel modification of bone grafts with antibiotics to render them bactericidal while maintaining biocompatibility. This antibiotic tethering shows clear advantages over current incorporation methods and may serve as a paradigm for development of a new generation of self-protecting bone grafts.

**Disclosures:** C. Ketonis, None.

This study received funding from: Musculoskeletal Transplant Foundation.

**M170**

**Assessment of Changes in Thoracic and Lumbar Vertebrae in T-type Cav3.2 (a1H) Voltage Sensitive Calcium Channel Knock Out Mice.** A. Kronbergs<sup>1</sup>, Y. Shao<sup>1</sup>, K. P. Campbell\*, R. L. Duncan<sup>1</sup>, M. C. Farach-Carson<sup>1</sup>. <sup>1</sup>Biology, University of Delaware, Newark, DE, USA, <sup>2</sup>Howard Hughes Medical Institute, University of Iowa, Iowa City, IA, USA.

Voltage sensitive calcium channels (VSCCs) are essential to the development of skeleton. We have also shown that inhibition of the L-type VSCC's significantly reduce the response of bone to exogenous mechanical loads. However, our lab has shown that two dominant types of VSCCs are found in bone, the L-type Ca<sub>v</sub>1.2 ( $\alpha_{1C}$ ) VSCC and the T-type Ca<sub>v</sub>3.2 ( $\alpha_{1H}$ ) VSCC. These channels are differently expressed in osteoblasts and osteocytes; with preosteoblasts and osteoblasts expressing both the L- and T-type VSCC while osteocytes only express the T-type Ca<sub>v</sub>3.2 ( $\alpha_{1H}$ ) VSCC. From these observations, we postulate that the loss of L-type VSCC signaling may act as the switch to induce a more differentiated phenotype in osteocytes. Further, we predict that the T-type VSCC may play a stronger role in the differentiated osteocyte function. In the current study, we used mice with conventional knockout of the T-type Ca<sub>v</sub>3.2  $\alpha_1$  subunit to examine changes in the skeletal phenotype of thoracic and lumbar vertebrae. These mice are characterized by constitutively constricted coronary arterioles, reduced relaxation of the coronary arteries and focal myocardial fibrosis. Alcian blue & alizarin red skeletal staining previously showed that the knock out animals exhibited abnormal osteochondral junction of the ribs. Using micro-CT scanning, we demonstrated that, compared to the wild-type controls, the Ca<sub>v</sub>3.2 null mice exhibited a lower bone mineral density and the vertebral foramen appeared to be larger. Using sodium fluorescein, we are extending our studies to include the density of osteocytes and osteocytic lacunae in thoracic and lumbar vertebrae of the control and knockout animals. These data together with the previous findings on the long bones suggest that the T-type Ca<sub>v</sub>3.2 knockout results in an altered bone mineralization process. We also hypothesize that the presence of Ca<sub>v</sub>3.2 channels in osteocytes may play a significant role of these channels in bone mechanotransduction.

**Disclosures:** A. Kronbergs, None.

This study received funding from: NIH.

**M171**

**Bone Marrow Cells Participate in Normal Endothelial, but not Epithelial or Mesenchymal Cell Renewal in Adult Rats.** K. I. Odoerfer<sup>\*1</sup>, N. Unger<sup>\*2</sup>, K. Weber<sup>\*2</sup>, I. Walter<sup>\*3</sup>, M. Egerbacher<sup>\*3</sup>, E. P. Sandgren<sup>\*4</sup>, R. G. Erben<sup>1</sup>.

<sup>1</sup>Dept. of Biomedical Sciences, University of Veterinary Medicine, Vienna, Austria, <sup>2</sup>Institute of Animal Physiology, University of Munich, Munich, Germany, <sup>3</sup>Dept. of Pathobiology, University of Veterinary Medicine, Vienna, Austria, <sup>4</sup>Department of Pathobiological Sciences, University of Wisconsin-Madison, Madison, WI, USA.

The extent to which bone marrow contributes to physiological cell renewal in various organs is still controversial. The current studies employs human placental alkaline phosphatase (hPLAP) as genetic marker, because this marker survives paraffin and methylmethacrylate embedding, and sets new standards in histological detection quality especially in hard tissues. Here we examined the role of bone marrow in physiological cell renewal by sequentially analyzing tissues from lethally irradiated, wild-type inbred Fischer 344 rats transplanted with bone marrow from transgenic F344 rats expressing hPLAP under the control of the ubiquitous R26 promoter. Bone marrow-transplanted rats were followed up to 6 months post-transplantation. Osteoblasts, osteocytes, and chondrocytes were exclusively of recipient origin at all time points post-transplantation. In contrast, the extent of hPLAP-labeled endothelial cells of donor origin profoundly increased with time in almost all organs. This finding was independently confirmed by a novel 5-bromo-2'-deoxyuridine (BrdU)-based method to directly assess the half life of cells. However, epithelial cells in the intestinal tract, kidney, liver, pancreas, and brain were of recipient origin at all time points. Similarly, muscle cells in skeletal muscle, heart, blood vessels or intestine were almost exclusively of recipient origin. Our analysis shows that physiological bone marrow-derived cell renewal in adult rats is restricted to endothelial cells, and casts doubt on the idea that adult bone marrow-derived precursor cells participate in physiological renewal of epithelial or mesenchymal cells.

**Disclosures:** R.G. Erben, None.

This study received funding from: German Research Foundation and University of Veterinary Medicine Vienna.

**M172**

**Cortical Bone Microstructure and Strength at the Mid-Diaphysis of Human Femurs: Influence of the Anatomical Position.** H. Beaupied<sup>\*1</sup>, A. Basillais<sup>1</sup>, J. Lepissier<sup>\*1</sup>, R. Hambli<sup>\*2</sup>, D. Soulat<sup>\*2</sup>, C. Chappard<sup>1</sup>, E. Dolléans<sup>\*1</sup>, C. Benhamou<sup>1</sup>. <sup>1</sup>Inserm U658, Orleans, France, <sup>2</sup>UMR CNRS 8106, Orleans, France.

The aim of this study was to assess the relationships between 3D microstructure and biomechanical parameters of human cortical bone in relation to their anatomical position around the medullary area.

Nine cadaveric femurs were removed from osteoporotic women at the anatomy department. Thirty six cortical bone samples were extracted from the anterior, lateral, posterior and medial mid-diaphysis of femurs. The samples were imaged by microcomputed tomography (skyscan 1072). The optical system was set to get a voxel size of 10.78  $\mu\text{m}$ . The cortical porosity (PoV/TV), the pore diameter (PoDm) and spacing (PoSp), the pore number (PoN), the pore surface (PoS) and the degree of anisotropy (DA) were calculated on these images. Compressive tests were performed on the samples in order to calculate their biomechanical properties (ultimate stress ( $\sigma_U$ ), yield stress ( $\sigma_Y$ ) and Young's modulus (E)). Spearman correlation coefficients were used to correlate the microstructure parameters with the mechanical parameters.

The linear regression analysis showed significant correlations between  $\sigma_U$  and PoV/TV ( $r = -0.84$ ), PoDm ( $r = -0.81$ ), PoN ( $r = -0.65$ ), PoSp ( $r = 0.51$ ) and DA ( $r = 0.42$ ) when the data were analyzed all together. The results showed significant correlations between  $\sigma_Y$  and PoV/TV ( $r = -0.81$ ), PoDm ( $r = -0.78$ ) and PoN ( $r = -0.63$ ) for the pooled data. The linear regression analysis showed significant correlations between E and PoV/TV ( $r = -0.85$ ), PoDm ( $r = -0.77$ ), PoN ( $r = -0.73$ ), PoSp ( $r = 0.66$ ) and DA ( $r = 0.39$ ). When the data were analyzed according to their location (anterior, posterior, medial and lateral)  $\sigma_U$ ,  $\sigma_Y$  and E were significantly correlated with PoV/TV and PoDm for the lateral, posterior and anterior positions. No correlation was significant between the biomechanical parameters and the microstructural parameters for the medial orientation. This study analyzed for the first time the correlations between the 3D structural parameters and the biomechanical parameters assessed by compressive testing of human cortical bone. Particularly, we showed that the relationships between the microstructure and the strength of cortical bone were different according to its position around the medullary area. The medial area seemed to have particular behaviour induced by a lower porosity (PoV/TV and PoDm lower than others sites).

**Disclosures:** H. Beaupied, None.

**M173**

**Low Magnitude Vibration can Inhibit Muscle Loss and Increase Mineralizing Bone Surfaces in Aging Mice.** J. Colantoni<sup>\*</sup>, D. Freeman<sup>\*</sup>, P. Arounleut<sup>\*</sup>, E. Kellum<sup>\*</sup>, K. Wenger, J. Yu<sup>\*</sup>, M. Hamrick. Medical College of Georgia, Augusta, GA, USA.

Previous studies using animal models have demonstrated that low magnitude, high frequency vibration can stimulate bone formation and increase bone mass. For example, vibration has been observed to produce a 26% increase in bone strength and a 10% increase in bone mineral content (BMC) in sheep. In a previous study we showed that C57BL/6 mice lose significant muscle mass, bone mass, and bone density between 18 and 24 months of age, suggesting that interventions aimed at preventing age-associated loss of muscle and bone strength in humans might be evaluated using this animal model. Here we test the hypothesis that vibration can increase bone formation and attenuate loss of muscle mass with aging in this mouse model. Approximately 25 mice, 18 months of age, were separated into three treatment groups: no vibration (control), low vibration (0.5 g; 31.7 Hz, 0.125 mm), or high vibration (1.5 g; 31.7 Hz, 0.375 mm). Mice exposed to either low or high vibration were vibrated for 30 min/day, 5 day/week, for 12 weeks, beginning at 18 months and finishing at 21 months. Results indicate that mice exposed to the low vibration regime showed significantly (~25%) greater cross-sectional areas for their extensor digitorum longus muscle fibers than either control mice or mice in the high vibration group. Soleus muscle fiber areas were significantly larger (~45%) in the control and low vibration groups compared to the high vibration group. Finally, calcein-labeled bone surfaces increased significantly (90%) in both the high and low vibration groups compared to controls. These findings suggest that low magnitude vibration may be effective at preserving musculoskeletal tissues with aging, and that higher magnitude vibration may actually have catabolic effects on skeletal muscle.

Funding for this research was provided in part by the National Institutes of Health (AR049717).

**Disclosures:** M. Hamrick, None.

**M174**

**Role of OPN in Beta-adrenergic Signaling Induced Bone Loss *in vivo*.** M. Nagao<sup>1</sup>, Y. Saita<sup>\*1</sup>, J. Nagata<sup>\*1</sup>, Y. Izu<sup>\*1</sup>, T. Hayata<sup>\*1</sup>, H. Hemmi<sup>\*1</sup>, Y. Ezura<sup>1</sup>, H. Kurosawa<sup>\*2</sup>, M. Noda<sup>1</sup>. <sup>1</sup>Dept Molecular Pharmacology, Medical Research Institute, Tokyo Medical and Dental University, Chiyoda-ku, Tokyo, Japan, <sup>2</sup>Dept Orthopedic Surgery, Juntendo University School of Medicine, Bunkyo-ku Tokyo, Japan.

Bone mass is regulated under the control of sympathetic nervous system. One of the pathways to induce changes in bone based on the nervous tone is through  $\beta$ -adrenergic receptors which are expressed on osteoblastic cells. OPN expression is observed on osteoblastic cells as well as osteoclastic cells which are both under the control of sympathetic nervous tone. As for the interaction between  $\beta$ -adrenergic signaling and OPN, we observed that ISO administration reduced trabecular bone mass while OPN deficiency prevented such bone loss. This was based on the reductions in the changes in bone formation activities as well as bone resorption activities altered by ISO treatment. However, the point of action of OPN has not yet been elucidated. To understand whether OPN action is through the cell autonomous mechanism or through indirect pathway mediated by its property such as extracellular matrix protein, involvement of OPN was tested *in vitro* and *in vivo*. To examine whether ISO treatment increase cell autonomous actions of OPN, MC3T3E-1 cells were exposed to 10uM ISO. C-fos expression was induced with its peak at 1h after the treatment with ISO. In the absence of OPN, based on the treatment of the cells with siOPN, resulted in the similar patterning, ie: peak at 1h, of the expression of the c-fos mRNA. With respect to bone resorption related cytokine, RANKL expression was induced by ISO treatment with its peak at 2hrs and reduced after 4 hrs in WT and this was also observed in presence of siOPN. As possible control OPN mRNA expression levels were reduced by 40% to 70% in the presence of si. To exclude the possibility that the observed changes were due to the treatment with siOPN, Both WT and KO mouse derived calvariae osteoblasts were exposed to 10uM ISO. RANKL mRNA expression was induced by the treatment with ISO with its peak at 2 hrs and reduced after 4hrs and similar pattern was observed both WT and OPN deficiency mouse derived osteoblast cells. We also examined *in vivo* setting and injected ISO into the peritoneum of the mice for 7 days and prepared RNA from the femur to examine the levels of TRAP. ISO treatment in WT increased expression levels of TRAP and this was blocked by the absence of OPN. As control expression of OPN per se was enhanced by the ISO treatment in bone marrow microenvironment.

In conclusion, OPN modulates the action of a ISO signaling *in vivo* while its function in cell autonomous pathway may not be a major part of the function of this molecule. Thus, OPN is a key molecule in the microenvironment of bone to regulate bone formation and bone resorption under the control of sympathetic nervous tone.

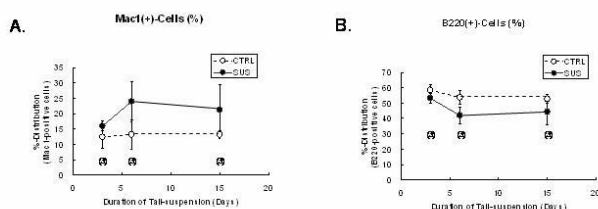
**Disclosures:** M. Nagao, None.

## M175

**Increased Expression of Osteopontin in Peripheral Blood Mononuclear Cells is Associated with Alteration in the Fractions of Lymphocytes in Hindlimb-unloaded Mice.** Y. Ezura, J. Nagata\*, H. Hemmi\*, T. Hayata, T. Nakamoto\*, M. Noda. Department of Molecular Pharmacology, Medical Research Institute, Tokyo Medical and Dental University, Tokyo, Japan.

Unloading induced bone loss analyzed by rodent "tail-suspension" has possible confounding factors related to sympathetic nervous tone, blood circulation, and immune function. To begin addressing with this problem, we investigated gene expression profiles and immunological lymphocyte surface markers of peripheral blood mononuclear cells in the mice subjected to 2-weeks of tail-suspension. Micro-array analysis revealed a reduced expression of B-cell specific genes in peripheral blood of tail-suspended mice, representatively indicated by Ebf1, Cd19, and Cd22. In contrast, genes characteristic for monocyte/macrophage lineage cells such as Msr2, Mrc1, C1q(s), and Itgam increased in parallel, implying proportional reduction and expansion in numbers of these leukocytes. Indeed, fluorescence activated cell sorting analysis for peripheral leukocytes revealed significant decrease of proportional numbers of B-cells and increased numbers of monocyte/macrophage lineage cells at day 3 of tail-suspension; these alterations continued until day-15 (Figure 1). However, since these fractional changes in lymphocytes remained small (less than 2-fold), we estimated the observed alterations in gene expression (greater than 2-fold) may not necessarily depend on the differences in cell numbers. Interestingly, we also observed significantly increased expression of osteopontin (also known as Spp1) in peripheral blood. Although it is not clear if the expression of osteopontin increased as a consequence of activation of peripheral blood macrophages, our data may imply that activation of peripheral blood macrophages and the increased expression of osteopontin may have some impact on bone metabolism in the hindlimb-unloaded mice.

Figure 1



**Disclosures:** Y. Ezura, None.

This study received funding from: Japan Science and Technology Agency.

## M176

**Cartilage Engineered with a Calcified Zone Enhances Interfacial Shear Strength to the Underlying Substrate.** J. St-Pierre\*, L. Gan\*, J. Wang\*, R. M. Pilliar\*, M. D. Grynblas, R. A. Kandel\*. University of Toronto, Toronto, ON, Canada.

The purpose of this study was to design bioengineered cartilage with improved attachment to a porous calcium polyphosphate (CPP) bone substitute by the formation of a zone of calcified cartilage (ZCC) at the cartilage-CPP interface zone. Cartilage-CPP biphasic implants were formed by seeding deep-zone chondrocytes onto the top surface of porous CPP substrates coated with a thin sol-gel-formed hydroxyapatite film. The cells were grown either in the absence or presence of  $\beta$ -glycerophosphate supplementation to induce mineralization. After 8 weeks, tissues were harvested and examined histologically, biochemically, by RT-PCR for gene expression and for the shear properties of the interface between cartilage and the substrate using a specifically designed shear test apparatus. Histological sections stained with toluidine blue and von Kossa demonstrated cartilage tissue with a thin ZCC when cultured in mineralization-inducing media. The ZCC was localized in the tissue directly above the substrate, mimicking osteochondral zonal organization. Previous work demonstrated that the mineral formed in cartilage *in vitro* under these conditions has similar composition and crystal size to that present in the ZCC of native cartilage [1]. Conversely, no calcification was observed in cartilage formed in the absence of  $\beta$ -glycerophosphate. Collagen and glycosaminoglycan contents were similar for tissues with and without a calcified zone. Expression levels of cartilage extracellular matrix genes including collagen type II and type X were not affected by the generation of a ZCC. Interestingly, the shear stiffness of the interface was increased by 2-fold in bioengineered cartilage with a ZCC compared to cartilage without a ZCC. This was associated with 240% improvement in the peak shear load and in 340% increase in energy to failure measurements. The maximal displacement prior to failure was similar in both tissues. In conclusion, this study demonstrates a significant increase in interfacial shear properties of biphasic cartilage constructs by mimicking the zonal organization of adult articular cartilage by generating a ZCC at the tissue/bone substitute interface. Generating biphasic cartilage constructs with a strong interface may be critical to the clinical success of biphasic constructs for repair of larger joint defects. [1] Tissue Eng. 5:25, 1999.

**Disclosures:** J. St-Pierre, None.

## M177

**Physiological Concentrations of Inhibin A Are Anabolic, Affecting both Trabecular and Cortical Bone in Normal Intact Mice.** K. M. Nicks, N. S. Akei\*, L. Liu\*, J. Aronson\*, L. J. Suva, D. Gaddy. Physiology and Biophysics & Orthopaedic Surgery, University of Arkansas for Medical Sciences, Little Rock, AR, USA.

Skeletal metabolism is regulated by many endocrine hormones, including non-steroidal hormones in the hypothalamic-pituitary-gonadal axis. We have previously demonstrated the skeletal anabolic actions of the gonadal peptide Inhibin A (InhA) in a transgenic (TG) model of systemic expression in intact mice. We have now extended our observations in the tibia and spine of Inh TG mice to demonstrate InhA affects both the trabecular and cortical compartments of the humerus in TG mice expressing 600-800 pg/ml human (h) InhA. The expression of InhA increases trabecular (Tb) bone volume (BV/TV), via increases in Tb thickness. InhA *in vivo* also altered cortical geometry, inducing increases in total and cortical cross-sectional area, medullary diameter, and both endocortical and periosteal perimeters. To determine if InhA treatment in adult wild-type outbred mice is similarly anabolic, 3 month old male Swiss-Webster mice were treated with continuous recombinant hInhA at physiological concentrations (serum levels of 30-80pg/ml) via osmotic minipump for 17d. Femoral bone marrow cultures were initiated at sacrifice for osteoblast (OB) differentiation; tibiae and humeri were used to quantify bone volume and trabecular architecture as well as all geometric indices using microCT. InhA treatment *in vivo* recruited more mesenchymal cells into the OB lineage in *ex vivo* culture (by increases in AP+ CFU-F), and increased the number of mineralized bone nodules (CFU-OB). Increases in BV/TV were observed in both the humerus and the tibia, due to increases in Tb thickness and number. Collectively, these data demonstrate that physiological concentrations of systemic hInhA (delivered either transgenically or by osmotic mini-pump) is anabolic in intact adult mice. The bone anabolism of continuous hInhA treatment in outbred mice confirms the regulation of bone metabolism by non-steroidal gonadal hormones. These observations suggest that modulation of the Inh signaling pathways may represent a new therapeutic target for the treatment of osteopenia.

**Disclosures:** K.M. Nicks, None.

This study received funding from: NIH R21-DK074024-A2 to DG; NIH NIH R21-DK074024-A2S and F31 DK079362-01A to KMN.

## M178

**PTH and not Vitamin D Predicts Age-Related Bone Loss in the Elderly: A Prospective Population Based Study.** A. Arabi<sup>1</sup>, R. Baddoura<sup>2</sup>, G. El-Hajj Fuleihan<sup>1</sup>. <sup>1</sup>Calcium Metabolism and Osteoporosis Program, American University of Beirut, Beirut, Lebanon, <sup>2</sup>Rheumatology, Saint Joseph University, Beirut, Lebanon.

Type I involutional osteoporosis is mediated by increased sensitivity to PTH whereas type II is also induced by primary changes in calciotropic hormones. Over the years, attention has focused, amongst others, on serum 25-hydroxy vitamin D (25-OHD) rather than parathyroid hormone (PTH), although PTH is the mediator for the deleterious effect of hypovitaminosis D on bone. Moreover, scarce are the studies that prospectively evaluated the impact of calciotropic hormones on bone loss rates. We had previously shown that the negative effect of low vitamin D on bone mineral density (BMD) is mediated by PTH in the elderly. We further examined these observations in a prospective follow-up of the same cohort.

195 ambulatory subjects (65 men and 130 women), age 72.3±5.0 years, participated in a prospective population based study assessing bone mass, bone loss and fractures in the elderly Lebanese. 25-OHD, PTH levels, and BMD of the spine, hip and forearm were measured at baseline and follow up 4.2±0.3 years later. The mean values of 25 OHD and PTH (baseline and follow up) were used in the analyses.

The annualized percent changes in BMD were 0.18±2.3 at the spine, -1.0±1.7 at the hip, -0.63±2.0 at the femoral neck, -1.12±2.1 at the trochanter and -0.58±1.3 at the forearm. A significant negative correlation between changes in BMD and PTH, but not 25 OHD, was observed at all skeletal sites (p<0.05). We divided the study subjects into subgroups according to three categories: 25-OHD> 20 ng/ml, 25-OHD< 20 ng/ml and normal PTH levels, and 25-OHD<20 ng/ml and high PTH levels (Table). There were too few subjects (N=5) with 25-OHD levels > 30 ng/ml to use this cut-off for analyses. There was no difference in annualized bone loss rates between subjects with 25-OHD> 20 ng/ml and those with low 25-OHD & normal PTH levels. Conversely, the annualized bone loss was higher in subjects with low 25-OHD and high PTH levels compared to the two other groups (Table). In multivariate analyses, the negative effect of PTH persisted after adjustment for age and changes in BMI (p< 0.05) except at the forearm (p=0.07). In conclusion, PTH levels rather than vitamin D predict bone loss rates in the elderly. Aiming at normalizing PTH, as opposed to targeting specific D levels, may be the best approach to optimize skeletal health in elderly with low vitamin D levels.

Annualized percent changes in BMD by categories of mean 25-OHD (ng/ml) and PTH (pg/ml) levels

	25OHD ≥20 n=30	25OHD<20 & PTH≤76(n=141)	25OHD<20 & PTH>76 (n=19)
Spine	1.28±2.2 <sup>a</sup>	0.17±2.2	-0.94±2.6 <sup>a</sup>
Total Hip	-0.85±1.2 <sup>a</sup>	-0.93±1.8 <sup>b</sup>	-1.92±2.0 <sup>a,b</sup>
Femoral neck	0.6±2.2 <sup>a</sup>	-0.7±1.9	-1.1±2.1 <sup>a</sup>
Trochanter	-0.85±1.5 <sup>a</sup>	-1.06±2.2 <sup>b</sup>	-2.2±2.1 <sup>a,b</sup>
Forearm	-0.49±1.4	-0.56±1.3	-1.09±1.6

Variables with same superscript are significantly different from each other (p< 0.05) by ANOVA post-hoc analyses.

**Disclosures:** A. Arabi, None.

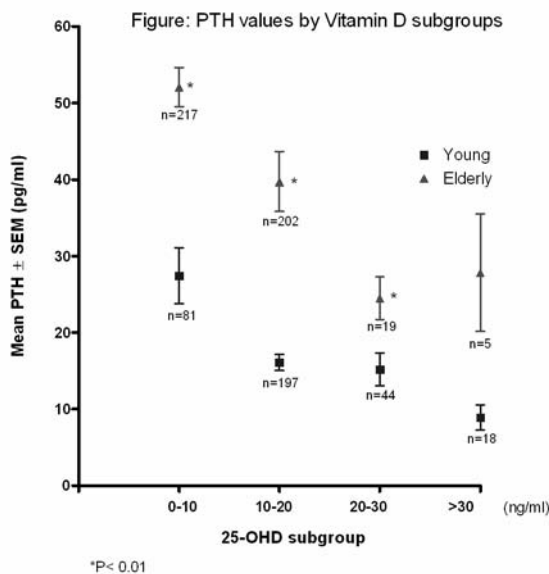
## M179

**The Negative Relationship between PTH and Vitamin D: Is There an Age and a Gender Effect?** A. ARABI, R. El-Rassi\*, G. El-Hajj Fuleihan. Calcium Metabolism and Osteoporosis Program, American University of Beirut, Beirut, Lebanon.

Hypovitaminosis D is prevalent worldwide and across age groups. In adults, optimal vitamin D levels are defined based on biological read outs of low vitamin D levels such as parathyroid hormone (PTH) levels. Sex steroids and aging affect calcium absorption and possibly PTH levels. Although the inverse relationship between vitamin D and PTH is well described, it is unclear whether the relationship is the same across genders and age groups. This study assessed the vitamin D-PTH relationship in 340 adolescents (age 13±3 years, mean±SD) and 443 elderly subjects (age 72±5 years) studied within the same period. Estimated calcium intake was 735±330mg in the young and 310±231 mg/day in the elderly. Female subjects consumed less calcium than male subjects in both age groups. PTH levels were measured with a second generation assay and 25 hydroxy vitamin D (25-OHD) levels with a radioimmunoassay (IDS Immunodiagnostics, Boldon, UK). Vitamin D sub-groups were created using 25-OHD levels <10 ng/ml, 10-20 ng/ml, 20-30 ng/ml, > 30 ng/ml.

In the overall group, mean 25-OHD levels were lower in the elderly compared to adolescents (11.4±4.9 vs 15.3±7.5,  $p < 0.001$ ), and in female compared to male subjects (10.9±5 vs 12.1±4 in elderly and 14.2±8 vs 16.5±6 in children,  $p < 0.05$ ). Mean PTH levels were higher in the elderly compared to adolescents (44.0±47 vs 18.4±20,  $p < 0.001$ ) but there were no gender differences in either age group. Within each vitamin D level subgroup, mean PTH levels were comparable across genders (data not shown). Within each vitamin D level subgroup, mean 25-OHD levels were comparable across age groups, but PTH levels were 1.5- two folds higher in the elderly ( $p < 0.0001$ , Figure). These age differences persisted in multivariate analyses adjusting for calcium intake.

The vitamin D-PTH relationship varies by age but not gender. For the same 25-OHD level subgroup, PTH levels are higher in elderly compared to young, possibly reflecting differences in calcium absorption and renal function. Optimal vitamin D levels derived from examining the 25-OHD-PTH relationship may differ between young and elderly subjects.



**Disclosures:** A. Arabi, None.

## M180

**Parathyroid Hormone Increases after Oral Peptones Administration in Obese Subjects Treated with Roux-En-Y Gastric Bypass Surgery: Role of Phosphate on the Rapid Control of Parathyroid Hormone Release.** M. Bevilacqua<sup>\*1</sup>, L. J. Dominguez<sup>\*2</sup>, V. Righini<sup>\*1</sup>, T. Vago<sup>\*1</sup>, D. Foschi<sup>\*1</sup>, E. Corsi<sup>\*1</sup>, E. Trabucchi<sup>\*1</sup>, E. Chebat<sup>\*1</sup>, E. Renesto<sup>\*1</sup>, M. Barrella<sup>\*1</sup>, M. Massarotti<sup>3</sup>, M. Barbagallo<sup>\*2</sup>. <sup>1</sup>Ospedale L. Sacco-Polo Universitario, Milan, Italy, <sup>2</sup>Internal Medicine and Geriatrics, University of Palermo, Palermo, Italy, <sup>3</sup>Rheumatology Unit, Humanitas, Milan, Italy.

**Introduction:** PTH is regulated by changes in circulating ionized calcium (iCa); its rapid regulation by P was recently demonstrated in low-P treated rats: duodenal infusion of sodium P increased PTH levels by twofold within 10 min, concomitantly with a 1 mg/dl increase of circulating P without changes of iCa. We previously demonstrated that oral peptones administration increases serum P and consequently PTH in hypophosphoremic primary hyperparathyroid patients but not in normal controls. We wonder whether the administration of peptones to patients after RYGB could be followed by a rise of PTH owing to the rapid absorption of P directly arriving into the jejunum. **Materials and Methods:** We recruited 24 obese subjects (18M/6F; 18-35 years) to study the effect of oral

peptones administration on PTH before and after 6 m of RYGB. Before and after RYGB we evaluated gastrin, P, PTH, iCa and pH before and during the oral administration of peptones (10 g Liebig meat extract in 250 ml NaCl 0.9%). **Results:** Before RYGB peptones elicited a significant increase of gastrin ( $P < 0.001$ ), and a slight increase of P, evident at 60-90 min ( $P < 0.05$ ), without changes of PTH; pH slightly increased perhaps as a mirror of the gastric acidification and iCa slightly decreased. After RYGB surgery, gastrin did not change, along with pH and iCa, maybe due to the lack of gastric remnant acidification. Serum P increased by 0.4-0.6 mg/dl in 15-30 min and remained elevated for 120 min, and PTH increased at 15 min ( $P < 0.05$ ) and remained elevated for 120 min ( $P < 0.01$ ). **Conclusions:** The marked difference in P and PTH response elicited by peptones observed in obese subjects before and after RYGB in the absence of changes of other possible regulators of PTH suggest that after RYGB there is a rapid arrive of P into the jejunum, with a rapid increase of serum P accompanied by a rapid release of PTH. Therefore we conclude that in some conditions, PTH is rapidly regulated also by P in man.

**Disclosures:** M. Bevilacqua, None.

## M181

**Hematopoietic Cells in the Bone Marrow Augment Anabolic Actions of PTH.** A. J. Koh\*, T. Wang\*, R. Taichman, L. K. McCauley. POM, University of Michigan, Ann Arbor, MI, USA.

PTH has potent anabolic effects on the skeleton and previous reports suggest that a cell in the hematopoietic lineage may be a critical mediator of this effect. The purpose of this study was to determine whether the ability of PTH to increase hematopoietic stem cells (HSCs) in the bone marrow niche is linked to its anabolic actions in bone. Total body irradiation (TBI) was performed to selectively target hematopoietic cell populations in the marrow. Preliminary studies of varied irradiation doses identified 325cGy as a sub-lethal dose in neonatal C57/B6 mice. Analysis of the bone marrow hematopoietic cells determined by flow cytometry at d3 and d21 post TBI revealed a significant reduction in B220 (B cells) and CD41 (megakaryocytes). Irradiation decreased the total numbers of bone marrow cells and hematopoietic cells after 3 days; however, there was a relative increase in the percentage of HSCs (lin-sca-1+c-kit+ cells). At day 3, histologic analysis of irradiated vertebrae and tibia confirmed a severe generalized decrease in nucleated hematopoietic cells within the marrow, but cells lining the trabecular bone appeared robust and selectively protected. Analysis of the effects of PTH treatment with and without irradiation was performed after 21 days (TBI performed on d1, then PTH treatment, 50µg/kg/d on d2). Femur length and width were significantly reduced with irradiation regardless of PTH treatment. As shown previously, PTH treatment significantly increased bone area in control, non-irradiated mice. Interestingly, PTH treatment in irradiated mice increased bone area to a greater extent than in non-irradiated mice. Osteoclast activity as revealed by TRAP+ staining was increased similarly with PTH in non-irradiated and irradiated mice. Immunostain for Von Willebrand factor on histologic sections identified reduced numbers of megakaryocytes in irradiated mice but no impact of PTH treatment. An in vitro model system was utilized to test the hypothesis that increased HSC's promote osteoblast differentiation. Coculture of osteoblastic cells with whole bone marrow cells typically inhibits mineralization. Whole bone marrow from irradiated mice partially blocked this effect, resulting in more mineralization vs. non-irradiated mice, and supporting the in vivo findings of hematopoietic cells supporting osteoblast differentiation. The mechanisms of PTH anabolic action are as yet unclear and complex. Sub lethal ablation of the bone marrow may increase osteoblast exposure to its target cells (which survive) and may thus increase its anabolic action. Alternatively, irradiation may decrease cell types which are inhibitory for the anabolic actions of PTH. The technique of irradiation provides valuable information about the cell types involved in anabolic actions of PTH.

**Disclosures:** A.J. Koh, None.

This study received funding from: NIH.

## M182

**A Novel and Sensitive Immunoassay for Parathyroid Hormone Related Protein.** L. J. Deftos<sup>1</sup>, A. Caston-Balderrama<sup>\*2</sup>, R. T. Dimayuga<sup>\*2</sup>, C. L. Chalberg<sup>\*1</sup>, K. C. Smith<sup>\*1</sup>, D. W. Burton<sup>\*1</sup>, R. E. Reitz<sup>2</sup>. <sup>1</sup>University of California, San Diego and San Diego VA Medical Center, San Diego, CA, USA, <sup>2</sup>Endocrine Division, Quest Diagnostics Nichols Institute, San Juan Capistrano, CA, USA.

The potential of parathyroid hormone-related protein (PTHrP) as a serum biomarker for common PTHrP-expressing tumors has not been realized, especially for the differential diagnosis of hypercalcemia of malignancy. Most available assays can detect only the markedly elevated levels of this oncoprotein present in the later stages of disease, and the circulation of this polypeptide in normal subjects remains controversial. The poor diagnostic value of many PTHrP assays seems to be due to inadequate specificity and sensitivity for circulating PTHrP species, as well as poor technical performance. Through a series of in vitro and in vivo biochemical and immunochemical studies, we identified PTHrP 107-138 as a candidate for clinical assay targeting, since this domain is less affected by proteolysis and thus more stable in biological fluids. We focused on this region to develop antibodies, tracers, standards, and assay matrices that would yield a diagnostically useful assay procedure. We developed rabbit antibodies to human PTHrP 107-138 and used the same peptide as the assay standards. Chloramine T iodination of Tyr108-PTHrP 109-138 yielded a peptide of high specific activity that was further enhanced by chromatographic purification. Assay conditions were optimized to produce a one-day immunoassay with a limit of detection of 0.3 pmol/L and limit of quantitation of 0.5 pmol/L. Inter-assay and intra-assay variations of 9.8% and 4.4% were achieved by appropriate modifications of assay reagents and incubation conditions. Clinical samples were collected from 110 apparently healthy adults for reference range studies and analyses of specimen

stability, specimen type comparisons, and interfering substances. The adult reference range for plasma samples collected in sodium heparin tubes was established as 1.4-2.7 pmol/L, with no age or gender dependencies; specimen comparison studies indicated that PTHrP-cocktail tube specimens are also acceptable. Because PTHrP overexpression can be seen in a majority of patients with common malignancies, such as breast and lung cancer, this novel assay should be useful for the diagnostic application of PTHrP measurement in patients with cancer-related hypercalcemia. Furthermore, since PTHrP is overexpressed in most patients with prostate cancer, who are not usually hypercalcemic, the assay could have wider application as a serum tumor biomarker.

**Disclosures:** L.J. Deftos, None.

## M183

**Parathyroid Hormone-gene Family in the Cartilaginous Fish, *Callorhynchus milii*.** Y. Liu<sup>\*1</sup>, S. J. Richardson<sup>\*1</sup>, A. S. Ibrahim<sup>\*1</sup>, T. I. Walker<sup>\*2</sup>, J. Bell<sup>\*2</sup>, S. Brenner<sup>\*3</sup>, B. Venkatesh<sup>\*3</sup>, J. A. Danks<sup>1</sup>. <sup>1</sup>School of Medical Sciences, RMIT University, Bundoora, Australia, <sup>2</sup>Marine and Freshwater Systems, Department of Primary Industries, Queenscliff, Australia, <sup>3</sup>Institute of Molecular and Cell Biology, Biopolis, Singapore, Singapore.

Parathyroid hormone (*pth*) and parathyroid hormone-related protein (*pthrp*) genes have been isolated and cloned in a number of bony vertebrates, including teleost fishes. Cartilaginous fishes are the most ancient living jawed vertebrates. They comprise of two groups: the elasmobranchs (sharks and rays) and the holocephalans. We have identified three members of the *pth* gene family (designated *EShpth1*, *EShpth2* and *EShpthrp*) in the genome of a holocephalan cartilaginous fish, *Callorhynchus milii*, commonly known as elephant shark or elephant fish. These animals are confined to south-eastern waters of Australia and New Zealand. *C. milii* has been recently targeted for whole-genome sequencing since its genome is the smallest among cartilaginous fishes (Venkatesh et al, *Science* 314:1892, 2006 and *PLoS Biol.* 5(4): e101, 2007). Initial bioinformatic analyses suggested that the three genes isolated were *EShpth1*, *EShpth2* and *EShpthrp* and this was confirmed by testing PTH-like biological activity in UMR106 cells. The expression pattern of the three genes were analyzed by RT-PCR and one gene, *EShpth2*, appeared to be confined to the brain. Immunohistochemistry was performed and strongest EShPthrp immunostaining was in the epidermis, kidney and gill while the strongest signals for EShPth1 and 2 were in the pancreas. This study confirms that *pth 1*, *2* and *pthrp* genes are present in the most ancient jawed vertebrates suggesting that the roles played by the parathyroid hormone family are fundamental and basic.

**Disclosures:** J.A. Danks, TeeleOstin Pty Ltd. 3, 4.

## M184

**A Continuous Rat Parathyroid Cell Line Expressing Parathyroid Hormone.** C. Mavilia<sup>\*</sup>, C. Mazzotta<sup>\*</sup>, L. Cavalli<sup>\*</sup>, T. Cavalli<sup>\*</sup>, M. Brandi. Department of Internal Medicine, University of Florence, Florence, Italy.

Development of a clonal parathyroid cell line capable to express parathyroid hormone (PTH) would represent an extraordinary achievement in the field of parathyroid biology. A PT-r cell strain was purified by successive colony isolation in 1995. However, PT-r cells secrete only PTH-related peptide (PTHrP) and this limited the use of the cell line for studies on regulatory mechanisms that control parathyroid cell differentiation. From primary cultures of hyperplastic parathyroid tissue we selectively recloned epithelial cell lines by limiting dilution using plastic surfaces coated with antibodies to the amino-terminal extracellular domain of the rat Ca(2+) receptor. The culture medium used was Coon's modified Ham's F12 containing 1.1 mM calcium and 10% FCS. Among the selected clones that we characterized one strain expressed *PTH* mRNA and it was, therefore, named PTHc1. The PTHc1 cells showed a polygonal morphology, with a doubling time of 25 hr, that did not vary over 8 months in culture. Over eighty five percent of PTHc1 cells exhibited a diploid chromosome number (2n=42) when analyzed over 5 months of serial culture. PTHc1 cell line expression profile was evaluated by RT-PCR. Parallel RT-PCR reactions, without added reverse transcriptase, were performed to confirm that the PCR products resulted from cDNA rather than from genomic DNA. PTHc1 cells expressed *PTH*, *CaSR*, *VDR*, *FGF23r4*, *ERα*, *ERβ*, and *GH-R*. Conversely, PTHc1 cells did not express *PTHrP*, *ENDO1*, *PTHr1*, *FGF23* and *Klotho*.

In conclusion, these results describe a novel PTH-secreting cell line derived from rat hyperplastic parathyroid tissue. The PTHc1 clone is ongoing an intensive characterization for both proliferative and differentiative features. We are confident that this cellular model will represent a unique opportunity for the understanding of either parathyroid physiology or the molecular bases of parathyroid disorders.

**Disclosures:** M. Brandi, None.

## M185

**Functional Induction of Target Genes in Parathyroid Cell by Direct Injection Technique.** K. Shiizaki<sup>1</sup>, I. Hatamura<sup>\*2</sup>, E. Nakazawa<sup>\*1</sup>, Y. Iwazu<sup>\*1</sup>, Y. Watanabe<sup>\*1</sup>, M. Fukagawa<sup>\*3</sup>, T. Akizawa<sup>\*4</sup>, E. Kusano<sup>\*1</sup>. <sup>1</sup>Division of Nephrology, Department of Internal Medicine, Jichi Medical University, Shimotsuke, Japan, <sup>2</sup>The First Department of Pathology, Wakayama Medical University, Wakayama, Japan, <sup>3</sup>Division of Nephrology & Dialysis Center, Kobe University School of Medicine, Kobe, Japan, <sup>4</sup>Department of Nephrology, Showa University School of Medicine, Tokyo, Japan.

Since there are not any available cell lines for studying parathyroid cell (PTC), it is difficult to adequately investigate the cellular effects of various factors in PTC. In the present study, the gene induction technique for PTC has been developed and this accuracy is also examined.

5/6-nephrectomized Sprague-Dawley rats were fed with a high-phosphate diet for eight weeks. LacZ-induced adenovirus (LacZ-Ad) was administered by the direct injection into parathyroid gland (PTG) (DI), the intravenously from jugular vein or directly applied on the PTG surface. The PTGs were excised at 48 hours after the treatment and were evaluated by X-Gal staining. Moreover, one of the PTGs was treated by DI of VDR- or CaSR-induced adenovirus (VDR-Ad and CaSR-Ad, respectively) and the other was treated with that of LacZ-Ad in the same rat. The VDR and CaSR expressions of PTCs at the same timing were examined immunohistochemically. Moreover, Ca-PTH response curves before and after treatment with CaSR-Ad were investigated.

Many X-gal-positive PTCs were observed in all over the PTG treated with DI of LacZ-Ad, however never in PTGs treated by the other administrations of LacZ-Ad. Marked increases in the number of both VDR- and CaSR-positive PTC were also confirmed in PTG treated by DI of VDR-Ad and CaSR-Ad, respectively. These findings were not observed in those with control treatment. The Ca-PTH response curve clearly sifted to the left side following the treatment with CaSR-Ad.

The functional gene induction in PTC of rat model with uremic secondary hyperparathyroidism has been established. This technique may make it possible to investigate the direct effects of various factors for PTC; in particular the signaling pathways and changes in cellular functions and proliferative activity in PTC.

**Disclosures:** K. Shiizaki, None.

## M186

**Selective Removal of PLC Signaling in Novel PTH(1-28) Analogs Abolishes Regulation of NaPi-IIc but not Napi-IIa.** S. Nagai, M. Mahon<sup>\*</sup>, M. Okazaki, J. T. Potts, H. Jüppner, T. Gardella. Endocrine Unit, Massachusetts General Hospital, Boston, MA, USA.

Last year we reported that the analog M-PTH(1-28) (M = Ala1,Aib3,Gln10,Har11,Ala12,Trp14,Arg19), a potent agonist for cAMP and IP3 signaling pathways, induces, when injected into mice, prolonged hypophosphatemic and hypercalcemic effects. The analog also induced prolonged reductions in NaPi-IIa immunoreactivity at the brush border membrane and cytoplasmic compartments of renal PT cells of injected mice. To help elucidate further the signaling mechanisms by which PTH ligands regulate renal phosphate transport, we developed a derivative of M-PTH(1-28) in which PLC/PKC signaling capacity is removed, but cAMP/PKA signaling activity is potentially retained. The new analog has alanine of M-PTH(1-28) replaced by tryptophan, in accordance with findings of Ferrari et. al (JBC 1999) showing that such bulky substitutions at position one selectively impair PLC signaling. In HEK-293 cells transiently transfected with the rat PTHR, Trp1-M-PTH(1-28) was about as potent as M-PTH(1-28) for stimulating cAMP formation, but at least 100-fold less potent than the parent peptide for stimulating IP3 formation. Trp1-M-PTH(1-28) retained the capacity to produce a prolonged cAMP response in MC3T3-E1 cells after ligand wash-out, as seen with M-PTH(1-28). When injected into mice (20 nmoles/kg) Trp1-M-PTH(1-28), like M-PTH(1-28), induced prolonged suppression of plasma phosphate levels, as compared to effects of PTH(1-34): maximal suppression at 2h for each analog; recovery to vehicle control levels at 4h for PTH(1-34), and at 6h for M-PTH(1-28) and Trp1-M-PTH(1-28). Apical and cytoplasmic NaPi-IIa staining was reduced in mice treated with each peptide at 2h, staining returned to vehicle control levels at 6h with PTH(1-34), it remained reduced for at least six hours in mice treated with either M-PTH(1-28) or Trp1-M-PTH(1-28). Reduction of NaPi-IIc surface expression required the more potent, PLC-sufficient analog M-PTH(1-28), and followed a slower kinetic loss of immunoreactivity than did reduction of NaPiIIa. Thus, immunostaining of NaPiIIc was reduced in mice treated with M-PTH(1-28) over the interval 4 to 6 h, and was unchanged in mice treated with Trp1-M-PTH(1-28) or PTH(1-34). M-PTH(1-28) inhibited 32P uptake in early passage LLC-PK1 cells (NHERF-1/ezrin positive) virally transduced to express NaPi-IIc, and the rat PTHR, but Trp1-M-PTH(1-28) failed to inhibit this activity. The combined findings in vivo and in vitro with the model PT cell system thus reveal that the selective elimination of PLC stimulation in the long-acting PTH analog Trp1-M-PTH(1-28) abolishes effects on NaPiIIc internalization, and indicate the importance of this signaling pathway in control of NaPiIIc, as distinct from NaPiIIa.

**Disclosures:** S. Nagai, None.

## M187

**Glial Cells Missing-2 (GCM2), the Regulator of Parathyroid Cell Fate, Transactivates the Calcium-sensing Receptor Gene (CASR): Identification of GCM-response Elements in CASR Promoters P1 and P2.** L. Canaff<sup>1</sup>, X. Zhou<sup>\*1</sup>, D. E. C. Cole<sup>\*2</sup>, G. N. Hendy<sup>1</sup>. <sup>1</sup>Medicine, McGill University, Montreal, QC, Canada, <sup>2</sup>University of Toronto, Toronto, ON, Canada.

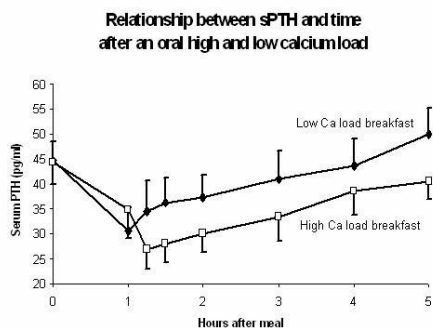
Glial cells missing-2 (GCM2) is a transcription factor expressed in the parathyroid hormone (PTH)-secreting cells of the parathyroid gland and is essential for their development. Thus far, downstream targets of GCM2 have not been identified. Here, we show that the promoters of the calcium-sensing receptor (CASR) gene, a differentiation marker for the parathyroid gland, are transactivated by wild-type GCM2. The human CASR gene has two promoters yielding transcripts with alternative 5'-untranslated regions but encoding the same receptor protein. Activities of P1 and P2 promoter-luciferase reporter constructs were stimulated ~2-3-fold over basal by cotransfection of a wild-type GCM2 expression vector in human embryonic kidney (HEK293) cells. Studies with mutated CASR promoter-reporter constructs as well as oligonucleotide precipitation assays identified GCM-response elements in CASR P1 (-451 to -441; relative to the transcription start site) and in CASR P2 (-166 to -156). Primary hypoparathyroidism is a heterogeneous group of conditions characterized by hypocalcemia and hyperphosphatemia due to deficient PTH secretion. In a few cases, homozygous or heterozygous inactivating mutations in the GCM2 gene have been implicated in familial isolated hypoparathyroidism inherited in an autosomal recessive or dominant manner, respectively. In co-transfection studies with either synthetic (3xgbs-lux; GCM-response element multimers) or natural (CASR) promoter-reporter constructs, a dominantly inherited mutant GCM2 exerted a dominant-negative effect on wild-type GCM2 activity, whereas recessively inherited mutants had little or no effect. These data support the notion that different functionality of the GCM2 mutants is sufficient to explain the different modes of inheritance. In addition, we have provided the mechanistic link for a previously noted association between GCM2 and CASR in the development of parathyroid glands of terrestrial vertebrates and evolutionarily related gills of bony fish.

**Disclosures:** L. Canaff, None.

## M188

**Serum Parathyroid Hormone Response to Oral Calcium Load in Asian Adolescents.** L. Wu<sup>\*1</sup>, B. Martin<sup>1</sup>, L. McCabe<sup>\*2</sup>, G. McCabe<sup>\*2</sup>, R. M. McClintock<sup>\*3</sup>, M. Peacock<sup>3</sup>, C. M. Weaver<sup>1</sup>. <sup>1</sup>Foods & Nutrition, Purdue University, West Lafayette, IN, USA, <sup>2</sup>Statistics, Purdue University, West Lafayette, IN, USA, <sup>3</sup>Indiana University School of Medicine, Indianapolis, IN, USA.

Measurement of calcium absorption is expensive and not routine. PTH suppression has been used as an indirect indicator of calcium absorption in adults, but not children. Thus, we investigated the calcium load effect on serum (s) PTH suppression in Asian adolescents. Sixteen healthy Chinese boys and girls, aged 12-15 years who had been in the USA for more than 8 months, participated in two 3-week metabolic calcium balance studies separated by a one week washout period. The subjects were randomly assigned to a pair of low (630-1008 mg/d) and high (1275-1602 mg/d) dietary calcium intakes in a cross-over design. Subjects ate a breakfast containing one-third of their daily calcium intake assignment on day 8 of each session. Blood was drawn before and at multiple times after the meal over a 5-hour period and sPTH was measured by radioimmunoassay. The sPTH nadir occurred 1.25 hours after the calcium load (Figure), earlier than the 3 hour nadir reported in adults. The high calcium load (425-534mg) led to significantly greater sPTH suppression ( $P<0.05$ ) than the low calcium load (210-336mg). The 5h sPTH 'area-under-the-curve' following the low calcium load was greater than that following the high calcium load, reflecting lesser suppression of sPTH. There was a significant calcium dose-effect on PTH suppression ( $P<0.05$ ). We also compared sPTH suppression and calcium absorption measured by the stable calcium isotope ratio method in the same subjects. The results suggest that PTH suppression reflects calcium absorption in Adolescents, but is limited to rather large calcium loads.



**Disclosures:** L. Wu, NIH 3.  
This study received funding from: NIH.

## M189

**Molecular Mechanisms Involved in PTH-induced Apoptosis in Caco-2 Intestinal Cells.** N. Calvo<sup>\*</sup>, R. L. Boland, A. Russo de Boland<sup>\*</sup>, C. Gentili<sup>\*</sup>. Dept. Biología, Bioquímica & Farmacia, Universidad Nacional del Sur, Bahía Blanca, Argentina.

Apoptosis, a form of programmed cell death, is a process fundamental to normal growth and development, immune response, tissue remodeling after injury or insult, and plays a critical role in maintaining homeostasis of the intestinal epithelium. Recently, it has become apparent that signaling by the PTH receptor can either promote or suppress apoptosis depending on the cellular context. In this study we show that stimulation of human colonic Caco-2 cells with PTH ( $10^{-8}$  M) results in the dephosphorylation and translocation of pro-apoptotic protein Bad from the cytosol to mitochondria and release of cytochrome c and Smac/Diablo. The hormone also triggers mitochondria cellular distribution to the perinuclear region, diminishes the number of viable cells, increases the enzymatic activity of caspase-3, that is also evidenced from the appearance of its cleaved fragments in western blot experiments, and degradation of its substrate PARP. Moreover, we found that the hormone induces disruption of actin filaments with changes of cellular shape, alteration of cell-to-cell junctions, externalization of membrane phosphatidylserine and also chromatin condensation and DNA fragmentation of the nucleus. Taken together, the present study suggests that the mitochondrial pathway may account for PTH promotion of apoptosis in Caco-2 intestinal cells.

**Disclosures:** R.L. Boland, None.

## M190

**Influence of Primary Hypoparathyroidism (PHp) on Bone Mineral Density (BMD) and Vertebral Morphometry.** F. J. A. de Paula<sup>\*</sup>, F. A. Pereira, L. M. Monsingnore<sup>\*</sup>, S. R. Teixeira<sup>\*</sup>, M. H. Nogueira-Barbosa<sup>\*</sup>. Internal Medicine, School of Medicine of Ribeirão Preto, University of São Paulo, Ribeirão Preto, Brazil.

The physiological role of PTH in the maintenance of bone mass and of the qualitative characteristics of this tissue is unknown. Our objective was to evaluate BMD and the prevalence of vertebral fractures by morphometric criteria in PHp, this being the first study evaluating vertebral morphometry in PHp. Thirty-three patients (27F:6M) with iatrogenic PHp and with a previous diagnosis of atoxic multinodular goiter were studied. Mean age was  $55.3 \pm 10.3$  years, weight =  $70.4 \pm 14.7$  kg, height =  $1.59 \pm 0.07$  m, BMI =  $25 \pm 7.4$  kg/m<sup>2</sup>, and duration of PHp  $13.3 \pm 11.8$  years. We determined calcium levels, Ca<sup>++</sup>, Pi, PTH, calciuria, BMD at L1-L4, femoral neck (FN) and hip and obtained thoracic and lumbar radiographies using rigid standardization criteria to measure the anterior (AH), middle (MH) and posterior (PH) height of each vertebral body from T4 to L4 using a digital caliper. The criteria of vertebral deformity were: 1) more than a 20% reduction between two of these measures and/or a 20% reduction in the relation between any one of these measures and the measure of the corresponding region of the vertebral body immediately superior or inferior to the vertebra analyzed, and 2) a reduction  $\geq 4$  mm in absolute value. Thus 228 measurements were made for each patient, for a total of 7980. In the diagnosis, calcium, Ca<sup>++</sup> and Pi levels were  $7.2 \pm 0.7$  mg/dl,  $0.89 \pm 0.1$  mol/l and  $5.3 \pm 0.8$  mg/dl, respectively. At last visit, the levels were: calcium =  $8.7 \pm 0.7$  mg/dl, Ca<sup>++</sup> =  $1.07 \pm 0.08$  mmol/L, Pi =  $4.4 \pm 0.9$  mg/dl, and calciuria =  $84 \pm 70$  mg/24 h. Densitometry values at L1-L4 were (BMD =  $1.138 \pm 0.3$  g/cm<sup>2</sup>; T-score =  $+0.8 \pm 2.4$  SD), FN (BMD =  $0.940 \pm 0.2$  g/cm<sup>2</sup>; T-score =  $+0.7 \pm 1.7$  SD), Hip (BMD =  $1.013 \pm 0.2$  g/cm<sup>2</sup>; T-score =  $+0.3 \pm 1.4$  SD). Seventeen patients (51%) presented at least one vertebral deformity and vertebral deformity were distributed as follows: T4 = 1, T5 = 5, T6 = 2, T7 = 7, T8 = 7, T9 = 5, T10 = 5, T11 = 9, T12 = 6, L1 = 5, L2 = 3, L3 = 2, L4 = 3, for a total of 60 vertebral deformity. Three patients had only one altered measure and 9 patients (27% of the total and 53% of the patients with vertebral deformity) had at least three deformities in different vertebral bodies. No other causes of vertebral deformity, such as neoplasias, were detected. This is the first study evaluating vertebral morphometry in PHp, showing that preservation or elevation of bone mass occurs in this condition. Nevertheless, a large number of vertebral deformity were observed in the study group, possibly indicating that the bone quality of these patients is compromised.

**Disclosures:** F.J.A. de Paula, None.

## M191

**Analysis of Chromosome Breaks in Osteoblasts and Non-osteoblastic Cells Treated with Intermittent PTH.** E. C. A. Oliveira<sup>\*</sup>, C. H. M. Castro<sup>\*</sup>, V. L. Szejnfeld. Rheumatology, Universidade Federal de São Paulo, São Paulo, Brazil.

Intermittent PTH has been approved for the treatment of osteoporosis as an anabolic agent. Toxicological studies have demonstrated that intermittent PTH is associated with osteosarcoma in Fischer rats. However, no solid evidence has been accumulated on the potential genotoxic and mutagenic effect of intermittent PTH and its safety remains controversial. In the present study we investigated the chromosome breaks formed by intermittent PTH on human and murine osteoblasts cells versus non-osteoblastic cells (Hep-2 and HeLa) using the Micronuclei (MN) assay. Osteoblastic cells were grown in  $\alpha$ MEM and non-osteoblastic cells in DMEM. All cell cultures were supplemented with 10% FBS, 100 IU/ml penicillin and 100  $\mu$ g/ml streptomycin. Cells were treated with PTH at 50 and 100 nM for 21 days. Cells were incubated with PTH for 6 hours a day and then were placed in new medium containing 10% FBS and antibiotics. Micronuclei assays were performed at different time points (6 hours, 7, 14 and 21 days). Non-treated cells and cultures exposed for 6 hours to methyl methane sulfonate at 0.1mg/ml were used as negative and positive controls, respectively. At the different time-points, cytochalasin B (4.5  $\mu$ g/ml) was added to the cultures

to inhibit cytokinesis at the end of mitosis. 36 hours after adding cytochalasin B, cells were fixed in methanol, stained with acridine orange and chromosome breaks were visualized by fluorescence microscopy. We observed a 2-3-fold increase in the prevalence of micronuclei in human and murine osteoblastic cells treated by PTH intermittent as compared to the controls. The effect was detectable 6 hours after PTH treatment and was more significant with the highest PTH concentration. Accordingly, the number of micronuclei increased significantly in the treated cells with time in culture and nucleoplasmic bridges were detected, suggesting that PTH treatment in osteoblastic cells induces genomic instability and can be considered clastogenic, at least *in vitro*. To non-osteoblastic cells chromosome breaks appeared only after three weeks of treatment, suggesting a delayed less potent effect in these cells. Our results demonstrate that intermittent PTH can interact with DNA, inducing chromosome breaks. The clastogenic effect is more accentuated in osteoblasts as compared to non-osteoblastic cells. These results are in agreement with our previous findings showing that intermittent PTH is also genotoxic to osteoblastic cells in an *in vivo* mice model.

**Disclosures:** E.C.A. Oliveira, None.

## M192

**The Role of Osteoprotegerin / Receptor Activator of Nuclear Factor kappa B Ligand System for Bone Loss in Primary Hyperparathyroidism.** N. G. Mokrysheva\*, S. S. Gulyaeva\*, Y. A. Dubrovina\*, L. G. Rostomyan\*, L. Y. Rozhinskaya, A. V. Ilyin\*, G. S. Kolesnikova\*, N. I. Sazonova\*. The National Research Centre for Endocrinology, Moscow, Russian Federation.

Pathogenesis of bone mineral density (BMD) loss in primary hyperparathyroidism (PHPT) has not been fully understood. The aim was to investigate the role of osteoprotegerin (OPG) / Receptor Activator of Nuclear factor kappa B ligand (RANKL) system in primary hyperparathyroidism (PHPT). Sixty seven patients with PHPT (62 women and 5 men, mean age 58 y) and 20 generally healthy people for control group were enrolled. Forty two of this patients received surgical treatment on parathyroid glands. Biochemical parameters, BMD (DXA), the markers of bone metabolism (osteocalcin and serum CTx), OPG and RANKL were measured in all subjects before and at the 6th, 12th months after surgical treatment. OPG and RANKL levels were significantly increased in patients with PHPT ( $p < 0.05$ ). Serum OPG correlated with PTH level ( $r = 0.33$ ,  $p < 0.009$ ). RANKL level did not correlate with PTH. Predictably, OPG level correlated with age ( $r = 0.5$ ,  $p < 0.05$ ) and duration of menopause ( $r = 0.36$ ,  $p = 0.007$ ). RANKL level showed negative correlation with duration of menopause ( $r = -0.36$ ,  $p < 0.05$ ). Correlation of OPG with osteocalcin level ( $r = 0.27$ ,  $p < 0.05$ ) was found. OPG level correlated with BMD T-score in L2-L4 ( $r = -0.48$ ,  $p < 0.001$ ), total hip ( $r = -0.37$ ,  $p < 0.005$ ) and radius total ( $r = -0.26$ ,  $p = 0.043$ ). PTH, CTx, osteocalcin, calcium levels were in the reference range 6 and 12 months after surgical treatment. However, OPG and RANKL levels did not decrease significantly even 1 year after surgical treatment, though some tendency to decrease of OPG was observed. OPG/RANKL system is involved in bone loss in PHPT. However the role of OPG/RANKL system is secondary to the effects of high PTH level on bone in patients with PHPT.

**Disclosures:** S.S. Gulyaeva, None.

## M193

**Nmp4-Knockout (KO) Mice Exhibit A Complex Phenotype.** A. G. Robling, J. Cottee\*, P. Childress\*, J. P. Bidwell. Anatomy and Cell Biology, Indiana University School of Medicine, Indianapolis, IN, USA.

The nucleocytoplasmic shuttling transcription factor Nmp4/CIZ (nuclear matrix protein 4/cas interacting zinc finger protein) is a ubiquitously expressed protein that regulates both cytoplasmic and nuclear activities in many cell types. In the nucleus, Nmp4/CIZ represses transcription of genes crucial to osteoblast differentiation (e.g., Runx2) and genes activated by a variety of anabolic stimuli, most notably PTH. We investigated the role of Nmp4/CIZ in PTH responsiveness by engineering mice with loss-of-function mutations in the Nmp4/CIZ gene, and treating those mice with intermittent PTH. Nmp4 knockout (Nmp4-KO) mice were prepared by replacing coding exons 4-7 with the Neo gene cassette. The progeny were backcrossed onto a pure C57BL/6 background (Nmp4-KO-N6) or left on a mixed B6/129 background (Nmp4-KO-F2). Bone mineral density (BMD), content (BMC), and body composition were collected by dual-energy X-ray absorptiometry (pdxMUS). To evaluate the response of Nmp4-KO-N6 mice to anabolic doses of human parathyroid hormone (hPTH 1-34), 10 wk-old female mice were injected with vehicle control or hormone at 30 µg/kg/day, 7 day/wk, for 6 wks.

The Nmp4 mutant alleles had no effect on body weight when expressed on a mixed background, but the same alleles on a pure B6 background yielded a significant, 15% increase in body weight among the KO mice, compared to their WT controls. Nmp4-KO mice exhibited significantly greater whole body, femur, and tibia BMD at 8 wks, regardless of genetic background, as compared to their WT counterparts. These differences were maintained at 16 wks, with the exception of femoral BMD, which returned to WT values in the mature skeleton.

Treatment of the backcrossed mice with PTH resulted in a significant increase in body weight among WT mice, but the same PTH regimen caused the KO mice to lose weight. PTH significantly enhanced femur BMD in both WT and Nmp4-KO-N6 animals however, the latter exhibited a significantly greater (~8%) PTH-induced gain in BMD than WT mice. These results suggest that femora from Nmp4-KO-N6 mice are more sensitive to anabolic PTH than femora from WT mice. The magnitude of PTH-response at other skeletal sites did not differ between the Nmp4-KO-N6 and WT mice.

These data suggest that Nmp4 plays a significant role in regulating tissue development, perhaps by altering differentiation of cells that contribute to lean and fat mass. Furthermore, Nmp4 appears to regulate site-specific skeletal response to PTH. The

differential effects of the Nmp4 null alleles on a pure B6 vs. mixed genetic background suggest the presence of modifier genes that alter the action of Nmp4. Nmp4 has distinct effects on the development, homeostasis, and PTH response at different skeletal sites.

**Disclosures:** J.P. Bidwell, None.

## M194

**Behavior of Circulating Rat(s) PTH Molecular Forms in Secondary Hyperparathyroidism Related to Vitamin D Deficiency and Renal Failure.**

P. D'Amour<sup>1</sup>, L. Rousseau<sup>\*1</sup>, S. C. Hornyak<sup>\*2</sup>, Y. Zang<sup>\*2</sup>, T. Cantor<sup>2</sup>.

<sup>1</sup>Department of Medicine, Université de Montréal, Centre de recherche du CHUM, Hôpital Saint-Luc, Montreal, QC, Canada, <sup>2</sup>Scantibodies Laboratory Inc., Santee, CA, USA.

The behavior of circulating PTH molecular forms has been well studied under a variety of clinical conditions and their immunoreactivity in second- (Intact or Total hPTH assays) and third- (Whole PTH assay) generation PTH assays well characterized. Little is known on similarity and possible differences between species concerning PTH molecular forms. The following study was thus performed to study the behavior of circulating PTH molecular forms in normal rats (N-r) and in rats with secondary hyperparathyroidism related to vitamin D deficiency (D-r) and advanced renal failure (RFr). rPTH assays similar to human assays were developed for this study. The rWhole PTH assay reacted with rPTH(1-84) but not with rPTH(7-84), demonstrating a 1-6 epitope. The rTotal PTH assay reacted equally well with rPTH(1-84) and (7-84) and could be saturated with PTH(7-34) indicating an epitope in the region 7-34. D-r had lower ionized calcium ( $\text{Ca}^{++}$ ) ( $p < 0.05$ ), 25(OH)D levels ( $p < 0.001$ ) and a 3-fold increase in Whole ( $15 \pm 17.6$  pmol/L;  $p < 0.001$ ) and Total rPTH ( $20.8 \pm 9.9$  pmol/L;  $p < 0.001$ ). RFr had a low  $\text{Ca}^{++}$  ( $p < 0.01$ ) and a 25 to 30-fold increase in Whole ( $140 \pm 70$  pmol/L;  $p < 0.001$ ) and Total ( $147 \pm 72$ ;  $p < 0.001$ ) rPTH levels. Pools of serum coming from 25 Nr, 13 D-r and 5 RFr were submitted to HPLC separation and analyzed with the 2r assays. Three regions were identified on HPLC profiles corresponding to tubes 28-37, 38-42 and 43-49. The first corresponded to non-(1-84) PTH fragments reacting in the rTotal PTH assay, the second to an aminoterminal (N) peak of PTH reacting slightly better in the rWhole PTH assay and the third to the election position of rPTH(1-84). With the rWhole PTH assay, rPTH(1-84) was 90.4% and N-PTH (8.4%) in D-r, 86.4 and 13.6% in NR and 67.5 and 29.9% in RFr. With the rTotal PTH assay, rPTH(1-84) was 82.5%, N-PTH 6.4% and non-(1-84) PTH 11.1% in D-r, 78.9, 9.6 and 11.5% in NR and 68.3, 19.5 and 12.2% in RFr. These results indicate that in rats adjustment of circulating PTH molecular forms are mainly made through rPTH(1-84) and N-PTH and less through non-(1-84) PTH fragments, with a decreased production of N-PTH in favor of rPTH(1-84) in D-r and with the accumulation of N-PTH in renal failure.

**Disclosures:** P. D'Amour, Scantibodies Laboratory Inc. 3.

This study received funding from: Scantibodies Laboratory Inc.

## M195

**The N-terminal Fragment of Parathyroid Hormone-related Protein (PTHrP) Promotes the Glucocorticoid-related Deficiency of Bone Regeneration after Bone Marrow Ablation in Mice.** L. F. de Castro<sup>\*1</sup>, D. Lozano<sup>\*1</sup>, E. Gómez-Barrena<sup>\*2</sup>, S. Dapia<sup>\*3</sup>, P. Esbrit<sup>1</sup>.

<sup>1</sup>Bone and Mineral Metabolism Laboratory, Fundación Jiménez Díaz, Madrid, Spain, <sup>2</sup>Dpt. of Traumatology, Fundación Jiménez Díaz, Madrid, Spain, <sup>3</sup>Trabeculae, S.L., Orense, Spain.

Glucocorticoids (GCs) inhibit osteoblast viability and function, and decrease bone formation. Osteoblastic expression of parathyroid hormone-related protein (PTHrP), an important modulator of bone formation, decreases by GCs. We here examined the effect of the PTH-like fragment of PTHrP on bone regeneration after bone marrow ablation in GC-treated mice. We administered 3-methylprednisolone (10 mg/Kg, s.c., every other day) or vehicle to C57BL/6 mice for 16 d. Some GC-treated mice were simultaneously injected with PTHrP (1-36) (100 µg/Kg, s.c., every other day). At day 5, bone marrow ablation was performed under anaesthesia. At the end of the study, bone marrow of one tibia was cultured for up to 21 days for evaluation of the abundance of cell colonies (by crystal violet staining), alkaline phosphatase (ALP) staining, and bone nodule formation (by alizarin red staining). Total RNA was isolated from the remaining hard tissue for mRNA analysis of several osteoblast-related genes (by real-time PCR). The other tibia was fixed, decalcified and included in paraffin for histological studies. Evaluation of femoral bone structure in these mice by µCT showed a 20% decrease in cortical thickness, and a trend to an increased porosity, with no changes in trabecular parameters. GC-treated mice had a moderate but significant weight loss (5%), but this was not observed in PTHrP (1-36)-administered mice. GC-treated mice showed a 25% decrease in both osteoid surface (by Masson's staining) and osteoblast number in the metaphysis, and a 2-fold higher number of adipocytes in the distal diaphysis, in the regenerating tibia, compared to those in control mice. Moreover, GC-treated mice exhibited a decreased gene expression of several osteoblastic products: Runx2, osterix, alkaline phosphatase, osteocalcin, vascular endothelial growth factor and its 1 and 2 receptors, and the osteoprotegerin/receptor activator of NF-κB ligand mRNA ratio; associated with a lower PTHrP gene expression in the regenerating tibia. These changes were totally or partially recovered by PTHrP (1-36) treatment. In addition, *in vivo* GC treatment induced a decrease in bone marrow-derived cell colonies and ALP staining, and also in their mineralization capacity. These *ex vivo* changes were also reversed by *in vivo* PTHrP (1-36) administration. In conclusion, the N-terminal fragment of PTHrP can restore the GC-induced alteration of osteoblastic function, and thus accelerates bone regeneration in mice.

**Disclosures:** L. F. de Castro, None.



## M196

**Metabolic Alkalosis Transition in Renal Proximal Tubule Cells Facilitates an Increase in CYP27B1, While Blunting Responsiveness to PTH.** M. A. Forster<sup>\*1</sup>, S. Masilamani<sup>\*2</sup>, T. A. Reinhardt<sup>3</sup>, M. J. Beckman<sup>\*4</sup>. <sup>1</sup>Physiology and Biophysics, Virginia Commonwealth University, Richmond, VA, USA, <sup>2</sup>Internal Medicine, Nephrology, Virginia Commonwealth University, Richmond, VA, USA, <sup>3</sup>Mineral Metabolism and Mastitis, ARS USDA National Animal Disease Center, Ames, IA, USA, <sup>4</sup>Biochemistry, Virginia Commonwealth University, Richmond, VA, USA.

Parathyroid hormone (PTH) is the central activator of renal proximal 1- $\alpha$ -hydroxylase (CYP27B1), the enzyme responsible for synthesis of 1,25-dihydroxyvitamin D<sub>3</sub> (1,25(OH)<sub>2</sub>D<sub>3</sub>). Past studies have documented a disruption of CYP27B1 activity in chronic metabolic acidosis *in vivo*, while simulated acidosis in cultured renal cells failed to demonstrate impairment of 1,25(OH)<sub>2</sub>D<sub>3</sub> synthesis. To determine the factors involved in regulating responsiveness of CYP27B1 to PTH in renal proximal tubule cells, we developed a dietary protocol to study the transition from metabolic acidosis (diet low in potassium) to metabolic alkalosis (diet high in potassium-bicarbonate) in young adult rats, n=9. Gene expression was determined in renal proximal tubules isolated from each group using Affymetrix GeneChip<sup>®</sup> microarray, n=3. The high potassium bicarbonate diet was found to induce metabolic alkalosis (> 7.5) by day 10 as tested by urine pH. The rats being fed the control diet were maintained at a slightly acidic urine pH (< 7.4) throughout the study. Blood concentrations of phosphate, calcium and 25-OH-D<sub>3</sub> were replete under the conditions effected by both acidic and basic diets, however, blood 1,25(OH)<sub>2</sub>D<sub>3</sub> concentrations were significantly increased by the switch to the high potassium-bicarbonate alkaline diet. This was matched by an increase in gene expression of 1- $\alpha$ -hydroxylase (CYP27B1), 9kDa-CaBP and NR4A2, and a decrease in VDR following alkalosis in renal proximal tubules. The orphan nuclear receptor family 4A, member 2 (NR4A2, also known as HZF-2, NURR1) was recently identified as a positive regulator of CYP27B1 transcription in renal proximal tubule epithelial cells. In the present study, intermediate components of PTH cell signaling such as adenylate cyclase and CREB were expressed at significantly higher levels in animals fed the acidic control diet, while NR4A2 was closely associated with the regulation pattern of CYP27B1 in metabolic alkalosis. These results indicate that the important link between PTH responsiveness and renal CYP27B1 gene expression is predisposed by levels of cAMP/PKA/CREB pathway intermediates, but CYP27B1 expression requires NR4A2. In conclusion, chronic acidosis suppressed CYP27B1 gene expression in proximal tubules but maintained enhanced responsiveness to PTH. In contrast, metabolic alkalosis displayed blunted PTH responsiveness.

**Disclosures:** M.J. Beckman, None.

This study received funding from: ARS USDA CRA 58-3625-6-103.

## M197

**Documented Response to Cinacalcet in Two Cases of Acquired Hypocalciuric Hypercalcemia.** A. Godbout<sup>\*1</sup>, G. Rondeau<sup>\*1</sup>, J. H. Brossard<sup>\*1</sup>, P. D'Amour<sup>1</sup>, R. Bélanger<sup>\*1</sup>, H. B. Lavoie<sup>\*1</sup>, G. N. Hendy<sup>2</sup>, N. Alos<sup>3</sup>, L. G. Ste-Marie<sup>1</sup>. <sup>1</sup>Endocrinology, Chum, Montreal, QC, Canada, <sup>2</sup>Department of Medicine, McGill University, Montreal, QC, Canada, <sup>3</sup>Endocrinology, Hôpital Ste-Justine, Montreal, QC, Canada.

Differential diagnosis of hypercalcemia (Hc) with inappropriately normal or elevated serum parathyroid hormone (PTH) includes primary hyperparathyroidism, rare cases of paraneoplastic PTH secretion and familial hypocalciuric hypercalcemia, which is caused by an inactivating mutation of the calcium-sensing receptor (CaSR). Only five cases of acquired hypocalciuric Hc due to CaSR autoantibodies have been reported. We present 2 cases of severe symptomatic Hc with hypocalciuria diagnosed in a girl and a man of respectively 15 and 75-year-old. Initially, they disclosed high serum Ca respectively of 3.20 and 5.10 mmol/L (N: 2.15-2.60). The teenager presented with 1 year history of weight loss. She was already treated for hypothyroidism and Myoclonic-Astatic Epilepsy. Being adopted, no information about her family was available. The old man was admitted for confusion and weight loss. His past medical history was negative. He took no medication. Family history was negative and his four daughters were normocalcemic. At presentation, both had inappropriate or elevated serum PTH (3.2 and 13.5 pmol/L N:1.4-6.8) and normal renal function. Serum phosphate (Pi) was normal for the girl but lowered in the old man. Serum 25(OH)vitamin D, 1,25(OH)<sub>2</sub>vitamin D and PTHrP were all normal. In both patients, 24h urinary Ca excretion was low at 3.7 and 2.4 mmol/d, with reduced Ca clearance to creatinine clearance ratio (CCa/CCreat) of 0.0042 and 0.0064. Mutation analysis of both patients DNA found all *CaSR* gene protein-coding exons to be normal. Serum Ca remained high despite alendronate for the girl and repeated pamidronate and zoledronic acid infusions in the man. However, after 2 weeks of prednisone (1mg/kg/d), Hc ameliorated in the first case decreasing from 3.00 to 2.71mmol/L whereas serum Ca, Pi and PTH normalized in the man but CCa/CCreat remained low in both. These responses, as previously published, suggest autoantibodies against the CaSR as the cause of the acquired hypocalciuric hypercalcemia. Prednisone was then tapered and cinacalcet, a calcimimetic, was administered and successfully controlled the Hc at a dosage of respectively 120 and 180 mg PO die. The CCa/CCreat normalized in both patients. Presence of circulating CaSR autoantibodies will now be sought. These are the first documented cases of successful control of acquired hypocalciuric hypercalcemia with cinacalcet, resulting in sustained normalization of calcemia and urinary calcium excretion. Cinacalcet should be considered as a first line treatment in acquired hypocalciuric hypercalcemia.

**Disclosures:** A. Godbout, None.

## M198

**Efficient Expression of the Full-Length Calcium-Sensing Receptor in Insect Cells.** Z. Ryan<sup>\*</sup>, R. Kumar. Nephrology Research, Mayo Clinic, Rochester, MN, USA.

The Calcium-Sensing Receptor (CaSR) is a 1078 amino acid cell surface G protein-coupled receptor that regulates calcium homeostasis by altering parathyroid hormone release and renal calcium transport. The receptor binds divalent and trivalent cations, amino acids, polyamines, and polycationic ligands and is involved in the sensing of serum calcium concentrations. The CaSR is localized in tissues involved in calcium homeostasis including the parathyroid gland, kidney, thyroid C-cells, bone (osteoclasts, osteoblasts), and intestine, as well as several other tissues without obvious roles in the maintenance of extracellular calcium such as nerve terminals, cardiac myocytes, and oligodendrocytes. The CaSR is composed of three domains: a large extracellular domain (ECD, amino acids 20-612), a seven-transmembrane-spanning segment (amino acids 613-867), and a cytoplasmic tail (amino acids 868-1078). The exact amino acid residues and molecular orientations which are responsible for Ca<sup>2+</sup> binding, Ca<sup>2+</sup> sensing, and signal transduction in response to changes in serum Ca<sup>2+</sup> concentrations are unknown.

In order to determine the biophysical properties of full-length CaSR, we have generated an efficient system for the expression of full-length CaSR in quantities sufficient for functional analysis and x-ray crystallography. Two CaSR constructs were created: one full length (amino acids 1-1078) and the other missing the CaSR signal sequence (amino acids 20-1078). Both constructs were cloned into a pIB/V5-His TOPO insect expression vector for transfection into the High-Five insect cell expression system (Invitrogen). The orientation of the inserts and DNA sequence were verified by DNA sequencing. *Trichoplusia ni* (High Five) cells were stably transfected with the pIB/V5-His CaSR constructs. After Blasticidin S selection for successful transfection, cells were harvested for SDS-PAGE and Western blot analysis using a V5-HRP antibody. Protein samples were made with and without DTT to determine whether the CaSR expressed by the insect cells formed dimers. Results indicate that the full-length (amino acids 1-1078) CaSR construct is highly expressed and is able to dimerize successfully. The CaSR lacking signal sequence (amino acids 20-1078) is poorly expressed and is unable to dimerize.

Conclusion: We have devised an efficient insect cell based system for the expression of the full-length CaSR which will permit the isolation of sufficient amounts of the receptor for biophysical and crystallization studies.

**Disclosures:** Z. Ryan, None.

## M199

**Dietary Normalization of Calcium Absorption in Mice Genetically Deficient in CaSR and 25-Hydroxyvitamin D-1 $\alpha$ -Hydroxylase Results in Non-Lethal, Severe Hyperparathyroidism with Reduced Osteoclastogenesis.** C. Richard<sup>1</sup>, D. Miao<sup>\*2</sup>, R. Huo<sup>\*1</sup>, G. N. Hendy<sup>1</sup>, D. Goltzman<sup>1</sup>. <sup>1</sup>Medicine Dept, Calcium Laboratory, McGill University, Royal Victoria Hospital, Montreal, QC, Canada, <sup>2</sup>Human Anatomy, Nanjing Medical University, Nanjing, China.

The calcium sensing receptor (CaSR) mediates the effect of high calcium to suppress PTH synthesis and secretion and also to promote renal calcium excretion. CaSR is also expressed in multiple bone cells, however the specific function of CaSR in bone is still controversial. These tissues are also the target sites for the action of 1,25-dihydroxyvitamin D [1,25(OH)<sub>2</sub>D]. To further delineate the specific *in vivo* interactions of CaSR and 1,25(OH)<sub>2</sub>D, we developed a mouse model in which the genes encoding CaSR and 1 $\alpha$ (OH)ase were inactivated. We investigated the effects of the combined deficiency of CaSR and 1,25(OH)<sub>2</sub>D on mice fed a diet high in lactose, calcium and phosphorus. This diet has been shown to normalize gastrointestinal calcium absorption in the absence of vitamin D. Study of genetic models showed that compared to CaSR<sup>+/+</sup>;1 $\alpha$ (OH)ase<sup>-/-</sup> and CaSR<sup>-/-</sup>;1 $\alpha$ (OH)ase<sup>-/-</sup>, CaSR<sup>-/-</sup>;1 $\alpha$ (OH)ase<sup>-/-</sup> mice had the lowest weight at weaning and the slowest initial growth rate but survived long-term. These mice were markedly hypercalcemic and hypophosphatemic (serum calcium and phosphorus of 5.0 mM and 0.6 mM respectively) in contrast to CaSR<sup>+/+</sup>;1 $\alpha$ (OH)ase<sup>-/-</sup> and CaSR<sup>-/-</sup>;1 $\alpha$ (OH)ase<sup>-/-</sup> which had normal serum calcium and phosphorus levels. Serum intact PTH levels were high in CaSR<sup>-/-</sup>;1 $\alpha$ (OH)ase<sup>-/-</sup> (3000 pg/ml) but normal in normocalcemic CaSR<sup>+/+</sup>;1 $\alpha$ (OH)ase<sup>-/-</sup> and CaSR<sup>-/-</sup>;1 $\alpha$ (OH)ase<sup>-/-</sup> mice. Bone volume over tissue volume of CaSR<sup>-/-</sup>;1 $\alpha$ (OH)ase<sup>-/-</sup> mice, and osteoid volume over bone volume, were both increased in the tibia (100%) and to a lesser extent in the lumbar spine compared to CaSR<sup>+/+</sup>;1 $\alpha$ (OH)ase<sup>-/-</sup>. Parathyroid gland size was clearly increased in CaSR<sup>-/-</sup>;1 $\alpha$ (OH)ase<sup>-/-</sup> but not in CaSR<sup>+/+</sup>;1 $\alpha$ (OH)ase<sup>-/-</sup> mice. Alkaline phosphatase staining of the femur revealed a large increase in osteoblast numbers in CaSR<sup>-/-</sup>;1 $\alpha$ (OH)ase<sup>-/-</sup> compared to CaSR<sup>+/+</sup>;1 $\alpha$ (OH)ase<sup>-/-</sup> and CaSR<sup>-/-</sup>;1 $\alpha$ (OH)ase<sup>-/-</sup> mice. TRAP staining showed a decrease in osteoclasts in both CaSR<sup>-/-</sup>;1 $\alpha$ (OH)ase<sup>-/-</sup> and CaSR<sup>+/+</sup>;1 $\alpha$ (OH)ase<sup>-/-</sup> mice. Bone mineral density (BMD) of 90 day old female CaSR<sup>+/+</sup>;1 $\alpha$ (OH)ase<sup>-/-</sup> and CaSR<sup>-/-</sup>;1 $\alpha$ (OH)ase<sup>-/-</sup> mice but not CaSR<sup>+/+</sup>;1 $\alpha$ (OH)ase<sup>-/-</sup> mice was higher than in male counterparts. Taken together these results suggest that CaSR activation is implicated in the control of bone resorption through osteoclastogenesis and that CaSR gene inactivation may result in a gender-specific effect on BMD.

**Disclosures:** C. Richard, None.

## M200

**Calcium Sensing Receptor Mediated Signaling In Human Vascular Smooth Muscle Cells.** R. Bland<sup>1</sup>, G. Molostvov<sup>\*2</sup>, J. Bennett<sup>\*1</sup>, D. Zehnder<sup>\*2</sup>.

<sup>1</sup>Biological Sciences, University of Warwick, Coventry, United Kingdom, <sup>2</sup>Clinical Sciences Research Institute, University of Warwick, Coventry, United Kingdom.

Vascular smooth muscle cells play a pivotal role in the pathogenesis of medial calcification. We have recently demonstrated expression of the calcium sensing receptor (CaSR) in human aortic smooth muscle cells (HAoSMC) and human arteries and demonstrated a correlation between CaSR expression and medial calcification. Here we have examined downstream CaSR-mediated signaling pathways in HAoSMC and investigated the role of the CaSR in regulating HAoSMC proliferation and apoptosis.

HAoSMC were incubated with CaSR agonists (neomycin or gentamycin) alone or in the presence of specific signaling inhibitors. Activation of the MEK1/ERK1,2 pathway was assessed by Western blot analysis. HAoSMC proliferation was assessed by BrdU incorporation and apoptotic cells were identified by flow cytometry following propidium iodide staining. CaSR knock-down was performed using siRNA technology.

Incubation of HAoSMC with the CaSR agonist neomycin (300µM), resulted in a 7.5 fold increase in ERK1,2 phosphorylation (p<0.05). This induction was attenuated by pre-treatment with PD98059 (10µM) an ERK1 inhibitor (p<0.01) and U73122 (5µM) a PLC inhibitor (p<0.01) suggesting that PLC-signaling was important for MEK1/ERK1,2 activation. No changes were seen with PKC and PI3K inhibitors. Further confirming PLC activation, IP3 production was increased by neomycin (p<0.05), which was reduced in the presence of U73122 (p<0.05). To confirm ERK1,2 stimulation and PLC signaling were mediated via the CaSR, responses were assessed in HAoSMC in which CaSR expression had been knocked-down. CaSR-knockdown resulted in attenuated ERK1,2 phosphorylation in response to neomycin (>50% of neomycin induction in control cells, p<0.01) and IP3 production was almost completely abolished. Gentamycin (300 µM, 15 min) induced similar, but less pronounced, effects. CaSR activation (neomycin treatment) increased HAoSMC proliferation 3.6 fold (p<0.01). This was inhibited by PD98059 and U73122 (p<0.05). Neomycin failed to induce proliferation in CaSR-knockdown cells confirming the importance CaSR-mediated MEK/ERK1,2 and PLC signaling in HAoSMC proliferation. Apoptosis was not affected by neomycin or expression of the CaSR, but inhibition of PLC signaling (incubation with 5µM U73122) increased apoptotic cell death 3.5 fold (p<0.05), which was further increased by CaSR-knockdown (4.8 fold vs. control siRNA, p<0.05).

In conclusion, stimulation of the CaSR results in activation of the MEK1/ERK1,2 and PLC-IP3 pathways and increases proliferation in HAoSMC independently of PKC and PI3K signaling. In addition, CaSR-mediated PLC activation protects against apoptosis in HAoSMC.

**Disclosures:** R. Bland, None.

This study received funding from: Coventry Kidney Research Fund, Coventry and Warwickshire Kidney Patient Association.

## M201

**Molecular Diagnostic Strategies for Mutations of the Calcium-Sensing Receptor Gene: Application to a Large Cohort of Patients with Different Hypercalcemic Syndromes.** V. Guarnieri<sup>\*1</sup>, A. Scillitani<sup>\*1</sup>, C. Battista<sup>\*1</sup>, L. A. Muscarella<sup>\*1</sup>, M. Coco<sup>\*1</sup>, L. D'Agruma<sup>\*1</sup>, M. Sacco<sup>\*1</sup>, L. Canaff<sup>2</sup>, F. Yun<sup>\*3</sup>, B. Y. L. Wong<sup>\*3</sup>, G. N. Hendy<sup>2</sup>, D. E. C. Cole<sup>2</sup>.

<sup>1</sup>IRCCS "Casa Sollievo della Sofferenza" Hospital, San Giovanni Rotondo, Italy, <sup>2</sup>Calcium Research Laboratory and Hormones and Cancer Research Unit, Royal Victoria Hospital, Montreal, QC, Canada, <sup>3</sup>Department of Laboratory Medicine and Pathobiology, University of Toronto, Toronto, ON, Canada.

Inactivating mutations of the calcium-sensing receptor (CASR) have been implicated in the genesis of different hypercalcemic syndromes, including familial hypocalciuric hypercalcemia (FHH), cases of primary hyperparathyroidism (PHPT), and familial isolated hyperparathyroidism (FIHP). However, assessment of the yield from molecular diagnostics applied to large cohorts from a single centre have not been reported. We describe our molecular findings for a series of cases with FHH (n=17), PHPT (n=173) and FIHP (n=3), and controls (n=200); all seen and prospectively evaluated at the "Casa Sollievo della Sofferenza" Hospital in southern Italy. CASR screening was conducted by denaturing high-performance liquid chromatography (dHPLC) using a fully validated series of primers to generate 12 amplicons covering the translated exons and exon/intron boundaries, with sequencing of the C-terminal amplicon to distinguish causative mutations from three common missense SNPs. Four novel missense variants were identified in the normocalcemic controls, suggesting that false positive tests will be uncommon but not rare. Mutations were identified in 2 PHPT cases - on follow-up, 1 was confirmed as PHPT, and 1 reclassified as FHH. Thus, CASR mutations are rare in PHPT. In hypocalciuric hypercalcemic probands, however, mutations were found in 8/17 (47%). With a hypercalcemic family member, mutation detection rate rose to 7/8 (87%), while only 1 of 9 sporadic cases was positive, and none of the 3 FIHP cases had detectable CASR mutations. Co-segregation of FHH and a novel intronic mutation (IVS4-19A>C) was noted in one family. A CASR fragment comprised of either mutant or wild-type IVS4, exonV and part of IVS5 was inserted into a minicassette with flanking PTHR1 and RAB1 exons and the construct expressed in HeLa cells. RT-PCR product from wild-type indicated normal splicing but the IVS4-19C mutant showed additional abnormal splicing into a cryptic site 118bp downstream of the wild-type exonV acceptor site. The importance of functional analyses for three novel missense mutations in this FHH cohort is accentuated by the identification of missense variants in the occasional control.

**Disclosures:** V. Guarnieri, None.

## M202

**Activation of the Calcium-Sensing Receptor by Beta-Aspartyl & Gamma-Glutamyl Peptides.** G. K. Broadhead<sup>\*1</sup>, S. C. Brennan<sup>\*1</sup>, H. Mun<sup>\*1</sup>, D. R. Hampson<sup>\*2</sup>, A. D. Conigrave<sup>1</sup>.

<sup>1</sup>School of Molecular and Microbial Biosciences, University of Sydney, Sydney, Australia, <sup>2</sup>Department of Pharmaceutical Sciences, University of Toronto, Toronto, ON, Canada.

The extracellular Ca<sup>2+</sup>-sensing receptor (CaR) is a class 3 G-protein coupled receptor that plays a major role in the regulation of whole body calcium homeostasis. The receptor is activated not only by Ca<sup>2+</sup>, various polycations and type-II calcimimetics, such as cinacalcet, but also L-amino acids in physiological relevant concentrations (L-Phe = L-Trp > L-Ala > L-Leu). Recent work has demonstrated that the receptor's promiscuity arises from the presence of multiple activator binding sites in the extracellular and transmembrane domain regions. L-amino acids have been shown to bind in the CaR's Venus Fly Trap (VFT) domain and molecular modeling of the amino acid binding site has indicated that the side-chain binding site is large enough to accommodate larger ligands, such as short peptides, in which the free α-amino and α-carboxylate functional groups are preserved. Consistent with this idea, the gamma-glutamyl tripeptide glutathione has recently been shown to activate the receptor. We have extended this analysis to test whether the receptor is activated by a series of glutathione related peptides. HEK-CaR cells, which stably express the CaR, and human parathyroid cells, which endogenously express the CaR, were loaded with fura-2AM and then exposed to various activators in the presence of Ca<sup>2+</sup> (0.5 - 5.0 mM). β-Aspartyl and γ-Glutamyl peptides activated the receptor. The following order of potency was observed: β-Asp-His > β-Asp-Phe ≥ GSH > γ-Glu-Cys ≥ γ-Glu-His > β-Asp-Leu > L-Phe. The most potent activator, β-Asp-His, was effective in the concentration range of 0.01 - 1 µmol L<sup>-1</sup>. The finding that β-Aspartyl and γ-Glutamyl peptides activate the CaR has potential physiological and pharmacological significance.

**Disclosures:** S.C. Brennan, None.

## M203

**Molecular Basis of Primary Hyperparathyroidism: Adenomatous Parathyroid Cells Are Resistant to L-Amino Acids.** H. C. Mun<sup>\*1</sup>, S. C. Brennan<sup>\*1</sup>, L. Delbridge<sup>\*2</sup>, M. Wilkinson<sup>\*3</sup>, E. M. Brown<sup>4</sup>, A. D. Conigrave<sup>1</sup>.

<sup>1</sup>School of Molecular and Microbial Biosciences, University of Sydney, NSW, Australia, <sup>2</sup>Department of Surgery, University of Sydney, Royal North Shore Hospital, St Leonards, NSW, Australia, <sup>3</sup>Department of Endocrinology, University of Sydney, Royal North Shore Hospital, St Leonards, NSW, Australia, <sup>4</sup>Division of Endocrinology, Diabetes and Hypertension, Brigham and Women's Hospital and Harvard Medical School, Boston, MA, USA.

Ca<sup>2+</sup>-sensing receptor (CaR) activation by L-amino acids suppresses PTH secretion and stimulates intracellular Ca<sup>2+</sup> mobilization in human parathyroid cells via enhanced sensitivity to extracellular Ca<sup>2+</sup> (Ca<sup>2+</sup><sub>o</sub>). Compared to normal cells, adenomatous cells exhibit reduced sensitivity to Ca<sup>2+</sup><sub>o</sub>, raising the possibility that impaired L-amino acid activation of the CaR disables the normal control of PTH secretion. In the current study, we compared the amino acid sensitivities of samples of normal and adenomatous human parathyroid tissue obtained under guidelines established by the Human Research Ethics Committees of Royal North Shore Hospital, St Leonards, NSW and the Mater Hospital, North Sydney, NSW, Australia. Human parathyroid cells were prepared by collagenase digestion and loaded with Fura-2 AM for analysis of intracellular Ca<sup>2+</sup> mobilization or perfused for analysis of PTH secretion as described previously (1). In normal cells (n = 9), PTH secretion was suppressed by Ca<sup>2+</sup><sub>o</sub> in the range 0.8 - 1.2 mM and the CaR-active amino acid L-Phe (5 mM) enhanced its Ca<sup>2+</sup><sub>o</sub> sensitivity such that the IC<sub>50</sub> for Ca<sup>2+</sup><sub>o</sub> fell from 1.16 ± 0.01 to 1.10 ± 0.01 mM. Adenomatous cells (n = 15), on the other hand, were unresponsive to L-Phe at Ca<sup>2+</sup><sub>o</sub> concentrations below 1.2 mM. In normal cells, L-Phe also markedly left-shifted Ca<sup>2+</sup><sub>o</sub>-dependent mobilization of intracellular Ca<sup>2+</sup> as described previously (1); however, adenomatous cells exhibited impaired amino acid sensitivity. The data support the hypothesis that impaired amino acid sensitivity in human adenomatous parathyroid cells is a significant factor in the loss of Ca<sup>2+</sup><sub>o</sub>-dependent feedback control of PTH secretion in primary hyperparathyroidism.

1. Conigrave *et al.*, J. Biol. Chem. 279:38151-9, 2004

**Disclosures:** H.C. Mun, None.

## M204

**Functional Characterization of Unreported Calcium Sensing Receptor in Four Italian Kindreds with Familial Hypocalciuric Hypercalcaemia.** E. Cetani<sup>\*1</sup>, S. Borsari<sup>\*2</sup>, M. Lemmi<sup>\*3</sup>, E. Pardi<sup>\*2</sup>, D. Cervia<sup>\*4</sup>, L. Cianferotti<sup>1</sup>, C. Banti<sup>\*1</sup>, E. Ambrogini<sup>\*1</sup>, E. Vignali<sup>\*1</sup>, P. Bagnoli<sup>\*5</sup>, A. Pinchera<sup>\*6</sup>, C. Marcocci<sup>6</sup>. <sup>1</sup>Endocrinology, University of Pisa, Pisa, Italy, <sup>2</sup>Endocrinology, University of Pisa, Pisa, Italy, <sup>3</sup>Endocrinology, University of Pisa, Pisa, Italy, <sup>4</sup>Biology, University of Pisa, Pisa, Italy, <sup>5</sup>Biology, University of Pisa, Pisa, Italy, <sup>6</sup>Endocrinology, University of Pisa, Pisa, Italy.

Familial hypocalciuric hypercalcaemia (FHH) is characterized by moderate and lifelong hypercalcaemia, relative hypocalciuria, and inappropriately normal serum PTH levels. Loss-of-function mutations of the CASR are responsible for this disease. We describe four unrelated FHH kindreds (A, B, C and D). Mutational analysis of the CASR gene was performed on genomic DNA of the probands. Functional studies on three mutations were performed in COS-7 cells transiently expressing the wild-type and mutant CASR. In family A, a novel heterozygous base substitution C to T was detected, determining a change of an histidine to a tyrosine at codon 595 (H595Y) of exon 7. In family B, a heterozygous mutation was found at codon 748, with a substitution of C to A in exon 7, leading to conversion of a proline to an histidine (P748H). In family C, an heterozygous C to G substitution determining a change of a cysteine to a tryptophan at codon 765 (C765W) of exon 7 was detected. In case D, direct sequencing showed a substitution of G to T in the donor splice site of intron 2 (IVS2+1G>T). The absence of these mutations in 50 unrelated healthy subjects could exclude their polymorphic nature. In fura-2-loaded COS-7 cells expressing the wild-type or mutant receptors, the P748H and H595Y mutants produced, in the cytosolic calcium response to increasing extracellular calcium concentrations, a shift to the right relative to the wild-type CASR. In contrast, the co-transfected WT/P748H and WT/H595Y had the same behaviour as the WT. The C765W mutant had a concentration-response curve shifted to the right and the co-transfected WT/C765W had the same EC<sub>50</sub> relative to that of WT. Immunofluorescence experiments revealed an equal quantity of WT, as well as mutant receptors, expressed in transfected COS-7 cells. In addition, COS-7 cells transfected with mutant CASR showed, in western blotting analysis, a response similar to the WT, with respect to intracellular signaling (MAPK activation) to increasing extracellular calcium concentrations. In conclusion, molecular analysis showed that all kindreds carried unreported CASR mutations, three of them functionally inactivate the receptor.

**Disclosures:** C. Marcocci, None.

## M205

**Dimerization and Trafficking of the Calcium-Sensing Receptor (CaSR) to the Plasma Membrane: Biochemical and Biophysical Evaluation of COOH-terminally Truncated CaSR Mutants.** M. Grant<sup>\*1</sup>, K. Schorr<sup>\*1</sup>, U. Kumar<sup>\*2</sup>, G. N. Hendy<sup>1</sup>. <sup>1</sup>McGill University, Montreal, QC, Canada, <sup>2</sup>University of British Columbia, Vancouver, BC, Canada.

Calcium homeostasis is critical to survival and in the functioning of numerous bodily processes. Due to its exquisite sensitivity to minute changes in extracellular calcium levels, the calcium-sensing receptor (CaSR) is a key player in this regard. Its primary function is to regulate parathyroid hormone secretion, a critical factor in calcium homeostasis. In addition to the parathyroid gland, CaSR plays important roles in kidney, gut and bone. The CaSR is a G-protein coupled receptor (GPCR) and in humans, the monomer comprises 1078 amino acids, 612 in the extracellular domain, 250 in the transmembrane domain (TMD) and 216 residues in the cytoplasmic tail (C-tail). The CaSR functions as a dimer at the plasma membrane and constitutive dimerization that occurs in the endoplasmic reticulum (ER) is necessary but may not be sufficient for exit from the ER and trafficking to the plasma membrane via the Golgi. Several different mechanisms contribute to receptor dimerization including covalent and noncovalent interactions occurring within the extracellular domain. However, other parts of the molecule, as yet uncharacterized, in the TMD and/or C-tail are likely to be important. In addition, the sequence requirements for exit of the CaSR from the ER are unclear. To address these issues we have generated and transiently transfected HEK-293 cells with a series of COOH-terminally truncated receptors, all based upon naturally occurring mutations identified in familial hypocalciuric hypercalcaemia and/or neonatal severe hyperparathyroidism patients. Although cell-surface expression was observed for truncation mutants where all or part of the C-tail was removed, the trafficking of mutants lacking all or part of the TMD was impaired. Furthermore, CaSR mutants deleted from TM4 onwards were retained in the ER and were not present in the Golgi. By Western blot and photobleaching fluorescence resonance energy transfer (pbFRET) microscopy techniques, the dimerization properties of each mutant were assessed. PbFRET analysis indicated constitutive dimerization for all cell-surface targeted receptors but not for TMD truncation mutants lacking TM5 onwards. Hence, with this particular set of CaSR mutants, the ability to undergo constitutive dimerization is correlated with exit from the ER to the Golgi but may not be sufficient for trafficking to the cell-surface. While dimerization is important for CaSR maturation, other factors are necessary to ensure its forward trafficking.

**Disclosures:** M. Grant, None.

## M206

**Skeletal Consequences of Familial Hypocalciuric Hypercalcaemia and Primary Hyperparathyroidism.** S. E. Christensen<sup>1</sup>, P. H. Nissen<sup>\*2</sup>, P. Vestergaard<sup>1</sup>, L. Heickendorff<sup>\*2</sup>, L. Rejnmark<sup>1</sup>, K. Brixen<sup>3</sup>, L. Mosekilde<sup>1</sup>. <sup>1</sup>Endocrinological Dept. C., Aarhus University Hospital, DK-8000 Aarhus C., Denmark, <sup>2</sup>Department of Clinical Biochemistry, Aarhus University Hospital, DK-8000 Aarhus C., Denmark, <sup>3</sup>Endocrinological Dept., Odense University Hospital, DK-5000 Odense C., Denmark.

Bone metabolism is well described in Primary Hyperparathyroidism (PHPT) but not in Familial Hypocalciuric Hypercalcaemia (FHH). We describe biochemical and osteodensitometric measurements in FHH and compare them with PHPT in a cross-sectional study.

We studied 66 hypercalcaemic FHH-patients with mutations in the CASR gene from 25 kindreds, 147 hypercalcaemic patients with surgically verified PHPT, and 48 controls matched to 48 of the FHH patients with respect to age (+/- 5 years), sex and season. All patients had a plasma creatinine level < 140 µmol/l. We measured plasma calcium, plasma ionized calcium, albumin, creatinine, phosphate, magnesium and intact PTH by standard laboratory methods. Plasma 25OHD and 1,25(OH)<sub>2</sub>D were measured by radio-immunoassay or enzyme-immunoassay. Plasma alkaline phosphatase (AP) was measured by the spectrophotometrical method, Aeroset. U-NTx was measured in morning spot urine by an immunometrical method and expressed as U-NTx/U-creatinine ratio (U-NTx), nmol/mmol. In FHH, all protein coding exons in the CASR were sequenced and aligned to GenBank reference sequence NM\_000388.

Osteodensitometry (DXA) was performed on the lumbar spine (L1-L4), the total hip, the forearm, and whole body using Hologic® equipment. In the PHPT, DXA was performed within the last year before surgery.

The FHH patients had normal Z-scores in all regions, and increased levels of PTH (p<0.01), AP (p<0.01) and U-NTx (p=0.02), compared to normal controls. Compared to PHPT, the FHH patients were younger, had a lower BMI, and lower levels of PTH (p<0.01), 1,25(OH)<sub>2</sub>D (p<0.01), 24h-U-calcium (p<0.01) and the calcium/creatinine clearance ratio (p<0.01). The PHPT patients exhibited lower BMD at all sites, higher plasma levels of AP (p<0.01), and U-NTx (p=0.03), compared to FHH. Plasma calcium and 25OHD did not differ between FHH and PHPT. PHPT patients had decreased Z-scores in the total hip (p=0.02), and in the forearm (p<0.01), compared to FHH, and normal controls (p<0.01, p<0.01, respectively). In FHH, increased severity of CASR mutations, as expressed by the severity of hypercalcaemia, was associated with increased BMD in the lumbar spine, but was not associated with bone markers.

FHH is not associated with increased bone loss. Inactivating CASR mutations do not cause deleterious effects on bone, as evaluated by DXA measurements, in spite of increased plasma levels of PTH, AP, and U-NTx. The levels of PTH, 1,25(OH)<sub>2</sub>D, AP, and U-NTx were significantly lower in FHH than in PHPT.

**Disclosures:** S.E. Christensen, None.

## M207

**In Vivo Longitudinal QCT Analysis PTH Efficacy in a Rat Cortical Defect Model.** D. E. Komatsu, K. A. Brune\*, A. L. Schmidt\*, H. Liu\*, B. Han\*, Y. Lu\*, M. S. Westmore\*, J. A. Wolos\*, Q. Q. Zeng\*, Y. L. Ma, M. Sato. Lilly Research Labs, Eli Lilly and Company, Indianapolis, IN, USA.

Osteoporotic patients with fracture could possibly benefit from therapies to accelerate bone healing. PTH has been shown to enhance fracture repair in numerous animal models; however, the spatial and kinetic efficacy of PTH in the bone healing process remains to be elucidated. Therefore, we conducted a longitudinal, region-specific analysis of bone regeneration in osteopenic rats using a new cortical defect model. Sprague Dawley rats were ovariectomized at 6 months of age and allowed to lose bone for 2 months prior to the generation of 2 mm circular defects through the anterior and posterior cortices of both femoral diaphyses. The animals were then treated for 5 weeks with hPTH1-38 at doses of 0, 3, 10 or 30 µg/kg/d sc, and scanned weekly by in vivo quantitative computed tomography (QCT, GE). Longitudinal, QCT analyses showed that the posterior cortices healed significantly faster than the anterior cortices regardless of treatment. The highest dose of PTH generated significant increases of 22% in BMD after 2wk within the posterior cortex and 56% after 3wk within the anterior cortex, with steady dose dependent increases observed until study termination. Slice by slice analyses (153 µm steps) from the anterior periosteal edges, through the defects to the posterior periosteal edges, showed dose dependent enhancement of mineral apposition along the endocortical edges and within the marrow cavities that was significant by 2wk, and continued to increase through 5wk for the two highest dose groups. Whole bone analyses of transverse cross-sections at the defect sites showed dose dependent gains of 39% cortical area by 2wk, as well as 25% BMD and 29% BMC by 3wk for the highest dose, but no significant changes in periosteal mineral apposition. Histomorphometry confirmed PTH stimulation of primarily endochondral bone formation activity. Post-necropsy 3-point bending tests showed that the ultimate moment of vehicle controls was 44% that of intact, non-drilled controls and that the highest dose of PTH significantly increased this to 63% of intact. Serum biomarker analyses identified a dose dependent elevation of PINP, with an 80% increase seen for the highest PTH dose along with an unexpected 60% reduction in Trap5b levels at 3wk. In summary, longitudinal QCT analyses demonstrated that PTH dose dependently induced new bone formation within the defects, along the endocortical surfaces and within the intramedullary spaces, resulting in stronger femora and some unexpected effects on serum markers. The effects of PTH were kinetic, region-specific, and most apparent at high doses which may not be clinically relevant.

**Disclosures:** D.E. Komatsu, Eli Lilly and Company 3. This study received funding from: Eli Lilly and Company.

## M208

**Marrow Ablation Induces Periosteal Bone Formation and Potentiates the Effect of PTH on Endosteal Bone Formation in Rat Femurs.** Q. Zhang<sup>1</sup>, J. Carlson<sup>2</sup>, M. Kim<sup>3</sup>, H. Ke<sup>3</sup>, J. Gilligan<sup>4</sup>, N. Mehta<sup>4</sup>, A. Vignery<sup>1</sup>. <sup>1</sup>Orthopaedics, Yale School of Medicine, New Haven, CT, USA, <sup>2</sup>Comparative Medicine, Yale School of Medicine, New Haven, CT, USA, <sup>3</sup>Pfizer Global Research, Groton, CT, USA, <sup>4</sup>Unigene Laboratories, Inc., Fairfield, NJ, USA.

During development and repair of bone, two distinct yet complementary mechanisms, intramembranous and endochondral, mediate bone formation via osteoblasts. Mechanical bone marrow ablation (BMX) leads to differentiation of osteoblasts, and transient formation of new intramembranous bone in lieu of bone marrow. We initially reported that systemic administration of parathyroid hormone (PTH) promotes the formation of new bone after BMX in a rapid and site-specific manner. We demonstrated that lamellar bone progressively fills the marrow cavity of ablated femoral shafts in animals treated daily with PTH for 3 weeks and that this newly formed bone endows femoral shafts with improved biomechanical properties when compared to those of contra lateral femurs as well as left femurs from control, sham operated and vehicle-treated rats (Tissue Eng. 14:237, 2008). Here we asked whether long-term treatment with PTH could maintain the new bone formed in lieu of marrow. We subjected the left femur of rats to sham operation or BMX, and treated the operated animals daily with PBS or the PTH analog PTH(1-34)NH<sub>2</sub> for 12 weeks (n = 8). Femurs were analyzed by soft X-ray, pQCT, microCT and histology, and serum osteocalcin concentration was determined.

The amount of new lamellar bone that had filled the marrow cavity in response to BMX and daily treatment with PTH for 3 weeks was substantially less after 3 months of treatment with PTH. Instead, the femoral shafts from these PTH-treated BMX rats demonstrated a 43% increase in cortical thickness when compared with controls, and 30% when compared with BMX alone. This 43% increase resulted for the most part from a 35% reduction in endosteal circumference. Marrow ablation alone led to an 8% increase in periosteal circumference. Our results thus demonstrate that BMX induces periosteal bone formation, and potentiates endosteal bone formation induced by PTH.

The spatial and time-dependent effect of PTH that follows marrow ablation is suggestive of an adaptation of bone to injury in the context of mechanical stress. While PTH is known to augment trabecular density, and to some extent endocortical bone density, we report here that PTH synergizes with the repair mechanism that takes place after marrow ablation to augment the thickness of cortical bone to a greater degree than previously seen with PTH treatment alone. These findings might be useful for investigations on the molecular mechanisms of periosteal versus endosteal cortical bone formation, and for preferential site-directed cortical bone growth.

**Disclosures:** A. Vignery, Unigene Laboratories, Inc. 2, 3.

This study received funding from: Unigene Laboratories, Inc.

## M209

**A New Intact Parathyroid Hormone (PTH) Assay on the IDS Automated Analyser 3X3™.** C. Dixon\*, C. E. Wynn\*, D. Laurie\*, C. J. Fox\*, M. J. Gardner\*, A. K. Barnes\*, M. L. Garrity\*. Immunodiagnostic Systems Ltd, Boldon, United Kingdom.

Abnormalities of bone and mineral metabolism are among the main complications in the treatment of patients with end-stage renal failure. Biologically active PTH (1-84) is secreted by the parathyroid gland and degraded within minutes into smaller N- and C-terminal fragments. The predominant mechanism for excretion of these fragments is via the kidneys and as a consequence, patients with renal impairment accumulate high levels of these fragments even when parathyroid activity is normal. Furthermore, recent data suggests the presence of novel, large C-terminal PTH fragments having unique biological mechanisms in bone. Intact PTH assays are therefore an important tool in the differentiation of renal bone disease from parathyroid gland activity-dependent conditions. We have developed a new Intact PTH assay that will be part of a comprehensive panel of bone and growth tests on the new IDS Automated Analyser 3X3™. This analyser will enable clinical laboratories to determine 25-hydroxy Vit D, PTH, Calcium and Phosphorus from a single specimen tube with integrated measurement modules for simultaneous analysis of different diagnostic tests, to include immunochemistry, biochemistry and coagulation.

The measurement of Intact PTH on the analyser is performed as a two-site chemiluminescent immunoassay. Biotinylated anti-PTH allows capture of PTH analyte by binding to streptavidin-coated magnetic particles. Captured PTH is then detected by an acridinium-conjugated second anti-PTH antibody. Following a wash step the signal generated by the acridinium conjugate is measured by a high sensitivity luminometer. The amount of analyte present is directly proportional to the Relative Light Units (RLU) quantitated by the luminometer.

The Intact PTH assay has a range of 5-1800pg/mL. The analytical sensitivity for this assay is 0.81pg/mL. Correlation by linear regression with a commercially-available Intact PTH EIA (n = 108) gave an R<sup>2</sup> value of 0.965. Analysis by Passing-Bablok gave an intercept of 3.29pg/mL and a slope of 0.853. No interference by small C-terminal PTH fragments including PTH (39-84), (39-68), (44-68) and (53-84) was observed up to 100,000pg/mL. Excellent correlation to existing manual assays combined with a reportable range covering the full likely clinical range of PTH demonstrate that this assay has the potential to provide a rapid and accurate automated measurement of full-length (1-84) and large C-terminal fragment PTH. This will form part of a comprehensive bone panel essential to the clinical laboratory.

**Disclosures:** C. Dixon, Dixon, C 2.

## M210

**Regulation of Nuclear Import of the Parathyroid Hormone Receptor.** E. Patterson<sup>\*1</sup>, B. Gaudet<sup>\*1</sup>, A. Hodsman<sup>1</sup>, R. Bringham<sup>2</sup>, L. Fraher<sup>1</sup>, P. H. Watson<sup>1</sup>. <sup>1</sup>Medicine, University of Western Ontario, London, ON, Canada, <sup>2</sup>Medicine, Harvard University, Boston, MA, USA.

**Introduction:** Previous studies in our lab have demonstrated that the PTH1R is able to traffic to the nucleus of expressing cells in a  $\beta$ -importin dependent manner and that it contains a bipartite type nuclear localization sequence (NLS). Our current studies revolve around determining the domains of the PTH1R which are responsible for regulating the nuclear import of the PTH1R.

**Hypothesis:** The amino acids sequence from 471-488 in the intracellular tail of the PTHR comprise a functional NLS, which can be regulated by other domains.

**Methods:** This study employed mutagenesis to produce plasmids coding for specific fragments of the C-terminal tail of the PTH1R fused to green fluorescent protein (GFP) for construct visualization. These constructs were then expressed in LLC-PK1 cells and the subcellular localization of the expressed proteins were studied by confocal microscopy. This allowed for the determination of the extent of nuclear localization via quantification of the relative fluorescent intensity in the nucleus versus cytoplasm.

**Results:** Constructs containing the NLS alone fused downstream of GFP were able to localize to the nucleus to a level of 12-fold that of the cytoplasm, compared to GFP alone (P<0.01). This capability was not seen when a mutated non-functional PTH1R NLS (i.e. K-A mutations) was fused to GFP. Sequences in the intracellular C-terminal tail of the PTH1R downstream of the NLS, when included in the construct, were shown to attenuate the nuclear localization activity of the NLS. The nuclear import of GFP was further diminished when only sequences directly adjacent to the NLS were included in the construct.

**Discussion:** The PTH1R NLS (residues 471-488) is a strong promoter of nuclear import as demonstrated by GFP fluorescence in our fusion constructs. However, this ability appears to be regulated (attenuated) by other downstream domains of the PTH1R. The amino acids directly downstream of the NLS comprise a binding site for a class of proteins known as 14-3-3 proteins, which have been shown to regulate the activity of NLSs in other proteins. Regulation of PTH1R NLS activity appears to be affected by still other, as yet undefined, domains in the distal C-terminal tail of the PTH1R.

**Disclosures:** E. Patterson, None.

## M211

**Relationship Between Vitamin D and PTH: Serum Calcium and Magnesium Are Major Determinants of PTH in Patients with Mild Chronic Kidney Disease.** S. Patel<sup>1</sup>, M. Mirzazadeh<sup>\*2</sup>, H. Gallagher<sup>\*3</sup>, S. Hyer<sup>\*4</sup>, W. Fraser<sup>5</sup>, T. Cantor<sup>6</sup>, J. Barron<sup>\*2</sup>. <sup>1</sup>Dept Rheumatology, St Helier University Hospital, Carshalton, United Kingdom, <sup>2</sup>Clinical Chemistry, St Helier University Hospital, Carshalton, United Kingdom, <sup>3</sup>South West Thames Renal Unit, St Helier University Hospital, Carshalton, United Kingdom, <sup>4</sup>Dept Endocrinology, St Helier University Hospital, Carshalton, United Kingdom, <sup>5</sup>Clinical Chemistry, University of Liverpool, Liverpool, United Kingdom, <sup>6</sup>R&D, Scantibodies Laboratory, Santee, CA, USA.

25-hydroxyvitamin D (25OHD) is known to be inversely related to parathyroid hormone levels (PTH). Previously we showed that estimated glomerular filtration rate (eGFR) is a major determinant of the PTH response for a given 25OHD level. In the present study we have examined this relationship in more detail using patients with varying degrees of chronic kidney disease (CKD).

We randomly recruited 165 adult patients from the Renal Unit database who were not being dialysed [CKD stage 1 (n=12), stage 2 (n=34), stage 3 (n=63), stage 4 (n=36) and stage 5 (n=20)]. PTH (1-84) and intact-PTH were measured by immunoassay (Scantibodies; California). We calculated C-PTH fragment levels by subtracting PTH (1-84) from intact-PTH. 25OHD levels were measured by HPLC-MS/MS (University of Liverpool).

No differences were found between the different PTH subtypes so data are presented only for intact-PTH. We found significant relationships between intact-PTH and eGFR (r = -0.71; p < 0.001), phosphate (r = 0.30; p < 0.001), Mg (r = 0.24; p = 0.003), age (r = 0.23; p = 0.003), albumin (r = -0.17; p = 0.03) and 25OHD (r = -0.16; p = 0.04). Multiple regression analysis showed that eGFR (r = -0.66; p < 0.001) and 25OHD (r = -0.14; p = 0.03) were determinants of intact-PTH. However for patients in the top tertile of eGFR (> 53 ml/min) we found that only Mg (r = 0.34; p = 0.01) and ionised Ca (r = -0.30; p = 0.03) were significantly associated with intact-PTH whereas only eGFR (r = -0.41; p = 0.001) and 25OHD (r = -0.31; p = 0.01) remained associated with intact-PTH for patients in the lowest tertile of eGFR (< 30ml/min).

There is a complex explanation for the PTH response for a given 25OHD level. Whilst eGFR and vitamin D are important determinants of PTH, in patients with normal eGFR or mild CKD, and therefore sufficient renal 1-alpha hydroxylase activity, serum ionised Ca and Mg have a more important role in determining PTH. Possible explanations include that in patients with adequate renal 1-alpha hydroxylase activity, PTH is able to maintain serum Ca in a tight range for cellular function through efficient 1-hydroxylation of 25OHD. Mg is essential for PTH release from chief cells hence a positive relationship with serum PTH levels. These findings need to be considered when interpreting vitamin D and PTH levels in clinical practice.

**Disclosures:** S. Patel, None.

This study received funding from: Epsom & St Helier University Hospitals R&D Department.

## M212

**Circulating Concentrations of 25-Hydroxyvitamin D after a Single Oral Dose of 100,000 IU of Vitamin D2 or Vitamin D3.** E. Cavalier<sup>1</sup>, A. M. Wallace<sup>2</sup>, S. Knox<sup>2</sup>, V. I. Mistretta<sup>1</sup>, J. Chapelle<sup>1</sup>, J. Souberbielle<sup>3</sup>.

<sup>1</sup>Clinical Chemistry, University Hospital of Liege, University of Liege, Liege, Belgium, <sup>2</sup>Clinical Biochemistry, Glasgow Royal Infirmary, Glasgow, United Kingdom, <sup>3</sup>Service d'Explorations Fonctionnelles, Hôpital Necker-Enfants Malades, AP-HP, Paris, France.

The aim of our study was to compare the evolution of circulating concentrations of 25-OH vitamin D (25VTD) in healthy subjects after a single oral dose of 100,000 IU of VTD2 or VTD3.

To determine 25VTD, we used a reference method (HPLC). We studied 18 young healthy volunteers who were randomly assigned to receive VTD2 (n=11) or VTD3 (n=7). The study involved subjects living in the area of Liege, Belgium during November, a time of year when UVB radiation is too low to increase circulating concentrations of 25VTD. Blood samples were drawn before giving VTD (D0) and after 1 (D1), 7 (D7) and 28 (D28) days. The serum 25VTD concentration at D0 was not significantly different in both groups (33.0±10.1 ng/mL vs 33.9±7.0 ng/mL respectively). At D1, the increase in 25VTD concentration was greater in the D3 group (+14.6 vs +7.4 ng/mL) but the difference was not significant. 8/11 and 7/7 subjects had a 25VTD level >30 ng/mL in the VTD2 and VTD3 group respectively. At D7, the difference between the two groups approached significance (p=0.07) with no change for the D2 group (-0.4 ng/mL) and a small increase in the D3 group (+4.7 ng/mL). At D28, the D3 group had significantly higher concentrations than the D2 group (40.9±6.4 vs 31.9±9.7 ng/mL respectively, p<0.05). The concentration of 25VTD in the D2 group fell to the pre-supplementation range whereas treatment with D3 resulted in a significant increase (+7.0 ng/mL, p<0.05) of the 25VTD level compared to baseline. At D28, 7/11 and 7/7 subjects had a 25VTD level >30 ng/mL in the VTD2 and VTD3 group respectively. In conclusion, our results indicate that initially both VTD2 and VTD3 increase 25VTD concentrations to a similar extent when given as a single 100,000 UI dose. VTD3, however, seems to maintain sufficient concentrations of 25VTD for a longer period than VTD2 as, at D28, subjects supplemented with D3 were the only ones to present a 25VTD level higher than before supplementation. This should be taken in consideration when prescribing monthly doses of vitamin D.

**Disclosures:** E. Cavalier, None.

## M213

**Distinctive Anabolic Roles of 1,25-Dihydroxyvitamin D<sub>3</sub> in Teeth and Mandible versus Long Bones.** H. Liu<sup>1</sup>, J. Guo<sup>2</sup>, L. Wang<sup>1</sup>, N. Chen<sup>1</sup>, D. Goltzman<sup>3</sup>, D. S. Miao<sup>1</sup>. <sup>1</sup>Institute of Dental Research, Nanjing Medical University, Nanjing, China, <sup>2</sup>The Research Center for Bone and Stem Cells, Nanjing Medical University, Nanjing, China, <sup>3</sup>Medicine, McGill University, Montreal, QC, Canada.

Elevated PTH in the secondary hyperparathyroidism of vitamin D deficiency is believed to be anabolic for long bones. We previously compared mice with targeted disruption of the gene encoding parathyroid hormone (PTH)(PTH<sup>-/-</sup> mice) or the gene encoding 25-hydroxyvitamin D 1 $\alpha$ -hydroxylase [1 $\alpha$ (OH)ase] [1 $\alpha$ (OH)ase<sup>-/-</sup> mice] with compound mutant PTH<sup>-/-</sup>1 $\alpha$ (OH)ase<sup>-/-</sup> mice. We found that PTH plays a predominant role in appositional bone growth, whereas 1,25(OH)<sub>2</sub>D<sub>3</sub> acts predominantly on endochondral bone formation in long bones. It is unknown, however, whether 1,25(OH)<sub>2</sub>D<sub>3</sub> or PTH plays a role in dentin and dental alveolar bone formation in the mandibles as it does in long bones. To determine whether 1,25(OH)<sub>2</sub>D<sub>3</sub> plays a distinctive role in flat bones such as mandibles, we examined the effect of 1,25(OH)<sub>2</sub>D<sub>3</sub> deficiency on dentin and dental alveolar bone formation and mineralization in the mandibles, and compared osteoblastic bone formation in the mandibles and tibiae in 1 $\alpha$ (OH)ase<sup>-/-</sup> mice. Compared to wild-type (WT) mice, the mineral density was decreased in the teeth and mandibles, and unmineralized dentin (predentin and biglycan immunopositive dentin) and unmineralized bone matrix in the dental alveolar bone were increased in 1 $\alpha$ (OH)ase<sup>-/-</sup> mice. The dental volume, reparative dentin volume and dentin sialoprotein immunopositive areas were reduced in 1 $\alpha$ (OH)ase<sup>-/-</sup> mice. The cortical thickness, dental alveolar bone volume and osteoblast numbers were all decreased significantly in the mandibles; in contrast, the osteoblast number and surface were increased in the trabecular bone of the tibiae in 1 $\alpha$ (OH)ase<sup>-/-</sup> mice consistent with their secondary hyperparathyroidism. The expression of parathyroid hormone receptor (PTHr) and insulin-like growth factor-1 (IGF-1) was reduced slightly in mandibles, but enhanced in the long bones in the 1 $\alpha$ (OH)ase<sup>-/-</sup> mice. These results indicate that 1,25(OH)<sub>2</sub>D<sub>3</sub> plays distinct roles in dentin and dental alveolar bone formation in the mandibles relative to trabecular bone formation in long bones, and suggests that 1,25(OH)<sub>2</sub>D<sub>3</sub> plays a more prominent anabolic role than does PTH in dentin and dental alveolar bone formation in mandibles.

**Disclosures:** D.S. Miao, None.

## M214

**25-Hydroxyvitamin D Acts on Calcium and Skeletal Homeostasis Independent of 1,25-Dihydroxyvitamin D *In Vivo*.** L. Nguyen-Yamamoto, I. Bolivar\*, M. Gratton\*, R. Kremer, G. Hendy, D. Goltzman. Medicine, Royal Victoria Hospital McGill University, Montreal, QC, Canada.

Previous studies in humans have demonstrated that increases in serum 25-Hydroxyvitamin D<sub>3</sub> (25OHD<sub>3</sub>), the most abundant circulating metabolite of vitamin D, are associated with increases in calcium absorption, and reductions in elevated parathyroid hormone (PTH) concentrations. Such bioactivity of 25OHD<sub>3</sub> has been ascribed to the renal and/or local conversion of 25OHD<sub>3</sub> to the active form, 1,25 dihydroxyvitamin D<sub>3</sub> [1,25(OH)<sub>2</sub>D<sub>3</sub>]. We assessed whether 25OHD<sub>3</sub> might exert direct actions on mineral and skeletal metabolism independent of 1,25(OH)<sub>2</sub>D<sub>3</sub>. 25OHD<sub>3</sub> has been reported to bind to the vitamin D receptor (VDR) with low affinity. We therefore first examined the capacity of 25OHD<sub>3</sub> to recruit the vitamin D receptor (VDR) to the promoter regions of the target genes osteopontin, osteocalcin and 24 hydroxylase in MC3T3-E1 osteoblastic cells *in vitro* using a chromatin immunoprecipitation (ChIP) assay in which 5  $\mu$ M ketoconazole had been added to inhibit 1 $\alpha$  hydroxylation. 1,25(OH)<sub>2</sub>D<sub>3</sub> 10<sup>-8</sup>M, significantly enhanced VDR and RXR binding to these promoters whereas 25OHD<sub>3</sub> at a concentration of 10<sup>-6</sup>M, also significantly stimulated binding suggesting that 25OHD<sub>3</sub> could function independent of prior 1 $\alpha$  hydroxylation at least *in vitro*. We next examined the bioactivity of 25OHD<sub>3</sub> *in vivo* in mice expressing the null mutation for the 25OHD<sub>3</sub>-1 $\alpha$  hydroxylase enzyme (1 $\alpha$  OHase<sup>-/-</sup>). We first injected 1 $\alpha$  OHase<sup>-/-</sup> mice, after weaning, with vehicle or 50 pg/g body weight, 10 ng/g, and 100 ng/g of 25OHD<sub>3</sub> intraperitoneally 3 times per week for 1 week while they were maintained on a high calcium diet. On this diet, mean serum calcium, phosphorus (P) and PTH concentrations in vehicle treated mice were 1.32 mM, 2.44 mM and 1.6 ng/ml respectively and values were not significantly different in mice treated with 50pg/g 25OHD<sub>3</sub>. In mice treated with 10 ng/g and 100ng/g of 25OHD<sub>3</sub> serum calcium rose to means of 1.71 and 2.77mM, respectively, serum P rose to means of 2.59 and 3.97 mM, respectively, and serum PTH decreased to means of 1.35 and 0.14 ng/ml, respectively. Serum calcium, phosphorus and PTH levels comparable to those achieved with a dose of 100ng/g 25OHD<sub>3</sub> were observed with a dose of 50 pg/g of 1,25(OH)<sub>2</sub>D<sub>3</sub>. After 3 months of treatment with 75ng/g of 25OHD<sub>3</sub> from the time of weaning, growth rates and mineralization of bones were increased and serum calcium and PTH levels were within the normal range. These results show that 25OHD<sub>3</sub> can exert effects on parathyroid, mineral and skeletal homeostasis independent of conversion to 1,25(OH)<sub>2</sub>D<sub>3</sub> *in vivo*.

**Disclosures:** L. Nguyen-Yamamoto, None.

## M215

**1,25-Dihydroxyvitamin D<sub>2</sub> Is as Effective as 1,25-Dihydroxyvitamin D<sub>3</sub> in Regulating Cellular Proliferation in Cultured Normal Human Keratinocytes and Transformed Prostate Cells.** X. Hung\*, I. S. Tsai\*, K. S. Persons\*, T. C. Chen\*, M. F. Holick. Boston University School of Medicine, Boston, MA, USA.

Recently it has been reported that vitamin D<sub>2</sub> is as effective as vitamin D<sub>3</sub> in maintaining serum levels of 25-hydroxyvitamin D. However, it remains unknown whether 1,25-dihydroxyvitamin D<sub>2</sub> [1,25(OH)<sub>2</sub>D<sub>2</sub>] is as effective as 1,25-dihydroxyvitamin D<sub>3</sub> [1,25(OH)<sub>2</sub>D<sub>3</sub>] in regulating cell growth and gene expression. We evaluated the antiproliferative activity of 1,25(OH)<sub>2</sub>D<sub>2</sub> and compared it to 1,25(OH)<sub>2</sub>D<sub>3</sub> in cultured human keratinocytes and in the human prostate cells PZ-HPV-7.

**Methods** Cultured human keratinocytes from neonatal foreskins and PZ-HPV-7 cells were cultured and exposed to varying concentrations of 1,25(OH)<sub>2</sub>D<sub>2</sub> and 1,25(OH)<sub>2</sub>D<sub>3</sub>. <sup>3</sup>H-thymidine incorporation and real time RT-PCR for 24-hydroxylase (24-OHase) was determined.

**Results** A dose dependent inhibition in proliferation was observed in human keratinocytes exposed to 1,25(OH)<sub>2</sub>D<sub>2</sub> and 1,25(OH)<sub>2</sub>D<sub>3</sub>. When compared to the placebo controlled treated keratinocytes, 1,25(OH)<sub>2</sub>D<sub>3</sub> reduced proliferative activity by 20±3, 36±4 and 60±5% at 10<sup>-10</sup>, 10<sup>-8</sup>, 10<sup>-6</sup> M 1,25(OH)<sub>2</sub>D<sub>3</sub>. In comparison, 1,25(OH)<sub>2</sub>D<sub>2</sub> reduced proliferative activity by 15±4, 32±6 and 82±2% at 10<sup>-10</sup>, 10<sup>-8</sup>, 10<sup>-6</sup> M 1,25(OH)<sub>2</sub>D<sub>2</sub>. A similar observation was made in PZ-HPV-7 human prostate cancer cells. There was a dose dependent inhibition in cellular proliferation with a reduction of 21±5 and 64±7% at 10<sup>-9</sup> and 10<sup>-7</sup> M 1,25(OH)<sub>2</sub>D<sub>3</sub>. In comparison, 1,25(OH)<sub>2</sub>D<sub>2</sub> decreased proliferative activity by 24±4% and 74±3% at 10<sup>-9</sup> and 10<sup>-7</sup> M 1,25(OH)<sub>2</sub>D<sub>2</sub>. An evaluation for the expression of the 24-OHase was performed in DU145 prostate cancer cells revealed that 1,25(OH)<sub>2</sub>D<sub>3</sub> enhanced the expression of the 24-OHase by 178, 104 and 11 fold at 10<sup>-7</sup>, 10<sup>-8</sup> and 10<sup>-9</sup> M compared to 34, 5 and 1 fold in cells treated with 1,25(OH)<sub>2</sub>D<sub>2</sub> at 10<sup>-7</sup> and 10<sup>-8</sup> and 10<sup>-9</sup> M respectively.

**Conclusion** The results from these studies suggest that 1,25(OH)<sub>2</sub>D<sub>2</sub> is as effective as 1,25(OH)<sub>2</sub>D<sub>3</sub> in its antiproliferative effect in both normal cultured human keratinocytes and in transformed human prostate cells. 1,25(OH)<sub>2</sub>D<sub>3</sub> may be effective in enhancing 24-OHase expression in a human prostate cancers cell line than 1,25(OH)<sub>2</sub>D<sub>2</sub>. Thus, vitamin D<sub>2</sub> is not only able to maintain vitamin D status as well as vitamin D<sub>3</sub>, but 1,25(OH)<sub>2</sub>D<sub>2</sub> is as effective as 1,25(OH)<sub>2</sub>D<sub>3</sub> in inhibiting proliferation of cultured human cells.

**Disclosures:** M.F. Holick, None.

## M216

**The Mechanism of Enhanced 19-nor-2a-(3-hydroxypropyl)-1 $\alpha$ ,25-Dihydroxyvitamin D<sub>3</sub> Anti-cancer Activity in Prostate Cancer Cells.** J. N. Flanagan<sup>\*1</sup>, A. Kittaka<sup>\*2</sup>, T. Sakaki<sup>\*3</sup>, Y. F. Lee<sup>\*4</sup>, M. F. Holick<sup>5</sup>, T. C. Chen<sup>5</sup>.  
<sup>1</sup>Karolinska Institute, Stockholm, Sweden, <sup>2</sup>Teikyo University, Sagamiko, Japan, <sup>3</sup>Toyama Prefectural University, Toyama, Japan, <sup>4</sup>University of Rochester, Rochester, NY, USA, <sup>5</sup>Boston University School of Medicine, Boston, MA, USA.

It has been shown that 19-nor-vitamin D derivatives are less calcemic when administered systemically and that C2- substituted 19-nor-2 $\alpha$ -(3-hydroxypropyl)-1 $\alpha$ ,25-dihydroxyvitamin D<sub>3</sub> (MART-10) was about 500- to 1000-fold more active than 1 $\alpha$ ,25-dihydroxyvitamin D<sub>3</sub> (1,25D) in inhibiting cell growth in the immortalized PZ-HPV-7 normal prostate cells. Based on the findings, we further compared its activities to 1,25D in PC3 prostate cancer cell model by examining (1) cell proliferation, (2) cell invasion, and (3) the induction of CYP24 and MMP-9 genes. We also studied the kinetics of their 24-hydroxylation by CYP24, and their vitamin D binding protein (DBP) binding affinities in cell-free systems. We showed that (1) MART-10 was more potent than 1,25D in inhibiting cell proliferation and invasion, (2) MART-10 induced CYP24 gene expression at lower concentrations and sustained the induction longer compared to 1,25D, (3) MART-10 inhibited MMP-9, a protease involved in cell invasion, at lower concentrations compared to 1,25D, (4) MART-10 has a much lower V<sub>max</sub> and a higher K<sub>m</sub> for CYP24, and (5) MART-10 has a much lower affinity for DBP compared to 1,25D. The down-regulation of MMP-9 expression in PC3 cells may provide a mechanism of how MART-10 can influence prostate cancer cell invasion. Most importantly, the findings that MART-10 was more resistant to CYP24 hydroxylation and had lower affinity for DBP may explain why MART-10 was more potent in inhibiting cell invasion and cellular proliferation. Taken together, our data suggest that MART-10 may be an effective vitamin D analog candidate for clinical trials to treat prostate cancer.

**Disclosures:** J.N. Flanagan, None.

## M217

**A Randomized Controlled Trial of Vitamin D3 Supplementation for the Prevention of Viral Upper Respiratory Tract Infections.** M. Mikhail, J. F. Aloia, S. Pollack\*, B. Cunha\*, J. Yeh\*, N. Berbari\*, M. Li-Ng\*. Winthrop University Hospital, Mineola, NY, USA.

**PURPOSE:** Vitamin D has been shown to be an important immune system regulator. Vitamin D insufficiency during the winter may cause increased susceptibility to infections, particularly viral upper respiratory tract infections (URIs). The purpose of the study is to determine whether vitamin D supplementation during the winter season prevents or decreases URI symptoms in adults.

**METHODS:** A randomized, double-blind, placebo-controlled trial was conducted in 162 adults. Participants were randomized to receive vitamin D3 50 mcg (2000 IU) daily or matching placebo for 12 weeks from December 2006 to March 2007. A biweekly questionnaire was used to record the incidence and severity of URI symptoms.

**RESULTS:** There was no difference in the incidence of URIs between the vitamin D and the placebo group (48 URIs out of 388 reports versus 50 URIs out of 363 reports respectively, p=0.57). There was no difference in the duration (or severity) of URI symptoms between the vitamin D and placebo group (5.4  $\pm$  4.8 days versus 5.3  $\pm$  3.1 days respectively, p=0.86). The mean 25-hydroxyvitamin D level at baseline was similar in both groups (64.3  $\pm$  25.4 nmol/L in the vitamin D group; 63.0  $\pm$  25.8 nmol/L in the placebo group, ns). The mean 25-OHD level increased to 88.5  $\pm$  23.2 nmol/L in the vitamin D group while remaining virtually constant in the placebo group.

**CONCLUSION:** There was no benefit of vitamin D3 supplementation in decreasing the incidence or severity of viral URI during the winter months. Further studies are needed to determine the role of vitamin D in infection.

Characteristics of URIs by group			
	VitaminD N = 78	Placebo N = 70	p-value
Reported URI, n	28 (37%)	29 (41%)	0.61
Duration of URI, days	5.4 $\pm$ 4.8	5.3 $\pm$ 3.1	0.86
Severity of URI, range 1-5 (1=healthy; 5=very ill)	2.6 $\pm$ 1.0	2.8 $\pm$ 1.2	0.4

**Disclosures:** M. Mikhail, None.

*This study received funding from: Empire Clinical Research Investigator Program (ECRIP).*

## M218

**Vitamin D and Physical Performance in African American Women.** M. Mikhail, J. F. Aloia, T. Bojadzievski\*, S. Pollack\*, J. Yeh\*, M. Li-Ng\*. Endocrinology, Winthrop University Hospital, Mineola, NY, USA.

**PURPOSE:** There is increasing evidence that vitamin D improves muscle strength in vitamin D-deficient elderly women. It also has been shown to improve body sway in ambulatory elderly women. The purpose of the study is to determine if vitamin D supplementation influences physical performance in postmenopausal African-American women.

**METHODS:** We performed a 4-month prospective cohort trial of vitamin D3 supplementation in 51 African-American postmenopausal women. Our goal in supplementation was to reach optimal levels of 25(OH)D > 75 nmol/L. Physical performance was measured by the Short Physical Performance Battery (SPPB) and grip strength. Subjects were asked to perform a balance assessment (open, semi-tandem, and tandem stance), a timed 4-meter walk, and a chair rise test (timed 5 rises). Each of these tests has a maximum score of 4 points (total SPPB maximum score is 12). Grip strength was measured using a handgrip dynamometer. The four physical tests were repeated one week later to account for any learning effect on subsequent measurements. This enabled us to measure the reliability of these four measures. Reliability ranged from 0.75 to 0.93.

**RESULTS:** A total of 48 women completed the study. The mean age of the women was 67.4 years and mean BMI was 30 kg/m<sup>2</sup>. Nine subjects were given no vitamin D3 as their baseline 25(OH)D was > 75 nmol/L, 23 subjects were given 70 mcg/day since their baseline 25(OH)D was between 45 and 75 nmol/L, and 20 subjects were given 100 mcg/day since their baseline 25(OH)D was < 45 nmol/L. Physical performance at baseline was exceptionally good in this cohort based on the four measures that we observed. Only the grip strength increased significantly. The increase was due to improvement in the subset with baseline 25(OH)D below 50 nmol/L with an increase in strength of 7%.

**CONCLUSION:** This study suggests that vitamin D benefit on physical performance was seen in grip strength in the subset with baseline 25(OH)D below 50 nmol/L. The high performance in this group on the SPPB may have precluded finding an improvement.

**Disclosures:** M. Mikhail, None.

*This study received funding from: Empire Clinical Research Investigator Program (ECRIP).*

## M219

**Effects of Alfacalcidol on Bone and Skeletal Muscle in Glucocorticoid-treated Rats.** H. Sasaki, N. Miyakoshi, Y. Kasukawa, S. Maekawa, K. Kamo, Y. Shimada. Orthopedic Surgery, Akita University School of Medicine, Akita, Japan.

Several recent studies have demonstrated that vitamin D prevents falls and osteoporotic fractures through its effects on bone and muscle. However, the effects of vitamin D on muscle and the mechanisms of fall-prevention have yet to be elucidated.

As glucocorticoids, which are prescribed as anti-inflammatory agents, are considered to cause secondary osteoporosis and skeletal muscle atrophy, the present study investigated whether alfacalcidol (1 $\alpha$ (OH)D<sub>3</sub>) could prevent skeletal muscle atrophy and osteoporosis induced by prednisolone (PSL).

Seven-week-old female Wistar rats were randomized into the following four groups: 1) control group, treated with vehicle of 1 $\alpha$ (OH)D<sub>3</sub> orally and daily s.c. injections of normal saline; 2) PSL group, administered PSL (10 mg/kg s.c., daily); 3) 1 $\alpha$ (OH)D<sub>3</sub> group, treated with alfacalcidol (0.1  $\mu$ g/kg/day, orally); and 4) 1 $\alpha$ (OH)D<sub>3</sub> + PSL group, treated with alfacalcidol plus PSL. After a 4-week treatment period, the left tibialis anterior (TA) muscle was removed for histological analysis and the cross sectional area (CSA) of muscle fiber was measured. In addition, the left femur was harvested in order to measure the bone mineral density (BMD) in the distal third of the femur by dual energy x-ray absorptiometry.

The CSA of the TA muscle in the PSL group was significantly smaller than that in the control group (-31%, p<0.05). However, the CSA in the 1 $\alpha$ (OH)D<sub>3</sub> and 1 $\alpha$ (OH)D<sub>3</sub> + PSL groups showed no significant difference compared to that in the control group (5% and -11%, respectively). The BMD in the PSL group was significantly lower than that in the control group (-11%, p<0.05). Furthermore, the BMD in the 1 $\alpha$ (OH)D<sub>3</sub> + PSL group was significantly higher than that in the PSL group (20%, p<0.05).

The present results suggest that in glucocorticoid-treated rats, alfacalcidol prevents not only decrease of BMD but also muscle atrophy. Therefore, administration of alfacalcidol might have positive effects on muscle in patients treated with glucocorticoids in addition to its known effects on bone metabolism.

**Disclosures:** H. Sasaki, None.

*This study received funding from: Chugai Pharmaceutical CO., LTD.*

## M220

**Expression of Vitamin D Receptor in the Developing Zebrafish Embryo.** T. Craig<sup>\*1</sup>, S. Sommer<sup>\*1</sup>, C. Sussman<sup>\*2</sup>, J. Grande<sup>\*3</sup>, R. Kumar<sup>1</sup>. <sup>1</sup>Nephrology Research, Mayo Clinic, Rochester, MN, USA, <sup>2</sup>Physiology, Mayo Clinic, Rochester, MN, USA, <sup>3</sup>Laboratory Medicine/Pathology, Mayo Clinic, Rochester, MN, USA.

The vitamin D receptor has been previously shown to be widely distributed in epithelial cells, cells of the central nervous system and skeleton of the adult zebrafish, *Danio rerio*. Little is known of the ontogeny of the VDR in the developing zebrafish embryo. We examined the distribution of the VDR in 48 h and 96 h post-fertilization zebrafish embryos. In the 48 h post-fertilization embryo, the VDR is seen in the developing brain (diencephalon) and in cells of the neural retina. The VDR immunostaining is also seen in the developing mandibular cartilage.

Figure 1A demonstrates results obtained with immune serum in 96 h post-fertilization (p.f.) embryos. VDR immunostaining is observed in the ganglion cells of the eye (E), portions of the brain (B), and the epithelium of the otic vesicle (O). Pre-immune serum does not demonstrate the presence of the VDR in these tissues (Figure 1B). A higher magnification view of the developing eye is seen in Figure 1C. Ganglion cells appear to immunostain for the VDR (G). Cells of the lens (L) do not immunostain. Rods (R) do not immunostain. Cells lining the otic vesicle (OE) immunostain for the VDR (Figure 1D). Conclusion. These data show that the VDR is expressed in the central nervous system, eye and ear of the developing zebrafish, and suggest that the receptor may play a role in the development of these organs in the zebrafish.

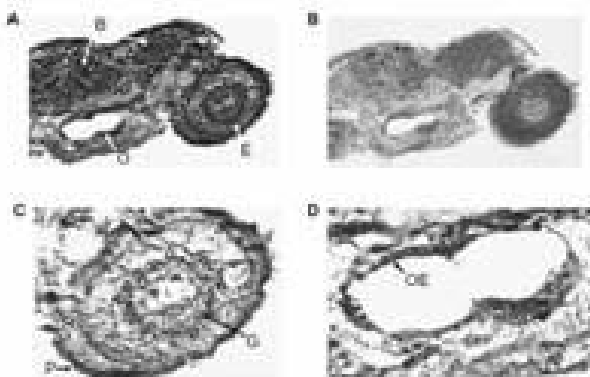


Figure 1. VDR in 96 h p.f. developing zebrafish embryo

**Disclosures:** T. Craig, None.

## M221

**High Prevalence of Vitamin D Insufficiency in a Young Adult Population.** M. Calatayud<sup>\*</sup>, R. Sánchez<sup>\*</sup>, S. Guadalix<sup>\*</sup>, E. Jódar, G. Martínez, F. Hawkins. Endocrinology, University Hospital 12 de Octubre, Madrid, Spain.

Recent studies have shown a wide range of beneficial skeletal and extra-skeletal effects of vitamin D. During the last years a high prevalence of vitamin D insufficiency (<30 ng/ml) and deficiency (<20 ng/ml) has been proved in aged and adult population. The main reasons for this high prevalence seem to be poor intake and low sun exposure. On the other hand, data related to the young adult population are scarce.

Our primary objective was to determine the prevalence of vitamin D insufficiency and deficiency in a young healthy population (physicians and nurses) and its relationship with calcium concentration, PTH, nutritional parameters and sun exposure. Data were obtained from 116 subjects (38 men and 78 women aged 26.56 ± 3.32 years), during the months of June and July in the year 2007.

Fasting blood sample was obtained and 25-hydroxyvitamin D, intact PTH, calcium, albumin and a basic biochemical study were measured. A questionnaire designed to assess sun exposure and sunshine protection during the previous 12 months was carried out. Average value of 25-hydroxyvitamin D obtained was 24.58 ± 6.98 ng/ml. Subjects were divided into three groups according to 25-hydroxyvitamin D levels: deficient, < 20 ng/ml (29.46% of the subjects); insufficient, 20 - 30 ng/ml (58.03% of the subjects) and sufficient, ≥ 30 ng/ml (16.96% of the subjects). There are no significant statistical differences between the groups and the study variables.

Our study shows a high prevalence of vitamin D insufficiency in a young healthy population without a clear relationship with sun exposure or sunshine protection. Just 1 in 6 subjects had the recommended levels of vitamin D. The lack of food fortification with vitamin D and the wide use of sunscreen could account for the low levels of vitamin D in this young population of southern of Europe.

**Disclosures:** M. Calatayud, None.

## M222

**Impaired Fracture Healing in the Absence of the Vitamin D-24-hydroxylase, Cyp24a1.** R. P. Naja<sup>\*</sup>, A. Arabian, R. St-Arnaud. Genetics Unit, Shriners Hospital for Children, Montreal, QC, Canada.

The Cyp24a1 enzyme (25-hydroxyvitamin D-24-hydroxylase) is involved in the catabolic breakdown of 1,25(OH)<sub>2</sub>D but also synthesizes the 24,25(OH)<sub>2</sub>D metabolite. Studies in chicken showed increases in serum levels of 24,25(OH)<sub>2</sub>D and of the renal mRNA levels of cyp24a1 following fracture, suggesting a role for 24,25(OH)<sub>2</sub>D in fracture repair. We used a cyp24a1-deficient mouse strain to determine the putative role of 24-hydroxylated vitamin D metabolites during mammalian fracture repair. In wild-type mice, we measured a significant increase in local expression of cyp24a1 mRNA in the tibiae subjected to an osteotomy as compared to the unfractured contralateral tibiae. We then subjected four-month-old wild-type and cyp24a1-deficient mice to a stabilized, transverse mid-diaphyseal fracture of the tibia. Bones were collected at days 14 and 21 post-fracture and analyzed for histology and gene expression. Examination of the callus sections stained by Goldner showed that the homozygous mutant animals had delayed hard callus formation when compared to wild-type littermates. Expression profiling using RT-qPCR showed that the levels of osteocalcin and type X collagen transcripts were reduced in mutant mice at 14 and 21 days post-fracture, reflecting the delayed healing. We attempted rescue of the impaired healing by subcutaneous injection of 24,25(OH)<sub>2</sub>D<sub>3</sub> (6.7 µg/kg) or 1α,25(OH)<sub>2</sub>D<sub>3</sub> (67 ng/kg). Control groups were injected with the vehicle (propylene glycol). Treatment with 1α,25(OH)<sub>2</sub>D<sub>3</sub> had no effect on fracture repair. Daily injection with 24,25(OH)<sub>2</sub>D<sub>3</sub> normalized the histological appearance of the callus and the measured static histomorphometric index (BV/TV). The treatment with 24,25(OH)<sub>2</sub>D<sub>3</sub> also rescued and normalized type X collagen mRNA expression at all time points studied. These results show that cyp24a1 deficiency delays fracture repair and strongly suggest that vitamin D metabolites hydroxylated at position 24, such as 24,25(OH)<sub>2</sub>D<sub>3</sub>, play an important role in the mechanisms leading to normal fracture healing.

**Disclosures:** R.P. Naja, None.

This study received funding from: Dairy Farmers of Canada and Shriners of North America.

## M223

**Vitamin D Status, Bone Mass, and Bone Metabolism in Postmenopausal Women and Men Older than 50 Attended in a Primary Care Center of Spain: The Camargo Cohort Study.** J. M. Olmos<sup>1</sup>, J. L. Hernández<sup>\*1</sup>, J. Martínez<sup>\*1</sup>, J. de Juan<sup>\*2</sup>, D. Nan<sup>\*1</sup>, C. Ramos<sup>\*2</sup>, C. Valero<sup>\*1</sup>, P. García<sup>\*2</sup>, J. González-Macías<sup>1</sup>. <sup>1</sup>Medicina Interna, Hospital Universitario M. Valdecilla, Santander, Spain, <sup>2</sup>Centro de Salud "José Barros", Camargo, Spain.

The objective of the present study was to determine the prevalence of vitamin D deficiency and insufficiency in a population of postmenopausal women and men older than 50 living in the North of Spain. People studied are part of a cohort that is being set up to study the prevalence and incidence of metabolic bone diseases and disorders of mineral metabolism attended in a primary care center of our region (The Camargo cohort study). We present results from 1.159 subjects (895 women, and 264 men). Serum levels of amino terminal propeptide of type I collagen (P1NP), C-terminal telopeptide of type I collagen (β-CrossLaps, β-CTX), 25-Hydroxyvitamin D<sub>3</sub> (25OHD), and intact parathyroid hormone (iPTH) were measured by a fully automated electrochemiluminescence system (Elecys 2010, Roche). BMD at lumbar spine (LS), femoral neck (FN) and total hip (TH) was determined by DXA. Studied women and men were 63±9 and 66±8 years old, respectively. Results are shown in the table 1 and 2.

Vitamin D deficiency (25OHD < 10 ng/ml) and insufficiency (25OHD < 30 ng/ml) were present in 3% and 74% of women, and in 4% and 74% of men. Serum 25OHD concentration was correlated with BMD at FN (r: 0.064; p<0.05) and TH (r: 0.068; p<0.05), but not at LS. Vitamin D levels were also correlated with P1NP (r: 0.063; p<0.05). Conversely, an inverse correlation between iPTH and 25OHD was found (r:-0.28; p<0.001). This relationship persisted after adjustment by age and sex.

Prevalence of hypovitaminosis D among Spanish adult population is similar to that described in other countries. The percentage of people with either vitamin D deficiency or insufficiency is the same in both sexes. An inverse relationship between serum vitamin D levels and PTH was observed.

Table 1				
	25OHD(ng/ml)	iPTH(pg/ml)	P1NP(ng/ml)	β-CTX(ng/ml)
Women	26±9	54±21	37±18	0.29±0.17
Men	25±9	52±22	47±20	0.38±0.18

Table 2			
	LS (g/cm <sup>2</sup> )	FN (g/cm <sup>2</sup> )	TH (g/cm <sup>2</sup> )
Women	0.91±0.13	0.72±0.11	0.87±0.12
Men	1.03±0.15	0.79±0.11	1.00±0.13

**Disclosures:** J.M. Olmos, None.

This study received funding from: a grant from the "Fondo de Investigación Sanitaria", Ministerio de Sanidad y Consumo, Spain (FIS: PI05 0125) and "Fundación Marqués de Valdecilla", Santander, Spain (IFIMAV: API/07/13).



## M224

**The Requirement of the Bone for Vitamin D for 1,25(OH)<sub>2</sub>D<sub>3</sub> Synthesis and Bone Mineralisation.** P. H. Anderson<sup>\*1</sup>, G. J. Atkins<sup>2</sup>, R. K. Sawyer<sup>\*3</sup>, D. M. Findlay<sup>2</sup>, P. D. O'Loughlin<sup>\*3</sup>, H. A. Morris<sup>3</sup>. <sup>1</sup>School of Medicine, University of Adelaide, Adelaide, Australia, <sup>2</sup>Department of Orthopaedics and Trauma, University of Adelaide, Adelaide, Australia, <sup>3</sup>Hanson Institute, IMVS, Adelaide, Australia.

*In vitro* evidence suggests that the 1,25-dihydroxyvitamin D<sub>3</sub> (1,25D) can exert effects during both the resorptive and synthetic phases of bone remodelling. However, the question as to whether the primary action of vitamin D on bone under normal circumstances is indirect by mediating changes in ECF calcium and phosphate concentrations or whether there is also a significant direct effect of vitamin D on bone is unclear. We hypothesise that 1,25D, synthesized by osteoblasts, regulates osteoblast differentiation and osteoclast activation, independently of changes to circulating 1,25D levels. In adult animals with stable mean 25-hydroxyvitamin D<sub>3</sub> (25D) levels ranging from 20 nmol/L to 115 nmol/L, a strong positive association occurred between femoral trabecular bone volume (BV/TV) and 25D levels ( $R^2=0.57$ ,  $P<0.01$ ). Interestingly, the loss of bone volume with vitamin D-insufficiency was as a consequence of increased osteoclast numbers and activity (via increased RANKL/OPG ratio) which is dependent on serum 25D levels ( $R^2=0.60$ ,  $P<0.01$ ) and not on circulating calcium, PTH or 1,25D levels. The autocrine actions of 1,25D may help explain why osteoclastogenesis occurs without an increase in circulating 1,25D levels. When the mRNA for CYP27B1 was reduced by 80% in HOS bone cells by RNAi, the production of 1,25D was markedly reduced when treated with 25D (100 to 400nm). The decline in 1,25D production almost completely abrogated the mRNA levels for osteocalcin and CYP24. Also, when primary human bone cells were treated with 25D (100 or 200nm) the anti-proliferative effects (as measured by CFSE fluorescent labelling of cells) and stimulation of *in vitro* mineralisation were comparable to cells treated with 1,25D (100pM). This *in vitro* mineralisation of osteoblasts is associated with a decline in RANKL mRNA expression. These results suggest that locally produced 1,25D is important for an intrinsic autocrine/paracrine signalling from pro-resorptive to pro-osteogenic activity as the osteoblast matures. Ultimately, the potential benefits of maintaining a healthy vitamin D status to limit bone loss due to reduced osteoclastic activity may be to enhance the osteogenic potential of osteoblasts.

**Disclosures:** P.H. Anderson, None.  
This study received funding from: NHMRC.

## M225

**Sunscreen Use and Vitamin D Status.** M. G. Kimlin, A. Brodie\*, C. Lang\*. Institute of Health and Biomedical Innovation, Queensland University of Technology, Brisbane, Australia.

Previous research suggests that the use of sunscreen reduces the skin's capability to synthesize Vitamin D to, in some cases, zero. Sunscreen has been demonstrated to be an important tool in the prevention of non-melanoma skin cancers and potentially in melanoma. This research poses the question, "Does sunscreen use impact on Vitamin D status in a population in a sunny climate such as Australia?". In this research we interviewed 127 participants (40 males / 87 females) with a median age 35 (18-87 years). A self reported questionnaire recorded a wide variety of demographic details along with sunscreen use. A blood sample was collected to assess 25(OH)D status. The application of sunscreen was varied. 43% of the sample rarely used sunscreen, 32% "usually" or "almost always" and 26% not at all. Sunscreen with an SPF of  $\geq 30$  was used by most (82%). Those who applied sunscreen, the face was the highest compliance site and other sites less frequently. In this sample, 24% had an adequate Vitamin D (blood serum 25[OH]D) level (50-75nmol/L), and 41% were Vitamin D deficient ( $<50$ nmol/L). Data was collected at the end of winter 2006 and in summer 2007. We found no association between Vitamin D (25[OH]D) status and sunscreen use. Of the participants who usually or almost always used sunscreen, 32% had Vitamin D levels of  $>75$ nmol/L, whilst 26% of participants were within the 51-75nmol/L range. This research suggests that individuals living in a sunny climate may have sufficient Vitamin D status even with the use of sunscreen. A potential factor that have led to this finding is that perhaps the sunscreen was not applied correctly, either through volume or application technique. This data, from a 'real-world' situation presents a differing message to research conducted under controlled conditions.

**Disclosures:** M.G. Kimlin, None.  
This study received funding from: Queensland Health.

## M226

**Vitamin D (Cholecalciferol) Production Does Not Increase Linearly with UV Dose: An in Vitro Model.** W. J. Olds<sup>1</sup>, M. R. Moore<sup>\*2</sup>, M. G. Kimlin<sup>1</sup>. <sup>1</sup>Australian Sun and Health Research Laboratory, Institute of Health and Biomedical Innovation, Queensland University of Technology, Kelvin Grove, Brisbane, Queensland, Australia, <sup>2</sup>National Research Centre for Environmental Toxicology (EnTox), University of Queensland, Brisbane, Queensland, Australia.

It is widely known that sun exposure initiates the synthesis of vitamin D (cholecalciferol) in human skin. The ultimate goal of current research is to arrive at a statement of what amount of time an individual should exposure himself to UV in order to receive adequate vitamin D. This is an important but complex question of public health, because excessive exposure to UV causes skin cancers and ocular conditions. It has been assumed that the amount of cholecalciferol produced will scale in proportion if the amount of exposure to UV is increased. However, we have used an *in vitro* model (Olds et al, 2008, J Photochem Photobiol B: Biol, in press) to demonstrate that, as the dose of UV radiation increases, the production of cholecalciferol actually decreases. This characteristic nonlinear dose-response relationship for cholecalciferol production will also apply to humans. Therefore, we conclude that if an individual increases his or her sun exposure, it cannot be assumed that a proportionate increase in serum vitamin D levels will result; that is, exposing oneself to twice the dose UV radiation will not produce twice the amount of cholecalciferol. Moreover, this may increase the risk of skin and eye conditions without justifiably benefiting vitamin D status. The *in vitro* model we used is a refinement of an existing model, where 7-dehydrocholesterol (the precursor to cholecalciferol) is dissolved in ethanol, placed into quartz cuvettes and exposed to UV and HPLC analysis of the photoproducts is undertaken. Our model uses a sound analytical methodology involving HPLC analysis and a computer-controlled UV dose system that is calibrated to the NIST international standard of irradiance. We discuss that this characteristic of cholecalciferol synthesis may arise because of a known reciprocity phenomenon, where additional UV actually degrades the cholecalciferol produced and creates other biologically inert photoproducts instead. This project shows that a vital key to understanding appropriate sun exposure for humans is to understand the reciprocity characteristic of cholecalciferol synthesis.

**Disclosures:** W.J. Olds, None.

## M227

**Silencing of PDIA3 (ERp60) Reduces the Rapid Membrane Response to 1,25-Dihydroxyvitamin D<sub>3</sub> in MC3T3-E1 Osteoblast-like Cells.** J. Chen\*, Y. Wang\*, R. Olivares-Navarrete\*, Z. Schwartz, B. D. Boyan. Biomedical Engineering, Georgia Institute of Technology, Atlanta, GA, USA.

Protein disulfide isomerase A3 (PDIA3), also known as ERp60, ERp57, Grp58, and 1,25-MARRS, is a multifunctional protein that has been associated with rapid membrane-initiated signaling by 1 $\alpha$ ,25-dihydroxyvitamin D<sub>3</sub> (1 $\alpha$ ,25(OH)<sub>2</sub>D<sub>3</sub>) in several cell types. Chondrocytes and osteoblasts isolated from mice lacking functional nuclear vitamin D receptors (VDR), retain 1 $\alpha$ ,25(OH)<sub>2</sub>D<sub>3</sub>-stimulated protein kinase C (PKC) activity and PKC-dependent responses to the vitamin D metabolite. To further elucidate the mechanism of PDIA3 action in the rapid response to 1 $\alpha$ ,25(OH)<sub>2</sub>D<sub>3</sub>, we assessed the effect of PDIA3 knockdown in the mouse osteoblastic cell line MC3T3-E1 on 1 $\alpha$ ,25(OH)<sub>2</sub>D<sub>3</sub> regulated PKC and phospholipase C (PLC) activity. The expression of PDIA3 in wild type MC3T3-E1 cells and its co-localization with caveolin-1 were detected both by immunofluorescence staining and by Western blot. The cells were then transfected with adenovirus-mediated siRNA against five different sequences of the PDIA3 gene. After selection in puromycin, silencing efficiency was evaluated at the mRNA level by RT-PCR as well as at the protein level by Western blot and flow cytometry. PKC and PLC specific activity were measured in wild type and PDIA3-silenced cells after 9 minutes treatment with different concentrations of 1 $\alpha$ ,25(OH)<sub>2</sub>D<sub>3</sub>. Immunofluorescence staining demonstrated abundant expression of PDIA3 in wild type MC3T3-E1 cells, which was localized to the caveolar fraction based on Western blot. A silencing efficiency of 80% was achieved in one of the five clones as determined by RT-PCR and confirmed by Western blot and flow cytometry. Treatment with 1 $\alpha$ ,25(OH)<sub>2</sub>D<sub>3</sub> for 9 minutes resulted in a dose dependent increase in PKC in wild type and silenced cells, but the effect was reduced in this clone. Furthermore, 1 $\alpha$ ,25(OH)<sub>2</sub>D<sub>3</sub> failed to induce a significant increase in PLC activity in silenced cells compared to wild type cells. These results suggest that knockdown of PDIA3 could decrease cell sensitivity to 1 $\alpha$ ,25(OH)<sub>2</sub>D<sub>3</sub>-regulated PKC and PLC activity. In addition, adenovirus-mediated siRNA can specifically and efficiently reduce PDIA3 expression in MC3T3-E1 cells, providing a useful model for further study on its function in caveolae and PKC-dependent responses to 1 $\alpha$ ,25(OH)<sub>2</sub>D<sub>3</sub>.

**Disclosures:** J. Chen, None.  
This study received funding from: the Price Gilbert, Jr. Foundation and Children's Healthcare of Atlanta.

## M228

**Thyroid Hormone Receptor Beta-Specific Agonist GC-1 Increases Bone Quality of Adult Female Mice.** C. C. Costa<sup>\*1</sup>, C. C. Wang<sup>\*2</sup>, K. O. Nonaka<sup>\*2</sup>, T. S. Scanlan<sup>\*3</sup>, C. H. A. Gouveia<sup>1</sup>. <sup>1</sup>Department of Anatomy, Institute of Biomedical Sciences, University of Sao Paulo, Sao Paulo, Brazil, <sup>2</sup>Department of Physiological Science, University of Sao Carlos, Sao Carlos, Brazil, <sup>3</sup>Department of Physiology and Pharmacology, Oregon Health and Science University, Portland, OR, USA.

It is well known that thyroid hormone excess is a risk factor for osteoporosis and bone fractures. Bone tissue expresses three isoforms of thyroid hormone receptors: TR $\alpha$ 1, TR $\alpha$ 2 and TR $\beta$ 1. In this study, we compared the effects of triiodothyronine (T3) and GC-1, a TR $\beta$ -selective agonist on biomechanical parameters of the tibia by the three-point bending test. 130-day old female C57BL/6J mice were divided in the following groups (n=6-7/group): (i) Euthyroid (EUT), untreated animals; (ii) Hypothyroid (HYPO), treated with methimazole and sodium perchlorate (MMI+P), to inactivate the thyroid function; (iii) 10xT3, (iv) 20xT3 and (v) 40xT3, treated with 10, 20 or 40 times the physiological dose of T3 (0.35 ug/100g BW/day), respectively; (vi) 10XGC-1; (vii) 20XGC-1 and (viii) 40XGC-1, treated with GC-1 in equimolar doses of T3. Groups ii-vii were also treated with MMI+P and all treatments lasted 60 days. Serum levels of thyroxine (T4) were decreased in all MMI+P-treated groups (vs. EUT) and were not affected by T3 or GC-1 treatment. Serum levels of T3 were reduced in MMI+P-treated groups and increased in a dose-dependent fashion by T3-treatment (above the EUT levels), but were not affected by GC-1 treatment. As expected, all T3 doses promoted cardiac hypertrophy, characterized by an increase in the dry mass of the heart, while GC-1 treatment had no effect. HYPO did not affect any biomechanical parameter of the tibia, while T3 treatment reduced bone resistance in 20% (evaluated by the maximum load applied to the bone) and bone stiffness in 17%. Surprisingly, all GC-1 doses promoted significant increases in bone resistance (36-45%), stiffness (14-30%) and resilience (75-83%). These findings show that bone tissue of mice is responsive to GC-1 in vivo and that its administration improves biomechanical parameters and, therefore, bone quality. Considering the selectiveness of GC-1 for TR $\beta$  and the positive effects of this analog on biomechanical parameters of the tibia, contrasting to the deleterious effects of high doses of T3, our results suggest that TR $\beta$  mainly mediates actions of T3 that improve bone quality.

**Disclosures:** C.C. Costa, None.

This study received funding from: FAPESP.

## M229

**Differential Cellular and Molecular Responses of Intestinal Epithelium to High Calcium Diet and 1,25(OH) $_2$ D $_3$ .** S. Peleg<sup>1</sup>, J. H. Sellin<sup>\*2</sup>, S. Umar<sup>\*2</sup>. <sup>1</sup>Endocrine Neoplasia & Hormonal Disorders, M. D. Anderson Cancer Center, Houston, TX, USA, <sup>2</sup>Gastroenterology & Hepatology, U. T. Medical Branch, Galveston, TX, USA.

Dietary calcium and the active metabolite of vitamin D (1,25(OH) $_2$ D $_3$ ), are essential for normal calcium homeostasis and skeletal health. While it is well established that a key component of their physiological action is adequate intestinal calcium absorption, little is known about how calcium and 1,25(OH) $_2$ D $_3$  affect the cellular dynamics in intestinal epithelium. To obtain a better understanding of epithelial responses to nutrients we used an infectious agent, *Citrobacter rodentium* (CR), which colonizes the distal colon of mice. CR infection induces a profound and sustained epithelial hyperplasia accompanied by a substantial activation of the  $\beta$ -catenin and NF- $\kappa$ B pathways. Because previous studies have shown that high calcium (hCa, 1%) diet inhibited the hyperplasia but had no effect on these pathways, we used this model to elucidate alternative molecular target/s for the protective action of hCa diet and to distinguish epithelial responses to calcium and 1,25(OH) $_2$ D $_3$ . First, we assessed the effect of infection on expression of several genes associated with calcium homeostasis in isolated colonic crypts and found a profound and sustained increase (up to 20-fold) in expression of the calcium channel TRPV6, but not in expression of TRPV5, calbindin D9K, calcium-sensing receptor, and vitamin D-metabolizing enzymes. Immunohistochemistry showed that in uninfected crypts TRPV6 was localized in the apical membrane of absorptive enterocytes, but in the infected crypts its abundance increased and its localization overlapped with the expanded proliferative zone. Expression of TRPV6 was diminished by hCa diet but increased substantially in both uninfected and infected crypts by intermittent administration of 1,25(OH) $_2$ D $_3$  (3  $\mu$ g/kg, 3 times per week). Likewise, hCa diet inhibited DNA synthesis (assessed by BrdU labeling) whereas 1,25(OH) $_2$ D $_3$  increased DNA synthesis and cellular mass in both uninfected and infected crypts. Furthermore, 1,25(OH) $_2$ D $_3$  blunted the anti-mitotic activity of hCa diet in both uninfected and infected crypts. This direct correlation between TRPV6 expression and cell proliferation in colonic crypts suggests that it promotes intestinal epithelial hyperplasia. This hypothesis was substantiated by finding that TRPV6 was over expressed in colon neoplasia. We conclude that in addition to its role in active calcium absorption, TRPV6 has the potential to regulate growth-promoting signaling in intestinal epithelium, and that intermittent 1,25(OH) $_2$ D $_3$  induces adverse cellular responses and attenuates the protective action of hCa diet in the intestine.

**Disclosures:** S. Peleg, None.

This study received funding from: M. D. Anderson Cancer Center.

## M230

**Pregnancy Upregulates Duodenal Calcium-Transport Genes and Normalizes Calcium Homeostasis In *Vdr* Null Mice.** N. J. Fudge<sup>\*</sup>, A. G. Green<sup>\*</sup>, C. S. Kovacs. Memorial University, St. John's, NL, Canada.

Without vitamin D receptors (VDR), intestinal calcium absorption is reduced, leading to hypocalcemia, rickets and osteomalacia. Pregnancy imposes a substantial demand on the mother to supply calcium to her fetuses, a demand met by doubling intestinal calcium absorption. Previous work has shown that *Vdr* null mice upregulated duodenal  $^{45}$ Ca absorption to normal during pregnancy, and increased their bone mineral content (BMC) to 158% of baseline, thus equalling wild-type (WT) by end of pregnancy (EP).

We investigated the impact of pregnancy on mineral homeostasis, histomorphometry, and duodenal gene expression in *Vdr* null versus WT.

*Vdr* null and WT siblings were raised on 1% calcium chow until 10 weeks of age, in order to induce rickets and secondary hyperparathyroidism in *Vdr* nulls. Both genotypes were then switched to a 2% calcium, 20% lactose "rescue" diet to maximize fertility in *Vdr* nulls. After confirming stability of baseline BMC by DXA (Piximus), mice were mated and followed to EP. Analyses included serum Ca and PTH; urine Ca and deoxypyridinoline/creatinine (DPD/Cr); histomorphometry of toluidine blue stained undecalcified sections of tibiae; and RNA expression analysis (SuperArray) of genes relevant to calcium and bone homeostasis.

By EP, serum Ca was normal in *Vdr* nulls ( $1.2 \pm 0.2$  versus  $1.3 \pm 0.2$  in WT), while serum PTH dropped from high pre-pregnancy levels to expected low-normal WT levels at EP. Urine DPD/Cr also fell in *Vdr* null from  $42.9 \pm 4.5$  to  $12.6 \pm 5.0$ , reaching the same value as WT at EP ( $12.2 \pm 5.0$ ). Urine calcium rose in *Vdr* nulls from  $1.6 \pm 2.6$  to  $10.8 \pm 3.2$  mM and equalled WT at EP. *Vdr* null tibiae revealed rachitic growth plates, substantial fibrosis and secondary hyperparathyroidism at baseline that was unchanged at EP, despite the 158% increase in BMC. Duodenal microarray revealed significantly altered expression of genes in *Vdr* null mice at EP versus baseline, including (fold change in brackets): 1 $\alpha$ -hydroxylase (11.3), Ca $^{2+}$ -ATPase (3.1), calmodulin (4.4), calbindin9K (2.6), and FGF-23 (0.1). Compared to WT mice at EP, significantly altered expression was noted in: calbindin 28K (2.1), calmodulin (1.8) and Ca $^{2+}$ -ATPase (1.8), but the expression of other calcium-binding proteins and channels was no different between pregnant *Vdr* null and WT.

In summary, pregnancy in *Vdr* nulls was associated with improved systemic mineral homeostasis and increased renal calcium excretion. The skeleton accrued more mineral but had not repaired the rachitic phenotype. Several genes involved in calcium transport were upregulated in the duodenum.

In conclusion, *Vdr* nulls upregulate duodenal genes independently of VDR, thus upregulating  $^{45}$ Ca absorption and leading in turn to improved mineral homeostasis and skeletal mineral content.

**Disclosures:** N.J. Fudge, None.

This study received funding from: Natural Sciences and Engineering Research Council of Canada, Dairy Farmers of Canada.

## M231

**CYP27A1 Mutations at Phe147 Confer 25-hydroxylase Activity Towards a Vitamin D $_2$ -type Sidechain.** D. E. Prosser<sup>\*</sup>, M. Kaufmann<sup>\*</sup>, R. C. Murchie<sup>\*</sup>, K. Vong<sup>\*</sup>, G. Jones<sup>\*</sup>. Biochemistry, Queen's University, Kingston, ON, Canada.

CYP27A1 is a mitochondrial cytochrome P450 which 25-hydroxylates vitamin D $_3$  but 24-hydroxylates vitamin D $_2$ . The objective of this study was to identify substrate contact residues responsible for this regioselectivity. A detailed examination of a CYP27A1 homology model suggested that steric and electronic interactions between the aromatic bonds in Phe147 and the  $\Delta^{22-23}$  and 24-methyl moieties in the vitamin D $_2$  sidechain preferentially positions C24 for hydroxylation. We also examined the ability of Ser56, a putative substrate A-ring contact residue or access channel determinant, to regulate regioselectivity at C24. Wildtype CYP27A1 and site-directed mutants S56A, S56G, F147A, and F147L were stably transfected into V79-4 cells cultured in DMEM and incubated with 10 $\mu$ M 1 $\alpha$ -OH-D $_3$  or DHT $_2$  (dihydrocholesterol-2, a model D $_2$  sidechain-containing analog) for 24 hours in BSA-supplemented media. HPLC analysis of total lipid extracts was used to identify hydroxylated products which were confirmed by LC-MS and co-migrational analysis with authentic standards. The wildtype CYP27A1 expressed C24:C25:C27 hydroxylase activities towards 1 $\alpha$ -OH-D $_3$  in the ratio of 0.1:1:0.4. The mutants gave similar product ratios but total enzymatic activities were reduced: S56A (70% of wildtype), S56G (50%), F147A (8%), and F147L (54%). By comparison, the wildtype and Ser56 mutants displayed barely detectable 24-, 27-, and 28-hydroxylase activity (<20ng total) towards DHT $_2$  and no detectable 25-OH-DHT $_2$ . The Phe147 mutations, however, exhibited substantial activity towards the DHT $_2$  sidechain and produced unprecedented amounts of 25-OH-DHT $_2$ : F147A (780ng) and F147L (560 ng). The lack of 25-OH-DHT $_2$  production for the wildtype CYP27A1 and Ser56 mutants is consistent with the view that Phe147 directs hydroxylation of vitamin D $_2$ -type sidechains away from C25. Overall, the F147A and F147L mutations conferred substantially larger total activity and 25-hydroxylase activity towards a vitamin D $_2$ -type sidechain.

**Disclosures:** D.E. Prosser, None.

## M232

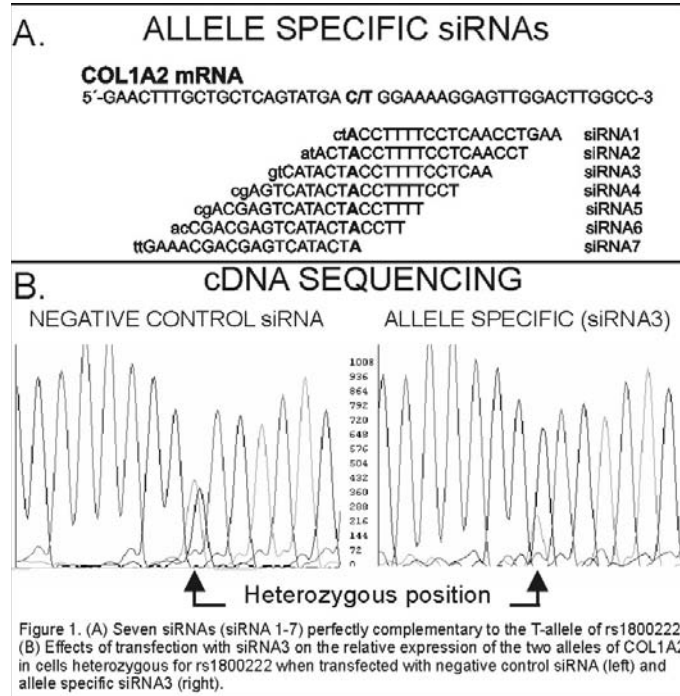
**Allele Specific Silencing of Collagen 1 Alpha Genes in Primary Human Bone Cells Using RNAi.** K. Lindahl\*, C. J. Rubin, A. Kindmark, Ö. Ljunggren. Dept. Med. Sciences, Uppsala University, Uppsala, Sweden.

Recent studies have reported successful allele specific gene silencing by RNA interference (RNAi) using small interfering RNA (siRNA) that discriminate between polymorphisms in mRNAs. These studies suggest that siRNAs may be interesting to explore as therapeutics in monogenic disorders, such as Osteogenesis Imperfecta, where the dysfunctional allele could be targeted specifically.

In the present study primary cultures of human bone derived cells were genotyped for a C/T single nucleotide polymorphism (SNP) in the coding region of COL1A2 (SNP ID rs1800222) (Allele frequencies: T=0.09 C=0.91). Heterozygous cells were transfected using the Magnet Assisted Transfection protocol (Promokine, Germany). Transfection was carried out for seven separate tiled siRNAs perfectly complementary to the T-allele of the COL1A2 mRNA (Figure 1A) and also with three separate scrambled negative control siRNAs. The transfected cells were incubated at 37°C until RNA was isolated 48h post-transfection and allele specific expression of COL1A2 mRNA was determined by cDNA-sequencing.

Cells transfected with negative control siRNA exhibited equal expression of the two alleles of rs1800222, whereas cells transfected with siRNA3 exhibited significant allelic imbalance of COL1A2, with lower relative abundance of the T-allele of rs1800222 (Figure 1B).

In conclusion: COL1A2 was silenced allele specifically in primary human bone cells using RNAi. The future aim is to design siRNAs that target mutated Collagen alleles in patients suffering from Osteogenesis Imperfecta (OI).



**Disclosures:** K. Lindahl, None.

## M233

**Stem Cell Antigen Positive (Sca-1<sup>+</sup>) Hematopoietic Cell-based Human Growth Hormone (hGH) Gene Therapy Enhanced Endosteal Bone Resorption in Mice.** S. L. Hall\*, S. T. Chen\*, S. Mohan, J. E. Wergedal, D. D. Strong, K. H. W. Lau. Pettis Mem. VAMC, Loma Linda, CA, USA.

Because hGH and its mediator, insulin growth factor-I (IGF-I), are key bone formation (BF) stimulators, this study tested the hypothesis that increasing hGH expression levels on the endocortical bone surface would increase trabecular BF in the marrow cavity. To increase hGH expression of cells at the endocortical surface, Sca-1<sup>+</sup> hematopoietic cells were transduced *ex vivo* to express hGH and transplanted into recipient mice. Sca-1<sup>+</sup> cells were used because of their ability to engraft into the marrow cavity and because the Sca-1<sup>+</sup> cell-based gene therapy approach has successfully been used to stimulate trabecular bone formation with FGF-2. Sublethally irradiated stem cell-deficient W<sup>41</sup>/W<sup>41</sup> mice were injected IV with GFP-expressing transgenic Sca-1<sup>+</sup> cells that were transduced with HIV-based vectors expressing hGH or  $\beta$ -galactosidase ( $\beta$ -gal). Engraftment, assessed by % GFP<sup>+</sup> cells in peripheral blood of recipients at 6 months post-transplantation, was high (70-80%) and stable, with no significant difference between the two groups. Consistent with successful hGH transgene transduction, engraftment and transcription, relative hGH mRNA levels (by real-time PCR) in bone marrow cells of hGH recipient mice were increased 20,000-fold ( $p < 0.001$ ) compared to the  $\beta$ -gal group. Serum IGF-1 levels were also significantly higher in the hGH group over the  $\beta$ -gal group ( $545 \pm 71$  vs.  $382 \pm 42$  ng/ml,  $p < 0.002$ ) and positively correlated with hGH expression ( $R = 0.86$ ,  $p < 0.01$ ), thus demonstrating high functional hGH levels in the hGH group.  $\mu$ CT analyses revealed that

trabecular bone volume fraction (BV/TV) of hGH-expressing Sca-1<sup>+</sup> recipient mice not only did not increase, but was significantly decreased, compared to the  $\beta$ -gal group ( $4.7 \pm 0.9$  vs.  $7.2 \pm 1.1$  %,  $p < 0.003$ ). hGH mice also had decreased trabecular number ( $2.6 \pm 0.3$  vs.  $3.5 \pm 0.2$  mm<sup>-1</sup>,  $p < 0.0002$ ) and increased trabecular separation ( $392 \pm 38$  vs.  $284 \pm 18$   $\mu$ m,  $p < 0.0003$ ). More importantly, trabecular connectivity density was drastically decreased in the hGH group compared to the  $\beta$ -gal group ( $20.9 \pm 4.5$  vs.  $58.1 \pm 17.9$  mm<sup>-3</sup>,  $p < 0.004$ ). Based on our findings that Sca-1<sup>+</sup> cell mediated hGH gene therapy results in loss of trabecular bone and previous findings that IGF-I stimulates bone resorption, we predict that continuous overexpression of hGH in Sca-1<sup>+</sup> cells at high levels at the endosteum leads to trabecular bone destruction presumably via increased formation/activity of osteoclasts. In conclusion, while the Sca-1<sup>+</sup> cell-based *ex vivo* gene therapy strategy is a powerful tool to deliver a therapeutic gene to marrow space, the choice of an appropriate growth factor gene is critical to effectively increase endosteal BF.

**Disclosures:** S.L. Hall, None.

This study received funding from: Veterans Administration.

## M234

**Proinflammatory Marker Values at Baseline and after a Fracture Are Distinctly Different Comparing a Mouse Model of Osteogenesis Imperfecta with Normal Controls.** A. I. Leet<sup>1</sup>, Y. Ni<sup>1,2</sup>, A. Jain<sup>1,2</sup>, T. Kazarian<sup>1</sup>, N. S. Fedarko<sup>1,2</sup>. <sup>1</sup>Orthopedic Surgery, Johns Hopkins University, Baltimore, MD, USA, <sup>2</sup>Geriatrics, Johns Hopkins University, Baltimore, MD, USA.

Patients with osteogenesis imperfecta (OI) can have high fevers after fracture or general anesthesia. The etiology of this response, we hypothesized, might be from an increased inflammatory response.

In this translational study, a mouse model of osteogenesis imperfecta (OIM), carrier, and normal (NL) mice were used to measure baseline inflammatory markers including IL-1 $\beta$ , TNF $\alpha$ , INF $\gamma$ , and IL-6, IL-8, IL-10, IL-12. OIM, carrier and NL mice underwent facial bleeding for a baseline pro-inflammatory profile. Tibia fractures were created in anesthetized OIM and NL mice using a closed model with a 3 point bend applied to the midshaft, followed by splinting. At short term time intervals (.25, .5, 1, 2, 4, 6 hrs.) and long term time intervals (1, 2, 3, 6 wk) mice underwent bleeding to obtain 1 ml of blood per animal that was spun to separate the serum layer. ELISA assays were performed using a 96 well 7 chamber multiplex plate for pro-inflammatory markers in mice (MSD Inc.).

Baseline values demonstrated greater variability in the OIM samples than either the NL or the carrier mice, which is to be expected given that OIM mice have spontaneous fractures. For TNF $\alpha$  and IL-10 the mean values for the OIM mouse was greater than NL controls with the carrier phenotype having an intermediate mean value compared to NL and OIM mice. For the other interleukins the means were not statistically different.

The short term fracture data showed a diminished initial elevation in INF $\gamma$ , IL-10, IL-12 in OIM versus NL mice; however, over time the amount of these pro-inflammatory markers increased such that by 6 hours the values were significantly higher in OIM than NL. For IL-6, the values at every time course were elevated in OIM compared to NL, while TNF $\alpha$ , IL-6, and IL-8 had similar slopes for OIM and NL mice when comparing the linear regression analysis of the data which started at baseline and then increased steadily as time elapsed from the fracture. The values of the pro-inflammatory markers at long term intervals were very similar comparing OIM to NL mice and tended to hover around baseline values.

The profile of inflammatory markers are very different comparing NL and OIM mice at baseline and then in the first few hours after a fracture. A week after a fracture there is not a large pro-inflammatory response as bone healing occurs, as would be expected since the inflammatory phase is generally the first stage in fracture healing. This model allows the study of only one genotype and phenotype, thus further study is warranted to determine if the high fevers seen clinically in some patients with OI can be explained by differences in cytokine production.

**Disclosures:** A.I. Leet, None.

This study received funding from: POSNA, OI Foundation.

## M235

**Analysis of Long Bone Fracture Nonunion by an Expression Profile of the Matrix Metalloproteinases and ADAMTS Enzyme Families.** M. Fajardo\*, K. Ego<sup>1</sup>, C. Liu. New York University, New York, NY, USA.

Skeletal tissue is one of the human tissues which can regenerate to its former biological state when injured. The ability to regenerate encompasses a complex interaction of many biological processes. When these processes are interrupted, a fracture nonunion can result. Fracture healing and osteosynthesis requires the constant remodeling of the extracellular matrix. The remodeling process is largely attributable to the matrix metalloproteinases (MMPs) and a disintegrin-like and metalloproteinase with thrombospondin type I motif (ADAMTS) enzymes. A variety of members from both these protease families have been found to be closely related to the fracture healing process. Delays in bone healing or even development of a nonunion could be related to the concentrations of these enzymes and their function. This study is aimed at defining an expression profile of most MMPs and ADAMTS enzymes and their inhibitors (TIMPs) in bone fracture nonunion tissue and correlating their expression with normal callus. Tissue samples taken from the nonunion site were prospectively collected from patients undergoing surgical treatment for an established bone fracture nonunion. Only long bone fracture nonunion tissue specimens were used. Visualized bone callus seen at the surgical site served as a control. 15 nonunion tissue samples of at least 6 months duration were compared to 15 matched site callus controls. The expression patterns of 45 different MMPs, ADAMTS, and TIMPs enzymes were determined in the nonunion/callus tissue using quantitative Real Time-PCR. The mean age of the patient cohort was 46 years (range 32-80). The anatomic sites involved included: 2 femoral shafts, 2 subtrochanteric femurs, 2 tibial shafts, 1 tibial plateau, 1 distal tibia, 2 fibular shafts, 3 mid shaft clavicles, 1 proximal humerus, and 1 ulnar shaft. Mean length of nonunion was determined to be 16 months. Comparison between both groups of tissue samples revealed significantly elevated concentrations of MMP-7, and MMP-12 in nonunion tissue when compared to normal callus ( $p < 0.01$ ). No correlation was found between the expression of these enzymes and other clinical parameters (i.e. patient smoking, use of a bone stimulator, number of previous surgeries, infection). Our findings indicate that nonunion tissue commonly expresses statistically significant levels of MMP-7 and MMP-12. The data suggests that these enzymes may play an integral role towards the development of a bone nonunion. These enzymes may likewise be used as biomarkers for the detection of a fracture nonunion in patients on one hand, and on the other hand they may be the potential therapeutic targets for development of novel treatments for bone fracture and nonunion.

**Disclosures:** C. Liu, None.

This study received funding from: OTA.

## M236

**Colistin-Impregnated Bone Cement Beads Prevent Multi-Drug Resistant *Acinetobacter* Osteomyelitis.** D. P. Crane<sup>\*1</sup>, K. Gromov<sup>\*1</sup>, C. K. Murray<sup>\*2</sup>, R. J. O'Keefe<sup>1</sup>, E. M. Schwarz<sup>1</sup>. <sup>1</sup>Orthopaedics, University of Rochester, Rochester, NY, USA, <sup>2</sup>Infectious Disease, Brooke Army Medical Center, Fort Sam Houston, San Antonio, TX, USA.

Current data of military operations in Iraq and Afghanistan demonstrate that the number of serious injuries greatly exceeds fatal casualties. Among these serious injuries, war wound infection and osteomyelitis (OM) appear to be of greatest concern, including multidrug-resistant (MDR) *Acinetobacter*. While *in vitro* studies have demonstrated that most *Acinetobacter* isolates are sensitive to colistin, bone void fillers containing this antibiotic are not available, and the high doses needed to treat some of the MDR strains cannot be achieved via parenteral administration. Thus, our goal was to develop a novel quantitative model of implant-associated *Acinetobacter* OM and evaluate the efficacy of parenteral colistin vs. colistin impregnated polymethylmethacrylate (PMMA) beads.

**Methods:** Six MDR strains of *Acinetobacter* were obtained from soldiers treated for OM at Brooke Army Medical Center. Over night cultures were used to contaminate insect pins that were surgically implanted transcorically through the tibial metaphysis of 6-8-week old C57B/6 mice. OM was assessed by longitudinal x-ray, micro-CT, histology and RTQ-PCR of the *parC* gene of *Acinetobacter* standardized to mouse *beta-actin*. In the efficacy study, mice (n=8 per group) were infected with the three most virulent strains and treated with parenteral colistinmethate (0.2mg i.m./day from day0-day7) or a 5mm PMMA bead containing 0 (bead control), 1 or 2mg of colistin sulfate and sacrificed on day 19. The data from the RTQ-PCR were used to determine the percentage of mice with OM in each group and the mean bacterial load in the infected tibiae in each group.

**Results:** The parenteral colistinmethate failed to protect the mice from OM as 70.8% of the mice were infected compared to 75% in the bead control group. However, the bead containing 1mg of colistin sulfate significantly reduced the infection rate down to 33.3% ( $p=0.004$  vs bead control). We also found that the colistin sulfate has a dose dependent effect on the bacterial load of the OM, as the mice with the 1mg bead had over ten times the number of *parC* genes per tibia compared to the 2mg group (423,300 +/- 214,700 vs. 41,160 +/- 25,870;  $p=0.02$ ).

**Conclusions:** These results demonstrate that implantation of colistin sulfate impregnated PMMA beads at the surgical site of an MDR *Acinetobacter* infection significantly prevents the establishment of OM. Further studies are warranted to see if a clinically relevant product can be made to treat war wound injuries associated with war in Iraq and Afghanistan.

**Disclosures:** D.P. Crane, None.

This study received funding from: US Dept. of Defense.

## M237

**Identification of a Novel Mutation (78dup27) of the *TNFRSF11A* Gene in a Chinese family with Early Onset Paget's Disease of Bone.** Z. Zhang, H. Zhang\*, W. Hu\*, J. He\*, J. Yu\*, J. Gu\*, G. Gao\*, Y. Hu\*, M. Li\*, Y. Liu\*, Y. Ke\*, W. Xiao\*, W. Fu\*. The Department of Osteoporosis, Osteoporosis Research Unit, Shanghai Jiao Tong University Affiliated Sixth People's Hospital, Shanghai, China.

Paget's disease of bone (PDB) is rare in China. Previous study showed affected individuals of early onset PDB from Japanese descent carried a 27-bp duplication at position 75 (75dup27) in *TNFRSF11A* gene. In here, we reported that a novel mutation (78dup27) in exon 1 of *TNFRSF11A* gene was identified in a Chinese unconsanguineous family with early onset PDB. Proposita of an unconsanguineous family and 3 affected familial individuals were admitted to our hospital because of deformity affecting the lower limbs and vertebral column with pain. Early onset PDB was diagnosed based on the clinical presentation with the characteristic of osteolysis and osteosclerosis with bone enlargement and deformity in their affected bones on x-ray, and elevated serum alkaline phosphatase levels. Genomic DNA was extracted from 4 affected individuals and 6 unaffected members in a Chinese family with early onset PDB. The entire coding region of the *TNFRSF11A* and *SOST* were amplified and sequenced directly. We did not find *SOST* gene mutations in proposita and her familial members. A novel 27-bp duplication in exon 1 (78dup27) in *TNFRSF11A* was found in four affected individuals and one unaffected individual. Although same 27-bp duplication, our mutation presented at bases 78-104, and on the protein level, this 78dup27 mutation resulted in nine amino acid insertions in the RANK signal peptide. However, the duplication of nine amino acids was LLLCALLA in our patients, rather than ALLLLCALL in affected individuals of Japanese family. The mutation was not detected in genomic DNA of 100 unrelated controls and five patients with sporadic PDB. The clinical findings in affected members of our family were similar to these bone presentations of previously reported early onset PDB of Japanese family, but different features were found in our patients. We presumed that the phenotypic differences between our affected subjects and Japanese early onset PDB were due to different sequence duplication. It is to be determined if it is a new typical form of PDB which is caused by a novel 78dup27 mutation in this familial PDB of Chinese descent.

**Disclosures:** Z. Zhang, None.

## M238

**Obesity Induced by High Dietary Fat Leads to Increased Bone Resorption Marker, TRAP, and Decreased Bone Mass in Mice.** J. J. Cao<sup>1</sup>, B. R. Gregoire<sup>\*1</sup>, H. Gao<sup>\*2</sup>. <sup>1</sup>USDA/ARS, GFHNR, Grand Forks, ND, USA, <sup>2</sup>Department of Biochemistry and Molecular Biology, University of North Dakota, Grand Forks, ND, USA.

Obesity, which is growing in prevalence, is a risk factor for such chronic health disorders as diabetes and cardiovascular diseases. However, it is thought to be a protective factor for osteoporosis and bone fractures in humans. Accumulating data in humans suggest that fat mass has a negative effect on bone when the confounding factor, mechanical loading of body weight in obesity, was removed. Furthermore, obesity is associated with the chronic up-regulation of inflammatory cytokines such as TNF- $\alpha$ , IL-1 $\beta$ , IL-6, and IL-7. These cytokines have been shown to be capable of stimulating osteoclast activity and bone resorption through regulating the RANKL/RANK/OPG pathway.

To determine how dietary fat might affect bone metabolism, we examined *in vitro* bone formation, blood markers of bone homeostasis, and bone structure in male C57BL/6 mice fed either a high-fat diet (HFD, 45% kcal as fat) or a normal fat control diet (NFD, 10%) for 14 weeks starting at 6 wk of age. Cancellous bone volume/total volume ratio decreased ( $P < 0.05$ ) in mice fed the HFD despite a greater average body weight (10 g) than those fed the NFD ( $P < 0.01$ ). Compared with mice fed the NFD, the numbers of colony forming units (CFU)-fibroblastic and CFU-alkaline phosphatase positive at d 14 and mineralization nodule at d 28 were higher in bone marrow stromal cells from mice fed the HFD. Serum osteocalcin was lower ( $P < 0.05$ ) with HFD as compared to NFD (71.2 $\pm$ 11.7 vs 53.4 $\pm$ 17.0 for NFD and HFD groups, respectively). Serum TRAP and OPG levels were higher in the HFD mice when compared to the NFD mice (TRAP: 1.74 $\pm$ 0.33 vs 2.54 $\pm$ 1.03 U/L; OPG: 1.39 $\pm$ 0.58 vs 2.81 $\pm$ 2.09 ng/ml, for NFD and HFD diet respectively). No significant differences were observed between the two groups for serum RANKL (3.07 $\pm$ 2.30 vs 3.87 $\pm$ 2.52 nmol/ml for NFD and HFD, respectively).

**Disclosures:** J.J. Cao, None.

## M239

**Bone Metabolism, Micro-architecture and Densitometric Measurement in Rat Femur after Chronic Alcohol Consumption.** D. B. Maurel<sup>\*1</sup>, G. Y. Rochefort<sup>\*1</sup>, N. Boisseau<sup>\*2</sup>, E. Lespessailles<sup>1</sup>, C. L. Benhamou<sup>1</sup>, C. Jaffre<sup>\*1</sup>.

<sup>1</sup>Rheumatology, INSERM U658, IPROS, CHR Orleans, Orleans, France, <sup>2</sup>Sport Sciences Faculty, LAPHAP, EA 3813, Poitiers, France.

It is well documented that chronic alcohol consumption weakens bone tissue, by decreasing bone density, and bone mineral content. Our objective has been to characterize bone micro architecture after alcohol consumption in rats. We have used a rat model that reproduces the human drinking pattern by separating food and beverage and by adding alcohol (20% v/v) into the drinking tap water (*ad libitum*). Forty eight male Wistar rats (8-

week-old) were randomly divided into four groups: Controls, Alcohol, Exercise and Alcohol-Exercise. Femoral bone mineral density (BMD) and content (BMC) were assessed by DXA (Discovery, Hologic, USA) at baseline and two months later. DXA has previously been validated on murine models in our lab. The femoral metaphysis micro-architecture was studied *post-mortem* by microCT (micro-scanner 1072, Skyscan, Belgium). Results are presented in table below. We observed no significant difference in BMD and BMC between groups. However, some micro architecture parameters were significantly different between groups as revealed by microCT: the Alcohol-Exercise group exhibited a lower percentage of bone in the entire sample (BV/TV) compared to both Controls and Alcohol groups. Both alcohol and exercise increased bone resorption (higher CTx concentrations vs. control), whereas exercise alone increased bone formation (higher osteocalcin concentrations in both exercise and alcohol-exercise groups vs. alcohol group). Alcohol alone decreased bone formation. In conclusion, a 20% (v/v) alcohol consumption seems to elicit a bone turnover change, with a bone resorption increase and bone formation decrease. A higher alcohol dose must be envisaged to better investigate the effects of alcohol with and without exercise.

(Mean +/- SD)	Controls (n=10)	Alcohol (n=10)	Exercise (n=8)	Alcohol-Exercise (n=10)
Weight gain (g)	249.2 +/- 24.8	183.9 +/- 37.6	208.5 +/- 40.3	211.7 +/- 31.0
Lean mass evolution (%)	40.0 +/- 6.1	29.4 +/- 6.5	38.1 +/- 6.3	38.5 +/- 6.6
BV/TV (%)	64.8 +/- 3.5	63.9 +/- 7.3	62.7 +/- 7.9	57.2 +/- 4.7
Osteocalcin (ng/mL)	1.46 +/- 0.07	1.40 +/- 0.08	1.49 +/- 0.07	1.50 +/- 0.11
CTx (ng/mL)	49.0 +/- 32.6	101.4 +/- 20.8	127.7 +/- 16.4	143.4 +/- 13.4

**Disclosures:** D.B. Maurel, None.

## M240

**A Morquio Syndrome Variant: Two siblings with Atypical Phenotype and Novel Compound Heterozygosity.** W. A. Baratela<sup>\*1</sup>, M. B. Bober<sup>2</sup>, S. Tomatsu<sup>\*3</sup>, W. Mackenzie<sup>\*4</sup>, L. Nicholson<sup>\*2</sup>, C. I. Scott<sup>\*2</sup>. <sup>1</sup>Setor de Genética Médica, Hospital das Clínicas de Ribeirão Preto - FMRP, Universidade de São Paulo, São Paulo, Brazil, <sup>2</sup>Division of Medical Genetics, AI duPont Hospital for Children, Wilmington, DE, USA, <sup>3</sup>Department of Pediatrics, St. Louis University, St. Louis, MO, USA, <sup>4</sup>Department of Orthopedics, AI duPont Hospital for Children, Wilmington, DE, USA.

Mucopolysaccharidosis type IVA (MPS IVA) or Morquio A syndrome is an autosomal recessively inherited lysosomal storage disease caused by a deficiency of the N-acetylgalactosamine-6-sulfate sulfatase (GALNS) enzyme with the resultant urinary excretion of keratan sulfate (KS). The classic form of Morquio syndrome is characterized by a progressive spondyloepiphyseal dysplasia (SED) and associated disproportionate short stature of short trunk type. Typical adult heights are 80-120 cm with the final height being reached prior to puberty. Orthopedic complications typically include odontoid hypoplasia with C1-C2 instability, genu valgus. Marked ligamentous laxity is typical as are soft tissue accumulation of GALNS substrate leading to corneal clouding and cardiac valvular disease.

We describe a brother and his younger sister born to non-consanguineous parents with compound heterozygosity for p.R61W and c.498delC mutations in the GALNS gene. Neither of these mutations had been described before. GALNS fibroblast activity from the older brother activity revealed activity 10-15% of control fibroblasts. This is substantially higher than is seen in classic Morquio patients. Clinically, the older brother was initially diagnosed with an unclassified (SED) at the 9 years of age. At that time, his height was 129.7 cm (~25th%ile), but his arm span exceeded his height by 10.5 cm. Thoraco-lumbar platyspondyly was noted as was odontoid hypoplasia without instability. Epiphyseal changes were present throughout. Genu valgus was also present. Ophthalmologic evaluation revealed corneal clouding and a storage disease was considered. Initial urine screening studies showed elevated keratan sulfate and further biochemical and molecular studies confirmed the abnormality in GALNS. Following this discovery the younger sister was studied and found to have the same Morquio variant. At the age of 8 she was 123.2 cm (~25th%ile) with an arm span of 125.6. Mild corneal clouding was seen. Growth in both of these children ceased before puberty and the final adult heights were 150.0 cm (height age 12.5 years) in the brother and 142.8 cm (height age 11years) in the sister. Neither of these children have exhibited cardiac valvular abnormalities. Both of them are obese and have had surgery to correct genu valgus. Psychiatric and learning problems are present in the brother.

**Disclosures:** M.B. Bober, None.

## M241

**Gene Transcripts Related to T-cell Activation, Proliferation, and Cytokine Signaling Show Significant Effects on BMD Variation in Baboons.** L. M. Havill<sup>1</sup>, A. Vinson<sup>\*1</sup>, J. Blangero<sup>\*1</sup>, J. E. Curran<sup>\*1</sup>, M. P. Johnson<sup>\*1</sup>, O. S. Platt<sup>\*2</sup>, C. Brugnara<sup>\*2</sup>, M. C. Mahaney<sup>\*1</sup>. <sup>1</sup>Genetics, Southwest Foundation for Biomedical Research, San Antonio, TX, USA, <sup>2</sup>Laboratory Medicine, Harvard University, Cambridge, MA, USA.

Interplay between the skeletal and immune systems is receiving increasing attention among researchers of bone metabolism as the extent and importance of osteoimmunological crosstalk to bone health becomes apparent. Research shows that many genes important to immune system function also play extremely influential roles in regulation of bone metabolism. Increasing evidence implicates T-cell mediated regulation of bone metabolism. The fact that activated T-cells of the express a key osteoclast

differentiation factor (TRANCE) demonstrates that normal immune cell function can affect bone homeostasis. To further characterize the nature of the relationship between T-cells and bone metabolism, we examined the effect of elements of a network of genes consisting of 57 gene transcripts related to t-cell activation, proliferation, and cytokine signaling on variation in bone mineral density (BMD). We used the Illumina Human Sentrix-6 BeadChip microarray system to measure mRNA levels in lymphocytes from 495 pedigreed baboons. Heritability of expression level was demonstrated for each of the 57 transcripts in a previous study in these baboons. We regressed forearm BMD of the radius shaft, ulna shaft, and ultradistal radius against the level of expression of each individual transcript to assess the degree to which variation in expression levels accounted for BMD variation. Five transcripts, NFKC, FYN, IRF1, IL-27R alpha, and LT alpha showed statistically significant (using a p<0.05) covariate effects on variation in forearm BMD. Each of these transcripts accounts for approximately 1% of the variation in BMD as measured at the radius shaft, ulna shaft, and ultradistal radius. The association of these transcripts related to BMD, an indicator of bone health that represents a lifetime of bone formation and resorption events, provides further support for the role of activated T-cells in bone metabolism.

**Disclosures:** L.M. Havill, None.

## M242

**Mecp2 Null Mice Display Multiple Skeletal Abnormalities.** R. D. O'Connor<sup>1</sup>, M. Zayzafoon<sup>2</sup>, M. C. Farach-Carson<sup>1</sup>, N. C. Schanen<sup>3</sup>. <sup>1</sup>Department of Biological Sciences, University of Delaware, Newark, DE, USA, <sup>2</sup>Department of Pathology, University of Alabama at Birmingham, Birmingham, AL, USA, <sup>3</sup>Laboratory for Human Genetics, Nemours/A.I. duPont Hospital for Children, Wilmington, DE, USA.

Rett Syndrome (RTT), a neurodevelopmental disorder, is most often caused by inactivating mutations in the X-linked gene encoding a regulator of epigenetic gene expression, methyl CpG binding protein, MeCP2. Clinical data show that, along with neurological defects, females with RTT frequently have marked decreases in Bone Mineral Density (BMD) beyond that expected from disuse atrophy. Our work with a Mecp2 null mouse model, *Mecp2*<sup>-yBIRD</sup>, reveals a difference between the wild-type and null mice, with the *Mecp2*<sup>-yBIRD</sup> mice having significantly shorter femurs and an overall reduced skeletal size. Histological studies have highlighted a shortened growth plate as well as decreased trabecular bone in the primary spongiosum of Mecp2 null femurs by 21 days of age, prior to the onset of neurological symptoms. Additionally, the trabeculae in the primary spongiosum of 60 day old *Mecp2*<sup>-yBIRD</sup> mice were abnormally shaped and hypercellularity was noted in the marrow space. Both histological and histomorphometrical analyses have shown reductions in the cortical bone parameters of Mecp2 null mice. It does not appear that these decreases in bone are owed to a primary effect on osteoclasts, as osteoclast numbers were comparable between wild-type and null animals. Also of note, serum calcium and phosphate levels were unchanged in *Mecp2*<sup>-yBIRD</sup> mice, consistent with that seen clinically in RTT patients. We speculate that Mecp2 deficiency leads to a primary dysregulation of genes critical for regulation of bone growth, differentiation and mineral homeostasis. Several genes essential to proper bone formation and maintenance of bone and calcium homeostasis have been identified as likely targets of Mecp2 in a differentiating osteoblast cell system. Current studies are underway to determine the functional significance of Mecp2 deficiency on candidate gene expression and function in osteoblastic cells.

**Disclosures:** R.D. O'Connor, None.

This study received funding from: Nemours, NIH P20 RR016458-06, and NIH P20 RR020173-04.

## M243

**Hypoxia Promotes Ligand-independent Activation of the ACVR1 (R206H) Mutant Receptor in C2C12 Cells.** H. Wang<sup>\*1</sup>, E. M. Shore<sup>1</sup>, F. S. Kaplan<sup>1</sup>, J. Groppe<sup>\*2</sup>, R. J. Pignolo<sup>1</sup>. <sup>1</sup>Department of Orthopaedic Surgery, University of Pennsylvania, Philadelphia, PA, USA, <sup>2</sup>Department of Biomedical Sciences, Texas A&M University Health Science Center, Dallas, TX, USA.

Fibrodysplasia ossificans progressiva (FOP) is a rare, autosomal dominant disorder of connective tissue that leads to progressive, disabling heterotopic ossification. A recurrent mutation in activin receptor IA/activin-like kinase 2 (ACVR1/ALK2) replaces an evolutionarily conserved arginine with histidine at residue 206 in all sporadic and familial cases of classic FOP. Protein modeling predicts that substitution with histidine, and only histidine, creates a pH-sensitive switch within the activation domain of the receptor that leads to ligand-independent activation of ACVR1. Clinically, a local hypoxic tissue microenvironment caused by trauma or minor injury could promote such signaling through the mutant ACVR1 receptor in FOP patients. Thus, we tested the hypothesis that low pO<sub>2</sub> can enhance ligand-independent activation of the mutant ACVR1 receptor. We performed transient transfections of the wild-type and mutant (FOP) ACVR1 receptor in the mouse myoblast cell line C2C12, which undergoes osteoblast differentiation in response to BMPs. We observed that ligand-independent activation of mutant ACVR1, including Smad 1/5/8 phosphorylation and inhibitor of differentiation 1 (ID1) expression, was enhanced under hypoxic conditions (1% or 5% O<sub>2</sub>) compared to ambient O<sub>2</sub> (normoxia or 21% O<sub>2</sub>). These studies provide the first evidence that hypoxia may be an important mediator of ACVR1 (R206H) activation in FOP, with important clinical implications for early lesion formation.

**Disclosures:** H. Wang, None.

## M244

**Common Genetic Factors Contribute to the Relationship of Body Composition and Bone Mass in Mouse Populations.** R. Li\*, P. C. Reifsnyder\*, B. L. King\*, L. B. Donahue, E. H. Leiter\*, G. A. Churchill\*. The Jackson Lab, Bar Harbor, ME, USA.

Osteoporosis and obesity, two disorders in body components, are growing in prevalence. Genetic studies for bone mineral density (BMD) and bone geometry in humans and mice are confronted with challenges because of the influence of body composition and many other confounders such as sex, age, and diet. In this study we will introduce a new multi-gene and multi-variable analytic approach to model the relationship between body composition and bone traits. Evidence of genetic studies from two mouse populations, C57BL/6J x DBA/2J intercross and NOD x 129.H2<sup>67</sup> backcross, shows that there are common QTLs for lean mass, fat mass, and bone mineral density. The parental strains C57BL/6J and DBA/2J show remarkable differences in body composition in response to a high-fat diet. The NOD strain has fragile bones. Strain 129.H2<sup>67</sup> is an MHC (Major Histocompatibility) congenic stock with normal bones. Linkage analysis indicates that one QTL on Chr 2 (with a LOD score peak at 164 Mb) affects both subcutaneous fat pad mass and BMD in the first intercross with 111 female mice on a high-fat diet. We also identified a QTL on Chr 3 (with a peak at 140 Mb) affecting lean mass, fat mass, and BMD in the second cross with 310 female mice on a standard chow diet. In addition, the Chr 3 QTL interacts with another QTL on Chr 15 (with a peak at 96 Mb) and this interaction has a significant effect on both fat mass and plasma leptin levels. Genome-wide gene expression profiling data and protein-protein interaction databases have shown promise to help identify the underlying candidate genes involved in the muscle-fat-bone system. We plan to expand these models to additional mouse strains and intercrosses, as well as human populations.

**Key words:** body composition, bone mineral density, gene interaction

**Disclosures:** R. Li, None.

## M245

**Phased Genome-Wide Association Study Identifies Probable New Gene Affecting Bone Mineral Density.** E. L. Duncan<sup>1</sup>, K. Addison<sup>\*1</sup>, M. Brugmans<sup>\*1</sup>, D. Irwin<sup>\*2</sup>, D. Evans<sup>\*3</sup>, J. Eisman<sup>4</sup>, G. Jones<sup>5</sup>, G. Nicholson<sup>6</sup>, R. Prince<sup>7</sup>, E. Seeman<sup>6</sup>, A. G. Uitterlinden<sup>8</sup>, J. Wark<sup>6</sup>, S. Ralston<sup>9</sup>, M. A. Brown<sup>1</sup>.

<sup>1</sup>Diamantina Institute, Brisbane, Australia, <sup>2</sup>Sequenom inc., Brisbane, Australia, <sup>3</sup>University of Bristol, Bristol, United Kingdom, <sup>4</sup>Garvan Institute of Medical Research, Sydney, Australia, <sup>5</sup>Menzies Research Institute, Hobart, Australia, <sup>6</sup>University of Melbourne, Victoria, Australia, <sup>7</sup>University of Western Australia, Perth, Australia, <sup>8</sup>Erasmus MC, Rotterdam, Netherlands, <sup>9</sup>FAMOS consortium, University of Edinburgh, Edinburgh, United Kingdom.

Genomewide association studies (GWAS) are a powerful method for identifying genes of small to moderate effect involved in common heritable diseases.

A phase 1 GWAS was performed in an Australian and UK cohort of postmenopausal female probands (age 50-85 years) with extreme truncate selection for FN BMD (1.5<|z-score|<4), with 317,000 SNPs genotyped using Illumina HumanHap300 chips. 130 SNPs, selected for further study based on the initial results, were genotyped in families selected from the FAMOS cohort (proband FN or LS BMD z-score <-1, n=429 families including 1286 individuals) using Sequenom MALDI-TOF technology. PLINK was used to test association in the GWA component, and QTDT to test total association controlling for linkage in the confirmation family study. For a range of different genetic models, the phase 1 component of 140 subjects has equivalent power to a cohort study of 850-920 unselected individuals. Overall genotyping success rate was 99.6% in phase 1 and 93.1% in phase 2. No gene achieved genomewide statistical significance in the phase 1 screen (as expected due to small sample size). However, 31 markers achieved p-values of 10<sup>-5</sup> to 10<sup>-7</sup>. One SNP, rs10904952, was associated with FN BMD in both phase 1 (P=0.0021) and phase 2 (P=0.00072) studies. Combining these findings, the overall level of significance for this SNP is 4.86x10<sup>-6</sup>. This SNP lies in the gene encoding ST8 alpha-n-acetyl-neuraminide alpha-2,8-sialyltransferase 6 (ST8SIA6), a protein that interacts with fetuin-alpha, which controls apatite formation and bone and tissue mineralisation. Four other SNPs lying in ST8SIA6 were associated with FN BMD with p-values of 0.0078-0.00048 in the phase 1 study.

This study suggests that polymorphisms of ST8SIA6 influence FN BMD in the general population. Whilst the finding did not achieve genomewide significance in the discovery cohort, association was confirmed in the replication cohort, despite modest study power. A much larger cohort of cases with extreme high and low BMD is being recruited for further studies. If confirmed, ST8SIA6 represents a novel gene associated with BMD. The mechanism underlying the association and its effect on fracture risk have yet to be determined.

**Disclosures:** E.L. Duncan, None.

## M246

**Screening the PHEX Gene in a Large Cohort of Hypophosphatemic Rickets Allowed the Description of a Missense Mutation not Responsible for the Disease on a Highly Conserve Amino Acid Residue.** C. Gaucher\*, O. Walrant-Debray\*, M. Nguyen\*, M. Garabedian\*, F. Jehan. Inserm U561, Paris, France.

Mutations responsible for hypophosphatemic rickets have been mostly found in the PHEX gene and 193 different mutations have been so far described in the PHEX database (www.phexdb.mcgill.ca). We have screened the 22 exons of the PHEX gene, by PCR amplification followed by sequencing, in a large cohort of 140 hypophosphatemic patients (97 families) selected on the following criteria: rickets with bone deformities, low serum phosphate with urinary phosphate wasting, normal PTH levels and hypocalciuria. PHEX mutations were found in 79 of the 97 probands (81%), representing 76 different mutations, 43 being de novo mutations (not found in the parents' probands), and 59 mutations not being reported in the PHEX database. PHEX mutations were not found in 18 probands, including 13 sporadic cases (23 % of total sporadic cases), one of whom with oncogenic hypophosphatemia, and 5 familial cases with dominant inheritance (12 % of total familial cases), one of whom bearing an activating FGF23 mutation.

Like in the PHEX database, missense mutations were found in 20% of the probands (n=16). Interestingly, two probands bore 2 distinct mutations, the first one on different exons (a splice site mutation near exon 18, c.1899+1 g>a, and a missense mutation A653D on exon 19), the second one on the same exon (a T deletion on c.538 and a missense mutation V169M on exon 5). Clinical and genetic analysis of all healthy and affected members of the latter family (3 generations) showed segregation of the two mutations on the same allele of exon 5, the T deletion appearing at generation 2. Only the T deletion, and not the V169M mutation, was associated with hypophosphatemia.

In conclusion, PHEX mutations are found in 8 out of 10 patients with hypophosphatemic rickets, normal PTH and hypocalciuria, even in sporadic cases. Findings of missense mutations, even at a very conserved amino acid, may not cause the disease and requires complete exploration of the entire coding sequence.

**Disclosures:** F. Jehan, None.

## M247

**An Integrative Genetics Approach to Identify Candidate Genes Regulating Bone Density: Combining Linkage, Gene Expression and Association.** C. R. Farber<sup>1</sup>, A. van Nas<sup>\*2</sup>, A. Ghazalpour<sup>\*1</sup>, J. E. Aten<sup>\*2</sup>, S. Doss<sup>\*1</sup>, B. Sos<sup>\*1</sup>, E. E. Schadt<sup>\*3</sup>, L. Ingram-Drake<sup>\*2</sup>, R. C. Davis<sup>\*2</sup>, S. Horvath<sup>\*2</sup>, D. J. Smith<sup>\*4</sup>, T. A. Drake<sup>\*5</sup>, A. J. Lusis<sup>\*1</sup>.

<sup>1</sup>Department of Medicine, David Geffen School of Medicine at University of California, Los Angeles, CA, USA, <sup>2</sup>Department of Human Genetics, David Geffen School of Medicine at University of California, Los Angeles, CA, USA, <sup>3</sup>Rosetta Inpharmatics/Merck, Inc., Seattle, WA, USA, <sup>4</sup>Molecular and Medical Pharmacology, David Geffen School of Medicine at University of California, Los Angeles, CA, USA, <sup>5</sup>Department of Pathology and Laboratory Medicine, David Geffen School of Medicine at University of California, Los Angeles, CA, USA.

Numerous quantitative trait loci (QTL) affecting bone traits have been identified in the mouse. However, few of the underlying genes have been discovered. To improve the process of transitioning from QTL to gene we describe an integrative genetics approach, which combines traditional linkage analysis, DNA microarray expression profiling and genetic association in outbred mice. In C57BL/6J and C3H/HeJ (BXH) F2 mice, QTL affecting bone mineral density (BMD) were identified using marker regression. To identify candidate genes, transcripts regulated by local expression QTL (eQTL) were identified using linkage analysis of microarray-generated gene expression profiles in individual F2 mice. Causal relationships between genes with local eQTL and BMD were predicted using network edge orienting (NEO), a recently developed R function for causality modeling. In order to fine-map QTL, regions regulating BMD in BXH mice were tested for association in outbred MF1 mice using ANOVA. Nine QTL regulating BMD were identified, three of which displayed male-biased expression. Additionally, 148 genes, located within BMD QTL support intervals, were correlated with BMD and regulated by local eQTL. Causal relationships for 18 of these genes and BMD were predicted using NEO. Integrating linkage, eQTL analysis, dense SNP maps, causality modeling and genetic association in outbred MF1 mice provided strong support for *Wnt9a*, *Rasd1* or both underlying *Bmd11*. Integration of multiple genetic and genomic data sets can substantially improve the efficiency of QTL fine-mapping and candidate gene identification.

**Disclosures:** C.R. Farber, None.

This study received funding from: a NIH Program Project Grant (HL28481) to AJL. CRF was supported by a Ruth L. Kirschstein NIH F32 Fellowship (SF32DK074317).

## M248

**Craniofacial Gene Discovery in Mice.** L. Donahue, M. Curtain\*, J. Hurd\*, C. Marden\*, S. Murray\*. The Jackson Laboratory, Bar Harbor, ME, USA.

The purpose of the Craniofacial Resource (CR) at The Jackson Laboratory (TJL) is to identify and characterize craniofacial disorders in mice that are potential genetic and physiological models for human craniofacial dysmorphologies and to share these models with the scientific public. We screen for spontaneous and induced mutations resulting in abnormal clinical presentations, do comprehensive genetic and characterization studies, and

identify gene mutations by candidate gene testing and positional cloning. We provide notification of new models via our website: <http://craniofacial.jax.org/>, offer information and training via our email: [faces@jax.org](mailto:faces@jax.org), and distribute live mice to investigators worldwide. We are currently seeking collaborations to exploit the collection of mutants we are holding and welcome inquiries for mutants at all stages of development.

We have tested the heritability and penetrance of over 200 craniofacial phenodeviants and found 50 with transmissible traits of acceptable penetrance. Mutant strains carrying these abnormal craniofacial phenotypes are at various stages of genetic and phenotypic development. We have new spontaneous models for: crystallin, alpha A (*Cryaa*); sclerostin domain containing 1 (*Sostdc1*); aristaless 4 (*Alx4*), and lamin A (*Lmna*), plus 3 remutations to bone morphogenetic protein 5 (*Bmp5*). A chromosomal location has been identified for 15 additional mutant strains (Chromosomes 2, 3, 4, 5, 7, 8, 11, 12, 13, 14, 19); mapping is underway for 17 strains, and heritability testing is being done for the remaining phenodeviants. Phenotypes include: cleft lip; abnormal ear pinnae shape, size, and placement; shortened snouts; shortened, domed and asymmetrical skulls; abnormal dentition; abnormal eye morphology, and deafness. Many deviants have more than one phenotype, and are potential models of human craniofacial syndromes. Recently, we have begun to test apparently dominant phenotypes for recessive expression during embryogenesis and have discovered several extremely interesting models of cleft palate and other facial dysmorphologies. We are keenly interested in working with experts in each of these areas to take full advantage of the opportunity represented by these new models.

Craniofacial dysmorphologies represent nearly 75% of all human congenital malformations visible in newborns and are a complication in over 700 known human genetic syndromes. Gene discovery in humans is difficult due to population heterogeneity and to the diversity of interacting environmental and nutritional variables. Consequently, animal models with defined genetic backgrounds maintained in controlled environments are critical for craniofacial gene discovery.

**Disclosures:** L. Donahue, None.

This study received funding from: NIH, NAEC, EY015073.

## M249

**Bivariate Whole Genome Linkage Analysis of Femoral Bone Geometric Traits and Leg Lean Mass: the Framingham Study.** D. Karasik<sup>1</sup>, Y. Zhou<sup>\*2</sup>, L. A. Cupples<sup>\*2</sup>, D. P. Kiel<sup>1</sup>, S. Demissie<sup>\*2</sup>. <sup>1</sup>IFAR, Hebrew SeniorLife, Harvard SM, Boston, MA, USA, <sup>2</sup>Dept Biostats, BUSPH, Boston, MA, USA.

The risk of osteoporotic fracture is a function of loading conditions and the ability of the bone to withstand load. Both spatial distribution of bone tissue and applied muscle mass are important contributors to fracture risk. DXA non-invasively measures leg lean mass (LLM) as well as femoral bone geometry (BG). Both LLM and BG are known to have a substantial genetic component. Therefore, we estimated shared heritability and performed linkage analysis to identify chromosomal regions governing both LLM and BG.

A genome-wide scan (with a set of 636 genome-wide markers with an average marker spacing of 5.7 cM) was performed on 1,362 adult individuals from 321 extended families of the Framingham study. DXA was used to measure LLM; femoral neck length (FNL), neck-shaft angle (NSA), as well as subperiosteal width (Wid), cross-sectional bone area (CSA), and section modulus (Z) were measured at the narrowest section of the femoral neck (NN) and shaft (S) regions.

Variance component analysis was performed on normalized residuals (adjusted for age, age<sup>2</sup>, height, BMI, and estrogen status/menopause in women) using SOLAR. The analysis provided substantial heritability for leg lean mass ( $h^2 = 0.42 \pm 0.07$ ). Heritability was also significant for all BG traits, ranging from 0.28 (NSA) to 0.63 (S\_Wid). Phenotypic correlations between covariate-adjusted LLM and BG phenotypes ranged from low (0.038 with NSA,  $p > 0.05$ ) to substantial (0.285 with S\_Z,  $p < 0.001$ ). Genetic correlations ( $\rho_g$ ) between covariate-adjusted LLM ranged from 0.113 (NSA,  $p > 0.05$ ) to 0.603 (S\_Z,  $p < 0.001$ ). Environmental correlations ( $\rho_e$ ) between LLM and some geometric traits were lower than  $\rho_g$ . Notably, an alternative adjustment for leg fat did not change correlation estimates. Univariate linkage analysis of adjusted LLM identified no chromosomal regions with LOD scores  $\geq 2.0$ ; bivariate analysis identified two QTLs with LOD scores  $> 3.0$ , shared by LLM with S\_CSA on chr. 12p12.3-p13.2, and with NSA, on 14q21.3-q22.1.

In conclusion, we identified chromosomal regions potentially linked to both leg lean mass and femoral bone geometry. Identification and subsequent characterization of these shared loci may further elucidate the genetic contributions to both osteoporosis and sarcopenia.

**Disclosures:** D. Karasik, None.

This study received funding from: R01-AR050066; R01-AR/AG 41398.

## M250

**Genetic Locus on Chromosome 1q Influences Bone Loss in Young Mexican American Adults.** J. R. Shaffer<sup>1</sup>, C. M. Kammerer<sup>1</sup>, J. M. Bruder<sup>2</sup>, S. A. Cole<sup>\*3</sup>, T. D. Dyer<sup>\*3</sup>, L. Almasy<sup>\*3</sup>, J. W. MacCluer<sup>\*3</sup>, J. Blangero<sup>\*3</sup>, R. L. Bauer<sup>\*2</sup>, B. D. Mitchell<sup>4</sup>. <sup>1</sup>Department of Human Genetics, University of Pittsburgh, Pittsburgh, PA, USA, <sup>2</sup>University of Texas Health Science Center, San Antonio, TX, USA, <sup>3</sup>Southwest Foundation for Biomedical Research, San Antonio, TX, USA, <sup>4</sup>Division of Endocrinology, Diabetes and Nutrition, University of Maryland School of Medicine, Baltimore, MD, USA.

Bone loss over the lifespan, eventually leading to low bone mineral density (BMD), is one of the major determinants of risk for osteoporosis. Most research has focused on BMD change in older individuals, however, substantial bone loss begins as early as the third decade and the factors affecting early adult bone loss are largely unknown. We investigated the influences of genes and environment on rate of BMD change in young adult participants of the San Antonio Family Osteoporosis Study.

Rate of BMD change, calculated from DXA measurements at two time points, 5.6 years apart, was analyzed in 300 Mexican Americans (ages 25-45 years) from 32 extended families. Family-based likelihood methods were used to estimate heritability ( $h^2$ , the proportion of trait variance due to genes) and perform genome-wide linkage analysis (using 460 genetic markers at 7.6 cM resolution) for BMD change of the proximal femur, while simultaneously adjusting for the effects of sex, baseline BMD, weight, interim change in weight, and interim menopause.

Rate of early adult BMD change was significantly heritable for the total hip ( $h^2 = 0.34$ ,  $p = 0.01$ ) and modestly heritable for the femoral neck ( $h^2 = 0.22$ ,  $p = 0.06$ ). Endogenous environmental covariates accounted for 16% and 24% of total hip and femoral neck variation, respectively. A genetic locus influencing early adult bone loss of the femoral neck was observed on chromosome 1q23 (LOD = 3.6,  $p = 0.00002$ ).

In conclusion, we observed that change in hip BMD in young adults was heritable, and performed one of the first linkage studies for BMD change. Evidence of linkage to chromosome 1q23 suggests this region may harbor one or more genes involved in regulating early bone loss of the femoral neck. Discovery of such genes could lead to new biological targets for the treatment of osteoporosis, and/or the identification of persons at risk who may benefit from preventative interventions.

**Disclosures:** J.R. Shaffer, None.

## M251

**Familial Humeraloradioulnar Synostosis Maps to Chromosome 7p15.** J. Jeong<sup>\*</sup>, I. Jeon<sup>\*</sup>, S. Choi<sup>\*</sup>, H. Kim<sup>\*</sup>, M. Han<sup>\*</sup>, K. Lim<sup>\*</sup>, S. Kim, U. Kim<sup>\*</sup>, J. Choi<sup>\*</sup>. Biochemistry & Cell Biology, Skeletal Diseases Genome Research Center, Kyungpook Natl. Univ. School of Medicine, Daegu, Republic of Korea.

Congenital bilateral humeraloradioulnar fusion of the elbow is rare. We found a rare familial humeraloradioulnar synostosis affecting the elbow and forearm among Koreans. To identify the gene causing this disorder, we have performed whole genome-wide linkage scan by 403 microsatellite markers with an average spacing of 10 cM from 16 out of 32 members in the family of whom DNA samples are available. We calculated the pairwise and multipoint LOD scores of these markers for both dominant and recessive models. The analysis with dominant model indicated LOD score of 2.3 at marker GGAA3F06 ( $\theta = 0.00$ ) on the short arm of chromosome 7. Fine mapping in the region of chromosome 7p15 with 17 microsatellite markers narrowed down the candidate region from 17 cM to 10 cM. This study provides a map location for isolation of a gene causing familial humeraloradioulnar synostosis. Also, it will aid future identification of the responsible gene, which will be useful for the understanding of the molecular mechanism of humeraloradioulnar synostosis.

**Disclosures:** J. Choi, None.

## M252

**Defining Epistasis in a Double Congenic Mouse: Implications for the Skeleton.** V. E. DeMambro, K. L. Shultz, J. A. Maynard<sup>\*</sup>, C. L. Ackert-Bicknell, W. G. Beamer, G. A. Churchill<sup>\*</sup>, C. J. Rosen. The Jackson Laboratory, Bar Harbor, ME, USA.

We have previously identified several QTLs for BMD and IGF-1 utilizing C57BL/6J X C3H/HeSnJ (B6 X C3H) F2 progeny. The strongest QTL for lowering IGF-1 was located on Chr 6 and analyses of the original cross showed an interacting locus on Chr 11. This interaction suggested that when there were fixed *c3* alleles on Chr 6 and heterozygous *c3* alleles on 11, then the lower IGF-1/BMD phenotype could be rescued. To test this interaction, we took the previously characterized B6.C3-6T mouse which has a 20% reduction in IGF-1, reduced bone mass, impaired osteoblast differentiation, and enhanced marrow and hepatic adiposity; and mated them to our B6.C3-11 congenic mouse. Once the alleles on Chr 6 were fixed for *c3* we then phenotyped and compared male mice carrying either the *b6* or *c3* alleles on Chr 11, by PIX1, pQCT, MicroCT and for serum IGF-1 levels. Mice Carrying the *c3c3* alleles on Chr 11 at 8wks of age had increased IGF-1 levels (*b6b6* =  $248 \pm 4$ , *c3c3* =  $273 \pm 7$ ;  $p = .004$ ) and increased whole body aBMD (*b6b6* =  $248 \pm 4$ , *c3c3* =  $273 \pm 7$ ;  $p = .004$ ) vs. *b6b6* mice. At 16 weeks of age *c3c3* mice had increased femur length (*b6b6* =  $15.6 \pm .05$ , *c3c3* =  $16.2 \pm .05$ ;  $p < .0001$ ), as well as increased total femur vBMD (*b6b6* =  $.592 \pm .005$ , *c3c3* =  $.612 \pm .008$ ;  $p = .02$ ) and cortical thickness (*b6b6* =  $.185 \pm .002$ , *c3c3* =  $.195 \pm .002$ ;  $p = .002$ ) as measured by pQCT. MicroCT of the distal femur revealed increased BV/TV (*b6b6* =  $.147 \pm .009$ , vs *c3c3* =  $.202 \pm .010$ ;  $p = .0007$ ) in *c3c3* mice which is attributable to increases in both trabecular # (*b6b6* =  $5.2 \pm .1$ , *c3c3* =  $5.7 \pm .1$ ;  $p = .002$ ) and thickness (*b6b6* =  $.047 \pm .001$ , *c3c3* =  $.053 \pm .002$ ;  $p = .001$ ). Thus there is an interaction between Chr 6 and 11 such that when *c3* alleles are present on the Chr 11 they rescue the 6T phenotype. Next, we looked at potential candidate genes in the Chr 11 locus using *in silico* haplotyping and gene expression. More than 50% of the SNP haplotype blocks between B6 and C3H in Chr 11 were found to be identical by descent (IBD). In previous expression data from the 6T mouse we identified 19 genes that were in the Chr 11 region that were differentially expressed and were not IBD. Two particular genes of interest *Srebp1c* (sterol regulatory element binding protein 1c: 60.01Mb on Chr 11) and *Per1* (period1: 68.92Mb, Chr 11) transcripts were two fold higher in 6T than B6 ( $p < .01$ ). Both genes are important in adipogenesis and skeletal homeostasis, particularly the former, *Srebp1c*, which is upstream of *Pparg*, the major candidate gene in our 6T mouse. *In sum*, we identified an epistatic locus on mouse Chr 11 that influences IGF-1 and bone mass in 6T. We narrowed the QTL through recombination and *in silico* mapping, and identified two potentially important candidate genes for adipogenesis and skeletal homeostasis.

**Disclosures:** V.E. DeMambro, None.

This study received funding from: NIAMS 45433.



## M253

**Epistasis Between QTLs for Bone Density Variation in Copenhagen X Dark Agouti F2 Rats.** D. L. Koller<sup>1</sup>, L. Liu<sup>\*1</sup>, I. Alam<sup>2</sup>, Q. Sun<sup>2</sup>, M. J. Econs<sup>3</sup>, T. Foroud<sup>\*1</sup>, C. H. Turner<sup>2</sup>. <sup>1</sup>Medical and Molecular Genetics, Indiana University School of Medicine, Indianapolis, IN, USA, <sup>2</sup>Orthopedics, Indiana University School of Medicine, Indianapolis, IN, USA, <sup>3</sup>Medicine, Indiana University School of Medicine, Indianapolis, IN, USA.

The variation in several of the risk factors for osteoporotic fracture, including bone mineral density, has been shown to be due largely to genetic differences. However, the genetic architecture of BMD is complex in both humans and in model organisms. We have previously reported QTL results for BMD from a genome screen of 828 F2 progeny of Copenhagen and dark agouti rats. These progeny also provide an excellent opportunity to search for epistatic effects, or interaction between genetic loci, that contribute to fracture risk.

Microsatellite marker data from a 20 cM genome screen was analyzed along with weight-adjusted bone density (DXA and pQCT) phenotypic data using the R/qtl software package. Genotype and phenotype data were permuted to determine a genome-wide significance threshold for the epistasis or interaction LOD score corresponding to an alpha level of 0.01.

Novel loci on chromosomes 5 and 13 demonstrated a strong epistatic effect on BMD at the femur by DEXA (LOD=5.6). A previously reported QTL on chromosome 14 was found to interact with a novel locus on chromosome 20 to affect whole BMD at the distal femur by pQCT (LOD=5.0), as well as to influence BMD at other skeletal sites. These results provide new information regarding the mode of action of previously identified rat QTL, as well as identifying novel loci that act in combination with known QTL or with other novel loci to contribute to the risk factors for osteoporotic fracture.

**Disclosures:** D.L. Koller, None.

## M254

**Nuclear Receptor Interacting Protein 1 (NR1P1), a Novel Osteoporosis Candidate Gene Identified by Expression and Association Analyses.** D. P. Kiel<sup>1</sup>, D. Karasik<sup>1</sup>, S. Demissie<sup>2</sup>, Y. Zhou<sup>\*2</sup>, E. Bianchi<sup>\*3</sup>, K. Cho<sup>\*2</sup>, L. A. Cupples<sup>2</sup>, Y. Hsu<sup>1</sup>, J. M. Zmuda<sup>\*4</sup>, S. Ferrari<sup>\*3</sup>. <sup>1</sup>Harvard Med, Sch, HSL, IFAR, Boston, MA, USA, <sup>2</sup>Boston Univ, Boston, MA, USA, <sup>3</sup>Geneva Univ Hosp, Geneva, Switzerland, <sup>4</sup>Univ of Pitts, Pittsburgh, PA, USA.

Three mouse gene expression databases using mRNA of PTH-differentiated primary osteoblasts from neonatal calvariae, mRNA of adult femoral diaphysis and metaphysis, and in situ mRNA hybridization of skeletal embryonic tissue were used to identify NR1P1 (Chrom 21) as a potential candidate gene for osteoporosis. NR1P1 encodes a pleiotropic factor that interacts and regulates multiple members of the nuclear receptor super-family, including the estrogen receptor. Thus, to corroborate these findings in humans, we selected tag SNPs in NR1P1 including exon/missense SNPs with minor allele frequency >5%. Genotyping was performed in a subset of 1493 unrelated individuals (792 females mean age 60.6 ± 9.1 yrs and 701 males mean age 62.1 ± 9.2 yrs) from the Framingham Offspring Cohort who had DXA measurements of the hip (total hip BMD) and spine (L2-L4 BMD) and/or calcaneal broadband ultrasound attenuation (BUA) performed 1996-2001 using a Lunar DPX-L and Hologic Sahara ultrasound device. Genotyping was performed using the SNPlex™ Genotyping System and ABI Taqman. Covariate data included: age, BMI, smoking, and for women, estrogen status (premenopausal or postmenopausal on estrogen vs postmenopausal not on estrogen). Sex-specific single SNP analyses (2-df) were performed using analysis of covariance adjusting for age, BMI, height, smoking, and estrogen status. Permutation tests were performed within each gender to account for multiple testing. HWE p-values were > 0.1 for all SNPs. Of the 12 SNPs only one (rs2229742) achieved nominal significance in women for BUA p=0.033. In men four SNPs were significantly associated with either hip BMD (rs2178894, rs2249465, rs2103466), and/or spine BMD (rs13050325 and rs2249465) (all p-values<0.05). After permutation testing, two SNPs remained significant (rs13050325 and rs2249465) for spine BMD in men (permutation p<0.05). These SNPs explained 3.3% of the variance in spine BMD among men (each contributed about 2% when evaluated individually). Replication is being performed by genotyping these two SNPs in 1,800 men who participated in the Tobago Bone Health Study. Our findings suggest that NR1P1 is a widely expressed skeletal gene that is associated with BMD, mostly in men. The use of gene expression databases to identify candidate genes for osteoporosis traits may be a fruitful approach. The prominent association with BMD in men for a gene that in women has been shown by others to interact with the estrogen receptor, adds to the growing body of information supporting a role for estrogen in the male skeleton.

**Disclosures:** D.P. Kiel, None.

This study received funding from: NIAMS.

## M255

**Calcium-Sensing Receptor Gene "A986S" Polymorphisms: Relation to Bone Loss and Urine Calcium in a Spanish Early Postmenopausal Women Population.** J. A. Blázquez<sup>\*1</sup>, L. Navarro<sup>\*2</sup>, C. Andrés<sup>\*2</sup>, J. Ontañón<sup>\*2</sup>, J. Solera<sup>\*1</sup>, J. Del Pino<sup>\*3</sup>. <sup>1</sup>Internal Medicine, Hospital General Universitario de Albacete, Albacete, Spain, <sup>2</sup>Clinical Chemistry, Hospital General Universitario de Albacete, Albacete, Spain, <sup>3</sup>Rheumatology, Hospital Universitario, Salamanca, Spain.

**Background.** Calcium-sensing receptor (CaSR) is a candidate gene for osteoporosis susceptibility. There are not studies regarding the relationship between CaSR gene A986S polymorphism and bone loss.

**Objectives.** 1) To assess the association between CaSR gene A986S polymorphisms and postmenopausal bone loss. 2) To evaluate whether urine calcium excretion depends of CaSR gene A986S polymorphisms.

**Subjects and methods.** 153 women with natural menopause were randomly selected in the province of Albacete, Spain (mean age 53.7±1.6 yr). They did not have any diseases to affect bone metabolism. Genomic DNA was extracted from peripheral blood leukocytes by the Higuchi method. A fragment of exon 7 of CaSR gene containing the A986S polymorphism was amplified by polymerase chain reaction (PCR). After amplification, all samples were digested with Bsa H1 restriction enzymes, and the fragments were separated by agarose gel electrophoresis. Calcium was measured in a fasting 2 hr morning urine (Ca/Cr). BMD was measured at lumbar spine (L<sub>2</sub>-L<sub>4</sub>) baseline and two years later. 119 women completed the study.

**Results.** The distribution of genotype frequencies of CaSR gene A986S polymorphisms was: AA, 93 (78.2%); AS, 24 (20.2%), and SS, 2 (1.7%). The mean of annual bone loss was 2.04±1.67%. We found no association between CaSR gene A986S polymorphisms and bone loss (p>0.05), but we found an association with urine calcium. Women with the AS genotype had higher urine calcium than those with AA genotype: AS, 0.21 ± 0.09 mg/mg; AA, 0.16 ± 0.07 mg/mg (p=0.017).

**Conclusions.** 1) We found no association between postmenopausal bone loss and CaSR gene A986S polymorphisms. 2) We found an association between CaSR gene A986S polymorphisms and urine calcium.

**Supported by grants from FIS 99/07059, JCCM98196 FISCAM, and Research Board of University Hospital, Albacete.**

**Disclosures:** J.A. Blázquez, None.

This study received funding from: FIS 99/07059, JCCM98196 FISCAM, and Research Board of University Hospital, Albacete.

## M256

**Association of Calcitonin Receptor Gene Polymorphisms with Bone Mineral Density and Fracture Risk in Postmenopausal Koreans.** S. H. Lee<sup>\*1</sup>, H. J. Lee<sup>\*2</sup>, S. Y. Kim<sup>\*3</sup>, Y. J. Kim<sup>\*2</sup>, B. Jung<sup>\*2</sup>, H. D. Shin<sup>\*4</sup>, B. L. Park<sup>\*4</sup>, T. H. Kim<sup>\*5</sup>, J. M. Hong<sup>\*6</sup>, E. K. Park<sup>\*5</sup>, H. L. Kim<sup>\*2</sup>, B. Oh<sup>\*2</sup>, J. M. Koh<sup>1</sup>, J. Y. Lee<sup>\*2</sup>, G. S. Kim<sup>1</sup>. <sup>1</sup>Division of Endocrinology and Metabolism, Asan Medical Center, University of Ulsan College of Medicine, Seoul, Republic of Korea, <sup>2</sup>The Center for Genome Science, National Institute of Health, Seoul, Republic of Korea, <sup>3</sup>Department of Orthopedic Surgery, Kyungpook National University School of Medicine, Daegu, Republic of Korea, <sup>4</sup>Department of Genetic Epidemiology, SNP Genetics, Inc., Seoul, Republic of Korea, <sup>5</sup>Department of Pathology and Regenerative Medicine, School of Dentistry, Kyungpook National University, Daegu, Republic of Korea, <sup>6</sup>Skeletal Diseases Genome Research Center, Kyungpook National University Hospital, Daegu, Republic of Korea.

Calcitonin inhibits osteoclast-mediated bone resorption and affects calcium ion excretion in the kidney via a specific receptor, the calcitonin receptor (CTR). We investigated the association between calcitonin receptor gene (CALCR) polymorphisms and osteoporotic phenotypes in postmenopausal Korean women, to identify genetic factors that may be involved in susceptibility to osteoporosis and development of the disease phenotype. We directly sequenced the coding region, portions of the 5'-flanking and 3'-flanking sequences, and the intron-exon boundaries, of the CALCR genes from 24 individuals. We discovered nine single nucleotide polymorphisms (SNPs), and found an additional two SNPs in public databases. We investigated the potential involvement of these SNPs in osteoporosis in postmenopausal women (n = 729). The subjects carrying AA genotypes with an SNP in the CALCR promoter (-89413G > A) had higher bone mass density (BMD) values at the femoral neck (P = 0.002) and other proximal femur sites (P = 0.002-0.006). The A allele of this SNP tended to protect against vertebral fracture (OR = 0.72, 95% CI = 0.50-1.04, in the co-dominant model). In particular, functional analyses showed that the CALCR -89413G > A SNP affected expression of CALCR. These results indicate that the CALCR gene may be a key regulator of bone metabolism, and the -89413G > A SNP in the CALCR promoter may genetically modulate bone phenotype.

**Disclosures:** S.H. Lee, None.

This study received funding from: intramural grants from the Korea National Institute of Health, the Korea Center for Disease Control of the Republic of Korea (Project No.: 347-6111-211), and a grant from the Korea Health 21 R&D Project, Ministry of Health.

## M257

**Effect of Raloxifene Treatment on Bone Mineral Density Might Be Influenced by UGT1A1\*28 Polymorphism.** A. Zavratnik<sup>\*1</sup>, J. Trontelj<sup>\*2</sup>, J. Marc<sup>\*3</sup>, M. Bogataj<sup>\*2</sup>, A. Mrhar<sup>\*2</sup>. <sup>1</sup>Endocrinology, University Clinic Centre Maribor, Maribor, Slovenia, <sup>2</sup>Department of Biopharmacy and Pharmacokinetics, Faculty of Pharmacy, Ljubljana, Slovenia, <sup>3</sup>Department of Clinical chemistry, Faculty of Pharmacy, Ljubljana, Slovenia.

**Objectives:** Raloxifene concentrations were reported to approximately correlate with serum bilirubin levels. Bilirubin is typical UGT1A1 substrate. Based on these facts, we postulated a hypothesis that UGT1A1\*28 polymorphism, significantly contributes to the large pharmacokinetic variability of raloxifene and results in different bone mineral density (BMD) gain.

**Methods:** Serum samples of 47 postmenopausal osteoporotic women treated with raloxifene were assayed for the concentrations of raloxifene and its glucuronides by LC-MS-MS. The same samples were also genotyped for the presence of UGT1A1\*28 polymorphism by SSCP method. The pharmacodynamic effect was evaluated by measuring the change in BMD of femoral neck, total hip and lumbar spine after 12 months of therapy.

**Results:** Women homozygous for the \*28 allele showed a significantly, 2.2-fold higher total raloxifene concentrations compared to patients homozygous for the wild-type allele (562 +/- 116 nmol/L compared to 256 +/- 53 nmol/L, respectively,  $p=0.029$ ). Likewise, a significantly greater increase in hip BMD was observed in subjects homozygous for the \*28 allele compared to the group carrying at least one copy of the wild-type allele (4.4 +/- 2.4% compared to 0.3 +/- 1.4%,  $p=0.035$ ).

**Conclusion:** Our data have shown that the relatively common UGT1A1\*28 polymorphism strongly influences total raloxifene concentration and was clearly identified as one of the factors contributing to the large interindividual pharmacokinetic variability of raloxifene that could effect BMD gain and could be of clinical importance.

**Funding:** The authors acknowledge financial support from the state budget through the Slovenian Research Agency (project "Pharmacogenetic study of raloxifene metabolism and transport").

**Disclosures:** A. Zavratnik, the Slovenian Research Agency 5.  
This study received funding from: the Slovenian Research Agency.

## M258

**Association between Polymorphisms in Tumor Necrosis Factor Receptor (TNFR) Genes and Circulating TNFR Levels, and Bone Mineral Density in Postmenopausal Korean Women.** J. Kim<sup>1</sup>, H. Kim<sup>\*1</sup>, S. Chun<sup>\*1</sup>, B. Jee<sup>\*2</sup>, C. Suh<sup>\*1</sup>, Y. Choi<sup>\*1</sup>. <sup>1</sup>Dept. of Obstetrics & Gynecology, Seoul National University Hospital, Seoul, Republic of Korea, <sup>2</sup>Dept. of Obstetrics & Gynecology, Seoul National University Bundang Hospital, Seongnam, Republic of Korea.

Tumor necrosis factor (TNF)- $\alpha$  is suggested to play a role in the increased osteoclastic bone resorption and skeletal response to TNF has been known to depend on a balance between expression and activation of the TNF receptor (TNFR)-1 and 2 gene products. We investigated the association between polymorphisms in TNFR genes and circulating soluble TNFR (sTNFR) levels, and bone mineral density (BMD) in postmenopausal Korean women

The TNFR1 A(36)G and TNFR2 T(676)G, A(1663)G, A(1668)G and C(1690)T polymorphisms were analyzed by polymerase chain reaction-restriction fragment length polymorphism or Taqman assay or DNA sequencing in 377 postmenopausal Korean women. Levels of serum sTNFR1, sTNFR2, osteocalcin, bone alkaline phosphatase, and C-telopeptide of type I collagen were measured. BMD at the lumbar spine and femoral neck was examined by dual energy X-ray absorptiometry.

TNFR2 A(1668)G polymorphism was not observed in study subjects. No significant associations were found between single genotypes of TNFR1, and TNFR2 polymorphisms and BMD of lumbar spine and femoral neck, but the prevalence of osteoporosis is significantly higher ( $p<0.05$ ) in GG genotype of TNFR2 A(1663)G polymorphism compared to other genotypes. Haplotype analysis of three TNFR2 polymorphisms did not show any significant association with BMD and the distributions of haplotype genotypes were not different among normal, osteopenic, and osteoporotic women. No significant differences in the levels of any bone turnover marker among single and haplotype genotypes of TNFR polymorphisms were found. Circulating sTNFR2 levels in TT genotype of TNFR2 T(676)G polymorphism and TT genotype of TNFR2 C(1690)T polymorphism were significantly lower compared to other genotypes, but sTNFR1 levels were not different according to TNFR1 polymorphism. The TNFR2 A(1663)G polymorphism are a genetic factor which may evaluate postmenopausal Korean women at risk of osteoporosis, and sTNFR2 level may be affected by TNFR2 T(676)G and C(1690)T polymorphisms.

**Disclosures:** J. Kim, None.

This study received funding from: the Korea Health 21 R&D project (A050005), Ministry of Health and Welfare, Republic of Korea.

## M259

**Is there any Association Between CYP 17-CYP 19 Polymorphisms and Bone Loss in Early Postmenopausal Women? Results of a Two-Years Study in a Spanish Population.** L. Navarro<sup>\*1</sup>, J. A. Blázquez<sup>\*2</sup>, C. Andrés<sup>\*1</sup>, J. Ontañón<sup>\*1</sup>, M. Cháfer<sup>\*1</sup>, M. Sosa<sup>\*3</sup>. <sup>1</sup>Clinical Chemistry, Hospital General Universitario de Albacete, Albacete, Spain, <sup>2</sup>Internal Medicine, Hospital General Universitario de Albacete, Albacete, Spain, <sup>3</sup>Internal Medicine, Hospital Universitario Insular, Las Palmas de Gran Canaria, Spain.

**Background.** Osteoporosis is a polygenic disorder resulting from the interaction of common polymorphic alleles and environmental factors. In contrast to the extensive studies on heritability of bone mass, few studies on heritability of bone loss have been reported. The CYP 17 and CYP 19 genes encode 17 $\alpha$ -hydroxylase/17,20-lyase and aromatase, respectively, both involved in androgens and estrogens synthesis, that they are important for the development and maintenance of bone mass.

**Objective.** To assess the association between CYP 17 and CYP19 polymorphisms and postmenopausal bone loss.

**Subjects and methods:** 153 women with natural menopause were randomly selected in the province of Albacete, Spain (mean age 53.7 $\pm$ 1.6 yr). They did not have any diseases to affect bone metabolism. Genomic DNA was extracted from peripheral blood leukocytes by the Higuchi method. The areas of interest were amplified with specific primers by polymerase chain reaction (PCR) technique. After amplification, all samples were digested with Msp A1 (CYP 17) and Rsa1 (CYP 19) restriction enzymes, and the fragments were separated by agarose gel electrophoresis. BMD was measured at lumbar spine (L<sub>2</sub>-L<sub>4</sub>) baseline and two years later. 119 women completed the study.

**Results.** The distribution of genotype frequencies of CYP 17 polymorphisms was: TT 45 (37.8%), TC 58 (48.7%) and CC 16 (13.4%). The distribution of genotype frequencies of CYP 19 polymorphisms was: AA 39 (38.8%), AG 61 (51.3%), GG 19 (16%). The mean of annual bone loss was 2.04 $\pm$ 1.67%. In the comparison between groups there was no difference in relation to bone loss for the CYP 17 or for the CYP19 polymorphisms ( $p>0.05$ ).

**Conclusion:** We found no association between postmenopausal bone loss and CYP 17-CYP 19 polymorphisms.

**Supported by grants from FIS 99/07059, JCCM98196 FISCAM, and Research Board of University Hospital, Albacete.**

**Disclosures:** L. Navarro, None.

This study received funding from: grants from FIS 99/07059, JCCM98196 FISCAM, and Research Board of University Hospital, Albacete.

## M260

**Association of HSD11B1 Polymorphisms with Vertebral Fracture Risk and Bone Mineral Density in Postmenopausal Korean Population.** J. Hwang<sup>\*1</sup>, G. Kim<sup>\*2</sup>, M. Go<sup>\*1</sup>, Y. Kim<sup>\*1</sup>, M. Park<sup>\*1</sup>, H. Shin<sup>\*3</sup>, B. Park<sup>\*3</sup>, E. Park<sup>\*2</sup>, T. Kim<sup>\*2</sup>, J. Hong<sup>\*2</sup>, S. Lee<sup>\*2</sup>, H. Kim<sup>\*1</sup>, J. Lee<sup>\*1</sup>, S. Kim<sup>\*2</sup>, J. Koh<sup>4</sup>. <sup>1</sup>Center for Genome Science, Korean National Institute of Health, Seoul, Republic of Korea, <sup>2</sup>Skeletal Diseases Genome Research Center, Kyungpook National University Hospital, Seoul, Republic of Korea, <sup>3</sup>Department of Genetic Epidemiology, SNP Genetics, Seoul, Republic of Korea, <sup>4</sup>Division of Endocrinology and Metabolism, University of Ulsan College of Medicine, Asan Medical Center, Seoul, Republic of Korea.

11 $\beta$ -hydroxysteroid dehydrogenase type 1 (HSD11B1) is a primary regulator that catalyze the reduction of inactive cortisone (E) to active cortisol (F). To examine the relationship between HSD11B1 polymorphism and osteoporosis, we investigated the potential involvement of five SNPs using the Illumina Golden Gate genotyping system in 729 postmenopausal women. Three SNPs, -19835G>A, +16374G>A and +27447G>C were associated with the risk of spinal fracture ( $p = 0.003$ -0.035) and vertebral fracture ( $p = 0.02$ -0.05). Two SNPs (LD) in intron 5, +16374G>A and +27447G>C were correspondently associated with bone mineral density (BMD) at the lumbar spine ( $p = 0.002$ -0.04) and femoral neck ( $p = 0.003$ -0.004). Particularly, the most significant -19835G>A (rs846908) was associated with the fracture risk on lumbar spine (OR = 2.14, 95% CI = 1.29-3.53, in the recessive model) including multiple comparison ( $p = 0.020$ ), and functionally correlated with Sox-5 (transcription factor, core matching score = 7.56). Also, +27447G>C was associated with protective effect (OR = 0.59, 95% CI = 0.41-0.86, in the dominant model) including multiple testing ( $p = 0.020$ ), and tended to be higher BMD value with independent. It suggest that the +27447G>C SNP acts as an intronic enhancer/silencer role with -19835G>A SNP in promoter sequence and genetically regulates glucocorticoid-induced osteoporosis. These results provide, for the first time, evidence supporting the association of HSD11B1 with osteoporosis in postmenopausal women.

**Disclosures:** J. Hwang, None.

## M261

**Associations of the Vitamin D Receptor and Calcitonin Receptor Genes with Bone Density, Bone Turnover Markers and Fracture Incidence with Regard to Calcium Intake Level in Slovak Postmenopausal Women.** R. Omelka<sup>1</sup>, M. Martiniakova<sup>\*1</sup>, V. Smolarikova<sup>\*1</sup>, D. Galbavy<sup>\*2</sup>, M. Bauerova<sup>\*1</sup>. <sup>1</sup>Constantine the Philosopher University, Nitra, Slovakia, <sup>2</sup>Private Orthopedic Ambulance, Nitra, Slovakia.

Osteoporosis is multifactorial in nature, and various genes, as well as insufficient diet have been reported to be involved in the pathology of the disease. The vitamin D receptor (VDR) and the calcitonin receptor (CALCR) genes code proteins that mediate an action of hormones involved in calcium homeostasis in target tissues. Therefore, genetic variability in the genes could affect the variability of bone mineral density (BMD), bone remodeling, and fracture risk.

We analyzed associations of FokI polymorphism in the VDR gene and AluI polymorphism in the CALCR gene with variability of femoral and spinal BMD, circulating alkaline phosphatase (ALP) and osteocalcin (OC; formation markers), beta-CrossLaps (CTX; resorption marker), and fracture incidence with regard to different amounts of calcium intake.

Our study involved 152 Slovak postmenopausal women (64.4±7.2 years) selected according to strict inclusion criteria. Genetic polymorphisms were detected by the PCR-RFLP method. The differences between the genotypes were analyzed by GLM procedure and covariance analysis after correction of the measurements for age and BMI. Gene-gene interactions were also evaluated within the statistical analysis. Frequencies of fractures were tested using the chi-square test. The fracture frequencies were also compared between groups with different daily calcium intake of <350 mg (group A), 350-650 mg (B), and >650 mg (C).

We found a significant effect of VDR-CALCR interaction on femoral BMD (P=0.033) and spine BMD (P<0.001). No polymorphism alone affected any of the analyzed traits significantly; however, effects of VDR gene on spine BMD (P=0.070) and ALP (P=0.086) were not far from the significance level. We did not find significant associations between the genes and OC, CTX. Comparison of fracture incidence between the genotype groups showed significant differences (P<0.05) for CALCR gene regardless of calcium intake level. The effect of the VDR gene was significant only in the C diet group (P<0.01). The ff-genotype carriers had higher frequency of fracture than the others.

The analysis of associations between candidate genes (interactions), diet, and BMD or bone turnover markers can extend our knowledge about molecular background of bone remodeling and loss. The results could be also applicable in predicting osteoporosis susceptibility. All procedures were approved by the Ethical Committee of the Specialized Hospital of St. Svorad in Nitra (Slovakia). This study was supported by the grant KEGA 3/4040/06.

**Disclosures:** R. Omelka, None.

## M262

**Significant Association Between Polymorphisms of CYP19A1, Fracture Incidence and Bone Mineral Density in Post-menopausal Women.** E. J. Payne<sup>\*1</sup>, S. G. Wilson<sup>1</sup>, E. Ingley<sup>\*2</sup>, R. L. Prince<sup>3</sup>. <sup>1</sup>Endocrinology and Diabetes, Sir Charles Gairdner Hospital, Perth, Australia, <sup>2</sup>Cancer Medicine, Western Australian Institute for Medical Research, Perth, Australia, <sup>3</sup>Medicine and Pharmacology, University of Western Australia, Perth, Australia.

The human aromatase gene (CYP19A1) plays a major role in the biosynthesis of estrogen in a tissue specific manner. In post-menopausal women, this aromatization of adrenal androgens is the primary source of estrogen, implicating CYP19A1 in many estrogen-dependant functions such as tumour progression, obesity and bone health. Polymorphisms in CYP19A1 have been shown to alter aromatase expression furthermore we and others have shown previously that in postmenopausal women certain polymorphisms in CYP19A1 are associated with serum estradiol concentrations, bone structure and fracture risk. Thus CYP19A1 variation is a strong candidate for the known effects of heredity on osteoporosis risk in postmenopausal women.

Study subjects were members of a population-based cohort comprising of 1,257 Caucasian women aged between 70 and 85 years recruited for the Calcium Intake Fracture Outcome Study (CAIFOS). BMD at the hip site was measured by DXA (Hologic QDR 4500). Serum estradiol was measured by RIA (Orion Diagnostica, Finland). 31 tag SNPs selected to represent variation in the CYP19A1 gene were genotyped using MALDI-ToF (Sequenom Inc.). Statistical analysis was performed using SPSSv15.

Eight of the 31 tag SNPs showed significant associations with hip BMD (rs8034835 P=0.009; rs767199 P=0.039; rs3889391 P=0.045; rs17523880 P=0.005; rs16964215 P=0.028; rs12439137 P=0.048). Two SNPs showed a significant association with incident fragility fracture (rs4646 P=0.019; rs12439137 P=0.036). For SNP rs12439137, an increase in fracture rate and a decrease in BMD was observed for individuals with the rarer GG genotype. None of the SNPs analyzed were associated with detectable differences in circulating estradiol levels.

These observations indicate that genetic variation in the CYP19A1 gene contributes to variation in BMD in postmenopausal women. The lack of effect on circulating estradiol levels may be due to lack of power in the study or local tissue specific splice variant effects not reflected in circulating estradiol levels. This study confirms effects of specific variants on bone structure and supports the importance of such variation on fracture prediction. Study of the LD bins represented by these tag SNPs will allow further insights into the mechanism of the gene variation effect. These variants may be of importance given the efforts being undertaken to establish diagnostic tools and molecular targets for treatment.

**Disclosures:** E.J. Payne, None.

This study received funding from: NHMRC Australia.

## M263

**Prediction of Osteoporotic Fracture Risk by 25-hydroxyvitamin D<sub>3</sub>-1 $\alpha$ -hydroxylase (CYP27B1) Gene.** B. H. Tran<sup>1</sup>, A. Au<sup>\*2</sup>, N. D. Nguyen<sup>1</sup>, R. Clifton-Bligh<sup>2</sup>, J. R. Center<sup>1</sup>, J. A. Eisman<sup>1</sup>, T. V. Nguyen<sup>1</sup>. <sup>1</sup>Bone and Mineral Research Program, Garvan Institute of Medical Research, Sydney, Australia, <sup>2</sup>Cancer Genetics Unit, Kolling Institute of Medical Research, Sydney, Australia.

Adult mice with knock-out CYP27B1 gene (which encodes the mitochondrial enzyme 1 $\alpha$ -hydroxylase) had an impairment of bone formation and bone mineralization. The present study was designed to test the hypothesis that variants within the CYP27B1 gene are associated with fracture risk.

The study was designed as a matched case-control investigation, with 295 women with fracture who were randomly matched for age with 295 women without a fracture. All women aged 60 or above as of 1989 (average age of participants was 71±7 years, mean±SD). Fracture was ascertained by X-ray reports between 1989 and 2007. Bone mineral density, lifestyle and clinical risk factors were obtained at baseline and in subsequent visits, which had taken place every two years. Genotypes of the CYP27B1 gene were determined in the promoter region (-1260 C to A) by restriction enzyme digestion. The conditional logistic regression was used to assess the association between the gene polymorphism and fracture.

Fracture cases as expected had significantly lower femoral neck BMD than controls (0.74±0.12 vs 0.8±0.12 g/cm<sup>2</sup>, p<0.001). The distribution of CYP27B1 genotypes was consistent with the Hardy Weinberg disequilibrium law: AA 18.4%, CA 38.0%, and CC 43.6%. There was no significant association between the CYP27B1 genotypes and BMD, body weight, or height. However, there was an over-representation of the heterozygous CA genotype in fracture cases (39%) compared to the non-fracture controls (32%). Thus, individuals with the CA genotype were associated with an increased risk of fracture (odds ratio [OR]: 1.35, 95%CI 1.63 - 2.40). Furthermore, after adjusting for age, BMD and lifestyle factors, individuals with polymorphic A allele was more likely to sustain a fracture than those homozygous with C allele (OR: 1.44, 95%CI 1.00 - 2.07). The CYP27B1 genotypes accounted for approximately 14% of fracture liability.

These results indicate that a common variation within the CYP27B1 gene contributes to an increased risk of fracture in the elderly independent of BMD. Genotypic information of this gene may improve the prognosis of fracture risk for an individual.

**Disclosures:** B.H. Tran, None.

This study received funding from: NHMRC.

## M264

**A BMD-Associated SNP Lies in a Runx2 Binding Site of the LRP5 Promoter.** D. Grinberg<sup>\*1</sup>, L. Agueda<sup>\*1</sup>, M. Bustamante<sup>\*1</sup>, S. Jurado<sup>\*2</sup>, N. Garcia-Giralte<sup>\*2</sup>, M. Ciria<sup>\*2</sup>, G. Salo<sup>\*2</sup>, R. Carreras<sup>\*2</sup>, X. Nogues<sup>2</sup>, L. Mellibovsky<sup>\*2</sup>, A. Diez-Perez<sup>1</sup>, S. Balcells<sup>\*1</sup>. <sup>1</sup>Genetics, University of Barcelona, CIBERER, IBUB, Barcelona, Spain, <sup>2</sup>URFOA, IMIM, Hospital del Mar, Autonomous University of Barcelona, Barcelona, Spain.

LRP5 encodes the low-density lipoprotein receptor-related protein 5, one of the co-receptors involved in Wnt signalling and an important regulator of osteoblast growth and differentiation. Implication of its common variation (SNPs) in the normal spectrum of bone phenotypes has been shown by several association analyses. The purpose of the present study was to assess the functionality of SNPs found to be associated with bone phenotypes in a haplotype based association analysis.

We analysed 24 SNPs spanning the LRP5 region in a cohort of 964 Spanish women. Association with osteoporosis related phenotypes (LS BMD, FN BMD and fracture) was tested at single SNP and haplotype level. Predictive tools were employed to search for putative functional variant/s within blocks associated with bone phenotypes. Functionality of an associated promoter SNP was assessed by gel-shift assays, using SAOS-2 nuclear extracts and radiolabeled probes for both alleles.

The SNP rs312009 in the LRP5 promoter was found associated with LS-BMD [recessive model, CC/CT vs TT 0.07 (0.02-0.13) g/cm<sup>2</sup>, p=0.011]. Association analysis of the haplotype containing this SNP gave equivalent results. A consensus binding-site for the bone transcription factor Runx2 was identified at the SNP site when the T allele was present. In EMSA analyses, a band shift was produced with the T-allele probe, which was competed by increasing amounts of the cold oligonucleotide. A clear competition by the oligonucleotide containing the described OSE in the osteocalcin promoter and a supershift produced by the Runx2 antibody confirmed Runx2 involvement. Experiments using the C allele, as labelled probe or as cold competitor, produced similar results.

In conclusion, EMSA analyses showed the existence of a Runx2 binding site in the LRP5 promoter, involving rs312009. This suggests a functional role for the SNP and is the first indication of the interregulation of Runx2 and LRP5. However, the lack of differential binding by the two alleles could argue against rs312009 being the functional variant, and suggests that it might tag another unidentified causal SNP. Alternatively, limitations in gel shift experiments to detect slight differences could be the cause of the failure to find allele-specific binding affinities. Further approaches, such as competitive chromatin immunoprecipitation and gene reporter assays are currently being undertaken to assess the importance of Runx2 in LRP5 regulation.

**Disclosures:** D. Grinberg, None.

## M265

**The -13910C>T LCT Promoter Polymorphism in the Spanish Population.** S. Balcells<sup>\*1</sup>, X. Nogues<sup>2</sup>, L. Agueda<sup>\*1</sup>, R. Urreiziti<sup>\*1</sup>, M. Bustamante<sup>\*1</sup>, S. Jurado<sup>\*2</sup>, N. Garcia-Giralte<sup>\*2</sup>, G. Yoskovitz<sup>\*2</sup>, L. Mellibovsky<sup>\*2</sup>, A. Diez-Perez<sup>2</sup>, D. Grinberg<sup>\*1</sup>. <sup>1</sup>Genetics, University of Barcelona, CIBERER, IBUB, Barcelona, Spain, <sup>2</sup>URFOA, IMIM, Hospital del Mar, Autonomous University of Barcelona, RETICEF, Barcelona, Spain.

Lactose tolerance is an autosomal dominant trait characterized by the persistence of high levels of the intestinal lactase-phlorizin hydrolase (LPH), encoded by lactase gene (*LCT*). A limited fraction of the human adult population retains LPH activity during adulthood (lactase tolerance, LT), which allows the consumption of large amounts of milk. This phenotype is especially common in Northern Europe and decreases in Southern Europe. Mutation -13910C>T at *LCT* has been previously associated with the lactase persistence trait in European population. Nevertheless, LPH persistence has been scarcely investigated in the Spanish population. Previous studies found association between lactose intolerance and bone mineral density (BMD), which might be due to reduced milk consumption and consequently reduced calcium intake.

The aim of this study was to establish the allele frequencies of the -13910C/T mutation at *LCT* gene in a Spanish population and to assess its relationship with anthropometrical markers and bone phenotypes.

The -13910C/T mutation at *LCT* gene was genotyped in 964 Spanish women (BARCOS cohort) by Taqman. Categorical parameters were analyzed by  $\chi^2$  and logistic regression. Continuous variables were analyzed by ANCOVA. The significance level was set at  $p < 0.05$ .

We found a T-allele frequency of 38.6%, which is significantly lower ( $p < 0.0001$ ) than in previously described North-European populations. No association between this polymorphism and BMD or fracture was found in our cohort. On the other hand, we found an association between it and increased body weight once adjusting for age ( $p = 0.037$ ). A stronger association was found when T-homozygotes were compared with the C-allele carriers (age-adjusted,  $p = 0.015$ ). Additionally, the T-allele carrier status was associated with higher stature (age-adjusted,  $p = 0.032$ ).

Our results confirm the previous observation of a cline in lactose tolerance across Europe, since Spanish allele frequencies are more similar to French (43.1%) or North Italian (35.7%), than to Swedish and Finnish (81.5%) or European American (77.2%). However, we have not found association between lactose tolerance and BMD.

The lack of association may be due to small effects that are below the power of this study. Alternatively, in this Spanish population, intolerant individuals may achieve equivalent calcium intake from food sources devoid of lactose. Finally, our results are in agreement with previous studies showing a tendency in milk consumers to higher stature.

**Disclosures:** S. Balcells, None.

## M266

**A Large Scale Candidate Gene Analysis Identifies an Association Between the Cyclin-Dependent Kinase 6 (CDK6) Locus and Trabecular Volumetric BMD at the Lumbar Spine in Older Men.** S. P. Moffett<sup>1</sup>, L. A. Yerges<sup>1</sup>, J. A. Cauley<sup>1</sup>, L. M. Marshall<sup>\*2</sup>, C. M. Kammerer<sup>\*1</sup>, R. E. Ferrell<sup>\*1</sup>, C. S. Nestlerode<sup>\*1</sup>, K. E. Ensrud<sup>\*3</sup>, A. R. Hoffman<sup>\*4</sup>, E. S. Orwoll<sup>\*2</sup>, J. M. Zmuda<sup>1</sup>.

<sup>1</sup>University of Pittsburgh, Pittsburgh, PA, USA, <sup>2</sup>Oregon Health and Science University, Portland, OR, USA, <sup>3</sup>Veterans Affairs Medical Center, Minneapolis, MN, USA, <sup>4</sup>Stanford University, Stanford, CA, USA.

Many candidate genes have been proposed to influence bone mineral density (BMD) and osteoporosis risk; however, until recently, thorough investigations of large panels of putative candidate genes were not possible. Moreover, most studies to date have relied on DXA measures of integral areal BMD and have not been able to separately assess the possible genetic determinants of trabecular volumetric BMD (tBMD). In the current study, we investigated the association between SNPs within or flanking physiologically defined candidate genes for bone metabolism and lumbar spine tBMD measured with QCT in 882 Caucasian American men aged  $\geq 65$  years in the Osteoporotic Fractures in Men (MrOS) Study. SNPs in each candidate gene region were comprehensively interrogated by first creating a reference SNP panel spanning 30kb upstream and 10kb downstream of each gene using HapMap genotype data and then identifying tagging SNPs from the reference SNP panel with a minor allele frequency (MAF)  $\geq 5\%$  using a pairwise correlation method ( $r^2 \geq 0.80$ ). In addition, non-synonymous coding SNPs with a MAF  $\geq 1\%$  and other potentially functional SNPs with a MAF  $\geq 2\%$  were also selected for genotyping. 4,108 SNPs in 371 genes were genotyped using the Illumina GoldenGate assay, met quality control criteria and were analyzed for their association with lumbar spine tBMD. Analyses adjusted for participant age and clinic site. Principal components eigenanalysis was used to account for population substructure. Nine SNPs within 8 genes were associated with spine tBMD at  $P < 0.001$ . A SNP (MAF, 0.47) in the intronic region of the cyclin-dependent kinase 6 (CDK6) gene showed the most significant association with tBMD (additive  $p = 0.00006$ ). Men who were homozygous for the minor alleles had a mean BMD 12% higher than men who were homozygous for the major alleles. Another SNP located in the 3' untranslated region of CDK6 was also significantly associated with tBMD ( $p = 0.0002$ ). Two additional SNPs in the CDK6 gene region were associated at  $p < 0.05$ . No SNPs in the CDK gene were associated with DXA measures of the lumbar spine, highlighting the importance of examining different measures of bone density. These results require confirmation, but reveal the potential importance of the cell-cycle regulator, CDK6, in the determination of trabecular BMD variation among healthy men.

**Disclosures:** S.P. Moffett, None.

This study received funding from: NIAMS.

## M267

**Characterization of a Promoter Polymorphism in Frizzled Homolog 1 (FZD1): Allele-Specific Regulation by Early Growth Response Factor 1 (Egr1) in Osteoblast-like Cells.** L. Yerges, Y. Zhang<sup>\*</sup>, J. Zmuda. University of Pittsburgh, Pittsburgh, PA, USA.

WNT signaling has emerged as an important regulator of bone formation. The WNT co-receptor, Frizzled homolog 1 (FZD1), initiates WNT signal transduction and is a biological candidate gene for osteoporosis. We recently identified an association between genetic variation in the FZD1 promoter region and bone mineral density and bone structural geometry. One associated variant of interest, a common G-to-C promoter polymorphism, was associated with greater bone size and mineral content and was predicted to create an early growth factor 1 (Egr1) binding site *in silico*. To further investigate this promoter variant *in vitro*, we characterized DNA-protein binding and promoter activity. Electrophoretic mobility shift assays (EMSA) and transcription factor ELISA assays were completed to investigate allele-specific DNA-protein binding at this polymorphic site in the MG63 and SaOS-2 osteosarcoma cell lines. The C allele, which was predicted to create an Egr1 binding site, was associated with greater Egr1 binding (as evidenced by EMSA band pattern) and with a 1.5 to 1.9-fold increase ( $P < 0.05$ ) in Egr1 binding (as evidenced by transcription factor ELISA). Investigation of allele-specific promoter activity using luciferase reporter plasmids revealed a 2.3 to 3.4-fold higher FZD1 activity for reporter constructs containing the C allele as opposed to the G allele ( $P < 0.05$ ). Our results suggest that a *cis*-regulatory polymorphism in the FZD1 promoter region has a novel role in influencing Egr1 transcription factor binding and FZD1 gene expression in osteoblast-like cells. Our findings also reveal a plausible molecular mechanism for our previous genetic association and underscore the importance of combining both population-based and molecular evidence when investigating genetic polymorphisms.

**Disclosures:** L. Yerges, None.

This study received funding from: National Institute of Arthritis and Musculoskeletal and Skin Diseases (NIAMS).

## M268

**Comprehensive Genetic Analysis of Bone Volume in Men: The Osteoporotic Fractures in Men Study (MrOS).** J. M. Zmuda<sup>1</sup>, L. M. Yerges<sup>1</sup>, L. M. Marshall<sup>2</sup>, C. M. Kammerer<sup>\*3</sup>, J. A. Cauley<sup>1</sup>, K. Ensrud<sup>4</sup>, C. Nestlerode<sup>\*1</sup>, R. Ferrell<sup>\*3</sup>, A. R. Hoffman<sup>\*5</sup>, E. S. Orwoll<sup>2</sup>. <sup>1</sup>Epidemiology, University of Pittsburgh, Pittsburgh, PA, USA, <sup>2</sup>Oregon Health & Sciences University, Portland, OR, USA, <sup>3</sup>Human Genetics, University of Pittsburgh, Pittsburgh, PA, USA, <sup>4</sup>VAMC & University of Minnesota, Minneapolis, MN, USA, <sup>5</sup>Stanford University, Stanford, CA, USA.

Bone size, an important determinant of bone strength, is a highly heritable trait. Animal and human studies suggest that the genetic determinants of bone size are to some extent distinct from those that regulate bone density. However, there is a paucity of information about the genetic factors that influence bone size in humans. Thus, we investigated the possible genetic determinants of femoral neck bone volume measured by quantitative computed tomography (QCT). To address this aim, we interrogated 371 candidate genes with 4108 tagging SNPs from HapMap Phase I and potentially functional SNPs from NCBI dbSNP in 871 men aged  $\geq 65$  years in the Osteoporotic Fractures in Men Study. Principal component eigenanalysis was used to account for population substructure. We initially adjusted for participant age and clinic site. The strongest association was with a tagging SNP (minor allele frequency=0.19) flanking the gene region encoding bone morphogenetic protein 2 inducible kinase (*BMP2K*) ( $P = 0.0001$ ), a serine/threonine protein kinase identified in 2001 as having a novel regulatory role in osteoblast differentiation. Compared to men who were homozygous for the major allele, men who were homozygous for the minor allele had 10% greater bone volume and 12% greater bone mineral content ( $P = 0.005$ ). Additional adjustments for body weight and height, to control for body size, did not alter these results. QCT volumetric and DXA areal BMD were not associated with this SNP. Three additional tagging SNPs in the *BMP2K* region were also associated with bone volume at  $P \leq 0.002$ . Our results suggest a potentially novel role of the *BMP2K* locus in the control of femoral bone size variation in men.

**Disclosures:** J.M. Zmuda, None.

This study received funding from: NIAMS.

## M269

**Haplotype Specific Promoter Activity of the Human Frizzled 1 (FZD1) Gene.** Y. Zhang<sup>1</sup>, L. M. Yerges<sup>2</sup>, C. S. Nestlerode<sup>\*2</sup>, S. E. Hagerty<sup>\*1</sup>, J. M. Zmuda<sup>1</sup>. <sup>1</sup>Medicine, University of Pittsburgh, Pittsburgh, PA, USA, <sup>2</sup>Epidemiology, University of Pittsburgh, Pittsburgh, PA, USA.

The Wnt signaling pathway has emerged as a therapeutic target in osteoporosis and influences human bone mass. Frizzled 1 (FZD1) is a trans-membrane receptor that mediates Wnt signaling. We have begun to characterize the human FZD1 sequence variants in the population by genetic association analysis and *in vitro* by functional analysis.

Bidirectional sequence analysis of the FZD1 promoter region identified two SNPs, a G/T and a G/C substitution, within 300 bp upstream from the translation start site in DNA from 48 men of African ancestry. These two SNPs are in high linkage disequilibrium ( $r^2=0.67$ ;  $D'=0.99$ ) and are both associated with DXA measures of BMD and cross-sectional area at the radius measured by peripheral quantitative computed tomography.

To begin to characterize the potential functional consequences of these common variants, we characterized the promoter activity associated with different haplotypes using a transient expression of a FZD1 reporter gene construct in osteoblast-like cell lines, MG63 and SaOS2. In agreement with our association study, the promoter consisting of both minor variants exhibited the highest activity while the promoter consisting of both major variants had the lowest level activity. To dissect the contribution of each polymorphism of this haplotype, we have begun to characterize allele specific promoter activities *in vitro*. We have identified Egr-1 dependent allele specific regulation of the FZD1 promoter associated with the G/C variant (see abstract by L Yerges et al at this meeting). For the G/T variant, enhanced protein binding was observed for the T allele specific DNA fragment in both MG63 and SaOS-2 cell lines using an electrophoretic mobility shift assay. *In silico* analysis of allele specific transcription factor binding revealed a high affinity consensus site for E2F1 for the minor T allele in comparison with the common G allele. The E2F family of transcription factors regulates an array of cellular functions including cell cycle progression, cell differentiation and apoptosis. E2F1, in particular, has been shown to be important in appendicular skeletal growth in transgenic mice. Thus, experimental verification of E2F1 binding to allele specific FZD1 promoter constructs is currently underway. Our results suggest that a common G/T polymorphism in the FZD1 promoter region may also contribute to the haplotype specific promoter activity of the FZD1 gene. Identification of the specific transcription factors that are responsible for this allele specific promoter regulation will be important for understanding the transcriptional regulation of FZD1 and its role in bone metabolism.

**Disclosures:** Y. Zhang, None.

This study received funding from: R01-AR049747, NIAMS.

## M270

**Differential Regulation of Gene Expression by SNPs in the Osteonectin/SPARC 3' Untranslated Region (UTR): a Mechanism for Modulation of Bone Mass.** K. Kapinas<sup>1</sup>, E. S. Kurland<sup>2</sup>, C. B. Kessler<sup>\*1</sup>, A. M. Delany<sup>1</sup>. <sup>1</sup>Center for Molecular Medicine, University of Connecticut Health Center, Farmington, CT, USA, <sup>2</sup>Division of Endocrinology, Columbia University College of Physicians & Surgeons, New York, NY, USA.

Osteonectin (ON) is a glycoprotein promoting matrix assembly, osteoblast differentiation, and survival. ON-null and -haploinsufficient mice display osteopenia and an aberrant response to intermittent PTH therapy. We reported 6 haplotypes (HAPs) consisting of 3 single nucleotide polymorphisms (SNPs) at cDNA bases 1046, 1599 and 1970 in the 3' UTR of the ON gene. The frequency of selected HAPs was associated with disease severity in Caucasian men with idiopathic osteoporosis (IOM). Here, we determined whether ON SNPs regulate gene expression, which may contribute to differences in bone density. Constitutively expressed luciferase-osteonectin 3' UTR reporter constructs were transiently transfected into the hFOB1.19 human osteoblastic cell line. The function of each HAP was assayed in the context of the entire 1.1 Kb ON 3' UTR (cDNA bases 1018-2123). The function of individual SNPs was assayed in the context of the 50 bases on either side of the SNP.

We found that HAP A (1046C\_1599G\_1970T), most frequent in severely affected IOM patients, showed the lowest level of reporter gene expression. In contrast, HAP B (1046C\_1599C\_1970T), more common in healthy controls ( $p < 0.01$ ) and associated with a higher tertile of bone density in IOM, had 2.5 fold greater gene expression compared with A ( $p < 0.01$ ). Individually, SNP 1599G, found in HAP A, repressed gene expression by 60% ( $p < 0.01$ ), whereas SNP 1599C, found in HAP B, stimulated gene expression by 50% ( $p = 0.05$ ). These data suggest that a negative regulatory element in the osteonectin 3' UTR is disrupted by a C at SNP1599.

HAP D (1046C\_1599C\_1970G) allowed slightly higher gene expression compared with HAP B (1046C\_1599C\_1970T) ( $p = \text{NS}$ ). Individually, SNP 1970T, found in HAP B, repressed gene expression by 85% ( $p < 0.01$ ), while SNP 1970G did not, suggesting that a negative regulatory element is disrupted by a G at SNP1970.

HAP E (1046G\_1599G\_1970T), associated with higher total hip density in IOM, had 3.5 fold greater gene expression than HAP A (1046C\_1599G\_1970T) ( $p < 0.01$ ). Individually, SNPs 1046C and 1046G each had modest, stimulatory effects on gene expression, suggesting that SNP1046 is not contained within an independent regulatory element. We hypothesize that it may modify the function of microRNA binding sites located 60 bases down stream in the UTR.

Overall, our data demonstrate that SNPs in the 3' UTR of the ON gene mediate differential regulation of gene expression. These findings suggest a genetic mechanism for the phenotypic association of ON 3' UTR SNP haplotypes with bone mass in IOM patients.

**Disclosures:** A.M. Delany, None.

## M271

**Osteoprotegerin Production by Breast Cancer Cells Is Modulated by Steroid Hormones and Confers Resistance Against TRAIL-Induced Apoptosis.** T. D. Rachner<sup>\*1</sup>, M. Schoppert<sup>\*2</sup>, L. C. Hofbauer<sup>\*3</sup>. <sup>1</sup>Department of Medicine, Division of Gastroenterology and Endocrinology, Philipps-University, Marburg, Germany, <sup>2</sup>Department of Medicine, Division of Cardiology, Philipps-University, Marburg, Germany, <sup>3</sup>Department of Medicine, Division of Endocrinology and Bone Diseases, Technical University, Dresden, Germany.

Osteoprotegerin (OPG) is a secreted glycoprotein that acts as a decoy receptor for receptor activator of NF- $\kappa$ B ligand (RANKL) and TNF- $\alpha$  related apoptosis inducing ligand (TRAIL). While RANKL is an essential stimulator of osteoclastogenesis and promotes breast cancer migration into bone, TRAIL induces apoptosis of breast cancer cells. The role of the OPG/RANKL/TRAIL system for bone metabolism has been characterized in detail. However, its importance on breast cancer biology has remained elusive. First, we analyzed the expression and modulation of OPG and TRAIL by steroid hormones in estrogen receptor-positive MCF-7 cells and receptor-negative MDA-MB-231 cells using quantitative real-time polymerase chain reaction and ELISA. While pro-inflammatory cytokines IL-1 $\beta$  and TNF- $\alpha$  dose- and time-dependently increased OPG mRNA levels and protein secretion, dexamethasone suppressed OPG expression irrespective of the estrogen receptor status. 17 $\beta$ -estradiol and testosterone inhibited OPG expression in receptor-positive MCF-7 cells, but not in receptor-negative MDA-MB-231 cells. This inhibitory effect was fully reversed by the pure anti-estrogen ICI 182,780 and an aromatase inhibitor. Second, TRAIL dose-dependently activated pro-apoptotic caspases 3, 7, and poly-ADP-ribose polymerase (PARP) and decreased cell numbers of MDA-MB-231, but had no effect in MCF-7 cells. Of note, MDA-MB-231 abundantly expressed TRAIL mRNA. While the presence of IL-1 $\beta$  enhanced TRAIL mRNA expression by MDA-MB-231 cells, it was suppressed by dexamethasone. Gene silencing of OPG using siRNA resulted in a 31% higher rate of apoptosis, compared to non-target siRNA treated controls in MDA-MB-231. By contrast, TRAIL-induced apoptosis rate significantly decreased from 24.1% (in fresh medium) to 13.6% (in conditioned medium that contained OPG at 12.4 pmol/l;  $p < 0.05$ ). Furthermore, a direct correlation between cell survival and OPG levels in the supernatant of MDA-MB-231 was observed, when OPG secretion was modulated using IL-1 $\beta$  (10 ng/ml) or dexamethasone ( $10^{-8}$  M) prior to TRAIL exposure ( $p < 0.05$ ). In conclusion, OPG secretion by breast cancer cells is modulated by cytokines and steroid hormones and may represent an important mechanism conferring resistance against the autocrine pro-apoptotic effect of TRAIL. Interference with the OPG/TRAIL system could become a novel therapeutic target.

**Disclosures:** T.D. Rachner, None.

This study received funding from: Wilhelm Sander Foundation and Deutsche Forschungsgemeinschaft.

## M272

**Microarray Analysis of Human Bone Metastases Evidenced a Set of Genes that Segregates Patients with Metastases only in Bone from Patients with Metastases also in Visceral Organs.** M. Capulli<sup>\*1</sup>, A. Angelucci<sup>\*2</sup>, N. Rucci<sup>1</sup>, F. Martella<sup>\*3</sup>, L. Ventura<sup>\*4</sup>, A. Jackson<sup>\*5</sup>, M. Bologna<sup>\*2</sup>, O. Moreschini<sup>\*6</sup>, S. Pelle<sup>\*6</sup>, K. Driouch<sup>\*7</sup>, T. Landemaine<sup>\*7</sup>, R. Lidereau<sup>\*7</sup>, P. Clement-Lacroix<sup>\*5</sup>, T. Garcia<sup>\*3</sup>, A. Teti<sup>1</sup>, E. Ricevuto<sup>\*3</sup>. <sup>1</sup>Experimental Medicine, University of L'Aquila, L'Aquila, Italy, <sup>2</sup>Basic Applied Biology, University of L'Aquila, L'Aquila, Italy, <sup>3</sup>U.O. Medical Oncology, University of L'Aquila, L'Aquila, Italy, <sup>4</sup>Pathology, S. Salvatore Hospital, L'Aquila, Italy, <sup>5</sup>Galapagos, Romainville, France, <sup>6</sup>Dep. of Orthopaedics and Traumatology, University of Rome, Rome, Italy, <sup>7</sup>Oncogenetic Laboratory, Centre René Huguenin, Institut de la Santé et de la Recherche Médicale, St.Cloud, France.

Bone is the preferential site of distant metastases in breast carcinoma (BrCa). It is possible, based on clinical features, to stratify bone metastatic breast cancer patients, in two groups: 1) patients with bone-only metastases (BO), who frequently have a better overall survival, and 2) patients with metastases in bone and visceral organs (BV), who have a worse clinical outcome. We performed a microarray analysis with the Affymetrix platform on bone metastasis samples from BO and BV patients. We evaluated the profiles obtained using an unsupervised clustering and showed that transcriptomes correlated with the clinical features, segregating BO from BV profiles. In order to obtain a BV gene signature, a statistical analysis was performed to identify the 2-fold regulated genes in BV samples relative to BO samples. This analysis revealed 100 up- and 18 down-regulated genes in BV vs. BO ( $p < 0.05$ ). However, this gene signature was validated by real time RT-PCR analysis only for 66% of the genes selected for evaluation. This result was unexpected and prompted us to perform another microarray analysis of BO and BV samples using the Agilent platform. We then matched the Affymetrix signature with the most regulated genes in the Agilent profiles and found 15 genes (13 up-, 2 down-regulated) commonly modulated in BV vs. BO in both platforms, also validated by real time RT-PCR. These genes perhaps represent the most reliable gene set segregating BV from BO. We clustered these genes by the Gene Ontology Tree Machine software, which allowed us to identify the related biological processes and molecular functions. We observed up-regulation of many processes involved in oxygen transport, plus additional processes associated with fatty acid metabolism, gametogenesis and circulation. In conclusion, this study evidenced a group of genes that are likely to characterize breast cancer patients with bone-only metastases from those who also developed multiple metastases. Our results provide a rationale for setting custom-made gene arrays for diagnostic and prognostic purposes.

**Disclosures:** M. Capulli, None.

**M273**

**A Humanized Model of Breast Cancer Metastasis Revealing a Human-Specific Metastasis Gene Signature.** R. Goldstein<sup>\*1</sup>, K. Anderson<sup>\*2</sup>, M. Rosenblatt<sup>2</sup>. <sup>1</sup>Genetics Program, Tufts University Sackler School of Biomedical Sciences, Boston, MA, USA, <sup>2</sup>Department of Physiology, Tufts University School of Medicine, Boston, MA, USA.

The skeletal complications of malignancy represent some of the most serious complications associated with cancer, signaling the entry of the disease into an incurable phase. Despite many recent advances in cancer research and therapy, there remains a need for a better understanding of the metastatic spread of cancer from its primary location to distant "soils" within the body. Animal models are critical to the understanding of the complexities of tumor metastasis. Through creation of an animal model that is more representative of human pathophysiology, it should be possible to elucidate the genetic alterations that are required for cancer migration from orthotopic locations to distant sites. Further, clinical observations indicate that organ and stromal environments greatly influence the response of tumors to chemotherapy, suggesting that orthotopic implantation of tumor cells in animal models can recapitulate the process of cancer metastasis to bone. Currently, orthotopic implantation of cancer cells is not widely used in animal modeling. Work in our lab has developed a humanized orthotopic injection model of breast cancer metastasis. We use SUM1315 breast cancer cells injected into the murine mammary fat pad. Subsequently, metastases to subcutaneously implanted human bone cores develop. When compared to results obtained from an intracardiac injection model of cancer metastasis to murine bone, results from our gene array studies and genetic profiling have illuminated a novel metastatic gene signature. While different in specific gene identities (intracardiac signature = MMP1, IL-11, CTGF, and CXCR4; orthotopic signature = MMP13, IL-17BR, and HUNK), the two signatures contain genes of overlapping function (ie homing, invasion, angiogenesis and osteolysis). Comparison of the expression levels of the specific gene signatures across different breast cancer cell lines used in the intracardiac or the orthotopic injection models of breast cancer metastasis using qRT-PCR, provides the basis for our hypothesis, suggesting that the humanized animal model of breast cancer metastasis provides a novel, human-species specific, metastatic gene signature.

**Disclosures:** R. Goldstein, None.

**M274**

**Local Administration with Paclitaxel-loaded Hydroxyapatite-alginate Beads for Metastatic Spine Cancer in Rats.** T. Abe<sup>1</sup>, M. Sakane<sup>1</sup>, T. Ikoma<sup>\*2</sup>, M. Kobayashi<sup>\*3</sup>, N. Ochiai<sup>\*1</sup>. <sup>1</sup>Orthopedic Surgery, University of Tsukuba, Tsukuba, Japan, <sup>2</sup>National Institute for Materials Science, Tsukuba, Japan, <sup>3</sup>Innovation Satellite Ibaraki, Japan Science and Technology Agency, Tsukuba, Japan.

Breast cancer is one of the most common cancers to develop metastasis to bone. Among these patients, 5-10% did not respond to treatment and developed metastatic epidural spinal cord compression. Paralysis caused by spinal cord compression is directly associated with survival and the quality of life of breast cancer patients. Thus, local control of metastatic site is very important for metastatic spine cancer. We have shown the anti-tumor effect of 2.4wt% of paclitaxel (PTX)-loaded Hydroxyapatite (HAP)-alginate beads, previously. This study was made to clarify the effects of the 21wt% of PTX-loaded HAP-alginate beads administered therapeutically in a rat model of metastatic spine cancer. Rat's mammary adenocarcinoma (the CRL-1666 cell line) and female Fischer 344 rats (8 weeks old) weighing 130-150 grams were used. The PTX-loaded HAP-alginate beads were prepared by a spray-drying method and the gelation with alginate acid followed by drying at room temperature for 24 h. A 21 wt% of PTX was contained in each HAP-alginate bead with a diameter of approximately 1.7 mm. We performed surgery to obtain metastatic spine cancer model in rats. Twelve animals with metastatic spine cancer were divided into 2 groups. We checked hind-limb motor function and survival time using the BBB scale. The mean disease-free time (DFT) of the local-treatment group (n = 6) and the control group (n = 6) was 15.6 days and 10.8 days, respectively. The DFT in the local-treatment group was significantly longer than that in the control group. The mean survival time of the local-control group and the control group was 21.8 days and 16.0 days, respectively. The survival time in the local-treatment group was also significantly longer than that in the control group. This report documents that the local administration of the PTX-loaded HAP-alginate beads showed significant delay in the DFT and survival time. But the anti-tumor effect was not correlated with increase of the amount of PTX loaded into HAP-alginate beads. PTX loaded into HAP-alginate beads offers promise as a local treatment for patients with metastatic spine cancer to improve the quality of life. Further investigation of pharmacokinetics of the PTX-loaded HAP-alginate beads is needed.

**Disclosures:** T. Abe, None.

**M275**

**c-Src-regulated Osteoblast-mimicry in Breast Cancer Bone Metastasis: The Role of RAMP2 and BSP2.** B. Peruzzi<sup>\*</sup>, A. Del Fattore<sup>\*</sup>, A. Cappariello<sup>\*</sup>, M. Longo<sup>\*</sup>, N. Rucci, A. Teti. Experimental Medicine, University of L'Aquila, L'Aquila, Italy.

Bone tissue represents the preferential target for metastatic colonization by breast cancer cells, which lead to osteolytic lesions. We compared data derived from large-scale gene expression profiles of bone versus visceral metastases of human breast ductal carcinomas, and identified two typical osteoblast genes (RAMP2 and BSP2) over-expressed in the former. Therefore we hypothesized that these genes could cause an osteoblast-mimicry of breast cancer cells. It is well known that the tyrosine-kinase c-Src plays a crucial role both in osteoblast physiology and in bone metastasis progression. Since we noted a modulation of the two genes in the transcriptomes of primary mouse calvarial osteoblasts treated with a c-Src inhibitor (PP1), we also investigated the involvement of c-Src in cancer cell osteoblast-mimicry. To this aim, we assessed expression of the two genes in highly (MDA-MB-231) and moderately (MCF-7) osteotropic human breast cancer cell lines in which c-Src was down-regulated by various treatments (PP1, small-interference RNA and transfection of a dominant negative variant). In each condition, we found modulation of the two genes in MDA but not in MCF-7 cells, indicating a c-Src regulation of osteoblast-mimicry only in tumor cells with high affinity to bone. To investigate whether the two genes were involved in typical osteoblast-like functions, we transfected MDA cells with expression vectors carrying BSP2 or RAMP2 cDNAs and found no modulation of genes involved in bone formation. However, the expression of cytokines, such as RANKL, osteoprotegerin, TNFalpha, IL6 and IL1beta, was changed in a manner favoring the osteoclastogenic process. Moreover, we treated mouse calvarial osteoblast cultures with conditioned media from transfected MDA cells and found the same pattern of modulation of osteoclastogenic cytokine expression. We then analyzed the osteoclastogenic potential in mouse bone marrow cell cultures treated with conditioned media from transfected MDA cells and found a significant increase of osteoclast number and activity in both BSP2- and RAMP2-transfected cells versus empty vector-transfected cells. Finally, we characterized the malignant phenotype of BSP2- and RAMP2-transfected MDA cells, finding no significant changes in proliferation, migration and cell survival versus empty vector-transfected MDA cells. In conclusion, we have obtained evidence of a c-Src-regulated osteoblast-mimicry in highly osteotropic breast cancer cells, in which the osteoclastogenic potential is enhanced by over-expression of RAMP2 and BSP2.

**Disclosures:** B. Peruzzi, None.

**M276**

**Potential Anti-Invasion Activity of Cathepsin K Inhibitors for the Treatment of Breast Cancer-Induced Bone Metastasis.** M. Pickarski, P. Leung<sup>\*</sup>, G. A. Wesolowski, L. T. Duong. Molecular Endocrinology, Merck & Co., Inc, West Point, PA, USA.

Cathepsin K (Cat K) is highly expressed in osteoclasts and plays a critical role in bone collagen degradation. Bone metastasis is often initiated by tumor-induced bone resorption, providing a favorable environment for cancer growth. It is widely accepted that MMPs and serine proteases degrade extracellular matrices and facilitate neoplastic progression. Recent evidence supports the role of the cysteine cathepsins during pericellular proteolysis in tumor invasion. In this study, we examine the direct role of Cat K in tissue invasion by breast cancer cells. We previously reported efficacy of the Cat K inhibitor (Cat Ki) L-006235 in the prevention of osteolysis and reduction of tumor burden in the intratibial engraftment model of MDA-MB-231 breast carcinoma in nude rats. In addition, L-006235 was found to inhibit local invasion of micrometastases. Here, Cat K protein is highly expressed in breast and prostate tumors at levels comparable in osteoclasts or osteoclastomas. From a cancer tissue array study, Cat K protein is detected in ~45% of breast and >75% of prostate primary tumors. Its mRNA expression increases 3-fold in metastatic tissue as compared to pair-matched primary tumors, implicating Cat K in tumor metastasis. We show that proliferation, senescence and migration in human breast and prostate cancer cell lines are not changed by selective inhibitors of Cat K, including odanacatib (MK-0822). While stable transfection of rabbit Cat K in MDA-231 cells (MDA-CatK) results in ~1000-fold increase in mRNA, protein levels increase merely 2-fold over parental cells. Moreover, Cat K is present in the pro-form (39kDa) as undetectable, mature, active enzyme (27kDa), suggesting that additional engagement is required for activation. Using a Cat K fluorogenic substrate, MDA-CatK shows punctate staining around cell nuclei while activity in parental cells is less abundant and more diffuse. In the matrigel invasion assay, MDA-CatK shows a significant increase (89%) in basal invasion compared to parental cells. While the non-selective cathepsin inhibitor E64d inhibits MDA-231 cell invasion with IC<sub>50</sub> of 4.4μM, L-006235 and MK-0822 inhibit cell invasion with IC<sub>50</sub>s of 4nM and 11nM, respectively, which is comparable to their potencies in blocking rabbit osteoclastic bone resorption, with IC<sub>50</sub>s of 5nM and 23nM, respectively. Overall, elevated expression of Cat K in subsets of breast and prostate cancers, and its putative role in tumor cell invasion suggest that Cat Ki therapy may reduce visceral metastasis in these patients. The data also suggest that an oral, potent and reversible Cat Ki with dual antiresorptive and anti-invasive properties may present a more effective therapy for the treatment of bone metastasis.

**Disclosures:** M. Pickarski, Merck & Co., Inc 3.

**M277**

**Opposing Effects on Bone Metastases of Tumor Adrenomedullin Expression in Breast and Prostate Cancer.** V. A. Siclari<sup>1</sup>, K. S. Mohammad<sup>2</sup>, T. A. Guise<sup>2</sup>, J. M. Chirgwin<sup>2</sup>. <sup>1</sup>Biochemistry and Molecular Genetics, University of Virginia, Charlottesville, VA, USA, <sup>2</sup>Endocrinology, University of Virginia, Charlottesville, VA, USA.

Adrenomedullin (AM) is a peptide secreted by cancer cells that stimulates osteoblasts and new bone formation. AM overexpression in prostate cancer cells increased bone metastases in mice, while siRNA knockdown (k/d) of AM in lung adenocarcinoma cells decreased bone lesions. We hypothesized that decreasing AM expression in breast cancer cells would similarly suppress bone metastases.

Bone-metastatic MDA-MB-231 breast cancer cells were transfected with an AM shRNA expression vector or scrambled control. Single-cell clones were tested for AM knockdown (>90%) by real-time PCR. Clonal stability was assured by culturing in the absence of antibiotic selection for 60d. Two stable AM k/d and two control clones were injected into the left cardiac ventricle (n=12/group) and the mammary fat pad (MFP) (n=10/group) of nude mice. Bone lesions were monitored by x-ray over 5 wks. AM k/d cells caused greater osteolytic lesion area (17.9 vs 4.8 mm<sup>2</sup> at 5 wks; p<0.0001) than scrambled control cells. However, AM k/d decreased tumor take (2.5% vs 64.3%; p<0.0001) and growth (0.5 vs 126.4 mm<sup>3</sup> on d 26) when injected into the MFP. These responses are opposite to those seen in a PC-3 prostate cancer model, where AM overexpression increased osteolytic lesions and decreased growth of subcutaneous xenografts.

MDA-MB-231 clones (2) with AM k/d showed decreased IL-11 and ET-1 mRNA expression *in vitro* but no change in Cyr61, CTGF, IL-8, PTHrP, or IL-6 mRNAs compared to 2 control clones. Decreased IL-11 or ET-1 mRNAs were not rescued by exogenous AM peptide, suggesting an intracrine action of AM. No significant cell morphological differences were noted by microscopy. Osteoclast, osteoblast and CD31+ endothelial cells numbers and tumor burden will be assessed by histomorphometry.

The responses of breast cancer cells to reduction of AM expression were opposite to those found previously with A549 lung and PC-3 prostate models. In addition, the effects of changed tumor expression of AM have opposite effects on tumor burden in bone versus at soft tissue sites. This converse effect was noted in both breast and prostate models, suggesting that AM is a Jeckle & Hyde factor, whose active personality changes with both tumor type and microenvironment. AM acts on many cell types, including bone, tumor and endothelial cells, altering angiogenesis, tumor growth, apoptosis, and bone, which may account for tumor-type-specific responses to AM in bone metastasis. AM receptor antagonists are in preclinical development. They may be effective only against certain tumor types in specific locations and will need to be used with caution.

**Disclosures:** V.A. Siclari, None.

This study received funding from: DOD, NIH.

**M278**

**Wnt Signaling Regulates Gli2 and PTHrP Expression in Human Breast Cancer Cells that cause Osteolysis.** R. W. Johnson<sup>\*1</sup>, J. A. Sterling<sup>1</sup>, X. Li<sup>\*2</sup>, A. Roberts<sup>\*1</sup>, N. Bhowmick<sup>\*2</sup>, G. R. Mundy<sup>1</sup>. <sup>1</sup>Center for Bone Biology, Vanderbilt University, Nashville, TN, USA, <sup>2</sup>Department of Urologic Surgery, Vanderbilt University, Nashville, TN, USA.

One of the major mediators of tumor-induced bone destruction is parathyroid hormone-related peptide, PTHrP. Our previous studies have demonstrated that tumor cells that stimulate osteoclast-mediated bone destruction and express PTHrP express the Hedgehog (Hh) signaling transcriptional activator, Gli2. However, our recent data has shown that Hh is not responsible for increasing Gli2 or PTHrP expression, indicating that Gli2 and PTHrP are regulated independently of Hh. Other laboratories have demonstrated that Gli2 expression can be regulated by Wnt signaling during development, and that Wnt signaling is important in metastasis and tumor progression. Based on these observations, we hypothesized that Wnt expression by tumor cells may regulate Gli2 expression and subsequent PTHrP expression in breast cancer cells that are associated with osteolysis. To test this hypothesis, we first examined the human metastatic breast cancer cell line, MDA-MB-231, for the effects of Wnt signaling on Gli2 and PTHrP expression. To do this, we over-expressed the downstream mediator,  $\beta$ -catenin, in the MDA-MB-231 cells and performed Real-time PCR using Gli2 specific primers to determine if Wnt signaling regulates Gli2 expression. We found that  $\beta$ -catenin expression increased Gli2 expression by 2-fold. In addition to assessing Gli2 expression, we also determined both PTHrP promoter activity and expression. We found that  $\beta$ -catenin increased PTHrP promoter activity by greater than 3.5-fold. Interestingly, ICAT expression decreased Gli2-mediated PTHrP promoter activity by 50%, suggesting that Gli2-mediated regulation of PTHrP is at least in part  $\beta$ -catenin dependent, and that  $\beta$ -catenin regulates basal PTHrP secretion by the tumor cells. Real-time PCR confirmed that  $\beta$ -catenin increased and ICAT decreased endogenous PTHrP expression. In addition, treatment with a virally expressed soluble frizzled receptor protein 2 (sFRP2) decreased PTHrP expression. Finally, we found that these cells expressed Wnt 3,3a, 5a, 7a, 7b, 10b, and 16, consistent with an autocrine role for Wnt signaling in these cells. Taken together, these studies are consistent with an important role for Wnt signaling in the regulation of Gli2 and PTHrP expression in human breast cancer cells, which in turn drives PTHrP expression and causes osteolytic bone destruction. Inhibition of Wnt signaling *in vivo* may be a rational therapeutic approach to decreasing Gli2 expression and subsequent PTHrP expression and tumor-induced osteolysis.

**Disclosures:** R.W. Johnson, None.

**M279**

**The Histone Deacetylase Inhibitor, Vorinostat, Blocks Growth and Associated Osteolysis of Cancer Cells within Bone, but Reduces Bone Volume in Non-Tumor Bearing Bones in Mice.** J. Pratap<sup>1</sup>, R. Dhillon<sup>\*2</sup>, X. Li<sup>\*2</sup>, J. J. Wixted<sup>\*1</sup>, J. Akech<sup>1</sup>, K. Bedard<sup>\*1</sup>, S. Hussain<sup>\*1</sup>, J. Colby<sup>\*1</sup>, A. J. van Wijnen<sup>1</sup>, J. L. Stein<sup>\*1</sup>, G. S. Stein<sup>1</sup>, J. J. Westendorf<sup>2</sup>, J. B. Lian<sup>1</sup>. <sup>1</sup>Depts. of Cell Biology, Orthopedic Surgery and Cancer Center, University of Massachusetts Medical School, Worcester, MA, USA, <sup>2</sup>Depts. of Orthopedic Surgery and Molecular Biology, Mayo Clinic, Rochester, MN, USA.

Histone deacetylase inhibitors (HDIs) suppress the expression and/or enzymatic activities of a subset of deacetylases. HDIs alter expression of genes that control cell survival, proliferation, differentiation and migration. Tumor cells with defects in the G2/M cell cycle checkpoint undergo apoptosis in response to HDIs. Vorinostat is an oral HDI with anti-tumor activity in preclinical cancer models and is in phase I and II clinical trials for hematological and solid tumors. The effects of Vorinostat on skeletal metastases and normal bone tissue have not been described. We and others previously showed that several HDIs promote *in vitro* osteoblastic differentiation. Here, we tested effects of Vorinostat on both tumor growth and osteolytic lesions formed by prostate (PC-3) and breast (MDA-MB-231) tumor cells injected into tibias of SCID mice, and on health of the normal skeleton. Tumors cells were injected into mouse tibia one week prior to administering Vorinostat (100 mg/kg, i.p., daily for three (PC3) to seven (MDA-231) weeks). Mice were sacrificed when osteolysis became severe. MRI studies showed that Vorinostat significantly reduced tumor growth within the bone by approximately 33%. Radiographs and micro-CT analysis showed that the osteolytic bone disease was also reduced in accord with lower tumor burden. These results are consistent with decreased expression of Runx2 and their metastatic target MMPs, demonstrated by *in vitro* treatment of TSA (at 50 nM) in both PC-3 and MDA-MB-231 which express high endogenous levels of Runx2 and metastatic related genes. Surprisingly, the contralateral femurs showed significant loss of bone volume density (50%) after just three weeks of Vorinostat therapy. We hypothesize that there are selective effects of HDIs on normal osteoblast lineage cells compared to metastatic cancer cells *in vitro* and within bone. Several mechanistic pathways can account for these findings that have clinical relevance in the long-term use of Vorinostat in cancer patients. For example, increased osteoclastic resorption could be related to stimulated osteoblast activity from the HDIs and/or HDIs might prevent survival or expansion of osteoblast progenitor cells. Our studies indicate that Vorinostat is effective at inhibiting cancer growth in bone and osteolytic disease. Anti-resorptive therapy could be used to prevent therapy-induced bone loss throughout the skeleton.

**Disclosures:** J. Pratap, None.

**M280**

**Effects of Extracellular Matrix Properties and Elastic Modulus on the Expression of parathyroid hormone-related peptide (PTHrP) by Human Breast Cancer Cells.** N. S. Ruppender<sup>\*1</sup>, J. A. Sterling<sup>2</sup>, J. S. Nyman<sup>2</sup>, J. F. O'Keefe<sup>\*1</sup>, G. R. Mundy<sup>2</sup>, S. A. Guelcher<sup>\*1</sup>. <sup>1</sup>Vanderbilt University Chemical Engineering, Nashville, TN, USA, <sup>2</sup>Vanderbilt University Center for Bone Biology, Nashville, TN, USA.

When breast cancer cells metastasize to bone, they change their gene expression patterns and express PTHrP (Southby et al, 1991). The reason is unknown. We hypothesized that in the bone microenvironment, expression of osteoclastogenic factors such as PTHrP by the tumor cells is up-regulated due to the increased stiffness of the mineralized bone ECM. To test this, we created substrates to mimic the biomechanical properties of bone, and tested these for effects on PTHrP expression by the human breast cancer cell line, MDA-MB-231. Model soft and hard polyurethane (PUR) substrates were synthesized with elastic moduli of 0.05 GPa and 1.2 GPa, which mimic the estimated moduli of soft tissue (such as breast and liver) and bone, respectively. Briefly, a lysine diisocyanate prepolymer was mixed with a polyester triol or diol for 15 s, cast in the wells of a 6-well tissue culture plate, and cured at 37C for 24h. The modulus was measured by compression testing. MDA-MB-231 human breast cancer cells were cultured on the PUR substrates in 1X DMEM containing 10% heat inactivated fetal calf serum (FCS) for 48 hours. Tissue culture polystyrene (TCPS, ~2 GPa) served as a control substrate which has a modulus near the low end of the range for cortical bone. Cell morphology was observed at the 4, 24 and 48 hour time points via microscopy. Expression of PTHrP was measured by real-time PCR. Since cell attachment to substrates may also influence expression patterns, some substrates were treated with fibronectin (Fn+) prior to cell seeding. While cells seeded on TCPS (Fn+ and Fn-) and PUR substrates treated with Fn exhibited a flat morphology, cells seeded on Fn- PUR substrates were more rounded and not as well attached. For the Fn- treatment groups, expression of PTHrP for TCPS and hard PUR substrates was greater than that observed for the soft PUR substrate. For the Fn+ treatment groups, PTHrP expression was also observed to be significantly less for soft PUR substrates compared to TCPS. These data suggest that the stiffness of the substrate has a significant effect on the expression of PTHrP, either in the presence or absence of Fn. In conclusion, MDA-MB-231 human breast cancer cells respond to substrates with increasing stiffness by increasing PTHrP expression. These effects may explain in part the enhanced expression of PTHrP described in breast cancer cells that have metastasized to bone.

**Disclosures:** N.S. Ruppender, None.



## M281

**A Plasma Proteomic Profile that Predicts Breast Cancer Metastasis to Bone.** S. Byrum<sup>1</sup>, K. Leitzel<sup>\*2</sup>, S. M. Ali<sup>\*2</sup>, A. Lipton<sup>\*2</sup>, L. J. Suva<sup>1</sup>.<sup>1</sup>Orthopaedic Surgery, UAMS, Little Rock, AR, USA, <sup>2</sup>Penn State/Hershey Medical Center, Hershey, PA, USA.

Bone is a common site for the spread of breast cancer. The identification of a highly discriminatory plasma protein profile could provide a tool for the early detection of bone metastasis. The purpose of this study was to identify a protein signature indicative of breast cancer metastasis to bone. Plasma was obtained from 76 breast cancer patients treated with second-line hormone therapy: 38 patients with clinical evidence of bone metastasis and high levels of the resorption marker N-Telopeptide (NTx), and 38 patients with no clinical evidence of bone metastasis and low levels of NTx. Samples were analyzed in duplicate on weak cation-exchange (CM10) arrays using surface-enhanced laser desorption ionization time-of-flight mass spectrometry (SELDI-TOF MS) in three mass ranges: low 1.5 - 10 KD, mid 7 - 30 KD, and high 25 - 150 KD. All spectra were baseline corrected, normalized to the total ion current, log<sub>2</sub> transformed, and analyzed by analysis of variance (ANOVA), principle component analysis (PCA), random forest (RF), classification and regression trees (CART), and See5. The multivariate statistical analysis and data mining procedures ultimately resulted in the detection of thirteen specific protein peaks (MW ranging from 4.1-39.1kDa) that optimally separated the two groups with a high degree of significance (p<0.05). In all, 11 peaks were increased and 2 peaks were decreased in plasma of breast cancer patients with bone metastasis compared to breast cancer patients without bone metastasis. The plasma protein profile identified was independently validated in a blinded fashion using a second set of anonymous plasma samples from 20 patients with and 20 patients without bone metastasis; 11 of the original 13 protein peaks identified were confirmed. Importantly, one protein peak found in the plasma of bone metastasis patients was identified as parathyroid hormone-related protein (PTHrP), a tumor-derived factor expressed in a majority of bone metastasis of breast cancer. SELDI-TOF MS analysis has identified and confirmed a plasma protein profile that distinguishes breast cancer patients with and without bone metastasis. Further elucidation of the identity of these proteins has value for the early diagnosis of breast cancer bone metastasis.

**Disclosures:** S. Byrum, None.

This study received funding from: AR Breast Cancer Research Fund.

## M282

**Zoledronate Protects Bone but not Soft Tissue from Prostate Cancer Progression in a Nude Mouse Model.** R. L. Fitzgerald<sup>1</sup>, D. W. Burton<sup>2</sup>, T. L. Griffin<sup>\*3</sup>, D. J. Hillegonds<sup>4</sup>, D. A. Herold<sup>\*1</sup>, L. J. Deftos<sup>2</sup>. <sup>1</sup>Pathology, VA Medical Center/UCSD, San Diego, CA, USA, <sup>2</sup>Medicine, VA Medical Center/UCSD, San Diego, CA, USA, <sup>3</sup>Pathology, VA Medical Center, San Diego, CA, USA, <sup>4</sup>Center for Accelerator Mass Spectrometry, Lawrence Livermore National Laboratories, Livermore, CA, USA.

**Background:** Metastatic bone disease is one of the major causes of morbidity and mortality in prostate cancer patients. Bisphosphonates are currently used to inhibit bone resorption and reduce tumor induced skeletal complications. While widely used with good clinical efficacy, the dynamics of prostate cancer growth and progression after bisphosphonate treatment are somewhat unclear, as there are reports in animal models that indicate the bisphosphonates can increase the incidence of metastases to soft tissues.

**Methods:** Prostate tumor growth was studied using PTHrP-expressing PC-3 GFP cells that were injected into the tibiae of immunocompromised mice. The controls received saline injections and no tumor implantation (Saline/Saline, N=6). The second group received saline and tumor implantation (Saline/Tumor, N=5) and the third group of animals received zoledronate and tumor implantation (ZOL/TumorN=4). The effects of zoledronate on tumor growth in bone and outside of the bone microenvironment were evaluated fluorometrically, radiologically and histologically.

**Results:** Zoledronate protected bone from tumor mediated destruction but demonstrated a significant increase in fluorescence once the cancer expanded beyond the bone as compared to the saline treated group (see Figure below). At the end of the study, x-ray data demonstrated a significant reduction in the severity of bone lesions in the zoledronate group compared to the saline group. The histology of the tumors demonstrated more condensed nuclei in the saline group compared to the zoledronate treated group.

**Conclusions:** We showed that zoledronate was effective in reducing the severity of the bone lesions but not tumor burden outside of the bone in animals treated with PTHrP-expressing prostate cancer cells

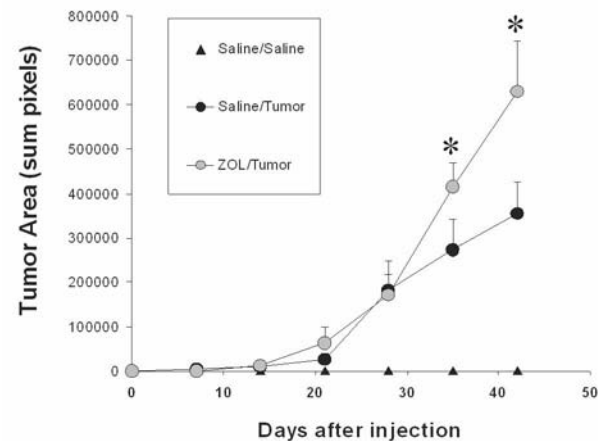


**Figure Legend:** Prostate cancer tumor growth curves in mice implanted with PC-3-GFP cells. Fluorescent images were quantitated for GFP (sum of the pixels) as an index of tumor mass and normalized to an external fluorescent standard. The asterisks represent significant differences ( $P < 0.05$ ) between the tumor bearing mice treated with zoledronate (ZOL) vs. saline.

**Disclosures:** R.L. Fitzgerald, None.

This study received funding from: NIH R21 CA118337-01.

## M283

**Prevention of Aromatase Inhibitor-Associated Bone Loss in Women with Breast Cancer: Practical Guidance.** P. Hadji<sup>1</sup>, M. Aapro<sup>\*2</sup>, A. Brufsky<sup>\*3</sup>, M. Tubiana-Hulin<sup>\*4</sup>, T. Guise<sup>5</sup>, J. Body<sup>\*6</sup>. <sup>1</sup>Philipps-University of Marburg, Marburg, Germany, <sup>2</sup>Institut Multidisciplinaire d'Oncologie, Genolier, Switzerland, <sup>3</sup>University of Pittsburgh, Pittsburgh, OH, USA, <sup>4</sup>Centre René Huguenin, St-Cloud, France, <sup>5</sup>University of Virginia, Charlottesville, VA, USA, <sup>6</sup>Université Libre de Bruxelles, Brussels, Belgium.

American Society of Clinical Oncology guidelines recommend that women with breast cancer (BC) and osteoporosis (T-score < -2.5) be treated with bisphosphonates and that osteopenic women (T-score -1 to -2.5) receive individualized therapy. However, the majority of fractures occur in osteopenic women. Therefore, the osteoporosis (T-score < -2.5) threshold may be inadequate to avert fractures in patients with BC, particularly those being treated with aromatase inhibitors (AIs). Because bone mineral density (BMD) testing is not readily available to all patients, guidance is required to assess fracture risk and select treatment with/without BMD scores. A systematic literature review was performed to identify factors contributing to elevated fracture risk in women with BC. Risk factors were evaluated by an evidence-based medicine approach to identify patients at high risk, to determine when to initiate bisphosphonate therapy, and to identify the appropriate bisphosphonate for use.

Fracture risk factors (other than AI therapy) were identified based on their validation in large, prospective, population-based studies. Risk factors in women with BC were AI therapy, T-score 65 yr, family history of hip fracture, personal history of fragility fracture after age 50, oral corticosteroid use for > 6 mo, or body mass index < 20. Additional risk factors for which guidance could not be provided because of insufficient data included diagnosis of BC, chemotherapy, radiotherapy, low weight, and smoking. Currently available data clearly suggest that combined risk factors indicate fracture risk independent of BMD and that osteoporosis need not precede fracture. BMD measurement should therefore not be the sole criterion to assess fracture risk in women with BC. Randomized clinical trials in patients at risk for fracture support the use of zoledronic acid (4 mg every 6 mo) to prevent AI-associated bone loss when a patient is identified to be at risk. Data with other bisphosphonates are emerging.

We recommend that any patient initiating AI therapy with T-score < -2.0 should receive zoledronic acid (4 mg every 6 mo) in addition to calcium and vitamin D supplements. Zoledronic acid should also be used in patients with any 2 of the following: T-score < -1.5, age > 65 yr, family history of hip fracture, personal history of fragility fracture after age 50, and oral corticosteroid therapy > 6 mo.

**Disclosures:** P. Hadji, Novartis 2, 3; Amgen 2, 3; AstraZeneca 2, 3; Eli Lilly 2, 3.

This study received funding from: Novartis.

## M284

**Phthalein Monophosphates Are Specific Substrates for Tartrate-Resistant Acid Phosphatase 5b.** B. Houston<sup>1</sup>, H. Ylipahkala<sup>2</sup>, J. M. Halleen<sup>3</sup>, D. Laurie<sup>1</sup>. <sup>1</sup>Immunodiagnostic Systems (IDS) Ltd, Boldon, United Kingdom, <sup>2</sup>SBA Sciences Ltd, Oulu, Finland, <sup>3</sup>Pharmatest Services Ltd, Turku, Finland.

Tartrate-resistant acid phosphatase 5b (TRACP5b) is secreted exclusively by osteoclasts. The level of TRACP5b in serum is a measure of osteoclast abundance and hence an indirect indicator of bone resorption. Measurement of TRACP5b in serum is complicated by the presence of an approximately 10-fold molar excess of TRACP5a, produced principally by macrophages and dendritic cells. An existing commercial immunoassay for TRACP5b involves the capture of TRACP5 by an immobilised antibody, followed by an activity measurement at a pH where the specific activity of TRACP5b is around 10x that of the TRACP5a. In seeking to transfer this assay onto the IDS Automated Analyser 3X3™, we encountered problems relating to the stability of the substrate pNPP. This led us to examine the utility of phthalein monophosphates (PMs) as TRACP5b substrates.

We examined the abilities of human serum-derived TRACP5a and TRACP5b (separated by chromatography on CM-Sepharose), and baculovirus-derived recombinant human TRACP5, to hydrolyse PMs. All TRACP5 preparations hydrolysed phenolphthalein monophosphate (PTMP) and thymolphthalein monophosphate (TTMP). We observed dramatic differences between the pH optima of these preparations with the PM substrates compared to those determined with pNPP. For example, using PTMP the pH optima of TRACP5a and TRACP5b were around 6.0 and 7.0 respectively. These values are markedly higher than those obtained using pNPP (4.9 and 5.9 respectively).

We next established an immunoassay for TRACP5 in which the enzyme activity was measured using PTMP at pH 7.0, and compared this with the commercial immunoassay using pNPP at pH 6.1. Typical specific activities obtained for the native TRACP5 forms were: TRACP5a (PTMP); 0.035 U/μg; TRACP5a (pNPP); 0.177 U/μg; TRACP5b (PTMP); 1.68 U/μg; TRACP5b (pNPP); 1.60 U/μg. These data indicate that while the PTMP- and pNPP-based assays detect similar amounts of TRACP5b, the PTMP-based assay detects only 20% of the TRACP5a detected by the pNPP-based assay. On a panel of 32 patient samples there was an excellent correlation between the PTMP and pNPP-based assays ( $R^2 = 0.96$ ). The values obtained with the PTMP-based assay were slightly lower than those obtained using the pNPP-based assay ( $y=1.09x-0.62$ ), consistent with the former experiencing less interference by TRACP5a.

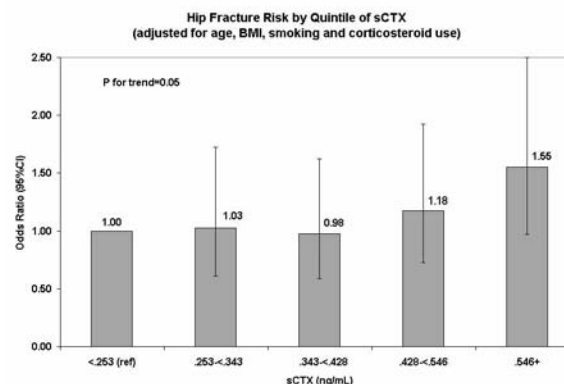
Our results demonstrate that phthalein monophosphates are more specific substrates for TRACP5b than pNPP and related compounds, by providing an assay where the specific activity of TRACP5b approaches 50x that of TRACP5a. They also reveal that TRACP5 is not intrinsically an acid phosphatase, but that the pH optimum of the enzyme is dependent upon the substrate.

**Disclosures:** B. Houston, IDS Ltd 2.

## M285

**Bone Turnover and Incident Hip Fracture Risk: The Women's Health Initiative (WHI).** D. C. Bauer<sup>1</sup>, S. Harrison<sup>2</sup>, R. Jackson<sup>3</sup>, M. LeBoff<sup>4</sup>, J. Robbins<sup>5</sup>, N. Greep<sup>6</sup>, A. LaCroix<sup>7</sup>, J. A. Cauley<sup>8</sup>. <sup>1</sup>UCSF, San Francisco, CA, USA, <sup>2</sup>CPMC, San Francisco, CA, USA, <sup>3</sup>Ohio State University, Columbus, OH, USA, <sup>4</sup>Brigham and Women's Hospital, Boston, MA, USA, <sup>5</sup>UC Davis, Sacramento, CA, USA, <sup>6</sup>UC Irving, Irving, CA, USA, <sup>7</sup>Fred Hutchinson, Seattle, WA, USA, <sup>8</sup>University of Pittsburgh, Pittsburgh, PA, USA.

Elevated bone turnover is associated with an increased risk of fracture in some, but not all, prospective studies of older women. To determine if bone turnover predicts hip fracture risk in community dwelling women, we performed a nested case-control study in the WHI Observational Study Cohort. We excluded women with previous hip fracture and those who used hormones or other osteoporosis medications. A total of 39,793 women met these criteria. We randomly chose 400 women with incident hip fractures confirmed by central review of medical records. A control was selected for each case, matched on baseline age, race/ethnicity and date of blood draw. A marker of bone resorption,  $\beta$ CTX (Roche Diagnostics), and a marker of bone formation, PINP (Roche Diagnostics), were measured in a single batch at a core laboratory (Synarc, Lyon) using archived fasting serum drawn at baseline. We used conditional logistic regression models that account for the matched case-control design to estimate the odds ratio (OR) and 95% confidence intervals (CI) per SD increase in marker, and across quintiles (defined by the distribution in controls) with p values for tests of linear trend. We adjusted for other risk factors associated with both hip fracture and bone turnover (age, BMI, smoking and corticosteroid use), but unadjusted results were similar. The mean age of cases and controls was 70.8 years; 95% were White. Mean  $\beta$ CTX levels were higher among cases than controls ( $0.446 \pm 0.206$  vs.  $0.412 \pm 0.187$  ng/ml,  $p=0.02$ ), but were similar for PINP ( $51.0 \pm 23.0$  vs.  $49.0 \pm 20.4$  ng/ml,  $p=0.2$ ). Higher quintiles of  $\beta$ CTX were associated with increased hip fracture risk ( $p$ -trend = 0.05)(Figure). Compared to women in the lower 4 quintiles of  $\beta$ CTX, hip fracture risk was elevated among those in the highest quintile ( $>0.546$  ng/ml, OR = 1.49, 95% CI: 1.04, 2.16). PINP was not associated with hip fracture risk ( $p$ -trend = 0.43). BMD was not available in the full cohort. Our results suggest that elevated  $\beta$ CTX, but not PINP, is associated with a modest increase in hip fracture risk in older women, but the relationship may be too weak to be useful as an independent clinical risk factor for hip fracture.



**Disclosures:** D.C. Bauer, Roche Diagnostics 4; Tethys 2. This study received funding from: NHLBI and NIAMS.

## M286

**Stability of TRACP 5b in Rat and Mouse Serum.** H. Ylipahkala<sup>1</sup>, L. Wahlberg<sup>2</sup>, J. M. Halleen<sup>2</sup>. <sup>1</sup>SBA Sciences Ltd, Oulu, Finland, <sup>2</sup>Pharmatest Services Ltd, Turku, Finland.

Osteoclasts secrete tartrate-resistant acid phosphatase (TRACP) 5b into the blood circulation, and serum TRACP 5b is a useful marker of osteoclast number in rat and mouse ovariectomy models. In human serum, TRACP 5b is otherwise stable enough for routine laboratory measurements, but long term storage at -20°C should be avoided. Here we have studied stability of TRACP 5b in rat and mouse serum samples. Rat and mouse serum samples were stored for up to one week at +37°C, room temperature and +4°C, and up to one month at -20°C and -70°C, and TRACP 5b activity was measured at various time points. At +37°C, TRACP 5b values decreased rapidly in both rat and mouse serum. The values decreased by 40% already after 2 hours. At room temperature, rat serum TRACP values did not change after 4 hours, but the values decreased by 40% after 8 hours. However, mouse serum TRACP 5b values did not change during 24 hours of storage at room temperature. At +4°C, rat serum TRACP values did not change during 3 days of storage, but the values were decreased by 40% after 7 days. Surprisingly, mouse serum TRACP 5b values increased by 34% after 4 hours, and stayed in the increased level for at least up to 7 days. Rat and mouse serum TRACP 5b values did not change during one month storage at -20°C and -70°C. When the samples were stored at -20°C and -70°C, after freezing and thawing, rat serum TRACP 5b values remained unchanged, but mouse serum TRACP 5b values increased by 75-85% already after 7 days. These results demonstrate that rat serum TRACP 5b is stable for 4 hours at room temperature, for 3 days at +4°C, and for up to one month when the samples are stored frozen at -20°C and -70°C both before and after freezing and thawing. Mouse serum TRACP 5b is stable at room temperature for up to 24 hours and at -20°C and -70°C for up to one month, but the values increase rapidly when the samples are stored at +4°C or frozen at -20°C and -70°C after freezing and thawing. As a conclusion, the handling and storing rat and mouse serum samples for subsequent TRACP 5b measurements should be done with care to avoid undesirable changes in the values.

**Disclosures:** H. Ylipahkala, SBA Sciences Ltd 2.

## M287

**The Bone Degradation Marker CTX Shows Unique Properties in Disease Monitoring Compared to NTX, ICTP and bALP in Multiple Myeloma.** T. Lund<sup>1</sup>, J. Delaisse<sup>1</sup>, N. Abildgaard<sup>2</sup>, K. Kupisiewicz<sup>1</sup>, T. L. Andersen<sup>1</sup>, K. Soe<sup>1</sup>, T. Plesner<sup>1</sup>. <sup>1</sup>Clinical Cell Biology, Vejle Hospital, Vejle, Denmark, <sup>2</sup>Hematology, Odense University Hospital, Odense, Denmark.

Multiple myeloma (MM) is a haematological malignancy with a high degree of skeletal morbidity. 80 % of the patients present with osteolyses, pathological fractures, vertebral compression fractures and/or osteopenia on skeletal survey at diagnosis. MM causes an unbalanced bone resorption and formation as the myeloma cell induces factors stimulating osteoclast activity and inhibiting osteoblast activity. Various markers of bone turnover have been tested for prognostic value in multiple myeloma. Here we tested if consecutive measurements of bone markers could detect progressive disease (1), development of osteolysis (2) and response to treatment (3) in the individual patient. In 106 patients the bone resorption markers ICTP (CTX-MMP), NTX-I, CTX-I and bALP as well as serum M-component and serum free light kappa/lambda chains (FLC), were measured every fourth week for up to 22 months. Disease progression and response to treatment were defined according to the International Uniform Response Criteria for Multiple Myeloma 2006. In case of disease progression, bone marker values at plateau phase were compared to values when progressive disease was first detected. Development of osteolysis was evaluated by conventional radiography or computed tomography. Patients who received new treatment were divided into responders and non-responders. Bone marker values prior to treatment were compared to values when treatment was stopped or when best response during treatment was achieved.

Progressive disease was observed in 40 cases (1). Bone morbidity was evaluated in 26 patients at the time of disease progression (2). A statistically significant mean increase in

CTX-I of 44 percent was found at the time of disease progression. No deterioration in renal function was seen. No significant changes were observed in ICTP, NTX-I or bALP. Patients developing osteolysis had a statistically significant higher increase in CTX-I of 344% compared to patients who had no new osteolytic lesions. New treatment was initiated in 50 cases (3), and 33 responded. A significant decline in CTX-I of 52 percent was observed in responding patients. No significant changes in CTX-I were observed in the non-responding group. NTX-I, ICTP or bALP showed no significant changes, neither in the responding patients nor in the non-responding patients. Our data indicate that CTX-I may be a useful marker of disease progression, development of osteolysis and response to treatment in multiple myeloma. CTX-I appears to be a better marker for monitoring disease activity and bone morbidity in multiple myeloma than NTX-I, ICTP and bALP.

**Disclosures:** T. Lund, None.

## M288

**Bone Resorption Markers in Saliva. Experimental Longitudinal Study.** G. G. Pellegrini<sup>\*1</sup>, M. M. Gonzales Chaves<sup>\*1</sup>, J. I. Somoza<sup>\*2</sup>, S. M. Friedman<sup>\*1</sup>, S. N. Zeni<sup>2</sup>. <sup>1</sup>Cátedra de Bioquímica General y Bucal, Facultad de Odontología, Universidad de Buenos Aires, Argentina, <sup>2</sup>Sección de Osteopatías Médicas, Hospital de Clínicas, Universidad de Buenos Aires, Argentina.

Previously, we measured terminal C-telopeptide of collagen type I (CTX) in saliva. The present longitudinal experimental study sought to determine whether salivary concentrations of CTX have the same response as in serum samples under different conditions: normal, increased, and reduced bone remodeling. Thirty rats were ovariectomized (OVX) and 10 rats were SHAM operated. The rats were divided into 4 groups (G) and treated as follows for 45 days: G1 = SHAM+vehicle; G2 = OVX + 8 mg olpadronate (OPD)/100 g body weight (BW); G3 = OVX + 4 mg OPD/100 g BW ;G4 = OVX +vehicle. Saliva and serum CTX (ng/ml) were determined by ELISA (Rat Laps. Osteometer BioTech, Denmark) at baseline (t=initial), at t=10, t=20 and t=45 days of surgery. Results (mean±SD): (table 1) There were no differences in salivary CTX levels at baseline. G4 presented the highest salivary CTX levels compared to the other 3 groups throughout the experience (P <0.05). Salivary CTX values remained unchanged in G1 and G2 and decreased in G3 (P <0.01). Salivary CTX levels were similar in G1 and G2 and significantly lower in G3 (p<0.05). Conclusions: Saliva samples responded like serum samples to changes in bone turnover. Then saliva may prove to be a practical and reliable sample to evaluate changes in bone remodeling and to monitor therapy with anticatabolic drugs.

**Disclosures:** G.G. Pellegrini, None.

This study received funding from: Grant M099: UBACyT and CONICET.

## M289

**Relationship Between Adipokines and Biochemical Bone Markers in Osteoporotic Women Before and After Growth Hormone Supplementation.** B. H. Durham<sup>1</sup>, F. Joseph<sup>\*2</sup>, R. Sodi<sup>\*1</sup>, J. P. Vora<sup>\*2</sup>, W. D. Fraser<sup>1</sup>. <sup>1</sup>Clinical Chemistry, Royal Liverpool University Hospital, Liverpool, United Kingdom, <sup>2</sup>Clinical Endocrinology, Royal Liverpool University Hospital, Liverpool, United Kingdom.

We have studied the relationship between adipokines and biochemical markers of bone formation and resorption in 14 post menopausal women with osteoporosis, average age 63.4 ± 2.1 yr, before and after 6m growth hormone supplementation [GH]. After an overnight fast, prior to and after 6m GH, serum/plasma was obtained and stored at -70C until analysed. The adipokines measured were adiponectin [Apn], ghrelin [Grn], leptin [Lpn] and the panel of bone markers were osteocalcin [OC], bone alkaline phosphatase [BoneALP], and amino terminal extension of type1 collagen [PINP] for formation and carboxy and amino telopeptides of type1 collagen [beta CTX, NTX], bone acid phosphatase [TRACP5b] and cathepsin K [CathK] for resorption. Also measured was osteoprotegerin [OPG]. All assays had CVs for the measurable range of 4-7%, correlations were calculated by Pearson's formula. There was no significant change in Lpn 28.6 ± 8.2 vs 28.4 ± 7.5 ng/mL or Grn 17.2 ± 3.7 vs 16.7 ± 4.0 ng/mL. Apn increased by 24% 9.9 ± 3.8 vs 12.3 ± 3.8ng/mL [ns]. There was no significant correlation between any of the adipokines or the change in them after 6m GH, also there was no significant correlations between the change in adipokines and that for any of the bone markers. Prior to GH there were significant negative correlations between Lpn and beta CTX, NTX, TRACP5b, CathK [p<0.05] and OC, PINP [p<0.01]; there was a significant negative correlation between Apn and OPG and beta CTX [p<0.05] but there were no significant correlations between Grn and any of the bone markers. After 6m GH only the correlations between Lpn v TRACP5b [p<0.01] and CathK [p<0.05] remained significant, also Apn v OPG [p<0.05]; significant positive correlations were found between Grn and NTX [p<0.05] and osteoclast activity [NTX/TRACP5b] [p<0.01]. The only significant correlations that were present prior to and after 6m GH were those for Lpn v TRACP5b, CathK and Apn v OPG. From this study it appears that in elderly osteoporotic women Lpn has a negative influence on bone formation and resorption; the stronger correlations were with formation markers. Grn has no effect on bone turnover whereas Apn has an inverse effect on OPG. After GH supplementation, which increases circulating IGF1 to pre-menopausal levels, the correlations between Lpn and collagen1 turnover markers disappear but the negative correlation with TRACP5b [ a marker of osteoclast number] remains. Grn has a positive influence on bone resorption whereas that of Apn is independent of IGF1 levels. The 3 adipokines studied have an inverse effect on aspects of bone turnover.

**Disclosures:** B.H. Durham, None.

## M290

**Changes of Biochemical Resorption Markers During Fracture Healing in Osteoporosis.** C. Heiss<sup>\*</sup>. Trauma and Experimental Surgery, University Hospital of Giessen-Marburg, Giessen, Germany.

**INTRODUCTION** The aim of this study was to evaluate the development of biochemical resorption markers during the fracture healing in patients with osteoporotic fractures of the proximal femur.

### METHODS

This prospective, explorative follow-up study included 33 patients who sustained a fracture of the proximal femur and 25 control persons without a fracture. We recruited 35 patients with a fracture of the distal forearm to compare typical osteoporosis-associated fracture locations. The concentration of the resorption markers N-terminal telopeptide (NTx), Desoxypyridinoline (D-Pyr) and Pyridinoline (Pyr) were measured in the first urine spot preoperatively and at day 2, 4, 10 and 14 postoperatively. Further the Bone Mineral Density (BMD) of the lumbar spine was determined in all patients with the qCT to diagnose an osteoporosis.

**RESULTS** Among the 33 study patients with a femur fracture were 60% women and 40% men, an osteoporosis was diagnosed in 90% of all the patients, while only 10% showed a normal bone density. We found a positive correlation between age and BMD in both sexes (female p=0.002; men p=0.01). It was noticed that peritrochanteric fractures were more common with 64% than femoral neck. A statistically significant increase was found in the three measured resorption markers NTx, D-Pyr and Pyr during the observing period of 14 days of fracture healing (p<0.001). Patients suffering from osteoporosis had higher concentrations of markers than non-osteoporotic patients during the fracture healing, and female patients showed a higher increase of markers than men. Patients who sustained a peritrochanteric femur fracture had higher concentrations of markers than patients with a femoral neck fracture. Women with a femur fracture showed higher concentrations of resorption markers than women who sustained a distal forearm fracture. Higher concentrations of the resorption markers in patients were found who underwent a cemented total hip replacement than in patients with an uncemented implantation of the prosthesis.

**DISCUSSION** NTx, D-Pyr and Pyr remained unchanged during the first 2 days after operation, reflecting Phase I of fracture healing (activation), and significantly increased from day 4 to 14 reflecting Phase II (resorption). Bonemarkers showed higher concentrations in individuals with osteoporosis. This may be due to the overall increased bone resorption associated with this disease. This study described trends in the development of biochemical markers during the early period of fracture healing. If we better understand the function, the postoperative development and the meaning of bone markers during the fracture healing, it should be possible to improve the treatment of osteoporotic fractures in the future.

**Disclosures:** C. Heiss, None.

## M291

**The Relationship Between Biochemical Bone Markers in Osteoporotic Women Before and After 6 Months Treatment with Either Growth Hormone, Strontium Ranelate or Growth Hormone Plus Strontium.** B. H. Durham<sup>1</sup>, F. Joseph<sup>\*2</sup>, A. A. Joshi<sup>\*2</sup>, J. P. Vora<sup>\*2</sup>, W. D. Fraser<sup>1</sup>. <sup>1</sup>Clinical Chemistry, Royal Liverpool University Hospital, Liverpool, United Kingdom, <sup>2</sup>Clinical Endocrinology, Royal Liverpool University Hospital, Liverpool, United Kingdom.

We have studied the relationship between biochemical bone markers in a group of 28 osteoporotic women, age 65 ± 4y, before and after 6 m treatment with either growth hormone supplementation [GH] or 2g/d of strontium ranelate [StR] or a combination of the two [GHSr]. Fourteen received GH, 8 StR and 6 GHSr. After an overnight fast, prior to and after 6m of treatment, serum/plasma was obtained and stored at -70C until analysed. Each marker was analysed in the same run. The markers were:- for formation osteocalcin [OC], bone alkaline phosphatase [Bone ALP], amino terminal extension of type1 collagen [PINP] and for resorption carboxy and amino telopeptides of type1 collagen [beta CTX, NTX], bone acid phosphatase [TRACP5b], osteoclast activity [OcAct] was calculated as [NTX/TRACP5b]; osteoprotegerin [OPG] was also measured. The significance of the correlations was calculated using Pearson's formula. Before treatment the correlations that showed statistical significance were: OC vs PINP, beta CTX, NTX, TRACP5b [p<0.01], BoneALP [p<0.05]; PINP vs OC, BoneALP, beta CTX [p<0.01], TRACP5b [p<0.05]; BoneALP vs OC, PINP, beta CTX, NTX, TRACP5b [p<0.01]; beta CTX vs Oc, PINP, BoneALP, TRACP5b [p<0.01]; TRACP5b vs OC, BalP, beta CTX, NTX, OPG [p<0.01], PINP [p<0.05]; OcAct vs -TRACP5b [p<0.01], -OPG [p<0.05]; OPG vs TRACP5b [p<0.01], -OcAct [p<0.05]. After GH treatment most of the significant correlations disappeared, OC vs PINP [p<0.01], BoneALP vs TRACP5b [p<0.01], OcAct vs NTX [p<0.01] remained but no significance vs TRACP5b, the other component of the calculation. A similar picture was seen after StR, the remaining significant correlations were: OC vs BoneALP, beta CTX [p<0.05]; beta CTX vs OC, TRACP5b [p<0.05], OcAct vs NTX [p<0.05]. After the combination GHSr most of the significant correlations remained, the main exceptions were TRACP5b vs PINP, BoneALP, beta CTX, NTX, OPG. In all 3 treatment regimes the significance of the correlations between TRACP5b and PINP, NTX, OPG and between OPG and OcAct disappeared. Pre-treatment there were significant correlations between formation and resorption values. After 6m of GH or StR treatment the significances between formation and resorption markers disappeared; only with the combination GHSr did most of the significant correlations remain. In the 3 treatments osteoclast numbers [TRACP5b] and osteoblast activity [BoneALP] were uncoupled from other markers of resorption and formation.

**Disclosures:** B.H. Durham, None.

## M292

**Vitamin D Insufficiency Together with High Serum Levels of Vitamin A Increase the Osteoporosis Risk in Postmenopausal Women.** J. Mata-Granados<sup>\*1</sup>, J. Cuenca-Acevedo<sup>\*2</sup>, I. Serrano-Alferez<sup>\*2</sup>, J. Caballero-Villaras<sup>\*2</sup>, M. Luque de Castro<sup>\*3</sup>, J. Quesada-Gómez<sup>\*4</sup>. <sup>1</sup>Sanyres I+D+i, Córdoba, Spain, <sup>2</sup>Mineral Metabolism Unit. Endocrinology, Hospital Reina Sofía, Córdoba, Spain, <sup>3</sup>Department of Analytical Chemistry, University of Córdoba, Córdoba, Spain, <sup>4</sup>Mineral metabolism Unit. Endocrinology, Hospital Reina Sofía, Córdoba, Spain.

Nutrition plays an important role in bone health. Hypovitaminosis D is a contributor factor both to development of osteopenia-osteoporosis and to muscle weakness and falls; therefore, vitamin D (25OHD) insufficiency is a determinant of osteoporosis fractures. An excess of vitamin A (retinol) stimulates bone resorption, inhibits bone formation, and antagonizes the ability of vitamin D to maintain normal serum calcium levels, which may also contribute to the accelerated bone loss and fracture risk.

We assessed the prevalence of low levels of 25OHD and high levels of vitamin A and their impact over the bone mineral density (BMD) in a cross-sectional study of 232 postmenopausal Spanish women referred to outpatient clinic of the Bone Mineral Metabolism Unit at the "Reina Sofía" Hospital (Córdoba, Spain) for osteoporosis screening.

Vitamin A and 25OHD were measured by a fully automated high performance liquid chromatography (HPLC) method. The BMD was measured at both the lumbar spine (LS) and the femoral neck (FN) by dual-energy X-ray absorptiometry with a Hologic QDR1000 densitometer.

The prevalence of high serum levels of vitamin A ( $\geq 2.8 \mu\text{M}$ ) was 36.4 %. Vitamin A concentration was higher in osteoporotic (3.33  $\mu\text{M}$ ) than non osteoporotic (3.04  $\mu\text{M}$ ) postmenopausal women ( $p < 0.05$ ) for bone mineral density measured in femoral neck (BMD-FN). The prevalence of vitamin D insufficiency ( $25\text{OHD}_3 < 50 \text{ nM}$ ) was 55.76%; meanwhile 14.29% showed deficiency of vitamin D ( $25\text{OHD}_3 < 25 \text{ nM}$ ) and only 29.95% postmenopausal women had normal level of vitamin D. The serum level of 25OHD<sub>3</sub> was lower in the osteoporotic group vs. non osteoporotic women, both in BMD-FN (44.92 nM vs. 51.83 nM;  $p < 0.01$ ), and BMD-LS (47.35 nM vs. 52.48;  $p < 0.05$ ). Among subjects with vitamin D below 50 nmol/L, 30.4% had high serum levels of retinol. Moreover, the group with high level of vitamin A showed low values of both BMD-FN ( $p < 0.0001$ ) and BMD-LS ( $p = 0.04$ ).

In conclusion, high levels of vitamin A, a known factor of bone loss, should be considered as a determinant factor of low BMD and bone fracture risk, mainly if it coexists with insufficiency of vitamin D. Since supplements contribute significantly to vitamin A intake, the amounts of retinol in fortified foods and vitamin supplements may need to be reassessed.

**Disclosures:** J. Mata-Granados, None.

This study received funding from: Grants P06-FQM-01515, CM0010/05 and SAF2005-05254; Teams PAI CTS-413, and PAI FQM-227 of Junta de Andalucía, and Sanyres (Grupo PRASA), Córdoba (Spain).

## M293

**Serum PINP is a Sensitive Marker of Bone Formation in Mouse Ovariectomy Model.** J. P. Rissanen<sup>1</sup>, Z. Peng<sup>1</sup>, M. I. Suominen<sup>1</sup>, C. Otto<sup>\*2</sup>, T. Wintermantel<sup>\*2</sup>, J. M. Halleen<sup>1</sup>. <sup>1</sup>Pharmatest Services Ltd, Turku, Finland, <sup>2</sup>Bayer Schering Pharma AG, Berlin, Germany.

We have previously shown that serum procollagen I N-terminal propeptide (PINP) is a sensitive marker of bone formation in rat ovariectomy (OVX) model. Here we have studied serum PINP as a bone formation marker in mouse OVX model. Three-month-old female mice from two different strains, C3H/HeN and C57Black/6J, were included in the study. Three study groups ( $n=12/\text{group}$ ) were included for both strains as follows: 1) Sham-operated control group receiving vehicle; 2) OVX group receiving vehicle; 3) OVX group receiving  $17\beta$ -estradiol (E2, 3  $\mu\text{g}/\text{kg}/\text{day}$  s.c.). PINP was determined as a marker of bone formation and C-terminal cross-linked telopeptides of type I collagen (CTX) as a marker of bone resorption. These two bone turnover markers were measured by immunoassays from fasting serum samples before the operations and at 2, 6, 10 and 14 days after the operations. Bone mineral density (BMD) values were determined from tibial metaphysis at 6 weeks after the operation using peripheral quantitative computed tomography (pQCT). Ovariectomized animals showed decreased uterus weight and total BMD compared to sham controls in both strains, demonstrating successful estrogen depletion and osteopenia by OVX. As expected, these effects were prevented by E2 application. Serum PINP was strongly elevated already at day 6 after OVX in both strains, and this elevation was prevented by E2. In C57Black/6J mice, CTX values showed similar changes, but not earlier than at day 14. In C3H/HeN mice, CTX values did not change as a result of OVX within 14 days after the operation. These results demonstrate that serum PINP is a sensitive marker of bone formation that describes changes in bone homeostasis in mouse OVX model. PINP values change rapidly after OVX, and short-term changes in PINP predict long-term changes in BMD in mouse OVX model.

**Disclosures:** J.P. Rissanen, None.

This study received funding from: Bayer Schering Pharma AG.

## M294

**Vitamin D Deficiency is Highly Prevalent in Irish Hip Fracture Patients.** J. G. Browne<sup>\*</sup>, B. Brennan<sup>\*</sup>, M. Healy<sup>\*</sup>, N. Maher<sup>\*</sup>, M. C. Casey<sup>\*</sup>, J. B. Walsh. Medicine for the Elderly, St James Hospital, Dublin, Ireland.

The purpose of the study was to assess the prevalence of hypovitaminosis D in acute hip fracture patients within a Dublin hospital. It is well established that vitamin D levels are sub-optimal in the elderly and that adults with fragility fracture are more likely to have serum vitamin D levels either lower than those of control patients of similar age.

This was a retrospective review of hip fracture patients admitted to St James Hospital, Dublin (Latitude 53° 20' N), reviewing levels of serum 25-hydroxyvitamin D (Vitamin D), parathyroid hormone, markers of bone turnover (CTX, Osteocalcin, PINP) and calculated glomerular filtration rates (GFRs).

Between October 2003 to October 2006, 449 hip fracture patients were admitted with 171 hip fracture patients having a serum 25 Vitamin D available. These patients were further analysed. Mean age was 78.49 ( $\pm 9.64$ ) years, with 76% of patients being female. 13.4% were on calcium and vitamin D supplementation at the time of fracture. Mean Vitamin D was 41.86 ( $\pm 25.17$ ) nmol/L and PTH was 51.76 ( $\pm 44.39$ ) pg/mL, with 18.6% of patients having a level of PTH above 75pg/mL. 25% of patients had a calculated GFR of less than 30mls/min with a further 52% with a GFR between 30 to 60 mls/min. Vitamin D levels were subdivided into 3 categories: Severe Vitamin D deficiency (50 nmol/L). Using these criteria, 28.5% had severe vitamin D deficiency and 37.4 % had vitamin D insufficiency. Patients who had been on vitamin D supplementation at the time of fracture were excluded.

Subgroups of Patients with Categories of Vitamin D compared to Bone Markers, PTH and GFR.

	Vitamin D Deficiency <20 nmol/L (n=42)	Vitamin D Insufficiency 20-50 nmol/L (n=55)	Vitamin D Replete >50 nmol/L (n=50)
Age (Yrs)	77.84 ( $\pm 7.84$ )	79.75 ( $\pm 9.69$ )	76.58 ( $\pm 9.31$ )
PTH (pg/mL)	65.98 ( $\pm 47.92$ )	48.02 ( $\pm 46.55$ )	39.64 ( $\pm 28.23$ )
GFR (ml/min)	36.94 ( $\pm 20.37$ )	31.21 ( $\pm 19.85$ )	52.17 ( $\pm 31.45$ )
CTX	0.653 ( $\pm 0.553$ )	0.592 ( $\pm 0.357$ )	0.594 ( $\pm 0.328$ )
Osteocalcin	32.2 ( $\pm 33.62$ )	28.17 ( $\pm 34.15$ )	24.41 ( $\pm 17.51$ )
PINP	149 ( $\pm 224.3$ )	78.79 ( $\pm 60.34$ )	101.78 ( $\pm 72.15$ )

In conclusion, vitamin D deficiency is highly prevalent in Irish patients with hip fracture, with almost a third demonstrating severe vitamin D deficiency. These patients showed increased levels of PTH, reduced renal function and increased bone turnover, as compared to those that were replete. One quarter of patients showed significant renal impairment, which suggests that standard oral replacement therapy of Vitamin D may not be sufficient.

**Disclosures:** J.G. Browne, None.

## M295

**Changes in Serum PINP in Orchidectomized Osteopenic Rats Treated with PTH and Alendronate.** J. Morko<sup>1</sup>, Z. Peng<sup>1</sup>, J. P. Rissanen<sup>1</sup>, M. I. Suominen<sup>1</sup>, L. Ravanti<sup>\*2</sup>, P. J. Kallio<sup>\*2</sup>, J. M. Halleen<sup>1</sup>. <sup>1</sup>Pharmatest Services Ltd, Turku, Finland, <sup>2</sup>Orion Corporation, Turku, Finland.

Serum procollagen I N-terminal propeptide (PINP) is a sensitive marker of bone formation in rat and mouse ovariectomy (OVX) models. Here we have studied changes in serum PINP in rat orchidectomy (ORX) model. Three-month-old male rats were orchidectomized and allowed to develop osteopenia for 3 months, after which the animals were treated for 3 months with PTH (1-34) or alendronate. The following study groups were included ( $n=12/\text{group}$ ): 1) Sham-operated control group receiving vehicle; 2) ORX group receiving vehicle; 3) ORX group receiving PTH (40  $\mu\text{g}/\text{kg}/\text{day}$  s.c.); 4) ORX group receiving alendronate (10  $\mu\text{g}/\text{kg}/\text{day}$  s.c.). PINP, mid-fragment of osteocalcin (OC) and C-terminal cross-linked telopeptides of type I collagen (CTX) were determined from fasting serum samples before the start of treatment (at 3 months) and at 4 and 6 months. Trabecular bone mineral density (BMD) was determined from tibial metaphysis before the operations, before the start of treatment and at the end of the study. Static and dynamic histomorphometry were determined from tibial metaphysis at the end of the study. Prostate weight was decreased by ORX, confirming that the operations were performed successfully. Trabecular BMD was decreased by ORX at 3 months, confirming the development of osteopenia. During the treatment period, bone formation rate (BFR/BS) was increased by PTH, confirming its anabolic effects, and decreased by alendronate, confirming its anti-resorptive effects. Trabecular BMD was increased by both PTH and alendronate at the end of the study. Trabecular bone volume (BV/TV) was strongly increased by PTH, but no changes were observed with alendronate. CTX and OC did not change by ORX at 3 months, but PINP decreased strongly. OC values were elevated by PTH and decreased by alendronate at both 4 and 6 months, but CTX values showed no changes. PINP values were strongly elevated by PTH and slightly decreased by alendronate at both 4 and 6 months. These results demonstrate that PINP is a sensitive marker of bone formation in rat ORX model. PINP shows a strong response to anabolic treatment, and it can also be used for monitoring anti-resorptive treatment. OC showed less strong response to anabolic treatment and more strong response to anti-resorptive treatment than PINP, suggesting that OC may reflect both bone formation and bone resorption. The CTX assay was not sensitive enough to detect changes in bone resorption in rat ORX model.

**Disclosures:** J. Morko, None.

**M296**

**Validation of an Immunoassay for the Determination of PINP in Rat Serum.** T. M. Gruetzner\*, P. Oldfield\*. Immunochemistry, Charles River Laboratories PCS-MTL, Senneville, QC, Canada.

Bone formation markers in rat osteoporosis models are limited. Recently, a new immunoassay (EIA) kit was developed for the determination of the n-terminal peptide of type 1 pro-collagen (PINP) from Immuno-Diagnostic Systems. In this study, we validated this EIA kit for use as a bone formation biomarker. The kit uses an immobilized rabbit polyclonal antibody specific for a peptide region of the analyte. PINP in the sample competes for a limited number of antibody binding sites with biotinylated PINP. The biotin is visualized with a streptavidin peroxidase system. The signal is inversely proportional to the PINP concentration in the sample. Samples require a minimum 3 fold dilution.

Parameters assessed included: working calibration range (9 standard curves consisting of 9 PINP concentration ranging from 0.6 to 75.0 ng/mL in duplicate), intra- and inter-assay precision and accuracy (5 quality control levels in 6 duplicate assessments in 3 separate assays) and in-process storage stability (room temperature and 4°C for ~ 11 hours, and 3 freeze thaw cycles). Dilution linearity and spike in selectivity tests were also performed. Long term stability at -20°C is ongoing. 24 lots of normal rat serum were assessed in order to define a normal range.

A 4 parameter logistic curve fit was applied to the standard curve. 6/9 standard curves required no reprocessing (all points within +/- 20% of the theoretical concentration) and 3 standard curves required deletion of a maximum of one standard.

Table 1: Precision and accuracy of PINP in Rat Serum (n = 18, 3 different assays).

	PINP concentration on plate (after dilution) (ng/mL)	Accuracy (% from endogenous assessment)	Precision % CV
LLOQ	0.77	106.2%	16.7
QC1	1.91	100.0%	14.5
QC2	4.41	96.2%	13.0
QC3	12.89	100.0%	13.2
ULOQ	36.30	108.5 %	22.8

Note: QCs were prepared from rat serum samples with endogenous PINP levels

In process stability samples recovered +/-12 % of the untreated control samples. Dilution linearity tests of up to 100 fold yielded acceptable levels of accuracy (+/- 25% of the undiluted theoretical concentration). Selectivity experiments (standard PINP spiked into 10 individual lots of rat serum) under-recovered (mean = 35.5% of the theoretical endogenous + spiked concentration). The mean serum PINP concentration in 24 normal adult rats was 136.1 ng/mL (range 24.7 to 293.4 ng/mL and standard deviation of 72.7).

The PINP kit performs well over the concentration range found in normal rats. Under-recovery of spike-in selectivity experiments may be a result of matrix differences between the standard curve diluent and rat serum. Validation of this method against established rat bone formation biomarkers and model endpoints will determine the full utility.

**Disclosures:** T.M. Gruetzner, None.

This study received funding from: Charles River Laboratories Montreal

**M297**

**Serum Sex Hormone-Binding Globulin Level to Predict Osteoporosis Severity.** E. Hoppé\*, B. Bouvard\*, E. Legrand, R. Levasseur, C. Masson\*, M. Audran. Rheumatology, CHU, Angers, France.

**Purpose:** Sex Hormone-Binding Globulin (SHBG) is a plasma glycoprotein that binds and regulates sex steroids. Several studies have shown a relation between serum SHBG levels and bone mineral density (BMD), bone turnover markers, and fracture risk among post-menopausal women. The aim of our study was to measure serum SHBG levels among post-menopausal women, and to assess its relationship with osteoporosis severity.

**Patients and methods:** We included 184 post-menopausal women who suffered from osteoporosis (T-score < -2.5) and/or presented osteoporotic fractures. We considered physical data (age, body mass index, weight, tobacco and alcohol intake, menopause age, hormonal replacement therapy duration, corticosteroid intake), biological parameters (albumin, prealbumin, estradiol, SHBG, serum C-telopeptide of type-I collagen, osteocalcin, serum bone specific alkaline phosphatase), the presence of vertebral or peripheral fractures, and lumbar and total hip bone mineral density.

**Results:** Mean age was 76.1 (+/- 9) years-old. Mean serum SHBG level was 80.2 (+/- 43) nmol/L (range: 10-297, or -1.6 to +5.4 standard deviations (SD)). We divided this population in 4 quartiles, according to an increasing serum SHBG level (Group I, II, III and IV). Lumbar BMD was lower in group III and group IV (respectively -3.2 SD and -3.1 SD) than in group I and group II (respectively -2.0 SD and -2.3 SD) (p<0.05). Total hip BMD was lower in group III and group IV (respectively -2.8 SD and -2.9 SD) than in group I and group II (respectively -1.6 SD and -2.2 SD) (p<0.05). Mean vertebral fracture number per women was higher in group III and group IV (respectively 2.8 and 3.5) than in group I and group II (respectively 1.5 and 2) (p<0.05). The rate of women suffering from severe osteoporosis (at least 2 vertebral fractures) was higher in group III and group IV (respectively 62.8 and 70%) than in group I and group II (respectively 35.7 and 50%) (p<0.05). After adjusting for age and body mass index, logistic regression analysis showed a significant association between serum SHBG level and the presence of severe osteoporosis. The Odds Ratio of having at least 2 vertebral fractures was 2.7 (95% confidence interval: 1.24-5.99) for an increase of 1 SD for SHBG.

**Conclusion:** There is a wide range of serum SHBG level among women suffering from post-menopausal osteoporosis. The higher is the SHBG level, the lower is the BMD and the higher is the number of vertebral fractures. These data strongly suggest that measuring serum SHBG level could be a new and reliable tool to predict post-menopausal osteoporosis severity.

**Disclosures:** E. Hoppé, None.

**M298**

**Optimization of Bone Turnover Marker Measurements in a Mouse Model of Glucocorticoid-Induced Osteoporosis.** M. I. Suominen, J. P. Rissanen, Z. Peng, J. M. Halleen. Pharmatest Services Ltd, Turku, Finland.

Glucocorticoids induce osteoporosis by increasing bone resorption and decreasing bone formation. A fast and reliable animal model of glucocorticoid-induced osteoporosis (GIOP) would allow rapid determination of side-effects of new glucocorticoid analogs on bone, and effects of new osteoporosis drug candidates on GIOP. We have studied the effects of 3-week administration of prednisolone on bones in intact 13-week old BALB/c mice. The following study groups were included (n=8/group): 1) Control group receiving vehicle; 2) Oral prednisolone (10 mg/kg/day); 3) Prednisolone pellets with a release rate of 24 µg/day ("low pellet", mean dose 1.1 mg/kg/day); 4) Prednisolone pellets with a release rate of 71 µg/day ("medium pellet", mean dose 3.4 mg/kg/day); 5) Prednisolone pellets with a release rate of 238 µg/day ("high pellet", mean dose 11.4 mg/kg/day). Histomorphometric analysis and peripheral quantitative computed tomography (pQCT) were performed from proximal tibia and tibial diaphysis at the end of the study. Intact osteocalcin, procollagen I N-terminal propeptide (PINP) and C-terminal cross-linked telopeptides of type I collagen (CTX) were measured from fasting serum samples before the start of treatment and at 1, 2 and 3 weeks. Parameters of dynamic histomorphometry decreased substantially in both trabecular and cortical bone by the oral prednisolone and the high pellet. However, prednisolone had no effects on trabecular bone parameters determined by pQCT or static histomorphometry, but cortical bone mineral content and cortical thickness were decreased by the oral prednisolone and the high pellet. The medium and high pellets increased CTX values and decreased PINP and osteocalcin values at one week, indicating increased bone resorption and decreased bone formation. After the first week, the CTX values decreased and the PINP values increased towards the levels obtained before the start of treatment, but the osteocalcin values stayed low. These results demonstrate that high doses of prednisolone induce an early increase in bone resorption and decrease in bone formation, and cortical bone loss at 3 weeks, while a low dose (1.1 mg/kg/day) has no effects on bone in this study setup. Although parameters of dynamic histomorphometry reveal decreased turnover in trabecular bone at 3 weeks, a longer study period is probably required to demonstrate trabecular bone loss. An optimal timepoint for measuring bone turnover markers is at one week after start of dosing, demonstrating highly elevated bone resorption and decreased bone formation. A one-week GIOP study with bone marker measurements could be a useful tool for rapid screening of a large number of compounds.

**Disclosures:** M.I. Suominen, None.

**M299**

**Clinical Significance of Undercarboxylated Osteocalcin (ucOC) in Glucocorticoid-induced Osteoporosis (GIO).** I. Tanaka<sup>1</sup>, S. Tamaki<sup>2,3</sup>, H. Oshima<sup>3</sup>, J. Ishii<sup>2,1</sup>. <sup>1</sup>Department of Laboratory Medicine, Fujita Health University School of Medicine, Toyoake, Japan, <sup>2</sup>Department of Rheumatology, National Hospital Organization, Mie Chuo Medical Center, Tsu, Japan, <sup>3</sup>Department of Rheumatology, National Hospital Organization, Tokyo Medical Center, Tokyo, Japan.

**[Objective]** In GIO, bone fractures are often seen even at high bone mineral density. This suggests bone quality is an important factor in GIO for bone strength, which is usually evaluated with bone markers on the clinical basis. In this study, we tried to clarify the clinical significance of various bone makers in predicting the bone quality in GIO.

**[Subjects & Methods]** one hundred thirty four patients (99 females and 35 males) with collagen diseases under glucocorticoid treatment were enrolled in this study. The mean of age and daily glucocorticoid dosage (prednisolone equivalent) were 52 years old and 9.0 mg/day, respectively. Serum undercarboxylated osteocalcin (ucOC) and NTX in the urine (uNTX) were measured by the ECLIA and ELISA methods, respectively. Vertebral compression fractures were evaluated with X-ray photography.

**[Results]** 1) uNTX were increased one month after the start of glucocorticoid therapy, but the ucOC decreased in that period. 2) Doses of glucocorticoids, were significantly correlated with uNTX positively and with ucOC negatively. 3) ucOC were significantly increased in patients with vertebral deformities. 4) In patients treated with menatetrenone, which is vit K analog, ucOC was lower in patients without menatetrenone. 5) uNTX seemed correlated with an incident fracture after corrected with risk factors. **[Conclusion]** It is suggested that serum ucOC levels decreased in dosage dependent manner after treatment with corticosteroids. Its shows that bone formation is inhibited by glucocorticoid in GIO.

**Disclosures:** I. Tanaka, None.

## M300

**Uncarboxylated Osteocalcin Level in Healthy Korean Women.** B. Choi<sup>\*1</sup>, D. Lee<sup>2</sup>, Y. Lee<sup>\*1</sup>. <sup>1</sup>Cha School of Medicine, Seoul, Republic of Korea, <sup>2</sup>Rheumatology Clinic, Cha School of Medicine, Seoul, Republic of Korea.

Uncarboxylated osteocalcin(ucOC) has been recognized to evaluate vitamin K status and inversely associated with bone mineral density. We have recruited 337 healthy women age group 20, 30, 40, 50, 60, 70 years 60 women in all age groups except 37 women in 70 years old age group. All women were healthy and postmenopausal women have ever taken hormone, drugs and supplements that may influence bone metabolism or stopped taking for the last six months.

Serum uncarboxylated osteocalcin was measured from the collected fasting venous blood samples as well as alkaline phosphatase, serum calcium. Mean body mass index was lowest ( $20.3 \pm 1.9 \text{ kg/m}^2$ ) in 20 years old group and highest ( $24.8 \pm 2.6 \text{ kg/m}^2$ ) in 60 years old group. BMD of the L2-4 vertebral bodies was measured by dual-energy X-ray absorptiometry (DEXA) using a Hologic QDR 2000 densitometer (Hologic Corp., MA, USA). The coefficients of variation (CVs) of the measurement were less than 1.0% for lumbar BMD. Data for BMD are expressed as g/cm<sup>2</sup>. The serum uncarboxylated osteocalcin concentration was assayed by an enzyme-linked immunosorbent assay (ELISA) system using two monoclonal antibodies, an anti-OC (21-31) antibody and a solid-phase anti-Glu 21, 24-OC (4-5) antibody, with recombinant human uncarboxylated osteocalcin (Biotechnology Research Laboratory, Takara Shuzo Co., Otsu, Shiga, Japan. The intra- and inter-assay coefficients of variation (CVs) were 7.3% and 9.7%, respectively, and the sensitivity of the assay was 0.5 ng/ml. Spine bone mineral density was highest in age group and lowest in age group. Hip bone mineral density was highest in age group and lowest in age group.

Serum mean alkaline phosphatase was lowest ( $122 \pm 30 \text{ IU/L}$ ) in 30 years old group and highest ( $190.3 \pm 55.8 \text{ IU/L}$ ) in 60 years old group. Serum mean uncarboxylated osteocalcin levels were ( $2.6 \pm 2.0 \text{ ng/ml}$ ), ( $1.9 \pm 1.3 \text{ ng/ml}$ ), ( $1.6 \pm 1.2 \text{ ng/ml}$ ), ( $2.2 \pm 1.5 \text{ ng/ml}$ ), ( $2.1 \pm 2.3 \text{ ng/ml}$ ), ( $1.8 \pm 1.3 \text{ ng/ml}$ ) respectively. Serum ucoc was inversely associated with BMI ( $-0.12 \text{ p} < 0.02$ ) and lumbar spine BMD ( $0.13 \text{ p} < 0.01$ ) and positively associated with alkaline phosphatase ( $0.19 \text{ p} < 0.00$ ). Serum mean uncarboxylated osteocalcin was highest in 20 years old group then 50 years old group suggesting vitamin K deficiency in these age groups.

**Disclosures:** B. Choi, None.

## M301

**High Level Dietary Phosphorus and Cadmium Exacerbate Ovariectomy-Induced Bone Loss.** S. Hooshmand<sup>1</sup>, N. Bakhshalian<sup>\*1</sup>, D. Y. Soung<sup>1</sup>, E. A. Lucas<sup>\*2</sup>, S. C. Chai<sup>\*1</sup>, B. H. Arjmandi<sup>1</sup>. <sup>1</sup>Nutrition, Food and Exercise Sciences, Florida State University, Tallahassee, FL, USA, <sup>2</sup>Nutritional Sciences, Oklahoma State University, Stillwater, OK, USA.

Cadmium is one of the most toxic contaminants present in the natural and occupational environment and is a serious threat to living organisms. Chronic exposure to cadmium is associated with a number of disorders including kidney injury and skeletal damage. This study was designed to investigate the extent to which combination of cadmium and phosphorus exacerbates the bone loss as a result of ovariectomy. We used five groups (n=5 rats per group) of 3-month old OVX Sprague Dawley rats to examine the dose-dependent deleterious effects of cadmium (Cd) on BMD of whole body, femoral, and forth lumbar vertebrae as well as micro-structural properties of femoral necks. The treatment groups were as follows: 1) Control; 2) 50 ppm cadmium (Cd); 3) 50 ppm Cd+1.2% phosphorous (P); 4) 200 ppm Cd, and 5) 200 ppm Cd+1.2% P. Five months postovariectomy, rats were sacrificed and whole body, femoral, and forth lumbar vertebrae were scanned using DXA. Additionally, femoral necks were analyzed for microstructural properties using micro-computed tomography ( $\mu\text{CT}$  35). OVX Controls gained 3.9 and 9.8% BMD in compression with baseline BMD value after three and five months, respectively. High dose of Cd (200 ppm) completely prevented the gain in BMD. When P was added to Cd, the harmful effect of Cd on bone was pronouncedly exacerbated. In terms of femoral neck micro-structural properties, Cd decreased bone volume to total volume ratio (BV/TV), trabecular number (Tb.N) and increased structural model index (SMI) by both doses of 50 and 200 ppm. Cadmium in the context of high level of P in the diet made all these parameters worsen. Our results indicated that 200 ppm Cd+1.2% P had the most deleterious effect on BMD (7% loss) and femoral structural properties (significant differences were observed in BV/TV and Tb.N). We conclude that cadmium exposure along with high intake of phosphorus may be a public health hazard particularly in term of bone mass. The bone loss due to Cd in this study may have been confounded by OVX-induced loss of bone. Intact animals are to be used to confirm our findings.

**Disclosures:** B.H. Arjmandi, None.

## M302

**Comparison of 2D and 3D Subchondral Bone Texture Parameters in Severe OA Knees.** A. Wong<sup>\*1</sup>, D. Inglis<sup>\*2</sup>, K. A. Beattie<sup>\*1</sup>, P. D. Emond<sup>\*1</sup>, A. Doan<sup>\*1</sup>, J. de Beer<sup>\*3</sup>, C. E. Webber<sup>\*4</sup>, J. D. Adachi<sup>1</sup>, A. Papaioannou<sup>1</sup>.

<sup>1</sup>Department of Medicine, McMaster University, Hamilton, ON, Canada,

<sup>2</sup>Department of Civil Engineering, McMaster University, Hamilton, ON,

Canada, <sup>3</sup>Department of Orthopaedics, St. Joseph's Healthcare, Hamilton, ON,

Canada, <sup>4</sup>Department of Radiology, McMaster University, Hamilton, ON, Canada.

**Objectives:** 1) To compare apparent subchondral bone texture (BTX) parameters from radiographs with 3D parameters from bone cores using micro-computed tomography ( $\mu\text{CT}$ ) and 2) to determine the potential of 2D and 3D BTX parameters for assessing OA.

**Methods:** A cohort of male and female total knee arthroplasty (TKA) participants (N=17) had posteroanterior fixed-flexion knee radiographs of each affected knee obtained. Radiographs were digitized and analyzed for BTX parameters: bone volume fraction (BTVF), connectivity index (CX), trabecular spacing (Tr.Sp) and trabecular thickness (Tr.Th) in the centre of the tibia, 2 mm below the tibial plateau at a region of interest (ROI) 10 mm in diameter. Minimum joint space width (mJSW) was computed from digitized radiographs using a semi-automated algorithm. Cylindrical bone cores removed from the mid-tibia were imaged using a  $\mu\text{CT}$  scanner at an isotropic spatial resolution of 47  $\mu\text{m}$ . The same BTX parameters were obtained from 3D reconstructions of bone cores at 2 mm below the proximal end in cylindrical ROIs sized 1 cm<sup>3</sup>.

2D and 3D BTX parameters were correlated using a linear regression analysis. BTX parameters were correlated with mJSW to investigate the relationship between bone texture and OA severity.

**Results:** In mid-subchondral tibia, 3D BTX parameters correlated poorly with their 2D analogues. All 2D measures demonstrated significant correlations with mJSW (Table 1). Meanwhile, none of the 3D BTX parameters exhibited correlations with mJSW.

**Table 1.** Correlation coefficients of 2D BTX parameters as predictors of mJSW

2D BTX	B Coefficient	Upper CI	Lower CI	P-value
BTVF	-14.83	-4.87	-24.80	0.005
BSTV	-16.46	-0.02	-32.90	0.05
Tr.Sp	8.35	14.50	2.20	0.009
Tr.Th	-34.98	-13.50	-56.45	0.002
CX	-0.163	-0.091	-0.235	<0.001

**Conclusions:** Despite their poor construct validity, we showed that 2D BTX parameters in the mid-subchondral tibia may be predictive of OA progression. However, the same correlations were not observed with 3D analyses of bone in the mid-subchondral tibia. Our results suggest mismatch between 2D and 3D BTX parameters. Certainly, differences in spatial resolution remain a factor. Nonetheless, mid-subchondral tibia BTX measures may provide information regarding the condition of subchondral bone and remain candidates for measuring longitudinal change.

**Disclosures:** A. Wong, None.

*This study received funding from: CIHR Strategic Training Program in Skeletal Health Research.*

## M303

**Trabecular 3D volumetric Density at Organ and Tissue Levels by Micro QCT Evaluation of Iliac Crest Biopsy: Relationship with Microstructure and DXA Measures.** R. Dai<sup>\*</sup>, J. Jacobson<sup>\*</sup>, J. Zhao<sup>\*</sup>, Y. Jiang. Osteoporosis and Arthritis Lab, Department of Radiology, University of Michigan, Ann Arbor, MI, USA.

QCT or DXA measures 3D or 2D bone mineral density at organ level (BMDog), calculated as amount of bone mineral content per 3D volume of interest consisting of bone and bone marrow and vascular space for QCT, or per projectional area with mixture of cortex and trabeculae (Tb) and marrow cavity and vasculature for DXA. Measurement of 3D BMD for Tb per se, or Tb 3D BMD at tissue level (BMDts) for Tb only, has not been reported. BMDts may improve our ability to understand pathophysiology and important mineralization changes underlying the mechanisms of bone fragility in osteoporosis and metabolic bone disorders, bone quality in terms of mechanical competence which is a function of bone mineral and 3D distribution, bone mineralization process as well as disorders such as hypomineralization in osteomalacia and initial administration of anabolic agents for osteoporosis, or hypermineralization in frozen bone with bisphosphonates, bony incorporation of metal, e.g., strontium, etc. We investigated the Tb 3D BMDog and BMDts and its relationship with Tb microstructure and DXA BMD.

Iliac crest bone biopsies from 35 postmenopausal women with osteoporotic vertebral fractures and the hip and lumbar DXA BMD T-score < -2.5 were scanned twice with 4-week interval using a Scanco micro CT and isotropic resolution of 20  $\mu\text{m}$ . A micro CT phantom is scanned weekly for quality control and examining conversion constants. For BMDts, partial volume effect at Tb interface with bone marrow was minimized by discarding 2 voxels on Tb surface. 3D Tb structural parameters were directly measured. The root mean square coefficient of variation (CV) as measurement error was 1.6% for BMDts and 2.7% for BMDog. Mean ( $\pm\text{SD}$ ) BMDts was 968 ( $\pm 14$ ) mg hydroxyapatite (HA)/cc, with 1.4% CV < measurement error, and could be considered constant, while BMDog was 154 ( $\pm 55$ ) mg HA/cc. BMDog is correlated with femoral neck DXA BMD ( $r = .55$ ) and lumbar spine DXA BMD ( $r = .59$ ) and with most structural parameters ( $p < .05$ ): 3D Tb bone volume fraction ( $15 \pm 6\%$ ,  $r = .98$ ), structure model index ( $1.4 \pm .5$ ,  $r = .85$ ), Tb number ( $1.1 \pm .2 / \text{mm}$ ,  $r = .66$ ), Tb thickness ( $178 \pm 46 \mu\text{m}$ ,  $r = .72$ ), Tb separation ( $887 \pm 143$

$\mu\text{m}$ ,  $r=-.79$ ), except ( $p>.05$ ) degree of anisotropy ( $1.6\pm.3$ ,  $r=.26$ ) and connectivity density ( $1.9\pm.5/\text{cm}$ ,  $r=.32$ ). BMDs was not correlated with any of them ( $r<.2$ ,  $p>.05$ ). Micro QCT can reproducibly measure iliac Tb BMDs and BMDog. BMDog is associated with microstructure and hip and lumbar DXA BMD. BMDs is constant and unassociated with other measures and may provide independent and unique information in studying bone metabolism, bone quality, metal incorporation or intoxication, mineralization process, hypo- and hyper-mineralization.

**Disclosures:** R. Dai, None.

## M304

**Femoral BMD and Femoral Structure, Assessed by DXA-Based Hip Structural Analysis, Contribute Independently to Femoral Strength.** B. J. Roberts\*, E. J. Thrall\*, J. A. Muller\*, M. L. Bouxsein. Orthopedic Surgery, Beth Israel Deaconess Medical Center / Harvard Medical School, Boston, MA, USA.

Measurement of areal BMD by DXA is the current gold standard for diagnosis of osteoporosis. However, aBMD has limitations with regard to fracture risk prediction, as up to half of fractures occur in individuals who are not osteoporotic by DXA-based criteria. Whole bone strength depends on bone size, macro- and microarchitecture, and the intrinsic properties of the bone matrix. Thus, we asked whether parameters of femoral structure, as assessed by DXA-based hip structural analysis (HSA), would add to aBMD in the prediction of femoral strength. We obtained 76 human cadaveric femurs (50 female and 26 male, aged  $74.2 \pm 8.7$ yr, range 55 to 98 yrs) with no evidence of prior fracture or metastatic lesions. We measured femoral neck (FN) and trochanteric (TR) aBMD, and indices of femoral structure by DXA-based HSA as implemented in the manufacturer's software (Hologic, Bedford, MA). Femora were then mechanically tested to failure in a sideways fall configuration. Bivariate and stepwise regression analyses were used to determine predictors of femoral failure load. The sample was representative of those at risk for hip fracture, as 80% of the femora had FN T-scores  $< -2.0$ . FN and TR aBMD were strong predictors of failure load ( $r = 0.84$  and  $0.86$ , respectively), as were narrow neck and intertrochanteric bone cross-sectional area (CSA) assessed by HSA ( $r=0.87$  and  $0.88$ , respectively). FN length, FN width, and intertrochanteric (IT) width were moderately correlated with failure load ( $r = 0.35$ ,  $0.37$ , and  $0.52$ , respectively). When added to FN BMD in a stepwise regression, FN width statistically significantly increased the correlation from  $r^2 = 0.70$  to  $0.75$ . Similarly, addition of IT width and avg. cortical thickness of the IT region to TR BMD statistically significantly increased  $r^2$  from  $0.74$  to  $0.80$ . Although limited by the fact that structural measures and BMD were derived from the same x-ray attenuation profile, these data show that aBMD and indices of femoral structure assessed by HSA contribute independently to femoral strength, and provide strong rationale for future studies that utilize 3D imaging to explore the contribution of femoral morphology to hip fracture risk.

**Disclosures:** M.L. Bouxsein, Merck & Co 3; Acceleron Pharma 2; Amgen 4.

This study received funding from: Merck & Co.

## M305

**Extended Lactation Is Associated with Failure to Restore BMD 6 Months after Resumption of Menstrual Cycle.** S. A. Brown<sup>1</sup>, T. A. Guise<sup>1</sup>, A. M. Siega-Riz<sup>2</sup>, M. J. Caminiti<sup>2</sup>, C. J. Rosen<sup>3</sup>. <sup>1</sup>UVA, Charlottesville, VA, USA, <sup>2</sup>UNC, Chapel Hill, NC, USA, <sup>3</sup>Maine Medical Research Institute, Scarborough, ME, USA.

This study examined 1) IGF-I & BMD recovery after extended lactation and 2) cortical & trabecular changes by pQCT in response to lactation and weaning. This on-going prospective study enrolled women with extended lactation ( $\geq 5$  mos) and women with little to no lactation period ( $< 1$  mo). The 4 timepoints are: baseline at delivery, 3 mos postpartum, time of menstrual cycle return and 6 mos after menses return. 60 of 88 subjects enrolled completed the final visit to date. Subjects had DXA (spine, hip & whole body) and pQCT (radius & tibia) at each visit. Subjects were mean  $31.7$  yo ( $22.9-40.1$ ) with normal Z-scores at term delivery & 56% primiparous. 44 subjects had extended lactation (mean 9.8 mos), 12 had  $< 1$ mo lactation and 4 had 1-5 mos of lactation. 77% of extended lactation subjects had almost or completely weaned at the final visit.

**DXA:** The extended lactation group lost spine BMD at 3 mos postpartum ( $-6.2\%$ ,  $P<0.05$ ) which was not fully recovered by the final visit at mean 55.2 wks postpartum ( $-2.4\%$  vs. baseline,  $P<0.05$ ) with no change in the comparison group. BMD loss at the FN was greatest at the return of menses mean 29 wks postpartum ( $-5.7\%$ ,  $P<0.05$ ) and did not recover by the final visit ( $-3.5\%$ ,  $P<0.05$ ). The comparison group had FN losses of  $-2.5\%$  ( $P<0.05$ ) at the return of menses which recovered by the final visit.

**IGF-I:** Compared to baseline, IGF-I decreased at 3 mos postpartum ( $153.5$  ng/mL vs.  $172.6$ ,  $P<0.05$ ) and increased at the final visit ( $198.3$ ,  $P<0.05$ ) with extended lactation. The comparison group had no significant changes in IGF-I. IGF-I was not correlated with change in BMD by DXA.

**pQCT:** Trabecular vBMD decreased from baseline to final (radius  $4\%$ :  $204.3\pm 35.5$  mg/cm<sup>3</sup> vs.  $198.5\pm 40.0$ ,  $P<0.05$ ,  $N=19$ ) and cortical vBMD did not significantly change (tibia  $38\%$ :  $1212.8\pm 16.8$  mg/cm<sup>3</sup> vs.  $1209.9\pm 21.2$ ,  $P=0.01$ ,  $N=23$ ) with extended lactation whereas no changes occurred in the comparison group. Cortical thickness and periosteal circumference (ext. lactation:  $67.4\pm 4.3$ mm baseline vs.  $67.5\pm 4.3$  final,  $P=0.01$ ,  $N=23$ ) did not change in either group. IGF-I was correlated with cortical thickness ( $r=0.42$ ,  $P=0.05$ ), cortical area ( $r=0.53$ ,  $P=0.01$ ) and periosteal circumference ( $r=0.36$ ,  $P=0.09$ ).

These data to date suggest that spine and FN aBMD by DXA did not fully recover by 6 mos after menstrual cycle return in women with extended lactation. Trabecular vBMD but

not cortical vBMD further decreased from baseline to the final visit with no significant changes in periosteal parameters by pQCT. IGF-I decreased at 3 mos postpartum and rose above baseline at the final visit with extended lactation but were not correlated with aBMD. IGF-I was positively correlated with cortical thickness and cortical area.

**Disclosures:** S.A. Brown, None.

This study received funding from: NIH/NIAMS.

## M306

**Hip Structural Analysis and Volumetric QCT in Postmenopausal Women from the PaTH Study: Mono- or Combination Therapy with Alendronate and Parathyroid Hormone.** G. J. van Londen<sup>1</sup>, L. Palermo<sup>2</sup>, T. J. Beck<sup>3</sup>, T. F. Lang<sup>2</sup>, J. M. Wagner<sup>1</sup>, D. Black<sup>2</sup>, J. P. Bilezikian<sup>4</sup>, K. E. Ensrud<sup>5</sup>, S. L. Greenspan<sup>1</sup>. <sup>1</sup>Department of Medicine, University of Pittsburgh, Pittsburgh, PA, USA, <sup>2</sup>University of California, San Francisco, CA, USA, <sup>3</sup>John Hopkins, Baltimore, MD, USA, <sup>4</sup>Columbia University College of Physicians, New York, NY, USA, <sup>5</sup>Minneapolis Veterans Affairs, Minneapolis, MN, USA.

Bone strength depends on bone mineral density (BMD) as well as material and structural properties. Hip Structural Analysis (HSA) and Quantitative Computed Tomography (QCT) methods provide quantitative information on bone structure. Our objectives were to 1) examine changes in HSA and QCT derived structural parameters following antiresorptive, anabolic or combination therapy and 2) correlate structural indices as assessed by HSA and QCT. In the 2 year, double-blind, placebo-controlled PaTH trial, 238 postmenopausal women (mean age 70 years) were randomized to: 1) PTH (100  $\mu\text{g}$  sc daily) in year 1 followed by ALN (10 mg po daily) in year 2 (PTH-ALN); 2) PTH in year 1 followed by placebo in year 2 (PTH-PLB); 3) PTH plus ALN in year 1 followed by alendronate in year 2 (PTH/ALN-ALN) or 4) ALN for 2 years (ALN-ALN). Outcomes included conventional BMD (bone mineral density) by DXA ( $\text{g}/\text{cm}^2$ ), HSA (DXA-derived) and volumetric QCT-derived parameters measured at the femoral neck [including cross-sectional area (CSA), buckling ratio (BR, an index of cortical instability, with a decrease suggesting improvement)]. After 2 years, femoral neck BMD, CSA and BR derived by HSA and QCT improved most in the PTH-ALN group compared to the PTH-PLB group (table,  $p<0.05$ ). Similar trends for BMD, HSA and QCT were observed for other groups. At baseline, HSA-BMD correlated with QCT-BMD ( $r=0.41$ ), HSA-CSA correlated with QCT-CSA ( $r=0.58$ ), and HSA-BR with QCT-BR ( $r=0.56$ ), all  $p<0.0001$ . We conclude that in postmenopausal women who received 1 year of PTH followed by 1 year of ALN, DXA-derived HSA and QCT-derived indices of structural geometry were significantly associated with each other at baseline and demonstrate similar improvements in CSA and stability at 2 years. HSA and QCT provide additional information on structure that may complement results from BMD changes alone.

Table: Mean (SE) percent change at 24 months

Parameter	PTH-PLB	PTH-ALN	PTH/ALN-ALN	ALN-ALN
DXA-BMD	1.14 (0.82)	5.19 (0.80)* †	3.19 (0.84)*	2.52 (0.82)* ¶
HSA-BMD	0.79 (0.75)	4.93 (0.73)* †	2.55 (0.77)*#	2.60 (0.75)* ¶
QCT-BMD	-1.27 (0.97)	1.19 (0.93)	0.59 (0.99)	-1.70 (0.97) ¶
HSA-CSA	2.63 (2.11)	13.50 (2.05)* †	7.60 (2.17)*#	8.88 (2.12)*~
QCT-CSA	-0.41 (1.37)	3.38 (1.32)* †	0.51(1.40)	0.27 (1.37)
HSA-BR	-19.7 (16.3)	-88.1 (15.7)* †	-54.6 (16.7)*	-39.6 (16.3)* ¶
QCT-BR	0.32 (1.00)	-3.72 (0.97)* †	-2.18 (1.02)*	-0.47 (1.00) ¶

\*  $p<0.05$  vs. baseline, †  $p<0.05$  PTH-PLB vs. PTH-ALN, ¶  $p<0.05$  PTH-ALN vs. ALN-ALN, #  $p<0.05$  PTH-ALN vs. PTH/ALN-ALN, ~  $p<0.05$  PTH-PLB vs. ALN-ALN.

**Disclosures:** S.L. Greenspan, Merck Inc., Amgen 4; Merck, Procter and Gamble, NPS 2; Lilly, Procter and Gamble, Novartis, Sanofi Aventis, Amgen 3.

This study received funding from: NIH/NIAMS.

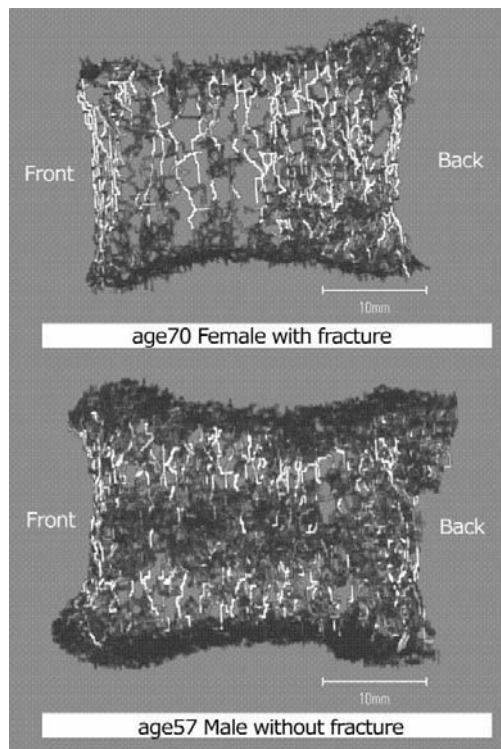


## M307

**Evaluation of Osteoporosis Vertebrae Fragility by Connecting Path Method.** N. Nango<sup>1</sup>, N. Endo<sup>\*2</sup>, T. Yamamoto<sup>\*3</sup>, H. Takahashi<sup>4</sup>, M. Machida<sup>\*5</sup>, Y. Suga<sup>\*6</sup>, T. Asai<sup>\*6</sup>. <sup>1</sup>Ratoc System Engineering Co., Ltd., Tokyo, Japan, <sup>2</sup>Niigata University, Niigata, Japan, <sup>3</sup>Niigata Bone Science Institute, Niigata, Japan, <sup>4</sup>Niigata University of Health and Welfare, Niigata, Japan, <sup>5</sup>Murayama Medecal Center, Tokyo, Japan, <sup>6</sup>Kawaguchi Municipal Medical Center, Saitama, Japan.

We suggested the Connecting Path Method (CP method) last ASBMR to quantify the fragility of human lumbar vertebrae and develop a bone morphometry index to predict stress fracture tolerance. This is done by quantifying the trabecular path, the part which transmits the load on endplates.

Presently, we have expanded the method and made it possible to quantize the fragility of vertebrae to include cortical bone. We divided the bone into a hexahedron mesh to create the network that connects the paths through the center of mass. For the elastic constant of the connecting path, we brought a Young's modulus obtained from a CT value and reflected the property on the bone. As a specimen, we analyzed a clinical CT-scanned image of the L3 vertebra taken from (A) 70-year-old woman with fractures (Sp.A) and (B) 57-year-old man without fracture (Sp.B) using 3D analytical software called TRI/3D-BON (RATOC). We extracted the bone, and calculated the apparent resistance force (app RF) generated against the outer pressure through the connecting path using the CP method. These figures show the amount of power generated by bone to counter the outer pressure. The white area indicates a large power generated, and the black area indicates less power. Counter to an external deformation, the app RF generated by Sp.A is calculated to be about 1/3 that of Sp.B. In the case of Sp.A, we can observe the bone parts around the void zone mixed together, some connecting trabecular bone generates strong app RF while others provides little. Cortical bone has strong resistance force generated in all areas. Conversely, Sp.B seems to be generating stronger app RF in the neighboring areas both above and beneath endplates while the center area is weak. The distribution of app RF within the Sp.B is likely with trabecular bone anatomy showing a three-layer zonal structure. Though, Sp.A has lost its original vertebral anatomy probably due to the trabecular bone resorption. Finally, we conclude that it is possible to analyze the strength and the change in the network and fragility of trabecular and cortical bone that is caused by osteoporosis by using this method.



**Disclosures:** N. Nango, None.

## M308

**Lumbar Spine TBS Complements BMD in the Discrimination Between Vertebral Fractured and Non-Fractured Subjects Postmenopausal Women: a Retrospective Case-Control Study.** B. Rabier<sup>\*1</sup>, R. Winzenrieth<sup>\*1</sup>, A. Heraud<sup>\*2</sup>, C. Grand-Lenoir<sup>\*3</sup>, P. Carceller<sup>\*1</sup>, D. Hans<sup>4</sup>, L. Pothuaud<sup>1</sup>. <sup>1</sup>PTIB - University Hospital of Bordeaux, Med-Imaps, Pessac Cedex, France, <sup>2</sup>Robert Boulin Hospital, Hospital Center of Libourne, Libourne, France, <sup>3</sup>Center of Radiology - Clinics of Lesparre, Lesparre, France, <sup>4</sup>Center of Bone Disease, Department of Bone and Joint Disease, Lausanne University Hospital, Switzerland.

Bone Mineral Density as assessed by DXA constitutes the gold standard in osteoporosis diagnosis. However, it does not take into account the bone microarchitecture deterioration. Trabecular Bone Score (TBS), a new grey-level texture measurement, based on a reanalysis of the image of DXA examination, correlates with 3D parameters of bone microarchitecture. The aim of our study was to evaluate the ability of lumbar spine TBS to complement BMD in the discrimination between vertebral fractured subjects and age-matched controls in Caucasian postmenopausal women with T-score  $\leq -1.0$ .

Included subjects, 50 to 80 years old, from a Rheumatology Department of a Hospital or the Radiology Department of a Clinic, have been measured on Prodigy GE-Lunar system and showed a BMD measurement T-score  $\leq -1.0$  at femoral neck, total hip or lumbar spine. Fractured subjects had low-energy vertebral fractures confirmed by X-rays. Non-fractured subjects had a matched age-paired in the fractured subject group ( $\pm 3$  years). Subjects with pathology, treatment known to affect bone metabolism were excluded. DXA scan files were exported onto a dedicated workstation for TBS calculation. A central database was constructed after cross-calibration.

42 vertebral fractured subjects of  $65.6 \pm 7.8$  years and 126 age-matched non-fractured subjects of  $63.5 \pm 8.3$  years were retained. The two groups were significantly different for BMD ( $p=0.0017$ ) and TBS ( $p<0.0001$ ) and not for basic anthropomorphic parameters (age, height, weight). Odds-ratios (OR) per standard deviation decrease is 1.95 [1.34-2.84] and Area Under the ROC Curve (AUC) is 0.662 [0.585-0.733] for BMD, and OR=2.96 [1.88-4.64] and AUC=0.729 [0.655-0.794] for region of interest matched TBS, with non-significant difference of the AUCs ( $p=0.243$ ). The comparison of a model combining (TBS, BMD) to (BMD) alone showed an OR of 3.40 [2.20-5.24] and AUC of 0.776 [0.705-0.836] versus an OR of 2.00 [1.39-2.87] and an AUC of 0.662 [0.705-0.836] respectively, with a significant difference in the AUCs ( $p=0.016$ ).

Combining bone microarchitecture index, TBS and BMD derived from the same spine DXA examination improved significantly the vertebral fracture discrimination in postmenopausal women. It would be of interest to test a case finding strategy using spine BMD then TBS to identify subjects at the highest risk of fracture especially in the osteopenic zone.

**Disclosures:** B. Rabier, None.

## M309

**In vivo Quantification of Intra-cortical Porosity in Human Cortical Bone using HR-pQCT in Patients with type II Diabetes.** A. J. Burghardt<sup>1</sup>, K. A. Dais<sup>\*1</sup>, U. Masharani<sup>\*2</sup>, T. M. Link<sup>1</sup>, S. Majumdar<sup>1</sup>. <sup>1</sup>Radiology, University of California, San Francisco, San Francisco, CA, USA, <sup>2</sup>UCSF Diabetes Research Center, University of California, San Francisco, San Francisco, CA, USA.

Cortical bone comprises a significant portion of overall bone mass and bears the bulk of axial loads in the peripheral skeleton. That metabolic disorders, including osteoporosis and type II diabetes, affect intra-cortical porosity is an emerging concept. Quantitative cortical microstructural and biomechanical endpoints are important for understanding structure-function relations in the context of fracture risk and therapeutic efficacy. In this study, novel image processing methods and  $\mu$ FE analysis applied to HR-pQCT were used to investigate intra-cortical macro-porosity in type II diabetes patients with and without a history of atraumatic fracture (Fx).

The distal radius and tibia of patients with type II diabetes and a history of Fx ( $n=2$ ), without Fx ( $n=7$ ), and age/BMI matched controls ( $n=6$ ) were imaged using HR-pQCT (XtremeCT, Scanco Medical). Segmentation of the cortical compartment was performed using manually drawn contours at the endosteal boundary. Segmentation of intra-cortical macro-porosity was achieved using a novel automated segmentation technique based on 2D component labeling and a hysteresis region growing process. Intra-cortical pore volume fraction (PVF) and cross sectional moment of inertia (CSMI) were calculated. Mechanical properties were determined by  $\mu$ FE. A 1% uniaxial compressive strain was simulated in the complete structure using a voxel based finite element technique. Apparent and compartmental parameters were calculated.

PVF was dramatically higher in diabetic Fx patients ( $p<0.01$  vs controls) but not in diabetics without Fx. Both diabetic groups tended to have higher BV/TV and Tb.N in the trabecular compartment. Accordingly, diabetes patients without Fx tended to have higher elastic modulus, stiffness, and estimated failure load, while Fx patients were similar to controls, though the cortical compartment tended to carry less load ( $p<0.01$  for tibia). CSMI tended to be lower in Fx patients compared to non-Fx and controls.

Despite limited numbers, these results suggest that loss of bone in the cortical compartment due to intra-cortical porosity is compensated for by increased trabecular bone mass in diabetics with Fx. This normalizes bone strength for axial loads, but likely results in compromised bending strength as evidenced by a lower CSMI. Non-Fx diabetes patients tended to have minimally increased porosity and higher mechanical indices for axial and bending loads. This indicates that cortical porosity metrics may be critical for differentiating patients at risk for fracture and evaluating treatment efficacy in this population profile.

**Disclosures:** A.J. Burghardt, None.

## M310

**Marked Abnormalities in Cortical and Trabecular Microarchitecture and Strength in Premenopausal Women with Idiopathic Osteoporosis: A Bone Biopsy Study.** A. Cohen<sup>1</sup>, R. R. Recker<sup>2</sup>, D. W. Dempster<sup>3</sup>, H. Zhou<sup>\*3</sup>, A. Wirth<sup>\*4</sup>, T. Kohler<sup>\*4</sup>, G. H. van Lenthe<sup>4</sup>, R. Müller<sup>4</sup>, J. LeMaster<sup>\*2</sup>, J. Lappe<sup>\*2</sup>, H. F. Eisenberg<sup>\*1</sup>, D. J. McMahon<sup>\*1</sup>, E. Shane<sup>1</sup>. <sup>1</sup>Columbia University, New York, NY, USA, <sup>2</sup>Creighton University, Omaha, NE, USA, <sup>3</sup>Helen Hayes Hospital, West Haverstraw, NY, USA, <sup>4</sup>University of Zürich, Zürich, Switzerland.

Idiopathic osteoporosis (IOP) in premenopausal women (PrM) is an uncommon and poorly understood entity in which young, otherwise healthy women present with one or more low trauma fractures (LTFX) or very low BMD. In the course of a prospective study to elucidate the cause of bone fragility in PrM with IOP, we performed transiliac crest bone biopsies (BX) in 27 normally menstruating women with LTFX (n=17) and/or low BMD (T-score  $\leq -2.5$ ; n=10) and 50 healthy PrM controls (C) with normal BMD and no history of LTFX. Secondary causes of osteoporosis were excluded by clinical and laboratory evaluation. IOP and C were of comparable age (mean  $37 \pm 8$  yrs), height, weight (mean  $68 \pm 15$  kg), serum calcium, PTH, 25-OHD, and urine calcium. BMD was significantly lower at the spine, hip and forearm in IOPs. BX were analyzed by both 2D histomorphometry (2DH) and 3D micro-computed tomography ( $\mu$ CT). In a subset (n=45; 27 Cs), we also assessed mechanical competence (strength) by finite element modeling based on  $\mu$ CT image data to calculate apparent E (in the BX direction). By 2DH, IOPs had 21% lower trabecular (Tb) bone volume fraction (BV/TV), 11% lower Tb number, 20% higher Tb separation, and a trend toward lower Tb width (by 8%). Cortical (Ct) width was 25% lower, while Ct porosity (CtPoNo/CtAr) did not differ. By  $\mu$ CT, IOPs had 23% lower BV/TV, Tb number was 21% lower and separation was 18% higher. The standard deviation (SD) of Tb separation (Tb network inhomogeneity) was 14% higher, while Tb thickness and connectivity density did not differ. Mechanical competence (E) was 33% lower in IOP (p=0.06), but quite variable. E correlated best with 2DH and  $\mu$ CT BV/TV and  $\mu$ CT Tb number (R 0.8-0.9; p<0.0001). Dynamic parameters of bone remodeling activity were variable, but did not differ significantly between IOP and C.

In summary, PrM with IOP have thinner cortices, fewer and more widely spaced trabeculae, and greater Tb network inhomogeneity than C. These structural characteristics likely account for decreased bone strength and resistance to FX. The pathogenesis of these structural differences is unknown and is the subject of ongoing investigation.

	2DH			$\mu$ CT		
	IOP	C	p	IOP	C	p
Ct width ( $\mu$ m)	698 $\pm$ 222	927 $\pm$ 213	<0.0001			
CtPoNo/CtAr (#/mm <sup>2</sup> )	5.0 $\pm$ 2.4	5.9 $\pm$ 2.4	0.6			
Tb BV/TV (%)	17.0 $\pm$ 4.8	21.4 $\pm$ 5.7	0.001	18.7 $\pm$ 6.1	24.3 $\pm$ 9.2	0.002
Tb BS/TV (1/mm)				3.4 $\pm$ 0.6	4.0 $\pm$ 0.6	<0.0001
Tb Number (#/mm)	1.6 $\pm$ 0.3	1.8 $\pm$ 0.3	<0.001	1.5 $\pm$ 0.3	1.9 $\pm$ 1.1	0.01
Tb Width/Thickness ( $\mu$ m)	108 $\pm$ 20	117 $\pm$ 24	0.08	161 $\pm$ 39	164 $\pm$ 42	0.8
Tb Separation ( $\mu$ m)	559 $\pm$ 150	445 $\pm$ 96	0.001	730 $\pm$ 87	602 $\pm$ 117	<0.0001
Tb Separation SD ( $\mu$ m)				204 $\pm$ 36	175 $\pm$ 26	<0.001
Tb Conn Density (1/mm <sup>3</sup> )				12.4 $\pm$ 18.6	17.6 $\pm$ 25.7	0.4
Tb Mechanical Competence (E)				332 $\pm$ 200	493 $\pm$ 359	0.06

**Disclosures:** A. Cohen, None.

This study received funding from: NIH/NIAMS

## M311

**Reproducibility of Mineral Density and Morphometric MicroCT Measurements at Different Voxel Size Scans.** K. Verdelis<sup>1</sup>, L. Lukashova<sup>\*1</sup>, E. Atti<sup>\*2</sup>, S. Tetradis<sup>\*2</sup>, A. L. Boskey<sup>1</sup>, M. C. H. van der Meulen<sup>3</sup>. <sup>1</sup>Mineralized Tissues Laboratory, Hospital for Special Surgery, New York, NY, USA, <sup>2</sup>Oral Biology, School of Dentistry, Univ. of California Los Angeles, Los Angeles, CA, USA, <sup>3</sup>Sibley School of Mechanical & Aerospace Engineering, Cornell Univ., Ithaca, NY, USA.

The purpose of this study was to examine the reproducibility of mineral density and morphometric measurements from microCT analysis of mouse femurs performed at two different voxel sizes. The distal halves of three femurs from 3 month-old normal mice were analyzed in triplicate at 12 $\mu$ m and 8 $\mu$ m voxel resolution, using three different microCT systems: eXplore Locus SP (GE Healthcare, Canada), Skyscan 1172 (Skyscan, Belgium) and Scanco mCT40 (Scanco Medical, Switzerland). The samples were scanned in alcohol and each manufacturer's recommendations were followed for KVP, uMA, binning mode conditions and scan length. The scanned volumes were reconstructed in 3D and processed for both densitometric and morphometric analyses using the respective manufacturer's software for each system. Scans at each voxel size were performed in succession, without sample repositioning so that cortical or trabecular regions of interest (ROIs) defined subsequently could be applied identically to the same voxel size and system scanned volumes. Boundaries of the cortical and trabecular ROIs for each bone were constant as possible between different voxel size and system scans. True mineral density (TMD) was calculated for cortical and trabecular bone and directly measured bone volume (BV), bone volume fraction (BV/TV), surface to volume ratio (BS/BV), trabecular thickness (Tb.Th),

trabecular number (Tb.N) and trabecular separation (Tb.Sp) were determined for trabecular bone. Coefficients of variation (%) for each parameter were calculated for each system from the results of 12 $\mu$ m or 8 $\mu$ m scans individually (COVwithin resolution=COVw) or from results of 12 $\mu$ m and 8 $\mu$ m scans combined (COVbetween resolutions=COVb). COVw values were not correlated to COVb values in any of the parameters examined. 8 $\mu$ m cortical bone TMD measurements showed the lowest COVw (0.15-0.22) and 8 $\mu$ m trabecular TMD measurements the highest COVw (0.39-1.59). Decrease of the voxel size resulted in lower COVw values for cortical TMDs, while the opposite was true for trabecular TMDs. For all the 3D analysis parameters examined, higher resolution in most systems resulted in increased COVw. For both voxel sizes, BV/TV measurements presented the lowest COVw but the highest COVb values, while for the Tb.Sp the reverse held true. Increased precision in mineral density and morphometry measurements resulting from higher resolutions used in microCT is not generally accompanied by increased reproducibility of the measurements. Supported by NIH AR 46121.

**Disclosures:** K. Verdelis, None.

This study received funding from: AR 46121.

## M312

**Evaluation of the Detection Sensitivity of Simulated Trabecular Bone Loss in  $\mu$ MRI at In Vivo Resolution.** C. Q. Li<sup>\*1</sup>, J. F. Magland<sup>\*1</sup>, C. S. Rajapakse<sup>\*1</sup>, X. E. Guo<sup>\*2</sup>, X. H. Zhang<sup>\*2</sup>, F. W. Wehrli<sup>1</sup>. <sup>1</sup>University of Pennsylvania, Philadelphia, PA, USA, <sup>2</sup>Columbia University, New York City, NY, USA.

The MRI-based "virtual bone biopsy" (VBB) is a method for quantifying structural signs of disease progression or treatment effectiveness using high-resolution in vivo images of trabecular bone. To evaluate VBB's detection sensitivity we created accurate models of trabecular structure from  $\mu$ CT images of human cadaveric bone samples acquired at 21x21x22 $\mu$ m<sup>3</sup> resolution. These images were binarized and inverted to generate bone and marrow phases. To simulate bone loss, the images were eroded by randomly generating pits 60 $\mu$ m in radius on bone surfaces to reduce bone volume by 1, 2, 3, 4 and 5%. The resulting pre- and post-erosion trabecular bone models were then subjected to simulated k-space scanning, assuming marrow spaces to contain MR-active material. Subsequently, the data were low-pass filtered and Fourier reconstructed analogous to in vivo image processing to result in effective resolutions of 137x137x410 $\mu$ m<sup>3</sup> and 160x160x160 $\mu$ m<sup>3</sup>. Gaussian noise was superimposed on the complex data to result in a signal-to-noise ratio (SNR) of 12 in the magnitude images, commensurate with typical resolutions and SNR achievable in vivo. BV/TV and topological parameters (surface density, curve density, junction density, surface-to-curve ratio, erosion index and skeleton density) were calculated for the pre-erosion (control) and eroded images using VBB processing, and ANOVA performed to determine if the various levels of erosion were detectable. At SNR = 12 and 137x137x410 $\mu$ m<sup>3</sup> resolution, 6 of the 7 parameters studied changed significantly (p < .05) after reducing bone volume by 2%. Four of these parameters (SD, CD, SD, S/C) were also significantly different after a bone volume reduction of 1%. BV/TV decreased linearly with increasing bone volume reduction while the erosion index increased as expected, more significantly than BV/TV (Fig). At SNR = 12 and 160x160x160 $\mu$ m<sup>3</sup> resolution, 5 of the 7 parameters changed significantly after a 2% erosion, but only BV/TV was significantly different after 1% bone loss. The data suggest that, even at limited resolution and SNR clinically achievable, the VBB can detect changes of topology and scale of the trabecular network caused by small, possibly subclinical bone loss. The results have implications for the method's potential to study the effects of aging and response to therapeutic intervention.

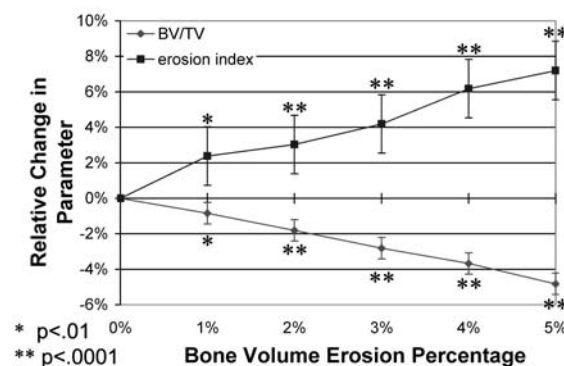


**Figure.** Relative change in parameter values after varying amounts of erosion, calculated with 137x137x410 $\mu$ m<sup>3</sup> voxel size and SNR=12. Error bars indicate 95% CI from Tukey HSD tests, relative to parameters of non-eroded images.

**Disclosures:** C.Q. Li, None.

This study received funding from: NIH RO1AR 41443 and NIH RO1 AR5315.

## M313

**Evidence of Increase in Vertebral Body Dimensions in Postmenopausal Women with Osteoporosis: A Three-Year Follow-Up Study.** K. Briot<sup>1</sup>, S. Kolta<sup>1</sup>, J. Fechtenbaum<sup>1</sup>, R. Said-Nahal<sup>\*1</sup>, C. Benhamou<sup>2</sup>, C. Roux<sup>1</sup>.<sup>1</sup>Rheumatology, Cochin Hospital, Paris, France, <sup>2</sup>Rheumatology, CHR d'Orléans, Unité INSERM U 658, Orléans, France.

Bone geometry plays a prominent role in the bone strength. Cross-sectional studies have shown that advancing age is associated with increasing diameter of long bones, related to both periosteal apposition and endosteal resorption. However, there are few data provided by prospective studies, especially concerning the changes in vertebral body dimensions. The objective here is to measure the changes occurring in the vertebral body size in a prospective study of women with postmenopausal osteoporosis.

Three-year data from placebo groups of the SOTI (1) and TROPOS (2) trials, performed in women with postmenopausal osteoporosis, were used for this current study. In these trials, patients underwent lateral radiographs of the thoracic and lumbar spine at baseline and annually over three years, according to standardized procedures. Six-point digitization method was used: the four corner points of the vertebral body from T4 to L4 are marked, as well as an additional point in the middle of the upper and lower endplates. From these 6 points, the vertebral body perimeter, area and depth were measured at baseline and at three years. The analysis excluded all vertebrae with prevalent or incident fracture.

A total of 2017 postmenopausal women (mean age 73.4±6.1 years) with a mean lumbar spine T score of -3.1±1.5, and a mean femoral neck T score of -3.0±0.7 are included in the analysis. Vertebral body dimensions increased over 3 years, by 0.5±1.1 mm (mean depth ± SD), by 11.4±49.2 mm<sup>2</sup> (mean area ±SD) and by 1.1±3.4 mm (mean perimeter ±SD) at the thoracic level (T4 to T12). At the lumbar level (L1 to L4), these dimensions increased as well: 0.5±1.3 mm (mean depth ± SD), 13.9±67mm<sup>2</sup> (mean area ±SD), 0.7±3.9 mm (mean perimeter ±SD). A significant increase in vertebral body size was observed for each vertebral level from T5 to L4 for each of these parameters (p<0.01).

These prospective results demonstrate that vertebral body dimensions increase over 3 years in women with postmenopausal osteoporosis.

1. Meunier PJ et al. N Engl J Med 2004;350(12):459-68.

2. Reginster JY et al. J Clin Endocrinol Metab 2005; 90(5) : 2816-22.

**Disclosures:** K. Briot, None.

## M314

**Radiographic Texture Analysis (RTA) of Densitometric Calcaneal Images Differs Between Subjects with and without Glucocorticoid (GC) Use.** T. J. Vokes<sup>1</sup>, M. Chinander<sup>\*2</sup>, M. Giger<sup>\*3</sup>. <sup>1</sup>Medicine/Endocrinology, University of Chicago, Chicago, IL, USA, <sup>2</sup>Radiology, University of Chicago, Chicago, IL, USA, <sup>3</sup>Radiology, University of Chicago, Chicago, IL, USA.

RTA is a method for non-invasive assessment of bone structure through computerized analysis of the pattern of radiographic images. We have previously shown that RTA performed on densitometric calcaneal images differentiated subjects with and without vertebral fractures even when controlling for age and BMD, suggesting that RTA captures an aspect of bone fragility that is not assessed by BMD. GC-associated increase in bone fragility is not fully explained by decrease in BMD, suggesting that GC also cause deterioration of bone structure. Therefore, we examined whether RTA differs between subjects who had received pharmacologic doses of GC and those who had not.

We recruited 800 subjects (age 19-95 years, mean±SD of 62.6±13.6 years, 82 males) referred for BMD testing. We used Prodigy to image the spine for VFA and to measure BMD at the lumbar spine and proximal femur, and PIXI to measure calcaneal BMD and to generate a high resolution image for RTA. RTA was performed on a 128x128 pixel ROI in the proximal calcaneus. RTA features analyzed include RMS (root mean square variation, a measure of coarseness of radiographic texture pattern) and its standard deviation across the 24 radial slices, sdRMS, which is a measure of the anisotropy of the textural pattern.

There were 126 subjects who had received more than 2800 mg of prednisone or equivalent and 674 subjects without history of GC use. Compared to non-users, GC users had higher prevalence of vertebral fractures (31 vs. 17%, p=0.001), despite their younger age (55.9 vs. 63.8 years, p<0.0001), and higher weight (165 vs. 153lbs, p=0.0005). Although BMD T-score (the lowest of hip or spine) did not differ between GC users and non-users (-2.4 vs. -2.3, p=0.5), both RMS and sdRMS were lower in GC users (4.34 vs. 4.46, p=0.001, and 0.11 vs. 0.12, p=0.03). In a multivariate logistic regression analysis with GC use as outcome, and age, weight, BMD T-score and RTA as predictors, both BMD and RTA had a significant effect with p<0.0001 for BMD T-score, p=0.002 for RMS and p=0.03 for sdRMS, respectively. In general, subjects with vertebral fractures (VFX) had lower RTA values than those without VFX. GC users without VFX had RTA values similar to non-GC users with VFX, while GC users who also had VFX had even lower values. No such relationship was observed for BMD.

These results suggest that RTA performed on densitometric calcaneal images captures changes in bone structure associated with GC-induced increase in bone fragility.

**Disclosures:** T.J. Vokes, Merck 1, 3; P&G 1, 3; Roche/GSK 1; Novartis 1. This study received funding from: NIH.

## M315

**Regional Differences in Femoral Neck Cortical Thickness Determine Hip Fragility: An in-Vivo CT Study.** P. M. Mayhew<sup>\*1</sup>, C. M. Rose<sup>\*1</sup>, K. Brown<sup>\*2</sup>, S. K. Kaptoge<sup>\*1</sup>, N. Loveridge<sup>\*1</sup>, J. Reeve<sup>1</sup>, K. E. S. Poole<sup>1</sup>. <sup>1</sup>Department of Medicine, University of Cambridge, CB2 2QQ, United Kingdom, <sup>2</sup>Austin, Mindways Software Inc, Texas, TX, USA.

This in vivo CT study examined the regional variability in the contra-lateral femoral neck cortical thickness (C.Th) of female patients that had fractured a hip, and an age matched group of control patients, to determine whether C.Th may be an indicator of hip fragility.

Sixteen pre-discharge patients with low/moderate trauma hip fracture (intracapsular (n=7), trochanteric (n=9) mean age 80.3 +/- 1.15) consented to a CT scan of the unfractured hip (Siemens 16, 1mm slice thickness, 0.59 mm pixel size) and analysis with Mindways software (v 4.1.3, Texas, USA). Forty eight healthy controls attending for a routine clinical CT scan of the abdomen and pelvis were also consented to hip CT (age 79.5 +/- 0.7; exclusions: malignancy, severe hip osteoarthritis, liver disease, Paget's ). Femoral neck T scores were <2.5 in 5 of the controls and 6 cases (3 intracapsular and 3 trochanteric). Six cross-sectional slices at 1mm intervals of the femoral neck were automatically extracted commencing from a reproducible mid-neck location (eccentricity/max-min ratio of 1.4) for analysis of the regional C.Th. Four anatomical quadrants for each slice were defined: supero-posterior, supero-anterior, infero-posterior and infero-anterior; using the centre of mineral mass and principal axes. There were no differences in C.Th between right and left hips in controls so mean values were used. Longitudinal drift by phantom measurement was <2%. Data was Log transformed to normalize distributions of the C.Th. A nested ANOVA with random effects was used to obtain least squares means and fracture case/control contrasts in quadrants.

Allowing for the expected effect of age (reducing cortical thickness), hip fracture cases exhibited significantly lower cortical thickness in all the quadrants, when compared to the controls: Supero-anterior 21% lower (mean 0.28mm, p=0.0007), Infero-anterior 21% (1.08mm, p=0.0008), Infero-posterior 21% (2.04mm, p=0.0007), and Supero-posterior 16% (0.18mm, p=0.0132). Although there were no statistically significant differences in C.Th estimates between the intracapsular and trochanteric fracture types (p=0.23), mean C.Th estimates were lower in the intracapsular group in all quadrants.

Technological advancements in tomography and analysis mean that cortical thickness measurements can be made at clinical CT resolution, and thus help direct appropriate therapy to those at risk of hip fracture.

**Disclosures:** P.M. Mayhew, None.

## M316

**In Vivo Measurements of Vertebral Body Dimensions by 3 Dimensional X-ray Absorptiometry (3D-XA) and Their Relation with Age: A Cross-Sectional and Longitudinal Study.** S. Kerkeni<sup>\*1</sup>, S. Kolta<sup>1</sup>, L. Gossec<sup>\*1</sup>, B. Billotet<sup>\*2</sup>, E. Sapin<sup>\*2</sup>, D. Mitton<sup>\*2</sup>, W. Skalli<sup>\*2</sup>, C. Roux<sup>1</sup>. <sup>1</sup>Cochin Hospital, Paris, France, <sup>2</sup>LBM, Arts et Métiers ParisTech ENSAM, CNRS, Paris, France.

Our study aimed to assess changes in vertebral geometric parameters with age using 3D-XA method in vivo. Subjects were women participating in the European population-based Osteoporosis and Ultrasound Study (OPUS) (1). This cross-sectional and longitudinal study was conducted in 3 subgroups of women without vertebral fracture. Group 1: 20-40 years (N=27), group 2: 55-60 years (N=29) and group 3: 70-79 years (N=29). All participants had an anterior-posterior and a lateral measurement of thoracic and lumbar spine using Instant Vertebral Assessment software on a standard Hologic QDR4500A device at baseline and 6 years later. All vertebrae from T4 to L4 were studied. 3D-XA was performed according to our previously published methodology (2). Several geometric parameters of vertebral bodies were measured from the 3D-XA including anterior, middle and posterior heights (aH, mH and pH), volume, minimal cross sectional area (CSA). At baseline, without any adjustment, vertebral body heights were not significantly different between groups. Mean CSA (T4-L4) was 701.5 ± 84.7, 740.9 ± 68.8 and 739.2 ± 67.2 mm<sup>2</sup> in groups 1, 2 and 3 respectively (p = 0.09). The difference was significant in thoracic vertebrae (p=0.04) but not in lumbar vertebrae. After adjustment for body height, aH, mH, pH, CSA and vertebral body volume were significantly different between the 3 groups in the thoracic vertebrae as well as the lumbar vertebrae (p<0.0001) except for thoracic aH. Six years follow-up revealed, in the whole population, a significant increase in thoracic vertebral body volume (+ 392.3 mm<sup>3</sup>, p=0.02) and a trend to an increase in CSA of thoracic vertebrae (+18.2 mm<sup>2</sup>, p=0.09). This study shows that vertebral dimensions vary with age and that these changes can be detected by the 3D-XA method. Bone geometry is known to be an important determinant of bone strength. Combined to bone density, it could improve fracture risk prediction.

(1) Gluer et al J Bone Miner Res 2004;19:782-93.

(2) Kolta et al Osteoporos Int 2008 ;19:185-92.

**Disclosures:** S. Kolta, None.

## M317

**Active Shape Modelling As a Predictor of Hip Fracture.** F. Jabbar<sup>\*1</sup>, R. J. Barr<sup>\*1</sup>, D. M. Reid<sup>1</sup>, R. M. Aspden<sup>1</sup>, I. R. Reid<sup>2</sup>, B. Mason<sup>\*2</sup>, A. N. Horne<sup>\*2</sup>, J. S. Gregory<sup>\*1</sup>. <sup>1</sup>University of Aberdeen, Aberdeen, United Kingdom, <sup>2</sup>University of Auckland, Auckland, New Zealand.

Osteoporosis (OP) is a common musculoskeletal disorder characterised by reduced Bone Mineral Density (BMD) and a disruption of bone microarchitecture, leading to an increased risk of fracture. Dual Energy Absorptiometry (DXA) is used to diagnose OP, however BMD alone has a poor efficacy in terms of hip fracture prediction. The shape of the hip is known to affect fracture risk. Active Shape Models (ASM) can quantify shape variation of the proximal femur and have been shown to relate to fracture in a cross sectional study. This study aimed to discover if the link between fracture risk and the shape of the proximal femur can be observed prospectively using ASM.

Images from DXA scans of 260 subjects from the baseline visit of 'The Auckland Calcium study', were used. All subjects were healthy postmenopausal women aged over 55 years with no major disease, or treatment for OP. The fracture group comprised 20 subjects who incurred a proximal femoral fracture during the 5 year study.

Each DXA image was processed using the 'Active Shape Modelling Toolkit' software. The shape was outlined using points at key anatomical landmarks. A 29 point model from a previous study was used to automate and train the model. Once all images had been processed a new ASM was produced which outputted 9 distinct shape modes for the dataset.

Three of the modes showed significant differences in the shape of the proximal femur in the fracture group. After adjusting for age and BMI with logistic regression, Mode 1 was no longer significant, due to a high correlation with age, Mode 4 was highly significant ( $P=0.003$ ) while Mode 9 became marginally insignificant, ( $P=0.049$  to  $P=0.066$ ) (Table). The shape changes associated with an increase in Mode 4 include an increase in neck-shaft angle and femoral neck length, which have individually been shown in geometrical studies to increase the risk of hip fracture. The odds ratio for mode 4 is 2.33 indicating that a 1 standard deviation increase from the mean will more than double the risk of hip fracture.

This study has demonstrated a link between the morphology of the proximal femur and prospective risk of hip fracture. It may be possible to improve hip fracture risk assessment by using methods such as ASM to examine the shape of the whole femur.

Mode		1	4	9
t-test#	P-value	0.014	<0.001	0.049
Age and BMIS				
Adjusted	P-value	0.154	0.003	0.066
Logistic	Odds-ratio	1.53	2.33	1.69
Regression*		(0.85-2.73)	(1.33-4.17)	(0.97-2.95)

#,\$ Comparison of fracture cases and controls (\$ after adjustment). \*Odds Ratio for a 1sd difference in mode score for predicting fracture

**Disclosures:** J.S. Gregory, None.

This study received funding from: University of Aberdeen.

## M318

**Calcaneal Quantitative Ultrasound Measurement of 2323 Healthy Adults in Southwest China.** J. Yang, X. Zhao\*, J. Sun\*, J. Rong\*, C. Li\*, L. Chen. Trauma Center, Institute of Surgery Research, Daping Hospital, Chongqing, China.

**Background:** In China, especially in Southwest China, the awareness of OP is not appreciated, and DEXA is not broadly used for the evaluation of bone health. As a non-invasive, radiation-free, and portable measurement, quantitative ultrasound (QUS) assessment of bone status is a reliable, fast and low-cost approach to evaluate the bone structure and bone quality.

**Objective:** To establish the reference QUS data and investigate the correlation among age, body size and ultrasound variables in healthy southwest chinese population.

**Materials and Methods:** Ultrasound bone densitometry of the calcaneus in 2323 healthy adults in southwest china (1459 men and 864 women) aged 20-95 years was carried out using SONOST2000 (Korea) in this study. QUS parameters represented as speed of sound (SOS), broadband ultrasound attenuation (BUA) and bone quality index (BQI) were determined at the right Calcaneus.

**Results:** The SOS, BUA and BQI peaked at 20-29 years old in both genders. Compared with the 20-29 years old group, there was a significant decrease in female SOS and BQI starting from the age of 50 years. The SOS and BQI in male, and BUA in female started to fall from the age of 60 years ( $P<0.05$ ). The male SOS, BUA and BQI were higher than that in the female in all age groups, but only significantly higher in groups over 60 ( $P<0.001$ ). Pearson's correlation analysis showed a significant correlation between SOS and BUA (for male,  $r=0.658$ , for female,  $r=0.610$ ,  $P<0.001$ ), which was higher than those found by other groups in mainland chinese men and women. We also observed significant correlation between BQI and SOS, or between BQI and BUA (for male,  $r=0.895$ ,  $0.870$ ; for female,  $r=0.915$ ,  $0.883$  respectively,  $P<0.001$ ). Age had the highest correlation coefficient with SOS, BUA and BQI ( $P<0.001$ ) especially in women ( $r=-0.475$ ,  $-0.317$  and  $-0.442$  respectively). The linear regression revealed that the mean decreasing rates of the QUS parameters in men ( $0.508$  m/s per year for SOS,  $0.177$  dB/MHz per year for BUA) and women ( $0.987$  m/s per year for SOS,  $0.224$  dB/MHz per year for BUA) were faster than those reported for the mainland chinese population. In the stepwise multiple linear regression analyses, the male BMI or female weight was the secondary positive factor influencing QUS parameters, which was different from the previous report, in which weight was found to be a less important factor affecting QUS parameters in mainland Chinese of both genders.

**Conclusion:** We established the normative QUS data for the adult southwest chinese of

both genders, which will provide the reference values for the screening of osteoporosis and prediction of fracture risk in local area.

This study received "973" program of China (No.2005CB522604), and NSFC (No.30470947, 30530410).

**Disclosures:** J. Yang, None.

## M319

**Assessment of Cortical Thickness and Bone Mineral Density in the Radius by Low-Frequency Guided-Wave Ultrasound.** P. Moilanen<sup>\*1</sup>, V. Kilappa<sup>\*1</sup>, T. Chen<sup>\*2</sup>, H. Ma<sup>\*2</sup>, J. Timonen<sup>\*1</sup>, S. Cheng<sup>2</sup>. <sup>1</sup>Department of Physics, University of Jyväskylä, Jyväskylä, Finland, <sup>2</sup>Department of Health Sciences, University of Jyväskylä, Jyväskylä, Finland.

Low-frequency quantitative guided-wave ultrasonics (Q-GWUS) based on the first arriving signal shows enhanced sensitivity to cortical thickness and osteoporotic changes deep in the endosteal region of cortical bone. A group of female subjects were measured on the tibia and radius shaft. Low-frequency ultrasound velocity ( $V_{LF}$ ) was recorded by a Q-GWUS device (0.4 MHz) with a bidirectional array of transducers. In addition, high-frequency ultrasound velocity ( $V_{HF}$ ) was recorded by an Omnisense® (Sunlight Medical Ltd; 1.25 MHz). Peripheral quantitative computed tomography (XCT 2000, Stratec Medizintechnik GmbH) was used to assess the volumetric bone mineral density (BMD) and cortical thickness (CTH) at the same bone locations. *In vivo* reproducibility of the Q-GWUS (RMS CV) across the subjects was 0.5% for the radius and tibia.

Preliminary results indicate that radius  $V_{LF}$  follows well the typical growth and loss curve of bone with aging, similarly as CTH and BMD (age 10-85 years;  $n=207$ ). In addition,  $V_{LF}$  appears to be more strongly correlated with CTH ( $r=0.61$ ,  $p<0.001$ ) and BMD ( $r=0.75$ ,  $p<0.001$ ) than  $V_{HF}$  (respectively:  $r=0.28$ ,  $p<0.05$ ;  $r=0.38$ ,  $p<0.01$ ) ( $n=59$  for the comparative correlations).

In conclusion, our results indicate that the low-frequency ultrasound device (Q-GWUS) had an enhanced sensitivity and yielded better prediction over that of the high-frequency device (Omnisense) with respect to changing of cortical thickness and bone mineral density with aging.

**Disclosures:** P. Moilanen, None.

## M320

**Relationship of Quantitative Ultrasound at Phalanges with Hand and Axial BMD, Sex Hormones and Bone Turnover Markers in Elderly Women.** S. Gonnelli, C. Caffarelli\*, L. Gennari, D. Merlotti, S. Campagna\*, B. Franci\*, R. Nuti. Institute of Internal Medicine, University of Siena, Siena, Italy.

Quantitative ultrasound (QUS) has been applied to the assessment of bone status for almost two decades. Some recent studies have reported that the quantitative analysis of the graphic trace of QUS signal at phalanges could improve our ability in evaluating bone status and in distinguishing different metabolic bone diseases. The literature data on the determinants of the QUS parameters derived from graphic trace analysis are scarce.

This study aimed to investigate for any possible relationships of QUS parameters at phalanges with hand and axial BMD, sex hormones and bone turnover markers in a cohort of elderly Italian women, who were participating in a larger epidemiological study. In 763 consecutive healthy women aged 55 years or more (mean age  $62.7 \pm 6.7$  yrs), living in the area of Siena (Italy), we evaluated: QUS at phalanges (amplitude dependent speed of sound [AD-SoS], bone transmission time [BTT]; ultrasound bone profile index [UBPI]) by Bone Profiler-IGEA. BMD at right hand, at lumbar spine and at femur was also assessed (Prodigy, GE-Lunar). In all subjects we also measured serum testosterone (T), estradiol (E), sex-hormone binding globulin (SHBG), 25-hydroxyvitamin D (25OHD), bone alkaline phosphatase (B-ALP), parathyroid hormone (PTH) and carboxy-terminal telopeptide of type I collagen (CTX). Dietary calcium intake was assessed by a validated Food Frequency Questionnaire.

Both AD-SoS and UBPI were inversely associated with age ( $r=-0.39$  and  $r=-0.44$  respectively). No significant correlation was found between BTT and age. Among QUS parameters BTT showed the highest correlation with hand-BMD ( $r=0.68$ ;  $p<0.001$ ). The correlation coefficients between AD-SoS, BTT and UBPI with hand and axial BMD were all significant ( $p<0.001$ ) but low, ranging from 0.25 to 0.44. Both AD-SoS and UBPI, but not BTT, showed a significant, even though marginal, correlation ( $p<0.05$ ) with serum 25OHD. SHBG serum levels were inversely correlated with AD-SoS, BTT and UBPI ( $r=-0.17$ ,  $r=-0.11$  and  $r=-0.20$ , respectively). All QUS parameters were inversely correlated with serum B-ALP, but not with serum CTX. Multiple regression analysis showed that age, E, PTH and 25OHD were significant determinants of AD-SoS; instead, only age, PTH and E were significant determinants of UBPI.

On the basis of our results we can conclude that BTT could improve the identifying of subjects with reduced BMD both at hand and axial skeleton. However, AD-SoS and UBPI seem to better reflect the changes in bone status induced by aging, sex hormones and vitamin D levels.

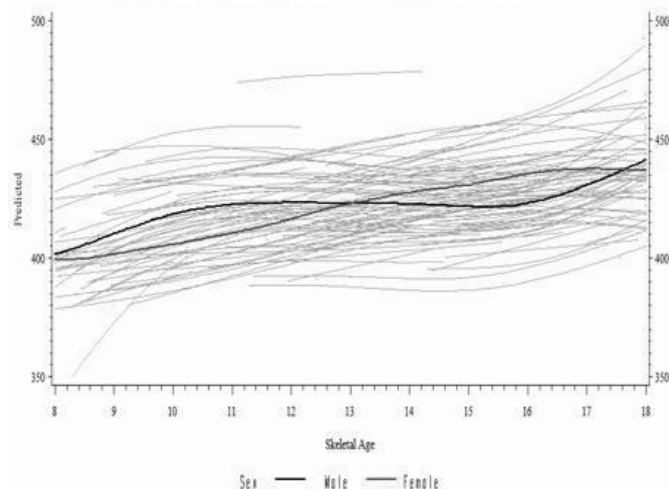
**Disclosures:** S. Gonnelli, None.

## M321

**Longitudinal Analysis of Calcaneal Quantitative Ultrasound Measures During Childhood.** M. Lee<sup>1</sup>, R. W. Nahhas<sup>\*1</sup>, A. C. Choh<sup>\*1</sup>, E. W. Demerath<sup>\*2</sup>, W. C. Chumlea<sup>\*1</sup>, D. L. Duren<sup>1</sup>, R. J. Sherwood<sup>\*1</sup>, K. D. Williams<sup>\*1</sup>, B. Towne<sup>\*1</sup>, R. M. Siervogel<sup>1</sup>, S. A. Czerwinski<sup>\*1</sup>. <sup>1</sup>Community Health, Wright State University, Dayton, OH, USA, <sup>2</sup>Epidemiology, University of Minnesota, Minneapolis, MN, USA.

Accrual of peak bone mass at the end of adolescence lays the foundation for bone in adulthood to manage the various challenges to the skeleton over one's lifetime. Quantitative ultrasound (QUS) technology has been used to estimate properties of bone in children and adults with the advantages of no radiation exposure. However, there are only a few studies that have examined longitudinal changes in calcaneal QUS measures in samples of children. We examined how QUS parameters change over time by examining both chronological age and skeletal age and determined whether changes in QUS measures differ by sex. The study sample consisted of a total of 219 Caucasian children and adolescents (112 males and 107 females) participating in the Fels Longitudinal Study. A total of 610 calcaneal QUS observations were obtained using Sahara ® bone sonometer (Hologic, Inc., Waltham, MA) from children aged between 7.6 and 18 years (skeletal ages between 6.4 to 18 y.). Broadband ultrasound attenuation (BUA, dM/Hz), and speed of sound (SOS, m/s) were collected twice in the dominant heel, and the average value of each QUS parameter was used in the analysis. Using statistical methods for linear mixed effect models, the best fitting models were selected. The results for log(BUA) indicate that there is a cubic growth curve that is best described using skeletal age rather than chronological age as the timing variable, and that the growth curves differ significantly by sex ( $p < 0.0001$ ). In particular, males experience their most rapid growth in BUA in early and late adolescence, while females experience their most rapid growth in BUA in mid-adolescence (Figure 1). For SOS, the growth trend is linear with respect to skeletal age with a significantly positive slope for females only; however there is no significant difference between the trends for males and females ( $p > 0.05$ ). This study documents significant sex differences in the pattern of change in QUS measures of bone strength (particularly BUA) during childhood and adolescence, demonstrating the utility of QUS for tracking bone development.

**Figure 1. Predicted log(BUA) over time, by sex**



**Disclosures:** M. Lee, None.

This study received funding from: NIH/NICHD (R01HD12252), NIH/NIAMS (R01AR52147).

## M322

**Post-Fracture Osteoporosis Intervention Strategy.** V. I. M. Elliot-Gibson<sup>\*1</sup>, R. Jain<sup>\*2</sup>, D. E. Beaton<sup>1</sup>, R. Sujic<sup>\*1</sup>, F. Jiwa<sup>\*2</sup>, E. R. Bogoch<sup>3</sup>, S. Richie<sup>\*4</sup>, E. Samji<sup>\*5</sup>. <sup>1</sup>Mobility Program Clinical Research Unit, St. Michael's Hospital, Toronto, ON, Canada, <sup>2</sup>Osteoporosis Canada, Toronto, ON, Canada, <sup>3</sup>Department of Surgery, St. Michael's Hospital, Toronto, ON, Canada, <sup>4</sup>Department of Surgery, McMaster University and Brantford General Hospital and Ontario Orthopaedic Association, Hamilton, ON, Canada, <sup>5</sup>Ministry of Health and Long-Term Care, Government of Ontario, Toronto, ON, Canada.

The Ontario Osteoporosis (OP) Strategy is a multifaceted initiative mandated and funded by the Ontario Government, Ministry of Health. The Post-Fracture OP Program is one of five components and was implemented by Osteoporosis Canada (OC) on behalf of the Ministry. The goals of this program are to improve OP diagnosis and treatment in this population, prevent future fractures, and improve OP knowledge among health professionals and patients. From January 3, 2007 to January 8, 2008 OC deployed 19 OP Screening Coordinators (OSCs) in 31 medium to high volume fracture clinics in Ontario. The OSC identifies fragility fracture patients, educates them on OP and their risks, and suggest follow up with the family physician (FP) for further investigation and treatment of

their bone health. OSC's also facilitate communication between the FP and surgeon by way of a standardized form letter recommending OP assessment with their patient. Quality assurance self-report data is collected on patients able to voluntarily complete the questionnaire and includes OP risk factors, prior OP treatment and adherence, prior bone mineral density (DXA) testing, OP knowledge and beliefs and socio-demographics characteristics. Patient review is conducted at three and six months. Data collection from January, 2007 to April, 2007 was completed on paper format and starting in May, 2007 data was collected using tablet PC's. From May 2, 2007 to January 11, 2008, 97,386 fracture clinic patient visits were screened, of which 16.97% were identified for OP screening and 58.92% were seen by the OSC. Out of the 9737 identified for screening, 45.65% did not meet inclusion criteria, 50.84% completed baseline screening, 2.72% refused intervention, and 0.8% missing data. From the electronic database (January 3, 2007 to January 7, 2008) and referring to the fragility fracture (target) population ( $n = 5330$ ), follow up with the FP was suggested for 85.5% patients, with 61.7% of FP's receiving the standardized form letter. Discussion about having a bone mineral density (DXA) test completed by their FP was suggested to 75.2%. It was suggested to 97.8% of patients to take 1500 mgs of calcium and 800 IU Vitamin D daily. The most common fracture sites were the wrist, ankle, shoulder and hip. Approval from each hospital's Research Ethics Board is currently underway to use the quality assurance data collected for research purposes.

**Disclosures:** V.I.M. Elliot-Gibson, None.

## M323

**LRP5 G171V Mutation and Tobacco Smoke Related Bone Fragility.** M. P. Akhter, A. S. Manolides<sup>\*</sup>, D. M. Cullen, R. R. Recker. Medicine, Creighton University, Omaha, NE, USA.

Tobacco smoking is a lifestyle choice that may cause bone loss and osteoporosis. In this study, we characterized bone structure and strength properties to determine if the LRP5 G171V mutation will protect against bone loss associated with tobacco smoking. Ninety adult (4 mo.) female mice representing three genotypes (all bred to C57BL/6 mice): WT (Lrp5<sup>+/+</sup>, wild type), KO (Lrp5<sup>-/-</sup> knockout), HBM (High bone mass with LRP5 G171V mutation) were randomly divided into control and tobacco exposure groups. Mice were subjected to whole body tobacco/cigarette (IR4F University of Kentucky Research) smoke at either smoke exposure of 129±38 mg/mm<sup>3</sup> (mean± SD) total suspended particulates (TSP/m<sup>3</sup>) or sham exposed (no smoke exposure, Control). A smoke exposure was for 3hrs (5 days/week) for 12 weeks. Mice were inspected daily to assure adequate food intake, and general health. Femurs were collected for biomechanical measurements. Trabecular bone structure in distal femurs was analyzed by micro-CT scans. Mid-shaft femurs were tested in 3-point bending. We used the General Linear Model for univariate analysis to test for differences due to smoking within each genotype. Bone volume fraction (BV/TV) and connectivity density (ConnD) declined in all three genotypes exposed to tobacco smoke (Table). While trabecular number (TbN) was lower in the HBM smoke exposed group as compared to their respective controls (Table). Apparent density (AppDens) was lower in the smoke exposed group for HBM and KO (Table) as compared to the controls. Smoking-related loss in trabecular structure (BV/TV) was 36%, 28% and 45% in HBM, WT and KO mice respectively. In addition, the mid shaft ultimate (ULT) load declined in the Smoke exposed group as compared to their respective controls. The trabecular bone structure (BV/TV, ConnD, TbN, AppDens) and femur strength in HBM mice remained elevated as compared to both WT and KO within each treatment group (Control & Smoke exposed). The already fragile KO had a large decrease in trabecular bone structure (45%), and the HBM losses were moderate with final bone structure and strength remaining well above that for the wild type mice. Mice with the LRP5 G171V mutation (HBM) did show a significant decline to smoke exposure demonstrating sensitivity to tobacco smoke exposure.

(Mean ± SEM)	Control			Smoke Exposed		
Trabecular structure	HBM	WT	KO	HBM	WT	KO
BVTV	35.2 ± 3.2	2.7 ± 0.5 <sup>b</sup>	3.4 ± 0.2 <sup>b</sup>	22.6 ± 2.7 <sup>a</sup>	1.9 ± 0.4 <sup>ab</sup>	1.9 ± 0.2 <sup>ab</sup>
ConnD (mg/mm <sup>3</sup> )	63.8 ± 2.4	6.7 ± 2.2 <sup>b</sup>	10.9 ± 2.1 <sup>b</sup>	54.7 ± 1.4 <sup>a</sup>	3.6 ± 1.0 <sup>ab</sup>	3.8 ± 0.5 <sup>ab</sup>
TbN (1/mm)	5.6 ± 0.6	1.8 ± 0.09 <sup>b</sup>	1.9 ± 0.09 <sup>b</sup>	4.0 ± 0.3 <sup>a</sup>	1.7 ± 0.1 <sup>b</sup>	1.8 ± 0.09 <sup>b</sup>
AppD(mg/mm <sup>3</sup> )	390 ± 28	97 ± 5	107 ± 3	277 ± 23 <sup>a</sup>	90 ± 4 <sup>b</sup>	92 ± 3 <sup>ab</sup>
ULT Load (N)	49 ± 2.0	21 ± 0.6	19 ± 0.6	36 ± 1.5 <sup>a</sup>	18 ± 0.6 <sup>ab</sup>	17 ± 0.5 <sup>ab</sup>

<sup>a</sup>Differences due to Smoke exposure ( $P < 0.05$ ); <sup>b</sup>Different from HBM within each group ( $P < 0.05$ )

**Disclosures:** M.P. Akhter, None.

This study received funding from: LB595 State of Nebraska.

## M324

**High Impact Exercise May Have a Protective Effect on BMD but Moderate Impact Exercise May Have Negative Effect in Young Women with Anorexia Nervosa.** E. J. Waugh<sup>1</sup>, D. E. Beaton<sup>\*2</sup>, P. Cote<sup>\*3</sup>, B. Woodside<sup>\*4</sup>, G. A. Hawker<sup>1</sup>. <sup>1</sup>Osteoporosis, Women's College Hospital, Toronto, ON, Canada, <sup>2</sup>Mobility Program, St. Michael's Hospital, Toronto, ON, Canada, <sup>3</sup>Rehabilitation Solutions, University Health Network, Toronto, ON, Canada, <sup>4</sup>Psychiatry, University Health Network, Toronto, ON, Canada.

We investigated the effect of exercise on BMD in a retrospective cohort study of patients aged 17-40 yrs who had received inpatient treatment for AN over a 12-yr time period. A detailed illness history was obtained by a Life History Calendar semi-structured interview. Lifetime exercise history was obtained by an adapted Minnesota Leisure Time Physical Activity interview. Exercise type was categorized as non/low (NL), moderate

(MOD) or high (HI) impact. Total lifetime hours for each category was converted to a lifetime percentage based on participants' age (NL%, MOD%, HI%). BMD at the lumbar spine L1-L4 (LSP), femoral neck (FN) and total body (TB) and body composition (fat, lean mass) was measured by DXA. Low BMD was defined as a Z-score value  $\leq -1.5$  at one or more sites. Participants were considered recovered if they both achieved a BMI  $\geq 18.5$  kg/m<sup>2</sup> and resumed regular menstruation for  $\geq 1$  year. Logistic regression was used to examine the association between exercise and BMD values adjusting for recovery status (no/yes), weight, and duration and severity (lowest lifetime BMI) of illness.

We recruited 190 participants from two centers (113 ill; 77 recovered). At interview, mean age was  $27.2 \pm 5.6$  yrs, mean BMI was  $19.4$  ( $11.1 - 35.5$ ) kg/m<sup>2</sup>, % fat was  $26.2$  ( $4.3 - 49.3$ ), lean mass was  $36.0$  ( $24.9 - 55.4$ ) kg, age at AN onset was  $18.2$  ( $10-32$ ) yrs, duration of illness was  $5.9$  ( $1 - 25$ ) yrs and lowest lifetime BMI was  $13.9$  ( $7.2 - 18.0$ ) kg/m<sup>2</sup>. Mean hrs/ wk of past year exercise was  $7.2$  ( $0 - 46.3$ ). Lifetime NL% was  $0.4$  ( $0 - 4.3$ ), MOD% was  $1.0$  ( $0 - 8.3$ ), HI% was  $0.7$  ( $0 - 9.2$ ). HI% was correlated with lean mass (Spearman  $r=0.29$ ,  $p<0.0001$ ). Descriptively, participants with high MOD% ( $> 2\%$ ) typically walked for  $\geq 3$  hrs/d while ill; those with high HI% ( $> 2\%$ ) participated in dance or gymnastics at a competitive level before AN onset during childhood and early adolescence. NL% was not associated with low BMD ( $p=0.8$ ), MOD% had a negative effect (OR =  $1.5$ , 95% CI  $1.11 - 2.08$ ,  $p=0.007$ ) and HI% had a positive effect (OR =  $0.49$ , 95% CI  $0.26 - 0.83$ ,  $p=0.005$ ). Lean mass also had a positive effect (OR =  $0.89$ , 95% CI  $0.8-0.98$ ,  $p=0.03$ ).

The results suggest that HI exercise prior to AN onset may have a protective effect on BMD which may be due to the associated increase in lean mass. Excessive MOD exercise often observed in AN patients appears to have a negative effect on BMD even after adjusting for weight and illness history.

**Disclosures:** E.J. Waugh, None.

## M325

**Physical Activity, BMD and Fragility Fracture: the Canadian Multicentre Osteoporosis Study (CaMos).** C. L. Hitchcock<sup>\*1</sup>, E. J. Kingwell<sup>\*1</sup>, M. A. Petit<sup>2</sup>, K. S. Davison<sup>3</sup>, S. Forsmo<sup>4</sup>, W. Zhou<sup>\*5</sup>, N. Kreiger<sup>\*6</sup>, J. C. Prior<sup>1</sup>. <sup>1</sup>UBC, Vancouver, BC, Canada, <sup>2</sup>U MN, Minneapolis, MN, USA, <sup>3</sup>Laval, Quebec City, QC, Canada, <sup>4</sup>NTNU, Trondheim, Norway, <sup>5</sup>McGill U, Montreal, QC, Canada, <sup>6</sup>U of T, Toronto, ON, Canada.

Physical activity has the potential to optimize bone mineral density (BMD) and reduce the risk of fractures. However, few studies have explored these relationships in a population-based data set. We explored the association with physical activity, BMD and fragility fracture at baseline and over 5 years using population-based data from the 9 regional centres in the Canadian Multicentre Osteoporosis Study (CaMos). Lumbar spine (LS) and total hip (hip) BMD were assessed at baseline and after 5-y using phantom-adjusted dual energy x-ray absorptiometry (DXA). Questionnaires were used to assess self-reported physical activity (PA) and prevalent and 5-yr incident fragility fractures (FFx) at any site (defined as a Fx with a fall from less than standing height).

PA was assessed by: (1) daily metabolic equivalents (METs in MET-min/day) and (2) self-report of Regular Activity (RgA). Multiple regression analysis included potential confounders (e.g., age, BMI, reproductive history, lifestyle). Descriptive statistics and regression coefficients are reported as mean $\pm$ SE and (95% CI), respectively; METs coefficients are per 1000-MET-min/day. Women's and men's data were analyzed separately. Average age was  $63.1\pm0.2$ ,  $59.9\pm0.3$  and BMI was  $26.9\pm0.1$ ,  $27.0\pm0.1$  for women and men, respectively. The Table shows that average METs were moderate (equivalent to 1.7 per min) and about half the participants reported RgA.

	Baseline (mean $\pm$ SE)		5-y change or Incident Fx (mean $\pm$ SE)	
	Women (n=5659)	Men (n=2560)	Women (n=4335)	Men (n=1859)
BMD-LS (g/cm <sup>2</sup> )	$0.94 \pm 0.002$	$1.05 \pm 0.003$	$0.013 \pm 0.001$	$0.022 \pm 0.001$
BMD-Total Hip (g/cm <sup>2</sup> )	$0.86 \pm 0.002$	$1.01 \pm 0.003$	$-0.012 \pm 0.001$	$-0.012 \pm 0.001$
Fragility Fracture	27.5%	24.2%	9.3%	4.2%
MET-min/day	$2,510 \pm 4$	$2,500 \pm 8$		
RgA (%)	54.9%	55.6%		

Results show that, for women at baseline, PA was positively associated with hip BMD (RgA: (0.005, 0.017), MET: (0.009, 0.026)), but with neither LS BMD nor FFx. For men at baseline, RgA and METs were positively associated with hip BMD (RgA: (0.026, 0.046), MET: (0.005, 0.028)). LS BMD was associated with RgA (0.009, 0.034), but no other PA measures in men.

None of the PA measures were associated with 5-year change in BMD or FFx in either men or women with the exception of METs (-0.008, -0.001) which had an unexpectedly negative association with change in hip BMD in women.

Overall, men and women who were more active had higher hip BMD at baseline, but activity level was not positively associated with change in BMD over 5 years or with incident fracture in our population-based Canadian sample.

**Disclosures:** J.C. Prior, None.

This study received funding from: Canadian Institutes for Health Research

## M326

**Osteopenia by High Alcohol Consumption in the Absence of ALDH2 Attribute to the Disturbance of the Differentiation in Osteoblasts.** Y. Shimizu<sup>\*</sup>, K. Menuki<sup>\*</sup>, T. Mori<sup>\*</sup>, A. Sakai<sup>\*</sup>, T. Isse<sup>\*</sup>, T. Oyama<sup>\*</sup>, T. Kawamoto<sup>\*</sup>, T. Nakamura<sup>\*</sup>. Orthopedics, University of Occupational Environmental Health, Kitakyusyu, Japan.

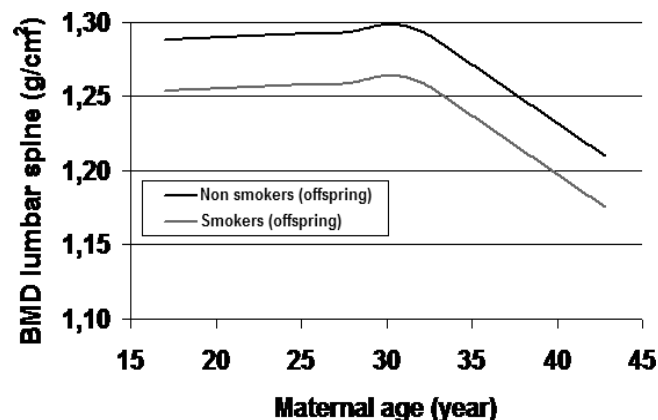
High consumption of alcohol is a risk factor of osteoporosis. Approximately 45% of Chinese and Japanese individuals are inactive ALDH2 phenotype. The absence of the ALDH2 Glu allele was found to adversely influence the risk of osteoporosis. The aim of this study is to clarify the effect of the alcohol consumption on bone metabolism with ALDH2 knock-out mice (ALDH2KO) after ethanol drinking. 8-week-old male ALDH2 knock-out mice and wild-type were free-ingested water (groups ALDH2KO/water and Wild/water) and 5% ethanol (groups ALDH2KO/alcohol and Wild/alcohol) for 4 weeks. At the age of 12 weeks, we evaluated the bone histomorphometry in trabecular bone in distal metaphysis of left tibias. Bone marrow cells from bilateral femurs and tibias were used for mRNA expressions analysis. In histomorphometry, Bone volume (BV/TV) was significantly decreased in ALDH2KO/alcohol compared with those in ALDH2KO/water and wild/water groups. Bone formation rate (BFR/BS) was significantly decreased in ALDH2KO/alcohol compared with those in the other three groups. The value of activation frequency (Ac.f) in ALDH2KO/alcohol significantly decreased, too. Quantitative RT-PCR revealed that typeI collagen, osteonin, osteopontin and osteocalcin mRNA expressions significant decreased in ALDH2KO/Alcohol mice. Our results suggested that osteopenia caused by high alcohol consumption in the absence of ALDH2, attribute to the disturbance of the differentiation in osteoblasts.

**Disclosures:** Y. Shimizu, None.

## M327

**Advancing Maternal Age Is Associated with Lower Peak Bone Mineral Density in the Male Offspring.** R. Rudäng<sup>\*</sup>, D. Mellström, C. Ohlsson, M. Lorentzon. Internal Medicine, Center for Bone Research at the Sahlgrenska Academy (CBS), Göteborg, Sweden.

In Sweden the maternal age in both primi- and multipara mothers has steadily increased during the last three decades. It has been previously reported that advancing maternal age increases the risk of fetal death, but also of morbidity in the offspring, such as chromosome abnormalities, leukemia, diabetes mellitus type 1 and schizophrenia. Whether or not maternal age influences bone mass and the subsequent risk of osteoporosis in the offspring has not been reported. The aim of the present study was to investigate whether a high maternal age was associated with lower peak bone mass, as measured using DXA in a large cohort of male offspring (the Gothenburg Osteoporosis and Obesity Determinants study (GOOD)). Through the Swedish multi-generation register, we identified the mothers of 1009 GOOD-study subjects. From the Swedish medical birth register, maternal parameters, including detailed information about the medical circumstances at the time of child birth, including maternal and offspring anthropometrics (birth height and weight), maternal age and smoking habits, parity and length of pregnancy. Maternal age was inversely correlated to areal BMD (aBMD) at the total body ( $r=-0.07$ ,  $p=0.03$ ) and the lumbar spine ( $r=-0.09$ ,  $p<0.01$ ). Using a linear regression model (including covariates that were correlated with lumbar spine BMD: GOOD-study subject current physical activity, smoking, height, total body lean mass), we found that maternal age negatively independently predicted lumbar spine aBMD ( $\beta=-0.08$ ,  $p<0.01$ ) in the male offspring (Fig.1). This association remained significant ( $\beta=-0.08$ ,  $p=0.025$ ), also after inclusion of additional covariates including GOOD-study subject age, total body fat mass, length of pregnancy, socio-economic index (of the GOOD-subjects' mothers and fathers), parity, smoking during pregnancy and paternal age. In conclusion, our results suggest that advancing maternal age negatively affects peak bone mass and could increase the risk of subsequent osteoporosis in the male offspring.



**Disclosures:** R. Rudäng, None.

This study received funding from: Swedish Research Council.



## M328

**Calcium Release from Bone in Postmenopausal Women: Effects of Low Level Cadmium Exposure.** M. Bhattacharyya, A. Ebert-McNeill\*, S. Clark\*, P. Birdsall\*, E. Cerny\*. Argonne National Laboratory, Lemont, IL, USA.

Our studies in mice and dogs demonstrate that cadmium (Cd) causes bone loss at low exposure levels - starting at 2 ng Cd/ml blood. Isotope studies show that calcium release from bone starts early - 8 to 16 hr after a single gavage dose in mice. Regarding mechanism, Cd at 10 nM causes extensive demineralization in fetal rat limb bone cultures, demonstrating a direct effect of Cd on bone, independent of kidney damage. Finally, bone cell culture and gene expression microarray results identify osteoclast formation and activation as a potential mechanism. This project grows from the above results; it examines whether low level Cd contributes to osteoporosis in humans, particularly postmenopausal women. Cd from cigarettes is the exposure source. STUDY I characterizes exposures in smoking vs. non-smoking postmenopausal women. Biological exposure measures include Cd concentrations in blood, the blood serum compartment, and urine. Cd intake from the total particulate matter of cigarette smoke vs. diet are also determined. STUDY I is nearly complete, and early results demonstrate that Cd exposures among smokers 1) were significantly higher than in non-smokers ( $p < 0.05$ ) and 2) showed a wide range of values. For example, mean blood Cd concentrations were  $1.29 \pm 0.28$  (15) in smokers vs.  $0.33 \pm 0.06$  ng/ml (10) in non-smokers [mean  $\pm$  SE (n)]. In addition, individual values for smokers ranged from 0.53 ng/ml, similar to non-smokers, to 2.74 ng/ml, a concentration at which a bone response to cadmium starts in both mice and dogs. In contrast to Cd, urine cotinine concentrations in smokers - a measure of exposure to the nicotine component of cigarette smoke - were similarly high in all smokers. This wide range of Cd exposure levels will be utilized to evaluate whether the Cd component is a causative agent in the bone response to smoking. Analogous to our studies with laboratory animals, STUDY II will use  $^{45}\text{Ca}$  labeling of the skeletons of women in STUDY I, to determine whether a relationship exists between Cd exposure and  $^{45}\text{Ca}$  release from bone.  $^{45}\text{Ca}$  measurements will be made over a 3-week period to generate a baseline level for smokers vs. non-smokers. During a time of non-smoking, ranging from 4 days (minimum required from Ca isotope studies in dogs) to 3 weeks (depending on each smoker's experiences with smoking cessation),  $^{45}\text{Ca}$  measurements will continue for a second 3-week period. Results should provide insight into which level of Cd exposure might stimulate bone loss in humans. Work supported by Philip Morris USA Inc and Philip Morris International.

**Disclosures:** M. Bhattacharyya, None.

## M329

**Suppression of Bone Resorption Markers by Calcium and Vitamin D Separately and in Combination.** S. D. C. Thomas\*, A. G. Need, B. E. C. Nordin. Clinical Biochemistry, Institute of Medical and Veterinary Science and Hanson Institute, Adelaide, Australia.

This study was designed to compare the effects of calcium and vitamin D separately and together on suppression of a bone resorption marker. Nineteen healthy ambulatory women aged 59-74 years were randomised to receive either 1000IU vitamin D3 (Ostelin) daily for 7 weeks or 1000mg Ca as carbonate (Calsup) daily for 1 week. The first group then received added calcium (1000mg/d) for 1 week and the second received added vitamin D (1000IU/d) for 7 weeks. Fasting blood samples were collected for biochemistry, parathyroid hormone (PTH) and beta crosslaps at baseline, after each of the supplements alone and after the combination period. The rise in mean serum ionised calcium was not significant after calcium ( $P=0.2$ ), however it rose significantly after vitamin D ( $P=0.03$ ) and after the combination ( $P=0.004$ ). The fall in serum PTH was not significant after calcium ( $P=0.4$ ), vitamin D ( $P=0.2$ ) alone but approached significance when Ca and vitamin D were taken together ( $P=0.09$ ). The fall in crosslaps was 34%, 8% and 40% on calcium, vitamin D and the combination ( $P=0.1$ , 0.2 and 0.001) respectively. The use of calcium with vitamin D is a more significant suppressor of bone resorption markers than either supplement alone. These findings are compatible with recent evidence that combined therapy reduces fracture risk more effectively than either agent alone.

**Disclosures:** S.D.C. Thomas, None.

## M330

**A Rodent Model to Evaluate the Effect of Dietary Protein on Intestinal Calcium Absorption.** E. G. Stomberg\*<sup>1</sup>, B. Sun\*<sup>2</sup>, C. Simpson\*<sup>2</sup>, J. Kerstetter\*<sup>3</sup>, K. Insogna\*<sup>2</sup>. <sup>1</sup>Nutritional Sciences, UConn, Storrs, CT, USA, <sup>2</sup>Internal Medicine, Yale, New Haven, CT, USA, <sup>3</sup>Allied Health, UConn, Storrs, CT, USA.

In humans, urinary calcium (UCa) increases with increasing dietary protein. As measured by dual stable calcium (Ca) isotopes, when healthy adults ingest a high protein diet (2.1 g/kg/day), skeletal turnover tends to be reduced and Ca absorption significantly increases almost entirely accounting for the observed hypercalciuria. In contrast, a low protein diet significantly impairs intestinal Ca absorption. To explore the mechanisms underlying dietary protein-induced increases in Ca absorption, 250 g female rats were randomly fed a control (20%), low (5%), or high (40%) protein diet for 7 days. All 3 diets were isocaloric and contained 0.45% Ca, 0.35% P. Twenty-four hour urines were collected both before and after the 7-day experimental period. Serum collections were made on day 7. A Ca balance study was performed during days 4-7. Dynamic and static bone histomorphometry were performed on tibiae.

UCa was not different between the 3 groups at baseline. By day 7, UCa was more than 2-fold higher in the 40% protein vs control group (4.2 mg/d vs 1.7 mg/d,  $p < 0.05$ ). In contrast,

UCa fell significantly in the 5% protein group compared to control (0.4 mg/d vs 1.7 mg/d,  $p < 0.01$ ). At day 7, there were no differences in serum Ca, 1,25(OH)<sub>2</sub>vit D, or 25(OH)vit D between the 5% and 40% protein groups. Serum PTH tended to be higher in the 5% protein group ( $p=0.07$ ). Serum osteocalcin was lower in the 40% protein group compared to the other two groups ( $p < 0.03$ ). Rats consuming the 40% protein diet absorbed and retained more Ca compared to the 5% protein group (see table). Pre-treating animals with pamidronate did not attenuate the impact of dietary protein on UCa consistent with the idea that increased bone resorption was not the basis for the increase in UCa. Histomorphometric analyses showed that rats consuming a 40% protein diet tended to have lower bone turnover.

This animal model recapitulates the key findings in humans ingesting a high protein diet in that: 1. Animals developed hypercalciuria on the high protein diet and hypocalciuria on the low protein diet. 2. During the high protein diet, increased Ca absorption, not bone resorption, is the source of the hypercalciuria. 3. Reducing levels of dietary protein leads to Ca malabsorption. Studies are ongoing to elucidate the cellular and molecular bases for the effect of dietary protein in Ca absorption.

**Disclosures:** E.G. Stomberg, None.

*This study received funding from: USDA.*

## M331

**OP Patients Behaviours and Understanding of the Importance of Calcium and Vitamin D Supplementation.** S. Boonen\*<sup>1</sup>, P. Fardellone\*<sup>2</sup>, J. Quesada\*<sup>3</sup>, L. Kalouche-Khalil\*<sup>4</sup>, J. Ringe\*<sup>5</sup>. <sup>1</sup>University Hospital Leuven, Leuven, Belgium, <sup>2</sup>Department of Rheumatology, CHU, Amiens, France, <sup>3</sup>Unidad de Metabolismo Mineral. Hospital Universitario Reina Sofía, Córdoba, Spain, <sup>4</sup>P & G Pharmaceuticals, Asnières, France, <sup>5</sup>Medizinische Klinik IV, Klinikum Leverkusen, Cologne, Germany.

National and international guidelines recommend the co-prescription of calcium (Ca) and vitamin D (Vit D) with osteoporosis (OP) treatment unless patients are Ca and Vit D replete. Among general practices, levels of co-prescription vary considerably. In addition, patients' compliance with Ca and Vit D supplementation may be poor.

The objective of the study was to evaluate on a pan-European basis, the treatment knowledge and behaviour of osteoporotic patients treated for OP.

A quantitative patient research survey was conducted in December 07 on women aged 50 years and older in four European countries: France, Germany, UK and Spain. All participants were post-menopausal females who have been diagnosed and treated for OP. A standardized 10 minute questionnaire was used, however, data collection methods varied across countries i.e. mail-in for France, face to face for Germany and an online interview for the UK and Spain. All patients gave consent to participate in the survey.

The survey included 383 patients equally distributed across the four countries. Main results are reported in Table 1. Further analysis showed that compared to patients who never forget taking their supplement, patients who declared missing supplements were mainly:

- those who declared not convinced of the importance of this supplementation,
- those who reported not to have detailed explanations by treating physician and,
- those who reported a need for a new tool/packaging to help taking both OP treatment and supplements.

Patients were more able to identify food sources of Ca than those of Vit D.

Patients were aware of the importance of Ca and Vit D in osteoporosis management. Continued efforts by physicians will help improve patients' understanding of the importance of Ca and Vit D supplementation.

**Table 1.** Number and percentage of patients in the different countries according to their current treatment knowledge and behaviours regarding Ca & Vit D supplementation.

	Total	FR	GE	UK	SP
<b>Number of Patients</b>	<b>383</b>	<b>97</b>	<b>98</b>	<b>94</b>	<b>94</b>
<b>Treated Patients (% of patients)</b>					
- Taking osteoporotic medication regularly and correctly	91	90	96	82	95
- Taking any supplementation	74	69	74	61	90
- Taking Ca & VitD supplements	43	46	49	37	43
<b>Patients' knowledge and behaviours regarding supplementation (% patients)</b>					
- Is part of the whole treatment regimen	81	61	94	74	95
- Has to be taken regularly	72	63	59	69	97
- Complete and detailed explanation was provided by treating physician	72	59	88	56	84
- Is not as important as OP medication	64	64	59	63	72
- Regularly missed a dose of any supplements	22	13	19	30	27

**Disclosures:** S. Boonen, P&G 5.

*This study received funding from: The Alliance for Better Bone Health (Procter & Gamble Pharmaceuticals and sanofi-aventis).*



## M332

**The Effects of Agave Inulin on Calcium Metabolism in Japanese Young Adults.** T. Koike<sup>1</sup>, Y. Kojima<sup>\*2</sup>, T. Okano<sup>\*1</sup>, M. Tada<sup>\*1</sup>, A. Ichimura<sup>\*3</sup>. <sup>1</sup>Orthopaedic Surgery, Osaka City University Medical School, Osaka, Japan, <sup>2</sup>Agave Inc., Osaka, Japan, <sup>3</sup>Molecular Inorganic Chemistry, Osaka City University Molecular Materials Science, Osaka, Japan.

Absorption of an adequate amount of calcium is particularly important during early adolescence to help achieve peak bone mass. In addition to dietary intake, intestinal absorption is a key factor that controls the retention of calcium. Numerous animal studies have shown that inulin-like fructans significantly increase calcium absorption. Inulins are a group of naturally occurring polysaccharides produced by many types of plants. Plants that contain high concentrations of inulin include chicory, wild yam, elecampane and agave. Agave inulin was found to consist of a few to >150 monosaccharide residues, with very much greater solubility than other known inulins. Therefore, it is feasible to obtain products of good quality with agave inulin since the high solubility facilitates homogeneity. The aim of this study is to investigate the effects of agave inulin on calcium metabolism in young adults. Calcium metabolism in 12 Japanese young adults was studied by using metabolic balance in a randomized, 12-days controlled dietary intervention: calcium gluconate (Ca 300mg, control), calcium gluconate with agave inulin (34% of volume) (high inulin) and calcium gluconate with agave inulin (11% of volume) (low inulin). The first 9 days of 12-day intervention was a period of equilibration to the diet. Days 10-12 made up the metabolic balance period, in which all urine and feces were collected. On days 1, 9 and 12, bone metabolic markers (intact PTH, osteocalcin, urinary NTX, deoxypyridinoline) were measured. Calcium absorption was significantly greater in high inulin group than in the control group (high inulin:  $45.7 \pm 5.4$ , low inulin:  $39.4 \pm 48.9$ , control:  $19.6 \pm 5.2\%$ ,  $P < 0.05$ , repeated-measures ANOVA). There was no significant difference between the supplements in calcium retention (high inulin:  $23.3$ , low inulin:  $11.7$ , control:  $4.9\%$ ). Although intact PTH significantly decreased on day 12 compared to baseline, there was no significant differences between groups. There was no significant change on other bone metabolic markers. These findings suggest that daily consumption of high dose of agave inulin significantly increases calcium absorption and enhances bone mineralization in young adults.

**Disclosures:** T. Koike, None.

*This study received funding from: Osaka City Health and Preventive Medicine Leading Project.*

## M333

**The Effect of the Dietary Ca/P Ratio on the Rate of Skeletal Accrual in Mice.** B. Sun<sup>1</sup>, C. Simpson<sup>\*1</sup>, T. Carpenter<sup>2</sup>, K. Insogna<sup>1</sup>. <sup>1</sup>Internal Medicine, Yale School of Medicine, New Haven, CT, USA, <sup>2</sup>Department of Paediatrics, Yale School of Medicine, New Haven, CT, USA.

Many studies have investigated dietary factors that affect skeletal health but the impact of the dietary calcium phosphate ratio (Ca/P) on rates of skeletal accrual has received relatively little recent attention. In many earlier studies, the appearance of secondary hyperparathyroidism represented a significant confounding variable. Since the osteocyte is known to play a key role both in regulating skeletal turnover and phosphate homeostasis, we revisited the impact of alterations in the dietary Ca/P ratio on rates of skeletal accrual in mice. Forty, 4-week old female CD-1 mice were divided into equal groups and fed one of five diets varying in Ca/P ratio. The diets were isocaloric and identical in all respects except for the amount of Ca and P and were as follows: **G1:** Ca/P= 1.5:1 (0.45% Ca/0.3% P); **G2** Ca/P= 1:1 (0.3% Ca/0.3% P); **G3** Ca/P= 2:1 (0.6% Ca/0.3% P); **G4** Ca/P= 2X 1:1; (0.6% Ca/0.6% P); **G5** Ca/P= 2X 2:1 (1.2% Ca/0.6% P). There were no inter-group differences in the rates of weight gain or food consumption after 4 weeks and 8 weeks of the diets. Although both BMD and BMC increased in each group there were significant differences observed among the five dietary groups when analyzed by one-way ANOVA at week 4. Thus, the **G5** animals, (2X 2:1), had a higher percentage increase in both femur and total BMD and BMC when compared to all other groups ( $p < 0.05$ ) except **G1** ( $p = NS$ ). This resulted in significantly higher femur and total body BMD values in **G5** compared to **G2**, (1X 1:1) and **G3** (1X 2:1) groups. Total body BMD in **G5** was also higher than the mean value in **G4**, (2X 1:1). During the second 4 weeks of the study, the rate of skeletal accrual remained higher in the femur in the **G5** group compared to **G1**, **G2** and **G4** and at 8 weeks **G5** had the highest femur BMD compared to all other groups ( $p < 0.05$ ). Serum concentrations of Ca, P, Alk Phos, and PTH were not significantly different among the groups. Interestingly, serum CTX tended to be lower, albeit not significantly so, in **G5** compared to the values in **G1**, **G2** and **G4** (10.0, vs. 12.1, 12.2 and 11.7 respectively). These data demonstrate that altering the dietary Ca/Pi ratio while keeping all other nutrients constant affects the rate of skeletal accrual in mice. This occurred without alteration in PTH activity in the **G5** group, which had the highest initial rates of skeletal accrual and had the highest mean femur BMD at study end. The molecular mechanisms that underlie these changes as well as the bases for the apparent differences in the regional skeletal response to the dietary Ca/P ratio are currently under investigation.

**Disclosures:** B. Sun, None.

## M334

**Low Dose Administration of Interferon  $\gamma$  Stimulates Osteoblastogenesis and Prevents Ovariectomy-Induced Osteoporosis in C57BL/6 Mice.** D. C. Huang<sup>1</sup>, G. Duque<sup>2</sup>, X. F. Yang<sup>1</sup>, F. T. Marino<sup>\*3</sup>, J. Barralet<sup>\*3</sup>, R. Kremer<sup>1</sup>. <sup>1</sup>Department of Medicine, Department of Medicine and Center for Bone and Periodontal Research, McGill University, Montreal, QC, Canada, <sup>2</sup>Aging Bone Research Program, Nepean Clinical School, University of Sydney, Penrith, NSW 2750, Australia, <sup>3</sup>Faculty of Dentistry, McGill University, Montreal, QC, Canada.

Interferon  $\gamma$  (IFN $\gamma$ ) exerts either an antiresorptive or pro-resorptive effect on bone *in vivo* depending on the model and dosage used. However, its effect on osteoblastogenesis and bone formation has not been reported. In this study, we administered 2000 units of recombinant IFN $\gamma$  or vehicle three times a week for 18 weeks to 10 week-old C57BL/6 ovariectomized (OVX) female mice. Ex-vivo cultures of bone marrow mesenchymal stem cells (BM-MSC) isolated from IFN $\gamma$  treated animals had an increased capacity to differentiate into osteoblasts as demonstrated by the higher number of CFU-OB stained with alkaline phosphatase or Alizarin red. In contrast, ex-vivo cultures of BM-MSC isolated from normal female C57BL/6 mice and treated with siRNA against IFN $\gamma$  had a reduced ability to form CFU-OB as compared to BM-MSC treated with control siRNA. Bone mineral density (BMD) was significantly higher in IFN $\gamma$ -treated animals as compared to control both at the lumbar spine and femur. Examination of bone microarchitecture by 3D- $\mu$ CT analysis demonstrated a significant increase in bone volume (BV/TV) ( $9.7 \pm 0.5$  vs  $7.2 \pm 0.5\%$ ,  $p < 0.01$ ), trabecular thickness ( $54 \pm 5$  vs  $49 \pm 5 \mu\text{m}$ ,  $p < 0.05$ ), trabecular number ( $3.2 \pm 0.05$  vs  $2.1 \pm 0.03 \text{ N/mm}$ ,  $p < 0.04$ ) and cortical width ( $172 \pm 6$  vs  $143 \pm 7 \mu\text{m}$ ,  $p < 0.01$ ) in IFN $\gamma$ -treated OVX animals as compared to vehicle-treated OVX animals. Furthermore, static histomorphometry showed a significant increase in osteoblast number in IFN $\gamma$ -treated mice as compared to controls. Finally, mechanical properties of bone were assessed in tibia with the three-point bending test. A significant increase in all mechanical indices was observed in IFN $\gamma$ -treated OVX animals compared to vehicle-treated OVX animals including stiffness (K) ( $53 \pm 5$  vs  $43 \pm 6 \text{ N/mm}$ ,  $p < 0.05$ ), Young's modulus (E) ( $13.2 \pm 2.1$  vs  $10.5 \pm 2.2 \text{ N/mm}^2$ ,  $p < 0.05$ ), ultimate force (N) ( $13.6 \pm 2.2$  vs  $11.9 \pm 2.3 \text{ N}$ ,  $p < 0.05$ ) and work to failure (U) ( $3.55 \pm 0.18$  vs  $3.13 \pm 0.15 \text{ mm x N}$ ,  $p < 0.01$ ). Overall, our data indicates that low dose administration of IFN $\gamma$  prevents bone loss, and restores skeletal microarchitecture and bone strength induced by estrogen deficiency.

**Disclosures:** D.C. Huang, None.

## M335

**A Selective p38alpha Inhibitor Prevents Bone Loss Induced by Estrogen Deficiency.** J. Caverzasio<sup>1</sup>, L. Higgins<sup>\*2</sup>, P. Ammann<sup>1</sup>. <sup>1</sup>Service of Bone Diseases, Dept of Rehabilitation and Geriatrics, University of Geneva, Geneva, Switzerland, <sup>2</sup>SCIOS, Fremont, CA, USA.

Increased bone remodelling with excess bone resorption over formation is the principal mechanism of bone loss with estrogen deficiency and increased bone fractures. Different mechanisms have been described to explain the enhanced osteoclast activity with estrogen deprivation such as an increased cytokines production by stromal cells and alteration in osteoclasts apoptosis. The p38 pathway is known to be involved in controlling both cytokines effects on osteoclastogenesis and osteoclast activity. Thus, in this study we investigated the effect of a selective p38alpha inhibitor (p38Inhib), on the prevention of bone loss induced by estrogen deficiency in an adult ovariectomized (OVX) rat model. Oral administration of 15 and 45 mg/kg BW of the p38Inhib for 8 weeks dose-dependently blunted the increase in urinary deoxypyridinoline (DPD) excretion level, a marker of bone resorption, induced by OVX in adult rats ( $p < 0.0001$ ). Interestingly, the p38Inhib did not reduce but significantly enhanced (2x,  $p < 0.001$ ) the rise in osteocalcin level, a marker of bone formation, observed in OVX animals. Associated with the blunted increase in DPD excretion, the p38Inhib completely prevented the vertebral bone loss associated with estrogen deficiency. A partial preventive effect was also observed in long bones (68%) with reduction of trabecular bone loss of the tibial metaphysis and enhancement of the cross sectional area of the tibial diaphysis ( $p < 0.02$ ). Finally, prevention of trabecular bone loss and increased in the cortical cross sectional area were associated with improvement of the biomechanical resistance.

In conclusion, chronic administration of a selective p38alpha inhibitor blunted the increased bone turnover induced by estrogen deficiency and differentially affected trabecular bone resorption and cortical bone formation. This effect resulted in a complete prevention of axial trabecular bone loss and alteration of bone microarchitecture induced by OVX. These data suggest that p38alpha is a critical pathway for regulation of bone resorption in response to estrogen deficiency. Selective inhibitors of this pathway are molecules of potential interest for prevention of bone loss in postmenopausal osteoporosis.

**Disclosures:** J. Caverzasio, SCIOS, Fremont, USA 3.

*This study received funding from: SCIOS Inc.*

## M336

**Effects of Different Extracts of Fructus Ligustri Lucidi on Ca Balance in Normal Female Rats.** X. Dong<sup>\*1</sup>, W. Chen<sup>\*1</sup>, C. Che<sup>\*2</sup>, M. Wong<sup>1</sup>. <sup>1</sup>Applied Biology and Chemical Technology, The Hong Kong Polytechnic University, Hong Kong, China, <sup>2</sup>School of Chinese Medicine, The Hong Kong Chinese University, Hong Kong, China.

Our previous studies indicated that ethanol extract of *Fructus Ligustri Lucidi* (FLL) could improve bone properties in aged rats through modulating Ca homeostasis in both ovary-intact as well as ovariectomized (OVX) aged female rats. The present study aims to search for the active fractions of FLL on Ca balance *in vivo*. The ethanol extract of FLL was separated into two fractions, the lipophilic fraction extracted with ethyl acetate (EA extract) and the hydrophilic fraction extracted with water (water extract). Four month old Sprague-Dawley female rats were orally administered with ethanol extract (700mg/kg/d), EA extract (574mg/kg/d), water extract (126mg/kg/d) or its vehicle for 12 weeks, respectively. Rat urine, feces and serum were collected every week for biochemical marker determination. Urinary Ca and Ca absorption efficiency were used as the biomarker for the identification of the active fractions in FLL. Rat kidney and intestine were collected at sacrifice for subsequent gene expression analysis by real-time PCR. Urinary Ca excretion significantly decreased from week 4 onward in young rats treated with water extract of FLL; while the suppressive effects on urinary Ca excretion by ethanol extract of FLL could only be detected by week 10. In contrast, EA extract of FLL did not suppress urinary Ca excretion in young rats. The water and ethanol extract, but not EA extract, of FLL exerted positive actions on Ca absorption efficiency in young rats from week 6 onward. Our results also showed that water extract of FLL increased duodenum Ca absorption in rats through inducing mRNA expression of the vitamin D receptor (VDR) and the enzymes involved in active epithelial transport (TRPV6 and PMCA). Rat duodenum TRPV6, PMCA, and VDR mRNA in water extract treatment group were increased by 41.8% (P<0.05), 66% (P<0.05) and 61.7% (P<0.01), respectively (vs those in vehicle treated rats). Water extract of FLL also appeared to increase renal TRPV6 and CaBP28k mRNA expression in rats (vs vehicle or EA extract treated rats). Our results indicated that the hydrophilic fraction of the ethanol extract of FLL was responsible for the active action of FLL on Ca balance.

**Disclosures:** X. Dong, None.

This study received funding from: CERG grant (POLYU 5402/04M) from the Hong Kong Research Grant Council, HK SAR as well as the niche area funding (1-BB8N) from the Hong Kong Polytechnic University for the State Key Laboratory of Chinese Medicine and Molecular Pharmacology.

## M337

**Bone Anabolic Effects of Icaritin and Total Flavonoid Fraction of *Herba Epimedii* in Ovariectomized Mice.** W. Chen<sup>\*1</sup>, X. Dong<sup>\*1</sup>, S. Mok<sup>\*1</sup>, X. Yao<sup>\*2</sup>, P. Leung<sup>\*3</sup>, M. Wong<sup>1</sup>. <sup>1</sup>Applied Biology and Chemical Technology, The Hongkong Polytechnic University, Hong Kong, China, <sup>2</sup>Pharmacology, Pharmacology, Shenyang Pharmaceutical University, Shenyang, China, <sup>3</sup>Orthopaedics and Traumatology, Orthopaedics and Traumatology, the Chinese University of Hong Kong, Hong Kong, China.

*Herba Epimedii* (HEP) is one of the most frequently used kidney-tonifying herbs in China over centuries. Flavonoids are considered as its active components and icaritin is a major flavonoid compound found in HEP. The present study aims to determine the osteoprotective effect of total flavonoid fraction of HEP and its active ingredient icaritin in ovariectomized (OVX) mice. Four-week-old sham-operated or OVX C57BL/6J mice were pair-fed and treated with total flavonoid fraction (TF, 100ug/g/day), icaritin (0.3 mg/g/day), or its vehicle by tube-feeding for 6 weeks. Body weight and uterus weight was recorded. Blood and urine sample were collected for Ca and P detection. BMD as well as bone microarchitecture of distal femur in mice were studied by using pQCT and microCT, respectively. The bone related gene expressions in femur were determined by real time RT-PCR. No significant changes were observed in uterus weight in TF-treated and icaritin-treated mice. TF and icaritin did not alter serum Ca and P in mice as compared with OVX mice. The increase in urinary Ca excretion by OVX was reduced in TF-treated and icaritin-treated mice (P<0.01). Ovariectomy produced bone loss and a global deterioration in trabecular 3D-microarchitecture. Treatment of OVX mice with TF or icaritin increased trabecular BMD in distal femur (P< 0.05 vs. vehicle-treated OVX mice). TF treatment prevented the decrease in trabecular thickness (Tb.Th), the increase in trabecular separation (Tb.Sp) as well as the decrease in bone volume/tissue volume (BV/TV) induced by OVX in mice. In addition, TF treatment significantly up-regulated the mRNA expression of type I collagen, osteocalcin and Cbfa1 in mice femur (P<0.05), suggesting that it might modulate osteoblastic functions *in vivo*. Both icaritin and TF increased the ratio of the mRNA expression of OPG/RANKL (P<0.05), indicating that HEP might suppress osteoclastogenesis *in vivo*. These data suggest that icaritin and TF of HEP could protect against bone loss induced by estrogen deficiency in OVX mice. Moreover, our study showed the total flavonoid fraction of HEP was more effective than icaritin alone in preserving bone in respect to its ability to improve bone microarchitecture and to induce osteoblast-related gene expressions in OVX mice.

**Disclosures:** W. Chen, None.

This study received funding from: The National Natural Science Foundation of China and the Research Grants Council of Hong Kong Joint Research Scheme (N PolyU536/04).

## M338

**Green Tea Polyphenols Protects Bone Microarchitecture in Female Rats with Chronic Inflammation-Induced Bone Loss.** C. Shen<sup>1</sup>, J. K. Yeh<sup>2</sup>, B. J. Stoecker<sup>3</sup>, C. Samathanam<sup>\*1</sup>, S. Graham<sup>\*1</sup>, D. M. Dunn<sup>\*1</sup>, T. Tatum<sup>\*4</sup>, R. Dagda<sup>\*1</sup>, M. Chyu<sup>\*5</sup>, X. Q. Liu<sup>\*2</sup>, C. Tubb<sup>\*4</sup>, X. Wang<sup>\*6</sup>, J. Wang<sup>\*6</sup>. <sup>1</sup>Pathology, Texas Tech University Health Sciences Center, Lubbock, TX, USA, <sup>2</sup>Medicine, Winthrop-University Hospital, Mienola, NY, USA, <sup>3</sup>Nutritional Sciences, Oklahoma State University, Stillwater, OK, USA, <sup>4</sup>Molecular Pathology Program, Texas Tech University Health Sciences Center, Lubbock, TX, USA, <sup>5</sup>Mechanical Engineering, Texas Tech University, Lubbock, TX, USA, <sup>6</sup>Institute of Environmental and Human Health, Texas Tech University, Lubbock, TX, USA.

Our recent study showed that green tea polyphenols (GTP) supplementation mitigated chronic-inflammation-induced bone loss in female rats. This study explored bioavailability, molecular mechanisms, and bone microarchitecture of GTP related to preventing bone loss in rats with and without chronic inflammation. A 2 (placebo vs. lipopolysaccharide, LPS) × 2 (no GTPs vs. 0.5% GTPs in drinking water) factorial design, 12-wk experiment using 40 female rats (3-month-old) assigned to 4 groups (n=10/group): placebo (P, placebo implantation), LPS implantation (L), P+0.5% GTP (PG), and LPS+0.5% GTP (LG) was performed. Concentrations of urinary GTP ingredients and 8-hydroxydeoxyguanosine were determined by high-pressure liquid chromatography-couarray detection. Efficacy was evaluated by examining changes in tibial and femoral microarchitecture using histomorphometric and µCT analysis, respectively. mRNA gene expression was determined by real-time RT-PCR. Status of fibrosis in heart vessels was evaluated by trichrome staining. GTP supplementation in drinking water increased concentrations of epigallocatechin in urine of rats, but decreased urinary 8-hydroxydeoxyguanosine level. The results of two-way ANOVA show that LPS lowered trabecular volume fraction, number, and thickness in proximal tibia, but increased eroded surface and osteoclast number in endocortical tibial shafts. GTP supplementation also increased trabecular volume fraction and number in both femur and tibia, but decreased eroded surface and osteoclast number in endocortical tibial shafts. Compared to the other treatments, the L group had a higher degree of fibrosis in heart vessels and gene expression of cyclooxygenase-2 in spleen. Neither LPS implementation nor GTP supplementation affected serum lipid profiles. This study demonstrates that GTP administered in drinking water for 12 weeks prevents trabecular bone loss through LPS-induced higher bone turnover. Such a protective role of GTP may, in part, be attributed to a decrease in oxidative stress DNA damage and expression of cyclooxygenase-2. This study suggests a potentially significant prophylactic role of green tea in bone health of women with chronic inflammation-induced bone loss.

**Disclosures:** C. Shen, None.

This study received funding from: Laura W. Bush Institute for Women's Health.

## M339

**Calcium Signaling Is a Major Target of OCT-1547, a Small Molecule Osteoporosis Drug Candidate.** H. Hwang<sup>\*1</sup>, H. Lee<sup>\*1</sup>, S. Kim<sup>\*1</sup>, S. Ko<sup>\*2</sup>, D. Kang<sup>\*3</sup>, S. Shim<sup>\*3</sup>, S. Kim<sup>1</sup>, J. Ko<sup>1</sup>, J. Kim<sup>\*1</sup>. <sup>1</sup>Dept. of Pharmacology and Mechanism, Oscotec Inc., Cheonan, Republic of Korea, <sup>2</sup>Dept. of Oral Biochemistry, College of Dentistry, Dankook University, Cheonan, Republic of Korea, <sup>3</sup>Dept. of Medicinal Chemistry, Oscotec Inc., Cheonan, Republic of Korea.

We have previously discovered OCT-1547, a small molecule anti-osteoporosis drug candidate, using our proprietary assay system for osteoclast activity, OAAST<sup>TM</sup>. OCT-1547 has been shown to inhibit osteoclast differentiation *in vitro* and loss of bone mineral density in ovariectomized rats. Preclinical safety evaluation for OCT-1547 was completed in Aputit (UK), and phase I clinical trial will start this year. To clarify the action mechanism of OCT-1547 in the inhibition of osteoclastogenesis, we examined the signaling pathways activated by RANK and immune receptor linked to ITAM-harboring adaptors. OCT-1547 drastically reduced the RANKL-induced expression of NFATc1, which is known to be essential for osteoclastogenesis. Importantly, RANKL-induced tyrosine phosphorylation of PLCγ2 was specifically suppressed when RAW264.7 and mouse bone marrow macrophages were treated with OCT-1547. In addition, OCT-1547 treatment resulted in moderate inhibition of IκB degradation and c-Fos induction, all of which are activated at downstream of RANK. OCT-1547 did not alter the interactions of signaling proteins at downstream of RANK including TRAF6, TRAF2, c-Src, TAB1, TAB2 and TAK1. Among the tested immune receptor-downstream signaling proteins, ZAP-70 activation was significantly inhibited by OCT-1547, suggesting that inhibition of PLCγ2 activity by OCT-1547 might be mediated through the inhibition of ZAP-70 activation. Current investigation is focused on the identification of signaling proteins whose activities are modulated by OCT-1547 and of molecular target of OCT-1547.

**Disclosures:** S. Kim, None.

## M340

**Effect of Cannabinoid CB1 Receptor Ligands on Body Weight and Bone Mass in Mice.** S. Park\*, C. Hwang\*, S. Choi\*, H. Kwak\*, M. Jeong\*, Y. Kang\*, C. Yim\*, H. Yoon, K. Han\*. Kwandong University College of Medicine, Cheil General Hospital, Seoul, Republic of Korea.

The cannabinoid CB1 receptor, one of the cannabinoid receptors has been known to regulate appetite, bone remodeling and bone mass. A few researches for CB1 receptor have revealed the different skeletal phenotypes according to the mouse strain and the method of gene ablation. Sympathetic CB1 signaling was suggested to stimulate bone formation. We investigated the effects of CB1 receptor agonist and antagonist on body weight and bone mass in mice with ad libitum feeding for 8 weeks. 6-week female Balb/c mice were received noladin ether (2-arachidonylglycerol ether) known as a CB1 specific agonist with or without the CB1 antagonist SR141716A intraperitoneally and injections were performed 6 times per week. CB1 agonist treatment caused a significant increase in body weight compared to placebo as well as SR141716A treatment. But, no significant weight differences were found between placebo and SR141716A treatment. Pharmacological activity for behavioral effect was evaluated with noladin ether and SR141716A. SR141716A treatment increased intestinal motility reflected by fecal numbers and this effect was counteracted by noladin ether. However, no specific difference in other tests for locomotor activity and antinociception was shown. The analysis of bone mineral density between groups showed that there was a tendency to increase in bone mineral density in femur with noladin ether and SR141716A treatment, respectively. In conclusion, the chronic treatment with CB1 receptor ligands affected body weight change and bone mineral density. Additional bone-protective effect of CB1 receptor agonist might be related to weight enhancement effect and sympathetic activity of noladin ether, which seems to overcome SR141716A effect. Further study is needed to look for molecular mechanism to delineate the role of CB1 signaling in the regulation of bone metabolism.

**Disclosures:** S. Park, None.

## M341

**Dried Plum Alters Bone Metabolism Via a Different Mechanism than PTH.** B. J. Smith<sup>1</sup>, D. M. Cullen<sup>2</sup>, S. Y. Bu<sup>1</sup>, S. L. Clarke\*, E. Rendina\*, Y. E. Lim\*, E. A. Lucas<sup>1</sup>. <sup>1</sup>Department of Nutritional Sciences, Oklahoma State University, Stillwater, OK, USA, <sup>2</sup>Osteoporosis Research Center, Creighton University, Omaha, NE, USA.

Previous studies have demonstrated that dietary supplementation with dried plum (*Prunus domestica* L.) prevents and reverses bone loss due to gonadal hormone deficiency in male and female models of osteoporosis. Despite these positive effects on bone mass and structural properties, the alterations in bone metabolism induced by dried plum supplementation remain in question. Therefore, this study was designed to assess the dose-dependent effects of dried plum on indices of dynamic bone histomorphometry. Six-month-old female Sprague Dawley rats (n=84) were either sham-operated or ovariectomized (OVX) and randomly assigned to one of 6 treatment groups: Sham-control diet (AIN-93M), OVX-control diet, OVX-5% (w/w) dried plum, OVX-15% dried plum, OVX-25% dried plum or OVX+PTH (80 µg/kg/d x 5 days/wk) used as a positive control. Animals were maintained on control diet for 6 wks with osteopenia confirmed by whole body DXA scans prior to the initiation of treatments. At the end of the 6 wk treatment period, bone specimens were collected for assessment of bone mass, microarchitectural properties and dynamic cortical and trabecular bone histomorphometry. Whole body, femur and spine BMD was restored by all 3 doses of dried plum to the level of the sham group, although as anticipated the magnitude of the restoration was not as great as that of PTH. Analysis of the proximal tibial metaphysis and the diaphysis by micro-computed tomography (µCT40 SCANCO) indicated that cortical thickness was maintained in all dried plum treated groups comparable to the sham, and that cortical porosity tended to be decreased by the two higher doses of dried plum. Although longer duration studies have demonstrated otherwise, trabecular structural parameters including BV/TV, TbTh and TbN as assessed by µCT and histology were not restored by dried plum by the end of the 6-wk treatment period. Dynamic histomorphometry revealed that dried plum significantly reduced the OVX-induced increase in trabecular MAR (15% dose only) and trabecular BFR (all doses), and all doses resulted in MAR and BFR comparable to the sham. Endocortical MAR was increased ( $p<0.05$ ) by dried plum, but periosteal BFR was not. As expected, PTH significantly increased endocortical MAR and BFR, periosteal BFR, and trabecular MAR and BFR beyond that of the OVX. These data suggest that although both dried plum and PTH increase endocortical MAR, dried plum acts via a different mechanism than PTH on trabecular bone in that it slows the OVX-induced increase in bone turnover in osteopenic animals.

**Disclosures:** B.J. Smith, None.  
This study received funding from: USDA.

## M342

**Risk Factors for Bone Fracture, Elevated by 90-Days of Bed Rest, Are Reduced by Daily Exposure to Low Magnitude Mechanical Stimuli (LMMS).** J. W. Muir\*, S. Judex, Y. Qin\*, C. Rubin. Biomedical Engineering, SUNY Stony Brook, Stony Brook, NY, USA.

Extended bed-rest causes a reduction of bone density, postural stability, and muscle strength. With increasing evidence of the anabolic effects of low magnitude mechanical stimulation (LMMS) to the musculoskeletal system, we hypothesized that these signals would serve to suppress the complications inherent to non-weight bearing, and thus contain

an aggregate increase in the risk factors for bone fracture. 29 healthy subjects underwent 90 days of 6-degree head down tilt bed-rest. Eleven subjects served as controls, 12 subjects received a daily 10 minute treatment of a 0.3g, 30 Hz LMMS, and six subjects received LMMS at 0.5g at same frequency. Performed at baseline and post bed-rest, BMD was quantified by CT scan of hip and spine, muscle strength was assessed using an isokinetic dynamometer, and postural control was evaluated through center of pressure analysis during four-minute quiet stance. Untreated controls realized significant decrements to BMD (2.1% decrease per month in the hip;  $p<0.01$ ), muscle strength (14.4% decrease in knee concentric flexion strength;  $p<0.01$ ), and postural control (66.9% per month increase in peak sway velocity;  $p<0.01$ ). While treatment did not significantly impact the loss of bone (1.4% per month decrease;  $p<0.01$ , 31% improved retention,  $p=0.08$ ), it did serve to help muscle strength (6.7% loss, 53% improved retention,  $p<0.01$ ), and postural control (9.6% per month increase, 85.6% improved retention of peak sway velocity,  $p<0.01$ , Fig. 1). No difference was seen between the 0.3 and 0.5g treatment groups, so the groups were pooled. These data provide evidence of a mechanically-based means of reducing bone fracture risk under the challenges of chronic bed rest, achieved by influencing the aggregate of distinct risk factors, and ultimately may represent a means of reducing the incidence of falls in the elderly and infirm.

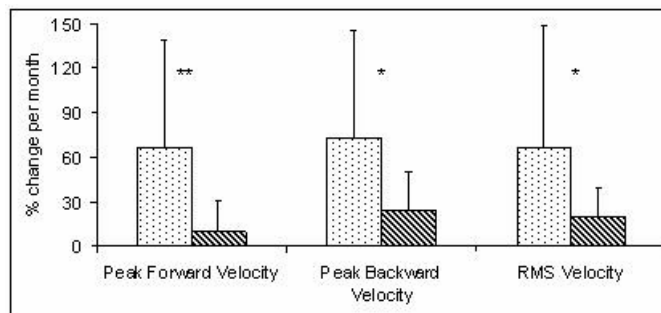


Fig 1: AP sway velocity in control subjects measured from COP increased significantly after bed-rest, as did the root-mean-square of the AP velocity. High sway velocity is strongly associated with high fall risk groups, indicating that subjects undergoing long term disuse are at an increased threat of fall related injury. \* =  $p<0.05$   
\*\* =  $p<0.01$

**Disclosures:** J.W. Muir, None.  
This study received funding from: NASA.

## M343

**Efficacy of Odanacatib in the Ovariectomized Rhesus Monkey as Measured with pQCT.** P.J. McCracken\*, R. Y. Jayakar\*, L. T. Duong<sup>2</sup>, T. N. Hangartner<sup>3</sup>, D. S. Williams\*. <sup>1</sup>Imaging, Merck Research Laboratories, West Point, PA, USA, <sup>2</sup>Department of Molecular Endocrinology, Merck Research Laboratories, West Point, PA, USA, <sup>3</sup>Biomedical Imaging Laboratory, Wright State University, Dayton, OH, USA.

Preclinical evaluation of disease burden and treatment efficacy is critical to the development of new therapies for osteoporosis. Clinically translatable modalities beyond DXA, such as pQCT and hrMRI, give us the advantage of studying *in-vivo* macro- and micro-architectural parameters relevant to bone strength. We have quantified effects of the Cathepsin K inhibitor for osteoporosis, odanacatib, using pQCT endpoints in the estrogen-deficient model of the ovariectomized (OVX) rhesus monkey as compared to intact animals to examine treatment effects as well as potential technological and model-based measurement limitations. pQCT (XtremeCT, Scanco Medical) in OVX, odanacatib-treated OVX, and intact anesthetized monkeys (10/group, age 14-20 years) was performed at 12, 15 and 18 months post-OVX to assess cortical and cancellous bone. BMD was also measured using a Hologic QDR Discovery. Distal radius, distal tibia, and one-third proximal locations in each were scanned and parameters derived including Cortical Thickness (CtTh), Bone Volume Fraction (BVf), Trabecular Number (TbN), Trabecular Thickness (TbTh), Trabecular Separation (TbSp), and Total Density (D100). After precubrication and scout imaging, animals were scanned using: 9mm slice pack, 220 slices, 1500 projections, 3072 points per projection, 3000x3000 matrix, 200 ms integration time, 41 µm voxel size, 8.3 min measurement time per site. The data were reconstructed at a 100 µm voxel size and processed using the manufacturer's 'clinical' and 'research' analysis protocols. Odanacatib treatment preserved the cortical thickness which remained significantly thicker at the 1/3 radial and tibial sites than the OVX cohort. Treatment effects of odanacatib also trended towards thicker trabeculae and higher vBMD. Radial and tibial measures of BVf, TbN, TbTh, TbSp, and D100 each trend towards a OVX model effect of thinning, fewer trabeculae, increased separation, and decreased vBMD, consistent with estrogen deficiency. Significant differences from intact to OVX cohorts were found in CtTh at the 1/3 site for the radius and tibia at each time point on the order of a 30% thinner cortex in the OVX animals. The longitudinal measurements over the six month period are robust. These results show that odanacatib treatment effects on bone morphometry of the OVX rhesus can be quantified by *in-vivo* pQCT. Measurable differences in the geometry of cancellous and cortical bone between normal, treated and estrogen deficient animals were observed adding value to the development of disease-modifying therapies.

**Disclosures:** P.J. McCracken, None.

## M344

**The Safe Zone for Percutaneous Extrapedicular Surgical Approach to the Lumbar Spine.** N. Karkare, A. Steever\*, L. Bogunovic\*, R. Parker\*, P. O'Loughlin\*, J. M. Lane. Metabolic Bone Disease, HSS, New York, NY, USA.

The objective of this study was to define the zone for safe placement of the targeting device for the surgical treatment of osteoporotic vertebral compression fractures of the thoracolumbar vertebrae.

29 CT scans of patients were studied. The optimal angle was calculated as the one furthest from the medial neural and the lateral peritoneal structures. The respective distance from the skin was measured from the midline.

The mean age of the patients was 64.6±16 years. The optimal angle for placement of the needle, the optimal skin entry from the midline for the left and right side are shown in table 1 for T12, L1, L2, L3, and L4 respectively.

The distance for insertion of the needle on the skin increased from T12 to L4. Our data show that this distance is the similar for L3 and L4. Optimal angles were different on the left and right side for T12 and L3 due to differences in local anatomy. The largest safe angle for safe placement of the targeting needle was at L3 on both left and right sides. This definition of the safe zone for the targeting device in percutaneous extrapedicular and far lateral surgical approach to the lumbar spine may guide surgeons intraoperatively and prevent potential complications.

		L Optimal Angle		L Skin Dist		R Optimal angle		R Skin Dist	
		Mean	Std Dev	Mean	Std Dev	Mean	Std Dev	Mean	Std Dev
T12	Mean	53.02	8.48	111.39	33.51	51.68	7.72	104.77	27.31
	Std Dev								
L1	Mean	54.98	6.28	127.49	26.79	54.40	7.04	120.83	26.53
	Std Dev								
L2	Mean	57.39	7.65	133.87	26.08	55.99	7.80	132.49	34.83
	Std Dev								
L3	Mean	64.73	9.30	173.04	49.39	62.30	7.67	161.99	38.66
	Std Dev								
L4	Mean	66.84	23.77	174.32	81.85	61.52	24.51	160.97	81.31
	Std Dev								

**Disclosures:** L. Bogunovic, None.

## M345

**Short Duration Pharmacokinetic Profile of ZT-031 (Cyclic PTH [1-31]), a Novel hPTH Analog.** D. Krause, R. Vaninwegen\*. Zelos Therapeutics, Inc, West Conshohocken, PA, USA.

Anabolic responses to human parathyroid hormone (hPTH) and hPTH analogs require intermittent, short duration stimulation of PTH receptors on osteoblasts. ZT-031 (cyclic PTH [1-31]) is a novel, cyclic 31 amino acid PTH analog in late clinical development; it has previously demonstrated clinically significant increases in bone mineral density (BMD) in a 12 month Phase 2 clinical study in postmenopausal women with low BMD.

The purpose of this analysis was to define the pharmacokinetic (PK) profile of ZT-031 in a series of clinical trials.

Samples were obtained at various time points in 4 clinical trials, including a single dose, dose rising trial in healthy adults (n=40), a multiple dose, dose rising trial in healthy adult women (n=40), a multiple dose, dose rising trial in healthy elderly women (n=18) and a Phase 2 dose-ranging parallel group trial in postmenopausal women with low BMD (subset, n=10). Doses ranging from 0 (placebo) to 160 µg, in volumes from 0.1 to 0.4 mL/dose, were administered subcutaneously once daily. Samples for PK were obtained pre-dose and at 0.25, 0.5, 1, 2, 4, hours post-dose in all trials and at various other time points up to 24 hours post-dose. Samples were analyzed by a validated ELISA with a limit of detection (LOD) of 10.0 pg/mL. Dose normalized data obtained on Day 1 and on repeat dosing (7 days or 12 weeks of dosing) are displayed in the TABLE.

	AUC <sub>(0-12h)</sub> (pg-h/mL)		AUC <sub>(0-24h)</sub> (pg-h/mL)		C <sub>max</sub> (pg/mL)		T <sub>max</sub> (h)*	T <sub>1/2</sub> (h)*	CL/F (L/h)*	Vz/F (L)*
	Day 1	Repeat	Day 1	Repeat	Day 1	Repeat				
Mean	74.0	75.0	108.0	131.0	56.8	63.5	0.40	1.02	283	412
STD	56.3	59.2	69.5	74.8	28.4	33.1	0.28	0.38	129	238
N	79	48	51	18	82	49	130	49	49	49

\* all data points combined

ZT-031 had a short duration PK profile with a T<sub>1/2</sub> of 1 hour. AUC and C<sub>max</sub> were linearly related to dose whereas T<sub>max</sub>, T<sub>1/2</sub>, CL/F and Vz/F were dose-independent. Correction of dose by patient bodyweight improved the correlation between dose and AUC and C<sub>max</sub> and explained slight gender related differences in these PK parameters.

The PK profile of ZT-031 is well suited to provide the intermittent stimulation of PTH receptors required for anabolic effects on bone. Bodyweight has a significant impact on the PK parameters for a fixed dose, suggesting that dosing strategies that limit the µg/kg dose range will improve the consistency of PK parameters in patients of different bodyweights, possibly leading to improved clinical response.

**Disclosures:** D. Krause, Employee of Zelos Therapeutics 5.  
This study received funding from: Zelos Therapeutics, Inc.

## M346

**The Effect of Bodyweight on Clinical Response to ZT-031: Development of a Simple, Improved Dosing Regimen for PTH Analogs.** B. MacDonald, J. Conlon\*, M. Stogniew\*. Zelos Therapeutics, Inc, West Conshohocken, PA, USA.

ZT-031 (Ostabolin-CTM) is a cyclic 31 an analogue of parathyroid hormone (PTH) that demonstrated rapid onset of bone formation and marked increases in bone mineral density (BMD) in a 12 month study in postmenopausal women. The BMD increase was greatest at the 45 µg/day dose (11% at lumbar spine) but the incidence of asymptomatic hypercalcemia and side effects causing discontinuation was also highest. At a lower dose (30 µg/day) tolerability concerns were minimal but efficacy was also reduced, though adequate. This raised the question of which dose was most appropriate for further study.

To address this question, we converted the daily dose for every patient to a µg/kg dose and regrouped all patients into 6 cohorts of ascending µg/kg dose. Mean change in biomarker and BMD endpoints and in serum calcium was increased with increasing µg/kg dose. Incidence of PTH class side effects (headache and nausea) and hypercalcemia >2.64 mM/L showed similar trends. Stepwise regression and backward elimination regression models confirmed that, in addition to dose, bodyweight was a highly significant predictor of change in lumbar spine BMD (P<0.0001) and that no other baseline variable (including age, height, LS-BMD, FN-BMD, creatinine, smoking and alcohol history) explained the effect of bodyweight. The optimal dose range to generate a large BMD increase while minimizing the occurrence of side effects and hypercalcemia was 0.45 to 0.65 µg/kg. With a fixed dose of PTH analog, patients at either extreme of the bodyweight range are under or over-treated, increasing the risk of treatment failure due to lack of efficacy or excessive side effects/hypercalcemia. The simplest way to maintain the administered dose within the desired µg/kg range for the maximum number of patients is to provide two or more dose strengths, each for use in patients in different bodyweight categories. A ZT-031 dose of 30 µg/day for patients weighing < 68 kg or 45 µg/day for those weighing ≥ 68 kg resulted in a profile that included high BMD responder rate (71% of patients with LS-BMD increase ≥ 5% [net of placebo]) with acceptable hypercalcemia incidence (9.1% with serum calcium >2.64 mM/L at any visit [net of placebo]).

These analyses illustrate the strong influence of bodyweight on clinical response to ZT-031. Extremes of bodyweight may lead to a suboptimal clinical profile for a fixed dose PTH analog, for example diminished BMD effects in males or troublesome side effects in women with low bodyweight. A simple, weight-based dosing regimen with two or more dose strengths can produce a consistent, optimized therapeutic effect regardless of bodyweight, reflected by a higher proportion of BMD responders without significant increase in hypercalcemia or side effect incidence.

**Disclosures:** B. MacDonald, Employee of Zelos Therapeutics, Inc 5.  
This study received funding from: Zelos Therapeutics, Inc

## M347

**An Active Controlled, Non-Inferiority Study to Compare the Effect of ZT-031 with Alendronate on the Incidence of New Vertebral Fractures: The PACE (cyclic PTH and Alendronate Comparative Efficacy) Study.** B. MacDonald<sup>1</sup>, E. Vittinghoff<sup>2</sup>, S. Cummings<sup>3</sup>, D. C. Bauer<sup>2</sup>, D. Krause<sup>1</sup>. <sup>1</sup>Zelos Therapeutics, Inc, West Conshohocken, PA, USA, <sup>2</sup>UC San Francisco Med Ctr, San Francisco, CA, USA, <sup>3</sup>California Pacific Med Ctr Res Inst, UC San Francisco, San Francisco, CA, USA.

In a 12 month study in postmenopausal women ZT-031 (cyclic PTH [1-31]) produced marked increases in bone mineral density with an acceptable safety profile, justifying further clinical development for the treatment of osteoporosis. Regulatory approval of new PTH analogs is complicated by usage restrictions to patients with severe disease (≥ 1 prevalent vertebral fracture [VF]). Such patients are generally excluded from placebo (PBO) controlled studies on ethical grounds. To address this issue we have designed the first active controlled non-inferiority (NI) Phase 3 trial for an investigational osteoporosis drug. The FIT-1 trial provides a reference database for the effect of alendronate (AL) (10 mg/day) versus PBO on the incidence of new VF in the target population (62% and 47% reduction at 2 and 3 years, respectively). The FIT trial (Neer et al 2001) provides a reference database on the likely effect size of a PTH analog (65-69% reduction versus PBO). The large effect size in both reference studies enables the use of NI margins defined as a percentage of the minimum risk difference (lower 95% CI bound) between AL and PBO, that maintain assay sensitivity because a PBO effect is implausible within the NI margin. Sample size calculation used these assumptions: predicted background PBO VF rate: 11.6% (2 year PBO rate in FIT-1), anticipated AL VF rate: ≥5.2% (55% reduction), ZT-031 VF rate: ≤3.8% (67% reduction), NI margin: 30% of the minimum risk difference between AL and PBO (1.17%). Using these parameters a total sample size of 3,255 patients has 90% power to reject the null hypothesis that the effect of ZT-031 is inferior to that of AL after 2 years of treatment, assuming 15% loss to follow up. To address the concern that low VF rates could diminish the validity of an NI margin based on absolute risk difference we confirmed 1) that a sample size of 3,255 could exclude a relative risk (RR) equivalent to the largest possible RR in FIT-1, and 2) that for a range of different effect sizes of AL and ZT-031, the risk difference margin never exceeds 50%, thus preserving assay sensitivity.

This Phase 3 registration study for the treatment of osteoporosis is the first to employ an active controlled design. The comparison is enabled by the existence of robust reference databases from PBO controlled studies in the target population. Sample size feasibility is maintained by establishing NI margins based on risk difference rather than risk ratio and the anticipation that the effect of ZT-031 on VF incidence will actually be greater than that of AL.

**Disclosures:** B. MacDonald, Employee of Zelos Therapeutics, Inc 5.  
This study received funding from: Zelos Therapeutics, Inc.

## M348

**Bone Mineral Density Response to Treatment with Recombinant Parathyroid Hormone in Patients Previously Treated with Bisphosphonates.** S. de Bhaldrath<sup>\*</sup>, A. Pazderska<sup>\*</sup>, K. Fitzgerald<sup>\*</sup>, C. Walsh<sup>\*</sup>, J. Walsh<sup>\*</sup>, M. Casey<sup>\*</sup>. St James Hospital Dublin, Dublin, Ireland.

Parathyroid hormone is the first anabolic agent available for the treatment of severe osteoporosis. Bisphosphonates, which had previously been the mainstay of treatment, act by shutting down bone turnover. We aimed to compare the bone mineral density (BMD) benefit of PTH in treatment naïve patients and patients previously treated with bisphosphonates.

We measured hip and lumbar spine BMD, at 0 and 18 months, in 52 consecutive patients treated with teriparatide.

Mean age was 74 (SD 10.1). 48 were female and 4 were male. 20 were previously treated with bisphosphonates (for a mean of 20 months), (range 4-60months). 32 did not previously receive bisphosphonates. Baseline BMD was comparable in both groups. BMD improved in both groups, however the increase in patients' BMD was significantly greater in patients who were bisphosphonate treatment naïve. See table 1. Treatment naïve patients made highly significantly greater BMD gains than previously bisphosphonate treated patients. Patients with severe established osteoporosis should be considered for PTH therapy before starting bisphosphonates to achieve maximal BMD benefit.

Table 1

	Bisphosphonate + (n=20)	Bisphosphonate - (n=32)	p
	Mean (95%CI)	Mean (95%CI)	
Baseline Spine BMD (g/cm <sup>2</sup> )	0.729	0.742	NS
Baseline Hip BMD (g/cm <sup>2</sup> )	0.646	0.691	NS
% Increase in Spine BMD	4.0 (1.6 - 8.0)	14.6 (10.6-19.0)	0.004
% Increase in Hip BMD	1.6 (0.4-3.1)	6.4 (3.8-9.2)	0.006

**Disclosures:** S. de Bhaldrath, None.

## M349

**Imaging the Spatial Distribution of Proximal Femoral Response to One Year of Teriparatide Therapy: The OPTAMISE Study.** W. Li<sup>1</sup>, J. H. Keyak<sup>2</sup>, P. D. Miller<sup>3</sup>, J. P. Bilezikian<sup>4</sup>, J. A. Stewart<sup>5</sup>, T. F. Lang<sup>1</sup>. <sup>1</sup>Radiology, University of California, San Francisco, San Francisco, CA, USA, <sup>2</sup>Department of Orthopaedic Surgery, University of California, Irvine, Irvine, CA, USA, <sup>3</sup>Colorado Center for Bone Research, Lakewood, CO, USA, <sup>4</sup>College of Physicians and Surgeons, Columbia University, New York, NY, USA, <sup>5</sup>Sanofi-Aventis, Laval, QC, Canada.

**Purpose:** Previous QCT studies of the hip in patients treated with teriparatide (TPTD) have shown differential effects on cortical and trabecular bone, with loss of cortical BMD and increases in trabecular BMD. However, these measurements do not address the spatial distribution of the response within the trabecular and cortical compartments. These data could be useful in understanding the therapeutic response in relevant hip fracture regions and in optimizing image-based treatment monitoring.

**Methods:** Subjects previously treated with alendronate (ALN, n=65) and risendronate (RIS, n=56) discontinued their bisphosphonate and were treated with TPTD (20 µg/d SQ) for 12 months. QCT images of the hip were obtained at baseline and 12 months. 121 pairs of QCT images were registered with satisfactory accuracy into a single population-based statistical image model for each time point, and treatment changes were computed for each voxel. Statistical significance of per-voxel changes were computed using paired T-tests, with false discovery rate (FDR) methods to correct for multiple comparisons. The distribution of voxels showing significant changes was superimposed on the image map and the mean BMD calculated. BMD changes were analyzed by ANCOVA and paired t-test.

**Results:** For this sample similar to the whole, analyses identified a group of voxels showing negative changes clustered in the inferior cortex, and a group showing positive changes clustered in dense trabecular bone. The percentage BMD changes within the trabecular and cortical bands were  $9.9 \pm 9.0\%$  and  $-4.3 \pm 4.9\%$  respectively ( $p < 0.0001$ ). In contrast to cortical changes, trabecular changes trended ( $P = 0.07$ ) towards a difference in favor of RIS.

**Conclusions:** The results showed distinct focal responses of trabecular and cortical bone to TPTD therapy. Cortical response was distributed throughout the inferior cortex, while trabecular response was found in the lateral aspect of the femoral head and in the lesser trochanter. The focal nature of these results may influence the selection of regions of interest for monitoring response to anabolic therapies.

**Disclosures:** W. Li, None.

This study received funding from: The Alliance for Better Bone Health (Procter & Gamble Pharmaceuticals and Sanofi-Aventis). ClinicalTrials.gov number; NCT00130403.

## M350

**Danish Patients Treated with Teriparatide. Results from a National Database Initiative.** L. Hyldstrup<sup>1</sup>, B. L. Langdahl<sup>2</sup>, J. Beck Jensen<sup>3</sup>, P. Schwarz<sup>4</sup>, P. Eiken<sup>5</sup>, K. T. Brixen<sup>6</sup>, A. Schmitz<sup>7</sup>, F. Bennedbak<sup>8</sup>, H. K. Brockstedt<sup>9</sup>, H. Rønne<sup>10</sup>, M. Kleis Møller<sup>11</sup>, A. Jarlov<sup>12</sup>, M. Mørch<sup>13</sup>, R. Pelck<sup>14</sup>, L. Mortensen<sup>15</sup>, O. R. Madsen<sup>16</sup>, B. Abrahamsen<sup>17</sup>, P. N. Andresen<sup>18</sup>, H. C. Hoec<sup>19</sup>. <sup>1</sup>Dept. of Endocrinology, Hvidovre Hospital, Hvidovre, Denmark, <sup>2</sup>Dept. of Endocrinology, Aarhus Sygehus, Aarhus, Denmark, <sup>3</sup>Dept. of Endocrinology, Hvidovre Hospital, 2650 Hvidovre, Denmark, <sup>4</sup>Dept of Geriatrics, Glostrup Hospital, Glostrup, Denmark, <sup>5</sup>Dept. of Cardiology and Endocrinology, Hillerød Hospital, Hillerød, Denmark, <sup>6</sup>Dept. of Endocrinology, Odense Hospital, Hvidovre, Denmark, <sup>7</sup>Dept. of Internal Medicine, Vejle Hospital, Vejle, Denmark, <sup>8</sup>Dept. of Endocrinology, Herlev Hospital, Hvidovre, Denmark, <sup>9</sup>Dept. of Internal Medicine, Silkeborg Centralsygehus, Silkeborg, Denmark, <sup>10</sup>Dept. of Internal Medicine, Farsø Sygehus, Farsø, Denmark, <sup>11</sup>Dept. of Internal Medicine, Regionshospital Horsens, Horsens, Denmark, <sup>12</sup>Cardio-endocrine Clinic E, Frederiksberg Hospital, Frederiksberg, Denmark, <sup>13</sup>Dept. of Geriatrics, Aarhus Sygehus, Aarhus, Denmark, <sup>14</sup>Dept. of Rheumatology, Holbæk Sygehus, Holbæk, Denmark, <sup>15</sup>Endocrine Clinic, Viborg Sygehus, Viborg, Denmark, <sup>16</sup>Osteoporosis Clinic, Gentofte Hospital, Gentofte, Denmark, <sup>17</sup>Osteoporosis Clinic, Gentofte Hospital, Gentofte, Denmark, <sup>18</sup>Dept. of Rheumatology, Graasten Hospital, Graasten, Denmark, <sup>19</sup>Osteoporosis Clinic, CCB, Aalborg, Denmark.

At the introduction of Teriparatide in 2003 a national database was established with the purpose of gaining information on the results obtained in Denmark. So far 608 patients from 17 different clinics have been included.

Compared to the inclusion criteria of the Neer-study the Danish patients chosen for PTH treatment seem have more severe osteoporosis with a lower T-score in the spine and hip, as well as a higher number of prevalent vertebral fractures. Male patients were significantly more likely to be treatment naïve, while most women had been on antiresorptive treatment before Teriparatide was instituted.

In women, treatment with Teriparatide caused a significant increase in BMDspine, reaching 8.8% at 18 months ( $p < 0.0001$ ), while BMDtotalhip did not change (0.3%, n.s.). In men BMD spine and hip increased by 9.6% /0.9%, respectively ( $p < 0.0001$ ). The increase in BMD spine and total hip in females and males was identical. The BMD response was neither influenced by age nor baseline BMD. Patients with steroid induced osteoporosis had the same BMD response as other patients. Previous bisphosphonate treatment did not blunt the BMD response. Side effects to treatment were mild.

Conclusion. Using a voluntary national database it has been possible to gain information on approximately 45% of all patients treated with Teriparatide in Denmark.

**Disclosures:** L. Hyldstrup, Eli-Lilly 1, 3.

This study received funding from: Eli-Lilly Denmark, Nycomed.

## M351

**Previous Antiresorptive Agents Use Did Not Hinder the Increase of Bone Turnover Marker in Teriparatide Use.** Y. Rhee, K. Kim<sup>\*</sup>, C. Ku<sup>\*</sup>, D. Shin<sup>\*</sup>, H. Choi<sup>\*</sup>, S. Lim. Internal Medicine, Yonsei University College of Medicine, Seoul, Republic of Korea.

**Purpose:** Parathyroid hormone (PTH) is an anabolic agent which increases bone remodeling and decrease fracture rate. Previous studies reported that in patients who have been treated previously with antiresorptive agents, the actions of PTH were delayed compared with treatment naïve patients. We compared the effects of teriparatide on bone turnover changes according to the previous treatment histories. **Method:** Patients with previous fracture or osteoporosis with high risk of fracture were included. They received subcutaneous injections of 20µg teriparatide daily. Serum levels of bone turnover markers (C-telopeptide(CTx), osteocalcin) were assessed at baseline and 3,6 months. **Result:** Total 46 osteoporosis patients were included. According to the cause, 31(67%) were postmenopausal, 8(17%) were glucocorticoid-related and 7(16%) were male with any other specific reason. Twenty seven (59%) patients were previous treated with bisphosphonate, 4(9%) with raloxifene and others were treatment-naïve patients. PTH increased CTx( $302.4 \pm 21.7\%$ ) and osteocalcin ( $133.4 \pm 5.8\%$ ). There was no significant difference among prior bisphosphonate treated, prior raloxifene treated and treatment naïve groups. **Conclusion:** Teriparatide treatment well stimulated bone turnover in all patients with osteoporosis regardless of causes. Moreover, prior treatment with antiresorptive agents did not hinder the expected short term effect of teriparatide comparable with treatment naïve patients. This early change on bone turnover suggests that teriparatide does show anabolic effect in various patients with low bone mass.

**Disclosures:** Y. Rhee, None.

## M352

**Formation of New Trabeculae in a Female Patient with Osteoporosis Treated with Teriparatide, Demonstrated with in-Vivo-Assessment of 3-Dimensional Bone Micro Architecture with HR-pQCT.** H. Radspieler<sup>1</sup>, M. A. Dambacher<sup>2</sup>, M. Neff<sup>3</sup>. <sup>1</sup>Osteoporosezentrum München, München, Germany, <sup>2</sup>ZORG International, Zürich, Switzerland, <sup>3</sup>Osteoporosezentrum Zürich, Zürich, Switzerland.

Teriparatide was the first osteoanabolic drug associated with real bone formation. This was shown in bone biopsies but as the location of bone biopsy before and after therapy differs only statistically analysis is possible. With the HR-pQCT (XtremeCT®, SCANCO Medical AG) for the first time it is possible to show 3-dimensional bone architecture and the changes in bone architecture during therapy in vivo with a very low radiation dose. Because of the high resolution of 80 µm trabecular and cortical bone micro-architecture can be visualized before and after therapy at the identical site in individuals and additionally a couple of parameters of bone-structure as number of trabeculae, trabecular thickness, trabecular separation, cortical thickness and trabecular bone volume can be measured. So this method offers quite new possibilities in diagnosis of osteoporosis and monitoring therapeutic effects.

In this case study we present a 80 years old woman with severe osteoporosis and already 4 vertebral fractures was treated with Teriparatide. Before starting therapy she showed extremely low trabecular and cortical bone densities and pronounced deterioration of trabecular and cortical bone microarchitecture. After 9 month therapy with Teriparatide trabecular bone densities and particularly number of trabeculae in the ultradistal radius and tibia not only showed a significant increase but the 3-dimensional images showed new trabeculae particularly in the inner regions where before starting therapy no more trabeculae were found.

The increase of trabecular bone density in the radius after nine month was 5,5% and 2,7% respectively in the tibia and the increase of number of trabeculae was 7,2% in the radius and 34,2% in the tibia respectively. According to these findings the decrease of the disparation distance (trabekular separation) in the radius was - 7,1% in the radius and - 25,7% in the tibia respectively.

So this is probably the first documented evidence in vivo to show the ability of Teriparatide to create new trabeculae in osteoporotic patients.

The images show the bone-microarchitecture in the tibia before and after therapy with Teriparatide. The images will show trabeculae after therapy which were not visible before therapy.

**Disclosures:** H. Radspieler, None.

## M353

**Evaluating the Effect of Soy and Isoflavones on Bone Mineral Density in Older Women; A Randomized Controlled Trial.** K. Mangano<sup>\*1</sup>, A. DiCioccio<sup>\*1</sup>, B. Ryan<sup>\*1</sup>, J. Dauz<sup>\*1</sup>, A. Kenny<sup>2</sup>, R. Abourizk<sup>\*1</sup>, R. Bruno<sup>\*3</sup>, D. Anamani<sup>\*1</sup>, P. Fall<sup>\*4</sup>, A. Kleppinger<sup>\*2</sup>, L. Kenyon Pesce<sup>\*2</sup>, S. Walsh<sup>\*5</sup>, D. Dauser<sup>\*5</sup>, K. Prestwood<sup>\*2</sup>, J. Kerstetter<sup>1</sup>, R. Lipsious<sup>\*1</sup>, S. Strand<sup>\*2</sup>. <sup>1</sup>Allied Health, University of Connecticut, Storrs, CT, USA, <sup>2</sup>Center on Aging, University of Connecticut Health Center, Farmington, CT, USA, <sup>3</sup>Nutritional Sciences, University of Connecticut, Storrs, CT, USA, <sup>4</sup>Clinical Research Center, University of Connecticut Health Center, Farmington, CT, USA, <sup>5</sup>Community Medicine and Health Care, University of Connecticut Health Center, Farmington, CT, USA.

Soy foods contain several components, such as isoflavones and a relative paucity of sulfur-containing amino acids that could potentially have positive effects on bone health. However, there are few long-term clinical trials evaluating soy's effect on bone mineral density (BMD). The purpose of this study was to provide a soy or an omnivorous protein supplement with or without added soy isoflavones to postmenopausal women  $\geq 60$  y.o. for 1 y and measure the effect on BMD. Ninety-seven women participated in this randomized, double-blind, placebo-controlled trial. Following a 1-mo adjustment period in which calcium and vitamin D intake were standardized, subjects were randomized to one of 4 intervention groups: soy protein (20 g) and isoflavone tablets (90 mg), soy protein and placebo tablets, control protein (20 g) and isoflavone tablets (90 mg), control protein and placebo tablets. The primary outcome measure was BMD (by DXA) and secondary outcome measures were changes in bone-specific alkaline phosphatase and urine N-telopeptide crosslinks of collagen. There were no significant differences in compliance between the 4 groups. There were no significant differences in change from baseline in L-spine, total femur or femoral neck BMD among the 4 groups. No statistically significant differences were seen in final BMD, or final bone marker values between the 4 groups at 12 mos. In the study group as a whole bone turnover tended to decline over the 12 mos of protein supplementation ( $p < 0.001$  for BSAP,  $p = 0.06$  for urine NTX). Among the study subjects randomized to isoflavone supplementation there was no difference in mean BMD based on whether or not individuals were equal producers. We conclude that there is no observable difference, as assessed by changes in bone mass, between supplementation with a soy vs. an omnivorous protein isolate, nor is there a discernable effect of adding isoflavones to these protein sources. The trend towards a reduced rate of bone turnover suggests that protein supplementation, at least at this level, does not increase skeletal catabolism. Future, controlled intervention trials might include a higher dose of isoflavones and/or specifically recruit women with a habitually low dietary protein intake.

**Disclosures:** K. Mangano, None.  
This study received funding from: NIH.

## M354

**Prevention of Postmenopausal Osteoporosis Using Nitroglycerine: NOVEL Clinical Study.** S. J. Wimalawansa<sup>1</sup>, J. Grimes<sup>\*1</sup>, A. Wilson<sup>\*1</sup>, N. Cosgrove<sup>\*1</sup>, D. Hoover<sup>\*2</sup>. <sup>1</sup>Medicine, Robert Wood Johnson Medical School, New Brunswick, NJ, USA, <sup>2</sup>Statistics, Rutgers University, New Brunswick, NJ, USA.

Several new drugs have been recently introduced to prevent and treat osteoporosis, but these agents are expensive and some have significant adverse effects. Many women previously relied on hormone replacement therapy (HRT) after menopause to reduce osteoporosis risk. However, use of HRT declined after a Women's Health-Initiative clinical trial showed that elevated risks of some cancers with HRT. This result prompted a search for cost-effective osteoporosis prevention regimens. The beneficial effects of estrogen on bone maintenance at least in part mediated via nitric oxide (NO)/cGMP pathway. At appropriate doses, nitroglycerine as a NO donor was shown to favorably affect both osteoblasts and osteoclasts (i.e., uncoupling these two cell types).

A three-year randomized, doubled-blind, controlled clinical trial was conducted to assess the efficacy nitroglycerine in preventing bone loss in early postmenopausal women. This Nitroglycerin as an Option: Value in Early Bone Loss (NOVEL) study, was funded by NIAMS. Over 200,000 women were contacted, 1,400 were interviewed, 215 were screened, and 186 were recruited. Women were randomized to receive either nitroglycerine ointment or placebo ointment. All women received calcium and vitamin D supplementation. There were no differences in the treatment arms in key baseline characteristics including BMD, BMI, smoking status, time since menopause, etc. Taking compliance (~75%) into consideration, the dose actually used by the study participants, only ~50% of that was originally intend to use in this study.

The intent to treat analysis did not reveal differences between the two treatment groups on the primary outcome of lumbar spine BMD. Change of BMD from the baseline in each group was only -0.023 (2.1% change over the three-year study period; was not significant). Except for the increase headaches in the active arm, all other adverse events had, similar profiles compared to placebo. Some of the secondary outcomes including biochemical markers of bone turnover have not been completed.

These results suggest that nitroglycerin at the dose used in this NOVEL clinical study was not effective. However, the NOVEL study subjects used only ~half the effective dose of nitroglycerine, in preventing bone loss. Taken the narrow therapeutic margin for beneficial effects of nitroglycerin on bone, this is likely to be the main reason for not having positive outcome. Therefore, we believe that an additional study using correct dose of nitroglycerine is warranted before eliminating nitroglycerine as a novel and cost-effective therapy for osteoporosis.

**Disclosures:** S.J. Wimalawansa, None.  
This study received funding from: NIAMS-NIH.

## M355

**Evaluation of BMD Changes in Women with Severe Osteoporosis after Teriparatide Treatment.** N. Malavolta<sup>1</sup>, A. Buffa<sup>\*1</sup>, G. Vukatana<sup>\*1</sup>, R. Mule<sup>\*1</sup>, M. Frigato<sup>\*1</sup>, S. Migliaccio<sup>2</sup>, G. Iolascon<sup>\*3</sup>, G. Resmini<sup>\*4</sup>, C. Borghi<sup>\*1</sup>. <sup>1</sup>UOS Reumatologia-UO Medicina Interna Borghi, Azienda Ospedaliero Universitaria Sant'Orsola-Malpighi, Bologna, Italy, <sup>2</sup>Università La Sapienza, Roma, Italy, <sup>3</sup>Ortopedia/Riabilitazione, Second University, Naples, Italy, <sup>4</sup>Ortopedia/Traumatologia, Ospedale Treviglio-Caravaggio, Treviglio, Italy.

Osteoporosis is a skeletal disorder characterised by altered bone strength predisposing to increased risk of fractures. Human parathyroid hormone fragment (1-34), teriparatide, is a new therapeutic approach for postmenopausal osteoporosis.

Aim of our study was to evaluate the change in bone mineral density (BMD) at the spine and hip in women with severe osteoporosis treated with teriparatide for 18-months.

We considered 105 postmenopausal women (mean age  $70.52 \pm 8.5$ ys) with severe osteoporosis (mean vertebral Tscore -3.25) and multiple vertebral fractures (mean of number of fractures:  $3.14 \pm 2.19$ ) who received daily, self-injections of teriparatide 20 microg/day, supplemented with 500-1000 mg/d calcium and 400-800 UI/d vitamin D. All patients previously received various antiresorptive drugs. BMD was measured by dual X-ray absorptiometry (DXA) at the spine and hip regions. Vertebral radiographs and DXA were performed at baseline and at the end of treatment. Biochemical markers were assessed at baseline and after 1, 6, 12 and 18 months. Physical examination and vital signs were recorded every six months, serious and non serious adverse events were registered.

The BMD of the spine and hip increased +1.09% and +5.52% respectively. This increase was statistically significant for the spine ( $p < 0.001$ ). We recorded neither new vertebral nor nonvertebral fractures. In 21.8 % of our patients we noted an increase in height ( $2.14 \text{ cm} \pm 1.07 \text{ cm}$ ).

According with literature, in our patients teriparatide treatment determined the expected increase in BMD at the axial skeleton, no new fractures were recorded and in some patients we noted an increase of height. The increased bone strength would be explained with the improvement in trabecular bone microarchitecture. These observational data indicate that teriparatide is useful in patients with severe osteoporosis.

**Disclosures:** N. Malavolta, None.

## M356

**Effectiveness of Bisphosphonate Therapy in a Real-World Setting.** A. C. Feldstein<sup>\*1</sup>, D. Weycker<sup>\*2</sup>, G. A. Nichols<sup>\*1</sup>, G. Oster<sup>\*2</sup>, G. Rosales<sup>\*1</sup>, N. Perrin<sup>\*1</sup>. <sup>1</sup>Center for Health Research, Kaiser Permanente Northwest, Portland, OR, USA, <sup>2</sup>Policy Analysis Inc., Brookline, MA, USA.

In randomized controlled trials, bisphosphonates--the most commonly prescribed treatment for osteoporosis--have been found to prevent fractures; it is unknown whether these agents are similarly effective in real-world clinical practice where patients may be less compliant with their treatment regimens.

To examine the effectiveness of bisphosphonate therapy in clinical practice, we employed a retrospective, matched cohort design to compare risk of clinical fracture in women with low BMD (T-score  $\leq -2.0$ ) or prior fracture who initiated such therapy versus those who did not. Data were obtained from the electronic medical records of a large US HMO. Beginning with the first month of patient accrual (7/96 through 6/06), women who initiated bisphosphonate therapy and had low BMD or clinical fracture in the prior 6 months ("treated patients") were matched (1:1 without replacement) to women with a similar clinical profile who did not initiate such therapy in that month or the next 6 months ("comparison patients"). New clinical fractures were identified from the day following therapy initiation for treated patients (and from the same date for matched comparison patients) through the end of observation; treated patients were followed for fracture irrespective of their compliance with therapy. Cox proportional hazards models were employed to estimate the hazard ratio of fracture for treated versus comparison patients, adjusting for differences in potential confounders (but not medication adherence). Mean ( $\pm$  SD) age of treated patients ( $n = 1,829$ ) and comparison patients was 72 ( $\pm 10$ ) years, 45% of each group had a prior clinical fracture, and mean BMD (for those with values) was  $-2.7 (\pm 0.5)$  and  $-2.6 (\pm 0.5)$ , respectively. Mean medication (ie, bisphosphonate) possession ratio (days of therapy  $\div$  days of follow-up) among treated patients was 0.60 ( $\pm 0.38$ ). A total of 198 (11%) treated patients experienced new clinical fracture over a mean follow-up of 2.7 ( $\pm 2.0$ ) years versus 179 (10%) comparison patients over a mean follow-up of 2.3 ( $\pm 1.8$ ) years. The adjusted hazard ratio for fracture among treated versus comparison patients was 0.91 (95% CI, 0.74 - 1.12;  $p = 0.39$ ). In this analysis of post-menopausal women with low BMD or prior clinical fracture in real-world clinical practice, risk of fracture did not differ significantly between those who began bisphosphonate therapy and those who did not. While we suspect that our findings may be attributable--at least in part--to poor drug adherence, further research in this area is warranted.

**Disclosures:** A.C. Feldstein, Amgen Inc. 3; Merck & Co. 3; Sanofi-Aventis 3. This study received funding from: Amgen Inc.

## M357

**Alendronate Treatment in Postmenopausal Romanian Women Followed by BMD- Digital X-Ray Radiogrammetry.** C. Galesanu<sup>1</sup>, M. R. Galesanu<sup>\*2</sup>. <sup>1</sup>Endocrinology, University of Medicine and Pharmacy, IASI, Romania, <sup>2</sup>Osteodensitometry, Centre of Imaging and Radiology Diagnosis, IASI, Romania.

The bisphosphonates have been shown to increase bone mineral density (BMD) and reduce bone turnover in postmenopausal osteoporotic women. Measuring BMD by Digital X-Ray Radiogrammetry was accepted for diagnosis and monitoring response to therapy. The aim of this study was to evaluate the effect of Alendronate (Fosamax®) treatment in a group of postmenopausal women, assessed by Digital X-Ray Radiogrammetry (DXR-BMD) in bone changes.

We studied 9,733 healthy women with ages between 20 and 89 years referred to our department of densitometry using DXR-BMD, 6,903 from them being in postmenopause. Using WHO - criteria for osteoporosis diagnosis, 792 from them presented osteoporosis and 1,450 osteopenia. Among 385 patients who were selected for Alendronate, 115 were under the treatment after five years or more. The patients received Alendronate 70 mg/weekly. The mean age of osteoporotic treated women was 61.3 $\pm$ 7.8 years. BMD by DXR was measured at each 12 months. Statistical analyses was "t" Test (Student - Fischer). The witness group, 35 women, received 1 mcg Alfacalcidol daily.

BMD mean changes after Alendronate was: +3.3% after one year; +4.4% after two years; +5.35% after three years; +6.3% after four years and +7.1% after five years. The BMD changes under Alfacalcidol was +1.89% after the first year and +3.2% after five years. Three patients (2.6%) suffered a fracture under the Alendronate: one hip fracture and two vertebral fractures recorded on X-Ray.

Under Alfacalcidol one patient presented a hip fracture.

We conclude that BMD increase significantly after Fosamax® treatment in postmenopausal women. Though Alendronate seemed to be good tolerated by the patients the therapy adherence after five years was only 29%. The postmenopausal osteoporosis rested untreated even if it was diagnosed. In our study, like in others, the adherence at treatment was lower.

**Disclosures:** C. Galesanu, None.

## M358

**Comparative Gastrointestinal Safety of Weekly Oral Bisphosphonates.** S. M. Cadarette, J. N. Katz\*, M. A. Brookhart\*, T. Stürmer\*, M. R. Stedman\*, D. H. Solomon. Brigham and Women's Hospital, Harvard Medical School, Boston, MA, USA.

Weekly bisphosphonates are the primary agents prescribed for osteoporosis. Prior evidence from endoscopic trials and observational studies suggests that daily risedronate has better gastrointestinal safety than daily alendronate. The purpose of our study was to compare the relative gastrointestinal safety of treatment with weekly bisphosphonates among older adults. We studied a population-based cohort of new users of weekly alendronate (70 mg) and weekly risedronate (35 mg) enrolled in the Pennsylvania Pharmaceutical Assistance Contract for the Elderly. Pharmacy and Medicare claims served as the primary data sources. Covariates included risk factors plausibly related to gastrointestinal disease and were assessed using information from the 12 months prior to bisphosphonate initiation. The primary outcome was hospitalization for upper gastrointestinal bleed. Secondary outcomes included outpatient diagnoses for upper gastrointestinal disease, symptoms, endoscopic procedures, and use of gastroprotective agents. We used Cox proportional hazard models to compare outcomes between agents within 120 days of treatment initiation, adjusting for covariates using risedronate propensity score quintiles. In sensitivity analysis, we examined composite outcomes and stratified results by gastrointestinal event history (yes or no) and age group (65-79 years or 80+ years). Alendronate was the reference group in all Cox proportional hazard models. We identified 10,420 new users of either agent who initiated treatment between June 2002 and August 2005, mean age=79 years (SD=6.9) and 95% female. We observed 31 hospitalizations for upper gastrointestinal bleed (0.91/100 person-years) within 120 days of treatment initiation. Adjusting for covariates, there was no large difference in hospitalization rates for upper gastrointestinal bleed among those treated with risedronate (HR=1.12, 95%CI=0.55-2.28) compared to alendronate. Similarly, no differences were observed for secondary or composite outcomes, or in stratified analyses. However, among those with a history of gastrointestinal disease, rates for upper gastrointestinal endoscopies were lower among risedronate (HR=0.70, 95%CI=0.49-0.99) compared with alendronate recipients. Nonetheless, when endoscopies were combined with upper gastrointestinal diseases and symptoms as the outcome, this finding was attenuated towards the null (HR=0.93; 95%CI=0.83-1.04).

In conclusion, we found no difference in hospitalizations for upper gastrointestinal bleed between weekly alendronate and weekly risedronate. Small differences between agents were observed for upper gastrointestinal endoscopy, but this is of unclear clinical importance.

**Disclosures:** S.M. Cadarette, None.

## M359

**Differences in Safety and Efficacy of Generic and Original Branded once weekly Bisphosphonates.** J. D. Ringe, P. Farahmand\*. Medizinische Klinik IV (Osteology/Rheumatology), Klinikum Leverkusen, University of Cologne, Leverkusen, Germany.

**Objective:** To compare the changes on bone mineral density (BMD), the effects on persistence and adverse events (AE), in patients treated for postmenopausal osteoporosis with either generic alendronate or with branded Fosamax® or Actonel®, once weekly. **Patients and methods:** In this retrospective patient chart analysis we reviewed the one year observational treatment results of 186 women (ITT population) with postmenopausal osteoporosis. Patients from our out-patient department having started with once weekly BP therapy between 36 to at least 12 months before this chart review were included in this comparative study with three arms according to their treatment: A: Generic Alendronate 70 mg products, B: Alendronate (Fosamax®) 70 mg and C: Risedronate (Actonel®) 35 mg. All patients received basic therapy with 1200 mg calcium and 800 IU Vit. D per day. Patients' BMD at lumbar spine and total hip was below - 2.5 T-score, with and without prevalent vert. and non-vert. fractures. **Results:** Analysis of the 186 patients' results shows an average increases in LS-BMD after 12 months of 2.8%, 5.2% and 4.8% for the groups A, B and C resp. The respective mean changes at total hip were 1.5%, 2.9%, and 3.1%. At both sites, the mean increases in BMD were not different between the two groups receiving original BP (B, C) but for both were significantly higher than for the group treated with generic alendronate (A). At 12 months 68% of group A, 84% of B and 94% of C were still on BP-therapy. The persistence of patients treated with generic alendronate was significantly lower as compared to each of the two original BP treated groups. The total number of patients with gastrointestinal AEs were 32, 15 and 9 for A, B and C resp. **Conclusions:** Significantly lower increases of lumbar spine and total hip BMD with generic alendronate once weekly as compared to the two branded originals (Fosamax, Actonel) were observed. We do not know the reason for the 40-50% lower BMD increase rates of the generic compounds. At least in part the lower efficacy can be explained by a significantly lower degree of compliance with generic alendronate, which could be related to a higher incidence of GI AE's. Other reasons could be lower bioavailability or potency of generic alendronate.

**Disclosures:** J.D. Ringe, None.



## M360

**Continued Evidence for Safety and Efficacy of Risedronate in Men with Osteoporosis: Outcome of the 2-year Open-Label Extension Study of MASTER.** S. Boonen<sup>1</sup>, E. Orwoll<sup>2</sup>, D. Wenderoth<sup>3</sup>, K. Stoner<sup>\*4</sup>, R. Eusebio<sup>5</sup>, P. Delmas<sup>6</sup>. <sup>1</sup>University Hospital, Leuven, Leuven, Belgium, <sup>2</sup>Oregon Health Sciences University, Portland, OR, USA, <sup>3</sup>P & G Pharmaceuticals, Schwalbach, Germany, <sup>4</sup>P & G Pharmaceuticals, Egham, United Kingdom, <sup>5</sup>P & G Pharmaceuticals, Mason, OH, USA, <sup>6</sup>INSERM Research Unit 403, Lyon, France.

The objective of this 2-year open-label extension to the 2-year, double-blind, placebo-controlled study (MASTER) was to continue to assess the safety of 35 mg once-a-week (OAW) risedronate in men with osteoporosis. 218 of the 284 men (67 of 93 placebo group [Pla/Ris]; 151 of 191 risedronate group [Ris/Ris]) from the initial blinded study were enrolled in this extension study. Safety variables included adverse events (AEs), laboratory data, vital signs, physical examinations, and changes in lumbar spine, total proximal femur, femoral neck, and femoral trochanter BMD and bone turnover markers (BTMs) including type I collagen C-telopeptide (CTX), type I collagen N-telopeptide/creatinine (NTX/Cr), and bone-specific alkaline phosphatase (BAP). BMD was measured at Months 36 and 48 of the 2-year extension; BTMs were measured at Months 27, 30, 36 and 48 of the 2-year extension.

The mean increase from baseline at Year 4 in lumbar spine BMD for patients receiving risedronate 35 mg OAW for all 4 years (Ris/Ris group) was 7.9% (6.6-9.1, 95% CI, n=128). These Ris/Ris patients also continued to show BMD response at other skeletal sites. The mean increase from baseline at Year 4 in lumbar spine BMD for the placebo patients that received risedronate 35 mg OAW for the 2 years of the open-label extension study (Pla/Ris group) was 6.2% (4.6-7.9, 95% CI, n=54), which is similar to the response observed in risedronate-treated patients during the initial 2-year, double-blind study period (5.98% [5.22-6.73, 95% CI], n=172). Similar patterns were observed in the Pla/Ris group at other skeletal sites.

Similar reductions in NTX/Cr, CTX, and BAP were found at Years 3 & 4 between the 2 groups. In general, greater decreases in BTMs were observed in the Pla/Ris group during the open-label extension study while taking risedronate 35 mg OAW than during the double-blind study while taking placebo.

The 2 groups were similar in overall percentages of patients with AEs (68.7% Pla/Ris, 66.9% Ris/Ris), serious AEs (11.9% Pla/Ris, 13.9% Ris/Ris), upper GI AEs (10.4% Pla/Ris, 8.6% Ris/Ris), and overall musculoskeletal AEs (11.9% Pla/Ris, 13.9% Ris/Ris).

In conclusion, the Pla/Ris group in the 2-year open-label extension study showed similar safety and efficacy results compared to the Ris/Ris group in the first 2 years of the study. Patients who received risedronate for 4 years in total showed similar safety and efficacy to that observed in women with postmenopausal osteoporosis treated with risedronate for 4 years.

**Disclosures:** S. Boonen, P&G 2.

This study received funding from: The Alliance for Better Bone Health (Procter & Gamble Pharmaceuticals and sanofi-aventis).

## M361

**Postmenopausal Women with Gastroesophageal Reflux Disease and Long Term Treatment with Bisphosphonates IV.** M. Cokolic\*. Endocrinology and Diabetology, UKC Maribor, Maribor, Slovenia.

The aim of this study was to assess the effectiveness of bisphosphonate (BP) iv (zoledronat 5 mg, pamidronate 30 mg, ibandronate 3 mg) therapy in treatment of postmenopausal osteoporosis in patients with gastroesophageal reflux disease (GERD). GERD occurs when the lower esophageal sphincter opens spontaneously, for varying periods of time, or does not close properly and stomach contents rise up into the esophagus and it can eventually lead to more serious health problems and unable take BP orally.

Fifteen women with osteoporosis (T-score at lumbar spine or hip <-2.5 SD) were enrolled in a prospective study between January 2003 and December 2007. Patients were 61 to 93 years old (mean: 72,3 years). They were treated with BP iv in combination with 500-mg elemental calcium and 800 IU vitamin D. The BMD in the lumbar spine (L1-L4) and left hip was measured in all patients using dual energy X-ray densitometry (Hologic 2000+) at the start of the treatment and at 12 to 48 months after initiation of the treatment. The serum levels of RBC, Hgb, WBC, Plt, TSH, Ca, P, Mg, Na, K, Cl, ALP, AST, ALT, BUN, creatinine, osteocalcin and  $\beta$  cross laps were measured every 12 months. Average baseline BMD was 0.698 g/cm<sup>2</sup> (n=15, range 0.602 to 0.787 g/cm<sup>2</sup>) at the lumbar spine and 0.676 g/cm<sup>2</sup> (n=15, range 0.499 to 0.862 g/cm<sup>2</sup>) at the hip.

After treating patients on average for 40 months, the average BMD was 0.722 g/cm<sup>2</sup> (n=15, range 0.600 to 0.966 g/cm<sup>2</sup>) at the lumbar spine and 0.704 g/cm<sup>2</sup> (n=15, range 0.494 to 0.901 g/cm<sup>2</sup>) at the hip. BMD thus increased on average by 3.4% at the lumbar spine and 4.1% at the hip. Serum levels remained within normal limits throughout the treatment, with no adverse events observed during the study. BP iv was well tolerated in all patients.

In our report of our on-going study we have shown that postmenopausal osteoporosis with GERD can be effectively and safely treated with BP iv in all patients for up to four years without new fractures.

**Disclosures:** M. Cokolic, None.

## M362

**Effect of a Single 5-mg Infusion of Zoledronic Acid on Bone Turnover Markers Versus Oral Risedronate (5 mg/day) Over 1 Year in Patients with Glucocorticoid-Induced Osteoporosis.** P. Sambrook<sup>1</sup>, J. Devogelaer<sup>2</sup>, J. Reginster<sup>3</sup>, K. Saag<sup>4</sup>, C. Roux<sup>5</sup>, C. Lau<sup>\*6</sup>, P. Papanastasiou<sup>\*7</sup>, O. Schoenborn-Kellenberger<sup>\*7</sup>, K. Maylandt<sup>\*7</sup>, T. Fashola<sup>\*7</sup>, P. Mesenbrink<sup>\*8</sup>, D. Reid<sup>9</sup>. <sup>1</sup>University of Sydney, Sydney, Australia, <sup>2</sup>Universite Catholique de Louvain, Brussels, Belgium, <sup>3</sup>University of Liege, Liege, Belgium, <sup>4</sup>University of Alabama at Birmingham, Birmingham, AL, USA, <sup>5</sup>Paris-Descartes University, Paris, France, <sup>6</sup>University of Dundee, Dundee, United Kingdom, <sup>7</sup>Novartis Pharma AG, Basel, Switzerland, <sup>8</sup>Novartis Pharmaceutical Corp., East Hanover, NJ, USA, <sup>9</sup>University of Aberdeen, Aberdeen, United Kingdom.

A single zoledronic acid (ZOL, 5 mg) infusion was compared with oral risedronate (RIS, 5 mg/d) in patients with glucocorticoid-induced osteoporosis (GIO) in a 1-yr, double-blind, double-dummy study. Randomized patients were divided into 2 subpopulations: treatment (>3 months glucocorticoid therapy [ZOL, n=272; RIS, n=273]) and prevention ( $\leq$ 3 months glucocorticoids [ZOL, n=144; RIS, n=144]). Bone mineral density (BMD) was evaluated at 6 and 12 months. Changes from baseline in fasting serum  $\beta$ -C-terminal telopeptides of type 1 collagen ( $\beta$ -CTX) and procollagen type 1 amino-terminal propeptide (PINP) were measured at 9-11 days and Months 3, 6, and 12. ZOL significantly increased lumbar spine (LS) BMD vs RIS in both the treatment (4.1% vs 2.7%; P=0.0001) and prevention (2.6% vs 0.6%; P<0.0001) subpopulations at 12 months. ZOL reduced  $\beta$ -CTX and PINP levels significantly more than RIS in the treatment (day 9-11 onwards) and prevention ( $\beta$ -CTX, day 9-11 onwards; PINP, Month 3 onwards) subpopulations (P<0.0001). There was a significant correlation between LS BMD change and some biomarkers at 12 months. In subgroups of patients with/without rheumatoid arthritis (RA), systemic lupus erythematosus (SLE) or asthma/chronic obstructive pulmonary disease (COPD), reductions in  $\beta$ -CTX for ZOL vs RIS were significant from day 9-11 onwards in the combined treatment and prevention subpopulations (P $\leq$ 0.0004 for all). Reductions in PINP for ZOL vs RIS were significant from day 9-11 onwards in patients without RA, SLE, and asthma/COPD. In subgroups with/without concomitant use of proton pump inhibitors (PPIs), selective serotonin inhibitors (SSRIs) or anti-tumor necrosis factor (anti-TNF) at baseline there was no difference in reductions in  $\beta$ -CTX levels for ZOL vs RIS (P<0.001). PINP levels were significantly reduced for ZOL vs RIS from day 9-11 onwards, regardless of PPI use (P $\leq$ 0.0002) or anti-TNF use (P $\leq$ 0.0001), but was only significantly reduced at all timepoints in patients not taking SSRIs (P<0.001). These results indicate that a single infusion of ZOL suppresses bone turnover significantly more than daily oral RIS for up to 1 yr in different subgroups of patients with GIO.

**Disclosures:** P. Sambrook, Merck 1, 4; Sanofi-Aventis 1, 4; Novartis 1, 4. This study received funding from: Novartis.

## M363

**Effect of Zoledronic Acid (Single 5-mg Infusion) on Lumbar Spine Bone Mineral Density Versus Oral Risedronate (5 mg/day) Over 1 Year in Subgroups of Patients Receiving Glucocorticoid Therapy.** C. Roux<sup>1</sup>, D. Reid<sup>2</sup>, J. Devogelaer<sup>3</sup>, K. Saag<sup>4</sup>, C. Lau<sup>\*5</sup>, J. Reginster<sup>6</sup>, P. Papanastasiou<sup>\*7</sup>, A. Ferreira<sup>\*7</sup>, F. Hartl<sup>8</sup>, T. Fashola<sup>\*7</sup>, P. Mesenbrink<sup>\*9</sup>, P. Sambrook<sup>10</sup>. <sup>1</sup>Paris-Descartes University, Paris, France, <sup>2</sup>University of Aberdeen, Aberdeen, United Kingdom, <sup>3</sup>Universite Catholique de Louvain, Brussels, Belgium, <sup>4</sup>University of Alabama at Birmingham, Birmingham, AL, USA, <sup>5</sup>University of Dundee, Dundee, United Kingdom, <sup>6</sup>University of Leige, Liege, Belgium, <sup>7</sup>Novartis Pharma AG, Basel, Switzerland, <sup>8</sup>F. Hoffmann-La Roche Ltd., Basel, Switzerland, <sup>9</sup>Novartis Pharmaceutical Corp., East Hanover, NJ, USA, <sup>10</sup>University of Sydney, Sydney, Australia.

The effects of intravenous zoledronic acid (ZOL, single 5-mg infusion) and oral risedronate (RIS, 5 mg/d) on lumbar spine (LS) bone mineral density (BMD) were evaluated in subgroups of glucocorticoid-treated patients in a 1-year, randomized, double-blind, double-dummy study. Patients were divided into two subpopulations according to glucocorticoid treatment duration at randomization (treatment subpopulation: >3 months [ZOL, n=272; RIS, n=273]; prevention subpopulation:  $\leq$ 3 months [ZOL, n=144; RIS, n=144]), then further divided into subgroups by gender, age (<35, 35-50, 51-64, 65-74,  $\geq$ 75 years), mean prednisone dose during the trial (<7.5,  $\geq$ 7.5 to <12,  $\geq$ 12 mg/d), and history of other medications. Increases in LS BMD from baseline to 12 months seen with ZOL were significantly greater than with RIS for: men (P<0.05) and women (P<0.01) for both treatment and prevention subpopulations; age 35-40 years (P=0.0041) and 51-64 years (P=0.0075) for the treatment subpopulation and 65-74 years (P<0.05) for both subpopulations (the difference between ZOL and RIS increased with age); mean prednisone dose  $\geq$ 7.5 to <12 mg/d (P<0.001) for both subpopulations; no history of proton pump inhibitor (PPI) (P<0.01), selective serotonin reuptake inhibitor (P<0.0001) or anti-tumor necrosis factor (TNF) therapies (P<0.01) for both subpopulations; and prior history of anti-TNF (P=0.0278) and PPI therapies (P=0.0148) for the treatment and prevention subpopulations, respectively. There was no significant difference in increase in LS BMD for ZOL vs RIS for the remaining subgroup parameters in either subpopulation. In the 3 days post treatment, AEs were more common with ZOL (mainly transient post-dose symptoms). From day 3, the 2 treatment groups had similar AE rates. These findings suggest that ZOL is effective in increasing LS BMD to a significantly greater extent than RIS in a wide range of patient subgroups.

**Disclosures:** C. Roux, Novartis, Amgen, MSD, Alliance, Roche, Servier, Lilly, Nycomed 3, 4. This study received funding from: Novartis

## M364

**Acute Phase Response and Bone Metabolism Marker after Intravenous Bisphosphonate in Osteoporotic Patients with Rheumatism.** W. Park<sup>1</sup>, M. Lim<sup>\*1</sup>, S. Kwon<sup>\*1</sup>, S. Kim<sup>\*1</sup>, S. Hong<sup>2</sup>. <sup>1</sup>Medicine/Rheumatology, IN-HA University Hospital, Incheon, Republic of Korea, <sup>2</sup>Endocrinology and Metabolism, IN-HA University Hospital, Incheon, Republic of Korea.

The side effects typically associated with the intermittent large dose bisphosphonate are myalgia and transient fever. Increase of cytokines in acute phase response was reported mostly in treatment for cancer and only few studies were reported for osteoporosis. The aim of this study is to evaluate cytokine change in acute phase response and bone metabolism shortly after single dose of intravenous pamidronate.

Nineteen patients with osteoporosis and rheumatism without prior bisphosphonate or immunosuppressant use were selected. They were given 30 mg of IV pamidronate and the venous blood samples were taken before and 48 hours after the infusion. Serum level of IL-6, TNF- $\alpha$  and C-telopeptide (CTX) were measured with an immunoenzymetric assay (serum IL-6 and TNF- $\alpha$ : R&D Systems, Minneapolis, Minn., USA; serum CTX: Nordic Bioscience Diagnostics, Bolden, UK). The real-time RT-PCR quantified the expression of the interferon (IFN)- $\gamma$  from peripheral blood mononuclear cells. Leukocyte count and serum calcium level were also determined at the same time. Acute phase reactants such as erythrocyte sedimentation rate (ESR) and C-reactive protein (CRP) were measured for three consecutive days.

At baseline, mean level of CRP was 0.14 mg/dL which rose to 0.30 mg/dL, 0.61 mg/dL and 1.58 mg/dL at 24hours, 48 hours and 72 hours, respectively. Their rise were all significant at all times comparing to baseline ( $p=0.049$ , 0.002, 0.004, respectively). ESR seemed to increase at 72 hours but it was not significant ( $p=0.413$ ). The WBC count and serum calcium level tend to decreased after the treatment. Serum TNF- $\alpha$  increased significantly ( $p=0.031$ ). Both serum IL-6 and IFN- $\gamma$  did not increase significantly but increment of IL-6 after treatment strongly correlated with that of CRP ( $p=0.023$ ). Serum CTX decreased markedly after the treatment ( $p=0.009$ ). The dose of bisphosphonate used in this study was smaller than previous studies. The marked decrease of serum CTX implies that osteoclastic activity is suppressed as early as 48 hours after the treatment. As inflammation occurs even with 30mg of intravenous pamidronate, we recommend smaller dose frequent therapy or slower infusion of bisphosphonate in contrary to the current trend of large dose intermittent therapy.

	Before treatment	48 hours after treatment	P value
WBC (/ $\mu$ l)	6763 $\pm$ 1778	6352 $\pm$ 2212	0.31
CRP (mg/dL)	0.14	0.61	0.002
IL-6 (pg/mL)	1.76 $\pm$ 1.03	2.54 $\pm$ 1.51	0.084
TNF- $\alpha$ (pg/mL)	1.11 $\pm$ 0.91	1.96 $\pm$ 2.11	0.031
IFN- $\gamma$	1.0 $\pm$ 0	2.23 $\pm$ 2.37	0.38
Serum CTX (ng/ml)	0.49 $\pm$ 0.40	0.14 $\pm$ 0.14	0.009

**Disclosures:** W. Park, None.

## M365

**Zoledronic Acid Prevents Accelerated Bone Loss after Discontinuation of Teriparatide.** C. Deal<sup>1</sup>, K. Tuthill<sup>\*1</sup>, A. Kriegman<sup>2</sup>. <sup>1</sup>Rheumatology, Cleveland Clinic, Cleveland, OH, USA, <sup>2</sup>Novartis Pharmaceuticals Corporation, East Hanover, NJ, USA.

Teriparatide (TPTD) is an anabolic agent approved for daily injection over a 2 year period in patients at high risk for fracture. After discontinuation of TPTD, rapid bone loss ensues. Treatment with antiresorptive agents prevents accelerated bone loss and may therefore maintain the increased bone mass following TPTD. Zoledronic acid 5mg (ZOL) is an IV bisphosphonate approved as a once-yearly infusion for the treatment of postmenopausal osteoporosis. In order to test the ability of ZOL to maintain bone mass after treatment with TPTD, we enrolled 35 postmenopausal women in a trial evaluating the effect of ZOL 5 mg given immediately after a 2-year course of TPTD. The primary endpoint was change in bone density (grams/cm<sup>2</sup>) in the lumbar spine (LS) (L1-4) at 12 months. Secondary endpoints were change in bone density (grams/cm<sup>2</sup>) at the total hip (TH), femoral neck (FN) and total body (TB); change in serum c-telopeptide type I collagen (CTX) and serum n-propeptide type I collagen (PINP). So far, 24 patients have completed 12-months of follow-up, and here we report on changes in bone density in these patients.

The study cohort had a mean age of 68.7  $\pm$  11.4 and a mean T-score at the time of TPTD discontinuation of -2.1 for both LS and TH. Table 1 summarizes the number of patients exhibiting either maintenance/increase or a decrease in BMD at LS, TH, FN and TB. Table 1. Number of patients (bone density change from baseline to 12 months)

Bone density	LS	TH	FN	TB
Maintained/ increased	21	24	22	23
Declined	3	0	2	1

**Decline = change  $>0.03$ g/cm<sup>2</sup>**

A single infusion of Zoledronic acid 5 mg appears to be a safe and effective therapy to maintain or increase bone mass in patients after TPTD treatment. It preserves, or increases bone mass in the lumbar spine, total hip, femoral neck and total body in 88%, 100%, 92% and 96% of patients, respectively.

**Disclosures:** C. Deal, Novartis 1, 3, 4.

This study received funding from: Novartis Pharmaceuticals.

## M366

**Alendronate Treatment for Juvenile Osteoporosis. A Double-Blind, Randomized, Placebo-controlled Cross-Over Clinical Trial.** L. L. Key, P. Madyastha<sup>\*</sup>, W. Ries, B. Hollis, F. Reed<sup>\*</sup>. Pediatrics, Medical University of South Carolina, Charleston, SC, USA.

A phase IIb, double-blind, crossover study was designed to demonstrate the efficacy and safety of alendronate treatment in juvenile osteoporosis. Twenty two children (age 5-13 years) with two or more fractures, associated with minimal or no trauma, were enrolled with a Z-score of  $\leq -2.0$  SD based upon dual energy x-ray analysis. They were randomized using a permuted block design. In the first year (12 months), eleven children (group 1) received alendronate (35mg if patients  $<40$ kg, and 70mg if  $\geq 40$ kg) along with calcium supplementation (500mg or 1000mg daily, using the same weight cutoffs and vitamin D 800 IU ). Another 11 children (group 2) received placebo, calcium and vitamin D. In the second year (12 months), they crossed over and received placebo (group 1) and alendronate (group 2) with calcium and vitamin supplements. Bone mineral density (BMD) of lumbar spine (LS) and hip were measured every 6 months. Biochemical markers of bone turnover (bone formation, serum bone-specific alkaline phosphatase, BSAP) and resorption (N-telopeptide, NTx) were also determined. At the end of first year, the BMD of LS increased significantly (11.6-45.6%) in group 1, as compared to a minimum increase in group 2 (3.9-10%). In the second year (crossover), group 1 continued to increase (13.8-49.5%) and group 2 increased to 8.2-46.5%. Although the BMD increased in all the participants at the end of two years, the increase in %BMD (group 1) was less than that over previous measurements (18.5% (6 mo), 6.5% (12 mo), 3.7% (18 mo), 1.8% (24 mo)). This pattern was observed in group 2. Bone marker analyses correlated with the BMD increase. There was no side effects and no reduction in the rate of height growth. Children with multiple fractures and low bone density should be treated with alendronate as soon as they are diagnosed. It is possible that alendronate may inhibit the osteoclast activity for a short period of time.

**Disclosures:** L.L. Key, None.

This study received funding from: Food and Drug Administration (FDA), Merck & Co.

## M367

**Fracture Risk in Women Aged 65 Years or Older with Once-Monthly Oral Ibandronate Compared with Weekly Bisphosphonates: Analyses From the eValuation of Ibandronate Efficacy (VIBE) Database Fracture Study.** S. L. Silverman<sup>1</sup>, W. A. Blumentals<sup>\*2</sup>, S. A. Poston<sup>\*3</sup>, S. T. Harris<sup>4</sup>. <sup>1</sup>Cedars-Sinai Medical Center/UCLA, Beverly Hills, CA, USA, <sup>2</sup>Roche, Nutley, NJ, USA, <sup>3</sup>GlaxoSmithKline, Research Triangle Park, NC, USA, <sup>4</sup>University of California, San Francisco, San Francisco, CA, USA.

The VIBE study compared fracture risk between patients treated with once-monthly and weekly oral bisphosphonates (BPs). This subanalysis focused on a higher-risk group of older women, aged  $\geq 65$  years.

Patients were newly prescribed once-monthly oral ibandronate or weekly oral alendronate or risedronate, adherent for  $\geq 90$  days, and without malignancy or Paget's disease. Data were censored at fracture, 12 months after BP initiation, end of health plan enrollment, BP brand switch, regimen switch, or treatment discontinuation. Fracture risk was compared using Cox regression models to calculate hazard ratio (HR) and adjusted for potential confounding factors (age, concomitant medications, estrogen use, outpatient visits, osteoporosis diagnosis, bone densitometry procedure, fracture history, glucocorticoid use, use of other non-estrogen osteoporosis medications). The analysis was repeated for the separate weekly alendronate or risedronate groups compared with ibandronate.

The analysis included 1,811 patients receiving once-monthly ibandronate and 14,648 patients receiving weekly BPs (alendronate 9,270, risedronate 5,378). Baseline characteristics included: mean (median) age 72.41 (72) years for ibandronate vs 72.82 (73) years for weekly BPs ( $p=0.0029$ ); pre-index fracture 6.29% for ibandronate vs 6.45% for weekly BPs ( $p=0.7979$ ); pre-index glucocorticoid use 15.52% for ibandronate vs 10.98% for weekly BPs ( $p<0.001$ ); pre-index rheumatoid arthritis diagnosis 5.36% for ibandronate vs 3.29% for weekly BPs ( $p<0.001$ ). The risks of hip fracture, and nonvertebral fracture (NVF) were not significantly different between groups (hip fracture adjusted HR 1.14,  $p=0.707$ ; NVF 0.75,  $p=0.172$ ), but the risks of vertebral fracture and all fractures were statistically lower in the ibandronate group (vertebral fracture adjusted HR 0.28,  $p=0.030$ ; all fractures 0.65,  $p=0.033$ ). Similarly, when comparing ibandronate vs individual weekly BPs, the risk of hip fracture or NVF was not significantly different from either alendronate or risedronate.

Women aged  $\geq 65$  years treated with oral once-monthly ibandronate or weekly BPs had similar risks of hip fracture or NVF. The risks of vertebral fracture and all fractures were statistically lower for ibandronate patients, though the clinical implications of these findings require further exploration and validation.

**Disclosures:** S.L. Silverman, Eli Lilly, Novartis, Merck, Procter & Gamble, Roche, Inc., Wyeth 3; Eli Lilly, Merck, Procter & Gamble, Roche 2; Merck, Novartis, Roche, Wyeth 1. This study received funding from: Roche and GlaxoSmithKline.

## M368

**Improving the Prediction of Medication Adherence: The Example of Bisphosphonates for Osteoporosis.** J. R. Curtis<sup>1</sup>, J. Xi<sup>\*1</sup>, A. O. Westfall<sup>\*2</sup>, H. Cheng<sup>\*3</sup>, K. Lyles<sup>\*4</sup>, K. G. Saag<sup>5</sup>, E. Delzell<sup>\*3</sup>. <sup>1</sup>Center for Education and Research on Therapeutics (CERTs), University of Alabama at Birmingham, Birmingham, AL, USA, <sup>2</sup>Department of Biostatistics, University of Alabama at Birmingham, Birmingham, AL, USA, <sup>3</sup>Department of Epidemiology, University of Alabama at Birmingham, Birmingham, AL, USA, <sup>4</sup>Department of Medicine, Duke University, Durham, NC, USA, <sup>5</sup>Division of Rheumatology, University of Alabama at Birmingham, Birmingham, AL, USA.

**Introduction** Administrative claims data have a limited ability to identify persons with high adherence to oral bisphosphonates. We tested whether adding information on adherence with other drugs used to treat chronic, asymptomatic conditions would improve the predictive ability of administrative data to identify adherent individuals.

**Methods** Using data from a large, U.S. healthcare organization, we identified new bisphosphonate users and their 1 year adherence to oral bisphosphonates, quantified by the Medication Possession Ratio (MPR). Multivariable logistic regression models evaluated the relationship between high bisphosphonate adherence (MPR  $\geq$  80%) and patient demographics, comorbidities, and health services utilization. To these logistic regression models, we evaluated the incremental change in the area under the receiver operator curve (AUC) after adding information regarding adherence with other drug classes. These included anti-hyperlipidemics (statins), anti-hypertensives, anti-depressants, oral diabetes agents, and glaucoma medications. Results from the logistic regression models were evaluated in parallel using recursive partitioning trees with 10-fold cross-validation.

**Results** Among 101,038 new bisphosphonate users, administrative data identified numerous non-medication factors (e.g. age, gender, use of preventive services) significantly associated with high bisphosphonate adherence at 1 year. However, all these factors in aggregate had low discriminant ability to identify persons highly adherent with bisphosphonates (AUC = 0.62). For persons who were new users of  $\geq$  1 of the other asymptomatic condition drugs, MPR data on the other drugs substantially improved the prediction of high bisphosphonate adherence. The impact on prediction was largest for concomitant statin users (AUC = 0.70).

**Conclusions** Information on adherence with drugs used to treat chronic asymptomatic conditions improves the prediction of adherence with oral bisphosphonates. This may help identify persons who should receive targeted interventions to promote adherence to osteoporosis medications.

**Disclosures:** J.R. Curtis, Roche, UCB, Proctor & Gamble 2; Merck, Proctor & Gamble, Eli Lilly, Roche, Novartis 1; Novartis, Amgen, Merck, Proctor & Gamble, Eli Lilly, Roche 3.

This study received funding from: Arthritis Foundation, a Pharma Foundation Research Grant in Health Outcomes, and Novartis Pharmaceuticals, National Institutes of Health (AR053351, AR052361).

## M369

**A Post-Fracture Initiative in a Rural Ontario Community Hospital.** J. E. M. Sale<sup>\*1</sup>, D. E. Beaton<sup>1</sup>, E. R. Bogoch<sup>1</sup>, V. Elliot-Gibson<sup>\*1</sup>, K. J. Ingram<sup>\*2</sup>.

<sup>1</sup>Mobility Program Clinical Research Unit, Keenan Research Centre, Li Ka Shing Knowledge Institute, St. Michael's Hospital, Toronto, ON, Canada,

<sup>2</sup>Peterborough Regional Health Centre, Peterborough, ON, Canada.

We evaluated a coordinator-based osteoporosis (OP) initiative in a regional community hospital fracture clinic in rural Ontario. A coordinator screened and identified fragility fracture patients, educated them about OP, and then referred them back to their family physician for further OP assessment and intervention. Eligible patients were males  $\geq$ 50 years and females  $\geq$  40 years presenting to an outpatient fracture clinic for follow up of a low trauma fracture of the distal radius, proximal humerus, proximal femur, or vertebrae over a 12-month period. Patients voluntarily completed a quality assurance survey with the coordinator and were contacted 6 months later for follow up. At baseline, 524 patients (mean age 74 years) met our eligibility criteria; 432 (82%) were female; 150 (29%) had a prior fracture, 205 (39%) had a previous OP diagnosis, and 120 (23%) were on first-line therapy for OP. Of these 524, 339 (65%) were successfully followed-up at 6 months. Compared with patients without follow-up data (n=185), patients with follow-up data were younger (73 vs. 76 years; t(522)=2.33, p=.02), more likely to be female (86% vs. 77%;  $\chi^2(1)=6.4$ , p=.011), more likely to report ever having a bone mineral density (BMD) test (56% vs. 35%;  $\chi^2(1)=20.7$ , p<.001), and more likely to be on first-line therapy at baseline (26% vs. 18%;  $\chi^2(1)=4.15$ , p=.042). Within 6-months of screening, 26% of follow-up patients had initiated, while 22% remained on, first-line therapy. Of those on first-line therapy at baseline, only 3% were not on therapy at follow-up. Fifty-one percent (n=174) of follow-up patients reported having a BMD in the past 6 months; the majority of these patients (n=139) had not been previously diagnosed and/or treated for OP. Approximately 20% of follow-up patients reporting a previous diagnosis and/or treatment of OP at baseline and a BMD between baseline and follow-up, did not report OP or osteopenia on their BMD at follow-up. An OP screening program with education, facilitation of testing, and communication with family doctors was associated with an increased prevalence of OP testing and care when compared to baseline prevalence of OP care. Given the risk that fracture could be perceived as treatment failure, discontinuation of therapy was low (3%). However, we need to understand why some patients previously diagnosed or treated for OP did not report OP or osteopenia on their BMD at follow-up.

**Disclosures:** J.E.M. Sale, None.

This study received funding from: Merck Frosst Canada Inc.

## M370

**Interventions to Improve Adherence and Persistence with Osteoporosis Medications: A Systematic Literature Review.** T. Gleeson<sup>\*</sup>, M. Iversen<sup>\*</sup>, D. H. Solomon. Brigham and Women's Hospital, Boston, MA, USA.

**BACKGROUND:** Adherence (% of time taking medication) and persistence (length of time from initiation to discontinuation of medication) with pharmacologic therapy for osteoporosis is poor. Prior studies have shown that adherence and persistence with osteoporosis medications decrease significantly within one year of initiation. With a rapidly growing aged population, there is strong impetus for the improvement of adherence and persistence with osteoporosis medications.

**METHODS:** A literature search of English language articles between 1990 and March 2008 was conducted using PubMed, EMBASE, CINAHL, and Cochrane Reviews. Search terms included: osteoporosis, adherence, persistence, compliance, treatment refusal, medication, and intervention. We selected papers according to the following criteria: 1) the study was an intervention to improve adherence/persistence with osteoporosis medication and 2) statistical results of adherence and/or persistence were reported for observational and intervention cohorts. Two reviewers independently reviewed the publications using a structured data abstraction form.

**RESULTS:** We found over 300 articles and reviewed their abstracts. Four articles met the inclusion criteria. These four studies are summarized in the table below. Two interventions provided patient education and counseling. One RCT (Guilera) reported a negative result. One NRHCT (Cook) reported significantly better adherence in the intervention cohort. The remaining two interventions utilized measurements of bone turnover markers (BTMs) to provide feedback to patients based on their response to therapy. One RCT (Clowes) had two intervention arms. Arm A (attention) showed statistically significant improvement in adherence over the observational cohort (no attention), whereas Arm B (attention and BTMs feedback) did not. The other RCT (Delmas) reported no significant difference in persistence between patients receiving BTMs feedback versus controls who did not receive such feedback.

**CONCLUSION:** Despite strong evidence of poor adherence and persistence with osteoporosis medications, few high quality interventions have been conducted. While some interventions produced encouraging findings, there is a need for new intervention types and rigorously controlled randomized trials to establish best practice for improving adherence and persistence with osteoporosis medications.

Article (Author/Yr)	Study Design <sup>*</sup>	Study Population Size (N) <sup>**</sup>		Description of Intervention <sup>***</sup>	Results <sup>****</sup>	
		Control	Intervention		Control	Intervention
Guilera, 2005	RCT	259	269	Attention, Counseling, Education	Adh: 53% Per: N/R	Adh: 47% Per: N/R
Cook, 2007	NRHCT	N/R	188	Attention, Counseling, Education	Adh: 41% Per: N/R	Adh: 69%† Per: N/R
Clowes, 2004	RCT	24	Arm A: 24 Arm B: 25	Arm A: Attention Arm B: Attention, BTMs feedback	Adh: 42% Per: 67%	Arm A: Adh = 68%† Per = 88% Arm B: Adh = 63% Per = 79%
Delmas, 2007	RCT	1113	1189	BTMs feedback	Adh: N/R Per: 77%	Adh: N/R Per: 80%

<sup>\*</sup>RCT=Randomized Controlled Trial, NRHCT=Non-randomized Historical Control Trial

<sup>\*\*</sup>N=population size analyzed at study endpoint, N/R=Not Reported

<sup>\*\*\*</sup>BTMs=Bone Turnover Markers

<sup>\*\*\*\*</sup>Adh=Adherence, Per=Persistence, N/R=Not Reported, †= P  $\leq$  0.05 for comparison with control outcome

**Disclosures:** T. Gleeson, None.

This study received funding from: NIH AR047782.

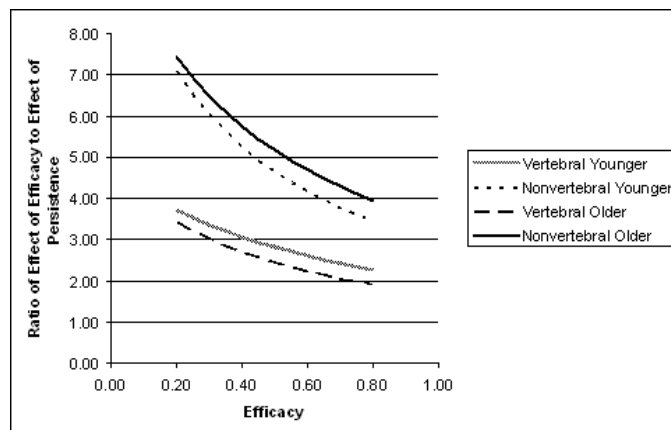
## M371

**The Relative Contributions of Nonvertebral Efficacy, Vertebral Efficacy, and Persistence in Determining Cost-Effectiveness: The Case of Osteoporosis and Implications for Payers.** C. M. L. Kelton<sup>\*1</sup>, M. K. Pasquale<sup>\*2</sup>. <sup>1</sup>College of Business, University of Cincinnati, Cincinnati, OH, USA, <sup>2</sup>Epidemiology & Pharmacoeconomics, Procter & Gamble Pharmaceuticals, Mason, OH, USA.

The cost-effectiveness literature on bisphosphonates to date has focused on the importance of improved persistence without placing its impact in the context of efficacy. The objective of this research was to determine the effects of persistence (the proportion of individuals who persist on treatment), vertebral efficacy, and nonvertebral efficacy, on incremental cost-effectiveness ratios (ICERs) for osteoporosis in order to enhance the payer's ability to evaluate the tradeoff between efficacy and persistence among competing treatments. We developed an ICER relative to Vitamin D plus calcium for postmenopausal osteoporotic women with BMD T-score  $\leq$  -2.5, completing one year of bisphosphonate treatment, and determined the relative contributions to the ICER of its inputs using a mathematical approach involving partial derivatives. Model inputs from the osteoporosis literature included fracture incidence rates for two age groups, 55-59 and 75-79, drug costs, and fracture treatment costs. Efficacy values were taken from randomized clinical trials. Outcomes were a series of effects of 1 percentage point changes in nonvertebral efficacy, vertebral efficacy, and persistence values on the ICER. The effects on the ICER of a 1 percentage point change in vertebral efficacy were 2.60 and 2.24 times the effect of a 1 percentage point change in persistence for the younger and older age groups, respectively; nonvertebral efficacy had 4.95 and 5.51 times the effect of persistence for the two groups,

respectively. As shown in Figure 1, these ratios are inversely related to the level of efficacy; however, even at 80 percent efficacy, the importance to the ICER of an increase in efficacy exceeds that of an increase in persistence. These results hold generally over a 3-year time period; for different discontinuation patterns; using cost-utility analysis; and in a generic-drug cost environment. In evaluating claims regarding enhanced persistence, formulary decision-makers need to exercise caution to ensure that efficacy, particularly nonvertebral efficacy, is not compromised.

Figure 1. Relative contribution of efficacy versus persistence for different levels of efficacy



**Disclosures:** C.M.L. Kelton, Christina M.L. Kelton 2.

This study received funding from: The Alliance for Better Bone Health.

## M372

**Preference and Satisfaction with a 6-Monthly Subcutaneous Injection Versus a Weekly Tablet for Treatment of Low Bone Mass.** D. T. Gold, R. Horne\*, J. Borenstein\*, S. Varon\*, D. Macarios\*. Amgen Inc., Thousand Oaks, CA, USA.

Preference and satisfaction are important for maintaining compliance and persistence with chronic therapies for treating bone loss. We compared subject preference and satisfaction between two bone loss agents: a subcutaneous (SC) injection of an investigational product (denosumab) administered every 6 months (Q6M) with an oral tablet (alendronate) taken weekly.

Preference and satisfaction were assessed as part of the ongoing development of a new questionnaire in a phase 3 international, randomized, double-blind, double-dummy, active-controlled study. Healthy postmenopausal women, T-score  $\leq -2.0$  (total hip or spine) were randomized 1:1 to receive: denosumab injection (SC, 60 mg Q6M) + placebo tablet (oral weekly) or placebo injection (SC Q6M) + oral alendronate (70 mg weekly). After 12 months of treatment, subjects were asked to complete a 34-item questionnaire to rate their preference for and satisfaction with each agent. Preference and satisfaction were assessed based on single items and were pre-specified endpoints. Subjects were asked to choose either: the pill, the injection, or neither, for preference ("Which do you prefer?") and satisfaction (With which frequency of administration have you been more satisfied?).

In total, 1189 subjects (594 denosumab; 595 alendronate) with a mean age of 64.4 yrs enrolled. 1100 (92.5%) subjects completed the questionnaire. Some subjects in each group did not report a preference (alendronate = 101; denosumab = 96) or satisfaction (alendronate = 123; denosumab = 125). Among those who reported a preference/satisfaction, more subjects preferred and were more satisfied with the Q6M injection over the weekly tablet (Table). Similar proportions of subjects in the alendronate group or denosumab group preferred or were more satisfied with the Q6M injection compared with the weekly tablet.

As reported by others,<sup>1,2</sup> subjects in this study preferred and were more satisfied with a therapeutic agent that was dosed less frequently. Preference for and greater satisfaction with the frequency of a subcutaneous injection given Q6M compared with current weekly oral agents for the treatment of bone loss in postmenopausal women may be an important factor in helping improve compliance and persistence with therapy.

1. Reginster et al. Bone. 38:S2-6, 2006.

2. Simon et al. Clin Ther. 24:1871-88, 2002.

Subject Preference For and Satisfaction With Q6M Injection or Weekly Tablet			
	Age (years) - Mean (SD)	Preference n (%)	Satisfaction with Frequency n (%)
Alendronate + Placebo injection (N = 545)	64.6 (8.3)	Q6M Injection 339 (77)	331 (80)
		Weekly Tablet 101 (23)	83 (20)
		Within group P-value	<0.0001 <0.0001
		Q6M Injection 352 (77)	338 (79)
Denosumab + Placebo tablet (N = 555)	64.1 (8.6)	Weekly Tablet 107 (23)	89 (21)
		Within group P-value	<0.0001 <0.0001
		Between group P-value	0.8329 0.9256

**Disclosures:** D.T. Gold, Amgen 1, 2; P&G/Sanofi-Aventis 1, 2, 4; Eli Lilly 1, 2, 4; Merck/Novartis 1, 4.

This study received funding from: Amgen Inc.

## M373

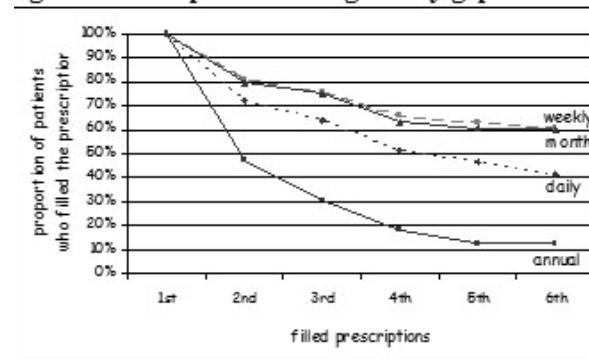
**Patient Refill Behavior among Select Daily, Weekly, Monthly, and Annual Dosing Regimens.** D. Gold<sup>1</sup>, N. Borisov<sup>2</sup>, W. Safi<sup>2</sup>. <sup>1</sup>Duke University Medical Center, Durham, NC, USA, <sup>2</sup>Procter & Gamble Pharmaceuticals, Mason, OH, USA.

Patient refill behavior follows the same trend across many different therapeutic classes suggesting many factors influence the refill trend. Less frequent dosing regimens have been introduced to impact this trend. This study explored patient refill trend among daily, weekly, monthly regimens of bisphosphonate therapy and explored annual dosing proxy using two integrated administrative medical claims databases (Ingenix Lab/Rx<sup>TM</sup> and Medstat MarketScan<sup>®</sup>).

The study included women 50+ years with a new prescription fill for either daily (risedronate 5mg, alendronate 5/10 mg), weekly (risedronate 35mg, alendronate 35/70 mg), or monthly (ibandronate 150 mg) treatment between July 1, 2000 and December 31, 2005. Data for the annual osteoporosis treatment (zoledronate 5mg/100 ml) were not available in the databases at the time of the study; thus, we used annual flu shot data as a proxy for the annual treatment regimen. Discontinuation was defined as either a gap between refills longer than a predefined number of days, switching between regimens, disenrollment from a plan, or end of database. Women were followed up to 6 continuous prescriptions of each treatment to measure proportion of patients refilling each script. Effect of various length of the allowable gap between prescriptions on the refill pattern was examined.

We identified 26,228 (6%) women who initiated daily, 404,149 (89%) women initiated weekly, and 24,854 (5%) initiated monthly bisphosphonate therapy. There were 2,534,860 patients who had a first flu shot during the study period. Varying the length of the gap between scripts from 15 to 90 days increased proportion of women who refilled the second script from 10 to 12 points among regimens. Figure 1 shows refill patterns using 45-day refill gap. Women who discontinued after 2 scripts had significantly less concomitant medications, specialist visits, hospitalizations, and fractures compared to women who filled all 6 scripts of either daily or monthly therapy. No difference between these groups was observed among women on monthly therapy. In this study, dosing regimens exhibited similar refill patterns among women 50+ years. Refill trend of weekly and monthly dosing regimens was observed to be nearly identical. The highest rate of discontinuation occurs within the first 3 to 4 script refills regardless of the dosing frequency.

Figure 1. Refill patterns using 45-day gap between refills



**Disclosures:** D. Gold, P&G 2.

This study received funding from: The Alliance for Better Bone Health (Procter & Gamble Pharmaceuticals and sanofi-aventis).

## M374

**The Impact of Dosing Frequency in Compliance with Bisphosphonates Among Postmenopausal Japanese Women for Osteoporosis Treatment.** Y. Nomura\*. Obstetrics and Gynecology, Yokohama City University, Yokohama, Japan.

[Object] Osteoporosis is an asymptomatic disease that increases fracture risk and results in considerable morbidity, mortality, and reduced quality of life. The main aim of osteoporosis management is to prevent the occurrence of fractures. To benefit, it appears that women must remain on therapy for an extended period. Bisphosphonate provides efficacious treatment for osteoporosis. However, side effects and dosing regimens often lead to patients discontinuing this treatment. Reducing oral Bisphosphonate dosing frequency is one measure available to increase therapy. This study compared compliance with weekly and daily Bisphosphonate regimens for postmenopausal osteoporosis.

[Method] Ninety postmenopausal Japanese women diagnosed with osteoporosis or osteopenia were enrolled in this study. These postmenopausal women (aged 66.2 years old) were asked some questions about their social background and treated with Alendronate 5mg/day and Alendronate 35mg/week, respectively. This study continued for 12 weeks after starting the given prescription. Explanations of anti resorptive therapy and study were done by professionals. Compliance was measured as a Medication possession ratio, defined as the proportion of days for which patients had prescription coverage prescription. [Results] The social background of the ninety postmenopausal Japanese women is different. 12(13.3%)patients live alone, 18(20%)patients have a job, 54(60%)patients have been taking other medicine. In their various lifestyles, weekly regimens had a higher compliance than those on daily regimens. Once-weekly dosing and daily dosing were well tolerated with a similar result. With regards to esophageal events, there were fewer upper GI and a trend toward a lower incidence in the once-weekly dosing compared to the daily dosing. After this, 78(87%)postmenopausal osteoporosis women want to prescribe a weekly Bisphosphonate dose. Dosing frequency was the strongest predictor of time to discontinuation.

[Conclusion] This study suggests that less frequent dosing intervals may provide an opportunity to further improve the consistent use of Bisphosphonate therapy. Without regard to any life style, dosing convenience is a key element to enhance compliance and long-term persistence with therapy.

**Disclosures:** Y. nomura, Kentaro Kurasawa Hiromi Yoshikata 1; Rituko Kikui 1; Osamu Chaki 1; Fumiki Hirahara 1.

## M375

**Correlates of Osteoporosis Treatment Persistence For Patients New to Therapy and Patients with Recent Switches: 6-Month Results from POSSIBLE US™.** A. N. A. Tosteson<sup>1</sup>, S. Wade<sup>\*2</sup>, M. Anthony<sup>3</sup>, C. Brancato<sup>\*4</sup>, S. Nichols<sup>\*4</sup>, R. W. Downs<sup>\*5</sup>. <sup>1</sup>Dartmouth Medical School, Hanover, NH, USA, <sup>2</sup>Wade Outcomes Research and Consulting, Salt Lake City, UT, USA, <sup>3</sup>Amgen Inc., Thousand Oaks, CA, USA, <sup>4</sup>REGISTRAT, Lexington, KY, USA, <sup>5</sup>Virginia Commonwealth University, Richmond, VA, USA.

Poor osteoporosis medication adherence has been associated with increased fracture incidence, yet few studies examine treatment persistence and its correlates in primary care settings. To study osteoporosis medication use, 134 US primary care physicians enrolled postmenopausal women in the Prospective Observational Scientific Study Investigating Bone Loss Experience (POSSIBLE US™). We report 6-month treatment persistence and related factors for 1217 women who (1) initiated pharmacologic therapy within 6 months of study entry and had no therapy in the prior 12 months (new), or (2) had transitioned between pharmacologic agents within 6 months of study entry (switch).

Physician and participant-reported study entry data on age, prior fracture, BMD, demographics, lifestyle/behaviors, medication class, medication side effects (none, mild, moderate, severe), treatment satisfaction using the Treatment Satisfaction Questionnaire for Medication (TSQM-efficacy, -convenience, -global subscales), and health status using EQ-5D and OPAQ were evaluated as correlates of treatment discontinuation using multiple logistic regression. We report odds ratios (OR) and 95% confidence intervals (CI) for factors related to 6-month treatment discontinuation.

At study entry, 825 women (68% of 1217) were new to pharmacologic therapy; 392 (32%) had recently switched. Most patients reported bisphosphonate use (new: 80%; switch: 73%). At entry, new and switch patients had similar health status, race, and education; however switch patients were older (67 y vs 64 y,  $p<0.001$ ) and more often had an osteoporosis diagnosis (56% vs 40%,  $p<0.001$ ). Follow-up (6-month) was available for 1106/1217 (91%). Overall, 84% (929/1106) continued the study entry agent at 6 months. Compared to those continuing therapy, discontinuers were older (67 y vs 65 y,  $p=0.019$ ), more likely to report severe side effects (29% vs 14%,  $p=0.003$ ) and have lower TSQM-convenience (70.0 vs 76.2,  $p<0.001$ ), -efficacy (60.9 vs 64.5,  $p=0.02$ ) and -global scores (58.3 vs 64.4,  $p<0.001$ ). In adjusted analyses, significant correlates [OR (95% CI)] of discontinuation at 6 months were age [1.02 (1.00, 1.04)], side effects [mild: 1.70 (1.02, 2.85); moderate: 2.12 (1.27, 3.54); severe: 4.68 (2.50, 8.78)], TSQM convenience [0.98 (0.97, 0.99)] and being new to therapy [1.75 (1.14, 2.71)]. In this 6-month period, age, side effects, perceived convenience and efficacy, and being new to therapy were related to early discontinuation.

**Disclosures:** A.N.A. Tosteson, Amgen 4; P&G Pharmaceuticals 2; GlaxoSmithKline 4. This study received funding from: Amgen Inc.

## M376

**Medication Switching in Postmenopausal Women on Osteoporosis Therapy: Six-Month Findings from the POSSIBLE US™ Study.** T. Do<sup>\*1</sup>, S. Wade<sup>\*2</sup>, M. Anthony<sup>3</sup>, R. B. Wagman<sup>4</sup>, R. W. Downs<sup>\*5</sup>. <sup>1</sup>Amgen Inc., Seattle, WA, USA, <sup>2</sup>Wade Outcomes Research and Consulting, Salt Lake City, UT, USA, <sup>3</sup>Amgen Inc., Thousand Oaks, CA, USA, <sup>4</sup>Amgen Inc. and Stanford University School of Medicine, San Francisco and Stanford, CA, USA, <sup>5</sup>Virginia Commonwealth University, Richmond, VA, USA.

Although research is accumulating on medication adherence in osteoporosis (OP) little is known about the occurrence and causes of medication switching.

The Prospective Observational Scientific Study Investigating Bone Loss Experience (POSSIBLE US™) follows 4994 postmenopausal US women on OP therapies for up to 3 years, with self-administered questionnaires every 6 months. From October 2005 to January 2007, 134 primary care physicians enrolled women with varying therapy history. Analysis cohorts were created for new (initiating pharmacologic therapy in last 6 months, no therapy prior 12 months), stable (at least 6 months on same pharmacologic regimen), switch (transitioned between pharmacologic agents within 6 months), augment (added a pharmacologic agent to existing regimen), or calcium/vitamin D use only. We examined the first patient-reported switch (discontinuation of agent used at entry then initiation of new agent) between study entry and first follow-up assessment (approximately 6-month), reasons for switching, and patient characteristics associated with switching.

Nearly 70% (n=3414) of patients reported OP therapy use at study entry and had follow-up data at 6 months. Most (n=1877) patients reported bisphosphonate (BP) use at entry. Three percent (n=102) of the cohort reported at least 1 switch. BP users comprised 81% of switchers and 64% (n=65) of switchers switched within the drug class reported at entry. Among BP switchers, patient-reported side effects were the most common reason for switching (40%). Women entering POSSIBLE US™ as new, switch or augment patients were somewhat more likely to switch than women on stable therapy. After adjusting for age, race, education, fracture history, report of severe side effects and number of comorbidities, the increased risk of switching persisted only for new patients (Table).

Side effects and recent therapy initiation were associated with a higher likelihood of medication switching, even during a short time window. The longitudinal data accumulating from POSSIBLE US™ will be used to further test these associations.

**Table. Hazard Ratios for Switching Pharmacologic Agents Between Study Entry and A1\***

	Unadjusted HR (95% CI)	Adjusted HR (95% CI)**
Status at study entry		
	3414 women	3331 women
	102 switchers	102 switchers
	1830.0 person-years	1783.9 person-years
Stable	1.0	1.0
New	1.66 (1.06, 2.60)	1.68 (1.07, 2.64)
Augment	2.40 (1.07, 5.39)	2.26 (1.00, 5.09)
Switch	1.37 (0.74, 2.53)	1.37 (0.74, 2.55)
Calcium/ Vitamin D	0.32 (0.11, 0.90)	0.31 (0.11, 0.89)

\*Stable patients are referent group. \*\*Adjusted for differences in age, race, education, fracture history, comorbidity, patient report of severe side effects.

**Disclosures:** T. Do, Amgen 5.

This study received funding from: Amgen Inc.

## M377

**Osteoporosis Therapy following Bone Densitometry - Patient Expectations as Determinants of Drug Initiation and Persistence.** D. Brask-Rasmussen<sup>\*1</sup>, S. M. Cadarette<sup>\*2</sup>, P. Eskildsen<sup>\*1</sup>, B. Abrahamsen<sup>3</sup>. <sup>1</sup>Department of Endocrinology, Køge University Hospital, Køge, Denmark, <sup>2</sup>Division of Pharmacoepidemiology and Pharmacoeconomics, Brigham and Women's Hospital, Harvard Medical School, Boston, MA, USA, <sup>3</sup>Department of Endocrinology, Copenhagen University Hospital, Gentofte, Denmark.

Persistence with osteoporosis therapy has been disappointingly low in the past, possibly related to poor patient perception of treatment benefits.

We assessed health beliefs among patients with osteoporosis in relation to initiation of and persistence with bisphosphonate treatment.

A mailed questionnaire was sent to 1000 consecutive patients, who had been referred to DXA-scanning in a Danish osteoporosis clinic one year earlier, to assess osteoporosis treatment, persistence and beliefs. Patients and GPs had received written information on diagnosis and treatment recommendations shortly after the DXA-exam. Of the 1000 patients, 717 responded to the questionnaire (72%).

Initiation of OT had been recommended to 146 patients with osteoporosis. Of these 83% began treatment, hereof 90% with a bisphosphonate. The self-reported persistence with bisphosphonate one year after DXA assessment was 86%.

The likelihood of initiating a recommended treatment was assessed by multivariate logistic regression demonstrating significant association with beliefs in treatment benefits (OR 1.6, 95% CI 1.2-2.2,  $p<0.01$ ) but not with treatment barrier beliefs, sex or age of the patient. No significant association with persistence and beliefs, sex or age could be established for discontinuation of treatment. Side effects were reported as the main reason for discontinuing treatment.

While the encouragingly low rate of discontinuation among respondents limited the information available on factors associated with persistence, the study suggest that initiation of bisphosphonate treatment is linked to patient perception of drug benefits. This highlights the need to improve communicative strategies, perhaps especially related to conveying the message of anti-fracture efficacy

**Disclosures:** D. Brask-Rasmussen, None.

## M378

**Predictors of Self-Reported Non-persistence with Oral Bisphosphonates Due to Perceived Side Effects or Other Reasons.** J. T. Schousboe, B. Dowd\*, M. Davison\*, P. Johnson\*, R. L. Kane\*. Univ of Minn, Minneapolis, MN, USA.

**Background:** Non-persistence with drug therapy to prevent fractures remains a major obstacle to reducing the population burden of osteoporotic fractures. Our objective was to estimate the association of attitudes to medication, the patient-perceived quality of the MD-patient relationship, medication use self-efficacy, and other predictors to self-reported non-persistence due to side effects or other reasons.

**Methods:** 1179 patients prescribed an oral bisphosphonate between 1/1/2006 & 3/31/2007 were mailed a survey to assess medication adherence and attitudes toward osteoporosis and medication to reduce fractures. 729 (63%) returned the survey and had complete data. Perceived medication need, concerns about dependence upon and long-term safety of medication, medication use self-efficacy, and medication cost concerns were assessed by Likert scales. Number of adverse drug reactions (ADRs), bone density, and use of proton pump inhibitors (PPI) (a marker of gastric acidity disorder) were extracted from the medical record. The associations of these predictors with non-persistence were assessed with logistic regression models.

**Results:** Self-reported non-persistence due to side effects were associated with perceived medication need (odds ratio (OR [95% C.I.]) of 0.20 [0.10-0.41] for the top vs bottom quartile), medication concerns (OR 1.41 [1.05-1.89] per unit increase), PPI use (OR 1.63 [1.06-2.52]),  $\geq 2$  ADRs (OR 3.24 [1.84-5.69] vs no ADRs). Non-persistence for reasons other than side effects were associated with perceived medication need (OR 0.24 [0.12-0.49] for top vs bottom quartile), with poor medication use self-efficacy (OR 1.74 [1.13-2.70] vs excellent self-efficacy) and with very high medication cost concerns (OR of 4.85 [1.96-12.0] vs no cost concerns). MD-patient relationship quality was not associated directly with non-persistence, adjusting for all of these other predictors.

**Conclusion:** Patients are less likely to stop taking medications due to side effects if they feel they need fracture prevention medication to preserve their health, do not have concerns about long-term safety or dependence on medications, have not had other adverse drug reactions, and are not on a PPI. Patients are less likely to discontinue oral bisphosphonates for reasons other than side effects if they have confidence they can execute medication use in their daily lives (medication self-efficacy), do not feel burdened by their out of pocket medication costs, and perceive need for fracture prevention therapy. These results are strongly consistent with most non-persistence with bisphosphonate medication being the result of deliberate discrete choices.

**Disclosures:** J.T. Schousboe, Roche, Inc 2.

## M379

**Attitudes to Fracture Prevention in Long-term Care Facilities: A Multi-centre Study Examining the Opinions of Nursing Home Staff.** A. M. Sawka<sup>1</sup>, M. Nixon<sup>2</sup>, L. Giangregorio<sup>3</sup>, L. Thabane<sup>4</sup>, J. D. Adachi<sup>2</sup>, A. Gafni<sup>4</sup>, P. Raina<sup>4</sup>, A. Papaioannou<sup>2</sup>. <sup>1</sup>Medicine, University Health Network and University of Toronto, Toronto, ON, Canada, <sup>2</sup>Medicine, McMaster University, Hamilton, ON, Canada, <sup>3</sup>Kinesiology, University of Waterloo, Waterloo, ON, Canada, <sup>4</sup>Clinical Epidemiology and Biostatistics, McMaster University, Hamilton, ON, Canada.

**Objectives:** In this secondary analysis, our objective was define attitudes of staff in long-term care facilities to strategies for prevention of hip fracture in residents.

**Design, Setting, and Participants:** We conducted a cross-sectional study that collected data using a self-administered, written questionnaire. We collected data from 160 staff in five nursing homes in the region of Hamilton, Ontario, Canada. For questions on opinions on fracture prevention strategies, questions were framed on a seven point Likert scale (1=strongly disagree, 7=strongly agree), with a check box for "don't know" responses.

**Results:** The most common job descriptions of respondents were: health care aide 56.9% (91/160) and registered or practical nursing 26.9% (43/160). Approximately a third of respondents were 50 years or older in age (52/160). Responses were mixed to a question asking if we are currently doing enough to prevent fractures in long-term care facilities, mean 4.4 on a seven point Likert scale with a standard deviation (SD) 1.8. Approximately sixty-one percent of respondents (97/160) indicated that they did not know if bisphosphonates decrease the risk of hip fracture. More than half of respondents indicated that they did not know if hip protectors decrease the risk of hip fracture (86/160, 54%). For statements suggesting that it is important to provide fracture-prevention interventions to all long-term care facility residents, the respondents scores according to intervention, were as follows: calcium supplements 5.4 (SD 1.6) (n=141 agreement responses), vitamin D supplements 5.4 (SD 1.6) (n=124), hip protectors 4.3 (SD 2.1) (n=114).

**Conclusions:** Knowledge translation strategies should be developed to improve the awareness of staff working in long-term care facilities on effective fracture prevention strategies for elderly residents, in an effort to improve uptake and adherence of such strategies.

**Disclosures:** A.M. Sawka, None.

*This study received funding from: Interdisciplinary Capacity Enhancement (ICE) (Grant #: ICH63069) Team Grant focused on Reducing the Burden of Injury in Canada from The Canadian Institutes of Health Research (CIHR) and the Ontario Ministry of Health Long-term Care Strategies Program.*

## M380

**Strategies for Hip Fracture Prevention in Long-term Care Facilities: A Survey of Canadian Geriatricians and Family Physicians.** A. M. Sawka<sup>1</sup>, L. Thabane<sup>2</sup>, J. D. Adachi<sup>3</sup>, A. Gafni<sup>4</sup>, P. Raina<sup>4</sup>, S. Straus<sup>5</sup>, A. Papaioannou<sup>3</sup>.

<sup>1</sup>Medicine, University Health Network and University of Toronto, Toronto, ON, Canada, <sup>2</sup>Clinical Epidemiology and Biostatistics, McMaster University, Hamilton, ON, Canada, <sup>3</sup>Medicine, McMaster University, Hamilton, ON, Canada, <sup>4</sup>Clinical Epidemiology, McMaster University, Hamilton, ON, Canada, <sup>5</sup>Medicine, University of Calgary and University of Toronto, Toronto, ON, Canada.

**Objectives:** Our primary objective is to identify strategies that Canadian physicians with expertise elder- or long-term care recommend for decreasing the risk of hip fracture in elderly in elderly nursing home residents. A secondary objective is to identify the barriers associated with the implementation of various strategies for prevention of hip fracture in elderly nursing home residents.

**Design, Setting, and Participants:** We are currently conducting a cross-sectional study, collecting data using a self-administered, written questionnaire. The written questionnaire was mailed on April 1, 2008 to more than two hundred Canadian Geriatricians in active practice as well as Ontario Family Physicians belonging to the Ontario Long-term Care Association. A case-based approach in a self-administered written questionnaire is being utilized. Anti-fracture strategies being examined include: calcium, vitamin D, other vitamin therapies, pharmacologic osteoporosis therapies, hormonal therapies, hip protectors, physical therapy, and environmental modification. The nature of barriers to implementation of such strategies in the long-term care setting will be identified.

**Results:** The final results of the survey will be presented. We hypothesize that strategies such as provision of hip protectors, bisphosphonates, vitamin D, or environmental modification may be recommended in decreasing the risk of hip fracture in elderly nursing home residents. We suspect that barriers to use of pharmacologic therapies will include side effect profiles of medications, poor compliance with proper administration of strategies, prescribing contra-indications and expense. We suspect that compliance may be a barrier for use of devices such as hip protectors.

**Disclosures:** A.M. Sawka, None.

*This study received funding from: Interdisciplinary Capacity Enhancement (ICE) (Grant #: ICH63069) Team Grant focused on Reducing the Burden of Injury in Canada from The Canadian Institutes of Health Research (CIHR) and the Ontario Ministry of Health Long-term Care Strategies Program.*

## M381

**Medication Prescription and Adherence after Hospitalization for Osteoporotic Vertebral Fracture.** H. Leydet-Quilici, M. Luc\*, Y. Grandgeorge\*, T. Pham\*, P. Lafforgue\*. Hopital la Conception, Marseille, France.

Several studies have demonstrated the lack of secondary prevention of osteoporotic non vertebral fractures, but treatment prevention of osteoporotic vertebral fractures (VF) is little assessed. Our study goal was to assess treatment prescription when patients got out from the hospital and medication adherence at least one year after.

We studied patients hospitalized between 2005 and 2006 for osteoporotic sacral or VF, in a Rheumatology Department in a tertiary referral hospital. From Sept. to Dec. 2007, all patients were interviewed, following a standardized questionnaire on treatment adherence. Patients dead, unreachable, or who wished not to answer were excluded from the analysis. Non-adherence was defined as absence of any ongoing antiosteoporosis treatment (i.e. calcium, calcitriol, raloxifen, oral or i.v. bisphosphonates, strontium or teriperatide) at the survey time. Patients were adherent if they were still carrying on an active treatment, even if this treatment was not the one prescribed during hospitalization. Calcium and calcitriol were assessed separately from the other treatments.

On 63 screened patients, 43 were analyzed : women 86%; mean age 77 years. 86% experienced previous insufficiency fractures and only 42% were previously treated for osteoporosis. All patients received a specific anti-osteoporotic treatment and 97% calcitriol and calcium prescription at the hospital leaving time. The mean time between prescription and survey was 16.7 months. Adherence was 69.8% for calcitriol and calcium and 86% for anti-osteoporotic specific treatment. The main treatment giving up reason was a GP care instead of a rheumatologist care (p=0.01). Daily treatment (calcium and calcitriol), maybe considered as compeller, had lesser observance and adherence.

Our study showed higher prescription and adherence levels compared to those usually reported. The main reasons are : the context (symptomatic VF requiring an hospitalization versus asymptomatic VF), the situation (tertiary referral hospital) and a rheumatologist care for nearly 50% of patients. These results can not be extrapolated to all prevalent osteoporotic VF.

**Disclosures:** H. Leydet-Quilici, None.

## M382

**The Influence of Bone Osteoporotic Fractures in the Past on the Persistence of Pharmacological Treatment in Osteoporosis. Pomost study.** J. Przedlaci, K. Ksiopolska-Orowska\*, A. Grodzki\*, T. Bartuszek\*, D. Bartuszek\*, A. Swirski\*, J. Musia\*, E. Luczak\*, E. Loth\*, P. Teter\*, A. Lasiewicki\*, A. Walkiewicz\*, I. Drozdowska-Rusinowicz\*. National Center of Osteoporosis, Warsaw, Poland.

The purpose of the study was to evaluate the influence of the past bone osteoporotic fracture on the persistence of pharmacological treatment in osteoporosis. The study, as a part of POMOST study (evaluation of different aspects of medical procedures in osteoporosis) was done in KCO with participation of 188 patients who signed informed consent (28 men and 160 women, aged 70.0±7.3 years). All patients were divided into 2 groups: 89 patients with the past bone osteoporotic fracture (spine, hip or/and forearm; no-one referred to KCO due to actual fracture) and 99 patients without fracture. Evaluation of the fracture risk, decision on the need of pharmacological treatment and the method of it, as well as the control visit after 3 months were done in KCO. Next, the follow up was done by specialists or GPs. The final evaluation of persistence of therapy after 12 months was planned in KCO. Persistence of treatment was evaluated on the basis of patients visit in KCO (after 3 and 12 months). Patients were treated with medicines of approved antifracture activity (mainly weekly oral bisphosphonates), vitamin D and calcium.

After 12 months 84 patients (68.3% of 123 patients who in accordance to visits schedule ought to finish the treatment, 58 with and 65 without fracture; NS) came to KCO. 31 patients continue the treatment (between 3. and 12. month). 50 patients (26.6% of all, 28 with and 22 without fracture; NS) stopped the treatment before 3 months. 17 patients (9.0% of all; 10 with and 7 without fracture; NS) stopped the treatment after 3. month. Adverse events were the primary reason of discontinuation of therapy in all groups. We called patients who did not visit our center after expected 12 months of treatment. Nine patients out of 14 who were reached by phone (4 with and 5 without past fracture) were still interested in the therapy and were referred to KCO once more. Next 3 consider it. The lack of easy contact with specialists and the lack of stimulation by their GPs to continue the treatment in the case of adverse events was important reason in patients opinion of discontinuation of therapy.

We conclude that, contrary to our expectations, there was not difference in persistence of pharmacological treatment in osteoporosis between patients with and without past bone osteoporotic fracture. Incidents of fractures in past, sometimes several years ago did not motivate patients to treatment. Closer contact with doctors (specialist or GPs) and referral to specialist center just after bone osteoporotic fracture could have stronger impact on persistence of the treatment.

**Disclosures:** J. Przedlaci, None.

## M383

**Ambiguity about Osteoporosis and Osteoporosis Care Exists Despite a Screening Program to Educate Fracture Patients.** J. E. M. Sale\*, D. E. Beaton, R. Sujic\*, E. R. Bogoch. Mobility Program Clinical Research Unit, Keenan Research Centre, Li Ka Shing Knowledge Institute, St. Michael's Hospital, Toronto, ON, Canada.

Behaviour change models suggest that people need to have clear information about their susceptibility to disease and treatment recommendations before they will successfully change their behaviour. We conducted a qualitative study to examine fracture patients' understanding of osteoporosis (OP) and OP care after being screened for OP in an urban hospital fracture clinic. English-speaking patients who were screened for OP through the fracture clinic in the previous 3-9 months and did not demonstrate any physical or cognitive impairments that would prevent them from participating were eligible. Forty-seven patients were identified by one of two screening coordinators and 24 (18 females, 6 males) aged 47-80 years old agreed to participate in 1 of 5 focus groups. During the focus groups, participants were asked about their awareness of OP and status of BMD testing and OP treatment. Twenty participants vocalized at least one expression of ambiguity regarding OP and/or treatment recommendations conveyed by the screening program staff. Participants were ambiguous about the cause of their fracture, the BMD test process and results, and the presentation of OP. They were also ambiguous about the amount and type of medication and supplements recommended. Despite a standardized screening program in which OP was addressed in fragility fracture patients, ambiguity about diagnosis, testing, and treatment were described. Efforts to clarify information relayed to fracture patients about their condition and recommended care need to extend beyond the fracture clinic so that health care providers can promote long-term adherence to these recommendations.

**Disclosures:** J.E.M. Sale, None.

This study received funding from: Ontario Ministry of Health and Long-Term Care.

## M384

**Adherence in Patients with Severe Osteoporosis Treated with Teriparatide.** V. Ziller\*, S. Zimmermann\*, P. Hadji. University Hospital Giessen and Marburg, Marburg, Germany.

Introduction: Medical interventions play a key role in the treatment of severe postmenopausal osteoporosis but patients adherence to medical therapy is essential for optimal clinical outcomes. While adherence in RCT's is usually around 70-90% we were

able to show that in clinical routine 12 months after therapy initiation only 27.8% and 46.5% of the women on oral daily vs. weekly Alendronate were still on treatment. Data on adherence with treatment of severe postmenopausal osteoporosis with subcutaneous Teriparatide (TPT) in daily clinical routine have not been published. The aim of the present analysis was to investigate adherence with TPT in women visiting our out-patient clinic.

**Material and Methods:** We investigated a sample of 50 postmenopausal women with severe postmenopausal osteoporosis on TPT in accordance to the German guidelines. Treatment was initiated at least 12-24 months before recruitment. We combined patient self report using a validated questionnaire and the medication possession ratio (MPR). To calculate MPR we performed a prescription control including all doctors who were treating the patients for any disease. Finally patients were classified adherent if self-reported adherence and a MPR of  $\geq 80\%$  was achieved.

**Results:** There were no significant differences in baseline demographics, except for age at menopause which was significantly lower in the compliant group (46.1 vs. 50.0;  $p<0.006$ ). Our results comprised that 80% of the patients treated with TPT in our clinic were compliant, while 20% were noncompliant after 12 months. A significant correlation to treatment adherence was found only for self-reported medication toleration ( $p<0.001$ ).

**Discussion:** In the past numerous studies have underlined, especially for Bisphosphonates, that an optimal compliance was necessary to ensure the therapeutic treatment effect. Concerning oral long-term treatment in postmenopausal Osteoporosis our results indicate that compliance with TPT seems to be higher than expected. Further prospective studies are needed to investigate possible factors influencing treatment adherence.

**Disclosures:** V. Ziller, Novartis Germany 2; Lilly Germany 2; Daiichi Sankyo Germany 2; Procter&Gamble Germany 2.

## M385

**Safety and Effectiveness Profile of Raloxifene in Long-term Prospective Observational Study; Interim Analysis.** A. Miyauchi<sup>1</sup>, E. Hamaya<sup>1</sup>, D. Tsuzuki<sup>1</sup>, H. Kishimoto<sup>1</sup>, F. Yoshiki<sup>1</sup>, H. Okada<sup>1</sup>, H. Kobayashi<sup>2</sup>, S. Yokoyama<sup>2</sup>, A. Tanaka<sup>2</sup>, H. Tara<sup>1</sup>. <sup>1</sup>Eli Lilly Japan K.K., Kobe, Japan, <sup>2</sup>Chugai Pharmaceutical Co., LTD., Tokyo, Japan.

Raloxifene (RLX) is the first launched selective estrogen receptor modulator (SERM) for the treatment of osteoporosis in Japan. This large scale post marketing surveillance of RLX was designed to assess the safety of RLX in Japanese postmenopausal osteoporosis patients in long term practical use (three years). The present interim analysis was conducted using data from 6846 patients (mean age: 70.5 years) completed for 6 months and up to 12 months survey after treatment with open-label RLX therapy. The persistence of RLX administration at 180 days after treatment was 72.9%. Overall RLX was well tolerated and exhibited a favorable safety profile. A total of 664 adverse drug reactions (ADRs) out of 561 patients (8.14%) were reported. Most frequently observed ADR was gastrointestinal disorder (201 events) including stomach discomfort. One serious and 6 non-serious events of venous thromboembolism (VTE) (total 7 cases 0.10%) were reported. All 6 cases with known outcomes have recovered. Regarding efficacy, lumbar spine bone mineral density (BMD) increased significantly ( $p<0.05$ , paired t-test) compared with baseline both at 6 (2.6%) and 12 months (2.8%), comparable to the result of the Japan registration trial (Morii H et al. (2003) Osteoporosis Int 14:793-800). Significant decreases in serum and urinary type I collagen N-terminal telopeptide (NTX), urinary deoxypyridinoline (DPD) levels from baseline were observed as early as 3 months, followed by a significant decrease of serum bone specific alkaline phosphatase (BAP) at 6 months ( $p<0.01$  for all comparisons, signed rank test), indicating typical pattern of bone marker changes by antiresorptive therapy. The incidence of any new clinical fractures within 1 year (mean administration period 274 days) was 0.4% (29 cases), possibly supporting the result from a post hoc analysis used pooled data of Japan and China registration trials (Nakamura T et al. (2006) J Bone Miner Metab 24:414-418).

In summary, from this interim analysis of a prospective large scale post marketing surveillance, no new signal in safety was observed in the daily use of RLX and the VTE observation suggests a lower incidence in Japanese than in Caucasian women. Moreover, RLX exhibited a stable antiresorptive action on bone turnover leading to BMD increases in real clinical settings.

**Disclosures:** A. Miyauchi, Eli Lilly Japan K.K. 3.

This study received funding from: Eli Lilly Japan K.K., Chugai Pharmaceutical Co., LTD.

## M386

**Effects of Arzoxifene on Bone Turnover and Safety in Postmenopausal Women with Low Bone Mass: Results from a 6-Month Phase 2 Study.** R. Downs<sup>1</sup>, A. H. Moffett<sup>2</sup>, A. Ghosh<sup>3</sup>, D. A. Cox<sup>4</sup>, K. Harper<sup>4</sup>. <sup>1</sup>Virginia Commonwealth University, Richmond, VA, USA, <sup>2</sup>OB-GYN Associates of Mid-Florida, PA, Leesburg, FL, USA, <sup>3</sup>Johnson and Johnson PRD, Raritan, NJ, USA, <sup>4</sup>Eli Lilly & Company, Indianapolis, IN, USA.

Preclinical studies suggest that arzoxifene (ARZ), a benzothioephene selective estrogen receptor modulator (SERM), has an improved bone efficacy and a similar endometrial safety profile to raloxifene (RLX) 60 mg/d. This 6-month, phase 2, multicenter, randomized, double-blind, placebo (PBO)- and active-controlled (RLX) study was designed to assess the effects of various doses of ARZ on bone turnover markers and overall safety in postmenopausal women with low bone mass.

Healthy postmenopausal women (N=219; mean age, 59 yrs) with a lumbar spine or femoral neck T-score between -1 and -2.5 were randomly assigned to ARZ 5 (N=34), 10 (N=33), 20 (N=34), or 40 mg (N=40), RLX 60 mg (N=37), or PBO (N=41). All women received daily oral calcium (400-600 mg). The primary endpoints were 6-month percent change in osteocalcin and overall safety; the primary analysis was ARZ compared with



PBO. Secondary endpoints included other bone turnover markers, BMD as an exploratory endpoint, and hot flush occurrence (assessed by electronic diary). Endometrial safety was assessed by transvaginal ultrasound and endometrial biopsy.

Baseline characteristics were similar across treatment groups. All ARZ doses significantly reduced osteocalcin levels vs PBO. At 6 months, median % changes in serum osteocalcin were -24%, -30%, -45%, -39%, -45%, and -44% in the PBO, RLX, and ARZ 5, 10, 20, and 40 mg groups, respectively. Compared with PBO, ARZ also significantly reduced serum bone specific alkaline phosphatase, CTX, and PINP at 6 months. The 6-month change in lumbar spine (LS) BMD was significantly greater with all ARZ doses vs PBO: 1.50%, 1.69%, 1.77% and 1.92% in ARZ 5, 10, 20, and 40 mg, compared to a 0.60% decrease in PBO. ARZ generally had greater effects on bone turnover and LS BMD than RLX at 6 months.

The proportion of women reporting  $\geq 1$  adverse event (AE) did not differ significantly among treatment groups. Muscle cramps were reported more frequently with ARZ vs PBO, with a similar frequency to RLX (pooled ARZ 7.1%, RLX 5.4%, PBO 0%). The frequency and severity of hot flushes did not differ significantly between ARZ and PBO, except for an increase in the ARZ 5 mg group by some measures. Change in endometrial thickness was not statistically significant for any ARZ group compared with PBO or RLX, and no cases of endometrial hyperplasia or adenocarcinoma were observed.

In postmenopausal women with low bone mass, all doses of ARZ were well tolerated, suppressed bone turnover and increased LS BMD. Within the limitations of this small Phase 2 study, the endometrial safety profile of ARZ was similar to RLX.

**Disclosures:** A.H. Moffett, Eli Lilly and Company 2, 3.

This study received funding from: Eli Lilly and Company.

## M387

**Assessment of Adherence to Treatment of Osteoporosis with Raloxifene and/or Alfacalcidol in Postmenopausal Japanese Women.** I. Gorai, Y. Tanaka\*, S. Hattisutari\*. Obstetrics and Gynecology, International University of Health and Welfare Atami Hospital, Atami, Japan.

Patients who are diagnosed and beginning treatment often do not persist with their osteoporosis medication relatively early after the start of the treatment because of their poor recognition of fracture risk and asymptomatic nature of osteoporosis. We have already reported that a more bone-sparing effect could be expected when estrogen was administered concomitantly with alfacalcidol rather than when used alone in postmenopausal Japanese women with osteoporosis or osteopenia. In this study we aimed to assess the adherence to the treatment of osteoporosis or osteopenia with 60mg raloxifene (R), 1µg alfacalcidol (D) or a combination of both (R+D) for 1 yr by defining precisely persistence and compliance in postmenopausal Japanese women. We defined persistence of R and D as continuing to take tablets for more than 7 of any 14 days immediately before the 1-yr visit. A total of 130 subjects aged 49 to 81 yrs (64.9±6.8 yrs, 18.8±13.3 YSM) were randomly assigned to each treatment group. There were significant increases in L-BMD (+3.3% in 6-mon and +5.0% in 1 yr,  $P<0.01$ ) in the combination-treated group and non-significant increases (+3.3% in 6-mon and +5.0% in 1 yr) in R-treated group. The increase of the R+D group at 1 yr was significant as compared with that in D-treated group (vs.+1.1%,  $P<0.05$ ). In D group one of seven subjects with adverse events (AE) was non-persistent with therapy whereas seven of seventeen subjects with AE discontinued therapy in R group. Six of thirteen subjects with AE stopped therapy in R+D group. In addition, four subjects discontinued therapy because of hypercalciuria in D group. The most common events reported were: climacteric symptoms including hot flash (n=4) and hypercalciuria (n=4). Of four subjects who had climacteric symptoms, two subjects were prescribed R alone and the other two were a combination of R and D. All the subjects who revealed hypercalciuria were treated with D alone. There were no significant differences in the number of subjects who discontinued treatment due to AE among each group. The proportions persisting with each treatment group at 1 yr were 62.8%, 67.6%, 56.7% for D, R and D+R groups, respectively whereas the compliance rates to each therapy were 97.7%, 96.6%, 97.4%, respectively. There were no significant differences in persistence and compliance among each group. In summary, the combination therapy was well tolerated compared with raloxifene or alfacalcidol alone.

**Disclosures:** I. Gorai, None.

## M388

**Replacing Testosterone in Male Cardiac Transplant Patients Exerts Multiple Benefits on Bone Mass, Libido and Sexual Activity: A 5-Year Prospective Study.** A. Fahrleitner-Pammer<sup>1</sup>, B. Obermayer-Pietsch<sup>1</sup>, M. Schweiger<sup>\*2</sup>, G. Prenner<sup>\*2</sup>, K. H. Tscheliessnigg<sup>\*2</sup>, J. C. Piswanger-Sölkner<sup>1</sup>, H. P. Dimai<sup>1</sup>, H. Dobnig<sup>1</sup>. <sup>1</sup>Endocrinology, Medical University, Graz, Austria, <sup>2</sup>Transplantation Surgery, Medical University, Graz, Austria.

**Background:** Hypogonadism is frequently encountered in cardiac transplant patients (CTX) with immunosuppressive treatment regimens and exerts negative effects on bone mass, libido and quality of sex life. Aim of the study was to investigate whether testosterone replacement therapy (TRT) of hypogonadal CTX recipients on top of intravenous bisphosphonate treatment confers positive effects on bone mass and quality of sex life compared to untreated hypogonadal and eugonadal CTX patients.

**Patients and Methods:** Parenteral ibandronate (2mg every 3 months) as well as 1200mg calcium and 880IU vitamin D3 was given to all patients. Fourteen out of 31 hypogonadal patients (45%) were treated with testosterone enanthate (250mg intramuscularly every 3-5 weeks).

**Results:** At baseline 77% of the hypogonadal patients admitted loss of libido (compared to 27% of eugonadal men,  $P=0.005$ ) and reported an average  $7\pm 6$  annual sexual activities (as

compared to  $15\pm 14$  of eugonadal men,  $P=0.005$ ). Hypogonadal men at baseline had also markedly lower Z-score values at the femoral neck (-1.54 vs. 0.15), and total hip (-1.34 vs. 0.01) (all  $P=0.0001$ ) as well as a higher percentage of prevalent vertebral fractures (63.3%; vs. 13.6%;  $P=0.0003$ ). After 1 and 5 years of treatment BMD had significantly increased in hypogonadal patients with TRT (neck 12.4 and 16.4%, total hip 9.2 and 12.4%, respectively, all  $P<0.001$ ) as compared to eugonadal patients (neck 2.9 and 3.4%, total hip 3.7 and 4.4%). A similarly low BMD increase was found in unreplaced hypogonadal patients (neck 2.3 and 3%, total hip 3.2 and 4.2%). Compared to baseline annual sexual activities had increased in patients with TRT after 1 year ( $29\pm 8$ ;  $p<0.0001$ ) and 5 years ( $25\pm 9$ ;  $p<0.0005$ ) and had remained unchanged in unreplaced hypogonadal ( $5\pm 4$  after 5 years) as well as eugonadal patients ( $16\pm 9$  and  $14\pm 8$ ). At 1 and 5 years the number of annual sexual activities in replaced hypogonadal patients was also higher when compared to eugonadal CTX patients.

**Conclusion:** Intravenous IBN therapy increases hip BMD in CTX patients on continuing immunosuppressive treatment. Hypogonadal patients clearly benefit from additional TRT over at least 5 years with respect to bone mass changes and a better quality of sex life.

**Disclosures:** A. Fahrleitner-Pammer, None.

## M389

**The Safety Profile of Bazedoxifene in Japanese Postmenopausal Women with Osteoporosis.** T. Sugimoto<sup>1</sup>, A. Itabashi<sup>2</sup>, H. Ohta<sup>3</sup>, H. Ochi<sup>\*4</sup>, A. A. Chines<sup>5</sup>, G. Constantine<sup>\*5</sup>. <sup>1</sup>Shimane University Faculty of Medicine, Shimane, Japan, <sup>2</sup>Saitama Center for Bone Research, Saitama, Japan, <sup>3</sup>Tokyo Women's Medical University, Tokyo, Japan, <sup>4</sup>Wyeth Research, Tokyo, Japan, <sup>5</sup>Wyeth Research, Collegeville, PA, USA.

Bazedoxifene (BZA) is a novel selective estrogen receptor modulator that has demonstrated bone-sparing effects without endometrial or breast stimulation in postmenopausal women. Here we report safety findings from a randomized, double-blind, phase 2 study that evaluated the efficacy and safety of 2 doses of BZA compared with placebo in Japanese postmenopausal women with osteoporosis.

Japanese postmenopausal women (aged  $\leq 85$  years) with osteoporosis were randomly assigned to treatment with BZA 20 or 40 mg or placebo (PBO) once daily for 2 years. All subjects received a daily supplement containing elemental calcium (610 mg), vitamin D<sub>3</sub> (400 IU), and magnesium (30 mg). Safety and tolerability assessments included adverse event (AE) reporting, physical and gynecologic examinations (including pelvic and breast), and transvaginal ultrasonography (TVU).

A total of 423 subjects (mean age, 63.7 years) receiving  $\geq 1$  dose of the study drug were included in analyses of safety data. No deaths occurred during the study. Overall, the incidence of AEs and serious AEs with BZA 20 or 40 mg was not significantly different from that with PBO. There were no reports of myocardial infarction, coronary occlusion, or venous thromboembolic events in any treatment group. As shown in the table below, the incidence of selected cardiac/cerebrovascular and gynecologic/breast-related AEs was low and similarly distributed among BZA- and PBO-treated subjects. There were 2 reports of cerebral infarction (1 each with BZA 20 and 40 mg), which were found incidentally on brain imaging; however, they were not considered drug related by the investigator. The incidence of hot flushes and muscle spasm was low among all treatment groups, but higher in the BZA 20-mg group.

AE, n (%)	Incidence of Selected AEs		
	BZA 20 mg (n = 143)	BZA 40 mg (n = 140)	PBO (n = 140)
Angina pectoris	1 (0.7)	1 (0.7)	1 (0.7)
Cerebral infarction	1 (0.7)	1 (0.7)	0
Carotid artery thrombosis	0	1 (0.7)	0
Hot flushes	6 (4.2)	0	2 (1.4)
Muscle spasm	8 (5.6)	5 (3.6)	2 (1.4)
Endometrial hypertrophy	1 (0.7)	0	0
Ovarian cyst	1 (0.7)	0	0
Uterine polyp	1 (0.7)	0	0
Breast cancer	1 (0.7)	0	1 (0.7)
Breast pain	0	2 (1.4)	1 (0.7)

TVU results demonstrated no differences in the change from baseline in endometrial thickness among treatment groups. No major changes in ovarian volume were observed in any treatment group.

In conclusion, BZA 20 or 40 mg was well tolerated and demonstrated a favorable safety profile that was overall similar to that of PBO in Japanese postmenopausal women with osteoporosis.

**Disclosures:** T. Sugimoto, Wyeth Research 2.

This study received funding from: Wyeth Research.

## M390

**Efficacy of Bazedoxifene In Reducing the Incidence of Nonvertebral Fractures in Postmenopausal Osteoporotic Women at Higher Fracture Risk.** S. L. Silverman<sup>1</sup>, C. Christiansen<sup>2</sup>, H. K. Genant<sup>3</sup>, J. R. Zanchetta<sup>4</sup>, S. Vukicevic<sup>5</sup>, I. Valter<sup>6</sup>, T. J. de Villiers<sup>7</sup>, M. Ciesielska<sup>8</sup>, A. A. Chines<sup>8</sup>. <sup>1</sup>Cedars-Sinai Medical Center and UCLA, Los Angeles, CA, USA, <sup>2</sup>Center for Clinical and Basic Research (CCBR), Ballerup, Denmark, <sup>3</sup>UCSF, and Synarc Inc, San Francisco, CA, USA, <sup>4</sup>Univ. of El Salvador, Metabolic Research Institute, Buenos Aires, Argentina, <sup>5</sup>Univ. of Zagreb School of Medicine, Zagreb, Croatia, <sup>6</sup>CCBR, Tallinn, Estonia, <sup>7</sup>Panorama MediClinic and Univ. of Stellenbosch, Cape Town, South Africa, <sup>8</sup>Wyeth Research, Collegeville, PA, USA.

In a recent phase 3 trial, treatment with bazedoxifene for 3 years effectively reduced the risk of new vertebral fracture relative to placebo in postmenopausal women with osteoporosis. Here we report the results of post hoc analyses of nonvertebral fracture (NVF) incidence among women at higher risk for fracture in that study.

Generally healthy postmenopausal women (N = 7,492; mean age, 66.4 y) with osteoporosis were randomized to daily therapy with bazedoxifene 20 or 40 mg, raloxifene 60 mg, or placebo; all subjects received supplemental elemental calcium (1,000-1,200 mg/d) and vitamin D (400-800 IU/d). Kaplan-Meier estimates of the incidence of NVFs at 36 months were evaluated for the overall population and for subgroups of women at higher fracture risk, based on known skeletal risk factors (low femoral neck [FN] T-score and/or prevalent vertebral fracture).

The overall incidence of NVFs was similar among groups. In a subgroup of women at higher risk for fracture (FN T-score  $\leq -3.0$  and/or  $\geq 2$  mild vertebral fractures; n = 1,772), NVF rates were 4.9%, 6.5%, 8.4%, and 9.1% with bazedoxifene 20 and 40 mg, raloxifene 60 mg, and placebo, respectively. Bazedoxifene 20 mg significantly reduced NVF incidence relative to placebo and raloxifene 60 mg (50% and 44%, respectively;  $P < 0.05$ ); a similar reduction was observed when NVF data for bazedoxifene 20 and 40 mg were combined (40% relative to placebo;  $P = 0.03$ ). Conversely, there were no significant between-group differences in NVF rates in the lower-risk subgroup (n = 5,710). Further evaluation of NVF incidence in subjects with FN T-scores  $\leq -2.5$  or  $\leq -2.0$  and/or  $\geq 1$  moderate or  $\geq 2$  mild vertebral fractures showed a trend toward NVF risk reduction with bazedoxifene treatment, supporting the robustness of the results. The selection of subjects at higher fracture risk was also supported by Cox regression analyses indicating a significant treatment by risk category interaction with bazedoxifene 20 mg ( $P = 0.025$ ) and of borderline significance with bazedoxifene 20 and 40 mg combined ( $P = 0.052$ ).

In conclusion, treatment with bazedoxifene significantly reduced the risk of NVF in postmenopausal osteoporotic women at higher risk for fracture.

**Disclosures:** S.L. Silverman, Wyeth Research and Eli Lilly 4; Eli Lilly 1.  
This study received funding from: Wyeth Research.

## M391

**A Double-blind, Placebo-controlled, Dose-response Study of Bazedoxifene in Japanese Postmenopausal Women with Osteoporosis.** A. Itabashi<sup>1</sup>, H. Ohta<sup>2</sup>, B. Ebende<sup>3</sup>, G. Constantine<sup>3</sup>, A. A. Chines<sup>3</sup>. <sup>1</sup>Saitama Center for Bone Research, Saitama, Japan, <sup>2</sup>Tokyo Women's Medical University, Tokyo, Japan, <sup>3</sup>Wyeth Research, Collegeville, PA, USA.

Bazedoxifene (BZA) is a novel selective estrogen receptor modulator under clinical development for the prevention and treatment of postmenopausal osteoporosis. This randomized, double-blind, placebo-controlled, dose-response phase 2 study evaluated the efficacy and safety of BZA in postmenopausal women with osteoporosis.

Japanese postmenopausal women (aged  $\leq 85$  y) with osteoporosis were randomized to treatment with daily oral doses of BZA 20 or 40 mg or placebo (PBO) for 2 years; all subjects were supplemented daily with elemental calcium (610 mg), vitamin D (400 IU), and magnesium (30 mg). The primary endpoint was the percent change from baseline in bone mineral density (BMD) at the lumbar spine (L1-L4) at 2 years. Secondary endpoints included BMD response at other skeletal sites, changes in serum bone marker levels, incidence of vertebral and nonvertebral fractures, and lipid parameters.

Of 429 subjects who were randomized to therapy, a total of 387 subjects (mean age, 63.5 y) were evaluable for primary efficacy analyses. At 2 years, the mean percent changes from baseline in lumbar spine BMD were significantly greater with BZA 20 and 40 mg (2.43% and 2.74%, respectively) than with PBO (-0.65%;  $P < 0.001$  for both). There was no difference in lumbar spine BMD response between BZA 20 and 40 mg. Treatment with BZA 20 and 40 mg was associated with increased lumbar spine BMD relative to baseline as early as 24 weeks ( $P < 0.001$  vs PBO), which was sustained through study end. Similarly, the mean percent changes in BMD of the total hip, femoral neck, and greater trochanter from baseline to 2 years were significantly greater with BZA 20 and 40 mg versus PBO ( $P < 0.001$  for all), with no differences between BZA 20 and 40 mg. Relative to PBO, treatment with BZA 20 and 40 mg conferred significantly greater reductions in levels of bone turnover markers (serum CTx, NTx, OC and urinary NTx) as early as 12 weeks ( $P < 0.05$  vs baseline for all), which were sustained through study end. The incidence of new vertebral fractures with BZA 20 and 40 mg and PBO was 3.8%, 2.4%, and 4.7%, respectively. The incidence of nonvertebral fractures was 3.8%, 2.4%, and 3.1% with BZA 20 and 40 mg and PBO, respectively. BZA 20 and 40 mg demonstrated significant decreases from baseline in total cholesterol ( $P < 0.001$ ) and LDL cholesterol ( $P < 0.05$ ). HDL cholesterol levels were increased from baseline with BZA 20 mg; no clear trend with BZA 40 mg or PBO was observed. In conclusion, BZA significantly improved BMD, reduced bone turnover, and had favorable effects on the lipid profile in Japanese postmenopausal women with osteoporosis.

**Disclosures:** A. Itabashi, Wyeth Research 2.  
This study received funding from: Wyeth Research.

## M392

**The Effects of Estrogen Therapy and Flucalcic Effervescent on the Bone Mineral Densities and Bone Metabolism of Surgical Menopause Women with Osteopenia.** H. Kim<sup>\*1</sup>, H. Choi<sup>\*2</sup>, H. Park<sup>\*3</sup>, T. Kim<sup>\*4</sup>, H. Jung<sup>\*5</sup>, D. Lee<sup>\*6</sup>. <sup>1</sup>Dept. of OB & GYN, College of Medicine, Kosin University, Busan, Republic of Korea, <sup>2</sup>Dept. of OB & GYN, College of Medicine, Inje University, Seoul, Republic of Korea, <sup>3</sup>Dept. of OB & GYN, College of Medicine, Chungang University, Seoul, Republic of Korea, <sup>4</sup>Dept. of OB & GYN, College of Medicine, Korea University, Seoul, Republic of Korea, <sup>5</sup>Dept. of OB & GYN, College of Medicine, Chosun University, Kwangju, Republic of Korea, <sup>6</sup>Dept. of OB & GYN, National Cancer Center, Koyang, Republic of Korea.

Introduction: Hormon therapy results in only modest increase in bone mineral density. Sodium fluoride stimulate bone formation and has been used to treat osteopenia for decades despite debate about the antifracture efficacy. However, for women with low bone mass, the ideal therapy should not only inhibit bone resorption but simultaneously stimulate bone formation to increase bone mass above the fracture threshold.

Objective: To evaluate the effects of estrogen therapy and flucalcic on the bone mineral density and bone metabolism in the surgically menopause women with osteopenia.

Methods: This prospective randomized clinical trial examined the effects of conjugated equine estrogen and flucalcic in combination and separately, on BMD and biochemical markers of bone turnover in 200 women with low bone mass. Treatment included 0.3mg CEE (group I, n=50), 0.625 CEE (group II, n=50), 0.3mg CEE plus flucalcic (group III, n=50), and 0.625mg CEE plus flucalcic (group IV, n=50) for 12 months. Bone density measurements were performed at months 6 and 12 months at the lumbar spine and femur neck. Biochemical markers of bone turnover were also measured every six months.

Results: BMD of lumbar spine, it increased significantly during the treatment in Group III and Group IV ( $p < 0.05$ ). As for BMD of femur neck, it increased slightly during the treatment in all Groups, but not significantly, and urinary deoxypyridinoline in Group III and Group IV decreased significantly at 12 months of treatment ( $p < 0.005$ ). But serum osteocalcin and total alkaline phosphatase decreased slightly during the treatment in all groups but not significance: \*  $p < 0.05$

Conclusion: The combined treatment with Conjugated equine estrogen and flucalcic is more effective in surgical menopause women with osteopenia by decreasing bone biochemical markers, by increasing the BMD and induces a synergistic effect on bone mass.

**Disclosures:** H. Kim, None.

## M393

**The Effects of Low Dose Estrogen Therapy on the Bone Mineral Densities and Bone Metabolism of Menopausal Women.** H. Kim<sup>\*1</sup>, H. Park<sup>\*2</sup>, H. Choi<sup>\*3</sup>, H. Jung<sup>\*4</sup>, T. Kim<sup>\*5</sup>. <sup>1</sup>Dept. of OB & GYN, College of Medicine, Kosin University, Busan, Republic of Korea, <sup>2</sup>Dept. of OB & GYN, College of Medicine, Chungang University, Seoul, Republic of Korea, <sup>3</sup>Dept. of OB & GYN, College of Medicine, Inje University, Seoul, Republic of Korea, <sup>4</sup>Dept. of OB & GYN, College of Medicine, Chosun University, Kwangju, Republic of Korea, <sup>5</sup>Dept. of OB & GYN, College of Medicine, Korea University, Seoul, Republic of Korea.

Introduction : Estrogen therapy(ET) is well established as an effective treatment of menopausal bone loss. There is less confidence about the minimum dose of estrogen required to prevent bone loss. Daily dosage in excess of 0.3mg conjugated equine estrogen prevents bone loss at the radius and at the spine as measured by computed tomography. Prospective studies have shown that doses equivalent to conjugated equine estrogens of 0.625mg/day are needed to produce a significant increase in bone mineral density of the lumbar spine. Safety concerns associating long-term use with endometrial and breast cancer, have prompted the search for the lowest effective dose for each indication of estrogen therapy.

Objective: To evaluate the effects of low dose estrogen therapy on the bone mineral densities and bone metabolism in the menopausal women.

Methods: This prospective randomized clinical trial examined the effects of low dose conjugated equine estrogen on BMD and biochemical markers of bone turnover in 140 women with low bone mass. Treatment included 0.625mg conjugated equine estrogen (group I, n=50) or 0.3mg conjugated equine estrogen (group II, n=50) for 12 months. Bone density measurements were performed at months 6 and 12 months at the lumbar spine and femur neck. Biochemical markers of bone turnover were also measured every six months.

Results: BMD of lumbar spine, it increased significantly during the treatment in Group I and Group II ( $p < 0.05$ ). As for BMD of femur neck, it increased slightly during the treatment in Group I and Group II, but not significantly. Urinary deoxypyridinoline in Group I and Group II decreased significantly at 12 months of treatment ( $p < 0.05$ ). But serum osteocalcin decreased during the treatment in but not significantly.

Conclusion: The low dose conjugated equine estrogen is also positive changes on bone densities and bone metabolism of menopausal women.

**Disclosures:** H. Kim, None.

## M394

### An Assessment of Serum Calcium and Bone Resorption Markers in Patients Transitioned from Alendronate to Denosumab. D. Padhi<sup>\*1</sup>, A. Kivitz<sup>\*2</sup>, T. J. Weber<sup>3</sup>, K. Lyles<sup>4</sup>, E. Lee<sup>\*1</sup>, B. Cooke<sup>\*1</sup>, H. Deng<sup>\*1</sup>, E. Posvar<sup>\*1</sup>.

<sup>1</sup>Amgen Inc., Thousand Oaks, CA, USA, <sup>2</sup>Altoona Arthritis and Osteoporosis Center, Duncansville, PA, USA, <sup>3</sup>Duke Univ Med Ctr, Durham, NC, USA, <sup>4</sup>Duke Univ Med Ctr and VA Med Ctr, Durham, NC, USA.

Denosumab, a fully human mAb with a high affinity and specificity for RANKL, neutralizes the activity of human RANKL and blocks osteoclastic bone resorption. The objective of this study was to evaluate changes in serum calcium and bone resorption markers in patients transitioned from alendronate to denosumab to aid in the design of an international, double-blind, active-controlled, double-dummy, parallel group study in postmenopausal women with low bone mineral density (BMD).

In this open-label, single-dose phase 1 study, 20 postmenopausal women with low BMD (t-score between -4 and -1) who were receiving alendronate therapy (70 mg weekly or equivalent) for at least 1 year were randomized to receive a single subcutaneous (SC) dose of denosumab (n=15) or to continue with their alendronate regimen (n=5). The first 3 subjects randomized to denosumab received a SC dose of 15 mg, and the remaining 12 subjects received 60 mg SC. Blood samples were collected at baseline and for up to 107 days for determination of serum calcium, serum CTx, and denosumab concentrations.

Although small transient decreases in calcium occurred in all treatment groups, mean total and ionized calcium concentrations remained within normal limits for all groups throughout the study. The maximum mean decrease from baseline in total serum calcium for the 15 and 60 mg denosumab groups and alendronate group was 11%, 9%, and 6% and for ionized calcium was 5%, 6%, and 5%, respectively.

Fourteen days after dosing, the mean percent change from baseline in sCTx was approximately -60% and -73% for subjects in the 15 mg and 60 mg denosumab groups, respectively. These changes were generally maintained from study day 14 through 84. The mean percent change from baseline for sCTx for subjects who continued on alendronate treatment ranged from approximately -40% to +20%, with no changes on average at study day 107.

Serum denosumab concentrations were within the ranges observed in previous studies in bisphosphonate-naïve subjects. Therefore, dose adjustments of denosumab are not required in patients previously treated with alendronate.

In conclusion, there were no notable differences between the serum (total and ionized) calcium profiles after subjects were transitioned from alendronate to denosumab. Denosumab serum concentrations were consistent with those from previous denosumab studies, indicating that prior treatment with alendronate did not alter the pharmacokinetics of denosumab. Transitioning postmenopausal patients from alendronate to denosumab resulted in further reductions in sCTx levels.

**Disclosures:** D. Padhi, Amgen 5.

This study received funding from: Amgen Inc.

## M395

### Effects of Denosumab vs Alendronate on Bone Mineral Density (BMD), Bone Turnover Markers (BTM), and Safety in Women Previously Treated with Alendronate. D. L. Kendler<sup>1</sup>, C. L. Benhamou<sup>2</sup>, J. P. Brown<sup>3</sup>, M. Lillestol<sup>\*4</sup>, C. Roux<sup>5</sup>, H. S. Man<sup>\*6</sup>, S. Siddhanti<sup>6</sup>, J. San Martin<sup>6</sup>, H. G. Bone<sup>7</sup>.

<sup>1</sup>Clinical Research Centre, Vancouver, BC, Canada, <sup>2</sup>Centre Hospitalier, Orleans, France, <sup>3</sup>CHUQ, Laval University, Quebec, QC, Canada, <sup>4</sup>Internal Medicine Associates, Fargo, ND, USA, <sup>5</sup>Hopital Cochin, Paris, France, <sup>6</sup>Amgen Inc., Thousand Oaks, CA, USA, <sup>7</sup>Michigan Bone and Mineral Clinic, Detroit, MI, USA.

Denosumab is a RANKL inhibitor in late-stage clinical development as a therapy for postmenopausal bone loss. Because many patients with osteoporosis are currently treated with bisphosphonates (BPs), it is important to understand the safety and efficacy of transitioning patients from BPs to denosumab. Cynomolgus monkeys treated with alendronate (ALN) followed by denosumab had significant reductions in BTMs and maintenance of BMD compared with monkeys remaining on ALN. In a phase 1 study in subjects who had received prior ALN therapy, serum calcium remained in the normal range following subcutaneous (SC) denosumab administration, while serum CTX decreased more than in subjects continuing to receive ALN. This phase 3 study in women previously treated with ALN was conducted to evaluate the effects of denosumab on BMD and BTM changes and safety compared with continuation of brand ALN therapy.

In this international, double-blind, active-controlled, double-dummy study, the primary efficacy endpoint was the percent change in total hip BMD from baseline to 12 mos. Secondary endpoints included percent changes in serum CTX at 3 mos and lumbar spine BMD at 12 mos. The study design allowed testing of the primary endpoint for superiority if non-inferiority was demonstrated.

Postmenopausal women  $\geq 55$  years old with a BMD measurement corresponding to a T-score of  $\leq -2.0$  and  $\geq -4.0$  at the lumbar spine or total hip who had received ALN therapy equivalent to 70 mg/week (QW) for  $\geq 6$  mos were eligible. After enrollment, all subjects received open-label ALN 70 mg QW for 1 mo, then subjects were randomized to continue receiving ALN 70 mg QW or to receive SC denosumab 60 mg Q6M. Randomization was stratified by length of prior ALN therapy. All subjects were given daily supplements of calcium (1000 mg) and vitamin D ( $\geq 400$  IU). Adverse events, serum calcium levels, and serum chemistry and hematology were evaluated to monitor safety.

A total of 504 women were enrolled from 46 study centers. The mean  $\pm$  SD age was 68  $\pm$  8 yrs, and the mean  $\pm$  SD length of prior BP therapy was 44  $\pm$  33 mos. The last subject visit occurred in March 2008, and the study remains blinded. The changes in BMD and BTM

observed in this study in subjects transitioning from ALN to denosumab may provide insights into the significance of the different mechanisms of action between denosumab, a RANKL inhibitor, and ALN, a BP.

**Disclosures:** D.L. Kendler, Merck 2, 3; Amgen 2, 3, 4; Eli Lilly, Novartis, Wyeth 1, 2, 3, 4; Takeda, GSK, Pfizer 3.

This study received funding from: Amgen Inc.

## M396

### The Efficacy of Whole-Body Vibration in Reducing Bone Loss in Postmenopausal Women: A Meta-Analysis. L. Slatkowska<sup>1</sup>, S. M. H. Alibhai<sup>\*2</sup>, J. Beyene<sup>\*2</sup>, A. M. Cheung<sup>2</sup>. <sup>1</sup>Institute of Medical Science, University of Toronto, Toronto, ON, Canada, <sup>2</sup>Department of Medicine, University of Toronto, Toronto, ON, Canada.

Whole-body vibration (WBV) has received attention recently due to its potential to improve bone mineral density (BMD). Animal models have shown anabolic bone effects of WBV, but small clinical trials in humans have produced variable results. Thus, we conducted a systematic review and meta-analysis of randomized controlled trials (RCTs) examining the effects of WBV on BMD in postmenopausal women. Eligible RCTs included randomized or quasi-randomized trials, with a minimum follow-up of six months, examining WBV effects on BMD in postmenopausal women without secondary osteoporosis. Blinding of patients and researchers was not a requirement. WBV therapy was defined as mechanical vibration, performed erect, with no restriction on the amount and magnitude of WBV. Control interventions included no treatment, anti-osteoporotic drugs (matched between groups), and physical activity. The effect measure was a weighted mean difference in absolute pre-post change in the areal BMD in the spine and hip (as measured by dual-energy x-ray absorptiometry), and in the volumetric tibial trabecular BMD (as measured by computed tomography). Intention-to-treat data were analyzed preferentially. Fixed versus random effect models were reported, unless significant heterogeneity was found. Subgroup analysis was performed to examine whether WBV magnitude and amount, and control intervention type modify WBV effects. From 1257 identified titles, five RCTs were included with a total of 209 patients. Study population consisted primarily of healthy osteopenic women of Caucasian and Southeast Asian origin, 47-88 years of age, and with low to moderate physical activity levels. Four RCTs obtained areal BMD measurements (spine, 4 RCTs; hip, 3 RCTs), and one trial obtained volumetric BMD measurements. No significant effect of WBV on spine BMD was found (-3.39 mg-cm<sup>2</sup>; 95% CI, -12.01, 5.24; n = 181). Decline in hip BMD was found to be significantly smaller in the WBV versus control group (14.32 mg-cm<sup>2</sup>; 95% CI, 6.69, 21.95; n = 131). No change in volumetric tibial trabecular BMD was found in one trial (-2.20 mg-cm<sup>3</sup>; 95% CI, -6.14, 1.74; n = 29). In subgroup analysis, only WBV magnitude was found to significantly modify the effect of WBV on hip BMD. However, this involved a comparison of two high-magnitude WBV trials (n = 98) with only one low-magnitude WBV trial (n = 33). In conclusion, WBV appeared to be efficacious in attenuating postmenopausal decline in hip but not spine BMD, suggesting that this therapy is a promising new candidate for prevention of bone loss in postmenopausal women. Larger trials will need to be conducted to examine whether WBV affects bone structure or fracture risk.

**Disclosures:** L. Slatkowska, None.

This study received funding from: The Physicians' Services Incorporated Foundation.

## M397

**The "Vibes" Trial: Low Magnitude Mechanical Stimulation (LMMS) to Improve Bone Mineral Density (BMD).** D. P. Kiel<sup>1</sup>, M. T. Hannan<sup>1</sup>, B. A. Barton<sup>2</sup>, T. F. Lang<sup>3</sup>, M. L. Bouxsein<sup>4</sup>, K. Brown<sup>2</sup>, E. Shane<sup>5</sup>, J. Magaziner<sup>6</sup>, S. Zimmerman<sup>7</sup>, T. Harris<sup>8</sup>, C. T. Rubin<sup>9</sup>. <sup>1</sup>IFAR, Hebrew Rehab Center, Boston, MA, USA, <sup>2</sup>Maryland Med Res Inst, Baltimore, MA, USA, <sup>3</sup>Radiology, UCSF, San Francisco, CA, USA, <sup>4</sup>Ortho Biomech Lab, BIDMC, Boston, MA, USA, <sup>5</sup>Medicine, Columbia Univ, New York, NY, USA, <sup>6</sup>Epidemiol & Prev Med, Univ MD, Baltimore, MD, USA, <sup>7</sup>Cecil G. Sheps Center for Health Services Research, UNC, Chapel Hill, NC, USA, <sup>8</sup>NIA, Washington, DC, USA, <sup>9</sup>Biomed Engin, SUNY Stony Brook, Stony Brook, NY, USA.

Treatment options for osteoporosis in older persons are primarily limited to pharmacologic therapy. The VIBES trial is evaluating the efficacy of a unique, biomechanically based treatment for bone loss and possibly for sarcopenia: low magnitude mechanical stimulations (LMMS) with the use of vibrating platforms that meet ISO safety standards for vibration exposure. To extend previous findings that LMMS improves BMD in young women, disabled children and postmenopausal women, VIBES is a 2 yr, double-blind, randomized, placebo-controlled trial of LMMS in 200 women and men  $\geq 60$  yrs of age, with T-scores at the hip or spine = -1 and -2.49. Investigators at Hebrew SeniorLife (Boston) are recruiting subjects from independent living settings and data are being managed by a Maryland Medical Research Institute. Following a multi-stage screening process, eligible participants are randomized to either daily exposure to LMMS on an active vibrating platform (10 min/d of 0.3g @ 30Hz; 1g = 9.8 m/s<sup>2</sup>) or a placebo platform that is located in a common area of the independent living setting, and is activated by a radiofrequency identification card provided to all randomized participants. Subjects are receiving 1000 mg calcium and 800 IU of vitamin D/day. The primary endpoints are changes in volumetric trabecular BMD of the spine and hip by QCT. Secondary outcomes are change in biochemical markers of bone formation (Procollagen type 1 N-terminal peptide and Bone Specific Alkaline Phosphatase) and resorption (C-terminal Telopeptide of type I collagen), change in muscle strength, balance, muscle cross sectional area, and falls. Adverse events are monitored. Adherence is obtained electronically from the platforms. As of April 1, 2008, 194 subjects had been screened, and 40 participants (28 females, 12 males) randomized. Major reasons for exclusion were low BMD and current use of osteoporosis medications. The mean age of participants is  $82 \pm 8$  yrs, the mean femoral neck T-score is -1.89, and the mean vitamin D concentration is  $29 \pm 7$  ng/ml. There have been no withdrawals and few adverse events attributable to the treatment. Adherence is currently 85%. This study will provide new and important information about the role of high frequency LMMS on the skeleton, muscle mass and balance in independently living seniors.

**Disclosures:** D.P. Kiel, None.  
This study received funding from: NIA.

## M398

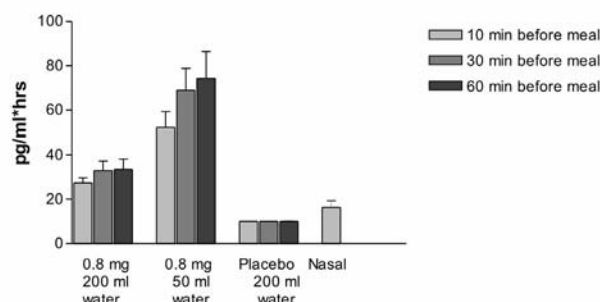
**Optimizing Bioavailability of Oral Administration of Small Peptides through Pharmacokinetic and Pharmacodynamic Parameters: The Effect of Water and Timing of Meal Intake on Oral Delivery of Salmon Calcitonin.** M. A. Karsdal, I. Byrjalsen, B. Riis\*, C. Christiansen. Nordic Bioscience, Herlev, Denmark.

**Purpose:** Oral delivery of peptides is hampered by an array of obstacles, including but not limited to proteolytic degradation in the gastrointestinal tract and uptake in the intestine. We investigated the influence of water intake and dose timing on the pharmacokinetic and pharmacodynamic parameters of an oral formulation of salmon calcitonin (sCT).

**Methods:** The study was a randomized, partially-blind, placebo-controlled, single dose, exploratory crossover phase I study of oral sCT. 56 healthy postmenopausal women, 56 to 70 years old were randomly assigned to receive five treatments according to pre-defined sequences. The treatments comprised a combination of study medication 0.8 mg sCT + 200 mg 5-CNAC, placebo, or 200 IU Miacalcic® NS nasal spray, water volume given with the tablet (50 or 200 ml water), and time between dosing and meal (10, 30, or 60 minutes pre-meal. Plasma sCT levels and changes in the bone resorption (C-terminal telopeptide of collagen type I) was investigated.

**Results:** Oral delivery of 0.8 mg of sCT with 50 ml of water resulted in a two-fold increase in maximum concentration ( $C_{max}$  and  $AUC_{0-4}$ ) of plasma sCT when compared to 200 ml water, but comparable time to reach maximum concentration ( $T_{max}$ ). The sCT  $AUC_{0-4}$  when SMC021 was given with 50 ml of water was 4-fold higher than that obtained with nasal calcitonin, as illustrated in the figure. The increased absorption of sCT resulted in increased suppression of the serum CTX-I levels calculated as AUC of the relative change of measured in the 6 hours following drug intake. A trend towards increased efficacy when dosing 30 minutes or 1 hour before meal intake was observed when comparing to dosing 10 minutes before meal.

**Conclusion:** 0.8 mg sCT with 50 ml of water taken 30 and 60 minutes prior to meal time resulted in optimal pharmacodynamic and pharmacokinetic parameters. These results appeared to be superior to those of the currently used Miacalcic® 200IU nasal spray calcitonin, although the study was not planned nor powered to compare the two sCT formulations. The data suggest that this novel oral formulation may have improved absorption and reduction of serum CTX-I over 24 hours compared to that of the nasal form.

AUC<sub>0-4 hrs</sub> of plasma CT

**Disclosures:** M.A. Karsdal, None.

## M399

**GLP-2 Acutely Uncouples Bone Resorption and Bone Formation in Postmenopausal Women.** D. B. Henriksen<sup>1</sup>, P. Alexandersen<sup>1</sup>, B. Hartmann<sup>1</sup>, C. Christiansen<sup>3</sup>. <sup>1</sup>Sanos Bioscience, Copenhagen, Denmark, <sup>2</sup>Center for Clinical and Basic Research, Ballerup, Denmark, <sup>3</sup>Nordic Bioscience, Herlev, Denmark.

We have previously shown that treatment with GLP-2 for 120 days results in a dose dependent and statistically significant increase in total hip BMD from baseline as compared to placebo.

We now report on the overall bone turnover marker response as well as TRAP-5b over the entire treatment period of 120 days. The study was a randomized, placebo-controlled 120-day trial including 160 postmenopausal women. The study subjects were osteopenic (BMD T-score,  $-2.5 < T \leq -1.0$ ) at one or more of the regions: lumbar spine, femoral neck, or total hip. Subjects received daily bedtime injections of 0.4, 1.6, or 3.2 mg GLP-2, or placebo. All subjects received supplements of calcium and vitamin D. Injection of 0.4, 1.6 and 3.2 mg GLP-2 resulted in acute and sustained reductions, of the nocturnal rise in s-CTX compared to placebo, at day 1 and day 120. At day 1 this effect was statistically significant compared to placebo for the 1.6 and 3.2 mg GLP-2 groups at all time points, but not for the 0.4 mg group. At day 120 all GLP-2 treatment groups had statistical significant and comparable reduction in s-CTX at all time points. S-osteocalcin levels were unaffected in the 10 hours following injection of GLP-2 at day 1 and day 120. There was an overall reduction in bone turnover following daily injections of 1.6 and 3.2 mg GLP-2 over the 120 days treatment period as assessed in morning fasting samples collected at day 2, 15, 30, 60, 90 and 121. This reduction resulted in a statistical significant decrease in s-CTX and s-osteocalcin between day 2 and day 121 for the 1.6 and 3.2 mg GLP-2 doses of 10-20% as compared to placebo. No reduction in s-CTX or s-osteocalcin was seen in the 0.4 mg GLP-2 group over the 120 days treatment period. TRAP-5b, which has been proposed as a biomarker for osteoclast number, showed a trend towards a decrease over the 120 days of treatment. The decrease was 10-15% compared to placebo for the 1.6 and 3.2 mg groups, whereas treatment with 0.4 mg GLP-2 did not result in any change of osteoclast number.

In conclusion, these results suggest that treatment with GLP-2 acutely uncouples the two processes of bone remodeling and thereby increases the bone calcium (ossification) balance particular at the hip. The decrease in TRAP-5b over the 120 day for the 1.6 and 3.2 mg groups suggests a reduction in osteoclast number and this might explain the overall reduction of 10-20% seen in bone turnover markers. This reduction in bone turnover markers was, however fully expressed during the first two week of treatment. An overall reduction in bone turnover markers during the 120 days treatment was not observed for the 0.4 mg GLP-2 group, whereas the acute effect on bone resorption on day 120 was identical for the three GLP-2 groups.

**Disclosures:** D.B. Henriksen, None.

## M400

**Vitamin D Supplementation Intake Among Osteoporosis Patients Aged 50 Years and Older at Various 25(OH)D Levels In the US.** D. T. Gold<sup>1</sup>, T. Fan<sup>2</sup>, S. G. Sajjan<sup>2</sup>, S. S. Sen<sup>2</sup>. <sup>1</sup>Departments of Psychiatry & Behavioral Science, Sociology, & Psychology, Duke Medical Center, Durham, NC, USA, <sup>2</sup>Merck & Co., Inc, Whitehouse Station, NJ, USA.

To assess the adequacy of the vitamin D supplement use and describe the characteristics of osteoporosis patients in a US national representative population from year 2001 - 2004, a cross-sectional analysis was conducted on combined data from the National Health and Nutrition Examination Survey (NHANES) 2001 - 2002 and NHANES 2003 - 2004. Descriptive analysis and multiple regression analyses were used to estimate the prevalence of vitamin D supplements intake and characteristics of osteoporosis patients with various 25(OH)D concentrations. Detailed vitamin, dietary supplements and multi-vitamin use were also collected in the surveys. A total of 3,002 subjects aged 50 years and older (mean age =  $64.2 \pm 0.29$ ) were included in the analysis. Self-reported prevalence of osteoporosis in the US was 7.1% (SD=0.01) from 2001-2004. Overall, the prevalence of vitamin D use did not differ between patients with osteoporosis and without osteoporosis (26.4% v.s.22.4%, P=0.297). Of 202 patients with self-reported osteoporosis, 22.5% reported taking vitamin D supplements. Vitamin D supplement rate was significantly higher for

patients aged 50-66 (16.1%) than those over 65 (31.0%,  $P=0.02$ ) but there were no gender differences (male=21.0%; female=23.7%,  $P=0.69$ ). Among osteoporosis patients in the US, 21.8% had serum 25(OH)D lower than 30ng/ml. The prevalence of vitamin D supplements use was 30.6% among osteoporotic patients with vitamin D insufficiency, and 19.9% among those patients whose serum 25(OH)D was at least 30 ng/ml ( $P=0.19$ ). In the logistic regression analysis, likelihood of taking vitamin D supplements was higher among Mexican American (OR=1.83 versus whites, 95% CI = 1.29 - 7.98) and increased with age (OR=1.03, 95% CI = 1.00 - 1.05). Patients with vitamin D insufficiency did not have significantly higher vitamin D supplements intake (OR=1.83, 95% CI = 0.74 - 4.52) when other factors were controlled. The most recent US national data revealed that vitamin D supplement intake was not higher among patients with osteoporosis than in the general population and was inadequate even among patients with insufficient serum vitamin D concentrations. Comprehensive strategies should target the improvement of overall vitamin D intake for patients with osteoporosis.

**Disclosures:** D.T. Gold, Merck & Co., Inc 5.

## M401

**Assessment of a Provincial Strategy for Osteoporosis Best Practices: Fracture Fighters - The Ontario Osteoporosis Strategy for Inpatient Rehabilitation.** S. B. Jaglal<sup>1</sup>, S. E. Munce<sup>\*2</sup>, V. Quan<sup>\*3</sup>, C. Evans<sup>\*3</sup>, V. Bansod<sup>\*2</sup>, G. Hawker<sup>2</sup>. <sup>1</sup>Rehabilitation Science, University of Toronto, Toronto, ON, Canada, <sup>2</sup>Health Policy, Management and Evaluation, University of Toronto, Toronto, ON, Canada, <sup>3</sup>Physical Therapy, University of Toronto, Toronto, ON, Canada.

**Purpose:** To assess the change in practices of osteoporosis care for fracture patients in 36 inpatient rehabilitation units across Ontario, Canada using a clinical coach intervention. **Methods:** Hospitals with inpatient rehabilitation units that treated at least 40 hip fractures per year were eligible for inclusion. Two clinical coaches (nurse and rehabilitation therapist) were identified from each unit and attended a one-day training session which included education on osteoporosis best practices, change management strategies, and the distribution of resource materials. Prior to implementation, a baseline survey was conducted on existing practices related to osteoporosis, including provision of education, recommendation of calcium and vitamin D supplements, prescription of medications, referral for bone mineral density (BMD) testing, and referral to a general practitioner for follow-up. Sites were asked to complete 10 audit checklists on fracture patients and complete a 6 month follow-up telephone survey to assess changes in osteoporosis practices. **Results:** Improvement in osteoporosis best practices was observed across all dimensions in 67% of the units. The areas of greatest improvement were provision of osteoporosis education (23% of sites at baseline vs. 77% of sites after training), recommendation of calcium and/or vitamin D supplements (17% of sites at baseline vs. 50% of sites after training), referral for BMD testing (9% of sites at baseline vs. 25% of sites after training), and referral to a general practitioner for osteoporosis follow-up (0% of sites at baseline vs. 42% of sites after training). Fourteen sites completed audit checklists on 165 fracture patients. Sixty-four percent had a hip fracture; 70% were female, with 43% older than 80 years of age. At the time of admission to the rehabilitation unit, 27% had had a previous fracture, 29% had a diagnosis of osteoporosis, 32% were already taking some type of bisphosphonate, and 37% were taking a calcium and/or vitamin D supplement. **Conclusions:** This strategy produced significant changes to post-fracture care in inpatient rehabilitation units across Ontario. Particular improvement was noted in referrals to general practitioners for osteoporosis follow-up. The clinical coach model (Fracture Fighters), can have a significant impact on the post-fracture care provided by inpatient rehabilitation units, and may help health care professionals make the link between fractures and osteoporosis.

**Disclosures:** S.B. Jaglal, None.

This study received funding from: Ministry of Health and Long-term Care.

## M402

**Possible Increased Risk of Fracture among South Florida White Hispanic Women \_ Characteristics of Women Screened for the Soy Phytoestrogen as Replacement Estrogen (SPARE) Study.** S. Levis<sup>1</sup>, N. Strickman-Stein<sup>\*2</sup>, A. Barrera<sup>\*2</sup>, O. Gomez-Marin<sup>\*3</sup>. <sup>1</sup>Medicine, Geriatric Research, Education, and Clinical Center, Miami VA Healthcare System, and Geriatrics Institute, University of Miami Miller School of Medicine, Miami, FL, USA, <sup>2</sup>University of Miami Miller School of Medicine, Miami, FL, USA, <sup>3</sup>Geriatric Research, Education, and Clinical Center, Miami VA Healthcare System, and Geriatrics Institute, University of Miami Miller School of Medicine, Miami, FL, USA.

The SPARE study is a 5-year trial to test the effectiveness of purified soy isoflavone tablets in preventing rapid bone loss and improving health-related quality of life and emotional health of women in the initial menopausal years. In this ongoing, randomized, double-blind, placebo-controlled clinical trial, subjects were randomized (50/50) to receive soy isoflavones 200 mg/day or placebo. Each participant is being followed for 2 years, undergoing serial measurements of spine and hip bone mineral density (BMD), thyroid function, and vaginal cytology and serial quality-of-life assessments. We here describe the characteristics of women screened for the study according to race and ethnicity. Potential study candidates were pre-screened by telephone, and those <45 or >60 years of age, or with BMI >32, or with known diagnosis of osteoporosis were excluded from further participation. Screening visits were performed in 524 women from the south Florida area; 283 met eligibility criteria and were enrolled into the study.

Mean age ( $\pm$  SD) of the 524 women screened was  $52.3 \pm 3.4$  years; there were no differences among ethnic / racial groups. Of those screened, 69% were white Hispanics

(WH), 20% white non-Hispanics (WNH), 8% African-American (AA), and 2% other race / ethnicity. At screening, 39% of WH had normal BMD, compared to 49% of WNH and 79% of AA; 54% of WH had osteopenia, compared to 41% WNH and 17% AA. Osteoporosis was diagnosed in 6% of WH compared to 9% WNH and 5% AA. WH had lower BMD in the spine compared to WNH and AA. The mean body mass index (BMI) for the entire screened population was  $26.2 (\pm 3.5)$ . AA women had significantly higher BMI than WH or WNH ( $p = 0.01$ ), and WH had significantly higher BMI than WNH women ( $p < 0.001$ ). Mean waist-hip ratio was significantly higher in WH (0.82) and AA (0.82) than in WNH (0.79) ( $p \leq 0.002$ ). The women screened for this study are representative of the general south Florida female population. AA and WH had significantly higher BMI than WNH. In spite of having higher BMI and waist-hip ratio, the WH women screened had the highest proportion of osteopenia and the lowest spine BMD. Due to behavioral, environmental, or genetic factors, WH women might be in a higher inflammatory state that could place them at higher risk of fractures and other comorbidities than their WNH and AA counterparts.

**Disclosures:** S. Levis, None.

This study received funding from: National Institute of Health.

## M403

**Cissus quadrangularis Attenuates Ovariectomy Induced Bone Loss in Mice.** J. Banu, R. Soomro<sup>\*</sup>, N. Kazi<sup>\*</sup>, G. Fernandes<sup>\*</sup>. Med/Clinical Immunology & Rheumatology, UT Health Science Center at San Antonio, San Antonio, TX, USA.

Bone loss during aging leads to osteoporosis, a disease characterized by low bone mass which increases the risk of fractures from minor trauma. Although both women and men are loose bone while aging, women lose bone drastically during and after menopause. Treatments for bone loss have been focused on hormone replacement therapy and other agents that can reduce bone resorption. However, all existing drugs have severe side-effects, therefore, the focus has turned towards identifying alternative medicines which can prevent and treat osteoporosis with minimal or no side-effects. *Cissus quadrangularis* (CQ) a medicinal herb used for bone fracture healing has shown bone forming properties. We studied the effects of CQ on bone loss after ovariectomy in young female C57Bl/6 mice.

Eight weeks old female C57Bl/6 mice were divided into the following groups: Group 1. Lab chow sham (LC S); Group 2. Lab chow ovariectomy (LC O); Group 3 CQ (500mg/kg b wt) sham (CQ S); and Group 4 CQ (500mg/kg b wt) ovariectomy (CQ O). One month after surgery mice were fed the respective diets for 11 weeks. After which the mice were sacrificed. Serum PINP and Trap5b were assayed. Femur and tibia were analyzed using pQCT densitometry.

Serum PINP decreased in LC O group, when compared to that of LC S group. There were no significant differences between CQ S and CQ O groups. No significant differences were seen in Trap5b levels in any of the groups studied.

In the distal femoral metaphysis (DFM), cancellous (Cn) BMC and BMD, cortical (Ct) BMC and BMD and cortical thickness (Ct Th) were significantly reduced in the LC O groups, when compared to that of the LC S groups. In the CQ O group, there were no significant differences in the Cn and Ct parameters studied, when compared to those of the CQ S group. In the FD, there were significant decreases in the Ct BMC and Ct Th in the LC O group, when compared to those of the LC S group while there were no significant differences between the CQ fed groups. In the proximal tibial metaphysis (PTM), Cn BMC, Cn BMD and Ct BMC decreased significantly in the LC O group when compared to those of LC S group. In the CQ O group, except for Ct BMC, there were no significant decreases in any of the parameters studied, when compared to that of the CQ S group. There were no significant differences in the tibia fibular junction between the shams and ovariectomized mice.

We conclude that CQ effectively attenuated ovariectomy induced bone loss in the cancellous and cortical bones of DFM and PTM as well as cortical bone of FD in young female mice mainly by increasing bone formation.

**Disclosures:** J. Banu, None.

This study received funding from: NIH.

## M404

**Genome-Wide Copy Number Variation Study Identified a Novel Susceptibility Gene *UGT2B17* for Osteoporosis.** T. L. Yang<sup>\*1</sup>, S. F. Lei<sup>\*2</sup>, Y. Guo<sup>\*1</sup>, F. Pan<sup>\*1</sup>, Q. Zhou<sup>\*1</sup>, Z. X. Zhang<sup>\*1</sup>, S. S. Dong<sup>\*1</sup>, X. H. Xu<sup>\*1</sup>, X. G. Liu<sup>\*1</sup>, H. Yan<sup>\*1</sup>, B. Drees<sup>\*2</sup>, J. Hamilton<sup>\*2</sup>, C. J. Papasian<sup>\*2</sup>, R. R. Recker<sup>3</sup>, H. W. Deng<sup>2</sup>. <sup>1</sup>School of Life Science and Technology, Xi'an Jiaotong University, Xi'an, China, <sup>2</sup>School of Medicine, University of Missouri - Kansas City, Kansas City, MO, USA, <sup>3</sup>Osteoporosis Research Center, Creighton University, Omaha, NE, USA.

DNA copy number variation (CNV) is a rich and important source of genetic diversity for human diseases. We conducted the first case-controlled, genome-wide CNV analyses for osteoporosis in 700 elderly Chinese Han subjects comprising 350 case subjects with a history of osteoporotic hip fractures (OF) and 350 matched healthy controls, using Affymetrix 500K array set. For the significant CNVs identified for OF, we further examined their relevance with hip BMD and bone geometry, in both Chinese (310 subjects) and Caucasian (1000 subjects) unrelated random samples. We constructed a genomic map containing 727 CNV regions (CNVR) covering 8.5% (254 Mb) of the human genome in Chinese. We found that CNV 4q13.2 duplication was strongly associated with OF ( $P < 0.001$ , Bonferroni corrected  $P = 0.041$ , odds ratio = 1.78). Real time PCR further identified that copy number change of *UGT2B17* located in 4q13.2 was associated with OF. Interestingly, *UGT2B17* gene duplication was also significantly associated with BMD and femoral neck bone geometry parameters (CT: cortical thickness; BR: buckling ratio) in Chinese, which were further confirmed in Caucasians. The contributions of this CNV to BMD, CT, BR variations in the Chinese and Caucasian were 1.91%, 1.50%, 1.47% and 0.63%, 0.65%, 0.84%, respectively. The phenotypic differences of subjects with various CNVs vary from 1.4%-7.0%. Our findings suggested that dosage of *UGT2B17* gene (via copy number variation), probably through affecting the extent of steroid hormone synthesis and metabolism, may be a novel genomic mechanism for etiology of osteoporosis.

**Disclosures:** T.L. Yang, None.

## M405

**Effect of Three Different Doses of Vitamin D<sub>2</sub> (Ergocalciferol) on Muscle Function and Strength in Women >65 years: A Preliminary Study.** S. R. Mastaglia<sup>\*</sup>, M. Seijo<sup>\*</sup>, D. Muzio<sup>\*</sup>, J. Somoza<sup>\*</sup>, B. Oliveri. Sección Osteopatías Médicas, Hospital de Clínica. Universidad de Buenos Aires, Buenos Aires, Argentina.

Vitamin D insufficiency is frequently observed in subjects aged  $\geq 65$  years. Serum levels of 25-hydroxyvitamin D (25OHD) $>20$ ng/ml would seem optimum for adequate muscle function and strength. In a previous study (*JBM 22: Suppl.1;2007*) we evaluated 40 postmenopausal women; 20 had mean 25OHD levels ( $X \pm DS$ ) at  $31.8 \pm 6$  ng/ml and exhibited improved muscle function compared to those with average 25OHD levels at  $12.9 \pm 3$  ng/ml ( $7.3 \pm 1$  vs.  $6.7 \pm 2$  scores;  $p < 0.02$ ). The aim of this study was to evaluate the effect of 3 different doses of vitamin D<sub>2</sub> administered for 6 months, on muscle function and strength in the group of women with levels of 25OHD $<20$ ng/ml. Twenty postmenopausal women from Buenos Aires (34°S), mean age ( $X \pm DS$ )  $70.5 \pm 4$  were randomly assigned to one of the following three groups (G) to receive: 800IU/day G 1 ( $n=6$ ); 5,000IU/day G2 ( $n=6$ ); and 10,000IU/day G3 ( $n=8$ ). All the subjects received calcium carbonate supplementation (500mg/day). Serum calcium, phosphate, 25OHD, bone alkaline phosphatase (BAP), and crosslaps (CTX) were determined, as well as 24-hours urine calciuria/creatininuria. Muscle function was assessed in terms of gait speed, balance, and stand-and-sit-test. Muscle strength of lower limbs was evaluated using a manual dynamometer. All determinations were performed at baseline and at 6 months. G2 and G3 were analyzed as a whole. Average baseline 25OHD of the whole group was 13 ng/ml. At 6 months, 25OHD levels reached  $18.4 \pm 2.5$  ng/ml in G1 and  $29.2 \pm 11.4$  ng/ml in G2+G3; G2 and G3 showed an improvement in their gait speed test (baseline:  $3.2 \pm 0.9$  vs. 6 months:  $3.6 \pm 0.9$  score;  $p < 0.05$ ) at 6 months. No significant changes in muscle strength were observed in any of the groups at the end of the study. Serum and urinary levels of calcium remained within reference values; no significant changes in BAP or CTX were observed. The dose of vitamin D supplementation for subjects in the age group at risk of suffering falls and osteoporotic fractures should be higher than the currently recommended dose.

**Disclosures:** S.R. Mastaglia, None.

This study received funding from: Grant PIP 6482, CONICET

## M406

**Circulating Osteoprotegerin and Its Ligand in Post Operative Biliary Atresia: Relationship with Metabolic Bone Disease.** S. Honsawek<sup>\*1</sup>, T. Chaiwatanarat<sup>\*2</sup>, P. Vejchapipat<sup>\*3</sup>, L. Wolfinbarger<sup>4</sup>, Y. Poovorawan<sup>\*5</sup>. <sup>1</sup>Biochemistry, Faculty of Medicine, Chulalongkorn University, Bangkok, Thailand, <sup>2</sup>Radiology, Faculty of Medicine, Chulalongkorn University, Bangkok, Thailand, <sup>3</sup>Surgery, Faculty of Medicine, Chulalongkorn University, Bangkok, Thailand, <sup>4</sup>Research and Development, LifeNet, Virginia Beach, VA, USA, <sup>5</sup>Pediatric, Faculty of Medicine, Chulalongkorn University, Bangkok, Thailand.

Osteodystrophy is a well-recognized complication of chronic liver disease. Biliary atresia (BA) is one of the typical cholestatic disorders that lead to end-stage liver disease in

children and severe cholestatic jaundice of BA is associated with a high prevalence of osteoporosis. Osteoprotegerin (OPG) and receptor activator of nuclear factor- $\kappa$ B ligand (RANKL) are proteins recently identified to play an essential role in the regulation of osteoclastogenesis. The purpose of this study has been to evaluate the relationships between circulating OPG and RANKL levels, bone mineral density (BMD), and clinical outcome in patients with BA.

We have investigated 50 patients with BA and 13 healthy controls. The mean age of BA patients and controls was  $7.3 \pm 0.6$  and  $8.0 \pm 1.1$  years. The study has been approved by the ethics committee on human research. Serum levels of OPG and RANKL were measured by sandwich enzyme-linked immunosorbent assay. BMD of the lumbar spine was determined by dual energy X-ray absorptiometry.

The results showed that BA patients had significantly elevated serum OPG levels compared with controls ( $4.0 \pm 0.3$  vs  $3.0 \pm 0.3$  pmol/l,  $P < 0.02$ ) and serum OPG levels in BA patients with jaundice were higher than in those without jaundice ( $4.6 \pm 0.4$  vs  $3.6 \pm 0.4$  pmol/l,  $P < 0.04$ ). Likewise, serum RANKL levels were significantly higher in BA patients than in controls ( $2.9 \pm 0.2$  vs  $1.2 \pm 0.7$  pmol/l,  $P < 0.001$ ). In addition, serum RANKL levels were increased in BA patients with jaundice compared to those without jaundice, but this difference was not statistically significant ( $3.2 \pm 0.3$  vs  $2.7 \pm 0.2$  pmol/l,  $P = 0.2$ ). Subgroup analysis in BA patients with normal BMD (Z score  $\geq -1.0$ ), with osteopenia ( $-2.5 < Z$  score  $< -1.0$ ), and with osteoporosis (Z score  $\leq -2.5$ ) revealed a gradual increase in OPG serum levels, with a significant increase observed in osteoporotic patients ( $P < 0.05$ ). There was an inverse correlation between OPG and BMD ( $R = -0.32$ ,  $P = 0.01$ ). Furthermore, there was a negative correlation between serum RANKL levels and BMD ( $R = -0.25$ ,  $P = 0.04$ ).

The present study showed significant differences in circulating OPG and RANKL levels between children with BA and healthy controls. High serum OPG and RANKL levels are associated with the severity of BA. The increase of serum OPG in BA patients with severe disease could reflect a compensatory response to bone loss.

**Disclosures:** S. Honsawek, None.

## M407

**A Study About the Association of Circulating MCP-1 Levels with Lumbar Bone Mineral Density in Korean Women.** S. Lee<sup>1</sup>, H. Baik<sup>\*2</sup>, K. Lee<sup>\*2</sup>, B. Kim<sup>\*3</sup>, Y. Jo<sup>\*3</sup>, H. Kim<sup>\*3</sup>, K. Park<sup>\*3</sup>, Y. Chung<sup>4</sup>. <sup>1</sup>Biochemistry and Internal Medicine, Eulji University School of Medicine, Daejeon, Republic of Korea, <sup>2</sup>Biochemistry, Eulji University School of Medicine, Daejeon, Republic of Korea, <sup>3</sup>Internal Medicine, Eulji University School of Medicine, Daejeon, Republic of Korea, <sup>4</sup>Endocrinology and Metabolism, Ajou University School of Medicine, Suwon, Republic of Korea.

Adipose tissue expresses chemotactic cytokine, monocyte chemoattractant protein-1 (MCP-1). MCP-1 has been known as adipocytokine initiating macrophage infiltration of the adipose tissue and inducing systemic insulin resistance. MCP-1 expression in adipose tissue and circulating MCP-1 levels have been known to have a positive correlation with the degree of obesity. In the field of bone and mineral research, previous studies have shown that parathyroid hormone or low-intensity pulsed ultrasound stimulates MCP-1 expression in osteoblast, receptor activator of NF kappa B ligand stimulates MCP-1 expression in human osteoclasts, and MCP-1 promotes osteoclast differentiation. However, there were no studies about the relationship of circulating MCP-1 levels with bone mineral density (BMD) in human, until now. In this study, we assessed the relationship of circulating MCP-1 levels with lumbar BMD in Korean pre- and post-menopausal women. 155 Korean women (109, premenopausal women; 46, postmenopausal women) who had no confounding diseases were recruited at the Eulji University Hospital, South Korea. We performed several anthropometric measurements and measured serum MCP-1 levels, various blood parameters, and lumbar spine L<sub>1</sub>-L<sub>4</sub> BMD using DXA. There were significant differences in age ( $39 \pm 6$  vs  $60 \pm 6$  years), body weight ( $55.5 \pm 7.0$  vs  $58.9 \pm 9.5$  kg), abdominal circumference ( $73 \pm 7$  vs  $84 \pm 8$  cm), percentage of body fat ( $28 \pm 5$  vs  $32 \pm 5$  %), BMI ( $22.2 \pm 2.7$  vs  $25.3 \pm 3.7$  kg/m<sup>2</sup>), systolic ( $116 \pm 13$  vs  $141 \pm 22$  mmHg) and diastolic ( $69 \pm 9$  vs  $79 \pm 13$  mmHg) blood pressure, serum total cholesterol ( $182 \pm 31$  vs  $215 \pm 42$  mg/dL), triglyceride ( $95 \pm 68$  vs  $119 \pm 48$  mg/dL), LDL-cholesterol ( $109 \pm 28$  vs  $137 \pm 40$  mg/dL), fasting glucose ( $83 \pm 8$  vs  $90 \pm 11$  mg/dL), MCP-1 ( $245.9 \pm 73.5$  vs  $336.5 \pm 101.7$  pg/mL) levels, and lumbar BMD ( $0.992 \pm 0.114$  vs  $0.772 \pm 0.113$  g/cm<sup>2</sup>) between pre- and post-menopausal women. Circulating MCP-1 levels increased and lumbar BMD decreased after menopause. However, circulating MCP-1 levels had no correlation with any anthropometric data, blood parameters and lumbar BMD in pre- or post-menopausal women. In conclusion, circulating MCP-1 levels had no association with lumbar BMD in Korean pre- or post-menopausal women, most of whom were not obese. Prospective studies in various populations, and involving a large number of obese subjects are required to reveal the association of circulating MCP-1 levels with BMD.

**Disclosures:** S. Lee, None.

This study received funding from: the Korea Research Foundation Grant funded by the Korean Government (MOEHRD) (KRF-2006-331-E00051).

## M408

**Bone Density Changes at the Non-operated Hip Following Total Hip Arthroplasty.** S. Ortolani<sup>1</sup>, G. Bianchi<sup>2</sup>, R. Cherubini<sup>\*1</sup>, C. Trevisan<sup>\*3</sup>, G. Isaia<sup>4</sup>, L. Massari<sup>\*5</sup>, D. Dallari<sup>\*6</sup>, P. Romano<sup>\*7</sup>. <sup>1</sup>Centre for Metabolic Bone Disease, Istituto Auxologico Italiano, Milan, Italy, <sup>2</sup>Department of Rheumatology, Ospedale La Colletta, Arenzano (GE), Italy, <sup>3</sup>Department of Orthopaedics, University of Milano-Bicocca, Milan, Italy, <sup>4</sup>Department of Internal Medicine, University of Turin, Turin, Italy, <sup>5</sup>Department of Orthopaedics, University of Ferrara, Ferrara, Italy, <sup>6</sup>VII Orthopaedic Division, Rizzoli Orthopaedic Institute, Bologna, Italy, <sup>7</sup>Medical Department, SPA-Società Prodotti Antibiotici, Milan, Italy.

As part of a multicentre randomized controlled study on bone density changes after total hip arthroplasty (THA), we measured the bone mineral density (BMD) of the contralateral (non-operated) hip using DXA. Forty-one patients (mean age 65.6±6.4 (SD), 24 male and 17 female) undergoing THA operation for severe osteoarthritis of the hip were enrolled in the untreated control group of the study. Baseline assessment was obtained no later than 2 weeks after the operation and 41, 36 and 26 patients respectively completed the follow-up with DXA measurements repeated at 3, 6 and 12 months.

Total hip and greater trochanter BMD of the non operated hip showed significant decreases at 3, 6 and 12-month follow-up (total hip BMD at 12 months -1.2%, p=0.05; greater trochanter at 12 months -1.6%, p<0.05). Intertrochanteric and femoral neck regions showed significant BMD reductions only at some of the time-points. When analyzing the data according to sex, only women showed significant hip bone loss (total hip BMD at 12 months -2.4%, p<0.05; femoral neck BMD at 12 months -4.5%, p<0.05; greater trochanter at 12 months -3.1%, p<0.05), while no changes were observed in men.

The observed bone loss at the non operated hip of patients undergoing THA for severe osteoarthritis may be a consequence of reduced mechanical load, or relative disuse, contrasting with an increased load prior to THA to compensate for the reduced joint function of the affected side. However, the gender difference may indicate that postmenopausal and age related bone loss, that is more pronounced in women, is also contributing to the observed BMD decreases.

Following THA, a significant bone loss in women at the non operated hip should be interpreted with caution in clinical practice and not necessarily indicates systemic bone loss.

**Disclosures:** S. Ortolani, None.

*This study received funding from: SPA-Società Prodotti Antibiotici, Italy.*

## M409

**Effect of Metabolic Acidosis on Bone Mineral Density and Bone Microarchitecture in Normal and Ovariectomized Rats.** R. Krapf<sup>1</sup>, J. A. Gasser<sup>2</sup>. <sup>1</sup>Medicine, Kantonsspital Bruderholz, Bruderholz/Basel, Switzerland, <sup>2</sup>Musculoskeletal Diseases, Novartis Institute for Biomedical Research, Basel, Switzerland.

Metabolic acidosis (MA) in vitro increases osteoclast, but decreases osteoblast activity and impairs bone matrix protein synthesis as well as bone mineralization. The dietary-induced MA typical of the Western diet may contribute to the current osteoporosis epidemic. We, therefore, wished to characterize the effects of MA on bone mass and microarchitecture in vivo in rats.

MA was induced in normal and ovariectomized (OVX) virgin Wistar rats by feeding 30 mEq/kg bw of NH<sub>4</sub>Cl. Rats were analysed at baseline and at weeks 6 and 10 using in vivo pQCT and in vivo uCT in proximal tibia metaphysis.

NH<sub>4</sub>Cl feeding resulted in MA of comparable severity in both groups, characterised by significant falls in the plasma [HCO<sub>3</sub><sup>-</sup>] and stable increases in urinary ammonium excretion.

Difference in % change of various bone parameters at week 10 compared to non-acidotic normal or non-acidotic ovx rats respectively

		Total BMD	Cortical thickness	Endosteal surface	BV/TV	TbN	Connectivity density
Normal NH <sub>4</sub> Cl	+	-5.7% *	-4.1%	+14.1% *	11.7%	-24.7% *	-24.4% *
OVX + NH <sub>4</sub> Cl		-5.7% *	-4.8%	+6.3%	-7.1%	-7.4%	-5.6%

\* denotes p at least < 0.5 by Dunnett

The table illustrates that MA significantly decreased total BMD and reduced cortical thickness in both normal and OVX rats at 10 weeks. Cortical thinning resulted from endosteal resorption without any change in periosteal circumference. MA also significantly diminished trabecular number (TbN) without any change in trabecular thickness (TbTh), and as a consequence, increased trabecular separation in normal rats. In addition, MA decreased connectivity density. In OVX rats, MA induced similar changes but most of the effects did not reach statistical significance. Increases in the structure model index (SMI) were seen in normal rats with MA at week 10, indicating progressive conversion of plate like structures into more rod like structures. MA also increased TRAP5b activity without any significant change in osteocalcin in the two groups.

MA significantly changes bone parameters in both, OVX and estrogen replete rats, primarily by a) increasing endosteal bone resorption and b) decreasing TbN. MA apparently increases endosteal bone resorption and induces impaired bone microarchitecture in rats in vivo.

**Disclosures:** R. Krapf, None.

*This study received funding from: Swiss National Science foundation grant 4053-110259.*

## M410

**Therapeutic Effects of One-year Alendronate Treatment in Three Cases of Osteoporosis with Parietal Thinning.** S. Takata<sup>1</sup>, N. Yasui<sup>1</sup>, S. Takao<sup>\*2</sup>, S. Yoshida<sup>\*2</sup>. <sup>1</sup>Orthopedics, Institute of Health Biosciences, The University of Tokushima Graduate School, Tokushima, Japan, <sup>2</sup>Radiology, The University of Tokushima, Tokushima, Japan.

Parietal thinning is defined as external thinning of the parietal bone of the skull. External thinning of the posteromedial part of the bilateral parietal bones is a morphological characteristic of the skulls of osteoporotic patients with parietal thinning. There are two types of parietal thinning of the skull, flat and grooved and most cases of parietal thinning are of the flat type. At this time, the reasons for excessive bone resorption in the skull, especially in the posteromedial part of the parietal bone in osteoporotic patients, as well as the reasons for enhanced external lamina bone resorption remain unclear.

We studied the therapeutic effects of one-year alendronate treatment in three cases (two males and one female) of osteoporosis with parietal thinning of skull. Plain radiography and three dimensional computed tomography revealed asymmetric external thinning of the posteromedial part of the bilateral parietal bones. Parietal thinning of our three cases was of the flat type.

Technetium-99m methylenediphosphate bone scintigraphy did not show any changes in these three cases. Pretreatment levels of urinary type I collagen cross-linked N-telopeptides (NTX) in all three cases were high compared to the normal range. Pretreatment levels of serum bone-specific alkaline phosphatase (BAP) in the two male patients were high in contrast to the normal values in the female patient. Pretreatment mean bone mineral density (BMD) values of the 2nd to 4th lumbar vertebrae (L2-4BMD), head BMD, femoral neck BMD, and whole body BMD of all three patients were low compared with the respective normal ranges.

One-year alendronate treatment increased the whole body BMD in all three cases, the L2-4BMD of the female patient, the femoral neck BMD of the female patient and one male patient, and the head BMD of the female patient when compared to pretreatment levels. This treatment decreased both urinary NTX and serum BAP in all three cases to normal values.

**Disclosures:** S. Takata, None.

## M411

**Different Influence of the Clinical Condition, Degree of Cholestasis, Alcohol Abuse and Serum Calcium on the Musculoskeletal System in Chronic Cirrhotics.** S. E. Ferretti<sup>\*1</sup>, R. F. Capozza<sup>\*2</sup>, G. R. Cointny<sup>\*2</sup>, S. Feldman<sup>\*2</sup>, M. R. Ulla<sup>2</sup>, H. Tanno<sup>\*2</sup>, J. L. Ferretti<sup>2</sup>. <sup>1</sup>Service of Gastroenterology & Hepatology, Univ Hospital, Faculty of Medicine, National University of Rosario, Rosario, Argentina, <sup>2</sup>CEMFOC, Faculty of Medicine, National University of Rosario, Rosario, Argentina.

This study analyzed the associations between indicators of the clinical condition (Child-Pugh Score -CPS, capturing bilirubinemia, albuminemia, prothrombin time, ascitis and encephalopathy-), degree of cholestasis (total bilirubinemia, plasma alkaline phosphatase -BRB, APase-), alcohol abuse, serum Ca and other biochemical variables, and tomographic (pQCT) indicators of bone mass (cortical CSA and BMC -CtA, CtC-, trabecular BMC and vBMD -TbC, vTbD-), cortical tissue mineralization (cortical vBMD -vCtD-), diaphyseal design (cross-sectional area moments of inertia -CSMI's-) and torsion strength (*Stress-Strain Index* -SSI-) and muscle mass (height-adjusted muscle CSA -mCSA-) of the radii (4% and 66% sites) and tibiae (4%, 14%, 38% & 66% sites) of 43 chronic cirrhotics (18 men) of alcoholic, viral, cryptogenetic, autoimmune or cholestatic etiology, aged 18-69 yr. Bone and muscle pQCT data were expressed as Z-scores calculated for every patient taking those of healthy men (60) and women (200) of comparable age as a control reference.

The cirrhotic sample showed reduced TbC, vTbD and mCSA, while CtA, CtC, vCtD, CSMI's and SSI were unaffected. The proportion between cortical bone mass (tibia + fibula CtA) and muscle CSA at the 66% site of the leg (calf) was reduced. Trabecular bone loss correlated with CPS (especially with its component, albuminemia) and with the degree of cholestasis only when alcohol abusers were excluded from the analyses. Muscle loss correlated with CPS but not with the degree of cholestasis. Alcohol abusers showed always these alterations, regardless of CPS and degree of cholestasis. Serum Ca did not correlate with any other indicator. No differences were detected in those analyses between forearm and leg pQCT data. The chronic cirrhosis condition reduced trabecular mass (and obviously the compressive strength of the trabecular network) in correlation with the severity of the disease and cholestasis, with little or no affection of cortical mass, design, or strength. It reduced also correlatively muscle mass, regardless of the degree of cholestasis. However, the metabolic disturbance seemed to have reduced the impact of muscle-bone interactions in terms of bone mass (not material quality, design, or strength) related to muscle mass in the studied sample. The generally negative impact of alcohol abuse on all those properties was unrelated to any other influence.

**Disclosures:** J.L. Ferretti, None.

*This study received funding from: CONICET (ARGENTINA).*



M412

**Detrimental Effects of Abdominal Irradiation on the Skeleton in Growing Mice.** D. Jia<sup>1</sup>, R. J. Griffin<sup>\*1</sup>, R. Halakatti<sup>\*1</sup>, L. J. Suva<sup>2</sup>, D. Gaddy<sup>3</sup>, N. S. Ake<sup>1\*3</sup>, C. Jackson<sup>\*1</sup>, C. Thompson<sup>\*4</sup>, P. M. Corry<sup>\*1</sup>. <sup>1</sup>Department of Radiation Oncology, U Arkansas for Medical Sciences, Little Rock, AR, USA, <sup>2</sup>Department of Orthopedics, U Arkansas for Medical Sciences, Little Rock, AR, USA, <sup>3</sup>Department of Physiology, U Arkansas for Medical Sciences, Little Rock, AR, USA, <sup>4</sup>U Arkansas at Little Rock, Little Rock, AR, USA.

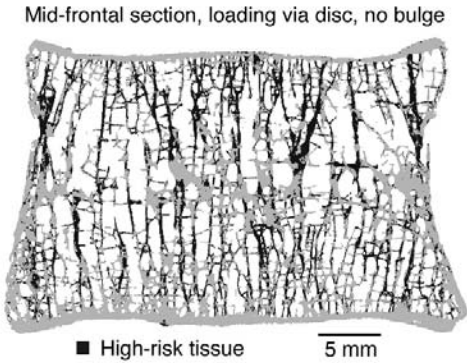
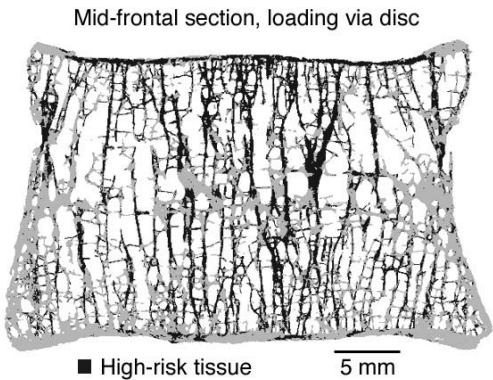
Partial abdominal ionizing irradiation (AI) is a common clinical anti-tumor modality. AI can induce responses in distant organs presumably through systemic mechanisms. The effects of AI on the skeleton of 10-week-old male C57BL/6 mice was evaluated following a single dose of 0 or 20 Gy x-ray irradiation to the abdomen, with the skeleton shielded. The mice were monitored daily for 8 days. Blood was collected at day 8 for measurement of bone turnover markers; bone marrow collected from tibiae and femora for *ex vivo* bone cell differentiation and stromal cell colony assay; lumbar vertebrae, femora and tibiae assessed by DEXA for baseline and final bone mineral content and density (BMC and BMD). The tibiae were analyzed by microCT to determine architectural properties of cancellous bone in the proximal metaphysis as well as cortical geometry in the mid-diaphysis. DEXA scanning of the proximal one-third of the tibia revealed a decrease in BMD in the irradiated mice, compared with an increase in the controls (-5.3% vs 7.9%, *p* < 0.001). This was accompanied by changes in BMC (-7.9% vs. 9.9%, *p* < 0.001). Similar effects on BMD and BMC in the distal femora, but not the lumbar vertebrae, were observed. MicroCT assessment of the proximal tibia revealed significantly lower BV/TV and Tb.Th in irradiated mice than in the controls (0.137 vs. 0.110, and 0.053 mm vs. 0.048 mm, respectively, *p* < 0.01). Decreased BMD and BMC in the tibial midshaft, but not femoral midshaft, were also detected by DEXA in the irradiated mice, compared with increased parameters in the controls (-1.79% vs 8.52%, -7.56% vs 13.85%, respectively, *p* < 0.001). Tibial midshaft geometry, assessed by microCT, showed no difference between the two groups. Serum TRAP5b increased while osteocalcin decreased in irradiated mice as compared with the controls (*p* < 0.05). *Ex vivo* bone marrow osteoblast differentiation and stromal cell colony formation were suppressed following AI (*p* < 0.01). By contrast, bone marrow osteoclast formation was similar between the two groups, suggesting differential cell responses to AI. Our data demonstrate that AI has adverse abscopal effects on both cancellous and cortical bone in growing mice in a site-specific manner. The effects are manifested by altered activity of mature osteoblasts and osteoclasts. The cellular effects may result from direct responses to AI-induced signals, or be mediated by osteoblast progenitors/stroma-derived molecules.

Disclosures: D. Jia, None.

M413

**Mechanisms of Endplate Failure in the Human Vertebral Body.** A. J. Fields\*, T. M. Keaveny. Mechanical Engineering, University of California, Berkeley, Berkeley, CA, USA.

Understanding the failure mechanisms associated with vertebral fracture is important for assessing fracture risk and may provide insight into fracture etiology. Recent work suggests that the cortical endplates should play a role in the clinical diagnosis of these fractures, and thus, this study focused on the biomechanical behavior of endplate tissue. Using micro-CT-based finite element analysis of 22 human T9 whole vertebral bodies (age range: 53-97 years, 81.5±9.6 years), we sought to quantify the amount of endplate tissue at high risk of failure during compressive loading and to identify the regions where this high-risk tissue occurs. Each model (posterior elements removed) was loaded through a simulated intervertebral disc. To isolate the cause of the high-risk tissue, we performed a second set of analyses in which we removed the ability of the disc to bulge when compressed. Results indicated that the high-risk endplate tissue was strained almost exclusively in tension, indicating a unique failure mechanism of the endplates since the high-risk tissue in the cortical shell and trabecular compartments was strained proportionately more in compression. Within both endplates, the largest concentrations of high-risk tissue were in the mid-sagittal and mid-frontal regions--the locations where the endplates are thinnest. The amount of high-risk tissue comprised 20.8±6.6% of the inferior endplate bony tissue and 27.8±7.7% of the superior endplate (*p*=0.002, paired t-test) tissue, representing 8.9±2.4% and 10.2±2.1% of the total amount of high-risk bone in the vertebrae, respectively. When the disc bulging effect was removed from the models, the amount of high-risk endplate tissue decreased by over 70% and was largely due to a reduction in tensile strains in the endplates (Figure). We conclude that the endplate tissue at high risk of initial failure is primarily loaded in tension and that the development of such tensile strains is associated with bulging of the intervertebral disc.



Disclosures: A.J. Fields, None.  
This study received funding from: NIH AR49828.

M414

**Acute Chronic Obstructive Pulmonary Disease (COPD) Exacerbations Are Associated with Uncoupling of Bone Resorption from Bone Formation.** A. Hutchinson<sup>\*1</sup>, M. Thompson<sup>\*1</sup>, D. Smallwood<sup>\*1</sup>, S. Bozinovski<sup>\*2</sup>, G. P. Anderson<sup>\*2</sup>, L. Irving<sup>\*1</sup>, P. R. Ebeling<sup>3</sup>. <sup>1</sup>Depts. Respiratory Medicine, CEHSEU and CCRED, The Royal Melbourne Hospital, Parkville, Australia, <sup>2</sup>Pharmacology Department, CRCID, University of Melbourne, Western Hospital, Footscray, Australia, <sup>3</sup>Dept. of Medicine (RMH/WH), University of Melbourne, Western Hospital, Footscray, Australia.

COPD is an independent risk factor for minimal trauma fractures and osteoporosis. Inhaled corticosteroids (ICS) reduce bone formation markers, while acute exacerbations (AECOPD) increase inflammatory markers. We first compared biochemical bone turnover markers in 61 patients with stable COPD on high-dose ICS with 58 sex-matched, healthy controls. Second, we measured acute changes in bone turnover markers, highly sensitive C-reactive protein (hsCRP), and insulin-like growth factor-1 (IGF-1) during AECOPD. Early morning, fasting samples were obtained during stable COPD and Day 1 to 7 after AECOPD onset. To assess the affect of maintenance ICS on bone turnover, we compared serum  $\beta$  C-telopeptide ( $\beta$ -CTX) and type 1 procollagen N-terminal propeptide (PINP) in stable COPD patients with sex-matched, healthy controls. Bone formation markers, serum osteocalcin and PINP; the bone resorption marker,  $\beta$ -CTX; hsCRP and IGF-1 were measured in AECOPD. In stable COPD, mean PINP (in men and women) and  $\beta$ -CTX levels (in men) were significantly lower than controls. For PINP: In men with COPD vs. controls 38 vs. 67 ng/mL, (*p* < 0.001); and in women with COPD vs. controls 33 vs. 51 ng/mL, (*p* < 0.002). For  $\beta$ -CTX: In men with COPD vs. controls 0.43 vs. 0.55 ng/mL, (*p*=0.03); and in women with COPD vs. controls 0.29 vs. 0.33 ng/mL (*p* = 0.52). At AECOPD onset (*n* = 17), there were significant acute decreases in both serum osteocalcin (-25%) and PINP (-32%) on day-3, after commencing high-dose systemic or oral corticosteroids. Significant increases in  $\beta$ -CTX (+24%; day-3; *p* < 0.01) and hsCRP (+30%; day-1; *p* < 0.01) occurred, the latter correlating with a decrease in bone formation, as measured by PINP. Uncoupling of bone formation from bone resorption occurs in stable COPD. In AECOPD bone formation decreases further, increasing the risk of bone loss and osteoporosis. This acute decrease in bone formation in AECOPD may be related to either inflammation or high-dose corticosteroids.

Table (n=17)				
% Change Median (range)	Day-1	Day-3	Day-5	Day-7
PINP	-41% (-78 to +267%)	-32% (-72% to 122%)	-30% (-72% to 62%)	-33% (-66% to 48%)
$\beta$ -CTX	+12.1% (-70% to 265%)	+24% (-63% to +200%)	+24% (-47% to +188%)	+50% (-100% to 236%)
IGF-1	-4.4 (-100 to +23%)	+40% (-100% to +44%)	-30% (-30% to +47%)	-30% (-34% to +72%)
Osteocalcin	-29% (-65 to 52)	-25% (-63% to 76%)	-67% (-100% to 44%)	-29% (-70% to +100%)
hsCRP	+30% (-70% to +3632%)	-8% (-100% to +2504)	-9% (-100 to +1012%)	+5% (-100% to +404%)

Disclosures: P.R. Ebeling, None.

M415

**Impact of Adjuvant Hormonal Therapy on Bone Loss Depending on Initial Adjuvant Chemotherapy and Menstrual Status.** F. A. Tremollieres<sup>1</sup>, C. Frayssinet<sup>\*1</sup>, P. Leguevague<sup>\*2</sup>, J. M. Pouilles<sup>\*1</sup>, J. Hoff<sup>\*2</sup>, C. Ribot<sup>1</sup>. <sup>1</sup>Menopause Center, Hôpital Paule de Viguier, Toulouse, France, <sup>2</sup>Department of General and Gynaecological Surgery, CHU Rangueil, Toulouse, France.

In intermediate or high risk hormone receptor-positive (HR+) breast cancer (BC) women, adjuvant chemotherapy is standard treatment and usually followed by hormonal therapy. Tamoxifen (Tam) and aromatase inhibitors have been shown to have opposite effects on bone remodeling and the risk of fracture. However, it is not clear whether their

respective effect on bone might be influenced by initial chemotherapy (CT) and/or changes in menstrual status. We thus conducted a prospective study to determine whether the effect of adjuvant tamoxifen vs anastrozole (Ana) on bone loss was influenced by initial CT and menstrual status changes in early stage BC women.

One hundred and twelve women with early stage BC were followed over an average 28.8 month-period of time. 97 women with HR+ BC received either adjuvant Tam (n=55) or Ana (n=42) therapy. Of these women, 60 had received adjuvant CT prior to the beginning of hormonal treatment. The remaining 15 women with HR- BC received adjuvant CT only. The effect of menstrual status on BMD was further studied.

A significantly higher rate of vertebral bone loss was noted in women who received initial adjuvant CT as compared to those who did not, irrespective of the type of further adjuvant hormonal treatment (-2.5% vs -1.4%,  $p=0.0205$ ). However, such effect appeared mainly the consequence of premature ovarian failure. In postmenopausal women, Ana was associated with a significantly greater rate of femoral and total body bone loss compared to Tam. Accordingly, opposite effects of biochemical markers of bone turnover were found with a significant increase in osteocalcin levels and a significant reduction in serum CTX levels from baseline in Ana-treated women and those who received Tam, respectively. On the other hand, in pre-menopausal women who developed amenorrhea (n=19), Tam had no effect in preventing bone loss at all bone sites while a protective effect was observed in initially postmenopausal women who were further treated with Tam (n=20) (lumbar spine: -3.4% vs -0.64%,  $p=0.0002$ ; femoral neck: -1.6% vs +0.3%,  $p=0.037$ ; total body: -0.82% vs +0.003%,  $p=0.02$ ). In initially postmenopausal women, Tam induced a significantly greater decrease in serum osteocalcin and CTX levels compared to that in women who developed amenorrhea throughout follow-up. In conclusion, the impact of CT and the apparent lack of prevention of Tam on ovarian failure-induced bone loss in premenopausal women must be considered in the long-term preventive strategy of the risk of fracture in BC women. An evaluation of the risk of fracture should be recommended in all women from the beginning of therapy.

**Disclosures:** F.A. Tremollieres, None.

## M416

### Sex Steroids Have Site Specific Effects on Muscle and Bone Geometry in Young Adult Males. L. Edwards<sup>1</sup>, J. E. Adams<sup>1</sup>, P. L. Selby<sup>2</sup>, K. A. Ward<sup>1</sup>.

<sup>1</sup>Imaging Science and Biomedical Engineering, University of Manchester, Manchester, United Kingdom, <sup>2</sup>Medicine, Central Manchester and Manchester Childrens University Hospital NHS Trust, Manchester, United Kingdom.

Sex steroids are essential for skeletal development and the maintenance of bone health. The current study aimed to establish whether there were relationships between sex hormones and bone mineral density (BMD) and the geometric properties of the peripheral bones of young adult males (YM).

European Caucasian YM (18-24 years) were recruited (n=95). Fasting venous blood samples were taken for analysis of serum sex steroids. Peripheral quantitative computed tomography (pQCT) measurements were taken at the 4 and 50% non-dominant radius and 65% tibia. Dependent variables (DV) at the 4% radius included: Total and trabecular BMD (TotBMD and TrabBMD respectively mg/cm<sup>3</sup>) and total area (TA mm<sup>2</sup>). DV at the 50% radius / 65% tibia included: radius / tibia area (RA / TibA mm<sup>2</sup>) muscle cross sectional area (MCSA mm<sup>2</sup>), cortical bone mineral content (CBMC mg/mm), cortical BMD (CBMD mg/cm<sup>3</sup>), cortical thickness (CT mm), stress strain index (SSI mm<sup>3</sup>) and medullary area (MA mm<sup>2</sup>). Serum DV included: total testosterone (T<sub>t</sub> nmol/L) Total estrogen (E<sub>t</sub> pmol/L) sex hormone binding globulin (SHBG nmol/L) and albumin (Al g/L). Bioavailable estrogen (BE pmol/L) bioavailable testosterone (BT nmol/L), free estrogen (FE pmol/L) and free testosterone (FT nmol/L) were calculated from serum measured variables using standard calculations.

The influence of sex hormones upon bone variables was tested using ANCOVA controlling for height (cm), weight (Kg). There were no significant findings for the sex hormones at the 4% radius. SHBG was significant for TA ( $p=0.022$ ) and TrabBMD ( $p=0.022$ ). At the 50% radius: T<sub>t</sub> was significant for MCSA ( $p=0.017$ ), RA ( $p=0.011$ ), SSI ( $p=0.027$ ) and MA ( $p=0.024$ ); SHBG was significant for RA ( $p=0.013$ ), MCSA ( $p=0.003$ ) CBMD ( $p=0.005$ ), SSI ( $p=0.013$ ) and MA (0.032). At the 65% tibia: E<sub>t</sub> was significant for CBMC ( $p=0.028$ ) and CT ( $p=0.026$ ); SHBG and T<sub>t</sub> were significant for MCSA ( $p=0.029$  and 0.010 respectively); bioavailable oestrogen and free oestrogen were significant for CT ( $p=0.049$  and 0.040 respectively). Bioavailable and free testosterone were not significant at any of the skeletal sites.

These data suggest that there are site specific differences in the effect of sex hormones and SHBG on bone. In the radius, total testosterone and SHBG are important in determining bone geometric parameters and MCSA. In the tibia, bone geometry and BMD are influenced by total, bioavailable and free estrogen; total testosterone and SHBG also have an effect on muscle. In conclusion, in young adult males an important determinant of the geometric properties of the radius is testosterone and for the tibia, estrogen.

**Disclosures:** L. Edwards, None.

## M417

### Homocysteine Accumulates in Bone Tissue by Collagen Binding and Adversely Affects Bone. M. Herrmann<sup>\*1</sup>, A. Tami<sup>\*2</sup>, B. Wildemann<sup>\*3</sup>, M. Wolny<sup>\*3</sup>, A. Wagner<sup>\*4</sup>, H. Schorr<sup>\*4</sup>, O. Taban-Shomal<sup>\*4</sup>, N. Umanskaya<sup>\*5</sup>, S. Ross<sup>\*5</sup>, P. Garcia<sup>\*4</sup>, U. Huebner<sup>\*4</sup>, W. Herrmann<sup>\*5</sup>. <sup>1</sup>Bone Research Program, ANZAC Research Institute, Concord, Australia, <sup>2</sup>AO Foundation, Davos, Switzerland, <sup>3</sup>Charite Universitaetsmedizin, Berlin, Germany, <sup>4</sup>University Hospital of Saarland, Homburg, Germany, <sup>5</sup>Bone Research Program, University Hospital of Saarland, Homburg, Germany.

Recently, hyperhomocysteinemia (HHCY) has been suggested to have adverse effects on bone. This study investigated if an experimental hyperhomocysteinemia (HHCY) in rats induces an accumulation of HCY in bone tissue that is accompanied by a reduced bone quality. HHCY was induced in healthy rats by either a methionine (Meth)- or a homocystine (Homo)-enriched diet and compared with controls. Tissue and plasma concentrations of homocysteine (HCY), S-adenosylhomocysteine (SAH) and S-adenosylmethionine (SAM) were measured. Bone quality was assessed by biomechanical testing, histomorphometry,  $\mu$ CT and the measurement of biochemical bone turnover markers in plasma. Meth and Homo animals developed a significant HHCY that was accompanied by a tissue specific accumulation of HCY (1300 to 2000% vs. controls). 65% of HCY in bone was bound to collagen of the extracellular matrix. The SAH / SAM-ratio in bone and plasma of Meth and Homo animals exhibited a tissue specific increase indicating a reduced methylation capacity. Accumulation of HCY in bone was characterized by a distinct reduction of trabecular bone (proximal femur: -25 to -35%; distal femur -56 to -58%, proximal tibia: -28 to -43%). Accordingly, bone strength was significantly reduced (-9 to -12%). A tissue specific accumulation of HCY in bone may be a promising mechanism explaining adverse effects of HHCY on bone. A reduced methylation capacity of bone cells might be another relevant pathomechanism.

**Disclosures:** M. Herrmann, None.

## M418

### Central Control of Bone Remodeling: The Neurohypophysial Hormone Oxytocin Is Decreased In Severe Post-menopausal Osteoporosis. V. Breuil<sup>1</sup>,

E. Amri<sup>\*2</sup>, J. Testa<sup>\*3</sup>, C. H. Roux<sup>\*1</sup>, P. Ferrari<sup>\*4</sup>, C. Albert-Sabonnadière<sup>\*1</sup>, C. Elabd<sup>\*2</sup>, G. Ailhaud<sup>\*2</sup>, C. Dani<sup>\*2</sup>, G. f. Carle<sup>5</sup>, L. Euler-Ziegler<sup>\*1</sup>. <sup>1</sup>Rheumatology, CHU de Nice, Nice, France, <sup>2</sup>ISBDC - Université Sophia-Antipolis, CNRS, Nice, France, <sup>3</sup>Statistics & Epidemiology, CHU de Nice, Nice, France, <sup>4</sup>Laboratory of Hormonology, CHU de Nice, Nice, France, <sup>5</sup>GEPITOS - Université Sophia-Antipolis, CNRS, Nice, France.

Oxytocin (OT) is a neurohypophysial hormone; its receptor is expressed on bone cells. In a study, we demonstrated in rodents that OT negatively modulates adipogenesis while promoting osteogenesis; in ovariectomized mice, OT serum levels were decreased and subcutaneous OT injection reversed bone loss.

**In this study** we measured OT serum levels in post-menopausal OP and its relationships with body composition and hormonal factors.

**Subjects and Methods** We measured serum levels of OT, high sensitive estradiol, testosterone, FSH, LH, SHBG, TSH, osteocalcin, crosslaps, leptin and body composition by DEXA in post-menopausal women with severe OP compared to non OP women.

**Results** Main results are presented in the following table as means  $\pm$  SEM.

group	age (years)	weight (kg)	fat mass (kg)	BMI (kg/m <sup>2</sup> )	OT pg/ml	leptin ng/ml	estradiol pg/ml	BMD femoral neck (T-score SD)
control (n=16)	67.31 $\pm$ 6.19	75.8 $\pm$ 17.5	31.8 $\pm$ 10.7	30.35 $\pm$ 6.58	110.64 $\pm$ 79.12	6.20 $\pm$ 2.70	21.51 $\pm$ 11.23	-0.069 $\pm$ 0.677
OP (n=20)	73.25 $\pm$ 9.17	61.1 $\pm$ 9.5	23.9 $\pm$ 7.1	26.24 $\pm$ 4.33	50.22 $\pm$ 39.16	3.71 $\pm$ 1.42	24.47 $\pm$ 7.68	-1.948 $\pm$ 0.748
p	0.04	0.002	0.03	0.08	<b>0.0001</b>	<b>0.002</b>	ns	<0.001

In OP women, fat mass and lean mass were significantly decreased in absolute values. OT serum level was significantly correlated to BMD (spine,  $r=0.64$  and hip,  $r=0.55$ ) but not to all others measured parameters. Leptin was significantly correlated to BMI ( $r=0.74$ ), fat mass ( $r=0.67$ ), lean mass ( $r=0.52$ ) and BMD (spine,  $r=0.48$ ) and hip  $r=0.55$ ). In logistic regression analysis, OP remains significantly correlated to OT ( $p<0.05$ ) and leptin levels ( $p<0.05$ ) regardless of age.

**Conclusion:** OT serum level is significantly decreased in OP, independently of leptin and estradiol, that are known to modulate OT secretion. Thus, OT appears as a new interesting factor in the OP pathophysiology.

**Disclosures:** V. Breuil, None.

This study received funding from: CNRS & PHRC régional du CHU de Nice.

**M419**

**Bridging Vascular Calcification and Osteoporosis: The Function of Receptor Activator of Nuclear Factor  $\kappa$ B.** C. Byon<sup>\*1</sup>, J. Chen<sup>\*2</sup>, J. McDonald<sup>2</sup>, Y. Chen<sup>2</sup>. <sup>1</sup>Cell Biology, University of Alabama at Birmingham, Birmingham, AL, USA, <sup>2</sup>Pathology, University of Alabama at Birmingham, Birmingham, AL, USA.

Clinical studies support an association between atherosclerosis/vascular calcification and osteoporosis, suggesting possible common pathophysiological mechanisms. Oxidative stress has been linked to both bone loss and vascular calcification. Our previous studies have demonstrated that hydrogen peroxide ( $H_2O_2$ ), at non-toxic concentrations, induces oxidative stress and promotes osteogenic differentiation and calcification of vascular smooth muscle cells (VSMC). Multinucleated tartrate-resistant acid phosphatase (TRAP)-positive osteoclast-like cells have been identified in calcified atherosclerotic lesions. Therefore, we sought to determine whether  $H_2O_2$ -induced VSMC calcification contributes to osteoclastogenesis.

We found a 33-fold increase in the transcripts of receptor activator of nuclear factor  $\kappa$ B (RANKL), as determined by real-time PCR, during  $H_2O_2$ -induced VSMC calcification. Further, increased expression of RANKL protein in VSMC under oxidative stress was demonstrated by ELISA and flow cytometry analysis. With the use of a series of deletion constructs of the murine RANKL promoter-driven luciferase reporter, we determined that  $H_2O_2$  responsive region is located between -200 to -400 in the 5'-flanking regions of RANKL gene. Analyses of the sequence of this region identified multiple binding sites of the key osteogenic transcript factor, Runx2, which we have reported to be essential for  $H_2O_2$ -induced VSMC calcification.  $H_2O_2$ -induced RANKL expression was blocked in VSMC with Runx2 knockdown by lentivirus-carrying shRNA for Runx2.

To determine whether  $H_2O_2$ -induced RANKL in VSMC is functionally active, we determined the effects of  $H_2O_2$ -induced RANKL in VSMC on osteoclastogenesis of bone marrow macrophages (BMM) in a co-culture system. After exposure to  $H_2O_2$  for two weeks, VSMC (wild-type) induced the differentiation of BMM into multinucleated TRAP-positive cells. Addition of osteoprotegerin (OPG) inhibited osteoclastogenesis of BMM when co-cultured with VSMC. By contrast, VSMC from RANKL deficient mice failed to induce differentiation of BMM into TRAP-positive multinucleated cells, which was restored when recombinant RANKL protein was added in culture media.

We have demonstrated that  $H_2O_2$  up-regulates the expression of RANKL during VSMC calcification and it is dependent upon the expression of Runx2. VSMC-derived RANKL induces osteoclastogenesis of BMM, which may contribute to the genesis of TRAP-positive multinucleated cells in atherosclerotic lesions and may provide a mechanism for oxidative stress-induced bone loss attributed to increased osteoclastogenesis.

**Disclosures:** C. Byon, None.

**M420**

**Effect of Risedronate on Osteocyte Viability in Paired Biopsies from Early Postmenopausal Women.** S. Qiu<sup>1</sup>, R. Phipps<sup>2</sup>, S. Palnitkar<sup>\*1</sup>, D. Rao<sup>1</sup>. <sup>1</sup>Bone and Mineral, Henry Ford Hospital, Detroit, MI, USA, <sup>2</sup>Procter & Gamble, Mason, OH, USA.

There is strong evidence that estrogen deficiency can accelerate osteocyte death by apoptosis. Increased osteocyte apoptosis may compromise bone quality for postmenopausal women. The purpose of this analysis was to determine whether 1 year risedronate treatment affected osteocyte viability in early postmenopausal women (within 1-5 years postmenopause).

Paired iliac bone biopsies were obtained from 19 postmenopausal women at baseline and after 1 year of treatment with placebo (n = 8; Age:  $52.9 \pm 3.44$  years) or risedronate (n = 11; Age:  $52.5 \pm 3.36$ ). From 5  $\mu$ m sections stained with goldner trichrome, we measured the following osteocyte related variables in trabecular bone: osteocyte density (Ot.Dn), empty lacunar density (EL.Dn), total lacunar density (TL.Dn) and the percent empty lacunae (EL/TL). Coefficient of variation [CV (%) = SD/mean \* 100] of each variable was computed from ten measured areas to determine the homogeneity of osteocyte and empty lacunar distribution. The difference in each variable between baseline and 1-year biopsies was compared for each group using paired t-test. ANCOVA was used to compare the difference in each variable between 1-year biopsies with placebo and risedronate treatment by adjusting for the corresponding variable from baseline biopsies.

In both placebo and risedronate groups, EL.Dn and EL/TL were significantly lower at 1 year compared to baseline, but there was no significant difference in TL.Dn and CV for each variable between baseline and 1 year (Table 1). In addition, there was no significant difference in any variable between placebo and risedronate treatment at 1 year.

In conclusion, the present study suggests that while risedronate effectively inhibits bone remodeling (data not shown), at least in early postmenopausal women it does not influence osteocyte death or impair osteocyte distribution. An unexpected observation was that the empty lacunae were significantly decreased at 1 year in the placebo treated group. Although a site-specific difference cannot be excluded (baseline and 1-year biopsies were obtained from right and left iliac crests), a possible explanation is that osteocyte apoptosis is a short-term, transient phenomenon after estrogen depletion.

Variables	Placebo (n = 8)		Risedronate (n = 11)	
	Baseline	1-Year	Baseline	1-Year
Ot.Dn (#/mm <sup>2</sup> )	134 (13.2)	162 (43.1)*	154 (31.3)	179 (28.9)
EL.Dn (#/mm <sup>2</sup> )	48.1 (13.2)	27.2 (9.31)**	39.0 (8.07)	27.9 (8.17)*
TL.Dn (#/mm <sup>2</sup> )	183 (22.0)	189 (48.4)	193 (28.4)	207 (27.1)
EL/TL.N (%)	26.6 (5.14)	14.9 (3.21)**	21.2 (6.17)	14.0 (5.37)*

Data expressed as mean (SD); Baseline vs 1-Year \*P<0.05 and \*\*P<0.005

**Disclosures:** S. Qiu, P&G 3.

This study received funding from: The Alliance for Better Bone Health (Procter & Gamble Pharmaceuticals and sanofi-aventis).

**M421**

**Serum Level of  $\gamma$ -glutamyltransferase (sGGT) Is One of the Factors That Determines the Response to Alendronate Treatment in Osteoporotic Women.** Y. Sakamoto<sup>\*1</sup>, M. Ishijima<sup>1</sup>, M. Yamanaka<sup>\*1</sup>, K. Kitahara<sup>\*1</sup>, A. Tokita<sup>\*2</sup>, H. Kurosawa<sup>\*1</sup>. <sup>1</sup>Orthopaedics, Juntendo University School of Medicine, Tokyo, Japan, <sup>2</sup>Pediatrics, Juntendo University School of Medicine, Tokyo, Japan.

Serum level of  $\gamma$ -glutamyltransferase ( $\gamma$ -GTP/GGT) is known as a marker for alcohol consumption, liver dysfunction and biliary tract disorders. Recently, GGT is reported to act as a bone-resorbing factor that stimulates osteoclast formation by animal studies. However, it is still remained obscure whether GGT regulates bone metabolism in human. The present study examined to determine whether sGGT is involved in the effect of alendronate (ALN) to increase in lumbar bone mineral density (L-BMD) in osteoporosis. A total of fifty-five postmenopausal women (age 58 to 86) with primary osteoporosis enrolled in this prospective study. All the patients of this study took 5mg of ALN daily for twelve months. L-BMD was measured at baseline and six and twelve months of the treatment. Serum levels of bone specific alkaline phosphatase (BAP), calcium, phosphate, creatinine, total protein (TP), lactate dehydrogenase, aminotransferases, GGT, intact-parathyroid hormone, 25-hydroxyvitamin D, 1,25-dihydroxyvitamin D and urinary N-terminal telopeptides of type I collagen (NTX) and deoxypyridinoline (DPD) were also measured. Multiple regression analysis was conducted to investigate the associations between the biochemical markers at six months and their percent change (%change) for six months as potential predictor variables listed above with the %change in L-BMD for twelve months as outcome variable. A p value less than 0.05 was considered to be statistically significant. Multiple regression analysis showed that, in addition to %change of NTX ( $\beta = -0.48$ ) and basal level of TP ( $\beta = -0.27$ ), basal level of sGGT ( $\beta = -0.33$ ) was one of the factors that determines the increase in L-BMD by ALN ( $R^2 = 0.35$ ,  $p < 0.05$ ). %change of sGGT for twelve months showed positive correlation with %change in BMD ( $r = 0.33$ ,  $p < 0.05$ ) and negative correlation with %changes of BAP and DPD for twelve months ( $r = -0.45$ ,  $p < 0.01$  and  $r = -0.39$ ,  $p < 0.01$ , respectively). Bisphosphonate is reported to increase bone mass via activation of OPG expression (Osteoporos Int 06). GGT stimulates RANKL expression and bone resorption (J Biol Chem 04). Combined with all these data and our result, GGT is speculated to activate bone resorption by stimulating RANK-RANKL-OPG system via unique pathway independent from that of bisphosphonate. This is a first report to suggest that sGGT is involved in bone metabolism in human and, furthermore, may be able to shed light on an unknown mechanism of bone resorption. In conclusion, basal level of sGGT was independent predictor of the increase in L-BMD by the ALN treatment.

**Disclosures:** Y. Sakamoto, None.

**M422**

**Solid-State <sup>31</sup>P MRI Quantifies Mineralization Changes in OVX Rat Bone.** S. Anumula<sup>1</sup>, D. Horng<sup>\*1</sup>, S. L. Wehrli<sup>\*2</sup>, F. W. Wehrli<sup>1</sup>. <sup>1</sup>Radiology, University of Pennsylvania Medical Center, Philadelphia, PA, USA, <sup>2</sup>NMR Core Facility, Children's Hospital of Philadelphia, Philadelphia, PA, USA.

Postmenopausal osteoporosis is characterized by lower bone volume fraction and reduced degree of mineralization of bone (DMB) resulting in an imbalance between bone formation and resorption. There is currently no noninvasive technique for measuring DMB. Here we examined the hypothesis that 3D <sup>31</sup>P solid-state magnetic resonance imaging (<sup>31</sup>P MRI) is able to detect the increase in mineralization upon treatment with alendronate (ALN) in the ovariectomized (OVX) rat. The study involved nine OVX rats (four month old) treated with ALN (5 $\mu$ g/kg/day) compared to eleven sham-operated rats (NO) and eleven OVX rats of the same age. All animals received standard chow and water *ad libitum* for 50 days at which time they were euthanized and cortical bones extracted from the right and left femurs. <sup>31</sup>P MRI was performed at 9.4 Tesla field strength on a vertical bore superconducting system (DMX-400, Bruker Instruments, USA) in conjunction with a home-built solenoid coil using a previously developed 3D radial imaging sequence. The specimens were co-imaged with a reference phantom of 2M  $K_2HPO_4$  in order to quantify mineral <sup>31</sup>P concentration. The k-space data were reconstructed off-line yielding an isotropic resolution of 157  $\mu$ m. MRI results were compared with ash weight and ultimate strength (US) derived from three-point bending. Phosphorus concentration obtained by <sup>31</sup>P MRI was found to return toward normal levels in ALN treated bones (Fig. 1). This result was paralleled by increased ash weight and US although the latter was not significant (Table 1).

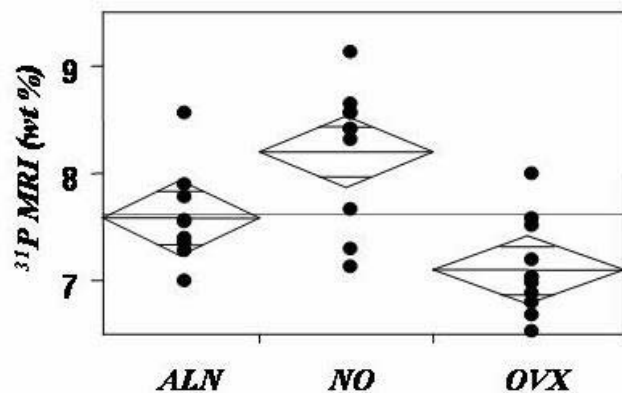


**Fig. 1 Phosphorus concentration indicating recovery of OVX bone after treatment with ALN.**

**Table 1 Measures of DMB and ultimate strength quantified by different modalities in NO, OVX and ALN groups (mean $\pm$  SD)**

Group	$^{31}\text{P MRI}$ (wt %)	Ash (wt %)	US (N/mm $^2$ )
NO	8.2 $\pm$ 0.6 <sup>a</sup>	65.4 $\pm$ 1.1 <sup>a</sup>	147.2 $\pm$ 17.6 <sup>b</sup>
OVX	7.1 $\pm$ 0.4	65.2 $\pm$ 1.2	137.9 $\pm$ 12.3
ALN	7.6 $\pm$ 0.5 <sup>a</sup>	66.5 $\pm$ 1.1 <sup>a</sup>	147.5 $\pm$ 15.5 <sup>b</sup>

<sup>a,b</sup>ALN, NO versus OVX ( $p \leq 0.01$ ;  $p > 0.05$ , respectively)

In conclusion, our data suggest that  $^{31}\text{P MRI}$  may have potential for noninvasive monitoring of the changes in mineral metabolism in response to hormonal changes and treatment

**Disclosures:** S. Anumula, None.

## M423

**Psychotropic Drugs Have Contrasting Skeletal Effects that Are Independent of Their Negative Effects On Activity Levels.** S. J. Warden<sup>1</sup>, S. M. Hassett<sup>1</sup>, J. L. Bond<sup>1</sup>, J. Rydberg<sup>1</sup>, J. D. Grogg<sup>1</sup>, E. L. Hilles<sup>1</sup>, R. K. Fuchs<sup>1</sup>, M. M. Bliziotis<sup>2</sup>, C. H. Turner<sup>3</sup>. <sup>1</sup>Department of Physical Therapy, Indiana University, Indianapolis, IN, USA, <sup>2</sup>Oregon Health and Science University, Portland, OR, USA, <sup>3</sup>Department of Biomedical Engineering, Indiana University-Purdue University, Indianapolis, IN, USA.

Psychotropic drugs (incl. selective serotonin reuptake inhibitors [SSRIs], tricyclic antidepressants [TCAs] and lithium) are prescribed to treat depression and other affective disorders. Preclinical studies have shown negative skeletal effects of psychotropic drugs; however, it is unclear whether these changes resulted from drug effects on animal physical activity levels. Psychotropic drugs act on the central nervous system and induce a hypoactive (skeletal unloading) phenotype in mice. This study removed this potential confounder by investigating psychotropic drug effects in animals with complete unloading. Eighty female Swiss-Webster mice were purchased at 4 wk of age and randomly divided into two activity groups: 1) cage control (ACTIVE), and; 2) tail suspended (INACTIVE). Animals within each activity group were randomly divided into four drug groups: 1) vehicle treated (VEH); 2) fluoxetine hydrochloride (20 mg/kg) treated (SSRI); 3) desipramine hydrochloride (20 mg/kg) treated (TCA), and; 4) lithium chloride (200 mg/kg) treated (LICL). *In vivo* assessments of hindlimb areal (aBMD) and proximal tibia volumetric (vBMD) BMD were performed at baseline and following 4 wk of intervention. Femurs and lumbar vertebrae were subsequently removed and assessed *ex vivo* for aBMD and vBMD, as well as trabecular bone architecture (bone volume fraction [BV/TV]). Drug reduced activity levels in ACTIVE, with LICL traveling half the total distance of VEH, SSRI and TCA. There were no differences in distance traveled between VEH, SSRI and TCA. There were no activity and drug interactions on skeletal measures indicating that their effects were independent. There were drug effects for most outcomes, with SSRI and LICL having inferior and superior bone properties than all other groups, respectively. For instance, SSRI gained 9.0% less proximal tibia vBMD and

had 3.1% less lumbar vertebrae BV/TV than VEH, whereas LICL gained 6.7% more proximal tibia vBMD than VEH. There were limited differences between TCA and VEH. These data indicate that psychotropic drugs have contrasting skeletal effects that are independent of any physical inactivity induced by these drugs. Of particular note is the inferior bone properties observed with SSRI. This observation is consistent with the recent findings of functional serotonin pathways in bone and clinical studies demonstrating accelerated bone loss with SSRIs.

**Disclosures:** S.J. Warden, None.

This study received funding from: NIH/NIAMS (AR-052018).

## M424

**Osteogenic Action of Exendin-4 in Normal and Insulin-Resistant State.** B. Nuche-Berenguer<sup>1</sup>, P. Moreno<sup>1</sup>, L. Arnés<sup>1</sup>, S. Dapía<sup>2</sup>, P. Esbrit<sup>3</sup>, M. Villanueva-Peñacarrillo<sup>1</sup>. <sup>1</sup>Metabolism, Nutrition & Hormones, Fundación Jiménez Díaz, Madrid, Spain, <sup>2</sup>Trabeculae, Orense, Spain, <sup>3</sup>Bone & Mineral Metabolism, Fundación Jiménez Díaz, Madrid, Spain.

**Background and Aims:** A role of incretins in changes in bone turnover, occurring after meals, was suggested. Exendin-4 (Ex-4) mimics GLP-1 (glucagon-like peptide 1) action on glucose metabolism in extrapancreatic tissues, is agonist of its specific receptors, and also has insulinotropic, antidiabetic and anorectic effects. We explored the possible *in vivo* effect of Ex-4 upon bone turnover markers in normal rats (N) and in an insulin-resistant model (IR).

**Materials and Methods:** IR was induced in adult Wistar rats by 8 weeks feeding with standard chow plus 20% D-fructose in the drinking water. N (n=21) and IR (n=20) were treated -osmotic pump- with saline (control) or Ex-4 (0.1 nmol/kg/h). In fed conditions, blood samples were taken before (basal) and by ending the treatment; femurs and tibiae were collected. Measurements: *in plasma*, osteocalcin (OC), tartrate-resistant acid phosphatase (TRAP) -ELISA-, insulin -RIA- and glucose. *In tibia*, osteocalcin, osteoprotegerin (OPG) and RANK ligand (RANKL) mRNA -rt-PCR-. Femoral bone structure was evaluated by  $\mu\text{CT}$  (n=3 rats/group).

**Results:** *In plasma* (n=10-15): Ex-4 did not modify basal OC in N (406.24 $\pm$ 16.6 ng/ml) or IR group (271.0 $\pm$ 12.3 ng/ml,  $p < 0.0001$  vs N); N basal TRAP (2.25 $\pm$ 0.23 U/l) was not modified by Ex-4, while in IR, with lower than N ( $p < 0.016$ ) value (1.50 $\pm$ 0.15 U/l), it reduced it (-33.5 $\pm$ 10.7%  $\Delta$  of basal,  $p < 0.05$ ); basal insulin and glucose were similar in all groups at any condition. *In tibia* (n=7-11): OC mRNA level in IR was 0.49 $\pm$ 0.09 times N ( $p < 0.001$ ), and Ex-4 increased it in N (1.7 $\pm$ 0.1 times control,  $p < 0.02$ ) and IR (3.6 $\pm$ 0.3 times control,  $p < 0.05$ , and  $p < 0.05$  vs N Ex-4-treated); OPG mRNA in IR was 0.66 $\pm$ 0.12 times that in N ( $p < 0.02$ ), and Ex-4 increased it in N (2.36 $\pm$ 0.20 times control,  $p < 0.001$ ), and even more in IR (4.76 $\pm$ 0.43 times control,  $p < 0.001$ ); RANKL mRNA was lower ( $p < 0.001$ ) in IR (0.56 $\pm$ 0.08 times N), and Ex-4 decreased the value in N (0.63 $\pm$ 0.07 times control,  $p < 0.01$ ), but stimulated it in IR (2.73 $\pm$ 0.49 times control,  $p < 0.02$ , and  $p < 0.0001$  vs N Ex-4-treated). In IR, OPG/RANKL mRNA ratio was 1.18-fold N, and Ex-4 increased it to 3.76 in N and to 1.74-fold in IR. *In femur*, trabecular thickness and anisotropy in IR were higher and lower, respectively, than in N, and no changes were observed after Ex-4; yet, both cortical thickness and momentum of inertia, higher than in N, were increased even further by Ex-4 treatment.

**Conclusion:** Several changes in bone markers and structure suggest a low bone turnover rate in this insulin-resistant model, and the results suggest that this situation can be ameliorated by an apparent osteogenic action of Ex-4.

**Disclosures:** B. Nuche-Berenguer, None.

This study received funding from: Research Grant from Ministerio de Sanidad y Consumo (FIS: 06/0076)

## M425

**Positive Effect of GLP-1 upon Bone Formation and Resistance in Insulin-Resistant Rats.** P. Moreno<sup>\*1</sup>, B. Nuche-Berenguer<sup>1</sup>, S. Dapia<sup>\*2</sup>, P. Esbrit<sup>3</sup>, M. Villanueva-Peñacarrillo<sup>\*1</sup>. <sup>1</sup>Metabolism, Nutrition & Hormones, Fundación Jiménez Díaz, Madrid, Spain, <sup>2</sup>Metabolism, Nutrition & Hormones, Trabeculae, Orense, Spain, <sup>3</sup>Bone & Mineral Metabolism, Fundación Jiménez Díaz, Madrid, Spain.

**Introduction:** The insulin-independent antidiabetic action of GLP-1 (Glucagon-like-peptide 1), insulinotropic and positive effect upon glucose metabolism in liver, muscle and fat, and neurotrophic and anorectic properties, are documented. It was proposed that incretins could participate in bone remodelling changes occurring after nutrients absorption. We searched for the possible *in vivo* modulating effect of GLP-1 upon bone turnover markers, in insulin-resistant rats (IR) compared to normal (N).

**Materials & Methods:** IR was induced in adult Wistar rats by 8 weeks feeding with standard chow plus 20% D-fructose in the drinking water. N (n=20 rats) and IR (n=20) were treated 3 days -osmotic pump- with saline (control) or GLP-1 (0.86 nmol/kg/h). In fed conditions, blood was taken before (basal) and by ending the treatment; femurs and tibiae were collected. Measurements: in plasma, osteocalcin (OC), tartrate-resistant acid phosphatase (TRAP) -ELISA-, insulin -RIA- and glucose; in tibia, OC, osteoprotegerin (OPG) and RANK ligand (RANKL) mRNA -rtPCR-. In femur: bone structure -μCT- (n=3 rats/group).

**Results:** In plasma: GLP-1 did not change the basal OC in N ( $407.9 \pm 16.1$  ng/ml, n=15) but decreased it in IR ( $-22.2 \pm 4\%$  Δ of basal,  $p < 0.03$ ), which was initially lower ( $p < 0.0001$ ) than N ( $289.40 \pm 16.64$  ng/ml, n= 15); N-basal TRAP ( $2.26 \pm 0.20$  U/l, n= 16) was not modified by GLP-1, while in IR, with lower than N ( $p < 0.0001$ ) basal value ( $1.14 \pm 0.16$  U/l, n= 15) GLP-1 normalized it ( $48.3 \pm 20.3\%$  Δ basal); basal insulin and glucose were similar in all groups at any condition. In tibia (n=7-11): control OC mRNA in IR was  $0.49 \pm 0.09$  times that in N ( $p < 0.001$ ), in which GLP-1 increased  $4.22 \pm 0.83$  times its control value ( $p < 0.01$ ), as it did, but less ( $p < 0.05$  vs N) in IR ( $1.82 \pm 0.18$  times control,  $p < 0.01$ ); control OPG mRNA in IR was lower than N ( $0.66 \pm 0.12$  times,  $p < 0.02$ ), and GLP-1 raised it in N ( $2.29 \pm 0.23$  times control,  $p < 0.01$ ) and also in IR ( $2.84 \pm 0.46$  times control,  $p < 0.01$ ); control RANKL mRNA was lower ( $p < 0.001$ ) in IR ( $0.56 \pm 0.09$  times N), and GLP-1 increased it only slightly in N and IR. In IR, OPG/RANKL mRNA ratio was 1.2 fold of N, and GLP-1 raised it in both (1.8 in N and 1.6 fold in IR). Femur trabecular thickness and anisotropy in IR were higher and lower, respectively, than in N, with no apparent changes after GLP-1; both femoral cortical thickness and momentum of inertia in IR were higher than in N, and further increased after GLP-1.

**Conclusion:** The insulin-resistance of this experimental model is associated to a low bone remodelling rate and in this state, GLP-1 treatment seems to favour both bone formation and resistance.

**Disclosures:** P. Moreno, None.

This study received funding from: Research Grant from Ministerio de Sanidad y Consumo (FIS: 06/0076)

## M426

**Does Dietary Phosphorus Influence FGF-23 Concentrations in Fibrous Dysplasia Patients?** C. Marotte<sup>\*</sup>, L. Guerrero<sup>\*</sup>, A. L. Sánchez<sup>\*</sup>, J. Somoza<sup>\*</sup>, A. Bagur<sup>\*</sup>, B. Oliveri<sup>\*</sup>, M. S. Parisi<sup>\*</sup>. Sección Osteopatías Médicas, Hospital de Clínicas, Universidad de Buenos Aires, Buenos Aires, Argentina.

High levels of fibroblast growth factor 23 (FGF-23) have been reported in Fibrous Dysplasia (FD) patients. However, whether or not phosphate physiological regulation mechanisms are maintained is unknown.

**Objective:** to determine whether serum FGF-23 concentrations are regulated by dietary phosphorus (P) in FD patients.

We studied 6 polyostotic FD patients (2M, 4W) aged  $31.5 \pm 11.2$  y (X±SD) (r: 20-50), and 6 healthy controls (1M, 5W) aged  $33.4 \pm 15.5$  y (r: 20-57).

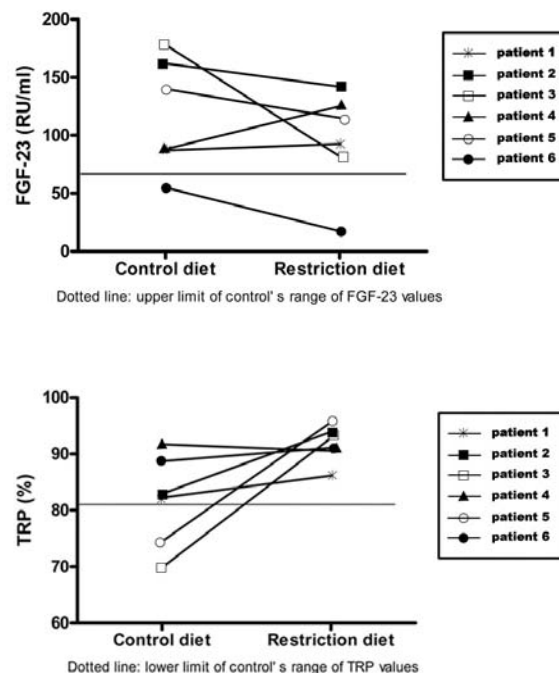
Patients and controls performed a 5 days control diet with 1500mg/d of P. After a free diet period (3-27d), FD patients performed a 5 days restriction diet with 625mg/d of P. All the subjects filled a daily meals record. P and calcium total intakes were calculated. Lab tests after each diet: serum FGF-23 (C-terminal, Inmutopics), 1,25(OH)2D, P, Ca, iPTH, and creatinine; and urinary P, Ca, and creatinine. Tubular reabsorption of P (TRP) was calculated.

After the control diet, P intakes were:  $1145 \pm 116$ mg/d in patients, and  $917 \pm 250$ mg/d in controls (ns). After the restriction diet, in FD patients, P intake was:  $712 \pm 67$ mg/d ( $p < 0.05$  vs control diet).

After control diet: FGF-23 levels were higher in FD patients ( $118.3 \pm 48.7$  vs  $40.0 \pm 25.6$  RU/ml,  $p < 0.02$ ). Only patient 6 had levels in the control's range (17.5 to 68 RU/ml). Mean TRP was lower in FD patients ( $81.7 \pm 8.3\%$ ) vs controls ( $86.7 \pm 5.6\%$ ) (ns). No differences were observed in the other studied parameters.

After the restriction diet, mean FGF-23 levels dropped to  $95.7 \pm 44.0$  RU/ml, (ns). FGF-23 values of 5 patients persisted above the control's range upper limit (fig 1). TRP values increased ( $92.2 \pm 3.4\%$ ,  $p < 0.05$ ). All patients had TRP >80% (fig 2). 1,25(OH)2D and iPTH did not correlate with FGF-23 or TRP levels.

Our observations may suggest that physiological mechanisms involved in P homeostasis could be preserved in some, but not all, FD patients. These results are in accordance with the wide clinical expression of FD. Further studies should be conducted to confirm these results.



**Disclosures:** M.S. Parisi, None.

This study received funding from: Agencia Nacional de Promoción Científica y Tecnológica, PICT 2005 / 38328.

## M427

**Association of Familial Hypocalciuric Hypercalcemia and Mandible Lesions in Two Kindreds.** M. V. Pedroni<sup>\*1</sup>, P. T. Gonçalves<sup>\*2</sup>, G. Guerra<sup>\*3</sup>, M. T. M. Baptista<sup>\*2</sup>, S. H. V. Lemos-Marini<sup>\*2</sup>, L. F. R. De Souza-Li<sup>3</sup>. <sup>1</sup>Center for Investigation in Pediatrics, State University of Campinas, Campinas, Brazil, <sup>2</sup>Pediatrics, State University of Campinas, Campinas, Brazil, <sup>3</sup>Pediatrics and Center for Investigation in Pediatrics, State University of Campinas, Campinas, Brazil.

Familial hypocalciuric hypercalcemia (FHH) is characterized by high normal serum calcium, low calcium clearance to creatinine clearance ratio ( $\text{Ca}^{++}/\text{Cr}$  ratio) and normal but not suppressed PTH. FHH is a benign disease with very few complications described. Unspecific symptoms such as fatigue, muscle pain, headache are found in some affected members. We report two families with FHH where lesions in mandible lead to their investigation. IDSS, female, 10 years old, was referred to the Pediatric Endocrinology unit due to recurrent episodes of swelling in the central part of mandible, looseness of lower central incisors and fever lasting 4 days followed spontaneous remission. After 1 year she had another episode with gingival bleeding requiring antibiotics and fixation of the loosened teeth. X-ray showed destruction of alveolar bone of the four inferior incisors. She referred Legg-Calvé-Perthes at 5 years old with persistent pain on the right leg. Her biochemical profile showed ionized calcium  $1.19$  mmol/L (reference values  $1.12-1.32$ ), serum calcium  $9.9$  mg/dL ( $8.6-10.0$ ), PTH  $30.66$  pg/mL ( $15-65$ ), Pi  $4.9$  mg/dL ( $2.7-4.5$ ) and  $\text{Ca}^{++}/\text{Cr}$  ratio of  $0.0037$ . Bone scanning showed increase uptake in mandible and decrease uptake in right femoral epiphysis. Her mother had a serum calcium of  $9.1$  mg/dL, PTH  $49.1$  pg/mL and  $\text{Ca}^{++}/\text{Cr}$  ratio of  $0.01$ , while her father presented with serum calcium of  $10.2$  mg/dL, PTH  $55.34$  pg/mL and  $\text{Ca}^{++}/\text{Cr}$  ratio of  $0.13$ . WHG, male, 11 years old, had a history of a mass in central mandible, dislocating the lower central incisors, which was removed and the pathology revealed giant cell granuloma. The mass recurred, being excised again after 2 years. Investigation after the third recurrence of the expansive lesion, showed increase ionized calcium of  $1.43$  mmol/L, total serum calcium  $10.8$  mg/dL, PTH  $51.3$  pg/mL, Pi  $4.3$  mg/dL and  $\text{Ca}^{++}/\text{Cr}$  ratio of  $0.019$ . He had a normal abdominal ultrasound, and a cranial CT scan showed an expansive lesion of soft tissue with bone involvement in anterior left mandible. His mother showed total serum calcium of  $10.9$  mg/dL, Pi  $2.2$  mg/dL, PTH  $99.3$  pg/mL and  $\text{Ca}^{++}/\text{Cr}$  ratio of  $0.0089$ . His father had a normal serum calcium ( $8.9$  mg/dL), Pi  $4.1$  mg/dL, and  $\text{Ca}^{++}/\text{Cr}$  ratio of  $0.012$ . Molecular genetics analyses of the patients have been pursued. Mandible is a sensitive target to PTH and bisphosphonates action. However, it has not been described mandible lesions associated with FHH. Whether this is a casual coincidence or a rare complication of the disease is unclear.

**Disclosures:** L.F.R. De Souza-Li, None.

## M428

### Bisphosphate Protect Cartilage by Reducing Chondrocyte Apoptosis and Reduce Bone Lose by Suppressing Osteoclast in Adjuvant Arthritis. C. Yongping\*. Orthopedic Surgery, Peking University, First Hospital, Beijing, China.

**Objective** To investigate the effects of bisphosphate on joint cartilage in rat adjuvant arthritis. **Method** 160 seven-week-old female Lewis rats were randomly allocated into 4 groups: normal group(NV), arthritic group(SV), low dose group(SI-10), and high dose group(SI-100). Except the normal control, the other groups were injected with Freund's complete adjuvant into the tail base. Immediately after sensitization, the rats were treated with vehicle or incadronate at 10 or 100µg/kg/d subcutaneously, three times per week. The animals were killed at 2, 4, 6 and 10 weeks after sensitization. The hind-paw and fore-paw joints were evaluated. Results At 4 weeks after sensitization, articular cartilage destruction and subchondral bone loss of the hind-paws were found in the SV group. But SI-10 and SI-100 groups showed less destruction in cartilage. The number of osteoclast and the serum IL-6, sialic acid levels obviously decreased. 2 weeks later, all groups had ruined hind-paws, even in the SI-100 group. In the fore-paw study, at 6 weeks, most severe articular cartilage destruction and subchondral bone loss were found in the SV group. The most apoptotic chondrocytes were found in the SV group when compare with others. And the SV group was significant difference with the NV, SI-100 groups ( $P < 0.05$ ), so did the SI-10 group. There was no significant difference ( $P > 0.05$ ) between the NV and the SI-100 groups. At 10 weeks, more severe articular cartilage destruction was detected in the arthritic control group than others. The apoptotic chondrocyte number in the SV group was still significant higher ( $P < 0.05$ ) than the other three groups. But among the NV, SI-10 and SI-100 groups, there was no significant difference ( $P > 0.05$ ). **Conclusion** Bisphosphates could not only inhibit osteoclast function to protect subchondral bone, but also decrease the serum inflammatory factors levels, chondrocyte apoptosis and cartilage matrix loss to protect articular cartilage in adjuvant arthritis.

**Disclosures:** C. Yongping, None.

## M429

### Bisphosphonates in Children with Hypercalciuria and Reduced Bone Mineral Density. U. S. Alon<sup>1</sup>, M. Freundlich<sup>2</sup>. <sup>1</sup>Nephrology, Bone and Mineral Disorders Clinic, Children's Mercy Hospital, Kansas City, MO, USA, <sup>2</sup>Pediatric Nephrology, University of Miami, Miami, FL, USA.

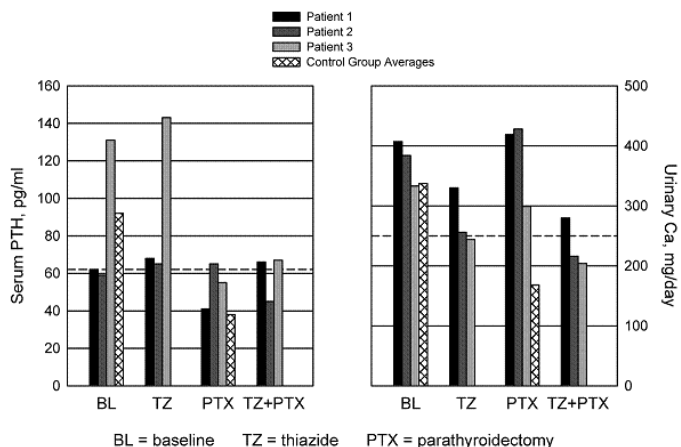
Previous studies have demonstrated reduced bone mineral density (BMD) and biochemical changes of excessive bone resorption in some patients with idiopathic hypercalciuria (IH). Consequently, bisphosphonates have been successfully employed in research animals and adults with IH and reduced BMD. We evaluated the effect of treatment with bisphosphonates in 7 patients, ages 10-16 years, with persistent IH and reduced BMD. In 5 children, preceding traditional therapy failed. All children received oral alendronate and one also IV Zoledronic acid, for 6-18 months (median 9.0, mean 10.7 months). With treatment, BMD Z-scores in the lumbar spine improved from  $-2.0 \pm 0.3$  to  $-0.8 \pm 0.8$  ( $p = 0.002$ ) and in the femoral neck from  $-1.8 \pm 0.4$  to  $-0.7 \pm 0.9$  ( $p = 0.01$ ); urine N-telopeptides/creatinine decreased from  $372 \pm 289$  to  $72 \pm 39$  nmol/mmol ( $p = 0.05$ ) and calcium/creatinine from  $0.29 \pm 0.12$  to  $0.13 \pm 0.06$  mg/mg ( $p = 0.009$ ). Height Z scores, normal at baseline in all, have remained unaffected, and no new stones or fractures were documented throughout the treatment period. Serum creatinine, electrolytes, Ca, P and PTH remained normal as well. In summary, in children with IH and decreased BMD, treatment with bisphosphonates normalized urine calcium excretion, eliminated urinary symptoms, and significantly improved reduced BMD. These beneficial effects indicate the need for larger prospective studies on the potential of bisphosphonates to serve as a new tool in treating children with IH and reduced BMD.

**Disclosures:** U.S. Alon, None.

## M430

### Renal Leak Hypercalciuria: A Potential Cause of Tertiary Hyperparathyroidism. P. Tondapu\*, C. V. Odvina. Charles and Jane Pak Center for Mineral Metabolism, UT Southwestern Medical Center, Dallas, TX, USA.

Tertiary hyperparathyroidism is commonly seen in chronic renal failure, after kidney transplant, hyperphosphatemia or during long-term oral phosphate therapy, and chronic vitamin D deficiency. It has also been reported in patients with renal leak hypercalciuria although not very common. In renal leak hypercalciuria, impaired renal tubular reabsorption of calcium is the primary abnormality. Serum PTH concentration is either high or high normal because of preexisting negative calcium balance. Chronic stimulation of parathyroid gland could lead to hyperplasia (secondary hyperparathyroidism). Eventually, the hyperplastic parathyroid gland could become autonomous leading to tertiary hyperparathyroidism. Regardless of the cause, the physiological sequelae are similar, with hypercalcemia coexisting with a raised PTH. This report is a retrospective analysis of data on three patients; 2 with nephrolithiasis and one with osteoporosis. All three patients had normal serum calcium, high or high normal serum PTH and increased urinary calcium (figure 1). Administration of thiazide diuretic to control urinary calcium loss resulted in slight decline in urinary calcium but patients became hypercalcemic with non-suppressed PTH. All three patients underwent parathyroidectomy. However, despite lower serum calcium after surgery, they remained hypercalciuric (figure 1)



When compared to patients with primary hyperparathyroidism, patients with renal leak hypercalciuria had significantly higher urinary calcium excretion postoperatively. These findings suggest that renal leak hypercalciuria is the primary problem which led to the hyperparathyroidism. This has previously been described in detail by Bordier et al. in 1977. To the best of our knowledge, after the publication of the study mentioned above and 1 case report in 1980, there has not been any published cases since. Our findings emphasize the need for continued follow up of these patients. Patients with tertiary hyperparathyroidism due to renal leak should receive thiazides postoperatively to decrease the possibility of recurrence. In addition, early diagnosis and treatment with thiazides before they develop tertiary hyperparathyroidism may alleviate the need for surgery.

**Disclosures:** C.V. Odvina, None.

## M431

### Prevalence and Demographics of Asymptomatic Normocalcemic Hyperparathyroidism in the United States. B. Misra, S. J. Silverberg, J. P. Bilezikian. College of Physicians and Surgeons, Columbia University, New York, NY, USA.

Normocalcemic primary hyperparathyroidism (NPHPT) is a disorder characterized by normal serum calcium concentration and elevated PTH in the absence of known secondary causes for hyperparathyroidism (HPT). Typically these patients are identified in referral centers when they are being evaluated for low bone density, kidney stones, or other target organ complications. These patients, therefore, do not necessarily reflect a variant of asymptomatic primary hyperparathyroidism (PHPT) but rather PHPT with symptoms. This led to the hypothesis that in order to identify asymptomatic NPHPT, one would have to screen a population of healthy individuals who have not been referred to a specialty center. To gain information on the putative incidence of asymptomatic NPHPT, therefore, we obtained data from the 2003-2004 National Health and Nutrition Examination Survey (NHANES) survey, in which parathyroid hormone (PTH), calcium, 25-hydroxyvitamin D [25(OH)D] levels and renal function were measured in over 6000 individuals. Weighting allowed calculations of national estimates. We sampled 1909 individuals from this NHANES database >45 years old with a creatinine clearance of  $\geq 60$  cc/min (to eliminate those with renal-based secondary elevations in PTH), in whom the corrected serum calcium was in the mid-normal range (9-10 mg/dL) and the 25(OH)D was  $\geq 30$  ng/dL. Using these criteria, we found that 1% of the population had PTH levels  $\geq 65$  pg/mL (mean PTH level of  $81 \pm 14$  pg/mL). The group with NPHPT was 65% female, 89% Caucasian, and 48% were between the ages 45-54. The estimated prevalence of NPHPT in this sample is similar to a reported incidence of 1.2% of parathyroid adenomas discovered incidentally during neck surgery for reasons other than PHPT. Although all secondary causes of HPT have not been ruled-out, these data suggest that in a free-living unscreened population, there is an appreciable incidence of NPHPT. These individuals may be the earliest forerunners of asymptomatic PHPT. Future prospective studies should permit direct estimates of the incidence of NPHPT as well as identification of predictors of disease progression to the hypercalcemic asymptomatic variant of PHPT.

**Disclosures:** B. Misra, None.

**M432**

**Immunohistochemical and Genetic Characterization of the Atypical Parathyroid Adenoma.** A. Scillitani<sup>\*1</sup>, V. Guarnieri<sup>\*2</sup>, M. Bisceglia<sup>\*3</sup>, C. Battista<sup>\*1</sup>, S. Minisola<sup>\*4</sup>, I. Chiodini<sup>\*5</sup>, L. A. Muscarella<sup>\*2</sup>, C. Vainicher-  
Eller<sup>\*5</sup>, D. E. C. Cole<sup>6</sup>. <sup>1</sup>U.O. of Endocrinology, IRCCS "Casa Sollievo della Sofferenza" Hospital, San Giovanni Rotondo, Italy, <sup>2</sup>Medical Genetics Service, IRCCS "Casa Sollievo della Sofferenza" Hospital, San Giovanni Rotondo, Italy, <sup>3</sup>U.O. of Pathology, IRCCS "Casa Sollievo della Sofferenza" Hospital, San Giovanni Rotondo, Italy, <sup>4</sup>Department of Clinical Sciences, "La Sapienza" University, Rome, Italy, <sup>5</sup>Department of Medical Sciences, University of Milan, Milan, Italy, <sup>6</sup>Department of Laboratory Medicine and Pathobiology, University of Toronto, Toronto, ON, Canada.

Molecular studies of non-malignant parathyroid tumours suggest that the atypical parathyroid adenoma (AA) may be an intermediate stage of progression to parathyroid carcinoma. Various investigators have suggested that HRPT2 mutations may be found in this sub-type of adenoma, but systematic immunohistochemical and molecular study of a single cohort has not been reported. Although parafibromin immunostaining has been proposed as an adjunct tool for the diagnosis of parathyroid carcinoma, its usefulness in AA has not yet been defined. From our centre, eleven cases of AA were available for study (5 women; 6 men; age 53 +/- 17 years). The criteria for AA classification were: (i) presence of fibrous bands and/or (ii) necrosis, and/or (iii) excess mitoses, and/or (iv) capsular invasion. Screening of exons and exon-intron boundaries for germline mutations in genomic DNA from peripheral blood showed: 2/11 patients with germline truncating mutations (c.679\_680delAG; c.685\_688delAGAG). Tumor tissue was subjected to LOH analysis and mutation screening of exons 1, 2 and 7, encompassing 85% of point mutations. One somatic mutation (c.231C>G) was identified in the patient with c.679\_680delAG and LOH was observed in another. Thus, in total, at least three of the 11 patients showed genetic alterations. Parafibromin immunoreactivity, assessed in 10/11 tumours, showed: complete (~100%) expression in 3; partial but diffuse expression in 3; patchy expression in 2; and none in 2. Although the loss of parafibromin immunostaining was prevalent in atypical adenomas, it was not clearly associated with the presence of genetic mutation, suggesting that immunohistochemistry cannot substitute for molecular analysis. Studies on larger case series will better define the place of this technique in AA assessment and help identify patients needing closer clinical follow-up.

**Disclosures:** A. Scillitani, None.

**M433**

**Body Composition Changes after Radioiodine Treatment of Hyperthyroidism.** H. Xu<sup>\*1</sup>, J. Wang<sup>\*1</sup>, Q. Wu<sup>\*1</sup>, H. S. Barden<sup>2</sup>, Q. Zhou<sup>3</sup>. <sup>1</sup>Department of Nuclear Medicine, The First Affiliated Hospital, Jinan University, Guangzhou, China, <sup>2</sup>GE Healthcare, Madison, WI, USA, <sup>3</sup>GE Healthcare, Shanghai, China.

Patients treated for thyrotoxicosis often complain of increases in body weight after radioiodine <sup>131</sup>I treatment of their thyroid disorder. The objective of this study was to estimate changes in body weight and composition following treatment of hyperthyroidism with radioiodine <sup>131</sup>I. Body composition (fat mass, lean mass, and bone mineral content), was determined by dual energy X-ray absorptiometry (DXA), (GE Healthcare, Prodigy) at baseline and 3 mo after radioiodine treatment in 92 previously untreated subjects with hyperthyroidism (59 women and 33 men, age 37±9 yrs). Suppressed serum TSH and high free serum thyroxine levels were found in all patients. All patients received radioiodine <sup>131</sup>I therapy. Sixty patients achieved a euthyroid status after 3 mo of radioiodine <sup>131</sup>I therapy, while 32 patients developed a hypothyroid status. DXA total body short-term precision was good (BMC 0.7%, fat mass 1.5%, and lean mass 0.7% and BMD ranged from 0.7% to 2.1%). Body composition results by DXA before and after radioiodine <sup>131</sup>I treatment in patients with hyperthyroidism are shown in following table. Results suggest that the body weight increase in hyperthyroid patients who achieved a euthyroid status after 3 mo of radioiodine <sup>131</sup>I therapy was mainly the result of their lean mass increase, while the body weight increase in subjects who became hypothyroid after treatment was due to increases in both lean mass and fat mass.

	Baseline (n=60)	euthyroidism after treatment	Baseline (n=32)	hypothyroidism after treatment
FT <sub>3</sub> (pmol/L)	20.99±13.84	7.75±6.57*	16.78±11.42	1.79±1.08*
FT <sub>4</sub> (pmol/L)	49.07±19.83	24.95±17.48*	46.31±22.80	6.02±3.46*
sTSH (mIU/L)	0.02±0.33	0.54±1.26*	0.45±1.61	19.52±9.77*
Weight (kg)	49.94±8.28	60.19±5.82*	49.94±9.11	53.78±10.40*
BMC (kg)	2.076±0.376	2.114±0.384	2.031±0.393	1.983±0.379
Fat mass (kg)	12.260±6.334	12.563±6.602	11.668±5.547	12.622±5.472*
Lean mass (kg)	35.599±6.664	38.334±7.386*	36.268±8.252	39.160±8.327*

\* P<0.05 vs before treatment

**Disclosures:** H. Xu, None.

**M434**

**Changes in Cardiovascular Function after Parathyroidectomy in Mild Primary Hyperparathyroidism.** M. D. Walker<sup>1</sup>, J. Fleischer<sup>1</sup>, S. Homma<sup>\*1</sup>, T. Rundek<sup>\*2</sup>, D. J. McMahon<sup>1</sup>, A. Tineo<sup>\*1</sup>, W. B. Inabnet<sup>\*1</sup>, J. Lee<sup>\*1</sup>, J. Udesky<sup>\*1</sup>, R. Lui<sup>\*1</sup>, R. Sacco<sup>\*2</sup>, S. J. Silverberg<sup>1</sup>. <sup>1</sup>College of Physicians and Surgeons, Columbia University, New York, NY, USA, <sup>2</sup>University of Miami, Miami, FL, USA.

Severe primary hyperparathyroidism (PHPT) is associated with cardiovascular (CV) calcification and increased CV mortality. This study is designed to determine whether subclinical cardiovascular abnormalities are present in mild PHPT and reversible with surgical correction (PTX).

Patients with PHPT, who had elected to have PTX, were evaluated with structural and functional cardiovascular tests pre-PTX and for 2-yr post-PTX. Patients (N=50) were typical of those with mild PHPT: 84% female, age ± SD 62 ± 8 yrs, serum calcium 10.5 ± 0.5 mg/dl, PTH 116 ± 50 pg/ml. In the total group (n=50), carotid intimal medial thickness (IMT) and carotid stiffness, an indicator of vascular stiffness were abnormal at baseline. In the subset of patients who completed 12 months of follow-up thus far (n=20), mean values for blood pressure, left ventricular (LV) mass, endothelial reactivity (FMD), vascular compliance and diastolic dysfunction were normal at baseline. After parathyroidectomy, some measures of diastolic dysfunction (deceleration time and tissue doppler E' velocity) improved, while others worsened (isovolumic relaxation time IVRT) within the normal range. Carotid intima-medial thickness (IMT) increased post-PTX.

CV Test	Baseline Mean ± SD	12 month Mean ± SD	Normal Range	p- value*
Blood pressure (mmHg)	121 ± 18/76 ± 11	131 ± 21/78 ± 11	≤140/90	NS
Heart Rate	71 ± 9	76 ± 8	60-99	NS
LV mass (g/m <sup>2</sup> )	98 ± 26	101 ± 25	43-115	NS
Mitral Pulse Wave E/A	1.2 ± .3	1.0 ± .3	.75-1.5	NS
Deceleration Time (DT) (msec)	165 ± 27	180 ± 32	>140	0.02
IVRT (msec)	79 ± 19	94 ± 15	50-102	0.02
Tissue Doppler E' Velocity (cm/sec)	11.7 ± 1.5	10 ± 2.1	<15	0.05
FMD (%)	5.9 ± 3.5	5.8 ± 5.1	3-7%	NS
IMT (mm)	0.938 ± 0.078	1.075 ± 0.336	0.7-0.9	0.04
Carotid STRAIN (%)	10 ± 0.0	10 ± 0.0	6-12%	NS
Carotid STIFFNESS	4.3 ± 0.9	7.7 ± 3.4	< 6	NS

\*Baseline vs. 12 months

The subset of patients who had abnormal baseline measures of diastolic function (DT:120 ± 29 msec; n = 10; and tissue doppler E' velocity: 16.1 ± 1.2 cm/sec; n = 8) had normalization of those parameters post-PTX (203 ± 53 msec and 9.1 ± 3.3 respectively, p<.003). Improvement in tissue doppler E' velocity strongly correlated with the change in PTH (r = 0.8, p < 0.0001) and calcium (r = 0.4, p = 0.001) levels.

In summary, in patients with mild PHPT, improvement in structural and functional CV measures post-PTX was inconsistent. However, in patients with evidence of diastolic dysfunction at the time of diagnosis, PTX may lead to improvement. In these patients, normalization of indices of diastolic function was associated with the extent of decline in serum calcium and PTH levels. Further studies are necessary to confirm these findings.

**Disclosures:** M.D. Walker, None.

**M435**

**Clinical Implications of Commercial Biotin-Based Detection Systems in PTH Assays.** S. M. Jan de Beur<sup>1</sup>, D. Meany<sup>\*2</sup>, L. Sokoll<sup>\*2</sup>. <sup>1</sup>Medicine, Johns Hopkins Medical Institute, Baltimore, MD, USA, <sup>2</sup>Pathology, Johns Hopkins Medical Institute, Baltimore, MD, USA.

Accurate measurement of serum parathyroid hormone (PTH) in patients with end-stage renal disease (ESRD) is critical for the proper management of the aberrant bone and mineral metabolism characteristic of renal failure. Adynamic bone disease (ABD) was suspected in a 63 year old female with ESRD because of low normal serum PTH levels, high normal serum calcium and severe osteoporosis. However, her mildly elevated serum alkaline phosphatase level was inconsistent with the low bone turnover observed in ABD. This discrepant clinical profile prompted investigation into the clinical PTH assay used at our institution which utilizes biotin-streptavidin detection. Simultaneous serum samples for PTH were analyzed on the Roche Elecsys 2010 at Johns Hopkins and on the Siemens Immulite 2000 analyzer at Quest Diagnostics, discrepant values of 48 pg/mL and 786 pg/mL were obtained respectively. Heterophile antibodies were eliminated as a cause of the inconsistency. Further review of the patient's medical history revealed that she was ingesting biotin 10 mg/day for restless leg syndrome. Biotin is recognized by the assay manufacturer as a potential interferent and it is recommended that samples be collected at least 8 hours after biotin administration. We hypothesized that serum biotin was competitively inhibiting the biotinylated anti-PTH antibody in the Roche assay thus preventing the binding of the sandwich complex to the streptavidin-coated microparticles yielding falsely low PTH results. Therefore, we 1) measured patient serum biotin levels, 2) performed serial serum dilutions and 3) pre-cleared the serum with streptavidin microparticles before measuring PTH. In support of our hypothesis, the patient's serum contained high levels of biotin [4784 pg/mL (200-500 pg/mL)]. Twenty-fold dilution of the serum sample yielded PTH values of 567 pg/mL and 465 pg/mL that were concordant with those obtained from Quest. Moreover, by pre-clearing with streptavidin microparticles, we obtained results similar to the Quest assay which is not based on streptavidin-biotin chemistry (PTH: 32 pg/mL pre-treatment vs. 419 pg/mL post-treatment).



Thus, biotin molecules present in specimens from patients taking high-dose biotin will interfere with the Roche PTH assay and provide falsely low results. In addition, excessive serum biotin may interfere with a wide range of immunoassays that are based on streptavidin-biotin chemistry. As in the case of this patient, the delay in initiating appropriate therapy for severe secondary hyperparathyroidism in ESRD has significant clinical consequences that can include tertiary hyperparathyroidism and progressive hyperparathyroid bone disease.

**Disclosures:** S.M. Jan de Beur, None.

## M436

**Mutational Analysis of Beta-catenin Exon 3 in Benign and Malignant Parathyroid Tumors.** C. Banti\*, F. Cetani\*, E. Pardi\*, S. Borsari\*, F. Saponaro\*, E. Vignali\*, G. Viccica\*, L. Cianferotti, E. Ambrogini\*, A. Pinchera\*, C. Marocci. Endocrinology, University of Pisa, Pisa, Italy.

Single benign adenoma is responsible for 80-85% of primary hyperparathyroidism (PHPT), while carcinoma accounts for 1% of all sporadic cases. In addition, tumours with histological aspects of carcinoma, but without distant metastasis, are defined atypical adenomas. Wnt signaling pathway abnormalities have been described in many human tumours and, recently, alterations and cytoplasmic accumulation of  $\beta$ -catenin, a key signal mediator of the Wnt signaling pathway, have been reported in a subset of sporadic parathyroid adenomas. The exon 3 of *CTNNB1* gene, encoding  $\beta$ -catenin, can be considered a "hotspot" for mutational activation of  $\beta$ -catenin in many human tumours, because it contains serine-threonine aminoacids, potential targets for GSK-3 $\beta$  phosphorylation.

The aim of the study was to investigate abnormalities of the regulation of  $\beta$ -catenin in parathyroid tumorigenesis. Genomic DNA from thirty sporadic parathyroid adenomas, 21 carcinomas and 6 atypical adenomas was extracted and the exon 3 of the *CTNNB1* gene was PCR-amplified and direct sequencing was performed using ABI Prism 310 sequencer. Potential mutations of target residues prevent degradation of  $\beta$ -catenin. Direct sequencing of exon 3 of the *CTNNB1* gene showed absence of stabilizing mutations in any pathologic specimens.

Our results suggest and confirm that Wnt/ $\beta$ -catenin signaling pathway abnormalities are rarely, if at all, involved in the development of sporadic benign as well as malignant parathyroid tumours.

**Disclosures:** C. Banti, None.

## M437

**A Clinically Useful Paradigm for Interpretation of Serum 25-hydroxyvitamin D (25-OHD) Levels with Simultaneously Measured PTH Levels.** D. Rao, S. Qiu, N. Parikh. Bone & Mineral Research Laboratory, Henry Ford Hospital, Detroit, MI, USA.

The prevailing practice is to measure serum 25-OHD, the best available index, to assess vitamin D nutritional status. However, single 25-OHD level alone does not give information either about the duration of vitamin D depletion or appropriate replacement strategy in patients with low 25-OHD. Accordingly, we analyzed simultaneously measured 25-OHD & PTH levels in all patients >50y of age seeking advice on osteoporosis in 2007. We excluded patients with hypercalcemia (Ca >10.2 mg/dl), renal dysfunction (Cr >1.5 mg/dl) or with known causes of vitamin D depletion.

There were 486 patients, 434 women and 52 men; mean age  $67 \pm 10$ y. The mean serum 25-OHD was  $26.6 \pm 11.7$  ng/ml and PTH  $66.0 \pm 47.6$  pg/ml with the expected inverse relationship between the two. However, there was no regression of PTH or 25-OHD on age or Cr (data not shown).

When the patients were classified based on low or normal 25-OHD (defined as < or > 30 ng/ml; a value now considered optimal), with or without high PTH (defined as < or > 75 pg/ml), 4 groups emerged that suggested different pathophysiologic basis (Table).

Group-1 had normal 25-OHD (>30 ng/ml) and PTH (<75 pg/ml) and Group-2 had normal 25-OHD but high PTH (>75 pg/ml) with no relationship between these two variables in either group. However, in the other 2 groups with low 25-OHD (<30 ng/ml) and either high (Group-3) or normal (Group-4) PTH, there was an inverse relationship between these 2 variables. Furthermore, the slope of regression, after "normalizing" the data for each group, was significantly steeper in Group-3 with high PTH compared to Group-4 with normal PTH ( $p < 0.001$ ). This suggests that vitamin D depletion may have been of longer duration in Group-3 compared to Group-4 and thus may require aggressive (? urgent) pharmacologic therapy. The Group-4 patients with low 25-OHD and normal PTH may represent seasonal variation, short duration vitamin D depletion or abnormal PTH response. Finally, Group-2 with normal 25-OHD and high PTH may represent patients with low calcium intake or incipient primary hyperparathyroidism and thus require further evaluation.

Conclusion: Simultaneously measured 25-OHD and PTH is useful to optimize proper interpretation of vitamin D nutritional status. This strategy offers a clinically useful tool to look for other causes of high PTH in those with normal 25-OHD and explore reasons for lack of PTH response in those with low 25-OHD and normal PTH.

Relationship Between 25-OHD & PTH				
Category	n (%)	Slope	r <sup>2</sup>	p value
Group-1	160 (33)	-0.153	0.011	NS
Group-2	26 (5)	0.596	0.035	NS
Group-3	87 (18)	-3.563	0.104	<0.001
Group-4	213 (44)	-0.368	0.032	0.022
Total	486 (100)	-1.227	0.091	<0.001

**Disclosures:** D. Rao, None.

## M438

**Increased Risk of Morphometric Vertebral Fracture in Postmenopausal Women with Primary Hyperparathyroidism.** G. Viccica\*, E. Vignali\*, L. Cianferotti\*, E. Ambrogini\*, F. Cetani\*, S. Chiavistelli\*, D. Diacinti\*, A. Pinchera\*, C. Marocci\*. <sup>1</sup>Endocrinology, University of Pisa, Pisa, Italy, <sup>2</sup>Clinical Sciences, University of Roma, Pisa, Italy.

An increased risk of vertebral fracture (VF) compared to general population has been reported in patients with primary hyperparathyroidism (pHPT), but the available data is still controversial. The aim of the present study was to prospectively evaluate the presence of VFs in a series of consecutive Caucasian postmenopausal women with sporadic PHPT referred to our outpatient clinic for management advice, and to compare its rate with that of a control group (C). One hundred and fifty patients underwent a standard clinical, biochemical and densitometric (DXA) evaluation. Patients were classified as symptomatic (n=21) or asymptomatic according to the presence or absence of HPT related symptoms. The latter were further grouped according to whether the met (non-mild, n=84) or not (mild, n=45) the criteria for surgery established by 2002 Workshop on Asymptomatic Primary Hyperparathyroidism. Morphometric X-ray absorptiometry (MXA) was used to assess the presence of a VF, classified by semiquantitative Genant's method. Each patient was compared with two age ( $\pm 2$ ) and menopausal age ( $\pm 5$ ) matched controls. There was no statistically significant difference in age, menopausal age, years since menopause. Vertebral fractures were detected 37 out of 150 patients (24.6%) and 12 out of 300 (4.0%) controls [ $\chi^2=44.0$ ,  $p < 0.01$ ; OR = 7.86; (95% CI, 3.96-15.61)]. The majority of VF were classified as mild. VF distribution was evaluated according to quartiles of BMD of lumbar spine (LS-BMD). Patients had an increased risk of VF in all quartiles even if VF risk decreased at increasing LS-BMD values. Stepwise multiple logistic regression analysis showed that BMD of lumbar spine ( $\beta$ -coefficient = -5.2311, SE ( $\beta$ ) 1.8382 and  $p=0.004$ ) was the only variable independently associated with the risk of VFs. The rate of VF was higher in all subgroups of patients compared to the controls: 27.6% ( $p > 0.01$ ; OR 14.7) in patients with symptomatic pHPT, 22.5% ( $p < 0.01$ ; OR 6.96) in asymptomatic ones, asymptomatic non-mild (28.6%;  $p < 0.01$ , OR 9.6) and asymptomatic mild (11.1%;  $p=NS$ , OR 3.0). In conclusion our study shows an increased rate of VF in postmenopausal women with PHPT compared to controls. Patients with asymptomatic pHPT have an increased risk of VF, even those without criteria for surgery. We suggest that an evaluation of VF should be included in the workout of postmenopausal women with pHPT.

**Disclosures:** G. Viccica, None.

## M439

**Serum Cathepsin K Levels in Ankylosing Spondylitis.** D. Wendling, J. Cedoz\*, E. Racador\*. Rheumatology, University Teaching Hospital, Besançon, France.

Ankylosing spondylitis (AS) is a chronic inflammatory disease associated with a reduction of BMD correlated with systemic inflammation, and reversible under anti TNF therapy. Cathepsin K is a recognized mediator of bone resorption.

The aim of this study was to evaluate serum levels of Cathepsin K levels in AS patients compared to controls, and their evolution under anti TNF treatment.

Methods: This prospective study included AS patients (modified New York criteria) and healthy volunteers as controls. Age, disease duration, BASDAI, ESR and CRP were recorded. Cathepsin K (Biomedica, France) were assessed by duplicate ELISA, as well as MMP-3 (Quantikine MMP-3, R&D Systems) and IL-17 (Quantikine IL-17, R&D). Patients treated with anti TNF were evaluated again after 10 weeks of therapy. Statistical analysis used Mann-Whitney test for comparisons between groups, Wilcoxon test for evaluation under treatment, and correlation test for correlations. Significance threshold was  $p$  less than 0.05.

Results: 23 ambulatory AS patients and 21 controls were included, mean age 39.9 and 41.2 years (ns). AS duration was 10.1 years, AS was mainly axial (n=21) and HLA-B27 positive (n=19). At inclusion, BASDAI was 44.1 (4.1), CRP 22.3 mg/l (4.7). In AS patients, serum levels of Cathepsin K (6.4 vs 3.6 pg/ml, ns), of MMP-3 (4.71 vs 2.79 ng/ml,  $p=0.04$ ) and of IL-17 (60.4 vs 32 pg/ml, ns) were higher compared to controls. No positive correlation was found between the several parameters assessed, except between ESR and CRP ( $p=0.0002$ ). 13 of the AS patients were evaluated after anti TNF (adalimumab: 7; etanercept: 4; infliximab: 2). A significative reduction of ESR, CRP, BASDAI ( $p=0.002$ ) and of MMP-3 ( $p=0.04$ ) was observed, but Cathepsin K showed tendency of increase ( $p=0.07$ ).

Conclusion: Serum Cathepsin K does not seem to be a good candidate for evaluation of bone resorption in AS.

**Disclosures:** D. Wendling, None.

**M440**

**Bone Fragility Is Increased in the MKR Type 2 Diabetic Mouse.** S. Epstein, Y. Kawashima\*, C. Fritton\*, K. Inagaki\*, H. Sun\*, K. Jepsen\*, S. Yakar\*, M. Schaffer, D. LeRoith\*. Mt Sinai School of Medicine, New York, NY, USA.

Both Type 1 and Type 2 diabetes patients may demonstrate changes in bone morphology. While Type 1 patients may develop osteoporosis when they age, Type 2 diabetic patients often demonstrate increased bone fragility leading to fractures. The latter effects may be worsened with the use of thiazolidinedione therapy for the diabetic state. The mechanisms involved in these changes are as yet undefined.

We have created a mouse model of Type 2 diabetes (called the MKR mice) and studied the effect of this model on bone morphogenesis. Compared to control mice, MKR diabetic mice demonstrate increased periosteal and endosteal bone resorption during ontogeny that correlates with increased osteoclastic activity. Because MKR diabetic mice show minor changes in longitudinal bone growth, the increased osteoclastic activity and the lack of a compensatory increase in periosteal bone formation during growth resulted in a 28% reduction ( $p < 0.001$ , t-test) in total cross-sectional area of the femoral mid-shaft (a measure of periosteal expansion) by 16 weeks of age. This reduced radial expansion of the mid-shaft led to a 24% increase ( $p < 0.001$ ) in slenderness (i.e., width relative to length) of adult femora. Trabecular bone mass decreased and spacing was also increased, consistent with greater osteoclastic activity. Overall, femora from adult MKR diabetic mice are more fragile, as measured by a 30% reduction ( $p < 0.001$ ) in whole bone stiffness and strength relative to femora from control mice. Marrow-derived osteoclast cultures revealed an increase in the number of differentiated osteoclasts in response to M-CSF and RANK-L. Additionally, marrow derived non-adherent cells treated with increasing concentrations of insulin, in the presence of M-CSF and RANK-L revealed an increased number of differentiated osteoclasts in vitro. Taken together, the MKR mouse model suggests that skeletal fragility may arise from the hyperinsulinemia that leads to increased osteoclastogenesis and likely uncoupling of bone resorption and formation.

**Disclosures:** S. Epstein, None.

This study received funding from: NIH.

**M441**

**The Effect of Aquatic Exercise and Education on Improving Indices of Fall Risk in Older Adults with Hip Osteoarthritis: A Randomized Controlled Clinical Trial.** C. M. Arnold\*, R. A. Faulkner<sup>2</sup>. <sup>1</sup>Kinesiology, Physical Therapy, University of Saskatchewan, Saskatoon, SK, Canada, <sup>2</sup>Kinesiology, University of Saskatchewan, Saskatoon, SK, Canada.

The purpose of this study was to evaluate the effect of aquatic exercise and aquatic exercise combined with an education group program on fall risk factors in adults aged 65 years or older with hip osteoarthritis (OA). Individuals with hip OA present with an increased risk of falls and the ideal type of intervention to decrease fall risk in this population is unknown. Seventy-nine older adults with hip OA and at least 1 fall risk factor were randomly assigned to one of three groups: Aquatic-Education, Aquatic or Control. Exercise interventions were twice per week for 11 weeks with Aquatic-Education receiving an additional one half hour education class once per week. Fall risk outcomes included primary and secondary measures of balance, falls-efficacy, lower body strength, walking endurance, dual task function, and mobility. The mean age was 74 years of age (range 65 - 88 years) with 71% of the sample female and 49% reported one or more falls in the past year. An intention to treat analysis was used. There was a significant group by time interaction for primary fall risk factors (repeated measures MANCOVA;  $p = 0.038$ ), using baseline measures as co-variables, where Aquatic-Education had a 8% improvement in balance confidence compared to a 4% decrease in Control and a 20% improvement in lower body strength and mobility (chair stands) compared to an 8% improvement in Aquatic and Control. Falls-efficacy specific to daily fall-related tasks was also significantly improved in Aquatic-Education compared to both Aquatic and Control (16% improvement compared to a 2% improvement and no change respectively). General health status was also significantly improved in Aquatic-Education compared to Control. The greatest benefit in reducing fall risk factors was realized for those who entered the Aquatic-Education program with lower levels of falls-efficacy. There were no significant differences in fall risk factors comparing Aquatic to Control. In conclusion, the addition of land-based education to reinforce fall prevention strategies, teach movement control and the purpose of exercise resulted in improvements in falls-efficacy and functional strength in conjunction with an aquatic exercise program for older adults with hip OA. Aquatic exercise on its own was not sufficient to decrease fall risk in this population. Intervention programs for older adults already at risk for falls due to conditions such as arthritis should include both exercise and education programs.

**Disclosures:** C.M. Arnold, None.

This study received funding from: Saskatchewan-Canadian Institute of Health Regional Partnership Program, Physiotherapy Foundation of Canada

**M442**

**Fracture Risk in Primary Biliary Cirrhosis: Role of Osteopenia and Severity of Cholestasis.** N. Guanabens<sup>1</sup>, D. Cerda<sup>\*1</sup>, A. Monegal<sup>\*1</sup>, F. Pons<sup>\*1</sup>, L. Caballeria<sup>\*2</sup>, P. Peris<sup>1</sup>, A. Pares<sup>\*3</sup>. <sup>1</sup>Metabolic Bone Diseases Unit, Hospital Clinic, IDIBAPS, Barcelona, Spain, <sup>2</sup>Liver Unit, Hospital Clinic, IDIBAPS, CIBEREHD, Barcelona, Spain, <sup>3</sup>Liver Unit, CIBEREHD, Hospital Clinic, IDIBAPS, Barcelona, Spain.

**Background and aims:** Osteoporosis, a frequent complication in patients with primary biliary cirrhosis (PBC) with severe and prolonged cholestasis, may result in a higher risk of vertebral and non vertebral fractures. However, the influence of osteoporosis and severity of liver disease on fracture risk in PBC are not well characterized and therefore, we have studied a large series of women with PBC with the aim of assessing the prevalence of fractures and their association with osteoporosis and the degree and duration of liver damage.

**Patients and methods:** 185 female patients with PBC (age  $55.7 \pm 0.7$  years, range: 28-79). Age, duration of PBC, menopausal status, histological stage and severity of liver disease were assessed in all the patients. Vertebral fractures were recorded by X-ray of spine in 170 patients while non vertebral fractures were recorded in 172 patients. Diagnosis of osteoporosis and osteopenia were established by densitometric criteria at the lumbar spine (180 patients) and femoral neck (140 patients).

**Results:** The prevalence of vertebral, nonvertebral and overall fractures were 11.2%, 12.2% y 20.8%, respectively. Osteoporosis was significantly higher in PBC than in normal Spanish women at the lumbar spine (30.6% vs 11.2%,  $p < 0.001$ ) and femoral neck (12.9 vs 4.3%,  $p < 0.001$ ). Osteoporosis was associated with age, weight, height, histological stage, and severity and duration of liver damage, while fractures were associated with osteoporosis, menopausal status, age, height but not with severity of liver disease. Osteoporosis was a risk factor for vertebral fracture (OR: 8.48, 95% CI: 2.67-26.95). Lumbar osteopenia with a T-score  $< -1.5$  (OR: 8.50, 95% CI 1.89-38.09 and femoral neck osteopenia with a T-score  $< -1.5$  (OR: 6.83, 95% CI: 1.48-31.63) were already significant risk factors for vertebral fracture. Thus 17 of the 19 patients (89.5%) with vertebral fracture had a lumbar T-score lower than -1.5, and 15 patients (86.7%) a femoral neck T-score lower than -1.5.

**Conclusions:** Fractures, particularly vertebral fractures, are associated with osteoporosis and osteopenia with a T-score lower than -1.5, whereas osteoporosis and osteopenia are associated with the severity of liver damage. The clear-cut correlation between vertebral fracture and a T-score  $< -1.5$ , may indicate that this densitometric measurement is a useful criteria for prescribing agents to prevent further loss of bone mass and development of new fractures in patients with PBC.

**Disclosures:** N. Guanabens, None.

**M443**

**Serum Undercarboxylated Osteocalcin Concentration are Related to Renal Function in Type 2 Diabetes Patients.** M. Shibata, S. Sekiguchi, Y. Umetani\*, S. Asano, T. Hara\*, H. Kakizawa\*, N. Hayakawa\*, N. Oda\*, A. Suzuki, M. Itoh\*. Div. Endocrinology, Dept of Internal Medicine, Fujita Health University, Aichi, Japan.

Vitamin K contributes to bone health, probably through its role as co-factor for the gamma-carboxylation of vitamin K-dependent proteins such as osteocalcin. Undercarboxylated osteocalcin (ucOC) is considered to be an "inactive" form osteocalcin, and does not contribute to bone formation. UcOC is a sensitive marker of vitamin K status, resulting in low bone formation. The patients with high ucOC levels have been reported to have higher risk for osteoporotic fracture. Type 2 diabetes mellitus is another risk factor of osteoporosis with low bone turn over, especially for the patients with renal dysfunction due to diabetic nephropathy. In the present study, we investigated serum ucOC concentrations in type 2 diabetes patients and its association with renal function estimated by new formula of glomerular filtration rate (GFR) for Japanese population. Serum ucOC, total homocysteine and bone-specific alkaline phosphatase (BAP) concentrations were measured by ELISA, HPLC and EIA, respectively. Subjects were outpatients with type 2 diabetes mellitus ( $n=56$ , M/F = 28/28, Age  $66.1 \pm 10.3$ ). Mean blood HbA1c levels were  $6.9 \pm 1.1\%$ . Subjects were divided into 4 groups according to estimated GFR (eGFR) by MDRD formula by Japanese Society of Nephrology. Serum ucOC and homocysteine concentrations were negatively associated with eGFR, while BAP was positively associated with eGFR in type 2 diabetes patients. On the contrary, HbA1c levels were not related to these bone markers. Serum ucOC levels higher than 4.5 ng/ml was defined as cut-off value for vitamin K deficiency. The patients with eGFR under 60 ml/min/1.73m<sup>2</sup> were defined as chronic kidney disease (CKD), and they have higher incidence of vitamin K deficiency (6/27) compared with the population without CKD (1/29). In summary, vitamin K deficiency seems to be an additional risk factor for osteoporotic fracture in type 2 diabetes patients especially for the subjects with renal dysfunction such as CKD.

**Disclosures:** M. Shibata, None.

## M444

**Stress Fracture and Vertebral Osteosclerosis Related to Fluorosis Induced by Excessive Gingival Topical Fluoride Application.** E. Toussiot<sup>\*1</sup>, P. Ornetti<sup>\*2</sup>, D. Wendling<sup>\*1</sup>, C. Tavernier<sup>\*2</sup>. <sup>1</sup>Rheumatology, University Hospital, Besancon, France, <sup>2</sup>Rheumatology, University Hospital, Dijon, France.

Fluorosis may induce ligamentous ossifications, osteosclerosis and bone fractures. It is reported in fluoridated area (endemic skeletal fluorosis) or caused by industrial water fluorification.

We report here one case of stress fracture and another case of vertebral osteosclerosis related to fluorosis which was explained by repeated fluoride gingival application. These patients lived in Franche-Comté and Bourgogne, 2 regions from France which are not endemic for fluorosis.

**Case 1:** A 49-year old premenopausal woman, without medical history complained of mechanical pain of her left foot. Physical examination showed swelling, warmth and tenderness of the dorsal region of her foot around the second metatarsus. X-rays revealed a fracture located at the second metatarsus and technetium bone scan an increased uptake at the same level. Serum calcemia, phosphate, alkaline phosphatases, Vitamine D levels, PTH and osteocalcin were normal. Bone densitometry (Lunar DPX-IQ) showed high BMD at the spine (T score = + 2.1) with normal values at the femoral neck (T score = 0). The patient reported that she had been receiving topical fluoride applications for 10 years for periodontal disease. Serum and urinary fluoride concentrations were found elevated (35 µg/L [N<29] and 1230 µg /24H [N<950]). A bone biopsy was not performed.

**Case 2:** a 54 year old man had had for pertinent medical history a cancer of the larynx treated by radiotherapy. During this treatment, he had received prophylactic treatment for dental caries using topical fluoride application. Thirteen years later, he was referred in rheumatology for mechanical low back pain with vertebral osteosclerosis on dorso-lumbar spine X-rays. Laboratory parameters of calcium homeostasis were normal and bone scintigraphy showed increased uptake of the spine. A bone biopsy did not show any neoplastic infiltrate while the histomorphometric analysis revealed osteomalacia. Serum and urinary fluor levels were increased (5.8 µm/L [N<1.5] and 91.7 µm/L (N< 26)) as well as fluor concentrations in calcined bone specimen (0.686 % N< 0.10). The patient reported that he had been continuing gingival fluoride application since the diagnosis of cancer.

**Conclusion:** Beside the classical causes (endemic or industrial fluorosis), fluorosis may be induced by certain mineral water or ice tea beverages. Fluoride ingestion from toothpaste leading to osteosclerosis has been exceptionally reported. Our two cases suggest that repeated or excessive gingival fluoride application for periodontal disease or for the prevention of dental caries in patients with a larynx cancer may also be an etiological factor for fluorosis.

**Disclosures:** E. Toussiot, None.

## M445

**Recombinant Human Bone Morphogenic Protein-2 (rhBMP-2) Accelerates Segmental Defect Healing in Diabetic Rats.** E. A. Breitbart<sup>\*1</sup>, V. Azad<sup>\*1</sup>, S. Yeh<sup>\*1</sup>, L. Al-Zube<sup>\*1</sup>, J. P. O'Connor<sup>\*2</sup>, S. S. Lin<sup>\*1</sup>. <sup>1</sup>Department of Orthopaedic Surgery, University of Medicine and Dentistry of New Jersey: New Jersey Medical School, Newark, NJ, USA, <sup>2</sup>Department of Biochemistry and Molecular Biology, University of Medicine and Dentistry of New Jersey: New Jersey Medical School, Newark, NJ, USA.

This study was designed to determine the bone healing capacity of rhBMP-2 in a non-critical size femoral defect in both healthy rats and rats with diabetes mellitus (DM). It was hypothesized that DM would result in impaired bone regeneration in this defect model due to reduced bone formation, and furthermore, that local delivery of rhBMP-2 would accelerate non-DM healing and normalize impaired bone healing in DM rats to the levels of Non-DM bone healing.

A total of 80 BB Wistar rats were used in the project. A 3mm defect was created during surgery and stabilized with a polyimide plate. Either a 0.05cc/11µg dose of rhBMP-2 or buffer in a collagen sponge was implanted into the defect at the time of surgery. Serial microradiographs were taken biweekly up to the day of sacrifice and processing of samples for PECAM-1 immunohistochemistry, histomorphometry, and mechanical testing was performed.

Both Non-DM and DM groups treated with rhBMP-2 demonstrated significantly higher radiographic scoring and total new bone formation (Table 1), and blood vessel quantification and mechanical testing parameters (Table 2) compared to those treated with buffer at all timepoints with the exception of 3 week radiographic scoring in the DM group and maximum shear stress. Moreover, no significance was noted between Non-DM and DM groups treated with rhBMP-2 in any of the above parameters.

In summary, decreased quantity and quality of new bone formation was seen in DM animals compared to Non-DM animals, showing the detrimental effects of DM upon bone healing. A single application of rhBMP-2 resulted in new bone formation in DM animals similar to Non-DM animals, suggesting a critical role for rhBMP-2 in ameliorating the deleterious effects of DM on bone regeneration and formation.

Radiographic scoring and total bone formation in DM and non-DM rats treated with rhBMP-2 / Buffer				
	Non-DM+Buffer	Non-DM + rhBMP-2 (p-value vs. Non-DM+Buffer)	DM+Buffer	DM + rhBMP-2 (p-value vs. DM+Buffer)
Sample Size (3 weeks/6 weeks)	5/6	6/6	6/6	6/6
3 weeks Radiographic Score (0-5)	1.3 ± 1.0	3.16 ± 0.68 p=0.006	1.5 ± 1.18	2.33 ± 0.4 p=0.134
6 weeks Radiographic Score (0-5)	1.75 ± 1.17	4.0 ± 0.35 p<0.001	1.16 ± 1.29	4.21 ± 0.9 p<0.001
3 weeks Total New Bone Formation (mm2)	2.07 ± 0.66	6.91 ± 1.42 p<0.001	0.84 ± 0.39	7.89 ± 1.0 p<0.001
6 weeks Total New Bone Formation (mm2)	3.22 ± 1.24	7.38 ± 0.86 p<0.001	3.01 ± 2.06	7.16 ± 2.44 p=0.006

Mechanical Testing Data and Blood Vessel Quantification in DM rats treated with rhBMP-2 vs. Buffer		
	DM+Buffer	DM+rhBMP-2
Sample Size (mechanical testing/BV quantification)	4/3	4/4
Torque to Failure (Nm)	0	393.57±233.3 p=0.03
Torsional Rigidity (Nm/rad)	0	29,711±6,224 p=0.002
Shear Modulus	0	1,978±1,467 p=0.05
Maximum Shear Stress (MPa)	0	89.6±94.9
Blood Vessel Density (BV/mm2)	4.50 ± 5.45	12.76 ± 1.90 p=0.034

**Disclosures:** E.A. Breitbart, None.

This study received funding from: Medtronic, Inc.

## M446

**Deficiency of the Nucleocytoplasmic Shuttling Protein CIZ Suppresses K/BxN Serum-Induced Model of Rheumatoid Arthritis.** T. Nakamoto<sup>1</sup>, E. Mizoguchi<sup>1</sup>, Y. Izu<sup>1</sup>, T. Hayata<sup>1</sup>, Y. Ezura<sup>1</sup>, D. Mathis<sup>\*2</sup>, C. Benoist<sup>\*2</sup>, N. Miyasaka<sup>\*3</sup>, M. Noda<sup>1</sup>. <sup>1</sup>Molecular Pharmacology, Tokyo Medical and Dental University, Tokyo, Japan, <sup>2</sup>Joslin Diabetes Center, Boston, MA, USA, <sup>3</sup>Medicine and Rheumatology, Tokyo Medical and Dental University, Tokyo, Japan.

CIZ (Cas interacting zinc finger protein) is a nucleocytoplasmic shuttling protein and regulates the transcription from the collagen type I alpha1 promoter and several matrix metalloproteinase promoters. It is also known as Nmp4 (Nuclear matrix protein 4) or Zfp384 (Zinc finger protein 384), and was first identified by binding to p130<sup>cas</sup>, a docking protein involved in integrin signaling. Overexpression of CIZ suppresses BMP-induced osteoblastic differentiation *in vitro*. CIZ-deficient mice show hyper-responsiveness of osteoblasts to BMP stimulation, increased bone mass, enhanced recovery from bone marrow ablation, and resistance to unloading-induced bone loss. These observations suggest that CIZ plays a pivotal role in the skeletal system. To further examine the possible pathological features of CIZ function in skeletal system, we applied the inflammatory arthritis model to CIZ-deficient mice. Sera from spontaneously arthritic K/BxN mice were transferred to CIZ-deficient- and wild-type mice (Background C57BL/6) to elicit serum-induced arthritis.

CIZ deficiency reduced arthritis severity in both ankle swelling and a clinical score by 50%. Histological analysis showed that CIZ deficiency reduced less severe invasion of inflammatory cells in periarticular tissues. Cartilage destruction levels were also reduced by CIZ deficiency. CIZ deficiency suppressed the arthritis-induced increase in the number of osteoclasts at the interface between bone and pannus at the joint. Systemic parameters such as accelerated levels of deoxypyridinoline were also reduced by CIZ deficiency.

Arthritis-induced increase in the levels of mRNA expression of MMP-3, IL-1beta, RANKL, Adams4 and CXCL16 was decreased by CIZ deficiency.

Thus CIZ plays a key role in the arthritis in this K/BxN model.

**Disclosures:** T. Nakamoto, None.

This study received funding from: JSPS.

## M447

**Prevalence and Factors Associated to the Presence of Vertebral Fractures in Patients with Type 2 Diabetes Mellitus.** P. Rozas-Moreno<sup>\*1</sup>, M. Muñoz-Torres<sup>2</sup>, G. Alonso<sup>\*1</sup>, P. Muñoz-Rueda<sup>\*1</sup>, R. Reyes-García<sup>\*1</sup>, M. Varsavsky<sup>\*1</sup>, J. Jiménez-Moleón<sup>\*3</sup>. <sup>1</sup>Endocrinology, Bone Metabolic Unit - Hospital Universitario San Cecilio, Granada, Spain, <sup>2</sup>Endocrinology, Bone Metabolic Unit - Hospital Universitario San Cecilio, Granada, Spain, <sup>3</sup>University of Granada, Department of Preventive Medicine and Public Health. RETICEF, Granada, Spain.

**Aim:** To analyse the prevalence and factors related to non-traumatic vertebral fractures (VF) in patients with type 2 diabetes mellitus (T2DM)

**Patients and methods:** Case-Control study including 118 subjects, 72 patients with T2DM and 46 healthy controls. The presence of prevalent VF was evaluated in lateral-view conventional X-Rays of the thoracic and lumbar spine (T4-L5). The severity of vertebral deformities was graded according to Genant's criteria. The relationship between the main risk factors of VF in general population (age, gender, bone mineral density, previous fragility fracture, smoking, body mass index) and the observed prevalent VF was determined. Likewise, the association between the presence of VF and the main cardiovascular risk factors linked to T2DM (arterial hypertension, dyslipidemia, abdominal obesity, diabetic retinopathy, ischemic heart disease, pathologic carotid intima-media thickness) was analyzed. Lumbar spine and femoral BMD were measured by dual X-Ray absorptiometry (Hologic QDR 4500).

**Results:** Mean age was 56.7± 6.8 yr (57.8± 6.4 and 55.1± 7.1 in T2DM and control group respectively; p=0.024). Among the T2DM patients (n=72), 47.2% were females (n=34) and 52.8% males (n=38). In the control group 56.5% were females (n=26) and 43.5% males (n=20). Prevalent VF were detected in 27.7% of T2DM group and 22.2% of controls (p=0.46). In the T2DM group prevalent VF were significantly related to the presence of diabetic retinopathy ( $\chi^2$  4.09; p=0.043) and ischemic heart disease ( $\chi^2$  5.02; p=0.025). The waist circumference was significantly greater in T2DM patients with VF compared to T2DM patients without VF (110.8 ± 11.76 vs 103.9 ± 11.18 cm respectively; p=0.024). No significant relationship was observed between the other analyzed variables and the presence of VF (age, gender, BMD, previous fragility fracture, smoking, body mass index, arterial hypertension, dyslipidemia, pathologic carotid intima-media thickness).

**Conclusions:** In patients with type 2 diabetes mellitus the presence of vascular complications was associated to increased risk of vertebral fractures. The classic vertebral fracture risk factors were not predictive of the presence of vertebral fractures in this group of patients.

**Disclosures:** M. Muñoz-Torres, None.

## M448

**Vitamin D Insufficiency is Common in Racially Diverse Postmenopausal Women with Human Immunodeficiency Virus (HIV).** E. M. Stein<sup>1</sup>, M. Yin<sup>1</sup>, A. Shu<sup>1</sup>, D. J. McMahon<sup>1</sup>, V. Thomas<sup>\*1</sup>, D. Ferris<sup>\*2</sup>, J. Laurence<sup>\*3</sup>, E. Shane<sup>1</sup>. <sup>1</sup>Columbia University, New York, NY, USA, <sup>2</sup>Bronx Lebanon Hospital Center, New York, NY, USA, <sup>3</sup>Weill Cornell Medical College, New York, NY, USA.

Postmenopausal minority women constitute a growing segment of the HIV positive (HIV+) population in the United States (US). We hypothesized that postmenopausal HIV+ women may be at risk for abnormal bone and mineral metabolism, because of older age, estrogen deficiency, and effects of HIV infection and antiretroviral therapy (ART) upon bone. As part of a longitudinal study of bone metabolism in HIV+ Hispanic and African American (AA) postmenopausal women in the northeastern US, we assessed the prevalence and effects of vitamin D insufficiency.

Of 203 women enrolled (101 HIV+ and 102 HIV- controls, mean age 58; range 43-78 years), 32% were AA and 68% were Hispanic. Hispanic subjects were predominantly from the Dominican Republic (59%) and Puerto Rico (22%). At baseline, 19% of HIV+ subjects were ART-naïve and 81% were receiving various ART regimens. Mean CD4 count was 509 ± 305 (range 67-1550) and 37% had a viral load < 50K.

We found sub-optimal serum 25OHD levels (<30 ng/ml) in the majority of HIV+ (69%) and HIV- (74%) women. Severe vitamin D deficiency (<10 ng/ml) was present in 10% of subjects in both groups. Among HIV+ women, serum 25OHD was significantly lower in AA than Hispanic subjects (21 ± 12 vs. 27 ± 15 ng/ml respectively; p<0.04). Use of calcium supplements (r=0.20, p<0.05) and multivitamins (MVI; r=0.19; p<0.06) were positively associated with serum 25OHD. In HIV- women, 25OHD was similarly associated with race and supplement use. Serum 1,25(OH)<sub>2</sub>D did not differ between groups. In HIV+ women, no relationship was found between serum 25OHD or 1,25(OH)<sub>2</sub>D and nadir CD4 count, history of AIDS defining illness, viral load, or protease inhibitor use.

Serum 25OHD and parathyroid hormone (PTH) levels were inversely associated (r=-0.33; p<0.001), regardless of HIV status. In HIV+ women, NTx was significantly greater than in HIV- women (21 ± 11 vs. 17 ± 6 nM BCE/l; p<0.0001) and was associated with higher PTH and lower estrone levels. In a multivariate regression model, PTH and estrone accounted for 16% of the variance in NTx (p overall model <0.001). This relationship was not observed among HIV- women.

In conclusion, vitamin D insufficiency is common and comparably prevalent among HIV+ and HIV- Hispanic and AA postmenopausal women living in the northeastern US. Lower serum 25OHD is associated with higher PTH levels, and in HIV+ women, is also associated with biochemical evidence of increased bone resorption. Whether these effects are associated with higher rates of bone loss remains to be determined.

**Disclosures:** E.M. Stein, None.

## M449

**Advanced Hip Assessment and Bone Mineral Density in Japanese Women with Osteoarthritis.** M. Takakuwa<sup>\*1</sup>, K. Ohtsuka<sup>\*1</sup>, M. Konishi<sup>\*2</sup>, W. Wacker<sup>\*3</sup>, H. S. Barden<sup>3</sup>, Q. Zhou<sup>2</sup>. <sup>1</sup>Takakuwa Orthopedic Nagayama Clinic, Asahikawa City, Hokkaido, Japan, <sup>2</sup>GE Healthcare, Shanghai, China, <sup>3</sup>GE Healthcare, Madison, WI, USA.

Osteoarthritis (OA) and osteoporosis (OP) are common, age-related, musculoskeletal diseases with complex, interrelated associations with bone mineral density (BMD) and fracture risk. Measurement of BMD with dual-energy X-ray absorptiometry (DXA) is an accepted method for diagnosing osteoporosis and assessing fracture risk. Femoral strength is a function of bone mass and its spatial distribution, which are incorporated in several Advanced Hip Assessment (AHA) structural variables, including: Hip Axis Length (HAL), Cross-Sectional Moment of Inertia (CSMI), Cross Sectional Area (CSA), and femur Strength Index (SI), a measure of the ability of the hip to withstand a fall on the greater trochanter. We measured BMD and AHA variables in 30 women with OA and 1291 controls, using Lunar Prodigy Advance (GE Healthcare). Controls and OA subjects were of similar age (70.0 vs. 69.2 yrs), height (148.7 vs. 147.7 cm) and weight (53.4 vs. 55.8 kg). Appropriate age-adjusted regression models for BMD and AHA variables were selected using TableCurve 2D. Minitab two-sample t-tests identified significant variation of mean values between subject groups. Age-related changes of AHA variables and femur neck BMD were strongly correlated. OA means were lower than controls for all variables except HAL. For OA subjects, age-adjusted femur neck and total femur BMD, and HAL and SI were significantly different from controls. Low SI and longer HAL, even after adjustment for femur neck BMD, were associated significantly with OA. We conclude that low SI and longer HAL appear to be predictors for OA, even after adjustment for femur neck BMD.

Femur BMD and Advanced Hip Assessment in Japanese Women with Osteoarthritis				
	Control Mean (SD)	OA Mean (SD)	p (Not Adjusted)	p (Adjusted for Neck BMD)
Femur Neck BMD*	0.813 (0.11)	0.766 (0.11)	<b>0.031</b>	-----
Total Femur BMD*	0.865 (0.12)	0.819 (0.11)	<b>0.036</b>	-----
Trochanter BMD*	0.710 (0.12)	0.689 (0.12)	0.360	-----
HAL	100.7 (5.41)	102.9 (5.82)	<b>0.049</b>	<b>0.029</b>
CSMI**	8.724 (0.29)	8.718 (0.39)	0.910	0.570
CSA	104.4 (19.2)	101.0 (20.8)	0.380	0.370
SI**	0.477 (0.31)	0.344 (0.28)	<b>0.016</b>	<b>0.029</b>

\* BMD values were adjusted for age. \*\* Variables were log transformed

**Disclosures:** M. Takakuwa, None.

## M450

**Effects of Serum Factors During Osteoblast Differentiation - Implication for the Pathogenesis of Osteoporosis in Crohn's Disease.** M. Blaschke<sup>\*1</sup>, A. Hell<sup>\*2</sup>, R. Koepf<sup>\*1</sup>, D. Raddatz<sup>1</sup>, N. Schuetz<sup>3</sup>, N. Miosge<sup>\*4</sup>, G. Salinas-Riester<sup>\*5</sup>, H. Siggelkow<sup>1</sup>. <sup>1</sup>Gastroenterology and Endocrinology, University Medicine of Goettingen, Goettingen, Germany, <sup>2</sup>Orthopedics, University Medicine of Goettingen, Goettingen, Germany, <sup>3</sup>Orthopaedic Center for Musculoskeletal Research, University of Wuerzburg, Wuezburg, Germany, <sup>4</sup>University Medicine of Goettingen, Goettingen, Germany, <sup>5</sup>Molecular Cell Biology, University Medicine of Goettingen, Goettingen, Germany.

Crohn's disease (CD) is associated with a higher prevalence of osteoporosis, a complication, which is increasingly recognized as a significant source of morbidity also in these patients. The pathogenesis is still controversial, yet disease activity is thought to be one of the main contributing factors. We used primary human mesenchymal progenitor cells directed to the osteoblastic phenotype to investigate the effect of serum of seven patients during the active phase in CD on expression of osteoblast related genes. Four of the investigated patients had osteoporosis or osteopenia (CD-OPO+), three showed no obvious bone disease (CD-OPO-).

Mesenchymal progenitor cells obtained from a healthy patient grown in regular media were used in first passage at confluence. Cells were switched to 1% human serum and stimulated with 10 mM beta-glycerol-phosphate and 10 µM ascorbic acid. After 24 h human serum was changed to eight different CD sera (four CD-OPO+, three CD-OPO-) and cells were analyzed at days 3 and 14. Global gene expression analysis was applied using the human 4x44k design array from Agilent Technologies. A subset of regulated genes were reevaluated at all time points by real-time PCR.

The quantitative changes in significantly altered genes were listed using different criteria using the principal component analysis (PCA). A group of 38 genes was identified showing a contrast of 2 for CD-OPO+ versus CD-OPO-. A second list including 236 genes could be generated showing a contrast of 1.5 between the two groups. Regulated genes participate in the actin cytoskeleton, many of them associated with cell adhesion and extra cellular matrix. In addition, we identified regulation of genes associated with bone diseases and repression of the Wnt and TGF-beta pathways. Genes coding for proteins involved in the lipid and fatty acid metabolism were strongly increased in CD-OPO+ treated samples. Serum from CD patients with osteoporosis compared to serum from CD patients with healthy bone induced a different set of genes, including multiple involved in bone differentiation and disease. Our results suggest, that serum factors contribute decisively to bone disease in CD patients probably mediated by mesenchymal progenitor cells

**Disclosures:** H. Siggelkow, MSD 1, 2; Novartis, Roche, Lilly, Procter and Gamble 1. This study received funding from: Elsbeth-Bonhoff-Foundation.

## M451

**Interactions between Obesity, Cardiovascular Disease and Bone Formation.** J. L. Stevens-Smith<sup>\*1</sup>, A. Scutt<sup>\*2</sup>, G. Reilly<sup>1</sup>. <sup>1</sup>Engineering Materials, University of Sheffield, Sheffield, United Kingdom, <sup>2</sup>Musculoskeletal Science Medical School, University of Sheffield, Sheffield, United Kingdom.

Cardiovascular and bone diseases are of great physiological and economic importance. Cardiovascular disease causes 17.5million deaths globally per annum. Osteoporosis is a metabolic bone disease characterised by a low bone mineral density (BMD). Obesity is a well known risk factor for cardiovascular disease but it is not generally associated with osteoporosis. Recent research, however, has suggested a link between osteoporosis and levels of adipocytokines and labelled osteoporosis the 'obesity of bone'. In this study we investigate the effect soluble products of adipose tissue on markers of bone formation. The effects of a cardiovascular disease on bone strength and density were investigated in a mouse model of cardiovascular disease.

Tibiae were isolated from a mouse model of cardiovascular disease (via a high fat Paigen diet<sup>1</sup>) and controls. The bone mineral density and structure were analysed by micro-CT and OCT (Optical Coherence Tomography). Bone strength was measured using the three-point bending test in an Electroforce 3200 (Bose) testing system. Mesenchymal Stem Cells (MSCs) were isolated from rat bone marrow and resuspended in 10ml cell culture medium. Fat from the abdomen, epididymus and kidneys was dissected from the same rats and 1.2g of fat was placed in 50mls of culture medium for 24 hrs in standard incubator conditions, the media was filtered and used as 'fat conditioned medium'. 2ml of fat conditioned medium was added to the cells' standard medium on day two of culture and on each subsequent media change. Cultures were stopped after 14 days and stained for alkaline phosphatase, Alizarin red (calcium), Sirius red (collagen), and methylene blue.

In the mouse model there were no differences in trabecular bone mineral density between mice on standard diets and mice fed the high cholesterol diet. However mechanical testing demonstrated a lower ultimate strength and Young's modulus of tibiae from the cardiovascular diseased mice. OCT demonstrated a corresponding decrease in optical scattering in the cortical bone. In the MSC cultures, alkaline phosphatase activity was 70% higher in the groups treated with abdominal and epididymal fat conditioned medium, compared to controls. Collagen and calcium deposition was also higher as was total colony number. These data suggest that higher body fat deposition associated with obesity and cardiovascular disease has strong effects on mesenchymal stem cell differentiation and whole bone properties.

1. **Diet and Murine Atherosclerosis** Godfrey S. Getz and Catherine A. Reardon *Arterioscler. Thromb. Vasc. Biol.* 2006;26:242-249

**Disclosures:** J.L. Stevens-Smith, None.  
This study received funding from: EPSRC.

## M452

**Diffuse Sclerosing Osteomyelitis of the Mandible: Case Report and Literature Review.** A. L. Schafer, R. Silva\*, M. Yafai\*, D. Shoback. San Francisco VA Medical Center and University of California, San Francisco, San Francisco, CA, USA.

Osteonecrosis of the jaw is a serious complication of bisphosphonate therapy and highlights the need for greater understanding of bisphosphonate effects on oral bone. We evaluated a patient with diffuse sclerosing osteomyelitis of the mandible (DSOM), for which there are reported dramatic improvements after IV bisphosphonate therapy. DSOM is a chronic inflammatory condition with intermittent, acute flares of pain and swelling in the absence of pus or fistulae. Response to conventional treatment with antibiotics is transient. Frequent flares lead to pain and progressive loss of oral function.

A 51 year-old man presented to the Oral and Maxillofacial Surgery Department with 3 years of recurrent pain and swelling of the left mandible. Repeated biopsies, debridements, and cultures failed to isolate a causative organism, although he had a modest clinical response to clindamycin. He had no history of endocrine or metabolic bone disorder. Examination showed diffuse left facial swelling, redness, warmth, and tenderness and marked trismus. CT showed cortical irregularity, destruction, and sclerosis of the left mandible. Technetium scan showed marked uptake in the left mandible. ESR and high-sensitivity CRP were elevated at 31 mm/hr (nl 0-15) and 41.9 mg/L (nl 0.2-7.5), respectively. Clindamycin and analgesics were increased, but symptoms continued unabated, and eventually he was admitted to the hospital for IV pain management. After literature review disclosed potential benefit from IV bisphosphonates, he received pamidronate 60mg IV. In 2 days, jaw swelling and pain decreased markedly. After 5 days, he had complete resolution of symptoms and remains without recurrence 3 months later.

There are 7 reports of DSO treated with IV or oral bisphosphonates, 6 of them cases of DSOM (3 children, 3 adults), and one trial with 10 patients. There are 3 cases of DSO of the femur and/or tibia. The 2 adults and 2 of the 3 children who received IV bisphosphonates for DSOM had resolution and lasting remissions. The third child developed mouth ulcers and increased pain and swelling. In the randomized trial of IV clodronate vs. placebo for DSOM, there was no difference in immediate pain relief between the 2 groups, but there was statistically significant decreased pain intensity 6 months after clodronate therapy (vs. placebo), without adverse events. Our patient with DSOM had a dramatic response to pamidronate, similar to patients in the literature. This case highlights the importance of accurate oral pathologic diagnosis and the need for greater understanding of mandibular bone disorders, especially the role of suppressing bone turnover in controlling inflammation and sclerosis in DSOM.

**Disclosures:** A.L. Schafer, None.

## M453

**Discordance in Femoral Neck Bone Density in Subjects with Osteoarthritis.** M. Tuteja<sup>\*1</sup>, J. Glowacki<sup>2</sup>, S. Hurwitz<sup>\*3</sup>, T. S. Thornhill<sup>\*2</sup>, M. S. LeBoff<sup>1</sup>. <sup>1</sup>Endocrine, Diabetes, and Hypertension Division, Brigham and Women's Hospital, Boston, MA, USA, <sup>2</sup>Department of Orthopedic Surgery, Brigham and Women's Hospital, Boston, MA, USA, <sup>3</sup>Biostatistics, Brigham and Women's Hospital, Boston, MA, USA.

Osteoarthritis (OA) is a common disease that increases with age and currently affects an estimated 27 million Americans. Although previous studies suggest that subjects with OA have elevated bone density, we found low bone mass in a subgroup of hip OA subjects<sup>1</sup>. In non-OA women, bilateral hip bone density measurements may show a discordance in the hip BMD that may result in differences in treatment classification and fracture risk assessments<sup>2</sup>. To determine whether site-specific hip BMD measures are confounded by the presence of OA, we measured BMD in 26 subjects who were scheduled for hip replacement for confirmed advanced OA and with no comorbidities or medications affecting bone. BMD was measured by dual X-ray absorptiometry (Hologic, Discovery) on the surgical (Surg) and non-surgical (Non-Surg) hip. There were 14 (54%) women. The mean age  $\pm$ SD of the subjects was 66.1  $\pm$  10.1 years. The median BMI was 25.9 (range 19.8 to 42.6). The mean 25-hydroxyvitamin D level  $\pm$ SD was 32.3  $\pm$  9.3 ng/ml (n=22). Vitamin D insufficiency (defined as a 25(OH) D level  $\leq$ 32 ng/mL) was present in 50% of subjects. Compared with the FN BMD on Surg hip with advanced OA (mean BMD 0.819  $\pm$  0.141 gm/cm<sup>2</sup>), FN BMD on the Non-Surg hip (0.756  $\pm$  0.139 gm/cm<sup>2</sup>) was lower by 8% (p=0.010), without differences in the TH measurements (p= 0.99). Osteopenia at the FN site (BMD, T-score between -1.0 and -2.5) was present in 35% of the Surg hips versus 50% of the Non-Surg hips. These data suggest that advanced OA can be associated with a higher bone density at the femoral neck but not the TH. Because the risks of OA and of low bone mass both increase with age, discrepancies in the femoral neck BMD, which is used for fracture risk assessment, may have an impact on patient treatment decisions.

**References:**

1. Glowacki J, Hurwitz S, Thornhill TS, Kelly M, LeBoff MS. Osteoporosis and vitamin-D deficiency among postmenopausal women with osteoarthritis undergoing total hip arthroplasty. *J Bone Joint Surg Am.* 2003;85-A:2371
2. Cole R, Larson J. The effect of measurement of the contralateral hip if the spine is not included in the bone mineral density analysis. *J Clin Densitom.* 2006;9:210

**Disclosures:** M. Tuteja, None.  
This study received funding from: NIH-NIA

## M454

**Unsymmetrical Beam Theory and Finite Element Method: Analysis of Murine Cortical Bone based on microCT Imaging.** T. Kummer<sup>\*1</sup>, N. Götzen<sup>\*2</sup>, M. M. Morlock<sup>\*2</sup>, M. Amling<sup>3</sup>. <sup>1</sup>Department of Emergency Medicine, Brown University School of Medicine, Providence, RI, USA, <sup>2</sup>Biomechanics Institute, Hamburg University of Technology, Hamburg, Germany, <sup>3</sup>Center for Biomechanics & Skeletal Biology, University Medical Center Hamburg Eppendorf, Hamburg, Germany.

We compared two methods for the numerical analysis of the murine femur. Our goal is to develop a tool that allows the routine calculation and visualization of important biomechanical parameters without the difficulties and time constraints of the more sophisticated FE analysis.

Femora of 19 10-week old female C57BL/6 mice were scanned using a  $\mu$ CT 40. MATLAB was used for the morphometrical analysis of the mid-diaphysis. To compensate for skewed bending, the principal moments of Inertia  $I_1$  and  $I_2$  were calculated. Ultimate load and displacement were recorded during a three-point bending test and the extrinsic stiffness of the bone was calculated from the slope of the load-displacement curve.

The surface stress was calculated using the beam theory for unsymmetrical bending and the results were mapped onto a polygonal surface. FE analysis based on a linear-elastic simulation with an iterative solver (Ansys, USA) and conventional meshing technique was used to calculate and visualize the surface stress. Standard approaches for both methods were used to determine Young's modulus.

Maximal tensile stresses were not significantly different using the Beam Theory and FE method ( $75.82 \pm 2.37$  vs.  $77.67 \pm 2.35$  MPa,  $p=0.58$ ), while FE analysis resulted in higher peak compressive surface stresses ( $-78.81 \pm 2.77$  vs.  $-98.23 \pm 2.84$  MPa,  $p<0.01$ ). Figure 1 and 2 show the mapped surface stress and the stress distribution along the midshaft. The Young's Moduli were not significantly different ( $3166 \pm 747$  vs.  $3326 \pm 755$  MPa,  $p=0.51$ ).

In conclusion, we found that the ultimate tensile stresses, which are crucial for fracture initiation, as well as the Young's moduli were calculated and displayed correctly compared to the FE analysis. The peak compressive stresses were underestimated by an average of 20%.

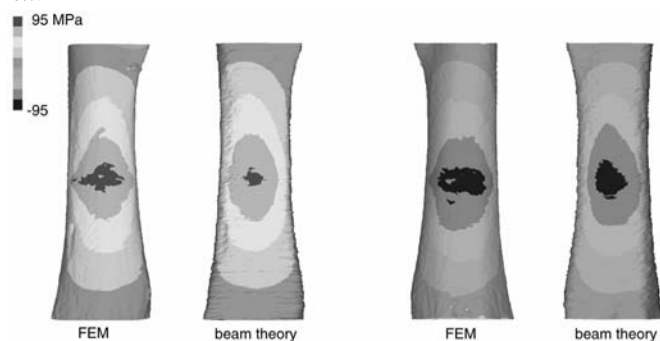


Fig. 1

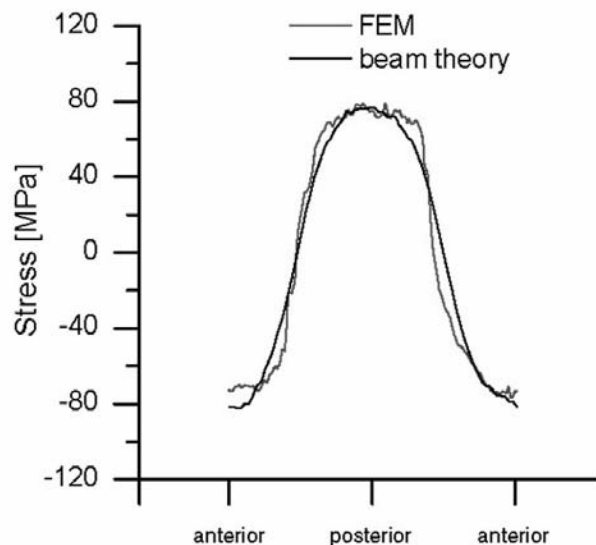


Fig. 2

**Disclosures:** T. Kummer, None.

## M455

**Contributions of Trabecular and Cortical components to Biomechanical Properties of Human Vertebrae.** J. P. Roux<sup>\*1</sup>, J. Wegrzyn<sup>\*1</sup>, M. E. Arlot<sup>1</sup>, Z. Merabet<sup>\*1</sup>, M. L. Bouxsein<sup>2</sup>, P. D. Delmas<sup>1</sup>. <sup>1</sup>INSERM unit 831, Université de Lyon, Lyon, France, <sup>2</sup>Orthopedic Biomechanics Laboratory, Beth Israel Deaconess Medical Center and Harvard Medical School, Boston, MA, USA.

Vertebral fractures are common in elderly persons, yet the mechanisms of injury underlying these fractures remain obscure. Whereas there is clear evidence for a strong influence of the quantity of bone (i.e., bone mass or BMD) on the mechanical behavior of vertebrae, there are less data addressing the relative influence of cortical and trabecular microarchitecture. Thus, the aim of this study was to determine the relative contributions of bone mass, trabecular microarchitecture and cortical thickness and curvature to the mechanical behavior of human lumbar vertebrae. We obtained 31 L3 vertebrae (16 men and 15 women, aged respectively  $75 \pm 10$  yrs and  $76 \pm 10$  yrs), and assessed BMD ( $\text{g}/\text{cm}^3$ ) of the vertebral body by lateral DXA; vBMD ( $\text{g}/\text{cm}^3$ , as BMC / directly measured vertebral body volume); 3D trabecular microarchitecture (BV/TV, trabecular thickness (Tb.Th), degree of anisotropy (DA), and structure model index (SMI)); thickness and curvature of the anterior cortex by  $\mu$ CT ( $35 \mu\text{m}$  voxel size, Skyscan1076). Then, compressive stiffness and failure load were measured on the whole vertebral body. No difference was found between sex, except for BMC, which was higher in men than women ( $5.99 \pm 1.25$  vs  $7.18 \pm 1.88$ , T-test  $p=0.05$ ). BMD was strongly correlated to compressive stiffness ( $r=0.60$ ) and failure load ( $r=0.70$ ). Except for DA, all trabecular parameters ( $r=0.36-0.58$ ,  $p=0.05-0.001$ ) and anterior cortex thickness or curvature ( $r=0.36-0.61$ ,  $p=0.05-0.0001$ ) were correlated with mechanical behavior. Stepwise and Multiple regression analyses indicated that the combination of BMD, SMI and Tb.Th was the best predictor of failure load ( $R=0.80$ ); BMD, Tb.Th and curvature of the anterior cortex were the best predictor of stiffness ( $R=0.82$ ) and anterior cortical thickness and BMD were the best predictor of work to failure (i.e. ability to absorb energy) ( $R=0.68$ ). Our data imply that measurements of cortical thickness and curvature may enhance predictions of vertebral fragility, and that therapies which improve both vertebral cortical as well as trabecular bone properties may provide a greater reduction in fracture risk.

**Disclosures:** J.P. Roux, None.

This study received funding from: INSERM-Lilly contract unrestricted research grant.

## M456

**Murine Bone Mechanics Is Determined by the Ultrastructural Canal Network in a Sex- and Strain-Specific Manner.** P. Schneider<sup>\*1</sup>, R. Voide<sup>\*1</sup>, L. R. Donahue<sup>2</sup>, R. Müller<sup>1</sup>. <sup>1</sup>Institute for Biomechanics, ETH Zurich, Zurich, Switzerland, <sup>2</sup>The Jackson Laboratory, Bar Harbor, ME, USA.

Previous results from our group revealed that the canal network is a major contributor to cortical tissue porosity on an ultrastructural level, and thus, may be linked to bone mechanics. Therefore, the goal of this study was to quantify the contribution of the canal network to murine bone mechanics. To this end, we designed a mouse model including strains derived from C57BL/6J (B6) and C3H/HeJ (C3H) mice characterizing low and high bone mass phenotypes, respectively, with physiological (*lit*+) and absent (*lit*lit) growth hormone (GH) levels. Femoral mid-diaphyses of the four resulting mouse strains B6-*lit*+, C3.B6-*lit*+, B6-*lit*lit, and C3.B6-*lit*lit (N=12 each, 4-mo-old) were scanned using synchrotron radiation-based micro-computed tomography at a nominal resolution of  $3.5 \mu\text{m}$ . For quantitative analysis, morphometric indices characterizing the macroscopic cortical bone compartment and the canal network were derived. For mechanical testing, three-point bending tests were performed and ultimate force ( $F_u$ ) was determined. Multiple linear regression models were built to explain the variation in  $F_u$  in terms of the morphometric indices. For both *lit*lit strains the absence of GH removed sex differences for bone size still present in the *lit*lit strains. However, sex differences in bone strength characterized by  $F_u$  were removed only in B6-*lit*lit. These differences in the mechanical properties could only be explained by sex differences in cannular morphometry found in the same animals. From this, we hypothesized that cannular parameters accounted for the variance in  $F_u$  unexplained by bone size alone. We verified this hypothesis for *lit*lit strains, which covered a broad range in bone strength. Multiple linear regression showed that bone size predicted bone strength to a great extent for C3.B6-*lit*lit ( $R^2_{adj} = 0.90$ ) but only moderately for B6-*lit*lit ( $R^2_{adj} = 0.51$ ). Moreover, bone strength prediction was increased by 6% and 75% for C3.B6-*lit*lit ( $R^2_{adj} = 0.95$ ) and B6-*lit*lit ( $R^2_{adj} = 0.89$ ), respectively, when including cannular parameters like canal volume density, canal spacing or mean canal length in addition to bone size. We consequently provided strong evidence for a significant influence of the canal network on murine bone mechanics in a sex- and strain-specific manner. The larger increase in the power to predict bone strength for low bone mass B6-*lit*lit (75%) compared to high bone mass C3.B6-*lit*lit (6%) was due to strong coupling of the canal network with bone size for C3.B6-*lit*lit, which was absent for B6-*lit*lit. Finally, we believe that morphometric analysis of ultrastructural phenotypes will give new insights in the assessment of bone quality and the mechanical competence of bone.

**Disclosures:** P. Schneider, None.

## M457

**Optimization of Failure Load Estimation using Radiographs of Human Cadaveric Femur.** C. D. Arnaud<sup>1</sup>, S. Liew<sup>\*1</sup>, E. Thrall<sup>\*2</sup>, B. Roberts<sup>\*2</sup>, R. Vargas-Voracek<sup>\*1</sup>, P. Hess<sup>\*1</sup>, M. L. Bouxsein<sup>2</sup>. <sup>1</sup>Imaging Therapeutics Inc., Redwood City, CA, USA, <sup>2</sup>Orthopedic Biomechanics Laboratory, Beth Israel Deaconess Medical Center, Harvard Medical School, Boston, MA, USA.

Measurement of BMD by DXA is the current gold standard for diagnosis of osteoporosis. However, several studies have been critical of BMD for not fully accounting for changes in hip fracture rate in osteoporosis therapies. Bone geometry and trabecular architecture have been proposed as factors that contribute to bone strength. In this study we tested the ability of an optimization approach using radiograph-based trabecular pattern and geometric parameters to predict femoral strength.

Human-cadaver femora from 51 donors (34 female, 17 male) 55 to 98 years old were selected as representative of the target population of individuals likely to suffer a hip fracture. DXA BMD and x-ray images were obtained on all femora following a predefined imaging and positioning protocol. Femoral strength was assessed in a sideways fall configuration simulating impact to the greater trochanter. X-Ray images were analyzed to obtain femoral geometry and trabecular micro-architecture measurements. Combinations of measurements that were most robust in estimating failure load were identified using stepwise linear regressions and cross-validation. The ability of x-ray based measurements to complement DXA-BMD for prediction of femoral strength was also investigated.

A combination of five radiograph-based measurements were strongly correlated to femoral failure load ( $r=0.87$ ). Cross-validation using repeated random selections of 34 cases for optimization and 27 for validation provided an average correlation value of  $r=0.85$ . DXA total hip BMD by itself correlated strongly with failure load ( $r=0.84$ ), but the association was significantly improved to  $r=0.93$  with the addition of 5 radiographic structural measurements.

Altogether, these results indicate that radiograph-based measurement of femoral geometry and projected trabecular bone micro-architecture has the potential of providing an alternative, non-invasive and widely accessible approach to the estimation of femoral strength and possibly hip fracture risk. The follow-on blinded validation phase of the study will provide further insights on the generalizability of this method, and its relative performance with other imaging modalities.

Method	Correlation with failure load, $r$ ( $r^2$ )
DXA BMD	0.84 (0.71)
Radiographic measurements	0.87 (0.76)
DXA BMD + radiographic measurements	0.93 (0.86)

**Disclosures:** C.D. Arnaud, None.

This study received funding from: Merck & Co. Inc.

## M458

**Overweight Children Are More at Risk to Sustain a Forearm Fracture due to Poor Bone Strength Relative to Body Weight.** G. Ducher<sup>1</sup>, R. Daly<sup>2</sup>, G. Naughton<sup>\*3</sup>, P. Eser<sup>\*4</sup>, R. English<sup>\*1</sup>, A. Patchett<sup>\*1</sup>, K. Gravenmaker<sup>\*5</sup>, M. Seibel<sup>6</sup>, A. Javai<sup>\*5</sup>, R. Telford<sup>\*7</sup>, S. Bass<sup>1</sup>. <sup>1</sup>Centre for Physical Activity and Nutrition Research, Deakin University, Burwood, Australia, <sup>2</sup>Department of Medicine, Western Hospital, The University of Melbourne, Melbourne, Australia, <sup>3</sup>Australian Catholic University, Melbourne, Australia, <sup>4</sup>Division of Clinical Epidemiology & Biostatistics, University of Bern, Bern, Switzerland, <sup>5</sup>The Canberra Hospital, Canberra, Australia, <sup>6</sup>ANZAC Research Institute, Sydney, Australia, <sup>7</sup>Australian National University, and The Commonwealth Institute (UK and Australia), Canberra, Australia.

Comparison of bone strength between overweight and normal-weight children using 3D imaging techniques has been conducted at the femur and tibia, but not the forearm, a site prone to fracture in children. The aim of this study was to investigate forearm bone strength in prepubertal children of different adiposity levels.

Bone mass (BMC), geometry (total area, ToA) and trabecular volumetric density (TrD) were measured by pQCT at the nondominant radius (4% and 66%; TrD: 4%) in 511 children (253 boys), mean age  $8.3 \pm 0.4$  years. Two bone strength indices combining bone size and volumetric density were calculated: BSI (ToA\*ToD<sup>2</sup>) at the 4% site and polar SSI at the 66% site. The ratio between fat and muscle cross-sectional areas (66% radius) was used as an indicator of adiposity. A total of 111 children (22%) were classified as overweight (BMI>equivalent to 25 kg/m<sup>2</sup> in adults). As expected, overweight children were heavier (+3SD) and fatter (adiposity +2SD), but were also taller (+0.7SD), had larger muscle CSA (+1.2SD) and greater values for all bone parameters than normal-weight peers (Z-scores +0.5 to +0.9SD,  $p < 0.0001$ ). Age was not different between the two groups. Compared to height or weight, muscle CSA was a better predictor of BMC, ToA, BSI and SSI ( $r=0.58-0.68$ ,  $p < 0.0001$ ) and TrD ( $r=0.2$ ,  $p < 0.0001$ ). The differences in BMC, ToA, BSI and SSI remained significant after adjustment for height (except for ToA at 4%). After adjustment for muscle CSA, these differences disappeared except for ToA at 4% that became lower in overweight children ( $p=0.035$ ). TrD was greater in overweight children before (+0.6 SD,  $p < 0.0001$ ) and after adjustment for muscle CSA. Adiposity (fat CSA/muscle CSA) was negatively correlated with BMC, ToA and BSI at the radius 4% only ( $r=-0.1$ ,  $p < 0.06$ ). After controlling for body weight, these correlations were stronger and significant for all bone parameters at both sites ( $r=-0.36$  to  $-0.55$ ,  $p < 0.0001$ ), except for TrD.

Overweight children have stronger bones due largely to greater muscle size. However, high adiposity is associated with lower bone mass, size and strength relative to body weight, placing overweight children at higher risk for forearm fracture.

**Disclosures:** G. Ducher, None.

This study received funding from: Commonwealth Education Trust and Commonwealth Institute (Australia).

## M459

**Temporal Trends in Vertebral Size and Shape from Medieval to Modern-Day.** J. A. Junno<sup>\*1</sup>, M. Nieminen<sup>\*2</sup>, M. Niskanen<sup>\*3</sup>, J. Tuukkanen<sup>1</sup>. <sup>1</sup>Anatomy and Cell Biology, University of Oulu, Oulu, Finland, <sup>2</sup>Radiology, University of Oulu, Oulu, Finland, <sup>3</sup>Anthropology, University of Oulu, Oulu, Finland.

Human lumbar vertebrae support the weight of upper body and loads lifted and carried by upper extremities causing significant loading stress to vertebral bodies. It is well known that trauma based vertebral fractures are common especially among elderly people. The aim of this study was to determine the factors that could have affected to the prevalence of trauma based vertebral fractures from medieval to present. According to this study there seems to be morphological change in size and shape of vertebral body from medieval period to modern days. In this study the vertebral size and shape was measured from the 4<sup>th</sup> lumbar vertebra in chronologically differentiating samples using magnetic resonance imaging (MRI) and standard measuring calipers. Densitometric analyses were performed using pQCT and uCT. Modern sample consisted of modern Finns and archaeological samples of medieval Swedes and Britons. This survey revealed that the shape and size of the 4<sup>th</sup> lumbar vertebra has changed significantly from medieval times affecting greatly to the biomechanical characteristics of the lumbar vertebra. These changes have possibly affected to the appearance of trauma based spine fractures in modern times.

**Disclosures:** J.A. Junno, None.

## M460

**Degradation of Allograft Bone Quality by Gamma Irradiation is Not Explained By Altered Enzymatic or Non-Enzymatic Cross-Links.** H. Nguyen<sup>\*1</sup>, E. Gyneys<sup>\*2</sup>, A. C. K. Wu<sup>1</sup>, A. I. Cassady<sup>2</sup>, M. B. Bennett<sup>\*1</sup>, D. A. F. Morgan<sup>\*4</sup>, P. D. Delmas<sup>2</sup>, M. R. Forwood<sup>1</sup>. <sup>1</sup>School of Biomedical Sciences, The University of Queensland, Brisbane, Australia, <sup>2</sup>INSERM Unit 831, University of Lyon, Lyon, France, <sup>3</sup>Institute of Molecular Biosciences, The University of Queensland, Brisbane, Australia, <sup>4</sup>Queensland Bone Bank, Brisbane Private Hospital, Brisbane, Australia.

Gamma irradiation is commonly used to sterilise bone allografts, with 25 kGy accepted as the Australian standard dose. Radiation causes dose-related degradation in mechanical properties of allograft bone, but it is not known if it affects allograft biocompatibility or enzymatic and non-enzymatic cross-links of collagen. Our aim was to investigate the mechanical properties of bone allografts irradiated at 25, 20, 15, 10, and 5 kGy; and to determine the activity of osteoblasts, osteoclasts and macrophages seeded onto this bone, and the content of pyridinoline (PYD), deoxypyridinoline (DPD) and pentosidine (PEN) in the bone samples. Sixteen femoral shafts from eight human donors were sectioned into six cortical bone beams (40x4x2mm) and irradiated at 0, 5, 10, 15, 20, and 25 kGy for three-point bending tests. 100µm-thick cortical bone slices were used for *in vitro* determination of macrophage activation (RAW264.7/ELAM-GFP cells), osteoblast (MC3T3E1 cells) proliferation and attachment assays, and osteoclast (Balb/c BMCs) formation and fusion assays. Samples of 0.3g of bone samples were hydrolysed for determination of PYD, DPD and PEN by HPLC. Irradiation up to 25 kGy did not affect the elastic properties of cortical bone, but the modulus of toughness was decreased from 87% to 74% ( $p < 0.05$ ) compared with controls from 15 to 25 kGy. Macrophage activation was not increased, and the proliferation and attachment of osteoblastic cells on irradiated bone was not affected. However, osteoclast formation and fusion were less than 40% of controls when cultured on bone irradiated at 25 kGy, and 80% at 15 kGy ( $p < 0.05$ ). Irradiation did not significantly alter the content of PYD, DPD or PEN. These data demonstrate that standard irradiation is not proinflammatory, but increases fragility of cortical allografts at doses above 15 kGy. Decreased osteoclast viability at these doses suggests a reduction in the capacity for remodelling of allograft bone. These changes cannot be explained by alterations in the enzymatic or non-enzymatic cross-links of collagen.

**Disclosures:** H. Nguyen, None.

This study received funding from: NHMRC (Aus), AINSE (Aus), INSERM (France).

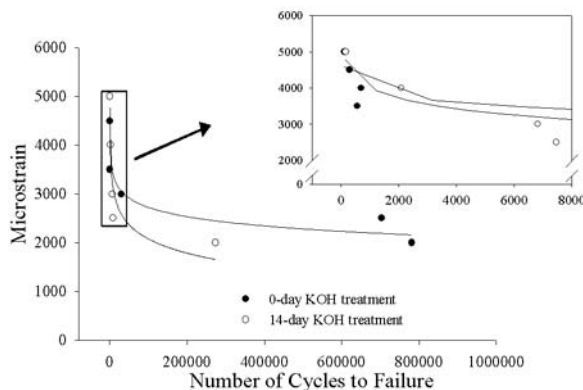


## M461

**The Effect of Collagen Degradation on the Fatigue Behaviour of Emu Bone.** C. A. Wynnyckyj<sup>1</sup>, S. Omelon<sup>2</sup>, J. Wang<sup>2</sup>, T. L. Willett<sup>2</sup>, M. D. Grynpas<sup>2</sup>. <sup>1</sup>Materials Science Engineering, University of Toronto, Toronto, ON, Canada, <sup>2</sup>Mount Sinai Hospital, Samuel Lunenfeld Research Institute, Toronto, ON, Canada.

We recently conducted a pilot study using an ex-vivo emu model to investigate the ability of the Mechanical Response Tissue Analyzer (MRTA) in detecting changes in the collagen matrix of emu bone and to evaluate the differences between male and female emu bone. The emu tibia was chosen due to its size and approximate cylindrical shape, making it ideal for devices designed to accommodate human long bones. Male and female emu tibiae were endocortically treated with 1 M potassium hydroxide (KOH) for 1-14 days, resulting in negligible mass loss (0.5 %), collagen loss (0.05 %) and a significant reduction in modulus (18%). The MRTA detected this change however, the change in bone quality measured after KOH treatment by conventional clinical tools such as DXA and QUS varied by less than 2%. Male emu tibiae had significantly decreased failure stress and increased failure strain and toughness compared to female tibiae with increasing KOH treatment time. This was a surprising result since a minimal amount of collagen was removed. We hypothesize that the significant changes in bone mechanical properties may be due to partial debonding between the mineral and organic matrix or *in situ* collagen degradation.

To further determine the contribution of collagen on the mechanical properties of bone, we investigated the effects of KOH treatment on the fatigue resistance of female emu bone. Five groups (n=10) of mature female emu tibiae were endocortically treated with 1M KOH for 0, 1, 3, 7 and 14 days and then subsequently fatigued as controlled cyclic loading of bone is known to result in accumulation of microdamage and significantly reduce bone stiffness. Emu tibiae were fatigued at a frequency of 2 Hz under load control, corresponding to a set of initial strains ranging from 2000 µε to 6000 µε peak-to-peak. Strain was measured directly using strain gauges. The strain versus number of cycles to failure (S/N) was determined for each group and we found that the 14-day KOH treated specimens appear to resist less cycles at low strain fatigue. This difference in fatigue life could be due to collagen mineral interface alterations or changes in the collagen matrix itself caused by KOH treatment.



**Disclosures:** C.A. Wynnyckyj, None.

## M462

**Non-invasive Detection of Bone Microdamage by Light Scattering.** J. H. Cole<sup>1</sup>, E. I. Waldorff<sup>2</sup>, M. V. Schulmerich<sup>1</sup>, K. A. Dooley<sup>1</sup>, S. A. Goldstein<sup>2</sup>, M. D. Morris<sup>1</sup>. <sup>1</sup>Department of Chemistry, University of Michigan, Ann Arbor, MI, USA, <sup>2</sup>Department of Orthopaedic Surgery, University of Michigan, Ann Arbor, MI, USA.

Microcracks develop in bone when loading rates, magnitudes, and/or cycles exceed the load-bearing capacity of the tissue. With increased loading (e.g., in athletes and military recruits) or degraded tissue properties (e.g., with osteoporosis), the repair mechanisms of bone may become insufficient, leading to microcrack accumulation and fracture. Current *in vivo* imaging tools cannot examine microdamage in bone tissue. Previous studies reported the use of optical techniques to assess bone demineralization and microdamage in excised bone tissue, as well as bone mineral and lipid content *in vivo* using idealized models. We recently developed a simple, non-invasive light scattering probe that allows us to detect microdamage in cortical bone tissue of excised limbs. Microcracks scatter light more than the undamaged native bone tissue, providing a direct means to evaluate the extent of damage. The objective of our study was to optimize probe sensitivity for detecting damage and to explore its capability for *in vivo* use. Here we report the probe's potential to assess aspects of bone quality. By using concentric paths to deliver light to the specimens (in a ring) and collect light scattered by the specimens (in a disk inside the ring), and by varying the separation between the ring and disk, we can examine tissue properties below the surface. This technique exploits the difference in tissue scattering properties between bone tissue and overlying skin, connective tissues, and the serum-based fluid between the microcracks. Using phantoms, we have tested the ability of the ring/disk light scattering probe to find boundaries between materials with different scattering properties, similar to what occurs *in vivo* with bone and surrounding soft tissues. These phantoms, which are widely used in tissue optics studies, include: a) layered composites made of engineering

polymers and b) excised murine cortical bone placed at known depths in an Intralipid® suspension. For these phantoms, an abrupt change in scattering behavior was observed, corresponding to the boundary between the dissimilar materials. For further analysis and development of the light scattering probe, we plan to take transcutaneous bone measurements in murine limbs both with and without microdamage and to compare those with exposed bone measurements. Because skin, connective tissue, and bone have different scattering properties, we can distinguish between the different scattering signals arising from these tissues. This non-invasive probe has great potential as an inexpensive and portable diagnostic tool.

**Disclosures:** J.H. Cole, None.

## M463

**Characterization and Genetic Mapping of Bone Size Phenotypes in GK and F344 Rats Using a New 3D CT Method.** S. Lagerholm, H. Luthman\*, M. Nilsson\*, K. Åkesson. Dept of Clinical Sciences, Malmö University Hospital, Lund University, Malmö, Sweden.

Evaluation of bone phenotypes requires methods with high resolution and precision, particularly when determining bone parameters in animal models. The aim of this study was to test reproducibility and precision of a new 3D CT method measuring bone size parameters in rats and identify quantitative trait loci (QTLs) regulating bone size phenotypes.

Tibia and femur from male and female diabetic GK and non-diabetic F344 rats, representing the parental (n= 39), F1 (n=37) and F2 (n=206) generations were examined with CT (Somatom Sensation 64, Siemens, Erlangen, Germany) and analyzed using Analyze® software version 5.0 for the parameters: Total and cortical volume (mm<sup>3</sup>), total and cortical BMC (mg/cm<sup>3</sup>), straight and curved length (mm), peri- and endosteal area at mid-shaft (mm<sup>2</sup>). CVs were calculated based on repeated measurements and repeated analyses. The F2 progeny (108 male and 98 female) were genotyped for 192 genome-wide microsatellite markers at an average distance of 10 cM. Genetic maps were generated using Mapmaker/EXP and QTLs were identified in MapManager/QTx.

The repeated measurement CV (%) was parameter dependent; total and cortical volume 0.0-0.0, length 1.8-5.9, mid-shaft peri- and endosteal area 2.9-4.5 and BMC (total and cortical) 0.0-0.0. Intra-observer analysis yielded variation between 0.4-9.2. The cross-sectional areal measurements had the largest variation due to small size and subsequent few pixels, nevertheless area and periosteal circumference were highly correlated (r=0.997). All bone size parameters were significantly lower in the F344 females (Table 1). In males, the findings were similar except for bone length, total volume and BMC. Several QTLs were identified in both males and females some of which were reciprocal-cross or sex specific; LOD scores >4.0 on Chr 1, 3, 4, 9, 10, 17.

We show that this new 3D CT analysis provides high precision measurements of bone size parameters in rat bone, improving the available methods for determining bone phenotypes. Observed differences in bone size and bone mineral content between GK and F344 strains, make these rats ideally suited for studying genetic regulation of skeletal phenotypes. Several unique QTLs linked to bone size were identified, many overlapping previously identified QTLs in rats and homologous with regions found in humans.

Table 1.

CT results	Female (Tibia/Femur)		P-value
	GK (n=10)	F344 (n=10)	
Bodyweight (g)	250±20	192±12	<10 <sup>-4</sup>
Total volume (mm <sup>3</sup> )	371±19 / 430±18	285±14 / 337±29	<10 <sup>-4</sup> / <10 <sup>-4</sup>
Cortical volume (mm <sup>3</sup> )	158±11 / 151±8.1	105±6.7 / 98±6.0	<10 <sup>-4</sup> / <10 <sup>-4</sup>
Length (straight) (mm)	39.7±1.1 / 35.1±0.6	38.4±1.2 / 33.5±1.0	0.02 / 0.0006
Cortical midshaft Periosteal Area (mm <sup>2</sup> )	9.4±0.5 / 13.9±1.7	6.1±0.3 / 10.6±1.2	<10 <sup>-4</sup> / <10 <sup>-4</sup>
Cortical midshaft Endosteal Area (mm <sup>2</sup> )	2.9±0.1 / 3.7±0.4	1.2±0.1 / 2.5±0.5	<10 <sup>-4</sup> / <10 <sup>-4</sup>
Total vBMC (mg/cm <sup>3</sup> )	1341±6 / 1324±16	1281±11 / 1258±32	<10 <sup>-4</sup> / <10 <sup>-4</sup>
Cortical vBMC (mg/cm <sup>3</sup> )	1819±16 / 1858±26	1795±25 / 1802±26	0.02 / 0.0002

**Disclosures:** S. Lagerholm, None.

## M464

**The Correlation between DXA Femur Strength Index and QUS Heel Stiffness Index in Chinese Women.** H. Xu<sup>1</sup>, J. Li<sup>1</sup>, Q. Wu<sup>2</sup>, H. S. Barden<sup>3</sup>, Q. Zhou<sup>4</sup>. <sup>1</sup>Department of Nuclear Medicine, The First Affiliated Hospital, Jinan University, Guangzhou, China, <sup>2</sup>Medical College, Jinan University, Guangzhou, China, <sup>3</sup>GE Healthcare, Madison, WI, USA, <sup>4</sup>GE Healthcare, Shanghai, China.

Hip strength analysis (HSA) is the new application for dual-energy X-ray absorptiometry (DXA) that allows the measurement of geometric contributions to bone strength in the proximal femur. The femur strength index (FSI) assessed by DXA may be an independent predictor of hip fracture risk. Quantitative ultrasound (QUS) bone measurement is a promising new technology for the screening diagnosis of osteoporosis. This study was aimed at assessing the correlations between the FSI calculated by DXA and SI of the heel calculated by QUS in Chinese women. We measured the bone mineral density (BMD) of the bilateral proximal femurs (i.e., total hip, femoral neck, Ward's

triangular area and trochanter) using DXA, and speed of sound (SOS), broadband ultrasound attenuation (BUA), and a calculated strength index (SI) of the left calcis in 90 Chinese females aged from 20-80 years. With HSA, a series of structural variables such as the femoral neck cross-sectional moment of inertia (CMSI), section modulus (Z), cross-sectional area (CSA), femoral neck shaft angle, and hip axis length (HAL) were assessed automatically. The BMD precision for bilateral proximal femur was 0.7-2.2%, depending on ROI. The precision for FSI was 2.6% for left side and 1.9% for right. The precision of SI, SOS and BUA was 1.8%, 0.4% and 2.9%, respectively. No significant differences ( $p>0.05$ ) in bilateral femoral BMDs (total hip, femoral neck, Ward's triangular area and trochanter) and FSI (left FSI  $1.69\pm0.45$  vs right FSI  $1.69\pm0.41$ ) were found. There were significant correlations ( $p<0.001$ ) for heel SI and femoral BMDs ( $r=0.44-0.61$ ), heel BUA and femoral BMDs ( $r=0.34-0.52$ ), and heel SOS and femoral BMDs ( $r=0.42-0.59$ ). Heel SI correlated significantly ( $p<0.001$ ) with CSA ( $r=0.52$ ), CSMI ( $r=0.36$ ), and Z ( $r=0.42$ ) for all subjects. The correlation between FSI assessed by DXA and heel SI calculated by QUS ( $r=0.18$ ) was not significant. The difference of the alignment of trabeculae in the stress orientation between femur neck and calcaneal bone may be one of reasons for no significant correlation between FSI and heel QUS. Understanding the reason for this lack of association requires further study.

**Disclosures:** H. Xu, None.

M465

**Cost-Effective Rack and Pinion System for Torsion Testing of Rodent Bones.** M. Saunders. Center for Biomedical Engineering, University of Kentucky, Lexington, KY, USA.

Thorough mechanical testing of rodent bones requires an understanding of bone behavior in a variety of loading modes including tension, compression, bending and shear. While these tests are easily conducted with single axis mechanical testing machines, it may also be desirable to determine torsional properties of bone. Although higher end biaxial materials testing machines will enable torsional and/or rotational testing, simpler, less expensive systems rarely offer these capabilities. This work illustrates the development of a torsion system that uses a simple rack and pinion concept to deliver a rotary motion to bones given the linear motion of a testing machine. While mechanical and biomechanical engineers may have high end equipment, as the bone field becomes more interdisciplinary more and more biologists will need cost-effective mechanical testing capabilities and this torsion system has proven to be more than adequate for our mechanical testing needs. Furthermore, given the small-scale size of the rodent long bones, a series of potting and testing fixtures that enable preparation and handling of the specimens without incurring damage to the bone shafts was also fabricated. Bones were potted in the testing fixtures using bone cement and kept hydrated with saline at all times during potting and testing. While the concept can be used to adapt to any linear loading system, the torsion system here was developed for a loading platform we developed in-house. A 25 in-oz torque cell and 25 mm displacement sensor were outfitted to the system to record torque-twist data with real-time data acquisition. Using simple geometry and a dial caliper, the rack and pinion was calibrated to convert linear motion of the slide to rotary motion (twist) experienced by the specimen. Once calibrated the system was used to destructively test four, three month old mice humeri and quantify torsional properties. Bones were tested to failure under displacement control at a constant linear rate of 2mm/sec (6.5 deg/sec). From destructive testing on the four bones, mean  $\pm$  standard deviations for stiffness, failure torque and failure twist were:  $8.24 \pm 3.7$  (Nmm/deg);  $12.00 \pm 5.1$  (Nmm); and,  $12.01 \pm 2.8$  (deg), respectively. Results are acceptable in comparison to published studies. Similar agreement was found for femurs tested to failure in torsion. The development of this simple rack and pinion torsion fixture enabled successful torsion testing of rodent limbs and the potting system enabled the bones to be aligned and tested along their neutral axis to guarantee pure torsion and increase testing accuracy and precision. As such, the system developed offers a cost-effective solution to adapt any axial testing machine to torsion testing.

**Disclosures:** M. Saunders, None.  
This study received funding from: Whitaker Foundation, NIH (Aging).

M466

**Comparison of HR-pQCT to DXA & QUS for the Assessment of Ex-Vivo Bone Strength.** I. Ally, J. Lau\*, C. Chan\*, A. M. Cheung. University Health Network, Toronto, ON, Canada.

Proper assessment of fracture risk depends on the ability to obtain a measure of the mechanical competence of bone, or bone strength. Current tools used to assess fracture risk, such as DXA and QUS, do not directly measure bone mechanical properties. Instead, they offer surrogate measures of bone strength based primarily on the bones' material properties (bone mineral content), and to some extent bone size. We conducted an ex-vivo emu study to examine how parameters measured by HR-pQCT, DXA, and QUS correlate with true bone mechanical properties. Forty emu tibiae were used for this study. Bone mineral content (BMC) and areal bone mineral density (aBMD) were measured by DXA, and the speed of sound through the bone (SOS) was measured by QUS. HR-pQCT was used to determine total volumetric density (TvBMD), cortical volumetric density (CvBMD), cortical thickness (CTh), total cross-sectional area (tCSA), and cortical cross-sectional area (cCSA). A bone strength index (BSI = CvBMD  $\times$  cCSA) was also calculated. To obtain the bones' mechanical properties, four-point bending tests were performed, and ultimate load, flexural cross-sectional bending stiffness (EI-4pt), and bone toughness were determined. We used Pearson correlations to examine the relationships between measures from mechanical bending tests and measures obtained from DXA, QUS, and HR-pQCT. Additionally, linear regression modeling was used to predict the mechanical properties of bone from parameters obtained

from DXA, QUS, and HR-pQCT measures. Results are shown in Table 1. We found that ultimate load correlates well with aBMD, BMC, CTh, and moderately with cCSA. Toughness correlates moderately with aBMD, CTh, and BMC. EI-4pt correlates strongly with BSI, BMC, cCSA, tCSA, and aBMD, and moderately with CvBMD and CTh. Measures of SOS had no significant relationship to any of the measures of bone mechanical competence. We also found that EI-4pt is best predicted by parameters obtained from HR-pQCT: cCSA, CvBMD, and CTh (adjusted  $r^2=0.83$ ,  $p<0.001$ ). Parameters obtained from HR-pQCT could not predict ultimate load better than DXA-based aBMD. Our results suggest that ultimate load and toughness are best predicted by aBMD. However, parameters measured by HR-pQCT are better able to predict true cross-sectional flexural stiffness than conventional measures obtained by DXA or QUS. HR-pQCT, then, provides unique information about bone mechanical competence that cannot be obtained by DXA or QUS.

Results are Pearson correlations (R <sup>2</sup> values followed by p-values in parentheses)				
		Ultimate Load	Toughness	EI-4pt
QUS	SOS	0.01822 (0.4191)	0.001859 (0.7972)	0.1084 (0.04353)
		0.5362 (1.737e-07)	0.3209 (0.0002093)	0.6877 (1.260e-10)
DXA	BMC	0.593 (1.582e-08)	0.3971 (2.236e-05)	0.5129 (4.297e-07)
	aBMD	0.05301 (0.1643)	0.009203 (0.5667)	0.5139 (4.128e-07)
	tCSA	0.3279 (0.0001719)	0.2334 (0.002122)	0.0737 (0.0991894)
	TvBMD	0.04229 (0.2155)	0.00373 (0.7157)	0.4723 (1.883e-06)
	CvBMD	0.5278 (2.421e-07)	0.3439 (0.0001091)	0.3284 (0.0001697)
HR-pQCT	CTh	0.4647 (1.479e-06)	0.2423 (0.001001)	0.6839 (9.535e-11)
	cCSA	0.4246 (5.631e-06)	0.2023 (0.0027)	0.7799 (1.330e-13)
	BSI			

**Disclosures:** I. Ally, None.

M467

**Generating 3D Finite Element Models of a Human Proximal Femur from 2D DXA Data.** T. L. Bredbenner, D. P. Nicoletta. Materials Engineering, Southwest Research Institute, San Antonio, TX, USA.

The clinical standard for assessing an individual's risk of fracture is based on using a population-level statistical correlation to interpret clinical DXA data; however, these methods have been proven to be non-specific in assessing bone strength. Although engineering models based on clinical (QCT) imaging data improve the prediction of fracture load by providing a physics-based approach rather than a correlative approach, QCT is not widely available and biomechanical models that accurately represent the complex morphology of a human skeletal structure are time-consuming to create. In previous work, statistical shape and density modeling methods were used to develop and implement a parametric description of the complex geometry and bone mineral density (BMD) distribution based on clinical (QCT) imaging data for a set of 6 human female proximal femurs [1,2]. In the present study, a high fidelity 3D finite element (FE) model of a previously unseen (not included in the parametric model) individual human proximal femur was generated from clinical DXA data using the parametric model of the human proximal femur. The "unknown" target femur geometry and BMD distribution were determined from QCT data and the corresponding DXA data was simulated by projecting the target femur geometry and BMD distribution onto the coronal plane. The geometry and BMD of the target femur were quantified from the DXA data using standard descriptors [3,4]. The parametric model was then optimized to match the DXA data for the unknown femur, thus determining the "most probable" FE model that matches the target model. Error between the optimized models and the target femur were quantified using Euclidean distance, Mahalanobis distance, and maximum Hausdorff distance. Quantitative comparison demonstrated that the most probable FE model was capable of matching the target femur and predictive success was generally related to the number of descriptors used to drive the optimization process. The results demonstrate that a high fidelity 3D geometry and density-based FE model of an individual proximal femur can be efficiently reconstructed from 2D data using our existing parametric Statistical Shape and Density FE model. The resulting engineering models can then be used to assess the structural strength of an individual's femur, allowing a sophisticated interpretation of widely available clinical DXA scans for application to a variety of aging and disease-related conditions. References: 1. Bredbenner and Nicoletta, ASBMR, 2007.; 2. Bredbenner and Nicoletta, ORS, 2008.; 3. Pulkkinen, et al., J. Bone Miner. Res., 2006; 4. Pulkkinen, et al., Osteoporos. Int., 2004.

**Disclosures:** T.L. Bredbenner, None.  
This study received funding from: Internal Research Program, Southwest Research Institute.

## M468

**Do Racial Differences Exist in Cortical and Trabecular Bone? A pQCT Study in Young Adult Females.** N. K. Pollock<sup>1</sup>, E. M. Laing<sup>1</sup>, R. G. Taylor<sup>\*1</sup>, M. W. Hamrick<sup>2</sup>, C. A. Baile<sup>1</sup>, R. D. Lewis<sup>1</sup>. <sup>1</sup>Foods and Nutrition, The University of Georgia, Athens, GA, USA, <sup>2</sup>Cellular Biology and Anatomy, The Medical College of Georgia, Augusta, GA, USA.

Most reports examining the racial differences in bone have used DXA and found that areal BMD (aBMD) and/or bone mineral content (BMC) is higher in blacks than whites, although many of the reports do not take into account bone and body size. Few studies have investigated racial differences in the structural indices of bone using 3-dimensional imaging. The purpose of this investigation was to determine whether there are racial differences in BMC, bone geometry and BMD at the tibia and radius in black (n=48) and white (n=98) females, using peripheral quantitative computed tomography (pQCT). Female college freshman, 18 to 19 years of age, participated in this cross-sectional study. Because of the importance of body size on bone, 25 whites and 25 blacks were individually matched on age (2%), height (1%), fat-free soft tissue mass (FFST; 2%), and weight (7%). Body composition [FFST, fat mass (FM) and %fat] was measured using DXA. Tibial and radial bone measurements were assessed at the 4%, 20% and 66% sites from the distal metaphyses, which reflect trabecular bone, cortical bone and muscle cross-sectional area (MCSA), respectively. Limb lengths were also measured at the tibia and radius. Given that racial differences in muscle size and body segment lengths can result in over- or under-estimates depending on which skeletal regions and races are compared, the data were adjusted for differences in MCSA and limb length at each respective bone site. Data were analyzed using independent samples t-tests and ANCOVA. Blacks vs. whites had greater tibial and radial length. MCSA differences were not observed between groups at the radius; however, at the tibia, blacks vs. whites had smaller MCSA. In the unadjusted data, blacks vs. whites had higher total volumetric BMD (tibia and radius), cortical BMD (Cort BMD; tibia only), cortical cross sectional area (tibia only), cortical BMC (tibia only), cortical thickness (tibia only), and lower trabecular BMD (tibia only), total cross sectional area (tibia and radius at 4% site only), and Cort BMD (radius only). After adjustment for MCSA and limb length, similar results were found within the unadjusted matched sample, except blacks vs. whites had higher polar strength-strain index at the tibia. Collectively, these results create a bone strength profile reflecting a stronger bone at the radius and tibia in young adult black vs. white females, possibly accounting for the lower fracture rates in older black females.

**Disclosures:** N.K. Pollock, None.

## M469

**Combined Cs-137 Gamma Irradiation and Hindlimb Unloading Rapidly Decreased Cancellous Bone Volume Fraction in the Mouse Lumbar Vertebrae.** J. S. Alwood<sup>\*1</sup>, K. Yumoto<sup>\*2</sup>, H. Kondo<sup>\*2</sup>, R. Mojarrah<sup>\*2</sup>, D. P. Lindsey<sup>\*3</sup>, G. S. Beaupre<sup>3</sup>, C. L. Limoli<sup>\*4</sup>, E. A. C. Almeida<sup>\*2</sup>, N. D. Searby<sup>\*2</sup>, R. K. Globus<sup>2</sup>. <sup>1</sup>Stanford University, Stanford, CA, USA, <sup>2</sup>NASA Ames Research Center, Moffett Field, CA, USA, <sup>3</sup>Bone and Joint Center of Excellence, VA Palo Alto Healthcare System, Palo Alto, CA, USA, <sup>4</sup>University of California Irvine, Irvine, CA, USA.

Spaceflight poses a risk to the skeletal system due to musculoskeletal unloading in microgravity and increased radiation exposure. As separate stimuli, unloading and irradiation each can reduce bone density and increase fracture risk, but combined effects have not been investigated. We hypothesize that skeletal integrity is further compromised when unloading and irradiation are combined. Sixteen-week old C57Bl6/J male mice were continuously hindlimb unloaded (HU) or normally loaded (NL) and either irradiated (IR) with gamma rays (Cs-137, ~1Gy/min) or sham irradiated. In the first experiment, NL and HU mice were irradiated (2 Gy) 3 days before tissue harvest on day 7. A longer duration experiment was carried out to test mechanical properties; NL and HU mice were irradiated (1 Gy) 10 days before tissue harvest on day 14. Cancellous tissue in tibiae and vertebrae were analyzed by microcomputed tomography and ultimate force determined by axial compression of the lumbar vertebral bodies (L1 and L3). Statistical significance was determined via 1-way ANOVA with Tukey-Kramer post-hoc comparison, with  $p < 0.05$ . In lumbar vertebrae, combined HU and IR caused a significant 13-15% decline in cancellous BV/TV compared to controls, a greater decrement than either HU or IR alone. However, in the tibiae, HU and IR alone and in combination caused a 14-22% decline in cancellous BV/TV. Lumbar BV/TV values strongly correlated with tibial BV/TV ( $r = 0.63 - 0.72$ ), although lumbar vertebrae displayed a more plate-like cancellous structure ( $SMI < 1.0$ ) than tibiae ( $SMI > 1.5$ ). In preliminary mechanical tests, combined HU and IR caused a 30% decrease in ultimate compressive force of L3 compared to controls, an effect greater than either HU or IR alone. However, L1 did not show such a large effect. In summary, HU and IR together caused a rapid decrease in cancellous BV/TV in lumbar vertebrae, which may reduce compressive strength. The more plate-like structure of cancellous tissue in lumbar vertebrae compared to the tibiae may account for the observed differences in sensitivity to HU and IR. We speculate microgravity together with radiation may increase fracture risk of the spine.

**Disclosures:** J.S. Alwood, None.

This study received funding from: NASA Grant # NNH04ZU0005N/RAD2004-0000-0110.

## M470

**Proton NMR Study of Transverse Relaxation in Rabbit and Rat Cortical Bone.** H. H. Ong<sup>\*1</sup>, S. L. Wehrli<sup>\*2</sup>, F. W. Wehrli<sup>1</sup>. <sup>1</sup>Radiology, Laboratory for Structural NMR Imaging, University of Pennsylvania School of Medicine, Philadelphia, PA, USA, <sup>2</sup>NMR Core Facility, Children's Hospital of Philadelphia, Philadelphia, PA, USA.

The NMR signal of bone is comprised of collagen matrix protons, collagen fibril bound water, and water in the Haversian canals and lacuno-canalicular system. Proton NMR relaxometry has the potential to provide nondestructively insight into cortical bone porosity due to its known dependence on pore size. Here, we quantified relaxation time constants  $T_1$  and  $T_2$  of rabbit and rat tibia cortical bone specimens from free induction decay (FID) and Carr-Purcell-Meiboom-Gill (CPMG) signals. Sections of cortical bone ( $10 \times 4 \times 1 \text{ mm}^3$ ) were harvested from demarrowed tibia mid-shafts of healthy 20 week-old New Zealand white rabbits (N=5). Whole tibia mid-shafts were harvested and demarrowed from healthy 16 week-old Sprague-Dawley rats (N=4). CPMG and FID experiments were performed on a vertical-bore 9.4T spectrometer (DMX-400, Bruker Instr.). Normalized CPMG signal decays and FIDs were fitted to the bi-exponential curve  $M_1 \exp(-t/T_1) + M_2 \exp(-t/T_2)$  (Levenberg-Marquadt algorithm in Matlab), where  $t$  is either TE or FID time axis,  $M_1$  and  $M_2$  are the magnitudes of the two components, and  $T_1$  and  $T_2$  represent either  $T_1$  or  $T_2$  (Figure 1). The short  $T_2$  represents protons in collagen.  $D_2O$  exchange experiments that removed unbound water indicate that the majority of the FID signal (65%) is from water (Table 1). The major difference in relaxation behavior between rat and rabbit specimens was an increased fraction of the short  $T_2$  component for rat bone. From the dependence of  $T_2$  on pore size, short and long  $T_2$  components likely originate from water in the lacunae and Haversian canals, respectively. Therefore, our results suggest a lower fraction of Haversian canals in rat. Previous studies have indicated a greater porosity in rabbit bone. In conclusion, our results suggest transverse relaxation properties provide insight into the bone NMR signal and can detect inter-species differences between rabbit and rat cortical bone porosity

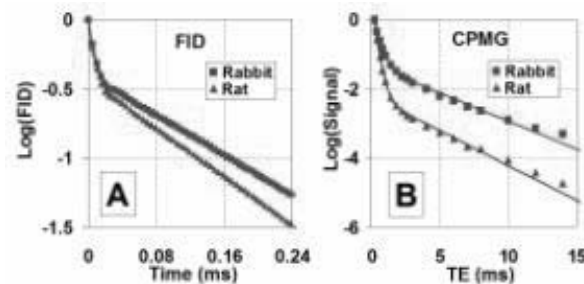


**Figure 1.** Sample rabbit and rat plots of (A) FIDs and (B) CPMG signal decay curves. Squares and triangles are the data points. Solid lines bi-exponential fits (all  $R^2 > 0.95$ ).

**Table 1.** Average values of bi-exponential fit parameters

Species	FID			CPMG		
	Short $T_2$ Magnitude	Short $T_2$ ( $\mu s$ )	Long $T_2$ Magnitude	Short $T_2$ Magnitude	Long $T_2$ Magnitude	Long $T_2$ ( $ms$ )
Rabbit	0.34 $\pm$ 0.002	7.9 $\pm$ 0.3	0.66 $\pm$ 0.002	307 $\pm$ 23	0.72 $\pm$ 0.01	422 $\pm$ 20
Rat	0.35 $\pm$ 0.002	7.1 $\pm$ 0.2	0.65 $\pm$ 0.002	240 $\pm$ 10	0.87 $\pm$ 0.05	319 $\pm$ 13

**Disclosures:** H.H. Ong, None.

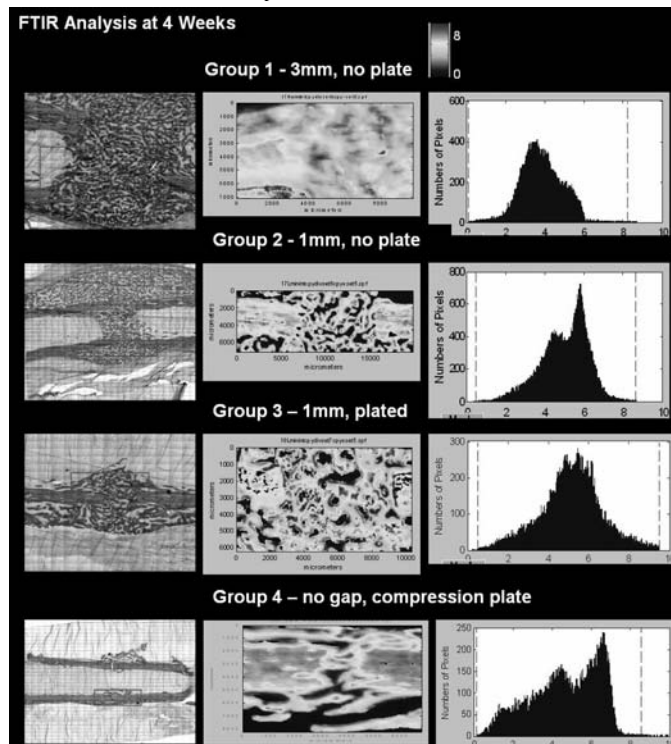
This study received funding from: R01 AR050068.

## M471

**Characterization of the Osteotomy Callus Using Fourier Transfer Infrared (FTIR) Imaging in a Rabbit Ulnar Model.** P. F. O'Loughlin<sup>\*</sup>, N. Karkare<sup>\*</sup>, J. B. Toro-Arbelaez<sup>\*</sup>, K. Voellmicke<sup>\*</sup>, E. Tomin<sup>\*</sup>, B. Shore<sup>\*</sup>, L. Spevak<sup>\*</sup>, A. L. Boskey, J. M. Lane. Orthopedic Surgery, Hospital for Special Surgery, New York, NY, USA.

The purpose of the present study was to test the hypothesis that the woven bone formed in four different models of fracture repair in the rabbit would have different matrix characteristics, based on Fourier transform infrared (FTIR) imaging. Non-unions account for greater than 10% of fracture complications encountered in the clinical setting. To prevent such complications, it is necessary to understand the biology of the processes involved. The process of mineralization is different in primary and secondary fracture healing due to the inherent rigidity of plate fixation as opposed to unfixed natural bone healing. The authors had previously demonstrated that fracture fixation accelerated the rate at which endochondral ossification progressed in terms of changes in matrix composition. A previously established rabbit ulnar fracture model was used. There were four groups each consisting of 21 mature male New Zealand white rabbits (6 mo. old). In an IACUC-approved study, both forelimbs were fractured in each rabbit, with limbs randomly assigned to each group. The groups were organized as follows: Group 1: uniplated 3mm gap, Group 2 - uniplated 1mm gap, Group 3 - plated 1mm gap, Group 4 - compression plate, no gap. Ulnae were harvested at 2, 4 and 8 weeks post-fracture and analyzed via histology and FTIR.

At 2 weeks and 4 weeks (see figure), mineral to matrix ratio, crystallinity and collagen cross-linking were not significantly different in lamellar or woven bone when comparing the four treatment groups, however the distribution of parameters did differ. At 8 weeks, a statistical difference in mineral quality was not found between the groups. Despite the mode of healing at 2, 4 and 8 weeks the mineral to matrix ratio, crystallinity and collagen cross-linking was not significantly different in either lamellar or woven bone. This study demonstrates that regardless of the mode of repair, there is no significant difference in the matrix characteristics of woven or lamellar bone whether produced by endochondral or intramembranous processes.



**Disclosures:** P.F. O'Loughlin, None

This study received funding from: Supported by a grant from the Orthopaedic Trauma Association. Imaging data was collected at the NIH sponsored Imaging Core (AR046312).

## M472

**Non-Steroidal Anti-Inflammatory Use and the Response of Bone to Exercise.** D. W. Barry<sup>1</sup>, R. E. Van Pelt<sup>2</sup>, C. M. Jankowski<sup>2</sup>, P. Wolfe<sup>3</sup>, W. M. Kohrt<sup>2</sup>. <sup>1</sup>General Internal Medicine, University of Colorado Denver, Aurora, CO, USA, <sup>2</sup>Geriatric Medicine, University of Colorado Denver, Aurora, CO, USA, <sup>3</sup>Preventive Medicine and Biometrics, University of Colorado Denver, Aurora, CO, USA.

The bone response to exercise is a prostaglandin-dependent process. Non-steroidal anti-inflammatory drugs (NSAIDs) inhibit prostaglandin synthesis and may affect the adaptation of bone to mechanical loading, particularly when administered before loading. The purpose of this study was to examine whether taking ibuprofen before or after exercise sessions influences the bone mineral density (BMD) response of premenopausal women to a 9-month bone-loading exercise program. We hypothesized that ibuprofen before exercise would diminish the BMD response more than ibuprofen use after exercise, and that the placebo group would exhibit the most robust response to exercise. Women were randomized (n=102) to 3 arms that took 2 study pills on exercise days as follows: 1) 400 mg ibuprofen before and placebo after exercise (ibuprofen/placebo), 2) placebo before and 400 mg ibuprofen after (placebo/ibuprofen), and 3) placebo before and after (placebo/placebo). The exercise program included progressive high-intensity resistance exercises, endurance exercises (primarily walking, running), and jumping/stepping exercises. DXA was used to measure BMD of the whole body, lumbar spine and proximal femur (total and subregions) at baseline and 9 months. Fifty-three percent of participants (n=54) exercised at 80% of the prescribed frequency ( $\geq 2.4$  times/wk); only data from these subjects were included in this analysis. The average age was  $32.1 \pm 5.5$  years. Relative changes from baseline BMD and bone mineral content (BMC) values are shown in Table 1. Contrary to our hypothesis, the placebo/placebo group did not have the largest increases in BMD; this may have been related to use of non-study NSAIDs. Rather, the most robust increases in BMD occurred in the placebo/ibuprofen group. It is possible that taking ibuprofen after exercise permits the activation of bone formation during exercise, but attenuates increases in pro-resorptive cytokines. Because this is the first study of the effects of NSAIDs on the adaptation of bone to exercise, findings should be considered preliminary. Further research is needed to confirm whether taking NSAIDs after exercise enhances the BMD response.

Table 1: Relative changes in BMD and BMC from baseline

		Percent change from baseline (mean $\pm$ SD)		
		Placebo/placebo (n=23)	Ibuprofen/placebo (n=17)	Placebo/ibuprofen (n=14)
Lumbar spine BMD		$0.3 \pm 2.1$	$-0.3 \pm 1.8$	$1.0 \pm 2.0$
Total hip BMD		$0.2 \pm 1.9$	$-0.2 \pm 1.3$	$2.1 \pm 1.7^{\dagger\dagger**}$
Femoral neck BMD		$-0.5 \pm 2.5$	$-0.4 \pm 1.9$	$1.6 \pm 2.9^{\dagger*}$
Trochanter BMD		$0.2 \pm 2.2$	$0.3 \pm 1.7$	$1.9 \pm 2.0^{\dagger*}$
Shaft BMD		$0.4 \pm 2.7$	$-0.4 \pm 2.0$	$2.1 \pm 1.6^{\dagger**}$
Total body BMC		$-0.4 \pm 1.4^*$	$0.2 \pm 1.5^{\dagger}$	$1.5 \pm 2.1^{\dagger\dagger}$

<sup>†</sup>Different from placebo/placebo at the 0.05 level <sup>††</sup>Different from placebo/placebo at the 0.01 level

<sup>\*</sup>Different from ibuprofen/placebo at the 0.05 level <sup>\*\*</sup>Different from ibuprofen/placebo at the 0.01 level

Statistical tests were done using an ANCOVA model on untransformed data at 9 months controlling for baseline.

**Disclosures:** D.W. Barry, None.

This study received funding from: Department of Defense.

## M473

**An Effective Progressive Resistive Exercise Program from Prone Position for Paravertebral Muscles to Reduce Risk of Vertebral Fractures.** M. Sinaki<sup>1</sup>, M. J. Borgo<sup>2</sup>, E. Itoi<sup>3</sup>. <sup>1</sup>Physical Medicine and Rehabilitation, Mayo Clinic College of Medicine; Mayo Clinic, Rochester, MN, USA, <sup>2</sup>Mayo Medical School, Mayo Clinic, Rochester, MN, USA, <sup>3</sup>Department of Orthopaedic Surgery, Tohoku University School of Medicine, Sendai, Japan.

In a previous communication, it was hypothesized that back strengthening from prone, rather than vertical position, can decrease the risk of vertebral fracture due to improvement of horizontal trabecular connections. In this communication, we discuss the method of a specific progressive resistive exercise (PRE) program that had been implemented in a two-year study to decrease the risk of vertebral fractures. Therefore, it is of great interest that we describe our methodology since we did not induce any vertebral fractures with this exercise program.

Sixty-seven Caucasian women ranging from age 49 to 65 (mean of 56 years) were randomly assigned to a control group (n=33) or an exercise group (n=34). All subjects were instructed in proper dynamic and static posture principles. The level of physical activity and back extensor strength was evaluated every four weeks for a period of two years. The study group performed PRE from the prone position against measured and progressively increasing resistance, up to four sessions a week; the control group did not. The isometric strength of the back extensor muscles was measured with a strain-gauge dynamometer. Thirty percent of the subject's maximum back extensor strength was prescribed for strengthening exercises.

A statistical analysis demonstrated significant increase in the strength of back extensors in the exercise group as compared with the control group. The participants in the exercise group experienced a 100 percent greater increase in the strength of the back extensors (mean increase of 18.5 kg) when compared with the control group (mean increase of 9.5 kg).

This method of PRE of the back extensors was effective in decreasing the risk of vertebral fractures.

**Disclosures:** M.J. Borgo, None.

## M474

**Mechanical Loading Prevents Bone Loss due to Hormone-Deficiency in Female Mice.** M. E. Lynch<sup>1</sup>, R. P. Main<sup>1</sup>, T. M. Wright<sup>2</sup>, M. C. H. van der Meulen<sup>1</sup>. <sup>1</sup>Cornell, Ithaca, NY, USA, <sup>2</sup>Hospital for Special Surgery, New York, NY, USA.

Cancellous bone adaptation to mechanical loading is poorly understood. Dynamic loading stimulates adaptation in healthy mice and prevents bone loss in hormone-compromised male mice at cancellous sites. We investigated the effects of loading on cancellous bone in hormone-compromised female mice. Twenty 10 week-old C57Bl/6 mice underwent ovariectomy (OVX) or sham surgery (n=10/group). Following surgery, cyclic compression was applied to the left tibia. The right tibia served as the unloaded control. Each cycle consisted of a triangle wave with a peak load of -11.5N followed by a static dwell of -2.3N. 1200 cycles were applied 5 days/week at 4 Hz for 2 weeks. Following euthanasia, all tibiae were scanned using quantitative microcomputed tomography with a 15  $\mu$ m voxel resolution. Cancellous bone from the proximal metaphysis was analyzed for bone volume fraction (BV/TV), tissue mineral density (tBMD), and trabecular thickness and separation (Tb.Th, Tb.Sp). OVX significantly reduced BV/TV and increased Tb.Th. Loading significantly affected both sham and OVX groups (Table 1). In sham mice, tBMD (+16%), BV/TV (+57%), and Tb.Th (+4%) were greater in loaded tibiae relative to controls (Fig. 1). Similarly in OVX mice, tBMD (+16%), BV/TV (+68%), and Tb.Th (+14%) were greater in loaded tibiae relative to controls. Tb.Sp decreased with loading in both groups. The response to loading was similar in OVX and sham groups. Mechanical loading prevented bone loss due to hormone-deficiency and in fact cancellous parameters in the loaded OVX mouse tibiae were increased relative to the unloaded sham tibiae. Our results show that mechanical loading is an anabolic stimulus in cancellous bone independent of estrogen status. This work was supported by NIH AG53571 and AR46121.

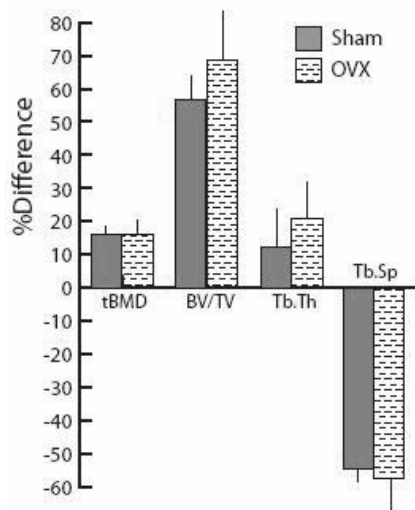


Figure 1: Percent difference in loaded tibiae relative to control tibiae (+/- sd)

Table 1: Cancellous parameters in the proximal metaphysis

	tBMD (mg/cc)	BV/TV	Tb.Th ( $\mu$ m)	Tb.Sp ( $\mu$ m)
OVX L	585 <sup>a,b</sup>	0.20 <sup>a,b,c</sup>	164 <sup>a,b,c</sup>	44 <sup>a,b,c</sup>
OVX R	497 <sup>c</sup>	0.10 <sup>c</sup>	189 <sup>c</sup>	24 <sup>c</sup>
OVX L-R	88	0.10	-25	20
Sham L	573 <sup>a,b</sup>	0.21 <sup>a,b</sup>	144 <sup>a,b</sup>	42 <sup>a,b</sup>
Sham R	489	0.12	161	24
Sham L-R	84	0.09	-17	18

<sup>a</sup>L vs R, paired t-test; <sup>b</sup>Loading effects, 2F ANOVA; <sup>c</sup>OVX effects, 2F ANOVA

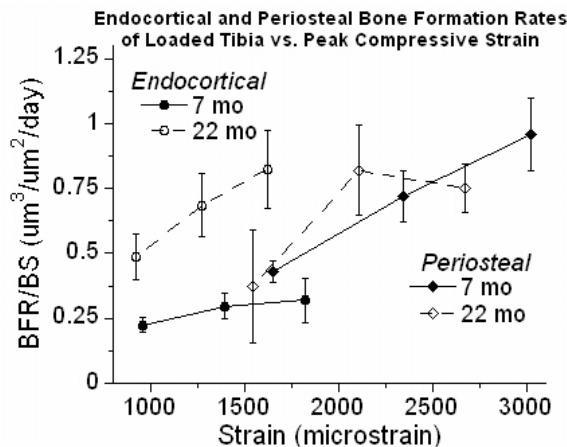
**Disclosures:** M.E. Lynch, None.  
This study received funding from: NIH.

## M475

**Aged and Young Adult BALB/c Male Mice Respond Similarly to In Vivo Tibial Compression.** M. D. Brodt<sup>1</sup>, R. Civitelli<sup>2</sup>, M. J. Silva<sup>1</sup>. <sup>1</sup>Orthopaedic Surgery, Washington University, St. Louis, MO, USA, <sup>2</sup>Division of Bone and Mineral Diseases, Washington University, St. Louis, MO, USA.

A decline in mechanoresponsiveness with aging may contribute to diminished rates of bone formation in senile osteoporosis. Recently, we established that "aged" 22-month male BALB/c mice are osteoporotic compared to "young adult" 7-month mice, as evidenced by increased tibial medullary area, and decreased cortical thickness, trabecular bone volume and endosteal bone formation. Our goal in the current study was to compare the response of 22 and 7 mo. mice to in vivo tibial compression, a non-invasive loading method that applies force across the knee and foot (along the tibial axis). Prior to in vivo loading, we determined the force-strain relationships using a combination of strain gage measurements, microCT imaging and beam theory. Because moments of inertia were not significantly different

between 22 and 7 mo. tibiae, the force-strain relationships were similar, with differences of ~10% for the peak endocortical strain at 12 N compression. We then performed in vivo tibial compression on 60 mice at 22 (n = 28) or 7 (n = 32) mos. age. Under anesthesia, the right legs were loaded to a peak force of 8, 10 or 12 N; 60 cycles/day (rest-inserted waveform) for 5 days; left legs were not loaded (control). Mice were injected with fluorochromes on days 4 and 9, and euthanized on day 11. Tibias were embedded in plastic, sectioned and histomorphometric analysis performed at the midshaft (site of peak bone strain). Data from non-loaded controls confirmed that marrow area was greater in 22 vs. 7 mo. tibiae ( $0.52 \pm 0.07$  vs.  $0.39 \pm 0.06$  mm<sup>2</sup>), while bone area ( $0.59 \pm 0.07$  vs.  $0.72 \pm 0.07$  mm<sup>2</sup>) and cortical thickness ( $0.15 \pm 0.02$  vs.  $0.20 \pm 0.01$  mm) were less ( $p < 0.001$ ). Analysis of relative differences between loaded and control tibiae revealed that, contrary to our hypothesis, aged mice did not exhibit diminished responsiveness to loading. On the endocortical surface, the increases in mineralizing surface ( $p < 0.001$ ), mineral apposition rate ( $p = 0.06$ ) and bone formation rate (BFR/BS,  $p < 0.001$ ; Figure) were actually greater in 22 mo. mice than in 7 mo. mice (two-way ANOVA). On the periosteal surface, there were no differences between the responses of 22 and 7 mo. mice ( $p > 0.05$ ). In conclusion, we found no deficit in the ability of aged mice to form bone in response to tibial compression, indicating that the aged skeleton can respond to mechanical stimuli with increased bone formation.



**Disclosures:** M.J. Silva, None.  
This study received funding from: NIH/NIAMS AR047867.

## M476

**Bone Length Was Differentially Promoted in the Left/Right Hindlimbs with Knee Loading and Administration of IGF2.** P. Zhang, H. Yokota. Biomedical Engineering, and Anatomy & Cell Biology, Indiana University Purdue University Indianapolis, Indianapolis, IN, USA.

Treatment of limb length discrepancy requires differential bone lengthening. In order to seek for its potential therapeutic strategy, we addressed a pair of questions: Does knee loading or local injection of IGF2 increase bone length in the treated hindlimb more than the contralateral hindlimb? If so, is their growth promotion identical in the femur and the tibia? Usage of C57BL/6 mice (~8 wks) was approved by the IACUC. In knee loading (21 mice), the left hindlimb was given 5-min bouts at 0.5 N, while the right hindlimb was used as contralateral control. Age matched controls were included. In IGF2 injection (30 mice), 5  $\mu$ l of PBS containing IGF2 was injected into the distal epiphysis of the left femur at 100  $\mu$ g/kg/day, while the right hindlimb was treated as contralateral control. Vehicle controls received an equal volume of PBS. Bone length was measured with a digital caliper, and BMD and BMC were determined with a PIXImus densitometer. First, knee loading lengthened both the femur and the tibia, but IGF2 injection was effective only in the femur. BMD and BMC were increased in the femur and the tibia with knee loading, while with IGF2 injection they were unchanged in the tibia. Second, the total increase in the length of the hindlimb was significantly higher with knee loading than IGF2 injection (femora with  $p < 0.05$  and tibiae with  $p < 0.001$ ). Third, in knee loading the measured values in Table for contralateral controls were closer to those for the loaded hindlimb than those for the age-matched controls, suggesting a possibility that knee loading on one hindlimb could affect on the other hindlimb. Fourth, an increase in body weight was elevated for mice with IGF2 injection compared to mice with vehicle injection ( $p < 0.001$ ).

We demonstrate herein enhancement of bone length by both knee loading and local administration of IGF2. The effects of knee loading are observed in the femur and the tibia. The IGF2 effects were localized in the femur, and a possibility of increasing body weight was identified. Further studies are necessary to examine efficacy of treatment conditions including magnitude/dosages and durations of applications.

Increase of bone length, BMD, and BMC

treatment	target control	length		BMD		BMC	
		femur	tibia	femur	tibia	femur	tibia
knee loading	contralateral	2.3%**	2.3%***	3.3%*	4.4%***	6.9%**	6.9%**
	age-matched	3.5%***	3.6%***	3.5%*	6.1%***	7.2%**	9.0%**
IGF2 injection	contralateral	1.7%*	n.s.	5.4%*	n.s.	9.3%*	n.s.
	vehicle	1.6%*	n.s.	3.6%*	n.s.	5.3%*	n.s.

\*:  $p < 0.05$ ; \*\*:  $p < 0.01$ ; \*\*\*:  $p < 0.001$ .

**Disclosures:** P. Zhang, None.  
This study received funding from: NIH

## M477

**Positive Influence of Physical Activity on BMD Measurements and Hip Geometry Parameters in Young Adults: a 2-year Prospective Study.** S. Breban\*, C. Chappard, C. Benhamou. IPROS - CHR Orleans, INSERM Unit 658, Orleans, France.

Weight-bearing physical activity induces higher BMD values and higher bone geometry parameters. The Hip Structural Analysis (HSA) software on DXA images has been poorly used in young athlete women. The aim of this work was to analyze in a prospective study, the effects of weight-bearing sports on BMD measurements, hip structure and peak bone geometry in young adult women. 70 women between 17 and 29 years participated in this 2-year prospective study. The sample included 40 athlete women participating in various weight-bearing sports ( $10.2 \pm 2.2$  hours/week of training) and 30 age matched control women. Each group was divided in 4 age-groups (18-20 years, 21-23 years, 24-26 years and 27-29 years). BMD ( $\text{g}/\text{cm}^2$ ) was measured by DXA (Delphi, Hologic ®), at whole body (WB), lumbar spine (L1-L4) and non dominant femoral neck (FN). The HSA software was applied to evaluate BMC, BMD, cross-sectional area (CSA), cross-sectional moment of inertia (CSMI), section modulus (Z) and cortical thickness of the FN. Age of menarche was similar in athletes and controls. BMD values were significantly higher in athletes compared to controls, at all bone sites. Moreover, bone gain was significantly greater in athletes compared to controls at LS and FN but not at WB ( $p > 0.05$ ). All the geometry parameters were significantly higher ( $p < 0.05$ ) in athletes compared to controls, at baseline and after one year. Maximal bone gain, for all geometry parameters, was observed for the 21-23 years age-group in athlete women and for the 18-20 years age-group in control women. The gain was significantly higher in athletes compared to controls for CSA ( $0.02 \pm 0.04 / -0.03 \pm 0.08 \text{ cm}^2$ ,  $p = 0.02$ ), CSMI ( $0.06 \pm 0.04 / -0.20 \pm 0.34 \text{ cm}^4$ ,  $p = 0.01$ ), Z ( $0.002 \pm 0.08 / -0.05 \pm 0.09 \text{ cm}^3$ ,  $p = 0.03$ ) but not for Cortical Thickness ( $0.003 \pm 0.002 / 0.001 \pm 0.020 \text{ cm}$ ,  $p = \text{NS}$ ). Intense weight-bearing sport induces a prolonged bone gain associated to a higher and later peak bone geometry in women. Athletes continue to optimize their femur macro architecture properties and their BMD peak whereas controls have already reached their maximal potential.

**Disclosures:** S. Breban, None.

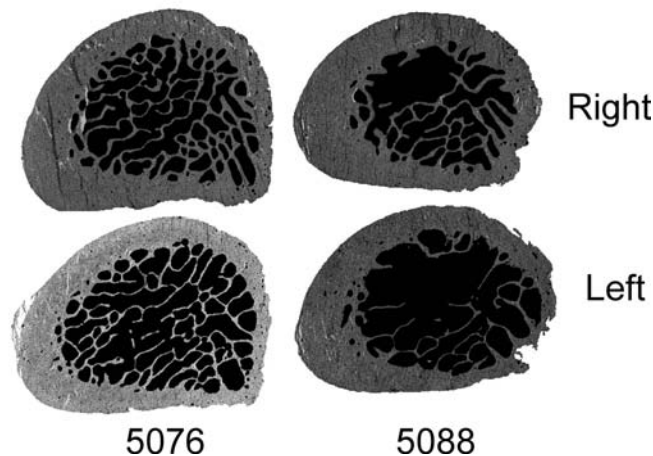
## M478

**Mechanical Underloading of the Sheep Calcaneus: A Model for Hip Fracture.** N. Loveridge\*, J. Power\*, E. Draper\*, M. Warren\*, J. Reeve\*, A. Goodship\*. <sup>1</sup>Medicine, University of Cambridge, Cambridge, United Kingdom, <sup>2</sup>Royal Veterinary College, London, United Kingdom.

The aetiology of hip fracture is associated with an age-related loss of cancellous bone, cortical thinning and an increase in cortical porosity through the formation of large pores, changes which indicate that mechanical underloading plays an important role. Currently there is no model of underloading in animals that undergo haversian remodelling in a manner similar to that in human bone. The artiodactyl calcaneus, like the human femoral neck is loaded in bending, so using fixators we have underloaded the left calcaneus of adult female sheep and analysed changes in cortical and cancellous bone after 2, 4, 8 & 16 weeks (n=6 in each group) using the contra-lateral bone as a control.

Fixing the calcaneus resulted in a significant reduction in maximum local loads as measured using surface mounted strain gauges (free:  $95.9 \mu\epsilon \pm 24.4 \text{ SD}$ ; fixed:  $48.0 \mu\epsilon \pm 9.9 \text{ S.D.}$ ) Left and right calcanei showed marked evidence of individual patterning that was unaffected by underloading (Fig). Analysis of cancellous bone (Densiscan XTREME) showed a significant loss in BV/TV at 8 (diff  $-0.043 \pm 0.011$   $p = 0.011$ ) and 16 (diff  $-0.77 \pm 0.01$ ;  $p = 0.001$ ) weeks. Histological analysis of cortical bone showed a marked increase in the mean area of canals in the fixated calcaneus at 16 weeks (diff  $-62.5 \pm 15$ ;  $p = 0.02$ ) while the number of pores showed no change.

In conclusion, underloading of the sheep calcaneus results in the anticipated loss of cancellous bone and changes in cortical bone analogous to that seen in hip fracture suggesting that this will prove to be a suitable model for the studying the aetiology of intracapsular hip fracture.

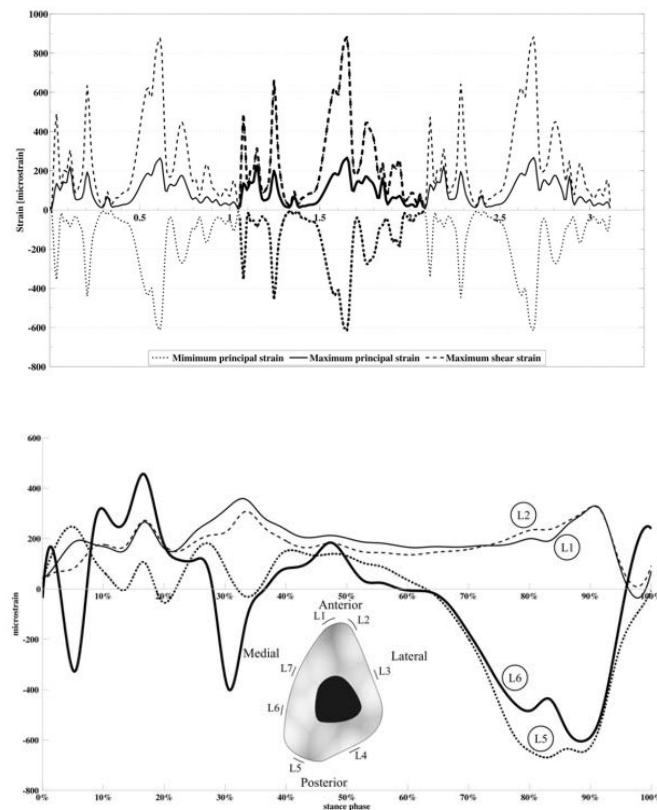


**Disclosures:** N. Loveridge, None.  
This study received funding from: BBSRC.

## M479

**Flexible Tibia Model Predicts Bone Strains During Walking.** A. Heinonen<sup>1</sup>, R. Al Nazer<sup>2</sup>, A. Klodowski<sup>2</sup>, T. Rantalainen<sup>3</sup>, H. Sievänen<sup>4</sup>, A. Mikkola<sup>2</sup>. <sup>1</sup>Department of Health Sciences, University of Jyväskylä, Jyväskylä, Finland, <sup>2</sup>Department of Mechanical Engineering, Lappeenranta University of Technology, Lappeenranta, Finland, <sup>3</sup>Neuromuscular Research Center, Department of Biology of Physical Activity, University of Jyväskylä, Jyväskylä, Finland, <sup>4</sup>Bone Research Group, UKK Institute, Tampere, Finland.

In vivo strain measurements requires invasive methodology which is challenging and limited to certain regions of superficial bones only such as the anterior surface of the tibia. Based on our previous study (Al Nazer R et al. J Biomech 2008), an alternative numerical approach to analyse in vivo strains based on the flexible multibody simulation approach was proposed. The purpose of this study was to use the flexible multibody approach in the analysis of bone strains during physical activity through integrating the MRI technique within the framework. A healthy male volunteer (28 years, 177 cm, 80 kg) served as a subject. The model was used in a forward dynamics simulation in order to predict the tibial strains during walking. The flexible tibial model was developed using the actual geometry of human tibia, which was obtained from 3-dimensional reconstruction of MRI. The walking test was recorded using four digital video cameras. The motion capture data obtained from walking at constant velocity was used to drive the model during the inverse dynamics simulation in order to teach the muscles to reproduce the motion in the forward dynamics simulation. Fig 1 shows the simulated maximum and minimum principal and maximum shear strains for four walking cycles (bolded line corresponds for one walking cycle). Fig 2 shows the simulated axial strain profiles at the middle of the tibia in four locations. Based on the agreement between the literature-based in vivo strain measurements and the simulated strain results, it can be concluded that the flexible multibody approach enables reasonable predictions of bone strain in response to dynamic loading.



**Disclosures:** A. Heinonen, None.  
This study received funding from: The Academy of Finland.



M480

**Osteoporosis in a Murine Model of Hemophilia A.** C. Vanek, D. Greenberg\*, E. Larson\*. Endocrinology, Oregon Health & Science University, Portland, OR, USA.

There is clinical evidence that patients with hemophilia A have reduced bone mineral density. This is a risk factor for osteoporosis and fragility fractures. Hemophilia A is a genetic disorder of coagulation due to a deficiency of factor VIII. Many patients with hemophilia A have multiple co-morbid conditions that could potentially adversely affect skeletal health: reduced physical activity, joint hemorrhage, HIV, and hepatitis C infection. It is therefore difficult to determine if the genetic defect in hemophilia A is the direct cause of decreased bone mass *per se* without also accounting for co-morbid health factors. To better explore this issue, we have examined factor VIII knockout mice (FVIII-KO) that mimic human hemophilia A. We assessed the skeletal phenotype of 11 female FVIII-KO and 8 female wild-type mice of the same genetic background (C57BL/6) at 20-22 weeks of age, when skeletal maturity has been achieved. Bone mineral density (BMD) was measured by dual energy x-ray absorptiometry (pisiMUS) and bone geometry was measured by desktop x-ray microtomographic CT (SkyScan model 1074). Femoral breaking strength (failure load) was measured by three-point bending until failure on a high resolution materials test apparatus (model 4442, Instron Corp.)

	L5 BMD (mg/cm <sup>3</sup> )	Femoral BMD (mg/cm <sup>2</sup> )	Cortical Area (mm <sup>2</sup> )	Femoral Failure Load(Newtons)
<b>FVIII-KO (11)</b>	39.6 +/- 1.2	49.2 +/- 1.2	0.664 +/- 0.01	16.35 +/- 0.61
<b>Wild-Type (8)</b>	44.0 +/- 1.8	53.1 +/- 1.5	0.709 +/- 0.02	19.29 +/- 0.82
<b>P Value</b>	<b>0.048</b>	<b>0.050</b>	0.056	<b>0.009</b>

The results show that FVIII-KO mice have reduced BMD, bone size, and femoral breaking strength compared to wild-type. Under these controlled conditions, the data indicates that factor VIII participates in normal skeletal development. Factor VIII deficiency is known to decrease thrombin generation. Thrombin receptors are present on osteoblasts and may play a role in skeletal development. Thus hemophilia A, through effects on thrombin generation, may directly impact skeletal integrity.

**Disclosures:** C. Vanek, Pfizer 1; Procter & Gamble 5.  
This study received funding from: Procter & Gamble.

M481

**Effects of Exercise Intensity on the Bone Metabolic Response to Running.** J. P. R. Scott\*<sup>1</sup>, J. P. Greeves<sup>1</sup>, C. Sale<sup>2</sup>, A. Casey\*<sup>1</sup>, J. Dutton\*<sup>3</sup>, W. D. Fraser<sup>3</sup>. <sup>1</sup>Human Protection and Performance Enhancement, QinetiQ, Farnborough, United Kingdom, <sup>2</sup>Sport, Exercise and Health Sciences, Nottingham Trent University, Nottingham, United Kingdom, <sup>3</sup>Department of Clinical Biochemistry, University of Liverpool, Liverpool, United Kingdom.

The aerobic fitness of recruits entering UK Army Phase 1 training varies considerably, and so, during standardised activities, training is conducted across a range of relative exercise intensities. Since low aerobic fitness is a risk factor for stress fracture injury, we examined the effect of different exercise intensities (EI) on the bone metabolic response to running. Eight physically-active men (mean (1SD) age 28 (3) y; maximal rate of oxygen uptake (VO<sub>2max</sub>) 55.7 (7.4) ml·min<sup>-1</sup>·kg<sup>-1</sup>) completed three, 8-day trials. On days 1 to 3 and 5 to 8, subjects consumed a prescribed diet and performed no exercise. On day 4, subjects completed 60 min of treadmill running at 55% (LOW), 65% (MOD) or 75% (HIGH) VO<sub>2max</sub>. Fasting blood and second void urine were obtained prior to exercise (BASE) and on four consecutive recovery days (R1 to R4). Serum was analysed for markers of bone resorption (β-CTX) and formation (PINP, OC, Bone-ALP). Urine samples were also analysed for pyridinolines (UfPYD and UfDPD), markers of bone resorption, which were corrected for creatinine concentration (Cr). There were no significant differences in the response of bone resorption or bone formation markers to different EI. Main effects of time from BASE were observed for UfDPD/Cr (P<0.001) and UfPYD/Cr (P<0.05), but not β-CTX, OC, PINP or Bone-ALP (P>0.05). Mean (1SD) values of pyridinolines are shown in Table 1. Both UfDPD/Cr (P<0.01) and UfPYD/Cr (P<0.05) increased significantly at R3 compared with BASE. UfDPD/Cr increased by 4(9)%, 10(9)%, and 10(18)%, and UfPYD/Cr increased by 4(11)%, 16(18)% and 7(18)% in LOW, MOD and HIGH.

Mean (1SD) UfDPD/Cr and UfPYD/Cr between different exercise intensities over time.					
	BASE	R1	R2	R3	R4
<b>DPD (μmol·mol<sup>-1</sup>/Cr)</b>					
LOW	4.5 (0.6)	4.2 (0.5)	4.6 (0.7)	4.7 (0.7)	4.4 (0.4)
MOD	4.4 (0.6)	4.3 (0.9)	4.7 (1.0)	4.9 (0.7)	4.4 (0.9)
HIGH	4.1 (0.7)	4.3 (0.8)	4.1 (0.7)	4.4 (0.5)	4.0 (0.7)
Mean (All Conditions)	4.3 (0.6)	4.3 (0.7)	4.4 (0.8)	4.7 (0.7)†	4.3 (0.7)
<b>PYD (μmol·mol<sup>-1</sup>/Cr)</b>					
LOW	16.2 (1.7)	14.3 (1.2)	17.6 (2.2)	16.7 (2.4)	16.7 (1.8)
MOD	15.9 (2.0)	16.1 (3.8)	18.2 (3.9)	18.5 (4.0)	16.2 (3.4)
HIGH	15.4 (2.2)	14.8 (3.4)	14.7 (3.0)	16.3 (2.9)	14.9 (2.9)
Mean (All Conditions)	15.8 (1.9)	15.0 (3.0)	16.8 (3.3)	17.2 (3.2)*	15.9 (2.8)

\* (P<0.05); † (P<0.01) significant increase from BASE. There was no effect of exercise intensity on the bone metabolic responses to 60 min of treadmill running. The increase in

pyridinolines but not in β-CTX during recovery suggests an increase in type I collagen metabolism, and not bone resorption, with exercise. Acute exercise of different intensity did not invoke a concomitant change in bone formation as indicated by OC, PINP and Bone-ALP.

**Disclosures:** J.P.R. Scott, None.  
This study received funding from: the Human Capability Domain of the UK Ministry of Defence Scientific Research Programme.

M482

**Bone Strength In Overweight Children Is Adapted to Mechanical Loads From Walking, But Is Low For Higher Loading Activities.** S. A. Novotny\*<sup>1</sup>, R. J. Wetzsteon<sup>2</sup>, K. A. Pickett\*<sup>1</sup>, J. M. Hughes<sup>1</sup>, J. M. Cousins\*<sup>1</sup>, M. A. Petit<sup>1</sup>. <sup>1</sup>Kinesiology, University of Minnesota, Minneapolis, MN, USA, <sup>2</sup>Pediatrics, Children's Hospital of Philadelphia, Philadelphia, PA, USA.

Areal bone mineral density (aBMD) assessed by DXA is typically higher in overweight than healthy-weight children, however it is not clear if bone strength is adequate for higher loads incurred during physical activity by overweight children. The purpose of the present study was to assess bone strength relative to mechanical load during physical activity in overweight and healthy-weight children. We measured bone geometry (Total Area, ToA, mm<sup>2</sup>), cortical volumetric density (vBMD, mg/mm<sup>3</sup>) and estimated bone bending strength (SSI<sub>p</sub>, mm<sup>3</sup>) by peripheral quantitative computed tomography (pQCT, Orthometrix XCT 3000) at 66% of tibia length in overweight (BMI ≥ 85th percentile, n = 22) and healthy-weight (BMI < 85th percentile, n = 37) children (8-15yr). Peak ground reaction force (GRF) was assessed with Pedar insoles during 5 activities, including a walk, active video game (Dance Dance Revolution, DDR), run, tuck jump and jump from a 30cm box. Height, tibia length and weight were measured by standard procedures. Relative bone strength [(SSI<sub>p</sub>/(tibia length\*0.66))/GRF] was calculated for each activity. We used ANCOVA adjusting for tibia length and sex to compare absolute bone outcomes, and independent t-tests to compare relative bone strength for each activity between groups. Compared to the healthy-weight group, overweight children had greater ToA (+23%, p < 0.001) and SSI<sub>p</sub> (+27%, p = 0.001), but similar cortical vBMD. Peak GRF were higher in overweight children for all activities (+37-60%, p < 0.05 for all). Relative bone strength was not different between groups for DDR (p = 0.113) or walking (p=0.235). However, relative bone strength from running (-17%, p = 0.010), tuck jump (-27%, p < 0.001) and box jump (-24%, p = 0.003) were all significantly lower in overweight children. Overall, bone strength in overweight children was high and appropriately adapted to loads from normal activities such as walking. However bone strength was low in overweight children for higher impact activities such as running and jumping, suggesting that excess body weight may not have a protective effect on bone as has been previously implied.

**Disclosures:** S.A. Novotny, None.

M483

**Intermittent, Short Duration Cyclic Loading Attenuates Disuse Osteoporosis Without Affecting Resorption.** R. K. Long\*, B. M. Boudignon\*, D. D. Bikle. Endocrine Unit, University of California, San Francisco, San Francisco, CA, USA.

Hindlimb unloading (HU) by tail suspension (a model of disuse osteoporosis) causes a rapid and profound loss of bone in the tibia and femur due to reduction in bone formation and enhanced bone resorption. On the other hand, mechanical loading of the tibia with intermittent cyclic loads stimulates bone formation. The purpose of this study is to determine whether intermittent cyclic axial compressive loading applied to the tibia concurrent with HU will prevent disuse osteoporosis, and if so, by what mechanism. Twelve-week-old male Sprague Dawley rats were subjected to a two-week period of HU or normal ambulation (controls). Concurrently, the right tibia of each animal was cyclically loaded, the left tibia served as non-loaded control. Cyclic loading with an Enduratec ELF3200 was achieved by the application of 40 trapezoidal loading cycles with a peak axial compressive load of 30 N, determined by load-strain calibrations to achieve ~2500 microstrain, each over 0.5 second with a 10 second rest inserted after each load. Six loading episodes were distributed equally over 2 weeks, totaling 42 minutes of cyclic load. Both tibiae were harvested for trabecular microCT and histomorphometric analysis, osteoclast activity and periosteal bone formation. MicroCT analysis of the proximal tibia revealed that 2 weeks of skeletal unloading caused a 54% decrease in BV/TV relative to controls (p < 0.001). These unloaded bones were more responsive to cyclic loading with a 62% increase in BV/TV (p < 0.01) relative to only a 15% increase seen in those from the controls (p < 0.05). Changes in connectivity density parallel those seen with BV/TV. Analysis of trabecular indices revealed a significant unloading induced decrease in number and thickness that normalized with cyclic loading. No cyclic loading induced trabecular changes were noted in the tibiae from controls. Resorption surfaces increased by 40% in the secondary spongiosa of unloaded bones as compared to those from controls and was unaffected by cyclic loading. However, the 25% reduction in periosteal bone formation induced by HU was mostly reversed by cyclic loading (p < 0.05). These results demonstrate that intermittent short duration cyclic loading totaling only 42 minutes over 2 weeks significantly blunts unloading induced trabecular bone loss. The mechanism of the enhanced response of the unloaded bones to cyclic loading is due to augmentation of bone formation rather than reduction in osteoclast activity. The threshold for mechanical stimulation induced bone formation in the unloaded state is lower than that required to prevent unloading induced osteoclast mediated bone loss.

**Disclosures:** R.K. Long, None.  
This study received funding from: National Space and Biomedical Research Institute.



**M484****The Effect of Exercise on Geometric Bone Structure and Bone Strength in Postmenopausal Women - A Systematic Review and Meta-Analysis of Randomized Controlled Trials.** I. Polidoulis<sup>1</sup>, J. Beyene<sup>2\*</sup>, A. Cheung<sup>3</sup>.<sup>1</sup>Family and Community Medicine, University of Toronto, Toronto, ON, Canada, <sup>2</sup>Biostatistics, University of Toronto, Toronto, ON, Canada, <sup>3</sup>Osteoporosis, University Health Network, Toronto, ON, Canada.

Current literature suggests that exercise in postmenopausal women can at best only slow bone mineral density loss by about 1% per year. Although randomized controlled trials have examined the effects of exercise on bone structure, most studies are small with variable results. Thus, we conducted a systematic review and meta-analysis of randomized controlled trials that examined effects of exercise on geometric structure of bone in postmenopausal women.

We systematically searched Medline, Pubmed, and Embase from 1950 to March 2008 using the following search terms: exercise, exercise movement techniques, motor activity, physical activity, sports, bone, microarchitecture, bone geometry or structure or histomorphometry, quantitative computed tomography. We limited to human studies and included only prospective randomized controlled trials that examined the effects of exercise on bone geometry in post-menopausal women. We excluded studies in children, men and secondary osteoporosis patients. Outcome variables were total volumetric BMD (Tv BMD), cortical volumetric BMD (Cv BMD), trabecular volumetric BMD (Trv BMD), total BMC, cortical BMC, Total Bone Area, cortical Area, Polar Stress Strain Index (PSSI), and Bone Strength Index (BSI), as measured by pQCT at the distal radius, radial shaft, distal tibia, and tibial shaft. Additional outcomes were three bone parameters as measured by DXA, including areal BMD, BMC and Section Modulus (Z), at the femoral neck, trochanter and lumbar spine.

A total of six studies satisfied inclusion and exclusion criteria with a total of 358 subjects in the exercise group and 279 in the control group. Average age was 65 years. Average duration of the exercise program was 8.8 months (range: 5-12 months). Lower extremity exercises resulted in small but significant improvements in Trv BMD of the distal tibia (0.87%, 95%CI: 0.37%-1.37%) and in Cv BMD of the tibial shaft (0.89%; 95%CI: 0.37%-1.41%). Site-specific exercises also resulted in a trend towards improvements in Tv BMD at the distal radius (1.7%; 95%CI: 0.63%-4.02%) and cortical area at the radial shaft (0.95%, 95%CI: 0.14%-2.03%). None of the other parameters had significant differences between exercise and non-exercise groups, although the number of studies and total number of subjects included are small.

Based on our data, we conclude that exercise in postmenopausal women can decrease bone loss by maintaining cortical and trabecular volumetric BMD. To better understand the effect of exercise on bone structure and strength, more and larger studies are needed.

**Disclosures:** I. Polidoulis, None.

**M485****Femur from C57BL/6 and DBA/2 Inbred Mice Display a Strain Dependent Response to Treadmill Running and Tower Climbing Exercise in Cortical and Trabecular Bone Architecture.** D. H. Lang, H. M. Preston\*, A. C. Henry\*, N. A. Sharkey. Kinesiology, Pennsylvania State University, University Park, PA, USA.

This study was designed to increase our understanding of the genetic architecture responsible for the maintenance of bone quality. By focusing efforts on defining interactions between genes and environmental loading, therapeutic interventions may someday be designed to target specific genotypes where differential responses are anticipated. We hypothesize that treadmill running and tower climbing exercise will produce a differential skeletal response as a function of inbred mouse strain.

B6 and D2 inbred female mice were subjected to treadmill running and tower climbing at 180 days of age. Ninety mice were used in a 2 x 3 experimental design with strain (B6 vs. D2), and treatment (treadmill running vs. tower climbing vs. control) as independent factors resulting in six groups with fifteen mice per group. The entire femur underwent micro-computed tomography (Scanco Medical, Zürich, Switzerland) using a 15.4µm voxel size. Separate evaluations were conducted for trabecular bone in the distal metaphysis, cortical bone at the mid-shaft and the whole bone. Strain and exercise group differences and interactions were evaluated using a three-way ANOVA.

Many of the skeletal measures had significant strain main effects. Of primary interest were those skeletal measures that displayed an exercise treatment main effect or an interaction effect with exercise treatment. Treadmill running produced thicker more closely spaced trabeculae in the distal femoral metaphysis compared to controls (Table 1). Tower climbers were intermediate to treadmill runners and controls. Several strain by treatment interactions were also identified. In general, D2 femurs were more responsive to treadmill running than B6 femur. Mid-shaft cortical BV/TV and density were greater in D2 treadmills compared to tower climbers and controls. However, no differences were identified in B6 femur. These results indicate that both strain and exercise are very important predictors of skeletal health. These data emphasize the importance of gene by environment interactions leading to future research that could provide the foundation on which to build effective means of assessing fracture risk due to osteoporosis and thereby enable early intervention.

Means and tukey pairwise comparisons. Levels not connected by same letter are significant.

	Main Effects	Treadmill Runners	Tower Climbers	Controls
Trabecular Thickness	Mean:	0.223 (A)	0.219 (A, B)	0.217 (B)
Trabecular Spacing	Mean:	0.604 (B)	0.713 (A, B)	0.797 (A)

**Disclosures:** D.H. Lang, None.

This study received funding from: NIH/NIA.

**M486****The Osteogenic Potential of Bone Marrow, Compromised by Disuse, is Normalized by Brief Exposure to a Low-Level Mechanical Signal.** E. Ozcivici, Y. K. Luu, C. T. Rubin, S. Judex. Biomedical Engineering, SUNY Stony Brook, Stony Brook, NY, USA.

Loss of functional weight bearing has devastating consequences for trabecular bone. Perhaps even worse, the lost skeletal tissue may never be fully recovered during reambulation. Here, it was hypothesized that disuse induces a reduction in the number of osteogenic cells within the bone marrow and that a high-frequency mechanical stimulus is able to rescue the cellular and morphological phenotype. Hindlimb unloaded male C57BL/6J either received a high-frequency mechanical stimulus (90Hz, 0.2g) induced by whole body vibration (WBV, n=12) for 15min/d, sham stimulation by allowing to bear weight for 15min/d (SHAM, n=12), or no stimulus at all (DC, n=12). An additional group of mice was not hindlimb suspended and served as normal age matched controls (AC, n=12). Three weeks into the protocol, half of the mice in each group were sacrificed while the remaining mice were allowed to ambulate freely for an additional 3wk. Upon sacrifice, bone marrow from each right hindlimb was extracted for fluorescence activated cell sorting (FACS) to identify cells with osteogenic potential as indicated by their positive expression of SCA-1 and CD90.2 surface antigens. Left hindlimbs were scanned by microCT. After 3wk of disuse, mice had 59% less BV/TV than age matched controls in the proximal tibia (p<0.05). Neither sham nor WBV loading was able to alleviate this loss during disuse. In contrast, FACS analysis demonstrated that AC, DC and SHAM groups had a similar percentage of total osteogenic cells while mice receiving the low-level mechanical signal had more osteogenic cells than DC (30%), SHAM (22%) and AC (30%, all p<0.05). The number of committed osteoprogenitors, a big and granulated sub-population of osteogenic cells that are SCA-1 positive, was 14% and 18% greater in AC than in SHAM and WBV mice and 55% greater than in DC mice (p<0.05). After reambulation, there were no significant differences in the number of osteogenic cells between groups. Nevertheless, trabecular BV/TV was greater (p<0.05) in WBV mice than in SHAM (18%) or DC (46%) mice but did not regain the levels of AC mice (-18%, p<0.05). These data showed that the hindlimbs of mice that received mechanical signals either by WBV or weightbearing during disuse, were able to preserve the number of osteoprogenitors, while only mice that received WBV also increased the number of cells that have the potential to commit to the osteogenic lineage. As the greater increase in BV/TV in WBV than in SHAM mice during reambulation may reflect the differences in their cell populations caused by disuse, the low-level mechanical signal may have provided long-term benefits in the absence of immediate tissue-level effects.

**Disclosures:** E. Ozcivici, None.

**M487****Bone Geometry and Bone Strength Are Compromised in Patients with Anterior Cruciate Ligament Reconstruction.** M. A. Petit<sup>1</sup>, S. L. Peart<sup>1\*</sup>, R. J. Wetzsteon<sup>2</sup>, T. J. Gaddie<sup>1</sup>, J. Rittweger<sup>3</sup>, S. D. Stovitz<sup>4\*</sup>, C. M. Larson<sup>4\*</sup>.<sup>1</sup>University of Minnesota, Minneapolis, MN, USA, <sup>2</sup>Children's Hospital of Philadelphia, Philadelphia, PA, USA, <sup>3</sup>Manchester Metropolitan University, Cheshire, United Kingdom, <sup>4</sup>Minnesota Sports Medicine, Minneapolis, MN, USA.

Loss of bone mineral content (BMC) and areal bone mineral density (aBMD), measured by dual energy x-ray absorptiometry, has been demonstrated following anterior cruciate ligament (ACL) reconstruction. However, due to the planar nature of aBMD and BMC measurements, it remains unclear whether ACL reconstruction results in alterations in volumetric bone mineral density, bone geometry and strength. Therefore, the purpose of this study was to assess leg side-to-side differences in bone volumetric density, bone geometry and bone strength in patients with a history of ACL reconstruction in the past 10 years. We used peripheral quantitative computed tomography (pQCT, Orthometrix XCT 3000) to assess bone geometry (total area, ToA, mm<sup>2</sup>), volumetric density (vBMD, mg/mm<sup>3</sup>), and an index of compressive bone strength (BSI) at trabecular sites close to the injury (patella and 4% distal femur). We assessed bone geometry (ToA and cortical area, CoA, mm<sup>2</sup>), vBMD, and an index of bone bending strength (polar strength strain index, SSIP, mm<sup>3</sup>) at the patella, 66% and 86% sites of the tibia, and at 20% of the femur. Muscle cross-sectional area (muscle CSA) was assessed at 66% tibia and 20% femur sites. We calculated differences in the surgical vs. non-surgical leg in 64 patients (41% male) aged 18-63 years (28.1±10.6yr) who had undergone a single-side ACL reconstruction in the past 1-10 years (mean 4.5yrs) and present data as mean difference (95% confidence intervals) between limbs. Bone strength (SSIP) was significantly lower in the surgical leg, particularly at sites closest to the injury from -12% (-17.4, -6.7) at the patella to -3% at 86% tibia (-5.2, -0.4) and 20% femur (-4.4, -1.3). There was no difference in bending strength at the 66% tibia site. BSI was also significantly lower at the patella (-10%; -4.4, -1.3) due largely to a significantly lower vBMD (-8.3%; -10.3, -6.4). Side-to-side muscle CSA was similar at both the tibia and femur. Further, side-to-side differences in bone strength were not associated with muscle CSA, time since surgery, surgical type, age or gender. These data suggest ACL reconstruction influences bone geometry and strength at sites closest to the injury and long-term bone deficits may exist despite post-surgical return of muscle mass.

**Disclosures:** M.A. Petit, None.

## M488

**Can Impact Exercise Mitigate the Adverse Effects of Oral Contraceptives on Bone?** J. M. Welch<sup>1</sup>, N. C. Laroche<sup>\*1</sup>, S. M. Kaiser<sup>2</sup>. <sup>1</sup>Kinesiology, Dalhousie University, Halifax, NS, Canada, <sup>2</sup>Endocrinology and Metabolism, Dalhousie University, Halifax, NS, Canada.

Oral contraceptive (OC) use may adversely affect bone status but whether exercise can mitigate this effect is unknown. We hypothesized that young women who habitually participate in impact exercise would not differ in bone status by OC use, while non-impact exercisers who take OCs would be disadvantaged. Two cross-sectional studies were conducted. In a pilot study, Study 1, 30 women 18-25 years old were recruited. Their use of OCs, exercise history, and factors such as smoking, diet and past medical problems were collected by questionnaire. Subjects were classified into four groups: OC use plus impact exercise (OC+I), OC use without impact exercise (OC+NI), no OC use plus impact exercise (NOC+I) or no OC use plus no impact exercise (NOC+NI). A Lunar Achilles InSight bone ultrasonometer was used to measure Stiffness Index (SI) at the calcaneus, in duplicate. Women in the OC+NI group had lower SI than those in other groups but 43% of them smoked compared to 0-17% in the other groups. Therefore, we undertook Study 2, in which smokers were excluded. 39 non-smoking women, aged 18-25 were recruited. They were placed into three of the previous categories: OC+I, OC+NI, and NOC+I. Women in the NOC+I group had the best bone status (SI=119±10), those in the OC+NI group had the poorest (SI=102±21), while women in the OC+I group were intermediate (SI=109±15). The results of both studies suggest that the repressive effect of oral contraceptives on skeletal health may be mitigated to some extent by habitual participation in impact exercise. If a larger study corroborates these results, then impact exercise should be recommended concomitantly with the prescription of oral contraceptives.

**Disclosures:** J.M. Welch, None.

## M489

**Contribution of Local Buckling to Femoral Neck Failure in Stance and Fall Mode Simulations: an Advanced FEA Analysis of Elderly Cadaver Femur Data.** A. Khaled<sup>\*1</sup>, B. Schafer<sup>\*2</sup>, J. Brown<sup>3</sup>, F. Eckstein<sup>4</sup>, V. Kuhn<sup>\*5</sup>, T. M. Link<sup>6</sup>, T. J. Beck<sup>1</sup>. <sup>1</sup>Department of Radiology and Radiological Sciences, Johns Hopkins School of Medicine, Baltimore, MD, USA, <sup>2</sup>Civil Engineering, Whiting School of Engineering, Baltimore, MD, USA, <sup>3</sup>Mindways Software Inc., Austin, TX, USA, <sup>4</sup>Institute of Anatomy and Musculoskeletal Research, Paracetus Private Medical University, Salzburg, Austria, <sup>5</sup>Medizinische Universität Innsbruck, Universitätsklinik für Unfallchirurgie und Sporttraumatologie, Innsbruck, Austria, <sup>6</sup>Department of Radiology, University of California San Francisco, San Francisco, CA, USA.

Results of several studies suggest that the mechanism underlying the ability of DXA BMD to predict hip fracture is local buckling failure but theoretical verification using continuum FEA methods are problematic since continuum methods do not accommodate local buckling failure. A specialized version of FEA called Finite Strip Method (FSM) was designed to evaluate failure in pure elastic buckling in thin-walled structures. We have developed a reliable method for deriving a smooth, geometrically accurate FSM model of the femoral neck cortex using CT scan data, without the necessity of employing the density modulus relationship. **Methods:** Six cadaver femurs from German subjects including 3 males aged 52, 66 and 93, and 3 females aged 65, 81 and 85 were scanned in a water bath using a 16 slice Siemens CT scanner with a slice spacing of 0.5 mm. Specialized software was used to extract the cross-section at the minimum neck diameter and FSM models of the cortex were derived and evaluated in the plane of the neck-shaft angle. Physiologic loads were simulated in a static one-legged stance including abductor forces acting on the outer margin of the greater trochanter. The fall mode was simulated without muscle forces and with impact on the greater trochanter, with the shaft at a fixed 10° angle from the impact surface. **Results:** In the stance mode, local buckling did not contribute to femoral neck failure in any model but it reduced strength in the fall mode in all models from 13% to 40%. **Conclusions:** The results of this preliminary analysis support the view that elderly femurs remain well adapted to physiologic loads but that the adaptation results in strength loss due to local buckling when subjected to unaccustomed loading conditions.

**Disclosures:** A. Khaled, None.

## M490

**The Loaded Distal Radius: Gymnastic-related Cross-sectional Asymmetry.** J. N. Dowthwaite, R. M. Hickman<sup>\*</sup>, J. A. Spadaro, T. A. Scerpella. Orthopedic Surgery, SUNY Upstate Medical University, Syracuse, NY, USA.

Mechanical loading during human growth generates adaptations in areal bone mineral density; these adaptations appear to occur via enlarged total bone and cortical dimensions, elevating theoretical bone strength. Few studies have assessed whether human bone adapts to mechanical loading symmetrically. The non-dominant radius is both a specific barometer of weight-bearing impact loading via gymnastics and a suitable site for pQCT evaluation of bone architecture. Therefore, we evaluated the non-dominant radius in post-menarcheal gymnasts and non-gymnasts, hypothesizing that the radius adapts asymmetrically to gymnastic loading during growth, with greater periosteal expansion in the medial-lateral plane than the antero-posterior plane. To test this hypothesis, we used pQCT to measure aspect ratios and bone widths from a cross-section of the radial diaphysis (33% region of interest, X plane= medial-lateral, Y plane= anteroposterior), comparing

output for post-menarcheal non-gymnasts versus girls exposed to gymnastic loading during growth.

Forearm pQCT scans were performed upon 48 post-menarcheal girls at the 33% distal radius. Maximum X (medial-lateral) and Y (anteroposterior) plane bone widths were measured using the XCT 2000 ruler function. Aspect ratios were calculated with X-plane width in the numerator and Y-plane width in the denominator. Girls were classed as gymnasts (n=27)(current or ex- gymnasts) or non-gymnasts (n=21) based upon childhood exposure to gymnastic loading. Height was measured using wall-mounted rulers. ANOVA compared aspect ratios for gymnasts versus non-gymnasts. ANCOVA compared X and Y plane widths, adjusting for gynecological age and height.

Subjects averaged 17.0 years old (gynecological age 3.9 years) and 162.0 cm tall. Girls exposed to gymnastics during growth exhibited 14% higher X-axis diameters than non-gymnasts, after adjustment for gynecological age and height (gymnasts= 14.6 mm; non-gymnasts=12.8 mm (ANCOVA p<0.02)). Although an 11% difference was found between gymnast and non-gymnast Y-axis diameters, this was not statistically significant after adjustment (gymnasts= 12.1 mm; non-gymnasts= 10.9 mm (ANCOVA p= 0.16). Similarly, the 3% gymnast versus non-gymnast aspect ratio difference was not statistically significant (gymnasts= 1.21; non-gymnasts= 1.17 (ANOVA p=0.10).

Exposure to weight-bearing impact loading during growth appears to yield larger periosteal dimensions along both medial-lateral and anteroposterior axes. Examination of aspect ratios is suggestive of loading-induced asymmetry; however aspect ratio differences did not achieve statistical significance in this limited sample.

**Disclosures:** J.N. Dowthwaite, None.

This study received funding from: SUNY Upstate Medical University.

## M491

**Prevention of Nutritional Rickets in Nigerian Children with Dietary Calcium Supplementation.** T. D. Thacher<sup>1</sup>, P. R. Fischer<sup>\*2</sup>, C. O. Isichei<sup>\*3</sup>, J. M. Pettifor<sup>4</sup>. <sup>1</sup>Family Medicine, Mayo Clinic, Rochester, MN, USA, <sup>2</sup>Pediatric and Adolescent Medicine, Mayo Clinic, Rochester, MN, USA, <sup>3</sup>Chemical Pathology, University of Jos, Jos, Nigeria, <sup>4</sup>Paediatrics, University of the Witwatersrand, Johannesburg, South Africa.

Most nutritional rickets in Nigerian children result from dietary calcium insufficiency. Typical dietary calcium intakes in African children are about 200 mg daily. We sought to determine if rickets could be prevented with supplemental calcium in at risk populations. We enrolled children ages 12 to 18 months from three urban Nigerian communities. Two communities were assigned to receive 400 mg calcium (Ca), either as calcium carbonate or ground dried fish daily, while children in all three communities received vitamin A (2500 IU) daily as a placebo. Serum markers of mineral homeostasis and forearm bone mass (pDXA) were measured and radiographs obtained at entry into the study and at the end of 18 months of supplementation.

The overall prevalence of radiographic rickets at baseline was 1.2 percent. Of 647 children enrolled, 387 (60%) completed the 18-month follow-up. Rickets developed in 1, 1, and 2 children assigned to the calcium tablet, ground fish, and control groups, respectively. Children who developed rickets in the calcium-supplemented groups had less than 50% adherence (P=0.04 for developing rickets with adherence less than 50%). Serum Ca did not differ between the children from the three groups at the end of the study (P=0.70). Final height was related positively to milk intake (P<0.01) and negatively to alkaline phosphatase (P<0.01) but not to supplemental calcium intake (P=0.89). At enrollment, serum calcium and weight independently predicted forearm bone mass. When adjusted for baseline bone mass and bone area, calcium supplementation did not have a significant effect on the increase in bone mass over time of either the proximal (P=0.88) or distal (P=0.18) forearm. Serum alkaline phosphatase values were negatively related to bone mass at 18 months (P<0.01). The relative risk of alkaline phosphatase >350 U/L was unaffected by supplemental calcium (RR=0.81, 95%CI 0.58-1.1). The change in 25OHD values did not differ between children who did and did not receive supplemental calcium (P=0.53). Overall, 5.4% (95%CI 3.8-7.7%) and 7.1% (95%CI 4.8-10%) had 25OHD values below 12 ng/mL at baseline and 18 months, respectively.

Adherence to calcium supplementation appeared to prevent rickets in Nigerian children. Calcium supplementation did not lead to greater bone mineral content or altered mineral homeostasis in young Nigerian children.

**Disclosures:** T.D. Thacher, None.

This study received funding from: Thrasher Research Fund.

## M492

**Contribution of Birth Status, Age at Menarche and Lifestyle Factors to Skeletal Formation in Junior and Senior High School Students.** Y. Onoe, T. Kuroda<sup>\*</sup>, Y. Miyabara<sup>\*</sup>, S. Orito, R. Yoshikata<sup>\*</sup>, M. Sakai<sup>\*</sup>, Y. Haruna<sup>\*</sup>, K. Ishitani<sup>\*</sup>, H. Okano, H. Ohta. Dpt. of Obstetrics and Gynecology, Tokyo Women's Medical University, Tokyo, Japan.

We investigated how birth status, age at menarche and lifestyle factors contributed to skeletal formation and bone mineral density (BMD) as skeletal indices in junior and senior high school students who were in growth and developmental stages.

The study enrolled 631 female students who were 12 to 18 years old and were attending junior and senior high school. We investigated birth-related data and age at menarche in these subjects. Height, body weight, and lumbar vertebra BMD were measured as skeletal indices. The total energy intake and intake of each nutrient were converted from answers to diet history-related questions in the DHQ, and current physical activity was investigated by using the JALS-PAQ. The skeletal indices were evaluated as z-scores as they reflected the influence of age and then were analyzed by using ANOVA and multivariate analysis.

The mean age of the subjects was  $14.4 \pm 1.7$  years old, and no significant correlation was found for birth-related data, presence of menarche, and time from menarche. A significant ( $P < 0.001$ ) correlation was seen between current height and boy weight, and gestational age showed a significant correlation with body weight and lumbar vertebra BMD ( $P = 0.012$ ,  $P = 0.031$ , respectively). Again, age at menarche showed a significant ( $P < 0.0001$ ) correlation with body weight and lumbar vertebra BMD. A significant ( $P = 0.023$ ) correlation was seen between calcium intake as a lifestyle factor and lumbar vertebra BMD. Lumbar vertebra BMD was shown to be significantly ( $P = 0.016$ ) higher in those who reported exercise ( $n = 370$ ) compared to those who reported no exercise ( $n = 261$ ). Moreover, lumbar vertebra BMD showed a significant ( $P = 0.0057$ ) positive correlation with time spent on exercise.

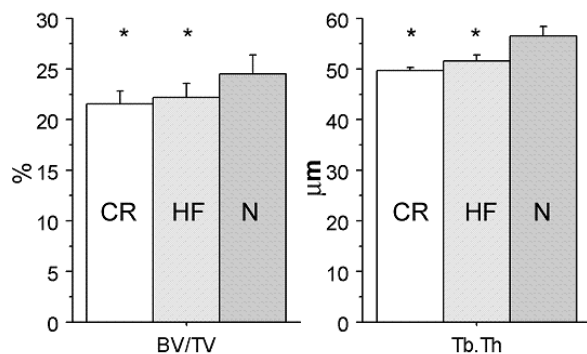
It was found that birth-related data and age at menarche independently influenced the skeletal indices, physique and lumbar vertebra BMD. It was also suggested that calcium intake, exercise and exercise time influenced lumbar vertebra BMD and that these lifestyle factors contribute markedly to BMD acquisition in adolescent girls who are in growth and developmental stages.

**Disclosures:** Y. Onoe, None.

## M493

**Both Excess and Restricted Energy Availability Negatively Influence Acquisition of Trabecular Bone Mass and Microarchitecture During Growth.** M. J. Devlin<sup>\*1</sup>, D. Panus<sup>\*1</sup>, C. J. Rosen<sup>2</sup>, M. L. Bouxsein<sup>1</sup>. <sup>1</sup>Orthopedic Surgery, Beth Israel Deaconess Medical Center / Harvard Medical School, Boston, MA, USA, <sup>2</sup>Maine Medical Center Research Institute, Scarborough, ME, USA.

This study tested the hypothesis that energy availability during the period of rapid skeletal growth affects bone mass and microarchitecture. At 3 wks of age we weaned male C57Bl/6J mice ( $N=4$  per group) onto normal (N, 10% calories/fat), 30% caloric restriction (CR, 10% calories/fat), or high fat diet (HF, 45% calories/fat). At 6 wks of age, we measured body weight, femoral length, serum IGF-1, total body BMD (TBBMD, g/cm<sup>3</sup>) using PIXImus, and trabecular bone architecture at the distal femur and cortical bone morphology at the femoral midshaft using  $\mu$ CT. CR mice were 54% lighter than N ( $p<0.0001$ ), had 12% shorter femurs and 18% lower TBBMD ( $p<0.0001$ ). Body mass, femur length, and BMD did not differ significantly between HF and N. Compared to N, both CR and HF diets were associated with lower distal femur trabecular bone volume (BV/TV) and thickness (Tb.Th, see Figure): BV/TV and Tb.Th were 14% lower in CR ( $p<0.03$  and  $p<0.0001$ ), and 11-12% lower in HF ( $p=0.057$  and  $p=0.0006$ ). In keeping with their lower body mass and shorter femurs, CR mice had 28-67% lower femoral cross-sectional area, cortical bone area, BA/TA, and cortical thickness ( $p<0.0001$ ), and 98-129% lower area moments of inertia ( $p<0.0001$ ), but HF and N did not differ. Serum IGF-1 was 14% lower in CR and 26% higher in HF vs. N ( $p<0.01$  for both). These results support the hypothesis that energy availability during growth affects cortical and trabecular bone mass and architecture, in some instances independently of effects on body mass. Young mice fed either HF or CR diet for a short period during growth had decreased trabecular bone volume and thickness but body mass-appropriate cortical bone parameters, suggesting cortical bone properties are driven primarily by body mass, but trabecular bone is more susceptible to metabolic disturbances.



**Disclosures:** M.L. Bouxsein, None.

## M494

**Maternal Nutrient Restriction During Pregnancy Results in Significant Alterations in Fetal Skeletal Development in the Baboon.** L. M. Havill<sup>1</sup>, M. R. Allen<sup>2</sup>, P. B. Higgins<sup>\*1</sup>, S. Amugongo<sup>\*3</sup>, J. A. K. Harris<sup>\*1</sup>, J. Mayeux<sup>\*1</sup>, N. E. Schlambitz-Loutsevitch<sup>\*4</sup>, P. W. Nathanielsz<sup>\*4</sup>, M. C. Mahaney<sup>\*1</sup>. <sup>1</sup>Genetics, Southwest Foundation for Biomedical Research, San Antonio, TX, USA, <sup>2</sup>Anatomy and Cell Biology, Indiana University School of Medicine, Indianapolis, IN, USA, <sup>3</sup>Dept. of Integrative Biology, University of California at Berkeley, Berkeley, CA, USA, <sup>4</sup>Dept. of Obstetrics and Gynecology, University of Texas Health Science Center San Antonio, San Antonio, TX, USA.

Bone development begins in utero and continues through the middle of the third decade of life in humans. Osteoporosis risk later in life is closely related to peak bone mineral density (BMD) attained at the end of this period of bone acquisition. Compromised nutrition in utero may effect changes in fetal skeletal development - e.g., alterations in the number and function of cells of the musculoskeletal system and/or expression of genes that regulate bone metabolism - that have long term consequences for skeletal growth, development, aging, resulting in increased risk of osteoporosis in adulthood. We assessed the effects of moderate global nutrient restriction in pregnant baboons, and hence fetal nutrient restriction, on fetal bone growth and development at 90% gestation (165 days). Nutrient-restricted (NR) mothers ate 70% of the amount of food eaten by ad lib controls. Whole body bone mineral density (BMD) was assessed for 6 NR fetuses and 8 control fetuses using DXA. NR fetuses showed significantly lower BMD than controls ( $p=0.02$ ). Proximal tibiae from all animals and a femurs from 4 NR fetuses and 4 controls were imaged using microCT. NR fetuses show a 26% reduction ( $p=0.007$ ) in amount of bone, which appears to be due to both thinner and fewer trabeculae. The femoral midshaft in NR fetuses is also smaller in size (smaller total and bone volume, cross-sectional area, and periosteal perimeter) and shows a lower cross-sectional moment of inertia, suggesting lower bending strength. Interestingly, however, the density of the bone tissue (pixels), specifically, in the NR cases is higher. While there is less bone, it is more highly mineralized, suggesting a compensatory mechanism in these animals. Nutrient restriction appears to result in an overall reduction in BMD and also an alteration in the localized tissue geometry and mineral density properties.

**Disclosures:** L.M. Havill, None.

## M495

**Increased Maternal Fat Intake Increases Skeletal Mass in Congenic Mice.** L. M. Cote<sup>\*1</sup>, H. F. Coombs<sup>\*2</sup>, C. J. Rosen<sup>2</sup>, J. M. Hock<sup>1</sup>, W. G. Beamer<sup>2</sup>, C. L. Ackert-Bicknell<sup>2</sup>. <sup>1</sup>Maine Institute for Human Genetics and Health, Brewer, ME, USA, <sup>2</sup>The Jackson Laboratory, Bar Harbor, ME, USA.

There is accumulating evidence that maternal environment has a significant impact upon the physiology of the progeny. In this study, we examined the effect of maternal dietary fat intake on the peak bone mass of the offspring. We chose the B6.C3H-6T congenic mouse strain for these studies as this strain is an excellent model of age related bone loss and we have previously used this strain to study the influence of dietary fat on peak bone mass. Mice were placed on either a high fat (HF, 60% KJ from fat) or a low fat (LF, 11% KJ from fat) diet when breeder pairs were established and the dams were maintained on that diet for the duration of pregnancy and lactation. When the offspring reached weaning age, they were either placed on the same diet as the mother or on the diet opposite that of the mother. At 16 weeks of age, the age of peak bone mass, whole body areal BMD (aBMD), volumetric density of the femur (vBMD) and femur size were assessed in the offspring. Stepwise ANCOVA analyses were performed to determine statistical significance. Body weight, femur length, maternal diet, wean diet and the interaction factor (maternal diet X wean diet) were considered as covariates in the statistical model. The covariates of body weight and femur length were not found to be significant for any of the phenotypes analyzed. For the phenotypes of total femoral mineral (Femoral BMC), total femoral volume and periosteal circumference the covariates maternal diet, wean diet and the interaction term: maternal diet X wean diet were found to be significant ( $p<0.05$ ) for both males and females. No effect of maternal diet was found for either femoral vBMD or whole body aBMD for females, but a significant effect was found for males. This data demonstrates a definite link between maternal dietary fat intake and bone physiology. It would be interesting to determine if the effects on bone mass were a consequence of the maternal environment during fetal development, or occurred postnatally due to transmission of key factors in breast milk.

**Disclosures:** L.M. Cote, None.

**M496****Elevated Systolic Blood Pressure is Positively Related to Bone Mass Measurements in Overweight Pre-pubertal and Pubertal Children.** F. A. Tylavsky<sup>1</sup>, M. Hare<sup>\*1</sup>, P. Richey<sup>\*1</sup>, P. Velasquez<sup>\*2</sup>, P. Cowan<sup>\*3</sup>, G. Somes<sup>\*1</sup>.

<sup>1</sup>Preventive Medicine, University of Tennessee Health Science Center, Memphis, TN, USA, <sup>2</sup>Pediatrics, University of Tennessee Health Science Center, Memphis, TN, USA, <sup>3</sup>Nursing, University of Tennessee Health Science Center, Memphis, TN, USA.

Human and animal studies have shown that total body sodium in excess of chloride is highly correlated with total body calcium, implicating a role for incorporating sodium in bones crystalline structure. In obesity induced hypertension, there is an increase of sodium retention due to concomitant reabsorption of calcium and sodium in the proximal tubule of the nephron. This results in a positive sodium and calcium balance leading to increases in extra cellular fluid and increases of calcium and sodium available for mineralizing the growing skeleton. We investigated the relationship between systolic (sys) blood pressure (BP) and bone area (BA), bone mineral content (BMC) and bone mineral density (BMD) in pre-pubertal (4-7 years, N=93, 96% African-American(AA)) and pubertal (11-18 years, N=48,72% AA) children. All participants were classified as at risk of or overweight as indicated by a BMI greater than 85<sup>th</sup> percentile for age and gender. BA, BMC and BMD of the whole body was determined by DXA (Hologic,Inc) using a standardized protocol. After sitting quietly for 5 minutes, sysBP were measured using a conventional mercury sphygmomanometer for the pre-pubertal children and dinamap for the pubertal children. Individuals were classified as having elevated BP if sysBP was greater than the 95<sup>th</sup> percentile for age, height and gender with the remaining being classified as normal. The average weight was 40.0± 11.6 and 98.2 ± 22 kg, and BMI was 25.7± 4.8 and 36.3± 7.7 kg/m<sup>2</sup> for pre-pubertal and pubertal participants respectively. SysBP had a moderate positive correlation to BA, BMC and BMD in both pre-pubertal and pubertal children  $r = 0.33-0.34$  and  $r = 0.59-0.66$ , respectively ( $p < 0.0001$ ). Pre-pubertal children with elevated sysBP had 4.1 % higher BA ( $p = 0.28$ ), 6.1% higher BMC ( $p = 0.27$ ), 2.6% higher BMD ( $p = 0.12$ ) while pubertal children with elevated sysBP had 10.3 % higher BA ( $p < 0.01$ ); 16.9% higher BMC, ( $p < 0.02$ ) and 6.9% higher BMD ( $p = 0.07$ ) than those with normal BP. Pubertal children with elevated sysBP also had higher lean body mass (58.2±2.1 kg) than those with normal sysBP (49.9±2.7 kg) ( $p < 0.02$ ) but similar fat and total mass. In pre-pubertal children similar but non-significant results were obtained for body composition. Our findings suggest that associations between elevated sysBP and BA, BMC and BMD in overweight children are evident in early childhood and magnify in puberty. How the skeleton is affected by elevated BP in overweight children as they mature and the mechanism behinds this warrants further investigation.

**Disclosures:** F.A. Tylavsky, None.  
This study received funding from: NIH.

**M497****Tracking of Femur Length during Intrauterine Growth.** A. Bjornerem<sup>\*1</sup>, T. Wilsgaard<sup>\*1</sup>, T. Kiserud<sup>\*2</sup>, E. Seeman<sup>3</sup>, S. L. Johnsen<sup>\*4</sup>. <sup>1</sup>Institute of Community Medicine, University of Tromso, Tromso, Norway, <sup>2</sup>Division of Obstetrics and Gynaecology, Department of Clinical Medicine, University of Bergen, Bergen, Norway, <sup>3</sup>Department of Medicine and Endocrinology, Austin Hospital and University of Melbourne, Melbourne, Australia, <sup>4</sup>Department of Obstetrics and Gynaecology, Haukeland University Hospital, Bergen, Norway.

The magnitude of the variance in traits such as bone size, mass and density is established in prepubertal life (Loro et al 2000). In addition, traits track in their percentile of origin during growth in most individuals. The aims of this study were (1) to determine whether the magnitude of variance in growth and adulthood is fully expressed in utero, (2) to determine whether individuals' traits grow at different rates establishing this variance or whether growth rate is similar from individual to individual - an observation supporting very early establishment of variance, and (3) determine whether traits track in their percentile of origin. We measured femur length (FL) in 650 low-risk pregnancies in Bergen, Norway using 2D ultrasound an average of 2.6 times (range 1-5) during weeks 10-41 gestational. The first measurement correlated the 2nd ( $r = 0.67$ ), 3rd ( $r = 0.53$ ) and the 4th ( $r = 0.26$ ) (all  $P < 0.001$ ), but not with the 5th ( $r = 0.05$ ). 42.8% of fetuses remained in the same FL quartile from the 1st to 2nd scan, 35.7% did so from 1st to the 3rd, and 33.5% from the 1st to 4th scan. Only 23.1% tracked from the 1st to 5th scan. Maternal height correlated weakly with FL at the 4th scan ( $r = 0.13$ ,  $P = 0.002$ ) and not at all with scans 1, 2 and 3. The variance in FL increased 2-3 fold in absolute terms as gestational age advanced but the standard deviation relative to age-specific mean (SD/mean) decreased as gestational age increased to 20 weeks and then remained constant and no different to their mothers SD/mean in height. We infer that variance is established in intrauterine life and tracking does occur but shifting between quartiles is more common than tracking and occurred in 77% of fetuses so that the tracking observed during postnatal growth may be set during the first years of life. The intrauterine, maternal or paternal factors operating before and shortly after birth that influence trait variance and tracking or change of tracking are unknown.

**Disclosures:** A. Bjornerem, None.

**M498****Birth Weight Predicts Bone Size, Adult Weight Predicts BMC and BMD In Young Gambian Adults.** S. de Bono<sup>\*1</sup>, I. Schoenmakers<sup>\*1</sup>, M. Ceesay<sup>\*2</sup>, M. Mendy<sup>\*2</sup>, M. Laskey<sup>\*1</sup>, T. Cole<sup>\*3</sup>, A. Prentice<sup>1</sup>. <sup>1</sup>Nutrition and Bone Health, MRC Human Nutrition Research, Cambridge, United Kingdom, <sup>2</sup>MRC, Keneba, Gambia, <sup>3</sup>UCL Institute of Child Health, MRC Centre of Epidemiology of Child Health, London, United Kingdom.

Fracture risk is determined by bone mass, size and architecture. Birth weight is reported to predict adult bone mass and density. Early life environment may therefore be a determinant of fracture risk in later life. However this evidence was obtained using dual-energy X-ray absorptiometry (DXA), which is known to be dependent on bone size. In this study we used peripheral quantitative computed tomography (pQCT) to investigate birth weight as a determinant of adult bone size, bone mineral content (BMC) and volumetric bone mineral density (vBMD) at trabecular and cortical sites, independent of adult weight, height and age. The results were compared to BMC and areal BMD (aBMD) measured by DXA. The study population had a high prevalence of factors likely to influence growth and skeletal development (poor nutrition, low calcium intake, delayed puberty and high physical activity).

Bone cross-sectional area, BMC and BMD were measured using pQCT (Stratec 2000; at 4 and 66% of the radius; 4 and 50% of the tibia length) and DXA (Lunar DPX; spine, hip, forearm and whole body) in 68 men and 52 nulliparous women aged 17.4 to 20.8 years from the rural village of Keneba, The Gambia. We used sequential univariable (influence of birth weight on each bone variable) and multivariable linear regression analyses (influence of birth weight on each bone variable after adjusting for adult height, weight and age) to investigate the independent effects of birth weight and adult size on adult skeletal status. Preliminary analyses showed significant interactions between birth weight by gender and bone variables. Therefore analyses were performed separately for both sexes. Birth weight was a significant positive predictor of total cross-sectional bone area (pQCT) at trabecular sites in females (total area radius:  $p = 0.003$ ; tibia:  $p = 0.05$ ) and cortical sites in males (total area radius:  $p = 0.01$ ; tibia:  $p = 0.005$ ), after adjustment for adult height, weight and age. Birth weight was not consistently related to BMC, vBMD or aBMD as measured by pQCT or DXA. Adult weight was a positive predictor of pQCT and DXA derived BMC and aBMD and adult height predicted aBMD at most sites in both males and females. In summary, birth weight significantly predicted adult bone size at trabecular sites in females, and cortical sites in males. Adult weight was a positive predictor of adult BMC and aBMD in both sexes. In conclusion, birth weight and hence prenatal factors affecting fetal growth may influence long-term bone health and fracture risk through their associations with adult skeletal size, independent of postnatal factors.

**Disclosures:** I. Schoenmakers, None.

**M499****Effects of Diet and Menstrual Cyclicity on Bone Mass Accumulation in Pubertal Monkeys.** C. J. Lees, M. Cline<sup>\*</sup>. Wake Forest University School of Medicine, Winston-Salem, NC, USA.

By end of puberty 80-90% of total adult bone mass is present. Anything that affects bone mass accumulation (such as diet) during this time period may have long term repercussions on skeletal health.

We examined the effects of dietary soy on bone mass accumulation during puberty in *Macaca fascicularis*. Twenty-nine 1.5 kg females were imported from Indonesia. The animals were divided into two groups that were fed a diet differing only in protein source (soy {n=17} vs. casein {n=12}). Vaginal swabs were performed daily to determine onset of menses and regularity of menstrual cycle. Whole body bone mineral content (WBBMC) and vertebral bone mineral density (LV24BMD) were determined by dual X-ray absorptiometry (DEXA) at baseline and then every 6 months for a total of 5 scans. Repeated measures analysis of variance showed no overall dietary effect on either WBBMC or LV24BMD. However, at scan time point 2, menstrual cyclicity had an impact on bone mass accumulation and this impact was dependent on diet. Within the soy group, cycling vs. non-cycling females did not differ in WBBMC or LV24BMD whereas in the casein fed group, cycling animals had higher WBBMC and LV24BMD compared to non-cycling females (see table below). The animals fed soy, regardless of cycling, did not acquire as much WBBMC or LV24BMD during this period compare to cycling casein animals. A similar trend was seen at the third scan.

Diet (D)	Soy		Casein		p-Values D/C/D*C
	Yes (N=11)	No (N=6)	Yes (N=6)	No (N=6)	
Cycling (C)					
WBBMC2	79 ± 5	78 ± 4	97 ± 7	69 ± 6	ns/0.02/0.03
LV24BMD2	0.460 ± 0.013	0.457 ± 0.012	0.520 ± 0.027	0.457 ± 0.014	ns/0.06/0.09

The groups are quite small in this study, especially when divided into cycling vs. non-cycling. However, it appears that soy may have differing effects on pubertal bone mass accumulation that is dependent on menstrual cyclicity.

**Disclosures:** C.J. Lees, None.

## M500

**Is Increased Bone Fragility During Adolescence a Result of Delayed Development in Bone Bending Strength?** S. A. Jackowski\*, R. A. Faulkner, A. Baxter-Jones. Kinesiology, University of Saskatchewan, Saskatoon, SK, Canada.

**Purpose:** The objective of this study was to investigate the sequential timing between the age of peak height velocity (APHV) and age of peak section modulus velocity (APZV) at the narrow neck and femoral shaft during the adolescent growth period.

**Methods:** 41 males and 42 females aged 8-18 years were selected from the Saskatchewan Pediatric Bone Mineral Accrual Study (1991-2005). Participants height and section modulus (Z) at the proximal femur were assessed annually using a wall-mounted stadiometer and hip structural analysis (HSA) program, respectively. Height and Z values were converted into whole year velocities and the maturational age of peak tissue velocities was determined using a cubic spline curve fitting procedure. Differences in APHV and APZV at the narrow neck and femoral shaft were compared using multiple t-tests with significance set at  $p < 0.05$ .

**Results:** APHV (males,  $13.15 \pm 0.89y$ ; females,  $11.70 \pm 0.98y$ ) preceded the APZV at the narrow neck ( $13.71 \pm 1.01y$ ;  $12.39 \pm 1.15y$ ) and femoral shaft ( $13.70 \pm 1.46y$ ;  $12.28 \pm 1.04y$ ) for both males and females ( $p < 0.05$ ).

**Discussion:** The timing of APHV and Z are in agreement with previous studies showing a sequential timing between APHV and bone mineral accrual. Thus these findings support in the conjecture that during adolescence there is a period of relative skeletal fragility that may partially explain the increased risk of fracture rate at this time of life.

**Disclosures:** S.A. Jackowski, None.

## M501

**Environmental Perturbations during Puberty and Bone strength.** R. N. Joshi, V. Yingling. Kinesiology, Temple University, Philadelphia, PA, USA.

Studies have reported bone densities in young athletic women similar to 51-year-old women. Fracture risk in the elderly has its origins during growth and development; both genetic and environmental factors (including secondary amenorrhea disordered eating and delayed pubertal development) have been found to correlate with low bone mass in young women. Pubertal timing is considered to be one of the key factors that predicts peak bone mass. Delayed puberty is observed in females with hypothalamic amenorrhea and energy deficiency. The purpose of this study was to determine the effect of delayed puberty on bone strength through two different physiological mechanisms. At 23 days of age, 16 female Sprague Dawley rats (Charles River) were randomly assigned into three groups: Aged match control group (C, n=4), Gonadotropin releasing hormone-antagonist (GnRH-a group, n=6), and Energy Restriction (ER, n=6). The animals in the GnRH-a group received daily injections (Antide, Bachem) at a dose of 2.5 mg/kg for 28 days. The animals in the ER group received 0.7 g for each 1 g of food consumed by control animals (Research Diets). All the animals were sacrificed on day 51. Vaginal opening (VO) was documented and considered to be the day of pubertal onset. After sacrifice, body weight, uterine weights and muscle weights were measured in all groups. Mechanical strength was measured using a 3-point bending test to failure at a loading rate of 0.05 mm/s. Differences were detected using a One-way ANOVA. Puberty was completely suppressed in the GnRH-a model as evidenced by a cessation of VO and suppressed uterine development however this group had similar body weights at sacrifice as control. The ER model had a moderate delay in puberty based on day of VO with no change in uterine development. ER resulted in a lower body weight at sacrifice and decreased muscle weight. However, there was a significant decrease in mechanical strength in the GnRH-a group and a trend towards decreased strength in the ER group. These results suggest that two physiologically different mechanisms during the pubertal period have a negative impact on bone strength.

Table 1. Outcome measures. Mean (SD) \*  $p < 0.05$

Parameters	C	GnRH-a	ER
Peak Moment Femur (Nmm)	202.9 (23.2)	156.8 (16.8)*	185.2 (18.6)
Peak Moment Tibia (Nmm)	163.1 (15.4)	133.7 (8.6)*	142.8 (14.7)
VO (days)	34 (0)	None of the animals reached puberty	38 (4.1)
Body Weight (g)	191.3 (17.7)	185.3 (6.8)	147.2 (4.6)*
Uterine Weight (g)	0.36 (0.04)	0.08 (0.05)*	0.30 (0.08)
Muscle Weight (g)	1.26 (0.1)	1.27 (0.08)	1.04 (0.04)*

**Disclosures:** R.N. Joshi, None.

## M502

**Ethnicity-specific Bone Changes During Adolescent Growth: pQCT Analysis of the Tibia.** S. Braid<sup>1</sup>, M. Burrows<sup>1</sup>, Y. Ahamed\*<sup>1</sup>, H. McKay<sup>2</sup>.

<sup>1</sup>Department of Orthopaedics; Centre for Hip Health and Musculoskeletal Research, University of British Columbia, Vancouver, BC, Canada,

<sup>2</sup>Department of Orthopaedics and Family Practice; Centre for Hip Health and Musculoskeletal Research, Vancouver Coastal Health Research Institute, Vancouver, BC, Canada.

Ethnicity, body habitus and lifestyle including physical activity (PA) and dietary calcium (Ca2+) are among the key determinants of peak bone mass. However, little is known about ethnic differences related to the development of bone strength in growing children. Thus, we used pQCT (Stratec XCT 2000) to assess the ethnicity-specific variation in bone total area (ToA, mm<sup>2</sup>), cortical density (CoD, mg/mm<sup>3</sup>), and SSI (mm<sup>3</sup>) at the 50% site of the tibia in 142 Asian (A) and Caucasian (C) girls (F) and boys (M) over 52-months (37AF, 22CF, 45AM, 38CM). Ages (SD) were 10.4 (0.6) and 14.7yrs (0.6) at baseline (T1) and final (T2), respectively. We evaluated a 2.5mm mid-diaphyseal slice of the tibia using pQCT. Height (Ht, cm) and weight (Wt, kg) were assessed using standard protocol and tibial length (TL, cm) was the distance from the tibial plateau to the medial malleolus. PA and Ca2+ were assessed by questionnaire. Ht, Wt and TL did not differ between AM and CM at T1 {141.1cm (7.3); 36.5kg (9.5); 32.7cm (2.4)} or T2 {167.5cm (8.7), 58.0kg (13.7), 40.8cm (2.6)}. AF were shorter and weighed less than CF at T1 and T2 ( $p < 0.05$  both). T1 values (AF v CF) were: Ht 139.0 (6.9) v 143.3cm (7.6); Wt 34.1 (7.1) v 38.0kg (10.2); and TL 32.0 (2.0) v 33.1cm (2.3). T2 values (AF v CF) were: Ht 157.6 (5.7) v 164.3cm (6.2); Wt 49.9 (7.6) v 57.4kg (12.0); and TL 36.9 (1.7) v 38.9cm (2.0). No significance (NS) indicated for PA between ethnicities (F: 3.8 (3.7) and M: 6.3 load hrs/wk (5.2)). At T1 Ca2+ was 781.8 (379.9) v 1009.8kcal (397.2) for AF and CF, respectively. For M, T1 Ca2+ was 895.3 (91.9) v 1111.46kcal (98.9) for AM and CM, respectively ( $p < 0.05$ ). All bone outcomes increased with age in A and C ( $p < 0.05$ ). ANCOVA was used to assess change in bone outcomes (covariates: TL, Wt and Ca2+). At T1, CF had greater ToA 303.2 (55.4) v 279.0mm<sup>2</sup> (43.0), CoD 1052.1 (23.7) v 1061.6mg/mm<sup>3</sup> (35.9) and SSI 1006.9 (260.2) v 893.3mm<sup>3</sup> (200.6) compared with AF ( $p < 0.05$ ). T2 values (CF v AF) were: ToA 394.6 (63.4) v 361.3mm<sup>2</sup> (47.2); CoD 1126.8 (23.8) v 1136.0mg/mm<sup>3</sup> (20.9) and SSI 1601.3 (375.6) v 1414.9mm<sup>3</sup> (256.6). However, these differences were explained by size and were NS once covariates introduced. For boys, A had greater ( $p < 0.05$ ) CoD only at T1 and T2, respectively [1051.8 (27.7) and 1078.2 (31.6)] compared with C [1052.7 (36.7) and 1053.7 (44.9)]. No other differences were noted between AM and CM. Although there were some differences in lifestyle factors (Ca2+) known to effect bone, A and C girls changed similarly as they matured. However, the difference in CoD between boys is notable and should be explored further.

**Disclosures:** S. Braid, None.

This study received funding from: CIHR, MSFHR, and NSERC

## M503

**Early Exposure to Soy Isoflavones Modulates Bone Mineral, Strength and Microarchitecture in CD-1 Mice.** J. Kaludjerovic\*, W. E. Ward. Nutritional Sciences, University of Toronto, Toronto, ON, Canada.

Neonatal exposure to the soy isoflavone genistein (GEN), at levels similar to that of infants consuming soy protein-based infant formula, favourably modulates bone mineral and bone strength in mice. The objective of this study was to determine if early exposure to a combination of soy isoflavones, daidzein (DAI) and GEN, results in greater benefits to bone at adulthood than either treatment alone. Male and female CD-1 mice (n = 8-16 pups/group/gender) were randomized to subcutaneous injections of DAI (2 µg/d), GEN (5 µg/d), DAI+GEN (7 µg/d), diethylstilbestrol (DES, positive control) (2 µg/d), or corn oil (CON) from postnatal day (PND) 1 to 5, and were followed to young adulthood (4 months old). Serum isoflavones were measured at PND 5, while bone mineral, strength and microarchitecture were analyzed at 4 months of age. Females treated with DAI, GEN, DAI+GEN or DES had higher ( $p < 0.001$ ) femur and lumbar vertebrae (LV1-3) BMD compared to the CON group, which translated into stronger ( $p < 0.010$ ) bones that were more resistant to fracture. Microstructural analysis demonstrated that females treated with DAI, GEN, DAI+GEN or DES had greater ( $p < 0.001$ ) cortical area at the femur midpoint compared to the CON group, with DAI providing added benefits. At the lumbar spine, females treated with DAI and DAI+GEN had higher ( $p < 0.001$ ) trabecular number and lower ( $p < 0.001$ ) trabecular separation compared to CON, suggesting that DAI alone or in combination with GEN improves the interconnectivity of trabecular bone. Females treated with GEN had higher ( $p = 0.031$ ) trabecular thickness at the lumbar spine compared to the CON group. Effects in males were modest, with DAI or DAI+GEN resulting in higher yield load ( $p = 0.030$ ) at the femur neck compared to the CON group. In conclusion, neonatal exposure to DAI and/or GEN had a positive effect on the skeleton of female mice but compared to individual treatments, DAI+GEN did not have a greater benefit to bone in females or males. Future research should determine if these positive effects protect against deterioration of bone tissue during aging.

**Disclosures:** J. Kaludjerovic, None.

This study received funding from: International Life Sciences Institute North America, Future Leader Award to W. Ward.

## M504

**Heel Ultrasound and Consolidation of Peak Bone Mass in Young Women - Bath Cohort Study.** S. Venkatachalam<sup>1</sup>, I. Reading<sup>\*2</sup>, C. Cooper<sup>2</sup>, D. Elvins<sup>\*3</sup>, A. Bhalla<sup>3</sup>. <sup>1</sup>Rheumatology, Cannock Chase Hospital, Cannock, United Kingdom, <sup>2</sup>MRC Environmental Epidemiology Unit, Southampton, United Kingdom, <sup>3</sup>Rheumatology, Royal National Hospital for Rheumatic Diseases, Bath, United Kingdom.

We had earlier identified that infant growth and physical activity in childhood are important determinants of peak bone mass in women at the age of 21 years, in a cohort of young women from Bath, UK born in 1968-69. Our longitudinal study showed continuing gain in BMD in the third decade at both the lumbar spine and the total hip in young women on DXA. Their weight at the age of 21 years was the only significant determinant of consolidation of peak bone mass. We explored the relationship of bone quality measured by heel ultrasound with consolidation of peak bone mass in these young women at the age of 31 years.

We traced 90 of 153 women from the initial cohort and 87 had heel ultrasound (Sahara) at 31 years of age. We ascertained lifestyle factors like calcium intake, physical activity, smoking and alcohol consumption by questionnaire. Data were analysed by multiple regression with changes in heel BMD, BUA (Bone Ultrasound Attenuation) and SOS (Speed of Sound) as dependent variables.

Significant determinants of heel BUA were weight at 21 years of age ( $\beta = 0.355$ ,  $p = 0.018$ ) and walking ( $\beta = 2.826$ ,  $p = 0.037$ ). Heel BMD was associated only with walking ( $\beta = 0.02$ ,  $p = 0.047$ ) while Heel SOS was not associated with any of the measures. Only weight at birth negatively predicted Heel SOS and BMD, but not BUA at age 31 years ( $p = 0.012$ ,  $p = 0.025$ ). The conditional weights at 1 year, 5, 10 or 21 years and life style factors did not predict bone quality on ultrasound in the women.

Walking is known to increase the impact on heel bone quality and is associated with consolidation of heel bone mass. Weight at 21 years of age not only determines consolidation of hip and spine BMD but also bone quality measured as heel BUA.

**Disclosures:** S. Venkatachalam, None.

## M505

**Vitamin K Intake Is Positively Related to Trabecular Bone Microarchitecture in Children.** C. M. Modlesky<sup>1</sup>, J. T. Kirby<sup>\*1</sup>, S. Kanoff<sup>†\*1</sup>, F. Miller<sup>\*2</sup>. <sup>1</sup>Health, Nutrition and Exercise Sciences, University of Delaware, Newark, DE, USA, <sup>2</sup>Orthopaedics, AI duPont Hospital for Children, Wilmington, DE, USA.

Vitamin K seems to play an important role in the development and maintenance of the skeleton. This idea is supported by studies reporting an inverse relationship between vitamin K intake and fracture. Interestingly, vitamin K status is not consistently related to areal bone mineral density (aBMD). The discordant relationship suggests that vitamin K is more closely connected to skeletal features not captured by aBMD, such as the trabecular microarchitecture and the geometric structure of bone. The purpose of this study was to determine if vitamin K intake is related to measures of trabecular bone microarchitecture and cortical bone geometry in the femur of children. Fifteen boys and 15 girls (Caucasian; 6 to 12 y) participated in the study. Pubertal development was determined using Tanner staging. Vitamin K and calcium intake were determined using 3-day diet records and the USDA Food and Nutrient Database for Dietary Studies (v.1.0). Physical activity was assessed using accelerometry (Actical; MiniMitter Co.). Magnetic resonance imaging (GE 1.5 T) was used to collect images of the distal femur and images of the thigh. Distal femur images were used to assess trabecular bone microarchitecture [i.e., apparent trabecular bone volume to total volume (appBV/TV), trabecular number (appTb.N), trabecular thickness (appTb.Th) and trabecular spacing (appTb.Sp)] in the lateral half of the bone. Thigh images were used to assess measures of cortical bone geometry (i.e., cortical volume, polar moment of inertia and section modulus) and muscle mass at the level of the middle-third of the femur. All images were processed using software created with Interactive Data Language (Research Systems, Inc). The relationships between vitamin K and measures of trabecular bone microarchitecture and cortical bone geometry were determined using linear regression analysis, with midthigh muscle mass, calcium intake and physical activity counts as covariates. Twenty five children were prepubertal (Tanner stage I) and 5 children were early pubertal (Tanner stage II). Vitamin K intake was not significantly related to any measure of cortical bone geometry in the middle-third of the femur ( $p > 0.05$ ); however, vitamin K intake was positively related to appBV/TV (partial  $r = 0.501$ ,  $p = 0.008$ ) and appTb.Th (partial  $r = 0.468$ ,  $p = 0.014$ ) and inversely related to appTb.Sp (partial  $r = -0.351$ ,  $p = 0.072$ ) in the distal femur. The findings suggest that vitamin K may be an important contributor to the development of trabecular bone microarchitecture in children.

**Disclosures:** C.M. Modlesky, None.

This study received funding from: National Osteoporosis Foundation; National Institutes of Health.

## M506

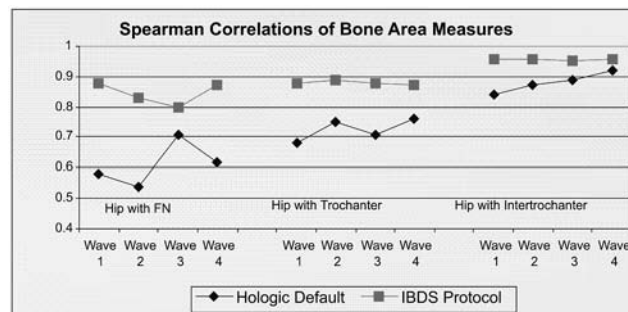
**A Protocol for Pediatric Proximal Femur DXA Analysis.** J. Eichenberger Gilmore<sup>\*1</sup>, C. A. Pauley<sup>\*2</sup>, T. L. Burns<sup>\*3</sup>, J. C. Torner<sup>\*3</sup>, E. M. Letuchy<sup>\*3</sup>, K. F. Janz<sup>\*4</sup>, M. C. Willing<sup>5</sup>, S. M. Levy<sup>1</sup>. <sup>1</sup>Preventive and Community Dentistry, University of Iowa, Iowa City, IA, USA, <sup>2</sup>Food and Nutrition, University of Iowa, Iowa City, IA, USA, <sup>3</sup>Epidemiology, University of Iowa, Iowa City, IA, USA, <sup>4</sup>Sports and Health Studies, University of Iowa, Iowa City, IA, USA, <sup>5</sup>Pediatrics, University of Iowa, Iowa City, IA, USA.

Pediatric proximal femur DXA scans present analytic challenges for both cross-sectional and longitudinal research due to lack of fully developed anatomical landmarks in the growing skeleton. The Iowa Bone Development Study (IBDS) developed a modified pediatric-specific proximal femur analysis protocol using Hologic software. Serial DXA measurements were obtained for 214 children at approximate ages 5, 8, 11, and 13 years (Waves 1 - 4). Standard analysis procedures as described by the manufacturer (Hologic Default) were compared to the IBDS protocol. The IBDS protocol yielded lower but more stable results for bone area (BA), bone mineral content (BMC) and bone mineral density (BMD) for total hip, femoral neck (FN), trochanter, and intertrochanter as a result of more precisely controlling the regions of interest (ROIs). Linear regression models with body size, age and gender as predictors were developed to examine variation in measurements. Coefficients of variation ( $R^2$ ) with the IBDS protocol were greater for each time point, demonstrating that the modified protocol was better aligned with body size (Table). Similarly, Spearman correlation coefficients between total hip and hip sub-regions were consistently higher for BMC and BA with the IBDS protocol with differences more notable among younger children (Figure). The IBDS protocol provides a reproducible method for evaluating pediatric proximal femur DXA scans during growth.

Table. Coefficients of Determination ( $R^2$ ) for Hip BMC (Hologic Default and IBDS Protocols) with Body Size (Height and Weight), Age, and Gender as Predictors.

	Protocol	Wave 1	Wave 2	Wave 3	Wave 4
Hip BMC	Default	0.57	0.68	0.67	0.63
	IBDS	0.62	0.72	0.70	0.67
Femoral Neck BMC	Default	0.41	0.50	0.64	0.61
	IBDS	0.58	0.63	0.68	0.66
Trochanter BMC	Default	0.33	0.51	0.49	0.53
	IBDS	0.54	0.66	0.66	0.62

Figure. Spearman Correlations of Total Hip Bone Area and Hip Sub-region Bone Area.



**Disclosures:** J. Eichenberger Gilmore, None.

This study received funding from: National Institutes of Health R01-DE12101, R01-DE09551 and General Clinical Research Centers Program, National Center for Research Resources M01-RR00059.

M507

**A Randomised Double Blinded Controlled Trial of Individual Response in Biochemical Markers of Bone Turnover to Lasofoxifene Therapy.** S. J. Glover, A. Rogers, F. Gossiel\*, R. Eastell. Academic Unit of Bone Metabolism, University of Sheffield, Sheffield, UK, United Kingdom.

Biochemical markers of bone turnover (BTMs) may be used to monitor the response to anti-resorptive therapy. It has been proposed that to be effective in the prevention of fracture, the goals of therapy in the individual are a decrease in BTMs > the least significant change (LSC), and to within the lower half of the reference interval (RI) for healthy, young pre-menopausal women.

The aim of this study was to evaluate the use of BTMs in monitoring the response to lasofoxifene (laso) therapy after 6 months by determining the % of women: a) with a decrease in BTMs >LSC b) with BTMs in the lower half of the RI for young pre-menopausal women.

51 postmenopausal osteopenic women, ages 55 to 77 (mean 63.7) years were randomized to receive either laso (0.25 mg/day) or placebo. 47 women (completed 6 months of therapy. All women received calcium and vitamin D throughout the study. We measured serum bone alkaline phosphatase (bone ALP), procollagen type I propeptide (PINP), serum beta crosslinked C-telopeptides of type I collagen (S-bCTX) and urinary crosslinked N-telopeptides of type I collagen (NTX) at weeks -1, 0 (baseline), 4, 8, 12, 24 and 25 (6 months) using standard techniques. BTMs were also measured at a single time point in 145 healthy pre-menopausal women ages 35 to 45 years. LSC was calculated from baseline duplicate measurements using the ISCD calculator (<http://www.iscd.org/visitors/resources/calc.cfm>). T scores for the patient population were calculated from the mean and SD of the log transformed reference data.

We observed a significant decrease in all BTMs in response to laso (p<0.0001 by ANOVA). For all BTMs the change from baseline was significant by 4 weeks post laso (p<0.0001) with the largest reduction observed at 6 months. The LSC for each marker was as follows; bone ALP, 14.14%, PINP 25.10%, S-bCTX 27.67 % and NTX 36.79%. The values for mean % change in BTMs in the laso (placebo) groups at 6 months were: bone ALP -26.6(-6.5) %, PINP -44.0(-8.6) %, S-bCTX -44.1(-3.5) % and NTX -29.1(-6.3) %. The number (%) of responders and women in the lower half of the RI at 6 months are shown below (table).

We conclude that almost all patients responded to laso therapy based on the values for LSC in the serum based BTMs. BTMs were reduced to the lower half of the RI in a large % of women suggesting that laso may be a useful therapy in the prevention of osteoporotic fracture.

	Laso	Placebo	Laso	Laso
	% Responders	% Responders	% Lower Half RI	% Lower Half RI
bone ALP	88	33	48	18
PINP	92	29	76	9
S-bCTX	92	4	52	9
NTX/Cr	39	9	36	27

**Disclosures:** *S.J. Glover, None.*  
*This study received funding from: Pfizer.*



## MUSCLE AND BONE WORKING GROUP

### WG1

**The Effect of Non-Ambulation on Bone Strength in Boys with Duchenne Muscular Dystrophy (DMD).** Crabtree NJ<sup>1</sup>, Ward KA<sup>2</sup>, Roper H<sup>3</sup>, Mughal Z<sup>4</sup>  
<sup>1</sup>Shaw, NJ <sup>1</sup>Birmingham Children's Hospital, <sup>2</sup>University of Manchester, <sup>3</sup>Heartlands Hospital, Birmingham, & <sup>4</sup>St Mary's Hospital for Women and Children, Manchester, UK

DMD is the most common childhood neuromuscular disorder causing loss of ambulation in early life. Steroids are currently used to improve muscle strength and prolong ambulation although the effect on bone health in this group of children is still unclear. The aim of this study was to compare bone strength in healthy children to bone strength in children with DMD and investigate the interaction between high dose oral steroids and diminished muscle function.

Forty-seven children were studied, 18 healthy boys (mean age 9.0±1.5 years) and 29 boys with DMD (mean age 9.1±2.5 years). Of the 29 boys with DMD 9 were ambulant and had not started on steroids, 14 were ambulant and had taken steroids for at least 12 months (mean 25.4 ±11.0 months) and 6 were no longer ambulant and had taken steroids for between 14 and 45 months (mean 37.2 ±11.7 months). Peripheral quantitative computed tomography was used to measure bone geometry, density and muscle mass of the non-dominant tibia. Measurements were made at the distal metaphysis and mid diaphysis sites taken as 4 & 66% of the tibial length, respectively. Data were adjusted for age & height and differences between the four groups evaluated.

In general, at the distal metaphysis, healthy boys had larger bones (21.3%, p<0.001) which were more dense (18.4%, p<0.001) than the boys with DMD. The greatest differences were observed between healthy and non-ambulant DMD boys, where bone area and bone density were reduced by 41.6% and 32.0%, respectively. No significant differences were observed between ambulant steroid and non steroid DMD boys, for these parameters. At the mid diaphysis, cross-sectional tibial area, cortical area, cortical bone mass and the stress-strain index (a surrogate measure for bone strength) were all reduced in DMD boys by 40.0%, 29.2%, 22.4% & 31.5%, respectively (p<0.001). Once again this effect was most striking in the boys who had lost ambulation, with no differences detected between ambulant steroid and non steroid DMD boys. In contrast, DMD boys had significantly greater muscle mass (48.4%, p<0.001) but with greatly diminished function. In addition, there were no significant differences in cortical density.

In summary, this data suggests that ambulation and hence muscle function & gravitational load has the greatest effect on bone strength and density in boys with DMD. In contrast, whilst they remain ambulant the effect of the relatively high dose steroids appears to be negligible. This information is likely to be useful when considering potential interventions for maximising bone strength as these boys go through puberty in to young adulthood.

### WG2

**Shared Genetics Within the Musculoskeletal System: A Pleiotropic Approach to Osteoporosis and Sarcopenia.** D. Karasik. IFAR Hebrew SeniorLife and Harvard Medical School, Boston, MA, USA

Osteoporotic fracture can be viewed as an outcome of loading conditions and the ability of the bone to withstand the load. Muscle action is the major mediator of skeletal load. Aging-related change in the musculoskeletal system manifests as bone loss (osteoporosis) and muscle wasting (sarcopenia). Recently, it has become clear that bone and muscle share genetic determinants (pleiotropy), which may be pertinent to etiology of osteoporosis and sarcopenia.

This report provides evidence of accumulating data for a shared genetic influence on bone and muscle. Thus, genetic correlations between lean mass (LM) and femoral geometry ranged from 0.28 to 0.69 (Deng et al JBMR 2007) and between LM and BMD from 0.30 - 0.41 (Videman et al JBMR 2007). Animal studies (in mouse intercrosses, sheep, and beef cattle) confirm the above observations. Our recent genome-wide studies in the Framingham study provide an important insight on the pleiotropy, as well as sex-specificity of the genetic associations. Several candidate genetic mechanisms, including *ESR1* and *IGF1* pathways, show sex-specific association with bone and muscle strength phenotypes.

Physical exercise produces larger effects on the adult skeleton (beyond puberty) in men compared to women. It is not obvious whether or not sex-specific genetic associations may be attributed to the modifying effects of sex chromosomes or other differences between the genders, such as the level of sex hormones and/or physical exercise. Therefore, we considered several related questions such as (a) what genetic factors modulate varying responses to the exercise in men and women, and (b) whether there is a sex-specific genetic predisposition, or (c) whether the environment/ hormonal milieu differs by sex. Finally, some insights and recommendations as to the value of studying shared genetic factors, and possible directions for future research, will be offered and explored.

We believe that further progress in understanding the shared genetic etiology of osteoporosis and sarcopenia will provide valuable insight into important biological underpinnings for both osteoporosis and sarcopenia. For example, selective androgen receptor modulators (SARMs) and low magnitude strains (vibration) are characterized by the anabolic activity on both muscles and bones. Knowledge of the general paradigm of bone responses to mechanical loading may translate into targeted new approaches to reduce the burden of both conditions affecting elderly women and men.

## WORKING GROUP ON MUSCULOSKELETAL REHABILITATION

### WG4

**Non-Steroidal Anti-Inflammatory Use and the Response of Bone to Exercise.** D. W. Barry<sup>1</sup>, R. E. Van Pelt<sup>\*2</sup>, C. M. Jankowski<sup>\*2</sup>, P. Wolfe<sup>\*3</sup>, W. M. Kohrt<sup>2</sup>. <sup>1</sup>General Internal Medicine, University of Colorado Denver, Aurora, CO, USA, <sup>2</sup>Geriatric Medicine, University of Colorado Denver, Aurora, CO, USA, <sup>3</sup>Preventive Medicine and Biometrics, University of Colorado Denver, Aurora, CO, USA.

For full text see presentation #M472

### WG5

**The Effect of a One Year Exercise Program on Markers of Bone Metabolism after Hip Fracture.** J. Yu-Yahiro<sup>1</sup>, E. Streeten<sup>2</sup>, M. Hochberg<sup>2</sup>, D. Orwig<sup>\*2</sup>, J. Magaziner<sup>2</sup>. <sup>1</sup>Department of Orthopaedics, Union Memorial Hospital, Baltimore, MD, USA, <sup>2</sup>Epidemiology and Preventive Medicine, University of Maryland School of Medicine, Baltimore, MD, USA.

For full text see presentation # SA432

### WG6

**An Effective Progressive Resistive Exercise Program from Prone Position for Paravertebral Muscles to Reduce Risk of Vertebral Fractures.** M. Sinaki<sup>1</sup>, M. J. Borgo<sup>\*2</sup>, E. Itoi<sup>\*3</sup>. <sup>1</sup>Physical Medicine and Rehabilitation, Mayo Clinic College of Medicine; Mayo Clinic, Rochester, MN, USA, <sup>2</sup>Mayo Medical School, Mayo Clinic, Rochester, MN, USA, <sup>3</sup>Department of Orthopaedic Surgery, Tohoku University School of Medicine, Sendai, Japan.

For full text see presentation #M473

### WG7

**The Influence of Muscle Size and Strength on Changes in Bone Mass and Size During Growth and in Response to Exercise: A Longitudinal Study.** G. Ducher<sup>1</sup>, R. Daly<sup>1</sup>, J. Black<sup>\*3</sup>, C. Turner<sup>\*4</sup>, S. Bass<sup>1</sup>. <sup>1</sup>Centre for Physical Activity and Nutrition Research, Deakin University, Burwood, Australia, <sup>2</sup>Department of Medicine, Western Hospital, The University of Melbourne, Melbourne, Australia, <sup>3</sup>Musculoskeletal Research Centre, La Trobe University, Heidelberg, Australia, <sup>4</sup>Biomedical Engineering, Indiana University-Purdue University, Indianapolis, IN, USA.

For full text see presentation #SA537

### WG8

**High Impact Exercise May Have a Protective Effect on BMD but Moderate Impact Exercise May Have Negative Effect in Young Women with Anorexia Nervosa.** E. J. Vaughn<sup>1</sup>, D. E. Beaton<sup>\*2</sup>, P. Cote<sup>\*3</sup>, B. Woodside<sup>\*4</sup>, G. A. Hawker<sup>1</sup>. <sup>1</sup>Osteoporosis, Women's College Hospital, Toronto, ON, Canada, <sup>2</sup>Mobility Program, St. Michael's Hospital, Toronto, ON, Canada, <sup>3</sup>Rehabilitation Solutions, University Health Network, Toronto, ON, Canada, <sup>4</sup>Psychiatry, University Health Network, Toronto, ON, Canada.

For full text see presentation #M324

### WG9

**Can Impact Exercise Mitigate the Adverse Effects of Oral Contraceptives on Bone?** J. M. Welch<sup>1</sup>, N. C. Laroche<sup>\*1</sup>, S. M. Kaiser<sup>2</sup>. <sup>1</sup>Kinesiology, Dalhousie University, Halifax, NS, Canada, <sup>2</sup>Endocrinology and Metabolism, Dalhousie University, Halifax, NS, Canada.

For full text see presentation #M488

### WG10

**Targeted Exercise against Hip Fragility.** R. Nikander<sup>1</sup>, P. Kannus<sup>\*1</sup>, P. Dastidar<sup>\*2</sup>, M. Hannula<sup>\*3</sup>, L. Harrison<sup>\*2</sup>, T. Cervinka<sup>\*3</sup>, N. G. Narra<sup>\*3</sup>, R. Aktour<sup>\*3</sup>, T. Arola<sup>\*3</sup>, H. Eskola<sup>\*3</sup>, S. Soimakallio<sup>\*4</sup>, A. Heinonen<sup>5</sup>, J. Hyttinen<sup>\*3</sup>, H. Sievänen<sup>1</sup>. <sup>1</sup>UKK Institute, Tampere, Finland, <sup>2</sup>Radiology, Regional Medical Imaging Center, Tampere University Hospital, Tampere, Finland, <sup>3</sup>Biomedical Engineering, Tampere University of Technology, Tampere, Finland, <sup>4</sup>Radiology, Regional Imaging Center, Tampere University Hospital, Tampere, Finland, <sup>5</sup>Health Sciences, University of Jyväskylä, Jyväskylä, Finland.

For full text see presentation #SA533



## VITAMIN D WORKING GROUP

### WG11

**Improved Motor Performance in Vitamin D Deficient Mice with VDRMs.** L. Porras\*, Q. Zeng\*, R. L. Cain\*, K. Stayrook\*, L. Burris\*, M. Carson\*, J. Dodge\*, J. Andrews\*, H. U. Bryant, M. Sato, Y. L. Ma. Eli Lilly and Company, Indianapolis, IN, USA.

For full text see presentation #SU196

### WG12

**The Protective Actions Of Vitamin D Analogs In The Vascular Calcification Of Chronic Kidney Disease (CKD).** S. Mathew\*, F. Strebeck\*, K. A. Hruska. Pediatrics, Washington University, St. Louis, MO, USA.

For full text see presentation #SU450

### WG13

**A Key Mechanism Underlying the Immunosuppressive Effects of Vitamin D: 1,25dihydroxyvitamin D<sub>3</sub> Is a Transcriptional Modulator of IL-17.** S. Joshi\*<sup>1</sup>, S. Youssef\*<sup>2</sup>, S. Gaffen\*<sup>3</sup>, L. Steinman\*<sup>2</sup>, S. Christakos\*<sup>1</sup>. <sup>1</sup>Biochemistry, UMDNJ-NJMS, Newark, NJ, USA, <sup>2</sup>Neurology, Stanford University, Stanford, CA, USA, <sup>3</sup>SUNY Buffalo School of Dental Medicine, Buffalo, NY, USA.

For full text see presentation #F246

## WORKING GROUP ON PATIENT EDUCATION AND ADHERENCE TO TREATMENT

### WG14

**Adherence in Patients with Severe Osteoporosis Treated with Teriparatide.** V. Ziller\*, S. Zimmermann\*, P. Hadji. University Hospital Giessen and Marburg, Marburg, Germany.

For full text see presentation #M384

### WG15

**Interventions to Improve Adherence and Persistence with Osteoporosis Medications: A Systematic Literature Review.** T. Gleeson\*, M. Iversen\*, D. H. Solomon. Brigham and Women's Hospital, Boston, MA, USA.

For full text see presentation #M370

### WG16

**Osteoporosis Therapy following Bone Densitometry - Patient Expectations as Determinants of Drug Initiation and Persistence.** D. Brask-Rasmussen\*<sup>1</sup>, S. M. Cadarette\*<sup>2</sup>, P. Eskildsen\*<sup>1</sup>, B. Abrahamsen\*<sup>3</sup>. <sup>1</sup>Department of Endocrinology, Køge University Hospital, Køge, Denmark, <sup>2</sup>Division of Pharmacoepidemiology and Pharmacoeconomics, Brigham and Women's Hospital, Harvard Medical School, Boston, MA, USA, <sup>3</sup>Department of Endocrinology, Copenhagen University Hospital, Gentofte, Denmark.

For full text see presentation #M377

### WG17

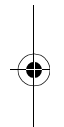
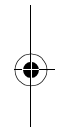
**8 year Fracture & Mortality Outcomes of the Fracture Liaison Service That Provides Systematic Assessment for Prevention of Secondary Fractures to All Patients Age 50+ With New Low-trauma Fractures.** A. R. McLellan, M. Fraser\*. Medical Sciences, Western Infirmary, Glasgow, United Kingdom.

For full text see presentation #SU324

### WG18

**Predictors of Self-Reported Non-Persistence with Oral Bisphosphonates Due to Perceived Side Effects or Other Reasons.** J. T. Schousboe, B. Dowd\*, M. Davison\*, P. Johnson\*, R. L. Kane\*. Univ of Minn, Minneapolis, MN, USA.

For full text see presentation #M378



## PEDIATRIC BONE AND MINERAL WORKING GROUP

### WG19

**Bone Status Evaluation in Pre-Pubertal Children with Cystic Fibrosis.** N. Haddad<sup>\*1</sup>, M. Howenstine<sup>\*1</sup>, M. Peacock<sup>2</sup>, L. A. DiMeglio<sup>1</sup>. <sup>1</sup>Pediatrics, Indiana School of Medicine, Indianapolis, IN, USA, <sup>2</sup>Medicine, Indiana School of Medicine, Indianapolis, IN, USA.

For full text see presentation #SU486

### WG20

**Bone Strength In Overweight Children Is Adapted to Mechanical Loads From Walking, But Is Low For Higher Loading Activities.** S. A. Novotny<sup>\*1</sup>, R. J. Wetzsteon<sup>2</sup>, K. A. Pickett<sup>\*1</sup>, J. M. Hughes<sup>1</sup>, J. M. Cousins<sup>\*1</sup>, M. A. Petit<sup>1</sup>. <sup>1</sup>Kinesiology, University of Minnesota, Minneapolis, MN, USA, <sup>2</sup>Pediatrics, Children's Hospital of Philadelphia, Philadelphia, PA, USA.

For full text see presentation #M482

### WG21

**Effects of Serum Factors During Osteoblast Differentiation - Implication for the Pathogenesis of Osteoporosis in Crohn's Disease.** M. Blaschke<sup>\*1</sup>, A. Hell<sup>\*2</sup>, R. Koepf<sup>\*1</sup>, D. Raddatz<sup>1</sup>, N. Schuetze<sup>3</sup>, N. Miosge<sup>\*4</sup>, G. Salinas-Riester<sup>\*5</sup>, H. Siggelkow<sup>1</sup>. <sup>1</sup>Gastroenterology and Endocrinology, University Medicine of Goettingen, Goettingen, Germany, <sup>2</sup>Orthopedics, University Medicine of Goettingen, Goettingen, Germany, <sup>3</sup>Orthopaedic Center for Musculoskeletal Research, University of Wuerzburg, Wuezburg, Germany, <sup>4</sup>University Medicine of Goettingen, Goettingen, Germany, <sup>5</sup>Molecular Cell Biology, University Medicine of Goettingen, Goettingen, Germany.

For full text see presentation #M450

### WG22

**Use of Bone Biomarkers as an Endpoint in a Pediatric Study of Alendronate.** E. von Scheven<sup>1</sup>, C. M. Gordon<sup>2</sup>, D. Wypij<sup>\*2</sup>, M. Chagomerana<sup>\*2</sup>, J. Shepherd<sup>3</sup>, M. Wertz<sup>\*1</sup>, L. Bachrach<sup>4</sup>. <sup>1</sup>Pediatrics, UCSF, San Francisco, CA, USA, <sup>2</sup>Pediatrics, Harvard University, Boston, MA, USA, <sup>3</sup>Radiology, UCSF, San Francisco, CA, USA, <sup>4</sup>Pediatrics, Stanford University, Stanford, CA, USA.

For full text see presentation #SU488

### WG23

**Advanced Vertebral Compression at Diagnosis among Children with Acute Lymphoblastic Leukemia.** L. M. Ward<sup>1</sup>, M. Matzinger<sup>\*1</sup>, N. Alos<sup>2</sup>, S. Atkinson<sup>3</sup>, C. Clarkson<sup>\*4</sup>, R. Couch<sup>\*5</sup>, E. Cummings<sup>\*6</sup>, F. H. Glorieux<sup>7</sup>, R. Grant<sup>\*8</sup>, J. Halton<sup>\*1</sup>, B. Lentle<sup>\*9</sup>, H. Nadel<sup>9</sup>, C. Rodd<sup>7</sup>, K. Siminoski<sup>\*5</sup>, D. Stephure<sup>\*10</sup>, S. Taback<sup>\*11</sup>, N. Shenouda<sup>\*1</sup>, F. Rauch<sup>7</sup>, ... and the Canadian STOPP Consortium<sup>\*12</sup>. <sup>1</sup>Univ of Ottawa, Ottawa, ON, Canada, <sup>2</sup>Univ de Montréal, Montréal, QC, Canada, <sup>3</sup>McMaster Univ, Hamilton, ON, Canada, <sup>4</sup>Univ of Western Ontario, London, ON, Canada, <sup>5</sup>Univ of Alberta, Edmonton, AB, Canada, <sup>6</sup>Dalhousie Univ, Halifax, NS, Canada, <sup>7</sup>McGill Univ, Montréal, QC, Canada, <sup>8</sup>Univ of Toronto, Toronto, ON, Canada, <sup>9</sup>Univ of British Columbia, Vancouver, BC, Canada, <sup>10</sup>Univ of Calgary, Calgary, AB, Canada, <sup>11</sup>University of Manitoba, Winnipeg, MB, Canada, <sup>12</sup>Canadian Pediatric Bone Health Working Group, Ottawa, ON, Canada.

For full text see presentation #SU478

## ADULT BONE AND MINERAL WORKING GROUP

### WG24

**A case presentation: Bisphosphonate induced Osteonecrosis of the Jaw in Pagetic Jaw Bone.** M. Adams<sup>1</sup>, K. Adams<sup>1</sup>, A. Freemont<sup>2</sup>. <sup>1</sup>Bolton NHS Primary Care Trust, Bolton, UK, <sup>2</sup>The University of Manchester, Manchester UK

Bisphosphonate induced Osteonecrosis of Jaw in is a rare condition in patients except for those who are on high doses in the treatment of malignancy. We would like to report what appears to be the first case of Bisphosphonate induced Osteonecrosis of Jaw in Pagetic bone. The patient was an 86-year-old lady who had been treated for pain related to Paget's disease of the bone. An isotope bone scan had shown polyostotic Paget's disease including involvement of the whole of the maxilla. She was treated with oral Risedronate 30 mg daily but had to stop after 6 weeks because of gastrointestinal adverse effects. She was then treated with IV Pamidronate but because of difficult venous access only two infusions of 60 mg were administered. A few months later she had difficulty removing a partial upper right denture, which was finally removed after 3 days. Shortly after, pieces of the upper jawbone began to come loose and fall out - two pieces with a tooth attached. (photograph). She also noted food appearing in the back of her nose. The patient attended the Department of Rheumatology at Bolton in 2006 when she produced the jaw fragments asking for someone to dispose of them. Histology of these dry fragments showed evidence of Paget's disease of bone. (photomicrograph). She refused any debridement there being visible loose bone in the gum. No further bisphosphonates were given and the maxillary defect slowly healed although a piece of jaw bone fell out about 2 years later. The defect to the palate closed and the patient has remained well now being able to eat comfortably although she cannot be fitted with any denture.

### WG25

**Diffuse Sclerosing Osteomyelitis of the Mandible: Case Report and Literature Review.** A. L. Schafer, R. Silva<sup>\*</sup>, M. Yafai<sup>\*</sup>, D. Shoback. San Francisco VA Medical Center and University of California, San Francisco, San Francisco, CA, USA.

Osteonecrosis of the jaw is a serious complication of bisphosphonate therapy and highlights the need for greater understanding of bisphosphonate effects on oral bone. We evaluated a patient with diffuse sclerosing osteomyelitis of the mandible (DSOM), for which there are reported dramatic improvements after IV bisphosphonate therapy. DSOM is a chronic inflammatory condition with intermittent, acute flares of pain and swelling in the absence of pus or fistulae. Response to conventional treatment with antibiotics is transient. Frequent flares lead to pain and progressive loss of oral function. A 51 year-old man presented to the Oral and Maxillofacial Surgery Department with 3 years of recurrent pain and swelling of the left mandible. Repeated biopsies, debridements, and cultures failed to isolate a causative organism, although he had a modest clinical response to clindamycin. He had no history of endocrine or metabolic bone disorder. Examination showed diffuse left facial swelling, redness, warmth, and tenderness and marked trismus. CT showed cortical irregularity, destruction, and sclerosis of the left mandible. Technetium scan showed marked uptake in the left mandible. ESR and high-sensitivity CRP were elevated at 31 mm/hr (nl 0-15) and 41.9 mg/L (nl 0.2-7.5), respectively. Clindamycin and analgesics were increased, but symptoms continued unabated, and eventually he was admitted to the hospital for IV pain management. After literature review disclosed potential benefit from IV bisphosphonates, he received pamidronate 60mg IV. In 2 days, jaw swelling and pain decreased markedly. After 5 days, he had complete resolution of symptoms and remains without recurrence 3 months later. There are 7 reports of DSO treated with IV or oral bisphosphonates, 6 of them cases of DSOM (3 children, 3 adults), and one trial with 10 patients. There are 3 cases of DSO of the femur and/or tibia. The 2 adults and 2 of the 3 children who received IV bisphosphonates for DSOM had resolution and lasting remissions. The third child developed mouth ulcers and increased pain and swelling. In the randomized trial of IV clodronate vs. placebo for DSOM, there was no difference in immediate pain relief between the 2 groups, but there was statistically significant decreased pain intensity 6 months after clodronate therapy (vs. placebo), without adverse events. Our patient with DSOM had a dramatic response to pamidronate, similar to patients in the literature. This case highlights the importance of accurate oral pathologic diagnosis and the need for greater understanding of mandibular bone disorders, especially the role of suppressing bone turnover in controlling inflammation and sclerosis in DSOM.

## WG26

**Bisphosphonate-associated Femoral Fracture: Implications for Management.** N Napoli, R Armamento-Villareal Div. of Bone and Mineral Diseases, Washington University Sch. Of Med.

Recent reports of femoral shaft fractures in patients on long-term bisphosphonates (BPs) with biopsy evidence of severely suppressed bone turnover raised important concerns on the safety for this class of drugs. Patients with malignant skeletal conditions, such as multiple myeloma are potentially especially at risk for this complication considering the dose and the duration of treatment with BPs that these patients are subjected to. In this report we describe the case of 56 year-old woman who was referred for evaluation at the Bone Clinic of Washington University because of a recent left femoral shaft fracture. Her history revealed that she had a stem cell transplant in Nov. 1999 for multiple myeloma. After the transplant, she was put on high dose steroids and pamidronate infusions at 30 mg monthly for 2 years followed by zoledronate infusions at 4 mg monthly for 4 years. This was discontinued because of concerns for osteonecrosis of the jaw and increasing serum creatinine. One and a half years later, she developed a left femoral shaft fracture (Figure 1A) while trying to get up from a squatting position. She underwent an intramedullary fixation of the left femur but insertion of the rod literally resulted in "splitting" of the fractured bone (Figure 1B). Follow-up x-rays showed poor healing and non-union of the fractured bones even at 6 months after surgery. Serum calcium, alkaline phosphatase, 25-hydroxyvitamin D, and thyroid stimulating hormone were normal. Serum creatinine was elevated at 1.9 ng/ml. Bone mineral density was normal in the femur and mildly low in the lumbar spine. An attempt to do a bone biopsy was unsuccessful due of the inability of the biopsy needle to penetrate the "rock-hard" iliac crest.

The above case illustrates a potential problem in the management of patients with skeletal fragility fractures from prolonged BPs. Bone X-rays from these patients may appear normal, as shown in our patients x-ray, but these bones appear to be biomechanically compromised. Our patient had a non-traumatic fracture of the left femur which was complicated by shattering of the fractured bones during surgical repair. Paradoxically, despite the apparent bone fragility, her bones were hard and impenetrable to a needle bone biopsy suggesting the likelihood of hypermineralized bone matrix perhaps superimposed on an inactive bone turnover as a possible etiology of this complication.



## WG27

**Mathematical Model of Remodelling Cycles with Feedback Mechanism for Maintaining the Balance between Bone Resorption and Formation.** D. Putra<sup>a</sup>, R.J. Patton<sup>b</sup>, P.G. Genever<sup>c</sup>, and M.J. Fagan<sup>a</sup> <sup>a</sup> Centre for Medical Engineering and Technology, University of Hull, Hull HU6 7RX, UK. <sup>b</sup> Department of Engineering, University of Hull, Hull HU6 7RX, UK. <sup>c</sup> Department of Biology, University of York, York YO10 5YW, UK.

Since Eriksen et. al.<sup>1</sup> published reconstructed curves of the remodelling process (RP) in trabecular bone of normal human adults, similar reconstructed remodelling curves have been made available for cortical bone and for some types of pathological conditions. Some dynamic interactions between osteoblasts and osteoclasts in RP have also been reported<sup>2</sup>. In this paper we describe the development of a new mathematical model that can replicate these reconstructed remodelling curves and the observed dynamic interaction between osteoclasts and osteoblasts in RP. This will facilitate our understanding of RP and provide insights into alternative therapeutics to treat bone loss diseases. The proposed RP model is given by equations (1-3), where  $\dot{x}_i = \frac{dx_i}{dt}$ ,  $x_{oc}$  and  $x_{ob}$  are the population of the osteoclasts and osteoblasts, respectively,  $x_b$  and  $\bar{x}_b$  are the bone thickness and its reference value, respectively, while  $a, b, c, d, e, f, K_{oc}$  and  $K_{ob}$  are positive scalar parameters.  $\bar{x}_b$  is the bone thickness at the end of modelling process or the one required to withstand the mechanical loads and serves as the initial value of  $x_b$ . The term  $\bar{x}_b - x_b$  in (3) represents the feedback mechanism responsible for maintaining bone thickness at  $\bar{x}_b$  at the end of normal RP. The dynamics interaction between  $x_{oc}$  and  $x_{ob}$  given by (1-2) belongs to the Gause-type predator-prey system<sup>3</sup>. Hence, this work introduces the link between bone cell dynamics and the ecological predator-prey systems. Kuang<sup>3</sup> proved that every trajectory of the subsystem (1-2) starting at positive values of  $x_{oc}$  and  $x_{ob}$  is a periodic orbit, except its unique positive equilibrium point. Hence, the cyclic coupling between osteoclastic and osteoblastic activities is preserved. The parameter values of the model have been estimated to match the reconstructed normal trabecular bone remodelling curve<sup>1</sup> and the response of the model is shown in Figure 1. The model is also able to replicate the reconstructed remodelling cycles in hyper- and hypothyroidism, primary hyperthyroidism and in normal cortical bone by altering the model parameter values. Currently, the link between the model parameters and the biochemical processes involved in the remodelling process are being established.

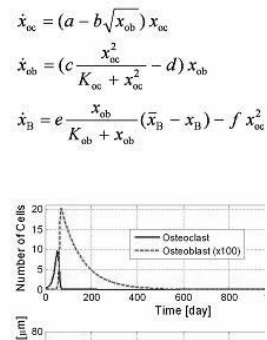


Figure 1 Remodelling cycles generated by the model

## WG28

**Non Steroid Responsive Hypercalcemia associated with Sarcoidosis- A Rapid Response to Hydroxychloroquine.** Sameera Daud MD, Sirinart Sirinvaravong MD, Angelo Licata MD

**INTRODUCTION:** Hypercalcemia is common in granulomatous disorders. About 10-20% of patients with sarcoidosis are hypercalcemic. Overproduction of 1,25-dihydroxyvitamin D [1,25(OH)<sub>2</sub>D<sub>3</sub>] by activated macrophages in the granulomas plays an important pathological role in hypercalcemia. The conventional treatment is corticosteroid therapy for a variable period of time. However, in the acute situation neither corticosteroid nor bisphosphonates work quickly enough to control the problem. Hydroxychloroquine/chloroquine (4- amino quinolone derivative), however has rapid onset as our case shows. **CASE:** 61 years old Caucasian female was transferred to The Cleveland Clinic with 3 week history of dyspnea and long standing polydipsia and polyuria. There was no significant past medical history. Physical examination was benign. Initial tests revealed Corrected calcium: 12.4 (8.5-10.5mg/dL), albumin 3.3 (3.5-5.0g/dL), creatinine 2.8 (0.7-1.4 mg/dL). Further investigations showed intact PTH <4 (10-60 pg/mL), PTH-rP <0.2, 25(OH) vitamin D 13.7 (31-80 pg/mL) and 1,25(OH)<sub>2</sub>D<sub>3</sub> 72 (22-67 pg/ml). CT chest showed extensive mediastinal and hilar lymphadenopathy with calcium deposition and scattered lung nodules (calcified nodes). Mediastinoscopy and hilar lymph node biopsy was performed. The pathology report revealed non-necrotizing granulomas, suggestive of sarcoidosis. The patient received pamidronate 60 mg intravenously on admission. Four days later prednisone (40 mg) was started. After 8 days no improvement in calcium occurred. The patient started hydroxychloroquine 100 mg to 200mg/day. After 2 days of hydroxychloroquine, calcium level decreased to 10.3 mg/dL and 1,25(OH)<sub>2</sub>D<sub>3</sub> to 60 pg/ml. The patient has reported symptomatic improvement in polyuria and polydipsia. **DISCUSSION:** We present a case of steroid nonresponsive hypercalcemia in a patient with sarcoidosis, who responded to low dose of hydroxychloroquine. The mechanism of action is not clear, but one proposed mechanism is the inhibition of ornithine decarboxylase that antagonizes the action of 1,25(OH)<sub>2</sub>D<sub>3</sub> in fusion of mononuclear cells to multinucleated giant cells. This results in impairment of granuloma formation. Regardless of mechanism of action, hydroxychloroquine has been reported to decrease the 1,25(OH)<sub>2</sub>D<sub>3</sub> levels. **SUMMARY:** The rapid response of hydroxychloroquine in these patients makes this a first line consideration since it antagonizes production of activated vitamin D, the underlying cause of the problem.

## WG29

**Hypoparathyroidism and Renal Insufficiency.** G. Palmieri<sup>1,2</sup>, T. Hodgkiss<sup>4,1</sup>, H. Williams<sup>3</sup>, J. Ahmed<sup>2,2</sup>. The West Clinic<sup>1</sup>, Endocrinology, University of Tennessee<sup>2</sup>, Methodist Hospital<sup>3</sup>, Memphis, TN, USA.

The skeletal and vascular effects of renal insufficiency in longstanding, preexisting, hypoparathyroidism (HpoP) are not well known. A 36 year (y) old African-American woman with diagnoses of primary hyperparathyroidism, diabetes mellitus, arterial hypertension and dyslipidemia developed HpoP after surgical removal of a parathyroid adenoma. The serum calcium (Ca) was 7.4 mg/dl (8.6 - 10.6) (normal ranges in parentheses), phosphorus (P) 5.9 mg/dl (2.5 - 4.5), creatinine (Creat) 0.8 mg/dl (0.8 - 1.4) and the Creat clearance 122 ml/min (91 - 130). For 14y she took ergocalciferol, calcitriol and Ca for control of paresthesias and cramps without strict medical supervision. At age 50y she was admitted with lethargy. Serum Ca was 18 mg/dl, P 4.1 mg/dl and Creat 11.6 mg/dl. She received hemodialysis resulting in some improvement of renal function. At the time of discharge, off dialysis, the serum Creat was 5.3 mg/dl and Ca 9.1 mg/dl. During the next 7y the Creat clearance ranged between 20-40 ml/min. At age 57y (Feb 2008) she was asymptomatic, her weight was 119 kg, the BMI was 45 and blood pressure 141/88. Medications: diuretics, phosphate binders, oral hypoglycemic agents, ergocalciferol 50,000 U/ month, calcitriol 0.25 mcg/bid and Ca 1,000 mg/bid. Serum electrolytes were normal, glucose was 195 mg/dl (65-110), Creat 4.4 mg/dl, ionized Ca 4.6 mg/dl (4.5-5.3), P 4 mg/dl, parathyroid hormone (PTH) <2 pg/ml (10-65), bone alkaline phosphatase 14 U/l (14-42.7), 25-hydroxyvitamin D 71 ng/ml (32-100), and urine N-telopeptide (NTX) 13 nM BCE/mM Creat (26-124). These results are compatible with a rather low degree of bone turnover. There is no history of fractures and the DXA bone densitometry was normal. A computerized tomography (CT) scan of the abdomen and pelvis showed no lithiasis or nephrocalcinosis. No calcifications were observed in the arteries of the abdomen and pelvis. Standard x-rays and CT scans of both forearms and hands showed normal bones and no evidence of Ca deposits in the arteries. Based on the known cellular Ca agonist effect of PTH, (Rasmussen et al. Ionic control of metabolism. Handbook of Physiology, section 7, vol VII: 225, 1976), which affects heart cells in uremia (Bogin et al. J Clin. Invest 67: 1215, 1981), we propose that the absence of the expected skeletal and vascular abnormalities in a patient with renal insufficiency and multiple risk factors for osteoporosis and arteriosclerosis was probably due to HpoP.

## WG30

**The potential role of Fibroblast Growth Factor -23 (FGF-23) in Chronic Kidney Disease-Mineral Bone Disorder (CKD-MBD).** P. Manghat<sup>1</sup>, J. Cheung<sup>1</sup>, D. MacDonald<sup>1</sup>, D.J.A. Goldsmith<sup>2</sup>, I. Fogelman<sup>3</sup>, A.S. Weirzbicki<sup>1</sup>, G. Hampson<sup>1</sup> <sup>1</sup> Chemical Pathology, St. Thomas' Hospital, London, <sup>2</sup> Renal Unit, Guy's Hospital, London, <sup>3</sup> Nuclear Medicine, Guy's Hospital, London, UK.

CKD-MBD is a clinical syndrome that develops as a systemic disorder of mineral and bone metabolism in CKD. FGF-23 is markedly elevated in CKD, although the driving stimulus for the increase in FGF-23 remains unclear. It is postulated that FGF-23 may play a central role in the regulation of phosphate and bone metabolism in CKD. The aim of this study was to assess firstly the predictors of circulating FGF-23 in early stage and pre-dialysis CKD and secondly the relationship between FGF-23 and bone metabolism. We studied 145 ambulant patients (85 M and 60 F) (age mean [SD] 53 [14] years). Forty one patients had CKD 1,2 (eGFR >60 ml/min; mean [SD] 78 [14]), 59 patients had CKD 3 (eGFR 30-59 ml/min; mean [SD] 45 [8]) and 45 patients had CKD 4 (eGFR <30 ml/min; mean [SD] 21[4]). Bone Mineral Density (BMD) and Bone Mineral Content (BMC) were measured at the lumbar spine (LS), femoral neck (FN), forearm (FA) and total hip (TH) by DXA. Serum PTH, FGF-23, 25 (OH) vitamin D, Bone Alkaline Phosphatase (BAP), Tartrate- Resistant Acid Phosphatase (TRAP), high sensitivity CRP (hs-CRP) were determined. Calcium Phosphate Product (CPP) was derived. Univariate analyses and multiple linear regression models were used. Non-parametric data were log-transformed. In the whole population, univariate analysis showed significant relationship between FGF-23 and CPP ( $r = 0.31$ ,  $p = 0.0002$ ), hs-CRP ( $r = 0.21$ ,  $p < 0.02$ ), Serum phosphate ( $r = 0.34$ ,  $p < 0.0001$ ), fractional excretion of phosphate ( $r = 0.29$ ,  $p = 0.0005$ ), eGFR ( $r = -0.40$ ,  $p < 0.0001$ ) and haemoglobin ( $r = -0.35$ ,  $p < 0.0001$ ). There was no significant correlation between PTH and FGF-23 ( $r = 0.15$ ,  $p = 0.08$ ). Following correction for confounders in a multivariate model, age ( $p < 0.05$ ), eGFR ( $p = 0.001$ ), CPP ( $p < 0.0001$ ) and hs-CRP ( $p < 0.0001$ ) remained significant independent predictors of FGF-23 and explained 45% of the variance in the circulating levels. Patients with CKD 3 and 4 had significantly higher FGF-23 ( $p < 0.002$ ), PTH ( $p < 0.0001$ ), BAP ( $p < 0.05$ ) and TRAP ( $p < 0.005$ ) compared to CKD 1 and 2. Univariate analysis between FGF-23 and bone metabolism showed significant negative association with BMD ( $r = -0.28$ ,  $p < 0.005$ ) and BMC ( $r = -0.24$ ,  $p = 0.008$ ) of the hip. No correlation was found between FGF-23 and the bone turnover markers. Significant correlations were observed between PTH and BAP ( $r = 0.45$ ,  $p < 0.0001$ ) and TRAP ( $r = 0.37$ ,  $p < 0.0001$ ). Multivariate analysis showed that FGF-23 ( $p < 0.05$ ) and TRAP ( $p = 0.057$ ) were associated with hip BMC.

In summary, circulating FGF-23 is significantly associated with the CPP and hip BMC in patients with CKD. FGF-23 may play a role in the pathogenesis of CKD-MBD.

## WG31

**Late Presentation of Autosomal Dominant Hypophosphatemic Rickets.** Nelson B. Watts<sup>1</sup>, Erik A. Imel<sup>2</sup>, Michael J. Econs<sup>2</sup> <sup>1</sup>Bone Health and Osteoporosis Center, Cincinnati, OH, USA, <sup>2</sup>Indiana University School of Medicine, Indianapolis, IN, USA.

A 34-year-old woman, previously healthy, complains of muscle and joint pain (8 on a scale of 10) and fatigue that began about 6 months ago. She is a member of large, previously published kindred with autosomal dominant hypophosphatemic rickets (ADHR), and her sister is affected. In 1994, this patient's serum phosphate was 2.6 mg/dL with tubular maximum reabsorption of phosphate per deciliter glomerular filtrate (TmP/GFR) 2.8 mg/dL. In 2002, she participated in continued evaluation of this kindred. She had grown normally without leg deformities (height was 63.5 inches). On a questionnaire, she reported a past history of tooth abscesses, root canal and chronic bone and joint pain. At that time her serum phosphorus was normal (2.8 mg/dL), (TmP/GFR) 2.5 mg/dL, alkaline phosphatase 81 U/L, C-terminal FGF23 97 RU/mL (normal <149 RU/mL), and intact FGF23 was 51 pg/mL (normal <71 pg/mL). Mutation detection indicated an FGF23 mutation resulting in an amino acid change, R176Q. She was not on treatment for ADHR. On current exam she appeared depressed and had mild proximal muscle weakness. Laboratory results revealed serum calcium 8.8 mg/dL, parathyroid hormone 79 pg/mL, serum magnesium 1.9 mg/dL, serum phosphorus 1.3 mg/dL, TmP/GFR 0.9 mg/dL, 25-hydroxyvitamin D 23 ng/mL, 1,25-dihydroxyvitamin D 19 pg/mL. During hypophosphatemia, intact FGF23 concentration was elevated at 117 pg/mL.

Treatment was started with calcitriol, ergocalciferol and phosphorus supplements. Within a month her serum phosphorus was normal but her symptoms were worse. Doses of calcitriol and phosphorus were increased. Within three months her serum phosphorus remained normal and her symptoms had completely resolved.

This case illustrates the variable nature of ADHR, with initial features sometimes occurring in childhood or adulthood. The biochemical and clinical phenotype appear to wax and wane, and may resolve completely for years. The clinical course of presentation is likely determined by the FGF23 concentrations at that particular time. The mechanism for alteration in FGF23 concentrations is unclear. Since the FGF23 mutation induces resistance to cleavage, the likely mechanism for the observed change in levels is altered gene expression or translation. One would therefore expect that all subjects would be able to down regulate FGF23 and avoid clinical disease. Since this is clearly not the case, there may be additional factors influencing the ability to

control FGF23 concentrations in this population.

A nuclear medicine bone scan, ordered by her rheumatologist, demonstrated multiple areas of increased uptake thought to be consistent with metastatic carcinoma, which caused considerable anxiety for the patient. Without a family history of ADHR, this patient's presentation might suggest tumor induced osteomalacia; however, considering FGF23 mutations in adult patients with hypophosphatemia and renal phosphate wasting may avoid a costly search for tumors.

## WG32

**Opioid-induced Osteoporosis: Delayed Bone Healing and Compression Fractures in a Man with Chronic Narcotic Use.** Rose Christian, MD, Endocrine Unit, University of Vermont College of Medicine, Burlington, VT.

History: Orthopedic surgery requested an endocrine consultation on a 60 yo white man with non-union after vertebral fusion surgery and vertebral compression fractures of T11 and T12 detected on CT scan performed post-operatively to assess integrity of hardware. The patient complained of back pain, depressed mood, low libido, fatigue and muscle weakness that had progressed in severity for one year prior to admission. He was unemployed due to disability, and ambulatory but sedentary. He had no history of height loss, falls, fractures or kidney stones. He took morphine sulfate and oxycodone daily for back pain, but denied alcohol or tobacco use. He denied past or present use of oral, iv, inhaled or intrathecal glucocorticoids. He had no history of malnutrition, malabsorption, malignancy, HIV infection, renal, pituitary or testicular disorders. His past medical history was notable for stable coronary disease post-CABG, obesity, hypertension and depression. Laboratory (serum, fasting morning values): Total T 56 ng/mL, LH 1.0 mIU/mL, FSH <0.3 mIU/mL, prolactin 10.6 ng/mL, total 25-OH- vitamin D 12 ng/mL, calcium 9.7 mg/dL, phosphorus 3.3 mg/dL, magnesium 2.3 mg/dL, creatinine 0.9 mg/dL, cortisol 24 mcg/dL, iPTH 57 pg/mL. Discussion: Hypogonadism in men is associated with low bone density and sarcopenia and is a risk factor for both falls and fractures. Hypogonadotropic hypogonadism is a recently recognized complication of chronic opioid use in both men and women (1, 2). Low bone density was detected in 83% of methadone users (3), and fracture risk was increased in a case-control study of oral narcotic users (4). Opioid-induced hypogonadotropic hypogonadism may contribute to poor bone quality and should be suspected in opioid-dependent patients with fracture non-union or bone graft failure.

## WG33

**Calciophylaxis in a patient with hypoparathyroidism and normal kidney function.** Leonardo P. J. Oliveira MD, Sameera Daud MD, Leann Olansky MD, Angelo Licata, MD, PhD

Introduction: Calciophylaxis (CP) has been known as a medical entity related to renal replacement therapy and hypercalcemic states. Recent reports demonstrate that poor kidney function and calcium abnormalities are not a requirement. Other reported etiologies include malignancy, alcoholic disease, and warfarin therapy. We wish to report a case of a 76 year old white female with type 2 diabetes (DM), post surgical hypothyroidism, coronary artery disease (CAD), atrial fibrillation (AF) on oral anticoagulation, transferred to our institution with a 3 month history of a painful ulcerative lesion in her left lower extremity. Patient (pt) was on warfarin, calcitriol, calcium carbonate, gemfibrozil, levothyroxine and insulin. Skin biopsy revealed extensive fat necrosis and calcium deposits in subcutaneous vessels compatible with CP. Laboratory tests revealed corrected calcium of 8.35 mg/dL (8.5-10.), phosphate 3.9 mg/dL (2.5-4.5), PTH 5 mg/dL (10-60), creatinine 1.1 mg/dL (0.7-1.4), PTH-rp < 0.2, 25(OH) vitamin D 57.3 pg/mL (31-80) and 1,25(OH)2D3 18 pg/mL (22-67), complement levels and rheumatologic workup was normal but homocysteine 22 umol/L (3.4-12.9), CRP 10.4 mg/dL (0 - 2), uric acid 11 mg/dL (2 - 7.0) and factor VIII assay 223% (49 - 134%) were elevated while Protein C was 66% (76-147%) although the patient was on coumadin. A CT of the abdomen revealed non-obstructing renal calculi and a CT of the brain demonstrated a small left parietal cortical infarct in addition to multiple paraneural calcifications. The pt was started on phosphate binders to reduce phosphate levels, Vit B and folic acid supplements to lower homocysteine and allopurinol for the elevated uric acid. Discussion: We present a case of rare disease in a unique context. This is the first case report of a patient with hypoparathyroidism and CP. Hypocalcemia, low calcium X phosphorus product, absence of rheumatological disease and malignancy, raises the question of the etiology of CP. Warfarin use could be a potential etiology however the prolonged use makes coumadin-induced skin necrosis unlikely. Despite a normal kidney function, elevated homocysteine and uric acid levels have been linked to arterial calcifications.

In summary: Calciophylaxis is an aggressive necrotic ulceration which may be related to novel factors such as hyperuricemia and homocysteinemia. Further studies are required to evaluate if therapy against directed against these metabolites will be beneficial.

## PHYSICAL ACTIVITY AND FALLS WORKING GROUP

### WG34

**Non-Steroidal Anti-Inflammatory Use and the Response of Bone to Exercise.** D. W. Barry<sup>1</sup>, R. E. Van Pelt<sup>\*2</sup>, C. M. Jankowski<sup>\*2</sup>, P. Wolfe<sup>\*3</sup>, W. M. Kohrt<sup>2</sup>. <sup>1</sup>General Internal Medicine, University of Colorado Denver, Aurora, CO, USA, <sup>2</sup>Geriatric Medicine, University of Colorado Denver, Aurora, CO, USA, <sup>3</sup>Preventive Medicine and Biometrics, University of Colorado Denver, Aurora, CO, USA.

For full text see presentation #M472

### WG35

**The Effect of Exercise on Geometric Bone Structure and Bone Strength in Postmenopausal Women - A Systematic Review and Meta-Analysis of Randomized Controlled Trials.** I. Polidoulis<sup>1</sup>, J. Beyene<sup>\*2</sup>, A. Cheung<sup>3</sup>. <sup>1</sup>Family and Community Medicine, University of Toronto, Toronto, ON, Canada, <sup>2</sup>Biostatistics, University of Toronto, Toronto, ON, Canada, <sup>3</sup>Osteoporosis, University Health Network, Toronto, ON, Canada.

For full text see presentation # M484

### WG36

**Femur from C57BL/6 and DBA/2 Inbred Mice Display a Strain Dependent Response to Treadmill Running and Tower Climbing Exercise in Cortical and Trabecular Bone Architecture.** D. H. Lang, H. M. Preston<sup>\*</sup>, A. C. Henry<sup>\*</sup>, N. A. Sharkey. Kinesiology, Pennsylvania State University, University Park, PA, USA.

For full text see presentation # M485

### WG37

**Treadmill Exercise Provides Only Short-Term Protection Against Cancellous Bone Loss with Reduced Dietary Energy Intake: Endocrine Mechanisms.** S. N. Swift<sup>1</sup>, K. Baek<sup>1</sup>, M. J. De Souza<sup>2</sup>, S. A. Bloomfield<sup>1</sup>. <sup>1</sup>Intercollegiate Faculty of Nutrition, Health & Kinesiology, Texas A&M University, College Station, TX, USA, <sup>2</sup>Kinesiology, Pennsylvania State University, University Park, PA, USA.

For full text see presentation # SA449

### WG38

**The Association Between Falls and Health-Related Quality of Life (HRQoL).** J. McPetridge<sup>\*1</sup>, E. Barrett-Connor<sup>2</sup>, S. G. Sajjan<sup>\*3</sup>, T. Fan<sup>\*3</sup>, P. D. Miller<sup>4</sup>, S. S. Sen<sup>\*3</sup>, E. S. Siris<sup>5</sup>. <sup>1</sup>Lehigh University, Bethlehem, PA, USA, <sup>2</sup>University of California, San Diego, La Jolla, CA, USA, <sup>3</sup>Merck & Co., Inc, Whitehouse Station, NJ, USA, <sup>4</sup>Colorado Center for Bone Research, Lakewood, CO, USA, <sup>5</sup>Columbia University Medical Center, New York, NY, USA.

For full text see presentation # SU420

## WORKING GROUP ON RHEUMATIC DISEASES AND BONE

### WG39

**Direct Correlation of Osteocyte Deformation with Calcium Influx in Response to Fluid Flow Shear Stress.** A. R. Bonivitch<sup>1</sup>, L. F. Bonewald<sup>2</sup>, J. Ling<sup>\*1</sup>, J. X. Jiang<sup>3</sup>, D. P. Nicolella<sup>1</sup>. <sup>1</sup>Southwest Research Institute, San Antonio, TX, USA, <sup>2</sup>University of Missouri at Kansas City School of Dentistry, Kansas City, MO, USA, <sup>3</sup>University of Texas Health Science Center, San Antonio, TX, USA.

For full text see presentation # SA057

### WG40

**Low Intensity Pulsed Ultrasound Synergistically Modulates SOST and OPG/RANKL Ratio in MLO-Y4 Osteocytes *in vitro*.** D. Liu. Orthodontics, Marquette University, Milwaukee, WI, USA.

For full text see presentation #M109

### WG41

**Multiple WNT Signaling Antagonists Are Differentially Expressed Over Time In Inflammatory Arthritis.** N.C. Walsh, C.A. Manning, S. Reinwald<sup>\*</sup>, K.W. Condon<sup>\*</sup>, S. Karmakar, D.B. Burr<sup>\*</sup>, E.M. Gravalles. Department of Medicine, University of Massachusetts Medical School, Worcester, MA 01605; <sup>\*</sup>Department of Anatomy and Cell Biology, Indiana University School of Medicine, Indianapolis, IN 46202

Rheumatoid Arthritis (RA) is characterized by inflammation of the joint lining (synovium) resulting in destruction of bone. Despite treatment, most RA patients do not repair erosive lesions. We have used the K/BxN serum transfer arthritis (STA) model to investigate the hypothesis: cells present within arthritic soft tissues produce factors that impact osteoblast differentiation and/or function, contributing to net bone loss. We have shown that formation of mineralized bone is reduced at bone surfaces adjacent to inflammation compared to bone surfaces adjacent to normal bone marrow, indicating that inflammation affects osteoblast capacity to form mineralized bone. Active WNT signaling is requisite for osteoblast differentiation and function. Recently, blockade of the WNT signaling antagonist DKK1 in mouse models of inflammatory arthritis resulted in protection from erosion<sup>1</sup>. We have previously shown that the WNT signaling antagonist sFRP1 is upregulated in arthritic soft tissues. We now demonstrate that additional WNT signaling antagonists are differentially expressed over time within arthritic soft tissues in STA. Expression of mRNAs for WNT signaling antagonists (assessed by quantitative RT-PCR) in arthritic soft tissues was compared to expression in tissues isolated from the same sites in non-arthritic mice. DKK1, DKK3, sFRP1, and sFRP2 mRNA expression was elevated in arthritic tissues. sFRP1 and sFRP2 mRNA expression was highest (20 fold, sFRP1; 35 fold, sFRP2) at days 7 and 8 post initial serum injection, corresponding to increasing inflammation and the onset of focal bone erosion within nearby bones. DKK1 mRNA expression peaked later in the time course of arthritis, with highest expression occurring around day 12 when inflammation and focal bone erosion is typically at its peak. DKK3 mRNA expression was elevated throughout the time course of arthritis. Interestingly, expression of mRNA for sFRP4, a WNT signaling antagonist that has been implicated in the inhibition of mineralization, was dramatically upregulated late in the time course of arthritis in tissues isolated from focal bone erosion sites. These studies demonstrate the expression of multiple WNT signaling antagonists within arthritic tissues over the course of STA. Thus inhibitors of the WNT signaling pathway are candidate factors for modulating osteoblast capacity to form mineralized bone, potentially limiting repair of focal bone erosions in RA.

## Key Word Index

## ASBMR 30th Annual Meeting

## Numeric

## 13910C&gt;T

13910C>T LCT promoter polymorphism in the Spanish population, M265

 $\alpha_v$ -/-

High dose of RANKL rescues integrin  $\alpha_v$ -/- osteoclast phenotype, F081

## 1p36

Linkage and association study of chromosome 1p36 with BMD in southern Chinese, SU295

## 1q

Genetic locus on chromosome 1q influences bone loss in young Mexican American adults, M250

## 2p

Childhood cortical bone and skeletal age show bivariate genetic linkage to chromosome 2p, 1177

## 3.6 Col I

Identification and characterization of 3.6 Col I positive cells from mouse temporomandibular joint, SU132

## 6b N-terminal

Enrichment of type XI collagen and 6b N-terminal domain at sites of mineral nucleation within osteoblastic cultures, SA070

## 7B2

7B2 protein mediated inhibition of DMP1 cleavage in osteoblasts enhances FGF-23 production in *Hyp*-mice, 1053

## 7F2

Characterization of osteoblastic properties of 7F2 and UMR-106 cultures after acclimation to reduced levels of fetal bovine serum, SU041

## 7p15

Familial humeroradioulnar synostosis maps to chromosome 7p15, M251

19-nor-2a-(3-hydroxypropyl)-1a,25-(OH)<sub>2</sub>D<sub>3</sub>

Mechanism of enhanced 19-nor-2a-(3-hydroxypropyl)-1a,25-(OH)<sub>2</sub>D<sub>3</sub> anti-cancer activity in prostate cancer cells, M216

## A

**A allele at Valine80 of the CYP19 gene is a risk factor for aromatase inhibitors associated bone loss, 1021**

**A disintegrating and metalloprotease (ADAM). See ADAM**

## a1H

Assessment of changes in thoracic and lumbar vertebrae in T-type Ca<sub>v</sub>3.2 (a1H) VSCC KO mice, M170

## A214V

G171V and A214V Lrp5 knock-in mice have increased bone mass and strength, and can help precisely define the in vivo functions of Lrp5 during bone growth and homeostasis, 1002

## A986S

CaSR gene A986S polymorphisms: relation to bone loss and urine Ca in a Spanish early postmenopausal women population, M255

## Abdominal aortic calcification (AAC)

AAC detected on lateral DXA spine images is associated with coronary artery disease, 1035

## Absorptiometry, 3D x-ray (3D-XA)

In vivo measurements of vertebral body dimensions by 3D-XA and their relation with age, M316

## Absorptiometry, dual energy x-ray (DXA)

AAC detected on lateral DXA spine images is associated with coronary artery disease,

1035

Accuracy of Cobb angle measurement with iDXA, SU484

Areal BMD by DXA may predict similar risk of fracture in elderly women and men due to offsetting effects of bone size and true volumetric BMD, SU267

BMD measurement by DXA after a fragility fracture increases the likelihood of subsequent osteoporosis treatment, SU296

Comparison of HR-pQCT to DXA and QUS for the assessment of ex-vivo bone strength, M466

Consistency in measurement assessments in different models of Norland DXA scanners, SA307

Contribution of the vertebral posterior elements in anterior-posterior DXA scans, 1180

Correlation between DXA Femur Strength Index and QUS Heel Stiffness Index in Chinese women, M464

Establishing healthy body composition values with DXA, SU366

Femoral BMD and femoral structure, assessed by DXA-based hip structural analysis, contribute independently to femoral strength, M304

Generating 3D finite element models of a human proximal femur from 2D DXA data, M467

HSA based on DXA data in women with postmenopausal osteoporosis receiving once-monthly oral IBN for 12 months, SA507

Low calcaneal BMD estimated by a peripheral DXA heel scanner is associated with a high risk to have had a distal radius fracture, SU262

Performance of QUS in comparison to DXA for prediction of prospective fractures among older men and women, 1240

Prevalence of vertebral compression fracture deformity by x-ray absorptiometry in patients selected according to simple clinical tests, SU261

Protocol for pediatric proximal femur DXA analysis, M506

Ten-year fracture risk assessment in Norland-based equipment in a Chinese population, SU253

Three methods of lumbar spine DXA analysis as a means to predict male fracture, 1131

Validation of bone mineral measurements on the new Norland Model XR-600 and XR-800 using the BMIL QA/QC Phantom, SU252

What happens to the availability of DXA if physicians stop performing them in their offices?, SU256

## Absorptiometry, radiographic

6819 analysis on measurement of BMD of phalanges by radiographic absorptiometry in Beijing, SA313

## AC-100

AC-100 promotes cartilage repair and subchondral bone healing in surgically induced cartilage defects, SA111

## Acanthopanax senticosus

Effects of *Acanthopanax senticosus* extract on bone metabolism in Korean postmenopausal women, SA431

## ACE-011

Soluble activin receptor type IIA fusion protein, ACE-011, increases bone mass by stimulating bone formation and inhibiting bone resorption in cynomolgus monkeys, SU376

## Acid excretion

Association of urine measures of diet-derived acid excretion with bone loss and fractures, SU283

## Acid-ash hypothesis

Osteoporosis and the acid-ash hypothesis, SA331

## Acidic, serine- and aspartate-rich motif (ASARM)

MEPE C-terminal ASARM-peptide, promotes hypophosphatemia, bone defects and increases adiposity, F207

PEHEX cleavage of SIBLING-ASARM peptides as a mechanism underlying osteomalacia in XLH, 1199

Transgenic ASARM-peptide overexpression with reduced serum phosphate and 1,25(OH)<sub>2</sub>D<sub>3</sub> leads to decreased BMD and obesity, F210

## Acidification, lysosomal

Acidosis augments the resorptive capacity of human osteoclasts by increasing lysosomal acidification, M122

## Acidosis

Acidosis augments the resorptive capacity of human osteoclasts by increasing lysosomal acidification, M122

## Acinetobacter

Colistin-impregnated bone cement beads prevent multi-drug resistant *Acinetobacter* osteomyelitis, M236

## Acini

Ectopic Runx2 expression disrupts normal acini structure in mammary epithelial cells, F279

## Activating transcription factor 4 (ATF4)

Role of ATF4 in osteoblast proliferation and survival, M079

## Activin

Activin A mediates MM bone disease which is reversed by RAP-011, a soluble activin receptor, 1231

Soluble activin receptor type IIA fusion protein, ACE-011, increases bone mass by stimulating bone formation and inhibiting bone resorption in cynomolgus monkeys, SU376

**Acute lymphoblastic leukemia (ALL). See Leukemia**

## ACVR1

ACVR1 knock-in mouse model for FOP, 1203

Hypoxia promotes ligand-independent activation of the ACVR1 (R206H) mutant receptor in C2C12 cells, M243

## ADAM8

Novel splicing variants of ADAM8 stimulate tumor-induced bone metastasis by increasing invasion and osteoclastogenesis, F286

## ADAM15

Deletion of ADAM15 decreases osteoblast differentiation and bone formation in vitro, M073

## ADAMTS

Analysis of long bone fracture nonunion by an expression profile of the MMPs and ADAMTS enzyme families, M235

## ADAMTS-7

ADAMTS-7, a direct targeting molecule of PTHrP, is a novel potent mediator of chondrogenesis, 1262

## ADAMTS18

GWAS and subsequent replication studies identified ADAMTS18 and TGFBR3 as novel osteoporosis risk genes, 1093

## Adenine

Altered regulation and expression of FGF-23 in the adenine-induced uremic rat model, SU178

Comparison of 1,25(OH)<sub>2</sub>D<sub>3</sub> and calcitriol effects in an adenine-induced model of CKD reveals differential control over serum Ca and phosphate, SU448

## Adenoma, atypical parathyroid

Immunohistochemical and genetic characterization of the atypical parathyroid adenoma, M432

## Adenomatous polyposis coli (Apc)

Apc-mediated control of  $\beta$ -catenin is essential for both chondrogenic and osteogenic differentiation of skeletal precursors, SA130



**Adenosine monophosphate, cyclic (cAMP)**

- Adenylyl cyclase 6 mediates primary cilia-regulated decreases in cAMP in bone cells exposed to dynamic fluid flow, 1040
- Association between Cx43 and  $\beta$ -arrestin is required for cAMP-dependent osteoblast survival induced by PTH, 1227
- Expression profiles of Wnt signaling pathway components in response to cAMP stimulation at different stages of osteoblast maturation, M040
- PTH induces COX-2 in MC3T3-E1 osteoblasts via cAMP-PKA and Ca-calciueurin pathways, SA033

**Adenovirus**

- Establishment of a murine model of HCa by overexpression of sRANKL using an adenovirus vector, SU082

**Adenylyl cyclase 6**

- Adenylyl cyclase 6 mediates primary cilia-regulated decreases in cAMP in bone cells exposed to dynamic fluid flow, 1040

**Adipocytes**

- Adipocyte-secreted protein URB is a potent stimulator of bone formation, F006
- Effect of resveratrol and flax oil on MC3T3-L1 pre-adipocyte and ST2 BMSC proliferation and differentiation, SU059
- Expression of NF- $\kappa$ B ligand and regulation of osteoclastogenesis by bone marrow adipocytes, SA078
- Mature human adipocytes differentiated from BMSCs, SA042
- Primary human bone marrow adipocytes stimulate osteoclast differentiation, M111
- Quantitative  $\mu$ CT imaging of adipocyte volume in bone marrow of mice with high and low bone mass, SU250
- TGF $\beta$  suppresses adipocytic differentiation and enhances accumulation of stromal cells in myeloma bone lesions, SA294
- Transactivation of RANKL by C/EBP $\beta$  and C/EBP $\delta$  in adipocyte lineage cells, SU092
- VEGF and PTEN regulate bone homeostasis via control of osteoblastogenesis, osteoclastogenesis and adipocyte differentiation, M029

**Adipocytokine**

- Model of high body mass: BMD, bone markers and adipocytokine levels in high level male rugby players, SA167

**Adipogenesis**

- Chemerin and CMKLR1 expression and function in human bone marrow MSC adipogenesis, SU165
- FGF-1 inhibits adipogenic differentiation and transdifferentiation of human MSCs, M075
- High concentrations of hydroxytyrosol and quercetin antioxidants enhance adipogenesis and inhibit osteoblastogenesis in MSCs, SA037
- Mapping the interrelationship of the adipogenic and osteogenic lineage with visual reporters, M097
- Targeted expression of SOX9 in hypertrophic chondrocytes leads to enhanced adipogenic activity and spontaneous OA in transgenic mice, SA115

**Adipokines**

- Obesity is associated with higher BMD, lower bone resorption and slower hip bone loss: are these associations mediated by adipokines?, SU369
- Relationship between adipokines and biochemical bone markers in osteoporotic women before and after GH supplementation, M289

**Adiponectin**

- Adiponectin inhibits osteoclast formation via AKT signaling pathway, SU110

**Adipose-derived stem cells (ASC). See Stem cells****Adiposity**

- MEPE C-terminal ASARM-peptide, promotes hypophosphatemia, bone defects and increases adiposity, F207

**Adrenergic receptors**

- Aging dependent and independent effects of b2 adrenergic receptor signaling on bone formation induced by intermittent PTH treatment in female mice, SA378
- Double deletion of  $\alpha$ 2a- and  $\alpha$ 2c-adrenergic receptors results in a phenotype of high bone mass and in resistance to the thyrotoxicosis-induced osteopenia, F244

**Adrenocorticotrophic hormone (ACTH)**

- Human osteoblasts synthesize VEGF in response to ACTH, SA236

**Adrenomedullin (ADM)**

- (22-52) ADM prevents systemic bone loss related to inflammation in mice, SA493
- Opposing effects on bone metastases of tumor ADM expression in breast and prostate cancer, M277

**Adynamic bone disease (ABD)**

- Association of the marker of ABD with malnutrition-inflammation complex in hemodialysis patients, SU446
- Kidney dysfunction disturbs collagen maturation in ABD as assessed by confocal laser Raman spectroscopy, SU439

**AEBSF**

- Serine protease inhibitor AEBSF blocks transcription of Phex by osteoblasts, M053

**AF-1**

- Specific inactivation of AF-1 in ER $\alpha$  results in growth plate closure while total inactivation of ER $\alpha$  results in increased growth plate width in elderly female mice, 1181

**AG490**

- AG490, a Jak2 specific inhibitor, induces osteoclast survival by activating Akt and ERK signaling pathway, SU108

**Age Gene/Environment Susceptibility (AGES) Study**

- Prediction of incidental low trauma limb fractures in older men and women with QCT variables of bone and muscles in mid-thigh, F369
- Proximal femoral fragility and age-related white matter lesions by brain MRI in elderly subjects, 1096

**Aggrecanases**

- Betulin down regulates IL-1 $\alpha$ -stimulated aggrecanases and MMP gene expression in human chondrocytes, M147

**Aging**

- AAC detected on lateral DXA spine images is associated with coronary artery disease, 1035
- Acute change in iCa directly affects bone formation independent of PTH action during hemodialysis, SU437
- Advanced hip assessment and BMD in Japanese women with OA, M449
- Age-related impairment of IGF-I receptor activation is associated with changes in integrin and SHP-2 expression, M096
- Aged and young adult BALB/c male mice respond similarly to in vivo tibial compression, M475
- Aging dependent and independent effects of b2 adrenergic receptor signaling on bone formation induced by intermittent PTH treatment in female mice, SA378
- Albuminuria, 25(OH)D, 1,25(OH) $_2$ D, and intact PTH in older adults, SU442
- Analysis of long bone fracture nonunion by an expression profile of the MMPs and ADAMTS enzyme families, M235
- Anti-fall efficacy of oral supplemental Vitamin D and active Vitamin D, SU423
- Antioxidants (phytoestrogens and quercetin) are potential agents against RA, SA487
- Application of a treatment algorithm to avoid BMD loss and limit bisphosphonate use after kidney and kidney/pancreas transplantation, SA497
- Association between several factors affecting aortic calcification and BMD in postmenopausal women, SA489

- Association between vascular calcification and low total femur BMD in elderly people community-dwelling, SU453
- Association of FHH and mandible lesions in two kindreds, M427
- Biomechanical impact of chronic hemodialysis on bones and muscles, SU269
- Bisphosphonates in children with hypercalciuria and reduced BMD, M429
- BMSC aging directly alters bone formation, 1252
- Bone fragility is increased in the MKR type 2 diabetic mouse, M440
- Bone histomorphometry in patients with Crohn's Disease, SU462
- Bone metabolism in long-term kidney transplantation recipients, SA499
- Bony symptoms and vertebral fractures in GD1: data from the 105 patients of the French Observatoire on Gaucher Disease, SA466
- Calorie restriction prevents age-related trabecular bone loss via SIRT-1, 1251
- Cardiovascular manifestations of mild PHPT, 1034
- Change of pathological bone lesion in recipients with renal osteopathy after renal transplantation, SA498
- Changes in cardiovascular function after parathyroidectomy in mild PHPT, M434
- Changes in marrow cell dynamics and bone geometry with aging in TSP-2 null mice, 1249
- Clinical outcome in elderly with proximal femur or humerus fractures in an orthogeriatric rehabilitation unit, SU329
- Clinical usefulness of measurement of FGF-23 in hypophosphatemic patients, SA470
- Clinically useful paradigm for interpretation of serum 25(OH)D levels with simultaneously measured PTH levels, M437
- Coactivator MBF1 binds to JunD and protects its transcriptional activity against oxidative stress to prevent age-related suppression of osteoblast differentiation, 1248
- Common genetic factors contribute to the relationship of body composition and bone mass in mouse populations, M244
- Comparison of 1,25(OH) $_2$ D $_3$  and calcitriol effects in an adenine-induced model of CKD reveals differential control over serum Ca and phosphate, SU448
- Comparison of 2D and 3D subchondral bone texture parameters in severe OA knees, M302
- Comparison of intravenous and intramuscular neridronate regimens for the treatment of PDB, SA481
- Cortical and trabecular microarchitecture in HIV-infected postmenopausal women, SU458
- Decreasing calcidiol (25OHD3) in serum is related to impaired function and increased mortality in the elderly, SU204
- Deficiency of the nucleocytoplasmic shuttling protein CIZ suppresses K/BxN serum-induced model of RA, M446
- Determinants of low BMD in HIV infected postmenopausal women, SU455
- Different influence of the clinical condition, degree of cholestasis, alcohol abuse and serum Ca on the musculoskeletal system in chronic cirrhotics, M411
- Diffuse sclerosing osteomyelitis of the mandible, WG25, M452
- Discordance in femoral neck bone density in subjects with OA, M453
- Does dietary P influence FGF-23 concentrations in FD patients?, M426
- Effect of aquatic exercise and education on improving indices of fall risk in older adults with hip OA, M441
- Effect of exercise on geometric bone structure and bone strength in postmenopausal women, M484
- Effects of 50,000 IU of Vitamin D $_2$  twice per month on circulating 25(OH)D and Ca levels, SU426

## Key Word Index

## ASBMR 30th Annual Meeting

- Effects of ADT on bone health in prostate cancer, SA280
- Effects of aromatase inhibitor therapy on BMD in hypogonadal elderly men, 1135
- Efficacy and safety of intravenous ZOL in the treatment of patients with resistant PDB, SA479
- Elevated SIF levels in post-menopausal women is due to the enhanced release of fluoride from bone, SA490
- Endogenous GC are critical for the development of skeletal fragility with aging in mice, 1250
- Evaluation of clinical utility of venous sampling for FGF-23 in identifying and confirming responsible tumors for TIO, F163
- Evidence of increase in vertebral body dimensions in postmenopausal women with osteoporosis, M313
- Femoral strength, bone density, and aging in women and men, 1165
- Fracture risk in primary biliary cirrhosis: role of osteopenia and severity of cholestasis, M442
- Glomerular filtration rate and physical function in community-dwelling Japanese frail elders, SA332
- Hemodialysis patients rapidly lose their bone minerals after 60 years of age, SU438
- Histomorphometric evaluation in an experimental model of hepatic osteodystrophy, M480
- Hormonal influences on volumetric bone density and geometric properties in obesity, SU367
- Improved forearm BMD after treatment with Vitamin D<sub>3</sub> in a patient 30 years after bariatric surgery, SA492
- Increased caloric intake in energy deficient exercising with functional hypothalamic amenorrhea women is associated with decreased ghrelin and increased bone formation, SU184
- Increased proinflammatory cytokines TNF $\alpha$  and IL-6 correlate with pathological bone turnover markers in diabetic patients with acute Charcot foot, F491
- Increased risk of morphometric vertebral fracture in postmenopausal women with PHPT, M438
- Influence of hip flexor or knee extensor muscle strength on spinal sagittal alignment or falls, SU454
- Interactions between obesity, CVD and bone formation, M451
- Interventions to prevent falls in the community-dwelling elderly, SU313
- Jumping mechanography safely evaluates muscle performance in older adults, SA535
- Kidney disease is associated with abnormal cortical geometry independent of age and gender, SU441
- Kidney dysfunction disturbs collagen maturation in ABD as assessed by confocal laser Raman spectroscopy, SU439
- Late presentation of ADHR, WG31
- Loss or gain of FoxO function in osteoclasts and osteoblasts alters the rate of apoptosis and BMD in mice, 1247
- MACD index is a strong predictor of cardiovascular death and include the predictive power of BMD, SU463
- Marked Vitamin D deficiency in recent heart and liver transplant recipients, SA501
- Mechanism of action of the anti-aging agent resveratrol on bone, 1136
- Muscle power and tibial bone strength in older women, SU362
- New data on the impact of renal function on the relationship between 25(OH)D and PTH, 1031
- Novel hypothesis explains the syndrome of chronic musculoskeletal pain and comorbid painful healed fracture sites in Vitamin D deficiency, SA474
- Osteopenia by high alcohol consumption in the absence of ALDH2 attribute to the disturbance of the differentiation in osteoblasts, M326
- Osteopenia in CKD: effects of Ca overload, SU449
- Osteoporosis in the aging males after hip fracture, SU436
- Osteoporosis in the old old: review of the evidence, SA437
- Overexpression of GSR in osteoblasts decreases bone formation and partially prevents OVX-induced bone loss, F024
- Patients with CKD and low 1/3 radius and femoral neck BMD have markedly abnormal cortical and trabecular microstructure by HR-pQCT, 1033
- PDB: a histologic and histomorphometric analysis of bone biopsies from 754 patients, 1133
- Plasma osteocalcin is inversely related to fat mass and plasma glucose in elderly Swedish men, SU459
- Possible role for the T<sub>H</sub>17 system in a mouse model of AS, SU460
- Postprandial hyperphosphatemia is a novel risk factor for CVD by involving endothelial dysfunction, SU443
- Premature aging-like phenotypes in Mta1 null mice, F494
- Pretransplant parathyroid function predicts laboratory and BMD changes after kidney and kidney/pancreas transplantation, 1032
- Prevalence and demographics of asymptomatic NPHPT in the United States, M431
- Prevalence and factors associated to the presence of vertebral fractures in patients with type 2 diabetes mellitus, M447
- Prevalence of Vitamin D deficiency among surgical orthopedic patients, SU205
- PTH increases bone turnover in HPT, F485
- PTH reverses abnormal bone remodeling and structure in HPT, 1036
- Randomized dose comparison of pamidronate in children with types III and IV OI, SU496
- Rare cases of XLH rickets/osteomalacia mimicking ARHR/osteomalacia, F469
- Recovery from HCAO following anti-viral treatment, F488
- Reduced serum osteocalcin and sex hormone binding globulin in men with type II diabetes, SU461
- Regional thinning of the femoral neck cortex with advancing age predisposes to hip fracture, SU275
- Rehabilitation after clinically-diagnosed osteoporotic vertebral fracture, SU411
- Relationship among nutritional status, oxidative stress and bone density in institutionalized elderly, SU310
- Relationship between low bone mass and aortic valve sclerosis in Korean men and women, SU452
- Renal leak hypercalciuria: a potential cause of tertiary hyperparathyroidism, M430
- rhBMP-2 accelerates segmental defect healing in diabetic rats, M445
- Risk factors for bone loss in the hip in 70-year-old women, SA374
- Scl-Ab increases bone mass by stimulating bone formation and inhibiting bone resorption in a hindlimb-immobilization rat model, 1138
- Serum 25(OH)D measurement and histomorphometric analysis of iliac crest biopsies from 1180 patients reveals a high prevalence of Vitamin D-dependent osteomalacia, 1134
- Serum Cathepsin K levels in AS, M439
- Serum uOC concentration are related to renal function in type 2 diabetes patients, M443
- Short-term deleterious skeletal response to hindlimb suspension involves multifaceted compromises in cells of the osteogenic lineage, F523
- SIF levels among hemodialysis patients are positively associated with levels of serum phosphate and intact PTH, SU440
- Stimulation of fracture healing by rhPDGF-BB combined with  $\beta$ TCP/collagen matrix in a diabetic rat fracture model, 1137
- Stress fracture and vertebral osteosclerosis related to fluorosis induced by excessive gingival topical fluoride application, M444
- Therapy with ALF leads to a significant increase in muscle power and balance, SU444
- TPTD treatment in a young man with IJO diagnosis, SU499
- Vitamin D deficiency is associated with diminished quality of life based on Qualeffo-41 questionnaire analysis, SU424
- Vitamin D deficiency, osteomalacia and high bone turnover in patients with NF-1, F465
- Vitamin D insufficiency is common in racially diverse postmenopausal women with HIV, M448
- Vitamin D status and bone remodeling marker CTx-I in patients with early RA: association with disease activity and joint damage, SA496
- Vitamin D status in severely obese individuals can be predicted by demographic and lifestyle factors, SU201
- Vitamin D toxicity due to a commonly available remedy from the Dominican Republic, SU195
- Ahnak**  
Ahnak regulates Ca signaling and ATP release in osteoblasts in response to mechanical stimulation, SA027
- Akp2-/-**  
Enzyme replacement therapy prevents dental defects in the Akp2-/- mouse model of infantile HPP, F107  
Relative efficacy of "treating" versus "preventing" infantile HPP in Akp2-/- mice by enzyme replacement therapy, 1054
- AKT**  
Adiponectin inhibits osteoclast formation via AKT signaling pathway, SU110
- Akt**  
AG490, a Jak2 specific inhibitor, induces osteoclast survival by activating Akt and ERK signaling pathway, SU108  
Akt regulates skeletal development through GSK3, mTOR, and FoxOs, 1151  
BMP-2-stimulated signaling niche in osteoblasts comprising of Smad and PI3K/ Akt regulates NFATc1 expression and its nuclear translocation, 1081
- (Ala-Gly)n**  
(Ala-Gly)<sub>n</sub> sequences configured silk protein scaffold induces osteoblast differentiation and bone formation via increased Cbfa1 and Osx expression, M167
- Ala459Pro**  
Functional polymorphism in COL1A2 (Ala459Pro) that is associated with intracranial aneurysms, shows heterozygous disadvantage concerning BMD and stroke in elderly men, SU219
- Albright's hereditary osteodystrophy**  
Hypothyroidism and autism combined with PHP in the absence of Albright's hereditary osteodystrophy and GNAS imprinting changes, SA259
- Albuminuria**  
Albuminuria, 25(OH)D, 1,25(OH)<sub>2</sub>D, and intact PTH in older adults, SU442
- Alcohol**  
Bone metabolism, microarchitecture and densitometric measurement in rat femur after chronic alcohol consumption, M239  
Different influence of the clinical condition, degree of cholestasis, alcohol abuse and serum Ca on the musculoskeletal system in chronic cirrhotics, M411  
Osteopenia by high alcohol consumption in the absence of ALDH2 attribute to the disturbance of the differentiation in osteoblasts, M326
- ALDH2**

Osteopenia by high alcohol consumption in the absence of ALDH2 attribute to the disturbance of the differentiation in osteoblasts, M326

#### **Alendronate (ALN)**

Active controlled, non-inferiority study to compare the effect of ZT-031 with ALN on the incidence of new vertebral fractures, M347

ALN affects cross-talk of osteoclasts and osteoblasts in vivo, SU392

ALN transiently impairs removal of alveolar bone and healing of the root socket after tooth extraction in rats, 1275

ALN treatment for juvenile osteoporosis, M366

ALN treatment in postmenopausal Romanian women followed by BMD-digital x-ray radiogrammetry, M357

Assessment of serum Ca and bone resorption markers in patients transitioned from ALN to DMAB, M394

Atypical osteoclast phenotype after long-term ALN therapy for osteoporosis, SU399

BMP/Wnt antagonists are upregulated by DEX in osteoblasts and reversed by ALN and PTH: potential therapeutic targets for GIO, M098

Changes in serum PINP in orchidectomized osteopenic rats treated with PTH and ALN, M295

Continuous local infusion of ALN prevents osteopenia of the lengthened segment during distraction osteogenesis, SU001

Cost-effectiveness of RIS vs. generic ALN, SA423

Does ALN use prevent kyphosis progression in older women?, SA410

Effect of DMAB vs ALN on bone turnover markers and BMD changes at 12 months based on baseline bone turnover level, 1285

Effects of ALN and RLX on the RANKL/OPG system in primary cultures of human osteoblasts, M101

Effects of ALN or DMAB on cortical and trabecular bone mass, bone strength, and bone mass-strength relationships in mice, 1139

Effects of co-treatment with an Scl-Ab and ALN in OVX rats, 1213

Effects of DMAB vs ALN on BMD, bone turnover markers, and safety in women previously treated with ALN, M395

Fracture reduction during two years of treatment with RIS or ALN, SA404

Hip structural analysis and volumetric QCT in postmenopausal women from the PaTH Study: mono- or combination therapy with ALN and PTH, M306

Histomorphometric changes by TPTD in ALN pre-treated women with osteoporosis, 1019

Increased non-enzymatic glycation of cancellous bone due to decrease in remodeling during ALN therapy of osteoporotic women, 1071

Monthly intravenous ZOL suppresses tissue-level remodeling significantly more than daily oral ALN in the mandible and rib of skeletally mature female dogs, SU388

Prevention of GC-induced osteoporosis with ALN or ALF in patients with ophthalmologic diseases, SA450

Reduced osteoclastogenesis and RANKL expression in marrow from women taking ALN, SU400

RIS has a more rapid onset of remodeling suppression than ALN in rabbit vertebral trabecular bone, SU387

sGGT is one of the factors that determines the response to ALN treatment in osteoporotic women, M421

Sites of femoral fractures in the Fracture Intervention Trial (FIT) of ALN and its Long-term Extension (FLEX), SU389

Subtrochanteric and diaphyseal femur fractures in patients treated with ALN, 1026

Therapeutic effects of one-year ALN treatment in three cases of osteoporosis with parietal thinning, M410

Towards an understanding of the mechanism of femur strength improvement by ALN in postmenopausal women, F323

TPTD versus ALN for treatment of GIO, 1171

Transition from ALN to DMAB in OVX cynomolgus monkeys maintained or improved cortical and trabecular bone mass, without altering the linear relationship between bone mass and bone strength, 1072

Transition from ALN to DMAB resulted in further reductions in local and systemic bone turnover parameters and reduced cortical porosity in OVX cynomolgus monkeys, 1216

Treatment discontinuation due to gastrointestinal adverse events and decreased BMD in patients switched from branded ALN to generic ALN, SA414

Use of bone biomarkers as an endpoint in a pediatric study of ALN, SU488

#### **ALERT System**

Electronic medical record based "ALERT System" improved diagnosis and treatment of osteoporosis in orthopaedic out-patient clinic, SU416

#### **Alfacalcidol (ALF)**

ALF ameliorates bone dynamics in senescence-accelerated SAMP6 mice and in fracture repair rat model, SU394

ALF prevents aromatase inhibitor (letrozole)-induced bone mineral loss in young growing female rats, SA570

Assessment of adherence to treatment of osteoporosis with RLX and/or ALF in postmenopausal Japanese women, M387

Effect of RLX and ALF on bone and joint pain assessed by fall of skin impedance (electroalgotometry), SA384

Effects of ALF on bone and skeletal muscle in GC-treated rats, M219

Prevention of GC-induced osteoporosis with ALN or ALF in patients with ophthalmologic diseases, SA450

Superiority of ALF over plain Vitamin D in men with osteoporosis, SU421

Therapy with ALF leads to a significant increase in muscle power and balance, SU444

#### **Alkaline phosphatase (ALP)**

C-telopeptide and bone ALP predict morphometric vertebral fracture risk in a pivotal Phase III trial of TOR in men on ADT, 1292

Development of a bone specific ALP assay on the IDS Automated Analyser 3x3™, SA302

Li affects matrix mineralization by decreasing tissue non-specific ALP levels in osteoblasts, SA071

Prostaglandins enhance extracellular matrix mineralization through the enhancement of both Na-dependent phosphate transport activity and ALP activity in osteoblast-like cells, SU031

Proteoliposomes carrying ALP and NPP1 as matrix vesicle mimetics, SA061

SOST blocks GSK3-beta inhibitor-induced ALP activity, SU036

Stable expression of constitutively active Ga12 in osteoblastic cells promotes matrix protein expression and ALP activity, M068

TNF $\alpha$  and IL-1 $\beta$  stimulate ALP activity and mineralization but decreases RUNX2 expression and osteocalcin secretion in human MSC, SU044

#### **Alkaline phosphatase, tissue-nonspecific (TNSALP)**

Altered TNSALP expression and phosphate regulation contribute to reduced mineralization in mice lacking androgen receptor, SU181

c.1250A>G, p.N417S is a common American TNSALP mutation involved in all clinical forms of HPP, including pseudo-HPP, SA566

Ca intake and serum bone formation markers are associated with the functional single nucleotide polymorphism in the TNSALP gene, SU308

Specific inhibitors of TNSAP's pyrophosphatase activity suppress medial arterial calcification, M142

#### **Alkalosis**

Metabolic alkalosis transition in renal proximal tubule cells facilitates an increase in CYP27B1, while blunting responsiveness to PTH, M196

#### **Alkaptonuria (AKU)**

Studies on the deposition of ochronotic pigment in AKU reveal tyrosine metabolism in human chondrocytes, M166

#### **All-trans-retinoic acid. See also Vitamin A**

All-trans-retinoic acid (Vitamin A) increases expression of MafB and inhibits osteoclast formation by interfering with differentiation of osteoclast progenitor cells, M117

#### **Allergies, nutritional**

Bone health impairment in children with chronic Ca and Vitamin D deficiency due to nutritional allergies, SU503

#### **ALOX12**

Polymorphisms of the ALOX12 gene are associated with increased risk of osteoporotic fracture, SU220

#### **Alternative medicine**

Use of alternative medicine for treating osteoporosis in Korea, SA390

#### **Alveolar bone**

ALN transiently impairs removal of alveolar bone and healing of the root socket after tooth extraction in rats, 1275

Enhanced osteogenic potential of alveolar vs. long bone derived BMSC, M095

Improvement of alveolar bone quality by local bFGF injection—histological and cellular biological analysis in a rabbit model, SA162

Isolation and characterization of osteoblasts from alveolar bones of aged donors, SU049

#### **Amenorrhea, hypothalamic**

Increased caloric intake in energy deficient exercising with functional hypothalamic amenorrhea women is associated with decreased ghrelin and increased bone formation, SU184

#### **Amino acids**

Screening the PHEX gene in a large cohort of hypophosphatemic rickets allowed the description of a missense mutation not responsible for the disease on a highly conserve amino acid residue, M246

Stable isotopic labeling of amino acids in cultured human BMSC: application to BMP-2 induced Wnt/ $\beta$ -catenin signaling, SA036

#### **AMP-activated protein kinase (AMPK)**

Neuroendocrine activation of AMPK in osteoblasts, SU037

Regulation of autophagy in the epiphyseal growth plate by AMPK and mTOR requires HIF-1, SU134

#### **Androgen deprivation therapy (ADT)**

C-telopeptide and bone ALP predict morphometric vertebral fracture risk in a pivotal Phase III trial of TOR in men on ADT, 1292

Effects of ADT on bone health in prostate cancer, SA280

#### **Androgen receptor**

Altered TNSALP expression and phosphate regulation contribute to reduced mineralization in mice lacking androgen receptor, SU181

Androgen receptor disruption increases the osteogenic response to mechanical loading in male mice, 1140

Crosstalk between androgen receptor and Wnt signaling mediates sexual dimorphism during bone mass accrual, 1121

Osteoblastic androgen receptor regulates cortical BMD, 1122

## Key Word Index

## ASBMR 30th Annual Meeting

Overexpression of androgen receptor in mature osteoblasts and osteocytes inhibits osteoblast differentiation, SU192

**Androgens**

Elevated androgens are associated with increased bone formation in premenopausal exercising oligomenorrheic women, SU191  
PINP, a new available rat bone formation marker: usefulness in osteopenia studies due to androgen lack and IBN treatment, SA299  
Treatment threshold in men on androgen deprivation therapy: T-score vs. FRAX, F308

**Angiogenesis**

Angiogenic potential of osteoclasts, SU075  
Identification and characterization of angiogenesis-inducing secretory molecules from osteogenically differentiated MSC, M163  
Impaired angiogenesis and compromised fluid volume accompanies increased osteoblast and osteocyte apoptosis with GC excess, SA453  
Inhibition of MM growth and preservation of bone with combined radiotherapy and anti-angiogenic agent, SA285  
Osteogenic cell lineages show differential responsiveness to angiogenic signals, SU061  
Overexpression of the transcriptional cofactor Lbh impairs angiogenesis and endochondral bone formation during fetal bone development in chickens, SU004  
Point mutation of endofin at PP1c-binding domain induces angiogenesis and bone formation in mice by sensitizing BMP signaling, I082

**Angiopoietin-1 (Ang-1)**

Ang-1 enhanced BMP-2 induced osteoblast differentiation, SU035

**Angiotensin II**

Angiotensin II type 2 receptor blockade increases bone mass, SU007

**ANKH**

ANKH mutation causing CMD inhibits osteoclast differentiation, SU214

**Ankylosing spondylitis (AS)**

Possible role for the T<sub>H</sub>17 system in a mouse model of AS, SU460  
Serum Cathepsin K levels in AS, M439

**Annexin II (AXII)**

Role of AXII and AXIIR in homing MM cells in the bone marrow, SA287

**Annexin II receptor (AXIIR)**

Role of AXII and AXIIR in homing MM cells in the bone marrow, SA287

**Anorexia nervosa**

BMD changes over time associated with illness and recovery in young women with anorexia nervosa, SA558  
Bone mass recovers in young women with anorexia nervosa who are both weight and menstrual recovered, F339  
Effect of bed rest on bone turnover in adolescents hospitalized for anorexia nervosa, SA559  
High impact exercise may have a protective effect on BMD but moderate impact exercise may have negative effect in young women with anorexia nervosa, M324

**Anterior cruciate ligament (ACL). See Ligament****Anti-resorptive treatment**

One year of TPTD treatment increases hip strength in subjects with recent history of anti-resorptive treatment, F396

**Anti-sclerostin monoclonal antibody (Scl-Ab)**

Effects of co-treatment with an Scl-Ab and ALN in OVX rats, I213  
Increases in BMD observed with Scl-Ab treatment are reversible, I211  
Scl-Ab increases bone formation and decreases bone resorption in distal tibial metaphyseal trabecular bone in OVX rats, F394  
Short treatment with Scl-ab can inhibit bone loss in an ongoing model of colitis, I212

**Antiaromatase therapy**

BMD and vertebral fracture in women with breast cancer and antiaromatase therapy, SA400

**Antioxidants**

Antioxidants (phytoestrogens and quercetin) are potentials agents against RA, SA487

**Antiresorptive agents**

Association between BMD change, use of antiresorptive agents and fragility fracture in women and men, SA364  
Previous antiresorptive agents use did not hinder the increase of bone turnover marker in TPTD use, M351

**Antiresorptive treatment**

Biomechanical and geometrical property changes in rat tibias with tumor-induced osteolysis after anti-resorptive or anti-cancer treatments, SU236

**AOD9604**

Anabolic skeletal effects of a GH-derived peptide (AOD9604) in the OVX rat model of osteoporosis, SU373

**Aortic calcification**

Association between several factors affecting aortic calcification and BMD in postmenopausal women, SA489

**AP-1**

AP-1 and Mitf interact with NFATc1 to stimulate Cat K promoter activity in osteoclast precursors, SA076

**aP2**

Tracking adipose differentiation in vitro with aP2-GFP reporters and flow cytometry: lipid staining and macrophage mimicry, SU057

**Apert Syndrome**

Dynamic morphological changes in the skulls of mice mimicking human Apert Syndrome resulting from gain-of-function mutation of FGFR2 (P253R), SA248

**Apheresis**

Frequent apheresis for platelet and plasma donations constitutes an independent risk factor for decreased BMD, F327

**Apoptosis**

bFGF induces the expression of a subset of Bcl-2 family genes to inhibit the apoptosis of ATDC5 chondroprogenitor cells, SU043  
Bisphosphonate protect cartilage by reducing chondrocyte apoptosis and reduce bone loss by suppressing osteoclast in adjuvant arthritis, M428  
Conditional knockout of the CaSR in osteoblasts alters regulators of Wnt signaling, delays cell differentiation, and promotes apoptosis in bone, I156  
Fat suppresses osteoblast differentiation by soluble factors that induce apoptosis, M003  
GIP inhibits glucose-induced apoptosis of bone cells, M011  
Impaired angiogenesis and compromised fluid volume accompanies increased osteoblast and osteocyte apoptosis with GC excess, SA453  
Lentiviral shRNA mediated inhibition of Grx5 expression induces apoptosis via a mechanism involving increased ROS and cardiolipin oxidation, and reduced SOD activity, M009  
Loss or gain of FoxO function in osteoclasts and osteoblasts alters the rate of apoptosis and BMD in mice, I247  
LPA enhances the viability of rat growth plate chondrocytes through the inhibition apoptosis and the promotion of cellular maturation, SU156  
Molecular mechanisms involved in PTH-induced apoptosis in Caco-2 intestinal cells, M189  
Osteoblasts apoptosis is mediated through GSK3 $\beta$ , M005  
Overexpression of CCN2/CTGF in cartilage shows prolonged bone length resulting from stimulation of chondrogenesis, chondrocyte growth, apoptosis, and bone mineralization during endochondral ossification, M153

Phosphate induced apoptosis in growth plate chondrocytes via a NO and JNK-dependent pat, SA113

Phosphate regulates chondrocyte differentiation, proliferation and apoptosis in a model of embryonic endochondral bone formation, SU124

Regulation of hypertrophic chondrocyte apoptosis, M158

Sr ranelate protects osteoblasts from apoptosis independently of the CaSR, M007

TGF $\beta$ 1 induces human osteoclast apoptosis, SU078

**Aromatase inhibitors**

A allele at Valine80 of the CYP19 gene is a risk factor for aromatase inhibitors associated bone loss, I021  
Effect of tamoxifen and aromatase inhibitors on the risk of fractures in women with breast cancer, SU227  
Effects of aromatase inhibitor therapy on BMD in hypogonadal elderly men, I135  
Prevention of aromatase inhibitor-associated bone loss in women with breast cancer, M283

 **$\beta$ -arrestin**

Association between Cx43 and  $\beta$ -arrestin is required for cAMP-dependent osteoblast survival induced by PTH, I227  
PTHr1 stimulates bone formation through a distinct  $\beta$ -arrestin dependent pathway independent of G protein activation, I226

**Arthritis**

In the absence of NF- $\kappa$ B, TNF induces osteoclast formation in vivo independent of RANKL/RANK and more severe arthritis in TNF-Tg mice, I009  
Subcutaneous administration of salmon calcitonin: bone protective effect in adjuvant arthritis prevention model in rats, SA193

**Arthritis, adjuvant**

Bisphosphonate protect cartilage by reducing chondrocyte apoptosis and reduce bone loss by suppressing osteoclast in adjuvant arthritis, M428

**Arthritis, collagen-induced (CIA)**

Grape seed extract suppresses IL-23/Th17 inflammatory pathways and bone destruction in CIA, SU093

**Arthritis, inflammatory**

IL-27/WSX-1 signaling inhibits RANKL-induced osteoclastogenesis through STAT1 activation: a possible involvement in TLR4/MyD88-mediated inflammatory arthritis, SU102

Multiple WNT signaling antagonists are differentially expressed over time in inflammatory arthritis, WG41

**Arthritis, psoriatic**

BMD and body composition in postmenopausal women with psoriasis and psoriatic arthritis, SU337

**Arthritis, rheumatoid (RA)**

Antioxidants (phytoestrogens and quercetin) are potentials agents against RA, SA487  
Deficiency of the nucleocytoplasmic shuttling protein CIZ suppresses K/BxN serum-induced model of RA, M446  
H4R is expressed by both OA and RA human tissues, SU159  
PLC $\gamma$ 2 as a promising therapeutic target in RA, F176  
Reduction of BMD in the patients with RA is more remarkable at proximal femur than at lumbar spine, SU451  
Relationship between focal erosions and generalized osteoporosis in postmenopausal women with RA, SA370  
Vitamin D status and bone remodeling marker CTx-I in patients with early RA: association with disease activity and joint damage, SA496

**Arthroplasty, total hip**

Bone density changes at the non-operated hip following total hip arthroplasty, M408

**Arthroplasty, total knee (TKA)**

Evaluation of tibial bone density surrounding Ta tibial implants in TKA, SU266

#### Arzoxifene (ARZ)

ARZ in postmenopausal women with normal or low bone mass, SA421

Effects of ARZ on bone turnover and safety in postmenopausal women with low bone mass, M386

#### Ascorbic acid

Osteoblast differentiation induced by Shh-expressing prostate cancer cells is enhanced by ascorbic acid, SA284

#### ASK-1

Antiapoptotic action of 17 $\beta$ -estradiol in skeletal muscle cells involves ERK 1/2, p38 MAPK, ASK-1 and HSP27, SU185

#### ATDC5

bFGF induces the expression of a subset of Bcl-2 family genes to inhibit the apoptosis of ATDC5 chondroprogenitor cells, SU043

TGF $\beta$  and Smad3-dependent repression of Runx2 function in ATDC5 chondrocytes, SU122

Vinculin is involved in hypertrophic differentiation through Raf/MEK/ERK pathway in chondrocytic ATDC5 cells, SA119

#### ATF2

BMP-2 inactivates TAK1-ATF2 signaling pathway in chondrocytes, F186

#### Atherosclerosis, carotid

Higher BMD is associated with increased odds of carotid atherosclerosis in postmenopausal women not currently using estrogen therapy, 1206

#### ATP

Ahnak regulates Ca signaling and ATP release in osteoblasts in response to mechanical stimulation, SA027

Role of cell surface ATP synthase in fluid shear stress induced ATP release in osteoblasts, SU039

#### Atresia, biliary

Circulating OPG and its ligand in post operative biliary atresia: relationship with metabolic bone disease, M406

#### Atypical parathyroid adenoma. See Adenoma

#### Autism

Hypothyroidism and autism combined with PHP in the absence of Albright's hereditary osteodystrophy and *GNAS* imprinting changes, SA259

#### Autophagy

Normal human osteoblasts internalize MSUM by phagocytosis and autophagy, M057

Regulation of autophagy in the epiphyseal growth plate by AMPK and mTOR requires HIF-1, SU134

#### Autosomal recessive hypophosphatemic rickets. See Rickets

## B

#### B cells

In vivo differential expression profiling study on human circulating B cells suggested a novel EGFR and CALM3 network underlying smoking and BMD, SU154

#### B.H-6

Recombinant congenic strain (B.H-6) establishes that trabecular bone mass and bone marrow adiposity are distinct and heritable phenotypes, F265

#### b2

Aging dependent and independent effects of b2 adrenergic receptor signaling on bone formation induced by intermittent PTH treatment in female mice, SA378

#### BAC

Engineering mice with multiple BAC fluorescent protein reporter gene elements, SU028

#### BALB/c

Aged and young adult BALB/c male mice respond similarly to in vivo tibial compression, M475

#### bALP

Bone degradation marker CTX shows unique properties in disease monitoring compared to NTX, ICTP and bALP in MM, M287

#### Baltimore Hip Studies

Serum Vitamin D levels do not modify the response to an exercise program following hip fracture, SA346

#### Bax

DEX triggers mitochondrial apoptosis through Bax in proliferative growth plate chondrocytes causing growth retardation, 1188

#### Bazedoxifene (BZA)

BZA in combination with conjugated estrogens improves bone mass and strength in the OVX rat, SA385

Double-blind, placebo-controlled, dose-response study of BZA in Japanese postmenopausal women with osteoporosis, M391

Efficacy of BZA in reducing the incidence of nonvertebral fractures in postmenopausal osteoporotic women at higher fracture risk, M390

Safety profile of BZA in Japanese postmenopausal women with osteoporosis, M389

#### BBB Study

TPTD in bisphosphonate-resistant osteoporosis—clinical and  $\mu$ CT data, 1172

#### Bcl-2

bFGF induces the expression of a subset of Bcl-2 family genes to inhibit the apoptosis of ATDC5 chondroprogenitor cells, SU043

#### bcl-2-/-

Loss of a single bim allele recovers the defective osteoclast function in bcl-2-/- mice but does not restore the anabolic action of PTH, 1217

#### Beam theory, unsymmetrical

Unsymmetrical beam theory and finite element method: analysis of murine cortical bone based on  $\mu$ CT imaging, M454

#### Beauvericin

Fungal secondary metabolites beauvericin and enniatin inhibit osteoclast differentiation and bone resorption, M130

#### Beta-adrenergic receptor

Beta-adrenergic receptor agonist administration during hindlimb unloading effectively mitigates reductions in cancellous bone formation, SA514

Low bone mass and decreased biomechanical response in beta 1 adrenergic receptor KO but not in beta 2 adrenergic receptor KO mice, 1141

Role of OPN in beta-adrenergic signaling induced bone loss in vivo, M174

#### Beta-aspartyl peptides

Activation of the CaSR by beta-aspartyl and gamma-glutamyl peptides, M202

#### beta-D-glucopyranoside

Effects of beta-D-glucopyranoside from *Phellodendron Amurense* on the production of inflammatory cytokines, growth factors, MMP, and on bone markers in human subchondral OA osteoblasts, SA117

#### Beta-tricalcium phosphate (b-TCP)

Microporosity in b-TCP ceramics may be detrimental to MSC survival and osteoblastic differentiation, SA015

#### Betulin

Betulin down regulates IL-1 $\alpha$ -stimulated aggrecanases and MMP gene expression in human chondrocytes, M147

#### bFGF. See Fibroblast growth factor

#### bim

Loss of a single bim allele recovers the defective osteoclast function in bcl-2-/- mice but does not restore the anabolic action of PTH, 1217

#### Biomechanics

Alteration of trabecular bone architecture following sciatic denervation and subsequent reinnervation in rat proximal tibiae, SA513

Anabolic response to skeletal loading in mice with targeted disruption of PTN gene, 1142

Androgen receptor disruption increases the osteogenic response to mechanical loading in male mice, 1140

Association between femoral neck BMD and the factor-of-risk for hip fracture derived from direct measurements of strength in human cadaveric femora, 1070

Bone density comparisons in young male rock climbers, weight lifters and sedentary controls, SA534

Bone geometry and bone strength are compromised in patients with ACL reconstruction, M487

Bone geometry, strength, and muscle mass in female distance runners with a history of stress fracture, SA540

Bone length was differentially promoted in the left/right hindlimbs with knee loading and administration of IGF-2, M476

Bone strength in overweight children is adapted to mechanical loads from walking, but is low for higher loading activities, M482

Bone strength measurement: new approach, SU249

Bone tissue quality is differently altered by PTH, bisphosphonates and SERMs, SA510

Bone volumetric density, geometry and strength in male and female collegiate runners, SA539

Can impact exercise mitigate the adverse effects of oral contraceptives on bone?, M488

Cartilage engineered with a calcified zone enhances interfacial shear strength to the underlying substrate, M176

Changes in bone matrix material properties due to OPN deficiency, F149

Combined effects of irradiation and unloading on murine bone, 1295

Comparison of HR-pQCT to DXA and QUS for the assessment of ex-vivo bone strength, M466

Comparison of voxel-based and smooth FEA to predict damage accumulation in vertebral bodies, SU474

Concentration of IGF-I in human cortex bone is highly correlated with fracture toughness of the bone, 1069

Contribution of local buckling to femoral neck failure in stance and fall mode simulations: an advanced FEA analysis of elderly cadaver femur data, M489

Contributions of trabecular and cortical components to biomechanical properties of human vertebrae, M455

Cost-effective rack and pinion system for torsion testing of rodent bones, M465

Degradation of allograft bone quality by gamma irradiation is not explained by altered enzymatic or non-enzymatic cross-links, M460

Dependence of endosseous implant anchorage on mechanostuctural determinants of peri-implant bone trabeculae, 1298

Development of empirical model using  $^{45}\text{Ca}$  for the study of bone remodeling in human, SA454

Disuse with a rapid bone loss affects the expression profile of osteoblastic and resorption genes, F516

Does adiposity affect bone strength indices in young adult black females?, SU318

Early exposure to soy isoflavones modulates bone mineral, strength and microarchitecture in CD1 mice, M503

Effect of collagen degradation on the fatigue behaviour of emu bone, M461

Effect of RIS on bone strength and work to failure determined by FEA and simulation of clinically-measured bone loss and mineralization changes, SA505

Effects of a high g environment on BMD in UK fast-jet trainee pilots, SU473

Effects of ALN or DMAb on cortical and trabecular bone mass, bone strength, and bone mass-strength relationships in mice, 1139

Effects of obesity on cortical bone, SA342

## Key Word Index

## ASBMR 30th Annual Meeting

- Effects of resorption cavities on strength of trabecular bone, SA512
- Effects of running exercise on bone quality after immobilization, SA518
- Effects of simulated resistive exercise on cortical bone in the tibia mid-diaphysis of hindlimb unloaded rats, SA521
- Efficacy of single-level instrumented posterolateral (intertransverse) lumbar spinal fusion in baboons with BMP-7 putty, SU146
- Environmental perturbations during puberty and bone strength, M501
- Estimation of relative stiffness contributions of cortical and trabecular compartments by MRI-based FEA, SU481
- Excessive erythropoiesis affects bone architecture, 1294
- FEA performed on radius and tibia HR-pQCT images provides new insights for fracture status assessment, 1067
- Feasibility and reproducibility of in-vivo assessment of trabecular bone architecture using  $\mu$ MRI-based method at multiple study centers, SA314
- Femoral BMD and femoral structure, assessed by DXA-based hip structural analysis, contribute independently to femoral strength, M304
- Femur from C57BL/6 and DBA/2 inbred mice display a strain dependent response to treadmill running and tower climbing exercise in cortical and trabecular bone architecture, M485
- First clinical application of electric stimulation on human distracted bone, SA568
- Flexible tibia model predicts bone strains during walking, M479
- Formation of new trabeculae in a female patient with osteoporosis treated with TPTD, demonstrated with in-vivo-assessment of 3D bone microarchitecture with HR-pQCT, M352
- Generating 3D finite element models of a human proximal femur from 2D DXA data, M467
- Geometric evidence of a modeling defect in type 2 diabetic women enrolled in the WHI as a potential explanation for increased fracture risk, 1068
- Geometric property QTLs in HcB/8 x HcB/23 F2 cross, F260
- Grayscale MRI based finite element mechanical modeling of trabecular bone at in vivo resolution, SU277
- Hip structural analysis and volumetric QCT in postmenopausal women from the PaTH Study: mono- or combination therapy with ALN and PTH, M306
- HSA and physical activity in boys and girls during puberty, SA538
- Implications of resolution isotropy on apparent topology of trabecular bone architecture in MRI, SU280
- Increased non-enzymatic glycation of cancellous bone due to decrease in remodeling during ALN therapy of osteoporotic women, 1071
- Inhibition of bone biomechanical response to physical activity and loading in mice lacking periostin, 1143
- Interfacial tissue response is influenced by local strain created during implant micromotion, SA531
- Investigation of the fatigue behaviour of rabbit tibiae: effects of sex and age, SU470
- Is increased bone fragility during adolescence a result of delayed development in bone bending strength?, M500
- Load induced changes in trabecular and cortical bone are dose dependent in both C57BL/6 and C3H/HeJ mice, F527
- Loading duration influences the degree of inhibition of bone loss using dynamic muscle stimulation in a disuse rat model, 1297
- Low bone mass and decreased biomechanical response in beta 1 adrenergic receptor KO but not in beta 2 adrenergic receptor KO mice, 1141
- Low systemic BMD increases implant migration in cementless hip replacement, F458
- LRP5 G171V mutation and tobacco smoke related bone fragility, M323
- LV best enhances fracture repair when administered one week post-fracture, 1300
- Marked abnormalities in cortical and trabecular microarchitecture and strength in premenopausal women with idiopathic osteoporosis, M310
- Measurement of T2\* relaxation time of the trabecular bone network at 7T and 3T compared to topological and structural measurements from HR-pQCT, F317
- Mechanical unloading of the sheep calcaneus: a model for hip fracture, M478
- Mediation of bone loss with ultrasound induced dynamic mechanical signals in an OVX rat model of osteopenia, F536
- Microdamage repair and remodeling requires mechanical loading, 1299
- Microstructural changes at the ultradistal radius in MGUS, SU238
- Murine bone mechanics is determined by the ultrastructural canal network in a sex- and strain-specific manner, M456
- NanoCT can be used to assess mechanically related modeling and remodeling in the mouse fibula, 1296
- NEG alters collagen fibrillar structure and energy dissipation characteristics, SU478
- New link between trabecular properties and T-score at the human femur, SU281
- Non-enzymatic glycation increases bone fragility through altered microdamage formation and propagation, F103
- Non-invasive detection of bone microdamage by light scattering, M462
- Non-invasive in vivo Raman spectroscopy in mice, SU480
- Non-steroidal anti-inflammatory use and the response of bone to exercise, M472
- ODN increases bone strength and maintains bone quality in estrogen deficient adult rhesus monkeys, F508
- Optimization of failure load estimation using radiographs of human cadaveric femur, M457
- Oral Sr ranelate treatment markedly improves implant osseointegration, SA506
- Positive influence of physical activity on BMD measurements and hip geometry parameters in young adults, M477
- Prediction of trabecular level microdamage and bone fracture through local strain, SU467
- Previous sport activity during childhood and adolescence is associated with bone geometry in young adult men, SA541
- Proton NMR study of transverse relaxation in rabbit and rat cortical bone, M470
- Reduction of MRI processing time for assessment of trabecular bone microarchitecture, SU282
- Regulation of parameters of bone quality by MMP-2 and MMP-9, 1144
- Reproducibility of mineral density and morphometric  $\mu$ CT measurements at different voxel size scans, M311
- Response of matrix synthesizing MLO-A5 cells to fluid shear, SA067
- RTA of densitometric calcaneal images differs between subjects with and without GC use, M314
- Sex steroids have site specific effects on muscle and bone geometry in young adult males, M416
- Subject-specific mechanical properties of trabecular bone using a low-dose imaging, SU471
- Targeted exercise against hip fragility, SA533
- Thermoreversible Pluronic F108 gel as a universal tissue immobilization material for  $\mu$ CT analyses, SU468
- Trabecular 3D volumetric density at organ and tissue levels by  $\mu$ QCT evaluation of iliac crest biopsy, M303
- Trabecular risk of fracture, caused by disuse, is strongly influenced by baseline morphology, 1293
- Transition from ALN to DMAb in OVX cynomolgus monkeys maintained or improved cortical and trabecular bone mass, without altering the linear relationship between bone mass and bone strength, 1072
- Transmenopausal changes in the trabecular bone intrinsic properties, SU479
- Unsymmetrical beam theory and finite element method: analysis of murine cortical bone based on  $\mu$ CT imaging, M454
- In vivo assessment of 3D bone microarchitecture with HR-pQCT in patients with and without fractures, SU276
- In vivo quantification of intra-cortical porosity in human cortical bone using HR-pQCT in patients with type II diabetes, M309
- Biotin**
- Clinical implications of commercial biotin-based detection systems in PTH assays, M435
- Birth weight**
- Born small is not bad for bone, SA551
- Preterm birth and BMD in young adulthood, 1103
- Self-reported weight at birth predicts measures of femoral size but not volumetric BMD in elderly men, SU338
- Bisphenol-A-diglycidyl ether (BADGE)**
- Inhibition of PPAR $\gamma$ 2 by BADGE and Vitamin D in male mice increases osteoblastogenesis and inhibits bone matrix mineralization leading to osteomalacia, SU374
- Bisphosphates**
- Bisphosphate protect cartilage by reducing chondrocyte apoptosis and reduce bone loss by suppressing osteoclast in adjuvant arthritis, M428
- Bisphosphonate-related osteonecrosis of the jaw (BRONJ)**
- Usefulness of alveolar bone density measurement in risk assessment for BRONJ, SA305
- Bisphosphonates**
- 1-year analysis of adherence with bisphosphonate treatments in osteoporotic patients, SA415
- Acute phase response and bone metabolism marker after intravenous bisphosphonate in osteoporotic patients with rheumatism, M364
- Application of a treatment algorithm to avoid BMD loss and limit bisphosphonate use after kidney and kidney/pancreas transplantation, SA497
- Application of preventive measures minimizes the occurrence of ONJ in patients with bone loss treated with bisphosphonates, F281
- Bisphosphonate, pamidronate, suppresses the pro-inflammatory response in a mouse model of OI as well as normal littermates, SU386
- Bisphosphonate-associated femoral fracture: implications for management, WG26
- Bisphosphonate-associated ONJ cases in South Korea, SA412
- Bisphosphonate-induced osteopetrosis: novel bone modeling defects, metaphyseal osteopenia, and osteosclerosis fractures after drug exposure ceases, F569
- Bisphosphonates and osteoporotic fractures in highly compliant/persistent postmenopausal women, 1025
- Bisphosphonates in children with hypercalciuria and reduced BMD, M429
- BMD response to treatment with rhPTH in patients previously treated with bisphosphonates, M348
- Bone tissue quality is differently altered by PTH, bisphosphonates and SERMs, SA510

Case presentation: bisphosphonate induced ONJ in Pagetic jaw bone, WG24

Combined TGF $\beta$  receptor I kinase inhibitor and bisphosphonates are additive to reduce breast cancer bone metastases, F275

Comparative antifracture efficacy of N-containing bisphosphonates, SU397

Comparative gastrointestinal safety of weekly oral bisphosphonates, M358

Development of an animal model of bisphosphonate-induced severe suppression of bone turnover, SA511

Differences in safety and efficacy of generic and original branded once weekly bisphosphonates, M359

Dkk-1 predicts the gain of BMD in osteoporotic women on bisphosphonates, SA300

Effect of 10-year fracture risk tool results on likelihood of bisphosphonate prescribing, SU402

Effect of bisphosphonate treatment of OA in a guinea pig model, M149

Effectiveness of bisphosphonate therapy in a real-world setting, M356

Fracture risk in women aged 65 years or older with once-monthly oral IBN compared with weekly bisphosphonates, M367

Fracture risk with once-monthly oral IBN compared with weekly bisphosphonates, SU408

Homocystinuria associated bone disease: effect of long term bisphosphonate treatment, SA406

Impact of dosing frequency in compliance with bisphosphonates among postmenopausal Japanese women for osteoporosis treatment, M374

Improving the prediction of medication adherence: example of bisphosphonates for osteoporosis, M368

Induction of Runx2 and Osx by bisphosphonate promote osteogenic differentiation, SU062

Long-term treatment with oral bisphosphonates in postmenopausal women: effects on the degree of mineralization and microhardness of bone, 1029

OPG and bisphosphonates had differential effects on osteoclast numbers, bone marrow fibrosis and cortical porosity in a mouse model of constitutive activation of the PTH/PTHrP receptor, M076

Patient persistence with weekly bisphosphonates for two years after initiation of therapy, SA418

Patients desire of administration form and dose interval in bisphosphonate therapy of osteoporosis, SA408

Postmenopausal women with GERD and long term treatment with bisphosphonates IV, M361

Predictors of patient perceived need for oral bisphosphonates to prevent fracture: the role of the MD-patient relationship, F416

Predictors of self-reported non-persistence with oral bisphosphonates due to perceived side effects or other reasons, M378

Premenopausal reference ranges of bone turnover markers and the effect of bisphosphonates in Korean postmenopausal women, SU406

Risk of hip fracture after bisphosphonate discontinuation, F409

Studying cellular uptake and distribution of bisphosphonate in vivo using fluorescently-labelled analogues of RIS, 1065

TPTD in bisphosphonate-resistant osteoporosis—clinical and  $\mu$ CT data, 1172

**Bisphosphonates, nitrogen containing (NBP)**

Role of active site Thr201 in the inhibition of farnesyl pyrophosphate synthase by NBPs, F407

**BL6**

Effect of Pb on bone mineral properties from female adult C57/BL6 mice, M146

**Bladder cancer.** See *Cancer*

**Blood donors**

Prevalence and incidence of viral infections among musculoskeletal tissue donors and first-time blood donors, SA549

**Blood pressure.** See also *Hypertension*

Elevated systolic blood pressure is positively related to bone mass measurements in overweight pre-pubertal and pubertal children, M496

**Bmi-1**

Defects in MSC self-renewal lead to an osteopenic phenotype in *Bmi-1* null mice, 1050

**BMP and activin membrane-bound inhibitor (BAMBI)**

BAMBI gene is epigenetically silenced in a subset of high-grade bladder cancer, SU245

**BMPR2**

BMPR2 is dispensable for formation of the limb skeleton, SU145

**Body composition**

Automatic estimation of body composition using  $\mu$ CT and a Gaussian mixture model, M139

BMD is associated with lean mass and not fat mass, SU273

Body composition changes after radioiodine treatment of hyperthyroidism, M433

Body fatness negatively associated with BMD and hip geometry indices in adolescents, F546

Bone size, volumetric bone density in relation to fat mass in healthy young men at age of PBM, SU477

Establishing healthy body composition values with DXA, SU366

How does body fat influence bone health in childhood? A Mendelian randomisation approach, 1175

Increased maternal fat intake increases skeletal mass in congenic mice, M495

Percentage body fat and risk of prospective hip fracture in older men and women, F363

Plasma osteocalcin is inversely related to fat mass and plasma glucose in elderly Swedish men, SU459

At similar plasma 25(OH)D levels, fat mass influence PTH levels in the state of Vitamin D insufficiency, SA218

Variation in the osteocalcin gene: association study of BMD, fracture and changes in body fat mass in elderly women, SU225

Vertebral fracture in men: level of trauma, BMD and lean body mass, SU360

Vitamin D status in young women is strongly negatively related to body weight, BMI and body fat, but is not associated to bone mass, SU203

**Body mass index (BMI).** See also *Obesity; Weight*

Dietary patterns in Canadian men and women ages 25 and older: relationship to BMI and BMD, SU309

Model of high body mass: BMD, bone markers and adipocytokine levels in high level male rugby players, SA167

Vitamin D status in young women is strongly negatively related to body weight, BMI and body fat, but is not associated to bone mass, SU203

Weight and BMI predict BMD and fractures in women 40 to 59 years, SA438

**Bone acquisition.** See also *Pediatric bone disease*

Accuracy of Cobb angle measurement with iDXA, SU484

ALF prevents aromatase inhibitor (letrozole)-induced bone mineral loss in young growing female rats, SA570

Autosomal recessive HPP manifesting in utero with long bone deformity but showing spontaneous postnatal improvement, SA562

Bisphosphonate-induced osteopetrosis: novel bone modeling defects, metaphyseal osteopenia, and osteosclerosis fractures after drug exposure ceases, F569

Bone formation in mice with variations in Lrp5 expression, F550

Bone size, volumetric bone density in relation to fat mass in healthy young men at age of PBM, SU477

Contribution of the vertebral posterior elements in anterior-posterior DXA scans, 1180

Cortical bone acquisition in the appendicular skeleton of healthy young females is reciprocally related to marrow adiposity, M074

Determinants of humeral bone volume in males, F122

Effects of diet and menstrual cyclicity on bone mass accumulation in pubertal monkeys, M499

Effects of GH on bone micro-architecture by in vivo  $\mu$ CT, SA547

Effects of long-term administration of high-dose GH on body composition and bone mineralization, SA571

Extracellular matrix protein periostin regulates periosteal apposition, 1178

Forearm pQCT measurements in males with DMD, SU492

Kenney-Caffey syndrome in a Caucasian man, SA464

Loaded distal radius: gymnastic-related cross-sectional asymmetry, M490

PBM is determined at 1 year-old: evidence from growth charts, F542

Prevalence and incidence of viral infections among musculoskeletal tissue donors and first-time blood donors, SA549

Transcriptional silencing of Frzb/sFRP3 by promoter methylation in osteogenic sarcoma, SU231

Valproate: a model for adverse psychoactive drug effects on BMD, SA556

**Bone architecture**

Alteration of trabecular bone architecture following sciatic denervation and subsequent reinnervation in rat proximal tibiae, SA513

Bone metabolism, microarchitecture and densitometric measurement in rat femur after chronic alcohol consumption, M239

Bone microarchitecture is dependent upon collagen  $\alpha 1$ (XI) expression during development, F135

Both excess and restricted energy availability negatively influence acquisition of trabecular bone mass and microarchitecture during growth, M493

Cortical and trabecular microarchitecture in HIV-infected postmenopausal women, SU458

Early exposure to soy isoflavones modulates bone mineral, strength and microarchitecture in CD1 mice, M503

Effect of luteolin on bone loss, microarchitecture and bone resorption in OVX mice, M128

Effect of metabolic acidosis on BMD and bone microarchitecture in normal and OVX rats, M409

Effects of GH on bone micro-architecture by in vivo  $\mu$ CT, SA547

Excessive erythropoiesis affects bone architecture, 1294

Feasibility and reproducibility of in-vivo assessment of trabecular bone architecture using  $\mu$ MRI-based method at multiple study centers, SA314

Femur from C57BL/6 and DBA/2 inbred mice display a strain dependent response to treadmill running and tower climbing exercise in cortical and trabecular bone architecture, M485

Formation of new trabeculae in a female patient with osteoporosis treated with TPTD, demonstrated with in-vivo-assessment of 3D bone microarchitecture with HR-pQCT, M352

Green tea polyphenols protect bone microarchitecture in female rats with chronic inflammation-induced bone loss, M338

Implications of resolution isotropy on apparent topology of trabecular bone architecture in MRI, SU280



## Key Word Index

## ASBMR 30th Annual Meeting

- Microarchitecture and tissue age influence in vivo bone resorption, M125
- Obesity and bone architecture in men—can we apportion the metabolic and the mechanical effect?, SA440
- Recovery of bone architecture after RANKL administration in rats is characterized by increased bone mass on existing trabeculae assessed by in vivo  $\mu$ CT, SU076
- Reduction of MRI processing time for assessment of trabecular bone microarchitecture, SU282
- Twelve month changes in trabecular microarchitecture assessed by  $\mu$ MRI in postmenopausal women on antiresorptive versus anabolic therapy, 1020
- Vitamin K intake is positively related to trabecular bone microarchitecture in children, M505
- In vivo assessment of 3D bone microarchitecture with HR-pQCT in patients with and without fractures, SU276
- Bone biomarkers**
- Effects of ODN on bone biomarkers in OVX non-human primates, F297
- Use of bone biomarkers as an endpoint in a pediatric study of ALN, SU488
- Bone degradation**
- Significant trabecular bone degradation occurs within five days of muscle paralysis, SA515
- Bone DESTINY**
- Assessment of fracture risk and treatment of osteoporosis in postmenopausal women: bone density vs. Bone DESTINY, SU251
- Bone DESTINY—a one step fracture risk predictor for clinicians, SU504
- Patients with fragility fracture assessed by BMD, Bone DESTINY and osteoporosis Canada guidelines, SA343
- Bone diseases. See also Pediatric bone disease**
- Circulating OPG and its ligand in post operative biliary atresia: relationship with metabolic bone disease, M406
- Tec kinases, therapeutic targets for bone destructive diseases, F083
- Bone disorders**
- 30IT/C of SCT modulates BMD by Wnt and estrogen signaling pathways, 1270
- 13910C>T LCT promoter polymorphism in the Spanish population, M265
- $\mu$ CT abnormalities in the th3 mouse model of thalassemia start at a young age and are associated with decreased bone turnover, SA128
- 7B2 protein mediated inhibition of DMP1 cleavage in osteoblasts enhances FGF-23 production in *Hyp*-mice, 1053
- Aberrant *Phex* function in osteocytes has limited effects on bone mineralization in XLH, 1051
- ACVR1 knock-in mouse model for FOP, 1203
- Additional clinical features of IMON, SU212
- Adult HPP treatment with TPTD, SA468
- Age-associated changes in the material properties of the G610C (Amish) OI mouse model, SA252
- Allele specific silencing of Collagen 1 Alpha genes in primary human bone cells using RNAi, M232
- ALN transiently impairs removal of alveolar bone and healing of the root socket after tooth extraction in rats, 1275
- ANKH mutation causing CMD inhibits osteoclast differentiation, SU214
- Archaeological skeletons support a North-West European origin for PDB, SA477
- Association between polymorphisms in TNFR genes and circulating TNFR levels, and BMD in postmenopausal Korean women, M258
- Association of *HSD11B1* polymorphisms with vertebral fracture risk and BMD in postmenopausal Korean population, M260
- Association study of the TF and IGFBP3 gene polymorphisms with an osteonecrosis of femoral head in Korean population, SU226
- Associations of the VDR and calcitonin receptor genes with bone density, bone turnover markers and fracture incidence with regard to Ca intake level in Slovak postmenopausal women, M261
- Beta-adrenergic receptor agonist administration during hindlimb unloading effectively mitigates reductions in cancellous bone formation, SA514
- Bi-allelic loss of *Nf1* in osteoblasts delays bone fracture healing, SU218
- Bisphosphonate, pamidronate, suppresses the pro-inflammatory response in a mouse model of OI as well as normal littermates, SU386
- BMD-associated SNP lies in a Runx2 binding site of the LRP5 promoter, M264
- Body composition changes after radioiodine treatment of hyperthyroidism, M433
- Bone metabolism, microarchitecture and densitometric measurement in rat femur after chronic alcohol consumption, M239
- Bone resorption and articular cartilage degenerative changes following performance of high repetition high force tasks are attenuated by secondary ibuprofen treatment, SA532
- Brain-derived serotonin positively regulates bone mass accrual, SA463
- c.1250A>G, p.N417S is a common American TNSALP mutation involved in all clinical forms of HPP, including pseudo-HPP, SA566
- Case presentation: bisphosphonate induced ONJ in Pagetic jaw bone, WG24
- CaSR gene A986S polymorphisms: relation to bone loss and urine Ca in a Spanish early postmenopausal women population, M255
- CED: a unique variant featuring a novel, heterozygous, leucine repeat mutation in *TGF $\beta$ 1* together with a novel, homozygous, missense change in *TNFSF11* encoding RANKL, F256
- CFTR regulates osteoblast bone formation independent of chloride conductance, 1274
- Changes of bone metabolism in immunosuppressant, FK506 treated rats, SU383
- Characterization and genetic mapping of bone size phenotypes in GK and F344 rats using a new 3D CT method, M463
- Characterization of the enthesopathy of XLH in the Hyp mouse, SA254
- Colistin-impregnated bone cement beads prevent multi-drug resistant *Acinetobacter* osteomyelitis, M236
- Connective tissue progenitor cell contribution to ectopic skeletogenesis, F044
- Controlled drug release from Ca phosphate-based orthopaedic implants, SU235
- Defects in MSC self-renewal lead to an osteopenic phenotype in *Bmi-1* null mice, 1050
- Defining epistasis in a double congenic mouse: implications for the skeleton, M252
- Deletion of the *GNAS* antisense transcript results in parent-of-origin specific *GNAS* imprinting defects and phenotypes including PTH-resistance, 1052
- Deprivation of Vitamin A results in a partial rescue of the mineralization defects in *Phex*-deficient Hyp mice, F202
- Differential effects of GH and 1  $\alpha$  calcidol on cancellous and cortical bone in hypophysectomized rats, SU501
- Differential regulation of gene expression by SNPs in the osteonectin/SPARC 3 untranslated region, M270
- Documented response to cinacalcet in two cases of acquired hypocalciuric HCa, M197
- Dynamic morphological changes in the skulls of mice mimicking human Apert Syndrome resulting from gain-of-function mutation of FGFR2 (P253R), SA248
- Dysosteosclerosis in a 2-year-old girl: investigation of a rare, sclerosing bone disorder, SA567
- Effect of hypercalciuria and diet on bone in genetic hypercalciuric stone-forming rats, SU213
- Effect of RLX treatment on BMD might be influenced by UGT1A1\*28 polymorphism, M257
- Effects of exercise and estrogen on OPG in premenopausal women, SU166
- Endothelial progenitor cell mobilization during DO in human, SA053
- Enzyme replacement therapy prevents dental defects in the *Akp2*<sup>-/-</sup> mouse model of infantile HPP, F107
- Epistasis between QTLs for bone density variation in Copenhagen X Dark Agouti F2 rats, M253
- Establishment of a murine model of HCa by overexpression of sRANKL using an adenovirus vector, SU082
- Evidence supporting the necessity of GalNac-T3 in the processing of FGF-23 in humans, SA200
- Familial humeroradioular synostosis maps to chromosome 7p15, M251
- FGF-2 stimulates RANKL expression in PDB, F480
- Functional characterization of unreported CaSR in four Italian kindreds with FHH, M204
- Functional polymorphism in COL1A2 (Ala459Pro) that is associated with intracranial aneurysms, shows heterozygous disadvantage concerning BMD and stroke in elderly men, SU219
- GCM2, the regulator of parathyroid cell fate, transactivates the CaSR gene, M187
- Gender specific effects of TRPV4 on osteoblast-osteoclast coupling and risk of osteoporotic fractures, SA355
- Gene expression in blast-injured muscle: insights into the mechanism of heterotopic ossification, SU163
- Genome-wide CNV study identified a novel susceptibility gene *UGT2B17* for osteoporosis, M404
- Genomic expression analysis of rat Chr 4 for skeletal traits at femoral neck, SA261
- Gut-derived serotonin is an inhibitor of bone formation, M069
- GWAS identified novel susceptibility loci for osteoporosis, SA267
- Haplotype specific promoter activity of the human *FZD1* gene, M269
- High levels of IL-6 and hyper-responsivity to 1,25(OH)<sub>2</sub>D<sub>3</sub> are both required for development of Pagetic osteoclasts, F478
- High-fat diet negatively regulates bone development in growing mice, SA441
- Homozygous threonine to methionine substitution in FGF-23 gene is associated with tumoral calcinosis in a 12 year-old girl, SU171
- Hotspot splicing mutation in *LEPRE1* affects P3H1 and causes recessive OI, SU215
- Human SLC34A3/NaPi-IIc mutations T137M and L527del uncouple Na-phosphate co-transport, F471
- Hyperphosphatasia: a unique type without mutations in *TNFRSF11A* (RANK), *TNFRSF11B* (OPG), or *SOSTM1* (sequestosome 1), SU210
- Hypothyroidism and autism combined with PHP in the absence of Albright's hereditary osteodystrophy and *GNAS* imprinting changes, SA259
- Hypoxia promotes ligand-independent activation of the ACVR1 (R206H) mutant receptor in C2C12 cells, M243
- Identification of a novel mutation (78dup27) of the *TNFRSF11A* gene in a Chinese family with early onset PDB, M237
- Identification of skin abnormalities in OI patients by MRI, SA561
- Impairment of osteoblast lineage differentiation leads to increased osteoclastogenesis in OI murine, 1202
- Immunohistochemical and genetic characterization of the atypical parathyroid adenoma, M432

- Immunohistochemical localisation of SCT in human trabecular bone from fragility hip fracture patients, SA148
- Impaired oxidative stress defense mechanism may reduce bone stiffness in diabetic Charcot neuroarthropathy, M002
- Integrative genetics approach to identify candidate genes regulating bone density: combining linkage, gene expression and association, M247
- Investigation into the impact of OA changes on BMD measurements in patients with high bone mass, SA257
- Is there any association between CYP 17-CYP 19 polymorphisms and bone loss in early postmenopausal women?, M259
- Large collaborative study on geographic variation of *SQSTM1* mutations in PDB in Italy, SA475
- Large osteoclasts in pediatric OI patients receiving intravenous pamidronate, SU497
- Loss of function polymorphisms in the P2X<sub>7</sub> receptor gene are associated with accelerated lumbar spine bone loss in postmenopausal women, SU224
- Lrp6 loss of function impacts bone homeostasis and responds to folate supplementation, F253
- Mecp2 null mice display multiple skeletal abnormalities, M242
- Molecular consequences of a mutant Dlx3 affecting bone homeostasis in TDO, 1272
- Molecular diagnostic strategies for mutations of the CaSR gene, M201
- Morquio Syndrome variant: two siblings with atypical phenotype and novel compound heterozygosity, M240
- Mouse with a Ser1386Pro mutation in the C-propeptide domain of *col2a1* provides a model for SEDC, 1269
- Mutational analysis of  $\beta$ -catenin Exon 3 in benign and malignant parathyroid tumors, M436
- Nonsteroid responsive HCa associated with sarcoidosis—a rapid response to hydroxychloroquine, WG28
- NR1P1*, a novel osteoporosis candidate gene identified by expression and association analyses, M254
- Obesity induced by high dietary fat leads to increased bone resorption marker, TRAP, and decreased bone mass in mice, M238
- OPG deficiency mimicked by a novel 15-base pair tandem duplication in *TNFRSF11A* encoding RANK: merging the juvenile PD and ESH phenotypes, F563
- OPG serum levels in shaft fractures healing and non-union, M013
- OPN deficiency reduces aortic calcification and oxidative stress in diabetic LDLR<sup>-/-</sup> mice, F109
- Osteoblast and osteoclast involvement in the pathogenesis of a mouse model for CMD, 1204
- Osteoporosis in a murine model of hemophilia A, M480
- Over-expression of CNP enhances the formation of long bone exostoses in *Ext1*<sup>+/-</sup> mice, SU130
- Oxytocin inhibits bone formation through the activation of the sympathetic tone, 1200
- P3H1 and CRTAP are mutually stabilizing in the endoplasmic reticulum collagen prolyl 3-hydroxylation complex, 1049
- Phased GWAS identifies probable new gene affecting BMD, M245
- PHEX cleavage of SIBLING-ASARM peptides as a mechanism underlying osteomalacia in XLH, 1199
- Polymorphisms in *CYP24A1*, the gene encoding 25(OH)D-24-hydroxylase, are associated with BMD, SA266
- Polymorphisms in the WIF1 gene are associated with BMD in elderly Swedish women, SA264
- Polymorphisms of the ALOX12 gene are associated with increased risk of osteoporotic fracture, SU220
- Polyostotic form of FD in a 13 year old Colombian girl exhibiting clinical and biochemical response to neridronate intravenous therapy, SU211
- Possible central function of the calcitonin receptor on bone mass, SA255
- Prediction of fracture risk by LRP5 gene haplotype, SU222
- Prediction of osteoporotic fracture risk by 25(OH)D3-1 $\alpha$ -hydroxylase (CYP27B1) gene, M263
- Proinflammatory marker values at baseline and after a fracture are distinctly different comparing a mouse model of OI with normal controls, M234
- Protective actions of Vitamin D analogs in the vascular calcification of CKD, SU450
- Proteins involved in mineralization expressions perturbations in bones and teeth of *Msx2* mutant mouse mandibles, SA150
- Quantitative  $\mu$ CT imaging of adipocyte volume in bone marrow of mice with high and low bone mass, SU250
- Rachitic defects in *tcirg1*-dependent osteopetrosis are caused by impaired gastric acidification, 1201
- Recalculation of genome scans on a common genetic map enhances our ability to identify common bone density QTL in new and historical data, 1276
- Recurring mutation causing severe/lethal recessive type VIII OI in African-Americans originated in West Africa more than 300 years ago, SA262
- Relative efficacy of “treating” versus “preventing” infantile HPP in *Akp2*<sup>-/-</sup> mice by enzyme replacement therapy, 1054
- Role of *Ostm1* in bone, hematopoiesis and neuronal development, 1271
- RsaI* polymorphism in *ESR2* is associated with postmenopausal fracture risk, SU221
- Safety and efficacy of long-term PTH replacement in a pediatric patient with inherited HPT, F217
- Screening the PHEX gene in a large cohort of hypophosphatemic rickets allowed the description of a missense mutation not responsible for the disease on a highly conserve amino acid residue, M246
- Serum FGF-23 level in term infants, SA165
- Significant association between polymorphisms of *CYP19A1*, fracture incidence and BMD in post-menopausal women, M262
- Significant trabecular bone degradation occurs within five days of muscle paralysis, SA515
- Single nucleotide polymorphisms in the P2X<sub>7</sub> receptor gene are associated with increased postmenopausal bone loss and fracture incidence, SU223
- Skeletal consequences of FHH and PHPT, M206
- Specific inhibitors of TNSAP's pyrophosphatase activity suppress medial arterial calcification, M142
- Spectrum of OI mutations in Sweden, SA247
- Strong and extensive epistatic interactions affect bone traits in a mouse reciprocal intercross of HcB/8 and HcB/23, SA125
- T $\beta$ RI inhibitor rescues uncoupled bone remodeling in two different animal disease models, 1273
- Three unrelated patients with a unique spondylo-epi-metaphyseal dysplasia, SU494
- Twist1 haploinsufficiency is associated with reduced IGF-1 levels and an osteoporotic phenotype, SU029
- Two novel *SQSTM1* mutations in American patients with PDB, SU216
- ucOC is an endocrine link between the skeleton and the glucose metabolism, F444
- Usefulness of *HRPT2* gene and parafibromin studies in two patients with PHPT and uncertain pathological assessment, SA482
- In utero stem cell therapy as treatment for classical OI using the knock in murine model *BrtlIV*, F500
- Variation in the osteocalcin gene: association study of BMD, fracture and changes in body fat mass in elderly women, SU225
- ### Bone formation
- (Ala-Gly)<sub>n</sub> sequences configured silk protein scaffold induces osteoblast differentiation and bone formation via increased *Cbfa1* and *Osx* expression, M167
- Ablation of IGF-I signaling in osteoprogenitors decreases bone formation and blunts the skeletal response to PTH, 1193
- Abnormality of bone formation in transgenic mice expressing *Osr1*, M144
- Acute change in iCa directly affects bone formation independent of PTH action during hemodialysis, SU437
- Acute COPD exacerbations are associated with uncoupling of bone resorption from bone formation, M414
- Adipocyte-secreted protein URB is a potent stimulator of bone formation, F006
- Aging dependent and independent effects of b2 adrenergic receptor signaling on bone formation induced by intermittent PTH treatment in female mice, SA378
- BMSC aging directly alters bone formation, 1252
- Bone formation in mice with variations in *Lrp5* expression, F550
- Bone tether formation in femoral and basicranial growth plates have similar responses to growth disruptions due to nuclear VDR genotype and mineral homeostasis, M164
- Ca intake and serum bone formation markers are associated with the functional single nucleotide polymorphism in the *TNSALP* gene, SU308
- Calcifications in children with JDM contain several bone formation markers, SA106
- Catecholamines accelerate BMP-induced osteoblastic differentiation and bone formation, SU137
- CFTR regulates osteoblast bone formation independent of chloride conductance, 1274
- Concentration of connective tissue progenitors in autologous cancellous bone graft enhances new bone formation in a canine femoral defect model, SA039
- Conditional disruption of *Pkd1* in osteoblasts results in osteopenia due to direct impairment of osteoblast-mediated bone formation, SA019
- Decreased bone formation, increased bone resorption, and osteopenia in mice lacking SP, SU160
- Deficiency of NCK1, an actin cytoskeletal modulator with SH2/SH3 motifs, induces bone loss via suppression of bone formation and induction of biochemical high bone turnover state, M026
- Deletion of the *Dkk-1* *Krm-1* and *Krm-2* in mice leads to increased bone formation and bone mass, 1004
- Deletion of the Wnt signaling antagonist sRFP4 in mice induces opposite bone formation phenotypes in trabecular and cortical bone, 1005
- Dlk1*/*FA1* is a novel factor enhancing osteoclastogenesis and inhibiting bone formation in vitro and in vivo, 1007
- Early osteocyte marker, *E11/gp38* is highly elevated in new bone formed in response to distraction as compared to existing bone, SA136
- Effects of Vitamin K2 and RIS on bone formation and resorption, osteocyte lacunar system and porosity in the cortical bone of GC-treated rats, SU385
- Elevated androgens are associated with increased bone formation in premenopausal exercising oligomenorrheic women, SU191
- Ephrin B1 reverse signaling regulates bone formation via influencing osteoblast activity in mice, 1194
- Fluoride effects on bone formation, mineralization and mechanical properties are influenced by genetics, SU465

## Key Word Index

## ASBMR 30th Annual Meeting

Fully human anti-DKK1 antibodies increase bone formation and resolve osteopenia in mouse models of estrogen-deficiency induced bone loss, 1214

Gastric proton pump inhibitors failed to affect bone resorption and formation, SA095

GLP-2 acutely uncouples bone resorption and bone formation in postmenopausal women, M399

Gut-derived serotonin is an inhibitor of bone formation, M069

High bone mass due to increased bone formation in mice lacking the CTR, SA192

Histomorphometric and biochemical bone formation responses to first and second cycles of TPTD treatment, 1169

IGFBP6 Is a negative regulator of osteoblast differentiation and bone formation, SA182

Impaired bone formation in mice lacking lamin A/C activation leads to severe osteopenia, F131

Increased caloric intake in energy deficient exercising with functional hypothalamic amenorrhea women is associated with decreased ghrelin and increased bone formation, SU184

Interaction of combined intervention of PTH and GH on trabecular and cortical bone formation and resorption in the hypophysectomized rats, SU502

Interactions between obesity, CVD and bone formation, M451

Long-acting PTH ligand that binds to a distinct PTH receptor conformation (R0) can stimulate increases in markers of both bone resorption and bone formation in mice, F221

Losartan<sup>®</sup> (Cozaar) increases appendicular bone formation by inhibiting osteoclastogenesis, M126

Marrow ablation induces periosteal bone formation and potentiates the effect of PTH on endosteal bone formation in rat femurs, M208

Mathematical model of remodeling cycles with feedback mechanism for maintaining the balance between bone resorption and formation, WG27

Mice lacking the Wnt receptor Frizzled-9 display osteopenia caused by decreased bone formation, 1006

Molecular mechanisms underlying matrix vesicle-induced mineralization during bone formation, SA063

Osteoblast-targeted deletion of the GC receptor has little impact on PBM but attenuates DEX-induced suppression of bone formation, F452

Osx, a positive regulator in adult bone formation, F008

Overexpression of GSR in osteoblasts decreases bone formation and partially prevents OVX-induced bone loss, F024

Overexpression of sFRP1 inhibits bone formation and attenuates PTH bone anabolic effects, 1100

Oxytocin inhibits bone formation through the activation of the sympathetic tone, 1200

PINP, a new available rat bone formation marker: usefulness in osteopenia studies due to androgen lack and IBN treatment, SA299

Point mutation of endofin at PP1c-binding domain induces angiogenesis and bone formation in mice by sensitizing BMP signaling, 1082

Positive effect of GLP-1 upon bone formation and resistance in insulin-resistant rats, M425

PTHr1 stimulates bone formation through a distinct  $\beta$ -arrestin dependent pathway independent of G protein activation, 1226

Rapid optical imaging of bone formation responses in the rodent skeleton, SU379

Regulation of bone formation by osteoclasts involves Wnt/BMP signaling and the chemokine S1P, M017

Ronacaleret, a novel CaSR antagonist, demonstrates potential as an oral bone-forming therapy in healthy postmenopausal women, 1174

Scl-Ab increases bone formation and decreases bone resorption in distal tibial metaphyseal trabecular bone in OVX rats, F394

Scl-Ab increases bone mass by stimulating bone formation and inhibiting bone resorption in a hindlimb-immobilization rat model, 1138

Serum PINP is a sensitive marker of bone formation in mouse OVX model, M293

Soluble activin receptor type IIA fusion protein, ACE-011, increases bone mass by stimulating bone formation and inhibiting bone resorption in cynomolgus monkeys, SU376

TGF $\beta$ 1 induces migration of Sca-1 and CD29-positive MSC in coupling bone resorption and formation, F188

Transgenic overexpression of the Wnt antagonist Krm-2 in osteoblasts leads to severe impairment of bone formation and increased bone resorption, 1003

In vivo demonstration that PTH acts on early osteoprogenitor cells to enhance bone formation during repair of critical-size calvarial defects, M062

**Bone formation, cortical**

Endogenous G $_i$  signaling in osteoblasts negatively regulates cortical bone formation, 1255

**Bone formation, endochondral**

Expression of an engineered G $_i$ -coupled receptor in osteoblasts affects intramembranous and endochondral bone formation during bone repair, F127

Marked induction of endochondral bone formation by overexpression of a constitutively active Gli2 in MSCs isolated from the healing site, SA049

Overexpression of the transcriptional cofactor Lbh impairs angiogenesis and endochondral bone formation during fetal bone development in chickens, SU004

Phosphate regulates chondrocyte differentiation, proliferation and apoptosis in a model of embryonic endochondral bone formation, SU124

Role of Wdr5 in endochondral bone formation during chicken limb development, SU121

Trps1 represses Runx2 during endochondral bone formation, SU126

**Bone formation, trabecular**

Ligand activation of the engineered G $_i$ -coupled receptor Rs1 in osteoblasts promotes trabecular bone formation, 1076

**Bone fragility**

Bone fragility is increased in the MKR type 2 diabetic mouse, M440

Is increased bone fragility during adolescence a result of delayed development in bone bending strength?, M500

Non-enzymatic glycation increases bone fragility through altered microdamage formation and propagation, F103

**Bone geometry**

Bivariate whole genome linkage analysis of femoral bone geometric traits and leg lean mass, M249

Bone geometry and bone strength are compromised in patients with ACL reconstruction, M487

Bone geometry, strength, and muscle mass in female distance runners with a history of stress fracture, SA540

Bone volumetric density, geometry and strength in male and female collegiate runners, SA539

Changes in marrow cell dynamics and bone geometry with aging in TSP-2 null mice, 1249

Effects of a targeted bone and muscle loading program on QCT bone geometry and strength, muscle size and function in older men, 1244

Previous sport activity during childhood and adolescence is associated with bone geometry in young adult men, SA541

Sex steroids have site specific effects on muscle and bone geometry in young adult males, M416

**Bone grafts**

Concentration of connective tissue progenitors in autologous cancellous bone graft enhances new bone formation in a canine femoral defect model, SA039

Downregulation of Cx43 expression and osteoclastogenesis by a bioceramic bone graft substitute, M119

Novel modification of bone grafts inhibits bacterial colonization, M169

**Bone growth**

Soy-based formula promotes bone growth in neonatal piglets by inducing osteoprogenitors to differentiate into osteoblasts via enhanced BMP-2 signaling, SA336

**Bone healing**

AC-100 promotes cartilage repair and subchondral bone healing in surgically induced cartilage defects, SA111

Accelerated fracture callus remodeling and membranous bone healing in STAT1 deficient mice, SA022

Impaired bone healing in a BMP-2 KO mouse model of DO, SA159

Opioid-induced osteoporosis: delayed bone healing and compression fractures in a man with chronic narcotic use, WG32

Roles of ZOL in bone healing and osteoblast functions, 1064

Use of endothelial progenitor cells to promote bone healing, SA104

**Bone homeostasis**

Lrp6 loss of function impacts bone homeostasis and responds to folate supplementation, F253

Molecular consequences of a mutant Dlx3 affecting bone homeostasis in TDO, 1272

Osx is required for skeletal growth and bone homeostasis after birth, 1074

Oxytocin directly regulates skeletal homeostasis, SA199

VEGF and PTEN regulate bone homeostasis via control of osteoblastogenesis, osteoclastogenesis and adipocyte differentiation, M029

**Bone length**

Bone length was differentially promoted in the left/right hindlimbs with knee loading and administration of IGF-2, M476

Overexpression of CCN2/CTGF in cartilage shows prolonged bone length resulting from stimulation of chondrogenesis, chondrocyte growth, apoptosis, and bone mineralization during endochondral ossification, M153

**Bone loss**

(22-52) ADM prevents systemic bone loss related to inflammation in mice, SA493

A allele at Valine80 of the CYP19 gene is a risk factor for aromatase inhibitors associated bone loss, 1021

Age-related bone loss in mice associated with ubiquitin ligase Smurf1 degradation of JunB protein and reduced osteoblast proliferation, 1113

ALF prevents aromatase inhibitor (letrozole)-induced bone mineral loss in young growing female rats, SA570

Application of preventive measures minimizes the occurrence of ONJ in patients with bone loss treated with bisphosphonates, F281

Association of urine measures of diet-derived acid excretion with bone loss and fractures, SU283

Bisphosphate protect cartilage by reducing chondrocyte apoptosis and reduce bone loss by suppressing osteoclast in adjuvant arthritis, M428

Bone loss with smoke exposure and Lrp5 expression, SA459

Calorie restriction prevents age-related trabecular bone loss via SIRT-1, 1251

Cannabinoid receptor ligands rescue bone loss and stimulate fracture healing, SU375

CaSR gene A986S polymorphisms: relation to bone loss and urine Ca in a Spanish early postmenopausal women population, M255

*Cissus quadrangularis* attenuates OVX induced bone loss in mice, M403

Deficiency of NCK1, an actin cytoskeletal modulator with SH2/SH3 motifs, induces bone loss via suppression of bone formation and induction of biochemical high bone turnover state, M026

DHT administration is effective for the prevention of hypogonadal bone loss, SU193

Disuse with a rapid bone loss affects the expression profile of osteoblastic and resorption genes, F516

Effect of luteolin on bone loss, microarchitecture and bone resorption in OVX mice, M128

Effect of RIS on bone strength and work to failure determined by FEA and simulation of clinically-measured bone loss and mineralization changes, SA505

Efficacy of whole-body vibration in reducing bone loss in postmenopausal women, M396

Evaluation of the detection sensitivity of simulated trabecular bone loss in  $\mu$ MRI at in vivo resolution, M312

Fully human anti-DKK1 antibodies increase bone formation and resolve osteopenia in mouse models of estrogen-deficiency induced bone loss, 1214

GC-induced bone loss in mice is dependent on beta 2-adrenergic signaling, M102

Genetic locus on chromosome 1q influences bone loss in young Mexican American adults, M250

Gondanotropins, bone loss and fracture in men, 1278

Green tea polyphenols protect bone microarchitecture in female rats with chronic inflammation-induced bone loss, M338

High level dietary P and Cd exacerbate OVX-induced bone loss, M301

IGFBP2 and bone loss in aging women and men, 1284

Impact of adjuvant hormonal therapy on bone loss depending on initial adjuvant chemotherapy and menstrual status, M415

Inhibition of bone loss and muscle atrophy by DHT in a mouse hindlimb disuse model, SU377

Injection of MSCs overexpressing both CXCR4 and RANK-Fc effectively prevented OVX-induced bone loss, F391

Intestinal-specific VDR null mice maintain normal calcemia but display severe bone loss, F238

Intravenous IBN for prevention of early bone loss after kidney transplantation, F413

Is there any association between CYP 17-CYP 19 polymorphisms and bone loss in early postmenopausal women?, M259

Lack of calcitonin accentuates bone loss during lactation by enhanced osteoclast formation and reduced osteoblast formation, SA194

Late pregnancy serum Vitamin D and longitudinal bone loss during pregnancy, F544

Loading duration influences the degree of inhibition of bone loss using dynamic muscle stimulation in a disuse rat model, 1297

Loop diuretic use and rates of hip bone loss, and risk of falls and fractures in older women, F371

Loss of function polymorphisms in the P2X<sub>7</sub> receptor gene are associated with accelerated lumbar spine bone loss in postmenopausal women, SU224

Low serum 25(OH)D is associated with higher rates of hip bone loss in older men, F367

Mechanical loading prevents bone loss due to hormone-deficiency in female mice, M474

Mediation of bone loss with ultrasound induced dynamic mechanical signals in an OVX rat model of osteopenia, F536

Melanoma-induced bone loss is mediated by the rapid recruitment of osteoclasts, SU233

Modeling pathways for bone loss in childhood malignancies, SU237

Neglected role of intracortical remodeling in age-related bone loss, 1101

Obesity is associated with higher BMD, lower bone resorption and slower hip bone loss: are these associations mediated by adipokines?, SU369

Overexpression of GSR in osteoblasts decreases bone formation and partially prevents OVX-induced bone loss, F024

Prevention of aromatase inhibitor-associated bone loss in women with breast cancer, M283

PTH and not Vitamin D predicts age-related bone loss in the elderly, M178

R-spondin 1 reduces bone loss in human TNF transgenic and OVX mice, 1215

Radiation-induced bone loss: description of dose, time course, age, strain and sex variables, SU368

Rate of bone loss is greater in young adult men than women, SU297

Reduced renal function is associated with increased rates of bone loss at the hip and spine, SU357

RIS prevents early radiation-induced bone loss at multiple skeletal sites, 1066

Risk factors for bone loss in the hip in 70-year-old women, SA374

Role of OPG/RANKL system for bone loss in PHPT, M192

Role of OPN in beta-adrenergic signaling induced bone loss in vivo, M174

Selective p38 $\alpha$  inhibitor prevents bone loss induced by estrogen deficiency, M335

Short treatment with Scl-ab can inhibit bone loss in an ongoing model of colitis, 1212

Single nucleotide polymorphisms in the P2X<sub>7</sub> receptor gene are associated with increased postmenopausal bone loss and fracture incidence, SU223

Strength training prevents bone loss at the spine in older breast cancer survivors, SA271

Trabecular bone loss in response to transient muscle paralysis is not gender dependent, SA462

ZOL prevents accelerated bone loss after discontinuation of TPTD, M365

#### Bone marrow

Bone marrow cells participate in normal endothelial, but not epithelial or mesenchymal cell renewal in adult rats, M171

*Ccrn4l*, a peripheral clock gene, influences stromal cell allocation, bone mass, and marrow adiposity in mice and humans, 1073

Changes in marrow cell dynamics and bone geometry with aging in TSP-2 null mice, 1249

Comparison of the effects of zoledronates on the differentiation of human bone marrow and amniotic fluid derived MSCs, SA045

Cortical bone acquisition in the appendicular skeleton of healthy young females is reciprocally related to marrow adiposity, M074

Diet induced obesity compromises the osteogenic potential of the bone marrow, F047

Effect of bone marrow transplantation in a child with malignant IO, SU498

Effect of osteoblast depletion on hematopoietic niches in the bone marrow, F041

Effect of vertebral marrow fat content on the diagnosis of osteoporosis, SA309

Hematopoietic cells in the bone marrow augment anabolic actions of PTH, M181

OPG and bisphosphonates had differential effects on osteoclast numbers, bone marrow fibrosis and cortical porosity in a mouse model of constitutive activation of the PTH/PTHrP receptor, M076

Osteogenic potential of bone marrow, compromised by disuse, is normalized by brief exposure to a low-level mechanical signal, M486

Osteogenic potential of human bone marrow and circulating Stro-1+/CD45<sup>low</sup> cells, M078

Primary human bone marrow adipocytes stimulate osteoclast differentiation, M111

Quantitation of bone marrow fat in long bones of mice using MRI or  $\mu$ CT, M145

Reciprocal relation between MR measures of marrow adiposity and cortical bone in the appendicular skeleton of healthy adults, SU042

Recombinant congenic strain (B.H-6) establishes that trabecular bone mass and bone marrow adiposity are distinct and heritable phenotypes, F265

Reconstituting marrow-derived extracellular matrix ex vivo: an optimal niche for retaining the properties of human MSCs, M165

Role of AXII and AXIIR in homing MM cells in the bone marrow, SA287

Selective retention of bone marrow cells in repair of canine femoral defect with polycaprolactone-tricalcium phosphate scaffolds, SU005

#### Bone marrow ablation

N-terminal fragment of PTHrP promotes the GC-related deficiency of bone regeneration after bone marrow ablation in mice, M195

#### Bone marrow stromal cells (BMSC)

Aging of human BMSC: role of WNT pathways, SA048

Anabolic PTH treatment mobilizes BMSC and osteoprogenitors towards bone surfaces, SA229

BMSC aging directly alters bone formation, 1252

BMSC and Osx contributing to osseointegration of dental implants, SA138

BMSC up-regulate M-CSF receptor in monocytes to disrupt dendritic cell differentiation while facilitating osteoclastogenesis in myeloma, SU242

BMSC-derived extracellular matrix promotes MSC motility, SA134

Different osteogenic properties of human BMSC from different skeletal site origin, SU055

Distinct modes of osteoblastic differentiation from BMSC and vascular smooth muscle cells: induction by BMP-2 and PKA and suppression by Vitamin D derivatives, SU060

DNA methylation analysis of osteogenic gene promoter regions in mouse BMSC, M035

Effect of resveratrol and flax oil on MC3T3-L1 pre-adipocyte and ST2 BMSC proliferation and differentiation, SU059

Enhanced osteogenic potential of alveolar vs. long bone derived BMSC, M095

Expression of 1 $\alpha$ -hydroxylase (CYP27B1) in BMSC, SA237

Loss of classical ERE signaling results in suppression of early commitment of BMSC to osteoblasts, F029

Mature human adipocytes differentiated from BMSCs, SA042

MKP-1 is an endogenous negative regulator of pro-inflammatory cytokines in BMSC, SU013

SP stimulates BMSC osteogenic activity and osteoclast differentiation and function in vitro, SU032

Stable isotopic labeling of amino acids in cultured human BMSC: application to BMP-2 induced Wnt/ $\beta$ -catenin signaling, SA036

WNT-4 acts through the non-canonical pathways to stimulate osteoblast and BMSC differentiation, F050

#### Bone mass

Angiotensin II type 2 receptor blockade increases bone mass, SU007

## Key Word Index

## ASBMR 30th Annual Meeting

ARZ in postmenopausal women with normal or low bone mass, SA421

Bone mass recovers in young women with anorexia nervosa who are both weight and menstrual recovered, F339

In bone, RPTP $\alpha$  is exclusively expressed in osteocytes and may affect bone mass, SA052

Both excess and restricted energy availability negatively influence acquisition of trabecular bone mass and microarchitecture during growth, M493

Brain-derived serotonin positively regulates bone mass accrual, SA463

BZA in combination with conjugated estrogens improves bone mass and strength in the OVX rat, SA385

Cannabinoid receptor GPR55 affects osteoclast function in vitro and bone mass in vivo, 1221

CCR2 receptor signaling is involved in bone mass regulation and mediates the response to anabolic but not catabolic regimens of PTH(1-34), SU158

*Ccrn4l*, a peripheral clock gene, influences stromal cell allocation, bone mass, and marrow adiposity in mice and humans, 1073

Central and peripheral leptin treatment produce similar increase in cortical and trabecular bone mass in ob/ob mice, SU164

Circulating DKK1 levels are reduced in young subjects with low bone mass, F455

Common genetic factors contribute to the relationship of body composition and bone mass in mouse populations, M244

Common single nucleotide polymorphism in the *HMGA2* gene is associated with bone mass in men, SA268

Cortical bone mass and structure in older Afro-Caribbean and Caucasian men, SU300

Critical role of Cx43 in postnatal skeletal growth and bone mass acquisition, 1257

Crosstalk between androgen receptor and Wnt signaling mediates sexual dimorphism during bone mass accrual, 1121

Deletion of *Mef2c* in osteocytes decreases *Sost* expression and increases bone mass, F054

Deletion of the *Dkk-1* *Krm-1* and *Krm-2* in mice leads to increased bone formation and bone mass, 1004

Double deletion of  $\alpha 2a$ - and  $\alpha 2c$ -adrenergic receptors results in a phenotype of high bone mass and in resistance to the thyrotoxicosis-induced osteopenia, F244

Effect of 12 months gymnastics participation on bone mass accrual in 4 to 7 year olds, SA555

Effect of cannabinoid CB1 receptor ligands on body weight and bone mass in mice, M340

Effect of RIS in liver transplantation patients with low bone mass, SA503

Effects of ALN or DMAb on cortical and trabecular bone mass, bone strength, and bone mass-strength relationships in mice, 1139

Effects of diet and menstrual cyclicity on bone mass accumulation in pubertal monkeys, M499

Effects of ODN on bone mass and turnover in estrogen deficient adult rhesus monkeys, SA072

Elevated systolic blood pressure is positively related to bone mass measurements in overweight pre-pubertal and pubertal children, M496

FOXO1 signaling in the control of bone mass, 1112

G171V and A214V *Lrp5* knock-in mice have increased bone mass and strength, and can help precisely define the in vivo functions of *Lrp5* during bone growth and homeostasis, 1002

High bone mass due to increased bone formation in mice lacking the CTR, SA192

High bone mass phenotype in the bone specific *Dlx3* KO mice, M027

IC162, a new flavonoid, preserves bone mass and microarchitecture without affecting uterine weight in OVX rats, SA386

Improved bone mass after co-administration of Sr ranelate and RIS in a rat model of osteoporosis using "in-vivo"  $\mu$ CT, SU393

Influence of long-term hormone replacement therapy on tibia bone mineral mass and mass distribution in postmenopausal women, F420

Influence of muscle size and strength on changes in bone mass and size during growth and in response to exercise, SA537

Inpp4b as a regulator of bone mass, F089

Intermittent PTH administration increases bone mass and strength in aged mice by antagonizing oxidative stress-induced osteoblast apoptosis via ERK-mediated attenuation of p66<sup>shc</sup> phosphorylation, SU380

Investigation into the impact of OA changes on BMD measurements in patients with high bone mass, SA257

Low bone mass and decreased biomechanical response in beta 1 adrenergic receptor KO but not in beta 2 adrenergic receptor KO mice, 1141

MKP-1 protects bone mass via negative regulation of osteoclast differentiation and activation, 1219

Obesity induced by high dietary fat leads to increased bone resorption marker, TRAP, and decreased bone mass in mice, M238

Overexpression of Lef-1 $\delta$ N increases bone mass in mice, 1258

Possible central function of the calcitonin receptor on bone mass, SA255

Preference and satisfaction with a 6-monthly subcutaneous injection versus a weekly tablet for treatment of low bone mass, M372

PTH receptor signaling in osteocytes increases bone mass and the rate of bone remodeling through Wnt/LRP5-dependent and -independent mechanisms, respectively, 1038

PTH-induced bone mass gain is blunted but not abolished in *SOST* overexpressing and deficient mice, 1039

Quantitative  $\mu$ CT imaging of adipocyte volume in bone marrow of mice with high and low bone mass, SU250

Randomized, placebo-controlled, double blind study on high frequency, low intensity vibration in bone mass, muscle strength and quality of life in children with motor disabilities, F435

Recombinant congenic strain (B.H-6) establishes that trabecular bone mass and bone marrow adiposity are distinct and heritable phenotypes, F265

Recovery of bone architecture after RANKL administration in rats is characterized by increased bone mass on existing trabeculae assessed by in vivo  $\mu$ CT, SU076

Regulation of bone mass and osteoclastogenesis by the CEACAM1, F091

Relationship between low bone mass and aortic valve sclerosis in Korean men and women, SU452

Replacing testosterone in male cardiac transplant patients exerts multiple benefits on bone mass, libido and sexual activity, M388

Scl-Ab increases bone mass by stimulating bone formation and inhibiting bone resorption in a hindlimb-immobilization rat model, 1138

Soluble activin receptor type IIA fusion protein, ACE-011, increases bone mass by stimulating bone formation and inhibiting bone resorption in cynomolgus monkeys, SU376

Telomerase deficiency leads to decrease bone mass and impaired MSCs functions in telomerase deficient (TERC<sup>-/-</sup>) mice, 1147

TGF $\beta$  receptor I kinase inhibitor increases bone mass in normal mice, SA172

TGIF regulation of bone mass: impaired osteoblast differentiation, SA018

Transition from ALN to DMAb in OVX cynomolgus monkeys maintained or improved cortical and trabecular bone mass, without altering the linear relationship between bone mass and bone strength, 1072

Vitamin D status in young women is strongly negatively related to body weight, BMI and body fat, but is not associated to bone mass, SU203

Vitamin D status, bone mass, and bone metabolism in postmenopausal women and men older than 50 attended in a primary care center of Spain, M223

Weight reduction is not deleterious for bone mass or strength in obese women, SA338

**Bone mass, peak (PBM)**

Augmentation of PBM occurs in female and male mice without progesterone nuclear receptors, F249

Bone size, volumetric bone density in relation to fat mass in healthy young men at age of PBM, SU477

Heel ultrasound and consolidation of PBM in young women, M504

Osteoblast-targeted deletion of the GC receptor has little impact on PBM but attenuates DEX-induced suppression of bone formation, F452

PBM is determined at 1 year-old: evidence from growth charts, F542

Volumetric bone parameters in relation to fracture history in healthy men at the age of PBM, SU302

**Bone mechanics**

Murine bone mechanics is determined by the ultrastructural canal network in a sex- and strain-specific manner, M456

**Bone metabolism**

Acute phase response and bone metabolism marker after intravenous bisphosphonate in osteoporotic patients with rheumatism, M364

Bone metabolism in long-term kidney transplantation recipients, SA499

Bone metabolism, microarchitecture and densitometric measurement in rat femur after chronic alcohol consumption, M239

Changes of bone metabolism in immunosuppressant, FK506 treated rats, SU383

DC-STAMP regulates bone metabolism through cell-cell fusion of osteoclasts, F087

Dried plum alters bone metabolism via a different mechanism than PTH, M341

Effect of a one year exercise program on markers of bone metabolism after hip fracture, SA432

Effects of *Acanthopanax senticosus* extract on bone metabolism in Korean postmenopausal women, SA431

Effects of estrogen therapy and fluocalcic effervescent on the BMD and bone metabolism of surgical menopause women with osteopenia, M392

Effects of exercise intensity on the bone metabolic response to running, M481

Effects of KHCO<sub>3</sub> on Ca and bone metabolism during high salt intake, SA446

Effects of low dose estrogen therapy on the BMD and bone metabolism of menopausal women, M393

FGF-23 and parameters of Ca and bone metabolism are positively influenced by GH replacement in adult GH deficiency patients from the KIMS survey, SU177

New automated multiplex assay for simultaneous measurements of four serum biochemical markers of bone metabolism in osteoporosis, SA295

Proteasome inhibition counteracts the negative effect of GC treatment on bone metabolism by stimulating osteoblasts and inhibiting osteoclasts in vitro, SA231

Vitamin D status, bone mass, and bone metabolism in postmenopausal women and men older than 50 attended in a primary care center of Spain, M223

**Bone mineral content (BMC)**

- Birth weight predicts bone size, adult weight predicts BMC and BMD in young Gambian adults, M498
- Differences in BMC at the lumbar spine and proximal femur in South American children of different ethnic groups, SU490
- Bone mineral density (BMD)**
- “Vibes” Trial: LMMs to improve BMD, M397
- 30IT/C of SCT modulates BMD by Wnt and estrogen signaling pathways, 1270
- 6819 analysis on measurement of BMD of phalanges by radiographic absorptiometry in Beijing, SA313
- Advanced hip assessment and BMD in Japanese women with OA, M449
- Advancing maternal age is associated with lower peak BMD in the male offspring, M327
- Age-related changes in BMD, cross-sectional area and the strength of rat femur; an involvement of suppression of GH-IGF-1 signaling, SA467
- ALN treatment in postmenopausal Romanian women followed by BMD-digital x-ray radiogrammetry, M357
- Application of a treatment algorithm to avoid BMD loss and limit bisphosphonate use after kidney and kidney/pancreas transplantation, SA497
- Are there any ethnic differences in BMD in a lupus cohort?, SU358
- Assessment of cortical thickness and BMD in the radius by low-frequency Q-GWUS, M319
- Assessment of fracture risk and treatment of osteoporosis in postmenopausal women: bone density vs. Bone DESTINY, SU251
- Assessment of the 10-year risk of fracture in Italian postmenopausal women using BMD and clinical risk factors, SU348
- Association between BMD change, use of antiresorptive agents and fragility fracture in women and men, SA364
- Association between femoral neck BMD and the factor-of-risk for hip fracture derived from direct measurements of strength in human cadaveric femora, 1070
- Association between polymorphisms in TNFR genes and circulating TNFR levels, and BMD in postmenopausal Korean women, M258
- Association between several factors affecting aortic calcification and BMD in postmenopausal women, SA489
- Association between vascular calcification and low total femur BMD in elderly people community-dwelling, SU453
- Association of CTR gene polymorphisms with BMD and fracture risk in postmenopausal Koreans, M256
- Association of *HSD11B1* polymorphisms with vertebral fracture risk and BMD in postmenopausal Korean population, M260
- Associations of the VDR and calcitonin receptor genes with bone density, bone turnover markers and fracture incidence with regard to Ca intake level in Slovak postmenopausal women, M261
- Bilateral bone density loss after unilateral disuse in the forearm, SA519
- Birth weight predicts bone size, adult weight predicts BMC and BMD in young Gambian adults, M498
- Bisphosphonates in children with hypercalciuria and reduced BMD, M429
- BMD and biochemical marker response rates in postmenopausal women after treatment with ZOL, F401
- BMD and body composition in postmenopausal women with psoriasis and psoriatic arthritis, SU337
- BMD and vertebral fracture in women with breast cancer and antiaromatase therapy, SA400
- BMD changes over time associated with illness and recovery in young women with anorexia nervosa, SA558
- BMD in children and adolescents with sickle cell disease, SU217
- BMD is associated with lean mass and not fat mass, SU273
- BMD measurement by DXA after a fragility fracture increases the likelihood of subsequent osteoporosis treatment, SU296
- BMD measurement: an independent risk factor of breast cancer recurrence?, SU265
- BMD response to treatment with rPTH in patients previously treated with bisphosphonates, M348
- BMD shows no peak from birth to youth as measured by QCT, F310
- BMD, fracture and survival in women in nursing/residential care, SA340
- BMD-associated SNP lies in a Runx2 binding site of the LRP5 promoter, M264
- Body fatness negatively associated with BMD and hip geometry indices in adolescents, F546
- Bone density changes at the non-operated hip following total hip arthroplasty, M408
- Bone density comparisons in young male rock climbers, weight lifters and sedentary controls, SA534
- Bone fragility beyond BMD: a French prospective experience, SU288
- Bone size, volumetric bone density in relation to fat mass in healthy young men at age of PBM, SU477
- Bone volumetric density, geometry and strength in male and female collegiate runners, SA539
- Carotid plaque causes low spinal BMD in Korean postmenopausal women with diabetes, SU359
- Changes in volumetric bone density and bone strength at the tibial midshaft in boys and girls 12-17 years of age, SU469
- Clinical prediction rule to identify women for BMD testing at menopause, SU271
- Clinical tool for adjusting BMD Z-scores for body size in growing children, 1105
- Comparison of the effects of IBN alone with IBN in combination with SNAC on bone density and bone strength in OVX rats, SU391
- Correlation of hip geometry and bone density with fragility fracture in Japanese postmenopausal women, SU466
- Correlations between panoramic radiomorphometric indices and BMD in postmenopausal women, SA311
- Deformity of the distal radius fractures resulting from falls in Japanese women over 50 years of age is closely associated with BMD of the lumbar spine, SU286
- Determinants of low BMD in HIV infected postmenopausal women, SU455
- Determinants of trabecular and cortical volumetric BMD differ in men of African ancestry, SU299
- Dietary patterns in Canadian men and women ages 25 and older: relationship to BMI and BMD, SU309
- Dkk-1 predicts the gain of BMD in osteoporotic women on bisphosphonates, SA300
- Early exposure to soy isoflavones modulates bone mineral, strength and microarchitecture in CD1 mice, M503
- Effect of a single infusion of ZOL 5 mg versus oral RIS 5 mg on BMD at lumbar spine, hip, femoral neck and trochanter in patients with GIO, F403
- Effect of DMAB vs ALN on bone turnover markers and BMD changes at 12 months based on baseline bone turnover level, 1285
- Effect of metabolic acidosis on BMD and bone microarchitecture in normal and OVX rats, M409
- Effect of once-yearly ZOL on integral BMD of the spine, SU405
- Effect of parity on BMD in premenopausal women, SA325
- Effect of RIS on bone density in HSC transplant patients, SU407
- Effect of RLX treatment on BMD might be influenced by UGT1A1\*28 polymorphism, M257
- Effect of ZOL (single 5-mg infusion) on lumbar spine BMD versus oral RIS (5 mg/day) over 1 year in subgroups of patients receiving GC therapy, M363
- Effects of a high g environment on BMD in UK fast-jet trainee pilots, SU473
- Effects of aromatase inhibitor therapy on BMD in hypogonadal elderly men, 1135
- Effects of diacylglycerol oil on body composition, BMD and bone strength in mice, SA442
- Effects of DMAB vs ALN on BMD, bone turnover markers, and safety in women previously treated with ALN, M395
- Effects of estrogen therapy and fluocalcic effervescent on the BMD and bone metabolism of surgical menopause women with osteopenia, M392
- Effects of low dose estrogen therapy on the BMD and bone metabolism of menopausal women, M393
- Effects of neurological impairment and functional mobility on BMD following stroke, SU364
- Efficacy and safety of monthly oral IBN in postmenopausal women with low bone density, SU384
- Epistasis between QTLs for bone density variation in Copenhagen X Dark Agouti F2 rats, M253
- Essential fatty acid and fish intake is associated with higher BMD in elderly women and men, F341
- Evaluating the effect of soy and isoflavones on BMD in older women, M353
- Evaluation of BMD changes in women with severe osteoporosis after TPTD treatment, M355
- Evaluation of BMD following an education intervention on osteoporosis offered to women after a fragility fracture, SU330
- Evaluation of tibial bone density surrounding Ta tibial implants in TKA, SU266
- Extended lactation is associated with failure to restore BMD 6 months after resumption of menstrual cycle, M305
- Femoral BMD and femoral structure, assessed by DXA-based hip structural analysis, contribute independently to femoral strength, M304
- Femoral strength, bone density, and aging in women and men, 1165
- FRAX™ and the assessment of ten-year fracture probability in Hong Kong Southern Chinese according to age and BMD femoral neck T-scores, SU264
- Frequent apheresis for platelet and plasma donations constitutes an independent risk factor for decreased BMD, F327
- Functional polymorphism in COL1A2 (Ala459Pro) that is associated with intracranial aneurysms, shows heterozygous disadvantage concerning BMD and stroke in elderly men, SU219
- Functionality outcomes including brisk walking speed are associated with BMD in postmenopausal women, SU418
- Gene transcripts related to T-cell activation, proliferation, and cytokine signaling show significant effects on BMD variation in baboons, M241
- GWAS of BMD and hip geometry indices, 1092
- GWAS reveals genetic variants associated with BMD, osteoporosis and osteoporotic fractures, SA263
- Hemodialysis patients rapidly lose their bone minerals after 60 years of age, SU438
- High impact exercise may have a protective effect on BMD but moderate impact exercise may have negative effect in young women with anorexia nervosa, M324
- High-fat diet facilitated decreases in BMD of OVX mice and suppressed the anabolic effects of PTH on bone, SA448
- Higher BMD is associated with increased odds of carotid atherosclerosis in postmenopausal women not currently using estrogen therapy, 1206

## Key Word Index

## ASBMR 30th Annual Meeting

Higher BMD loss in older men with diabetes, 1209

Hormonal influences on volumetric bone density and geometric properties in obesity, SU367

Impact of varying BMD resources on prediction of hip fracture using FRAX™, SU257

Impaired methylation capacity is associated with low BMD, SU317

Improved forearm BMD after treatment with Vitamin D<sub>3</sub> in a patient 30 years after bariatric surgery, SA492

Increases in BMD observed with Scl-Ab treatment are reversible, 1211

Influence of PHP on BMD and vertebral morphometry, M190

Influence of sex hormones on BMD in middle aged and elderly men, SU335

Integrative genetics approach to identify candidate genes regulating bone density: combining linkage, gene expression and association, M247

Interaction between the skeletal parameter BMD and lifestyle factors in 390 adolescent daughter-mother pairs, F548

Investigation into the impact of OA changes on BMD measurements in patients with high bone mass, SA257

Lack of correlation between glycemic control and BMD in type 2 diabetic women, SU255

Large scale candidate gene analysis identifies an association between the CDK6 locus and trabecular volumetric BMD at the lumbar spine in older men, M266

Lean body mass is a better predictor of BMD than leg power or grip strength in healthy caucasian adults, SU290

Linkage and association study of chromosome 1p36 with BMD in southern Chinese, SU295

Loss or gain of FoxO function in osteoclasts and osteoblasts alters the rate of apoptosis and BMD in mice, 1247

Low calcaneal BMD estimated by a periferal DXA heel scanner is associated with a high risk to have had a distal radius fracture, SU262

Low systemic BMD increases implant migration in cementless hip replacement, F458

Lumbar spine TBS complements BMD in the discrimination between vertebral fractured and non-fractured subject, M308

MACD index is a strong predictor of cardiovascular death and include the predictive power of BMD, SU463

Model of high body mass: BMD, bone markers and adipocytokine levels in high level male rugby players, SA167

Negative association between the metabolic syndrome and BMD in Korean adults, SU304

Obesity is associated with higher BMD, lower bone resorption and slower hip bone loss: are these associations mediated by adipokines?, SU369

Osteoblastic androgen receptor regulates cortical BMD, 1122

Patients with CKD and low 1/3 radius and femoral neck BMD have markedly abnormal cortical and trabecular microstructure by HR-pQCT, 1033

Patients with fragility fracture assessed by BMD, Bone DESTINY and osteoporosis Canada guidelines, SA343

Percutaneous injection of GEM OS2 increases vertebral BMD in geriatric female baboons, F376

Phased GWAS identifies probable new gene affecting BMD, M245

Physical activity, BMD and fragility fracture, M325

Physician practices in bone density testing among Medicare patients, SA428

Polymorphisms in *CYP24A1*, the gene encoding 25(OH)D-24-hydroxylase, are associated with BMD, SA266

Polymorphisms in the WIF1 gene are associated with BMD in elderly Swedish women, SA264

Poor peripheral nerve function is related to lower BMD, SA328

Positive Celiac disease serology and BMD in adult women, SA366

Positive influence of physical activity on BMD measurements and hip geometry parameters in young adults, M477

Post-fracture mortality in men: contributions of sex hormones and BMD as risk factors, 1280

Predictive validity of the WHO FRAX model, BMD and prevalent vertebral fracture for incident radiographic vertebral fractures, 1127

Preterm birth and BMD in young adulthood, 1103

Pretransplant parathyroid function predicts laboratory and BMD changes after kidney and kidney/pancreas transplantation, 1032

QUS, BMD and QCT in women with established osteoporosis treated with TPTD, SA393

Randomized, double-blind, placebo-controlled study of ODN (MK-822) in the treatment of postmenopausal women with low BMD, 1291

Recalculation of genome scans on a common genetic map enhances our ability to identify common bone density QTL in new and historical data, 1276

Reduction of BMD in the patients with RA is more remarkable at proximal femur than at lumbar spine, SU451

Regional differences of femoral BMD changes after one year once-monthly IBN as measured by 3D QCT, SU260

Reimbursement for BMD testing among US Medicare beneficiaries, SA326

Relationship among nutritional status, oxidative stress and bone density in institutionalized elderly, SU310

Relationship between BMD of the lumbar spine and knee OA in South Korean, SU298

Relationship between clinical risk factors for osteoporosis and BMD in women aged less than 50 years, SU355

Relationship between the metabolic syndrome and BMD in Korean middle-aged women, SU291

Relationship of bone turnover marker (PINP) and changes in femoral neck BMD to fracture risk in women with postmenopausal osteoporosis treated with once-yearly ZOL 5 mg, 1027

Relationship of QUS at phalanges with hand and axial BMD, sex hormones and bone turnover markers in elderly women, M320

Reproducibility of mineral density and morphometric  $\mu$ CT measurements at different voxel size scans, M311

Retrospective study evaluating the relationship of Vitamin D 25 OH and free testosterone levels with changes in hip bone density after liver transplantation, SA502

Risk factors for low BMD in healthy men age 50 years or older, SU341

Rosiglitazone-induced change in BMD among African Americans with type 2 diabetes mellitus or impaired glucose tolerance, SU315

Self-reported weight at birth predicts measures of femoral size but not volumetric BMD in elderly men, SU338

Significant association between polymorphisms of *CYP19A1*, fracture incidence and BMD in post-menopausal women, M262

Smoking is an independent predictor of low BMD, prevalent vertebral fractures and incident fractures in elderly men, SU349

Socioeconomic status, BMD testing and hip fracture rates in a universal health-care system, SU293

Study about the association of circulating MCP-1 levels with lumbar BMD in Korean women, M407

Ten-year change in BMD in a representative sample of Japanese women, SA330

Three year school-curriculum-based exercise program in prepubertal children increases bone mineral accrual and bone size but do not influence femoral neck structure, 1107

Timed Up and Go test and BMD as predictors of fracture, F373

Timing of repeated BMD measurements: development of an absolute risk-based prognostic model, F347

Transgenic ASARM-peptide overexpression with reduced serum phosphate and 1,25(OH)2D3 leads to decreased BMD and obesity, F210

Treatment discontinuation due to gastrointestinal adverse events and decreased BMD in patients switched from branded ALN to generic ALN, SA414

Type 1 diabetes is associated with lower BMD in premenopausal women but not in middle-aged men, SU456

Usefulness of alveolar bone density measurement in risk assessment for BRONJ, SA305

Validation of bone mineral measurements on the new Norland Model XR-600 and XR-800 using the BMIL QA/QC Phantom, SU252

Valproate: a model for adverse psychoactive drug effects on BMD, SA556

Variation in the osteocalcin gene: association study of BMD, fracture and changes in body fat mass in elderly women, SU225

Vertebral fracture in men: level of trauma, BMD and lean body mass, SU360

In vivo bone matrix density measurements by water and fat suppressed projection MRI (WASPI), SA102

In vivo differential expression profiling study on human circulating B cells suggested a novel EGFR and CALM3 network underlying smoking and BMD, SU154

Weight and BMI predict BMD and fractures in women 40 to 59 years, SA438

**Bone mineral density (BMD), volumetric**

Areal BMD by DXA may predict similar risk of fracture in elderly women and men due to offsetting effects of bone size and true volumetric BMD, SU267

Compartment specific genetic analysis of trabecular and cortical volumetric BMD in men, SU284

**Bone mineralization**

Aberrant *Phex* function in osteocytes has limited effects on bone mineralization in XLH, 1051

Altered TNSALP expression and phosphate regulation contribute to reduced mineralization in mice lacking androgen receptor, SU181

Deletion of the oxygen-sensor PHD2 in chondrocytes results in increased cartilage and bone mineralization, 1153

Deletion of Zfp521, an antagonist to Runx2 and Ebf1 transcriptional activity, leads to osteopenia and a defect in matrix mineralization in mice, 1109

Effect of RIS on bone strength and work to failure determined by FEA and simulation of clinically-measured bone loss and mineralization changes, SA505

Effects of long-term administration of high-dose GH on body composition and bone mineralization, SA571

FGF-23 and FGF-2 share a common but also have distinct signaling pathways for negative regulation of bone nodule mineralization in cultured osteoblasts, SA206

Fluoride effects on bone formation, mineralization and mechanical properties are influenced by genetics, SU465

Human skeletal muscle cells undergo matrix mineralization in an osteogenic pellet culture assay, M135

Imaging of mineralization kinetics suggests that the transition from osteoblast to osteocyte initiates prior to mineral deposition, F062



Inactivation of the ILK in osteoblasts increases mineralization, M061

Inhibition of PPAR $\gamma$ 2 by BADGE and Vitamin D in male mice increases osteoblastogenesis and inhibits bone matrix mineralization leading to osteomalacia, SU374

Inhibition of the mevalonate pathway rescues the DEX-induced suppression of the mineralization of osteoblastic cells, SA230

Li affects matrix mineralization by decreasing tissue non-specific ALP levels in osteoblasts, SA071

Long-term treatment with oral bisphosphonates in postmenopausal women: effects on the degree of mineralization and microhardness of bone, 1029

Low magnitude vibration can inhibit muscle loss and increase mineralizing bone surfaces in aging mice, M173

Mineralization is related to collagen cross-links in growing cancellous and cortical bone, SA110

Mineralization potential and orientational aspects of osteogenic cell cultures by Raman spectroscopy, M084

Molecular mechanisms underlying matrix vesicle-induced mineralization during bone formation, SA063

Notch signaling regulates osteoblast maturation transition to mineralization phase, SA068

Novel screening system for bone matrix proteins that control bone mineralization, SA108

Overexpression of CCN2/CTGF in cartilage shows prolonged bone length resulting from stimulation of chondrogenesis, chondrocyte growth, apoptosis, and bone mineralization during endochondral ossification, M153

Phex binds to SNARE-associated protein snapin and co-localizes in vesicle-enriched, extracellular matrix micro-environment mediating mineral crystal nucleation, F066

Prostaglandins enhance extracellular matrix mineralization through the enhancement of both Na-dependent phosphate transport activity and ALP activity in osteoblast-like cells, SU031

Proteins involved in mineralization expressions perturbations in bones and teeth of Msx2 mutant mouse mandibles, SA150

Requirement of the bone for Vitamin D for 1,25(OH) $_2$ D $_3$  synthesis and bone mineralization, M224

Solid-state  $^{31}$ P MRI quantifies mineralization changes in OVX rat bone, M422

**Bone morphogenetic protein (BMP)**

BMP/Wnt antagonists are upregulated by DEX in osteoblasts and reversed by ALN and PTH: potential therapeutic targets for GIO, M098

Catecholamines accelerate BMP-induced osteoblastic differentiation and bone formation, SU137

Dual roles of Smad proteins in the conversion from myoblasts to osteoblastic cells by BMPs, SA161

Estrogens reverse a potentiating effect of the unliganded estrogen receptor on BMP-induced transcription and osteoblastogenesis by promoting ERK-dependent Smad1 phosphorylation at the linker region, SU189

Expression of BMP antagonists during fracture healing, SA160

Icariin induces osteogenic differentiation in vitro in a BMP- and Runx2- dependent manner and bone regeneration in vivo, M089

Inhibition of BMP pathway and osteoclast activity in osteoblastic prostate cancer lesion in bone, F283

Integrin-associated protein upregulates osteogenesis-related transcription factors via TGF $\beta$  and BMP pathways, SA028

Interplay between BMP and TGF $\beta$  signaling in osteoblast differentiation, SA031

Negative regulation of Tcf/Lef-dependent transcription by the BMP/Smad4 signaling axis, SU144

Point mutation of endofin at PP1c-binding domain induces angiogenesis and bone formation in mice by sensitizing BMP signaling, 1082

Regulation of bone formation by osteoclasts involves Wnt/BMP signaling and the chemokine S1P, M017

Regulation of chondrogenesis and bone development by neogenin via BMP pathway, SU127

Regulatory signaling pathways in BMP mediated osteogenesis of adult human MSC cultures, M060

Runx2 and canonical Wnt signaling cooperatively regulate BMP-induced differentiation pathways of adult dural cells into osteoblasts or chondrocytes, M043

TGF $\beta$  inhibits BMP signaling and osteogenesis through the TGF $\beta$  and BMP R-Smad direct interaction, 1080

TGF $\beta$ -and BMP-signaling pathways have antagonistic effects during chondrogenesis, F158

Traf2 regulates BMP signaling pathway in osteoblastic cells, M063

Transcription factor NFATp regulates BMP-induced chondrocyte differentiation in a tissue-specific manner, SU020

Wnt pathway regulation by demineralized bone requires TGF $\beta$ /BMP signaling, SU138

**Bone morphogenetic protein-1 (BMP-1)**

Circulating BMP-1 isoforms: novel diagnostic and therapeutic challenges for bone fracture repair, SU142

**Bone morphogenetic protein-2 (BMP-2)**

Ang-1 enhanced BMP-2 induced osteoblast differentiation, SU035

BMP-2 inactivates TAK1-ATF2 signaling pathway in chondrocytes, F186

BMP-2 induces Osx expression through up-regulation of Dlx5 and its phosphorylation by p38 MAPK, F020

BMP-2 stimulates a feedback activation loop for expression of NFATc1 in osteoblasts, F002

BMP-2-stimulated signaling niche in osteoblasts comprising of Smad and PI3K/Akt regulates NFATc1 expression and its nuclear translocation, 1081

Both the Smad and ERK MAP kinase pathway play critical roles in BMP-2-induced osteogenic transcription factors expression, M050

Conditional deletion of BMP-2 gene in early osteoblasts leads to reduction in the total bone marrow MSCs and their capacity to form osteoblast precursors, 1114

Coordinate regulation of PTHrP and PTHR1 in the osteoblast differentiation of C2C12 cells promoted by BMP-2, SA157

Dependence of post natal osteogenic differentiation on BMP-2, SA001

Distinct modes of osteoblastic differentiation from BMSC and vascular smooth muscle cells: induction by BMP-2 and PKA and suppression by Vitamin D derivatives, SU060

Effects of statins on eNOS and BMP-2 in osteoblasts, SU378

Identification of IRX3 a novel transcription factor during BMP-2 mediated osteoblast differentiation, SU024

Impaired bone healing in a BMP-2 KO mouse model of DO, SA159

INF $\gamma$  attenuates BMP-2 signaling via Stat-1 binding of Smad4 in the cytoplasm, SU139

Lxn is a novel effector of BMP-2 signaling in modulation of chondrocyte differentiation, SU117

Mechanism of BMP-2 enhancement of PGE $_2$  stimulated osteoclastogenesis, SU085

MEPE expression is regulated by BMP-2 signaling through the activation of its downstream transcription factors, Dlx3, Dlx5 and Runx2, SA064

Osteogenesis effect of human ligamentum flavum, myoblast, osteoblast and MSC by DBM and BMP-2, SU135

PKD regulates HDAC7 localization and interaction with Runx2 during BMP-2-stimulated osteogenesis, SU027

Program of miRNAs control BMP-2 induced bone phenotype development, M090

Regulation of the BMP-2 distant osteoblast enhancer by FGF-2, SU150

Soy-based formula promotes bone growth in neonatal piglets by inducing osteo-progenitors to differentiate into osteoblasts via enhanced BMP-2 signaling, SA336

Stable isotopic labeling of amino acids in cultured human BMSC: application to BMP-2 induced Wnt/ $\beta$ -catenin signaling, SA036

**Bone morphogenetic protein-2, recombinant human (rhBMP-2)**

Functionalization of a PLGA/PEG-PLA composite electrospun scaffold with rhBMP-2 plasmid DNA for bone regeneration, SA124

rhBMP-2 accelerates segmental defect healing in diabetic rats, M445

**Bone morphogenetic protein-3 (BMP-3)**

BMP-3-null aged mice display increased trabecular bone volume and reduced cross sectional area at the mid-femoral diaphysis, SU143

**Bone morphogenetic protein-4 (BMP-4)**

Canonical Wnt signaling suppresses BMP-4 accumulation from C3H10T1/2 cells transfected with BMP-4 expression vector, SA156

**Bone morphogenetic protein-6 (BMP-6)**

BMP-6 from bone regulates serum glucose via IGF-1 released from pancreas, SU141

BMP-6 stimulated osteogenesis of HOB cultures is associated with suppression of PYK2, SU048

**Bone morphogenetic protein-7 (BMP-7)**

BMP-7 is not required for fracture healing, SU148

Efficacy of single-level instrumented posterolateral (intertransverse) lumbar spinal fusion in baboons with BMP-7 putty, SU146

Safety and efficacy of BMP-7 putty in a rabbit model of posterolateral vertebral lumbar fusion, SU149

**Bone quality**

Bone quality in Chinese-American and Caucasian women, SU464

Degradation of allograft bone quality by gamma irradiation is not explained by altered enzymatic or non-enzymatic cross-links, M460

Effects of running exercise on bone quality after immobilization, SA518

ODN increases bone strength and maintains bone quality in estrogen deficient adult rhesus monkeys, F508

QCT and FEA assessment of proximal femur bone quality and strength in women with postmenopausal osteoporosis receiving once-monthly oral IBN for 12 months, SA509

Regulation of parameters of bone quality by MMP-2 and MMP-9, 1144

TR $\beta$ -specific agonist GC-1 increases bone quality of adult female mice, M228

**Bone regeneration**

Clinical application of resorbable polymers in guided bone regeneration, SA003

Functionalization of a PLGA/PEG-PLA composite electrospun scaffold with rhBMP-2 plasmid DNA for bone regeneration, SA124

Icariin induces osteogenic differentiation in vitro in a BMP- and Runx2- dependent manner and bone regeneration in vivo, M089

N-terminal fragment of PTHrP promotes the GC-related deficiency of bone regeneration after bone marrow ablation in mice, M195

## Key Word Index

## ASBMR 30th Annual Meeting

SATB2 overexpression promotes osteoblast differentiation and enhances regeneration of bone defects, SU058

**Bone remodeling**

Central control of bone remodeling: neurohypophyseal hormone oxytocin is decreased in severe postmenopausal osteoporosis, M418

CT-1 is an osteoclast-derived coupling factor required for normal bone remodeling, M014

Development of empirical model using  $^{41}\text{Ca}$  for the study of bone remodeling in human, SA454

Do type I collagen homotrimers contribute to osteoporosis by altering bone remodeling?, SA146

Increased non-enzymatic glycation of cancellous bone due to decrease in remodeling during ALN therapy of osteoporotic women, 1071

Influence of IM on bone remodeling in juvenile mice, SA292

Mathematical model of remodeling cycles with feedback mechanism for maintaining the balance between bone resorption and formation, WG27

MEPE regulates bone remodelling independent of serum phosphate and alters renal vascularization, F205

Mice deficient in BSP display impaired modeling and remodeling and respond to ovariectomy but not to the cortical anabolic effect of PTH, 1191

Mice lacking the novel transmembrane protein Opt develop catastrophic defects in bone modeling, 1075

Microdamage repair and remodeling requires mechanical loading, 1299

NanoCT can be used to assess mechanically related modeling and remodeling in the mouse fibula, 1296

Neglected role of intracortical remodeling in age-related bone loss, 1101

PTH receptor signaling in osteocytes increases bone mass and the rate of bone remodeling through Wnt/LRP5-dependent and -independent mechanisms, respectively, 1038

PTH reverses abnormal bone remodeling and structure in HPT, 1036

Role of LIMK1 in osteoclast cytoskeletal remodeling and bone resorption, 1116

Secretomic analysis of Ca supplement-mediated bone remodeling, M022

T $\beta$ RI inhibitor rescues uncoupled bone remodeling in two different animal disease models, 1273

Vitamin D status and bone remodeling marker CTx-I in patients with early RA: association with disease activity and joint damage, SA496

**Bone repair**

Bone defect model in mouse femur to challenge biomaterials, cells and molecules for bone repair, SA126

Expression of an engineered G $_i$ -coupled receptor in osteoblasts affects intramembranous and endochondral bone formation during bone repair, F127

Inhibition of MMP activity delays bone repair whereas inhibition of osteoclast function and formation does not, SA075

**Bone resorption**

Acid-induced stimulation of bone resorption is decreased in OGR1 KO mouse calvariae, M021

Acute COPD exacerbations are associated with uncoupling of bone resorption from bone formation, M414

Are all anti-resorptive treatments the same? Lessons learned from inhibition of human osteoclastic bone resorption by alternative pathways, M129

Assessment of serum Ca and bone resorption markers in patients transitioned from ALN to DMAB, M394

Bone resorption and articular cartilage degenerative changes following performance of high repetition high force tasks are attenuated by secondary ibuprofen treatment, SA532

Bone resorption markers in saliva, M288

Cat K inhibitor, MIV-701, suppresses bone resorption markers in healthy postmenopausal women, F433

Changes of biochemical resorption markers during fracture healing in osteoporosis, M290

Decreased bone formation, increased bone resorption, and osteopenia in mice lacking SP, SU160

Disuse with a rapid bone loss affects the expression profile of osteoblastic and resorption genes, F516

Dock5, an essential Rac exchange factor in osteoclasts that controls adhesion structure organization and bone resorbing activity, SU064

Effect of luteolin on bone loss, microarchitecture and bone resorption in OVX mice, M128

Effects of resorption cavities on strength of trabecular bone, SA512

Effects of the Cat K inhibitor ODN on osteoclast-mediated bone resorption, M127

Effects of Vitamin K2 and RIS on bone formation and resorption, osteocyte lacunar system and porosity in the cortical bone of GC-treated rats, SU385

Exploring the effect of food intake on bone resorption for optimal drug delivery and efficacy in osteoporosis with oral calcitonin, SA436

Formation of podosome belts by osteoclasts on plastic correlates with resorptive activity, SU068

Fungal secondary metabolites beauvericin and enniatin inhibit osteoclast differentiation and bone resorption, M130

Gastric proton pump inhibitors failed to affect bone resorption and formation, SA095

GLP-2 acutely uncouples bone resorption and bone formation in postmenopausal women, M399

Identification of the regulatory mechanism(s) of PTP-PEST associating with the sealing ring formation and bone resorption in osteoclasts, SU065

Inactivation of *Dlx5* gene results in altered osteoblast-osteoclast coupling inducing increased bone resorption and reduced cortical thickness in male mice, F010

Increased osteoclast differentiation and bone resorption during spaceflight, SU094

Interaction of combined intervention of PTH and GH on trabecular and cortical bone formation and resorption in the hypophysectomized rats, SU502

Intermittent, short duration cyclic loading attenuates disuse osteoporosis without affecting resorption, M483

Lack of seasonal variation of bone resorption in elderly women in relation to periodicity of sunlight exposure at a northerly latitude, F337

Long-acting PTH ligand that binds to a distinct PTH receptor conformation (R0) can stimulate increases in markers of both bone resorption and bone formation in mice, F221

Mathematical model of remodeling cycles with feedback mechanism for maintaining the balance between bone resorption and formation, WG27

Menopausal and postmenopausal women have significantly higher bone resorption and oxidative stress parameters than premenopausal women, SU336

Mice deficient in *Pyk-2* have impaired OVX-induced bone resorption, F098

Microarchitecture and tissue age influence in vivo bone resorption, M125

Obesity induced by high dietary fat leads to increased bone resorption marker, TRAP, and decreased bone mass in mice, M238

Obesity is associated with higher BMD, lower bone resorption and slower hip bone loss: are these associations mediated by adipokines?, SU369

Proteasome inhibitors attenuate osteoclastogenesis and bone resorption via the modulation of RANK-mediated TRAF6, p62 and I $\kappa$ B- $\alpha$  signaling cascades, SA099

Pyrophosphates stimulates osteoclast differentiation and bone resorption, SA084

Resorption mechanism of HA and  $\beta$ TCP coating layer, SA100

Role of LIMK1 in osteoclast cytoskeletal remodeling and bone resorption, 1116

Sca-1 $^{+}$  HSC-based hGH gene therapy enhanced endosteal bone resorption in mice, M233

Scl-Ab increases bone formation and decreases bone resorption in distal tibial metaphyseal trabecular bone in OVX rats, F394

Scl-Ab increases bone mass by stimulating bone formation and inhibiting bone resorption in a hindlimb-immobilization rat model, 1138

SHBG levels in older patients with acute hip fracture are correlated with worse function and increased bone resorption, SU363

Soluble activin receptor type IIA fusion protein, ACE-011, increases bone mass by stimulating bone formation and inhibiting bone resorption in cynomolgus monkeys, SU376

Suppression of bone resorption markers by Ca and Vitamin D separately and in combination, M329

Systemic IL-8 increases bone resorption in vivo, 1234

TGF $\beta$ 1 induces migration of Sca-1 and CD29-positive MSC in coupling bone resorption and formation, F188

TOR inhibits osteoclast activity in vitro and prevents orchietomy-induced bone resorption in male rats, SA381

Toward a physiologically-based definition of hypogonadism in men: dose-response relationship between testosterone and bone resorption, 1102

Transgenic overexpression of the Wnt antagonist Krm-2 in osteoblasts leads to severe impairment of bone formation and increased bone resorption, 1003

TSG-6 acts synergistically with OPG to inhibit bone resorption, SA097

**Bone restricted ifitm-like (Bril)**

Bril localization in mouse and rat bones, M025

**Bone sialoprotein (BSP)**

BSP deficiency impairs osteoclast differentiation and resorption in vitro, SA142

Mice deficient in BSP display impaired modeling and remodeling and respond to ovariectomy but not to the cortical anabolic effect of PTH, 1191

**Bone sialoprotein 2 (BSP2)**

c-Src-regulated osteoblast-mimicry in breast cancer bone metastasis: the role of RAMP2 and BSP2, M275

**Bone size**

Areal BMD by DXA may predict similar risk of fracture in elderly women and men due to offsetting effects of bone size and true volumetric BMD, SU267

Birth weight predicts bone size, adult weight predicts BMC and BMD in young Gambian adults, M498

Bone size, volumetric bone density in relation to fat mass in healthy young men at age of PBM, SU477

Characterization and genetic mapping of bone size phenotypes in GK and F344 rats using a new 3D CT method, M463

Is GH/IGF-I mediated mechanism involved in regulating gender differences in bone size?, SA180

Serum IGF-1 is a developmental determinant of bone size, SA183

Targeted disruption of Nrf1 in osteoblasts leads to reduced bone size and dramatic alterations in trabecular bone microstructure in mice, 1190

Three year school-curriculum-based exercise program in prepubertal children increases bone mineral accrual and bone size but do not influence femoral neck structure, 1107

**Bone strength**

12 months of TPTD therapy increases ultradistal radius bone strength in severely osteoporotic postmenopausal women, SA504

Age at menarche associated with bone strength in girls, SU493

Arterial compliance is associated with change in bone strength in children, F552

Blocking TGF $\beta$  signaling reduces gammopathy and improves bone volume and strength in vivo, F293

Bone geometry and bone strength are compromised in patients with ACL reconstruction, M487

Bone geometry, strength, and muscle mass in female distance runners with a history of stress fracture, SA540

Bone strength in overweight children is adapted to mechanical loads from walking, but is low for higher loading activities, M482

Bone strength measurement: new approach, SU249

Bone volumetric density, geometry and strength in male and female collegiate runners, SA539

BZA in combination with conjugated estrogens improves bone mass and strength in the OVX rat, SA385

Changes in volumetric bone density and bone strength at the tibial midshaft in boys and girls 12-17 years of age, SU469

Comparison of HR-pQCT to DXA and QUS for the assessment of ex-vivo bone strength, M466

Comparison of the effects of IBN alone with IBN in combination with SNAC on bone density and bone strength in OVX rats, SU391

Does adiposity affect bone strength indices in young adult black females?, SU318

Early exposure to soy isoflavones modulates bone mineral, strength and microarchitecture in CD1 mice, M503

Effect of 1,25(OH) $_2$ D $_3$  and 25(OH)D $_3$  on osteoblastogenesis and bone strength in Vitamin D sufficient growing mice, SU207

Effect of exercise on geometric bone structure and bone strength in postmenopausal women, M484

Effect of non-ambulation on bone strength in boys with DMD, WG1

Effect of RIS on bone strength and work to failure determined by FEA and simulation of clinically-measured bone loss and mineralization changes, SA505

Effects of a targeted bone and muscle loading program on QCT bone geometry and strength, muscle size and function in older men, 1244

Effects of ALN or DMAB on cortical and trabecular bone mass, bone strength, and bone mass-strength relationships in mice, 1139

Effects of diacylglycerol oil on body composition, BMD and bone strength in mice, SA442

Environmental perturbations during puberty and bone strength, M501

Femoral BMD and femoral structure, assessed by DXA-based hip structural analysis, contribute independently to femoral strength, M304

G171V and A214V Lrp5 knock-in mice have increased bone mass and strength, and can help precisely define the in vivo functions of Lrp5 during bone growth and homeostasis, 1002

GWAS identified RTP3 as a novel gene for bone strength, SU331

Intermittent PTH administration increases bone mass and strength in aged mice by antagonizing oxidative stress-induced osteoblast apoptosis via ERK-mediated attenuation of p66<sup>shc</sup> phosphorylation, SU380

Is increased bone fragility during adolescence a result of delayed development in bone bending strength?, M500

Mouse-to-human strategy to identify bone strength QTL genes, SA120

Muscle power and tibial bone strength in older women, SU362

ODN increases bone strength and maintains bone quality in estrogen deficient adult rhesus monkeys, F508

Overweight children are more at risk to sustain a forearm fracture due to poor bone strength relative to body weight, M458

OVX-induced hyperphagia does not modulate bone mineral or bone strength in female Sprague-Dawley rats, SA447

QCT and FEA assessment of proximal femur bone quality and strength in women with postmenopausal osteoporosis receiving once-monthly oral IBN for 12 months, SA509

Transition from ALN to DMAB in OVX cynomolgus monkeys maintained or improved cortical and trabecular bone mass, without altering the linear relationship between bone mass and bone strength, 1072

Women who fractured their hips experience greater loss of geometric strength in the contralateral hip during the year following fracture compared to age-matched controls, F345

#### Bone structure

Alterations in bone structure and growth in dwarf rats with a depressed GH/IGF-I axis, SA178

Cortical bone mass and structure in older Afro-Caribbean and Caucasian men, SU300

Deleterious effect of late menarcheal age on bone microstructure in both distal radius and tibia, 1239

Effect of exercise on geometric bone structure and bone strength in postmenopausal women, M484

Evaluating bone microstructure at the distal tibia in children, F315

GC signaling in osteoblasts maintains normal bone structure in mice, F233

Gender-specific changes in bone microstructure of mice lacking ribosomal protein L29/HIP, SA133

Non-invasive detection of bone microdamage by light scattering, M462

PTH reverses abnormal bone remodeling and structure in HPT, 1036

Target ablation of PPR in osteocytes induces hypocalcemia and impairs bone structure, 1158

#### Bone turnover

$\mu$ CT abnormalities in the th3 mouse model of thalassemia start at a young age and are associated with decreased bone turnover, SA128

Associations of the VDR and calcitonin receptor genes with bone density, bone turnover markers and fracture incidence with regard to Ca intake level in Slovak postmenopausal women, M261

Bone turnover and incident hip fracture risk, M285

Bone turnover evaluated by a combined Ca balance and  $^{45}$ Ca kinetic study, and dynamic histomorphometry, M137

Deficiency of NCK1, an actin cytoskeletal modulator with SH2/SH3 motifs, induces bone loss via suppression of bone formation and induction of biochemical high bone turnover state, M026

Development of an animal model of bisphosphonate-induced severe suppression of bone turnover, SA511

Effect of a single 5-mg infusion of ZOL on bone turnover markers versus oral RIS (5 mg/day) over 1 year in patients with GIO, M362

Effect of bed rest on bone turnover in adolescents hospitalized for anorexia nervosa, SA559

Effect of DMAB vs ALN on bone turnover markers and BMD changes at 12 months based on baseline bone turnover level, 1285

Effects of ARZ on bone turnover and safety in postmenopausal women with low bone mass, M386

Effects of DMAB vs ALN on BMD, bone turnover markers, and safety in women previously treated with ALN, M395

Effects of intermediate doses of GCs on bone turnover and circulating Dkk-1, MIF, sRANKL and OPG in patients with interstitial lung disease, SA451

Effects of LASO on bone turnover markers, 1287

Effects of ODN on bone mass and turnover in estrogen deficient adult rhesus monkeys, SA072

High bone turnover in mice lacking the growth factor Mdk, 1198

Impact of physical inactivity (10 days bed rest) on markers of bone turnover in young men with low and normal birth weight, SA456

Increased proinflammatory cytokines TNF- $\alpha$  and IL-6 correlate with pathological bone turnover markers in diabetic patients with acute Charcot foot, F491

Influence of markers of bone turnover on calcaneal QUS, SA457

Longitudinal relationships between cartilage and bone turnover in OA, SA129

Optimization of bone turnover marker measurements in a mouse model of GC-induced osteoporosis, M298

Osteosclerotic prostate cancer metastasis to murine bone: enhanced with increased bone turnover, SA269

Predictive capacity of biochemical markers of bone turnover and endogenous hormones for osteoporosis in men, SU334

Premenopausal reference ranges of bone turnover markers and the effect of bisphosphonates in Korean postmenopausal women, SU406

Previous antiresorptive agents use did not hinder the increase of bone turnover marker in TPTD use, M351

PTH increases bone turnover in HPT, F485

Randomized double blinded controlled trial of individual response in biochemical markers of bone turnover to LASO therapy, M507

Relationship between serum levels of inflammatory cytokines and bone turnover markers in the year following hip fracture, SU073

Relationship of bone turnover marker (PINP) and changes in femoral neck BMD to fracture risk in women with postmenopausal osteoporosis treated with once-yearly ZOL 5 mg, 1027

Relationship of QUS at phalanges with hand and axial BMD, sex hormones and bone turnover markers in elderly women, M320

Skeletal plasma clearance, as measured by quantitative radionuclide studies, is correlated with bone turnover markers at 3 months of TPTD therapy, F398

Transition from ALN to DMAB resulted in further reductions in local and systemic bone turnover parameters and reduced cortical porosity in OVX cynomolgus monkeys, 1216

Vitamin D deficiency, osteomalacia and high bone turnover in patients with NF-1, F465

Wintertime Vitamin D supplementation inhibits seasonal variation of calcitropic hormones and maintains bone turnover in healthy men, SU433

**Bone turnover, severe suppression of (SSBT)**

Effect of SSBT on osteocyte viability, F405

## Key Word Index

## ASBMR 30th Annual Meeting

**Bone volume**

- Abrogation of Cbl-PI3K interaction in mice results in increased bone volume and osteoblast proliferation, 1150
- Blocking TGF $\beta$  signaling reduces gammopathy and improves bone volume and strength in vivo, F293
- BMP-3-null aged mice display increased trabecular bone volume and reduced cross sectional area at the mid-femoral diaphysis, SU143
- Comprehensive genetic analysis of bone volume in men, M268
- Determinants of humeral bone volume in males, F122
- HDI, Vorinostat, blocks growth and associated osteolysis of cancer cells within bone, but reduces bone volume in non-tumor bearing bones in mice, M279
- Increased bone volume and correction of HYP mouse hypophosphatemia in the Klotho/HYP Mouse, 1017
- Mice lacking the GH receptor in liver have normal skeletal growth and bone volume despite virtual absence of circulating IGF-1, F181

**Boron (B)**

- Carborane BE360, one of the carbon-containing polyhedral boron-cluster compounds, is a new type of selective estrogen receptor modulator., SU187

**Bortezomib (Bzb)**

- Bzb, a proteasome inhibitor, prevents metastatic breast cancer osteolysis and reduces mammary fat pad tumor growth in mice, F277

**Brachy-syndactyly**

- Brachy-syndactyly caused by loss of *Sfrp2* function, F118

**Breast cancer. See Cancer****Breastfeeding**

- Vitamin D supplementation in breast fed infants, SU500

**BRM**

- Depletion of the chromosome remodeling subunit BRM accelerates differentiation of osteoblast precursors, M038

**BrtlIV**

- In utero stem cell therapy as treatment for classical OI using the knock in murine model BrtlIV, F500

**BT-201**

- BT-201, a butanol extract of *Panax notoginseng* inhibits progression of joint degeneration in a rat model of OA, M152

**Butanol**

- BT-201, a butanol extract of *Panax notoginseng* inhibits progression of joint degeneration in a rat model of OA, M152

**Butyrate**

- Butyrate stimulates mineralized nodule formation and OPG expression by osteoblasts, M012

**C****C-fms**

- Recombinant mouse M-CSF receptor C-fms inhibits TNF $\alpha$ -induced osteoclastogenesis, M112

**c-Fms**

- Vimentin binds c-Fms in an M-CSF dependent manner and regulates osteoclast differentiation, SU097

**c-Fos**

- c-Fos is associated with renal FGF-23-mediated signaling, SU173

**c-Jun N-terminal kinase (JNK)**

- JNK activation is involved in TNF $\alpha$ -stimulated Smurf1 expression, SA016
- Phosphate induced apoptosis in growth plate chondrocytes via a NO and JNK-dependent pat, SA113

- Stimulation of macrophage TNF $\alpha$  production by orthopaedic wear particles requires activation of the ERK 1/2/Egr-1 pathway but is independent of p38 and JNK, SA177

**C-propeptides**

- Interaction of Ciz, a nucleocytoplasmic shuttling transcription factor with C-propeptides of type I collagen, M044
- Mouse with a Ser1386Pro mutation in the C-propeptide domain of *col2a1* provides a model for SEDC, 1269

**c-Src**

- c-Src-regulated osteoblast-mimicry in breast cancer bone metastasis: the role of RAMP2 and BSP2, M275
- Lyn, opposite to c-Src, negatively regulates osteoclastogenesis in vitro and in vivo via its interaction with SHP-1 and Gab2, 1119

**C-telopeptides**

- C-telopeptide and bone ALP predict morphometric vertebral fracture risk in a pivotal Phase III trial of TOR in men on ADT, 1292
- Relationship of urinary excretion of C-telopeptides to growth in children, F301

**C-terminus**

- C-terminal fragment of PTHrP (107-139), exerts osteogenic features in both regenerating and nonregenerating bone in mice with diabetes-related osteopenia, SA223
- MEPE C-terminal ASARM-peptide, promotes hypophosphatemia, bone defects and increases adiposity, F207
- PTHrP nuclear localization sequence and C-terminus regulate craniofacial development, 1264

**C/EBP $\alpha$** 

- Ghrelin inhibits early osteogenic differentiation of C3H10T1/2 cells by suppressing Runx2 expression and enhancing PPAR $\gamma$  and C/EBP $\alpha$  expression, M086

**C/EBP $\beta$** 

- Transactivation of RANKL by C/EBP $\beta$  and C/EBP $\delta$  in adipocyte lineage cells, SU092

**C/EBP $\delta$** 

- Transactivation of RANKL by C/EBP $\beta$  and C/EBP $\delta$  in adipocyte lineage cells, SU092

**c.1250A>G**

- c.1250A>G, p.N417S is a common American TNSALP mutation involved in all clinical forms of HPP, including pseudo-HPP, SA566

**C1**

- Evidence of a role for the human Vitamin D response element binding protein, hnRNP C1/C2 in chromatin remodeling and transcript splicing, F240

**C2**

- Evidence of a role for the human Vitamin D response element binding protein, hnRNP C1/C2 in chromatin remodeling and transcript splicing, F240

**C2C12**

- Coordinate regulation of PTHrP and PTHR1 in the osteoblast differentiation of C2C12 cells promoted by BMP-2, SA157
- Effect of 1 $\alpha$ ,25-dihydroxy Vitamin D3 on proliferation and differentiation of C2C12 myoblast, SA245
- Hypoxia promotes ligand-independent activation of the ACVR1 (R206H) mutant receptor in C2C12 cells, M243

**C3H/Hej**

- Load induced changes in trabecular and cortical bone are dose dependent in both C57BL/6 and C3H/Hej mice, F527

**C3H10T1/2**

- Canonical Wnt signaling suppresses BMP-4 accumulation from C3H10T1/2 cells transfected with BMP-4 expression vector, SA156
- Enhanced mitochondrial biogenesis contributes to Wnt induced osteogenic differentiation of C3H10T1/2 cells, SA043
- Ghrelin inhibits early osteogenic differentiation of C3H10T1/2 cells by suppressing Runx2 expression and enhancing PPAR $\gamma$  and C/EBP $\alpha$  expression, M086

- Overexpression of  $\alpha$ -catenin in C3H10T1/2 cells increases osteoblast differentiation, SA046

**C4**

- Isoform-specific expression of PPARs and gene regulation during osteoclastogenesis in RAW/C4 cells, M118

**C57**

- Effect of Pb on bone mineral properties from female adult C57/BL6 mice, M146

**C57BL/6**

- Femur from C57BL/6 and DBA/2 inbred mice display a strain dependent response to treadmill running and tower climbing exercise in cortical and trabecular bone architecture, M485
- Load induced changes in trabecular and cortical bone are dose dependent in both C57BL/6 and C3H/Hej mice, F527
- Low dose administration of INF $\gamma$  stimulates osteoblastogenesis and prevents ovariectomy-induced osteoporosis in C57BL/6 mice, M334

**Caco-2**

- Molecular mechanisms involved in PTH-induced apoptosis in Caco-2 intestinal cells, M189

**Cadmium (Cd)**

- Ca release from bone in postmenopausal women: effects of low level Cd exposure, M328
- High level dietary P and Cd exacerbate OVX-induced bone loss, M301

**Calcaneus**

- Calcaneal QUS measurement of 2323 healthy adults in southwest China, M318
- Longitudinal analysis of calcaneal QUS measures during childhood, M321
- Mechanical unloading of the sheep calcaneus: a model for hip fracture, M478
- Normal reference values for QUS bone densitometry of the calcaneus in Chinese children and adolescents, SU489
- RTA of densitometric calcaneal images differs between subjects with and without GC use, M314

**Calcein**

- Intestinal-specific VDR null mice maintain normal calcein but display severe bone loss, F238

**Calciol**

- Decreasing calciol (25OHD3) in serum is related to impaired function and increased mortality in the elderly, SU204
- Differential effects of GH and 1  $\alpha$  calciol on cancellous and cortical bone in hypophysectomized rats, SU501

**Calcification**

- Calcifications in children with JDM contain several bone formation markers, SA106
- Cartilage engineered with a calcified zone enhances interfacial shear strength to the underlying substrate, M176
- Strain-induced fluid flow in a 3D porous matrix promotes osteoblastic calcification in vitro, SA525

**Calcification, arterial**

- OPN deficiency reduces aortic calcification and oxidative stress in diabetic LDLR $^{-/-}$  mice, F109
- Specific inhibitors of TNSAP's pyrophosphatase activity suppress medial arterial calcification, M142

**Calcification, coronary artery**

- Ca intake is not associated with increased coronary artery calcification, 1207

**Calcification, renal**

- High expression of the Ca/phosphate-regulating hormone STC2 is associated with renal calcification in the Klotho mutant mice, SA201

**Calcification, vascular**

- Association between vascular calcification and low total femur BMD in elderly people community-dwelling, SU453
- Bridging vascular calcification and osteoporosis: the function of receptor activator of nuclear factor  $\kappa$ B, M419

Protective actions of Vitamin D analogs in the vascular calcification of CKD, SU450

**Calcineurin**

Nicotine induces chondrogenesis via calcineurin/NFAT, SU133

PTH induces COX-2 in MC3T3-E1 osteoblasts via cAMP-PKA and Ca-calcineurin pathways, SA033

**Calcinosis, tumoral**

Homozygous threonine to methionine substitution in FGF-23 gene is associated with tumoral calcinosis in a 12 year-old girl, SU171

**Calciophylaxis**

Calciophylaxis in a patient with HPT and normal kidney function, WG33

**Calcitonin**

Associations of the VDR and calcitonin receptor genes with bone density, bone turnover markers and fracture incidence with regard to Ca intake level in Slovak postmenopausal women, M261

Calcitonin attenuates the anabolic effect of PTH in vivo and rapidly upregulates SCT expression, F195

Calcitonin intramuscular administration for treating acute pain of osteoporotic vertebral compression fractures, SA196

Calcitonin receptor on osteoclasts plays a physiological role to protect against HCa in mice, SA197

Exploring the effect of food intake on bone resorption for optimal drug delivery and efficacy in osteoporosis with oral calcitonin, SA436

Lack of calcitonin accentuates bone loss during lactation by enhanced osteoclast formation and reduced osteoblast formation, SA194

Possible central function of the calcitonin receptor on bone mass, SA255

Subcutaneous administration of salmon calcitonin: bone protective effect in adjuvant arthritis prevention model in rats, SA193

**Calcitonin receptor (CTR)**

Association of CTR gene polymorphisms with BMD and fracture risk in postmenopausal Koreans, M256

High bone mass due to increased bone formation in mice lacking the CTR, SA192

**Calcitonin-gene related peptide (CGRP)**

CGRP stimulates osteogenesis and inhibits osteoclastogenesis in vitro, SU033

**Calcitriol**

Comparison of 1,25(OH)<sub>2</sub>D<sub>2</sub> and calcitriol effects in an adenine-induced model of CKD reveals differential control over serum Ca and phosphate, SU448

**Calcium (Ca)**

25(OH)D acts on Ca and skeletal homeostasis independent of 1,25(OH)<sub>2</sub>D in vivo, M214

Activation of FGF receptors is a novel mechanism by which extracellular Ca stimulates the proliferation of osteoblasts, M088

Ahnak regulates Ca signaling and ATP release in osteoblasts in response to mechanical stimulation, SA027

Alpha-Ca/CaMKII controls osteosarcoma cell migration, SU234

Assessment of serum Ca and bone resorption markers in patients transitioned from ALN to DMAB, M394

Associations of the VDR and calcitonin receptor genes with bone density, bone turnover markers and fracture incidence with regard to Ca intake level in Slovak postmenopausal women, M261

Bone health impairment in children with chronic Ca and Vitamin D deficiency due to nutritional allergies, SU503

Bone turnover evaluated by a combined Ca balance and <sup>45</sup>Ca kinetic study, and dynamic histomorphometry, M137

Ca intake and serum bone formation markers are associated with the functional single nucleotide polymorphism in the TNSALP gene, SU308

Ca intake is not associated with increased coronary artery calcification, 1207

Ca release from bone in postmenopausal women: effects of low level Cd exposure, M328

Ca signaling is a major target of OCT-1547, a small molecule osteoporosis drug candidate, M339

Comparison of 1,25(OH)<sub>2</sub>D<sub>2</sub> and calcitriol effects in an adenine-induced model of CKD reveals differential control over serum Ca and phosphate, SU448

Controlled drug release from Ca phosphate-based orthopaedic implants, SU235

Development of empirical model using <sup>41</sup>Ca for the study of bone remodeling in human, SA454

Dietary normalization of Ca absorption in mice genetically deficient in CaSR and 25(OH)D-1 $\alpha$ -hydroxylase results in non-lethal, severe hyperparathyroidism with reduced osteoclastogenesis, M199

Different influence of the clinical condition, degree of cholestasis, alcohol abuse and serum Ca on the musculoskeletal system in chronic cirrhotics, M411

Differential cellular and molecular responses of intestinal epithelium to high Ca diet and 1,25(OH)<sub>2</sub>D<sub>3</sub>, M229

Direct correlation of osteocyte deformation with Ca influx in response to fluid flow shear stress, SA057

Effect of particle size of Ca carbonate supplement on Ca retention in adolescent girls, SA545

Effect of the dietary Ca/P ratio on the rate of skeletal accrual in mice, M333

Effect of Vitamin D<sub>3</sub> and Vitamin D<sub>2</sub> on intestinal Ca absorption in Nigerian children with rickets, SA560

Effects of 50,000 IU of Vitamin D<sub>2</sub> twice per month on circulating 25(OH)D and Ca levels, SU426

Effects of agave inulin on Ca metabolism in Japanese young adults, M332

Effects of different extracts of *Fructus ligustri lucidi* on Ca balance in normal female rats, M336

Effects of KHCO<sub>3</sub> on Ca and bone metabolism during high salt intake, SA446

Endocytotic processes underlying Ca-induced inhibition of plasma membrane V-ATPase in murine osteoclasts, SU101

Evidence for a role of prolactin in Ca homeostasis: regulation of intestinal TRPV6 and intestinal Ca absorption by prolactin, 1223

FGF-23 and parameters of Ca and bone metabolism are positively influenced by GH replacement in adult GH deficiency patients from the KIMS survey, SU177

Goettingen minipigs—a model for Ca/Vitamin D-deficiency osteomalacia and steroid-induced osteoporosis, SA445

High expression of the Ca/phosphate-regulating hormone STC2 is associated with renal calcification in the Klotho mutant mice, SA201

Impact of dietary protein on Ca homeostasis and nitrogen excretion in the presence and absence of KHCO<sub>3</sub>, SU305

Infantile HCa: relationship of dietary intake of Ca and Vitamin D to serum and urine levels, SU491

Is it time to update normative values for ionized Ca and urine Ca? Creatinine ratios in healthy Canadian infants, SU487

Medullary carcinoma of the thyroid and anomalies of the Ca metabolism, SU246

Osteocytic perilacunar remodeling as a significant source of Ca during lactation, M110

Osteofornin increases the levels of intracellular Ca of human preosteoblast cells in culture, SU051

Osteopenia in CKD: effects of Ca overload, SU449

Osteoporosis patients behaviours and understanding of the importance of Ca and Vitamin D supplementation, M331

Pediatric Crohn's Disease is associated with negative Ca balance and increased renal losses of Ca, SA565

Pregnancy upregulates duodenal Ca-transport genes and normalizes Ca homeostasis in *Vdr* null mice, M230

Prevention of nutritional rickets in Nigerian children with dietary Ca supplementation, M491

PTH induces COX-2 in MC3T3-E1 osteoblasts via cAMP-PKA and Ca-calcineurin pathways, SA033

RANKL induces Ca channel activation in human osteoclasts, SU107

Relationship between physical fitness and bone and physical activity and Ca retention in adolescent girls, SA553

Relationship between Vitamin D and PTH: serum Ca and Mg are major determinants of PTH in patients with mild CKD, M211

Rodent model to evaluate the effect of dietary protein on intestinal Ca absorption, M330

Secretomic analysis of Ca supplement-mediated bone remodeling, M022

Serum PTH response to oral Ca load in Asian adolescents, M188

Stat3 induces osteoblastic bone metastases through up-regulating the expression of Shh and a Ca channel TRPM8 in the LNCaP human prostate cancer cells, 1089

Suppression of bone resorption markers by Ca and Vitamin D separately and in combination, M329

**Calcium channels, voltage sensitive (VSCC)**

Assessment of changes in thoracic and lumbar vertebrae in T-type Ca<sub>v</sub>3.2 (a1H) VSCC KO mice, M170

**Calcium, serum ionized (iCa)**

Acute change in iCa directly affects bone formation independent of PTH action during hemodialysis, SU437

**Calcium-sensing receptor (CaSR)**

Activation of the CaSR by beta-aspartyl and gamma-glutamyl peptides, M202

Bone-building effects of the oral CaSR antagonist, ronacaleret, in OVX rats, SU372

CaSR gene A986S polymorphisms: relation to bone loss and urine Ca in a Spanish early postmenopausal women population, M255

CaSR mediated signaling in human vascular smooth muscle cells, M200

Conditional knockout of the CaSR in osteoblasts alters regulators of Wnt signaling, delays cell differentiation, and promotes apoptosis in bone, 1156

Dietary normalization of Ca absorption in mice genetically deficient in CaSR and 25(OH)D-1 $\alpha$ -hydroxylase results in non-lethal, severe hyperparathyroidism with reduced osteoclastogenesis, M199

Dimerization and trafficking of the CaSR to the plasma membrane, M205

Efficient expression of the full-length CaSR in insect cells, M198

Functional characterization of unreported CaSR in four Italian kindreds with FHH, M204

GCM2, the regulator of parathyroid cell fate, transactivates the CaSR gene, M187

Molecular diagnostic strategies for mutations of the CaSR gene, M201

Novel CaSR antagonist leads to dose-dependent transient release of PTH after oral administration to healthy volunteers, 1173

Ronacaleret, a novel CaSR antagonist, demonstrates potential as an oral bone-forming therapy in healthy postmenopausal women, 1174

Sr ranelate decreases osteoblast-induced osteoclastogenesis through the involvement of the CaSR, F389

Sr ranelate protects osteoblasts from apoptosis independently of the CaSR, M007

## Key Word Index

## ASBMR 30th Annual Meeting

Tissue-specific KO of the CaSR in chondrocytes inhibits IGF-1 signaling and delays differentiation in the growth plate, 1261

***Callorhinchus milii***  
PTH-gene family in the cartilaginous fish, *Callorhinchus milii*, M183

**Calmodulin 3 (CALM3)**  
In vivo differential expression profiling study on human circulating B cells suggested a novel EGFR and CALM3 network underlying smoking and BMD, SU154

**Calmodulin dependent kinase II (CaMKII)**  
Alpha-Ca/CaMKII controls osteosarcoma cell migration, SU234

**Calpain**  
Impact of calpain inhibition on chondrocyte development, M150

**Camargo Cohort Study**  
Vitamin D status, bone mass, and bone metabolism in postmenopausal women and men older than 50 attended in a primary care center of Spain, M223

**CaMOS Study**. See *Canadian Multicentre Osteoporosis Study*

**cAMP**. See *Adenosine monophosphate, cyclic*

**cAMP response element binding (CREB) protein**  
Cloning and functional analysis of human Nurrl (NR4A2) promoter: critical role in the regulation of CYP27B1 by PTH and CREB phosphorylation, 1161

**Camurati-Engelmann disease (CED)**  
CED: a unique variant featuring a novel, heterozygous, leucine repeat mutation in *TGFβ1* together with a novel, homozygous, missense change in *TNFSF11* encoding RANKL, F256

**Canadian Multicentre Osteoporosis (CaMOS) Study**  
10-year probability of recurrent osteoporotic fractures after a primary wrist fracture in postmenopausal women enrolled in the CaMOS cohort, F358  
Association of urine measures of diet-derived acid excretion with bone loss and fractures, SU283  
Fractures of the spine and hip increase the risk of death in Canadians, SU351  
Normative Z-scores from the CaMOS youth cohort, SU292  
Physical activity, BMD and fragility fracture, M325  
Population burden of first and repeat low-trauma fractures, 1056  
Reduced renal function is associated with increased rates of bone loss at the hip and spine, SU357

**Canadian Quality Circle (CQC) National Project**  
Family physician characteristics that predict appropriate x-ray ordering, SA359

**Cancellous bone**  
Beta-adrenergic receptor agonist administration during hindlimb unloading effectively mitigates reductions in cancellous bone formation, SA514  
Combined Cs-137 gamma irradiation and hindlimb unloading rapidly decreased cancellous bone volume fraction in the mouse lumbar vertebrae, M469  
Differential effects of GH and 1 alpha calcidol on cancellous and cortical bone in hypophysectomized rats, SU501  
Effects of intermittent human PTH administration on bone union with hydroxyapatite blocks at the site of cancellous bone osteotomy in OVX rats, SA214  
Increased non-enzymatic glycation of cancellous bone due to decrease in remodeling during ALN therapy of osteoporotic women, 1071  
Mineralization is related to collagen cross-links in growing cancellous and cortical bone, SA110

Treadmill exercise provides only short-term protection against cancellous bone loss with reduced dietary energy intake: endocrine mechanisms, SA449

**Cancer**  
2ME2 alters eIF4E activity and causes protein synthesis inhibition in osteosarcoma cells, SU240  
Activin A mediates MM bone disease which is reversed by RAP-011, a soluble activin receptor, 1231  
Alpha-Ca/CaMKII controls osteosarcoma cell migration, SU234  
Biomechanical and geometrical property changes in rat tibias with tumor-induced osteolysis after anti-resorptive or anti-cancer treatments, SU236  
Blocking TGFβ signaling reduces gammopathy and improves bone volume and strength in vivo, F293  
BMSC up-regulate M-CSF receptor in monocytes to disrupt dendritic cell differentiation while facilitating osteoclastogenesis in myeloma, SU242  
Bone degradation marker CTX shows unique properties in disease monitoring compared to NTX, ICTP and bALP in MM, M287  
CXCL12 expression is regulated by HIF-2α in MM plasma cells, SU080  
CXCL13 stimulates RANK ligand expression in SCC, SU247  
Disruption of the syndecan-1/integrin axis is a novel target for myeloma therapy, 1229  
DKK1 is regulated by mRNA stability and epigenetic mechanisms in bone metastasis, 1090  
Drugs which inhibit osteoclast function suppress tumor growth and alter hematopoietic cell populations in bone, F270  
EphB4 expression in osteoblasts is regulated by myeloma cells and the Wnt signaling pathway, SU232  
FGFR signaling in the pathogenesis of osteosarcoma, 1233  
Fracture risk in patients with different types of cancer, SA290  
HDI, Vorinostat, blocks growth and associated osteolysis of cancer cells within bone, but reduces bone volume in non-tumor bearing bones in mice, M279  
Hedgehog pathway is activated in osteosarcoma and cyclopamine prevents osteosarcoma growth by cell cycle regulation, SU241  
Hfg inhibits melanoma bone metastases and TGFβ signaling, F190  
Host bone marrow-derived stromal cells promote myeloma initiation and development of osteolysis, 1088  
Identification of RhoB as a key target involved in cell motility and bone metastasis, F291  
Important contribution of the immune system in regulating the tumor/bone vicious cycle independent from osteoclasts, 1086  
Increased signaling through p62 in the MM microenvironment increases myeloma cell growth and osteoclast formation, SA289  
Influence of IM on bone remodeling in juvenile mice, SA292  
Inhibition of HIF-1α alone or combined with TGFβ blockade prevents breast cancer bone metastases, 1085  
Inhibition of MM growth and preservation of bone with combined radiotherapy and anti-angiogenic agent, SA285  
Melanoma-induced bone loss is mediated by the rapid recruitment of osteoclasts, SU233  
Microarray analysis of human bone metastases evidenced a set of genes that segregates patients with metastases only in bone from patients with metastases also in visceral organs, M272  
Monoclonal antibody to TGFβ inhibits tumor burden and osteolysis in a pre-clinical model of bone metastasis, SA187  
Monthly intravenous ZOL suppresses tissue-level remodeling significantly more than daily oral ALN in the mandible and rib of skeletally mature female dogs, SU388

Notch pathway is activated in osteosarcoma and inhibitors of γ-secretase inhibit osteosarcoma growth by cell cycle regulation, SU229  
Novel splicing variants of ADAM8 stimulate tumor-induced bone metastasis by increasing invasion and osteoclastogenesis, F286  
Opposing effects on bone metastases of tumor ADM expression in breast and prostate cancer, M277  
PGE receptor EP4 antagonist attenuates growth and metastases of cancer, 1230  
Platelets contribute to circulating levels of Dkk-1: clinical implications in MM, SU228  
Preclinical validation of a novel Dkk1 neutralizing antibody for the treatment of MM related bone disease, SU239  
Role of AXII and AXIIR in homing MM cells in the bone marrow, SA287  
Role of FAP and DPP4 in myeloma bone disease and tumor growth, F288  
Systemic IL-8 increases bone resorption in vivo, 1234  
TGFβ suppresses adipocytic differentiation and enhances accumulation of stromal cells in myeloma bone lesions, SA294  
TSP-1 and CD47 regulate osteoclastogenesis but have distinct effects on bone metastasis, 1232  
Wnt/β-catenin/TCF is a constitutive repressor pathway interfering with Foxo3-mediated induction of synd2, a tumor suppressor in osteosarcoma cells, SU243  
ZOL inhibits the capacity of myeloid-immune suppressor cells in myeloma to form osteoclasts, SU230

**Cancer, bladder**  
BAMBI gene is epigenetically silenced in a subset of high-grade bladder cancer, SU245

**Cancer, breast**  
BMD and vertebral fracture in women with breast cancer and antiaromatase therapy, SA400  
BMD measurement: an independent risk factor of breast cancer recurrence?, SU265  
Breast cancer cell conditioned media stimulates osteoblastic cells to attract breast cancer cells, SA276  
Breast cancer derived factors synergize with TGFβ to induce phosphorylation of ERK1/2 and to stimulate osteoclastogenesis, SU115  
Bzb, a proteasome inhibitor, prevents metastatic breast cancer osteolysis and reduces mammary fat pad tumor growth in mice, F277  
c-Src-regulated osteoblast-mimicry in breast cancer bone metastasis: the role of RAMP2 and BSP2, M275  
Combined TGFβ receptor I kinase inhibitor and bisphosphonates are additive to reduce breast cancer bone metastases, F275  
Ectopic Runx2 expression disrupts normal acini structure in mammary epithelial cells, F279  
Effect of tamoxifen and aromatase inhibitors on the risk of fractures in women with breast cancer, SU227  
Effects of extracellular matrix properties and elastic modulus on the expression of PTHrP by human breast cancer cells, M280  
Effects of LASO on fractures and breast cancer, 1288  
Humanized model of breast cancer metastasis revealing a human-specific metastasis gene signature, M273  
Inhibition of HIF-1α alone or combined with TGFβ blockade prevents breast cancer bone metastases, 1085  
KO of the PTHrP gene in breast cancer cells inhibits tumor progression and metastatic spread in vivo, 1016  
Low plasma 25(OH)D and VDR polymorphisms are associated with increased breast cancer risk, SU202

OPG production by breast cancer cells is modulated by steroid hormones and confers resistance against TRAIL-induced apoptosis, M271

Osteoclast precursors play a role in recruiting breast cancer cells and osteoblasts onto the bone in vitro, SA278

Plasma proteomic profile that predicts breast cancer metastasis to bone, M281

Potential anti-invasion activity of Cat K inhibitors for the treatment of breast cancer-induced bone metastasis, M276

Prevention of aromatase inhibitor-associated bone loss in women with breast cancer, M283

PTHrP blockade inhibits tumor progression in a model of human breast cancer, F213

Quantitative image analysis method for measuring whole-body tumor burden in a mouse model of breast cancer bone metastasis, SA282

Strength training prevents bone loss at the spine in older breast cancer survivors, SA271

Vitamin D delays breast cancer progression in the PyVMT transgenic mouse model, 1185

Wnt signaling regulates Gli2 and PTHrP expression in human breast cancer cells that cause osteolysis, M278

**Cancer, prostate**

2ME2 blocks prostate cancer bone metastases, F272

Effects of ADT on bone health in prostate cancer, SA280

Inhibition of BMP pathway and osteoclast activity in osteoblastic prostate cancer lesion in bone, F283

Mechanism of enhanced 19-nor-2a-(3-hydroxypropyl)-1a,25-(OH)<sub>2</sub>D<sub>3</sub> anti-cancer activity in prostate cancer cells, M216

Osteoblast differentiation induced by Shh-expressing prostate cancer cells is enhanced by ascorbic acid, SA284

Osteosclerotic prostate cancer metastasis to murine bone: enhanced with increased bone turnover, SA269

Stat3 induces osteoblastic bone metastases through up-regulating the expression of Shh and a Ca channel TRPM8 in the LNCaP human prostate cancer cells, 1089

TGF $\beta$  activates prostate cancer bone metastases, pro-osteolytic gene expression and the new TGF $\beta$  signaling regulator PMEPA1, SA273

TGF $\beta$  blockade inhibits osteolytic but not osteoblastic prostate cancer metastases, SA274

TGF $\beta$  signaling in stromal cells facilitates osteoblastic lesions in prostate cancer, 1087

Zoledronate protects bone but not soft tissue from prostate cancer progression in a nude mouse model, M282

**Cancer, spine**

Local administration with PTX-loaded HA-alginate beads for metastatic spine cancer in rats, M274

**Cancer, thyroid**

Medullar carcinoma of the thyroid and anomalies of the Ca metabolism, SU246

**Cannabinoid receptors**

Cannabinoid receptor ligands rescue bone loss and stimulate fracture healing, SU375

**Cannabinoids**

Cannabinoid receptor GPR55 affects osteoclast function in vitro and bone mass in vivo, 1221

Effect of cannabinoid CB1 receptor ligands on body weight and bone mass in mice, M340

**Carbon nanotubes.** See *Nanotechnology*

**Carborane BE360**

Carborane BE360, one of the carbon-containing polyhedral boron-cluster compounds, is a new type of selective estrogen receptor modulator., SU187

**Carcino-embryonic antigen related cell adhesion molecule 1 (CEACAM1)**

Regulation of bone mass and osteoclastogenesis by the CEACAM1, F091

**Carcinoma, medullar**

Medullar carcinoma of the thyroid and anomalies of the Ca metabolism, SU246

**Carcinoma, squamous cell (SCC)**

CXCL13 stimulates RANK ligand expression in SCC, SU247

**Cardiac transplantation**

Replacing testosterone in male cardiac transplant patients exerts multiple benefits on bone mass, libido and sexual activity, M388

**Cardiolipin**

Lentiviral shRNA mediated inhibition of Grx5 expression induces apoptosis via a mechanism involving increased ROS and cardiolipin oxidation, and reduced SOD activity, M009

**Cardiotrophin-1 (CT-1)**

CT-1 is an osteoclast-derived coupling factor required for normal bone remodeling, M014

**Cardiovascular disease (CVD)**

CVD as forecasters of hip fracture: a nationwide cohort study in twins, 1205

Postprandial hyperphosphatemia is a novel risk factor for CVD by involving endothelial dysfunction, SU443

**Cardiovascular Health Study**

Subclinical thyroid disease predicts risk of hip fracture, 1208

**Cardiovascular system**

Arterial compliance is associated with change in bone strength in children, F552

Cardiovascular manifestations of mild PHPT, 1034

Changes in cardiovascular function after parathyroidectomy in mild PHPT, M434

MACD index is a strong predictor of cardiovascular death and include the predictive power of BMD, SU463

**Cartilage**

AC-100 promotes cartilage repair and subchondral bone healing in surgically induced cartilage defects, SA111

Biomarker discovery for bone and cartilage based on metabolic reconstruction bioinformatics, M134

Bone resorption and articular cartilage degenerative changes following performance of high repetition high force tasks are attenuated by secondary ibuprofen treatment, SA532

Cartilage engineered with a calcified zone enhances interfacial shear strength to the underlying substrate, M176

Continuous culture of tissue engineered cartilage, SU131

Deletion of the oxygen-sensor PHD2 in chondrocytes results in increased cartilage and bone mineralization, 1153

Identification of a transcription factor p63 for transactivation of Wnt9a and Gdf5 causing joint cartilage formation, F116

Longitudinal relationships between cartilage and bone turnover in OA, SA129

Overexpression of CCN2/CTGF in cartilage shows prolonged bone length resulting from stimulation of chondrogenesis, chondrocyte growth, apoptosis, and bone mineralization during endochondral ossification, M153

PTH has direct anabolic effects on OA articular cartilage in vitro and in vivo, M155

PTH-gene family in the cartilaginous fish, *Callorhynchus milii*, M183

In vivo knockdown of GEP, a novel growth factor in cartilage, led to defects in cartilage and OA, 1048

Widespread expression of SCT in adult and embryonic cartilage and bone, cells of the developing central nervous system and epithelia of the embryonic kidney and intestine, SA055

**Cartilage associated protein (CRTAP)**

P3H1 and CRTAP are mutually stabilizing in the endoplasmic reticulum collagen prolyl 3-hydroxylation complex, 1049

**Cartoid plague**

Carotid plague causes low spinal BMD in Korean postmenopausal women with diabetes, SU359

**Cas interacting zinc finger protein (CIZ)**

Deficiency of the nucleocytoplasmic shuttling protein CIZ suppresses K/BxN serum-induced model of RA, M446

**Catecholamines**

Catecholamines accelerate BMP-induced osteoblastic differentiation and bone formation, SU137

**$\alpha$ -catenin**

Overexpression of  $\alpha$ -catenin in C3H10T1/2 cells increases osteoblast differentiation, SA046

**$\beta$ -catenin**

Activation of  $\beta$ -catenin signaling in articular chondrocytes leads to OA-like phenotype in adult  $\beta$ -catenin conditional activation mice, 1047

Apc-mediated control of  $\beta$ -catenin is essential for both chondrogenic and osteogenic differentiation of skeletal precursors, SA130

Availability of cytoplasmic  $\beta$ -catenin impacts mechanical signaling in osteoblasts, 1253

$\beta$ -catenin directly binds to a specific intracellular domain of PTH/PTHrP receptor and regulates the signaling in chondrocytes during endochondral ossification, 1013

$\beta$ -catenin protects osteoblasts from oxidative stress by co-activating the expression of pro-survival, but not pro-apoptotic, target genes of the FoxO transcription factors, M010

FHL2 mediates DEX-induced MSC osteogenic differentiation by activating Wnt/ $\beta$ -catenin signaling and Runx2 expression, M048

hPTHrP 1-36 stimulates PKA-dependent phosphorylation and nuclear translocation of  $\beta$ -catenin in neonatal mouse calvarial bone cells, F032

Induction of oxidative stress and diversion of  $\beta$ -catenin from TCF- to FOXO-mediated transcription by GCs or TNF $\alpha$  in osteoblastic cells, SA185

Kinase activation and osteocyte survival promoted by mechanical stimulation require LRP5/6 signaling and  $\beta$ -catenin accumulation, but not  $\beta$ -catenin/TCF-dependent transcription, M108

Mechanical strain prevents adipogenesis in MSC by stimulating a durable  $\beta$ -catenin signal, SA522

Mutational analysis of  $\beta$ -catenin Exon 3 in benign and malignant parathyroid tumors, M436

Oxidative stress stimulates the synthesis of PPAR $\gamma$ 2, and ligand-activated PPAR $\gamma$ 2 sequesters  $\beta$ -catenin leading to suppression of TCF-mediated transcription, 1099

PPAR $\gamma$ 2-mediated proteolytic degradation of  $\beta$ -catenin determines an anti-osteoblastic effect of anti-diabetic TZDs, SU023

Stable isotopic labeling of amino acids in cultured human BMSC: application to BMP-2 induced Wnt/ $\beta$ -catenin signaling, SA036

Transcriptional regulation of Cx43 by  $\beta$ -catenin, a pathway activated by PGE<sub>2</sub>-PI3K-GSK3 signaling in mechanically loaded osteocytes, 1042

In vivo load activated propagation of  $\beta$ -catenin signaling in osteocytes through coordinated downregulation of inhibitors of Lrp, 1041

Wnt/ $\beta$ -catenin/TCF is a constitutive repressor pathway interfering with Foxo3-mediated induction of synd2, a tumor suppressor in osteosarcoma cells, SU243

**Cathepsin K (Cat K)**

AP-1 and Mitf interact with NFATc1 to stimulate Cat K promoter activity in osteoclast precursors, SA076



## Key Word Index

## ASBMR 30th Annual Meeting

Cat K expression during enamel formation, SA154

Cat K inhibitor, MIV-701, suppresses bone resorption markers in healthy postmenopausal women, F433

Effects of the Cat K inhibitor ODN on osteoclast-mediated bone resorption, M127

Osteoclast-independent function of Cat K: regulation of TLR-9 signaling in autoimmunity, F074

Potential anti-invasion activity of Cat K inhibitors for the treatment of breast cancer-induced bone metastasis, M276

Serum Cathepsin K levels in AS, M439

**Ca<sub>3.2</sub>, T-type**

Assessment of changes in thoracic and lumbar vertebrae in T-type Ca<sub>3.2</sub> (a1H) VSCC KO mice, M170

**Caveolae**

Congenetic mouse models provide novel evidence of caveolae-1 $\alpha$  domain regulation of osteoblast differentiation, SU147

Involvement of caveolae in 1 $\alpha$ ,25(OH)<sub>2</sub>D<sub>3</sub>-dependent activation of MAPKs in skeletal muscle cells, SA243

**CB1**

Effect of cannabinoid CB1 receptor ligands on body weight and bone mass in mice, M340

**Cbfa1**

(Ala-Gly)<sub>n</sub> sequences configured silk protein scaffold induces osteoblast differentiation and bone formation via increased Cbfa1 and Osx expression, M167

**Cbl-PI3K**

Abrogation of Cbl-PI3K interaction in mice results in increased bone volume and osteoblast proliferation, I150

Cbl-PI3K interaction regulates osteoclast function, differentiation and survival, I011

**CCAAT/enhancer binding protein  $\beta$  (C/EBP $\beta$ )**

C/EBP $\beta$  overexpression causes osteopenia, SA005

C/EBP $\beta$ /p57<sup>Kip2</sup> signaling maintains transition from proliferation to hypertrophic differentiation of chondrocytes during skeletal growth, I187

**CCN2**

Overexpression of CCN2/CTGF in cartilage shows prolonged bone length resulting from stimulation of chondrogenesis, chondrocyte growth, apoptosis, and bone mineralization during endochondral ossification, M153

**CCR2**

CCR2 receptor signaling is involved in bone mass regulation and mediates the response to anabolic but not catabolic regimens of PTH(1-34), SU158

**Ccrn4l**

*Ccrn4l*, a peripheral clock gene, influences stromal cell allocation, bone mass, and marrow adiposity in mice and humans, I073

**CD1**

Early exposure to soy isoflavones modulates bone mineral, strength and microarchitecture in CD1 mice, M503

Over-expression of RAGE prevents OVX-mediated bone loss in CD1 mice, M132

**CD4<sup>+</sup>**

IL-12 stimulates the OIP-1 gene expression in CD4<sup>+</sup> T-cells, SA173

**CD29**

TGF $\beta$ 1 induces migration of Sca-1 and CD29-positive MSC in coupling bone resorption and formation, F188

**CD34**

Expression of bone-related genes by peripheral blood CD34 cells, M083

**CD45<sup>low</sup>**

Osteogenic potential of human bone marrow and circulating Stro-1+/CD45<sup>low</sup> cells, M078

**CD47**

CD47 (IAP) is an important modulator of osteoclast and osteoblast differentiation in vitro and in vivo, F093

TSP-1 and CD47 regulate osteoclastogenesis but have distinct effects on bone metastasis, I232

**Celiac disease**

Positive Celiac disease serology and BMD in adult women, SA366

**Cellular nucleic acid binding protein (CNBP)**

CNBP conditional KO mice show severe osteoporosis-like phenotype, F014

**Cerebral palsy**

Is Vitamin D deficiency more common in children with cerebral palsy than in healthy children?, SU194

**Cesium (Cs)**

Combined Cs-137 gamma irradiation and hindlimb unloading rapidly decreased cancellous bone volume fraction in the mouse lumbar vertebrae, M469

**CFK2**

Intracellular PTHR2 alters cell proliferation and pattern of gene expression while antagonizing PTHR1 signaling in chondrocytic CFK2 cells, SA121

**Charcot foot**

Increased proinflammatory cytokines TNF- $\alpha$  and IL-6 correlate with pathological bone turnover markers in diabetic patients with acute Charcot foot, F491

**Charcot neuroarthropathy**

Impaired oxidative stress defense mechanism may reduce bone stiffness in diabetic Charcot neuroarthropathy, M002

**Chemerin**

Chemerin and CMKLR1 expression and function in human bone marrow MSC adipogenesis, SU165

Chemerin and CMKLR1 targeted gene delivery identifies a novel molecular switch in the treatment of osteoporosis, M071

**Chemokines**

DARC regulates osteoclast differentiation via modulating chemokine effects on migration/fusion of osteoclast precursors, M115

**Chemotherapy**

Impact of adjuvant hormonal therapy on bone loss depending on initial adjuvant chemotherapy and menstrual status, M415

**Chloride**

CFTR regulates osteoblast bone formation independent of chloride conductance, I274

Chloride channel CIC-7 mediates acidification of the resorption lacuna in osteoclasts, M123

**Cholecalciferol**. See also *Vitamin D*

Efficacy and safety of short term treatment with different doses of cholecalciferol on 25(OH)D levels in postmenopausal females with osteoporosis, SU434

Ergocalciferol is not bioequivalent to cholecalciferol in Vitamin D insufficient hip fracture cases, I289

Vitamin D (cholecalciferol) production does not increase linearly with UV dose, M226

**Cholestasis**

Different influence of the clinical condition, degree of cholestasis, alcohol abuse and serum Ca on the musculoskeletal system in chronic cirrhotics, M411

Fracture risk in primary biliary cirrhosis: role of osteopenia and severity of cholestasis, M442

**Cholesterol**

Low density lipoprotein-cholesterol levels affect vertebral fracture risk in female patients with PHPT, SA484

**Chondrocytes**

Activation of  $\beta$ -catenin signaling in articular chondrocytes leads to OA-like phenotype in adult  $\beta$ -catenin conditional activation mice, I047

Betulin down regulates IL-1 $\alpha$ -stimulated aggrecanases and MMP gene expression in human chondrocytes, M147

Bisphosphate protect cartilage by reducing chondrocyte apoptosis and reduce bone loss by suppressing osteoclast in adjuvant arthritis, M428

BMP-2 inactivates TAK1-ATF2 signaling pathway in chondrocytes, F186

C/EBP $\beta$ /p57<sup>Kip2</sup> signaling maintains transition from proliferation to hypertrophic differentiation of chondrocytes during skeletal growth, I187

$\beta$ -catenin directly binds to a specific intracellular domain of PTH/PTHrP receptor and regulates the signaling in chondrocytes during endochondral ossification, I013

Chondrocyte differentiation is differentially affected by COX-2 and 5-LO during fracture healing, SU123

Chondrocyte-derived Ihh is required for osteoblast differentiation despite reconstitution of a normal growth plate, I154

Deletion of the oxygen-sensor PHD2 in chondrocytes results in increased cartilage and bone mineralization, I153

DEX triggers mitochondrial apoptosis through Bax in proliferative growth plate chondrocytes causing growth retardation, I188

HDAC inhibitors suppress IL-1 $\beta$ -induced NO and PGE<sub>2</sub> production in human chondrocytes, SU116

Hedgehog signaling regulates growth plate chondrocyte proliferation and growth factor expression, SU161

Impact of calpain inhibition on chondrocyte development, M150

Intracellular PTHR2 alters cell proliferation and pattern of gene expression while antagonizing PTHR1 signaling in chondrocytic CFK2 cells, SA121

LPA enhances the viability of rat growth plate chondrocytes through the inhibition of apoptosis and the promotion of cellular maturation, SU156

Lxn is a novel effector of BMP-2 signaling in modulation of chondrocyte differentiation, SU117

Nkx3.2 is an important mediator of hypoxia-induced chondrocytic differentiation, F112

Notch signaling inhibits chondrogenesis and subsequently promotes chondrocyte maturation, I268

Overcoming the zone of chondrocyte death associated with osteochondral harvest by sequential treatment with collagenase and IGF-1, SU129

Overexpression of CCN2/CTGF in cartilage shows prolonged bone length resulting from stimulation of chondrogenesis, chondrocyte growth, apoptosis, and bone mineralization during endochondral ossification, M153

PGD2 downregulates MMP-1 and MMP-13 expression in human OA chondrocytes, SA152

Phosphate induced apoptosis in growth plate chondrocytes via a NO and JNK-dependent path, SA113

Phosphate regulates chondrocyte differentiation, proliferation and apoptosis in a model of embryonic endochondral bone formation, SU124

Postnatal deletion of PTH/PTHrP receptor in growth plate chondrocytes leads to growth plate fusion, F114

Protein sulfation is required to prevent chondrocytes autophagy and growth factor signaling during endochondral ossification, SU119

PTHrP prevents chondrocyte premature hypertrophy by inducing cyclin D1-dependent Runx2 and 3 phosphorylation and degradation, I044

Regulation of hypertrophic chondrocyte apoptosis, M158

Runx2 and canonical Wnt signaling cooperatively regulate BMP-induced differentiation pathways of adult dural cells into osteoblasts or chondrocytes, M043

Studies on the deposition of ochronotic pigment in AKU reveal tyrosine metabolism in human chondrocytes, M166

- Targeted expression of SOX9 in hypertrophic chondrocytes leads to enhanced adipogenic activity and spontaneous OA in transgenic mice, SA115
- TGF $\beta$  and Smad3-dependent repression of Runx2 function in ATDC5 chondrocytes, SU122
- Thyroid hormone activates Wnt signaling pathways in rat growth plate chondrocytes, M157
- Tissue-specific KO of the CaSR in chondrocytes inhibits IGF-1 signaling and delays differentiation in the growth plate, 1261
- Transcription factor NFATp regulates BMP-induced chondrocyte differentiation in a tissue-specific manner, SU020
- Transcription factor Znf219 regulates chondrocyte differentiation through forming transcription factory complex with Sox9, 1265
- Chondrodysplasia**
- Reduced cell proliferation and chondrodysplasia in mice lacking the mitotic protein NuSAP, SU120
- Chondrogenesis**
- ADAMTS-7, a direct targeting molecule of PTHrP, is a novel potent mediator of chondrogenesis, 1262
- Apc-mediated control of  $\beta$ -catenin is essential for both chondrogenic and osteogenic differentiation of skeletal precursors, SA130
- MIA3, a novel secreted factor, regulates chondrogenic differentiation in the developing mouse embryo, 1043
- Nicotine induces chondrogenesis via calcineurin/NFAT, SU133
- Notch signaling inhibits chondrogenesis and subsequently promotes chondrocyte maturation, 1268
- Overexpression of CCN2/CTGF in cartilage shows prolonged bone length resulting from stimulation of chondrogenesis, chondrocyte growth, apoptosis, and bone mineralization during endochondral ossification, M153
- Regulation of chondrogenesis and bone development by neogenin via BMP pathway, SU127
- TGF $\beta$ - and BMP-signaling pathways have antagonistic effects during chondrogenesis, F158
- Wnt target gene Twist1 inhibits Sox9, the master regulator of chondrogenesis, 1266
- Chondroprogenitor cells**
- bFGF induces the expression of a subset of Bcl-2 family genes to inhibit the apoptosis of ATDC5 chondroprogenitor cells, SU043
- Chromatin**
- Evidence of a role for the human Vitamin D response element binding protein, hnRNP C1/C2 in chromatin remodeling and transcript splicing, F240
- Functional association of MAPK and Runx2 on osteoblast chromatin, SU025
- Wdr5 is required for chromatin modifications at the Runx2 promoter, M039
- Chromosome 4 (Chr 4)**
- Genomic expression analysis of rat Chr 4 for skeletal traits at femoral neck, SA261
- Chromosome breaks**
- Analysis of chromosome breaks in osteoblasts and non-osteoblastic cells treated with intermittent PTH, M191
- Chronic kidney disease (CKD). See Kidney disease**
- Chronic obstructive pulmonary disease (COPD). See Pulmonary disease**
- Cinacalcet**
- Documented response to cinacalcet in two cases of acquired hypocalciuric HCa, M197
- Cirrhosis**
- Different influence of the clinical condition, degree of cholestasis, alcohol abuse and serum Ca on the musculoskeletal system in chronic cirrhotics, M411
- Fracture risk in primary biliary cirrhosis: role of osteopenia and severity of cholestasis, M442
- Cis**
- Cis-regulatory motifs and computationally-derived transcriptional networks predict dynamic motions for osteocytes, M103
- Cissus quadrangularis**
- Cissus quadrangularis* attenuates OVX induced bone loss in mice, M403
- Ciz**
- Interaction of Ciz, a nucleo-cytoplasmic shuttling transcription factor with C-propeptides of type I collagen, M044
- CIC-7**
- Chloride channel CIC-7 mediates acidification of the resorption lacuna in osteoclasts, M123
- Cleidocranial dysplasia. See Dysplasia**
- Cloning**
- Cloning and functional analysis of human Nurr1 (NR4A2) promoter: critical role in the regulation of CYP27B1 by PTH and CREB phosphorylation, 1161
- Clozapine**
- Atypical antipsychotic clozapine reduces rat osteoblast proliferation and osteoclastogenesis at therapeutic levels, SU030
- CMKLR1**
- Chemerin and CMKLR1 expression and function in human bone marrow MSC adipogenesis, SU165
- Chemerin and CMKLR1 targeted gene delivery identifies a novel molecular switch in the treatment of osteoporosis, M071
- CNP**
- Over-expression of CNP enhances the formation of long bone exostoses in Ext1<sup>-/-</sup> mice, SU130
- Cobb angle**
- Accuracy of Cobb angle measurement with iDXA, SU484
- COL1A2**
- Functional polymorphism in COL1A2 (Ala459Pro) that is associated with intracranial aneurysms, shows heterozygous disadvantage concerning BMD and stroke in elderly men, SU219
- col2a1**
- Mouse with a Ser1386Pro mutation in the C-propeptide domain of *col2a1* provides a model for SEDC, 1269
- Col10a1**
- Transcription factor Dmrt2 controls endochondral ossification through regulating type 10 collagen (Col10a1) gene expression, 1045
- Colistin**
- Colistin-impregnated bone cement beads prevent multi-drug resistant *Acinetobacter* osteomyelitis, M236
- Colitis**
- Short treatment with Scl-ab can inhibit bone loss in an ongoing model of colitis, 1212
- Collagen**
- 1,25(OH)<sub>2</sub>D<sub>3</sub> regulates collagen maturation in osteoblastic cell culture system, SU208
- Do type I collagen homotrimers contribute to osteoporosis by altering bone remodeling?, SA146
- Effect of collagen degradation on the fatigue behaviour of emu bone, M461
- Fusion protein of PTH and a collagen binding domain shows superior efficacy and longer duration of action compared to PTH(1-34) as an anabolic bone agent in normal female mice, 1063
- Homocysteine accumulates in bone tissue by collagen binding and adversely affects bone, M417
- Interaction of Ciz, a nucleo-cytoplasmic shuttling transcription factor with C-propeptides of type I collagen, M044
- Kidney dysfunction disturbs collagen maturation in ABD as assessed by confocal laser Raman spectroscopy, SU439
- Mineralization is related to collagen cross-links in growing cancellous and cortical bone, SA110
- NEG alters collagen fibrillar structure and energy dissipation characteristics, SU478
- P3H1 and CRTAP are mutually stabilizing in the endoplasmic reticulum collagen prolyl 3-hydroxylation complex, 1049
- Collagen  $\alpha$ 1(XI)**
- Bone microarchitecture is dependent upon collagen  $\alpha$ 1(XI) expression during development, F135
- Collagen 1 Alpha**
- Allele specific silencing of Collagen 1 Alpha genes in primary human bone cells using RNAi, M232
- Collagen, type XI**
- Enrichment of type XI collagen and 6b N-terminal domain at sites of mineral nucleation within osteoblastic cultures, SA070
- Collagen-induced arthritis (CIA). See Arthritis**
- Collagenase**
- Overcoming the zone of chondrocyte death associated with osteochondral harvest by sequential treatment with collagenase and IGF-1, SU129
- Colony stimulating factor-1 (CSF-1)**
- Sim induces Wnt signaling and reduces CSF-1 secretion and RANKL/OPG ratio to block osteoclast differentiation, SU096
- Computed tomography (CT)**
- Characterization and genetic mapping of bone size phenotypes in GK and F344 rats using a new 3D CT method, M463
- Evaluating bone microstructure at the distal tibia in children, F315
- Computed tomography, micro ( $\mu$ CT)**
- $\mu$ CT abnormalities in the th3 mouse model of thalassemia start at a young age and are associated with decreased bone turnover, SA128
- Automatic estimation of body composition using  $\mu$ CT and a Gaussian mixture model, M139
- Characterization through  $\mu$ CT of the bone phenotype of mice showing impaired gait and motor skills, SA250
- Effects of GH on bone micro-architecture by in vivo  $\mu$ CT, SA547
- Improved bone mass after co-administration of Sr ranelate and RIS in a rat model of osteoporosis using "in-vivo"  $\mu$ CT, SU393
- Quantification of non-mineralized tissue via  $\mu$ CT as a readout for GC effects on rat growth plate, M136
- Quantitation of bone marrow fat in long bones of mice using MRI or  $\mu$ CT, M145
- Quantitative  $\mu$ CT imaging of adipocyte volume in bone marrow of mice with high and low bone mass, SU250
- Recovery of bone architecture after RANKL administration in rats is characterized by increased bone mass on existing trabeculae assessed by in vivo  $\mu$ CT, SU076
- Reproducibility of mineral density and morphometric  $\mu$ CT measurements at different voxel size scans, M311
- Thermoreversible Pluronic F108 gel as a universal tissue immobilization material for  $\mu$ CT analyses, SU468
- TPTD improves trabecular architecture as measured by  $\mu$ CT at simulated in vivo resolution in the femoral neck of OVX monkeys, SA375
- TPTD in bisphosphonate-resistant osteoporosis—clinical and  $\mu$ CT data, 1172
- Trabecular 3D volumetric density at organ and tissue levels by  $\mu$ QCT evaluation of iliac crest biopsy, M303
- Unsymmetrical beam theory and finite element method: analysis of murine cortical bone based on  $\mu$ CT imaging, M454
- Computed tomography, nano (nanoCT)**

## Key Word Index

## ASBMR 30th Annual Meeting

- NanoCT can be used to assess mechanically related modeling and remodeling in the mouse fibula, 1296
- Computed tomography, peripheral quantitative (pQCT)**
- Efficacy of ODN in the OVX rhesus monkey as measured with pQCT, M343
- Ethnicity-specific bone changes during adolescent growth: pQCT analysis of the tibia, M502
- FEA performed on radius and tibia HR-pQCT images provides new insights for fracture status assessment, 1067
- Forearm pQCT measurements in males with DMD, SU492
- Formation of new trabeculae in a female patient with osteoporosis treated with TPTD, demonstrated with in-vivo-assessment of 3D bone microarchitecture with HR-pQCT, M352
- Measurement of T2\* relaxation time of the trabecular bone network at 7T and 3T compared to topological and structural measurements from HR-pQCT, F317
- Patients with CKD and low 1/3 radius and femoral neck BMD have markedly abnormal cortical and trabecular microstructure by HR-pQCT, 1033
- pQCT predicts vertebral fractures in osteoporotic postmenopausal women, SU472
- Precision of pQCT measurements of bone and muscle area in the forearm and lower limb, SU279
- Validating pQCT MCSA measurement, SU278
- In vivo assessment of 3D bone microarchitecture with HR-pQCT in patients with and without fractures, SU276
- In vivo quantification of intra-cortical porosity in human cortical bone using HR-pQCT in patients with type II diabetes, M309
- Computed tomography, quantitative (QCT)**
- BMD shows no peak from birth to youth as measured by QCT, F310
- Comparison of HR-pQCT to DXA and QUS for the assessment of ex-vivo bone strength, M466
- Composite bone score with QCT bone measurements and fracture history, SU289
- Effects of a targeted bone and muscle loading program on QCT bone geometry and strength, muscle size and function in older men, 1244
- FEA of proximal femur QCT scans for the assessment of hip fracture risk in older men, F321
- Hip structural analysis and volumetric QCT in postmenopausal women from the PaTH Study: mono- or combination therapy with ALN and PTH, M306
- Prediction of incidental low trauma limb fractures in older men and women with QCT variables of bone and muscles in mid-thigh, F369
- QCT and FEA assessment of proximal femur bone quality and strength in women with postmenopausal osteoporosis receiving once-monthly oral IBN for 12 months, SA509
- QUS, BMD and QCT in women with established osteoporosis treated with TPTD, SA393
- Regional differences of femoral BMD changes after one year once-monthly IBN as measured by 3D QCT, SU260
- Subject-specific mechanical properties of trabecular bone using a low-dose imaging, SU471
- In vivo longitudinal QCT analysis PTH efficacy in a rat cortical defect model, M207
- Confocal laser scanning microscopy (CLSM)**
- Human osteoprogenitor cell adhesion and spreading on functionalized Ti surfaces followed by QCM and CLSM, SA101
- Connecting Path method**
- Evaluation of osteoporosis vertebrae fragility by Connecting Path method, M307
- Connective tissue growth factor (CTGF)**
- Evaluation of two novel bone growth factors to enhance fracture healing, SU012
- Induction of CTGF by TGF $\beta$ 1 in osteoblasts: independent effects of Src and Erk on Smad signaling, M066
- Overexpression of CCN2/CTGF in cartilage shows prolonged bone length resulting from stimulation of chondrogenesis, chondrocyte growth, apoptosis, and bone mineralization during endochondral ossification, M153
- Connective tissues.** See also *Cartilage; Collagen*
- Abnormality of bone formation in transgenic mice expressing Osr1, M144
- AC-100 promotes cartilage repair and subchondral bone healing in surgically induced cartilage defects, SA111
- Activation of  $\beta$ -catenin signaling in articular chondrocytes leads to OA-like phenotype in adult  $\beta$ -catenin conditional activation mice, 1047
- ADAMTS-7, a direct targeting molecule of PTHrP, is a novel potent mediator of chondrogenesis, 1262
- Akt regulates skeletal development through GSK3, mTOR, and FoxOs, 1151
- Apc-mediated control of  $\beta$ -catenin is essential for both chondrogenic and osteogenic differentiation of skeletal precursors, SA130
- Assessment of changes in thoracic and lumbar vertebrae in T-type Ca $_v$ 3.2 (a1H) VSCC KO mice, M170
- Betulin down regulates IL-1 $\alpha$ -stimulated aggrecanases and MMP gene expression in human chondrocytes, M147
- Biological activation of biomaterials by rAAV vector, SU136
- Bisphosphate protect cartilage by reducing chondrocyte apoptosis and reduce bone loss by suppressing osteoclast in adjuvant arthritis, M428
- BMSC and Osx contributing to osseointegration of dental implants, SA138
- BMSC-derived extracellular matrix promotes MSC motility, SA134
- Bone defect model in mouse femur to challenge biomaterials, cells and molecules for bone repair, SA126
- Bone marrow cells participate in normal endothelial, but not epithelial or mesenchymal cell renewal in adult rats, M171
- Bone tether formation in femoral and basicranial growth plates have similar responses to growth disruptions due to nuclear VDR genotype and mineral homeostasis, M164
- Both excess and restricted energy availability negatively influence acquisition of trabecular bone mass and microarchitecture during growth, M493
- Brachy-syndactyly caused by loss of *Sfrp2* function, F118
- BT-201, a butanol extract of *Panax notoginseng* inhibits progression of joint degeneration in a rat model of OA, M152
- C/EBP $\beta$ /p57<sup>Kip2</sup> signaling maintains transition from proliferation to hypertrophic differentiation of chondrocytes during skeletal growth, 1187
- Calcifications in children with JDM contain several bone formation markers, SA106
- Cat K expression during enamel formation, SA154
- Changes in chemical, mechanical, and structural properties of lamellar bone during young adulthood, SU475
- Characterization of the osteotomy callus using FTIR imaging in a rabbit ulnar model, M471
- Characterization through  $\mu$ CT of the bone phenotype of mice showing impaired gait and motor skills, SA250
- Chondrocyte differentiation is differentially affected by COX-2 and 5-LO during fracture healing, SU123
- Chondrocyte-derived Ihh is required for osteoblast differentiation despite reconstitution of a normal growth plate, 1154
- Circulating fibronectin affects bone matrix, SA151
- Clinical application of resorbable polymers in guided bone regeneration, SA003
- Co-expression of p62<sup>P392L</sup> and MVNP in osteoclast precursors increases the formation of osteoclasts that express a pagetic phenotype, F476
- Combined Cs-137 gamma irradiation and hindlimb unloading rapidly decreased cancellous bone volume fraction in the mouse lumbar vertebrae, M469
- Comparison of cPTH(1-31) to PTH(1-34) in the enhancement of experimental fracture healing, M161
- Concentration of connective tissue progenitors in autologous cancellous bone graft enhances new bone formation in a canine femoral defect model, SA039
- Conditional deletion of fibronectin results in a scoliosis-like phenotype, 1046
- Conditional disruption of *Pkd1* in osteoblasts results in osteopenia due to direct impairment of osteoblast-mediated bone formation, SA019
- Conditional knockout of the CaSR in osteoblasts alters regulators of Wnt signaling, delays cell differentiation, and promotes apoptosis in bone, 1156
- Connective tissue progenitor cell contribution to ectopic skeletogenesis, F044
- Cortical bone microstructure and strength at the mid-diaphysis of human femurs, M172
- Craniofacial gene discovery in mice, M248
- Development of OA and its relationship to meniscal ossification in Dunkin Hartley guinea pigs, M154
- Development of pharmacological HIF activators for fracture healing, SU052
- DEX triggers mitochondrial apoptosis through Bax in proliferative growth plate chondrocytes causing growth retardation, 1188
- DHCR24 gene is mandatory for the proper growth of long bone, SU118
- Diet induced obesity compromises the osteogenic potential of the bone marrow, F047
- Differences in femoral bone structure between juvenile non-transgenic and transgenic rabbits with the WAP-hFVIII gene construct, SA132
- DMP1 fragments interact differently with HA: insights into mechanism of action, SA140
- Do racial differences exist in cortical and trabecular bone?, M468
- Dwarfism and osteopenia in mice with inactivated HRE in the VEGF gene promoter, 1152
- Dynamic histomorphometry of mineralized tissue using cryosections of murine bone and teeth, M138
- Early osteocyte marker, E11/gp38 is highly elevated in new bone formed in response to distraction as compared to existing bone, SA136
- Effect of bisphosphonate treatment of OA in a guinea pig model, M149
- Effects of beta-D-glucopyranoside from *Phellodendron Amurense* on the production of inflammatory cytokines, growth factors, MMP, and on bone markers in human subchondral OA osteoblasts, SA117
- Effects of Pt group metals treatment on the bone of developing chick embryos, M141
- Essential Hox gene function in limb skeletal and synovial joint formation, M151
- Expansion of mesenchymal progenitors in an in vivo model of constitutive activation of the PTH/PTHrP receptor, 1263
- Expression of an engineered G $_i$ -coupled receptor in osteoblasts affects intramembranous and endochondral bone formation during bone repair, F127

- Expression of BMP antagonists during fracture healing, SA160
- Fluoride effects on bone formation, mineralization and mechanical properties are influenced by genetics, SU465
- Functionalization of a PLGA/PEG-PLA composite electrospun scaffold with rhBMP-2 plasmid DNA for bone regeneration, SA124
- GC signaling through osteoblasts is essential for cranial skeletal development, 1267
- Gender-specific changes in bone microstructure of mice lacking ribosomal protein L29/HIP, SA133
- Gene expression profiling within murine growth plates using DNA microarrays, M156
- GIP inhibits glucose-induced apoptosis of bone cells, M011
- HDAC inhibitors suppress IL-1 $\beta$ -induced NO and PGE<sub>2</sub> production in human chondrocytes, SU116
- Histologic and radiographic analysis of osteopromotive property of demineralized allogenic dentin matrix in parietal bone defects in rabbit, M168
- Human skeletal muscle cells undergo matrix mineralization in an osteogenic pellet culture assay, M135
- Hypothyroidism is not deleterious to the skeleton during early fetal development, SA123
- Identification and characterization of 3.6 Col I positive cells from mouse temporomandibular joint, SU132
- Identification and characterization of angiogenesis-inducing secretory molecules from osteogenically differentiated MSC, M163
- Identification of DPP-I as a potential activator of KLK-4, SA155
- Identification of DSP-phosphoryn cleavage site, SA144
- IGFBP6 Is a negative regulator of osteoblast differentiation and bone formation, SA182
- Immediate abnormalities at the chondro-osseous junction due to severe spinal cord injury in growing rats, SA520
- Impact of calpain inhibition on chondrocyte development, M150
- Impaired bone formation in mice lacking lamin A/C activation leads to severe osteopenia, F131
- Impaired bone healing in a BMP-2 KO mouse model of DO, SA159
- Impaired fracture healing in the absence of the Vitamin D-24-hydroxylase, Cyp24a1, M222
- Increased maternal fat intake increases skeletal mass in congenic mice, M495
- Increased osteoclasts in Brl mouse model for OI are independent of decreased osteoblast matrix production and RANKL/OPG ratio, but are associated with increased osteoclast precursors in marrow, SU209
- Induction of ESC-related pluripotency genes in post natal stem cells during fracture healing, F038
- Influence of muscle size and strength on changes in bone mass and size during growth and in response to exercise, SA537
- Intracellular PTHR2 alters cell proliferation and pattern of gene expression while antagonizing PTHR1 signaling in chondrocytic CFK2 cells, SA121
- LMP-1, positive regulator in osteolineage differentiation of human PDL fibroblasts, M051
- Loss of *MMP-9* results in improved healing, and remodeling of adhesions in a murine model of flexor tendon repair, F153
- Low magnitude vibration can inhibit muscle loss and increase mineralizing bone surfaces in aging mice, M173
- Lxn is a novel effector of BMP-2 signaling in modulation of chondrocyte differentiation, SU117
- Marked induction of endochondral bone formation by overexpression of a constitutively active Gli2 in MSCs isolated from the healing site, SA049
- MIA3, a novel secreted factor, regulates chondrogenic differentiation in the developing mouse embryo, 1043
- Mice deficient in BSP display impaired modeling and remodeling and respond to ovariectomy but not to the cortical anabolic effect of PTH, 1191
- Mineralization is related to collagen cross-links in growing cancellous and cortical bone, SA110
- Mineralization potential and orientational aspects of osteogenic cell cultures by Raman spectroscopy, M084
- Modulation of skeletal modeling by silica-based nanoparticles, SU014
- Musculoskeletal disuse worsens the acute detrimental effects of heavy particle radiation on osteoblastogenesis, SA517
- Nanogel cross-linking hydrogel as a drug delivery system for TNF $\alpha$  antagonist, M121
- Nanotechnological scaffold with combination of PGE<sub>2</sub> receptor EP4 agonist and rhBMP2, enhances bone repair in the defect of mouse calvarium bone, SA105
- Nicotine induces chondrogenesis via calcineurin/NFAT, SU133
- Nkx3.2 is an important mediator of hypoxia-induced chondrocytic differentiation, F112
- Notch signaling inhibits chondrogenesis and subsequently promotes chondrocyte maturation, 1268
- Nov induces gremlin expression by post transcriptional mechanisms, F141
- Novel MMP-13-derived peptides demonstrate non-covalent interaction of MMP-13 with the TGF $\beta$  large latent complex, 1189
- Novel model system for drug discovery in OA: monitoring whole tissue turnover in murine femur heads, SU125
- Novel screening system for bone matrix proteins that control bone mineralization, SA108
- OAH19, an ethanol extract from combined two herbs, inhibits IL-1 $\alpha$ -induced expression of MMP-1 and MMP-13 in OA human cartilage and synovial fibroblast, M148
- Overexpression of the transcriptional cofactor Lbh impairs angiogenesis and endochondral bone formation during fetal bone development in chickens, SU004
- PGD2 downregulates MMP-1 and MMP-13 expression in human OA chondrocytes, SA152
- Phosphate induced apoptosis in growth plate chondrocytes via a NO and JNK-dependent pat, SA113
- Phosphate regulates chondrocyte differentiation, proliferation and apoptosis in a model of embryonic endochondral bone formation, SU124
- Postnatal deletion of PTH/PTHrP receptor in growth plate chondrocytes leads to growth plate fusion, F114
- Proinflammatory mediators downregulate PPAR $\gamma$ 1 expression and activity in OA synovial fibroblasts, M159
- Protein hydrolyzate directly modulates the expression of GIP by osteoprogenitor cells, SU010
- Protein sulfation is required to prevent chondrocytes autophagy and growth factor signaling during endochondral ossification, SU119
- Proteoliposomes carrying ALP and NPPI as matrix vesicle mimetics, SA061
- PTHrP nuclear localization sequence and C-terminus regulate craniofacial development, 1264
- PTHrP prevents chondrocyte premature hypertrophy by inducing cyclin D1-dependent Runx2 and 3 phosphorylation and degradation, 1044
- Quantification of non-mineralized tissue via  $\mu$ CT as a readout for GC effects on rat growth plate, M136
- Quantitation of bone marrow fat in long bones of mice using MRI or  $\mu$ CT, M145
- Rapid EDTA microwave decalcification of rabbit osteochondral samples preserves enzyme activity and antigen epitopes, M140
- Reconstituting marrow-derived extracellular matrix ex vivo: an optimal niche for retaining the properties of human MSCs, M165
- Reduced cell proliferation and chondrodysplasia in mice lacking the mitotic protein NuSAP, SU120
- Regulation of autophagy in the epiphyseal growth plate by AMPK and mTOR requires HIF-1, SU134
- Regulation of chondrogenesis and bone development by neogenin via BMP pathway, SU127
- Regulation of hypertrophic chondrocyte apoptosis, M158
- Regulation of intracellular signaling of MC3T3-E1 osteoblasts by the extracellular matrix, SA139
- Regulation of osteonectin/SPARC by miRNA-29, 1155
- Regulation of the BMP-2 distant osteoblast enhancer by FGF-2, SU150
- Role of gal-3 in OA, M162
- Role of pyrophosphate and inorganic phosphate in PKA-mediated osteoblastic differentiation and mineralization of primary murine aortic cells, M143
- Role of Wdr5 in endochondral bone formation during chicken limb development, SU121
- Specific forms of DMP1 support attachment and haptotactic migration via  $\alpha$ V $\beta$ 3 but not  $\alpha$ V $\beta$ 5 integrin, F145
- Studies on the deposition of ochronotic pigment in AKU reveal tyrosine metabolism in human chondrocytes, M166
- Study of hGH and IGF-1 receptors in the human fetal femoral growth plate, SU128
- Targeted disruption of Nrf1 in osteoblasts leads to reduced bone size and dramatic alterations in trabecular bone microstructure in mice, 1190
- Targeted expression of SOX9 in hypertrophic chondrocytes leads to enhanced adipogenic activity and spontaneous OA in transgenic mice, SA115
- TGF $\beta$  and Smad3-dependent repression of Runx2 function in ATDC5 chondrocytes, SU122
- TGF $\beta$ -and BMP-signaling pathways have antagonistic effects during chondrogenesis, F158
- Thyroid hormone activates Wnt signaling pathways in rat growth plate chondrocytes, M157
- TIEG1 KO mice display defects in the molecular structure of tendon fibers, M133
- TiO<sub>2</sub>-scaffolds for use in bone tissue engineering, SA137
- Tissue-specific KO of the CaSR in chondrocytes inhibits IGF-1 signaling and delays differentiation in the growth plate, 1261
- Transcription factor Dmrt2 controls endochondral ossification through regulating type 10 collagen (Col10a1) gene expression, 1045
- Transcription factor Znf219 regulates chondrocyte differentiation through forming transcription factory complex with Sox9, 1265
- Trps1 represses Runx2 during endochondral bone formation, SU126
- Use of endothelial progenitor cells to promote bone healing, SA104
- Use of GFP reporter mice for assessing osteoprogenitor cell activity in a critical size calvarial defect, SA007

## Key Word Index

## ASBMR 30th Annual Meeting

- Vinculin is involved in hypertrophic differentiation through Raf/MEK/ERK pathway in chondrocytic ATDC5 cells, SA119
- In vivo bone matrix density measurements by water and fat suppressed projection MRI (WASPI), SA102
- In vivo demonstration that PTH acts on early osteoprogenitor cells to enhance bone formation during repair of critical-size calvarial defects, M062
- In vivo downregulation of *Mustn1* mRNA leads to musculoskeletal defects, 1192
- Wnt target gene *Twist1* inhibits Sox9, the master regulator of chondrogenesis, 1266
- Connexin 43 (Cx43)**
- Altered long bone structure in recessive null and dominant negative Cx43 (*Gja1*) mouse mutants, 1110
- Association between Cx43 and  $\beta$ -arrestin is required for cAMP-dependent osteoblast survival induced by PTH, 1227
- Critical role of Cx43 in postnatal skeletal growth and bone mass acquisition, 1257
- Downregulation of Cx43 expression and osteoclastogenesis by a bioceramic bone graft substitute, M119
- FGF-2 signaling in osteoblasts: Cx43 is a docking platform for PKC $\delta$ , F026
- Mechanical perturbation of integrin  $\alpha 5$  with or without association with fibronectin opens Cx43-hemichannels in osteocytes, SA060
- Transcriptional regulation of Cx43 by  $\beta$ -catenin, a pathway activated by PGE $_2$ -PI3K-GSK3 signaling in mechanically loaded osteocytes, 1042
- Contraceptives, oral**
- Can impact exercise mitigate the adverse effects of oral contraceptives on bone?, M488
- Copy number variation (CNV)**
- Genome-wide CNV study identified a novel susceptibility gene *UGT2B17* for osteoporosis, M404
- Coronary artery disease**
- AAC detected on lateral DXA spine images is associated with coronary artery disease, 1035
- Coronary syndrome, acute**
- Increased circulating DKK1 in acute coronary syndrome—association with platelet release and endothelial inflammatory response, SU167
- Cortical bone**
- Assessment of cortical thickness and BMD in the radius by low-frequency Q-GWUS, M319
- Childhood cortical bone and skeletal age show bivariate genetic linkage to chromosome 2p, 1177
- Contributions of trabecular and cortical components to biomechanical properties of human vertebrae, M455
- Cortical bone acquisition in the appendicular skeleton of healthy young females is reciprocally related to marrow adiposity, M074
- Cortical bone microstructure and strength at the mid-diaphysis of human femurs, M172
- Cortical cross sectional area in young adult men is inversely related to risk of hip fracture in their older relatives, 1281
- Deletion of the Wnt signaling antagonist sFRP4 in mice induces opposite bone formation phenotypes in trabecular and cortical bone, 1005
- Differential effects of GH and 1  $\alpha$  calcidol on cancellous and cortical bone in hypophysectomized rats, SU501
- Do racial differences exist in cortical and trabecular bone?, M468
- Effects of obesity on cortical bone, SA342
- Effects of simulated resistive exercise on cortical bone in the tibia mid-diaphysis of hindlimb unloaded rats, SA521
- Estimation of relative stiffness contributions of cortical and trabecular compartments by MRI-based FEA, SU481
- Inactivation of *Dlx5* gene results in altered osteoblast-osteoclast coupling inducing increased bone resorption and reduced cortical thickness in male mice, F010
- Juvenile murine model of OVX-induced trabecular and cortical osteoporosis, SA387
- Kidney disease is associated with abnormal cortical geometry independent of age and gender, SU441
- Load induced changes in trabecular and cortical bone are dose dependent in both C57BL/6 and C3H/HeJ mice, F527
- Low serum IGF-I alters the cortical bone response to estrogen deficiency, SU190
- Marked abnormalities in cortical and trabecular microarchitecture and strength in premenopausal women with idiopathic osteoporosis, M310
- Microfinite element modeling reveals that transient deficits in cortical bone may underlie the adolescent peak in forearm fractures, 1179
- Mineralization is related to collagen cross-links in growing cancellous and cortical bone, SA110
- Physiological concentrations of inhibin A are anabolic, affecting both trabecular and cortical bone in normal intact mice, M177
- Proton NMR study of transverse relaxation in rabbit and rat cortical bone, M470
- Reciprocal relation between MR measures of marrow adiposity and cortical bone in the appendicular skeleton of healthy adults, SU042
- In vivo quantification of intra-cortical porosity in human cortical bone using HR-pQCT in patients with type II diabetes, M309
- COX-2. See Cyclooxygenase-2**
- Cozaar. See Losartan®**
- CPT2**
- In vivo differential expression profiling study on human circulating monocytes suggested a novel CRAT and CPT2 network underlying smoking and BMD, SU155
- Craniofacial disorders**
- Craniofacial gene discovery in mice, M248
- Cranio metaphyseal dysplasia. See Dysplasia; Dysplasia, craniometaphyseal**
- CRAT**
- In vivo differential expression profiling study on human circulating monocytes suggested a novel CRAT and CPT2 network underlying smoking and BMD, SU155
- Creatine**
- Brain-type creatine kinase is required for RANKL-induced osteoclastogenesis, M116
- Creatinine**
- Is it time to update normative values for ionized Ca and urine Ca? Creatinine ratios in healthy Canadian infants, SU487
- Crohn's Disease**
- Bone histomorphometry in patients with Crohn's Disease, SU462
- Effects of serum factors during osteoblast differentiation—implication for the pathogenesis of osteoporosis in Crohn's Disease, M450
- Pediatric Crohn's Disease is associated with negative Ca balance and increased renal losses of Ca, SA565
- CTX**
- Bone degradation marker CTX shows unique properties in disease monitoring compared to NTX, ICTP and bALP in MM, M287
- CTx-I**
- Vitamin D status and bone remodeling marker CTx-I in patients with early RA: association with disease activity and joint damage, SA496
- CXC**
- Transient expression of CXC receptor 2 in human MSC stimulates chemotaxis toward CXC ligand 8 and increased mineralization in the presence of osteogenic medium, SA170
- Cxcl2**
- Roles of Cxcl2 in osteoclast precursor cells, SU086
- CXCL12**
- CXCL12 expression is regulated by HIF-2 $\alpha$  in MM plasma cells, SU080
- Elevated serum levels of CXCL12 is associated with increased osteoclast activity and osteolytic bone disease in MM patients, SU079
- CXCL13**
- CXCL13 stimulates RANK ligand expression in SCC, SU247
- CXCR4**
- Injection of MSCs overexpressing both CXCR4 and RANK-Fc effectively prevented OVX-induced bone loss, F391
- CXCR7**
- Analysis of CXCR7-deficient mice reveals CXCR7 expression in osteocytes but no apparent bone phenotype, M104
- Cyclin D1**
- PTHrP prevents chondrocyte premature hypertrophy by inducing cyclin D1-dependent Runx2 and 3 phosphorylation and degradation, 1044
- Cyclin-dependent kinase 6 (CDK6)**
- Large scale candidate gene analysis identifies an association between the CDK6 locus and trabecular volumetric BMD at the lumbar spine in older men, M266
- Cyclooxygenase-2 (COX-2)**
- Chondrocyte differentiation is differentially affected by COX-2 and 5-LO during fracture healing, SU123
- Effect of MKP-1 deletion on the fluid shear stress induction of COX-2 expression in osteoblasts, SA529
- Mechanical loading upregulates expression of the transcription factor EGR2/Krox-20 by a COX-2-mediated mechanism, SA526
- PTH induces COX-2 in MC3T3-E1 osteoblasts via cAMP-PKA and Ca-calceineurin pathways, SA033
- Cyclopamine**
- Hedgehog pathway is activated in osteosarcoma and cyclopamine prevents osteosarcoma growth by cell cycle regulation, SU241
- CYP17**
- Is there any association between CYP 17-CYP 19 polymorphisms and bone loss in early postmenopausal women?, M259
- CYP19**
- A allele at Valine80 of the CYP19 gene is a risk factor for aromatase inhibitors associated bone loss, 1021
- Is there any association between CYP 17-CYP 19 polymorphisms and bone loss in early postmenopausal women?, M259
- CYP19A1**
- Significant association between polymorphisms of CYP19A1, fracture incidence and BMD in post-menopausal women, M262
- CYP24A1**
- 25(OH)D $_3$ -24-hydroxylase (CYP24A1): mutagenesis and activity studies reveal important residues involved in regioselectivity and substrate access, SU199
- Impaired fracture healing in the absence of the Vitamin D-24-hydroxylase, Cyp24a1, M222
- Polymorphisms in *CYP24A1*, the gene encoding 25(OH)D-24-hydroxylase, are associated with BMD, SA266
- CYP27A1**
- CYP27A1 mutations at Phe147 confer 25-hydroxylase activity towards a Vitamin D $_2$ -type sidechain, M231
- CYP27B1**
- Cloning and functional analysis of human Nurrl (NR4A2) promoter: critical role in the regulation of CYP27B1 by PTH and CREB phosphorylation, 1161
- Deletion of CYP27B1 reverts the premature aging phenotype of the Klotho-null mice, F069
- Expression of 1 $\alpha$ hydroxylase (CYP27B1) in BMSC, SA237

Metabolic alkalosis transition in renal proximal tubule cells facilitates an increase in CYP27B1, while blunting responsiveness to PTH, M196

Prediction of osteoporotic fracture risk by 25(OH)D3-1 $\alpha$ -hydroxylase (CYP27B1) gene, M263

**Cystic fibrosis (CF)**  
Bone status evaluation in pre-pubertal children with CF, SU486

**Cystic fibrosis transmembrane regulator (CFTR)**  
CFTR regulates osteoblast bone formation independent of chloride conductance, 1274

**Cytokines**  
Comparison of direct osteoclastogenic potential on osteoclast precursor cells among proinflammatory cytokines, SU077

Effects of beta-D-glucopyranoside from *Phellodendron Amurense* on the production of inflammatory cytokines, growth factors, MMP, and on bone markers in human subchondral OA osteoblasts, SA117

Gene transcripts related to T-cell activation, proliferation, and cytokine signaling show significant effects on BMD variation in baboons, M241

Increased proinflammatory cytokines TNF- $\alpha$  and IL-6 correlate with pathological bone turnover markers in diabetic patients with acute Charcot foot, F491

MKP-1 is an endogenous negative regulator of pro-inflammatory cytokines in BMSC, SU013

MSC enhance fracture healing: essential role for cytokines in homing and anti-inflammatory response, SA169

Proinflammatory cytokine TWEAK induces SCT expression in human immature osteoblasts in a MAPK dependent fashion, M046

Relationship between serum levels of inflammatory cytokines and bone turnover markers in the year following hip fracture, SU073

Suppression of TREM-2 expression and TREM-2-mediated costimulation of RANK signaling by cytokines that inhibit human osteoclast differentiation, SU114

**D**

**DANCE.** See *Direct Assessment of Non-vertebral Fracture in Community Experience*

**DAP12**  
Modeled microgravity sensitizes osteoclast precursors to RANKL mediated osteoclastogenesis by increasing DAP12, M114

**Dasatinib**  
Tyrosine kinase inhibitor dasatinib decreases osteoclast formation and activity in vitro, SU074

**DBA/2**  
Femur from C57BL/6 and DBA/2 inbred mice display a strain dependent response to treadmill running and tower climbing exercise in cortical and trabecular bone architecture, M485

**DBP**  
Vitamin D deficiency in inner city infants: impact of DBP genotype, SA472

**DC-STAMP**  
DC-STAMP regulates bone metabolism through cell-cell fusion of osteoclasts, F087

**Decalcification, microwave**  
Rapid EDTA microwave decalcification of rabbit osteochondral samples preserves enzyme activity and antigen epitopes, M140

**Deminerlized bone matrix (DBM)**  
Osteogenesis effect of human ligamentum flavum, myoblast, osteoblast and MSC by DBM and BMP-2, SU135

**Denosumab (DMab)**

Assessment of serum Ca and bone resorption markers in patients transitioned from ALN to DMab, M394

Effect of DMab vs ALN on bone turnover markers and BMD changes at 12 months based on baseline bone turnover level, 1285

Effects of ALN or DMab on cortical and trabecular bone mass, bone strength, and bone mass-strength relationships in mice, 1139

Effects of DMab vs ALN on BMD, bone turnover markers, and safety in women previously treated with ALN, M395

Phase III study of the effects of DMab on vertebral, nonvertebral, and hip fracture in women with osteoporosis, 1286

Transition from ALN to DMab in OVX cynomolgus monkeys maintained or improved cortical and trabecular bone mass, without altering the linear relationship between bone mass and bone strength, 1072

Transition from ALN to DMab resulted in further reductions in local and systemic bone turnover parameters and reduced cortical porosity in OVX cynomolgus monkeys, 1216

**Densitometry**  
Bone metabolism, microarchitecture and densitometric measurement in rat femur after chronic alcohol consumption, M239

Densitometric vertebral fracture assessment in postmenopausal women, SU254

Do different densitometers, or use of T-score vs. Z-score, affect fracture risk estimation?, SU258

Improving the diagnostic yield of bone densitometry, F361

Influence of body weight on cost-effectiveness of bone densitometry and treatment for osteoporosis among older women and men without prior fracture, F426

Normal reference values for QUS bone densitometry of the calcaneus in Chinese children and adolescents, SU489

Osteoporosis therapy following bone densitometry—patient expectations as determinants of drug initiation and persistence, M377

RTA of densitometric calcaneal images differs between subjects with and without GC use, M314

**Dentin matrix**  
Histologic and radiographic analysis of osteopromotive property of demineralized allogenic dentin matrix in parietal bone defects in rabbit, M168

**Dentin matrix protein-1 (DMP1)**  
DMP1 fragments interact differently with HA: insights into mechanism of action, SA140

Specific forms of DMP1 support attachment and haptotactic migration via  $\alpha$ V $\beta$ 3 but not  $\alpha$ V $\beta$ 5 integrin, F145

**Dentin sialoprotein (DSP)**  
Identification of DSP-phosphophoryn cleavage site, SA144

**Deoxyribonucleic acid (DNA)**  
DNA demethylation for hormone-induced transcriptional derepression, 1182

DNA methylation analysis of osteogenic gene promoter regions in mouse BMSC, M035

Functionalization of a PLGA/PEG-PLA composite electrospun scaffold with rhBMP-2 plasmid DNA for bone regeneration, SA124

Gene expression profiling within murine growth plates using DNA microarrays, M156

**Derepression**  
DNA demethylation for hormone-induced transcriptional derepression, 1182

**Dermatomyositis, juvenile (JDM)**  
Calcifications in children with JDM contain several bone formation markers, SA106

**Dermo1**  
Dermo1 lineage tracing identifies early osteoprogenitor cells in adult murine bone marrow MSC cultures, SA051

**DESTINY.** See *Bone DESTINY*

**Dexamethasone (DEX)**  
BMP/Wnt antagonists are upregulated by DEX in osteoblasts and reversed by ALN and PTH: potential therapeutic targets for GIO, M098

DEX triggers mitochondrial apoptosis through Bax in proliferative growth plate chondrocytes causing growth retardation, 1188

FHL2 mediates DEX-induced MSC osteogenic differentiation by activating Wnt/ $\beta$ -catenin signaling and Runx2 expression, M048

Inhibition of the mevalonate pathway rescues the DEX-induced suppression of the mineralization of osteoblastic cells, SA230

Osteoblast-targeted deletion of the GC receptor has little impact on PBM but attenuates DEX-induced suppression of bone formation, F452

**DHCR24**  
DHCR24 gene is mandatory for the proper growth of long bone, SU118

**Diabetes mellitus**  
C-terminal fragment of PTHrP (107-139), exerts osteogenic features in both regenerating and nonregenerating bone in mice with diabetes-related osteopenia, SA223

Carotid plaque causes low spinal BMD in Korean postmenopausal women with diabetes, SU359

Impaired oxidative stress defense mechanism may reduce bone stiffness in diabetic Charcot neuroarthropathy, M002

Increased proinflammatory cytokines TNF- $\alpha$  and IL-6 correlate with pathological bone turnover markers in diabetic patients with acute Charcot foot, F491

OPN deficiency reduces aortic calcification and oxidative stress in diabetic LDLR-/- mice, F109

rhBMP-2 accelerates segmental defect healing in diabetic rats, M445

Stimulation of fracture healing by rhPDGF-BB combined with  $\beta$ TCP/collagen matrix in a diabetic rat fracture model, 1137

**Diabetes mellitus, type 1**  
Type 1 diabetes is associated with lower BMD in premenopausal women but not in middle-aged men, SU456

**Diabetes mellitus, type 2**  
Bone fragility is increased in the MKR type 2 diabetic mouse, M440

Geometric evidence of a modeling defect in type 2 diabetic women enrolled in the WHI as a potential explanation for increased fracture risk, 1068

Lack of correlation between glycemic control and BMD in type 2 diabetic women, SU255

Prevalence and factors associated to the presence of vertebral fractures in patients with type 2 diabetes mellitus, M447

Reduced serum osteocalcin and sex hormone binding globulin in men with type II diabetes, SU461

Rosiglitazone-induced change in BMD among African Americans with type 2 diabetes mellitus or impaired glucose tolerance, SU315

Serum ucOC concentration are related to renal function in type 2 diabetes patients, M443

In vivo quantification of intra-cortical porosity in human cortical bone using HR-pQCT in patients with type II diabetes, M309

**Diacylglycerol oil**  
Effects of diacylglycerol oil on body composition, BMD and bone strength in mice, SA442

**Diasorin Liaison (LIA)**  
Analytical validation of LIA and ELEC methods for the determination of osteocalcin, SA191

**Dickkopf-1 (DKK-1)**  
Circulating DKK1 levels are reduced in young subjects with low bone mass, F455

## Key Word Index

## ASBMR 30th Annual Meeting

Deletion of the Dkk-1 Krm-1 and Krm-2 in mice leads to increased bone formation and bone mass, 1004

Dkk-1 predicts the gain of BMD in osteoporotic women on bisphosphonates, SA300

DKK1 is regulated by mRNA stability and epigenetic mechanisms in bone metastasis, 1090

Effects of intermediate doses of GCs on bone turnover and circulating Dkk-1, MIF, sRANKL and OPG in patients with interstitial lung disease, SA451

Fully human anti-DKK1 antibodies increase bone formation and resolve osteopenia in mouse models of estrogen-deficiency induced bone loss, 1214

Increased circulating DKK1 in acute coronary syndrome—association with platelet release and endothelial inflammatory response, SU167

Platelets contribute to circulating levels of Dkk-1: clinical implications in MM, SU228

Preclinical validation of a novel Dkk1 neutralizing antibody for the treatment of MM related bone disease, SU239

Regulation of Dkk-1 and Dkk-2 is needed for osteoblast terminal differentiation on microstructured Ti surfaces, SU006

Suppression of canonical wnt signaling by Dkk1 attenuates PTH-mediated peritrabecular stromal cell response and new bone formation in a model of HPT2, F215

**Dickkopf-2 (DKK-2)**

Regulation of Dkk-1 and Dkk-2 is needed for osteoblast terminal differentiation on microstructured Ti surfaces, SU006

**Diet**

Association of the marker of ABD with malnutrition-inflammation complex in hemodialysis patients, SU446

Bone health impairment in children with chronic Ca and Vitamin D deficiency due to nutritional allergies, SU503

Calorie restriction prevents age-related trabecular bone loss via SIRT-1, 1251

Diet induced obesity compromises the osteogenic potential of the bone marrow, F047

Dietary patterns in Canadian men and women ages 25 and older: relationship to BMI and BMD, SU309

Dietary Sr in a model of established osteopenic rats reduce the levels of 25(OH)D, SA377

Differential cellular and molecular responses of intestinal epithelium to high Ca diet and 1,25(OH)<sub>2</sub>D<sub>3</sub>, M229

Does dietary protein reduce hip fracture risk in elderly men and women?, SU319

Dried plum alters bone metabolism via a different mechanism than PTH, M341

Effect of hypercalciuria and diet on bone in genetic hypercalciuric stone-forming rats, SU213

Effect of the dietary Ca/P ratio on the rate of skeletal accrual in mice, M333

Effects of diacylglycerol oil on body composition, BMD and bone strength in mice, SA442

Effects of diet and menstrual cyclicity on bone mass accumulation in pubertal monkeys, M499

Effects of exercise and milk intake on bone in adolescents, SU301

Effects of KHCO<sub>3</sub> on Ca and bone metabolism during high salt intake, SA446

Essential fatty acid and fish intake is associated with higher BMD in elderly women and men, F341

Evaluating the effect of soy and isoflavones on BMD in older women, M353

Exploring the effect of food intake on bone resorption for optimal drug delivery and efficacy in osteoporosis with oral calcitonin, SA436

Green tea polyphenols protect bone microarchitecture in female rats with chronic inflammation-induced bone loss, M338

High level dietary P and Cd exacerbate OVX-induced bone loss, M301

High-fat diet facilitated decreases in BMD of OVX mice and suppressed the anabolic effects of PTH on bone, SA448

High-fat diet negatively regulates bone development in growing mice, SA441

Impact of dietary protein on Ca homeostasis and nitrogen excretion in the presence and absence of KHCO<sub>3</sub>, SU305

Increased caloric intake in energy deficient exercising with functional hypothalamic amenorrhea women is associated with decreased ghrelin and increased bone formation, SU184

Infantile HCa: relationship of dietary intake of Ca and Vitamin D to serum and urine levels, SU491

Maternal nutrient restriction during pregnancy results in significant alterations in fetal skeletal development in the baboon, M494

Obesity induced by high dietary fat leads to increased bone resorption marker, TRAP, and decreased bone mass in mice, M238

Prevention of the metabolic syndrome together with osteoporosis in young men, SU314

Relationship among nutritional status, oxidative stress and bone density in institutionalized elderly, SU310

Rodent model to evaluate the effect of dietary protein on intestinal Ca absorption, M330

Treadmill exercise provides only short-term protection against cancellous bone loss with reduced dietary energy intake: endocrine mechanisms, SA449

**Dihydrotestosterone (DHT)**

DHT administration is effective for the prevention of hypogonadal bone loss, SU193

Inhibition of bone loss and muscle atrophy by DHT in a mouse hindlimb disuse model, SU377

**1,25-dihydroxyvitamin D (1,25(OH)<sub>2</sub>D)**

25(OH)D acts on Ca and skeletal homeostasis independent of 1,25(OH)<sub>2</sub>D in vivo, M214

Albuminuria, 25(OH)D, 1,25(OH)<sub>2</sub>D, and intact PTH in older adults, SU442

Effects of hPTH(1-34) infusion on circulating serum phosphate, 1,25(OH)<sub>2</sub>D and FGF-23 levels in healthy men, SU169

Genetic model to study 1,25(OH)<sub>2</sub>D action in classical and non-classical target tissues, 1184

**1,25-dihydroxyvitamin D<sub>2</sub> (1,25(OH)<sub>2</sub>D<sub>2</sub>)**

1,25(OH)<sub>2</sub>D<sub>2</sub> is as effective as 1,25(OH)<sub>2</sub>D<sub>3</sub> in regulating cellular proliferation in cultured normal human keratinocytes and transformed prostate cells, M215

Comparison of 1,25(OH)<sub>2</sub>D<sub>2</sub> and calcitriol effects in an adenine-induced model of CKD reveals differential control over serum Ca and phosphate, SU448

Effect of 1,25(OH)<sub>2</sub>D<sub>3</sub> and 25(OH)D<sub>3</sub> on osteoblastogenesis and bone strength in Vitamin D sufficient growing mice, SU207

**1,25-dihydroxyvitamin D<sub>3</sub> (1,25(OH)<sub>2</sub>D<sub>3</sub>)**

1,25(OH)<sub>2</sub>D<sub>3</sub> is as effective as 1,25(OH)<sub>2</sub>D<sub>2</sub> in regulating cellular proliferation in cultured normal human keratinocytes and transformed prostate cells, M215

1,25(OH)<sub>2</sub>D<sub>3</sub> can directly induce osteoclast formation in osteoclast precursors in the absence of RANKL, SU070

1,25(OH)<sub>2</sub>D<sub>3</sub> regulates collagen maturation in osteoblastic cell culture system, SU208

Differential cellular and molecular responses of intestinal epithelium to high Ca diet and 1,25(OH)<sub>2</sub>D<sub>3</sub>, M229

Distinctive anabolic roles of 1,25(OH)<sub>2</sub>D<sub>3</sub> in teeth and mandible versus long bones, M213

High levels of IL-6 and hyper-responsivity to 1,25(OH)<sub>2</sub>D<sub>3</sub> are both required for development of Pagetic osteoclasts, F478

Key mechanism underlying the immunosuppressive effects of Vitamin D: 1,25(OH)<sub>2</sub>D<sub>3</sub> is a transcriptional modulator of IL-17, F246

Rapid-nontranscriptional action of 1,25(OH)<sub>2</sub>D<sub>3</sub> induces IL-6 production in osteoclast precursors expressing MVNP, 1186

Requirement of the bone for Vitamin D for 1,25(OH)<sub>2</sub>D<sub>3</sub> synthesis and bone mineralization, M224

Silencing of PDIA3 (ERp60) reduces the rapid membrane response to 1,25(OH)<sub>2</sub>D<sub>3</sub> in MC3T3-E1 osteoblast-like cells, M227

Transgenic ASARM-peptide overexpression with reduced serum phosphate and 1,25(OH)<sub>2</sub>D<sub>3</sub> leads to decreased BMD and obesity, F210

**1α,25-dihydroxyvitamin D<sub>3</sub> (1α,25(OH)<sub>2</sub>D<sub>3</sub>)**

IFN-β is a key molecule in inhibition of human osteoclast differentiation by 1α,25-dihydroxyvitamin D<sub>3</sub>, SU090

Involvement of caveolae in 1α,25(OH)<sub>2</sub>D<sub>3</sub>-dependent activation of MAPKs in skeletal muscle cells, SA243

**DIOS Study**

Type 1 diabetes is associated with lower BMD in premenopausal women but not in middle-aged men, SU456

**Dipeptidyl peptidase 4 (DPP4)**

Role of FAP and DPP4 in myeloma bone disease and tumor growth, F288

**Dipeptidyl peptidase I (DPP-I)**

Identification of DPP-I as a potential activator of KLK-4, SA155

**Direct Assessment of Non-vertebral Fracture in Community Experience (DANCE)**

TPTD therapy in a community setting: persistence and use of other osteoporosis medications in DANCE, SA395

**Direct injection**

Functional induction of target genes in parathyroid cell by direct injection technique, M185

**Disabilities, motor**

Randomized, placebo-controlled, double blind study on high frequency, low intensity vibration in bone mass, muscle strength and quality of life in children with motor disabilities, F435

**Disc regeneration**

Tissue-engineering and co-culture system based disc regeneration MSC's role, SA189

**Distal radius**

Loaded distal radius: gymnastic-related cross-sectional asymmetry, M490

**Distraction osteogenesis (DO). See Osteogenesis**

**Diuretics**

Loop diuretic use and rates of hip bone loss, and risk of falls and fractures in older women, F371

**Dlk1**

Dlk1/FA1 is a novel factor enhancing osteoclastogenesis and inhibiting bone formation in vitro and in vivo, 1007

**Dlx3**

High bone mass phenotype in the bone specific Dlx3 KO mice, M027

MEPE expression is regulated by BMP-2 signaling through the activation of its downstream transcription factors, Dlx3, Dlx5 and Runx2, SA064

Molecular consequences of a mutant Dlx3 affecting bone homeostasis in TDO, 1272

**Dlx5**

BMP-2 induces Osx expression through up-regulation of Dlx5 and its phosphorylation by p38 MAPK, F020

Dlx5 overexpression stimulates odontoblast differentiation and function, M054

Inactivation of Dlx5 gene results in altered osteoblast-osteoclast coupling inducing increased bone resorption and reduced cortical thickness in male mice, F010

MEPE expression is regulated by BMP-2 signaling through the activation of its downstream transcription factors, Dlx3, Dlx5 and Runx2, SA064

**Dmp1**

Local osteocyte defect in *Dmp1* null mice causes overproduction of FGF-23, 1225



- Mechanical unloading partially rescues hypophosphatemic rickets in *Dmp1*-null mice, 1162
- DMP1**  
7B2 protein mediated inhibition of DMP1 cleavage in osteoblasts enhances FGF-23 production in *Hyp*-mice, 1053
- Dmrt2**  
Transcription factor Dmrt2 controls endochondral ossification through regulating type 10 collagen (*Col10a1*) gene expression, 1045
- DNA**. See *Deoxyribonucleic acid*
- Dock5**  
Dock5, an essential Rac exchange factor in osteoclasts that controls adhesion structure organization and bone resorbing activity, SU064
- Dual energy x-ray absorptiometry (DXA)**. See *Absorptiometry*
- Duchenne muscular dystrophy (DMD)**. See *Muscular dystrophy*
- Duffy antigen receptor for chemokines (DARC)**  
DARC regulates osteoclast differentiation via modulating chemokine effects on migration/fusion of osteoclast precursors, M115
- Dwarfism**  
Dwarfism and osteopenia in mice with inactivated HRE in the VEGF gene promoter, 1152
- Dynorphin**  
Endorphins regulate bone material properties by actions through dynorphin, 1195
- Dysosteosclerosis**  
Dysosteosclerosis in a 2-year-old girl: investigation of a rare, sclerosing bone disorder, SA567
- Dysplasia, cleidocranial (CCD)**  
Runx2 threshold for the CCD phenotype, M041
- Dysplasia, craniometaphyseal (CMD)**  
ANKH mutation causing CMD inhibits osteoclast differentiation, SU214  
Osteoblast and osteoclast involvement in the pathogenesis of a mouse model for CMD, 1204
- Dysplasia, fibrous (FD)**  
Does dietary P influence FGF-23 concentrations in FD patients?, M426  
Polyostotic form of FD in a 13 year old Colombian girl exhibiting clinical and biochemical response to neridronate intravenous therapy, SU211
- Dysplasia, progressive diaphyseal**. See *Camurati-Engelmann disease*
- Dysplasia, spondylo-epi-metaphyseal**  
Three unrelated patients with a unique spondylo-epi-metaphyseal dysplasia, SU494
- E**
- E. coli***  
Expression of human SCT in heterologous eukaryotic insect and *E. coli* expression systems, SA059
- E11**  
Early osteocyte marker, E11/gp38 is highly elevated in new bone formed in response to distraction as compared to existing bone, SA136
- Early growth response factor 1 (EGR-1)**  
Characterization of a promoter polymorphism in FZD1: allele-specific regulation by Egr-1 in osteoblast-like cells, M267  
Stimulation of macrophage TNF $\alpha$  production by orthopaedic wear particles requires activation of the ERK 1/2/Egr-1 pathway but is independent of p38 and JNK, SA177
- Early growth response factor 2 (EGR2)**  
Mechanical loading upregulates expression of the transcription factor EGR2/Krox-20 by a COX-2-mediated mechanism, SA526
- Ebf1**  
Deletion of Zfp521, an antagonist to Runx2 and Ebf1 transcriptional activity, leads to osteopenia and a defect in matrix mineralization in mice, 1109
- EDTA**  
Rapid EDTA microwave decalcification of rabbit osteochondral samples preserves enzyme activity and antigen epitopes, M140
- eIF3i**  
TRIP-1 is eIF3i: a key regulator of osteoblast activity, 1259
- eIF4E**  
2ME2 alters eIF4E activity and causes protein synthesis inhibition in osteosarcoma cells, SU240
- ELEC**. See *Roche Elecsys*
- Electroalgotomy**  
Effect of RLX and ALF on bone and joint pain assessed by fall of skin impedance (electroalgotomy), SA384
- Electromagnetism**  
Brief pulsing electromagnetic field exposure differentially effects cell cycle in proliferating and confluent osteoblasts, M004
- Embryonic stem cells (ESC)**. See *Stem cells*
- Emdogain**  
Enamel matrix derivative (emdogain) enhance osteoblast differentiation on Ti surfaces, M030
- Enamel**  
Cat K expression during enamel formation, SA154
- Endofin**  
Point mutation of endofin at PP1c-binding domain induces angiogenesis and bone formation in mice by sensitizing BMP signaling, 1082
- Endorphins**  
Endorphins regulate bone material properties by actions through dynorphin, 1195
- Endothelial cells**  
Postprandial hyperphosphatemia is a novel risk factor for CVD by involving endothelial dysfunction, SU443
- Endothelial nitric oxide synthase (eNOS)**. See *Nitric oxide synthase*
- Enniatin**  
Fungal secondary metabolites beauvericin and enniatin inhibit osteoclast differentiation and bone resorption, M130
- Enzyme replacement therapy**  
Enzyme replacement therapy prevents dental defects in the *Akp2*<sup>-/-</sup> mouse model of infantile HPP, F107  
Relative efficacy of "treating" versus "preventing" infantile HPP in *Akp2*<sup>-/-</sup> mice by enzyme replacement therapy, 1054
- EP4**  
Nanotechnological scaffold with combination of PGE<sub>2</sub> receptor EP4 agonist and rhBMP2, enhances bone repair in the defect of mouse calvarium bone, SA105  
PGE receptor EP4 antagonist attenuates growth and metastases of cancer, 1230
- Epac**  
PTH/PTHrP mediated stimulation of osteoblast differentiation involves Epac-Rap1 dependent processes, SA025
- EphB4**  
Blockade of Ephrin/EphB4 signaling within the osteoblast lineage reduces osteoblast differentiation and mineralization, SU046  
EphB4 expression in osteoblasts is regulated by myeloma cells and the Wnt signaling pathway, SU232  
Inhibition of major bone catabolic mediators in human subchondral bone osteoblasts upon EphB4 receptor activation by Ephrin-B2 ligand, SU003
- Ephrin**  
Blockade of Ephrin/EphB4 signaling within the osteoblast lineage reduces osteoblast differentiation and mineralization, SU046
- Ephrin B1 reverse signaling regulates bone formation via influencing osteoblast activity in mice, 1194
- EPIC-Norfolk Study**. See *European Prospective Investigation into Cancer-Norfolk Study*
- Epidermal growth factor receptor (EGFR)**  
In vivo differential expression profiling study on human circulating B cells suggested a novel EGFR and CALM3 network underlying smoking and BMD, SU154
- Epigenetics**  
DKK1 is regulated by mRNA stability and epigenetic mechanisms in bone metastasis, 1090
- Epistasis**  
Defining epistasis in a double congenic mouse: implications for the skeleton, M252
- ERE**  
Loss of classical ERE signaling results in suppression of early commitment of BMSC to osteoblasts, F029
- Ergocalciferol**. See also *Vitamin D<sub>2</sub>*  
Effect of three different doses of Vitamin D<sub>2</sub> (ergocalciferol) on muscle function and strength in women > 65 years, M405  
Ergocalciferol is not bioequivalent to cholecalciferol in Vitamin D insufficient hip fracture cases, 1289
- ERK**. See *Extracellular-regulated protein kinase*
- ERp60**  
Silencing of PDIA3 (ERp60) reduces the rapid membrane response to 1,25(OH)<sub>2</sub>D<sub>3</sub> in MC3T3-E1 osteoblast-like cells, M227
- Erythropoiesis**  
Excessive erythropoiesis affects bone architecture, 1294
- ESR2**  
RsaI polymorphism in ESR2 is associated with postmenopausal fracture risk, SU221
- Estradiol**  
Ethanol alters estrogen receptor signaling and activates senescence pathways in osteoblasts while estradiol attenuates ethanol effects, SU182  
Older men with low serum estradiol and high serum SHBG have an increased risk of fractures, 1279  
Serum estradiol and fracture reduction during treatment with hormone therapy, F383
- 17 $\beta$ -estradiol (E<sub>2</sub>)**  
Antiapoptotic action of 17 $\beta$ -estradiol in skeletal muscle cells involves ERK 1/2, p38 MAPK, ASK-1 and HSP27, SU185  
ER $\alpha$  deletion in cells of the monocyte/macrophage lineage increases osteoclastogenesis and abrogates the pro-apoptotic effect of E<sub>2</sub> on osteoclasts, 1097
- Estrogen**  
30IT/C of SCT modulates BMD by Wnt and estrogen signaling pathways, 1270  
BZA in combination with conjugated estrogens improves bone mass and strength in the OVX rat, SA385  
Cell type specific regulation of transcription by estrogen, SU180  
Combination of flaxseed and estrogen benefits bone health in the OVX rat model of postmenopausal osteoporosis, SU381  
Effects of exercise and estrogen on OPG in premenopausal women, SU166  
ER $\alpha$  expression in mesenchymal cells is crucial for the bone protective effects of estrogen, 1123  
Estrogen suppresses RANKL-induced osteoclastic differentiation of human monocytes via an ER $\alpha$  associated cytoplasmic signaling complex, but ER $\alpha$  is downregulated during osteoclastic differentiation, 1125  
Estrogens reverse a potentiating effect of the unliganded estrogen receptor on BMP-induced transcription and osteoblastogenesis by promoting ERK-dependent Smad1 phosphorylation at the linker region, SU189

## Key Word Index

## ASBMR 30th Annual Meeting

Ethanol alters estrogen receptor signaling and activates senescence pathways in osteoblasts while estradiol attenuates ethanol effects, SU182

Genetic variations in sex steroid-related genes as predictors of serum estrogen levels in men, SU183

Role of GPR30 in effects of estrogen in OVX mice, SU179

**Estrogen deficiency**

Effects of ODN on bone mass and turnover in estrogen deficient adult rhesus monkeys, SA072

Estrogen deficiency alters the localized material properties of the peri-lacunar bone matrix in old rats, M107

Fully human anti-DKK1 antibodies increase bone formation and resolve osteopenia in mouse models of estrogen-deficiency induced bone loss, 1214

Low serum IGF-I alters the cortical bone response to estrogen deficiency, SU190

ODN increases bone strength and maintains bone quality in estrogen deficient adult rhesus monkeys, F508

Selective p38 $\alpha$  inhibitor prevents bone loss induced by estrogen deficiency, M335

**Estrogen receptor**

Carborane BE360, one of the carbon-containing polyhedral boron-cluster compounds, is a new type of selective estrogen receptor modulator., SU187

Estrogens reverse a potentiating effect of the unliganded estrogen receptor on BMP-induced transcription and osteoblastogenesis by promoting ERK-dependent Smad1 phosphorylation at the linker region, SU189

**Estrogen receptor- $\alpha$  (ER $\alpha$ )**

Biochemical characterization of ER $\alpha$  co-regulators in multinucleated mature osteoclasts, 1126

ER $\alpha$  deletion in cells of the monocyte/macrophage lineage increases osteoclastogenesis and abrogates the pro-apoptotic effect of E $_2$  on osteoclasts, 1097

ER $\alpha$  expression in mesenchymal cells is crucial for the bone protective effects of estrogen, 1123

Estrogen suppresses RANKL-induced osteoclastic differentiation of human monocytes via an ER $\alpha$  associated cytoplasmic signaling complex, but ER $\alpha$  is downregulated during osteoclastic differentiation, 1125

Multinuclear expression of ER $\alpha$  in mature osteoclasts, SU186

Novel ER $\alpha$  variant signals rapidly from the caveolae of traditional ER $\alpha$ -negative cells, 1124

Regulation of renal Klotho: the importance of ER $\alpha$ , SA211

Specific inactivation of AF-1 in ER $\alpha$  results in growth plate closure while total inactivation of ER $\alpha$  results in increased growth plate width in elderly female mice, 1181

**Estrogen therapy**

Effects of estrogen therapy and fluocalcic effervescent on the BMD and bone metabolism of surgical menopause women with osteopenia, M392

Effects of low dose estrogen therapy on the BMD and bone metabolism of menopausal women, M393

Higher BMD is associated with increased odds of carotid atherosclerosis in postmenopausal women not currently using estrogen therapy, 1206

**Ethanol**

Ethanol alters estrogen receptor signaling and activates senescence pathways in osteoblasts while estradiol attenuates ethanol effects, SU182

OAH19, an ethanol extract from combined two herbs, inhibits IL-1 $\alpha$ -induced expression of MMP-1 and MMP-13 in OA human cartilage and synovial fibroblast, M148

**European Forsteo Observational Study (EFOS)**

Back pain is reduced in postmenopausal women with severe osteoporosis treated with rhPTH(1-34) regardless of incident fractures, SU413

Women with severe osteoporosis treated with rhPTH(1-34) improve quality of life regardless of incident fractures, SU412

**European Male Ageing Study (EMAS)**

Influence of markers of bone turnover on calcaneal QUS, SA457

**European Prospective Investigation into Cancer (EPIC)-Norfolk Study**

Percentage body fat and risk of prospective hip fracture in older men and women, F363

Performance of QUS in comparison to DXA for prediction of prospective fractures among older men and women, 1240

**EUROQOL (EQ-5)**

Quality of life in Mexican hip fractures patients using EUROQOL (EQ-5) after discharge from hip fracture and 6 months of followup, SU419

**eValuation of IBN Efficacy (VIBE) Database Fracture Study**

"Vibes" Trial: LMMS to improve BMD, M397

Fracture risk in women aged 65 years or older with once-monthly oral IBN compared with weekly bisphosphonates, M367

Fracture risk with once-monthly oral IBN compared with weekly bisphosphonates, SU408

**Exendin-4 (Ex-4)**

Osteogenic action of Ex-4 in normal and insulin-resistant state, M424

**Exercise**

Bone density comparisons in young male rock climbers, weight lifters and sedentary controls, SA534

Bone geometry, strength, and muscle mass in female distance runners with a history of stress fracture, SA540

Bone volumetric density, geometry and strength in male and female collegiate runners, SA539

Can impact exercise mitigate the adverse effects of oral contraceptives on bone?, M488

Effect of 12 months gymnastics participation on bone mass accrual in 4 to 7 year olds, SA555

Effect of a one year exercise program on markers of bone metabolism after hip fracture, SA432

Effect of aquatic exercise and education on improving indices of fall risk in older adults with hip OA, M441

Effect of exercise on geometric bone structure and bone strength in postmenopausal women, M484

Effective progressive resistive exercise program from prone position for paravertebral muscles to reduce risk of vertebral fractures, M473

Effects of exercise and estrogen on OPG in premenopausal women, SU166

Effects of exercise and milk intake on bone in adolescents, SU301

Effects of exercise intensity on the bone metabolic response to running, M481

Effects of running exercise on bone quality after immobilization, SA518

Effects of simulated resistive exercise on cortical bone in the tibia mid-diaphysis of hindlimb unloaded rats, SA521

Femur from C57BL/6 and DBA/2 inbred mice display a strain dependent response to treadmill running and tower climbing exercise in cortical and trabecular bone architecture, M485

Flexible tibia model predicts bone strains during walking, M479

Functionality outcomes including brisk walking speed are associated with BMD in postmenopausal women, SU418

High impact exercise may have a protective effect on BMD but moderate impact exercise may have negative effect in young women with anorexia nervosa, M324

HSA and physical activity in boys and girls during puberty, SA538

Impact of physical inactivity (10 days bed rest) on markers of bone turnover in young men with low and normal birth weight, SA456

Increased caloric intake in energy deficient exercising with functional hypothalamic amenorrhea women is associated with decreased ghrelin and increased bone formation, SU184

Increasing the number of steps taken per day leads to a greater weight loss and more favorable body composition in overweight postmenopausal women, SU311

Influence of muscle size and strength on changes in bone mass and size during growth and in response to exercise, SA537

Inhibition of bone biomechanical response to physical activity and loading in mice lacking periostin, 1143

Model of high body mass: BMD, bone markers and adipocytokine levels in high level male rugby players, SA167

Non-steroidal anti-inflammatory use and the response of bone to exercise, M472

Physical activity, BMD and fragility fracture, M325

Positive influence of physical activity on BMD measurements and hip geometry parameters in young adults, M477

Prevention of the metabolic syndrome together with osteoporosis in young men, SU314

Previous sport activity during childhood and adolescence is associated with bone geometry in young adult men, SA541

Relationship between physical fitness and bone and physical activity and Ca retention in adolescent girls, SA553

Serum Vitamin D levels do not modify the response to an exercise program following hip fracture, SA346

Strength training prevents bone loss at the spine in older breast cancer survivors, SA271

Targeted exercise against hip fragility, SA533

Three year school-curriculum-based exercise program in prepubertal children increases bone mineral accrual and bone size but do not influence femoral neck structure, 1107

Treadmill exercise provides only short-term protection against cancellous bone loss with reduced dietary energy intake: endocrine mechanisms, SA449

**Exon 3**

Mutational analysis of  $\beta$ -catenin Exon 3 in benign and malignant parathyroid tumors, M436

**Expansile skeletal hyperphosphatasia (ESH).**

See *Hyperphosphatasia*

**Ext1<sup>+/-</sup>**

Over-expression of CNP enhances the formation of long bone exostoses in Ext1<sup>+/-</sup> mice, SU130

**Extracellular-regulated protein kinase (ERK)**

AG490, a Jak2 specific inhibitor, induces osteoclast survival by activating Akt and ERK signaling pathway, SU108

Both the Smad and ERK MAP kinase pathway play critical roles in BMP-2-induced osteogenic transcription factors expression, M050

Estrogens reverse a potentiating effect of the unliganded estrogen receptor on BMP-induced transcription and osteoblastogenesis by promoting ERK-dependent Smad1 phosphorylation at the linker region, SU189

Induction of CTGF by TGF $\beta$ 1 in osteoblasts: independent effects of Src and Erk on Smad signaling, M066

Intermittent PTH administration increases bone mass and strength in aged mice by antagonizing oxidative stress-induced osteoblast apoptosis via ERK-mediated attenuation of p66<sup>shc</sup> phosphorylation, SU380

Vinculin is involved in hypertrophic differentiation through Raf/MEK/ERK pathway in chondrocytic ATDC5 cells, SA119

**Extracellular-regulated protein kinase 1/2 (ERK1/2)**

- Antiapoptotic action of 17 $\beta$ -estradiol in skeletal muscle cells involves ERK 1/2, p38 MAPK, ASK-1 and HSP27, SU185
- Breast cancer derived factors synergize with TGF $\beta$  to induce phosphorylation of ERK1/2 and to stimulate osteoclastogenesis, SU115
- Stimulation of macrophage TNF $\alpha$  production by orthopaedic wear particles requires activation of the ERK 1/2/Egr-1 pathway but is independent of p38 and JNK, SA177

**Extracellular-regulated protein kinase 5 (ERK5)**

- MEK5/ERK5 signal regulates RANKL-induced osteoclastogenesis, SU103

**F****F2**

- Geometric property QTLs in HcB/8 x HcB/23 F2 cross, F260

**F344**

- Characterization and genetic mapping of bone size phenotypes in GK and F344 rats using a new 3D CT method, M463

**FA1**

- Dlk1/FA1 is a novel factor enhancing osteoclastogenesis and inhibiting bone formation in vitro and in vivo, 1007

**Familial hypocalciuric hypercalcemia (FHH).**

See *Hypercalcemia*

**Familial humeroradioulnar synostosis.** See *Synostosis***Farnesoid X receptor (FXR)**

- Deletion of FXR leads to an osteopenic phenotype in mice, F439

**Farnesyl pyrophosphate synthase**

- Role of active site Thr201 in the inhibition of farnesyl pyrophosphate synthase by NBPs, F407

**Fatty acids**

- Essential fatty acid and fish intake is associated with higher BMD in elderly women and men, F341
- Modulation of osteoclastogenesis by fatty acids, SU071

**Femoral neck structure**

- Contribution of local buckling to femoral neck failure in stance and fall mode simulations: an advanced FEA analysis of elderly cadaver femur data, M489
- Discordance in femoral neck bone density in subjects with OA, M453
- Morphometric determinants of 3D femoral neck structure and strength in older postmenopausal women, SA320
- Regional differences in femoral neck cortical thickness determine hip fragility, M315
- Regional thinning of the femoral neck cortex with advancing age predisposes to hip fracture, SU275
- Three year school-curriculum-based exercise program in prepubertal children increases bone mineral accrual and bone size but do not influence femoral neck structure, 1107

**Femur**

- BMP-3-null aged mice display increased trabecular bone volume and reduced cross sectional area at the mid-femoral diaphysis, SU143
- Differences in BMC at the lumbar spine and proximal femur in South American children of different ethnic groups, SU490
- Femoral strength, bone density, and aging in women and men, 1165
- Generating 3D finite element models of a human proximal femur from 2D DXA data, M467
- Imaging the spatial distribution of proximal femoral response to one year of TPTD therapy, M349
- New link between trabecular properties and T-score at the human femur, SU281

- Optimization of failure load estimation using radiographs of human cadaveric femur, M457
- Protocol for pediatric proximal femur DXA analysis, M506
- Reduction of BMD in the patients with RA is more remarkable at proximal femur than at lumbar spine, SU451
- Tracking of femur length during intrauterine growth, M497
- Vitamin K treatment for one year does not alter femur geometry in postmenopausal women, SA443

**Femur Strength Index**

- Correlation between DXA Femur Strength Index and QUS Heel Stiffness Index in Chinese women, M464

**FHL2**

- FHL2 mediates DEX-induced MSC osteogenic differentiation by activating Wnt/ $\beta$ -catenin signaling and Runx2 expression, M048

**Fibroblast activation protein (FAP)**

- Role of FAP and DPP4 in myeloma bone disease and tumor growth, F288

**Fibroblast growth factor (FGF)**

- Activation of FGF receptors is a novel mechanism by which extracellular Ca stimulates the proliferation of osteoblasts, M088

**Fibroblast growth factor agonist (F2A)**

- Skeletal effects of a F2A in OVX rats, SA388

**Fibroblast growth factor receptor (FGFR)**

- FGFR signaling in the pathogenesis of osteosarcoma, 1233

**Fibroblast growth factor receptor 2 (FGFR2)**

- Dynamic morphological changes in the skulls of mice mimicking human Apert Syndrome resulting from gain-of-function mutation of FGFR2 (P253R), SA248

- Permanent FGFR2 activation promotes osteoblast differentiation in MSCs through activation of PKC signaling, M093

**Fibroblast growth factor, basic (bFGF)**

- bFGF induces the expression of a subset of Bcl-2 family genes to inhibit the apoptosis of ATDC5 chondroprogenitor cells, SU043
- Improvement of alveolar bone quality by local bFGF injection—histological and cellular biological analysis in a rabbit model, SA162
- NARS induced by bFGF regulates the proliferation and survival of osteoblasts, SA164

**Fibroblast growth factor-1 (FGF-1)**

- FGF-1 inhibits adipogenic differentiation and transdifferentiation of human MSCs, M075

**Fibroblast growth factor-2 (FGF-2)**

- FGF-2 signaling in osteoblasts: Cx43 is a docking platform for PKC $\delta$ , F026
- FGF-2 stimulates RANKL expression in PDB, F480
- FGF-23 and FGF-2 share a common but also have distinct signaling pathways for negative regulation of bone nodule mineralization in cultured osteoblasts, SA206
- Regulation of the BMP-2 distant osteoblast enhancer by FGF-2, SU150
- Targeted overexpression of the nuclear FGF-2 isoforms in osteoblasts induces hypophosphatemia via modulation of FGF-23 and Klotho in mice, 1084

**Fibroblast growth factor-23 (FGF-23)**

- 7B2 protein mediated inhibition of DMP1 cleavage in osteoblasts enhances FGF-23 production in *Hyp*-mice, 1053
- Ablation of the Galnt3 gene in mice leads to low circulating FGF-23 concentrations and hyperphosphatemia despite increased FGF-23 gene expression, 1018
- Altered regulation and expression of FGF-23 in the adenine-induced uremic rat model, SU178
- Association of urinary GGT and serum FGF-23 with prevalent fracture, SA296
- c-Fos is associated with renal FGF-23-mediated signaling, SU173

- Clinical usefulness of measurement of FGF-23 in hypophosphatemic patients, SA470
- Does dietary P influence FGF-23 concentrations in FD patients?, M426
- Effect of treating Vitamin D deficiency on FGF-23 levels in humans, SA209
- Effects of hPTH(1-34) infusion on circulating serum phosphate, 1,25(OH) $_2$ D and FGF-23 levels in healthy men, SU169
- Evaluation of clinical utility of venous sampling for FGF-23 in identifying and confirming responsible tumors for TIO, F163
- Evidence supporting the necessity of GalNac-T3 in the processing of FGF-23 in humans, SA200
- FGF-23 and FGF-2 share a common but also have distinct signaling pathways for negative regulation of bone nodule mineralization in cultured osteoblasts, SA206
- FGF-23 and parameters of Ca and bone metabolism are positively influenced by GH replacement in adult GH deficiency patients from the KIMS survey, SU177
- FGF-23 and post-transplant hypophosphatemia: evidence for a causative link, SU168
- FGF-23 in Vitamin D deficient older persons, SA203
- Homozygous threonine to methionine substitution in FGF-23 gene is associated with tumoral calcinosis in a 12 year-old girl, SU171
- Local osteocyte defect in *Dmp1* null mice causes overproduction of FGF-23, 1225
- Potential role of FGF-23 in CKD-MBD, WG30
- Rapid detection of intact FGF-23 in tumor tissue from patients with OOM, SA204
- Role of FGF-23 in the early response to the PTH analogue: TPTD, SU174
- Serum FGF-23 level in term infants, SA165
- Signaling of extracellular inorganic phosphate mediated via Na-phosphate co-transporters influences FGF-23 signaling in renal tubular cells, SU172
- Significance of O-linked glycosylation of FGF-23 protein, SA208
- Targeted overexpression of the nuclear FGF-2 isoforms in osteoblasts induces hypophosphatemia via modulation of FGF-23 and Klotho in mice, 1084

**Fibroblasts**

- LMP-1, positive regulator in osteolineage differentiation of human PDL fibroblasts, M051

**Fibroblasts, synovial**

- OAH19, an ethanol extract from combined two herbs, inhibits IL-1 $\alpha$ -induced expression of MMP-1 and MMP-13 in OA human cartilage and synovial fibroblast, M148

**Fibrodysplasia ossificans progressiva (FOP)**

- ACVR1 knock-in mouse model for FOP, 1203

**Fibronectin**

- Circulating fibronectin affects bone matrix, SA151
- Conditional deletion of fibronectin results in a scoliosis-like phenotype, 1046
- Extracellular matrix protein fibronectin positively regulates the osteoclast function, SU069
- Mechanical perturbation of integrin  $\alpha$ 5 with or without association with fibronectin opens Cx43-hemichannels in osteocytes, SA060

**Fibrous dysplasia.** See *Dysplasia***Finite element analysis (FEA)**

- Comparison of voxel-based and smooth FEA to predict damage accumulation in vertebral bodies, SU474
- Contribution of local buckling to femoral neck failure in stance and fall mode simulations: an advanced FEA analysis of elderly cadaver femur data, M489
- Effect of RIS on bone strength and work to failure determined by FEA and simulation of clinically-measured bone loss and mineralization changes, SA505
- Estimation of relative stiffness contributions of cortical and trabecular compartments by MRI-based FEA, SU481

## Key Word Index

## ASBMR 30th Annual Meeting

FEA of proximal femur QCT scans for the assessment of hip fracture risk in older men, F321

FEA performed on radius and tibia HR-pQCT images provides new insights for fracture status assessment, 1067

Generating 3D finite element models of a human proximal femur from 2D DXA data, M467

Grayscale MRI based finite element mechanical modeling of trabecular bone at in vivo resolution, SU277

Hip strength estimates by FEA and fracture prediction in women and men, 1167

Microfinite element modeling reveals that transient deficits in cortical bone may underlie the adolescent peak in forearm fractures, 1179

QCT and FEA assessment of proximal femur bone quality and strength in women with postmenopausal osteoporosis receiving once-monthly oral IBN for 12 months, SA509

Unsymmetrical beam theory and finite element method: analysis of murine cortical bone based on  $\mu$ CT imaging, M454

**FIP200**

Role of FIP200 in osteoblast differentiation, M091

**FIT Long-term Extension (FLEX)**

Sites of femoral fractures in the Fracture Intervention Trial (FIT) of ALN and its Long-term Extension (FLEX), SU389

**FK506**

Changes of bone metabolism in immunosuppressant, FK506 treated rats, SU383

**Flavonoids**

IC162, a new flavonoid, preserves bone mass and microarchitecture without affecting uterine weight in OVX rats, SA386

**Flaxseed oil**

Combination of flaxseed and estrogen benefits bone health in the OVX rat model of postmenopausal osteoporosis, SU381

Effect of resveratrol and flax oil on MC3T3-L1 pre-adipocyte and ST2 BMSC proliferation and differentiation, SU059

**FLEX.** See *FIT Long-term Extension*

**Fluid flow**

Adenylyl cyclase 6 mediates primary cilia-regulated decreases in cAMP in bone cells exposed to dynamic fluid flow, 1040

Direct correlation of osteocyte deformation with Ca influx in response to fluid flow shear stress, SA057

Effect of MKP-1 deletion on the fluid shear stress induction of COX-2 expression in osteoblasts, SA529

Primary bone cells of pregnant mice exposed to oscillatory fluid flow, M015

Response of matrix synthesizing MLO-A5 cells to fluid shear, SA067

Role of cell surface ATP synthase in fluid shear stress induced ATP release in osteoblasts, SU039

Strain-induced fluid flow in a 3D porous matrix promotes osteoblastic calcification in vitro, SA525

Tracking adipose differentiation in vitro with aP2-GFP reporters and flow cytometry: lipid staining and macrophage mimicry, SU057

**Fluorescence imaging**

Quantitative image analysis method for measuring whole-body tumor burden in a mouse model of breast cancer bone metastasis, SA282

**Fluoride**

Fluoride effects on bone formation, mineralization and mechanical properties are influenced by genetics, SU465

Stress fracture and vertebral osteosclerosis related to fluorosis induced by excessive gingival topical fluoride application, M444

**Fluoride, serum ionic (SIF)**

Elevated SIF levels in post-menopausal women is due to the enhanced release of fluoride from bone, SA490

SIF levels among hemodialysis patients are positively associated with levels of serum phosphate and intact PTH, SU440

**Fluorosis**

Stress fracture and vertebral osteosclerosis related to fluorosis induced by excessive gingival topical fluoride application, M444

**Focal adhesion kinase (FAK)**

Investigations into the role of FAK in bone marrow-derived osteoclasts, SU111

**Folate**

Lrp6 loss of function impacts bone homeostasis and responds to folate supplementation, F253

**Fourier transfer infrared (FTIR) imaging**

Characterization of the osteotomy callus using FTIR imaging in a rabbit ulnar model, M471

**FoxO**

$\beta$ -catenin protects osteoblasts from oxidative stress by co-activating the expression of pro-survival, but not pro-apoptotic, target genes of the FoxO transcription factors, M010

Loss or gain of FoxO function in osteoclasts and osteoblasts alters the rate of apoptosis and BMD in mice, 1247

**FOXO**

Induction of oxidative stress and diversion of  $\beta$ -catenin from TCF- to FOXO-mediated transcription by GCs or TNF $\alpha$  in osteoblastic cells, SA185

**FOXO1**

FOXO1 signaling in the control of bone mass, 1112

**Foxo3**

Wnt/ $\beta$ -catenin/TCF is a constitutive repressor pathway interfering with Foxo3-mediated induction of synd2, a tumor suppressor in osteosarcoma cells, SU243

**FoxOs**

Akt regulates skeletal development through GSK3, mTOR, and FoxOs, 1151

**Fra1**

Progressive lipodystrophy in the osteosclerotic mice over-expressing Fra1, 1149

**Fracture healing**

ALF ameliorates bone dynamics in senescence-accelerated SAMP6 mice and in fracture repair rat model, SU394

Bi-allelic loss of *Nf1* in osteoblasts delays bone fracture healing, SU218

BMP-7 is not required for fracture healing, SU148

Cannabinoid receptor ligands rescue bone loss and stimulate fracture healing, SU375

Changes of biochemical resorption markers during fracture healing in osteoporosis, M290

Chondrocyte differentiation is differentially affected by COX-2 and 5-LO during fracture healing, SU123

Circulating BMP-1 isoforms: novel diagnostic and therapeutic challenges for bone fracture repair, SU142

Comparison of cPTH(1-31) to PTH(1-34) in the enhancement of experimental fracture healing, M161

Development of pharmacological HIF activators for fracture healing, SU052

Effects of PTH on fracture repair in GC treated mice, 1062

Evaluation of circulating osteoprogenitor cells during fracture healing using parabiotic mice, 1260

Evaluation of two novel bone growth factors to enhance fracture healing, SU012

Expression of BMP antagonists during fracture healing, SA160

Impaired fracture healing in the absence of the Vitamin D-24-hydroxylase, Cyp24a1, M222

Induction of ESC-related pluripotency genes in post natal stem cells during fracture healing, F038

LV best enhances fracture repair when administered one week post-fracture, 1300

MSC enhance fracture healing: essential role for cytokines in homing and anti-inflammatory response, SA169

Normal intramembranous fracture healing in mice with transgenic osteoblast-targeted disruption of GC signaling, SA234

OPG serum levels in shaft fractures healing and non-union, M013

Stimulation of fracture healing by rhPDGF-BB combined with  $\beta$ TCP/collagen matrix in a diabetic rat fracture model, 1137

**Fracture Intervention Trial (FIT)**

Sites of femoral fractures in the Fracture Intervention Trial (FIT) of ALN and its Long-term Extension (FLEX), SU389

**Fracture prevention**

8-year fracture and mortality outcomes of the fracture liaison service that provides systematic assessment for prevention of secondary fractures to all patients age 50+ with new low-trauma fractures, SU324

Attitudes to fracture prevention in long-term care facilities, M379

Predictors of patient perceived need for oral bisphosphonates to prevent fracture: the role of the MD-patient relationship, F416

Prevention of non-vertebral fractures with oral Vitamin D is dose dependent, 1242

Strategies for hip fracture prevention in long-term care facilities: a survey of Canadian geriatricians and family physicians, M380

**Fracture risk**

10-year probability of recurrent osteoporotic fractures after a primary wrist fracture in postmenopausal women enrolled in the CaMos cohort, F358

Absolute risk for subsequent fractures fluctuates over time, 1060

Age is the key to assessing fracture risk: FRAX, F306

Areal BMD by DXA may predict similar risk of fracture in elderly women and men due to offsetting effects of bone size and true volumetric BMD, SU267

Assessment of absolute fracture risk and osteoporosis in Chinese, F312

Assessment of fracture risk and treatment of osteoporosis in postmenopausal women: bone density vs. Bone DESTINY, SU251

Assessment of the 10-year risk of fracture in Italian postmenopausal women using BMD and clinical risk factors, SU348

Association between femoral neck BMD and the factor-of-risk for hip fracture derived from direct measurements of strength in human cadaveric femora, 1070

Association of CTR gene polymorphisms with BMD and fracture risk in postmenopausal Koreans, M256

Association of *HSD11B1* polymorphisms with vertebral fracture risk and BMD in postmenopausal Korean population, M260

Bone DESTINY—a one step fracture risk predictor for clinicians, SU504

Bone turnover and incident hip fracture risk, M285

C-telopeptide and bone ALP predict morphometric vertebral fracture risk in a pivotal Phase III trial of TOR in men on ADT, 1292

Comparative antifracture efficacy of N-containing bisphosphonates, SU397

Comparison between logistic regression and artificial neural networks for vertebral fracture risk assessment, SU345

Cortical cross sectional area in young adult men is inversely related to risk of hip fracture in their older relatives, 1281

Development a nomogram for individualizing the absolute risk and time to recurrent fracture, F349

Distribution of risk factors for fracture in women with and without a fracture history, SU342

Do different densitometers, or use of T-score vs. Z-score, affect fracture risk estimation?, SU258

Does dietary protein reduce hip fracture risk in elderly men and women?, SU319

Effect of 10-year fracture risk tool results on likelihood of bisphosphonate prescribing, SU402

Effect of aquatic exercise and education on improving indices of fall risk in older adults with hip OA, M441

Effect of tamoxifen and aromatase inhibitors on the risk of fractures in women with breast cancer, SU227

Effective progressive resistive exercise program from prone position for paravertebral muscles to reduce risk of vertebral fractures, M473

Efficacy of BZA in reducing the incidence of nonvertebral fractures in postmenopausal osteoporotic women at higher fracture risk, M390

Failure to perceive increased risk of fracture in women 55 years, SA360

FEA of proximal femur QCT scans for the assessment of hip fracture risk in older men, F321

Fracture risk and incidence of falls in younger postmenopausal women, 1236

Fracture risk in patients with different types of cancer, SA290

Fracture risk in primary biliary cirrhosis: role of osteopenia and severity of cholestasis, M442

Fracture risk in women aged 65 years or older with once-monthly oral IBN compared with weekly bisphosphonates, M367

Fracture risk in young patients with chronic diseases, SU371

Fracture risk with once-monthly oral IBN compared with weekly bisphosphonates, SU408

FRAX™ and the assessment of ten-year fracture probability in Hong Kong Southern Chinese according to age and BMD femoral neck T-scores, SU264

Geometric evidence of a modeling defect in type 2 diabetic women enrolled in the WHI as a potential explanation for increased fracture risk, 1068

Hip fracture patients at high risk of second hip fracture, 1163

Hip strength estimates by FEA and fracture prediction in women and men, 1167

Inflammatory markers and the risk of hip fracture, F333

Loop diuretic use and rates of hip bone loss, and risk of falls and fractures in older women, F371

Low calcaneal BMD estimated by a peripheral DXA heel scanner is associated with a high risk to have had a distal radius fracture, SU262

Low density lipoprotein-cholesterol levels affect vertebral fracture risk in female patients with PHPT, SA484

No fracture is a poor predictor of fracture risk, SU356

Older men with low serum estradiol and high serum SHBG have an increased risk of fractures, 1279

Once-a-month RIS 150 mg reduced vertebral fracture risk at one year in a historical control analysis, SU403

Osteoporosis diagnosis and incident fracture as a function of prior fractures site in a large clinical cohort, 1235

Overweight children are more at risk to sustain a forearm fracture due to poor bone strength relative to body weight, M458

Percentage body fat and risk of prospective hip fracture in older men and women, F363

Polymorphisms of the ALOX12 gene are associated with increased risk of osteoporotic fracture, SU220

Poor peripheral sensorimotor nerve function is associated with high fall risk, SU323

Possible increased risk of fracture among South Florida White Hispanic women, M402

Post-fracture mortality in men: contributions of sex hormones and BMD as risk factors, 1280

Prediction of fracture risk by LRP5 gene haplotype, SU222

Prediction of osteoporotic fracture risk by 25(OH)D3-1 $\alpha$ -hydroxylase (CYP27B1) gene, M263

Relationship of bone turnover marker (PINP) and changes in femoral neck BMD to fracture risk in women with postmenopausal osteoporosis treated with once-yearly ZOL 5 mg, 1027

Risk factors for bone fracture, elevated by 90-days of bed rest, are reduced by daily exposure to LMMS, M342

Risk factors for fragility fracture in a multiracial cohort of US women, SA362

Risk factors for subsequent fractures within the next year in patients presenting with a clinical fracture, 1237

Risk of hip fracture after bisphosphonate discontinuation, F409

Risks and outcomes for hip fractures in a predominantly African-American male veteran population, SA352

RsaI polymorphism in ESR2 is associated with postmenopausal fracture risk, SU221

Serum estradiol and fracture reduction during treatment with hormone therapy, F383

Simply ask them about their balance—fracture prediction in a nationwide cohort study in twins, 1095

SSRI use and risk of fracture in older women, F351

Subclinical thyroid disease predicts risk of hip fracture, 1208

Ten-year fracture risk assessment in Norland-based equipment in a Chinese population, SU253

Thoracic kyphosis index as a risk factor for incident vertebral fractures and alteration of quality of life in postmenopausal women with osteoporosis, 1130

Three methods of lumbar spine DXA analysis as a means to predict male fracture, 1131

Timed Up and Go test and BMD as predictors of fracture, F373

Trabecular risk of fracture, caused by disuse, is strongly influenced by baseline morphology, 1293

Weight and BMI predict BMD and fractures in women 40 to 59 years, SA438

#### Fractures

“Pathologic” fractures: to include or exclude?, SU321

Accelerated fracture callus remodeling and membranous bone healing in STAT1 deficient mice, SA022

Ambiguity about osteoporosis and osteoporosis care exists despite a screening program to educate fracture patients, M383

Analysis of long bone fracture nonunion by an expression profile of the MMPs and ADAMTS enzyme families, M235

Association of stiffness index and cross-linked NTx with any clinical fractures differs with age and gender, SU350

Association of urinary GGT and serum FGF-23 with prevalent fracture, SA296

Associations of the VDR and calcitonin receptor genes with bone density, bone turnover markers and fracture incidence with regard to Ca intake level in Slovak postmenopausal women, M261

Back pain is reduced in postmenopausal women with severe osteoporosis treated with rPHT(1-34) regardless of incident fractures, SU413

Bisphosphonates and osteoporotic fractures in highly compliant/persistent postmenopausal women, 1025

BMD, fracture and survival in women in nursing/residential care, SA340

Comparison of prediction models for hip, osteoporotic, and any clinical fracture in older women: is more better?, 1057

Concentration of IGF-I in human cortex bone is highly correlated with fracture toughness of the bone, 1069

Cost-effectiveness of IBN therapy for women with postmenopausal osteoporosis with respect to nonvertebral fracture efficacy, SA429

Deformity of the distal radius fractures resulting from falls in Japanese women over 50 years of age is closely associated with BMD of the lumbar spine, SU286

Direct medical costs associated with the treatment of NHNV, hip, and vertebral fractures in a managed care setting, F356

Distribution and rate of clinical fractures in older men without osteoporosis, 1282

Effect of once-yearly ZOL 5 mg infusion on fracture incidence in postmenopausal osteoporosis, 1028

Effects of LASO on fractures and breast cancer, 1288

Excess of post-fracture mortality among men and women, SA348

FEA performed on radius and tibia HR-pQCT images provides new insights for fracture status assessment, 1067

Femoral neck and trochanteric fractures and Vitamin D, SU353

Fracture reduction during two years of treatment with RIS or ALN, SA404

Gender specific effects of TRPV4 on osteoblast-osteoclast coupling and risk of osteoporotic fractures, SA355

Gondanotropins, bone loss and fracture in men, 1278

GWAS reveals genetic variants associated with BMD, osteoporosis and osteoporotic fractures, SA263

Increase in risk of atypical subtrochanteric fractures with ZOL?, F411

Incremental costs associated with selected skeletal fractures, 1024

Influence of bone osteoporotic fractures in the past on the persistence of pharmacological treatment in osteoporosis, M382

Is the association between hypertension and bone osteoporotic fracture expressing a real interdependence?, SU346

Microfinite element modeling reveals that transient deficits in cortical bone may underlie the adolescent peak in forearm fractures, 1179

No fracture is a poor predictor of fracture risk, SU356

Novel hypothesis explains the syndrome of chronic musculoskeletal pain and comorbid painful healed fracture sites in Vitamin D deficiency, SA474

Opioid-induced osteoporosis: delayed bone healing and compression fractures in a man with chronic narcotic use, WG32

Osteoporosis diagnosis and incident fracture as a function of prior fractures site in a large clinical cohort, 1235

In osteoporotic other than in healthy bone, thoracolumbar fractures spare the adjacent discs, SU415

Performance of QUS in comparison to DXA for prediction of prospective fractures among older men and women, 1240

Population burden of first and repeat low-trauma fractures, 1056

Post-fracture initiative in a rural Ontario community hospital, M369

Prediction of incidental low trauma limb fractures in older men and women with QCT variables of bone and muscles in mid-thigh, F369

Prediction of trabecular level microdamage and bone fracture through local strain, SU467

Predictors of poor outcomes following osteoporotic fractures in elderly women and men, 1210

Prevalence of subtrochanteric fractures in patients older than 50 years presenting with a clinical vertebral or non-vertebral fracture, SU390

Proinflammatory marker values at baseline and after a fracture are distinctly different comparing a mouse model of OI with normal controls, M234

## Key Word Index

## ASBMR 30th Annual Meeting

- Significant association between polymorphisms of CYP19A1, fracture incidence and BMD in post-menopausal women, M262
- Single nucleotide polymorphisms in the P2X7 receptor gene are associated with increased postmenopausal bone loss and fracture incidence, SU223
- Smoking is an independent predictor of low BMD, prevalent vertebral fractures and incident fractures in elderly men, SU349
- Use of genetic markers in prediction of fractures, 1094
- Variation in the osteocalcin gene: association study of BMD, fracture and changes in body fat mass in elderly women, SU225
- Volumetric bone parameters in relation to fracture history in healthy men at the age of PBM, SU302
- WHO absolute fracture models in older women: how does prediction vary for incident hip and non-spine fractures across T-scores?, 1055
- Women with severe osteoporosis treated with rhPTH(1-34) improve quality of life regardless of incident fractures, SU412
- Fractures, femoral**
- Bisphosphonate-associated femoral fracture: implications for management, WG26
- Clinical outcome in elderly with proximal femur or humerus fractures in an orthogeriatric rehabilitation unit, SU329
- Sites of femoral fractures in the Fracture Intervention Trial (FIT) of ALN and its Long-term Extension (FLEX), SU389
- Subtrochanteric and diaphyseal femur fractures in patients treated with ALN, 1026
- Fractures, fragility**
- Association between BMD change, use of antiresorptive agents and fragility fracture in women and men, SA364
- BMD measurement by DXA after a fragility fracture increases the likelihood of subsequent osteoporosis treatment, SU296
- Correlation of hip geometry and bone density with fragility fracture in Japanese postmenopausal women, SU466
- Evaluation of BMD following an education intervention on osteoporosis offered to women after a fragility fracture, SU330
- Excess medical cost after a fragility fracture during 3-year follow-up, SA422
- Fragility fractures and health status in a multinational cohort, SU340
- Impact of an educational intervention on knowledge about osteoporosis following a fragility fracture, SA353
- Patients with fragility fracture assessed by BMD, Bone DESTINY and osteoporosis Canada guidelines, SA343
- Physical activity, BMD and fragility fracture, M325
- Prevalence of osteoporosis and osteopenia in men and women according to the fragility fracture type, SU294
- Risk factors for fragility fracture in a multiracial cohort of US women, SA362
- Substantial adverse outcomes follow NHNV fragility fractures, 1059
- Targeted exercise against hip fragility, SA533
- Fractures, hip**
- Active shape modeling as a predictor of hip fracture, M317
- Association between femoral neck BMD and the factor-of-risk for hip fracture derived from direct measurements of strength in human cadaveric femora, 1070
- Bone turnover and incident hip fracture risk, M285
- Comparison of prediction models for hip, osteoporotic, and any clinical fracture in older women: is more better?, 1057
- CVD as forecasters of hip fracture: a nationwide cohort study in twins, 1205
- Direct medical costs associated with the treatment of NHNV, hip, and vertebral fractures in a managed care setting, F356
- Disability in patients with osteoporotic pertrochanteric hip fracture, SA357
- Does dietary protein reduce hip fracture risk in elderly men and women?, SU319
- Effect of a one year exercise program on markers of bone metabolism after hip fracture, SA432
- Elevated production of IL-1 $\beta$  and TNF $\alpha$  by PBMC is associated with increased hip fracture risk in elders, 1283
- Ergocalciferol is not bioequivalent to cholecalciferol in Vitamin D insufficient hip fracture cases, 1289
- FEA of proximal femur QCT scans for the assessment of hip fracture risk in older men, F321
- Fractures of the spine and hip increase the risk of death in Canadians, SU351
- High mortality in male nursing home residents with hip fracture, SU326
- Hip fracture patients at high risk of second hip fracture, 1163
- Hip fracture patients with vertebral fractures have more severe osteoporosis and are candidates for more active treatment including PTH, SU274
- Immunohistochemical localisation of SCT in human trabecular bone from fragility hip fracture patients, SA148
- Impact of varying BMD resources on prediction of hip fracture using FRAX™, SU257
- Independent contribution of hip geometry to incident fracture prediction in a large clinical cohort, 1238
- Inflammatory markers and the risk of hip fracture, F333
- Mechanical unloading of the sheep calcaneus: a model for hip fracture, M478
- Osteoporosis in the aging males after hip fracture, SU436
- Pattern of death after hip fracture among institutionalized older people, 1164
- Phase III study of the effects of DMAB on vertebral, nonvertebral, and hip fracture in women with osteoporosis, 1286
- Potential mediators of the reduction in mortality with ZOL after hip fracture, 1030
- Prevalence of vertebral fractures in aging women suffering from hip fracture, SU322
- Protective effect of total and supplemental Vitamin C intake on the risk of hip fracture, 1168
- Quality of life in Mexican hip fractures patients using EUROQOL (EQ-5) after discharge from hip fracture and 6 months of followup, SU419
- RANKL/OPG in primary cultures of osteoblasts from patients with osteoporotic hip fractures, SU009
- Red flags are missed in the prevention of hip fractures, SU432
- Regional thinning of the femoral neck cortex with advancing age predisposes to hip fracture, SU275
- Relationship between serum levels of inflammatory cytokines and bone turnover markers in the year following hip fracture, SU073
- Risk of hip fracture after bisphosphonate discontinuation, F409
- Risks and outcomes for hip fractures in a predominantly African-American male veteran population, SA352
- Role of the lean muscle and fat mass in hip fractures production, SU263
- Secular trends in Swedish hip fracture incidence 1987-2002, 1166
- Serum 25(OH)D and the risk of hip and non-spine fractures in older men, 1277
- Serum Vitamin D levels do not modify the response to an exercise program following hip fracture, SA346
- SHBG levels in older patients with acute hip fracture are correlated with worse function and increased bone resorption, SU363
- Socioeconomic status, BMD testing and hip fracture rates in a universal health-care system, SU293
- Vitamin D deficiency is highly prevalent in Irish hip fracture patients, M294
- WHO absolute fracture models in older women: how does prediction vary for incident hip and non-spine fractures across T-scores?, 1055
- Women who fractured their hips experience greater loss of geometric strength in the contralateral hip during the year following fracture compared to age-matched controls, F345
- Fractures, non-hip non-vertebral (NHNV)**
- Costs associated with NHNV fractures in a managed care setting, SU320
- Efficacy of BZA in reducing the incidence of nonvertebral fractures in postmenopausal osteoporotic women at higher fracture risk, M390
- Trauma type of NHNV fractures in postmenopausal women being treated for osteoporosis in Europe, SU325
- Fractures, proximal humerus**
- Incidence and costs of proximal humerus and wrist fractures in women in France, SU327
- Proximal humerus fractures in men: epidemiology and costs, SU328
- Fractures, rib**
- Epidemiology of rib fractures in older men, F354
- Fractures, spinal**
- Fractures of the spine and hip increase the risk of death in Canadians, SU351
- Fractures, stress**
- Stress fracture and vertebral osteosclerosis related to fluorosis induced by excessive gingival topical fluoride application, M444
- Fractures, tibial**
- Diffuse osteopenia after tibia fracture: benefits of early mobilization and weight bearing, F461
- Use of GFP reporters to assess cell lineage in a murine model of tibial fracture repair, M077
- Fractures, vertebral**
- Active controlled, non-inferiority study to compare the effect of ZT-031 with ALN on the incidence of new vertebral fractures, M347
- To avoid underdiagnosis of vertebral fracture, recognition of true fracture line including multiple Schmorl's Node is necessary, SA324
- BMD and vertebral fracture in women with breast cancer and antiaromatase therapy, SA400
- Bony symptoms and vertebral fractures in GD1: data from the 105 patients of the French Observatoire on Gaucher Disease, SA466
- Calcitonin intramuscular administration for treating acute pain of osteoporotic vertebral compression fractures, SA196
- Comparison between logistic regression and artificial neural networks for vertebral fracture risk assessment, SU345
- Cortical porosity is increased in male osteoporosis with vertebral fracture, 1132
- Densitometric vertebral fracture assessment in postmenopausal women, SU254
- Effective progressive resistive exercise program from prone position for paravertebral muscles to reduce risk of vertebral fractures, M473
- Height loss, vertebral fractures and misclassification of osteoporosis, SU259
- Hip fracture patients with vertebral fractures have more severe osteoporosis and are candidates for more active treatment including PTH, SU274
- Incident vertebral fracture is predicted by prevalent vertebral fracture as identified by the algorithm-based qualitative method, but not by non-osteoporotic short vertebral height, 1128
- Increased risk of morphometric vertebral fracture in postmenopausal women with PHPT, M438
- Lumbar spine TBS complements BMD in the discrimination between vertebral fractured and non-fractured subject, M308

Medication prescription and adherence after hospitalization for osteoporotic vertebral fracture, M381

Once-a-month RIS 150 mg reduced vertebral fracture risk at one year in a historical control analysis, SU403

pQCT predicts vertebral fractures in osteoporotic postmenopausal women, SU472

Predictive validity of the WHO FRAX model, BMD and prevalent vertebral fracture for incident radiographic vertebral fractures, 1127

Prevalence and factors associated to the presence of vertebral fractures in patients with type 2 diabetes mellitus, M447

Prevalence of subtrochanteric fractures in patients older than 50 years presenting with a clinical vertebral or non-vertebral fracture, SU390

Prevalence of vertebral compression fracture deformity by x-ray absorptiometry in patients selected according to simple clinical tests, SU261

Prevalence of vertebral fractures in aging women suffering from hip fracture, SU322

Randomized trial of balloon kyphoplasty and nonsurgical care for acute vertebral fracture, 1243

Smoking is an independent predictor of low BMD, prevalent vertebral fractures and incident fractures in elderly men, SU349

Spine shape predicts vertebral fractures in postmenopausal women, 1129

Vertebral fracture in men: level of trauma, BMD and lean body mass, SU360

ZOL treatment of osteoporosis: effects in men, SU398

**Fractures, wrist**

10-year probability of recurrent osteoporotic fractures after a primary wrist fracture in postmenopausal women enrolled in the CaMos cohort, F358

Incidence and costs of proximal humerus and wrist fractures in women in France, SU327

**Framingham Osteoporosis Study**

Bivariate whole genome linkage analysis of femoral bone geometric traits and leg lean mass, M249

Does dietary protein reduce hip fracture risk in elderly men and women?, SU319

Elevated production of IL-1 $\beta$  and TNF $\alpha$  by PBMC is associated with increased hip fracture risk in elders, 1283

Essential fatty acid and fish intake is associated with higher BMD in elderly women and men, F341

GWAS of BMD and hip geometry indices, 1092

Protective effect of total and supplemental Vitamin C intake on the risk of hip fracture, 1168

**Framingham QCT Study**

Ca intake is not associated with increased coronary artery calcification, 1207

**Framingham SHARe Project**

GWAS pleiotropic associations of bone phenotypes, SA251

**FRAX**

Age is the key to assessing fracture risk: FRAX, F306

Case finding for the management of osteoporosis with FRAX—assessment and intervention thresholds for the UK, 1290

FRAX<sup>TM</sup> and the assessment of ten-year fracture probability in Hong Kong Southern Chinese according to age and BMD femoral neck T-scores, SU264

Impact of varying BMD resources on prediction of hip fracture using FRAX<sup>TM</sup>, SU257

Incorporating FRAX<sup>TM</sup> algorithms in models of cost-effectiveness, 1023

Predictive validity of the WHO FRAX model, BMD and prevalent vertebral fracture for incident radiographic vertebral fractures, 1127

Treatment threshold in men on androgen deprivation therapy: T-score vs. FRAX, F308

**FREEDOM Trial**

Phase III study of the effects of DMAB on vertebral, nonvertebral, and hip fracture in women with osteoporosis, 1286

**Frizzled homolog 1 (FZD1)**

Characterization of a promoter polymorphism in FZD1: allele-specific regulation by Egr-1 in osteoblast-like cells, M267

**Frizzled-9**

Mice lacking the Wnt receptor Frizzled-9 display osteopenia caused by decreased bone formation, 1006

**Fructus ligustri lucidi**

Effects of different extracts of *Fructus ligustri lucidi* on Ca balance in normal female rats, M336

**Frzb/sFRP3**

Transcriptional silencing of Frzb/sFRP3 by promoter methylation in osteogenic sarcoma, SU231

**FSH**

Transgenic expression of human FSH in female mice has an anabolic effect on bone, 1224

**FZD1**

Haplotype specific promoter activity of the human *FZD1* gene, M269

**G**

**G protein**

Deletion of the G protein subunit G $\alpha$  in early osteoblasts leads to accelerated osteoblast maturation and formation of woven bone with abnormal osteocytes, resulting in severe osteoporosis, 1254

PTHr1 stimulates bone formation through a distinct  $\beta$ -arrestin dependent pathway independent of G protein activation, 1226

Small G protein Rap1 promotes osteoblast differentiation, M080

XXLs acts as a novel heterotrimeric G protein subunit with an ability to transduce receptor activation into intracellular signaling, F226

**G protein-coupled receptor (GPR30)**

Role of GPR30 in effects of estrogen in OVX mice, SU179

**Ga11**

Effects of Ga11 overexpression on osteoblast signaling and function in transgenic mice, M067

**Ga12**

Stable expression of constitutively active Ga12 in osteoblastic cells promotes matrix protein expression and ALP activity, M068

**Gaq**

Inhibitory role of Gaq/PKC $\delta$  signal in the bone anabolic action of PTH, 1228

**G171V**

G171V and A214V Lrp5 knock-in mice have increased bone mass and strength, and can help precisely define the in vivo functions of Lrp5 during bone growth and homeostasis, 1002

LRP5 G171V mutation and tobacco smoke related bone fragility, M323

**G610C**

Age-associated changes in the material properties of the G610C (Amish) OI mouse model, SA252

**Gab2**

Lyn, opposite to c-Src, negatively regulates osteoclastogenesis in vitro and in vivo via its interaction with SHP-1 and Gab2, 1119

**Galectin-3 (gal-3)**

Role of gal-3 in OA, M162

**GalNac-T3**

Evidence supporting the necessity of GalNac-T3 in the processing of FGF-23 in humans, SA200

**Galnt3**

Ablation of the Galnt3 gene in mice leads to low circulating FGF-23 concentrations and hyperphosphatemia despite increased FGF-23 gene expression, 1018

**Gamma-glutamyl peptides**

Activation of the CaSR by beta-aspartyl and gamma-glutamyl peptides, M202

**Gammopathy**

Blocking TGF $\beta$  signaling reduces gammopathy and improves bone volume and strength in vivo, F293

**Gastric acidification**

Rachitic defects in tcirg1-dependent osteopetrosis are caused by impaired gastric acidification, 1201

**Gastric bypass surgery**

PTH increases after oral peptones administration in obese subjects treated with roux-en-y gastric bypass surgery: role of phosphate on the rapid control of PTH release, M180

**Gastroesophageal reflux disease (GERD)**

Postmenopausal women with GERD and long term treatment with bisphosphonates IV, M361

**Gastrointestinal events**

Treatment discontinuation due to gastrointestinal adverse events and decreased BMD in patients switched from branded ALN to generic ALN, SA414

**Gaucher disease type 1 (GD1)**

Bony symptoms and vertebral fractures in GD1: data from the 105 patients of the French Observatoire on Gaucher Disease, SA466

**GC-1**

TR $\beta$ -specific agonist GC-1 increases bone quality of adult female mice, M228

**GCMB**

Dominant-negative GCMB mutants causing autosomal-dominant HPT—protein expression and cellular localization, SA225

**GDF-8**

Myostatin (GDF-8) regulates the secretion of growth factors localized to the muscle-bone interface, SU153

**Gdf5**

Identification of a transcription factor p63 for transactivation of Wnt9a and Gdf5 causing joint cartilage formation, F116

**GEFOS Consortium**

Large-scale meta-analysis of genome-wide association scans for osteoporosis traits, 1091

**GEM OS2**

Percutaneous injection of GEM OS2 increases vertebral BMD in geriatric female baboons, F376

Stimulation of fracture healing by rhPDGF-BB combined with  $\beta$ TCP/collagen matrix in a diabetic rat fracture model, 1137

**Genome analysis**

Bivariate whole genome linkage analysis of femoral bone geometric traits and leg lean mass, M249

**Genome-wide association study (GWAS)**

GWAS and subsequent replication studies identified ADAMTS18 and TGFBR3 as novel osteoporosis risk genes, 1093

GWAS identified novel susceptibility loci for osteoporosis, SA267

GWAS identified RTP3 as a novel gene for bone strength, SU331

GWAS of BMD and hip geometry indices, 1092

GWAS pleiotropic associations of bone phenotypes, SA251

GWAS reveals genetic variants associated with BMD, osteoporosis and osteoporotic fractures, SA263

Phased GWAS identifies probable new gene affecting BMD, M245

**GERD. See Gastroesophageal reflux disease**

**GFP**

Tracking adipose differentiation in vitro with ap2-GFP reporters and flow cytometry: lipid staining and macrophage mimicry, SU057

Use of GFP reporter mice for assessing osteoprogenitor cell activity in a critical size calvarial defect, SA007



## Key Word Index

## ASBMR 30th Annual Meeting

- Use of GFP reporters to assess cell lineage in a murine model of tibial fracture repair, M077
- Use of GFP reporters to map the progression of multipotential progenitor cells into the osteoblast lineage, SU053
- Ghrelin**
- Ghrelin inhibits early osteogenic differentiation of C3H10T1/2 cells by suppressing Runx2 expression and enhancing PPAR $\gamma$  and C/EBP $\alpha$  expression, M086
- Increased caloric intake in energy deficient exercising with functional hypothalamic amenorrhea women is associated with decreased ghrelin and increased bone formation, SU184
- G $_i$**
- Endogenous G $_i$  signaling in osteoblasts negatively regulates cortical bone formation, 1255
- GISMO Lombardia Database**
- Comparison between logistic regression and artificial neural networks for vertebral fracture risk assessment, SU345
- Is the association between hypertension and bone osteoporotic fracture expressing a real interdependence?, SU346
- Gja1**
- Altered long bone structure in recessive null and dominant negative Cx43 (*Gja1*) mouse mutants, 1110
- GK**
- Characterization and genetic mapping of bone size phenotypes in GK and F344 rats using a new 3D CT method, M463
- Gli2**
- Marked induction of endochondral bone formation by overexpression of a constitutively active Gli2 in MSCs isolated from the healing site, SA049
- Wnt signaling regulates Gli2 and PTHrP expression in human breast cancer cells that cause osteolysis, M278
- Glial cells missing-2 (GCM2)**
- GCM2, the regulator of parathyroid cell fate, transactivates the CaSR gene, M187
- Global Longitudinal Registry of Osteoporosis in Women (GLOW)**
- Distribution of risk factors for fracture in women with and without a fracture history, SU342
- Failure to perceive increased risk of fracture in women 55 years, SA360
- Fragility fractures and health status in a multinational cohort, SU340
- Multinational comparison of bone health in women 55 years of age and older, SU344
- Regional differences in the management of osteoporosis, SU287
- Risk factors for fragility fracture in a multiracial cohort of US women, SA362
- Globulin**
- Reduced serum osteocalcin and sex hormone binding globulin in men with type II diabetes, SU461
- Globulin, sex hormone-binding (SHBG)**
- Genetic variation of the SHBG gene, SHBG levels and bone parameters, SU188
- Older men with low serum estradiol and high serum SHBG have an increased risk of fractures, 1279
- Serum SHBG level to predict osteoporosis severity, M297
- SHBG levels in older patients with acute hip fracture are correlated with worse function and increased bone resorption, SU363
- GLOW**. See *Global Longitudinal Registry of Osteoporosis in Women*
- Glucagon-like peptide-1 (GLP-1)**
- Positive effect of GLP-1 upon bone formation and resistance in insulin-resistant rats, M425
- Glucagon-like peptide-2 (GLP-2)**
- GLP-2 acutely uncouples bone resorption and bone formation in postmenopausal women, M399
- Glucocorticoid-induced leucine zipper (GILZ)**
- GILZ promotes osteoblast development and modulates RANKL/OPG levels, M049
- Glucocorticoid-induced osteoporosis (GIO)**. See *Osteoporosis*
- Glucocorticoids (GC)**
- Challenge of continuous exogenous GC administration in mice, M100
- Effect of a dissociating GC receptor modulator on bone cells, SA232
- Effect of ZOL (single 5-mg infusion) on lumbar spine BMD versus oral RIS (5 mg/day) over 1 year in subgroups of patients receiving GC therapy, M363
- Effects of ALF on bone and skeletal muscle in GC-treated rats, M219
- Effects of intermediate doses of GCs on bone turnover and circulating Dkk-1, MIF, sRANKL and OPG in patients with interstitial lung disease, SA451
- Effects of PTH on fracture repair in GC treated mice, 1062
- Effects of Vitamin K2 and RIS on bone formation and resorption, osteocyte lacunar system and porosity in the cortical bone of GC-treated rats, SU385
- Endogenous GC are critical for the development of skeletal fragility with aging in mice, 1250
- GC signaling in osteoblasts maintains normal bone structure in mice, F233
- GC signaling through osteoblasts is essential for cranial skeletal development, 1267
- GC-induced bone loss in mice is dependent on beta 2-adrenergic signaling, M102
- Impaired angiogenesis and compromised fluid volume accompanies increased osteoblast and osteocyte apoptosis with GC excess, SA453
- Induction of oxidative stress and diversion of  $\beta$ -catenin from TCF- to FOXO-mediated transcription by GCs or TNF $\alpha$  in osteoblastic cells, SA185
- N-terminal fragment of PTHrP promotes the GC-related deficiency of bone regeneration after bone marrow ablation in mice, M195
- Normal intramembranous fracture healing in mice with transgenic osteoblast-targeted disruption of GC signaling, SA234
- Optimization of bone turnover marker measurements in a mouse model of GC-induced osteoporosis, M298
- Osteoblast-targeted deletion of the GC receptor has little impact on PBM but attenuates DEX-induced suppression of bone formation, F452
- Prevention of GC-induced osteoporosis with ALN or ALF in patients with ophthalmologic diseases, SA450
- Proteasome inhibition counteracts the negative effect of GC treatment on bone metabolism by stimulating osteoblasts and inhibiting osteoclasts in vitro, SA231
- Quantification of non-mineralized tissue via  $\mu$ CT as a readout for GC effects on rat growth plate, M136
- RTA of densitometric calcaneal images differs between subjects with and without GC use, M314
- Glucose**
- BMP-6 from bone regulates serum glucose via IGF-1 released from pancreas, SU141
- GIP inhibits glucose-induced apoptosis of bone cells, M011
- Intermittent injection of recombinant osteocalcin improves glucose tolerance and insulin sensitivity, F168
- Plasma osteocalcin is inversely related to fat mass and plasma glucose in elderly Swedish men, SU459
- Rosiglitazone-induced change in BMD among African Americans with type 2 diabetes mellitus or impaired glucose tolerance, SU315
- ucOC is an endocrine link between the skeleton and the glucose metabolism, F444
- Glucose-dependent insulinotropic peptide (GIP)**
- Cloning and functional expression of the full length mouse GIP receptor and the regulation of its expression in osteoblasts by the Sp1 transcription factor, SU026
- GIP inhibits glucose-induced apoptosis of bone cells, M011
- Protein hydrolyzate directly modulates the expression of GIP by osteoprogenitor cells, SU010
- $\gamma$ -glutamyltransferase (GGT)**
- Association of urinary GGT and serum FGF-23 with prevalent fracture, SA296
- $\gamma$ -glutamyltransferase, serum level of (sGGT)**
- sGGT is one of the factors that determines the response to ALN treatment in osteoporotic women, M421
- Glutathione reductase (GSR)**
- Overexpression of GSR in osteoblasts decreases bone formation and partially prevents OVX-induced bone loss, F024
- Glycation**
- Non-enzymatic glycation increases bone fragility through altered microdamage formation and propagation, F103
- Glycation, non-enzymatic (NEG)**
- NEG alters collagen fibrillar structure and energy dissipation characteristics, SU478
- Glycogen synthase kinase-3 $\beta$  (GSK3 $\beta$ )**
- Osteoblasts apoptosis is mediated through GSK3 $\beta$ , M005
- GNAS**
- Deletion of the *GNAS* antisense transcript results in parent-of-origin specific *GNAS* imprinting defects and phenotypes including PTH-resistance, 1052
- Hypothyroidism and autism combined with PHP in the absence of Albright's hereditary osteodystrophy and *GNAS* imprinting changes, SA259
- Gondanotropins**
- Gondanotropins, bone loss and fracture in men, 1278
- Gothenburg Osteoporosis and Obesity Determinants (GOOD) Study**
- Cortical cross sectional area in young adult men is inversely related to risk of hip fracture in their older relatives, 1281
- gp38**
- Early osteocyte marker, E11/gp38 is highly elevated in new bone formed in response to distraction as compared to existing bone, SA136
- Gpr30**
- Non-genomic estrogen receptor Gpr30 is a Runx2 responsive gene that is required for osteoblast proliferation, F572
- GPR55**
- Cannabinoid receptor GPR55 affects osteoclast function in vitro and bone mass in vivo, 1221
- GPRC6A**
- GPRC6A null mice exhibit osteopenia and feminization, F004
- Granulin/epithelin precursor (GEP)**
- In vivo knockdown of GEP, a novel growth factor in cartilage, led to defects in cartilage and OA, 1048
- Grape seed extract**
- Grape seed extract suppresses IL-23/Th17 inflammatory pathways and bone destruction in CIA, SU093
- Gremlin**
- Nov induces gremlin expression by post transcriptional mechanisms, F141
- Growth factor, vascular endothelial (VEGF)**
- Dwarfism and osteopenia in mice with inactivated HRE in the VEGF gene promoter, 1152
- Human osteoblasts synthesize VEGF in response to ACTH, SA236
- VEGF and PTEN regulate bone homeostasis via control of osteoblastogenesis, osteoclastogenesis and adipocyte differentiation, M029
- VEGF induction provides evidence for different signaling pathway activation by large and small osteoclasts, SU106

**Growth factors**

- Ablation of IGF-I signaling in osteoprogenitors decreases bone formation and blunts the skeletal response to PTH, 1193
- Adipocyte-secreted protein URB is a potent stimulator of bone formation, F006
- Age-related changes in BMD, cross-sectional area and the strength of rat femur; an involvement of suppression of GH-IGF-1 signaling, SA467
- Alterations in bone structure and growth in dwarf rats with a depressed GH/IGF-I axis, SA178
- Anabolic PTH treatment mobilizes BMSC and osteoprogenitors towards bone surfaces, SA229
- bFGF induces the expression of a subset of Bcl-2 family genes to inhibit the apoptosis of ATDC5 chondroprogenitor cells, SU043
- BMP-2 inactivates TAK1-ATF2 signaling pathway in chondrocytes, F186
- BMP-2-stimulated signaling niche in osteoblasts comprising of Smad and PI3K/Akt regulates NFATc1 expression and its nuclear translocation, 1081
- BMP-3-null aged mice display increased trabecular bone volume and reduced cross sectional area at the mid-femoral diaphysis, SU143
- BMP-6 from bone regulates serum glucose via IGF-1 released from pancreas, SU141
- BMP-7 is not required for fracture healing, SU148
- BMPR2 is dispensable for formation of the limb skeleton, SU145
- Canonical Wnt signaling suppresses BMP-4 accumulation from C3H10T1/2 cells transfected with BMP-4 expression vector, SA156
- Catecholamines accelerate BMP-induced osteoblastic differentiation and bone formation, SU137
- CCR2 receptor signaling is involved in bone mass regulation and mediates the response to anabolic but not catabolic regimens of PTH(1-34), SU158
- CD47 (IAP) is an important modulator of osteoclast and osteoblast differentiation in vitro and in vivo, F093
- Central and peripheral leptin treatment produce similar increase in cortical and trabecular bone mass in ob/ob mice, SU164
- Characterization of Jab1-interacting motif in LMP-1, SA023
- Chemerin and CMKLR1 expression and function in human bone marrow MSC adipogenesis, SU165
- Circulating BMP-1 isoforms: novel diagnostic and therapeutic challenges for bone fracture repair, SU142
- Circulating OPG and its ligand in post operative biliary atresia: relationship with metabolic bone disease, M406
- CPTH; prediction of novel functions, structural features and potential receptor, SU072
- Craniofacial bone defect in Nell-1 mutant mice associated with dysregulated Runx2 and Osx expression, F174
- Critical role of TGF $\beta$  signaling pathways in skeletal development, 1079
- Decreased bone formation, increased bone resorption, and osteopenia in mice lacking SP, SU160
- Dependence of post natal osteogenic differentiation on BMP-2, SA001
- Distinct biological activity of IL-8 isoforms, SU162
- Effects of beta-D-glucopyranoside from *Phellodendron Amurense* on the production of inflammatory cytokines, growth factors, MMP, and on bone markers in human subchondral OA osteoblasts, SA117
- Effects of IL-27 on regulation of osteoclastogenesis by way of T cells, SU081
- Endocrine IGF-I maintains linear growth in the total absence of tissue IGF-1, SA184
- Endorphins regulate bone material properties by actions through dynorphin, 1195
- Ephrin B1 reverse signaling regulates bone formation via influencing osteoblast activity in mice, 1194
- FGF-23 and parameters of Ca and bone metabolism are positively influenced by GH replacement in adult GH deficiency patients from the KIMS survey, SU177
- Gene transcripts related to T-cell activation, proliferation, and cytokine signaling show significant effects on BMD variation in baboons, M241
- Grape seed extract suppresses IL-23/Th17 inflammatory pathways and bone destruction in CIA, SU093
- H4R is expressed by both OA and RA human tissues, SU159
- Hedgehog signaling regulates growth plate chondrocyte proliferation and growth factor expression, SU161
- High bone turnover in mice lacking the growth factor Mdk, 1198
- Identification and analysis of human LMP gene promoter region, M034
- IFN- $\gamma$  inhibits TNF $\alpha$ -induced osteoclastogenesis in vitro and in vivo, SU152
- IGF-I secreted from osteoblasts as a major chemotactic factor for osteoblasts, SA179
- IL-1 $\beta$ -induced hepcidin expression in synovial membranes of patients with OA is associated with TNF $\alpha$  repression, SU157
- IL-12 induces apoptosis in TNF $\alpha$ -mediated osteoclastogenesis in vivo, SA166
- IL-12 stimulates the OIP-1 gene expression in CD4<sup>+</sup> T-cells, SA173
- IL-27/WSX-1 signaling inhibits RANKL-induced osteoclastogenesis through STAT1 activation: a possible involvement in TLR4/MyD88-mediated inflammatory arthritis, SU102
- Importance of melastatin-like transient receptor potential 7 and Mg in the stimulation of osteoblast proliferation and migration by platelet-derived growth factor, M008
- Improvement of alveolar bone quality by local bFGF injection—histological and cellular biological analysis in a rabbit model, SA162
- Increased circulating DKK1 in acute coronary syndrome—association with platelet release and endothelial inflammatory response, SU167
- Increased expression of OPN in PBMC is associated with alteration in the fractions of lymphocytes in hindlimb-unloaded mice, M175
- Induction of CTGF by TGF $\beta$ 1 in osteoblasts: independent effects of Src and Erk on Smad signaling, M066
- Inhibition of PPAR $\gamma$ 2 by BADGE and Vitamin D in male mice increases osteoblastogenesis and inhibits bone matrix mineralization leading to osteomalacia, SU374
- Intermittent injection of recombinant osteocalcin improves glucose tolerance and insulin sensitivity, F168
- Interplay between BMP and TGF $\beta$  signaling in osteoblast differentiation, SA031
- Is GH/IGF-I mediated mechanism involved in regulating gender differences in bone size?, SA180
- JNK activation is involved in TNF $\alpha$ -stimulated Smurf1 expression, SA016
- Low serum IGF-I alters the cortical bone response to estrogen deficiency, SU190
- LPA enhances the viability of rat growth plate chondrocytes through the inhibition apoptosis and the promotion of cellular maturation, SU156
- Mechanism of action of lactoferrin's bone anabolic activity, SA175
- Mice lacking the GH receptor in liver have normal skeletal growth and bone volume despite virtual absence of circulating IGF-1, F181
- MKP-1 is an endogenous negative regulator of pro-inflammatory cytokines in BMSC, SU013
- Model of high body mass: BMD, bone markers and adipocytokine levels in high level male rugby players, SA167
- MSC enhance fracture healing: essential role for cytokines in homing and anti-inflammatory response, SA169
- Myostatin (GDF-8) regulates the secretion of growth factors localized to the muscle-bone interface, SU153
- NADPH oxidase/Nox signaling stimulates myofibroblast Mx2 transcription via H<sub>2</sub>O<sub>2</sub>, 1083
- Negative regulation of Tcf/Lef-dependent transcription by the BMP/Smad4 signaling axis, SU144
- OPG production by breast cancer cells is modulated by steroid hormones and confers resistance against TRAIL-induced apoptosis, M271
- Osteocalcin is a stress hormone: interaction with the sympathetic nervous system, M059
- Osteogenesis effect of human ligamentum flavum, myoblast, osteoblast and MSC by DBM and BMP-2, SU135
- Osteotropic peptides: anabolic and osteogenic effects, M045
- Permanent FGFR2 activation promotes osteoblast differentiation in MSCs through activation of PKC signaling, M093
- PGE2 as a potential mediator of PTH-dependent regulation of HSCs, F171
- Physiological concentrations of inhibin A are anabolic, affecting both trabecular and cortical bone in normal intact mice, M177
- PKD regulates HDAC7 localization and interaction with Runx2 during BMP-2-stimulated osteogenesis, SU027
- PLC $\gamma$ 2 as a promising therapeutic target in RA, F176
- Point mutation of endofin at PP1c-binding domain induces angiogenesis and bone formation in mice by sensitizing BMP signaling, 1082
- Protein sulfation is required to prevent chondrocytes autophagy and growth factor signaling during endochondral ossification, SU119
- PTHrP is processed by skin keratinocytes and has immunomodulation properties, SA216
- Real time oscillations in TNF-induced gene expression MAPK phosphorylation and promoter binding, SU087
- Recombinant congenic strain (B.H-6) establishes that trabecular bone mass and bone marrow adiposity are distinct and heritable phenotypes, F265
- Recovery of bone architecture after RANKL administration in rats is characterized by increased bone mass on existing trabeculae assessed by in vivo  $\mu$ CT, SU076
- Relationship between serum levels of inflammatory cytokines and bone turnover markers in the year following hip fracture, SU073
- Rheumatoid synoviocytes are stimulated with IL-23 to enhance osteoclastogenesis through upregulation of RANKL expression, SU084
- Runx2 and canonical Wnt signaling cooperatively regulate BMP-induced differentiation pathways of adult dural cells into osteoblasts or chondrocytes, M043
- Safety and efficacy of BMP-7 putty in a rabbit model of posterolateral vertebral lumbar fusion, SU149
- Serum IGF-1 is a developmental determinant of bone size, SA183
- Stimulation of macrophage TNF $\alpha$  production by orthopaedic wear particles requires activation of the ERK 1/2/Egr-1 pathway but is independent of p38 and JNK, SA177
- Sympathetic tone mediates leptin's inhibition of insulin secretion by modulating osteocalcin bioactivity, F034

## Key Word Index

## ASBMR 30th Annual Meeting

Synergistic activation of osteogenesis in MLPC by oxysterols, SU038

T cells amplify the anabolic action of PTH through Wnt10b signaling, 1197

Targeted overexpression of the nuclear FGF-2 isoforms in osteoblasts induces hypophosphatemia via modulation of FGF-23 and Klotho in mice, 1084

Tcf is required for Wnt11 mediated osteoblast differentiation, M058

TGF $\beta$  inhibits BMP signaling and osteogenesis through the TGF $\beta$  and BMP R-Smad direct interaction, 1080

TGF $\beta$  receptor I kinase inhibitor increases bone mass in normal mice, SA172

TGF $\beta$ 1 induces migration of Sca-1 and CD29-positive MSC in coupling bone resorption and formation, F188

Tissue-engineering and co-culture system based disc regeneration MSC's role, SA189

Transcription factor NFATp regulates BMP-induced chondrocyte differentiation in a tissue-specific manner, SU020

Transient expression of CXCR2 in human MSC stimulates chemotaxis toward CXCR2 ligand 8 and increased mineralization in the presence of osteogenic medium, SA170

In vivo knockdown of GEP, a novel growth factor in cartilage, led to defects in cartilage and OA, 1048

Wnt pathway regulation by demineralized bone requires TGF $\beta$ /BMP signaling, SU138

Wnt7a and Wnt7b evoke overlapping yet distinct transcriptional responses during the osteogenic programming of mesenchymal progenitors by Msx2, 1196

**Growth hormone (GH)**

Alterations in bone structure and growth in dwarf rats with a depressed GH/IGF-I axis, SA178

Anabolic skeletal effects of a GH-derived peptide (AOD9604) in the OVX rat model of osteoporosis, SU373

Differential effects of GH and 1  $\alpha$  calcidol on cancellous and cortical bone in hypophysectomized rats, SU501

Effects of GH on bone micro-architecture by in vivo  $\mu$ CT, SA547

Effects of long-term administration of high-dose GH on body composition and bone mineralization, SA571

FGF-23 and parameters of Ca and bone metabolism are positively influenced by GH replacement in adult GH deficiency patients from the KIMS survey, SU177

Interaction of combined intervention of PTH and GH on trabecular and cortical bone formation and resorption in the hypophysectomized rats, SU502

Is GH/IGF-I mediated mechanism involved in regulating gender differences in bone size?, SA180

Mice lacking the GH receptor in liver have normal skeletal growth and bone volume despite virtual absence of circulating IGF-1, F181

Relationship between adipokines and biochemical bone markers in osteoporotic women before and after GH supplementation, M289

Relationship between biochemical bone markers in osteoporotic women before and after 6 months treatment with either GH, Sr ranelate or GH plus Sr, M291

**Growth hormone, human (hGH)**

Sca-1<sup>+</sup> HSC-based hGH gene therapy enhanced endosteal bone resorption in mice, M233

Study of hGH and IGF-1 receptors in the human fetal femoral growth plate, SU128

**Growth plates**

Bone tether formation in femoral and basicranial growth plates have similar responses to growth disruptions due to nuclear VDR genotype and mineral homeostasis, M164

Chondrocyte-derived Ihh is required for osteoblast differentiation despite reconstitution of a normal growth plate, 1154

Gene expression profiling within murine growth plates using DNA microarrays, M156

Hedgehog signaling regulates growth plate chondrocyte proliferation and growth factor expression, SU161

Mechanisms of endplate failure in the human vertebral body, M413

Postnatal deletion of PTH/PTHrP receptor in growth plate chondrocytes leads to growth plate fusion, F114

Quantification of non-mineralized tissue via  $\mu$ CT as a readout for GC effects on rat growth plate, M136

Regulation of autophagy in the epiphyseal growth plate by AMPK and mTOR requires HIF-1, SU134

Specific inactivation of AF-1 in ER $\alpha$  results in growth plate closure while total inactivation of ER $\alpha$  results in increased growth plate width in elderly female mice, 1181

Study of hGH and IGF-1 receptors in the human fetal femoral growth plate, SU128

Thyroid hormone activates Wnt signaling pathways in rat growth plate chondrocytes, M157

Tissue-specific KO of the CaSR in chondrocytes inhibits IGF-1 signaling and delays differentiation in the growth plate, 1261

**Grx5**

Lentiviral shRNA mediated inhibition of Grx5 expression induces apoptosis via a mechanism involving increased ROS and cardiolipin oxidation, and reduced SOD activity, M009

**G $\alpha$**

Expression of an engineered G $\alpha$ -coupled receptor in osteoblasts affects intramembranous and endochondral bone formation during bone repair, F127

Expression of an engineered G $\alpha$ -coupled receptor, Rs1, in mature osteoblasts is sufficient to drive a dramatic anabolic skeletal response, 1077

Ligand activation of the engineered G $\alpha$ -coupled receptor Rs1 in osteoblasts promotes trabecular bone formation, 1076

**Gsa**

Deletion of the G protein subunit Gsa in early osteoblasts leads to accelerated osteoblast maturation and formation of woven bone with abnormal osteocytes, resulting in severe osteoporosis, 1254

**GSK3**

Akt regulates skeletal development through GSK3, mTOR, and FoxOs, 1151

Transcriptional regulation of Cx43 by  $\beta$ -catenin, a pathway activated by PGE $_2$ -PI3K-GSK3 signaling in mechanically loaded osteocytes, 1042

**GSK3-beta**

SOST blocks GSK3-beta inhibitor-induced ALP activity, SU036

**GTPase**

Proteomic identification and characterization of the small GTPase Rab18 in human osteoclasts, SU109

**GWAS**. See *Genome-wide association study*

**H**

**H3**

Snail downregulates VDR expression by recruiting Sin3A, HDAC1 and HDAC2 to multiple regions of VDR promoter and deacetylating histone H3/H4, F242

**H4**

Snail downregulates VDR expression by recruiting Sin3A, HDAC1 and HDAC2 to multiple regions of VDR promoter and deacetylating histone H3/H4, F242

**Halofuginone (Hfg)**

Hfg inhibits melanoma bone metastases and TGF $\beta$  signaling, F190

**Hardness**

Long-term treatment with oral bisphosphonates in postmenopausal women: effects on the degree of mineralization and microhardness of bone, 1029

**HcB/8**

Geometric property QTLs in HcB/8 x HcB/23 F2 cross, F260

Strong and extensive epistatic interactions affect bone traits in a mouse reciprocal intercross of HcB/8 and HcB/23, SA125

**HcB/23**

Geometric property QTLs in HcB/8 x HcB/23 F2 cross, F260

Strong and extensive epistatic interactions affect bone traits in a mouse reciprocal intercross of HcB/8 and HcB/23, SA125

**Health care**. See also *Alternative medicine; Medicare*

Costs associated with NHNV fractures in a managed care setting, SU320

Designing a Latino osteoporosis awareness campaign, SU312

Do physicians who practice together provide similar osteoporosis care?, SU401

Falls predict higher medical costs among osteoporosis patients in community setting, SA430

Incorporating FRAX<sup>TM</sup> algorithms in models of cost-effectiveness, 1023

Incremental costs associated with selected skeletal fractures, 1024

Osteoporosis: evaluation of screening patterns primary care group practice, SU272

Predictors of osteoporosis management among residents living in long-term care, SA368

Quarterly intravenous IBN acid in the community setting in England, SU409

Questionnaire-based osteoporosis risk assessment in a rural area primary care setting, SU354

Relative contributions of nonvertebral efficacy, vertebral efficacy, and persistence in determining cost-effectiveness: the case of osteoporosis and implications for payers, M371

Socioeconomic status, BMD testing and hip fracture rates in a universal health-care system, SU293

Treating osteoporosis in the elderly: an environmental scan of nursing home prescribing in Ontario, Canada, SU404

**Heart transplant**

Marked Vitamin D deficiency in recent heart and liver transplant recipients, SA501

**Hedgehog proteins**

Hedgehog pathway is activated in osteosarcoma and cyclopamine prevents osteosarcoma growth by cell cycle regulation, SU241

Hedgehog signaling regulates growth plate chondrocyte proliferation and growth factor expression, SU161

**Heel Stiffness Index**

Correlation between DXA Femur Strength Index and QUS Heel Stiffness Index in Chinese women, M464

**Height loss**

Height loss, vertebral fractures and misclassification of osteoporosis, SU259

**Helsinki Study of Very Low Birth Weight**

Preterm birth and BMD in young adulthood, 1103

**Hematopoiesis**

Impact of PTH on cells of the hematopoietic lineage, 1159

PTH stimulates hematopoiesis and increases survival in irradiated mice, 1015

Role of Ostm1 in bone, hematopoiesis and neuronal development, 1271

**Hematopoietic cells**

Drugs which inhibit osteoclast function suppress tumor growth and alter hematopoietic cell populations in bone, F270

Hematopoietic cells in the bone marrow augment anabolic actions of PTH, M181

**Hematopoietic stem cells (HSC).** See *Stem cells*  
**Hemodialysis**

- Acute change in iCa directly affects bone formation independent of PTH action during hemodialysis, SU437
- Association of the marker of ABD with malnutrition-inflammation complex in hemodialysis patients, SU446
- Biomechanical impact of chronic hemodialysis on bones and muscles, SU269
- Hemodialysis patients rapidly lose their bone minerals after 60 years of age, SU438
- Parathyroidectomy improves quality of life in hemodialysis patients with HPT2, SA212
- Serum intact PTH of 100 to 150 pg/ml is associated with greatest survival in maintenance hemodialysis patients, SU445
- SIF levels among hemodialysis patients are positively associated with levels of serum phosphate and intact PTH, SU440

**Hemophilia A**

- Osteoporosis in a murine model of hemophilia A, M480

**Heparan sulfate proteoglycans (HSPG)**

- HSPG modulate osteogenic differentiation through heparan sulfate chains, M094

**Hepatic osteodystrophy.** See *Osteodystrophy***Hepatitis C-associated osteosclerosis (HCAO)**

- Recovery from HCAO following anti-viral treatment, F488

**Hepcidin**

- IL-1 $\beta$ -induced hepcidin expression in synovial membranes of patients with OA is associated with TNF $\alpha$  repression, SU157

***Herba epimedii***

- Bone anabolic effects of icariin and total flavonoid fraction of *Herba epimedii* in OVX mice, M337

**Heterochromatin**

- TZD modify nuclear heterochromatin architecture, SU056

**Heterogeneous nuclear ribonucleoproteins (hnRNP).** See *Ribonucleoproteins***Heterozygosity**

- Morquio Syndrome variant: two siblings with atypical phenotype and novel compound heterozygosity, M240

**hFVIII**

- Differences in femoral bone structure between juvenile non-transgenic and transgenic rabbits with the WAP-hFVIII gene construct, SA132

**High g environments**

- Effects of a high g environment on BMD in UK fast-jet trainee pilots, SU473
- Increased osteoclast differentiation and bone resorption during spaceflight, SU094

**High mobility group AT-hook 2 (HMGA2)**

- Common single nucleotide polymorphism in the HMGA2 gene is associated with bone mass in men, SA268

**High mobility group box protein (HMGB)**

- TSH inhibits the expression of HMGB, a regulator of TNF $\alpha$  transcription, in osteoclastogenesis, 1117

**HIP**

- Gender-specific changes in bone microstructure of mice lacking ribosomal protein L29/HIP, SA133

**Hip replacement**

- Low systemic BMD increases implant migration in cementless hip replacement, F458

**Hip structure analysis (HSA)**

- HSA and physical activity in boys and girls during puberty, SA538
- HSA based on DXA data in women with postmenopausal osteoporosis receiving once-monthly oral IBN for 12 months, SA507
- HSA for RLX treatment in Japanese women with osteoporosis, SA419
- HSA in women, SU270

**Hiroshima Cohort Study**

- Association of urinary GGT and serum FGF-23 with prevalent fracture, SA296

**Histamine H4 receptor (H4R)**

- H4R is expressed by both OA and RA human tissues, SU159

**Histomorphometry**

- Bone histomorphometry in patients with Crohn's Disease, SU462
- Bone turnover evaluated by a combined Ca balance and <sup>45</sup>Ca kinetic study, and dynamic histomorphometry, M137
- Dynamic histomorphometry of mineralized tissue using cryosections of murine bone and teeth, M138
- Histomorphometric evaluation in an experimental model of hepatic osteodystrophy, M480
- Long term safety of oral RIS treatment in men with osteoporosis as assessed by histomorphometry, SA344

**Histone deacetylase (HDAC)**

- HDAC inhibitors suppress IL-1 $\beta$ -induced NO and PGE<sub>2</sub> production in human chondrocytes, SU116
- NFATc1 mediates HDAC-dependent transcriptional repression of osteocalcin expression during osteoblast differentiation, 1145

**Histone deacetylase 1 (HDAC1)**

- Snail downregulates VDR expression by recruiting Sin3A, HDAC1 and HDAC2 to multiple regions of VDR promoter and deacetylating histone H3/H4, F242

**Histone deacetylase 2 (HDAC2)**

- Snail downregulates VDR expression by recruiting Sin3A, HDAC1 and HDAC2 to multiple regions of VDR promoter and deacetylating histone H3/H4, F242

**Histone deacetylase 7 (HDAC7)**

- PKD regulates HDAC7 localization and interaction with Runx2 during BMP-2-stimulated osteogenesis, SU027

**Histone deacetylase inhibitors (HDI)**

- HDI, Vorinostat, blocks growth and associated osteolysis of cancer cells within bone, but reduces bone volume in non-tumor bearing bones in mice, M279

**Homocysteine**

- Homocysteine accumulates in bone tissue by collagen binding and adversely affects bone, M417
- Homocysteine levels in relation to physical performance, SA372

**Homocystinuria**

- Homocystinuria associated bone disease: effect of long term bisphosphonate treatment, SA406

**Horizon Pivotal Fracture Trial**

- Effect of once-yearly ZOL 5 mg infusion on fracture incidence in postmenopausal osteoporosis, 1028
- Effect of once-yearly ZOL on integral BMD of the spine, SU405
- Increase in risk of atypical subtrochanteric fractures with ZOL?, F411

**Hormone deficiency**

- Mechanical loading prevents bone loss due to hormone-deficiency in female mice, M474

**Hormone therapy**

- Impact of adjuvant hormonal therapy on bone loss depending on initial adjuvant chemotherapy and menstrual status, M415
- Influence of long-term hormone replacement therapy on tibia bone mineral mass and mass distribution in postmenopausal women, F420
- Serum estradiol and fracture reduction during treatment with hormone therapy, F383
- Treatment threshold in men on androgen deprivation therapy: T-score vs. FRAX, F308

**Hormones**

- Hormonal influences on volumetric bone density and geometric properties in obesity, SU367

**Hormones, calcitropic and phosphotropic**

- Ablation of the Galnt3 gene in mice leads to low circulating FGF-23 concentrations and hyperphosphatemia despite increased FGF-23 gene expression, 1018

- Activation of the CaSR by beta-aspartyl and gamma-glutamyl peptides, M202
- Altered regulation and expression of FGF-23 in the adenine-induced uremic rat model, SU178
- Analysis of chromosome breaks in osteoblasts and non-osteoblastic cells treated with intermittent PTH, M191
- Analytical validation of LIA and ELEC methods for the determination of osteocalcin, SA191
- Angiotensin II type 2 receptor blockade increases bone mass, SU007
- Association between Cx43 and  $\beta$ -arrestin is required for cAMP-dependent osteoblast survival induced by PTH, 1227
- Association of the marker of ABD with malnutrition-inflammation complex in hemodialysis patients, SU446
- Behavior of circulating rat(s) PTH molecular forms in HPT2 related to Vitamin D deficiency and renal failure, M194
- Bone turnover evaluated by a combined Ca balance and <sup>45</sup>Ca kinetic study, and dynamic histomorphometry, M137
- c-Fos is associated with renal FGF-23-mediated signaling, SU173
- C-terminal fragment of PTHrP (107-139), exerts osteogenic features in both regenerating and nonregenerating bone in mice with diabetes-related osteopenia, SA223
- Calciphylaxis in a patient with HPT and normal kidney function, WG33
- Calcitonin attenuates the anabolic effect of PTH in vivo and rapidly upregulates SCT expression, F195
- Calcitonin receptor on osteoclasts plays a physiological role to protect against HCa in mice, SA197
- CaSR mediated signaling in human vascular smooth muscle cells, M200
- $\beta$ -catenin directly binds to a specific intracellular domain of PTH/PTHrP receptor and regulates the signaling in chondrocytes during endochondral ossification, 1013
- Circulating concentrations of 25(OH)D after a single oral dose of 100,000 IU of Vitamin D2 or Vitamin D3, M212
- Clinical implications of commercial biotin-based detection systems in PTH assays, M435
- Cloning and functional analysis of human Nurrl (NR4A2) promoter: critical role in the regulation of CYP27B1 by PTH and CREB phosphorylation, 1161
- Continuous rat parathyroid cell line expressing PTH, M184
- Deletion of CYP27B1 reverts the premature aging phenotype of the Klotho-null mice, F069
- Development of nephrotic in transgenic rats over expressing Type III Na-dependent phosphate transporter, SU170
- Dietary normalization of Ca absorption in mice genetically deficient in CaSR and 25(OH)D-1 $\alpha$ -hydroxylase results in non-lethal, severe hyperparathyroidism with reduced osteoclastogenesis, M199
- Dimerization and trafficking of the CaSR to the plasma membrane, M205
- Dominant tissue accumulation of MIBI in parathyroid glands in uremic rats, SA222
- Dominant-negative GCMB mutants causing autosomal-dominant HPT—protein expression and cellular localization, SA225
- Effect of treating Vitamin D deficiency on FGF-23 levels in humans, SA209
- Effects of hPTH(1-34) infusion on circulating serum phosphate, 1,25(OH)<sub>2</sub>D and FGF-23 levels in healthy men, SU169
- Effects of intermittent human PTH administration on bone union with hydroxyapatite blocks at the site of cancellous bone osteotomy in OVX rats, SA214
- Effects of KHCO<sub>3</sub> on Ca and bone metabolism during high salt intake, SA446

## Key Word Index

## ASBMR 30th Annual Meeting

Efficient expression of the full-length CaSR in insect cells, M198

Evidence for a role of prolactin in Ca homeostasis: regulation of intestinal TRPV6 and intestinal Ca absorption by prolactin, 1223

Extended lactation is associated with failure to restore BMD 6 months after resumption of menstrual cycle, M305

FGF-23 and FGF-2 share a common but also have distinct signaling pathways for negative regulation of bone nodule mineralization in cultured osteoblasts, SA206

FGF-23 and post-transplant hypophosphatemia: evidence for a causative link, SU168

FGF-23 in Vitamin D deficient older persons, SA203

Functional induction of target genes in parathyroid cell by direct injection technique, M185

Hematopoietic cells in the bone marrow augment anabolic actions of PTH, M181

High bone mass due to increased bone formation in mice lacking the CTR, SA192

High expression of the Ca/phosphate-regulating hormone STC2 is associated with renal calcification in the Klotho mutant mice, SA201

HPT and renal insufficiency, WG29

Identification and optimization of residues in PTH and PTHrP that determine altered modes of binding to the PTH/PTHrP receptor, F224

Impact of PTH on cells of the hematopoietic lineage, 1159

Increased bone volume and correction of HYP mouse hypophosphatemia in the Klotho/HYP Mouse, 1017

Influence of PHP on BMD and vertebral morphometry, M190

Inhibitory role of Gαq/PKCδ signal in the bone anabolic action of PTH, 1228

Interaction of combined intervention of PTH and GH on trabecular and cortical bone formation and resorption in the hypophysectomized rats, SU502

Intermittent PTH administration increases bone mass and strength in aged mice by antagonizing oxidative stress-induced osteoblast apoptosis via ERK-mediated attenuation of p66<sup>shc</sup> phosphorylation, SU380

Intestinal-specific VDR null mice maintain normal calcemia but display severe bone loss, F238

KO of the PTHrP gene in breast cancer cells inhibits tumor progression and metastatic spread in vivo, 1016

Lack of calcitonin accentuates bone loss during lactation by enhanced osteoclast formation and reduced osteoblast formation, SA194

Local osteocyte defect in *Dmp1* null mice causes overproduction of FGF-23, 1225

Long-acting PTH ligand that binds to a distinct PTH receptor conformation (R0) can stimulate increases in markers of both bone resorption and bone formation in mice, F221

Low density lipoprotein-cholesterol levels affect vertebral fracture risk in female patients with pHPT, SA484

Low serum osteocalcin predicts carotid plaques and indicators of the metabolic syndrome, SA198

Marrow ablation induces periosteal bone formation and potentiates the effect of PTH on endosteal bone formation in rat femurs, M208

Mechanical unloading partially rescues hypophosphatemic rickets in *Dmp1*-null mice, 1162

Mechanism of enhanced 19-nor-2a-(3-hydroxypropyl)-1a,25-(OH)<sub>2</sub>D<sub>3</sub> anti-cancer activity in prostate cancer cells, M216

MEPE C-terminal ASARM-peptide, promotes hypophosphatemia, bone defects and increases adiposity, F207

MEPE regulates bone remodelling independent of serum phosphate and alters renal vascularization, F205

Metabolic alkalosis transition in renal proximal tubule cells facilitates an increase in CYP27B1, while blunting responsiveness to PTH, M196

Molecular basis of PHPT: adenomatous parathyroid cells are resistant to L-amino acids, M203

Molecular mechanisms involved in PTH-induced apoptosis in Caco-2 intestinal cells, M189

N-terminal fragment of PTHrP promotes the GC-related deficiency of bone regeneration after bone marrow ablation in mice, M195

Negative relationship between PTH and Vitamin D: is there an age and a gender effect?, M179

New intact PTH assay on the IDS Automated Analyser 3x3™, M209

New long-acting PTH/PTHrP hybrid analog that binds to a distinct PTHR conformation has superior efficacy in a rat model of HPT, F483

Nmp4-KO mice exhibit a complex phenotype, M193

Normocalcemic PHPT: update on a new clinical phenotype, SA486

Novel and sensitive immunoassay for PTHrP, M182

Osteogenic action of Ex-4 in normal and insulin-resistant state, M424

Osteopenia in CKD: effects of phosphate overload, SU447

Parathyroidectomy improves quality of life in hemodialysis patients with HPT2, SA212

Phex binds to SNARE-associated protein snapin and co-localizes in vesicle-enriched, extracellular matrix micro-environment mediating mineral crystal nucleation, F066

Phosphatonins and liver resection-related hypophosphatemia, SU176

Positive effect of GLP-1 upon bone formation and resistance in insulin-resistant rats, M425

Possible pathogenic role of aberrant Klotho expression in PHPT and HPT2, SA227

Post-mitotic preosteoblasts are the targets of the anabolic actions of intermittent PTH on periosteal bone, 1157

Potential role of FGF-23 in CKD-MBD, WG30

PTH and not Vitamin D predicts age-related bone loss in the elderly, M178

PTH increases after oral peptones administration in obese subjects treated with roux-en-y gastric bypass surgery: role of phosphate on the rapid control of PTH release, M180

PTH induces COX-2 in MC3T3-E1 osteoblasts via cAMP-PKA and Ca-calceineurin pathways, SA033

PTH signaling through LRP5/6 in osteoblasts, 1014

PTH stimulates hematopoiesis and increases survival in irradiated mice, 1015

PTH-gene family in the cartilaginous fish, *Callorhynchus milii*, M183

PTHrP1 mutations associated with Ollier Disease result in receptor loss of function, SA258

PTHrP1 stimulates bone formation through a distinct β-arrestin dependent pathway independent of G protein activation, 1226

PTHrP blockade inhibits tumor progression in a model of human breast cancer, F213

PTHrP regulates mammary gland ductal elongation during puberty, F228

PTHrP-induced Wnt signaling specifies the mammary mesenchyme, F219

Rapid detection of intact FGF-23 in tumor tissue from patients with OOM, SA204

Regulation of nuclear import of the PTHR, M210

Regulation of renal Klotho: the importance of ERα, SA211

Relationship between Vitamin D and PTH: serum Ca and Mg are major determinants of PTH in patients with mild CKD, M211

Requirement of the bone for Vitamin D for 1,25(OH)<sub>2</sub>D<sub>3</sub> synthesis and bone mineralization, M224

Role of FGF-23 in the early response to the PTH analogue: TPTD, SU174

Role of OPG/RANKL system for bone loss in PHPT, M192

Role of the transcription factor SOX4 in the skeletal response to intermittent PTH, SA220

Selective removal of PLC signaling in novel PTH(1-28) analogs abolishes regulation of NaPi-IIc but not NaPi-IIa, M186

Serum intact PTH of 100 to 150 pg/ml is associated with greatest survival in maintenance hemodialysis patients, SU445

Serum PTH response to oral Ca load in Asian adolescents, M188

Signaling of extracellular inorganic phosphate mediated via Na-phosphate co-transporters influences FGF-23 signaling in renal tubular cells, SU172

Significance of O-linked glycosylation of FGF-23 protein, SA208

At similar plasma 25(OH)D levels, fat mass influence PTH levels in the state of Vitamin D insufficiency, SA218

Skeletal dysmorphology of mice lacking the mid-region, nuclear localization sequence and C-terminus of PTHrP, 1160

Subcutaneous administration of salmon calcitonin: bone protective effect in adjuvant arthritis prevention model in rats, SA193

Synergistic role of Npt2a and Npt2c in inorganic phosphate metabolism of mice, F473

Target ablation of PPR in osteocytes induces hypocalcemia and impairs bone structure, 1158

Transgenic ASARM-peptide overexpression with reduced serum phosphate and 1,25(OH)<sub>2</sub>D<sub>3</sub> leads to decreased BMD and obesity, F210

Transgenic expression of human FSH in female mice has an anabolic effect on bone, 1224

Vitamin D deficiency in inner city infants: impact of DBP genotype, SA472

Vitamin D status in young women is strongly negatively related to body weight, BMI and body fat, but is not associated to bone mass, SU203

In vivo longitudinal QCT analysis PTH efficacy in a rat cortical defect model, M207

What is your patient's Vitamin D status? Clinical consideration of variability in a 25(OH)D measurement, SU427

Wintertime Vitamin D supplementation inhibits seasonal variation of calcitropic hormones and maintains bone turnover in healthy men, SU433

XXLαs acts as a novel heterotrimeric G protein subunit with an ability to transduce receptor activation into intracellular signaling, F226

**Hormones, endogenous**

Predictive capacity of biochemical markers of bone turnover and endogenous hormones for osteoporosis in men, SU334

**Hormones, sex**

Influence of sex hormones on BMD in middle aged and elderly men, SU335

Post-fracture mortality in men: contributions of sex hormones and BMD as risk factors, 1280

Reduced serum osteocalcin and sex hormone binding globulin in men with type II diabetes, SU461

Relationship of QUS at phalanges with hand and axial BMD, sex hormones and bone turnover markers in elderly women, M320

**Hormones, stress**

Osteocalcin is a stress hormone: interaction with the sympathetic nervous system, M059

**Hox**

Essential Hox gene function in limb skeletal and synovial joint formation, M151

**HOXA10**  
PBX1 interaction with HOXA10 regulates timing and expression of phenotypic bone genes during osteoblastogenesis, SU019

**HRPT2**  
Usefulness of *HRPT2* gene and parafibromin studies in two patients with PHPT and uncertain pathological assessment, SA482

**HSD11B1**  
Association of *HSD11B1* polymorphisms with vertebral fracture risk and BMD in postmenopausal Korean population, M260

**HSP27**  
Antiapoptotic action of 17 $\beta$ -estradiol in skeletal muscle cells involves ERK 1/2, p38 MAPK, ASK-1 and HSP27, SU185

**Human immunodeficiency virus (HIV)**  
Cortical and trabecular microarchitecture in HIV-infected postmenopausal women, SU458  
Determinants of low BMD in HIV infected postmenopausal women, SU455  
Efficient and stable gene expression into human osteoclasts using an HIV-1 based lentiviral vector, SU113  
Vitamin D insufficiency is common in racially diverse postmenopausal women with HIV, M448

**Hydrogels**  
Nanogel cross-linking hydrogel as a drug delivery system for TNF $\alpha$  antagonist, M121  
Sequestration, proliferation and differentiation of osteoblasts in hydrogels for tissue engineering applications, SA143

**Hydrogen peroxide (H<sub>2</sub>O<sub>2</sub>)**  
NADPH oxidase/Nox signaling stimulates myofibroblast Msx2 transcription via H<sub>2</sub>O<sub>2</sub>, 1083

**Hydroxyapatite (HA)**  
DMP1 fragments interact differently with HA: insights into mechanism of action, SA140  
Effects of intermittent human PTH administration on bone union with hydroxyapatite blocks at the site of cancellous bone osteotomy in OVX rats, SA214  
Local administration with PTX-loaded HA-alginate beads for metastatic spine cancer in rats, M274  
Resorption mechanism of HA and  $\beta$ TCP coating layer, SA100

**Hydroxychloroquine**  
Nonsteroid responsive HCa associated with sarcoidosis—a rapid response to hydroxychloroquine, WG28

**1 $\alpha$ -hydroxylase**  
Expression of 1 $\alpha$ -hydroxylase (CYP27B1) in BMSC, SA237

**25-hydroxylase**  
CYP27A1 mutations at Phe147 confer 25-hydroxylase activity towards a Vitamin D<sub>2</sub>-type sidechain, M231

**11 $\beta$ -hydroxysteroid dehydrogenase**  
Expression of 11 $\beta$ -hydroxysteroid dehydrogenase during murine osteoclast formation, SA235

**5-hydroxytryptamine**. See *Serotonin*

**Hydroxytyrosol**  
High concentrations of hydroxytyrosol and quercetin antioxidants enhance adipogenesis and inhibit osteoblastogenesis in MSCs, SA037

**25-hydroxyvitamin D (25(OH)D)**  
25(OH)D acts on Ca and skeletal homeostasis independent of 1,25(OH)<sub>2</sub>D in vivo, M214  
25(OH)D levels in children with CKD as measured by tandem mass spectrometry, SU485  
Albuminuria, 25(OH)D, 1,25(OH)<sub>2</sub>D, and intact PTH in older adults, SU442  
Circulating concentrations of 25(OH)D after a single oral dose of 100,000 IU of Vitamin D2 or Vitamin D3, M212

Clinically useful paradigm for interpretation of serum 25(OH)D levels with simultaneously measured PTH levels, M437

Dietary normalization of Ca absorption in mice genetically deficient in CaSR and 25(OH)D-1 $\alpha$ -hydroxylase results in non-lethal, severe hyperparathyroidism with reduced osteoclastogenesis, M199

Dietary Sr in a model of established osteopenic rats reduce the levels of 25(OH)D, SA377

Effect of skin color and oral Vitamin D supplementation on serum 25(OH)D in adolescent girls, SU395

Effect of Vitamin D2 or Vitamin D3 supplementation on serum 25(OH)D, SU425

Effects of 50,000 IU of Vitamin D<sub>2</sub> twice per month on circulating 25(OH)D and Ca levels, SU426

Efficacy and safety of short term treatment with different doses of cholecalciferol on 25(OH)D levels in postmenopausal females with osteoporosis, SU434

Evaluation of automated methods for quantifying serum 25(OH)D, SU206

Low plasma 25(OH)D and VDR polymorphisms are associated with increased breast cancer risk, SU202

Low serum 25(OH)D is associated with higher rates of hip bone loss in older men, F367

New 25(OH)D assay on the IDS Automated Analyser 3x3™, SU200

New data on the impact of renal function on the relationship between 25(OH)D and PTH, 1031

Polymorphisms in *CYP24A1*, the gene encoding 25(OH)D-24-hydroxylase, are associated with BMD, SA266

Seasonal genetic influence on serum 25(OH)D levels, SA334

Serum 25(OH)D and the risk of hip and non-spine fractures in older men, 1277

Serum 25(OH)D measurement and histomorphometric analysis of iliac crest biopsies from 1180 patients reveals a high prevalence of Vitamin D-dependent osteomalacia, 1134

At similar plasma 25(OH)D levels, fat mass influence PTH levels in the state of Vitamin D insufficiency, SA218

Single dose of 100,000 IU D3 appears to be insufficient to achieve desirable levels of 25(OH)D in patients with hypovitaminosis D, SU430

Vitamin D supplementation intake among osteoporosis patients aged 50 years and older at various 25(OH)D levels in the US, M400

What is your patient's Vitamin D status? Clinical consideration of variability in a 25(OH)D measurement, SU427

**25-hydroxyvitamin D<sub>3</sub> (25(OH)D<sub>3</sub>)**  
25(OH)D<sub>3</sub>-24-hydroxylase (CYP24A1): mutagenesis and activity studies reveal important residues involved in regioselectivity and substrate access, SU199

Decreasing calcidiol (25OHD<sub>3</sub>) in serum is related to impaired function and increased mortality in the elderly, SU204

Effect of 1,25(OH)<sub>2</sub>D<sub>3</sub> and 25(OH)D<sub>3</sub> on osteoblastogenesis and bone strength in Vitamin D sufficient growing mice, SU207

Prediction of osteoporotic fracture risk by 25(OH)D<sub>3</sub>-1 $\alpha$ -hydroxylase (CYP27B1) gene, M263

**Hyp**  
7B2 protein mediated inhibition of DMP1 cleavage in osteoblasts enhances FGF-23 production in *Hyp*-mice, 1053

**HYP**  
Increased bone volume and correction of HYP mouse hypophosphatemia in the *Klotho*/HYP Mouse, 1017

**Hypercalcemia (HCa)**  
Calcitonin receptor on osteoclasts plays a physiological role to protect against HCa in mice, SA197

Documented response to cinacalcet in two cases of acquired hypocalciuric HCa, M197

Establishment of a murine model of HCa by overexpression of sRANKL using an adenovirus vector, SU082

Infantile HCa: relationship of dietary intake of Ca and Vitamin D to serum and urine levels, SU491

Nonsteroid responsive HCa associated with sarcoidosis—a rapid response to hydroxychloroquine, WG28

**Hypercalcemia, familial hypocalciuric (FHH)**  
Association of FHH and mandible lesions in two kindreds, M427  
Functional characterization of unreported CaSR in four Italian kindreds with FHH, M204  
Skeletal consequences of FHH and PHPT, M206

**Hypercalciuria**  
Bisphosphonates in children with hypercalciuria and reduced BMD, M429  
Effect of hypercalciuria and diet on bone in genetic hypercalciuric stone-forming rats, SU213  
Renal leak hypercalciuria: a potential cause of tertiary hyperparathyroidism, M430

**Hypercalciuria, idiopathic (IHC)**  
ALN and indapamid alone or in combination in the management of IHC associated with osteoporosis, 1245

**Hyperhomocysteinemia**  
RLX ameliorates detrimental collagen cross-link formation in bone from an OVX rabbits with or without hyperhomocysteinemia, SA382

**Hyperparathyroidism**  
Dietary normalization of Ca absorption in mice genetically deficient in CaSR and 25(OH)D-1 $\alpha$ -hydroxylase results in non-lethal, severe hyperparathyroidism with reduced osteoclastogenesis, M199

**Hyperparathyroidism, normocalcemic primary (NPHPT)**  
Prevalence and demographics of asymptomatic NPHPT in the United States, M431

**Hyperparathyroidism, primary (PHPT)**  
Cardiovascular manifestations of mild PHPT, 1034  
Changes in cardiovascular function after parathyroidectomy in mild PHPT, M434  
Increased risk of morphometric vertebral fracture in postmenopausal women with PHPT, M438  
Low density lipoprotein-cholesterol levels affect vertebral fracture risk in female patients with PHPT, SA484  
Molecular basis of PHPT: adenomatous parathyroid cells are resistant to L-amino acids, M203  
Normocalcemic PHPT: update on a new clinical phenotype, SA486  
Possible pathogenic role of aberrant *Klotho* expression in PHPT and HPT2, SA227  
Role of OPG/RANKL system for bone loss in PHPT, M192  
Skeletal consequences of FHH and PHPT, M206  
Usefulness of *HRPT2* gene and parafibromin studies in two patients with PHPT and uncertain pathological assessment, SA482

**Hyperparathyroidism, secondary (HPT2)**  
Behavior of circulating rat(s) PTH molecular forms in HPT2 related to Vitamin D deficiency and renal failure, M194  
Efficacy of the Vitamin D supplementation in patients with hypovitaminosis D and HPT2, SU431  
Parathyroidectomy improves quality of life in hemodialysis patients with HPT2, SA212  
Possible pathogenic role of aberrant *Klotho* expression in PHPT and HPT2, SA227  
Suppression of canonical wnt signaling by *Dkk1* attenuates PTH-mediated peritrabecular stromal cell response and new bone formation in a model of HPT2, F215

**Hyperparathyroidism, tertiary**

## Key Word Index

## ASBMR 30th Annual Meeting

Renal leak hypercalciuria: a potential cause of tertiary hyperparathyroidism, M430

**Hyperphagia**

OVX-induced hyperphagia does not modulate bone mineral or bone strength in female Sprague-Dawley rats, SA447

**Hyperphosphatasia**

Hyperphosphatasia: a unique type without mutations in *TNFRSF11A* (RANK), *TNFRSF11B* (OPG), or *SQSTM1* (sequestosome 1), SU210

**Hyperphosphatasia, expansile skeletal (ESH)**

OPG deficiency mimicked by a novel 15-base pair tandem duplication in *TNFRSF11A* encoding RANK: merging the juvenile PD and ESH phenotypes, F563

**Hyperphosphatemia**

Ablation of the Galnt3 gene in mice leads to low circulating FGF-23 concentrations and hyperphosphatemia despite increased FGF-23 gene expression, 1018

Postprandial hyperphosphatemia is a novel risk factor for CVD by involving endothelial dysfunction, SU443

**Hyperphosphatemia, transient (TH)**

Prevalence of TH among healthy infants and toddlers, SA564

**Hyperpolarization-activated cyclic nucleotide (HCN)**

Pacemaker channel, HCN, controls functions of osteoclasts, SU100

**Hypertension.** See also *Blood pressure*

Is the association between hypertension and bone osteoporotic fracture expressing a real interdependence?, SU346

**Hyperthyroidism**

Body composition changes after radioiodine treatment of hyperthyroidism, M433

**Hypocalcemia**

Target ablation of PPR in osteocytes induces hypocalcemia and impairs bone structure, 1158

**Hypogonadism**

DHT administration is effective for the prevention of hypogonadal bone loss, SU193

Effects of aromatase inhibitor therapy on BMD in hypogonadal elderly men, 1135

Toward a physiologically-based definition of hypogonadism in men: dose-response relationship between testosterone and bone resorption, 1102

**Hypoparathyroidism (HPT)**

Calciophylaxis in a patient with HPT and normal kidney function, WG33

Circulating osteoblast lineage cells increase with PTH treatment of HPT, 1146

Dominant-negative GCMB mutants causing autosomal-dominant HPT—protein expression and cellular localization, SA225

HPT and renal insufficiency, WG29

New long-acting PTH/PTHrP hybrid analog that binds to a distinct PTHR conformation has superior efficacy in a rat model of HPT, F483

PTH increases bone turnover in HPT, F485

PTH reverses abnormal bone remodeling and structure in HPT, 1036

Safety and efficacy of long-term PTH replacement in a pediatric patient with inherited HPT, F217

**Hypoparathyroidism, primary (PHP)**

Influence of PHP on BMD and vertebral morphometry, M190

**Hypophosphatasia (HPP)**

Adult HPP treatment with TPTD, SA468

Autosomal recessive HPP manifesting in utero with long bone deformity but showing spontaneous postnatal improvement, SA562

c.1250A>G, p.N417S is a common American

Enzyme replacement therapy prevents dental defects in the *Akp2*<sup>-/-</sup> mouse model of infantile HPP, F107

Relative efficacy of “treating” versus “preventing” infantile HPP in *Akp2*<sup>-/-</sup> mice by enzyme replacement therapy, 1054

**Hypophosphatasia, pseudo**

c.1250A>G, p.N417S is a common American TNSALP mutation involved in all clinical forms of HPP, including pseudo-HPP, SA566

**Hypophosphatemia**

Clinical usefulness of measurement of FGF-23 in hypophosphatemic patients, SA470

FGF-23 and post-transplant hypophosphatemia: evidence for a causative link, SU168

Increased bone volume and correction of HYP mouse hypophosphatemia in the *Klotho*/HYP Mouse, 1017

MEPE C-terminal ASARM-peptide, promotes hypophosphatemia, bone defects and increases adiposity, F207

Phosphatonins and liver resection-related hypophosphatemia, SU176

Targeted overexpression of the nuclear FGF-2 isoforms in osteoblasts induces hypophosphatemia via modulation of FGF-23 and *Klotho* in mice, 1084

**Hypophosphatemia, X-linked (XLH)**

Aberrant *PheX* function in osteocytes has limited effects on bone mineralization in XLH, 1051

Characterization of the enthesopathy of XLH in the Hyp mouse, SA254

PHEX cleavage of SIBLING-ASARM peptides as a mechanism underlying osteomalacia in XLH, 1199

Rare cases of XLH rickets/osteomalacia mimicking ARHR/osteomalacia, F469

**Hypothalamic amenorrhea.** See *Amenorrhea***Hypothyroidism**

Hypothyroidism and autism combined with PHP in the absence of Albright's hereditary osteodystrophy and *GNAS* imprinting changes, SA259

Hypothyroidism is not deleterious to the skeleton during early fetal development, SA123

**Hypovitaminosis D**

Air pollution might be a neglected risk-factor of hypovitaminosis D, SU306

Efficacy of the Vitamin D supplementation in patients with hypovitaminosis D and HPT2, SU431

Single dose of 100,000 IU D3 appears to be insufficient to achieve desirable levels of 25(OH)D in patients with hypovitaminosis D, SU430

Which is the best oral high-dose Vitamin D<sub>3</sub> regimen for postmenopausal women with hypovitaminosis D?, SU429

**Hypoxia**

Hypoxia promotes ligand-independent activation of the ACVR1 (R206H) mutant receptor in C2C12 cells, M243

**Hypoxia inducible factor (HIF)**

Development of pharmacological HIF activators for fracture healing, SU052

**Hypoxia inducible factor-1 (HIF-1)**

Regulation of autophagy in the epiphyseal growth plate by AMPK and mTOR requires HIF-1, SU134

**Hypoxia inducible factor-1 $\alpha$  (HIF-1 $\alpha$ )**

Evidence that differentiated bone cells display an autophagic response regulated by HIF-1 $\alpha$ , F058

Inhibition of HIF-1 $\alpha$  alone or combined with TGF $\beta$  blockade prevents breast cancer bone metastases, 1085

**Hypoxia-inducible factor-2 $\alpha$  (HIF-2 $\alpha$ )**

CXCL12 expression is regulated by HIF-2 $\alpha$  in MM plasma cells, SU080

**Hypoxia-responsive element (HRE)**

Dwarfism and osteopenia in mice with inactivated HRE in the VEGF gene promoter, 1152

**1 $\alpha$ -hydroxylase**

Dietary normalization of Ca absorption in mice genetically deficient in CaSR and 25(OH)D-1 $\alpha$ -hydroxylase results in non-lethal, severe hyperparathyroidism with reduced osteoclastogenesis, M199

Prediction of osteoporotic fracture risk by 25(OH)D3-1 $\alpha$ -hydroxylase (CYP27B1) gene, M263

**I****I $\kappa$ B kinase  $\beta$  (IKK $\beta$ )**

Ubiquitin-like domain of IKK $\beta$  is critical for osteoclastogenesis, SU112

**I $\kappa$ B- $\alpha$** 

Proteasome inhibitors attenuate osteoclastogenesis and bone resorption via the modulation of RANK-mediated TRAF6, p62 and I $\kappa$ B- $\alpha$  signaling cascades, SA099

**Ibandronate (IBN)**

Comparison of the effects of IBN alone with IBN in combination with SNAC on bone density and bone strength in OVX rats, SU391

Cost-effectiveness of IBN therapy for women with postmenopausal osteoporosis with respect to nonvertebral fracture efficacy, SA429

Cost-effectiveness of RIS versus IBN at one year: the case of the United Kingdom, SA424

Cost-effectiveness of RIS versus IBN at one year: the case of Germany, SA425

Efficacy and safety of monthly oral IBN in postmenopausal women with low bone density, SU384

Fracture risk in women aged 65 years or older with once-monthly oral IBN compared with weekly bisphosphonates, M367

Fracture risk with once-monthly oral IBN compared with weekly bisphosphonates, SU408

HSA based on DXA data in women with postmenopausal osteoporosis receiving once-monthly oral IBN for 12 months, SA507

Intravenous IBN for prevention of early bone loss after kidney transplantation, F413

Modeled cost-effectiveness of RIS versus IBN: the case of Italy, SA427

PINP, a new available rat bone formation marker: usefulness in osteopenia studies due to androgen lack and IBN treatment, SA299

QCT and FEA assessment of proximal femur bone quality and strength in women with postmenopausal osteoporosis receiving once-monthly oral IBN for 12 months, SA509

Quarterly intravenous IBN acid in the community setting in England, SU409

Regional differences of femoral BMD changes after one year once-monthly IBN as measured by 3D QCT, SU260

**Ibuprofen**

Bone resorption and articular cartilage degenerative changes following performance of high repetition high force tasks are attenuated by secondary ibuprofen treatment, SA532

**IC162**

IC162, a new flavonoid, preserves bone mass and microarchitecture without affecting uterine weight in OVX rats, SA386

**Icariin**

Bone anabolic effects of icariin and total flavonoid fraction of *Herba epimedii* in OVX mice, M337

Icariin induces osteogenic differentiation in vitro in a BMP- and Runx2- dependent manner and bone regeneration in vivo, M089

**ICTP**

Bone degradation marker CTX shows unique properties in disease monitoring compared to NTX, ICTP and bALP in MM, M287



**Idiopathic juvenile osteoporosis (IJO).** See*Osteoporosis***Idiopathic multicentric osteolysis with****nephropathy (IMON).** See *Osteolysis***IDS Automated Analyser 3x3™**

Development of a bone specific ALP assay on the IDS Automated Analyser 3x3™, SA302

Development of a new N-Mid® osteocalcin immunoassay on the IDS Automated Analyser 3x3™, SA303

New 25(OH)D assay on the IDS Automated Analyser 3x3™, SU200

New intact PTH assay on the IDS Automated Analyser 3x3™, M209

**IFN-β**IFN-β is a key molecule in inhibition of human osteoclast differentiation by 1α,25-dihydroxyvitamin D<sub>3</sub>, SU090**IFN-γ**

IFN-γ inhibits TNFα-induced osteoclastogenesis in vitro and in vivo, SU152

**Ihh**

Chondrocyte-derived Ihh is required for osteoblast differentiation despite reconstitution of a normal growth plate, 1154

**IL6**Genetic variation in *IL6* and *LRP5* is associated with osteoporosis in the Marshfield Clinic Personalized Medicine Project, SU365**Iliac crest**

Serum 25(OH)D measurement and histomorphometric analysis of iliac crest biopsies from 1180 patients reveals a high prevalence of Vitamin D-dependent osteomalacia, 1134

**Imatinib (IM)**

Influence of IM on bone remodeling in juvenile mice, SA292

**Immune system**

Important contribution of the immune system in regulating the tumor/bone vicious cycle independent from osteoclasts, 1086

Key mechanism underlying the immunosuppressive effects of Vitamin D: 1,25(OH)<sub>2</sub>D<sub>3</sub> is a transcriptional modulator of IL-17, F246

PTHrP is processed by skin keratinocytes and has immunomodulation properties, SA216

**Indapamid**

ALN and indapamid alone or in combination in the management of IHC associated with osteoporosis, 1245

**Indolent systemic mastocytosis (ISM).** See*Mastocytosis***Infantile osteopetrosis (IO).** See *Osteopetrosis***Infections, bacterial**

Novel modification of bone grafts inhibits bacterial colonization, M169

**Infections, viral**

Cortical and trabecular microarchitecture in HIV-infected postmenopausal women, SU458

Determinants of low BMD in HIV infected postmenopausal women, SU455

Prevalence and incidence of viral infections among musculoskeletal tissue donors and first-time blood donors, SA549

Randomized controlled trial of Vitamin D3 supplementation for the prevention of viral upper respiratory tract infections, M217

Vitamin D insufficiency is common in racially diverse postmenopausal women with HIV, M448

**Inhibin**

Inhibin directly targets suppression of isolated human osteoclast precursor development and activity, SA086

Physiological concentrations of inhibin A are anabolic, affecting both trabecular and cortical bone in normal intact mice, M177

**Inpp4b**

Inpp4b as a regulator of bone mass, F089

**Insulin**

Intermittent injection of recombinant osteocalcin improves glucose tolerance and insulin sensitivity, F168

Sympathetic tone mediates leptin's inhibition of insulin secretion by modulating osteocalcin bioactivity, F034

**Insulin-like growth factor binding protein 2 (IGFBP2)**

IGFBP2 and bone loss in aging women and men, 1284

**Insulin-like growth factor binding protein 3 (IGFBP3)**

Association study of the TF and IGFBP3 gene polymorphisms with an osteonecrosis of femoral head in Korean population, SU226

**Insulin-like growth factor binding protein 5 (IGFBP5)**

NFI transcription factors regulate IGFBP5 gene transcription in human osteoblasts, SU015

**Insulin-like growth factor binding protein 6 (IGFBP6)**

IGFBP6 Is a negative regulator of osteoblast differentiation and bone formation, SA182

**Insulin-like growth factor-1 (IGF-1)**

Age-related changes in BMD, cross-sectional area and the strength of rat femur; an involvement of suppression of GH-IGF-1 signaling, SA467

Alterations in bone structure and growth in dwarf rats with a depressed GH/IGF-I axis, SA178

BMP-6 from bone regulates serum glucose via IGF-1 released from pancreas, SU141

Endocrine IGF-1 maintains linear growth in the total absence of tissue IGF-1, SA184

IGF-1 secreted from osteoblasts as a major chemotactic factor for osteoblasts, SA179

Mice lacking the GH receptor in liver have normal skeletal growth and bone volume despite virtual absence of circulating IGF-1, F181

Overcoming the zone of chondrocyte death associated with osteochondral harvest by sequential treatment with collagenase and IGF-1, SU129

Serum IGF-1 is a developmental determinant of bone size, SA183

Study of hGH and IGF-1 receptors in the human fetal femoral growth plate, SU128

Tissue-specific KO of the CaSR in chondrocytes inhibits IGF-1 signaling and delays differentiation in the growth plate, 1261

Twist1 haploinsufficiency is associated with reduced IGF-1 levels and an osteoporotic phenotype, SU029

**Insulin-like growth factor-2 (IGF-2)**

Bone length was differentially promoted in the left/right hindlimbs with knee loading and administration of IGF-2, M476

**Insulin-like growth factor-I (IGF-I)**

Ablation of IGF-I signaling in osteoprogenitors decreases bone formation and blunts the skeletal response to PTH, 1193

Age-related impairment of IGF-I receptor activation is associated with changes in integrin and SHP-2 expression, M096

Concentration of IGF-I in human cortex bone is highly correlated with fracture toughness of the bone, 1069

Dried plum polyphenols increase IGF-I production in osteoblast-like cells, SU002

Is GH/IGF-I mediated mechanism involved in regulating gender differences in bone size?, SA180

Low serum IGF-I alters the cortical bone response to estrogen deficiency, SU190

**Integrin**

Age-related impairment of IGF-I receptor activation is associated with changes in integrin and SHP-2 expression, M096

Disruption of the syndecan-1/integrin axis is a novel target for myeloma therapy, 1229

Integrin mediated mechanical forces stimulate differentiation of MSCs, SA528

Integrin-associated protein upregulates osteogenesis-related transcription factors via TGFβ and BMP pathways, SA028

Mechanical perturbation of integrin α5 with or without association with fibronectin opens Cx43-hemichannels in osteocytes, SA060

**Integrin associated protein (IAP)**

CD47 (IAP) is an important modulator of osteoclast and osteoblast differentiation in vitro and in vivo, F093

**Integrin-linked kinase (ILK)**

Inactivation of the ILK in osteoblasts increases mineralization, M061

**Interferon γ (INFγ)**

INFγ attenuates BMP-2 signaling via Stat-1 binding of Smad4 in the cytoplasm, SU139

Low dose administration of INFγ stimulates osteoblastogenesis and prevents ovariectomy-induced osteoporosis in C57BL/6 mice, M334

**Interleukin-1 (IL-1)**Three RANK cytoplasmic motifs, IVVY<sup>535-538</sup>, PVQEET<sup>559-564</sup> and PVQEQQ<sup>604-609</sup>, play a critical role in TNFα/IL-1-mediated osteoclastogenesis, 1118**Interleukin-1α (IL-1α)**

Betulin down regulates IL-1α-stimulated aggrecanases and MMP gene expression in human chondrocytes, M147

OAH19, an ethanol extract from combined two herbs, inhibits IL-1α-induced expression of MMP-1 and MMP-13 in OA human cartilage and synovial fibroblast, M148

**Interleukin-1β (IL-1β)**

Elevated production of IL-1β and TNFα by PBMC is associated with increased hip fracture risk in elders, 1283

HDAC inhibitors suppress IL-1β-induced NO and PGE<sub>2</sub> production in human chondrocytes, SU116

IL-1β-induced hepcidin expression in synovial membranes of patients with OA is associated with TNFα repression, SU157

TNFα and IL-1β stimulate ALP activity and mineralization but decreases RUNX2 expression and osteocalcin secretion in human MSC, SU044

**Interleukin-6 (IL-6)**High levels of IL-6 and hyper-responsivity to 1,25(OH)<sub>2</sub>D<sub>3</sub> are both required for development of Pagetic osteoclasts, F478

Increased proinflammatory cytokines TNF-α and IL-6 correlate with pathological bone turnover markers in diabetic patients with acute Charcot foot, F491

Mab21 suppresses the osteogenic markers by recruiting Sin3A and stimulates osteoclast by up-regulation of IL-6 and LIF, SU022

Rapid-nontranscriptional action of 1,25(OH)<sub>2</sub>D<sub>3</sub> induces IL-6 production in osteoclast precursors expressing MVNP, 1186**Interleukin-8 (IL-8)**

Distinct biological activity of IL-8 isoforms, SU162

Systemic IL-8 increases bone resorption in vivo, 1234

**Interleukin-12 (IL-12)**

IL-12 induces apoptosis in TNFα-mediated osteoclastogenesis in vivo, SA166

IL-12 stimulates the OIP-1 gene expression in CD4<sup>+</sup> T-cells, SA173**Interleukin-17 (IL-17)**Key mechanism underlying the immunosuppressive effects of Vitamin D: 1,25(OH)<sub>2</sub>D<sub>3</sub> is a transcriptional modulator of IL-17, F246**Interleukin-23 (IL-23)**

Grape seed extract suppresses IL-23/Th17 inflammatory pathways and bone destruction in CIA, SU093

Rheumatoid synoviocytes are stimulated with IL-23 to enhance osteoclastogenesis through upregulation of RANKL expression, SU084

**Interleukin-27 (IL-27)**

Effects of IL-27 on regulation of osteoclastogenesis by way of T cells, SU081

## Key Word Index

## ASBMR 30th Annual Meeting

IL-27/WSX-1 signaling inhibits RANKL-induced osteoclastogenesis through STAT1 activation: a possible involvement in TLR4/MyD88-mediated inflammatory arthritis, SU102

**Inulin, agave**

Effects of agave inulin on Ca metabolism in Japanese young adults, M332

**Iron (Fe)**

PGC-1 $\beta$  and iron uptake in the mitochondrial activation of osteoclasts, L222

**IRX3**

Identification of IRX3 a novel transcription factor during BMP-2 mediated osteoblast differentiation, SU024

**Isoflavones**

Early exposure to soy isoflavones modulates bone mineral, strength and microarchitecture in CD1 mice, M503  
Evaluating the effect of soy and isoflavones on BMD in older women, M353  
Neonatal exposure to soy isoflavones attenuates deterioration of bone tissue in female but not male mice after cessation of sex steroid production, SU476

**Isotropy, resolution**

Implications of resolution isotropy on apparent topology of trabecular bone architecture in MRI, SU280

**IVVY**

Three RANK cytoplasmic motifs, IVVY<sup>535-538</sup>, PVQEET<sup>559-564</sup> and PVQEQG<sup>604-609</sup>, play a critical role in TNF $\alpha$ /IL-1-mediated osteoclastogenesis, L118

**J****Jagged1**

Jagged1 stimulation by PTH(1-34) in mature osteoblasts is not required for HSC expansion, L078

**Jak2**

AG490, a Jak2 specific inhibitor, induces osteoclast survival by activating Akt and ERK signaling pathway, SU108

**Japanese Population-based Osteoporosis (JPOS) Cohort Study**

Effect of parity on BMD in premenopausal women, SA325  
Ten-year change in BMD in a representative sample of Japanese women, SA330

**JDM. See Dermatomyositis****JNK. See c-Jun N-terminal kinase****Jumonji**

Regulation of the osteoblast-specific transcription factor Osx by NO66, a Jumonji family histone demethylase, F017

**Jun activation-domain binding protein (Jab1)**

Characterization of Jab1-interacting motif in LMP-1, SA023

**JunB**

Age-related bone loss in mice associated with ubiquitin ligase Smurf1 degradation of JunB protein and reduced osteoblast proliferation, L113

**JunD**

Coactivator MBF1 binds to JunD and protects its transcriptional activity against oxidative stress to prevent age-related suppression of osteoblast differentiation, L248

**K****K/BxN**

Deficiency of the nucleocytoplasmic shuttling protein CIZ suppresses K/BxN serum-induced model of RA, M446

**Kallikrein-4 (KLK-4)**

Identification of DPP-I as a potential activator of KLK-4, SA155

**Kenney-Caffey syndrome**

Kenney-Caffey syndrome in a Caucasian man, SA464

**Keratinocytes**

1,25(OH)<sub>2</sub>D<sub>3</sub> is as effective as 1,25(OH)<sub>2</sub>D<sub>3</sub> in regulating cellular proliferation in cultured normal human keratinocytes and transformed prostate cells, M215

PTHrP is processed by skin keratinocytes and has immunomodulation properties, SA216

**Kidney disease, chronic (CKD)**

25(OH)D levels in children with CKD as measured by tandem mass spectrometry, SU485

Comparison of 1,25(OH)<sub>2</sub>D<sub>3</sub> and calcitriol effects in an adenine-induced model of CKD reveals differential control over serum Ca and phosphate, SU448

Glomerular filtration rate and physical function in community-dwelling Japanese frail elderly, SA332

Interactions between obesity, CVD and bone formation, M451

Kidney disease is associated with abnormal cortical geometry independent of age and gender, SU441

Osteopenia in CKD: effects of Ca overload, SU449

Osteopenia in CKD: effects of phosphate overload, SU447

Patients with CKD and low 1/3 radius and femoral neck BMD have markedly abnormal cortical and trabecular microstructure by HR-pQCT, L033

Potential role of FGF-23 in CKD-MBD, WG30

Protective actions of Vitamin D analogs in the vascular calcification of CKD, SU450

Relationship between Vitamin D and PTH: serum Ca and Mg are major determinants of PTH in patients with mild CKD, M211

**Kidney dysfunction**

Kidney dysfunction disturbs collagen maturation in ABD as assessed by confocal laser Raman spectroscopy, SU439

**Kidney transplantation**

Application of a treatment algorithm to avoid BMD loss and limit bisphosphonate use after kidney and kidney/pancreas transplantation, SA497

Bone metabolism in long-term kidney transplantation recipients, SA499

Change of pathological bone lesion in recipients with renal osteopathy after renal transplantation, SA498

Intravenous IBN for prevention of early bone loss after kidney transplantation, F413

Pretransplant parathyroid function predicts laboratory and BMD changes after kidney and kidney/pancreas transplantation, L032

**KIMS Survey**

FGF-23 and parameters of Ca and bone metabolism are positively influenced by GH replacement in adult GH deficiency patients from the KIMS survey, SU177

**Kremen-1 (Krm-1)**

Deletion of the Dkk-1 Krm-1 and Krm-2 in mice leads to increased bone formation and bone mass, L004

**Kremen-2 (Krm-2)**

Deletion of the Dkk-1 Krm-1 and Krm-2 in mice leads to increased bone formation and bone mass, L004

Transgenic overexpression of the Wnt antagonist Krm-2 in osteoblasts leads to severe impairment of bone formation and increased bone resorption, L003

**Krox-20**

Mechanical loading upregulates expression of the transcription factor EGR2/Krox-20 by a COX-2-mediated mechanism, SA526

**Kyphoplasty, balloon**

Randomized trial of balloon kyphoplasty and nonsurgical care for acute vertebral fracture, L243

**Kyphosis**

Does ALN use prevent kyphosis progression in older women?, SA410

Factors associated with kyphosis progression in older age, F365

**Kyphosis, thoracic**

Sr ranelate prevents the progression of thoracic kyphosis in postmenopausal women with osteoporosis, L241

Thoracic kyphosis index as a risk factor for incident vertebral fractures and alteration of quality of life in postmenopausal women with osteoporosis, L130

**L****L-amino acids**

Molecular basis of PHPT: adenomatous parathyroid cells are resistant to L-amino acids, M203

**L-serine (L-Ser)**

Novel role of L-Ser for the activation of RANKL-RANK signaling machinery in osteoclastogenesis in vitro, SA082

**L29**

Gender-specific changes in bone microstructure of mice lacking ribosomal protein L29/HIP, SA133

**L527del**

Human SLC34A3/NaPi-IIc mutations T137M and L527del uncouple Na-phosphate co-transport, F471

**Lactation**

Extended lactation is associated with failure to restore BMD 6 months after resumption of menstrual cycle, M305

Lack of calcitonin accentuates bone loss during lactation by enhanced osteoclast formation and reduced osteoblast formation, SA194

Osteocytic perilacunar remodeling as a significant source of Ca during lactation, M110

**Lactoferrin**

Mechanism of action of lactoferrin's bone anabolic activity, SA175

**Lactose intolerance**

Lactose intolerance does not have effect on bone status in adolescence, SU285

**Lamellar bone**

Changes in chemical, mechanical, and structural properties of lamellar bone during young adulthood, SU475

**Lamin A/C**

Impaired bone formation in mice lacking lamin A/C activation leads to severe osteopenia, F131

Inhibition of lamin A/C attenuates osteoblast differentiation and stimulates osteoclastogenesis through enhanced RANKL signaling, M070

**Lasofloxifene (LASO)**

Effects of LASO on bone turnover markers, L287

Effects of LASO on fractures and breast cancer, L288

Randomized double blinded controlled trial of individual response in biochemical markers of bone turnover to LASO therapy, M507

**Latexin (Lxn)**

Lxn is a novel effector of BMP-2 signaling in modulation of chondrocyte differentiation, SU117

**LCT**

13910C>T LCT promoter polymorphism in the Spanish population, M265

**LDLR-/-**

OPN deficiency reduces aortic calcification and oxidative stress in diabetic LDLR-/- mice, F109

**Lead (Pb)**

Effect of Pb on bone mineral properties from female adult C57/BL6 mice, M146

**Lef**

Negative regulation of Tcf/Lef-dependent transcription by the BMP/Smad4 signaling axis, SU144

**Leg lean mass**

Bivariate whole genome linkage analysis of femoral bone geometric traits and leg lean mass, M249

**LEPREI**

Hotspot splicing mutation in *LEPRE1* affects P3H1 and causes recessive OI, SU215

**Leptin**  
Central and peripheral leptin treatment produce similar increase in cortical and trabecular bone mass in ob/ob mice, SU164  
Sympathetic tone mediates leptin's inhibition of insulin secretion by modulating osteocalcin bioactivity, F034

**Letrozole**  
ALF prevents aromatase inhibitor (letrozole)-induced bone mineral loss in young growing female rats, SA570

**Leukemia, acute lymphoblastic (ALL)**  
Advanced vertebral compression at diagnosis among children with ALL, SU483

**LIA.** See *Diasorin Liaison*

**LIF**  
Mab21 suppresses the osteogenic markers by recruiting Sin3A and stimulates osteoclast by up-regulation of IL-6 and LIF, SU022

**Ligament, anterior cruciate (ACL)**  
Bone geometry and bone strength are compromised in patients with ACL reconstruction, M487

**Ligamentum flavum**  
Osteogenesis effect of human ligamentum flavum, myoblast, osteoblast and MSC by DBM and BMP-2, SU135

**Light scattering**  
Non-invasive detection of bone microdamage by light scattering, M462

**LIM kinase 1 (LIMK1)**  
Role of LIMK1 in osteoclast cytoskeletal remodeling and bone resorption, 1116

**LIM mineralization protein (LMP)**  
Identification and analysis of human LMP gene promoter region, M034

**LIM mineralization protein-1 (LMP-1)**  
Characterization of Jab1-interacting motif in LMP-1, SA023  
LMP-1, positive regulator in osteolineage differentiation of human PDL fibroblasts, M051

**Limb-bud and heart (Lbh)**  
Overexpression of the transcriptional cofactor Lbh impairs angiogenesis and endochondral bone formation during fetal bone development in chickens, SU004

**Lipodystrophy**  
Progressive lipodystrophy in the osteosclerotic mice over-expressing Fra1, 1149

**Lipopolysaccharide (LPS)**  
Differential contribution of osteoclast- and osteoblast-lineage cells to LPS modulation of osteoclastogenesis, SU088  
LPS suppresses RANK gene through the down-regulation of PU.1 and MITF, SU083  
LPS-induced inhibition of osteogenesis is TNF $\alpha$  dependent, M019  
RANKL-mediated osteoclast lineage commitment dictates the role of LPS in osteoclast differentiation, SA088

**Lipoproteins**  
Low density lipoprotein-cholesterol levels affect vertebral fracture risk in female patients with PHPT, SA484

**5-lipoxygenase (5-LO)**  
Chondrocyte differentiation is differentially affected by COX-2 and 5-LO during fracture healing, SU123

**Lithium (Li)**  
Li affects matrix mineralization by decreasing tissue non-specific ALP levels in osteoblasts, SA071

**Lithocholic acid**  
Lithocholic acid downregulates the effects of Vitamin D<sub>3</sub> on primary human osteoblasts, SA030

**Liver transplantation**  
Effect of RIS in liver transplantation patients with low bone mass, SA503  
Marked Vitamin D deficiency in recent heart and liver transplant recipients, SA501

Retrospective study evaluating the relationship of Vitamin D 25 OH and free testosterone levels with changes in hip bone density after liver transplantation, SA502

**Liver X receptors**  
Cholesterol sensing receptors, Liver X receptor  $\alpha$  and  $\beta$ , have novel and distinct roles in osteoclast differentiation and activation in bone, F085

**Liver-enriched inhibitory protein (LIP)**  
Cooperativity between VDR and LIP in the regulation of TRPV6 identifies a novel function for LIP as a transcriptional activator, SU198

**LMMS.** See *Low magnitude mechanical stimulations*

**LNcaP**  
Stat3 induces osteoblastic bone metastases through up-regulating the expression of Shh and a Ca channel TRPM8 in the LNcaP human prostate cancer cells, 1089

**Long bones**  
Altered long bone structure in recessive null and dominant negative Cx43 (*Gjal*) mouse mutants, 1110  
Autosomal recessive HPP manifesting in utero with long bone deformity but showing spontaneous postnatal improvement, SA562  
DHCR24 gene is mandatory for the proper growth of long bone, SU118  
Distinctive anabolic roles of 1,25(OH)<sub>2</sub>D<sub>3</sub> in teeth and mandible versus long bones, M213  
Enhanced osteogenic potential of alveolar vs. long bone derived BMSC, M095  
Over-expression of CNP enhances the formation of long bone exostoses in Ext1<sup>+/+</sup> mice, SU130  
Quantitation of bone marrow fat in long bones of mice using MRI or  $\mu$ CT, M145

**Losartan®**  
Losartan® (Cozaar) increases appendicular bone formation by inhibiting osteoclastogenesis, M126

**Lovastatin (LV)**  
LV best enhances fracture repair when administered one week post-fracture, 1300

**Low intensity pulsed ultrasound (LIPUS).** See *Ultrasound*

**Low magnitude mechanical stimulations (LMMS)**  
"Vibes" Trial: LMMS to improve BMD, M397

**Low-density lipoprotein receptor related protein 5 (LRP5)**  
BMD-associated SNP lies in a Runx2 binding site of the LRP5 promoter, M264  
Bone formation in mice with variations in Lrp5 expression, F550  
Bone loss with smoke exposure and Lrp5 expression, SA459  
Bone response to mechanical loads and Lrp5 genotype, M020  
G171V and A214V Lrp5 knock-in mice have increased bone mass and strength, and can help precisely define the in vivo functions of Lrp5 during bone growth and homeostasis, 1002  
Kinase activation and osteocyte survival promoted by mechanical stimulation require LRP5/6 signaling and  $\beta$ -catenin accumulation, but not  $\beta$ -catenin/TCF-dependent transcription, M108  
LRP5 G171V mutation and tobacco smoke related bone fragility, M323  
Prediction of fracture risk by LRP5 gene haplotype, SU222  
PTH receptor signaling in osteocytes increases bone mass and the rate of bone remodeling through Wnt/LRP5-dependent and -independent mechanisms, respectively, 1038  
PTH signaling through LRP5/6 in osteoblasts, 1014  
In vivo load activated propagation of  $\beta$ -catenin signaling in osteocytes through coordinated downregulation of inhibitors of Lrp, 1041

Wnt/LRP5-independent inhibition of osteoblastic cell differentiation by SCT, 1256

**Low-density lipoprotein receptor related protein 6 (LRP6)**  
Kinase activation and osteocyte survival promoted by mechanical stimulation require LRP5/6 signaling and  $\beta$ -catenin accumulation, but not  $\beta$ -catenin/TCF-dependent transcription, M108  
Lrp6 loss of function impacts bone homeostasis and responds to folate supplementation, F253  
PTH signaling through LRP5/6 in osteoblasts, 1014

**LRP5**  
Genetic variation in *IL6* and *LRP5* is associated with osteoporosis in the Marshfield Clinic Personalized Medicine Project, SU365  
Genetic variation in *LRP5* associates with metabolic characteristics in healthy prepubertal children, 1176

**Lrp5**  
Osteoblast-specific deletion of *Lrp6* reveals distinct roles for *Lrp5* and *Lrp6* in bone development, 1001

**Lrp6**  
Osteoblast-specific deletion of *Lrp6* reveals distinct roles for *Lrp5* and *Lrp6* in bone development, 1001

**Lung disease**  
Effects of intermediate doses of GCs on bone turnover and circulating Dkk-1, MIF, sRANKL and OPG in patients with interstitial lung disease, SA451

**Lupus**  
Are there any ethnic differences in BMD in a lupus cohort?, SU358

**Luteolin**  
Effect of luteolin on bone loss, microarchitecture and bone resorption in OVX mice, M128

**Lymphocytes**  
Increased expression of OPN in PBMC is associated with alteration in the fractions of lymphocytes in hindlimb-unloaded mice, M175

**Lymphoid enhancer binding factor-1 $\delta$ N (Lef-1 $\delta$ N)**  
Overexpression of Lef-1 $\delta$ N increases bone mass in mice, 1258

**Lyn**  
Lyn, opposite to c-Src, negatively regulates osteoclastogenesis in vitro and in vivo via its interaction with SHP-1 and Gab2, 1119

**Lysophosphatidic acid (LPA)**  
LPA enhances the viability of rat growth plate chondrocytes through the inhibition apoptosis and the promotion of cellular maturation, SU156  
LPA regulates osteoclast survival and retraction, SU105

**Lysosomal proteins**  
Identification of osteoclast lysosomal proteins by mass spectrometry, SA077

## M

**M-CSF**  
BMSC up-regulate M-CSF receptor in monocytes to disrupt dendritic cell differentiation while facilitating osteoclastogenesis in myeloma, SU242  
Recombinant mouse M-CSF receptor C-fms inhibits TNF $\alpha$ -induced osteoclastogenesis, M112  
Vimentin binds c-Fms in an M-CSF dependent manner and regulates osteoclast differentiation, SU097

**Mab21**  
Mab21 suppresses the osteogenic markers by recruiting Sin3A and stimulates osteoclast by up-regulation of IL-6 and LIF, SU022

**MafB**

## Key Word Index

## ASBMR 30th Annual Meeting

All-*trans*-retinoic acid (Vitamin A) increases expression of MafB and inhibits osteoclast formation by interfering with differentiation of osteoclast progenitor cells, M117

**Magnesium (Mg)**  
Importance of melastatin-like transient receptor potential 7 and Mg in the stimulation of osteoblast proliferation and migration by platelet-derived growth factor, M008  
Relationship between Vitamin D and PTH: serum Ca and Mg are major determinants of PTH in patients with mild CKD, M211

**Magnetic resonance imaging (MRI)**  
Estimation of relative stiffness contributions of cortical and trabecular compartments by MRI-based FEA, SU481  
Grayscale MRI based finite element mechanical modeling of trabecular bone at in vivo resolution, SU277  
Identification of skin abnormalities in OI patients by MRI, SA561  
Implications of resolution isotropy on apparent topology of trabecular bone architecture in MRI, SU280  
Proximal femoral fragility and age-related white matter lesions by brain MRI in elderly subjects, 1096  
Quantitation of bone marrow fat in long bones of mice using MRI or  $\mu$ CT, M145  
Reciprocal relation between MR measures of marrow adiposity and cortical bone in the appendicular skeleton of healthy adults, SU042  
Reduction of MRI processing time for assessment of trabecular bone microarchitecture, SU282  
Solid-state  $^{31}\text{P}$  MRI quantifies mineralization changes in OVX rat bone, M422  
In vivo bone matrix density measurements by water and fat suppressed projection MRI (WASPI), SA102

**Magnetic resonance imaging, micro ( $\mu$ MRI)**  
Evaluation of the detection sensitivity of simulated trabecular bone loss in  $\mu$ MRI at in vivo resolution, M312  
Feasibility and reproducibility of in-vivo assessment of trabecular bone architecture using  $\mu$ MRI-based method at multiple study centers, SA314  
Twelve month changes in trabecular microarchitecture assessed by  $\mu$ MRI in postmenopausal women on antiresorptive versus anabolic therapy, 1020

**Malnutrition**  
Association of the marker of ABD with malnutrition-inflammation complex in hemodialysis patients, SU446

**Mammary glands.** See also *Cancer, breast*  
Bzb, a proteasome inhibitor, prevents metastatic breast cancer osteolysis and reduces mammary fat pad tumor growth in mice, F277  
Ectopic Runx2 expression disrupts normal acini structure in mammary epithelial cells, F279  
PTHrP regulates mammary gland ductal elongation during puberty, F228  
PTHrP-induced Wnt signaling specifies the mammary mesenchyme, F219

**Mandible**  
Distinctive anabolic roles of  $1,25(\text{OH})_2\text{D}_3$  in teeth and mandible versus long bones, M213

**MAP kinase**  
Both the Smad and ERK MAP kinase pathway play critical roles in BMP-2-induced osteogenic transcription factors expression, M050

**MAP kinase phosphatase-1 (MKP-1)**  
Effect of MKP-1 deletion on the fluid shear stress induction of COX-2 expression in osteoblasts, SA529  
MKP-1 is an endogenous negative regulator of pro-inflammatory cytokines in BMSC, SU013

MKP-1 protects bone mass via negative regulation of osteoclast differentiation and activation, 1219

**MAPK.** See *Mitogen-activated protein kinase*

**Marrow.** See *Bone marrow*

**Marshfield Clinic Personalized Medicine Project**  
Genetic variation in *IL6* and *LRP5* is associated with osteoporosis in the Marshfield Clinic Personalized Medicine Project, SU365

**MASTER**  
Continued evidence for safety and efficacy of RIS in men with osteoporosis, M360

**Mastocytosis, indolent systemic (ISM)**  
Prevalence of osteoporosis in ISM, SU268

**Matrix extracellular phosphoglycoprotein (MEPE)**  
MEPE C-terminal ASARM-peptide, promotes hypophosphatemia, bone defects and increases adiposity, F207  
MEPE expression is regulated by BMP-2 signaling through the activation of its downstream transcription factors, *Dlx3*, *Dlx5* and *Runx2*, SA064  
MEPE regulates bone remodelling independent of serum phosphate and alters renal vascularization, F205

**Matrix metalloproteinase (MMP)**  
Analysis of long bone fracture nonunion by an expression profile of the MMPs and ADAMTS enzyme families, M235  
Betulin down regulates *IL-1 $\alpha$* -stimulated aggrecanases and MMP gene expression in human chondrocytes, M147  
Effects of beta-D-glucopyranoside from *Phellodendron Amurense* on the production of inflammatory cytokines, growth factors, MMP, and on bone markers in human subchondral OA osteoblasts, SA117  
Inhibition of MMP activity delays bone repair whereas inhibition of osteoclast function and formation does not, SA075

**Matrix metalloproteinase-1 (MMP-1)**  
OAH19, an ethanol extract from combined two herbs, inhibits *IL-1 $\alpha$* -induced expression of MMP-1 and MMP-13 in OA human cartilage and synovial fibroblast, M148  
PGD2 downregulates MMP-1 and MMP-13 expression in human OA chondrocytes, SA152

**Matrix metalloproteinase-2 (MMP-2)**  
Regulation of parameters of bone quality by MMP-2 and MMP-9, 1144

**Matrix metalloproteinase-9 (MMP-9)**  
Regulation of parameters of bone quality by MMP-2 and MMP-9, 1144

**Matrix metalloproteinase-13 (MMP-13)**  
Novel MMP-13-derived peptides demonstrate non-covalent interaction of MMP-13 with the TGF $\beta$  large latent complex, 1189  
OAH19, an ethanol extract from combined two herbs, inhibits *IL-1 $\alpha$* -induced expression of MMP-1 and MMP-13 in OA human cartilage and synovial fibroblast, M148  
PGD2 downregulates MMP-1 and MMP-13 expression in human OA chondrocytes, SA152

**MBF1**  
Coactivator MBF1 binds to JunD and protects its transcriptional activity against oxidative stress to prevent age-related suppression of osteoblast differentiation, 1248

**MC3T3-E1**  
Chemical composition and nanoscale structure of RIS-treated mineralizing MC3T3-E1 cells, M023  
PTH induces COX-2 in MC3T3-E1 osteoblasts via cAMP-PKA and Ca-calcineurin pathways, SA033  
Regulation of intracellular signaling of MC3T3-E1 osteoblasts by the extracellular matrix, SA139  
Silencing of PDIA3 (ERp60) reduces the rapid membrane response to  $1,25(\text{OH})_2\text{D}_3$  in MC3T3-E1 osteoblast-like cells, M227

**MC3T3-L1**

Effect of resveratrol and flax oil on MC3T3-L1 pre-adipocyte and ST2 BMSC proliferation and differentiation, SU059

**MCSA.** See *Muscle cross-sectional area*

**Measles virus nucleocapsid protein (MVNP)**  
Co-expression of p62<sup>392L</sup> and MVNP in osteoclast precursors increases the formation of osteoclasts that express a pagetic phenotype, F476  
Rapid-nontranscriptional action of  $1,25(\text{OH})_2\text{D}_3$  induces *IL-6* production in osteoclast precursors expressing MVNP, 1186

**Mechanical loading**  
Anabolic response to skeletal loading in mice with targeted disruption of PTN gene, 1142  
Androgen receptor disruption increases the osteogenic response to mechanical loading in male mice, 1140  
Bone cell response to neurotransmitters and mechanical loading, SA009  
Bone strength in overweight children is adapted to mechanical loads from walking, but is low for higher loading activities, M482  
Cost-effective rack and pinion system for torsion testing of rodent bones, M465  
Effects of a targeted bone and muscle loading program on QCT bone geometry and strength, muscle size and function in older men, 1244  
Inhibition of bone biomechanical response to physical activity and loading in mice lacking periostin, 1143  
Intermittent, short duration cyclic loading attenuates disuse osteoporosis without affecting resorption, M483  
Kinase activation and osteocyte survival promoted by mechanical stimulation require LRP5/6 signaling and  $\beta$ -catenin accumulation, but not  $\beta$ -catenin/TCF-dependent transcription, M108  
Load induced changes in trabecular and cortical bone are dose dependent in both C57BL/6 and C3H/HeJ mice, F527  
Loading duration influences the degree of inhibition of bone loss using dynamic muscle stimulation in a disuse rat model, 1297  
Mechanical loading prevents bone loss due to hormone-deficiency in female mice, M474  
Mechanical loading upregulates expression of the transcription factor *EGR2/Krox-20* by a COX-2-mediated mechanism, SA526  
Mechanical unloading partially rescues hypophosphatemic rickets in *Dmp1*-null mice, 1162  
Microdamage repair and remodeling requires mechanical loading, 1299  
Osteogenic potential of bone marrow, compromised by disuse, is normalized by brief exposure to a low-level mechanical signal, M486  
SDF-1 is expressed in osteocytes and periosteal cells in response to mechanical loading, M105  
Transcriptional regulation of *Cx43* by  $\beta$ -catenin, a pathway activated by PGE $_2$ -PI3K-GSK3 signaling in mechanically loaded osteocytes, 1042

**Mechanical stimuli, low magnitude (LMMS)**  
Risk factors for bone fracture, elevated by 90-days of bed rest, are reduced by daily exposure to LMMS, M342

**Mechanography**  
Jumping mechanography safely evaluates muscle performance in older adults, SA535

**Mecp2**  
Mecp2 null mice display multiple skeletal abnormalities, M242

**Medical records, electronic**  
Electronic medical record based "ALERT System" improved diagnosis and treatment of osteoporosis in orthopaedic out-patient clinic, SU416

**Medicare**  
Excess medical cost after a fragility fracture during 3-year follow-up, SA422

Physician practices in bone density testing among Medicare patients, SA428  
 Reimbursement for BMD testing among US Medicare beneficiaries, SA326

**Medications**  
 Comparative gastrointestinal safety of weekly oral bisphosphonates, M358  
 Differences in safety and efficacy of generic and original branded once weekly bisphosphonates, M359  
 Exploring the effect of food intake on bone resorption for optimal drug delivery and efficacy in osteoporosis with oral calcitonin, SA436  
 Influence of bone osteoporotic fractures in the past on the persistence of pharmacological treatment in osteoporosis, M382  
 Interventions to improve adherence and persistence with osteoporosis medications: a systematic literature review, M370  
 Medication prescription and adherence after hospitalization for osteoporotic vertebral fracture, M381  
 Medication switching in postmenopausal women on osteoporosis, M376  
 Optimizing bioavailability of oral administration of small peptides through pharmacokinetic and pharmacodynamic parameters, M398  
 Osteoporosis therapy following bone densitometry—patient expectations as determinants of drug initiation and persistence, M377  
 Patient refill behavior among select daily, weekly, monthly, and annual dosing regimens, M373  
 Patients desire of administration form and dose interval in bisphosphonate therapy of osteoporosis, SA408  
 Predictors of self-reported non-persistence with oral bisphosphonates due to perceived side effects or other reasons, M378  
 Preference and satisfaction with a 6-monthly subcutaneous injection versus a weekly tablet for treatment of low bone mass, M372  
 Prospective observational study of osteoporosis medication use in postmenopausal women in the European Union, SU347  
 Psychotropic drugs have contrasting skeletal effects that are independent of their negative effects on activity levels, M423  
 Vitamin D<sub>3</sub> treatment of elderly people—twice a day or every four months? A comparative study of efficacy and safety of two oral dosages with same annual dose of 292,000 units, SU422

**Mef2c**  
 Deletion of *Mef2c* in osteocytes decreases *Sost* expression and increases bone mass, F054

**MEK**  
 Vinculin is involved in hypertrophic differentiation through Raf/MEK/ERK pathway in chondrocytic ATDC5 cells, SA119

**MEK5**  
 MEK5/ERK5 signal regulates RANKL-induced osteoclastogenesis, SU103

**Melanoma**  
 Hfg inhibits melanoma bone metastases and TGF $\beta$  signaling, F190  
 Melanoma-induced bone loss is mediated by the rapid recruitment of osteoclasts, SU233

**Melastatin**  
 Importance of melastatin-like transient receptor potential 7 and Mg in the stimulation of osteoblast proliferation and migration by platelet-derived growth factor, M008

**Menaquinone-4 (MK-4)**  
 Conversion of Vitamin K analogues to MK-4 in osteoblastic cells, M064  
 Effect of low dose Vitamin K2 (MK-4) supplementation on bio-indices in postmenopausal Japanese women, SU307  
 Menaquinone-4 derived from phyloquinone regulates osteoblast function, SU034

**Menarche.** See also *Menstruation*

Age at menarche associated with bone strength in girls, SU493  
 Contribution of birth status, age at menarche and lifestyle factors to skeletal formation in junior and senior high school students, M492  
 Deleterious effect of late menarcheal age on bone microstructure in both distal radius and tibia, 1239  
 Influence of pubertal timing on bone trait acquisition: predetermined trajectory detectable five years before menarche, 1106

**Menin**  
 Possible physiological function of menin protein as transcriptional factor that modulates miRNA expression during osteogenesis, M036

**Menstruation.** See also *Menarche*  
 Bone mass recovers in young women with anorexia nervosa who are both weight and menstrual recovered, F339  
 Effects of diet and menstrual cyclicity on bone mass accumulation in pubertal monkeys, M499  
 Elevated androgens are associated with increased bone formation in premenopausal exercising oligomenorrheic women, SU191  
 Extended lactation is associated with failure to restore BMD 6 months after resumption of menstrual cycle, M305  
 Impact of adjuvant hormonal therapy on bone loss depending on initial adjuvant chemotherapy and menstrual status, M415

**Mesenchymal stem cells (MSC).** See *Stem cells*

**Metabolic acid**  
 Activation of P2X7 nucleotide receptors increases metabolic acid production by osteoblastic cells, M065

**Metabolic acidosis**  
 Effect of metabolic acidosis on BMD and bone microarchitecture in normal and OVX rats, M409

**Metabolic syndrome**  
 Low serum osteocalcin predicts carotid plaques and indicators of the metabolic syndrome, SA198  
 Negative association between the metabolic syndrome and BMD in Korean adults, SU304  
 Prevention of the metabolic syndrome together with osteoporosis in young men, SU314  
 Relationship between the metabolic syndrome and BMD in Korean middle-aged women, SU291

**Metastasis-associated protein 1 (Mta1)**  
 Premature aging-like phenotypes in Mta1 null mice, F494

**Methionine**  
 Homozygous threonine to methionine substitution in FGF-23 gene is associated with tumoral calcinosis in a 12 year-old girl, SU171

**2-methoxyestradiol (2ME2)**  
 2ME2 alters eIF4E activity and causes protein synthesis inhibition in osteosarcoma cells, SU240  
 2ME2 blocks prostate cancer bone metastases, F272

**Mevalonate**  
 Inhibition of the mevalonate pathway rescues the DEX-induced suppression of the mineralization of osteoblastic cells, SA230

**MIA3**  
 MIA3, a novel secreted factor, regulates chondrogenic differentiation in the developing mouse embryo, 1043

**MIBI**  
 Dominant tissue accumulation of MIBI in parathyroid glands in uremic rats, SA222

**Microgravity**  
 Combined effects of irradiation and unloading on murine bone, 1295  
 Deciphering the cellular defects of osteoblasts in microgravity, SA013

Modeled microgravity sensitizes osteoclast precursors to RANKL mediated osteoclastogenesis by increasing DAP12, M114  
 Silencing of RhoGTPases counteract microgravity-induced effects on osteoblasts, SA011

**Microporosity.** See *Porosity*

**Midkine (Mdk)**  
 High bone turnover in mice lacking the growth factor Mdk, 1198

**MIF**  
 Effects of intermediate doses of GCs on bone turnover and circulating Dkk-1, MIF, sRANKL and OPG in patients with interstitial lung disease, SA451

**Mineral bone disorder (MBD)**  
 Potential role of FGF-23 in CKD-MBD, WG30

**mir-206**  
 Noncanonical Wnt signaling is involved mir-206 expression in osteoblastic differentiation, SA021

**miRNA.** See *Ribonucleic acid*

**Mitf**  
 AP-1 and Mitf interact with NFATc1 to stimulate Cat K promoter activity in osteoclast precursors, SA076

**MITF**  
 LPS suppresses RANK gene through the down-regulation of PU.1 and MITF, SU083

**Mitochondria**  
 Enhanced mitochondrial biogenesis contributes to Wnt induced osteogenic differentiation of C3H10T1/2 cells, SA043  
 PGC-1 $\beta$  and iron uptake in the mitochondrial activation of osteoclasts, 1222

**Mitogen-activated protein kinase (MAPK)**  
 Antiapoptotic action of 17 $\beta$ -estradiol in skeletal muscle cells involves ERK 1/2, p38 MAPK, ASK-1 and HSP27, SU185  
 BMP-2 induces *Osx* expression through up-regulation of Dlx5 and its phosphorylation by p38 MAPK, F020  
 Functional association of MAPK and Runx2 on osteoblast chromatin, SU025  
 Involvement of caveolae in 1 $\alpha$ ,25(OH)<sub>2</sub>D<sub>3</sub>-dependent activation of MAPKs in skeletal muscle cells, SA243  
 MAPK-dependent inhibition of osteocalcin gene expression by TGF $\beta$ , M033  
 Proinflammatory cytokine TWEAK induces SCT expression in human immature osteoblasts in a MAPK dependent fashion, M046  
 Real time oscillations in TNF-induced gene expression MAPK phosphorylation and promoter binding, SU087

**MIV-701**  
 Cat K inhibitor, MIV-701, suppresses bone resorption markers in healthy postmenopausal women, F433

**MK-822**  
 Randomized, double-blind, placebo-controlled study of ODN (MK-822) in the treatment of postmenopausal women with low BMD, 1291

**MLO-A5**  
 Response of matrix synthesizing MLO-A5 cells to fluid shear, SA067

**MLO-Y4**  
 LIPUS synergistically modulates SCT and OPG/RANKL ratio in MLO-Y4 osteocytes in vitro, M109

**MMP-9**  
 Loss of *MMP-9* results in improved healing, and remodeling of adhesions in a murine model of flexor tendon repair, F153

**Monoclonal gammopathy of undetermined significance (MGUS)**  
 Microstructural changes at the ultradistal radius in MGUS, SU238

**Monocyte chemoattractant protein-1 (MCP-1)**  
 Study about the association of circulating MCP-1 levels with lumbar BMD in Korean women, M407

**Monocytes**

## Key Word Index

## ASBMR 30th Annual Meeting

BMSC up-regulate M-CSF receptor in monocytes to disrupt dendritic cell differentiation while facilitating osteoclastogenesis in myeloma, SU242

In vivo differential expression profiling study on human circulating monocytes suggested a novel CRAT and CPT2 network underlying smoking and BMD, SU155

**Monosodium urate monohydrate crystals (MSUM)**

Normal human osteoblasts internalize MSUM by phagocytosis and autophagy, M057

**Morphological atherosclerosis calcification distribution (MACD)**

MACD index is a strong predictor of cardiovascular death and include the predictive power of BMD, SU463

**Morquio Syndrome**

Morquio Syndrome variant: two siblings with atypical phenotype and novel compound heterozygosity, M240

**Mortality**

Pattern of death after hip fracture among institutionalized older people, 1164

**mRNA.** See *Ribonucleic acid*

Effect of  $\text{Sr}^{2+}$  on PTHrP, OPG and RANKL mRNA expression in osteoblastic-like cells UMR 106.1, SU016

**MrOS Study.** See *Osteoporotic Fractures in Men Study*

**Msx1**

Msx1 homeogene specific and non-redundant function in oral bones, M016

**Msx2**

NADPH oxidase/Nox signaling stimulates myofibroblast Msx2 transcription via  $\text{H}_2\text{O}_2$ , 1083

Post-translational regulation of Msx2 protein, SU021

Proteins involved in mineralization expressions perturbations in bones and teeth of Msx2 mutant mouse mandibles, SA150

Wnt7a and Wnt7b evoke overlapping yet distinct transcriptional responses during the osteogenic programming of mesenchymal progenitors by Msx2, 1196

**mTOR**

Akt regulates skeletal development through GSK3, mTOR, and FoxOs, 1151

Regulation of autophagy in the epiphyseal growth plate by AMPK and mTOR requires HIF-1, SU134

**Multilineage progenitor cells (MLPC).** See *Progenitor cells*

**Multiple myeloma (MM).** See *Myeloma*

**Muscle atrophy**

Inhibition of bone loss and muscle atrophy by DHT in a mouse hindlimb disuse model, SU377

**Muscle cells**

Antiapoptotic action of  $17\beta$ -estradiol in skeletal muscle cells involves ERK 1/2, p38 MAPK, ASK-1 and HSP27, SU185

CaSR mediated signaling in human vascular smooth muscle cells, M200

Distinct modes of osteoblastic differentiation from BMSC and vascular smooth muscle cells: induction by BMP-2 and PKA and suppression by Vitamin D derivatives, SU060

Human skeletal muscle cells undergo matrix mineralization in an osteogenic pellet culture assay, M135

Involvement of caveolae in  $1\alpha,25(\text{OH})_2\text{D}_3$ -dependent activation of MAPKs in skeletal muscle cells, SA243

**Muscle cross-sectional area (MCSA)**

Validating pQCT MCSA measurement, SU278

**Muscle function**

Effect of three different doses of Vitamin D<sub>3</sub> (ergocalciferol) on muscle function and strength in women > 65 years, M405

Effects of a targeted bone and muscle loading program on QCT bone geometry and strength, muscle size and function in older men, 1244

Gene expression in blast-injured muscle: insights into the mechanism of heterotopic ossification, SU163

Influence of hip flexor or knee extensor muscle strength on spinal sagittal alignment or falls, SU454

Muscle power and tibial bone strength in older women, SU362

Musculoskeletal disuse worsens the acute detrimental effects of heavy particle radiation on osteoblastogenesis, SA517

Randomised controlled trial of the effects of Vitamin D supplementation upon muscle function in adolescent girls, SU428

Therapy with ALF leads to a significant increase in muscle power and balance, SU444

Vitamin D and physical performance in African American women, M218

**Muscle loss**

Low magnitude vibration can inhibit muscle loss and increase mineralizing bone surfaces in aging mice, M173

**Muscle mass**

Bone geometry, strength, and muscle mass in female distance runners with a history of stress fracture, SA540

**Muscle paralysis**

Significant trabecular bone degradation occurs within five days of muscle paralysis, SA515

Trabecular bone loss in response to transient muscle paralysis is not gender dependent, SA462

**Muscle size**

Effects of a targeted bone and muscle loading program on QCT bone geometry and strength, muscle size and function in older men, 1244

Influence of muscle size and strength on changes in bone mass and size during growth and in response to exercise, SA537

**Muscular dystrophy, Duchenne (DMD)**

Effect of non-ambulation on bone strength in boys with DMD, WG1

Forearm pQCT measurements in males with DMD, SU492

**Mustn1**

In vivo downregulation of *Mustn1* mRNA leads to musculoskeletal defects, 1192

**MVNP.** See *Measles virus nucleocapsid protein*

**Myoblasts**

Osteogenesis effect of human ligamentum flavum, myoblast, osteoblast and MSC by DBM and BMP-2, SU135

**MyD88**

IL-27/WSX-1 signaling inhibits RANKL-induced osteoclastogenesis through STAT1 activation: a possible involvement in TLR4/MyD88-mediated inflammatory arthritis, SU102

**Myeloma**

Anti-myeloma effects of osteoblasts is mediated through production of SLRPs, M001

BMSC up-regulate M-CSF receptor in monocytes to disrupt dendritic cell differentiation while facilitating osteoclastogenesis in myeloma, SU242

Disruption of the syndecan-1/integrin axis is a novel target for myeloma therapy, 1229

EphB4 expression in osteoblasts is regulated by myeloma cells and the Wnt signaling pathway, SU232

Host bone marrow-derived stromal cells promote myeloma initiation and development of osteolysis, 1088

Role of FAP and DPP4 in myeloma bone disease and tumor growth, F288

TGF $\beta$  suppresses adipocytic differentiation and enhances accumulation of stromal cells in myeloma bone lesions, SA294

ZOL inhibits the capacity of myeloid-immune suppressor cells in myeloma to form osteoclasts, SU230

**Myeloma, multiple (MM)**

Activin A mediates MM bone disease which is reversed by RAP-011, a soluble activin receptor, 1231

Bone degradation marker CTX shows unique properties in disease monitoring compared to NTX, ICTP and bALP in MM, M287

CXCL12 expression is regulated by HIF-2 $\alpha$  in MM plasma cells, SU080

Elevated serum levels of CXCL12 is associated with increased osteoclast activity and osteolytic bone disease in MM patients, SU079

Increased signaling through p62 in the MM microenvironment increases myeloma cell growth and osteoclast formation, SA289

Inhibition of MM growth and preservation of bone with combined radiotherapy and anti-angiogenic agent, SA285

Platelets contribute to circulating levels of Dkk-1: clinical implications in MM, SU228

Preclinical validation of a novel Dkk1 neutralizing antibody for the treatment of MM related bone disease, SU239

Role of AXII and AXIIR in homing MM cells in the bone marrow, SA287

**Myoblasts**

Dual roles of Smad proteins in the conversion from myoblasts to osteoblastic cells by BMPs, SA161

**Myostatin**

Myostatin (GDF-8) regulates the secretion of growth factors localized to the muscle-bone interface, SU153

## N

## N-Mid®

Development of a new N-Mid® osteocalcin immunoassay on the IDS Automated Analyser 3x3™, SA303

## N-telopeptides of type I collagen (NTx)

Association of stiffness index and cross-linked NTx with any clinical fractures differs with age and gender, SU350

## N-terminally extended XLas (XXLas)

XXLas acts as a novel heterotrimeric G protein subunit with an ability to transduce receptor activation into intracellular signaling, F226

## NADPH

NADPH oxidase/Nox signaling stimulates myofibroblast Msx2 transcription via  $\text{H}_2\text{O}_2$ , 1083

## Nanotechnology

Adipose tissue derived MSCs: differentiation into osteoblastic phenotype and interaction with nanostructured Ti alloys, SU050

Chemical composition and nanoscale structure of RIS-treated mineralizing MC3T3-E1 cells, M023

Modulation of skeletal modeling by silica-based nanoparticles, SU014

Multi-walled carbon nanotubes inhibit osteoclast differentiation by inhibiting nuclear translocation of NFATc1, M113

Nanogel cross-linking hydrogel as a drug delivery system for TNF $\alpha$  antagonist, M121

Nanotechnological scaffold with combination of PGE<sub>2</sub> receptor EP4 agonist and rhBMP2, enhances bone repair in the defect of mouse calvarium bone, SA105

## NaPi-IIa

Selective removal of PLC signaling in novel PTH(1-28) analogs abolishes regulation of NaPi-IIc but not NaPi-IIa, M186

## NaPi-IIc

Selective removal of PLC signaling in novel PTH(1-28) analogs abolishes regulation of NaPi-IIc but not NaPi-IIa, M186

## Narcotics

Opioid-induced osteoporosis: delayed bone healing and compression fractures in a man with chronic narcotic use, WG32

## NARS

NARS induced by bFGF regulates the proliferation and survival of osteoblasts, SA164

## National Osteoporosis Foundation (NOF)

What proportion of older women would receive drug treatment under the new NOF guidelines?, 1022

**National Osteoporosis Risk Assessment (NORA) Survey**  
Fracture risk and incidence of falls in younger postmenopausal women, 1236

**NCK1**  
Deficiency of NCK1, an actin cytoskeletal modulator with SH2/SH3 motifs, induces bone loss via suppression of bone formation and induction of biochemical high bone turnover state, M026

**Nell-1**  
Craniofacial bone defect in Nell-1 mutant mice associated with dysregulated Runx2 and Osx expression, F174

**Neogenin**  
Regulation of chondrogenesis and bone development by neogenin via BMP pathway, SU127

**Nephroblastoma overexpressed (Nov)**  
Nov induces gremlin expression by post transcriptional mechanisms, F141

**Nephrotic syndrome**  
Development of nephrotic in transgenic rats over expressing Type III Na-dependent phosphate transporter, SU170

**Neridronate**  
Comparison of intravenous and intramuscular neridronate regimens for the treatment of PDB, SA481  
Polyostotic form of FD in a 13 year old Colombian girl exhibiting clinical and biochemical response to neridronate intravenous therapy, SU211

**Nervous system, sympathetic**  
Osteocalcin is a stress hormone: interaction with the sympathetic nervous system, M059

**Neural networks, artificial**  
Comparison between logistic regression and artificial neural networks for vertebral fracture risk assessment, SU345

**Neurofibromatosis 1 (NF-1)**  
Vitamin D deficiency, osteomalacia and high bone turnover in patients with NF-1, F465

**Neuronal development**  
Role of Ostm1 in bone, hematopoiesis and neuronal development, 1271

**Neuropeptide Y (NPY)**  
NPY effect on osteoblast cells, SU011  
Osteocytes can modulate osteoblastic activity via NPY signaling, SA056

**Neurotransmitters**  
Bone cell response to neurotransmitters and mechanical loading, SA009

**Neutrophil**  
Neutrophil-like PLB-985 cells induce differentiation of human blood monocytic precursors into functional osteoclasts via a RANKL-dependent mechanism, SA092

**NF- $\kappa$ B**  
Expression of NF- $\kappa$ B ligand and regulation of osteoclastogenesis by bone marrow adipocytes, SA078

**NfI**  
Bi-allelic loss of *NfI* in osteoblasts delays bone fracture healing, SU218

**NFAT**  
Nicotine induces chondrogenesis via calcineurin/NFAT, SU133

**NFATc1**  
AP-1 and Mitf interact with NFATc1 to stimulate Cat K promoter activity in osteoclast precursors, SA076  
BMP-2 stimulates a feedback activation loop for expression of NFATc1 in osteoblasts, F002  
BMP-2-stimulated signaling niche in osteoblasts comprising of Smad and PI3K/Akt regulates NFATc1 expression and its nuclear translocation, 1081  
Multi-walled carbon nanotubes inhibit osteoclast differentiation by inhibiting nuclear translocation of NFATc1, M113

NFATc1 mediates HDAC-dependent transcriptional repression of osteocalcin expression during osteoblast differentiation, 1145

**NFATp**  
Transcription factor NFATp regulates BMP-induced chondrocyte differentiation in a tissue-specific manner, SU020

**NHNV fractures. See Fractures**

**Nicotine**  
Nicotine induces chondrogenesis via calcineurin/NFAT, SU133

**Nitric oxide (NO)**  
Effects of electrical stimulation on NO expression and osteocyte viability in OVX rats, SA524  
HDAC inhibitors suppress IL-1 $\beta$ -induced NO and PGE<sub>2</sub> production in human chondrocytes, SU116  
NO has a powerful effect of osteoclast cells, M131  
Phosphate induced apoptosis in growth plate chondrocytes via a NO and JNK-dependent pat, SA113

**Nitric oxide synthase, endothelial (eNOS)**  
Effects of statins on eNOS and BMP-2 in osteoblasts, SU378

**Nitrogen**  
Impact of dietary protein on Ca homeostasis and nitrogen excretion in the presence and absence of KHCO<sub>3</sub>, SU305

**Nitroglycerin**  
Prevention of postmenopausal osteoporosis using nitroglycerin, M354

**Nitroglycerin as an Option: Value in Early Bone Loss (NOVEL) Study**  
Prevention of postmenopausal osteoporosis using nitroglycerin, M354

**Nkx3.2**  
Nkx3.2 is an important mediator of hypoxia-induced chondrocytic differentiation, F112

**NMDA**  
Mice lacking NMDA receptor expression in osteoblasts have pronounced vertebral bone abnormalities, F012

**Nmp4**  
Nmp4-KO mice exhibit a complex phenotype, M193

**NO66**  
Regulation of the osteoblast-specific transcription factor Osx by NO66, a Jumonji family histone demethylase, F017

**Non-steroidal anti-inflammatory drugs (NSAIDs)**  
Non-steroidal anti-inflammatory use and the response of bone to exercise, M472

**NORA Survey. See National Osteoporosis Risk Assessment Survey**

**Notch**  
Notch inhibits NFAT transactivation in osteoblast cultures, 1111  
Notch pathway is activated in osteosarcoma and inhibitors of  $\gamma$ -secretase inhibit osteosarcoma growth by cell cycle regulation, SU229  
Notch signaling inhibits chondrogenesis and subsequently promotes chondrocyte maturation, 1268  
Notch signaling regulates osteoblast maturation transition to mineralization phase, SA068

**NOVEL Study. See Nitroglycerin as an Option: Value in Early Bone Loss Study**

**Nox**  
NADPH oxidase/Nox signaling stimulates myofibroblast *Msx2* transcription via H<sub>2</sub>O<sub>2</sub>, 1083

**Npt2a**  
Synergistic role of Npt2a and Npt2c in inorganic phosphate metabolism of mice, F473

**Npt2c**  
Synergistic role of Npt2a and Npt2c in inorganic phosphate metabolism of mice, F473

**NR4A2**

Cloning and functional analysis of human Nurr1 (NR4A2) promoter: critical role in the regulation of CYP27B1 by PTH and CREB phosphorylation, 1161

**NTX**  
Bone degradation marker CTX shows unique properties in disease monitoring compared to NTX, ICTP and bALP in MM, M287

**Nuclear factor  $\kappa$ B (NF- $\kappa$ B)**  
Bridging vascular calcification and osteoporosis: the function of receptor activator of nuclear factor  $\kappa$ B, M419  
Matrix PRELP interferes with the NF- $\kappa$ B pathway and impairs osteoclast formation and activity, SU089

**Nuclear factor  $\kappa$ B2 (NF- $\kappa$ B2)**  
In the absence of NF- $\kappa$ B2, TNF induces osteoclast formation in vivo independent of RANKL/RANK and more severe arthritis in TNF-Tg mice, 1009

**Nuclear factor I (NFI)**  
NFI transcription factors regulate IGFBP5 gene transcription in human osteoblasts, SU015

**Nuclear factor of activated T-cells (NFAT)**  
Notch inhibits NFAT transactivation in osteoblast cultures, 1111

**Nuclear factor-E2 related factor-1 (Nrf1)**  
Targeted disruption of Nrf1 in osteoblasts leads to reduced bone size and dramatic alterations in trabecular bone microstructure in mice, 1190

**Nuclear magnetic resonance (NMR)**  
Proton NMR study of transverse relaxation in rabbit and rat cortical bone, M470

**Nuclear receptor interacting protein 1 (NRIP1)**  
*NRIP1*, a novel osteoporosis candidate gene identified by expression and association analyses, M254

**Nucleotide pyrophosphatase/phosphodiesterase-1 (NPP1)**  
Proteoliposomes carrying ALP and NPP1 as matrix vesicle mimetics, SA061

**Nurr1**  
Cloning and functional analysis of human Nurr1 (NR4A2) promoter: critical role in the regulation of CYP27B1 by PTH and CREB phosphorylation, 1161

**NuSAP**  
Reduced cell proliferation and chondrodysplasia in mice lacking the mitotic protein NuSAP, SU120

## O

**OAH19**  
OAH19, an ethanol extract from combined two herbs, inhibits IL-1 $\alpha$ -induced expression of MMP-1 and MMP-13 in OA human cartilage and synovial fibroblast, M148

**ob/ob**  
Central and peripheral leptin treatment produce similar increase in cortical and trabecular bone mass in ob/ob mice, SU164

**Obesity. See also Body composition; Weight**  
Diet induced obesity compromises the osteogenic potential of the bone marrow, F047  
Effects of obesity on cortical bone, SA342  
Hormonal influences on volumetric bone density and geometric properties in obesity, SU367  
Interactions between obesity, CVD and bone formation, M451  
Obesity and bone architecture in men—can we apportion the metabolic and the mechanical effect?, SA440  
Obesity induced by high dietary fat leads to increased bone resorption marker, TRAP, and decreased bone mass in mice, M238  
Obesity is associated with higher BMD, lower bone resorption and slower hip bone loss: are these associations mediated by adipokines?, SU369  
Overweight children are more at risk to sustain a forearm fracture due to poor bone strength relative to body weight, M458



## Key Word Index

## ASBMR 30th Annual Meeting

PTH increases after oral peptones administration in obese subjects treated with roux-en-y gastric bypass surgery: role of phosphate on the rapid control of PTH release, M180

Transgenic ASARM-peptide overexpression with reduced serum phosphate and 1.25(OH)2D3 leads to decreased BMD and obesity, F210

Vitamin D insufficiency in obesity, SA239

Vitamin D status in severely obese individuals can be predicted by demographic and lifestyle factors, SU201

Weight reduction is not deleterious for bone mass or strength in obese women, SA338

**OCT-1547**

Ca signaling is a major target of OCT-1547, a small molecule osteoporosis drug candidate, M339

**Odanacatib (ODN)**

Bone effects of ODN in adult OVX rabbits, SA073

Effects of ODN on bone biomarkers in OVX non-human primates, F297

Effects of ODN on bone mass and turnover in estrogen deficient adult rhesus monkeys, SA072

Effects of the Cat K inhibitor ODN on osteoclast-mediated bone resorption, M127

Efficacy of ODN in the OVX rhesus monkey as measured with pQCT, M343

ODN increases bone strength and maintains bone quality in estrogen deficient adult rhesus monkeys, F508

Randomized, double-blind, placebo-controlled study of ODN (MK-822) in the treatment of postmenopausal women with low BMD, 1291

**Odd-skipped related 1 (Osr1)**

Abnormality of bone formation in transgenic mice expressing Osr1, M144

**Odd-skipped related 2 (Osr2)**

Functional role of Osr2 in preosteoblastic cells, M006

**Odontoblasts**

Dlx5 overexpression stimulates odontoblast differentiation and function, M054

**Oleuropein**

Oleuropein from olive stimulates the differentiation and mineralization of cultured osteoblasts and inhibits the formation of osteoclasts in culture, M081

**Oligomenorrhea**

Elevated androgens are associated with increased bone formation in premenopausal exercising oligomenorrheic women, SU191

**Ollier Disease**

PTHR1 mutations associated with Ollier Disease result in receptor loss of function, SA258

**Oncogenic osteomalacia (OOM). See Osteomalacia**

**Ontario Osteoporosis Strategy for Inpatient Rehabilitation**

Assessment of a provincial strategy for osteoporosis best practices, M401

Post-fracture osteoporosis intervention strategy, M322

**Ophthalmologic diseases**

Prevention of GC-induced osteoporosis with ALN or ALF in patients with ophthalmologic diseases, SA450

**OPTAMISE Study**

Imaging the spatial distribution of proximal femoral response to one year of TPTD therapy, M349

One year of TPTD treatment increases hip strength in subjects with recent history of anti-resorptive treatment, F396

**Oral bones**

Mxs1 homeogene specific and non-redundant function in oral bones, M016

**Osseointegration**

Oral Sr ranelate treatment markedly improves implant osseointegration, SA506

**Ossification, endochondral**

$\beta$ -catenin directly binds to a specific intracellular domain of PTH/PTHrP receptor and regulates the signaling in chondrocytes during endochondral ossification, 1013

Overexpression of CCN2/CTGF in cartilage shows prolonged bone length resulting from stimulation of chondrogenesis, chondrocyte growth, apoptosis, and bone mineralization during endochondral ossification, M153

Protein sulfation is required to prevent chondrocytes autophagy and growth factor signaling during endochondral ossification, SU119

Transcription factor Dmrt2 controls endochondral ossification through regulating type 10 collagen (Col10a1) gene expression, 1045

**Ossification, heterotopic**

Gene expression in blast-injured muscle: insights into the mechanism of heterotopic ossification, SU163

**Ossification, meniscal**

Development of OA and its relationship to meniscal ossification in Dunkin Hartley guinea pigs, M154

**Osteoactivin**

Evaluation of two novel bone growth factors to enhance fracture healing, SU012

**Osteoarthritis (OA)**

Activation of  $\beta$ -catenin signaling in articular chondrocytes leads to OA-like phenotype in adult  $\beta$ -catenin conditional activation mice, 1047

Advanced hip assessment and BMD in Japanese women with OA, M449

BT-201, a butanol extract of *Panax notoginseng* inhibits progression of joint degeneration in a rat model of OA, M152

Comparison of 2D and 3D subchondral bone texture parameters in severe OA knees, M302

Development of OA and its relationship to meniscal ossification in Dunkin Hartley guinea pigs, M154

Discordance in femoral neck bone density in subjects with OA, M453

Effect of aquatic exercise and education on improving indices of fall risk in older adults with hip OA, M441

Effect of bisphosphonate treatment of OA in a guinea pig model, M149

Effects of beta-D-glucopyranoside from *Phellodendron Amurense* on the production of inflammatory cytokines, growth factors, MMP, and on bone markers in human subchondral OA osteoblasts, SA117

H4R is expressed by both OA and RA human tissues, SU159

IL-1 $\beta$ -induced hepcidin expression in synovial membranes of patients with OA is associated with TNF $\alpha$  repression, SU157

Investigation into the impact of OA changes on BMD measurements in patients with high bone mass, SA257

Longitudinal relationships between cartilage and bone turnover in OA, SA129

Novel model system for drug discovery in OA: monitoring whole tissue turnover in murine femur heads, SU125

OAH19, an ethanol extract from combined two herbs, inhibits IL-1 $\alpha$ -induced expression of MMP-1 and MMP-13 in OA human cartilage and synovial fibroblast, M148

PGD2 downregulates MMP-1 and MMP-13 expression in human OA chondrocytes, SA152

Proinflammatory mediators downregulate PPAR $\gamma$ 1 expression and activity in OA synovial fibroblasts, M159

PTH has direct anabolic effects on OA articular cartilage in vitro and in vivo, M155

Relationship between BMD of the lumbar spine and knee OA in South Korean, SU298

Role of gal-3 in OA, M162

Targeted expression of SOX9 in hypertrophic chondrocytes leads to enhanced adipogenic activity and spontaneous OA in transgenic mice, SA115

In vivo knockdown of GEP, a novel growth factor in cartilage, led to defects in cartilage and OA, 1048

**Osteoblastic differentiation**

(Ala-Gly) $_n$  sequences configured silk protein scaffold induces osteoblast differentiation and bone formation via increased Cbfa1 and Osx expression, M167

Adipose tissue derived MSCs: differentiation into osteoblastic phenotype and interaction with nanostructured Ti alloys, SU050

Ang-1 enhanced BMP-2 induced osteoblast differentiation, SU035

Blockade of Ephrin/EphB4 signaling within the osteoblast lineage reduces osteoblast differentiation and mineralization, SU046

Catecholamines accelerate BMP-induced osteoblastic differentiation and bone formation, SU137

CD47 (IAP) is an important modulator of osteoclast and osteoblast differentiation in vitro and in vivo, F093

Chondrocyte-derived Ihh is required for osteoblast differentiation despite reconstitution of a normal growth plate, 1154

Coactivator MBF1 binds to JunD and protects its transcriptional activity against oxidative stress to prevent age-related suppression of osteoblast differentiation, 1248

Congenetic mouse models provide novel evidence of caveolae-1 $\alpha$  domain regulation of osteoblast differentiation, SU147

Coordinate regulation of PTHrP and PTHR1 in the osteoblast differentiation of C2C12 cells promoted by BMP-2, SA157

Deletion of ADAM15 decreases osteoblast differentiation and bone formation in vitro, M073

Depletion of the chromosome remodeling subunit BRM accelerates differentiation of osteoblast precursors, M038

Distinct modes of osteoblastic differentiation from BMSC and vascular smooth muscle cells: induction by BMP-2 and PKA and suppression by Vitamin D derivatives, SU060

Effect of a novel splice-site mutation of PHEX gene during osteoblast differentiation, M092

Effects of serum factors during osteoblast differentiation—implication for the pathogenesis of osteoporosis in Crohn's Disease, M450

Enamel matrix derivative (emdogain) enhance osteoblast differentiation on Ti surfaces, M030

Enhanced mitochondrial biogenesis contributes to Wnt induced osteogenic differentiation of C3H10T1/2 cells, SA043

Fat suppresses osteoblast differentiation by soluble factors that induce apoptosis, M003

FGF-1 inhibits adipogenic differentiation and transdifferentiation of human MSCs, M075

FHL2 mediates DEX-induced MSC osteogenic differentiation by activating Wnt/ $\beta$ -catenin signaling and Runx2 expression, M048

Ghrelin inhibits early osteogenic differentiation of C3H10T1/2 cells by suppressing Runx2 expression and enhancing PPAR $\gamma$  and C/EBP $\alpha$  expression, M086

Icariin induces osteogenic differentiation in vitro in a BMP- and Runx2- dependent manner and bone regeneration in vivo, M089

Identification of IRX3 a novel transcription factor during BMP-2 mediated osteoblast differentiation, SU024

IGFBP6 Is a negative regulator of osteoblast differentiation and bone formation, SA182

Impairment of osteoblast lineage differentiation leads to increased osteoclastogenesis in OI murine, 1202

- Induction of Runx2 and Osx by bisphosphonate promote osteogenic differentiation, SU062
- Inhibition of lamin A/C attenuates osteoblast differentiation and stimulates osteoclastogenesis through enhanced RANKL signaling, M070
- Interplay between BMP and TGF $\beta$  signaling in osteoblast differentiation, SA031
- Mature human adipocytes differentiated from BMSCs, SA042
- Microporosity in b-TCP ceramics may be detrimental to MSC survival and osteoblastic differentiation, SA015
- NFATc1 mediates HDAC-dependent transcriptional repression of osteocalcin expression during osteoblast differentiation, 1145
- Noncanonical Wnt signaling is involved mir-206 expression in osteoblastic differentiation, SA021
- Oleuropein from olive stimulates the differentiation and mineralization of cultured osteoblasts and inhibits the formation of osteoclasts in culture, M081
- Osteoblast differentiation induced by Shh-expressing prostate cancer cells is enhanced by ascorbic acid, SA284
- Osteopenia by high alcohol consumption in the absence of ALDH2 attribute to the disturbance of the differentiation in osteoblasts, M326
- Overexpression of  $\alpha$ -catenin in C3H10T1/2 cells increases osteoblast differentiation, SA046
- Overexpression of androgen receptor in mature osteoblasts and osteocytes inhibits osteoblast differentiation, SU192
- Permanent FGFR2 activation promotes osteoblast differentiation in MSCs through activation of PKC signaling, M093
- PTH/PTHrP mediated stimulation of osteoblast differentiation involves Epac-Rap1 dependent processes, SA025
- Pulse treatment with ZOL causes sustained commitment of bone marrow derived MSC for osteogenic differentiation, M072
- R-spondin 2 is a novel osteogenic factor required for Wnt11 mediated osteoblast differentiation, SU063
- Regulation of Dkk-1 and Dkk-2 is needed for osteoblast terminal differentiation on microstructured Ti surfaces, SU006
- Regulation of osteoblast differentiation by miRNA, M087
- Role of FIP200 in osteoblast differentiation, M091
- Role of pyrophosphate and inorganic phosphate in PKA-mediated osteoblastic differentiation and mineralization of primary murine aortic cells, M143
- Runx2 and canonical Wnt signaling cooperatively regulate BMP-induced differentiation pathways of adult dural cells into osteoblasts or chondrocytes, M043
- SATB2 overexpression promotes osteoblast differentiation and enhances regeneration of bone defects, SU058
- Small G protein Rap1 promotes osteoblast differentiation, M080
- T-box 3 negatively regulates osteoblast differentiation by inhibiting expression of Osx and Runx2, SU018
- Tcf is required for Wnt11 mediated osteoblast differentiation, M058
- TGIF regulation of bone mass: impaired osteoblast differentiation, SA018
- TIEG: a key regulator of Runx2 and Osx gene expression and osteoblast differentiation, M052
- WNT-4 acts through the non-canonical pathways to stimulate osteoblast and BMSC differentiation, F050
- Osteoblastogenesis**
- Effect of 1,25(OH) $_2$ D $_3$  and 25(OH)D $_3$  on osteoblastogenesis and bone strength in Vitamin D sufficient growing mice, SU207
- Estrogens reverse a potentiating effect of the unliganded estrogen receptor on BMP-induced transcription and osteoblastogenesis by promoting ERK-dependent Smad1 phosphorylation at the linker region, SU189
- High concentrations of hydroxytyrosol and quercetin antioxidants enhance adipogenesis and inhibit osteoblastogenesis in MSCs, SA037
- Inhibition of PPAR $\gamma$ 2 by BADGE and Vitamin D in male mice increases osteoblastogenesis and inhibits bone matrix mineralization leading to osteomalacia, SU374
- Low dose administration of INF $\gamma$  stimulates osteoblastogenesis and prevents ovariectomy-induced osteoporosis in C57BL/6 mice, M334
- Musculoskeletal disuse worsens the acute detrimental effects of heavy particle radiation on osteoblastogenesis, SA517
- PBX1 interaction with HOXA10 regulates timing and expression of phenotypic bone genes during osteoblastogenesis, SU019
- VEGF and PTEN regulate bone homeostasis via control of osteoblastogenesis, osteoclastogenesis and adipocyte differentiation, M029
- Osteoblasts**
- (Ala-Gly) $_n$  sequences configured silk protein scaffold induces osteoblast differentiation and bone formation via increased Cbfa1 and Osx expression, M167
- 1,25(OH) $_2$ D $_3$  regulates collagen maturation in osteoblastic cell culture system, SU208
- 7B2 protein mediated inhibition of DMP1 cleavage in osteoblasts enhances FGF-23 production in *Hyp*-mice, 1053
- Abrogation of Cbl-PI3K interaction in mice results in increased bone volume and osteoblast proliferation, 1150
- Accelerated fracture callus remodeling and membranous bone healing in STAT1 deficient mice, SA022
- Acid-induced stimulation of bone resorption is decreased in OGR1 KO mouse calvariae, M021
- Activation of FGF receptors is a novel mechanism by which extracellular Ca stimulates the proliferation of osteoblasts, M088
- Activation of P2X7 nucleotide receptors increases metabolic acid production by osteoblastic cells, M065
- Age-related bone loss in mice associated with ubiquitin ligase Smurf1 degradation of JunB protein and reduced osteoblast proliferation, 1113
- Aging of human BMSC: role of WNT pathways, SA048
- Ahnak regulates Ca signaling and ATP release in osteoblasts in response to mechanical stimulation, SA027
- ALN affects cross-talk of osteoclasts and osteoblasts in vivo, SU392
- Altered long bone structure in recessive null and dominant negative Cx43 (*Gjal*) mouse mutants, 1110
- Analysis of chromosome breaks in osteoblasts and non-osteoblastic cells treated with intermittent PTH, M191
- Anti-myeloma effects of osteoblasts is mediated through production of SLRPs, M001
- Association between Cx43 and  $\beta$ -arrestin is required for cAMP-dependent osteoblast survival induced by PTH, 1227
- Atypical antipsychotic clozapine reduces rat osteoblast proliferation and osteoclastogenesis at therapeutic levels, SU030
- Availability of cytoplasmic  $\beta$ -catenin impacts mechanical signaling in osteoblasts, 1253
- Bi-allelic loss of *Nf1* in osteoblasts delays bone fracture healing, SU218
- BMP-2 induces Osx expression through up-regulation of Dlx5 and its phosphorylation by p38 MAPK, F020
- BMP-2 stimulates a feedback activation loop for expression of NFATc1 in osteoblasts, F002
- BMP-2-stimulated signaling niche in osteoblasts comprising of Smad and PI3K/Akt regulates NFATc1 expression and its nuclear translocation, 1081
- BMP-6 stimulated osteogenesis of HOB cultures is associated with suppression of PYK2, SU048
- BMP/Wnt antagonists are upregulated by DEX in osteoblasts and reversed by ALN and PTH: potential therapeutic targets for GIO, M098
- Bone cell response to neurotransmitters and mechanical loading, SA009
- Bone response to mechanical loads and Lrp5 genotype, M020
- Both the Smad and ERK MAP kinase pathway play critical roles in BMP-2-induced osteogenic transcription factors expression, M050
- Breast cancer cell conditioned media stimulates osteoblastic cells to attract breast cancer cells, SA276
- Brief pulsing electromagnetic field exposure differentially effects cell cycle in proliferating and confluent osteoblasts, M004
- Bril localization in mouse and rat bones, M025
- Butyrate stimulates mineralized nodule formation and OPG expression by osteoblasts, M012
- c-Src-regulated osteoblast-mimicry in breast cancer bone metastasis: the role of RAMP2 and BSP2, M275
- C/EBP $\beta$  overexpression causes osteopenia, SA005
- $\beta$ -catenin protects osteoblasts from oxidative stress by co-activating the expression of pro-survival, but not pro-apoptotic, target genes of the FoxO transcription factors, M010
- Ccrn4l*, a peripheral clock gene, influences stromal cell allocation, bone mass, and marrow adiposity in mice and humans, 1073
- CFTR regulates osteoblast bone formation independent of chloride conductance, 1274
- CGRP stimulates osteogenesis and inhibits osteoclastogenesis in vitro, SU033
- Characterisation of an antigen found in giant cell tumor and osteosarcoma cells, SU244
- Characterization of a promoter polymorphism in FZD1: allele-specific regulation by Egr-1 in osteoblast-like cells, M267
- Characterization of osteoblastic properties of 7F2 and UMR-106 cultures after acclimation to reduced levels of fetal bovine serum, SU041
- Chemerin and CMKLR1 targeted gene delivery identifies a novel molecular switch in the treatment of osteoporosis, M071
- Chemical composition and nanoscale structure of RIS-treated mineralizing MC3T3-E1 cells, M023
- Circulating osteoblast lineage cells increase with PTH treatment of HPT, 1146
- Cloning and functional expression of the full length mouse GIP receptor and the regulation of its expression in osteoblasts by the Sp1 transcription factor, SU026
- CNBP conditional KO mice show severe osteoporosis-like phenotype, F014
- Comparison of gene expression in osteocytes versus osteoblasts, M056
- Comparison of the effects of zoledronates on the differentiation of human bone marrow and amniotic fluid derived MSCs, SA045
- Concentration of connective tissue progenitors in autologous cancellous bone graft enhances new bone formation in a canine femoral defect model, SA039
- Conditional deletion of BMP-2 gene in early osteoblasts leads to reduction in the total bone marrow MSCs and their capacity to form osteoblast precursors, 1114

## Key Word Index

## ASBMR 30th Annual Meeting

- Conditional disruption of *Pkd1* in osteoblasts results in osteopenia due to direct impairment of osteoblast-mediated bone formation, SA019
- Conditional knockout of the CaSR in osteoblasts alters regulators of Wnt signaling, delays cell differentiation, and promotes apoptosis in bone, 1156
- Continuous local infusion of ALN prevents osteopenia of the lengthened segment during distraction osteogenesis, SU001
- Conversion of Vitamin K analogues to MK-4 in osteoblastic cells, M064
- Critical role of Cx43 in postnatal skeletal growth and bone mass acquisition, 1257
- CT-1 is an osteoclast-derived coupling factor required for normal bone remodeling, M014
- Deciphering the cellular defects of osteoblasts in microgravity, SA013
- Deficiency of NCK1, an actin cytoskeletal modulator with SH2/SH3 motifs, induces bone loss via suppression of bone formation and induction of biochemical high bone turnover state, M026
- Deletion of the Dkk-1 Krm-1 and Krm-2 in mice leads to increased bone formation and bone mass, 1004
- Deletion of the G protein subunit G $\alpha$  in early osteoblasts leads to accelerated osteoblast maturation and formation of woven bone with abnormal osteocytes, resulting in severe osteoporosis, 1254
- Deletion of the Wnt signaling antagonist sFRP4 in mice induces opposite bone formation phenotypes in trabecular and cortical bone, 1005
- Deletion of Zfp521, an antagonist to Runx2 and Ebf1 transcriptional activity, leads to osteopenia and a defect in matrix mineralization in mice, 1109
- Dermo1 lineage tracing identifies early osteoprogenitor cells in adult murine bone marrow MSC cultures, SA051
- Development of high-throughput screening system for osteogenic drugs using cell-based sensor, M082
- Different osteogenic properties of human BMSC from different skeletal site origin, SU055
- Differential contribution of osteoclast- and osteoblast-lineage cells to LPS modulation of osteoclastogenesis, SU088
- Disuse with a rapid bone loss affects the expression profile of osteoblastic and resorption genes, F516
- Dlx5 overexpression stimulates odontoblast differentiation and function, M054
- DNA methylation analysis of osteogenic gene promoter regions in mouse BMSC, M035
- Dried plum polyphenols increase IGF-I production in osteoblast-like cells, SU002
- Dual roles of Smad proteins in the conversion from myoblasts to osteoblastic cells by BMPs, SA161
- Effect of MKP-1 deletion on the fluid shear stress induction of COX-2 expression in osteoblasts, SA529
- Effect of osteoblast depletion on hematopoietic niches in the bone marrow, F041
- Effect of resveratrol and flax oil on MC3T3-L1 pre-adipocyte and ST2 BMSC proliferation and differentiation, SU059
- Effect of Sr<sup>2+</sup> on PTHrP, OPG and RANKL mRNA expression in osteoblastic-like cells UMR 106.1, SU016
- Effects of ALN and RLX on the RANKL/OPG system in primary cultures of human osteoblasts, M101
- Effects of Ga11 overexpression on osteoblast signaling and function in transgenic mice, M067
- Effects of statins on eNOS and BMP-2 in osteoblasts, SU378
- Endogenous G $\beta$  signaling in osteoblasts negatively regulates cortical bone formation, 1255
- Engineering mice with multiple BAC fluorescent protein reporter gene elements, SU028
- Enhanced osteogenic potential of alveolar vs. long bone derived BMSC, M095
- Enrichment of type XI collagen and 6b N-terminal domain at sites of mineral nucleation within osteoblastic cultures, SA070
- EphB4 expression in osteoblasts is regulated by myeloma cells and the Wnt signaling pathway, SU232
- Ephrin B1 reverse signaling regulates bone formation via influencing osteoblast activity in mice, 1194
- Ethanol alters estrogen receptor signaling and activates senescence pathways in osteoblasts while estradiol attenuates ethanol effects, SU182
- Evaluation of circulating osteoprogenitor cells during fracture healing using parabiotic mice, 1260
- Evaluation of two novel bone growth factors to enhance fracture healing, SU012
- Expression of an engineered G $\gamma$ -coupled receptor in osteoblasts affects intramembranous and endochondral bone formation during bone repair, F127
- Expression of an engineered G $\gamma$ -coupled receptor, Rs1, in mature osteoblasts is sufficient to drive a dramatic anabolic skeletal response, 1077
- Expression of bone-related genes by peripheral blood CD34 cells, M083
- Expression profiles of Wnt signaling pathway components in response to cAMP stimulation at different stages of osteoblast maturation, M040
- FGF-2 signaling in osteoblasts: Cx43 is a docking platform for PKC $\delta$ , F026
- FGF-23 and FGF-2 share a common but also have distinct signaling pathways for negative regulation of bone nodule mineralization in cultured osteoblasts, SA206
- FOXO1 signaling in the control of bone mass, 1112
- Functional association of MAPK and Runx2 on osteoblast chromatin, SU025
- Functional role of Osr2 in preosteoblastic cells, M006
- G171V and A214V Lrp5 knock-in mice have increased bone mass and strength, and can help precisely define the in vivo functions of Lrp5 during bone growth and homeostasis, 1002
- GC signaling in osteoblasts maintains normal bone structure in mice, F233
- GC signaling through osteoblasts is essential for cranial skeletal development, 1267
- Gender specific effects of TRPV4 on osteoblast-osteoclast coupling and risk of osteoporotic fractures, SA355
- Gene expression analysis of in vitro-aged and immortalized human MSCs, M047
- GILZ promotes osteoblast development and modulates RANKL/OPG levels, M049
- Global transcriptome analysis in mouse osteoblasts identifies a mechanosensing osteoblast gene signature, SU017
- GPRC6A null mice exhibit osteopenia and feminization, F004
- High bone mass phenotype in the bone specific Dlx3 KO mice, M027
- High concentrations of hydroxytyrosol and quercetin antioxidants enhance adipogenesis and inhibit osteoblastogenesis in MSCs, SA037
- Hormonal control of RANKL expression is independent of Runx family proteins: evidence that commitment to the osteoblast lineage is not a requirement for the stromal cells that support osteoclast differentiation, SU047
- hPTHrP 1-36 stimulates PKA-dependent phosphorylation and nuclear translocation of  $\beta$ -catenin in neonatal mouse calvarial bone cells, F032
- HSPG modulate osteogenic differentiation through heparan sulfate chains, M094
- Human osteoblasts synthesize VEGF in response to ACTH, SA236
- Human osteoprogenitor cell adhesion and spreading on functionalized Ti surfaces followed by QCM and CLSM, SA101
- Imaging of mineralization kinetics suggests that the transition from osteoblast to osteocyte initiates prior to mineral deposition, F062
- Impaired angiogenesis and compromised fluid volume accompanies increased osteoblast and osteocyte apoptosis with GC excess, SA453
- Importance of melastatin-like transient receptor potential 7 and Mg in the stimulation of osteoblast proliferation and migration by platelet-derived growth factor, M008
- Inactivation of Dlx5 gene results in altered osteoblast-osteoclast coupling inducing increased bone resorption and reduced cortical thickness in male mice, F010
- Inactivation of the ILK in osteoblasts increases mineralization, M061
- Increased osteoclasts in Brl mouse model for OI are independent of decreased osteoblast matrix production and RANKL/OPG ratio, but are associated with increased osteoclast precursors in marrow, SU209
- Induction of CTGF by TGF $\beta$ 1 in osteoblasts: independent effects of Src and Erk on Smad signaling, M066
- Induction of oxidative stress and diversion of  $\beta$ -catenin from TCF- to FOXO-mediated transcription by GCs or TNF $\alpha$  in osteoblastic cells, SA185
- INF $\gamma$  attenuates BMP-2 signaling via Stat-1 binding of Smad4 in the cytoplasm, SU139
- Inhibition of BMP pathway and osteoclast activity in osteoblastic prostate cancer lesion in bone, F283
- Inhibition of major bone catabolic mediators in human subchondral bone osteoblasts upon EphB4 receptor activation by Ephrin-B2 ligand, SU003
- Inhibition of the mevalonate pathway rescues the DEX-induced suppression of the mineralization of osteoblastic cells, SA230
- Integrin mediated mechanical forces stimulate differentiation of MSCs, SA528
- Integrin-associated protein upregulates osteogenesis-related transcription factors via TGF $\beta$  and BMP pathways, SA028
- Interaction of Ciz, a nucleocytoplasmic shuttling transcription factor with C-propeptides of type I collagen, M044
- Isolation and characterization of osteoblasts from alveolar bones of aged donors, SU049
- Jagged1 stimulation by PTH(1-34) in mature osteoblasts is not required for HSC expansion, 1078
- Lack of calcitonin accentuates bone loss during lactation by enhanced osteoclast formation and reduced osteoblast formation, SA194
- Lentiviral shRNA mediated inhibition of Grx5 expression induces apoptosis via a mechanism involving increased ROS and cardiolipin oxidation, and reduced SOD activity, M009
- Li affects matrix mineralization by decreasing tissue non-specific ALP levels in osteoblasts, SA071
- Ligand activation of the engineered G $\gamma$ -coupled receptor Rs1 in osteoblasts promotes trabecular bone formation, 1076
- Lithocholic acid downregulates the effects of Vitamin D $_3$  on primary human osteoblasts, SA030
- Longevity gene *SIRT-1* independently controls both osteoblast and osteoclast function, 1098
- Loss of classical ERE signaling results in suppression of early commitment of BMSC to osteoblasts, F029
- Loss or gain of FoxO function in osteoclasts and osteoblasts alters the rate of apoptosis and BMD in mice, 1247

- LPS-induced inhibition of osteogenesis is TNF $\alpha$  dependent, M019
- Mab21 suppresses the osteogenic markers by recruiting Sin3A and stimulates osteoclast by up-regulation of IL-6 and LIF, SU022
- MAPK-dependent inhibition of osteocalcin gene expression by TGF $\beta$ , M033
- Mapping the interrelationship of the adipogenic and osteogenic lineage with visual reporters, M097
- Mechanical loading upregulates expression of the transcription factor EGR2/Krox-20 by a COX-2-mediated mechanism, SA526
- Mechanical strain prevents adipogenesis in MSC by stimulating a durable  $\beta$ -catenin signal, SA522
- Menaquinone-4 derived from phyloquinone regulates osteoblast function, SU034
- Mice lacking NMDA receptor expression in osteoblasts have pronounced vertebral bone abnormalities, F012
- Mice lacking the novel transmembrane protein Opt develop catastrophic defects in bone modeling, 1075
- Mice lacking the Wnt receptor Frizzled-9 display osteopenia caused by decreased bone formation, 1006
- Molecular mechanisms underlying matrix vesicle-induced mineralization during bone formation, SA063
- Molecular phenotyping of osteoblastic and osteocytic cell fractions isolated from mouse calvaria, M106
- Msx1 homegene specific and non-redundant function in oral bones, M016
- NARS induced by bFGF regulates the proliferation and survival of osteoblasts, SA164
- Neuroendocrine activation of AMPK in osteoblasts, SU037
- NFI transcription factors regulate IGFBP5 gene transcription in human osteoblasts, SU015
- Non-genomic estrogen receptor Gpr30 is a Runx2 responsive gene that is required for osteoblast proliferation, F572
- Normal human osteoblasts internalize MSUM by phagocytosis and autophagy, M057
- Normal intramembranous fracture healing in mice with transgenic osteoblast-targeted disruption of GC signaling, SA234
- Notch inhibits NFAT transactivation in osteoblast cultures, 1111
- Notch signaling regulates osteoblast maturation transition to mineralization phase, SA068
- Novel modification of bone grafts inhibits bacterial colonization, M169
- NPY effect on osteoblast cells, SU011
- Osteoblast and osteoclast involvement in the pathogenesis of a mouse model for CMD, 1204
- Osteoblast-specific deletion of *Lrp6* reveals distinct roles for *Lrp5* and *Lrp6* in bone development, 1001
- Osteoblast-targeted deletion of the GC receptor has little impact on PBM but attenuates DEX-induced suppression of bone formation, F452
- Osteoblastic androgen receptor regulates cortical BMD, 1122
- Osteoblasts apoptosis is mediated through GSK3 $\beta$ , M005
- Osteoclast precursors play a role in recruiting breast cancer cells and osteoblasts onto the bone in vitro, SA278
- Osteocytes can modulate osteoblastic activity via NPY signaling, SA056
- Osteoformin increases the levels of intracellular Ca of human preosteoblast cells in culture, SU051
- Osteogenesis effect of human ligamentum flavum, myoblast, osteoblast and MSC by DBM and BMP-2, SU135
- Osteogenic cell lineages show differential responsiveness to angiogenic signals, SU061
- Osteogenic potential of human bone marrow and circulating Stro-1<sup>+</sup>/CD45<sup>low</sup> cells, M078
- Osteogenic potential of PDL cells in vivo, SU054
- Osx is required for skeletal growth and bone homeostasis after birth, 1074
- Osx, a positive regulator in adult bone formation, F008
- Overexpression of GSR in osteoblasts decreases bone formation and partially prevents OVX-induced bone loss, F024
- Overexpression of Lef-1 $\delta$ N increases bone mass in mice, 1258
- P2X<sub>7</sub> receptor activation mediates PKC $\alpha$  translocation in osteoblasts through alteration in actin cytoskeletal organization, SU040
- P2Y<sub>2</sub> receptor activation regulates RhoA-mediated stress fiber formation in osteoblasts, SA035
- PAR-2 activation induces bone resorption via RANKL upregulation in human OA subchondral bone osteoblasts, M018
- PBX1 interaction with HOXA10 regulates timing and expression of phenotypic bone genes during osteoblastogenesis, SU019
- PIAS3 negatively regulated RANKL-mediated osteoclastogenesis directly in osteoclast precursors and indirectly via osteoblasts, F079
- Possible physiological function of menin protein as transcriptional factor that modulates miRNA expression during osteogenesis, M036
- Post-mitotic preosteoblasts are the targets of the anabolic actions of intermittent PTH on periosteal bone, 1157
- Post-translational regulation of Msx2 protein, SU021
- PPAR $\gamma$ 2-mediated proteolytic degradation of  $\beta$ -catenin determines an anti-osteoblastic effect of anti-diabetic TZDs, SU023
- Primary bone cells of pregnant mice exposed to oscillatory fluid flow, M015
- Program of miRNAs control BMP-2 induced bone phenotype development, M090
- Progressive lipodystrophy in the osteosclerotic mice over-expressing Fra1, 1149
- Proinflammatory cytokine TWEAK induces SCT expression in human immature osteoblasts in a MAPK dependent fashion, M046
- Prostaglandins enhance extracellular matrix mineralization through the enhancement of both Na-dependent phosphate transport activity and ALP activity in osteoblast-like cells, SU031
- Proteasome inhibition counteracts the negative effect of GC treatment on bone metabolism by stimulating osteoblasts and inhibiting osteoclasts in vitro, SA231
- PTH induces COX-2 in MC3T3-E1 osteoblasts via cAMP-PKA and Ca-calcineurin pathways, SA033
- PTH regulation of Osx transcription in osteoblasts, M042
- PTH signaling through LRP5/6 in osteoblasts, 1014
- RANKL suppression by siRNAs in rat primary osteoblasts, M032
- RANKL/OPG in primary cultures of osteoblasts from patients with osteoporotic hip fractures, SU009
- RBP1 is critical for Runx2 expression, transcriptional activity and nodule formation in osteoblasts, M037
- Regulation of bone formation by osteoclasts involves Wnt/BMP signaling and the chemokine S1P, M017
- Regulation of intracellular signaling of MC3T3-E1 osteoblasts by the extracellular matrix, SA139
- Regulation of osteogenesis by Wnt signaling in rat MSC and human ASC, SU045
- Regulation of RUNX2 at the nuclear lamina, M055
- Regulation of Runx2 function in osteoblasts by sex steroid receptors, M099
- Regulation of the BMP-2 distant osteoblast enhancer by FGF-2, SU150
- Regulation of the osteoblast-specific transcription factor Osx by NO66, a Jumonji family histone demethylase, F017
- Regulatory signaling pathways in BMP mediated osteogenesis of adult human MSC cultures, M060
- Role of ATF4 in osteoblast proliferation and survival, M079
- Role of cell surface ATP synthase in fluid shear stress induced ATP release in osteoblasts, SU039
- Roles of ZOL in bone healing and osteoblast functions, 1064
- Runx2 threshold for the CCD phenotype, M041
- Selective retention of bone marrow cells in repair of canine femoral defect with polycaprolactone-tricalcium phosphate scaffolds, SU005
- Sequestration, proliferation and differentiation of osteoblasts in hydrogels for tissue engineering applications, SA143
- Serine protease inhibitor AEBSF blocks transcription of Phex by osteoblasts, M053
- Silencing of RhoGTPases counteract microgravity-induced effects on osteoblasts, SA011
- SIRT1 is a regulator of MSC lineage allocation, M085
- SOST blocks GSK3-beta inhibitor-induced ALP activity, SU036
- Soy-based formula promotes bone growth in neonatal piglets by inducing osteo-progenitors to differentiate into osteoblasts via enhanced BMP-2 signaling, SA336
- SP stimulates BMSC osteogenic activity and osteoclast differentiation and function in vitro, SU032
- Sr ranelate decreases osteoblast-induced osteoclastogenesis through the involvement of the CaSR, F389
- Sr ranelate protects osteoblasts from apoptosis independently of the CaSR, M007
- Stable expression of constitutively active G $\alpha$ 12 in osteoblastic cells promotes matrix protein expression and ALP activity, M068
- Stable isotopic labeling of amino acids in cultured human BMSC: application to BMP-2 induced Wnt/ $\beta$ -catenin signaling, SA036
- Stat3 induces osteoblastic bone metastases through up-regulating the expression of Shh and a Ca channel TRPM8 in the LNCaP human prostate cancer cells, 1089
- Strain-induced fluid flow in a 3D porous matrix promotes osteoblastic calcification in vitro, SA525
- Suppression of canonical wnt signaling by Dkk1 attenuates PTH-mediated peritrabecular stromal cell response and new bone formation in a model of HPT2, F215
- Targeted disruption of Nrf1 in osteoblasts leads to reduced bone size and dramatic alterations in trabecular bone microstructure in mice, 1190
- Targeted disruption of PPAR $\gamma$  in BMSC reveals its role in aging-induced bone loss, 1148
- Targeted overexpression of the nuclear FGF-2 isoforms in osteoblasts induces hypophosphatemia via modulation of FGF-23 and Klotho in mice, 1084
- Telomerase deficiency leads to decrease bone mass and impaired MSCs functions in telomerase deficient (TERC<sup>-/-</sup>) mice, 1147
- TGF $\beta$  blockade inhibits osteolytic but not osteoblastic prostate cancer metastases, SA274
- TGF $\beta$  signaling in stromal cells facilitates osteoblastic lesions in prostate cancer, 1087
- TNF $\alpha$  and IL-1 $\beta$  stimulate ALP activity and mineralization but decreases RUNX2 expression and osteocalcin secretion in human MSC, SU044
- Towards development of a PSi-based hybrid biomaterial with osteoconductivity and osteoinductivity, M028

## Key Word Index

## ASBMR 30th Annual Meeting

Tracking adipose differentiation in vitro with aP2-GFP reporters and flow cytometry: lipid staining and macrophage mimicry, SU057

Traf2 regulates BMP signaling pathway in osteoblastic cells, M063

Transcriptional activation of osteocalcin by Runx2 during osteoblast development is controlled at the post-translational level, M031

Transgenic mice over-expressing TIEG in osteoblasts display a gender specific bone phenotype, M024

Transgenic overexpression of the Wnt antagonist Krm-2 in osteoblasts leads to severe impairment of bone formation and increased bone resorption, 1003

TRIP-1 is eIF3i: a key regulator of osteoblast activity, 1259

TZD modify nuclear heterochromatin architecture, SU056

Use of  $\alpha$ -SMA-GFP transgene to identify periodontium derived osteoprogenitors, SA040

Use of GFP reporters to assess cell lineage in a murine model of tibial fracture repair, M077

Use of GFP reporters to map the progression of multipotential progenitor cells into the osteoblast lineage, SU053

Various roles of syndecan family in osteoblastic cells, SA147

VEGF and PTEN regulate bone homeostasis via control of osteoblastogenesis, osteoclastogenesis and adipocyte differentiation, M029

Wdr5 is required for chromatin modifications at the Runx2 promoter, M039

Wnt/LRP5-independent inhibition of osteoblastic cell differentiation by SCT, 1256

**Osteocalcin**

Analytical validation of LIA and ELEC methods for the determination of osteocalcin, SA191

Development of a new N-Mid<sup>®</sup> osteocalcin immunoassay on the IDS Automated Analyser 3x3<sup>TM</sup>, SA303

Intermittent injection of recombinant osteocalcin improves glucose tolerance and insulin sensitivity, F168

Low serum osteocalcin predicts carotid plaques and indicators of the metabolic syndrome, SA198

MAPK-dependent inhibition of osteocalcin gene expression by TGF $\beta$ , M033

NFATc1 mediates HDAC-dependent transcriptional repression of osteocalcin expression during osteoblast differentiation, 1145

Osteocalcin is a stress hormone: interaction with the sympathetic nervous system, M059

Plasma osteocalcin is inversely related to fat mass and plasma glucose in elderly Swedish men, SU459

Reduced serum osteocalcin and sex hormone binding globulin in men with type II diabetes, SU461

Sympathetic tone mediates leptin's inhibition of insulin secretion by modulating osteocalcin bioactivity, F034

TNF $\alpha$  and IL-1 $\beta$  stimulate ALP activity and mineralization but decreases RUNX2 expression and osteocalcin secretion in human MSC, SU044

Transcriptional activation of osteocalcin by Runx2 during osteoblast development is controlled at the post-translational level, M031

Variation in the osteocalcin gene: association study of BMD, fracture and changes in body fat mass in elderly women, SU225

**Osteocalcin, uncarboxylated (ucOC)**

Clinical significance of ucOC in GIO, M299

Serum ucOC concentration are related to renal function in type 2 diabetes patients, M443

ucOC is an endocrine link between the skeleton and the glucose metabolism, F444

ucOC level in healthy Korean women, M300

**Osteoclast inhibitory peptide-1 (OIP-1)**

IL-12 stimulates the OIP-1 gene expression in CD4<sup>+</sup> T-cells, SA173

**Osteoclastic differentiation**

All-*trans*-retinoic acid (Vitamin A) increases expression of MafB and inhibits osteoclast formation by interfering with differentiation of osteoclast progenitor cells, M117

ANKH mutation causing CMD inhibits osteoclast differentiation, SU214

CD47 (IAP) is an important modulator of osteoclast and osteoblast differentiation in vitro and in vivo, F093

Cholesterol sensing receptors, Liver X receptor  $\alpha$  and  $\beta$ , have novel and distinct roles in osteoclast differentiation and activation in bone, F085

DARC regulates osteoclast differentiation via modulating chemokine effects on migration/fusion of osteoclast precursors, M115

Estrogen suppresses RANKL-induced osteoclastic differentiation of human monocytes via an ER $\alpha$  associated cytoplasmic signaling complex, but ER $\alpha$  is downregulated during osteoclastic differentiation, 1125

Fungal secondary metabolites beauvericin and enniatin inhibit osteoclast differentiation and bone resorption, M130

IFN- $\beta$  is a key molecule in inhibition of human osteoclast differentiation by 1 $\alpha$ ,25-dihydroxyvitamin D<sub>3</sub>, SU090

Increased osteoclast differentiation and bone resorption during spaceflight, SU094

MKP-1 protects bone mass via negative regulation of osteoclast differentiation and activation, 1219

Multi-walled carbon nanotubes inhibit osteoclast differentiation by inhibiting nuclear translocation of NFATc1, M113

Primary human bone marrow adipocytes stimulate osteoclast differentiation, M111

Pyrophosphates stimulates osteoclast differentiation and bone resorption, SA084

RANKL-mediated osteoclast lineage commitment dictates the role of LPS in osteoclast differentiation, SA088

Sim induces Wnt signaling and reduces CSF-1 secretion and RANKL/OPG ratio to block osteoclast differentiation, SU096

SP stimulates BMSC osteogenic activity and osteoclast differentiation and function in vitro, SU032

Suppression of TREM-2 expression and TREM-2-mediated costimulation of RANK signaling by cytokines that inhibit human osteoclast differentiation, SU114

Vimentin binds c-Fms in an M-CSF dependent manner and regulates osteoclast differentiation, SU097

Wnt5a regulates osteoclast differentiation in physiological and pathological conditions, 1012

**Osteoclastogenesis**

Atypical antipsychotic clozapine reduces rat osteoblast proliferation and osteoclastogenesis at therapeutic levels, SU030

BMSC up-regulate M-CSF receptor in monocytes to disrupt dendritic cell differentiation while facilitating osteoclastogenesis in myeloma, SU242

Brain-type creatine kinase is required for RANKL-induced osteoclastogenesis, M116

Breast cancer derived factors synergize with TGF $\beta$  to induce phosphorylation of ERK1/2 and to stimulate osteoclastogenesis, SU115

CGRP stimulates osteogenesis and inhibits osteoclastogenesis in vitro, SU033

Comparison of direct osteoclastogenic potential on osteoclast precursor cells among proinflammatory cytokines, SU077

Dietary normalization of Ca absorption in mice genetically deficient in CaSR and 25(OH)D-1 $\alpha$ -hydroxylase results in non-lethal, severe hyperparathyroidism with reduced osteoclastogenesis, M199

Differential contribution of osteoclast- and osteoblast-lineage cells to LPS modulation of osteoclastogenesis, SU088

DLK1/FA1 is a novel factor enhancing osteoclastogenesis and inhibiting bone formation in vitro and in vivo, 1007

Downregulation of Cx43 expression and osteoclastogenesis by a bioceramic bone graft substitute, M119

Effects of IL-27 on regulation of osteoclastogenesis by way of T cells, SU081

ER $\alpha$  deletion in cells of the monocyte/macrophage lineage increases osteoclastogenesis and abrogates the pro-apoptotic effect of E<sub>2</sub> on osteoclasts, 1097

Expression and function of synoviolin in human osteoclastogenesis, SA080

Expression of NF- $\kappa$ B ligand and regulation of osteoclastogenesis by bone marrow adipocytes, SA078

IFN- $\gamma$  inhibits TNF $\alpha$ -induced osteoclastogenesis in vitro and in vivo, SU152

IL-12 induces apoptosis in TNF $\alpha$ -mediated osteoclastogenesis in vivo, SA166

IL-27/WSX-1 signaling inhibits RANKL-induced osteoclastogenesis through STAT1 activation: a possible involvement in TLR4/MyD88-mediated inflammatory arthritis, SU102

Impairment of osteoblast lineage differentiation leads to increased osteoclastogenesis in OI murine, 1202

Inhibition of lamin A/C attenuates osteoblast differentiation and stimulates osteoclastogenesis through enhanced RANKL signaling, M070

Isoform-specific expression of PPARs and gene regulation during osteoclastogenesis in RAW/C4 cells, M118

Losartan<sup>®</sup> (Cozaar) increases appendicular bone formation by inhibiting osteoclastogenesis, M126

Lyn, opposite to c-Src, negatively regulates osteoclastogenesis in vitro and in vivo via its interaction with SHP-1 and Gab2, 1119

Mechanism of BMP-2 enhancement of PGE<sub>2</sub> stimulated osteoclastogenesis, SU085

MEK5/ERK5 signal regulates RANKL-induced osteoclastogenesis, SU103

Modeled microgravity sensitizes osteoclast precursors to RANKL mediated osteoclastogenesis by increasing DAP12, M114

Modulation of osteoclastogenesis by fatty acids, SU071

Novel role of L-Ser for the activation of RANKL-RANK signaling machinery in osteoclastogenesis in vitro, SA082

Novel splicing variants of ADAM8 stimulate tumor-induced bone metastasis by increasing invasion and osteoclastogenesis, F286

PIAS3 negatively regulated RANKL-mediated osteoclastogenesis directly in osteoclast precursors and indirectly via osteoblasts, F079

Proteasome inhibitors attenuate osteoclastogenesis and bone resorption via the modulation of RANK-mediated TRAF6, p62 and I $\kappa$ B- $\alpha$  signaling cascades, SA099

Recombinant mouse M-CSF receptor C-fms inhibits TNF $\alpha$ -induced osteoclastogenesis, M112

Reduced osteoclastogenesis and RANKL expression in marrow from women taking ALN, SU400

Regulation of bone mass and osteoclastogenesis by the CEACAM1, F091

- Rheumatoid synoviocytes are stimulated with IL-23 to enhance osteoclastogenesis through upregulation of RANKL expression, SU084
- S100 protein directly and indirectly affects RANKL-stimulated osteoclastogenesis, SA090
- Sr ranelate decreases osteoblast-induced osteoclastogenesis through the involvement of the CaSR, F389
- Three RANK cytoplasmic motifs, IVVY<sup>535-538</sup>, PVQEE<sup>559-564</sup> and PVQEQG<sup>604-609</sup>, play a critical role in TNF $\alpha$ /IL-1-mediated osteoclastogenesis, 1118
- TSH inhibits the expression of HMGB, a regulator of TNF $\alpha$  transcription, in osteoclastogenesis, 1117
- TSP-1 and CD47 regulate osteoclastogenesis but have distinct effects on bone metastasis, 1232
- Ubiquitin-like domain of IKK $\beta$  is critical for osteoclastogenesis, SU112
- VEGF and PTEN regulate bone homeostasis via control of osteoblastogenesis, osteoclastogenesis and adipocyte differentiation, M029
- In vitro aging of young bone enhances osteoclastogenesis, SU091
- Osteoclasts**
- 1,25(OH)<sub>2</sub>D<sub>3</sub> can directly induce osteoclast formation in osteoclast precursors in the absence of RANKL, SU070
- In the absence of NF- $\kappa$ B2, TNF induces osteoclast formation in vivo independent of RANKL/RANK and more severe arthritis in TNF-Tg mice, 1009
- Acidosis augments the resorptive capacity of human osteoclasts by increasing lysosomal acidification, M122
- Adiponectin inhibits osteoclast formation via AKT signaling pathway, SU110
- AG490, a Jak2 specific inhibitor, induces osteoclast survival by activating Akt and ERK signaling pathway, SU108
- ALN affects cross-talk of osteoclasts and osteoblasts in vivo, SU392
- Angiogenic potential of osteoclasts, SU075
- AP-1 and Mitf interact with NFATc1 to stimulate Cat K promoter activity in osteoclast precursors, SA076
- Are all anti-resorptive treatments the same? Lessons learned from inhibition of human osteoclastic bone resorption by alternative pathways, M129
- Atypical osteoclast phenotype after long-term ALN therapy for osteoporosis, SU399
- Biochemical characterization of ER $\alpha$  co-regulators in multinucleated mature osteoclasts, 1126
- Bisphosphate protect cartilage by reducing chondrocyte apoptosis and reduce bone loss by suppressing osteoclast in adjuvant arthritis, M428
- Brain-type creatine kinase is required for RANKL-induced osteoclastogenesis, M116
- Breast cancer derived factors synergize with TGF $\beta$  to induce phosphorylation of ERK1/2 and to stimulate osteoclastogenesis, SU115
- Bridging vascular calcification and osteoporosis: the function of receptor activator of nuclear factor  $\kappa$ B, M419
- BSP deficiency impairs osteoclast differentiation and resorption in vitro, SA142
- Calcitonin receptor on osteoclasts plays a physiological role to protect against HCa in mice, SA197
- Cannabinoid receptor GPR55 affects osteoclast function in vitro and bone mass in vivo, 1221
- Cbl-PI3K interaction regulates osteoclast function, differentiation and survival, 1011
- Cell cycle-arrested QOP are cells committed to the osteoclast lineage, SU098
- Chloride channel CIC-7 mediates acidification of the resorption lacuna in osteoclasts, M123
- Class IA PI3Ks are indispensable for osteoclast function by regulating cytoskeletal organization and cell death, 1115
- Co-expression of p62<sup>P392L</sup> and MVNP in osteoclasts precursors increases the formation of osteoclasts that express a pagetic phenotype, F476
- Comparison of direct osteoclastogenic potential on osteoclast precursor cells among proinflammatory cytokines, SU077
- CT-1 is an osteoclast-derived coupling factor required for normal bone remodeling, M014
- DC-STAMP regulates bone metabolism through cell-cell fusion of osteoclasts, F087
- Differential contribution of osteoclast- and osteoblast-lineage cells to LPS modulation of osteoclastogenesis, SU088
- Dkl1/FA1 is a novel factor enhancing osteoclastogenesis and inhibiting bone formation in vitro and in vivo, 1007
- Dock5, an essential Rac exchange factor in osteoclasts that controls adhesion structure organization and bone resorbing activity, SU064
- Downregulation of Cx43 expression and osteoclastogenesis by a bioceramic bone graft substitute, M119
- Drugs which inhibit osteoclast function suppress tumor growth and alter hematopoietic cell populations in bone, F270
- Effect of luteolin on bone loss, microarchitecture and bone resorption in OVX mice, M128
- Effect of MSCs in coculture with osteoclasts: a contact mediated and dose-dependent effect?, SA094
- Effects of exercise intensity on the bone metabolic response to running, M481
- Effects of the Cat K inhibitor ODN on osteoclast-mediated bone resorption, M127
- Efficient and stable gene expression into human osteoclasts using an HIV-1 based lentiviral vector, SU113
- Elevated serum levels of CXCL12 is associated with increased osteoclast activity and osteolytic bone disease in MM patients, SU079
- Endocytotic processes underlying Ca-induced inhibition of plasma membrane V-ATPase in murine osteoclasts, SU101
- Expression and function of synoviolin in human osteoclastogenesis, SA080
- Expression of 11 $\beta$ -hydroxysteroid dehydrogenase during murine osteoclast formation, SA235
- Extracellular matrix protein fibronectin positively regulates the osteoclast function, SU069
- Formation of podosome belts by osteoclasts on plastic correlates with resorptive activity, SU068
- Gastric proton pump inhibitors failed to affect bone resorption and formation, SA095
- Gender specific effects of TRPV4 on osteoblast-osteoclast coupling and risk of osteoporotic fractures, SA355
- High dose of RANKL rescues integrin  $\alpha_v$ <sup>-/-</sup> osteoclast phenotype, F081
- High levels of IL-6 and hyper-responsivity to 1,25(OH)<sub>2</sub>D<sub>3</sub> are both required for development of Pagetic osteoclasts, F478
- Hormonal control of RANKL expression is independent of Runx family proteins: evidence that commitment to the osteoblast lineage is not a requirement for the stromal cells that support osteoclast differentiation, SU047
- Identification of osteoclast lysosomal proteins by mass spectrometry, SA077
- Identification of the regulatory mechanism(s) of PTP-PEST associating with the sealing ring formation and bone resorption in osteoclasts, SU065
- Identification, characterization and isolation of peripheral osteoclast progenitors, SU099
- Implication of PGD<sub>2</sub> in the birth and death of human osteoclasts, SU095
- Important contribution of the immune system in regulating the tumor/bone vicious cycle independent from osteoclasts, 1086
- Inactivation of Dlx5 gene results in altered osteoblast-osteoclast coupling inducing increased bone resorption and reduced cortical thickness in male mice, F010
- Increased osteoclasts in Brl mouse model for OI are independent of decreased osteoblast matrix production and RANKL/OPG ratio, but are associated with increased osteoclast precursors in marrow, SU209
- Increased signaling through p62 in the MM microenvironment increases myeloma cell growth and osteoclast formation, SA289
- Inhibin directly targets suppression of isolated human osteoclast precursor development and activity, SA086
- Inhibition of BMP pathway and osteoclast activity in osteoblastic prostate cancer lesion in bone, F283
- Inhibition of MMP activity delays bone repair whereas inhibition of osteoclast function and formation does not, SA075
- Inpp4b as a regulator of bone mass, F089
- Investigations into the role of FAK in bone marrow-derived osteoclasts, SU111
- Isoform-specific expression of PPARs and gene regulation during osteoclastogenesis in RAW/C4 cells, M118
- Lack of calcitonin accentuates bone loss during lactation by enhanced osteoclast formation and reduced osteoblast formation, SA194
- Large osteoclasts in pediatric OI patients receiving intravenous pamidronate, SU497
- Longevity gene *SIRT-1* independently controls both osteoblast and osteoclast function, 1098
- Losartan<sup>®</sup> (Cozaar) increases appendicular bone formation by inhibiting osteoclastogenesis, M126
- Loss of a single bim allele recovers the defective osteoclast function in bcl-2<sup>-/-</sup> mice but does not restore the anabolic action of PTH, 1217
- Loss or gain of FoxO function in osteoclasts and osteoblasts alters the rate of apoptosis and BMD in mice, 1247
- LPA regulates osteoclast survival and retraction, SU105
- LPS suppresses RANK gene through the down-regulation of PU.1 and MITF, SU083
- Lyn, opposite to c-Src, negatively regulates osteoclastogenesis in vitro and in vivo via its interaction with SHP-1 and Gab2, 1119
- Mab21 suppresses the osteogenic markers by recruiting Sin3A and stimulates osteoclast by up-regulation of IL-6 and LIF, SU022
- Matrix PRELP interferes with the NF- $\kappa$ B pathway and impairs osteoclast formation and activity, SU089
- Mechanism of BMP-2 enhancement of PGE<sub>2</sub> stimulated osteoclastogenesis, SU085
- MEK5/ERK5 signal regulates RANKL-induced osteoclastogenesis, SU103
- Melanoma-induced bone loss is mediated by the rapid recruitment of osteoclasts, SU233
- Mice deficient in Pyk-2 have impaired OVX-induced bone resorption, F098
- Microarchitecture and tissue age influence in vivo bone resorption, M125
- Modeled microgravity sensitizes osteoclast precursors to RANKL mediated osteoclastogenesis by increasing DAP12, M114
- Modulation of osteoclastogenesis by fatty acids, SU071
- Multinuclear expression of ER $\alpha$  in mature osteoclasts, SU186
- Neutrophil-like PLB-985 cells induce differentiation of human blood monocytic precursors into functional osteoclasts via a RANKL-dependent mechanism, SA092
- NO has a powerful effect of osteoclast cells, M131
- Novel role for TPO in regulating osteoclast development, SU104

## Key Word Index

## ASBMR 30th Annual Meeting

Novel role of L-Ser for the activation of RANKL-RANK signaling machinery in osteoclastogenesis in vitro, SA082

Novel selective P2X<sub>7</sub> receptor antagonist inhibits human osteoclast formation in vitro, M120

Oleuropein from olive stimulates the differentiation and mineralization of cultured osteoblasts and inhibits the formation of osteoclasts in culture, M081

OPG and bisphosphonates had differential effects on osteoclast numbers, bone marrow fibrosis and cortical porosity in a mouse model of constitutive activation of the PTH/PTHrP receptor, M076

Osteoblast and osteoclast involvement in the pathogenesis of a mouse model for CMD, 1204

Osteoclast precursors play a role in recruiting breast cancer cells and osteoblasts onto the bone in vitro, SA278

Osteoclast-independent function of Cat K: regulation of TLR-9 signaling in autoimmunity, F074

Over-expression of RAGE prevents OVX-mediated bone loss in CD1 mice, M132

Pacemaker channel, HCN, controls functions of osteoclasts, SU100

PGC-1 $\beta$  and iron uptake in the mitochondrial activation of osteoclasts, 1222

Phthalein monophosphates are specific substrates for TRACP5b, M284

PIAS3 negatively regulated RANKL-mediated osteoclastogenesis directly in osteoclast precursors and indirectly via osteoblasts, F079

PKC $\delta$  is important for acidification of the lysosomes and resorption lacuna in osteoclasts, M124

Proteasome inhibition counteracts the negative effect of GC treatment on bone metabolism by stimulating osteoblasts and inhibiting osteoclasts in vitro, SA231

Proteasome inhibitors attenuate osteoclastogenesis and bone resorption via the modulation of RANK-mediated TRAF6, p62 and I $\kappa$ B- $\alpha$  signaling cascades, SA099

Proteomic identification and characterization of the small GTPase Rab18 in human osteoclasts, SU109

R740S, a dominant V-ATPase a3 mutation, causes osteopetrosis in mice, 1218

Rac 1 and 2, in combination, mediate osteoclast function and survival, 1220

RANKL induces Ca channel activation in human osteoclasts, SU107

Rapid-nontranscriptional action of 1,25(OH)<sub>2</sub>D<sub>3</sub> induces IL-6 production in osteoclast precursors expressing MVNP, 1186

Recombinant mouse M-CSF receptor C-fms inhibits TNF $\alpha$ -induced osteoclastogenesis, M112

Reduced osteoclastogenesis and RANKL expression in marrow from women taking ALN, SU400

Regulation of bone mass and osteoclastogenesis by the CEACAM1, F091

Resorption mechanism of HA and  $\beta$ TCP coating layer, SA100

Role of alpha gene tropomyosins in osteoclast function, SU067

Role of LIMK1 in osteoclast cytoskeletal remodeling and bone resorption, 1116

Roles of Cxcl2 in osteoclast precursor cells, SU086

S100 protein directly and indirectly affects RANKL-stimulated osteoclastogenesis, SA090

SLP-76 couples Syk to the osteoclast cytoskeleton in vitro and in vivo, 1010

Syk tyrosine 317 negatively regulates osteoclast function, 1120

Tec kinases, therapeutic targets for bone destructive diseases, F083

TGF $\beta$ 1 induces human osteoclast apoptosis, SU078

Three RANK cytoplasmic motifs, IVVY<sup>535-538</sup>, PVQEET<sup>559-564</sup> and PVQEQQ<sup>604-609</sup>, play a critical role in TNF $\alpha$ /IL-1-mediated osteoclastogenesis, 1118

Transactivation of RANKL by C/EBP $\beta$  and C/EBP $\delta$  in adipocyte lineage cells, SU092

TRIP-6 regulates osteoclast formation, adhesion, and resorptive capacity, SU066

TSG-6 acts synergistically with OPG to inhibit bone resorption, SA097

TSH inhibits the expression of HMGB, a regulator of TNF $\alpha$  transcription, in osteoclastogenesis, 1117

Twisted gastrulation-deficient mice exhibit osteopenia through enhanced osteoclast function, 1008

Tyrosine kinase inhibitor dasatinib decreases osteoclast formation and activity in vitro, SU074

Ubiquitin-like domain of IKK $\beta$  is critical for osteoclastogenesis, SU112

Ucn strongly suppresses the formation and function of osteoclasts via a novel mechanism, SA096

VEGF induction provides evidence for different signaling pathway activation by large and small osteoclasts, SU106

In vitro aging of young bone enhances osteoclastogenesis, SU091

ZOL inhibits the capacity of myeloid-immune suppressor cells in myeloma to form osteoclasts, SU230

**Osteoconductivity**

Towards development of a PSi-based hybrid biomaterial with osteoconductivity and osteoinductivity, M028

**Osteocytes**

Aberrant *Phex* function in osteocytes has limited effects on bone mineralization in XLH, 1051

Adenylyl cyclase 6 mediates primary cilia-regulated decreases in cAMP in bone cells exposed to dynamic fluid flow, 1040

Analysis of CXCR7-deficient mice reveals CXCR7 expression in osteocytes but no apparent bone phenotype, M104

In bone, RPTP $\mu$  is exclusively expressed in osteocytes and may affect bone mass, SA052

Cis-regulatory motifs and computationally-derived transcriptional networks predict dynamic motions for osteocytes, M103

Comparison of gene expression in osteocytes versus osteoblasts, M056

Deletion of *Mef2c* in osteocytes decreases *Sost* expression and increases bone mass, F054

Direct correlation of osteocyte deformation with Ca influx in response to fluid flow shear stress, SA057

Early osteocyte marker, E11/gp38 is highly elevated in new bone formed in response to distraction as compared to existing bone, SA136

Effect of RIS on osteocyte viability in paired biopsies from early postmenopausal women, M420

Effect of SSBT on osteocyte viability, F405

Effect of the dietary Ca/P ratio on the rate of skeletal accrual in mice, M333

Effects of electrical stimulation on NO expression and osteocyte viability in OVX rats, SA524

Effects of Vitamin K2 and RIS on bone formation and resorption, osteocyte lacunar system and porosity in the cortical bone of GC-treated rats, SU385

Estrogen deficiency alters the localized material properties of the peri-lacunar bone matrix in old rats, M107

Evidence that differentiated bone cells display an autophagic response regulated by HIF-1 $\alpha$ , F058

Expression of human SCT in heterologous eukaryotic insect and *E. coli* expression systems, SA059

Imaging of mineralization kinetics suggests that the transition from osteoblast to osteocyte initiates prior to mineral deposition, F062

Impaired angiogenesis and compromised fluid volume accompanies increased osteoblast and osteocyte apoptosis with GC excess, SA453

Kinase activation and osteocyte survival promoted by mechanical stimulation require LRP5/6 signaling and  $\beta$ -catenin accumulation, but not  $\beta$ -catenin/TCF-dependent transcription, M108

LIPUS synergistically modulates SCT and OPG/RANKL ratio in MLO-Y4 osteocytes in vitro, M109

Local osteocyte defect in *Dmp1* null mice causes overproduction of FGF-23, 1225

Mechanical perturbation of integrin  $\alpha$ 5 with or without association with fibronectin opens Cx43-hemichannels in osteocytes, SA060

MEPE expression is regulated by BMP-2 signaling through the activation of its downstream transcription factors, Dlx3, Dlx5 and Runx2, SA064

Molecular phenotyping of osteoblastic and osteocytic cell fractions isolated from mouse calvaria, M106

Notch signaling regulates osteoblast maturation transition to mineralization phase, SA068

Osteocyte-specific ablation of canonical Wnt signaling induces severe osteoporosis, 1037

Osteocytes can modulate osteoblastic activity via NPY signaling, SA056

Osteocytic perilacunar remodeling as a significant source of Ca during lactation, M110

Overexpression of androgen receptor in mature osteoblasts and osteocytes inhibits osteoblast differentiation, SU192

PTH receptor signaling in osteocytes increases bone mass and the rate of bone remodeling through Wnt/LRP5-dependent and -independent mechanisms, respectively, 1038

PTH-induced bone mass gain is blunted but not abolished in *SOST* overexpressing and deficient mice, 1039

SDF-1 is expressed in osteocytes and periosteal cells in response to mechanical loading, M105

Target ablation of PPR in osteocytes induces hypocalcemia and impairs bone structure, 1158

TIEG1 KO mice display defects in the bone matrix immediately surrounding osteocytes, SA065

Transcriptional regulation of Cx43 by  $\beta$ -catenin, a pathway activated by PGE<sub>2</sub>-PI3K-GSK3 signaling in mechanically loaded osteocytes, 1042

Validation of an immunoassay for the determination of PINP in rat serum, M296

In vivo load activated propagation of  $\beta$ -catenin signaling in osteocytes through coordinated downregulation of inhibitors of Lrp, 1041

**Osteodistraction**

First clinical application of electric stimulation on human distracted bone, SA568

**Osteodystrophy**

Hypothyroidism and autism combined with PHP in the absence of Albright's hereditary osteodystrophy and *GNAS* imprinting changes, SA259

**Osteodystrophy, hepatic**

Histomorphometric evaluation in an experimental model of hepatic osteodystrophy, M480

**Osteoformin**

Osteoformin increases the levels of intracellular Ca of human preosteoblast cells in culture, SU051

**Osteogenesis**

Androgen receptor disruption increases the osteogenic response to mechanical loading in male mice, 1140

Apc-mediated control of  $\beta$ -catenin is essential for both chondrogenic and osteogenic differentiation of skeletal precursors, SA130



BMP-6 stimulated osteogenesis of HOB cultures is associated with suppression of PYK2, SU048

Both the Smad and ERK MAP kinase pathway play critical roles in BMP-2-induced osteogenic transcription factors expression, M050

C-terminal fragment of PTHrP (107-139), exerts osteogenic features in both regenerating and nonregenerating bone in mice with diabetes-related osteopenia, SA223

CGRP stimulates osteogenesis and inhibits osteoclastogenesis in vitro, SU033

Continuous local infusion of ALN prevents osteopenia of the lengthened segment during distraction osteogenesis, SU001

Dependence of post natal osteogenic differentiation on BMP-2, SA001

Development of high-throughput screening system for osteogenic drugs using cell-based sensor, M082

Diet induced obesity compromises the osteogenic potential of the bone marrow, F047

Different osteogenic properties of human BMSC from different skeletal site origin, SU055

DNA methylation analysis of osteogenic gene promoter regions in mouse BMSC, M035

Enhanced mitochondrial biogenesis contributes to Wnt induced osteogenic differentiation of C3H10T1/2 cells, SA043

Enhanced osteogenic potential of alveolar vs. long bone derived BMSC, M095

FHL2 mediates DEX-induced MSC osteogenic differentiation by activating Wnt/ $\beta$ -catenin signaling and Runx2 expression, M048

Ghrelin inhibits early osteogenic differentiation of C3H10T1/2 cells by suppressing Runx2 expression and enhancing PPAR $\gamma$  and C/EBP $\alpha$  expression, M086

HSPG modulate osteogenic differentiation through heparan sulfate chains, M094

Icariin induces osteogenic differentiation in vitro in a BMP- and Runx2- dependent manner and bone regeneration in vivo, M089

Identification and characterization of angiogenesis-inducing secretory molecules from osteogenically differentiated MSC, M163

Induction of Runx2 and Osx by bisphosphonate promote osteogenic differentiation, SU062

Integrin-associated protein upregulates osteogenesis-related transcription factors via TGF $\beta$  and BMP pathways, SA028

LPS-induced inhibition of osteogenesis is TNF $\alpha$  dependent, M019

Mab21 suppresses the osteogenic markers by recruiting Sin3A and stimulates osteoclast by up-regulation of IL-6 and LIF, SU022

Mapping the interrelationship of the adipogenic and osteogenic lineage with visual reporters, M097

Mineralization potential and orientational aspects of osteogenic cell cultures by Raman spectroscopy, M084

Osteogenesis effect of human ligamentum flavum, myoblast, osteoblast and MSC by DBM and BMP-2, SU135

Osteogenic action of Ex-4 in normal and insulin-resistant state, M424

Osteogenic potential of bone marrow, compromised by disuse, is normalized by brief exposure to a low-level mechanical signal, M486

Osteogenic potential of human bone marrow and circulating Stro-1<sup>+</sup>/CD45<sup>low</sup> cells, M078

Osteogenic potential of PDL cells in vivo, SU054

Osteotropic peptides: anabolic and osteogenic effects, M045

PKD regulates HDAC7 localization and interaction with Runx2 during BMP-2-stimulated osteogenesis, SU027

Possible physiological function of menin protein as transcriptional factor that modulates miRNA expression during osteogenesis, M036

Pulse treatment with ZOL causes sustained commitment of bone marrow derived MSC for osteogenic differentiation, M072

R-spondin 2 is a novel osteogenic factor required for Wnt11 mediated osteoblast differentiation, SU063

Regulation of osteogenesis by Wnt signaling in rat MSC and human ASC, SU045

Regulatory signaling pathways in BMP mediated osteogenesis of adult human MSC cultures, M060

Short-term deleterious skeletal response to hindlimb suspension involves multifaceted compromises in cells of the osteogenic lineage, F523

SP stimulates BMSC osteogenic activity and osteoclast differentiation and function in vitro, SU032

Synergistic activation of osteogenesis in MLPC by oxysterols, SU038

TGF $\beta$  inhibits BMP signaling and osteogenesis through the TGF $\beta$  and BMP R-Smad direct interaction, 1080

Transient expression of CXC receptor 2 in human MSC stimulates chemotaxis toward CXC ligand 8 and increased mineralization in the presence of osteogenic medium, SA170

Wnt7a and Wnt7b evoke overlapping yet distinct transcriptional responses during the osteogenic programming of mesenchymal progenitors by Msx2, 1196

**Osteogenesis imperfecta (OI)**

Bisphosphonate, pamidronate, suppresses the pro-inflammatory response in a mouse model of OI as well as normal littermates, SU386

Hotspot splicing mutation in *LEPRE1* affects P3H1 and causes recessive OI, SU215

Identification of skin abnormalities in OI patients by MRI, SA561

Impairment of osteoblast lineage differentiation leads to increased osteoclastogenesis in OI murine, 1202

Increased osteoclasts in Brl mouse model for OI are independent of decreased osteoblast matrix production and RANKL/OPG ratio, but are associated with increased osteoclast precursors in marrow, SU209

Large osteoclasts in pediatric OI patients receiving intravenous pamidronate, SU497

Proinflammatory marker values at baseline and after a fracture are distinctly different comparing a mouse model of OI with normal controls, M234

Randomized dose comparison of pamidronate in children with types III and IV OI, SU496

Recurring mutation causing severe/lethal recessive type VIII OI in African-Americans originated in West Africa more than 300 years ago, SA262

Spectrum of OI mutations in Sweden, SA247

In utero stem cell therapy as treatment for classical OI using the knock in murine model BrlIV, F500

**Osteogenesis, distraction (DO)**

Endothelial progenitor cell mobilization during DO in human, SA053

Impaired bone healing in a BMP-2 KO mouse model of DO, SA159

Reconstruction of massive skeletal defects due to osteomyelitis by DO, M160

**Osteogenic sarcoma. See Sarcoma**

**Osteoinductivity**

Towards development of a PSi-based hybrid biomaterial with osteoconductivity and osteoinductivity, M028

**Osteolysis**

Biomechanical and geometrical property changes in rat tibias with tumor-induced osteolysis after anti-resorptive or anti-cancer treatments, SU236

Bzb, a proteasome inhibitor, prevents metastatic breast cancer osteolysis and reduces mammary fat pad tumor growth in mice, F277

Elevated serum levels of CXCL12 is associated with increased osteoclast activity and osteolytic bone disease in MM patients, SU079

HDI, Vorinostat, blocks growth and associated osteolysis of cancer cells within bone, but reduces bone volume in non-tumor bearing bones in mice, M279

Host bone marrow-derived stromal cells promote myeloma initiation and development of osteolysis, 1088

Monoclonal antibody to TGF $\beta$  inhibits tumor burden and osteolysis in a pre-clinical model of bone metastasis, SA187

TGF $\beta$  blockade inhibits osteolytic but not osteoblastic prostate cancer metastases, SA274

Wnt signaling regulates Gli2 and PTHrP expression in human breast cancer cells that cause osteolysis, M278

**Osteolysis, idiopathic multicentric with nephropathy (IMON)**

Additional clinical features of IMON, SU212

**Osteomalacia**

Goettingen minipigs—a model for Ca/Vitamin D-deficiency osteomalacia and steroid-induced osteoporosis, SA445

Inhibition of PPAR $\gamma$ 2 by BADGE and Vitamin D in male mice increases osteoblastogenesis and inhibits bone matrix mineralization leading to osteomalacia, SU374

PHEX cleavage of SIBLING-ASARM peptides as a mechanism underlying osteomalacia in XLH, 1199

Rare cases of XLH rickets/osteomalacia mimicking ARHR/osteomalacia, F469

Serum 25(OH)D measurement and histomorphometric analysis of iliac crest biopsies from 1180 patients reveals a high prevalence of Vitamin D-dependent osteomalacia, 1134

Vitamin D deficiency, osteomalacia and high bone turnover in patients with NF-1, F465

**Osteomalacia, oncogenic (OOM)**

Rapid detection of intact FGF-23 in tumor tissue from patients with OOM, SA204

**Osteomalacia, tumor-induced (TIO)**

Evaluation of clinical utility of venous sampling for FGF-23 in identifying and confirming responsible tumors for TIO, F163

**Osteomyelitis**

Colistin-impregnated bone cement beads prevent multi-drug resistant *Acinetobacter* osteomyelitis, M236

Reconstruction of massive skeletal defects due to osteomyelitis by DO, M160

**Osteomyelitis, sclerosing**

Diffuse sclerosing osteomyelitis of the mandible, WG25, M452

**Osteonecrosis**

Usefulness of alveolar bone density measurement in risk assessment for BRONJ, SA305

**Osteonecrosis of the jaw (ONJ)**

Application of preventive measures minimizes the occurrence of ONJ in patients with bone loss treated with bisphosphonates, F281

Bisphosphonate-associated ONJ cases in South Korea, SA412

Case presentation: bisphosphonate induced ONJ in Pagetic jaw bone, WG24

ONJ: ZOL 5 mg experience in a variety of osteoporosis indications, 1246

**Osteonectin**

Differential regulation of gene expression by SNPs in the osteonectin/SPARC 3 untranslated region, M270

Regulation of osteonectin/SPARC by miRNA-29, 1155

**Osteopathy, renal**

## Key Word Index

## ASBMR 30th Annual Meeting

- Change of pathological bone lesion in recipients with renal osteopathy after renal transplantation, SA498
- Osteopenia**
- Bisphosphonate-induced osteopetrosis: novel bone modeling defects, metaphyseal osteopenia, and osteosclerosis fractures after drug exposure ceases, F569
- C-terminal fragment of PTHrP (107-139), exerts osteogenic features in both regenerating and nonregenerating bone in mice with diabetes-related osteopenia, SA223
- C/EBP $\beta$  overexpression causes osteopenia, SA005
- Changes in serum PINP in orchidectomized osteopenic rats treated with PTH and ALN, M295
- Conditional disruption of *Pkd1* in osteoblasts results in osteopenia due to direct impairment of osteoblast-mediated bone formation, SA019
- Continuous local infusion of ALN prevents osteopenia of the lengthened segment during distraction osteogenesis, SU001
- Decreased bone formation, increased bone resorption, and osteopenia in mice lacking SP, SU160
- Defects in MSC self-renewal lead to an osteopenic phenotype in *Bmi-1* null mice, 1050
- Deletion of Zfp521, an antagonist to Runx2 and Ebf1 transcriptional activity, leads to osteopenia and a defect in matrix mineralization in mice, 1109
- Dietary Sr in a model of established osteopenic rats reduce the levels of 25(OH)D, SA377
- Diffuse osteopenia after tibia fracture: benefits of early mobilization and weight bearing, F461
- Dwarfism and osteopenia in mice with inactivated HRE in the VEGF gene promoter, 1152
- Effects of estrogen therapy and fluocalcic effervescent on the BMD and bone metabolism of surgical menopause women with osteopenia, M392
- Fracture risk in primary biliary cirrhosis: role of osteopenia and severity of cholestasis, M442
- Fully human anti-DKK1 antibodies increase bone formation and resolve osteopenia in mouse models of estrogen-deficiency induced bone loss, 1214
- GPRC6A null mice exhibit osteopenia and feminization, F004
- Mediation of bone loss with ultrasound induced dynamic mechanical signals in an OVX rat model of osteopenia, F536
- Mice lacking the Wnt receptor Frizzled-9 display osteopenia caused by decreased bone formation, 1006
- Osteopenia by high alcohol consumption in the absence of ALDH2 attribute to the disturbance of the differentiation in osteoblasts, M326
- Osteopenia in CKD: effects of Ca overload, SU449
- Osteopenia in CKD: effects of phosphate overload, SU447
- PINP, a new available rat bone formation marker: usefulness in osteopenia studies due to androgen lack and IBN treatment, SA299
- Prevalence of osteoporosis and osteopenia in men and women according to the fragility fracture type, SU294
- Twisted gastrulation-deficient mice exhibit osteopenia through enhanced osteoclast function, 1008
- Osteopenia, thyrotoxicosis-induced**
- Double deletion of  $\alpha 2a$ - and  $\alpha 2c$ -adrenergic receptors results in a phenotype of high bone mass and in resistance to the thyrotoxicosis-induced osteopenia, F244
- Osteopetrosis**
- R740S, a dominant V-ATPase  $\alpha 3$  mutation, causes osteopetrosis in mice, 1218
- Rachitic defects in *tcirg1*-dependent osteopetrosis are caused by impaired gastric acidification, 1201
- Osteopetrosis, infantile (IO)**
- Effect of bone marrow transplantation in a child with malignant IO, SU498
- Osteopontin (OPN)**
- Changes in bone matrix material properties due to OPN deficiency, F149
- Increased expression of OPN in PBMC is associated with alteration in the fractions of lymphocytes in hindlimb-unloaded mice, M175
- OPN deficiency reduces aortic calcification and oxidative stress in diabetic LDLR $^{-/-}$  mice, F109
- Role of OPN in beta-adrenergic signaling induced bone loss in vivo, M174
- Osteoporosis**
- Bisphosphonate-induced osteopetrosis: novel bone modeling defects, metaphyseal osteopenia, and osteosclerosis fractures after drug exposure ceases, F569
- Bridging vascular calcification and osteoporosis: the function of receptor activator of nuclear factor  $\kappa B$ , M419
- Chemerin and CMKLR1 targeted gene delivery identifies a novel molecular switch in the treatment of osteoporosis, M071
- CNBP conditional KO mice show severe osteoporosis-like phenotype, F014
- Deletion of the G protein subunit G $\alpha$  in early osteoblasts leads to accelerated osteoblast maturation and formation of woven bone with abnormal osteocytes, resulting in severe osteoporosis, 1254
- Do type I collagen homotrimers contribute to osteoporosis by altering bone remodeling?, SA146
- Evidence of increase in vertebral body dimensions in postmenopausal women with osteoporosis, M313
- Formation of new trabeculae in a female patient with osteoporosis treated with TPTD, demonstrated with in-vivo-assessment of 3D bone microarchitecture with HR-pQCT, M352
- Genome-wide CNV study identified a novel susceptibility gene *UGT2B17* for osteoporosis, M404
- GWAS identified novel susceptibility loci for osteoporosis, SA267
- Increased non-enzymatic glycation of cancellous bone due to decrease in remodeling during ALN therapy of osteoporotic women, 1071
- NRIP1*, a novel osteoporosis candidate gene identified by expression and association analyses, M254
- Osteocyte-specific ablation of canonical Wnt signaling induces severe osteoporosis, 1037
- Osteoporosis in a murine model of hemophilia A, M480
- Osteoporosis in the aging males after hip fracture, SU436
- Platelet VDR levels are reduced in osteoporotic patients, SA241
- Prevention of GC-induced osteoporosis with ALN or ALF in patients with ophthalmologic diseases, SA450
- Rehabilitation after clinically-diagnosed osteoporotic vertebral fracture, SU411
- Twist1 haploinsufficiency is associated with reduced IGF-1 levels and an osteoporotic phenotype, SU029
- Osteoporosis in Rheumatoid Arthritis (OPiRA) Cohort Study**
- Relationship between focal erosions and generalized osteoporosis in postmenopausal women with RA, SA370
- Osteoporosis, assessment**
- 6819 analysis on measurement of BMD of phalanges by radiographic absorptiometry in Beijing, SA313
- A allele at Valine80 of the CYP19 gene is a risk factor for aromatase inhibitors associated bone loss, 1021
- Active shape modeling as a predictor of hip fracture, M317
- Age is the key to assessing fracture risk: FRAX, F306
- ALN treatment in postmenopausal Romanian women followed by BMD-digital x-ray radiogrammetry, M357
- Ambiguity about osteoporosis and osteoporosis care exists despite a screening program to educate fracture patients, M383
- Areal BMD by DXA may predict similar risk of fracture in elderly women and men due to offsetting effects of bone size and true volumetric BMD, SU267
- Assessment of a provincial strategy for osteoporosis best practices, M401
- Assessment of absolute fracture risk and osteoporosis in Chinese, F312
- Assessment of cortical thickness and BMD in the radius by low-frequency Q-GWUS, M319
- Assessment of fracture risk and treatment of osteoporosis in postmenopausal women: bone density vs. Bone DESTINY, SU251
- Automatic estimation of body composition using  $\mu$ CT and a Gaussian mixture model, M139
- To avoid underdiagnosis of vertebral fracture, recognition of true fracture line including multiple Schmorl's Node is necessary, SA324
- BMD and body composition in postmenopausal women with psoriasis and psoriatic arthritis, SU337
- BMD measurement by DXA after a fragility fracture increases the likelihood of subsequent osteoporosis treatment, SU296
- Bone density changes at the non-operated hip following total hip arthroplasty, M408
- Bone DESTINY—a one step fracture risk predictor for clinicians, SU504
- Ca release from bone in postmenopausal women: effects of low level Cd exposure, M328
- Calcaneal QUS measurement of 2323 healthy adults in southwest China, M318
- Changes in serum PINP in orchidectomized osteopenic rats treated with PTH and ALN, M295
- Changes of biochemical resorption markers during fracture healing in osteoporosis, M290
- Clinical prediction rule to identify women for BMD testing at menopause, SU271
- Collecting bone out of the medial condyle of tibia, SA318
- Comparison of the TRACP 5b specificity of two commercial TRACP 5b assays, SA298
- Computer-based measure using normalized heights predicts vertebral fracture independent of BMD in post-menopausal women, SU361
- Consistency in measurement assessments in different models of Norland DXA scanners, SA307
- Correlation between DXA Femur Strength Index and QUS Heel Stiffness Index in Chinese women, M464
- Correlation of hip geometry and bone density with fragility fracture in Japanese postmenopausal women, SU466
- Cortical porosity is increased in male osteoporosis with vertebral fracture, 1132
- Deleterious effect of late menarcheal age on bone microstructure in both distal radius and tibia, 1239
- Densitometric vertebral fracture assessment in postmenopausal women, SU254
- Development of a bone specific ALP assay on the IDS Automated Analyser 3x3<sup>TM</sup>, SA302
- Development of a new N-Mid<sup>®</sup> osteocalcin immunoassay on the IDS Automated Analyser 3x3<sup>TM</sup>, SA303
- Development of a point-of-care clinical decision support tool for osteoporosis disease management, SU343

Direct medical costs associated with the treatment of NHNV, hip, and vertebral fractures in a managed care setting, F356

Dkk-1 predicts the gain of BMD in osteoporotic women on bisphosphonates, SA300

Do different densitometers, or use of T-score vs. Z-score, affect fracture risk estimation?, SU258

Effect of 10-year fracture risk tool results on likelihood of bisphosphonate prescribing, SU402

Effect of RLX and ALF on bone and joint pain assessed by fall of skin impedance (electroalgotometry), SA384

Effect of vertebral marrow fat content on the diagnosis of osteoporosis, SA309

Establishing healthy body composition values with DXA, SU366

Evaluation of osteoporosis vertebrae fragility by Connecting Path method, M307

Evaluation of the detection sensitivity of simulated trabecular bone loss in  $\mu$ MRI at in vivo resolution, M312

Evaluation of tibial bone density surrounding Ta tibial implants in TKA, SU266

Family physician characteristics that predict appropriate x-ray ordering, SA359

FEA of proximal femur QCT scans for the assessment of hip fracture risk in older men, F321

Fracture risk and incidence of falls in younger postmenopausal women, 1236

FRAX<sup>TM</sup> and the assessment of ten-year fracture probability in Hong Kong Southern Chinese according to age and BMD femoral neck T-scores, SU264

Height loss, vertebral fractures and misclassification of osteoporosis, SU259

Hip fracture patients with vertebral fractures have more severe osteoporosis and are candidates for more active treatment including PTH, SU274

Histomorphometric changes by TPTD in ALN pre-treated women with osteoporosis, 1019

HSA for RLX treatment in Japanese women with osteoporosis, SA419

Improving the diagnostic yield of bone densitometry, F361

Incident vertebral fracture is predicted by prevalent vertebral fracture as identified by the algorithm-based qualitative method, but not by non-osteoporotic short vertebral height, 1128

Incorporating FRAX<sup>TM</sup> algorithms in models of cost-effectiveness, 1023

Incremental costs associated with selected skeletal fractures, 1024

Independent contribution of hip geometry to incident fracture prediction in a large clinical cohort, 1238

Influence of body weight on cost-effectiveness of bone densitometry and treatment for osteoporosis among older women and men without prior fracture, F426

Lumbar spine TBS complements BMD in the discrimination between vertebral fractured and non-fractured subject, M308

Measurement equivalence of osteoporosis-specific and general quality of life instruments in Aboriginal and non-Aboriginal women, SU410

Morphometric determinants of 3D femoral neck structure and strength in older postmenopausal women, SA320

New automated multiplex assay for simultaneous measurements of four serum biochemical markers of bone metabolism in osteoporosis, SA295

Optimization of bone turnover marker measurements in a mouse model of GC-induced osteoporosis, M298

Osteoporosis diagnosis and incident fracture as a function of prior fractures site in a large clinical cohort, 1235

Osteoporosis risk assessment: a composite index combining clinical risk factors and biophysical parameters, F319

Osteoporosis: evaluation of screening patterns primary care group practice, SU272

In osteoporotic other than in healthy bone, thoracolumbar fractures spare the adjacent discs, SU415

Patients with fragility fracture assessed by BMD, Bone DESTINY and osteoporosis Canada guidelines, SA343

Performance characteristics of a workflow tool for the assessment of vertebral shape, SA350

Performance of QUS in comparison to DXA for prediction of prospective fractures among older men and women, 1240

pQCT predicts vertebral fractures in osteoporotic postmenopausal women, SU472

Precision of pQCT measurements of bone and muscle area in the forearm and lower limb, SU279

Prediction of incidental low trauma limb fractures in older men and women with QCT variables of bone and muscles in mid-thigh, F369

Predictive validity of the WHO FRAX model, BMD and prevalent vertebral fracture for incident radiographic vertebral fractures, 1127

Predictors of patient perceived need for oral bisphosphonates to prevent fracture: the role of the MD-patient relationship, F416

Prevalence of vertebral compression fracture deformity by x-ray absorptiometry in patients selected according to simple clinical tests, SU261

Quality of life in Mexican hip fractures patients using EUROQOL (EQ-5) after discharge from hip fracture and 6 months of followup, SU419

QUS, BMD and QCT in women with established osteoporosis treated with TPTD, SA393

Rapid optical imaging of bone formation responses in the rodent skeleton, SU379

Red flags are missed in the prevention of hip fractures, SU432

Regional differences in femoral neck cortical thickness determine hip fragility, M315

Regional differences of femoral BMD changes after one year once-monthly IBN as measured by 3D QCT, SU260

Reimbursement for BMD testing among US Medicare beneficiaries, SA326

Relationship of QUS at phalanges with hand and axial BMD, sex hormones and bone turnover markers in elderly women, M320

Risk factors for subsequent fractures within the next year in patients presenting with a clinical fracture, 1237

Role of the lean muscle and fat mass in hip fractures production, SU263

Serum PINP is a sensitive marker of bone formation in mouse OVX model, M293

Serum SHBG level to predict osteoporosis severity, M297

Shared genetics within the musculoskeletal system: a pleiotropic approach to osteoporosis and sarcopenia, WG2

Skeletal plasma clearance, as measured by quantitative radionuclide studies, is correlated with bone turnover markers at 3 months of TPTD therapy, F398

Spine shape predicts vertebral fractures in postmenopausal women, 1129

Stability of TRACP 5b in rat and mouse serum, M286

Ten-year fracture risk assessment in Norland-based equipment in a Chinese population, SU253

Thoracic kyphosis index as a risk factor for incident vertebral fractures and alteration of quality of life in postmenopausal women with osteoporosis, 1130

Three methods of lumbar spine DXA analysis as a means to predict male fracture, 1131

Treatment threshold in men on androgen deprivation therapy: T-score vs. FRAX, F308

Twelve month changes in trabecular microarchitecture assessed by  $\mu$ MRI in postmenopausal women on antiresorptive versus anabolic therapy, 1020

Use of conductivity for the correction of uNTx, SA304

Usefulness of alveolar bone density measurement in risk assessment for BRONJ, SA305

Usefulness of SpinalMouse<sup>®</sup> as a screening tool for the presence of vertebral wedge deformity, SA316

Validating pQCT MCSA measurement, SU278

Validation of bone mineral measurements on the new Norland Model XR-600 and XR-800 using the BMIL QA/QC Phantom, SU252

In vivo measurements of vertebral body dimensions by 3D-XA and their relation with age, M316

What happens to the availability of DXA if physicians stop performing them in their offices?, SU256

What proportion of older women would receive drug treatment under the new NOF guidelines?, 1022

**Osteoporosis, epidemiology**

“Pathologic” fractures: to include or exclude?, SU321

“Vibes” Trial: LMMS to improve BMD, M397

8-year fracture and mortality outcomes of the fracture liaison service that provides systematic assessment for prevention of secondary fractures to all patients age 50+ with new low-trauma fractures, SU324

10-year probability of recurrent osteoporotic fractures after a primary wrist fracture in postmenopausal women enrolled in the CaMos cohort, F358

Absolute risk for subsequent fractures fluctuates over time, 1060

Advancing maternal age is associated with lower peak BMD in the male offspring, M327

Air pollution might be a neglected risk-factor of hypovitaminosis D, SU306

Are there any ethnic differences in BMD in a lupus cohort?, SU358

Assessment of the 10-year risk of fracture in Italian postmenopausal women using BMD and clinical risk factors, SU348

Association between BMD change, use of antiresorptive agents and fragility fracture in women and men, SA364

Association between falls and health-related quality of life, SU420

Association of CTR gene polymorphisms with BMD and fracture risk in postmenopausal Koreans, M256

Association of stiffness index and cross-linked NTx with any clinical fractures differs with age and gender, SU350

Association of urinary GGT and serum FGF-23 with prevalent fracture, SA296

Association of urine measures of diet-derived acid excretion with bone loss and fractures, SU283

Baseline assessment of osteoporosis risk in Oklahoma Native American women, SU303

Baseline characteristics of women taking part in an osteoporosis intervention, SU370

Bivariate whole genome linkage analysis of femoral bone geometric traits and leg lean mass, M249

BMD changes over time associated with illness and recovery in young women with anorexia nervosa, SA558

BMD is associated with lean mass and not fat mass, SU273

BMD measurement: an independent risk factor of breast cancer recurrence?, SU265

BMD, fracture and survival in women in nursing/residential care, SA340

Bone fragility beyond BMD: a French prospective experience, SU288

Bone mass recovers in young women with anorexia nervosa who are both weight and menstrual recovered, F339

## Key Word Index

## ASBMR 30th Annual Meeting

- Bone turnover and incident hip fracture risk, M285
- Ca intake and serum bone formation markers are associated with the functional single nucleotide polymorphism in the TNSALP gene, SU308
- Ca intake is not associated with increased coronary artery calcification, 1207
- Carotid plaque causes low spinal BMD in Korean postmenopausal women with diabetes, SU359
- Casual decomposition of risk factors in osteoporosis burden, SU339
- Circulating DKK1 levels are reduced in young subjects with low bone mass, F455
- Common single nucleotide polymorphism in the *HMG2* gene is associated with bone mass in men, SA268
- Comparison between logistic regression and artificial neural networks for vertebral fracture risk assessment, SU345
- Comparison of prediction models for hip, osteoporotic, and any clinical fracture in older women: is more better?, 1057
- Compartment specific genetic analysis of trabecular and cortical volumetric BMD in men, SU284
- Composite bone score with QCT bone measurements and fracture history, SU289
- Comprehensive genetic analysis of bone volume in men, M268
- Correlations between panoramic radiomorphometric indices and BMD in postmenopausal women, SA311
- Cortical bone acquisition in the appendicular skeleton of healthy young females is reciprocally related to marrow adiposity, M074
- Cortical bone mass and structure in older Afro-Caribbean and Caucasian men, SU300
- Cortical cross sectional area in young adult men is inversely related to risk of hip fracture in their older relatives, 1281
- Cost-effectiveness of RIS versus IBN at one year: the case of the United Kingdom, SA424
- Costs associated with NHNV fractures in a managed care setting, SU320
- CVD as forecasters of hip fracture: a nationwide cohort study in twins, 1205
- Deformity of the distal radius fractures resulting from falls in Japanese women over 50 years of age is closely associated with BMD of the lumbar spine, SU286
- Designing a Latino osteoporosis awareness campaign, SU312
- Determinants of trabecular and cortical volumetric BMD differ in men of African ancestry, SU299
- Development a nomogram for individualizing the absolute risk and time to recurrent fracture, F349
- Dietary patterns in Canadian men and women ages 25 and older: relationship to BMI and BMD, SU309
- Differences in fall rates and predictors of falls by sex, 1058
- Disability in patients with osteoporotic peritrochanteric hip fracture, SA357
- Distribution and rate of clinical fractures in older men without osteoporosis, 1282
- Distribution of risk factors for fracture in women with and without a fracture history, SU342
- Does dietary protein reduce hip fracture risk in elderly men and women?, SU319
- Effect of a one year exercise program on markers of bone metabolism after hip fracture, SA432
- Effect of metabolic acidosis on BMD and bone microarchitecture in normal and OVX rats, M409
- Effect of parity on BMD in premenopausal women, SA325
- Effects of exercise and milk intake on bone in adolescents, SU301
- Effects of neurological impairment and functional mobility on BMD following stroke, SU364
- Elevated production of IL-1 $\beta$  and TNF $\alpha$  by PBMC is associated with increased hip fracture risk in elders, 1283
- Epidemiology of rib fractures in older men, F354
- Essential fatty acid and fish intake is associated with higher BMD in elderly women and men, F341
- Evaluation of BMD following an education intervention on osteoporosis offered to women after a fragility fracture, SU330
- Excess medical cost after a fragility fracture during 3-year follow-up, SA422
- Excess of post-fracture mortality among men and women, SA348
- Factors associated with kyphosis progression in older age, F365
- Failure to perceive increased risk of fracture in women 55 years, SA360
- Falls predict higher medical costs among osteoporosis patients in community setting, SA430
- Femoral neck and trochanteric fractures and Vitamin D, SU353
- Femoral strength, bone density, and aging in women and men, 1165
- Fracture risk in young patients with chronic diseases, SU371
- Fractures of the spine and hip increase the risk of death in Canadians, SU351
- Fragility fractures and health status in a multinational cohort, SU340
- Frequent apheresis for platelet and plasma donations constitutes an independent risk factor for decreased BMD, F327
- Genetic locus on chromosome 1q influences bone loss in young Mexican American adults, M250
- Genetic variation in *IL6* and *LRP5* is associated with osteoporosis in the Marshfield Clinic Personalized Medicine Project, SU365
- Genetic variations in sex steroid-related genes as predictors of serum estrogen levels in men, SU183
- Gondanotropins, bone loss and fracture in men, 1278
- GWAS and subsequent replication studies identified ADAMTS18 and TGFBR3 as novel osteoporosis risk genes, 1093
- GWAS identified RTP3 as a novel gene for bone strength, SU331
- GWAS of BMD and hip geometry indices, 1092
- GWAS pleiotropic associations of bone phenotypes, SA251
- GWAS reveals genetic variants associated with BMD, osteoporosis and osteoporotic fractures, SA263
- High impact exercise may have a protective effect on BMD but moderate impact exercise may have negative effect in young women with anorexia nervosa, M324
- High mortality in male nursing home residents with hip fracture, SU326
- Higher BMD is associated with increased odds of carotid atherosclerosis in postmenopausal women not currently using estrogen therapy, 1206
- Higher BMD loss in older men with diabetes, 1209
- Hip fracture patients at high risk of second hip fracture, 1163
- Hip strength estimates by FEA and fracture prediction in women and men, 1167
- Homocysteine levels in relation to physical performance, SA372
- HSA in women, SU270
- IGFBP2 and bone loss in aging women and men, 1284
- Impact of an educational intervention on knowledge about osteoporosis following a fragility fracture, SA353
- Impact of physical inactivity (10 days bed rest) on markers of bone turnover in young men with low and normal birth weight, SA456
- Incidence and costs of proximal humerus and wrist fractures in women in France, SU327
- Inflammatory markers and the risk of hip fracture, F333
- Influence of markers of bone turnover on calcaneal QUS, SA457
- Influence of sex hormones on BMD in middle aged and elderly men, SU335
- Is the association between hypertension and bone osteoporotic fracture expressing a real interdependence?, SU346
- Lack of correlation between glycemic control and BMD in type 2 diabetic women, SU255
- Lack of seasonal variation of bone resorption in elderly women in relation to periodicity of sunlight exposure at a northerly latitude, F337
- Lactose intolerance does not have effect on bone status in adolescence, SU285
- Large scale candidate gene analysis identifies an association between the CDK6 locus and trabecular volumetric BMD at the lumbar spine in older men, M266
- Large-scale meta-analysis of genome-wide association scans for osteoporosis traits, 1091
- Late pregnancy serum Vitamin D and longitudinal bone loss during pregnancy, F544
- Lean body mass is a better predictor of BMD than leg power or grip strength in healthy caucasian adults, SU290
- Linkage and association study of chromosome 1p36 with BMD in southern Chinese, SU295
- Loop diuretic use and rates of hip bone loss, and risk of falls and fractures in older women, F371
- Low calcaneal BMD estimated by a peripheral DXA heel scanner is associated with a high risk to have had a distal radius fracture, SU262
- Low serum 25(OH)D is associated with higher rates of hip bone loss in older men, F367
- Low Vitamin D levels and risk of death in older men, F335
- Mathematical model of remodeling cycles with feedback mechanism for maintaining the balance between bone resorption and formation, WG27
- Menopausal and postmenopausal women have significantly higher bone resorption and oxidative stress parameters than premenopausal women, SU336
- Mouse-to-human strategy to identify bone strength QTL genes, SA120
- Multinational comparison of bone health in women 55 years of age and older, SU344
- Negative association between the metabolic syndrome and BMD in Korean adults, SU304
- Neglected role of intracortical remodeling in age-related bone loss, 1101
- No fracture is a poor predictor of fracture risk, SU356
- Normative Z-scores from the CaMOS youth cohort, SU292
- Obesity and bone architecture in men—can we apportion the metabolic and the mechanical effect?, SA440
- Obesity is associated with higher BMD, lower bone resorption and slower hip bone loss: are these associations mediated by adipokines?, SU369
- Older men with low serum estradiol and high serum SHBG have an increased risk of fractures, 1279
- Opioid-induced osteoporosis: delayed bone healing and compression fractures in a man with chronic narcotic use, WG32
- Osteoporosis in elderly fallers, underdiagnosed and undertreated, SU248
- Osteoporosis in men: still under-screened and under-treated, SA329
- Pattern of death after hip fracture among institutionalized older people, 1164
- Physical activity, BMD and fragility fracture, M325
- Physician practices in bone density testing among Medicare patients, SA428
- Poor peripheral nerve function is related to lower BMD, SA328

Poor peripheral sensorimotor nerve function is associated with high fall risk, SU323

Population burden of first and repeat low-trauma fractures, 1056

Positive Celiac disease serology and BMD in adult women, SA366

Post-fracture initiative in a rural Ontario community hospital, M369

Post-fracture mortality in men: contributions of sex hormones and BMD as risk factors, 1280

Post-fracture osteoporosis intervention strategy, M322

Predictive capacity of biochemical markers of bone turnover and endogenous hormones for osteoporosis in men, SU334

Predictors of osteoporosis management among residents living in long-term care, SA368

Predictors of poor outcomes following osteoporotic fractures in elderly women and men, 1210

Prevalence of osteoporosis and osteopenia in men and women according to the fragility fracture type, SU294

Prevalence of osteoporosis in ISM, SU268

Prevalence of subtrochanteric fractures in patients older than 50 years presenting with a clinical vertebral or non-vertebral fracture, SU390

Prevalence of vertebral fractures in aging women suffering from hip fracture, SU322

Prospective observational study of osteoporosis medication use in postmenopausal women in the European Union, SU347

Protective effect of total and supplemental Vitamin C intake on the risk of hip fracture, 1168

Proximal femoral fragility and age-related white matter lesions by brain MRI in elderly subjects, 1096

Proximal humerus fractures in men: epidemiology and costs, SU328

Questionnaire-based osteoporosis risk assessment in a rural area primary care setting, SU354

Radiation-induced bone loss: description of dose, time course, age, strain and sex variables, SU368

Rate of bone loss is greater in young adult men than women, SU297

Reciprocal relation between MR measures of marrow adiposity and cortical bone in the appendicular skeleton of healthy adults, SU042

Recognition and treatment of male osteoporosis is low, SU332

Reduced renal function is associated with increased rates of bone loss at the hip and spine, SU357

Reduction of BMD in the patients with RA is more remarkable at proximal femur than at lumbar spine, SU451

Regional differences in the management of osteoporosis, SU287

Relationship between BMD of the lumbar spine and knee OA in South Korean, SU298

Relationship between clinical risk factors for osteoporosis and BMD in women aged less than 50 years, SU355

Relationship between focal erosions and generalized osteoporosis in postmenopausal women with RA, SA370

Relationship between the metabolic syndrome and BMD in Korean middle-aged women, SU291

Retrospective study evaluating the relationship of Vitamin D 25 OH and free testosterone levels with changes in hip bone density after liver transplantation, SA502

Risk factors for fragility fracture in a multiracial cohort of US women, SA362

Risk factors for low BMD in healthy men age 50 years or older, SU341

Risks and outcomes for hip fractures in a predominantly African-American male veteran population, SA352

Rosiglitazone-induced change in BMD among African Americans with type 2 diabetes mellitus or impaired glucose tolerance, SU315

Seasonal genetic influence on serum 25(OH)D levels, SA334

Secular trends in Swedish hip fracture incidence 1987-2002, 1166

Self-reported weight at birth predicts measures of femoral size but not volumetric BMD in elderly men, SU338

Serum 25(OH)D and the risk of hip and non-spine fractures in older men, 1277

Serum Vitamin D levels do not modify the response to an exercise program following hip fracture, SA346

Simply ask them about their balance—fracture prediction in a nationwide cohort study in twins, 1095

Smoking is an independent predictor of low BMD, prevalent vertebral fractures and incident fractures in elderly men, SU349

Socioeconomic status, BMD testing and hip fracture rates in a universal health-care system, SU293

SSRI use and risk of fracture in older women, F351

Study about the association of circulating MCP-1 levels with lumbar BMD in Korean women, M407

Subclinical thyroid disease predicts risk of hip fracture, 1208

Substantial adverse outcomes follow NHNV fragility fractures, 1059

Temporal trends in vertebral size and shape from medieval to modern-day, M459

Ten-year change in BMD in a representative sample of Japanese women, SA330

Timed Up and Go test and BMD as predictors of fracture, F373

Timing of repeated BMD measurements: development of an absolute risk-based prognostic model, F347

Trauma type of NHNV fractures in postmenopausal women being treated for osteoporosis in Europe, SU325

Type 1 diabetes is associated with lower BMD in premenopausal women but not in middle-aged men, SU456

ucOC level in healthy Korean women, M300

Use of genetic markers in prediction of fractures, 1094

Vertebral fracture in men: level of trauma, BMD and lean body mass, SU360

Very high frequency of poor Vitamin D status in French women with bone fragility, SU352

Vitamin D concentrations of healthy children living in the Calgary health region, SU396

Vitamin D deficiency is highly prevalent in Irish hip fracture patients, M294

Vitamin D insufficiency together with high serum levels of Vitamin A increase the osteoporosis risk in postmenopausal women, M292

Vitamin D supplementation intake among osteoporosis patients aged 50 years and older at various 25(OH)D levels in the US, M400

In vivo differential expression profiling study on human circulating B cells suggested a novel EGFR and CALM3 network underlying smoking and BMD, SU154

In vivo differential expression profiling study on human circulating monocytes suggested a novel CRAT and CPT2 network underlying smoking and BMD, SU155

Volumetric bone parameters in relation to fracture history in healthy men at the age of PBM, SU302

Weight and BMI predict BMD and fractures in women 40 to 59 years, SA438

Weight reduction is not deleterious for bone mass or strength in obese women, SA338

WHO absolute fracture models in older women: how does prediction vary for incident hip and non-spine fractures across T-scores?, 1055

Women who fractured their hips experience greater loss of geometric strength in the contralateral hip during the year following fracture compared to age-matched controls, F345

#### **Osteoporosis, glucocorticoid-induced (GIO)**

BMP/Wnt antagonists are upregulated by DEX in osteoblasts and reversed by ALN and PTH: potential therapeutic targets for GIO, M098

Clinical significance of ucOC in GIO, M299

Effect of a single 5-mg infusion of ZOL on bone turnover markers versus oral RIS (5 mg/day) over 1 year in patients with GIO, M362

Effect of a single infusion of ZOL 5 mg versus oral RIS 5 mg on BMD at lumbar spine, hip, femoral neck and trochanter in patients with GIO, F403

TPTD versus ALN for treatment of GIO, 1171

#### **Osteoporosis, idiopathic**

Marked abnormalities in cortical and trabecular microarchitecture and strength in premenopausal women with idiopathic osteoporosis, M310

#### **Osteoporosis, idiopathic juvenile (IJO)**

TPTD treatment in a young man with IJO diagnosis, SU499

#### **Osteoporosis, juvenile**

ALN treatment for juvenile osteoporosis, M366

#### **Osteoporosis, opioid-induced**

Opioid-induced osteoporosis: delayed bone healing and compression fractures in a man with chronic narcotic use, WG32

#### **Osteoporosis, pathophysiology**

(22-52) ADM prevents systemic bone loss related to inflammation in mice, SA493

Acute COPD exacerbations are associated with uncoupling of bone resorption from bone formation, M414

Age at menarche associated with bone strength in girls, SU493

Bilateral bone density loss after unilateral disuse in the forearm, SA519

BMP/Wnt antagonists are upregulated by DEX in osteoblasts and reversed by ALN and PTH: potential therapeutic targets for GIO, M098

Bone is more susceptible to Vitamin K deficiency than liver, SU316

Bone loss with smoke exposure and Lrp5 expression, SA459

Bone resorption markers in saliva, M288

Central control of bone remodeling: neurohypophysial hormone oxytocin is decreased in severe postmenopausal osteoporosis, M418

Changes in histomorphometric parameters after menopause, SU333

Clinical significance of ucOC in GIO, M299

Deletion of FXR leads to an osteopenic phenotype in mice, F439

Detrimental effects of abdominal irradiation on the skeleton in growing mice, M412

Double deletion of  $\alpha 2a$ - and  $\alpha 2c$ -adrenergic receptors results in a phenotype of high bone mass and in resistance to the thyrotoxicosis-induced osteopenia, F244

Effect of Pb on bone mineral properties from female adult C57/BL6 mice, M146

Effects of diacylglycerol oil on body composition, BMD and bone strength in mice, SA442

Effects of intermediate doses of GCs on bone turnover and circulating Dkk-1, MIF, sRANKL and OPG in patients with interstitial lung disease, SA451

Effects of serum factors during osteoblast differentiation—implication for the pathogenesis of osteoporosis in Crohn's Disease, M450

ER $\alpha$  deletion in cells of the monocyte/macrophage lineage increases osteoclastogenesis and abrogates the pro-apoptotic effect of E<sub>2</sub> on osteoclasts, 1097

Expression of NF- $\kappa$ B ligand and regulation of osteoclastogenesis by bone marrow adipocytes, SA078

## Key Word Index

## ASBMR 30th Annual Meeting

GC-induced bone loss in mice is dependent on beta 2-adrenergic signaling, M102  
 Goettingen minipigs—a model for Ca/Vitamin D-deficiency osteomalacia and steroid-induced osteoporosis, SA445  
 High level dietary P and Cd exacerbate OVX-induced bone loss, M301  
 High-fat diet facilitated decreases in BMD of OVX mice and suppressed the anabolic effects of PTH on bone, SA448  
 Homocysteine accumulates in bone tissue by collagen binding and adversely affects bone, M417  
 Impact of adjuvant hormonal therapy on bone loss depending on initial adjuvant chemotherapy and menstrual status, M415  
 Impact of dietary protein on Ca homeostasis and nitrogen excretion in the presence and absence of  $\text{KHCO}_3$ , SU305  
 Impaired angiogenesis and compromised fluid volume accompanies increased osteoblast and osteocyte apoptosis with GC excess, SA453  
 Impaired methylation capacity is associated with low BMD, SU317  
 Longevity gene *SIRT-1* independently controls both osteoblast and osteoclast function, 1098  
 Mechanisms of endplate failure in the human vertebral body, M413  
 Osteoporosis and the acid-ash hypothesis, SA331  
 Overexpression of sFRP1 inhibits bone formation and attenuates PTH bone anabolic effects, 1100  
 OVX-induced hyperphagia does not modulate bone mineral or bone strength in female Sprague-Dawley rats, SA447  
 Oxidative stress stimulates the synthesis of PPAR $\gamma$ 2, and ligand-activated PPAR $\gamma$ 2 sequesters  $\beta$ -catenin leading to suppression of TCF-mediated transcription, 1099  
 Oxytocin directly regulates skeletal homeostasis, SA199  
 Percentage body fat and risk of prospective hip fracture in older men and women, F363  
 Psychotropic drugs have contrasting skeletal effects that are independent of their negative effects on activity levels, M423  
 RLX ameliorates detrimental collagen cross-link formation in bone from an OVX rabbits with or without hyperhomocysteinemia, SA382  
 Role of OPN in beta-adrenergic signaling induced bone loss in vivo, M174  
 SHBG levels in older patients with acute hip fracture are correlated with worse function and increased bone resorption, SU363  
 Toward a physiologically-based definition of hypogonadism in men: dose-response relationship between testosterone and bone resorption, 1102  
 Trabecular bone loss in response to transient muscle paralysis is not gender dependent, SA462  
 Treadmill exercise provides only short-term protection against cancellous bone loss with reduced dietary energy intake: endocrine mechanisms, SA449  
**Osteoporosis, treatment (clinical)**  
 1-year analysis of adherence with bisphosphonate treatments in osteoporotic patients, SA415  
 12 months of TPTD therapy increases ultradistal radius bone strength in severely osteoporotic postmenopausal women, SA504  
 Active controlled, non-inferiority study to compare the effect of ZT-031 with ALN on the incidence of new vertebral fractures, M347  
 Acute phase response and bone metabolism marker after intravenous bisphosphonate in osteoporotic patients with rheumatism, M364  
 Adherence in patients with severe osteoporosis treated with TPTD, M384

ALN and indapamid alone or in combination in the management of IHC associated with osteoporosis, 1245  
 ALN treatment for juvenile osteoporosis, M366  
 Application of preventive measures minimizes the occurrence of ONJ in patients with bone loss treated with bisphosphonates, F281  
 ARZ in postmenopausal women with normal or low bone mass, SA421  
 Assessment of adherence to treatment of osteoporosis with RLX and/or ALF in postmenopausal Japanese women, M387  
 Assessment of serum Ca and bone resorption markers in patients transitioned from ALN to DMAB, M394  
 Attitudes to fracture prevention in long-term care facilities, M379  
 Atypical osteoclast phenotype after long-term ALN therapy for osteoporosis, SU399  
 Back pain is reduced in postmenopausal women with severe osteoporosis treated with rhPTH(1-34) regardless of incident fractures, SU413  
 Bisphosphonate-associated femoral fracture: implications for management, WG26  
 Bisphosphonate-associated ONJ cases in South Korea, SA412  
 Bisphosphonates and osteoporotic fractures in highly compliant/persistent postmenopausal women, 1025  
 BMD and biochemical marker response rates in postmenopausal women after treatment with ZOL, F401  
 BMD response to treatment with rhPTH in patients previously treated with bisphosphonates, M348  
 C-telopeptide and bone ALP predict morphometric vertebral fracture risk in a pivotal Phase III trial of TOR in men on ADT, 1292  
 Calcitonin intramuscular administration for treating acute pain of osteoporotic vertebral compression fractures, SA196  
 Case finding for the management of osteoporosis with FRAX—assessment and intervention thresholds for the UK, 1290  
 Cat K inhibitor, MIV-701, suppresses bone resorption markers in healthy postmenopausal women, F433  
 Comparative antifracture efficacy of N-containing bisphosphonates, SU397  
 Comparative gastrointestinal safety of weekly oral bisphosphonates, M358  
 Continued evidence for safety and efficacy of RIS in men with osteoporosis, M360  
 Correlates of osteoporosis treatment persistence for patients new to therapy and patients with recent switches, M375  
 Cost-effectiveness of IBN therapy for women with postmenopausal osteoporosis with respect to nonvertebral fracture efficacy, SA429  
 Cost-effectiveness of RIS versus IBN at one year: the case of Germany, SA425  
 Cost-effectiveness of RIS vs. generic ALN, SA423  
 Danish patients treated with TPTD, M350  
 Development, reliability, and validity of a new PSQ, SA417  
 Differences in safety and efficacy of generic and original branded once weekly bisphosphonates, M359  
 Do physicians who practice together provide similar osteoporosis care?, SU401  
 Does ALN use prevent kyphosis progression in older women?, SA410  
 Double-blind, placebo-controlled, dose-response study of BZA in Japanese postmenopausal women with osteoporosis, M391  
 Effect of a single 5-mg infusion of ZOL on bone turnover markers versus oral RIS (5 mg/day) over 1 year in patients with GIO, M362  
 Effect of a single infusion of ZOL 5 mg versus oral RIS 5 mg on BMD at lumbar spine, hip, femoral neck and trochanter in patients with GIO, F403

Effect of bodyweight on clinical response to ZT-031: development of a simple, improved dosing regimen for PTH analogs, M346  
 Effect of DMAB vs ALN on bone turnover markers and BMD changes at 12 months based on baseline bone turnover level, 1285  
 Effect of low dose Vitamin K2 (MK-4) supplementation on bio-indices in postmenopausal Japanese women, SU307  
 Effect of once-yearly ZOL 5 mg infusion on fracture incidence in postmenopausal osteoporosis, 1028  
 Effect of once-yearly ZOL on integral BMD of the spine, SU405  
 Effect of RIS in liver transplantation patients with low bone mass, SA503  
 Effect of RIS on bone density in HSC transplant patients, SU407  
 Effect of skin color and oral Vitamin D supplementation on serum 25(OH)D in adolescent girls, SU395  
 Effect of SSBT on osteocyte viability, F405  
 Effect of three different doses of Vitamin D<sub>2</sub> (ergocalciferol) on muscle function and strength in women > 65 years, M405  
 Effect of Vitamin D2 or Vitamin D3 supplementation on serum 25(OH)D, SU425  
 Effect of ZOL (single 5-mg infusion) on lumbar spine BMD versus oral RIS (5 mg/day) over 1 year in subgroups of patients receiving GC therapy, M363  
 Effective progressive resistive exercise program from prone position for paravertebral muscles to reduce risk of vertebral fractures, M473  
 Effectiveness of bisphosphonate therapy in a real-world setting, M356  
 Effects of a targeted bone and muscle loading program on QCT bone geometry and strength, muscle size and function in older men, 1244  
 Effects of *Acanthopanax senticosus* extract on bone metabolism in Korean postmenopausal women, SA431  
 Effects of ARZ on bone turnover and safety in postmenopausal women with low bone mass, M386  
 Effects of DMAB vs ALN on BMD, bone turnover markers, and safety in women previously treated with ALN, M395  
 Effects of estrogen therapy and fluocalcic effervescent on the BMD and bone metabolism of surgical menopause women with osteopenia, M392  
 Effects of LASO on bone turnover markers, 1287  
 Effects of LASO on fractures and breast cancer, 1288  
 Effects of low dose estrogen therapy on the BMD and bone metabolism of menopausal women, M393  
 Efficacy and safety of monthly oral IBN in postmenopausal women with low bone density, SU384  
 Efficacy and safety of short term treatment with different doses of cholecalciferol on 25(OH)D levels in postmenopausal females with osteoporosis, SU434  
 Efficacy of BZA in reducing the incidence of nonvertebral fractures in postmenopausal osteoporotic women at higher fracture risk, M390  
 Efficacy of the Vitamin D supplementation in patients with hypovitaminosis D and HPT2, SU431  
 Efficacy of whole-body vibration in reducing bone loss in postmenopausal women, M396  
 Electronic medical record based "ALERT System" improved diagnosis and treatment of osteoporosis in orthopaedic out-patient clinic, SU416  
 Ergocalciferol is not bioequivalent to cholecalciferol in Vitamin D insufficient hip fracture cases, 1289  
 Evaluating the effect of soy and isoflavones on BMD in older women, M353

- Evaluation of BMD changes in women with severe osteoporosis after TPTD treatment, M355
- Exploring the effect of food intake on bone resorption for optimal drug delivery and efficacy in osteoporosis with oral calcitonin, SA436
- Fracture reduction during two years of treatment with RIS or ALN, SA404
- Fracture risk in women aged 65 years or older with once-monthly oral IBN compared with weekly bisphosphonates, M367
- Fracture risk with once-monthly oral IBN compared with weekly bisphosphonates, SU408
- Functionality outcomes including brisk walking speed are associated with BMD in postmenopausal women, SU418
- Gastrointestinal side effects in postmenopausal U.S. women on osteoporosis therapies, SU417
- GLP-2 acutely uncouples bone resorption and bone formation in postmenopausal women, M399
- Histomorphometric and biochemical bone formation responses to first and second cycles of TPTD treatment, 1169
- Homocystinuria associated bone disease: effect of long term bisphosphonate treatment, SA406
- HSA based on DXA data in women with postmenopausal osteoporosis receiving once-monthly oral IBN for 12 months, SA507
- Imaging the spatial distribution of proximal femoral response to one year of TPTD therapy, M349
- Impact of dosing frequency in compliance with bisphosphonates among postmenopausal Japanese women for osteoporosis treatment, M374
- Impact of varying BMD resources on prediction of hip fracture using FRAX™, SU257
- Improvement in quality of life among women treated with RIS, SU414
- Improving the prediction of medication adherence: example of bisphosphonates for osteoporosis, M368
- Increase in risk of atypical subtrochanteric fractures with ZOL?, F411
- Increasing the number of steps taken per day leads to a greater weight loss and more favorable body composition in overweight postmenopausal women, SU311
- Influence of bone osteoporotic fractures in the past on the persistence of pharmacological treatment in osteoporosis, M382
- Influence of long-term hormone replacement therapy on tibia bone mineral mass and mass distribution in postmenopausal women, F420
- Interventions to improve adherence and persistence with osteoporosis medications: a systematic literature review, M370
- Intravenous IBN for prevention of early bone loss after kidney transplantation, F413
- Long term safety of oral RIS treatment in men with osteoporosis as assessed by histomorphometry, SA344
- Long-term treatment with oral bisphosphonates in postmenopausal women: effects on the degree of mineralization and microhardness of bone, 1029
- Male perspectives on osteoporosis suggest that continuous followup and tailored groups for patient education are important issues, SA434
- Medication prescription and adherence after hospitalization for osteoporotic vertebral fracture, M381
- Medication switching in postmenopausal women on osteoporosis, M376
- Modeled cost-effectiveness of RIS versus IBN: the case of Italy, SA427
- Novel CaSR antagonist leads to dose-dependent transient release of PTH after oral administration to healthy volunteers, 1173
- Once-a-month RIS 150 mg reduced vertebral fracture risk at one year in a historical control analysis, SU403
- One year of TPTD treatment increases hip strength in subjects with recent history of anti-resorptive treatment, F396
- ONJ: ZOL 5 mg experience in a variety of osteoporosis indications, 1246
- Optimizing bioavailability of oral administration of small peptides through pharmacokinetic and pharmacodynamic parameters, M398
- Osteoporosis patients behaviours and understanding of the importance of Ca and Vitamin D supplementation, M331
- Osteoporosis therapy following bone densitometry—patient expectations as determinants of drug initiation and persistence, M377
- Patient persistence with weekly bisphosphonates for two years after initiation of therapy, SA418
- Patient refill behavior among select daily, weekly, monthly, and annual dosing regimens, M373
- Patients desire of administration form and dose interval in bisphosphonate therapy of osteoporosis, SA408
- Phase 1, randomized, double-blind, placebo controlled trial of the PK/PD effect and safety of ZT-031, a hPTH analog, in healthy elderly women, SA399
- Phase III study of the effects of DMAB on vertebral, nonvertebral, and hip fracture in women with osteoporosis, 1286
- Possible increased risk of fracture among South Florida White Hispanic women, M402
- Postmenopausal women with GERD and long term treatment with bisphosphonates IV, M361
- Potential mediators of the reduction in mortality with ZOL after hip fracture, 1030
- Predictors of self-reported non-persistence with oral bisphosphonates due to perceived side effects or other reasons, M378
- Preference and satisfaction with a 6-monthly subcutaneous injection versus a weekly tablet for treatment of low bone mass, M372
- Premenopausal reference ranges of bone turnover markers and the effect of bisphosphonates in Korean postmenopausal women, SU406
- Prevention of GC-induced osteoporosis with ALN or ALF in patients with ophthalmologic diseases, SA450
- Prevention of non-vertebral fractures with oral Vitamin D is dose dependent, 1242
- Prevention of postmenopausal osteoporosis using nitroglycerin, M354
- Prevention of the metabolic syndrome together with osteoporosis in young men, SU314
- Previous antiresorptive agents use did not hinder the increase of bone turnover marker in TPTD use, M351
- QCT and FEA assessment of proximal femur bone quality and strength in women with postmenopausal osteoporosis receiving once-monthly oral IBN for 12 months, SA509
- Quarterly intravenous IBN acid in the community setting in England, SU409
- Randomized double blinded controlled trial of individual response in biochemical markers of bone turnover to LASO therapy, M507
- Randomized trial of balloon kyphoplasty and nonsurgical care for acute vertebral fracture, 1243
- Randomized, double-blind, placebo-controlled study of ODN (MK-822) in the treatment of postmenopausal women with low BMD, 1291
- Randomized, placebo-controlled, double blind study on high frequency, low intensity vibration in bone mass, muscle strength and quality of life in children with motor disabilities, F435
- Relationship between adipokines and biochemical bone markers in osteoporotic women before and after GH supplementation, M289
- Relationship between biochemical bone markers in osteoporotic women before and after 6 months treatment with either GH, Sr ranelate or GH plus Sr, M291
- Relationship of bone turnover marker (PINP) and changes in femoral neck BMD to fracture risk in women with postmenopausal osteoporosis treated with once-yearly ZOL 5 mg, 1027
- Relative contributions of nonvertebral efficacy, vertebral efficacy, and persistence in determining cost-effectiveness: the case of osteoporosis and implications for payers, M371
- Renal safety across a wide range of dosing regimens of RIS, SA402
- Repetitive rapid delivery of pharmacologically-active hPTH 1-34 across human skin without injection, SA397
- Replacing testosterone in male cardiac transplant patients exerts multiple benefits on bone mass, libido and sexual activity, M388
- Risk factors for bone fracture, elevated by 90-days of bed rest, are reduced by daily exposure to LMMS, M342
- Risk of hip fracture after bisphosphonate discontinuation, F409
- Ronacaleret, a novel CaSR antagonist, demonstrates potential as an oral bone-forming therapy in healthy postmenopausal women, 1174
- Safe zone for percutaneous extrapedicular surgical approach to the lumbar spine, M344
- Safety and effectiveness profile of RLX in long-term prospective observational study, M385
- Safety profile of BZA in Japanese postmenopausal women with osteoporosis, M389
- Serum estradiol and fracture reduction during treatment with hormone therapy, F383
- sGGT is one of the factors that determines the response to ALN treatment in osteoporotic women, M421
- Short duration pharmacokinetic profile of ZT-031 (cyclic PTH [1-31]), a novel hPTH analog, M345
- Short treatment with Scl-ab can inhibit bone loss in an ongoing model of colitis, 1212
- Single dose of 100,000 IU D3 appears to be insufficient to achieve desirable levels of 25(OH)D in patients with hypovitaminosis D, SU430
- Sites of femoral fractures in the Fracture Intervention Trial (FIT) of ALN and its Long-term Extension (FLEX), SU389
- Sr ranelate prevents the progression of thoracic kyphosis in postmenopausal women with osteoporosis, 1241
- Strategies for hip fracture prevention in long-term care facilities: a survey of Canadian geriatricians and family physicians, M380
- Subtrochanteric and diaphyseal femur fractures in patients treated with ALN, 1026
- Superiority of ALF over plain Vitamin D in men with osteoporosis, SU421
- Suppression of bone resorption markers by Ca and Vitamin D separately and in combination, M329
- Therapeutic effects of one-year ALN treatment in three cases of osteoporosis with parietal thinning, M410
- Towards an understanding of the mechanism of femur strength improvement by ALN in postmenopausal women, F323
- TPTD in bisphosphonate-resistant osteoporosis—clinical and  $\mu$ CT data, 1172
- TPTD therapy in a community setting: persistence and use of other osteoporosis medications in DANCE, SA395
- TPTD versus ALN for treatment of GIO, 1171



## Key Word Index

## ASBMR 30th Annual Meeting

- Treating osteoporosis in the elderly: an environmental scan of nursing home prescribing in Ontario, Canada, SU404
- Treatment discontinuation due to gastrointestinal adverse events and decreased BMD in patients switched from branded ALN to generic ALN, SA414
- Treatment with daily subcutaneous PTH (1-84) in women with severe postmenopausal osteoporosis, 1170
- Vitamin D<sub>3</sub> treatment of elderly people—twice a day or every four months? A comparative study of efficacy and safety of two oral dosages with same annual dose of 292,000 units, SU422
- Vitamin K treatment for one year does not alter femur geometry in postmenopausal women, SA443
- Which is the best oral high-dose Vitamin D<sub>3</sub> regimen for postmenopausal women with hypovitaminosis D?, SU429
- Wintertime Vitamin D supplementation inhibits seasonal variation of calcitropic hormones and maintains bone turnover in healthy men, SU433
- Women with severe osteoporosis treated with rhPTH(1-34) improve quality of life regardless of incident fractures, SU412
- ZOL prevents accelerated bone loss after discontinuation of TPTD, M365
- ZOL treatment of osteoporosis: effects in men, SU398
- Osteoporosis, treatment (preclinical)**
- ALF ameliorates bone dynamics in senescence-accelerated SAMP6 mice and in fracture repair rat model, SU394
- Anabolic daily intermittent PTH 1-84 reduces bone blood vascular bed and induces dramatic changes in the bone/vessel spatial relationship, 1061
- Anabolic skeletal effects of a GH-derived peptide (AOD9604) in the OVX rat model of osteoporosis, SU373
- Bone anabolic effects of icariin and total flavonoid fraction of *Herba epimedii* in OVX mice, M337
- Bone effects of ODN in adult OVX rabbits, SA073
- Bone-building effects of the oral CaSR antagonist, ronacaleret, in OVX rats, SU372
- BZA in combination with conjugated estrogens improves bone mass and strength in the OVX rat, SA385
- Ca signaling is a major target of OCT-1547, a small molecule osteoporosis drug candidate, M339
- Cannabinoid receptor ligands rescue bone loss and stimulate fracture healing, SU375
- Carborane BE360, one of the carbon-containing polyhedral boron-cluster compounds, is a new type of selective estrogen receptor modulator., SU187
- Cissus quadrangularis* attenuates OVX induced bone loss in mice, M403
- Combination of flaxseed and estrogen benefits bone health in the OVX rat model of postmenopausal osteoporosis, SU381
- Comparison of the effects of IBN alone with IBN in combination with SNAC on bone density and bone strength in OVX rats, SU391
- Development of an animal model of bisphosphonate-induced severe suppression of bone turnover, SA511
- Dietary Sr in a model of established osteopenic rats reduce the levels of 25(OH)D, SA377
- Diffuse osteopenia after tibia fracture: benefits of early mobilization and weight bearing, F461
- Dried plum alters bone metabolism via a different mechanism than PTH, M341
- Effect of cannabinoid CB1 receptor ligands on body weight and bone mass in mice, M340
- Effects of agave inulin on Ca metabolism in Japanese young adults, M332
- Effects of co-treatment with an Scl-Ab and ALN in OVX rats, 1213
- Effects of different extracts of *Fructus ligustri lucidi* on Ca balance in normal female rats, M336
- Effects of ODN on bone biomarkers in OVX non-human primates, F297
- Effects of ODN on bone mass and turnover in estrogen deficient adult rhesus monkeys, SA072
- Effects of PTH on fracture repair in GC treated mice, 1062
- Effects of Vitamin K2 and RIS on bone formation and resorption, osteocyte lacunar system and porosity in the cortical bone of GC-treated rats, SU385
- Efficacy of ODN in the OVX rhesus monkey as measured with pQCT, M343
- Fully human anti-DKK1 antibodies increase bone formation and resolve osteopenia in mouse models of estrogen-deficiency induced bone loss, 1214
- Fusion protein of PTH and a collagen binding domain shows superior efficacy and longer duration of action compared to PTH(1-34) as an anabolic bone agent in normal female mice, 1063
- Green tea polyphenols protect bone microarchitecture in female rats with chronic inflammation-induced bone loss, M338
- IC162, a new flavonoid, preserves bone mass and microarchitecture without affecting uterine weight in OVX rats, SA386
- Improved bone mass after co-administration of Sr ranelate and RIS in a rat model of osteoporosis using “in-vivo”  $\mu$ CT, SU393
- Increases in BMD observed with Scl-Ab treatment are reversible, 1211
- Inhibition of bone loss and muscle atrophy by DHT in a mouse hindlimb disuse model, SU377
- Injection of MSCs overexpressing both CXCR4 and RANK-Fc effectively prevented OVX-induced bone loss, F391
- Intermittent, short duration cyclic loading attenuates disuse osteoporosis without affecting resorption, M483
- Juvenile murine model of OVX-induced trabecular and cortical osteoporosis, SA387
- Low dose administration of INF $\gamma$  stimulates osteoblastogenesis and prevents ovariectomy-induced osteoporosis in C57BL/6 mice, M334
- Male and female cynomolgus monkey models of osteoporosis, SU435
- Mechanical loading prevents bone loss due to hormone-deficiency in female mice, M474
- Neonatal exposure to soy isoflavones attenuates deterioration of bone tissue in female but not male mice after cessation of sex steroid production, SU476
- Osteogenic potential of bone marrow, compromised by disuse, is normalized by brief exposure to a low-level mechanical signal, M486
- Percutaneous injection of GEM OS2 increases vertebral BMD in geriatric female baboons, F376
- PINP, a new available rat bone formation marker: usefulness in osteopenia studies due to androgen lack and IBN treatment, SA299
- Prior treatment with Vitamin K<sub>2</sub> significantly improves the efficacy of RIS, SA379
- Profile analysis of rodent metaphyseal trabecular bone reveals a biphasic dose-dependent response to administered bone active agents, SA460
- Proteasome inhibition counteracts the negative effect of GC treatment on bone metabolism by stimulating osteoblasts and inhibiting osteoclasts in vitro, SA231
- R-spondin 1 reduces bone loss in human TNF transgenic and OVX mice, 1215
- RIS has a more rapid onset of remodeling suppression than ALN in rabbit vertebral trabecular bone, SU387
- RIS prevents early radiation-induced bone loss at multiple skeletal sites, 1066
- Rodent model to evaluate the effect of dietary protein on intestinal Ca absorption, M330
- Role of active site Thr201 in the inhibition of farnesyl pyrophosphate synthase by NBP, F407
- Roles of ZOL in bone healing and osteoblast functions, 1064
- Sca-1<sup>+</sup> HSC-based hGH gene therapy enhanced endosteal bone resorption in mice, M233
- Scl-Ab increases bone formation and decreases bone resorption in distal tibial metaphyseal trabecular bone in OVX rats, F394
- Secretomic analysis of Ca supplement-mediated bone remodeling, M022
- Selective p38 $\alpha$  inhibitor prevents bone loss induced by estrogen deficiency, M335
- Short-term effect of ZOL on the superficial vascularisation of membranous bone sites, SU382
- Skeletal effects of a F2A in OVX rats, SA388
- Solid-state <sup>31</sup>P MRI quantifies mineralization changes in OVX rat bone, M422
- Soluble activin receptor type IIA fusion protein, ACE-011, increases bone mass by stimulating bone formation and inhibiting bone resorption in cynomolgus monkeys, SU376
- Sr ranelate decreases osteoblast-induced osteoclastogenesis through the involvement of the CaSR, F389
- Studying cellular uptake and distribution of bisphosphonate in vivo using fluorescently-labelled analogues of RIS, 1065
- TOR inhibits osteoclast activity in vitro and prevents orchietomy-induced bone resorption in male rats, SA381
- TPTD improves trabecular architecture as measured by  $\mu$ CT at simulated in vivo resolution in the femoral neck of OVX monkeys, SA375
- Transition from ALN to DMAb resulted in further reductions in local and systemic bone turnover parameters and reduced cortical porosity in OVX cynomolgus monkeys, 1216
- Use of alternative medicine for treating osteoporosis in Korea, SA390
- Osteoporotic Fractures in Men (MrOS) Study**
- Comprehensive genetic analysis of bone volume in men, M268
- Distribution and rate of clinical fractures in older men without osteoporosis, 1282
- Epidemiology of rib fractures in older men, F354
- Functional polymorphism in COL1A2 (Ala459Pro) that is associated with intracranial aneurysms, shows heterozygous disadvantage concerning BMD and stroke in elderly men, SU219
- Gondanotropins, bone loss and fracture in men, 1278
- Higher BMD loss in older men with diabetes, 1209
- Poor peripheral nerve function is related to lower BMD, SA328
- Self-reported weight at birth predicts measures of femoral size but not volumetric BMD in elderly men, SU338
- Smoking is an independent predictor of low BMD, prevalent vertebral fractures and incident fractures in elderly men, SU349
- Osteopotential (Opt)**
- Mice lacking the novel transmembrane protein Opt develop catastrophic defects in bone modeling, 1075
- Osteoprogenitor cells**
- Ablation of IGF-I signaling in osteoprogenitors decreases bone formation and blunts the skeletal response to PTH, 1193
- All-trans-retinoic acid (Vitamin A) increases expression of MafB and inhibits osteoclast formation by interfering with differentiation of osteoclast progenitor cells, M117
- Anabolic PTH treatment mobilizes BMSC and osteoprogenitors towards bone surfaces, SA229

Dermo1 lineage tracing identifies early osteoprogenitor cells in adult murine bone marrow MSC cultures, SA051

Evaluation of circulating osteoprogenitor cells during fracture healing using parabiotic mice, 1260

Identification, characterization and isolation of peripheral osteoclast progenitors, SU099

Protein hydrolyzate directly modulates the expression of GIP by osteoprogenitor cells, SU010

Use of  $\alpha$ -SMA-GFP transgene to identify periodontium derived osteoprogenitors, SA040

Use of GFP reporter mice for assessing osteoprogenitor cell activity in a critical size calvarial defect, SA007

In vivo demonstration that PTH acts on early osteoprogenitor cells to enhance bone formation during repair of critical-size calvarial defects, M062

#### Osteoprotegerin (OPG)

Butyrate stimulates mineralized nodule formation and OPG expression by osteoblasts, M012

Circulating OPG and its ligand in post operative biliary atresia: relationship with metabolic bone disease, M406

Effect of  $\text{Sr}^{2+}$  on PTHrP, OPG and RANKL mRNA expression in osteoblastic-like cells UMR 106.1, SU016

Effects of ALN and RLX on the RANKL/OPG system in primary cultures of human osteoblasts, M101

Effects of exercise and estrogen on OPG in premenopausal women, SU166

Effects of intermediate doses of GCs on bone turnover and circulating Dkk-1, MIF, sRANKL and OPG in patients with interstitial lung disease, SA451

GILZ promotes osteoblast development and modulates RANKL/OPG levels, M049

Hyperphosphatasia: a unique type without mutations in *TNFRSF11A* (RANK), *TNFRSF11B* (OPG), or *SOST* (sequestosome 1), SU210

Increased osteoclasts in Brl mouse model for OI are independent of decreased osteoblast matrix production and RANKL/OPG ratio, but are associated with increased osteoclast precursors in marrow, SU209

LIPUS synergistically modulates SCT and OPG/RANKL ratio in MLO-Y4 osteocytes in vitro, M109

OPG and bisphosphonates had differential effects on osteoclast numbers, bone marrow fibrosis and cortical porosity in a mouse model of constitutive activation of the PTH/PTHrP receptor, M076

OPG deficiency mimicked by a novel 15-base pair tandem duplication in *TNFRSF11A* encoding RANK: merging the juvenile PD and ESH phenotypes, F563

OPG production by breast cancer cells is modulated by steroid hormones and confers resistance against TRAIL-induced apoptosis, M271

OPG serum levels in shaft fractures healing and non-union, M013

RANKL/OPG in primary cultures of osteoblasts from patients with osteoporotic hip fractures, SU009

Role of OPG/RANKL system for bone loss in PHPT, M192

Sim induces Wnt signaling and reduces CSF-1 secretion and RANKL/OPG ratio to block osteoclast differentiation, SU096

TSG-6 acts synergistically with OPG to inhibit bone resorption, SA097

#### Osteosarcoma

2ME2 alters eIF4E activity and causes protein synthesis inhibition in osteosarcoma cells, SU240

Alpha-Ca/CaMKII controls osteosarcoma cell migration, SU234

Characterisation of an antigen found in giant cell tumor and osteosarcoma cells, SU244

FGFR signaling in the pathogenesis of osteosarcoma, 1233

Hedgehog pathway is activated in osteosarcoma and cyclopamine prevents osteosarcoma growth by cell cycle regulation, SU241

Notch pathway is activated in osteosarcoma and inhibitors of  $\gamma$ -secretase inhibit osteosarcoma growth by cell cycle regulation, SU229

#### Osteosclerosis

Bisphosphonate-induced osteopetrosis: novel bone modeling defects, metaphyseal osteopenia, and osteosclerosis fractures after drug exposure ceases, F569

Osteosclerotic prostate cancer metastasis to murine bone: enhanced with increased bone turnover, SA269

Progressive lipodystrophy in the osteosclerotic mice over-expressing Fra1, 1149

Recovery from HCAO following anti-viral treatment, F488

Stress fracture and vertebral osteosclerosis related to fluorosis induced by excessive gingival topical fluoride application, M444

#### Osteotropic peptides. See Peptides

#### Osterix (Osx)

(Ala-Gly)n sequences configured silk protein scaffold induces osteoblast differentiation and bone formation via increased Cbfa1 and Osx expression, M167

BMP-2 induces Osx expression through up-regulation of Dlx5 and its phosphorylation by p38 MAPK, F020

BMSC and Osx contributing to osseointegration of dental implants, SA138

Craniofacial bone defect in Nell-1 mutant mice associated with dysregulated Runx2 and Osx expression, F174

Induction of Runx2 and Osx by bisphosphonate promote osteogenic differentiation, SU062

Osx is required for skeletal growth and bone homeostasis after birth, 1074

Osx, a positive regulator in adult bone formation, F008

PTH regulation of Osx transcription in osteoblasts, M042

Regulation of the osteoblast-specific transcription factor Osx by NO66, a Jumonji family histone demethylase, F017

T-box 3 negatively regulates osteoblast differentiation by inhibiting expression of Osx and Runx2, SU018

TIEG: a key regulator of Runx2 and Osx gene expression and osteoblast differentiation, M052

#### Ostm1

Role of Ostm1 in bone, hematopoiesis and neuronal development, 1271

#### Oxysterols

Synergistic activation of osteogenesis in MLPC by oxysterols, SU038

#### Oxytocin

Central control of bone remodeling: neurohypophyseal hormone oxytocin is decreased in severe postmenopausal osteoporosis, M418

Oxytocin directly regulates skeletal homeostasis, SA199

Oxytocin inhibits bone formation through the activation of the sympathetic tone, 1200

## P

#### p.N417S

c.1250A>G, p.N417S is a common American TNSALP mutation involved in all clinical forms of HPP, including pseudo-HPP, SA566

#### P2X<sub>7</sub>

Activation of P2X<sub>7</sub> nucleotide receptors increases metabolic acid production by osteoblastic cells, M065

Loss of function polymorphisms in the P2X<sub>7</sub> receptor gene are associated with accelerated lumbar spine bone loss in postmenopausal women, SU224

Novel selective P2X<sub>7</sub> receptor antagonist inhibits human osteoclast formation in vitro, M120

P2X<sub>7</sub> receptor activation mediates PKC $\alpha$  translocation in osteoblasts through alteration in actin cytoskeletal organization, SU040

Single nucleotide polymorphisms in the P2X<sub>7</sub> receptor gene are associated with increased postmenopausal bone loss and fracture incidence, SU223

#### P2Y<sub>2</sub>

P2Y<sub>2</sub> receptor activation regulates RhoA-mediated stress fiber formation in osteoblasts, SA035

#### p38

Antiapoptotic action of 17 $\beta$ -estradiol in skeletal muscle cells involves ERK 1/2, p38 MAPK, ASK-1 and HSP27, SU185

BMP-2 induces Osx expression through up-regulation of Dlx5 and its phosphorylation by p38 MAPK, F020

Stimulation of macrophage TNF $\alpha$  production by orthopaedic wear particles requires activation of the ERK 1/2/Egr-1 pathway but is independent of p38 and JNK, SA177

#### p38 $\alpha$

Selective p38 $\alpha$  inhibitor prevents bone loss induced by estrogen deficiency, M335

#### p57<sup>Kip2</sup>

C/EBP $\beta$ /p57<sup>Kip2</sup> signaling maintains transition from proliferation to hypertrophic differentiation of chondrocytes during skeletal growth, 1187

#### p62

Increased signaling through p62 in the MM microenvironment increases myeloma cell growth and osteoclast formation, SA289

Proteasome inhibitors attenuate osteoclastogenesis and bone resorption via the modulation of RANK-mediated TRAF6, p62 and I $\kappa$ B- $\alpha$  signaling cascades, SA099

#### p62<sup>P392L</sup>

Co-expression of p62<sup>P392L</sup> and MVNP in osteoclast precursors increases the formation of osteoclasts that express a pagetic phenotype, F476

#### p63

Identification of a transcription factor p63 for transactivation of Wnt9a and Gdf5 causing joint cartilage formation, F116

#### p66<sup>shc</sup>

Intermittent PTH administration increases bone mass and strength in aged mice by antagonizing oxidative stress-induced osteoblast apoptosis via ERK-mediated attenuation of p66<sup>shc</sup> phosphorylation, SU380

#### P253R

Dynamic morphological changes in the skulls of mice mimicking human Apert Syndrome resulting from gain-of-function mutation of FGFR2 (P253R), SA248

#### Paclitaxel (PTX)

Local administration with PTX-loaded HA-alginate beads for metastatic spine cancer in rats, M274

#### Paget's Disease (PD)

High levels of IL-6 and hyper-responsivity to 1,25(OH)<sub>2</sub>D<sub>3</sub> are both required for development of Pagetic osteoclasts, F478

OPG deficiency mimicked by a novel 15-base pair tandem duplication in *TNFRSF11A* encoding RANK: merging the juvenile PD and ESH phenotypes, F563

#### Paget's Disease of bone (PDB)

Archaeological skeletons support a North-West European origin for PDB, SA477

Case presentation: bisphosphonate induced ONJ in Pagetic jaw bone, WG24

Comparison of intravenous and intramuscular neridronate regimens for the treatment of PDB, SA481

Efficacy and safety of intravenous ZOL in the treatment of patients with resistant PDB, SA479

FGF-2 stimulates RANKL expression in PDB, F480

## Key Word Index

## ASBMR 30th Annual Meeting

Identification of a novel mutation (78dup27) of the *TNFRSF11A* gene in a Chinese family with early onset PDB, M237  
 Large collaborative study on geographic variation of *SQSTM1* mutations in PDB in Italy, SA475  
 PDB: a histologic and histomorphometric analysis of bone biopsies from 754 patients, 1133  
 Two novel *SQSTM1* mutations in American patients with PDB, SU216

**Pain**

Back pain is reduced in postmenopausal women with severe osteoporosis treated with rhPTH(1-34) regardless of incident fractures, SU413  
 Effect of RLX and ALF on bone and joint pain assessed by fall of skin impedance (electroalgotometry), SA384  
 Novel hypothesis explains the syndrome of chronic musculoskeletal pain and comorbid painful healed fracture sites in Vitamin D deficiency, SA474

**Pamidronate**

Bisphosphonate, pamidronate, suppresses the pro-inflammatory response in a mouse model of OI as well as normal littermates, SU386  
 Large osteoclasts in pediatric OI patients receiving intravenous pamidronate, SU497  
 Randomized dose comparison of pamidronate in children with types III and IV OI, SU496

***Panax notoginseng***

BT-201, a butanol extract of *Panax notoginseng* inhibits progression of joint degeneration in a rat model of OA, M152

**Pancreas transplantation**

Application of a treatment algorithm to avoid BMD loss and limit bisphosphonate use after kidney and kidney/pancreas transplantation, SA497  
 Pretransplant parathyroid function predicts laboratory and BMD changes after kidney and kidney/pancreas transplantation, 1032

**Parafibromin**

Usefulness of *HRPT2* gene and parafibromin studies in two patients with PHPT and uncertain pathological assessment, SA482

**Parathyroid**

Continuous rat parathyroid cell line expressing PTH, M184  
 Dominant tissue accumulation of MIB1 in parathyroid glands in uremic rats, SA222  
 Pretransplant parathyroid function predicts laboratory and BMD changes after kidney and kidney/pancreas transplantation, 1032

**Parathyroid cells**

Functional induction of target genes in parathyroid cell by direct injection technique, M185  
 GCM2, the regulator of parathyroid cell fate, transactivates the CaSR gene, M187  
 Molecular basis of PHPT: adenomatous parathyroid cells are resistant to L-amino acids, M203

**Parathyroid hormone (PTH)**

Ablation of IGF-I signaling in osteoprogenitors decreases bone formation and blunts the skeletal response to PTH, 1193  
 Acute change in iCa directly affects bone formation independent of PTH action during hemodialysis, SU437  
 Aging dependent and independent effects of b2 adrenergic receptor signaling on bone formation induced by intermittent PTH treatment in female mice, SA378  
 Albuminuria, 25(OH)D, 1,25(OH)<sub>2</sub>D, and intact PTH in older adults, SU442  
 Anabolic daily intermittent PTH 1-84 reduces bone blood vascular bed and induces dramatic changes in the bone/vessel spatial relationship, 1061  
 Anabolic PTH treatment mobilizes BMSC and osteoprogenitors towards bone surfaces, SA229

Analysis of chromosome breaks in osteoblasts and non-osteoblastic cells treated with intermittent PTH, M191  
 Association between Cx43 and  $\beta$ -arrestin is required for cAMP-dependent osteoblast survival induced by PTH, 1227  
 Behavior of circulating rat(s) PTH molecular forms in HPT2 related to Vitamin D deficiency and renal failure, M194  
 BMP/Wnt antagonists are upregulated by DEX in osteoblasts and reversed by ALN and PTH: potential therapeutic targets for GIO, M098  
 Bone tissue quality is differently altered by PTH, bisphosphonates and SERMs, SA510  
 Calcitonin attenuates the anabolic effect of PTH in vivo and rapidly upregulates SCT expression, F195  
 $\beta$ -catenin directly binds to a specific intracellular domain of PTH/PTHrP receptor and regulates the signaling in chondrocytes during endochondral ossification, 1013  
 CCR2 receptor signaling is involved in bone mass regulation and mediates the response to anabolic but not catabolic regimens of PTH(1-34), SU158  
 Changes in serum PINP in orchidectomized osteopenic rats treated with PTH and ALN, M295  
 Circulating osteoblast lineage cells increase with PTH treatment of HPT, 1146  
 Clinical implications of commercial biotin-based detection systems in PTH assays, M435  
 Clinically useful paradigm for interpretation of serum 25(OH)D levels with simultaneously measured PTH levels, M437  
 Cloning and functional analysis of human Nurr1 (NR4A2) promoter: critical role in the regulation of CYP27B1 by PTH and CREB phosphorylation, 1161  
 Comparison of cPTH(1-31) to PTH(1-34) in the enhancement of experimental fracture healing, M161  
 Continuous rat parathyroid cell line expressing PTH, M184  
 Deletion of the *GNAS* antisense transcript results in parent-of-origin specific *GNAS* imprinting defects and phenotypes including PTH-resistance, 1052  
 Dried plum alters bone metabolism via a different mechanism than PTH, M341  
 Effect of bodyweight on clinical response to ZT-031: development of a simple, improved dosing regimen for PTH analogs, M346  
 Effects of intermittent human PTH administration on bone union with hydroxyapatite blocks at the site of cancellous bone osteotomy in OVX rats, SA214  
 Effects of PTH on fracture repair in GC treated mice, 1062  
 Expansion of mesenchymal progenitors in an in vivo model of constitutive activation of the PTH/PTHrP receptor, 1263  
 Fusion protein of PTH and a collagen binding domain shows superior efficacy and longer duration of action compared to PTH(1-34) as an anabolic bone agent in normal female mice, 1063  
 Hematopoietic cells in the bone marrow augment anabolic actions of PTH, M181  
 High-fat diet facilitated decreases in BMD of OVX mice and suppressed the anabolic effects of PTH on bone, SA448  
 Hip fracture patients with vertebral fractures have more severe osteoporosis and are candidates for more active treatment including PTH, SU274  
 Hip structural analysis and volumetric QCT in postmenopausal women from the PaTH Study: mono- or combination therapy with ALN and PTH, M306  
 Identification and optimization of residues in PTH and PTHrP that determine altered modes of binding to the PTH/PTHrP receptor, F224

Impact of PTH on cells of the hematopoietic lineage, 1159  
 Inhibitory role of *Gaq*/PKC $\delta$  signal in the bone anabolic action of PTH, 1228  
 Interaction of combined intervention of PTH and GH on trabecular and cortical bone formation and resorption in the hypophysectomized rats, SU502  
 Intermittent PTH administration increases bone mass and strength in aged mice by antagonizing oxidative stress-induced osteoblast apoptosis via ERK-mediated attenuation of p66<sup>shc</sup> phosphorylation, SU380  
 Jagged1 stimulation by PTH(1-34) in mature osteoblasts is not required for HSC expansion, 1078  
 Long-acting PTH ligand that binds to a distinct PTH receptor conformation (R0) can stimulate increases in markers of both bone resorption and bone formation in mice, F221  
 Loss of a single bim allele recovers the defective osteoclast function in *bcl-2*<sup>-/-</sup> mice but does not restore the anabolic action of PTH, 1217  
 Marrow ablation induces periosteal bone formation and potentiates the effect of PTH on endosteal bone formation in rat femurs, M208  
 Metabolic alkalosis transition in renal proximal tubule cells facilitates an increase in CYP27B1, while blunting responsiveness to PTH, M196  
 Mice deficient in BSP display impaired modeling and remodeling and respond to ovariectomy but not to the cortical anabolic effect of PTH, 1191  
 Molecular mechanisms involved in PTH-induced apoptosis in Caco-2 intestinal cells, M189  
 Negative relationship between PTH and Vitamin D: is there an age and a gender effect?, M179  
 New data on the impact of renal function on the relationship between 25(OH)D and PTH, 1031  
 New intact PTH assay on the IDS Automated Analyser 3x3<sup>TM</sup>, M209  
 New long-acting PTH/PTHrP hybrid analog that binds to a distinct PTHrP conformation has superior efficacy in a rat model of HPT, F483  
 Novel CaSR antagonist leads to dose-dependent transient release of PTH after oral administration to healthy volunteers, 1173  
 OPG and bisphosphonates had differential effects on osteoclast numbers, bone marrow fibrosis and cortical porosity in a mouse model of constitutive activation of the PTH/PTHrP receptor, M076  
 Overexpression of sFRP1 inhibits bone formation and attenuates PTH bone anabolic effects, 1100  
 PGE2 as a potential mediator of PTH-dependent regulation of HSCs, F171  
 Post-mitotic preosteoblasts are the targets of the anabolic actions of intermittent PTH on periosteal bone, 1157  
 Postnatal deletion of PTH/PTHrP receptor in growth plate chondrocytes leads to growth plate fusion, F114  
 PTH and not Vitamin D predicts age-related bone loss in the elderly, M178  
 PTH has direct anabolic effects on OA articular cartilage in vitro and in vivo, M155  
 PTH increases after oral peptones administration in obese subjects treated with roux-en-y gastric bypass surgery: role of phosphate on the rapid control of PTH release, M180  
 PTH increases bone turnover in HPT, F485  
 PTH induces COX-2 in MC3T3-E1 osteoblasts via cAMP-PKA and Ca-calceineurin pathways, SA033

PTH receptor signaling in osteocytes increases bone mass and the rate of bone remodeling through Wnt/LRP5-dependent and -independent mechanisms, respectively, 1038

PTH regulation of *Osx* transcription in osteoblasts, M042

PTH reverses abnormal bone remodeling and structure in HPT, 1036

PTH signaling through LRP5/6 in osteoblasts, 1014

PTH stimulates hematopoiesis and increases survival in irradiated mice, 1015

PTH-gene family in the cartilaginous fish, *Callorhynchus milii*, M183

PTH-induced bone mass gain is blunted but not abolished in *SOST* overexpressing and deficient mice, 1039

PTH/PTHrP mediated stimulation of osteoblast differentiation involves Epac-Rap1 dependent processes, SA025

Relationship between Vitamin D and PTH: serum Ca and Mg are major determinants of PTH in patients with mild CKD, M211

Role of FGF-23 in the early response to the PTH analogue; TPTD, SU174

Role of the transcription factor SOX4 in the skeletal response to intermittent PTH, SA220

Safety and efficacy of long-term PTH replacement in a pediatric patient with inherited HPT, F217

Selective removal of PLC signaling in novel PTH(1-28) analogs abolishes regulation of NaPi-IIc but not NaPi-IIa, M186

Serum intact PTH of 100 to 150 pg/ml is associated with greatest survival in maintenance hemodialysis patients, SU445

Serum PTH response to oral Ca load in Asian adolescents, M188

SIF levels among hemodialysis patients are positively associated with levels of serum phosphate and intact PTH, SU440

At similar plasma 25(OH)D levels, fat mass influence PTH levels in the state of Vitamin D insufficiency, SA218

Suppression of canonical wnt signaling by Dkk1 attenuates PTH-mediated peritrabecular stromal cell response and new bone formation in a model of HPT2, F215

T cells amplify the anabolic action of PTH through Wnt10b signaling, 1197

Treatment with daily subcutaneous TPTD (1-34) compared with daily subcutaneous PTH (1-84) in women with severe postmenopausal osteoporosis, 1170

In vivo demonstration that PTH acts on early osteoprogenitor cells to enhance bone formation during repair of critical-size calvarial defects, M062

In vivo longitudinal QCT analysis PTH efficacy in a rat cortical defect model, M207

**Parathyroid hormone receptor (PTHrP)**

New long-acting PTH/PTHrP hybrid analog that binds to a distinct PTHR conformation has superior efficacy in a rat model of HPT, F483

Regulation of nuclear import of the PTHR, M210

**Parathyroid hormone receptor 1 (PTHr1)**

Coordinate regulation of PTHrP and PTHR1 in the osteoblast differentiation of C2C12 cells promoted by BMP-2, SA157

Intracellular PTHR2 alters cell proliferation and pattern of gene expression while antagonizing PTHR1 signaling in chondrocytic CFK2 cells, SA121

PTHr1 mutations associated with Ollier Disease result in receptor loss of function, SA258

PTHr1 stimulates bone formation through a distinct  $\beta$ -arrestin dependent pathway independent of G protein activation, 1226

**Parathyroid hormone receptor 2 (PTHr2)**

Intracellular PTHR2 alters cell proliferation and pattern of gene expression while antagonizing PTHR1 signaling in chondrocytic CFK2 cells, SA121

**Parathyroid hormone related protein (PTHrP)**

ADAMTS-7, a direct targeting molecule of PTHrP, is a novel potent mediator of chondrogenesis, 1262

C-terminal fragment of PTHrP (107-139), exerts osteogenic features in both regenerating and nonregenerating bone in mice with diabetes-related osteopenia, SA223

$\beta$ -catenin directly binds to a specific intracellular domain of PTH/PTHrP receptor and regulates the signaling in chondrocytes during endochondral ossification, 1013

Coordinate regulation of PTHrP and PTHR1 in the osteoblast differentiation of C2C12 cells promoted by BMP-2, SA157

Effect of  $\text{Sr}^{2+}$  on PTHrP, OPG and RANKL mRNA expression in osteoblastic-like cells UMR 106.1, SU016

Effects of extracellular matrix properties and elastic modulus on the expression of PTHrP by human breast cancer cells, M280

Expansion of mesenchymal progenitors in an in vivo model of constitutive activation of the PTH/PTHrP receptor, 1263

hPTHrP 1-36 stimulates PKA-dependent phosphorylation and nuclear translocation of  $\beta$ -catenin in neonatal mouse calvarial bone cells, F032

Identification and optimization of residues in PTH and PTHrP that determine altered modes of binding to the PTH/PTHrP receptor, F224

KO of the PTHrP gene in breast cancer cells inhibits tumor progression and metastatic spread in vivo, 1016

N-terminal fragment of PTHrP promotes the GC-related deficiency of bone regeneration after bone marrow ablation in mice, M195

New long-acting PTH/PTHrP hybrid analog that binds to a distinct PTHR conformation has superior efficacy in a rat model of HPT, F483

Novel and sensitive immunoassay for PTHrP, M182

OPG and bisphosphonates had differential effects on osteoclast numbers, bone marrow fibrosis and cortical porosity in a mouse model of constitutive activation of the PTH/PTHrP receptor, M076

Postnatal deletion of PTH/PTHrP receptor in growth plate chondrocytes leads to growth plate fusion, F114

PTH/PTHrP mediated stimulation of osteoblast differentiation involves Epac-Rap1 dependent processes, SA025

PTHrP blockade inhibits tumor progression in a model of human breast cancer, F213

PTHrP is processed by skin keratinocytes and has immunomodulation properties, SA216

PTHrP nuclear localization sequence and C-terminus regulate craniofacial development, 1264

PTHrP prevents chondrocyte premature hypertrophy by inducing cyclin D1-dependent Runx2 and 3 phosphorylation and degradation, 1044

PTHrP regulates mammary gland ductal elongation during puberty, F228

PTHrP-induced Wnt signaling specifies the mammary mesenchyme, F219

Skeletal dysmorphology of mice lacking the mid-region, nuclear localization sequence and C-terminus of PTHrP, 1160

Wnt signaling regulates Gli2 and PTHrP expression in human breast cancer cells that cause osteolysis, M278

**Parathyroid hormone, carboxyl-terminal (CPTH)**

CPTH; prediction of novel functions, structural features and potential receptor, SU072

**Parathyroid hormone, cyclic (cPTH)**

Comparison of cPTH(1-31) to PTH(1-34) in the enhancement of experimental fracture healing, M161

**Parathyroid hormone, human (hPTH)**

Effects of hPTH(1-34) infusion on circulating serum phosphate, 1,25(OH)<sub>2</sub>D and FGF-23 levels in healthy men, SU169

Phase 1, randomized, double-blind, placebo controlled trial of the PK/PD effect and safety of ZT-031, a hPTH analog, in healthy elderly women, SA399

Repetitive rapid delivery of pharmacologically-active hPTH 1-34 across human skin without injection, SA397

Short duration pharmacokinetic profile of ZT-031 (cyclic PTH [1-31]), a novel hPTH analog, M345

**Parathyroid hormone, recombinant human (rhPTH)**

Back pain is reduced in postmenopausal women with severe osteoporosis treated with rhPTH(1-34) regardless of incident fractures, SU413

BMD response to treatment with rhPTH in patients previously treated with bisphosphonates, M348

Women with severe osteoporosis treated with rhPTH(1-34) improve quality of life regardless of incident fractures, SU412

**Parathyroidectomy**

Changes in cardiovascular function after parathyroidectomy in mild PHPT, M434

Parathyroidectomy improves quality of life in hemodialysis patients with HPT2, SA212

**Paravertebral muscles**

Effective progressive resistive exercise program from prone position for paravertebral muscles to reduce risk of vertebral fractures, M473

**Parietal bone**

Histologic and radiographic analysis of osteopromotive property of demineralized allogenic dentin matrix in parietal bone defects in rabbit, M168

Therapeutic effects of one-year ALN treatment in three cases of osteoporosis with parietal thinning, M410

**PaTH Study**

Hip structural analysis and volumetric QCT in postmenopausal women from the PaTH Study: mono- or combination therapy with ALN and PTH, M306

**Pathogenesis**

Effects of serum factors during osteoblast differentiation—implication for the pathogenesis of osteoporosis in Crohn's Disease, M450

**PBMC. See Peripheral blood mononuclear cells**

**PBX1**

PBX1 interaction with HOXA10 regulates timing and expression of phenotypic bone genes during osteoblastogenesis, SU019

**PEARL Trial. See Postmenopausal Evaluation and Risk-reduction with Lasofoxifene Trial**

**Pediatric bone disease. See also Bone acquisition**

25(OH)D levels in children with CKD as measured by tandem mass spectrometry, SU485

Advanced vertebral compression at diagnosis among children with ALL, SU483

Arterial compliance is associated with change in bone strength in children, F552

Background UVB exposure in pregnancy and skeletal development in childhood, 1104

Birth weight predicts bone size, adult weight predicts BMC and BMD in young Gambian adults, M498

BMD in children and adolescents with sickle cell disease, SU217

BMD shows no peak from birth to youth as measured by QCT, F310

Body fatness negatively associated with BMD and hip geometry indices in adolescents, F546

Bone health impairment in children with chronic Ca and Vitamin D deficiency due to nutritional allergies, SU503

Bone status evaluation in pre-pubertal children with CF, SU486

Born small is not bad for bone, SA551

## Key Word Index

## ASBMR 30th Annual Meeting

Changes in volumetric bone density and bone strength at the tibial midshaft in boys and girls 12-17 years of age, SU469

Childhood cortical bone and skeletal age show bivariate genetic linkage to chromosome 2p, 1177

Clinical tool for adjusting BMD Z-scores for body size in growing children, 1105

Comparison of the effect of puberty on hip structure in boys and girls, F554

Contribution of birth status, age at menarche and lifestyle factors to skeletal formation in junior and senior high school students, M492

Differences in BMC at the lumbar spine and proximal femur in South American children of different ethnic groups, SU490

Dysosteosclerosis in a 2-year-old girl: investigation of a rare, sclerosing bone disorder, SA567

Effect of 12 months gymnastics participation on bone mass accrual in 4 to 7 year olds, SA555

Effect of bed rest on bone turnover in adolescents hospitalized for anorexia nervosa, SA559

Effect of bone marrow transplantation in a child with malignant IO, SU498

Effect of non-ambulation on bone strength in boys with DMD, WG1

Effect of particle size of Ca carbonate supplement on Ca retention in adolescent girls, SA545

Effect of Vitamin D<sub>2</sub> and Vitamin D<sub>3</sub> on intestinal Ca absorption in Nigerian children with rickets, SA560

Elevated systolic blood pressure is positively related to bone mass measurements in overweight pre-pubertal and pubertal children, M496

Ethnicity-specific bone changes during adolescent growth: pQCT analysis of the tibia, M502

Evaluating bone microstructure at the distal tibia in children, F315

Genetic variation in *LRP5* associates with metabolic characteristics in healthy prepubertal children, 1176

Heel ultrasound and consolidation of PBM in young women, M504

How does body fat influence bone health in childhood? A Mendelian randomisation approach, 1175

Infantile HCa: relationship of dietary intake of Ca and Vitamin D to serum and urine levels, SU491

Influence of pubertal timing on bone trait acquisition: predetermined trajectory detectable five years before menarche, 1106

Interaction between the skeletal parameter BMD and lifestyle factors in 390 adolescent daughter-mother pairs, F548

Is it time to update normative values for ionized Ca and urine Ca? Creatinine ratios in healthy Canadian infants, SU487

Is Vitamin D deficiency more common in children with cerebral palsy than in healthy children?, SU194

Longitudinal analysis of calcaneal QUS measures during childhood, M321

Maternal nutrient restriction during pregnancy results in significant alterations in fetal skeletal development in the baboon, M494

Microfinite element modeling reveals that transient deficits in cortical bone may underlie the adolescent peak in forearm fractures, 1179

Modeling pathways for bone loss in childhood malignancies, SU237

Newborn infant bone mineralization is affected by their umbilical cord length, SU495

Normal reference values for QUS bone densitometry of the calcaneus in Chinese children and adolescents, SU489

Overweight children are more at risk to sustain a forearm fracture due to poor bone strength relative to body weight, M458

Path analysis (structural equation modeling) and covariation of bone traits following delayed puberty, SA543

Pediatric Crohn's Disease is associated with negative Ca balance and increased renal losses of Ca, SA565

Preterm birth and BMD in young adulthood, 1103

Prevalence of TH among healthy infants and toddlers, SA564

Prevention of nutritional rickets in Nigerian children with dietary Ca supplementation, M491

Protocol for pediatric proximal femur DXA analysis, M506

Randomised controlled trial of the effects of Vitamin D supplementation upon muscle function in adolescent girls, SU428

Relationship between physical fitness and bone and physical activity and Ca retention in adolescent girls, SA553

Relationship of urinary excretion of C-telopeptides to growth in children, F301

Suboptimal Vitamin D status in pregnant adolescents is associated with neonatal Vitamin D insufficiency, F557

Three year school-curriculum-based exercise program in prepubertal children increases bone mineral accrual and bone size but do not influence femoral neck structure, 1107

Tracking of femur length during intrauterine growth, M497

Use of bone biomarkers as an endpoint in a pediatric study of ALN, SU488

Vitamin D dose response study in Canadian infants, 1108

Vitamin D insufficiency: seasonal variation in healthy 6-12 year old African American and Caucasian children, SU482

Vitamin D supplementation in breast fed infants, SU500

Vitamin K intake is positively related to trabecular bone microarchitecture in children, M505

**PEG-PLA**  
Functionalization of a PLGA/PEG-PLA composite electrospon scaffold with rhBMP-2 plasmid DNA for bone regeneration, SA124

**Peptide of type 1 pro-collagen (P1NP)**  
Validation of an immunoassay for the determination of P1NP in rat serum, M296

**Peptides**  
Optimizing bioavailability of oral administration of small peptides through pharmacokinetic and pharmacodynamic parameters, M398

**Peptides, osteotropic**  
Osteotropic peptides: anabolic and osteogenic effects, M045

**Peptones**  
PTH increases after oral peptones administration in obese subjects treated with roux-en-y gastric bypass surgery: role of phosphate on the rapid control of PTH release, M180

**Periodontal ligament (PDL)**  
LMP-1, positive regulator in osteolineage differentiation of human PDL fibroblasts, M051  
Osteogenic potential of PDL cells in vivo, SU054

**Periodontium**  
Use of  $\alpha$ -SMA-GFP transgene to identify periodontium derived osteoprogenitors, SA040

**Periosteal bone**  
Post-mitotic preosteoblasts are the targets of the anabolic actions of intermittent PTH on periosteal bone, 1157

**Periosteal cells**  
Extracellular matrix protein periostin regulates periosteal apposition, 1178  
SDF-1 is expressed in osteocytes and periosteal cells in response to mechanical loading, M105

**Periostin**

Extracellular matrix protein periostin regulates periosteal apposition, 1178

Inhibition of bone biomechanical response to physical activity and loading in mice lacking periostin, 1143

**Peripheral blood mononuclear cells (PBMC)**  
Elevated production of IL-1 $\beta$  and TNF $\alpha$  by PBMC is associated with increased hip fracture risk in elders, 1283  
Increased expression of OPN in PBMC is associated with alteration in the fractions of lymphocytes in hindlimb-unloaded mice, M175

**Peroxisome proliferator-activated receptor (PPAR)**  
Isoform-specific expression of PPARs and gene regulation during osteoclastogenesis in RAW/C4 cells, M118

**Peroxisome proliferator-activated receptor gamma (PPAR $\gamma$ )**  
Ghrelin inhibits early osteogenic differentiation of C3H10T1/2 cells by suppressing Runx2 expression and enhancing PPAR $\gamma$  and C/EBP $\alpha$  expression, M086

**Peroxisome proliferator-activated receptor gamma-1 (PPAR $\gamma$ 1)**  
Proinflammatory mediators downregulate PPAR $\gamma$ 1 expression and activity in OA synovial fibroblasts, M159

**Peroxisome proliferator-activated receptor gamma-2 (PPAR $\gamma$ 2)**  
Inhibition of PPAR $\gamma$ 2 by BADGE and Vitamin D in male mice increases osteoblastogenesis and inhibits bone matrix mineralization leading to osteomalacia, SU374  
Oxidative stress stimulates the synthesis of PPAR $\gamma$ 2, and ligand-activated PPAR $\gamma$ 2 sequesters  $\beta$ -catenin leading to suppression of TCF-mediated transcription, 1099  
PPAR $\gamma$ 2-mediated proteolytic degradation of  $\beta$ -catenin determines an anti-osteoblastic effect of anti-diabetic TZDs, SU023  
Targeted disruption of PPAR $\gamma$  in BMSC reveals its role in aging-induced bone loss, 1148

**PGC-1 $\beta$**   
PGC-1 $\beta$  and iron uptake in the mitochondrial activation of osteoclasts, 1222

**Phagocytosis**  
Normal human osteoblasts internalize MSUM by phagocytosis and autophagy, M057

**PHD2**  
Deletion of the oxygen-sensor PHD2 in chondrocytes results in increased cartilage and bone mineralization, 1153

**Phe147**  
CYP27A1 mutations at Phe147 confer 25-hydroxylase activity towards a Vitamin D<sub>2</sub>-type sidechain, M231

**Phellodendron Amurensis**  
Effects of beta-D-glucopyranoside from *Phellodendron Amurensis* on the production of inflammatory cytokines, growth factors, MMP, and on bone markers in human subchondral OA osteoblasts, SA117

**Phex**  
Aberrant *Phex* function in osteocytes has limited effects on bone mineralization in XLH, 1051

**Phex**  
Deprivation of Vitamin A results in a partial rescue of the mineralization defects in *Phex*-deficient Hyp mice, F202  
Effect of a novel splice-site mutation of *PHEX* gene during osteoblast differentiation, M092  
*Phex* binds to SNARE-associated protein snapin and co-localizes in vesicle-enriched, extracellular matrix micro-environment mediating mineral crystal nucleation, F066  
*PHEX* cleavage of SIBLING-ASARM peptides as a mechanism underlying osteomalacia in XLH, 1199

Screening the PHEX gene in a large cohort of hypophosphatemic rickets allowed the description of a missense mutation not responsible for the disease on a highly conserve amino acid residue, M246

Serine protease inhibitor AEBSF blocks transcription of PheX by osteoblasts, M053

**Phosphates**

Altered TNSALP expression and phosphate regulation contribute to reduced mineralization in mice lacking androgen receptor, SU181

Comparison of 1,25(OH)<sub>2</sub>D<sub>2</sub> and calcitriol effects in an adenine-induced model of CKD reveals differential control over serum Ca and phosphate, SU448

Controlled drug release from Ca phosphate-based orthopaedic implants, SU235

High expression of the Ca/phosphate-regulating hormone STC2 is associated with renal calcification in the Klotho mutant mice, SA201

Human SLC34A3/NaPi-IIc mutations T137M and L527del uncouple Na-phosphate co-transport, F471

MEPE regulates bone remodelling independent of serum phosphate and alters renal vascularization, F205

Osteopenia in CKD: effects of phosphate overload, SU447

Phosphate regulates chondrocyte differentiation, proliferation and apoptosis in a model of embryonic endochondral bone formation, SU124

PTH increases after oral peptones administration in obese subjects treated with roux-en-y gastric bypass surgery: role of phosphate on the rapid control of PTH release, M180

SIF levels among hemodialysis patients are positively associated with levels of serum phosphate and intact PTH, SU440

Transgenic ASARM-peptide overexpression with reduced serum phosphate and 1,25(OH)<sub>2</sub>D<sub>3</sub> leads to decreased BMD and obesity, F210

**Phosphates, inorganic**

Role of pyrophosphate and inorganic phosphate in PKA-mediated osteoblastic differentiation and mineralization of primary murine aortic cells, M143

Signaling of extracellular inorganic phosphate mediated via Na-phosphate co-transporters influences FGF-23 signaling in renal tubular cells, SU172

Synergistic role of Npt2a and Npt2c in inorganic phosphate metabolism of mice, F473

**Phosphatidylinositol 3-kinases (PI3K)**

BMP-2-stimulated signaling niche in osteoblasts comprising of Smad and PI3K/Akt regulates NFATc1 expression and its nuclear translocation, 1081

Class IA PI3Ks are indispensable for osteoclast function by regulating cytoskeletal organization and cell death, 1115

Transcriptional regulation of Cx43 by  $\beta$ -catenin, a pathway activated by PGE<sub>2</sub>-PI3K-GSK3 signaling in mechanically loaded osteocytes, 1042

**Phosphatonins**

Phosphatonins and liver resection-related hypophosphatemia, SU176

**Phospholipase C (PLC)**

Selective removal of PLC signaling in novel PTH(1-28) analogs abolishes regulation of NaPi-IIc but not NaPi-IIa, M186

**Phospholipase C gamma 2 (PLC $\gamma$ 2)**

PLC $\gamma$ 2 as a promising therapeutic target in RA, F176

**Phosphorus (P)**

Does dietary P influence FGF-23 concentrations in FD patients?, M426

Effect of the dietary Ca/P ratio on the rate of skeletal accrual in mice, M333

High level dietary P and Cd exacerbate OVX-induced bone loss, M301

Solid-state <sup>31</sup>P MRI quantifies mineralization changes in OVX rat bone, M422

### Phthalein monophosphates

Phthalein monophosphates are specific substrates for TRACP5b, M284

**Phylloquinone**

Menaquinone-4 derived from phylloquinone regulates osteoblast function, SU034

**Phytoestrogens**

Antioxidants (phytoestrogens and quercetin) are potentials agents against RA, SA487

**Pkd1**

Conditional disruption of *Pkd1* in osteoblasts results in osteopenia due to direct impairment of osteoblast-mediated bone formation, SA019

**Plasma clearance**

Skeletal plasma clearance, as measured by quantitative radionuclide studies, is correlated with bone turnover markers at 3 months of TPTD therapy, F398

**Platelets**

Platelet VDR levels are reduced in osteoporotic patients, SA241

Platelets contribute to circulating levels of Dkk-1: clinical implications in MM, SU228

**Platinum (Pt)**

Effects of Pt group metals treatment on the bone of developing chick embryos, M141

**PLB-985**

Neutrophil-like PLB-985 cells induce differentiation of human blood monocytic precursors into functional osteoclasts via a RANKL-dependent mechanism, SA092

**Pleiotrophin (PTN)**

Anabolic response to skeletal loading in mice with targeted disruption of PTN gene, 1142

**PLGA**

Functionalization of a PLGA/PEG-PLA composite electrospun scaffold with rhBMP-2 plasmid DNA for bone regeneration, SA124

**Plums**

Dried plum alters bone metabolism via a different mechanism than PTH, M341

Dried plum polyphenols increase IGF-I production in osteoblast-like cells, SU002

**Pluronic F108**

Thermoreversible Pluronic F108 gel as a universal tissue immobilization material for  $\mu$ CT analyses, SU468

**PMEPA1**

TGF $\beta$  activates prostate cancer bone metastases, pro-osteolytic gene expression and the new TGF $\beta$  signaling regulator PMEPA1, SA273

**Podosome**

Formation of podosome belts by osteoclasts on plastic correlates with resorptive activity, SU068

**Pollution**

Air pollution might be a neglected risk-factor of hypovitaminosis D, SU306

**Polycaprolactone-tricalcium phosphate**

Selective retention of bone marrow cells in repair of canine femoral defect with polycaprolactone-tricalcium phosphate scaffolds, SU005

**Polymers, resorbable**

Clinical application of resorbable polymers in guided bone regeneration, SA003

**Polyomamiddle T antigen (PyMT)**

Vitamin D delays breast cancer progression in the PyVMT transgenic mouse model, 1185

**Polyphenols**

Green tea polyphenols protect bone microarchitecture in female rats with chronic inflammation-induced bone loss, M338

**POMOST Study**

Influence of bone osteoporotic fractures in the past on the persistence of pharmacological treatment in osteoporosis, M382

**POROS Study. See Primary Care Osteoporosis Risk of Fracture Screening Study**

**Porosity**

Cortical porosity is increased in male osteoporosis with vertebral fracture, 1132

Effects of Vitamin K2 and RIS on bone formation and resorption, osteocyte lacunar system and porosity in the cortical bone of GC-treated rats, SU385

Microporosity in b-TCP ceramics may be detrimental to MSC survival and osteoblastic differentiation, SA015

OPG and bisphosphonates had differential effects on osteoclast numbers, bone marrow fibrosis and cortical porosity in a mouse model of constitutive activation of the PTH/PTHrP receptor, M076

Transition from ALN to DMAb resulted in further reductions in local and systemic bone turnover parameters and reduced cortical porosity in OVX cynomolgus monkeys, 1216

In vivo quantification of intra-cortical porosity in human cortical bone using HR-pQCT in patients with type II diabetes, M309

**POSSIBLE EU®**

Prospective observational study of osteoporosis medication use in postmenopausal women in the European Union, SU347

**POSSIBLE US™**

Correlates of osteoporosis treatment persistence for patients new to therapy and patients with recent switches, M375

Gastrointestinal side effects in postmenopausal U.S. women on osteoporosis therapies, SU417

Medication switching in postmenopausal women on osteoporosis, M376

**Postmenopausal Evaluation and Risk-reduction with Lasofoxifene (PEARL) Trial**

Effects of LASO on bone turnover markers, 1287

**Potassium bicarbonate (KHCO<sub>3</sub>)**

Effects of KHCO<sub>3</sub> on Ca and bone metabolism during high salt intake, SA446

Impact of dietary protein on Ca homeostasis and nitrogen excretion in the presence and absence of KHCO<sub>3</sub>, SU305

**PP1c**

Point mutation of endofin at PP1c-binding domain induces angiogenesis and bone formation in mice by sensitizing BMP signaling, 1082

**Preference satisfaction questionnaire (PSQ)**

Development, reliability, and validity of a new PSQ, SA417

**Pregnancy**

Advancing maternal age is associated with lower peak BMD in the male offspring, M327

Background UVB exposure in pregnancy and skeletal development in childhood, 1104

Late pregnancy serum Vitamin D and longitudinal bone loss during pregnancy, F544

Maternal nutrient restriction during pregnancy results in significant alterations in fetal skeletal development in the baboon, M494

Pregnancy upregulates duodenal Ca-transport genes and normalizes Ca homeostasis in *Vdr* null mice, M230

Suboptimal Vitamin D status in pregnant adolescents is associated with neonatal Vitamin D insufficiency, F557

**Preosteoblast cells**

Osteonin increases the levels of intracellular Ca of human preosteoblast cells in culture, SU051

**Primary Care Osteoporosis Risk of Fracture Screening (POROS) Study**

Baseline characteristics of women taking part in an osteoporosis intervention, SU370

**Procollagen I N-terminal propeptide (PINP)**

Changes in serum PINP in orchidectomized osteopenic rats treated with PTH and ALN, M295

PINP, a new available rat bone formation marker: usefulness in osteopenia studies due to androgen lack and IBN treatment, SA299

## Key Word Index

## ASBMR 30th Annual Meeting

Relationship of bone turnover marker (PINP) and changes in femoral neck BMD to fracture risk in women with postmenopausal osteoporosis treated with once-yearly ZOL 5 mg, 1027  
Serum PINP is a sensitive marker of bone formation in mouse OVX model, M293

**Progenitor cells**

Use of endothelial progenitor cells to promote bone healing, SA104  
Use of GFP reporters to map the progression of multipotential progenitor cells into the osteoblast lineage, SU053

**Progenitor cells, multilineage (MLPC)**

Synergistic activation of osteogenesis in MLPC by oxysterols, SU038

**Progesterone**

Augmentation of PBM occurs in female and male mice without progesterone nuclear receptors, F249

**Progressive diaphyseal dysplasia. See Camurati-Engelmann disease****Prolactin**

Evidence for a role of prolactin in Ca homeostasis: regulation of intestinal TRPV6 and intestinal Ca absorption by prolactin, 1223

**Proline/arginine-rich end leucine-rich repeat protein (PRELP)**

Matrix PRELP interferes with the NF- $\kappa$ B pathway and impairs osteoclast formation and activity, SU089

**Prolyl 3-hydroxylase 1 (P3H1)**

Hotspot splicing mutation in *LEPRE1* affects P3H1 and causes recessive OI, SU215  
P3H1 and CRTAP are mutually stabilizing in the endoplasmic reticulum collagen prolyl 3-hydroxylation complex, 1049

**Prostaglandin**

Prostaglandins enhance extracellular matrix mineralization through the enhancement of both Na-dependent phosphate transport activity and ALP activity in osteoblast-like cells, SU031

**Prostaglandin D<sub>2</sub> (PGD<sub>2</sub>)**

Implication of PGD<sub>2</sub> in the birth and death of human osteoclasts, SU095  
PGD<sub>2</sub> downregulates MMP-1 and MMP-13 expression in human OA chondrocytes, SA152

**Prostaglandin E (PGE)**

PGE receptor EP4 antagonist attenuates growth and metastases of cancer, 1230

**Prostaglandin E<sub>2</sub> (PGE<sub>2</sub>)**

HDAC inhibitors suppress IL-1 $\beta$ -induced NO and PGE<sub>2</sub> production in human chondrocytes, SU116  
Mechanism of BMP-2 enhancement of PGE<sub>2</sub> stimulated osteoclastogenesis, SU085  
Nanotechnological scaffold with combination of PGE<sub>2</sub> receptor EP4 agonist and rhBMP2, enhances bone repair in the defect of mouse calvarium bone, SA105  
PGE<sub>2</sub> as a potential mediator of PTH-dependent regulation of HSCs, F171  
Transcriptional regulation of Cx43 by  $\beta$ -catenin, a pathway activated by PGE<sub>2</sub>-PI3K-GSK3 signaling in mechanically loaded osteocytes, 1042

**Prostate**

1,25(OH)<sub>2</sub>D<sub>3</sub> is as effective as 1,25(OH)<sub>2</sub>D<sub>3</sub> in regulating cellular proliferation in cultured normal human keratinocytes and transformed prostate cells, M215

**Prostate cancer. See Cancer****Proteasome**

Bzb, a proteasome inhibitor, prevents metastatic breast cancer osteolysis and reduces mammary fat pad tumor growth in mice, F277

Proteasome inhibition counteracts the negative effect of GC treatment on bone metabolism by stimulating osteoblasts and inhibiting osteoclasts in vitro, SA231

Proteasome inhibitors attenuate osteoclastogenesis and bone resorption via the modulation of RANK-mediated TRAF6, p62 and I $\kappa$ B- $\alpha$  signaling cascades, SA099

**Protein disulfide isomerase A3 (PDIA3)**

Silencing of PDIA3 (ERp60) reduces the rapid membrane response to 1,25(OH)<sub>2</sub>D<sub>3</sub> in MC3T3-E1 osteoblast-like cells, M227

**Protein hydrolyzate**

Protein hydrolyzate directly modulates the expression of GIP by osteoprogenitor cells, SU010

**Protein inhibitor of activated STAT3 (PIAS3)**

PIAS3 negatively regulated RANKL-mediated osteoclastogenesis directly in osteoclast precursors and indirectly via osteoblasts, F079

**Protein kinase A (PKA)**

Distinct modes of osteoblastic differentiation from BMSC and vascular smooth muscle cells: induction by BMP-2 and PKA and suppression by Vitamin D derivatives, SU060

hPTHrP 1-36 stimulates PKA-dependent phosphorylation and nuclear translocation of  $\beta$ -catenin in neonatal mouse calvarial bone cells, F032

PTH induces COX-2 in MC3T3-E1 osteoblasts via cAMP-PKA and Ca-calcineurin pathways, SA033

Role of pyrophosphate and inorganic phosphate in PKA-mediated osteoblastic differentiation and mineralization of primary murine aortic cells, M143

**Protein kinase C (PKC)**

Inhibitory role of G $\alpha$ /PKC $\delta$  signal in the bone anabolic action of PTH, 1228

Permanent FGFR2 activation promotes osteoblast differentiation in MSCs through activation of PKC signaling, M093

PKC $\delta$  is important for acidification of the lysosomes and resorption lacuna in osteoclasts, M124

**Protein kinase C $\alpha$  (PKC $\alpha$ )**

P2X<sub>7</sub> receptor activation mediates PKC $\alpha$  translocation in osteoblasts through alteration in actin cytoskeletal organization, SU040

**Protein kinase C $\delta$  (PKC $\delta$ )**

FGF-2 signaling in osteoblasts: Cx43 is a docking platform for PKC $\delta$ , F026

**Protein kinase D (PKD)**

PKD regulates HDAC7 localization and interaction with Runx2 during BMP-2-stimulated osteogenesis, SU027

**Protein tyrosine phosphatase (PTP)**

Identification of the regulatory mechanism(s) of PTP-PEST associating with the sealing ring formation and bone resorption in osteoclasts, SU065

**Proteinase-activated receptor-2 (PAR-2)**

PAR-2 activation induces bone resorption via RANKL upregulation in human OA subchondral bone osteoblasts, M018

**Proteoliposomes**

Proteoliposomes carrying ALP and NPP1 as matrix vesicle mimetics, SA061

**Proton pump inhibitors**

Gastric proton pump inhibitors failed to affect bone resorption and formation, SA095

**Pseudohypoparathyroidism (PHP)**

Hypothyroidism and autism combined with PHP in the absence of Albright's hereditary osteodystrophy and *GNAS* imprinting changes, SA259

**Psoriasis**

BMD and body composition in postmenopausal women with psoriasis and psoriatic arthritis, SU337

**Psoriatic arthritis. See Arthritis****PTEN**

VEGF and PTEN regulate bone homeostasis via control of osteoblastogenesis, osteoclastogenesis and adipocyte differentiation, M029

**PTH and Alendronate Comparative Efficacy****(PACE) Study**

Active controlled, non-inferiority study to compare the effect of ZT-031 with ALN on the incidence of new vertebral fractures, M347

**PTH/PTHrP receptor (PPR)**

Target ablation of PPR in osteocytes induces hypocalcemia and impairs bone structure, 1158

**PU.1**

LPS suppresses RANK gene through the down-regulation of PU.1 and MITF, SU083

**Puberty, delayed**

Path analysis (structural equation modeling) and covariation of bone traits following delayed puberty, SA543

**Pulmonary disease, chronic obstructive (COPD)**

Acute COPD exacerbations are associated with uncoupling of bone resorption from bone formation, M414

**PVQEET<sup>559-564</sup>**

Three RANK cytoplasmic motifs, IVVY<sup>535-538</sup>, PVQEET<sup>559-564</sup> and PVQEQQ<sup>604-609</sup>, play a critical role in TNF $\alpha$ /IL-1-mediated osteoclastogenesis, 1118

**PVQEQQ<sup>604-609</sup>**

Three RANK cytoplasmic motifs, IVVY<sup>535-538</sup>, PVQEET<sup>559-564</sup> and PVQEQQ<sup>604-609</sup>, play a critical role in TNF $\alpha$ /IL-1-mediated osteoclastogenesis, 1118

**Pyk-2**

Mice deficient in Pyk-2 have impaired OVX-induced bone resorption, F098

**PYK2**

BMP-6 stimulated osteogenesis of HOB cultures is associated with suppression of PYK2, SU048

**Pyrophosphates**

Pyrophosphates stimulates osteoclast differentiation and bone resorption, SA084

Role of pyrophosphate and inorganic phosphate in PKA-mediated osteoblastic differentiation and mineralization of primary murine aortic cells, M143

**Q****Q-GWUS. See Ultrasound****Qualeffo-41**

Vitamin D deficiency is associated with diminished quality of life based on Qualeffo-41 questionnaire analysis, SU424

**Quality of life, health-related**

Association between falls and health-related quality of life, SU420

**Quantitative computed tomography (QCT). See Computed tomography****Quantitative trait loci (QTL)**

Epistasis between QTLs for bone density variation in Copenhagen X Dark Agouti F2 rats, M253

Geometric property QTLs in HcB/8 x HcB/23 F2 cross, F260

Mouse-to-human strategy to identify bone strength QTL genes, SA120

Recalculation of genome scans on a common genetic map enhances our ability to identify common bone density QTL in new and historical data, 1276

**Quantitative ultrasound (QUS). See Ultrasound****Quartz crystal microbalance (QCM)**

Human osteoprogenitor cell adhesion and spreading on functionalized Ti surfaces followed by QCM and CLSM, SA101

**Quercetin**

Antioxidants (phytoestrogens and quercetin) are potential agents against RA, SA487

High concentrations of hydroxytyrosol and quercetin antioxidants enhance adipogenesis and inhibit

osteoblastogenesis in MSCs, SA037

**Quiescent osteoclast precursors (QOP)**

Cell cycle-arrested QOP are cells committed to the osteoclast lineage, SU098



**R****R-Smad**

TGF $\beta$  inhibits BMP signaling and osteogenesis through the TGF $\beta$  and BMP R-Smad direct interaction, 1080

**R-spondin 1**

R-spondin 1 reduces bone loss in human TNF transgenic and OVX mice, 1215

**R-spondin 2**

R-spondin 2 is a novel osteogenic factor required for Wnt11 mediated osteoblast differentiation, SU063

**R0**

Long-acting PTH ligand that binds to a distinct PTH receptor conformation (R0) can stimulate increases in markers of both bone resorption and bone formation in mice, F221

**R206H**

Hypoxia promotes ligand-independent activation of the ACVR1 (R206H) mutant receptor in C2C12 cells, M243

**R740S**

R740S, a dominant V-ATPase  $\alpha 3$  mutation, causes osteopetrosis in mice, 1218

**Rab18**

Proteomic identification and characterization of the small GTPase Rab18 in human osteoclasts, SU109

**Rac**

Dock5, an essential Rac exchange factor in osteoclasts that controls adhesion structure organization and bone resorbing activity, SU064

Rac 1 and 2, in combination, mediate osteoclast function and survival, 1220

**Radiation therapy**

Combined Cs-137 gamma irradiation and hindlimb unloading rapidly decreased cancellous bone volume fraction in the mouse lumbar vertebrae, M469

Combined effects of irradiation and unloading on murine bone, 1295

Degradation of allograft bone quality by gamma irradiation is not explained by altered enzymatic or non-enzymatic cross-links, M460

Detrimental effects of abdominal irradiation on the skeleton in growing mice, M412

Musculoskeletal disuse worsens the acute detrimental effects of heavy particle radiation on osteoblastogenesis, SA517

Radiation-induced bone loss: description of dose, time course, age, strain and sex variables, SU368

RIS prevents early radiation-induced bone loss at multiple skeletal sites, 1066

**Radiation, ultraviolet (UV)**

Vitamin D (cholecalciferol) production does not increase linearly with UV dose, M226

**Radiogrammetry, digital x-ray**

ALN treatment in postmenopausal Romanian women followed by BMD-digital x-ray radiogrammetry, M357

**Radiographic texture analysis (RTA)**

RTA of densitometric calcaneal images differs between subjects with and without GC use, M314

**Radioiodine**

Body composition changes after radioiodine treatment of hyperthyroidism, M433

**Radiomorphometry**

Correlations between panoramic radiomorphometric indices and BMD in postmenopausal women, SA311

**Radiotherapy**

Inhibition of MM growth and preservation of bone with combined radiotherapy and anti-angiogenic agent, SA285

**Radius**

Deleterious effect of late menarcheal age on bone microstructure in both distal radius and tibia, 1239

FEA performed on radius and tibia HR-pQCT images provides new insights for fracture status assessment, 1067

Microstructural changes at the ultradistal radius in MGUS, SU238

**Raf**

Vinculin is involved in hypertrophic differentiation through Raf/MEK/ERK pathway in chondrocytic ATDC5 cells, SA119

**Raloxifene (RLX)**

Assessment of adherence to treatment of osteoporosis with RLX and/or ALF in postmenopausal Japanese women, M387

Effect of RLX and ALF on bone and joint pain assessed by fall of skin impedance (electroalgotometry), SA384

Effect of RLX treatment on BMD might be influenced by UGT1A1\*28 polymorphism, M257

Effects of ALN and RLX on the RANKL/OPG system in primary cultures of human osteoblasts, M101

HSA for RLX treatment in Japanese women with osteoporosis, SA419

RLX ameliorates detrimental collagen cross-link formation in bone from an OVX rabbits with or without

hyperhomocysteinemia, SA382

Safety and effectiveness profile of RLX in long-term prospective observational study, M385

**RAMP2**

c-Src-regulated osteoblast-mimicry in breast cancer bone metastasis: the role of RAMP2 and BSP2, M275

**Rancho Bernardo Study**

Albuminuria, 25(OH)D, 1,25(OH) $_2$ D, and intact PTH in older adults, SU442

Incident vertebral fracture is predicted by prevalent vertebral fracture as identified by the algorithm-based qualitative method, but not by non-osteoporotic short vertebral height, 1128

Lean body mass is a better predictor of BMD than leg power or grip strength in healthy caucasian adults, SU290

**RAP-011**

Activin A mediates MM bone disease which is reversed by RAP-011, a soluble activin receptor, 1231

**Rap1**

PTH/PTHrP mediated stimulation of osteoblast differentiation involves Epac-Rap1 dependent processes, SA025

Small G protein Rap1 promotes osteoblast differentiation, M080

**RAW**

Isoform-specific expression of PPARs and gene regulation during osteoclastogenesis in RAW/C4 cells, M118

**Receptor activator of nuclear factor- $\kappa$ B (RANK)**

In the absence of NF- $\kappa$ B2, TNF induces osteoclast formation in vivo independent of RANKL/RANK and more severe arthritis in TNF-Tg mice, 1009

CXCL13 stimulates RANK ligand expression in SCC, SU247

Hyperphosphatasia: a unique type without mutations in *TNFRSF11A* (RANK), *TNFRSF11B* (OPG), or *SOST* (sequestosome 1), SU210

Injection of MSCs overexpressing both CXCR4 and RANK-Fc effectively prevented OVX-induced bone loss, F391

LPS suppresses RANK gene through the down-regulation of PU.1 and MTF, SU083

Novel role of L-Ser for the activation of RANKL-RANK signaling machinery in osteoclastogenesis in vitro, SA082

OPG deficiency mimicked by a novel 15-base pair tandem duplication in *TNFRSF11A* encoding RANK: merging the juvenile PD and ESH phenotypes, F563

Proteasome inhibitors attenuate osteoclastogenesis and bone resorption via the modulation of RANK-mediated TRAF6, p62 and I $\kappa$ B- $\alpha$  signaling cascades, SA099

Suppression of TREM-2 expression and TREM-2-mediated costimulation of RANK signaling by cytokines that inhibit human osteoclast differentiation, SU114

Three RANK cytoplasmic motifs, IVVY<sup>535-538</sup>, PVQEET<sup>559-564</sup> and PVQEQQ<sup>604-609</sup>, play a critical role in TNF $\alpha$ /IL-1-mediated osteoclastogenesis, 1118

**Receptor activator of nuclear factor- $\kappa$ B ligand (RANKL)**

1,25(OH) $_2$ D $_3$  can directly induce osteoclast formation in osteoclast precursors in the absence of RANKL, SU070

In the absence of NF- $\kappa$ B2, TNF induces osteoclast formation in vivo independent of RANKL/RANK and more severe arthritis in TNF-Tg mice, 1009

Brain-type creatine kinase is required for RANKL-induced osteoclastogenesis, M116

CED: a unique variant featuring a novel, heterozygous, leucine repeat mutation in *TGF $\beta$ 1* together with a novel, homozygous, missense change in *TNFSF11* encoding RANKL, F256

Effect of Sr<sup>2+</sup> on PTHrP, OPG and RANKL mRNA expression in osteoblastic-like cells UMR 106.1, SU016

Effects of ALN and RLX on the RANKL/OPG system in primary cultures of human osteoblasts, M101

**Receptor activator of nuclear factor- $\kappa$ B ligand, soluble (sRANKL)**

Effects of intermediate doses of GCs on bone turnover and circulating Dkk-1, MIF, sRANKL and OPG in patients with interstitial lung disease, SA451

Establishment of a murine model of HCa by overexpression of sRANKL using an adenovirus vector, SU082

**Receptor activator of nuclear factor- $\kappa$ B ligand (RANKL)**

Estrogen suppresses RANKL-induced osteoclastic differentiation of human monocytes via an ER $\alpha$  associated cytoplasmic signaling complex, but ER $\alpha$  is downregulated during osteoclastic differentiation, 1125

FGF-2 stimulates RANKL expression in PDB, F480

GILZ promotes osteoblast development and modulates RANKL/OPG levels, M049

High dose of RANKL rescues integrin  $\alpha_v$ -osteoclast phenotype, F081

Hormonal control of RANKL expression is independent of Runx family proteins: evidence that commitment to the osteoblast lineage is not a requirement for the stromal cells that support osteoclast differentiation, SU047

IL-27/WSX-1 signaling inhibits RANKL-induced osteoclastogenesis through STAT1 activation: a possible involvement in TLR4/MyD88-mediated inflammatory arthritis, SU102

Increased osteoclasts in Brl mouse model for OI are independent of decreased osteoblast matrix production and RANKL/OPG ratio, but are associated with increased osteoclast precursors in marrow, SU209

Inhibition of lamin A/C attenuates osteoblast differentiation and stimulates osteoclastogenesis through enhanced RANKL signaling, M070

LIPUS synergistically modulates SCT and OPG/RANKL ratio in MLO-Y4 osteocytes in vitro, M109

MEK5/ERK5 signal regulates RANKL-induced osteoclastogenesis, SU103

Modeled microgravity sensitizes osteoclast precursors to RANKL mediated osteoclastogenesis by increasing DAP12, M114

Neutrophil-like PLB-985 cells induce differentiation of human blood monocytic precursors into functional osteoclasts via a RANKL-dependent mechanism, SA092

## Key Word Index

## ASBMR 30th Annual Meeting

Novel role of L-Ser for the activation of RANKL-RANK signaling machinery in osteoclastogenesis in vitro, SA082

PAR-2 activation induces bone resorption via RANKL upregulation in human OA subchondral bone osteoblasts, M018

PIAS3 negatively regulated RANKL-mediated osteoclastogenesis directly in osteoclast precursors and indirectly via osteoblasts, F079

RANKL induces Ca channel activation in human osteoclasts, SU107

RANKL suppression by siRNAs in rat primary osteoblasts, M032

RANKL-mediated osteoclast lineage commitment dictates the role of LPS in osteoclast differentiation, SA088

RANKL/OPG in primary cultures of osteoblasts from patients with osteoporotic hip fractures, SU009

Recovery of bone architecture after RANKL administration in rats is characterized by increased bone mass on existing trabeculae assessed by in vivo  $\mu$ CT, SU076

Reduced osteoclastogenesis and RANKL expression in marrow from women taking ALN, SU400

Rheumatoid synoviocytes are stimulated with IL-23 to enhance osteoclastogenesis through upregulation of RANKL expression, SU084

Role of OPG/RANKL system for bone loss in PHPT, M192

S100 protein directly and indirectly affects RANKL-stimulated osteoclastogenesis, SA090

Sim induces Wnt signaling and reduces CSF-1 secretion and RANKL/OPG ratio to block osteoclast differentiation, SU096

Transactivation of RANKL by C/EBP $\beta$  and C/EBP $\delta$  in adipocyte lineage cells, SU092

**Receptor for advanced glycation endproducts (RAGE)**

Over-expression of RAGE prevents OVX-mediated bone loss in CD1 mice, M132

**Receptor transporting protein 3 (RTP3)**

GWAS identified RTP3 as a novel gene for bone strength, SU331

**Receptor-like protein tyrosine phosphatase  $\mu$  (RPTP $\mu$ )**

In bone, RPTP $\mu$  is exclusively expressed in osteocytes and may affect bone mass, SA052

**Recombinant adeno-associated virus (rAAV)**

Biological activation of biomaterials by rAAV vector, SU136

**Recombinant human platelet-derived growth factor BB (rhPDGF-BB)**

Percutaneous injection of GEM OS2 increases vertebral BMD in geriatric female baboons, F376

Stimulation of fracture healing by rhPDGF-BB combined with  $\beta$ TCP/collagen matrix in a diabetic rat fracture model, I137

**Renal function**

Behavior of circulating rat(s) PTH molecular forms in HPT2 related to Vitamin D deficiency and renal failure, M194

c-Fos is associated with renal FGF-23-mediated signaling, SU173

HPT and renal insufficiency, WG29

MEPE regulates bone remodelling independent of serum phosphate and alters renal vascularization, F205

New data on the impact of renal function on the relationship between 25(OH)D and PTH, I031

Pediatric Crohn's Disease is associated with negative Ca balance and increased renal losses of Ca, SA565

Reduced renal function is associated with increased rates of bone loss at the hip and spine, SU357

Regulation of renal Klotho: the importance of ER $\alpha$ , SA211

Renal leak hypercalciuria: a potential cause of tertiary hyperparathyroidism, M430

Renal safety across a wide range of dosing regimens of RIS, SA402

Serum uOC concentration are related to renal function in type 2 diabetes patients, M443

Signaling of extracellular inorganic phosphate mediated via Na-phosphate co-transporters influences FGF-23 signaling in renal tubular cells, SU172

**Resveratrol**

Effect of resveratrol and flax oil on MC3T3-L1 pre-adipocyte and ST2 BMSC proliferation and differentiation, SU059

Mechanism of action of the anti-aging agent resveratrol on bone, I136

**Retinoblastoma binding protein-1 (RBP1)**

RBP1 is critical for Runx2 expression, transcriptional activity and nodule formation in osteoblasts, M037

**Rheumatism**

Acute phase response and bone metabolism marker after intravenous bisphosphonate in osteoporotic patients with rheumatism, M364

**Rheumatoid arthritis (RA). See Arthritis**

**RhoA**

P2Y<sub>2</sub> receptor activation regulates RhoA-mediated stress fiber formation in osteoblasts, SA035

**RhoB**

Identification of RhoB as a key target involved in cell motility and bone metastasis, F291

**RhoGTPases**

Silencing of RhoGTPases counteract microgravity-induced effects on osteoblasts, SA011

**Ribonucleic acid interference (RNAi)**

Allele specific silencing of Collagen 1 Alpha genes in primary human bone cells using RNAi, M232

**Ribonucleic acid, messenger (mRNA)**

DKK1 is regulated by mRNA stability and epigenetic mechanisms in bone metastasis, I090

In vivo downregulation of *Mustn1* mRNA leads to musculoskeletal defects, I192

**Ribonucleic acid, micro (miRNA)**

Possible physiological function of menin protein as transcriptional factor that modulates miRNA expression during osteogenesis, M036

Program of miRNAs control BMP-2 induced bone phenotype development, M090

Regulation of osteoblast differentiation by miRNA, M087

Regulation of osteonectin/SPARC by miRNA-29, I155

**Ribonucleic acid, short hairpin (shRNA)**

Lentiviral shRNA mediated inhibition of Grx5 expression induces apoptosis via a mechanism involving increased ROS and cardiolipin oxidation, and reduced SOD activity, M009

**Ribonucleic acid, small interfering (siRNA)**

RANKL suppression by siRNAs in rat primary osteoblasts, M032

**Ribonucleoproteins, heterogeneous nuclear (hnRNP)**

Evidence of a role for the human Vitamin D response element binding protein, hnRNP C1/C2 in chromatin remodeling and transcript splicing, F240

**Rickets**

Effect of Vitamin D<sub>2</sub> and Vitamin D<sub>3</sub> on intestinal Ca absorption in Nigerian children with rickets, SA560

Prevention of nutritional rickets in Nigerian children with dietary Ca supplementation, M491

Rare cases of XLH rickets/osteomalacia mimicking ARHR/osteomalacia, F469

**Rickets, autosomal recessive hypophosphatemic (ARHR)**

Late presentation of ADHR, WG31

Rare cases of XLH rickets/osteomalacia mimicking ARHR/osteomalacia, F469

**Rickets, hypophosphatemic**

Mechanical unloading partially rescues hypophosphatemic rickets in *Dmp1*-null mice, I162

Screening the PHEX gene in a large cohort of hypophosphatemic rickets allowed the description of a missense mutation not responsible for the disease on a highly conserve amino acid residue, M246

**Risedronate (RIS)**

Chemical composition and nanoscale structure of RIS-treated mineralizing MC3T3-E1 cells, M023

Continued evidence for safety and efficacy of RIS in men with osteoporosis, M360

Cost-effectiveness of RIS versus IBN at one year: the case of the United Kingdom, SA424

Cost-effectiveness of RIS versus IBN at one year: the case of Germany, SA425

Cost-effectiveness of RIS vs. generic ALN, SA423

Effect of a single 5-mg infusion of ZOL on bone turnover markers versus oral RIS (5 mg/day) over 1 year in patients with GIO, M362

Effect of a single infusion of ZOL 5 mg versus oral RIS 5 mg on BMD at lumbar spine, hip, femoral neck and trochanter in patients with GIO, F403

Effect of RIS in liver transplantation patients with low bone mass, SA503

Effect of RIS on bone density in HSC transplant patients, SU407

Effect of RIS on bone strength and work to failure determined by FEA and simulation of clinically-measured bone loss and mineralization changes, SA505

Effect of RIS on osteocyte viability in paired biopsies from early postmenopausal women, M420

Effect of ZOL (single 5-mg infusion) on lumbar spine BMD versus oral RIS (5 mg/day) over 1 year in subgroups of patients receiving GC therapy, M363

Effects of Vitamin K2 and RIS on bone formation and resorption, osteocyte lacunar system and porosity in the cortical bone of GC-treated rats, SU385

Fracture reduction during two years of treatment with RIS or ALN, SA404

Improved bone mass after co-administration of Sr ranelate and RIS in a rat model of osteoporosis using "in-vivo"  $\mu$ CT, SU393

Improvement in quality of life among women treated with RIS, SU414

Long term safety of oral RIS treatment in men with osteoporosis as assessed by histomorphometry, SA344

Modeled cost-effectiveness of RIS versus IBN: the case of Italy, SA427

Once-a-month RIS 150 mg reduced vertebral fracture risk at one year in a historical control analysis, SU403

Prior treatment with Vitamin K<sub>2</sub> significantly improves the efficacy of RIS, SA379

Renal safety across a wide range of dosing regimens of RIS, SA402

RIS has a more rapid onset of remodeling suppression than ALN in rabbit vertebral trabecular bone, SU387

RIS prevents early radiation-induced bone loss at multiple skeletal sites, I066

Studying cellular uptake and distribution of bisphosphonate in vivo using fluorescently-labelled analogues of RIS, I065

**RNA. See Ribonucleic acid**

**Roche Elecsys (ELEC)**

Analytical validation of LIA and ELEC methods for the determination of osteocalcin, SA191

**Ronacaleret**

Bone-building effects of the oral CaSR antagonist, ronacaleret, in OVX rats, SU372

Ronacaleret, a novel CaSR antagonist, demonstrates potential as an oral bone-forming therapy in healthy postmenopausal women, I174

**ROS**

Lentiviral shRNA mediated inhibition of Grx5 expression induces apoptosis via a mechanism involving increased ROS and cardiolipin oxidation, and reduced SOD activity, M009

**Rosiglitazone**

Rosiglitazone-induced change in BMD among African Americans with type 2 diabetes mellitus or impaired glucose tolerance, SU315

**Rsl1**

Expression of an engineered G<sub>s</sub>-coupled receptor, Rsl1, in mature osteoblasts is sufficient to drive a dramatic anabolic skeletal response, 1077

Ligand activation of the engineered G<sub>s</sub>-coupled receptor Rsl1 in osteoblasts promotes trabecular bone formation, 1076

**RsaI**

RsaI polymorphism in ESR2 is associated with postmenopausal fracture risk, SU221

**Runx**

Hormonal control of RANKL expression is independent of Runx family proteins: evidence that commitment to the osteoblast lineage is not a requirement for the stromal cells that support osteoclast differentiation, SU047

**Runx2**

BMD-associated SNP lies in a Runx2 binding site of the LRP5 promoter, M264

Craniofacial bone defect in Nell-1 mutant mice associated with dysregulated Runx2 and Osx expression, F174

Deletion of Zfp521, an antagonist to Runx2 and Ebf1 transcriptional activity, leads to osteopenia and a defect in matrix mineralization in mice, 1109

Ectopic Runx2 expression disrupts normal acini structure in mammary epithelial cells, F279

FHL2 mediates DEX-induced MSC osteogenic differentiation by activating Wnt/ $\beta$ -catenin signaling and Runx2 expression, M048

Functional association of MAPK and Runx2 on osteoblast chromatin, SU025

Ghrelin inhibits early osteogenic differentiation of C3H10T1/2 cells by suppressing Runx2 expression and enhancing PPAR $\gamma$  and C/EBP $\alpha$  expression, M086

Icariin induces osteogenic differentiation in vitro in a BMP- and Runx2- dependent manner and bone regeneration in vivo, M089

Induction of Runx2 and Osx by bisphosphonate promote osteogenic differentiation, SU062

MEPE expression is regulated by BMP-2 signaling through the activation of its downstream transcription factors, Dlx3, Dlx5 and Runx2, SA064

Non-genomic estrogen receptor Gpr30 is a Runx2 responsive gene that is required for osteoblast proliferation, F572

PKD regulates HDAC7 localization and interaction with Runx2 during BMP-2-stimulated osteogenesis, SU027

PTHrP prevents chondrocyte premature hypertrophy by inducing cyclin D1-dependent Runx2 and 3 phosphorylation and degradation, 1044

RBP1 is critical for Runx2 expression, transcriptional activity and nodule formation in osteoblasts, M037

Regulation of RUNX2 at the nuclear lamina, M055

Regulation of Runx2 function in osteoblasts by sex steroid receptors, M099

Runx2 and canonical Wnt signaling cooperatively regulate BMP-induced differentiation pathways of adult dural cells into osteoblasts or chondrocytes, M043

Runx2 threshold for the CCD phenotype, M041

T-box 3 negatively regulates osteoblast differentiation by inhibiting expression of Osx and Runx2, SU018

TGF $\beta$  and Smad3-dependent repression of Runx2 function in ATDC5 chondrocytes, SU122

TIEG: a key regulator of Runx2 and Osx gene expression and osteoblast differentiation, M052

TNF $\alpha$  and IL-1 $\beta$  stimulate ALP activity and mineralization but decreases RUNX2 expression and osteocalcin secretion in human MSC, SU044

Transcriptional activation of osteocalcin by Runx2 during osteoblast development is controlled at the post-translational level, M031

Trps1 represses Runx2 during endochondral bone formation, SU126

Wdr5 is required for chromatin modifications at the Runx2 promoter, M039

**Runx3**

PTHrP prevents chondrocyte premature hypertrophy by inducing cyclin D1-dependent Runx2 and 3 phosphorylation and degradation, 1044

**S****S100**

S100 protein directly and indirectly affects RANKL-stimulated osteoclastogenesis, SA090

**Saliva**

Bone resorption markers in saliva, M288

**Salt**

Effects of KHCO<sub>3</sub> on Ca and bone metabolism during high salt intake, SA446

**SAMP6**

ALF ameliorates bone dynamics in senescence-accelerated SAMP6 mice and in fracture repair rat model, SU394

**Sarcoidosis**

Nonsteroid responsive HCa associated with sarcoidosis—a rapid response to hydroxychloroquine, WG28

**Sarcoma, osteogenic**

Transcriptional silencing of Frzb/sFRP3 by promoter methylation in osteogenic sarcoma, SU231

**Sarcopenia**

Shared genetics within the musculoskeletal system: a pleiotropic approach to osteoporosis and sarcopenia, WG2

**SATB2**

SATB2 overexpression promotes osteoblast differentiation and enhances regeneration of bone defects, SU058

**Schmorl's Node**

To avoid underdiagnosis of vertebral fracture, recognition of true fracture line including multiple Schmorl's Node is necessary, SA324

**Sciatic denervation**

Alteration of trabecular bone architecture following sciatic denervation and subsequent reinnervation in rat proximal tibiae, SA513

**Scl-Ab. See Anti-sclerostin monoclonal antibody****Sclerosis, aortic valve**

Relationship between low bone mass and aortic valve sclerosis in Korean men and women, SU452

**Sclerostin (SCT)**

30IT/C of SCT modulates BMD by Wnt and estrogen signaling pathways, 1270

Calcitonin attenuates the anabolic effect of PTH in vivo and rapidly upregulates SCT expression, F195

Expression of human SCT in heterologous eukaryotic insect and *E. coli* expression systems, SA059

Immunohistochemical localisation of SCT in human trabecular bone from fragility hip fracture patients, SA148

LIPUS synergistically modulates SCT and OPG/RANKL ratio in MLO-Y4 osteocytes in vitro, M109

Proinflammatory cytokine TWEAK induces SCT expression in human immature osteoblasts in a MAPK dependent fashion, M046

Widespread expression of SCT in adult and embryonic cartilage and bone, cells of the developing central nervous system and epithelia of the embryonic kidney and intestine, SA055

Wnt/LRP5-independent inhibition of osteoblastic cell differentiation by SCT, 1256

**Scoliosis**

Conditional deletion of fibronectin results in a scoliosis-like phenotype, 1046

 **$\gamma$ -secretase**

Notch pathway is activated in osteosarcoma and inhibitors of  $\gamma$ -secretase inhibit osteosarcoma growth by cell cycle regulation, SU229

**Secreted frizzled-related protein 1 (sFRP1)**

Overexpression of sFRP1 inhibits bone formation and attenuates PTH bone anabolic effects, 1100

**Secreted frizzled-related protein 4 (sFRP4)**

Deletion of the Wnt signaling antagonist sFRP4 in mice induces opposite bone formation phenotypes in trabecular and cortical bone, 1005

**Sensorimotor nerves**

Poor peripheral sensorimotor nerve function is associated with high fall risk, SU323

**Sequestosome 1**

Hyperphosphatasia: a unique type without mutations in *TNFRSF11A* (RANK), *TNFRSF11B* (OPG), or *SOSTM1* (sequestosome 1), SU210

**Ser1386Pro**

Mouse with a Ser1386Pro mutation in the C-propeptide domain of *col2a1* provides a model for SEDC, 1269

**SERM**

Bone tissue quality is differently altered by PTH, bisphosphonates and SERMs, SA510

**Serotonin**

Brain-derived serotonin positively regulates bone mass accrual, SA463

Gut-derived serotonin is an inhibitor of bone formation, M069

**Serum ionic fluoride (SIF). See Fluoride****Serum level of  $\gamma$ -glutamyltransferase. See  $\gamma$ -glutamyltransferase****Severe suppression of bone turnover (SSBT).**

See *Bone turnover*

**Sex hormone-binding globulin (SHBG). See Globulin****Sexual dimorphism**

Crosstalk between androgen receptor and Wnt signaling mediates sexual dimorphism during bone mass accrual, 1121

**Sfrp2**

Brachy-syndactyly caused by loss of *Sfrp2* function, F118

**SH2**

Deficiency of NCK1, an actin cytoskeletal modulator with SH2/SH3 motifs, induces bone loss via suppression of bone formation and induction of biochemical high bone turnover state, M026

**SH3**

Deficiency of NCK1, an actin cytoskeletal modulator with SH2/SH3 motifs, induces bone loss via suppression of bone formation and induction of biochemical high bone turnover state, M026

**Shh**

Osteoblast differentiation induced by Shh-expressing prostate cancer cells is enhanced by ascorbic acid, SA284

Stat3 induces osteoblastic bone metastases through up-regulating the expression of Shh and a Ca channel TRPM8 in the LNCaP human prostate cancer cells, 1089

**SHP-1**

Lyn, opposite to c-Src, negatively regulates osteoclastogenesis in vitro and in vivo via its interaction with SHP-1 and Gab2, 1119

## Key Word Index

## ASBMR 30th Annual Meeting

**SHP-2**

Age-related impairment of IGF-I receptor activation is associated with changes in integrin and SHP-2 expression, M096

**shRNA. See Ribonucleic acid****Sickle cell disease**

BMD in children and adolescents with sickle cell disease, SU217

**Signal transducer and activator of transcription 1 (STAT1)**

Accelerated fracture callus remodeling and membranous bone healing in STAT1 deficient mice, SA022

IL-27/WSX-1 signaling inhibits RANKL-induced osteoclastogenesis through STAT1 activation: a possible involvement in TLR4/MyD88-mediated inflammatory arthritis, SU102

INF $\gamma$  attenuates BMP-2 signaling via Stat-1 binding of Smad4 in the cytoplasm, SU139

**Signal transducer and activator of transcription 3 (STAT3)**

Stat3 induces osteoblastic bone metastases through up-regulating the expression of Shh and a Ca channel TRPM8 in the LNCaP human prostate cancer cells, 1089

**Silicon, porous (PSi)**

Towards development of a PSi-based hybrid biomaterial with osteoconductivity and osteoinductivity, M028

**Silk protein**

(Ala-Gly) $_n$  sequences configured silk protein scaffold induces osteoblast differentiation and bone formation via increased Cbfa1 and Osx expression, M167

**Simvastatin (Sim)**

Sim induces Wnt signaling and reduces CSF-1 secretion and RANKL/OPG ratio to block osteoclast differentiation, SU096

**Sin3A**

Mab21 suppresses the osteogenic markers by recruiting Sin3A and stimulates osteoclast by up-regulation of IL-6 and LIF, SU022

Snail downregulates VDR expression by recruiting Sin3A, HDAC1 and HDAC2 to multiple regions of VDR promoter and deacetylating histone H3/H4, F242

**Single nucleotide polymorphisms (SNP)**

BMD-associated SNP lies in a Runx2 binding site of the LRP5 promoter, M264

Differential regulation of gene expression by SNPs in the osteonectin/SPARC 3 untranslated region, M270

**siRNA. See Ribonucleic acid****SIRT-1**

Longevity gene *SIRT-1* independently controls both osteoblast and osteoclast function, 1098

**Sirtuin 1 (SIRT1)**

Calorie restriction prevents age-related trabecular bone loss via SIRT-1, 1251

SIRT1 is a regulator of MSC lineage allocation, M085

**Skeletal development**

Akt regulates skeletal development through GSK3, mTOR, and FoxOs, 1151

Background UVB exposure in pregnancy and skeletal development in childhood, 1104

Bone microarchitecture is dependent upon collagen  $\alpha 1$ (XI) expression during development, F135

Childhood cortical bone and skeletal age show bivariate genetic linkage to chromosome 2p, 1177

Connective tissue progenitor cell contribution to ectopic skeletogenesis, F044

Contribution of birth status, age at menarche and lifestyle factors to skeletal formation in junior and senior high school students, M492

Critical role of Cx43 in postnatal skeletal growth and bone mass acquisition, 1257

Critical role of TGF $\beta$  signaling pathways in skeletal development, 1079

Defining epistasis in a double congenic mouse: implications for the skeleton, M252

Detrimental effects of abdominal irradiation on the skeleton in growing mice, M412

Effect of the dietary Ca/P ratio on the rate of skeletal accrual in mice, M333

Effects of Pt group metals treatment on the bone of developing chick embryos, M141

Endogenous GC are critical for the development of skeletal fragility with aging in mice, 1250

Essential Hox gene function in limb skeletal and synovial joint formation, M151

GC signaling through osteoblasts is essential for cranial skeletal development, 1267

High-fat diet negatively regulates bone development in growing mice, SA441

Hypothyroidism is not deleterious to the skeleton during early fetal development, SA123

Increased maternal fat intake increases skeletal mass in congenic mice, M495

Maternal nutrient restriction during pregnancy results in significant alterations in fetal skeletal development in the baboon, M494

Mecp2 null mice display multiple skeletal abnormalities, M242

Mice lacking the GH receptor in liver have normal skeletal growth and bone volume despite virtual absence of circulating IGF-1, F181

Modulation of skeletal modeling by silica-based nanoparticles, SU014

Osx is required for skeletal growth and bone homeostasis after birth, 1074

PTHrP nuclear localization sequence and C-terminus regulate craniofacial development, 1264

Skeletal consequences of FHH and PHPT, M206

Skeletal dysmorphology of mice lacking the mid-region, nuclear localization sequence and C-terminus of PTHrP, 1160

ucOC is an endocrine link between the skeleton and the glucose metabolism, F444

In vivo downregulation of *MyoD* mRNA leads to musculoskeletal defects, 1192

**Skin abnormalities**

Identification of skin abnormalities in OI patients by MRI, SA561

**Skin color**

Effect of skin color and oral Vitamin D supplementation on serum 25(OH)D in adolescent girls, SU395

**SLC34A3**

Human SLC34A3/NaPi-IIc mutations T137M and L527del uncouple Na-phosphate co-transport, F471

**SLP-76**

SLP-76 couples Syk to the osteoclast cytoskeleton in vitro and in vivo, 1010

 **$\alpha$ -SMA-GFP**

Use of  $\alpha$ -SMA-GFP transgene to identify periodontium derived osteoprogenitors, SA040

**Smad**

BMP-2-stimulated signaling niche in osteoblasts comprising of Smad and PI3K/ Akt regulates NFATc1 expression and its nuclear translocation, 1081

Both the Smad and ERK MAP kinase pathway play critical roles in BMP-2-induced osteogenic transcription factors expression, M050

Dual roles of Smad proteins in the conversion from myoblasts to osteoblastic cells by BMPs, SA161

Induction of CTGF by TGF $\beta$ 1 in osteoblasts: independent effects of Src and Erk on Smad signaling, M066

**Smad1**

Estrogens reverse a potentiating effect of the unliganded estrogen receptor on BMP-induced transcription and osteoblastogenesis by promoting ERK-dependent Smad1 phosphorylation at the linker region, SU189

**Smad3**

TGF $\beta$  and Smad3-dependent repression of Runx2 function in ATDC5 chondrocytes, SU122

**Smad4**

INF $\gamma$  attenuates BMP-2 signaling via Stat-1 binding of Smad4 in the cytoplasm, SU139

Negative regulation of Tcf/Lef-dependent transcription by the BMP/Smad4 signaling axis, SU144

**Small integrin-binding ligand N-linked****glycoproteins (SIBLING)**

PHEX cleavage of SIBLING-ASARM peptides as a mechanism underlying osteomalacia in XLH, 1199

**Small leucine-rich proteoglycans (SLRP)**

Anti-myeloma effects of osteoblasts is mediated through production of SLRPs, M001

**Smoking**

Bone loss with smoke exposure and Lrp5 expression, SA459

Genetic variation in *IL6* and *LRP5* is associated with osteoporosis in the Marshfield Clinic Personalized Medicine Project, SU365

LRP5 G171V mutation and tobacco smoke related bone fragility, M323

Smoking is an independent predictor of low BMD, prevalent vertebral fractures and incident fractures in elderly men, SU349

In vivo differential expression profiling study on human circulating B cells suggested a novel EGFR and CALM3 network underlying smoking and BMD, SU154

In vivo differential expression profiling study on human circulating monocytes suggested a novel CRAT and CPT2 network underlying smoking and BMD, SU155

**Smurf1**

Age-related bone loss in mice associated with ubiquitin ligase Smurf1 degradation of JunB protein and reduced osteoblast proliferation, 1113

JNK activation is involved in TNF $\alpha$ -stimulated Smurf1 expression, SA016

**Snail**

Snail downregulates VDR expression by recruiting Sin3A, HDAC1 and HDAC2 to multiple regions of VDR promoter and deacetylating histone H3/H4, F242

**Snapin**

Phex binds to SNARE-associated protein snapin and co-localizes in vesicle-enriched, extracellular matrix micro-environment mediating mineral crystal nucleation, F066

**SNARE**

Phex binds to SNARE-associated protein snapin and co-localizes in vesicle-enriched, extracellular matrix micro-environment mediating mineral crystal nucleation, F066

**Sodium (Na)**

Human SLC34A3/NaPi-IIc mutations T137M and L527del uncouple Na-phosphate co-transport, F471

Prostaglandins enhance extracellular matrix mineralization through the enhancement of both Na-dependent phosphate transport activity and ALP activity in osteoblast-like cells, SU031

Signaling of extracellular inorganic phosphate mediated via Na-phosphate co-transporters influences FGF-23 signaling in renal tubular cells, SU172

**Sodium N-[8-(2-****hydroxybenzoyl)amino]caprylate (SNAC)**

Comparison of the effects of IBN alone with IBN in combination with SNAC on bone density and bone strength in OVX rats, SU391

**Sost**

Deletion of *Mef2c* in osteocytes decreases *Sost* expression and increases bone mass, F054

**SOST**

PTH-induced bone mass gain is blunted but not abolished in *SOST* overexpressing and deficient mice, 1039

**SOST**

SOST blocks GSK3-beta inhibitor-induced ALP activity, SU036

**Southampton Womens Survey**  
Late pregnancy serum Vitamin D and longitudinal bone loss during pregnancy, F544

**SOX4**  
Role of the transcription factor SOX4 in the skeletal response to intermittent PTH, SA220

**Sox9**  
Targeted expression of SOX9 in hypertrophic chondrocytes leads to enhanced adipogenic activity and spontaneous OA in transgenic mice, SA115  
Transcription factor Znf219 regulates chondrocyte differentiation through forming transcription factory complex with Sox9, 1265  
Wnt target gene Twist1 inhibits Sox9, the master regulator of chondrogenesis, 1266

**Soy**  
Early exposure to soy isoflavones modulates bone mineral, strength and microarchitecture in CD1 mice, M503  
Evaluating the effect of soy and isoflavones on BMD in older women, M353  
Neonatal exposure to soy isoflavones attenuates deterioration of bone tissue in female but not male mice after cessation of sex steroid production, SU476  
Soy-based formula promotes bone growth in neonatal piglets by inducing osteoprogenitors to differentiate into osteoblasts via enhanced BMP-2 signaling, SA336

**Soy Phytoestrogen as Replacement Estrogen (SPARE) Study**  
Possible increased risk of fracture among South Florida White Hispanic women, M402

**Sp1**  
Cloning and functional expression of the full length mouse GIP receptor and the regulation of its expression in osteoblasts by the Sp1 transcription factor, SU026

**SPARC**  
Regulation of osteonectin/SPARC by miRNA-29, 1155

**SPARC 3**  
Differential regulation of gene expression by SNPs in the osteonectin/SPARC 3 untranslated region, M270

**SPARE Study.** See *Soy Phytoestrogen as Replacement Estrogen Study*

**Spectrometry, mass**  
Identification of osteoclast lysosomal proteins by mass spectrometry, SA077

**Spectrometry, tandem mass**  
25(OH)D levels in children with CKD as measured by tandem mass spectrometry, SU485

**Spectroscopy, confocal laser Raman**  
Kidney dysfunction disturbs collagen maturation in ABD as assessed by confocal laser Raman spectroscopy, SU439

**Spectroscopy, Raman**  
Mineralization potential and orientational aspects of osteogenic cell cultures by Raman spectroscopy, M084  
Non-invasive in vivo Raman spectroscopy in mice, SU480

**Sphingosine-1-phosphate (S1P)**  
Regulation of bone formation by osteoclasts involves Wnt/BMP signaling and the chemokine S1P, M017

**Spinal alignment**  
Influence of hip flexor or knee extensor muscle strength on spinal sagittal alignment or falls, SU454

**Spinal cord injury**  
Immediate abnormalities at the chondro-osseous junction due to severe spinal cord injury in growing rats, SA520

**SpinalMouse®**  
Usefulness of SpinalMouse® as a screening tool for the presence of vertebral wedge deformity, SA316

**Spine cancer.** See *Cancer*

**Spine, lumbar**  
Deformity of the distal radius fractures resulting from falls in Japanese women over 50 years of age is closely associated with BMD of the lumbar spine, SU286  
Differences in BMC at the lumbar spine and proximal femur in South American children of different ethnic groups, SU490  
Effect of ZOL (single 5-mg infusion) on lumbar spine BMD versus oral RIS (5 mg/day) over 1 year in subgroups of patients receiving GC therapy, M363  
Efficacy of single-level instrumented posterolateral (intertransverse) lumbar spinal fusion in baboons with BMP-7 putty, SU146  
Large scale candidate gene analysis identifies an association between the CDK6 locus and trabecular volumetric BMD at the lumbar spine in older men, M266  
Loss of function polymorphisms in the P2X<sub>7</sub> receptor gene are associated with accelerated lumbar spine bone loss in postmenopausal women, SU224  
Lumbar spine TBS complements BMD in the discrimination between vertebral fractured and non-fractured subject, M308  
Reduction of BMD in the patients with RA is more remarkable at proximal femur than at lumbar spine, SU451  
Relationship between BMD of the lumbar spine and knee OA in South Korean, SU298  
Safe zone for percutaneous extrapedicular surgical approach to the lumbar spine, M344

**Spondylitis, ankylosing (AS).** See *Ankylosing spondylitis*

**Spondylo-epi-metaphyseal dysplasia.** See *Dysplasia*

**Spondyloepiphyseal dysplasia congenita (SEDC)**  
Mouse with a Ser1386Pro mutation in the C-propeptide domain of *col2a1* provides a model for SEDC, 1269

**SQSTM1**  
Hyperphosphatasia: a unique type without mutations in *TNFRSF11A* (RANK), *TNFRSF11B* (OPG), or *SQSTM1* (sequestosome 1), SU210  
Large collaborative study on geographic variation of *SQSTM1* mutations in PDB in Italy, SA475

**SQSTM1**  
Two novel SQSTM1 mutations in American patients with PDB, SU216

**Squamous cell carcinoma (SCC).** See *Carcinoma*

**Src**  
Induction of CTGF by TGFβ1 in osteoblasts: independent effects of Src and Erk on Smad signaling, M066

**SSRI**  
SSRI use and risk of fracture in older women, F351

**ST2**  
Effect of resveratrol and flax oil on MC3T3-L1 pre-adipocyte and ST2 BMSC proliferation and differentiation, SU059

**Stanniocalcin 2 (STC2)**  
High expression of the Ca/phosphate-regulating hormone STC2 is associated with renal calcification in the Klotho mutant mice, SA201

**Stem cell antigen (Sca-1)**  
TGFβ1 induces migration of Sca-1 and CD29-positive MSC in coupling bone resorption and formation, F188

**Stem cell antigen positive (Sca-1<sup>+</sup>)**  
Sca-1<sup>+</sup> HSC-based hGH gene therapy enhanced endosteal bone resorption in mice, M233

**Stem cell therapy**  
In utero stem cell therapy as treatment for classical OI using the knock in murine model BrtlIV, F500

**Stem cells, adipose-derived (ASC)**  
Adipose tissue derived MSCs: differentiation into osteoblastic phenotype and interaction with nanostructured Ti alloys, SU050

Regulation of osteogenesis by Wnt signaling in rat MSC and human ASC, SU045

**Stem cells, embryonic (ESC)**  
Induction of ESC-related pluripotency genes in post natal stem cells during fracture healing, F038

**Stem cells, hematopoietic (HSC)**  
Effect of RIS on bone density in HSC transplant patients, SU407  
Jagged1 stimulation by PTH(1-34) in mature osteoblasts is not required for HSC expansion, 1078  
PGE2 as a potential mediator of PTH-dependent regulation of HSCs, F171  
Sca-1<sup>+</sup> HSC-based hGH gene therapy enhanced endosteal bone resorption in mice, M233

**Stem cells, mesenchymal (MSC)**  
Adipose tissue derived MSCs: differentiation into osteoblastic phenotype and interaction with nanostructured Ti alloys, SU050  
BMSC-derived extracellular matrix promotes MSC motility, SA134  
Chemerin and CMKLR1 expression and function in human bone marrow MSC adipogenesis, SU165  
Comparison of the effects of zoledronates on the differentiation of human bone marrow and amniotic fluid derived MSCs, SA045  
Conditional deletion of BMP-2 gene in early osteoblasts leads to reduction in the total bone marrow MSCs and their capacity to form osteoblast precursors, 1114  
Defects in MSC self-renewal lead to an osteopenic phenotype in *Bmi-1* null mice, 1050  
Dermo1 lineage tracing identifies early osteoprogenitor cells in adult murine bone marrow MSC cultures, SA051  
Effect of MSCs in coculture with osteoclasts: a contact mediated and dose-dependent effect?, SA094  
ERα expression in mesenchymal cells is crucial for the bone protective effects of estrogen, 1123  
FGF-1 inhibits adipogenic differentiation and transdifferentiation of human MSCs, M075  
FHL2 mediates DEX-induced MSC osteogenic differentiation by activating Wnt/β-catenin signaling and Runx2 expression, M048  
Gene expression analysis of in vitro-aged and immortalized human MSCs, M047  
High concentrations of hydroxytyrosol and quercetin antioxidants enhance adipogenesis and inhibit osteoblastogenesis in MSCs, SA037  
Identification and characterization of angiogenesis-inducing secretory molecules from osteogenically differentiated MSC, M163  
Injection of MSCs overexpressing both CXCR4 and RANK-Fc effectively prevented OVX-induced bone loss, F391  
Integrin mediated mechanical forces stimulate differentiation of MSCs, SA528  
Marked induction of endochondral bone formation by overexpression of a constitutively active Gli2 in MSCs isolated from the healing site, SA049  
Mechanical strain prevents adipogenesis in MSC by stimulating a durable β-catenin signal, SA522  
Microporosity in b-TCP ceramics may be detrimental to MSC survival and osteoblastic differentiation, SA015  
MSC enhance fracture healing: essential role for cytokines in homing and anti-inflammatory response, SA169  
Osteogenesis effect of human ligamentum flavum, myoblast, osteoblast and MSC by DBM and BMP-2, SU135  
Permanent FGFR2 activation promotes osteoblast differentiation in MSCs through activation of PKC signaling, M093  
Pulse treatment with ZOL causes sustained commitment of bone marrow derived MSC for osteogenic differentiation, M072

## Key Word Index

## ASBMR 30th Annual Meeting

Reconstituting marrow-derived extracellular matrix *ex vivo*: an optimal niche for retaining the properties of human MSCs, M165

Regulation of osteogenesis by Wnt signaling in rat MSC and human ASC, SU045

Regulatory signaling pathways in BMP mediated osteogenesis of adult human MSC cultures, M060

SIRT1 is a regulator of MSC lineage allocation, M085

Telomerase deficiency leads to decrease bone mass and impaired MSCs functions in telomerase deficient (TERC<sup>-/-</sup>) mice, I147

TGFβ1 induces migration of Sca-1 and CD29-positive MSC in coupling bone resorption and formation, F188

Tissue-engineering and co-culture system based disc regeneration MSC's role, SA189

TNFα and IL-1β stimulate ALP activity and mineralization but decreases RUNX2 expression and osteocalcin secretion in human MSC, SU044

Transient expression of CXC receptor 2 in human MSC stimulates chemotaxis toward CXC ligand 8 and increased mineralization in the presence of osteogenic medium, SA170

**Steroids**

1,25(OH)<sub>2</sub>D<sub>3</sub> is as effective as 1,25(OH)<sub>2</sub>D<sub>3</sub> in regulating cellular proliferation in cultured normal human keratinocytes and transformed prostate cells, M215

25(OH)D acts on Ca and skeletal homeostasis independent of 1,25(OH)<sub>2</sub>D *in vivo*, M214

25(OH)D<sub>3</sub>-24-hydroxylase (CYP24A1): mutagenesis and activity studies reveal important residues involved in regioselectivity and substrate access, SU199

Altered TNSALP expression and phosphate regulation contribute to reduced mineralization in mice lacking androgen receptor, SU181

Antipapoptotic action of 17β-estradiol in skeletal muscle cells involves ERK 1/2, p38 MAPK, ASK-1 and HSP27, SU185

Augmentation of PBM occurs in female and male mice without progesterone nuclear receptors, F249

Biochemical characterization of ERα co-regulators in multinucleated mature osteoclasts, I126

Cell type specific regulation of transcription by estrogen, SU180

Challenge of continuous exogenous GC administration in mice, M100

Characterization of interactions between the unliganded VDR and effectors of the canonical Wnt signaling pathway, I183

Cholesterol sensing receptors, Liver X receptor α and β, have novel and distinct roles in osteoclast differentiation and activation in bone, F085

Cooperativity between VDR and LIP in the regulation of TRPV6 identifies a novel function for LIP as a transcriptional activator, SU198

Crosstalk between androgen receptor and Wnt signaling mediates sexual dimorphism during bone mass accrual, I121

CYP27A1 mutations at Phe147 confer 25-hydroxylase activity towards a Vitamin D<sub>2</sub>-type sidechain, M231

DHT administration is effective for the prevention of hypogonadal bone loss, SU193

Differential cellular and molecular responses of intestinal epithelium to high Ca diet and 1,25(OH)<sub>2</sub>D<sub>3</sub>, M229

Distinctive anabolic roles of 1,25(OH)<sub>2</sub>D<sub>3</sub> in teeth and mandible versus long bones, M213

DNA demethylation for hormone-induced transcriptional derepression, I182

Effect of 1,25(OH)<sub>2</sub>D<sub>3</sub> and 25(OH)D<sub>3</sub> on osteoblastogenesis and bone strength in Vitamin D sufficient growing mice, SU207

Effect of 1α,25-dihydroxy Vitamin D3 on proliferation and differentiation of C2C12 myoblast, SA245

Effect of a dissociating GC receptor modulator on bone cells, SA232

Effects of ALF on bone and skeletal muscle in GC-treated rats, M219

Elevated androgens are associated with increased bone formation in premenopausal exercising oligomenorrheic women, SU191

ERα expression in mesenchymal cells is crucial for the bone protective effects of estrogen, I123

Estrogen suppresses RANKL-induced osteoclastic differentiation of human monocytes via an ERα associated cytoplasmic signaling complex, but ERα is downregulated during osteoclastic differentiation, I125

Estrogens reverse a potentiating effect of the unliganded estrogen receptor on BMP-induced transcription and osteoblastogenesis by promoting ERK-dependent Smad1 phosphorylation at the linker region, SU189

Ethanol alters estrogen receptor signaling and activates senescence pathways in osteoblasts while estradiol attenuates ethanol effects, SU182

Evaluation of automated methods for quantifying serum 25(OH)D, SU206

Evidence of a role for the human Vitamin D response element binding protein, hnRNP C1/C2 in chromatin remodeling and transcript splicing, F240

Expression of 1α-hydroxylase (CYP27B1) in BMSC, SA237

Expression of 11β-hydroxysteroid dehydrogenase during murine osteoclast formation, SA235

Expression of VDR in the developing zebrafish embryo, M220

GC signaling in osteoblasts maintains normal bone structure in mice, F233

Genetic model to study 1,25(OH)<sub>2</sub>D action in classical and non-classical target tissues, I184

Genetic variation of the SHBG gene, SHBG levels and bone parameters, SU188

Genetic variations in sex steroid-related genes as predictors of serum estrogen levels in men, SU183

Goettingen minipigs—a model for Ca/Vitamin D-deficiency osteomalacia and steroid-induced osteoporosis, SA445

High prevalence of Vitamin D insufficiency in a young adult population, M221

Improved motor performance in Vitamin D deficient mice with VDRMs, SU196

Involvement of caveolae in 1α,25(OH)<sub>2</sub>D<sub>3</sub>-dependent activation of MAPKs in skeletal muscle cells, SA243

Key mechanism underlying the immunosuppressive effects of Vitamin D: 1,25(OH)<sub>2</sub>D<sub>3</sub> is a transcriptional modulator of IL-17, F246

Loss of classical ERE signaling results in suppression of early commitment of BMSC to osteoblasts, F029

Measurements of Vitamin D do not necessarily reflect what you give to your patients, SU197

Multinuclear expression of ERα in mature osteoclasts, SU186

Neonatal exposure to soy isoflavones attenuates deterioration of bone tissue in female but not male mice after cessation of sex steroid production, SU476

New 25(OH)D assay on the IDS Automated Analyser 3x3™, SU200

Normal intramembranous fracture healing in mice with transgenic osteoblast-targeted disruption of GC signaling, SA234

Novel ERα variant signals rapidly from the caveolae of traditional ERα-negative cells, I124

OPG production by breast cancer cells is modulated by steroid hormones and confers resistance against TRAIL-induced apoptosis, M271

Osteoblast-targeted deletion of the GC receptor has little impact on PBM but attenuates DEX-induced suppression of bone formation, F452

Osteoblastic androgen receptor regulates cortical BMD, I122

Overexpression of androgen receptor in mature osteoblasts and osteocytes inhibits osteoblast differentiation, SU192

Platelet VDR levels are reduced in osteoporotic patients, SA241

Pregnancy upregulates duodenal Ca-transport genes and normalizes Ca homeostasis in *Vdr* null mice, M230

Randomized controlled trial of Vitamin D3 supplementation for the prevention of viral upper respiratory tract infections, M217

Rapid-nontranscriptional action of 1,25(OH)<sub>2</sub>D<sub>3</sub> induces IL-6 production in osteoclast precursors expressing MVNP, I186

Reconstruction of massive skeletal defects due to osteomyelitis by DO, M160

Regulation of Runx2 function in osteoblasts by sex steroid receptors, M099

Role of GPR30 in effects of estrogen in OVX mice, SU179

Sex steroids have site specific effects on muscle and bone geometry in young adult males, M416

Silencing of PDIA3 (ERp60) reduces the rapid membrane response to 1,25(OH)<sub>2</sub>D<sub>3</sub> in MC3T3-E1 osteoblast-like cells, M227

Snail downregulates VDR expression by recruiting Sin3A, HDAC1 and HDAC2 to multiple regions of VDR promoter and deacetylating histone H3/H4, F242

Specific inactivation of AF-1 in ERα results in growth plate closure while total inactivation of ERα results in increased growth plate width in elderly female mice, I181

Sunscreen use and Vitamin D status, M225

TRβ-specific agonist GC-1 increases bone quality of adult female mice, M228

Vitamin D (cholecalciferol) production does not increase linearly with UV dose, M226

Vitamin D and physical performance in African American women, M218

Vitamin D delays breast cancer progression in the PyVMT transgenic mouse model, I185

Vitamin D insufficiency in obesity, SA239

Vitamin D status, bone mass, and bone metabolism in postmenopausal women and men older than 50 attended in a primary care center of Spain, M223

**Stress, oxidative**

β-catenin protects osteoblasts from oxidative stress by co-activating the expression of pro-survival, but not pro-apoptotic, target genes of the FoxO transcription factors, M010

Menopausal and postmenopausal women have significantly higher bone resorption and oxidative stress parameters than premenopausal women, SU336

Relationship among nutritional status, oxidative stress and bone density in institutionalized elderly, SU310

**Stro-1+**

Osteogenic potential of human bone marrow and circulating Stro-1+/CD45<sup>low</sup> cells, M078

**Stroke**

Effects of neurological impairment and functional mobility on BMD following stroke, SU364

**Stromal cell-derived factor-1 (SDF-1)**

SDF-1 is expressed in osteocytes and periosteal cells in response to mechanical loading, M105

**Stromal cells.** See also *Bone marrow stromal cells*

*Ccrn4l*, a peripheral clock gene, influences stromal cell allocation, bone mass, and marrow adiposity in mice and humans, I073

Hormonal control of RANKL expression is independent of Runx family proteins: evidence that commitment to the osteoblast lineage is not a requirement for the stromal cells that support osteoclast differentiation, SU047

Host bone marrow-derived stromal cells promote myeloma initiation and development of osteolysis, 1088

Suppression of canonical wnt signaling by Dkk1 attenuates PTH-mediated peritrabecular stromal cell response and new bone formation in a model of HPT2, F215

TGF $\beta$  signaling in stromal cells facilitates osteoblastic lesions in prostate cancer, 1087

TGF $\beta$  suppresses adipocytic differentiation and enhances accumulation of stromal cells in myeloma bone lesions, SA294

**Strontium (Sr)**

Dietary Sr in a model of established osteopenic rats reduce the levels of 25(OH)D. SA377

Effect of Sr<sup>2+</sup> on PTHrP, OPG and RANKL mRNA expression in osteoblastic-like cells UMR 106.1, SU016

**Strontium ranelate**

Improved bone mass after co-administration of Sr ranelate and RIS in a rat model of osteoporosis using "in-vivo"  $\mu$ CT, SU393

Oral Sr ranelate treatment markedly improves implant osseointegration, SA506

Relationship between biochemical bone markers in osteoporotic women before and after 6 months treatment with either GH, Sr ranelate or GH plus Sr, M291

Sr ranelate decreases osteoblast-induced osteoclastogenesis through the involvement of the CaSR, F389

Sr ranelate prevents the progression of thoracic kyphosis in postmenopausal women with osteoporosis, 1241

Sr ranelate protects osteoblasts from apoptosis independently of the CaSR, M007

**Subchondral bone**

PAR-2 activation induces bone resorption via RANKL upregulation in human OA subchondral bone osteoblasts, M018

**Substance P (SP)**

Decreased bone formation, increased bone resorption, and osteopenia in mice lacking SP, SU160

SP stimulates BMSC osteogenic activity and osteoclast differentiation and function in vitro, SU032

**Sunlight**

Lack of seasonal variation of bone resorption in elderly women in relation to periodicity of sunlight exposure at a northerly latitude, F337

**Sunscreens**

Sunscreens use and Vitamin D status, M225

**Superoxide dismutase (SOD)**

Lentiviral shRNA mediated inhibition of Grx5 expression induces apoptosis via a mechanism involving increased ROS and cardiolipin oxidation, and reduced SOD activity, M009

**Syk**

SLP-76 couples Syk to the osteoclast cytoskeleton in vitro and in vivo, 1010

Syk tyrosine 317 negatively regulates osteoclast function, 1120

**Syndecan**

Various roles of syndecan family in osteoblastic cells, SA147

**Syndecan-1**

Disruption of the syndecan-1/integrin axis is a novel target for myeloma therapy, 1229

**Syndecan-2 (synd2)**

Wnt/ $\beta$ -catenin/TCF is a constitutive repressor pathway interfering with Foxo3-mediated induction of synd2, a tumor suppressor in osteosarcoma cells, SU243

**Synostosis, familial humeroradioulnar**

Familial humeroradioulnar synostosis maps to chromosome 7p15, M251

**Synoviocytes, rheumatoid**

Rheumatoid synoviocytes are stimulated with IL-23 to enhance osteoclastogenesis through upregulation of RANKL expression, SU084

**Synoviolin**

Expression and function of synoviolin in human osteoclastogenesis, SA080

**T****T cells**

Effects of IL-27 on regulation of osteoclastogenesis by way of T cells, SU081

Gene transcripts related to T-cell activation, proliferation, and cytokine signaling show significant effects on BMD variation in baboons, M241

IL-12 stimulates the OIP-1 gene expression in CD4<sup>+</sup> T-cells, SA173

T cells amplify the anabolic action of PTH through Wnt10b signaling, 1197

**T-box 3**

T-box 3 negatively regulates osteoblast differentiation by inhibiting expression of Osx and Runx2, SU018

**T-scores**

Do different densitometers, or use of T-score vs. Z-score, affect fracture risk estimation?, SU258

FRAX<sup>TM</sup> and the assessment of ten-year fracture probability in Hong Kong Southern Chinese according to age and BMD femoral neck T-scores, SU264

WHO absolute fracture models in older women: how does prediction vary for incident hip and non-spine fractures across T-scores?, 1055

**T $\beta$ RI**

T $\beta$ RI inhibitor rescues uncoupled bone remodeling in two different animal disease models, 1273

**T2\***

Measurement of T2\* relaxation time of the trabecular bone network at 7T and 3T compared to topological and structural measurements from HR-pQCT, F317

**T137M**

Human SLC34A3/NaPi-IIc mutations T137M and L527del uncouple Na-phosphate co-transport, F471

**TAK1**

BMP-2 inactivates TAK1-ATF2 signaling pathway in chondrocytes, F186

**Tamoxifen**

Effect of tamoxifen and aromatase inhibitors on the risk of fractures in women with breast cancer, SU227

**Tantalum (Ta)**

Evaluation of tibial bone density surrounding Ta tibial implants in TKA, SU266

**Tartrate-resistant acid phosphatase 5b (TRACP5b)**

Comparison of the TRACP 5b specificity of two commercial TRACP 5b assays, SA298

Phthalein monophosphates are specific substrates for TRACP5b, M284

Stability of TRACP 5b in rat and mouse serum, M286

**TCF**

Induction of oxidative stress and diversion of  $\beta$ -catenin from TCF- to FOXO-mediated transcription by GCs or TNF $\alpha$  in osteoblastic cells, SA185

Kinase activation and osteocyte survival promoted by mechanical stimulation require LRP5/6 signaling and  $\beta$ -catenin accumulation, but not  $\beta$ -catenin/TCF-dependent transcription, M108

Negative regulation of Tcf/Lef-dependent transcription by the BMP/Smad4 signaling axis, SU144

Tcf is required for Wnt11 mediated osteoblast differentiation, M058

Wnt/ $\beta$ -catenin/TCF is a constitutive repressor pathway interfering with Foxo3-mediated induction of synd2, a tumor suppressor in osteosarcoma cells, SU243

**tcirg1**

Rachitic defects in tcirg1-dependent osteopetrosis are caused by impaired gastric acidification, 1201

**Tec**

Tec kinases, therapeutic targets for bone destructive diseases, F083

**Teeth**

ALN transiently impairs removal of alveolar bone and healing of the root socket after tooth extraction in rats, 1275

BMSC and Osx contributing to osseointegration of dental implants, SA138

Distinctive anabolic roles of 1,25(OH)<sub>2</sub>D<sub>3</sub> in teeth and mandible versus long bones, M213

Enzyme replacement therapy prevents dental defects in the *Akp2*<sup>-/-</sup> mouse model of infantile HPP, F107

**Telomerase**

Telomerase deficiency leads to decrease bone mass and impaired MSCs functions in telomerase deficient (TERC<sup>-/-</sup>) mice, 1147

**Tendon repair**

Loss of *MMP-9* results in improved healing, and remodeling of adhesions in a murine model of flexor tendon repair, F153

**Tendons**

TIEG1 KO mice display defects in the molecular structure of tendon fibers, M133

**TERC<sup>-/-</sup>**

Telomerase deficiency leads to decrease bone mass and impaired MSCs functions in telomerase deficient (TERC<sup>-/-</sup>) mice, 1147

**Teriparatide (TPTD)**

12 months of TPTD therapy increases ultradistal radius bone strength in severely osteoporotic postmenopausal women, SA504

Adherence in patients with severe osteoporosis treated with TPTD, M384

Adult HPP treatment with TPTD, SA468

Danish patients treated with TPTD, M350

Evaluation of BMD changes in women with severe osteoporosis after TPTD treatment, M355

Formation of new trabeculae in a female patient with osteoporosis treated with TPTD, demonstrated with in-vivo-assessment of 3D bone microarchitecture with HR-pQCT, M352

Histomorphometric and biochemical bone formation responses to first and second cycles of TPTD treatment, 1169

Histomorphometric changes by TPTD in ALN pre-treated women with osteoporosis, 1019

Imaging the spatial distribution of proximal femoral response to one year of TPTD therapy, M349

One year of TPTD treatment increases hip strength in subjects with recent history of anti-resorptive treatment, F396

Previous antiresorptive agents use did not hinder the increase of bone turnover marker in TPTD use, M351

QUS, BMD and QCT in women with established osteoporosis treated with TPTD, SA393

Role of FGF-23 in the early response to the PTH analogue; TPTD, SU174

Skeletal plasma clearance, as measured by quantitative radionuclide studies, is correlated with bone turnover markers at 3 months of TPTD therapy, F398

TPTD improves trabecular architecture as measured by  $\mu$ CT at simulated in vivo resolution in the femoral neck of OVX monkeys, SA375

TPTD in bisphosphonate-resistant osteoporosis—clinical and  $\mu$ CT data, 1172

TPTD therapy in a community setting: persistence and use of other osteoporosis medications in DANCE, SA395



## Key Word Index

## ASBMR 30th Annual Meeting

- TPTD treatment in a young man with IJO diagnosis, SU499
- TPTD versus ALN for treatment of GIO, 1171
- Treatment with daily subcutaneous TPTD (1-34) compared with daily subcutaneous PTH (1-84) in women with severe postmenopausal osteoporosis, 1170
- ZOL prevents accelerated bone loss after discontinuation of TPTD, M365
- Testosterone**
- Replacing testosterone in male cardiac transplant patients exerts multiple benefits on bone mass, libido and sexual activity, M388
- Retrospective study evaluating the relationship of Vitamin D 25 OH and free testosterone levels with changes in hip bone density after liver transplantation, SA502
- Toward a physiologically-based definition of hypogonadism in men: dose-response relationship between testosterone and bone resorption, 1102
- TG interacting factor (TGIF)**
- TGIF regulation of bone mass: impaired osteoblast differentiation, SA018
- TGF $\beta$  inducible early gene (TIEG)**
- TIEG: a key regulator of Runx2 and Osx gene expression and osteoblast differentiation, M052
- Transgenic mice over-expressing TIEG in osteoblasts display a gender specific bone phenotype, M024
- TGF $\beta$  inducible early gene 1 (TIEG1)**
- TIEG1 KO mice display defects in the bone matrix immediately surrounding osteocytes, SA065
- TIEG1 KO mice display defects in the molecular structure of tendon fibers, M133
- TGF $\beta$ I**
- CED: a unique variant featuring a novel, heterozygous, leucine repeat mutation in *TGF $\beta$ I* together with a novel, homozygous, missense change in *TNFSF11* encoding RANKL, F256
- TGFBFR3**
- GWAS and subsequent replication studies identified ADAMTS18 and TGFBFR3 as novel osteoporosis risk genes, 1093
- th3**
- $\mu$ CT abnormalities in the th3 mouse model of thalassemia start at a young age and are associated with decreased bone turnover, SA128
- T<sub>H</sub>17**
- Possible role for the T<sub>H</sub>17 system in a mouse model of AS, SU460
- Th17**
- Grape seed extract suppresses IL-23/Th17 inflammatory pathways and bone destruction in CIA, SU093
- Thalassemia intermedia (TI)**
- $\mu$ CT abnormalities in the th3 mouse model of thalassemia start at a young age and are associated with decreased bone turnover, SA128
- Thiazolidinediones (TZD)**
- PPAR $\gamma$ 2-mediated proteolytic degradation of  $\beta$ -catenin determines an anti-osteoblastic effect of anti-diabetic TZDs, SU023
- TZD modify nuclear heterochromatin architecture, SU056
- Threonine**
- Homozygous threonine to methionine substitution in FGF-23 gene is associated with tumoral calcinosis in a 12 year-old girl, SU171
- Threonine (Thr201)**
- Role of active site Thr201 in the inhibition of farnesyl pyrophosphate synthase by NBPs, F407
- Thrombopoietin (TPO)**
- Novel role for TPO in regulating osteoclast development, SU104
- Thrombospondin-1 (TSP-1)**
- TSP-1 and CD47 regulate osteoclastogenesis but have distinct effects on bone metastasis, 1232
- Thrombospondin-2 (TSP-2)**
- Changes in marrow cell dynamics and bone geometry with aging in TSP-2 null mice, 1249
- Thyroid cancer.** See *Cancer*
- Thyroid disease**
- Subclinical thyroid disease predicts risk of hip fracture, 1208
- Thyroid hormone**
- Thyroid hormone activates Wnt signaling pathways in rat growth plate chondrocytes, M157
- Thyroid hormone  $\beta$  (TR $\beta$ )**
- TR $\beta$ -specific agonist GC-1 increases bone quality of adult female mice, M228
- Thyroid hormone receptor-interacting protein 1 (TRIP-1)**
- TRIP-1 is eIF3i: a key regulator of osteoblast activity, 1259
- Thyroid hormone receptor-interacting protein 6 (TRIP-6)**
- TRIP-6 regulates osteoclast formation, adhesion, and resorptive capacity, SU066
- Thyroid stimulating hormone (TSH)**
- TSH inhibits the expression of HMGB, a regulator of TNF $\alpha$  transcription, in osteoclastogenesis, 1117
- Tibia**
- Aged and young adult BALB/c male mice respond similarly to in vivo tibial compression, M475
- Changes in volumetric bone density and bone strength at the tibial midshaft in boys and girls 12-17 years of age, SU469
- Collecting bone out of the medial condyle of tibia, SA318
- Deleterious effect of late menarcheal age on bone microstructure in both distal radius and tibia, 1239
- Ethnicity-specific bone changes during adolescent growth: pQCT analysis of the tibia, M502
- FEA performed on radius and tibia HR-pQCT images provides new insights for fracture status assessment, 1067
- Flexible tibia model predicts bone strains during walking, M479
- Investigation of the fatigue behaviour of rabbit tibiae: effects of sex and age, SU470
- Timed Up and Go test**
- Timed Up and Go test and BMD as predictors of fracture, F373
- Tissue donors**
- Prevalence and incidence of viral infections among musculoskeletal tissue donors and first-time blood donors, SA549
- Tissue engineering**
- Continuous culture of tissue engineered cartilage, SU131
- Sequestration, proliferation and differentiation of osteoblasts in hydrogels for tissue engineering applications, SA143
- TiO<sub>2</sub>-scaffolds for use in bone tissue engineering, SA137
- Tissue-engineering and co-culture system based disc regeneration MSC's role, SA189
- Tissue-nonspecific alkaline phosphatase (TNSALP).** See *Alkaline phosphatase*
- Tissue-specific alkaline phosphatase.** See *Alkaline phosphatase*
- Titanium (Ti)**
- Adipose tissue derived MSCs: differentiation into osteoblastic phenotype and interaction with nanostructured Ti alloys, SU050
- Enamel matrix derivative (emdogain) enhance osteoblast differentiation on Ti surfaces, M030
- Human osteoprogenitor cell adhesion and spreading on functionalized Ti surfaces followed by QCM and CLSM, SA101
- Regulation of Dkk-1 and Dkk-2 is needed for osteoblast terminal differentiation on microstructured Ti surfaces, SU006
- Titanium oxide (TiO<sub>2</sub>)**
- TiO<sub>2</sub>-scaffolds for use in bone tissue engineering, SA137
- TLR4**
- IL-27/WSX-1 signaling inhibits RANKL-induced osteoclastogenesis through STAT1 activation: a possible involvement in TLR4/MyD88-mediated inflammatory arthritis, SU102
- TNF- $\alpha$  related apoptosis inducing ligand (TRAIL)**
- OPG production by breast cancer cells is modulated by steroid hormones and confers resistance against TRAIL-induced apoptosis, M271
- TNF-like weak inducer of apoptosis (TWEAK)**
- Proinflammatory cytokine TWEAK induces SCT expression in human immature osteoblasts in a MAPK dependent fashion, M046
- TNF-stimulated gene-6 (TSG-6)**
- TSG-6 acts synergistically with OPG to inhibit bone resorption, SA097
- TNFRSF11A**
- Hyperphosphatasia: a unique type without mutations in *TNFRSF11A* (RANK), *TNFRSF11B* (OPG), or *SQSTM1* (sequestosome 1), SU210
- Identification of a novel mutation (78dup27) of the *TNFRSF11A* gene in a Chinese family with early onset PDB, M237
- OPG deficiency mimicked by a novel 15-base pair tandem duplication in *TNFRSF11A* encoding RANK: merging the juvenile PD and ESH phenotypes, F563
- TNFRSF11B**
- Hyperphosphatasia: a unique type without mutations in *TNFRSF11A* (RANK), *TNFRSF11B* (OPG), or *SQSTM1* (sequestosome 1), SU210
- TNFSF11**
- CED: a unique variant featuring a novel, heterozygous, leucine repeat mutation in *TGF $\beta$ I* together with a novel, homozygous, missense change in *TNFSF11* encoding RANKL, F256
- Tobacco.** See *Smoking*
- Toll-like receptor-9 (TLR-9)**
- Osteoclast-independent function of Cat K: regulation of TLR-9 signaling in autoimmunity, F074
- Tomography (CT).** See *Computed tomography*
- Toremifene (TOR)**
- C-telopeptide and bone ALP predict morphometric vertebral fracture risk in a pivotal Phase III trial of TOR in men on ADT, 1292
- TOR inhibits osteoclast activity in vitro and prevents orchietomy-induced bone resorption in male rats, SA381
- Total knee arthroplasty (TKA).** See *Arthroplasty*
- Trabecular bone**
- Contributions of trabecular and cortical components to biomechanical properties of human vertebrae, M455
- Deletion of the Wnt signaling antagonist sFRP4 in mice induces opposite bone formation phenotypes in trabecular and cortical bone, 1005
- Dependence of endosseous implant anchorage on mechanostuctural determinants of peri-implant bone trabeculae, 1298
- Do racial differences exist in cortical and trabecular bone?, M468
- Effects of resorption cavities on strength of trabecular bone, SA512
- Estimation of relative stiffness contributions of cortical and trabecular compartments by MRI-based FEA, SU481
- Feasibility and reproducibility of in-vivo assessment of trabecular bone architecture using  $\mu$ MRI-based method at multiple study centers, SA314
- Grayscale MRI based finite element mechanical modeling of trabecular bone at in vivo resolution, SU277
- Immunohistochemical localisation of SCT in human trabecular bone from fragility hip fracture patients, SA148
- Juvenile murine model of OVX-induced trabecular and cortical osteoporosis, SA387

Load induced changes in trabecular and cortical bone are dose dependent in both C57BL/6 and C3H/HeJ mice, F527

Marked abnormalities in cortical and trabecular microarchitecture and strength in premenopausal women with idiopathic osteoporosis, M310

Measurement of T2\* relaxation time of the trabecular bone network at 7T and 3T compared to topological and structural measurements from HR-pQCT, F317

Physiological concentrations of inhibin A are anabolic, affecting both trabecular and cortical bone in normal intact mice, M177

Prediction of trabecular level microdamage and bone fracture through local strain, SU467

Profile analysis of rodent metaphyseal trabecular bone reveals a biphasic dose-dependent response to administered bone active agents, SA460

RIS has a more rapid onset of remodeling suppression than ALN in rabbit vertebral trabecular bone, SU387

Scl-Ab increases bone formation and decreases bone resorption in distal tibial metaphyseal trabecular bone in OVX rats, F394

Significant trabecular bone degradation occurs within five days of muscle paralysis, SA515

Subject-specific mechanical properties of trabecular bone using a low-dose imaging, SU471

Targeted disruption of Nrf1 in osteoblasts leads to reduced bone size and dramatic alterations in trabecular bone microstructure in mice, I190

Transmenopausal changes in the trabecular bone intrinsic properties, SU479

**Trabecular Bone Score (TBS)**

Lumbar spine TBS complements BMD in the discrimination between vertebral fractured and non-fractured subject, M308

**Traf2**

Traf2 regulates BMP signaling pathway in osteoblastic cells, M063

**TRAF6**

Proteasome inhibitors attenuate osteoclastogenesis and bone resorption via the modulation of RANK-mediated TRAF6, p62 and I $\kappa$ B- $\alpha$  signaling cascades, SA099

**Transcriptome analysis**

Global transcriptome analysis in mouse osteoblasts identifies a mechanosensing osteoblast gene signature, SU017

**Transferrin (TF)**

Association study of the TF and IGFBP3 gene polymorphisms with an osteonecrosis of femoral head in Korean population, SU226

**Transforming growth factor  $\beta$  (TGF $\beta$ )**

Blocking TGF $\beta$  signaling reduces gammopathy and improves bone volume and strength in vivo, F293

Breast cancer derived factors synergize with TGF $\beta$  to induce phosphorylation of ERK1/2 and to stimulate osteoclastogenesis, SU115

Combined TGF $\beta$  receptor I kinase inhibitor and bisphosphonates are additive to reduce breast cancer bone metastases, F275

Critical role of TGF $\beta$  signaling pathways in skeletal development, 1079

Hfg inhibits melanoma bone metastases and TGF $\beta$  signaling, F190

Inhibition of HIF-1 $\alpha$  alone or combined with TGF $\beta$  blockade prevents breast cancer bone metastases, I085

Integrin-associated protein upregulates osteogenesis-related transcription factors via TGF $\beta$  and BMP pathways, SA028

Interplay between BMP and TGF $\beta$  signaling in osteoblast differentiation, SA031

MAPK-dependent inhibition of osteocalcin gene expression by TGF $\beta$ , M033

Monoclonal antibody to TGF $\beta$  inhibits tumor burden and osteolysis in a pre-clinical model of bone metastasis, SA187

Novel MMP-13-derived peptides demonstrate non-covalent interaction of MMP-13 with the TGF $\beta$  large latent complex, I189

TGF $\beta$  activates prostate cancer bone metastases, pro-osteolytic gene expression and the new TGF $\beta$  signaling regulator PMEPA1, SA273

TGF $\beta$  and Smad3-dependent repression of Runx2 function in ATDC5 chondrocytes, SU122

TGF $\beta$  blockade inhibits osteolytic but not osteoblastic prostate cancer metastases, SA274

TGF $\beta$  inhibits BMP signaling and osteogenesis through the TGF $\beta$  and BMP R-Smad direct interaction, I080

TGF $\beta$  receptor I kinase inhibitor increases bone mass in normal mice, SA172

TGF $\beta$  signaling in stromal cells facilitates osteoblastic lesions in prostate cancer, I087

TGF $\beta$  suppresses adipocytic differentiation and enhances accumulation of stromal cells in myeloma bone lesions, SA294

TGF $\beta$ - and BMP-signaling pathways have antagonistic effects during chondrogenesis, F158

*Wnt* pathway regulation by demineralized bone requires TGF $\beta$ /BMP signaling, SU138

**Transforming growth factor  $\beta$ 1 (TGF $\beta$ 1)**

Induction of CTGF by TGF $\beta$ 1 in osteoblasts: independent effects of Src and Erk on Smad signaling, M066

TGF $\beta$ 1 induces human osteoclast apoptosis, SU078

TGF $\beta$ 1 induces migration of Sca-1 and CD29-positive MSC in coupling bone resorption and formation, F188

**Transient receptor potential 7**

Importance of melastatin-like transient receptor potential 7 and Mg in the stimulation of osteoblast proliferation and migration by platelet-derived growth factor, M008

**TRAP**

Obesity induced by high dietary fat leads to increased bone resorption marker, TRAP, and decreased bone mass in mice, M238

**$\beta$ -tricalcium phosphate ( $\beta$ TCP)**

Percutaneous injection of GEM OS2 increases vertebral BMD in geriatric female baboons, F376

Resorption mechanism of HA and  $\beta$ TCP coating layer, SA100

Stimulation of fracture healing by rhPDGF-BB combined with  $\beta$ TCP/collagen matrix in a diabetic rat fracture model, I137

**Tricho-dento-osseous syndrome (TDO)**

Molecular consequences of a mutant Dlx3 affecting bone homeostasis in TDO, I272

**Triggering receptor expressed on myeloid cells 2 (TREM-2)**

Suppression of TREM-2 expression and TREM-2-mediated costimulation of RANK signaling by cytokines that inhibit human osteoclast differentiation, SU114

**Tropomyosins**

Role of alpha gene tropomyosins in osteoclast function, SU067

**TRPM8**

Stat3 induces osteoblastic bone metastases through up-regulating the expression of Shh and a Ca channel TRPM8 in the LNCaP human prostate cancer cells, I089

**Trps1**

Trps1 represses Runx2 during endochondral bone formation, SU126

**TRPV4**

Gender specific effects of TRPV4 on osteoblast-osteoclast coupling and risk of osteoporotic fractures, SA355

**TRPV6**

Cooperativity between VDR and LIP in the regulation of TRPV6 identifies a novel function for LIP as a transcriptional activator, SU198

Evidence for a role of prolactin in Ca homeostasis: regulation of intestinal TRPV6 and intestinal Ca absorption by prolactin, I223

**Tumor necrosis factor (TNF)**

In the absence of NF- $\kappa$ B2, TNF induces osteoclast formation in vivo independent of RANKL/RANK and more severe arthritis in TNF-Tg mice, I009

R-spondin 1 reduces bone loss in human TNF transgenic and OVX mice, I215

Real time oscillations in TNF-induced gene expression MAPK phosphorylation and promoter binding, SU087

**Tumor necrosis factor  $\alpha$  (TNF $\alpha$ )**

Elevated production of IL-1 $\beta$  and TNF $\alpha$  by PBMC is associated with increased hip fracture risk in elders, I283

IFN- $\gamma$  inhibits TNF $\alpha$ -induced osteoclastogenesis in vitro and in vivo, SU152

IL-1 $\beta$ -induced hepcidin expression in synovial membranes of patients with OA is associated with TNF $\alpha$  repression, SU157

IL-12 induces apoptosis in TNF $\alpha$ -mediated osteoclastogenesis in vivo, SA166

Increased proinflammatory cytokines TNF- $\alpha$  and IL-6 correlate with pathological bone turnover markers in diabetic patients with acute Charcot foot, F491

Induction of oxidative stress and diversion of  $\beta$ -catenin from TCF- to FOXO-mediated transcription by GCs or TNF $\alpha$  in osteoblastic cells, SA185

JNK activation is involved in TNF $\alpha$ -stimulated Smurf1 expression, SA016

LPS-induced inhibition of osteogenesis is TNF $\alpha$  dependent, M019

Nanogel cross-linking hydrogel as a drug delivery system for TNF $\alpha$  antagonist, M121

Recombinant mouse M-CSF receptor C-fms inhibits TNF $\alpha$ -induced osteoclastogenesis, M112

Stimulation of macrophage TNF $\alpha$  production by orthopaedic wear particles requires activation of the ERK 1/2/Egr-1 pathway but is independent of p38 and JNK, SA177

Three RANK cytoplasmic motifs, IVVY<sup>535-538</sup>, PVQEET<sup>559-564</sup> and PVQEQQ<sup>604-609</sup>, play a critical role in TNF $\alpha$ /IL-1-mediated osteoclastogenesis, I118

TNF $\alpha$  and IL-1 $\beta$  stimulate ALP activity and mineralization but decreases RUNX2 expression and osteocalcin secretion in human MSC, SU044

TSH inhibits the expression of HMGB, a regulator of TNF $\alpha$  transcription, in osteoclastogenesis, I117

**Tumor necrosis factor receptor (TNFR)**

Association between polymorphisms in TNFR genes and circulating TNFR levels, and BMD in postmenopausal Korean women, M258

**Tumor necrosis factor Tg (TNF-Tg)**

In the absence of NF- $\kappa$ B2, TNF induces osteoclast formation in vivo independent of RANKL/RANK and more severe arthritis in TNF-Tg mice, I009

**Tumor-induced osteomalacia (TIO). See Osteomalacia**

**Tumors. See also Cancer**

Drugs which inhibit osteoclast function suppress tumor growth and alter hematopoietic cell populations in bone, F270

**Tumors, parathyroid**

Mutational analysis of  $\beta$ -catenin Exon 3 in benign and malignant parathyroid tumors, M436

**Twist1**

Twist1 haploinsufficiency is associated with reduced IGF-1 levels and an osteoporotic phenotype, SU029

Wnt target gene Twist1 inhibits Sox9, the master regulator of chondrogenesis, I266

**Type III Na-dependent phosphate transporter**

## Key Word Index

## ASBMR 30th Annual Meeting

Development of nephrotic in transgenic rats over expressing Type III Na-dependent phosphate transporter, SU170

**Tyrosine**  
Studies on the deposition of ochronotic pigment in AKU reveal tyrosine metabolism in human chondrocytes, M166  
Tyrosine kinase inhibitor dasatinib decreases osteoclast formation and activity in vitro, SU074

**Tyrosine 317**  
Syk tyrosine 317 negatively regulates osteoclast function, 1120

**U**

**UGT1A1\*28**  
Effect of RLX treatment on BMD might be influenced by UGT1A1\*28 polymorphism, M257

**UGT2B17**  
Genome-wide CNV study identified a novel susceptibility gene *UGT2B17* for osteoporosis, M404

**Ultrasound**  
Heel ultrasound and consolidation of PBM in young women, M504  
Mediation of bone loss with ultrasound induced dynamic mechanical signals in an OVX rat model of osteopenia, F536

**Ultrasound, low intensity pulsed (LIPUS)**  
LIPUS synergistically modulates SCT and OPG/RANKL ratio in MLO-Y4 osteocytes in vitro, M109

**Ultrasound, quantitative (QUS)**  
Calcaneal QUS measurement of 2323 healthy adults in southwest China, M318  
Comparison of HR-pQCT to DXA and QUS for the assessment of ex-vivo bone strength, M466  
Correlation between DXA Femur Strength Index and QUS Heel Stiffness Index in Chinese women, M464  
Influence of markers of bone turnover on calcaneal QUS, SA457  
Longitudinal analysis of calcaneal QUS measures during childhood, M321  
Normal reference values for QUS bone densitometry of the calcaneus in Chinese children and adolescents, SU489  
Performance of QUS in comparison to DXA for prediction of prospective fractures among older men and women, 1240  
QUS, BMD and QCT in women with established osteoporosis treated with TPTD, SA393  
Relationship of QUS at phalanxes with hand and axial BMD, sex hormones and bone turnover markers in elderly women, M320

**Ultrasound, quantitative guided-wave (Q-GWUS)**  
Assessment of cortical thickness and BMD in the radius by low-frequency Q-GWUS, M319

**Ultraviolet radiation**  
Background UVB exposure in pregnancy and skeletal development in childhood, 1104

**Umbilical cord**  
Newborn infant bone mineralization is affected by their umbilical cord length, SU495

**UMR 106.1**  
Effect of  $\text{Sr}^{2+}$  on PTHrP, OPG and RANKL mRNA expression in osteoblastic-like cells UMR 106.1, SU016

**UMR-106**  
Characterization of osteoblastic properties of 7F2 and UMR-106 cultures after acclimation to reduced levels of fetal bovine serum, SU041

**Uncarboxylated osteocalcin (unOC).** See *Osteocalcin*

**URB**  
Adipocyte-secreted protein URB is a potent stimulator of bone formation, F006

**Urinary N-telopeptide (uNTx)**

Use of conductivity for the correction of uNTx, SA304

**Urocoitin (Ucn)**  
Ucn strongly suppresses the formation and function of osteoclasts via a novel mechanism, SA096

## V

**Vacuolar-type  $\text{H}^+$ -ATPase (V-ATPase)**  
Endocytotic processes underlying Ca-induced inhibition of plasma membrane V-ATPase in murine osteoclasts, SU101  
R740S, a dominant V-ATPase  $\alpha 3$  mutation, causes osteopetrosis in mice, 1218

**Valine80**  
A allele at Valine80 of the CYP19 gene is a risk factor for aromatase inhibitors associated bone loss, 1021

**Valproate**  
Valproate: a model for adverse psychoactive drug effects on BMD, SA556

**Vascular endothelial growth factor (VEGF).** See *Growth factor*

**Vascular system**  
Anabolic daily intermittent PTH 1-84 reduces bone blood vascular bed and induces dramatic changes in the bone/vessel spatial relationship, 1061

**Vdr**  
Pregnancy upregulates duodenal Ca-transport genes and normalizes Ca homeostasis in *Vdr* null mice, M230

**VDRM**  
Improved motor performance in Vitamin D deficient mice with VDRMs, SU196

**Vertebrae**  
Advanced vertebral compression at diagnosis among children with ALL, SU483  
Assessment of changes in thoracic and lumbar vertebrae in T-type  $\text{Ca}_v3.2$  (a1H) VSCC KO mice, M170  
Comparison of voxel-based and smooth FEA to predict damage accumulation in vertebral bodies, SU474  
Contributions of trabecular and cortical components to biomechanical properties of human vertebrae, M455  
Evaluation of osteoporosis vertebrae fragility by Connecting Path method, M307  
Evidence of increase in vertebral body dimensions in postmenopausal women with osteoporosis, M313  
Influence of PHP on BMD and vertebral morphometry, M190  
Mechanisms of endplate failure in the human vertebral body, M413  
Mice lacking NMDA receptor expression in osteoblasts have pronounced vertebral bone abnormalities, F012  
Performance characteristics of a workflow tool for the assessment of vertebral shape, SA350  
Temporal trends in vertebral size and shape from medieval to modern-day, M459  
In vivo measurements of vertebral body dimensions by 3D-XA and their relation with age, M316

**Vertebral wedge deformities**  
Usefulness of SpinalMouse® as a screening tool for the presence of vertebral wedge deformity, SA316

**Very low birth weight (VLBW).** See *Birth weight*

**VIBE Study.** See *eValuation of IBN Efficacy Database Fracture Study*

**Vibration**  
Randomized, placebo-controlled, double blind study on high frequency, low intensity vibration in bone mass, muscle strength and quality of life in children with motor disabilities, F435

**Vimentin**  
Vimentin binds c-Fms in an M-CSF dependent manner and regulates osteoclast differentiation, SU097

**Vinculin**

Vinculin is involved in hypertrophic differentiation through Raf/MEK/ERK pathway in chondrocytic ATDC5 cells, SA119

**Vitamin A.** See also *All-trans-retinoic acid*  
*All-trans-retinoic acid* (Vitamin A) increases expression of MafB and inhibits osteoclast formation by interfering with differentiation of osteoclast progenitor cells, M117  
Deprivation of Vitamin A results in a partial rescue of the mineralization defects in Phex-deficient Hyp mice, F202  
Vitamin D insufficiency together with high serum levels of Vitamin A increase the osteoporosis risk in postmenopausal women, M292

**Vitamin C**  
Protective effect of total and supplemental Vitamin C intake on the risk of hip fracture, 1168

**Vitamin D.** See also *Cholecalciferol*  
Anti-fall efficacy of oral supplemental Vitamin D and active Vitamin D, SU423  
Distinct modes of osteoblastic differentiation from BMSC and vascular smooth muscle cells: induction by BMP-2 and PKA and suppression by Vitamin D derivatives, SU060  
Effect of 1,25(OH) $_2$ D $_3$  and 25(OH)D $_3$  on osteoblastogenesis and bone strength in Vitamin D sufficient growing mice, SU207  
Effect of skin color and oral Vitamin D supplementation on serum 25(OH)D in adolescent girls, SU395  
Efficacy of the Vitamin D supplementation in patients with hypovitaminosis D and HPT2, SU431  
Evidence of a role for the human Vitamin D response element binding protein, hnRNP C1/C2 in chromatin remodeling and transcript splicing, F240  
Femoral neck and trochanteric fractures and Vitamin D, SU353  
Impaired fracture healing in the absence of the Vitamin D-24-hydroxylase, Cyp24a1, M222  
Infantile HCa: relationship of dietary intake of Ca and Vitamin D to serum and urine levels, SU491  
Inhibition of PPAR $\gamma$ 2 by BADGE and Vitamin D in male mice increases osteoblastogenesis and inhibits bone matrix mineralization leading to osteomalacia, SU374  
Key mechanism underlying the immunosuppressive effects of Vitamin D: 1,25(OH) $_2$ D $_3$  is a transcriptional modulator of IL-17, F246  
Late pregnancy serum Vitamin D and longitudinal bone loss during pregnancy, F544  
Low Vitamin D levels and risk of death in older men, F335  
Measurements of Vitamin D do not necessarily reflect what you give to your patients, SU197  
Negative relationship between PTH and Vitamin D: is there an age and a gender effect?, M179  
Osteoporosis patients behaviours and understanding of the importance of Ca and Vitamin D supplementation, M331  
Prevention of non-vertebral fractures with oral Vitamin D is dose dependent, 1242  
Protective actions of Vitamin D analogs in the vascular calcification of CKD, SU450  
PTH and not Vitamin D predicts age-related bone loss in the elderly, M178  
Randomised controlled trial of the effects of Vitamin D supplementation upon muscle function in adolescent girls, SU428  
Relationship between Vitamin D and PTH: serum Ca and Mg are major determinants of PTH in patients with mild CKD, M211  
Requirement of the bone for Vitamin D for 1,25(OH) $_2$ D $_3$  synthesis and bone mineralization, M224

Retrospective study evaluating the relationship of Vitamin D 25 OH and free testosterone levels with changes in hip bone density after liver transplantation, SA502

Serum 25(OH)D measurement and histomorphometric analysis of iliac crest biopsies from 1180 patients reveals a high prevalence of Vitamin D-dependent osteomalacia, 1134

Serum Vitamin D levels do not modify the response to an exercise program following hip fracture, SA346

Sunscreen use and Vitamin D status, M225

Superiority of ALF over plain Vitamin D in men with osteoporosis, SU421

Suppression of bone resorption markers by Ca and Vitamin D separately and in combination, M329

Very high frequency of poor Vitamin D status in French women with bone fragility, SU352

Vitamin D (cholecalciferol) production does not increase linearly with UV dose, M226

Vitamin D and physical performance in African American women, M218

Vitamin D concentrations of healthy children living in the Calgary health region, SU396

Vitamin D delays breast cancer progression in the PyVMT transgenic mouse model, 1185

Vitamin D dose response study in Canadian infants, 1108

Vitamin D status and bone remodeling marker CTx-I in patients with early RA: association with disease activity and joint damage, SA496

Vitamin D status in severely obese individuals can be predicted by demographic and lifestyle factors, SU201

Vitamin D status in young women is strongly negatively related to body weight, BMI and body fat, but is not associated to bone mass, SU203

Vitamin D status, bone mass, and bone metabolism in postmenopausal women and men older than 50 attended in a primary care center of Spain, M223

Vitamin D supplementation in breast fed infants, SU500

Vitamin D supplementation intake among osteoporosis patients aged 50 years and older at various 25(OH)D levels in the US, M400

Vitamin D toxicity due to a commonly available remedy from the Dominican Republic, SU195

What is your patient's Vitamin D status? Clinical consideration of variability in a 25(OH)D measurement, SU427

Wintertime Vitamin D supplementation inhibits seasonal variation of calcitropic hormones and maintains bone turnover in healthy men, SU433

#### Vitamin D deficiency

Behavior of circulating rat(s) PTH molecular forms in HPT2 related to Vitamin D deficiency and renal failure, M194

Bone health impairment in children with chronic Ca and Vitamin D deficiency due to nutritional allergies, SU503

Effect of treating Vitamin D deficiency on FGF-23 levels in humans, SA209

Ergocalciferol is not bioequivalent to cholecalciferol in Vitamin D insufficient hip fracture cases, 1289

FGF-23 in Vitamin D deficient older persons, SA203

Goettingen minipigs—a model for Ca/Vitamin D-deficiency osteomalacia and steroid-induced osteoporosis, SA445

High prevalence of Vitamin D insufficiency in a young adult population, M221

Improved motor performance in Vitamin D deficient mice with VDRMs, SU196

Is Vitamin D deficiency more common in children with cerebral palsy than in healthy children?, SU194

Marked Vitamin D deficiency in recent heart and liver transplant recipients, SA501

Novel hypothesis explains the syndrome of chronic musculoskeletal pain and comorbid painful healed fracture sites in Vitamin D deficiency, SA474

Prevalence of Vitamin D deficiency among surgical orthopedic patients, SU205

At similar plasma 25(OH)D levels, fat mass influence PTH levels in the state of Vitamin D insufficiency, SA218

Suboptimal Vitamin D status in pregnant adolescents is associated with neonatal Vitamin D insufficiency, F557

Vitamin D deficiency in inner city infants: impact of DBP genotype, SA472

Vitamin D deficiency is associated with diminished quality of life based on Qaleffo-41 questionnaire analysis, SU424

Vitamin D deficiency is highly prevalent in Irish hip fracture patients, M294

Vitamin D deficiency, osteomalacia and high bone turnover in patients with NF-1, F465

Vitamin D insufficiency in obesity, SA239

Vitamin D insufficiency is common in racially diverse postmenopausal women with HIV, M448

Vitamin D insufficiency together with high serum levels of Vitamin A increase the osteoporosis risk in postmenopausal women, M292

Vitamin D insufficiency: seasonal variation in healthy 6-12 year old African American and Caucasian children, SU482

#### Vitamin D receptor (VDR)

Associations of the VDR and calcitonin receptor genes with bone density, bone turnover markers and fracture incidence with regard to Ca intake level in Slovak postmenopausal women, M261

Bone tether formation in femoral and basicranial growth plates have similar responses to growth disruptions due to nuclear VDR genotype and mineral homeostasis, M164

Characterization of interactions between the unliganded VDR and effectors of the canonical Wnt signaling pathway, 1183

Cooperativity between VDR and LIP in the regulation of TRPV6 identifies a novel function for LIP as a transcriptional activator, SU198

Expression of VDR in the developing zebrafish embryo, M220

Intestinal-specific VDR null mice maintain normal calcemia but display severe bone loss, F238

Low plasma 25(OH)D and VDR polymorphisms are associated with increased breast cancer risk, SU202

Platelet VDR levels are reduced in osteoporotic patients, SA241

Snail downregulates VDR expression by recruiting Sin3A, HDAC1 and HDAC2 to multiple regions of VDR promoter and deacetylating histone H3/H4, F242

#### Vitamin D<sub>2</sub>. See also Ergocalciferol

Circulating concentrations of 25(OH)D after a single oral dose of 100,000 IU of Vitamin D<sub>2</sub> or Vitamin D<sub>3</sub>, M212

CYP27A1 mutations at Phe147 confer 25-hydroxylase activity towards a Vitamin D<sub>2</sub>-type sidechain, M231

Effect of three different doses of Vitamin D<sub>2</sub> (ergocalciferol) on muscle function and strength in women > 65 years, M405

Effect of Vitamin D<sub>2</sub> and Vitamin D<sub>3</sub> on intestinal Ca absorption in Nigerian children with rickets, SA560

Effect of Vitamin D<sub>2</sub> or Vitamin D<sub>3</sub> supplementation on serum 25(OH)D, SU425

Effects of 50,000 IU of Vitamin D<sub>2</sub> twice per month on circulating 25(OH)D and Ca levels, SU426

#### Vitamin D<sub>3</sub>

Circulating concentrations of 25(OH)D after a single oral dose of 100,000 IU of Vitamin D<sub>2</sub> or Vitamin D<sub>3</sub>, M212

Effect of 1 $\alpha$ ,25-dihydroxy Vitamin D<sub>3</sub> on proliferation and differentiation of C2C12 myoblast, SA245

Effect of Vitamin D<sub>2</sub> and Vitamin D<sub>3</sub> on intestinal Ca absorption in Nigerian children with rickets, SA560

Effect of Vitamin D<sub>2</sub> or Vitamin D<sub>3</sub> supplementation on serum 25(OH)D, SU425

Improved forearm BMD after treatment with Vitamin D<sub>3</sub> in a patient 30 years after bariatric surgery, SA492

Lithocholic acid downregulates the effects of Vitamin D<sub>3</sub> on primary human osteoblasts, SA030

Randomized controlled trial of Vitamin D<sub>3</sub> supplementation for the prevention of viral upper respiratory tract infections, M217

Single dose of 100,000 IU D<sub>3</sub> appears to be insufficient to achieve desirable levels of 25(OH)D in patients with hypovitaminosis D, SU430

Vitamin D<sub>3</sub> treatment of elderly people—twice a day or every four months? A comparative study of efficacy and safety of two oral dosages with same annual dose of 292,000 units, SU422

Which is the best oral high-dose Vitamin D<sub>3</sub> regimen for postmenopausal women with hypovitaminosis D?, SU429

#### Vitamin K

Bone is more susceptible to Vitamin K deficiency than liver, SU316

Conversion of Vitamin K analogues to MK-4 in osteoblastic cells, M064

Vitamin K intake is positively related to trabecular bone microarchitecture in children, M505

Vitamin K treatment for one year does not alter femur geometry in postmenopausal women, SA443

#### Vitamin K<sub>2</sub>

Effect of low dose Vitamin K<sub>2</sub> (MK-4) supplementation on bio-indices in postmenopausal Japanese women, SU307

Effects of Vitamin K<sub>2</sub> and RIS on bone formation and resorption, osteocyte lacunar system and porosity in the cortical bone of GC-treated rats, SU385

Prior treatment with Vitamin K<sub>2</sub> significantly improves the efficacy of RIS, SA379

#### Voltage sensitive calcium channels (VSCC). See Calcium channels

#### Vorinostat

HDI, Vorinostat, blocks growth and associated osteolysis of cancer cells within bone, but reduces bone volume in non-tumor bearing bones in mice, M279

## W

#### WAP

Differences in femoral bone structure between juvenile non-transgenic and transgenic rabbits with the WAP-hFVIII gene construct, SA132

#### WASPI. See Magnetic resonance imaging

#### Wdr5

Role of Wdr5 in endochondral bone formation during chicken limb development, SU121

Wdr5 is required for chromatin modifications at the Runx2 promoter, M039

#### Weight. See also Body composition; Obesity

Birth weight predicts bone size, adult weight predicts BMC and BMD in young Gambian adults, M498

Bone mass recovers in young women with anorexia nervosa who are both weight and menstrual recovered, F339

Bone strength in overweight children is adapted to mechanical loads from walking, but is low for higher loading activities, M482

Effect of bodyweight on clinical response to ZT-031: development of a simple, improved dosing regimen for PTH analogs, M346

Effect of cannabinoid CB1 receptor ligands on body weight and bone mass in mice, M340

## Key Word Index

## ASBMR 30th Annual Meeting

Elevated systolic blood pressure is positively related to bone mass measurements in overweight pre-pubertal and pubertal children, M496

Increasing the number of steps taken per day leads to a greater weight loss and more favorable body composition in overweight postmenopausal women, SU311

Influence of body weight on cost-effectiveness of bone densitometry and treatment for osteoporosis among older women and men without prior fracture, F426

Overweight children are more at risk to sustain a forearm fracture due to poor bone strength relative to body weight, M458

Vitamin D status in young women is strongly negatively related to body weight, BMI and body fat, but is not associated to bone mass, SU203

Weight and BMI predict BMD and fractures in women 40 to 59 years, SA438

Weight reduction is not deleterious for bone mass or strength in obese women, SA338

**WHI.** See *Women's Health Initiative*

**Whole-body vibration**

Efficacy of whole-body vibration in reducing bone loss in postmenopausal women, M396

**Wnt**

*Wnt* pathway regulation by demineralized bone requires TGF $\beta$ /BMP signaling, SU138

**Wnt**

30IT/C of SCT modulates BMD by Wnt and estrogen signaling pathways, 1270

Aging of human BMSC: role of WNT pathways, SA048

BMP/Wnt antagonists are upregulated by DEX in osteoblasts and reversed by ALN and PTH: potential therapeutic targets for GIO, M098

Canonical Wnt signaling suppresses BMP-4 accumulation from C3H10T1/2 cells transfected with BMP-4 expression vector, M098

Characterization of interactions between the unliganded VDR and effectors of the canonical Wnt signaling pathway, 1183

Conditional knockout of the CaSR in osteoblasts alters regulators of Wnt signaling, delays cell differentiation, and promotes apoptosis in bone, 1156

Crosstalk between androgen receptor and Wnt signaling mediates sexual dimorphism during bone mass accrual, 1121

Deletion of the Wnt signaling antagonist sFRP4 in mice induces opposite bone formation phenotypes in trabecular and cortical bone, 1005

Enhanced mitochondrial biogenesis contributes to Wnt induced osteogenic differentiation of C3H10T1/2 cells, SA043

EphB4 expression in osteoblasts is regulated by myeloma cells and the Wnt signaling pathway, SU232

Expression profiles of Wnt signaling pathway components in response to cAMP stimulation at different stages of osteoblast maturation, M040

FHL2 mediates DEX-induced MSC osteogenic differentiation by activating Wnt/ $\beta$ -catenin signaling and Runx2 expression, M048

Mice lacking the Wnt receptor Frizzled-9 display osteopenia caused by decreased bone formation, 1006

Multiple WNT signaling antagonists are differentially expressed over time in inflammatory arthritis, WG41

Noncanonical Wnt signaling is involved mir-206 expression in osteoblastic differentiation, SA021

Osteocyte-specific ablation of canonical Wnt signaling induces severe osteoporosis, 1037

PTH receptor signaling in osteocytes increases bone mass and the rate of bone remodeling through Wnt/LRP5-dependent and -independent mechanisms, respectively, 1038

PTHrP-induced Wnt signaling specifies the mammary mesenchyme, F219

Regulation of bone formation by osteoclasts involves Wnt/BMP signaling and the chemokine S1P, M017

Regulation of osteogenesis by Wnt signaling in rat MSC and human ASC, SU045

Runx2 and canonical Wnt signaling cooperatively regulate BMP-induced differentiation pathways of adult dural cells into osteoblasts or chondrocytes, M043

Sim induces Wnt signaling and reduces CSF-1 secretion and RANKL/OPG ratio to block osteoclast differentiation, SU096

Stable isotopic labeling of amino acids in cultured human BMSC: application to BMP-2 induced Wnt/ $\beta$ -catenin signaling, SA036

Suppression of canonical wnt signaling by Dkk1 attenuates PTH-mediated peritrabecular stromal cell response and new bone formation in a model of HPT2, F215

Thyroid hormone activates Wnt signaling pathways in rat growth plate chondrocytes, M157

Transgenic overexpression of the Wnt antagonist Krm-2 in osteoblasts leads to severe impairment of bone formation and increased bone resorption, 1003

Wnt signaling regulates Gli2 and PTHrP expression in human breast cancer cells that cause osteolysis, M278

Wnt target gene Twist1 inhibits Sox9, the master regulator of chondrogenesis, 1266

Wnt/ $\beta$ -catenin/TCF is a constitutive repressor pathway interfering with Foxo3-mediated induction of synd2, a tumor suppressor in osteosarcoma cells, SU243

Wnt/LRP5-independent inhibition of osteoblastic cell differentiation by SCT, 1256

**Wnt inhibitory factor 1 (WIF1)**

Polymorphisms in the WIF1 gene are associated with BMD in elderly Swedish women, SA264

**WNT-4**

WNT-4 acts through the non-canonical pathways to stimulate osteoblast and BMSC differentiation, F050

**Wnt5a**

Wnt5a regulates osteoclast differentiation in physiological and pathological conditions, 1012

**Wnt7a**

Wnt7a and Wnt7b evoke overlapping yet distinct transcriptional responses during the osteogenic programming of mesenchymal progenitors by Msx2, 1196

**Wnt7b**

Wnt7a and Wnt7b evoke overlapping yet distinct transcriptional responses during the osteogenic programming of mesenchymal progenitors by Msx2, 1196

**Wnt9a**

Identification of a transcription factor p63 for transactivation of Wnt9a and Gdf5 causing joint cartilage formation, F116

**Wnt10b**

T cells amplify the anabolic action of PTH through Wnt10b signaling, 1197

**Wnt11**

R-spondin 2 is a novel osteogenic factor required for Wnt11 mediated osteoblast differentiation, SU063

Tcf is required for Wnt11 mediated osteoblast differentiation, M058

**Women's Health Initiative (WHI)**

Bone turnover and incident hip fracture risk, M285

Geometric evidence of a modeling defect in type 2 diabetic women enrolled in the WHI as a potential explanation for increased fracture risk, 1068

Inflammatory markers and the risk of hip fracture, F333

Serum estradiol and fracture reduction during treatment with hormone therapy, F383

**World Health Organization (WHO)**

Predictive validity of the WHO FRAX model, BMD and prevalent vertebral fracture for incident radiographic vertebral fractures, 1127

WHO absolute fracture models in older women: how does prediction vary for incident hip and non-spine fractures across T-scores?, 1055

**WSX-1**

IL-27/WSX-1 signaling inhibits RANKL-induced osteoclastogenesis through STAT1 activation: a possible involvement in TLR4/MyD88-mediated inflammatory arthritis, SU102

**X**

**X-linked hypophosphatemia (XLH).** See *Hypophosphatemia*

**X-ray**

Family physician characteristics that predict appropriate x-ray ordering, SA359

**X-ray absorptiometry (DXA).** See *Absorptiometry*

**X-tremeCT.** See also *Computed tomography*

Evaluating bone microstructure at the distal tibia in children, F315

**Z****Z-scores**

Clinical tool for adjusting BMD Z-scores for body size in growing children, 1105

Do different densitometers, or use of T-score vs. Z-score, affect fracture risk estimation?, SU258

**Zinc-finger protein 521 (Zfp521)**

Deletion of Zfp521, an antagonist to Runx2 and Ebf1 transcriptional activity, leads to osteopenia and a defect in matrix mineralization in mice, 1109

**Znf219**

Transcription factor Znf219 regulates chondrocyte differentiation through forming transcription factory complex with Sox9, 1265

**Zoledronates**

Comparison of the effects of zoledronates on the differentiation of human bone marrow and amniotic fluid derived MSCs, SA045

Zoledronate protects bone but not soft tissue from prostate cancer progression in a nude mouse model, M282

**Zoledronic acid (ZOL)**

BMD and biochemical marker response rates in postmenopausal women after treatment with ZOL, F401

Effect of a single 5-mg infusion of ZOL on bone turnover markers versus oral RIS (5 mg/day) over 1 year in patients with GIO, M362

Effect of a single infusion of ZOL 5 mg versus oral RIS 5 mg on BMD at lumbar spine, hip, femoral neck and trochanter in patients with GIO, F403

Effect of once-yearly ZOL 5 mg infusion on fracture incidence in postmenopausal osteoporosis, 1028

Effect of once-yearly ZOL on integral BMD of the spine, SU405

Effect of ZOL (single 5-mg infusion) on lumbar spine BMD versus oral RIS (5 mg/day) over 1 year in subgroups of patients receiving GC therapy, M363

Efficacy and safety of intravenous ZOL in the treatment of patients with resistant PDB, SA479

Increase in risk of atypical subtrochanteric fractures with ZOL?, F411

Monthly intravenous ZOL suppresses tissue-level remodeling significantly more than daily oral ALN in the mandible and rib of skeletally mature female dogs, SU388



ONJ: ZOL 5 mg experience in a variety of osteoporosis indications, 1246  
Potential mediators of the reduction in mortality with ZOL after hip fracture, 1030  
Pulse treatment with ZOL causes sustained commitment of bone marrow derived MSC for osteogenic differentiation, M072  
Relationship of bone turnover marker (PINP) and changes in femoral neck BMD to fracture risk in women with postmenopausal osteoporosis treated with once-yearly ZOL 5 mg, 1027  
Roles of ZOL in bone healing and osteoblast functions, 1064  
Short-term effect of ZOL on the superficial vascularisation of membranous bone sites, SU382  
ZOL inhibits the capacity of myeloid-immune suppressor cells in myeloma to form osteoclasts, SU230  
ZOL prevents accelerated bone loss after discontinuation of TPTD, M365  
ZOL treatment of osteoporosis: effects in men, SU398

**ZT-031**

Active controlled, non-inferiority study to compare the effect of ZT-031 with ALN on the incidence of new vertebral fractures, M347  
Effect of bodyweight on clinical response to ZT-031: development of a simple, improved dosing regimen for PTH analogs, M346  
Phase 1, randomized, double-blind, placebo controlled trial of the PK/PD effect and safety of ZT-031, a hPTH analog, in healthy elderly women, SA399



## Author Index

## ASBMR 30th Annual Meeting

**A**

Aapro, M.	M283	Ahn, K.	SA431	Amano, H.	1117, SU100	Arlot, M. E.	M455
Aarum, S.	SU422	Ahn, Y. Heun	SA489	Amano, K.	1045, 1265	Armas, L. A. G.	SU333
Abbaspour, A.	SU001	Ailhaud, G.	M418	Ambati, S.	SU164	Armamento-Villarea, R.	WG26
Abboud, M.	SU237	Aino, M.	SU049	Ambia-Sobhan, H.	SU367	Armstrong, J. K.	SU468
Abdallah, B.	1007, 1147	Aiyer, A.	M169	Ambrogini, E.	1097, 1099, 1247,	Arnaud, C. Donald	M457
Abdelmagid, S.	SA084	Ajibade, D. V.	1223		F024, M010, M204, M436, M438,	Arnés, L.	M424
Abdul Raheem, K. Ghazi	F260,	Akashi, Y.	M035		SA024, SA185, SA482, SU189	Arnold, C. M.	M441
	SA125, SA260	Akech, J.	M279	Amedee, J.	SA101, SA126	Arnott, J. A.	M066
Abe, E.	1117	Akel, N.	F288, SA288	Amerika, D.	F413, SA413	Aro, H. T.	F458, SA458
Abe, M.	SA294, SU242	Akel, N. S.	1234, F523, M177, M412,	Amiable, N.	M018, SU003	Arola, T.	SA533, WG10
Abe, T.	M274		SA086, SA523, SU162	Amin, M.	1011	Aronson, J.	M177
Abe, Y.	SA316	Akerstrom, G.	SA227	Amin, M.	SA532	Arora, T.	SU401
Abed, E.	M008	Åkesson, K.	M463, SU225	Amin, S.	1165, 1167, 1179, 1284,	Arounleut, P.	M173
Aberman, H.	SA111	Akhavan, P. S.	SU271		SU238, SU267	Arp, P.	SA263, SU188
Abildgaard, N.	M287	Akhter-Danesh, N.	SU351	Amizuka, N.	F473, SA473	Arroyo, J. Erica	SA173
Abo, A.	1215	Akhter, M. P.	M020, M323, SA459,	Amling, C.	SA280	Arsenault, M.	F089, SA089
Abott, J.	SA280		SU479	Amling, M.	1003, 1006, 1007, 1133,	Arteaga, E.	SU119
Abou-Samra, A. B.	SA025	Akiba, T.	SA498		1134, 1198, 1201, F202, F465,	Asagiri, M.	F074, SA074
Abourizk, R.	M353	Akimitsu, N.	F494, SA494		M454, SA192, SA202, SA465	Asai, T.	M307
Abrahamsen, B.	1026, M350, M377,	Akiyama, H.	F008, SA008	Ammann, P.	M335, SA506, SA510,	Asakura, T.	M167
	WG16	Akiyama, T.	1217		SU329	Asano, S.	M443, SA499, SU031,
Abramovitz, E.	M085	Akiyoshi, K.	M121, SA105	Amou, H.	SU242		SU170
Abrams, S. A.	SA560, SU305	Akizawa, T.	M185	Amrein, K.	F327, SA327	Ascani, L.	F281, SA281
Abu-Amer, Y.	SU112	Akter, R.	F131, SA131	Amri, E.	M418	Ascenzi, M.	SU281
Abukhaled, M. K.	SU496	Aktour, R.	SA533, WG10	Amsden, B. A.	SU129	Asensio, C.	SA493
Aburatani, H.	1222	Akune, T.	SU334	Amugongo, S.	M494	Ashe, M. C.	SU362
Achenbach, S.	1284, SU238	Al Nazer, R.	M479	An, J.	SA045	Ashida, S.	M035
Açil, Y.	SA445	Al-Dayeh, L.	SA313	An, J. Hyun	SA043	Ashley, L. A.	SU041
Ackerman, J. L.	SA102	Al-Zube, L.	1137, M445	An, Z.	1214	Aspden, R. M.	M317
Ackert-Bicknell, C.	1073, 1276, F265,	Alam, I.	M253., SA261	Anamani, D.	M353	Aspelund, T.	1094, F369, SA369
	M252, M495, SA120, SA265	Alam, J.	SA421	Anastasopoulou, C.	SA329	Assor, E.	SU491, SU503
Acosta, F.	SU269	Alam, N.	SA159	Anastassiades, T.	F358, SA358,	Aston, C. E.	SU303
Adachi, J.	SA362, SU340	Alamanou, M.	SU089		SU309, SU351	Asuncion, F.	1139, 1213, M076
Adachi, J. D.	1056, M302, M379,	Alander, C.	SU085	Anders, O.	1023	Aten, J. E.	M247
	M380, SA343, SA359, SA414,	Alaoui-Ishmaili, M. Hicham	SU146,	Andersen, T. Levin	M287, SA231	Atesok, K.	SA104
	SU251, SU292, SU342, SU351,		SU149	Anderson, F. A.	SU340, SU344	Atkins, G. J.	M046, M224
	SU404, SU504	Albera, C.	SA451	Anderson, G. P.	M414	Atkinson, E.	1167, 1284, SU267
Adachi, R.	F358, SA358	Albers, J.	1006	Anderson, J. L.	F081, SA081	Atkinson, S.	SU292, SU483, WG23
Adami, S.	1286, F401, SA401,	Albert-Sabonnadière, C.	M418	Anderson, K.	M273	Atroshi, I.	SU262
	SU340, SU344	Alén, M.	F420, F542, SA420, SA542,	Anderson, K. C.	1231, SU239	Atsawasuwan, P.	SU208
Adams, C. S.	F058, M169, SA058		SA551	Anderson, P. H.	M224	Attalah, L. Habiba	SU159
Adams, D.	1260, M027, M077,	Alexandersen, P.	M399	Anderson, R.	SA399	Atti, E.	M095, M311, SU468
	M145, SU250	Ali, A.	SU377	Andersson, B.	M119	Au, A.	M263
Adams, G.	M074	Ali, A. Afshan	1157	Andersson, G.	F085, SA085	Aubin, J.	1191, 1218, SA142, SA206
Adams, J. E.	M416, SA457, SU335,	Ali, F.	SU485	Andersson, N.	SU179	Audran, M.	M297, SA400
	SU428, SU473	Ali, S. M.	M281	Andersson, S.	1103	Audran, M. J. Y.	SU056
Adams, J. S.	F240, SA240	Alibegovic, A.	SA456	Ando, K.	M063	Augat, P.	SA392
Adams, K.	WG24	Alibhai, S. M. H.	M396	Andreeva, V.	SU029	Aukrust, P.	SU167
Adams, M.	WG24	Allaelys, I.	M057	Andrés, C.	M255, M259	Ausk, B. J.	SA462, SA515
Adamson, S. L.	1218	Allan, C. M.	1224	Andresen, P. N.	M350	Austin, M.	1285
Adamson, I.	F413, SA413	Allan, E. H.	M014, SU046	Andresen, R.	SU354	Avanzati, A.	F455, SA455, SA481
Adapala, N.	1011, 1150	Allen, M. J.	SU161	Andrew, T.	SA263	Awad, H. A.	F153, SA153
Addison, K.	M245	Allen, M. R.	M494, SU387, SU388	Andrews, J.	SU196, WG11	Awdishu, S.	SU166, SU184, SU191
Addison, W. N.	1199	Alles, N.	M019, M121	Ang, E. S.	SA099	Aya, K.	SA165
Adesanya, A. T. M.	F242, SA242	Allison, M. A.	F333, SA333	Angel, P.	1123	Aydin, C.	F226, SA226
Adler, R. A.	1171, F308, F426,	Alliston, T.	F149, SA149, SA172,	Angeli, A.	SA451	Ayres, F. J.	M139
	SA308, SA426, SU398		SA342, SU122	Angelucci, A.	M272	Azad, V.	M445
Afghani, A.	SU290	Ally, I.	M466	Anginot, A.	SA142	Azimi, H.	M168
Afif, H.	M159, SA152, SU116	Alm, J. J.	F458, SA458	Antal, M.	1123, 1181	Aziz, N.	F288, SA288
Afif, N.	F488, SA488	Almasy, L.	M250	Anter, J.	SA037	Azizi, N.	SU069
Agalliu, A.	SA150	Almeida, E. A. C.	M469, SA517	Anthony, M.	M375, M376	Azria, M.	SA193
Ager, J. W.	F149, SA149, SA342	Almeida, M.	1097, 1099, 1247, F024,	Antón, I.	F291, SA291		
Aghaloo, T.	M095		M010, M108, SA024, SA185,	Anumula, S.	M422		
Agorreta, J.	F291, SA291		SU189, SU380	Aoe, T.	SU314		
Aguado, P.	SA496	Aloia, A.	SA475	Aoki, K.	F074, M019, M121, SA074		
Agueda, L.	M264, M265	Aloia, J. F.	M217, M218, SU501,	Aoyagi, K.	SA316, SU350	Bab, I.	1121, 1298, F527, SA199,
Aguila, H.	SA040		SU502	Aoyama, E.	M153		SA527, SU375
Aguila, H. L.	F041, SA041, SU099	Alon, U. S.	M429	Arabi, A.	M178, M179, SU237	Babajko, S.	M016
Aguirre, J. Ignacio	1275, SA388	Alonso, G.	M447	Arabian, A.	M061, M222	Babarykin, D.	F413, SA413
Ah-Kioon, M.	SA493	Alos, N.	M197, SU483, WG23	Aragon, A. B.	SU163	Bachrach, L.	SU488, WG22
Ahamed, Y.	F315, M502, SA315,	Alshits, V.	SU088	Arai, A.	SU098	Badamgarav, E.	F356, SA356, SU320
	SU469, SU493	Altman, M. K.	1275, SA178, SA388	Arai, K.	F083, SA083	Baddoura, R.	M178
Ahlander, F.	SU262	Alvarez, G. K.	F550, M020, SA459,	Arakaki, J.	SA517	Badger, T. M.	SA336, SU182
Ahlborg, H. G.	1107, 1166, SU262		SA550	Aranami, F.	F473, SA473	Bae, E.	SA390
Ahmad, J.	WG29	Alvarez, L.	SA030	Arango-Hisijara, I.	SU012	Bae, I.	SU035
Ahmedi, K. R.	SA263	Alwis, G.	1107	Arden, N.	F544, SA544	Bae, Y.	SU024
Ahn, J.	SA036	Alwood, J. S.	M469	Ardeshipour, L.	M110	Baecker, N.	SA446
		Amagasa, T.	M019, SA105	Arjmandi, B. H.	M168, M301, SU002,	Baek, J.	SA064, SU021
		Amano, A.	M006, M144		SU273	Baek, J. H.	M050, SA016

(Key: 1001-1300 = Oral, F = Friday Plenary poster, SA = Saturday poster, SU = Sunday poster, M = Monday poster, WG = Working Group Abstract)



## ASBMR 30th Annual Meeting

## Author Index

Baek, K.	SA449, SU407, WG37	Barrett-Connor, E.	1035, 1058, 1128,	Bellou, A.	SU288	Binkley, N.	SA443, SA535, SU195,
Baek, W.	F008, SA008		1206, 1209, 1236, 1277, F335,	Bemben, D. A.	SA534		SU258, SU425, SU427
Baek, Y.	M147, M148, SA117		F354, F367, F426, SA335,	Bemben, M. G.	SA534	Binnerts, M.	1215
Baeyens, N.	SA302, SA303		SA354, SA367, SA410,	Benasciutti, E.	F176, SA176	Birdsall, P.	M328
Baghdadi, T.	SU001		SA426, SU290, SU338, SU420,	Bendre, M. S.	1234	Bisceglia, M.	M432
Bagnoli, P.	M204		SU442, WG38	Benedikt, M.	SA143	Bischoff, D. S.	SA170
Bagur, A.	M426, SU429, SU430,	Barron, J.	M211	Benhamou, C.	1130, 1241, F319,	Bischoff-Ferrari, H. A.	1242, SU363,
	SU499	Barry, C. V.	1102		M172, M239, M313, M395,		SU423, SU432
Bahtiar, A.	SA082	Barry, D. W.	M472		M477, SA167, SA319, SA538	Bishop, G.	M161
Bai, X.	1262, F069, SA069	Bartell, S. M.	SU164, WG4, WG34	Benisch, P.	M047	Bishop, N. J.	F301, SA301
Baik, H.	M407	Bartfai, G.	SA457, SU335	Benn, B. S.	1223, SU198	Bisson, M.	SU078, SU107
Baile, C. A.	M468, SU164, SU318	Barth, H. Dana	SA342	Bennedbaek, F.	M350	Biswas, S.	SA187
Bailey-Wilson, J.	SA262	Barthe, N.	SA322	Benneteau-Pelissero, C.	SA487	Bjorklund, P.	SA227
Baim, S.	SU258	Barthel, T. K.	F277, SA277	Bennett, A.	1219	Bjornerem, A.	M497
Bain, S. D.	SA462, SA515	Bartholin, L.	SA018	Bennett, C.	SU279	Black, A. J.	F337, SA337
Bais, M. V.	F038, SA001, SA038	Bartlett, J. D.	SA154, SA155	Bennett, J.	M200	Black, D.	1027, 1057, 1246, M306
Bajayo, A.	SU375	Barton, B. A.	M397	Bennett, J. A.	SA271	Black, D. M.	1022, 1028, 1055, F411,
Baker, M. Z.	SU303	Bartuszek, D.	M382	Bennett, M. B.	M460		SA411, SU389, SU405
Bakhshalian, N.	M168, M301	Bartuszek, T.	M382	Benoist, C.	M446	Black, J.	M126, SA537, WG7
Bakker, A.	1140	Baruffaldi, F.	F500, SA500	Bensamoun, S.	M133, SA065	Black, W. Cameron	M127
Bakker, N. E. C.	M104	Barvencik, F.	F202, SA202	Bensen, W.	SU251, SU504	Blackburn, M. L.	SA336
Bala, J. F.	1065	Basillais, A.	M172	Bensen, W. G.	SA343, SU504	Blackwell, K. A.	SU085
Bala, Y.	1029	Bass, S.	1244, M458, SA537, WG7	Bentmann, A.	SA151	Blackwell, T.	F351, F371, SA351,
Balcells, S.	M264, M265	Bassit, A. C. F.	1275, SA178	Beppu, H.	SU145		SA371
Baldock, P. A.	1195	Bastepe, M.	1052, F226, SA226,	Berberi, N.	M217	Blackwell, T. L.	1282
Balian, G.	M045		SA259	Berdal, A.	M016, SA150	Blair, H. C.	1125, SA236
Baliram, R.	1117	Bastian, L.	1243	Bergamaschi, C.	SA524	Blake, G. M.	F398, SA309, SA398,
Balkan, W.	SA076	Bateman, T. A.	1066, 1295, SU368	Bergemann, C.	SA528		SU355
Ballabio, A.	SU119	Bates, A. L.	SU232	Bergenstock, M. K.	F050, SA050	Bland, R.	M200
Ballanti, P.	SU210	Batista, D. G.	SU447, SU449	Berger, C.	SA364, SU292	Blaner, W. S.	SU195
Ballock, R. T.	M157	Battaglini, R. A.	SA520	Bergmann, P. J. M.	SU016	Blangero, J.	1177, M241, M250
Balooch, G.	SA172	Battista, C.	M201, M432, SU210	Bergwitz, C.	F471, SA471	Blangy, A.	SU064
Balsa, A.	SA496	Bauer, A.	SU036	Bernard, P. J.	F452, SA452	Blank, R. D.	1131, F260, SA125,
Bandstra, E. R.	1295	Bauer, D. C.	1022, 1055, 1209, 1277,	Berry, J.	1159		SA260
Baniwal, S. K.	M031, M099		1278, F333, F354, F411, M285,	Berry, J. L.	SU428	Blanton, C.	1005
Bank, R. A.	SA110		M347, SA333, SA354, SA411,	Berry, S. D.	1207, SU319, SU326	Blaschke, M.	M450, WG21
Banse, X.	SU465		SU389	Berryhill, S.	1038, SA453	Blatter, T. R.	SU415
Bansod, V.	M401	Bauer, R. L.	M250, SU297	Bertholon, C.	1071	Blázquez, J. Antonio	M255, M259
Banti, C.	M204, M436, SA482	Bauerova, M.	M261, SA132	Bertin, T.	F118, F158, M055, SA118,	Bluc, D.	1059, 1210
Banu, J.	M403	Baumann, A.	SU048		SA158,, SU024, SU126	Blizotes, M. M.	M423
Baptista, M. Tereza M.	M427	Bauss, F.	SA299, SU391	Bertrand, G.	SA258	Bloomfield, S. A.	SA449, SA514,
Baqi, L.	SU261	Baxter-Jones, A.	M500, SA555	Bessette, L.	SA353, SU330		SA521, WG37
Bar-Shavit, Z.	SU088	Bazarra-Fernandez, A.	SU249	Bevilacqua, M.	1170, M180, SU345,	Blumberg, J.	1168
Baranci, M.	SA353, SU330	Bazille, C.	SA493		SU346	Blumentals, W. A.	M367, SU408
Baranowsky, A.	1201	Beamer, B.	SU205	Beyene, J.	M396, M484, WG35	Bluml, S.	SU042
Baratela, W. AR.	M240	Beamer, W. G.	1276, F093, M252,	Beyer, I.	SU016	Bober, M. B.	M240, SU494
Barbagallo, M.	1170, M180		M495, SA093, SA120, SU029,	Bezouglaia, O.	M095	Bockman, R.	SU201
Barbara, A.	M007		SU147	Bhalla, A.	M504	Boden, S.	SA023
Barbe, M.	1011, 1150, SA532	Bearcroft, P.	SU275	Bhattacharya, R. K.	SA502	Boden, S. D.	M034
Barbieri, S.	M073	Beaton, D. E.	F339, M322, M324,	Bhattacharyya, M.	M328	Bodine, P.	F439, SA399
Barbour, K.	F333, SA333		M369, M383, SA339, SA558,	Bhattacharyya, N.	SA200	Body, J.	M283
Barclay, C. L.	SA399		WG8	Bhowmick, N.	1087, M278	Boehm, C.	SA039, SU005
Barden, H. S.	M433, M449, M464,	Beattie, K.	M302, SA343, SU251,	Bi, L. X.	SU051	Boehme, J.	SA292
	SU366, SU484, SU489		SU504	BI, X.	SA313	Bogataj, M.	M257
Bareggi, C.	F281, SA281	Beaulieu, M.	SA353, SU330	Bi, Y.	SU132	Bogoch, E. R.	M322, M369, M383
Bareille, R.	SA101	Beaupied, H.	M172	Bianchi, E.	1092, M254	Bogunovic, L.	M344, SU205
Barengolts, E. I.	SA352	Beaupré, G. S.	M469	Bianchi, G.	1245, M408, SU348,	Bohensky, J.	SU134
Bargouti, M.	M034	Beber, E. Henrique	SA123		SU405	Bohte, A.	1101
Barisic-Dujmovic, T.	1260	Beck, G.	M045	Bianchi, M. L.	SU371	Boileau, C.	1054, M018, M162,
Barker, C.	SU412, SU413	Beck, G. R.	M038, SU014	Bianco, A. C.	SA123		SU003
Barkmann, R.	SU270	Beck, T.	1068, F345, SA345	Bianco, E.	SA451	Boisclair, J.	1037
Barnes, A. K.	M209, SA302, SA303	Beck, T. J.	F323, M306, M489,	Bidwell, J. P.	M193	Boisseau, N.	M239
	SU200		SA323, SA419	Biebler, K.	SU354	Boivin, G.	1029, 1071
Barnes, A. M.	1049, SA262	Beck Jensen, J.	M350	Bierme, H.	F319, SA319	Bojadzievski, T.	M218
Barnes, C. L. T.	SU104	Becker, D. J.	1024, SA326, SU256,	Biggioggero, M.	SU371	Boland, R. L.	M189, SA243, SU185
Barnett, B. L.	F407, SA407		SU321	Bikle, D.	1156, 1261	Bolano, A.	SA150
Barnette, G.	1292	Beckman, M. J.	1161, M196	Bikle, D. D.	1193, M483	Bolivar, I.	M214
Baron, R.	1004, 1005, 1109, F098,	Bedard, K.	M279	Bilezikian, J. P.	1031, 1036, 1112,	Bollag, R. J.	SU026
	SA098, SU376	Beerli, R.	1173		F396, F485, M306, M349, M431,	Bollag, W. B.	M011, SU010, SU026
Barone, A.	1245, SU348	Beidelschies, M. A.	SA177		SA396, SA485, SA486, SU195,	Bollerslev, J.	M049, M123, SU167
Barr, A. E.	SA532	Beil, F. Timo	1133, F465, SA465		SU464	Bologna, M.	M272
Barr, R. J.	M317	Beisiegel, U.	SA042	Bilgin, A.	SU130	Bolognese, M.	SA421, SU384
Barr, S.	SU309	Beiyun, X.	SA138	Bilic-Curcic, I.	1202	Bond, J. L.	M423
Barralet, J.	M334, SU207	Bélanger, R.	M197	Billotet, B.	M316	Bonduel, M.	SU498
Barrella, M.	1170, M180	Bell, J.	M183	Billsten, M.	SU262	Bone, H.	1291, M395
Barrera, A.	M402	Belleli, R.	1173	Bindels, R. J. M.	SA355	Bonel, E.	SU263
Barrero, M.	1139	Bellido, T.	1038, 1097, 1227, SA185,	Bingham, S.	1240, F363, SA363		
			M108				

(Key: 1001-1300 = Oral, F = Friday Plenary poster, SA = Saturday poster, SU = Sunday poster, M = Monday poster, WG = Working Group Abstract)

## Author Index

## ASBMR 30th Annual Meeting

- Bonewald, L. 1042, 1157, 1162, F062, M103, M110, SA057, SA060, SA062, SA136, WG39
- Bonfa, E. SU453
- Bonivitch, A. Rath SA057, WG39
- Bonjour, J. P. 1106, 1239
- Bonnet, N. 1141, 1143
- Bonnette, P. SU048
- Bonor, J. SU147
- Boon, L. SA258
- Boonen, A. SU390
- Boonen, S. 1027, 1028, 1030, 1140, 1243, F411, M331, M360, SA344, SA360, SA411, SA457, SU287, SU335, SU405
- Booth, S. L. 1207
- Borah, B. SA314, SA505
- Boras-Granic, K. F228, SA228
- Bordes, M. SU326
- Borenstein, J. M372, SA417
- Borges, L. F. 1102
- Borghii, C. M355
- Borghs, H. SA457, SU335
- Borgo, M. J. M473, WG6
- Borgström, F. 1023, 1290
- Borisov, N. M373, SA418, SA422, SA423, SU414
- Börjesson, A. E. 1123, 1181
- Bornhäuser, M. SA292
- Bornikolas, V. SU475
- Bornstein, S. A. M003
- Borsari, S. M204, M436, SA482
- Bosch, C. A. J. SA130
- Boskey, A. M146, M311, M471, SA133, SA140
- Bosley, A. L. SA128
- Bostrom, M. 1169
- Böttiger, D. F433, SA433
- Boudiffa, M. 1191, SA142
- Boudignon, B. 1076, 1077, 1252, 1255, M096, M483
- Boudreau, R. F333, SA333
- Boudreau, R. M. 1209
- Bougoussa, M. SA302, SA303
- Bouillon, R. 1140, 1152, 1153, F238, SA238, SU120
- Bouin, O. SA427
- Bourland, J. Daniel 1066, SU368
- Bouton, A. H. SU111
- Boutroy, S. 1067, SA440
- Bouvard, B. M297, SA400
- Bouxsein, M. 1038, 1070, 1179, F277, M304, M397, M455, M457, M493, SA277, SU143, SU190, SU376
- Bowers, K. M120
- Bowman, L. C. 1066, SU368
- Boyan, B. D. 1124, M164, M227, SA113, SU006, SU156
- Boyce, B. F. 1009, 1113
- Boyd, S. K. M139, SA504, SA547, SU076
- Boykin, C. F081, SA081
- Bozinovski, S. M414
- Bracey, J. M. 1234
- Bradford, E. SU500
- Bradica, G. 1137, F376, SA376
- Bragdon, B. SU147
- Brahim, J. S. F217, SA200, SA217
- Braid, S. F315, M502, SA315, SU469, SU493
- Brancato, C. M375
- Brander Weber, P. 1037
- Brandi, M. M036, M092, M184, SA393, SU050, SU211
- Brandish, P. E. M136
- Brandoli, C. F122, SA122
- Brändström, H. SU219
- Branski, L. K. SA571
- Brask-Rasmussen, D. M377, WG16
- Bravenboer, N. SU462
- Brazier, H. SU064
- Brazier, M. SA487
- Breban, S. M477, SA167
- Brecht, J. SA425
- Bredbenner, T. L. M467
- Breitbart, E. A. 1137, M445
- Breitenstein, W. 1173
- Brennan, B. M294
- Brennan, E. 1174
- Brennan, S. Catherine M202
- Brennan, S. C. M203
- Brennan, T. A. 1150
- Brennan, T. C. F389, SA389, SA510
- Brenner, S. M183
- Bretschner, B. SU432
- Brett, A. SA350
- Breuil, V. M418
- Brewer, E. SA138, SU058, SU110
- Bringham, F. 1158, F215, SA215
- Bringham, R. M210, SU072
- Briot, K. 1130, 1241, M313, SU471
- Brisette, L. SA250
- Brixen, K. 1163, F310, M206, SA310, SA434, SU221
- Brixen, K. T. M350, SU270
- Brixner, D. SA422, SU414
- Broadhead, G. K. M202
- Brochu, E. R. SU216
- Brockstedt, H. K. M350
- Brodie, A. M225
- Brodth, M. D. 1110, M475
- Brody, L. SA262
- Broe, K. E. 1207, SU319, SU326
- Brookhart, M. Alan M358, SA370
- Brooks, E. R. SU485
- Brossard, J. H. SU176
- Brossard, J. Hugues M197
- Broux, O. SU044
- Brown, A. C. M003
- Brown, E. M. M203
- Brown, H. A. 1160, 1264
- Brown, J. M489, SU403
- Brown, J. P. 1285, M395, SA353, SU216, SU292, SU330, SU341, SU351
- Brown, K. M315, M397, SU275
- Brown, M. 1091, 1269, SU180, SU460
- Brown, M. A. M245
- Brown, R. SA501
- Brown, S. 1269
- Brown, S. A. M305
- Brown, T. A. F098, SA098, SU158
- Browne, J. SU274
- Browne, J. Gerard M294
- Browner, W. 1057
- Brownstein, C. 1017
- Broy, S. SA421
- Bruder, J. M. M250, SU297
- Brüel, A. F310, M149, M154, SA310
- Brufsky, A. M283
- Brugmans, M. M245
- Brugnara, C. M241
- Bruijine, M. 1129, SU361
- Bruin, G. 1173
- Brum, P. Chakur F244, SA244
- Brunden, K. R. F004, SA004
- Brune, K. A. M207
- Brunelli, C. F281, SA281
- Bruno, R. M353
- Brunski, J. B. SA531
- Bryan, A. F032, SA032
- Bryant, H. U. SU196, WG11
- Bu, S. Young M341
- Bucci-Rechtweg, C. 1246
- Buck, K. SU012
- Buckbinder, L. F098, SA098, SU048, SU158
- Buckingham, D. K. SA307, SU252
- Buckley, K. Anne M120
- Budden, F. H. N. SU353
- Buehlmeier, J. SA446
- Buehring, B. SA535
- Buettner, C. SA199
- Buffa, A. M355
- Buford, W., Jr. SU051
- Buhl, T. 1173
- Buitrago, C. SA243
- Bukulmez, H. SU130
- Bunker, C. H. SA268, SU299, SU300
- Burghardt, A. J. F317, M309, SA317
- Burnett-Bowie, S. M. 1102, 1135, SA209, SU169
- Burns, T. L. M506
- Burr, D. B. 1019, 1178, SU387, SU388, WG41
- Burra, S. SA060
- Burris, L. SU196, WG11
- Burrows, M. F315, M502, SA315, SU469, SU493
- Burton, D. SA216
- Burton, D. W. M182, M282
- Buschmann, M. D. M140
- Bushinsky, D. M021, SU213
- Busse, C. 1100, F249, SA249
- Bustamante, M. M264, M265
- Butler, W. T. SA140
- Butt, D. A. SU254, SU313
- Buttgereit, F. M100, SA234
- Buttke, P. C. SA269
- Buzkova, P. 1208
- Byberg, L. 1205
- Byers, P. H. SA146
- Byford, V. SU199
- Byon, C. M419
- Byrjalsen, I. M398, SA129, SA436, SU091
- Byrne, J. L. B. SA562
- Byrum, S. M281
- Byun, D. SU359
- Byun, J. SA164
- Caballeria, L. M442
- Caballero-Villaraso, J. M292
- Cabazon, A. SA496
- Cabral, S. SU455, SU458
- Cabral, W. A. 1049, SA262, SU209
- Cackowski, F. F081, SA081
- Cackowski, F. C. SU075
- Cacucci, B. M. SA239
- Cadarette, S. M. M358, M377, WG16
- Caffarelli, C. M320
- Cai, J. F109, SA109
- Cai, M. H. SU426
- Cain, R. L. SU196, WG11
- Calatayud, M. M221
- Callewaert, F. 1140
- Callon, K. SU030
- Callon, K. E. SA175, SU071
- Calvi, L. M. 1078, F171, SA171
- Calvo, N. M189
- Camacho, A. SU419
- Camacho, P. M. SA468, SU424
- Camalier, C. E. SU014
- Camerino, C. 1200, SA199, SU094
- Cameron, I. D. 1164
- Caminiti, M. J. M305
- Camp, J. 1284
- Campa, T. F281, SA281
- Campagna, S. F455, M320, SA455
- Campbell, G. SU404
- Campbell, G. M. M139, SU076
- Campbell, K. SU312, SU370
- Campbell, K. P. M170
- Campbell, P. 1180, SU203
- Campbell, P. P. M074, SU042
- Can, U. SU432
- Canaff, L. M187, M201
- Canalis, E. 1111, F141, F265, M145, SA005, SA141, SA183, SA265
- Cantley, L. C. 1115
- Cantor, T. M194, M211
- Cao, H. SA102
- Cao, J. J. M238
- Cao, L. SA019
- Cao, R. M022
- Cao, X. 1014, 1082, 1273, F188, SA188
- Cao, Z. 1048
- Caparbo, V. Falco SU453
- Capelo, L. P. SA123
- Capozza, R. Francisco M411, SU269
- Cappariello, A. M275
- Cappola, A. R. 1208
- Capriotti, C. A. SU372
- Capulli, M. M272, SU017, SU089
- Caracchini, G. SA393
- Carbone, L. SA326, SU256
- Carbone, L. D. 1208
- Carceller, P. M308, SA322
- Carey, J. C. SA562
- Carle, G. Francis M418
- Carlilse, S. SA304
- Carlisi, A. SA191
- Carlos, F. SU419
- Carlson, A. Elizabeth 1008
- Carlson, J. 1219, M208
- Carlsten, H. 1123, SU179
- Carly, B. SU265
- Carmeliet, G. 1152, 1153, F238, SA238, SU120
- Carmeliet, P. 1152, 1153, SU120
- Carmona, G. A. SU329
- Carossino, A. Maria SU050
- Carpenter, T. 1017, 1084, F471, M333, SA254, SA471, SA472, SU171
- Carreras, R. M264
- Carroll, W. 1297
- Carson, M. SU196, WG11
- Carsote, M. SU246
- Carstens, M. SU220
- Carter, E. M. SA561
- Carver, A. SA018
- Carver, A. A. 1234
- Casado, E. SA357, SU431
- Casado-Díaz, A. SA037
- Casanueva, F. SA457, SU335
- Casasco, M. F500, SA500
- Casco, C. SU498
- Case, N. 1253, SA522
- Casey, A. M481
- Casey, M. M348
- Casey, M. Catherine M294, SU274
- Casillas, L. N. SU372
- Cassady, A. I. M118, M460
- Castaneda, B. SA150
- Castellini, S. SU269
- Castillo, A. B. M105
- Castle, L. D. SU041
- Caston-Balderrama, A. M182
- Castro, C. H. M. M191
- Castro-Magana, M. SU501, SU502
- Catala-Lehnen, P. 1198, SA192

(Key: 1001-1300 = Oral, F = Friday Plenary poster, SA = Saturday poster, SU = Sunday poster, M = Monday poster, WG = Working Group Abstract)

## ASBMR 30th Annual Meeting

## Author Index

Cauley, J.	1022, 1028, 1055, 1057, 1068, 1209, 1277, 1278, 1282, F323, F333, F351, F354, F367, F383, M266, M268, M285, SA268, SA328, SA333, SA323, SA351, SA354, SA367, SA383, SU284, SU299, SU300, SU323, SU405	Cavaliere, E.	M212, SA191, SU197	Cavalli, L.	M184	Cavalli, T.	M184	Caverzasio, J.	1256, M088, M335	Cawley, J.	M141	Cawthon, P.	SU338	Cawthon, P. M.	1022, 1058, F335, F367, SA335, SA367	Cazer, P.	1038	Cedoz, J.	M439	Ceesay, M.	M498	Ceglia, L.	SU305	Cella, M.	F176, SA176	Center, J. R.	1059, 1210, F347, F349, M263, SA347, SA348, SA349, SU222, SU461	Cepollaro, C.	SA393	Cerda, D.	M442	Cerny, E.	M328	Cervia, D.	M204	Cervinka, T.	SA533, WG10	Cetani, F.	M204, M436, M438, SA482	Cetta, G.	F500, SA500	Chabane, N.	M159, SA152, SU116	Cháfer, M.	M259	Chagin, A.	SU179	Chagin, A. S.	F114, SA114	Chagomerana, M.	SU488, WG22	Chai, S. C.	M301, SU002, SU273	Chai, T.	SA099	Chai, Y.	1121	Chaiban, J.	SU237	Chaichanasakul, N.	M095	Chaiwatanarat, T.	M406	Chakkalakal, S. A.	1203	Chakravarti, A.	SA092	Chalberg, C.	SA216	Chalberg, C. L.	M182	Chambers, L. J.	SU217	Chambers, T. J.	F433, SA096, SA433, SU068	Chambon, P.	1123, 1181, SA211	Chamoux, E.	SU078, SU107	Chan, C.	1269, M466	Chan, G. M.	SU495	Chan, J.	1190	Chan, J. A.	SU073	Chan, W. W.	1025	Chan, Y. Huak	SU236	Chandler, R. L.	SU150	Chandrasekaran, S.	SA329	Chang, C.	1014	Chang, J.	SA100	Chang, S.	M152	Chang, W.	1049, 1156, 1261	Chao, W.	F188, SA188	Chaoying, C.	SA070	Chapelle, J.	M212, SA191	Chappard, C.	F319, M172, M477, SA167, SA319	Chappard, D.	1132, F516, SA400, SA516, SU056	Chappel, J.	SA077, SU097	Chapurlat, R. D.	1029	Charatcharoenwittaya, N.	SU238	Charbord, P.	M048	Chassande, O.	SA126	Chatziioannou, A. F.	F283, SA283	Chaudhri, R. A.	1124	Chaudhry, A. A.	SU501	Chauveau, C.	SA015, SU044	Chavassieux, P.	1071, SA524	Che, C.	M336	Chebat, E.	1170, M180	Checovich, M.	SA535	Cheeseman, M.	1269	Chel, V.	SA203	Chellaiah, M. A.	SU065	Chen, C.	F149, SA149, SA172	Chen, D.	1044, 1047, 1113, F186, F253, SA115, SA186, SA253	Chen, F.	1214, F174, M136, SA174	Chen, H.	1052, F240, SA240, SU062	Chen, H. Y.	F394, SA394	Chen, I.	1204, M027	Chen, J.	1064, F444, M116, M164, M227, M419, SA138, SA444, SU058, SU110, SU132	Chen, J. R.	SA336, SU182	Chen, J. Sheng	1164	Chen, L.	F004, F014, M318, SA004, SA014, SA248	Chen, M.	1047, 1254, M028	Chen, N.	M213	Chen, P. F.	F398, SA375, SA395, SA398	Chen, Q.	1046	Chen, S.	M126, SU018	Chen, S. Tai	M233	Chen, S. X.	1272	Chen, T.	1156, 1261	Chen, T.	M319	Chen, T. C.	M215, M216, SU482	Chen, W.	F014, M336, M337, SA014	Chen, X.	1114, M165, SA134, SA177, SU331	Chen, X. Ding	SU154, SU155	Chen, Y.	F118, F158, M055, M116, M126, M419, SA118, SA158, SU154, SU155	Chen, Z.	1068, 1208, F383, SA248, SA383	Cheng, H.	F409, M368, SA409	Cheng, S.	1196, F420, F542, M319, SA420, SA542, SA551	Cheng, Z.	1100, F249, SA249	Chenu, C. C.	SU037	Cheon, S.	SU298	Chérin, P.	SA466	Chernoff, A.	SA329	Cherubini, R.	M408	Cheung, A.	M484, SU313, WG35	Cheung, A. M.	M396, SU254	Cheung, A. Man-Wei	M466	Cheung, M.	SU497	Chevalier, Y.	SU474	Chevalley, T.	1106, 1239	Chew, G. T.	1289	Chhana, A.	SA175	Chiavistelli, S.	M438	Chikazu, D.	SA033	Childress, P.	M193	Chillambhi, S.	1052	Chin, E. N.	SU122	Chin, H.	M054	Chin-queue, K. Patrice	SA276	Chinander, M.	M314	Chines, A. A.	M389, M390, M391	Chiodini, I.	M432, SU345, SU346	Chirgwin, J.	F190, SA018, SA190	Chirgwin, J. M.	1085, 1090, F272, M277, SA272, SA273, SA274	Chirita, C.	SU246	Chittur, S. V.	M053, SA070	Chiu, W. S. M.	SA197	Chiusaroli, R.	M076	Chmielewski, P.	SA314, SA505	Cho, D.	SU406	Cho, E.	SU022	Cho, H. Young	SA043	Cho, J.	SA036, SU021, SU022, SU055	Cho, K.	1092, M254	Cho, S.	M086, SA046	Cho, S. Wook	F391, SA043, SA391	Cho, T.	SA053	Cho, Y.	SA064, SU021	Cho, Y. Min	SA043	Choh, A. C.	1177, M321	Choi, B.	M300	Choi, D.	M147, M148, SA117	Choi, H.	M351, M392, M393, SA164, SA442, SU291, SU452	Choi, H. Jin	F391, SA391	Choi, I.	SA053	Choi, J.	M163, M251, SU043, SU214	Choi, O.	M086	Choi, S.	M251, M340	Choi, W. Hwan	SA489	Choi, Y.	M258	Choksi, R. J.	SU075	Chon, S.	SA431	Chonchol, M.	SU442	Choo, M. Kyung	1145	Choudhary, S.	SA529	Choudhry, K.	SU126	Choudhury, G. Ghosh	1081, F002, SA002	Chouinard, L.	SA385	Chrenek, P.	SA132	Christakos, S.	F246, SA246, SU198, WG13	Christakos, S. S.	1223	Christen, D.	1179	Christensen, S. E.	M206	Christenson, K. B.	1299	Christenson, L.	F004, SA004	Christian, R.	WG32	Christiansen, C.	1286, M390, M398, M399, SA129, SA436, SU091, SU204, SU361, SU463	Chrysis, D.	1188	Chu, B.	SA124	Chu, E. Yuet Wah	F312, SA312	Chu, K.	SU113	Chumlea, W. Cameron	1177, M321	Chun, H.	SA189, SU135, SU416	Chun, S.	M258	Chung, D.	SU406	Chung, H.	SA431	Chung, J.	SA046, SU406	Chung, M.	SU406	Chung, N.	SU452	Chung, U.	1013, 1187, 1228, F116, M082, M089, SA116	Chung, Y.	M005, M407, SA412	Churchill, G. A.	1276, F265, M244, M252, SA265	Chutkan, N.	M011, SU010, SU026	Chyu, M.	M338	Ciancaglini, P.	SA061, SA063	Cianferotti, L.	M204, M436, M438	Cierny, D.	SU261	Ciesielska, M.	M390	Cintas, H. L.	SU496	Cioppi, F.	SA393	Ciria, M.	M264	Cirstea, D.	1231, SU239	Cislighi, E.	F281, SA281	Ciuffi, S.	SU050, SU211	Civitelli, R.	1110, 1257, M475, SU144	Clafin, D.	1035	Clark, P.	SU419	Clark, S.	M328	Clark, S. H.	1260	Clarke, S. L.	M341	Clarson, C.	SU483, WG23	Claudon, A.	SA295	Clemens, T.	1082, SU052	Clemens, T. L.	1001, F181, SA181, SA453	Clément-Lacroix, P.	1004, M272	Clements, K. L.	F569, SA569	Clemmons, D. R.	F093, SA093	Clézardin, P.	SU228	Clifton-Bligh, R.	M263, SU224	Cline, M.	M499	Clines, G. A.	1090, 1274, SA273	Clines, K. L.	1090, 1274	Cobaleda, B.	SA503	Coburn, S. P.	SA562	Coco, M.	M201	Cody, D.	1005	Cody, K.	SU312, SU402	Coenegrachts, L.	1152	Coetzee, G.	M099	Coffin, J.	1084	Cogan, J.	1121	Cohen, A.	M310, SA501	Cohen, K.	SU272	Cohen, R.	1083, F109, SA109	Cohen-Kfir, E.	M085	Cohen-Solal, M.	1132	Cohen-Solal, M. E.	SA493	Cohet, N.	F279, SA279	Cointry, G. R.	M411, SU269	Cokolic, M.	M361	Colaianne, G.	SA199, SU094	Colantoni, J.	M173	Colby, J.	M041, M279	Cole, D. E. C.	M201, M432, M187, SA472	Cole, J. H.	M462, SU480	Cole, S. A.	1177, M250	Cole, T.	M498	Collet, C.	SA493	Colli, J.	SA280	Collin-Osdoby, P.	SU209	Collins, M. T.	F217, SA200, SA217	Colnot, C.	F127, SA127	Colombo, C.	SU371	Colón-Emeric, C.	1030, SU401	Colucci, S.	SA199	Combaila, A.	SA030	Combs, C. E.	SA096	Combs, J. A.	1249	Compston, J.	1290, SU340, SU342	Conaway, H. H.	M117	Condel, L.	F376, SA376	Condon, K. W.	WG41	Conen, K. L.	SU004	Confavreux, C. B.	SA255	Conigrave, A. D.	F389, SA389	Conigrave, A. David	M202, M203	Conklin, B.	1076, 1077, 1255, F127, SA127	Conlon, J.	M346	Connerney, J.	SU029	Conrads, T. P.	SU014	Considine, R. V.	SA239	Constantine, G.	M389, M391	Conway, S.	1143	Conway, S. J.	1178	Cooke, B.	M394	Coombes, M. M.	F017, SA017	Coombs, H. F.	M495	Cooper, C.	F544, M504, SA360, SA544, SU325, SU338, SU340, SU347	Cooper, D. M. L.	SU362	Cooper, D. Michael L.	SU469	Cooper, E.	F557, SA557	Copeland, N. G.	1109	Cormier, C.	SU197, SU352	Cornetta, K. G.	SU113
------------	---	---------------	--------------------	-------------	------	-------------	------	----------------	------------------	------------	------	-------------	-------	----------------	--------------------------------------	-----------	------	-----------	------	------------	------	------------	-------	-----------	-------------	---------------	---	---------------	-------	-----------	------	-----------	------	------------	------	--------------	-------------	------------	-------------------------	-----------	-------------	-------------	--------------------	------------	------	------------	-------	---------------	-------------	-----------------	-------------	-------------	--------------------	----------	-------	----------	------	-------------	-------	--------------------	------	-------------------	------	--------------------	------	-----------------	-------	--------------	-------	-----------------	------	-----------------	-------	-----------------	---------------------------	-------------	-------------------	-------------	--------------	----------	------------	-------------	-------	----------	------	-------------	-------	-------------	------	---------------	-------	-----------------	-------	--------------------	-------	-----------	------	-----------	-------	-----------	------	-----------	------------------	----------	-------------	--------------	-------	--------------	-------------	--------------	--------------------------------	--------------	---------------------------------	-------------	--------------	------------------	------	--------------------------	-------	--------------	------	---------------	-------	----------------------	-------------	-----------------	------	-----------------	-------	--------------	--------------	-----------------	-------------	---------	------	------------	------------	---------------	-------	---------------	------	----------	-------	------------------	-------	----------	--------------------	----------	---	----------	-------------------------	----------	--------------------------	-------------	-------------	----------	------------	----------	---	-------------	--------------	----------------	------	----------	---------------------------------------	----------	------------------	----------	------	-------------	---------------------------	----------	------	----------	-------------	--------------	------	-------------	------	----------	------------	----------	------	-------------	-------------------	----------	-------------------------	----------	---------------------------------	---------------	--------------	----------	--	----------	--------------------------------	-----------	-------------------	-----------	---	-----------	-------------------	--------------	-------	-----------	-------	------------	-------	--------------	-------	---------------	------	------------	-------------------	---------------	-------------	--------------------	------	------------	-------	---------------	-------	---------------	------------	-------------	------	------------	-------	------------------	------	-------------	-------	---------------	------	----------------	------	-------------	-------	----------	------	------------------------	-------	---------------	------	---------------	------------------	--------------	--------------------	--------------	--------------------	-----------------	---	-------------	-------	----------------	-------------	----------------	-------	----------------	------	-----------------	--------------	---------	-------	---------	-------	---------------	-------	---------	----------------------------	---------	------------	---------	-------------	--------------	--------------------	---------	-------	---------	--------------	-------------	-------	-------------	------------	----------	------	----------	-------------------	----------	--	--------------	-------------	----------	-------	----------	--------------------------	----------	------	----------	------------	---------------	-------	----------	------	---------------	-------	----------	-------	--------------	-------	----------------	------	---------------	-------	--------------	-------	---------------------	-------------------	---------------	-------	-------------	-------	----------------	--------------------------	-------------------	------	--------------	------	--------------------	------	--------------------	------	-----------------	-------------	---------------	------	------------------	--	-------------	------	---------	-------	------------------	-------------	---------	-------	---------------------	------------	----------	---------------------	----------	------	-----------	-------	-----------	-------	-----------	--------------	-----------	-------	-----------	-------	-----------	---	-----------	-------------------	------------------	-------------------------------	-------------	--------------------	----------	------	-----------------	--------------	-----------------	------------------	------------	-------	----------------	------	---------------	-------	------------	-------	-----------	------	-------------	-------------	--------------	-------------	------------	--------------	---------------	-------------------------	------------	------	-----------	-------	-----------	------	--------------	------	---------------	------	-------------	-------------	-------------	-------	-------------	-------------	----------------	--------------------------	---------------------	------------	-----------------	-------------	-----------------	-------------	---------------	-------	-------------------	-------------	-----------	------	---------------	-------------------	---------------	------------	--------------	-------	---------------	-------	----------	------	----------	------	----------	--------------	------------------	------	-------------	------	------------	------	-----------	------	-----------	-------------	-----------	-------	-----------	-------------------	----------------	------	-----------------	------	--------------------	-------	-----------	-------------	----------------	-------------	-------------	------	---------------	--------------	---------------	------	-----------	------------	----------------	-------------------------	-------------	-------------	-------------	------------	----------	------	------------	-------	-----------	-------	-------------------	-------	----------------	--------------------	------------	-------------	-------------	-------	------------------	-------------	-------------	-------	--------------	-------	--------------	-------	--------------	------	--------------	--------------------	----------------	------	------------	-------------	---------------	------	--------------	-------	-------------------	-------	------------------	-------------	---------------------	------------	-------------	-------------------------------	------------	------	---------------	-------	----------------	-------	------------------	-------	-----------------	------------	------------	------	---------------	------	-----------	------	----------------	-------------	---------------	------	------------	--	------------------	-------	-----------------------	-------	------------	-------------	-----------------	------	-------------	--------------	-----------------	-------

(Key: 1001-1300 = Oral, F = Friday Plenary poster, SA = Saturday poster, SU = Sunday poster, M = Monday poster, WG = Working Group Abstract)

## Author Index

## ASBMR 30th Annual Meeting

- Cornish, J. SA175, SU030, SU071  
 Corona, F. SU371  
 Corradini, C. Francesco M013  
 Correa, D. 1109  
 Corry, P. M. M412, SA285  
 Corsi, F. M180  
 Corsi, K. A. M135  
 Cortet, B. SU382  
 Cosgrove, N. M354  
 Cosman, F. 1027, 1169, 1291  
 Costa, C. C. F244, M228, SA244  
 Costa, J. Lynn SU030  
 Costan, R. SU310  
 Costinescu, A. SU358  
 Cote, J. François SU064  
 Cote, L. M. M495  
 Cote, P. F339, M324, SA339, SA558, WG8  
 Cotté, F. E. SA415  
 Cotte, N. 1255  
 Cottee, J. M193  
 Cottrell, J. A. SU123  
 Couch, R. SU483, WG23  
 Coucke, P. SU215  
 Coudane, H. SU288  
 Courteix, D. SA538  
 Cousins, J. M. F552, M482, SA552, WG20  
 Couvineau, A. SA258  
 Cowan, P. M496  
 Cox, A. 1276  
 Cox, D. A. M386  
 Cox, K. SU145, SU148  
 Cox, R. 1269  
 Cox, R. G. SU396  
 Coxon, F. SU109  
 Coxon, F. P. 1065  
 Crabtree, N. J. WG1  
 Craig, T. M220  
 Craig, T. A. SA059  
 Crane, D. P. M236  
 Crane, E. 1269  
 Cranney, A. SU341  
 Crapanzano, C. M013  
 Crawford, D. T. F098, SA098, SU158  
 Cremasco, V. F176, SA176  
 Cremers, S. 1146, F485, SA485, SU202, SU455  
 Crew, K. D. SU202  
 Crine, P. 1054, 1199, F107, SA107  
 Cristofaro, M. Angela SA241  
 Criswell, B. 1121  
 Croce, C. M. M090  
 Croke, M. R. 1220  
 Crombie, A. P. SU311, SU418  
 Crook, M. K. SA018  
 Croucher, P. 1269  
 Cuenca-Acevedo, J. M292  
 Cuerrier, D. SU178, SU448  
 Cui, Y. 1002, 1114  
 Culiati, C. T. F174, SA174  
 Cullen, D. F032, SA032  
 Cullen, D. M. F550, M020, M323, M341, SA459, SA550  
 Cumming, R. G. 1164  
 Cummings, E. SU483, WG23  
 Cummings, S. 1057, 1243, 1277, F383, M347, SA383, SU338  
 Cummings, S. R. 1022, 1028, 1055, 1058, 1127, 1278, 1286, 1287, 1288, F321, F333, F335, F365, F367, F411, F426, SA321, SA333, SA335, SA365, SA367, SA410, SA411, SA426, SU183, SU389, SU405  
 Cunha, B. M217  
 Cupples, A. 1091  
 Cupples, L. A. 1092, 1168, 1207, 1283, F341, M249, M254, SA120, SA251, SA341, SU319  
 Curran, J. E. 1177, M241  
 Currey, J. A. SA531  
 Curtain, M. M248  
 Curtis, J. R. 1024, F409, M368, SA280, SA326, SA409, SU256, SU321, SU401  
 Cusick, T. 1214, SA072  
 Cusick, T. Elyse SA073  
 Czernik, P. SU023  
 Czerwinski, S. A. 1177, M321  
 Czymmek, K. SU039, SU040
- D**  
 D'Agruma, L. M201  
 D'Amelio, P. SA241  
 D'Amour, P. M194, M197, SU176  
 D'Amours, M. SA406  
 D'Angelo, M. 1189, SA568  
 D'Elia, G. SA393  
 D'Silva, N. J. SA025  
 Dadsetan, M. SA143  
 Dagda, R. M338  
 Dahl, R. M142  
 Dai, R. M303  
 Dai, S. SU112  
 Dais, K. A. M309  
 Dakin, G. SU201  
 Daley, E. L. H. SA252  
 Dallal, G. SU305  
 Dallari, D. M408  
 Dallas, M. M110  
 Dallas, S. 1162  
 Dallas, S. L. 1046, F062, SA062  
 Dalsky, G. P. 1171  
 Dalton, J. T. SA381  
 Daly, R. M458, SA537, WG7  
 Daly, R. M. 1244  
 Dam, E. SU463  
 Dam, E. B. SA129  
 Dambacher, M. A. M352, SU276  
 Dammers, K. SA132  
 Damron, T. A. SU161  
 Damulewicz, M. M060  
 Dani, C. M418  
 Danielsen, C. Christian M149, M154  
 Danilevicius, C. Figueiredo SU453  
 Danks, J. A. M183  
 Dapia, S. M195, M424, M425, SA223  
 Darnay, B. G. 1074  
 Darpo, B. F433, SA433  
 Darrington, S. SU409  
 Das, G. SU428  
 Das De, S. SU236  
 Dasic, G. SA509  
 DaSilva, C. 1291  
 Dastidar, P. SA533, WG10  
 Datema, R. M134  
 Datta, N. S. SA025  
 Daud, S. WG28, WG33  
 Dauser, D. M353  
 Daut, J. M353  
 Davey, R. A. SA197, SA255  
 Davey-Smith, G. 1175  
 David, J. 1149  
 David, M. SA329  
 David, V. F205, F207, F210, SA205, SA207, SA210  
 Davie, M. W. J. SA340, SU360  
 Davis, A. N. SU074  
 Davis, M. Jonathon SU353  
 Davis, R. C. M247  
 Davis, R. Y. SU260  
 Davis, S. SU173  
 Davison, K. Shawn M325, SA364, SU292, SU351  
 Davison, M. F416, M378, SA416, WG18  
 Davison, S. K. SA353, SU330  
 Dawson, B. M055, M126  
 Dawson, B. Christopher SU024  
 Dawson, J. SA193  
 Dawson-Hughes, B. SU305, SU363, SU423, SU432  
 Day, A. J. SA097  
 Day, R. E. F233, SA233  
 Day, S. E. SU473  
 de Beer, J. M302  
 de Bhalldraithe, S. M348  
 de Bono, S. M498  
 de Brum-Fernandes, A. J. SU095  
 de Castro, L. F. SA223  
 de Crombrughe, B. 1074, F008, F017, SA008, SA017  
 De Filippo, G. SA481  
 de Gorter, D. J. J. SA031  
 de Gregorio, L. H. 1285  
 de Jong, F. H. SU188  
 de Jonge, R. SU317  
 de Juan, J. M223  
 De la Piedra, C. SA299  
 de Landeta, M. C. SA377  
 de Monchy, J. G. R. SU268  
 De Paep, A. SU215  
 De Paola, V. F455, SA455, SA475, SA481  
 de Papp, A. SU389  
 de Paula, F. J. A. M190  
 de Rooij, K. E. SA052  
 de Roux Serratrice, C. SA466  
 De Souza, M. Jane SA449, SU166, SU184, SU191, WG37  
 De Souza-Li, L. F. R. M427  
 de Vernejoul, M. F488, SA488  
 de Vernejoul, M. Christine 1132, F010, SA010  
 de Villiers, T. J. M390  
 de Wilt, E. SA052  
 Deal, C. 1285, M365  
 Dean, A. K. M103  
 Dean, D. F376, SA376  
 Dean, D. Brian SA160  
 Dechering, K. J. M104  
 Deckers, M. M. L. SA052  
 Dedhar, S. M061  
 Dedrick, R. SA360, SU287, SU340, SU342, SU344  
 Defetos, L. SA216  
 Defetos, L. J. M182, M282  
 Del Carpio-Cano, F. SU012  
 Del Fattore, A. M275, SU089  
 Del Pino, J. M255  
 Del Prete, D. F081, SA081, SA287  
 del Rio, L. SU263  
 Dela, F. SA456  
 Delaissé, J. M287, SA231  
 Delanaye, P. SA191  
 Delaney, J. 1202  
 Delany, A. M. 1155, M270  
 Delbridge, L. M203  
 Della-Fera, M. A. SU164  
 Delmas, P. D. 1027, 1028, 1029, 1030, 1067, 1071, 1286, 1287, 1288, F401, M360, M455, M460, SA080, SA401, SA404, SA440, SA524, SU287, SU344, SU405  
 Delmas, V. F190, SA190  
 DeLong, W. G. M066, SU012  
 DeLoose, A. 1157  
 Deloukas, P. SA263  
 Delzell, E. 1024, F409, M368, SA326, SA409, SU256, SU321, SU401  
 DeMambro, V. E. F093, M252, SA093  
 Demant, P. F260, SA125, SA260  
 Demay, M. B. 1183, M039, M158, SU124  
 Demer, L. L. M143  
 Demerath, E. W. 1177, M321  
 Demissie, S. 1091, 1092, M249, M254, SA120, SA251  
 DeMoss, D. L. SU041  
 Dempster, D. W. 1036, 1146, 1169, F217, F476, F478, F485, M310, SA217, SA476, SA478, SA485  
 Dencker, M. 1107  
 Deng, H. 1093, 1232, M394, SU331  
 Deng, H. Wen M404, SA267, SU154, SU155  
 Dent, S. Y. R. F017, SA017  
 DePapp, A. F323, SA323  
 DePinho, R. A. 1112, 1247  
 Dere, M. 1135  
 Dere, M. E. SU169  
 DeRidder, A. M. SA146  
 Derynck, R. SA172  
 Descamps, M. SA015  
 DeSimone, D. SA060  
 Devaney, J. F122, SA122  
 Devedjian, J. SU044  
 Devine, A. F373, SA373  
 Devlin, M. J. M493  
 Devogelaer, J. F403, M362, M363, SA403  
 Devogelaer, J. P. SU465  
 Devogelaer, J. Pierre 1171, SU306  
 Dew, T. F491, SA491  
 Dewar, A. L. SU074  
 Dhawan, P. 1223  
 Dhillon, R. M279  
 Di Bella, S. SA241  
 Di Benedetto, A. SU094  
 Di Gregorio, S. SU263  
 Di Iorgi, N. M074  
 Di Stefano, M. SA475  
 Di Benedetto, A. SA199  
 Diacinti, D. M438  
 Diamond, P. SU079, SU080  
 Diaz, D. SA239  
 Diaz-Curiel, M. SA299  
 Diaz-Doran, V. SU250  
 DiCioccio, A. M353  
 Dick, J. SA456  
 Diederichs, G. F317, SA317  
 Diem, S. F351, SA351  
 Dieudonné, F. SU243  
 Diez- Pérez, A. M264, M265, SA360, SU287, SU325, SU342  
 Diffey, B. L. F337, SA337  
 DiGirolamo, D. James F181, SA181  
 Dijkstra, G. SU462  
 Dijkstra, J. E. SA203  
 Dijkstra, H. SA203  
 Dilley, J. D. 1234  
 Dimai, H. Peter M388  
 Dimayuga, R. T. M182  
 DiMeglio, L. A. SU486, WG19  
 Dimitri, P. F301, SA301  
 Ding, J. 1050  
 Ding, K. 1148, F452, M132, SA441, SA452, SU010  
 Ding, Y. SA154  
 Dion, M. SU159  
 Dion, N. SU399  
 Ditzel, N. 1007  
 DiVasta, A. D. SA559  
 Divieti, P. P. 1158  
 Dixon, A. 1121  
 Dixon, C. M209  
 Dixon, G. SA387, SA460  
 Dixon, J. F435, SA435  
 Dixon, S. Jeffrey M065, SU105  
 Djennane, S. SU352

(Key: 1001-1300 = Oral, F = Friday Plenary poster, SA = Saturday poster, SU = Sunday poster, M = Monday poster, WG = Working Group Abstract)

## ASBMR 30th Annual Meeting

## Author Index

Do, S. H.	SA342	Duncan, R. Lyle	SU039	El Hage, R.	SA538	Evdokiou, A.	M046, SU079
Do, T.	M376	Dunford, J. E.	F407, SA407, SU071	El-Hajj Fuleihan, G.	M178, M179, SU237	Everett, E. T.	F093, SA093, SU465
Doan, A.	M302	Dunn, D. M.	M338	El-Hoss, J.	M061	Ezaki, J.	SU307
Dobbelaere, D.	SA466	Dunstan, C. R.	1224, 1267, F233, M100, SA233, SA234	El-Onsi, L.	SU237	Ezura, Y.	M026, M044, M174, M175, M446, SA105, SA378, SU007
Dobek, J.	SA271	Duong, L. T.	M343	El-Rassi, R.	M179		
Dobnig, H.1019, F327, M388, SA327		Duong, L. Thi	F297, M127, M276, SA297	Elabdi, C.	M418		
Dodge, J.	SU196, WG11	Dupont-Versteegden, E. E.	F523, SA523	Elalieh, H.	1261		
Dodge-Kafka, K.	SA033			Elalieh, H. Z.	1193	<b>F</b>	
Dolléans, E.	M172			Elble, A. E.	SA545, SA553, SU395	F de Castro, L.	M195
Domae, E.	M094, SA147	Duque, G.	F131, M003, M334, SA131, SU374	Elder, G. J.	1032, SA497	Faber, P.	F004, SA004
Dominguez, L. Juliana	1170, M180	Duquesnoy, B.	SU382	Elefteriou, F.	1098, M102, SU218	Facchini, A.	SU050
Donahue, H. J.	SA276	Durand, M.	SU095	Elenich, L.	1005	Faccio, R.	1086, 1119, F176, SA176, SA199
Donahue, L.	M248	Duren, D. L.	1177, M321	Elis, S.	SA184	Facincani, I.	SU457
Donahue, L. B.	M244	Durham, B. H.	M289, M291	Ell, B.	1229	Facon, T.	SU228
Donaldson, M.	1057	Dusevich, V.	1157, M110	Elliot-Gibson, V.	M369	Fadeel, B.	1188
Donaldson, M. G.	1022, 1127	Dutton, G. R.	SU311	Elliot-Gibson, V. I. M.	M322	Fagerlund, K. M.	SA298
Donescu, O. S.	SU293	Dutton, J.	M481	Ellis, B.	SA472	Fagan, M. J.	WG27
Dong, S. Shan	M404	Duval, N.	M018, SU003	Ellis, M.	1021	Fagnoni, E.	F281, SA281
Dong, X.	M336, M337	Duverger, O.	1272	Ellwanger, K.	1004	Fahmi, H.	M159, SA152, SU116
Dong, Y.	1268	Dvorkin, L.	SU248	Elvins, D.	M504	Fahrleitner-Pammer, A.	M388, 'SU412, SU413
Dooley, K. A.	M462, SU480	Dworakowski, E.	SU202	Emerton, K. B.	SU190	Fajardo, M.	M235
Dorado, G.	SA037	Dwyer, D.	1139, 1211, 1213	Emond, P. D.	M302	Fajardo, R. Jose	SU376
Dorschner, R.	SA216	Dyer, T.	1177, M250	Enders, J. Tyler	SA160	Falchetti, A.	M036, SA393, SU211
dos Reis, L. M.	SU447, SU449, SU457			Endo, I.	SA470	Falchi, M.	SA263
Doschak, M. R.	SU393	<b>E</b>		Endo, M.	M113	Fall, P.	M353
Doss, S.	M247	Ea, H.	SA493	Endo, N.	M307	Fan, J.	M079
Doty, S. B.	SA128	Earnshaw, S.	SA429	Endo, Y.	SU187	Fan, T.	1236, M400, SA430, SU420, WG38
Doucet, J.	M133	Easley, S. K.	SA512	Engelke, J.	SU425, SU427	Fan, Y.	F181, SA181
Dougall, W. C.	F283, SA283	Eastell, R.	1026, 1027, 1028, 1128, 1243, 1287, 1288, F301, F401, F411, M507, SA301, SA401, SA411, SA571, SU369, SU405	Engelke, K.	SA507, SA509, SU260	Farach-Carson, M. C.	M170, M242, SA027, SA133
Douglas, C. C.	SU059, SU311, SU418			English, R.	M458	Farahmand, P.	M359, SU421
Dovio, A.	SA451			Enjuanes, A.	SA030	Farber, C. R.	M247
Dowd, B.F416, M378, SA416, WG18				Enomoto, T.	SU082	Fardellone, P.	F319, M331, SA319, SA487
Dowd, T.	M146			Enright, G.	SU259	Farias, A.	1089
Dowell, K.	SU029			Enriquez, R. F.	1195	Farias, M. L. F.	SA212
Downs, R.	M386	Easton, V.	SU325, SU347	Enslin, M.	SA507, SU260	Farina, A.	F500, SA500
Downs, R. W.	M375, M376	Ebede, B.	M391	Ensrud, K.	1022, 1055, 1057, 1058, 1277, 1288, 1127, 1282, F323, F335, F351, F367, F371, F426, M266, M268, SA268, SA323, SA335, SA351, SA367, SA371, SA410, SA426, M306, SU284, SU300, SU389	Farina, E.	F341, SA341
Dowthwaite, J. N.	M490	Ebeling, P. R.	M414	Epstein, S.	M440	Farquhar, D.	SA424
Doyle, J.	1178	Eberhardt, C.	SA392	Erben, R. G.	M171	Farquharson, C.	SA063
Doyle, N.	SA381, SU435	Ebert, D.	1005	Ergun, D.	SU366, SU484	Farrow, E.	SU173
Doyon, A. Robert	1062	Ebert, R.	M047, M072	Erich, L.	SA408	Fashola, T.	F403, M362, M363, SA403
Draheim, B.	SU194	Ebert-McNeill, A.	M328	Ericson, K. L.	SA562	Fassbender, W. J.	SU177
Drake, M. T.	SU238	Ebetino, F. Hal	1065, F407, SA407	Eriksen, E.	1030, 1027, 1246, F401, SA401, SU405	Fassler, R.	1046
Drake, T. A.	M247	Ebraheim, N.	F091, SA091	Eriksson, A.	SU183	Fauchet, P. M.	M028
Draper, E.	M478	Eckstein, F.	M489	Eriksson, J. G.	1103	Faulkner, K. A.	1058, SA328, SU323
Drees, B.	M404, SA267	Economides, A. N.	F141, SA141, SU143, SU148	Erlandson, M. C.	SA555	Faulkner, R. A.	M441, M500
Dresner-Pollak, R.	M085	Econs, M. J.	1018, M253, SA261, SU113, WG31	Esapa, C. T.	1269	Faure, C.	SA011
Drezner, M. K.	1051, 1053, 1162, SA165, SU425, SU427	Edderkaoui, B.	M115	Escobar, R.	F435, SA435	Favia, A.	SU281
Driban, J. B.	SA532	Eddleston, A.	1212	Eser, P.	M458	Favus, M. J.	F242, SA242
Driessler, F.	1149	Edefonti, A.	SU371	Eskildsen, P.	M377, WG16	Fazzalari, N. L.	SA148
Driouch, K.	M272	Edenberg, H. J.	SA261	Esko, J. D.	SU130	Fechtenbaum, J.	1130, 1241, M313
Drissi, H.	M052, SA033	Edger, J. Thomas	SU282	Eskola, H.	SA533, WG10	Fedarko, N. S.	M234, SU386
Driver, K.	SA314	Edmonds, M.	F491, SA491	Eslami, B.	SU400	Feig, D. S.	SU254
Drozdzowska-Rusinowicz, I.	M382	Edwards, C. M.	1088, F293, SA293, SU230, SU232	Espandar, R.	SU001	Feldman, H. A.	SA559, SA564
Du, X.	SA248	Edwards, J. R.	1098, 1136, 1251, SU233, SU378	Esposito, T.	SA475	Feldman, R.	SA421
Dubrovina, Y. Alekseevna	M192	Edwards, L.	M416	Essley, B. V.	F557, SA557	Feldstein, A. C.	M356
Ducher, G.	M458, SA537, WG7	Edwards, M.	SU128	Esteve, F.	SA287	Feng, J.	1162
Ducy, P.	F168, M069, SA168, SA463	Efstathopoulos, E.	SU472	Estrada, K.	1091	Feng, J. Q.	1037, 1048, 1051, 1053, 1074
Dudzek, C. A.	SA307	Egerbacher, M.	M171	Ethgen, D.	1174, SU260	Feng, X.	1118, F188, SA088, SA188, SA278
Dudzek, K. M.	SU252	Egli, A.	SU363, SU423	Ettinger, B.	SU402	Fenton, T. R.	SA331, SU283
Duerksen, D.	SA366	Egol, K.	M235	Euler, D. H.	M136	Ferchak, M.	SU259
Duffin, M.	M027	Eguchi, T.	M112, SA166, SU152	Eulert, J.	M072	Fernandes, G.	M403
Dufour, C.	M093	Egusa, H.	M035	Euller-Ziegler, L.	M418	Fernandez, C.	SU036
Dufresne, T.	SA314	Eichenberger Gilmore, J.	M506	Eusebio, R.	M360, SA344	Fernández, M. Candela	SU430
Dufresne, T. E.	SA505	Eiken, P.	1026, M350, SU221, SU223	Evans, C.	M401	Fernando, C.	SU130
Dugard, M. Naomi	SA340	Einhorn, T. A.	F038, M161, SA001, SA038, SU061	Evans, D.	M245	Ferrari, L.	1128
Dukas, L. C.	SU444			Evans, G.	1258	Ferrari, P.	M418
Duke, M. J. M.	SU393	Eiriksdottir, G.	1094, SU289	Evans, S. F.	SU360	Ferrari, S.	1106, 1141, 1143, 1239
Dumitrescu, C. E.	SA200	Eisenberg, H.	SU455, SU458	Evdokimov, A.	F407, SA407	Ferrari, S.	M254
Dumitrescu, L. Caneel	SU233	Eisenberg, H. F.	1033, M310, SU441			Ferrari, S. L.	1092, SA220
Dumitriu, M.	SU465	Eisman, J. A.	1059, 1195, 1210, 1280, F347, F349, M245, M263, SA347, SA348, SA349, SU222, SU461				
Dunbar, M.	F228, SA228	Ekker, G.	SU252				

(Key: 1001-1300 = Oral, F = Friday Plenary poster, SA = Saturday poster, SU = Sunday poster, M = Monday poster, WG = Working Group Abstract)

## Author Index

## ASBMR 30th Annual Meeting

- Ferreira, A. F403, M363, SA403  
 Ferrell, R. M268, SU284  
 Ferrell, R. E. M266  
 Ferrer, V. SA040  
 Ferrer, V. Lea S. M054  
 Ferreri, S. F536, SA536  
 Ferretti, J. Luis M411, SU269  
 Ferretti, S. Eduardo M411  
 Ferries, I. Kenneth 1062  
 Ferris, A. 1041  
 Ferris, D. M448, SU455, SU458  
 Ferro, M. Veronica SU430  
 Ferron, M. F089, F168, SA089, SA168  
 Fidalgo, J. M118  
 Fields, A. J. M413  
 Figueiredo, P. T. S. SA311  
 Figueroa, C. SU498  
 Findlay, D. M. M046, M224, SA197  
 Finigan, J. SU369  
 Fink, H. 1057, 1058  
 Fink, H. A. 1131, 1208, 1278, 1282, F367, F371, F426, SA367, SA371, SA426  
 Finkelstein, J. S. 1102, SA209, SA370  
 Finn, J. D. SA457, SU335  
 Fiorani, L. SU288  
 Fischer, P. R. 1179, M491  
 Fischer, R. SA292  
 Fishbein, K. W. SA561  
 Fisher, J. 1214  
 Fisher, J. E. M136  
 Fisher, L. W. F145, SA145  
 Fitch, J. L. SU061  
 Fitter, S. SU074  
 Fitzgerald, K. M348  
 Fitzgerald, R. L. M282  
 Fitzpatrick, L. A. 1174, SA507, SA509, SU260  
 Fiveash, J. B. SA280  
 Flanagan, J. N. M216  
 Flannery, P. J. 1226  
 Fleet, J. 1184  
 Flegler, A. SA090  
 Fleischer, J. 1034, M434  
 Fleming, N. L. F376, SA376  
 Flenniken, A. M. 1218  
 Fletcher, B. M118  
 Flipon, E. SA487  
 Flores, O. 1214  
 Flowers, S. M038  
 Focil, A. SU312  
 Fodde, R. SA130  
 Fogelholm, M. SA338  
 Fogelman, I. F398, SA309, SA398, SU174, SU355, WG30  
 Foisner, R. M070  
 Foley, J. 1160  
 Foley, K. F356, SA356, SU320  
 Folkmane, I. F413, SA413  
 Fomin, V. P. SA027, SU040  
 Fong-Yee, C. 1267  
 Fonseca, P. M. M055  
 Fonseca, T. Lourde F244, SA244  
 Fontaine, R. M161  
 Foo, A. SA437  
 Førde, A. SA137  
 Forlino, A. F500, SA500  
 Forman, S. F471, SA471  
 Foroud, T. M253, SA261  
 Forsdahl, S. M130  
 Forsmo, S. M325  
 Forster, M. Ann 1161, M196  
 Forti, G. SA457, SU335  
 Forwood, M. R. M460  
 Foschi, D. M180  
 Fostad, G. SA137  
 Foster, J. SU393  
 Fourman, L. T. SA565  
 Fournier, P. G. J. F275, SA273, SA274, SA275  
 Fowler, J. Aaron 1088, F293, SA293  
 Fox, C. J. M209, SU200  
 Fox, C. S. 1207  
 Fradinger, E. SU498  
 Fraher, L. M210  
 Fraisl, P. 1153  
 Franceschelli, F. SU211  
 Franceschi, R. T. SU025, SU035  
 Franchimont, N. SU325  
 Franci, B. F455, M320, SA455  
 Francke, U. 1006  
 Franco, F. M. SA212  
 Franco, R. M095  
 Franco-Marina, F. SU419  
 Franke, S. SU456  
 Franz, S. E. 1275, SA178, SA388  
 Franzson, L. SA374  
 Fraser, D. G. F029, SA029  
 Fraser, M. SU324, WG17  
 Fraser, W. M211  
 Fraser, W. D. 1289, F337, M166, M289, M291, M481, SA337, SU174, SU224  
 Frattini, A. F500, SA500  
 Frayssinet, C. M415  
 Frazier, W. A. 1232  
 Frederick, D. M041  
 Frederick, M. 1105  
 Freeby, M. SA501  
 Freeman, D. M173  
 Freemantle, N. SU325, SU347  
 Freemont, A. WG24  
 Freitas, F. Rodrigues Souza F244, SA244  
 Frenkel, B. 1121, M031, M099  
 Frera, G. 1227, M108  
 Freundlich, M. M429  
 Fricain, J. SA126  
 Friedman, M. S. M058, SU063  
 Friedman, P. A. 1274  
 Friedman, S. M. M288, SA377  
 Friedrich, F. 1006  
 Frieling, I. SU276  
 Fries, M. SA507, SA509  
 Frigato, M. M355  
 Frings-Meuthen, P. SA446  
 Frisch, B. 1078, F171, SA171  
 Fritton, C. M440  
 Fritton, J. Christopher SU190  
 Fritz, T. A. 1018  
 Frohn, M. SU159  
 Fromigué, O. M007, M048  
 Frost, M. L. SU355  
 Frost, S. A. F347, F349, SA347, SA348, SA349  
 Fu, C. 1015  
 Fu, Q. SU047  
 Fu, W. M237  
 Fuchs, R. K. 1178, M423  
 Fudge, N. J. M230  
 Fuerst, T. SA507, SA509, SU260  
 Fujii, N. SU079  
 Fujii, Y. SA384  
 Fujimura, Y. M112, SA166, SU152  
 Fujioka, T. SU438, SU440  
 Fujishima, M. SU438, SU440  
 Fujishima, Y. SU438, SU440  
 Fujita, T. 1151, F163, F469, M094, SA147, SA163, SA208, SA305, SA384, SA469  
 Fujiwara, S. SA296  
 Fukagawa, M. M185, SU439  
 Fukawa, T. SU081  
 Fukaya, M. SA201  
 Fukayama, S. F006, SA006  
 Fukuda, M. SU316  
 Fukuda, T. SA161  
 Fukumoto, S. F163, F469, SA163, SA208, SA469, SA470  
 Fulford, A. D. SA239  
 Fuller, K. SA096, SU068  
 Fullman, R. L. 1058  
 Fultz, M. E. SU041  
 Fumoto, T. SU092  
 Funase, Y. SA222  
 Furber, M. M120  
 Furukawa, M. F079, SA079, SU090, SU102, SU103  
 Furutani, J. F473, SA473  
 Furuya, Y. SU082
- G**
- Gabet, Y. 1121, 1298, M099, SU375  
 Gabriel, S. E. 1274  
 Gaddam, D. R. SU164  
 Gaddie, T. J. M487  
 Gaddy, D. 1234, F288, F523, M177, M412, SA086, SA288, SA523, SU162  
 Gaffen, S. F246, SA246, WG13  
 Gafni, A. M379, M380, SA359, SU351  
 Gafni, R. I. SA200  
 Gagari, E. SU145  
 Gagel, R. F. SA194  
 Gagnon, D. R. 1168  
 Gagnon, Z. E. M141  
 Gaillard, T. SU315  
 Gajic-Veljanoski, O. SU254, SU313  
 Galbavy, D. M261  
 Galesanu, C. M357, SU310  
 Galesanu, M. Romeo M357  
 Galindo, M. F572, SA572  
 Galisteo, C. SA357  
 Gallagher, H. M211  
 Gallagher, J. A. M120, M166, SU224, SU244  
 Gallant, M. A. SU095  
 Galley, M. 1178  
 Galli, C. 1038, SU047  
 Galli, G. M036, M092, SU050  
 Gallo, R. SA216  
 Gallo, S. 1108, SU487  
 Gallone, S. SA475  
 Galson, D. L. M079  
 Galvin, R. J. SU045  
 Gamble, G. F358, SA358  
 Gamer, L. SU145  
 Gammon, M. D. SU202  
 Gamse, R. 1173  
 Gan, B. M091  
 Gan, L. M176  
 Ganapathy, S. 1081  
 Gandolini, G. SU345, SU346  
 Ganguly, S. SU041  
 Ganz, M. SU463  
 Gao, G. M237, SU417  
 Gao, H. M238  
 Gao, K. M032  
 Gao, L. F186, SA186  
 Gao, N. F034, SA034  
 Gao, S. SA068  
 Garabedian, M. M246  
 Garcia, G. F376, SA376  
 Garcia, M. SU263  
 Garcia, P. M223, M417  
 Garcia, T. M272  
 Garcia-Giralt, N. M264, M265  
 García-Manrique, M. SU431  
 Gardella, T. M186  
 Gardella, T. J. F221, F224, SA221, SA224  
 Gardella, T. James F483, SA483  
 Gardinier, J. SA035  
 Gardner, B. M. M043, SU020  
 Gardner, M. J. M209, SU200  
 Gardsell, P. 1107  
 Garg, R. 1068, SU255  
 Garnero, P. SA295, SU228  
 Garrett, I. Ross 1136  
 Garrity, M. L. M209, SU200  
 Garrity, M. Louise SA302, SA303  
 Gartland, A. M120, SU224  
 Gary, L. C. 1024, SU321  
 Gasser, J. A. M409, SA193, SA292  
 Gaucher, C. M246  
 Gaudet, B. M210  
 Gaudin, A. F. SA415  
 Gaur, T. M041  
 Gaustad, D. SA143  
 Gauthier, J. Yves M127  
 Gaw, A. M120  
 Ge, C. SU025  
 Gebauer, M. 1006, 1201  
 Gedeberg, R. 1095, 1205, SA334  
 Gehlbach, S. SA362, SU344  
 Geiser, A. G. SU045  
 Gemar, D. SU425  
 Genant, H. M390, SA507, SA509, SU260, SU389  
 Genever, P. G. WG27  
 Geng, W. SA511  
 Gennari, L. F455, M320, SA455, SA475, SA481  
 Gensure, R. C. 1063, SU500  
 Gentili, C. M189  
 Geoffroy, V. F010, SA010  
 Gérard, B. SA258  
 Gerdhem, P. SU225  
 Gericke, A. SA140  
 Gerrits, H. M104  
 Gersch, R. P. 1192  
 Gerstenfeld, L. C. F038, M161, SA001, SA038, SU061  
 Gesty-Palmer, D. 1226  
 Geusens, P. 1060, 1237, SU390  
 Gevaert, K. SU215  
 Ghali, O. SU044  
 Ghasem, A. 1101  
 Ghazalpour, A. M247  
 Ghebranious, N. SU365  
 Ghio, L. SU371  
 Ghosh, A. 1129, M386, SU361  
 Ghosh-Choudhury, N. 1081, F002, SA002, SU096  
 Giampietro, P. SU365  
 Gianfrancesco, F. SA475  
 Giangregorio, L. M379, SA368, SU404  
 Giannobile, W. V. M051  
 Giardina, P. J. SA128  
 Giger, M. M314  
 Gigliotti, B. 1078  
 Gilbert, S. R. SU052  
 Gillespie, M. T. F195, M014, SA157, SA195, SU046  
 Gillett, M. J. 1289  
 Gilligan, J. M208  
 Gilsanz, V. 1105, 1180, M074, SU042, SU203  
 Gimeno, R. F006, SA006  
 Gindre, M. SA101  
 Giner, M. M101, SU009  
 Gineys, E. 1071  
 Gioe, T. J. SU266  
 Gioia, R. F500, SA500  
 Girasole, G. 1245, SU348  
 Giusti, A. 1245, SU348  
 Giwerzman, A. SA457, SU335  
 Glant, T. SU460  
 Glantschnig, H. 1214  
 Glaser, D. L. F044, SA044  
 Glass, R. SA370

(Key: 1001-1300 = Oral, F = Friday Plenary poster, SA = Saturday poster, SU = Sunday poster, M = Monday poster, WG = Working Group Abstract)

## ASBMR 30th Annual Meeting

## Author Index

Gleeson, T.	M370, WG15	Goto, H.	M111	Griffiths, A.	1271	<b>H</b>	
Glendenning, P.	1289	Goto, T.	M081	Grigoriadis, A. E.	1233	Ha, H.	SU108
Glimcher, M. J.	SA102	Götzen, N.	M454	Grima, D.	SA414, SA423	Ha, J.	SU086
Globus, R. K.	M469, SA517	Gourlay, M.	F426, SA426	Grimes, J.	M354	Ha, M.	M128
Glorieux, F. H.	SU483, SU497, WG23	Gouveia, C. Helena A.	F244, M228, SA123, SA244	Grimston, S.	1257	Ha, S.	SU014
Glover, S. J.	M507	Gouveia, V. C. N.	SU449	Grimston, S. K.	1110	Habermann, B.	SA392
Glowacki, J.	M453, SA048, SA237, SU138, SU400	Govoni, K.	M009	Grinberg, D.	M264, M265	Habersetzer, F.	F488, SA488
Glüer, C. C.	SA445, SU270	Govoni, K. E.	SA180, SU018	Grisanti, M.	1139, 1211, 1213, F394, SA394	Hachulla, E.	SA466
Gluhak-Heinrich, J.	M103	Gozzini, A.	M092	Griswold, R. D.	1125	Hackfort, B. T.	F550, M020, SA459, SA550
Go, C.	SU464	Grabenstaetter, T.	SU036	Grodzki, A.	M382	Hadaya, K.	SU168
Go, M.	M260	Grabowska, U.	F433, SA433	Grogg, J. D.	M423	Haddad, N.	SU486, WG19
Goad, M.	SU146, SU149	Gracioli, F. G.	SU447, SU449	Grol, M. W.	M065	Haddad, O.	SA065
Gober, H. Jurgen	F074, SA074	Gracious, B. L.	SA556	Gromov, K.	M236	Hadji, P.	M283, M384, WG14
Goda, S.	M094, SA147	Grady, R. W.	SA128	Gronowicz, G. A.	SU209	Hadjiargyrou, M.	1192, SA124
Godbout, A.	M197	Graell, E.	SA357	Gronthos, S.	SU079, SU080	Hafell, B.	SA137
Godfrey, K.	F544, SA544	Graf, D.	SU148	Groppe, J.	M243	Hagan, M.	SA502
Goehrig, D.	SU228	Graf, J. Daniel	SU168	Grosbois, B.	SA466	Hagelstein, C.	SA303
Goellner, J.	1247, F024, SA024	Graham, D. Bartholomew	F176, SA176	Gross, C.	SU402	Hagerty, S. E.	M269
Goellner, J. J.	1038	Graham, S.	M338	Gross, G. J.	SA505	Hagiwara, F.	SU451
Goemaere, S.	SU302, SU477	Gram, J.	M123	Gross, T. S.	1253, SA462, SA515	Hagiwara, H.	M081
Goh, J. Cho Hong	SU236	Gramoun, A.	SU069	Grossi, E.	SU345, SU346	Hagiwara, K.	M081
Gold, D.	M373, SA418, SU414	Grand-Lenoir, C.	M308	Grosskopf, B.	SA132	Hahn, C. W.	1102
Gold, D. T.	M372, M400, SA395, SA417	Grandchamp, B.	SA258	Gruetznier, T. M.	M296	Hajibeigi, A.	SA211
Goldberg, L.	SU209	Grande, J.	M220	Grünheid, T.	SA110	Häkansson, C.	1123
Goldberg, V. M.	SA177	Grande, J. P.	SA055	Grynepas, M.	SU213	Hakozaki, A.	F079, SA079, SU103
Goldsmith, D. J. A.	WG30	Grandgeorge, Y.	M381	Grynepas, M. D.	M176, M461, SU465, SU470	Halakatti, R.	M412, SA285
Goldstein, A.	SU246	Granero-Molto, F.	F444, SA169, SA444	Grynepas, M. Daniel	SU373	Halén, M.	M117
Goldstein, R.	M273	Granhölm, S.	M117	Gu, J.	M237	Haley, R. Lynn	SU182
Goldstein, S. A.	1299, F500, M462, SA252, SA500, SU480	Grano, A.	SU094	Gu, S.	1266	Haliga, R.	SU310
Goldswain, P.	1289	Grano, M.	SA199	Guadalix, S.	M221, SA503	Hall, S. L.	M233
Goltzman, D.	1056, F069, F358, M199, M213, M214, SA069, SA121, SA358, SA364, SU292, SU309, SU351, SU357	Grant, D.	1043	Guan, J.	M091	Halldórsson, B.	1091
Gomberg, B.	SA375	Grant, M.	M205	Guan, Y.	M079	Halleen, J. M.	M284, M286, M293, M295, M298, SA282, SA298
Gomberg, B. R.	1020, SA314	Grant, R.	SU483, WG23	Guanabens, N.	M442, SA030	Halleux, C.	1037, M106, SU036
Gomes, Jr, R. R.	SA269	Grappiolo, I.	SU269	Guarente, L.	1098, 1251	Hallgrímsson, B.	SA547
Gómez, A.	SA357	Grasemann, C.	SU491, SU503	Guarnieri, V.	M201, M432, SU210	Halloran, B.	1076
Gómez-Barrena, E.	M195, SA223	Grasser, W.	SU048	Gudmundsdottir, S. Lara	SA374	Halloran, B. P.	1077, 1252, 1255, M096
Gomez-Marin, O.	M402	Gratacós, J.	SA357, SU431	Gudnason, V.	1094, 1096, F369, SA369, SU289	Halton, J.	SU483, WG23
Gonçalves, M. D. C.	SA212	Gratton, M.	M214	Guelcher, S. A.	M280	Halvorsen, B.	SU167
Gonçalves, P. Tatiana	M427	Grauer, A.	SA314	Guerra, G.	M427	Hämäläinen, E.	SU422
Gong, A. J.	1252	Gravallese, E. M.	SA370, WG41	Guerrero, L.	M426	Hamamoto, H.	F494, SA494
Gonnelli, S.	M320	Gravenmaker, K.	M458	Guevarra, M. N.	SU502	Hamanishi, C.	SA450
Gonzales Chaves, M. M. S.	M288, SA377	Graves, D.	SA001	Gugala, Z.	SU051	Hamaya, E.	M385
Gonzalez, B.	SA030	Graves, L.	SA502	Guglielmi, G.	SU210	Hambli, R.	M172
González, D.	SU430	Grbic, J.	1246	Guia, C. M.	SA311	Hamdani, G.	M085
Gonzalez, F.	1148	Greasley, P.	1221	Guiglia, G.	M106	Hamdy, R. C.	SA159
Gonzalez-Bofill, N.	SU221	Greco, G.	SA199, SU094	Guignandon, A.	1061, SA011, SA142	Hamidi, Z.	SU339
Gonzalez-Casaús, M. L.	SA496	Greeley, P.	1020	Guise, T. F190, M283, SA018, SA190		Hamidouche, Z.	M048
González-Macías, J.	M223	Green, A. G.	M230	Guise, T. A.	1085, 1090, F272, F275, M277, M305, SA172, SA272, SA273, SA274, SA275	Hamilton, D.	M030
Gooding, L. M.	1160	Green, C. B.	1073	Gulberg, R. E.	M164	Hamilton, J.	M404, SA267
Goodship, A.	M478	Green, D.	SU473	Gullestad, L.	SU167	Hampson, D. R.	M202
Goodyer, C. Gates	SU128	Green, V. J.	SU244	Gulyaeva, S. Sergeevna	M192	Hampson, G.	SU174, WG30
Gooi, J.	M155	Greenbaum, C.	F306, SA306	Gumez, L.	M133	Hampton, R.	1214
Gooi, J. H.	F195, SA195, SU046	Greenberg, D.	M480	Gundberg, C.	1017	Hamrick, M.	1148, F452, M132, M173, SA441, SA452, SU010, SU153, SU164
Gopalakrishnan, R.	1008, SU027	Greenfield, D. M.	SU369	Gundberg, C. M.	M146	Hamrick, M. W.	M468, SU318
Gorai, I.	M387	Greenfield, E. M.	SA177	Günther, C.	SA408	Han, B.	M207
Gordish-Dressman, H.	F122, SA122	Greenspan, S. L.	1020, M306, SA314, SA360, SA362, SU259, SU482	Guo, E.	SU280	Han, H.	SA489
Gordon, C.	SU367	Greenwald, M.	F306, SA306	Guo, F.	1048	Han, J.	M152, SU407
Gordon, C. L.	SA268, SU299, SU300	Greep, N.	F333, M285, SA333	Guo, J.	F215, M213, SA215	Han, K.	M340
Gordon, C. M.	SA559, SA564, SU488, WG22	Greer, P. A.	M150	Guo, L.	SA236	Han, L.	1099, 1247, F024, M010, SA024, SA185, SU189, SU380
Gordon, J. A. R.	SU019	Greeves, J. P.	M481, SU473	Guo, R.	1113	Han, M.	M251
Gori, F.	M039, SU121	Gregoire, B. R.	M238	Guo, T. Zhi	F461, SA461	Han, S.	SA146, SA390
Gorski, J. P.	F066, M053, SA066, SA070	Gregory, J. S.	M317	Guo, X. Edward	M312	Hancock, M. L.	1292
Gortazar, A. R.	M108	Gregson, C. L.	SA257	Guo, X. E.	SU277, SU481	Handelsman, D. J.	1224
Goseki-Sone, M.	SU308	Gremlich, H.	SU379	Guo, Y.	M404, SA267, SU331	Haney, E.	F351, SA351
Gossec, L.	M316	Grethen, E. R.	SA239	Gupta, C. E.	SA239	Hangartner, T. N.	M343
Gossen, J. A.	M104	Grewal, J. S.	SU130	Gupta, V.	SU156	Hankenson, K. D.	1203, 1249, M058, SU063
Gossiel, F.	F301, M507, SA301, SU369	Grey, A. B.	SU071	Gusev, E.	SU115	Hanley, D. A.	SU357, 1056, SA331, SA364, SA504, SU283, SU292, SU309, SU351
Gössl, M.	M083	Grey, R. D.	SU041	Gustafsson, J.	F085, SA085		
		Grgurevic, L.	SU141, SU142	Gutierrez, G. E.	1300, SU378		
		Gridley, T.	1268	Gutierrez, S. E.	SU062		
		Griffin, R. J.	M412, SA285	Gwilliam, R.	SA263		
		Griffin, T. L.	M282	Gyau, S.	1173		
		Griffith, J. F.	SA309	Gyneys, E.	M460		
		Griffith, L.	SU005				

(Key: 1001-1300 = Oral, F = Friday Plenary poster, SA = Saturday poster, SU = Sunday poster, M = Monday poster, WG = Working Group Abstract)



## Author Index

## ASBMR 30th Annual Meeting

Hannan, M. T.	1168, 1207, 1283, M397, SU319	Hawse, J. R.	M024, M037, M052, M133, SA065	Hetzer, N.	SU281	Hojo, H.	M082
Hannon, R. Anne	F301, SA301	Haÿ, E.	M007, M048, SU243	Hewer, T.	F361, SA361	Holets, M. F.	SU238, M215, M216, SU426, SU482
Hannon, R. A.	SU369	Hayakawa, N.	M443, SU031, SU170	Hewison, M.	F240, SA240	Holladay, B.	1041
Hannula, M.	SA533, WG10	Hayashi, K.	M098, SA230	Heyer, D.	SA556	Hollinger, J. O.	F376, SA376
Hans, D.	M308, SA322	Hayata, T.	M026, M044, M174, M175, M446, SU007	Hiasa, M.	SA294, SU242	Hollis, B.	M366
Hansen, K. E.	1131	Haycock, J. W.	SA067	Hickman, R. M.	M490, SA519	Holmberg, A. H.	1279, SU219
Hansma, P. Kenneth	SU467	Haykowsky, M. J.	F552, SA552	Hickok, N. J.	M169	Holmgren, J.	F435, SA435
Hanson, N. A.	F098, SA098, SU158	Haynes, D. R.	M046	Hicks, G. E.	SU073	Holmyard, D.	SU213, SU465
Hanwell, H. E. C.	SU206	He, J.	M237	Hideshima, T.	1231, SU239	Holzmann, P.	SU462
Hanyu, R.	SA378	He, Q.	SA248	Higgins, L.	F275, M335, SA275	Homma, S.	1034, M434
Hao, Y.	M032	He, X.	1014	Higgins, P. B.	M494	Hong, H.	SA505
Haque, T.	SA159	Head, R.	1269	Higgs, K.	SA304	Hong, J.	M128, M260, SU226
Hara, T.	M443	Healy, M.	M294, SU274	Hikasa, T.	SA162	Hong, J. Min	M256
Harada, A.	SU466	Heaney, R.	M022	Hikata, T.	F079, SA079, SU103	Hong, S.	M062, M364
Harada, N.	SU443	Hebel, J. Richard	SU073	Hill, C.	SA417	Hong, S. H. H.	M042
Haralam, M.	SU482	Hebel, R.	F345, SA345, SA346	Hill, K. M.	SA545, SA553, SU395	Hong, S. Mo	SA489
Hardouin, P.	SA015, SU044	Hedge, A. M.	F205, F207, F210, SA205, SA207, SA210	Hill, W.	SU153	Hong, X.	F546, SA546
Hare, M.	M496	Heer, M.	SA446	Hille, E. L.	M423	Hongo, M.	SU454
Harland, R. M.	1075	Heeren, J.	SA042	Hillier, T.	1057, F351, SA351	Honjo, T.	1268
Harmon, B.	F122, SA122	Heersche, J. N. M.	SU106	Hillier, T. A.	1022, 1055	Honsawek, S.	M406
Harnish, D.	F439, SA439	Hefferan, T. E.	1258, SA143	Hillman, L.	SU217	Hood, B.	SU014
Harper, K.	M386	Heft, R.	1054, F107, SA107	Hilton, D.	SA517	Hooshmand, S.	M301, SU002, SU273
Harrington, J. J.	F004, SA004	Hegedus, E.	SU411	Hilton, M. J.	1268	Hooven, F.	SA362, SU342
Harris, J. A. K.	M494	Hegge, O.	SA568	Himeno, M.	SU316	Hoover, D.	M354
Harris, M.	F091, SA091, SA532	Heickendorff, L.	M206	Himeno, Y.	SU437	Hopman, W. M.	SU351
Harris, M. A.	1114, M103, SA060	Heidari, P.	SU001	Hinkle, R.	1005	Hoppé, E.	M297, SA400
Harris, S.	1042, 1158	Heine-Geldern, A.	SA143	Hinoi, E.	F034, SA034	Horne, A. N.	M317
Harris, S. E.	1081, 1114, M056, M103, SA060	Heinegard, D.	SU089	Hiort, O.	F471, SA471	Horne, R.	M372, SA417, SU325, SU347
Harris, S. S.	SU305	Heinonen, A.	F420, M479, SA420, SA533, WG10	Hiraga, T.	M080, SU054	Horne, W. C.	1109
Harris, S. T.	M367, SU408	Heiss, C.	M290	Hirai, T.	F074, F114, SA074, SA114	Hornez, J.	SA015
Harris, T.	M397, SU289	Held, N.	SA472	Hirao, M.	F112, SA112	Horng, D.	M422
Harris, T. B.	1094, 1096, F369, SA369	Hellmich, M.	1172	Hirasawa, H.	SA448	Hornig, S. C.	M194
Harris, Z. L.	F557, SA557	Helms, J. A.	M105, SA531	Hirata, M.	1187, M167, SU187	Horowitz, M.	F265, M003, M145, SA265, SU104
Harrison, A.	SU266	Helvig, C.	SU178, SU448	Hirbe, A.	1086	Horowitz, Z.	SU405
Harrison, J. R.	M097, SA235, SU057	Hemmelmann, C.	SU456	Hirde, J.	SA368	Horton, B.	SU473
Harrison, L.	SA533, WG10	Hemmi, H.	M026, M174, M175, SA378	Hiremath, M.	F219, SA219	Horton, J. A.	SU161
Harrison, S.	M285	Hempel, U.	M070	Hirota, K.	SU314	Hortopan, D.	SU246
Harrison, S. Litwack	1278	Henao, M. P.	SA209, SU169	Hirota, T.	SU314	Hortschansky, P.	SU085
Harslöf, T.	SU220	Henderson, J. E.	1218, F131, SA131, SU374	Hirotsu, M.	SU229, SU241	Horvath, S.	M247
Hart, A. J.	F293, SA293	Hendy, G.	M214	Hiruma, Y.	1186, F081, F476, F478, SA081, SA289, SA476, SA478, SU070	Hoshinaga, K.	SA499
Hart, C. E.	1137, F376, SA376	Hendy, G. N.	M201, M187, M197, M199, M205	Hisa, I.	SA484	Hoshino, Y.	SU117
Hart, D.	SA263	Henneicke, H.	M100	Hisanori, N.	SU451	Hosking, D.	SU473
Hartl, F.	F403, M363, SA403	Hennings, L.	SA285	Hitchcock, C. L.	M325	Hoskins, N. J.	F135, SA135
Hartmann, A.	SA466	Henriksen, D. B.	M399	Ho, H.	SU133	Hosoi, T.	SU308
Hartmann, B.	M399	Henriksen, K.	M122, M123, M124, M129, SU091, SU125	Ho, P. W. M.	SA157	Hosoya, A.	SU054
Hartmann, L.	SU036	Henry, A. C.	M485, WG36	Hoak, D.	SU133	Hotton, D.	SA150
Hartzell, D. L.	SU164	Henry-Desailly, I.	SA487	Hochberg, M.	F345, SA345, SA432, SU417, WG5	Hou, S.	SU160
Haruna, Y.	F548, M492, SA548	Henschkowski, J.	1242, SU363, SU423	Hock, J.	1127, SA346, SU073, SU397	Hou, W.	1044
Harvey, N.	F544, SA544	Heo, S.	SU022	Hocking, L. J.	M495, SA068	Houde, N.	SU078
Harvey, R. L.	SU364	Heraud, A.	M308	Hodgkiss, T.	WG29	Hough, T.	1269
Hasegawa, H.	SA222	Héraud, C.	1271	Hodsman, A.	F358, M210, SA358, SA359	Houlihan, M. J.	SA125
Hasegawa, U.	M121	Hermanns, P.	F118, SA118	Hoeck, H. C.	M350	Houlihan, M. Jean	F260, SA260
Hashimoto, J.	F112, SA112	Hernandez, C. J.	SA512	Hoeck, H. Chr	SU434	Houston, B.	M284
Hashimoto, T.	SA294	Hernández, I.	F286, F291, SA286, SA291	Hoemann, C. D.	M140	Hovi, P.	1103
Hashimoto, Y.	SU137	Hernández, J. Luis	M223	Hoenderop, J. G. J.	SA355	Howard, G. C.	SU041
Hashizume, E.	SU307	Hernandez, M.	F435, SA076, SA435	Hoenig, H.	SU411	Howard, K.	SU015
Hashmi, R. U.	SA352	Herndon, D. N.	SA571	Hoepfner, L. H.	1258	Howenstine, M.	SU486, WG19
Hassan, M. Q.	1272, M090, SU019	Herold, D. A.	M282	Hofbauer, L. C.	1285, M070, M271, M415	Hoylaerts, M. F.	M142, SA061, SA063
Hassett, S. M.	M423	Herreros, F.	SA472	Hoff, J.	M415	Hozumi, A.	M111, SA078
Hata, K.	1045, 1265, SA095	Herrick, J.	SA143	Hoffman, A.	1277, 1278, SU284	Hrovat, M. I.	SA102
Hatamura, I.	M185	Herrmann, M.	M100, M417	Hoffman, A. R.	F335, M266, M268, SA268, SA335	Hruska, K. A.	SU450, WG12
Hatori, M.	SA245	Herrmann, W.	M417	Hoffman, E.	F122, SA122	Hsiao, B.	SA124
Hattori, T.	M153	Hershey, J. C.	M136	Hoffman, S. J.	SU372	Hsiao, E.	1076, F127, SA127
Hattisuturi, S.	M387	Hershman, D. L.	SU202	Hoffmann, O.	M130	Hsu, Y.	1091, F546, M254, SA546
Haug, E.	SU204	Herzog, H.	1195	Hoffmann, P. F.	1165, F321, SA321	Hsu, Y. H.	1092, SA120, SA251
Hauge, E. M.	F310, SA310	Hess, P.	M457	Hofman, A.	SA263, SU188, SU317	Hu, J. C.	1264
Haugen, H.	SA137	Hesse, E.	1004, 1109	Hogan, E. A.	SA453	Hu, W.	M237
Haug, D.	1185			Hogan, H. A.	SA521	Hu, Y.	M237
Havill, L. M.	M241, M494			Hogue, W. R.	1234	Huang, C.	SU181
Hawa, G.	M134, SA300			Hoiseth, A.	SU356	Huang, D.	M045
Hawker, G. A.	F339, M324, M401, SA339, SA558, SU271, SU293, SU341, WG8			Højbjørre, L.	SA456	Huang, D. C.	M334
Hawkes, W.	F345, SA345, SA346, SU073					Huang, D. Chao	F213, SA213, SU207
Hawkins, F.	M221, SA503					Huang, E.	1083
						Huang, H.	SA033, SA177
						Huang, J.	1113

(Key: 1001-1300 = Oral, F = Friday Plenary poster, SA = Saturday poster, SU = Sunday poster, M = Monday poster, WG = Working Group Abstract)



## Author Index

## ASBMR 30th Annual Meeting

Joseph, F.	M289, M291	Kanatani, N.	1151	Katzenbeisser, J.	1215	Khaw, K. Tee	1240, F363, SA363
Joseph, L.	SA364	Kanayama, D.	SA021	Kaufman, B.	SA539	Khosla, S.	1165, 1167, 1179, 1284,
Joshi, A. A.	M291	Kanazawa, I.	SA230	Kaufman, J.	SU302, SU477		F029, M017, M078, M083,
Joshi, R. N.	M501	Kanda, J.	SU383	Kaufmann, M.	M231, SU199		SA029, SU267
Joshi, S.	F246, SA246, WG13	Kandel, R. A.	M176, SU131	Kavanagh, K. L.	F407, SA407	Kida, Y.	SA382
Josse, R.	SA364, SU292	Kane, R. L.	F416, M378, SA416,	Kavvoura, F.	1091	Kido, S. 1248, SA294, SU242, SU316	
Josse, R. G.	1056, SU336, SU351,		WG18	Kaw, M.	F091, SA091	Kiehintopf, M.	SU456
	SU357	Kaneko, H.	SU090	Kawabe, Y.	F483, SA483	Kiel, D.	1091
Jost, B.	SA193	Kaneko, I.	F473, SA473	Kawaguchi, H.	1013, 1187, 1228,	Kiel, D. P.	1092, 1168, 1207, 1242,
Josten, C.	SU415	Kang, B.	M095, SU010, SU026		F116, M082, SA116, SU334		1283, F341, M249, M254, M397,
Ju, J.	SU077	Kang, D.	M339	Kawahara, I.	SU098		SA120, SA251, SA341, SU319,
Juárez, P.	F190, SA190	Kang, H.	SU181	Kawai, M.	1073, M003		SU326
Judex, S.	1293, F047, M342, M486,	Kang, M.	SU407	Kawai, S.	M006, M144	Kiiskilä, E.	SA232
	SA047, SU377, SU475	Kang, Y.	M340	Kawamata, A.	SA105, SU007	Kilappa, V.	M319
Jules, J.	1118	Kanis, J. & the National Osteoporosis	1290	Kawamata, R.	SA379	Kilgore, M.	SA326, SU256, SU321
Jung, B.	M256	Guideline Group		Kawamoto, A.	M094, SA147	Kilgore, M. L.	1024
Jung, D.	F034, M152, SA034	Kanis, J. A.	1023, SU257, SU264	Kawamoto, K.	SA028	Killinger, Z.	SU261
Jung, H.	M392, M393	Kann, P.	SU177	Kawamoto, T.	M326	Kim, B.	1101, M407, SA036
Jung, J.	M128	Kannus, P.	SA338, SA533, WG10	Kawamura, N.	1187	Kim, B. G.	M015, SA009
Jung, J. Yeon	SA043	Kanoff, S.	M505	Kawana, H.	F087, SA087	Kim, C.	SU359
Jung, W.	SA442	Kanomata, K.	SA161	Kawanabe, N.	SA173	Kim, C. H.	M015, SA009
Jung, Y.	SU214	Kanzaki, H.	1089	Kawano, T.	1116	Kim, D.M147, M148, SA046, SA117,	
Jungmann, R.	SU467	Kao, R. Shih-Hsuan	M040	Kawano, Y.	M054		SA412
Junno, J. Antti	M459	Kapila, Y.	1159	Kawasaki, I.	SU314	Kim, D. Hee	F391, SA391
Jüppner, H.	1052, F471, M186,	Kapinas, K.	1155, M270	Kawasaki, Y.	1013, 1187	Kim, E.	SA036, SA431
	SA204, SA225, SA259, SA471	Kaplan, F. S.	1203, F044, M243,	Kawashima, Y.M440, SA183, SA184,		Kim, G.	M260, SA016, SU407
			SA044		SU190	Kim, G. S.	SU304
Jurado, S.	M264, M265	Kaplanoglou, T.	SU472	Kawato, T.	M012	Kim, G. Su	M256
Jurdic, P.	SA142	Kapner, A.	SA408	Kawato, Y.	F112, SA112	Kim, H.	1119, M128, M251, M258,
Jutberger, H.	SU349	Kappil, M.	SU202	Kawawaki, J.	SU101		M260, M392, M393, M407,
		Kaprio, J.	F420, SA420	Kawelke, N.	SA151		SA189, SA189, SA189, SU043,
		Kaptoge, S.	1240	Kazarian, T.	M234, SU386		SU077, SU086, SU108, SU135,
		Kaptoge, S. K.	M315, SU275	Kazi, N.	M403		SU135, SU214, SU407, SU416
		Karaplis, A. C.	1016, F069, SA069,	Ke, H.	M208	Kim, H. K.	SU304
			SA121	Ke, H. Z.	1138, 1139	Kim, H. Lae	M256
		Karasik, D.	1091, 1092, M249, M254,	Ke, H. Zhu	1211, 1213, F394, SA394	Kim, H. Young	SU304
			SA120, SA251, WG2	Ke, Y.	M237	Kim, I.	SA045
		Karkare, N.	M344, M471, SU205	Keaveny, T.	1167	Kim, J.	1074, 1190, 1194, F008,
		Karlsson, M.	SU349	Keaveny, T. M.	1165, F321, M413,		M163, M163, M258, M339,
		Karlsson, M. K.	1107, 1166, 1279,		SA321, SA509, SA512		SA008, SA036, SA100, SA431,
			SU183, SU219, SU262, SU459	Keightley, J. A.	SA070		SU022, SU055, SU178, SU359,
		Karlsson, S.	1079	Keller, B.	F158, SA158		SU448
		Karmakar, S.	WG4	Keller, H.	1037, 1039, F054, SA054	Kim, J. K.	F034, SA034
		Karmali, R.	SU016	Keller, J. H.	SA192	Kim, K.	1215, M152, M351, 1182
		Karnik, K.	SA456	Kellum, E.	M173	Kim, M.	M208, SA561, SU407
		Karperien, M.	SA130	Kelly, M. H.	SA200	Kim, S.	F008, M086, M086, M128,
		Karras, D.	SU412, SU413	Kelly, O. J.	SU311, SU059, SU418		M152, M251, M260, M339,
		Karsdal, M. A.	M122, M123, M124,	Kelton, C. M. L.	M371		M339, M364, SA008, SA046,
			M129, M155, M398, SA129,	Kemi, V.	SU433		SA046, SA431, SA442, SU214,
			SA436, SU091, SU125, SU361,	Kenan, Y.	SA397		SU226, SU291, SU359, SU452
			SU463	Kendler, D.	1027, SU405	Kim, S. Wan	F391, SA043, SA391
		Karsenty, G.	F034, F168, M069,	Kendler, D. L.	M395	Kim, S. Yeon	F391, M256, SA391
			SA034, SA168, SA255, SA463,	Kennedy, C. C.	SU341, SU351,	Kim, T.	M128, M260, M392, M393,
			SU119		SU404		SU226
		Kasahara, H.	SA222	Kenny, A.	M353	Kim, T. Ho Kim	M256
		Kashemirov, B. A.	1065	Kent, T.	F557, SA557	Kim, U.	M251
		Kashima, I.	SA379	Kentenich, M.	F317, SA317	Kim, Y.M163, M260, SA045, SA390,	
		Kashima, T.	1233	Kenyon Pesce, L.	M353		SA431, SU035, SU043, SU059,
		Kashiwagi, A.	M150	Kerckhofs, G.	SA387		SU359
		Kassem, M.	1007, 1147, M047,	Kerkeni, S.	M316	Kim, Y. Jung	M256
			SA042	Kerstetter, J.	M330, M353	Kim-Weroha, N. A.	1041
		Kasten, A.	SA528	Kerzberg, E.	SU405	Kimlin, M. G.	M225, M226
		Kastner, M.	SU343	Kesavan, C.	1142	Kimmel, D.	1214, SA072
		Kasukawa, Y.	M219, SA214, SU454	Kessler, C. B.	1155, M270	Kimmel, D. B.	F508, SA508, SA073
		Katae, Y.	SA448	Kessler, S.	1134	Kimura, A.	M087
		Katagiri, T.	SA161	Ketonis, C.	M169	Kimura, T.	F079, SA079
		Katayanagi, E.	SU383	Key, L. L.	M366	Kindblom, J.	SA198
		Katikaneni, R.	1063	Key, L. Lyndon	SA173	Kindblom, J. M.	SU459
		Kato, H.	M113	Keyak, J.	F396, SA396	Kindmark, A.	M232, SA247, SA264,
		Kato, K.	SU438, SU440	Keyak, J. H.	M349		SU219
		Kato, S.1012, 1115, 1122, 1126, 1182,		Khaled, A.	M489	King, B. L.	M244
			F074, SA074, SU186	Khalid, O.	M099	King, W.	SU492
		Katono, T.	M012	Khamessan, A.	1108, SU487	Kingery, W. S.	SU032, SU033, SU160
		Katschnig, C.	F327, SA327	Khan, A. A.	SU131	Kingery, W. Steven	F461, SA461
		Katsimbri, P.	SU472	Khan, F.	SU130	Kingsley, L.	F272, F275, SA272,
		Kattappuram, R. Simon	F260, SA260,	Khan, K. M.	SU362		SA275
			SA125	Kharebov, A.	SU178, SU448	Kingsley, L. A.	1085, 1274
		Katz, J. N.	M358	Kharode, Y. P.	F439, SA439	Kingwell, E. J.	M325
		Katz, L. D.	SA254	Khatib, A.	SU157	Kirby, B. J.	SA194

(Key: 1001-1300 = Oral, F = Friday Plenary poster, SA = Saturday poster, SU = Sunday poster, M = Monday poster, WG = Working Group Abstract)

## ASBMR 30th Annual Meeting

## Author Index

Kirby, J. T.	M505, SU282	Kolesnikova, G. Sergeevna	M192	Krueger, D.	SA443, SA535, SU258, SU425, SU427	<b>L</b>	
Kirimoto, H.	SA513	Koller, D. L.	M253., SA261	Krug, R.	F317, M072, SA317	L'Abbe, M.	1108, SU487
Kirkland, S.	SU292	Kolta, S.	1130, 1241, M313, M316, SU471	Krum, S. A.	SU180	La Croix, A.	SA410
Kirkwood, K. L.	SU013	Komarov, S. V.	SU115	Kruse, H.	SA425	La Vallee, T.	F272, SA272
Kirmani, S.	1179	Komasa, Y.	M094, SA147	Krust, A.	1123, 1181	Labrie, F.	1279, SU183
Kirmizitas, A.	1192	Komatsu, D. E.	M207	Ksiopolska-Orowska, K.	M382	Labrinidis, A.	SU079
Kirn-Safran, C. B.	SA133	Komiya, S.	SU229, SU241	Ku, C.	M351	Lacativa, P. G. S.	SA212
Kiserud, T.	M497	Komiyama, Y.	M082, M089	Kubek, D. J.	SU388	Lacey, T.	SA350
Kishimoto, H.	M385	Komm, B.	SA385	Kuboki, T.	SA162	LaCroix, A.	1068, 1288, F333, F383, M285, SA360, SA333, SA362, SA383
Kishimoto, M.	SU316	Komori, T.	1151	Kueffner, R.	M075	Lafage-Proust, M.	1061, 1191, SA142
Kissel, J.	SU492	Konda, R.	SU438, SU440	Kugimiya, F.	1187	Lafforgue, P.	M381
Kitada, K.	SA513	Kondo, H.	M469	Kuhn, G.	1294	LaFleur, J.	SU332, SU398
Kitahara, K.	M421	Kondo, T.	SU083, SU245	Kuhn, V.	M489	Lagerholm, S.	M463
Kitaori, T.	SU136	Kondoh, S.	1122	Kuhstoss, S.	SU239	Lagerquist, M. K.	1123, SU179
Kitaura, H.	M112, SA166, SU152	Kondou, S.	SU186	Kuipers, A. L.	SA268	Lah, T.	SA075
Kitazawa, R.	SU083, SU245	Kong, L.	1048	Kujala, U. M.	F420, SA420	Lahiji, P.	1234
Kitazawa, S.	SU083, SU245	Konishi, M.	M449, SU285, SU301	Kukkonen-Harjula, K.	SA338	Lai, C.	1083, F109, SA109
Kitchner, T.	SU365	Kontulainen, S.	SU278, SU279	Kukreja, S. C.	SA352	Lai, M.	SA437
Kittaka, A.	M216	Kopan, R.	1268	Kukuljan, S.	1244	Lai, Y.	1114, M165, SA134
Kiviranta, R.	1109	Kopperdahl, D.	1167, F321, SA321, SA509	Kula, K.	SA457, SU335	Laing, E. M.	M468, SU318
Kivitz, A.	M394	Korach, K.	SA211	Kuliwaba, J. S.	SA148	Laitinen, E. Kalevi A.	SU433
Klatte, T. Orla	1134	Korbonits, M.	SU037	Kulkarni, A. B.	1079	Lakshmanan, M.	SA421
Klause, U.	SA295	Korchynskiy, O.	1080	Kulp, G.	SA571	Lam, M.	SU271
Klaushofer, K.	F217, SA217	Kordalis, N.	SU472	Kumagai, K.	SA039, SA467, SU005	Lamberg-Allardt, C.	SU433
Kleerekoper, M.	1020	Koretzky, G.	1010	Kumanduri, V.	SA263	Lambert, E. V.	SU490
Klein, G. L.	SA571	Korstanje, R.	1276	Kumar, R.	M198, M220, SA055, SA059, SU176	Lamghari, M.	SU011
Klein-Hitpass, L.	M047, M075	Kosaki, N.	SA022	Kumar, S.	1174, SU238, SU372	Lamm, M. L. G.	SA284
Kleis Møller, M.	M350	Koshimizu, T.	SA119	Kumar, U.	M205	Lamothe, K.	F041, SA041, SU099
Klemes, A.	SA402, SU403	Koskenvuo, M.	F420, SA420	Kummer, T.	M454	Lamy, O.	SU294, SU296
Klene, F.	1178	Kostenuik, P.	1072, 1139, 1211, 1213, 1216, M076	Kung, A.	SU295	Lancaster, J. L.	F376, SA376
Kleppinger, A.	M353	Kotadiya, P.	SU067	Kung, A. W. C.	1270	Landais, P.	SU327, SU328
Klickstein, L.	1173	Kotha, S. P.	1041	Kung, A. Wai Chee	F312, SA312, SU264	Landemaine, T.	M272
Klodowski, A.	M479	Kotsioprifitis, M.	SA159	Kunigami, T.	F074, SA074	Landis, B.	SA169
Kluin-Nelemans, J. C.	SU268	Kotton, D. N.	F038, SA038, SU061	Kuno, M.	SU100, SU101	Landoll, J.	SU492
Kneissel, M.1037, 1039, F054, M106, SA054, SU036, SU379		Kouda, K.	SA330	Kuntz, J.	F488, SA488	Landy, H.	1054
Kneuer, R.	SU379	Kousteni, S.	1112, 1146	Kuo, L.	M056	Lane, B.	SU259
Knierim, D. A.	M020	Kovacs, C. S.	1056, M230, SA194	Kupisiewicz, K.	M287	Lane, J. M.	M344, M471, SU205
Knox, S.	M212	Kovanen, V.	F420, SA420	Kuribayashi, T.	SA490	Lane, N.	1100, F249, M107, SA249, SU338
Ko, J.	M152, M339	Koyama, E.	M151	Kurihara, N.	1186, F476, F478, SA289, SA476, SA478, SU070	Lane, T. F.	1197
Ko, S.	1136, M339	Kozai, Y.	SA379	Kurimoto, P.	M096	Lang, C.	M225
Ko, T.	F174, SA174	Krajisnik, T.	SA227	Kuriwaka, R.	1248	Lang, D. H.	M485, WG36
Kobayashi, E.	SU117	Krajnc-Franken, M. A. M.	M104	Kurland, E. S.	M270	Lang, T.	F396, SA396, SU284, SU289, SU338, SU405
Kobayashi, H.	M385	Kramer, I.	1037, 1039, F054, M106, SA054	Kuroda, T.	F548, M492, SA548	Lang, T. F.	1094, 1096, F369, M306, M349, M397, SA369
Kobayashi, M.	M035, M167, M274	Krapf, R.	M409	Kuroishi, M. Etsuko	SU453	Langdahl, B.	M350, SU220, SU221, SU223, SU412, SU413
Kobayashi, T.	1158, 1262, F114, M156, SA114, SA130	Krasnoperov, V.	SU046	Kuromaru, O.	F483, SA483	Lange, J.	SA404
Kobayashi, Y.	1012, M113, SU098	Krause, D.	M345, M347, SA399	Kurosawa, H.	M174, M421, SA378	Langenbach, G. E. J.	SA110
Kocjan, T.	SA300	Kream, B.	1114, 1148, SA235	Kurth, A. A.	SA392	Langman, C. B.	SU485
Kockeritz, L.	1121	Krebill, R.	SA502	Kusano, E.	M185	Langsetmo, L.	1056, SA364, SU309
Koczon-Jaremko, B.	1204	Krege, J.	1171, SA421	Kutahov, A.	SU412, SU413	Lankinen, P.	F458, SA458
Kodama, M.	SU285, SU301	Kreider, J.	F500, SA500, SU480	Kutilek, S.	1286	Lanske, B.	1154
Kodani, N.	SA165	Kreiger, N.	1056, M325, SA364, SU292	Kuwabara, A.	SU316	Lanyon, L.	1296, SA526
Koedam, M.	SA355	Kremer, R.	1016, 1185, F213, M214, M334, SA213, SU203, SU207	Kuwahara, S.	F473, SA473	Lanzer, G.	F327, SA327
Koehler, S.	SA540	Kremke, B.	F471, SA471	Kuziez, M.	SU112	Lapauw, B.	SU302, SU477
Koepf, R.	M450, WG21	Krieger, N.	F358, SA358, SU309	Kuznetsova, N. V.	SA252, SA146	Laperre, K.	1153
Koga, T.	F083, SA083	Krieger, N. S.	M021	Kvern, B.	SA359	Lapierre, D. M.	SU105
Koh, A.	1159, F270, SA270	Kriegman, A.	M365	Kvetnansky, R.	M059	Lapointe, R. W.	SU176
Koh, A. J.	1264, M181	Krishnan, V.	SU377	Kwaasi, A.	F407, SA407	Lappalainen, S.	1176
Koh, G.	SU035	Krishnankutty, A.	SA304	Kwag, J. H.	M015, SA009	Lappe, J.	1105, M022, M310, SU333
Koh, J.	M260, SU035	Kristensen, E.	SA547	Kwak, H.	M340, SU108	Larche, M.	SA343, SU251, SU504
Koh, J. M.	SU304	Kristo, C.	M049	Kwan Tat, S.	M018, SU003	Larijani, B.	SU339
Koh, J. Min	M256	Krizko, M.	SU261	Kwon, D.	SU055	Laroche, N.	1191, M488, SA011, WG9
Kohara, H.	M112, SA166, SU152	Kroenke, G.	1215	Kwon, E.	SA189	Larrosa, M.	SA357, SU431
Kohavi, D.	1298	Kröger, H.	SU433	Kwon, I.	SA189, SU135, SU416	Larson, C. M.	M487
Kohler, T.	1121, M310	Krohn, K.	1171, SA375, SA395	Kwon, M.	SA431	Larson, E.	M480
Kohrt, W. M.	M472, WG4, WG34	Kronbergs, A.	M170	Kwon, R. Y.	1040	Larson, J.	F383, SA383
Koide, M.	SA173	Kronenberg, H. M.	1254, 1262, F114, F215, M156, SA114, SA130, SA215, SU004	Kwon, S.	M364	Larsson, T.	SA227
Koike, T.	M332	Kronenberg, M.	M027, SA051	Kwon, U.	SU135	Larue, L.	F190, SA190
Koitaya, N.	SU307	Kronenberg, M. S.	M056, M097, SU057	Kwon, Y.	SA412	Lascau-Coman, V.	M140
Koivuniemi, A. S.	SU387			Kyle, R. A.	SU238	Lasiewicki, A.	M382
Koivuniemi, M. C.	SU387					Laskey, M.	M498
Kojima, Y.	M332						
Kokolus, S.	SA501						
Kola, B.	SU037						
Kolb, F.	M073						

(Key: 1001-1300 = Oral, F = Friday Plenary poster, SA = Saturday poster, SU = Sunday poster, M = Monday poster, WG = Working Group Abstract)

## Author Index

## ASBMR 30th Annual Meeting

Lassalle, C.	SA400	Lees, C. J.	M499	Li-Ng, M.	M217, M218	Liu, M.	F215, SA215, SU013
Laster, A.	SA326, SU256	Leet, A. I.	M234, SU386	Lian, J. B.	1272, F277, F279, F572, M037, M041, M052, M090, M279, SA277, SA279, SA572, SU019	Liu, N. Q.	F283, SA283
Lau, C.	M362, M363	Lefauveau, P.	SA487			Liu, P. SA068, SU059, SU311, SU418	
Lau, C. S.	F403, SA403	Legrand, E.	M297, SA400			Liu, P. Y.	F233, SA233
Lau, J.	M466	Leguevague, P.	M415	Liang, B.	SA115	Liu, Q.	SA453
Lau, K. H. W.	M233	Lei, S.	SU331	Liang, G.	SA254	Liu, S.	1225, F066, M053, SA066
Lau, S.	1189	Lei, S. Feng	M404	Liang, X.	SU372	Liu, W.	SA314
Laud, P. W.	SA428	Lei, W.	1273, F188, SA188	Liao, E.	SA386	Liu, X. M028, SA199, SU331, SU385	
Laughlin, G. A.	1206	Leikin, S.	SA146, SA252	Liao, J.	F270, SA270	Liu, X. Gang	M404, SA267
Laugier, P.	SA101	Leite, A. F.	SA311	Libanati, C.	1285, 1286	Liu, X. Q.	F394, M338, SA394, SA570, SU501, SU502
Launay, J.	SA493	Leiter, E. H.	M244	Libouban, H.	F516, SA516, SU056	Liu, Y.	M029, M034, M183, M237, SA007, SA023, SA051, SA261, SU028, SU127, SU253, SU331, SU331
Launer, L.	1094, 1096, F369, SA369	Leitzel, K.	M281	Licata, A. A.	SA492, WG28, WG33		
Laurence, J.	M448, SU455	Lekva, T.	M049, SU167	Lichtler, A.	1114, M027, M054, M082, SU028		
Laurie, D.	M209, M284, SU200	Lelliott, C. J.	1222	Lidereau, R.	M272	Liu, Z.	SA313
Laurin, M.	SU064	LeMaster, J.	M310	Lie, A.	M117	Liu-Ambrose, T. Y. L.	SU362
Lauzier, D.	SA159	Lemire, I.	1054, F107, SA107	Lieben, L.	F238, SA238	Livesay, B.	SU218
LaVallee, T.	1085	Lemmens-Gruber, R.	M130	Liebens, F.	SU265	Livingston, E. W.	1066, SU368
Lavi, J.	M085	Lemmi, M.	M204	Lieberman, J. R.	F283, SA283	Lix, L. M.	1235, SU410
Lavoie, H. B.	M197	Lemos-Marini, S. Helena V.	M427	Lieu, S.	F127, SA127	Ljunggren, Ö.	1279, M232, SA247, SA264, SU183, SU219, SU262, SU349, SU412, SU413, SU459
Lawrence, K. M.	SA096	Lems, W.	SU412, SU413	Liew, S.	M457	Lloyd, D.	SU409
Lawrence, S.	SA259	Lencel, P.	SU044	Lifton, R.	1017, SU171	Lloyd, S. A. J.	1295
Lawson, M.	SA259	Lenhart, G.	F356, SA356, SU320	Lillestol, M.	M395	Lodes, S.	SU456
Lazarenko, O. P.	SA336, SU182	Lentle, B.	SU483, WG23	Lim, D.	SU407	Loeffler, R.	SA193
Lazaretti-Castro, M.	SA524	Leonard, M. B.	1033, SU441	Lim, K.	M251	Lofgren, B.	1107
Le Drévo, M.	F516, SA516	Leonard, P.	1054	Lim, L. S.	F371, SA371	Loisel, T. P.	1054, 1199
Le Guillou-Buffello, D.	SA101	Lepage, R.	SU176	Lim, M.	M364	Loiselle, A. E.	F153, SA153
Leal, M. E.	SA178, SA388	Lepissier, J.	M172	Lim, S. M351, SA164, SA442, SU452		Lomashvili, K. A.	M142
Leblanc, M. M.	SU105	Lerman, A.	M083	Lim, Y. F.	M341	Lomecky, M.	SA203
Leblon, J. Vincent	SA302	Lerner, U.	M117, SA198	Lima, F.	1252, F026, M096, SA026	Lomovtsev, A.	SU281
LeBoff, M.		LeRoith, D.	M440	Limoli, C.	M469, SA517	Lomri, A.	SU157
LeBoff, M. S.	1068, M285, M453, SA370, SU255	Leslie, W. D.	1235, 1238, SA366, SA438, SU341, SU410	Limonta, C.	SU371	Long, R. K.	1193, M483
LeBoff, M. Susan	SA237, SU400	Lespessailles, E. F319, M239, SA319, SA538		Lin, J.	SU071	Longhi, M.	SU345, SU346
Leboy, P. S.	M060	Letocha, A. D.	SU496	Lin, J. Ming	SA175, SU030	Longo, M.	M275
Lecanda, F.	F286, F291, SA286, SA291	Letuchy, E. M.	M506	Lin, S.	1137	Longobardi, L.	SA169
Lecka-Czernik, B.	1073, F091, SA091, SU023	Leucht, P.	M105, SA531	Lin, S. Sutton	M445	Lonning, S.	SA187
LeClerc, N.	M099	Leung, P. M127, M276, M337, SU405		Lin, X.	SA388	Looser, S.	SU432
Leder, B. Z.	1102, 1135, SA209, SU169	Leung, P. C.	SA309	Lin, Y.	SU482	Loots, G. G.	1039
LeDuc, R. D.	SA077	Leupin, O.	F054, SA054, SU036	Linares, G.	SU018	Lopes, J. Barros	SU453
Lee, B.	F118, F158, M055, M126, M132, M152, SA115, SA118, SA158, SA412, SU024, SU126	Levasseur, J.	SU365	Linares, G. R.	M009	Lopez, R.	SA280
Lee, B. S.	SU066, SU067	Levasseur, R.	M297, SA400	Lincoln, M.	SA565	Lopez Franco, G.	F260, SA260
Lee, C.	SA100, SA189, SU135, SU416	Levi, G.	F010, SA010	Lind, L.	SA264	Lora, D.	SA503
Lee, C. S. D.	M164	Levin, A.	M085	Lindahl, K.	M232, SA247, SU219	Lorberg, A.	SU278, SU279
Lee, C. T.	SU393	Levis, S.	M402	Lindemans, J.	SU317	Loredo, R.	F376, SA376
Lee, D.	1272, M300, M392, SA053, SA100, SU042, SU127	Levy, S. M.	M506	Lindén, C.	1107	Lorente, C.	SA204
Lee, D. Choen	1180	Levy-Weil, F. E.	SU352	Lindersson, M.	SU183	Lorentzon, M.	1279, 1281, M327, SA541, SU183, SU349
Lee, E.	M394, SA442, SU452	Lewanczurk, R. Z.	F552, SA552	Lindley, P.	F376, SA376	Lorenzo, J.	SU099
Lee, H.	F174, M339, SA016, SA053, SA174, SA189, SU135, SU169, SU416	Lewiecki, E. Michael	1025, SA507, SA509, SU258	Lindner, B.	SA300	Lorenzo, J. A.	SU070
Lee, H. G.	M015, SA009	Lewis, B.	1068	Lindsay, R.	1169, SA362, SA404, SU287, SU344	Loth, E.	M382
Lee, H. Ja	M256	Lewis, R. D.	M468, SU318	Lindsey, D. P.	M469	Lotinun, S.	SU376
Lee, J.	M147, M148, M260, M434, SA036, SA117, SA189, SA412, SU014, SU055, SU108, SU135, SU416	Leydet-Quilici, H.	M381	Lindvall, C.	1001	Lottridge, D.	SU343
Lee, J. S.	1208, F333, SA333, SU183	Leyva, M.	SU303	Ling, J.	SA057, SA134, WG39	Lou, Y.	M041
Lee, J. Young	M256	Lézet, F.	SA150	Link, T. M.	F317, M309, M489, SA317	Louie, A.	1076, 1077, 1255, M040
Lee, K. M407, SA100, SA189, SU135		Li, B.	1015, F004, SA004, SU434	Linkhart, T.	SA182, SU015	Lounev, V. Y.	F044, SA044
Lee, M.	1177, F008, M321, SA008	Li, C.	M132, M318, SA441	Linossier, M.	SA011, SA142	Loveridge, N.	M315, M478, SU275
Lee, R. W.	1004	Li, C. Qingchuan	M312	Liote, F.	SA493	Low, V. H. S.	SA320
Lee, S.	M128, M260, M407, SA412, SU407	Li, G.	F233, SA233, SA234, SU393	Liou, M.	1124	Lowe, H.	SA486, SU195
Lee, S. H.	SU304	Li, G. H. Y.	1270	Lippard, S. J.	SU235	Löwik, C. W. G. M.	SA031, SA052, SA130
Lee, S. Hun	M256	Li, H.	M027, M054, M138, SA040, SU295	Lippuner, K.	SU294, SU296		
Lee, T.	SU236	Li, H. Tao	1202, SA056	Lips, P.	SA203, SA372, SU462	Löytniemi, E.	SU422
Lee, W.	F131, M137, SA131, SU374	Li, J.	1014, 1016, 1019, 1062, 1185, F376, M464, SA071, SA199, SA376, SU343, SU489	Lipsious, R.	M353	Lozano, D.	M195, SA223
Lee, Y.	M300, SU291	Leydet-Quilici, H.	M381	Lipton, A.	M281	Lu, C.	SU036
Lee, Y. F.	M216	Lézet, F.	SA150	Liquin, D.	M160	Lu, G.	F081, SA081, SA287
Lee, Z.	SU108	Li, M.	F473, M237, SA473	Lirani-Galvao, A. Paula R.	SA524	Lu, J.	M143
Leeb-Lundberg, L. M. F.	SU179	Li, N.	F014, SA014	Lisbona, P.	SA357	Lu, L.	SA143
Leeming, D.	SU091, SU361	Li, R.	M244, SA104	Litscher, S.	F260, SA125, SA260	Lu, Q.	M043, SU020
		Li, T.	F186, SA186	Little, D. G.	1195, SA075	Lu, W.	1076, 1077, 1255, M040
		Li, W.	M349	Liu, C.	1048, 1262, M235	Lu, X.	SA248, SU133
		Li, X.	1087, 1138, 1139, 1211, 1213, F270, F288, F394, M001, M278, M279, SA270, SA285, SA288, SA394	Liu, D.	F315, M109, SA315, SU493, WG40	Lu, Y.	1010, F062, M207, SA062
		Li, Y.	F014, F242, SA014, SA242, SU025	Liu, F.	M091	Lu, Z.	1276
		Li, Y. Ping	SA154	Liu, G.	SU464	Luan, Y.	1262
		Li, Z.	M090, M160	Liu, H.	M207, M213	Luben, R.	1240
				Liu, J.	SA088, SA266, SU331	Luben, R. N.	F363, SA363
				Liu, J. C.	F277, SA277	Luc, M.	M381
				Liu, L.	M177, M253, SA236, SA261	Luca, V.	SU310

(Key: 1001-1300 = Oral, F = Friday Plenary poster, SA = Saturday poster, SU = Sunday poster, M = Monday poster, WG = Working Group Abstract)

## ASBMR 30th Annual Meeting

## Author Index

Lucani, B.	F455, SA455	Magaziner, J.	1030, F345, M397,	Martínez, G.	M221, SA503	McCabe, L.	M188
Lucas, E. A.	M301, M341		SA345, SA346, SA432,	Martínez, J.	M223	McCarty, C.	SU365
Luciani, F.	F190, SA190		SU073, WG5	Martínez, L.	SU347	McCauley, L. K.	1159, 1160, 1264,
Luczak, E.	M382	Maggi, S.	SA427	Martínez, R. X.	F006, SA006		F270, M181, SA025, SA270
Lüder, M.	SU354	Magland, J. F.	M312, SU277, SU280,	Martínez de Osaba, M.	Jesus. SA030	McClintock, R.	SA239
Luderer, H. F.	1183		SU481	Martínez-Bautista, S.	F012, SA012	McClintock, R. M.	M188
Lui, L.	1057, SU338	Magne, D.	SA015, SU044	Martínez-Ferrer, A.	SA030	McCloskey, E.	1023, 1290, SU257
Lui, R.	1034, M434	Magyar, C. E.	SU468	Martini, G.	F455, SA455, SA475,	McClung, M.	1291
Luis-Ravelo, D.	F291, SA291	Mah, J. K.	SU396		SA481	McClung, M. R.	1286, SU384
Lujan, V.	SU312	Mahadevan-Jansen, A.	1144	Martiniakova, M.	M261, SA132	McCracken, P. J.	M343
Lukashova, L.	F253, M311, SA253	Mahaney, M. C.	M241, M494	Marty, C.	1132, F010, SA010, SA493	McCrea, J. D.	F361, SA361
Lukert, B.	SA502	Mahboubi, S.	1105	Marumo, K.	1012, SA382	McCready, L.	1179, SU238
Lund, T.	M287, SA231	Maher, J. J.	1234	Maruyama, R.	SU308	McDaniel, L. J.	SU267
Lundy, M. W.	1065	Maher, N.	M294, SU274	Masarachia, P.	1230	McDonald, J.	M419
Luo, J.	1115, F004, SA004	Mahlum, E.	SU231, SU240	Mascia, M. Lucia	M127	McDonald, J. M.	M114
Luo, M.	M079	Mahon, M.	M186	Masharani, U.	SU210	McDonald, M. M.	1195, SA075
Luo, W.	M058, SU063	Mahon, M. J.	1013, F226, SA226	Masi, L.	M092, SA393, SU211	McDonough, A. K.	SA280
Lupi, A.	F500, SA500	Mahoney, D.	SA097	Masilamani, S.	M196	McFetridge, J.	SU420, WG38
Luque, L.	SA037	Maier, D.	SU272	Mason, B.	M317	McGavock, J. M.	F552, SA552
Luque de Castro, M.	M292	Maile, L. A.	F093, SA093	Mason, R. S.	F389, SA389	McGibbon, A.	SU071
Lusis, A. J.	M247	Maimoun, L.	SA506	Mason, Z.	M161	McGovern, E.	SU274
Luther, J.	1149	Main, R. P.	M474	Massari, L.	M408	McGregor, A. J.	SU129
Luthman, H.	M463, SU225	Mainard, D.	SU288	Massaro, J. M.	1207	McGregor, N. E.	F195, M014, SA195
Luu, Y. K.	F047, M486, SA047	Mainous, E. G.	SU051	Massarotti, M.	1170, M180, SU345,	McGuigan, F.	SU225
Luzi, E.	M036	Mainra, R.	1032, SA497		SU346	McHugh, K. P.	SU083
Lwin, S. T.	1088, 1098, 1251, F293,	Maire, T.	SU288	Masson, C.	M297	McInerney, M.	F091, SA091
	SA293, SU230, SU232, SU233	Maiti, A.	1161	Mastaglia, S. R.	M405, SU429	McIntyre, A. W.	F557, SA557
Lyles, K.	1030, 1246, M368, M394	Maitzen, S.	SA300	Masuda, M.	SA201	McKay, H.	M502
Lynch, C. C.	1144	Majdzadeh, R.	SU339	Masunari, N.	SA296	McKay, H. A.	F315, F552, SA315,
Lynch, M. E.	M474	Majumdar, S.	F317, M309, SA035,	Masuyama, R.	F238, SA238		SA552, SU362, SU469, SU493
Lynch, S. E.	F376, SA376		SA317, SU039	Mata-Granados, J.	M292	McKee, M. D.	1199, F107, SA107,
Lyngstadaas, S.	SA137	Mak, W.	1267		1174		SU119
Lyon, A. W.	SA331, SU283	Makareeva, E.	SA146	Matheny, C.	SU450, WG12	McKenna, C. E.	1065
Lyon, M.	SU396	Makhijani, N. S.	SA170	Mathew, S.	M446	McKenna, C. R.	SA274
Lyytikäinen, A.	F542, SA542, SA551	Mäkinen, T. J.	F458, SA458	Mathis, D.	SU248	McKenna, C. Ryan	F275, SA275
		Mäkitie, O.	1103, 1176	Mative, N.	SU492	McKenna, R.	F190, SA190
		Malaval, L.	1061, 1191, SA126,	Matkovic, V.	1265	McKibbin, C. R.	1274
			SA142	Matsuda, A.	SA162	McKiernan, F.	SU365
		Malavolta, N.	M355	Matsuka, Y.	SU187	McKinney, B.	SU194
Ma, C.	1021	Malbari, M.	1297	Matsumoto, C.	SU385	McLaughlin, M.	1174
Ma, D.	1162	Malfait, F.	SU215	Matsumoto, H.	F079, F473, SA022,	McLean, J.	F038, SA038
Ma, D. W.L.	SU381	Malik, M.	SU039		SA079, SA473, SU102, SU103	McLean, R. R.	1207, 1283
Ma, H.	M319	Mallmin, H.	1279, SU219	Matsumoto, T.	1122, 1248, SA294,	McLellan, A. R.	SU324, WG17
Ma, J.	SU404	Maltry, N.	1004		SA397, SA470, SU242	McMahon, A. P.	M150
Ma, L.	SA529	Man, H. S.	M395	Matsumoto, Y.	SA379	McMahon, D. J.	1031, 1033, 1034,
Ma, M.	1253, SA522	Man, Z.	SU405	Matsunobu, T.	1079		1036, 1146, F485, M310, M434,
Ma, Y.	M102	Manacu, C.	SU159	Matsushita, O.	1063		M448, SA485, SA486, SA501,
Ma, Y. L.	1019, M207, SU196,	Manalac, C.	1076, 1255, F127, SA127	Matsusue, K.	F494, SA494		SU201, SU441, SU455, SU458,
	SU377, WG11	Manavalan, J. Sanil.	1146		SU090		SU464
Mac, A.	SU281	Mancini, D.	SA501	Matsuzaki, K.	SU090	McMichael, B. K.	SU066
Macarios, D.	M372, SA417	Mancini, L.	SA199, SU094	Matthews, R.	1024, SA326, SU256,	McMullen, M. R.	SA177
MacCluer, J. W.	M250	Mandair, G. S.	M084		SU321	McNanley, T.	F557, SA557
MacDonald, B.	M346, M347, SA399	Mandal, C. Charan	1081, F002,	Mattocks, M.	M067	McNeil, P.	SU153
MacDonald, D.	SU174, WG30		SA002, SU096	Matzinger, M.	SU483, WG23	McPeake, J.	SU409
Macdonald, H. M.	F337, F552,	Mandic, V.	1149	Maurel, D. B.	M239	McTavish, K. J.	1224
	SA337, SA504, SA552	Mangano, K.	M353	Mautalen, C.	SU498	Meany, D.	M435
Macek, B.	SU142	Manghat, P.	SU174, WG30	Mautner, V. Felix	F465, SA465	Meary, F.	M016
Machida, M.	M307	Manicourt, D. H.	SU306	Mauviel, A.	F190, SA190	Meats, D. L.	SA421
Macica, C. M.	SA254	Maniezzo, M.	F281, SA281	Mavalli, M.	F181, SA181	Mechoulam, R.	SU375
Mackem, S.	F114, SA114	Mann, M.	SU142	Mavilia, C.	M184	Medich, D. L.	1020, SU259
MacKenzie, B.	1008	Manning, C. A.	WG41	Mavroeidi, A.	F337, SA337	Megges, M.	1149
Mackenzie, D. S.	1018	Mannstadt, M.	SA204, SA225	Maxwell, C. J.	SA368	Mehrotra, M.	SA529
Mackenzie, W.	M240, SU494	Manolagas, S. C.	1038, 1097, 1099,	Maye, P.	SA007, SA051, SU028	Mehta, N.	M208
Mackie, E.	1101		1157, 1227, 1247, 1250, F024,	Mayeux, J.	M494	Mei, L.	SU127
Mackie, K.	1221		M010, M108, SA024, SA185,	Mayhew, P. M.	M315, SU275	Meier, C.	1280
Mackinnon, E. S.	SU336		SA453, SU047, SU189, SU380	Maylandt, K.	M362	Meier, M.	1294
Madhu, V.	M045	Manolides, A. S.	M323	Maynard, J. A.	M252	Meier, S.	1134
Madsen, O. R.	M350	Manolson, M. F.	1218, SU069, SU106	Mayr, A.	SA295	Meissner-Weigl, J.	M072
Madsen, S. H.	M155, SU125	Mansky, K. Carpenter	1008	Mays, S.	SA477	Mejia, W.	SA183, SU190
Madyastha, P.	M366	Manwani, B.	SU255	Mazhari, A. M.	SU424, SA468	Melamed, E.	SU375
Maeda, K.	1012, M113	Manzarbeitia, F.	SA22, SA195,	Mazzetti, M.	SA475	Melhus, H.	1095, 1205, SA264,
Maeda, N.	SA206		SU046	Mazzotta, C.	M184		SA334
Maeda, Y.	1154	Martin, T. John	M014, SA157	Mbalaviele, G.	SU144	Mellibovsky, L.	M264, M265
Maekawa, S.	M219	Martin-Millan, M.	1097, 1247, F024,	McAdam-Marx, C.	SU332	Mellström, D.	1166, 1279, 1281,
Maeno, M.	M012, M063, SA028		M010, M108, SA024,	McAlister, W. H.	F563, F569, SA563,		M327, SA198, SA541, SU183,
Maes, C.	1152, 1254		SA185, SU189		SA566, SA567, SA569, SU212		SU204, SU219, SU262, SU349,
Magalhães, A. O.	SU449	Martin-Mola, E.	SA496	McBride, D.	SA146, SA252, SA266		SU459
		Martineau, C.	SA250	McCabe, G.	M188	Melo, N. S.	SA311

(Key: 1001-1300 = Oral, F = Friday Plenary poster, SA = Saturday poster, SU = Sunday poster, M = Monday poster, WG = Working Group Abstract)

## Author Index

## ASBMR 30th Annual Meeting

Melsen, F.	F310, SA310	Min, J.	SU084, SU093	Monaghan, J.	F253, SA253	Muglia, L. J.	F452, SA452
Melton, L. J.	1165, 1167, 1284, SU267	Minagawa, M.	SA470	Monegal, A.	M442, SA030	Muir, J. W.	M342
Melton, L. Joseph	1179, F426, SA426	Minami, Y.	1012	Monfoulet, L.	SA126	Mukesh, B.	SU365
Mencej, S.	SA300	Minamizaki, T.	SA206	Monir, A.	M146	Mukherjee, S.	1231, F277, SA277, SU239
Mendoza, N. T.	SA209	Minamizawa, T.	SA222	Moniz, C.	F491, SA491	Mulay, S.	F277, SA277
Mendy, M.	M498	Minck, D.	SA385	Monroe, D. G.	M024, M037, M052	Mulder, L.	SA110
Meneu, J.	SA503	Mineau, F.	M018	Monsingnore, L. M.	M190	Mulè, R.	M355
Menezes, P. Rossi	SU453	Minisola, S.	M432, SU210	Montemurro, G.	SA199	Muller, J. A.	M304
Meng, D.	M132	Minne, H.	1133	Montero, M.	SA299	Müller, P.	SA528
Menuki, K.	M326	Miosge, N.	M450, WG21	Montoya, M. José	M101, SU009	Müller, R.	1121, 1179, 1294, 1298, M310, M456
Merabet, Z.	M455	Miossec, P.	SA080	Montuenga, L.	F286, F291, SA286, SA291	Müller, U.	SU456
Mercan, F.	1219	Miraoui, H.	M093	Moon, E.	SA189, SU135, SU416, SA189, SU135, SU416	Muller, W.	1185
Mercante, L.	SA451	Miron, R.	M030	Moore, A.	1212	Muller, W. J.	1016
Mercer, L. M.	F135, SA135	Mirza, R.	SU118	Moore, A. E. B.	F398, SA398	Mullin, B. H.	SA263
Mercier, F.	SA415	Mirzazadeh, M.	M211	Moore, A. F.	1102	Mumm, S.	F256, F563, SA256, SA562, SA563, SA566, SA567, SU210
Merdes, M.	SU379	Mishina, Y.	1114	Moore, A. J.	SA197	Mun, H.	M202
Merle, B.	SA080	Misiorowski, W.	SU436	Moore, M. M.	1098, SU378	Mun, H. Chang	M203
Merlotti, D.	F455, M320, SA455, SA475, SA481	Misra, B.	1031, M431	Moore, M. R.	M226	Munce, S. Elizabeth Patricia	M401
Mesenbrink, P.	1027, 1028, 1030, 1246, F401, F403, F411, M362, M363, SA401, SA403, SA411, SU405	Misra, D.	SU319	Moran, E.	M038	Mundlos, S.	F054, SA054
Messing, S.	SA556	Mistretta, V. I.	M212	Morandi, L.	SU371	Mundy, G. R.	1087, 1088, 1098, 1136, 1144, 1251, 1300, F293, M278, M280, SA187, SA293, SU230, SU232, SU233, SU378, SA158, SU024, SU126
Metania, E.	SU472	Mitchell, B. D.	M250, SU297	Morasso, M.	M027	Munivez, E.	F118, F158, SA118, SA158, SU024, SU126
Metge, C.	SU410	Mitchell, J.	M042, M067, SU487	Morasso, M. I.	1272	Munoz, F.	1027, 1067
Metz-Estrella, D. M.	1259	Mitrovic, D.	SU157	Mørch, M.	M350	Munoz, S.	1098
Meudt, J.	1051, 1053	Mitten, D. J.	F153, SA153	Morck, D. W.	SA547	Munoz, S. A.	1087, 1251, 1300, F293, SA187, SA293
Meyer, M. B.	1223, SU198	Mitton, D.	M316, SU471	Moreau, M.	SU056	Muñoz-Rueda, P.	M447
Mi, Q.	M011, M132, SA441	Miyabara, Y.	F548, M492, SA548	Moreau, R.	M008, SA250	Muñoz-Torres, M.	M447
Mian, A.	M121	Miyagawa, K.	SA379	Morello, R.	F118, SA118	Murakami, T.	SU117
Miao, D.	1015, M199	Miyai, K.	M026	Moreno, E.	SA503	Muraki, S.	SU334
Miao, D. S.	1050, M213	Miyai, T.	SA165	Moreno, J. L.	F286, SA286	Muramatsu, S.	1265
Miayamoto, K.	F473, SA473	Miyakoshi, N.	M219, SA214, SU454	Moreno, M.	SA357	Murata, Y.	SU118
Michaëlsson, K.	1095, 1205, SA264, SA334	Miyamoto, T.	1217, F087, SA087, 'SU090, SU118	Moreno, P.	M424, M425	Murchie, R. C.	M231
Michalek, J.	SA318	Miyasaka, N.	M446	Moreschini, O.	M272	Murphy, A.	SU143
Michalek, S. M.	SA088	Miyauchi, A.	M385	Morgan, D. A. F.	M460	Murphy-Ullrich, J. E.	SU052
Michalenska, A. C.	M021	Miyaura, C.	1230, M167, SU187	Morgan, E. F.	M161, SA001	Murray, C. K.	M236
Michigami, T.	SA119, SA470, SU172	Miyazaki, J.	SU082	Mori, K.	SU082, SU083, SU245	Murray, S.	M248
Michou, L.	SU216	Mizoguchi, F.	M446, SU007	Mori, T.	M326	Murshed, M.	SA071
Micklesfield, L. K.	SU490	Mizoguchi, T.	M113, SU098	Morimoto, N.	M121	Muruganandan, S.	M071
Miclea, R. Lucian	SA130	Mizuno, A.	1151	Morin, S. N.	SA438	Muscarella, L. Anna	M201, M432
Miday, R.	SA402	Mizutani, S.	M026	Morishima, T.	SA165	Muscat, G.	M118
Middlemist, S.	SU200	Mladenovic, Z.	M119	Morishita, K.	SU307	Muschler, G. F.	SA039, SU005
Middleton-Hardie, C. A.	SA111	Moayyeri, A.	1240, F363, SA363	Morissette, J.	SU216	Musia, J.	M382
Midura, R. J.	M053, SA070	Mobley, S. L.	SA553	Morita, A.	SA325, SA330	Musk, A.	1289
Miedlich, S. U.	M158	Mocanu, V.	SU310	Morita, Y.	M112, SA166, SU152	Musto, R.	F491, SA491
Miga, M. I.	SA169	Mochida, Y.	SU208	Moritz, N.	F458, SA458	Muto, A.	SU098
Migliaccio, S.	M355	Modlesky, C. M.	M505, SU282	Moriura, Y.	SU101	Muwakkitt, S.	SU237
Mihara, M.	SU394	Modrowski, D.	SU243	Moriyama, K.	M093	Muzio, D.	M405
Mikawa, K.	SA316	Modzelewski, J.	F233, M100, SA233	Morko, J.	M295	Muzylak, M.	1212
Mikhail, M.	M217, M218	Moedder, U. I. L.	M083	Morlock, M. M.	M454	Myoui, A.	F112, SA112
Miki, H.	SA294, SU242	Moehrke, W.	SA425	Morris, H. Arthur	M224		
Miki, T.	M094, SA147, SA222, SA305, SA419	Moen, S.	F550, SA550	Morris, H. A.	SA197		
Mikkola, A.	M479	Moermans, K.	F238, SA238	Morris, H. L.	SA067		
Mikkola, T. M.	F420, SA420	Moffatt, P.	M025	Morris, M. D.	M084, M462, SU480		
Mikulec, K.	SA075	Moffett, A. H.	M386	Morrisey, M. A.	1024, SA326, SU256, SU321		
Mikuni-Takagaki, Y.	SA379	Moffett, S.	M266, SU284	Morrissey, M. M.	SU282		
Milanesi, L.	SU185	Mogensen, B.	F369, SA369	Morse, L. R.	SA520		
Millan, J.	F107, SA107	Moh, A.	1018	Mortensen, L.	M350		
Millan, J. Luis	1054, M142, SA061, SA063	Mohammad, K.	F190, SA018, SA190	Mortlock, D. P.	M031, SU150		
Millard, S.	1076	Mohammad, K. S.	1085, F272, F275, M277, SA172, SA272, SA274, SA275	Morton, R. A.	1292		
Millard, S. M.	1077, 1255	Mohand, S.	1142, 1190, 1194, M009, M115, M233, SA180, SA182, SU018	Morvan, F.	M073		
Miller, E.	1063, M505	Mohr, A.	1075	Mosekilde, L.	M206, SA218, SA290, SU227		
Miller, L.	SU475	Moiilanen, P.	M319	Moskowitz, G.	1021		
Miller, L. M.	M023	Mojarrab, R.	M469, SA517	Moss, D.	SA151		
Miller, P.	F396, SA395, SA396, SA402	Mok, J.	SU359	Mossetti, G.	SA475, SA481		
Miller, P. D.	1236, M349, SU258, SU384, SU420, WG38	Mok, S.	M337	Motokawa, S.	SA467		
Miller, R.	SA346	Mokrysheva, N. Georgievna	M192	Moulatlet, A. Carolina Bernardini	F244, SA244		
Miller, R. Ron	SU073	Moldovan, F.	SU157, SU159	Mousny, M.	SU465		
Miller, T. A.	SU038	Moldovan, I.	SU358	Moverare-Skrtic, S.	SA460		
Milligan, C.	F439, SA439	Mole, D.	SU288	Moysés, R. M. A.	SU447, SU449		
Milner, C. M.	SA097	Molinolo, A. A.	SA200	Mrhar, A.	M257		
		Molla, M.	SA150	Muche, B.	1172		
		Molloy, C.	SU409	Mudford, L. A.	SU200		
		Molostvov, G.	M200	Mueller, R.	F527, SA527		
		Monaco, R.	SA393	Mueller, T. L.	1298		
				Mughal, Z.	SU428, WG1		

(Key: 1001-1300 = Oral, F = Friday Plenary poster, SA = Saturday poster, SU = Sunday poster, M = Monday poster, WG = Working Group Abstract)



## ASBMR 30th Annual Meeting

## Author Index

Nair, S. K.	M033	Neumann, T.	SU456	Nogueira-Barbosa, M. H.	M190	Ogawa, T.	SA082
Naja, R. P.	M222	Neunaber, C.	1198	Nogues, X.	M264, M265	Ogawa, Y.	SU316
Naji, L.	M101, SU009	Neuner, J. M.	SA428	Noguti, T.	SU049	Ogita, F.	SA513
Najjar, S.	F091, SA091	Neutsky-Wulff, A. V.	M123, M129, SU125	Noh, T.	1121	Ogita, M.	1112
Naka, H.	SA419	Neves, K. R.	SU447, SU449	Nohe, A.	SU147	Oh, B.	M256
Nakagawa, C.	F483, SA483	Nevitt, M.	SU338	Nojima, J.	SA161	Oh, H.	SU077, SU291
Nakagawa, K.	M064, SU034	Nevitt, M. C.	1058	Nomura, Y.	M374	Oh, J.	F008, SA008
Nakagawa, T.	F087, SA087	Newmark, R.	1285	Nonaka, K. Okino	M228	Oh, K.	SU407
Nakajima, K.	M082	Ng, G. Y.	SU159	Norbury, W. B.	SA571	Oh, S.	SA431
Nakajima, M.	SA305	Ngouala, G.	SU157	Nordin, B. E. C.	M329	Ohba, S.	1187, M082, M089
Nakamoto, T.	M026, M044, M175, M446, SU007	Nguemo, J.	M130	Norgård, M.	F085, SA085	Ohishi, M.	1263, M076
Nakamura, A.	SA161	Nguyen, H.	M460	Norris, S. A.	SU490	Ohishi, W.	SA296
Nakamura, C.	SU081	Nguyen, J.	SU205	Notomi, T.	SU100, SU101	Ohlsson, C.	1123, 1181, 1279, 1281, F085, M327, SA085, SA198, SA460, SA541, SU179, SU183, SU219, SU262, SU349, SU459
Nakamura, E.	1045	Nguyen, M.	M246	Novack, D.	1086, F256, F569, SA256, SA569	Ohsawa, M.	SA490, SU438, SU440
Nakamura, H.	M113, SU054	Nguyen, N. D.	1210, 1280, F347, F349, M263, SA347, SA348, SA349, SU222, SU461	Novince, C. M.	1160, 1264	Ohta, H.	F548, M389, M391, M492, SA548
Nakamura, K.	1115, 1187, 1217, 1228, F116, M082, SA116, SU334	Nguyen, T. V.	1059, 1210, 1280, F347, F349, M263, SA347, SA348, SA349, SU222, SU461	Novotny, S. A.	M482, SA540, WG20	Ohta, Y.	SU137
Nakamura, M.	1115, 1217, SU114	Nguyen-Yamamoto, L.	M214	Nowson, C.	1244	Ohtake, F.	1182
Nakamura, S.	SA294, SU242	Ni, Y.	M234, SU386	Nozaka, K.	SA214	Ohtsuka, K.	M449
Nakamura, T.	1115, 1122, M326, SA448, SU136, SU286	Nichols, G. A.	M356	Nozaki, T.	SA498	Ohue, M.	SA384
Nakanishi, M.	1045, SA095	Nichols, S.	M375	Nucci, A.	SU482	Ohya, K.	F074, M019, M121, SA074
Nakano, T.	SA196	Nicholson, G. C.	1244, M245	Nuche-Berenguer, B.	M424, M425	Oie, E.	SU167
Nakano, Y.	1199	Nicholson, L.	M240, SU494	Nunes, A.	SU011	Oka, H.	SU334
Nakao, Y.	SU137	Nickerson, J.	F279, SA279	Nuti, R.	F455, M320, SA455, SA475, SA481	Okada, H.	M385
Nakasaka, M.	SA179	Nickolas, T.	1033, 1036, F485, SA485, SU441	Nyman, J. S.	1144, 1251, 1300, F293, M102, M280, SA293, SU218	Okada, T.	SU172
Nakashima, T.	SA108	Nicks, K. M.	F523, M177, SA086, SA523, SU162			Okada, Y.	F079, SA079
Nakatsuka, K.	SA419	Nicola, G.	SU269			Okamoto, K.	F074, F083, SA074, SA083
Nakaya, Y.	SU443	Nicolella, D. P.	M107, M467, SA057, WG39			Okamoto, S.	SA324, SA324
Nakazawa, E.	M185	Nie, S.	1014			Okamoto, Y.	SA162
Nakchbandi, I.	SA151	Niedermeyer, J.	1004			Okano, H.	F548, M492, SA548
Namba, N.	SA470	Niehs, C.	1004			Okano, T.	M064, M332, SU034, SU308, SU316
Nampei, A.	F112, SA112	Nielsen, C.	F354, SA354			Okayama, A.	SA490, SU440
Nan, D.	M223	Nielsen, D. Susanne	SA434			Okazaki, J.	M094, SA147
Nan, M.	SA189, SU135	Nielsen, M.	1129, SU270, SU361, SU463			Okazaki, M.	F221, F224, F483, M186, SA221, SA224, SA483
Nanci, A.	M025, SA531	Nielson, C. M.	F321, SA321			Okazaki, R.	SU060
Nanes, M.	1197, F240, M042, SA240	Niemeier, A. C.	SA042			Okazaki, Y.	SA161
Nango, N.	M307	Nieminen, M.	M459			Okuno, H.	SA245
Nantermet, P.	1214	Nieves, J.	1169			Okuno, J.	SA332
Naot, D.	SA175, SU071	Niewolna, M.	1085, F190, F275, SA190, SA275			Okura, T.	SA332
Napierala, D.	M126, SU126	Niger, C.	F026, SA026			Olaboro, F.	SU482
Napoli, N.	1021, WG26	Nijs-Dewolf, N.	SU016			Olansky, L.	WG33
Narayanan, R.	SA381	Nikander, R.	SA533, WG10			Olde, B.	SU179
Narisawa, S.	M142, SA061, SA063	Nilsen, A.	SA232			Oldfield, P.	M296
Narita, N.	M113	Nilsson, M.	M463, SA521, SA541			Olds, W. J.	M226
Narra, N. G.	SA533, WG10	Ninomiya, T.	SU054			Olender, G.	SA392
Naruse, K.	SA379	Nishikawa, K.	F074, SA074			Olivares-Navarrete, R.	1124, M227, SU006
Nashimoto, M.	SA021	Nishimori, K.	SA199			Oliveira, E. Cláudia A.	M191
Naski, M.	1266	Nishimori, S.	M156, SU004			Oliveira, I. Regina S.	SU453
Nasser, P.	SA183	Nishimura, R.	1045, 1265, F079, SA079			Olivera, L.	WG33
Nasu, T.	SU136	Nishimuta, M.	SU307			Oliveri, B.	M405, M426, SU429, SU430, SU499
Nathanielsz, P. W.	M494	Nishisho, T.	SA095			Olm-Shipman, A.	1078, F171, SA171
Nattinger, A. Butler	SA428	Nishita, M.	1012			Olmos, J. M.	M223
Nattiv, A.	SU281	Nishizawa, Y.	SA222			Olofsson, S.	SA334
Naughton, G.	M458	Niskanen, M.	M459			Olsen, B. R.	M029, SU047
Navarro, L.	M255, M259	Nissen, N.	SU223			Olson, S.	F260, SA125, SA260
Navarro, N.	SA357	Nissen, P. H.	M206			Olstad, O. Kristoffer	M049
Nawata, K.	SU285, SU301	Nissen-Meyer, L. Sofie	SA220			Olszynski, W. P.	1056, SU292, SU351
Naylor, K. E.	SA571	Nissenson, R.	1076, 1077, 1255, F127, M040, SA127			Omella, R.	M261, SA132
Nebbia, G.	SU371	Nissinen, M.	SA232			Omelson, S.	M461, SU465
Nebeker, J.	SU332	Niu, Q. Tian	1211, 1213, F394, SA394			Ominsky, M.	1213, M076
Need, A. G.	M329	Nixon, M.	M379			Ominsky, M. S.	1072, 1139, 1216, SU076
Neer, R.	SA397	Niziolek, P. J.	1002			Omizo, M.	SA421
Neff, L.	1109	Noda, H.	F483, SA483, M026, M044, M174, M175, M446, SA105, SA378, SU007			Ong, H. H.	M470
Neff, M.	M352, SU276	Noël, E.	SA466			Ong, J.	F376, SA376, SU374
Nefussi, J.	M016	Noguchi, H.	SA324, SU454			Onitsuka, A.	F473, SA473
Nelo, K.	SA232					Ono, K.	1045
Nelson, D.	1068					Ono, M.	SA162
Nelson, G. A.	1295					Onoda, T.	SA490, SU438, SU440
Nelson-Williams, C.	SU171					Onodera, J.	SU163
Nemeckova, A.	SA318						
Nesti, L. J.	SU163						
Nestlerode, C.	M266, M268, M269, SU284, SA268						
Netelenbos, J. C.	SU340, SU342						
Netter, C.	1134						
Neugut, A. I.	SU202						

(Key: 1001-1300 = Oral, F = Friday Plenary poster, SA = Saturday poster, SU = Sunday poster, M = Monday poster, WG = Working Group Abstract)

## Author Index

## ASBMR 30th Annual Meeting

Onodera, K.	SU383	Paigen, B.	1276, SA120	Patano, N.	SA199	Perrin, N.	M356
Onoe, Y.	F548, M492, SA548	Paik, I.	SA442	Patchett, A.	M458	Persons, K. S.	M215
Ontañón, J.	M255, M259	Paik, J.	1247	Patel, S.	M211	Persson, E.	M117
Ooshima, T.	M144	Pajares, M. José	F291, SA291	Pathmanathan, D.	F174, SA174	Peruzzi, B.	M275
Oostlander, A.	SU462	Palculict, T. Blake	F523, SA523	Patil, C. A.	1144	Pescarmona, G. Piero	SA241
Oppermann, U.	F407, SA407	Palermo, L.	1028, 1127, 1131, F365, F411, M306, SA365, SA411	Patkar, N.	SU321	Pessin, J. E.	F047, SA047
Orav, J. E.	1242, SU423	Palmas, E.	SA451	Patrene, K.	F081, SA081	Peter, Z.	1061
Ordoñez, M. C.	SA496	Palmieri, G.	WG29	Patricio Filho, P. J. M.	SA212	Peters, H. Charlie	SA160
Orellana, C.	SU431	Palnitkar, S.	F405, M420, SA405	Patrick, A. L.	SA268, SU300	Peters, K. D.	M024
Orito, S.	F548, M492, SA548	Palummeri, E.	1245, SU348	Patterson, E.	M210	Peterson, A.	1043
Orlic, I.	SU141	Pamuklar, Z. Nurgul	F444, SA444	Patterson, S.	SU153	Peterson, J.	1179
Ornetti, P.	M444	Pan, F.	M404, SA267, SU154, SU155, SU331	Patterson-Buckendahl, P. E.	M059	Petit, J. Luc	SU399
Ornitz, D.	1257	Pan, G.	M114	Patton, R. J.	WG27	Petit, M.	F552, M325, M482, M487, SA328, SA539, SA540, SA552, SU300, WG20
Ortiz, D.	SU201	Panaroni, C.	F500, SA500	Paudel, M. L.	F367, SA367	Petkovich, M.	SU178, SU448
Ortolani, S.	M408, SU325	Panda, D.	F069, SA069	Paul, E. M.	SA269	Petrigliano, F. A.	F283, SA283
Ortuño, M. J.	F020, SA020	Panda, D. K.	SA121	Paul, S.	SU496	Petrosky, K.	SU379
Orwall, E.	1131	Pang, M.	SA076	Paula, A. P.	SA311	Petrova, N.	F491, SA491
Orwig, D.	F345, SA345, SA346, SA432, SU073, WG5	Panton, L. B.	SU418	Pauley, C. A.	M506	Petryk, A.	1008
Orwoll, E. S.	1058, 1209, 1246, 1277, 1278, 1279, 1282, F321, F335, F354, F367, F426, M266, M268, M360, SA268, SA321, SA328, SA335, SA354, SA367, SA426, SU183, SU219, SU284, SU300, SU338, SU349	Panus, D.	M493, SU143	Pavel, I. Emilia	M141	Pettersen, P.	1129, SU361
Osaki, M.	M111	Papadimitropoulos, E.	SU351	Pavlos, N.	SA099	Petterson, U.	M117
Osborne, L. R.	1218	Papadopoulos, A.	SA148	Pawlak, G.	SU064	Pettifor, J.	SU490
Osdoby, P.	SU209	Papaioannou, A.	1056, F358, M302, M379, M380, SA343, SA358, SA359, SA368, SA414, SU251, SU292, SU341, SU351, SU357, SU404, SU504	Payer, J.	SU261	Pettifor, J. M.	M491
Osei, K.	SU315	Papanastasiou, P.	F403, M362, M363, SA403	Payet, M.	SU107	Petto, H.	1019
Oshige, T.	SU286	Papasian, C. J.	M404, SA267	Payne, E. J.	M262	Peyrin, F.	1061
Oshima, H.	M299	Paralkar, V.	SU048	Payne, T. R.	M135	Peyton, D. K.	SU041
Oshima, M.	SA162	Pardi, E.	M204, M436, SA482	Pazderska, A.	M348	Pfeilschifter, J.	SU340, SU344
Oshima, Y.	1217	Pares, A.	M442, SA030	Peacock, L.	SA075	Pfister, T.	SU391
Oskarsdottir, D.	SA374	Parikh, N.	M437	Peacock, M.	M188, SA239, SU395, SU486, WG19	Pham, A.	1100, F249, SA249
Osses, N.	F020, SA020	Parimi, N.	1277, F335, SA335	Pearsall, R. Scott	SU376	Pham, C. T.	SA155
Oste, L.	SA387, SA460	Parisi, M. S.	M426, SU430, SU499	Pearson, D.	SU473	Pham, T.	M381
Oster, G.	M356	Park, B.	M260	Pear, S. Lynn	M487	Phamluong, K.	1043
Ostertag, A.	1132	Park, B. Lae	M256	Pecaut, M. J.	1295	Phillips, C. L.	SA146
Ostroff, R. L.	SU150	Park, C. Y.	SA545, SA553, SU395	Pedersen, J.	SU194	Phillips, J.	1174
Oszyczka, A. M.	M060	Park, D.	M147, M148, SA117	Pedersen, N.	1095, 1205, SA334	Phipps, R.	M023, M420, SA344, SA505, SU387
Ota, N.	SA022	Park, E.M128, M260, SA036, SU214, SU226		Pederson, L.	M017	Pi, M.	F004, SA004
Otero, J.	SU112	Park, E. Kyun	M256	Pedracini, A.	F135, SA135	Pichon, C.	M133, SA065
Otonichar, J.	SA039, SU005	Park, H.	M392, M393, SA036, SU055, SU359	Pedrazzoni, M.	SU348	Pickard, L.	SU351
Otterdal, K.	SU167	Park, I.	SU298	Pedreira, P. G.	SU337	Pickard, S.	SU332
Otto, C.	M293	Park, J. M050, M152, SA064, SA390, SU077		Pedroni, M. Vinicius	M427	Pickarski, M.	F297, M127, M276, SA297
Ou, G.	1148	Park, K.	M086, M407	Pedula, K. L.	1055	Pickett, K. A.	M482, WG20
Oursler, M.	F029, M017, M052, SA029	Park, M.	M260	Peet, D.	SU080	Pienta, K. J.	F270, SA270
Oury, F.	SA255, SA463	Park, N.	SU214	Pegurri, M.	SU379	Pieper, C.	1030
Ovchinnikov, D.	M118	Park, S. F242, M340, SA036, SA164, SA189, SA242, SU077, SU416		Pei, F.	M032	Pieper, C. F.	SU411
Overgaard, S.	1163	Park, W.	M364	Pekkarinen, T.	SU422	Pierce, A.	SU146, SU149
Owen, C.	1218	Park, Y.	SA390	Pela, I.	M092	Pieroz, D.	1141
Oxford, J. T.	F135, SA070, SA135	Park-Min, K.	SU114	Pelck, R.	M350	Pierroz, D. D.	SA220
Oxlund, H.	M149, M154	Parker, K. T.	SU491, SU503	Peleg, S.	M229	Pietras, S. M.	SU426
Oyama, T.	M326	Parker, R.	M344	Pelle, S.	M272	Pietrogrande, L.	SU345, SU346
Oyersman, S. M.	M058, SU063	Parkhurst, M.	SA556	Pellegrini, G. G.	M288, SA377	Pietschmann, P.	M070
Oz, O. K.	SA211	Parra Prada, E.	SU211	Pelletier, J.	M018, M162, SA152, SU003	Pighin, A.	SA377
Ozaki, S.	SA294, SU242	Parravicini, L.	M013	Pelletier, J. Pierre	M159, SU116	Pigni, A.	F281, SA281
Ozanian, T.	SA350	Parrini, S.	M092	Pellisa, E.	SU498	Pignolo, R. J.	M243
Ozawa, H.	M113	Parsons, C.	SU224	Pendergrass, M.	SU255	Pike, J. W.	1223, SU198
Ozcivici, E.	1293, M486	Parsons, H. K.	M002	Pendleton, C. M.	SU041	Pikner, R.	SA318
Ozono, K.	SA119, SA470, SU172	Partridge, N. C.	F050, M033, SA050, SA229, SU392	Penel, G.	SU382	Pilbeam, C.	SA033, SA529, SU085
Paccou, J.	SU382	Parvizi, J.	M169	Peng, D.	M160	Pilka, E.	F407, SA407
Pace, J. M.	SA146	Pasanen, M.	SA338	Peng, X.	F188, F275, SA188, SA274, SA275	Pilliar, R. M.	M176
Pachman, L. M.	SA106	Pascal-Vigneron, V.	SU288	Peng, Z.	M293, M295, M298, SA518	Pinchera, A.	M204, M436, M438, SA482
Pacicca, D.	1046, SA136	Pascual-Salcedo, D.	SA496	Pennisi, A.	F288, M001, SA288	Pinessi, L.	SA475
Pacifici, M.	M151	Pasquale, M.	M371, SA424, SA425, SA427	Penny, S. J.	SU266	Pinheiro, M. M.	SU337
Pacifici, R.	1197	Passeri, G.	SU348	Pennypacker, B.	1214, F508, SA072, SA073, SA508	Pino, A. M.	1073
Pactrick, A. L.	SU299	Pastinen, T.	SA263	Percival, D.	M127	Pinto, T.	SA259
Padhi, D.	M394	Pastor, F.	1134	Pereira, F. A.	M190, SU457	Pinz, I.	M145
Page, K.	F471, SA471	Paszy, C.	1138, 1211, 1213, F394, SA394	Pereira, R. Maria R.	SU453	Pioli, G.	1245, SU348
Pahlavan, P.	1238	Pata, M.	1271, F089, SA089	Perera, S.	1020, SU259	Pirens, G.	SA302, SA303
Pahr, D.	SU474			Pereverzev, A.	SU105	Pirih, F.	1159
Paic, F.	M056, SA056			Perez, F. P.	SA352	Pirrello, J.	F439, SA439
				Pérez, L. A.	SU015	Piswanger-Sölkner, J. Claudia	M388
				Pérez-Cano, R.	M101, SU009	Pitsillides, A.	SA460
				Perilli, E.	F500, SA500	Pittenger, G.	M002
				Peris, P.	M442, SA030	Piwnica-Worms, D.	1232
				Perkins, S. M.	SA239	Platt, O. S.	M241
				Perrien, D. S.	1137, F376, SA376	Platz, A.	SU432
						Pleshko, N.	SA561

(Key: 1001-1300 = Oral, F = Friday Plenary poster, SA = Saturday poster, SU = Sunday poster, M = Monday poster, WG = Working Group Abstract)

## ASBMR 30th Annual Meeting

## Author Index

Plesner, T.	M287, SA231	Purcell, D.	M099	Randall, D. L.	SA035	Reynolds, J. C.	F217, SA217, SU496
Plotkin, L.	1038, 1227, M108, SA185	Purev, E.	F098, SA098	Ranganath, L. R.	M166	Reza-Lopez, S.	SU381
Plouffe, L.	SA421	Purple, C.	SA422	Ransjö, M.	M119	Rhee, Y.	M351, SA164, SA442, SU452
Pluijm, S. M. F.	SA372	Purton, L. Elizabeth	1263	Ranstam, J.	1243	Rianon, N.	SU289
Plum, L. A.	SU195	Purvis, D. R.	SA307, SU252	Rantalainen, T.	M479	Ribot, C.	M415
Poiana, C.	SU246	Püschel, K.	1133, 1134	Rantanen, T.	F420, SA420	Riccardi, K.	SU048
Poliachik, S. L.	SA462, SA515	Putra, D.	WG27	Rao, A. V.	SU336	Ricevuto, E.	M272
Polidoulis, I.	M484, WG35	Puzas, E. J.		Rao, D. Sudhaker.	F405, F480, M420, M437, SA405, SA480	Richa, J.	1203
Poliquin, S.	SU309	Puzas, J. Edward	1259, M025, M028,, SA556, SU133	Rao, L. G.	SU336	Richard, C.	M199
Pollack, S.	M217, M218	Pye, S. R.	SA457, SU335	Rapraeger, A. C.	1229	Richard, F.	F319, SA319
Pollock, M.	SA320			Rashed, M.	F089, SA089	Richards, B.	1091
Pollock, N. K.	M468, SU318			Rasmussen, H. M.	SU305	Richards, G.	F012, SA012
Polly, B. J.	SU479			Rastelli, A.	1021	Richards, J.	SA263
Pols, H.	1091, SA263, SU188, SU317			Ratajczak, T.	SA099	Richardson, J. K.	SU411
Pomp, A.	SU201			Rattner, A.	SA011	Richardson, S. Jane	M183
Pompolo, S.	F195, M014, SA195, SU046			Rauch, F.	SA259, SU483, SU497, WG23	Richert, L.	SU168
Ponnapakkam, A.	1063			Rauner, M.	M070	Richey, P.	M496
Ponnapakkam, T.	1063, SU500			Ravanti, L.	M295	Richie, S.	M322
Pons, F.	M442			Ravazzoli, M.	SA241	Ridge, S.	1221
Poole, K. E. S.	M315, SU275			Rawadi, G.	1004, SA130	Riera, H.	SU157
Poovorawan, Y.	M406			Ray, B. J.	SU111	Ries, W.	M366, SU247
Popa, N.	M115			Rayalam, S.	SU164	Riffle, S. E.	1295
Popoff, S.	1011, 1150, M066, SU012			Raz, R.	SU143	Riggs, B. L.	1167, 1179, 1284, SU267
Popp, A. Werner	SU296			Rea, S.	SA099	Righini, V.	1170, M180
Popp, K. L.	SA539, SA540			Reading, I.	F544, M504, SA544	Riis, B.	M398
Porrás, L.	SU196, WG11			Reboul, P.	M162	Riis, B. J.	SA436
Porter, A.	SA342			Recker, R. R.	1093, M022, M310, M323, M404, SA267, SA344, SU154, SU155, SU331, SU333, SU384, SU479	Rikkonen, T.	SU433
Porter, F. D.	SA262			Redfern, D.	SA140	Riley, S.	M136
Porter, R.	1078, F171, SA171			Reed, F.	M366	Ringe, J.	M331
Portero-Muzy, N.	SA524			Reed, K. E.	F552, SA552	Ringe, J. D.	M359, SU421
Poss, J. W.	SA368			Reens, D.	M141	Ringhofer, B.	F004, SA004
Poston, S.	M367, SA429, SU408			Reese, T. G.	SA102	Rios, M. José.	M101, SU009
Posvar, E.	M394			Reeve, J.	1010, 1120, 1240, M315, M478, SU275	Rios, S.	1073
Pothuaud, L.	M308, SA322			Refetoff, S.	F242, SA242	Ripamonti, C.	F281, SA281
Potts, J. T.	M186, F221, F224, F483, SA221, SA224, SA483			Reginster, J.	F403, M362, M363, SA403	Rissanen, J. P.	M293, M295, M298, SA282
Poubelle, P. E.	M057, SA092			Regmi, A.	SU045	Risteli, J.	SA232
Pouilles, J. Michel	M415			Rehman, S.	M066, SU012	Ritchie, H. H.	SA144
Poulton, I. J.	M014			Reichenberger, E.	1204, M027	Ritchie, J. P.	1229
Poundarik, A. Abhay	SU478			Reid, D.	1246, M362, M363	Ritchie, R. O.	F149, SA149, SA342
Pourteymoor, S.	SU018			Reid, D. M.	1287, 1288, F337, F403, M317, SA257, SA337, SA403, SU224	Rittweger, J.	M487
Powell, K.	SA039, SU005			Reid, I.	F401, SA401	Rivadeneira, F.	1091, SA263, SA355, SU188, SU317
Powell, W. F.	1158			Reid, I. R.	1286, M317, SA175, SU071	Rivas, D.	F131, SA131, SU374
Power, J.	M478			Reider, L.	F345, SA345	Rivella, S.	SA128
Pozzi, S.	1231, SU239			Reifsnyder, P. C.	M244	Rizzo, J. H.	1055
Praeda, M.	M145			Reilly, G.	M451	Rizzoli, R.	1106, 1239, F401, SA401, SA506, SA510, SU168, SU329
Pratap, J.	F279, F572, M041, M279, SA279, SA572			Reilly, G. Clair	SA067	Robanus-Maandag, E. C.	SA130
Prawitt, J.	SA042			Reina, P. Soledad	SU269	Robb, R.	1284
Pregizer, S.	M031			Reiner, A.	SA271	Robbins, J.	1208, F383, M285, SA383
Prenner, G.	M388			Reinhardt, T.	1185, M196, SU203	Robbins, J. A.	F333, SA333
Prenovost, K.	F365, SA365			Reinhold, M.	1266	Robbins, M. E.	1066, SU368
Prentice, A.	M498			Reinwald, S.	WG41	Roberson, P.	1157
Preston, H. M.	M485, WG36			Reitz, R. E.	M182	Roberson, P. K.	1250
Prestwood, K.	M353			Rejnmark, L.	1163, M206, SA218, SA290, SU227	Robert, B.	SA150
Prezelj, J.	SA300			Rendina, D.	SA475, SA481	Roberta, N. J.	1025
Price, C.	1249			Rendina, E.	M341	Roberts, A.	M278
Price, H. E.	SU485			Renesto, E.	M180	Roberts, B.	M457
Price, J. Susan	SA526			Renlund, R.	SU373	Roberts, B. J.	1070, M304
Price, R.	1101			Renous, R.	SU159	Roberts, S. A.	SU428
Price, T.	SU409			Reseland, J.	SA137	Robertson, K.	F085, SA085
Priemel, M.	1006, 1133, 1134, 1201			Resmini, G.	M355	Robinson, B.	SU048
Prince, R.	F373, M245, M262, SA320, SA373			Restaino, S.	SA501	Robinson, J. A.	F439, SA439
Prior, H. J.	1238			Reszka, A.	1214	Robinson, L. J.	1125
Prior, J.F358, SA358, SU292, SU309, SU357				Reyes, M. Loreto	F435, SA435	Robling, A.	1002, 1038, M193
Prior, J. C.	M325, SU351			Reyes-García, R.	M447	Rocheffort, G. Y.	M239, SA538
Prior, J. L.	1232			Reynolds, C.	1173	Rodd, C.	1108, SU483, SU487, WG23
Prisby, R.	1061					Rodova, M.	M043, SU020
Proksch, N.	1134					Rodriguez, D.	1292
Prosser, D. E.	M231, SU199					Rodriguez, J. Pablo	1073
Provot, S.	SU004, SU121					Rodriguez, M.	SA076
Przedlacki, J.	M382					Roelofs, A. J.	1065
Pulusani, S. R.	SA225					Roemer, F.	1075
Punab, M.	SA457, SU335					Roesel, T. R.	SA474
Puolakka, J.	F420, SA420					Roffe, C. M.	SU200

(Key: 1001-1300 = Oral, F = Friday Plenary poster, SA = Saturday poster, SU = Sunday poster, M = Monday poster, WG = Working Group Abstract)

## Author Index

## ASBMR 30th Annual Meeting

Rogers, A.	M507	Rowe, P. S.	1051, F066, F205,	Said-Nahal, R.	1130, 1241, M313	Sasaki, T.	1121
Rogers, M.	SU109		F207, F210, SA066,	Saini, S.	SU019	Sasov, A.	1296
Rogers, M. B.	SU150		SA205, SA207, SA210	Sainsbury, A.	1195	Sassi, A.	SU265
Rogers, M. J.	1065, 1221	Rozas-Moreno, P.	M447	saita, Y.	M174, SA378	Sato, M.	M207, SA021, SA375,
Roh, M.	SU359	Rozenberg, S.	SU265	Saito, H.	1004, 1005, 1109		SU196, WG11
Rokutanda, S.	1151	Rozental, R.	F413, SA413	Saito, M.	SA382, SU049	Sato, T.	1122, SA201, SA490
Romagnoli, E.	SU210	Rozhinskaya, L. Yakovlevna	M192	Saito, N.	M113	Sato, Y.	SA325, SA330
Roman, A.	M071	Rozic, R.	SA039, SU005	Saito, T.	F116, F163, F469, SA039,	Saunders, M.	M465
Roman, A. A.	SU165	Ruan, J.	M103		SA116, SA163, SA469	Savage, P. M.	F523, SA523
Romano, P.	M408	Ruan, M.	M017	Saito, T.	SU005	Sävendahl, L.	1188, SU179
Ronda, A. Carolina	SU185	Rubert, M.	SA299	Sajjan, S. G.	1236, M400, SU420,	Savoye, M.	SA472
Rondeau, G.	M197	Ruberte-Thiele, R. A.	1249		WG38	Sawada, N.	SU034
Rong, J.	M318	Rubin, C.	M342, SA247, SA522	Sakai, A.	M326, SA448, SU286	Sawada, S.	M121
Ronis, M. J. J.	SA336, SU182	Rubin, C. Johan	M232, SA264	Sakai, H. SU101, F548, M492, SA548		Sawka, A. M.	M379, M380
Ronkainen, P.	F420, SA420	Rubin, C. T.	F047, M397, M486,	Sakai, S.	SU090, SU102, SU394	Sawyer, R. Kay	M224
Rønne, H.	M350		SA047	Sakai, T.	SA082	Saxena, R.	M114
Roodman, D.	SU075	Rubin, J.	1253, SA522	Sakaki, T.	M216	Saxon, L.	1296, SA526
Roodman, G. David1186, F081, F476,		Rubin, M.	SA486	Sakamoto, K.	M111, SU117	Saxon, S. H.	SU364
F478, SA081, SA287, SA289,		Rubin, M. Ruth	1036, 1146, F485,	Sakamoto, Y.	M421	Sayers, A.	1104, 1175, F554, SA554
SA476, SA478, SU070			SA485	Sakane, M.	M274	Sazonova, N. Ivanovna	M192
Roopenian, D.	M003	Rucci, N.	M272, M275, SU017,	Sakane, Y.	SU036	Sbaiz, F.	SU050
Ropper, H.	WG1		SU089	Sakashita, I.	SA513	Scadden, D.	1231, SU239
Rosa, J. Luis	F020, SA020	Rudäng, R.	1281, M327	Sakata, K.	SA490, SU438, SU440	Scamuffa, N.	SU157
Rosales, G.	M356	Rude, R.	SU281	Sakon, J.	1063	Scanlan, T. S.	M228, SA232
Rosales, J.	SU263	Rudkin, G. H.	SU038	Sakurai, T.	SA379	Sczufca, M.	SU453
Roschger, P.	F217, SA217	Rufo, A.	SU017, SU089	Salazar, V. S.	SU144	Scerpella, T. A.	M490
Rose, C.	SA466	Ruiz, S.	F020, SA020	Salbene, G.	F281, SA281	Schacht, E.	SU421, SU444
Rose, C. M.	M315, SU275	Ruiz-Gaspà, S.	SA030	Sale, C.	M481	Schadt, E. E.	M247
Rosen, C. J. 1073, F093, F265, M003,		Rundek, T.	1034, M434	Sale, J. E. M.	M369, M383	Schaefer, E. J.	F341, SA341
M145, M252, M305, M493,		Rundle, C. H.	SA182	Saless, N.	F260, SA125, SA260	Schafer, A. L.	M452, WG25
M495, SA093, SA120, SA265,		Runge, M.	SU444	Salhab, I.	SA084	Schafer, B.	M489
SU029, SU190		Ruppel, M.	M023, SU475	Salinas-Riester, G.	M450, WG21	Schäfer, V.	SA408
Rosen, D. M.	SA111	Ruppender, N. S.	M280	Salmon, P. L.	1296, SA387, SA460	Schaffer, M.	M440
Rosen, V.	SA159, SU143, SU145,	Russell, R. Graham G.	F407, SA407	Salo, G.	M264	Schaffler, M. B.	SU190
	SU148	Russo de Boland, A.	M189, SU185	Samadfan, R.	1072, 1216, SA385,	Schaller, M. D.	SU065
Rosenberg, C.	SU352	Ryan, B.	M353		SU391	Schanen, N. Carolyn	M242
Rosenberg, E.	SU389	Ryan, K.	SA266	Samadfan, R.	F508, SA508	Scheid, J. L.	SU166, SU184, SU191
Rosenblatt, M.	M273	Ryan, Z.	M198, SA059	Sämann, A.	SU456	Schemitsch, E. H.	SA104
Rosengren, B. E.	1166	Rybchyn, M. S.	F389, SA389	Samathanam, C.	M338	Schett, G.	1149, 1215
Rosier, R. N.	1047	Ryberg, E.	1221	Sambrook, P.	F401, F403, M362,	Schiavi, S.	SU173
Rosol, M.	M074	Rychly, J.	SA528		M363, SA401, SA403, SU342,	Schilling, A. F.	1007, 1201
Rosol, T. J.	1160, 1264	Rydborg, J.	M423		SU344	Schilling, T.	M047, M075
Ross, F.	1119	Ryder, K.	SU178, SU448	Sambrook, P. N.	1164	Schiltz, C.	F010, SA010
Ross, F. Patrick	1010, 1120, 1220,	Rydzik, R.	SU250	Samee, N. M.	F010, SA010	Schinke, T.	1003, 1006, 1133, 1198,
	SA077, SU097	Ryg, J.	1163, SU270	Samelson, E. J.	1207, SU326		1201, F202, SA192, SA202
Ross, J. L.	SU068	Ryoo, H.	M050, SA016, SA064,	Samji, F.	M322	Schipani, E.	1038, 1154, 1263, F215,
Ross, M. Elizabeth	F253, SA253		SU021, SU022	Samuelsson, B.	F433, SA433		M076, M150, SA215
Ross, R.	1221	Ryu, J.	M069, SA463	San Martin, J.	1285, 1286, M395	Schirtzinger, L.	SU239
Ross, S.	M417, SA331, SU283	Ryu, S.	M163	San Miguel, S. Marquez	SA040,	Schitter, G.	SU467
Rossa, C.	SU013				SA056	Schlabritz-Loutsevitch, N. E.	M494
Rossant, J.	1218	<b>S</b>		Sánchez, A. Laura	M426	Schlaubit, S.	F118, SA118
Rossdeutscher, L.	1185	Saadat, R. L.	SU273	Sánchez, R.	M221	Schlie, J.	1134
Rossdeutscher, L.	SU207	Saadia, M.	SU235	Sanchez, T. V. SA307, SU252, SU253		Schlüssel, Y.	SU367
Rosser, J. L.	F062, SA062	Saag, K. G.	1024, 1171, F403, F409,	Sanda Khin, S.	SU245	Schmidt, A. L.	M207
Rossi, A.	F500, SA500		M362, M363, M368, SA280,	Sandberg, W.	SU167	Schmidt, C.	F376, SA376
Rostomyan, L. Grantovna	M192		SA326, SA360, SA362, SA403,	Sanders, A. K.	1001	Schmidt, H.	F465, SA465
Roth, E. J.	SU364		SA409, SU256, SU287, SU321,	Sanders, K.	1244	Schmitz, A.	M350
Rothenberg, E.	SU204		SU401	Sanderson, R. D.	1229	Schmitz, S.	SU177
Rotimi, C. N.	SA262	Saarinén, A.	1176	Sandgren, E. P.	M171	Schnabel, C.	F465, SA465
Roubenoff, R.	1283, F341, SA341	Saba, L.	SA451	Sandhu, P.	1214	Schneebauer, M.	1003
Rousseau, L.	M194	Sabastiani, P.	F038, SA038	Sangadala, S.	M034, SA023	Schnegelsberg, B.	SA111
Routson, S. M.	1189	Sabatatos, G.	1005	Sanhueza, E.	F435, SA435	Schneider, D.	1128, M072, SU370
Roux, C.	1130, 1241, 1291, F319,	Saberi, S.	SU001	Sanjay, A.	1011, 1150, M066	Schneider, P.	1294, M456
	F403, M313, M316, M362, M363,	Sabetrasekh, R.	SA137	Sano, H.	SA222	Schneider, S.	SU367
	M395, SA319, SA403, SA415,	Sabokbar, A.	SA097	Sanovic, S.	SU085	Schnitzer, T. J.	SU364
	SA466, SU325, SU327, SU328,	Sabsovich, I.	F461, SA461, SU160	Santella, R. M.	SU202	Schober, H.	SU354
	SU342, SU344, SU471	Sacco, M.	M201	Santi, I.	SU345, SU346	Schoeller, M. C.	SU266
Roux, C. Hubert	M418	Sacco, R.	1034, M434	Santiago-Mora, R.	SA037	Schoenborn-Kellenberger, O.	M362
Roux, J. Paul	M455	Sacco, S. M.	SA447, SU381	Santo, L.	1231, SU239	Schoenecker, P. L.	F569, SA569
Roux, S.	SU078, SU107	Saeed, H.	1147	Santora, A.	1291, SU389	Schoenmakers, I.	M498
Rouyer, C.	SA258	Safadi, F.	1011, 1150, M066, SA532,	Saoji, N.	SU062	Scholz-Ahrens, K. E.	SA445
Rowe, D.	F041, SA041, SA051,		SU012	Sapin, E.	M316, SU471	Schoonmaker, J.	F277, SA277
	SU028	Safi, W.	M373	Saponaro, F.	M436	Schoppet, M.	M271
Rowe, D. W.	1202, F062, M062,	Saftig, P.	F074, SA074	Sapountzi, P.	SU424	Schorr, H.	M417
	M077, M082, M097, M103,	Sage, A. P.	M143	Sarkar, G.	SU231	Schorr, K.	M205
	M138, SA007, SA062, SU053,	Sahni, S.	1168	Sarlet, G.	SA302, SA303	Schousboe, J. T.	1022, 1035, 1057,
	SU057	Said-Al-Naief, N.	SU062	Sasaki, H.	M219, SA214, SA499,		1127, F416, F426, M378, SA416,
Rowe, G. Cameron	1109				SU229, SU241, SU454		SA426, WG18
				Sasaki, S.	SU307	Schrezenmeir, J.	SA445

(Key: 1001-1300 = Oral, F = Friday Plenary poster, SA = Saturday poster, SU = Sunday poster, M = Monday poster, WG = Working Group Abstract)

## ASBMR 30th Annual Meeting

## Author Index

Schrier, D.	SU146, SU149	Shah, A.	M059, SA136	Shiraishi, A.	SU090, SU394	Sitruk-Khalfon, D.	SU352
Schrooten, J.	1140	Shah, J.	1146	Shiroo, M.	F433, SA433	Sittichokechaiwut, A.	SA067
Schuetze, N.	M075, M450, WG21	Shah, M.	SU037	Shoback, D.	1156, 1261, M452, WG25	Sittitavornwong, S.	SU062
Schuler, B.	1294	Shahid, M.	M059			Skalli, W.	M316, SU471
Schulmerich, M. V.	M462, SU480	Shahnazari, M.	1100, M137	Shockley, K. R.	F265, SA265	Skarantavos, G.	SU472
Schultz, N.	SU125	Shane, E.	1033, M310, M397, M448, SA501, SU202, SU441, SU455, SU458	Shogren, K. L.	SU231, SU240	Skarratt, K. K.	SU224
Schulz, A.	1201			Shohami, E.	SU375	Skarzynska, J.	M060
Schulze, J.	1003, 1006			Shore, B.	M471	Skerry, T. M.	F012, SA012, SU100
Schwartz, A.	1209, SA271, SA328	Shanmugarajan, S.	SA173	Shore, E. M.	1203, F044, M243, SA044	Skinner, C.	1114
Schwartz, M. A.	SA060	Shao, J.	1083, 1196, F109, SA109			Skinner, C. M.	M165, SA134
Schwartz, Z.	1124, M164, M227, SA113, SU006, SU156	Shao, Y.	M170, SA027	Short, W. H.	SA519	Skinner, R. A.	1234
		Shao, Y. Y.	M157	Shu, A.	M448	Skordos, L.	1174
Schwartz, U.	SA146	Shapiro, I. M.	F058, M169, SA058	Shu, A. D.	SU458	Skrzypek, L.	M060
Schwarz, E. M.	F153, F186, M236, SA153, SA186, SU136	Shapses, S. A.	SU367	Shu, S. T.	1160	Skurla, C. T.	SA511
		Shardell, M. D.	SU073	Shuldiner, A.	SA266, SU365	Slatkovska, L.	M396
Schwarz, P.	M350, SU223	Sharkey, N. A.	M485, WG36	Shultz, K. L.	M252, SU147	Sliney, J.	1036, 1146, F485, SA485
Schwarz, T.	1008	Sharma, A.	SU487	Shuto, E.	SU443	Sloofman, L. G.	SA133
Schwarzer, C.	1195	Sharma, M.	SA454	Sibai, T.	M126	Slowinska, B.	F253, SA253
Schweiger, M.	M388	Sharp, C. A.	SU360	Sibilia, J.	F488, SA488	Smallwood, D.	M414
Scillitani, A.	M201, M432, SU210	Sharp, M.	F439, SA439	Siccardi, V.	1245	Smerdel-Ramoya, A.	1111, F141, SA005, SA141
Scott, C. I.	M240, SU494	Shaw, C. A.	F118, SA118	Sicliari, V. A.	M277		
Scott, J. M.	F552, SA552	Shaw, N.J.	WG1	Siddhanti, S.	1286, M395	Smets, N.	1152
Scott, J. Paul R.	M481	She, J.	SU164	Siega-Riz, A. Maria	M305	Smith, A. V.	1094
Scott, K.	1214	Sheeche, P. R.	SA519	Siegel, P. M.	1016, SU115	Smith, B. J.	M341, SU303
Scott, K. R.	F508, SA508	Sheer, R.	SA418	Sierra, O.	1083	Smith, D. J.	M247
Scutt, A.	M451	Shelton, R. Shane	1097, 1247, F024, SA024, SA185	Siervogel, R. M.	1177, M321	Smith, E.	1121, F098, SA098
Seaman, P.	1020, SA314			Sievänen, H.	M479, SA338, SA533, WG10	Smith, E. A.	SU158
Searby, N. D.	M469, SA517	Shen, C.	M338			Smith, G.	SU030
Secreto, F.	1258	Shen, J.	F242, SA242	Siggeirsdottir, K.	1094, 1096, F369, SA369, SU289	Smith, J.	1078
Sedarati, F.	SU384	Shen, L.	SA048			Smith, J. Jermaine	SU282
See, K.	1171	Shen, R.	1044	Siggelkow, H.	M450, WG21	Smith, K.	SA216
Seefried, L.	M072	Shen, X.	SU052, WG23	Sigurdsson, G.	1096, F369, SA369, SA374, SU289	Smith, K. C.	M182
Seehra, J.	1231	Shenouda, N.	SU483, WG23	Sigurdsson, S.	1096, F369, SA369, SU289	Smith, M. R.	1292
Seeman, E.	1101, F542, M245, M497, SA542, SA551	Shepherd, J.	1105, SU488, WG22			Smith, M. V.	SA177
		Shepherd, P.	SU030			Smith, R.	1276
Segal, E.	SU248	Sherk, V. D.	SA534	Sikes, R. A.	SA269	Smith, S. Y.	F508, SA508, 1072, 1216, SA381, SA385, SU391, SU435
Segawa, H.	F473, SA473	Sherwood, R. J.	1177, M321	Silberman, C.	SA429		
Segev, E.	1121	Sheu, T.	1259, F186, M028, SA186	Siller-Jackson, A. J.	SA060	Smith, T.	F038, SA038
Segre, G. V.	1013, 1228	Sheu, Y.	SU299, SU300	Silman, A. J.	SA457, SU335	Smith, U.	SA198, SU459
Seibel, M. J.	1164, 1224, 1267, 1280, F233, M458, M100, SA233, SA234	Shi, N.	F356, SA356, SU320	Silva, M. J.	1110, M475	Smith, W.	1024
Seidah, N. G.	M053	Shi, W.	1082	Silva, O. L.	SA524	Smolarikova, V.	M261
Seijo, M.	M405, SU429	Shi, W. Y.	SU253	Silva, R.	M452, WG25	Smulders, Y.	SA372
Seitz, S.	1003, 1133, F202, F465, SA202, SA465	Shi, X.	1148, M011, SA266, SU010, SU032, SU033	Silve, C.	SA225, SA258	Snellman, G.	SA334
		Shi, Z.	1118, F188, SA188, SA278	Silver, A. G.	SU401	Sochett, E. B.	SU491, SU503
Sekiguchi, S.	M443, SA499, SU031, SU170	Shibata, M.	M443, SA499, SU031, SU170	Silverberg, S. J.	1031, 1034, M4341, M431, SA486, SU201	Sodek, J.	SU069
				Silverman, L. D.	SU235	Sodi, R.	M289
Sekimizu, K.	F494, SA494	Shibuya, H.	1182	Silverman, S.	M367, M390, SA360, SA362, SA404, SU340, SU344, SU408	Søe, K.	M287, SA231
Selby, P. Leslie	M416	Shih, M.	1297			Sogabe, N.	SU308
Selim, A. A.	1189, SA568, SU072	Shiizaki, K.	M185	Simao, A. Maria S.	SA061, SA063	Sohaskey, M. L.	1075
Selim, H.	SA568	Shikany, J.	1277, F335, SA335	Simic, P.	SU141	Soimakallio, S.	SA533, WG10
Selim, S.	F439, SA439	Shikany, J. M.	F367, SA367	Siminoski, K.	SU483, WG23	Sokoll, L.	M435
Selkov, E.	M134	Shim, S.	M152, M339	Simon, A. M.	1137	Sole, C.	SU263
Sellin, J. H.	M229	Shimada, K.	M063, SA028	Simon, T.	SA111	Solera, J.	M255
Selvamurugan, N.	M033	Shimada, M.	M150	Simonelli, C.	SU266	Solloway, M. J.	1043
Semirale, A. A.	SU193	Shimada, Y.	M219, SA214, SU454	Simonet, W. S.	1139, 1211, 1213, F394, SA394	Solomon, B.	SA520
Semler, J.	1172	Shimizu, E.	SU392			Solomon, D. H.	M370, M358, SA370, WG15
Semmler, J.	1133	Shimizu, M.	F483, SA483	Simpson, C.	M330, M333, SA472	Soltani, A.	SU339
Sen, B.	1253, SA522	Shimizu, Y.	F163, M326, SA163	Simpson, J. M.	1164	Somes, G.	M496
Sen, S. S.	1236	Shimohata, N.	1222	Sims, N. A.	F195, M014, M155, SA194, SA195, SU046	Sommer, S.	M220, SA055
Sen, S. Sankar	M400, SA430	Shimokawa, H.	M019			Somoza, J.	M405, M426, SU429
Sen, S. S.	SU420, WG38	Shimokawa, I.	SA467	Sims, S. M.	SU105	Somoza, J. Isabel	M288
Senn, C.	SU296	Shimono, K.	SA162	Simsek, S.	SA372	Son, M.	M152
Senn, J.	F480, SA480	Shin, C.	M086	Sinacore, J.	SU424	Sondergaard, B. C.	M155
Sennerby, U.	1205	Shin, C. S.	SA046	Sinaki, M.	M473, WG6	Sonne, M.	SA456
Seo, H.	SU118	Shin, C. Soo	F391, SA043, SA391	Sinal, C.	M071, SU165	Sonoyama, W.	SA162
Serrano-Alferez, I.	M292	Shin, D.	M056, M351	Sinha, K. M.	F017, SA017	Soo, C.	F174, SA174
Setoguchi, T.	SU229, SU241	Shin, H.	M260, SU059, SU311, SU418	Sinha, N.	SU201	Soomro, R.	M403
Settembre, C.	SA255, SU119			Sinnot, L. T.	SU315	Soong, R. Chuan Teck	SU236
Seul, K.	SU022	Shin, H. Doo	M256	Sinofsky, A.	SU190	Sorace, S.	M092, SU050
Seuwen, K.	1173	Shindich, D.	SA512	Sipilä, S.	F420, SA420	Soranzo, N.	SA263
Sewing, A.	SA101	Shindle, L.	SU205	Sipos, A.	1019	Sorensen, M. G.	1129, M122, M124, M129, SU091
Sexton, B.	SU424	Shindo, H.	M111, SA467	Sipos, W.	M070		
Seymour, H.	1289	Shinohara, A.	SA382	Sirinvaravong, S.	WG28	Sorenson, A. H.	1018
Sha, B. Yong	SU154, SU155	Shinohara, M.	F083, SA083	Siris, E. S.	1236, 1286, SA360, SA362, SU216, SU420, WG38	Sornay-Rendu, E.	1067
Shabe, P.	1243	Shinomiyu, K.	M087	Sisler, J. D.	1161	Sos, B.	M247
Shadick, N.	SA370	Shiozawa, Y.	SA287			Sosa, M.	M259, SU322
Shaffer, J. R.	M250, SU297	Shipp, K. M.	SU411				

(Key: 1001-1300 = Oral, F = Friday Plenary poster, SA = Saturday poster, SU = Sunday poster, M = Monday poster, WG = Working Group Abstract)

## Author Index

## ASBMR 30th Annual Meeting

Soshi, S.	SA382	Stockmans, I.	1152	Sun, J.	M318	Takata, S.	M410, SU001
Sotillo, J.	1008	Stoecker, B. J.	M338	Sun, L.	SA199, SU087	Takayama, L.	SU453
Souberbielle, J. M212, SU197, SU352		Stogniew, M.	M346	Sun, Q.	M253., SA248, SA261	Takayanagi, H.	F074, F083, SA074, SA083, SA108
Soucacos, P. Nikolaos	SU472	Stoian, C. A.	SU396	Sun, W.	M028	Takeda, E.	SA201, SU443
Souen, S.	SA450	Stokes, L.	SU224	Sun, Y.	M165, SA140	Takeda, S.	M087
Soulat, D.	M172	Stolina, M.	1139	Sundaram, K.	F480, SA480, SU247	Takeda, T.	SU385
Soung, D. Y.	M301	Stolina, M.	1211, 1213	SunTERS, A.	SA526, SU037	Takei, Y.	SA201
Sousa, M.	SU011	Stolk, L.	SU188	Sunycz, J. A.	SA429	Takekura, H.	SA513
Soysa, N. S.	M121	Stomberg, E. G.	M330	Suominen, H.	F420, SA420	Takenoshita, S.	1045
Spadaro, J. A.	M004, M490, SA519	Stone, K. F351, F365, SA351, SA365		Suominen, M. I.	M293, M295, M298, SA282	Takeshita, S.	1222, SU092
Spagnoli, A.	F444, SA169, SA444	Stone, K. L.	1058	Supanwanid, P.	SU364	Taketani, S.	1222
Spanier, C.	SA408	Stoner, K.	M360	Surcel, H. Maria	SA232	Taketani, Y.	SA201, SU443
Sparapani, R.	SA428	Stouch, B.	F394, SA394	Surdhar, M. S.	SU355	Takeuchi, K.	SA294, SU242
Spector, T.	1091, SA263	Stout, D.	F283, SA283	Susan, J.	SU271	Takeya, T.	SA082
Spelsberg, T. C.	M024, M037, M052, M133, SA065, SA143	Stover, M. Louise	SU028	Susperregui, A. R. G.	F020, SA020, SA157	Takeyama, K.	1182
Spencer, R. G.	SA561	Stovitz, S. D.	M487, SA539, SA540	Sussman, C.	M220	Takigawa, M.	1188, M153
Sperling, M. A.	F181, SA181	Straarup, T. Simonsen	M149, M154	Sutter, M. B.	SA146	Takigawa, Y.	1045, 1265
Spevak, L.	M471, SA133	Strain, G.	SU201	Suttie, J. W.	SA443	Takiguchi, S.	F494, SA494
Spicer, D. B.	SU029	Strand, S.	M353	Sutton, D. A.	SU271	Takita, M.	1230, SU187
Spiro, R. C.	SA111	Strang-Karlsson, S.	1103	Suttorp, M.	SA292	Takito, J.	F079, SA022, SA079, SU102, SU103
Sprague, E.	1042, SA060	Straus, S.	M380	Suva, L.	1234, F523, M177, M281, M412, SA018, SA086, SA172, SA285, SA523, SU162	Talbot, D.	SA456
Sprague, S.	SU445, SU446	Straus, S. E.	SU343	Suzuki, A.	M443, SA499, SU031, SU170	Taleb, H.	SA140
Spurney, R. F.	1226	Strazzullo, P.	SA475, SA481	Suzuki, H.	F163, F469, SA163, SA208, SA324, SA469, SA498	Talish, R. J.	F536, SA536
Sridhar, S.	M011, SU010	Strebeck, F.	SU450, WG12	Suzuki, K.	SU437	Talmdage, K.	1243
Sridharan, M.	SU174	Street, J.	1267, F233, M100, SA233, SA234	Suzuki, M.	SA355, SU286	Tam, J.	1121
Srinivas, I. M.	SU134	Streeten, E.	SA266, SA346, SA432, SU073, WG5	Suzuki, N.	M012	Tamai, N.	F112, SA112
Srinivas, V.	F058, SA058, SU134	Streichert, T.	1134	Suzuki, S.	SA206	Tamaki, H.	SA513
Srinivasan, B.	M078, SU267	Strickman-Stein, N.	M402	Svensson, O.	M117	Tamaki, J.	SA325, SA330
Srinivasan, N.	M033	Strigoli, D.	SU211	Swain, F. L.	1234	Tamaki, S.	M299
Srinivasan, S.	SA462, SA515	Strippoli, M.	SA199, SU094	Swaminathan, R.	F544, SA544	Tamasi, J.	F050, SA050, SU392
Sriram, U.	1288	Strobbach, C. A.	SA182	Swanson, C.	SU179	Tami, A.	M417
Sroga, G.	1069	Strohl, W.	1214	Sweetwyne, M.	SU052	Tamma, R.	SA199, SU094
St-Arnaud, R.	M061, M222, SA159	Ström, O.	1023, 1290	Swift, J. M.	SA514, SA521	Tamura, I.	M094, SA147
St-Pierre, J.	M176	Strong, D.	M233, SA182, SU015	Swift, S. Nichole	SA449, SA514, WG37	Tamura, M.	SA021
St. Jeanos, A.	SU147	Strotmeyer, E. S.	1209, SA328, SU323	Swirski, A.	M382	Tamura, T.	F483, SA483
Stabley, J. N.	SA388	Stroup, G. B.	SU372	Syed, F. Asad	F029, SA029	Tan, H.	1139, 1211, 1213, F394, SA394
Staciuk, R.	SU498	Stuck, A.	1242, SU423	Syed, F. A.	M024, M052	Tanabe, K.	SA498
Stadmeyer, L.	SA005	Studenski, S.	SU323	Sylvester, F.	SA565, SU139, SU194	Tanabe, N.	M012
Stachelin, H. B.	1242, SU363, SU423, SU432	Studer, A.	SU379	Symoens, S.	SU215	Tanaka, A.	M385
Stahl, T.	SU367	Stumpf, U. C.	SU177	Syvänen, A.	SU183	Tanaka, H.	SA165, SA470
Stains, J. P.	F026, SA026	Stürmer, T.	M358	Szejnfeld, V. L.	M191, SU337	Tanaka, I.	M299
Stallcup, M.	M099	Styrkarsdóttir, U.	1091	Szulc, P.	SA440	Tanaka, K.	SA332, SA448, SU316
Stallknecht, B.	SA456	Su, N.	SA248			Tanaka, M.	SU229
Stashenko, P.	SA520	Su, Q.	1214			Tanaka, O.	SA294, SU242
Stathopoulos, K. D.	SU472	Su, Y.	M142			Tanaka, R.	SU443
Stayrook, K.	SU196, WG11	Subler, M. A.	F476, F478, SA476, SA478			Tanaka, S.	1115, 1217, SA448
Ste-Marie, L.	M197, SA353, SA406, SU330, SU399	Subramaniam, M.	M024, M037, M052, M133, SA065			Tanaka, S. M.	SA525
Stebbins, E.	F275, SA172, SA275	Suchitra, R.	SU409			Tanaka, Y.	M387
Stedman, M.	M358, SA370	Suda, N.	M069, SA463			Tang, A. A.	SU200
Steel, S.	SA257	Suda, T.	F087, SA087, SU090			Tang, D.	1047
Steenhuis, P.	M084	Sudhakaran, S.	F260, SA125, SA260			Tang, J.	M105, SU058
Steever, A.	M344	Suematsu, A.	SA108			Tang, L. Y.	F439, SA439
Steiger, P.	SA350	Suer, F.	F122, SA122			Tang, R.	SU467
Stein, E. A.	1033, SU441	Suga, Y.	M307			Tang, S.	F103, SA103
Stein, E. M.	1036, F485, M448, SA485, SA501, SU201	Sugai, J. V.	M051			Tang, W.	1225
Stein, G. S.	F277, F279, F572, M037, M041, M052, M090, M279, SA277, SA279, SA572, SU019	Sugimoto, T.	M098, M389, SA230, SA470, SA484, SU437			Tang, Y.	1273, F188, SA188
Stein, J. L.	F279, F572, M041, M090, M279, SA279, SA572, SU019	Sugita, A.	1045			Tang, Z.	SU331
Steinbuch, M.	SU370, SU414	Suh, C.	M258			Tanigawa, T.	SA448
Steiner, M.	1292	Suh, K.	SU359			Tanimoto, Y.	M093
Steinman, L.	F246, SA246, WG13	Suh, P.	M163			Tanimura, A.	SU443
Stenkjaer, L.	SU220	Suhara, Y.	M064, SU034			Tanini, A.	M092, SA393, SU050, SU211
Stensgard, B.	1258	Suhm, N.	SU294, SU296			Tank, A.	1121
Stepan, J. J.	1019	Suits, J. M.T.	SU131			Tanner, S. Bobo	SA326, SU256
Stephens, L. D.	SU303	Sujic, R.	M322, M383			Tanno, H.	M411
Stephens, P.	1212	Sukumar, D.	SU367			Tanno, K.	SA490, SU438, SU440
Stephure, D.	SU396, SU483, WG23	Sul, N.	SU416			Tara, H.	M385
Sterling, J. A.	1087, M278, M280, SA187, SU233	Sumi, M.	SU437			Taranto, M.	1289
Stern, P. H.	M068, SA090	Summers, L.	SU173			Tatum, T.	M338
Stevens-Smith, J. L.	M451	Sun, B.	M330, M333			Tau, C.	F563, SA563, SU498
Stevenson, D. A.	SA562	Sun, H.	M440, SA183, SA184, SU108, SU190			Taupin, P.	SU327, SU328
Stewart, J.	F396, M349, SA396	Sun, H. Jin	F391, SA391			Tavernier, C.	M444
						Tawfeek, H. A. W.	1013
						Taylor, A.	SU109
						Taylor, A. F.	SU104
						Taylor, A. M.	M166

(Key: 1001-1300 = Oral, F = Friday Plenary poster, SA = Saturday poster, SU = Sunday poster, M = Monday poster, WG = Working Group Abstract)

(Key: 1001-1300 = Oral, F = Friday Plenary poster, SA = Saturday poster, SU = Sunday poster, M = Monday poster, WG = Working Group Abstract)



## Author Index

## ASBMR 30th Annual Meeting

- Venkatachalam, S. M504, SU409  
Venkatesh, B. M183  
Venken, K. 1140  
Venners, S. F546, SA546  
Veno, P. A. F062, SA062  
Ventura, F. F020, SA020, SA157  
Ventura, L. M272  
Venturiere, A. SA193  
Verbruggen, N. 1291  
Verdelis, K. M311  
Verdoia, C. Alberto M013  
Vergari, R. SA199, SU094  
Verghese, J. SU323  
Vergnaud, P. SA295  
Verhoeven, G. 1140  
Verlaan, D. J. SA263  
Vervloet, M. SA203  
Vesco, K. K. 1055  
Vesterby, A. F310, SA310  
Vestergaard, P. 1163, M206, SA218, SA290, SU221, SU227  
Veverka, K. A. 1292, SA381, SU435  
Vezzoni, P. F500, SA500  
Viacava, P. SA482  
Viccica, G. M436, M438  
Vicent, S. F291, SA291  
Vicente, F. B. SU485  
Vico, L. 1061, 1191, SA011, SA142  
Vidal-Puig, A. 1222  
Vieillard, M. SU382  
Vieth, R. SU206  
Vieux-Rochas, M. F010, SA010  
Viggeswarapu, M. M034, SA023  
Vignali, E. M204, M436, M438  
Vignery, A. 1219, M208  
Vikkula, M. SA258  
Vilayphiou, N. 1067  
Viljakainen, H. T. SU433  
Villa, A. 1201  
Villa, I. F500, SA500  
Villanueva-Peñacarrillo, M. M424, M425  
Villareal, R. C. 1021  
Viñals, F. SA157  
Vincent, C. M046  
Vinik, A. I. M002  
Vinson, A. M241  
Virbalas, J. SU205  
Virk, M. S. F283, SA283  
Visse, R. SA146  
Visser, M. SA372  
Vitenzon, A. M059  
Vittinghoff, E. M347  
Vives, V. SU064  
Vlasseros, F. 1072, 1216, SA385  
Voellmicke, K. M471  
Vogel, J. 1294  
Voges, A. K. F376, SA376  
Vogiatzi, M. G. SA128  
Voide, R. 1298, M456  
Vokes, T. J. M314  
von Domarus, C. 1134  
von Marschall, Z. F145, SA145  
von Muhlen, D. SU442  
von Scheven, E. SU488, WG22  
Vong, K. M231  
Voorzanger-Rousselot, N. SU228  
Vora, J. P. M289, M291  
Voroniu, O. SU310  
Voutilainen, R. 1176  
Voznesensky, O. SA033  
Vu, J. A. 1208  
Vujevich, K. T. 1020  
Vukatana, G. M355  
Vukicevic, S. 1287, 1288, M390, SU141, SU142  
Vyas, K. 1038, 1227, M108  
Vyskocil, V. SA318
- W**  
Waarsing, E. SA052  
Wacker, W. M449  
Wactawski-Wende, J. F383, SA383  
Wada, H. SA419  
Wada, S. SU081  
Wada, Y. F494, SA494  
Wade, S. M375, M376, SU417  
Wade-Gueye, N. 1191, SA142  
Wadhwa, S. SU132  
Waern, E. SA198, SU204  
Wagman, R. B. 1285, M376  
Wagner, A. M417  
Wagner, D. SU206  
Wagner, H. 1095  
Wagner, J. M. 1020, M306  
Wagner, L. SU403  
Wahlberg, L. M286  
Wakabayashi, H. SU383  
Wakao, H. SA379  
Wakao, N. SU466  
Wakefield, D. SU390  
Wald, M. J. SU277, SU280, SU481  
Waldman, S. SU213  
Waldman, S. D. SU129, SU131  
Waldorff, E. I. 1299, M462  
Walker, E. F195, SA195  
Walker, E. C. M014  
Walker, M. D. 1034, M434, SA486, SU464  
Walker, T. Ian M183  
Walkiewicz, A. M382  
Wallace, A. M. M212  
Wallace, R. B. F333, SA333  
Walrant-Debray, O. M246  
Walsh, A. SA359  
Walsh, A. A. SU244  
Walsh, C. M348  
Walsh, J. M294, M348, SU274, SU412, SU413  
Walsh, N. C. WG41  
Walsh, S. M353  
Walter, I. M171  
Walton, H. F190, SA190  
Wan, C. 1001, 1082, F181, SA181, SA453, SU052  
Wan, M. 1014, 1082, 1273, F188, SA188  
Wang, A. 1286, SA517  
Wang, C. Chenwe M228  
Wang, D. 1262  
Wang, F. 1214  
Wang, H. 1285, F242, F323, M056, M243, SA242, SA323  
Wang, J. 1204, M043, M068, M176, M338, M433, M461, SA313, SU020, SU253, SU470  
Wang, J. Tang SA267  
Wang, L. 1260, F461, M054, M062, M077, M157, M213, SA007, SA051, SA095, SA441, SA461, SU032, SU033, SU053, SU160, SU331  
Wang, M. M116, SA441, SU312  
Wang, N. F012, SA012  
Wang, Q. 1044, F542, SA049, SA313, SA542, SA551  
Wang, T. M181  
Wang, T. J. 1207  
Wang, W. SU047, SU218  
Wang, X. 1015, F546, M338, SA546, SU015  
Wang, Y. 1082, 1193, M164, M227, SA453, SU364  
Wang, Y. Hsiung M062, SU053  
Warburton, D. E. R. F552, SA552  
Ward, K. A. M416, SA457, SU335, SU428, WG1
- Ward, L. M. SA259, SU483, WG23  
Ward, W. Elizabeth M503, SA447, SU381, SU476  
Warden, S. J. 1178, M423  
Wardlaw, D. 1243  
Wareham, N. J. 1240, F363, SA363  
Wark, J. M245  
Warman, M. L. 1002, SU130  
Warming, S. 1109  
Warmington, K. 1139, 1211, 1213, F394, SA394  
Warner, M. R. 1171  
Warren, A. 1097, 1247, F024, M010, SA024, SA185, SU189  
Warren, M. M478  
Warriner, A. H. SU321  
Wasserman, E. F527, SA527  
Watanabe, Y. M185  
Watkins, M. 1110  
Watkins, M. P. 1257  
Watson, J. Tracy SA160  
Watson, M. SU030, SU071  
Watson, P. H. M210  
Watts, N. 1027, SA314, SA360, SA362, SA404, SU342, SU403, WG31  
Waugh, E. J. F339, M324, SA339, SA558, SU271, WG8  
Wazen, R. M025  
Wazen, R. M. SA531  
Weaver, C. M. M137, M188, SA545, SA553, SU395  
Webb, W. 1038  
Webber, C. M302, SU292  
Weber, A. J. SA234  
Weber, F. F527, SA527  
Weber, G. SA060  
Weber, J. 1078, F171, SA171  
Weber, K. M171  
Weber, T. J. M394, SU411  
Webster, D. J. F527, SA527  
Weekes, D. 1233  
Wegrzyn, J. M455  
Wehrli, F. W. M312, M422, M470, SU277, SU280, SU481  
Wehrli, S. L. M422, M470  
Wei, N. 1214  
Wei, T. F461, SA461, SU160  
Weilbaecher, K. 1086, 1232  
Weiler, H. 1108, SU487  
Weinans, H. SA355  
Weinblatt, M. E. SA370  
Weinstein, L. S. 1254  
Weinstein, R. S. 1038, 1097, 1157, 1250, F024, SA024, SA185, SA453, SU380  
Weirzbicki, A. S. WG30  
Weis, J. A. SA169  
Weiss, R. E. F242, SA242  
Weitzmann, M. 1197, 1197, SU014  
Welch, J. M. M488, WG9  
Welldon, K. J. M046  
Wellik, D. M151  
Wenderoth, D. M360  
Wendling, D. M439, M444  
Wenger, K. M173  
Wenkert, D. F256, F569, SA256, SA566, SA567, SA569, SU212  
Werbeck, J. L. 1160  
Wergedal, J. 1194, 1276, M233, SA180, SA182  
Wertheimer, A. I. SA430  
Wertz, M. SU488, WG22  
Weryha, G. SU288  
Wesolowski, G. A. F297, M127, M276, SA297  
West, J. F323, SA323  
West, S. L. SU166, SU184, SU191
- Westendorf, J. J. 1258, M017, M279, SU027  
Westfall, A. O. F409, M368, SA409, SU401  
Westin, G. SA227  
Westmore, M. S. M207, SA375  
Westphal, H. 1004  
Wettschureck, N. 1228  
Wetzsteon, R. J. M482, M487, SA539, WG20  
Weycker, D. M356  
Wheeler, V. W. SA268, SU299, SU300  
White, H. SU411  
White, K. SU173  
Whittaker, P. SA263  
Whyte, L. 1221  
Whyte, M. P. 1054, F256, F563, F569, SA256, SA562, SA563, SA566, SA567, SA569, SU210, SU212  
Widler, L. 1173  
Wieland, M. M030, SA138, SU006  
Wierzbicki, A. S. SU174  
Wigner, N. F038, SA001, SA038  
Wijenayaka, A. R. M046  
Wilburn, C. SA187  
Wildemann, B. M417  
Wiley, J. S. SU224  
Wilkes, M. M. 1025  
Wilkinson, M. M203  
Willaert, A. SU215  
Willems, G. 1237  
Willems, N. M. B. K. SA110  
Willett, T. L. M461, SU470  
Willett, W. C. 1242  
Willey, J. S. 1066, 1295, SU368  
Williams, B. O. 1001  
Williams, D. A. 1220  
Williams, D. S. M343  
Williams, G. A. SU071  
Williams, H. WG29  
Williams, J. K. M164  
Williams, K. D. M321  
Williams, M. I. SU398  
Williams, N. I. SU184  
Williams, P. 1089  
Williams, S. E. SA492  
Williams, V. SA183  
Willing, M. C. M506  
Wilsgaard, T. M497  
Wilson, A. M354  
Wilson, D. SU365  
Wilson, P. J. M. M166  
Wilson, P. W. SU244  
Wilson, S. G. M262, SA263  
Wimalawansa, S. J. M131, M354  
Winalski, C. SA370  
Windahl, S. F085, SA085  
Windahl, S. H. 1181, SU179  
Windahl, S. Helena 1123  
Windle, J. J. F081, F476, F478, SA081, SA476, SA478, SU075  
Winer, K. 1105  
Winer, K. K. F217, SA217  
Wintermantel, T. M293  
Winters-Stone, K. M. SA271  
Winzenrieth, R. M308  
Wiren, K. SU192  
Wiren, K. M. SU193  
Wirth, A. M310  
Wise, L. SU465  
Wit, J. M. SA130  
Witter, F. R. F557, SA557  
Witzke, K. A. M002  
Wixted, J. J. M279  
Wojtowicz, A. M060  
Wolenski, M. J. F153, SA153  
Wolf, G. SU456  
Wolfe, P. M472, WG4, WG34

(Key: 1001-1300 = Oral, F = Friday Plenary poster, SA = Saturday poster, SU = Sunday poster, M = Monday poster, WG = Working Group Abstract)

## ASBMR 30th Annual Meeting

## Author Index

- Wolfinbarger, L. M406  
 Wolk, A. SA334  
 Wolny, M. M417  
 Wolos, J. A. M207  
 Woloszczuk, W. M134  
 Wong, A. M302  
 Wong, B. Y. L. M201  
 Wong, D. F275, SA172, SA275  
 Wong, I. 1195  
 Wong, J. B. 1242  
 Wong, M. M336, M337, SA395  
 Wong Pack, W. SA343, SU251, SU504  
 Woo, C. SU417  
 Woo, J. SA431  
 Woo, J. Tea M082  
 Woo, K. SA016  
 Woo, K. SA064, SU021  
 Woo, K. M. M050  
 Wood, D. SA549  
 Woodgett, J. 1121  
 Woodrow, J. P. SA194  
 Woods, A. SA535, SU258, SU425  
 Woodside, B. F339, M324, SA339, SA558, WG8  
 Working Group on Osteoporosis SU322  
 Worley, K. SU370  
 Wotton, D. SA018  
 Wouters, V. SA258  
 Wren, T. SU042  
 Wren, T. A. L. 1180  
 Wright, D. SU495  
 Wright, J. SU005  
 Wright, T. M. M474  
 Wronski, T. J. 1275, SA178, SA388  
 Wu, A. C. K. M460  
 Wu, F. C. SA457, SU335  
 Wu, G. 1068  
 Wu, H. M116  
 Wu, J. Y. 1254  
 Wu, L. M188  
 Wu, Q. 1047, M433, M464, SU489  
 Wu, R. SA019  
 Wu, X. 1014, 1082, 1273, F188, SA188  
 Wu, Y. SA102, SA183, SA184, SU190  
 Wutzi, A. M070  
 Wyman, A. SA362  
 Wynn, C. E. M209  
 Wynnkyj, C. A. M461  
 Wypij, D. SU488, WG22  
 Wysocki, N. M. SU364  
 Wysolmerski, J. J. F219, F228, M110, SA219, SA228  
 Wyzga, N. SU139  
  
**X**  
 Xi, J. M027, M077, M368, SU250, SU401  
 Xia, X. 1042  
 Xiang, J. SU489  
 Xiao, G. M079  
 Xiao, G. Guishan M022  
 Xiao, J. M022  
 Xiao, L. 1084  
 Xiao, P. SU154, SU155  
 Xiao, W. M237  
 Xiao, Z. F066, SA019, SA066  
 Xie, C. 1047, SA049  
 Xie, H. SA386  
 Xie, J. SU127  
 Xie, R. 1044, M041  
 Xie, Y. 1048, 1162  
 Xie, Z. 1253, SA522  
 Xing, L. 1009, 1113  
 Xing, W. 1190, 1194, M009  
 Xing, Y. 1051  
 Xiong, D. 1093, SU331  
 Xiong, W. SU127  
 Xu, B. SU110  
 Xu, H. M433, M464, SU489  
 Xu, J. M132, SA099, SA441, SU026  
 Xu, L. F542, SA542  
 Xu, S. SA344  
 Xu, W. SU259  
 Xu, X. F546, SA546  
 Xu, X. Hong M404  
 Xue, M. SA049  
 Xue, Y. 1184, SU143  
  
**Y**  
 Yabushita, N. SA332  
 Yaccoby, S. F288, M001, SA285, SA288  
 Yadav, M. C. M142, SA061, SA063  
 Yadav, V. K. M069, SA463  
 Yafai, M. M452, WG25  
 Yagerman, S. M146  
 Yaguchi, M. F494, SA494  
 Yakar, S. M440, SA183, SA184, SU190  
 Yamada, K. SU098  
 Yamada, Y. 1079  
 Yamaguchi, A. SA108, SU117  
 Yamaguchi, D. T. SA170, SU038  
 Yamaguchi, T. M098, SA230, SU437  
 Yamakoshi, K. SA525  
 Yamamoto, H. SA201, SU443  
 Yamamoto, M. M098  
 Yamamoto, S. SA499, SU285, SU301  
 Yamamoto, T. M307  
 Yamamoto, Y. SA105  
 Yamanaka, M. M421  
 Yamanaka, Y. SU286  
 Yamasaki, N. F112, SA112  
 Yamashiro, T. M153  
 Yamashita, T. SA419  
 Yamato, H. SU439  
 Yamauchi, F. SU438, SU440  
 Yamauchi, J. SU307  
 Yamauchi, M. M006, M098, M144, SA230, SA470, SU208  
 Yamaura, T. SU285, SU301  
 Yamazaki, M. SU172  
 Yamoah, K. 1117  
 Yan, H. M404, SU239, SU331  
 Yan, S. M132, SA441  
 Yan, X. M031  
 Yan-Clasen, W. SA445  
 Yanagi, H. SA332  
 Yancopoulos, G. D. SU143  
 Yang, C. 1014  
 Yang, D. F215, SA215  
 Yang, G. SA199, SU087  
 Yang, J. M086, M318, SA046  
 Yang, J. Yeon SA043  
 Yang, J. Yun F391, SA391  
 Yang, K. SU416  
 Yang, M. SA235  
 Yang, Q. SU025  
 Yang, S. 1148, F014, SA014  
 Yang, T. M055, M126, SU331  
 Yang, T. Lin M404, SA267  
 Yang, W. 1114, M103  
 Yang, W. Dong SA035  
 Yang, X. SU045  
 Yang, X. F. M334  
 Yang, X. Fang F213, SA213, SU207  
 Yang, Y. 1229  
 Yano, F. 1013, 1228, M082  
 Yano, S. M098, SA230, SU437  
 Yao, F. SA549  
 Yao, M. M153  
 Yao, W. 1100, F249, M107, SA249  
 Yao, X. M337  
 Yao, Z. 1009  
 Yaroslavkiy, B. B. SA236  
 Yaroslavskiy, B. B. 1125  
 Yarramaneni, J. 1021  
 Yasuda, H. F017, SA017, SU082  
 Yasui, N. M410, SA095, SU001  
 Yasui, T. 1217  
 Yasuyo, A. SU350  
 Yaszemski, M. SU231  
 Yaszemski, M. J. 1258, SA143, SU240  
 Yata, K. SA294, SU242  
 Yatani, H. M035  
 Yates, III, J. SA036  
 Yawaka, Y. SA021  
 Yazdanpanah, N. SU317  
 Yee, J. A. F032, SA032, SA459  
 Yeh, J. M217, M218  
 Yeh, J. K. M338, SA570, SU385, SU501, SU502  
 Yeh, S. M445  
 Yeo, H. 1145  
 Yerges, L. M267, SU284  
 Yerges, L. A. M266  
 Yerges, L. M. M268, M269  
 Yeung, D. K. W. SA309  
 Yi, B. 1174  
 Yi, S. M005  
 Yi, T. SA016  
 Yigit, S. SU194  
 Yim, C. M340  
 Yin, M. M448  
 Yin, M. T. SU455, SU458  
 Yingling, V. 1150, M501  
 Yingling, V. R. SA543  
 Yip, K. SA099  
 Ylipahkala, H. M284, M286, SA298  
 Yoda, M. SA022, SU102, SU103  
 Yoda, T. SA161  
 Yokota, H. M476  
 Yokoyama, A. SU031, SU170  
 Yokoyama, M. SA165  
 Yokoyama, S. 1230, M385  
 Yoneda, T. 1045, 1089, 1265, M080, SA095, SU049  
 Yoneshima, H. SA325, SA330  
 Yonezawa, T. M082  
 Yongping, C. M428  
 Yono, H. 1089  
 Yoo, J. SA036  
 Yoo, M. SU359  
 Yoo, W. SA053  
 Yoon, H. M005, M340  
 Yoon, S. SA431  
 Yoon, W. SA064, SU021  
 Yoshida, A. M167  
 Yoshida, C. A. 1151  
 Yoshida, K. SA257, SA498  
 Yoshida, N. M112, SA166, SU152  
 Yoshida, S. M410  
 Yoshida, T. M068, SA090  
 Yoshii, T. 1144  
 Yoshikata, R. F548, M492, SA548  
 Yoshikawa, H. F112, SA112, SA179  
 Yoshikawa, Y. M094, SA147  
 Yoshiki, F. M385  
 Yoshiko, Y. SA206  
 Yoshimatsu, M. M112, SA166, SU152  
 Yoshimoto, T. SU081  
 Yoshimura, N. SU334  
 Yoshioka, K. SA179  
 Yoshizaki, T. SA419  
 Yoshizawa, T. F034, SA034  
 Yost, J. G. M265  
 Yotani, K. SA513  
 Youn, M. 1126, SU186  
 Young, C. S. 1137, F376, SA376  
 Young, L. SA199  
 Young, M. F038, SA001, SA038  
 Young, M. F. SU132  
 Young, M. L. M161  
 Youngner, J. M. 1102  
 Youssef, S. F246, SA246, WG13  
 Yu, J. M173, M237  
 Yu, S. 1162, M079  
 Yu, Y. F127, SA127  
 Yu-Yahiro, J. SA346, SA432, WG5  
 Yu-Yahiro, J. A. SU073  
 Yuan, B. 1051, 1053, 1162, SA165  
 Yuan, H. 1014  
 Yuan, K. SU234  
 Yuan, L. 1226  
 Yuki, A. SA513  
 Yumoto, K. M469, SA517  
 Yun, F. M201  
 Yun, H. 1024  
 Yun, S. M005  
 Yura, A. SA330  
 Yuvaraj, S. SU247  
 Yu-Yahiro, J. F345, SA345  
  
**Z**  
 Zabel, B. F118, F158, SA118, SA158  
 Zadorozny, E. D. 1125  
 Zahm, A. M. F058, SA058  
 Zaidi, A. SA136  
 Zaidi, M. SA199, SA236, SU087  
 Zainabadi, K. 1098, 1251  
 Zajac, A. SA084  
 Zajac, J. D. SA197, SA255  
 Zak, K. SA304  
 Zallone, A. SA199, SU094  
 Zalutskaya, A. A. SU124  
 Zaman, F. 1188  
 Zaman, G. SA526  
 Zamora, P. O. SA388  
 Zanchetta, J. R. 1171, 1286, M390  
 Zanduetta, C. F286, F291, SA286, SA291  
 Zanetti, N. SU185  
 Zang, Y. M194  
 Zannettino, A. C. W. SU074, SU079, SU080  
 Zanolli, S. 1111, F141, SA005, SA141  
 Zappoli Thyron, G. Donata SU050  
 Zavratinik, A. M257  
 Zayafoon, M. 1197  
 Zayed, N. M159, SA152, SU116  
 Zayzafoon, M. 1145, M242, SU234  
 Zdunek, K. M060  
 Zebaze, R. 1101  
 Zech, C. 1149  
 Zeck, S. M072  
 Zehnder, D. M200  
 Zelnier, I. M065  
 Zemel, B. 1105  
 Zeng, Q. SU196, SU377, WG11  
 Zeng, Q. Q. M207  
 Zeng, Y. SU051  
 Zeni, S. Noemí M288  
 Zeni, S. N. SA377  
 Zenke, Y. SU286  
 Zentner, A. SA110  
 Zerwekh, J. SA211  
 Zerwekh, J. E. SA511  
 Zgliczynski, W. SU436  
 Zhai, G. SA263  
 Zhang, D. 1203  
 Zhang, F. 1082, SA267  
 Zhang, H. F004, M032, M237, SA004  
 Zhang, H. W. 1050

(Key: 1001-1300 = Oral, F = Friday Plenary poster, SA = Saturday poster, SU = Sunday poster, M = Monday poster, WG = Working Group Abstract)



## Author Index

## ASBMR 30th Annual Meeting

Zhang, J.	1064, M079, SA138, SU058, SU110, SU230	Zongyu, M.	M032
Zhang, J. Hongyuan	SA472	Zorn, T. Maria T.	SA123
Zhang, K.	1086	Zou, W.	1010, 1120
Zhang, M.	1044	Zubko, G.	SA350
Zhang, P.	M476	Zunich, S. M.	SA284
Zhang, Q.	1219, M208	Zuscik, M.	1047
Zhang, R.	1162	Zuscik, M. J.	F186, SA186, SU133
Zhang, S.	SA019	Zustin, J.	1133, 1201
Zhang, X.	F174, F256, F563, M066, M079, M160, SA049, SA174, SA256, SA428, SA563, SU192, SU210	Zuvic, M.	SU141
Zhang, X. H.	SU277, SU280, SU481	Zylstra, C. R.	1001
Zhang, X. Henry	M312	Zysset, P. Kurt	SU474
Zhang, Y.	1048, F186, M267, M269, SA186, SU112		
Zhang, Y. E.	1113		
Zhang, Z.	1015, 1074, M237, SA160, SA313		
Zhang, Z. Xin	M404, SA267		
Zhao, H.	1046, 1220, SA077, SU097		
Zhao, J.	1046, 1075, 1214, 1215, M089, M303, SA441		
Zhao, L.	1093, 1113, F188, SA188, SA248, SU331		
Zhao, M.	1136		
Zhao, R.	F461, SA461, SU032, SU033, SU160		
Zhao, X.	M318, SA124, SA248		
Zhao, Y.	M022, SA106		
Zhen, Y. Y.	SU253		
Zheng, M.	SA099, SA549		
Zheng, T. S.	M046		
Zheng, Y.	1267		
Zhong, M.	SA113		
Zhong, P.	SA313		
Zhong, Q.	SU010		
Zhou, G.	M055, SA115		
Zhou, H.	1036, 1146, 1169, 1224, 1267, F217, F233, F476, F478, F485, M310, SA217, SA233, SA234, SA476, SA478, SA485		
Zhou, J.	1225		
Zhou, L.	M132, SA441, SU127		
Zhou, Q.	M404, M433, M449, M464, SA267, SU285, SU301, SU489		
Zhou, S.	SA048, SA237, SU138, SU400		
Zhou, W.	M325, SU292		
Zhou, X.	1074, M187		
Zhou, Y.	1092, M127, M249, M254, SA251		
Zhou, Z.	SU127		
Zhu, E.	SU121		
Zhu, G.	SU235		
Zhu, J.	SA229		
Zhu, K.	F373, SA320, SA373		
Zhu, L.	SA199, SU087		
Zhu, M.	1044, 1047, 1116		
Zhu, S.	SU121		
Zhu, T.	1044		
Zhu, W.	F004, SA004		
Zhuang, J.	SU230		
Ziller, V.	M384, WG14		
Zillikens, C.	1091, SU317		
Zillikens, M. C.	SU188		
Zimmer, R.	M075		
Zimmerman, S.	M397		
Zimmermann, S.	M384, WG14		
Zirngibl, R. A.	1218		
Zivkovic, S.	SU323		
Zmierzak, H.	SU302, SU477		
Zmuda, J.	M267, SU284		
Zmuda, J. M.	1093, F367, M254, M266, M268, M269, SA268, SA328, SA367, SU183, SU299, SU300		
Zonefrati, R.	SU050		

(Key: 1001-1300 = Oral, F = Friday Plenary poster, SA = Saturday poster, SU = Sunday poster, M = Monday poster, WG = Working Group Abstract)

